CHEM 210D: MODERN APPLICATIONS OF CHEMISTRY



LibreTexts™

CHEM 210D: Modern Applications of Chemistry

This text is disseminated via the Open Education Resource (OER) LibreTexts Project (https://LibreTexts.org) and like the thousands of other texts available within this powerful platform, it is freely available for reading, printing, and "consuming."

The LibreTexts mission is to bring together students, faculty, and scholars in a collaborative effort to provide an accessible, and comprehensive platform that empowers our community to develop, curate, adapt, and adopt openly licensed resources and technologies; through these efforts we can reduce the financial burden born from traditional educational resource costs, ensuring education is more accessible for students and communities worldwide.

Most, but not all, pages in the library have licenses that may allow individuals to make changes, save, and print this book. Carefully consult the applicable license(s) before pursuing such effects. Instructors can adopt existing LibreTexts texts or Remix them to quickly build course-specific resources to meet the needs of their students. Unlike traditional textbooks, LibreTexts' web based origins allow powerful integration of advanced features and new technologies to support learning.



LibreTexts is the adaptable, user-friendly non-profit open education resource platform that educators trust for creating, customizing, and sharing accessible, interactive textbooks, adaptive homework, and ancillary materials. We collaborate with individuals and organizations to champion open education initiatives, support institutional publishing programs, drive curriculum development projects, and more.

The LibreTexts libraries are Powered by NICE CXone Expert and was supported by the Department of Education Open Textbook Pilot Project, the California Education Learning Lab, the UC Davis Office of the Provost, the UC Davis Library, the California State University Affordable Learning Solutions Program, and Merlot. This material is based upon work supported by the National Science Foundation under Grant No. 1246120, 1525057, and 1413739.

Any opinions, findings, and conclusions or recommendations expressed in this material are those of the author(s) and do not necessarily reflect the views of the National Science Foundation nor the US Department of Education.

Have questions or comments? For information about adoptions or adaptions contact info@LibreTexts.org or visit our main website at https://LibreTexts.org.

This text was compiled on 01/11/2026

TABLE OF CONTENTS

Licensing

1: AGENDA

2: Core Learning Goals

- 2.1: 1. MAT- States of Matter, Interactions, Bonding, and Energy
  - Magic Day of Chemistry
- 2.2: 2. SOL- Solutions
- 2.3: 3. AB1- Equilibrium Acids and Bases
- 2.4: 4. AB2- Quantitative Properties of Acid/Base Systems
- 2.5: 5. ECHEM- Electrochemistry and RedOx Reactions
- 2.6: 6. TMC- Transition Metals and their Complexes
- 2.7: 7. APP- Applications in Modern Chemistry

Textbook- Modern Applications of Chemistry

- Licensing
- 1: Primer
  - 1.1: The Structure of Atoms
    - 1.1.1: Prelude to Atomic Structure
    - 1.1.2: Groups of Related Elements
    - 1.1.3: The Periodic Table
    - 1.1.4: Valence
    - 1.1.5: Exceptions to the Periodic Law
    - 1.1.6: Implications of Periodicity for Atomic Theory
    - 1.1.7: Radiation
    - 1.1.8: The Electron
    - 1.1.9: The Nucleus
  - 1.2: Chemical Bonding - Electron Pairs and Octets
    - 1.2.1: Prelude to Chemical Bonding
    - 1.2.2: Ionic Bonding
    - 1.2.3: Energy and the Formation of Ions
    - 1.2.4: The Ionic Crystal Lattice
    - 1.2.5: Ions and Noble-Gas Electron Configurations
    - 1.2.6: Ionization Energies
    - 1.2.7: Ionization of Transition and Inner Transition Elements
    - 1.2.8: Electron Affinities
    - 1.2.9: Binary Ionic Compounds and Their Properties
    - 1.2.10: The Octet Rule
    - 1.2.11: Physical Properties
      - 1.2.11.1: Lecture Demonstrations
    - 1.2.12: Chemical Properties
    - 1.2.13: The Covalent Bond
    - 1.2.14: Covalent Molecules and the Octet Rule
    - 1.2.15: Writing Lewis Structures for Molecules

- 1.2.15: Writing Lewis Structures for Molecules
  - 1.2.15.1: An Excess of Bonds
  - 1.2.15.2: Deciding on a Skeleton Structure
  - 1.2.15.3: Multiple Bonds
- 1.2.16: Examples of Lewis Structures
- 1.2.17: Polyatomic Ions
- 1.2.18: Ionic Compounds Containing Polyatomic Ions
- 1.2.19: Atomic Sizes
- 1.2.20: Ionic Sizes
- 1.2.21: Periodic Variation of IE and EA
  - 1.2.21.1: Lecture Demonstrations
- 1.3: Further Aspects of Covalent Bonding
  - 1.3.1: Prelude to Covalent Bonding
  - 1.3.2: Exceptions to the Octet Rule
    - 1.3.2.1: Biology- Biologically Active Exceptions to the Octet Rule
  - 1.3.3: The Shapes of Molecules
    - 1.3.3.1: Lecture Demonstrations
  - 1.3.4: Molecules with Lone Pairs
    - 1.3.4.1: Lecture Demonstrations
  - 1.3.5: Multiple Bonds and Molecular Shapes
  - 1.3.6: Hybrid Orbitals
  - 1.3.7: Orbital Descriptions of Multiple Bonds
  - 1.3.8: Sigma and Pi Bonds
  - 1.3.9: Polarizability
    - 1.3.9.1: Biology - Polarizability of Biologically Significant Atoms
  - 1.3.10: Polar Covalent Bonds
    - 1.3.10.1: Biology- Nonpolar Iodine and Polar Hydrogen Iodide
    - 1.3.10.2: Lecture Demonstrations
  - 1.3.11: Electronegativity
  - 1.3.12: Polarity in Polyatomic Molecules
    - 1.3.12.1: Biology- The Hydrophobic Effect and Properties of Small Polyatomic Molecules
    - 1.3.12.2: Lecture Demonstrations
  - 1.3.13: Formal Charge and Oxidation Numbers
  - 1.3.14: Resonance
- 1.4: Properties of Organic Compounds
  - 1.4.1: Prelude to Organic Compounds
  - 1.4.2: Covalent Compounds and Intermolecular Forces
  - 1.4.3: Dipole Forces
  - 1.4.4: London Forces
    - 1.4.4.1: Chapter 8 page 3.jpg
    - 1.4.4.2: Atomic Radii
    - 1.4.4.3: Atomic sizes on periodic table.jpg
    - 1.4.4.4: Ionization Energies
      - 1.4.4.4.1: IonizationEnergyAtomicWeight.PNG
    - 1.4.4.5: Ionization Energies and Electron Affinities
      - 1.4.4.5.1: Electron Affinities
        - 1.4.4.5.1.1: Ionization Energies and Electron Affinities.jpg

- 1.4.4.6: Polarizability on London Forces.jpg
- 1.4.5: Hydrogen Bonding- Water
  - 1.4.5.1: Atomic Radii and Ionic Radii
  - 1.4.5.2: H-Bonding Between 2 HF Molecules.jpg
  - 1.4.5.3: Nonmetal hydride bp.jpg
- 1.4.6: Ice and Water
  - 1.4.6.1: Ice; a hexagonal crystal.jpg
  - 1.4.6.2: Boiling Points of Hydrides
- 1.4.7: Macromolecular Substances
- 1.4.8: Diamond and Graphite
- 1.4.9: Silicon Dioxide
- 1.4.10: Synthetic Macromolecules- Some Applied Organic Chemistry
- 1.4.11: Addition Polymers
- 1.4.12: Condensation Polymers
- 1.4.13: Cross-Linking
- 1.5: Acid and Base Naming
  - 1.5.1: Polyatomic Ions
  - 1.5.2: Naming Acids
  - 1.5.3: Names and Formulas of Bases
- 2: Nuclear Chemistry
  - 2.1: Components of the Nucleus
  - 2.2: The Nuclear Atom
  - 2.3: Atomic Structure and Isotopes
  - 2.4: Isotopes
  - 2.5: Transmutation and Radioactivity
  - 2.6: Average Atomic Weights
  - 2.7: Measurement of Atomic Weights
  - 2.8: Nuclear Reactions
  - 2.9: Nuclear Radiation
  - 2.10: Rates of Radioactive Decay
  - 2.11: Stability of the Atomic Nucleus
  - 2.12: The Origin of the Elements
  - 2.13: Transmutation of the Elements
  - 2.14: Nuclear Fission
  - 2.15: Nuclear Fusion
  - 2.16: Nuclear Chemistry (Exercises)
- 3: Physical Properties of Gases
  - 3.1: Properties of Gases
  - 3.2: Gas Pressure
  - 3.3: Relationships among Pressure, Temperature, Volume, and Amount
  - 3.4: The Ideal Gas Law
  - 3.5: Gas Volumes and Stoichiometry
  - 3.6: Kinetic Molecular Theory of Gases
  - 3.7: Connecting Gas Properties to Kinetic Molecular Theory
  - 3.8: Chapter Problems
- 4: Intermolecular Forces
  - 4.1: Intermolecular Forces
  - 4.2: Properties of Liquids

- 4.3: Intermolecular Forces and the Solution Process
- 5: Solids
  - 5.1: Prelude to Liquids and Solids
  - 5.2: Carbon and Silicon- Network Atomic Solids
  - 5.3: The Solid State of Matter
  - 5.4: Lattice Structures in Crystalline Solids
  - 5.5: Bonding in Metals and Semiconductors
  - 5.6: Liquids and Solids (Exercises)
- 6: Phases and Phase Transitions
  - 6.1: Prelude to Liquids and Solids
  - 6.2: Intermolecular Forces Review
  - 6.3: Properties of Liquids
  - 6.4: Phase Transitions- Overview
  - 6.5: Phase Transitions
  - 6.6: Vaporization and Vapor Pressure
  - 6.7: Sublimation and Fusion
  - 6.8: Heating Curve for Water
  - 6.9: Phase Diagrams
  - 6.10: Water - An Extraordinary Substance
- 7: Solutions and their Physical Properties
  - 7.1: Types of Solutions- Some Terminology
  - 7.2: Mixtures of Gases
  - 7.3: Solution Concentration
  - 7.4: Intermolecular Forces and the Solution Process
  - 7.5: Solution Formation and Equilibrium
  - 7.6: Solubilities of Gases
  - 7.7: Vapor Pressures of Solutions
  - 7.8: Osmotic Pressure
  - 7.9: Freezing-Point Depression and Boiling-Point Elevation of Nonelectrolyte Solutions
  - 7.10: Solutions of Electrolytes
  - 7.11: Colloidal Mixtures
  - 7.12: Solubility and Complex-Ion Equilibria
    - 7.12.1: Solubility Product Constant, Ksp
    - 7.12.2: Relationship Between Solubility and Ksp
    - 7.12.3: Common-Ion Effect in Solubility Equilibria
    - 7.12.4: Limitations of the Ksp Concept
    - 7.12.5: Criteria for Precipitation and its Completeness
    - 7.12.6: Fractional Precipitation
    - 7.12.7: Solubility and pH
    - 7.12.8: Equilibria Involving Complex Ions
    - 7.12.9: Qualitative Cation Analysis
- 8: Acids and Bases
  - 8.1: Acids and Bases at Equilibrium
    - 8.1.1: Arrhenius Theory- A Brief Review
    - 8.1.2: Brønsted-Lowry Theory of Acids and Bases
    - 8.1.3: Self-Ionization of Water and the pH Scale
    - 8.1.4: Introduction to Strong Acids and Bases
    - 8.1.5: Strong Acids and Strong Bases

- 8.1.6: Weak Acids and Weak Bases
- 8.1.7: Conjugate Acid-Base Pairs and pH
- 8.1.8: Polyprotic Acids
- 8.1.9: Ions as Acids and Bases
- 8.1.10: Molecular Structure and Acid-Base Behavior
- 8.1.11: Lewis Acids and Bases
- 8.1.12: Common-Ion Effect in Acid–Base Equilibria
- 8.2: Additional Aspects of Acid-Base Equilibria
  - 8.2.1: Buffer Solutions
  - 8.2.2: Acid–Base Indicators
  - 8.2.3: Neutralization Reactions and Titration Curves
  - 8.2.4: Solutions of Salts of Polyprotic Acids
  - 8.2.5: Acid–Base Equilibrium Calculations- A Summary
  - 8.2.6: Exercises on Acids and Bases II
  - 8.2.7: E3. Solubility Constants for Compounds at 25°C Data Table
  - 8.2.8: pH Calculations for Acid–Base Titrations
- 9: Electrochemistry
  - 9.1: Oxidation-Reduction Reactions
  - 9.2: Balancing Redox Reactions
  - 9.3: Galvanic Cells
  - 9.4: Standard Electrode Potentials
  - 9.5: Strengths of Oxidants and Reductants
  - 9.6: E, ΔG, and K (The Big Triangle of Chemistry)
  - 9.7: Cell Potential as a Function of Concentrations
  - 9.8: Batteries- Producing Electricity Through Chemical Reactions
  - 9.9: Corrosion- Unwanted Voltaic Cells
  - 9.10: Electrolysis- Causing Nonspontaneous Reactions to Occur
- 10: Coordination Chemistry
  - 10.1: Werner’s Theory of Coordination Compounds
  - 10.2: Ligands
  - 10.3: Nomenclature
  - 10.4: Isomerism
  - 10.5: Optical Isomerism in Metal Complexes
  - 10.6: Stability Aspects of Complex-Ion Equilibria
  - 10.7: Chelation
  - 10.8: Bonding in Octahedral Complex Ions- Crystal Field Theory
  - 10.9: Bonding in Non-Octahedral Complex Ions- Crystal Field Theory
  - 10.10: High Spin and Low Spin Complexes
  - 10.11: Magnetic Behavior of Atoms, Molecules, and Materials
  - 10.12: Magnetic Behavior of Complex Ions
  - 10.13: Optical Properties of Coordination Compounds (Color)
- 11: Applications in Polymer and Biological Chemistry
  - 11.1: Bioinorganic Chemistry
    - 11.1.1: A Molecular Depot- Human Serum Albumin Carries Essential Cu and Zn in Serum
    - 11.1.2: Iron acquisition in bacteria- Siderophores
    - 11.1.3: Fe Wars- Lactoferrin
    - 11.1.4: Iron Storage- Ferritin
    - 11.1.5: Antioxidant- Cu/Zn Superoxide dismutase (SOD1)

- 11.1.6: Keep Cu Safe- Intracellular Copper Chaperones
- 11.1.7: Cytochrome C
- 11.1.8: Cytochrome Oxidase
- 11.1.9: Potassium Channels
- 11.1.10: Chemotherapy- Pt anticancer agents

- 11.2: Bioinorganic Chemistry (Bertini et al.)
  - Licensing
  - Preface
  - 11.2.1: Transition-Metal Storage, Transport, and Biomineralization
    - 11.2.1.1: Biological Significance of Iron, Zinc, Copper, Molybdenum, Cobalt, Chromium, Vanadium, and Nickel
    - 11.2.1.2: Biological Systems of Metal Storage
    - 11.2.1.3: Chemical Properties Relative to Storage and Transport
    - 11.2.1.4: Iron Biomineralization
    - 11.2.1.5: Transport of Iron
    - 11.2.1.6: Transport of Zinc, Copper, Vanadium, Chromium, Molybdenum, and Cobalt
  - 11.2.2: The Reaction Pathways of Zinc Enzymes and Related Biological Catalysts
    - 11.2.2.1: About Carbonic Anhydrase
    - 11.2.2.2: Acid-base Equilibria
    - 11.2.2.3: Catalytic Mechanism
    - 11.2.2.4: Coordinated Water and NMR
    - 11.2.2.5: Coordination Geometries
    - 11.2.2.6: Ester Hydrolysis and Phosphoryl Transfer
    - 11.2.2.7: Group Transfer and Vitamin B-12
    - 11.2.2.8: Metal Substitution
    - 11.2.2.9: Model Chemistry
    - 11.2.2.10: Nucleophilic Addition of \(OH^{-}\) and \(H^{-}\)
    - 11.2.2.11: Peptide Hydrolysis
    - 11.2.2.12: pH Dependence of Inhibitor Binding
    - 11.2.2.13: Selecting Zinc
    - 11.2.2.14: Steady-State and Equilibrium Kinetics of Carbonic Anhydrase-Catalyzed \(CO_{2}/HCO_{3}^{-}\) Interconversion
    - 11.2.2.15: Strategies for the Investigation of Zinc Enzymes
    - 11.2.2.16: The Natural Catalysts
    - 11.2.2.17: What Do We Learn?
  - 11.2.3: Calcium in Biological Systems
    - 11.2.3.1: Ca^{2+}-binding Proteins in Microorganisms- The Search for a Prokaryotic Calmodulin
    - 11.2.3.2: Basic Facts About Calcium- Its Compounds and Reactions
    - 11.2.3.3: Calcium in Mineralized Tissues
    - 11.2.3.4: Calmodulin
    - 11.2.3.5: Extracellular Calcium Ion-binding Proteins
    - 11.2.3.6: Inositol Trisphosphate and the Calcium Ion Messenger System
    - 11.2.3.7: Intracellular Calcium Ion Transport
    - 11.2.3.8: Measurements of "Free" Calcium Concentrations
    - 11.2.3.9: Measurements of Total Calcium Concentrations
    - 11.2.3.10: Mitochondrial Calcium Ion Transport
    - 11.2.3.11: Molecular Aspects of Calcium Ion-Regulated Intracellular Processes (Part 1)
    - 11.2.3.12: Molecular Aspects of Calcium Ion-regulated Intracellular Processes (Part 2)
    - 11.2.3.13: Paravalbumin and Calbindins \(D_{9K}\) and \(D_{28K}\)

- 11.2.3.14: The Transport and Regulation of Ca^{2+} Ions in Higher Organisms
- 11.2.3.15: Troponin C
- 11.2.4: Biological and Synthetic Dioxygen Carriers
  - 11.2.4.1: Biological Dioxygen Transport Systems
  - 11.2.4.2: Biological Oxygen Carriers
  - 11.2.4.3: Detailed Structures of Hemoglobins and Model Systems
  - 11.2.4.4: Dioxygen Carriers and Bioinorganic Chemistry
  - 11.2.4.5: General Aspects of the Chemistry of Cobalt
  - 11.2.4.6: General Aspects of the Chemistry of Copper
  - 11.2.4.7: General Aspects of the Chemistry of Dioxygen
  - 11.2.4.8: General Aspects of the Chemistry of Iron
  - 11.2.4.9: General Structural Features that Modulate Ligand Activity
  - 11.2.4.10: Hazards of Life with Dioxygen
  - 11.2.4.11: Nature of the Metal-Dioxygen Linkage in Biological Systems
  - 11.2.4.12: Other Ligands for Biological Oxygen Carriers
  - 11.2.4.13: Requirements for a Model System for Hemoglobin
  - 11.2.4.14: Requirements for Effective Oxygen Carriers
  - 11.2.4.15: Role of the Protein in Effecting Biological Oxygen Transport
  - 11.2.4.16: Selected Chemistry of Dioxygen, Iron, Copper, and Cobalt
  - 11.2.4.17: Stereochemical Changes Upon Ligation
  - 11.2.4.18: Structural Basis of Ligand Affinities of Oxygen Carriers
  - 11.2.4.19: Structures Relevant to Liganded Hemoglobins
  - 11.2.4.20: Thermodynamic Factors
  - 11.2.4.21: Ch. 4 References and Abbreviations
- 11.2.5: Dioxygen Reactions
  - 11.2.5.1: Catalase and Peroxidase
  - 11.2.5.2: Chemistry of Dioxygen
  - 11.2.5.3: Copper-zinc Superoxide Dismutase
  - 11.2.5.4: Cytochrome c Oxidase
  - 11.2.5.5: Dioxygen Toxicity
  - 11.2.5.6: Monooxygenases
  - 11.2.5.7: Oxygenases
- 11.2.6: Electron Transfer
  - 11.2.6.1: Biological Redox Components
  - 11.2.6.2: Coupling Electron Transfers and Substrate Activation
  - 11.2.6.3: Electron-transfer Rates
  - 11.2.6.4: Electron-Transfer Theory
  - 11.2.6.5: Energy Storage and Release
  - 11.2.6.6: Long-range Electron Transfer in Proteins (Part 1)
  - 11.2.6.7: Long-range Electron Transfer in Proteins (Part 2)
  - 11.2.6.8: Marcus Theory
- 11.2.7: Ferrodoxins, Hydrogenases, and Nitrogenases - Metal-Sulfide Proteins
  - 11.2.7.1: Iron-sulfur Proteins and Models
  - 11.2.7.2: Iron-sulfur Proteins and Models (Part 2)
  - 11.2.7.3: Iron-sulfur Proteins and Models (Part 3)
  - 11.2.7.4: Iron-sulfur Proteins and Models (Part 4)
  - 11.2.7.5: Multisite Redox Enzymes
  - 11.2.7.6: Multisite Redox Enzymes (Part 2)

- 11.2.7.7: Multisite Redox Enzymes (Part 3)
- 11.2.7.8: Multisite Redox Enzymes (Part 4)
- 11.2.7.9: Multisite Redox Enzymes (Part 5)
- 11.2.7.10: Multisite Redox Enzymes (Part 6)
- 11.2.7.11: Report on the Nitrogenase Crystal Structure\(\;^{378-381}\)
- 11.2.7.12: Rubredoxin- A Single-Fe Tetrathiolate Protein

11.2.8: Metal/Nucleic Acid Interactions

- 11.2.8.1: The Basics
- 11.2.8.2: The Basics (Part 2)
- 11.2.8.3: A Case Study- Tris(phenanthroline) Metal Complexes
- 11.2.8.4: Applications of Different Metal Complexes that Bind Nucleic Acids
- 11.2.8.5: Applications of Different Metal Complexes that Bind Nucleic Acids (Part 2)
- 11.2.8.6: Nature's Use of Metal/Nucleic-acid Interactions

11.2.9: Metals in Medicine

- 11.2.9.1: Metal Deficiency and Disease
- 11.2.9.2: Toxic Effects of Metals
- 11.2.9.3: Aspects of Platinum Binding to DNA
- 11.2.9.4: Survey of Metals Used for Diagnosis and Chemotherapy
- 11.2.9.5: Platinum Anticancer Drugs- A Case Study
- 11.2.9.6: Mapping the Major Adducts of cis- and trans-DDP on DNA; Sequence Specificity
- 11.2.9.7: Structure of Platinum-DNA Complexes
- 11.2.9.8: Site-specifically Platinated DNA \(\;^{154}\)
- 11.2.9.9: Bioinorganic Chemistry of Platinum Anticancer Drugs- How Might They Work?
- 11.2.9.10: Bioinorganic Chemistry of Platinum Anticancer Drugs; How Might They Work? (Part 2)
- 11.2.9.11: Design of New Inorganic Anticancer Drugs

Detailed Licensing

11.3: Cisplatin - The Invention of an Anticancer Drug

- 11.3.1: Cisplatin 1. Study of the Effect of Electric Fields on E. coli
- 11.3.2: Cisplatin 2. Control Experiments for the Effect of Electric Fields on E. coli
- 11.3.3: Cisplatin 3. Redox Chemistry
- 11.3.4: Cisplatin 4. Electrochemistry
- 11.3.5: Cisplatin 5. The Role of Platinum Electrodes
- 11.3.6: Cisplatin 6. Transition Metal Chemistry
- 11.3.7: Cisplatin 7. Bioinorganic Chemistry
- 11.3.8: Cisplatin 8. Discovery of Cisplatin
- 11.3.9: Cisplatin 9. The Discovery - One Scientist's Story
- 11.3.10: Cisplatin 10. Research as a Career
- 11.3.11: Cisplatin 11. Cisplatin as an Anticancer Drug
- 11.3.12: Cisplatin 12. Modes of Action of Cisplatin
- 11.3.13: Cisplatin 13. Further Studies/Recent Developments
- 11.3.14: Cisplatin 14. DNA
- 11.3.15: Cisplatin 15. FDA Drug Approval Process
- 11.3.16: Cisplatin 16. Profits from Cisplatin
- 11.3.17: Cisplatin 17. Drug Resistance
- 11.3.18: Cisplatin 18. Toxicity
- 11.3.19: Cisplatin 19. Cancer
- 11.3.20: Cisplatin 20. Other Treatments for Cancer

11.4: Polymeric Materials and Soft Condensed Matter

- 11.4.1: Polymerization Reactions for Synthetic Polymers
- 11.4.2: Natural Polymers
- 11.5: Polymer Chemistry (Schaller)
  - Licensing
  - 11.5.1: Monomers and Polymers
    - 11.5.1.1: Difunctional Carboxyloids
    - 11.5.1.2: Cyclic Carboxyloids
    - 11.5.1.3: Olefins
    - 11.5.1.4: Cyclic Olefins
    - 11.5.1.5: Coordination Polymers
    - 11.5.1.6: Supramolecular Assemblies
    - 11.5.1.7: Other Polymers
    - 11.5.1.8: Polymer Topology
    - 11.5.1.E: Solutions for Selected Problems
  - 11.5.2: Synthetic Methods in Polymer Chemistry
    - 11.5.2.1: Ziegler-Natta Polymerization
    - 11.5.2.2: Solutions to Selected Problems
    - 11.5.2.3: Step Growth and Chain Growth
    - 11.5.2.4: Cationic Polymerization
    - 11.5.2.5: Living Cationic Polymerization
    - 11.5.2.6: Anionic Polymerization
    - 11.5.2.7: Living Anionic Polymerization
    - 11.5.2.8: Ring-Opening Polymerization
    - 11.5.2.9: Radical Polymerization
    - 11.5.2.10: Living Radical Polymerization- RAFT
    - 11.5.2.11: Living Radical Polymerization- ATRP
  - 11.5.3: Kinetics and Thermodynamics of Polymerization
    - 11.5.3.1: Thermodynamics of Polymerization
    - 11.5.3.2: Kinetics of Step-Growth Polymerization
    - 11.5.3.3: Kinetics of Chain Polymerization
    - 11.5.3.4: Kinetics of Catalytic Polymerization
    - 11.5.3.5: Solutions to Selected Problems
  - 11.5.4: Polymer Properties
    - 11.5.4.1: Molecular Weight of Polymers
    - 11.5.4.2: Viscosity of Polymers
    - 11.5.4.3: Rheology
    - 11.5.4.4: Glass Transition
    - 11.5.4.5: Crystallinity in Polymers
    - 11.5.4.6: Microphase Separation
    - 11.5.4.7: Stress-Strain Relationships
    - 11.5.4.8: Storage and Loss Modulus
    - 11.5.4.9: Modulus, Temperature, Time
    - 11.5.4.10: Chapter Solutions
  - Detailed Licensing
- 11.6: Synthetic Polymers
  - 11.6.1: Introduction
  - 11.6.2: Chain-Growth Polymers—Addition Polymers

- 11.6.3: Anionic Polymerization of Epoxides
- 11.6.4: Ziegler–Natta Catalysts and Polymer Stereochemistry
- 11.6.5: Natural and Synthetic Rubbers
- 11.6.6: Step-Growth Polymers—Condensation Polymers
- 11.6.7: Polymer Structure and Properties
- 11.6.8: Green Polymer Synthesis
- 11.6.9: Polymer Recycling and Disposal
- 12: Reading
- Index
- Glossary
- Detailed Licensing

Index

Glossary

Detailed Licensing

Licensing

*A detailed breakdown of this resource's licensing can be found in **Back Matter/Detailed Licensing**.*

1: AGENDA

Duke University: Modern Applications of Chemistry
Prof. Justin M. Shorb

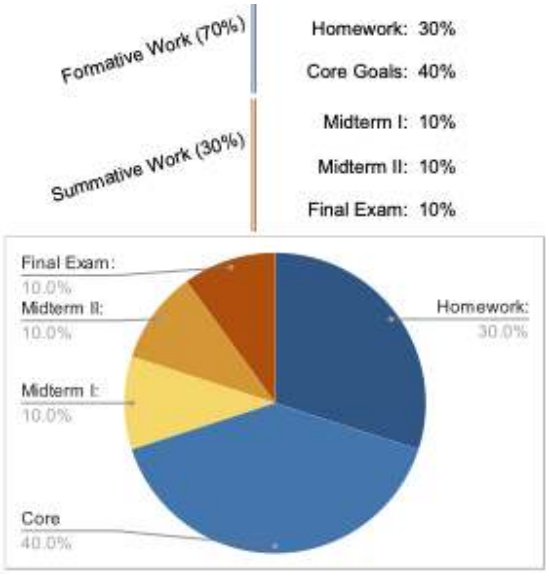
Template:HideTOC

Organization of the CHEM 210 Course

The title of this course "Modern Applications of Chemistry" embraces the fact that there are essential underlying principles that can be found in what seem to be radically complicated systems. Much of Modern Chemistry appears to be quite different from what you have seen in prior chemistry courses, but at the end of this course you should begin to see how even complicated systems can be interpreted through essentially simple concepts and models.

This course is assessed in two main ways: Formative and Summative assessments. Formative Assessments are meant to be a place where you receive detailed feedback to help you to improve and to master certain critical ideas - things we call "**Core Goals**" in this course. There are 7 Core Goals listed below.

Additionally, There will be **two midterms and one final exam** that will focus on approximately 1/3 of the material each. **It is important to note that the last third of the material is on applications of the prior 2/3 of the course in new situations, so it very much still will seem to be cumulative.** These summative assessments will evaluate your ability to demonstrate your ability on longer more complicated problems, as well as on basic Learning Objectives.



Formative Assessments for Demonstrating Skill on Core Goals:

Instead of a Homework or Quiz grade that gives points based on effort or ability, you will be given multiple tries to try to pass each of the Core Goals above. Your work will be graded on a rubric and be given either a mark of "M" for Meets Expectations or an "N" for Not yet. The schedule for these assessments is below:

Core Goal Attempt Date	First Attempt	Second Attempt	Third Attempt	Duration
Thur: 5/18/2023	(MAT)	—	—	30 min
Tue: 5/23/2023	MAT	—	—	20 min
Wed: 5/24/2023	SOL	MAT	—	30 min
Tue: 5/30/2023	AB1	SOL	—	30 min
Midterm I Thur: 6/1/2023	—	—	MAT / SOL	30 min
Tue: 6/6/2023	AB2	AB1	—	30 min
Wed: 6/7/2023	ECHEM	AB2	—	30 min
Tue: 6/13/2023	—	ECHEM	—	20 min
Midterm II Thur: 6/15/2023	—	—	AB1/AB2/ECHEM	45 min
Tue: 6/20/2023	TMC	—	—	20 min
Wed: 6/21/2023	APP	TMC	—	40 min
Final Exam Wed: 6/28/2023	—	APP	TMC	40 min

Note that only two attempts at the APP Core Goal attempts are given as these are cumulative applications of other materials. They are slightly longer than the others and time has been allocated for those. Note that the APP Core Goal is the 7th of the 7 goals, and is really intended to distinguish between an A- ability and an A ability in the course demonstrating an in-depth understanding of the applications of the other 6 Core Goals.

You only need to earn an "M" on a Core Goal ONCE. Once you have received a mark of "M" then you do not need to study for, nor take the subsequent attempts at that Core Goal!

Your grade on the Core Goals will be determined by the following Rubric:

- Earning an "M" on all 7 Core Goals: 100%
- 6 out of 7: 95%
- 5 out of 7: 80%
- 4 out of 7: 65%
- 3 out of 7: 50%
- 2 out of 7: 35%
- 1 out of 7: 20%
- 0 out of 7: 0%

Summative Assessments: Midterms and Final

The course has three summative assessments: Midterm I, Midterm II, and the Final Exam. Note that the Final Exam is the same duration as the standard exams (~1.5 hours), and just like the other exams, will have the time allotted at the end for Core Goal Assessments (recall that if you already met the Core Goal with an "M", then you will not need to stay to complete an additoinal attempt).

Midterm I: Matter and Interactions	Midterm II: Solutions and Electrochemistry	Final Exam: Applications of Modern Chemistry
1. Lecture 1: Matter of Scale 2. Lecture 2: Interactions & Energy 3. Lecture 3: Physical Properties of Solutions 4. Lecture 4: Chemical Properties of Solutions 5. Midterm I: Matter and Interactions (MAT/SOL)	1. Lecture 5: Equilibrium Acids and Bases 2. Lecture 6: Acids and Bases as Dynamic Solutions 3. Lecture 7: Harnessing RedOx Reactions 4. Lecture 8: Electrochemistry 5. Lecture 9: Magical Day of Chemistry 6. Midterm II: Acids/Bases and Electrochemistry (AB1/AB2/ECHEM)	1. Lecture 10: Properties of Transition Metals 2. Lecture 11: Transition Metal Complexes 3. Lecture 12: Polymers and Biological Molecules as Polymers 4. Lecture 13: Reactions of Biological Molecules 5. Final Exam: Applied Modern Chemistry (TMC/APP)

Supplemental Resources:

Table of Thermodynamic Properites that is a little longer than the LibreTexts one: https://www.chm.uri.edu/weuler/chm112/refmater/thermtable.html

Core Goal MAT: States of Matter, Interactions, Bonding, and Energy

- To gain a fundamental understanding of the composition of atoms with an emphasis on the atom's nucleus.
- To develop chemical literacy regarding isotopes, nuclear stability, radioactive decay, fission, fusion, and applications involving nuclear transformation.
- To develop chemical literacy regarding phases of matter including gases, liquids, and solids with an emphasis on:
    1. the gas phase and the origins and relative strengths of different contributions to intermolecular forces in the condensed phases,
    2. phase changes and phase diagrams,
    3. the properties of liquids and especially how they reflect intermolecular forces,
    4. the properties of solids, especially crystal structures and metallic conduction.
- To gain a fundamental understanding of the gaseous state of matter and the ideal and non-ideal behavior of gases.

Lectures	Readings	Assessments
1. Lecture 1: Matter of Scale 2. Lecture 2: Matter of Interaction	• List of Learning Objectives: MAT • Nuclear Chemistry • Physical Properties of Gases • Intermolecular Forces • Solids	1. MAT-1 2. MAT-2 3. MAT-3 4. Midterm I

Assumed Knowledge from the Primer

- The Structure of Atoms
- Chemical Bonding
- Further Aspects of Covalent Bonding
- Properties of Organic Molecules

Core Goal SOL: Solutions

- To develop chemical literacy regarding the properties of solutions, with an emphasis on
  1. the miscibility of liquids and the solubility of gases and solids in liquids,
  2. the vapor pressure of solutions,
  3. colligative properties, and
  4. how these properties reflect the underlying intermolecular forces and thermodynamics.
- To develop chemical literacy regarding chemical equilibrium as it applies to:
  1. solubility of ionic compounds and
  2. the formation of complex ions.

The SOL Core Goal Skill:

It is the expectation that you should be able to relate ΔG, ΔS, and ΔH for a system, determine whether it is spontaneous and whether it is for enthalpic or entropic driven reasons. Then: you should be able to use the relationship between K and $\Delta G°$ to relate this to an equilibrium process.

Finally: you should be able to determine equilibrium concentrations or pressures from a given K (or a calculated K).

Lectures	Readings	Assessments
• Lecture 3: Solutions I • Lecture 4: Solutions II	• List of Learning Objectives: SOL • Phases of Matter • Solutions	1. SOL-1 2. SOL-2 3. SOL-3 4. Midterm I

Assumed Knowledge from the Primer

- Temperature Conversion and Dimensional Analysis

Core Goal AB1: Equilibrium Acids and Bases

Demonstrate chemical literacy regarding chemical equilibrium with an emphasis on:

1. how chemical systems change as they move toward a state of equilibrium;
2. how the equilibrium condition itself can be characterized;
3. how a system at equilibrium will respond to changes in conditions;
4. the relationship chemical equilibrium to chemical kinetics and thermodynamics;
5. the relative reactivity of acids and bases;
6. quantitative calculations involving chemical equilibria & aqueous solutions of acids, bases, and salts.

The AB1 Core Goal Skill:

Given any concentration of any strong acid, strong base, weak acids, weak bases, or a salt with *either* an acidic cation or a basic anion, be able to determine the pH and any of the other requested quantities including pOH, K_a, K_b, pK_a, pK_b and/or percent ionization.

Lectures	Readings	Assessments
• Lecture 5: Acids and Bases	• List of Learning Objectives: AB1 • Acids and Bases at Equilibrium	1. AB1-1 2. AB1-2 3. AB1-3 4. Midterm II

Assumed Knowledge from the Primer

- Nomenclature of Acids
- Polyatomic Ions

Core Goal AB2: Quantitative Properties of Acid/Base Systems

To develop chemical literacy regarding mixtures of acids, bases, and buffers with an emphasis on the principles of chemical equilibrium as applied to (1) neutralization reactions, (2) buffered solutions, and (3) acid-base titrations.

The AB2 Core Goal Skill:

Given a known concentration and volume of a diprotic weak acid or base, and a known concentration of the opposite strong base/acid, be able to draw a titration curve including: (1) Initial pH, (2) first midpoint, (3) first equivalence point, (4) second midpoint, (5) second equivalence point, (6) strong titrant dilution (XS).

Lectures	Readings	Assessments
• Lecture 6: Acids and Bases • Lecture 9: Magical Day of Chemistry (part of)	• List of Learning Objectives: AB2 • Additional Aspects of Acid-Base Equilibria	1. AB2-1 2. AB2-2 3. AB2-3 4. Midterm II

Core Goal ECHEM: Electrochemistry and RedOx Chemistry

To develop chemical literacy regarding electron transfer reactions and their applications with an emphasis on (1) galvanic, electrolytic, and concentration cells, and (2) cell potentials and their relationship to chemical equilibrium and thermodynamics.

The ECHEM Core Goal Skill:

Be able to draw a galvanic or electrolytic cell, label it, and determine the spontaneous voltage (galvanic) or needed voltage (electrolytic) to get the cell to run.

Lectures	Readings	Assessments
• Lecture 7: Electrochemistry • Lecture 8: Electrochemistry • Lecture 9: Magical Day of Chemistry (part of)	• List of Learning Objectives: ECHEM • RedOx and Electrochemistry	1. ECHEM-1 2. ECHEM-2 3. ECHEM-3 4. Midterm II

Core Goals TMC: Transition Metals and their Complexes

To develop chemical literacy regarding transition metals and coordination chemistry with emphasis on: (1) formation of and bonding in coordination compounds and the characterization of their isomers; (2) electronic structure and properties (magnetic, optical) of transition metals and their ions; (3) the application of crystal field theory in interrelating molecular geometry, magnetic properties, and color for coordination compounds; (4) combining coordination chemistry concepts with previous knowledge, such as acid-base chemistry and equilibrium.

The TMC Core Goal Skill:

Given a pair of complexes, be able to predict each of their magnetism (diamagnetic or paramagnetic), high spin/low spin, which will be more blue-shifted or red-shifted in UV-VIS Spectroscopy, and all possible isomers of the structures.

Lectures	Readings	Assessments
• Lecture 10: Transition Metals • Lecture 11: Transition Metals	• List of Learning Objectives: TMC • Transition Metal Complexes	1. TMC-1 2. TMC-2 3. TMC-3 After Final Exam: 6/28/23 4. Final Exam: 6/28/23

Core Goals APP: Applications in Modern Chemistry

Unstable Nuclei: To gain a fundamental understanding of the composition of atoms with an emphasis on the atom's nucleus. • To develop chemical literacy regarding isotopes, nuclear stability, radioactive decay, fission, fusion, and applications involving nuclear transformation.

The APP Core Goal Skill:

Given a complex system (polymer, materials, or biochemical), be able to make a list of concepts that need to be considered in order to fully understand/describe the system by analysis via MAT/SOL/AB/ECHEM/TMC Core Goals. These Assessments will be open note and open internet.

Lectures	Readings	Assessments
• Lecture 12: Unstable Nuclei • Lecture 13: Biomolecules and Polymers	• List of Learning Objectives: APP • Add in Links to Pages	1. APP-1: 6/21/23 2. APP-2 After Final Exam: 6/28/23 3. Final Exam: 6/28/23

Lecture 1: 5/17/2023

Introduction to each other and general goals of the course were discussed. The full walk-through General Chemistry prior knowledge was done focusing on energy, scale, and the way matter and electromagnetic radiation interact with each other. The conceptual focus for this lecture was on: Scale Matters. Think about waves of light (electromagnetic radiation), waves of matter (electronic orbitals), and the Coulombic interaction of these as the basis for understanding interactions. Moving charges have electromagnetic properties. The nucleus has charged particles (protons) so changing the number of protons *greatly* changes the reactivity and properites of an atom. Electrons have a charge and a very much lighter mass, so they have larger space to occupy with their wavelengths (based on deBroglie's wavelength equation). A review of the components of the atom was highlighted and the chart of Nuclides to discuss stable vs unstable nuclei. Nuclear reactions were discussed and how to balance them. Finally, a discussion of Einstein's famous equation

$$E = mc^2 \tag{1.1}$$

was shown to be the source of immense amounts of energy from the Mass Deficit when nucleons combine to form atomic nuclei.

Readings	ADAPT Homework
• No expected Readings before class started. See MAT for list of material to review. • Nuclear Chemistry	• Lecture 1 Homework Due: Mon, 5/22/2023 11:55 PM

Final Exam: 6/28/2023 @ 2:00 p.m.-5:00 p.m in the DISCUSSION room

- TBD

This page titled 1: AGENDA is shared under a CC BY-SA 4.0 license and was authored, remixed, and/or curated by .

CHAPTER OVERVIEW

2: Core Learning Goals

Duke University: Modern Applications of Chemistry
Prof. Justin M. Shorb

Template:HideTOC

The course is made up of 7 Core Learning Goals ("Core Goals" or "CG"s). The pages below break these down into specific Learning Objectives.

Core Goals

2.1: 1. MAT- States of Matter, Interactions, Bonding, and Energy
Magic Day of Chemistry
2.2: 2. SOL- Solutions
2.3: 3. AB1- Equilibrium Acids and Bases
2.4: 4. AB2- Quantitative Properties of Acid/Base Systems
2.5: 5. ECHEM- Electrochemistry and RedOx Reactions
2.6: 6. TMC- Transition Metals and their Complexes
2.7: 7. APP- Applications in Modern Chemistry

2: Core Learning Goals is shared under a not declared license and was authored, remixed, and/or curated by LibreTexts.

2.1: 1. MAT- States of Matter, Interactions, Bonding, and Energy

Duke University: Modern Applications of Chemistry
Prof. Justin M. Shorb

Template:HideTOC

Summary:

- To gain a fundamental understanding of the composition of atoms with an emphasis on the atom's nucleus.
- To develop chemical literacy regarding isotopes, nuclear stability, radioactive decay, fission, fusion, and applications involving nuclear transformation.
- To develop chemical literacy regarding phases of matter including gases, liquids, and solids with an emphasis on:
    1. the gas phase and the origins and relative strengths of different contributions to intermolecular forces in the condensed phases,
    2. phase changes and phase diagrams,
    3. the properties of liquids and especially how they reflect intermolecular forces,
    4. the properties of solids, especially crystal structures and metallic conduction.
- To gain a fundamental understanding of the gaseous state of matter and the ideal and non-ideal behavior of gases.

Review of Key Concepts in Periodic Trends, Bonding, and Concentrations

- Determine whether the force of interaction is positive or negative for a pair of charged particles.
- Use Coulomb's Law to arrange a series of charged particle systems from the most attractive system to the most repulsive system.
- Describe the difference between the actual nuclear charge, Z, and the effective nuclear charge, Z_{eff}, experienced by a particular electron in an atom. Explain the reason for the periodic trend observed in the Z_{eff} for the outermost electron in the elements. Calculate Z_{eff} for the outermost electrons in the elements.
- Rank atoms and/or ions in order of increasing electronegativity, ionization energy, and/or atomic radius.
- Describe an ionic bond, which particular attention to the location of the electrons. Describe a covalent bond. Judge whether a covalent bond is polar or nonpolar.
- Determine if the bonding in a molecule would be best categorized as ionic, polar covalent, or nonpolar covalent. (This requires a synthesis of analyzing the position of the elements on the periodic table and applying knowledge of electronegativity trends, definitions of bond types, and recognition of polyatomic ions).
- Write chemical formulae from the names of ionic and molecular compounds and vice versa using chemical nomenclature conventions.
- Predict how to combine ions to make neutral ionic compounds by analyzing the charges and determining the number of each type of species needed.

Atomic Structure and Nuclear Reactions

- Describe atomic structures using the sub-atomic particles most relevant to chemists (protons, neutrons, and electrons), including charges, normal relative locations, and approximate masses of all species.
- Define the word isotope and provide examples of important radioactive isotopes in environmental chemistry, carbon-14 dating, and other applications.

- Calculate relative abundances of isotopes, exact isotopic masses, and/or average atomic mass from provided data.
- Write balanced chemical reaction equations for nuclear reactions.
- Define and provide symbols for some species that can be emitted in nuclear reactions: positron, neutron, alpha particle, beta particle, gamma ray.
- Define and be able to calculate binding energy and mass decrement or mass defect.
- Define fission and fusion and describe similarities and differences between these processes.
- Perform quantitative calculations for the half-life involved in radioactive decay.

Be sure you are logged in to your ADAPT Homework system so that you can see the assignment.



Login with LibreOne to view this question

NOTE: If you typically access ADAPT assignments through an LMS like Canvas, you should open this page there.

Login

Gases

- Explain Boyle's Law, Charles' Law and Avogadro's Law as empirical descriptions of the behavior of gases under certain conditions.
- Understand what is meant by an ideal gas, the assumptions made in describing an ideal gas, and the ideal gas equation as a combination of Boyle's Law, Charles' Law and Avogadro's Law.
- Adeptly convert between units of pressure if given the conversion factors.
- Relate pressure, volume, and/or temperature for a gas sample in a closed container using the ideal gas law.
- Define standard temperature and pressure (STP).
- Apply Dalton's Law of partial pressures to problems that involve mixtures of gases. (moved to SOL)
- Define mole fraction. Apply mole fraction in calculations. (moved to SOL)
- Synthesize previous knowledge of density, reaction stoichiometry, and gram-mole conversions with new knowledge about ideal gas behavior and partial pressures to construct solutions to quantitative problems that combine these concepts.
- Explain the key differences between real gases and the ideal gas.
- Explain the difference between effusion and diffusion, and apply knowledge to quantitative problems.
- Describe the differences between gases, liquids, and solids, both in terms of their macroscopic properties and molecular scale structure and dynamics.
- Describe the different kinds of intermolecular forces in terms of their origins and relative strengths.
- Describe the effect of intermolecular forces on a substance's properties like the boiling point or heat of vaporization. Rank substances by these properties.
- Recall and define 3 types of intermolecular forces. Apply this knowledge to various substances, and then combine this knowledge with that of phase changes to arrange those substances by increasing boiling point.
- For a given molecule or set of molecules, identify which intermolecular forces are most important.
- Apply the Clausius-Clapeyron equation to problems involving the vapor pressures of liquids. (moved to SOL)

Liquids, Solids, and Transitions

- Describe the differences between gases, liquids, and solids, both in terms of their macroscopic properties and molecular scale structure and dynamics.
- Describe the different kinds of intermolecular forces in terms of their origins and relative strengths.
- Describe the effect of intermolecular forces on physical properties like the boiling point or heat of vaporization. Rank substances by these properties.
- For a given molecule or set of molecules, identify which intermolecular forces are most important.
- Interpret heating curves and how they relate to phase diagrams. (moved to SOL)
- Use heat capacities and the enthalpies of vaporization and fusion to calculate the heat necessary to raise the temperature of a substance a given amount. (moved to SOL)
- Read and interpret a phase diagram, and identify special points on the diagram like the triple and critical points. (moved to SOL)
- Use a phase diagram to identify the sequence of phases that would be observed when changing temperature and/or pressure. (moved to SOL)
- Apply the Clausius-Clapeyron equation to problems involving the vapor pressures of liquids and solids. (moved to SOL)
- Explain how phase equilibria and phase transformations reflect the rate of transfer of molecules between different phases. (moved to SOL)
- Explain how intermolecular forces affect the microscopic and macroscopic properties of liquids, including boiling point, ΔH°_{vap}, surface tension, capillary action, and viscosity.
- Distinguish between the different classes of solids (atomic, molecular, ionic, metallic, and network), and describe the kinds of attractive forces and properties that are characteristic of each.
- Identify and describe the essential features of cubic unit cells (scc, bcc, and fcc) and closest packing structures (hcp and ccp).
- Relate densities and atomic radii using geometrical parameters for cubic unit cells.
- Identify the stoichiometry of crystalline compounds given information on the kinds of sites occupied by the atoms or ions in the unit cell.
- Rank the relative melting points of ionic solids using knowledge about atomic radius trends and the force of attraction between charge particles.

Matter and Energy

- Predict energy changes that result from the interaction of charged particles at different distances.
- Explain the essence of each of the following thermodynamic terms: enthalpy, entropy, and free energy.
- Calculate the amount of energy given off in a nuclear reaction.
- Understand and explain the difference between a law and a theory.
- Understand the Kinetic Molecular Theory (KMT) as a scientific theory and how it “explains” the behavior of ideal gases.
- Explain the meaning of root mean square speed for a collection of gas molecules.
- Understand what is meant by the temperature of a gas and its relationship to the average kinetic energy of a collection of gas molecules.
- Construct a Born Haber cycle to calculate lattice energies of ionic compounds. (moved to SOL)

2.1: 1. MAT- States of Matter, Interactions, Bonding, and Energy is shared under a not declared license and was authored, remixed, and/or curated by LibreTexts.

Magic Day of Chemistry

Core Learning Goals Learning Objectives Reviewed during Magic Day of Chemistry

MAT:

- Describe the effect of intermolecular forces on a substance's properties like the boiling point or heat of vaporization.
- Apply the Clausius-Clapeyron equation to problems involving the vapor pressures of liquids.
- Explain the essence of each of the following thermodynamic terms: enthalpy, entropy, and free energy.
- Understand what is meant by the temperature of a gas and its relationship to the average kinetic energy of a collection of gas molecules.

SOL

- Use heat capacities and the enthalpies of vaporization and fusion to calculate the heat necessary to raise the temperature of a substance a given amount.
- Construct a Born Haber cycle to calculate lattice energies of ionic compounds.
- Describe the important factors in the energetics of solution formation, both in terms of intermolecular interactions and thermodynamic variables.
- Relate the equilibrium constant to the rate constants for the forward and reverse reactions
- Define reaction quotient, *Q*, relate *Q* to the equilibrium constant, *K*, and explain how *Q* can be used to predict whether a system is at equilibrium, and if not, the direction a chemical system will move to establish equilibrium
- Given a chemical equation, write the expression for the reaction quotient and/or equilibrium constant
- Apply equilibrium concepts to calculations involving chemical reactions, concentrations, gas pressures, free energy, and other variables.
- Interpret the magnitudes of equilibrium constants regarding the extent of reaction that has occurred in the forward direction once equilibrium has been established
- Identify factors that can stress a system that is in a state of equilibrium and explain why these factors stress the equilibrium system
- Of the above factors, identify those that will alter the magnitude of the equilibrium constant, and how the constant will change as a result of the stress
- Apply Le Châtelier's principle to predict the direction a system, originally in a state of equilibrium, will shift when stressed by adding or removing reactants, adding or removing products, or heating or cooling the system

AB1/AB2

- Write the equation for the auto-ionization of water and relate to K_w, $[H^+]$, $[OH^-]$, pH, and pOH
- Describe changes in K_w, $[H^+]$, $[OH^-]$, pH, and pOH as a solution increases in acidity or in alkalinity
- Characterize acids and bases in terms of their strength using the following properties: K_a, pK_a, K_b, pK_b, $[H^+]$, pH, $[OH^-]$, pOH, % ionization in water, and strength relative to water
- Perform quantitative calculations related to water solutions of acids, bases, and salts (K_a, pK_a, K_b, pK_b, $[H^+]$, pH, $[OH^-]$, pOH, and % ionization) including polyprotic acids, mixtures of weak acids or bases, and very dilute solutions of acids or bases

ECHEM

- Calculate the standard cell potential from a table of reduction potentials and interpret the meaning of the sign of the calculated potential.
- Calculate the cell potential when the system is not at standard state conditions.
- Relate the cell potential when the system is in a state of equilibrium and calculate the value of the equilibrium constant from the standard state cell potential or vice-versa.
- Relate the cell potential to the change in free energy.
- Explain what concentration cells are and how they are able to produce electrical energy, and calculate the cell potential for a concentration cell.

Magic Day of Chemistry is shared under a not declared license and was authored, remixed, and/or curated by LibreTexts.

2.2: 2. SOL- Solutions

Duke University: *Modern Applications of Chemistry*
Prof. Justin M. Shorb

Template:HideTOC

Summary:

- To develop chemical literacy regarding the properties of solutions, with an emphasis on
  1. the miscibility of liquids and the solubility of gases and solids in liquids,
  2. the vapor pressure of solutions,
  3. colligative properties, and
  4. how these properties reflect the underlying intermolecular forces and thermodynamics.
- To develop chemical literacy regarding chemical equilibrium as it applies to:
  1. solubility of ionic compounds and
  2. the formation of complex ions.

SOL: Solutions

- Describe the important factors in the energetics of solution formation, both in terms of intermolecular interactions and thermodynamic variables
- Describe and apply the "like dissolves like" rule to solubility and miscibility
- Determine the concentration of a solution in different common units, including molarity, molality, mole fraction, and mass percent, and be able to convert between these units
- Explain the terms dilute, saturated, and supersaturated solutions, and describe how the concentration in each case relates to the solubility
- Describe the effects of temperature (T) and pressure (P) on the solubility of solids in liquids
- Describe the effects of T and P on the solubility of gases in liquids
- Use Henry’s law to relate the partial pressure of a gas to the amount of gas dissolved in solution
- Explain why the vapor pressure decreases when a non-volatile solute is dissolved in a volatile solvent
- Describe the vapor pressures of solution composed of two miscible, volatile liquids for the cases of ideal and non-ideal solutions
- Relate positive and negative deviations from ideal behavior in a general way to intermolecular forces and the enthalpy of mixing, and for specific pairs of liquids predict which behavior would be observed based on their molecular structure and intermolecular interactions
- Describe the origin of boiling point elevation and freezing point depression in terms of the vapor pressure lowering and the resulting shift in the phase diagram
- Calculate the boiling point elevation and freezing point depression for specific solutions, and be able to use them to determine the concentration and/or molecular mass of a solute
- Describe the phenomenon of osmotic pressure and its thermodynamic origin
- Calculate the osmotic pressure of a solution, and be able to use osmotic pressure to determine the concentration and/or molecular mass of a solute
- Describe why the values of colligative properties for electrolyte solutions differ from those for non-electrolyte solutions
- Use the van’t Hoff factor to predict the values of colligative properties for electrolyte solutions, and explain differences between the predicted and observed values in terms of ion pairing

2.2: 2. SOL- Solutions is shared under a not declared license and was authored, remixed, and/or curated by LibreTexts.

2.3: 3. AB1- Equilibrium Acids and Bases

Duke University: *Modern Applications of Chemistry*
Prof. Justin M. Shorb

Template:HideTOC

Summary of AB1 and AB2:

Acid and base chemistry has so many applications and so many essential properties throughout chemistry that it is broken down into two Core Goals:

AB1: Equilibrium Acids and Bases - focused on the qualitative nature of acid/base chemistry and the equilibrium between them.
AB2: Quantitative understanding of the various properties of complex acid/base systems.

AB1: Equilibrium Acids and Bases

Demonstrate chemical literacy regarding chemical equilibrium with an emphasis on:

1. how chemical systems change as they move toward a state of equilibrium;
2. how the equilibrium condition itself can be characterized;
3. how a system at equilibrium will respond to changes in conditions;
4. the relationship chemical equilibrium to chemical kinetics and thermodynamics;
5. the relative reactivity of acids and bases;
6. quantitative calculations involving chemical equilibria & aqueous solutions of acids, bases, and salts.

- Relate the equilibrium constant to the rate constants for the forward and reverse reactions (moved to SOL)
- Define reaction quotient, *Q*, relate *Q* to the equilibrium constant, *K*, and explain how *Q* can be used to predict whether a system is at equilibrium, and if not, the direction a chemical system will move to establish equilibrium (moved to SOL)
- Given a chemical equation, write the expression for the reaction quotient and/or equilibrium constant (moved to SOL)
- Apply equilibrium concepts to calculations involving chemical reactions, concentrations, gas pressures, free energy, and other variables. (moved to SOL)
- Interpret the magnitudes of equilibrium constants regarding the extent of reaction that has occurred in the forward direction once equilibrium has been established (moved to SOL)
- Identify factors that can stress a system that is in a state of equilibrium and explain why these factors stress the equilibrium system (moved to SOL)
- Of the above factors, identify those that will alter the magnitude of the equilibrium constant, and how the constant will change as a result of the stress (moved to SOL)
- Apply Le Châtelier's principle to predict the direction a system, originally in a state of equilibrium, will shift when stressed by adding or removing reactants, adding or removing products, or heating or cooling the system (moved to SOL)
- Identify common strong acids and bases by name and formula
- Characterize acids and bases according to the Arrhenius and Bronsted-Lowry definitions (model)
- Identify Bronsted-Lowry Acid-Base pairs (acid and conjugate base, base and conjugate acid) in a given reaction
- Write chemical reaction equations and equilibrium expressions for the ionization of an acid and for the ionization of a base in water
- Write the equation for the auto-ionization of water and relate to K_w, $[H^+]$, $[OH^-]$, pH, and pOH
- Describe changes in K_w, $[H^+]$, $[OH^-]$, pH, and pOH as a solution increases in acidity or in alkalinity
- Characterize acids and bases in terms of their strength using the following properties: K_a, pK_a, K_b, pK_b, $[H^+]$, pH, $[OH^-]$, pOH, % ionization in water, and strength relative to water

- Identify structural factors that influence the strength of a substance as an acid or as a base and use that information to predict/rank the relative strengths of another given group of substances
- Use K_a, pK_a, K_b, or pK_b to predict the extent of an acid-base reaction
- In terms of Le Châtelier's Principle, explain why the addition of a salt containing the conjugate base of a weak acid, or the conjugate acid of a weak base, suppresses the ionization of the acid or base respectively

---

2.3: 3. AB1- Equilibrium Acids and Bases is shared under a not declared license and was authored, remixed, and/or curated by LibreTexts.

2.4: 4. AB2- Quantitative Properties of Acid/Base Systems

Duke University: *Modern Applications of Chemistry*
Prof. Justin M. Shorb

Template:HideTOC

Summary of AB1 and AB2:

Acid and base chemistry has so many applications and so many essential properties throughout chemistry that it is broken down into two Core Goals:

AB1: Equilibrium Acids and Bases - focused on the qualitative nature of acid/base chemistry and the equilibrium between them.
AB2: Quantitative understanding of the various properties of complex acid/base systems.

AB2: Quantitative Properties of Acid/Base Systems

- Recall how to use K_a, pK_a, K_b, or pK_b, to predict the extent of an acid-base reaction and the value of the equilibrium constant for a reaction such as the mixture of a weak acid with a weak base.
- Perform quantitative calculations related to water solutions of acids, bases, and salts (K_a, pK_a, K_b, pK_b, $[H^+]$, pH, $[OH^-]$, pOH, and % ionization) including polyprotic acids, mixtures of weak acids or bases, and very dilute solutions of acids or bases
- In terms of Le Chatelier's Principle, explain why the addition of a salt containing the conjugate base of a weak acid, or the conjugate acid of a weak base, suppresses the ionization of the acid or base respectively.
- Distinguish between a solution that is buffered and one that is not in terms of composition and response to addition of small quantities of a strong acid or strong base
- Describe two distinctly different methods of preparing a buffered solution and the decisions one must make in preparing a buffered solution.
- Define and apply the following concepts to buffered solutions: buffer capacity, buffer range, acidic buffer, and basic buffer
- From a molecular perspective, use chemical reaction equations to describe what happens when small quantities of a strong acid or strong base is added to a buffered solution
- Calculate the initial pH of a buffered solution and the pH after addition of a strong acid or base
- Compare and contrast acid-base titrations:
    1. strong acid-strong base
    2. weak acid-strong base
    3. weak base-strong acid
    4. polyprotic acids with strong base
- Explain why the pH at the equivalence point in an acid-base titration is not always 7 even though the acid has been completely neutralized
- Interpret titration curves:
    1. initial pH
    2. equivalence point
    3. end-point
    4. buffered region and
    5. pKa values
- Calculate the pH at any point in an acid-base titration, especially:
    1. initially
    2. at 50% of the equivalence point (the midpoint)

3. near the midpoint point
4. at the equivalence point and
5. *much* beyond the equivalence point

- Explain the role of acid-base indicators in a titration, how they work, their limitations, and the factors that one must consider in the selection of an appropriate indicator for a titration

---

2.4: 4. AB2- Quantitative Properties of Acid/Base Systems is shared under a not declared license and was authored, remixed, and/or curated by LibreTexts.

2.5: 5. ECHEM- Electrochemistry and RedOx Reactions

Duke University: *Modern Applications of Chemistry*
Prof. Justin M. Shorb

Template:HideTOC

- Review concepts: Assign oxidation states to all atoms in a compound or element. Explain the difference between oxidation states and formal charges.
- Provide definitions for the following terms: oxidation state, oxidation, reduction, oxidizing agent, reducing agent, redox reaction, anode, and cathode.
- Identify the redox reactions from a given list of reactions and compare and contrast this type of reaction to other types of reactions, such as acid-base reactions, precipitations, etc.
- For a given redox reaction, decide which species is the reducing agent and explain why it is the reducing agent rather than some other species in the reaction.
- Write balanced redox reactions and determine the number of electrons transferred in a balanced chemical reaction.
- If any two given species are mixed, determine whether or not a spontaneous redox reaction will occur using tables of standard reduction potentials.
- Compare and contrast galvanic and electrolytic cells.
- For a given galvanic cell, identify (and define) the electrodes (anode and cathode), the positive (+) and negative (-) poles; the electrode where oxidation occurs, the electrode where reduction occurs, the "flow" of electrons through the external circuit, the flow of the ions through the solutions, and the salt bridge.
- If an electrode is changing size over the course of reaction, determine whether it is getting larger or smaller over time and explain why this is happening.
- Explain what the SHE half-cell is and how it is used to determine standard state reduction potentials for other species.
- Interpret cell diagrams to determine: 1) which species is the anode and which is the cathode and 2) the resulting voltage at that point in time.
- Calculate the standard cell potential from a table of reduction potentials and interpret the meaning of the sign of the calculated potential.
- Calculate the cell potential when the system is not at standard state conditions.
- Relate the cell potential when the system is in a state of equilibrium and calculate the value of the equilibrium constant from the standard state cell potential or vice-versa.
- Relate the cell potential to the change in free energy.
- Explain how a galvanic cell maintains overall electrical neutrality at all times.
- Explain what concentration cells are and how they are able to produce electrical energy, and calculate the cell potential for a concentration cell.
- Perform calculations involving Faradays' equation for electrolysis; i.e. finding needed electrical current, time current needs to operate, mass of substance electrolyzed, or volume of gaseous substance produced by electrolysis at a given T and P.
- Create a list of real world applications or processes that involve redox reactions.

2.5: 5. ECHEM- Electrochemistry and RedOx Reactions is shared under a not declared license and was authored, remixed, and/or curated by LibreTexts.

2.6: 6. TMC- Transition Metals and their Complexes

Duke University: *Modern Applications of Chemistry*
Prof. Justin M. Shorb

Template:HideTOC

To develop chemical literacy regarding transition metals and coordination chemistry with emphasis on:

1. formation of and bonding in coordination compounds and the characterization of their isomers;
2. electronic structure and properties (magnetic, optical) of transition metals and their ions;
3. the application of crystal field theory in interrelating molecular geometry, magnetic properties, and color for coordination compounds;
4. combining coordination chemistry concepts with previous knowledge, such as acid-base chemistry and equilibrium.

TMC: Transition Metals and their Complexes

- Write ground state electronic configurations for the first row of d-block transition metal atoms and their ions.
- Recall how to name ionic compounds that combine transition metal cations with monatomic anions (e.g. iron(III) oxide)
- Define coordination compound, complex ion, ligand, oxidation number, coordination number, Lewis acid-Lewis base interaction, & coordinate covalent
- bond
- Define Lewis acids and Lewis bases in the context of organometallic compounds
- Define and recognize ligands as being monodentate, bidentate, polydentate, or chelating
- Describe the geometries of complex ions with coordination numbers of 2, 4, and 6
- Define the different types of isomerism exhibited by coordination compounds, including structural isomerism, coordination isomerism, linkage isomerism, stereoisomerism, geometric and optical isomerism
- Define what is meant by trans and cis isomers, chiral compounds, and enantiomers
- Determine which types of isomerism are possible for a given coordination compound or complex ion
- Synthesize organometallic concepts with other course material, such as solution chemistry, concentrations, acid-base chemistry, and/or precipitation from aqueous solution, to solve quantitative problems
- Describe how the magnetic behavior of transition metals relates to their electronic structure and whether they are diamagnetic or paramagnetic
- Recognize from the demonstrations the wide variety of colors and magnetic properties exhibited by coordination compounds
- Describe the properties that are interrelated by theories of bonding in complex ions, including magnetic, optical, molecular geometry, and spectrochemical series
- Describe the crystal field model, the assumptions that underlie the model, the properties that can be predicted or interrelated by the model (along with the input required to make such predictions), and the limitations of the model
- Describe the splitting pattern of 3d orbital energies predicted for an octahedral complex ion by crystal field theory, and explain how these result from and correlate to the 3d atomic orbitals on the metal; identify the levels as eg or t2g and identify the energy splitting
- Use crystal field theory and the spectrochemical series to predict for an octahedral complex ion whether the splitting corresponds to a weak-field or strong-field case, to determine whether the electron configuration will be high-spin or low-spin, to determine the number of unpaired electrons and whether the complex will be paramagnetic or diamagnetic, and finally how all these parameters and properties related to the color of the ion and it’s absorption energy and wavelength
- Describe how these same principles of crystal field theory can be applied to other geometries, such as tetrahedral and square planar complexes

- Describe how the molecular orbital/ligand field models give rise to an alternate and more comprehensive picture of the geometry, bonding, stability, magnetic and optical properties of complex ions, and how molecular orbital energy diagrams for complex ions result in the same characteristic splitting pattern predicted by the crystal field model
- Describe how the absorption of light results in colored compounds, and relate the frequency and wavelength of the absorbed light to the absorption energy

---

2.6: 6. TMC- Transition Metals and their Complexes is shared under a not declared license and was authored, remixed, and/or curated by LibreTexts.

2.7: 7. APP- Applications in Modern Chemistry

Duke University: Modern Applications of Chemistry
Prof. Justin M. Shorb

Template:HideTOC

Polymers

- Define the following terms: repeat unit, molecular weight distribution, homopolymer, copolymer, topology, morphology, crosslink, thermoplastic, thermoset.
- List some of the positive impacts of synthetic polymers on society.
- Name at least three synthetic plastics that can be recycled.
- Name at least three naturally occurring polymers.
- Describe the similarities and differences in the following: random copolymer, alternating copolymer, block copolymer
- Determine if a polymer is formed via a free radical or acid-base polymerization process

Biological Polymers

- Describe the essential polymers: DNA, RNA, Proteins, Cellulose, and Glycogen
- Be able to identify the linkages in these biopolymers and how they can be forrmed and broken

Applications

- Identify transition metal properties in synthetic polymers
- Titrations amino acids with strong base including protonation states
- Describe states of proteins (and therefore the amino acids) at biolgogical pH
- Describe the coordination of bioinorganic (transition metal-containing) proteins
- Quantify reduction/oxidation processes in both synthetic and biological systems

2.7: 7. APP- Applications in Modern Chemistry is shared under a not declared license and was authored, remixed, and/or curated by LibreTexts.

CHAPTER OVERVIEW

Front Matter

TitlePage

InfoPage

Table of Contents

Licensing

CHEM 2010D: Modern Applications of Chemistry

This text is disseminated via the Open Education Resource (OER) LibreTexts Project (https://LibreTexts.org) and like the thousands of other texts available within this powerful platform, it is freely available for reading, printing, and "consuming."

The LibreTexts mission is to bring together students, faculty, and scholars in a collaborative effort to provide an accessible, and comprehensive platform that empowers our community to develop, curate, adapt, and adopt openly licensed resources and technologies; through these efforts we can reduce the financial burden born from traditional educational resource costs, ensuring education is more accessible for students and communities worldwide.

Most, but not all, pages in the library have licenses that may allow individuals to make changes, save, and print this book. Carefully consult the applicable license(s) before pursuing such effects. Instructors can adopt existing LibreTexts texts or Remix them to quickly build course-specific resources to meet the needs of their students. Unlike traditional textbooks, LibreTexts' web based origins allow powerful integration of advanced features and new technologies to support learning.



LibreTexts is the adaptable, user-friendly non-profit open education resource platform that educators trust for creating, customizing, and sharing accessible, interactive textbooks, adaptive homework, and ancillary materials. We collaborate with individuals and organizations to champion open education initiatives, support institutional publishing programs, drive curriculum development projects, and more.

The LibreTexts libraries are Powered by NICE CXone Expert and was supported by the Department of Education Open Textbook Pilot Project, the California Education Learning Lab, the UC Davis Office of the Provost, the UC Davis Library, the California State University Affordable Learning Solutions Program, and Merlot. This material is based upon work supported by the National Science Foundation under Grant No. 1246120, 1525057, and 1413739.

Any opinions, findings, and conclusions or recommendations expressed in this material are those of the author(s) and do not necessarily reflect the views of the National Science Foundation nor the US Department of Education.

Have questions or comments? For information about adoptions or adaptions contact info@LibreTexts.org or visit our main website at https://LibreTexts.org.

This text was compiled on 01/11/2026

TABLE OF CONTENTS

Licensing

1: Primer

- 1.1: The Structure of Atoms
  - 1.1.1: Prelude to Atomic Structure
  - 1.1.2: Groups of Related Elements
  - 1.1.3: The Periodic Table
  - 1.1.4: Valence
  - 1.1.5: Exceptions to the Periodic Law
  - 1.1.6: Implications of Periodicity for Atomic Theory
  - 1.1.7: Radiation
  - 1.1.8: The Electron
  - 1.1.9: The Nucleus
- 1.2: Chemical Bonding - Electron Pairs and Octets
  - 1.2.1: Prelude to Chemical Bonding
  - 1.2.2: Ionic Bonding
  - 1.2.3: Energy and the Formation of Ions
  - 1.2.4: The Ionic Crystal Lattice
  - 1.2.5: Ions and Noble-Gas Electron Configurations
  - 1.2.6: Ionization Energies
  - 1.2.7: Ionization of Transition and Inner Transition Elements
  - 1.2.8: Electron Affinities
  - 1.2.9: Binary Ionic Compounds and Their Properties
  - 1.2.10: The Octet Rule
  - 1.2.11: Physical Properties
    - 1.2.11.1: Lecture Demonstrations
  - 1.2.12: Chemical Properties
  - 1.2.13: The Covalent Bond
  - 1.2.14: Covalent Molecules and the Octet Rule
  - 1.2.15: Writing Lewis Structures for Molecules
    - 1.2.15.1: An Excess of Bonds
    - 1.2.15.2: Deciding on a Skeleton Structure
    - 1.2.15.3: Multiple Bonds
  - 1.2.16: Examples of Lewis Structures
  - 1.2.17: Polyatomic Ions
  - 1.2.18: Ionic Compounds Containing Polyatomic Ions
  - 1.2.19: Atomic Sizes
  - 1.2.20: Ionic Sizes
  - 1.2.21: Periodic Variation of IE and EA
    - 1.2.21.1: Lecture Demonstrations
- 1.3: Further Aspects of Covalent Bonding
  - 1.3.1: Prelude to Covalent Bonding
  - 1.3.2: Exceptions to the Octet Rule

- 1.3.2.1: Biology- Biologically Active Exceptions to the Octet Rule
- 1.3.3: The Shapes of Molecules
  - 1.3.3.1: Lecture Demonstrations
- 1.3.4: Molecules with Lone Pairs
  - 1.3.4.1: Lecture Demonstrations
- 1.3.5: Multiple Bonds and Molecular Shapes
- 1.3.6: Hybrid Orbitals
- 1.3.7: Orbital Descriptions of Multiple Bonds
- 1.3.8: Sigma and Pi Bonds
- 1.3.9: Polarizability
  - 1.3.9.1: Biology - Polarizability of Biologically Significant Atoms
- 1.3.10: Polar Covalent Bonds
  - 1.3.10.1: Biology- Nonpolar Iodine and Polar Hydrogen Iodide
  - 1.3.10.2: Lecture Demonstrations
- 1.3.11: Electronegativity
- 1.3.12: Polarity in Polyatomic Molecules
  - 1.3.12.1: Biology- The Hydrophobic Effect and Properties of Small Polyatomic Molecules
  - 1.3.12.2: Lecture Demonstrations
- 1.3.13: Formal Charge and Oxidation Numbers
- 1.3.14: Resonance
- 1.4: Properties of Organic Compounds
  - 1.4.1: Prelude to Organic Compounds
  - 1.4.2: Covalent Compounds and Intermolecular Forces
  - 1.4.3: Dipole Forces
  - 1.4.4: London Forces
    - 1.4.4.1: Chapter 8 page 3.jpg
    - 1.4.4.2: Atomic Radii
    - 1.4.4.3: Atomic sizes on periodic table.jpg
    - 1.4.4.4: Ionization Energies
      - 1.4.4.4.1: IonizationEnergyAtomicWeight.PNG
    - 1.4.4.5: Ionization Energies and Electron Affinities
      - 1.4.4.5.1: Electron Affinities
        - 1.4.4.5.1.1: Ionization Energies and Electron Affinities.jpg
    - 1.4.4.6: Polarizability on London Forces.jpg
  - 1.4.5: Hydrogen Bonding- Water
    - 1.4.5.1: Atomic Radii and Ionic Radii
    - 1.4.5.2: H-Bonding Between 2 HF Molecules.jpg
    - 1.4.5.3: Nonmetal hydride bp.jpg
  - 1.4.6: Ice and Water
    - 1.4.6.1: Ice; a hexagonal crystal.jpg
    - 1.4.6.2: Boiling Points of Hydrides
  - 1.4.7: Macromolecular Substances
  - 1.4.8: Diamond and Graphite
  - 1.4.9: Silicon Dioxide
  - 1.4.10: Synthetic Macromolecules- Some Applied Organic Chemistry
  - 1.4.11: Addition Polymers

- 1.4.12: Condensation Polymers
- 1.4.13: Cross-Linking
- 1.5: Acid and Base Naming
  - 1.5.1: Polyatomic Ions
  - 1.5.2: Naming Acids
  - 1.5.3: Names and Formulas of Bases

2: Nuclear Chemistry

- 2.1: Components of the Nucleus
- 2.2: The Nuclear Atom
- 2.3: Atomic Structure and Isotopes
- 2.4: Isotopes
- 2.5: Transmutation and Radioactivity
- 2.6: Average Atomic Weights
- 2.7: Measurement of Atomic Weights
- 2.8: Nuclear Reactions
- 2.9: Nuclear Radiation
- 2.10: Rates of Radioactive Decay
- 2.11: Stability of the Atomic Nucleus
- 2.12: The Origin of the Elements
- 2.13: Transmutation of the Elements
- 2.14: Nuclear Fission
- 2.15: Nuclear Fusion
- 2.16: Nuclear Chemistry (Exercises)

3: Physical Properties of Gases

- 3.1: Properties of Gases
- 3.2: Gas Pressure
- 3.3: Relationships among Pressure, Temperature, Volume, and Amount
- 3.4: The Ideal Gas Law
- 3.5: Gas Volumes and Stoichiometry
- 3.6: Kinetic Molecular Theory of Gases
- 3.7: Connecting Gas Properties to Kinetic Molecular Theory
- 3.8: Chapter Problems

4: Intermolecular Forces

- 4.1: Intermolecular Forces
- 4.2: Properties of Liquids
- 4.3: Intermolecular Forces and the Solution Process

5: Solids

- 5.1: Prelude to Liquids and Solids
- 5.2: Carbon and Silicon- Network Atomic Solids
- 5.3: The Solid State of Matter
- 5.4: Lattice Structures in Crystalline Solids
- 5.5: Bonding in Metals and Semiconductors
- 5.6: Liquids and Solids (Exercises)

6: Phases and Phase Transitions

- 6.1: Prelude to Liquids and Solids
- 6.2: Intermolecular Forces Review
- 6.3: Properties of Liquids
- 6.4: Phase Transitions- Overview
- 6.5: Phase Transitions
- 6.6: Vaporization and Vapor Pressure
- 6.7: Sublimation and Fusion
- 6.8: Heating Curve for Water
- 6.9: Phase Diagrams
- 6.10: Water - An Extraordinary Substance

7: Solutions and their Physical Properties

- 7.1: Types of Solutions- Some Terminology
- 7.2: Mixtures of Gases
- 7.3: Solution Concentration
- 7.4: Intermolecular Forces and the Solution Process
- 7.5: Solution Formation and Equilibrium
- 7.6: Solubilities of Gases
- 7.7: Vapor Pressures of Solutions
- 7.8: Osmotic Pressure
- 7.9: Freezing-Point Depression and Boiling-Point Elevation of Nonelectrolyte Solutions
- 7.10: Solutions of Electrolytes
- 7.11: Colloidal Mixtures
- 7.12: Solubility and Complex-Ion Equilibria
  - 7.12.1: Solubility Product Constant, Ksp
  - 7.12.2: Relationship Between Solubility and Ksp
  - 7.12.3: Common-Ion Effect in Solubility Equilibria
  - 7.12.4: Limitations of the Ksp Concept
  - 7.12.5: Criteria for Precipitation and its Completeness
  - 7.12.6: Fractional Precipitation
  - 7.12.7: Solubility and pH
  - 7.12.8: Equilibria Involving Complex Ions
  - 7.12.9: Qualitative Cation Analysis

8: Acids and Bases

- 8.1: Acids and Bases at Equilibrium
  - 8.1.1: Arrhenius Theory- A Brief Review
  - 8.1.2: Brønsted-Lowry Theory of Acids and Bases
  - 8.1.3: Self-Ionization of Water and the pH Scale
  - 8.1.4: Introduction to Strong Acids and Bases
  - 8.1.5: Strong Acids and Strong Bases
  - 8.1.6: Weak Acids and Weak Bases
  - 8.1.7: Conjugate Acid-Base Pairs and pH
  - 8.1.8: Polyprotic Acids
  - 8.1.9: Ions as Acids and Bases
  - 8.1.10: Molecular Structure and Acid-Base Behavior
  - 8.1.11: Lewis Acids and Bases

- 8.1.12: Common-Ion Effect in Acid–Base Equilibria
- 8.2: Additional Aspects of Acid-Base Equilibria
  - 8.2.1: Buffer Solutions
  - 8.2.2: Acid–Base Indicators
  - 8.2.3: Neutralization Reactions and Titration Curves
  - 8.2.4: Solutions of Salts of Polyprotic Acids
  - 8.2.5: Acid–Base Equilibrium Calculations- A Summary
  - 8.2.6: Exercises on Acids and Bases II
  - 8.2.7: E3. Solubility Constants for Compounds at 25°C Data Table
  - 8.2.8: pH Calculations for Acid–Base Titrations

9: Electrochemistry

- 9.1: Oxidation-Reduction Reactions
- 9.2: Balancing Redox Reactions
- 9.3: Galvanic Cells
- 9.4: Standard Electrode Potentials
- 9.5: Strengths of Oxidants and Reductants
- 9.6: E, ΔG, and K (The Big Triangle of Chemistry)
- 9.7: Cell Potential as a Function of Concentrations
- 9.8: Batteries- Producing Electricity Through Chemical Reactions
- 9.9: Corrosion- Unwanted Voltaic Cells
- 9.10: Electrolysis- Causing Nonspontaneous Reactions to Occur

10: Coordination Chemistry

- 10.1: Werner’s Theory of Coordination Compounds
- 10.2: Ligands
- 10.3: Nomenclature
- 10.4: Isomerism
- 10.5: Optical Isomerism in Metal Complexes
- 10.6: Stability Aspects of Complex-Ion Equilibria
- 10.7: Chelation
- 10.8: Bonding in Octahedral Complex Ions- Crystal Field Theory
- 10.9: Bonding in Non-Octahedral Complex Ions- Crystal Field Theory
- 10.10: High Spin and Low Spin Complexes
- 10.11: Magnetic Behavior of Atoms, Molecules, and Materials
- 10.12: Magnetic Behavior of Complex Ions
- 10.13: Optical Properties of Coordination Compounds (Color)

11: Applications in Polymer and Biological Chemistry

- 11.1: Bioinorganic Chemistry
  - 11.1.1: A Molecular Depot- Human Serum Albumin Carries Essential Cu and Zn in Serum
  - 11.1.2: Iron acquisition in bacteria- Siderophores
  - 11.1.3: Fe Wars- Lactoferrin
  - 11.1.4: Iron Storage- Ferritin
  - 11.1.5: Antioxidant- Cu/Zn Superoxide dismutase (SOD1)
  - 11.1.6: Keep Cu Safe- Intracellular Copper Chaperones
  - 11.1.7: Cytochrome C
  - 11.1.8: Cytochrome Oxidase

- 11.1.9: Potassium Channels
- 11.1.10: Chemotherapy- Pt anticancer agents
- 11.2: Bioinorganic Chemistry (Bertini et al.)
  - Licensing
  - Preface
  - 11.2.1: Transition-Metal Storage, Transport, and Biomineralization
    - 11.2.1.1: Biological Significance of Iron, Zinc, Copper, Molybdenum, Cobalt, Chromium, Vanadium, and Nickel
    - 11.2.1.2: Biological Systems of Metal Storage
    - 11.2.1.3: Chemical Properties Relative to Storage and Transport
    - 11.2.1.4: Iron Biomineralization
    - 11.2.1.5: Transport of Iron
    - 11.2.1.6: Transport of Zinc, Copper, Vanadium, Chromium, Molybdenum, and Cobalt
  - 11.2.2: The Reaction Pathways of Zinc Enzymes and Related Biological Catalysts
    - 11.2.2.1: About Carbonic Anhydrase
    - 11.2.2.2: Acid-base Equilibria
    - 11.2.2.3: Catalytic Mechanism
    - 11.2.2.4: Coordinated Water and NMR
    - 11.2.2.5: Coordination Geometries
    - 11.2.2.6: Ester Hydrolysis and Phosphoryl Transfer
    - 11.2.2.7: Group Transfer and Vitamin B-12
    - 11.2.2.8: Metal Substitution
    - 11.2.2.9: Model Chemistry
    - 11.2.2.10: Nucleophilic Addition of OH^{-} and H^{-}
    - 11.2.2.11: Peptide Hydrolysis
    - 11.2.2.12: pH Dependence of Inhibitor Binding
    - 11.2.2.13: Selecting Zinc
    - 11.2.2.14: Steady-State and Equilibrium Kinetics of Carbonic Anhydrase-Catalyzed CO_{2}/HCO_{3}^{-} Interconversion
    - 11.2.2.15: Strategies for the Investigation of Zinc Enzymes
    - 11.2.2.16: The Natural Catalysts
    - 11.2.2.17: What Do We Learn?
  - 11.2.3: Calcium in Biological Systems
    - 11.2.3.1: Ca^{2+}-binding Proteins in Microorganisms- The Search for a Prokaryotic Calmodulin
    - 11.2.3.2: Basic Facts About Calcium- Its Compounds and Reactions
    - 11.2.3.3: Calcium in Mineralized Tissues
    - 11.2.3.4: Calmodulin
    - 11.2.3.5: Extracellular Calcium Ion-binding Proteins
    - 11.2.3.6: Inositol Trisphosphate and the Calcium Ion Messenger System
    - 11.2.3.7: Intracellular Calcium Ion Transport
    - 11.2.3.8: Measurements of "Free" Calcium Concentrations
    - 11.2.3.9: Measurements of Total Calcium Concentrations
    - 11.2.3.10: Mitochondrial Calcium Ion Transport
    - 11.2.3.11: Molecular Aspects of Calcium Ion-Regulated Intracellular Processes (Part 1)
    - 11.2.3.12: Molecular Aspects of Calcium Ion-regulated Intracellular Processes (Part 2)
    - 11.2.3.13: Paravalbumin and Calbindins D_{9K} and D_{28K}
    - 11.2.3.14: The Transport and Regulation of Ca^{2+} Ions in Higher Organisms
    - 11.2.3.15: Troponin C
  - 11.2.4: Biological and Synthetic Dioxygen Carriers

- 11.2.4.1: Biological Dioxygen Transport Systems
- 11.2.4.2: Biological Oxygen Carriers
- 11.2.4.3: Detailed Structures of Hemoglobins and Model Systems
- 11.2.4.4: Dioxygen Carriers and Bioinorganic Chemistry
- 11.2.4.5: General Aspects of the Chemistry of Cobalt
- 11.2.4.6: General Aspects of the Chemistry of Copper
- 11.2.4.7: General Aspects of the Chemistry of Dioxygen
- 11.2.4.8: General Aspects of the Chemistry of Iron
- 11.2.4.9: General Structural Features that Modulate Ligand Activity
- 11.2.4.10: Hazards of Life with Dioxygen
- 11.2.4.11: Nature of the Metal-Dioxygen Linkage in Biological Systems
- 11.2.4.12: Other Ligands for Biological Oxygen Carriers
- 11.2.4.13: Requirements for a Model System for Hemoglobin
- 11.2.4.14: Requirements for Effective Oxygen Carriers
- 11.2.4.15: Role of the Protein in Effecting Biological Oxygen Transport
- 11.2.4.16: Selected Chemistry of Dioxygen, Iron, Copper, and Cobalt
- 11.2.4.17: Stereochemical Changes Upon Ligation
- 11.2.4.18: Structural Basis of Ligand Affinities of Oxygen Carriers
- 11.2.4.19: Structures Relevant to Liganded Hemoglobins
- 11.2.4.20: Thermodynamic Factors
- 11.2.4.21: Ch. 4 References and Abbreviations

- 11.2.5: Dioxygen Reactions
  - 11.2.5.1: Catalase and Peroxidase
  - 11.2.5.2: Chemistry of Dioxygen
  - 11.2.5.3: Copper-zinc Superoxide Dismutase
  - 11.2.5.4: Cytochrome c Oxidase
  - 11.2.5.5: Dioxygen Toxicity
  - 11.2.5.6: Monooxygenases
  - 11.2.5.7: Oxygenases
- 11.2.6: Electron Transfer
  - 11.2.6.1: Biological Redox Components
  - 11.2.6.2: Coupling Electron Transfers and Substrate Activation
  - 11.2.6.3: Electron-transfer Rates
  - 11.2.6.4: Electron-Transfer Theory
  - 11.2.6.5: Energy Storage and Release
  - 11.2.6.6: Long-range Electron Transfer in Proteins (Part 1)
  - 11.2.6.7: Long-range Electron Transfer in Proteins (Part 2)
  - 11.2.6.8: Marcus Theory
- 11.2.7: Ferrodoxins, Hydrogenases, and Nitrogenases - Metal-Sulfide Proteins
  - 11.2.7.1: Iron-sulfur Proteins and Models
  - 11.2.7.2: Iron-sulfur Proteins and Models (Part 2)
  - 11.2.7.3: Iron-sulfur Proteins and Models (Part 3)
  - 11.2.7.4: Iron-sulfur Proteins and Models (Part 4)
  - 11.2.7.5: Multisite Redox Enzymes
  - 11.2.7.6: Multisite Redox Enzymes (Part 2)
  - 11.2.7.7: Multisite Redox Enzymes (Part 3)
  - 11.2.7.8: Multisite Redox Enzymes (Part 4)
  - 11.2.7.9: Multisite Redox Enzymes (Part 5)
  - 11.2.7.10: Multisite Redox Enzymes (Part 6)

- 11.2.7.11: Report on the Nitrogenase Crystal Structure\(\;^{378-381}\)
- 11.2.7.12: Rubredoxin- A Single-Fe Tetrathiolate Protein
- 11.2.8: Metal/Nucleic Acid Interactions
  - 11.2.8.1: The Basics
  - 11.2.8.2: The Basics (Part 2)
  - 11.2.8.3: A Case Study- Tris(phenanthroline) Metal Complexes
  - 11.2.8.4: Applications of Different Metal Complexes that Bind Nucleic Acids
  - 11.2.8.5: Applications of Different Metal Complexes that Bind Nucleic Acids (Part 2)
  - 11.2.8.6: Nature's Use of Metal/Nucleic-acid Interactions
- 11.2.9: Metals in Medicine
  - 11.2.9.1: Metal Deficiency and Disease
  - 11.2.9.2: Toxic Effects of Metals
  - 11.2.9.3: Aspects of Platinum Binding to DNA
  - 11.2.9.4: Survey of Metals Used for Diagnosis and Chemotherapy
  - 11.2.9.5: Platinum Anticancer Drugs- A Case Study
  - 11.2.9.6: Mapping the Major Adducts of cis- and trans-DDP on DNA; Sequence Specificity
  - 11.2.9.7: Structure of Platinum-DNA Complexes
  - 11.2.9.8: Site-specifically Platinated DNA \(\;^{154}\)
  - 11.2.9.9: Bioinorganic Chemistry of Platinum Anticancer Drugs- How Might They Work?
  - 11.2.9.10: Bioinorganic Chemistry of Platinum Anticancer Drugs; How Might They Work? (Part 2)
  - 11.2.9.11: Design of New Inorganic Anticancer Drugs
- Detailed Licensing

- 11.3: Cisplatin - The Invention of an Anticancer Drug
  - 11.3.1: Cisplatin 1. Study of the Effect of Electric Fields on E. coli
  - 11.3.2: Cisplatin 2. Control Experiments for the Effect of Electric Fields on E. coli
  - 11.3.3: Cisplatin 3. Redox Chemistry
  - 11.3.4: Cisplatin 4. Electrochemistry
  - 11.3.5: Cisplatin 5. The Role of Platinum Electrodes
  - 11.3.6: Cisplatin 6. Transition Metal Chemistry
  - 11.3.7: Cisplatin 7. Bioinorganic Chemistry
  - 11.3.8: Cisplatin 8. Discovery of Cisplatin
  - 11.3.9: Cisplatin 9. The Discovery - One Scientist's Story
  - 11.3.10: Cisplatin 10. Research as a Career
  - 11.3.11: Cisplatin 11. Cisplatin as an Anticancer Drug
  - 11.3.12: Cisplatin 12. Modes of Action of Cisplatin
  - 11.3.13: Cisplatin 13. Further Studies/Recent Developments
  - 11.3.14: Cisplatin 14. DNA
  - 11.3.15: Cisplatin 15. FDA Drug Approval Process
  - 11.3.16: Cisplatin 16. Profits from Cisplatin
  - 11.3.17: Cisplatin 17. Drug Resistance
  - 11.3.18: Cisplatin 18. Toxicity
  - 11.3.19: Cisplatin 19. Cancer
  - 11.3.20: Cisplatin 20. Other Treatments for Cancer
- 11.4: Polymeric Materials and Soft Condensed Matter
  - 11.4.1: Polymerization Reactions for Synthetic Polymers
  - 11.4.2: Natural Polymers
- 11.5: Polymer Chemistry (Schaller)
  - Licensing

- 11.5.1: Monomers and Polymers
  - 11.5.1.1: Difunctional Carboxyloids
  - 11.5.1.2: Cyclic Carboxyloids
  - 11.5.1.3: Olefins
  - 11.5.1.4: Cyclic Olefins
  - 11.5.1.5: Coordination Polymers
  - 11.5.1.6: Supramolecular Assemblies
  - 11.5.1.7: Other Polymers
  - 11.5.1.8: Polymer Topology
  - 11.5.1.E: Solutions for Selected Problems
- 11.5.2: Synthetic Methods in Polymer Chemistry
  - 11.5.2.1: Ziegler-Natta Polymerization
  - 11.5.2.2: Solutions to Selected Problems
  - 11.5.2.3: Step Growth and Chain Growth
  - 11.5.2.4: Cationic Polymerization
  - 11.5.2.5: Living Cationic Polymerization
  - 11.5.2.6: Anionic Polymerization
  - 11.5.2.7: Living Anionic Polymerization
  - 11.5.2.8: Ring-Opening Polymerization
  - 11.5.2.9: Radical Polymerization
  - 11.5.2.10: Living Radical Polymerization- RAFT
  - 11.5.2.11: Living Radical Polymerization- ATRP
- 11.5.3: Kinetics and Thermodynamics of Polymerization
  - 11.5.3.1: Thermodynamics of Polymerization
  - 11.5.3.2: Kinetics of Step-Growth Polymerization
  - 11.5.3.3: Kinetics of Chain Polymerization
  - 11.5.3.4: Kinetics of Catalytic Polymerization
  - 11.5.3.5: Solutions to Selected Problems
- 11.5.4: Polymer Properties
  - 11.5.4.1: Molecular Weight of Polymers
  - 11.5.4.2: Viscosity of Polymers
  - 11.5.4.3: Rheology
  - 11.5.4.4: Glass Transition
  - 11.5.4.5: Crystallinity in Polymers
  - 11.5.4.6: Microphase Separation
  - 11.5.4.7: Stress-Strain Relationships
  - 11.5.4.8: Storage and Loss Modulus
  - 11.5.4.9: Modulus, Temperature, Time
  - 11.5.4.10: Chapter Solutions
- Detailed Licensing

- 11.6: Synthetic Polymers
  - 11.6.1: Introduction
  - 11.6.2: Chain-Growth Polymers—Addition Polymers
  - 11.6.3: Anionic Polymerization of Epoxides
  - 11.6.4: Ziegler–Natta Catalysts and Polymer Stereochemistry
  - 11.6.5: Natural and Synthetic Rubbers
  - 11.6.6: Step-Growth Polymers—Condensation Polymers
  - 11.6.7: Polymer Structure and Properties

- 11.6.8: Green Polymer Synthesis
- 11.6.9: Polymer Recycling and Disposal

12: Reading

Index

Glossary

Detailed Licensing

Licensing

*A detailed breakdown of this resource's licensing can be found in **Back Matter/Detailed Licensing**.*

CHAPTER OVERVIEW

1: Primer

Chemistry is all around us "from the air we breathe to the food we eat" to the items at the super market that say “no chemicals added”. In fact, it is impossible to create something without using chemistry because chemistry consists of all matter. It allows us to answer questions as simple as why a candle goes out when a glass is placed over it to more complex questions such as does a candle actually burn in zero gravity? Chemistry is the study of matter and the changes it undergoes such as ice changing from the solid to liquid to gas phase. People have used it for things such as creating metal from an ore, dying fabric, and making cheese. Chemistry deals with different substances and how they can interact with each other to create a product.

As you begin your study of college chemistry, those of you who do not intend to become professional chemists may well wonder why you need to study chemistry. You will soon discover that a basic understanding of chemistry is useful in a wide range of disciplines and career paths. You will also discover that an understanding of chemistry helps you make informed decisions about many issues that affect you, your community, and your world. A major goal of this text is to demonstrate the importance of chemistry in your daily life and in our collective understanding of both the physical world we occupy and the biological realm of which we are a part.

1.1: The Structure of Atoms

1.1.1: Prelude to Atomic Structure

1.1.2: Groups of Related Elements

1.1.3: The Periodic Table

1.1.4: Valence

1.1.5: Exceptions to the Periodic Law

1.1.6: Implications of Periodicity for Atomic Theory

1.1.7: Radiation

1.1.8: The Electron

1.1.9: The Nucleus

1.2: Chemical Bonding - Electron Pairs and Octets

1.2.1: Prelude to Chemical Bonding

1.2.2: Ionic Bonding

1.2.3: Energy and the Formation of Ions

1.2.4: The Ionic Crystal Lattice

1.2.5: Ions and Noble-Gas Electron Configurations

1.2.6: Ionization Energies

1.2.7: Ionization of Transition and Inner Transition Elements

1.2.8: Electron Affinities

1.2.9: Binary Ionic Compounds and Their Properties

1.2.10: The Octet Rule

1.2.11: Physical Properties

1.2.11.1: Lecture Demonstrations

1.2.12: Chemical Properties

1.2.13: The Covalent Bond

1.2.14: Covalent Molecules and the Octet Rule

1.2.15: Writing Lewis Structures for Molecules

1.2.15.1: An Excess of Bonds

1.2.15.2: Deciding on a Skeleton Structure
1.2.15.3: Multiple Bonds
1.2.16: Examples of Lewis Structures
1.2.17: Polyatomic Ions
1.2.18: Ionic Compounds Containing Polyatomic Ions
1.2.19: Atomic Sizes
1.2.20: Ionic Sizes
1.2.21: Periodic Variation of IE and EA
1.2.21.1: Lecture Demonstrations
1.3: Further Aspects of Covalent Bonding
1.3.1: Prelude to Covalent Bonding
1.3.2: Exceptions to the Octet Rule
1.3.2.1: Biology- Biologically Active Exceptions to the Octet Rule
1.3.3: The Shapes of Molecules
1.3.3.1: Lecture Demonstrations
1.3.4: Molecules with Lone Pairs
1.3.4.1: Lecture Demonstrations
1.3.5: Multiple Bonds and Molecular Shapes
1.3.6: Hybrid Orbitals
1.3.7: Orbital Descriptions of Multiple Bonds
1.3.8: Sigma and Pi Bonds
1.3.9: Polarizability
1.3.9.1: Biology - Polarizability of Biologically Significant Atoms
1.3.10: Polar Covalent Bonds
1.3.10.1: Biology- Nonpolar Iodine and Polar Hydrogen Iodide
1.3.10.2: Lecture Demonstrations
1.3.11: Electronegativity
1.3.12: Polarity in Polyatomic Molecules
1.3.12.1: Biology- The Hydrophobic Effect and Properties of Small Polyatomic Molecules
1.3.12.2: Lecture Demonstrations
1.3.13: Formal Charge and Oxidation Numbers
1.3.14: Resonance
1.4: Properties of Organic Compounds
1.4.1: Prelude to Organic Compounds
1.4.2: Covalent Compounds and Intermolecular Forces
1.4.3: Dipole Forces
1.4.4: London Forces
1.4.4.1: Chapter 8 page 3.jpg
1.4.4.2: Atomic Radii
1.4.4.3: Atomic sizes on periodic table.jpg
1.4.4.4: Ionization Energies
1.4.4.4.1: IonizationEnergyAtomicWeight.PNG
1.4.4.5: Ionization Energies and Electron Affinities
1.4.4.5.1: Electron Affinities

1.4.4.5.1.1: Ionization Energies and Electron Affinities.jpg
1.4.4.6: Polarizability on London Forces.jpg
1.4.5: Hydrogen Bonding- Water
1.4.5.1: Atomic Radii and Ionic Radii
1.4.5.2: H-Bonding Between 2 HF Molecules.jpg
1.4.5.3: Nonmetal hydride bp.jpg
1.4.6: Ice and Water
1.4.6.1: Ice; a hexagonal crystal.jpg
1.4.6.2: Boiling Points of Hydrides
1.4.7: Macromolecular Substances
1.4.8: Diamond and Graphite
1.4.9: Silicon Dioxide
1.4.10: Synthetic Macromolecules- Some Applied Organic Chemistry
1.4.11: Addition Polymers
1.4.12: Condensation Polymers
1.4.13: Cross-Linking
1.5: Acid and Base Naming
1.5.1: Polyatomic Ions
1.5.2: Naming Acids
1.5.3: Names and Formulas of Bases

1: Primer is shared under a not declared license and was authored, remixed, and/or curated by LibreTexts.

SECTION OVERVIEW

1.1: The Structure of Atoms

Knowledge of chemical reactivity and properties may be approached on both the macroscopic and microscopic levels. Macroscopically this involves what is called **descriptive chemistry**. The person who first carries out a chemical reaction describes what happened, usually in terms of a balanced equation, and lists properties of any new substances. This enables other scientists to repeat the experiment if they wish. Even if the work is not carried out again, the descriptive report allows prediction of what would happen if it were repeated.

Topic hierarchy

1.1.1: Prelude to Atomic Structure

1.1.2: Groups of Related Elements

1.1.3: The Periodic Table

1.1.4: Valence

1.1.5: Exceptions to the Periodic Law

1.1.6: Implications of Periodicity for Atomic Theory

1.1.7: Radiation

1.1.8: The Electron

1.1.9: The Nucleus

This page titled 1.1: The Structure of Atoms is shared under a CC BY-NC-SA 4.0 license and was authored, remixed, and/or curated by Ed Vitz, John W. Moore, Justin Shorb, Xavier Prat-Resina, Tim Wendorff, & Adam Hahn.

1.1.1: Prelude to Atomic Structure

We have examined the theoretical implications and practical applications of John Dalton's ideas about atoms in our discussion on atoms, molecules and chemical reactions, and using chemical equations in calculations. Clearly the atomic theory is a powerful tool which aids our thinking about how much of one substance can combine with (or be produced from) a given quantity of another. The theory is much less helpful, however, when we try to speculate about what holds the atoms together in molecules such as Br_2, $HgBr_2$ and Hg_2Br_2. As you have seen, techniques are available for *experimental* determination of the formula of a new compound, but Dalton's theory is of little value in *predicting* formulas. Neither does it tell us which elements are likely to combine with which, nor indicate what chemical and physical properties are to be expected of the compounds which form.

The ability to make predictions about chemical reactivity and properties is very important because it guides chemists' efforts to synthesize new substances which are of value to society at large. Medicines, metals, transistors, plastics, textiles, fertilizers, and many other things that we take for granted today have been made possible by detailed knowledge of chemical and physical properties. Such knowledge also permits greater understanding of how the natural world works and what changes (favorable or detrimental) may be brought about by human activities.

Knowledge of chemical reactivity and properties may be approached on both the macroscopic and microscopic levels. Macroscopically this involves what is called **descriptive chemistry**. The person who first carries out a chemical reaction describes what happened, usually in terms of a balanced equation, and lists properties of any new substances. This enables other scientists to repeat the experiment if they wish. Even if the work is not carried out again, the descriptive report allows prediction of what would happen if it were repeated.

The microscopic approach uses theory to predict which substances will react with which. During the past century Dalton's atomic theory has been modified so that it can help us to remember the properties of elements and compounds. We now attribute structure to each kind of atom and expect atoms having similar structures to undergo similar reactions. Such work has led to the classification of groups of elements, for instance the alkali metals, halogens, alkaline earth metals, and many more. The additional complication of learning about atomic structure is repaid many fold by the increased ability of our microscopic model to predict macroscopic properties.

In the following sections, you will see that a number of quite different kinds of experiments contributed to the extension of Dalton's atomic theory to include subatomic particles and atomic structure. The periodic variation of valence and the periodic table's successful correlation of macroscopic properties indicate that atoms must have certain specific ways of connecting to other atoms. It is reasonable to assume that valence depends on some underlying atomic structure. Atoms which are similar in structure should exhibit the same valence and have similar chemical and physical properties. While the periodicity was initially based upon atomic weight, exceptions to periodic law based upon weight implied some other property led to periodicity.

The property on which periodicity is based is the *electronic structure* of atoms. Our model for electronic structure is both scientifically and philosophically interesting, because it is based on a wave model for electrons. To learn more about our current electronic structure for atoms and the discoveries that led to this understanding, watch the video below.



The discovery of radioactivity and transmutation implied that one kind of atom could change into another. This can he explained if atoms have structure. A change in that structure may produce a new kind of atom. Experiments with cathode-ray tubes indicated that electrons, which are very light and carry a negative charge, are present in all atoms. Rutherford's interpretation of the Geiger-Marsden experiment suggested that electrons occupy most of the volume of the atom while most of the mass is concentrated in a small positively charged nucleus. Moseley's x-ray spectra and the existence of isotopes made it quite clear that Dalton's emphasis on the importance of atomic weight would have to he dropped. The chemical behavior of an atom is determined by how many protons are in the nucleus. Changing the number of neutrons changes the atomic mass but has very little effect on chemistry. The identity of an element depends on its atomic number, not on its atomic weight. If the periodic law is restated as "When the elements are listed in order of increasing atomic *number*, their properties vary periodically," there are no exceptions.

This page titled 1.1.1: Prelude to Atomic Structure is shared under a CC BY-NC-SA 4.0 license and was authored, remixed, and/or curated by Ed Vitz, John W. Moore, Justin Shorb, Xavier Prat-Resina, Tim Wendorff, & Adam Hahn.

- **4.1: Prelude to Atomic Structure** by Ed Vitz, John W. Moore, Justin Shorb, Xavier Prat-Resina, Tim Wendorff, & Adam Hahn is licensed CC BY-NC-SA 4.0.

1.1.2: Groups of Related Elements

The macroscopic, descriptive approach to chemical knowledge has led to a great deal of factual information. Right now more than 100 million chemical compounds and their properties are on file at the Chemical Abstracts Service of the American Chemical Society[1]. Anyone who wants information about these substances can look it up, although in practice it helps to have a computer do the looking! Even with a computer's memory it is hard to keep track of so many facts–no single person can remember more than a fraction of the total.

Fortunately these millions of facts are interrelated in numerous ways, and the relationships are helpful in remembering the facts. To illustrate this point, we shall present part of the descriptive chemistry of about 20 elements. Although each element has unique physical and chemical properties, it will be obvious that certain groups of elements are closely related. Members of each group are more like each other than they are like any member of another group. Because of this close relationship a special name has been assigned to these collections of elements. It is also possible to write general equations which apply to *all* members of a family of elements. Practical laboratory experience with one member gives a fairly accurate indication of how each of the others will behave.

Because of their similarities, lithium, sodium, potassium, rubidium, and cesium are grouped together and called the **alkali metals**. What do we mean when we say these elements are similar? The following video of lithium, sodium, and potassium reacting in water demonstrates the similarities quite well.



In the video, each metal is added to a dish containing water. All three metals react with the water, flying over the surface as H_2 is produced (albeit at different rates). LiOH, NaOH, and KOH, are each produced respectively. These hydroxides are evidenced through the use of phenolphthalein indicator, which turns pink in the presence of OH^- ions. While the reactivity of each metal differs (potassium is clearly more reactive with water than sodium, which is more reactive than lithium) all three are undergoing the same reaction. The three reactions are:

$$2\mathrm{Li}(s) + 2\mathrm{H_2O}(l) \rightarrow 2\mathrm{LiOH}(aq) + \mathrm{H_2}(g)$$

$$2\mathrm{Na}(s) + 2\mathrm{H_2O}(l) \rightarrow 2\mathrm{NaOH}(aq) + \mathrm{H_2}(g)$$

$$2\mathrm{K}(s) + 2\mathrm{H_2O}(l) \rightarrow 2\mathrm{KOH}(aq) + \mathrm{H_2}(g)$$

Indeed, all alkali metals react with water in this exact way, according to a general equation:

$$2\mathrm{M}(s) + 2\mathrm{H_2O}(l) \rightarrow 2\mathrm{MOH}(aq) + \mathrm{H_2}(g) \qquad \mathrm{M = Li, Na, K, Rb, or\ Cs}$$

Physical similarities are also apparent in the video. All three are metallic, silver-gray in color, and all three metals are less dense than water. All float on the surface while they react. Other properties not obvious in the video exist. Alkali metals are soft and easily cut. All are solid at room temperature, but melt below 200°C, low for a metal.

Beyond similar reactions with water, all alkali metals undergo analogous reactions with oxygen from the atmosphere, forming oxides, M_2O. Alkali metals react with hydrogen to form hydrides, MH, and sulfur to form sulfides, M_2S. In all of these compounds, the alkali metals are positive ions, Li^+, Na^+, K^+, Rb^+ or Cs^+.

Each member of the chemical family of alkali metals has physical and chemical properties very similar to all the others. In most cases *all alkali metals behave the same with regard to the formulas of their compounds.* The peroxides and superoxides are exceptions to this rule, but formulas for oxides and each of the other types of compounds we have described are identical except for the chemical symbol of each alkali metal.

For a demonstration of alkali metals on a larger (and more exciting scale), check out what Mythbusters did with Alkali metals.

Another set of elements with similar properties are fluorine, chlorine, bromine, and iodine, known collectively as the **halogens**. All four elements exist as diatomic molecules, in the form of: X_2, where X=F, Cl , Br, and I. Further, all the halogens react with the alkali metals to form salts according to the reaction:

$$\mathbf{2M + X_2 \rightarrow 2MX} \qquad \mathbf{M = Li, Na, K, Rb, or Cs \text{ and } X = F, Cl, Br, I}$$

All of the resulting compounds have similar properties as well, such as tasting "salty".

Another example of similarity in chemical properties is with mercury, whose reaction with bromine was discussed in the section covering macroscopic and microscopic views of a chemical reaction. Mercury reacts with other halogens in the same way:

$$\mathbf{Hg}(l) + \mathbf{X_2}(g, l, \text{or} s) \rightarrow \mathbf{HgX_2}(s) \qquad \mathbf{X = F, Cl, Br, \text{or } I}$$

The halogens also react directly with hydrogen, yielding the hydrogen halides:

$$\mathbf{H_2 + X_2 \rightarrow 2HX} \qquad \mathbf{X = F, Cl, Br, I}$$



Even though they differ in phase (F and Cl are gases, Br is a liquid, and I is a solid), all are water soluble, and, except for HF, are strong acids in aqueous solution.

In all these examples, the halogens are anions, F^-, Cl^-, Br^-, and I^-. From these examples, it should be clear that the halogens, like the alkali metals, represent a grouping of elements which share a number of chemical and physical properties.

There are several other examples of related groups of elements. Beryllium, magnesium, calcium, strontium, barium, and radium all show similarities, and are called **alkaline earth metals**. All alkaline earths are silvery-gray metals which are ductile and relatively soft. However, they are much denser than the alkali metals, and their melting points are significantly higher. They are also harder than the alkali metals. Further, they all form form hydrides, MH_2; oxides, MO; halides, MX_2; with M = Mg, Ca, Sr, Ba, or Ra and X = F, Cl, Br, I. In all these compounds the alkaline-earth elements occur as dipositive ions, Mg^{2+}, Ca^{2+}, Sr^{2+}, or Ba^{2+}.



Another example of related elements are the **coinage metals**, copper, silver, and gold, which often occur naturally as elements, not in compounds. They have been used throughout history to make coins because they do not combine rapidly with atmospheric oxygen. The reddish brown and golden colors of copper and gold are distinctive among the metals, and the electrical conductivities of the coinage metals are greater than those of any other elements. The **chalcogens** (sulfur, selenium, and tellurium) are another related group of nonmetallic elements. Their hydrogen compounds (hydrogen sulfide, hydrogen selenide, and hydrogen telluride) are all gases which have revolting odors. The familiar smell of rotten eggs is due to hydrogen sulfide and the other two are even worse. These compounds are also highly poisonous and more dense than air. Numerous cases are known where persons working in ditches or other low-lying areas have been rendered unconscious or even killed by hydrogen sulfide resulting from natural sources or from industrial activities such as petroleum refining.

One group of elements, the **noble gases** (helium, neon, argon, krypton, xenon, and radon), forms almost no chemical compounds. Although small concentrations of the noble gases are present in the earth's atmosphere, they were not discovered until 1894, largely because they underwent no reactions. Fluorine is sufficiently reactive to combine with pure samples of xenon, radon, and (under special conditions) krypton. The only other element that has been shown conclusively to occur in compounds with the noble gases is oxygen, and no more than a couple of dozen noble-gas compounds of all types are known. This group of elements is far less reactive chemically than any other.



1. ↑ "Substance and Registry Number Counter." Chemical Abstracts Service-American Chemical Society. 1 July 2009.www.cas.org/cgi-bin/cas/regreport.pl

---

This page titled 1.1.2: Groups of Related Elements is shared under a CC BY-NC-SA 4.0 license and was authored, remixed, and/or curated by Ed Vitz, John W. Moore, Justin Shorb, Xavier Prat-Resina, Tim Wendorff, & Adam Hahn.

- **4.2: Groups of Related Elements** by Ed Vitz, John W. Moore, Justin Shorb, Xavier Prat-Resina, Tim Wendorff, & Adam Hahn is licensed CC BY-NC-SA 4.0.

1.1.3: The Periodic Table

The similarities among macroscopic properties within each of the chemical families just described lead one to expect microscopic similarities as well. Atoms of sodium ought to be similar in some way to atoms of lithium, potassium, and the other alkali metals. This could account for the related chemical reactivities and analogous compounds of these elements.

According to Dalton's atomic theory, different kinds of atoms may be distinguished by their relative masses (atomic weights). Therefore it seems reasonable to expect some correlation between this microscopic property and macroscopic chemical behavior. You can see that such a relationship exists by listing symbols for the first dozen elements in order of increasing relative mass. Obtaining atomic weights, we have

At Wt	1.0	4.0	6.9	9.0	10.8	12.0	14.0	16.0	19.0	20.2	23.0	24.3
Symbol	H	He	Li	Be	B	C	N	O	F	Ne	Na	Mg

Elements which belong to families we have already discussed are indicated by shading around their symbols. The second, third, and forth elements on the list (He, Li, and Be) are a noble gas, an alkali metal, and an alkaline-earth metal, respectively. Exactly the same sequence is repeated eight elements later (Ne, Na, and Mg), but this time a halogen (F) precedes the noble gas. If a list were made of all elements, we would find the sequence halogen, noble gas, alkali metal, and alkaline-earth metal several more times.

In 1871 the Russian chemist Dmitri Ivanovich Mendeleev (1834 to 1907) proposed the **periodic law**. This law states that *when the elements are listed in order of increasing atomic weights, their properties vary periodically*. That is, similar elements do not have similar atomic weights. Rather, as we go down a list of elements in order of atomic weights, corresponding properties are observed at regular intervals. To emphasize this periodic repetition of similar properties, Mendeleev arranged the symbols and atomic weights of the elements in the table shown below. Each vertical column of this **periodic table** contains a **group** or **family** of related elements. The alkali metals are in group I (*Gruppe* I), alkaline earths in group II, chalcogens in group VI, and halogens in group VII. Mendeleev was not quite sure where to put the coinage metals, and so they appear twice. Each time, however, copper, silver, and gold are arranged in a vertical column. The noble gases were discovered nearly a quarter century after Mendeleev's first periodic table was published, but they, too, fit the periodic arrangement. In constructing his table, Mendeleev found that sometimes there were not enough elements to fill all the available spaces in each horizontal row or **period**. When this was true, he assumed that eventually someone would discover the element or elements needed to complete a period. Mendeleev therefore left blank spaces for undiscovered elements and predicted their properties by averaging the characteristics of other elements in the same group.

Reihen	Gruppe I. R^2O	Gruppe II. RO	Gruppe III. R^2O^3	Gruppe IV. RH^4 RO^2	Gruppe V. RH^3 R^2O^5	Gruppe VI. RH^2 RO^3	Gruppe VII. RH R^2O^7	Gruppe VIII. RO^4
1	H=1							
2	Li=7	Be=9,4	B=11	C=12	N=14	O=16	F=19	
3	Na=23	Mg=24	Al=27,3	Si=28	P=31	S=32	Cl=35,5	
4	K=39	Ca=40	—=44	Ti=48	V=51	Cr=52	Mn=55	Fe=56, Co=59, Ni=59, Cu=63
5	(Cu=63)	Zn=65	—=68	—=72	As=75	Se=78	Br=80	
6	Rb=85	Sr=87	?Yt=88	Zr=90	Nb=94	Mo=96	—=100	Ru=104, Rh=104, Pd=106, Ag=108
7	(Ag=108)	Cd=112	In=113	Sn=118	Sb=122	Te=125	J=127	
8	Cs=133	Ba=137	?Di=138	?Ce=140	—	—	—	— — — —
9	(—)	—	—	—	—	—	—	
10	—	—	?Er=178	?La=180	Ta=182	W=184	—	Os=195, Ir=197, Pt=198, Au=199
11	(Au=199)	Hg=200	Tl=204	Pb=207	Bi=208	—	—	
12	—	—	—	Th=231	—	U=240	—	— — — —

Figure **1.1.3.1**. Mendeleev's periodic table, redrawn from Annalen der Chemie, supplemental volume 8, 1872. The German words Gruppe and Reihen indicate, respectively, the groups and rows (or periods) in the table. Mendeleev also used the European convention of a comma instead of a period for the decimal and J instead I for iodine. The noble gases had not yet been discovered when Mendeleev devised the periodic table, and are thus not displayed.

As an example of this process, look at the fourth numbered row (*Reihen*). Scandium (Sc) was unknown in 1872; so titanium (Ti) followed calcium (Ca) in order of atomic weights. This would have placed titanium below boron (B) in group III, but Mendeleev knew that the most common oxide of titanium, TiO_2, had a formula similar to an oxide of carbon CO_2, rather than of boron, B_2O_3. Therefore he placed titanium below carbon in group IV. He proposed that an undiscovered element, ekaboron, would eventually be

found to fit below boron. (The prefix *eka* means “below.”) Properties predicted for ekaboron are shown in the following table. They agreed remarkably with those measured experimentally for scandium when it was discovered 7 years later. This agreement was convincing evidence that a periodic table is a good way to summarize a great many macroscopic, experimental facts. **Table 1.1.3.1** Comparison of Mendeleev’s Predictions with the Observed Properties of the Element Scandium.

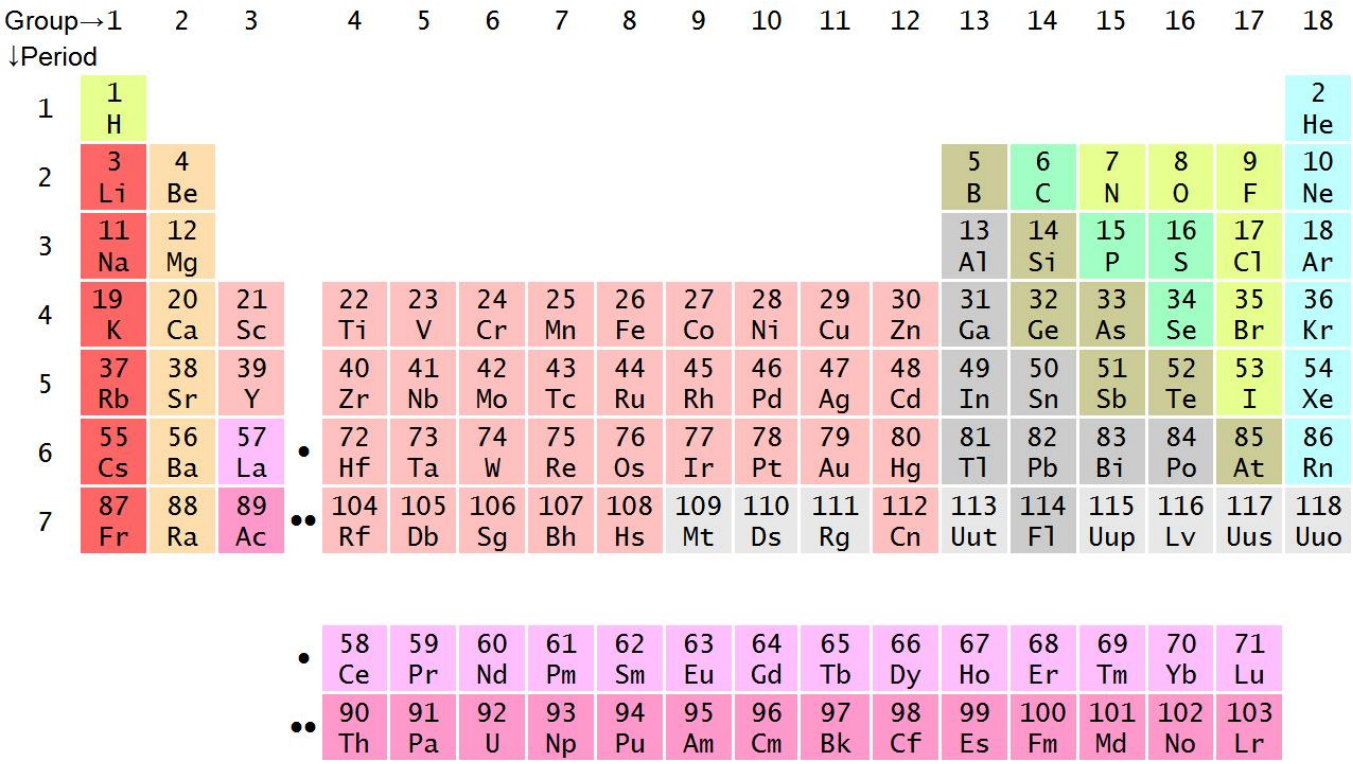
Comparison of Mendeleev’s Predictions with the Observed Properties of the Element Scandium.

	Properties Predicted for Ekaboron (Eb)* by Mendeleev 1872	Properties Found for Scandium after its Discovery in 1879
Atomic weight	44	44†
Formula of oxide	Eb_2O_3	Sc_2O_3
Density of oxide	3.5	3.86
Acidity of oxide	Greater than MgO	Greater than MgO
Formula of chloride	$EbCl_3$	$ScCl_3$
Color of compounds	Colorless	Colorless

* Mendeleev used the name "eka"boron because the blank space into which the element should fit was "below" boron in his periodic table.

† The modern value of the atomic weight of scandium is 44.96.

The modern periodic table differs in some ways from Mendeleev’s original version. It contains more than 40 additional elements, and its rows are longer instead of being squeezed under one another in staggered columns. For example, Mendeleev’s fourth and fifth rows are both contained in the fourth period of the modern table. This ends up placing gallium, not scandium underneath boron in the periodic table. This rearrangement is due to theory on the electronic structure of atoms, in particular ideas about orbitals and the relation of electronic configuration to the periodic table. The extremely important idea of vertical groups of related elements is still retained, as are Mendeleev’s group numbers. The latter appear as roman numerals at the top of each column in the modern table.



To end on a very practical note, there are a variety of sites with interactive periodic tables listed below. These tables can be helpful for understanding periodic trends and learning cool facts about the elements themselves.

Periodic Table [www.ptable.com]

Periodic Table [www.rsc.org]

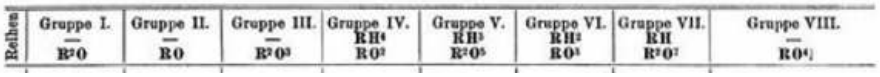
Periodic Table of Elements [www.webelements.com]

This page titled 1.1.3: The Periodic Table is shared under a CC BY-NC-SA 4.0 license and was authored, remixed, and/or curated by Ed Vitz, John W. Moore, Justin Shorb, Xavier Prat-Resina, Tim Wendorff, & Adam Hahn.

- **4.3: The Periodic Table** by Ed Vitz, John W. Moore, Justin Shorb, Xavier Prat-Resina, Tim Wendorff, & Adam Hahn is licensed CC BY-NC-SA 4.0.

1.1.4: Valence

Perhaps the most important function of the periodic table is that it helps us to predict the chemical formulas of commonly occurring compounds. At the top of each group, Mendeleev provided a general formula for oxides of the elements in the group.



Reihen	Gruppe I.	Gruppe II.	Gruppe III.	Gruppe IV.	Gruppe V.	Gruppe VI.	Gruppe VII.	Gruppe VIII.
	—	—	—	RH^4	RH^3	RH^2	RH	—
	R^2O	RO	R^2O^3	RO^2	R^2O^5	RO^3	R^2O^7	RO^4

Row and column headings from Mendeleev's original periodic table. This includes group number but also general formula for the oxides and hydrides it formed as well.

The heading R^2O above group I, for example, means that we can expect to find compounds such as H_2O, Li_2O, Na_2O etc. Similarly, the general formula RH^3 above group V suggests that the compounds NH_3, PH_3,VH_3, and AsH_3(among others) should exist. To provide a basis for checking this prediction, formulas are shown in the following table for compounds in which H, O, or Cl is combined with each of the first two dozen elements (in order of atomic weights). Even among groups of elements whose descriptive chemistry we have not discussed, you can easily confirm that most of the predicted formulas correspond to compounds which actually exist. Conversely, more than 40 percent of the formulas for known O compounds agree with Mendeleev's general formulas, and are shaded in color in the table.

Table **1.1.4.1**: Molecular Formulas for Hydrogen, Oxygen, and Chlorine Compounds of the First Twenty-Four Elements in Order of Atomic Weight.*

Element	Atomic Weight	Hydrogen Compounds	Oxygen Compounds	Chlorine Compounds
Hydrogen	1.01	H_2	H_2O, H_2O_2	HCl
Helium	4.00	None formed	None formed	None formed
Lithium	6.94	LiH	Li_2O, Li_2O_2	LiCl
Beryllium	9.01	BeH_2	BeO	$BeCl_2$
Boron	10.81	B_2H_6	B_2O_3	BCl_3
Carbon	12.01	CH_4, C_2H_6, C_3H_8†	CO_2, CO, C_2O_3	CCl_4, C_2Cl_6
Nitrogen	14.01	NH_3, N_2H_4, HN_3	N_2O, NO, NO_2, N_2O_5	NCl_3
Oxygen	16.00	H_2O, H_2O_2	O_2, O_3	<Cl_2O, ClO_2, Cl_2O_7
Fluorine	19.00	HF	OF_2, O_2F_2	ClF, ClF_3, ClF_5
Neon	20.18	None formed	None formed	None formed
Sodium	22.99	NaH	Na_2O, Na_2O_2	NaCl
Magnesium	24.31	MgH_2	MgO	$MgCl_2$
Aluminum	26.98	AlH_3	Al_2O_3	$AlCl_3$
Silicon	28.09	SiH_4, Si_2H_6	SiO_2	$SiCl_4$, Si_2Cl_6
Phosphorus	30.97	PH_3, P_2H_4	P_4O_{10}, P_4O_6	PCl_3, PCl_5, P_2Cl_4
Sulfur	32.06	H_2S, H_2S_2	SO_2, SO_3	S_2Cl_2, SCl_2, SCl_4
Chlorine	35.45	HCl	Cl_2O, ClO_2, Cl_2O_7	Cl_2
Potassium	39.10	KH	K_2O, K_2O_2, KO_2	KCl
Argon	39.95	None formed	None formed	None formed
Calcium	40.08	CaH_2	CaO, CaO_2	$CaCl_2$
Scandium	44.96	Relatively Unstable	Sc_2O_3	$ScCl_3$
Titanium	47.90	TiH_2	TiO_2, Ti_2O_3, TiO	$TiCl_4$, $TiCl_3$, $TiCl_2$
Vanadium	50.94	VH_2	V_2O_5, V_2O_3, VO_2, VO	VCl_4, VCl_3, VCl_2
Chromium	52.00	CrH_2	Cr_2O_3, CrO_2, CrO_3	$CrCl_3$, $CrCl_2$

* For each element compounds are listed in order of decreasing stability. In some cases additional compounds are known, but these are relatively unstable.

† A great many stable compounds of carbon and hydrogen are known, but space limitations prevent listing all of them.

The periodic repetition of similar formulas is even more pronounced in the case of Cl compounds. This is evident when a list is made of subscripts for Cl in combination with each of the first 24 elements. Consulting the above table, we find HCl (subscript 1), no compound with He (subscript 0), LiCl (subscript 1),and so on.

Element	H	He	Li	Be	B	C	N	O	F	Ne	Na	Mg	Al	Si	P	S	Cl	*K*	*Ar*	Ca	Sc	Ti	V	Cr
Subscript of Cl	1	0	1	2	3	4	3	2	1	0	1	2	3	4	3	2	1	*1*	*0*	2	3	4	3	2

List of the first twenty four elements and their subscripts with Cl. The subscripts of Cl in order of the element is 1, 0, 1, 2, 3, 4, 3, 2, 1, 0, 1, 2, 3, 4, 3, 2, 1, 1, 0, 2, 3, 4, 3, and 2 respectively.

With only the two exceptions indicated in italics, at least one formula for a compound of each element fits a sequence of subscripts which fluctuate regularly from 0 up to 4 and back to 0 again. (The unusual behavior of K and Ar will be discussed a bit later.) The number of Cl atoms which combines with one atom of each other element varies quite regularly as the atomic weight of the other element increases. The experimentally determined formulas in the first table and the general formulas in Mendeleev's periodic table both imply that each element has a characteristic chemical combining capacity. This capacity is called **valence**, and it varies periodically with increasing atomic weight. The noble gases all have valences of 0 because they almost never combine with any other element. H and Cl both have the same valence. They combine with each other in a 1:1 ratio to form HCl, each combines with Li in the same 1:1 ratio (LiH and LiCl), each combines with Be in the same ratio (BeH_2, $BeCl_2$), and so on. Because H and Cl have the same valence, we can predict that a large number of H compounds will have formulas identical to those of Cl compounds, except, of course, that the symbol H would replace the symbol Cl. The correctness of this prediction can be verified by studying the formulas surrounded by gray shading in the first table. The combining capacity, or valence, of O is apparently twice that of H or Cl. *Two* H atoms combine with one O atom in H_2O So do two Cl atoms or two Li atoms (Cl_2O and Li_2O). The number of atoms combining with a single O atom is usually *twice as great* as the number which combined with a single H or Cl atom. (Again, consulting the gray shaded formulas in the first table will confirm this statement.) After careful study of the formulas in the table, it is also possible to conclude that none of the elements (except the unreactive noble gases) have smaller valences than H or Cl. Hence we assign a valence of 1 to H and to Cl. The valence of O is twice as great, and so we assign a value of 2.

Example 1.1.4.1: Formula Predictions

Use the data in the first table to predict what formula would be expected for a compound containing (a) sodium and fluorine; (b) calcium and fluorine.

Solution

a) From the table we can obtain the following formulas for the most common sodium compounds:

$NaH\ Na_2O\ NaCl$

All of these would imply that sodium has a valence of 1. For fluorine compounds we have

$HF\ OF_2\ ClF$

which imply that fluorine also has a valence of 1. Therefore the formula is probably

NaF

b) We already know that the valence of fluorine is 1. For calcium the formulas

$CaH_2\ CaO\ CaCl_2$

argue in favor of a valence of 2. Therefore the formula is most likely

CaF_2

In some cases one element can combine in more than one way with another. For example, you have already encountered the compounds $HgBr_2$ and Hg_2Br_2. There are many other examples of such variable valence in the first table. Nevertheless in its most common compounds, each element usually exhibits one characteristic valence, no matter what its partner is. Therefore it is possible to use that valence to predict formulas. Variable valence of an element may be looked upon as an exception to the rule of a specific combining capacity for each element. The experimental observation that a given element usually has a specific valence can be explained if we assume that each of its atoms has a fixed number of valence sites. One of these sites would be required to connect with one site on another atom. In other words, a noble-gas atom such as Ar or Ne would not have any combining sites, H and Cl atoms would have one valence site each, an O atom would have two, and so on. Variable valence must involve atoms in which some valence sites are more readily used than others. In the case of the F compounds of Cl (ClF, ClF_3, ClF_5), for example, the formulas imply that at least five valence sites are available on Cl. Only one of these is used in ClF and in most of the chlorine

compounds in the table. The others are apparently less readily available. Mendeleev's inclusion of general formulas above the columns of his periodic table indicates that the table may be used to predict valences of the elements and formulas for their compounds. Two general rules may be followed:

1. In periodic groups I to IV, the group number is the most common valence.
2. In periodic groups V to VII, the most common valence is equal to 8 minus the group number, or to the group number itself.

For groups V to VII, the group number gives the valence only when the element in question is combined with oxygen, fluorine, or perhaps one of the other halogens. Otherwise 8 minus the group number is the rule.

✔ Example 1.1.4.2: Compound Formulas

Use the modern periodic to predict the formulas of compounds formed from (a) aluminum and chlorine; (b) phosphorus and chlorine. Use the table on this page to verify your prediction.

Solution

a) Aluminum is in group III and so rule 1 predicts a valence of 3. Chlorine is in group VII and is not combined with oxygen or fluorine, and so its valence is 8 – 7 = 1 by rule 2. Each aluminum has three valence sites, while each chlorine has only one, and so it requires three chlorine atoms to satisfy one aluminum, and the formula is $AlCl_3$.

b) Again chlorine has a valence of 1. Phosphorus is in group V and might have a valence of 5 or of 8 – 5 = 3. Therefore we predict formulas PCl_5 or PCl_3. *Note:* All three predicted formulas appear in the table on this page.

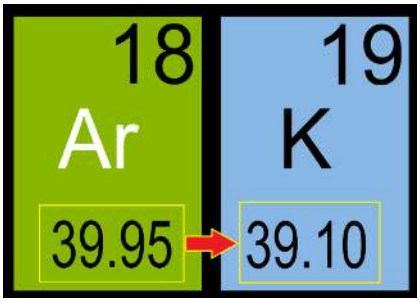
This page titled 1.1.4: Valence is shared under a CC BY-NC-SA 4.0 license and was authored, remixed, and/or curated by Ed Vitz, John W. Moore, Justin Shorb, Xavier Prat-Resina, Tim Wendorff, & Adam Hahn.

- **4.4: Valence** by Ed Vitz, John W. Moore, Justin Shorb, Xavier Prat-Resina, Tim Wendorff, & Adam Hahn is licensed CC BY-NC-SA 4.0.

1.1.5: Exceptions to the Periodic Law

In the process of constructing the first periodic table, Mendeleev encountered several situations where the properties of elements were incompatible with the positions they would be forced to occupy in order of increasing atomic weight. In such a case, Mendeleev chose to emphasize the properties, because in the 1870s it was difficult to determine atomic weights accurately. He assumed that some atomic weights were in error and that ordering of elements ought to be changed to agree with chemical behavior.

One example occurs when looking at the valence of potassium(K) and argon(Ar). While potassium has a smaller atomic weight than argon(39.10 vs. 39.95) the valence properties of potassium suggest that it should follow argon in the periodic table. Mendeleev did not have to contend with this because argon, one of the noble gases, had not been discovered in 1872, but it illustrates the difficulty nicely. There is a break in the regular sequence of valences of the first 24 elements when we come to K and Ar.



Comparison of Argon and potassium. Argon, atomic number of 18 has atomic mass of 39.95 u. Potassium, atomic number 19 has an atomic mass of 39.10 u.

The alkali metal has a *smaller* atomic weight than the noble gas and appears before the noble gas in the sequence of atomic weights. All other alkali metals immediately follow noble gases (they have slightly *larger* atomic weights). Unless we make an exception to the order of increasing atomic weight for Ar and K, the periodic table would contain a strange anomaly. One of the elements in the vertical column of noble gases would be the extremely reactive silver metal pictured below, Potassium (K). Likewise, the reactive group of alkali metals would contain the gas Argon, pictured below, which is not a metal and is very unreactive.



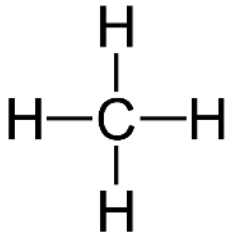
Mendeleev's assumption that more accurate atomic weight determinations would eliminate situations such as we have just described has turned out to be incorrect. The atomic weights used for K before Ar are modern, highly accurate values, but they still predict the wrong order for Ar and K. The same problem occurs in the case of Co and Ni and of Te and I. Apparently atomic weight, although related to chemical behavior, is not as fundamental as Mendeleev and other early developers of the periodic table thought.

This page titled 1.1.5: Exceptions to the Periodic Law is shared under a CC BY-NC-SA 4.0 license and was authored, remixed, and/or curated by Ed Vitz, John W. Moore, Justin Shorb, Xavier Prat-Resina, Tim Wendorff, & Adam Hahn.

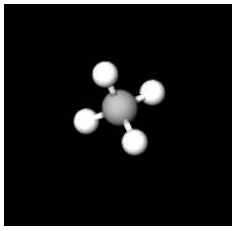
- **4.5: Exceptions to the Periodic Law** by Ed Vitz, John W. Moore, Justin Shorb, Xavier Prat-Resina, Tim Wendorff, & Adam Hahn is licensed CC BY-NC-SA 4.0.

1.1.6: Implications of Periodicity for Atomic Theory

The concept of valence implies that atoms of each element have a characteristic number of sites by which they can be connected to atoms of other elements. Carbon, as seen below, has 4 'connection' or valence sites. Here Carbon is connected to 4 Hydrogen atoms, forming CH_4, better known as methane. Note that the symbolic and 3D representations below both depict the same molecule, but the symbolic representation clearly shows the valence sites, while the 3D representation accurately shows how those valence sites are arranged in 3D space.



A central C atom is bonded to H atoms on the top, bottom, left and right making it a total of four bonds.



Three dimensional structure shows a central grey sphere connected to four white spheres in a tetrahedral shape.

The number of valence sites repeats periodically as atomic weight increases, and occasionally even this regular repetition is imperfect. Atoms of similar atomic weight often have quite different properties, while some which differ widely in relative mass behave almost the same. Dalton's atomic theory considers atoms to be indestructible spheres whose most important property is mass. This is clearly inadequate to account for the macroscopic observations of the elements. In order to continue using the atomic theory, we must attribute some underlying structure to atoms. If both valence and atomic weight are determined by that structure, we should be able to account for the close but imperfect relationship between these two properties. The next section will describe some of the experiments which led to current theories about just what this atomic structure is like.

This page titled 1.1.6: Implications of Periodicity for Atomic Theory is shared under a CC BY-NC-SA 4.0 license and was authored, remixed, and/or curated by Ed Vitz, John W. Moore, Justin Shorb, Xavier Prat-Resina, Tim Wendorff, & Adam Hahn.

- **4.6: Implications of Periodicity for Atomic Theory** by Ed Vitz, John W. Moore, Justin Shorb, Xavier Prat-Resina, Tim Wendorff, & Adam Hahn is licensed CC BY-NC-SA 4.0.

1.1.7: Radiation

Just prior to the turn of the twentieth century, additional observations were made which contradicted parts of Dalton's atomic theory. The French physicist Henri Becquerel (1852 to 1928) discovered by accident that compounds of uranium and thorium emitted *rays* which, like rays of sunlight, could darken photographic films. Seen in Figure **1.1.7.2** is the photographic Becquerel used, darkened by the *rays* emitted by Uranium. Becquerel's rays differed from light in that they could even pass through the black paper wrappings in which his films were stored.



Figure **1.1.7.1**: Image of Becquerel's photographic plate which has been fogged by exposure to radiation from a uranium salt. The shadow of a metal Maltese Cross placed between the plate and the uranium salt is clearly visible (Public Domain).

Black and white picture of a photographic film with two areas of dark spots. One is rectangular in shape and the other has an imprint of a Maltese Cross.

Detecting Radiation

Although themselves invisible to the human eye, the rays could be detected easily because they produced visible light when they struck phosphors such as impure zinc sulfide. Such luminescence is similar to the glow of a psychedelic poster when invisible ultraviolet (black light) rays strike it. Further experimentation showed that if the rays were allowed to pass between the poles of a magnet, they could be separated into the three groups shown in Figure **1.1.7.2**.

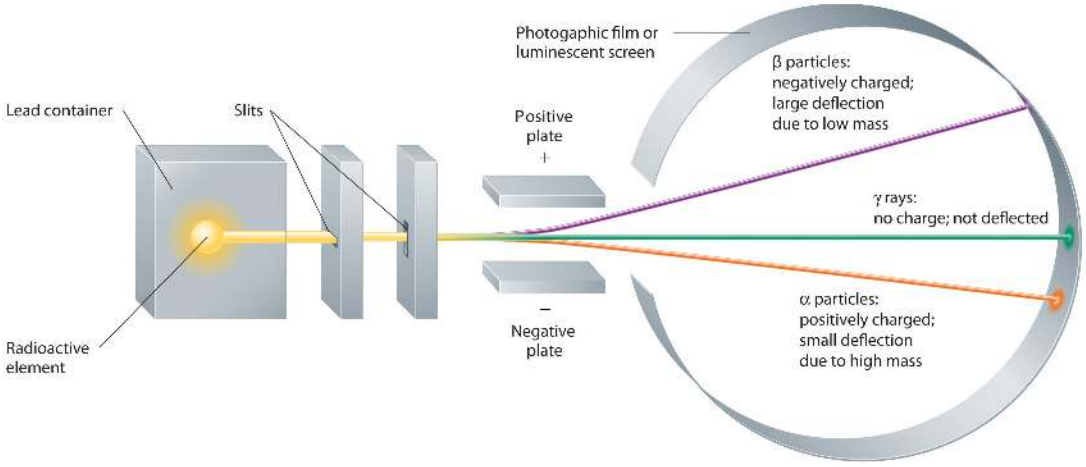


Figure **1.1.7.2**: Behavior of α particles, β particles, and γ rays upon passing through a magnetic field.

The experimental setup shows a lead container on the left containing a radioactive element inside it. The rays from this element first passes through a horizontal slit and then through a vertical slit. The ray then continues to pass between a positive plate at the top and a negative plate below. The rays are then allowed to hit a photographic film or a luminescent screen. The Beta particles's pathway is curved upwards. Gamma rays are not deflected and continues in a straight path. Alpha particles's pathway is curved downwards but to a less degree than the beta particle.

Properties of α, β and γ Particles

Because little or nothing was known about these rays, they were labeled with the first three letters of the Greek alphabet. Upon passing through the magnetic field, the alpha rays (α rays) were deflected slightly in one direction, beta rays (β rays) were deflected to a much greater extent in the opposite direction, and gamma rays (γ rays) were not deflected at all (Figure **1.1.7.2**). Deflection by a

magnet is a characteristic of electrically charged *particles* (as opposed to rays of light). From the direction and extent of deflection it was concluded that the β particles had a negative charge and were much less massive than the positively charged α particles. The γ rays did not behave as electrically charged particles would, and so the name *rays* was retained for them. Taken together the α particles, β particles, and γ rays were referred to as **radioactivity**, and the compounds which emitted them as **radioactive**.

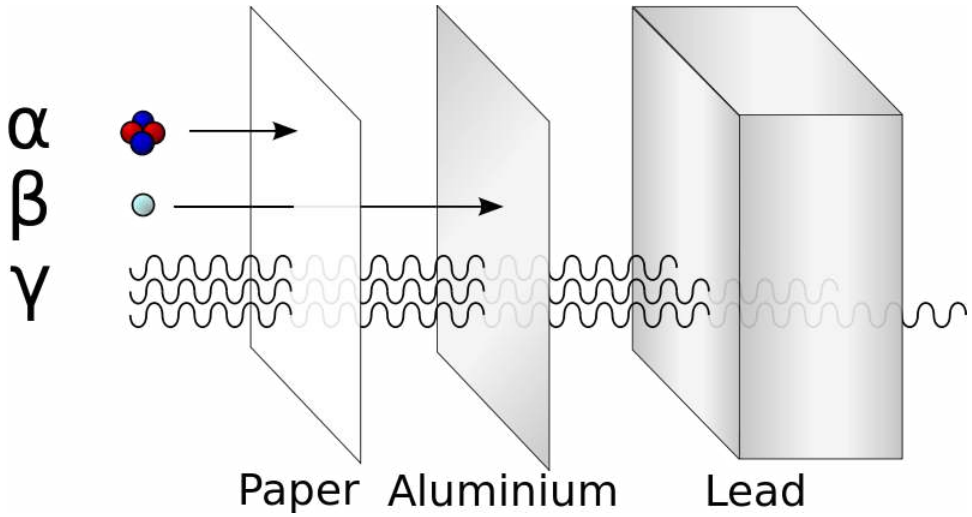


Figure **1.1.7.3**: This diagram demonstrates the ability to penetrate matter of different kinds of ionizing radiation. Alpha particles are stopped by a sheet of paper whilst beta particles halt to an aluminium plate. Gamma radiation is dampened when it penetrates matter. (CC BY-SA 2.5; Stannered).

Illustration of alpha particle, beta particle and gamma rays aligned on the left, starting at the same position. A piece of paper, aluminum, and lead is spaced apart and placed in that order. The alpha particle has an arrow that stops at the sheet of paper while the beta particles has arrows which pass through paper but stop at aluminum, and gamma rays are represented by multiple waves passing through paper, aluminum, and lead. However the number of rays is reduced as it exits the block of lead.

The three types of particle differ greatly in penetrating power Figure **1.1.7.3**. While γ particles may penetrate several millimeters of lead, β particles are may penetrate 1 mm of aluminum, but α particles do not penetrate thin paper, or a centimeter or two of air. The high penetrating power of γs does not make them more dangerous, because if they penetrate matter they do not cause changes in it. On the other hand, if an α source is a few inches away, it is not harmful at all; but if an α emitter like radon is inhaled, the α particles are very dangerous. Because they do not penetrate matter, their energy is absorbed in the alveoli of the lung where it causes molecular damage, sometimes leading to lung cancer.

Transmutation

Study of radioactive compounds by the French chemist Marie Curie (1867 to 1934) revealed the presence of several previously undiscovered elements (radium, polonium, actinium, and radon). These elements, and any compounds they formed, were intensely radioactive. When thorium and uranium compounds were purified to remove the newly discovered elements, the level of radioactivity decreased markedly. It increased again over a period of months or years, however. Even if the uranium or thorium compounds were carefully protected from contamination, it was possible to find small quantities of radium, polonium, actinium, or radon in them after such a time. To chemists, who had been trained to accept Dalton's indestructible atoms, these results were intellectually distasteful. The inescapable conclusion was that some of the uranium or thorium atoms were spontaneously changing their structures and becoming atoms of the newly discovered elements. A change in atomic structure which produces a different element is called transmutation.

Transmutation of uranium into the more radioactive elements could explain the increased emission of radiation by a carefully sealed sample of a uranium compound. During these experiments with radioactive compounds it was observed that minerals containing uranium or thorium always contained lead as well.

$$^{238}_{92}\mathrm{U} \rightarrow {}^{234}_{90}\mathrm{Th} + \alpha$$

This lead apparently resulted from further transmutation of the highly radioactive elements radium, polonium, actinium, and radon. The lead found in uranium ores always had a significantly lower atomic weight than lead from most other sources (as low as 206.4 compared with 207.2, the accepted value). Lead associated with thorium always had an unusually high atomic weight.

Nevertheless, all three forms of lead had the same chemical properties. Once mixed together, they could not be separated. Such results, as well as the reversed order of elements such as Ar and K in the periodic table, implied that atomic weight is not the fundamental determinant of chemical behavior.

This page titled 1.1.7: Radiation is shared under a CC BY-NC-SA 4.0 license and was authored, remixed, and/or curated by Ed Vitz, John W. Moore, Justin Shorb, Xavier Prat-Resina, Tim Wendorff, & Adam Hahn.

- **4.8: Radiation** by Ed Vitz, John W. Moore, Justin Shorb, Xavier Prat-Resina, Tim Wendorff, & Adam Hahn is licensed CC BY-NC-SA 4.0.

1.1.8: The Electron

Near the middle of the nineteenth century the English chemist and physicist Michael Faraday (1791 to 1867) established a connection between electricity and chemical reactions. He already knew that an electric current flowing into certain molten compounds through metal plates called **electrodes** could cause reactions to occur. Samples of different elements would deposit on the electrodes. Faraday found that the same quantity of electric charge was required to produce 1 mol of any element whose valence was 1. Twice that quantity of charge would deposit 1 mol of an element whose valence was 2, and so on.

Electric charge is measured in units called **coulombs**, abbreviated C. One coulomb is the quantity of charge which corresponds to a current of one ampere flowing for one second. In the image below, electrons (the blue particles) can be seen flowing through a metal wire. The coulomb then is the total charge of all electrons that flow through the wire in a given second.

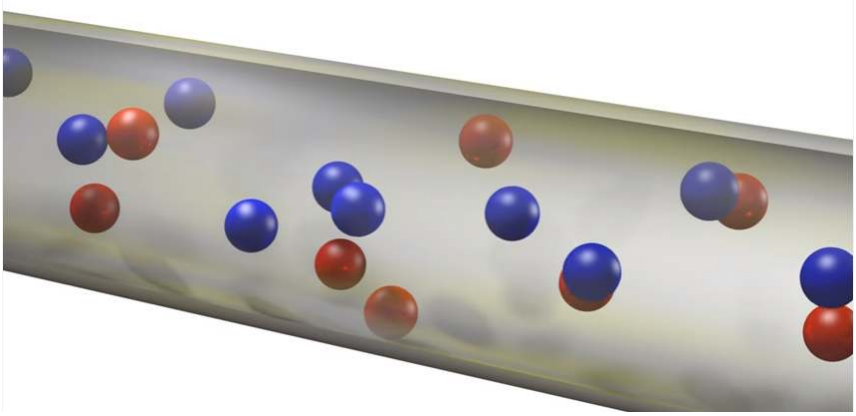


Image Credits: Physics Videos by Eugene Khutoryansky

The relationship between electricity and atomic structure was further clarified by experiments involving **cathode-ray tubes** in the 1890s. A cathode-ray tube can be made by pumping most of the air or other gas out of a glass tube and applying a high voltage to two metal electrodes inside. If ZnS or some other phosphor is placed on the glass at the end of the tube opposite the negatively charged electrode (**cathode**), the ZnS emits light. This indicates that some kind of rays are streaming away from the cathode. When passed between the poles of a magnet, these cathode rays behave the same way as the β particles described earlier. The fact that they were very small electrically charged particles led the English physicist J. J. Thomson (1856 to 1940) to identify them with the electrons of Faraday's experiments. Thus cathode rays are a beam of electrons which come out of the solid metal of the cathode. They behave exactly the same way no matter what the electrode is made of or what gas is in the tube. These observations allow one to conclude that *electrons must be constituents of all matter*.



In addition to being deflected by a magnet, the electron beam in a cathode-ray tube can be attracted toward a positively charged metal plate or repelled from a negative plate. By adjusting such electrodes to exactly cancel the deflection produced by a magnet of known strength, Thomson was able to determine that the ratio of charge to mass for an electron is 1.76×10^8 C/g. This is a rather

large ratio. Either each electron has a very large charge, or each has a very small mass. We can see which by using Faraday's result that there are 96 500 C mol^{-1} of electrons

$$\frac{96\ 500\ \text{C mol}^{-1}}{1.76\ \times\ 10^{8}\ \text{C g}^{-1}} = 5.48\ \times\ 10^{-4}\ \text{g mol}^{-1}$$

Thus the molar mass of an electron is 5.48×10^{-4} g mol^{-1}, and if we think of the electron as an "atom"(or indivisible particle) of electricity, its atomic weight would be 0.000548—only $\frac{1}{1837}$ that of hydrogen, the lightest element known. In 1909 the American physicist Robert A. Millikan (1863 to 1953) was able to determine the charge on an electron independently of its mass. His value of 1.6×10^{-19} C can be combined with Thomson's charge-to-mass ratio to give an independent check on the molar mass for the electron

$$\frac{1.60\ \times\ 10^{-19}\ \text{C}}{1.76\ \times\ 10^{8}\ \text{C g}^{-1}}\ \times\ 6.022\ \times\ 10^{23}\ \text{mol}^{-1} = 5.47\ \times\ 10^{-4}\ \text{g mol}^{-1}$$

thus confirming that the electron has much less mass than the lightest atom. (The quantity 1.6×10^{-19} C is often represented by the symbol *e*. Thus the charge on a single electron is $-e = -1.6 \times 10^{-19}$ C. The minus sign indicates that the electron is a *negatively* charged particle.)

This page titled 1.1.8: The Electron is shared under a CC BY-NC-SA 4.0 license and was authored, remixed, and/or curated by Ed Vitz, John W. Moore, Justin Shorb, Xavier Prat-Resina, Tim Wendorff, & Adam Hahn.

- **4.9: The Electron** by Ed Vitz, John W. Moore, Justin Shorb, Xavier Prat-Resina, Tim Wendorff, & Adam Hahn is licensed CC BY-NC-SA 4.0.

1.1.9: The Nucleus

The results of Thomson's and other experiments implied that electrons were constituents of all matter and hence of all atoms. Since macroscopic samples of the elements are found to be electrically neutral, this meant that each atom probably contained a positively charged portion to balance the negative charge of its electrons. In an attempt to learn more about how positive and negative charges were distributed in atoms, Ernest Rutherford (1871 to 1937) and his coworkers performed numerous experiments in which α particles emitted from a radioactive element such as polonium were allowed to strike thin sheets of metals such as gold or platinum.

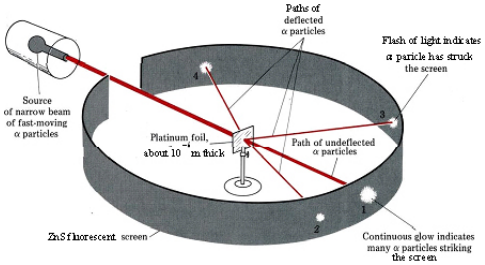
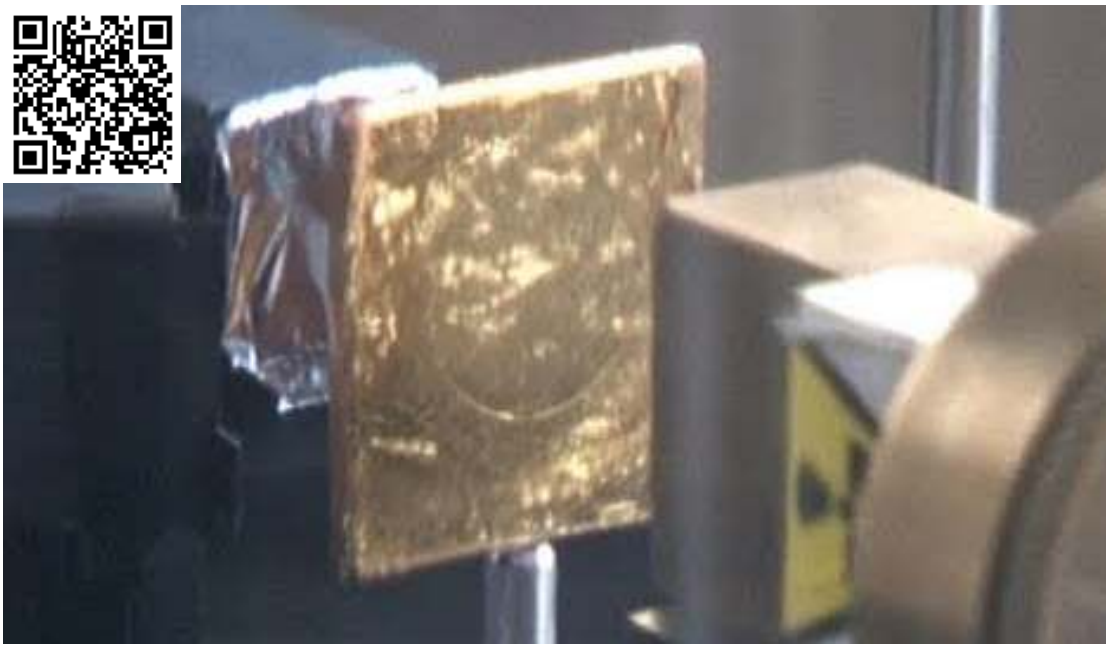


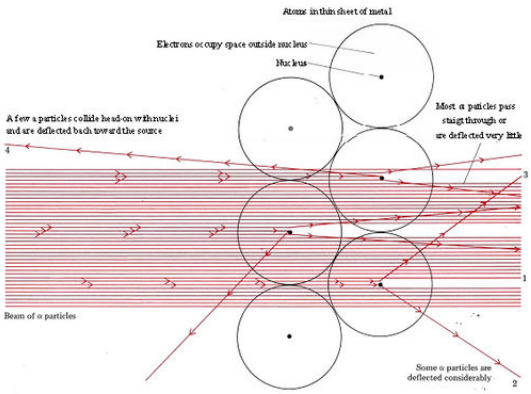
Figure **1.1.9.1** : A schematic diagram of the apparatus used by Geiger and Marsden to study deflection of α particles by thin metal foil. When an α particle strikes the ZnS screen, a flash of light is observed. Most of the flashes occurred at position 1, indicating the most α particles passed through the metal with little or no deflection. The few flashes at positions such as number 4 were interpreted to mean that a few α particles had struck something massive in the metal foil and hence had bounced almost straight back.

It was already known that the α particles carried a positive charge and traveled rapidly through gases in straight lines. Rutherford reasoned that in a solid, where the atoms were packed tightly together, there would be numerous collisions of α particles with electrons or with the unknown positive portions of the atoms. Since the mass of an individual electron was quite small, a great many collisions would be necessary to deflect an α particle from its original path, and Rutherford's preliminary calculations indicated that most would go right through the metal targets or be deflected very little by the electrons. In 1909, confirmation of this expected result was entrusted to Hans Geiger and a young student, Ernest Marsden, who was working on his first research project.



Video 1.1.9.1 *Rutherford Gold Foil Experiment*

The results of Geiger and Marsden's work (using apparatus whose design is shown schematically in Figure **1.1.9.1** were quite striking. Most of the α particles went straight through the sample or were deflected very little. These were observed by means of continuous luminescence of the ZnS screen at position 1 in the diagram. Observations made at greater angles from the initial path of the a particles (positions 2 and 3) revealed fewer and fewer flashes of light, but even at an angle nearly 180° from the initial path (position 4) *a few α particles were detected coming backward from the target*. This result amazed Rutherford. In his own words, "It was quite the most incredible event that has ever happened to me in my life. It was almost as incredible as if you fired a 15-inch shell at a piece of tissue paper and it came back and hit you. On consideration, I realized that this scattering backwards must be the result of a single collision, and when I made calculations I saw that it was impossible to get anything of that order of magnitude unless you took a system in which the greater part of the mass of an atom was concentrated in a minute nucleus."[1] Rutherford's interpretation of Geiger and Marsden's experiment is shown schematically in Fig **1.1.9.2**.



Beam of alpha particles are shown as multiple red parallel lines pointing to the right. Two columns of three circles each represent the atoms in the thin sheet of metal. Most of the lines are seen passing straight through or are deflected very little. Only a few alpha particles collide head on with nuclei and are deflected back towards the source. Some alpha particles are deflected considerably.

Figure **1.1.9.2 :** Rutherford's microscopic interpretation of the results of Geiger and Marsden's experiment.

Quantitative calculations using these experimental results showed that the diameter of the nucleus was about one ten-thousandth that of the atom. The positive charge on the nucleus was found to be + *Ze*, where *Z* is the number which indicates the position of an element in the periodic table. (For example, H is the first element and has *Z* = 1. Helium is the second element and *Z* = 2. The twentieth element in the valence table constructed earlier is Ca, and the nucleus of each Ca atom therefore has a charge of + 20*e* = 20 × 1.60 × 10^{-19} C = 32.0 × 10^{-19} C.) In order for an atom to remain electrically neutral, it must have a total of *Z* electrons outside the nucleus. These provide a charge of –*Ze* to balance the positive nuclear charge. The number *Z*, which indicates the positive charge on the nucleus and the number of electrons in an atom, is called the **atomic number**.

The significance of the atomic number was firmly established in 1914 when H. G. Moseley (1888 to 1915) published the results of experiments in which he bombarded a large number of different metallic elements with electrons in a cathode-ray tube. Wilhelm Roentgen (1845 to 1923) had discovered earlier that in such an experiment, rays were given off which could penetrate black paper or other materials opaque to visible light. He called this unusual radiation x-rays, the x indicating *unknown*. Moseley found that the frequency of the x-rays was unique for each different metal. It depended on the atomic number (but not on the atomic weight) of the metal. (If you are not familiar with electromagnetic radiation or the term *frequency*, read The Nature of Electromagnetic Radiation where they are discussed more fully.) Using his x-ray frequencies, Moseley was able to establish the correct ordering in the periodic table for elements such as Co and Ni whose atomic weights disagreed with the positions to which Mendeleev had assigned them. His work confirmed the validity of Mendeleev's assumption that chemical properties were more important than atomic weights.

[1] Ernest Rutherford, the Development of the Theory of Atomic Structure, in J. Needham and W. Pagel (eds.) "Background to Modern Science," The Macmillan Company, New York, 1938.

This page titled 1.1.9: The Nucleus is shared under a CC BY-NC-SA 4.0 license and was authored, remixed, and/or curated by Ed Vitz, John W. Moore, Justin Shorb, Xavier Prat-Resina, Tim Wendorff, & Adam Hahn.

- **4.10: The Nucleus** by Ed Vitz, John W. Moore, Justin Shorb, Xavier Prat-Resina, Tim Wendorff, & Adam Hahn is licensed CC BY-NC-SA 4.0.

SECTION OVERVIEW

1.2: Chemical Bonding - Electron Pairs and Octets

Theories of chemical bonding invariably involve electrons. When one atom approaches another, the valence electrons, found in the outermost regions of the atoms, interact long before the nuclei can come close together. Electrons are the least massive components of an atom, and so they can relocate to produce electrostatic forces which hold atoms together. According to Coulomb's law, such electrostatic or Coulombic forces are quite large when charges are separated by distances of a few hundred picometers—the size of an atom. Coulombic forces, then, are quite capable of explaining the strengths of the bonds by which atoms are held together.

1.2.1: Prelude to Chemical Bonding

1.2.2: Ionic Bonding

1.2.3: Energy and the Formation of Ions

1.2.4: The Ionic Crystal Lattice

1.2.5: Ions and Noble-Gas Electron Configurations

1.2.6: Ionization Energies

1.2.7: Ionization of Transition and Inner Transition Elements

1.2.8: Electron Affinities

1.2.9: Binary Ionic Compounds and Their Properties

1.2.10: The Octet Rule

1.2.11: Physical Properties

- 1.2.11.1: Lecture Demonstrations

1.2.12: Chemical Properties

1.2.13: The Covalent Bond

1.2.14: Covalent Molecules and the Octet Rule

1.2.15: Writing Lewis Structures for Molecules

- 1.2.15.1: An Excess of Bonds
- 1.2.15.2: Deciding on a Skeleton Structure
- 1.2.15.3: Multiple Bonds

1.2.16: Examples of Lewis Structures

1.2.17: Polyatomic Ions

1.2.18: Ionic Compounds Containing Polyatomic Ions

1.2.19: Atomic Sizes

1.2.20: Ionic Sizes

1.2.21: Periodic Variation of IE and EA

1.2.21.1: Lecture Demonstrations

This page titled 1.2: Chemical Bonding - Electron Pairs and Octets is shared under a CC BY-NC-SA 4.0 license and was authored, remixed, and/or curated by Ed Vitz, John W. Moore, Justin Shorb, Xavier Prat-Resina, Tim Wendorff, & Adam Hahn.

1.2.1: Prelude to Chemical Bonding

We have covered the basic ideas of atomic structure, but it is worth realizing that of all the elements only the noble gases are found naturally in a form such that their atoms occur as individuals, widely separated from all other atoms. Under the conditions that prevail on the surface of the earth, almost all atoms are linked by chemical bonds to other atoms. Oxygen, for example, is the most common element on earth. It is found in combination with metals in rocks, with hydrogen in water, with carbon and hydrogen in living organisms, or as the diatomic molecule O_2 in the atmosphere, but individual oxygen atoms are quite rare. Most other elements behave in a similar way. Thus, if we want to understand the chemistry of everyday matter, we need to understand the nature of the chemical bonds which hold atoms together.

Theories of chemical bonding invariably involve electrons. When one atom approaches another, the valence electrons, found in the outermost regions of the atoms, interact long before the nuclei can come close together. Electrons are the least massive components of an atom, and so they can relocate to produce electrostatic forces which hold atoms together. According to Coulomb's law, such electrostatic or Coulombic forces are quite large when charges are separated by distances of a few hundred picometers—the size of an atom. Coulombic forces, then, are quite capable of explaining the strengths of the bonds by which atoms are held together.

An important piece of evidence relating electrons and chemical bonding was noted by G. N. Lewis shortly after the discovery that the atomic number indicated how many electrons were present in each kind of atom. *Most chemical formulas correspond to an even number of electrons summed over all constituent atoms*. Thus H_2O has 2 electrons from the 2 H's and 8 from O for a total of 10, NCl_3 has $7 + (3 \times 17) = 58$ electrons, and so on. This is a bit surprising when you consider that half the elements have odd atomic numbers so that their atoms have an odd number of electrons. Lewis suggested that *when atoms are bonded together, the electrons occur in pairs*, thus accounting for the predominance of even numbers of electrons in chemical formulas. These pairs often leave bonded atoms with eight electrons in the outer most shell, known as the octet rule. The orbital shown below gives a visual example of the octet rule, as it has a full octet, or 8 valence electrons.

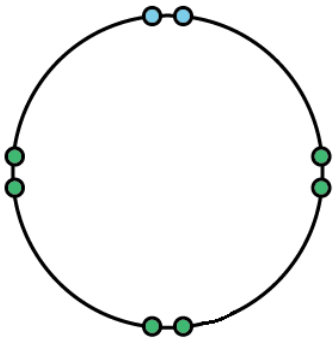


Figure 6.0.1 The octet above is considered full because it contains 8 valence electrons, depicted by circles.

Image s

There are two important ways in which the valence shells of different atoms can interact to produce electron pairs and chemical bonds. When two atoms have quite different degrees of attraction for their outermost electrons, one or more electrons may transfer their allegiance from one atom to another, pairing with electrons already present on the second atom. The atom to which electrons are transferred will acquire excess negative charge, becoming a negative ion, while the atom which loses electrons will become a positive ion. These oppositely charged ions will be held together by the coulombic forces of attraction between them, forming an **ionic bond**. Since electrons are shifted so that one neutral atom becomes positively charged, and the other becomes negatively charged, substances formed from ionic bonding are often in pairs and are then referred to as binary ionic compounds. Binary ionic compounds are not too common, but the existence of polyatomic ions greatly extends the number of ionic substances. Oppositely charged ions are held in crystal lattices by strong coulombic forces, an example of which is pictured below.

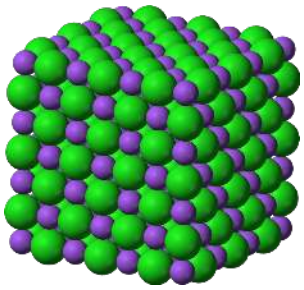


Figure 6.0.2 An example of a crystal lattice structure, in this case the lattice structure of NaCl, or table salt.

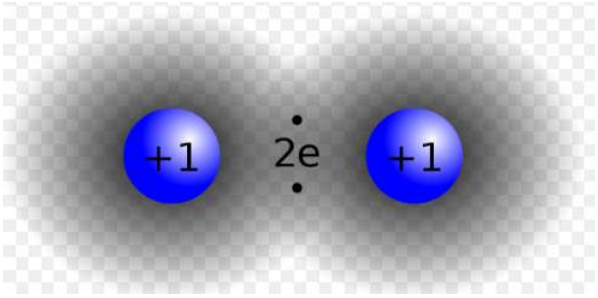
A three dimensional cubic structure is made up of an alternating pattern of green and purple spheres. The green sphere is slightly larger than the purple sphere.

This crystal lattice structure means the physical properties of ionic compounds include hardness, brittleness, and having high melting and boiling points. The majority of them dissolve in water, and in solution each ion exhibits its own chemical properties. Ionic compounds obey the octet rule, which explains why ions are generally in noble-gas electron configurations. An everyday example of an ionic compound, salt, can be seen below.



Figure 6.0.3 Table Salt, an example of an ionic compound. Like most ionic compounds, table salt is hard and brittle and dissolves easily in water.

On the other hand, when two atoms have the same degree of attraction for their valence electrons, it is possible for them to *share* pairs of electrons in the region between their nuclei. Such shared pairs of electrons attract *both* nuclei, holding them together with a **covalent bond**. Sharing one or more pairs of electrons between two atoms attracts the nuclei together and usually results in an octet around each atom. This process of sharing electrons is demonstrated below, where two Hydrogen atoms share their only electrons with each other, thus forming a covalent bond.



There are two identical blue circles. One is on the left and the other on the right. Inside the circles are label "Plus 1". Right in the center between these two circles are two tiny black dots with the label "2 e".

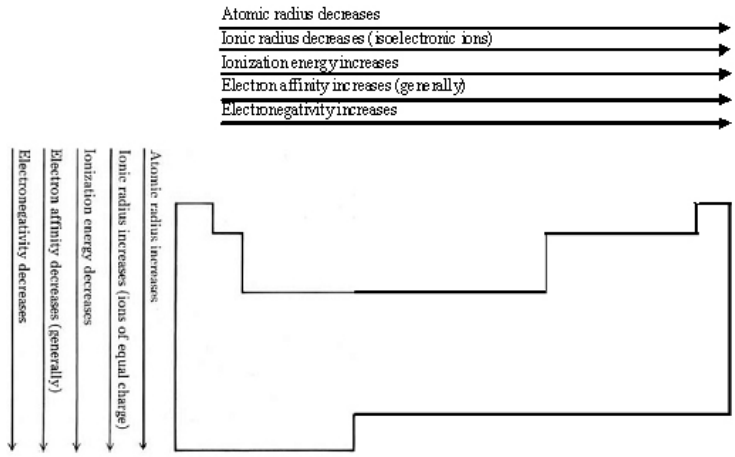
Figure 6.0.4 *The bond shown above is covalent because the 2 electrons are shared between atoms.*

Covalent bonding often produces individual molecules, like CO_2 or CH_3CH_2OH, which have no net electrical charge and little attraction for each other. Thus covalent substances often have low melting and boiling points and are liquids or gases at room

temperature. Occasionally, as in the case of SiO_2, an extended network of covalent bonds is required to satisfy the octet rule. Such giant molecules result in solid compounds with high melting points. A common (if expensive) covalent solid, known for its hardness, is the diamond, pictured below.



A number of atomic properties, such as ionization energy, electron affinity, van der Waals radii, covalent atomic radii, and ionic radii, are important in determining whether certain elements will form covalent or ionic compounds and what properties those compounds will have. In the next sections we will consider the formation of covalent and ionic bonds and the properties of some substances containing each type of bond. The figure below previews how each atomic property important to understanding bonding varies according to an atom's position in the periodic table. The figure also includes one atomic property, electronegativity, which will be covered when we explore further aspects of covalent bonding in more depth.



The trends of atomic properties down a group and across a period are shown. Across a period, atomic radius and ionic radius for isoelectronic ions decreases while ionization energy, electron affinity, and electronegativity increases. Down a group, Atomic radius and ionic radius for ions of equal charge increases. However, the ionization energy, electron affinity, and electronegativity decreases.

This page titled 1.2.1: Prelude to Chemical Bonding is shared under a CC BY-NC-SA 4.0 license and was authored, remixed, and/or curated by Ed Vitz, John W. Moore, Justin Shorb, Xavier Prat-Resina, Tim Wendorff, & Adam Hahn.

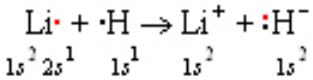
- **6.1: Prelude to Chemical Bonding** by Ed Vitz, John W. Moore, Justin Shorb, Xavier Prat-Resina, Tim Wendorff, & Adam Hahn is licensed CC BY-NC-SA 4.0.

1.2.2: Ionic Bonding

Ionic bonding involves transfer of an electron from one atom (which becomes a positively charged *cation*) to another (which becomes a negatively charged *anion*). The two ions attract strongly to form a *crystal lattice*.

Since ionic bonding requires that the atoms involved have unequal attraction for their valence electrons, an ionic compound must involve atoms of two quite different elements. Attraction for electrons depends on the distance of the electrons from the nucleus (which in turn depends on the amount of shielding by inner electrons). Ionic compounds generally form between metals toward the left and bottom of the periodic table, and nonmetals toward the right and top of the periodic table.

The simplest example of a binary ionic compound is provided by the combination of elements number 1 (H) and number 3 (Li) in lithium hydride, LiH. On a microscopic level the formula LiH contains four electrons. In separate Li and H atoms these electrons are arranged as shown in part *a* of the following figure. The H atom has the electron configuration $1s^1$, and Li is $1s^2 2s^1$. When the two atoms are brought close enough together, however, the striking rearrangement of the electron clouds shown part *b* takes place. Here the color coding shows clearly that the electron density which was associated with the 2*s* orbital in the individual Li atom has been transferred to a 1*s* orbital surrounding the H atom. As a result, two new microscopic species are formed. The extra electron transforms the H atom into a *negative ion* or **anion**, written H^- and called the *hydride ion*. The two electrons left on the Li atom are not enough to balance the charge of +3 on the Li nucleus, and so removal of an electron produces a *positive ion* or **cation**, written Li^+ and called the *lithium ion*. The electron-transfer process can be summarized in of Lewis diagrams as follows:



L i with a red dot beside it. This reacts with H with a black dot beside it. This produces a L i positive ion with no dots beside it as well as a H negative ion with a black dot and a red dot beside it.

The opposite charges of Li^+ and H^-attract each other strongly, and the ions form an **ion pair** (see image below) in which the two nuclei are separated by a distance of 160 pm (1.60 Å).

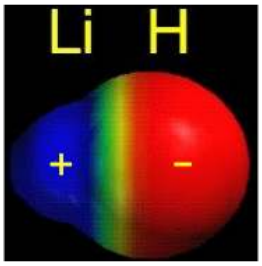
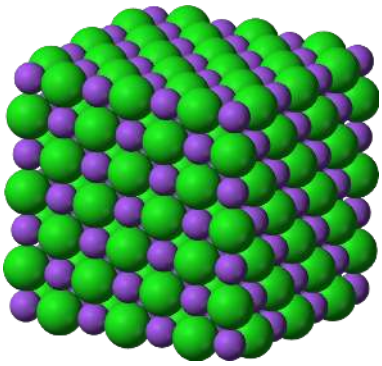


Diagram of a smaller blue sphere merging with a larger red sphere. The blue sphere is labeled as L i positive ion and the red sphere is H negative ion. The region in the middle is green in color.

The image above shows an ion pair of Lithium Hydride. Notice how Lithium has a strong positive charge (cation) and Hydrogen has a strong negative charge (anion).

Multiple **ion pairs** (as seen in the image above) connect to form a **crystal lattice**, pictured below. All ionic solids form a crystal lattice and the shape of the lattice determines the properties and look of the solid.



A three dimensional cubic structure is made up of an alternating pattern of green and purple spheres. The green sphere is slightly larger than the purple sphere.

This page titled 1.2.2: Ionic Bonding is shared under a CC BY-NC-SA 4.0 license and was authored, remixed, and/or curated by Ed Vitz, John W. Moore, Justin Shorb, Xavier Prat-Resina, Tim Wendorff, & Adam Hahn.

- **6.2: Ionic Bonding** by Ed Vitz, John W. Moore, Justin Shorb, Xavier Prat-Resina, Tim Wendorff, & Adam Hahn is licensed CC BY-NC-SA 4.0.

1.2.3: Energy and the Formation of Ions

Formation of an ion pair by transfer of an electron from an Li atom to an H atom results in an overall *lowering of the total energy* of the two nuclei and four electrons involved. How and why this occurs is best seen if we break ion-pair formation into three simpler steps and consider the energy change involved in each. The three steps are

1. Removal of the 2*s* electron from an Li atom to form an Li^+ ion.
2. Addition of that same electron to an H atom to form an H^- ion.
3. The coming together of the two ions to form an ion pair.

The energy required in step 1 to remove an electron completely from an isolated atom is called the **ionization energy**. The ionization energy of lithium is 520 kJ mol^{-1}. In other words, 520 kJ of energy is needed to remove a mole of 2*s* electrons from a mole of isolated lithium atoms in order to form a mole of isolated lithium ions. Alternatively we can say that 520 kJ is needed to **ionize** a mole of lithium atoms. See Figure **1.2.3.1** for a visual representation of the energy "cost" of ionization.

While energy is needed to accomplish step 1, we find that energy is *released* in step 2 when a hydrogen atom accepts an electron and becomes a hydride ion. The reason for this can be seen in the formation of LiH ion pair dot density diagram. The second electron acquired by the hydrogen atom can pair up with the electron already in the 1*s* orbital without contradicting the Pauli exclusion principle. As a result, the new electron can move in close enough to the hydrogen nucleus to be held fairly firmly, lowering its energy significantly. Although the paired electrons repel each other somewhat, this is not enough to offset the attraction of the nucleus for both.

Since the energy of the electron is *lowered*, the law of conservation of energy requires that the same quantity of energy must be *released* when a hydrogen atom is transformed into a hydride ion. The energy released when an electron is acquired by an atom is called the **electron affinity**. The electron affinity of hydrogen is 73 kJ mol^{-1} indicating that 73 kJ of energy is released when 1 mol of isolated hydrogen atoms each accepts an electron and is converted into a hydride ion.

Since 520 kJ mol^{-1} is *required* to remove an electron from a lithium atom, while 73 kJ mol^{-1} is *released* when the electron is donated to a hydrogen atom, it follows that transfer of an electron from a lithium to a hydrogen atom requires (520 – 73) kJ mol^{-1} = 447 kJ mol^{-1}. This net energy change can best be seen in Figure **1.2.3.1**.

At room temperature processes which require such a large quantity of energy are extremely unlikely. Indeed the transfer of the electron would be impossible if it were not for step 3, the close approach of the two ions. When oppositely charged particles move closer to each other, their potential energy decreases and they release energy. The energy released when lithium ions and hydride ions come together to 160 pm under the influence of their mutual attraction is 690 kJ mol^{-1}, more than enough to offset the 447 kJ mol^{-1} needed to transfer the electron. Thus there is a net release of (690 – 447) kJ mol^{-1} = 243 kJ mol^{-1} from the overall process. The transfer of the electron from lithium to hydrogen and the formation of an Li^+H^- ion pair results in an overall lowering of energy, as seen in Figure **1.2.3.1** below.

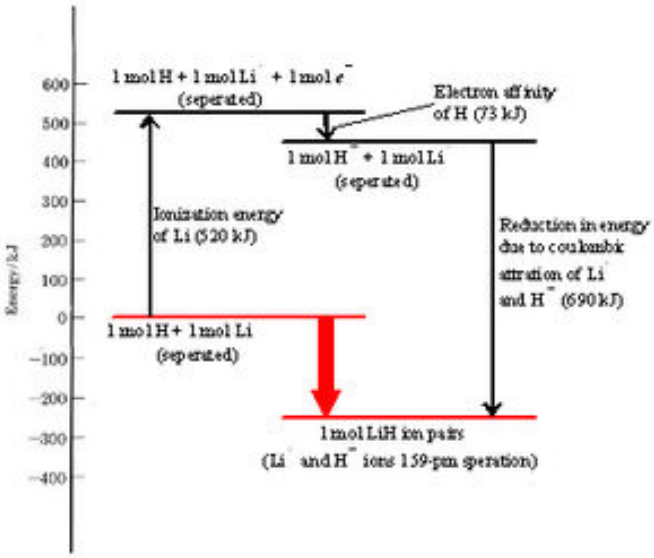


Figure **1.2.3.1**: Energy changes, which occur when 1 mol H atoms and 1 mol Li atoms are transformed into 1 mol LiH solid.

An energy level diagram in kilojoules is shown for the different steps involved in the formation of 1 mol of L i positive ion H negative ion pair from a separated set of 1 mol of H and 1 mol of Li.

In the above figure, the energy change in each step and the overall change are illustrated diagrammatically. As in the case of atomic structure, where electrons occupy orbitals having the lowest allowable energy, a collection of atoms tends to rearrange its constituent electrons so as to minimize its total energy. Formation of a lithium hydride ion pair is energetically “downhill” and therefore favored.

A more complete picture of the energies involved is provided by the "Born-Haber Cycle" diagram of LiF_2 below. It emphasizes that the EA and IP apply to single atoms in the gas phase, and that other energies may be more important in determining the exothermicity of formation of ionic compounds. The greatest energy released is not the EA, but the lattice energy. Other energy costs involve formation of single atoms in the gas phase by vaporization of Li (s) (ΔH_{vap}) to give Li (g), and the dissociation energy of F_2 ($\Delta H_{dissociation}$) to give 2F. The sum of all the energies is the energy of formation of the ionic compound, according to Hess' Law. Basically, the Born Haber Cycle shows all the details of the formation of LiF_2, while the diagram we looked at earlier takes a big picture view.

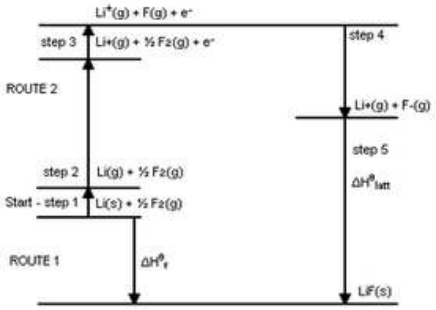


Figure **1.2.3.2**: Energy changes, which occur when 1 mol F_2 gas and 1 mol Li metal are transformed into 1 mol LiF_2 solid.[1]

Energy level diagram shown for two routes of Lithium fluoride ion formation. The energy levels are represented by horizontal lines and each step of energy exchanges is represented by arrows pointing either up or down. The second route breaks down all the steps involved. The starting level is 1 mol of solid lithium plus half a mole of fluorine gas. Step 1 points up to level of 1 mol of lithium gas plus half mol of fluorine gas. Step 2 points up to next level which is 1 mol of lithium ion gas plus half mole of fluorine gas plus 1 mol of electron. Step 3 points up to highest level which is 1 mol of lithium ion gas plus 1 mol of gaseous fluorine atom plus 1 mol of electrons. Step 4 points down to 1 mol of lithium ion gas plus fluoride ion gas. Step 5 labeled delta H latt, points to the lowest level showing a solid lithium fluoride. The first route involves 1 step, labeled delta H formation, pointing from the starting level to the lowest final level.

References

1. Haber Cycle [en.Wikipedia.org]

This page titled 1.2.3: Energy and the Formation of Ions is shared under a CC BY-NC-SA 4.0 license and was authored, remixed, and/or curated by Ed Vitz, John W. Moore, Justin Shorb, Xavier Prat-Resina, Tim Wendorff, & Adam Hahn.

- **6.3: Energy and the Formation of Ions** by Ed Vitz, John W. Moore, Justin Shorb, Xavier Prat-Resina, Tim Wendorff, & Adam Hahn is licensed CC BY-NC-SA 4.0.

1.2.4: The Ionic Crystal Lattice

Up to this point we have been considering what would happen if a single Li atom and a single H atom were combined. When a large number of atoms of each kind combine, the result is somewhat different. Electrons are again transferred, and ions are formed, but the ions no longer pair off in twos. Instead, under the influence of their mutual attractions and repulsions, they collect together in much larger aggregates, eventually forming a three-dimensional array like that shown in the Figure **1.2.4.1.** On the macroscopic level a crystal of solid lithium hydride is formed.

The formation of such an **ionic crystal lattice** results in a lower potential energy than is possible if the ions only group into pairs. It is easy to see from the figure of the crystal lattice why this should be so. In an ion pair each Li^+ ion is close to only one H^- ion, whereas in the crystal lattice it is close to no less than *six* ions of opposite charge. Conversely each H^- ion is surrounded by six Li^+ ions. In the crystal lattice therefore, more opposite charges are brought closer together than is possible for separate ion pairs and the potential energy is lower by an additional 227 kJ mol^{-1}. The arrangement of the ions in a crystal of LiH corresponds to the lowest possible energy. If there were an alternative geometrical arrangement bringing even more ions of opposite charge even closer together than that shown in the figure, the Li^+ ions and H^- ions would certainly adopt it.

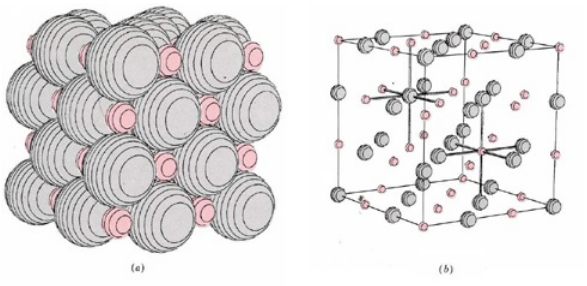


Figure **1.2.4.1**: A portion of the ionic crystal lattice of lithium hydride, LiH. (a) Lithium ions, Li^+, (color) and hydride ions, H^-, (gray) are shown full size. In a macroscopic crystal the regular array of ions extends indefinitely in all directions. (b) "Exploded" view of the lattice, showing that each Li^+ ion (color) is surrounded by six H^- ions (gray), and vice versa. (Computer-generated). (Copyright © 1976 by W. G. Davies and J. W. Moore.)

This page titled 1.2.4: The Ionic Crystal Lattice is shared under a CC BY-NC-SA 4.0 license and was authored, remixed, and/or curated by Ed Vitz, John W. Moore, Justin Shorb, Xavier Prat-Resina, Tim Wendorff, & Adam Hahn.

- **6.4: The Ionic Crystal Lattice** by Ed Vitz, John W. Moore, Justin Shorb, Xavier Prat-Resina, Tim Wendorff, & Adam Hahn is licensed CC BY-NC-SA 4.0.

1.2.5: Ions and Noble-Gas Electron Configurations

When considering the formation of LiH, one aspect deserves explanation. If the transfer of one electron from Li to H is energetically favorable, why is the same not true for the transfer of a second electron to produce $Li^{2+}H^{2-}$? Certainly the double charges on Li^{2+} and H^{2-} would attract more strongly than the single charges on Li^{+} and H^{-}, and the doubly charged ions would be held more tightly in the crystal lattice. The answer to this question can be found by looking back at the diagram below.

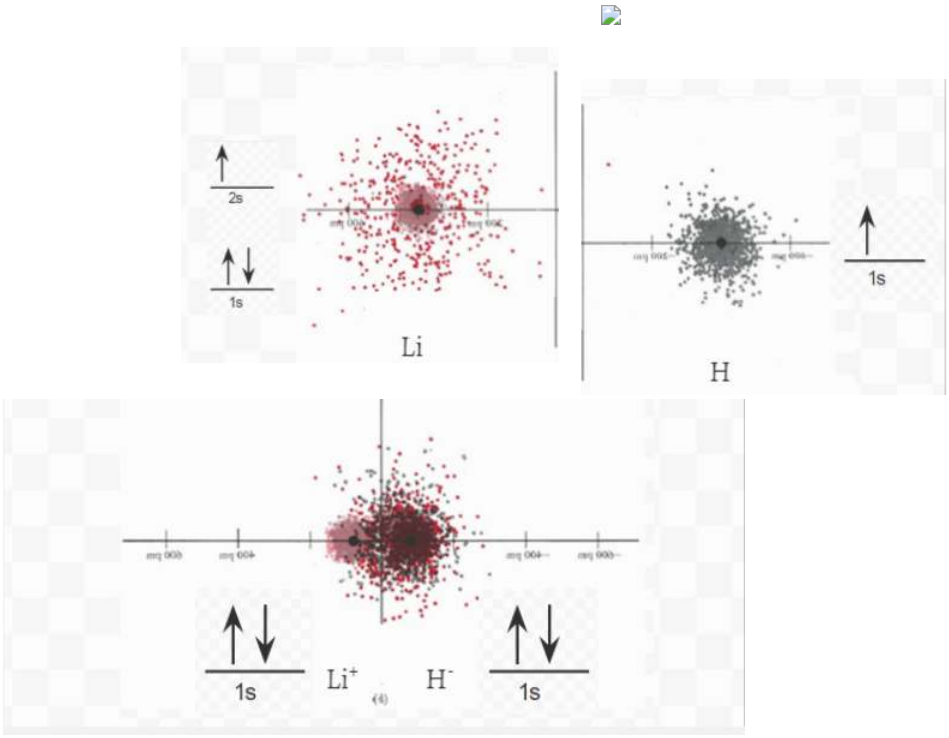
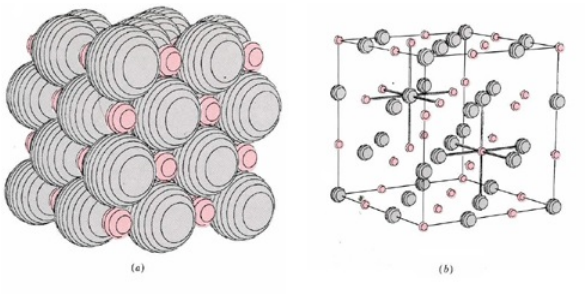


Figure 6.5.1 *The image above shows electron density diagrams for Lithium, Hydrogen, and the ionic compound LiH. Next to each element is the electron orbital diagram, which shows the symbolic form of the electron density diagram.*

Removal of a second electron from Li would require much more energy than the removal of the first because this second electron would be a 1*s* *(from the smaller circle in the image above, closer to the nucleus)* electron rather than a 2*s* electron. Not only is this second electron much closer to the nucleus, but it also is very poorly shielded from the nucleus, meaning it's attraction to the nucleus is strong. It is not surprising, therefore, that the **second ionization energy** of Li (the energy required to remove this second electron) is 7297 kJ mol^{-1} almost 14 times as large as the first ionization energy! Such a colossal energy requirement is enough to insure that only the outermost electron (the *valence* electron) of Li will be removed and that the inner 1*s* kernel with its helium-type electron configuration will remain intact.

A similar argument applies to the acceptance of a second electron by the H atom to form the H^{2-} ion. If such an ion were to be formed, the extra electron would have to occupy the 2*s* orbital (outside the mix of red and grey dots of the H^- ion pictured above). Its electron cloud would extend far from the nucleus (even farther than for the 2*s* electron in Li, because the nuclear charge in H^{2-} would only be +1, as opposed to +3 in Li), and it would be quite high in energy. So much energy would be needed to force a second electron to move around the H nucleus in this way, that only one electron is transferred. The ion formed has the formula H^- and a helium-type $1s^2$ electronic structure instead of an H^{2-} ion with a $1s^2 2s^1$ electronic structure.

The simple example of lithium hydride is typical of all ionic compounds which can be formed by combination of two elements. Invariably we find that one of the two elements has a relatively *low ionization energy* and is capable of easily losing one or more electrons. The other element has a relatively *high electron affinity* and is able to accept one or more electrons into its structure. The ions formed by this transfer of electrons almost always have an electronic structure which is the same as that of *noble gas*, and all electrons are paired in each ion. The resulting compound is *always a solid* in which the ions are arranged in a three-dimensional array or crystal lattice similar to, though not always identical with, that shown in the LiH crystal lattice below.



In such a solid the nearest neighbors of each anion are always cations and vice versa, and the solid is held together by the forces of attraction between the ions of opposite sign. An everyday example of such an ionic compound is ordinary table salt, sodium chloride, whose formula is NaCl. As we shall see in the next section, sodium is an element with a low ionization energy, and chlorine is an element with a high electron affinity.

On the microscopic level crystals of sodium chloride consist of an array of sodium ions, Na^+, and chloride ions, Cl^-, packed together in a lattice like that shown for lithium hydride. The chloride ions are chlorine atoms which have gained an electron and thus have the electronic structure $1s^2 2s^2 2p^6 3s^2 3p^6$, the same as that of the noble-gas argon. The sodium ions are sodium atoms which have lost an electron, giving them the structure $1s^2 2s^2 2p^6$, the same as that of the noble-gas neon. All electrons in both kinds of ions are paired.

This page titled 1.2.5: Ions and Noble-Gas Electron Configurations is shared under a CC BY-NC-SA 4.0 license and was authored, remixed, and/or curated by Ed Vitz, John W. Moore, Justin Shorb, Xavier Prat-Resina, Tim Wendorff, & Adam Hahn.

- **6.5: Ions and Noble-Gas Electron Configurations** by Ed Vitz, John W. Moore, Justin Shorb, Xavier Prat-Resina, Tim Wendorff, & Adam Hahn is licensed CC BY-NC-SA 4.0.

1.2.6: Ionization Energies

Figure **1.2.6.1** plots the the ionization energies of the elements are plotted against atomic number. An obvious feature of this figure is that the elements with the highest ionization energies are the noble gases. Since the ionization energy measures the energy which must be *supplied* to remove an electron, these high values mean that it is difficult to remove an electron from an atom of a noble gas.

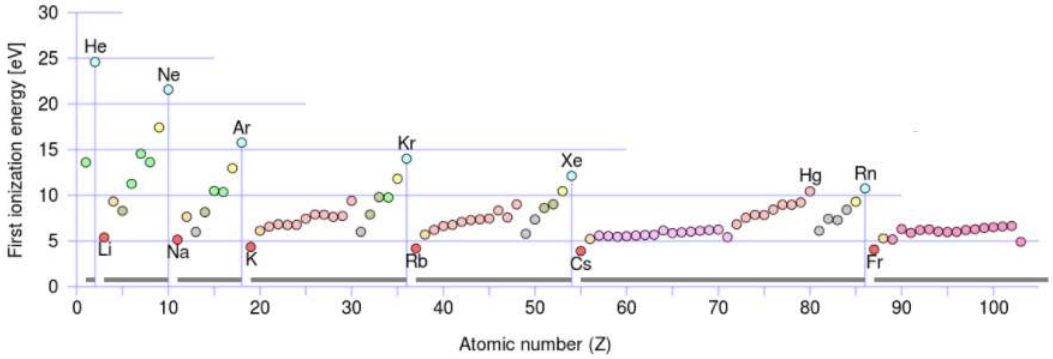


Figure **1.2.6.1**: Periodic trends for ionization energy (IE) vs. atomic number: note that within each of the seven periods the IE (colored circles) of an element begins at a minimum for the first column of the Periodic table (the alkali metals), and progresses to a maximum for the last column (the noble gases) which are indicated by vertical lines and labeled with a noble gas element symbol, and which also serve as lines dividing the 7 periods. Note that the maximum ionization energy for each row diminishes as one progresses from row 1 to row 7 in a given column, due to the increasing distance of the outer electron shell from the nucleus as inner shells are added. (CC-SA_BY-3.0; Sponk).

A second obvious feature is that the elements with the lowest ionization energies are the alkali metals. This means that it is easier to remove electrons from atoms of this group of elements than from any other group. Closer inspection also reveals the following two general tendencies:

1. As one moves *down a given group in the periodic table, the ionization energy decreases*. In group I, for example, the ionization energies decrease in the order Li > Na > K > Rb > Cs. The reason for this is a steady increase in size of the valence electron cloud as the principal quantum number n increases. The 6*s* valence electron of Cs, for instance, is further from the nucleus and hence easier to remove than the 5*s* valence electron of Rb.
2. As one moves from *left to right across the periodic table* (from an alkali-metal atom to a noble gas), *the ionization energy increases* on the whole. In such a move the *n* value of the outermost electrons remains the same, but the nuclear charge increases steadily. This increased nuclear attraction requires that more work he done to remove an electron, and so ionization energy goes up.

One can confirm these general trends by inspecting Figure **1.2.6.1**. As one moves from He to Ne to Ar one can see marked decreases in the ionization energy, confirming the trend of decreasing ionization energy as you move down a group. Moving from left to right across the periodic table produces an increase in the ionization energy, as can be observed by the upward trend as you go from Li to Ne.

Ionization energies can be measured quite accurately for atoms, and the values obtained show some additional features which are less important than the two major trends mentioned above. For example, consider the data for elements in the second row of the periodic table. Numerical values for the relevant ionization energies are shown in Figure **1.2.6.2** of ionization energies and electron affinities below.

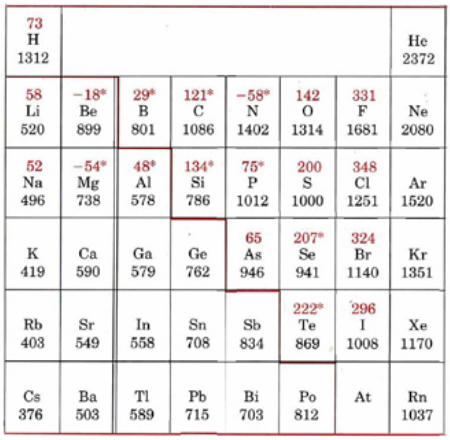


Figure 6.6.2: The image above displays the ionization energies of various elements, with the transition metals excluded.

The general trend of increasing ionization energy across the table is broken at two points. Boron has a smaller value than beryllium, and oxygen has a smaller value than nitrogen. The first break occurs when the first electron is added to a *p* subshell. As was mentioned several times in the previous chapter, a 2*p* electron is higher in energy and hence easier to remove than a 2*s* electron because it is more efficiently shielded from the nuclear charge. Thus the 2*p* electron in boron is easier to remove than a 2*s* electron in beryllium.

The second exception to the general trend occurs in the case of oxygen, which has one more 2*p* electron than the half-filled subshell of nitrogen. The last electron in the oxygen atom is forced into an already occupied orbital where it is kept close to another electron. The repulsion between these two electrons makes one of them easier to remove, and so the ionization energy of oxygen is lower than might be expected.

These discontinuities also appear periodically, as would be expected since they arise from the structure of the valence electrons. Sulfur and selenium, in the same group as oxygen, show the discontinuity in the trend of increasing ionization energy, which arises from the same half-filled *subshell effect*. Aluminum and gallium, both in the same group as boron, similarly show a decrease in ionization energy compared to magnesium and calcium.

While this trend does not seem to apply for indium, and thallium, it is important to remember that the chart is missing the transition metals. Looking at the graph of ionization energies, it is clear that indium(atomic number 49) *does* have a lower ionization energy than cadmium (atomic number 48), and the same is true of mercury, the element preceding thallium (atomic number 81).

Below is a full periodic table, with shading to demonstrate the periodic trend of ionization energy. The darker the shading, the higher the ionization energy. Notice the general trend of increasing darkness (or ionization energy) as one moves to the right and up. Take a moment to write down why this is so.

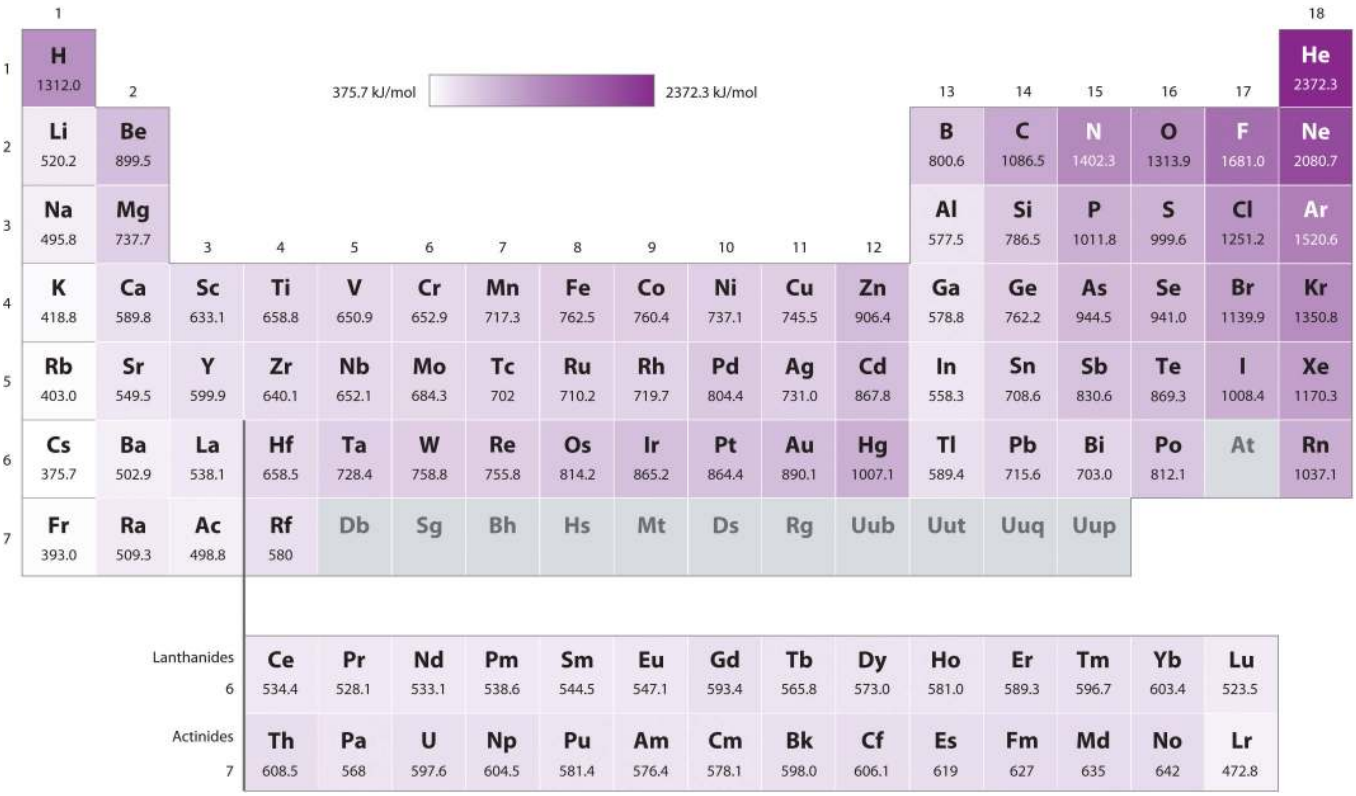


Figure **1.2.6.3**: The darkness of the shading inside the cells of the table indicates the relative magnitudes of the ionization energies. Elements in gray have undetermined first ionization energies. Source: Data from CRC Handbook of Chemistry and Physics (2004). (CC-SA_BY-NC 3.0; anonymous).

This page titled 1.2.6: Ionization Energies is shared under a CC BY-NC-SA 4.0 license and was authored, remixed, and/or curated by Ed Vitz, John W. Moore, Justin Shorb, Xavier Prat-Resina, Tim Wendorff, & Adam Hahn.

- **6.6: Ionization Energies** by Ed Vitz, John W. Moore, Justin Shorb, Xavier Prat-Resina, Tim Wendorff, & Adam Hahn is licensed CC BY-NC-SA 4.0.

1.2.7: Ionization of Transition and Inner Transition Elements

On the graph of ionization energies, it can be seen that ionization energies increase much more slowly across the transition and inner transition elements than for the representative elements. For example, the ionization energy of the representative-element boron is 800 kJ mol^{-1}. Five elements later we find neon, whose ionization energy is 2080 kJ mol^{-1}, an increase of 160 percent. In the fourth period, the transition-element scandium has an ionization energy of 631 kJ mol^{-1}. Five elements later we find iron at 759 kJ mol^{-1}, an increase of only 20 percent. All the lanthanoids have ionization energies from 500 to 600 kJ mol^{-1}, and the actinoids are all between 580 and 680 kJ mol^{-1}.

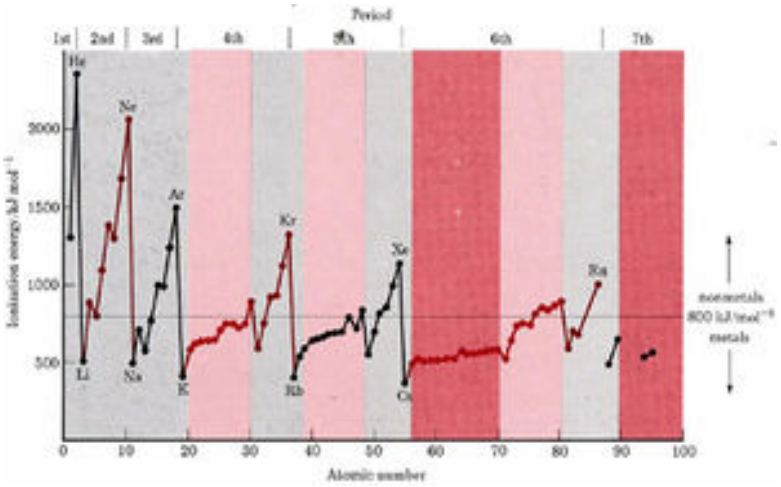


Figure 6.7.1 Graph of ionization energies of the elements versus atomic number. Rows in the periodic table are indicated at the top of the graph. Transition elements appear in a light color and inner transition elements are in the dark-colored areas of the chart.

These similarities among the transition and especially the inner transition elements illustrate statements made about electron configurations and the periodic table. The distinguishing electron for a transition element enters a *d* subshell in the *next-to-outermost* shell, while for an inner transition element it usually enters an *f* subshell in the *third-from-outermost* shell.

Thus the distinction between an element and the one preceding it in the periodic table is much smaller than among the representative elements. Furthermore, experimental measurements show that for transition and inner transition elements the electrons lost when ionization occurs are *not* the *last* ones which were added to build up the atomic electron configuration. Instead, *electrons are usually removed first from the subshell having the largest principal quantum number*.

Example 6.7.1 : Electron Configuration

Determine the electron configuration of the Fe^{3+} ion.

Solution

Since the charge on the ion is +3, three electrons must have been removed from a neutral iron atom (Fe). The electron configuration of Fe is

Fe: $1s^2 2s^2 2p^6 3s^2 3p^6 3d^6 4s^2$ or $[Ar]3d^6 4s^2$

We now remove electrons successively from subshells having the largest principal quantum number:

Fe^+ : $[Ar]3d^6 4s^1$ one 4s electron removed

Fe^{2+}: $[Ar]3d^6$ a second 4*s* electron removed

Fe^{3+}: $[Ar]3d^5$ since no electrons are left in the $n = 4$ shell, one 3*d* electron is removed

The behavior described in the previous paragraph and the example may be better understood by comparing the 3d and 4s shells, as in the following figure.

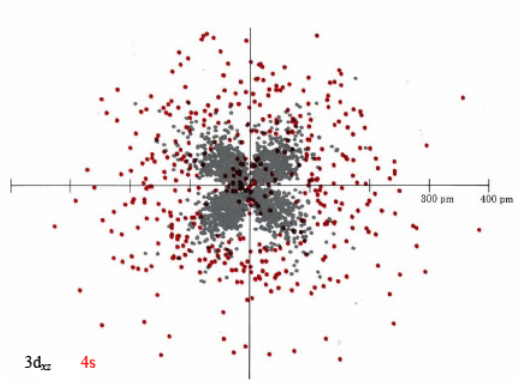


Figure 6.7.2 Comparison of 3d (gray) and 4s (color) electron clouds.

There is a vertical and horizontal axes. The axis has the units picometers. Around the origin is a four lobe shaped region forming an "X" shape around the origin. This region is highly concentrated with grey dots. A circular area around the origin is also filled with red dots. A ring shaped region just beyond the outer edges of the lobed region is filled with red dots. The number of grey and red dots decreases as we move further away from the origin.

Electrons in the subshell having the largest principal quantum number (4*s* in the example and the figure above) are, on the average, farther from the nucleus, and they are first to be removed. The first ionization energy of iron is not much larger than that of scandium because in each case a 4*s* electron is being removed. The iron atom has five more protons in the nucleus, but it also has five more 3*d* electrons which spend most of their time *between* the nucleus and the 4*s* electrons. The screening effect of such 3*d* electrons causes the *effective* nuclear charge to increase very slowly from one transition element to the next. The attraction for 4*s* electrons, and hence ionization energy, also increases very slowly.

Metals

Macroscopic properties such as high thermal and electric conductivity, malleability, and ductility were mentioned in a brief introduction to the elements as characteristics of **metals**. In addition, most metals have low ionization energies, usually below 800 kJ mol^{-1}. In other words, a metal consists of atoms, each of which has at least one loosely held electron.

When such atoms pack close together in a solid metal, the loosely held electrons are relatively free to move from one atom to another. If excess electrons are forced into one end of a metal wire, it is relatively easy for electrons to flow out of the other end. Thus an electric current may be carried through the wire, and the high conductivity of all metals may be understood.

More detailed microscopic interpretations of metallic properties are given for Metals later, but for the time being we are primarily interested in the location of metallic elements in the periodic table. Ionization energies are smallest near the bottom and on the left of the periodic table, and so this is where metals are found. Moreover, ionization energies increase slowly from one transition element to the next and hardly at all across the inner transition elements. Therefore *all* transition and inner transition elements are metals.

In periodic groups IIIA, IVA, and VA elements near the top of the table have large ionization energies and little metallic character. Ionization energies decrease as one moves downward, however. For example, Al is quite metallic, although the element above it, B, is not. A heavy “stairstep” line is usually drawn on the periodic table to separates the nonmetals (above and to the right) from the metals. Elements such as B, Si, Ge, As, Sb, and Te, which are adjacent to the stairstep, have intermediate properties and are called **semimetals**. This same class is also referred to as **metalloids**.

This page titled 1.2.7: Ionization of Transition and Inner Transition Elements is shared under a CC BY-NC-SA 4.0 license and was authored, remixed, and/or curated by Ed Vitz, John W. Moore, Justin Shorb, Xavier Prat-Resina, Tim Wendorff, & Adam Hahn.

- **6.7: Ionization of Transition and Inner Transition Elements** by Ed Vitz, John W. Moore, Justin Shorb, Xavier Prat-Resina, Tim Wendorff, & Adam Hahn is licensed CC BY-NC-SA 4.0.

1.2.8: Electron Affinities

Electron affinities are more difficult to measure experimentally than are ionization energies, and far fewer values are available. The relationship of the periodic table with those electron affinities that have been measured or estimated from calculations can be seen on the table of ionization energies and electron affinities (in the red), seen below.

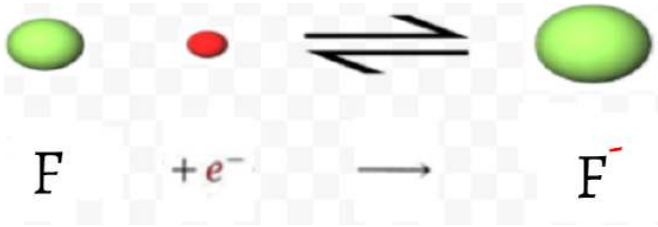
Table 1.2.8.1 Ionization Energies and Electron Affinities. The electron affinities are the red values above the atomic symbol.

73 H 1312							He 2372
58 Li 520	−18* Be 899	29* B 801	121* C 1086	−58* N 1402	142 O 1314	331 F 1681	Ne 2080
52 Na 496	−54* Mg 738	48* Al 578	134* Si 786	75* P 1012	200 S 1000	348 Cl 1251	Ar 1520
K 419	Ca 590	Ga 579	Ge 762	65 As 946	207* Se 941	324 Br 1140	Kr 1351
Rb 403	Sr 549	In 558	Sn 708	Sb 834	222* Te 869	296 I 1008	Xe 1170
Cs 376	Ba 503	Tl 589	Pb 715	Bi 703	Po 812	At	Rn 1037

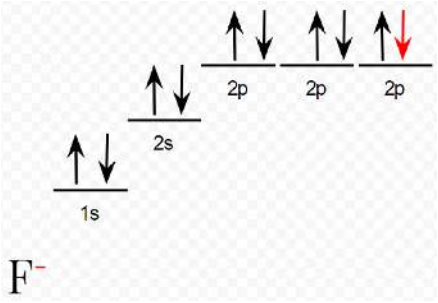
** Electron affinities marked with an asterisk (*) have been obtained from theoretical calculations rather than experimental measurements. The heavy colored line separates metals (ionization energy usually below about 800 kJ mol–1) from nonmetals.*

It is not easy to discern many obvious regularities in this table, especially since some of the electron-affinity values quoted are negative, indicating that energy is sometimes *required* to force an extra electron onto an atom. Nevertheless, it is quite obvious which of the periodic groups correspond to the highest electron affinities. All the halogens have values of about 300 kJ mol^{-1} while the group VI nonmetals have somewhat lower values, in the region of 200 kJ mol^{-1} or less. The high electron affinities of the halogens are a result of their having an almost complete outer shell of electrons.

The element fluorine, for example, has the structure $1s^2 2s^2 2p^5$, in which one of the 2*p* orbitals contains but one electron. If an extra electron (in the red in both diagrams below) is added to this atom to form a fluoride ion, the electron can pair with the electron in the half-filled 2*p* orbital (as seen in the orbital diagram below).



Macroscopic view of a Fluorine atom shown as a green sphere reacting with a single electron represented by a small red sphere. The resulting product is a larger green sphere labeled F superscript negative sign.



The orbital diagram for a fluoride ion has three separate levels. The lowest level, labeled "1 s" has two opposite pointing arrows. The next higher level, labeled "2 s" also has two opposite pointing arrows. The highest level has three identical levels adjacent to one another, each labeled "2 p". The first two levels have two opposite pointing arrows respectively. The last level has one upward pointing arrow with one downward pointing arrow in a different color than the rest of the arrows in the entire orbital.

The added electron will be shielded from the nucleus by the 1*s* electrons, but the 2*s* and 2*p* electrons are in the same shell and will shield it rather poorly. There will thus be quite a large effective nuclear charge (a rough estimate is +5) attracting the added electron. Because of this overall attraction, energy will be *released* when the electron is captured by the fluorine atom. Similar reasoning also explains why oxygen also has a high electron affinity. Here, though, the nuclear charge is smaller, and the attraction for the added electron distinctly less.

This page titled 1.2.8: Electron Affinities is shared under a CC BY-NC-SA 4.0 license and was authored, remixed, and/or curated by Ed Vitz, John W. Moore, Justin Shorb, Xavier Prat-Resina, Tim Wendorff, & Adam Hahn.

- **6.8: Electron Affinities** by Ed Vitz, John W. Moore, Justin Shorb, Xavier Prat-Resina, Tim Wendorff, & Adam Hahn is licensed CC BY-NC-SA 4.0.

1.2.9: Binary Ionic Compounds and Their Properties

All ionic compounds have numerous properties in common. Consequently, the ability to recognize an ionic compound from its formula will allow you to predict many of its properties. This is often possible in the case of a **binary compound** (one which contains only two elements), because formation of a binary ionic compound places quite severe restrictions on the elements involved. One element must be a metal and must have a very low ionization energy (see Figure **1.2.9.1** for the IE of various metals). The other element must be a nonmetal and must have a very high electron affinity.

In the following paragraphs, many references will be made to groups on the periodic table. Use the figure below for reference to keep track of the groups referred to in the paragraph.

Even though metals in general have low ionization energies, not all of them are low enough to form binary ionic compounds with a large fraction of the nonmetals. Although it is impossible to draw an exact line of demarcation, a good working rule is that essentially all binary compounds involving metals from periodic group 1, group 2, group 3 (Sc, Y, Lu), and the lanthanoids will be ionic. (Hydrogen is not a metal and is, therefore, an exception to the rule for group 1. Beryllium, whose ionization energy of 899 kJ mol^{-1} is quite high for a metal, also forms many binary compounds which are not ionic. Beryllium is the only exception to the rule from group 2.)

The transition metals to the right of group 3 in the periodic table form numerous binary compounds which involve covalent bonding, so they cannot be included in our rule. The same is true of the metals in periodic groups 13, 14, and 15.

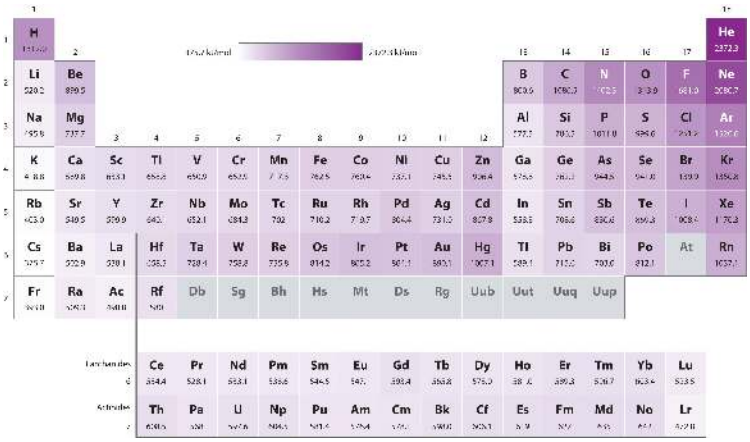


Figure **1.2.9.1** The image above shows the ionization energy of elements, with darker shades representing higher ionization energies. (CC-SA_BY-NC 3.0; anonymous)

The periodic table is colored with different shades of purple. The general trend observed here is that the purple gets darker across a period. All of the lightest colors are found on the left side of the periodic table and the darkest colors are found among the noble gas group.

The number of nonmetals with which a group 1, 2, 3, or lanthanoid metal can combine to form a binary ionic compound is even more limited than the number of appropriate metals. Such nonmetals are found mainly in periodic groups 16 and 17. The only other elements which form monatomic anions under normal circumstances are hydrogen (which forms H^- ions) and nitrogen (which forms N^{3-} ions).

In addition to combining with metals to form ionic compounds, all of the nonmetals can combine with other nonmetals to form covalent compounds as well. Therefore, presence of a particular nonmetal does not guarantee that a binary compound is ionic. It is necessary, however, for a group 16 or 17 nonmetal, nitrogen, or hydrogen to be present if a binary compound is to be classified as definitely ionic.

✔ Example 1.2.9.1 : Ionic Compounds

Which of the following compounds can be identified as definitely ionic? Which are definitely not ionic?

a) CuO **d)** $HgBr_2$ **g)** H_2S

b) CaO **e)** $BaBr_2$ **h)** InF_3

c) MgH_2 **f)** B_2H_2 **i)** BrCl

Solution

According to the guidelines in the previous two paragraphs, only compounds containing metals from groups IA, IIA, and IIIB, or the lanthanoids are definitely ionic, as long as the metal is combined with an appropriate nonmetal. CaO, MgH_2 and $BaBr_2$ fall into this category.

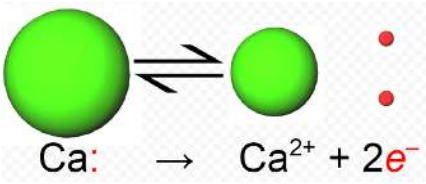
Compounds which do not contain a metallic element, such as B_2H_6, H_2S, and BrCl, cannot possibly be ionic. This leaves CuO, $HgBr_2$, and InF_3 in the category of possibility, but not definitely, ionic.

This page titled 1.2.9: Binary Ionic Compounds and Their Properties is shared under a CC BY-NC-SA 4.0 license and was authored, remixed, and/or curated by Ed Vitz, John W. Moore, Justin Shorb, Xavier Prat-Resina, Tim Wendorff, & Adam Hahn.

- **6.9: Binary Ionic Compounds and Their Properties** by Ed Vitz, John W. Moore, Justin Shorb, Xavier Prat-Resina, Tim Wendorff, & Adam Hahn is licensed CC BY-NC-SA 4.0.

1.2.10: The Octet Rule

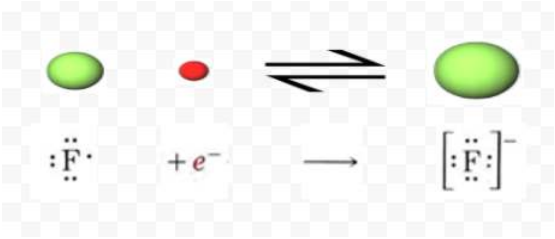
Because binary ionic compounds are confined mainly to group 1 and group 2 elements on the one hand and group VI and VII elements on the other, we find that they consist mainly of ions having an electronic structure which is the same as that of a noble gas. In calcium fluoride, for example, the calcium atom has lost *two* electrons in order to achieve the electronic structure of argon, and thus has a charge of +2:



Left side of the equation shows a large green sphere labeled C a with two red dots representing valence electron. This turns into a smaller green sphere labeled C a superscript 2 positive in addition to two red dots labeled as 2 e.

$$1s^2 2s^2 2p^6 3s^2 3p^6 4s^2 \rightarrow 1s^2 2s^2 2p^6 3s^2 3p^6 + 2e^-$$

By contrast, a fluorine atom needs to acquire but *one* electron in order to achieve a neon structure. The resulting fluoride ion has a charge of –1:



$$1s^2 2s^2 2p^5 + e^- \longrightarrow 1s^2 2s^2 2p^6$$

1 s superscript 2, 2 s superscript 2, 2 p superscript 5, plus an electron produces 1 s superscript 2, 2 s superscript 2, 2 p superscript 6.

Left side of the equation shows a green sphere labeled F with seven dots representing the seven valence electrons. This F reacts with a small red sphere labeled e superscript negative. The resulting product is a larger green sphere labeled F with 8 electrons in a square bracket with a superscript negative sign.

The outermost shell of each of these ions has the electron configuration ns^2np^6, where n is 3 for Ca^{2+} and 2 for F^-. Such an ns^2np^6 noble-gas electron configuration is encountered quite often. It is called an **octet** because it contains eight electrons. In a crystal of calcium fluoride, the Ca^{2+} and F^- ions are packed together in the lattice shown below. Careful study of the diagram shows that each F^- ion is surrounded by *four* Ca^{2+} ions, while each Ca^{2+} ion has *eight* F^- ions as nearest neighbors.

Thus there must be twice as many F^- ions as Ca^{2+} ions in the entire crystal lattice. Only a small portion of the lattice is shown, but if it were extended indefinitely in all directions, you could verify the ratio of two F^- for every Ca^{2+}. This ratio makes sense if you consider that two F^- ions (each with a –1 charge) are needed to balance the +2 charge of each Ca^{2+} ion, making the net charge on the crystal zero. The formula for calcium fluoride is thus CaF_2.

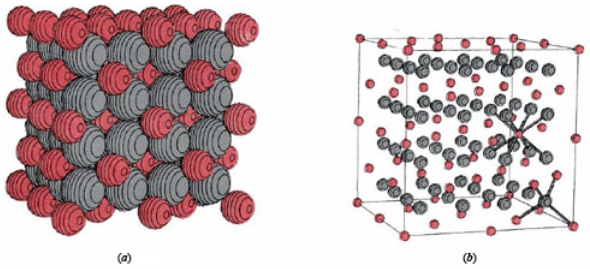


Figure **1.2.10.1**: A portion of the ionic crystal lattice of fluorite, calcium fluoride. (a) Ca^{2+} ions (color) and F^- ions (gray) are shown full size. "Exploded" view shows that each F^- surrounded by four Ca^{2+} ions, while each Ca^{2+} ion is surrounded by eight F^- ions. The ratio of Ca^{2+} ions to F^- ions is thus 4:8 or 1:2, and the formula is CaF_2. (Computer-generated). (Copyright © 1976 by W. G. Davies and J. W. Moore.)

Newcomers to chemistry often have difficulty in deciding what the formula of an ionic compound will be. A convenient method for doing this is to regard the compound as being formed from its atoms and to use Lewis diagrams. The **octet rule** can then be applied. Each atom must lose or gain electrons in order to achieve an octet. Furthermore, all electrons lost by one kind of atom must be gained by the other.

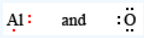
An exception to the octet rule occurs in the case of the three ions having the He $1s^2$ structure, that is, H^-, Li^+ and Be^{2+}. In these cases *two* rather than eight electrons are needed in the outermost shell to comply with the rule.

Example 1.2.10.1: Ionic Formula

Find the formula of the ionic compound formed from O and Al.

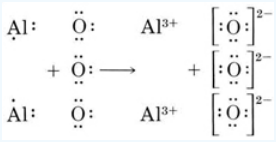
Solution

We first write down Lewis diagrams for each atom involved:



A l symbol with 2 red dots on its right and one red dot at the bottom. O symbol with two black dots on the top, left and bottom respectively.

We now see that each O atom needs 2 electrons to make up an octet, while each Al atom has 3 electrons to donate. In order that the same number of electrons would be donated as accepted, we need 2 Al atoms ($2 \times 3e^-$ donated) and 3 O atoms ($3 \times 2e^-$ accepted). The whole process is then



Equation shown in terms of lewis diagrams. There are 2 A l symbols with three black dots to represent the valence electrons. These reacts with three O symbols with six valence electrons each. The resulting product is 2 moles of Al 3 positive ion and three moles of oxygen anion, shown with a full set of octet electrons with superscript of 2 negative.

The resultant oxide consists of aluminum ions, Al^{3+}, and oxide ions, O^{2-}, in the ratio of 2:3. The formula is Al_2O_3.

This page titled 1.2.10: The Octet Rule is shared under a CC BY-NC-SA 4.0 license and was authored, remixed, and/or curated by Ed Vitz, John W. Moore, Justin Shorb, Xavier Prat-Resina, Tim Wendorff, & Adam Hahn.

- **6.10: The Octet Rule** by Ed Vitz, John W. Moore, Justin Shorb, Xavier Prat-Resina, Tim Wendorff, & Adam Hahn is licensed CC BY-NC-SA 4.0.

1.2.11: Physical Properties

Binary ionic compounds have many macroscopic properties in common, some of which are easy to explain in terms of the microscopic picture just presented. Because each ion in a crystal lattice, like those shown for lithium hydride and calcium fluoride, is surrounded by many oppositely charged nearest neighbors, each ion is held fairly tightly in its allotted position. At room temperature each ion can vibrate slightly about its mean position, but much more energy must be added before an ion can move fast enough and far enough to begin to escape the attraction of its neighbors. Therefore a fairly high temperature is needed to melt an ionic compound. The melting points of some substances we have considered are: LiH, 680°C; NaCl, 801°C; CaF_2, 1360°C. Once an ionic solid melts, the individual ions can move around, though most of the nearest neighbors of each anion will still be cations and vice versa. A characteristic feature of such a molten ionic compound is that it *conducts electricity*. If two wires are placed in the melt and are connected to a battery, the positive ions in the melt will gradually move toward the negatively charged wire, while the negative ions will move toward the positively charged wire. Movement of charged ions through the melt constitutes *passage of an electrical current* just as movement of electrons through a metal wire does. Its occurrence can be detected by an appropriate electrical meter.

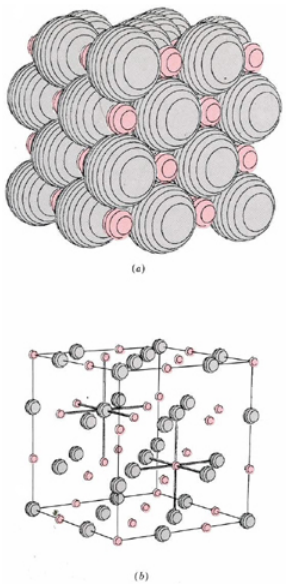


Figure **1.2.11.1** A portion of the ionic crystal lattice of lithium hydride, LiH. (a) Lithium ions, Li^+, (color) and hydride ions, H^-, (gray) are shown full size. In a macroscopic crystal the regular array of ions extends indefinitely in all directions. (b) "Exploded" view of the lattice, showing that each Li^+ ion (color) is surrounded by six H^- ions (gray), and vice versa. (Computer-generated). (Copyright © 1976 by W. G. Davies and J. W. Moore.)

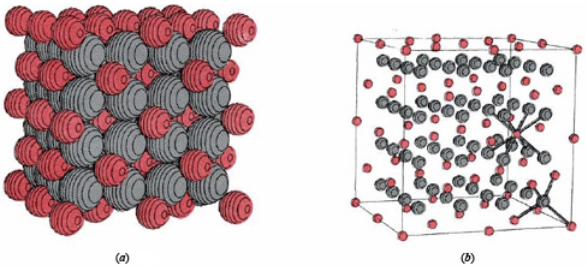


Figure **1.2.11.2** A portion of the ionic crystal lattice of fluorite, calcium fluoride. (a) Ca^{2+} ions (color) and F^- ions (gray) are shown full size. "Exploded" view shows that each F^- surrounded by four Ca^{2+} ions, while each Ca^{2+} ion is surrounded by eight F^- ions. The ratio of Ca^{2+} ions to F^- ions is thus 4:8 or 1:2, and the formula is CaF_2. (Computer-generated). (Copyright © 1976 by W. G. Davies and J. W. Moore.)

Both the melting point of the solid and the electrical conductivity of the liquid provide valuable clues for deciding whether a compound is ionic or not. An interesting example of this is a comparison between aluminum fluoride, AlF_3, and aluminum bromide, $AlBr_3$. We find that AlF_3 has a melting point of 1040°C, and the melt conducts electricity. By contrast $AlBr_3$ melts at

97.5°C, and the melt does not conduct electricity. The obvious inference is that the former compound is ionic, while the latter is not.

The crystals of ionic substances are transparent, hard, brittle, and have characteristic shapes. They also are easily cleaved. This means that if a wedge-shaped instrument (such as a knife blade) is properly placed on a crystal and tapped sharply, the crystal will break cleanly in two. This can be seen in the following video:

When the knife is placed parallel to the planes of the crystal, it breaks the first crystal into two new crystals, with faces that are nearly perfect planes. Further, when the knife is not placed in line with the plane, but at a 45° angle, the crystal shatters instead of breaking evenly. Still, the cleanest break occurs along the plane of the crystal. Hardness of ionic crystals is a consequence of the strong coulombic forces which hold each ion in its allotted position. The shape and cleavage of a crystal are the result of the specific geometric arrangement of the ions in a crystal lattice. For example, since 90° angles occur between layers of ions in the microscopic lattice of NaCl (and LiH), 90° angles are also reasonable in the macroscopic crystals of NaCl.(If you examine a few small crystals from a salt shaker, you will see that this is true-some are almost perfect cubes!) Thus characteristic shapes and cleavages may often be used to distinguish one ionic compound from another.

The following animation shows what is occurring on the atomic scale when the crystal of NaCl is cleaved.

When a large force is applied parallel to a layer of ions in the crystal lattice, it can shift that layer with respect to the next. Only a small shift is needed before positive ions in one layer are adjacent to positive ions in the other, and negative ions similarly become nearest neighbors. The two portions of the lattice repel one another and fall apart. On a macroscopic level the crystal cleaves, leaving flat faces corresponding to each layer of ions.

Perhaps the most important property of ionic solids is that most of them dissolve in water. Mute testimony to this is provided by the rows and rows of bottles in the average chemistry laboratory which contain aqueous ionic solutions. A characteristic feature of these solutions is that they all *conduct electricity*, showing that the ions retain their charges in solution and are also free to move about in it. When barium chloride, $BaCl_2$, dissolves in water, for example, the Ba^{2+} and Cl^- ions which were held tightly together in the crystal lattice become separated from each other in solution and can move about independently. If two wires are now immersed in this solution and attached to a battery, much the same thing happens as in the case of a molten salt. The Ba^{2+} ions are attracted by the negative charge on the one wire and move toward it, while the Cl^- ions move toward the positive charge on the other wire. This flow of charges in the body of the solution is matched by a flow of electrons in the wire and can be measured by an appropriate meter.

This page titled 1.2.11: Physical Properties is shared under a CC BY-NC-SA 4.0 license and was authored, remixed, and/or curated by Ed Vitz, John W. Moore, Justin Shorb, Xavier Prat-Resina, Tim Wendorff, & Adam Hahn.

- **6.11: Physical Properties** by Ed Vitz, John W. Moore, Justin Shorb, Xavier Prat-Resina, Tim Wendorff, & Adam Hahn is licensed CC BY-NC-SA 4.0.

1.2.11.1: Lecture Demonstrations

Conductivity of Molten Salt

Many salts can be melted in test tubes, and the conductivity of their melts measured with a low voltage device and either graphite "leads" from pencils, or TIG welding rods[1].

Conductivity of Salt Solutions

Compare solution conductivity of ionic and covalent compounds[2]. Besides the traditional 120 V light bulb with probes in series (available from scientific suppliers), many conductivity devices have been suggested.[3][4][5][6]

References

1. J. Chem. Educ., 2001, 78 (8), p 1052
2. J. Chem. Educ., 1962, 39 (10), p 531
3. Daniel T. Haworth , Mark R. Bartelt and Michael J. Kenney , Reed Howald. J. Chem. Educ., 1999, 76 (5), p 625
4. J. Chem. Educ., 1995, 72 (8), p 728
5. J. Chem. Educ., 1987, 64 (7), p 628
6. John W. Havrilla. J. Chem. Educ., 1991, 68 (1), p 80

This page titled 1.2.11.1: Lecture Demonstrations is shared under a CC BY-NC-SA 4.0 license and was authored, remixed, and/or curated by Ed Vitz, John W. Moore, Justin Shorb, Xavier Prat-Resina, Tim Wendorff, & Adam Hahn.

- **6.11.1: Lecture Demonstrations** by Ed Vitz, John W. Moore, Justin Shorb, Xavier Prat-Resina, Tim Wendorff, & Adam Hahn is licensed CC BY-NC-SA 4.0.

1.2.12: Chemical Properties

The most important chemical characteristic of ionic compounds is that *each ion has its own properties*. *Such properties are different from those of the atom from which the ion was derived*. In other words, an Na^+ ion is quite different from an Na atom, and a Cl^- ion is unlike an isolated Cl atom or either of the Cl atoms in a Cl_2 molecule. You eat a considerable quantity of Na^+ and Cl^- ions in table salt every day, but Na atoms or Cl_2 molecules would be quite detrimental to your health. The unique chemical properties of each type of ion are quite evident in aqueous solutions. Most of the reactions of $BaCl_2(aq)$, for example, can be classified as reactions of the Ba^{2+} (aq) ion or the $Cl^-(aq)$ ion. If sulfuric acid, H_2SO_4, is added to a solution of $BaCl_2$, the solution turns milky and very fine crystals of $BaSO_4(s)$ eventually settle out. The reaction can be written as:

$$\mathbf{Ba^{2+}}(aq) + \mathbf{H_2SO_4}(aq) \rightarrow \mathbf{BaSO_4}(s) + \mathbf{2H^+}(aq)$$

Below is a video of this reaction.



The solution of $BaCl_2$ is clear and colorless, but when H_2SO_4 is added through the the thin glass tube, the contents become white and opaque, as insoluble $BaSO_4(s)$ come out of solution.

This reaction is characteristic of the *barium ion*. It will also occur if H_2SO_4 is added to solutions such as $BaI_2(aq)$ or $BaBr_2(aq)$ which contain barium ions but no chloride ions. By contrast, if a solution of silver nitrate, $AgNO_3$, [which contains silver ions, Ag^+ (aq)] is added to a $BaCl_2$ solution, a reaction characteristic of the *chloride ion* occurs. A white curdy precipitate of $AgCl(s)$ forms according to the equation:

$$\mathbf{Ag^+}(aq) + \mathbf{Cl^-}(aq) \rightarrow \mathbf{AgCl}(s)$$

Other ionic solutions containing chloride ions, such as $LiCl(aq)$, $NaCl(aq)$, or $MgCl_2(aq)$, give an identical reaction. Below is a video of the reaction of a sodium chloride solution with a silver nitrate solution.



Both the NaCl(aq) solution and the $AgNO_3$(aq) solution begin clear and colorless. When the NaCl(aq) solution is added to the $AgNO_3$(aq) solution, a cloudy white precipitate of AgCl(s) is formed. The same result would have occurred had $BaCl_2$ been used, as the reaction is only between the Ag^+ and Cl^- ions, as seen:

$$Ag^+(aq) + Cl^-(aq) \rightarrow AgCl(s)$$

Many binary ionic solids not only dissolve in water, they also react with it. When the compound contains an anion such as N^{3-}, O^{2-}, or S^{2-}, which has more than one negative charge, the reaction with water produces hydroxide ions, OH^-:

$$O^{2-} + H_2O \rightarrow OH^-(aq) + OH^-(aq)$$

$$S^{2-} + H_2O \rightarrow HS^-(aq) + OH^-(aq)$$

$$N^{3-} + 3H_2O \rightarrow NH_3(aq) + 3OH^-(aq)$$

Thus, when sodium oxide, Na_2O, is added to water, the resulting solution contains sodium ions and hydroxide ions but no oxide ions:

$$Na_2O + H_2O \rightarrow 2Na^+(aq) + 2OH^-(aq)$$

The hydride ion also reacts with water to form hydroxide ions. When lithium hydride, LiH, is dissolved in water, for example, the following reaction occurs:

$$LiH(s) + H_2O \rightarrow Li^+(aq) + OH^-(aq) + H_2(g)$$

Note that hydrogen gas is evolved in this reaction. Lithium hydride crystals provide a very compact, if somewhat expensive, method for storing hydrogen.

Among the *halide ions* (F^-, Cl^-, Br^-, I^-) only the fluoride ion shows any tendency to react with water, and that only to a limited extent. When sodium fluoride is dissolved in water, for example, faint traces of hydroxide ion can be detected in the solution owing to the reaction

$$F^- + H_2O \rightarrow HF + OH^-$$

With sodium chloride, by contrast, no such reaction occurs.

This page titled 1.2.12: Chemical Properties is shared under a CC BY-NC-SA 4.0 license and was authored, remixed, and/or curated by Ed Vitz, John W. Moore, Justin Shorb, Xavier Prat-Resina, Tim Wendorff, & Adam Hahn.

- **6.12: Chemical Properties** by Ed Vitz, John W. Moore, Justin Shorb, Xavier Prat-Resina, Tim Wendorff, & Adam Hahn is licensed CC BY-NC-SA 4.0.

1.2.13: The Covalent Bond

Formation of an ionic bond by complete transfer of an electron from one atom to another is possible only for a fairly restricted set of elements. Covalent bonding, in which neither atom loses complete control over its valence electrons, is much more common. In a **covalent bond** the electrons occupy a region of space *between* the two nuclei and are said to be *shared* by them.

The simplest example of a covalent bond is the bond between the two H atoms in a molecule of H_2. Suppose that two H atoms approach each other until their two 1*s* electron clouds interpenetrate. You can see what would happen to each 1s electron in the figure below by clicking on 1s left atom to show a 1s atomic orbital on the left H atom.

In such a situation the electron does not continue to move about its own nucleus only. The electron initially associated with the left-hand H atom, for example, will feel the attractive pull of the right-hand nucleus as well as the left-hand nucleus. Since both nuclei have the same charge, the electron is unable to discriminate between them. Accordingly it adopts a new *symmetrical* probability cloud. You can see this by clicking on the Sigma 1 button in *the third row* of the figure. (Also click on the 1s button to remove the 1s atomic orbital.)

The same argument applies to the electron initially associated with the right-hand H atom. (Use the figure to show what happens to that electron when it is attracted by two H nuclei.) Each electron is said to be *delocalized* over both nuclei and each electron has an equal probability of being found in the vicinity of either nucleus.

An orbital, like Sigma 1, that extends over a whole molecule rather than being restricted to a single atom is called a molecular orbital. We can consider it to be the result of a combination or overlap of the two 1s atomic orbitals. In fact, if you follow the instructions for part c of the figure, you can see how the overall molecular orbital overlaps with the densities of the two Sigma electrons, and how the molecular orbital has adopted a new shape from the densities shown by the two 1s orbitals.

A molecular orbital formed in this way must conform to the Pauli exclusion principle. Only two electrons of opposite spin can occupy each orbital, denoted here as the two electrons in the Sigma orbital. Since the second electron (seen by clicking on the "Sigma 2" button) from the other H atom is available, it occupies the molecular orbital together with the original (Sigma 1) electron. The result is a shared pair of electrons moving around both nuclei and holding them together (the orange color).

The overlap of two 1*s* electron clouds and their spreading over both nuclei when the H_2 molecule forms has the effect of concentrating the electron density *between* the protons. When the molecule forms, the negative charges move *closer* to positive charges than before. This is represented by the fact that the extent of dots in the molecular orbital is less than the spread due to the individual 1*s* electrons. There is thus a reduction in potential energy.

Since the virial theorem guarantees that a reduction in the *potential* energy means that the total energy (kinetic + potential) is also reduced, we can conclude that the H_2 molecule is *lower in energy* and hence more stable under normal conditions than two separate H atoms. Alternatively we can say that energy is *required* to break apart an H_2 molecule and separate it into two H atoms. This energy (called the **bond energy**) can be measured experimentally. It is found to have a value of 436 kJ mol^{-1} for the H_2 molecule.

✔ Example 1.2.13.1 : Molecular Orbitals

Below is a Jmol applet, a 3-D interactive view of H_2. There are a set of commands to the left where you can play around with appearances, viewing the molecule as ball and stick, a wire, or see the van der Waals radii. You can also label the atoms, radii, and bond length. Take a bit to play around with the applet if you are unfamiliar with Jmol.

Now focus on the molecular orbital commands to the right. These allow you to visual the orbitals discussed earlier on this page. Set the MO cut off to 0.05. This will produce a surface that encloses 95% (0.95) of the electron density.

(a) Click on HOMO. This stands for **H**ighest **O**ccupied **M**olecular **O**rbital. This is the highest-energy orbital with any electrons in it. The HOMO contains two electrons, one from each H atom.

Try to see the relationship between the two-dimensional dot-density diagram above and the three-dimensional representation in the Jmol window. The Jmol shows a surface that encloses 95% of the electron density (95% of the dots in the figure above).

Rotate the HOMO diagram until you are looking along a line that passes through both H atoms (end-on to the molecule). What can you observe about the shape of the MO? Now rotate the diagram so that you are looking along a line perpendicular to the

H-H bond. What do you observe now?

What does the shape of the HOMO tell you about H_2?

(b) Now click on LUMO. this stands for **L**owest **U**noccupied **M**olecular **O**rbital. This is the next higher energy molecular orbital in the molecule--the orbital that electrons would fill if more electrons were added. Based on the shape of the LUMO, what would be the consequence of placing electrons in this orbital?

Solution

a) The orbital is symmetrical about the center of the H_2 molecule. As was discussed on this page, the two electrons in this orbital are now equally shared by both atoms. The orbital is centered between the two atoms, so electron density is highest there. Again, as said above, this reduced the total energy of the system, and electrons in this orbital will thus lead to a covalent bond between the two atoms. This orbital is referred to as a bonding orbital.

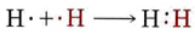
b)With the LUMO of H_2 there is *zero* electron density half way between the two hydrogen atoms. The two protons repel each other, and without much electron density between them to attract them together the LUMO has a higher energy than the two separate hydrogen atoms. If electrons occupied this orbital, it would lead to the repulsion of the atoms and breaking of the covalent bond. The point exactly half way the two atoms where the electron denisty is zero is called a node. Because the atoms would fly apart if the LUMO were occupied, this molecular orbital with a node is referred to as an anti-bonding orbital.

This page titled 1.2.13: The Covalent Bond is shared under a CC BY-NC-SA 4.0 license and was authored, remixed, and/or curated by Ed Vitz, John W. Moore, Justin Shorb, Xavier Prat-Resina, Tim Wendorff, & Adam Hahn.

- **6.13: The Covalent Bond** by Ed Vitz, John W. Moore, Justin Shorb, Xavier Prat-Resina, Tim Wendorff, & Adam Hahn is licensed CC BY-NC-SA 4.0.

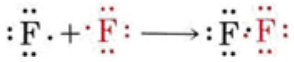
1.2.14: Covalent Molecules and the Octet Rule

The idea that a molecule could be held together by a shared pair of electrons was first suggested by Lewis in 1916. Although Lewis never won the Nobel prize for this or his many other theories, the shared pair of electrons is nevertheless one of the most significant contributions to chemistry of all time. Wave mechanics was still 10 years in the future, and so Lewis was unable to give any mathematical description of exactly how electron sharing was possible. Instead of the detailed picture presented in the previous section, Lewis indicated the formation of a hydrogen molecule from two hydrogen atoms with the aid of his electron-dot diagrams as follows:



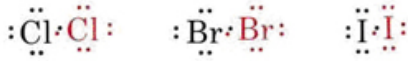
One H with a small dot plus another H with a small dot forms covalently bonded H that are bonded together through 2 shared dots in the center of the 2 H.

Lewis also suggested that the tendency to acquire a noble-gas structure is not confined to ionic compounds but occurs among covalent compounds as well. In the hydrogen molecule, for example, each hydrogen atom acquires some control over *two* electrons, thus achieving something resembling the helium structure. Similarly the formation of a fluorine molecule from its atoms can be represented by



There are two F symbols shown with seven dots drawn around it. They react to form a covalently bonded Fluorine gas molecule with a complete octet set of electrons around each of the bonded F.

Again a pair of electrons is shared, enabling each atom to attain a neon structure with eight electrons (i.e., an octet) in its valence shell. Similar diagrams can be used to describe the other halogen molecules:

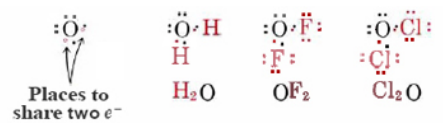


Lewis diagrams showing a complete octet among each of the bonded atoms in a diatomic molecule such as chlorine, fluorine, and iodine.

In each case a shared pair of electrons contributes to a noble-gas electron configuration on *both* atoms. Since only the valence electrons are shown in these diagrams, the attainment of a noble-gas structure is easily recognized as the attainment of a full complement of eight electron dots (an *octet*) around each symbol. In other words *covalent* as well as ionic compounds obey the octet rule.

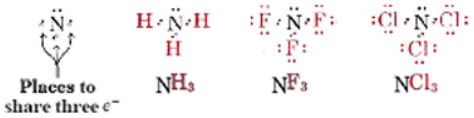
The octet rule is very useful, though by no means infallible, for predicting the formulas of many covalent compounds, and it enables us to explain the usual valence exhibited by many of the representative elements. According to Lewis' theory, hydrogen and the halogens each exhibit a valence of 1 because the atoms of hydrogen and the halogens each contain one less electron than a noble-gas atom. In order to attain a noble-gas structure, therefore, they need only to participate in the sharing of *one* pair of electrons. If we identify a shared pair of electrons with a chemical bond, these elements can only form *one* bond.

A similar argument can be extended to oxygen and the group VI elements to explain their valence of 2. Here *two* electrons are needed to complete a noble-gas configuration. By sharing two pairs of electrons, i.e., by forming two bonds, an octet is attained:



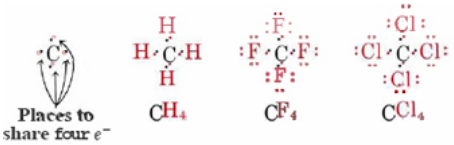
Lewis diagram of O is shown with an arrow pointing to two vacant spots around the atom which are places to share two electrons. The sharing of the electrons to fill the vacant spots are highlighted with examples showing lewis diagrams of H 2 O, O F subscript 2, and C l subscript 2 O.

Nitrogen and the group V elements likewise require three electrons to complete their octets, and so can participate in three shared pairs:



Lewis diagram of N is shown with an arrow pointing to three vacant spots around the atom which are places to share three electrons. The sharing of the electrons to fill the vacant spots are highlighted with examples showing lewis diagrams of N H subscript 3, N F subscript 3, and N C l subscript 3.

Finally, since carbon and the group IV elements have four vacancies in their valence shells, they are able to form four bonds:



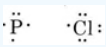
Lewis diagram of C is shown with an arrow pointing to four vacant spots around the atom which are places to share four electrons. The sharing of the electrons to fill the vacant spots are highlighted with examples showing lewis diagrams of C H subscript 4, C F subscript 4, and "C" "C l" subscript 4.

Example 1.2.14.1 : Lewis Structures

Draw Lewis structures and predict the formulas of compounds containing (a) P and Cl; (b) Se and H.

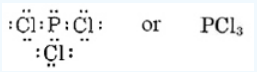
Solution:

a) Draw Lewis diagrams for each atom.



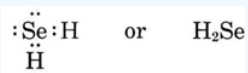
P symbol with two dots on the top and one dot on the left, right, and bottom respectively. C l symbol with two dots on the top, right, and bottom respectively as well as one dot on the left.

Since the P atom can share three electrons and the Cl atom only one, three Cl atoms will be required, and the formula is



Lewis diagram of P Cl subscript 3. Each of the atom is drawn with a complete octet, meaning 8 dots around each atom.

b) Since Se is in periodic group VI, it lacks two electrons of a noble-gas configuration and thus has a valence of 2. The formula is



Lewis diagram of H subscript 2 S e. The s e symbol has eight electrons around it while the two H bonded to S e has two electrons each, completing the duplet rule for hydrogen.

In drawing Lewis structures, the bonding pairs of electrons are often indicated by a **bond line** connecting the atoms they hold together. Electrons which are not involved in bonding are usually referred to as **lone pairs** or **unshared pairs**. Lone pairs are often

omitted from Lewis diagrams, or they may also be indicated by lines. Here are some of the alternative ways in which H_2, F_2, and PCl_3 can be written.

Full Diagram	With Bond Line	With Lone-Pair Lines	Omitting Lone Pairs
H:H	H—H	H—H	H—H
:F:F:	:F—F:	|F—F|	F—F
:Cl:P:Cl: :Cl:	:Cl—P—Cl: :Cl:	|Cl—P—Cl| |Cl|	Cl—P—Cl Cl

A table shows the four different ways a lewis structure can be drawn. There is a full diagram with all electrons shown as dots. There is also with bond line which represents shared electrons as a line, while the unbonded electrons are still drawn out as dots. There is with lone pair lines which shows unpaired electrons as shorts lines around each atom. Finally there is omitting lone pairs which only shows a single line between two atoms that are bonded. Examples are shown for H 2, F 2, and P C l 3.

This page titled 1.2.14: Covalent Molecules and the Octet Rule is shared under a CC BY-NC-SA 4.0 license and was authored, remixed, and/or curated by Ed Vitz, John W. Moore, Justin Shorb, Xavier Prat-Resina, Tim Wendorff, & Adam Hahn.

- **6.14: Covalent Molecules and the Octet Rule** by Ed Vitz, John W. Moore, Justin Shorb, Xavier Prat-Resina, Tim Wendorff, & Adam Hahn is licensed CC BY-NC-SA 4.0.

1.2.15: Writing Lewis Structures for Molecules

Because Lewis diagrams are widely used to describe the structures of molecules, it is important that you be able to construct them. The first step in this process is to draw a **skeleton structure** to show which atoms are linked to which. Next, determine how many valence electrons are available by adding the periodic group numbers for all atoms in the molecule. Finally, allocate the available electrons either as shared pairs or as lone pairs so that each atom has an octet (or in the case of H, a $1s^2$ pair).

Deciding on a Skeleton Structure

Multiple Bonds

An Excess of Bonds

Resonance

This page titled 1.2.15: Writing Lewis Structures for Molecules is shared under a CC BY-NC-SA 4.0 license and was authored, remixed, and/or curated by Ed Vitz, John W. Moore, Justin Shorb, Xavier Prat-Resina, Tim Wendorff, & Adam Hahn.

- **6.15: Writing Lewis Structures for Molecules** by Ed Vitz, John W. Moore, Justin Shorb, Xavier Prat-Resina, Tim Wendorff, & Adam Hahn is licensed CC BY-NC-SA 4.0.

1.2.15.1: An Excess of Bonds

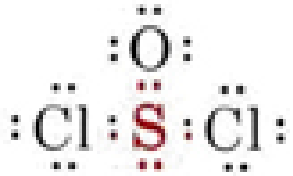
Back to Writing Lewis Structures for Molecules

There are a number of cases where the normal valences of the atoms involved do not predict the correct skeleton structure. For example, thionyl chloride, $SOCl_2$, is found *experimentally* to have both chlorines and the oxygen atom bonded to sulfur:



This exceeds the usual valence of 2 for sulfur, while oxygen has one less bond than we might have expected. Molecules which deviate in this way from the usual valence rules often contain at least one atom (such as S) from the third row or below in the periodic table. One or more oxygen atoms are usually bonded just to that third-row atom instead of linking a pair of other atoms. Usually the atom which occupies the central position in the skeleton is written first in the molecular formula, although sometimes H (which forms only one bond and cannot be the central atom) precedes it. Some examples (with the central atom in italics) are: $SOCl_2$, $POCl_3$, $HClO_4$, SO_2Br_2, and N_2O. (In the last case, one of the two nitrogens occupies the central position.)

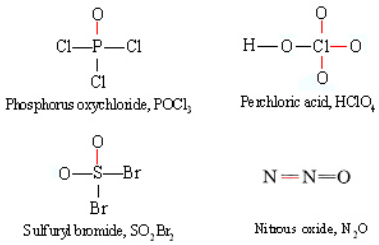
In such molecules the deviation from the normal valence occurs because at least one electron-pair bond contains two electrons which were originally associated with the *same* atom. Such a bond is called a coordinate **covalent bond** or a **dative bond**. An example is the bond between sulfur and oxygen in $SOCl_2$:



Lewis diagram shows a central S with two electrons on the top shared with oxygen. 2 electrons are shared between each of the S and C l bond. The other two electrons of S are not bonded to any atoms.

Both electrons in the S—O bond were originally valence electrons of sulfur. Therefore the sharing of this electron pair adds nothing to the valence shell of sulfur, and sulfur can form one more bond than would be predicted by its normal valence. Neither electron in the coordinate covalent bond was originally associated with oxygen, and a single bond (both electrons) is sufficient to provide an octet when added to oxygen's six valence electrons. Hence oxygen forms one less bond than expected.

It should be noted that there is nothing to distinguish a coordinate covalent bond from any other covalent bond once a structural formula has been drawn. A pair of electrons is still a pair of electrons no matter where it came from. The distinction is merely one we make when trying to fit electron pairs into octets around each atom. Structural formulas for the other examples of unusual valence we have mentioned are shown below with coordinate covalent bonds indicated in color:



Phosphorous oxychloride, P O C l subscript 3 is drawn as a central P atom bonded to three C l and one oxygen. Perchloric acid or H C l O subscript 4 is drawn out as one C l in the center bonded to four surrounding oxygen. One of the oxygen is also bonded to H. Sulfuryl bromide or S O subscript 2 B r subscript 2 is shown as a central S bonded to two oxygens as well as two bromine. Nitrous oxide or N subscript 2 O is shown as a central N with double bonds to N and also another double bond to O.

It is good practice to draw out the complete Lewis diagram for each of these molecules, differentiating electrons from different nuclei with different symbols such as × and ●, and satisfy yourself that they obey the octet rule.

Back to Writing Lewis Structures for Molecules

This page titled 1.2.15.1: An Excess of Bonds is shared under a CC BY-NC-SA 4.0 license and was authored, remixed, and/or curated by Ed Vitz, John W. Moore, Justin Shorb, Xavier Prat-Resina, Tim Wendorff, & Adam Hahn.

- **6.15.1: An Excess of Bonds** by Ed Vitz, John W. Moore, Justin Shorb, Xavier Prat-Resina, Tim Wendorff, & Adam Hahn is licensed CC BY-NC-SA 4.0.

1.2.15.2: Deciding on a Skeleton Structure

Back to Writing Lewis Structures for Molecules

The skeleton structure of a covalent molecule can often be determined by considering the valences of the constituent atoms. Usually the atom which forms the largest number of bonds is found in the center of the skeleton, where it can connect to the maximum number of other atoms.

✔ Example 1: Hypochlorous acid has the molecular formula HOCl. Draw a structural formula.

Solution There are several possible ways to link the atoms together

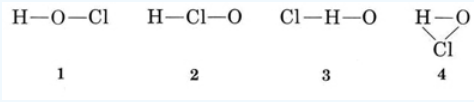
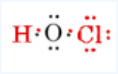


Diagram 1 shows a central O atom bonded to H and C l. Second diagram shows a central C l atom bonded to H and O. Diagram 3 shows a central H atom bonded to C l and O. Fourth diagram shows H, O, and C l bonded in triangular cyclic structure.

The usual valence of H is *1*, and so structures 3 and 4, which have *two* bonds to H, may be eliminated. The usual valence of Cl is also 1, and so structure 2 may also be ruled out. Structure 1 shows H forming one bond, Cl forming one, and O forming two, in agreement with the usual valences, and so it is chosen.

The total number of valence electrons available is 1 from H plus 6 from O plus 7 from Cl, or 14. Filling these into the skeleton we have



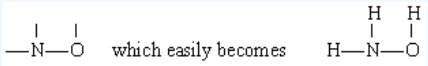
A central O atom with two unpaired electrons on the top and bottom respectively. On the left, it shares a pair of electrons with H. On the right, it shares a pair of electrons with C l which has six other electrons in its outer shell.

Note that O, which had the largest valence, is in the center of the skeleton.

✔ Example 2:

Draw a structural formula for hydroxylamine, NH_3O.

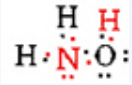
Solution In this case N has the largest valence (3), followed by O (2) and H (1). Both N and O can form “bridges” between other atoms, but H cannot. Therefore we place N and O in the center of the skeleton to give



The first diagram shows a central N bonded to O. The N atom has two other bonds available to be shared and the O has one electron. For this reason the central N and O can easily form three bonds with three hydrogen. Two is bonded to N and one is bonded to O.

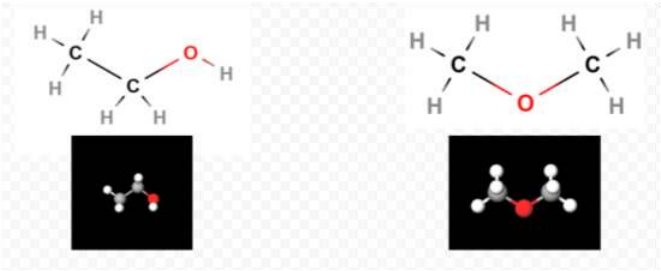
by addition of the three H atoms.

There are a total of 5 + 3 + 6 = 14 valence electrons from N, 3H’s and O. These can be placed as follows:



A central N shares two electrons each with the two H. A pair is shared with oxygen. A pair of electrons from N are unpaired. O shares a pair with another H. Two pairs of electrons from O are unpaired.

Once the Lewis diagram has been determined, the molecular formula is often rewritten to remind us of what the structural formula is. For example, the molecular formula for hydroxylamine is usually written NH_2OH instead of NH_3O to remind us that two H's are bonded to N and one to O. It is assumed that the person reading the formula will realize that N and O each have one valence electron left to share with each other, connecting —NH_2 with —OH. In some cases more than one skeleton structure will satisfy the valence of each atom and the octet rule as well. For example, you can verify that the molecular formula C_2H_6O corresponds to both of the following:



Ethyl alcohol starts with a C bonded to three H. This is bonded to another C with two hydrogens bonded to it. This central C is also connected to O which is also bonded to H. Dimethyl ether has a central O bonded to a C H 3 group on each side.

In such a case we can only decide which molecular structure we have by experiment. The properties of ethyl alcohol when diluted with water and consumed are well known. Dimethyl ether is a gas. Like the diethyl ether used in operating rooms, it is highly explosive and can put you to sleep. Two molecules, such as dimethyl ether and ethyl alcohol, which have the same molecular formula but different structural formulas are said to be isomers.

Back to Writing Lewis Structures for Molecules

Acknowledgements:

The C_2H_6O molecules and their skeletal structures were created using MolView.

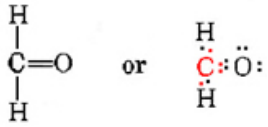
This page titled 1.2.15.2: Deciding on a Skeleton Structure is shared under a CC BY-NC-SA 4.0 license and was authored, remixed, and/or curated by Ed Vitz, John W. Moore, Justin Shorb, Xavier Prat-Resina, Tim Wendorff, & Adam Hahn.

- **6.15.2: Deciding on a Skeleton Structure** by Ed Vitz, John W. Moore, Justin Shorb, Xavier Prat-Resina, Tim Wendorff, & Adam Hahn is licensed CC BY-NC-SA 4.0.

1.2.15.3: Multiple Bonds

Back to Writing Lewis Structures for Molecules

In order to meet the requirements of normal valence, it is sometimes necessary to have *more than one bond*, that is, more than one shared pair of electrons between two atoms. A case in point is formaldehyde, CH_2O. In order to provide carbon with four bonds in this molecule, we must consider carbon as forming two bonds to the oxygen as well as one to each of the two hydrogens. At the same time the oxygen atom is also provided with the two bonds its normal valence requires:



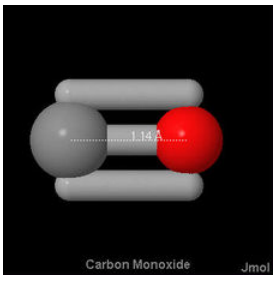
A central C double bonded to O and single bonded to two hydrogen. Another diagram shows the same molecule with each of the valence electrons shown. There are two pairs of electrons between C and O and a single pair shared between each of the C H bonds.

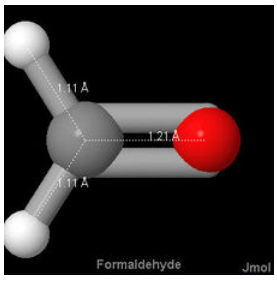
Note that all four of the shared electrons in the carbon-oxygen bond are included both in the octet of carbon and in the octet of oxygen. A bond involving two electron pairs is called a **double bond**.

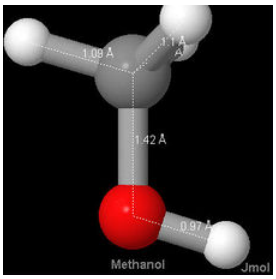
Occasionally the usual valences of the atoms in a molecule do not tell us what the skeleton structure should be. For example, in carbon monoxide, CO, it is hard to see how one carbon atom (usual valence of 4) can be matched with a single oxygen atom (usual valence of 2). In a case like this, where the valences appear to be incompatible, counting valence electrons usually leads to a structure which satisfies the octet rule. Carbon has 4 valence electrons and oxygen has 6, for a total of *10*. We want to arrange these 10 electrons in two octets, but two separate groups of 8 electrons would require 16 electrons. Only by *sharing* 16 – 10, or 6, electrons (so that those 6 electrons are part of *each* octet, and, in effect, count twice) can we satisfy the octet rule. This leads to the structure



Here three pairs of electrons are shared between two atoms, and we have a **triple bond**. Double and triple bonds are not merely devices for helping to fit Lewis diagrams into the octet theory. They have an objective existence, and their presence in a molecule often has a profound effect on how it reacts with other molecules. Triple bonds are invariably shorter than double bonds, which in turn are shorter than single bonds. In $C{\equiv}O$, for instance, the carbon-oxygen distance is 114 pm, in $H_2C{=}O$ it is 121 pm, while in both ethyl alcohol and dimethyl ether and methanol it is 142 pm. Below are 3-D Jmol images of carbon monoxide, formaldehyde, and methanol, to compare the difference in bond length with.







This agrees with the wave-mechanical picture of the chemical bond as being caused by the concentration of electron density between the nuclei. The more pairs of electrons which are shared, the greater this density and the more closely the atoms are pulled together. In line with this, we would also expect multiple bonds to be stronger than single bonds. Indeed, the bond energy of **C—O** is found experimentally to be 360 kJ mol^{-1}, while that of $C{=}O$ is 736 kJ mol^{-1}, and that of $C{\equiv}O$ is a gigantic 1072 kJ mol^{-1}. The $C{\equiv}O$ triple bond in carbon monoxide turns out to be the strongest known covalent bond.

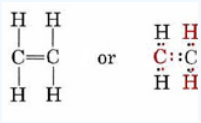
The formation of double and triple bonds is not as widespread among the atoms of the periodic table as one might expect. At least one of the atoms involved in a multiple bond is almost always C, N, or O, and in most cases both atoms are members of this trio. Other elements complete their octets by forming *additional single bonds* rather than multiple bonds.

✔ $2H_4$.

Solution Since hydrogen atoms are univalent, they must certainly all be bonded to carbon atoms, presumably two to each carbon. Each carbon atom thus has the situation



in which two bonds must still be accounted for. By assuming that the two carbon atoms are joined by a double bond, all the valence requirements are satisfied, and we can draw a Lewis structure containing satisfactory octets:

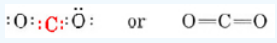


two C are double bonded to one another. Each of the C is also single bonded to two H, completing the octet rule for the C.

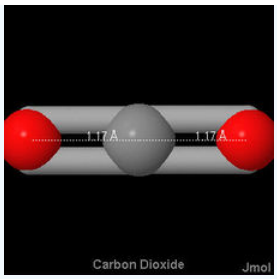
✔ Draw structural formulas for (a) CO and SiO . 22

Solution:

a) Carbon requires four bonds, and each oxygen requires two bonds, and so two $C{=}O$ double bonds will satisfy the normal valences. The structure is



Looking at the Jmol image for this molecule, the $C{=}O$ double bonds have a shorter distance than those seen in formaldehyde, but the are longer than the triple bond in carbon monoxide:

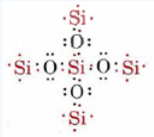


b) Silicon also has a normal valence of 4, but it is not an element which readily forms double bonds. Each silicon can form single bonds to four oxygen atoms however,



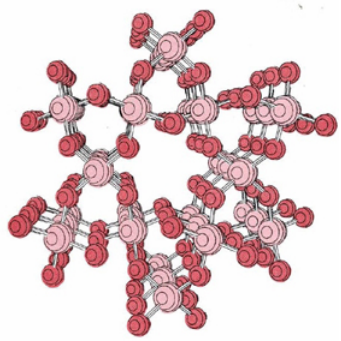
a central S i shares each of its valence electrons with the four oxygen. However, each of the four O atoms have a single unpaired electron.

Now the silicon is satisfied, but each oxygen lacks one electron and has only formed one bond. If each of the oxygens link to another silicon, they will be satisfied, but then the added silicon atoms will have unused valences:



A central S i is bonded to four O on each side. Each of the O atom is also bonded to another S i. However each of the four S i bonded to the O has 3 unpaired electrons in its valence.

The process of adding oxygen or silicon atoms can continue indefinitely, producing a giant lattice of covalently bonded atoms. In this giant molecule each silicon is bonded to four oxygens and each oxygen to two silicons, and so there are as many oxygen atoms as silicon. The molecular formula could be written $(SiO_2)_n$ where n is a very large number. A portion of this giant molecule is shown below.



A portion of the giant covalent molecule (SiO2)n. The lattice shown would extend indefinitely in all directions in a macroscopic crystal. Each silicon atom (light color) is covalently bonded to four oxygen atoms (dark color). Each oxygen bonds to two silicons. The ratio of silicon to oxygen is 2:4 or 1:2, in accord with the formula.

The difference in the abilities of carbon and silicon atoms to form double bonds has important consequences in the natural environment. Because $C{=}O$ double bonds form readily, carbon dioxide consists of individual molecules—there are no “empty spaces” on either the carbon or oxygen atoms where additional electrons may be shared. Hence there is little to hold one carbon dioxide molecule close to another, and at ordinary temperatures the molecules move about independently. On a macroscopic scale this means that carbon dioxide has the properties of a gas. In silicon dioxide, on the other hand, strong covalent bonds link all

silicon and oxygen atoms together in a three-dimensional network. At ordinary temperatures the atoms cannot vibrate far from their allotted positions, and silicon dioxide has the macroscopic properties of a solid.

As a gas, carbon dioxide is much freer than silicon dioxide to circulate through the environment. It can be removed from the atmosphere by plants in the photosynthetic process and eventually returned to the air by means of respiration. This is one of the reasons that terrestrial life is based on carbon compounds. If a supply of carbon from atmospheric carbon dioxide were not available, living organisms would be quite different in form and structure from the ones we know on earth.

Science-fiction authors are fond of suggesting, because of the periodic relationship of carbon and silicon, that life on some distant planet might be based on silicon. It is rather hard to imagine, though, the mechanism by which such life forms would obtain silicon from the rocks and soil of their planet's surface. Certainly they would face major difficulties if the combination of silicon with oxygen to form silicon dioxide were to be used as a source of energy. Imagine breathing out a solid instead of the gaseous carbon dioxide which forms when carbon combines with oxygen during respiration in terrestrial organisms! Macroscopic properties which are determined by microscopic structure and bonding are crucial in even such fundamental activities as living and breathing.

Back to Writing Lewis Structures for Molecules

This page titled 1.2.15.3: Multiple Bonds is shared under a CC BY-NC-SA 4.0 license and was authored, remixed, and/or curated by Ed Vitz, John W. Moore, Justin Shorb, Xavier Prat-Resina, Tim Wendorff, & Adam Hahn.

- **6.15.3: Multiple Bonds** by Ed Vitz, John W. Moore, Justin Shorb, Xavier Prat-Resina, Tim Wendorff, & Adam Hahn is licensed CC BY-NC-SA 4.0.

1.2.16: Examples of Lewis Structures

Here are a set of examples showing 3D twirlymol molecular models of from other sections in the text, along with Lewis structures of these molecules as well. It is useful to see what can be conveyed via 3D models, molecular geometry for instance, and what is conveyed by Lewis structure models, an example being the assignment of electrons around atoms and assignment of electrons for bonding. An important clarification, is that the twirlymols display *connections*, not bonds, so double and triple bonds do not show up. Double and triple bonds are shown in the Lewis structures. Molecules from a common page are grouped together, with a link back to the original page.

From Deciding on a Skeleton Structure

Hypochlorous Acid: HOCl

From Multiple Bonds

Formaldehyde: CH_2O

Carbon Monoxide: CO

Methanol: CH_3OH

Ethene: C_2H_4

Carbon Dioxide: CO_2

From An Excess of Bonds

Perchloric Acid: $HClO_4$

Nitrous Oxide: N_2O

From Resonance

Ozone: O_3

Carbonate Ion: CO_3^{2-}

From Polyatomic Ions

Sulfate Ion: SO_4^{2-}

Hydroxide Ion: OH^-

Hydronium Ion: H_3O^+

Ammonium Ion: NH_4^+

Sulfite Ion: SO_3^{2-}

Miscellaneous

Acetic Acid: CH_3COOH

Ammonia: NH_3

Contributors

- Ed Vitz (Kutztown University), John W. Moore (UW-Madison), Justin Shorb (Hope College), Xavier Prat-Resina (University of Minnesota Rochester), Tim Wendorff, and Adam Hahn.

This page titled 1.2.16: Examples of Lewis Structures is shared under a CC BY-NC-SA 4.0 license and was authored, remixed, and/or curated by Ed Vitz, John W. Moore, Justin Shorb, Xavier Prat-Resina, Tim Wendorff, & Adam Hahn.

- **6.16: Examples of Lewis Structures** by Ed Vitz, John W. Moore, Justin Shorb, Xavier Prat-Resina, Tim Wendorff, & Adam Hahn is licensed CC BY-NC-SA 4.0.

1.2.17: Polyatomic Ions

Our discussion of ionic compounds was confined to monatomic ions. However, more complex ions, containing several atoms *covalently bonded* to one another, but having a positive or negative charge, occur quite frequently in chemistry. The charge arises because the total number of valence electrons from the atoms cannot produce a stable structure. With one or more electrons added or removed, a stable structure results. Well-known examples of such **polyatomic ions** are the sulfate ion (SO_4^{2-}),

the hydroxide ion (OH^-),

the hydronium ion (H_3O^+),

and the ammonium ion (NH_4^+).

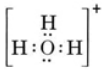
The atoms in these ions are joined together by covalent electron-pair bonds, and we can draw Lewis structures for the ions just as we can for molecules. The only difference is that the number of electrons in the ion does not exactly balance the sum of the nuclear charges. Either there are too many electrons, in which case we have an anion, or too few, in which case we have a cation.

Consider, for example, the hydroxide ion (OH^-) for which the Lewis structure is



O shares a pair of electrons with H. Three pairs of unpaired electrons is also shown. The entire O H molecules is enclosed in a square bracket with a superscript of negative sign.

A neutral molecule containing one O and one H atom would contain only seven electrons, six from O and one from H. The hydroxide ion, though, contains an *octet* of electrons, *one more* than the neutral molecule. The hydroxide ion must thus carry a single negative charge. In order to draw the Lewis structure for a given ion, we must first determine how many valence electrons are involved. Suppose the structure of H_3O^+ is required. The total number of electrons is obtained by adding the valence electrons for each atom, 6 + 1 + 1 + 1 = 9 electrons. We must now subtract 1 electron since the species under consideration is not H_3O but H_3O^+. The total number of electrons is thus 9 – 1 = 8. Since this is an octet of electrons, we can place them all around the O atom. The final structure then follows very easily:

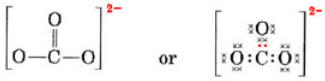


A central O shares three pairs of electrons with three H on the left top and right side. The bottom pair of electron from O is unpaired. The entire O H 3 molecule is enclosed in a square bracket which has a superscript positive sign.

In more complicated cases it is often useful to calculate the number of *shared electron pairs* before drawing a Lewis structure. This is particularly true when the ion in question is an *oxyanion* (i.e., a central atom is surrounded by several O atoms). A well-known oxyanion is the carbonate ion, which has the formula CO_3^{2-}. (Note that the central atom C is written first, as was done earlier for molecules.) The total number of valence electrons available in CO_3^{2-} is

$$4(\text{for C}) + 3 \times 6(\text{for O}) + 2(\text{for the } -2 \text{ charge}) = 24$$

We must distribute these electrons over 4 atoms, giving each an octet, a requirement of 4 × 8 = 32 electrons. This means that 32 – 24 = 8 electrons need to he counted twice for octet purposes; i.e., 8 electrons are shared. The a ion thus contains *four* electron-pair bonds. Presumably the C atom is double-bonded to one of the O's and singly bonded to the other two:



A central C is double bonded to one O and single bonded to two other O. The entire structure is enclosed in a square bracket with superscript of negative 2.

In this diagram the 4C electrons have been represented by dots, the 18 O electrons by ×'s, and the 2 extra electrons by colored dots, for purposes of easy reference. Real electrons do not carry labels like this; they are all the same.

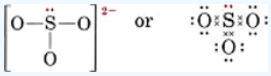
There is a serious objection to the Lewis structure just drawn. How do the electrons know which oxygen atom to single out and form a double bond with, since there is otherwise nothing to differentiate the oxygens? The answer is that they do not. To explain the bonding in the CO_3^{2-} ion and some other molecules requires an extension of the Lewis theory. We pursue this matter further when we discuss resonance. Now we end with an example.

Example 1.2.17.1 : Lewis Structure

Draw a Lewis structure for the sulfite ion, SO_3^{2-}.

Solution The safest method here is to count electrons. The total number of valence electrons available is

6(for S) + 3 × 6(for O) + 2(for the charge) = 26 To make four octets for the four atoms would require 32 electrons, and so the difference, 32 – 26 = 6, gives the number of shared electrons. There are thus only *three* electron-pair bonds in the ion. The central S atom must be linked by a single bond to each O atom.



A central S is single bonded to three O. There is a lone pair from S that is not bonded to any other atom. As a result, the overall charge of the molecule is negative 2.

Note that each of the S—O bonds is coordinate covalent.

This page titled 1.2.17: Polyatomic Ions is shared under a CC BY-NC-SA 4.0 license and was authored, remixed, and/or curated by Ed Vitz, John W. Moore, Justin Shorb, Xavier Prat-Resina, Tim Wendorff, & Adam Hahn.

- **6.17: Polyatomic Ions** by Ed Vitz, John W. Moore, Justin Shorb, Xavier Prat-Resina, Tim Wendorff, & Adam Hahn is licensed CC BY-NC-SA 4.0.

1.2.18: Ionic Compounds Containing Polyatomic Ions

When polyatomic ions are included, the number of ionic compounds increases significantly. Indeed, most ionic compounds contain polyatomic ions. Well-known examples are sodium hydroxide (NaOH) with OH^- as the polyatomic anion, calcium carbonate ($CaCO_3$), and ammonium nitrate (NH_4NO_3), which contains two polyatomic ions: NH^+ and NO_3^-.

A list of the more important polyatomic ions is given in the following table, which can be used for reference while learning the charges of polyatomic ions. A great many of them are oxyanions (polyatomic ions that contain oxygen).

Table 1.2.18.1 *Ions*

Ions

Charge	Name	Formula
-3	Phosphate	PO_4^{3-}
	Arsenate	AsO_4^{3-}
-2	Carbonate	CO_3^{2-}
	Peroxide	O_2^{2-}
	Sulfate	SO_4^{2-}
	Sulfite	SO_3^{2-}
	Chromate	CrO_4^{2-}
	Dichromate	$Cr_2O_7^{2-}$
	Hydrogen phosphate	HPO_4^{2-}
-1	Hydrogen carbonate (bicarbonate)	HCO_3^-
	Superoxide	O_2^-
	Hydrogen sulfate	HSO_4^-
	Dihydrogen phosphate	$H_2PO_4^-$
	Hydroxide	OH^-
	Nitrate	NO_3^-
	Nitrite	NO_2^-
	Acetate	$C_2H_3O_2^-$ or CH_3COO^-
	Cyanide	CN^-
	Permanganate	MnO_4^-
	Perchlorate	ClO_4^-
	Chlorate	ClO_3^-
	Chlorite	ClO_2^-
	Hypochlorite	ClO^-
+1	Ammonium	NH_4^+
	Hydronium	H_3O^+

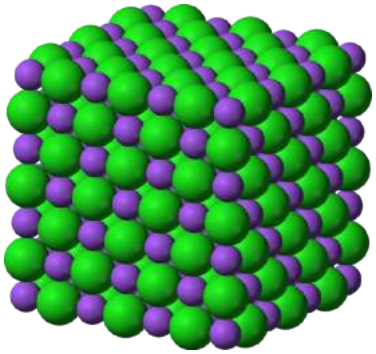
The properties of compounds containing polyatomic ions are very similar to those of binary ionic compounds. The ions are arranged in a regular lattice and held together by coulombic forces of attraction. The resulting crystalline solids usually have high melting points (1500 °F for $CaCO_3$) and all conduct electricity when molten.

Most are soluble in water and form conducting solutions in which the ions can move around as independent entities. In general polyatomic ions are colorless, unless, like CrO_4^{2-} or MnO_4^-, they contain a transition-metal atom. The more negatively charged polyatomic ions, like their monatomic counterparts, show a distinct tendency to react with water, producing hydroxide ions; for example,

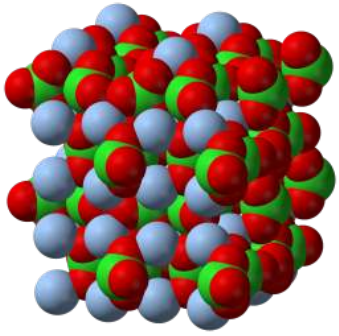
$$\mathbf{PO_4^{3-} + H_2O \rightarrow HPO_4^{2-} + OH^-}$$

It is important to realize that compounds containing polyatomic ions must be *electrically neutral*. In a crystal of calcium sulfate, for instance, there must be equal numbers of Ca^{2+} and SO_4^{2-} ions in order for the charges to balance. The formula is thus $CaSO_4$. In the case of sodium sulfate, by contrast, the Na^+ ion has only a single charge. In this case we need *two* Na^+ ions for each SO_4^{2-}ion in order to achieve electroneutrality. The formula is thus Na_2SO_4.

Structurally, polyatomic ions are similar to the ionic solids we saw earlier. An example of a simple ionic compound, NaCl, is seen below, alongside a more complex ionic solid, $AgClO_3^-$. Notice how both are tightly packed and form a repeating pattern, which lends both compounds strength and brittleness. In the Silver Chlorate ($AgClO_3^-$), however, polyatomic ions are present where the Cl^- ions are present in the Sodium Chloride (NaCl).



A cubic sodium chloride lattice made up of stacked green and purple spheres. The spheres are stacked in an alternating pattern. The green sphere is slightly larger than the purple sphere.



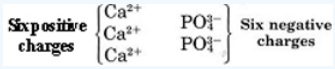
The three dimensional lattice of silver chlorate is complex because each silver sphere arranged in a regular cubic lattice is connected to a one green sphere which is connected to three red spheres.

On the left is the lattice structure of the ionic solid NaCl, with Na represented by the green spheres and Cl represented by the purple spheres. On the right is the lattice structure of $AgClO_3$, with the silver spheres representing Ag and the red and green molecules representing the polyatomic ion ClO_3

Example 1.2.18.1 : Ionic Formula

What is the formula of the ionic compound calcium phosphate?

Solution It is necessary to have the correct ratio of calcium ions, Ca^{2+}, and phosphate ions, PO_4^{3-}, in order to achieve electroneutrality. The required ratio is the *inverse* of the ratio of the charges on ions. Since the charges are in the ratio of 2:3, the numbers must be in the ratio of 3:2. In other words the solid salt must contain three calcium ions for every two phosphate ions:



Composition of calcium phosphate is three moles of Ca ions which make up a total of six positive charges as well as two phosphate ions which has a total of six negative charges.

The formula for calcium phosphate is thus $Ca_3(PO_4)_2$.

This page titled 1.2.18: Ionic Compounds Containing Polyatomic Ions is shared under a CC BY-NC-SA 4.0 license and was authored, remixed, and/or curated by Ed Vitz, John W. Moore, Justin Shorb, Xavier Prat-Resina, Tim Wendorff, & Adam Hahn.

- **6.18: Ionic Compounds Containing Polyatomic Ions** by Ed Vitz, John W. Moore, Justin Shorb, Xavier Prat-Resina, Tim Wendorff, & Adam Hahn is licensed CC BY-NC-SA 4.0.

1.2.19: Atomic Sizes

The sizes of atoms and ions are important in determining the properties of both covalent and ionic compounds. You should already have some appreciation of the factors which govern atomic sizes from the color-coded dot-density diagrams of Hydrogen, Helium, and Lithium and of Beryllium, Boron and Carbon. From the leftmost diagram below, one can see that Hydrogen seems to have a larger atomic radius than Helium, but not larger than Lithium (although it's "radius" is quite spread out). On the right side, one can see that the atomic radius steadily decreases as you go down the line. Note the relative locations of these elements on the periodic table and predict what the trend might be.

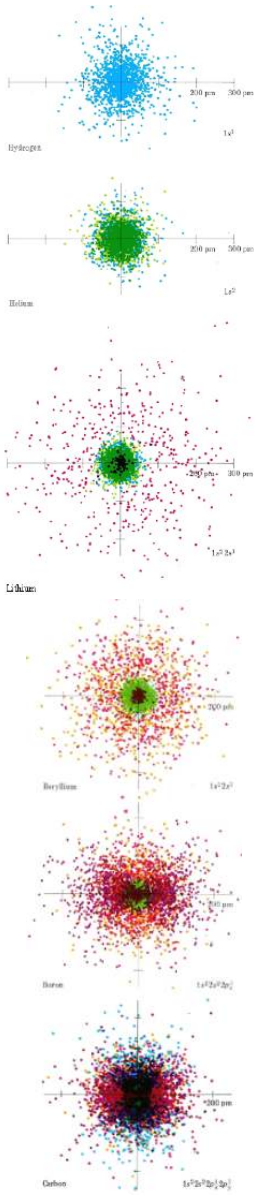


Figure **1.2.19.1** The figures above show the electron density of different elements. On the left from top to bottom are Hydrogen, Helium, and Lithium. On the right from top to bottom are Beryllium, Boron, and Carbon.

Hydrogen has a larger circular area concentrated with dots when compared to helium. Lithium has a 2 s orbital which translates to a significantly larger circular area in which the electrons are dispersed. The electron density diagram of Hydrogen and helium are superimposed on the diagram for lithium to better highlight the difference in sizes.

The circular area for beryllium is the largest since the electrons are more spread apart. The electron density for boron shows a circular area concentrated with dots but there are also two lobed area symmetrical about the vertical axis. This lobed region is also highly concentrated with dots. The electron density diagram for Carbon has four lobed shape region pointing to each side of the axis that are highly concentrated with dots. It also has the circular area in the center which is highly concentrated with dots. The area covered by electrons in boron is larger than carbon but still smaller than beryllium.

By far the largest atom illustrated in these color plates is Li. Because Li has an electron in the $n = 2$ shell, it is larger than H or He whose 1*s* electron clouds are much closer to the nucleus. Li is also larger than Be, B, or C. In the latter atoms, the 2*s* and 2*p* electron clouds are attracted by a greater nuclear charge and hence are held closer to the center of the atom than the 2*s* cloud in Li. Thus two important rules may be applied to the prediction of atomic sizes.

1 As one moves from top to bottom of the periodic table, the principal quantum number *n* increases and electrons occupy orbitals whose electron clouds are successively farther from the nucleus. The atomic radii increase.

2 As one moves from left to right across a horizontal period, then *n* value of the outermost electron clouds remains the same, but the nuclear charge increases steadily. The increased nuclear attraction contracts the electron cloud, and hence the atomic size decreases.

It is difficult to measure the size of an atom very exactly. As the dot-density diagrams show, an atom is not like a billiard ball which has a definite radius. Instead of stopping suddenly, an electron cloud gradually fades out so that one cannot point to a definite radius at which it ends. One way out of this difficulty is to find out how closely atoms are packed together in a crystal lattice. Figure **1.2.19.2** illustrates part of a crystal of solid Cl_2 at a very low temperature. The distance AA′ has the value of 369 pm. Since this represents the distance between adjacent atoms in *different* Cl_2 molecules, we can take it as the distance at which different Cl atoms just "touch." Half this distance, 184 pm, is called the **van der Waals radius** of Cl. The van der Waals radius gives an approximate idea of how closely atoms in *different* molecules can approach each other.

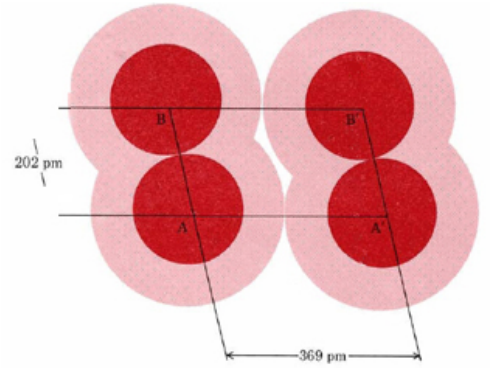


Figure **1.2.19.2** The relationship between van der Waals radii and covalent radii for Cl_2(s). In solid chlorine the molecules pack together so that the shortest distance between chlorine nuclei in different molecules (AA′ or BB′) or is 369 pm. The van der Waals radius of chlorine is defined as half that distance or 184 pm. The covalent radius of chlorine is half the distance (one-half AB or A′B′) between two chlorine nuclei in the same molecule. This is smaller than the van der Waals radius because of the covalent bond in each Cl_2 molecule.

Commonly accepted values of the van der Waals radii for the representative elements are shown in the Figure **1.2.19.3**. Note how these radii *decrease across* and *increase down* the periodic table.

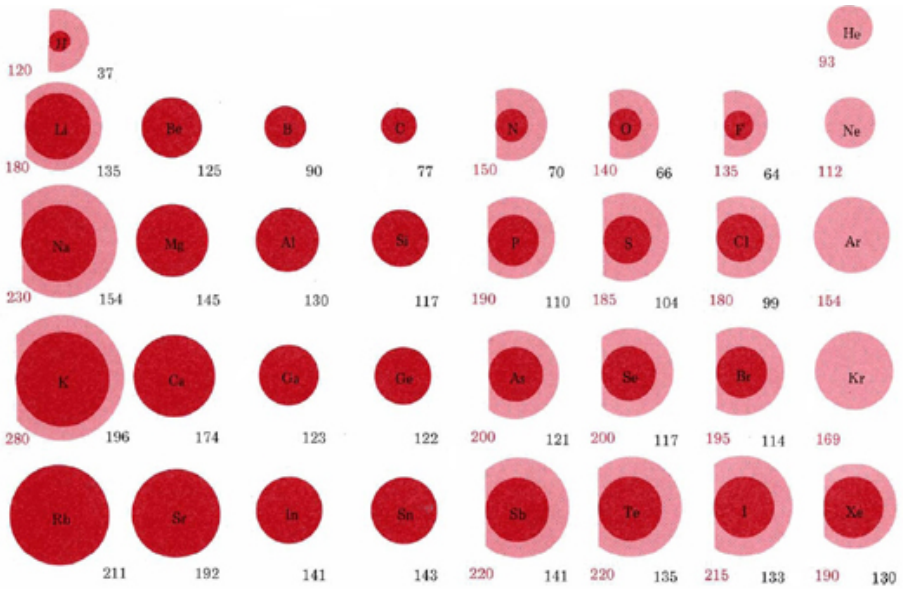


Figure **1.2.19.3** Sizes of atoms of the representative elements as a function of their position in the periodic table. Outer (lightly shaded) circles indicate van der Waals radii, while inner (darkly shaded) circles represent covalent radii. Colored numbers are van der Waals radii, and black numbers are covalent radii, both expressed in picometers.

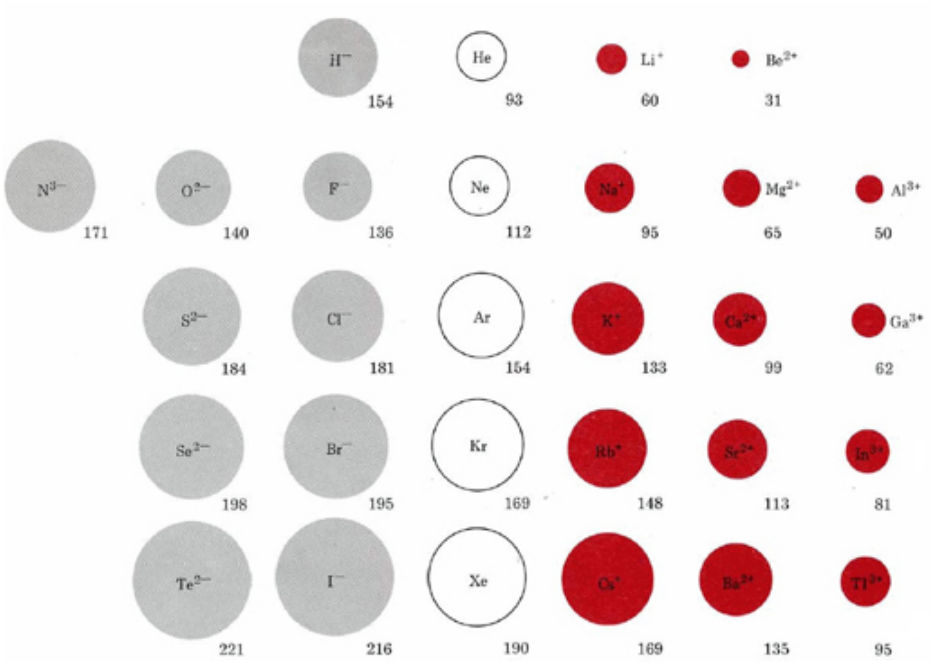
Also given are values for the **covalent radius** of each atom. Returning to the figure of Cl_2 (**Figure 1.2.19.2**, we see that the distance AB between two Cl atoms in the *same* molecule (i.e., the Cl—Cl **bond length**) has a value of 202 pm. The covalent radius is one-half of this bond length, or 101 pm. Covalent radii are approximately additive and enable us to predict rough values for the internuclear distances in a variety of molecules. For example, if we add the covalent radius of C (77 pm) to that of O (66 pm), we obtain an estimate for the length of the C—O bond, namely, 143 pm. This is in exact agreement with the measured value in ethyl alcohol and dimethyl ether seen previously.

This page titled 1.2.19: Atomic Sizes is shared under a CC BY-NC-SA 4.0 license and was authored, remixed, and/or curated by Ed Vitz, John W. Moore, Justin Shorb, Xavier Prat-Resina, Tim Wendorff, & Adam Hahn.

- **6.19: Atomic Sizes** by Ed Vitz, John W. Moore, Justin Shorb, Xavier Prat-Resina, Tim Wendorff, & Adam Hahn is licensed CC BY-NC-SA 4.0.

1.2.20: Ionic Sizes

The size of an ion is governed not only by its electronic structure but also by its *charge*. This relationship is evident in the following figure comparing ionic radii. Ions in the first row of this figure, H^-, Li^+, and Be^{2+}, all have the same $1s^2$ electronic structure as the helium (He) atom, but differ in size due to the different number of protons each has in their nucleus.



The elements of the periodic table are shown as circles with different radius. Each row consists of elements as well as ions which have the same number of electrons. The first row is H negative to B e superscript 2 positive. The second row is N superscript 3 negative to Al superscript 3 positive. Third row has S superscript 2 negative to G a superscript 3 positive. Fourth row has S e superscript 2 negative to I n superscript 3 positive. The final row has T e superscript 2 negative to T l superscript 3 positive. As we move across each row, the radius of each circle decreases.

Species which have the same electronic structure but different charges are said to be *isoelectronic*. For any electronic series, such as H^-, He, Li^+, Be^{2+}, in which the nuclear charge increases by 1 each time, we find a progressive decrease in size due to the increasingly strong attraction of the nucleus for the electron cloud. Each row in the figure corresponds to an isoelectronic series involving a different noble-gas electron configuration.

As we move from the more negative to the more positive ions in each row, there is a steady decrease in size. If we move *down* any of the columns, ionic sizes increase due to the increasing principal quantum number of the outermost electrons. The sizes of singly charged cations, for example, increase in the following order: $Li^+ < Na^+ < K^+ < Rb^+ < Cs^+$.

A further point of interest is the size of an ion relative to the atom from which it was formed. Recall the electron dot density diagram showing the formation of LiH. when the Li atom lost its electron and became a Li^+ ion, its size decreased dramatically. Comparing atomic radii to the ionic radii above reveals that this is also true for the other alkali metals. For example, check out the image below, which compares the atomic radii of the uncharged element to its ion. On the left are cations, which have lost an electron to become an ion and show decreases in size.

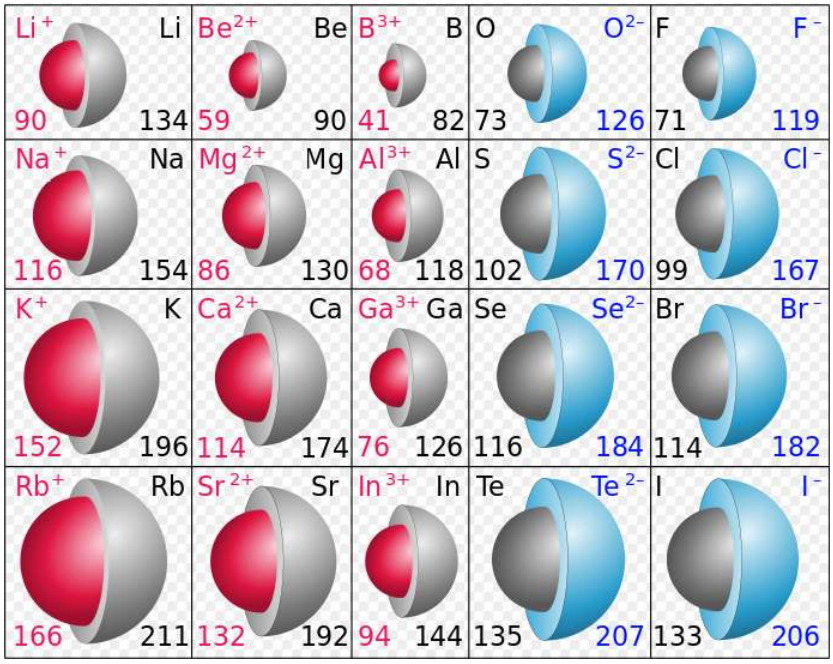


Image Credit: By Popnose [CC BY-SA 3.0 (Creative Commons [creativecommons.org]) or GFDL (GNU [www.gnu.org])], via Wikimedia Commons

On the right side of the figure are the anions, which form when an element gains an electron. The added electron, as can be observed from the pattern above, increases the atomic radii. Since the added electron goes into a subshell that already has occupants, rather than starting on a new subshell, there is often very little change in size. This is clearly seen in the electron dot density diagram mentioned above, where the formation of an H^- ion from an H atom produces no perceptible increase in size. Comparing the figure of atomic radii to ionic radii above, we also find that the van der Waals radii of nonmetals are only slightly smaller than the radii of their anions. However, some ions still experience fairly significant size changes, as can be seen in the figure above (anions are on the right side).

The sizes of the ions involved have a considerable influence on both the chemical and physical properties of ionic compounds. There is a strong correlation, for example, between ionic size and the melting point of an ionic compound. Among the halides of sodium the melting point decreases in the order of NaF (995°C) > NaCl (808°C) > NaBr (750°C) > NaI (662°C). The larger the anion, the farther it is from the sodium ion, and the weaker the coulombic force of attraction between them. Hence the lower the melting point. When a very small cation combines with a very large anion, the resulting compound is less likely to exhibit the characteristic macroscopic properties of an ionic substance.

This page titled 1.2.20: Ionic Sizes is shared under a CC BY-NC-SA 4.0 license and was authored, remixed, and/or curated by Ed Vitz, John W. Moore, Justin Shorb, Xavier Prat-Resina, Tim Wendorff, & Adam Hahn.

- **6.20: Ionic Sizes** by Ed Vitz, John W. Moore, Justin Shorb, Xavier Prat-Resina, Tim Wendorff, & Adam Hahn is licensed CC BY-NC-SA 4.0.

1.2.21: Periodic Variation of IE and EA

This page is a placeholder created because the page was deleted, but has sub-pages.

This page titled 1.2.21: Periodic Variation of IE and EA is shared under a CC BY-NC-SA 4.0 license and was authored, remixed, and/or curated by Ed Vitz, John W. Moore, Justin Shorb, Xavier Prat-Resina, Tim Wendorff, & Adam Hahn.

1.2.21.1: Lecture Demonstrations

Add small pieces of Li, K, Na to water, with universal indicator if desired, to show relative activities.

Hazards: K forms a peroxide coating that may explode when cut with a knife.

Activities of the Halogens[1][2][3][4]

Displace I, Br from NaI and NaBr solutions with Cl_2 (extract halogens into nonpolar solvent like hexane to make them more visible)[5].

Show that I_2 does not displace Cl_2 from NaCl, etc.

Reaction of Antimony with Halogens [6]

References

1. Furse, A. J. Chem. Educ., 1947, 24 (9), p 445
2. J. Chem. Educ., 1969, 46 (2), p A108
3. Alyea, H. J. Chem. Educ., 1969, 46 (2), p A108
4. J. Chem. Educ., 1933, 10 (10), p 637
5. J. Chem. Educ., 1969, 46 (2), p A108
6. J. Chem. Educ., 1969, 46 (2), p A108

This page titled 1.2.21.1: Lecture Demonstrations is shared under a CC BY-NC-SA 4.0 license and was authored, remixed, and/or curated by Ed Vitz, John W. Moore, Justin Shorb, Xavier Prat-Resina, Tim Wendorff, & Adam Hahn.

- **6.21.1: Lecture Demonstrations** by Ed Vitz, John W. Moore, Justin Shorb, Xavier Prat-Resina, Tim Wendorff, & Adam Hahn is licensed CC BY-NC-SA 4.0.

SECTION OVERVIEW

1.3: Further Aspects of Covalent Bonding

In the following sections, we will develop a more detailed picture of molecules—including some which do not obey the octet rule. You will learn how both the shapes and bonding of molecules may be described in terms of orbitals. In addition it will become apparent that the distinction between covalent and ionic bonding is not so sharp as it may have seemed. You will find that many covalent molecules are electrically unbalanced, causing their properties to tend toward those of ion pairs. Rules will be developed so that you can predict which combinations of atoms will exhibit this kind of behavior.

Topic hierarchy

1.3.1: Prelude to Covalent Bonding

1.3.2: Exceptions to the Octet Rule

1.3.2.1: Biology- Biologically Active Exceptions to the Octet Rule

1.3.3: The Shapes of Molecules

1.3.3.1: Lecture Demonstrations

1.3.4: Molecules with Lone Pairs

1.3.4.1: Lecture Demonstrations

1.3.5: Multiple Bonds and Molecular Shapes

1.3.6: Hybrid Orbitals

1.3.7: Orbital Descriptions of Multiple Bonds

1.3.8: Sigma and Pi Bonds

1.3.9: Polarizability

1.3.9.1: Biology - Polarizability of Biologically Significant Atoms

1.3.10: Polar Covalent Bonds

1.3.10.1: Biology- Nonpolar Iodine and Polar Hydrogen Iodide

1.3.10.2: Lecture Demonstrations

1.3.11: Electronegativity

1.3.12: Polarity in Polyatomic Molecules

1.3.12.1: Biology- The Hydrophobic Effect and Properties of Small Polyatomic Molecules

1.3.12.2: Lecture Demonstrations

1.3.13: Formal Charge and Oxidation Numbers

1.3.14: Resonance

This page titled 1.3: Further Aspects of Covalent Bonding is shared under a CC BY-NC-SA 4.0 license and was authored, remixed, and/or curated by Ed Vitz, John W. Moore, Justin Shorb, Xavier Prat-Resina, Tim Wendorff, & Adam Hahn.

1.3.1: Prelude to Covalent Bonding

While other sections concentrate on the octet rule and Lewis diagrams for simple covalent molecules, there are numerous examples of molecules which are quite stable, but contain one or more atoms which do not have a noble-gas electron configuration. Furthermore, structural formulas like those from sections under "Chemical Bonding - Electron Pairs and Octets" only show which atoms are connected to which. They do not tell us how the atoms are arranged in three-dimensional space. In other words a Lewis diagram does not show the shape of a molecule. It may actually be misleading because most molecules don't have the 90° or 180° bond angles that are conventionally used in the Lewis Diagram.

In the following sections, we will develop a more detailed picture of molecules—including some which do not obey the octet rule. You will learn how both the shapes and bonding of molecules may be described in terms of orbitals. In addition it will become apparent that the distinction between covalent and ionic bonding is not so sharp as it may have seemed. You will find that many covalent molecules are electrically unbalanced, causing their properties to tend toward those of ion pairs. Rules will be developed so that you can predict which combinations of atoms will exhibit this kind of behavior.

Lewis diagrams are used as the first step in predicting the structures for covalently bonded molecules. We will see what supplemental information is required to describe covalent molecules. We will describe some molecules which do not obey the octet rule and some which contain multiple bonds, as well as simple molecules. The structure of a molecule is determined by the positions of atomic nuclei in three-dimensional space, but it is repulsions among electron pairs—bonding pairs and lone pairs—which determine molecular geometry.

When dealing with molecular shapes, it is often convenient to think in terms of sp, sp^2, sp^3, or other hybrid orbitals. These correspond to the same overall electron density and to the same physical reality as do the *s* and *p* atomic orbitals considered earlier, but hybrid orbitals emphasize the directions in which electron density is concentrated. Hybrid orbitals may also be used to describe multiple bonding, in which case bonds must be bent so that two or three of them can link the same pair of atoms. A second equivalent approach to multiple bonding involves sigma and pi bonds. Electron density in a sigma bond is concentrated directly between the bonded nuclei, while that of the pi bond is divided in two—half on one side and half on the other side of the sigma bond.

No chemical bond can be 100 percent ionic, and, except for those between identical atoms, 100 percent covalent bonds do not exist either. Electron clouds—especially large, diffuse ones—are easily polarized, affecting the electrical balance of atoms, ions, or molecules. Large negative ions are readily polarized by small positive ions, increasing the covalent character of the bond between them. Electron density in covalent bonds shifts toward the more electronegative atom, producing partial charges on each atom and hence a dipole. In a polyatomic molecule, bond dipoles must be added as vectors to obtain a resultant which indicates molecular polarity. In the case of symmetric molecules, the effects of individual bond dipoles cancel and a nonpolar molecule results.

Macroscopic physical properties such as melting and boiling points depend on the strengths of the forces which hold microscopic particles together. In the case of molecules whose atoms are connected by covalent bonds, such intermolecular forces may be of three types. All molecules are attracted together by weak London forces. These depend on instantaneous polarization and increase in strength with the size of the molecular electron cloud. When a molecule contains atoms whose electronegativities differ significantly and the resulting bond dipoles do not cancel each other's effects, dipole forces occur. This results in higher melting and boiling points than for nonpolar substances.

The third type of intermolecular force, the hydrogen bond, occurs when one molecule contains a hydrogen atom connected to a highly electronegative partner. The other molecule must contain an electronegative atom, like fluorine, oxygen, or nitrogen, which has a lone pair. Although each hydrogen bond is weak compared with a covalent bond, large numbers of hydrogen bonds can have very significant effects. One example of this is in the properties of water. This highly unusual liquid plays a major role in making living systems and the earth's environment behave as they do.

Oxidation numbers are used by chemists to keep track of electrons during the course of a chemical reaction. They may be obtained by arbitrarily assigning valence electrons to the more electronegative of two bonded atoms and calculating the resulting charge as if the bond were 100 percent ionic. Alternatively, some simple rules are available to predict the oxidation number of each atom in a formula. Oxidation numbers are used in the names of compounds and are often helpful in predicting formulas and writing Lewis diagrams.

In addition to deficiency of electrons and expansion of the valence shell, the octet rule is violated by species which have one or more unpaired electrons. Such free radicals are usually quite reactive. A difficulty of another sort occurs in benzene and other molecules for which more than one Lewis diagram can be drawn. Rearranging electrons (but not atomic nuclei) results in several structures which are referred to collectively as a resonance hybrid. Like an *sp* hybrid, a resonance hybrid is a combination of the contributing structures and has properties intermediate between them.

This page titled 1.3.1: Prelude to Covalent Bonding is shared under a CC BY-NC-SA 4.0 license and was authored, remixed, and/or curated by Ed Vitz, John W. Moore, Justin Shorb, Xavier Prat-Resina, Tim Wendorff, & Adam Hahn.

- **7.1: Prelude to Covalent Bonding** by Ed Vitz, John W. Moore, Justin Shorb, Xavier Prat-Resina, Tim Wendorff, & Adam Hahn is licensed CC BY-NC-SA 4.0.

1.3.2: Exceptions to the Octet Rule

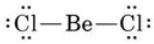
Considering the tremendous variety in properties of elements and compounds in the periodic system, it is asking a great deal to expect a rule as simple as Lewis' octet theory to be able to predict all formulas or to account for all molecular structures involving covalent bonds. Lewis' theory concentrates on resemblances to noble-gas ns^2np^6 valence octets. Therefore it is most successful in accounting for formulas of compounds of the representative elements, whose distinguishing electrons are also *s* and *p* electrons. The octet rule is much less useful in dealing with compounds of the transition elements or inner transition elements, most of which involve some participation of *d* or *f* orbitals in bonding.

Even among the representative elements there are some exceptions to the Lewis theory. These fall mainly into three categories:

1. Some stable molecules simply do not have enough electrons to achieve octets around all atoms. This usually occurs in compounds containing Be or B.
2. Elements in the third period and below can accommodate more than an octet of electrons. Although elements such as Si, P, S, Cl, Br, and I obey the octet rule in many cases, under other circumstances they form more bonds than the rule allows.
3. Free Radicals

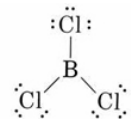
Electron Deficient Species

Good examples of the first type of exception are provided by $BeCl_2$ and BCl_3. Beryllium dichloride, $BeCl_2$, is a covalent rather than an ionic substance. Solid $BeCl_2$ has a relatively Complex structure at room temperature, but when it is heated to 750°C, a vapor which consists of separate $BeCl_2$ molecules is obtained. Since Cl atoms do not readily form multiple bonds, we expect the Be atom to be joined to each Cl atom by a single bond. The structure is



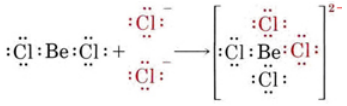
A central Be structure is single bonded to two chlorine atom. The three pairs of unpaired electrons on each chlorine is shown as dots.

Instead of an octet the valence shell of Be contains only *two* electron pairs. Similar arguments can be applied to boron trichloride, BCl_3, which is a stable gas at room temperature. We are forced to write its structure as



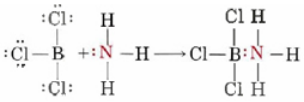
A central B atom is single bonded to three chlorine atoms. The three chlorine atoms are 60 degrees from one another and form a triangular shape with boron in the center. The three pairs of unpaired electrons on chlorine are shown as dots.

in which the valence shell of boron has only three pairs of electrons. Molecules such as $BeCl_2$ and BCl_3 are referred to as **electron deficient** because some atoms do not have complete octets. Electron-deficient molecules typically react with species containing lone pairs, acquiring octets by formation of coordinate covalent bonds. Thus $BeCl_2$ reacts with Cl^- ions to form $BeCl_4^-$;



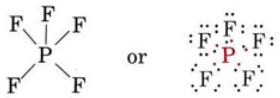
A B e C l 2 molecule reacts with two chlorine anions to give B e C l 4 with a complete octet set. The overall charge of the molecule is negative 2.

BCl_3 reacts with NH_3 in the following way:



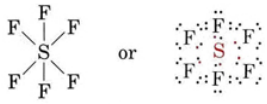
Species with Expanded Octets

Examples of molecules with more than an octet of electrons are phosphorus pentafluoride (PF_5) and sulfur hexafluoride (SF_6). Phosphorus pentafluoride is a gas at room temperature. It consists of PF_5 molecules in which each fluorine atom is bonded to the phosphorus atom. Since each bond corresponds to a shared pair of electrons, the Lewis structure is



P is connected to two equally spaced F atoms below it and three equally spaced F atoms above it. The dot diagram shows that P has a total of ten electrons on its valence.

Instead of an octet the phosphorus atom has 10 electrons in its valence shell. Sulfur hexafluoride (also a gas) consists of SF_6 molecules. Its structure is



Sulfur bonded to six Fluorine that are equally spaced out from one another. The dot diagram shows that sulfur has 12 electrons in its valence shell.

Here the sulfur atom has six electron pairs in its valence shell.

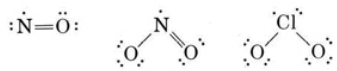
An atom like phosphorus or sulfur which has more than an octet is said to have *expanded its valence shell*. This can only occur when the valence shell has enough orbitals to accommodate the extra electrons. For example, in the case of phosphorus, the valence shell has a principal quantum number $n = 3$. An octet would be $3s^2 3p^6$. However, the $3d$ subshell is also available, and some of the $3d$ orbitals may also be involved in bonding. This permits the extra pair of electrons to occupy the valence ($n = 3$) shell of phosphorus in PF_5.

Expansion of the valence shell is impossible for an atom in the second period because there is no such thing as a $2d$ orbital. The valence ($n = 2$) shell of nitrogen, for example, consists of the $2s$ and $2p$ subshells only. Thus nitrogen can form NF_3 (in which nitrogen has an octet) but not NF_5. Phosphorus, on the other hand, forms both PF_3 and PF_5, the latter involving expansion of the valence shell to include part of the $3d$ subshell.

Free Radicals

The majority of molecules or complex ions discussed in general chemistry courses are demonstrated to have *pairs* of electrons. However, there are a few stable molecules which contain an odd number of electrons. These molecules, called ***"free radicals"***, contain at least one unpaired electron, a clear violation of the octet rule. Free radicals play many important roles a wide range of applied chemistry fields, including biology, medicine, and astrochemistry.

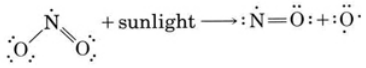
Three well-known examples of such molecules are nitrogen (II) oxide, nitrogen(IV) oxide, and chlorine dioxide. The most plausible Lewis structures for these molecules are



The N in nitrogen 2 oxide is double bonded to O, has one pair of unpaired electrons and one unpaired electron in its valence. The Nitrogen in nitrogen 4 oxide has one double bond with O, one single bond with O, and one unpaired electron. The Chlorine in chlorine dioxide is single bonded to two O which leaves one pair of unpaired electrons and one unpaired electrons in its valence.

Free radicals are usually more reactive than the average molecule in which all electrons are paired. In particular they tend to combine with other molecules so that their unpaired electron finds a partner of opposite spin. Since most molecules have all electrons paired, such reactions usually produce a new free radical. This is one reason why automobile emissions which cause even small concentrations of NO and NO_2 to be present in the air can be a serious pollution problem. When one of these free radicals

reacts with other automobile emissions, the problem does not go away. Instead a different free radical is produced which is just as reactive as the one which was consumed. To make matters worse, when sunlight interacts with NO_2, it produces *two* free radicals for each one destroyed:



In this way a bad problem is made very much worse.

A fourth very interesting example of a free radical is oxygen gas. The Lewis structure for Oxygen usually hides the fact that it is a ***"diradical"***, containing two unpaired electrons. This is often cited as a *serious flaw in Lewis bond theory*, and was a major impetus for development of molecular orbital theory. We know oxygen is a diradical because of its paramagnetic character, which is easily demonstrated by attraction of oxygen to an external magnet.

This page titled 1.3.2: Exceptions to the Octet Rule is shared under a CC BY-NC-SA 4.0 license and was authored, remixed, and/or curated by Ed Vitz, John W. Moore, Justin Shorb, Xavier Prat-Resina, Tim Wendorff, & Adam Hahn.

- **7.2: Exceptions to the Octet Rule** by Ed Vitz, John W. Moore, Justin Shorb, Xavier Prat-Resina, Tim Wendorff, & Adam Hahn is licensed CC BY-NC-SA 4.0.

1.3.2.1: Biology- Biologically Active Exceptions to the Octet Rule

Lewis' octet theory correctly predicts formulas for nearly all ionic compounds and accounts for most covalent bonding schemes for biologically important molecules. But the ones that are exceptions are among the most biologically interesting compounds.

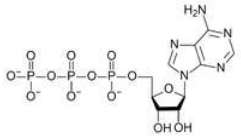
Lewis' theory concentrates on resemblances to noble-gas ns^2np^6 valence octets. Therefore it is most successful in accounting for formulas of compounds of the representative elements (especially in periods 1 and 2), whose distinguishing electrons are also *s* and *p* electrons. The octet rule is much less useful in dealing with compounds of the transition elements or inner transition elements, most of which involve some participation of *d* or *f* orbitals in bonding.

Even among the representative elements there are some interesting exceptions to the Lewis theory. These fall mainly into three categories:

1. ***"Expanded Valence Shell"*** compounds formed by elements in the third period and below which can accommodate more than an octet of electrons. Although elements such as Si, P, S, Cl, Br, and I obey the octet rule in many cases, under other circumstances they form more bonds than the rule allows because the third shell has s, pm, *and* d orbitals.
2. ***"Free Radicals"*** which have unpaired electrons, like the key vertebrate biological messenger nitric oxide, NO, which plays a role in a variety of biological processes. The 1998 Nobel Prize in Medicine was awarded for discoveries concerning nitric oxide as a signalling molecule in the cardiovascular system.
3. ***"Electron deficient"*** compounds do not have enough electrons to achieve octets around all atoms, but still have stable molecules. They often contain Be, B, or Al.

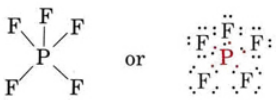
Expansion of Valence Shell

The typical structural formula for ATP (adenosine triphosphate) shows three single bonds and one double bond on the phosphorus atom, for a total of 5 electron pairs. This is possible because P has 3d orbitals as well as 3s and 3p orbitals to accommodate the electrons. The bonding is shown in the simple phosphate ion $[PO_4]^{3-}$:



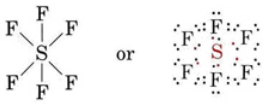
ATP

Other examples of molecules with more than an octet of electrons are phosphorus pentafluoride (PF_5) and sulfur hexafluoride (SF_6). Phosphorus pentafluoride is a gas at room temperature. It consists of PF_5 molecules in which each fluorine atom is bonded to the phosphorus atom. Since each bond corresponds to a shared pair of electrons, the Lewis structure is Expansion of the valence shell is impossible for an atom in the second period because there is no such thing as a 2*d* orbital. The valence (n = 2) shell of nitrogen, for example, consists of the 2*s* and 2*d* subshells only. Thus nitrogen can form NF_3 (in which nitrogen has an octet) but not NF_5. Phosphorus, on the other hand, forms both PF_3 and PF_5, the latter involving expansion of the valence shell to include part of the 3*d* subshell.



P is connected to two equally spaced F atoms below it and three equally spaced F atoms above it. The dot diagram shows that P has a total of ten electrons on its valence.

Instead of an octet the phosphorus atom has 10 electrons in its valence shell. Sulfur hexafluoride (also a gas) consists of SF_6 molecules. Its structure is



Sulfur bonded to six Fluorine that are equally spaced out from one another. The dot diagram shows that sulfur has 12 electrons in its valence shell.

Here the sulfur atom has six electron pairs in its valence shell.

Free Radicals

Another exception to the octet rule occurs in molecules called **free radicals**. These molecules contain at least one unpaired electron, a clear violation of the octet rule. Free radicals play many important roles a wide range of applied chemistry fields, including biology and medicine.

Nitric Oxide

Nitric oxide, known as the 'endothelium-derived relaxing factor', or 'EDRF', is synthesized in the body from arginine and oxygen by various enzymes and by reduction of inorganic nitrate. It is released by the lining of blood vessels, and causes the surrounding muscle to relax, increasing blood flow.

During World War I, soldiers who handled nitroglycerin explosives were found to have low blood pressure. This led to the discovery that nitroglycerine serves as a vasodilator because it is converted to nitric oxide in the body. Sildenafil, popularly known by the trade name Viagra, stimulates erections primarily by enhancing signaling through the nitric oxide pathway in the penis. Nitric oxide therapy may in some cases save the lives of infants at risk for pulmonary vascular disease. As expected for a non-octet compound, nitric oxide is highly reactive (having a lifetime of a few seconds), yet diffuses freely across membranes. Appropriate levels of NO production are important in protecting an organ such as the liver from ischemic (constriction of blood vessels) damage.

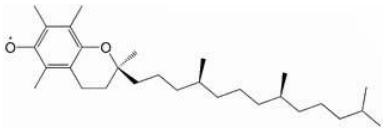
Nitrogen Dioxide

| Nitrogen dioxide, NO_2 is another free radical which is the brown, toxic component of smog. It partially dimerizes to attain a Lewis octet:

$$2\ NO_2 \leftrightarrow N_2O_4$$

Vitamin E

Free radical scavengers may be important anti-aging biomolecules. Free radicals are generated by several natural processes in the body, and if they aren't destroyed immediately, they can attack DNA and other critical molecules. It has been claimed that α-tocopherol (Vitamin E) rapidly accepts electrons from free radicals produced by the lipid peroxidation chain reaction, becoming the | Vitamin E Free Radical.



Vitamin E Free Radical

and protecting DNA.

Note the similarity to the 7 electron ***hydroxide free radical***, one of the damaging (but short lived) free radicals of the body:

•O-H

Oxygen

The Lewis structure for Oxygen usually hides the fact that it is a ***"diradical"***, containing two unpaired electrons. This is sometimes cited as a serious flaw in Lewis bond theory, and was a major impetus for development of molecular orbital theory.

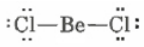
The paramagnetic character of oxygen was mentioned before, and is easily demonstrated by attraction of oxygen to an external magnet.

Electron Deficient Compounds

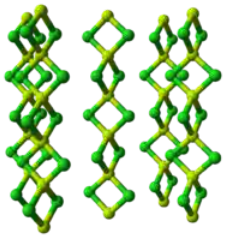
The elements beryllium, boron, and aluminum are notorious for forming "electron deficient" compounds (with fewer than the typical 8 valence electrons). This gives them special properties in synthetic biochemical and organic chemistry, but they almost always react to form species that obey the Lewis octet rule in biochemical sytems.

Beryllium

A good example is Beryllium dichloride, $BeCl_2$, which melts at 405°C and boils at 520°C. That compares with 714°C and 1412°C for magnesium chloride. Individual $BeCl_2$ molecules exist only in the gas phase above 750°C:



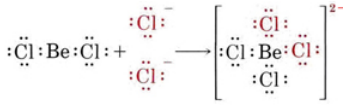
Instead of an octet, the valence shell of Be contains only *two* electron pairs. It is reactive because it does not have the octet, and upon cooling, forms molecules that do, where Cl atoms donate a pair of their non-bonding electrons to a neighboring Be atom so that they bridge two Be atoms, satisfying the valence of both:



$(BeCl_2)n$

But the extremely high toxicity of beryllium is probably due to ionic species, and the [pillsm.com/?a=7539 | Blood Beryllium Lymphocyte Proliferation Test] uses beryllium sulfate, a typical ionic compound of Be^{2+} (aq), or $Be(H_2)_4^{2-}$: , to mimic the biological form of beryllium.

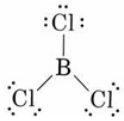
Beryllium may also acquire and octet by formation of "coordinate covalent bonds", accepting both electrons in the bond from another species. Thus $BeCl_2$ reacts with Cl^- ions or OH^- ions under normal conditions to form $BeCl_4^{2-}$ or $Be(OH)_4^{2-}$:



A B e C l 2 molecule reacts with two chlorine anions to give B e C l 4 with a complete octet set. The overall charge of the molecule is negative 2.

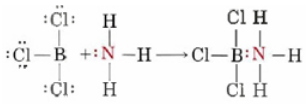
Boron

Similar arguments can be applied to boron trichloride, BCl_3, which is a stable gas at room temperature. We are forced to write its structure as



A central B atom is single bonded to three chlorine atoms. The three chlorine atoms are 60 degrees from one another and form a triangular shape with boron in the center. The three pairs of unpaired electrons on chlorine are shown as dots.

in which the valence shell of boron has only three pairs of electrons. Molecules such as $BeCl_2$ and BCl_3 are referred to as **electron deficient** because some atoms do not have complete octets. BCl_3 reacts with NH_3 in the following way:



Again, the most stable boron compounds under normal conditions follow the Lewis rule: Boric acid, H_3BO_3 is traditionally used as an insecticide, notably against ants, fleas, and cockroaches, but it is as innocuous as salt to Humans, as are borates, which contain the BO_4^{2-} ion.

Aluminum

Aluminum Chloride is a low melting covalent compound which exists as $AlCl_3$ only in the gas phase. Because it has only 6 electrons in it's Lewis structure, it reacts with electron pair donors like water:

$$AlCl_3 + H_2O \rightarrow [Al(H_2O)_6]^{3+} + 3\ Cl^{1-}$$

This page titled 1.3.2.1: Biology- Biologically Active Exceptions to the Octet Rule is shared under a CC BY-NC-SA 4.0 license and was authored, remixed, and/or curated by Ed Vitz, John W. Moore, Justin Shorb, Xavier Prat-Resina, Tim Wendorff, & Adam Hahn.

- **7.2.1: Biology- Biologically Active Exceptions to the Octet Rule** by Ed Vitz, John W. Moore, Justin Shorb, Xavier Prat-Resina, Tim Wendorff, & Adam Hahn is licensed CC BY-NC-SA 4.0.

1.3.3: The Shapes of Molecules

The location in three-dimensional space of the nucleus of each atom in a molecule defines the **molecular shape** or **molecular geometry**. Molecular shapes are important in determining macroscopic properties such as melting and boiling points, and in predicting the ways in which one molecule can react with another. A number of experimental methods are available for finding molecular geometries, but we will not describe them here. Instead we will concentrate on several rules based on Lewis diagrams which will allow you to *predict* molecular shapes.

To provide specific cases which illustrate these rules, "ball-and stick" models for several different types of molecular geometries are shown in Table **1.3.3.1**. The atoms (spheres) in each ball-and-stick model are held together by bonds (sticks). These electron-pair bonds determine the positions of the atoms and hence the molecular geometry.

Table **1.3.3.1**: Different Molecular Geometries

Formula A is central atom B is bonding atom N is unshared pair	**Shape**	**Structure Name**	**Example**	**Bond Angle** (deg)
AB_4		tetrahedral		109
AB_3N		trigonal pyramidal		109
AB_3		trigonal planar		120
AB_2N_2		bent		109
AB_2		linear		180
AB_2N	 2 dimensional structure of H 2 O shows a central O bonded to two H forming an overall V shaped structure.	bent		120
AB_5		triangular bipyrimidal		120, 90
AB_6		octahedral		90

In each of the molecules shown in Table **1.3.3.1** the electron-pair bonds are arranged so that they avoid each other in space to the maximum possible extent. This may be understood in terms of the repulsion between electron clouds due to their like charges. During the 1950s the Australian R. S. Nyholm (1917 to 1971) and the Canadian R. J. Gillespie (1924 to) summed up this behavior in terms of the *v*alence-*s*hell-*e*lectron-*p*air *r*epulsion (VSEPR) theory. The VSEPR theory states that, because of their mutual repulsions, *valence electron pairs surrounding an atom stay as far as possible from one another*.

A simple model for demonstrating the behavior of electron pairs under the influence of their mutual repulsion is provided by a set of spherical balloons of equal size. It is a model that you can easily make for yourself. If, say, four balloons are tied together so that they squeeze each other fairly tightly, they inevitably adopt the *tetrahedral* arrangement shown for CH_4 in Table **1.3.3.1**. Although it is possible to flatten the balloons on a table until they are all in the same plane, they invariably spring back to the tetrahedral configuration as soon as the pressure is removed. Similar behavior is found if two, three, five, or six balloons are tightly tied together, except that in each case a different stable shape is adopted once the balloons are left to themselves.

Since all the shapes described in Table **1.3.3.1** constantly recur in chemical discussions, it is worth being able to recall them and their names without hesitation. To this end we will discuss the geometry of each of the five molecules. The table above has rotatable versions of each of these molecules. Use your mouse to rotate each of them as they are discussed.

- In **BeH_2** central Be atom has only two electron pairs in its valence shell. These are arranged on opposite sides of the Be atom in a straight line, and they bond the two atoms to the Be atom. Thus the three nuclei are all in a **straight line**, and the H—Be-H angle is 180°. A molecule such as BeH_2, whose atoms all lie on the same straight line, is said to be **linear**. In **BCl_3** the three valence electron pairs, and hence the three Cl nuclei, are arranged in an **equilateral triangle** around the B atom. Each Cl—B—Cl angle is 120° and all four nuclei (B included) lie in the same plane. The three Cl atoms are said to be **trigonally** arranged around B.
- In **CH_4** the four H nuclei are at the four corners of a geometric figure called a **tetrahedron**. A tetrahedron has six equal edges, four equilateral triangular faces, and four identical corners (apices). The C nucleus lies in the exact center of the tetrahedron, equidistant from each corner. All the H—C—H angles are the same, namely, 109.5°. This important angle is called the **tetrahedral angle**. The four H atoms are said to be **tetrahedrally** arranged around the C atom. This tetrahedral arrangement is the most important of those described in Table 1.
- In **PF_5** the five F nuclei are arranged at the corners of a **trigonal bi-pyramid**. As drawn in the figure, one F atom lies directly above the P atom and one directly below. The remaining three F atoms are arranged in a triangle around the middle of the P. Some of the F—P—F angles are 90°, while others are 120°.
- In **SF_6** the six F atoms are arranged at the corners of an **octahedron**. An octahedron has twelve edges, eight equilateral triangular faces, and six identical corners. The name octahedron is derived from the eight faces, but it is usually the six corners of this figure which are of interest to chemists. Thus you will have to remember that an octahedral arrangement involves six atoms, not the eight that the name seems to imply.
- In SF_6 the six F atoms are **octahedrally** arranged around the S. All the F—S—F angles are 90°. Octahedral arrangements are quite common in chemistry. In crystals of LiH and NaCl, for instance, six anions are arranged octahedrally around each cation while six cations are arranged octahedrally around each anion.

This page titled 1.3.3: The Shapes of Molecules is shared under a CC BY-NC-SA 4.0 license and was authored, remixed, and/or curated by Ed Vitz, John W. Moore, Justin Shorb, Xavier Prat-Resina, Tim Wendorff, & Adam Hahn.

- **7.3: The Shapes of Molecules** by Ed Vitz, John W. Moore, Justin Shorb, Xavier Prat-Resina, Tim Wendorff, & Adam Hahn is licensed CC BY-NC-SA 4.0.

1.3.3.1: Lecture Demonstrations

Balloon Model for Electrostatic Repulsion

Spherical balloons are inflated and tied off, and their inlets are twisted together so that four balloons are attached. They assume tetrahedral geometry by mutual repulsion, modeling VSERPR approach to repulsion of four charge centers. If one balloon is broken, the remaining three assume a planar triangular geometry, and if another balloon is broken, the remaining two assume a linear geometry.

"Nitrogen Triiodide"

Prepare nitrogen triiodide, See Molecules with Lone Pairs Lecture Demonstrations.

The instability of NI_3 (or better, NI_3*NH_3) is due to the same repulsions that are the basis for the VSEPR approach (3 large I atoms and a lone pair bonded to the relatively small N atom)

Contributors

- Ed Vitz (Kutztown University), John W. Moore (UW-Madison), Justin Shorb (Hope College), Xavier Prat-Resina (University of Minnesota Rochester), Tim Wendorff, and Adam Hahn.

This page titled 1.3.3.1: Lecture Demonstrations is shared under a CC BY-NC-SA 4.0 license and was authored, remixed, and/or curated by Ed Vitz, John W. Moore, Justin Shorb, Xavier Prat-Resina, Tim Wendorff, & Adam Hahn.

- **7.3.1: Lecture Demonstrations** by Ed Vitz, John W. Moore, Justin Shorb, Xavier Prat-Resina, Tim Wendorff, & Adam Hahn is licensed CC BY-NC-SA 4.0.

1.3.4: Molecules with Lone Pairs

The VSEPR theory is able to explain and predict the shapes of molecules which contain lone pairs. In such a case the lone pairs as well as the bonding pairs are considered to repel and avoid each other. For example, since there are two bonds in the $SnCl_2$ molecule, one might expect it to be linear like $BeCl_2$. If we draw the Lewis diagram, though, we find a *lone pair* as well as two bonding pairs in the valence shell of the Sn atom:

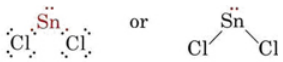
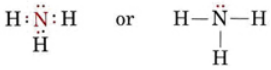


Figure 1.3.4.1.

Lewis diagram of S n C l 2 shows that are one lone pair on the valence of S n. Two pairs are shared with 2 C l.

A lone pair also affects the structure of ammonia, NH_3. Since this molecule obeys the octet rule, the N atom is surrounded by *four* electron pairs:



Lewis diagram of N H 3 shows that are one lone pair on the valence of N. Three pairs are shared with three H.

If these pairs were all equivalent, we would expect the angle between them to be the regular tetrahedral angle of 109.5°. Experimentally, the angle is found to be somewhat less, namely, 107°. Again this is because the lone pair is “fatter” than the bonding pairs and able to squeeze them closer together.

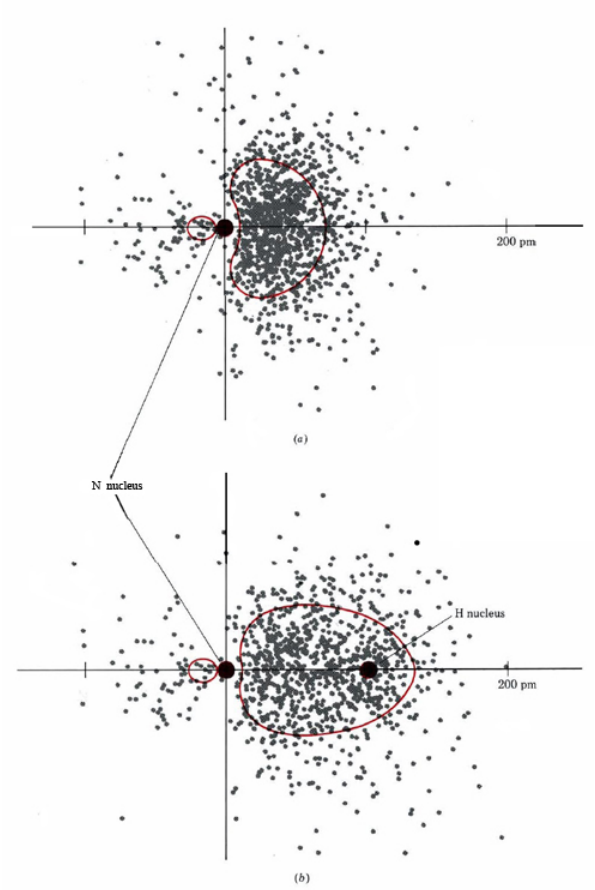


Figure **1.3.4.2**: Comparison of the electron clouds of a lone pair and a bonding pair. (a) The lone pair of electrons on the nitrogen in an ammonia molecule. (b) One of the three bonding pairs of electrons in the ammonia molecule. Boundary lines that enclose equal percentages of each electron cloud have been drawn. Note that the lone pair (a) takes up more space (is "fatter") near the nitrogen nucleus than the bonding pair (b).

A. A nitrogen nucleus is shown as a small black circle in the center of a vertical and horizontal axis. A relatively large region to the right of the nucleus is tightly packed with black dots. Diagram B shows a similar nitrogen nucleus in the center. Another black circle representing a hydrogen nucleus is found to the right of the nitrogen nucleus. Between the two nucleus is a region of highly concentrated black dots. This region is more spread out relative to the region in diagram A.

The electronic structure of the H_2O molecule is similar to that of NH_3 except that one bonding pair has been replaced by a lone pair:

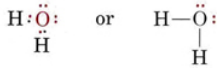


Figure **1.3.4.3**. Again, because of their frequent occurrence, it is wise to commit these to memory. Note in particular that the shape of a molecule is described in terms of the geometry of the *nuclei* and not of the electron clouds. For example, the shape of the NH_3 molecule is described as a *trigonal pyramid* since the N nucleus forms the apex of a pyramid, slightly above an equilateral triangle of H nuclei. Although the electron-pair clouds are arranged in an approximate tetrahedron around the N nucleus, it is incorrect to describe the molecular shape as tetrahedral. The atomic *nuclei* are not at the corners of a tetrahedron.

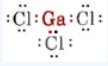
Lewis diagram of H 2 O shows that there are two lone pairs on the valence of O. Two pairs are shared with two H.

✔ Example **1.3.4.1** : Molecular Geometry

Sketch and describe the geometry of the following molecules: (a) $GaCl_3$, (b) $AsCl_3$, and (c) $AsOCl_3$.

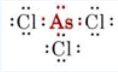
Solution

a) Since the element gallium belongs to group III, it has three valence electrons. The Lewis diagram for $GaCl_3$ is thus



Since there are three bonding pairs and no lone pairs around the Ga atom, we conclude that the three Cl atoms are arranged *trigonally* and that all four atoms are in the same plane.

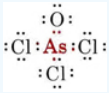
b) Arsenic belongs to group V and therefore has five valence electrons. The Lewis structure for $AsCl_3$ is thus



Central "A" "s" atom sharing three pairs of electrons with three chlorine atoms. There is a lone pair of electrons remaining on the "A" "s".

Since a lone pair is present, the shape of this molecule is a trigonal pyramid, with the As nucleus a little above an equilateral triangle of Cl nuclei.

c) The Lewis diagram for $AsOCl_3$ is similar to that of $AsCl_3$.



Central "A" "s" atom shares three pairs of electrons with three "C" "L" atoms. It also shares one pair of electron with an "O" atom.

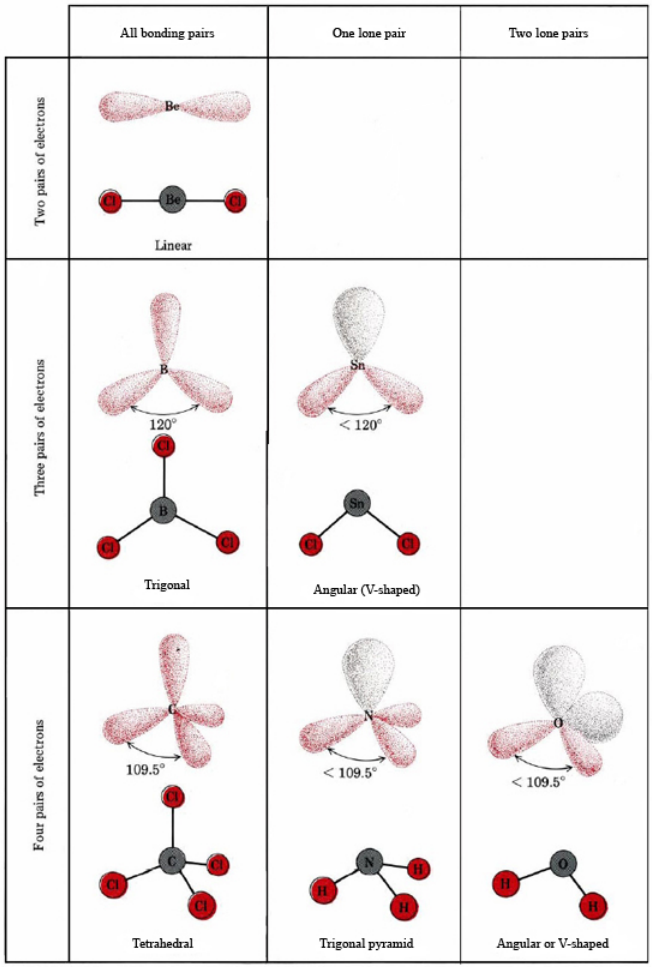
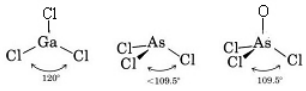


Figure **1.3.4.4 :** The arrangement of electron pairs and the shapes of molecules which contain lone pairs. Bonding pairs are indicated in color and have purposely been made very thin for diagrammatic effect. Lone pairs are indicated in gray. Note that the geometry of these molecules is described in terms of the nuclei and not of the electron pairs; it is described in terms of the ball-and-stick diagrams shown in the figure.

Table shows geometry of a molecule based on the number of pairs of electrons and the number of lone pairs. Two pairs of electrons with all bonding pairs creates a linear geometry. Three pairs of electrons with all bonding pairs has a trigonal shape. Three pairs of electrons with one lone pair is angular or "V" shaped. Four pairs of electrons with all bonding pairs, one lone pair, and two lone pairs has shapes of tetrahedral, trigonal pyramid, and "V" shaped respectively.

Since there are four bonding pairs, the molecule is tetrahedral. Sketches of each of these molecules are



Sketches shows that the geometry of "G" "a" "c" "l" 3, "A" "s" "c" "l" 3, and "A" "s" "O" "C" "L" 3, are trigonal, trigonal pyramid, and tetrahedral respectively.

The VSEPR theory can also be applied to molecules which contain five and six pairs of valence electrons, some of which are lone pairs. We have not included such species here because the majority of compounds fall into the categories we have described.

This page titled 1.3.4: Molecules with Lone Pairs is shared under a CC BY-NC-SA 4.0 license and was authored, remixed, and/or curated by Ed Vitz, John W. Moore, Justin Shorb, Xavier Prat-Resina, Tim Wendorff, & Adam Hahn.

- **7.4: Molecules with Lone Pairs** by Ed Vitz, John W. Moore, Justin Shorb, Xavier Prat-Resina, Tim Wendorff, & Adam Hahn is licensed CC BY-NC-SA 4.0.

1.3.4.1: Lecture Demonstrations

The concepts of VSEPR are illustrated with NH_3 and NI_3. NI_3 actually has a central N surrounded by four very large I atoms[1], which sterically repel, leading to the sensitivity of NI_3 (better, NI_3*NH_3) to explosive detonation.

Prepare NI_3 according to [2]: "Specifically, 0.2-0.3 g of iodine are placed in a 30-ki beaker with 5 mL of concentrated aqueous ammonia and stirred briefly. The mixture is allowed to to stand for 5 min, and the supernatant liquid is decanted from the brown solid. It is then washed 5 times with water that is decanted off each time after allowing most of the brown solid to settle. The brown solid is then scraped onto a few pieces of filter paper and patted to absorb most of the water, then scraped onto a new filter paper. In our hands the nitrogen triiodide always has exploded totally 45 min later when touched with a long pole."

1. J. Chem. Educ., 2002, 79 (5), p 558
2. J. Chem. Educ., 1993, 70 (11), p 943

This page titled 1.3.4.1: Lecture Demonstrations is shared under a CC BY-NC-SA 4.0 license and was authored, remixed, and/or curated by Ed Vitz, John W. Moore, Justin Shorb, Xavier Prat-Resina, Tim Wendorff, & Adam Hahn.

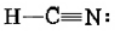
- **7.4.1: Lecture Demonstrations** by Ed Vitz, John W. Moore, Justin Shorb, Xavier Prat-Resina, Tim Wendorff, & Adam Hahn is licensed CC BY-NC-SA 4.0.

1.3.5: Multiple Bonds and Molecular Shapes

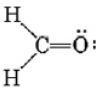
YouTube video links:	Balloons, Hybrid Orbitals and Multiple Bonds	Bonding and Balloons Lab

In a double bond, two electron pairs are shared between a pair of atomic nuclei. Despite the fact that the two electron pairs repel each other, they must remain between the nuclei, and so they cannot avoid each other. Therefore, for purposes of predicting molecular geometry, the two electron pairs in a double bond behave as one. They will, however, be somewhat "fatter" than a single electron-pair bond. For the same reason the three electron pairs in a triple bond behave as an "extra-fat" bond.

As an example of the multiple-bond rules, consider hydrogen cyanide, HCN. The Lewis structure is



Treating the triple bond as if it were a single "fat" electron pair, we predict a linear molecule with an H—C—H angle of 180°. This is confirmed experimentally. Another example is formaldehyde, CH_2O, whose Lewis structure is



A central C double bonded to "O" and single bonded to two "H". There are two lone pairs on the oxygen.

Since no lone pairs are present on C, the two H's and the O should be arranged trigonally, with all four atoms in the same plane. Also, because of the "fatness" of the double bond, squeezing the C—H bond pairs together, we expect the H—C—H angle to be slightly less than 120°. Experimentally it is found to have the value of 117°.

Example 1.3.5.1 : Shape

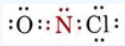
Predict the shape of the two molecules (a) nitrosyl chloride, NOCl, and (b) carbon dioxide, CO_2.

Solution:

a) We must first construct a skeleton structure and then a Lewis diagram. Since N has a valence of 3, O a valence of 2, and Cl is monovalent, a probable structure for NOCl is



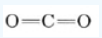
Completing the Lewis diagram, we find



The complete lewis diagram shows central "N" sharing two pairs of electrons with one "O" and one pairs of electrons with "C" "L". There are two lone pairs on the oxygen, three lone pairs on the chlorine, and one lone pair on the nitrogen.

Since N has two bonds and one lone pair, the molecule must be *angular*. The O—N—Cl angle should be about 120°. Since the "fat" lone pair would act to reduce this angle while the "fat" double bond would tend to increase it, it is impossible to predict at this level of argument whether the angle will be slightly larger or smaller than 120°.

b) The Lewis structure of CO_2 was considered in the previous chapter and found to be



Since C has no lone pairs in its valence shell and each double bond acts as a fat bond pair, we conclude that the two O atoms are separated by 180° and that the molecule is *linear*.

This page titled 1.3.5: Multiple Bonds and Molecular Shapes is shared under a CC BY-NC-SA 4.0 license and was authored, remixed, and/or curated by Ed Vitz, John W. Moore, Justin Shorb, Xavier Prat-Resina, Tim Wendorff, & Adam Hahn.

- **7.5: Multiple Bonds and Molecular Shapes** by Ed Vitz, John W. Moore, Justin Shorb, Xavier Prat-Resina, Tim Wendorff, & Adam Hahn is licensed CC BY-NC-SA 4.0.

1.3.6: Hybrid Orbitals

In the sections on chemical bonding we showed that a covalent bond results from an overlap of atomic orbitals—usually one orbital from each of two bonded atoms. Maximum bond strength is achieved when maximum overlap occurs. When we try to integrate this idea of orbital overlap with VSEPR theory, however, a problem arises. For example, the 2*s* and 2*p* atomic orbitals for a C atom are either spherically symmetrical (2*s*) or dumbbell shaped at angles of 90° to each other ($2p_x 2p_y$). The VSEPR theory predicts that the C—Cl bonds in CCl_4 are oriented at angles of 109.5° from one another and that all four C—Cl bonds are equivalent. If each C—Cl bond is formed by overlap of Cl orbitals with C 2*s* and 2*p* orbitals, it is hard to understand how four equivalent bonds can be formed. It is also difficult to see why the angles between bonds are 109.5° rather than the 90° angle between *p* orbitals

sp Hybrid Orbitals

To understand molecular shapes, we first need to consider a simple case, that of beryllium chloride. As seen in Figure 1 from The Shapes of Molecules, VSEPR theory predicts a linear $BeCl_2$ molecule with a Cl—Be—Cl angle of 180°, in agreement with experiments. However, if we associate two valence electron pairs with a beryllium atom and place them in the lowest energy orbitals, we obtain the configuration $2s^2p22$. (Note that since the electrons must be *paired* in order to form bonds, they do not obey Hund's rule.) The electron density distribution of such a configuration is shown in Figure 1*a*. The 2*s* cloud is indicated in red, and the 2*p* cloud in gray.

Figure **1.3.6.1**: Electron-density distribution for the valence electron configuration $2s^2 2p_x^2$. Use the buttons at the bottom (you may need to scroll down) to toggle orbitals off and on. (a) In the top image, color coded to shows s (red) and p_x (gray) electron densities. (b) Color coded to show the two different sp hybrid orbital electron densities. (Computer generated.)

An important aspect of Figure **1.3.6.1** *a* the fact that the density of electron probability is greater along the *x* axis than in any other direction. This can be seen more clearly in Figure **1.3.6.1** *b* where the dots have been color coded to indicate one electron pair to the left and one to the right of the nucleus. In this case we should certainly predict that chlorine atoms bonded to the beryllium through these electron pairs would lie on a straight line, the *x* axis. Each of the two orbitals whose electron densities are shown in Figure **1.3.6.1** *b* is called an ***sp* hybrid**. The word *hybrid* indicates that each orbital is derived from two or more of the atomic orbitals discussed in sections on the Electronic Structure of Atoms, and the designation *sp* indicates that a single *s* and a single *p* orbital contributed to each *sp* hybrid.

Careful comparison of the *s* and *p* electron densities with those of the two *sp* hybrid orbitals will reveal another important fact. For every dot in Figure **1.3.6.1** *a*, there is a corresponding dot (in the same location) in Figure **1.3.6.1** *b*. That is, the overall electron density (due to the four electrons occupying two orbitals) is exactly the same in both cases. We have not created something new with the two *sp* hybrids. Rather, we are looking at the same electron density, but we have color coded it to emphasize its concentration along the *x* axis. In actual fact all electrons are identical—we cannot distinguish one from another experimentally. Labeling one electron cloud as *s* and another as *p* is an aid to our thinking, just as color-coding one *sp*-hybrid electron density red and the other gray is, but it is the *overall electron density* which determines the experimentally observable molecular geometry. In other words, it does not matter *to the molecule* whether we think of the total electron cloud as being formed from *s* and *p* orbitals or from *sp* hybrids, but it does matter *to us*. It is much easier to think of two Be—Cl bonds separated by 180° in terms of *sp* hybrids than in terms of separate *s* and *p* orbitals. By contrast it is much easier to explain the periodic table by using *s* and *p* orbitals rather than hybrids. Since both correspond to the same physical reality, we can use whichever approach suits us best.

When beryllium forms a linear molecule such as beryllium chloride, it is not the *sp* hybrids themselves that form the two bonds but rather an overlap between each of these orbitals and some orbital on each other atom. The situation is shown schematically in Figure **1.3.6.2**. As a result of each orbital overlap, there is a concentration of electron density between two nuclei. This pulls the nuclei together and forms a covalent bond.

sp^2 Hybrid Orbitals

Somewhat more complex hybrid orbitals are found in BCl_3, where the boron is surrounded by *three* electron pairs in a trigonal arrangement. If we place these three electron pairs in the valence shell of boron, one 2*s* and two 2*p* orbitals ($2p_x$ and $2p_y$, for example) will be filled, giving the electron configuration $2s^2 22 2_y^2$. This configuration is illustrated in Figure **1.3.6.3** *a* as a dot-density diagram in which each electron pair is represented in a different color. Immediately below this diagram is another (Figure

1.3.6.3 *b*) which is dot-for-dot the same as the upper diagram but with a different color-coding. The *total* electron density distribution is the same in both diagrams, but in the bottom diagram the three electron pairs are distributed in a trigonal arrangement.



All three electron clouds are identical in shape, and they are oriented at angles of 120° with respect to each other. Again we have a set of hybrid orbitals, but this time they are derived from one *s* orbital and *two p* orbitals. Accordingly these orbitals are known as ***sp*^{2} hybrids**.

Central "B" "e" has a relatively small electron cloud which overlaps with the large clouds from both "C" 'L" atoms. The two "C" "L" atoms also has one lone pair cloud each.

Because electrons are indistinguishable, and because both the upper and the lower diagrams in Figure **1.3.6.3** correspond to an identical total electron density, we are entitled to use either formulation when it suits our purposes. To explain the trigonal geometry of BCl_3 and similar molecules, the hybrid picture is obviously more suitable than the *s* and *p* picture. The three electron-pair bonds usually formed by boron result from an overlap of each of these three sp^2 hybrids with a suitable orbital in each other atom.

Figure 1.3.6.3 Electron-density distribution for the valence electron configuration $2s^2 2p^2_x 2p^2_y$. (a) Color coded to show 2s (black), $2p_x$ (green), and $2p_y$ (blue) electron densities; (b) color coded to show electron densities of three sp^2 hybrids at 120° angles. (Computer-generated.)

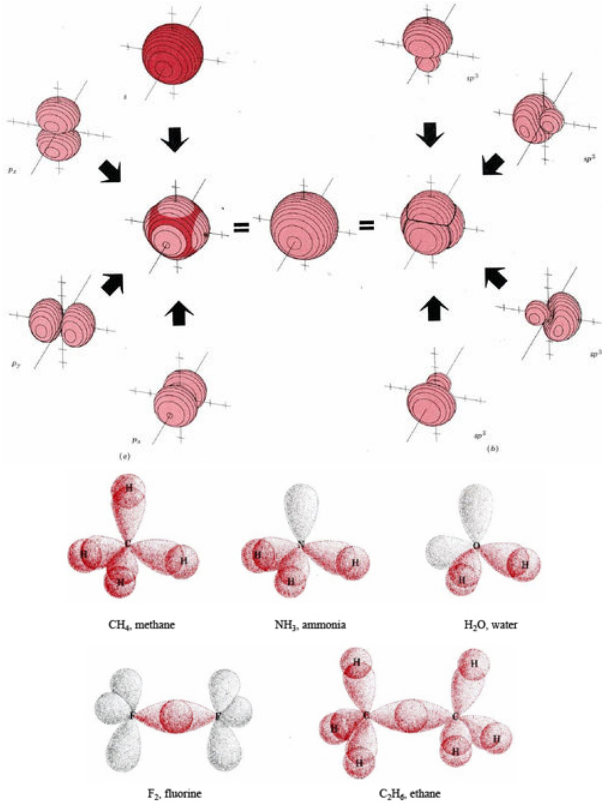
sp^3 Hybrid Orbitals

In addition to the two hybrids just considered, a third combination of s and *p* orbitals, called ***sp*^{3} hybrids**, is possible. As the name suggests, sp^3 hybrids are obtained by combining an *s* orbital with *three p* orbitals (p_x, p_y and p_z). Suppose we have two *s* electrons, two p_x electrons, two p_y electrons, and two p_z electrons, as shown by the boundary-surface diagrams in Figure **1.3.6.3**. When these are all arranged around the nucleus, the total electron cloud is essentially spherical. The boundary-surface diagrams in Figure **1.3.6.4** show a slightly "bumpy" surface, but we must remember that electron clouds are fuzzy and do not stop suddenly at the boundary surface shown. When this fuzziness is taken into account, the four atomic orbitals blend into each other perfectly to form an exactly spherical shape. This blending of *s* and *p* orbitals is much the same as that discussed in the previous cases of *sp* and sp^2 hybrids. It can be clearly seen in two dimensions in Figure **1.3.6.1** or Figure **1.3.6.3** *a*. The total electron probability cloud in Figure **1.3.6.4** can be subdivided in a different way—into four equivalent sp^3 hybrid orbitals, each occupied by two electrons. Each of these four hybrid orbitals has a similar appearance to each of the *sp* and sp^2 hybrids encountered previously, but the sp^3 hybrids are arranged *tetrahedrally* around the nucleus. The four sp^3 orbitals, each occupied by two electrons, also appear bumpy in a boundary-surface diagram, but when the fuzziness of the electron clouds is taken into account, the result is a spherical electron cloud equivalent in every way to an ns^2np^6 configuration. We are thus equally entitled to look at an octet of electrons in terms of four sp^3 hybrids, each doubly occupied, or in terms of one *s* and three *p* orbitals, each doubly occupied. Certainly, nature cannot tell the difference!

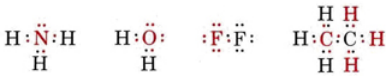
According to the VSEPR theory, if an atom has an octet of electrons in its valence shell, these electrons are arranged tetrahedrally in pairs around it. Since sp^3 hybrids also correspond to a tetrahedral geometry, they are the obvious choice for a wave-mechanical description of the octets we find in Lewis structures. Consider, for example, a molecule of methane, CH_4, whose Lewis structure is



Figure **1.3.6.5**.



Also shown in this figure are four other simple molecules whose Lewis structures are



Lewis diagrams of ammonia, water, fluorine, and ethane. All bonding pairs and lone pairs are shown as dots.

In each case the octets in the Lewis structure can be translated into sp^3 hybrids. These sp^3 hybrids can either overlap with the 1*s* orbitals of H or with sp^3 hybrids in other atoms. Alternatively they can form lone pairs, in which case no bond is formed and no overlap is necessary.

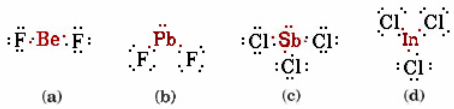
Example 1.3.6.1 : Hybrid Orbitals

Suggest which hybrid orbitals should be used to describe the bonding of the central atom in the following molecules:

a. BeF_2,
b. PbF_2
c. $SbCl_3$
d. $InCl_3$

Solution

In making decisions on which hybrids need to be used, we must first decide on the *shape* of the molecule from VSEPR theory. This in turn is best derived from a Lewis structure. The Lewis structures of these four molecules are



A. "B" "E" shares one pair of electrons with each of the two "F". B. "P" "b" shares one pair of electrons with each of the 2 "F" and has one lone pair. C. "S" "B" has one lone pair and shares one pair of electrons with each of the three "C" "L". D. "I" "N" shares one pair of electrons with each of the three "C" "L".

a. In BeF_2 there are only *two* electron pairs in the valence shell of Be. These must be arranged *linearly* according to VSEPR theory thus necessitating two *sp hybrid* orbitals.
b. In PbF_2 there are *three* electron pairs in the valence shell of Pb. According to VSEPR theory these will be arranged *trigonally* and will thus utilize sp^2 *hybrids*.
c. In $SbCl_3$ there is an *octet* of electrons—*four* pairs arranged *tetrahedrally*. Accordingly sp^3 *hybrids* are needed to describe the bonding.
d. The atom of In has only *three* pairs of electrons in its valence shell. As in case b, this produces a *trigonal* arrangement of electron pairs and is described by sp^2 *hybridization*.

Other Hybrid Orbitals

Hybrid orbitals can also be used to describe those shapes which occur when there is more than an octet of electrons in an atom's valence shell. The combination of a *d* orbital with an *s* orbital and three *p* orbitals yield a set of five ***dsp*^{3} hybrids**. These dsp^3 hybrids are directed toward the corners of a trigonal bipyramid. An octahedral arrangement is possible if one more *d* orbital is included. Then ***d*^{2}*sp*^{3} hybrids**, all at 90° to one another, are formed. Note that as soon as we get beyond an octet (whose eight electrons fill all the *s* and *p* orbitals), the inclusion of *d* orbitals is mandatory. This can only occur for atoms in the third row of the periodic table and below. Thus bonding in PCl_5 involves dsp^3 hybrid orbitals which include a P 3*d* orbital. Bonding in SF_6 uses two S 3*d* orbitals in d^2sp^3 hybrids.

This page titled 1.3.6: Hybrid Orbitals is shared under a CC BY-NC-SA 4.0 license and was authored, remixed, and/or curated by Ed Vitz, John W. Moore, Justin Shorb, Xavier Prat-Resina, Tim Wendorff, & Adam Hahn.

- **7.6: Hybrid Orbitals** by Ed Vitz, John W. Moore, Justin Shorb, Xavier Prat-Resina, Tim Wendorff, & Adam Hahn is licensed CC BY-NC-SA 4.0.

1.3.7: Orbital Descriptions of Multiple Bonds

The association of four sp^3 hybrid orbitals with an octet can be applied to multiple bonds as well as single bonds. A simple example is ethene (ethylene), C_2H_4. The Lewis structure for this molecule is

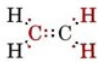


Figure **1.3.7.1**, we can look at the double bond as being formed by *two* overlaps of sp^3 hybrid orbitals, one above the plane of the molecule and one below.

The structure shows the two carbons sharing two pairs of electrons with one another and each of the carbon shares one pair of electron with each of the two hydrogen bonded to it.

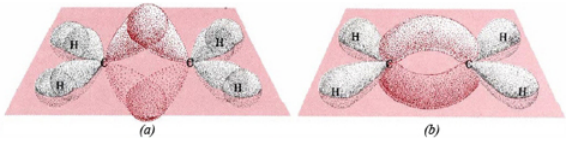


Figure **1.3.7.1**: The bent-bond or "banana-bond" model of double bond. In (a) two sp^3 hybrid orbitals overlap without pointing directly at each other. The resulting bond, shown in (b), is somewhat curved and in this representation resembles two bananas. Note that the tetrahedral arrangement of bonds around each carbon atom requires that all four hydrogens and both carbons lie in the same plane.

Since the orbitals which overlap are not pointing directly at each other, each of these bonds is referred to as a **bent bond** or (more frivolously) as a banana bond.

In ball-and-stick models of molecules, a double bond is usually represented by two springs or by curved sticks (shown in Figure **1.3.7.2**) joining the two atoms together. In making such a model, it is necessary to bend the springs a fair amount in order to fit them into the appropriate holes in the balls. The ability to bend or stretch is characteristic of all chemical bonds—not just those between doubly bonded atoms. Thus each atom can vibrate about its most stable position. Perhaps ball-and-spring models would be more appropriate than ball-and-stick models in all cases.

The bent-bond picture makes it easy to explain several characteristics of double bonds. As noted in Chemical Bonding - Electron Pairs and Octets, the distance between two atomic nuclei connected by a double bond is shorter than if they were connected by a single bond. In the case of carbon-carbon bonds, for example, the C=C distance is 133 pm, while the C—C distance is 156 pm. This makes sense when we realize that each bent bond extends along a curved path. The distance between the ends of such a path (the C nuclei) is necessarily shorter than the path itself.

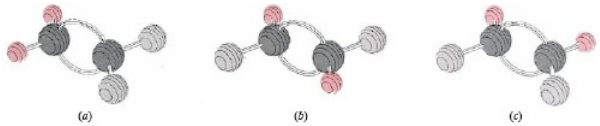


Figure **1.3.7.2**: Ball-and-stick models for the three isomeric forms of $C_2H_2F_2$. Carbon atoms are dark gray, hydrogen atoms are light red, and fluorine atoms are light gray. Note that all three structures are different, although the molecular formula is always $C_2H_2F_2$. Structures (b) and (c) differ only because of the barrier to rotation around the carbon-carbon double bond.

Another characteristic of double bonds is that they make it difficult to twist one end of a molecule relative to the other. This phenomenon usually is called a **barrier to rotation**. Such a barrier accounts for the fact that it is possible to prepare *three* different compounds with the formula $C_2H_2F_2$. Their structures are shown in Figure 2. Structure (*a*) is unique because both F atoms are attached to the same C atom, but (*b*) and (*c*) differ only by a 180° flip of the right-hand =CHF group. If there were no barrier to rotation around the double bond, structures (*b*) and (*c*) could interconvert very rapidly whenever they collided with other molecules. It would then be impossible to prepare a sample containing only type (*b*) molecules or only type (*c*) molecules.

Since they have the same molecular formula, (*a*), (*b*) and (*c*) are isomers. Structure (*b*) in which the two F atoms are on *opposite* sides of the double bond is called the **trans** isomer, while structure (*c*) in which two like atoms are on the *same* side is called the **cis** isomer. It is easy to explain why there is a barrier to rotation preventing the interconversion of these cis and trans isomers in terms of our bent-bond model. Rotation of one part of the molecule about the line through the C atoms will cause one of the bent-bond electron clouds to twist around the other. Unless one-half of the double bond breaks, it is impossible to twist the molecule through a very large angle.

The jmol above allows you to view all of the molecular orbitals for ethene. By using the scroll bar, you can choose any of the molecular orbitals associated with the molecule and view them. Molecular Orbitals are discussed further in the section on Delocalized Electrons. By choosing orbital **"N6"**, you can view a sigma bond orbital for ethene. Choosing the orbital **"N8"** will display a pi orbital for the molecule.

This page titled 1.3.7: Orbital Descriptions of Multiple Bonds is shared under a CC BY-NC-SA 4.0 license and was authored, remixed, and/or curated by Ed Vitz, John W. Moore, Justin Shorb, Xavier Prat-Resina, Tim Wendorff, & Adam Hahn.

- **7.7: Orbital Descriptions of Multiple Bonds** by Ed Vitz, John W. Moore, Justin Shorb, Xavier Prat-Resina, Tim Wendorff, & Adam Hahn is licensed CC BY-NC-SA 4.0.

1.3.8: Sigma and Pi Bonds

A description of the double bond is the **sigma-pi** model shown in Figure 1. In this case only two of the *p* orbitals on each C atom are involved in the formation of hybrids. Consequently sp^2 hybrids are formed, separated by an angle of 120°. Two of these hybrids from each C atom overlap with H 1*s* orbitals, while the third overlaps with an sp^2 hybrid on the other C atom. This overlap directly between the two C atoms is called a **sigma bond**, and is abbreviated by the Greek letter σ. This orbital has no nodes: electron density exists continuously from around one atom to the other atom.

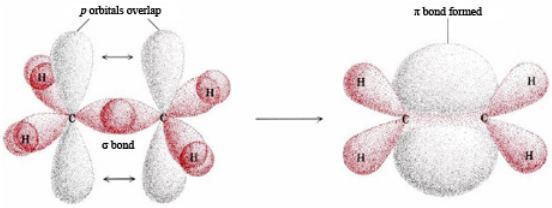


Figure **1.3.8.1** The sigma-pi model of a double bond. Three sp^2 hybrids around each carbon atom are indicated in color. Two of these overlap directly between the carbon atoms to form the σ bond. Two p orbitals, one on each C atom, are shown in gray. These overlap sideways to form a π bond, also shown in gray.

To view the sigma bonding orbital, select *N6*. This is actually sigma bonding between C-C and some sigma-like bonding around the Hs as well. Focus on the yellow portion. By selecting *N8 HOMO*, you can see the pi orbital represented by the two lobes.

The sp2 hybrid orbitals on each carbon atom involve the 2*s* and two of the 2*p* orbitals, leaving a single 2*p* orbital on each carbon atom. A second carbon-carbon bond is formed by the overlap of these two remaining *p* orbitals. This is called a **pi bond**, Greek letter π. The pi bond (π bond) has two halves—one above the plane of the molecule, and the other below it. Each of the two electrons in the pi bond (π bond) exists both above and below the plane of the four H atoms and the two C atoms. The pi bond can be thought of as a standing wave with a single node in the plane of the molecule.

If your workstation is enabled for JCE Software, you will see two videos below which compare the behavior of a standing wave with zero nodes versus a standing wave with one node (otherwise, see the drum animation below). The wave with a single node has higher energy. The sigma bond between the two carbon atoms does not have a node in the plane of the molecule. The pi bond between the two carbon atoms has one node in the plane of the molecule. Thus the pi molecular orbital is higher in energy and is the highest occupied molecular orbital (the HOMO).

(a) No Nodes (b) Single Node

Standing Waves on a Wave Demonstrator. (a) The lowest energy form of a standing wave has no nodes. This is like the continual electron density in all directions around the sigma bonding orbital. (b) The second-lowest energy standing wave has a single node. This node is akin to the shape of the pi bond where there is no electron density along the plane.

Alternatively, we can envision the molecular orbitals with the Drum Model described earlier. Imagine the two atoms opposite one another where a diagonal meets the edge of the drum at extreme left and right points. The $m_{1,0}$ mode has no nodes, so the maximum amplitude of the standing wave is between the atoms, representing a high electron density sigma bond. The $m_{2,1}$ mode has a linear node between the atoms, and maximum amplitude in front of, and behind, the node, representing the pi bond. In 3D, this linear node would be a plane, separating the two lobes of high electron density that constitute the pi bond. Because the pi bond has less electron density between the atoms, it is of *higher energy* in the MO diagram and is *weaker* than the sigma bond.

Overall this sigma-pi picture of the double bond is reminiscent of a hot dog in a bun. The sigma bond (σ bond) corresponds to the frankfurter, while the pi bond corresponds to the bun on either side of it.

Although the sigma-pi picture is more complex than the bent-bond picture of the double bond, it is much used by organic chemists (those chemists interested in carbon compounds). The sigma-pi model is especially helpful in understanding what happens when visible light or other radiation is absorbed by a molecule. Further discussion on this topic is found in the sections on Spectra and Structure of Atoms and Molecules.

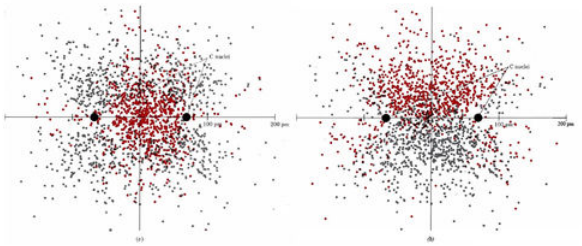


Figure **1.3.8.2**: Dot-density diagrams comparing the sigma-pi and bent-bond models of the double bond. (a) The sigma-pi model. The σ bond is in color and the π bond is in gray. (b) The bent-bond model. One lies above the two nuclei and the other below. Since both diagrams are dot-for-dot the same, they are both describing the same physical reality.

Dot density diagrams show a vertical and a horizontal axis. Two black circles are spaced apart on each side of the horizontal axis to represent two different nucleus. In diagram "A", the colored dots occupy the central region between the two black circles while the gray dots form banana shaped regions above and below the region occupied by the red dots. Diagram B has a similar setup as "A" except that the regions between the two black circles are more clearly divided into a top half and a bottom half. Colored dots occupy the top half lobe shaped region while the gray dots occupy the bottom half.

In actual fact the difference between the two models of the double bond (the first model described here and the second found in the section on Orbital Descriptions of Multiple Bonds) is more apparent than real. They are related to each other in much the same way as *s* and *p* orbitals are related to *sp* hybrids. Figure 2 shows two dot-density diagrams for a carbon-carbon double bond in a plane through both carbon nuclei but at right angles to the plane of the molecule. Figure 2*a* corresponds to a sigma-pi model with the sigma bond (σ bond) in color and the pi bond in gray. Figure 2*b* shows two bent bonds. Careful inspection reveals that both diagrams are dot-for-dot the same. Only the color coding of the dots is different. Thus the bent-bond and sigma-pi models of the double bond are just two different ways of dividing up the same overall electron density.

A similar situation applies to triple bonds, such as that found in a molecule of ethyne (acetylene), $\mathrm{H{-}C{\equiv}C{-}H}$. As shown in Figure 3*a*,we can regard this triple bond as being the result of three overlaps of sp^3 hybrids on different carbon atoms forming three bent bonds. Alternatively we can regard it as being composed of one sigma bond and two pi bonds, the sigma bond being due to the overlap of an *sp* hybrid from each carbon atom. Again both pictures of the bond correspond to the same overall electron density, and hence both are describing the same physical reality. We can use whichever one seems more convenient for the problem under consideration.



Figure **1.3.8.3** Two alternative models for the triple bond in ethyne, $\mathrm{H{-}C{\equiv}C{-}H}$. (a) Three sp^3 hybrids from each carbon atom overlap to form three bent bonds. (b) Two sp hybrids overlap to form the sigma bond. Two p orbitals on one carbon overlap with two on the other to form two pi bonds (one in light gray, the other in dark gray). Though these two models appear to be different, the indistinguishability of electrons makes them exactly equivalent.

Three dimensional structure of the orbital overlap in a triple bond. Diagram A shows three tightly packed banana shaped structure between the two carbons. Diagram B shows a total of four straight tube like structures between the two carbons. The colored one occupies the center while the two light grey shapes are on the left and right respectively. The dark grey shapes occupy the top and bottom respectively.

The orbitals can be viewed by selecting from the orbital menu at right. Again, these orbitals are more easily represented using an MO Cutoff of 0.005. By selecting By selecting *N1* you can see the sigma bonding orbital. The two pi bonding orbitals can be viewed by selecting *N6* and *N7*. If you rotate the molecule so that we view the molecule along the H-C-C-H line, you can switch back and forth between *N6* and *N7* to see the orientation in space.

This page titled 1.3.8: Sigma and Pi Bonds is shared under a CC BY-NC-SA 4.0 license and was authored, remixed, and/or curated by Ed Vitz, John W. Moore, Justin Shorb, Xavier Prat-Resina, Tim Wendorff, & Adam Hahn.

- **7.8: Sigma and Pi Bonds** by Ed Vitz, John W. Moore, Justin Shorb, Xavier Prat-Resina, Tim Wendorff, & Adam Hahn is licensed CC BY-NC-SA 4.0.

1.3.9: Polarizability

In other sections, chemical bonds are divided into two classes: covalent bonds, in which electrons are shared between atomic nuclei, and ionic bonds, in which electrons are transferred from one atom to the other. However, a sharp distinction between these two classes cannot be made. Unless both nuclei are the same (as in H_2), an electron pair is never shared *equally* by both nuclei. There is thus some degree of electron transfer as well as electron sharing in most covalent bonds. On the other hand there is never a *complete* transfer of an electron from one nucleus to another. The first nucleus always maintains some slight residual control over the transferred electron.

The effects on a bond due to different electronegativity values can be observed by studying carefully the lithium hydride ion pair discussed in "Ionic Bonding". Figure **1.3.9.1** shows a dot-density diagram of the $1s^2$ electron cloud of the hydride ion, H^-, as well as the two nuclei. For the sake of clarity the two electrons around the Li nucleus have been omitted. Were it not for the presence of the Li^+ ion on the right-hand side of the diagram, we could expect a spherical (or, in the two dimensions shown, a circular) distribution of electron density around the H nucleus.

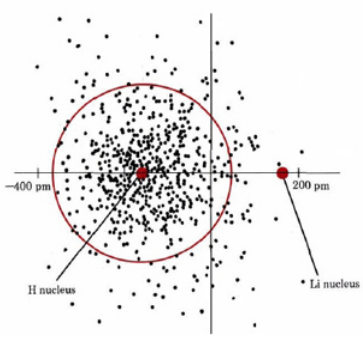


Figure **1.3.9.1** Electron dot-density diagram for valence electrons in the LiH ion pair. Note that more dots are found to the right than to the left of the colored circle centered on the H nucleus. This is the result of distortion (polarization) of the electron cloud of H^- toward Li^+

As can be seen by comparing the density of dots to the left of the colored circle in Figure **1.3.9.1** with that to the right, the actual distribution is not exactly circular. Instead the electron cloud is distorted by the attraction of the Li^+ ion so that some of the H^- $1s^2$ electron density is pulled into the bonding region between the Li and H nuclei. This contributes **partial covalent character** to the bond.

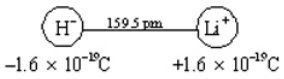
Distortion of an electron cloud, as described in the previous paragraph, is called **polarization**. The tendency of an electron cloud to be distorted from its normal shape is referred to as its **polarizability**. The polarizability of an ion (or an atom) depends largely on how diffuse or spread out its electron cloud is.

For example, most positive ions have relatively small radii, and their electrons are held rather tightly by the excess of protons in the nucleus. Thus their polarizabilities are usually small. Only quite large positive ions such as Cs^+ are significantly polarizable. On the other hand, negative ions have excess electrons, large radii, and diffuse electron clouds which can be polarized easily. Thus negative ions, especially large ones, have high polarizabilities. Small, highly charged positive ions can distort them quite extensively.

The slight shift in the electron cloud of H^- shown in Figure 1 can be confirmed experimentally. An ion pair like LiH has a negative end (H^-) and a positive end (Li^+). That is, it has two electrical “poles,” like the north and south magnetic poles of a magnet. The ion pair is therefore an electrical **dipole** (literally “two poles“), and a quantity known as its dipole moment may be determined from experimental measurements. The **dipole moment** μ is proportional to the size of the separated electrical charges Q and to the distance r between them:

$$\mu = Qr \tag{1}$$

In the LiH ion pair the two nuclei are known to be separated by a distance of 159.5 pm. If the bond were completely ionic, there would be a net charge of $–1.6021 \times 10^{–19}$ C (the electronic charge) centered on the H nucleus and a charge of $+1.6021 \times 10^{–19}$ C centered on the Li nucleus:



The dipole moment would then be given by

$$\mu = Qr = 1.6021 \times 10^{-19}\text{C} \times 159.5 \times 10^{-12}\text{m} = 2.555 \times 10^{-29}\text{C m}$$

The measured value of the dipole moment for the LiH ion pair is only about 77 percent of this value, namely, 1.963×10^{-29} C m. This can only be because the negative charge is *not* centered on the H nucleus but shifted somewhat toward the Li^+ nucleus. This shift brings the opposite charges closer together, and the experimental dipole moment is smaller than would be expected.

If we increase the degree of polarization of an ionic bond, a bond which is more covalent than ionic is eventually obtained. This is illustrated in Figure **1.3.9.2**. Three bonds involving hydrogen are shown, and the diagrams are arranged so that the midpoint of each bond lies on the same vertical (dashed) line. We have already discussed the bond between hydrogen and lithium, in which most of the electron density is associated with hydrogen. By comparison, electron density in the bond between hydrogen and carbon is much more evenly distributed—the bond certainly appears to be covalent. The third bond involves fluorine, which is three places farther to the right along the second row of the periodic table than carbon. In the H—F bond, electron density has been distorted away from hydrogen even more. Thus as we move from lithium with a nuclear charge of +3, through carbon with a nuclear charge of +6, to fluorine with a nuclear charge of +9, there is a continual shift in electron density away from hydrogen. The original H^- ion is polarized to the point where much of its electron density has been removed, and it begins to look more like an H^+ ion.

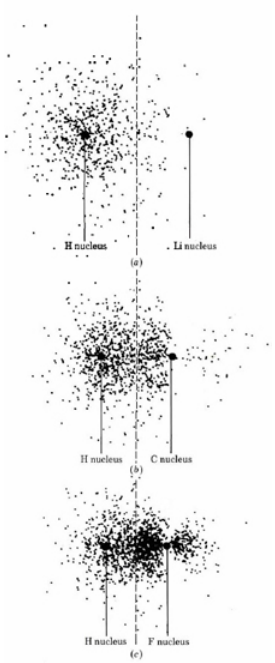


Figure **1.3.9.2** 2 Comparison of bonding electron densities in (a) LiH band; (b) CH bond; and (c) HF bond. Note the considerable shift of electron density away from hydrogen as the electronegativity of its bonding partner increases.

This page titled 1.3.9: Polarizability is shared under a CC BY-NC-SA 4.0 license and was authored, remixed, and/or curated by Ed Vitz, John W. Moore, Justin Shorb, Xavier Prat-Resina, Tim Wendorff, & Adam Hahn.

- **7.9: Polarizability** by Ed Vitz, John W. Moore, Justin Shorb, Xavier Prat-Resina, Tim Wendorff, & Adam Hahn is licensed CC BY-NC-SA 4.0.

1.3.9.1: Biology - Polarizability of Biologically Significant Atoms

Our next goal is to understand ***"noncovalent interactions"***. Noncovalent interactions hold together the two strands DNA in the double helix, convert linear proteins to 3D structures that are necessary for enzyme activity, and are the basis for antibody-antigen association. More importantly, noncovalent interactions between water molecules are probably the feature of water that is most important for ***biogenesis*** (the beginnings of life in the aqueous environment). Obviously, the topics of the next few sections, are of crucial importance to Biology. But in order to understand *noncovalent interactions*, we first need to develop a better understanding of the nature of bonds ranging from ***purely covalent*** to ***ionic***.

In other sections, chemical bonds are divided into two classes: covalent bonds, in which electrons are shared between atomic nuclei, and ionic bonds, in which electrons are transferred from one atom to the other. However, a sharp distinction between these two classes cannot be made. Unless both nuclei are the same (as in H_2), an electron pair is never shared *equally* by both nuclei. There is thus some degree of electron transfer as well as electron sharing in most covalent bonds. On the other hand there is never a *complete* transfer of an electron from one nucleus to another in ionic compounds. The first nucleus always maintains some slight residual control over the transferred electron.

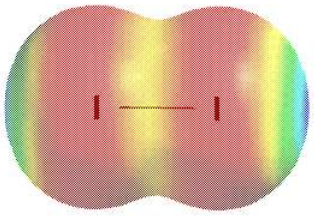
Pure Covalent Bonds

Pure Covalent Bonds are those in which electrons are shared equally between the two atoms involved. This can only happen for pairs of identical atoms. Iodine is a purple/black solid made up of \(\ce{I_2}\) molecules, which should have a pure covalent bond by sharing 5p electrons. It's toxic and, in solution, used as a bacteriocide. The net charge on each atom is 0, meaning that the charge is the same as if it were an isolated **I** atom.



The element iodine$_2$

Another way of showing charge distribution is with an ***electrostatic potential map***, where blue indicates positive charge and red indicates negative charge in regions of space around the two nuclei. Notice that the charge distribution is identical on the two iodines, although it is not uniformly distributed on either one (there's a positive region on the ends of the molecule, which probably results from electrons along the axis being drawn into the bond between the nuclei:



Electrostatic surface map for $\mathbf{I_2}$

Diagram of two spheres merging. There is a gradient of colors spread throughout the sphere. The color is blue on the end of each sphere. This transitions to green then to a minor strip of yellow then to a major portion which is red. The area around where the two sphere merges is yellow.

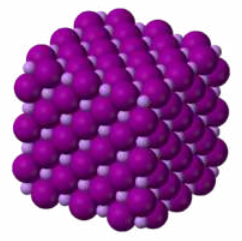
It is curious that the iodine molecule, with no net charges on either atom, should attract other iodine molecules to make a solid. This exemplifies one kind of attraction important in biomolecules, the *van der Waals attraction*, and we'll discuss that a lot more later. It's not the most important kind of attraction, however. To see how stronger attractions between molecules arise, we need to see what happens when we change the $\mathbf{I_2}$ molecule slightly.

Polarizability of iodine atoms

Suppose we now change one **I** atom to atoms in Group I: a **Li** atom, **Na** atom, and **Cs** atom in succession. The products, lithium iodide (**LiI**), sodium iodide (**NaI**), and cesium iodide (**CsI**) look like typical ionic compounds; they are all white crystalline solids. **NaI** is used as a source of "iodine" (actually iodide) for "iodized salt", and looks just like **NaCl**. But the relatively low melting point of **LiI** (459°C) is suggestive of covalent bonding. It is important to realize that all of these compounds exist as crystal lattices, not individual molecules, under ordinary conditions. The individual molecules that we're discussing are gas phase species, modeled in a vacuum. **LiI** and its crystal lattice are shown here:



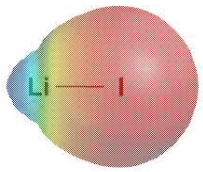
Lithium iodide crystals



LiI crystal lattice

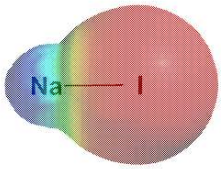
Three dimensional lithium iodide lattice is made up of a regular pattern of alternating dark purple spheres and light purple spheres. The light purple sphere is significantly smaller than the darker purple sphere.

The electrostatic potential surface confirms that there is sharing of electrons in **LiF**, because there is only a slight minimum in electron density between the atoms, and **Li** has clearly distorted the spherical distribution of electrons on **I**, showing that electrons are shared. In a purely ionic compound, there would be virtually no electron density between the two *spherical* electron clouds of the ions.



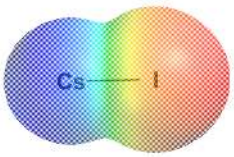
Electrostatic surface map for LiI

A small sphere in blue, labeled "L" "i" merges with a larger sphere, labeled "I", which is red. The region in between has a greenish yellow hue.



Electrostatic surface map for NaI

A small sphere in blue, labeled "N" "a" merges with a larger sphere, labeled "I", which is red. The region in between has a greenish yellow hue.



Electrostatic surface map for CsI

A sphere in blue, labeled "C" "s" merges with a slightly larger sphere, labeled "I", which is red. The region in between has a greenish yellow hue.

We say that the small $\mathbf{Li^+}$ ion distorts, or ***polarizes*** the large electron cloud of $\mathbf{I^-}$. Large anions (negative ions) are easily polarized, while smaller ones, like F^- are much less polarizable because the electrons are held more tightly. We see that small cations (positive ions) like $\mathbf{Li^+}$ are strong polarizers, while larger cations, like $\mathbf{Na^+}$ or $\mathbf{Cs^+}$ are less effective polarizers.

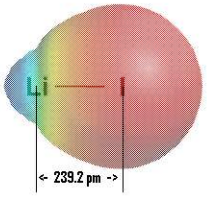
Because $\mathbf{Cs^+}$ is least effective in polarizing $\mathbf{I^-}$, **CsI** is the most ionic of the three. The electron cloud around the $\mathbf{I^-}$ is almost spherical (undistorted), and there is a definite decrease in electron density in the region between **Cs** and **I**. But there is still some sharing of electrons in **CsI**, because we do not see a region of zero electron density between two spherical ions. This is, in part, due to the fact that **Cs** is large (near the bottom of Group I), so it is also slightly polarized by the iodine core.

Dipole Moments

The extent of polarization in **LiI** can be confirmed experimentally. An ion pair like **LiI** has a negative end ($\mathbf{I^-}$) and a positive end ($\mathbf{Li^+}$). That is, it has two electrical “poles,” like the north and south magnetic poles of a magnet. The ion pair is therefore an electrical **dipole** (literally “two poles“), and a quantity known as its dipole moment may be determined from experimental measurements. The **dipole moment** μ is proportional to the size of the separated electrical charges Q and to the distance r between them:

$$\mu = Qr \tag{1.3.9.1.1}$$

In the **LiI** ion pair the two nuclei are known to be separated by a distance of 239.2 pm.



Li-I bond distance

If the bond were completely ionic, there would be a net charge of –1.6021 × 10^{-19} C (the electronic charge) centered on the **I** nucleus and a charge of +1.6021 × 10^{-19} C centered on the Li nucleus:

The dipole moment would then be given (via Equation 1.3.9.1.1):

$$\begin{aligned}\mu &= Qr \\ &= 1.6021 \times 10^{-19} C \times 239.2 \times 10^{-12}\, m \\ &= 3.832 \times 10^{-29}\, C\, m\end{aligned}$$

The measured value of the dipole moment for the **LiH** ion pair is 2.43× 10^{-29} C m, which is only about 64% of this value. This can only be because the negative charge is *not* centered on the **I** nucleus but shifted somewhat toward the Li^+ nucleus. This shift brings the opposite charges closer together, and the experimental dipole moment is smaller than would be expected.

As the bond becomes less polarized, there is less electron sharing and the bond becomes more ionic. In the case of **CsI**, the charge is 0.822 e, so the dipole moment is 82% of the theoretical value for a totally ionic species. The bond distance is 270.0 pm, so the dipole moment is

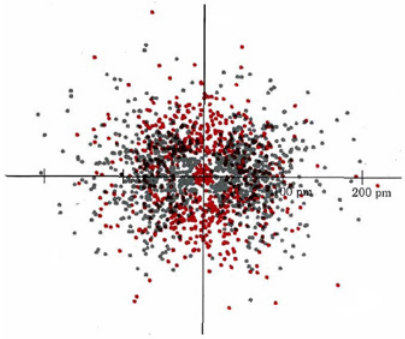
$$\begin{aligned}\mu &= Qr \\ &= 0.822\, e \times 1.6021 \times 10^{-19} C/e \times 270.0 \times 10^{-12} m \\ &= 3.56 \times 10^{-29}\, C\, m\end{aligned}$$

The polarization of the bond in **LiI** gives it very different properties than the nonpolar I_2. It's interesting that the blood/brain barrier allows nonpolar molecules, like O_2 to pass freely, while more polar molecules may be prohibited. Ionic species, like the Li^+ and I^- that result from dissolving **LiI** in water, require special carrier-mediated transport mechanism which moderates the ion levels in the brain, even when plasma levels fluctuate significantly.

This page titled 1.3.9.1: Biology - Polarizability of Biologically Significant Atoms is shared under a CC BY-NC-SA 4.0 license and was authored, remixed, and/or curated by Ed Vitz, John W. Moore, Justin Shorb, Xavier Prat-Resina, Tim Wendorff, & Adam Hahn.

- **7.9.1: Biology - Polarizability of Biologically Significant Atoms** by Ed Vitz, John W. Moore, Justin Shorb, Xavier Prat-Resina, Tim Wendorff, & Adam Hahn is licensed CC BY-NC-SA 4.0.

1.3.10: Polar Covalent Bonds



While other sections concentrate on the octet rule and Lewis diagrams for simple covalent molecules, there are numerous examples of molecules which are quite stable but contain one or more atoms which do not have a noble-gas electron configuration. Furthermore, structural formulas like those from sections under "Chemical Bonding - Electron Pairs and Octets" only show which atoms are connected to which. They do not tell us how the atoms are arranged in three-dimensional space. In other words a Lewis diagram does not show the shape of a molecule. It may actually be misleading because most molecules don't have the 90° or 180° bond angles that are conventionally used in the Lewis Diagram.

In the following sections, we will develop a more detailed picture of molecules—including some which do not obey the octet rule. You will learn how both the shapes and bonding of molecules may be described in terms of orbitals. In addition it will become apparent that the distinction between covalent and ionic bonding is not so sharp as it may have seemed. You will find that many covalent molecules are electrically unbalanced, causing their properties to tend toward those of ion pairs. Rules will be developed so that you can predict which combinations of atoms will exhibit this kind of behavior.

Lewis diagrams are used as the first step in predicting the structures for covalently bonded molecules. We will see what supplemental information is required to describe covalent molecules. We will describe some molecules which do not obey the octet rule and some which contain multiple bonds, as well as simple molecules. The structure of a molecule is determined by the positions of atomic nuclei in three-dimensional space, but it is repulsions among electron pairs—bonding pairs and lone pairs—which determine molecular geometry.

When dealing with molecular shapes, it is often convenient to think in terms of sp, sp^2, sp^3, or other hybrid orbitals. These correspond to the same overall electron density and to the same physical reality as do the *s* and *p* atomic orbitals considered earlier, but hybrid orbitals emphasize the directions in which electron density is concentrated. Hybrid orbitals may also be used to describe multiple bonding, in which case bonds must be bent so that two or three of them can link the same pair of atoms. A second equivalent approach to multiple bonding involves sigma and pi bonds. Electron density in a sigma bond is concentrated directly between the bonded nuclei, while that of the pi bond is divided in two—half on one side and half on the other side of the sigma bond.

No chemical bond can be 100 percent ionic, and, except for those between identical atoms, 100 percent covalent bonds do not exist either. Electron clouds—especially large, diffuse ones—are easily polarized, affecting the electrical balance of atoms, ions, or molecules. Large negative ions are readily polarized by small positive ions, increasing the covalent character of the bond between them. Electron density in covalent bonds shifts toward the more electronegative atom, producing partial charges on each atom and hence a dipole. In a polyatomic molecule, bond dipoles must be added as vectors to obtain a resultant which indicates molecular polarity. In the case of symmetric molecules, the effects of individual bond dipoles cancel and a nonpolar molecule results.

Macroscopic physical properties such as melting and boiling points depend on the strengths of the forces which hold microscopic particles together. In the case of molecules whose atoms are connected by covalent bonds, such intermolecular forces may be of three types. All molecules are attracted together by weak London forces. These depend on instantaneous polarization and increase in strength with the size of the molecular electron cloud. When a molecule contains atoms whose electronegativities differ significantly and the resulting bond dipoles do not cancel each other’s effects, dipole forces occur. This results in higher melting and boiling points than for nonpolar substances.

The third type of intermolecular force, the hydrogen bond, occurs when one molecule contains a hydrogen atom connected to a highly electronegative partner. The other molecule must contain an electronegative atom, like fluorine, oxygen, or nitrogen, which has a lone pair. Although each hydrogen bond is weak compared with a covalent bond, large numbers of hydrogen bonds can have very significant effects. One example of this is in the properties of water. This highly unusual liquid plays a major role in making living systems and the earth's environment behave as they do.

Oxidation numbers are used by chemists to keep track of electrons during the course of a chemical reaction. They may be obtained by arbitrarily assigning valence electrons to the more electronegative of two bonded atoms and calculating the resulting charge as if the bond were 100 percent ionic. Alternatively, some simple rules are available to predict the oxidation number of each atom in a formula. Oxidation numbers are used in the names of compounds and are often helpful in predicting formulas and writing Lewis diagrams.

In addition to deficiency of electrons and expansion of the valence shell, the octet rule is violated by species which have one or more unpaired electrons. Such free radicals are usually quite reactive. A difficulty of another sort occurs in benzene and other molecules for which more than one Lewis diagram can be drawn. Rearranging electrons (but not atomic nuclei) results in several structures which are referred to collectively as a resonance hybrid. Like an *sp* hybrid, a resonance hybrid is a combination of the contributing structures and has properties intermediate between them.

This page titled 1.3.10: Polar Covalent Bonds is shared under a CC BY-NC-SA 4.0 license and was authored, remixed, and/or curated by Ed Vitz, John W. Moore, Justin Shorb, Xavier Prat-Resina, Tim Wendorff, & Adam Hahn.

- **7.10: Polar Covalent Bonds** by Ed Vitz, John W. Moore, Justin Shorb, Xavier Prat-Resina, Tim Wendorff, & Adam Hahn is licensed CC BY-NC-SA 4.0.

1.3.10.1: Biology- Nonpolar Iodine and Polar Hydrogen Iodide

Pure Covalent Bonds are those in which electrons are shared equally between the two atoms involved, as we saw earlier, where the iodine molecule was given as an example:

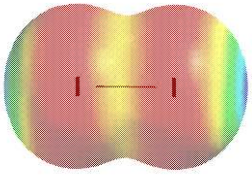


Diagram of two spheres merging. There is a gradient of colors spread throughout the sphere. The color is blue on the end of each sphere. This transitions to green then to a minor strip of yellow then to a major portion which is red. The area around where the two sphere merges is yellow.

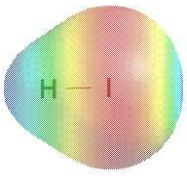
Electrostatic surface map for I_2

It was also shown that replacing an I atom with a group I metal decreased the covalent nature of the bond, while increasing its percent ionic character. The molecule is changed from a poisonous and bactericidal substance to salt-like white crystalline solids which may be more or less toxic depending on the particular metal chosen. IWC replica Réplica de reloj

Polar Covalent Compounds

But replacing one I atom in the purple solid I_2 with another nonmetal also makes a significant difference. Replacing one of the iodine atoms with a hydrogen atom to make HI (hydrogen iodide) changes the chemistry significantly. HI is a colorless gas, and reacts with NaOH to give sodium iodide (used in iodized salt). Aqueous solution of HI are called hydroiodic acid, because HI dissolves extensively and readily in water to make acidic solutions by increasing the hydrogen ion (H^+) concentration, while I_2 is barely soluble in water. The polarity of the bond clearly has biological significance.

The Jmol model and electrostatic potential surfaces differ from those of I_2 in several ways. Charge is no longer equally distributed between the atoms; the I atom has an excess of about 0.05 electrons, on the average, over the number of electrons in the neutral atom, so it has a charge of -0.05e. Even with electron shielding, the highly positive iodine nucleus pulls electrons toward itself more than the single proton of the hydrogen nucleus attracts electrons. The H atom has lost 0.05 of an electron, so it has an electrostatic charge of +0.05 e. The molecule has two electrical "poles", and is called a ***dipole***. The bond, in which electrons are not equally shared, is called a ***polar covalent bond***.



A small sphere in blue, labeled "L" "i" merges with a much larger sphere, labeled "I", which is mostly red in color. The region in between has a greenish yellow hue.

Electrostatic surface map for HI

In the H—I bond the I has an excess of 0.05 electrons and hence has a negative charge. This situation is often indicated as follows:

δ+ δ-

H----I δ=0.05

or $H^{\delta+}\ I^{\delta-}$

The Greek letter δ (delta) is used here to indicate that electron transfer is not complete and that some sharing takes place. If the transfer had been complete, δ would have been 1.0. Because the Li—H bond is only *partially* negative at the one end and *partially* positive at the other, we often say that the bond is **polar** or **polar covalent**, rather than 100 percent ionic.

Elements in the upper right of the periodic table, which are small because the large nucleus contracts the valence shell, form much more polar bonds with H. For example, HF has a δ value of 0.43, compared with δ = 0.05 for HI.

δ+ δ-

H----F δ=0.43

Lets see how to calculate the δ value for HI. The data for this example could be obtained from the Jmol model above, but there are a number of different methods for calculating charges, and the one used here may not be appropriate for this calculation. Nonetheless, the bond distance in HI can be measured by right clicking one the Jmol model, choosing "measurements", then clicking on the atoms in sequence. We'll use empirically (from experiment) measured values here:

EXAMPLE 1 The dipole moment of the HI molecule is found to be 1.34×10^{-30} C m, while the H—I distance is 165.0 pm. Find the partial charge on the H and F atoms.

Solution Rearranging Eq. (1) from Polarizability, we have

$$Q = \frac{\mu}{r}$$

Thus the apparent charge on each end of the molecule is given by

$$Q = \frac{1.34 \times 10^{-30}\ \text{C m}}{165.0 \times 10^{-12}\ \text{m}} = 8.10 \times 10^{-21}\ \text{C}$$

Since the charge on a single electron is 1.6021×10^{-19} C, we have

$$\delta = \frac{8.10 \times 10^{-21}}{1.6021 \times 10^{-19}} = 0.051$$

So δ = 0.051.

It is worth noting in the above example that the dipole moment measures the electrical imbalance of the *whole molecule* and not just that of the H—I bonding pair. In the HI molecule there are four valence electron pairs, with the three lone pairs on the right of the I atom also contributing to the overall negative charge of I.

This page titled 1.3.10.1: Biology- Nonpolar Iodine and Polar Hydrogen Iodide is shared under a CC BY-NC-SA 4.0 license and was authored, remixed, and/or curated by Ed Vitz, John W. Moore, Justin Shorb, Xavier Prat-Resina, Tim Wendorff, & Adam Hahn.

- **7.10.1: Biology- Nonpolar Iodine and Polar Hydrogen Iodide** by Ed Vitz, John W. Moore, Justin Shorb, Xavier Prat-Resina, Tim Wendorff, & Adam Hahn is licensed CC BY-NC-SA 4.0.

1.3.10.2: Lecture Demonstrations

Sublimation of Non-Polar Iodine

Add iodine crystals to a pre-heated 2 L Erlenmeyer flask on a hotplate and observe the sublimation and subsequent formation of beautiful crystals.

Easy sublimation is due to ***lack*** of permanent charge.

Solubility of Polar vs. NonPolar Gases in Water

An HCl fountain can be used[1][2][3][4] to demonstrate the high solubility of HCl in polar water. Compare to oxygen, nitrogen.

References

1. Alyea, H.N.; Duton, F.B. "Tested Demonstrations in Chemistry", J. Chem. Educ., Easton, PA 1965, p. 13-14
2. Ned Steadman. J. Chem. Educ., 1992, 69 (9), p 764
3. Nicholas C. Thomas and Stephen Faulk , Randy Sullivan J. Chem. Educ., 2008, 85 (8), p 1063
4. J. Chem. Educ., 1995, 72 (9), p 828

Contributors

- Ed Vitz (Kutztown University), John W. Moore (UW-Madison), Justin Shorb (Hope College), Xavier Prat-Resina (University of Minnesota Rochester), Tim Wendorff, and Adam Hahn.

This page titled 1.3.10.2: Lecture Demonstrations is shared under a CC BY-NC-SA 4.0 license and was authored, remixed, and/or curated by Ed Vitz, John W. Moore, Justin Shorb, Xavier Prat-Resina, Tim Wendorff, & Adam Hahn.

- **7.10.2: Lecture Demonstrations** by Ed Vitz, John W. Moore, Justin Shorb, Xavier Prat-Resina, Tim Wendorff, & Adam Hahn is licensed CC BY-NC-SA 4.0.

1.3.11: Electronegativity

The ability of an atom in a molecule to attract a shared electron pair to itself, forming a polar covalent bond, is called its **electronegativity**. The negative side of a polar covalent bond corresponds to the *more electronegative* element. Furthermore the more polar a bond, the larger the *difference* in electronegativity of the two atoms forming it.

Unfortunately there is no direct way of measuring electronegativity. Dipole-moment measurements tell us about the electrical behavior of *all* electron pairs in the molecule, not just the bonding pair in which we are interested. Also, the polarity of a bond depends on whether the bond is a single, double, or triple bond and on what the other atoms and electron pairs in a molecule are. Therefore the dipole moment cannot tell us quantitatively the difference between the electronegativities of two bonded atoms. Various attempts have been made over the years to derive a scale of electronegativities for the elements, none of which is entirely satisfactory. Nevertheless most of these attempts agree in large measure in telling us which elements are more electronegative than others. The best-known of these scales was devised by the Nobel prize-winning California chemist Linus Pauling (1901 to 1994) and is shown in the periodic table found below. In this scale a value of 4.0 is arbitrarily given to the most electronegative element, fluorine, and the other electronegativities are scaled relative to this value.

Periodic Table

→ Atomic radius decreases → Ionization energy increases → Electronegativity increases →																		
Group (vertical)	**1**	**2**	**3**	**4**	**5**	**6**	**7**	**8**	**9**	**10**	**11**	**12**	**13**	**14**	**15**	**16**	**17**	**18**
Period (horizontal)																		
1	H 2.20																	He
2	Li 0.98	Be 1.57											B 2.04	C 2.55	N 3.04	O 3.44	F 3.98	Ne
3	Na 0.93	Mg 1.31											Al 1.61	Si 1.90	P 2.19	S 2.58	Cl 3.16	Ar
4	K 0.82	Ca 1.00	Sc 1.36	Ti 1.54	V 1.63	Cr 1.66	Mn 1.55	Fe 1.83	Co 1.88	Ni 1.91	Cu 1.90	Zn 1.65	Ga 1.81	Ge 2.01	As 2.18	Se 2.55	Br 2.96	Kr 3.00
5	Rb 0.82	Sr 0.95	Y 1.22	Zr 1.33	Nb 1.6	Mo 2.16	Tc 1.9	Ru 2.2	Rh 2.28	Pd 2.20	Ag 1.93	Cd 1.69	In 1.78	Sn 1.96	Sb 2.05	Te 2.1	I 2.66	Xe 2.60
6	Cs 0.79	Ba 0.89	*	Hf 1.3	Ta 1.5	W 2.36	Re 1.9	Os 2.2	Ir 2.20	Pt 2.28	Au 2.54	Hg 2.00	Tl 1.62	Pb 2.33	Bi 2.02	Po 2.0	At 2.2	Rn 2.2
7	Fr 0.7	Ra 0.9	**	Rf	Db	Sg	Bh	Hs	Mt	Ds	Rg	Cn	Uut	Uuq	Uup	Uuh	Uus	Uuo
Lanthanoids	*	La 1.1	Ce 1.12	Pr 1.13	Nd 1.14	Pm 1.13	Sm 1.17	Eu 1.2	Gd 1.2	Tb 1.1	Dy 1.22	Ho 1.23	Er 1.24	Tm 1.25	Yb 1.1	Lu 1.27		
Actinoids	**	Ac 1.1	Th 1.3	Pa 1.5	U 1.38	Np 1.36	Pu 1.28	Am 1.13	Cm 1.28	Bk 1.3	Cf 1.3	Es 1.3	Fm 1.3	Md 1.3	No 1.3	Lr 1.3		

As can be seen from this table, elements with electronegativities of 2.5 or more are all nonmetals in the top right-hand comer of the periodic table. These have been color-coded dark red. By contrast, elements with negativities of 1.3 or less are all metals on the lower left of the table. These elements have been coded in dark gray. They are often referred to as the most **electropositive** elements, and they are the metals which invariably form binary ionic compounds. Between these two extremes we notice that most of the remaining metals (largely transition metals) have electronegativities between 1.4 and 1.9 (light gray), while most of the remaining nonmetals have electronegativities between 2.0 and 2.4 (light red). Another feature worth noting is the very large differences in electronegativities in the top right-hand comer of the table. Fluorine, with an electronegativity of 4, is by far the most electronegative element. At 3.5 oxygen is a distant second, while chlorine and nitrogen are tied for third place at 3.0.

If the electronegativity values of two atoms are very different, the bond between those atoms is largely ionic. In most of the typical ionic compounds discussed in the previous chapter, the difference is greater than 1.5, although it is dangerous to attach too much significance to this figure since electronegativity is only a semiquantitative concept. As the electronegativity difference becomes

smaller, the bond becomes more covalent. An important example of an almost completely covalent bond between two different atoms is that between carbon (2.5) and hydrogen (2.1).

The properties of numerous compounds of hydrogen and carbon (hydrocarbons) are described in sections on organic chemistry. These properties indicate that the C—H bond has almost no polar character.

Example 1.3.11.1 : Bond Polarity

Without consulting the table of electronegativities (use the periodic table), arrange the following bonds in order of decreasing polarity: B—Cl, Ba—Cl, Be—Cl, Br—Cl, Cl—Cl.

Solution

We first need to arrange the elements in order of increasing electronegativity. Since the electronegativity increases in going up a column of the periodic table, we have the following relationships:

Ba < Be and Br < Cl

Also since the electronegativity increases across the periodic table, we have

Be < B

Since B is a group III element on the borderline between metals and non-metals, we easily guess that

B < Br

which gives us the complete order

Ba < Be < B < Br < Cl

Among the bonds listed, therefore, the Ba—Cl bond corresponds to the largest difference in electronegativity, i.e., to the most nearly ionic bond. The order of bond polarity is thus

Ba—Cl > Br—Cl > B—Cl > Br—Cl > Cl—Cl

where the final bond, Cl—Cl,is, of course, purely covalent.

This page titled 1.3.11: Electronegativity is shared under a CC BY-NC-SA 4.0 license and was authored, remixed, and/or curated by Ed Vitz, John W. Moore, Justin Shorb, Xavier Prat-Resina, Tim Wendorff, & Adam Hahn.

- **7.11: Electronegativity** by Ed Vitz, John W. Moore, Justin Shorb, Xavier Prat-Resina, Tim Wendorff, & Adam Hahn is licensed CC BY-NC-SA 4.0.

1.3.12: Polarity in Polyatomic Molecules

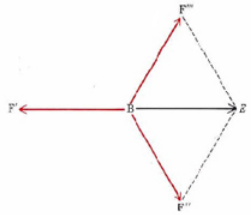


Figure **1.3.12.1** Although all three BF bonds in BF_3 are very polar, they are arranged at 120° to each other. The net result is that the three dipole moments (indicated by colored arrows) cancel each other and there is zero dipole moment.

When more than one polar bond is present in the same molecule, the polarity of one bond may cancel that of another. Thus the presence of polar bonds in a polyatomic molecule does not *guarantee* that the molecule as a whole will have a dipole moment. In such a case it is necessary to treat each polar bond mathematically as a *vector* and represent it with an arrow. The *length* of such an arrow shows how large the bond dipole moment is, while the *direction* of the arrow is a line drawn from the positive to the negative end of the bond. Adding the individual bond dipole moments as vectors will give the overall molecular dipole moment.

As an example of this vector addition, consider the BF_3 molecule in Figure **1.3.12.1**. The dipole moments of the three B—F bonds are represented by the arrows BF′ (pointing straight left), BF″ (pointing down to the right), and BF‴ (pointing up to the right). The sum of vectors BF″ and BF‴ may be obtained by the parallelogram law—a line from F‴ drawn parallel to BF″ intersects a line from F″ drawn parallel to BF‴ at point *E*. Thus the resultant vector BE (the diagonal of the parallelogram BF‴*E*F″) is the sum of BF″ and BF‴. The resultant BE is exactly equal in length and exactly opposite in direction to bond dipole BF″. Therefore the net result is zero dipole moment.

Those arrangements of equivalent bonds that give zero dipole moment in this way are shown in Figure **1.3.12.2**. In addition to the trigonal arrangement just discussed, there is the obvious case of two equal bonds 180° apart. The other is much less obvious, namely, a tetrahedral arrangement of equal bonds. Any combination of these arrangements will also be nonpolar. The molecule PF_5 for example, is nonpolar since the bonds are arranged in a trigonal bipyramid, as discussed in "The Shapes of Molecules." Since three of the five bonds constitute a trigonal arrangement, they will have no resultant dipole moment. The remaining two bonds have equal but opposite dipoles which will likewise cancel.

If we replace any of the bonds shown in Figure **1.3.12.2** with a different bond, or with a lone pair, the vectors will no longer cancel and the molecule will have a resultant dipole moment.

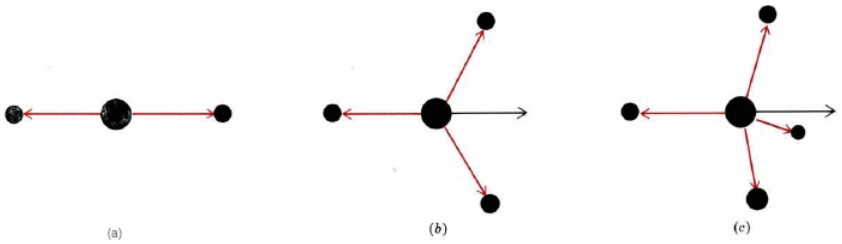


Figure 1.3.12.2 The simplest arrangements of equivalent bonds around a central atom which produce a resultant dipole moment of zero: (a) linear; (b) trigonal. The two right-hand bonds (black resultant) cancel the left-hand bond. (c) Tetrahedral. The three right-hand bonds (black resultant) cancel the left-hand bond.

The following jmols further illustrate the dipole moment concept. Click the Magnetic Dipole check box to see the dipole in place on the jmol. The first jmol of methane shows a molecule with no dipole. Each bond's dipole moment cancels, leading to a molecule without any net dipole.

This second jmol demonstrates the dipole when one hydrogen atom in methane is replaced by a highly electronegative fluorine. Fluorine pulls the electron strongly away from the carbon atom, creating a dipole moment pointing from carbon to fluorine.

The third jmol depicts the dipole moment when two hydrogen atoms in methane have been replaced by fluorine atoms. Each fluorine pulls the electrons in the carbon-fluorine bonds away from the carbon, creating a net dipole pointing between the two fluorine atoms.

Using this rule together with VSEPR theory, you can predict whether a molecule is polar or not. You can also make a rough estimate of how polar it will be.

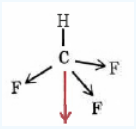
Example 1.3.12.1 : Polar Molecules

Which of the following molecules are polar? About how large a dipole moment would you expect for each? (a) CF_4; (b) CHF_3; (c) H_2O; (d)NF_3.

Solution:

a) VSEPR theory predicts a tetrahedral geometry for CF_4. Since all four bonds are the same, this molecule corresponds to Figure 2*c*. It has zero dipole moment.

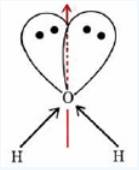
b) For CHF_3, VSEPR theory again predicts a tetrahedral geometry. However, all the bonds are not the same, and so there must be a resultant dipole moment. The C—H bond is essentially nonpolar, but the three C—F bonds are very polar and negative on the F side. Thus the molecule should have quite a large dipole moment:



A central "C" has a H bond above it. The three "F" is below the "C" forming a tetrahedral. Each "C" "F" bond is represented by an arrow pointing downward to form a tetrahedral shape. The resultant dipole moment is shown in color and is opposite to the "C" H" bond and is longer than the "C" "H" bond.

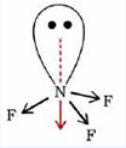
The resultant dipole is shown in color.

c) The O atom in H_2O is surrounded by four electron pairs, two bonded to H atoms and two lone pairs. All four pairs are not equivalent, and so there is a resultant dipole. Since O is much more electronegative than H, the two O—H bonds will produce a partial negative charge on the O. The two lone pairs will only add to this effect.



The two "O" "H" bonds are represented by an arrow pointing from "H" towards "O". The two "H" are below "O" and are at an angle from one another. The two lone pairs are above "O" and represented by two pairs of dots. The resultant dipole is shown by a colored arrow pointing straight upwards from "O", right in the middle of the two lone pairs as well as the two "O" "H" bonds.

d) In NF_3 the N atom is surrounded by four electron pairs in an approximately tetrahedral arrangement. Since all four pairs are not equivalent, the molecule is polar. The dipole moment, though, is surprisingly small because the lone pair cancels much of the polarity of the N—F bonds:



Above "N" is a pair of black dots. The three "F" below N form an overall tetrahedral shape. Each "N" "F" bond is represented by an arrow pointing from "N" to "F". The resultant arrow points straight downwards.

This page titled 1.3.12: Polarity in Polyatomic Molecules is shared under a CC BY-NC-SA 4.0 license and was authored, remixed, and/or curated by Ed Vitz, John W. Moore, Justin Shorb, Xavier Prat-Resina, Tim Wendorff, & Adam Hahn.

- **7.12: Polarity in Polyatomic Molecules** by Ed Vitz, John W. Moore, Justin Shorb, Xavier Prat-Resina, Tim Wendorff, & Adam Hahn is licensed CC BY-NC-SA 4.0.

1.3.12.1: Biology- The Hydrophobic Effect and Properties of Small Polyatomic Molecules

The biological properties of molecules depends strongly on their polarity, because ***bond* polarity** and ***molecular* polarity** play a large part in "noncovalent attractions" between molecules. Noncovalent attractions which are responsible for the DNA double helix, and antibody-antigen bonding can be understood in terms of *Polar Covalent Bonds* alone, but sometimes the polarity of the whole molecule must be considered.

For example, the suitability of water for biogenesis depends on the polarity of the whole molecule, and often involves the critically important "hydrophobic effect". The polarity of the molecule leads to extensive "hydrogen bonding" between molecules:

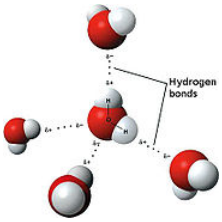


Figure 1:Hydrogen bonds between polar water molecules[1]

The hydrophobic effect accounts for the insolubility of nonpolar molecules, like CH_4. Note that nonpolar molecules may contain polar bonds!



Figure 2:Hydrophobic effect.



Figure 3: Magic Sand models hydrophobic effect [2]

The goal of this section is to differentiate between *bond polarity* and *molecular polarity*. To do that, we start with important biological, chemical, and physical properties of a few small molecules:

Physical Properties and Molecular Structure

First, look at the melting points and boiling points of substances in the table below. Surprisingly, they are not related in any way to the molecular weights. This makes sense if you remember that molecular weight is a nuclear property. Melting and boiling involve breaking bonds between molecules, so like all bonding, they involve electronic structure. They depend on the size of atoms and molecules, but by size we mean *volume*, not *mass*.

Second, notice that the small water molecule is exceptional. It has the largest dipole moment, and a boiling point that is over 100°C higher than molecules of similar size.

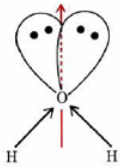
Molecules of very low boiling points have zero polarity, indicated by the molecular dipole moment in debyes[3]

The molecular dipole moments determine all the biological properties mentioned above, so we must explain why water is so polar, and methane, CH_4, is a *nonpolar molecule*, even though it contains *polar bonds*.

Molecule	MW	MP°C	BP °C	dipole moment, D[4]	Significance
H_2	2	-259.14	-252.87	0	Used to reduce "bends"[5]
CH_4	16	-182.5	-161.6	0	methane, "hydrophobic effect"
NH_3	17	-77.73	-33.4	1.46	ammonia, very soluble
H_2O	18	0	100	1.84	liquid,
CO	28	-205	-191.5	0.12	toxic carbon monoxide
O_2	32	-218.79	-182.95	0	20% of air
CO_2	44	-78[6]	[7]	0	
SO_3	80	16.9	45	0	acid rain

H_2O

First, let's look at the water molecule. The O atom in H_2O is surrounded by four electron pairs, two bonded to H atoms and two lone pairs. Oxygen has a higher electronegativity (3.34) than hydrogen (2.2), so we have two dipole bond vectors pointing from H to O. There are also two lone pairs on O, enhancing its negative charge, so there is a resultant dipole.



The two "O" "H" bonds are represented by an arrow pointing from "H" towards "O". The two "H" are below "O" and are at an angle from one another. The two lone pairs are above "O" and represented by two pairs of dots. The resultant dipole is shown by a colored arrow pointing straight upwards from "O", right in the middle of the two lone pairs as well as the two "O" "H" bonds.

This option will not work correctly. Unfortunately, your browser does not support inline frames.

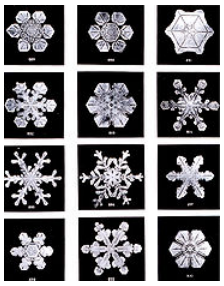


Figure 4 snowflake crystals.

The polarity of water leads to hydrogen bond networks in ice or snowflakes, which leads to destruction of plant tissue when water freezes. Snowflake crystals have shapes dictated by the angles between hydrogen bonded water molecules in Figure 1. Plants have several mechanisms to avoid ice damage. More important ramifications of water's polarity are mentioned later.

Vector Addition of Bond Dipoles

If water were linear, the dipole moment vectors of the two bonds would cancel each other by vector addition, as shown in Figure 5(a) below:

When more than one polar bond is present in the same molecule, the polarity of one bond may cancel that of another. Thus the presence of polar bonds in a polyatomic molecule does not *guarantee* that the molecule as a whole will have a dipole moment. In such a case it is necessary to treat each polar bond mathematically as a *vector* and represent it with an arrow. The *length* of such an arrow shows how large the bond dipole moment is, while the *direction* of the arrow is a line drawn from the positive to the negative end of the bond. Adding the individual bond dipole moments as vectors will give the overall molecular dipole moment.

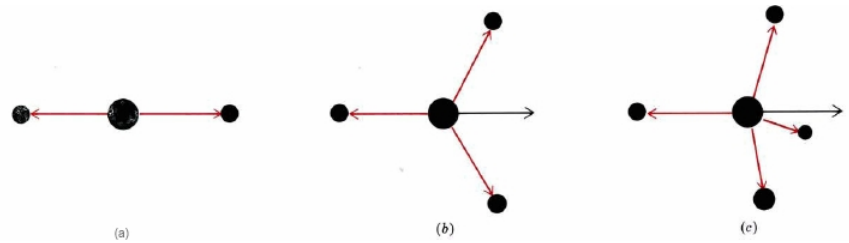


Figure 5: The simplest arrangements of equivalent bonds around a central atom which produce a resultant dipole moment of zero: (a) linear; (b) trigonal. The two right-hand bonds (black resultant) cancel the left-hand bond. (c) Tetrahedral. The three right-hand bonds (black resultant) cancel the left-hand bond.

Other arrangements of equivalent bonds that give zero dipole moment in this way are shown in Figure 5. The case of three equal bonds 120° apart, or a tetrahedral arrangement of equal bonds at 109° bond angles. Any combination of these arrangements will also be nonpolar. The molecule PF_5 for example, is nonpolar since the bonds are arranged in a trigonal bipyramid, as discussed in "The Shapes of Molecules." Since three of the five bonds constitute a trigonal arrangement, they will have no resultant dipole moment. The remaining two bonds have equal but opposite dipoles which will likewise cancel. If we replace any of the bonds shown in Figure 5 with a different bond, or with a lone pair, the vectors will no longer cancel and the molecule will have a resultant dipole moment.

CH_4

In methane, there are four C - H bonds, all slightly polar (the electronegativities of C and H are 2.55 and 2.20 respectively), but they are arranged so that the vectors cancel one another because methane is tetrahedral as shown in the Jmol model below. You may click the Magnetic Dipole check box to see the dipole in place on the model of methane.

Because methane is nonpolar, it does not dissolve in water. Other hydrocarbons and oils, like vegetable oil, can be made to dissolve by adding "amphiphilic" molecules (like soap), which have a polar ("hydrophilic", water loving) end that dissolves in water, and a nonpolar (hydrophobic, "water fearing") end that dissolves the oil. Amphiphilic molecules often make up cell walls, where the hydrophilic end of the molecule can face outward:





Figure 6 Lipid Bilayer.

SO_3

As another example of this vector addition, consider the SO_3 molecule. The dipole moments of the three S—O bonds are represented by the three arrows in Figure 6 below, at "1:00 o'clock", "5:00 o'clock", and "9:00 o'clock".

The sum of vectors at "2:00 o'clock" and "5:00 o'clock" may be obtained by the parallelogram law—lines parallel to the original vectors intersect at the tip of their resultant, a horizontal line ending at "3:00 o'clock". The resultant is exactly equal in length and exactly opposite in direction to the bond dipole at "9:00 o'clock". Therefore the net result is zero dipole moment.

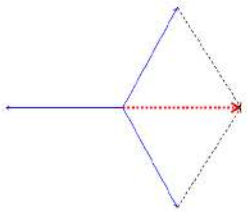


Figure 7: Parallelogram vector addition.

Note, however, that the melting point and boiling point of SO_3 are very high for a nonpolar substance. This is because it does not exist as a simple molecule in the solid state , but rather as a covalently bonded trimer (Figure 7), so covalent bonds need to be broken to melt or boil SO_3.

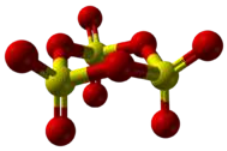
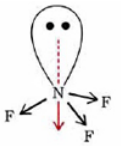


Figure 8: Solid form of sulfur trioxide [8]

NH_3

At first glance, you might expect NH_3 to have a zero molecular dipole moment, like SO_3. But in NH_3 or NF_3, the N atom is surrounded by four electron pairs in an approximately tetrahedral arrangement. Since all four pairs are not equivalent, the molecule is polar.

This option will not work correctly. Unfortunately, your browser does not support inline frames.



Above "N" is a pair of black dots. The three "F" below N form an overall tetrahedral shape. Each "N" "F" bond is represented by an arrow pointing from "N" to "F". The resultant arrow points straight downwards.

In NF_3, the dipole moment, though, is surprisingly small because the lone pair on N cancels much of the polarity of the N—F bonds, which place electron density on the more electronegative (4.0) F atoms.

Biomolecular Properties

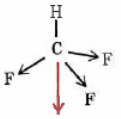
Note that polar NH_3 is soluble in water, because each has charges which can attract one another, but nonpolar CH_4 is insoluble in water. The insolubility of CH_4 is due to the fact that it has no charges for water to attract, but also because water bonds to itself so well. A full explanation requires the concept of entropy, because it's a rearrangement of the liquid water structure, shown in the first figure, which prevents nonpolar molecules from dissolving. This is called the "hydrophobic effect", and it has a lot to do with formation of cell walls and other biological structures like the lipid bilayers shown above, as well as forcing proteins into specific conformations. The "structure creating" results of the hydrophobic effect can be seen with the "Magic Sand" model shown in the second Figure, and in several YouTube videos.

EXAMPLE 1 Which of the following molecules are polar? About how large a dipole moment would you expect for each? (a) CF_4; (b) CHF_3; (c) CH_3F; (d) CH_2F_2.;

Solution

a) VSEPR theory predicts a tetrahedral geometry for CF_4. Since all four bonds are the same, this molecule corresponds to Figure 2*c*. It has zero dipole moment.

This option will not work correctly. Unfortunately, your browser does not support inline frames.



A central "C" has a H bond above it. The three "F" is below the "C" forming a tetrahedral. Each "C" "F" bond is represented by an arrow pointing downward to form a tetrahedral shape. The resultant dipole moment is shown in color and is opposite to the "C" H" bond and is longer than the "C" "H" bond.

b) For CHF_3, VSEPR theory again predicts a tetrahedral geometry. However, all the bonds are not the same, and so there must be a resultant dipole moment. The C—H bond is essentially nonpolar, but the three C—F bonds are very polar and negative on the F side. Thus the molecule should have quite a large dipole moment:

This option will not work correctly. Unfortunately, your browser does not support inline frames.

The resultant dipole is shown in color.

c) This second jmol demonstrates the dipole when one hydrogen atom in methane is replaced by a highly electronegative fluorine. Fluorine pulls the electron strongly away from the carbon atom, creating a dipole moment pointing from carbon to fluorine.

d)The third jmol depicts the dipole moment when two hydrogen atoms in methane have been replaced by fluorine atoms. Each fluorine pulls the electrons in the carbon-fluorine bonds away from the carbon, creating a net dipole pointing between the two fluorine atoms.

References

1. Water [en.Wikipedia.org]
2. YouTube [www.youtube.com]
3. 1 debye = 1 D = 3.34 x 10⁻³⁰ C m.
4. 1 D (debye) = 3.34 x 10⁻³⁰ C m
5. en.Wikipedia.org/wiki/Decompression_sickness
6. sublimes
7. liquid only exists under pressure

8. en.Wikipedia.org/wiki/Sulfur_trioxide

This page titled 1.3.12.1: Biology- The Hydrophobic Effect and Properties of Small Polyatomic Molecules is shared under a CC BY-NC-SA 4.0 license and was authored, remixed, and/or curated by Ed Vitz, John W. Moore, Justin Shorb, Xavier Prat-Resina, Tim Wendorff, & Adam Hahn.

- **7.12.1: Biology- The Hydrophobic Effect and Properties of Small Polyatomic Molecules** by Ed Vitz, John W. Moore, Justin Shorb, Xavier Prat-Resina, Tim Wendorff, & Adam Hahn is licensed CC BY-NC-SA 4.0.

1.3.12.2: Lecture Demonstrations

Magic Sand

Add Magic Sand to water and observe "rabbit guts" like formations that suggest the importance of water in biogenesis. Add magic sand to isopropanol or hexane to demonstrate that it is the water, not the sand, that is "magical".[1] [2] [3] [4]

Flipping Graphite Card

A 2 cm x 2 cm square of index card is coated thoroughly on one side with graphite from a #2 pencil. About 100 mL each of water and carbon tetrachloride are added to a 250 mL beaker. If the square held in tweezers and is released at the interface of the water and carbon tetrachloride, it will invariable flip so that the bare paper side is toward the polar water, and the nonpolar graphite side is toward the nonpolar liquid. This is not a gravity effect, as proven by using hexane (floats on water) and water in the same experiment.

References

1. J. Chem. Educ., 1982, 59 (2), p 155
2. J. Chem. Educ., 1990, 67 (6), p 512
3. J. Chem. Educ., 2000, 77 (1), p 40A
4. J. Chem. Educ., 2000, 77 (1), p 41

Contributors

- Ed Vitz (Kutztown University), John W. Moore (UW-Madison), Justin Shorb (Hope College), Xavier Prat-Resina (University of Minnesota Rochester), Tim Wendorff, and Adam Hahn.

This page titled 1.3.12.2: Lecture Demonstrations is shared under a CC BY-NC-SA 4.0 license and was authored, remixed, and/or curated by Ed Vitz, John W. Moore, Justin Shorb, Xavier Prat-Resina, Tim Wendorff, & Adam Hahn.

- **7.12.2: Lecture Demonstrations** by Ed Vitz, John W. Moore, Justin Shorb, Xavier Prat-Resina, Tim Wendorff, & Adam Hahn is licensed CC BY-NC-SA 4.0.

1.3.13: Formal Charge and Oxidation Numbers

Formal Charge

On the page discussing the covalent bond, it is shown that the density of electrons in a covalent bond is shared between both atoms. When drawing Lewis Structures it is sometimes useful to see which structure can be deemed the best. The **Formal Charge** is a somewhat artificial device that exists in the minds of chemists (not within the molecules, themselves) to help keep track of electrons in their bonding configurations. The ***Formal Charge*** **is the charge an atom in a molecule or polyatomic ion would have if all of the bonding electrons were divided equally between atoms in the bond.**

Formal Charge "Rules"

Here are some rules for determining the Formal Charge on each atom in a molecule or polyatomic ion:

1. Electrons within a Lone Pair on an atom are assigned exclusively to that atom.
2. Half of the electrons in each bond around an atom are assigned to that atom.
3. The Formal Charges on all atoms in a molecule must sum to zero; for a polyatomic ion the Formal Charges must sum to the charge on the ion (which may be positive or negative).

The Formal Charge is defined by the relationship:

Formal Charge = [*number of valence electrons in an isolated atom*] - [(*number of lone pair electrons*) + ½ (*number of bonding electrons*)]

With the definitions above, we can calculate the Formal Charge on the thiocyanate Ion, SCN^-:

Table **1.3.13.1**

	**S**	**C**	**N**
Valence electrons	6	4	5
Lone pair electrons	6	0	2
Shared electrons (bonds)	2 (1)	8 (4)	6 (3)
Formal Charge =	6 - (6 + ½·2)	4 - (0 + ½·8)	5 - (2 + ½·6)
Formal Charge	-1	0	0

Notice how the sum of all of the formal charges adds up to the charge of the thiocyanate ion (-1). When drawing Lewis Structures, we use this information to determine which structure would be the most likely. The following rules apply:

1. Smaller absolute Formal Charges are more favorable (recall that the absolute value of a number is > 0)
2. Negative Formal Charges should be on the most electronegative atoms
3. Like charges should not be on adjacent atoms

Oxidation Numbers

We have also discussed electronegativity, which gives rise to polarity in bonds and molecules. Thus, sometimes it is helpful for us to define another somewhat artificial device - invented by chemists, not by molecules - which enables us to keep track of electrons in complicated reactions where electrons rearrange into new bonds.

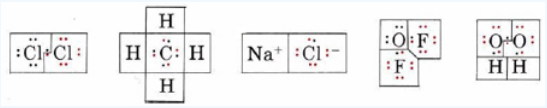
We can obtain oxidation numbers by arbitrarily assigning the electrons of each covalent bond to the more electronegative atom in the bond. This is in contrast to the Formal Charge which divides each bonding pair equally without concern for which atom may be more electronegative. When this division has been done for all bonds, the charge remaining on each atom is said to be its oxidation number. If two like atoms are joined, each atom is assigned half the bonding electrons.

Example 1.3.13.1: Oxidation Number

Determine the oxidation number of each atom in each of the following formulas: (a) Cl_2; (b) CH_4; (c) NaCl; (d) OF_2; (e) H_2O_2.

Solution:

In each case we begin by drawing a Lewis diagram:



In each Lewis diagram, electrons have been color coded to indicate the atom from which they came originally. The boxes enclose electrons assigned to a given atom by the rules for determining oxidation number.

a) Since the bond in Cl_2 is purely covalent and the electrons are shared equally, one electron from the bond is assigned to each Cl, giving the same number of valence electrons (7) as a neutral Cl atom. Thus neither atom has lost any electrons, and the oxidation number is 0. This is indicated by writing a 0 above the symbol for chlorine in the formula

$$\overset{0}{\mathrm{Cl}}_2$$

b) Since C is more electronegative than H, the pair of electrons in each C—H bond is assigned to C. Therefore each H has *lost* the one valence electron it originally had, giving an oxidation number of +1. The C atom has *gained* four electrons, giving it a negative charge and hence an oxidation number of – 4:

$$\overset{-4}{\mathrm{C}}\,\overset{+1}{\mathrm{H}}_4$$

c) In NaCl each Na atom has lost an electron to form an Na^+ ion, and each Cl atom has gained an electron to form $Cl^–$. The oxidation numbers therefore correspond to the ionic charges:

$$\overset{+1}{\mathrm{Na}}\,\overset{-1}{\mathrm{Cl}}$$

d) Since F is more electronegative than O, the bonding pairs are assigned to F in oxygen difluoride (OF_2). The O is left with four valence electrons, and each F has eight. The oxidation numbers are

$$\overset{+2}{\mathrm{O}}\,\overset{-1}{\mathrm{F}}_2$$

e) In Hydrogen peroxide (H_2O_2) the O—H bond pairs are assigned to the more electronegative O's, but the O—O bond is purely covalent, and the electron pair is divided equally. This gives each O seven electrons, a gain of 1 over the neutral atom. The oxidation numbers are

$$\overset{+1}{\mathrm{H}}_2\,\overset{-1}{\mathrm{O}}_2$$

Although one could always work out Lewis diagrams to obtain oxidation numbers as shown in Example **1.3.13.1**, it is often easier to use a few simple rules to obtain them. The rules summarize the properties of oxidation numbers illustrated in Example **1.3.13.2**.

Oxidation Number "Rules"

1. The oxidation *number of an atom in an uncombined element is 0*. Since atoms of the same element always form pure covalent bonds, they share electrons equally, neither losing nor gaining, e.g., Cl_2.
2. *The oxidation number of a monatomic ion equals the charge on that ion*, e.g., Na^+ and $Cl^–$.
3. *Some elements have the same oxidation number in nearly all their compounds.*
    a. Elements in periodic group IA have oxidation numbers of +1, and elements in periodic group IIA have oxidation numbers of +2, e.g., Na^+.
    b. The most electronegative element, fluorine, is always assigned both electrons from any bond in which it participates. This gives fluorine an oxidation number of –1 in all its compounds, e.g., OF_2.

c. Oxygen usually exhibits an oxidation number of –2, but exceptions occur in peroxides, superoxides, and when oxygen combines with fluorine.
d. Hydrogen exhibits an oxidation number of +1 unless it is combined with an element more electropositive than itself, e.g., with lithium, in which case its oxidation number is –1.

4. *The sum of the oxidation numbers of all atoms in a complete formula must be 0*; that is, when an electron is lost by one atom (+1 contribution to oxidation number), the same electron must be gained by another atom (–1 contribution to oxidation number).
5. *If a polyatomic ion is considered by itself, the sum of the oxidation numbers of its constituent atoms must equal the charge on the ion.*

As an illustration of these rules, let us consider a few more examples.

Example 1.3.13.2 : Oxidation Number

Determine the oxidation number of each element in each of the following formulas: (a) NaClO; (b) ClO_4^-; and (c) MgH_2.

Solution:

a) Since Na is a group IA element, its oxidation number is +1 (rule 3*a*). The oxidation number of O is usually –2 (rule 3*c*). Therefore (rule 4), +1 + oxidation number of Cl + (–2) = 0.

$$\text{Oxidation number of Cl} = 2–1 = +1$$

Thus we write the formula

$$\overset{+1}{\text{Na}}\ \overset{+1}{\text{Cl}}\ \overset{-2}{\text{O}}$$

if oxidation numbers are to be included.

b) In this case the oxidation numbers must add to –1, the charge on the polyatomic ion. Since O is usually –2, we have

$$\text{Oxidation number of Cl} + 4(–2) = –1$$

$$\text{Oxidation number of Cl} = –1 + 8 = +7$$

c) In MgH_2, H is combined with an element more electropositive than itself, and so its oxidation number is –1. Mg is in group IIA,and so its oxidation number is +2:

$$\overset{+2}{\text{Mg}}\ \overset{-1}{\text{H}}_2$$

As a check on these assignments, it is wise to make sure that the oxidation numbers sum to 0:

$$+2 + 2(–1) = 0 \qquad \text{OK}$$

Oxidation numbers are mainly used by chemists to identify and handle a type of chemical reaction called a **redox reaction**, or an **oxidation-reduction reaction**. This type of reaction can be recognized because it involves a *change in oxidation number* of at least one element. More information on these reactions is found in the section on redox reactions. Oxidation numbers are also used in the names of compounds. The internationally recommended rules of nomenclature involve roman numerals which represent oxidation numbers. For example, the two bromides of mercury, Hg_2Br_2 and $HgBr_2$, are called mercury(I) bromide and mercury(II) bromide, respectively. Here the numeral I refers to an oxidation number of +1 for mercury, and II to an oxidation number of +2. Oxidation numbers can sometimes also be useful in writing Lewis structures, particularly for oxyanions. In the sulfite ion, SO_3^{2-} for example, the oxidation number of sulfur is +4, suggesting that only *four* sulfur electrons are involved in the bonding. Since sulfur has six valence electrons, we conclude that two electrons are not involved in the bonding, i.e., that there is a *lone* pair. With this clue, a plausible Lewis structure is much easier to draw:



Central S has one lone pair and three bonding pairs with each of the three oxygen. Two of the bonding pairs comes directly from the electrons on the valence of sulfur. The other bonding pair comes from two additional electrons added to the oxygen. The overall structure is enclosed in a square bracket with superscript of 2 negative.

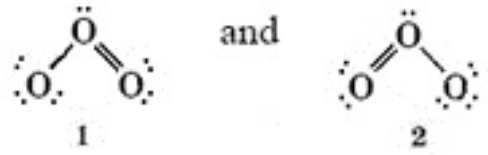
This page titled 1.3.13: Formal Charge and Oxidation Numbers is shared under a CC BY-NC-SA 4.0 license and was authored, remixed, and/or curated by Ed Vitz, John W. Moore, Justin Shorb, Xavier Prat-Resina, Tim Wendorff, & Adam Hahn.

- **7.13: Formal Charge and Oxidation Numbers** by Ed Vitz, John W. Moore, Justin Shorb, Xavier Prat-Resina, Tim Wendorff, & Adam Hahn is licensed CC BY-NC-SA 4.0.

1.3.14: Resonance

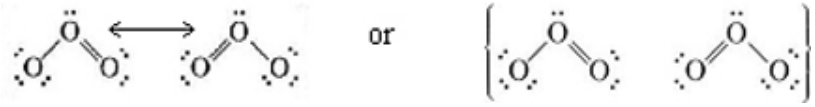
In addition to molecules containing odd numbers of electrons, there is another class of molecules which does not fit easily into the electron-pair theory of the covalent bond. For these molecules it is possible to draw *more than one* Lewis structure which obeys the octet rule but which is unsatisfactory in other ways. A simple example of such a molecule is ozone, an unusual form of oxygen, whose molecular formula is O_3. Like the oxides of nitrogen, ozone is important in a discussion of atmospheric-pollution problems, but for the moment we will confine ourselves to its structure.

We can draw two Lewis diagrams for O_3, both of which obey the octet rule:



Structure 1 suggests that there is an O—O single bond on the left and an O=O double bond on the right side of the molecule. Structure 2 suggests the opposite placement of the double bond. However, it seems unlikely that electrons should be able to distinguish left from right in this way, and experimental evidence confirms this suspicion. Both bonds are found to have the same length, namely, 128 pm. This is intermediate between the O=O double-bond length of 121 pm in O_2 and the O—O single-bond length of 147 pm in H_2O_2. In other words the structure of O_2 is somehow intermediate in character between the two structures shown.

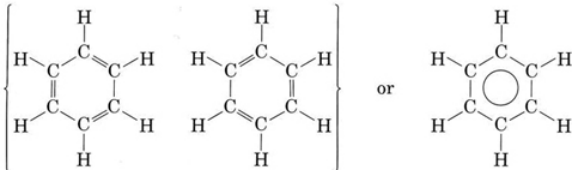
On a mathematical level, we can satisfactorily account for the properties of ozone by regarding its structure as a *hybrid* of the two structures shown above, the term hybrid having exactly the same sense as for hybrids. We then obtain an electron probability distribution in which both bonds receive equal treatment and are intermediate in character between double and single bonds. Such a structure is called a **resonance hybrid** and is indicated in one of the following ways:



Two resonance structures of "O" 3 are either shown with double headed arrows in between or with both structures enclosed in a bracket.

The term resonance and the use of a double-headed arrow, ↔, are both unfortunate since they suggest that the structure is continually oscillating between the two alternatives, so that if only you were fast enough, you could “catch” the double bond on one side or the other. One can no more do this than “catch” an *sp* hybrid orbital instantaneously in the form of an *s* or a *p* orbital.

The most important example of resonance is undoubtedly the compound benzene, C_6H_6, which has the structure



The two resonance structures of benzene are shown enclosed in a bracket. The double bonds are located on every other carbon and each double bonds moves to the next carbon between each resonance structure. The alternate way to express this resonance shows a benzene ring with a circle in the middle of the cyclic structure.

The circle within the second formula indicates that all C—C bonds in the hexagon are equivalent. This hexagonal ring of six carbon atoms is called a **benzene ring**. Each carbon-carbon bond is 139 pm long, intermediate between the length of a C—C single bond (154 pm) and a C=C double bond (135 pm). Whereas a double bond between two carbon atoms is normally quite reactive, the bonding between the carbons in the benzene ring is difficult to alter. In virtually all its chemical reactions, the ring structure of benzene remains intact.

Even when a molecule exhibits resonance, it is still possible to predict its shape. Any bonds which are intermediate in character can be treated as though they were single bonds, though perhaps a bit fatter. On this basis one would predict that the ozone molecule is angular rather than linear because of the lone pair on the central oxygen atom, with an angle slightly less than 120°. Experimentally the angle is 117°. In the same way each carbon atom in benzene can be expected to be surrounded by three atoms in a plane around it, separated by angles of approximately 120°. Again this agrees with experiment. All the atoms in C_6H_6 lie in the same plane, and all bond angles are 120°.

Example 1.3.14.1 : Resonance Structures

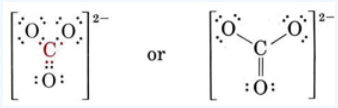
Write resonance structures to indicate the bonding in the carbonate ion, CO_3^{2-}. Predict the O—C—O angle and the carbon-oxygen bond length.

Solution

We must first write a plausible Lewis structure for the ion. Counting valence electrons, we have a total of

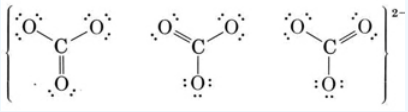
$$4(\text{from C}) + 3 \times 6(\text{from O}) + 2(\text{from charge}) = 24 \text{ electrons}$$

There are 4 octets to be filled, making a total of $4 \times 8 = 32$ electrons. We must thus count $32 - 24 = 8$ electrons twice, and so there are 4 shared pairs. Since there are only three oxygen atoms, one must be double bonded to the carbon atom:



Central carbon is double bonded to one oxygen and single bonded to two oxygen. The total charge of the structure is negative 2.

Two other equivalent structures can also be drawn, and so the carbonate ion corresponds to the following resonance hybrid:



The resonance structure of carbonate ion shows the double bonds with three different oxygen. The charge of each structure is negative 2.

Since the carbon has no lone pairs in its valence shell, the three oxygens should be arranged trigonally around the carbon and all four atoms should lie in a plane. As we saw in the previous chapter, the C—O single-bond length is 143 pm, while the C=O double-bond length is 122 pm. We can expect the carbon-oxygen distance in the carbonate ion to lie somewhere in between these values. Experimentally it is found to be 129 pm.

This page titled 1.3.14: Resonance is shared under a CC BY-NC-SA 4.0 license and was authored, remixed, and/or curated by Ed Vitz, John W. Moore, Justin Shorb, Xavier Prat-Resina, Tim Wendorff, & Adam Hahn.

- **7.14: Resonance** by Ed Vitz, John W. Moore, Justin Shorb, Xavier Prat-Resina, Tim Wendorff, & Adam Hahn is licensed CC BY-NC-SA 4.0.

SECTION OVERVIEW

1.4: Properties of Organic Compounds

Hydrogen, oxygen, nitrogen, and a number of other elements also bond strongly to carbon, and a tremendous variety of compounds can result. In the early days of chemistry such compounds were obtained from plants or animals rather than being synthesized by chemists, and so they came to be known as organic compounds. This distinguished them from the inorganic compounds available from nonliving portions of the earth's surface. Today literally millions of carbon compounds can be synthesized in laboratories, and so this historical distinction is no longer valid. Nevertheless, the study of carbon compounds is still referred to as organic chemistry.

1.4.1: Prelude to Organic Compounds

1.4.2: Covalent Compounds and Intermolecular Forces

1.4.3: Dipole Forces

1.4.4: London Forces

- 1.4.4.1: Chapter 8 page 3.jpg
- 1.4.4.2: Atomic Radii
- 1.4.4.3: Atomic sizes on periodic table.jpg
- 1.4.4.4: Ionization Energies
  - 1.4.4.4.1: IonizationEnergyAtomicWeight.PNG
- 1.4.4.5: Ionization Energies and Electron Affinities
  - 1.4.4.5.1: Electron Affinities
    - 1.4.4.5.1.1: Ionization Energies and Electron Affinities.jpg
- 1.4.4.6: Polarizability on London Forces.jpg

1.4.5: Hydrogen Bonding- Water

- 1.4.5.1: Atomic Radii and Ionic Radii
- 1.4.5.2: H-Bonding Between 2 HF Molecules.jpg
- 1.4.5.3: Nonmetal hydride bp.jpg

1.4.6: Ice and Water

- 1.4.6.1: Ice; a hexagonal crystal.jpg
- 1.4.6.2: Boiling Points of Hydrides

1.4.7: Macromolecular Substances

1.4.8: Diamond and Graphite

1.4.9: Silicon Dioxide

1.4.10: Synthetic Macromolecules- Some Applied Organic Chemistry

1.4.11: Addition Polymers

1.4.12: Condensation Polymers

1.4.13: Cross-Linking

This page titled 1.4: Properties of Organic Compounds is shared under a CC BY-NC-SA 4.0 license and was authored, remixed, and/or curated by Ed Vitz, John W. Moore, Justin Shorb, Xavier Prat-Resina, Tim Wendorff, & Adam Hahn.

1.4.1: Prelude to Organic Compounds

In our discussion of ionic substances, we described a number of macroscopic properties, such as electrical conductivity, crystal shape and cleavage, and characteristic chemical behavior of ions. These were understandable in terms of the microscopic picture of individual ions packed into a crystal lattice in a solid ionic compound or able to move past one another in a liquid or solution. The macroscopic properties of covalent and polar covalent substances can likewise be attributed to microscopic structure. We will see how the nature of the molecules in a covalently bonded substance influences its behavior.

The number of covalent substances is far larger than the number of ionic compounds, largely because of the ability of one element, carbon, to form strong bonds with itself, as in ethane, the compound shown below.

Hydrogen, oxygen, nitrogen, and a number of other elements also bond strongly to carbon, and a tremendous variety of compounds can result. In the early days of chemistry such compounds were obtained from plants or animals rather than being synthesized by chemists, and so they came to be known as organic compounds. This distinguished them from the inorganic compounds available from nonliving portions of the earth's surface. Today literally millions of carbon compounds can be synthesized in laboratories, and so this historical distinction is no longer valid. Nevertheless, the study of carbon compounds is still referred to as organic chemistry. Since organic compounds all involve covalent bonds, we will describe a number of them as we discuss covalent substances. Many are of considerable commercial importance, and you probably encounter them, perhaps without knowing it, every day.

Macroscopic physical properties such as melting and boiling points depend on the strengths of the forces which hold microscopic particles together. In the case of molecules whose atoms are connected by covalent bonds, such intermolecular forces may be of three types. All molecules are attracted together by weak London forces. These depend on instantaneous polarization and increase in strength with the size of the molecular electron cloud. When a molecule contains atoms whose electronegativities differ significantly and the resulting bond dipoles do not cancel each other's effects, dipole forces occur. This results in higher melting and boiling points than for nonpolar substances.

The third type of intermolecular force, the hydrogen bond, occurs when one molecule contains a hydrogen atom connected to a highly electronegative partner. The other molecule must contain an electronegative atom, like fluorine, oxygen, or nitrogen, which has a lone pair. Although each hydrogen bond is weak compared with a covalent bond, large numbers of hydrogen bonds can have very significant effects. One example of this is in the properties of water. This highly unusual liquid plays a major role in making living systems and the earth's environment behave as they do.

Carbon normally forms four bonds, and carbon-carbon bonds are quite strong, allowing formation of long chains to which side branches and a variety of functional groups may be attached. Hence the number of molecular structures which can be adopted by organic compounds is extremely large. Functional groups containing oxygen atoms, nitrogen atoms, and multiple bonds often determine the chemical and physical properties of carbon compounds. Therefore organic chemistry may be systematized by studying related groups of compounds such as alkanes, cycloalkanes, aromatic compounds, alkenes and alkynes, alcohols, ethers, aldehydes and ketones, carboxylic acids, esters, amines, and so on. Within each of these categories chemical and physical behaviors are closely related to molecular structures. Some covalently bonded substances do not consist of individual small molecules. Instead, giant macromolecules form. Examples include most of the rocks in the crust of the earth as well as modern plastics. Properties of such substances depend on whether the macromolecules are three dimensional (like diamond), two dimensional (like graphite or sheets of mica) or one dimensional (like polyethylene). In the latter two cases the strengths of forces between adjacent macromolecules have a significant effect on the properties of the substances.

This page titled 1.4.1: Prelude to Organic Compounds is shared under a CC BY-NC-SA 4.0 license and was authored, remixed, and/or curated by Ed Vitz, John W. Moore, Justin Shorb, Xavier Prat-Resina, Tim Wendorff, & Adam Hahn.

- **8.1: Prelude to Organic Compounds** by Ed Vitz, John W. Moore, Justin Shorb, Xavier Prat-Resina, Tim Wendorff, & Adam Hahn is licensed CC BY-NC-SA 4.0.

1.4.2: Covalent Compounds and Intermolecular Forces

The ionic compounds are almost all solids with melting temperatures above 600°C. By contrast, most substances which contain simple molecules are either gases or liquids at room temperature. They can only be persuaded to solidify at rather low temperatures. The reason for this contrasting behavior is easily explained on the microscopic level. Oppositely charged ions attract each other very strongly and usually require energies of 400 kJ mol^{-1} or more in order to be separated. On the other hand, molecules are electrically neutral and scarcely attract each other at all. The energy needed to separate two simple molecules is usually less than a hundredth of that needed to separate ions.

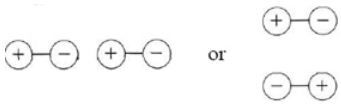
For example, only 1.23 kJ mol^{-1} is needed to separate two molecules of methane, CH_4. At room temperature virtually all molecules are moving around with energies in excess of this, so that methane is ordinarily a gas. Only if we cool the gas to quite a low temperature can we slow down the molecules to a point where they find it difficult to acquire an energy of 1.23 kJ mol^{-1}. At such a temperature, the molecules will be difficult to separate and the substance will become a liquid or a solid. Experimentally, we find that methane condenses to a liquid at –162°C, and this liquid freezes at –182°C.

This page titled 1.4.2: Covalent Compounds and Intermolecular Forces is shared under a CC BY-NC-SA 4.0 license and was authored, remixed, and/or curated by Ed Vitz, John W. Moore, Justin Shorb, Xavier Prat-Resina, Tim Wendorff, & Adam Hahn.

- **8.2: Covalent Compounds and Intermolecular Forces** by Ed Vitz, John W. Moore, Justin Shorb, Xavier Prat-Resina, Tim Wendorff, & Adam Hahn is licensed CC BY-NC-SA 4.0.

1.4.3: Dipole Forces

You may be wondering, why should neutral molecules attract each other at all? If the molecules are polar, the explanation is fairly obvious. When two polar molecules approach each other, they can arrange themselves in such a way that the negative side of one molecule is close to the positive end of the other:



Two arrangements of polar molecules are shown. One involves the head on attraction between opposite charges. The other arrangement shows one polar molecule on top of another molecule. The positive side of one molecule attracts the negative side of the other molecule and vice versa.

The molecules will then attract each other because the charges which are closest together are opposite in sign. (This behavior is very similar to the attraction between two bar magnets placed end to end or side by side with the north poles opposite the south poles.) Forces between polar molecules which arise in this way are called **dipole forces**. The existence of dipole forces explains why polar molecules have higher boiling points and melting points than do nonpolar molecules. In the following table, we compare the boiling points of several pairs of molecules. In each pair, one molecule is polar and the other is nonpolar, but otherwise they are as similar as possible. The polar substance always has the higher boiling point, indicating greater attractive forces between separate molecules, that is, larger intermolecular forces.

Table **1.4.3.1** Boiling Points of Otherwise Similar Polar and Nonpolar Substances.

Nonpolar Molecules				**Polar Molecules**			
Molecule	Molar Mass / g mol^{-1}	Total Number of Electrons	Boiling Point (in degrees C)	Molecule	Molar Mass / g mol^{-1}	Total Number of Electrons	Boiling Point (in degrees C)
N_2	28	14	-196	CO	28	14	-192
SiH_4	32	18	-112	PH_3	34	18	-85
GeH_4	77	36	-90	AsH_3	78	36	-55
Br_2	160	70	59	ICl	162	70	97

This page titled 1.4.3: Dipole Forces is shared under a CC BY-NC-SA 4.0 license and was authored, remixed, and/or curated by Ed Vitz, John W. Moore, Justin Shorb, Xavier Prat-Resina, Tim Wendorff, & Adam Hahn.

- **8.3: Dipole Forces** by Ed Vitz, John W. Moore, Justin Shorb, Xavier Prat-Resina, Tim Wendorff, & Adam Hahn is licensed CC BY-NC-SA 4.0.

1.4.4: London Forces

Dipole forces explain how polar molecules can attract each other, but it is a bit harder to account for the forces of attraction which exist between completely nonpolar molecules. Even the noble gases, whose atoms do not form chemical bonds with each other, can be condensed to liquids at sufficiently low temperatures. This indicates that the atoms attract each other, though only feebly. An explanation of these attractive forces was first given in 1930 by the Austrian physicist Fritz London (1900 to 1954). According to his theory, when two molecules approach each other very closely, the motion of the electrons in one of the molecules interferes with the motion of the electrons in the other, and the net result is an attractive force. In order to understand London's ideas better, let us start by considering the hypothetical situation shown in Figure **1.4.4.1**. When a dipole approaches a helium atom, the electron cloud of the helium atom is attracted toward the positive end of the dipole.

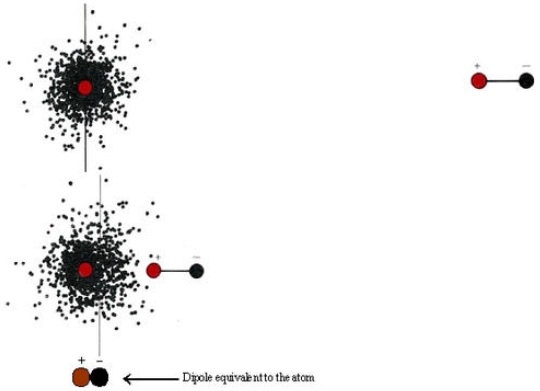


Figure **1.4.4.1**: The polarization and attraction of a helium atom by a dipole. The close approach of the positive side of the dipole attracts the electron cloud toward it. This makes the helium atom electrically lopsided and equivalent to the dipole shown below it. There is then a net force of attraction between this induced dipole and the permanent dipole. The two lines drawn in the figure go through the center of charge of the electron cloud.

The first electron dot diagram shows a small red circle with a circular area around it concentrated with many black dots. There is also a straight vertical line going straight through the middle of this circle. Far in the right there is another red circle, labeled positive, connected to a black circle which is labeled negative. In the next electron dot diagram, the red and black circle is now close to the electrons. The positive side faces the electrons. The vertical line shifted its position towards the right, no longer going through the center of the nucleus. Dipole shown below is a positive circle in contact with a negative circle on its right.

The helium atom becomes polarized and behaves electrically as though it were a second dipole, with its negative side pointed toward the positive side of the first dipole. As we have already seen, two dipoles oriented in this fashion *attract* each other.

If instead of a dipole, we now bring up another helium atom, a similar effect occurs. The electrons moving about the nucleus in this second atom will often both be found momentarily on one side of the nucleus or both on the other side. At any given instant, therefore, the approaching helium atom is likely to be slightly polar. It can then behave like the dipole used in the above figure, inducing a dipole in the first atom, and attraction will result. Thus, as the electrons in one atom move around it, they will tend to synchronize to some extent with the motion of the electrons in the other atom. Overall there will be a force of attraction between the two helium atoms.

An argument similar to that just presented can be applied to pairs of atoms of the other noble gases as well. Indeed, it explains why there must be forces of attraction, albeit quite small, between two molecules of *any* kind. Forces caused by the mutual instantaneous polarization of two molecules are called **London forces**, or sometimes **dispersion forces**. When referring to intermolecular forces in general, to either London or dipole forces or both, the term **van der Waals forces** is generally used. Johannes van der Waals (1837 to 1923) was a Dutch scientist who first realized that neutral molecules must attract each other, even though he was unable to explain these attractions himself.

In general, when we compare substances whose molecules have similar electronic structures, it is always the larger molecules which correspond to the stronger London forces. This rule is illustrated by the physical properties shown in the following table for the noble gases and the halogens. Both melting points and boiling points increase in the order He < Ne < Ar < Kr < Xe and F_2 < Cl_2 < Br_2 < I_2. This corresponds with the order of increasing van der Waals radius, showing that in each case the larger molecules are more strongly attracted to each other.

Table 1.4.4.1: Some Physical Properties of Nonpolar Substances.

Substance	van der Waals Radius* / pm	Melting Point (in °C)	Boiling Point (in °C)
He	93	†	-269
Ne	112	-248	-246
Ar	154	-189	-186
Kr	169	-157	-153
Xe	190	-112	-108
F_2	135	-220	-188
Cl_2	180	-101	-34
Br_2	195	-47	58
I_2	215	114	183

** From figure of atomic radii. Note that the halogen molecules are not spherical. Nevertheless the van Waals radius of the halogen atoms is in proportion to molecular size.*

† Only forms a solid at very high pressures.

This dependence on the size of the molecule is readily explained by London's theory. In larger molecules, the valence electrons are on the whole farther from the nuclei. The electron cloud is more diffuse, less tightly held, and hence *more easily polarizable* than for smaller molecules. The ionization energy for Xe is 1170 kJ mol^{-1}, for example, much less than for Ne (2080 kJ mol^{-1} as seen in the table of ionization energies). This indicates that the outermost octet in Xe is much less tightly held than in Ne. Thus when two Xe atoms approach each other closely, the motion of the electrons in the one atom can synchronize with the motion in the other more effectively than in the case of two Ne atoms.

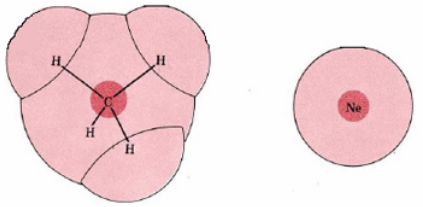


Figure 1.4.4.2: The effect of polarizability on London forces. Both CH_4 and Ne have eight electrons in the valence shell. In these CH_4 these electrons form a more diffuse, larger, and less tightly held cloud than in Ne. This makes the CH_4 electrons more easily polarizable and the intermolecular forces larger.

The magnitude of London forces is often said to depend on the molar mass of the molecules involved; if we compare molecules of similar electronic structure, the larger molecules are usually the heavier ones. But this is a coincidence rather than a cause-and-effect relationship, and is not always true. If we compare methane, CH_4 (M = 16 g mol^{-1}) with Ne (M = 20.2 g mol^{-1}), for example, we find that the lighter molecule has the stronger London forces. Both molecules contain 10 electrons, of which 8 are in valence shell. In an Ne atom, the electrons are tightly held by a single nucleus of charge +10, while in CH_4, this same total positive charge is spread out over one C nucleus of charge +6 and four H nuclei of charge +1. As can be seen from Figure 2, the electrons in CH_4 occupy a much larger electron cloud and are not so tightly constrained as in Ne. They are thus easier to polarize, and the London forces between two CH_4 molecules are expected to be larger than between two Ne molecules. In agreement with this we find a much higher boiling point for CH_4 (–162°C) than for Ne (–246°C).

✔ Example 1.4.4.1 : Boiling Point

Decide which substance in each of the following pairs will have the higher boiling point:

a. SiH_4 vs. SnH_4
b. CF_4 vs. CCl_4

c. Kr vs. HBr
d. C_2H_6 vs.F_2

Solution

a. Both SiH_4 and SnH_4 correspond to the same Lewis diagram. In SnH_4 though, the valence octet is in the $n = 5$ shell, as opposed to the $n = 3$ shell for SiH_4. SnH_4 is the larger molecule and should have the higher boiling point.
b. Again the two molecules have similar Lewis diagrams. Since Cl is larger than F, we conclude that electrons in CCl_4 are more easily polarized, and the boiling point will be higher for this compound.
c. Both Kr and HBr have the same number of electrons. HBr, however, is polar and thus has the higher boiling point.
d. Both molecules have the same total number of electrons, namely, 18, but in C_2H_6 the electron cloud is distributed around eight nuclei rather than two. This larger cloud is more easily polarized so that we can expect stronger London forces. C_2H_6, F_2 will thus have the higher boiling point.

Note that it is not always possible to decide which of two substances has the higher boiling point even though their electronic structures are very similar. A case in point is the pair of substances HCl and HI. We can expect HCl to be more polar than HI so that the dipole forces between HCl molecules should be greater than for HI molecules. The London forces, however, will be the other way around since HI is so much larger in size than HCl. It happens that the effect of the London forces is larger—HI is found to have a higher boiling point (–38°C) than HCl (–88°C).

This page titled 1.4.4: London Forces is shared under a CC BY-NC-SA 4.0 license and was authored, remixed, and/or curated by Ed Vitz, John W. Moore, Justin Shorb, Xavier Prat-Resina, Tim Wendorff, & Adam Hahn.

- **8.4: London Forces** by Ed Vitz, John W. Moore, Justin Shorb, Xavier Prat-Resina, Tim Wendorff, & Adam Hahn is licensed CC BY-NC-SA 4.0.

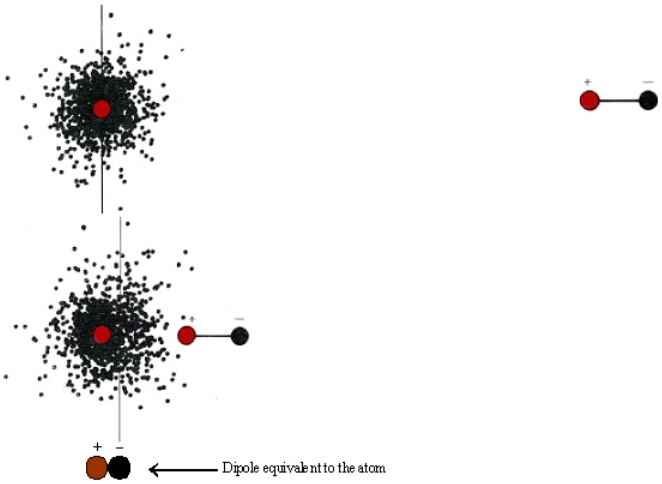
1.4.4.1: Chapter 8 page 3.jpg

File:Chapter 8 page 3.jpg

From ChemPRIME

Jump to: navigation, search

- File
- File history
- File links
- Metadata



The first electron dot diagram shows a small red circle with a circular area around it concentrated with many black dots. There is also a straight vertical line going straight through the middle of this circle. Far in the right there is another red circle, labeled positive, connected to a black circle which is labeled negative. In the next electron dot diagram, the red and black circle is now close to the electrons. The positive side faces the electrons. The vertical line shifted its position towards the right, no longer going through the center of the nucleus. Dipole shown below is a positive circle in contact with a negative circle on its right.

No higher resolution available.

Chapter_8_page_3.jpg (554 × 415 pixels, file size: 72 KB, MIME type: image/jpeg)

Description	The Polarization and Attraction of a Helium Atom by a Dipole
Keywords	Atomic Properties / Structure
Date	1978
Source	From Moore, Collins, Davies. "Chemistry" McGraw-Hill Companies. 1978.
Author	Moore, Collins, Davies
Permission	Attribution-Noncommercial-Share Alike 3.0 Unported

File history

Click on a date/time to view the file as it appeared at that time.

(Latest | Earliest) View (newer 50) (older 50) (20 | 50 | 100 | 250 | 500)

	Date/Time	Thumbnail	Dimensions	User	Comment
current	15:59, 16 March 2009		554×415 (72 KB)	WikiSysop (Talk | contribs)	

(Latest | Earliest) View (newer 50) (older 50) (20 | 50 | 100 | 250 | 500)

- Edit this file using an external application (See the setup instructions for more information)

File links

The following page links to this file:

- CoreChem:London Forces

Metadata

This file contains additional information, probably added from the digital camera or scanner used to create or digitize it. If the file has been modified from its original state, some details may not fully reflect the modified file.

Orientation	Normal
Horizontal resolution	72 dpi
Vertical resolution	72 dpi
Software used	Adobe Photoshop CS3 Windows
File change date and time	12:25, 22 September 2008
Color space	sRGB

Retrieved from "wiki.chemprime.chemeddl.org/i...r_8_page_3.jpg"
Category: Atomic Properties / Structure

Views

- File
- Talk
- View source
- History

Personal tools

- Log in

Navigation

- Main Page
- Site News
- Collaboration
- Student Assignments
- Recent changes
- Random page
- ChemEd DL
- Find Resources
- Help

Search

Toolbox

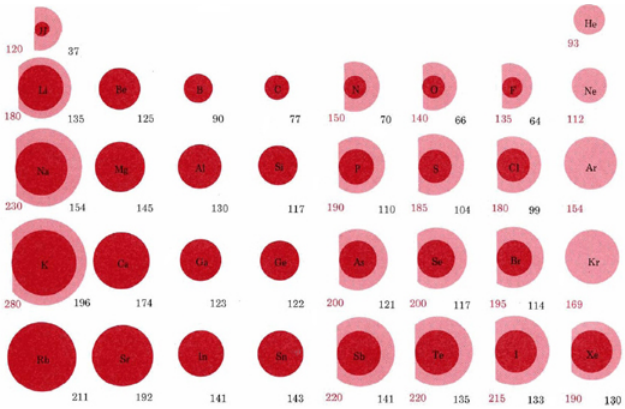
- What links here
- Related changes
- Upload file
- Special pages
- Printable version
- Permanent link

- This page was last modified on 22 March 2010, at 21:10.
- This page has been accessed 2,771 times.
- Content is available under Attribution-Noncommercial-Share Alike 3.0 Unported.
- Privacy policy
- About ChemPRIME
- Disclaimers

This page titled 1.4.4.1: <pic>Chapter 8 page 3.jpg is shared under a CC BY-NC-SA 4.0 license and was authored, remixed, and/or curated by Ed Vitz, John W. Moore, Justin Shorb, Xavier Prat-Resina, Tim Wendorff, & Adam Hahn.

- **8.4.1: Chapter 8 page 3.jpg** by Ed Vitz, John W. Moore, Justin Shorb, Xavier Prat-Resina, Tim Wendorff, & Adam Hahn is licensed CC BY-NC-SA 4.0.

1.4.4.2: Atomic Radii



No higher resolution available.

Atomic_sizes_on_periodic_table.jpg (521 × 337 pixels, file size: 143 KB, MIME type: image/jpeg)

Description	Sizes of Atoms of the Representative Elements as a Function of Their Position in the Periodic Table
Keywords	Atomic Properties / Structure , Periodicity / Periodic Table
Date	1978
Source	From Moore, Collins, Davies. "Chemistry" McGraw-Hill Companies. 1978.
Author	Moore, Collins, Davies
Permission	Attribution-Noncommercial-Share Alike 3.0 Unported

This page titled 1.4.4.2: Atomic Radii is shared under a CC BY-NC-SA 4.0 license and was authored, remixed, and/or curated by Ed Vitz, John W. Moore, Justin Shorb, Xavier Prat-Resina, Tim Wendorff, & Adam Hahn.

- **8.4.2: Atomic Radii** by Ed Vitz, John W. Moore, Justin Shorb, Xavier Prat-Resina, Tim Wendorff, & Adam Hahn is licensed CC BY-NC-SA 4.0.

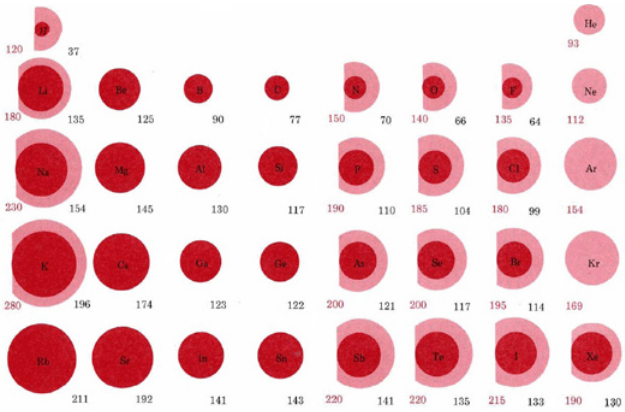
1.4.4.3: Atomic sizes on periodic table.jpg

File:Atomic sizes on periodic table.jpg

From ChemPRIME

(Redirected from File:Chapter 6 page 34.jpg) Jump to: navigation, search

- File
- File history
- File links
- Metadata



No higher resolution available.

Atomic_sizes_on_periodic_table.jpg (521 × 337 pixels, file size: 143 KB, MIME type: image/jpeg)

Description	Sizes of Atoms of the Representative Elements as a Function of Their Position in the Periodic Pable
Keywords	Atomic Properties / Structure , Periodicity / Periodic Table
Date	1978
Source	From Moore, Collins, Davies. "Chemistry" McGraw-Hill Companies. 1978.
Author	Moore, Collins, Davies
Permission	Attribution-Noncommercial-Share Alike 3.0 Unported

File history

Click on a date/time to view the file as it appeared at that time.

(Latest | Earliest) View (newer 50) (older 50) (20 | 50 | 100 | 250 | 500)

	Date/Time	Thumbnail	Dimensions	User	Comment
current	15:59, 16 March 2009		521×337 (143 KB)	WikiSysop (Talk | contribs)	

(Latest | Earliest) View (newer 50) (older 50) (20 | 50 | 100 | 250 | 500)

- Edit this file using an external application (See the setup instructions for more information)

File links

The following file redirects to this file:

- File:Chapter 6 page 34.jpg

The following 2 pages link to this file:

- CoreChem:Atomic Sizes
- Atomic Radii and Ionic Radii

Metadata

This file contains additional information, probably added from the digital camera or scanner used to create or digitize it. If the file has been modified from its original state, some details may not fully reflect the modified file.

Orientation	Normal
Horizontal resolution	72 dpi
Vertical resolution	72 dpi
Software used	Adobe Photoshop CS3 Windows
File change date and time	11:14, 12 September 2008
Color space	65535

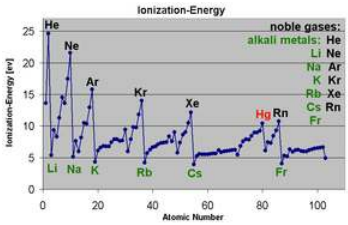
Retrieved from "wiki.chemprime.chemeddl.org/i...odic_table.jpg"
Categories: Atomic Properties / Structure | Periodicity / Periodic Table

- This page was last modified on 23 April 2010, at 16:55.
- This page has been accessed 4,772 times.
- Content is available under Attribution-Noncommercial-Share Alike 3.0 Unported.
- Privacy policy
- About ChemPRIME
- Disclaimers

This page titled 1.4.4.3: Atomic sizes on periodic table.jpg is shared under a CC BY-NC-SA 4.0 license and was authored, remixed, and/or curated by Ed Vitz, John W. Moore, Justin Shorb, Xavier Prat-Resina, Tim Wendorff, & Adam Hahn.

- **8.4.3: Atomic sizes on periodic table.jpg** by Ed Vitz, John W. Moore, Justin Shorb, Xavier Prat-Resina, Tim Wendorff, & Adam Hahn is licensed CC BY-NC-SA 4.0.

1.4.4.4: Ionization Energies



Above are the ionization energies of the elements are plotted against atomic number. An obvious feature of this graph is that the elements with the highest ionization energies are the noble gases. Since the ionization energy measures the energy which must be *supplied* to remove an electron, these high values mean that it is difficult to remove an electron from an atom of a noble gas. A second obvious feature is that the elements with the lowest ionization energies are the alkali metals. This means that it is easier to remove electrons from atoms of this group of elements than from any other group. Closer inspection also reveals the following two general tendencies:

1 As one moves *down a given group in the periodic table, the ionization energy decreases*. In group I, for example, the ionization energies decrease in the order Li > Na > K > Rb > Cs. The reason for this is a steady increase in size of the valence electron cloud as the principal quantum number n increases. The 6*s* valence electron of Cs, for instance, is further from the nucleus and hence easier to remove than the 5*s* valence electron of Rb.

2 As one moves from *left to right across the periodic table* (from an alkali-metal atom to a noble gas), *the ionization energy increases* on the whole. In such a move the *n* value of the outermost electrons remains the same, but the nuclear charge increases steadily. This increased nuclear attraction requires that more work he done to remove an electron, and so ionization energy goes up.

Ionization energies can be measured quite accurately for atoms, and the values obtained show some additional features which are less important than the two major trends mentioned above. For example, consider the data for elements in the second row of the periodic table. Numerical values for the relevant ionization energies are shown in the table of ionization energies and electron affinities below.

73 H 1312							He 2372
58 Li 520	−18* Be 899	29* B 801	121* C 1086	−58* N 1402	142 O 1314	331 F 1681	Ne 2080
52 Na 496	−54* Mg 738	48* Al 578	134* Si 786	75* P 1012	200 S 1000	348 Cl 1251	Ar 1520
K 419	Ca 590	Ga 579	Ge 762	65 As 946	207* Se 941	324 Br 1140	Kr 1351
Rb 403	Sr 549	In 558	Sn 708	Sb 834	222* Te 869	296 I 1008	Xe 1170
Cs 376	Ba 503	Tl 589	Pb 715	Bi 703	Po 812	At	Rn 1037

*** Electron affinities marked with an asterisk (*) have been obtained from theoretical calculations rather than experimental measurements. The heavy colored line separates metals (ionization energy usually below about 800 kJ mol^{-1}) from nonmetals.**

The general trend of increasing ionization energy across the table is broken at two points. Boron has a smaller value than beryllium, and oxygen has a smaller value than nitrogen. The first break occurs when the first electron is added to a *p* subshell. As was mentioned several times in the previous chapter, a 2*p* electron is higher in energy and hence easier to remove than a 2*s* electron because it is more efficiently shielded from the nuclear charge. Thus the 2*p* electron in boron is easier to remove than a 2*s* electron in beryllium. The second exception to the general trend occurs in the case of oxygen, which has one more 2*p* electron than the half-filled subshell of nitrogen. The last electron in the oxygen atom is forced into an already occupied orbital where it is kept close to another electron. The repulsion between these two electrons makes one of them easier to remove, and so the ionization energy of oxygen is lower than might be expected.

These discontinuities also appear periodically, as would be expected since they arise from the structure of the valence electrons. Sulfur and selenium, in the same group as oxygen, show the discontinuity in the trend of increasing ionization energy, which arises from the same half-filled subshell effect. Aluminum and gallium, both in the same group as boron, similarly show a decrease in ionization energy compared to magnesium and calcium. While this trend does not seem to apply for indium, and thallium, it is important to remember that the chart is missing the transition metals. Looking at the graph of ionization energies, it is clear that indium(atomic number 49) *does* have a lower ionization energy than cadmium(atomic number 48), and the same is true of mercury, the element preceding thallium(atomic number 81).

This page titled 1.4.4.4: Ionization Energies is shared under a CC BY-NC-SA 4.0 license and was authored, remixed, and/or curated by Ed Vitz, John W. Moore, Justin Shorb, Xavier Prat-Resina, Tim Wendorff, & Adam Hahn.

- **8.4.4: Ionization Energies** by Ed Vitz, John W. Moore, Justin Shorb, Xavier Prat-Resina, Tim Wendorff, & Adam Hahn is licensed CC BY-NC-SA 4.0.

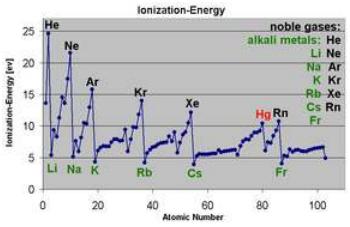
1.4.4.4.1: IonizationEnergyAtomicWeight.PNG

File:IonizationEnergyAtomicWeight.PNG

From ChemPRIME

Jump to: navigation, search

- File
- File history
- File links



Size of this preview: 800 × 499 pixels
Full resolution (856 × 534 pixels, file size: 13 KB, MIME type: image/png)

Description	Ionization Energy by Atomic Weight
Keywords	Physical Properties
Date	27 September 2007
Source	en.Wikipedia.org
Author	JJnoDog
Permission	Attribution-Noncommercial-Share Alike 3.0 Unported

File history

Click on a date/time to view the file as it appeared at that time.

(Latest | Earliest) View (newer 50) (older 50) (20 | 50 | 100 | 250 | 500)

	Date/Time	Thumbnail	Dimensions	User	Comment
current	17:43, 4 March 2010		856×534 (13 KB)	Arhahn (Talk | contribs)	

(Latest | Earliest) View (newer 50) (older 50) (20 | 50 | 100 | 250 | 500)

- Edit this file using an external application (See the setup instructions for more information)

File links

The following page links to this file:

- CoreChem:Ionization Energies

Retrieved from "wiki.chemprime.chemeddl.org/i...omicWeight.PNG"
Category: Physical Properties

Views

- File
- Talk
- View source

- History

Personal tools

- Log in

Navigation

- Main Page
- Site News
- Collaboration
- Student Assignments
- Recent changes
- Random page
- ChemEd DL
- Find Resources
- Help

Search

Toolbox

- What links here
- Related changes
- Upload file
- Special pages
- Printable version
- Permanent link



- This page was last modified on 4 March 2010, at 17:48.
- This page has been accessed 2,209 times.
- Content is available under Attribution-Noncommercial-Share Alike 3.0 Unported.
- Privacy policy
- About ChemPRIME
- Disclaimers

This page titled 1.4.4.4.1: <pic> IonizationEnergyAtomicWeight.PNG is shared under a CC BY-NC-SA 4.0 license and was authored, remixed, and/or curated by Ed Vitz, John W. Moore, Justin Shorb, Xavier Prat-Resina, Tim Wendorff, & Adam Hahn.

- **8.4.4.1: IonizationEnergyAtomicWeight.PNG** by Ed Vitz, John W. Moore, Justin Shorb, Xavier Prat-Resina, Tim Wendorff, & Adam Hahn is licensed CC BY-NC-SA 4.0.

1.4.4.5: Ionization Energies and Electron Affinities

73 H 1312							He 2372
58 Li 520	−18* Be 899	29* B 801	121* C 1086	−58* N 1402	142 O 1314	331 F 1681	Ne 2080
52 Na 496	−54* Mg 738	48* Al 578	134* Si 786	75* P 1012	200 S 1000	348 Cl 1251	Ar 1520
K 419	Ca 590	Ga 579	Ge 762	65 As 946	207* Se 941	324 Br 1140	Kr 1351
Rb 403	Sr 549	In 558	Sn 708	Sb 834	222* Te 869	296 I 1008	Xe 1170
Cs 376	Ba 503	Tl 589	Pb 715	Bi 703	Po 812	At	Rn 1037

*** Electron affinities marked with an asterisk (*) have been obtained from theoretical calculations rather than experimental measurements. The heavy colored line separates metals (ionization energy usually below about 800 kJ mol^{-1}) from nonmetals.**

This table gives ionization energies and electron affinities for common elements, and displays the information in terms of the periodic table. Ionization energies are in black, with electron affinities in red. For ionization energies, two general tendencies arise. First, as one moves down a given group in the periodic table, the ionization energy decreases. Second, as one moves from left to right across the periodic table (from an alkali-metal atom to a noble gas), the ionization energy increases on the whole. While electron affinities display fewer regularities on the table, trends do exist. All the halogens have values of about 300 kJ mol–1 while the group VI nonmetals have somewhat lower values, in the region of 200 kJ mol–1 or less.

To Ionization Energies | To Electron Affinities

This page titled 1.4.4.5: Ionization Energies and Electron Affinities is shared under a CC BY-NC-SA 4.0 license and was authored, remixed, and/or curated by Ed Vitz, John W. Moore, Justin Shorb, Xavier Prat-Resina, Tim Wendorff, & Adam Hahn.

- **8.4.5: Ionization Energies and Electron Affinities** by Ed Vitz, John W. Moore, Justin Shorb, Xavier Prat-Resina, Tim Wendorff, & Adam Hahn is licensed CC BY-NC-SA 4.0.

1.4.4.5.1: Electron Affinities

Electron affinities are more difficult to measure experimentally than are ionization energies, and far fewer values are available. The relationship of the periodic table with those electron affinities that have been measured or estimated from calculations can be seen on the table of ionization energies and electron affinities, seen below.

73 H 1312							He 2372
58 Li 520	−18* Be 899	29* B 801	121* C 1086	−58* N 1402	142 O 1314	331 F 1681	Ne 2080
52 Na 496	−54* Mg 738	48* Al 578	134* Si 786	75* P 1012	200 S 1000	348 Cl 1251	Ar 1520
K 419	Ca 590	Ga 579	Ge 762	65 As 946	207* Se 941	324 Br 1140	Kr 1351
Rb 403	Sr 549	In 558	Sn 708	Sb 834	222* Te 869	296 I 1008	Xe 1170
Cs 376	Ba 503	Tl 589	Pb 715	Bi 703	Po 812	At	Rn 1037

** Electron affinities marked with an asterisk (*) have been obtained from theoretical calculations rather than experimental measurements. The heavy colored line separates metals (ionization energy usually below about 800 kJ mol–1) from nonmetals.*

It is not easy to discern many obvious regularities in this table, especially since some of the electron-affinity values quoted are negative, indicating that energy is sometimes *required* to force an extra electron onto an atom. Nevertheless, it is quite obvious which of the periodic groups correspond to the highest electron affinities. All the halogens have values of about 300 kJ mol^{-1} while the group VI nonmetals have somewhat lower values, in the region of 200 kJ mol^{-1} or less. The high electron affinities of the halogens are a result of their having an almost complete outer shell of electrons. The element fluorine, for example, has the structure $1s^2 2s^2 2p^5$, in which one of the 2*p* orbitals contains but one electron. If an extra electron is added to this atom to form a fluoride ion, the electron can pair with the electron in the half-filled 2*p* orbital. The added electron will be shielded from the nucleus by the 1*s* electrons, but the 2*s* and 2*p* electrons are in the same shell and will shield it rather poorly. There will thus be quite a large effective nuclear charge (a rough estimate is +5) attracting the added electron. Because of this overall attraction, energy will be *released* when the electron is captured by the fluorine atom. Similar reasoning also explains why oxygen also has a high electron affinity. Here, though, the nuclear charge is smaller, and the attraction for the added electron distinctly less.

Contributors

- Ed Vitz (Kutztown University), John W. Moore (UW-Madison), Justin Shorb (Hope College), Xavier Prat-Resina (University of Minnesota Rochester), Tim Wendorff, and Adam Hahn.

This page titled 1.4.4.5.1: Electron Affinities is shared under a CC BY-NC-SA 4.0 license and was authored, remixed, and/or curated by Ed Vitz, John W. Moore, Justin Shorb, Xavier Prat-Resina, Tim Wendorff, & Adam Hahn.

- **8.4.5.1: Electron Affinities** by Ed Vitz, John W. Moore, Justin Shorb, Xavier Prat-Resina, Tim Wendorff, & Adam Hahn is licensed CC BY-NC-SA 4.0.

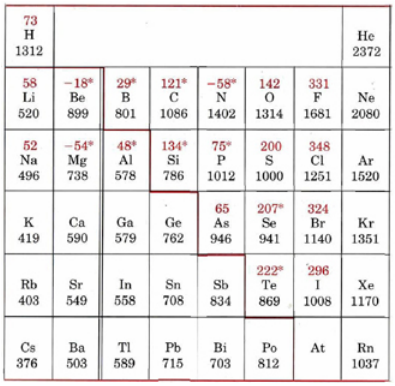
1.4.4.5.1.1: Ionization Energies and Electron Affinities.jpg

File:Ionization Energies and Electron Affinities.jpg

From ChemPRIME

Jump to: navigation, search

- File
- File history
- File links
- Metadata



No higher resolution available.

Ionization_Energies_and_Electron_Affinities.jpg (328 × 318 pixels, file size: 96 KB, MIME type: image/jpeg)

Description	Table of Ionization Energies and Electron Affinities
Keywords	Atomic Properties / Structure
Date	1978
Source	From Moore, Collins, Davies. "Chemistry" McGraw-Hill Companies. 1978.
Author	Moore, Collins, Davies
Permission	Attribution-Noncommercial-Share Alike 3.0 Unported

File history

Click on a date/time to view the file as it appeared at that time.

(Latest | Earliest) View (newer 50) (older 50) (20 | 50 | 100 | 250 | 500)

	Date/Time	Thumbnail	Dimensions	User	Comment
current	15:59, 16 March 2009		328×318 (96 KB)	WikiSysop (Talk | contribs)	

(Latest | Earliest) View (newer 50) (older 50) (20 | 50 | 100 | 250 | 500)

- Edit this file using an external application (See the setup instructions for more information)

File links

The following file redirects to this file:

- File:Chapter 6 page 10small.jpg

The following 3 pages link to this file:

- CoreChem:Ionization Energies
- CoreChem:Electron Affinities
- Ionization Energies and Electron Affinities

Metadata

This file contains additional information, probably added from the digital camera or scanner used to create or digitize it. If the file has been modified from its original state, some details may not fully reflect the modified file.

Orientation	Normal
Horizontal resolution	72 dpi
Vertical resolution	72 dpi
Software used	Adobe Photoshop CS3 Windows
File change date and time	13:44, 10 September 2008
Color space	65535

Retrieved from "wiki.chemprime.chemeddl.org/i...Affinities.jpg"
Category: Atomic Properties / Structure

Views

- File
- Talk
- View source
- History

Personal tools

- Log in

Navigation

- Main Page
- Site News
- Collaboration
- Student Assignments
- Recent changes
- Random page
- ChemEd DL
- Find Resources
- Help

Search

Toolbox

- What links here
- Related changes
- Upload file
- Special pages
- Printable version
- Permanent link



- This page was last modified on 29 April 2010, at 16:31.

- This page has been accessed 2,864 times.
- Content is available under Attribution-Noncommercial-Share Alike 3.0 Unported.
- Privacy policy
- About ChemPRIME
- Disclaimers

This page titled 1.4.4.5.1.1: <pic> Ionization Energies and Electron Affinities.jpg is shared under a CC BY-NC-SA 4.0 license and was authored, remixed, and/or curated by Ed Vitz, John W. Moore, Justin Shorb, Xavier Prat-Resina, Tim Wendorff, & Adam Hahn.

- **8.4.5.1.1: Ionization Energies and Electron Affinities.jpg** by Ed Vitz, John W. Moore, Justin Shorb, Xavier Prat-Resina, Tim Wendorff, & Adam Hahn is licensed CC BY-NC-SA 4.0.

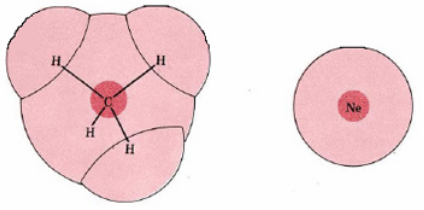
1.4.4.6: Polarizability on London Forces.jpg

File:Polarizability on London Forces.jpg

From ChemPRIME

Jump to: navigation, search

- File
- File history
- File links
- Metadata



No higher resolution available.

Polarizability_on_London_Forces.jpg (352 × 174 pixels, file size: 49 KB, MIME type: image/jpeg)

Description	The Effect of Polarizability on London Forces
Keywords	Atomic Properties / Structure
Date	1978
Source	From Moore, Collins, Davies. "Chemistry" McGraw-Hill Companies. 1978.
Author	Moore, Collins, Davies
Permission	Attribution-Noncommercial-Share Alike 3.0 Unported

File history

Click on a date/time to view the file as it appeared at that time.

(Latest | Earliest) View (newer 50) (older 50) (20 | 50 | 100 | 250 | 500)

	Date/Time	Thumbnail	Dimensions	User	Comment
current	15:59, 16 March 2009		352×174 (49 KB)	WikiSysop (Talk | contribs)	

(Latest | Earliest) View (newer 50) (older 50) (20 | 50 | 100 | 250 | 500)

- Edit this file using an external application (See the setup instructions for more information)

File links

The following file redirects to this file:

- File:Chapter 8 page 5.jpg

The following page links to this file:

- CoreChem:London Forces

Metadata

This file contains additional information, probably added from the digital camera or scanner used to create or digitize it. If the file has been modified from its original state, some details may not fully reflect the modified file.

Orientation	Normal
Horizontal resolution	72 dpi
Vertical resolution	72 dpi
Software used	Adobe Photoshop CS3 Windows
File change date and time	12:58, 22 September 2008
Color space	sRGB

Retrieved from "wiki.chemprime.chemeddl.org/i...don_Forces.jpg"
Category: Atomic Properties / Structure

Views

- File
- Talk
- View source
- History

Personal tools

- Log in

Navigation

- Main Page
- Site News
- Collaboration
- Student Assignments
- Recent changes
- Random page
- ChemEd DL
- Find Resources
- Help

Search

Toolbox

- What links here
- Related changes
- Upload file
- Special pages
- Printable version
- Permanent link

- This page was last modified on 13 May 2010, at 05:41.
- This page has been accessed 2,739 times.
- Content is available under Attribution-Noncommercial-Share Alike 3.0 Unported.
- Privacy policy
- About ChemPRIME
- Disclaimers

This page titled 1.4.4.6: Polarizability on London Forces.jpg is shared under a CC BY-NC-SA 4.0 license and was authored, remixed, and/or curated by Ed Vitz, John W. Moore, Justin Shorb, Xavier Prat-Resina, Tim Wendorff, & Adam Hahn.

- **8.4.6: Polarizability on London Forces.jpg** by Ed Vitz, John W. Moore, Justin Shorb, Xavier Prat-Resina, Tim Wendorff, & Adam Hahn is licensed CC BY-NC-SA 4.0.

1.4.5: Hydrogen Bonding- Water

It would seem that the London forces and dipole forces discussed in the earlier sections of this chapter should be adequate to account for macroscopic properties of covalently bonded substances. Certainly they can be successfully applied to hydrocarbons and many polar substances. There are some experimental data, however, which cannot be explained by London and dipole forces alone. An example appears below, where boiling points are plotted for hydrogen compounds (**hydrides**) of most of the nonmetals.

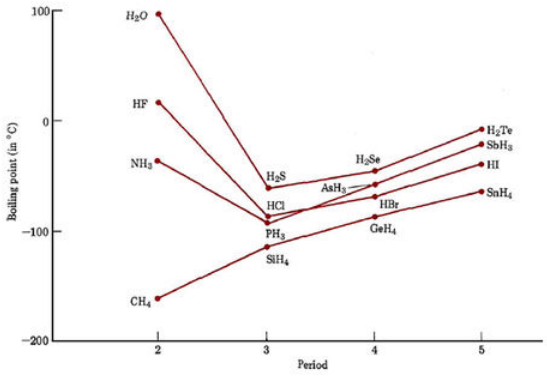


Figure **1.4.5.1** The boiling points of the hydrides of the nonmetals plotted against the period in which they occur in the periodic table. Note the anomalously high boiling points of H2O, HF, and NH3 in the second period.

Hydrides of elements in the fifth period behave as we might predict. SnH_4, which consists of nonpolar molecules, boils at the lowest temperature. SbH_3, H_2Te and HI, all of which are polar, have somewhat higher boiling points, but all lie within a range of 50°C. Similar behavior occurs among the hydrides of elements in the fourth and third periods. In the second period, however, the polar hydrides NH_3, H_2O, and HF all have boiling points more than 100°C above that of the nonpolar compound CH_4. Clearly these second-row hydrides must have particularly strong intermolecular forces.

In order to see why this happens, let us consider the simplest second-row hydride—HF. Suppose that two HF molecules approach each other, as shown in the following figure. In each HF molecule, the hydrogen nucleus is rather poorly shielded by a thin electron cloud (only two electrons), and much of that electron cloud has been distorted toward the highly electronegative fluorine atom.

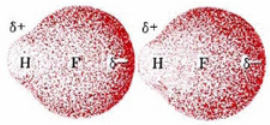
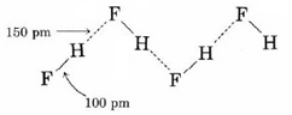


Diagram of two distorted spheres. One on the left and one on the right. The left sphere has a bulge on its left side corresponding to "H" and a partially positive charge. Most of the sphere corresponds to cloud of "F". The sphere on the right is oriented the same way with the positive side attracted to the "F" side of the first sphere.

Consequently, the hydrogen nucleus in the HF on the right can approach much closer to the fluorine side of the left-hand molecule than could any other kind of nucleus. Also, because fluorine is such an electronegative atom, its partial negative charge is particularly large. The attractive force between the electrons of the left-hand fluorine and the right-hand hydrogen nucleus will be unusually strong, and there will be considerable distortion of the electron clouds. Some covalent-bond character develops between fluorine in one molecule and hydrogen in the other.

The close approach of oppositely charged ends of molecular dipoles combines with this small degree of covalent-bond character to produce an abnormally strong intermolecular force called a **hydrogen bond**. In order for hydrogen bonding to occur, there must be a hydrogen atom connected to a small, highly electronegative atom (usually fluorine, oxygen, or nitrogen) in one molecule. The other molecule must have a very electronegative atom (again usually fluorine, oxygen, or nitrogen) which has one or more lone pairs of electrons. Separation of two molecules joined by a hydrogen bond requires 10 to 30 kJ mol^{-1}, roughly 10 times the energy needed to overcome dipole forces. Thus hydrogen bonding can account for the unusually high boiling points of NH_3, H_2O, and HF.

Hydrogen bonding between HF molecules is particularly evident in solid HF, where the atoms are arranged in a zigzag pattern:



Here the distance between hydrogen and fluorine nuclei in different molecules is only 150 pm. If we add the van der Waals radii for hydrogen and fluorine, we obtain an expected hydrogen to fluorine distance of (120 + 135) pm = 255 pm, over 100 pm larger than that observed. Obviously the hydrogen and fluorine atoms in adjacent molecules are not just “touching,” but must be associated in a much more intimate way.

Provisional Redefinition of the Hydrogen Bond

A task force of the International Union of Pure and Applied Chemistry (IUPAC) is proposing a redefinition of the hydrogen bond:

"The hydrogen bond is an attractive interaction between a hydrogen atom from a molecule or a molecular fragment X-H in which X is more electronegative than H, and an atom or a group of atoms in the same or a different molecule, in which there is evidence of bond formation." [1]

This proposed redefinition would include many more situations where hydrogen bonding appears to be important, including cases where the hydrogen atom is attracted to atoms other than F,O, and N. For example, there appears to be an attraction between the d subshell electrons in the central platinum atom in the complex shown in the Figure below, and the hydrogen atoms of an adjacent H_2O or the NH_3 group on an adjacent platinum complex[2].

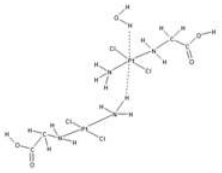


Figure **1.4.5.2** Two hydrogen bonds in trans-[$PtCl_2$ (NH_3)N-glycine)]•H_2O

The new formulation recognizes that the hydrogen bond may have some covalent character[3][4]. It recognizes that hydrogen bonds may be significant in H_2S at higher pressures and low temperatures, or that a "dihydrogen bond" may form (where metal hydrides like LiH are the H bond acceptors).

References

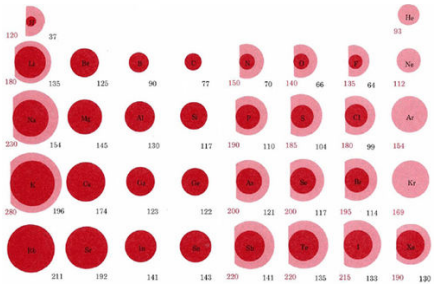
1. media.iupac.org/reports/provisional/abstract11/arunan_310311.html
2. Kozelka, J. et al, Angew. Chem. Int. Ed., DOI:10.1002/anie.201001892
3. Hydrogen Bond [en.Wikipedia.org]
4. Kemsley, Jyllian, "Hydrogen Bond Formation", Chemical & Engineering News, November 22, 2010, p. 32

This page titled 1.4.5: Hydrogen Bonding- Water is shared under a CC BY-NC-SA 4.0 license and was authored, remixed, and/or curated by Ed Vitz, John W. Moore, Justin Shorb, Xavier Prat-Resina, Tim Wendorff, & Adam Hahn.

- **8.11: Hydrogen Bonding- Water** by Ed Vitz, John W. Moore, Justin Shorb, Xavier Prat-Resina, Tim Wendorff, & Adam Hahn is licensed CC BY-NC-SA 4.0.

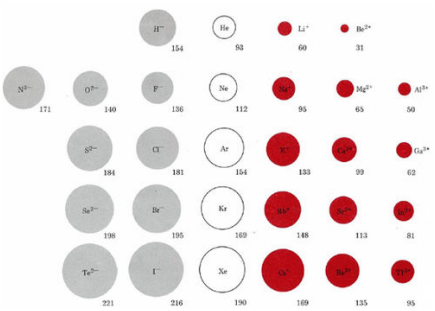
1.4.5.1: Atomic Radii and Ionic Radii

Atomic radii



This first figure is found on Atomic Sizes.

Ionic radii



This second figure is found on Ionic Sizes.

This page titled 1.4.5.1: Atomic Radii and Ionic Radii is shared under a CC BY-NC-SA 4.0 license and was authored, remixed, and/or curated by Ed Vitz, John W. Moore, Justin Shorb, Xavier Prat-Resina, Tim Wendorff, & Adam Hahn.

- **8.11.1: Atomic Radii and Ionic Radii** by Ed Vitz, John W. Moore, Justin Shorb, Xavier Prat-Resina, Tim Wendorff, & Adam Hahn is licensed CC BY-NC-SA 4.0.

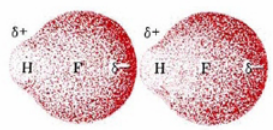
1.4.5.2: H-Bonding Between 2 HF Molecules.jpg

File:H-Bonding Between 2 HF Molecules.jpg

From ChemPRIME

Jump to: navigation, search

- File
- File history
- File links
- Metadata



No higher resolution available.

H-Bonding_Between_2_HF_Molecules.jpg (230 × 110 pixels, file size: 50 KB, MIME type: image/jpeg)

Description	Hydrogen Bonding Between the Two HF Molecules
Keywords	Hydrogen Bonding
Date	1978
Source	From Moore, Collins, Davies. "Chemistry" McGraw-Hill Companies. 1978.
Author	Moore, Collins, Davies
Permission	Attribution-Noncommercial-Share Alike 3.0 Unported

File history

Click on a date/time to view the file as it appeared at that time.

(Latest | Earliest) View (newer 50) (older 50) (20 | 50 | 100 | 250 | 500)

	Date/Time	Thumbnail	Dimensions	User	Comment
current	15:59, 16 March 2009		230×110 (50 KB)	WikiSysop (Talk | contribs)	

(Latest | Earliest) View (newer 50) (older 50) (20 | 50 | 100 | 250 | 500)

- Edit this file using an external application (See the setup instructions for more information)

File links

The following file redirects to this file:

- File:Chapter 8 page 18-1.jpg

The following page links to this file:

- CoreChem:Hydrogen Bonding: Water

Metadata

This file contains additional information, probably added from the digital camera or scanner used to create or digitize it. If the file has been modified from its original state, some details may not fully reflect the modified file.

Orientation	Normal
Horizontal resolution	72 dpi
Vertical resolution	72 dpi
Software used	Adobe Photoshop CS3 Windows
File change date and time	15:36, 23 September 2008
Color space	65535

Retrieved from "wiki.chemprime.chemeddl.org/i..._Molecules.jpg"
Category: Hydrogen Bonding

Views

- File
- Talk
- View source
- History

Personal tools

- Log in

Navigation

- Main Page
- Site News
- Collaboration
- Student Assignments
- Recent changes
- Random page
- ChemEd DL
- Find Resources
- Help

Search

Toolbox

- What links here
- Related changes
- Upload file
- Special pages
- Printable version
- Permanent link

- This page was last modified on 29 April 2010, at 19:28.
- This page has been accessed 2,420 times.
- Content is available under Attribution-Noncommercial-Share Alike 3.0 Unported.
- Privacy policy
- About ChemPRIME
- Disclaimers

This page titled 1.4.5.2: H-Bonding Between 2 HF Molecules.jpg is shared under a CC BY-NC-SA 4.0 license and was authored, remixed, and/or curated by Ed Vitz, John W. Moore, Justin Shorb, Xavier Prat-Resina, Tim Wendorff, & Adam Hahn.

- **8.11.2: H-Bonding Between 2 HF Molecules.jpg** by Ed Vitz, John W. Moore, Justin Shorb, Xavier Prat-Resina, Tim Wendorff, & Adam Hahn is licensed CC BY-NC-SA 4.0.

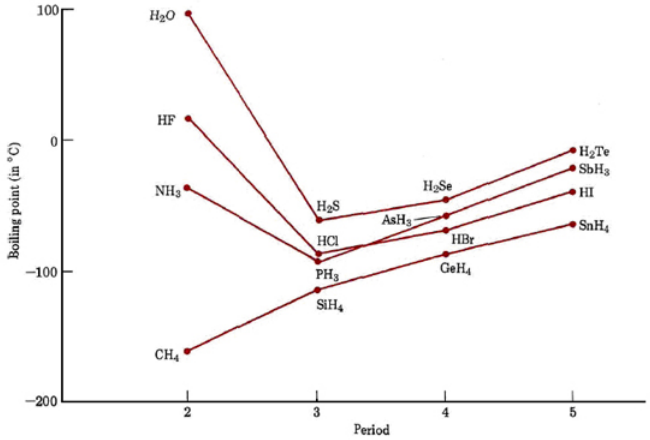
1.4.5.3: Nonmetal hydride bp.jpg

File:Nonmetal hydride bp.jpg

From ChemPRIME

Jump to: navigation, search

- File
- File history
- File links
- Metadata



No higher resolution available.

Nonmetal_hydride_bp.jpg (582 × 370 pixels, file size: 78 KB, MIME type: image/jpeg)

Description	The Boiling Points of the Hydrides of the Nonmetals Plotted Against the Period in Which They Occur in the Periodic Table
Keywords	Periodicity / Periodic Table , Physical Properties
Date	1978
Source	From Moore, Collins, Davies. "Chemistry" McGraw-Hill Companies. 1978.
Author	Moore, Collins, Davies
Permission	Attribution-Noncommercial-Share Alike 3.0 Unported

File history

Click on a date/time to view the file as it appeared at that time.

(Latest | Earliest) View (newer 50) (older 50) (20 | 50 | 100 | 250 | 500)

	Date/Time	Thumbnail	Dimensions	User	Comment
current	15:59, 16 March 2009		582×370 (78 KB)	WikiSysop (Talk | contribs)	

(Latest | Earliest) View (newer 50) (older 50) (20 | 50 | 100 | 250 | 500)

- Edit this file using an external application (See the setup instructions for more information)

File links

The following file redirects to this file:

- File:Chapter 8 page 17small.jpg

The following 3 pages link to this file:

- CoreChem:Hydrogen Bonding: Water
- Boiling Points of Hydrides
- Hydrogen Bonding: Water in Sports, Physiology & Health/Home Run Distance and Humidity

Metadata

This file contains additional information, probably added from the digital camera or scanner used to create or digitize it. If the file has been modified from its original state, some details may not fully reflect the modified file.

Orientation	Normal
Horizontal resolution	72 dpi
Vertical resolution	72 dpi
Software used	Adobe Photoshop CS3 Windows
File change date and time	15:40, 23 September 2008
Color space	sRGB

Retrieved from "wiki.chemprime.chemeddl.org/i...hydride_bp.jpg"
Categories: Periodicity / Periodic Table | Physical Properties

Views

- File
- Talk
- View source
- History

Personal tools

- Log in

Navigation

- Main Page
- Site News
- Collaboration
- Student Assignments
- Recent changes
- Random page
- ChemEd DL
- Find Resources
- Help

Search

Toolbox

- What links here
- Related changes
- Upload file
- Special pages
- Printable version

- Permanent link



- This page was last modified on 29 April 2010, at 19:33.
- This page has been accessed 3,501 times.
- Content is available under Attribution-Noncommercial-Share Alike 3.0 Unported.
- Privacy policy
- About ChemPRIME
- Disclaimers

This page titled 1.4.5.3: Nonmetal hydride bp.jpg is shared under a CC BY-NC-SA 4.0 license and was authored, remixed, and/or curated by Ed Vitz, John W. Moore, Justin Shorb, Xavier Prat-Resina, Tim Wendorff, & Adam Hahn.

- **8.11.3: Nonmetal hydride bp.jpg** by Ed Vitz, John W. Moore, Justin Shorb, Xavier Prat-Resina, Tim Wendorff, & Adam Hahn is licensed CC BY-NC-SA 4.0.

1.4.6: Ice and Water

The next simplest, and by far the most important, example of hydrogen bonding is that which occurs in H_2O. Again there is clear evidence of hydrogen bonding in the structure of the solid. Figure 1 shows two computer-drawn diagrams of the crystal lattice of ice. In the model we can clearly see that each O atom is surrounded by four H atoms arranged tetrahedrally. Two of these are at a distance of 99 pm and are clearly covalently bonded to the O atom. The other two are at a distance of 177 pm.

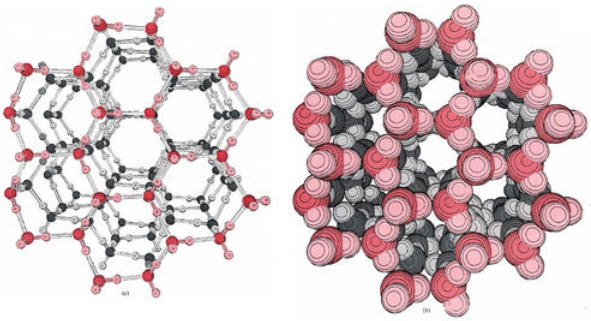
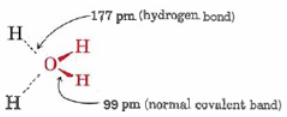


Figure 1.4.6.1 . Two computer images of the structure of ice. The water molecules have been arranged, so that each oxygen atom is surrounded by four hydrogen atoms in tetrahedral geometry. Two of these atoms are covalently bound to oxygen, while the other two are hydrogen bonding with the oxygen.

They are covalently bonded to other O atoms but are hydrogen bonded to the one in question. The situation is thus:



As in the case of HF, the distance between molecules is abnormally short. The sum of the van der Waals radii of H and O is 260 pm, considerably larger than the observed 177 pm.

The tetrahedral orientation of H atoms around O atoms which results from hydrogen-bond formation has a profound effect on the properties of ice and of liquid water. In the space-filling diagram of ice, most of the electron density of each H and O atom is enclosed by a boundary surface. As you can see, hydrogen bonding causes the H_2O molecules to adopt a rather open structure with hexagonal channels running through it. These channels contain an almost perfect vacuum-in them there is a little electron density from the surrounding atoms, but nothing else.

When ice melts, some of the hydrogen bonds are broken and the rigid crystal lattice collapses somewhat. The hexagonal channels become partially filled, and the volume of a given amount of H_2O decreases. This is the reason that ice is less dense than water and will float on it. As the temperature is raised above 0°C, more hydrogen bonds are broken, more empty space becomes occupied, and the volume continues to decrease. By the time 4°C has been reached, increased molecular velocities allow each H_2O molecule to push its neighbors farther away. This counteracts the effect of breaking hydrogen bonds, and the volume of a given amount of H_2O begins to increase with temperature.

Most solids expand when they melt, and the corresponding liquids expand continually with increasing temperature, so the behavior of water is rather unusual. It is also extremely important in the environment. When water freezes in small cracks in a rock, the greater volume of the ice can split the rock into smaller pieces. These eventually become able to support plant life, and so water contributes to the formation of fertile soil. The same process happens to roadways, and is the reason for new cracks and potholes seen on roads after a cold winter. The ice bomb experiment, seen below, is perhaps the the most dramatic example of water expanding when frozen.

In the video, water is poured into a cast iron container, which is tightly sealed. The container is then placed in a acetone/dry ice sludge, which is at a temperature of -77°C. After a short period of time, the ice freezes, expands, and causes the cast iron container to explode, blasting off the cover of the acetone/dry ice bath, and spraying the bath itself everywhere. Even though the cast iron container had ⅛ inch thick sides, the pressure of the expanding ice was still able to blow it apart.

Since water has maximum density at 4°C, water at that temperature sinks to the bottom of a deep lake, providing a relatively uniform environment all year around. If ice sank to the bottom, as most freezing liquids would, the surface of a lake would not be insulated from cold winter air. The remaining water would crystallize much more rapidly than it actually does. In a world where ice was denser than water, fish and other aquatic organisms would have to be able to withstand freezing for long periods.

Hydrogen bonding also contributes to the abnormally large quantities of heat that are required to melt, boil, or raise the temperature of a given quantity of water. Heat energy is required to break hydrogen bonds as well as to make water molecules move faster, and so a given quantity of heat raises the temperature of a gram of water less than for almost any other liquid. Even at 100°C there are still a great many unbroken hydrogen bonds, and almost 4 times as much heat is required to vaporize a mole of water than would be expected if there were no hydrogen bonding. This extra-large energy requirement is the reason that water has a higher boiling point than any of the other hydrides.

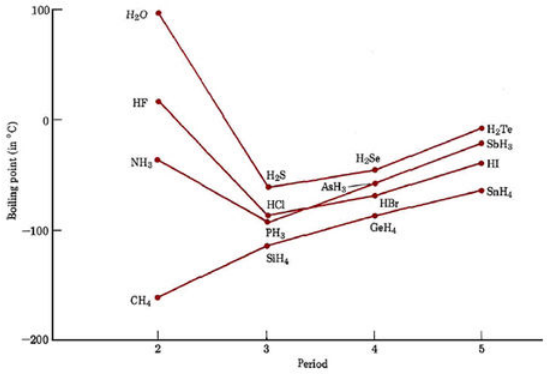


Figure **1.4.6.2** The boiling points of the hydrides of the nonmetals plotted against the period in which they occur in the periodic table. Note the anomalously high boiling points of H_2O, HF, and NH_3 in the second period.

The fact that it takes a lot of heat to melt, boil, or increase the temperature of water, makes this liquid ideal for transferring heat from one place to another. Water is used by engineers in automobile radiators, hot-water heating systems, and solar-energy collectors. More significantly, circulation (in the bloodstream) and evaporation (from the skin) of water regulate the temperature of the human body. (You are between 55 and 65 percent water if female and between 65 and 75 percent water if male.) Because of this (as well as for many other reasons) water is an important component of living systems. Water's ability to store heat energy is also a major factor affecting world climate. Persons who live near large lakes or oceans experience smaller fluctuations in temperature between winter and summer than those who inhabit places like Siberia, thousands of kilometers from a sizable body of water. Ocean currents, such as the Gulf Stream, convey heat from the tropics to areas which otherwise would be quite cold. It is interesting to ask, for example, whether European civilization could have developed without the aid of warmth transported by the common, but highly unusual, liquid—water.

This page titled 1.4.6: Ice and Water is shared under a CC BY-NC-SA 4.0 license and was authored, remixed, and/or curated by Ed Vitz, John W. Moore, Justin Shorb, Xavier Prat-Resina, Tim Wendorff, & Adam Hahn.

- **8.12: Ice and Water** by Ed Vitz, John W. Moore, Justin Shorb, Xavier Prat-Resina, Tim Wendorff, & Adam Hahn is licensed CC BY-NC-SA 4.0.

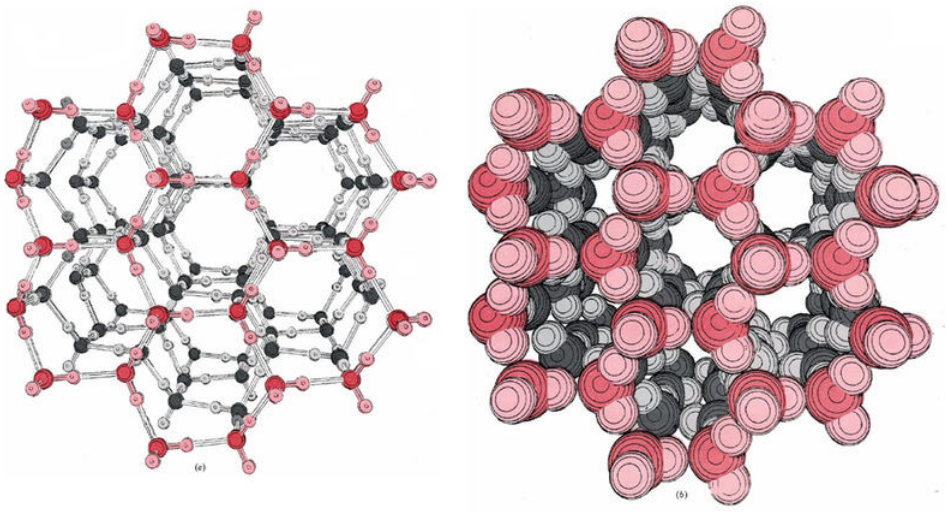
1.4.6.1: Ice; a hexagonal crystal.jpg

File:Ice; a hexagonal crystal.jpg

From ChemPRIME

Jump to: navigation, search

- File
- File history
- File links
- Metadata



Size of this preview: 800 × 444 pixels

Full resolution (900 × 500 pixels, file size: 343 KB, MIME type: image/jpeg)

Description	Ice; a Hexagonal Crystal
Keywords	Crystals / Crystallography , Water / Water Chemistry
Date	1978
Source	From Moore, Collins, Davies. "Chemistry" McGraw-Hill Companies. 1978.
Author	Moore, Collins, Davies
Permission	Attribution-Noncommercial-Share Alike 3.0 Unported

File history

Click on a date/time to view the file as it appeared at that time.

(Latest | Earliest) View (newer 50) (older 50) (20 | 50 | 100 | 250 | 500)

	Date/Time	Thumbnail	Dimensions	User	Comment
current	15:59, 16 March 2009		900×500 (343 KB)	WikiSysop (Talk | contribs)	

(Latest | Earliest) View (newer 50) (older 50) (20 | 50 | 100 | 250 | 500)

- Edit this file using an external application (See the setup instructions for more information)

File links

The following file redirects to this file:

- File:Chapter 8 page 19-1sum.jpg

The following 8 pages link to this file:

- CoreChem:Ice and Water
- UAVU Water and Ice
- User:Dzygas
- User:Vitz/play
- Ice and Water in Sports, Physiology & Health/Home Run Distance and Humidity
- User:Vitz/WaterIce
- Ice and Water in the Environment/Burning Ice: Clathrate Hydrates
- User talk:Vitz/play

Metadata

This file contains additional information, probably added from the digital camera or scanner used to create or digitize it. If the file has been modified from its original state, some details may not fully reflect the modified file.

Orientation	Normal
Horizontal resolution	72 dpi
Vertical resolution	72 dpi
Software used	Adobe Photoshop CS3 Windows
File change date and time	15:49, 23 September 2008
Color space	sRGB

Retrieved from "wiki.chemprime.chemeddl.org/i...al_crystal.jpg"
Categories: Crystals / Crystallography | Water / Water Chemistry

LibreTexts

Toolbox

- What links here
- Related changes
- Upload file
- Special pages
- Printable version
- Permanent link

- This page was last modified on 29 April 2010, at 19:04.
- This page has been accessed 4,308 times.
- Content is available under Attribution-Noncommercial-Share Alike 3.0 Unported.
- Privacy policy
- About ChemPRIME
- Disclaimers

This page titled 1.4.6.1: <pic> Ice; a hexagonal crystal.jpg is shared under a CC BY-NC-SA 4.0 license and was authored, remixed, and/or curated by Ed Vitz, John W. Moore, Justin Shorb, Xavier Prat-Resina, Tim Wendorff, & Adam Hahn.

- **8.12.1: Ice; a hexagonal crystal.jpg** by Ed Vitz, John W. Moore, Justin Shorb, Xavier Prat-Resina, Tim Wendorff, & Adam Hahn is licensed CC BY-NC-SA 4.0.

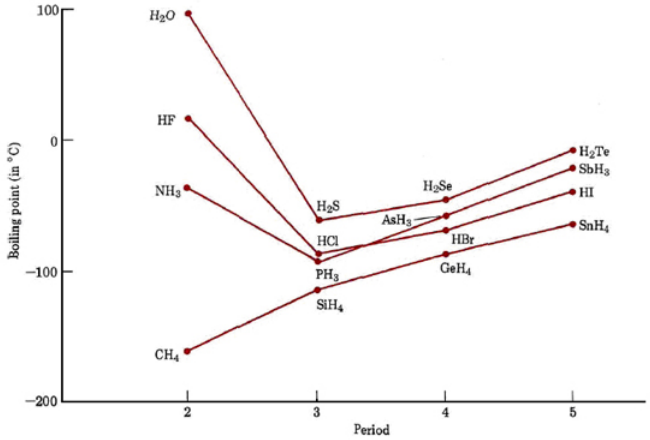
1.4.6.2: Boiling Points of Hydrides

File:Nonmetal hydride bp.jpg

From ChemPRIME

Jump to: navigation, search

- File
- File history
- File links
- Metadata



No higher resolution available.

Nonmetal_hydride_bp.jpg (582 × 370 pixels, file size: 78 KB, MIME type: image/jpeg)

Description	The Boiling Points of the Hydrides of the Nonmetals Plotted Against the Period in Which They Occur in the Periodic Table
Keywords	Periodicity / Periodic Table , Physical Properties
Date	1978
Source	From Moore, Collins, Davies. "Chemistry" McGraw-Hill Companies. 1978.
Author	Moore, Collins, Davies
Permission	Attribution-Noncommercial-Share Alike 3.0 Unported

File history

Click on a date/time to view the file as it appeared at that time.

(Latest | Earliest) View (newer 50) (older 50) (20 | 50 | 100 | 250 | 500)

	Date/Time	Thumbnail	Dimensions	User	Comment
current	15:59, 16 March 2009		582×370 (78 KB)	WikiSysop (Talk | contribs)	

(Latest | Earliest) View (newer 50) (older 50) (20 | 50 | 100 | 250 | 500)

- Edit this file using an external application (See the setup instructions for more information)

File links

The following file redirects to this file:

- File:Chapter 8 page 17small.jpg

The following 3 pages link to this file:

- CoreChem:Hydrogen Bonding: Water
- Boiling Points of Hydrides
- Hydrogen Bonding: Water in Sports, Physiology & Health/Home Run Distance and Humidity

Metadata

This file contains additional information, probably added from the digital camera or scanner used to create or digitize it. If the file has been modified from its original state, some details may not fully reflect the modified file.

Orientation	Normal
Horizontal resolution	72 dpi
Vertical resolution	72 dpi
Software used	Adobe Photoshop CS3 Windows
File change date and time	15:40, 23 September 2008
Color space	sRGB

Retrieved from "wiki.chemprime.chemeddl.org/i...hydride_bp.jpg"
Categories: Periodicity / Periodic Table | Physical Properties

Views

- File
- Talk
- View source
- History

Personal tools

- Log in

Navigation

- Main Page
- Site News
- Collaboration
- Student Assignments
- Recent changes
- Random page
- ChemEd DL
- Find Resources
- Help

Search

Toolbox

- What links here
- Related changes
- Upload file
- Special pages
- Printable version

- Permanent link



- This page was last modified on 29 April 2010, at 19:33.
- This page has been accessed 3,502 times.
- Content is available under Attribution-Noncommercial-Share Alike 3.0 Unported.
- Privacy policy
- About ChemPRIME
- Disclaimers

This page titled 1.4.6.2: Boiling Points of Hydrides is shared under a CC BY-NC-SA 4.0 license and was authored, remixed, and/or curated by Ed Vitz, John W. Moore, Justin Shorb, Xavier Prat-Resina, Tim Wendorff, & Adam Hahn.

- **8.12.2: Boiling Points of Hydrides** by Ed Vitz, John W. Moore, Justin Shorb, Xavier Prat-Resina, Tim Wendorff, & Adam Hahn is licensed CC BY-NC-SA 4.0.

1.4.7: Macromolecular Substances

Up to this point we have confined our discussion to covalently bonded substances consisting of small discrete molecules. The forces between these molecules are quite weak compared with covalent bonds. There are some covalently bonded substances, however, in which no small individual molecules exist. These substances contain extremely large molecules, and so they are called **macromolecular substances**. They are invariably solids at room temperature. Quite often we can regard each crystal of the substance as a *single molecule*.

This page titled 1.4.7: Macromolecular Substances is shared under a CC BY-NC-SA 4.0 license and was authored, remixed, and/or curated by Ed Vitz, John W. Moore, Justin Shorb, Xavier Prat-Resina, Tim Wendorff, & Adam Hahn.

- **8.20: Macromolecular Substances** by Ed Vitz, John W. Moore, Justin Shorb, Xavier Prat-Resina, Tim Wendorff, & Adam Hahn is licensed CC BY-NC-SA 4.0.

1.4.8: Diamond and Graphite

The simplest example of a macromolecular solid is *diamond*. Crystals of diamond contain only carbon atoms, and these are linked to each other by covalent bonds in a giant three-dimensional network, as shown below. Note how each carbon atom is surrounded tetrahedrally by four bonds.

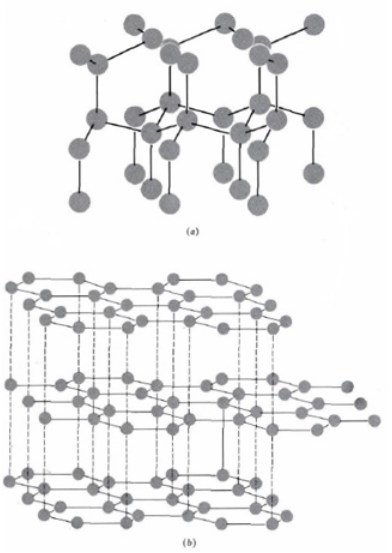


Figure **1.4.8.1** The crystal structure of (a) diamond and (b) graphite.

Such a network of carbon atoms extends throughout the crystal so that the whole diamond is one extremely large covalently bonded entity, i.e., a macromolecule.

Because strong covalent bonds, rather than London forces or dipole forces, hold the carbon atoms together in this crystal, it takes a great deal of energy to separate them. Accordingly, diamond has an extremely high melting point, 3550°C—much higher than any ionic solid. Diamond is also the hardest substance known. Each carbon atom is held firmly in its place from all sides and is thus very difficult to displace or remove.

Carbon also exists in a second, more familiar, crystalline form called *graphite*, whose crystal structure is also shown in part *b* of the figure. You use graphite every time you write with a pencil. (Pencil leads consist of C, not Pb!) The structure of graphite consists of flat layers. In each layer the carbon atoms are arranged in a regular hexagonal array. We can regard each layer as a large number of benzene rings fused together to form a gigantic honeycomb. All carbon-carbon bonds in this honeycomb are equivalent and intermediate in character between a single and a double bond.

While there are strong covalent bonds between the carbon atoms in a given plane, only weak London forces attract the planes together. The various layers can therefore slide past each other quite easily. When a pencil lead rubs across paper, the planes slide past each other and thin plates of crystal are left behind on the paper. These sliding plates also make graphite useful as a lubricant.

When an element can exist in more than one crystalline form, as carbon can in diamond and graphite, each form is said to be an **allotrope**. Other elements, such as sulfur and phosphorus, also form allotropes.

This page titled 1.4.8: Diamond and Graphite is shared under a CC BY-NC-SA 4.0 license and was authored, remixed, and/or curated by Ed Vitz, John W. Moore, Justin Shorb, Xavier Prat-Resina, Tim Wendorff, & Adam Hahn.

- **8.21: Diamond and Graphite** by Ed Vitz, John W. Moore, Justin Shorb, Xavier Prat-Resina, Tim Wendorff, & Adam Hahn is licensed CC BY-NC-SA 4.0.

1.4.9: Silicon Dioxide

Silicon dioxide, or silica, (SiO_2) is another important example of a macromolecular solid. Silica can exist in six different crystalline forms. The best known of these is *quartz*, whose crystal structure shown previously is shown again below.

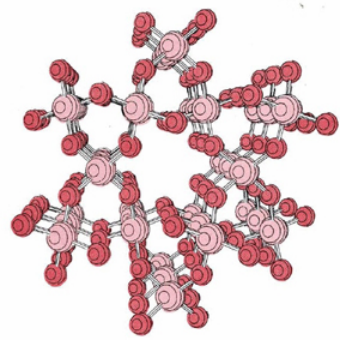
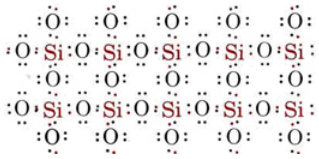


Figure **1.4.9.1** A portion of the giant covalent molecule $(SiO_2)_n$. The lattice shown would extend indefinitely in all directions in a macroscopic crystal. Each silicon atom (light color) is covalently bonded to four oxygen atoms (dark color). Each oxygen bonds to two silicons. The ratio of silicon to oxygen is 2:4 or 1:2, in accord with the formula. Computer-generated. (Copyright © 1976 by W. G. Davies and J. W. Moore.)

Sand consists mainly of small fragments of quartz crystals. Quartz has a very high melting point, though not so high as diamond.

If you refer back to the examples on silicon, you can remind yourself of the reason that SiO_2 is macromolecular. Silicon is reluctant to form multiple bonds, and so discrete $O{=}Si{=}O$ molecules, analogous to $O{=}C{=}O$, do not occur. In order to satisfy silicon's valence of 4 and oxygen's valence of 2, each silicon must be surrounded by four oxygens and each oxygen by two silicons. This can be represented schematically by the Lewis diagram



This page titled 1.4.9: Silicon Dioxide is shared under a CC BY-NC-SA 4.0 license and was authored, remixed, and/or curated by Ed Vitz, John W. Moore, Justin Shorb, Xavier Prat-Resina, Tim Wendorff, & Adam Hahn.

- **8.22: Silicon Dioxide** by Ed Vitz, John W. Moore, Justin Shorb, Xavier Prat-Resina, Tim Wendorff, & Adam Hahn is licensed CC BY-NC-SA 4.0.

1.4.10: Synthetic Macromolecules- Some Applied Organic Chemistry

Other important classes of substances containing very large molecules are the plastics and artificial fibers, which are such a conspicuous, though not always a positive, feature of modern life.

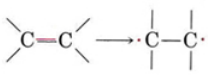
Most of these materials are made in the same basic way. The starting materials or monomers are relatively simple molecules—usually carbon compounds derived from petroleum—which can be persuaded to link up with each other in order to form a long chain of repeating units called a **polymer**. If we think of the monomer as a bead, then the polymer corresponds to a string of beads. Polymers are usually classified into two types: **addition polymers** and **condensation polymers**, according to the kind of reaction by which they are made.

This page titled 1.4.10: Synthetic Macromolecules- Some Applied Organic Chemistry is shared under a CC BY-NC-SA 4.0 license and was authored, remixed, and/or curated by Ed Vitz, John W. Moore, Justin Shorb, Xavier Prat-Resina, Tim Wendorff, & Adam Hahn.

- **8.23: Synthetic Macromolecules- Some Applied Organic Chemistry** by Ed Vitz, John W. Moore, Justin Shorb, Xavier Prat-Resina, Tim Wendorff, & Adam Hahn is licensed CC BY-NC-SA 4.0.

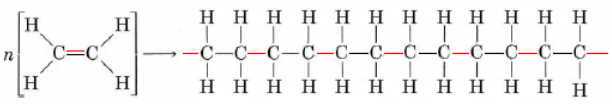
1.4.11: Addition Polymers

Addition polymers are usually made from a monomer containing a double bond. We can think of the double bond as "opening out" in order to participate in two new single bonds in the following way:



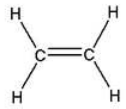
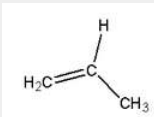
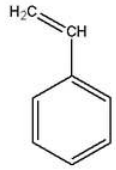
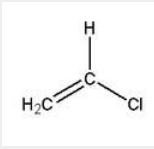
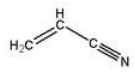
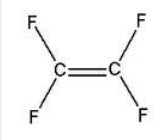
One of the lines in a double bond is highlighted in red. An arrow points from this double bond to a single bond in which each carbon now has one free electron each.

Thus, if ethene is heated at moderate temperature and pressure in the presence of an appropriate catalyst, it polymerizes:



Polymerization of ethene equation shows an indefinite amount of repeating ethene structure forming a long carbon chain.

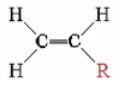
Table **1.4.11.1**: Some Common Addition Polymers.

Monomer	Nonsystematic Name	Polymer	Some Typical Uses
	Ethylene	Polyethylene	Film for packaging and bags, toys, bottles, coatings
	Propylene	Polypropylene	Milk cartons, rope, outdoor carpeting
	Styrene	Polystyrene	Transparent containers, plastic glasses, refrigerators, styrofoam
	Vinyl chloride	Polyvinyl chloride, PVC	Pipe and tubing, raincoats, curtains, phonograph records, luggage, floor tiles
	Acrylonitrile	Polyacrylonitrile (Orlon, Acrilan)	Textiles, ruga
	Tetrafluoroethylene	Teflon	Nonstick pan coatings, bearings, gaskets

The result is the familiar waxy plastic called polyethylene, which at a molecular level consists of a collection of long-chain alkane molecules, most of which contain tens of thousands of carbon atoms. There is only an occasional short branch chain.

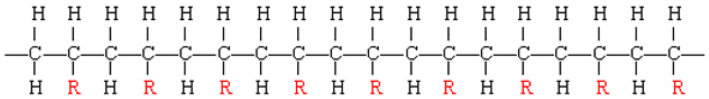
Polyethylene is currently manufactured on a very large scale, larger than any other polymer, and is used for making plastic bags, cheap bottles, toys, etc. Many of its properties are what we would expect from its molecular composition. The fact that it is a mixture of molecules each of slightly different chain length (and hence slightly different melting point) explains why it softens over a range of temperatures rather than having a single melting point. Because the molecules are only held together by London forces, this melting and softening occurs at a rather low temperature. (Some of the cheaper varieties of polyethylene with shorter chains and more branch chains will even soften in boiling water.) The same weak London forces explain why polyethylene is soft and easy to scratch and why it is not very ‘strong mechanically.'

The table above lists some other well-known addition polymers and also some of their uses. You can probably find at least one example of each of them in your home. Except for Teflon, all these polymers derive from a monomer of the form.



Structure shows "C" double bond "C". One "C" is single bonded to two "H". The other "C" is bonded to 1 "H" and one other "R" group.

The resulting polymer thus has the general form:



Repeating pattern in polymer show "C" "H" 2 single bond "C" "H" "R" single bond "C" "H" 2 and so on.

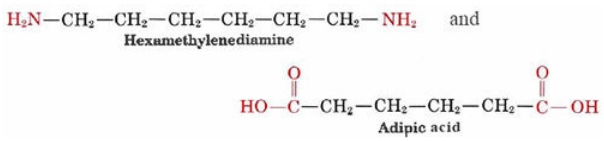
By varying the nature of the R group, the physical properties of the polymer can be controlled rather precisely.

This page titled 1.4.11: Addition Polymers is shared under a CC BY-NC-SA 4.0 license and was authored, remixed, and/or curated by Ed Vitz, John W. Moore, Justin Shorb, Xavier Prat-Resina, Tim Wendorff, & Adam Hahn.

- **8.24: Addition Polymers** by Ed Vitz, John W. Moore, Justin Shorb, Xavier Prat-Resina, Tim Wendorff, & Adam Hahn is licensed CC BY-NC-SA 4.0.

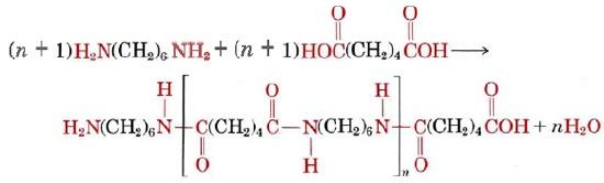
1.4.12: Condensation Polymers

When addition polymers are formed, no by-products result. Formation of a condensation polymer, on the other hand, produces H_2O, HCl, or some other simple molecule which escapes as a gas. A familiar example of a condensation polymer is *nylon*, which is obtained from the reaction of two monomers



Structure of hexamethylenediamine. Its "N" "H" 2 groups are highlighted in color. Structure of adipic acid is also shown with its "C" double bond "O" single bond "O" "H" highlighted in color.

These two molecules can link up with each other because each contains a reactive functional group, either an amine or a carboxylic acid which reacts to form an amide linkage. They combine as follows:



Equation shows the "N" "H" 2 functional group of an amine reacting with a "C" "O" "O" "H" group from a carboxylic acid. This forms a "N" "H" "C" double bond "O" group linkage between the two reactants. Water is a byproduct.

Below is a video of the reaction to form nylon. This reaction is slightly modified from the one described above, as adipoyl chloride, not adipic acid, is used as a reactant. Thus HCl, not H_2O is produced. This also means that the chain terminates in an acid chloride, rather than the carboxylic acid shown above. Note that an amide linkage is still formed.

A solution of adipoyl chloride in cyclohexane is poured on top of an aqueous solution of 1,6-diaminohexane in a beaker. Nylon (6,6) polyamide is formed at the interface of the two immiscible liquids and is carefully drawn from the solution and placed on a glass rod. The rod is then spun, and the Nylon (6,6) polyamide is spun onto the rod.

Well-known condensation polymers other than nylon are Dacron, Bakelite, melamine, and Mylar. Nylon makes extremely strong threads and fibers because its long-chain molecules have stronger intermolecular forces than the London forces of polyethylene. Each N—H group in a nylon chain can hydrogen bond to the O of a C=O group in a neighboring chain, as shown below. Therefore the chains cannot slide past one another easily.

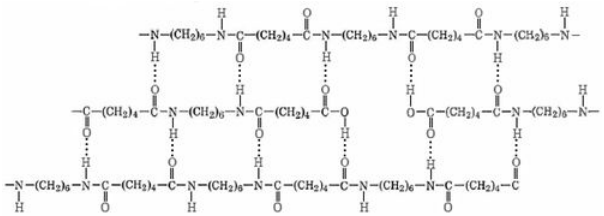


Figure **1.4.12.1**: The three nylon molecules are held together by hydrogen bonding. The N-H group of one chain hydrogen bonds to the C=O group of another chain. This makes nylon quite strong and difficult to pull apart.

If you pull on both ends of a nylon thread, for example, it will only stretch slightly. After that it will strongly resist breaking because a large number of hydrogen bonds are holding overlapping chains together. The same is not true of a polyethylene thread in which only London forces attract overlapping chains together, and this is one reason that polyethylene is not used to make thread.

This page titled 1.4.12: Condensation Polymers is shared under a CC BY-NC-SA 4.0 license and was authored, remixed, and/or curated by Ed Vitz, John W. Moore, Justin Shorb, Xavier Prat-Resina, Tim Wendorff, & Adam Hahn.

- **8.25: Condensation Polymers** by Ed Vitz, John W. Moore, Justin Shorb, Xavier Prat-Resina, Tim Wendorff, & Adam Hahn is licensed CC BY-NC-SA 4.0.

1.4.13: Cross-Linking

The formation of covalent bonds which hold portions of several polymer chains together is called **cross-linking**. Extensive cross-linking results in a random three-dimensional network of interconnected chains, as shown in the figure. As one might expect, extensive cross-linking produces a substance which has more rigidity, hardness, and a higher melting point than the equivalent polymer without cross-linking. Almost all the hard and rigid plastics we use are cross-linked. These include *Bakelite*, which is used in many electric plugs and sockets, *melamine*, which is used in plastic crockery, and epoxy resin glues.

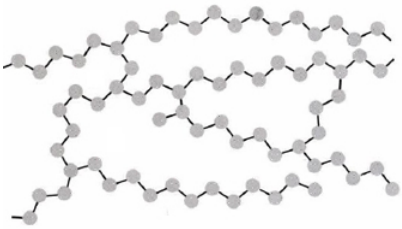
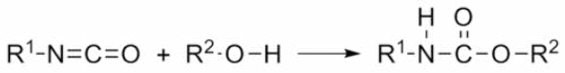


Figure **1.4.13.1**: A cross-linked polymer. For purposes of clarity, hydrogen atoms and side chains have been omitted, and only the carbon atoms in the chains are shown. Note that the cross links between chains occur at random.

Below is a video of the formation of Polyurethane Foam.



Polyether polyol, a blowing agent, which adds a gas to the mixture to produce a foam, silicone surfactant, and a catalyst is mixed with a second liquid contains a polyfunctional isocyanate. The polyol and the polyfunctional isocyanate react to form polyurethane - a very hard substance when dried. The general reaction is shown below:



isocyanate group **hydroxyl group urethane linkage**

"R" 1 single bond "N" double bond "C" double bond "O" reacts with "R" 2 single bond "O" single bond "H" to give "R" 1 single bond "N" "H" single bond "C" double bond "O" single bond "O" single bond "R" 2.

In the reaction in the video, each R^1 group has multiple isocyanate groups; the reactants are polyfunctional. Thus there is a high degree of cross-linking in the polyurethane. This causes the foam to become rigid after cooling.

This page titled 1.4.13: Cross-Linking is shared under a CC BY-NC-SA 4.0 license and was authored, remixed, and/or curated by Ed Vitz, John W. Moore, Justin Shorb, Xavier Prat-Resina, Tim Wendorff, & Adam Hahn.

- **8.26: Cross-Linking** by Ed Vitz, John W. Moore, Justin Shorb, Xavier Prat-Resina, Tim Wendorff, & Adam Hahn is licensed CC BY-NC-SA 4.0.

1.5: Acid and Base Naming

1.5: Acid and Base Naming is shared under a not declared license and was authored, remixed, and/or curated by LibreTexts.

1.5.1: Polyatomic Ions



Figure 1.5.1.1 (Public Domain; Huhu via Wikipedia)

Have you ever read the story of Romeo and Juliet?

Shakespeare wrote, "A rose by any other name would smell as sweet" as part of the romantic balcony scene between Romeo and Juliet in the famous play. The two families were bitter rivals, but Juliet meant this statement to mean that she loved Romeo no matter what his name was. Some names are simple—we know Romeo mainly as Romeo. Most of us have a first name, middle name (often not used), and last name. In some cultures, names will be much more complex. The full name of the famous 20th century artist Pablo Picasso is Pablo Diego José Francisco de Paula Juan Neponuceno María de los Remedios Cipriano de la Santísima Trinidad Martyr Patricio Clito Ruíz y Picasso.

Many materials exist as simply binary compounds composed of a metal cation and a nonmetal anion, with each ion consisting of only one type of atom. Other combinations of atoms also exist, either as larger ionic complexes or complete molecules. Some of the most useful materials we work with contain polyatomic ions.

Polyatomic Ions

A **polyatomic** ion is an ion composed of more than one atom. The ammonium ion consists of one nitrogen atom and four hydrogen atoms. Together, they comprise a single ion with a $1+$ charge and a formula of $\mathrm{NH_4^+}$. The carbonate ion consists of one carbon atom and three oxygen atoms, and carries an overall charge of $2-$. The formula of the carbonate ion is $\mathrm{CO_3^{2-}}$. The atoms of a polyatomic ion are tightly bonded together, and so the entire ion behaves as a single unit. The figures below show several models.

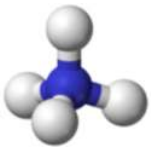


Figure 1.5.1.2: The ammonium ion ($\mathrm{NH_4^+}$) is a nitrogen atom (blue) bonded to four hydrogen atoms (white). (Public Domain; Ben Mills (Wikimedia: Benjah-bmm27) via Wikipedia)



Figure 1.5.1.3: The hydroxide ion ($\mathrm{OH^-}$) is an oxygen atom (red) bonded to a hydrogen atom. (Public Domain; Ben Mills (Wikimedia: Benjah-bmm27) via Wikipedia)

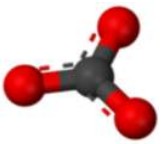


Figure 1.5.1.4: The carbonate ion ($\mathrm{CO_3^{2-}}$) is a carbon atom (black) bonded to three oxygen atoms. (Public Domain; Ben Mills (Wikimedia: Benjah-bmm27) via Wikipedia)

The table below lists a number of polyatomic ions by name and by formula. The heading for each column indicates the charge on the polyatomic ions in that group. Note that the vast majority of the ions listed are anions—there are very few polyatomic cations.

Table 1.5.1.1: Common Polyatomic Ions

1−	2−	3−	1+	2+
acetate, CH_3COO^-	carbonate, CO_3^{2-}	arsenate, AsO_3^{3-}	ammonium, NH_4^+	dimercury, Hg_2^{2+}
bromate, BrO_3^-	chromate, CrO_4^{2-}	phosphite, PO_3^{3-}		
chlorate, ClO_3^-	dichromate, $Cr_2O_7^{2-}$	phosphate, PO_4^{3-}		
chlorite, ClO_2^-	hydrogen phosphate, HPO_4^{2-}			
cyanide, CN^-	oxalate, $C_2O_4^{2-}$			
dihydrogen phosphate, $H_2PO_4^-$	peroxide, O_2^{2-}			
hydrogen carbonate, HCO_3^-	silicate, SiO_3^{2-}			
hydrogen sulfate, HSO_4^-	sulfate, SO_4^{2-}			
hydrogen sulfide, HS^-	sulfite, SO_3^{2-}			
hydroxide, OH^-				
hypochlorite, ClO^-				
nitrate, NO_3^-				
nitrite, NO_2^-				
perchlorate, ClO_4^-				
permanganate, MnO_4^-				

The vast majority of polyatomic ions are anions, many of which end in *-ate* or *-ite*. Notice that in some cases, such as nitrate (NO_3^-) and nitrite (NO_2^-), there are multiple anions that consist of the same two elements. In these cases, the difference between the ions is in the number of oxygen atoms present, while the overall charge is the same. As a class, these are called oxoanions. When there are two oxoanions for a particular element, the one with the greater number of oxygen atoms gets the *-ate* suffix, while the one with the fewer number of oxygen atoms gets the *-ite* suffix. The four oxoanions of chlorine are as follows:

- ClO^-, hypochlorite
- ClO_2^-, chlorite
- ClO_3^-, chlorate
- ClO_4^-, perchlorate

In cases such as this, the ion with one more oxygen atom than the *-ate* anion is given a *per-* prefix. The ion with one fewer oxygen atom than the *-ite* anion is given a *hypo-* prefix.



Summary

- Polyatomic ions contain more than one type of atom in the ion.
- The majority of polyatomic ions are anions that are named ending in *-ate* or *-ite*.
- Some anions have multiple forms and are named accordingly.

Review

1. Write the formulas for the following ions:
    a. ammonium
    b. carbonate
    c. sulfate
    d. phosphate
2. Name the following ions:
    1. PO_3^{3-}
    2. SiO_3^{2-}
    3. OH^-
    4. MnO_4^-

1.5.1: Polyatomic Ions is shared under a CC BY-NC license and was authored, remixed, and/or curated by LibreTexts.

- **7.9: Polyatomic Ions** by CK-12 Foundation is licensed CK-12. Original source: https://flexbooks.ck12.org/cbook/ck-12-chemistry-flexbook-2.0/.

1.5.2: Naming Acids



Figure 1.5.2.1 (CK-12 Curriculum Materials license; CK-12 Foundation via CK-12 Foundation)

How is gold tested?

A spot test for gold has been in use for decades. The sample is first treated with nitric acid. Other metals may react or dissolve in this acid, but gold will not. Then the sample is added to a mixture of nitric acid and hydrochloric acid. Gold will only dissolve in this mixture. The term "acid test" arose from the California gold rush in the late 1840s, when this combination was used to test for the presence of real gold. It has since come to mean "tested and approved" in a number of fields.

Acids

An **acid** can be defined in several ways. The most straightforward definition is that an acid is a molecular compound that contains one or more hydrogen atoms and produces hydrogen ions (H^+) when dissolved in water.



Figure 1.5.2.2: (A) Vinegar comes in a variety of types, but all contain acetic acid. (B) Citrus fruits like grapefruit contain citric and ascorbic acids. (CC BY 2.0; (A) Becky Cortino; (B) Flickr: isox4 via (A) http://www.flickr.com/photos/mediasavvy/8239231530; (B) http://www.flickr.com/photos/isox4/5167980026)

This is a different type of compound than the others we have seen so far. Acids are molecular, which means that in their pure state they are individual molecules and do not adopt the extended three-dimensional structures of ionic compounds like $NaCl$. However, when these molecules are dissolved in water, the chemical bond between the hydrogen atom and the rest of the molecule breaks, leaving a positively-charged hydrogen ion and an anion. This can be symbolized in a chemical equation:

$$HCl \rightarrow H^+ + Cl^-$$

Since acids produce H^+ cations upon dissolving in water, the H of an acid is written first in the formula of an inorganic acid. The remainder of the acid (other than the H) is the anion after the acid dissolves. Organic acids are also an important class of compounds, but will not be discussed here. A **binary acid** is an acid that consists of hydrogen and one other element. The most common binary acids contain a halogen. An **oxoacid** is an acid that consists of hydrogen, oxygen, and a third element. The third element is usually a nonmetal.

Naming Acids

Since all acids contain hydrogen, the name of an acid is based on the anion that goes with it. These anions can either be monatomic or polyatomic. The name of all monatomic ions ends in *-ide*. The majority of polyatomic ions end in either *-ate* or *-ite*, though there are a few exceptions such as the cyanide ion (CN^-). It is the suffix of the anion that determines how the acid is named, as displayed in the rules and table below.

Table 1.5.2.1: Naming System for Acids

Anion Suffix	Example	Name of Acid	Example
-ide	chloride (Cl^-)	hydro_____ic acid	hydrochloric acid (HCl)
-ate	sulfate (SO_4^{2-})	_____ic acid	sulfuric acid (H_2SO_4)
-ite	nitrite (NO_2^-)	____ous acid	nitrous acid (HNO_2)

The three different suffixes that are possible for the anions lead to three rules:

1. When the anion ends in *-ide*, the acid name begins with the prefix *hydro-*. The root of the anion name goes in the blank (*chlor* for chloride), followed by the suffix *-ic*. HCl is hydrochloric acid because Cl^- is the chloride ion. HCN is hydrocyanic acid because CN^- is the cyanide ion.
2. When the anion ends in *-ate*, the name of the acid is the root of the anion followed by the suffix *-ic*. There is no prefix. H_2SO_4 is sulfuric acid (not sulfic) because SO_4^{2-} is the sulfate ion.
3. When the anion ends in *-ite*, the name of the acid is the root of the anion followed by the suffix *-ous*. Again, there is no prefix. HNO_2 is nitrous acid because NO_2^- is the nitrite ion.

Note how the root for a sulfur-containing oxoacid is *sulfur-* instead of just *sulf-*. The same is true for a phosphorus-containing oxoacid. The root is *phosphor-* instead of simply *phosph-*.

Many foods and beverages contain citric acid. Vinegar is a dilute solution of acetic acid. Car batteries contain sulfuric acid that helps in the release of electrons to create electricity.

Writing Formulas for Acids

Like other compounds that we have studied, acids are electrically neutral. Therefore, the charge of the anion part of the formula must be exactly balanced out by the H^+ ions. Since H^+ ions carry a single positive charge, the number of H^+ ions in the formula is equal to the quantity of negative charge on the anion. Two examples from the table above illustrate this point. The chloride ion carries a $1-$ charge, so only one H is needed in the formula of the acid (HCl). The sulfate ion carries a $2-$ charge, so two Hs are needed in the formula of the acid (H_2SO_4). Another way to write the correct formula is to utilize the crisscross method, shown below for sulfuric acid.

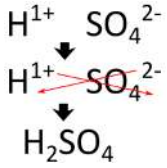
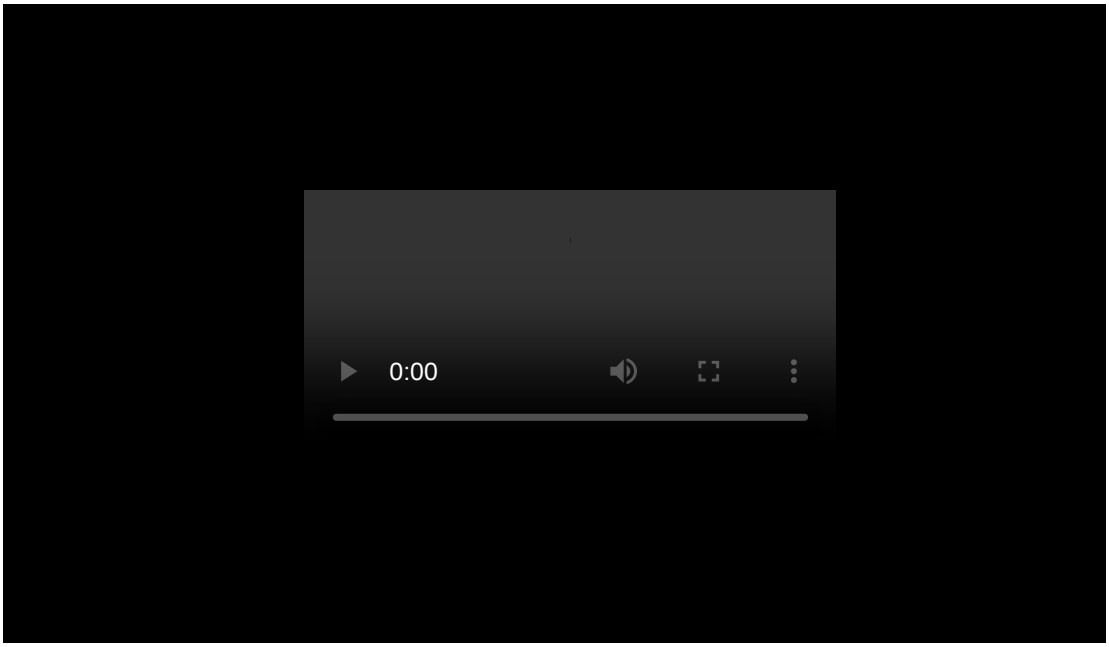


Figure **1.5.2.3**: Crisscross approach to writing the formula for sulfuric acid. (CC BY-NC 3.0; Joy Sheng via CK-12 Foundation)



Summary

- Acids are molecular compounds that release hydrogen ions.
- A binary acid consists of hydrogen and one other element.
- Oxoacids contain hydrogen, oxygen, and one other element.
- The name of the acid is based on the anion attached to the hydrogen.
- Writing formulas for acids follows the same rules as for binary ionic compounds.

Review

1. Define “acid.”
2. What is a binary acid?
3. What is an oxoacid?

4. Name the following acids:
    a. H_2SO_4
    b. HCN
    c. HCl
    d. H_3PO_4
5. Write formulas for the following acids:
    a. hydrobromic acid
    b. perchloric acid
    c. nitrous acid

1.5.2: Naming Acids is shared under a CC BY-NC license and was authored, remixed, and/or curated by LibreTexts.

- **7.12: Acids - Naming and Formulas** by CK-12 Foundation is licensed CK-12. Original source: https://flexbooks.ck12.org/cbook/ck-12-chemistry-flexbook-2.0/.

1.5.3: Names and Formulas of Bases



Figure 1.5.3.1 (Public Domain; Unknown Author via Wikipedia)

What different things are these workers doing to make soap?

Soap making has a long history. Until recently, soap was made using animal fats and lye from wood ashes. The lye served as a base to break down the fats and help form the soap. Needless to say, unless the soap was washed to remove the lye, it was very harsh on the skin. Many families would make their own soap by boiling the lye and fat in a large kettle over an open fire—a long and hot task.

Bases

A **base** can be simply defined as an ionic compound that produces **hydroxide ions** when dissolved in water. One of the most commonly used bases is sodium hydroxide, illustrated below.

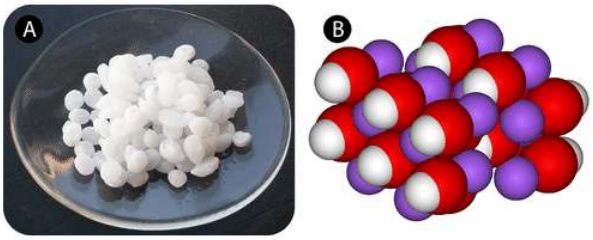


Figure 1.5.3.2: (A) Sodium hydroxide, a base, is a solid that is typically produced as small white pellets. (B) The structure of sodium hydroxide is an extended three-dimensional network. The purple spheres are the sodium ions (Na^+). The red and white spheres are oxygen and hydrogen atoms, respectively, which are bonded together to form hydroxide ions (OH^-). (Public Domain; (A) Martin Walker (Wikimedia: Walkerma); (B) Ben Mills (Wikimedia: Benjah-bmm27) via (A) http://commons.wikimedia.org/wiki/File:SodiumHydroxide.jpg; (B) http://commons.wikimedia.org/wiki/File:Sodium-hydroxide-crystal-3D-vdW.png)

Names and Formulas of Bases

There is no special system for naming bases. Since they all contain the OH^- anion, names of bases end in *hydroxide*. The cation is simply named first. Some examples of names and formulas for bases are shown in the table below.

Names and Formulas of Bases

Table 1.5.3.1

Formula	Name
$NaOH$	sodium hydroxide
$Ca(OH)_2$	calcium hydroxide
NH_4OH	ammonium hydroxide

Notice that because bases are ionic compounds, the number of hydroxides in the formula does not affect the name. The compound must be neutral, so the charges of the ions are balanced just as for other ionic compounds. The sodium ion (Na^+) requires one OH^-

ion to balance the charge, so the formula is $NaOH$. Calcium (Ca^{2+}) requires two OH^- ions to balance the charge, so the formula is $Ca(OH)_2$. Hydroxide ion is a polyatomic ion, and must be in parentheses when there is more than one in a formula.

Summary

- Bases are ionic compounds that produce hydroxide ions when dissolved in water.
- The cation is named first followed by "*hydroxide*."

Review

1. What is a base?
2. What is the charge on the hydroxide anion?
3. Name the following bases:
    a. LiOH
    b. $Mg(OH)_2$
    c. $Fe(OH)_3$
4. Write the formulas for the following bases:
    a. nickel (II) hydroxide
    b. aluminum hydroxide
    c. silver hydroxide

1.5.3: Names and Formulas of Bases is shared under a CC BY-NC license and was authored, remixed, and/or curated by LibreTexts.

- **7.13: Bases: Naming and Formulas** by CK-12 Foundation is licensed CK-12. Original source: https://flexbooks.ck12.org/cbook/ck-12-chemistry-flexbook-2.0/.

CHAPTER OVERVIEW

2: Nuclear Chemistry

Nuclear reactions differ from other chemical processes in one critical way: in a nuclear reaction, the identities of the elements change. In addition, nuclear reactions are often accompanied by the release of enormous amounts of energy, as much as a billion times more than the energy released by chemical reactions. Moreover, the yields and rates of a nuclear reaction are generally unaffected by changes in temperature, pressure, or the presence of a catalyst.

2.1: Components of the Nucleus
2.2: The Nuclear Atom
2.3: Atomic Structure and Isotopes
2.4: Isotopes
2.5: Transmutation and Radioactivity
2.6: Average Atomic Weights
2.7: Measurement of Atomic Weights
2.8: Nuclear Reactions
2.9: Nuclear Radiation
2.10: Rates of Radioactive Decay
2.11: Stability of the Atomic Nucleus
2.12: The Origin of the Elements
2.13: Transmutation of the Elements
2.14: Nuclear Fission
2.15: Nuclear Fusion
2.16: Nuclear Chemistry (Exercises)

2: Nuclear Chemistry is shared under a not declared license and was authored, remixed, and/or curated by LibreTexts.

2.1: Components of the Nucleus

24.03: Components of the Nucleus

2.1: Components of the Nucleus is shared under a not declared license and was authored, remixed, and/or curated by LibreTexts.

2.2: The Nuclear Atom

It should be clear by now that elements follow a periodic law, but atomic weight is inadequate for fully explaining this phenomenon. If ordered by atomic weight, chemical and physical properties will repeat at regular intervals, but there are clear exceptions to this behavior, for instance, K has a smaller atomic weight than Ar, but its properties would place it after Ar in terms of periodic behavior. All of this implies that there is another aspect to atomic structure to explain this law. Today, we know that such properties arise from a nuclear model of organization for atomic structure. The atom is not indivisible as Dalton suggested, but rather made up of a small, dense nucleus containing neutrons and protons, as well as rapidly moving electrons which take up the greater volume of an atom.

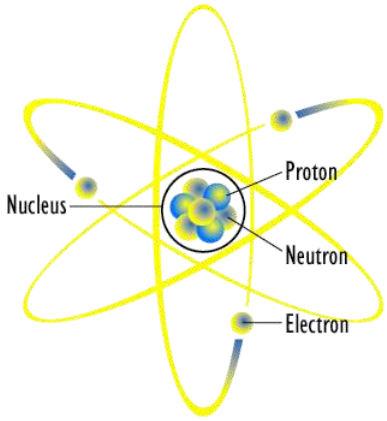


Diagram of atomic model shows a central circle representing the nucleus which contains the protons and neutrons. Outside of the nucleus are a few orbitals. Electrons are shown occupying these orbitals.

What led to this model? Beginning in the late 19th century a number of major experiments were performed. The results of these experiments helped scientists to formulate the current view of atomic structure. From this model of atomic structure, the origin of the periodicity of the elements can be more deeply explained. The order of the elements in the periodic table is dictated mostly by atomic weight which is directly related to the number of protons in the nucleus and the number of electrons surrounding the nucleus. The model of the Nuclear Atom reveals how the arrangement of electrons dictates the Periodic Law.

This page titled 2.2: The Nuclear Atom is shared under a CC BY-NC-SA 4.0 license and was authored, remixed, and/or curated by Ed Vitz, John W. Moore, Justin Shorb, Xavier Prat-Resina, Tim Wendorff, & Adam Hahn.

- **4.7: The Nuclear Atom** by Ed Vitz, John W. Moore, Justin Shorb, Xavier Prat-Resina, Tim Wendorff, & Adam Hahn is licensed CC BY-NC-SA 4.0.

2.3: Atomic Structure and Isotopes

The experimental facts described in the preceding section can be accounted for by assuming that any atom is made up of three kinds of **subatomic particles**.

1. The **electron** carries a charge of $-e$, has a mass about $\frac{1}{1837}$ that of a hydrogen atom, and occupies most of the volume of the atom.
2. The **proton** carries a charge of $+e$, has a mass about the same as a hydrogen atom, and is found within the very small volume of the nucleus.
3. The **neutron** carries no electric charge, has about the same mass as a hydrogen atom, and is found in the nucleus.

Some important properties of the three kinds of subatomic particles are listed in the following table. Experimental evidence for the existence of the neutron was first correctly interpreted in 1932 by James Chadwick (1891 to 1974), a discovery for which he was awarded the Nobel Prize in 1935.

Table **2.3.1**: Important Subatomic Particles and Some of Their Properties.

Particle	Mass (kg)	Electric Charge (C)	Location
Electron	9.1095×10^{-31}	-1.6022×10^{-19}	Outside nucleus
Proton	1.6726×10^{-27}	$+1.6022 \times 10^{-19}$	In nucleus
Neutron	1.6750×10^{-27}	0	In nucleus

The modern picture of a helium atom, which is made up of two electrons, two protons, and two neutrons, is shown below. Because each proton and each neutron has more than 1800 times the mass of an electron, nearly all the mass of the helium atom is accounted for by the nucleus. This agrees with Rutherford's interpretation of the Geiger-Marsden experiment.

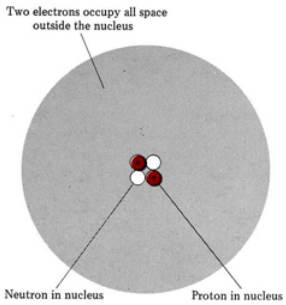


Figure **2.3.1**: The atomic structure of a helium atom. Two electrons, two protons, and two neutrons are arranged as shown.

A large circle with four significantly smaller circles in the center. The smaller circles with the positive sign shows the protons and the two other circles represent the neutrons. Two electrons occupy all space outside the nucleus.

The number of units of positive charge on the nucleus is usually about half the number of units of mass because about half the nuclear particles are uncharged neutrons. The two electrons move about rapidly, occupying all the volume of the atom outside the nucleus. Their negative charge neutralizes the positive charge of the two protons, producing a neutral or uncharged atom.

The protons and neutrons in the nucleus of an atom such as helium are held very tightly by strong nuclear forces. It is very difficult either to separate the nuclear particles or to add extra ones. The electrons, on the other hand, are held to the atom by their electrostatic attraction for the positively charged protons in the nucleus. This force is strong, but not so strong that an atom cannot lose or gain electrons. When the number of electrons is not the same as the number of protons, an atom has a net electric charge and is called an **ion**. The α particles emitted by radioactive elements consist of two protons and two neutrons tightly bound together. Thus an α particle is the same as a helium nucleus; that is, a helium atom that has lost its two electrons or a helium ion whose charge is $+2e$. When particles are emitted into a closed container, they slowly pick up electrons from their surroundings, and eventually the container becomes filled with helium.

The structure of any atom may be specified by indicating how many electrons, protons, and neutrons it contains. The number of protons is the same as the number of electrons and is given by the atomic number Z. Instead of directly specifying how many

neutrons are present, we use the **mass number** A. This is the total number of particles in the nucleus; hence

$$\begin{aligned} A &= \text{number of protons} + \text{number of neutrons} \\ &= Z + N \end{aligned}$$

where N represents the number of neutrons. To symbolize a particular atom, the mass number and atomic number are written as a superscript and subscript preceding the chemical symbol (**Sy**) as follows:

$$^{A}_{Z}\mathrm{Sy}$$

The helium atom, whose structure was represented above, has 2 protons and 2 electrons (Z = 2)as well as 2 neutrons. Hence $A = Z + N = 2 + 2 = 4$, and the atom is represented by

$$^{4}_{2}\mathrm{He}$$

In the case of an ion the positive or negative charge is indicated as a superscript to the right of the chemical symbol. Thus a helium atom which had lost two electrons (a helium ion with two more protons than electrons) would be written as

$$^{4}_{2}\mathrm{He}^{2+}$$

Example 2.3.1 : Atomic Numbers

How many electrons, protons, and neutrons are there in each of the atoms represented below?

a. $^{12}_{6}\mathrm{C}$
b. $^{40}_{20}\mathrm{Ca}$
c. $^{206}_{82}\mathrm{Pb}$
d. $^{40}_{20}\mathrm{Ca}^{2+}$

Solution

For an atom the number of electrons equals the number of protons and is given by Z. For an ion the atomic number gives the number of protons, but the number of electrons must be determined from the charge. Thus

a. $^{12}_{6}\mathrm{C}$ contains 6 electrons and 6 protons.
b. $^{40}_{20}\mathrm{Ca}$ contains 20 electrons and 20 protons.
c. $^{206}_{82}\mathrm{Pb}$ contains 82 electrons and 82 protons.
d. $^{40}_{20}\mathrm{Ca}^{2+}$ has lost two electrons. Therefore it contains 18 electrons and 20 protons.

The number of neutrons can be obtained by subtracting the number of protons (Z) from the total number of particles in the nucleus (A):

a. $^{12}_{6}\mathrm{C}$: N = A – Z = 12 – 6 = 6 neutrons
b. $^{40}_{20}\mathrm{Ca}$: N = 40 – 20 = 20 neutrons
c. (The same applies to $^{40}_{20}\mathrm{Ca}^{2+}$. Only electrons are gained or lost when an ion forms.)
d. $^{206}_{82}\mathrm{Pb}$: N = 206 – 82 = 124 neutrons

This page titled 2.3: Atomic Structure and Isotopes is shared under a CC BY-NC-SA 4.0 license and was authored, remixed, and/or curated by Ed Vitz, John W. Moore, Justin Shorb, Xavier Prat-Resina, Tim Wendorff, & Adam Hahn.

- **4.11: Atomic Structure and Isotopes** by Ed Vitz, John W. Moore, Justin Shorb, Xavier Prat-Resina, Tim Wendorff, & Adam Hahn is licensed CC BY-NC-SA 4.0.

2.4: Isotopes

The presence of neutrons in atomic nuclei accounts for the occurrence of **isotopes—** samples of an element whose atoms contain different numbers of neutrons and hence exhibit different "nuclidic masses". The ***nuclidic mass*** is the mass of a "nuclide", where a nuclide is the term used for any atom whose nuclear composition (Number of protons and neutrons) is defined. For example, naturally occurring hydrogen has two stable nuclides, $^{1}_{1}\mathbf{H}$ and $^{2}_{1}\mathbf{H}$, which also are isotopes of one another. More than 99.98 percent is “light” hydrogen, $^{1}_{1}\mathrm{H}$. This consists of atoms each of which has one proton, one electron, and zero neutrons. The rest is “heavy” hydrogen or deuterium, $^{2}_{1}\mathbf{H}$, which consists of atoms which contain one electron, one proton, and one neutron. Hence the nuclidic mass of deuterium is almost exactly twice as great as for light hydrogen. By transmutation of lithium, it is also possible to obtain a third isotope, tritium, $^{3}_{1}\mathbf{H}$. It consists of atoms whose nuclei contain two neutrons and one proton. Its nuclidic mass is about 3 times that of light hydrogen.

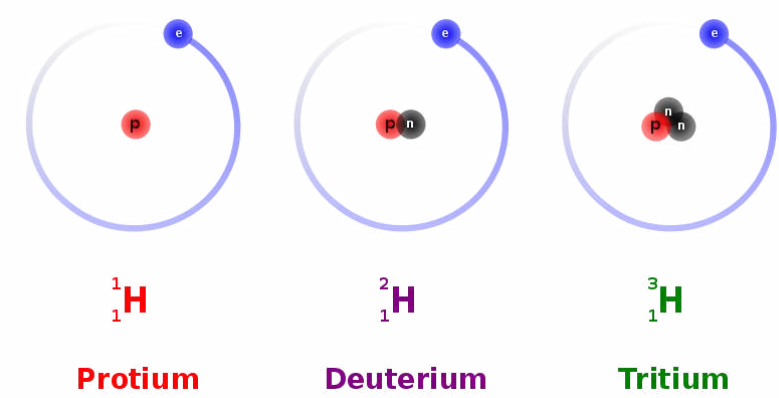


Figure **2.4.1**: Above are the 3 isotopes of Hydrogen. Each have the same number of protons, but have different numbers of neutrons in the nucleus.

The discovery of isotopes and its explanation on the basis of an atomic structure built up from electrons, protons, and neutrons required a change in the ideas about atoms which John Dalton had proposed. For a given element all atoms are *not quite* identical in all respects—especially with regard to mass. It is the number and distribution of electrons which occupy most of the volume of an atom which determines the chemical behavior of atoms. The number of protons in the nucleus of each element is important in determining its chemical properties, because the total positive charge of the nucleus determines how the electrons are distributed. *All atoms of the same element have the same atomic number*, but different isotopes have different nuclidic masses.

This page titled 2.4: Isotopes is shared under a CC BY-NC-SA 4.0 license and was authored, remixed, and/or curated by Ed Vitz, John W. Moore, Justin Shorb, Xavier Prat-Resina, Tim Wendorff, & Adam Hahn.

- **4.12: Isotopes** by Ed Vitz, John W. Moore, Justin Shorb, Xavier Prat-Resina, Tim Wendorff, & Adam Hahn is licensed CC BY-NC-SA 4.0.

2.5: Transmutation and Radioactivity

Transmutation of one element into another requires a change in the structures of the *nuclei* of the atoms involved. For example, the first step in the spontaneous radioactive decay of uranium is emission of an α particle, $^{4}_{2}\mathrm{He}^{2+}$, from the nucleus $^{238}_{92}\mathrm{U}$ Since the α particle consists of two protons and two neutrons, the atomic number must be reduced by 2 and the mass number by 4. The product of this nuclear reaction is therefore $^{234}_{90}\mathrm{Th}$. In other words, loss of an α particle changes (transmutes) uranium into thorium. In the equation for the decay, the sum of the atomic numbers on the left and right are equal, as is the sum of the mass numbers on the left and right:

$$^{238}_{92}\mathrm{U} \rightarrow {}_{90}{}^{234}\mathrm{Th}^{*} + {}^{4}_{2}\alpha \tag{2.5.1}$$

Alpha decay (Figure 4.12.1) is typical for large nuclei, because it reduces their size rapidly. Every element above Z = 83 (Bi) is radioactive, apparently because no number of neutrons can stabilize the nucleus against the repulsions between large numbers of protons.

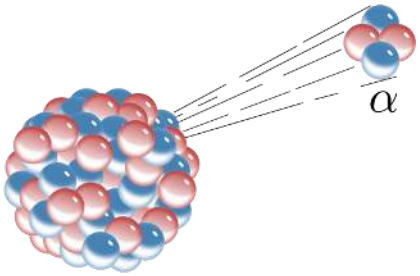


Figure 2.5.1: The figure above shows the process of alpha decay.

Loss of a β particle (electron) from an atomic nucleus leaves the nucleus with an extra unit of positive charge, that is, an extra proton. This increases the atomic number by 1 and also changes one element to another. For example, the $^{234}_{90}\mathrm{Th}$ mentioned above emits β particles. Its atomic number increases by 1, but its mass number remains the same. (The β particle is an electron and has a very small mass.) In effect one neutron is converted to a proton and an electron. Thus the thorium transmutes to protactinium $^{234}_{91}\mathrm{Pa}$. (Note carefully that the β particle is an electron emitted from the *nucleus* of the thorium atom, not one of the electrons from outside the nucleus (Figure 2.5.2) Using the standard symbol

$$^{234}_{90}\mathrm{Th} \rightarrow {}^{234}_{91}\mathrm{Pa} + {}^{0}_{-1}\beta$$

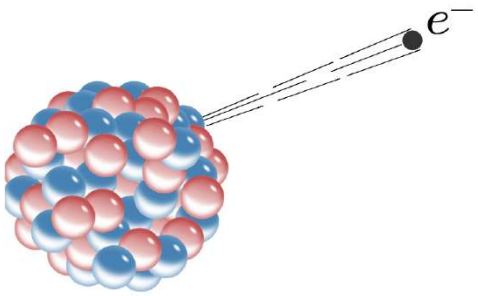


Figure 2.5.2: The image above shows beta decay, which is the release of an electron from the nucleus after the conversion of a neutron into a proton and electron. The proton remains in the nucleus while the electron (or beta particle) is ejected.

Beta decay increases the number of protons, so it occurs when a nucleus has a high n/p ratio, compared to the stable nuclei of that element. If the nucleus has a low n/p ratio, it can reduce the number of protons by "positron" emission:

$$^{11}_{6}\mathrm{C} \rightarrow {}^{11}_{5}\mathrm{B} + {}^{0}_{+1}\beta$$

Positrons (${}^{0}_{+1}\beta$) are the basis of medical "PET (Positron Emission Tomography) Scans", in which they *annihilate* their antiparticle, the beta:

$$ {}^{0}_{+1}\beta + {}^{0}_{-1}\beta \rightarrow 2\ {}^{0}_{0}\gamma $$

The two gammas leave in opposite directions from the point of the annihilation, so the PET machine can "trace" their origin to create an image.

A gamma ray is not a particle, and so its emission from a nucleus does not involve a change in atomic number or mass number. Rather it involves a change in the way the same protons and neutrons are packed together in the nucleus. In Equation 2.5.1, the product Th is shown with an asterisk, indicating that the decay leaves it in an excited state. It releases its extra energy in the form of a gamma (Figure 2.5.3):

$$ {}^{234}_{90}\mathrm{Th}^{*} \rightarrow {}^{234}_{90}\mathrm{Th} + {}^{0}_{0}\gamma $$

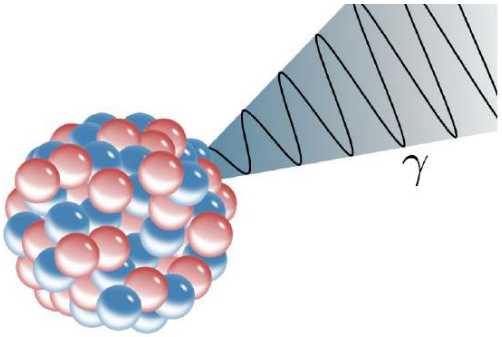


Figure 2.5.3*: The* image above depicts gamma ray emission. The rearrangement of neutrons and protons in the nucleus causes the release of energy in the form of a gamma ray, seen above.

It is important to note, however, that radioactivity and transmutation both involve changes *within the atomic nucleus*. Such **nuclear reactions** will be discussed in more detail in the section devoted to Nuclear Chemistry. Because protons and neutrons are held tightly in the nucleus, nuclear reactions are much less common in everyday life than chemical reactions. The latter involve electrons surrounding the nucleus, and these are much less rigidly held.

This page titled 2.5: Transmutation and Radioactivity is shared under a CC BY-NC-SA 4.0 license and was authored, remixed, and/or curated by Ed Vitz, John W. Moore, Justin Shorb, Xavier Prat-Resina, Tim Wendorff, & Adam Hahn.

- **4.13: Transmutation and Radioactivity** by Ed Vitz, John W. Moore, Justin Shorb, Xavier Prat-Resina, Tim Wendorff, & Adam Hahn is licensed CC BY-NC-SA 4.0.

2.6: Average Atomic Weights

There are 21 elements with only one isotope, so all their atoms have identical masses. All other elements have two or more isotopes, so their atoms have at least two different masses. But all elements obey the law of definite proportions when they combine with other elements, so they *behave as if* they had just one kind of atom with a definite mass. In order to solve this dilemma, we define the atomic weight as the weighted average mass of all naturally occurring (occasionally radioactive) isotopes of the element.

A weighted average is defined as

$$\text{Atomic Weight} = \left(\frac{\%\text{ abundance isotope 1}}{100}\right) \times (\text{mass of isotope 1}) + \left(\frac{\%\text{ abundance isotope 2}}{100}\right) \times (\text{mass of isotope 2}) \quad + \quad ...$$

Similar terms would be added for all the isotopes. The calculation is analogous to the method used to calculate grade point averages in most colleges:

$$\text{GPA} = \left(\frac{\text{Credit Hours Course 1}}{\text{total credit hours}}\right) \times (\text{Grade in Course 1}) + \left(\frac{\text{Credit Hours Course 2}}{\text{total credit hours}}\right) \times (\text{Grade in Course 2}) \quad + \quad ...$$

Some Conventions

The term ***"Average Atomic Weight"*** or simply ***"Atomic Weight"*** is commonly used to refer to what is properly called a ***"relative atomic mass"***. Atomic Weights are technically dimensionless, because they cannot be determined as absolute values. They were historically calculated from mass ratios (early chemists could say that magnesium atoms have atoms of mass 24.305/15.999 times as heavy as oxygen atoms, because that is the mass ratio of magnesium to oxygen in MgO). Now atomic weights are calculated from the position of peaks in a mass spectrum.

While the peak positions may be labeled in amu, that is only possible if the mass spectrometer is calibrated with a standard, whose mass can only be known relative to another, and it is also technically dimensionless. To solve this dilemma, we ***define*** an amu as 1/12 the mass of a $^{12}_{6}\text{C}$ atom. $^{12}_{6}\text{C}$ can then be used to calibrate a mass spectrometer. For convenience, we often use "token" dimensions of *amu/average atom* for atomic weight, or *g/mol* for molar mass.

The calculation of an atomic weight includes "naturally occurring isotopes", which are defined by the Commission on Isotopic Aundances and Atomic Weights of IUPAC (IUPAC/CIAAW) to include radioactive isotopes with half lives greater than 1 x 10^{10} years. Thus thorium, protactinium, and uranium are assigned atomic weights of 232.0, 231.0, and 238.0, but no other radioactive elements have isotopes with long enough lifetimes to be assigned atomic weights.

✔ Example 2.6.1: Isotopes

Naturally occurring lead is found to consist of four isotopes:

- 1.40% $^{204}_{82}\text{Pb}$ whose isotopic weight is 203.973.
- 24.10% $^{206}_{82}\text{Pb}$ whose isotopic weight is 205.974.
- 22.10% $^{207}_{82}\text{Pb}$ whose isotopic weight is 206.976.
- 52.40% $^{208}_{82}\text{Pb}$ whose isotopic weight is 207.977.

Calculate the atomic weight of an average naturally occurring sample of lead.

Solution

Suppose that you had 1 mol lead. This would contain 1.40% ($\frac{1.40}{100}$ × 1 mol) $^{204}_{82}\text{Pb}$ whose molar mass is 203.973 g mol^{-1}. The mass of $^{204}_{82}\text{Pb}$ would be

$$\begin{aligned} m_{204} &= n_{204} \times M_{204} \\ &= \left(\frac{1.40}{100} \times 1\text{ mol}\right)\ (203.973\text{ g mol}^{-1}) \\ &= 20.86\text{ g} \end{aligned}$$

Similarly for the other isotopes

$$\begin{aligned} m_{206} &= n_{206} \times M_{206} \\ &= \left(\frac{24.10}{100} \times 1 \text{ mol}\right) (205.974 \text{ g mol}^{-1}) \\ &= 490.64 \text{ g} \\ m_{207} &= n_{207} \times M_{207} \\ &= \left(\frac{22.10}{100} \times 1 \text{ mol}\right) (206.976 \text{ g mol}^{-1}) \\ &= 450.74 \text{ g} \\ m_{208} &= n_{208} \times M_{208} \\ &= \left(\frac{52.40}{100} \times 1 \text{ mol}\right) (207.977 \text{ g mol}^{-1}) \\ &= 1080.98 \text{ g} \end{aligned}$$

Upon summing all four results, the mass of 1 mol of the mixture of isotopes is to be found

$$2.86\,g + 49.64\,g + 45.74\,g + 108.98\,g = 207.22\,g$$

Thus the atomic weight of lead is 207.2 g/mol, as mentioned earlier in the discussion.

An important corollary to the existence of isotopes should be emphasized at this point. When highly accurate results are obtained, atomic weights may vary slightly depending on where a sample of an element was obtained. For this reason, the IUPAC CIAAW has recently redefined the atomic weights of 10 elements having two or more isotopes [1]. The percentages of different isotopes often depends on the source of the element.

For example, oxygen in Antarctic precipitation has an atomic weight of 15.99903, but oxygen in marine N_2O has an atomic weight of 15.9997. *"Fractionation"* of the isotopes results from slightly different rates of chemical and physical processes caused by small differences in their masses. The difference can be more dramatic when an isotope is derived from transmutation.

For example, lead produced by decay of uranium contains a much larger percentage of $^{206}_{82}\mathrm{Pb}$ than the 24.1 percent given in the example for the average sample. Consequently the atomic weight of lead found in uranium ores is less than 207.2 and is much closer to 205.974, the isotopic weight of $^{206}_{82}\mathrm{Pb}$.

After the discovery of isotopes of the elements by J.J. Thompson in 1913 [2], it was suggested that the scale of relative masses of the atoms (the atomic weights) should use as a reference the mass of an atom of a particular isotope of one of the elements. The standard that was eventually chosen was $^{12}_{6}\mathrm{C}$, and it was assigned an atomic-weight value of exactly 12.000 000.

Thus the atomic weights given in the Table of Atomic Weights are the ratios of weighted averages (calculated as in the Example) of the masses of atoms of all isotopes of each naturally occurring element to the mass of a single $^{12}_{6}\mathrm{C}$ atom. Since carbon consists of two isotopes, 98.99% $^{12}_{6}\mathrm{C}$ isotopic weight 12.000 and 1.11% $^{13}_{6}\mathrm{C}$ of isotopic weight 13.003, the average atomic weight of carbon is

$$\frac{98.89}{100.00} \times 12.000 + \frac{1.11}{100.00} \times 13.003 = 12.011$$

for example.

Conventional Atomic Weights and "Intervals"

Deviations from average isotopic composition are usually not large, and so the ***Conventional Atomic Weight Values*** were defined by the IUPAC/CIAAW for the elements showing the most variation in abundance. They can be used for nearly all chemical calculations. But at the same time, ***Atomic Weights*** were redefined for those elements as ranges, or ***"intervals"***, for any work where small differences may be important[3]. The table below gives typical values.

Table **2.6.1** Atomic Weights

Element Name	Symbol	Conventional Atomic Weight	Atomic Weight
Boron	B	10.81	[10.806; 10.821]
Carbon	C	12.011	[12.0096; 12.0116]
Chlorine	Cl	35.45	[35.446; 35.457]
Hydrogen	H	1.008	[1.00784; 1.00811]
Lithium	Li	6.94	[6.938; 6.997]
Nitrogen	N	14.007	[14.00643; 14.00728]
Oxygen	O	15.999	[15.99903; 15.99971]
Silicon	Si	28.085	[28.084; 28.086]
Sulfur	S	32.06	[32.059; 32.076]
Thallium	Tl	204.38	[204.382; 204.385]

In the study of nuclear reactions, however, one must be concerned about isotopic weights. This is discussed further in the section on Nuclear Chemistry.

SI Definition of the Mole

The SI definition of the mole also depends on the isotope $^{12}_{6}C$ and can now be stated. One mole is defined as the amount of substance of a system which contains as many elementary entities as there are atoms in exactly 0.012 kg of $^{12}_{6}C$. The *elementary entities* may be atoms, molecules, ions, electrons, or other microscopic particles.

This definition of the mole makes the mass of 1 mole of an element in grams numerically equal to the average mass of the atoms in grams. This official definition of the mole makes possible a more accurate determination of the Avogadro constant than was reported earlier. The currently accepted value is $N_A = 6.02214179 \times 10^{23}\ mol^{-1}$. This is accurate to 0.00000001 percent and contains five more significant figures than $6.022 \times 10^{23}\ mol^{-1}$, the number used to define the mole previously. It is very seldom, however, that more than four significant digits are needed in the Avogadro constant. The value $6.022 \times 10^{23}\ mol^{-1}$ will certainly suffice for most calculations needed.

This page titled 2.6: Average Atomic Weights is shared under a CC BY-NC-SA 4.0 license and was authored, remixed, and/or curated by Ed Vitz, John W. Moore, Justin Shorb, Xavier Prat-Resina, Tim Wendorff, & Adam Hahn.

- **4.14: Average Atomic Weights** by Ed Vitz, John W. Moore, Justin Shorb, Xavier Prat-Resina, Tim Wendorff, & Adam Hahn is licensed CC BY-NC-SA 4.0.

2.7: Measurement of Atomic Weights

You may have wondered why we have been so careful to define atomic weights and isotopic weights as *ratios* of masses. The reason will be clearer once the most important and accurate experimental technique by which isotopic weights are measured has been described. This technique, called **mass spectrometry**, has developed from the experiments with cathode-ray tubes mentioned earlier in this chapter. It depends on the fact that an electrically charged particle passing through a magnetic field of constant strength moves in a circular path. The radius *r* of such a path is directly proportional to the mass *m* and the speed *u* of the particle, and inversely proportional to the charge *Q*. Thus the greater the mass or speed of the particle, the greater the radius of its path. The greater the charge, the smaller the radius. In a mass spectrometer, as seen below, atoms or molecules in the gaseous phase are bombarded by a beam of electrons. Occasionally one of these electrons will strike another electron in a particular atom, and both electrons will have enough energy to escape the attraction of the positive nucleus. This leaves behind a positive ion since the atom now has one more proton than it has electrons. For example,

$$^{12}_{6}\mathrm{C} + \mathrm{e}^- \text{ (high speed electron)} \rightarrow {}^{12}_{6}\mathrm{C}^+ + 2\,\mathrm{e}^-$$

Once positive ions are produced in a mass spectrometer, they are accelerated by the attraction of a negative electrode and pass through a slit. This produces a narrow beam of ions traveling parallel to one another. The beam then passes through electric and magnetic fields. The fields deflect away all ions except those traveling at a certain speed.

The beam of ions is then passed between the poles of a large electromagnet. Since the speed and charge are the same for all ions, the radii of their paths depend only on their masses. For different ions of masses m_1 and m_2

$$\frac{r_2}{r_1} = \frac{m_2}{m_1}$$

and the ratio of masses may be obtained by measuring the ratio of radii, The paths of the ions are determined either by a photographic plate (which darkens where the ions strike it, as in Figure **2.7.1**) or a metal plate connected to a galvanometer (a device which detects the electric current due to the beam of charged ions).

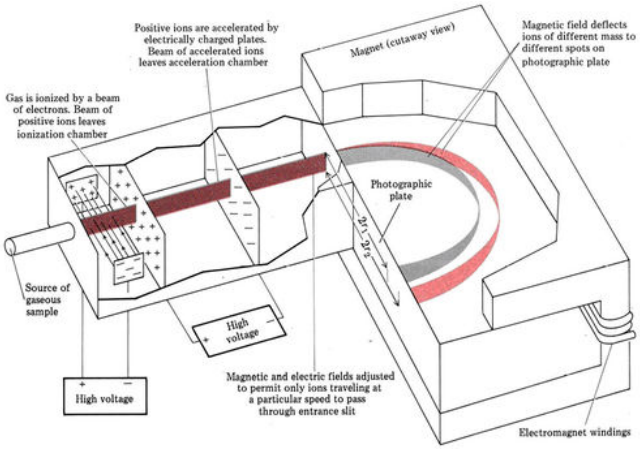


Figure **2.7.1**: A schematic for a mass spectrometer. Gas is ionized an accelerated through an electric potential. A magnetic field is applied, which causes particles to deflect to differing degrees dependent upon their mass to charge ratio.

Example **2.7.1**: Relative Atomic Masses

When a sample of carbon is vaporized in a mass spectrometer, two lines are observed on the photographic plate. The darker line is 27.454 cm, and the other is 29.749 cm from the entrance slit. Determine the relative atomic masses (isotopic weights) of the two isotopes of carbon.

Solution

Since the distance from the entrance slit to the line on the photographic plate is twice the radius of the circular path of the ions, we have

$$\frac{m_2}{m_1} = \frac{r_2}{r_1} = \frac{2r_2}{2r_1} = \frac{29.749\ \text{cm}}{27.454\ \text{cm}} = 1.083\ 59$$

Thus $m_2 = 1.083m_1$. If we assume that the darker mark on the photographic plate is produced because there are a greater number of

12^+ ions than of the less common13^+, then m_1 may be equated with the relative mass of ${}^{12}_{6}\text{C}$ and may be assigned a value of 12.000 000 exactly. The isotopic weight of ${}^{12}_{6}\text{C}$ is then

$$m_2 = (1.08359)(12.000000) = 13.0031$$

Note

Notice that in mass spectrometry all that is required is that the charge and speed of the two ions whose relative masses are to be determined be *the same*. If the mass of an individual ion were to be measured accurately, its actual speed upon entering the magnetic field and the exact magnitude of its electric charge would have to be known very accurately. Therefore it is easier to measure the ratio of two masses than to determine a single absolute mass, and so atomic weights are reported as pure numbers.

This page titled 2.7: Measurement of Atomic Weights is shared under a CC BY-NC-SA 4.0 license and was authored, remixed, and/or curated by Ed Vitz, John W. Moore, Justin Shorb, Xavier Prat-Resina, Tim Wendorff, & Adam Hahn.

- **4.15: Measurement of Atomic Weights** by Ed Vitz, John W. Moore, Justin Shorb, Xavier Prat-Resina, Tim Wendorff, & Adam Hahn is licensed CC BY-NC-SA 4.0.

2.8: Nuclear Reactions

Learning Objectives

- To know the different kinds of radioactive decay.
- To balance a nuclear reaction.

The two general kinds of nuclear reactions are nuclear decay reactions and nuclear transmutation reactions**.** In a **nuclear decay reaction**, also called radioactive decay, an unstable nucleus emits radiation and is transformed into the nucleus of one or more other elements. The resulting daughter nuclei have a lower mass and are lower in energy (more stable) than the parent nucleus that decayed. In contrast, in a **nuclear transmutation reaction**, a nucleus reacts with a subatomic particle or another nucleus to form a product nucleus that is *more massive* than the starting material. As we shall see, nuclear decay reactions occur spontaneously under all conditions, but nuclear transmutation reactions occur only under very special conditions, such as the collision of a beam of highly energetic particles with a target nucleus or in the interior of stars. We begin this section by considering the different classes of radioactive nuclei, along with their characteristic nuclear decay reactions and the radiation they emit.

> *Nuclear decay reactions occur spontaneously under all conditions, whereas nuclear transmutation reactions are induced.*

Classes of Radioactive Nuclei

The three general classes of radioactive nuclei are characterized by a different decay process or set of processes:

1. **Neutron-rich nuclei.** The nuclei on the upper left side of the band of stable nuclei have a neutron-to-proton ratio that is too high to give a stable nucleus. These nuclei decay by a process that *converts a neutron to a proton*, thereby *decreasing* the neutron-to-proton ratio.
2. **Neutron-poor nuclei.** Nuclei on the lower right side of the band of stable nuclei have a neutron-to-proton ratio that is too low to give a stable nucleus. These nuclei decay by processes that have the net effect of *converting a proton to a neutron*, thereby *increasing* the neutron-to-proton ratio.
3. **Heavy nuclei.** With very few exceptions, heavy nuclei (those with $A \geq 200$) are intrinsically unstable regardless of the neutron-to-proton ratio, and all nuclei with $Z > 83$ are unstable. This is presumably due to the cumulative effects of electrostatic repulsions between the large number of positively charged protons, which cannot be totally overcome by the strong nuclear force, regardless of the number of neutrons present. Such nuclei tend to decay by emitting an α particle (a helium nucleus, $^{4}_{2}\mathrm{He}$, which decreases the number of protons and neutrons in the original nucleus by 2. Because the neutron-to-proton ratio in an α particle is 1, the net result of alpha emission is an increase in the neutron-to-proton ratio.

> *Nuclear decay reactions always produce daughter nuclei that have a more favorable neutron-to- proton ratio and hence are more stable than the parent nucleus.*

Nuclear Decay Reactions

Just as we use the number and type of atoms present to balance a chemical equation, we can use the number and type of nucleons present to write a balanced nuclear equation for a nuclear decay reaction. This procedure also allows us to predict the identity of either the parent or the daughter nucleus if the identity of only one is known. Regardless of the mode of decay, the total number of nucleons is conserved in all nuclear reactions.

To describe nuclear decay reactions, chemists have extended the $^{A}_{Z}\mathrm{X}$ notation for nuclides to include radioactive emissions. Table 2.8.1 lists the name and symbol for each type of emitted radiation. The most notable addition is the **positron**, a particle that has the same mass as an electron but a positive charge rather than a negative charge.

Table **2.8.1**: Nuclear Decay Emissions and Their Symbols

Identity	Symbol	Charge	Mass (amu)
helium nucleus	${}^{4}_{2}\alpha$	+2	4.001506
electron	${}^{0}_{-1}\beta$ or β^{-}	−1	0.000549
photon	${}^{0}_{0}\gamma$	—	—
neutron	${}^{1}_{0}\mathrm{n}$	0	1.008665
proton	${}^{1}_{1}\mathrm{p}$	+1	1.007276
positron	${}^{0}_{+1}\beta$ or β^{+}	+1	0.000549

Like the notation used to indicate isotopes, the upper left superscript in the symbol for a particle gives the mass number, which is the total number of protons and neutrons. For a proton or a neutron, $A = 1$. Because neither an electron nor a positron contains protons or neutrons, its mass number is 0. The numbers should not be taken literally, however, as meaning that these particles have zero mass; ejection of a beta particle (an electron) simply has a negligible effect on the mass of a nucleus.

Similarly, the lower left subscript gives the charge of the particle. Because protons carry a positive charge, $Z = +1$ for a proton. In contrast, a neutron contains no protons and is electrically neutral, so $Z = 0$. In the case of an electron, $Z = -1$, and for a positron, $Z = +1$. Because γ rays are high-energy photons, both A and Z are 0. In some cases, two different symbols are used for particles that are identical but produced in different ways. For example, the symbol ${}^{0}_{-1}\mathrm{e}$, which is usually simplified to e^{-}, represents a free electron or an electron associated with an atom, whereas the symbol ${}^{0}_{-1}\beta$, which is often simplified to β^{-}, denotes an electron that originates from within the nucleus, which is a β particle. Similarly, ${}^{4}_{2}\mathrm{He}^{2+}$ refers to the nucleus of a helium atom, and ${}^{4}_{2}\alpha$ denotes an identical particle that has been ejected from a heavier nucleus.

There are six fundamentally different kinds of nuclear decay reactions, and each releases a different kind of particle or energy. The essential features of each reaction are shown in Figure **2.8.1**. The most common are alpha and beta decay and gamma emission, but the others are essential to an understanding of nuclear decay reactions.

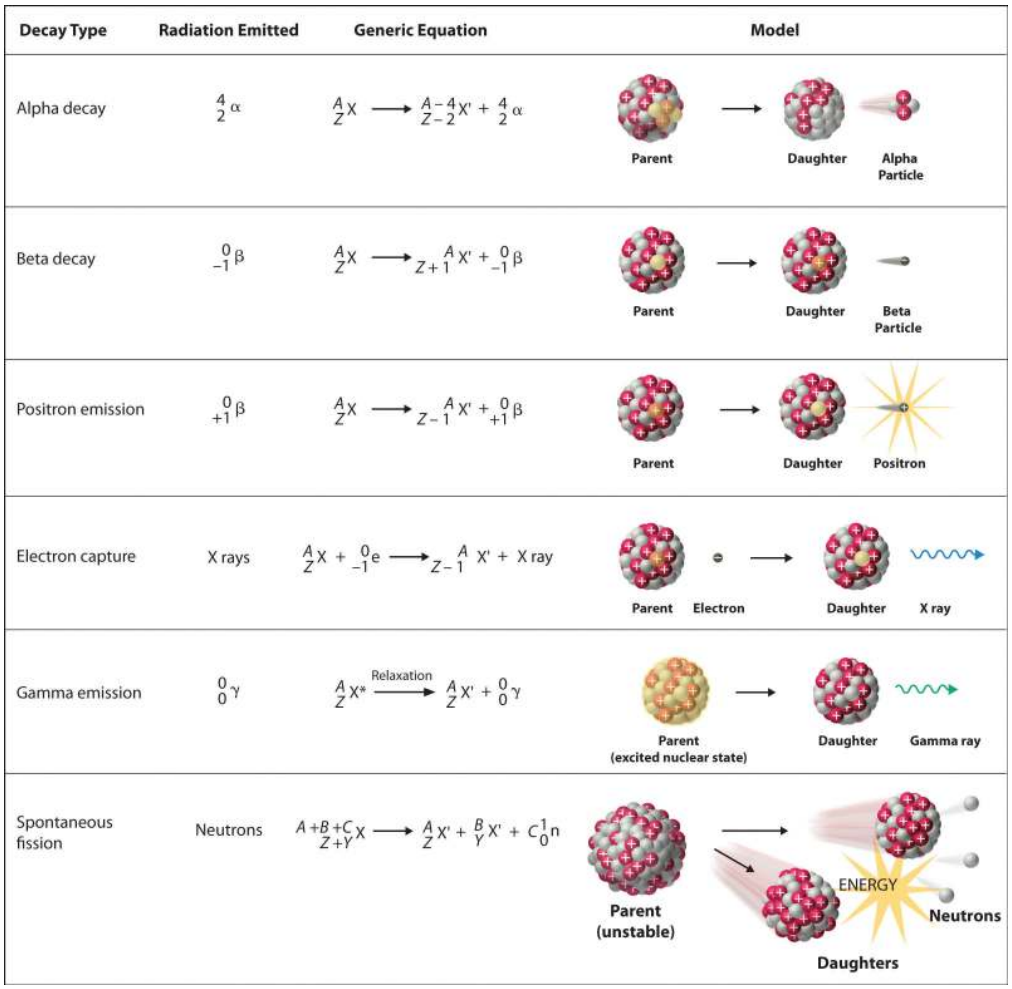


Figure **2.8.1**: Common Modes of Nuclear Decay

Alpha Decay

Many nuclei with mass numbers greater than 200 undergo **alpha (α) decay**, which results in the emission of a helium-4 nucleus as an **alpha (α) particle**, $^4_2\alpha$. The general reaction is as follows:

$$\underset{\text{parent}}{^A_Z\text{X}} \rightarrow \underset{\text{daughter}}{^{A-4}_{Z-2}\text{X}'} + \underset{\substack{\text{alpha}\\\text{particle}}}{^4_2\alpha} \tag{2.8.1}$$

The daughter nuclide contains two fewer protons and two fewer neutrons than the parent. Thus α-particle emission produces a daughter nucleus with a mass number $A - 4$ and a nuclear charge $Z - 2$ compared to the parent nucleus. Radium-226, for example, undergoes alpha decay to form radon-222:

$$^{226}_{88}\text{Ra} \rightarrow ^{222}_{86}\text{Rn} + ^4_2\alpha \tag{2.8.2}$$

Because nucleons are conserved in this and all other nuclear reactions, the sum of the mass numbers of the products, 222 + 4 = 226, equals the mass number of the parent. Similarly, the sum of the atomic numbers of the products, 86 + 2 = 88, equals the atomic number of the parent. Thus the nuclear equation is balanced.

> Just as the total number of atoms is conserved in a chemical reaction, the total number of nucleons is conserved in a nuclear reaction.

Beta Decay

Nuclei that contain too many neutrons often undergo **beta (β) decay**, in which a neutron is converted to a proton and a high-energy electron that is ejected from the nucleus as a β particle:

$$\underset{\text{unstable neutron in nucleus}}{{}^{1}_{0}\text{n}} \rightarrow \underset{\text{proton retained by nucleus}}{{}^{1}_{1}\text{p}} + \underset{\text{beta particle emitted by nucleus}}{{}^{0}_{-1}\beta} \tag{2.8.3}$$

The general reaction for beta decay is therefore

$$\underset{\text{parent}}{{}^{A}_{Z}\text{X}} \rightarrow \underset{\text{daughter}}{{}^{A}_{Z+1}\text{X}'} + \underset{\text{beta particle}}{{}^{0}_{-1}\beta} \tag{2.8.4}$$

Although beta decay does not change the mass number of the nucleus, it does result in an increase of +1 in the atomic number because of the addition of a proton in the daughter nucleus. Thus beta decay decreases the neutron-to-proton ratio, moving the nucleus toward the band of stable nuclei. For example, carbon-14 undergoes beta decay to form nitrogen-14:

$${}^{14}_{6}\text{C} \rightarrow {}^{14}_{7}\text{N} + {}^{0}_{-1}\beta \tag{2.8.5}$$

Once again, the number of nucleons is conserved, and the charges are balanced. The parent and the daughter nuclei have the same mass number, 14, and the sum of the atomic numbers of the products is 6, which is the same as the atomic number of the carbon-14 parent.

Positron Emission

Because a positron has the same mass as an electron but opposite charge, **positron emission** is the opposite of beta decay. Thus positron emission is characteristic of neutron-poor nuclei, which decay by transforming a proton to a neutron and emitting a high-energy positron:

$${}^{1}_{1}\text{p}^{+} \rightarrow {}^{1}_{0}\text{n} + {}^{0}_{+1}\beta^{+} \tag{2.8.6}$$

The general reaction for positron emission is therefore

$$\underset{\text{parent}}{{}^{A}_{Z}\text{X}} \rightarrow \underset{\text{daughter}}{{}^{A}_{Z-1}\text{X}'} + \underset{\text{positron}}{{}^{0}_{+1}\beta^{+}} \tag{2.8.7}$$

Like beta decay, positron emission does not change the mass number of the nucleus. In this case, however, the atomic number of the daughter nucleus is lower by 1 than that of the parent. Thus the neutron-to-proton ratio has increased, again moving the nucleus closer to the band of stable nuclei. For example, carbon-11 undergoes positron emission to form boron-11:

$${}^{11}_{6}\text{C} \rightarrow {}^{11}_{5}\text{B} + {}^{0}_{+1}\beta^{+} \tag{2.8.8}$$

Nucleons are conserved, and the charges balance. The mass number, 11, does not change, and the sum of the atomic numbers of the products is 6, the same as the atomic number of the parent carbon-11 nuclide.

Electron Capture

A neutron-poor nucleus can decay by either positron emission or **electron capture (EC)**, in which an electron in an inner shell reacts with a proton to produce a neutron:

$${}^{1}_{1}\text{p} + {}^{0}_{-1}\text{e} \rightarrow {}^{1}_{0}\text{n} \tag{2.8.9}$$

When a second electron moves from an outer shell to take the place of the lower-energy electron that was absorbed by the nucleus, an x-ray is emitted. The overall reaction for electron capture is thus

$$\underset{\text{parent}}{{}^{A}_{Z}\text{X}} + \underset{\text{electron}}{{}^{0}_{-1}\text{e}} \rightarrow \underset{\text{daughter}}{{}^{A}_{Z-1}\text{X}'} + \text{x-ray} \tag{2.8.10}$$

Electron capture does not change the mass number of the nucleus because both the proton that is lost and the neutron that is formed have a mass number of 1. As with positron emission, however, the atomic number of the daughter nucleus is lower by 1 than that of

the parent. Once again, the neutron-to-proton ratio has increased, moving the nucleus toward the band of stable nuclei. For example, iron-55 decays by electron capture to form manganese-55, which is often written as follows:

$$^{55}_{26}\text{Fe} \xrightarrow{\text{EC}} {}^{55}_{25}\text{Mn} + \text{x-ray} \tag{2.8.11}$$

The atomic numbers of the parent and daughter nuclides differ in Equation 20.2.11, although the mass numbers are the same. To write a balanced nuclear equation for this reaction, we must explicitly include the captured electron in the equation:

$$^{55}_{26}\text{Fe} + {}^{0}_{-1}\text{e} \rightarrow {}^{55}_{25}\text{Mn} + \text{x-ray} \tag{2.8.12}$$

Both positron emission and electron capture are usually observed for nuclides with low neutron-to-proton ratios, but the decay rates for the two processes can be very different.

Gamma Emission

Many nuclear decay reactions produce daughter nuclei that are in a nuclear excited state, which is similar to an atom in which an electron has been excited to a higher-energy orbital to give an electronic excited state. Just as an electron in an electronic excited state emits energy in the form of a photon when it returns to the ground state, a nucleus in an excited state releases energy in the form of a photon when it returns to the ground state. These high-energy photons are γ rays. **Gamma (γ) emission** can occur virtually instantaneously, as it does in the alpha decay of uranium-238 to thorium-234, where the asterisk denotes an excited state:

$$^{238}_{92}\text{U} \rightarrow \underbrace{^{234}_{90}\text{Th}^*}_{\substack{\text{excited}\\ \text{nuclear}\\ \text{state}}} + {}^{4}_{2}\alpha \xrightarrow{\text{relaxation}} {}^{234}_{90}\text{Th} + {}^{0}_{0}\gamma \tag{2.8.13}$$

If we disregard the decay event that created the excited nucleus, then

$$^{234}_{88}\text{Th}^* \rightarrow {}^{234}_{88}\text{Th} + {}^{0}_{0}\gamma \tag{2.8.14}$$

or more generally,

$$^{A}_{Z}\text{X}^* \rightarrow {}^{A}_{Z}\text{X} + {}^{0}_{0}\gamma \tag{2.8.15}$$

Gamma emission can also occur after a significant delay. For example, technetium-99*m* has a half-life of about 6 hours before emitting a γ ray to form technetium-99 (the *m* is for metastable). Because γ rays are energy, their emission does not affect either the mass number or the atomic number of the daughter nuclide. Gamma-ray emission is therefore the only kind of radiation that does not necessarily involve the conversion of one element to another, although it is almost always observed in conjunction with some other nuclear decay reaction.

Spontaneous Fission

Only very massive nuclei with high neutron-to-proton ratios can undergo **spontaneous fission**, in which the nucleus breaks into two pieces that have different atomic numbers and atomic masses. This process is most important for the transactinide elements, with $Z \geq 104$. Spontaneous fission is invariably accompanied by the release of large amounts of energy, and it is usually accompanied by the emission of several neutrons as well. An example is the spontaneous fission of $^{254}_{98}\text{Cf}$, which gives a distribution of fission products; one possible set of products is shown in the following equation:

$$^{254}_{98}\text{Cf} \rightarrow {}^{118}_{46}\text{Pd} + {}^{132}_{52}\text{Te} + 4{}^{1}_{0}\text{n} \tag{2.8.16}$$

Once again, the number of nucleons is conserved. Thus the sum of the mass numbers of the products (118 + 132 + 4 = 254) equals the mass number of the reactant. Similarly, the sum of the atomic numbers of the products [46 + 52 + (4 × 0) = 98] is the same as the atomic number of the parent nuclide.

✔ Example 2.8.1

Write a balanced nuclear equation to describe each reaction.

a. the beta decay of $^{35}_{16}\text{S}$
b. the decay of $^{201}_{80}\text{Hg}$ by electron capture

c. the decay of $^{30}_{15}\mathrm{P}$ by positron emission

Given: radioactive nuclide and mode of decay

Asked for: balanced nuclear equation

Strategy:

A Identify the reactants and the products from the information given.

B Use the values of *A* and *Z* to identify any missing components needed to balance the equation.

Solution

a.

A We know the identities of the reactant and one of the products (a β particle). We can therefore begin by writing an equation that shows the reactant and one of the products and indicates the unknown product as $^{A}_{Z}\mathrm{X}$:

$$^{35}_{16}\mathrm{S} \rightarrow {}^{A}_{Z}\mathrm{X} + {}^{0}_{-1}\beta \tag{2.8.17}$$

B Because both protons and neutrons must be conserved in a nuclear reaction, the unknown product must have a mass number of $A = 35 - 0 = 35$ and an atomic number of $Z = 16 - (-1) = 17$. The element with $Z = 17$ is chlorine, so the balanced nuclear equation is as follows:

$$^{35}_{16}\mathrm{S} \rightarrow {}^{35}_{17}\mathrm{Cl} + {}^{0}_{-1}\beta \tag{2.8.18}$$

b.

A We know the identities of both reactants: $^{201}_{80}\mathrm{Hg}$ and an inner electron, $^{0}_{-1}\mathrm{e}$. The reaction is as follows:

$$^{201}_{80}\mathrm{Hg} + {}^{0}_{-1}\mathrm{e} \rightarrow {}^{A}_{Z}\mathrm{X}$$

B Both protons and neutrons are conserved, so the mass number of the product must be $A = 201 + 0 = 201$, and the atomic number of the product must be $Z = 80 + (-1) = 79$, which corresponds to the element gold. The balanced nuclear equation is thus

$$^{201}_{80}\mathrm{Hg} + {}^{0}_{-1}\mathrm{e} \rightarrow {}^{201}_{79}\mathrm{Au}$$

c.

A As in part (a), we are given the identities of the reactant and one of the products—in this case, a positron. The unbalanced nuclear equation is therefore

$$^{30}_{15}\mathrm{P} \rightarrow {}^{A}_{Z}\mathrm{X} + {}^{0}_{+1}\beta$$

B The mass number of the second product is $A = 30 - 0 = 30$, and its atomic number is $Z = 15 - 1 = 14$, which corresponds to silicon. The balanced nuclear equation for the reaction is as follows:

$$^{30}_{15}\mathrm{P} \rightarrow {}^{30}_{14}\mathrm{Si} + {}^{0}_{+1}\beta$$

? Exercise 2.8.1

Write a balanced nuclear equation to describe each reaction.

a. $^{11}_{6}\mathrm{C}$ by positron emission
b. the beta decay of molybdenum-99
c. the emission of an α particle followed by gamma emission from $^{185}_{74}\mathrm{W}$

Answer

a. $^{11}_{6}\mathrm{C} \rightarrow {}^{11}_{5}\mathrm{B} + {}^{0}_{+1}\beta$
b. $^{99}_{42}\mathrm{Mo} \rightarrow {}^{99m}_{43}\mathrm{Tc} + {}^{0}_{-1}\beta$
c. $^{185}_{74}\mathrm{W} \rightarrow {}^{181}_{72}\mathrm{Hf} + {}^{4}_{2}\alpha + {}^{0}_{0}\gamma$

Example 2.8.2

Predict the kind of nuclear change each unstable nuclide undergoes when it decays.

a. $^{45}_{22}\mathrm{Ti}$
b. $^{242}_{94}\mathrm{Pu}$
c. $^{12}_{5}\mathrm{B}$
d. $^{256}_{100}\mathrm{Fm}$

Given: nuclide

Asked for: type of nuclear decay

Strategy:

Based on the neutron-to-proton ratio and the value of *Z*, predict the type of nuclear decay reaction that will produce a more stable nuclide.

Solution

a. This nuclide has a neutron-to-proton ratio of only 1.05, which is much less than the requirement for stability for an element with an atomic number in this range. Nuclei that have low neutron-to-proton ratios decay by converting a proton to a neutron. The two possibilities are positron emission, which converts a proton to a neutron and a positron, and electron capture, which converts a proton and a core electron to a neutron. In this case, both are observed, with positron emission occurring about 86% of the time and electron capture about 14% of the time.
b. Nuclei with $Z > 83$ are too heavy to be stable and usually undergo alpha decay, which decreases both the mass number and the atomic number. Thus $^{242}_{94}\mathrm{Pu}$ is expected to decay by alpha emission.
c. This nuclide has a neutron-to-proton ratio of 1.4, which is very high for a light element. Nuclei with high neutron-to-proton ratios decay by converting a neutron to a proton and an electron. The electron is emitted as a β particle, and the proton remains in the nucleus, causing an increase in the atomic number with no change in the mass number. We therefore predict that $^{12}_{5}\mathrm{B}$ will undergo beta decay.
d. This is a massive nuclide, with an atomic number of 100 and a mass number much greater than 200. Nuclides with $A \geq 200$ tend to decay by alpha emission, and even heavier nuclei tend to undergo spontaneous fission. We therefore predict that $^{256}_{100}\mathrm{Fm}$ will decay by either or both of these two processes. In fact, it decays by both spontaneous fission and alpha emission, in a 97:3 ratio.

Exercise 2.8.2

Predict the kind of nuclear change each unstable nuclide undergoes when it decays.

a. $^{32}_{14}\mathrm{Si}$
b. $^{43}_{21}\mathrm{Sc}$
c. $^{231}_{91}\mathrm{Pa}$

Answer

a. beta decay
b. positron emission or electron capture
c. alpha decay

Radioactive Decay Series

The nuclei of all elements with atomic numbers greater than 83 are unstable. Thus all isotopes of all elements beyond bismuth in the periodic table are radioactive. Because alpha decay decreases *Z* by only 2, and positron emission or electron capture decreases *Z* by only 1, it is impossible for any nuclide with $Z > 85$ to decay to a stable daughter nuclide in a single step, except via nuclear fission. Consequently, radioactive isotopes with $Z > 85$ usually decay to a daughter nucleus that is radiaoctive, which in turn decays to a second radioactive daughter nucleus, and so forth, until a stable nucleus finally results. This series of sequential alpha- and

beta-decay reactions is called a **radioactive decay series**. The most common is the uranium-238 decay series, which produces lead-206 in a series of 14 sequential alpha- and beta-decay reactions (Figure **2.8.2**). Although a radioactive decay series can be written for almost any isotope with $Z > 85$, only two others occur naturally: the decay of uranium-235 to lead-207 (in 11 steps) and thorium-232 to lead-208 (in 10 steps). A fourth series, the decay of neptunium-237 to bismuth-209 in 11 steps, is known to have occurred on the primitive Earth. With a half-life of "only" 2.14 million years, all the neptunium-237 present when Earth was formed decayed long ago, and today all the neptunium on Earth is synthetic.

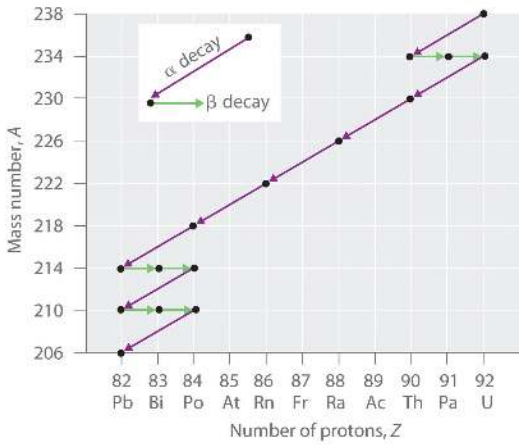


Figure **2.8.1**: A Radioactive Decay Series. Three naturally occurring radioactive decay series are known to occur currently: the uranium-238 decay series, the decay of uranium-235 to lead-207, and the decay of thorium-232 to lead-208.

Due to these radioactive decay series, small amounts of very unstable isotopes are found in ores that contain uranium or thorium. These rare, unstable isotopes should have decayed long ago to stable nuclei with a lower atomic number, and they would no longer be found on Earth. Because they are generated continuously by the decay of uranium or thorium, however, their amounts have reached a steady state, in which their rate of formation is equal to their rate of decay. In some cases, the abundance of the daughter isotopes can be used to date a material or identify its origin.

Induced Nuclear Reactions

The discovery of radioactivity in the late 19th century showed that some nuclei spontaneously transform into nuclei with a different number of protons, thereby producing a different element. When scientists realized that these naturally occurring radioactive isotopes decayed by emitting subatomic particles, they realized that—in principle—it should be possible to carry out the reverse reaction, converting a stable nucleus to another more massive nucleus by bombarding it with subatomic particles in a nuclear transmutation reaction.

The first successful nuclear transmutation reaction was carried out in 1919 by Ernest Rutherford, who showed that α particles emitted by radium could react with nitrogen nuclei to form oxygen nuclei. As shown in the following equation, a proton is emitted in the process:

$$^{4}_{2}\alpha + {}^{14}_{7}\mathrm{N} \rightarrow {}^{17}_{8}\mathrm{O} + {}^{1}_{1}\mathrm{p} \tag{2.8.19}$$

Rutherford's nuclear transmutation experiments led to the discovery of the neutron. He found that bombarding the nucleus of a light target element with an α particle usually converted the target nucleus to a product that had an atomic number higher by 1 and a mass number higher by 3 than the target nucleus. Such behavior is consistent with the emission of a proton after reaction with the α particle. Very light targets such as Li, Be, and B reacted differently, however, emitting a new kind of highly penetrating radiation rather than a proton. Because neither a magnetic field nor an electrical field could deflect these high-energy particles, Rutherford concluded that they were electrically neutral. Other observations suggested that the mass of the neutral particle was similar to the mass of the proton. In 1932, James Chadwick (Nobel Prize in Physics, 1935), who was a student of Rutherford's at the time, named these neutral particles neutrons and proposed that they were fundamental building blocks of the atom. The reaction that Chadwick initially used to explain the production of neutrons was as follows:

$$^{4}_{2}\alpha + {}^{9}_{4}\mathrm{Be} \rightarrow {}^{12}_{6}\mathrm{C} + {}^{1}_{0}\mathrm{n} \tag{2.8.20}$$

Because α particles and atomic nuclei are both positively charged, electrostatic forces cause them to repel each other. Only α particles with very high kinetic energy can overcome this repulsion and collide with a nucleus (Figure **2.8.3**). Neutrons have no electrical charge, however, so they are not repelled by the nucleus. Hence bombardment with neutrons is a much easier way to prepare new isotopes of the lighter elements. In fact, carbon-14 is formed naturally in the atmosphere by bombarding nitrogen-14 with neutrons generated by cosmic rays:

$$^{1}_{0}\mathrm{n} + {}^{14}_{7}\mathrm{N} \rightarrow {}^{14}_{6}\mathrm{C} + {}^{1}_{1}\mathrm{p} \tag{2.8.21}$$

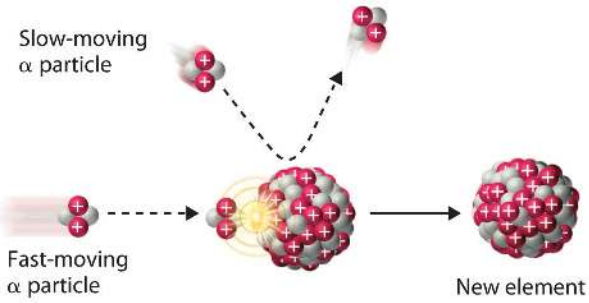


Figure **2.8.3**: A Nuclear Transmutation Reaction. Bombarding a target of one element with high-energy nuclei or subatomic particles can create new elements. Electrostatic repulsions normally prevent a positively charged particle from colliding and reacting with a positively charged nucleus. If the positively charged particle is moving at a very high speed, however, its kinetic energy may be great enough to overcome the electrostatic repulsions, and it may collide with the target nucleus. Such collisions can result in a nuclear transmutation reaction.

Example 2.8.3

In 1933, Frédéric Joliot and Iréne Joliot-Curie (daughter of Marie and Pierre Curie) prepared the first artificial radioactive isotope by bombarding aluminum-27 with α particles. For each ^{27}Al that reacted, one neutron was released. Identify the product nuclide and write a balanced nuclear equation for this transmutation reaction.

Given: reactants in a nuclear transmutation reaction

Asked for: product nuclide and balanced nuclear equation

Strategy:

A Based on the reactants and one product, identify the other product of the reaction. Use conservation of mass and charge to determine the values of *Z* and *A* of the product nuclide and thus its identity.

B Write the balanced nuclear equation for the reaction.

Solution

A Bombarding an element with α particles usually produces an element with an atomic number that is 2 greater than the atomic number of the target nucleus. Thus we expect that aluminum (Z = 13) will be converted to phosphorus (Z = 15). With one neutron released, conservation of mass requires that the mass number of the other product be 3 greater than the mass number of the target. In this case, the mass number of the target is 27, so the mass number of the product will be 30. The second product is therefore phosphorus-30, $^{30}_{15}\mathrm{P}$.

B The balanced nuclear equation for the reaction is as follows:

$$^{27}_{13}\mathrm{Al} + {}^{4}_{2}\alpha \rightarrow {}^{30}_{15}\mathrm{P} + {}^{1}_{0}\mathrm{n} \tag{2.8.22}$$

Exercise 2.8.1

Because all isotopes of technetium are radioactive and have short half-lives, it does not exist in nature. Technetium can, however, be prepared by nuclear transmutation reactions. For example, bombarding a molybdenum-96 target with deuterium nuclei ($^{2}_{1}\mathrm{H}$) produces technetium-97. Identify the other product of the reaction and write a balanced nuclear equation for this transmutation reaction.

Answer

neutron, ${}^{1}_{0}\text{n}$; ${}^{96}_{42}\text{Mo} + {}^{2}_{1}\text{H} \rightarrow {}^{97}_{43}\text{Tc} + {}^{1}_{0}\text{n}$

We noted earlier in this section that very heavy nuclides, corresponding to $Z \geq 104$, tend to decay by spontaneous fission. Nuclides with slightly lower values of Z, such as the isotopes of uranium (Z = 92) and plutonium (Z = 94), do not undergo spontaneous fission at any significant rate. Some isotopes of these elements, however, such as ${}^{235}_{92}\text{U}$ and ${}^{239}_{94}\text{Pu}$ undergo induced nuclear fission when they are bombarded with relatively low-energy neutrons, as shown in the following equation for uranium-235 and in Figure **2.8.3**:

$$ {}^{235}_{92}\text{U} + {}^{1}_{0}\text{n} \rightarrow {}^{236}_{92}\text{U} \rightarrow {}^{141}_{56}\text{Ba} + {}^{92}_{36}\text{Kr} + 3{}^{1}_{0}\text{n} \tag{2.8.23}$$

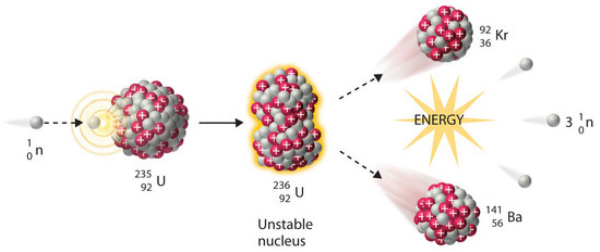


Figure **2.8.4**: Neutron-Induced Nuclear Fission. Collision of a relatively slow-moving neutron with a fissile nucleus can split it into two smaller nuclei with the same or different masses. Neutrons are also released in the process, along with a great deal of energy.

Any isotope that can undergo a nuclear fission reaction when bombarded with neutrons is called a **fissile isotope**.

During nuclear fission, the nucleus usually divides asymmetrically rather than into two equal parts, as shown in Figure **2.8.4**. Moreover, every fission event of a given nuclide does not give the same products; more than 50 different fission modes have been identified for uranium-235, for example. Consequently, nuclear fission of a fissile nuclide can never be described by a single equation. Instead, as shown in Figure **2.8.5**, a distribution of many pairs of fission products with different yields is obtained, but the mass ratio of each pair of fission products produced by a single fission event is always roughly 3:2.

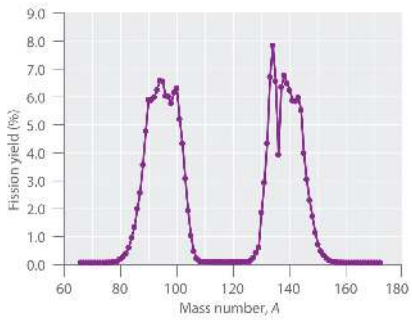


Figure **2.8.5**: Mass Distribution of Nuclear Fission Products of ^{235}U. Nuclear fission usually produces a range of products with different masses and yields, although the mass ratio of each pair of fission products from a fission event is approximately 3:2. As shown in this plot, more than 50 different fission products are known for235U. Data source: T. R. England and B. F. Rider, Los Alamos National Laboratory, LA-UR-94-3106, ENDF-349 (1993).

Synthesis of Transuranium Elements

Uranium (Z = 92) is the heaviest naturally occurring element. Consequently, all the elements with Z > 92, the **transuranium elements**, are artificial and have been prepared by bombarding suitable target nuclei with smaller particles. The first of the transuranium elements to be prepared was neptunium (Z = 93), which was synthesized in 1940 by bombarding a ^{238}U target with neutrons. As shown in Equation 20.21, this reaction occurs in two steps. Initially, a neutron combines with a ^{238}U nucleus to form ^{239}U, which is unstable and undergoes beta decay to produce ^{239}Np:

$$ {}^{238}_{92}\text{U} + {}^{1}_{0}\text{n} \rightarrow {}^{239}_{92}\text{U} \rightarrow {}^{239}_{93}\text{Np} + {}^{0}_{-1}\beta $$

Subsequent beta decay of ^{239}Np produces the second transuranium element, plutonium (Z = 94):

$$ {}^{239}_{93}\text{Np} \rightarrow {}^{239}_{94}\text{Pu} + {}^{0}_{-1}\beta $$

Bombarding the target with more massive nuclei creates elements that have atomic numbers significantly greater than that of the target nucleus (Table **2.8.2**). Such techniques have resulted in the creation of the superheavy elements 114 and 116, both of which lie in or near the “island of stability."

Table **2.8.2**: Some Reactions Used to Synthesize Transuranium Elements

$^{239}_{94}\text{Pu} + {}^{4}_{2}\alpha \rightarrow {}^{242}_{96}\text{Cm} + {}^{1}_{0}\text{n}$
$^{239}_{94}\text{Pu} + {}^{4}_{2}\alpha \rightarrow {}^{241}_{95}\text{Am} + {}^{1}_{1}\text{p} + {}^{1}_{0}\text{n}$
$^{242}_{96}\text{Cm} + {}^{4}_{2}\alpha \rightarrow {}^{243}_{97}\text{Bk} + {}^{1}_{1}\text{p} + 2{}^{1}_{0}\text{n}$
$^{253}_{99}\text{Es} + {}^{4}_{2}\alpha \rightarrow {}^{256}_{101}\text{Md} + {}^{1}_{0}\text{n}$
$^{238}_{92}\text{U} + {}^{12}_{6}\text{C} \rightarrow {}^{246}_{98}\text{Cf} + 4{}^{1}_{0}\text{n}$
$^{252}_{98}\text{Cf} + {}^{10}_{5}\text{B} \rightarrow {}^{256}_{103}\text{Lr} + 6{}^{1}_{0}\text{n}$

A device called a particle accelerator is used to accelerate positively charged particles to the speeds needed to overcome the electrostatic repulsions between them and the target nuclei by using electrical and magnetic fields. Operationally, the simplest particle accelerator is the linear accelerator (Figure **2.8.6**), in which a beam of particles is injected at one end of a long evacuated tube. Rapid alternation of the polarity of the electrodes along the tube causes the particles to be alternately accelerated toward a region of opposite charge and repelled by a region with the same charge, resulting in a tremendous acceleration as the particle travels down the tube. A modern linear accelerator such as the Stanford Linear Accelerator (SLAC) at Stanford University is about 2 miles long.

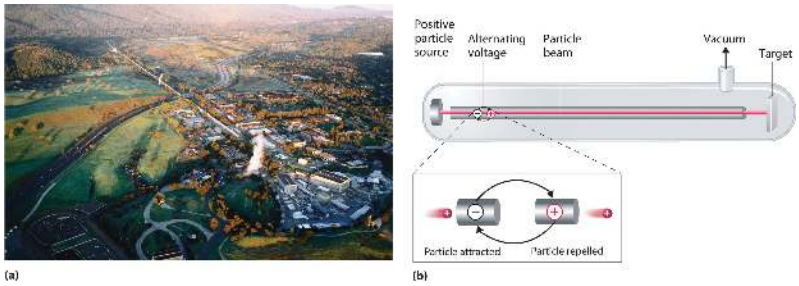


Figure **2.8.6**: A Linear Particle Accelerator. (a) An aerial view of the SLAC, the longest linear particle accelerator in the world; the overall length of the tunnel is 2 miles. (b) Rapidly reversing the polarity of the electrodes in the tube causes the charged particles to be alternately attracted as they enter one section of the tube and repelled as they leave that section. As a result, the particles are continuously accelerated along the length of the tube.

To achieve the same outcome in less space, a particle accelerator called a cyclotron forces the charged particles to travel in a circular path rather than a linear one. The particles are injected into the center of a ring and accelerated by rapidly alternating the polarity of two large D-shaped electrodes above and below the ring, which accelerates the particles outward along a spiral path toward the target.

The length of a linear accelerator and the size of the D-shaped electrodes in a cyclotron severely limit the kinetic energy that particles can attain in these devices. These limitations can be overcome by using a synchrotron, a hybrid of the two designs. A synchrotron contains an evacuated tube similar to that of a linear accelerator, but the tube is circular and can be more than a mile in diameter. Charged particles are accelerated around the circle by a series of magnets whose polarities rapidly alternate.

Summary

In **nuclear decay reactions (or radioactive decay)**, the parent nucleus is converted to a more stable daughter nucleus. Nuclei with too many neutrons decay by converting a neutron to a proton, whereas nuclei with too few neutrons decay by converting a proton to a neutron. Very heavy nuclei (with $A \geq 200$ and $Z > 83$) are unstable and tend to decay by emitting an **α particle**. When an unstable nuclide undergoes radioactive decay, the total number of nucleons is conserved, as is the total positive charge. Six different kinds of nuclear decay reactions are known. *Alpha decay* results in the emission of an α particle, $^{4}_{2}\alpha$, and produces a daughter nucleus with a mass number that is lower by 4 and an atomic number that is lower by 2 than the parent nucleus. **Beta decay** converts a neutron to a proton and emits a high-energy electron, producing a daughter nucleus with the same mass number as

the parent and an atomic number that is higher by 1. **Positron emission** is the opposite of beta decay and converts a proton to a neutron plus a positron. Positron emission does not change the mass number of the nucleus, but the atomic number of the daughter nucleus is lower by 1 than the parent. In **electron capture (EC)**, an electron in an inner shell reacts with a proton to produce a neutron, with emission of an x-ray. The mass number does not change, but the atomic number of the daughter is lower by 1 than the parent. In **gamma emission**, a daughter nucleus in a nuclear excited state undergoes a transition to a lower-energy state by emitting a γ ray. Very heavy nuclei with high neutron-to-proton ratios can undergo **spontaneous fission**, in which the nucleus breaks into two pieces that can have different atomic numbers and atomic masses with the release of neutrons. Many very heavy nuclei decay via a **radioactive decay series**—a succession of some combination of alpha- and beta-decay reactions. In **nuclear transmutation reactions**, a target nucleus is bombarded with energetic subatomic particles to give a product nucleus that is more massive than the original. All **transuranium elements**—elements with $Z > 92$—are artificial and must be prepared by nuclear transmutation reactions. These reactions are carried out in particle accelerators such as linear accelerators, cyclotrons, and synchrotrons.

Key Takeaway

Nuclear decay reactions occur spontaneously under all conditions and produce more stable daughter nuclei, whereas nuclear transmutation reactions are induced and form a product nucleus that is more massive than the starting material.

Key Equations

alpha decay

Equation 20.1: ${}^{A}_{Z}\mathrm{X} \rightarrow {}^{A-4}_{Z-2}\mathrm{X}' + {}^{4}_{2}\alpha$

beta decay

Equation 20.4: ${}^{A}_{Z}\mathrm{X} \rightarrow {}^{A}_{Z+1}\mathrm{X}' + {}^{0}_{-1}\beta$

positron emission

Equation 20.7: ${}^{A}_{Z}\mathrm{X} \rightarrow {}^{A}_{Z-1}\mathrm{X}' + {}^{0}_{+1}\beta$

electron capture

Equation 20.10: ${}^{A}_{Z}\mathrm{X} + {}^{0}_{-1}\mathrm{e} \rightarrow {}^{A}_{Z-1}\mathrm{X}' + \text{x-ray}$

gamma emission

Equation 20.15: ${}^{A}_{Z}\mathrm{X}^{*} \rightarrow {}^{A}_{Z}\mathrm{X} + {}^{0}_{0}\gamma$

2.8: Nuclear Reactions is shared under a not declared license and was authored, remixed, and/or curated by LibreTexts.

- **24.3: Nuclear Reactions** by Anonymous is licensed CC BY-NC-SA 3.0.

2.9: Nuclear Radiation

Learning Objectives

- Write and balance nuclear equations
- To know the different kinds of radioactive decay.
- To balance a nuclear reaction.

Nuclear chemistry is the study of reactions that involve changes in nuclear structure. The chapter on atoms, molecules, and ions introduced the basic idea of nuclear structure, that the nucleus of an atom is composed of protons and, with the exception of $^{1}_{1}\mathrm{H}$, neutrons. Recall that the number of protons in the nucleus is called the atomic number (Z) of the element, and the sum of the number of protons and the number of neutrons is the mass number (A). Atoms with the same atomic number but different mass numbers are isotopes of the same element. When referring to a single type of nucleus, we often use the term nuclide and identify it by the notation:

$$^{A}_{Z}\mathrm{X} \tag{2.9.1}$$

where

- X is the symbol for the element,
- A is the mass number, and
- Z is the atomic number.

Often a nuclide is referenced by the name of the element followed by a hyphen and the mass number. For example, $^{14}_{6}\mathrm{C}$ is called "carbon-14."

Protons and neutrons, collectively called nucleons, are packed together tightly in a nucleus. With a radius of about 10^{-15} meters, a nucleus is quite small compared to the radius of the entire atom, which is about 10^{-10} meters. Nuclei are extremely dense compared to bulk matter, averaging 1.8×10^{14} grams per cubic centimeter. For example, water has a density of 1 gram per cubic centimeter, and iridium, one of the densest elements known, has a density of 22.6 g/cm^3. If the earth's density were equal to the average nuclear density, the earth's radius would be only about 200 meters (earth's actual radius is approximately 6.4×10^6 meters, 30,000 times larger).

Changes of nuclei that result in changes in their atomic numbers, mass numbers, or energy states are nuclear reactions. To describe a nuclear reaction, we use an equation that identifies the nuclides involved in the reaction, their mass numbers and atomic numbers, and the other particles involved in the reaction.

Nuclear Equations

A balanced chemical reaction equation reflects the fact that during a chemical reaction, bonds break and form, and atoms are rearranged, but the total numbers of atoms of each element are conserved and do not change. A balanced nuclear reaction equation indicates that there is a rearrangement during a nuclear reaction, but of subatomic particles rather than atoms. Nuclear reactions also follow conservation laws, and they are balanced in two ways:

1. The sum of the mass numbers of the reactants equals the sum of the mass numbers of the products.
2. The sum of the charges of the reactants equals the sum of the charges of the products.

If the atomic number and the mass number of all but one of the particles in a nuclear reaction are known, we can identify the particle by balancing the reaction. For instance, we could determine that $^{17}_{8}\mathrm{O}$ is a product of the nuclear reaction of $^{14}_{7}\mathrm{N}$ and $^{4}_{2}\mathrm{He}$ if we knew that a proton, $^{1}_{1}\mathrm{H}$, was one of the two products. Example 2.9.1 shows how we can identify a nuclide by balancing the nuclear reaction.

Example 2.9.1: Balancing Equations for Nuclear Reactions

The reaction of an α particle with magnesium-25 ($^{25}_{12}\mathrm{Mg}$) produces a proton and a nuclide of another element. Identify the new nuclide produced.

Solution

The nuclear reaction can be written as:

$$^{25}_{12}\mathrm{Mg} + {}^{4}_{2}\mathrm{He} \rightarrow {}^{1}_{1}\mathrm{H} + {}^{A}_{Z}\mathrm{X}$$

where

- **A** is the mass number and
- **Z** is the atomic number of the new nuclide, **X**.

Because the sum of the mass numbers of the reactants must equal the sum of the mass numbers of the products:

$$25 + 4 = A + 1$$

so

$$A = 28$$

Similarly, the charges must balance, so:

$$12 + 2 = Z + 1$$

so

$$Z = 13$$

Check the periodic table: The element with nuclear charge = +13 is aluminum. Thus, the product is $^{28}_{13}\mathrm{Al}$.

Exercise 2.9.1

The nuclide $^{125}_{53}\mathrm{I}$ combines with an electron and produces a new nucleus and no other massive particles. What is the equation for this reaction?

Answer

$$^{125}_{53}\mathrm{I} + {}^{0}_{-1}\mathrm{e} \rightarrow {}^{125}_{52}\mathrm{Te}$$

The two general kinds of nuclear reactions are nuclear decay reactions and nuclear transmutation reactions**.** In a **nuclear decay reaction**, also called radioactive decay, an unstable nucleus emits radiation and is transformed into the nucleus of one or more other elements. The resulting daughter nuclei have a lower mass and are lower in energy (more stable) than the parent nucleus that decayed. In contrast, in a **nuclear transmutation reaction**, a nucleus reacts with a subatomic particle or another nucleus to form a product nucleus that is *more massive* than the starting material. As we shall see, nuclear decay reactions occur spontaneously under all conditions, but nuclear transmutation reactions occur only under very special conditions, such as the collision of a beam of highly energetic particles with a target nucleus or in the interior of stars. We begin this section by considering the different classes of radioactive nuclei, along with their characteristic nuclear decay reactions and the radiation they emit.

> *Nuclear decay reactions occur spontaneously under all conditions, whereas nuclear transmutation reactions are induced.*

Nuclear Decay Reactions

Just as we use the number and type of atoms present to balance a chemical equation, we can use the number and type of nucleons present to write a balanced nuclear equation for a nuclear decay reaction. This procedure also allows us to predict the identity of

either the parent or the daughter nucleus if the identity of only one is known. Regardless of the mode of decay, the total number of nucleons is conserved in all nuclear reactions.

To describe nuclear decay reactions, chemists have extended the ${}^{A}_{Z}\mathrm{X}$ notation for nuclides to include radioactive emissions. Table **2.9.1** lists the name and symbol for each type of emitted radiation. The most notable addition is the **positron**, a particle that has the same mass as an electron but a positive charge rather than a negative charge.

Table **2.9.1**: Nuclear Decay Emissions and Their Symbols

Identity	Symbol	Charge	Mass (amu)
helium nucleus	${}^{4}_{2}\alpha$	+2	4.001506
electron	${}^{0}_{-1}\beta$ or β^{-}	−1	0.000549
photon	${}^{0}_{0}\gamma$	—	—
neutron	${}^{1}_{0}\mathrm{n}$	0	1.008665
proton	${}^{1}_{1}\mathrm{p}$	+1	1.007276
positron	${}^{0}_{+1}\beta$ or β^{+}	+1	0.000549

Like the notation used to indicate isotopes, the upper left superscript in the symbol for a particle gives the mass number, which is the total number of protons and neutrons. For a proton or a neutron, $A = 1$. Because neither an electron nor a positron contains protons or neutrons, its mass number is 0. The numbers should not be taken literally, however, as meaning that these particles have zero mass; ejection of a beta particle (an electron) simply has a negligible effect on the mass of a nucleus.

Similarly, the lower left subscript gives the charge of the particle. Because protons carry a positive charge, $Z = +1$ for a proton. In contrast, a neutron contains no protons and is electrically neutral, so $Z = 0$. In the case of an electron, $Z = -1$, and for a positron, $Z = +1$. Because γ rays are high-energy photons, both A and Z are 0. In some cases, two different symbols are used for particles that are identical but produced in different ways. For example, the symbol ${}^{0}_{-1}\mathrm{e}$, which is usually simplified to e^{-}, represents a free electron or an electron associated with an atom, whereas the symbol ${}^{0}_{-1}\beta$, which is often simplified to β^{-}, denotes an electron that originates from within the nucleus, which is a β particle. Similarly, ${}^{4}_{2}\mathrm{He}^{2+}$ refers to the nucleus of a helium atom, and ${}^{4}_{2}\alpha$ denotes an identical particle that has been ejected from a heavier nucleus.

There are six fundamentally different kinds of nuclear decay reactions, and each releases a different kind of particle or energy. The essential features of each reaction are shown in Figure **2.9.1**. The most common are alpha and beta decay and gamma emission, but the others are essential to an understanding of nuclear decay reactions.

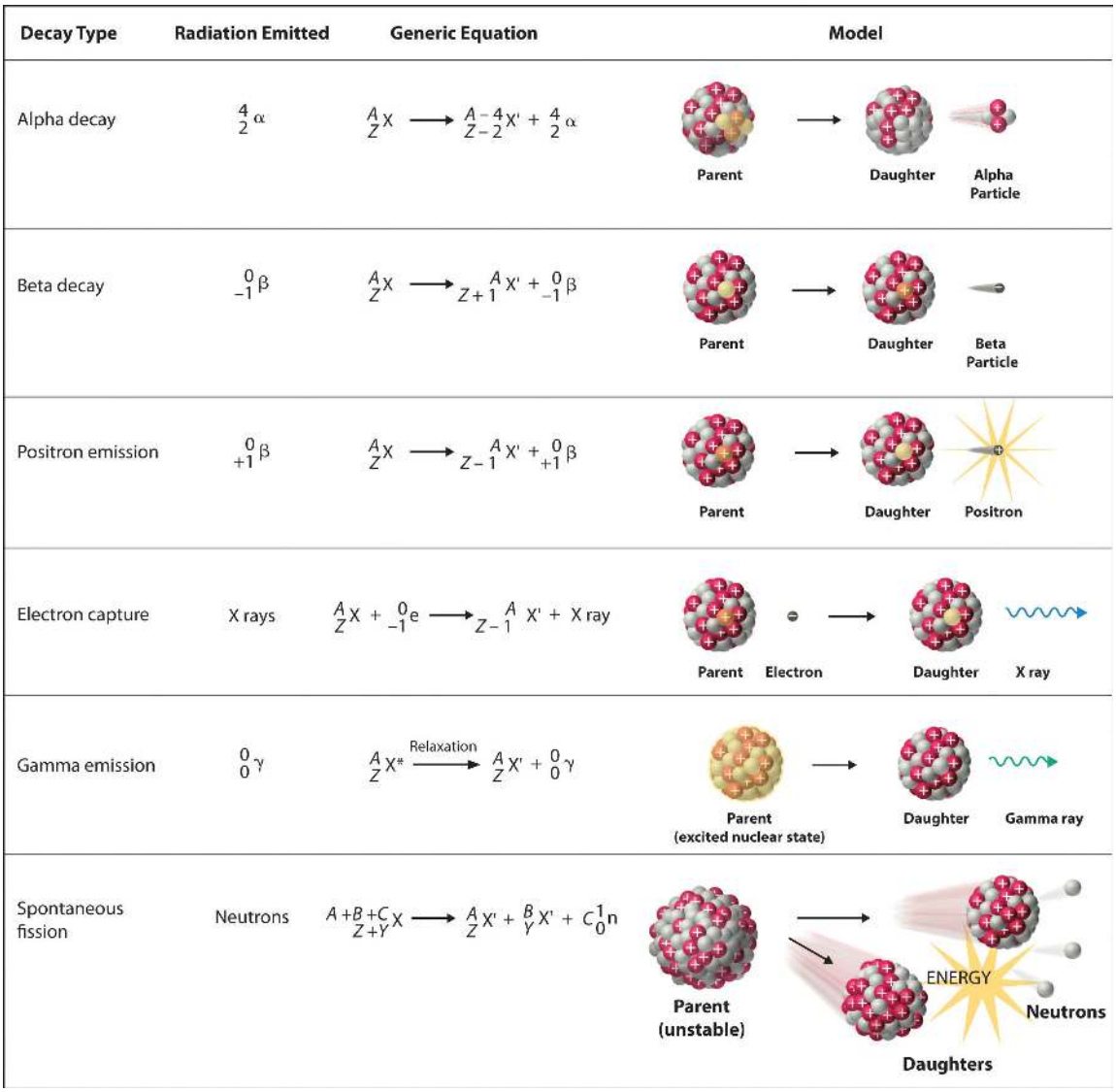


Figure **2.9.1**: Common Modes of Nuclear Decay

The different types of decay are alpha, beta, positron emission, electron capture, gamma emission, and spontaneous fission.

Alpha α Decay

Many nuclei with mass numbers greater than 200 undergo **alpha (α) decay**, which results in the emission of a helium-4 nucleus as an **alpha (α) particle**, ${}^{4}_{2}\alpha$. The general reaction is as follows:

$$\underset{\text{parent}}{{}^{A}_{Z}\mathrm{X}} \rightarrow \underset{\text{daughter}}{{}^{A-4}_{Z-2}\mathrm{X}'} + \underset{\text{particle}}{{}^{4}_{2}\alpha} \tag{2.9.2}$$

The daughter nuclide contains two fewer protons and two fewer neutrons than the parent. Thus α-particle emission produces a daughter nucleus with a mass number $A - 4$ and a nuclear charge $Z - 2$ compared to the parent nucleus. Radium-226, for example, undergoes alpha decay to form radon-222:

$${}^{226}_{88}\mathrm{Ra} \rightarrow {}^{222}_{86}\mathrm{Rn} + {}^{4}_{2}\alpha \tag{2.9.3}$$

Because nucleons are conserved in this and all other nuclear reactions, the sum of the mass numbers of the products, 222 + 4 = 226, equals the mass number of the parent. Similarly, the sum of the atomic numbers of the products, 86 + 2 = 88, equals the atomic number of the parent. Thus the nuclear equation is balanced.

> *Just as the total number of atoms is conserved in a chemical reaction, the total number of nucleons is conserved in a nuclear reaction.*

Beta β^- Decay

Nuclei that contain too many neutrons often undergo **beta (β) decay**, in which a neutron is converted to a proton and a high-energy electron that is ejected from the nucleus as a β particle:

$$\underset{\substack{\text{unstable}\\\text{neutron in}\\\text{nucleus}}}{{}^{1}_{0}\text{n}} \rightarrow \underset{\substack{\text{proton}\\\text{retained}\\\text{by nucleus}}}{{}^{1}_{1}\text{p}} + \underset{\substack{\text{beta particle}\\\text{emitted by}\\\text{nucleus}}}{{}^{0}_{-1}\beta} \tag{2.9.4}$$

The general reaction for beta decay is therefore

$$\underset{\text{parent}}{{}^{A}_{Z}\text{X}} \rightarrow \underset{\text{daughter}}{{}^{A}_{Z+1}\text{X}'} + \underset{\text{beta particle}}{{}^{0}_{-1}\beta} \tag{2.9.5}$$

Although beta decay does not change the mass number of the nucleus, it does result in an increase of +1 in the atomic number because of the addition of a proton in the daughter nucleus. Thus beta decay decreases the neutron-to-proton ratio, moving the nucleus toward the band of stable nuclei. For example, carbon-14 undergoes beta decay to form nitrogen-14:

$${}^{14}_{6}\text{C} \rightarrow {}^{14}_{7}\text{N} + {}^{0}_{-1}\beta$$

Once again, the number of nucleons is conserved, and the charges are balanced. The parent and the daughter nuclei have the same mass number, 14, and the sum of the atomic numbers of the products is 6, which is the same as the atomic number of the carbon-14 parent.

Positron β^+ Emission

Because a positron has the same mass as an electron but opposite charge, **positron emission** is the opposite of beta decay. Thus positron emission is characteristic of neutron-poor nuclei, which decay by transforming a proton to a neutron and emitting a high-energy positron:

$${}^{1}_{1}\text{p}^{+} \rightarrow {}^{1}_{0}\text{n} + {}^{0}_{+1}\beta^{+} \tag{2.9.6}$$

The general reaction for positron emission is therefore

$$\underset{\text{parent}}{{}^{A}_{Z}\text{X}} \rightarrow \underset{\text{daughter}}{{}^{A}_{Z-1}\text{X}'} + \underset{\text{positron}}{{}^{0}_{+1}\beta^{+}}$$

Like beta decay, positron emission does not change the mass number of the nucleus. In this case, however, the atomic number of the daughter nucleus is lower by 1 than that of the parent. Thus the neutron-to-proton ratio has increased, again moving the nucleus closer to the band of stable nuclei. For example, carbon-11 undergoes positron emission to form boron-11:

$${}^{11}_{6}\text{C} \rightarrow {}^{11}_{5}\text{B} + {}^{0}_{+1}\beta^{+}$$

Nucleons are conserved, and the charges balance. The mass number, 11, does not change, and the sum of the atomic numbers of the products is 6, the same as the atomic number of the parent carbon-11 nuclide.

Electron Capture

A neutron-poor nucleus can decay by either positron emission or **electron capture (EC)**, in which an electron in an inner shell reacts with a proton to produce a neutron:

$${}^{1}_{1}\text{p} + {}^{0}_{-1}\text{e} \rightarrow {}^{1}_{0}\text{n} \tag{2.9.7}$$

When a second electron moves from an outer shell to take the place of the lower-energy electron that was absorbed by the nucleus, an x-ray is emitted. The overall reaction for electron capture is thus

$$\underset{\text{parent}}{{}^{A}_{Z}\text{X}} + \underset{\text{electron}}{{}^{0}_{-1}\text{e}} \rightarrow \underset{\text{daughter}}{{}^{A}_{Z-1}\text{X}'} + \text{x-ray}$$

Electron capture does not change the mass number of the nucleus because both the proton that is lost and the neutron that is formed have a mass number of 1. As with positron emission, however, the atomic number of the daughter nucleus is lower by 1 than that of the parent. Once again, the neutron-to-proton ratio has increased, moving the nucleus toward the band of stable nuclei. For example, iron-55 decays by electron capture to form manganese-55, which is often written as follows:

$$^{55}_{26}\text{Fe} \xrightarrow{\text{EC}} {}^{55}_{25}\text{Mn} + \text{x-ray}$$

The atomic numbers of the parent and daughter nuclides differ in Equation 20.2.11, although the mass numbers are the same. To write a balanced nuclear equation for this reaction, we must explicitly include the captured electron in the equation:

$$^{55}_{26}\text{Fe} + {}^{0}_{-1}\text{e} \rightarrow {}^{55}_{25}\text{Mn} + \text{x-ray}$$

Both positron emission and electron capture are usually observed for nuclides with low neutron-to-proton ratios, but the decay rates for the two processes can be very different.

Gamma γ Emission

Many nuclear decay reactions produce daughter nuclei that are in a nuclear excited state, which is similar to an atom in which an electron has been excited to a higher-energy orbital to give an electronic excited state. Just as an electron in an electronic excited state emits energy in the form of a photon when it returns to the ground state, a nucleus in an excited state releases energy in the form of a photon when it returns to the ground state. These high-energy photons are γ rays. **Gamma (γ) emission** can occur virtually instantaneously, as it does in the alpha decay of uranium-238 to thorium-234, where the asterisk denotes an excited state:

$$^{238}_{92}\text{U} \rightarrow \underset{\substack{\text{excited}\\ \text{nuclear}\\ \text{state}}}{^{234}_{90}\text{Th}^*} + {}^{4}_{2}\alpha \xrightarrow{\text{relaxation}} {}^{234}_{90}\text{Th} + {}^{0}_{0}\gamma$$

If we disregard the decay event that created the excited nucleus, then

$$^{234}_{88}\text{Th}^* \rightarrow {}^{234}_{88}\text{Th} + {}^{0}_{0}\gamma$$

or more generally,

$$^{A}_{Z}\text{X}^* \rightarrow {}^{A}_{Z}\text{X} + {}^{0}_{0}\gamma$$

Gamma emission can also occur after a significant delay. For example, technetium-99*m* has a half-life of about 6 hours before emitting a γ ray to form technetium-99 (the *m* is for metastable). Because γ rays are energy, their emission does not affect either the mass number or the atomic number of the daughter nuclide. Gamma-ray emission is therefore the only kind of radiation that does not necessarily involve the conversion of one element to another, although it is almost always observed in conjunction with some other nuclear decay reaction.

Spontaneous Fission

Only very massive nuclei with high neutron-to-proton ratios can undergo **spontaneous fission**, in which the nucleus breaks into two pieces that have different atomic numbers and atomic masses. This process is most important for the transactinide elements, with $Z \geq 104$. Spontaneous fission is invariably accompanied by the release of large amounts of energy, and it is usually accompanied by the emission of several neutrons as well. An example is the spontaneous fission of $^{254}_{98}\text{Cf}$, which gives a distribution of fission products; one possible set of products is shown in the following equation:

$$^{254}_{98}\text{Cf} \rightarrow {}^{118}_{46}\text{Pd} + {}^{132}_{52}\text{Te} + 4{}^{1}_{0}\text{n}$$

Once again, the number of nucleons is conserved. Thus the sum of the mass numbers of the products (118 + 132 + 4 = 254) equals the mass number of the reactant. Similarly, the sum of the atomic numbers of the products [46 + 52 + (4 × 0) = 98] is the same as the atomic number of the parent nuclide.

Example 2.9.2

Write a balanced nuclear equation to describe each reaction.

a. the beta decay of $^{35}_{16}\mathrm{S}$
b. the decay of $^{201}_{80}\mathrm{Hg}$ by electron capture
c. the decay of $^{30}_{15}\mathrm{P}$ by positron emission

Given: radioactive nuclide and mode of decay

Asked for: balanced nuclear equation

Strategy:

A Identify the reactants and the products from the information given.

B Use the values of *A* and *Z* to identify any missing components needed to balance the equation.

Solution

a.

A We know the identities of the reactant and one of the products (a β particle). We can therefore begin by writing an equation that shows the reactant and one of the products and indicates the unknown product as $^{A}_{Z}\mathrm{X}$:

$$^{35}_{16}\mathrm{S} \rightarrow {}^{A}_{Z}\mathrm{X} + {}^{0}_{-1}\beta$$

B Because both protons and neutrons must be conserved in a nuclear reaction, the unknown product must have a mass number of $A = 35 - 0 = 35$ and an atomic number of $Z = 16 - (-1) = 17$. The element with $Z = 17$ is chlorine, so the balanced nuclear equation is as follows:

$$^{35}_{16}\mathrm{S} \rightarrow {}^{35}_{17}\mathrm{Cl} + {}^{0}_{-1}\beta$$

b.

A We know the identities of both reactants: $^{201}_{80}\mathrm{Hg}$ and an inner electron, $^{0}_{-1}\mathrm{e}$. The reaction is as follows:

$$^{201}_{80}\mathrm{Hg} + {}^{0}_{-1}\mathrm{e} \rightarrow {}^{A}_{Z}\mathrm{X}$$

B Both protons and neutrons are conserved, so the mass number of the product must be $A = 201 + 0 = 201$, and the atomic number of the product must be $Z = 80 + (-1) = 79$, which corresponds to the element gold. The balanced nuclear equation is thus

$$^{201}_{80}\mathrm{Hg} + {}^{0}_{-1}\mathrm{e} \rightarrow {}^{201}_{79}\mathrm{Au}$$

c.

A As in part (a), we are given the identities of the reactant and one of the products—in this case, a positron. The unbalanced nuclear equation is therefore

$$^{30}_{15}\mathrm{P} \rightarrow {}^{A}_{Z}\mathrm{X} + {}^{0}_{+1}\beta$$

B The mass number of the second product is $A = 30 - 0 = 30$, and its atomic number is $Z = 15 - 1 = 14$, which corresponds to silicon. The balanced nuclear equation for the reaction is as follows:

$$^{30}_{15}\mathrm{P} \rightarrow {}^{30}_{14}\mathrm{Si} + {}^{0}_{+1}\beta$$

Exercise 2.9.2

Write a balanced nuclear equation to describe each reaction.

a. $^{11}_{6}\mathrm{C}$ by positron emission
b. the beta decay of molybdenum-99
c. the emission of an α particle followed by gamma emission from $^{185}_{74}\mathrm{W}$

Answer a

$$^{11}_{6}\text{C} \rightarrow {}^{11}_{5}\text{B} + {}^{0}_{+1}\beta$$

Answer d

$$^{99}_{42}\text{Mo} \rightarrow {}^{99m}_{43}\text{Tc} + {}^{0}_{-1}\beta$$

Answer c

$$^{185}_{74}\text{W} \rightarrow {}^{181}_{72}\text{Hf} + {}^{4}_{2}\alpha + {}^{0}_{0}\gamma$$

Example 2.9.3

Predict the kind of nuclear change each unstable nuclide undergoes when it decays.

a. $^{45}_{22}\text{Ti}$
b. $^{242}_{94}\text{Pu}$
c. $^{12}_{5}\text{B}$
d. $^{256}_{100}\text{Fm}$

Given: nuclide

Asked for: type of nuclear decay

Strategy:

Based on the neutron-to-proton ratio and the value of *Z*, predict the type of nuclear decay reaction that will produce a more stable nuclide.

Solution

a. This nuclide has a neutron-to-proton ratio of only 1.05, which is much less than the requirement for stability for an element with an atomic number in this range. Nuclei that have low neutron-to-proton ratios decay by converting a proton to a neutron. The two possibilities are positron emission, which converts a proton to a neutron and a positron, and electron capture, which converts a proton and a core electron to a neutron. In this case, both are observed, with positron emission occurring about 86% of the time and electron capture about 14% of the time.
b. Nuclei with $Z > 83$ are too heavy to be stable and usually undergo alpha decay, which decreases both the mass number and the atomic number. Thus $^{242}_{94}\text{Pu}$ is expected to decay by alpha emission.
c. This nuclide has a neutron-to-proton ratio of 1.4, which is very high for a light element. Nuclei with high neutron-to-proton ratios decay by converting a neutron to a proton and an electron. The electron is emitted as a β particle, and the proton remains in the nucleus, causing an increase in the atomic number with no change in the mass number. We therefore predict that $^{12}_{5}\text{B}$ will undergo beta decay.
d. This is a massive nuclide, with an atomic number of 100 and a mass number much greater than 200. Nuclides with $A \geq 200$ tend to decay by alpha emission, and even heavier nuclei tend to undergo spontaneous fission. We therefore predict that $^{256}_{100}\text{Fm}$ will decay by either or both of these two processes. In fact, it decays by both spontaneous fission and alpha emission, in a 97:3 ratio.

Exercise 2.9.3

Predict the kind of nuclear change each unstable nuclide undergoes when it decays.

a. $^{32}_{14}\text{Si}$
b. $^{43}_{21}\text{Sc}$
c. $^{231}_{91}\text{Pa}$

Answer a

beta decay

Answer d

positron emission or electron capture

Answer c

alpha decay

Radioactive Decay Series

The nuclei of all elements with atomic numbers greater than 83 are unstable. Thus all isotopes of all elements beyond bismuth in the periodic table are radioactive. Because alpha decay decreases Z by only 2, and positron emission or electron capture decreases Z by only 1, it is impossible for any nuclide with $Z > 85$ to decay to a stable daughter nuclide in a single step, except via nuclear fission. Consequently, radioactive isotopes with $Z > 85$ usually decay to a daughter nucleus that is radiaoctive, which in turn decays to a second radioactive daughter nucleus, and so forth, until a stable nucleus finally results. This series of sequential alpha- and beta-decay reactions is called a **radioactive decay series**. The most common is the uranium-238 decay series, which produces lead-206 in a series of 14 sequential alpha- and beta-decay reactions (Figure **2.9.2**). Although a radioactive decay series can be written for almost any isotope with $Z > 85$, only two others occur naturally: the decay of uranium-235 to lead-207 (in 11 steps) and thorium-232 to lead-208 (in 10 steps). A fourth series, the decay of neptunium-237 to bismuth-209 in 11 steps, is known to have occurred on the primitive Earth. With a half-life of "only" 2.14 million years, all the neptunium-237 present when Earth was formed decayed long ago, and today all the neptunium on Earth is synthetic.

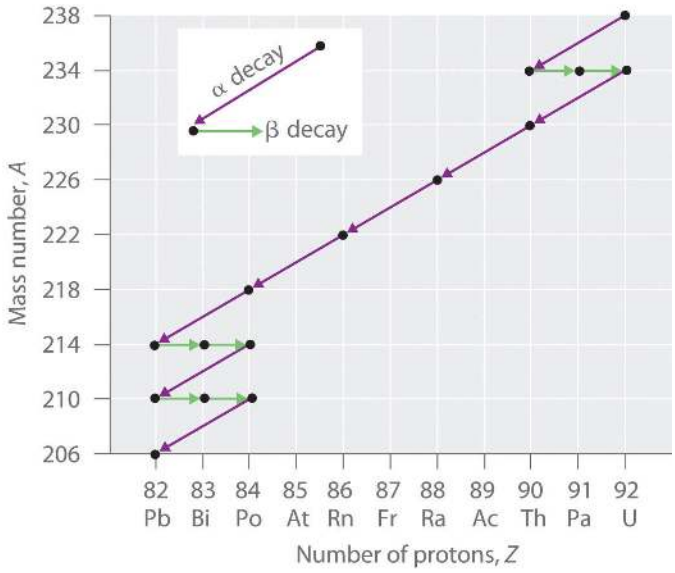


Figure **2.9.2** A Radioactive Decay Series. Three naturally occurring radioactive decay series are known to occur currently: the uranium-238 decay series, the decay of uranium-235 to lead-207, and the decay of thorium-232 to lead-208.

Graph of mass number against number of protons. The purple lines are alpha decay which are linear while the green lines are beta decay and are horizontal and parallel to the x axis.

Due to these radioactive decay series, small amounts of very unstable isotopes are found in ores that contain uranium or thorium. These rare, unstable isotopes should have decayed long ago to stable nuclei with a lower atomic number, and they would no longer be found on Earth. Because they are generated continuously by the decay of uranium or thorium, however, their amounts have reached a steady state, in which their rate of formation is equal to their rate of decay. In some cases, the abundance of the daughter isotopes can be used to date a material or identify its origin.

Induced Nuclear Reactions

The discovery of radioactivity in the late 19th century showed that some nuclei spontaneously transform into nuclei with a different number of protons, thereby producing a different element. When scientists realized that these naturally occurring radioactive isotopes decayed by emitting subatomic particles, they realized that—in principle—it should be possible to carry out the reverse reaction, converting a stable nucleus to another more massive nucleus by bombarding it with subatomic particles in a nuclear transmutation reaction.

The first successful nuclear transmutation reaction was carried out in 1919 by Ernest Rutherford, who showed that α particles emitted by radium could react with nitrogen nuclei to form oxygen nuclei. As shown in the following equation, a proton is emitted in the process:

$$^{4}_{2}\alpha + {}^{14}_{7}\mathrm{N} \rightarrow {}^{17}_{8}\mathrm{O} + {}^{1}_{1}\mathrm{p}$$

Rutherford's nuclear transmutation experiments led to the discovery of the neutron. He found that bombarding the nucleus of a light target element with an α particle usually converted the target nucleus to a product that had an atomic number higher by 1 and a mass number higher by 3 than the target nucleus. Such behavior is consistent with the emission of a proton after reaction with the α particle. Very light targets such as Li, Be, and B reacted differently, however, emitting a new kind of highly penetrating radiation rather than a proton. Because neither a magnetic field nor an electrical field could deflect these high-energy particles, Rutherford concluded that they were electrically neutral. Other observations suggested that the mass of the neutral particle was similar to the mass of the proton. In 1932, James Chadwick (Nobel Prize in Physics, 1935), who was a student of Rutherford's at the time, named these neutral particles neutrons and proposed that they were fundamental building blocks of the atom. The reaction that Chadwick initially used to explain the production of neutrons was as follows:

$$^{4}_{2}\alpha + {}^{9}_{4}\mathrm{Be} \rightarrow {}^{12}_{6}\mathrm{C} + {}^{1}_{0}\mathrm{n} \tag{2.9.8}$$

Because α particles and atomic nuclei are both positively charged, electrostatic forces cause them to repel each other. Only α particles with very high kinetic energy can overcome this repulsion and collide with a nucleus (Figure **2.9.3**). Neutrons have no electrical charge, however, so they are not repelled by the nucleus. Hence bombardment with neutrons is a much easier way to prepare new isotopes of the lighter elements. In fact, carbon-14 is formed naturally in the atmosphere by bombarding nitrogen-14 with neutrons generated by cosmic rays:

$$^{1}_{0}\mathrm{n} + {}^{14}_{7}\mathrm{N} \rightarrow {}^{14}_{6}\mathrm{C} + {}^{1}_{1}\mathrm{p} \tag{2.9.9}$$

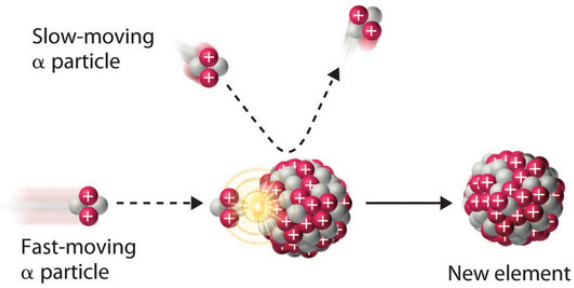


Figure **2.9.3**: A Nuclear Transmutation Reaction. Bombarding a target of one element with high-energy nuclei or subatomic particles can create new elements. Electrostatic repulsions normally prevent a positively charged particle from colliding and reacting with a positively charged nucleus. If the positively charged particle is moving at a very high speed, however, its kinetic energy may be great enough to overcome the electrostatic repulsions, and it may collide with the target nucleus. Such collisions can result in a nuclear transmutation reaction.

✔ Example 2.9.4

In 1933, Frédéric Joliot and Iréne Joliot-Curie (daughter of Marie and Pierre Curie) prepared the first artificial radioactive isotope by bombarding aluminum-27 with α particles. For each ^{27}Al that reacted, one neutron was released. Identify the product nuclide and write a balanced nuclear equation for this transmutation reaction.

Given: reactants in a nuclear transmutation reaction

Asked for: product nuclide and balanced nuclear equation

Strategy:

A Based on the reactants and one product, identify the other product of the reaction. Use conservation of mass and charge to determine the values of *Z* and *A* of the product nuclide and thus its identity.

B Write the balanced nuclear equation for the reaction.

Solution

A Bombarding an element with α particles usually produces an element with an atomic number that is 2 greater than the atomic number of the target nucleus. Thus we expect that aluminum (Z = 13) will be converted to phosphorus (Z = 15). With one neutron released, conservation of mass requires that the mass number of the other product be 3 greater than the mass number of the target. In this case, the mass number of the target is 27, so the mass number of the product will be 30. The second product is therefore phosphorus-30, $^{30}_{15}\mathrm{P}$.

B The balanced nuclear equation for the reaction is as follows:

$$^{27}_{13}\mathrm{Al} + {}^{4}_{2}\alpha \rightarrow {}^{30}_{15}\mathrm{P} + {}^{1}_{0}\mathrm{n}$$

? Exercise 2.9.4

Because all isotopes of technetium are radioactive and have short half-lives, it does not exist in nature. Technetium can, however, be prepared by nuclear transmutation reactions. For example, bombarding a molybdenum-96 target with deuterium nuclei ($^{2}_{1}\mathrm{H}$) produces technetium-97. Identify the other product of the reaction and write a balanced nuclear equation for this transmutation reaction.

Answer

neutron, $^{1}_{0}\mathrm{n}$; $^{96}_{42}\mathrm{Mo} + {}^{2}_{1}\mathrm{H} \rightarrow {}^{97}_{43}\mathrm{Tc} + {}^{1}_{0}\mathrm{n}$:

We noted earlier in this section that very heavy nuclides, corresponding to $Z \geq 104$, tend to decay by spontaneous fission. Nuclides with slightly lower values of Z, such as the isotopes of uranium (Z = 92) and plutonium (Z = 94), do not undergo spontaneous fission at any significant rate. Some isotopes of these elements, however, such as $^{235}_{92}\mathrm{U}$ and $^{239}_{94}\mathrm{Pu}$ undergo induced nuclear fission when they are bombarded with relatively low-energy neutrons, as shown in the following equation for uranium-235 and in Figure 2.9.4:

$$^{235}_{92}\mathrm{U} + {}^{1}_{0}\mathrm{n} \rightarrow {}^{236}_{92}\mathrm{U} \rightarrow {}^{141}_{56}\mathrm{Ba} + {}^{92}_{36}\mathrm{Kr} + 3{}^{1}_{0}\mathrm{n} \tag{2.9.10}$$

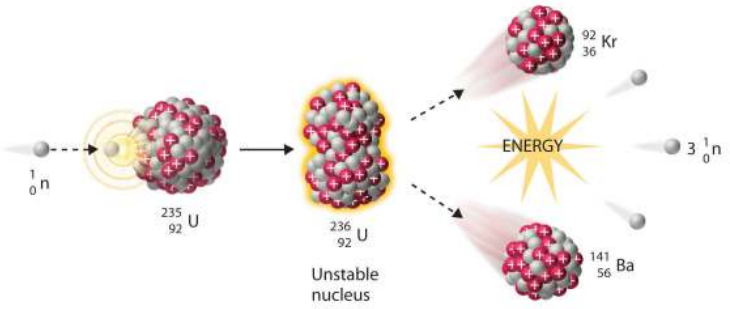


Figure 2.9.4 Neutron-Induced Nuclear Fission. Collision of a relatively slow-moving neutron with a fissile nucleus can split it into two smaller nuclei with the same or different masses. Neutrons are also released in the process, along with a great deal of energy.

Any isotope that can undergo a nuclear fission reaction when bombarded with neutrons is called a **fissile isotope**.

During nuclear fission, the nucleus usually divides asymmetrically rather than into two equal parts, as shown in Figure 2.9.4. Moreover, every fission event of a given nuclide does not give the same products; more than 50 different fission modes have been identified for uranium-235, for example. Consequently, nuclear fission of a fissile nuclide can never be described by a single equation. Instead, as shown in Figure 2.9.5, a distribution of many pairs of fission products with different yields is obtained, but the mass ratio of each pair of fission products produced by a single fission event is always roughly 3:2.

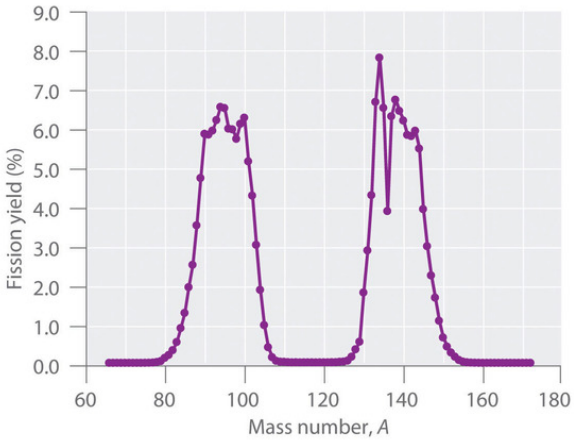


Figure **2.9.5**: Mass Distribution of Nuclear Fission Products of ^{235}U. Nuclear fission usually produces a range of products with different masses and yields, although the mass ratio of each pair of fission products from a fission event is approximately 3:2. As shown in this plot, more than 50 different fission products are known for^{235}U. Data source: T. R. England and B. F. Rider, Los Alamos National Laboratory, LA-UR-94-3106, ENDF-349 (1993).

Synthesis of Transuranium Elements

Uranium (Z = 92) is the heaviest naturally occurring element. Consequently, all the elements with Z > 92, the **transuranium elements**, are artificial and have been prepared by bombarding suitable target nuclei with smaller particles. The first of the transuranium elements to be prepared was neptunium (Z = 93), which was synthesized in 1940 by bombarding a ^{238}U target with neutrons. As shown in Equation 20.21, this reaction occurs in two steps. Initially, a neutron combines with a ^{238}U nucleus to form ^{239}U, which is unstable and undergoes beta decay to produce ^{239}Np:

$$^{238}_{92}\mathrm{U} + {}^{1}_{0}\mathrm{n} \rightarrow {}^{239}_{92}\mathrm{U} \rightarrow {}^{239}_{93}\mathrm{Np} + {}^{0}_{-1}\beta$$

Subsequent beta decay of ^{239}Np produces the second transuranium element, plutonium (Z = 94):

$$^{239}_{93}\mathrm{Np} \rightarrow {}^{239}_{94}\mathrm{Pu} + {}^{0}_{-1}\beta$$

Bombarding the target with more massive nuclei creates elements that have atomic numbers significantly greater than that of the target nucleus (Table **2.9.2**). Such techniques have resulted in the creation of the superheavy elements 114 and 116, both of which lie in or near the “island of stability."

Table **2.9.2**: Some Reactions Used to Synthesize Transuranium Elements

$^{239}_{94}\mathrm{Pu} + {}^{4}_{2}\alpha \rightarrow {}^{242}_{96}\mathrm{Cm} + {}^{1}_{0}\mathrm{n}$
$^{239}_{94}\mathrm{Pu} + {}^{4}_{2}\alpha \rightarrow {}^{241}_{95}\mathrm{Am} + {}^{1}_{1}\mathrm{p} + {}^{1}_{0}\mathrm{n}$
$^{242}_{96}\mathrm{Cm} + {}^{4}_{2}\alpha \rightarrow {}^{243}_{97}\mathrm{Bk} + {}^{1}_{1}\mathrm{p} + 2{}^{1}_{0}\mathrm{n}$
$^{253}_{99}\mathrm{Es} + {}^{4}_{2}\alpha \rightarrow {}^{256}_{101}\mathrm{Md} + {}^{1}_{0}\mathrm{n}$
$^{238}_{92}\mathrm{U} + {}^{12}_{6}\mathrm{C} \rightarrow {}^{246}_{98}\mathrm{Cf} + 4{}^{1}_{0}\mathrm{n}$
$^{252}_{98}\mathrm{Cf} + {}^{10}_{5}\mathrm{B} \rightarrow {}^{256}_{103}\mathrm{Lr} + 6{}^{1}_{0}\mathrm{n}$

A device called a particle accelerator is used to accelerate positively charged particles to the speeds needed to overcome the electrostatic repulsions between them and the target nuclei by using electrical and magnetic fields. Operationally, the simplest particle accelerator is the linear accelerator (Figure **2.9.6**), in which a beam of particles is injected at one end of a long evacuated tube. Rapid alternation of the polarity of the electrodes along the tube causes the particles to be alternately accelerated toward a region of opposite charge and repelled by a region with the same charge, resulting in a tremendous acceleration as the particle travels down the tube. A modern linear accelerator such as the Stanford Linear Accelerator (SLAC) at Stanford University is about 2 miles long.

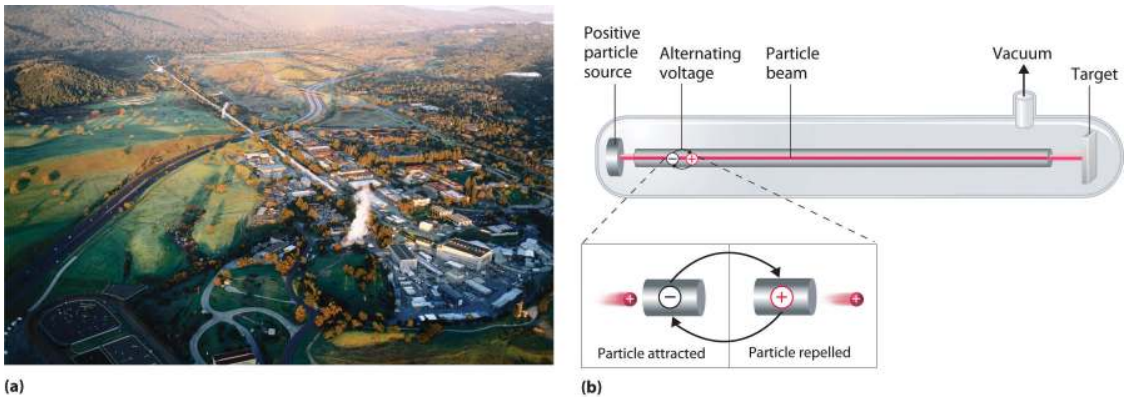


Figure **2.9.6**: A Linear Particle Accelerator. (a) An aerial view of the SLAC, the longest linear particle accelerator in the world; the overall length of the tunnel is 2 miles. (b) Rapidly reversing the polarity of the electrodes in the tube causes the charged particles to be alternately attracted as they enter one section of the tube and repelled as they leave that section. As a result, the particles are continuously accelerated along the length of the tube.

To achieve the same outcome in less space, a particle accelerator called a cyclotron forces the charged particles to travel in a circular path rather than a linear one. The particles are injected into the center of a ring and accelerated by rapidly alternating the polarity of two large D-shaped electrodes above and below the ring, which accelerates the particles outward along a spiral path toward the target.

The length of a linear accelerator and the size of the D-shaped electrodes in a cyclotron severely limit the kinetic energy that particles can attain in these devices. These limitations can be overcome by using a synchrotron, a hybrid of the two designs. A synchrotron contains an evacuated tube similar to that of a linear accelerator, but the tube is circular and can be more than a mile in diameter. Charged particles are accelerated around the circle by a series of magnets whose polarities rapidly alternate.

Summary and Key Takeaway

- Nuclear decay reactions occur spontaneously under all conditions and produce more stable daughter nuclei, whereas nuclear transmutation reactions are induced and form a product nucleus that is more massive than the starting material.

In **nuclear decay reactions (or radioactive decay)**, the parent nucleus is converted to a more stable daughter nucleus. Nuclei with too many neutrons decay by converting a neutron to a proton, whereas nuclei with too few neutrons decay by converting a proton to a neutron. Very heavy nuclei (with $A \geq 200$ and $Z > 83$) are unstable and tend to decay by emitting an **α particle**. When an unstable nuclide undergoes radioactive decay, the total number of nucleons is conserved, as is the total positive charge. Six different kinds of nuclear decay reactions are known. *Alpha decay* results in the emission of an α particle, $^{4}_{2}\alpha$, and produces a daughter nucleus with a mass number that is lower by 4 and an atomic number that is lower by 2 than the parent nucleus. **Beta decay** converts a neutron to a proton and emits a high-energy electron, producing a daughter nucleus with the same mass number as the parent and an atomic number that is higher by 1. **Positron emission** is the opposite of beta decay and converts a proton to a neutron plus a positron. Positron emission does not change the mass number of the nucleus, but the atomic number of the daughter nucleus is lower by 1 than the parent. In **electron capture (EC)**, an electron in an inner shell reacts with a proton to produce a neutron, with emission of an x-ray. The mass number does not change, but the atomic number of the daughter is lower by 1 than the parent. In **gamma emission**, a daughter nucleus in a nuclear excited state undergoes a transition to a lower-energy state by emitting a γ ray. Very heavy nuclei with high neutron-to-proton ratios can undergo **spontaneous fission**, in which the nucleus breaks into two pieces that can have different atomic numbers and atomic masses with the release of neutrons. Many very heavy nuclei decay via a **radioactive decay series**—a succession of some combination of alpha- and beta-decay reactions. In **nuclear transmutation reactions**, a target nucleus is bombarded with energetic subatomic particles to give a product nucleus that is more massive than the original. All **transuranium elements**—elements with $Z > 92$—are artificial and must be prepared by nuclear transmutation reactions. These reactions are carried out in particle accelerators such as linear accelerators, cyclotrons, and synchrotrons.

Key Equations

alpha decay

$$^{A}_{Z}\mathrm{X} \rightarrow {}^{A-4}_{Z-2}\mathrm{X}' + {}^{4}_{2}\alpha$$

beta decay

$$ {}^{A}_{Z}\mathrm{X} \rightarrow {}^{A}_{Z+1}\mathrm{X}' + {}^{0}_{-1}\beta $$

positron emission

$$ {}^{A}_{Z}\mathrm{X} \rightarrow {}^{A}_{Z-1}\mathrm{X}' + {}^{0}_{+1}\beta $$

electron capture

$$ {}^{A}_{Z}\mathrm{X} + {}^{0}_{-1}\mathrm{e} \rightarrow {}^{A}_{Z-1}\mathrm{X}' + \text{x-ray} $$

gamma emission

$$ {}^{A}_{Z}\mathrm{X}^{*} \rightarrow {}^{A}_{Z}\mathrm{X} + {}^{0}_{0}\gamma $$

2.9: Nuclear Radiation is shared under a not declared license and was authored, remixed, and/or curated by LibreTexts.

- **21.1: Radioactivity** is licensed CC BY-NC-SA 3.0.

2.10: Rates of Radioactive Decay

Learning Objectives

- To know how to use half-lives to describe the rates of first-order reactions

The rate of radioactive decay is an intrinsic property of each radioactive isotope that is independent of the chemical and physical form of the radioactive isotope. The rate is also independent of temperature. In this section, we will describe radioactive decay rates and how half-lives can be used to monitor radioactive decay processes.

A Quick Primer from Chemical Kinetics

As discussed previously, the half-life of a first-order reaction is independent of the concentration of the reactants. This becomes evident when we rearrange the integrated rate law for a first-order reaction to produce the following equation:

$$\ln \frac{[\mathrm{A}]_0}{[\mathrm{A}]} = kt \tag{2.10.1}$$

Substituting $[\mathrm{A}]_{0/2}$ for [A] and $t_{1/2}$ for t (to indicate a half-life) into Equation 2.10.1 gives

$$\ln \frac{[\mathrm{A}]_0}{[\mathrm{A}]_0/2} = \ln 2 = kt_{1/2} \tag{2.10.2}$$

Substituting $\ln 2 \approx 0.693$ into the equation results in the expression for the half-life of a first-order reaction:

$$t_{1/2} = \frac{0.693}{k} \tag{2.10.3}$$

Thus, for a first-order reaction, each successive half-life is the same length of time. Since radioactivity follows first order decay kinetics, these equations are also applicable for this type of nuclear reactions.

In any sample of a given radioactive substance, the number of atoms of the radioactive isotope must decrease with time as their nuclei decay to nuclei of a more stable isotope. Using N to represent the number of atoms of the radioactive isotope, we can define the **rate of decay** of the sample, which is also called its **activity** (A) as the decrease in the number of the radioisotope's nuclei per unit time:

$$A = -\frac{\Delta N}{\Delta t} \tag{2.10.4}$$

Activity is usually measured in disintegrations per second (dps) or disintegrations per minute (dpm).

The activity of a sample is directly proportional to the number of atoms of the radioactive isotope in the sample:

$$A = kN \tag{2.10.5}$$

Here, the symbol k is the radioactive decay constant, which has units of inverse time (e.g., s^{-1}, yr^{-1}) and a characteristic value for each radioactive isotope. If we combine Equation 2.10.4 and Equation 2.10.5, we obtain the relationship between the number of decays per unit time and the number of atoms of the isotope in a sample:

$$-\frac{\Delta N}{\Delta t} = kN \tag{2.10.6}$$

Equation 2.10.6 is the same as the equation for the reaction rate of a first-order reaction, except that it uses numbers of atoms instead of concentrations. In fact, radioactive decay is a first-order process and can be described in terms of either the differential rate law (Equation 2.10.6) or the integrated rate law:

$$N = N_0 e^{-kt} \tag{2.10.7}$$

$$\ln \frac{N}{N_0} = -kt \tag{2.10.8}$$

Because radioactive decay is a first-order process, the time required for half of the nuclei in any sample of a radioactive isotope to decay is a constant, called the half-life of the isotope. The half-life tells us how radioactive an isotope is (the number of decays per unit time); thus it is the most commonly cited property of any radioisotope. For a given number of atoms, isotopes with shorter half-lives decay more rapidly, undergoing a greater number of radioactive decays per unit time than do isotopes with longer half-lives. The half-lives of several isotopes are listed in Table **2.10.1**, along with some of their applications.

Table **2.10.1**: Half-Lives and Applications of Some Radioactive Isotopes

Radioactive Isotope	Half-Life	Typical Uses
hydrogen-3 (tritium)	12.32 yr	biochemical tracer
carbon-11	20.33 min	positron emission tomography (biomedical imaging)
carbon-14	5.70×10^3 yr	dating of artifacts
sodium-24	14.951 h	cardiovascular system tracer
phosphorus-32	14.26 days	biochemical tracer
potassium-40	1.248×10^9 yr	dating of rocks
iron-59	44.495 days	red blood cell lifetime tracer
cobalt-60	5.2712 yr	radiation therapy for cancer
technetium-99*m**	6.006 h	biomedical imaging
iodine-131	8.0207 days	thyroid studies tracer
radium-226	1.600×10^3 yr	radiation therapy for cancer
uranium-238	4.468×10^9 yr	dating of rocks and Earth's crust
americium-241	432.2 yr	smoke detectors

*The *m* denotes metastable, where an excited state nucleus decays to the ground state of the same isotope.

Radioisotope Dating Techniques

In our earlier discussion, we used the half-life of a first-order reaction to calculate how long the reaction had been occurring. Because nuclear decay reactions follow first-order kinetics and have a rate constant that is independent of temperature and the chemical or physical environment, we can perform similar calculations using the half-lives of isotopes to estimate the ages of geological and archaeological artifacts. The techniques that have been developed for this application are known as radioisotope dating techniques.

The most common method for measuring the age of ancient objects is carbon-14 dating. The carbon-14 isotope, created continuously in the upper regions of Earth's atmosphere, reacts with atmospheric oxygen or ozone to form $^{14}CO_2$. As a result, the CO_2 that plants use as a carbon source for synthesizing organic compounds always includes a certain proportion of $^{14}CO_2$ molecules as well as nonradioactive $^{12}CO_2$ and $^{13}CO_2$. Any animal that eats a plant ingests a mixture of organic compounds that contains approximately the same proportions of carbon isotopes as those in the atmosphere. When the animal or plant dies, the carbon-14 nuclei in its tissues decay to nitrogen-14 nuclei by a radioactive process known as beta decay, which releases low-energy electrons (β particles) that can be detected and measured:

$$^{14}C \rightarrow {}^{14}N + \beta^- \tag{2.10.9}$$

The half-life for this reaction is 5700 ± 30 yr.

The $^{14}C/^{12}C$ ratio in living organisms is 1.3×10^{-12}, with a decay rate of 15 dpm/g of carbon (Figure **2.10.1**). Comparing the disintegrations per minute per gram of carbon from an archaeological sample with those from a recently living sample enables

scientists to estimate the age of the artifact, illustrated below. Using this method implicitly assumes that the $^{14}CO_2/^{12}CO_2$ ratio in the atmosphere is constant, which is not strictly correct. Other methods, such as tree-ring dating, have been used to calibrate the dates obtained by radiocarbon dating, and all radiocarbon dates reported are now corrected for minor changes in the $^{14}CO_2/^{12}CO_2$ ratio over time.

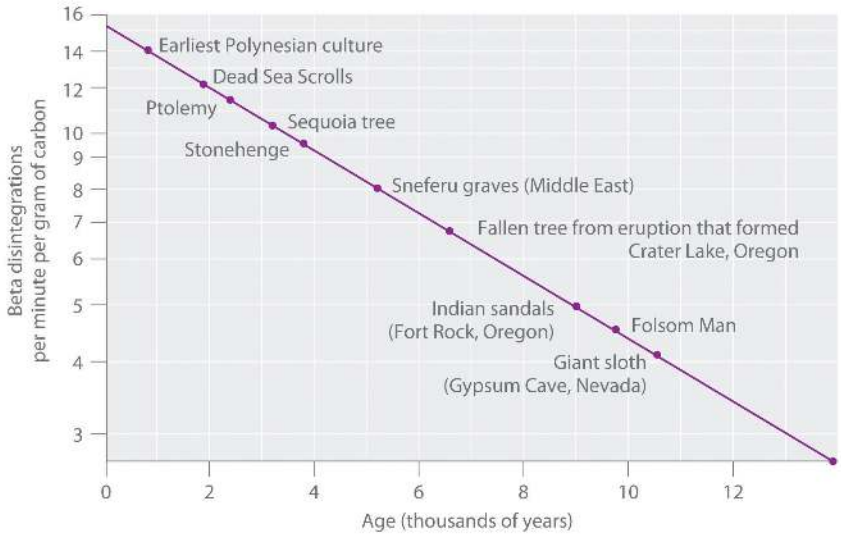


Figure 2.10.1: Radiocarbon Dating. A plot of the specific activity of ^{14}C versus age for a number of archaeological samples shows an inverse linear relationship between ^{14}C content (a log scale) and age (a linear scale).

Example 2.10.1

In 1990, the remains of an apparently prehistoric man were found in a melting glacier in the Italian Alps. Analysis of the ^{14}C content of samples of wood from his tools gave a decay rate of 8.0 dpm/g carbon. How long ago did the man die?

Given: isotope and final activity

Asked for: elapsed time

Strategy:

A Use Equation 2.10.5 to calculate N_0/N. Then substitute the value for the half-life of ^{14}C into Equation 2.10.3 to find the rate constant for the reaction.

B Using the values obtained for N_0/N and the rate constant, solve Equation 2.10.8 to obtain the elapsed time.

Solution

We know the initial activity from the isotope's identity (15 dpm/g), the final activity (8.0 dpm/g), and the half-life, so we can use the integrated rate law for a first-order nuclear reaction (Equation 2.10.8) to calculate the elapsed time (the amount of time elapsed since the wood for the tools was cut and began to decay).

$$\ln \frac{N}{N_0} = -kt$$

$$\frac{\ln(N/N_0)}{k} = t$$

A From Equation 2.10.5, we know that $A = kN$. We can therefore use the initial and final activities (A_0 = 15 dpm and A = 8.0 dpm) to calculate N_0/N:

$$dfrac A_0 A = \frac{kN_0}{kN} = \frac{N_0}{N} = \frac{15}{8.0}$$

Now we need only calculate the rate constant for the reaction from its half-life (5730 yr) using Equation 2.10.3:

$$t_{1/2} = \frac{0.693}{k}$$

This equation can be rearranged as follows:

$$k = \frac{0.693}{t_{1/2}} = \frac{0.693}{5730\ \text{yr}} = 1.22 \times 10^{-4}\ \text{yr}^{-1}$$

B Substituting into the equation for *t*,

$$t = \frac{\ln(N_0/N)}{k} = \frac{\ln(15/8.0)}{1.22 \times 10^{-4}\ \text{yr}^{-1}} = 5.2 \times 10^{3}\ \text{yr}$$

From our calculations, the man died 5200 yr ago.

Exercise 2.10.1

It is believed that humans first arrived in the Western Hemisphere during the last Ice Age, presumably by traveling over an exposed land bridge between Siberia and Alaska. Archaeologists have estimated that this occurred about 11,000 yr ago, but some argue that recent discoveries in several sites in North and South America suggest a much earlier arrival. Analysis of a sample of charcoal from a fire in one such site gave a ^{14}C decay rate of 0.4 dpm/g of carbon. What is the approximate age of the sample?

Answer

30,000 yr

Summary

- The half-life of a first-order reaction is independent of the concentration of the reactants.
- The half-lives of radioactive isotopes can be used to date objects.

The half-life of a reaction is the time required for the reactant concentration to decrease to one-half its initial value. The half-life of a first-order reaction is a constant that is related to the rate constant for the reaction: $t_{1/2} = 0.693/k$. Radioactive decay reactions are first-order reactions. The rate of decay, or activity, of a sample of a radioactive substance is the decrease in the number of radioactive nuclei per unit time.

This page titled 2.10: Rates of Radioactive Decay is shared under a CC BY-NC-SA 4.0 license and was authored, remixed, and/or curated by Anonymous.

2.11: Stability of the Atomic Nucleus

Learning Objectives

- To calculate a mass-energy balance and a nuclear binding energy.
- To understand the differences between nuclear fission and fusion.

Nuclear reactions, like chemical reactions, are accompanied by changes in energy. The energy changes in nuclear reactions, however, are enormous compared with those of even the most energetic chemical reactions. In fact, the energy changes in a typical nuclear reaction are so large that they result in a measurable change of mass. In this section, we describe the relationship between mass and energy in nuclear reactions and show how the seemingly small changes in mass that accompany nuclear reactions result in the release of enormous amounts of energy.

Mass–Energy Balance

The relationship between mass (m) and energy (E) is expressed in the following equation:

$$E = mc^2 \tag{2.11.1}$$

where c is the speed of light (2.998×10^8 m/s), and E and m are expressed in units of joules and kilograms, respectively. Albert Einstein first derived this relationship in 1905 as part of his special theory of relativity: the mass of a particle is directly proportional to its energy. Thus according to Equation 20.27, every mass has an associated energy, and similarly, any reaction that involves a change in energy must be accompanied by a change in mass. This implies that all exothermic reactions should be accompanied by a decrease in mass, and all endothermic reactions should be accompanied by an increase in mass. Given the law of conservation of mass, how can this be true? The solution to this apparent contradiction is that chemical reactions are indeed accompanied by changes in mass, but these changes are simply too small to be detected. As you may recall, all particles exhibit wavelike behavior, but the wavelength is inversely proportional to the mass of the particle (actually, to its momentum, the product of its mass and velocity). Consequently, wavelike behavior is detectable only for particles with very small masses, such as electrons. For example, the chemical equation for the combustion of graphite to produce carbon dioxide is as follows:

$$\mathrm{C(graphite)} + \frac{1}{2}\mathrm{O_2(g)} \rightarrow \mathrm{CO_2(g)} \quad \Delta H^\circ = -393.5\ \mathrm{kJ/mol} \tag{2.11.2}$$

Combustion reactions are typically carried out at constant pressure, and under these conditions, the heat released or absorbed is equal to ΔH. When a reaction is carried out at constant volume, the heat released or absorbed is equal to ΔE. For most chemical reactions, however, ΔE ≈ ΔH. If we rewrite Einstein's equation as

$$\Delta E = (\Delta m)c^2 \tag{2.11.3}$$

we can rearrange the equation to obtain the following relationship between the change in mass and the change in energy:

$$\Delta m = \frac{\Delta E}{c^2} \tag{2.11.4}$$

Because 1 J = 1 $(\mathrm{kg \cdot m^2})/\mathrm{s^2}$, the change in mass is as follows:

$$\Delta m = \frac{-393.5\ \mathrm{kJ/mol}}{(2.998 \times 10^8\ \mathrm{m/s})^2} = \frac{-3.935 \times 10^5 (\mathrm{kg \cdot m^2})/(\mathrm{s^2 \cdot mol})}{(2.998 \times 10^8\ \mathrm{m/s})^2} = -4.38 \times 10^{-12}\ \mathrm{kg/mol} \tag{2.11.5}$$

This is a mass change of about 3.6×10^{-10} g/g carbon that is burned, or about 100-millionths of the mass of an electron per atom of carbon. In practice, this mass change is much too small to be measured experimentally and is negligible.

In contrast, for a typical nuclear reaction, such as the radioactive decay of ^{14}C to ^{14}N and an electron (a β particle), there is a much larger change in mass:

$$^{14}\mathrm{C} \rightarrow {}^{14}\mathrm{N} + {}^{0}_{-1}\beta \tag{2.11.6}$$

We can use the experimentally measured masses of subatomic particles and common isotopes to calculate the change in mass directly. The reaction involves the conversion of a neutral ^{14}C atom to a positively charged ^{14}N ion (with six, not seven, electrons)

and a negatively charged β particle (an electron), so the mass of the products is identical to the mass of a neutral ^{14}N atom. The total change in mass during the reaction is therefore the difference between the mass of a neutral ^{14}N atom (14.003074 amu) and the mass of a ^{14}C atom (14.003242 amu):

$$\Delta m = \text{mass}_{\text{products}} - \text{mass}_{\text{reactants}} \tag{2.11.7}$$
$$= 14.003074 \text{ amu} - 14.003242 \text{ amu} = -0.000168 \text{ amu} \tag{2.11.8}$$

The difference in mass, which has been released as energy, corresponds to almost one-third of an electron. The change in mass for the decay of 1 mol of ^{14}C is −0.000168 g = -1.68×10^{-4} g = -1.68×10^{-7} kg. Although a mass change of this magnitude may seem small, it is about 1000 times larger than the mass change for the combustion of graphite. The energy change is as follows:

$$\Delta E = (\Delta m)c^2 = (-1.68 \times 10^{-7} \text{ kg})(2.998 \times 10^8 \text{ m/s})^2 \tag{2.11.9}$$
$$= -1.51 \times 10^{10} (\text{kg} \cdot \text{m}^2)/\text{s}^2 = -1.51 \times 10^{10} \text{ J} = -1.51 \times 10^7 \text{ kJ} \tag{2.11.10}$$

The energy released in this nuclear reaction is more than 100,000 times greater than that of a typical chemical reaction, even though the decay of ^{14}C is a relatively low-energy nuclear reaction.

Because the energy changes in nuclear reactions are so large, they are often expressed in kiloelectronvolts (1 keV = 10^3 eV), megaelectronvolts (1 MeV = 10^6 eV), and even gigaelectronvolts (1 GeV = 10^9 eV) per atom or particle. The change in energy that accompanies a nuclear reaction can be calculated from the change in mass using the relationship 1 amu = 931 MeV. The energy released by the decay of one atom of ^{14}C is thus

$$(-1.68 \times 10^{-4} \text{ amu}) \left(\frac{931 \text{ MeV}}{\text{amu}} \right) = -0.156 \text{ MeV} = -156 \text{ keV} \tag{2.11.11}$$

Example 2.11.1

Calculate the changes in mass (in atomic mass units) and energy (in joules per mole and electronvolts per atom) that accompany the radioactive decay of ^{238}U to ^{234}Th and an α particle. The α particle absorbs two electrons from the surrounding matter to form a helium atom.

Given: nuclear decay reaction

Asked for: changes in mass and energy

Strategy:

A Use the mass values in Table 20.1 to calculate the change in mass for the decay reaction in atomic mass units.

B Use Equation 20.30 to calculate the change in energy in joules per mole.

C Use the relationship between atomic mass units and megaelectronvolts to calculate the change in energy in electronvolts per atom.

Solution

A Using particle and isotope masses from Table 20.1, we can calculate the change in mass as follows:

$$\Delta m = \text{mass}_{\text{products}} - \text{mass}_{\text{reactants}} = (\text{mass } ^{234}\text{Th} + \text{mass } ^4_2\text{He}) - \text{mass } ^{238}\text{U} \tag{2.11.12}$$
$$= (234.043601 \text{ amu} + 4.002603 \text{ amu}) - 238.050788 \text{ amu} = -0.004584 \text{ amu} \tag{2.11.13}$$

B Thus the change in mass for 1 mol of ^{238}U is −0.004584 g or -4.584×10^{-6} kg. The change in energy in joules per mole is as follows:

$$\Delta E = (\Delta m)c^2 = (-4.584 \times 10^{-6} \text{ kg})(2.998 \times 10^8 \text{ m/s})^2 = -4.120 \times 10^{11} \text{ J/mol}$$

C The change in energy in electronvolts per atom is as follows:

$$\Delta E = -4.584 \times 10^{-3} \text{ amu} \times \frac{931 \text{ MeV}}{\text{amu}} \times \frac{1 \times 10^6 \text{ eV}}{1 \text{ MeV}} = -4.27 \times 10^6 \text{ eV/atom}$$

Exercise 2.11.1

Calculate the changes in mass (in atomic mass units) and energy (in kilojoules per mole and kiloelectronvolts per atom) that accompany the radioactive decay of tritium (^{3}H) to ^{3}He and a β particle.

Answer

$\Delta m = -2.0 \times 10^{-5}$ amu; $\Delta E = -1.9 \times 10^6$ kJ/mol = −19 keV/atom

Nuclear Binding Energies

We have seen that energy changes in both chemical and nuclear reactions are accompanied by changes in mass. Einstein's equation, which allows us to interconvert mass and energy, has another interesting consequence: The mass of an atom is always less than the sum of the masses of its component particles. The only exception to this rule is hydrogen-1 (^{1}H), whose measured mass of 1.007825 amu is identical to the sum of the masses of a proton and an electron. In contrast, the experimentally measured mass of an atom of deuterium (^{2}H) is 2.014102 amu, although its calculated mass is 2.016490 amu:

$$m_{^2\mathrm{H}} = m_{\text{neutron}} + m_{\text{proton}} + m_{\text{electron}} \tag{2.11.14}$$

$$= 1.008665 \text{ amu} + 1.007276 \text{ amu} + 0.000549 \text{ amu} = 2.016490 \text{ amu} \tag{2.11.15}$$

The difference between the sum of the masses of the components and the measured atomic mass is called the **mass defect** of the nucleus. Just as a molecule is more stable than its isolated atoms, a nucleus is more stable (lower in energy) than its isolated components. Consequently, when isolated nucleons assemble into a stable nucleus, energy is released. According to Equation 2.11.4, this release of energy must be accompanied by a decrease in the mass of the nucleus.

The amount of energy released when a nucleus forms from its component nucleons is the **nuclear binding energy** (Figure 21.2.1). In the case of deuterium, the mass defect is 0.002388 amu, which corresponds to a nuclear binding energy of 2.22 MeV for the deuterium nucleus. Because the magnitude of the mass defect is proportional to the nuclear binding energy, both values indicate the stability of the nucleus.

Just as a molecule is more stable (lower in energy) than its isolated atoms, a nucleus is more stable than its isolated components.

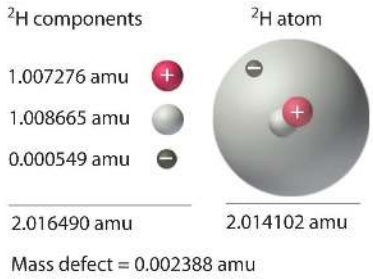


Figure 2.11.1: Nuclear Binding Energy in Deuterium. *The mass of a ^{2}H atom is less than the sum of the masses of a proton, a neutron, and an electron by 0.002388 amu; the difference in mass corresponds to the nuclear binding energy. The larger the value of the mass defect, the greater the nuclear binding energy and the more stable the nucleus.*

Not all nuclei are equally stable. Chemists describe the relative stability of different nuclei by comparing the binding energy per nucleon, which is obtained by dividing the nuclear binding energy by the mass number (A) of the nucleus. As shown in Figure 2.11.2, the binding energy per nucleon increases rapidly with increasing atomic number until about Z = 26, where it levels off to about 8–9 MeV per nucleon and then decreases slowly. The initial increase in binding energy is not a smooth curve but exhibits sharp peaks corresponding to the light nuclei that have equal numbers of protons and neutrons (e.g., ^{4}He, ^{12}C, and ^{16}O). As mentioned earlier, these are particularly stable combinations.

Because the maximum binding energy per nucleon is reached at ^{56}Fe, all other nuclei are thermodynamically unstable with regard to the formation of ^{56}Fe. Consequently, heavier nuclei (toward the right in 2.11.2) should spontaneously undergo reactions such as alpha decay, which result in a decrease in atomic number. Conversely, lighter elements (on the left in Figure 2.11.2) should spontaneously undergo reactions that result in an increase in atomic number. This is indeed the observed pattern.

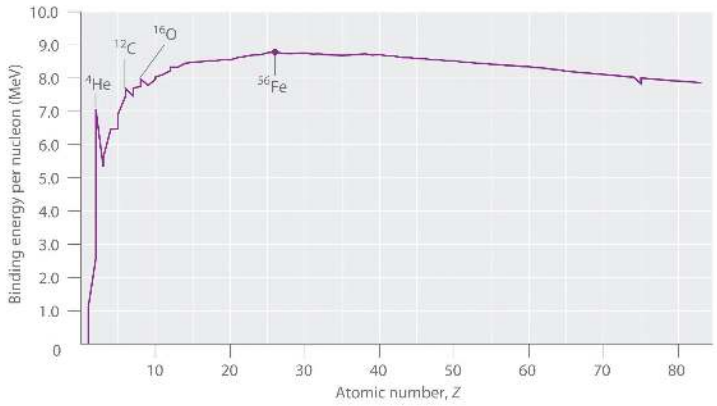


Figure **2.11.3**: The Curve of Nuclear Binding Energy. This plot of the average binding energy per nucleon as a function of atomic number shows that the binding energy per nucleon increases with increasing atomic number until about Z = 26, levels off, and then decreases. The sharp peaks correspond to light nuclei that have equal numbers of protons and neutrons.

Heavier nuclei spontaneously undergo nuclear reactions that *decrease* their atomic number. Lighter nuclei spontaneously undergo nuclear reactions that *increase* their atomic number.

Example 2.11.2

Calculate the total nuclear binding energy (in megaelectronvolts) and the binding energy per nucleon for ^{56}Fe. The experimental mass of the nuclide is given in Table A4.

Given: nuclide and mass

Asked for: nuclear binding energy and binding energy per nucleon

Strategy:

A Sum the masses of the protons, electrons, and neutrons or, alternatively, use the mass of the appropriate number of ^{1}H atoms (because its mass is the same as the mass of one electron and one proton).

B Calculate the mass defect by subtracting the experimental mass from the calculated mass.

C Determine the nuclear binding energy by multiplying the mass defect by the change in energy in electronvolts per atom. Divide this value by the number of nucleons to obtain the binding energy per nucleon.

Solution

A An iron-56 atom has 26 protons, 26 electrons, and 30 neutrons. We could add the masses of these three sets of particles; however, noting that 26 protons and 26 electrons are equivalent to 26 ^{1}H atoms, we can calculate the sum of the masses more quickly as follows:

$$\text{calculated mass} = 26(\text{mass } {}^{1}_{1}\text{H}) + 30(\text{mass } {}^{1}_{0}\text{n}) \tag{2.11.16}$$

$$= 26(1.007825)\text{amu} + 30(1.008665)\text{amu} = 56.463400 \text{ amu} \tag{2.11.17}$$

$$\text{experimental mass} = 55.934938 \tag{2.11.18}$$

B We subtract to find the mass defect:

$$\text{mass defect} = \text{calculated mass} - \text{experimental mass} \tag{2.11.19}$$

$$= 56.463400 \text{ amu} - 55.934938 \text{ amu} = 0.528462 \text{ amu} \tag{2.11.20}$$

C The nuclear binding energy is thus 0.528462 amu × 931 MeV/amu = 492 MeV. The binding energy per nucleon is 492 MeV/56 nucleons = 8.79 MeV/nucleon.

Exercise 2.11.2

Calculate the total nuclear binding energy (in megaelectronvolts) and the binding energy per nucleon for ^{238}U.

Answer 1800 MeV/^{238}U; 7.57 MeV/nucleon

Nuclear Fission and Fusion

N**uclear fission** is the splitting of a heavy nucleus into two lighter ones. Fission was discovered in 1938 by the German scientists Otto Hahn, Lise Meitner, and Fritz Strassmann, who bombarded a sample of uranium with neutrons in an attempt to produce new elements with Z > 92. They observed that lighter elements such as barium (Z = 56) were formed during the reaction, and they realized that such products had to originate from the neutron-induced fission of uranium-235:

$$^{235}_{92}\mathrm{U} + {}^{1}_{0}\mathrm{n} \rightarrow {}^{141}_{56}\mathrm{Ba} + {}^{92}_{36}\mathrm{Kr} + 3{}^{1}_{0}\mathrm{n} \tag{2.11.21}$$

This hypothesis was confirmed by detecting the krypton-92 fission product. The nucleus usually divides asymmetrically rather than into two equal parts, and the fission of a given nuclide does not give the same products every time.

In a typical nuclear fission reaction, more than one neutron is released by each dividing nucleus. When these neutrons collide with and induce fission in other neighboring nuclei, a self-sustaining series of nuclear fission reactions known as a **nuclear chain reaction** can result (Figure **2.11.3**). For example, the fission of ^{235}U releases two to three neutrons per fission event. If absorbed by other ^{235}U nuclei, those neutrons induce additional fission events, and the rate of the fission reaction increases geometrically. Each series of events is called a generation. Experimentally, it is found that some minimum mass of a fissile isotope is required to sustain a nuclear chain reaction; if the mass is too low, too many neutrons are able to escape without being captured and inducing a fission reaction. The minimum mass capable of supporting sustained fission is called the **critical mass**. This amount depends on the purity of the material and the shape of the mass, which corresponds to the amount of surface area available from which neutrons can escape, and on the identity of the isotope. If the mass of the fissile isotope is greater than the critical mass, then under the right conditions, the resulting supercritical mass can release energy explosively. The enormous energy released from nuclear chain reactions is responsible for the massive destruction caused by the detonation of nuclear weapons such as fission bombs, but it also forms the basis of the nuclear power industry.

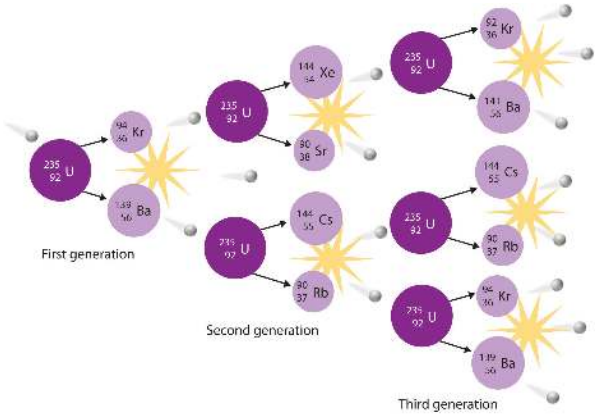


Figure **2.11.3**: A Nuclear Chain Reaction. The process is initiated by the collision of a single neutron with a ^{235}U nucleus, which undergoes fission, as shown in Figure 20.6. Because each neutron released can cause the fission of another ^{235}U nucleus, the rate of a fission reaction accelerates geometrically. Each series of events is a generation.

Nuclear fusion, in which two light nuclei combine to produce a heavier, more stable nucleus, is the opposite of nuclear fission. As in the nuclear transmutation reactions discussed in Section 20.2, the positive charge on both nuclei results in a large electrostatic energy barrier to fusion. This barrier can be overcome if one or both particles have sufficient kinetic energy to overcome the electrostatic repulsions, allowing the two nuclei to approach close enough for a fusion reaction to occur. The principle is similar to adding heat to increase the rate of a chemical reaction. As shown in the plot of nuclear binding energy per nucleon versus atomic number in Figure 21.2.3, fusion reactions are most exothermic for the lightest element. For example, in a typical fusion reaction, two deuterium atoms combine to produce helium-3, a process known as deuterium–deuterium fusion (D–D fusion):

$$2{}^{2}_{1}\mathrm{H} \rightarrow {}^{3}_{2}\mathrm{He} + {}^{1}_{0}\mathrm{n} \tag{2.11.22}$$

In another reaction, a deuterium atom and a tritium atom fuse to produce helium-4 (Figure **2.11.4**), a process known as deuterium–tritium fusion (D–T fusion):

$${}^{2}_{1}\mathrm{H} + {}^{3}_{1}\mathrm{H} \rightarrow {}^{4}_{2}\mathrm{He} + {}^{1}_{0}\mathrm{n} \tag{2.11.23}$$

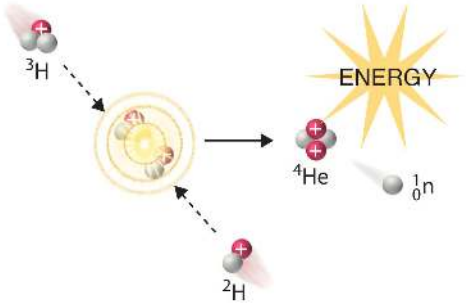


Figure **2.11.4**: Nuclear Fusion. In a nuclear fusion reaction, lighter nuclei combine to produce a heavier nucleus. As shown, fusion of ^{3}H and ^{2}H to give ^{4}He and a neutron releases an enormous amount of energy. In principle, nuclear fusion can produce much more energy than fission, but very high kinetic energy is required to overcome electrostatic repulsions between the positively charged nuclei and initiate the fusion reaction.

Initiating these reactions, however, requires a temperature comparable to that in the interior of the sun (approximately 1.5×10^7 K). Currently, the only method available on Earth to achieve such a temperature is the detonation of a fission bomb. For example, the so-called hydrogen bomb (or H bomb) is actually a deuterium–tritium bomb (a D–T bomb), which uses a nuclear fission reaction to create the very high temperatures needed to initiate fusion of solid lithium deuteride (^{6}LiD), which releases neutrons that then react with ^{6}Li, producing tritium. The deuterium-tritium reaction releases energy explosively. Example 9 and its corresponding exercise demonstrate the enormous amounts of energy produced by nuclear fission and fusion reactions. In fact, fusion reactions are the power sources for all stars, including our sun.

Example 2.11.3

Calculate the amount of energy (in electronvolts per atom and kilojoules per mole) released when the neutron-induced fission of ^{235}U produces ^{144}Cs, ^{90}Rb, and two neutrons:

$$^{235}_{92}\text{U} + {}^{1}_{0}\text{n} \rightarrow {}^{144}_{55}\text{Cs} + {}^{90}_{37}\text{Rb} + 2{}^{1}_{0}\text{n}$$

Given: balanced nuclear reaction

Asked for: energy released in electronvolts per atom and kilojoules per mole

Strategy:

A Following the method used in Example **2.11.1**, calculate the change in mass that accompanies the reaction. Convert this value to the change in energy in electronvolts per atom.

B Calculate the change in mass per mole of ^{235}U. Then use Equation **2.11.3** to calculate the change in energy in kilojoules per mole.

Solution

A The change in mass that accompanies the reaction is as follows:

$$\Delta m = \text{mass}_{\text{products}} - \text{mass}_{\text{reactants}} = \text{mass}({}^{144}_{55}\text{Cs} + {}^{90}_{37}\text{Rb} + {}^{1}_{0}\text{n}) - \text{mass } {}^{235}_{92}\text{U} \quad (2.11.24)$$

$$= (143.932077 \text{ amu} + 89.914802 \text{ amu} + 1.008665 \text{ amu}) - 235.043930 \text{ amu} \quad (2.11.25)$$

$$= -0.188386 \text{ amu} \quad (2.11.26)$$

The change in energy in electronvolts per atom is as follows:

$$\Delta E = (-0.188386 \text{ amu})(931 \text{ MeV/amu}) = -175 \text{ MeV}$$

B The change in mass per mole of $^{235}_{92}$U is −0.188386 g = -1.88386×10^{-4} kg, so the change in energy in kilojoules per mole is as follows:

$$\Delta E = (\Delta m)c^2 = (-1.88386 \times 10^{-4} \text{ kg})(2.998 \times 10^8 \text{ m/s})^2 \quad (2.11.27)$$

$$= -1.693 \times 10^{13} \text{ J/mol} = -1.693 \times 10^{10} \text{ kJ/mol} \quad (2.11.28)$$

Exercise 2.11.3

Calculate the amount of energy (in electronvolts per atom and kilojoules per mole) released when deuterium and tritium fuse to give helium-4 and a neutron:

$$^{2}_{1}\mathrm{H} + {}^{3}_{1}\mathrm{H} \rightarrow {}^{4}_{2}\mathrm{He} + {}^{1}_{0}\mathrm{n}$$

Answer

$\Delta E = -17.6$ MeV/atom $= -1.697 \times 10^{9}$ kJ/mol

Summary

Unlike a chemical reaction, a nuclear reaction results in a significant change in mass and an associated change of energy, as described by Einstein's equation. Nuclear reactions are accompanied by large changes in energy, which result in detectable changes in mass. The change in mass is related to the change in energy according to Einstein's equation: $\Delta E = (\Delta m)c^2$. Large changes in energy are usually reported in kiloelectronvolts or megaelectronvolts (thousands or millions of electronvolts). With the exception of ^{1}H, the experimentally determined mass of an atom is always less than the sum of the masses of the component particles (protons, neutrons, and electrons) by an amount called the mass defect of the nucleus. The energy corresponding to the mass defect is the nuclear binding energy, the amount of energy released when a nucleus forms from its component particles. In nuclear fission, nuclei split into lighter nuclei with an accompanying release of multiple neutrons and large amounts of energy. The critical mass is the minimum mass required to support a self-sustaining nuclear chain reaction. Nuclear fusion is a process in which two light nuclei combine to produce a heavier nucleus plus a great deal of energy.

2.11: Stability of the Atomic Nucleus is shared under a not declared license and was authored, remixed, and/or curated by LibreTexts.

- **24.5: Thermodynamic Stability of the Atomic Nucleus** by Anonymous is licensed CC BY-NC-SA 4.0.

2.12: The Origin of the Elements

Learning Objectives

- To understand how nuclear transmutation reactions lead to the formation of the elements in stars and how they can be used to synthesize transuranium elements.

The relative abundances of the elements in the known universe vary by more than 12 orders of magnitude. For the most part, these differences in abundance cannot be explained by differences in nuclear stability. Although the ^{56}Fe nucleus is the most stable nucleus known, the most abundant element in the known universe is not iron, but hydrogen (^{1}H), which accounts for about 90% of all atoms. In fact, ^{1}H is the raw material from which all other elements are formed. In this section, we explain why ^{1}H and ^{2}He together account for at least 99% of all the atoms in the known universe. We also describe the nuclear reactions that take place in stars, which transform one nucleus into another and create all the naturally occurring elements.

Relative Abundances of the Elements on Earth and in the Known Universe

The relative abundances of the elements in the known universe and on Earth relative to silicon are shown in Figure **2.12.1**. The data are estimates based on the characteristic emission spectra of the elements in stars, the absorption spectra of matter in clouds of interstellar dust, and the approximate composition of Earth as measured by geologists. The data in Figure **2.12.1** illustrate two important points. First, except for hydrogen, the most abundant elements have even atomic numbers. Not only is this consistent with the known trends in nuclear stability, but it also suggests that heavier elements are formed by combining helium nuclei (Z = 2). Second, the relative abundances of the elements in the known universe and on Earth are often very different, as indicated by the data in Table **2.12.1** for some common elements.

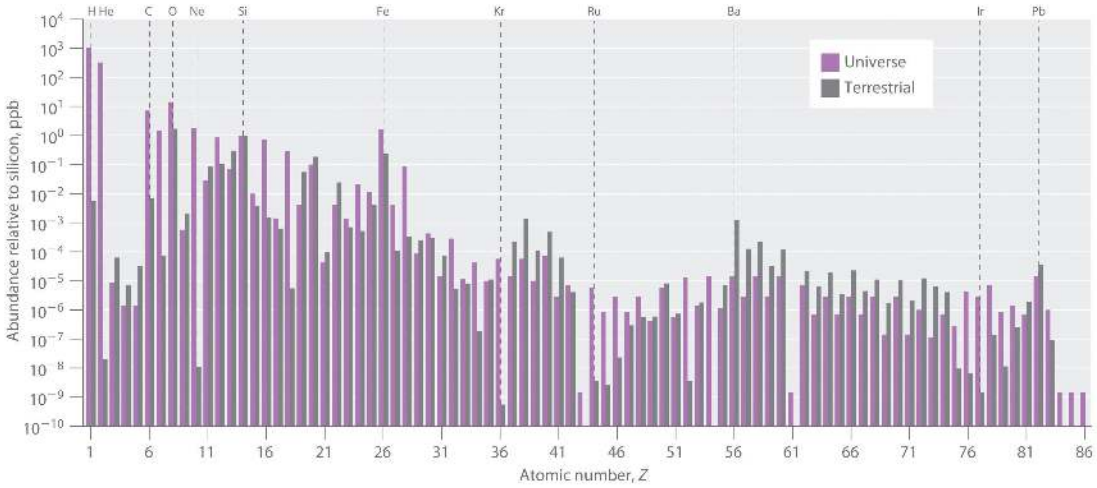


Figure **2.12.1**: The Relative Abundances of the Elements in the Universe and on Earth. In this logarithmic plot, the relative abundances of the elements relative to that of silicon (arbitrarily set equal to 1) in the universe (green bars) and on Earth (purple bars) are shown as a function of atomic number. Elements with even atomic numbers are generally more abundant in the universe than elements with odd atomic numbers. Also, the relative abundances of many elements in the universe are very different from their relative abundances on Earth. (CC BY-NC-SA 3.0; anonymous)

Bar graph of abundance realtive to silicon in pbb against atomic number. The purple bars are universe elements while the gray bars are terrestrial elements.

Some of these differences are easily explained. For example, nonmetals such as H, He, C, N, O, Ne, and Kr are much less abundant relative to silicon on Earth than they are in the rest of the universe. These elements are either noble gases (He, Ne, and Kr) or elements that form volatile hydrides, such as NH_3, CH_4, and H_2O. Because Earth's gravity is not strong enough to hold such light substances in the atmosphere, these elements have been slowly diffusing into outer space ever since our planet was formed. Argon is an exception; it is relatively abundant on Earth compared with the other noble gases because it is continuously produced in rocks by the radioactive decay of isotopes such as ^{40}K. In contrast, many metals, such as Al, Na, Fe, Ca, Mg, K, and Ti, are relatively abundant on Earth because they form nonvolatile compounds, such as oxides, that cannot escape into space. Other metals, however,

are much less abundant on Earth than in the universe; some examples are Ru and Ir. This section explains some of the reasons for the great differences in abundances of the metallic elements.

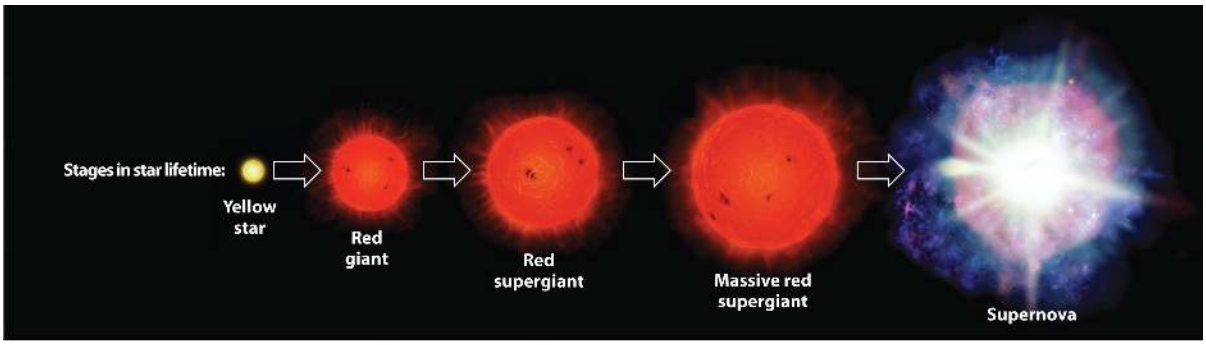
Table **2.12.1**: Relative Abundances of Elements on Earth and in the Known Universe

Terrestrial/Universal Element	Abundance Ratio
H	0.0020
He	2.4×10^{-8}
C	0.36
N	0.02
O	46
Ne	1.9×10^{-6}
Na	1200
Mg	48
Al	1600
Si	390
S	0.84
K	5000
Ca	710
Ti	2200
Fe	57

All the elements originally present on Earth (and on other planets) were synthesized from hydrogen and helium nuclei in the interiors of stars that have long since exploded and disappeared. Six of the most abundant elements in the universe (C, O, Ne, Mg, Si, and Fe) have nuclei that are integral multiples of the helium-4 nucleus, which suggests that helium-4 is the primary building block for heavier nuclei.

Synthesis of the Elements in Stars

Elements are synthesized in discrete stages during the lifetime of a star, and some steps occur only in the most massive stars known (Figure **2.12.2**). Initially, all stars are formed by the aggregation of interstellar “dust,” which is mostly hydrogen. As the cloud of dust slowly contracts due to gravitational attraction, its density eventually reaches about 100 g/cm^3, and the temperature increases to about 1.5×10^7 K, forming a dense plasma of ionized hydrogen nuclei. At this point, self-sustaining nuclear reactions begin, and the star “ignites,” creating a yellow star like our sun.



Core Temperature:	1.5×10^7 K	2×10^8 K	7×10^8 K	3×10^9 K	1×10^{11} K
Primary Nuclear Reaction:	^{1}H fusion	^{4}He fusion	$^4He + ^{12}C$ $^{12}C + ^{12}C$ $^{12}C + ^{16}O$	Proton–neutron exchange reactions	Multiple neutron captures
Elements Formed:	He	C, O, Ne, Mg	Na, Si, S, Ar, Ca	Fe, Ni	Elements with $Z \geq 28$

Figure **2.12.2**: Nuclear Reactions during the Life Cycle of a Massive Star. At each stage in the lifetime of a star, a different fuel is used for nuclear fusion, resulting in the formation of different elements. Fusion of hydrogen to give helium is the primary fusion reaction in young stars. As the star ages, helium accumulates and begins to "burn," undergoing fusion to form heavier elements such as carbon and oxygen. As the adolescent star matures, significant amounts of iron and nickel are formed by fusion of the heavier elements formed previously. The heaviest elements are formed only during the final death throes of the star—the formation of a nova or supernova.

The stages in a stare lifetime are yellow star, red giant, red supergiant, massive red supergiant and finally supernova.

In the first stage of its life, the star is powered by a series of nuclear fusion reactions that convert hydrogen to helium:

$$\begin{aligned} {}^1_1\mathrm{H} + {}^1_1\mathrm{H} &\rightarrow {}^2_1\mathrm{H} + {}^0_{+1}\beta \\ {}^2_1\mathrm{H} + {}^1_1\mathrm{H} &\rightarrow {}^3_2\mathrm{He} + {}^0_0\gamma \\ {}^3_2\mathrm{He} + {}^3_2\mathrm{He} &\rightarrow {}^4_2\mathrm{He} + 2{}^1_1\mathrm{H} \end{aligned} \tag{2.12.1}$$

The overall reaction is the conversion of four hydrogen nuclei to a helium-4 nucleus, which is accompanied by the release of two positrons, two γ rays, and a great deal of energy:

$$4{}^1_1\mathrm{H} \rightarrow {}^4_2\mathrm{He} + 2{}^0_{+1}\beta + 2{}^0_0\gamma \tag{2.12.2}$$

These reactions are responsible for most of the enormous amount of energy that is released as sunlight and solar heat. It takes several billion years, depending on the size of the star, to convert about 10% of the hydrogen to helium.

Once large amounts of helium-4 have been formed, they become concentrated in the core of the star, which slowly becomes denser and hotter. At a temperature of about 2×10^8 K, the helium-4 nuclei begin to fuse, producing beryllium-8:

$$2{}^4_2\mathrm{He} \rightarrow {}^8_4\mathrm{Be} \tag{2.12.3}$$

Although beryllium-8 has both an even mass number and an even atomic number, its also has a low neutron-to-proton ratio (and other factors beyond the scope of this text) that makes it unstable; it decomposes in only about 10^{-16} s. Nonetheless, this is long enough for it to react with a third helium-4 nucleus to form carbon-12, which is very stable. Sequential reactions of carbon-12 with helium-4 produce the elements with even numbers of protons and neutrons up to magnesium-24:

$${}^8_4\mathrm{Be} \xrightarrow{{}^4_2\mathrm{He}} {}^{12}_6\mathrm{C} \xrightarrow{{}^4_2\mathrm{He}} {}^{16}_8\mathrm{O} \xrightarrow{{}^4_2\mathrm{He}} {}^{20}_{10}\mathrm{Ne} \xrightarrow{{}^4_2\mathrm{He}} {}^{24}_{12}\mathrm{Mg} \tag{2.12.4}$$

So much energy is released by these reactions that it causes the surrounding mass of hydrogen to expand, producing a red giant that is about 100 times larger than the original yellow star.

As the star expands, heavier nuclei accumulate in its core, which contracts further to a density of about 50,000 g/cm3, so the core becomes even hotter. At a temperature of about 7×10^8 K, carbon and oxygen nuclei undergo nuclear fusion reactions to produce sodium and silicon nuclei:

$${}^{12}_6\mathrm{C} + {}^{12}_6\mathrm{C} \rightarrow {}^{23}_{11}\mathrm{Na} + {}^1_1\mathrm{H} \tag{2.12.5}$$

$${}^{12}_6\mathrm{C} + {}^{16}_8\mathrm{O} \rightarrow {}^{28}_{14}\mathrm{Si} + {}^0_0\gamma \tag{2.12.6}$$

At these temperatures, carbon-12 reacts with helium-4 to initiate a series of reactions that produce more oxygen-16, neon-20, magnesium-24, and silicon-28, as well as heavier nuclides such as sulfur-32, argon-36, and calcium-40:

$$^{12}_{6}\text{C} \xrightarrow{^{4}_{2}\text{He}} {}^{16}_{8}\text{O} \xrightarrow{^{4}_{2}\text{He}} {}^{20}_{10}\text{Ne} \xrightarrow{^{4}_{2}\text{He}} {}^{24}_{12}\text{Mg} \xrightarrow{^{4}_{2}\text{He}} {}^{28}_{14}\text{Si} \xrightarrow{^{4}_{2}\text{He}} {}^{32}_{16}\text{S} \xrightarrow{^{4}_{2}\text{He}} {}^{36}_{18}\text{Ar} \xrightarrow{^{4}_{2}\text{He}} {}^{40}_{20}\text{Ca} \tag{2.12.7}$$

The energy released by these reactions causes a further expansion of the star to form a red supergiant, and the core temperature increases steadily. At a temperature of about 3×10^9 K, the nuclei that have been formed exchange protons and neutrons freely. This equilibration process forms heavier elements up to iron-56 and nickel-58, which have the most stable nuclei known.

The Formation of Heavier Elements in Supernovas

None of the processes described so far produces nuclei with Z > 28. All naturally occurring elements heavier than nickel are formed in the rare but spectacular cataclysmic explosions called supernovas (Figure **2.12.2**). When the fuel in the core of a very massive star has been consumed, its gravity causes it to collapse in about 1 s. As the core is compressed, the iron and nickel nuclei within it disintegrate to protons and neutrons, and many of the protons capture electrons to form neutrons. The resulting neutron star is a dark object that is so dense that atoms no longer exist. Simultaneously, the energy released by the collapse of the core causes the supernova to explode in what is arguably the single most violent event in the universe. The force of the explosion blows most of the star's matter into space, creating a gigantic and rapidly expanding dust cloud, or nebula (Figure **2.12.3**). During the extraordinarily short duration of this event, the concentration of neutrons is so great that multiple neutron-capture events occur, leading to the production of the heaviest elements and many of the less stable nuclides. Under these conditions, for example, an iron-56 nucleus can absorb as many as 64 neutrons, briefly forming an extraordinarily unstable iron isotope that can then undergo multiple rapid β-decay processes to produce tin-120:

$$^{56}_{26}\text{Fe} + 64\,^{1}_{0}\text{n} \rightarrow {}^{120}_{26}\text{Fe} \rightarrow {}^{120}_{50}\text{Sn} + 24\,^{0}_{-1}\beta \tag{2.12.8}$$

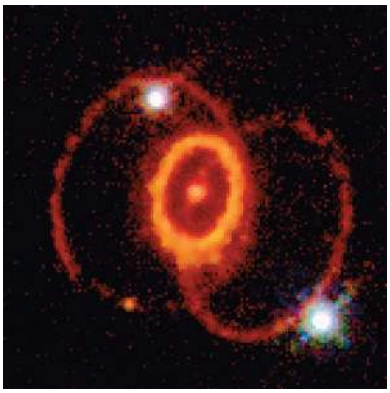


Figure **2.12.3**: A Supernova. A view of the remains of Supernova 1987A, located in the Large Magellanic Cloud, showing the circular halo of expanding debris produced by the explosion. Multiple neutron-capture events occur during a supernova explosion, forming both the heaviest elements and many of the less stable nuclides.

Although a supernova occurs only every few hundred years in a galaxy such as the Milky Way, these rare explosions provide the only conditions under which elements heavier than nickel can be formed. The force of the explosions distributes these elements throughout the galaxy surrounding the supernova, and eventually they are captured in the dust that condenses to form new stars. Based on its elemental composition, our sun is thought to be a second- or third-generation star. It contains a considerable amount of cosmic debris from the explosion of supernovas in the remote past.

✔ Example **2.12.1**: Carbon Burning Stars

The reaction of two carbon-12 nuclei in a carbon-burning star can produce elements other than sodium. Write a balanced nuclear equation for the formation of

a. magnesium-24.
b. neon-20 from two carbon-12 nuclei.

Given: reactant and product nuclides

Asked for: balanced nuclear equation

Strategy:

Use conservation of mass and charge to determine the type of nuclear reaction that will convert the reactant to the indicated product. Write the balanced nuclear equation for the reaction.

Solution

a. A magnesium-24 nucleus (Z = 12, A = 24) has the same nucleons as two carbon-12 nuclei (Z = 6, A = 12). The reaction is therefore a fusion of two carbon-12 nuclei, and no other particles are produced: $^{12}_{6}\mathrm{C} + {}^{12}_{6}\mathrm{C} \rightarrow {}^{24}_{12}\mathrm{Mg}$.

b. The neon-20 product has Z = 10 and A = 20. The conservation of mass requires that the other product have A = (2 × 12) − 20 = 4; because of conservation of charge, it must have Z = (2 × 6) − 10 = 2. These are the characteristics of an α particle. The reaction is therefore $^{12}_{6}\mathrm{C} + {}^{12}_{6}\mathrm{C} \rightarrow {}^{20}_{10}\mathrm{Ne} + {}^{4}_{2}\alpha$.

? Exercise 2.12.1

How many neutrons must an iron-56 nucleus absorb during a supernova explosion to produce an arsenic-75 nucleus? Write a balanced nuclear equation for the reaction.

Answer

19 neutrons; $^{56}_{26}\mathrm{Fe} + 19\,^{1}_{0}\mathrm{n} \rightarrow {}^{75}_{26}\mathrm{Fe} \rightarrow {}^{75}_{33}\mathrm{As} + 7\,^{0}_{-1}\beta$

Summary

Hydrogen and helium are the most abundant elements in the universe. Heavier elements are formed in the interior of stars via multiple neutron-capture events. By far the most abundant element in the universe is hydrogen. The fusion of hydrogen nuclei to form helium nuclei is the major process that fuels young stars such as the sun. Elements heavier than helium are formed from hydrogen and helium in the interiors of stars. Successive fusion reactions of helium nuclei at higher temperatures create elements with even numbers of protons and neutrons up to magnesium and then up to calcium. Eventually, the elements up to iron-56 and nickel-58 are formed by exchange processes at even higher temperatures. Heavier elements can only be made by a process that involves multiple neutron-capture events, which can occur only during the explosion of a supernova.

2.12: The Origin of the Elements is shared under a not declared license and was authored, remixed, and/or curated by LibreTexts.

- **21.3: Nuclear Transmutations** by Anonymous is licensed CC BY-NC-SA 3.0.

2.13: Transmutation of the Elements

Although the conversion of one element to another is the basis of natural radioactive decay, it is also possible to convert one element to another experimentally. The conversion of one element to another is the process of transmutation. In 1919 Rutherford converted a stable isotope to an unstable one. By bombarding $^{14}\mathrm{N}$ with α particles he created $^{17}\mathrm{O}$, which is an unstable isotope of oxygen. Transmutation may also be accomplished by bombardment with neutrons.

$$^{14}_{7}\mathrm{N} + {}^{4}_{2}\mathrm{He} \rightarrow {}^{17}_{8}\mathrm{O} + {}^{1}_{1}\mathrm{H} \tag{2.13.1}$$

Historically, part of Alchemy was the study of methods of creating gold from base metals, such lead. Where the Alchemists failed in this quest, we can now succeed. Thus, bombardment of platinum-198 with a neutron creates an unstable isotope of platinum that undergoes beta decay to gold-199. Unfortunately, while we may succeed in making gold, the platinum we make it from is actually worth more than the gold making this particular transmutation economically non-viable!

$$^{198}_{78}\mathrm{Pt} + {}^{1}_{0}\mathrm{n} \rightarrow {}^{199}_{78}\mathrm{Pt} \rightarrow {}^{199}_{79}\mathrm{Au} + {}^{0}_{-1}\beta \tag{2.13.2}$$

Transuranium Elements

Uranium (Z = 92) is the heaviest naturally occurring element. Consequently, all the elements with Z > 92, the **transuranium elements**, are artificial and have been prepared by bombarding suitable target nuclei with smaller particles. The first of the transuranium elements to be prepared was neptunium (Z = 93), which was synthesized in 1940 by bombarding a ^{238}U target with neutrons. As shown in Equation \(\ref{20.41}\) this reaction occurs in two steps. Initially, a neutron combines with a ^{238}U nucleus to form ^{239}U, which is unstable and undergoes beta decay to produce ^{239}Np:

$$^{238}_{92}\mathrm{U} + {}^{1}_{0}\mathrm{n} \rightarrow {}^{239}_{92}\mathrm{U} \rightarrow {}^{239}_{93}\mathrm{Np} + {}^{0}_{-1}\beta \tag{2.13.3}$$

Subsequent beta decay of ^{239}Np produces the second transuranium element, plutonium (Z = 94):

$$^{239}_{93}\mathrm{Np} \rightarrow {}^{239}_{94}\mathrm{Pu} + {}^{0}_{-1}\beta \tag{2.13.4}$$

Bombarding the target with more massive nuclei creates elements that have atomic numbers significantly greater than that of the target nucleus (Table **2.13.1**). Such techniques have resulted in the creation of the superheavy elements 114 and 116, both of which lie in or near the “island of stability." As of this writing, 22 transuranium elements have been produced and officially recognized by IUPAC; several other elements have formation claims that are waiting for approval.

Table 2.13.1: Preparation of Some of the Transuranium Elements

	Name			Symbol			Atomic Number			Reaction
americium	Am	95	$^{239}_{94}\mathrm{Pu} + {}^{1}_{0}\mathrm{n} \longrightarrow {}^{240}_{95}\mathrm{Am} + {}^{0}_{-1}\mathrm{e}$							
curium	Cm	96	$^{239}_{94}\mathrm{Pu} + {}^{4}_{2}\mathrm{He} \longrightarrow {}^{242}_{96}\mathrm{Cm} + {}^{1}_{0}\mathrm{n}$							
californium	Cf	98	$^{242}_{96}\mathrm{Cm} + {}^{4}_{2}\mathrm{He} \longrightarrow {}^{243}_{97}\mathrm{Bk} + 2{}^{1}_{0}\mathrm{n}$							
einsteinium	Es	99	$^{238}_{92}\mathrm{U} + 15{}^{1}_{0}\mathrm{n} \longrightarrow {}^{253}_{99}\mathrm{Es} + 7{}^{0}_{-1}\mathrm{e}$							
mendelevium	Md	101	$^{253}_{99}\mathrm{Es} + {}^{4}_{2}\mathrm{He} \longrightarrow {}^{256}_{101}\mathrm{Md} + {}^{1}_{0}\mathrm{n}$							
nobelium	No	102	$^{246}_{96}\mathrm{Cm} + {}^{12}_{6}\mathrm{C} \longrightarrow {}^{254}_{102}\mathrm{No} + 4\,{}^{1}_{0}\mathrm{n}$							
rutherfordium	Rf	104	$^{249}_{98}\mathrm{Cf} + {}^{12}_{6}\mathrm{C} \longrightarrow {}^{257}_{104}\mathrm{Rf} + 4\,{}^{1}_{0}\mathrm{n}$							
seaborgium	Sg	106	$^{206}_{82}\mathrm{Pb} + {}^{54}_{24}\mathrm{Cr} \longrightarrow {}^{257}_{106}\mathrm{Sg} + 3\,{}^{1}_{0}\mathrm{n}$ $^{249}_{98}\mathrm{Cf} + {}^{18}_{8}\mathrm{O} \longrightarrow {}^{263}_{106}\mathrm{Sg} + 4\,{}^{1}_{0}\mathrm{n}$							
meitnerium	Mt	107	$^{209}_{83}\mathrm{Bi} + {}^{58}_{26}\mathrm{Fe} \longrightarrow {}^{266}_{109}\mathrm{Mt} + {}^{1}_{0}\mathrm{n}$							

Particle Accelerators

A device called a particle accelerator is used to accelerate positively charged particles to the speeds needed to overcome the electrostatic repulsions between them and the target nuclei by using electrical and magnetic fields. Operationally, the simplest particle accelerator is the linear accelerator (Figure **2.13.2**), in which a beam of particles is injected at one end of a long evacuated tube. Rapid alternation of the polarity of the electrodes along the tube causes the particles to be alternately accelerated toward a region of opposite charge and repelled by a region with the same charge, resulting in a tremendous acceleration as the particle travels down the tube. A modern linear accelerator such as the Stanford Linear Accelerator (SLAC) at Stanford University is about 2 miles long.

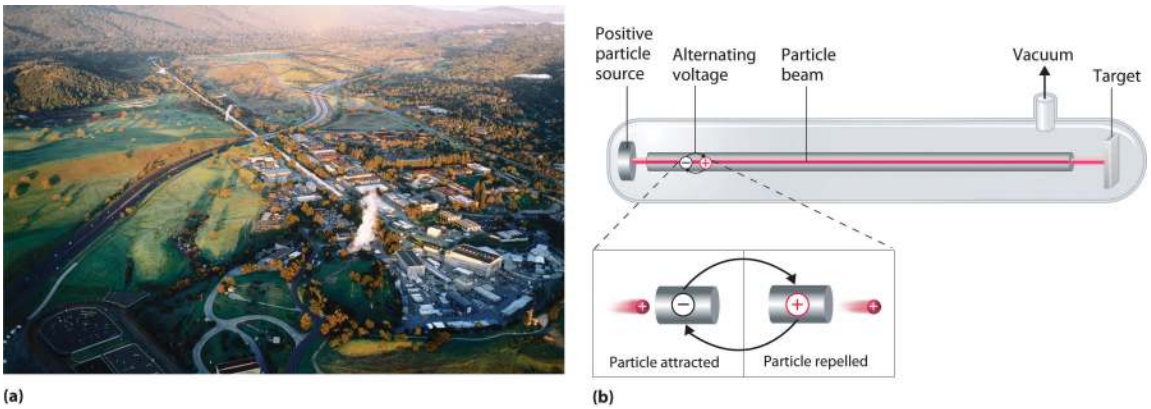


Figure **2.13.2**: A Linear Particle Accelerator. (a) An aerial view of the SLAC, the longest linear particle accelerator in the world; the overall length of the tunnel is 2 miles. (b) Rapidly reversing the polarity of the electrodes in the tube causes the charged particles to be alternately attracted as they enter one section of the tube and repelled as they leave that section. As a result, the particles are continuously accelerated along the length of the tube.

To achieve the same outcome in less space, a particle accelerator called a cyclotron forces the charged particles to travel in a circular path rather than a linear one. The particles are injected into the center of a ring and accelerated by rapidly alternating the

polarity of two large D-shaped electrodes above and below the ring, which accelerates the particles outward along a spiral path toward the target.

The length of a linear accelerator and the size of the D-shaped electrodes in a cyclotron severely limit the kinetic energy that particles can attain in these devices. These limitations can be overcome by using a synchrotron, a hybrid of the two designs. A synchrotron contains an evacuated tube similar to that of a linear accelerator, but the tube is circular and can be more than a mile in diameter. Charged particles are accelerated around the circle by a series of magnets whose polarities rapidly alternate.

Contributors and Attributions

- Paul Flowers (University of North Carolina - Pembroke), Klaus Theopold (University of Delaware) and Richard Langley (Stephen F. Austin State University) with contributing authors. Textbook content produced by OpenStax College is licensed under a Creative Commons Attribution License 4.0 license. Download for free at http://cnx.org/contents/85abf193-2bd...a7ac8df6@9.110).
- ◦ Hans Lohninger (Epina eBook Team)

  Template:HideTOC
- Andrew R. Barron

2.13: Transmutation of the Elements is shared under a not declared license and was authored, remixed, and/or curated by LibreTexts.

2.14: Nuclear Fission

Skills to Develop

- Explain nuclear fission
- Relate the concepts of critical mass and nuclear chain reactions
- Summarize basic requirements for nuclear fission

Many heavier elements with smaller binding energies per nucleon can decompose into more stable elements that have intermediate mass numbers and larger binding energies per nucleon—that is, mass numbers and binding energies per nucleon that are closer to the "peak" of the binding energy graph near 56. Sometimes neutrons are also produced. This decomposition is called fission, the breaking of a large nucleus into smaller pieces. The breaking is rather random with the formation of a large number of different products. Fission usually does not occur naturally, but is induced by bombardment with neutrons. The first reported nuclear fission occurred in 1939 when three German scientists, Lise Meitner, Otto Hahn, and Fritz Strassman, bombarded uranium-235 atoms with slow-moving neutrons that split the U-238 nuclei into smaller fragments that consisted of several neutrons and elements near the middle of the periodic table. Since then, fission has been observed in many other isotopes, including most actinide isotopes that have an odd number of neutrons. A typical nuclear fission reaction is shown in Figure **2.14.1**.

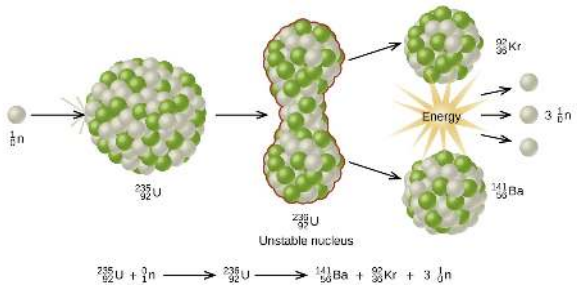


Figure **2.14.1**: When a slow neutron hits a fissionable U-235 nucleus, it is absorbed and forms an unstable U-236 nucleus. The U-236 nucleus then rapidly breaks apart into two smaller nuclei (in this case, Ba-141 and Kr-92) along with several neutrons (usually two or three), and releases a very large amount of energy.

Among the products of Meitner, Hahn, and Strassman's fission reaction were barium, krypton, lanthanum, and cerium, all of which have nuclei that are more stable than uranium-235. Since then, hundreds of different isotopes have been observed among the products of fissionable substances. A few of the many reactions that occur for U-235, and a graph showing the distribution of its fission products and their yields, are shown in Figure **2.14.2**.. Similar fission reactions have been observed with other uranium isotopes, as well as with a variety of other isotopes such as those of plutonium.

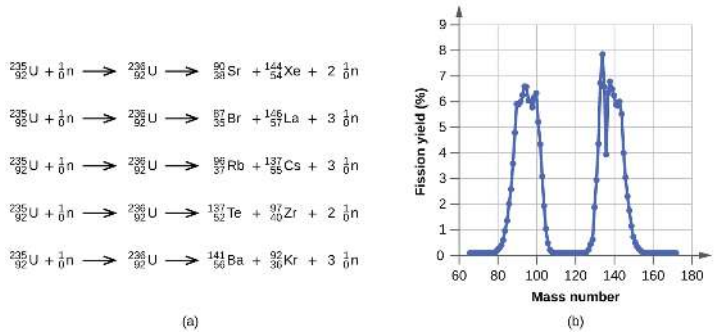


Figure **2.14.2**: (a) Nuclear fission of U-235 produces a range of fission products. (b) The larger fission products of U-235 are typically one isotope with a mass number around 85–105, and another isotope with a mass number that is about 50% larger, that is, about 130–150.

A tremendous amount of energy is produced by the fission of heavy elements. For instance, when one mole of U-235 undergoes fission, the products weigh about 0.2 grams less than the reactants; this "lost" mass is converted into a very large amount of energy, about 1.8×10^{10} kJ per mole of U-235. Nuclear fission reactions produce incredibly large amounts of energy compared to chemical reactions. The fission of 1 kilogram of uranium-235, for example, produces about 2.5 million times as much energy as is produced by burning 1 kilogram of coal.

As described earlier, when undergoing fission U-235 produces two "medium-sized" nuclei, and two or three neutrons. These neutrons may then cause the fission of other uranium-235 atoms, which in turn provide more neutrons that can cause fission of even more nuclei, and so on. If this occurs, we have a nuclear chain reaction (Figure **2.14.3**). On the other hand, if too many neutrons escape the bulk material without interacting with a nucleus, then no chain reaction will occur.

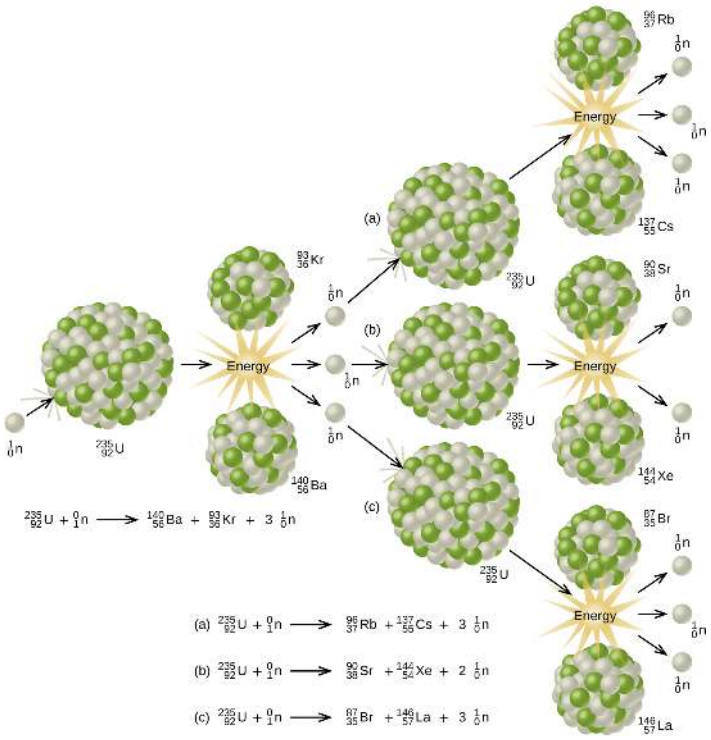


Figure **2.14.3**: The fission of a large nucleus, such as U-235, produces two or three neutrons, each of which is capable of causing fission of another nucleus by the reactions shown. If this process continues, a nuclear chain reaction occurs.

Material that can sustain a nuclear fission chain reaction is said to be fissile or fissionable. (Technically, fissile material can undergo fission with neutrons of any energy, whereas fissionable material requires high-energy neutrons.) Nuclear fission becomes self-sustaining when the number of neutrons produced by fission equals or exceeds the number of neutrons absorbed by splitting nuclei plus the number that escape into the surroundings. The amount of a fissionable material that will support a self-sustaining chain reaction is a critical mass. An amount of fissionable material that cannot sustain a chain reaction is a subcritical mass. An amount of material in which there is an increasing rate of fission is known as a supercritical mass. The critical mass depends on the type of material: its purity, the temperature, the shape of the sample, and how the neutron reactions are controlled (Figure **2.14.4**).

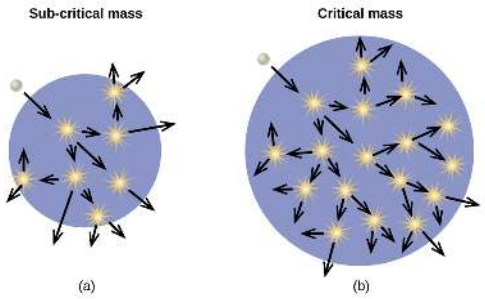


Figure **2.14.4**: (a) In a subcritical mass, the fissile material is too small and allows too many neutrons to escape the material, so a chain reaction does not occur. (b) In a critical mass, a large enough number of neutrons in the fissile material induce fission to create a chain reaction.

An atomic bomb (Figure **2.14.5**) contains several pounds of fissionable material, $^{235}_{92}\mathbf{U}$ or $^{239}_{94}\mathbf{Pu}$, a source of neutrons, and an explosive device for compressing it quickly into a small volume. When fissionable material is in small pieces, the proportion of neutrons that escape through the relatively large surface area is great, and a chain reaction does not take place. When the small pieces of fissionable material are brought together quickly to form a body with a mass larger than the critical mass, the relative number of escaping neutrons decreases, and a chain reaction and explosion result.

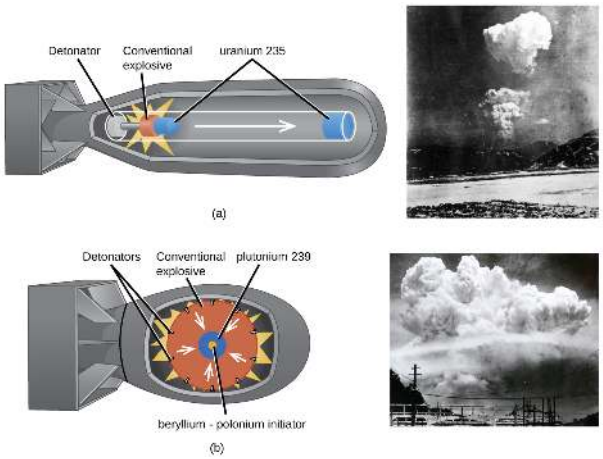


Figure **2.14.5**: (a) The nuclear fission bomb that destroyed Hiroshima on August 6, 1945, consisted of two subcritical masses of U-235, where conventional explosives were used to fire one of the subcritical masses into the other, creating the critical mass for the nuclear explosion. (b) The plutonium bomb that destroyed Nagasaki on August 12, 1945, consisted of a hollow sphere of plutonium that was rapidly compressed by conventional explosives. This led to a concentration of plutonium in the center that was greater than the critical mass necessary for the nuclear explosion.

Fission Reactors

Chain reactions of fissionable materials can be controlled and sustained without an explosion in a nuclear reactor (Figure **2.14.6**). Any nuclear reactor that produces power via the fission of uranium or plutonium by bombardment with neutrons must have at least five components: nuclear fuel consisting of fissionable material, a nuclear moderator, reactor coolant, control rods, and a shield and containment system. We will discuss these components in greater detail later in the section. The reactor works by separating the fissionable nuclear material such that a critical mass cannot be formed, controlling both the flux and absorption of neutrons to allow shutting down the fission reactions. In a nuclear reactor used for the production of electricity, the energy released by fission reactions is trapped as thermal energy and used to boil water and produce steam. The steam is used to turn a turbine, which powers a generator for the production of electricity.

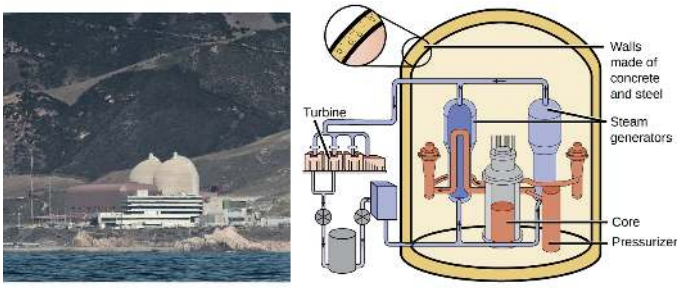


Figure **2.14.6**: (a) The Diablo Canyon Nuclear Power Plant near San Luis Obispo is the only nuclear power plant currently in operation in California. The domes are the containment structures for the nuclear reactors, and the brown building houses the turbine where electricity is generated. Ocean water is used for cooling. (b) The Diablo Canyon uses a pressurized water reactor, one of a few different fission reactor designs in use around the world, to produce electricity. Energy from the nuclear fission reactions in the core heats water in a closed, pressurized system. Heat from this system produces steam that drives a turbine, which in turn produces electricity. (credit a: modification of work by “Mike” Michael L. Baird; credit b: modification of work by the Nuclear Regulatory Commission)

Nuclear Fuels

Nuclear fuel consists of a fissionable isotope, such as uranium-235, which must be present in sufficient quantity to provide a self-sustaining chain reaction. In the United States, uranium ores contain from 0.05–0.3% of the uranium oxide U_3O_8; the uranium in the ore is about 99.3% nonfissionable U-238 with only 0.7% fissionable U-235. Nuclear reactors require a fuel with a higher concentration of U-235 than is found in nature; it is normally enriched to have about 5% of uranium mass as U-235. At this concentration, it is not possible to achieve the supercritical mass necessary for a nuclear explosion. Uranium can be enriched by gaseous diffusion (the only method currently used in the US), using a gas centrifuge, or by laser separation.

In the gaseous diffusion enrichment plant where U-235 fuel is prepared, UF_6 (uranium hexafluoride) gas at low pressure moves through barriers that have holes just barely large enough for UF_6 to pass through. The slightly lighter $^{235}UF_6$ molecules diffuse through the barrier slightly faster than the heavier $^{238}UF_6$ molecules. This process is repeated through hundreds of barriers, gradually increasing the concentration of $^{235}UF_6$ to the level needed by the nuclear reactor. The basis for this process, Graham’s law, is described in the chapter on gases. The enriched UF_6 gas is collected, cooled until it solidifies, and then taken to a fabrication facility where it is made into fuel assemblies. Each fuel assembly consists of fuel rods that contain many

thimble-sized, ceramic-encased, enriched uranium (usually UO_2) fuel pellets. Modern nuclear reactors may contain as many as 10 million fuel pellets. The amount of energy in each of these pellets is equal to that in almost a ton of coal or 150 gallons of oil.

Nuclear Moderators

Neutrons produced by nuclear reactions move too fast to cause fission (Figure **2.14.4**). They must first be slowed to be absorbed by the fuel and produce additional nuclear reactions. A nuclear moderator is a substance that slows the neutrons to a speed that is low enough to cause fission. Early reactors used high-purity graphite as a moderator. Modern reactors in the US exclusively use heavy water ($^{2}_{1}\mathbf{H_2O}$) or light water (ordinary H_2O), whereas some reactors in other countries use other materials, such as carbon dioxide, beryllium, or graphite.

Reactor Coolants

A nuclear reactor coolant is used to carry the heat produced by the fission reaction to an external boiler and turbine, where it is transformed into electricity. Two overlapping coolant loops are often used; this counteracts the transfer of radioactivity from the reactor to the primary coolant loop. All nuclear power plants in the US use water as a coolant. Other coolants include molten sodium, lead, a lead-bismuth mixture, or molten salts.

Control Rods

Nuclear reactors use control rods (Figure **2.14.8**) to control the fission rate of the nuclear fuel by adjusting the number of slow neutrons present to keep the rate of the chain reaction at a safe level. Control rods are made of boron, cadmium, hafnium, or other elements that are able to absorb neutrons. Boron-10, for example, absorbs neutrons by a reaction that produces lithium-7 and alpha particles:

$$^{10}_{5}\mathrm{B} + {}^{1}_{0}\mathrm{n} \longrightarrow {}^{7}_{3}\mathrm{Li} + {}^{4}_{2}\mathrm{He} \tag{2.14.1}$$

When control rod assemblies are inserted into the fuel element in the reactor core, they absorb a larger fraction of the slow neutrons, thereby slowing the rate of the fission reaction and decreasing the power produced. Conversely, if the control rods are removed, fewer neutrons are absorbed, and the fission rate and energy production increase. In an emergency, the chain reaction can be shut down by fully inserting all of the control rods into the nuclear core between the fuel rods.

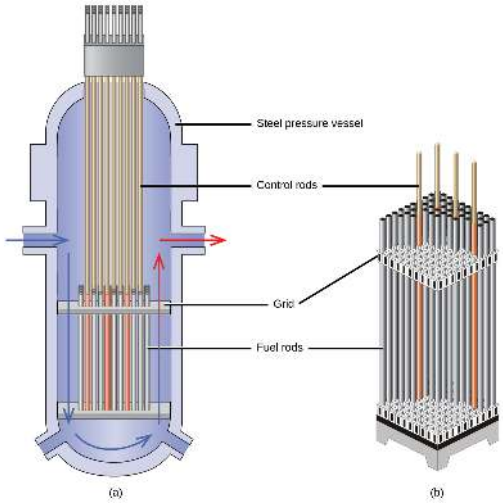


Figure **2.14.7**: The nuclear reactor core shown in (a) contains the fuel and control rod assembly shown in (b). (credit: modification of work by E. Generalic)

Shield and Containment System

During its operation, a nuclear reactor produces neutrons and other radiation. Even when shut down, the decay products are radioactive. In addition, an operating reactor is thermally very hot, and high pressures result from the circulation of water or another coolant through it. Thus, a reactor must withstand high temperatures and pressures, and must protect operating personnel from the radiation. Reactors are equipped with a containment system (or shield) that consists of three parts:

1. The reactor vessel, a steel shell that is 3–20-centimeters thick and, with the moderator, absorbs much of the radiation produced by the reactor
2. A main shield of 1–3 meters of high-density concrete
3. A personnel shield of lighter materials that protects operators from γ rays and X-rays

In addition, reactors are often covered with a steel or concrete dome that is designed to contain any radioactive materials might be released by a reactor accident.



Video* 2.14.1*: *Click here to watch a 3-minute video from the Nuclear Energy Institute on how nuclear reactors work.*

Nuclear power plants are designed in such a way that they cannot form a supercritical mass of fissionable material and therefore cannot create a nuclear explosion. But as history has shown, failures of systems and safeguards can cause catastrophic accidents, including chemical explosions and nuclear meltdowns (damage to the reactor core from overheating). The following Chemistry in Everyday Life feature explores three infamous meltdown incidents.

Nuclear Accidents

The importance of cooling and containment are amply illustrated by three major accidents that occurred with the nuclear reactors at nuclear power generating stations in the United States (Three Mile Island), the former Soviet Union (Chernobyl), and Japan (Fukushima).

In March 1979, the cooling system of the Unit 2 reactor at Three Mile Island Nuclear Generating Station in Pennsylvania failed, and the cooling water spilled from the reactor onto the floor of the containment building. After the pumps stopped, the reactors overheated due to the high radioactive decay heat produced in the first few days after the nuclear reactor shut down. The temperature of the core climbed to at least 2200 °C, and the upper portion of the core began to melt. In addition, the zirconium alloy cladding of the fuel rods began to react with steam and produced hydrogen:

$$\mathrm{Zr}(s) + 2\,\mathrm{H_2O}(g) \longrightarrow \mathrm{ZrO_2}(s) + 2\,\mathrm{H_2}(g) \tag{2.14.2}$$

The hydrogen accumulated in the confinement building, and it was feared that there was danger of an explosion of the mixture of hydrogen and air in the building. Consequently, hydrogen gas and radioactive gases (primarily krypton and xenon) were vented from the building. Within a week, cooling water circulation was restored and the core began to cool. The plant was closed for nearly 10 years during the cleanup process.

Although zero discharge of radioactive material is desirable, the discharge of radioactive krypton and xenon, such as occurred at the Three Mile Island plant, is among the most tolerable. These gases readily disperse in the atmosphere and thus do not produce highly radioactive areas. Moreover, they are noble gases and are not incorporated into plant and animal matter in the food chain. Effectively none of the heavy elements of the core of the reactor were released into the environment, and no cleanup of the area outside of the containment building was necessary (Figure 2.14.8).

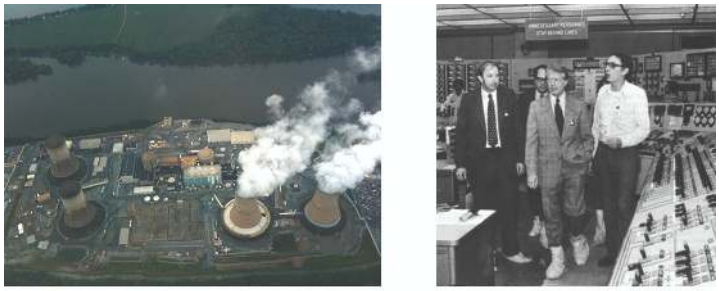


Figure 2.14.8: (a) In this 2010 photo of Three Mile Island, the remaining structures from the damaged Unit 2 reactor are seen on the left, whereas the separate Unit 1 reactor, unaffected by the accident, continues generating power to this day (right). (b) President Jimmy Carter visited the Unit 2 control room a few days after the accident in 1979.

Another major nuclear accident involving a reactor occurred in April 1986, at the Chernobyl Nuclear Power Plant in Ukraine, which was still a part of the former Soviet Union. While operating at low power during an unauthorized experiment with some of its safety devices shut off, one of the reactors at the plant became unstable. Its chain reaction became uncontrollable and increased to a level far beyond what the reactor was designed for. The steam pressure in the reactor rose to between 100 and 500 times the full power pressure and ruptured the reactor. Because the reactor was not enclosed in a containment building, a large amount of radioactive material spewed out, and additional fission products were released, as the graphite (carbon) moderator of the core ignited and burned. The fire was controlled, but over 200 plant workers and firefighters developed acute radiation sickness and at least 32 soon died from the effects of the radiation. It is predicted that about 4000 more deaths will occur among emergency workers and former Chernobyl residents from radiation-induced cancer and leukemia. The reactor has since been encapsulated in steel and concrete, a now-decaying structure known as the sarcophagus. Almost 30 years later, significant radiation problems still persist in the area, and Chernobyl largely remains a wasteland.

In 2011, the Fukushima Daiichi Nuclear Power Plant in Japan was badly damaged by a 9.0-magnitude earthquake and resulting tsunami. Three reactors up and running at the time were shut down automatically, and emergency generators came online to power electronics and coolant systems. However, the tsunami quickly flooded the emergency generators and cut power to the pumps that circulated coolant water through the reactors. High-temperature steam in the reactors reacted with zirconium alloy to produce hydrogen gas. The gas escaped into the containment building, and the mixture of hydrogen and air exploded. Radioactive material was released from the containment vessels as the result of deliberate venting to reduce the hydrogen pressure, deliberate discharge of coolant water into the sea, and accidental or uncontrolled events.

An evacuation zone around the damaged plant extended over 12.4 miles away, and an estimated 200,000 people were evacuated from the area. All 48 of Japan's nuclear power plants were subsequently shut down, remaining shuttered as of December 2014. Since the disaster, public opinion has shifted from largely favoring to largely opposing increasing the use of nuclear power plants, and a restart of Japan's atomic energy program is still stalled (Figure 2.14.10).



Figure 2.14.9: (a) After the accident, contaminated waste had to be removed, and (b) an evacuation zone was set up around the plant in areas that received heavy doses of radioactive fallout. (credit a: modification of work by "Live Action Hero"/Flickr)

The energy produced by a reactor fueled with enriched uranium results from the fission of uranium as well as from the fission of plutonium produced as the reactor operates. As discussed previously, the plutonium forms from the combination of neutrons and the uranium in the fuel. In any nuclear reactor, only about 0.1% of the mass of the fuel is converted into energy. The other 99.9% remains in the fuel rods as fission products and unused fuel. All of the fission products absorb neutrons, and after a period of several months to a few years, depending on the reactor, the fission products must be removed by changing the fuel rods. Otherwise, the concentration of these fission products would increase and absorb more neutrons until the reactor could no longer operate.

Spent fuel rods contain a variety of products, consisting of unstable nuclei ranging in atomic number from 25 to 60, some transuranium elements, including plutonium and americium, and unreacted uranium isotopes. The unstable nuclei and the transuranium isotopes give the spent fuel a dangerously high level of radioactivity. The long-lived isotopes require thousands of years to decay to a safe level. The ultimate fate of the nuclear reactor as a significant source of energy in the United States probably rests on whether or not a politically and scientifically satisfactory technique for processing and storing the components of spent fuel rods can be developed.

Contributors and Attributions

- Paul Flowers (University of North Carolina - Pembroke), Klaus Theopold (University of Delaware) and Richard Langley (Stephen F. Austin State University) with contributing authors. Textbook content produced by OpenStax College is licensed under a Creative Commons Attribution License 4.0 license. Download for free at http://cnx.org/contents/85abf193-2bd...a7ac8df6@9.110).

2.14: Nuclear Fission is shared under a not declared license and was authored, remixed, and/or curated by LibreTexts.

2.15: Nuclear Fusion

Skills to Develop

- Describe the nuclear reactions in a nuclear fusion reaction
- Quantify the energy released or absorbed in a fusion reaction

The process of converting very light nuclei into heavier nuclei is also accompanied by the conversion of mass into large amounts of energy, a process called fusion. The principal source of energy in the sun is a net fusion reaction in which four hydrogen nuclei fuse and produce one helium nucleus and two positrons. This is a net reaction of a more complicated series of events:

$$\underbrace{4{}_1^1\mathrm{H}}_{4\times 1.00794\ u} \longrightarrow \underbrace{{}_2^4\mathrm{He}}_{4.0012\ u} + \underbrace{2{}_1^0\beta^+}_{2\times 0.0005487\ u} \tag{2.15.1}$$

A helium nucleus has a mass that is 0.7% less than that of four hydrogen nuclei; this lost mass is converted into thermal energy during the fusion via Einstein's $E = mc^2$ equation. This reaction produces about 3.6×10^{11} kJ of energy per mole of ${}_2^4\mathrm{He}$ produced. This is somewhat larger than the energy produced by the nuclear fission of one mole of ${}^{235}\mathrm{U}$ (1.8×10^{10} kJ), and over **3 million times larger** than the energy produced by the (chemical) combustion of one mole of octane ($\Delta H = -5471\ kJ$):

$$2C_8H_{18} + 25O_2 \rightarrow 16CO_2 + 18H_2O \tag{2.15.2}$$

It has been determined that the nuclei of the heavy isotopes of hydrogen, a deuteron, ${}_1^2\mathrm{H}$ and a triton, ${}_1^3\mathrm{H}$, undergo fusion at extremely high temperatures (thermonuclear fusion). They form a helium nucleus and a neutron:

$${}_1^2\mathrm{H} + {}_1^3\mathrm{H} \longrightarrow {}_2^4\mathrm{He} + 2{}_0^1\mathrm{n} \tag{2.15.3}$$

This change proceeds with a mass loss of 0.0188 amu, corresponding to the release of 1.69×10^9 kilojoules per mole of ${}_2^4\mathrm{He}$ formed. The very high temperature is necessary to give the nuclei enough kinetic energy to overcome the very strong repulsive forces resulting from the positive charges on their nuclei so they can collide.

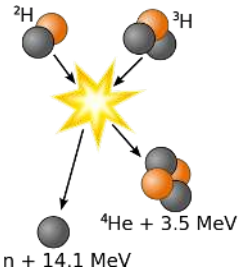


Figure **2.15.1**: Fusion of deuterium with tritium creating helium-4, freeing a neutron, and releasing 17.59 MeV of energy, as an appropriate amount of mass changing forms to appear as the kinetic energy of the products, in agreement with kinetic $E = \Delta mc^2$, where Δm is the change in rest mass of particles.[Image use with permission via Wikipedia (Wykis)

The most important fusion process in nature is the one that powers stars. In the 20th century, it was realized that the energy released from nuclear fusion reactions accounted for the longevity of the Sun and other stars as a source of heat and light. The fusion of nuclei in a star, starting from its initial hydrogen and helium abundance, provides that energy and synthesizes new nuclei as a byproduct of that fusion process. The prime energy producer in the Sun is the fusion of hydrogen to form helium, which occurs at a solar-core temperature of 14 million kelvin. The net result is the fusion of four protons into one alpha particle, with the release of two positrons, two neutrinos (which changes two of the protons into neutrons), and energy (Figure **2.15.2**).

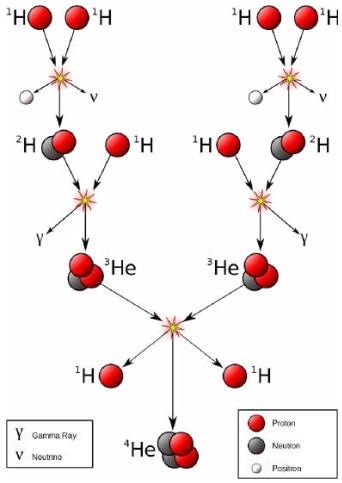


Figure **2.15.2**: (left) The Sun is a main-sequence star, and thus generates its energy by nuclear fusion of hydrogen nuclei into helium. In its core, the Sun fuses 620 million metric tons of hydrogen each second. (right) The proton-proton chain dominates in stars the size of the Sun or smaller.

Example 2.15.1

Calculate the energy released in each of the following hypothetical processes.

a. $3\,{}^4_2\mathrm{He} \rightarrow {}^{12}_6\mathrm{C}$
b. $6\,{}^1_1\mathrm{H} + 6\,{}^1_0\mathrm{n} \rightarrow {}^{12}_6\mathrm{C}$
c. $6\,{}^2_1\mathrm{D} \rightarrow {}^{12}_6\mathrm{C}$

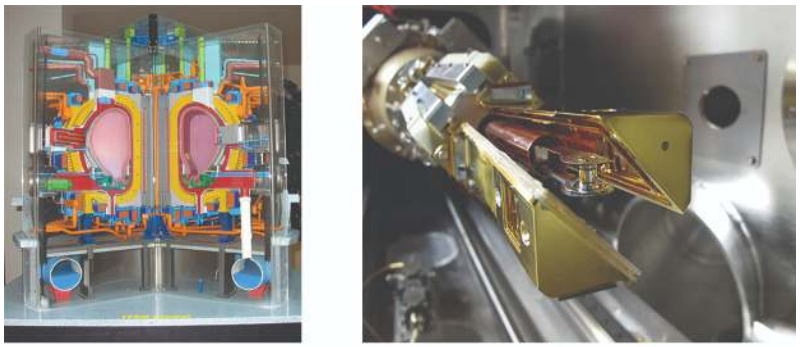
Discuss your results.

a. *Q*a = 3 * 4.0026 - 12.000) amu * (1.4924E-10 J/amu)
= 1.17E-12 J
b. *Q*b = (6*(1.007825 + 1.008665) - 12.00000) amu * (1.4924E-10 J/amu)
= 1.476E-11 J
c. *Q*c = 6*2.014102 - 12.00000 amu * (1.4924E-10 J/amu)
= 1.263E-11 J

Fusion of He to give C releases the least amount of energy, because the fusion to produce He has released a large amount. The difference between the second and the third is the binding energy of deuterium. The conservation of mass-and-energy is well illustrated in these calculations. On the other hand, the calculation is based on the conservation of mass-and-energy.

Nuclear Reactors

Useful fusion reactions require very high temperatures for their initiation—about 15,000,000 K or more. At these temperatures, all molecules dissociate into atoms, and the atoms ionize, forming plasma. These conditions occur in an extremely large number of locations throughout the universe—stars are powered by fusion. Humans have already figured out how to create temperatures high enough to achieve fusion on a large scale in thermonuclear weapons. A thermonuclear weapon such as a hydrogen bomb contains a nuclear fission bomb that, when exploded, gives off enough energy to produce the extremely high temperatures necessary for fusion to occur.



(a) (b)

Figure **2.15.3**: (a) This model is of the International Thermonuclear Experimental Reactor (ITER) reactor. Currently under construction in the south of France with an expected completion date of 2027, the ITER will be the world's largest experimental Tokamak nuclear fusion reactor with a goal of achieving large-scale sustained energy production. (b) In 2012, the National Ignition Facility at Lawrence Livermore National Laboratory briefly produced over 500,000,000,000 watts (500 terawatts, or 500 TW) of peak power and delivered 1,850,000 joules (1.85 MJ) of energy, the largest laser energy ever produced and 1000 times the power usage of the entire United States in any given moment. Although lasting only a few billionths of a second, the 192 lasers attained the conditions needed for nuclear fusion ignition. This image shows the target prior to the laser shot. (credit a: modification of work by Stephan Mosel)

Another much more beneficial way to create fusion reactions is in a fusion reactor, a nuclear reactor in which fusion reactions of light nuclei are controlled. Because no solid materials are stable at such high temperatures, mechanical devices cannot contain the plasma in which fusion reactions occur. Two techniques to contain plasma at the density and temperature necessary for a fusion reaction are currently the focus of intensive research efforts: containment by a magnetic field and by the use of focused laser beams (Figure **2.15.3**). A number of large projects are working to attain one of the biggest goals in science: getting hydrogen fuel to ignite and produce more energy than the amount supplied to achieve the extremely high temperatures and pressures that are required for fusion. At the time of this writing, there are no self-sustaining fusion reactors operating in the world, although small-scale controlled fusion reactions have been run for very brief periods.

Contributors

- Paul Flowers (University of North Carolina - Pembroke), Klaus Theopold (University of Delaware) and Richard Langley (Stephen F. Austin State University) with contributing authors. Textbook content produced by OpenStax College is licensed under a Creative Commons Attribution License 4.0 license. Download for free at http://cnx.org/contents/85abf193-2bd...a7ac8df6@9.110).

2.15: Nuclear Fusion is shared under a not declared license and was authored, remixed, and/or curated by LibreTexts.

2.16: Nuclear Chemistry (Exercises)

These are homework exercises to accompany the Textmap created for "Chemistry: The Central Science" by Brown et al. Complementary General Chemistry question banks can be found for other Textmaps and can be accessed here. In addition to these publicly available questions, access to private problems bank for use in exams and homework is available to faculty only on an individual basis; please contact Delmar Larsen for an account with access permission.

21.1: Radioactivity

Q21.1.1

Why are many radioactive substances warm to the touch? Why do many radioactive substances glow?

Q21.1.2

Describe the differences between nonionizing and ionizing radiation in terms of the intensity of energy emitted and the effect each has on an atom or molecule after collision. Which nuclear decay reactions are more likely to produce ionizing radiation? nonionizing radiation?

Q21.1.3

Would you expect nonionizing or ionizing radiation to be more effective at treating cancer? Why?

S21.1.3

Ionizing radiation is higher in energy and causes greater tissue damage, so it is more likely to destroy cancerous cells.

Q21.1.4

Historically, concrete shelters have been used to protect people from nuclear blasts. Comment on the effectiveness of such shelters.

Q21.1.5

Gamma rays are a very high-energy radiation, yet α particles inflict more damage on biological tissue. Why?

Q21.1.6

List the three primary sources of naturally occurring radiation. Explain the factors that influence the dose that one receives throughout the year. Which is the largest contributor to overall exposure? Which is the most hazardous?

S21.1.6

Three primary naturally occurring radiations are radium, uranium and thorium, each all having long half lives. Inhalation of air, ingestion of food and water,terrestrial radation from the ground and cosmic radiation from space are all factors tat influence the does that a person receives throughout the year. Inhalation of the air is the largest contributor to exposure. Radiation can damage DNA or kill cells. When radiation is exposed to your body, it will collide with atoms and this will change and damage your DNA.

Q21.1.7

Because radon is a noble gas, it is inert and generally unreactive. Despite this, exposure to even low concentrations of radon in air is quite dangerous. Describe the physical consequences of exposure to radon gas. Why are people who smoke more susceptible to these effects?

Q21.1.8

Most medical imaging uses isotopes that have extremely short half-lives. These isotopes usually undergo only one kind of nuclear decay reaction. Which kind of decay reaction is usually used? Why? Why would a short half-life be preferred in these cases?

Beta decay. Alfa decay can be easily stopped by paper, which means it can not be used to see inside people's body. Also, Gamma rays are really dangerous for human, that even a short period of time exploding to it will have negative effect on human body. Thus,

Beta decay is the perfect choice. It can be used to see through human's body and stopped by aluminum or some other metals.

Since all these radioactive decays are harmful for human body, if the half time of these reactions are short, the time exploding to these reactions will be short too.

Q21.1.9

Which would you prefer: one exposure of 100 rem, or 10 exposures of 10 rem each? Explain your rationale.

S21.1.9

Ten exposures of 10 rem are less likely to cause major damage.

Q21.1.10

A 2.14 kg sample of rock contains 0.0985 g of uranium. How much energy is emitted over 25 yr if 99.27% of the uranium is ^{238}U, which has a half-life of 4.46×10^9 yr, if each decay event is accompanied by the release of 4.039 MeV? If a 180 lb individual absorbs all of the emitted radiation, how much radiation has been absorbed in rads?

Q21.1.11

There is a story about a “radioactive boy scout” who attempted to convert thorium-232, which he isolated from about 1000 gas lantern mantles, to uranium-233 by bombarding the thorium with neutrons. The neutrons were generated via bombarding an aluminum target with α particles from the decay of americium-241, which was isolated from 100 smoke detectors. Write balanced nuclear reactions for these processes. The “radioactive boy scout” spent approximately 2 h/day with his experiment for 2 yr. Assuming that the alpha emission of americium has an energy of 5.24 MeV/particle and that the americium-241 was undergoing 3.5×10^6 decays/s, what was the exposure of the 60.0 kg scout in rads? The intrepid scientist apparently showed no ill effects from this exposure. Why?

241/95 Am---> 4/2 He + 237/93Np---> 4/2He + 233/91Pa----> 1/0n+ 232/91Th---> 1/1 H + 233/92 U

By adding alpha particles to the products side of the reaction, he was able to reduce the mass number by 4 and the atomic number by 2 to get the products he wanted. Bombardment with neutrons and 1 H was required to lower to the mass number to get Th and then raise both the mass number and the atomic number to yield Uranium.

2 hours*365*2= 1460 hours of exposure.*60min/1hr*60s/1min= 5.26*10^6s of exposure

1MeV= (1.6022*10^-13 Joules) * (5.24 MeV/particle)*2 particles= 1.679*10^-12 Joules.

(1.679*10^-12 Joules) * (1 amu/ 1.4924*10^-10 Joules)= 2.51*10^-13 amu

E=mc^2

E=(2.51*10^-13 amu)(1.66*10^-22kg/amu)(2.9998*10^8m/s)^2= (3.75*10^-18 kgm^2/s)*(3.5*10^6 decays/s)= 1.31*10^-11 joules of exposure per second.

The scientist showed no ill effects from this exposure because if we multiple the energy in joules of exposure per second, 1.31*10^-11, by the total amount of seconds of exposure, 5.26*10^6s, we find that he was only exposed to 6.9*10^-5 joules of radiation throughout the span of two years. This is a very small amount of radiation for such a long span of time.

In order to plug in the values for this equation, we must convert the given MeV to Joules with the known conversion rate. Similarly, we must convert Joules to amu with another known conversion rate. Then we can plug in the values and multiply by c^2 but we must not forget to multiple the amu by the conversion rate to kg in order to yield Joules. After all of this is done, we multiple the

amount of Joules of exposure per second by the total amount of exposure in seconds in order to find out the total amount of exposure over the two year span.

21.2: Patterns of Nuclear Stability

Q21.2.1

How do chemical reactions compare with nuclear reactions with respect to mass changes? Does either type of reaction violate the law of conservation of mass? Explain your answers.

Q21.2.2

Why is the amount of energy released by a nuclear reaction so much greater than the amount of energy released by a chemical reaction?

Q21.2.3

Explain why the mass of an atom is less than the sum of the masses of its component particles.

Q21.2.4

The stability of a nucleus can be described using two values. What are they, and how do they differ from each other?

Q21.2.5

In the days before true chemistry, ancient scholars (alchemists) attempted to find the philosopher's stone, a material that would enable them to turn lead into gold. Is the conversion of Pb → Au energetically favorable? Explain why or why not.

Q21.2.6

Describe the energy barrier to nuclear fusion reactions and explain how it can be overcome.

Q21.2.7

Imagine that the universe is dying, the stars have burned out, and all the elements have undergone fusion or radioactive decay. What would be the most abundant element in this future universe? Why?

Q21.2.8

Numerous elements can undergo fission, but only a few can be used as fuels in a reactor. What aspect of nuclear fission allows a nuclear chain reaction to occur?

Q21.2.9

How are transmutation reactions and fusion reactions related? Describe the main impediment to fusion reactions and suggest one or two ways to surmount this difficulty.

Q21.2.10

Using the information provided in Chapter 33, complete each reaction and calculate the amount of energy released from each in kilojoules.

a. $^{238}\text{Pa} \rightarrow ? + \beta^-$
b. $^{216}\text{Fr} \rightarrow ? + \alpha$
c. $^{199}\text{Bi} \rightarrow ? + \beta^+$

Q21.2.22

Using the information provided in Chapter 33, complete each reaction and calculate the amount of energy released from each in kilojoules.

a. $^{194}\text{Tl} \rightarrow ? + \beta^+$
b. $^{171}\text{Pt} \rightarrow ? + \alpha$
c. $^{214}\text{Pb} \rightarrow ? + \beta^-$

Q21.2.23

Using the information provided in Chapter 33, complete each reaction and calculate the amount of energy released from each in kilojoules per mole.

a. $^{234}_{91}\mathrm{Pa} \rightarrow ? + {}^{0}_{-1}\beta$
b. $^{226}_{88}\mathrm{Ra} \rightarrow ? + {}^{4}_{2}\alpha$

Q21.2.24

Using the information provided in Chapter 33, complete each reaction and then calculate the amount of energy released from each in kilojoules per mole.

a. $^{60}_{27}\mathrm{Co} \rightarrow ? + {}^{0}_{-1}\beta$ (The mass of cobalt-60 is 59.933817 amu.)
b. technicium-94 (mass = 93.909657 amu) undergoing fission to produce chromium-52 and potassium-40

Q21.2.25

Using the information provided in Chapter 33, predict whether each reaction is favorable and the amount of energy released or required in megaelectronvolts and kilojoules per mole.

a. the beta decay of bismuth-208 (mass = 207.979742 amu)
b. the formation of lead-206 by alpha decay

Q21.2.26

Using the information provided, predict whether each reaction is favorable and the amount of energy released or required in megaelectronvolts and kilojoules per mole.

a. alpha decay of oxygen-16
b. alpha decay to produce chromium-52

Q21.2.27

Calculate the total nuclear binding energy (in megaelectronvolts) and the binding energy per nucleon for ^{87}Sr if the measured mass of ^{87}Sr is 86.908877 amu.

a. the calculated mass
b. the mass defect
c. the nuclear binding energy
d. the nuclear binding energy per nucleon

Q21.2.30

The experimentally determined mass of ^{29}S is 28.996610 amu. Find each of the following.

a. the calculated mass
b. the mass defect
c. the nuclear binding energy
d. the nuclear binding energy per nucleon

Q21.2.31

Calculate the amount of energy that is released by the neutron-induced fission of ^{235}U to give ^{141}Ba, ^{92}Kr (mass = 91.926156 amu), and three neutrons. Report your answer in electronvolts per atom and kilojoules per mole.

Q21.2.31

Calculate the amount of energy that is released by the neutron-induced fission of ^{235}U to give ^{90}Sr, ^{143}Xe, and three neutrons. Report your answer in electronvolts per atom and kilojoules per mole.

Q21.2.33

Calculate the amount of energy released or required by the fusion of helium-4 to produce the unstable beryllium-8 (mass = 8.00530510 amu). Report your answer in kilojoules per mole. Do you expect this to be a spontaneous reaction?

Q21.2.34

Calculate the amount of energy released by the fusion of ^{6}Li and deuterium to give two helium-4 nuclei. Express your answer in electronvolts per atom and kilojoules per mole.

Q21.2.35

How much energy is released by the fusion of two deuterium nuclei to give one tritium nucleus and one proton? How does this amount compare with the energy released by the fusion of a deuterium nucleus and a tritium nucleus, which is accompanied by ejection of a neutron? Express your answer in megaelectronvolts and kilojoules per mole. Pound for pound, which is a better choice for a fusion reactor fuel mixture?

Numerical Answers

1

a. $^{238}_{91}\mathrm{Pa} \rightarrow {}^{238}_{92}\mathrm{U} + {}^{0}_{-1}\beta$; -5.540×10^{-16} kJ
b. $^{216}_{87}\mathrm{Fr} \rightarrow {}^{212}_{85}\mathrm{At} + {}^{4}_{2}\alpha$; -1.470×10^{-15} kJ
c. $^{199}_{83}\mathrm{Bi} \rightarrow {}^{199}_{82}\mathrm{Pb} + {}^{0}_{+1}\beta$; -5.458×10^{-16} kJ

3.

a. $^{234}_{91}\mathrm{Pa} \rightarrow {}^{234}_{92}\mathrm{U} + {}^{0}_{-1}\beta$; 2.118×10^{8} kJ/mol
b. $^{226}_{88}\mathrm{Ra} \rightarrow {}^{222}_{86}\mathrm{Rn} + {}^{4}_{2}\alpha$; 4.700×10^{8} kJ/mol

5.

a. The beta decay of bismuth-208 to polonium is endothermic (ΔE = 1.400 MeV/atom, 1.352×10^{8} kJ/mol).
b. The formation of lead-206 by alpha decay of polonium-210 is exothermic (ΔE = −5.405 MeV/atom, -5.218×10^{8} kJ/mol).

7. 757 MeV/atom, 8.70 MeV/nucleon

9.

a. 53.438245 amu
b. 0.496955 amu
c. 463 MeV/atom
d. 8.74 MeV/nucleon

11. −173 MeV/atom; 1.67×10^{10} kJ/mol

13. $\Delta E = +9.0 \times 10^{6}$ kJ/mol beryllium-8; no

15. D–D fusion: ΔE = −4.03 MeV/tritium nucleus formed = -3.89×10^{8} kJ/mol tritium; D–T fusion: ΔE = −17.6 MeV/tritium nucleus = -1.70×10^{9} kJ/mol; D–T fusion

21.3: Nuclear Transmutations

Q21.3.1

Why do scientists believe that hydrogen is the building block of all other elements? Why do scientists believe that helium-4 is the building block of the heavier elements?

Q21.3.2

How does a star produce such enormous amounts of heat and light? How are elements heavier than Ni formed?

Q21.3.3

Propose an explanation for the observation that elements with even atomic numbers are more abundant than elements with odd atomic numbers.

S21.3.3

The raw material for all elements with Z > 2 is helium (Z = 2), and fusion of helium nuclei will always produce nuclei with an even number of protons.

Q21.3.4

During the lifetime of a star, different reactions that form different elements are used to power the fusion furnace that keeps a star "lit." Explain the different reactions that dominate in the different stages of a star's life cycle and their effect on the temperature of the star.

Q21.3.5

A line in a popular song from the 1960s by Joni Mitchell stated, "We are stardust…." Does this statement have any merit or is it just poetic? Justify your answer.

Q21.3.6

If the laws of physics were different and the primary element in the universe were boron-11 (Z = 5), what would be the next four most abundant elements? Propose nuclear reactions for their formation.

Q21.3.7

Write a balanced nuclear reaction for the formation of each isotope.

a. ^{27}Al from two ^{12}C nuclei
b. ^{9}Be from two ^{4}He nuclei

Q21.3.8

At the end of a star's life cycle, it can collapse, resulting in a supernova explosion that leads to the formation of heavy elements by multiple neutron-capture events. Write a balanced nuclear reaction for the formation of each isotope during such an explosion.

a. ^{106}Pd from nickel-58
b. selenium-79 from iron-56

Q21.3.9

When a star reaches middle age, helium-4 is converted to short-lived beryllium-8 (mass = 8.00530510 amu), which reacts with another helium-4 to produce carbon-12. How much energy is released in each reaction (in megaelectronvolts)? How many atoms of helium must be "burned" in this process to produce the same amount of energy obtained from the fusion of 1 mol of hydrogen atoms to give deuterium?

21.4: Rates of Radioactive Decay

Q21.4.1

What do chemists mean by the half-life of a reaction?

Q21.4.2

If a sample of one isotope undergoes more disintegrations per second than the same number of atoms of another isotope, how do their half-lives compare?

Q21.4.3

Half-lives for the reaction A + B → C were calculated at three values of $[A]_0$, and [B] was the same in all cases. The data are listed in the following table:

$[A]_0$ (M)	$t_{½}$ (s)
0.50	420
0.75	280
1.0	210

Does this reaction follow first-order kinetics? On what do you base your answer?

S21.4.3

1. No; the reaction is second order in A because the half-life decreases with increasing reactant concentration according to $t_{1/2} = 1/k[A_0]$.

Q21.4.4

Ethyl-2-nitrobenzoate ($NO_2C_6H_4CO_2C_2H_5$) hydrolyzes under basic conditions. A plot of $[NO_2C_6H_4CO_2C_2H_5]$ versus t was used to calculate $t½$, with the following results:

$[NO_2C_6H_4CO_2C_2H_5]$ (M/cm^3)	$t_{½}$ (s)
0.050	240
0.040	300
0.030	400

Is this a first-order reaction? Explain your reasoning.

Q21.4.5

Azomethane ($CH_3N_2CH_3$) decomposes at 600 K to C_2H_6 and N_2. The decomposition is first order in azomethane. Calculate $t½$ from the data in the following table:

Time (s)	$P_{CH_3N_2CH_3}$ (atm)
0	8.2×10^{-2}
2000	3.99×10^{-2}
4000	1.94×10^{-2}

How long will it take for the decomposition to be 99.9% complete?

S21.4.5

$t_{1/2} = 1.92 \times 10^3$ s or 1920 s; 19100 s or 5.32 hrs.

Q21.4.6

The first-order decomposition of hydrogen peroxide has a half-life of 10.7 h at 20°C. What is the rate constant (expressed in s^{-1}) for this reaction? If you started with a solution that was 7.5×10^{-3} M H_2O_2, what would be the initial rate of decomposition (M/s)? What would be the concentration of H_2O_2 after 3.3 h?

2.16: Nuclear Chemistry (Exercises) is shared under a not declared license and was authored, remixed, and/or curated by LibreTexts.

CHAPTER OVERVIEW

3: Physical Properties of Gases

Here, we explore the relationships among pressure, temperature, volume, and the amount of gases. You will learn how to use these relationships to describe the physical behavior of a sample of both a pure gaseous substance and mixtures of gases. By the end of this chapter, your understanding of the gas laws and the model used to explain the behavior of gases will allow you to explain how straws and hot-air balloons work, why hand pumps cannot be used in wells beyond a certain depth, why helium-filled balloons deflate so rapidly, and how a gas can be liquefied for use in preserving biological tissue.

3.1: Properties of Gases
3.2: Gas Pressure
3.3: Relationships among Pressure, Temperature, Volume, and Amount
3.4: The Ideal Gas Law
3.5: Gas Volumes and Stoichiometry
3.6: Kinetic Molecular Theory of Gases
3.7: Connecting Gas Properties to Kinetic Molecular Theory
3.8: Chapter Problems

Thumbnail: Motion of gas molecules. The randomized thermal vibrations of fundamental particles such as atoms and molecules—gives a substance its "kinetic temperature." Here, the size of helium atoms relative to their spacing is shown to scale under 1950 atmospheres of pressure. (CC BY-SA 3.0; Greg L).

3: Physical Properties of Gases is shared under a not declared license and was authored, remixed, and/or curated by LibreTexts.

3.1: Properties of Gases

Learning Objectives

- To describe the characteristics of a gas.

The three common phases (or states) of matter are gases, liquids, and solids. Gases have the lowest density of the three, are highly compressible, and completely fill any container in which they are placed. Gases behave this way because their intermolecular forces are relatively weak, so their molecules are constantly moving independently of the other molecules present. Solids, in contrast, are relatively dense, rigid, and incompressible because their intermolecular forces are so strong that the molecules are essentially locked in place. Liquids are relatively dense and incompressible, like solids, but they flow readily to adapt to the shape of their containers, like gases. We can therefore conclude that the sum of the intermolecular forces in liquids are between those of gases and solids. Figure **3.1.1** compares the three states of matter and illustrates the differences at the molecular level.

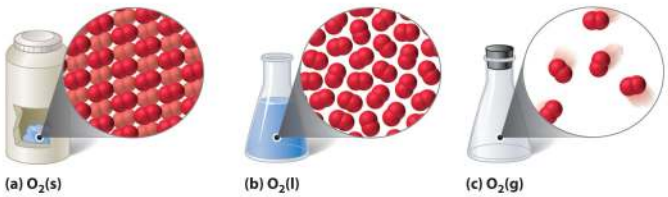


Figure **3.1.1**: A Diatomic Substance (O_2) in the Solid, Liquid, and Gaseous States: (a) Solid O_2 has a fixed volume and shape, and the molecules are packed tightly together. (b) Liquid O_2 conforms to the shape of its container but has a fixed volume; it contains relatively densely packed molecules. (c) Gaseous O_2 fills its container completely—regardless of the container's size or shape—and consists of widely separated molecules.

The state of a given substance depends strongly on conditions. For example, H_2O is commonly found in all three states: solid ice, liquid water, and water vapor (its gaseous form). Under most conditions, we encounter water as the liquid that is essential for life; we drink it, cook with it, and bathe in it. When the temperature is cold enough to transform the liquid to ice, we can ski or skate on it, pack it into a snowball or snow cone, and even build dwellings with it. Water vapor (the term *vapor* refers to the gaseous form of a substance that is a liquid or a solid under normal conditions so nitrogen (N_2) and oxygen (O_2) are referred to as gases, but gaseous water in the atmosphere is called water vapor) is a component of the air we breathe, and it is produced whenever we heat water for cooking food or making coffee or tea. Water vapor at temperatures greater than 100°C is called steam. Steam is used to drive large machinery, including turbines that generate electricity. The properties of the three states of water are summarized in Table **3.1.1**.

Table **3.1.1**: Properties of Water at 1.0 atm

Temperature	State	Density (g/cm^3)
≤0°C	solid (ice)	0.9167 (at 0.0°C)
0°C–100°C	liquid (water)	0.9997 (at 4.0°C)
≥100°C	vapor (steam)	0.005476 (at 127°C)

The geometric structure and the physical and chemical properties of atoms, ions, and molecules usually do *not* depend on their physical state; the individual water molecules in ice, liquid water, and steam, for example, are all identical. In contrast, the macroscopic properties of a substance depend strongly on its physical state, which is determined by intermolecular forces and conditions such as temperature and pressure.

Figure **3.1.2** shows the locations in the periodic table of those elements that are commonly found in the gaseous, liquid, and solid states. Except for hydrogen, the elements that occur naturally as gases are on the right side of the periodic table. Of these, all the noble gases (group 18) are monatomic gases, whereas the other gaseous elements are diatomic molecules (**H_2, N_2, O_2, F_2, and Cl_2**). Oxygen can also form a second allotrope, the highly reactive triatomic molecule ozone (**O_3**), which is also a gas. In contrast, bromine (as Br_2) and mercury (Hg) are liquids under normal conditions (25°C and 1.0 atm, commonly referred to as "room temperature and pressure"). Gallium (Ga), which melts at only 29.76°C, can be converted to a liquid simply by holding a container

of it in your hand or keeping it in a non-air-conditioned room on a hot summer day. The rest of the elements are all solids under normal conditions.

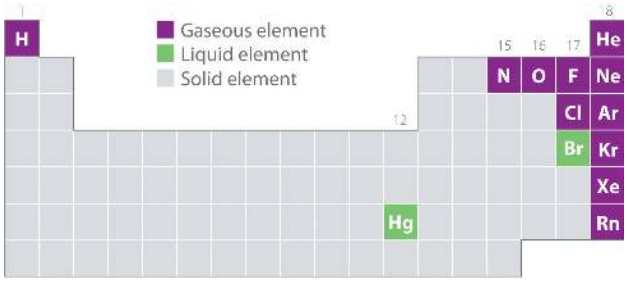


Figure **3.1.2**: Elements That Occur Naturally as Gases, Liquids, and Solids at 25°C and 1 atm. The noble gases and mercury occur as monatomic species, whereas all other gases and bromine are diatomic molecules.

All of the gaseous elements (other than the monatomic noble gases) are molecules. Within the same group (1, 15, 16 and 17), the lightest elements are gases. All gaseous substances are characterized by weak interactions between the constituent molecules or atoms.



Defining Gas Pressure: https://youtu.be/_CRn3cFs2CI

Summary

Bulk matter can exist in three states: gas, liquid, and solid. Gases have the lowest density of the three, are highly compressible, and fill their containers completely. Elements that exist as gases at room temperature and pressure are clustered on the right side of the periodic table; they occur as either monatomic gases (the noble gases) or diatomic molecules (some halogens, N_2, O_2).

3.1: Properties of Gases is shared under a not declared license and was authored, remixed, and/or curated by LibreTexts.

- **6.1: Properties of Gases: Gas Pressure** is licensed CC BY-NC-SA 4.0.

3.2: Gas Pressure

Learning Objectives

- to describe and measure the pressure of a gas.

At the macroscopic level, a complete physical description of a sample of a gas requires four quantities:

- ***temperature*** (expressed in kelvins),
- ***volume*** (expressed in liters),
- ***amount*** (expressed in moles), and
- ***pressure*** (in atmospheres).

As we demonstrated below, these variables are *not* independent (i.e., they cannot be arbitrarily be varied). If we know the values of any *three* of these quantities, we can calculate the fourth and thereby obtain a full physical description of the gas. Temperature, volume, and amount have been discussed in previous chapters. We now discuss pressure and its units of measurement.

Units of Pressure

Any object, whether it is your computer, a person, or a sample of gas, exerts a force on any surface with which it comes in contact. The air in a balloon, for example, exerts a force against the interior surface of the balloon, and a liquid injected into a mold exerts a force against the interior surface of the mold, just as a chair exerts a force against the floor because of its mass and the effects of gravity. If the air in a balloon is heated, the increased kinetic energy of the gas eventually causes the balloon to burst because of the increased pressure (P) of the gas, the force (F) per unit area (A) of surface:

$$P = \frac{\text{Force}}{\text{Area}} = \frac{F}{A} \tag{3.2.1}$$

Pressure is dependent on *both* the force exerted *and* the size of the area to which the force is applied. We know from Equation 3.2.1 that applying the same force to a smaller area produces a higher pressure. When we use a hose to wash a car, for example, we can increase the pressure of the water by reducing the size of the opening of the hose with a thumb.

The units of pressure are derived from the units used to measure force and area. The SI unit for pressure, derived from the SI units for force (newtons) and area (square meters), is the newton per square meter (N/m^2), which is called the **Pascal (Pa)**, after the French mathematician Blaise Pascal (1623–1662):

$$1\ \text{Pa} = 1\ \text{N/m}^2 \tag{3.2.2}$$

Example 3.2.1

Assuming a paperback book has a mass of 2.00 kg, a length of 27.0 cm, a width of 21.0 cm, and a thickness of 4.5 cm, what pressure does it exert on a surface if it is

a. lying flat?
b. standing on edge in a bookcase?

Given: mass and dimensions of object

Asked for: pressure

Strategy:

A. Calculate the force exerted by the book and then compute the area that is in contact with a surface.
B. Substitute these two values into Equation 3.2.1 to find the pressure exerted on the surface in each orientation.

Solution:

The force exerted by the book does *not* depend on its orientation. Recall that the force exerted by an object is $F = ma$, where m is its mass and a is its acceleration. In Earth's gravitational field, the acceleration is due to gravity (9.8067 m/s^2 at Earth's surface). In SI units, the force exerted by the book is therefore

$$F = ma = 2.00\ \text{kg} \times 9.8067 \frac{\text{m}}{\text{s}^2} = 19.6 \frac{\text{kg} \cdot \text{m}}{\text{s}^2} = 19.6\ \text{N}$$

A We calculated the force as 19.6 N. When the book is lying flat, the area is

$$A = 0.270\ \text{m} \times 0.210\ \text{m} = 0.0567\ \text{m}^2.$$

B The pressure exerted by the text lying flat is thus

$$P = \frac{F}{A} = \frac{19.6\ \text{N}}{0.0567\ \text{m}^2} = 3.46 \times 10^2 \text{Pa}$$

A If the book is standing on its end, the force remains the same, but the area decreases:

$$\text{A} = 21.0\ \text{cm} \times 4.5\ \text{cm} = 0.210\ \text{m} \times 0.045\ \text{m} = 9.5 \times 10^{-3}\ \text{m}^2$$

B The pressure exerted by the text lying flat is thus

$$P = \frac{19.6\ \text{N}}{9.5 \times 10^{-3}\ \text{m}^2} = 2.06 \times 10^3\ \text{Pa}$$

? Exercise 3.2.1

What pressure does a 60.0 kg student exert on the floor

a. when standing flat-footed in the laboratory in a pair of tennis shoes (the surface area of the soles is approximately 180 cm^2)?
b. as she steps heel-first onto a dance floor wearing high-heeled shoes (the area of the heel = 1.0 cm^2)?

Answer a

3.27×10^4 Pa

Answer b

5.9×10^6 Pa

Barometric Pressure

Just as we exert pressure on a surface because of gravity, so does our atmosphere. We live at the bottom of an ocean of gases that becomes progressively less dense with increasing altitude. Approximately 99% of the mass of the atmosphere lies within 30 km of Earth's surface (Figure **3.2.1**). Every point on Earth's surface experiences a net pressure called ***barometric pressure***. The pressure exerted by the atmosphere is considerable: a 1 m^2 column, measured from sea level to the top of the atmosphere, has a mass of about 10,000 kg, which gives a pressure of about 101 kPa:

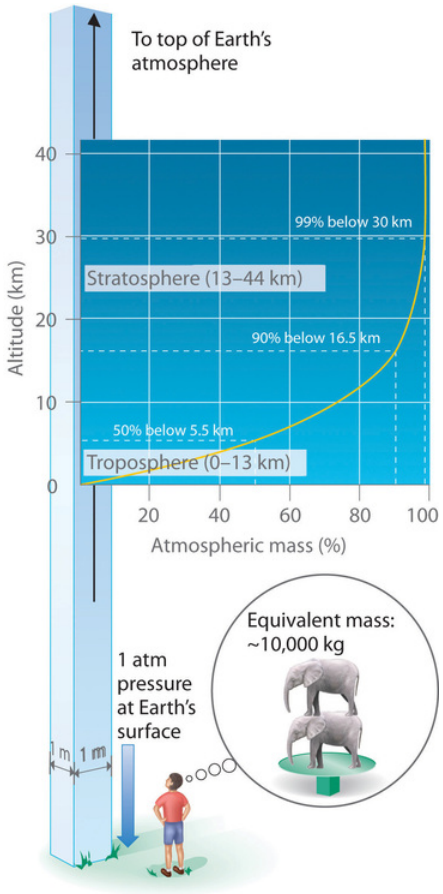


Figure **3.2.1**: Barometric Pressure. Each square meter of Earth's surface supports a column of air that is more than 200 km high and weighs about 10,000 kg at Earth's surface.

Barometric pressure can be measured using a barometer, a device invented in 1643 by one of Galileo's students, Evangelista Torricelli (1608–1647). A barometer may be constructed from a long glass tube that is closed at one end. It is filled with mercury and placed upside down in a dish of mercury without allowing any air to enter the tube. Some of the mercury will run out of the tube, but a relatively tall column remains inside (Figure **3.2.2**). Why doesn't all the mercury run out? Gravity is certainly exerting a downward force on the mercury in the tube, but it is opposed by the pressure of the atmosphere pushing down on the surface of the mercury in the dish, which has the net effect of pushing the mercury up into the tube. Because there is no air above the mercury inside the tube in a properly filled barometer (it contains a vacuum), there is no pressure pushing down on the column. Thus the mercury runs out of the tube until the pressure exerted by the mercury column itself exactly balances the pressure of the atmosphere. The pressure exerted by the mercury column can be expressed as:

$$P = \frac{F}{A} \tag{3.2.3}$$

$$= \frac{mg}{A} \tag{3.2.4}$$

$$= \frac{\rho V \cdot g}{A} \tag{3.2.5}$$

$$= \frac{\rho \cdot Ah \cdot g}{A} \tag{3.2.6}$$

$$= \rho gh \tag{3.2.7}$$

with

- g is the gravitational acceleration,
- m is the mass,
- ρ is the density,
- V is the volume,

- A is the bottom area, and
- h is height of the mercury column.

Under normal weather conditions at sea level, the two forces are balanced when the top of the mercury column is approximately 760 mm above the level of the mercury in the dish, as shown in Figure **3.2.2**. This value varies with meteorological conditions and altitude. In Denver, Colorado, for example, at an elevation of about 1 mile, or 1609 m (5280 ft), the height of the mercury column is 630 mm rather than 760 mm.

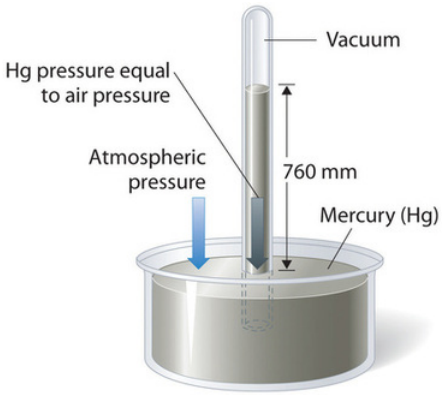


Figure **3.2.2**: A Mercury Barometer. The pressure exerted by the atmosphere on the surface of the pool of mercury supports a column of mercury in the tube that is about 760 mm tall. Because the boiling point of mercury is quite high (356.73°C), there is very little mercury vapor in the space above the mercury column.

Mercury barometers have been used to measure barometric pressure for so long that they have their own unit for pressure: the millimeter of mercury (mmHg), often called the torr, after Torricelli. Standard barometric pressure is the barometric pressure required to support a column of mercury exactly 760 mm tall; this pressure is also referred to as 1 atmosphere (atm). These units are also related to the pascal:

$$1\ \text{atm} = 760\ mmHg \tag{3.2.8}$$
$$= 760\ torr \tag{3.2.9}$$
$$= 1.01325 \times 10^5\ Pa \tag{3.2.10}$$
$$= 101.325\ kPa \tag{3.2.11}$$

Thus a pressure of 1 atm equals 760 mmHg exactly.

We are so accustomed to living under this pressure that we never notice it. Instead, what we notice are *changes* in the pressure, such as when our ears pop in fast elevators in skyscrapers or in airplanes during rapid changes in altitude. We make use of barometric pressure in many ways. We can use a drinking straw because sucking on it removes air and thereby reduces the pressure inside the straw. The barometric pressure pushing down on the liquid in the glass then forces the liquid up the straw.

✔ Example 3.2.2: Barometric Pressure

One of the authors visited Rocky Mountain National Park several years ago. After departing from an airport at sea level in the eastern United States, he arrived in Denver (altitude 5280 ft), rented a car, and drove to the top of the highway outside Estes Park (elevation 14,000 ft). He noticed that even slight exertion was very difficult at this altitude, where the barometric pressure is only 454 mmHg. Convert this pressure to

a. atmospheres (atm).
b. bar.

Given: pressure in millimeters of mercury

Asked for: pressure in atmospheres and bar

Strategy:

Use the conversion factors in Equation 3.2.11 to convert from millimeters of mercury to atmospheres and kilopascals.

Solution:

From Equation 3.2.11, we have 1 atm = 760 mmHg = 101.325 kPa. The pressure at 14,000 ft in atm is thus

$$P = 454 \text{ mmHg} \times \frac{1 \text{ atm}}{760 \text{ mmHg}} \tag{3.2.12}$$
$$= 0.597 \text{ atm}$$

The pressure in bar is given by

$$P = 0.597 \text{ atm} \times \frac{1.01325 \text{ bar}}{1 \text{ atm}} \tag{3.2.13}$$
$$= 0.605 \text{ bar}$$

? Exercise 3.2.2: Barometric Pressure

Mt. Everest, at 29,028 ft above sea level, is the world's tallest mountain. The normal barometric pressure at this altitude is about 0.308 atm. Convert this pressure to

a. millimeters of mercury.
b. bar.

Answer a

234 mmHg;

Answer b

0.312 bar

Manometers

Barometers measure barometric pressure, but manometers measure the pressures of samples of gases contained in an apparatus. The key feature of a manometer is a U-shaped tube containing mercury (or occasionally another nonvolatile liquid). A closed-end manometer is shown schematically in part (a) in Figure **3.2.3**. When the bulb contains no gas (i.e., when its interior is a near vacuum), the heights of the two columns of mercury are the same because the space above the mercury on the left is a near vacuum (it contains only traces of mercury vapor). If a gas is released into the bulb on the right, it will exert a pressure on the mercury in the right column, and the two columns of mercury will no longer be the same height. The *difference* between the heights of the two columns is equal to the pressure of the gas.

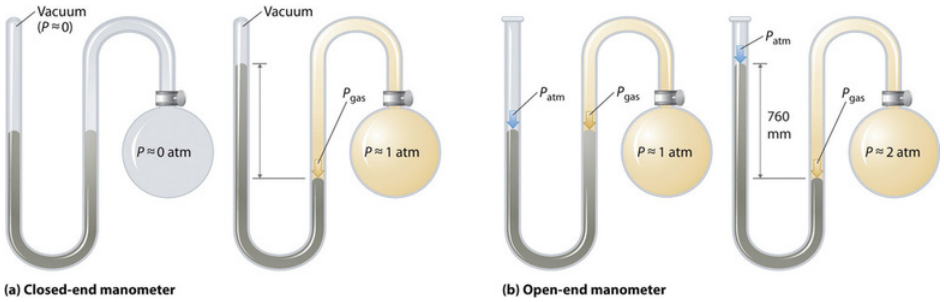


Figure **3.2.3**: The Two Types of Manometer. (a) In a closed-end manometer, the space above the mercury column on the left (the reference arm) is essentially a vacuum ($P \approx 0$), and the difference in the heights of the two columns gives the pressure of the gas contained in the bulb directly. (b) In an open-end manometer, the left (reference) arm is open to the atmosphere ($P \approx 1$ atm), and the difference in the heights of the two columns gives the *difference* between barometric pressure and the pressure of the gas in the bulb.

If the tube is open to the atmosphere instead of closed, as in the open-end manometer shown in part (b) in Figure **3.2.3**, then the two columns of mercury have the same height only if the gas in the bulb has a pressure equal to the barometric pressure. If the gas in the bulb has a *higher* pressure, the mercury in the open tube will be forced up by the gas pushing down on the mercury in the other arm of the U-shaped tube. The pressure of the gas in the bulb is therefore the sum of the barometric pressure (measured with a barometer) and the difference in the heights of the two columns. If the gas in the bulb has a pressure *less* than that of the

atmosphere, then the height of the mercury will be greater in the arm attached to the bulb. In this case, the pressure of the gas in the bulb is the barometric pressure minus the difference in the heights of the two columns.

Example 3.2.3

Suppose you want to construct a closed-end manometer to measure gas pressures in the range 0.000–0.200 atm. Because of the toxicity of mercury, you decide to use water rather than mercury. How tall a column of water do you need? (The density of water is 1.00 g/cm^3; the density of mercury is 13.53 g/cm^3.)

Given: pressure range and densities of water and mercury

Asked for: column height

Strategy:

A. Calculate the height of a column of mercury corresponding to 0.200 atm in millimeters of mercury. This is the height needed for a mercury-filled column.

B. From the given densities, use a proportion to compute the height needed for a water-filled column.

Solution:

A In millimeters of mercury, a gas pressure of 0.200 atm is

$$P = 0.200\ \text{atm} \times \frac{760\ \text{mmHg}}{1\ \text{atm}} = 152\ \text{mmHg}$$

Using a mercury manometer, you would need a mercury column at least 152 mm high.

B Because water is less dense than mercury, you need a *taller* column of water to achieve the same pressure as a given column of mercury. The height needed for a water-filled column corresponding to a pressure of 0.200 atm is proportional to the ratio of the density of mercury to the density of water

$$P = d_{\text{wat}} g h_{\text{wat}} = d_{\text{Hg}} g h_{\text{Hg}}$$

$$h_{\text{wat}} = h_{\text{Hg}} \times \frac{d_{\text{Hg}}}{g_{\text{wat}}} = 152\ \text{mm} \times \frac{13.53\ \text{g/cm}^3}{1.00\ \text{g/cm}^3} = 2070\ \text{mm}$$

The answer makes sense: it takes a taller column of a less dense liquid to achieve the same pressure.

Exercise 3.2.3

Suppose you want to design a barometer to measure barometric pressure in an environment that is always hotter than 30°C. To avoid using mercury, you decide to use gallium, which melts at 29.76°C; the density of liquid gallium at 25°C is 6.114 g/cm^3. How tall a column of gallium do you need if P = 1.00 atm?

Answer

1.68 m

The answer to Example **3.2.3** also tells us the maximum depth of a farmer's well if a simple suction pump will be used to get the water out. The 1.00 atm corresponds to a column height of

$$\begin{aligned} h_{\text{wat}} &= h_{\text{Hg}} \times \frac{d_{\text{Hg}}}{g_{\text{wat}}} \\ &= 760\ \text{mm} \times \frac{13.53\ \text{g/cm}^3}{1.00\ \text{g/cm}^3} \\ &= 1.03 \times 10^4\ mm \\ &= 10.3\ m \end{aligned}$$

A suction pump is just a more sophisticated version of a straw: it creates a vacuum above a liquid and relies on barometric pressure to force the liquid up a tube. If 1 atm pressure corresponds to a 10.3 m (33.8 ft) column of water, then it is physically impossible for barometric pressure to raise the water in a well higher than this. Until electric pumps were invented to push water mechanically from greater depths, this factor greatly limited where people could live because obtaining water from wells deeper than about 33 ft was difficult.

Summary

Pressure is defined as the force exerted per unit area; it can be measured using a barometer or manometer. Four quantities must be known for a complete physical description of a sample of a gas: *temperature*, *volume*, *amount*, and *pressure*. **Pressure** is force per unit area of surface; the SI unit for pressure is the **pascal (Pa)**, defined as 1 newton per square meter (N/m^2). The pressure exerted by an object is proportional to the force it exerts and inversely proportional to the area on which the force is exerted. The pressure exerted by Earth's atmosphere, called *barometric pressure*, is about 101 kPa or 14.7 $lb/in.^2$ at sea level. barometric pressure can be measured with a **barometer**, a closed, inverted tube filled with mercury. The height of the mercury column is proportional to barometric pressure, which is often reported in units of **millimeters of mercury (mmHg)**, also called **torr**. **Standard barometric pressure**, the pressure required to support a column of mercury 760 mm tall, is yet another unit of pressure: 1 **atmosphere (atm)**. A **manometer** is an apparatus used to measure the pressure of a sample of a gas.



3.2: Gas Pressure is shared under a not declared license and was authored, remixed, and/or curated by LibreTexts.

- **10.2: Pressure** is licensed CC BY-NC-SA 3.0.

3.3: Relationships among Pressure, Temperature, Volume, and Amount

Learning Objectives

- To understand the relationships among pressure, temperature, volume, and the amount of a gas.

Early scientists explored the relationships among the pressure of a gas (P) and its temperature (T), volume (V), and amount (n) by holding two of the four variables constant (amount and temperature, for example), varying a third (such as pressure), and measuring the effect of the change on the fourth (in this case, volume). The history of their discoveries provides several excellent examples of the scientific method.

The Relationship between Pressure and Volume: Boyle's Law

As the pressure on a gas increases, the volume of the gas decreases because the gas particles are forced closer together. Conversely, as the pressure on a gas decreases, the gas volume increases because the gas particles can now move farther apart. Weather balloons get larger as they rise through the atmosphere to regions of lower pressure because the volume of the gas has increased; that is, the atmospheric gas exerts less pressure on the surface of the balloon, so the interior gas expands until the internal and external pressures are equal.

The Irish chemist Robert Boyle (1627–1691) carried out some of the earliest experiments that determined the quantitative relationship between the pressure and the volume of a gas. Boyle used a J-shaped tube partially filled with mercury, as shown in Figure **3.3.1**. In these experiments, a small amount of a gas or air is trapped above the mercury column, and its volume is measured at atmospheric pressure and constant temperature. More mercury is then poured into the open arm to increase the pressure on the gas sample. The pressure on the gas is atmospheric pressure plus the difference in the heights of the mercury columns, and the resulting volume is measured. This process is repeated until either there is no more room in the open arm or the volume of the gas is too small to be measured accurately. Data such as those from one of Boyle's own experiments may be plotted in several ways (Figure **3.3.2**). A simple plot of V versus P gives a curve called a hyperbola and reveals an inverse relationship between pressure and volume: as the pressure is doubled, the volume decreases by a factor of two. This relationship between the two quantities is described as follows:

$$PV = \text{constant} \tag{3.3.1}$$

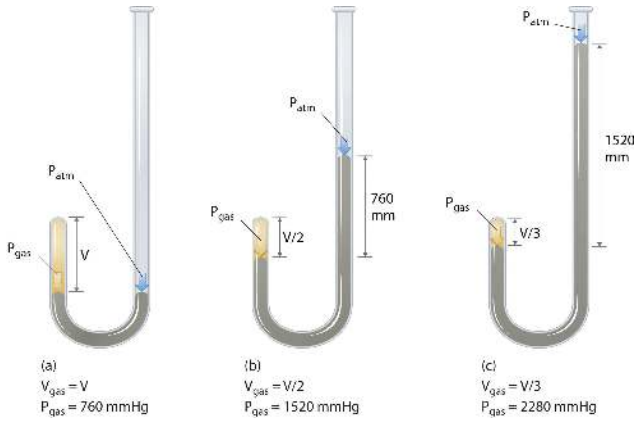


Figure **3.3.1**: Boyle's Experiment Using a J-Shaped Tube to Determine the Relationship between Gas Pressure and Volume. (a) Initially the gas is at a pressure of 1 atm = 760 mmHg (the mercury is at the same height in both the arm containing the sample and the arm open to the atmosphere); its volume is V. (b) If enough mercury is added to the right side to give a difference in height of 760 mmHg between the two arms, the pressure of the gas is 760 mmHg (atmospheric pressure) + 760 mmHg = 1520 mmHg and the volume is $V/2$. (c) If an additional 760 mmHg is added to the column on the right, the total pressure on the gas increases to 2280 mmHg, and the volume of the gas decreases to $V/3$.

Dividing both sides by P gives an equation illustrating the inverse relationship between P and V:

$$V = \frac{\text{const.}}{P} = \text{const.}\left(\frac{1}{P}\right) \tag{3.3.2}$$

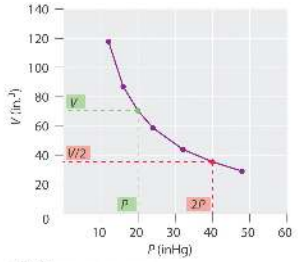
or

$$V \propto \frac{1}{P} \tag{3.3.3}$$

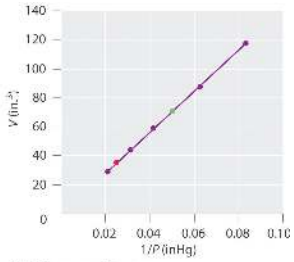
where the ∝ symbol is read “is proportional to.” A plot of V versus $1/P$ is thus a straight line whose slope is equal to the constant in Equation 6.2.1 and Equation 6.2.3. Dividing both sides of Equation 6.2.1 by V instead of P gives a similar relationship between P and $1/V$. The numerical value of the constant depends on the amount of gas used in the experiment and on the temperature at which the experiments are carried out. This relationship between pressure and volume is known as Boyle’s law, after its discoverer, and can be stated as follows: *At constant temperature, the volume of a fixed amount of a gas is inversely proportional to its pressure.*

P (inHg)	V (in.^{3})	PV
12.0	117.5	1410
16.0	87.2	1400
20.0	70.7	1410
24.0	58.8	1410
32.0	44.2	1410
40.0	35.3	1410
48.0	29.1	1400

(a) Data from Boyle's experiment



(b) Volume vs. pressure



(c) Volume vs. 1/pressure

Figure **3.3.2**: Plots of Boyle’s Data. (a) Here are actual data from a typical experiment conducted by Boyle. Boyle used non-SI units to measure the volume (in.^{3} rather than cm^3) and the pressure (in. Hg rather than mmHg). (b) This plot of pressure versus volume is a hyperbola. Because PV is a constant, decreasing the pressure by a factor of two results in a twofold increase in volume and vice versa. (c) A plot of volume versus 1/pressure for the same data shows the inverse linear relationship between the two quantities, as expressed by the equation V = constant/P.



Boyle’s Law: https://youtu.be/lu86VSupPO4

The Relationship between Temperature and Volume: Charles's Law

Hot air rises, which is why hot-air balloons ascend through the atmosphere and why warm air collects near the ceiling and cooler air collects at ground level. Because of this behavior, heating registers are placed on or near the floor, and vents for air-conditioning are placed on or near the ceiling. The fundamental reason for this behavior is that gases expand when they are heated. Because the same amount of substance now occupies a greater volume, hot air is less dense than cold air. The substance with the lower density —in this case hot air—rises through the substance with the higher density, the cooler air.

The first experiments to quantify the relationship between the temperature and the volume of a gas were carried out in 1783 by an avid balloonist, the French chemist Jacques Alexandre César Charles (1746–1823). Charles’s initial experiments showed that a plot of the volume of a given sample of gas versus temperature (in degrees Celsius) at constant pressure is a straight line. Similar but more precise studies were carried out by another balloon enthusiast, the Frenchman Joseph-Louis Gay-Lussac (1778–1850), who showed that a plot of V versus T was a straight line that could be extrapolated to a point at zero volume, a theoretical condition now known to correspond to −273.15°C (Figure **3.3.3**).A sample of gas cannot really have a volume of zero because any sample of matter must have some volume. Furthermore, at 1 atm pressure all gases liquefy at temperatures well above −273.15°C. Note from

part (a) in Figure **3.3.3** that the slope of the plot of V versus T varies for the same gas at different pressures but that the intercept remains constant at −273.15°C. Similarly, as shown in part (b) in Figure **3.3.3**, plots of V versus T for different amounts of varied gases are straight lines with different slopes but the same intercept on the T axis.

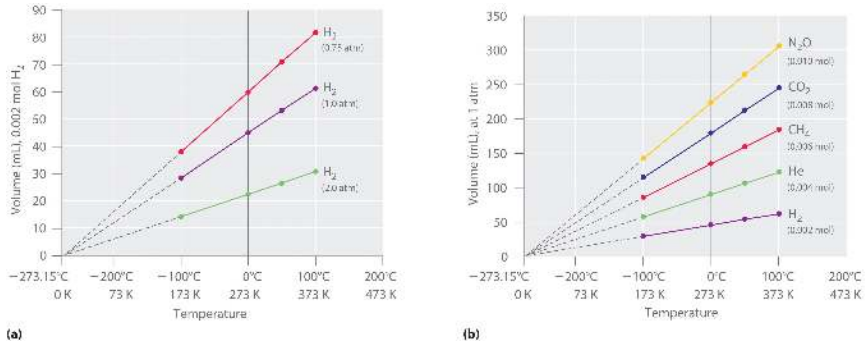


Figure **3.3.3**: The Relationship between Volume and Temperature. (a) In these plots of volume versus temperature for equal-sized samples of H_2 at three different pressures, the solid lines show the experimentally measured data down to −100°C, and the broken lines show the extrapolation of the data to $V = 0$. The temperature scale is given in both degrees Celsius and kelvins. Although the slopes of the lines decrease with increasing pressure, all of the lines extrapolate to the same temperature at $V = 0$ (−273.15°C = 0 K). (b) In these plots of volume versus temperature for different amounts of selected gases at 1 atm pressure, all the plots extrapolate to a value of $V = 0$ at −273.15°C, regardless of the identity or the amount of the gas.

The significance of the invariant T intercept in plots of V versus T was recognized in 1848 by the British physicist William Thomson (1824–1907), later named Lord Kelvin. He postulated that −273.15°C was the lowest possible temperature that could theoretically be achieved, for which he coined the term absolute zero (0 K).

We can state Charles's and Gay-Lussac's findings in simple terms: At constant pressure, the volume of a fixed amount of gas is directly proportional to its absolute temperature (in kelvins). This relationship, illustrated in part (b) in Figure **3.3.3** is often referred to as Charles's law and is stated mathematically as

$$V = \text{const.}\, T \tag{3.3.4}$$

or

$$V \propto T \tag{3.3.5}$$

with *temperature expressed in kelvins*, not *in degrees Celsius*. Charles's law is valid for virtually all gases at temperatures well above their boiling points.



Charles's Law: https://youtu.be/NBf510ZnlR0

The Relationship between Amount and Volume: Avogadro's Law

We can demonstrate the relationship between the volume and the amount of a gas by filling a balloon; as we add more gas, the balloon gets larger. The specific quantitative relationship was discovered by the Italian chemist Amedeo Avogadro, who recognized

the importance of Gay-Lussac's work on combining volumes of gases. In 1811, Avogadro postulated that, at the same temperature and pressure, equal volumes of gases contain the same number of gaseous particles (Figure **3.3.4**). This is the historic "Avogadro's hypothesis."

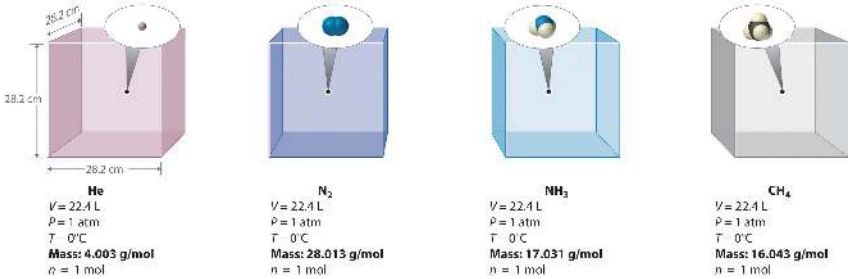


Figure **3.3.4**: Avogadro's Hypothesis. Equal volumes of four different gases at the same temperature and pressure contain the same number of gaseous particles. Because the molar mass of each gas is different, the *mass* of each gas sample is different even though all contain 1 mol of gas.

A logical corollary to Avogadro's hypothesis (sometimes called Avogadro's law) describes the relationship between the volume and the amount of a gas: *At constant temperature and pressure, the volume of a sample of gas is directly proportional to the number of moles of gas in the sample.* Stated mathematically,

$$V = \text{const.}\ (n) \tag{3.3.6}$$

or

$$V \propto .n@\ \text{constant T and P} \tag{3.3.7}$$

This relationship is valid for most gases at relatively low pressures, but deviations from strict linearity are observed at elevated pressures.

Note

For a sample of gas,

- V increases as P decreases (and vice versa)
- V increases as T increases (and vice versa)
- V increases as n increases (and vice versa)

The relationships among the volume of a gas and its pressure, temperature, and amount are summarized in Figure **3.3.5**. Volume *increases* with increasing temperature or amount but *decreases* with increasing pressure.

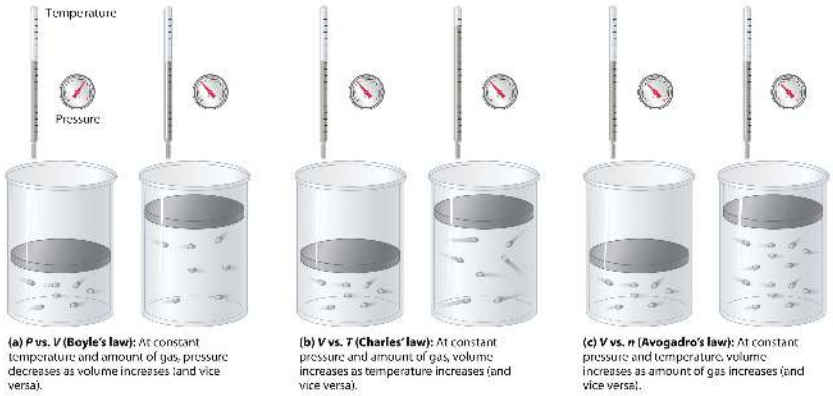


Figure **3.3.5**: The Empirically Determined Relationships among Pressure, Volume, Temperature, and Amount of a Gas. The thermometer and pressure gauge indicate the temperature and the pressure qualitatively, the level in the flask indicates the volume, and the number of particles in each flask indicates relative amounts.



Avogadro's Law: https://youtu.be/dRY3Trl4T24

Summary

The volume of a gas is inversely proportional to its pressure and directly proportional to its temperature and the amount of gas. Boyle showed that the volume of a sample of a gas is inversely proportional to its pressure (**Boyle's law**), Charles and Gay-Lussac demonstrated that the volume of a gas is directly proportional to its temperature (in kelvins) at constant pressure (**Charles's law**), and Avogadro postulated that the volume of a gas is directly proportional to the number of moles of gas present (**Avogadro's law**). Plots of the volume of gases versus temperature extrapolate to zero volume at −273.15°C, which is **absolute zero (0 K)**, the lowest temperature possible. Charles's law implies that the volume of a gas is directly proportional to its absolute temperature.

3.3: Relationships among Pressure, Temperature, Volume, and Amount is shared under a not declared license and was authored, remixed, and/or curated by LibreTexts.

- **6.2: The Simple Gas Laws** is licensed CC BY-NC-SA 4.0.

3.4: The Ideal Gas Law

Learning Objectives

- To use the ideal gas law to describe the behavior of a gas.

In this module, the relationship between Pressure, Temperature, Volume, and Amount of a gas are described and how these relationships can be combined to give a general expression that describes the behavior of a gas.

Deriving the Ideal Gas Law

Any set of relationships between a single quantity (such as V) and several other variables (P, T, and n) can be combined into a single expression that describes all the relationships simultaneously. The three individual expressions are as follows:

- **Boyle's law**

$$V \propto \frac{1}{P} \text{ @ constant n and T} \tag{3.4.1}$$

- **Charles's law**

$$V \propto T \text{ @ constant n and P} \tag{3.4.2}$$

- **Avogadro's law**

$$V \propto n \text{ @ constant T and P} \tag{3.4.3}$$

Combining these three expressions gives

$$V \propto \frac{nT}{P} \tag{6.3.1}$$

which shows that the volume of a gas is proportional to the number of moles and the temperature and inversely proportional to the pressure. This expression can also be written as

$$V = \text{Cons.}\left(\frac{nT}{P}\right) \tag{6.3.2}$$

By convention, the proportionality constant in Equation 6.3.1 is called the gas constant, which is represented by the letter R. Inserting R into Equation 6.3.2 gives

$$V = \frac{Rnt}{P} = \frac{nRT}{P} \tag{6.3.3}$$

Clearing the fractions by multiplying both sides of Equation 6.3.4 by P gives

$$PV = nRT \tag{6.3.4}$$

This equation is known as the **ideal gas law**.

An ideal gas is defined as a hypothetical gaseous substance whose behavior is independent of attractive and repulsive forces and can be completely described by the ideal gas law. In reality, there is no such thing as an ideal gas, but an ideal gas is a useful conceptual model that allows us to understand how gases respond to changing conditions. As we shall see, under many conditions, most real gases exhibit behavior that closely approximates that of an ideal gas. The ideal gas law can therefore be used to predict the behavior of real gases under most conditions. The ideal gas law does not work well at very low temperatures or very high pressures, where deviations from ideal behavior are most commonly observed.

Note

Significant deviations from ideal gas behavior commonly occur at low temperatures and very high pressures.

Before we can use the ideal gas law, however, we need to know the value of the gas constant R. Its form depends on the units used for the other quantities in the expression. If V is expressed in liters (L), P in atmospheres (atm), T in kelvins (K), and n in moles (mol), then

$$R = 0.08206 \frac{\text{L} \cdot \text{atm}}{\text{K} \cdot \text{mol}} \tag{6.3.5}$$

Because the product PV has the units of energy, R can also have units of J/(K•mol):

$$R = 8.3145 \frac{\text{J}}{\text{K} \cdot \text{mol}} \tag{6.3.6}$$

Standard Conditions of Temperature and Pressure

Scientists have chosen a particular set of conditions to use as a reference: 0°C (273.15 K) and $1 \text{ bar} = 100 \text{ kPa} = 10^5 \text{ Pa}$ pressure, referred to as standard temperature and pressure (**STP**).

$$\text{STP:} \qquad T = 273.15 \text{ K and } P = 1 \text{ bar} = 10^5 \text{ Pa} \tag{3.4.4}$$

Please note that STP was defined differently in the part. The old definition was based on a standard pressure of 1 atm.

We can calculate the volume of 1.000 mol of an ideal gas under standard conditions using the variant of the ideal gas law given in Equation 6.3.4:

$$V = \frac{nRT}{P} \tag{6.3.7}$$

Thus the volume of 1 mol of an ideal gas is **22.71 L at STP** and **22.41 L at 0°C and 1 atm**, approximately equivalent to the volume of three basketballs. The molar volumes of several real gases at 0°C and 1 atm are given in Table 10.3, which shows that the deviations from ideal gas behavior are quite small. Thus the ideal gas law does a good job of approximating the behavior of real gases at 0°C and 1 atm. The relationships described in Section 10.3 as Boyle's, Charles's, and Avogadro's laws are simply special cases of the ideal gas law in which two of the four parameters (P, V, T, and n) are held fixed.

Table **3.4.1**: Molar Volumes of Selected Gases at 0°C and 1 atm

Gas	Molar Volume (L)
He	22.434
Ar	22.397
H_2	22.433
N_2	22.402
O_2	22.397
CO_2	22.260
NH_3	22.079

Applying the Ideal Gas Law

The ideal gas law allows us to calculate the value of the fourth variable for a gaseous sample if we know the values of any three of the four variables (*P*, *V*, *T*, and *n*). It also allows us to predict the *final state* of a sample of a gas (i.e., its final temperature, pressure, volume, and amount) following any changes in conditions if the parameters (*P*, *V*, *T*, and *n*) are specified for an *initial state*. Some applications are illustrated in the following examples. The approach used throughout is always to start with the same equation—the ideal gas law—and then determine which quantities are given and which need to be calculated. Let's begin with simple cases in which we are given three of the four parameters needed for a complete physical description of a gaseous sample.

Example 3.4.1

The balloon that Charles used for his initial flight in 1783 was destroyed, but we can estimate that its volume was 31,150 L (1100 ft^3), given the dimensions recorded at the time. If the temperature at ground level was 86°F (30°C) and the atmospheric pressure was 745 mmHg, how many moles of hydrogen gas were needed to fill the balloon?

Given: volume, temperature, and pressure

Asked for: amount of gas

Strategy:

A. Solve the ideal gas law for the unknown quantity, in this case *n*.
B. Make sure that all quantities are given in units that are compatible with the units of the gas constant. If necessary, convert them to the appropriate units, insert them into the equation you have derived, and then calculate the number of moles of hydrogen gas needed.

Solution:

A We are given values for *P*, *T*, and *V* and asked to calculate *n*. If we solve the ideal gas law (Equation 6.3.4) for *n*, we obtain

$$745\ \text{mmHg} \times \frac{1\ \text{atm}}{760\ \text{mmHg}} = 0.980\ \text{atm} \tag{3.4.5}$$

B *P* and *T* are given in units that are not compatible with the units of the gas constant [*R* = 0.08206 (L•atm)/(K•mol)]. We must therefore convert the temperature to kelvins and the pressure to atmospheres:

$$T = 273 + 30 = 303\text{K} \tag{3.4.6}$$

Substituting these values into the expression we derived for *n*, we obtain

$$n = \frac{PV}{RT} = \frac{0.980\ \text{atm} \times 31150\ \text{L}}{0.08206 \frac{\text{atm} \cdot \text{L}}{\text{mol} \cdot \text{K}} \times 303\ \text{K}} = 1.23 \times 10^3\ \text{mol} \tag{3.4.7}$$

Exercise 3.4.1

Suppose that an “empty” aerosol spray-paint can has a volume of 0.406 L and contains 0.025 mol of a propellant gas such as CO_2. What is the pressure of the gas at 25°C?

Answer: 1.5 atm

In Example **3.4.1**, we were given three of the four parameters needed to describe a gas under a particular set of conditions, and we were asked to calculate the fourth. We can also use the ideal gas law to calculate the effect of *changes* in any of the specified conditions on any of the other parameters, as shown in Example **3.4.5**.



The Ideal Gas Law: https://youtu.be/rHGs23368mE

General Gas Equation

When a gas is described under two different conditions, the ideal gas equation must be applied twice - to an initial condition and a final condition. This is:

$$\underset{P_iV_i = n_iRT_i}{\text{Initial condition } (i)} \quad \underset{P_fV_f = n_fRT_f}{\text{Final condition}(f)} \tag{3.4.8}$$

Both equations can be rearranged to give:

$$R = \frac{P_iV_i}{n_iT_i} \qquad R = \frac{P_fV_f}{n_fT_f} \tag{3.4.9}$$

The two equations are equal to each other since each is equal to the same constant R. Therefore, we have:

$$\frac{P_iV_i}{n_iT_i} = \frac{P_fV_f}{n_fT_f} \tag{6.3.8}$$

The equation is called the **general gas equation**. The equation is particularly useful when one or two of the gas properties are held constant between the two conditions. In such cases, the equation can be simplified by eliminating these constant gas properties.

Example 3.4.2

Suppose that Charles had changed his plans and carried out his initial flight not in August but on a cold day in January, when the temperature at ground level was −10°C (14°F). How large a balloon would he have needed to contain the same amount of hydrogen gas at the same pressure as in Example **3.4.1**?

Given: temperature, pressure, amount, and volume in August; temperature in January

Asked for: volume in January

Strategy:

A. Use the results from Example **3.4.1** for August as the initial conditions and then calculate the *change in volume* due to the change in temperature from 30°C to −10°C. Begin by constructing a table showing the initial and final conditions.
B. Simplify the general gas equation by eliminating the quantities that are held constant between the initial and final conditions, in this case P and n.
C. Solve for the unknown parameter.

Solution:

A To see exactly which parameters have changed and which are constant, prepare a table of the initial and final conditions:

Initial (August)	Final (January)
$T_i = 30$°C = 303 K	$T_f =$−10°C = 263 K
$P_i =$0.980 atm	$P_f =$0.980 atm
$n_i =$1.23 × 103 mol	$n_f =$1.23 × 103 mol
$V_i = 31150$ L	$V_f =$?

B Both n and P are the same in both cases ($n_i = n_f, P_i = P_f$). Therefore, Equation can be simplified to:

$$\frac{V_i}{T_i} = \frac{V_f}{T_f} \tag{3.4.10}$$

This is the relationship first noted by Charles.

C Solving the equation for V_f, we get:

$$V_f = V_i \times \frac{T_f}{T_i} = 31150\ \text{L} \times \frac{263\ \text{K}}{303\ \text{K}} = 2.70 \times 10^4\ \text{L} \tag{3.4.11}$$

It is important to check your answer to be sure that it makes sense, just in case you have accidentally inverted a quantity or multiplied rather than divided. In this case, the temperature of the gas decreases. Because we know that gas volume decreases with decreasing temperature, the final volume must be less than the initial volume, so the answer makes sense. We could have calculated the new volume by plugging all the given numbers into the ideal gas law, but it is generally much easier and faster to focus on only the quantities that change.

? Exercise 3.4.2

At a laboratory party, a helium-filled balloon with a volume of 2.00 L at 22°C is dropped into a large container of liquid nitrogen (T = −196°C). What is the final volume of the gas in the balloon?

Answer: 0.52 L

Example **3.4.1** illustrates the relationship originally observed by Charles. We could work through similar examples illustrating the inverse relationship between pressure and volume noted by Boyle (PV = constant) and the relationship between volume and amount observed by Avogadro (V/n = constant). We will not do so, however, because it is more important to note that the historically important gas laws are only special cases of the ideal gas law in which two quantities are varied while the other two remain fixed. The method used in Example **3.4.1** can be applied in *any* such case, as we demonstrate in Example **3.4.2** (which also shows why heating a closed container of a gas, such as a butane lighter cartridge or an aerosol can, may cause an explosion).

✔ Example 3.4.3

Aerosol cans are prominently labeled with a warning such as “Do not incinerate this container when empty.” Assume that you did not notice this warning and tossed the “empty” aerosol can in Exercise 5 (0.025 mol in 0.406 L, initially at 25°C and 1.5 atm internal pressure) into a fire at 750°C. What would be the pressure inside the can (if it did not explode)?

Given: initial volume, amount, temperature, and pressure; final temperature

Asked for: final pressure

Strategy:

Follow the strategy outlined in Example **3.4.5**.

Solution:

Prepare a table to determine which parameters change and which are held constant:

Initial	Final
$V_i = 0.406\ \text{L}$	$V_f = 0.406\ \text{L}$
$n_i = 0.025\ \text{mol}$	$n_f = 0.025\ \text{mol}$
$T_i = 25\ ^\circ\text{C} = 298\ \text{K}$	$T_i = 750\ ^\circ\text{C} = 1023\ \text{K}$
$P_i = 1.5\ \text{atm}$	$P_f = ?$

Both V and n are the same in both cases ($V_i = V_f, n_i = n_f$). Therefore, Equation can be simplified to:

$$P_i T_i = P_f T_f \tag{3.4.12}$$

By solving the equation for P_f, we get:

$$P_f = P_i \times \frac{T_i}{T_f} = 1.5\ \text{atm} \times \frac{1023\ \text{K}}{298\ \text{K}} = 5.1\ \text{atm} \tag{3.4.13}$$

This pressure is more than enough to rupture a thin sheet metal container and cause an explosion!

? Exercise 3.4.3

Suppose that a fire extinguisher, filled with CO_2 to a pressure of 20.0 atm at 21°C at the factory, is accidentally left in the sun in a closed automobile in Tucson, Arizona, in July. The interior temperature of the car rises to 160°F (71.1°C). What is the internal pressure in the fire extinguisher?

Answer: 23.4 atm

In Example **3.4.1** and Example **3.4.2**, two of the four parameters (*P*, *V*, *T*, and *n*) were fixed while one was allowed to vary, and we were interested in the effect on the value of the fourth. In fact, we often encounter cases where two of the variables *P*, *V*, and *T* are allowed to vary for a given sample of gas (hence *n* is constant), and we are interested in the change in the value of the third under the new conditions.

✔ Example 3.4.4

We saw in Example **3.4.1** that Charles used a balloon with a volume of 31,150 L for his initial ascent and that the balloon contained 1.23×10^3 mol of H_2 gas initially at 30°C and 745 mmHg. Suppose that Gay-Lussac had also used this balloon for his record-breaking ascent to 23,000 ft and that the pressure and temperature at that altitude were 312 mmHg and −30°C, respectively. To what volume would the balloon have had to expand to hold the same amount of hydrogen gas at the higher altitude?

Given: initial pressure, temperature, amount, and volume; final pressure and temperature

Asked for: final volume

Strategy:

Follow the strategy outlined in Example **3.4.5**.

Solution:

Begin by setting up a table of the two sets of conditions:

Initial	Final
$P_i = 745\ \text{mmHg} = 0.980\ \text{atm}$	$P_f = 312\ \text{mmHg} = 0.411\ \text{atm}$
$T_i = 30\ ^\circ\text{C} = 303\ \text{K}$	$T_f = 750 - 30\ ^\circ\text{C} = 243\ \text{K}$
$n_i = 1.2 \times 10^3\ \text{mol}$	$n_i = 1.2 \times 10^3\ \text{mol}$
$V_i = 31150\ \text{L}$	$V_f = ?$

By eliminating the constant property (n) of the gas, Equation 6.3.8 is simplified to:

$$\frac{P_i V_i}{T_i} = \frac{P_f V_f}{T_f} \tag{3.4.14}$$

By solving the equation for V_f, we get:

$$V_f = V_i \times \frac{P_i}{P_f}\frac{T_f}{T_i} = 3.115 \times 10^4\ \text{L} \times \frac{0.980\ \text{atm}}{0.411\ \text{atm}}\frac{243\ \text{K}}{303\ \text{K}} = 5.96 \times 10^4\ \text{L} \tag{3.4.15}$$

Does this answer make sense? Two opposing factors are at work in this problem: decreasing the pressure tends to *increase* the volume of the gas, while decreasing the temperature tends to *decrease* the volume of the gas. Which do we expect to predominate? The pressure drops by more than a factor of two, while the absolute temperature drops by only about 20%. Because the volume of a gas sample is directly proportional to both *T* and 1/*P*, the variable that changes the most will have the

greatest effect on *V*. In this case, the effect of decreasing pressure predominates, and we expect the volume of the gas to increase, as we found in our calculation.

We could also have solved this problem by solving the ideal gas law for *V* and then substituting the relevant parameters for an altitude of 23,000 ft:

Except for a difference caused by rounding to the last significant figure, this is the same result we obtained previously. *There is often more than one "right" way to solve chemical problems.*

? Exercise 3.4.4

A steel cylinder of compressed argon with a volume of 0.400 L was filled to a pressure of 145 atm at 10°C. At 1.00 atm pressure and 25°C, how many 15.0 mL incandescent light bulbs could be filled from this cylinder? (Hint: find the number of moles of argon in each container.)

Answer: 4.07×10^3



Second Type of Ideal Gas Law Problems: https://youtu.be/WQDJOqddPI0

Using the Ideal Gas Law to Calculate Gas Densities and Molar Masses

The ideal gas law can also be used to calculate molar masses of gases from experimentally measured gas densities. To see how this is possible, we first rearrange the ideal gas law to obtain

$$\frac{n}{V} = \frac{P}{RT} \tag{6.3.9}$$

The left side has the units of moles per unit volume (mol/L). The number of moles of a substance equals its mass (m, in grams) divided by its molar mass (M, in grams per mole):

$$n = \frac{m}{M} \tag{6.3.10}$$

Substituting this expression for n into Equation 6.3.9 gives

$$\frac{m}{MV} = \frac{P}{RT} \tag{6.3.11}$$

Because m/V is the density d of a substance, we can replace m/V by d and rearrange to give

$$\rho = \frac{m}{V} = \frac{MP}{RT} \tag{6.3.12}$$

The distance between particles in gases is large compared to the size of the particles, so their densities are much lower than the densities of liquids and solids. Consequently, gas density is usually measured in grams per liter (g/L) rather than grams per milliliter (g/mL).

Example 3.4.5

Calculate the density of butane at 25°C and a pressure of 750 mmHg.

Given: compound, temperature, and pressure

Asked for: density

Strategy:

A. Calculate the molar mass of butane and convert all quantities to appropriate units for the value of the gas constant.
B. Substitute these values into Equation 6.3.12 to obtain the density.

Solution:

A The molar mass of butane (C_4H_{10}) is

$$M = (4)(12.011) + (10)(1.0079) = 58.123 \text{g/mol} \tag{3.4.16}$$

Using 0.08206 (L•atm)/(K•mol) for R means that we need to convert the temperature from degrees Celsius to kelvins (T = 25 + 273 = 298 K) and the pressure from millimeters of mercury to atmospheres:

$$P = 750 \text{ mmHg} \times \frac{1 \text{ atm}}{760 \text{ mmHg}} = 0.987 \text{ atm} \tag{3.4.17}$$

B Substituting these values into Equation 6.3.12 gives

$$\rho = \frac{58.123 \text{ g/mol} \times 0.987 \text{ atm}}{0.08206 \frac{\text{L} \cdot \text{atm}}{\text{K} \cdot \text{mol}} \times 298 \text{ K}} = 2.35 \text{ g/L} \tag{3.4.18}$$

Exercise 3.4.5

Radon (Rn) is a radioactive gas formed by the decay of naturally occurring uranium in rocks such as granite. It tends to collect in the basements of houses and poses a significant health risk if present in indoor air. Many states now require that houses be tested for radon before they are sold. Calculate the density of radon at 1.00 atm pressure and 20°C and compare it with the density of nitrogen gas, which constitutes 80% of the atmosphere, under the same conditions to see why radon is found in basements rather than in attics.

Answer: radon, 9.23 g/L; N_2, 1.17 g/L

A common use of Equation 6.3.12 is to determine the molar mass of an unknown gas by measuring its density at a known temperature and pressure. This method is particularly useful in identifying a gas that has been produced in a reaction, and it is not difficult to carry out. A flask or glass bulb of known volume is carefully dried, evacuated, sealed, and weighed empty. It is then filled with a sample of a gas at a known temperature and pressure and reweighed. The difference in mass between the two readings is the mass of the gas. The volume of the flask is usually determined by weighing the flask when empty and when filled with a liquid of known density such as water. The use of density measurements to calculate molar masses is illustrated in Example **3.4.6**.

Example 3.4.6

The reaction of a copper penny with nitric acid results in the formation of a red-brown gaseous compound containing nitrogen and oxygen. A sample of the gas at a pressure of 727 mmHg and a temperature of 18°C weighs 0.289 g in a flask with a volume of 157.0 mL. Calculate the molar mass of the gas and suggest a reasonable chemical formula for the compound.

Given: pressure, temperature, mass, and volume

Asked for: molar mass and chemical formula

Strategy:

A. Solve Equation 6.3.12 for the molar mass of the gas and then calculate the density of the gas from the information given.

B. Convert all known quantities to the appropriate units for the gas constant being used. Substitute the known values into your equation and solve for the molar mass.

C. Propose a reasonable empirical formula using the atomic masses of nitrogen and oxygen and the calculated molar mass of the gas.

Solution:

A Solving Equation 6.3.12 for the molar mass gives

$$M = \frac{mRT}{PV} = \frac{dRT}{P} \tag{3.4.19}$$

Density is the mass of the gas divided by its volume:

$$\rho = \frac{m}{V} = \frac{0.289\text{g}}{0.17\text{L}} = 1.84\text{g/L} \tag{3.4.20}$$

B We must convert the other quantities to the appropriate units before inserting them into the equation:

$$T = 18 + 273 = 291K \tag{3.4.21}$$

$$P = 727\text{mmHg} \times \frac{1\text{atm}}{760\text{mmHg}} = 0.957\text{atm} \tag{3.4.22}$$

The molar mass of the unknown gas is thus

$$\rho = \frac{1.84\text{ g/L} \times 0.08206\frac{\text{L}\cdot\text{atm}}{\text{K}\cdot\text{mol}} \times 291\text{ K}}{0.957\text{ atm}} = 45.9\text{g/mol} \tag{3.4.23}$$

C The atomic masses of N and O are approximately 14 and 16, respectively, so we can construct a list showing the masses of possible combinations:

$$M(\text{NO}) = 14 + 16 = 30\text{ g/mol} \tag{3.4.24}$$

$$M(\text{N}_2\text{O}) = (2)(14) + 16 = 44\text{ g/mol} \tag{3.4.25}$$

$$M(\text{NO}_2) = 14 + (2)(16) = 46\text{ g/mol} \tag{3.4.26}$$

The most likely choice is NO_2 which is in agreement with the data. The red-brown color of smog also results from the presence of NO_2 gas.

? Exercise 3.4.6

You are in charge of interpreting the data from an unmanned space probe that has just landed on Venus and sent back a report on its atmosphere. The data are as follows: pressure, 90 atm; temperature, 557°C; density, 58 g/L. The major constituent of the atmosphere (>95%) is carbon. Calculate the molar mass of the major gas present and identify it.

Answer: 44 g/mol; CO_2



Density and the Molar Mass of Gases: https://youtu.be/gnkGBsvUFVk

Summary

The ideal gas law is derived from empirical relationships among the pressure, the volume, the temperature, and the number of moles of a gas; it can be used to calculate any of the four properties if the other three are known.

Ideal gas equation: $PV = nRT$,

where $R = 0.08206 \frac{\text{L} \cdot \text{atm}}{\text{K} \cdot \text{mol}} = 8.3145 \frac{\text{J}}{\text{K} \cdot \text{mol}}$

General gas equation: $\frac{P_i V_i}{n_i T_i} = \frac{P_f V_f}{n_f T_f}$

Density of a gas: $\rho = \frac{MP}{RT}$

The empirical relationships among the volume, the temperature, the pressure, and the amount of a gas can be combined into the **ideal gas law**, *PV* = *nRT*. The proportionality constant, *R*, is called the **gas constant** and has the value 0.08206 (L•atm)/(K•mol), 8.3145 J/(K•mol), or 1.9872 cal/(K•mol), depending on the units used. The ideal gas law describes the behavior of an **ideal gas**, a hypothetical substance whose behavior can be explained quantitatively by the ideal gas law and the kinetic molecular theory of gases. **Standard temperature and pressure (STP)** is 0°C and 1 atm. The volume of 1 mol of an ideal gas at STP is 22.41 L, the **standard molar volume**. All of the empirical gas relationships are special cases of the ideal gas law in which two of the four parameters are held constant. The ideal gas law allows us to calculate the value of the fourth quantity (*P*, *V*, *T*, or *n*) needed to describe a gaseous sample when the others are known and also predict the value of these quantities following a change in conditions if the original conditions (values of *P*, *V*, *T*, and *n*) are known. The ideal gas law can also be used to calculate the density of a gas if its molar mass is known or, conversely, the molar mass of an unknown gas sample if its density is measured.

3.4: The Ideal Gas Law is shared under a not declared license and was authored, remixed, and/or curated by LibreTexts.

- **6.3: Combining the Gas Laws: The Ideal Gas Equation and the General Gas Equation** is licensed CC BY-NC-SA 4.0.

3.5: Gas Volumes and Stoichiometry

Learning Objectives

- To relate the amount of gas consumed or released in a chemical reaction to the stoichiometry of the reaction.
- To understand how the ideal gas equation and the stoichiometry of a reaction can be used to calculate the volume of gas produced or consumed in a reaction.

Introduction

With the ideal gas law, we can use the relationship between the amounts of gases (in moles) and their volumes (in liters) to calculate the stoichiometry of reactions involving gases, if the pressure and temperature are known. This is important for several reasons. Many reactions that are carried out in the laboratory involve the formation or reaction of a gas, so chemists must be able to quantitatively treat gaseous products and reactants as readily as they quantitatively treat solids or solutions. Furthermore, many, if not most, industrially important reactions are carried out in the gas phase for practical reasons. Gases mix readily, are easily heated or cooled, and can be transferred from one place to another in a manufacturing facility via simple pumps and plumbing. As a chemical engineer said to one of the authors, "Gases always go where you want them to, liquids sometimes do, but solids almost never do."

Example 3.5.1

Sulfuric acid, the industrial chemical produced in greatest quantity (almost 45 million tons per year in the United States alone), is prepared by the combustion of sulfur in air to give SO_2, followed by the reaction of SO_2 with O_2 in the presence of a catalyst to give SO_3, which reacts with water to give H_2SO_4. The overall chemical equation is as follows:

$$2S_{(s)} + 3O_{2(g)} + 2H_2O_{(l)} \rightarrow 2H_2SO_{4(aq)} \tag{3.5.1}$$

What volume of O_2 (in liters) at 22°C and 745 mmHg pressure is required to produce 1.00 ton (907.18 kg) of H_2SO_4?

Given: reaction, temperature, pressure, and mass of one product

Asked for: volume of gaseous reactant

Strategy:

A Calculate the number of moles of H_2SO_4 in 1.00 ton. From the stoichiometric coefficients in the balanced chemical equation, calculate the number of moles of O_2 required.

B Use the ideal gas law to determine the volume of O_2 required under the given conditions. Be sure that all quantities are expressed in the appropriate units.

Solution:

mass of H_2SO_4 → moles H_2SO_4 → moles O_2 → liters O_2

A We begin by calculating the number of moles of H_2SO_4 in 1.00 ton:

$$\frac{907.18 \times 10^3 \text{ g } H_2SO_4}{(2 \times 1.008 + 32.06 + 4 \times 16.00) \text{ g/mol}} = 9250 \text{ mol } H_2SO_4 \tag{3.5.2}$$

We next calculate the number of moles of O_2 required:

$$9250 \text{ mol } H_2SO_4 \times \frac{3 \text{mol } O_2}{2 \text{mol } H_2SO_4} = 1.389 \times 10^4 \text{ mol } O_2 \tag{3.5.3}$$

B After converting all quantities to the appropriate units, we can use the ideal gas law to calculate the volume of O_2:

$$V = \frac{nRT}{P} = \frac{1.389 \times 10^4 \text{ mol} \times 0.08206 \frac{\text{L} \cdot \text{atm}}{\text{mol} \cdot \text{K}} \times (273 + 22) \text{ K}}{745 \text{ mmHg} \times \frac{1 \text{ atm}}{760 \text{ mmHg}}} = 3.43 \times 10^5 \text{ L} \tag{3.5.4}$$

The answer means that more than 300,000 L of oxygen gas are needed to produce 1 ton of sulfuric acid. These numbers may give you some appreciation for the magnitude of the engineering and plumbing problems faced in industrial chemistry.

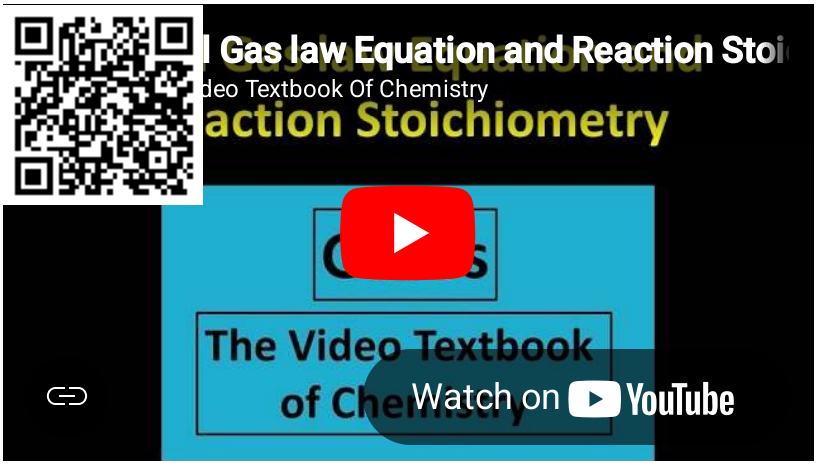
? Exercise 3.5.1

In Example 5, we saw that Charles used a balloon containing approximately 31,150 L of H_2 for his initial flight in 1783. The hydrogen gas was produced by the reaction of metallic iron with dilute hydrochloric acid according to the following balanced chemical equation:

$$Fe_{(s)} + 2HCl_{(aq)} \rightarrow H_{2(g)} + FeCl_{2(aq)} \tag{3.5.5}$$

How much iron (in kilograms) was needed to produce this volume of H_2 if the temperature was 30°C and the atmospheric pressure was 745 mmHg?

Answer: 68.6 kg of Fe (approximately 150 lb)



Ideal Gas law Equation and Reaction Stoichiometry: https://youtu.be/8pPlW8MRhgI

Collecting gases over water

As shown in Figure **3.5.1**, a common laboratory method of collecting the gaseous product of a chemical reaction is to conduct it into an inverted tube or bottle filled with water, the opening of which is immersed in a larger container of water. Because the gas is less dense than liquid water, it bubbles to the top of the bottle, displacing the water. Eventually, all the water is forced out and the bottle contains only gas. If a calibrated bottle is used (i.e., one with markings to indicate the volume of the gas) and the bottle is raised or lowered until the level of the water is the same both inside and outside, then the pressure within the bottle will exactly equal the atmospheric pressure measured separately with a barometer ($P_{bar.}$).

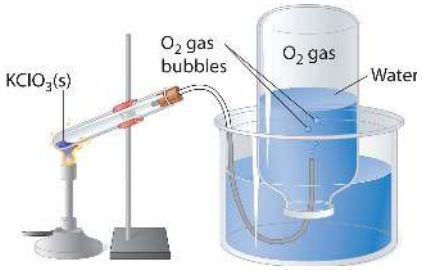


Figure **3.5.1**: An Apparatus for Collecting Gases by the Displacement of Water

Remember, however, when calculating the amount of gas formed in the reaction, the gas collected inside the bottle is *not* pure. Instead, it is a mixture of the product gas and water vapor. All liquids (including water) have a measurable amount of vapor in equilibrium with the liquid because molecules of the liquid are continuously escaping from the liquid's surface, while other molecules from the vapor phase collide with the surface and return to the liquid. The vapor thus exerts a pressure above the liquid,

which is called the liquid's ***vapor pressure***. In the case shown in Figure **3.5.1**, the bottle is therefore actually filled with a mixture of O_2 and water vapor, and the total pressure is, by **Dalton's law** of partial pressures, the sum of the pressures of the two components:

$$P_{tot} = P_{gas} + P_{H_2O} = P_{bar.} \tag{3.5.6}$$

If we want to know the pressure of the gas generated in the reaction to calculate the amount of gas formed, we must first subtract the pressure due to water vapor from the total pressure. This is done by referring to tabulated values of the vapor pressure of water as a function of temperature (Table **3.5.1**).

Table **3.5.1**: Vapor Pressure of Water at Various Temperatures

T (°C)	*P* (in mmHg)
0	4.58
15	12.79
17	14.53
19	16.48
21	18.65
23	21.07
25	23.76
30	31.82
50	92.51
70	233.8
100	760.0

As shown in Figure **3.5.2**, the vapor pressure of water increases rapidly with increasing temperature, and at the normal boiling point (100°C), the vapor pressure is exactly 1 atm. The methodology is illustrated in Example **3.5.2**. The only gases that cannot be collected using this technique are those that readily dissolve in water (e.g., NH_3, H_2S, and CO_2) and those that react rapidly with water (such as F_2 and NO_2).

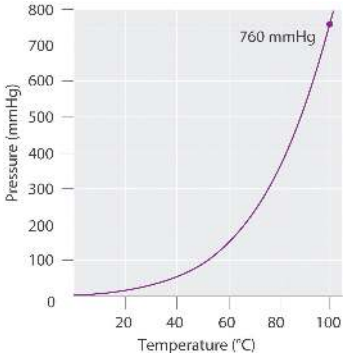


***Figure* 3.5.2:** *A Plot of the Vapor Pressure of Water versus Temperature. The vapor pressure is very low (but not zero) at 0°C and reaches 1 atm = 760 mmHg at the normal boiling point, 100°C.*

Example 3.5.2

Sodium azide (NaN_3) decomposes to form sodium metal and nitrogen gas according to the following balanced chemical equation:

$$2NaN_3 \rightarrow 2Na_{(s)} + 3N_{2\ (g)} \tag{3.5.7}$$

This reaction is used to inflate the air bags that cushion passengers during automobile collisions. The reaction is initiated in air bags by an electrical impulse and results in the rapid evolution of gas. If the N_2 gas that results from the decomposition of a 5.00 g sample of NaN_3 could be collected by displacing water from an inverted flask, as in Figure **3.5.1**, what volume of gas would be produced at 21°C and 762 mmHg?

Given: reaction, mass of compound, temperature, and pressure

Asked for: volume of nitrogen gas produced

Strategy:

A Calculate the number of moles of N_2 gas produced. From the data in Table **3.5.1**, determine the partial pressure of N_2 gas in the flask.

B Use the ideal gas law to find the volume of N_2 gas produced.

Solution:

A Because we know the mass of the reactant and the stoichiometry of the reaction, our first step is to calculate the number of moles of N_2 gas produced:

$$\frac{5.00\ \text{g NaN}_3}{(22.99 + 3 \times 14.01)\ \text{g/mol}} \times \frac{3\text{mol N}_2}{2\text{mol NaN}_3} = 0.115\ \text{mol N}_2 \tag{3.5.8}$$

The pressure given (762 mmHg) is the *total* pressure in the flask, which is the sum of the pressures due to the N_2 gas and the water vapor present. Table **3.5.1** tells us that the vapor pressure of water is 18.65 mmHg at 21°C (294 K), so the partial pressure of the N_2 gas in the flask is only

$$(762 - 18.65)\ \text{mmHg} \times \frac{1\ \text{atm}}{760\ \text{atm}} = 743.4\ \text{mmHg} \times \frac{1\ \text{atm}}{760\ \text{atm}} = 0.978\ \text{atm}. \tag{3.5.9}$$

B Solving the ideal gas law for V and substituting the other quantities (in the appropriate units), we get

$$V = \frac{nRT}{P} = \frac{0.115\ \text{mol} \times 0.08206 \frac{\text{atm} \cdot \text{L}}{\text{mol} \cdot \text{K}} \times 294\ \text{K}}{0.978\ \text{atm}} = 2.84\ \text{L} \tag{3.5.10}$$

? Exercise 3.5.2

A 1.00 g sample of zinc metal is added to a solution of dilute hydrochloric acid. It dissolves to produce H_2 gas according to the equation Zn(s) + 2 HCl(aq) → H_2(g) + $ZnCl_2$(aq). The resulting H_2 gas is collected in a water-filled bottle at 30°C and an atmospheric pressure of 760 mmHg. What volume does it occupy?

Answer: 0.397 L



Collecting a Product Gas over Water: https://youtu.be/zFuy3t81vjQ

Summary

The relationship between the amounts of products and reactants in a chemical reaction can be expressed in units of moles or masses of pure substances, of volumes of solutions, or of volumes of gaseous substances. The ideal gas law can be used to calculate the volume of gaseous products or reactants as needed. In the laboratory, gases produced in a reaction are often collected by the displacement of water from filled vessels; the amount of gas can then be calculated from the volume of water displaced and the atmospheric pressure. A gas collected in such a way is not pure, however, but contains a significant amount of water vapor. The measured pressure must therefore be corrected for the vapor pressure of water, which depends strongly on the temperature.

Conceptual Problems

1. Why are so many industrially important reactions carried out in the gas phase?
2. The volume of gas produced during a chemical reaction can be measured by collecting the gas in an inverted container filled with water. The gas forces water out of the container, and the volume of liquid displaced is a measure of the volume of gas. What additional information must be considered to determine the number of moles of gas produced? The volume of some gases cannot be measured using this method. What property of a gas precludes the use of this method?
3. Equal masses of two solid compounds (A and B) are placed in separate sealed flasks filled with air at 1 atm and heated to 50°C for 10 hours. After cooling to room temperature, the pressure in the flask containing A was 1.5 atm. In contrast, the pressure in the flask containing B was 0.87 atm. Suggest an explanation for these observations. Would the masses of samples A and B still be equal after the experiment? Why or why not?

Numerical Problems

1. Balance each chemical equation and then determine the volume of the indicated reactant at STP that is required for complete reaction. Assuming complete reaction, what is the volume of the products?
    1. $SO_2(g) + O_2(g) \rightarrow SO_3(g)$ given 2.4 mol of O_2
    2. $H_2(g) + Cl_2(g) \rightarrow HCl(g)$ given 0.78 g of H_2
    3. $C_2H_6(g) + O_2(g) \rightarrow CO_2(g) + H_2O(g)$ given 1.91 mol of O_2

- During the smelting of iron, carbon reacts with oxygen to produce carbon monoxide, which then reacts with iron(III) oxide to produce iron metal and carbon dioxide. If 1.82 L of CO_2 at STP is produced,
    1. what mass of CO is consumed?
    2. what volume of CO at STP is consumed?
    3. how much O_2 (in liters) at STP is used?
    4. what mass of carbon is consumed?
    5. how much iron metal (in grams) is produced?
- Complete decomposition of a sample of potassium chlorate produced 1.34 g of potassium chloride and oxygen gas.
    1. What is the mass of $KClO_3$ in the original sample?
    2. What mass of oxygen is produced?
    3. What is the volume of oxygen produced at STP?
- The combustion of a 100.0 mg sample of an herbicide in excess oxygen produced 83.16 mL of CO_2 and 72.9 mL of H_2O vapor at STP. A separate analysis showed that the sample contained 16.44 mg of chlorine. If the sample is known to contain only C, H, Cl, and N, determine the percent composition and the empirical formula of the herbicide.
- The combustion of a 300.0 mg sample of an antidepressant in excess oxygen produced 326 mL of CO_2 and 164 mL of H_2O vapor at STP. A separate analysis showed that the sample contained 23.28% oxygen. If the sample is known to contain only C, H, O, and N, determine the percent composition and the empirical formula of the antidepressant.

Answers

1.
2.

3. 1. 2.20 g $KClO_3$
   2. 0.863 g O_2
   3. 604 mL O_2
4.
5. Percent composition: 58.3% C, 4.93% H, 23.28% O, and 13.5% N; empirical formula: $C_{10}H_{10}O_3N_2$

3.5: Gas Volumes and Stoichiometry is shared under a not declared license and was authored, remixed, and/or curated by LibreTexts.

- **6.5: Gases in Chemical Reactions** is licensed CC BY-NC-SA 4.0.

3.6: Kinetic Molecular Theory of Gases

Learning Objectives

- To understand the significance of the kinetic molecular theory of gases.

The laws that describe the behavior of gases were well established long before anyone had developed a coherent model of the properties of gases. In this section, we introduce a theory that describes why gases behave the way they do. The theory we introduce can also be used to derive laws such as the ideal gas law from fundamental principles and the properties of individual particles.

A Molecular Description

The kinetic molecular theory of gases explains the laws that describe the behavior of gases. Developed during the mid-19th century by several physicists, including the Austrian Ludwig Boltzmann (1844–1906), the German Rudolf Clausius (1822–1888), and the Englishman James Clerk Maxwell (1831–1879), who is also known for his contributions to electricity and magnetism, this theory is based on the properties of individual particles as defined for an ideal gas and the fundamental concepts of physics. Thus the kinetic molecular theory of gases provides a molecular explanation for observations that led to the development of the ideal gas law. The kinetic molecular theory of gases is based on the following five postulates:

1. A gas is composed of a large number of particles called molecules (whether monatomic or polyatomic) that are in constant random motion.
2. Because the distance between gas molecules is much greater than the size of the molecules, the volume of the molecules is negligible.
3. Intermolecular interactions, whether repulsive or attractive, are so weak that they are also negligible.
4. Gas molecules collide with one another and with the walls of the container, but these collisions are perfectly elastic; that is, they do not change the average kinetic energy of the molecules.
5. The average kinetic energy of the molecules of any gas depends on only the temperature, and at a given temperature, all gaseous molecules have exactly the same average kinetic energy.

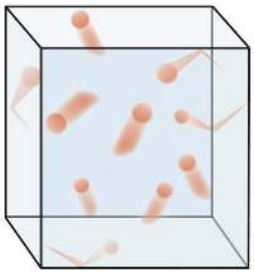


Figure **3.6.1** Visualizing molecular motion. Molecules of a gas are in constant motion and collide with one another and with the container wall.

Although the molecules of real gases have nonzero volumes and exert both attractive and repulsive forces on one another, for the moment we will focus on how the kinetic molecular theory of gases relates to the properties of gases we have been discussing. In Section 10.8, we explain how this theory must be modified to account for the behavior of real gases.

Postulates 1 and 4 state that gas molecules are in constant motion and collide frequently with the walls of their containers. The collision of molecules with their container walls results in a **momentum transfer** (impulse) from molecules to the walls (Figure **3.6.2**).

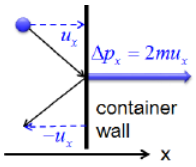


Figure **3.6.2** Momentum transfer (Impulse) from a molecule to the container wall as it bounces off the wall. u_x and Δp_x are the x component of the molecular velocity and the momentum transfered to the wall, respectively. The wall is perpendicular to x axis. Since the collisions are elastic, the molecule bounces back with the same velocity in the opposite direction.

The **momentum transfer** to the wall perpendicular to x axis as a molecule with an initial velocity u_x in x direction hits is expressed as:

$$\Delta p_x = 2mu_x \tag{3.6.1}$$

The **collision frequency**, a number of collisions of the molecules to the wall per unit area and per second, increases with the molecular speed and the number of molecules per unit volume.

$$f \propto (u_x) \times \left(\frac{N}{V}\right) \tag{3.6.2}$$

The pressure the gas exerts on the wall is expressed as the product of impulse and the collision frequency.

$$P \propto (2mu_x) \times (u_x) \times \left(\frac{N}{V}\right) \propto \left(\frac{N}{V}\right) mu_x^2 \tag{3.6.3}$$

At any instant, however, the molecules in a gas sample are traveling at different speed. Therefore, we must replace u_x^2 in the expression above with the average value of u_x^2, which is denoted by $\overline{u_x^2}$. The overbar designates the average value over all molecules.

The exact expression for pressure is given as :

$$P = \frac{N}{V} m\overline{u_x^2} \tag{3.6.4}$$

Finally, we must consider that there is nothing special about x direction. We should expect that $\overline{u_x^2} = \overline{u_y^2} = \overline{u_z^2} = \frac{1}{3}\overline{u^2}$. Here the quantity $\overline{u^2}$ is called the **mean-square speed** defined as the average value of square-speed (u^2) over all molecules. Since $u^2 = u_x^2 + u_y^2 + u_z^2$ for each molecule, $\overline{u^2} = \overline{u_x^2} + \overline{u_y^2} + \overline{u_z^2}$. By substituting $\frac{1}{3}\overline{u^2}$ for $\overline{u_x^2}$ in the expression above, we can get the final expression for the pressure:

$$P = \frac{1}{3}\frac{N}{V} m\overline{u^2} \tag{3.6.5}$$

Because volumes and intermolecular interactions are negligible, postulates 2 and 3 state that all gaseous particles behave identically, regardless of the chemical nature of their component molecules. This is the essence of the ideal gas law, which treats all gases as collections of particles that are identical in all respects except mass. Postulate 2 also explains why it is relatively easy to compress a gas; you simply decrease the distance between the gas molecules.

Postulate 5 provides a molecular explanation for the temperature of a gas. Postulate 5 refers to the *average translational* kinetic energy of the molecules of a gas ($\overline{e_K}$), which can be represented as *and states that at a given Kelvin temperature* (T), *all gases have the same value of*

$$\overline{e_K} = \frac{1}{2} m\overline{u^2} = \frac{3}{2}\frac{R}{N_A} T \tag{3.6.6}$$

where N_A is the Avogadro's constant. The total translational kinetic energy of 1 mole of molecules can be obtained by multiplying the equation by N_A:

$$N_A\overline{e_K} = \frac{1}{2} M\overline{u^2} = \frac{3}{2} RT \tag{3.6.7}$$

where M is the molar mass of the gas molecules and is related to the molecular mass by $M = N_A m$.

By rearranging the equation, we can get the relationship between the root-mean square speed (u_{rms}) and the temperature.

The rms speed (u_{rms}) is the square root of the sum of the squared speeds divided by the number of particles:

$$u_{rms} = \sqrt{\overline{u^2}} = \sqrt{\frac{u_1^2 + u_2^2 + \cdots u_N^2}{N}} \tag{3.6.8}$$

where N is the number of particles and u_i is the speed of particle i.

The relationship between u_{rms} and the temperature is given by:

$$u_{rms} = \sqrt{\frac{3RT}{M}} \tag{3.6.9}$$

In this equation, u_{rms} has units of meters per second; consequently, the units of molar mass M are kilograms per mole, temperature T is expressed in kelvins, and the ideal gas constant R has the value 8.3145 J/(K•mol).

The equation shows that u_{rms} of a gas is proportional to the square root of its Kelvin temperature and inversely proportional to the square root of its molar mass. The root mean-square speed of a gas increase with increasing temperature. At a given temperature, heavier gas molecules have slower speeds than do lighter ones.

The rms speed and the average speed do not differ greatly (typically by less than 10%). The distinction is important, however, because the rms speed is the speed of a gas particle that has average kinetic energy. Particles of different gases at the same temperature have the same average kinetic energy, not the same average speed. In contrast, the most probable speed (v_p) is the speed at which the greatest number of particles is moving. If the average kinetic energy of the particles of a gas increases linearly with increasing temperature, then Equation 6.7.8 tells us that the rms speed must also increase with temperature because the mass of the particles is constant. At higher temperatures, therefore, the molecules of a gas move more rapidly than at lower temperatures, and v_p increases.

Note

At a given temperature, all gaseous particles have the same average kinetic energy but not the same average speed.

Example 3.6.1

The speeds of eight particles were found to be 1.0, 4.0, 4.0, 6.0, 6.0, 6.0, 8.0, and 10.0 m/s. Calculate their average speed (v_{av}) root mean square speed (v_{rms}), and most probable speed (v_m).

Given: particle speeds

Asked for: average speed (v_{av}), root mean square speed (v_{rms}), and most probable speed (v_m)

Strategy:

Use Equation 6.7.6 to calculate the average speed and Equation 6.7.8 to calculate the rms speed. Find the most probable speed by determining the speed at which the greatest number of particles is moving.

Solution:

The average speed is the sum of the speeds divided by the number of particles:

$$v_{av} = \frac{(1.0 + 4.0 + 4.0 + 6.0 + 6.0 + 6.0 + 8.0 + 10.0)\ \text{m/s}}{8} = 5.6\ \text{m/s} \tag{3.6.10}$$

The rms speed is the square root of the sum of the squared speeds divided by the number of particles:

$$v_{rms} = \sqrt{\frac{(1.0^2 + 4.0^2 + 4.0^2 + 6.0^2 + 6.0^2 + 6.0^2 + 8.0^2 + 10.0^2)\ \text{m}^2/\text{s}^2}{8}} = 6.2\ \text{m/s} \tag{3.6.11}$$

The most probable speed is the speed at which the greatest number of particles is moving. Of the eight particles, three have speeds of 6.0 m/s, two have speeds of 4.0 m/s, and the other three particles have different speeds. Hence $v_m = 6.0$ m/s. The v_{rms} of the particles, which is related to the average kinetic energy, is greater than their average speed.

Boltzmann Distributions

At any given time, what fraction of the molecules in a particular sample has a given speed? Some of the molecules will be moving more slowly than average, and some will be moving faster than average, but how many in each situation? Answers to questions such as these can have a substantial effect on the amount of product formed during a chemical reaction, as you will learn in Chapter 14. This problem was solved mathematically by Maxwell in 1866; he used statistical analysis to obtain an equation that describes the distribution of molecular speeds at a given temperature. Typical curves showing the distributions of speeds of molecules at several temperatures are displayed in Figure **3.6.1**. Increasing the temperature has two effects. First, the peak of the curve moves to the right because the most probable speed increases. Second, the curve becomes broader because of the increased spread of the speeds. Thus increased temperature increases the *value* of the most probable speed but decreases the relative number of molecules that have that speed. Although the mathematics behind curves such as those in Figure **3.6.1** were first worked out by Maxwell, the curves are almost universally referred to as Boltzmann distributions, after one of the other major figures responsible for the kinetic molecular theory of gases.

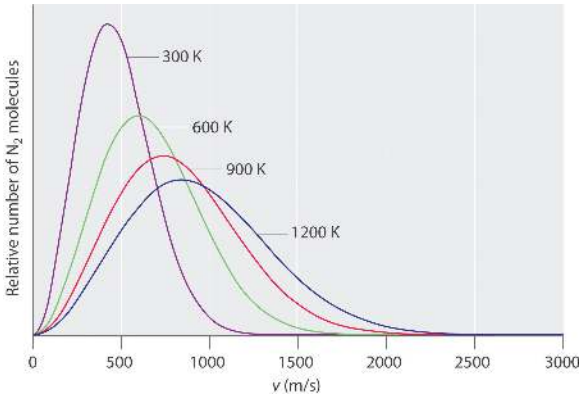


Figure **3.6.2** The Distributions of Molecular Speeds for a Sample of Nitrogen Gas at Various Temperatures. Increasing the temperature increases both the most probable speed (given at the peak of the curve) and the width of the curve.

The Relationships among Pressure, Volume, and Temperature

We now describe how the kinetic molecular theory of gases explains some of the important relationships we have discussed previously.

- **Pressure versus Volume**: At constant temperature, the kinetic energy of the molecules of a gas and hence the rms speed remain unchanged. If a given gas sample is allowed to occupy a larger volume, then the speed of the molecules does not change, but the density of the gas (number of particles per unit volume) decreases, and the average distance between the molecules increases. Hence the molecules must, on average, travel farther between collisions. They therefore collide with one another and with the walls of their containers less often, leading to a decrease in pressure. Conversely, increasing the pressure forces the molecules closer together and increases the density, until the collective impact of the collisions of the molecules with the container walls just balances the applied pressure.
- **Volume versus Temperature**: Raising the temperature of a gas increases the average kinetic energy and therefore the rms speed (and the average speed) of the gas molecules. Hence as the temperature increases, the molecules collide with the walls of their containers more frequently and with greater force. This increases the pressure, *unless* the volume increases to reduce the pressure, as we have just seen. Thus an increase in temperature must be offset by an increase in volume for the net impact (pressure) of the gas molecules on the container walls to remain unchanged.
- **Pressure of Gas Mixtures**: Postulate 3 of the kinetic molecular theory of gases states that gas molecules exert no attractive or repulsive forces on one another. If the gaseous molecules do not interact, then the presence of one gas in a gas mixture will have no effect on the pressure exerted by another, and Dalton's law of partial pressures holds.

Example 3.6.2

The temperature of a 4.75 L container of N_2 gas is increased from 0°C to 117°C. What is the qualitative effect of this change on the

1. average kinetic energy of the N_2 molecules?
2. rms speed of the N_2 molecules?
3. average speed of the N_2 molecules?
4. impact of each N_2 molecule on the wall of the container during a collision with the wall?
5. total number of collisions per second of N_2 molecules with the walls of the entire container?
6. number of collisions per second of N_2 molecules with each square centimeter of the container wall?
7. pressure of the N_2 gas?

Given: temperatures and volume

Asked for: effect of increase in temperature

Strategy:

Use the relationships among pressure, volume, and temperature to predict the qualitative effect of an increase in the temperature of the gas.

Solution:

1. Increasing the temperature increases the average kinetic energy of the N_2 molecules.
2. An increase in average kinetic energy can be due only to an increase in the rms speed of the gas particles.
3. If the rms speed of the N_2 molecules increases, the average speed also increases.
4. If, on average, the particles are moving faster, then they strike the container walls with more energy.
5. Because the particles are moving faster, they collide with the walls of the container more often per unit time.
6. The number of collisions per second of N_2 molecules with each square centimeter of container wall increases because the total number of collisions has increased, but the volume occupied by the gas and hence the total area of the walls are unchanged.
7. The pressure exerted by the N_2 gas increases when the temperature is increased at constant volume, as predicted by the ideal gas law.

Exercise 3.6.2

A sample of helium gas is confined in a cylinder with a gas-tight sliding piston. The initial volume is 1.34 L, and the temperature is 22°C. The piston is moved to allow the gas to expand to 2.12 L at constant temperature. What is the qualitative effect of this change on the

1. average kinetic energy of the He atoms?
2. rms speed of the He atoms?
3. average speed of the He atoms?
4. impact of each He atom on the wall of the container during a collision with the wall?
5. total number of collisions per second of He atoms with the walls of the entire container?
6. number of collisions per second of He atoms with each square centimeter of the container wall?
7. pressure of the He gas?

Answer: a. no change; b. no change; c. no change; d. no change; e. decreases; f. decreases; g. decreases



Kinetic-Molecular Theory of Gases: https://youtu.be/9f83XAYfXAg

Summary

- The kinetic molecular theory of gases provides a molecular explanation for the observations that led to the development of the ideal gas law.
- **Average kinetic energy:**

$$\overline{e_K} = \frac{1}{2} m {u_{\text{rms}}}^2 = \frac{3}{2} \frac{R}{N_A} T, \tag{3.6.12}$$

- **Root mean square speed:**

$$u_{\text{rms}} = \sqrt{\frac{u_1^2 + u_2^2 + \cdots u_N^2}{N}}, \tag{3.6.13}$$

- **Kinetic molecular theory of gases:**

$$u_{\text{rms}} = \sqrt{\frac{3RT}{M}}. \tag{3.6.14}$$

The behavior of ideal gases is explained by the **kinetic molecular theory of gases**. Molecular motion, which leads to collisions between molecules and the container walls, explains pressure, and the large intermolecular distances in gases explain their high compressibility. Although all gases have the same average kinetic energy at a given temperature, they do not all possess the same **root mean square (rms) speed (v_{rms})**. The actual values of speed and kinetic energy are not the same for all particles of a gas but are given by a **Boltzmann distribution**, in which some molecules have higher or lower speeds (and kinetic energies) than average.

3.6: Kinetic Molecular Theory of Gases is shared under a not declared license and was authored, remixed, and/or curated by LibreTexts.

- **6.7: Kinetic-Molecular Theory of Gases** is licensed CC BY-NC-SA 4.0.

3.7: Connecting Gas Properties to Kinetic Molecular Theory

Learning Objectives

- To understand the significance of the kinetic molecular theory of gases

We now describe how the kinetic molecular theory of gases explains some of the important relationships we have discussed previously.

Diffusion and Effusion

As you have learned, the molecules of a gas are *not* stationary but in constant and random motion. If someone opens a bottle of perfume in the next room, for example, you are likely to be aware of it soon. Your sense of smell relies on molecules of the aromatic substance coming into contact with specialized olfactory cells in your nasal passages, which contain specific receptors (protein molecules) that recognize the substance. How do the molecules responsible for the aroma get from the perfume bottle to your nose? You might think that they are blown by drafts, but, in fact, molecules can move from one place to another even in a draft-free environment.

Diffusion is the gradual mixing of gases due to the motion of their component particles even in the absence of mechanical agitation such as stirring. The result is a gas mixture with uniform composition. Diffusion is also a property of the particles in liquids and liquid solutions and, to a lesser extent, of solids and solid solutions. The related process, effusion, is the escape of gaseous molecules through a small (usually microscopic) hole, such as a hole in a balloon, into an evacuated space.

The phenomenon of effusion had been known for thousands of years, but it was not until the early 19th century that quantitative experiments related the rate of effusion to molecular properties. The rate of effusion of a gaseous substance is inversely proportional to the square root of its molar mass. This relationship *is referred to as Graham's law*, after the Scottish chemist Thomas Graham (1805–1869). The ratio of the effusion rates of two gases is the square root of the inverse ratio of their molar masses*:*

$$\frac{\text{rate of effusion A}}{\text{rate of effusion B}} = \sqrt{\frac{M_B}{M_A}} \tag{3.7.1}$$



Ethylene oxide

Figure **3.7.1** for ethylene oxide and helium. Helium (M = 4.00 g/mol) effuses much more rapidly than ethylene oxide (M = 44.0 g/mol). Because helium is less dense than air, helium-filled balloons "float" at the end of a tethering string. Unfortunately, rubber balloons filled with helium soon lose their buoyancy along with much of their volume. In contrast, rubber balloons filled with air tend to retain their shape and volume for a much longer time. Because helium has a molar mass of 4.00 g/mol, whereas air has an average molar mass of about 29 g/mol, pure helium effuses through the microscopic pores in the rubber balloon $\sqrt{\frac{29}{4.00}} = 2.7$ times faster than air. For this reason, high-quality helium-filled balloons are usually made of Mylar, a dense, strong, opaque material with a high molecular mass that forms films that have many fewer pores than rubber. Hence, mylar balloons can retain their helium for days.

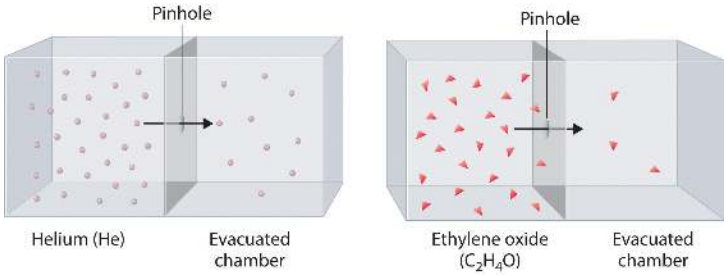


Figure **3.7.1**: The Relative Rates of Effusion of Two Gases with Different Masses. The lighter He atoms (M = 4.00 g/mol) effuse through the small hole more rapidly than the heavier ethylene oxide (C_2H_4O) molecules (M = 44.0 g/mol), as predicted by Graham's law.

Note

At a given temperature, heavier molecules move more slowly than lighter molecules.

Example 3.7.1

During World War II, scientists working on the first atomic bomb were faced with the challenge of finding a way to obtain large amounts of $^{235}\mathrm{U}$. Naturally occurring uranium is only 0.720% $^{235}\mathrm{U}$, whereas most of the rest (99.275%) is $^{238}\mathrm{U}$, which is not fissionable (i.e., it will not break apart to release nuclear energy) and also actually poisons the fission process. Because both isotopes of uranium have the same reactivity, they cannot be separated chemically. Instead, a process of gaseous effusion was developed using the volatile compound UF_6 (boiling point = 56°C).

1. Calculate the ratio of the rates of effusion of $^{235}UF_6$ and $^{238}UF_6$ for a single step in which UF_6 is allowed to pass through a porous barrier. (The atomic mass of ^{235}U is 235.04, and the atomic mass of ^{238}U is 238.05.)
2. If n identical successive separation steps are used, the overall separation is given by the separation in a single step (in this case, the ratio of effusion rates) raised to the nth power. How many effusion steps are needed to obtain 99.0% pure $^{235}UF_6$?

Given: isotopic content of naturally occurring uranium and atomic masses of ^{235}U and ^{238}U

Asked for: ratio of rates of effusion and number of effusion steps needed to obtain 99.0% pure $^{235}UF_6$

Strategy:

A. Calculate the molar masses of $^{235}UF_6$ and $^{238}UF_6$, and then use Graham's law to determine the ratio of the effusion rates. Use this value to determine the isotopic content of $^{235}UF_6$ after a single effusion step.
B. Divide the final purity by the initial purity to obtain a value for the number of separation steps needed to achieve the desired purity. Use a logarithmic expression to compute the number of separation steps required.

Solution:

1. The molar mass of $^{238}UF_6$ is 238.05 + (6)(18.998) = 352.04 g/mol

   The difference is only 3.01 g/mol (less than 1%). The ratio of the effusion rates can be calculated from Graham's law using Equation 6.8.1:

$$\frac{\text{rate } ^{235}\mathrm{UF_6}}{\text{rate } ^{238}\mathrm{UF_6}} = \sqrt{\frac{352.04\ \text{g/mol}}{349.03\ \text{g/mol}}} = 1.0043 \tag{3.7.2}$$

2.

   Thus passing UF_6 containing a mixture of the two isotopes through a single porous barrier gives an enrichment of 1.0043, so after one step the isotopic content is (0.720%)(1.0043) = 0.723% $^{235}UF_6$.

3. **B** To obtain 99.0% pure $^{235}UF_6$ requires many steps. We can set up an equation that relates the initial and final purity to the number of times the separation process is repeated: final purity = (initial purity)(separation)^n

   In this case, 0.990 = (0.00720)(1.0043)^n, which can be rearranged to give

$$1.0043^n = \frac{0.990}{0.00720} = 137.50 \tag{3.7.3}$$

4. Taking the logarithm of both sides gives

$$n \ln(1.0043) = \ln(137.50) \tag{3.7.4}$$

$$n = \frac{\ln(137.50)}{\ln(1.0043)} = 1148 \tag{3.7.5}$$

Thus at least a thousand effusion steps are necessary to obtain highly enriched ^{235}U. Figure **3.7.2** shows a small part of a system that is used to prepare enriched uranium on a large scale.



Figure **3.7.2**: A Portion of a Plant for Separating Uranium Isotopes by Effusion of UF_6. The large cylindrical objects (note the human for scale) are so-called diffuser (actually effuser) units, in which gaseous UF_6 is pumped through a porous barrier to partially separate the isotopes. The UF_6 must be passed through multiple units to become substantially enriched in ^{235}U.

? Exercise 3.7.1

Helium consists of two isotopes: ^{3}He (natural abundance = 0.000134%) and ^{4}He (natural abundance = 99.999866%). Their atomic masses are 3.01603 and 4.00260, respectively. Helium-3 has unique physical properties and is used in the study of ultralow temperatures. It is separated from the more abundant ^{4}He by a process of gaseous effusion.

a. Calculate the ratio of the effusion rates of ^{3}He and ^{4}He and thus the enrichment possible in a single effusion step.
b. How many effusion steps are necessary to yield 99.0% pure ^{3}He?

Answer: a. ratio of effusion rates = 1.15200; one step gives 0.000154% ^{3}He; b. 96 steps

Rates of Diffusion or Effusion

Graham's law is an empirical relationship that states that the ratio of the rates of diffusion or effusion of two gases is the square root of the inverse ratio of their molar masses. The relationship is based on the postulate that all gases at the same temperature have the same average kinetic energy. We can write the expression for the average kinetic energy of two gases with different molar masses:

$$KE = \frac{1}{2}\frac{M_\mathrm{A}}{N_A} v_{\mathrm{rms,A}}^2 = \frac{1}{2}\frac{M_\mathrm{B}}{N_A} v_{\mathrm{rms,B}}^2 \tag{3.7.6}$$

Multiplying both sides by 2 and rearranging give

$$\frac{v_{\mathrm{rms,B}}^2}{v_{\mathrm{rms,A}}^2} = \frac{M_\mathrm{A}}{M_\mathrm{B}} \tag{3.7.7}$$

Taking the square root of both sides gives

$$\frac{v_{\mathrm{rms,B}}}{v_{\mathrm{rms,A}}} = \sqrt{\frac{M_\mathrm{A}}{M_\mathrm{B}}} \tag{3.7.8}$$

Thus the rate at which a molecule, or a mole of molecules, diffuses or effuses is directly related to the speed at which it moves. Equation 6.8.4 shows that Graham's law is a direct consequence of the fact that gaseous molecules at the same temperature have the same average kinetic energy.

Typically, gaseous molecules have a speed of hundreds of meters per second (hundreds of miles per hour). The effect of molar mass on these speeds is dramatic, as illustrated in Figure **3.7.3** for some common gases. Because all gases have the same average kinetic energy, according to the Boltzmann distribution, molecules with lower masses, such as hydrogen and helium, have a wider distribution of speeds.

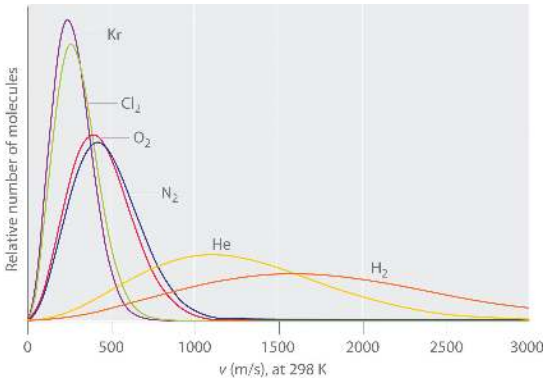


Figure **3.7.3**: The Wide Variation in Molecular Speeds Observed at 298 K for Gases with Different Molar Masses

The lightest gases have a wider distribution of speeds and the highest average speeds.

Note

Molecules with lower masses have a wider distribution of speeds and a higher average speed.

Gas molecules do not diffuse nearly as rapidly as their very high speeds might suggest. If molecules actually moved through a room at hundreds of miles per hour, we would detect odors faster than we hear sound. Instead, it can take several minutes for us to detect an aroma because molecules are traveling in a medium with other gas molecules. Because gas molecules collide as often as 10^{10} times per second, changing direction and speed with each collision, they do not diffuse across a room in a straight line, as illustrated schematically in Figure **3.7.4**.

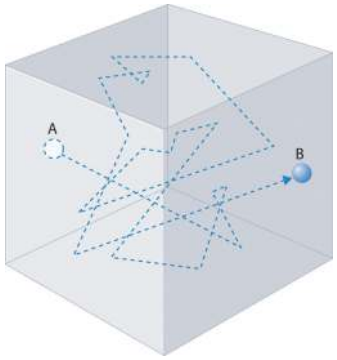


Figure **3.7.4**: The Path of a Single Particle in a Gas Sample. The frequent changes in direction are the result of collisions with other gas molecules and with the walls of the container.

The average distance traveled by a molecule between collisions is the mean free path. The denser the gas, the shorter the mean free path; conversely, as density decreases, the mean free path becomes longer because collisions occur less frequently. At 1 atm pressure and 25°C, for example, an oxygen or nitrogen molecule in the atmosphere travels only about 6.0×10^{-8} m (60 nm) between collisions. In the upper atmosphere at about 100 km altitude, where gas density is much lower, the mean free path is about 10 cm; in space between galaxies, it can be as long as 1×10^{10} m (about 6 million miles).

Note

The **denser** the gas, the **shorter** the mean free path.

Example 3.7.2

Calculate the rms speed of a sample of *cis*-2-butene (C_4H_8) at 20°C.

Given: compound and temperature

Asked for: rms speed

Strategy:

Calculate the molar mass of cis-2-butene. Be certain that all quantities are expressed in the appropriate units and then use Equation 6.8.5 to calculate the rms speed of the gas.

Solution:

To use Equation 6.8.4, we need to calculate the molar mass of *cis*-2-butene and make sure that each quantity is expressed in the appropriate units. Butene is C_4H_8, so its molar mass is 56.11 g/mol. Thus

$$u_{\text{rms}} = \sqrt{\frac{3RT}{M}} = \sqrt{\frac{3 \times 8.3145 \ \frac{\text{J}}{\text{K} \cdot \text{mol}} \times (20 + 273) \ \text{K}}{56.11 \times 10^{-3} \ \text{kg}}} = 361 \ \text{m/s} \tag{3.7.9}$$

or approximately 810 mi/h.

Exercise 3.7.2

Calculate the rms speed of a sample of radon gas at 23°C.

Answer: 1.82×10^2 m/s (about 410 mi/h)

The kinetic molecular theory of gases demonstrates how a successful theory can explain previously observed empirical relationships (laws) in an intuitively satisfying way. Unfortunately, the actual gases that we encounter are not “ideal,” although their behavior usually approximates that of an ideal gas. In Section 10.8, we explore how the behavior of real gases differs from that of ideal gases.



Graham’s law of Diffusion and Effusion: https://youtu.be/9HO-qgh-iGI

Summary

- The kinetic molecular theory of gases provides a molecular explanation for the observations that led to the development of the ideal gas law.

- **Average kinetic energy:**

$$\overline{e_K} = \frac{1}{2} m {u_{\text{rms}}}^2 = \frac{3}{2} \frac{R}{N_A} T, \tag{3.7.10}$$

- **Root mean square speed:**

$$u_{\text{rms}} = \sqrt{\frac{u_1^2 + u_2^2 + \cdots u_N^2}{N}}, \tag{3.7.11}$$

- **Kinetic molecular theory of gases**:

$$u_{\text{rms}} = \sqrt{\frac{3RT}{M}}. \tag{3.7.12}$$

- **Graham's law for effusion:**

$$\frac{v_{\text{rms,B}}}{v_{\text{rms,A}}} = \sqrt{\frac{M_{\text{A}}}{M_{\text{B}}}} \tag{3.7.13}$$

Diffusion is the gradual mixing of gases to form a sample of uniform composition even in the absence of mechanical agitation. In contrast, **effusion** is the escape of a gas from a container through a tiny opening into an evacuated space. The rate of effusion of a gas is inversely proportional to the square root of its molar mass (**Graham's law**), a relationship that closely approximates the rate of diffusion. As a result, light gases tend to diffuse and effuse much more rapidly than heavier gases. The **mean free path** of a molecule is the average distance it travels between collisions.

3.7: Connecting Gas Properties to Kinetic Molecular Theory is shared under a not declared license and was authored, remixed, and/or curated by LibreTexts.

- **6.8: Gas Properties Relating to the Kinetic-Molecular Theory** is licensed CC BY-NC-SA 4.0.

3.8: Chapter Problems

Application Problems

Be sure you are familiar with the material in Essential Skills 5 (Section 10.9 "Essential Skills 5") before proceeding to the Application Problems. Problems marked with a ♦ involve multiple concepts.

1. ♦ Oxalic acid ($C_2H_2O_4$) is a metabolic product of many molds. Although oxalic acid is toxic to humans if ingested, many plants and vegetables contain significant amounts of oxalic acid or oxalate salts. In solution, oxalic acid can be oxidized by air via the following chemical equation:

   $H_2C_2O_4(aq) + O_2(g) \rightarrow H_2O_2(l) + 2\ CO_2(g)$

   If a plant metabolized enough oxalic acid to produce 3.2 L of CO_2 on a day when the temperature was 29°C and the pressure was 752 mmHg, how many grams of oxalic acid were converted to CO_2? Given that air is 21% oxygen, what volume of air was needed for the oxidation?

2. ♦ The decomposition of iron oxide is used to produce gas during the manufacture of porous, expanded materials. These materials have very low densities due to the swelling that occurs during the initial rapid heating. Consequently, they are used as additives to provide insulation in concrete, road building, and other construction materials. Iron oxide decomposes at 1150°C according to the following chemical equation:

   $6\ Fe_2O_3(s) \rightarrow 4\ Fe_3O_4(s) + O_2(g)$

   1. Explain how this reaction could cause materials containing Fe_2O_3 to swell on heating.
   2. If you begin with 15.4 g of Fe_2O_3, what volume of O_2 gas at STP is produced?
   3. What is the volume of the same amount of O_2 gas at 1200°C, assuming a constant pressure of 1.0 atm?
   4. If 6.3 L of gas were produced at 1200°C and 1 atm, how many kilograms of Fe_2O_3 were initially used in the reaction? How many kilograms of Fe_3O_4 are produced?

3. ♦ A 70 kg man expends 480 kcal of energy per hour shoveling snow. The oxidation of organic nutrients such as glucose during metabolism liberates approximately 3.36 kcal of energy per gram of oxygen consumed. If air is 21% oxygen, what volume of air at STP is needed to produce enough energy for the man to clear snow from a walkway that requires 35 minutes of shoveling?

4. ♦ Calcium carbonate is an important filler in the processing industry. Its many uses include a reinforcing agent for rubber and improving the whiteness and hiding power of paints. When calcium nitrate is used as a starting material in the manufacture of fertilizers, calcium carbonate is produced according to the following chemical reaction:

   $Ca(NO_3)_2 + 2\ NH_3 + CO_2 + H_2O \rightarrow CaCO_3 + 2\ NH_4NO_3$

   1. What volume of CO_2 at STP is needed to react completely with 28.0 g of calcium nitrate?
   2. What volume of ammonia at STP is needed to react with the amount of calcium nitrate?
   3. If this reaction were carried out in Denver, Colorado (pressure = 630 mmHg), what volumes of CO_2 and NH_3 at room temperature (20°C) would be needed?

5. ♦ Calcium nitrate used in the process described in Problem 4 is produced by the reaction of fluoroapatite—$Ca_5[(PO_4)_3(F)]$—with nitric acid:

   $Ca_5[(PO_4)_3(F)] + 10\ HNO_3 \rightarrow 5\ Ca(NO_3)_2 + HF + 3\ H_3PO_4\ Ca(NO_3)_2 + 2\ NH_3 + CO_2 + H_2O \rightarrow CaCO_3 + 2\ NH_4NO_3$

   1. Your lab is in Denver, Colorado, and you have a cylinder with 8.40 L of CO_2 at room temperature (20°C) and 4.75 atm pressure. What would be the volume of the CO_2 gas at 630 mmHg? How many grams of fluoroapatite could be converted to $CaCO_3$ using the two reactions and this amount of CO_2?
   2. If 3.50 L of a 0.753 M HF solution was produced during the conversion of fluoroapatite to calcium nitrate, how many grams of calcium carbonate could you produce, assuming 100% efficiency?
   3. How many liters of ammonia gas at this higher altitude and 20°C are required to convert the calcium nitrate to calcium carbonate *and* to neutralize all of the HF solution?

4. If the reaction of fluoroapatite with nitric acid takes place at 330 atm and 80°C, what volumes of NH_3 and CO_2 are needed to convert 20.5 kg of fluoroapatite to calcium carbonate?

6. Mars has an average temperature of −47°C; a surface pressure of 500 Pa; and an atmosphere that is 95% carbon dioxide, 3% nitrogen, and 2% argon by mass, with traces of other gases. What is the partial pressure (in atmospheres) of each gas in this atmosphere? A 5.0 L sample is returned to Earth and stored in a laboratory at 19°C and 1 atm. What is the volume of this sample?

7. ♦ Chlorofluorocarbons (CFCs) are inert substances that were long used as refrigerants. Because CFCs are inert, when they are released into the atmosphere they are not rapidly destroyed in the lower atmosphere. Instead, they are carried into the stratosphere, where they cause ozone depletion. A method for destroying CFC stockpiles passes the CFC through packed sodium oxalate ($Na_2C_2O_4$) powder at 270°C. The reaction for Freon-12 (CF_2Cl_2) is as follows:

   $CF_2Cl_2(g) + 2\ Na_2C_2O_4(s) \rightarrow 2\ NaF(s) + 2\ NaCl + C(s) + 4\ CO_2(g)$

   1. If this reaction produced 11.4 L of CO_2 gas at 21°C and 752 mmHg, what mass of sodium oxalate was consumed in the reaction?
   2. If you had to design a reactor to carry out the reaction at a maximum safe pressure of 10.0 atm while destroying 1.0 kg of Freon-12, what volume reactor would you need?
   3. A 2.50 L reaction vessel is charged with 20.0 atm of Freon-12 and excess sodium oxalate at 20°C. The temperature is increased to 270°C, and the pressure is monitored as the reaction progresses. What is the initial pressure at 270°C? What is the final pressure when the reaction has gone to completion?

8. ♦ The exhaust from a typical six-cylinder car contains the following average compositions of CO and CO_2 under different conditions (data reported as percent by volume; rpm = rotations per minute):

Species	Idling (1000 rpm)	Accelerating (4000 rpm)	Decelerating (800 rpm)
CO	1.0	1.2	0.60
CO_2	0.80	0.40	0.40

   1. What are the mole fractions of CO and CO_2 under each set of conditions?
   2. If the engine takes in 4.70 L of air at STP mixed with fine droplets of gasoline (C_8H_{18}) with each rotation, how many grams of gasoline are burned per minute?

9. Automobile airbags inflate by the decomposition of sodium azide (NaN_3), which produces sodium metal and nitrogen gas according to the following chemical equation:

   $2\ NaN_3 \rightarrow 2\ Na(s) + 3\ N_2(g)$

   How many grams of sodium azide are needed to inflate a 15.0 L airbag at 20°C and 760 mmHg? The density of NaN_3 is 1.847 g/cm^3. What is the volume of the gas produced compared to the solid reactant? Suggest a plausible reason to explain why skin burns can result from the inflation of an airbag during an automobile accident.

10. Under basic conditions, the reaction of hydrogen peroxide (H_2O_2) and potassium permanganate ($KMnO_4$) produces oxygen and manganese dioxide. During a laboratory exercise, you carefully weighed out your sample of $KMnO_4$. Unfortunately, however, you lost your data just before mixing the $KMnO_4$ with an H_2O_2 solution of unknown concentration. Devise a method to determine the mass of your sample of $KMnO_4$ using excess H_2O_2.

11. Carbonated beverages are pressurized with CO_2. In an attempt to produce another bubbly soda beverage, an intrepid chemist attempted to use three other gases: He, N_2, and Xe. Rank the four beverages in order of how fast the drink would go “flat” and explain your reasoning. Which beverage would have the shortest shelf life (i.e., how long will an *unopened* bottle still be good)? Explain your answer.

12. ♦ Urea is synthesized industrially by the reaction of ammonia and carbon dioxide to produce ammonium carbamate, followed by dehydration of ammonium carbamate to give urea and water. This process is shown in the following set of chemical equations:

$2\ NH_3(g) + CO_2(g) \rightarrow NH_2CO_2NH_4(s)$ $NH_2CO_2NH_4(s) \rightarrow NH_2CONH_2(s) + H_2O(g)$

1. A 50.0 L reaction vessel is charged with 2.5 atm of ammonia and 2.5 atm of CO_2 at 50°C, and the vessel is then heated to 150°C. What is the pressure in the vessel when the reaction has gone to completion? If the vessel is then cooled to 20°C, what is the pressure?
2. An aqueous solution of urea and water is drained from the reaction vessel. What is the molarity of the urea solution? Industrially, this reaction is actually carried out at pressures ranging from 130 to 260 atm and temperatures of approximately 180°C. Give a plausible reason for using these extreme conditions.

13. Explain what happens to the temperature, the volume, or the pressure of a gas during each operation and give the direction of heat flow, if any.

    1. The gas is allowed to expand from V_1 to V_2; a heat transfer occurs to maintain a constant gas temperature.
    2. The gas is allowed to expand from V_2 to V_3 with no concomitant heat transfer.
    3. The gas is compressed from V_3 to V_4; a heat transfer occurs to maintain a constant gas temperature.
    4. The gas is compressed from V_4 to V_1; no heat transfer occurs.

    These four processes constitute the cycle used in refrigeration, in which a gas such as Freon is alternately compressed and allowed to expand in the piston of a compressor. Which step eventually causes the food in a refrigerator to cool? Where does the thermal energy go that was removed in the cooling process?

Answers

1. 5.9 g oxalic acid, 7.8 L
2.
3. 278 L

3.8: Chapter Problems is shared under a not declared license and was authored, remixed, and/or curated by LibreTexts.

CHAPTER OVERVIEW

4: Intermolecular Forces

4.1: Intermolecular Forces

4.2: Properties of Liquids

4.3: Intermolecular Forces and the Solution Process

4: Intermolecular Forces is shared under a not declared license and was authored, remixed, and/or curated by LibreTexts.

4.1: Intermolecular Forces

Learning Objectives

- Describe the types of intermolecular forces possible between atoms or molecules in condensed phases (dispersion forces, dipole-dipole attractions, and hydrogen bonding)
- Identify the types of intermolecular forces experienced by specific molecules based on their structures
- Explain the relation between the intermolecular forces present within a substance and the temperatures associated with changes in its physical state

As was the case for gaseous substances, the kinetic molecular theory may be used to explain the behavior of solids and liquids. In the following description, the term *particle* will be used to refer to an atom, molecule, or ion. Note that we will use the popular phrase "intermolecular attraction" to refer to attractive forces between the particles of a substance, regardless of whether these particles are molecules, atoms, or ions.

Consider these two aspects of the molecular-level environments in solid, liquid, and gaseous matter:

- Particles in a solid are tightly packed together and often arranged in a regular pattern; in a liquid, they are close together with no regular arrangement; in a gas, they are far apart with no regular arrangement.
- Particles in a solid vibrate about fixed positions and do not generally move in relation to one another; in a liquid, they move past each other but remain in essentially constant contact; in a gas, they move independently of one another except when they collide.

The differences in the properties of a solid, liquid, or gas reflect the strengths of the attractive forces between the atoms, molecules, or ions that make up each phase. The phase in which a substance exists depends on the relative extents of its intermolecular forces (IMFs) and the kinetic energies (KE) of its molecules. IMFs are the various forces of attraction that may exist between the atoms and molecules of a substance due to electrostatic phenomena, as will be detailed in this module. These forces serve to hold particles close together, whereas the particles' KE provides the energy required to overcome the attractive forces and thus increase the distance between particles. Figure **4.1.1** illustrates how changes in physical state may be induced by changing the temperature, hence, the average KE, of a given substance.

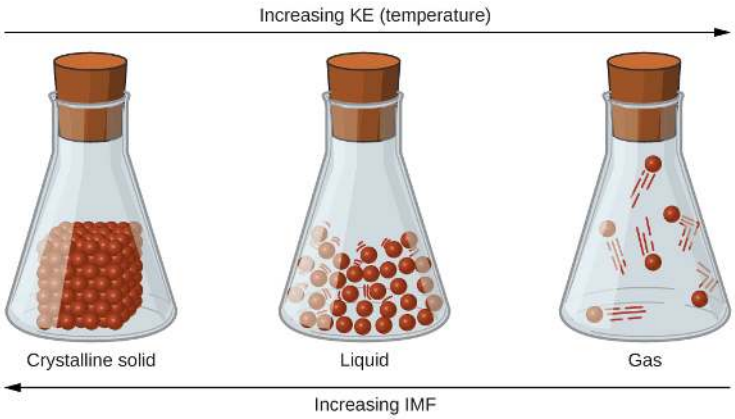


Figure **4.1.1**: Transitions between solid, liquid, and gaseous states of a substance occur when conditions of temperature or pressure favor the associated changes in intermolecular forces. (Note: The space between particles in the gas phase is much greater than shown.)

As an example of the processes depicted in this figure, consider a sample of water. When gaseous water is cooled sufficiently, the attractions between H_2O molecules will be capable of holding them together when they come into contact with each other; the gas condenses, forming liquid H_2O. For example, liquid water forms on the outside of a cold glass as the water vapor in the air is cooled by the cold glass, as seen in Figure **4.1.2**.



Figure **4.1.2**: Condensation forms when water vapor in the air is cooled enough to form liquid water, such as (a) on the outside of a cold beverage glass or (b) in the form of fog. (credit a: modification of work by Jenny Downing; credit b: modification of work by Cory Zanker)

We can also liquefy many gases by compressing them, if the temperature is not too high. The increased pressure brings the molecules of a gas closer together, such that the attractions between the molecules become strong relative to their KE. Consequently, they form liquids. Butane, C_4H_{10}, is the fuel used in disposable lighters and is a gas at standard temperature and pressure. Inside the lighter's fuel compartment, the butane is compressed to a pressure that results in its condensation to the liquid state, as shown in Figure **4.1.3**.



Figure **4.1.3**: Gaseous butane is compressed within the storage compartment of a disposable lighter, resulting in its condensation to the liquid state. (credit: modification of work by "Sam-Cat"/Flickr)

Finally, if the temperature of a liquid becomes sufficiently low, or the pressure on the liquid becomes sufficiently high, the molecules of the liquid no longer have enough KE to overcome the IMF between them, and a solid forms. A more thorough discussion of these and other changes of state, or phase transitions, is provided in a later module of this chapter.

4.1.1: Forces between Molecules

Under appropriate conditions, the attractions between all gas molecules will cause them to form liquids or solids. This is due to intermolecular forces, not *intra*molecular forces. *Intra*molecular forces are those *within* the molecule that keep the molecule together, for example, the bonds between the atoms. *Inter*molecular forces are the attractions *between* molecules, which determine many of the physical properties of a substance. Figure **4.1.4** illustrates these different molecular forces. The strengths of these attractive forces vary widely, though usually the IMFs between small molecules are weak compared to the intramolecular forces that bond atoms together within a molecule. For example, to overcome the IMFs in one mole of liquid HCl and convert it into

gaseous HCl requires only about 17 kilojoules. However, to break the covalent bonds between the hydrogen and chlorine atoms in one mole of HCl requires about 25 times more energy—430 kilojoules.

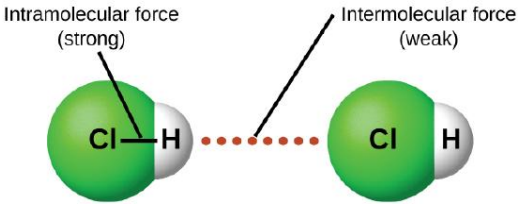


Figure **4.1.4**: Intramolecular forces keep a molecule intact. Intermolecular forces hold multiple molecules together and determine many of a substance's properties.

All of the attractive forces between neutral atoms and molecules are known as van der Waals forces, although they are usually referred to more informally as intermolecular attraction. We will consider the various types of IMFs in the next three sections of this module.

4.1.2: Dispersion Forces

One of the three van der Waals forces is present in all condensed phases, regardless of the nature of the atoms or molecules composing the substance. This attractive force is called the London dispersion force in honor of German-born American physicist Fritz London who, in 1928, first explained it. This force is often referred to as simply the dispersion force. Because the electrons of an atom or molecule are in constant motion (or, alternatively, the electron's location is subject to quantum-mechanical variability), at any moment in time, an atom or molecule can develop a temporary, instantaneous dipole if its electrons are distributed asymmetrically. The presence of this dipole can, in turn, distort the electrons of a neighboring atom or molecule, producing an induced dipole. These two rapidly fluctuating, temporary dipoles thus result in a relatively weak electrostatic attraction between the species—a so-called dispersion force like that illustrated in Figure **4.1.5**.

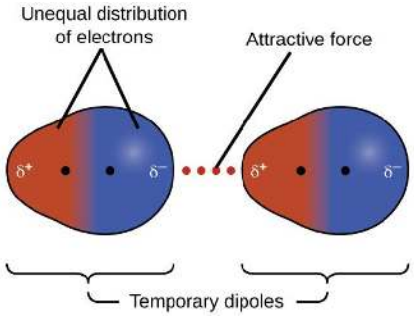


Figure **4.1.5**: Dispersion forces result from the formation of temporary dipoles, as illustrated here for two nonpolar diatomic molecules.

Dispersion forces that develop between atoms in different molecules can attract the two molecules to each other. The forces are relatively weak, however, and become significant only when the molecules are very close. Larger and heavier atoms and molecules exhibit stronger dispersion forces than do smaller and lighter atoms and molecules. F_2 and Cl_2 are gases at room temperature (reflecting weaker attractive forces); Br_2 is a liquid, and I_2 is a solid (reflecting stronger attractive forces). Trends in observed melting and boiling points for the halogens clearly demonstrate this effect, as seen in Table **4.1.1**.

Table **4.1.1**: Melting and Boiling Points of the Halogens

Halogen	Molar Mass	Atomic Radius	Melting Point	Boiling Point
fluorine, F_2	38 g/mol	72 pm	53 K	85 K
chlorine, Cl_2	71 g/mol	99 pm	172 K	238 K
bromine, Br_2	160 g/mol	114 pm	266 K	332 K
iodine, I_2	254 g/mol	133 pm	387 K	457 K
astatine, At_2	420 g/mol	150 pm	575 K	610 K

The increase in melting and boiling points with increasing atomic/molecular size may be rationalized by considering how the strength of dispersion forces is affected by the electronic structure of the atoms or molecules in the substance. In a larger atom, the valence electrons are, on average, farther from the nuclei than in a smaller atom. Thus, they are less tightly held and can more easily form the temporary dipoles that produce the attraction. The measure of how easy or difficult it is for another electrostatic charge (for example, a nearby ion or polar molecule) to distort a molecule's charge distribution (its electron cloud) is known as polarizability. A molecule that has a charge cloud that is easily distorted is said to be very polarizable and will have large dispersion forces; one with a charge cloud that is difficult to distort is not very polarizable and will have small dispersion forces.

Example 4.1.1: London Forces and Their Effects

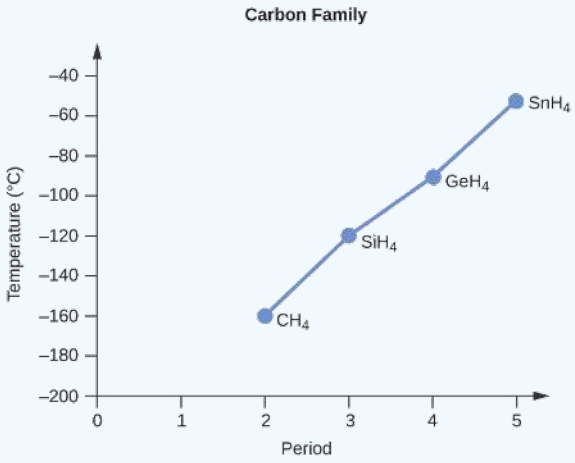
Order the following compounds of a group 14 element and hydrogen from lowest to highest boiling point: CH_4, SiH_4, GeH_4, and SnH_4. Explain your reasoning.

Solution

Applying the skills acquired in the chapter on chemical bonding and molecular geometry, all of these compounds are predicted to be nonpolar, so they may experience only dispersion forces: the smaller the molecule, the less polarizable and the weaker the dispersion forces; the larger the molecule, the larger the dispersion forces. The molar masses of CH_4, SiH_4, GeH_4, and SnH_4 are approximately 16 g/mol, 32 g/mol, 77 g/mol, and 123 g/mol, respectively. Therefore, CH_4 is expected to have the lowest boiling point and SnH_4 the highest boiling point. The ordering from lowest to highest boiling point is expected to be

$$CH_4 < SiH_4 < GeH_4 < SnH_4$$

A graph of the actual boiling points of these compounds versus the period of the group 14 elements shows this prediction to be correct:



Exercise 4.1.1

Order the following hydrocarbons from lowest to highest boiling point: C_2H_6, C_3H_8, and C_4H_{10}.

Answer

All of these compounds are nonpolar and only have London dispersion forces: the larger the molecule, the larger the dispersion forces and the higher the boiling point. The ordering from lowest to highest boiling point is therefore

$$C_2H_6 < C_3H_8 < C_4H_{10}.$$

The shapes of molecules also affect the magnitudes of the dispersion forces between them. For example, boiling points for the isomers *n*-pentane, isopentane, and neopentane (shown in Figure **4.1.6**) are 36 °C, 27 °C, and 9.5 °C, respectively. Even though these compounds are composed of molecules with the same chemical formula, C_5H_{12}, the difference in boiling points suggests that dispersion forces in the liquid phase are different, being greatest for *n*-pentane and least for neopentane. The elongated shape of *n*-

pentane provides a greater surface area available for contact between molecules, resulting in correspondingly stronger dispersion forces. The more compact shape of isopentane offers a smaller surface area available for intermolecular contact and, therefore, weaker dispersion forces. Neopentane molecules are the most compact of the three, offering the least available surface area for intermolecular contact and, hence, the weakest dispersion forces. This behavior is analogous to the connections that may be formed between strips of VELCRO brand fasteners: the greater the area of the strip's contact, the stronger the connection.

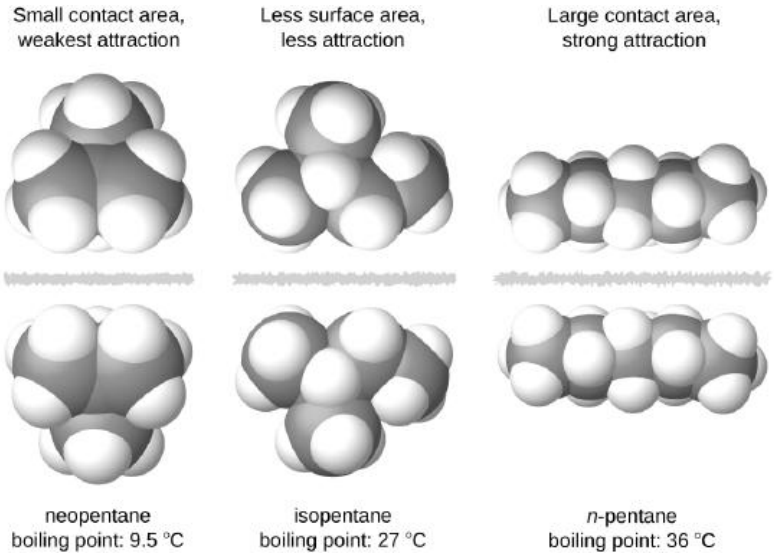


Figure **4.1.6**: The strength of the dispersion forces increases with the contact area between molecules, as demonstrated by the boiling points of these pentane isomers.

Applications: Geckos and Intermolecular Forces

Geckos have an amazing ability to adhere to most surfaces. They can quickly run up smooth walls and across ceilings that have no toe-holds, and they do this without having suction cups or a sticky substance on their toes. And while a gecko can lift its feet easily as it walks along a surface, if you attempt to pick it up, it sticks to the surface. How are geckos (as well as spiders and some other insects) able to do this? Although this phenomenon has been investigated for hundreds of years, scientists only recently uncovered the details of the process that allows geckos' feet to behave this way.

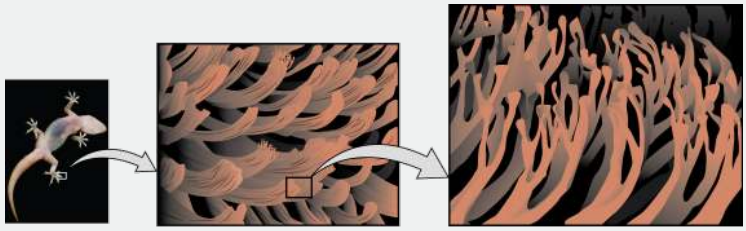


Figure **4.1.7**: Geckos' toes contain large numbers of tiny hairs (setae), which branch into many triangular tips (spatulae). Geckos adhere to surfaces because of van der Waals attractions between the surface and a gecko's millions of spatulae. By changing how the spatulae contact the surface, geckos can turn their stickiness "on" and "off." (credit photo: modification of work by "JC*+A!"/Flickr)

Geckos' toes are covered with hundreds of thousands of tiny hairs known as *setae*, with each seta, in turn, branching into hundreds of tiny, flat, triangular tips called *spatulae*. The huge numbers of spatulae on its setae provide a gecko, shown in Figure **4.1.7**, with a large total surface area for sticking to a surface. In 2000, Kellar Autumn, who leads a multi-institutional gecko research team, found that geckos adhered equally well to both polar silicon dioxide and nonpolar gallium arsenide. This proved that geckos stick to surfaces because of dispersion forces—weak intermolecular attractions arising from temporary, synchronized charge distributions between adjacent molecules. Although dispersion forces are very weak, the total attraction over millions of spatulae is large enough to support many times the gecko's weight.

In 2014, two scientists developed a model to explain how geckos can rapidly transition from “sticky” to “non-sticky.” Alex Greaney and Congcong Hu at Oregon State University described how geckos can achieve this by changing the angle between their spatulae and the surface. Geckos’ feet, which are normally nonsticky, become sticky when a small shear force is applied. By curling and uncurling their toes, geckos can alternate between sticking and unsticking from a surface, and thus easily move across it. Further investigations may eventually lead to the development of better adhesives and other applications.



Watch this video to learn more about Kellar Autumn’s research that determined that van der Waals forces are responsible for a gecko’s ability to cling and climb.

4.1.3: Dipole-Dipole Attractions

Recall from the chapter on chemical bonding and molecular geometry that *polar* molecules have a partial positive charge on one side and a partial negative charge on the other side of the molecule—a separation of charge called a *dipole*. Consider a polar molecule such as hydrogen chloride, HCl. In the HCl molecule, the more electronegative Cl atom bears the partial negative charge, whereas the less electronegative H atom bears the partial positive charge. An attractive force between HCl molecules results from the attraction between the positive end of one HCl molecule and the negative end of another. This attractive force is called a dipole-dipole attraction—the electrostatic force between the partially positive end of one polar molecule and the partially negative end of another, as illustrated in Figure **4.1.8**.

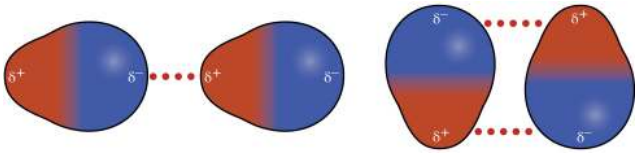


Figure **4.1.8**: This image shows two arrangements of polar molecules, such as HCl, that allow an attraction between the partial negative end of one molecule and the partial positive end of another.

The effect of a dipole-dipole attraction is apparent when we compare the properties of HCl molecules to nonpolar F_2 molecules. Both HCl and F_2 consist of the same number of atoms and have approximately the same molecular mass. At a temperature of 150 K, molecules of both substances would have the same average KE. However, the dipole-dipole attractions between HCl molecules are sufficient to cause them to “stick together” to form a liquid, whereas the relatively weaker dispersion forces between nonpolar F_2 molecules are not, and so this substance is gaseous at this temperature. The higher normal boiling point of HCl (188 K) compared to F_2 (85 K) is a reflection of the greater strength of dipole-dipole attractions between HCl molecules, compared to the attractions between nonpolar F_2 molecules. We will often use values such as boiling or freezing points, or enthalpies of vaporization or fusion, as indicators of the relative strengths of IMFs of attraction present within different substances.

✔ Example **4.1.2**: Dipole-Dipole Forces and Their Effects

Predict which will have the higher boiling point: N_2 or CO. Explain your reasoning.

Solution

CO and N_2 are both diatomic molecules with masses of about 28 amu, so they experience similar London dispersion forces. Because CO is a polar molecule, it experiences dipole-dipole attractions. Because N_2 is nonpolar, its molecules cannot exhibit dipole-dipole attractions. The dipole-dipole attractions between CO molecules are comparably stronger than the dispersion forces between nonpolar N_2 molecules, so CO is expected to have the higher boiling point.

A common method for preparing oxygen is the decomposition

? Exercise 4.1.2

Predict which will have the higher boiling point: **ICl** or **Br_2**. Explain your reasoning.

Answer

ICl. ICl and Br_2 have similar masses (~160 amu) and therefore experience similar London dispersion forces. ICl is polar and thus also exhibits dipole-dipole attractions; Br_2 is nonpolar and does not. The relatively stronger dipole-dipole attractions require more energy to overcome, so ICl will have the higher boiling point.

4.1.4: Hydrogen Bonding

Nitrosyl fluoride (ONF, molecular mass 49 amu) is a gas at room temperature. Water (H_2O, molecular mass 18 amu) is a liquid, even though it has a lower molecular mass. We clearly cannot attribute this difference between the two compounds to dispersion forces. Both molecules have about the same shape and ONF is the heavier and larger molecule. It is, therefore, expected to experience more significant dispersion forces. Additionally, we cannot attribute this difference in boiling points to differences in the dipole moments of the molecules. Both molecules are polar and exhibit comparable dipole moments. The large difference between the boiling points is due to a particularly strong dipole-dipole attraction that may occur when a molecule contains a hydrogen atom bonded to a fluorine, oxygen, or nitrogen atom (the three most electronegative elements). The very large difference in electronegativity between the H atom (2.1) and the atom to which it is bonded (4.0 for an F atom, 3.5 for an O atom, or 3.0 for a N atom), combined with the very small size of a H atom and the relatively small sizes of F, O, or N atoms, leads to *highly concentrated partial charges* with these atoms. Molecules with F-H, O-H, or N-H moieties are very strongly attracted to similar moieties in nearby molecules, a particularly strong type of dipole-dipole attraction called hydrogen bonding. Examples of hydrogen bonds include HF···HF, H_2O···HOH, and H_3N···HNH_2, in which the hydrogen bonds are denoted by dots. Figure **4.1.9** illustrates hydrogen bonding between water molecules.

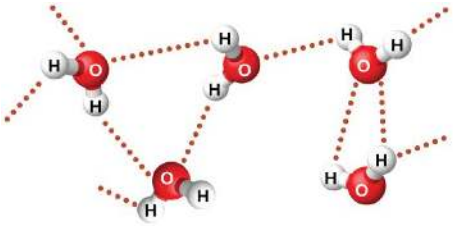


Figure **4.1.9**: Water molecules participate in multiple hydrogen-bonding interactions with nearby water molecules.

Despite use of the word “bond,” keep in mind that hydrogen bonds are *intermolecular* attractive forces, not *intramolecular* attractive forces (covalent bonds). Hydrogen bonds are much weaker than covalent bonds, only about 5 to 10% as strong, but are generally much stronger than other dipole-dipole attractions and dispersion forces.

Hydrogen bonds have a pronounced effect on the properties of condensed phases (liquids and solids). For example, consider the trends in boiling points for the binary hydrides of group 15 (NH_3, PH_3, AsH_3, and SbH_3), group 16 hydrides (H_2O, H_2S, H_2Se, and H_2Te), and group 17 hydrides (HF, HCl, HBr, and HI). The boiling points of the heaviest three hydrides for each group are plotted in Figure **4.1.10**. As we progress down any of these groups, the polarities of the molecules decrease slightly, whereas the sizes of the molecules increase substantially. The effect of increasingly stronger dispersion forces dominates that of increasingly weaker dipole-dipole attractions, and the boiling points are observed to increase steadily. For the group 15, 16, and 17 hydrides, the boiling points for each class of compounds increase with increasing molecular mass for elements in periods 3, 4, and 5.

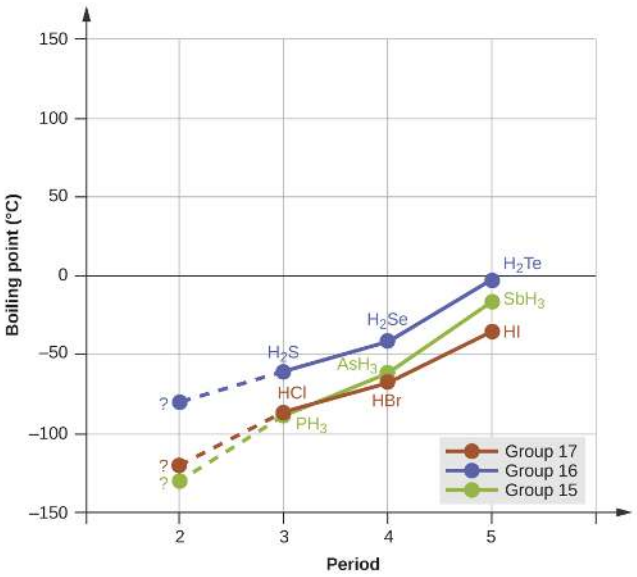


Figure 4.1.10: In comparison to periods 3−5, the binary hydrides of period 2 elements in groups 17, 16 and 15 (F, O and N, respectively) exhibit anomalously high boiling points due to hydrogen bonding.

If we use this trend to predict the boiling points for the lightest hydride for each group, we would expect NH_3 to boil at about −120 °C, H_2O to boil at about −80 °C, and HF to boil at about −110 °C. However, when we measure the boiling points for these compounds, we find that they are dramatically higher than the trends would predict, as shown in Figure 4.1.10. The stark contrast between our naïve predictions and reality provides compelling evidence for the strength of hydrogen bonding.

✔ Example 4.1.3: Effect of Hydrogen Bonding on Boiling Points

Consider the compounds dimethylether (CH_3OCH_3), ethanol (CH_3CH_2OH), and propane ($CH_3CH_2CH_3$). Their boiling points, not necessarily in order, are −42.1 °C, −24.8 °C, and 78.4 °C. Match each compound with its boiling point. Explain your reasoning.

Solution

The VSEPR-predicted shapes of CH_3OCH_3, CH_3CH_2OH, and $CH_3CH_2CH_3$ are similar, as are their molar masses (46 g/mol, 46 g/mol, and 44 g/mol, respectively), so they will exhibit similar dispersion forces. Since $CH_3CH_2CH_3$ is nonpolar, it may exhibit *only* dispersion forces. Because CH_3OCH_3 is polar, it will also experience dipole-dipole attractions. Finally, CH_3CH_2OH has an −OH group, and so it will experience the uniquely strong dipole-dipole attraction known as hydrogen bonding. So the ordering in terms of strength of IMFs, and thus boiling points, is $CH_3CH_2CH_3 < CH_3OCH_3 < CH_3CH_2OH$. The boiling point of propane is −42.1 °C, the boiling point of dimethylether is −24.8 °C, and the boiling point of ethanol is 78.5 °C.

? Exercise 4.1.2

Ethane (CH_3CH_3) has a melting point of −183 °C and a boiling point of −89 °C. Predict the melting and boiling points for methylamine (CH_3NH_2). Explain your reasoning.

Answer

The melting point and boiling point for methylamine are predicted to be significantly greater than those of ethane. CH_3CH_3 and CH_3NH_2 are similar in size and mass, but methylamine possesses an −NH group and therefore may exhibit hydrogen bonding. This greatly increases its IMFs, and therefore its melting and boiling points. It is difficult to predict values, but the known values are a melting point of −93 °C and a boiling point of −6 °C.

4.1.5: Hydrogen Bonding and DNA

Deoxyribonucleic acid (DNA) is found in every living organism and contains the genetic information that determines the organism's characteristics, provides the blueprint for making the proteins necessary for life, and serves as a template to pass this information on to the organism's offspring. A DNA molecule consists of two (anti-)parallel chains of repeating nucleotides, which form its well-known double helical structure, as shown in Figure 4.1.10.

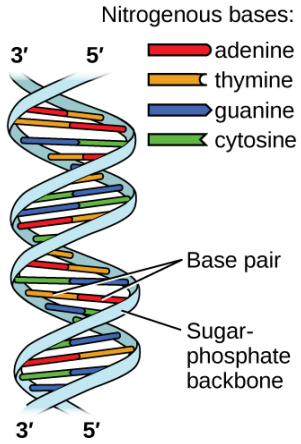


Figure 4.1.11: Two separate DNA molecules form a double-stranded helix in which the molecules are held together via hydrogen bonding. (credit: modification of work by Jerome Walker, Dennis Myts)

Each nucleotide contains a (deoxyribose) sugar bound to a phosphate group on one side, and one of four nitrogenous bases on the other. Two of the bases, cytosine (C) and thymine (T), are single-ringed structures known as pyrimidines. The other two, adenine (A) and guanine (G), are double-ringed structures called purines. These bases form complementary base pairs consisting of one purine and one pyrimidine, with adenine pairing with thymine, and cytosine with guanine. Each base pair is held together by hydrogen bonding. A and T share two hydrogen bonds, C and G share three, and both pairings have a similar shape and structure Figure 4.1.12

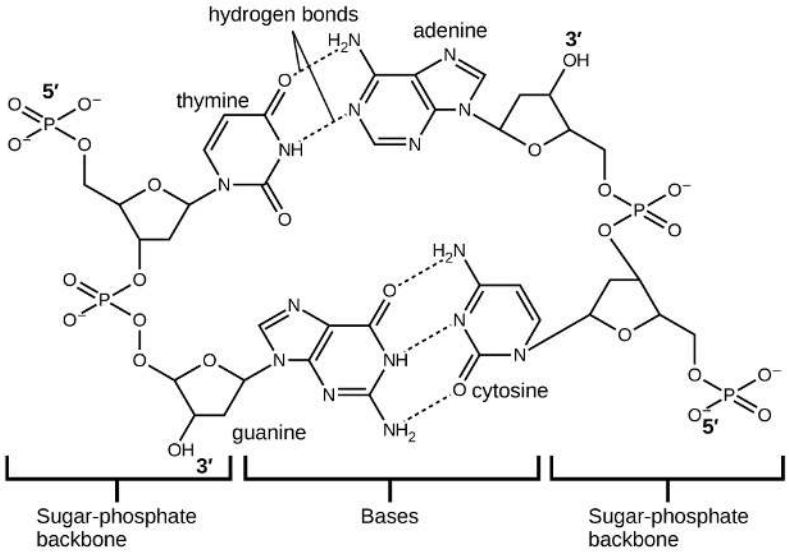


Figure 4.1.12: The geometries of the base molecules result in maximum hydrogen bonding between adenine and thymine (AT) and between guanine and cytosine (GC), so-called "complementary base pairs."

The cumulative effect of millions of hydrogen bonds effectively holds the two strands of DNA together. Importantly, the two strands of DNA can relatively easily "unzip" down the middle since hydrogen bonds are relatively weak compared to the covalent bonds that hold the atoms of the individual DNA molecules together. This allows both strands to function as a template for replication.

Contributors and Attributions

Summary

The physical properties of condensed matter (liquids and solids) can be explained in terms of the kinetic molecular theory. In a liquid, intermolecular attractive forces hold the molecules in contact, although they still have sufficient kinetic energy to move past each other. Intermolecular attractive forces, collectively referred to as van der Waals forces, are responsible for the behavior of liquids and solids and are electrostatic in nature. Dipole-dipole attractions result from the electrostatic attraction of the partial negative end of one dipolar molecule for the partial positive end of another. The temporary dipole that results from the motion of the electrons in an atom can induce a dipole in an adjacent atom and give rise to the London dispersion force. London forces increase with increasing molecular size. Hydrogen bonds are a special type of dipole-dipole attraction that results when hydrogen is bonded to one of the three most electronegative elements: F, O, or N.

Glossary

dipole-dipole attraction
: intermolecular attraction between two permanent dipoles

dispersion force
: (also, London dispersion force) attraction between two rapidly fluctuating, temporary dipoles; significant only when particles are very close together

hydrogen bonding
: occurs when exceptionally strong dipoles attract; bonding that exists when hydrogen is bonded to one of the three most electronegative elements: F, O, or N

induced dipole
: temporary dipole formed when the electrons of an atom or molecule are distorted by the instantaneous dipole of a neighboring atom or molecule

instantaneous dipole
: temporary dipole that occurs for a brief moment in time when the electrons of an atom or molecule are distributed asymmetrically

intermolecular force
: noncovalent attractive force between atoms, molecules, and/or ions

polarizability
: measure of the ability of a charge to distort a molecule’s charge distribution (electron cloud)

van der Waals force
: attractive or repulsive force between molecules, including dipole-dipole, dipole-induced dipole, and London dispersion forces; does not include forces due to covalent or ionic bonding, or the attraction between ions and molecules

Contributors and Attributions

- Paul Flowers (University of North Carolina - Pembroke), Klaus Theopold (University of Delaware) and Richard Langley (Stephen F. Austin State University) with contributing authors. Textbook content produced by OpenStax College is licensed under a Creative Commons Attribution License 4.0 license. Download for free at http://cnx.org/contents/85abf193-2bd...a7ac8df6@9.110).

This page titled 4.1: Intermolecular Forces is shared under a CC BY license and was authored, remixed, and/or curated by OpenStax.

- **10.2: Intermolecular Forces** by OpenStax is licensed CC BY 4.0. Original source: https://openstax.org/details/books/chemistry-2e.

4.2: Properties of Liquids

Learning Objectives

- Distinguish between adhesive and cohesive forces
- Define viscosity, surface tension, and capillary rise
- Describe the roles of intermolecular attractive forces in each of these properties/phenomena

When you pour a glass of water, or fill a car with gasoline, you observe that water and gasoline flow freely. But when you pour syrup on pancakes or add oil to a car engine, you note that syrup and motor oil do not flow as readily. The viscosity of a liquid is a measure of its resistance to flow. Water, gasoline, and other liquids that flow freely have a low viscosity. Honey, syrup, motor oil, and other liquids that do not flow freely, like those shown in Figure **4.2.1**, have higher viscosities. We can measure viscosity by measuring the rate at which a metal ball falls through a liquid (the ball falls more slowly through a more viscous liquid) or by measuring the rate at which a liquid flows through a narrow tube (more viscous liquids flow more slowly).



Figure **4.2.1**: (a) Honey and (b) motor oil are examples of liquids with high viscosities; they flow slowly. (credit a: modification of work by Scott Bauer; credit b: modification of work by David Nagy)

Two photographs are shown and labeled “a” and “b.” Photo a shows a jar of honey with a dipper drizzling it onto a biscuit. More biscuits are shown in a basket in the background. Photo b shows the engine of a car and a person adding motor oil to the engine.

The IMFs between the molecules of a liquid, the size and shape of the molecules, and the temperature determine how easily a liquid flows. As Table **4.2.1** shows, the more structurally complex are the molecules in a liquid and the stronger the IMFs between them, the more difficult it is for them to move past each other and the greater is the viscosity of the liquid. As the temperature increases, the molecules move more rapidly and their kinetic energies are better able to overcome the forces that hold them together; thus, the viscosity of the liquid decreases.

Table **4.2.1**: Viscosities of Common Substances at 25 °C

Substance	Formula	Viscosity (mPa·s)
water	H_2O	0.890
mercury	Hg	1.526
ethanol	C_2H_5OH	1.074
octane	C_8H_{18}	0.508
ethylene glycol	$CH_2(OH)CH_2(OH)$	16.1
honey	variable	~2,000–10,000
motor oil	variable	~50–500

The various IMFs between identical molecules of a substance are examples of cohesive forces. The molecules within a liquid are surrounded by other molecules and are attracted equally in all directions by the cohesive forces within the liquid. However, the molecules on the surface of a liquid are attracted only by about one-half as many molecules. Because of the unbalanced molecular

attractions on the surface molecules, liquids contract to form a shape that minimizes the number of molecules on the surface—that is, the shape with the minimum surface area. A small drop of liquid tends to assume a spherical shape, as shown in Figure **4.2.2**, because in a sphere, the ratio of surface area to volume is at a minimum. Larger drops are more greatly affected by gravity, air resistance, surface interactions, and so on, and as a result, are less spherical.

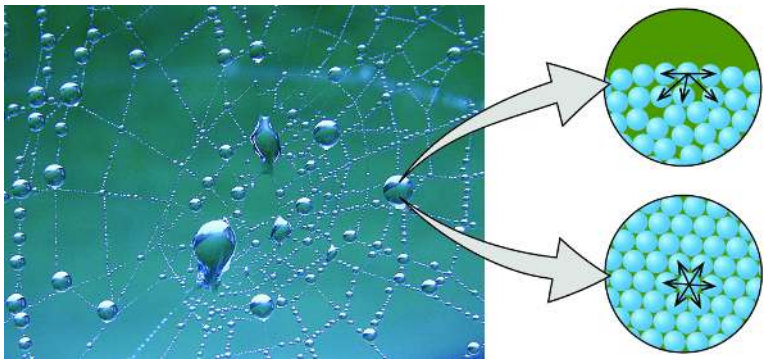


Figure **4.2.2**: Attractive forces result in a spherical water drop that minimizes surface area; cohesive forces hold the sphere together; adhesive forces keep the drop attached to the web. (credit photo: modification of work by "OliBac"/Flickr)

A photo of a spider's web with droplets of water attached to it is shown. Two images are shown the right of the photo and arrows lead from the photo to the images. The upper image shows twenty eight blue spheres stacked one atop the other in the bottom of a circular background. Five arrows are drawn pointing to the sides and downward from the sphere in the top middle of the drawing. The lower image shows another circular background of the same size as the first, but this time the blue spheres fill the image and are packed closely together. A sphere in the middle has six arrows pointing in all directions away from it.

Surface tension is defined as the energy required to increase the surface area of a liquid, or the force required to increase the length of a liquid surface by a given amount. This property results from the cohesive forces between molecules at the surface of a liquid, and it causes the surface of a liquid to behave like a stretched rubber membrane. Surface tensions of several liquids are presented in Table **4.2.2**.

Table **4.2.2**: Surface Tensions of Common Substances at 25 °C

Substance	Formula	Surface Tension (mN/m)
water	H_2O	71.99
mercury	Hg	458.48
ethanol	C_2H_5OH	21.97
octane	C_8H_{18}	21.14
ethylene glycol	$CH_2(OH)CH_2(OH)$	47.99

Among common liquids, water exhibits a distinctly high surface tension due to strong hydrogen bonding between its molecules. As a result of this high surface tension, the surface of water represents a relatively "tough skin" that can withstand considerable force without breaking. A steel needle carefully placed on water will float. Some insects, like the one shown in Figure **4.2.3**, even though they are denser than water, move on its surface because they are supported by the surface tension.

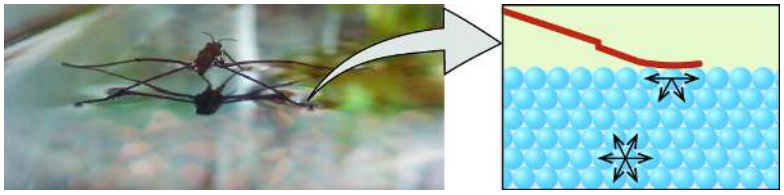


Figure **4.2.3**: Surface tension (right) prevents this insect, a "water strider," from sinking into the water.

A photo and a diagram as shown and a right-facing arrow leads from the photo to the image. The photo shows an insect standing on the surface of a sample of water. The image shows a square background that is two thirds covered in blue spheres that are closely packet together. A brown line starts at the upper left corner of the background and rests on top of the first row of spheres. The sphere directly under this low point of the line has four arrows drawn on it that face to both sides and downward. A sphere in the bottom center of the image has six arrows drawn on it that all face outward in different directions.

The IMFs of attraction between two *different* molecules are called adhesive forces. Consider what happens when water comes into contact with some surface. If the adhesive forces between water molecules and the molecules of the surface are weak compared to the cohesive forces between the water molecules, the water does not “wet” the surface. For example, water does not wet waxed surfaces or many plastics such as polyethylene. Water forms drops on these surfaces because the cohesive forces within the drops are greater than the adhesive forces between the water and the plastic. Water spreads out on glass because the adhesive force between water and glass is greater than the cohesive forces within the water. When water is confined in a glass tube, its meniscus (surface) has a concave shape because the water wets the glass and creeps up the side of the tube. On the other hand, the cohesive forces between mercury atoms are much greater than the adhesive forces between mercury and glass. Mercury therefore does not wet glass, and it forms a convex meniscus when confined in a tube because the cohesive forces within the mercury tend to draw it into a drop (Figure **4.2.4**).

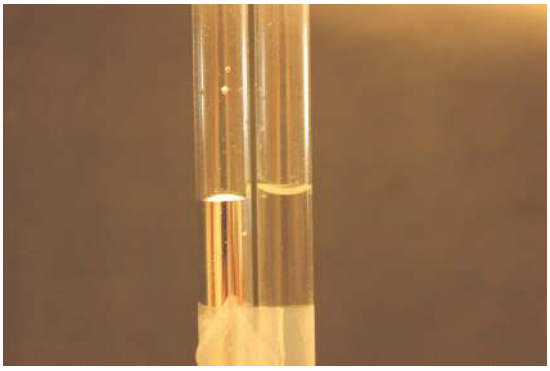


Figure **4.2.4**: Differences in the relative strengths of cohesive and adhesive forces result in different meniscus shapes for mercury (left) and water (right) in glass tubes. (credit: Mark Ott)

This figure shows two test tubes. The test tube on the left contains mercury with a meniscus that rounds up. The test tube on the right contains water with a meniscus that rounds down.

If you place one end of a paper towel in spilled wine, as shown in Figure **4.2.5**, the liquid wicks up the paper towel. A similar process occurs in a cloth towel when you use it to dry off after a shower. These are examples of capillary action—when a liquid flows within a porous material due to the attraction of the liquid molecules to the surface of the material and to other liquid molecules. The adhesive forces between the liquid and the porous material, combined with the cohesive forces within the liquid, may be strong enough to move the liquid upward against gravity.

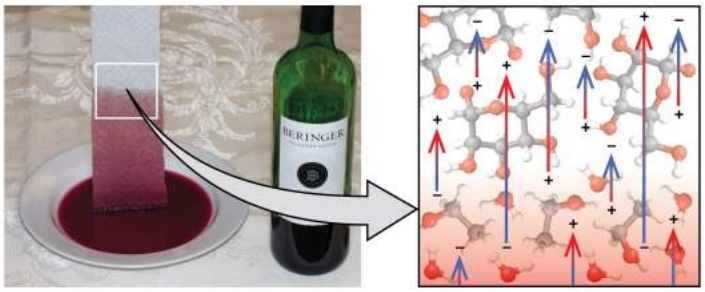


Figure **4.2.5**: Wine wicks up a paper towel (left) because of the strong attractions of water (and ethanol) molecules to the −OH groups on the towel’s cellulose fibers and the strong attractions of water molecules to other water (and ethanol) molecules (right). (credit photo: modification of work by Mark Blaser)

A photo and a diagram are shown. In the photo, a paper towel is dipped into a bowl full of a red liquid sitting on a countertop. The red liquid is traveling up the lower part of the paper towel, and this section of the photo has a square drawn around it. A right-facing arrow leads from this square to the image. The image is square and has a background of two types of molecules, mixed together. The first type of molecule is composed of two bonded black spheres, one of which is single bonded to three white spheres and one of which is single bonded to two white spheres and a red sphere that is itself bonded to a white sphere. The other type of molecule is composed of six black spheres bonded together in a row and bonded to other red and white spheres. Six upward-facing arrows are drawn on top of this background. They have positive signs on their lower ends and negative signs on their heads. Four upward-facing arrows are drawn with their signs reversed.

Towels soak up liquids like water because the fibers of a towel are made of molecules that are attracted to water molecules. Most cloth towels are made of cotton, and paper towels are generally made from paper pulp. Both consist of long molecules of cellulose

that contain many −OH groups. Water molecules are attracted to these −OH groups and form hydrogen bonds with them, which draws the H_2O molecules up the cellulose molecules. The water molecules are also attracted to each other, so large amounts of water are drawn up the cellulose fibers.

Capillary action can also occur when one end of a small diameter tube is immersed in a liquid, as illustrated in Figure **4.2.6**. If the liquid molecules are strongly attracted to the tube molecules, the liquid creeps up the inside of the tube until the weight of the liquid and the adhesive forces are in balance. The smaller the diameter of the tube is, the higher the liquid climbs. It is partly by capillary action occurring in plant cells called xylem that water and dissolved nutrients are brought from the soil up through the roots and into a plant. Capillary action is the basis for thin layer chromatography, a laboratory technique commonly used to separate small quantities of mixtures. You depend on a constant supply of tears to keep your eyes lubricated and on capillary action to pump tear fluid away.

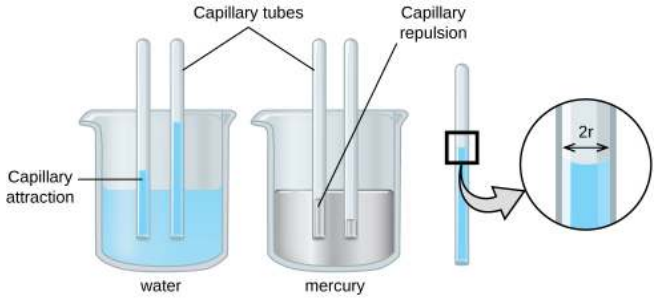


Figure **4.2.6**: Depending upon the relative strengths of adhesive and cohesive forces, a liquid may rise (such as water) or fall (such as mercury) in a glass capillary tube. The extent of the rise (or fall) is directly proportional to the surface tension of the liquid and inversely proportional to the density of the liquid and the radius of the tube.

An image of two beakers and a tube is shown. The first beaker, drawn on the left and labeled “Water,” is drawn half-full of a blue liquid. Two tubes are placed vertically in the beaker and inserted into the liquid. The liquid is shown higher in the tubes than in the beaker and is labeled “Capillary attraction.” The second beaker, drawn in the middle and labeled “Mercury,” is drawn half-full of a gray liquid. Two tubes are placed vertically in the beaker and inserted into the liquid. The liquid is shown lower in the tubes than in the beaker and is labeled “Capillary repulsion.” Lines point to the vertical tubes and label them “Capillary tubes.” A separate drawing of one of the vertical tubes from the first beaker is shown on the right. A right-facing arrow leads from the liquid in the tube to a square call-out box that shows a close-up view of the liquid’s surface. The distance across the tube is labeled “2 r” in this image.

The height to which a liquid will rise in a capillary tube is determined by several factors as shown in the following equation:

$$h = \frac{2T\cos\theta}{r\rho g} \tag{4.2.1}$$

where

- h is the height of the liquid inside the capillary tube relative to the surface of the liquid outside the tube,
- T is the surface tension of the liquid,
- θ is the contact angle between the liquid and the tube,
- r is the radius of the tube, ρ is the density of the liquid, and
- g is the acceleration due to gravity, 9.8 m/s^2.

When the tube is made of a material to which the liquid molecules are strongly attracted, they will spread out completely on the surface, which corresponds to a contact angle of 0°. This is the situation for water rising in a glass tube.

Example 4.2.1: Capillary Rise

At 25 °C, how high will water rise in a glass capillary tube with an inner diameter of 0.25 mm?

For water, T = 71.99 mN/m and ρ = 1.0 g/cm^3.

Solution

The liquid will rise to a height h given by Equation 4.2.1 :

$$h = \frac{2T\cos\theta}{r\rho g}$$

The Newton is defined as a kg m/s^2, and so the provided surface tension is equivalent to 0.07199 kg/s^2. The provided density must be converted into units that will cancel appropriately: ρ = 1000 kg/m^3. The diameter of the tube in meters is 0.00025 m, so the radius is 0.000125 m. For a glass tube immersed in water, the contact angle is θ = 0°, so cos θ = 1. Finally, acceleration due to gravity on the earth is g = 9.8 m/s^2. Substituting these values into the equation, and cancelling units, we have:

$$h = \frac{2(0.07199\ \text{kg/s}^2)}{(0.000125\ \text{m})(1000\ \text{kg/m}^3)(9.8\ \text{m/s}^2)} = 0.12\ \text{m} = 12\ \text{cm}$$

? Exercise 4.2.1

Water rises in a glass capillary tube to a height of 8.4 cm. What is the diameter of the capillary tube?

Answer

diameter = 0.36 mm

Applications: Capillary Action is Used to Draw Blood

Many medical tests require drawing a small amount of blood, for example to determine the amount of glucose in someone with diabetes or the hematocrit level in an athlete. This procedure can be easily done because of capillary action, the ability of a liquid to flow up a small tube against gravity, as shown in Figure **4.2.7**. When your finger is pricked, a drop of blood forms and holds together due to surface tension—the unbalanced intermolecular attractions at the surface of the drop. Then, when the open end of a narrow-diameter glass tube touches the drop of blood, the adhesive forces between the molecules in the blood and those at the glass surface draw the blood up the tube. How far the blood goes up the tube depends on the diameter of the tube (and the type of fluid). A small tube has a relatively large surface area for a given volume of blood, which results in larger (relative) attractive forces, allowing the blood to be drawn farther up the tube. The liquid itself is held together by its own cohesive forces. When the weight of the liquid in the tube generates a downward force equal to the upward force associated with capillary action, the liquid stops rising.



Figure **4.2.7**:: Blood is collected for medical analysis by capillary action, which draws blood into a small diameter glass tube. (credit: modification of work by Centers for Disease Control and Prevention)

A photograph shows a person's hand being held by a person wearing medical gloves. A thin glass tube is pressed against the persons finger and blood is moving up the tube.

4.2.1: Key Concepts and Summary

The intermolecular forces between molecules in the liquid state vary depending upon their chemical identities and result in corresponding variations in various physical properties. Cohesive forces between like molecules are responsible for a liquid's viscosity (resistance to flow) and surface tension (elasticity of a liquid surface). Adhesive forces between the molecules of a liquid and different molecules composing a surface in contact with the liquid are responsible for phenomena such as surface wetting and capillary rise.

4.2.2: Key Equations

- $h = \frac{2T\cos\theta}{r\rho g}$

Glossary

adhesive force

force of attraction between molecules of different chemical identities

capillary action

flow of liquid within a porous material due to the attraction of the liquid molecules to the surface of the material and to other liquid molecules

cohesive force

force of attraction between identical molecules

surface tension

energy required to increase the area, or length, of a liquid surface by a given amount

viscosity

measure of a liquid’s resistance to flow

This page titled 4.2: Properties of Liquids is shared under a CC BY license and was authored, remixed, and/or curated by OpenStax.

- **10.3: Properties of Liquids** by OpenStax is licensed CC BY 4.0. Original source: https://openstax.org/details/books/chemistry-2e.

4.3: Intermolecular Forces and the Solution Process

Learning Objectives

- To understand the relationship between solubility and molecular structure.
- To demonstrate how the strength of intramolecular bonding determines the solubility of a solute in a given solvent.

The interactions that determine the solubility of a substance in a liquid depend largely on the chemical nature of the solute (such as whether it is ionic or molecular) rather than on its physical state (solid, liquid, or gas). We will first describe the general case of forming a solution of a molecular species in a liquid solvent and then describe the formation of a solution of an ionic compound.

The Role of Enthalpy in Solution Formation

Energy is required to overcome the intermolecular interactions in a solute, which can be supplied only by the new interactions that occur in the solution, when each solute particle is surrounded by particles of the solvent in a process called **solvation**, or hydration when the solvent is water. Thus all of the solute–solute interactions and many of the solvent–solvent interactions must be disrupted for a solution to form. In this section, we describe the role of enthalpy in this process.

Because enthalpy is a state function, we can use a thermochemical cycle to analyze the energetics of solution formation. The process occurs in three discrete steps, indicated by ΔH_1, ΔH_2, and ΔH_3 in Figure **4.3.1**. The overall enthalpy change in the formation of the solution (ΔH_{soln}) is the sum of the enthalpy changes in the three steps:

$$\Delta H_{soln} = \Delta H_1 + \Delta H_2 + \Delta H_3 \tag{4.3.1}$$

When a solvent is added to a solution, steps 1 and 2 are both endothermic because energy is required to overcome the intermolecular interactions in the solvent (ΔH_1) and the solute (ΔH_2). Because ΔH is positive for both steps 1 and 2, the solute–solvent interactions (ΔH_3) must be stronger than the solute–solute and solvent–solvent interactions they replace in order for the dissolution process to be exothermic ($\Delta H_{soln} < 0$). When the solute is an ionic solid, ΔH_2 corresponds to the lattice energy that must be overcome to form a solution. The higher the charge of the ions in an ionic solid, the higher the lattice energy. Consequently, solids that have very high lattice energies, such as MgO (−3791 kJ/mol), are generally insoluble in all solvents.

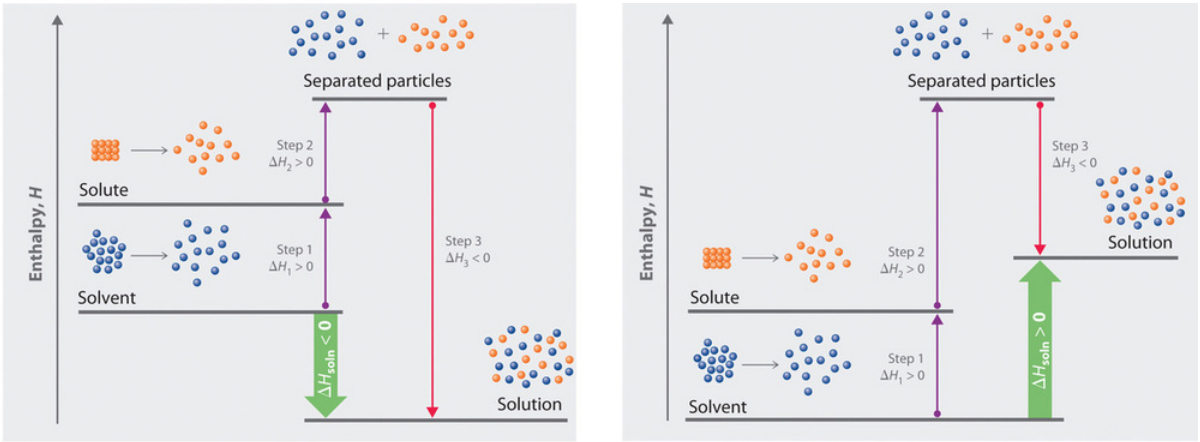


Figure **4.3.1**: Enthalpy Changes That Accompany the Formation of a Solution. Solvation can be an exothermic or endothermic process depending on the nature of the solute and solvent. In both cases, step 1, separation of the solvent particles, is energetically uphill ($\Delta H_1 > 0$), as is step 2, separation of the solute particles ($\Delta H_2 > 0$). In contrast, energy is released in step 3 ($\Delta H_3 < 0$) because of interactions between the solute and solvent. (a) When ΔH_3 is larger in magnitude than the sum of ΔH_1 and ΔH_2, the overall process is exothermic ($\Delta H_{soln} < 0$), as shown in the thermochemical cycle. (b) When ΔH_3 is smaller in magnitude than the sum of ΔH_1 and ΔH_2, the overall process is endothermic ($\Delta H_{soln} > 0$).

A positive value for ΔH_{soln} does not mean that a solution will not form. Whether a given process, including formation of a solution, occurs spontaneously depends on whether the total energy of the system is lowered as a result. Enthalpy is only one of the contributing factors. A high ΔH_{soln} is usually an indication that the substance is not very soluble. Instant cold packs used to treat

athletic injuries, for example, take advantage of the large positive ΔH_{soln} of ammonium nitrate during dissolution (+25.7 kJ/mol), which produces temperatures less than 0°C (Figure **4.3.2**).



Figure **4.3.2**: Commercial Cold Packs for Treating Injuries. These packs contain solid NH_4NO_3 and water in separate compartments. When the seal between the compartments is broken, the NH_4NO_3 dissolves in the water. Because ΔH_{soln} for NH_4NO_3 is much greater than zero, heat is absorbed by the cold pack during the dissolution process, producing local temperatures less than 0°C.

Solutions of Molecular Substances in Liquids

The London dispersion forces, dipole–dipole interactions, and hydrogen bonds that hold molecules to other molecules are generally weak. Even so, energy is required to disrupt these interactions. Unless some of that energy is recovered in the formation of new, favorable solute–solvent interactions, the increase in entropy on solution formation is not enough for a solution to form.

For solutions of gases in liquids, we can safely ignore the energy required to separate the solute molecules ($\Delta H_2 = 0$) because the molecules are already separated. Thus we need to consider only the energy required to separate the solvent molecules (ΔH_1) and the energy released by new solute–solvent interactions (ΔH_3). Nonpolar gases such as N_2, O_2, and Ar have no dipole moment and cannot engage in dipole–dipole interactions or hydrogen bonding. Consequently, the only way they can interact with a solvent is by means of London dispersion forces, which may be weaker than the solvent–solvent interactions in a polar solvent. It is not surprising, then, that nonpolar gases are most soluble in nonpolar solvents. In this case, ΔH_1 and ΔH_3 are both small and of similar magnitude. In contrast, for a solution of a nonpolar gas in a polar solvent, ΔH_1 is far greater than ΔH_3. As a result, nonpolar gases are less soluble in polar solvents than in nonpolar solvents. For example, the concentration of N_2 in a saturated solution of N_2 in water, a polar solvent, is only $7.07 \times 10^{-4}\ M$ compared with $4.5 \times 10^{-3}\ M$ for a saturated solution of N_2 in benzene, a nonpolar solvent.

The solubilities of nonpolar gases in water generally increase as the molecular mass of the gas increases, as shown in Table **4.3.1**. This is precisely the trend expected: as the gas molecules become larger, the strength of the solvent–solute interactions due to London dispersion forces increases, approaching the strength of the solvent–solvent interactions.

Table **4.3.1**: Solubilities of Selected Gases in Water at 20°C and 1 atm Pressure

Gas	Solubility (M) × 10^{-4}
He	3.90
Ne	4.65
Ar	15.2
Kr	27.9
Xe	50.2
H_2	8.06
N_2	7.07
CO	10.6
O_2	13.9
N_2O	281
CH_4	15.5

Virtually all common organic liquids, whether polar or not, are miscible. The strengths of the intermolecular attractions are comparable; thus the enthalpy of solution is expected to be small ($\Delta H_{soln} \approx 0$), and the increase in entropy drives the formation of a solution. If the predominant intermolecular interactions in two liquids are very different from one another, however, they may be immiscible. For example, organic liquids such as benzene, hexane, CCl_4, and CS_2 (S=C=S) are nonpolar and have no ability to act as hydrogen bond donors or acceptors with hydrogen-bonding solvents such as H_2O, HF, and NH_3; hence they are immiscible in these solvents. When shaken with water, they form separate phases or layers separated by an interface (Figure **4.3.3**), the region between the two layers. Just because two liquids are immiscible, however, does not mean that they are completely insoluble in each other. For example, 188 mg of benzene dissolves in 100 mL of water at 23.5°C. Adding more benzene results in the separation of an upper layer consisting of benzene with a small amount of dissolved water (the solubility of water in benzene is only 178 mg/100 mL of benzene).



Figure **4.3.3**: Immiscible Liquids. Separatory funnel demonstrating the separation of oil and colored water. from Wikipedia

The solubilities of simple alcohols in water are given in Table **4.3.2**.

Table **4.3.2**: Solubilities of Straight-Chain Organic Alcohols in Water at 20°C

Alcohol	Solubility (mol/100 g of H_2O)
methanol	completely miscible
ethanol	completely miscible
n-propanol	completely miscible
n-butanol	0.11
n-pentanol	0.030
n-hexanol	0.0058
n-heptanol	0.0008

Only the three lightest alcohols (methanol, ethanol, and n-propanol) are completely miscible with water. As the molecular mass of the alcohol increases, so does the proportion of hydrocarbon in the molecule. Correspondingly, the importance of hydrogen bonding and dipole–dipole interactions in the pure alcohol decreases, while the importance of London dispersion forces increases, which leads to progressively fewer favorable electrostatic interactions with water. Organic liquids such as acetone, ethanol, and tetrahydrofuran are sufficiently polar to be completely miscible with water yet sufficiently nonpolar to be completely miscible with all organic solvents.



Tetrahydrofuran (THF)

The same principles govern the solubilities of molecular solids in liquids. For example, elemental sulfur is a solid consisting of cyclic S_8 molecules that have no dipole moment. Because the S_8 rings in solid sulfur are held to other rings by London dispersion forces, elemental sulfur is insoluble in water. It is, however, soluble in nonpolar solvents that have comparable London dispersion forces, such as CS_2 (23 g/100 mL). In contrast, glucose contains five –OH groups that can form hydrogen bonds. Consequently, glucose is very soluble in water (91 g/120 mL of water) but essentially insoluble in nonpolar solvents such as benzene. The structure of one isomer of glucose is shown here.



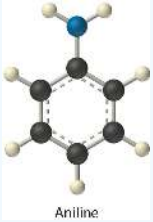
D-Glucose

Low-molecular-mass hydrocarbons with highly electronegative and polarizable halogen atoms, such as chloroform ($CHCl_3$) and methylene chloride (CH_2Cl_2), have both significant dipole moments and relatively strong London dispersion forces. These hydrocarbons are therefore powerful solvents for a wide range of polar and nonpolar compounds. Naphthalene, which is nonpolar, and phenol (C_6H_5OH), which is polar, are very soluble in chloroform. In contrast, the solubility of ionic compounds is largely determined not by the polarity of the solvent but rather by its dielectric constant, a measure of its ability to separate ions in solution, as you will soon see.

Example 4.3.1

Identify the most important solute–solvent interactions in each solution.

a. iodine in benzene
b. aniline ($C_6H_5NH_2$) in dichloromethane (CH_2Cl_2)


Aniline

c. iodine in water

Given: components of solutions

Asked for: predominant solute–solvent interactions

Strategy:

Identify all possible intermolecular interactions for both the solute and the solvent: London dispersion forces, dipole–dipole interactions, or hydrogen bonding. Determine which is likely to be the most important factor in solution formation.

Solution

a. Benzene and $I2$ are both nonpolar molecules. The only possible attractive forces are London dispersion forces.
b. Aniline is a polar molecule with an $-NH_2$ group, which can act as a hydrogen bond donor. Dichloromethane is also polar, but it has no obvious hydrogen bond acceptor. Therefore, the most important interactions between aniline and CH_2Cl_2 are likely to be London interactions.
c. Water is a highly polar molecule that engages in extensive hydrogen bonding, whereas I_2 is a nonpolar molecule that cannot act as a hydrogen bond donor or acceptor. The slight solubility of I_2 in water ($1.3 \times 10^{-3}\ mol/L$ at 25°C) is due to London dispersion forces.

Exercise 4.3.1

Identify the most important interactions in each solution:

a. ethylene glycol ($HOCH_2CH_2OH$) in acetone
b. acetonitrile ($CH_3C{\equiv}N$) in acetone
c. n-hexane in benzene

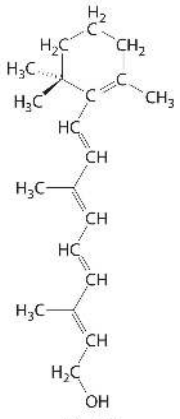
Answer:

a. hydrogen bonding
b. London interactions
c. London dispersion forces

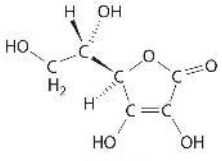
Hydrophilic and Hydrophobic Solutes

A solute can be classified as hydrophilic (literally, “water loving”), meaning that it has an electrostatic attraction to water, or hydrophobic (“water fearing”), meaning that it repels water. A hydrophilic substance is polar and often contains O–H or N–H groups that can form hydrogen bonds to water. For example, glucose with its five O–H groups is hydrophilic. In contrast, a hydrophobic substance may be polar but usually contains C–H bonds that do not interact favorably with water, as is the case with naphthalene and n-octane. Hydrophilic substances tend to be very soluble in water and other strongly polar solvents, whereas hydrophobic substances are essentially insoluble in water and soluble in nonpolar solvents such as benzene and cyclohexane.

The difference between hydrophilic and hydrophobic substances has substantial consequences in biological systems. For example, vitamins can be classified as either fat soluble or water soluble. Fat-soluble vitamins, such as vitamin A, are mostly nonpolar, hydrophobic molecules. As a result, they tend to be absorbed into fatty tissues and stored there. In contrast, water-soluble vitamins, such as vitamin C, are polar, hydrophilic molecules that circulate in the blood and intracellular fluids, which are primarily aqueous. Water-soluble vitamins are therefore excreted much more rapidly from the body and must be replenished in our daily diet. A comparison of the chemical structures of vitamin A and vitamin C quickly reveals why one is hydrophobic and the other hydrophilic.



Vitamin A
(*trans*-Retinol)

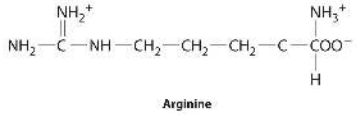


Vitamin C
(L-Ascorbic acid)

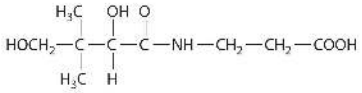
Because water-soluble vitamins are rapidly excreted, the risk of consuming them in excess is relatively small. Eating a dozen oranges a day is likely to make you tired of oranges long before you suffer any ill effects due to their high vitamin C content. In contrast, fat-soluble vitamins constitute a significant health hazard when consumed in large amounts. For example, the livers of polar bears and other large animals that live in cold climates contain large amounts of vitamin A, which have occasionally proven fatal to humans who have eaten them.

✔ Example 4.3.2

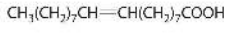
The following substances are essential components of the human diet:



Arginine



Pantothenic acid



Oleic acid

Using what you know of hydrophilic and hydrophobic solutes, classify each as water soluble or fat soluble and predict which are likely to be required in the diet on a daily basis.

a. arginine
b. pantothenic acid
c. oleic acid

Given: chemical structures

Asked for: classification as water soluble or fat soluble; dietary requirement

Strategy:

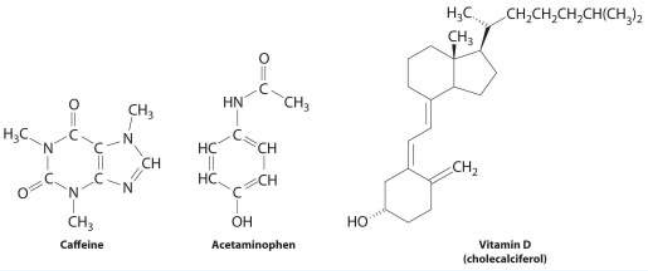
Based on the structure of each compound, decide whether it is hydrophilic or hydrophobic. If it is hydrophilic, it is likely to be required on a daily basis.

Solution:

a. Arginine is a highly polar molecule with two positively charged groups and one negatively charged group, all of which can form hydrogen bonds with water. As a result, it is hydrophilic and required in our daily diet.
b. Although pantothenic acid contains a hydrophobic hydrocarbon portion, it also contains several polar functional groups ($-OH$ and $-CO_2H$) that should interact strongly with water. It is therefore likely to be water soluble and required in the diet. (In fact, pantothenic acid is almost always a component of multiple-vitamin tablets.)
c. Oleic acid is a hydrophobic molecule with a single polar group at one end. It should be fat soluble and not required daily.

? Exercise 4.3.2

These compounds are consumed by humans: caffeine, acetaminophen, and vitamin D. Identify each as primarily hydrophilic (water soluble) or hydrophobic (fat soluble), and predict whether each is likely to be excreted from the body rapidly or slowly.



Answer: Caffeine and acetaminophen are water soluble and rapidly excreted, whereas vitamin D is fat soluble and slowly excreted

Solid Solutions

Solutions are not limited to gases and liquids; solid solutions also exist. For example, amalgams, which are usually solids, are solutions of metals in liquid mercury. Because most metals are soluble in mercury, amalgams are used in gold mining, dentistry, and many other applications. A major difficulty when mining gold is separating very small particles of pure gold from tons of crushed rock. One way to accomplish this is to agitate a suspension of the crushed rock with liquid mercury, which dissolves the gold (as well as any metallic silver that might be present). The very dense liquid gold–mercury amalgam is then isolated and the mercury distilled away.

An alloy is a solid or liquid solution that consists of one or more elements in a metallic matrix. A solid alloy has a single homogeneous phase in which the crystal structure of the solvent remains unchanged by the presence of the solute. Thus the microstructure of the alloy is uniform throughout the sample. Examples are substitutional and interstitial alloys such as brass or solder. Liquid alloys include sodium/potassium and gold/mercury. In contrast, a partial alloy solution has two or more phases that can be homogeneous in the distribution of the components, but the microstructures of the two phases are not the same. As a liquid solution of lead and tin is cooled, for example, different crystalline phases form at different cooling temperatures. Alloys usually have properties that differ from those of the component elements.

Network solids such as diamond, graphite, and $ceSiO_2$ are insoluble in all solvents with which they do not react chemically. The covalent bonds that hold the network or lattice together are simply too strong to be broken under normal conditions. They are certainly much stronger than any conceivable combination of intermolecular interactions that might occur in solution. Most metals are insoluble in virtually all solvents for the same reason: the delocalized metallic bonding is much stronger than any favorable metal atom–solvent interactions. Many metals react with solutions such as aqueous acids or bases to produce a solution. However, in these instances the metal undergoes a chemical transformation that cannot be reversed by simply removing the solvent.

Solids with very strong intermolecular bonding tend to be insoluble.

Solubilities of Ionic Substances in Liquids

Ionic substances are generally most soluble in polar solvents; the higher the lattice energy, the more polar the solvent must be to overcome the lattice energy and dissolve the substance. Because of its high polarity, water is the most common solvent for ionic compounds. Many ionic compounds are soluble in other polar solvents, however, such as liquid ammonia, liquid hydrogen fluoride, and methanol. Because all these solvents consist of molecules that have relatively large dipole moments, they can interact favorably with the dissolved ions.

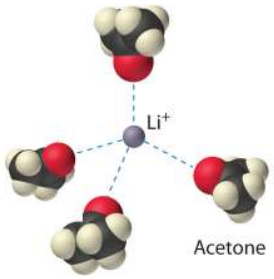


Figure **4.3.4**: Ion–Dipole Interactions in the Solvation of Li+ Ions by Acetone, a Polar Solvent

The interaction of water with Na+ and Cl− ions in an aqueous solution of **NaCl** was illustrated in Figure 4.3. The ion–dipole interactions between Li+ ions and acetone molecules in a solution of LiCl in acetone are shown in Figure **4.3.4**. The energetically favorable Li+–acetone interactions make ΔH_3 in Figure 13.1 sufficiently negative to overcome the positive ΔH_1 and ΔH_2. Because the dipole moment of acetone (2.88 D), and thus its polarity, is actually larger than that of water (1.85 D), one might even expect that LiCl would be more soluble in acetone than in water. In fact, the opposite is true: 83 g of LiCl dissolve in 100 mL of water at 20°C, but only about 4.1 g of LiCl dissolve in 100 mL of acetone. This apparent contradiction arises from the fact that the dipole moment is a property of a single molecule in the gas phase. A more useful measure of the ability of a solvent to dissolve ionic compounds is its dielectric constant (ε), which is the ability of a bulk substance to decrease the electrostatic forces between two charged particles. By definition, the dielectric constant of a vacuum is 1. In essence, a solvent with a high dielectric constant causes the charged particles to behave as if they have been moved farther apart. At 25°C, the dielectric constant of water is 80.1, one of the highest known, and that of acetone is only 21.0. Hence water is better able to decrease the electrostatic attraction between Li+ and Cl− ions, so LiCl is more soluble in water than in acetone. This behavior is in contrast to that of molecular substances, for which polarity is the dominant factor governing solubility.

A solvent's dielectric constant is the most useful measure of its ability to dissolve ionic compounds. A solvent's polarity is the dominant factor in dissolving molecular substances.

Summary

The solubility of a substance is the maximum amount of a solute that can dissolve in a given quantity of solvent; it depends on the chemical nature of both the solute and the solvent and on the temperature and pressure. The solubility of a substance in a liquid is determined by intermolecular interactions, which also determine whether two liquids are miscible. Solutes can be classified as hydrophilic (water loving) or hydrophobic (water fearing). Vitamins with hydrophilic structures are water soluble, whereas those with hydrophobic structures are fat soluble. Many metals dissolve in liquid mercury to form amalgams. Covalent network solids and most metals are insoluble in nearly all solvents. The solubility of ionic compounds is largely determined by the dielectric constant (ε) of the solvent, a measure of its ability to decrease the electrostatic forces between charged particles. Solutions of many ionic compounds in organic solvents can be dissolved using crown ethers, cyclic polyethers large enough to accommodate a metal ion in the center, or cryptands, compounds that completely surround a cation.

4.3: Intermolecular Forces and the Solution Process is shared under a not declared license and was authored, remixed, and/or curated by LibreTexts.

- **13.3: Intermolecular Forces and the Solution Process** is licensed CC BY-NC-SA 4.0.

CHAPTER OVERVIEW

5: Solids

A general chemistry Libretexts Textbook remixed and remastered from OpenStax's textbook:

General Chemistry

The great distances between atoms and molecules in a gaseous phase, and the corresponding absence of any significant interactions between them, allows for simple descriptions of many physical properties that are the same for all gases, regardless of their chemical identities. As described in the final module of the chapter on gases, this situation changes at high pressures and low temperatures—conditions that permit the atoms and molecules to interact to a much greater extent. In the liquid and solid states, these interactions are of considerable strength and play an important role in determining a number of physical properties that *do* depend on the chemical identity of the substance. In this chapter, the nature of these interactions and their effects on various physical properties of liquid and solid phases will be examined.

5.1: Prelude to Liquids and Solids

5.2: Carbon and Silicon- Network Atomic Solids

5.3: The Solid State of Matter

5.4: Lattice Structures in Crystalline Solids

5.5: Bonding in Metals and Semiconductors

5.6: Liquids and Solids (Exercises)

Contributors and Attributions

- Paul Flowers (University of North Carolina - Pembroke), Klaus Theopold (University of Delaware) and Richard Langley (Stephen F. Austin State University) with contributing authors. Textbook content produced by OpenStax College is licensed under a Creative Commons Attribution License 4.0 license. Download for free at http://cnx.org/contents/85abf193-2bd...a7ac8df6@9.110).

This page titled 5: Solids is shared under a CC BY license and was authored, remixed, and/or curated by OpenStax.

5.1: Prelude to Liquids and Solids

The great distances between atoms and molecules in a gaseous phase, and the corresponding absence of any significant interactions between them, allows for simple descriptions of many physical properties that are the same for all gases, regardless of their chemical identities. As described in the final module of the chapter on gases, this situation changes at high pressures and low temperatures—conditions that permit the atoms and molecules to interact to a much greater extent.



Figure **5.1.1**: Solid carbon dioxide (“dry ice”, left) sublimes vigorously when placed in a liquid (right), cooling the liquid and generating a fog of condensed water vapor above the cylinder. (credit: modification of work by Paul Flowers)

This figure shows pieces of a white substance which appear to be sublimating. To the right of these pieces are three graduated cylinders. Each cylinder holds a different color liquid, and above the liquid, the cylinders are filled with a fog-like substance. This fog-like substance swirls out of the top and around the outside of the cylinders.

In the liquid and solid states, these interactions are of considerable strength and play an important role in determining a number of physical properties that *do* depend on the chemical identity of the substance. In this chapter, the nature of these interactions and their effects on various physical properties of liquid and solid phases will be examined.

This page titled 5.1: Prelude to Liquids and Solids is shared under a CC BY license and was authored, remixed, and/or curated by OpenStax.

- **10.1: Prelude to Liquids and Solids** by OpenStax is licensed CC BY 4.0. Original source: https://openstax.org/details/books/chemistry-2e.

5.2: Carbon and Silicon- Network Atomic Solids

Learning Objectives

- To understand the correlation between bonding and the properties of solids.
- To classify solids as ionic, molecular, covalent (network), or metallic, where the general order of increasing strength of interactions.

Crystalline solids fall into one of four categories. All four categories involve packing discrete molecules or atoms into a lattice or repeating array, though *network solids* are a special case. The categories are distinguished by the nature of the interactions holding the discrete molecules or atoms together. Based on the nature of the forces that hold the component atoms, molecules, or ions together, solids may be formally classified as ionic, molecular, covalent (network), or metallic. The variation in the relative strengths of these four types of interactions correlates nicely with their wide variation in properties.

Table **5.2.1**: Solids may be formally classified as ionic, molecular, covalent (network), or metallic

Type of Solid	Interaction	Properties	Examples
Ionic	Ionic	High Melting Point, Brittle, Hard	NaCl, MgO
Molecular	Hydrogen Bonding, Dipole-Dipole, London Dispersion	Low Melting Point, Nonconducting	H_2, CO_2
Metallic	Metallic Bonding	Variable Hardness and Melting Point (depending upon strength of metallic bonding), Conducting	Fe, Mg
Network	Covalent Bonding	High Melting Point, Hard, Nonconducting	C (diamond), SiO_2 (quartz)

In ionic and molecular solids, there are no chemical bonds between the molecules, atoms, or ions. The solid consists of discrete chemical species held together by intermolecular forces that are **electrostatic** or **Coulombic** in nature. This behavior is most obvious for an ionic solid such as $NaCl$, where the positively charged Na^+ ions are attracted to the negatively charged Cl^- ions. Even in the absence of ions, however, electrostatic forces are operational. For polar molecules such as CH_2Cl_2, the positively charged region of one molecular is attracted to the negatively charged region of another molecule (dipole-dipole interactions). For a nonpolar molecule such as CO_2, which has no permanent dipole moment, the random motion of electrons gives rise to temporary polarity (a temporary dipole moment). Electrostatic attractions between two temporarily polarized molecules are called London Dispersion Forces.

Hydrogen bonding is a term describing an attractive interaction between a hydrogen atom from a molecule or a molecular fragment X–H in which X is more electronegative than H, and an atom or a group of atoms in the same or a different molecule, in which there is evidence of bond formation. (See the IUPAC Provisional Recommendation on the definition of a hydrogen bond.) Dots are employed to indicate the presence of a hydrogen bond: X–H•••Y. The attractive interaction in a hydrogen bond typically has a strong electrostatic contribution, but dispersion forces and weak covalent bonding are also present.

In metallic solids and network solids, however, chemical bonds hold the individual chemical subunits together. The crystal is essential a single, macroscopic molecule with continuous chemical bonding throughout the entire structure. In metallic solids, the valence electrons are no longer exclusively associated with a single atom. Instead these electrons exist in molecular orbitals that are delocalized over many atoms, producing an electronic band structure. The metallic crystal essentially consists of a set of metal cations in a sea of electrons. This type of chemical bonding is called metallic bonding.

Ionic Solids

You learned previously that an ionic solid consists of positively and negatively charged ions held together by electrostatic forces. The strength of the attractive forces depends on the charge and size of the ions that compose the lattice and determines many of the physical properties of the crystal.

The **lattice energy** (i.e., the energy required to separate 1 mol of a crystalline ionic solid into its component ions in the gas phase) is directly proportional to the product of the ionic charges and inversely proportional to the sum of the radii of the ions. For example, NaF and CaO both crystallize in the face-centered cubic (fcc) sodium chloride structure, and the sizes of their component ions are about the same: Na^+ (102 pm) versus Ca^{2+} (100 pm), and F^- (133 pm) versus O^{2-} (140 pm). Because of the higher charge on the ions in CaO, however, the lattice energy of CaO is almost four times greater than that of NaF (3401 kJ/mol versus 923 kJ/mol). The forces that hold Ca and O together in CaO are much stronger than those that hold Na and F together in NaF, so the heat of fusion of CaO is almost twice that of NaF (59 kJ/mol versus 33.4 kJ/mol), and the melting point of CaO is 2927°C versus 996°C for NaF. In both cases, however, the values are large; that is, simple ionic compounds have high melting points and are relatively hard (and brittle) solids.

Molecular Solids

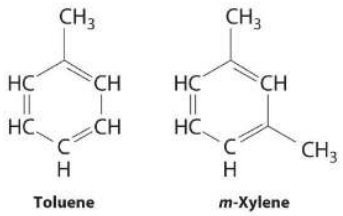
Molecular solids consist of atoms or molecules held to each other by dipole–dipole interactions, London dispersion forces, or hydrogen bonds, or any combination of these. The arrangement of the molecules in solid benzene is as follows:



The structure of solid benzene. In solid benzene, the molecules are not arranged with their planes parallel to one another but at 90° angles. (CC BY-NC-SA; Anonymous by request).

Because the intermolecular interactions in a molecular solid are relatively weak compared with ionic and covalent bonds, molecular solids tend to be soft, low melting, and easily vaporized (ΔH_{fus} and ΔH_{vap} are low). For similar substances, the strength of the London dispersion forces increases smoothly with increasing molecular mass. For example, the melting points of benzene (C_6H_6), naphthalene ($C_{10}H_8$), and anthracene ($C_{14}H_{10}$), with one, two, and three fused aromatic rings, are 5.5°C, 80.2°C, and 215°C, respectively. The enthalpies of fusion also increase smoothly within the series: benzene (9.95 kJ/mol) < naphthalene (19.1 kJ/mol) < anthracene (28.8 kJ/mol). If the molecules have shapes that cannot pack together efficiently in the crystal, however, then the melting points and the enthalpies of fusion tend to be unexpectedly low because the molecules are unable to arrange themselves to optimize intermolecular interactions. Thus toluene ($C_6H_5CH_3$) and m-xylene [m-$C_6H_4(CH_3)_2$] have melting points of −95°C and −48°C, respectively, which are significantly lower than the melting point of the lighter but more symmetrical analog, benzene.

Self-healing rubber is an example of a molecular solid with the potential for significant commercial applications. The material can stretch, but when snapped into pieces it can bond back together again through reestablishment of its hydrogen-bonding network without showing any sign of weakness. Among other applications, it is being studied for its use in adhesives and bicycle tires that will self-heal.



Toluene and m-xylene. The methyl groups attached to the phenyl ring in toluene and m-xylene prevent the rings from packing together as in solid benzene. (CC BY-NC-SA; Anonymous by request).

Covalent Network Solids

Covalent solids are formed by networks or chains of atoms or molecules held together by covalent bonds. A perfect single crystal of a covalent solid is therefore a single giant molecule. For example, the structure of diamond, shown in part (a) in Figure **5.2.1**, consists of sp3 hybridized carbon atoms, each bonded to four other carbon atoms in a tetrahedral array to create a giant network. The carbon atoms form six-membered rings.

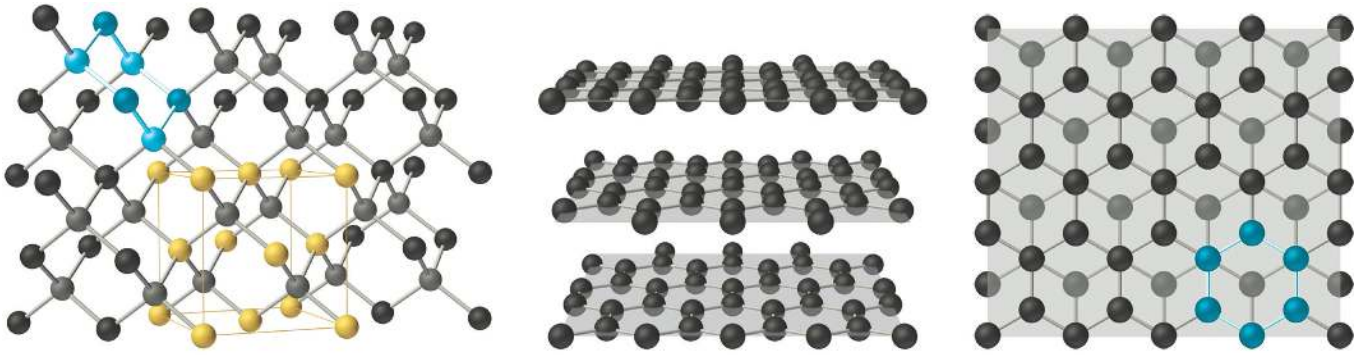


Figure **5.2.1**: The Structures of Diamond and Graphite. (a) Diamond consists of sp3 hybridized carbon atoms, each bonded to four other carbon atoms. The tetrahedral array forms a giant network in which carbon atoms form six-membered rings. This is easier to see in the rotating cube shown in Figure **5.2.2** below. (b) These side (left) and top (right) views of the graphite structure show the layers of fused six-membered rings and the arrangement of atoms in alternate layers of graphite. The rings in alternate layers are staggered, such that every other carbon atom in one layer lies directly under (and above) the center of a six-membered ring in an adjacent layer. (CC BY-NC-SA; Anonymous by request).

The unit cell of diamond can be described as an fcc array of carbon atoms with four additional carbon atoms inserted into four of the tetrahedral holes. It thus has the zinc blende structure described in Section 12.3, except that in zinc blende the atoms that compose the fcc array are sulfur and the atoms in the tetrahedral holes are zinc. Elemental silicon has the same structure, as does silicon carbide (SiC), which has alternating C and Si atoms. The structure of crystalline quartz (SiO_2), shown in Section 12.1, can be viewed as being derived from the structure of silicon by inserting an oxygen atom between each pair of silicon atoms.

All compounds with the diamond and related structures are hard, high-melting-point solids that are not easily deformed. Instead, they tend to shatter when subjected to large stresses, and they usually do not conduct electricity very well. In fact, diamond (melting point = 3500°C at 63.5 atm) is one of the hardest substances known, and silicon carbide (melting point = 2986°C) is used commercially as an abrasive in sandpaper and grinding wheels. It is difficult to deform or melt these and related compounds because strong covalent (C–C or Si–Si) or polar covalent (Si–C or Si–O) bonds must be broken, which requires a large input of energy.

Other covalent solids have very different structures. For example, graphite, the other common allotrope of carbon, has the structure shown in part (b) in Figure **5.2.1**. It contains planar networks of six-membered rings of sp2 hybridized carbon atoms in which each carbon is bonded to three others. This leaves a single electron in an unhybridized 2pz orbital that can be used to form C=C double bonds, resulting in a ring with alternating double and single bonds. Because of its resonance structures, the bonding in graphite is best viewed as consisting of a network of C–C single bonds with one-third of a π bond holding the carbons together, similar to the bonding in benzene.

To completely describe the bonding in graphite, we need a molecular orbital approach similar to the one used for benzene in Chapter 9. In fact, the C–C distance in graphite (141.5 pm) is slightly longer than the distance in benzene (139.5 pm), consistent with a net carbon–carbon bond order of 1.33. In graphite, the two-dimensional planes of carbon atoms are stacked to form a three-dimensional solid; only London dispersion forces hold the layers together. As a result, graphite exhibits properties typical of both covalent and molecular solids. Due to strong covalent bonding within the layers, graphite has a very high melting point, as expected for a covalent solid (it actually sublimes at about 3915°C). It is also very soft; the layers can easily slide past one another because of the weak interlayer interactions. Consequently, graphite is used as a lubricant and as the “lead” in pencils; the friction between graphite and a piece of paper is sufficient to leave a thin layer of carbon on the paper. Graphite is unusual among covalent solids in that its electrical conductivity is very high parallel to the planes of carbon atoms because of delocalized C–C π bonding. Finally, graphite is black because it contains an immense number of alternating double bonds, which results in a very small energy

difference between the individual molecular orbitals. Thus light of virtually all wavelengths is absorbed. Diamond, on the other hand, is colorless when pure because it has no delocalized electrons. Table **5.2.2** compares the strengths of the intermolecular and intramolecular interactions for three covalent solids, showing the comparative weakness of the interlayer interactions.

Table **5.2.2**: A Comparison of Intermolecular (ΔH_{sub}) and Intramolecular Interactions

Substance	ΔH_{sub} (kJ/mol)	Average Bond Energy (kJ/mol)
phosphorus (s)	58.98	201
sulfur (s)	64.22	226
iodine (s)	62.42	149

Carbon: An example of an Covalent Network Solid

In network solids, conventional chemical bonds hold the chemical subunits together. The bonding between chemical subunits, however, is identical to that within the subunits, resulting in a continuous network of chemical bonds. One common examples of network solids are diamond (a form of pure carbon) Carbon exists as a pure element at room temperature in three different forms: graphite (the most stable form), diamond, and fullerene.

Diamonds

The structure of diamond is shown at the right in a "ball-and-stick" format. The balls represent the carbon atoms and the sticks represent a covalent bond. Be aware that in the "ball-and-stick" representation the size of the balls do not accurately represent the size of carbon atoms. In addition, a single stick is drawn to represent a covalent bond irrespective of whether the bond is a single, double, or triple bond or requires resonance structures to represent. In the diamond structure, all bonds are single covalent bonds (σ bonds). The "space-filling" format is an alternate representation that displays atoms as spheres with a radius equal to the van der Waals radius, thus providing a better sense of the size of the atoms.

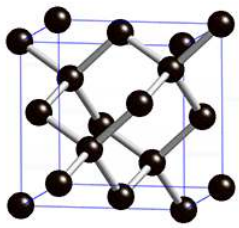


Figure **5.2.2**: Rotating model of diamond cubic. (CC0; H.K.D.H. Bhadeshia via Wikipedia)

Notice that diamond is a network solid. The entire solid is an "endless" repetition of carbon atoms bonded to each other by covalent bonds. (In the display at the right, the structure is truncated to fit in the display area.)

Questions to consider

- What is the bonding geometry around each carbon?
- What is the hybridization of carbon in diamond?
- The diamond structure consists of a repeating series of rings. How many carbon atoms are in a ring?
- Diamond are renowned for its hardness. Explain why this property is expected on the basis of the structure of diamond.

Graphite

The most stable form of carbon is graphite. Graphite consists of sheets of carbon atoms covalently bonded together. These sheets are then stacked to form graphite. Figure **5.2.3** shows a ball-and-stick representation of graphite with sheets that extended "indefinitely" in the xy plane, but the structure has been truncated for display purposed. Graphite may also be regarded as a

network solid, even though there is no bonding in the z direction. Each layer, however, is an "endless" bonded network of carbon atoms.

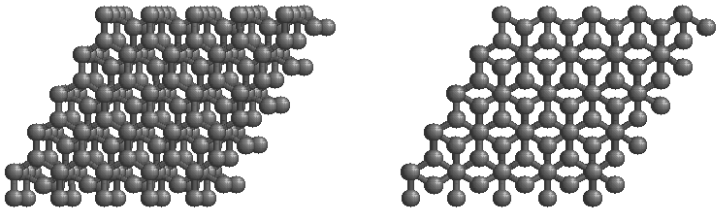


Figure **5.2.3**: Animation of a rotating graphite structure. This is a stereogram and can be viewed in 3D if a viewer's eyes are crossed slightly to overlap the two panels. Images used with permission from Wikipedia.

Questions to consider

- What is the bonding geometry around each carbon?
- What is the hybridization of carbon in graphite?
- The a layer of the graphite structure consists of a repeating series of rings. How many carbon atoms are in a ring?
- What force holds the carbon sheets together in graphite?
- Graphite is very slippery and is often used in lubricants. Explain why this property is expected on the basis of the structure of graphite.
- The slipperiness of graphite is enhanced by the introduction of impurities. Where would such impurities be located and why would they make graphite a better lubricant?

Fullerenes

Until the mid 1980's, pure carbon was thought to exist in two forms: graphite and diamond. The discovery of C_{60} molecules in interstellar dust in 1985 added a third form to this list. The existence of C_{60}, which resembles a soccer ball, had been hypothesized by theoreticians for many years. In the late 1980's synthetic methods were developed for the synthesis of C_{60}, and the ready availability of this form of carbon led to extensive research into its properties.

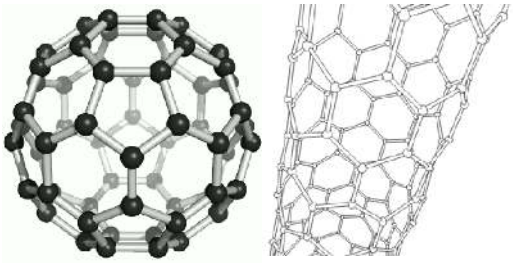


Figure **5.2.4**: Example of fullerenes: a buckyball (C_{60} on left and an extended bucktube. Images used with permission from Wikipedia.

The C_{60} molecule (Figure **5.2.4**; left), is called buckminsterfullerene, though the shorter name fullerene is often used. The name is a tribute to the American architect R. Buckminster Fuller, who is famous for designing and constructing geodesic domes which bear a close similarity to the structure of C_{60}. As is evident from the display, C_{60} is a sphere composed of six-member and five-member carbon rings. These balls are sometimes fondly referred to as "Bucky balls". It should be noted that fullerenes are an entire class of pure carbon compounds rather than a single compound. A distorted sphere containing more than 60 carbon atoms have also been found, and it is also possible to create long tubes (Figure **5.2.4**; right). All of these substances are pure carbon.

Questions to Consider

- What is the bonding geometry around each carbon? (Note that this geometry is distorted in C_{60}.)
- What is the hybridization of carbon in fullerene?
- A single crystal of C60 falls into which class of crystalline solids?
- It has been hypothesized that C60 would make a good lubricant. Why might C60 make a good lubricant?

Metallic Solids

Metallic solids such as crystals of copper, aluminum, and iron are formed by metal atoms Figure 5.2.5. The structure of metallic crystals is often described as a uniform distribution of atomic nuclei within a “sea” of delocalized electrons. The atoms within such a metallic solid are held together by a unique force known as *metallic bonding* that gives rise to many useful and varied bulk properties. All exhibit high thermal and electrical conductivity, metallic luster, and malleability. Many are very hard and quite strong. Because of their malleability (the ability to deform under pressure or hammering), they do not shatter and, therefore, make useful construction materials.

Metals are characterized by their ability to reflect light, called luster, their high electrical and thermal conductivity, their high heat capacity, and their malleability and ductility. Every lattice point in a pure metallic element is occupied by an atom of the same metal. The packing efficiency in metallic crystals tends to be high, so the resulting metallic solids are dense, with each atom having as many as 12 nearest neighbors.

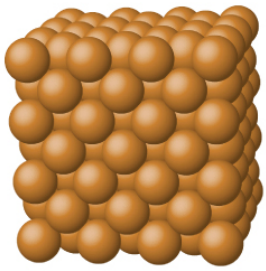


Figure 5.2.5: Copper is a metallic solid. (CC BY 4.0; OpenStax).

Bonding in metallic solids is quite different from the bonding in the other kinds of solids we have discussed. Because all the atoms are the same, there can be no ionic bonding, yet metals always contain too few electrons or valence orbitals to form covalent bonds with each of their neighbors. Instead, the valence electrons are delocalized throughout the crystal, providing a strong cohesive force that holds the metal atoms together.

> *Valence electrons in a metallic solid are delocalized, providing a strong cohesive force that holds the atoms together.*

The strength of metallic bonds varies dramatically. For example, cesium melts at 28.4°C, and mercury is a liquid at room temperature, whereas tungsten melts at 3680°C. Metallic bonds tend to be weakest for elements that have nearly empty (as in Cs) or nearly full (Hg) valence subshells, and strongest for elements with approximately half-filled valence shells (as in W). As a result, the melting points of the metals increase to a maximum around group 6 and then decrease again from left to right across the d block. Other properties related to the strength of metallic bonds, such as enthalpies of fusion, boiling points, and hardness, have similar periodic trends.

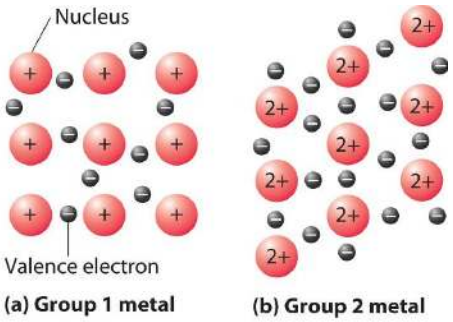


Figure 5.2.6: The Electron-Sea Model of Bonding in Metals. Fixed, positively charged metal nuclei from group 1 (a) or group 2 (b) are surrounded by a “sea” of mobile valence electrons. Because a group 2 metal has twice the number of valence electrons as a group 1 metal, it should have a higher melting point.

A somewhat oversimplified way to describe the bonding in a metallic crystal is to depict the crystal as consisting of positively charged nuclei in an electron sea (Figure 5.2.6). In this model, the valence electrons are not tightly bound to any one atom but are distributed uniformly throughout the structure. Very little energy is needed to remove electrons from a solid metal because they are

not bound to a single nucleus. When an electrical potential is applied, the electrons can migrate through the solid toward the positive electrode, thus producing high electrical conductivity. The ease with which metals can be deformed under pressure is attributed to the ability of the metal ions to change positions within the electron sea without breaking any specific bonds. The transfer of energy through the solid by successive collisions between the metal ions also explains the high thermal conductivity of metals. This model does not, however, explain many of the other properties of metals, such as their metallic luster and the observed trends in bond strength as reflected in melting points or enthalpies of fusion. Some general properties of the four major classes of solids are summarized in Table 5.2.2.

Table 5.2.2: Properties of the Major Classes of Solids

Ionic Solids	Molecular Solids	Covalent Solids	Metallic Solids
poor conductors of heat and electricity	poor conductors of heat and electricity	poor conductors of heat and electricity*	good conductors of heat and electricity
relatively high melting point	low melting point	high melting point	melting points depend strongly on electron configuration
hard but brittle; shatter under stress	soft	very hard and brittle	easily deformed under stress; ductile and malleable
relatively dense	low density	low density	usually high density
dull surface	dull surface	dull surface	lustrous

*Many exceptions exist. For example, graphite has a relatively high electrical conductivity within the carbon planes, and diamond has the highest thermal conductivity of any known substance.

The general order of increasing strength of interactions in a solid is:

$$\textit{molecular solids} < \textit{ionic solids} \approx \textit{metallic solids} < \textit{covalent solids}$$

Example 5.2.1

Classify Ge, RbI, $C_6(CH_3)_6$, and Zn as ionic, molecular, covalent, or metallic solids and arrange them in order of increasing melting points.

Given: compounds

Asked for: classification and order of melting points

Strategy:

A. Locate the component element(s) in the periodic table. Based on their positions, predict whether each solid is ionic, molecular, covalent, or metallic.
B. Arrange the solids in order of increasing melting points based on your classification, beginning with molecular solids.

Solution:

A Germanium lies in the p block just under Si, along the diagonal line of semimetallic elements, which suggests that elemental Ge is likely to have the same structure as Si (the diamond structure). Thus Ge is probably a covalent solid. RbI contains a metal from group 1 and a nonmetal from group 17, so it is an ionic solid containing Rb^+ and I^- ions. The compound C6(CH3)6 is a hydrocarbon (hexamethylbenzene), which consists of isolated molecules that stack to form a molecular solid with no covalent bonds between them. Zn is a d-block element, so it is a metallic solid.

B Arranging these substances in order of increasing melting points is straightforward, with one exception. We expect $C_6(CH_3)_6$ to have the lowest melting point and Ge to have the highest melting point, with RbI somewhere in between. The melting points of metals, however, are difficult to predict based on the models presented thus far. Because Zn has a filled valence shell, it should not have a particularly high melting point, so a reasonable guess is $C_6(CH_3)_6$ < Zn ~ RbI < Ge. The actual melting points are $C_6(CH_3)_6$, 166°C; Zn, 419°C; RbI, 642°C; and Ge, 938°C. This agrees with our prediction.

? Exercise 5.2.1

Classify C_{60}, $BaBr_2$, GaAs, and AgZn as ionic, covalent, molecular, or metallic solids and then arrange them in order of increasing melting points.

Answer

C_{60} (molecular) < AgZn (metallic) ~ $BaBr_2$ (ionic) < GaAs (covalent). The actual melting points are C60, about 300°C; AgZn, about 700°C; $BaBr_2$, 856°C; and GaAs, 1238°C.

Summary

The major types of solids are ionic, molecular, covalent, and metallic. Ionic solids consist of positively and negatively charged ions held together by electrostatic forces; the strength of the bonding is reflected in the lattice energy. Ionic solids tend to have high melting points and are rather hard. Molecular solids are held together by relatively weak forces, such as dipole–dipole interactions, hydrogen bonds, and London dispersion forces. As a result, they tend to be rather soft and have low melting points, which depend on their molecular structure. Covalent solids consist of two- or three-dimensional networks of atoms held together by covalent bonds; they tend to be very hard and have high melting points. Metallic solids have unusual properties: in addition to having high thermal and electrical conductivity and being malleable and ductile, they exhibit luster, a shiny surface that reflects light. An alloy is a mixture of metals that has bulk metallic properties different from those of its constituent elements. Alloys can be formed by substituting one metal atom for another of similar size in the lattice (substitutional alloys), by inserting smaller atoms into holes in the metal lattice (interstitial alloys), or by a combination of both. Although the elemental composition of most alloys can vary over wide ranges, certain metals combine in only fixed proportions to form intermetallic compounds with unique properties.

Contributors and Attributions

- Mike Blaber (Florida State University)
- Prof. David Blauch (Davidson College)
- Paul Flowers (University of North Carolina - Pembroke), Klaus Theopold (University of Delaware) and Richard Langley (Stephen F. Austin State University) with contributing authors. Textbook content produced by OpenStax College is licensed under a Creative Commons Attribution License 4.0 license. Download for free at http://cnx.org/contents/85abf193-2bd...a7ac8df6@9.110).

5.2: Carbon and Silicon- Network Atomic Solids is shared under a not declared license and was authored, remixed, and/or curated by LibreTexts.

- **11.8: Bonding in Solids** is licensed CC BY-NC-SA 3.0.

5.3: The Solid State of Matter

Learning Objectives

- Define and describe the bonding and properties of ionic, molecular, metallic, and covalent network crystalline solids
- Describe the main types of crystalline solids: ionic solids, metallic solids, covalent network solids, and molecular solids
- Explain the ways in which crystal defects can occur in a solid

When most liquids are cooled, they eventually freeze and form crystalline solids, solids in which the atoms, ions, or molecules are arranged in a definite repeating pattern. It is also possible for a liquid to freeze before its molecules become arranged in an orderly pattern. The resulting materials are called amorphous solids or noncrystalline solids (or, sometimes, glasses). The particles of such solids lack an ordered internal structure and are randomly arranged (Figure **5.3.1**).

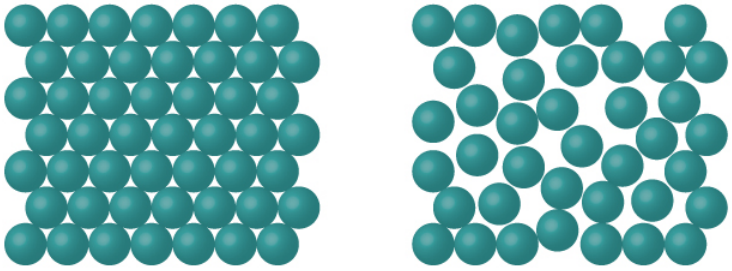


Figure **5.3.1**: The entities of a solid phase may be arranged in a regular, repeating pattern (crystalline solids) or randomly (amorphous).

The crystalline arrangement shows many circles drawn in rows and stacked together tightly. The amorphous arrangement shows many circles spread slightly apart and in no organized pattern.

Metals and ionic compounds typically form ordered, crystalline solids. Substances that consist of large molecules, or a mixture of molecules whose movements are more restricted, often form amorphous solids. For examples, candle waxes are amorphous solids composed of large hydrocarbon molecules. Some substances, such as boron oxide (Figure **5.3.2**), can form either crystalline or amorphous solids, depending on the conditions under which it is produced. Also, amorphous solids may undergo a transition to the crystalline state under appropriate conditions.

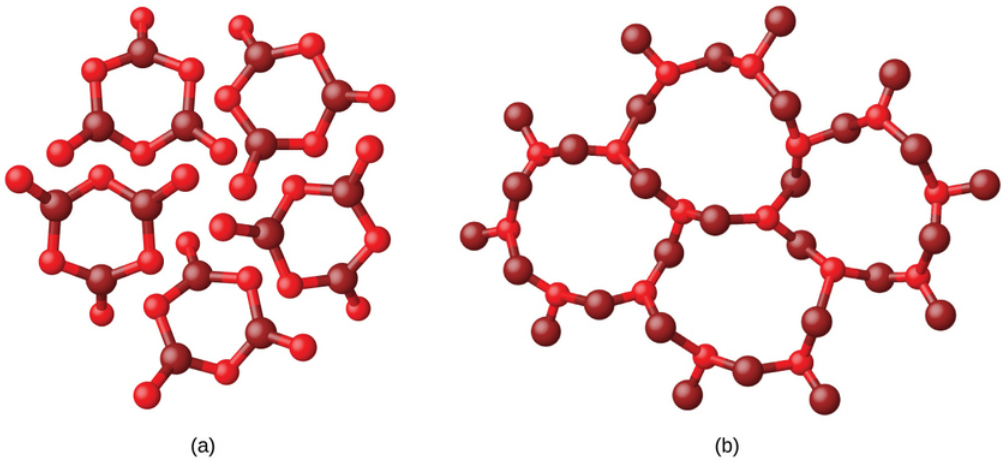


Figure **5.3.2**: (a) Diboron trioxide, B_2O_3, is normally found as a white, amorphous solid (a glass), which has a high degree of disorder in its structure. (b) By careful, extended heating, it can be converted into a crystalline form of B_2O_3, which has a very ordered arrangement.

The first structure of diboron trioxide shows five identical and separated hexagonal rings. The second structure of diboron trioxide shows a more interconnected structure with four large rings forming a more stable structure.

Crystalline solids are generally classified according the nature of the forces that hold its particles together. These forces are primarily responsible for the physical properties exhibited by the bulk solids. The following sections provide descriptions of the major types of crystalline solids: ionic, metallic, covalent network, and molecular.

5.3.1: Ionic Solids

Ionic solids, such as sodium chloride and nickel oxide, are composed of positive and negative ions that are held together by electrostatic attractions, which can be quite strong (Figure **5.3.3**). Many ionic crystals also have high melting points. This is due to the very strong attractions between the ions—in ionic compounds, the attractions between full charges are (much) larger than those between the partial charges in polar molecular compounds. This will be looked at in more detail in a later discussion of lattice energies. Although they are hard, they also tend to be brittle, and they shatter rather than bend. Ionic solids do not conduct electricity; however, they do conduct when molten or dissolved because their ions are free to move. Many simple compounds formed by the reaction of a metallic element with a nonmetallic element are ionic.

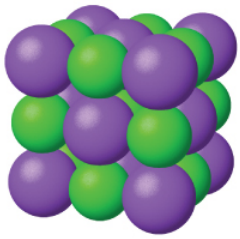


Figure **5.3.3**: Sodium chloride is an ionic solid.

A cube composed of purple and green spheres is shown. The cube has dimensions of three by three spheres. The purple spheres are slightly larger than the green spheres.

5.3.2: Metallic Solids

Metallic solids such as crystals of copper, aluminum, and iron are formed by metal atoms Figure **5.3.4**. The structure of metallic crystals is often described as a uniform distribution of atomic nuclei within a “sea” of delocalized electrons. The atoms within such a metallic solid are held together by a unique force known as *metallic bonding* that gives rise to many useful and varied bulk properties. All exhibit high thermal and electrical conductivity, metallic luster, and malleability. Many are very hard and quite strong. Because of their malleability (the ability to deform under pressure or hammering), they do not shatter and, therefore, make useful construction materials. The melting points of the metals vary widely. Mercury is a liquid at room temperature, and the alkali metals melt below 200 °C. Several post-transition metals also have low melting points, whereas the transition metals melt at temperatures above 1000 °C. These differences reflect differences in strengths of metallic bonding among the metals.

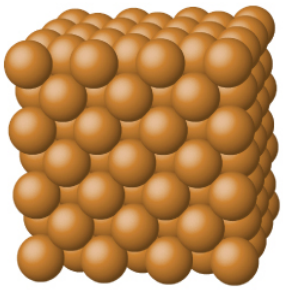


Figure **5.3.4**: Copper is a metallic solid.

5.3.3: Covalent Network Solids

Covalent network solids include crystals of diamond, silicon, some other nonmetals, and some covalent compounds such as silicon dioxide (sand) and silicon carbide (carborundum, the abrasive on sandpaper). Many minerals have networks of covalent bonds. The atoms in these solids are held together by a network of covalent bonds, as shown in Figure **5.3.5**. To break or to melt a covalent network solid, covalent bonds must be broken. Because covalent bonds are relatively strong, covalent network solids are typically characterized by hardness, strength, and high melting points. For example, diamond is one of the hardest substances known and melts above 3500 °C.

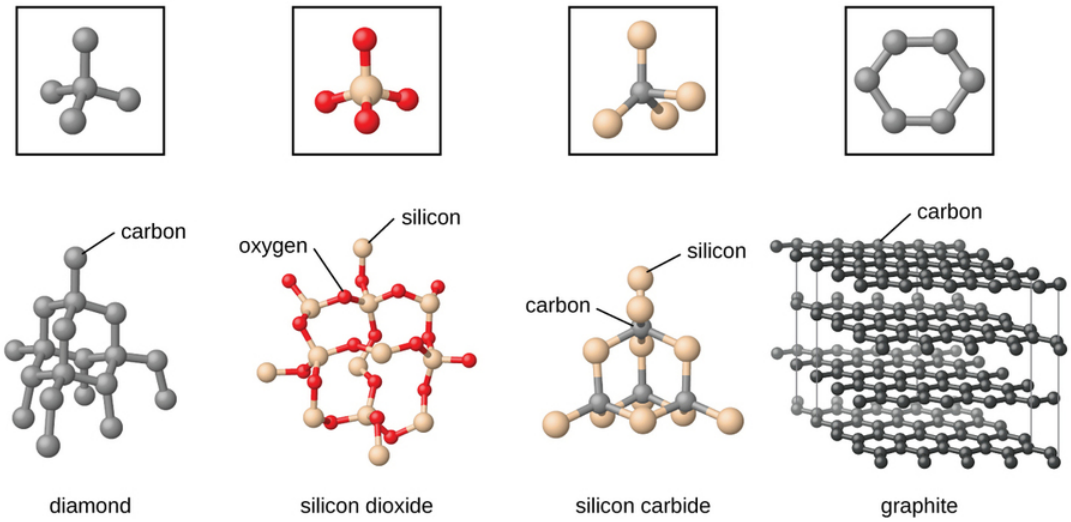


Figure **5.3.5**. A covalent crystal contains a three-dimensional network of covalent bonds, as illustrated by the structures of diamond, silicon dioxide, silicon carbide, and graphite. Graphite is an exceptional example, composed of planar sheets of covalent crystals that are held together in layers by noncovalent forces. Unlike typical covalent solids, graphite is very soft and electrically conductive.

The complex three dimensional structure of diamond, silicon dioxide, silicon carbide and graphite is shown along with a a smaller repeating unit of the structure shown above each structure.

5.3.4: Molecular Solids

Molecular solids, such as ice, sucrose (table sugar), and iodine, as shown in Figure **5.3.6**, are composed of neutral molecules. The strengths of the attractive forces between the units present in different crystals vary widely, as indicated by the melting points of the crystals. Small symmetrical molecules (nonpolar molecules), such as H_2, N_2, O_2, and F_2, have weak attractive forces and form molecular solids with very low melting points (below −200 °C). Substances consisting of larger, nonpolar molecules have larger attractive forces and melt at higher temperatures. Molecular solids composed of molecules with permanent dipole moments (polar molecules) melt at still higher temperatures. Examples include ice (melting point, 0 °C) and table sugar (melting point, 185 °C).

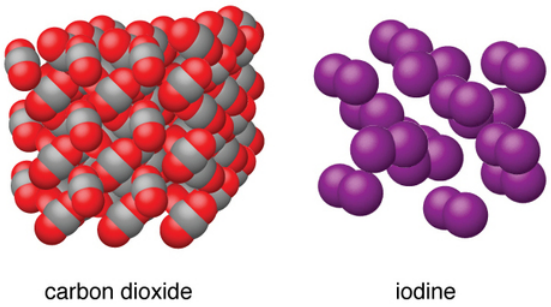


Figure **5.3.6**: Carbon dioxide (CO_2) consists of small, nonpolar molecules and forms a molecular solid with a melting point of −78 °C. Iodine (I_2) consists of larger, nonpolar molecules and forms a molecular solid that melts at 114 °C.

On the left, many red and grey molecules are densely stacked in a 3-D drawing to represent carbon dioxide. On the right, purple molecules are scattered randomly to represent iodine.

5.3.5: Properties of Solids

A crystalline solid, like those listed in Table **5.3.1** has a precise melting temperature because each atom or molecule of the same type is held in place with the same forces or energy. Thus, the attractions between the units that make up the crystal all have the same strength and all require the same amount of energy to be broken. The gradual softening of an amorphous material differs dramatically from the distinct melting of a crystalline solid. This results from the structural nonequivalence of the molecules in the amorphous solid. Some forces are weaker than others, and when an amorphous material is heated, the weakest intermolecular attractions break first. As the temperature is increased further, the stronger attractions are broken. Thus amorphous materials soften over a range of temperatures.

Table **5.3.1**: Types of Crystalline Solids and Their Properties

Type of Solid	Type of Particles	Type of Attractions	Properties	Examples
ionic	ions	ionic bonds	hard, brittle, conducts electricity as a liquid but not as a solid, high to very high melting points	NaCl, Al_2O_3
metallic	atoms of electropositive elements	metallic bonds	shiny, malleable, ductile, conducts heat and electricity well, variable hardness and melting temperature	Cu, Fe, Ti, Pb, U
covalent network	atoms of electronegative elements	covalent bonds	very hard, not conductive, very high melting points	C (diamond), SiO_2, SiC
molecular	molecules (or atoms)	IMFs	variable hardness, variable brittleness, not conductive, low melting points	H_2O, CO_2, I_2, $C_{12}H_{22}O_{11}$

Graphene: Material of the Future

Carbon is an essential element in our world. The unique properties of carbon atoms allow the existence of carbon-based life forms such as ourselves. Carbon forms a huge variety of substances that we use on a daily basis, including those shown in Figure **5.3.7**. You may be familiar with diamond and graphite, the two most common *allotropes* of carbon. (Allotropes are different structural forms of the same element.) Diamond is one of the hardest-known substances, whereas graphite is soft enough to be used as pencil lead. These very different properties stem from the different arrangements of the carbon atoms in the different allotropes.

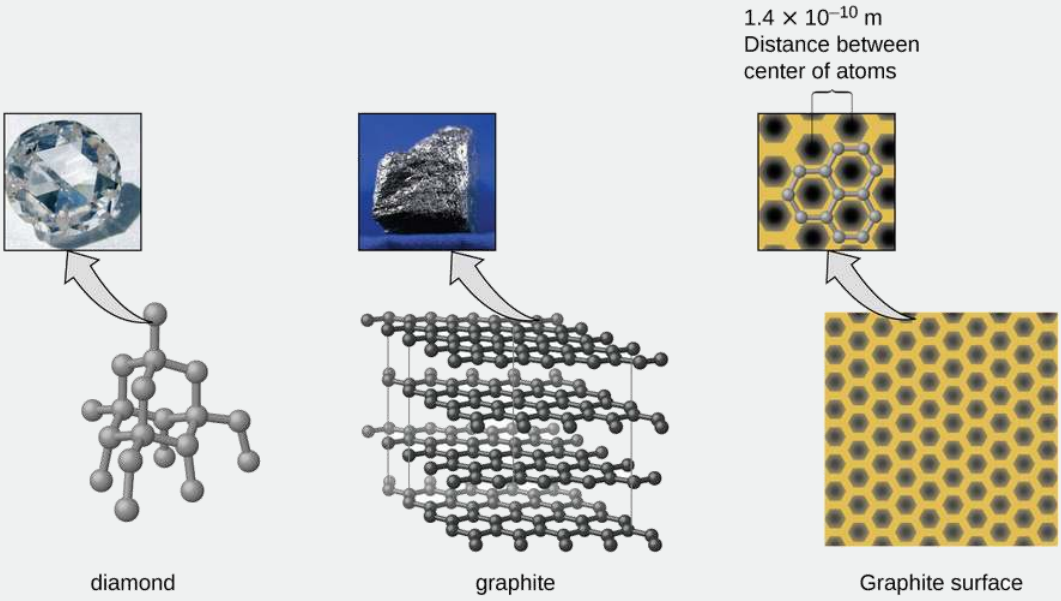


Figure **5.3.7**: Diamond is extremely hard because of the strong bonding between carbon atoms in all directions. Graphite (in pencil lead) rubs off onto paper due to the weak attractions between the carbon layers. An image of a graphite surface shows the distance between the centers of adjacent carbon atoms. (credit left photo: modification of work by Steve Jurvetson; credit middle photo: modification of work by United States Geological Survey)

A close up of a piece of diamond shows a three dimensional sturcture of a complex network of well bonded carbon atoms. A close up of a graphite shows several layers of carbon sheets. Each sheet is composed of a repeated and connected hexagonal structure of carbon atoms. The third diagram shows that the distance between the center of atoms is 1.4 times 10 to the power of negative 10 meters.

You may be less familiar with a recently discovered form of carbon: graphene. Graphene was first isolated in 2004 by using tape to peel off thinner and thinner layers from graphite. It is essentially a single sheet (one atom thick) of graphite. Graphene, illustrated in Figure **5.3.8**, is not only strong and lightweight, but it is also an excellent conductor of electricity and heat. These properties may prove very useful in a wide range of applications, such as vastly improved computer chips and circuits, better batteries and solar cells, and stronger and lighter structural materials. The 2010 Nobel Prize in Physics was awarded to Andre Geim and Konstantin Novoselov for their pioneering work with graphene.

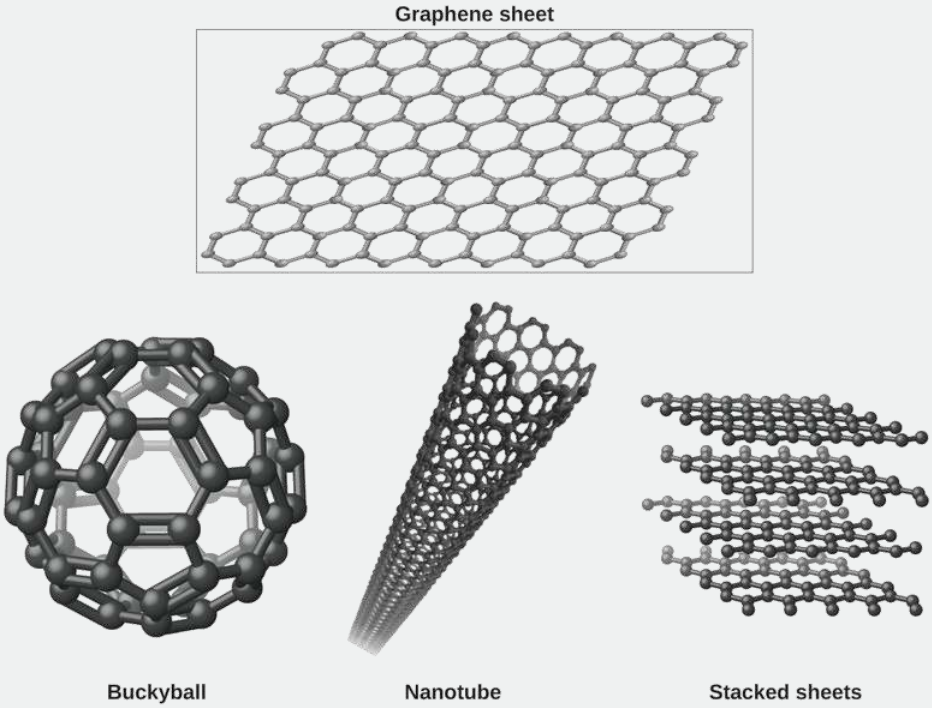


Figure **5.3.8**: Graphene sheets can be formed into buckyballs, nanotubes, and stacked layers.

A sheet of interconnected hexagonal rings is shown at the top. Below it, a bukcyball is shown which is a sphere is composed of hexagonal rings. In the lower middle image, a nanotube is shown that is made by rolling a graphene sheet into a tube. In the lower right image, stacked sheets made up of four horizontal sheets composed of joined, hexagonal rings is shown.

5.3.6: Crystal Defects

In a crystalline solid, the atoms, ions, or molecules are arranged in a definite repeating pattern, but occasional defects may occur in the pattern. Several types of defects are known, as illustrated in Figure **5.3.9**. Vacancies are defects that occur when positions that should contain atoms or ions are vacant. Less commonly, some atoms or ions in a crystal may occupy positions, called interstitial sites, located between the regular positions for atoms. Other distortions are found in impure crystals, as, for example, when the cations, anions, or molecules of the impurity are too large to fit into the regular positions without distorting the structure. Trace amounts of impurities are sometimes added to a crystal (a process known as *doping)* in order to create defects in the structure that yield desirable changes in its properties. For example, silicon crystals are doped with varying amounts of different elements to yield suitable electrical properties for their use in the manufacture of semiconductors and computer chips.

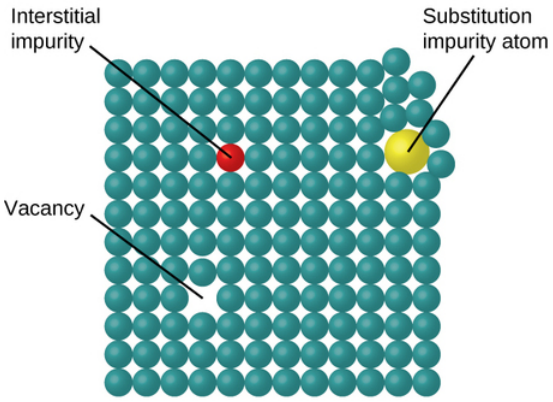


Figure **5.3.9**: Types of crystal defects include vacancies, interstitial atoms, and substitutions impurities.

Summary

Some substances form crystalline solids consisting of particles in a very organized structure; others form amorphous (noncrystalline) solids with an internal structure that is not ordered. The main types of crystalline solids are ionic solids, metallic

solids, covalent network solids, and molecular solids. The properties of the different kinds of crystalline solids are due to the types of particles of which they consist, the arrangements of the particles, and the strengths of the attractions between them. Because their particles experience identical attractions, crystalline solids have distinct melting temperatures; the particles in amorphous solids experience a range of interactions, so they soften gradually and melt over a range of temperatures. Some crystalline solids have defects in the definite repeating pattern of their particles. These defects (which include vacancies, atoms or ions not in the regular positions, and impurities) change physical properties such as electrical conductivity, which is exploited in the silicon crystals used to manufacture computer chips.

Glossary

amorphous solid

(also, noncrystalline solid) solid in which the particles lack an ordered internal structure

covalent network solid

solid whose particles are held together by covalent bonds

crystalline solid

solid in which the particles are arranged in a definite repeating pattern

interstitial sites

spaces between the regular particle positions in any array of atoms or ions

ionic solid

solid composed of positive and negative ions held together by strong electrostatic attractions

metallic solid

solid composed of metal atoms

molecular solid

solid composed of neutral molecules held together by intermolecular forces of attraction

vacancy

defect that occurs when a position that should contain an atom or ion is vacant

---

This page titled 5.3: The Solid State of Matter is shared under a CC BY license and was authored, remixed, and/or curated by OpenStax.

- **10.6: The Solid State of Matter** by OpenStax is licensed CC BY 4.0. Original source: https://openstax.org/details/books/chemistry-2e.

5.4: Lattice Structures in Crystalline Solids

Learning Objectives

- Describe the arrangement of atoms and ions in crystalline structures
- Compute ionic radii using unit cell dimensions
- Explain the use of X-ray diffraction measurements in determining crystalline structures

Over 90% of naturally occurring and man-made solids are crystalline. Most solids form with a regular arrangement of their particles because the overall attractive interactions between particles are maximized, and the total intermolecular energy is minimized, when the particles pack in the most efficient manner. The regular arrangement at an atomic level is often reflected at a macroscopic level. In this module, we will explore some of the details about the structures of metallic and ionic crystalline solids, and learn how these structures are determined experimentally.

5.4.1: The Structures of Metals

We will begin our discussion of crystalline solids by considering elemental metals, which are relatively simple because each contains only one type of atom. A pure metal is a crystalline solid with metal atoms packed closely together in a repeating pattern. Some of the properties of metals in general, such as their malleability and ductility, are largely due to having identical atoms arranged in a regular pattern. The different properties of one metal compared to another partially depend on the sizes of their atoms and the specifics of their spatial arrangements. We will explore the similarities and differences of four of the most common metal crystal geometries in the sections that follow.

5.4.2: Unit Cells of Metals

The structure of a crystalline solid, whether a metal or not, is best described by considering its simplest repeating unit, which is referred to as its unit cell. The unit cell consists of lattice points that represent the locations of atoms or ions. The entire structure then consists of this unit cell repeating in three dimensions, as illustrated in Figure **5.4.1**.

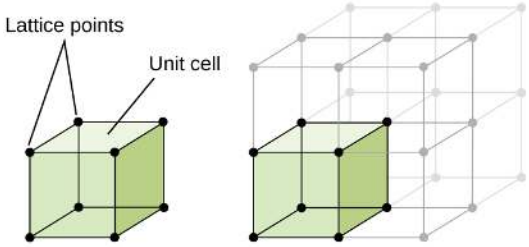


Figure **5.4.1**: A unit cell shows the locations of lattice points repeating in all directions.

A diagram of two images is shown. In the first image, a cube with a sphere at each corner is shown. The cube is labeled “Unit cell” and the spheres at the corners are labeled “Lattice points.” The second image shows the same cube, but this time it is one cube amongst eight that make up a larger cube. The original cube is shaded a color while the other cubes are not.

Let us begin our investigation of crystal lattice structure and unit cells with the most straightforward structure and the most basic unit cell. To visualize this, imagine taking a large number of identical spheres, such as tennis balls, and arranging them uniformly in a container. The simplest way to do this would be to make layers in which the spheres in one layer are directly above those in the layer below, as illustrated in Figure **5.4.2**. This arrangement is called simple cubic structure, and the unit cell is called the simple cubic unit cell or primitive cubic unit cell.

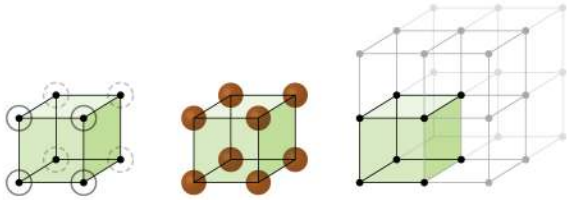


Figure 5.4.2: .When metal atoms are arranged with spheres in one layer directly above or below spheres in another layer, the lattice structure is called simple cubic. Note that the spheres are in contact.

A diagram of three images is shown. In the first image, a cube with a sphere at each corner is shown. The spheres at the corners are circled. The second image shows the same cube, but this time the spheres at the corners are larger and shaded in. In the third image, the cube is one cube amongst eight that make up a larger cube. The original cube is shaded a color while the other cubes are not.

In a simple cubic structure, the spheres are not packed as closely as they could be, and they only "fill" about 52% of the volume of the container. This is a relatively inefficient arrangement, and only one metal (polonium, Po) crystallizes in a simple cubic structure. As shown in Figure 5.4.3, a solid with this type of arrangement consists of planes (or layers) in which each atom contacts only the four nearest neighbors in its layer; one atom directly above it in the layer above; and one atom directly below it in the layer below. The number of other particles that each particle in a crystalline solid contacts is known as its coordination number. For a polonium atom in a simple cubic array, the coordination number is, therefore, six.

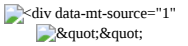


Figure 5.4.3: An atom in a simple cubic lattice structure contacts six other atoms, so it has a coordination number of six.

In a simple cubic lattice, the unit cell that repeats in all directions is a cube defined by the centers of eight atoms, as shown in Figure 5.4.4. Atoms at adjacent corners of this unit cell contact each other, so the edge length of this cell is equal to two atomic radii, or one atomic diameter. A cubic unit cell contains only the parts of these atoms that are within it. Since an atom at a corner of a simple cubic unit cell is contained by a total of eight unit cells, only one-eighth of that atom is within a specific unit cell. And since each simple cubic unit cell has one atom at each of its eight "corners," there is $8 \times \frac{1}{8} = 1$ atom within one simple cubic unit cell.

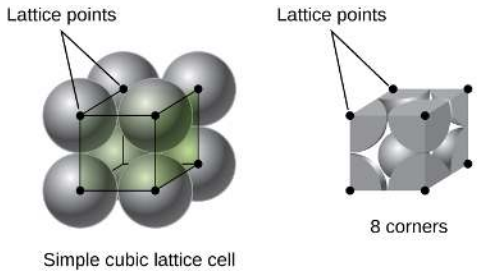


Figure 5.4.4: A simple cubic lattice unit cell contains one-eighth of an atom at each of its eight corners, so it contains one atom total.

A diagram of two images is shown. In the first image, eight spheres are stacked together to form a cube and dots at the center of each sphere are connected to form a cube shape. The dots are labeled "Lattice points" while a label under the image reads "Simple cubic lattice cell." The second image shows the portion of each sphere that lie inside the cube. The corners of the cube are shown with small circles labeled "Lattice points" and the phrase "8 corners" is written below the image.

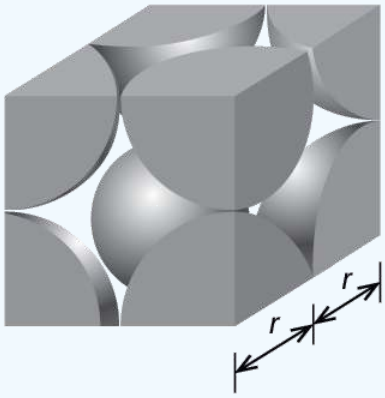
✔ Example 5.4.1: Calculating Atomic Radius and Density for Metals (Part 1)

The edge length of the unit cell of alpha polonium is 336 pm.

a. Determine the radius of a polonium atom.
b. Determine the density of alpha polonium.

Solution

Alpha polonium crystallizes in a simple cubic unit cell:



(a) Two adjacent Po atoms contact each other, so the edge length of this cell is equal to two Po atomic radii: $l = 2r$. Therefore, the radius of Po is

$$r = \frac{l}{2} = \frac{336\ \text{pm}}{2} = 168\ \text{pm}$$

(b) Density is given by

$$\text{density} = \frac{\text{mass}}{\text{volume}}.$$

The density of polonium can be found by determining the density of its unit cell (the mass contained within a unit cell divided by the volume of the unit cell). Since a Po unit cell contains one-eighth of a Po atom at each of its eight corners, a unit cell contains one Po atom.

The mass of a Po unit cell can be found by:

$$1\ \text{Po unit cell} \times \frac{1\ \text{Po atom}}{1\ \text{Po unit cell}} \times \frac{1\ \text{mol Po}}{6.022 \times 10^{23}\ \text{Po atoms}} \times \frac{208.998\ \text{g}}{1\ \text{mol Po}} = 3.47 \times 10^{-22}\ \text{g}$$

The volume of a Po unit cell can be found by:

$$V = l^3 = (336 \times 10^{-10}\ \text{cm})^3 = 3.79 \times 10^{-23}\ \text{cm}^3$$

(Note that the edge length was converted from pm to cm to get the usual volume units for density.)

Therefore, the density of

$$\text{Po} = \frac{3.471 \times 10^{-22}\ \text{g}}{3.79 \times 10^{-23}\ \text{cm}^3} = 9.16\ \text{g/cm}^3$$

? Exercise 5.4.1

The edge length of the unit cell for nickel is 0.3524 nm. The density of Ni is 8.90 g/cm^3. Does nickel crystallize in a simple cubic structure? Explain.

Answer

No. If Ni were simple cubic, its density would be given by:

$$1\ \text{Ni atom} \times \frac{1\ \text{mol Ni}}{6.022 \times 10^{23}\ \text{Ni atoms}} \times \frac{58.693\ \text{g}}{1\ \text{mol Ni}} = 9.746 \times 10^{-23}\ \text{g}$$

$$V = l^3 = (3.524 \times 10^{-8}\ \text{cm})^3 = 4.376 \times 10^{-23}\ \text{cm}^3$$

Then the density of Ni would be

$$(= \frac{9.746 \times 10^{-23}\ \text{g}}{4.376 \times 10^{-23}\ \text{cm}^3} = 2.23\ \text{g/cm}^3$$

Since the actual density of Ni is not close to this, Ni does not form a simple cubic structure.

Most metal crystals are one of the four major types of unit cells. For now, we will focus on the three cubic unit cells: simple cubic (which we have already seen), body-centered cubic unit cell, and face-centered cubic unit cell—all of which are illustrated in Figure 5.4.5. (Note that there are actually seven different lattice systems, some of which have more than one type of lattice, for a total of 14 different types of unit cells. We leave the more complicated geometries for later in this module.)

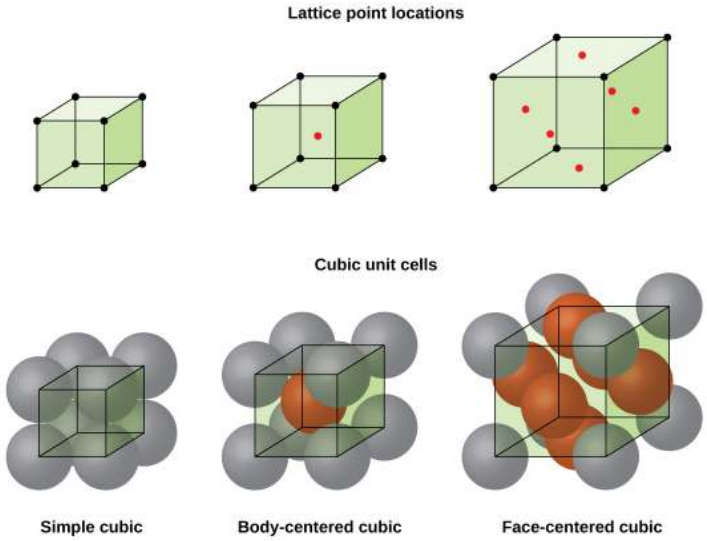


Figure 5.4.5: Cubic unit cells of metals show (in the upper figures) the locations of lattice points and (in the lower figures) metal atoms located in the unit cell.

Three pairs of images are shown. The first three images are in a row and are labeled “Lattice point locations” while the second three images are in a row labeled “Cubic unit cells.” The first image in the top row shows a cube with black dots at each corner while the first image in the second row is composed of eight spheres that are stacked together to form a cube and dots at the center of each sphere are connected to form a cube shape. The name under this image reads “Simple cubic.” The second image in the top row shows a cube with black dots at each corner and a red dot in the center while the second image in the second row is composed of eight spheres that are stacked together to form a cube with one sphere in the center of the cube and dots at the center of each corner sphere connected to form a cube shape. The name under this image reads “Body-centered cubic.” The third image in the top row shows a cube with black dots at each corner and red dots in the center of each face while the third image in the second row is composed of eight spheres that are stacked together to form a cube with six more spheres located in the center of each face of the cube. Dots at the center of each corner sphere are connected to form a cube shape. The name under this image reads “Face-centered cubic.”

Some metals crystallize in an arrangement that has a cubic unit cell with atoms at all of the corners and an atom in the center, as shown in Figure 5.4.6. This is called a body-centered cubic (BCC) solid. Atoms in the corners of a BCC unit cell do not contact each other but contact the atom in the center. A BCC unit cell contains two atoms: one-eighth of an atom at each of the eight corners ($8 \times \frac{1}{8} = 1$ atom from the corners) plus one atom from the center. Any atom in this structure touches four atoms in the layer above it and four atoms in the layer below it. Thus, an atom in a BCC structure has a coordination number of eight.

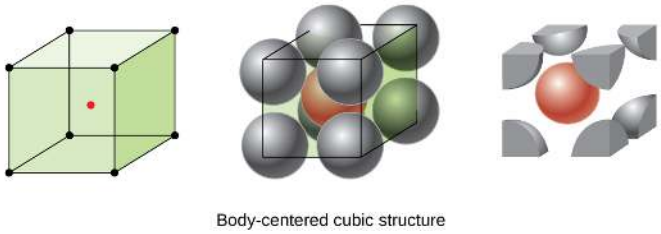


Figure 5.4.6: In a body-centered cubic structure, atoms in a specific layer do not touch each other. Each atom touches four atoms in the layer above it and four atoms in the layer below it.

Three images are shown. The first image shows a cube with black dots at each corner and a red dot in the center while the second image is composed of eight spheres that are stacked together to form a cube with one sphere in the center of the cube and dots at the center of each corner sphere connected to form a cube shape. The name under this image reads “Body-centered cubic structure.” The third image is the same as the second, but only shows the portions of the spheres that lie inside the cube shape.

Atoms in BCC arrangements are much more efficiently packed than in a simple cubic structure, occupying about 68% of the total volume. Isomorphous metals with a BCC structure include K, Ba, Cr, Mo, W, and Fe at room temperature. (Elements or compounds that crystallize with the same structure are said to be isomorphous.)

Many other metals, such as aluminum, copper, and lead, crystallize in an arrangement that has a cubic unit cell with atoms at all of the corners and at the centers of each face, as illustrated in Figure **5.4.7**. This arrangement is called a face-centered cubic (FCC) solid. A FCC unit cell contains four atoms: one-eighth of an atom at each of the eight corners ($8 \times \frac{1}{8} = 1$ atom from the corners) and one-half of an atom on each of the six faces ($6 \times \frac{1}{2} = 3$ atoms from the faces). The atoms at the corners touch the atoms in the centers of the adjacent faces along the face diagonals of the cube. Because the atoms are on identical lattice points, they have identical environments.

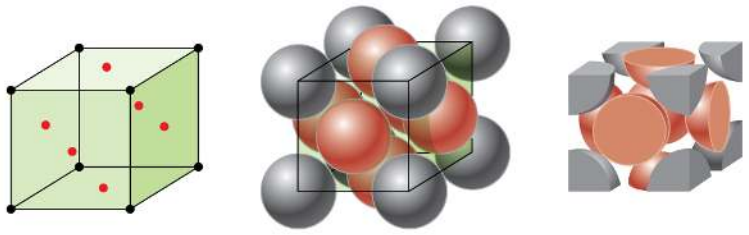


Figure **5.4.7**:A face-centered cubic solid has atoms at the corners and, as the name implies, at the centers of the faces of its unit cells.

Three images are shown. The first image shows a cube with black dots at each corner and red dots in the center of each face of the cube while the second image is composed of eight spheres that are stacked together to form a cube with six more spheres, one located on each face of the structure. Dots at the center of each corner sphere are connected to form a cube shape. The name under this image reads “Face-centered cubic structure.” The third image is the same as the second, but only shows the portions of the spheres that lie inside the cube shape.

Atoms in an FCC arrangement are packed as closely together as possible, with atoms occupying 74% of the volume. This structure is also called cubic closest packing (CCP). In CCP, there are three repeating layers of hexagonally arranged atoms. Each atom contacts six atoms in its own layer, three in the layer above, and three in the layer below. In this arrangement, each atom touches 12 near neighbors, and therefore has a coordination number of 12. The fact that FCC and CCP arrangements are equivalent may not be immediately obvious, but why they are actually the same structure is illustrated in Figure **5.4.8**.

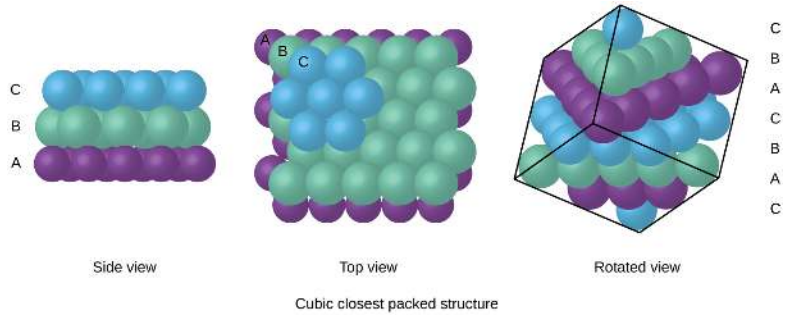


Figure **5.4.8**: A CCP arrangement consists of three repeating layers (ABCABC…) of hexagonally arranged atoms. Atoms in a CCP structure have a coordination number of 12 because they contact six atoms in their layer, plus three atoms in the layer above and three atoms in the layer below. By rotating our perspective, we can see that a CCP structure has a unit cell with a face containing an atom from layer A at one corner, atoms from layer B across a diagonal (at two corners and in the middle of the face), and an atom from layer C at the remaining corner. This is the same as a face-centered cubic arrangement.

Three images are shown. In the first image, a side view shows a layer of blue spheres, labeled “C” stacked on top of, and sitting in between the gaps in a second layer that is composed of green spheres, labeled “B,” which are sitting atop a purple layer of spheres labeled “A.” A label below this image reads “Side view.” The second image shows a top view of the same layers of spheres, where the top layer is “C,” the second layer is “B” and the lowest layer is “C.” This image is labeled “Top view” and written under this is the phrase “Cubic closest packed structure.” The third image shows an upper view of the side of a cube composed of two sets of the repeating layers shown in the other images. The layers are arranged “C, B, A, C, B, A, C” and the phrase written under this image reads “Rotated view.”

Because closer packing maximizes the overall attractions between atoms and minimizes the total intermolecular energy, the atoms in most metals pack in this manner. We find two types of closest packing in simple metallic crystalline structures: CCP, which we have already encountered, and hexagonal closest packing (HCP) shown in Figure **5.4.9**. Both consist of repeating layers of hexagonally arranged atoms. In both types, a second layer (B) is placed on the first layer (A) so that each atom in the second layer is in contact with three atoms in the first layer. The third layer is positioned in one of two ways. In HCP, atoms in the third layer are directly above atoms in the first layer (i.e., the third layer is also type A), and the stacking consists of alternating type A and type B close-packed layers (i.e., ABABAB⋯). In CCP, atoms in the third layer are not above atoms in either of the first two layers (i.e., the third layer is type C), and the stacking consists of alternating type A, type B, and type C close-packed layers (i.e., ABCABCABC⋯). About two–thirds of all metals crystallize in closest-packed arrays with coordination numbers of 12. Metals that crystallize in an HCP structure include Cd, Co, Li, Mg, Na, and Zn, and metals that crystallize in a CCP structure include Ag, Al, Ca, Cu, Ni, Pb, and Pt.

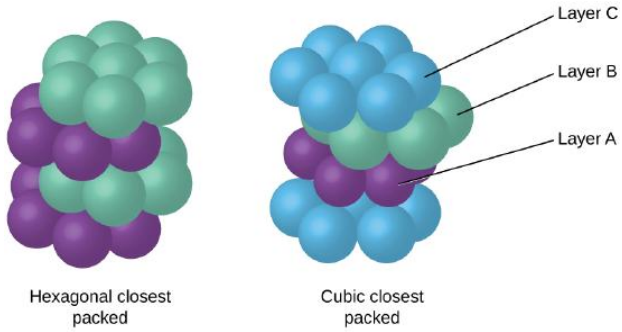


Figure **5.4.9**: In both types of closest packing, atoms are packed as compactly as possible. Hexagonal closest packing consists of two alternating layers (ABABAB…). Cubic closest packing consists of three alternating layers (ABCABCABC…).

Two images are shown. The first image, labeled “Hexagonal closest packed,” shows seven green spheres arranged in a circular sheet lying atop another sheet that is the same except the spheres are purple. The second sheet is offset just a bit so that the spheres of the top sheet lie in the grooves of the second sheet. Two more alternating green and purple layers of spheres lie below the first pair. The second image shows seven blue spheres, labeled “Layer C,” arranged in a circular sheet laying atop another sheet, labeled “Layer B” that is the same except the spheres are green. The second sheet is offset just a bit so that the spheres of the top sheet lie in the grooves of the second sheet. Two more alternating purple and then blue layers of spheres lie below the first pair. The purple layer is labeled “Layer A” and the phrase written below this image reads “Cubic closest packed.”

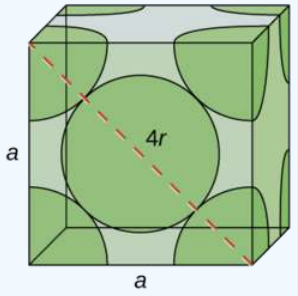
✔ Example 5.4.2: Calculating Atomic Radius and Density for Metals (Part 2)

Calcium crystallizes in a face-centered cubic structure. The edge length of its unit cell is 558.8 pm.

a. What is the atomic radius of Ca in this structure?
b. Calculate the density of Ca.

Solution

(a) In an FCC structure, Ca atoms contact each other across the diagonal of the face, so the length of the diagonal is equal to four Ca atomic radii (d = 4*r*).



Two adjacent edges and the diagonal of the face form a right triangle, with the length of each side equal to 558.8 pm and the length of the hypotenuse equal to four Ca atomic radii:

$$a^2 + a^2 = d^2$$

$$(558.8\ \text{pm})^2 + (558.5\ \text{pm})^2 = (4r)^2$$

Solving this gives

$$r = \sqrt{\frac{(558.8\ \text{pm})^2 + (558.5\ \text{pm})^2}{16}} = 197.6\ \text{pmg for a Ca radius.}$$

(b) Density is given by $\textbf{density} = \frac{\textbf{mass}}{\textbf{volume}}$. The density of calcium can be found by determining the density of its unit cell: for example, the mass contained within a unit cell divided by the volume of the unit cell. A face-centered Ca unit cell has one-eighth of an atom at each of the eight corners ($8 \times \frac{1}{8} = 1$atom) and one-half of an atom on each of the six faces $6 \times \frac{1}{2} = 3$ atoms), for a total of four atoms in the unit cell.

The mass of the unit cell can be found by:

$$1\ \text{Ca unit cell} \times \frac{4\ \text{Ca atoms}}{1\ \text{Ca unit cell}} \times \frac{1\ \text{mol Ca}}{6.022 \times 10^{23}\ \text{Ca atoms}} \times \frac{40.078\ \text{g}}{1\ \text{mol Ca}} = 2.662 \times 10^{-22}\ \text{g}$$

The volume of a Ca unit cell can be found by:

$$V = a^3 = (558.8 \times 10^{-10}\ \text{cm})^3 = 1.745 \times 10^{-22}\ \text{cm}^3$$

(Note that the edge length was converted from pm to cm to get the usual volume units for density.)

Then, the density of polonium:

$$\text{Po} = \frac{2.662 \times 10^{-22}\ \text{g}}{1.745 \times 10^{-22}\ \text{cm}^3} = 1.53\ \text{g/cm}^3$$

Exercise 5.4.2

Silver crystallizes in an FCC structure. The edge length of its unit cell is 409 pm.

a. What is the atomic radius of Ag in this structure?
b. Calculate the density of Ag.

Answer a

144 pm

Answer b

10.5 g/cm^3

In general, a unit cell is defined by the lengths of three axes (*a*, *b*, and *c*) and the angles (α, β, and γ) between them, as illustrated in Figure **5.4.10**. The axes are defined as being the lengths between points in the space lattice. Consequently, unit cell axes join points with identical environments.

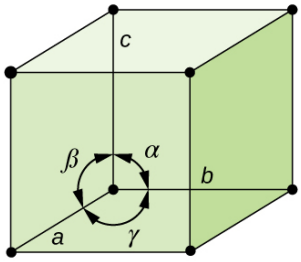


Figure 5.4.10: A unit cell is defined by the lengths of its three axes (a, b, and c) and the angles (α, β, and γ) between the axes.

A cube is shown where each corner has a black dot drawn on it. A circle in the bottom of the cube is composed of three double-ended arrows. The left top of this circle is labeled “alpha,” the top right is labeled “beta” and the bottom is labeled “gamma.” The bottom left corner of the cube is labeled “a” while the bottom of the back face is labeled “b” and the top, back, left corner is labeled “c.”

There are seven different lattice systems, some of which have more than one type of lattice, for a total of fourteen different unit cells, which have the shapes shown in Figure 5.4.11.

https://chem.libretexts.org/@go/page/362305

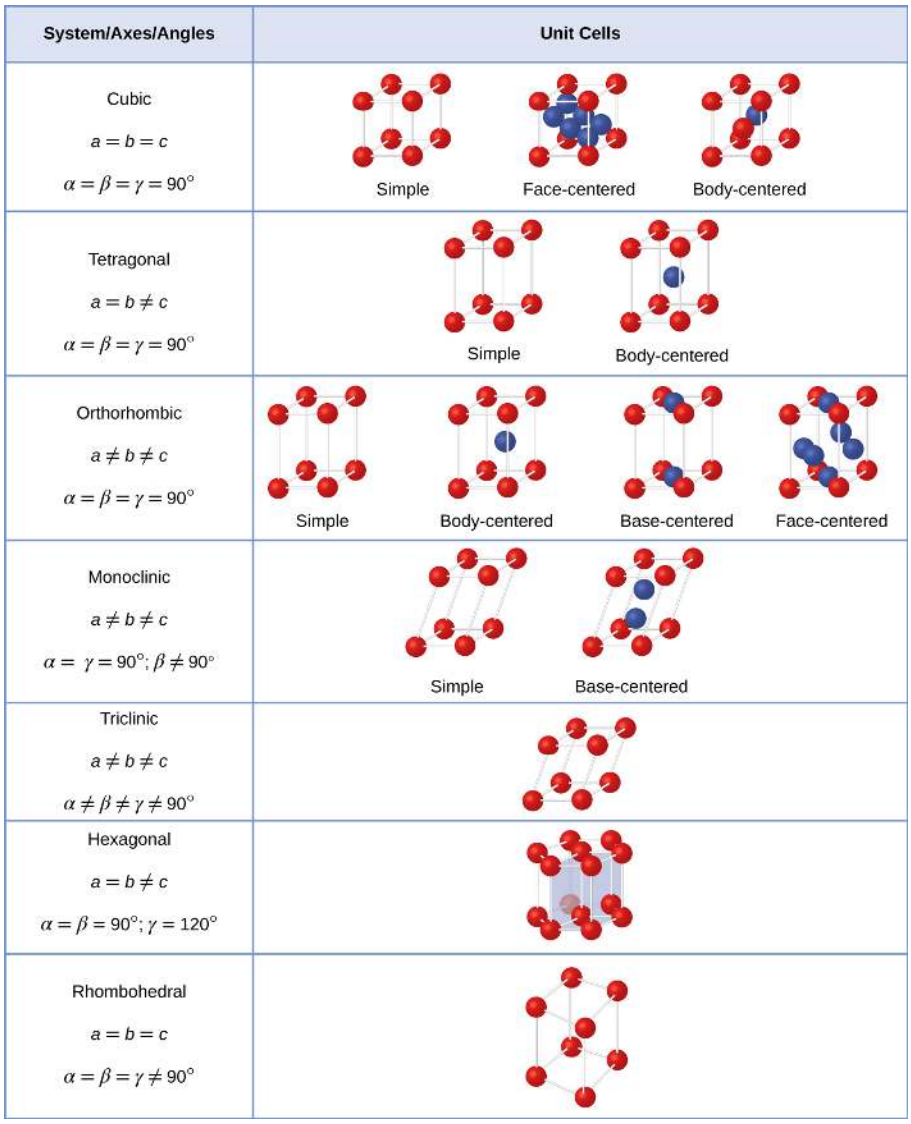


Figure **5.4.11**:There are seven different lattice systems and 14 different unit cells.

A table is composed of two columns and eight rows. The header row reads “System / Axes / Angles” and “Unit Cells .” The first column reads “Cubic, a equals b equals c, alpha equals beta equals gamma equals 90 degrees,” “Tetragonal, a equals b does not equal c, alpha equals beta equals gamma equals 90 degrees,” “Orthorhombic, a does not equal b does not equal c, alpha equals beta equals gamma equals 90 degrees,” “Monoclinic, a does not equal b does not equal c, alpha equals gamma equals 90 degrees, beta does not equal 90 degrees,” “Triclinic, a does not equal b does not equal c, alpha does not equal beta does not equal gamma does not equal 90 degrees,” “Hexagonal, a equals b does not equal c, alpha equals beta equals 90 degrees, gamma equals 120 degrees,” “Rhombohedral, a equals b equals c, alpha equals beta equals gamma does not equal 90 degrees.” The second column is composed of diagrams. The first set of diagrams in the first cell show a cube with spheres at each corner labeled “Simple,” a cube with spheres in each corner and on each face labeled “Face-centered” and a cube with spheres in each corner and one in the center labeled “Body-centered.” The second set of diagrams in the second cell show a vertical rectangle with spheres at each corner labeled “Simple” and a vertical rectangle with spheres in each corner and one in the center labeled “Body-centered.” The third set of diagrams in the third cell show a vertical rectangle with spheres at each corner labeled “Simple,” a vertical rectangle with spheres in each corner and one in the center labeled “Body-centered,” a vertical rectangle with spheres in each corner and one on the top and bottom faces labeled “Base-centered,” and a vertical rectangle with spheres in each corner and one on each face labeled “Face-centered.” The fourth set of diagrams in the fourth cell show a vertical rectangle with spheres at each corner that is slanted to one side labeled “Simple” and a vertical rectangle with spheres in each corner that is slanted to one side and has two spheres in the center is labeled “Body-centered.” The fifth diagrams in the fifth cell show a cube that is slanted with spheres at each corner while the sixth diagram in the sixth cell shows a pair of hexagonal rings that are connected together to form a six-sided shape with spheres at each corner. The seventh diagram in the seventh cell shows a rectangle that is slanted with spheres at each corner.

5.4.3: The Structures of Ionic Crystals

Ionic crystals consist of two or more different kinds of ions that usually have different sizes. The packing of these ions into a crystal structure is more complex than the packing of metal atoms that are the same size. Most monatomic ions behave as charged spheres, and their attraction for ions of opposite charge is the same in every direction. Consequently, stable structures for ionic compounds result (1) when ions of one charge are surrounded by as many ions as possible of the opposite charge and (2) when the cations and anions are in contact with each other. Structures are determined by two principal factors: the relative sizes of the ions and the ratio of the numbers of positive and negative ions in the compound.

In simple ionic structures, we usually find the anions, which are normally larger than the cations, arranged in a closest-packed array. (As seen previously, additional electrons attracted to the same nucleus make anions larger and fewer electrons attracted to the same nucleus make cations smaller when compared to the atoms from which they are formed.) The smaller cations commonly occupy one of two types of holes (or interstices) remaining between the anions. The smaller of the holes is found between three anions in one plane and one anion in an adjacent plane. The four anions surrounding this hole are arranged at the corners of a tetrahedron, so the hole is called a tetrahedral hole. The larger type of hole is found at the center of six anions (three in one layer and three in an adjacent layer) located at the corners of an octahedron; this is called an octahedral hole. Figure **5.4.12** illustrates both of these types of holes.

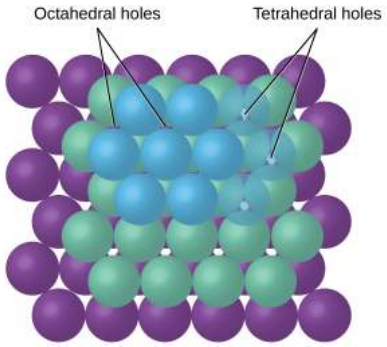


Figure **5.4.12**: Cations may occupy two types of holes between anions: octahedral holes or tetrahedral holes.

An image shows a top-view of a layer of blue spheres arranged in a sheet lying atop another sheet that is the same except the spheres are green. The second sheet is offset just a bit so that the spheres of the top sheet lie in the grooves of the second sheet. A third sheet composed of purple spheres lies at the bottom. The spaces created between the spheres in each layer are labeled “Octahedral holes” and “Tetrahedral holes.”

Depending on the relative sizes of the cations and anions, the cations of an ionic compound may occupy tetrahedral or octahedral holes, as illustrated in Figure **5.4.13**. Relatively small cations occupy tetrahedral holes, and larger cations occupy octahedral holes. If the cations are too large to fit into the octahedral holes, the anions may adopt a more open structure, such as a simple cubic array. The larger cations can then occupy the larger cubic holes made possible by the more open spacing.

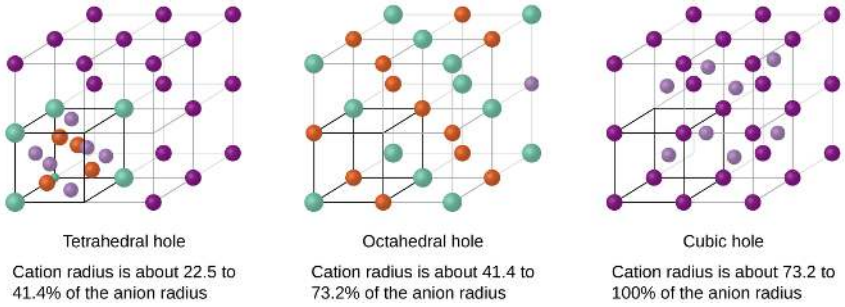


Figure 5.4.13:A cation's size and the shape of the hole occupied by the compound are directly related.

A diagram of three images is shown. In the first image, eight stacked cubes, with purple spheres at each corner, that make up one large cube are shown. The bottom left cube is different. It has green spheres at each corner and has four orange and six light purple spheres located on the faces of the cube. Labels below this structure read "Tetrahedral hole" and "Cation radius is about 22.5 to 41.4 percent of the anion radius. In the second image, eight stacked cubes, with alternating orange and green spheres at each corner, make up one large cube that is shown. The bottom left cube has darker lines that connect the spheres together. Labels below this structure read "Octahedral hole" and "Cation radius is about 41.4 to 73.2 percent of the anion radius. In the third image, eight stacked cubes, with purple spheres at each corner and light purple spheres on their interior faces, make up one large cube that is shown. Labels below this structure read "Cubic hole" and "Cation radius is about 73.2 to 100 percent of the anion radius."

There are two tetrahedral holes for each anion in either an HCP or CCP array of anions. A compound that crystallizes in a closest-packed array of anions with cations in the tetrahedral holes can have a maximum cation:anion ratio of 2:1; all of the tetrahedral holes are filled at this ratio. Examples include Li_2O, Na_2O, Li_2S, and Na_2S. Compounds with a ratio of less than 2:1 may also crystallize in a closest-packed array of anions with cations in the tetrahedral holes, if the ionic sizes fit. In these compounds, however, some of the tetrahedral holes remain vacant.

✔ Example 5.4.3: Occupancy of Tetrahedral Holes

Zinc sulfide is an important industrial source of zinc and is also used as a white pigment in paint. Zinc sulfide crystallizes with zinc ions occupying one-half of the tetrahedral holes in a closest-packed array of sulfide ions. What is the formula of zinc sulfide?

Solution

Because there are two tetrahedral holes per anion (sulfide ion) and one-half of these holes are occupied by zinc ions, there must be $\frac{1}{2} \times 2$, or 1, zinc ion per sulfide ion. Thus, the formula is ZnS.

? Exercise 5.4.3: Lithium selenide

Lithium selenide can be described as a closest-packed array of selenide ions with lithium ions in all of the tetrahedral holes. What it the formula of lithium selenide?

Answer

Li_2Se

The ratio of octahedral holes to anions in either an HCP or CCP structure is 1:1. Thus, compounds with cations in octahedral holes in a closest-packed array of anions can have a maximum cation:anion ratio of 1:1. In NiO, MnS, NaCl, and KH, for example, all of the octahedral holes are filled. Ratios of less than 1:1 are observed when some of the octahedral holes remain empty.

✔ Example 5.4.4: Stoichiometry of Ionic Compounds Sapphire

Aluminum oxide crystallizes with aluminum ions in two-thirds of the octahedral holes in a closest-packed array of oxide ions. What is the formula of aluminum oxide?

Solution

Because there is one octahedral hole per anion (oxide ion) and only two-thirds of these holes are occupied, the ratio of aluminum to oxygen must be $\frac{2}{3}$:1, which would give $\mathbf{Al_{2/3}O}$. The simplest whole number ratio is 2:3, so the formula is Al_2O_3.

? Exercise 5.4.4

The white pigment titanium oxide crystallizes with titanium ions in one-half of the octahedral holes in a closest-packed array of oxide ions. What is the formula of titanium oxide?

Answer

$\mathbf{TiO_2}$

In a simple cubic array of anions, there is one cubic hole that can be occupied by a cation for each anion in the array. In CsCl, and in other compounds with the same structure, all of the cubic holes are occupied. Half of the cubic holes are occupied in SrH_2, UO_2, $SrCl_2$, and CaF_2.

Different types of ionic compounds often crystallize in the same structure when the relative sizes of their ions and their stoichiometries (the two principal features that determine structure) are similar.

5.4.4: Unit Cells of Ionic Compounds

Many ionic compounds crystallize with cubic unit cells, and we will use these compounds to describe the general features of ionic structures. When an ionic compound is composed of cations and anions of similar size in a 1:1 ratio, it typically forms a simple cubic structure. Cesium chloride, CsCl, (Figure **5.4.14**) is an example of this, with Cs^+ and Cl^- having radii of 174 pm and 181 pm, respectively. We can think of this as chloride ions forming a simple cubic unit cell, with a cesium ion in the center; or as cesium ions forming a unit cell with a chloride ion in the center; or as simple cubic unit cells formed by Cs^+ ions overlapping unit cells formed by Cl^- ions. Cesium ions and chloride ions touch along the body diagonals of the unit cells. One cesium ion and one chloride ion are present per unit cell, giving the l:l stoichiometry required by the formula for cesium chloride. Note that there is no lattice point in the center of the cell, and CsCl is not a BCC structure because a cesium ion is not identical to a chloride ion.



Figure **5.4.14**: Ionic compounds with similar-sized cations and anions, such as CsCl, usually form a simple cubic structure. They can be described by unit cells with either cations at the corners or anions at the corners.

Three images are shown. The first image shows a cube with black dots at each corner and a red dot in the center. This cube is stacked with seven others that are not colored to form a larger cube. The second image is composed of eight spheres that are grouped together to form a cube with one smaller sphere in the center. The name under this image reads “Body-centered simple cubic structure.” The third image shows five horizontal layers of purple spheres with layers of smaller green spheres in between.

We have said that the location of lattice points is arbitrary. This is illustrated by an alternate description of the CsCl structure in which the lattice points are located in the centers of the cesium ions. In this description, the cesium ions are located on the lattice points at the corners of the cell, and the chloride ion is located at the center of the cell. The two unit cells are different, but they describe identical structures.

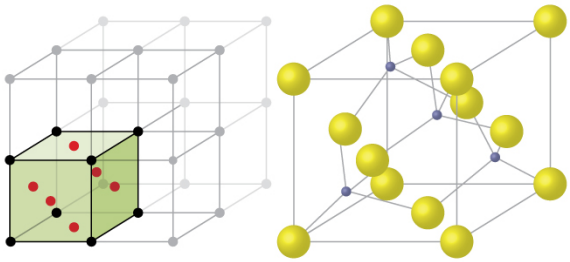
When an ionic compound is composed of a 1:1 ratio of cations and anions that differ significantly in size, it typically crystallizes with an FCC unit cell, like that shown in Figure **5.4.15**. Sodium chloride, NaCl, is an example of this, with Na^+ and Cl^- having radii of 102 pm and 181 pm, respectively. We can think of this as chloride ions forming an FCC cell, with sodium ions located in the octahedral holes in the middle of the cell edges and in the center of the cell. The sodium and chloride ions touch each other along the cell edges. The unit cell contains four sodium ions and four chloride ions, giving the 1:1 stoichiometry required by the formula, NaCl.



Figure 5.4.15: Ionic compounds with anions that are much larger than cations, such as NaCl, usually form an FCC structure. They can be described by FCC unit cells with cations in the octahedral holes.

Three images are shown. The first image shows a cube with black dots at each corner and a red dot in the center. This cube is stacked with seven others that are not colored to form a larger cube. The second image is composed of eight spheres that are grouped together to form a cube with one much larger sphere in the center. The name under this image reads “Body-centered simple cubic structure.” The third image shows seven horizontal layers of alternating purple and green spheres that are slightly offset with one another and form a large cube.

The cubic form of zinc sulfide, zinc blende, also crystallizes in an FCC unit cell, as illustrated in Figure 5.4.16. This structure contains sulfide ions on the lattice points of an FCC lattice. (The arrangement of sulfide ions is identical to the arrangement of chloride ions in sodium chloride.) The radius of a zinc ion is only about 40% of the radius of a sulfide ion, so these small Zn^{2+} ions are located in alternating tetrahedral holes, that is, in one half of the tetrahedral holes. There are four zinc ions and four sulfide ions in the unit cell, giving the empirical formula ZnS.

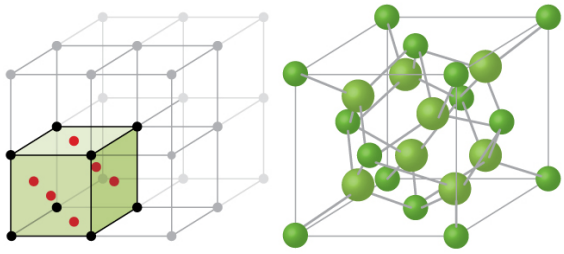


ZnS face-centered unit cell

Figure 5.4.16: ZnS, zinc sulfide (or zinc blende) forms an FCC unit cell with sulfide ions at the lattice points and much smaller zinc ions occupying half of the tetrahedral holes in the structure.

Two images are shown. The first image shows a cube with black dots at each corner and a red dot in the center of each face of the cube. This cube is stacked with seven others that are not colored to form a larger cube. The second image is composed of eight spheres that form the corners of a cube with six other spheres located in the face of the cube. The spheres are connected to one another by lines. The name under this image reads “Z n S, face-centered unit cell.”

A calcium fluoride unit cell, like that shown in Figure 5.4.17, is also an FCC unit cell, but in this case, the cations are located on the lattice points; equivalent calcium ions are located on the lattice points of an FCC lattice. All of the tetrahedral sites in the FCC array of calcium ions are occupied by fluoride ions. There are four calcium ions and eight fluoride ions in a unit cell, giving a calcium:fluorine ratio of 1:2, as required by the chemical formula, CaF_2. Close examination of Figure 5.4.17 will reveal a simple cubic array of fluoride ions with calcium ions in one half of the cubic holes. The structure cannot be described in terms of a space lattice of points on the fluoride ions because the fluoride ions do not all have identical environments. The orientation of the four calcium ions about the fluoride ions differs.



CaF_2 face-centered unit cell

Figure 5.4.17: Calcium fluoride, CaF_2, forms an FCC unit cell with calcium ions (green) at the lattice points and fluoride ions (red) occupying all of the tetrahedral sites between them.

Two images are shown. The first image shows a cube with black dots at each corner and a red dot in the center of each face of the cube. This cube is stacked with seven others that are not colored to form a larger cube. The second image is composed of eight small green spheres that form the corners of a cube with six other small green spheres located in the faces of the cube. Eight larger green spheres are spaced inside the cube and all of the spheres are connect to one another by lines. The name under this image reads “C a F, subscript 2, face-centered unit cell.”

5.4.5: Calculation of Ionic Radii

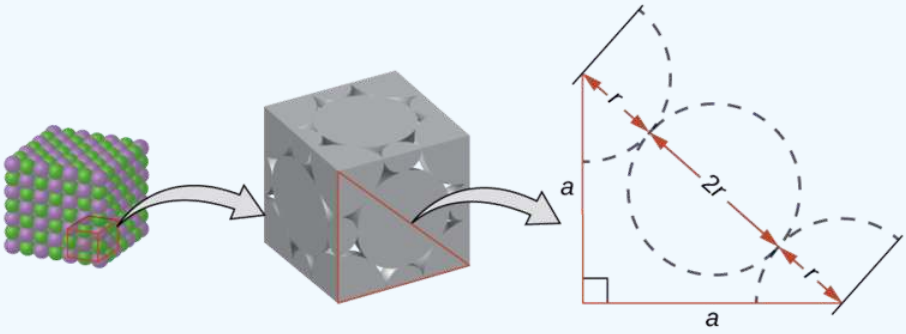
If we know the edge length of a unit cell of an ionic compound and the position of the ions in the cell, we can calculate ionic radii for the ions in the compound if we make assumptions about individual ionic shapes and contacts.

Example 5.4.5: Calculation of Ionic Radii

The edge length of the unit cell of LiCl (NaCl-like structure, FCC) is 0.514 nm or 5.14 Å. Assuming that the lithium ion is small enough so that the chloride ions are in contact, calculate the ionic radius for the chloride ion. Note: The length unit angstrom, Å, is often used to represent atomic-scale dimensions and is equivalent to 10^{-10} m.

Solution

On the face of a LiCl unit cell, chloride ions contact each other across the diagonal of the face:



Drawing a right triangle on the face of the unit cell, we see that the length of the diagonal is equal to four chloride radii (one radius from each corner chloride and one diameter—which equals two radii—from the chloride ion in the center of the face), so $d = 4r$. From the Pythagorean theorem, we have:

$$a^2 + a^2 = d^2$$

which yields:

$$(0.514\ \text{nm})^2 + (0.514\ \text{nm})^2 = (4r)^2 = 16r^2$$

Solving this gives:

$$r = \sqrt{\frac{(0.514\ \text{nm})^2 + (0.514\ \text{nm})^2}{16}} = 0.182\ \text{nm}\ (1.82\ \text{Å})\ \text{for a}\ Cl^-\ \text{radius.}$$

Exercise 5.4.6

The edge length of the unit cell of KCl (NaCl-like structure, FCC) is 6.28 Å. Assuming anion-cation contact along the cell edge, calculate the radius of the potassium ion. The radius of the chloride ion is 1.82 Å.

Answer

The radius of the potassium ion is 1.33 Å.

It is important to realize that values for ionic radii calculated from the edge lengths of unit cells depend on numerous assumptions, such as a perfect spherical shape for ions, which are approximations at best. Hence, such calculated values are themselves approximate and comparisons cannot be pushed too far. Nevertheless, this method has proved useful for calculating ionic radii from experimental measurements such as X-ray crystallographic determinations.

5.4.6: X-Ray Crystallography

The size of the unit cell and the arrangement of atoms in a crystal may be determined from measurements of the *diffraction* of X-rays by the crystal, termed X-ray crystallography. Diffraction is the change in the direction of travel experienced by an electromagnetic wave when it encounters a physical barrier whose dimensions are comparable to those of the wavelength of the light. X-rays are electromagnetic radiation with wavelengths about as long as the distance between neighboring atoms in crystals (on the order of a few Å).

When a beam of monochromatic X-rays strikes a crystal, its rays are scattered in all directions by the atoms within the crystal. When scattered waves traveling in the same direction encounter one another, they undergo *interference*, a process by which the waves combine to yield either an increase or a decrease in amplitude (intensity) depending upon the extent to which the combining waves' maxima are separated (Figure 5.4.18).

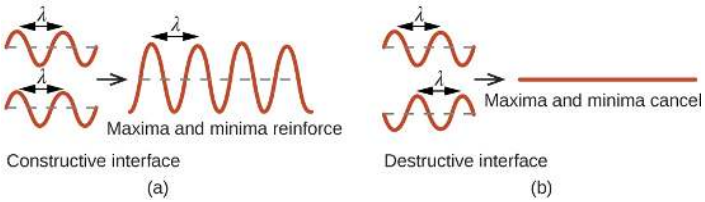


Figure 5.4.18: Light waves occupying the same space experience interference, combining to yield waves of greater (a) or lesser (b) intensity, depending upon the separation of their maxima and minima.

A pair of images is shown that has four sections. In the first section, two sinusoidal waves are shown, one drawn above the other, and a section from the top of one curve to the top of the next curve is labeled "lambda." The curves align with one another. The phrase below this reads "Constructive interference." A right facing arrow leads from the first section to the second, which shows one larger sinusoidal curve that has higher and lower peaks and troughs. A section from the top of one curve to the top of the next curve is labeled "lambda" and the phrase below this reads "Maxima and minima reinforce." In the second section, two sinusoidal waves are shown, one drawn above the other, and a section from the top of one curve to the top of the next curve is labeled "lambda." The curves do not align with one another. The phrase below this reads "Destructive interference." A right facing arrow leads from the first section to the second, which shows one flat line. The phrase below this reads "Maxima and minima cancel."

When X-rays of a certain wavelength, λ, are scattered by atoms in adjacent crystal planes separated by a distance, d, they may undergo constructive interference when the difference between the distances traveled by the two waves prior to their combination is an integer factor, n, of the wavelength. This condition is satisfied when the angle of the diffracted beam, θ, is related to the wavelength and interatomic distance by the equation:

$$n\lambda = 2d\sin\theta \tag{5.4.1}$$

This relation is known as the Bragg equation in honor of W. H. Bragg, the English physicist who first explained this phenomenon. Figure 5.4.18 illustrates two examples of diffracted waves from the same two crystal planes. The figure on the left depicts waves diffracted at the Bragg angle, resulting in constructive interference, while that on the right shows diffraction and a different angle that does not satisfy the Bragg condition, resulting in destructive interference.

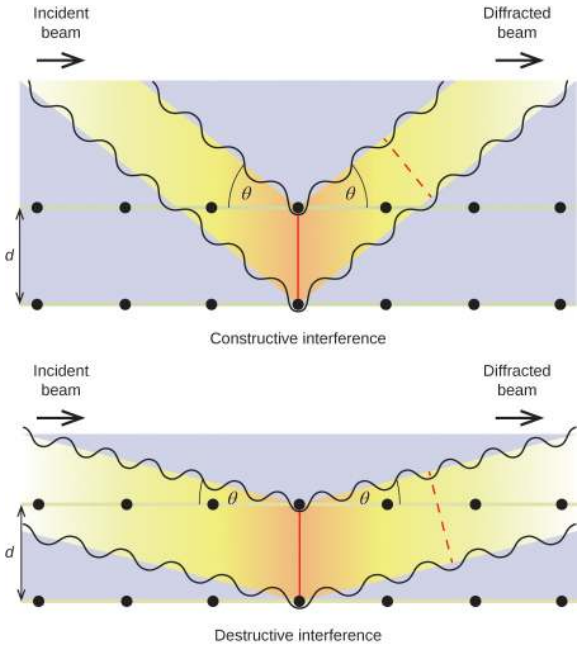


Figure 5.4.19: The diffraction of X-rays scattered by the atoms within a crystal permits the determination of the distance between the atoms. The top image depicts constructive interference between two scattered waves and a resultant diffracted wave of high intensity. The bottom image depicts destructive interference and a low intensity diffracted wave.

Two similar figures are shown. The first figure, labeled “Constructive Interference,” shows two horizontal rows of seven black dots with a line passing through them. The fourth dots of each row have a vertical line connecting them. The distance between these rows is labeled “d.” A beam labeled “Incident beam” descends at an angle labeled “theta” until it hits the line connecting the fourth dots, after which a diffracted beam ascends at the same angle “theta.” A dotted line is drawn across the diffracted beam. The second figure, labeled “Destructive interference,” is very similar, except that the angles “theta” are far more acute, making the slopes of the beams more shallow.

An X-ray diffractometer, such as the one illustrated in Figure 5.4.20, may be used to measure the angles at which X-rays are diffracted when interacting with a crystal as described earlier. From such measurements, the Bragg equation may be used to compute distances between atoms as demonstrated in the following example exercise.

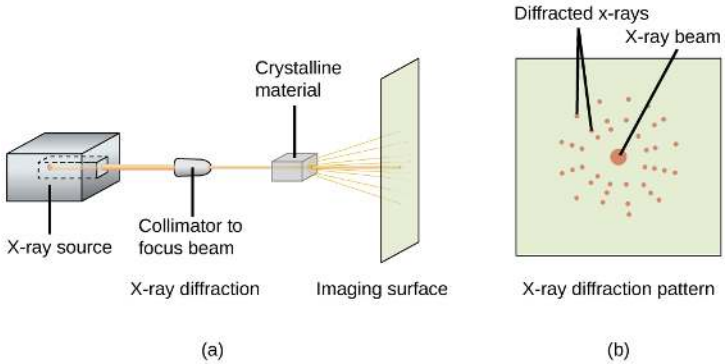


Figure 5.4.20: (a) In a diffractometer, a beam of X-rays strikes a crystalline material, producing (b) an X-ray diffraction pattern that can be analyzed to determine the crystal structure.

A diagram, labeled “a” shows a cube on the left with a channel bored into its right side labeled “X dash ray source.” A beam is leaving from this channel and traveling in a horizontal line toward an oval-shaped, short tube, labeled “Collimator to focus beam” and “X dash ray diffraction,” where it passes through a cube labeled “Crystalline material” and scatters onto a vertical sheet labeled “Imaging surface.” A second diagram, labeled “b,” shows a square sheet with a large dot in the center labeled “X dash ray beam,” that is surrounded by smaller dots arranged in rings and labeled “Diffracted X dash rays.”

Example 5.4.6: Using the Bragg Equation

In a diffractometer, X-rays with a wavelength of 0.1315 nm were used to produce a diffraction pattern for copper. The first order diffraction ($n = 1$) occurred at an angle $\theta = 25.25°$. Determine the spacing between the diffracting planes in copper.

https://chem.libretexts.org/@go/page/362305

Solution

The distance between the planes is found by solving the Bragg equation (Equation 5.4.1) for d.

This gives

$$d = \frac{n\lambda}{2\sin\theta} = \frac{1(0.1315\ \text{nm})}{2\sin(25.25°)} = 0.154\ \text{nm}$$

? Exercise 5.4.6

A crystal with spacing between planes equal to 0.394 nm diffracts X-rays with a wavelength of 0.147 nm. What is the angle for the first order diffraction?

Answer

21.9°

X-ray Crystallographer Rosalind Franklin

The discovery of the structure of DNA in 1953 by Francis Crick and James Watson is one of the great achievements in the history of science. They were awarded the 1962 Nobel Prize in Physiology or Medicine, along with Maurice Wilkins, who provided experimental proof of DNA's structure. British chemist Rosalind Franklin made invaluable contributions to this monumental achievement through her work in measuring X-ray diffraction images of DNA. Early in her career, Franklin's research on the structure of coals proved helpful to the British war effort. After shifting her focus to biological systems in the early 1950s, Franklin and doctoral student Raymond Gosling discovered that DNA consists of two forms: a long, thin fiber formed when wet (type "B") and a short, wide fiber formed when dried (type "A"). Her X-ray diffraction images of DNA provided the crucial information that allowed Watson and Crick to confirm that DNA forms a double helix, and to determine details of its size and structure. Franklin also conducted pioneering research on viruses and the RNA that contains their genetic information, uncovering new information that radically changed the body of knowledge in the field. After developing ovarian cancer, Franklin continued to work until her death in 1958 at age 37. Among many posthumous recognitions of her work, the Chicago Medical School of Finch University of Health Sciences changed its name to the Rosalind Franklin University of Medicine and Science in 2004, and adopted an image of her famous X-ray diffraction image of DNA as its official university logo.

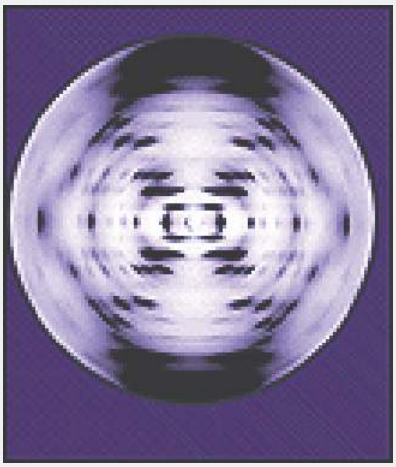


Figure 5.4.7.This illustration shows an X-ray diffraction image similar to the one Franklin found in her research. (credit: National Institutes of Health)

5.4.7: Key Concepts and Summary

The structures of crystalline metals and simple ionic compounds can be described in terms of packing of spheres. Metal atoms can pack in hexagonal closest-packed structures, cubic closest-packed structures, body-centered structures, and simple cubic structures.

The anions in simple ionic structures commonly adopt one of these structures, and the cations occupy the spaces remaining between the anions. Small cations usually occupy tetrahedral holes in a closest-packed array of anions. Larger cations usually occupy octahedral holes. Still larger cations can occupy cubic holes in a simple cubic array of anions. The structure of a solid can be described by indicating the size and shape of a unit cell and the contents of the cell. The type of structure and dimensions of the unit cell can be determined by X-ray diffraction measurements.

Glossary

body-centered cubic (BCC) solid
crystalline structure that has a cubic unit cell with lattice points at the corners and in the center of the cell

body-centered cubic unit cell
simplest repeating unit of a body-centered cubic crystal; it is a cube containing lattice points at each corner and in the center of the cube

Bragg equation
equation that relates the angles at which X-rays are diffracted by the atoms within a crystal

coordination number
number of atoms closest to any given atom in a crystal or to the central metal atom in a complex

cubic closest packing (CCP)
crystalline structure in which planes of closely packed atoms or ions are stacked as a series of three alternating layers of different relative orientations (ABC)

diffraction
redirection of electromagnetic radiation that occurs when it encounters a physical barrier of appropriate dimensions

face-centered cubic (FCC) solid
crystalline structure consisting of a cubic unit cell with lattice points on the corners and in the center of each face

face-centered cubic unit cell
simplest repeating unit of a face-centered cubic crystal; it is a cube containing lattice points at each corner and in the center of each face

hexagonal closest packing (HCP)
crystalline structure in which close packed layers of atoms or ions are stacked as a series of two alternating layers of different relative orientations (AB)

hole
(also, interstice) space between atoms within a crystal

isomorphous
possessing the same crystalline structure

octahedral hole
open space in a crystal at the center of six particles located at the corners of an octahedron

simple cubic unit cell
(also, primitive cubic unit cell) unit cell in the simple cubic structure

simple cubic structure
crystalline structure with a cubic unit cell with lattice points only at the corners

space lattice

all points within a crystal that have identical environments

tetrahedral hole

tetrahedral space formed by four atoms or ions in a crystal

unit cell

smallest portion of a space lattice that is repeated in three dimensions to form the entire lattice

X-ray crystallography

experimental technique for determining distances between atoms in a crystal by measuring the angles at which X-rays are diffracted when passing through the crystal

Paul Flowers (University of North Carolina - Pembroke), Klaus Theopold (University of Delaware) and Richard Langley (Stephen F. Austin State University) with contributing authors. Textbook content produced by OpenStax College is licensed under a Creative Commons Attribution License 4.0 license. Download for free at http://cnx.org/contents/85abf193-2bd...a7ac8df6@9.110).

This page titled 5.4: Lattice Structures in Crystalline Solids is shared under a CC BY license and was authored, remixed, and/or curated by OpenStax.

- **10.7: Lattice Structures in Crystalline Solids** by OpenStax is licensed CC BY 4.0. Original source: https://openstax.org/details/books/chemistry-2e.

5.5: Bonding in Metals and Semiconductors

In the early 1900's, Paul Drüde came up with the "sea of electrons" metallic bonding theory by modeling metals as a mixture of atomic cores (atomic cores = positive nuclei + inner shell of electrons) and valence electrons. Metallic bonds occur among metal atoms. Whereas ionic bonds join metals to non-metals, *metallic bonding joins a bulk of metal atoms*. A sheet of aluminum foil and a copper wire are both places where you can see metallic bonding in action.

Metals tend to have high melting points and boiling points suggesting strong bonds between the atoms. Even a soft metal like sodium (melting point 97.8°C) melts at a considerably higher temperature than the element (neon) which precedes it in the Periodic Table. Sodium has the electronic structure $1s^2 2s^2 2p^6 3s^1$. When sodium atoms come together, the electron in the 3s atomic orbital of one sodium atom shares space with the corresponding electron on a neighboring atom to form a molecular orbital - in much the same sort of way that a covalent bond is formed.

The difference, however, is that each sodium atom is being touched by eight other sodium atoms - and the sharing occurs between the central atom and the 3s orbitals on all of the eight other atoms. Each of these eight is in turn being touched by eight sodium atoms, which in turn are touched by eight atoms - and so on and so on, until you have taken in all the atoms in that lump of sodium. *All* of the 3s orbitals on all of the atoms overlap to give a vast number of molecular orbitals that extend over the whole piece of metal. There have to be huge numbers of molecular orbitals, of course, because any orbital can only hold two electrons.

The electrons can move freely within these molecular orbitals, and so each electron becomes detached from its parent atom. The electrons are said to be delocalized. The metal is held together by the strong forces of attraction between the positive nuclei and the delocalized electrons (Figure **5.5.1**).

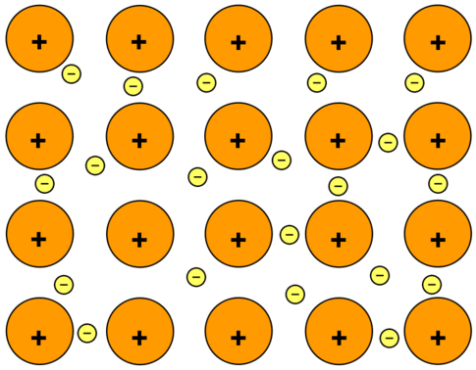


Figure **5.5.1**: Metallic Bonding: The Electron Sea Model: Positive atomic nuclei (orange circles) surrounded by a sea of delocalized electrons (yellow circles).

This is sometimes described as "an array of positive ions in a sea of electrons". If you are going to use this view, beware! Is a metal made up of atoms or ions? It is made of atoms**.** Each positive center in the diagram represents all the rest of the atom apart from the outer electron, but that electron has not been lost - it may no longer have an attachment to a particular atom, but it's still there in the structure. Sodium metal is therefore written as **Na**, not $\mathbf{Na^+}$.

✔ Example 5.5.1: Metallic bonding in magnesium

Use the sea of electrons model to explain why Magnesium has a higher melting point (650 °C) than sodium (97.79 °C).

Solution

If you work through the same argument above for sodium with magnesium, you end up with stronger bonds and hence a higher melting point.

Magnesium has the outer electronic structure $3s^2$. Both of these electrons become delocalized, so the "sea" has twice the electron density as it does in sodium. The remaining "ions" also have twice the charge (if you are going to use this particular view of the metal bond) and so there will be more attraction between "ions" and "sea".

More realistically, each magnesium atom has 12 protons in the nucleus compared with sodium's 11. In both cases, the nucleus is screened from the delocalized electrons by the same number of inner electrons - the 10 electrons in the $1s^2$ $2s^2$ $2p^6$ orbitals.

That means that there will be a net pull from the magnesium nucleus of 2+, but only 1+ from the sodium nucleus.

So not only will there be a greater number of delocalized electrons in magnesium, but there will also be a greater attraction for them from the magnesium nuclei. Magnesium atoms also have a slightly smaller radius than sodium atoms, and so the delocalized electrons are closer to the nuclei. Each magnesium atom also has twelve near neighbors rather than sodium's eight. Both of these factors increase the strength of the bond still further.

Note: Transition metals tend to have particularly high melting points and boiling points. The reason is that they can involve the 3d electrons in the delocalization as well as the 4s. The more electrons you can involve, the stronger the attractions tend to be.

Bulk properties of metals

Metals have several qualities that are unique, such as the ability to conduct electricity and heat, a low ionization energy, and a low electronegativity (so they will give up electrons easily to form cations). Their physical properties include a lustrous (shiny) appearance, and they are malleable and ductile. Metals have a crystal structure but can be easily deformed. In this model, the valence electrons are free, delocalized, mobile, and not associated with any particular atom. This model may account for:

- **Conductivity**: Since the electrons are free, if electrons from an outside source were pushed into a metal wire at one end (Figure 5.5.2), the electrons would move through the wire and come out at the other end at the same rate (conductivity is the movement of charge).

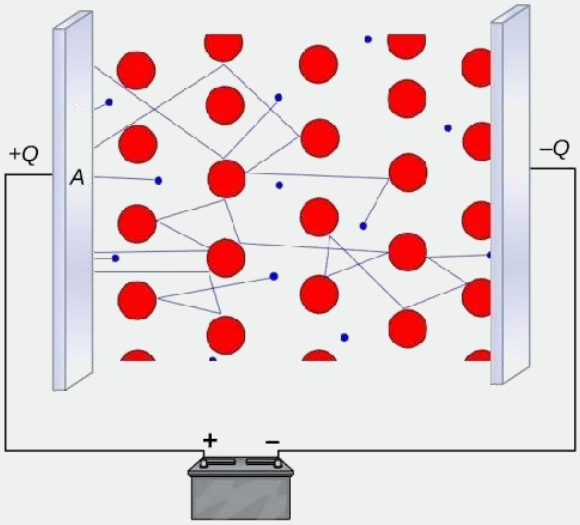


Figure 5.5.2: The "sea of electrons" is free to flow about the crystal of positive metal ions. These flowing electron can conduct electrical change when an electric field is applied (e.g., a battery). (CC-BY-SA; OpenStax and Rafaelgarcia).

- **Malleability** and **Ductility**: The electron-sea model of metals not only explains their electrical properties but their malleability and ductility as well. The sea of electrons surrounding the protons acts like a cushion, and so when the metal is hammered on, for instance, the overall composition of the structure of the metal is not harmed or changed. The protons may be rearranged but the sea of electrons with adjust to the new formation of protons and keep the metal intact. When one layer of ions in an electron sea moves along one space with respect to the layer below it, the crystal structure does not fracture but is only deformed (Figure 5.5.3).



Figure 5.5.3: Malleability of metals originate from each of moving layer of atoms with respect to each other. The final situation is much the same as the initial. Thus if we hit a metal with a hammer, the crystals do not shatter, but merely change their shape, This is very different from the behavior of ionic crystals.

- **Heat capacity**: This is explained by the ability of free electrons to move about the solid.
- **Luster**: The free electrons can absorb photons in the "sea," so metals are opaque-looking. Electrons on the surface can bounce back light at the same frequency that the light hits the surface, therefore the metal appears to be shiny.

> However, these observations are only qualitative, and not quantitative, so they cannot be tested. The "Sea of Electrons" theory stands today only as an oversimplified model of how metallic bonding works.

In a molten metal, the metallic bond is still present, although the ordered structure has been broken down. The metallic bond is not fully broken until the metal boils. That means that boiling point is actually a better guide to the strength of the metallic bond than melting point is. On melting, the bond is loosened, not broken. The strength of a metallic bond depends on three things:

1. The number of electrons that become delocalized from the metal
2. The charge of the cation (metal).
3. The size of the cation.

A **strong** metallic bond will be the result of more delocalized electrons, which causes the effective nuclear charge on electrons on the cation to increase, in effect making the size of the cation smaller. Metallic bonds are strong and require a great deal of energy to break, and therefore **metals have high melting and boiling points.** A metallic bonding theory must explain how so much bonding can occur with such few electrons (since metals are located on the left side of the periodic table and do not have many electrons in their valence shells). The theory must also account for all of a metal's unique chemical and physical properties.

Expanding the Range of Bonding Possible

Previously, we argued that bonding between atoms can classified as range of possible bonding between **ionic bonds** (fully charge transfer) and **covalent bonds** (fully shared electrons). When two atoms of slightly differing electronegativities come together to form a covalent bond, one atom attracts the electrons more than the other; this is called a polar covalent bond. However, simple “ionic” and “covalent” bonding are idealized concepts and most bonds exist on a two-dimensional continuum described by the van Arkel-Ketelaar Triangle (Figure **5.5.4**).

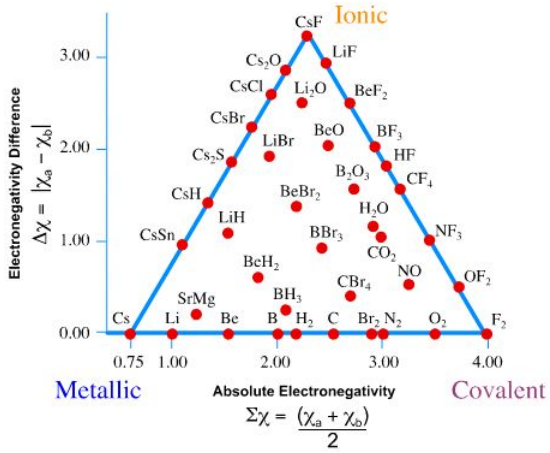


Figure **5.5.4**: van Arkel-Ketelaar Triangle plots the difference in electronegativity ($\Delta\chi$) and the average electronegativity in a bond ($\sum\chi$). the top region is where bonds are mostly ionic, the lower left region is where bonding is metallic, and the lower right region is where the bonding is covalent.

Bond triangles or **van Arkel–Ketelaar** triangles (named after Anton Eduard van Arkel and J. A. A. Ketelaar) are triangles used for showing different compounds in varying degrees of ionic, metallic and covalent bonding. In 1941 van Arkel recognized three extreme materials and associated bonding types. Using 36 main group elements, such as metals, metalloids and non-metals, he placed ionic, metallic and covalent bonds on the corners of an equilateral triangle, as well as suggested intermediate species. The bond triangle shows that chemical bonds are not just particular bonds of a specific type. Rather, bond types are interconnected and different compounds have varying degrees of different bonding character (for example, polar covalent bonds).



Video 5.5.1: What is the van Arkel-Ketelaar Triangle of Bonding?

Using electronegativity - two compound average electronegativity on x-axis of Figure 5.5.4.

$$\sum\chi = \frac{\chi_A + \chi_B}{2} \tag{5.5.1}$$

and electronegativity difference on y-axis,

$$\Delta\chi = |\chi_A - \chi_B| \tag{5.5.2}$$

we can rate the dominant bond between the compounds. On the right side of Figure 5.5.4 (from ionic to covalent) should be compounds with varying difference in electronegativity. The compounds with equal electronegativity, such as Cl_2 (chlorine) are placed in the covalent corner, while the ionic corner has compounds with large electronegativity difference, such as NaCl (table salt). The bottom side (from metallic to covalent) contains compounds with varying degree of directionality in the bond. At one extreme is metallic bonds with delocalized bonding and at the other are covalent bonds in which the orbitals overlap in a particular direction. The left side (from ionic to metallic) is meant for delocalized bonds with varying electronegativity difference.

The Three Extremes in bonding

In general:

- Metallic bonds have low $\Delta\chi$ **and** low average $\sum\chi$.
- Ionic bonds have moderate-to-high $\Delta\chi$ and moderate values of average $\sum\chi$.
- Covalent bonds have moderate to high average $\sum\chi$ and can exist with moderately low $\Delta\chi$.

Example 5.5.2

Use the tables of electronegativities (Table A2) and Figure 5.5.4 to estimate the following values

- difference in electronegativity ($\Delta\chi$)
- average electronegativity in a bond ($\sum\chi$)
- percent ionic character
- likely bond type

for the selected compounds:

a. AsH (e.g., in arsine AsH)
b. SrLi
c. KF.

Solution

a: AsH

- The electronegativity of As is 2.18

- The electronegativity of **H** is 2.22

Using Equations 5.5.1 and 5.5.2:

$$\begin{aligned}\sum\chi &= \frac{\chi_A + \chi_B}{2} \\ &= \frac{2.18 + 2.22}{2} \\ &= 2.2\end{aligned}$$

$$\begin{aligned}\Delta\chi &= \chi_A - \chi_B \\ &= 2.18 - 2.22 \\ &= 0.04\end{aligned}$$

- From Figure 5.5.4, the bond is fairly nonpolar and has a low ionic character (10% or less)
- The bonding is in the middle of a covalent bond and a metallic bond

b: **SrLi**

- The electronegativity of **Sr** is 0.95
- The electronegativity of **Li** is 0.98

Using Equations 5.5.1 and 5.5.2:

$$\begin{aligned}\sum\chi &= \frac{\chi_A + \chi_B}{2} \\ &= \frac{0.95 + 0.98}{2} \\ &= 0.965\end{aligned}$$

$$\begin{aligned}\Delta\chi &= \chi_A - \chi_B \\ &= 0.98 - 0.95 \\ &= 0.025\end{aligned}$$

- From Figure 5.5.4, the bond is fairly nonpolar and has a low ionic character (~3% or less)
- The bonding is likely metallic.

c: **KF**

- The electronegativity of **K** is 0.82
- The electronegativity of **F** is 3.98

Using Equations 5.5.1 and 5.5.2:

$$\begin{aligned}\sum\chi &= \frac{\chi_A + \chi_B}{2} \\ &= \frac{0.82 + 3.98}{2} \\ &= 2.4\end{aligned}$$

$$\begin{aligned}\Delta\chi &= \chi_A - \chi_B \\ &= |0.82 - 3.98| \\ &= 3.16\end{aligned}$$

- From Figure 5.5.4, the bond is fairly polar and has a high ionic character (~75%)
- The bonding is likely ionic.

? Exercise 5.5.2

Contrast the bonding of **NaCl** and silicon tetrafluoride.

Answer

> **NaCl** is an ionic crystal structure, and an electrolyte when dissolved in water; $\Delta\chi = 1.58$, average $\sum\chi = 1.79$, while silicon tetrafluoride is covalent (molecular, non-polar gas; $\Delta\chi = 2.08$, average $\sum\chi = 2.94$.

Contributors and Attributions

- Jim Clark (Chemguide.co.uk)
- Daniel James Berger
- Wikipedia
- Ed Vitz (Kutztown University), John W. Moore (UW-Madison), Justin Shorb (Hope College), Xavier Prat-Resina (University of Minnesota Rochester), Tim Wendorff, and Adam Hahn.

5.5: Bonding in Metals and Semiconductors is shared under a not declared license and was authored, remixed, and/or curated by LibreTexts.

- **Metallic Bonding** by Jim Clark is licensed CC BY-NC 4.0.

5.6: Liquids and Solids (Exercises)

5.6.1: 10.1: Intermolecular Forces

5.6.1.1: Q10.1.1

In terms of their bulk properties, how do liquids and solids differ? How are they similar?

5.6.1.2: S10.1.1

Liquids and solids are similar in that they are matter composed of atoms, ions, or molecules. They are incompressible and have similar densities that are both much larger than those of gases. They are different in that liquids have no fixed shape, and solids are rigid.

5.6.1.3: Q10.1.2

In terms of the kinetic molecular theory, in what ways are liquids similar to solids? In what ways are liquids different from solids?

5.6.1.4: Q10.1.3

In terms of the kinetic molecular theory, in what ways are liquids similar to gases? In what ways are liquids different from gases?

5.6.1.5: S10.1.3

They are similar in that the atoms or molecules are free to move from one position to another. They differ in that the particles of a liquid are confined to the shape of the vessel in which they are placed. In contrast, a gas will expand without limit to fill the space into which it is placed.

5.6.1.6: Q10.1.4

Explain why liquids assume the shape of any container into which they are poured, whereas solids are rigid and retain their shape.

5.6.1.7: Q10.1.5

What is the evidence that all neutral atoms and molecules exert attractive forces on each other?

5.6.1.8: S10.1.5

All atoms and molecules will condense into a liquid or solid in which the attractive forces exceed the kinetic energy of the molecules, at sufficiently low temperature.

5.6.1.9: Q10.1.6

Open the PhET States of Matter Simulation to answer the following questions:

a. Select the Solid, Liquid, Gas tab. Explore by selecting different substances, heating and cooling the systems, and changing the state. What similarities do you notice between the four substances for each phase (solid, liquid, gas)? What differences do you notice?
b. For each substance, select each of the states and record the given temperatures. How do the given temperatures for each state correlate with the strengths of their intermolecular attractions? Explain.
c. Select the Interaction Potential tab, and use the default neon atoms. Move the Ne atom on the right and observe how the potential energy changes. Select the Total Force button, and move the Ne atom as before. When is the total force on each atom attractive and large enough to matter? Then select the Component Forces button, and move the Ne atom. When do the attractive (van der Waals) and repulsive (electron overlap) forces balance? How does this relate to the potential energy versus the distance between atoms graph? Explain.

5.6.1.10: Q10.1.7

Define the following and give an example of each:

a. dispersion force
b. dipole-dipole attraction

c. hydrogen bond

5.6.1.11: S10.1.7

a. Dispersion forces occur as an atom develops a temporary dipole moment when its electrons are distributed asymmetrically about the nucleus. This structure is more prevalent in large atoms such as argon or radon. A second atom can then be distorted by the appearance of the dipole in the first atom. The electrons of the second atom are attracted toward the positive end of the first atom, which sets up a dipole in the second atom. The net result is rapidly fluctuating, temporary dipoles that attract one another (example: Ar).
b. A dipole-dipole attraction is a force that results from an electrostatic attraction of the positive end of one polar molecule for the negative end of another polar molecule (example: ICI molecules attract one another by dipole-dipole interaction).
c. Hydrogen bonds form whenever a hydrogen atom is bonded to one of the more electronegative atoms, such as a fluorine, oxygen, nitrogen, or chlorine atom. The electrostatic attraction between the partially positive hydrogen atom in one molecule and the partially negative atom in another molecule gives rise to a strong dipole-dipole interaction called a hydrogen bond (example: $\mathbf{HF\cdots HF}$).

5.6.1.12: Q10.1.8

The types of intermolecular forces in a substance are identical whether it is a solid, a liquid, or a gas. Why then does a substance change phase from a gas to a liquid or to a solid?

5.6.1.13: Q10.1.9

Why do the boiling points of the noble gases increase in the order He < Ne < Ar < Kr < Xe?

5.6.1.14: S10.1.9

The London forces typically increase as the number of electrons increase.

5.6.1.15: Q10.1.10

Neon and HF have approximately the same molecular masses.

a. Explain why the boiling points of Neon and HF differ.
b. Compare the change in the boiling points of Ne, Ar, Kr, and Xe with the change of the boiling points of HF, HCl, HBr, and HI, and explain the difference between the changes with increasing atomic or molecular mass.

5.6.1.16: Q10.1.11

Arrange each of the following sets of compounds in order of increasing boiling point temperature:

a. HCl, H_2O, SiH_4
b. F_2, Cl_2, Br_2
c. CH_4, C_2H_6, C_3H_8
d. O_2, NO, N_2

5.6.1.17: S10.1.11

(a) SiH_4 < HCl < H_2O; (b) F_2 < Cl_2 < Br_2; (c) CH_4 < C_2H_6 < C_3H_8; (d) N_2 < O_2 < NO

5.6.1.18: Q10.1.12

The molecular mass of butanol, C_4H_9OH, is 74.14; that of ethylene glycol, $CH_2(OH)CH_2OH$, is 62.08, yet their boiling points are 117.2 °C and 174 °C, respectively. Explain the reason for the difference.

5.6.1.19: Q10.1.13

On the basis of intermolecular attractions, explain the differences in the boiling points of *n*–butane (−1 °C) and chloroethane (12 °C), which have similar molar masses.

5.6.1.20: S10.1.13

Only rather small dipole-dipole interactions from C-H bonds are available to hold *n*-butane in the liquid state. Chloroethane, however, has rather large dipole interactions because of the Cl-C bond; the interaction is therefore stronger, leading to a higher boiling point.

5.6.1.21: Q10.1.14

On the basis of dipole moments and/or hydrogen bonding, explain in a qualitative way the differences in the boiling points of acetone (56.2 °C) and 1-propanol (97.4 °C), which have similar molar masses.

5.6.1.22: Q10.1.15

The melting point of $H_2O(s)$ is 0 °C. Would you expect the melting point of $H_2S(s)$ to be −85 °C, 0 °C, or 185 °C? Explain your answer.

5.6.1.23: S10.1.15

−85 °C. Water has stronger hydrogen bonds so it melts at a higher temperature.

5.6.1.24: Q10.1.16

Silane (SiH_4), phosphine (PH_3), and hydrogen sulfide (H_2S) melt at −185 °C, −133 °C, and −85 °C, respectively. What does this suggest about the polar character and intermolecular attractions of the three compounds?

5.6.1.25: Q10.1.17

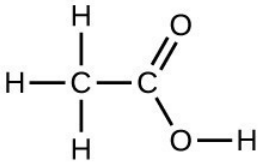
Explain why a hydrogen bond between two water molecules is weaker than a hydrogen bond between two hydrogen fluoride molecules.

5.6.1.26: S10.1.17

The hydrogen bond between two hydrogen fluoride molecules is stronger than that between two water molecules because the electronegativity of F is greater than that of O. Consequently, the partial negative charge on F is greater than that on O. The hydrogen bond between the partially positive H and the larger partially negative F will be stronger than that formed between H and O.

5.6.1.27: Q10.1.18

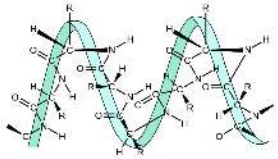
Under certain conditions, molecules of acetic acid, CH_3COOH, form “dimers,” pairs of acetic acid molecules held together by strong intermolecular attractions:



Draw a dimer of acetic acid, showing how two CH_3COOH molecules are held together, and stating the type of IMF that is responsible.

5.6.1.28: Q10.1.19

Proteins are chains of amino acids that can form in a variety of arrangements, one of which is a helix. What kind of IMF is responsible for holding the protein strand in this shape? On the protein image, show the locations of the IMFs that hold the protein together:



5.6.1.29: S10.1.19

H-bonding is the principle IMF holding the DNA strands together. The H-bonding is between the $\mathbf{N-H}$ and $\mathbf{C=O}$.

5.6.1.30: Q10.1.20

The density of liquid NH_3 is 0.64 g/mL; the density of gaseous NH_3 at STP is 0.0007 g/mL. Explain the difference between the densities of these two phases.

5.6.1.31: Q10.1.21

Identify the intermolecular forces present in the following solids:

a. CH_3CH_2OH
b. $CH_3CH_2CH_3$
c. CH_3CH_2Cl

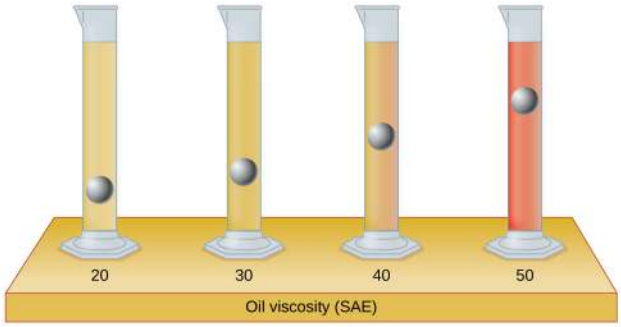
5.6.1.32: S10.1.21

(a) hydrogen bonding and dispersion forces; (b) dispersion forces; (c) dipole-dipole attraction and dispersion forces

5.6.2: 10.2: Properties of Liquids

5.6.2.1: Q10.2.1

The test tubes shown here contain equal amounts of the specified motor oils. Identical metal spheres were dropped at the same time into each of the tubes, and a brief moment later, the spheres had fallen to the heights indicated in the illustration. Rank the motor oils in order of increasing viscosity, and explain your reasoning:



5.6.2.2: Q10.2.2

Although steel is denser than water, a steel needle or paper clip placed carefully lengthwise on the surface of still water can be made to float. Explain at a molecular level how this is possible:



(credit: Cory Zanker)

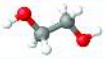
5.6.2.3: S10.2.2

The water molecules have strong intermolecular forces of hydrogen bonding. The water molecules are thus attracted strongly to one another and exhibit a relatively large surface tension, forming a type of “skin” at its surface. This skin can support a bug or

paper clip if gently placed on the water.

5.6.2.4: Q10.2.3

The surface tension and viscosity values for diethyl ether, acetone, ethanol, and ethylene glycol are shown here.

Compound	Molecule	Surface Tension (mN/m)	Viscosity (mPa s)
diethyl ether $C_2H_5OC_2H_5$		17	0.22
acetone $C_2H_5OC_2H_5$		23	0.31
ethanol C_2H_5OH		22	1.07
ethylene glycol $CH_2(OH)CH_2(OH)$		48	16.1

a. Explain their differences in viscosity in terms of the size and shape of their molecules and their IMFs.
b. Explain their differences in surface tension in terms of the size and shape of their molecules and their IMFs:

5.6.2.5: Q10.2.4

You may have heard someone use the figure of speech “slower than molasses in winter” to describe a process that occurs slowly. Explain why this is an apt idiom, using concepts of molecular size and shape, molecular interactions, and the effect of changing temperature.

5.6.2.6: S10.2.4

Temperature has an effect on intermolecular forces: the higher the temperature, the greater the kinetic energies of the molecules and the greater the extent to which their intermolecular forces are overcome, and so the more fluid (less viscous) the liquid; the lower the temperature, the lesser the intermolecular forces are overcome, and so the less viscous the liquid.

5.6.2.7: Q10.2.5

It is often recommended that you let your car engine run idle to warm up before driving, especially on cold winter days. While the benefit of prolonged idling is dubious, it is certainly true that a warm engine is more fuel efficient than a cold one. Explain the reason for this.

5.6.2.8: Q10.2.6

The surface tension and viscosity of water at several different temperatures are given in this table.

Water	Surface Tension (mN/m)	Viscosity (mPa s)
0 °C	75.6	1.79
20 °C	72.8	1.00
60 °C	66.2	0.47
100 °C	58.9	0.28

a. As temperature increases, what happens to the surface tension of water? Explain why this occurs, in terms of molecular interactions and the effect of changing temperature.
b. As temperature increases, what happens to the viscosity of water? Explain why this occurs, in terms of molecular interactions and the effect of changing temperature.

5.6.2.9: S10.2.6

(a) As the water reaches higher temperatures, the increased kinetic energies of its molecules are more effective in overcoming hydrogen bonding, and so its surface tension decreases. Surface tension and intermolecular forces are directly related. (b) The same

trend in viscosity is seen as in surface tension, and for the same reason.

5.6.2.10: Q10.2.7

At 25 °C, how high will water rise in a glass capillary tube with an inner diameter of 0.63 mm? Refer to Example for the required information.

5.6.2.11: Q10.2.8

Water rises in a glass capillary tube to a height of 17 cm. What is the diameter of the capillary tube?

5.6.2.12: S10.2.8

9.5×10^{-5} m

5.6.3: 10.3: Phase Transitions

5.6.3.1: Q10.3.1

Heat is added to boiling water. Explain why the temperature of the boiling water does not change. What does change?

5.6.3.2: Q10.3.2

Heat is added to ice at 0 °C. Explain why the temperature of the ice does not change. What does change?

5.6.3.3: S10.3.2

The heat is absorbed by the ice, providing the energy required to partially overcome intermolecular attractive forces in the solid and causing a phase transition to liquid water. The solution remains at 0 °C until all the ice is melted. Only the amount of water existing as ice changes until the ice disappears. Then the temperature of the water can rise.

5.6.3.4: Q10.3.3

What feature characterizes the dynamic equilibrium between a liquid and its vapor in a closed container?

5.6.3.5: Q10.3.4

Identify two common observations indicating some liquids have sufficient vapor pressures to noticeably evaporate?

5.6.3.6: S10.3.4

We can see the amount of liquid in an open container decrease and we can smell the vapor of some liquids.

5.6.3.7: Q10.3.5

Identify two common observations indicating some solids, such as dry ice and mothballs, have vapor pressures sufficient to sublime?

5.6.3.8: Q10.3.6

What is the relationship between the intermolecular forces in a liquid and its vapor pressure?

5.6.3.9: S10.3.7

The vapor pressure of a liquid decreases as the strength of its intermolecular forces increases.

5.6.3.10: Q10.3.7

What is the relationship between the intermolecular forces in a solid and its melting temperature?

5.6.3.11: Q10.3.8

Why does spilled gasoline evaporate more rapidly on a hot day than on a cold day?

5.6.3.12: S10.3.8

As the temperature increases, the average kinetic energy of the molecules of gasoline increases and so a greater fraction of molecules have sufficient energy to escape from the liquid than at lower temperatures.

5.6.3.13: Q10.3.9

Carbon tetrachloride, CCl_4, was once used as a dry cleaning solvent, but is no longer used because it is carcinogenic. At 57.8 °C, the vapor pressure of CCl_4 is 54.0 kPa, and its enthalpy of vaporization is 33.05 kJ/mol. Use this information to estimate the normal boiling point for CCl_4.

5.6.3.14: Q10.3.10

When is the boiling point of a liquid equal to its normal boiling point?

5.6.3.15: S10.3.10

When the pressure of gas above the liquid is exactly 1 atm

5.6.3.16: Q10.3.11

How does the boiling of a liquid differ from its evaporation?

5.6.3.17: Q10.3.12

Use the information in Figure to estimate the boiling point of water in Denver when the atmospheric pressure is 83.3 kPa.

5.6.3.18: S10.3.12

approximately 95 °C

5.6.3.19: Q10.3.13

A syringe at a temperature of 20 °C is filled with liquid ether in such a way that there is no space for any vapor. If the temperature is kept constant and the plunger is withdrawn to create a volume that can be occupied by vapor, what would be the approximate pressure of the vapor produced?

5.6.3.20: Q10.3.14

Explain the following observations:

a. It takes longer to cook an egg in Ft. Davis, Texas (altitude, 5000 feet above sea level) than it does in Boston (at sea level).
b. Perspiring is a mechanism for cooling the body.

5.6.3.21: S10.3.14

(a) At 5000 feet, the atmospheric pressure is lower than at sea level, and water will therefore boil at a lower temperature. This lower temperature will cause the physical and chemical changes involved in cooking the egg to proceed more slowly, and a longer time is required to fully cook the egg. (b) As long as the air surrounding the body contains less water vapor than the maximum that air can hold at that temperature, perspiration will evaporate, thereby cooling the body by removing the heat of vaporization required to vaporize the water.

5.6.3.22: Q10.3.15

The enthalpy of vaporization of water is larger than its enthalpy of fusion. Explain why.

5.6.3.23: Q10.3.16

Explain why the molar enthalpies of vaporization of the following substances increase in the order $CH_4 < C_2H_6 < C_3H_8$, even though all three substances experience the same dispersion forces when in the liquid state.

5.6.3.24: S10.3.16

Dispersion forces increase with molecular mass or size. As the number of atoms composing the molecules in this homologous series increases, so does the extent of intermolecular attraction via dispersion forces and, consequently, the energy required to overcome these forces and vaporize the liquids.

5.6.3.25: Q10.3.17

Explain why the enthalpies of vaporization of the following substances increase in the order $CH_4 < NH_3 < H_2O$, even though all three substances have approximately the same molar mass.

5.6.3.26: Q10.3.18

The enthalpy of vaporization of $CO_2(l)$ is 9.8 kJ/mol. Would you expect the enthalpy of vaporization of $CS_2(l)$ to be 28 kJ/mol, 9.8 kJ/mol, or −8.4 kJ/mol? Discuss the plausibility of each of these answers.

5.6.3.27: S10.3.18

The boiling point of CS_2 is higher than that of CO_2 partially because of the higher molecular weight of CS_2; consequently, the attractive forces are stronger in CS_2. It would be expected, therefore, that the heat of vaporization would be greater than that of 9.8 kJ/mol for CO_2. A value of 28 kJ/mol would seem reasonable. A value of −8.4 kJ/mol would indicate a release of energy upon vaporization, which is clearly implausible.

5.6.3.28: Q10.3.19

The hydrogen fluoride molecule, HF, is more polar than a water molecule, H_2O (for example, has a greater dipole moment), yet the molar enthalpy of vaporization for liquid hydrogen fluoride is lesser than that for water. Explain.

5.6.3.29: Q10.3.20

Ethyl chloride (boiling point, 13 °C) is used as a local anesthetic. When the liquid is sprayed on the skin, it cools the skin enough to freeze and numb it. Explain the cooling effect of liquid ethyl chloride.

5.6.3.30: S10.3.20

The thermal energy (heat) needed to evaporate the liquid is removed from the skin.

5.6.3.31: Q10.3.21

Which contains the compounds listed correctly in order of increasing boiling points?

a. $N_2 < CS_2 < H_2O < KCl$
b. $H_2O < N_2 < CS_2 < KCl$
c. $N_2 < KCl < CS_2 < H_2O$
d. $CS_2 < N_2 < KCl < H_2O$
e. $KCl < H_2O < CS_2 < N_2$

5.6.3.32: Q10.3.22

How much heat is required to convert 422 g of liquid H_2O at 23.5 °C into steam at 150 °C?

5.6.3.33: S10.3.22

1130 kJ

5.6.3.34: Q10.3.22

Evaporation of sweat requires energy and thus take excess heat away from the body. Some of the water that you drink may eventually be converted into sweat and evaporate. If you drink a 20-ounce bottle of water that had been in the refrigerator at 3.8 °C, how much heat is needed to convert all of that water into sweat and then to vapor?? (Note: Your body temperature is 36.6 °C. For the purpose of solving this problem, assume that the thermal properties of sweat are the same as for water.)

5.6.3.35: Q10.3.24

Titanium tetrachloride, $TiCl_4$, has a melting point of −23.2 °C and has a $\Delta H_{\text{fusion}} = 9.37$ kJ/mol.

a. How much energy is required to melt 263.1 g $TiCl_4$?
b. For $TiCl_4$, which will likely have the larger magnitude: ΔH_{fusion} or $\Delta H_{\text{vaporization}}$? Explain your reasoning.

5.6.3.36: S10.3.24

(a) 13.0 kJ; (b) It is likely that the heat of vaporization will have a larger magnitude since in the case of vaporization the intermolecular interactions have to be completely overcome, while melting weakens or destroys only some of them.

5.6.4: 10.4: Phase Diagrams

5.6.4.1: Q10.4.1

From the phase diagram for water, determine the state of water at:

a. 35 °C and 85 kPa
b. −15 °C and 40 kPa
c. −15 °C and 0.1 kPa
d. 75 °C and 3 kPa
e. 40 °C and 0.1 kPa
f. 60 °C and 50 kPa

5.6.4.2: Q10.4.2

What phase changes will take place when water is subjected to varying pressure at a constant temperature of 0.005 °C? At 40 °C? At −40 °C?

5.6.4.3: S10.4.2

At low pressures and 0.005 °C, the water is a gas. As the pressure increases to 4.6 torr, the water becomes a solid; as the pressure increases still more, it becomes a liquid. At 40 °C, water at low pressure is a vapor; at pressures higher than about 75 torr, it converts into a liquid. At −40 °C, water goes from a gas to a solid as the pressure increases above very low values.

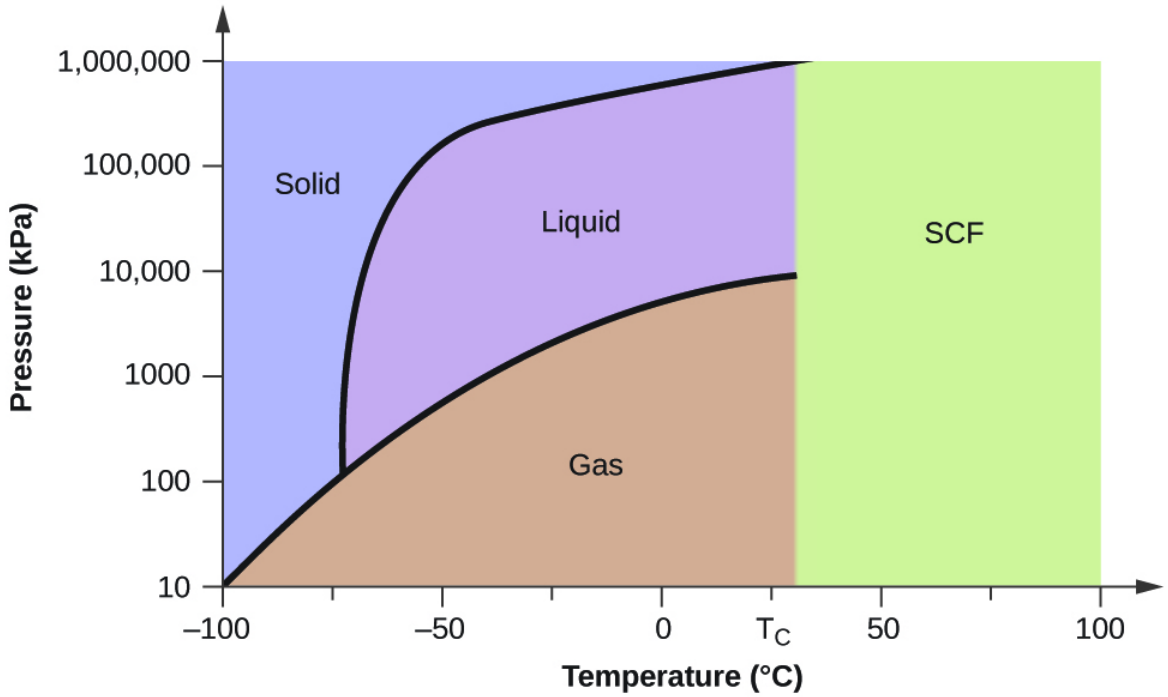
5.6.4.4: Q10.4.3

Pressure cookers allow food to cook faster because the higher pressure inside the pressure cooker increases the boiling temperature of water. A particular pressure cooker has a safety valve that is set to vent steam if the pressure exceeds 3.4 atm. What is the approximate maximum temperature that can be reached inside this pressure cooker? Explain your reasoning.

5.6.4.5: Q10.4.4

From the phase diagram for carbon dioxide, determine the state of CO_2 at:

a. 20 °C and 1000 kPa
b. 10 °C and 2000 kPa
c. 10 °C and 100 kPa
d. −40 °C and 500 kPa
e. −80 °C and 1500 kPa
f. −80 °C and 10 kPa



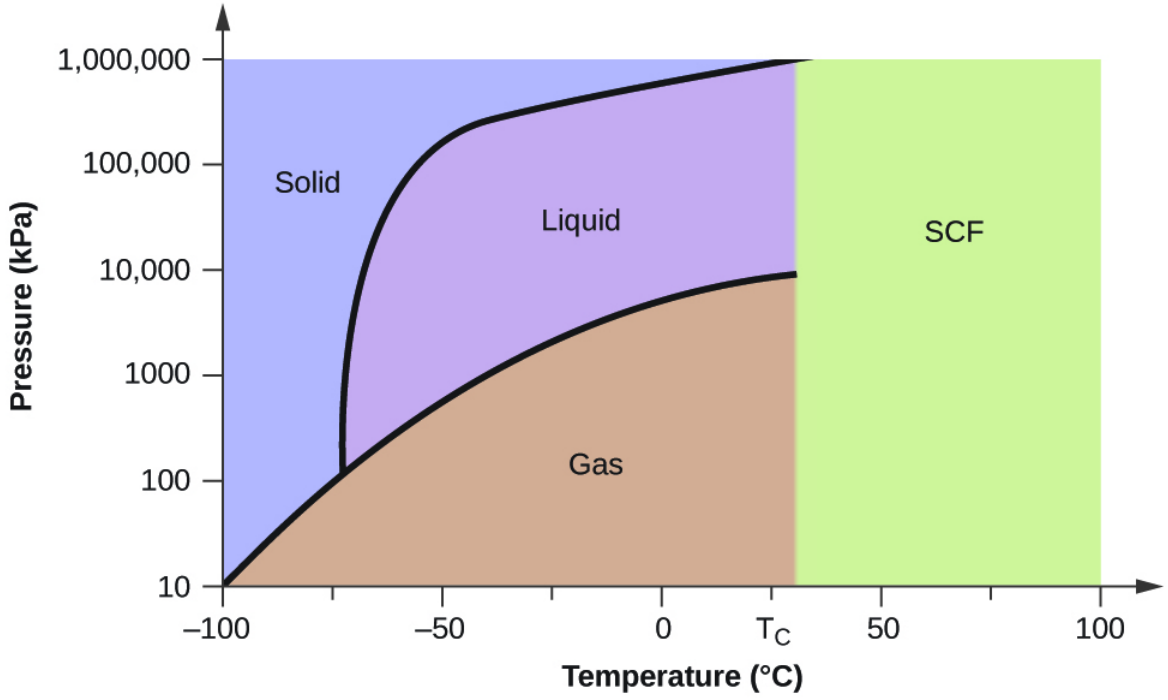
The pressure and temperature axes on this phase diagram of carbon dioxide are not drawn to constant scale in order to illustrate several important properties.

5.6.4.6: S10.4.4

(a) liquid; (b) solid; (c) gas; (d) gas; (e) gas; (f) gas

5.6.4.7: Q10.4.5

Determine the phase changes that carbon dioxide undergoes as the pressure changes if the temperature is held at −50 °C? If the temperature is held at −40 °C? At 20 °C?



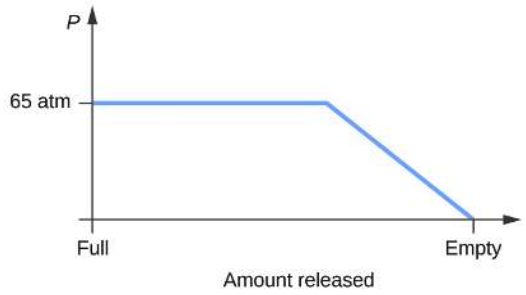
https://chem.libretexts.org/@go/page/362306

The pressure and temperature axes on this phase diagram of carbon dioxide are not drawn to constant scale in order to illustrate several important properties.

5.6.4.8: Q10.4.6

Consider a cylinder containing a mixture of liquid carbon dioxide in equilibrium with gaseous carbon dioxide at an initial pressure of 65 atm and a temperature of 20 °C. Sketch a plot depicting the change in the cylinder pressure with time as gaseous carbon dioxide is released at constant temperature.

5.6.4.9: S10.4.6



5.6.4.10: Q10.4.7

Dry ice, $CO_2(s)$, does not melt at atmospheric pressure. It sublimes at a temperature of −78 °C. What is the lowest pressure at which $CO_2(s)$ will melt to give $CO_2(l)$? At approximately what temperature will this occur? (See Figure for the phase diagram.)

5.6.4.11: S10.4.7

Dry ice, $CO_2(s)$, will melt to give $CO_2(l)$ at 5.11 atm at −56.6 °C, the triple point of carbon dioxide.

5.6.4.12: Q10.4.8

If a severe storm results in the loss of electricity, it may be necessary to use a clothesline to dry laundry. In many parts of the country in the dead of winter, the clothes will quickly freeze when they are hung on the line. If it does not snow, will they dry anyway? Explain your answer.

5.6.4.13: S10.4.8

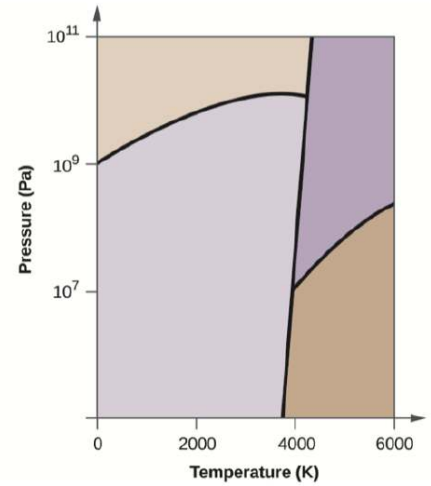
Yes, ice will sublime, although it may take it several days. Ice has a small vapor pressure, and some ice molecules form gas and escape from the ice crystals. As time passes, more and more solid converts to gas until eventually the clothes are dry.

5.6.4.14: Q10.4.9

Is it possible to liquefy nitrogen at room temperature (about 25 °C)? Is it possible to liquefy sulfur dioxide at room temperature? Explain your answers.

5.6.4.15: Q10.4.10

Elemental carbon has one gas phase, one liquid phase, and three different solid phases, as shown in the phase diagram:



a. On the phase diagram, label the gas and liquid regions.
b. Graphite is the most stable phase of carbon at normal conditions. On the phase diagram, label the graphite phase.
c. If graphite at normal conditions is heated to 2500 K while the pressure is increased to 10^{10} Pa, it is converted into diamond. Label the diamond phase.
d. Circle each triple point on the phase diagram.
e. In what phase does carbon exist at 5000 K and 10^{8} Pa?
f. If the temperature of a sample of carbon increases from 3000 K to 5000 K at a constant pressure of 10^{6} Pa, which phase transition occurs, if any?

5.6.5: 10.5: The Solid State of Matter

5.6.5.1: Q10.5.1

What types of liquids typically form amorphous solids?

5.6.5.2: S10.5.1

Amorphous solids lack an ordered internal structure. Liquid materials that contain large, cumbersome molecules that cannot move readily into ordered positions generally form such solids.

5.6.5.3: Q10.5.2

At very low temperatures oxygen, O_2, freezes and forms a crystalline solid. Which best describes these crystals?

a. ionic
b. covalent network
c. metallic
d. amorphous
e. molecular crystals

5.6.5.4: S10.5.3

(e) molecular crystals

5.6.5.5: Q10.5.4

As it cools, olive oil slowly solidifies and forms a solid over a range of temperatures. Which best describes the solid?

a. ionic
b. covalent network
c. metallic
d. amorphous

e. molecular crystals

5.6.5.6: S10.5.4

(d) amorphous

5.6.5.7: Q10.5.5

Explain why ice, which is a crystalline solid, has a melting temperature of 0 °C, whereas butter, which is an amorphous solid, softens over a range of temperatures.

5.6.5.8: S10.5.6

Ice has a crystalline structure stabilized by hydrogen bonding. These intermolecular forces are of comparable strength and thus require the same amount of energy to overcome. As a result, ice melts at a single temperature and not over a range of temperatures. The various, very large molecules that compose butter experience varied van der Waals attractions of various strengths that are overcome at various temperatures, and so the melting process occurs over a wide temperature range.

5.6.5.9: Q10.5.7

Identify the type of crystalline solid (metallic, network covalent, ionic, or molecular) formed by each of the following substances:

a. SiO_2
b. KCl
c. Cu
d. CO_2
e. C (diamond)
f. $BaSO_4$
g. NH_3
h. NH_4F
i. C_2H_5OH

5.6.5.10: S10.5.7

(a) SiO_2, covalent network; (b) KCl, ionic; (c) Cu, metallic; (d) CO, molecular; (e) C (diamond), covalent network; (f) $BaSO_4$, ionic; (g) NH_3, molecular; (h) NH_4F, ionic; (i) C_2H_5OH, molecular

5.6.5.11: Q10.5.8

Identify the type of crystalline solid (metallic, network covalent, ionic, or molecular) formed by each of the following substances:

a. $CaCl_2$
b. SiC
c. N_2
d. Fe
e. C (graphite)
f. $CH_3CH_2CH_2CH_3$
g. HCl
h. NH_4NO_3
i. K_3PO_4

5.6.5.12: S10.5.8

(a) $CaCl_2$, ionic; (b) SiC, covalent network; (c) N_2, molecular; (d) Fe, metallic; (e) C (graphite), covalent network; (f) $CH_3CH_2CH_2CH_3$, molecular; (g) HCl, molecular; (h) NH_4NO_3, ionic; (i) K_3PO_4, ionic

5.6.5.13: Q10.5.9

Classify each substance in the table as either a metallic, ionic, molecular, or covalent network solid:

Substance	Appearance	Melting Point	Electrical Conductivity	Solubility in Water
X	lustrous, malleable	1500 °C	high	insoluble
Y	soft, yellow	113 °C	none	insoluble
Z	hard, white	800 °C	only if melted/dissolved	soluble

5.6.5.14: S10.5.9

X = metallic; Y = covalent network; Z = ionic

5.6.5.15: Q10.5.10

Classify each substance in the table as either a metallic, ionic, molecular, or covalent network solid:

Substance	Appearance	Melting Point	Electrical Conductivity	Solubility in Water
X	brittle, white	800 °C	only if melted/dissolved	soluble
Y	shiny, malleable	1100 °C	high	insoluble
Z	hard, colorless	3550 °C	none	insoluble

5.6.5.16: S10.5.10

X = ionic; Y = metallic; Z = covalent network

5.6.5.17: Q10.5.11

Identify the following substances as ionic, metallic, covalent network, or molecular solids:

Substance A is malleable, ductile, conducts electricity well, and has a melting point of 1135 °C. Substance B is brittle, does not conduct electricity as a solid but does when molten, and has a melting point of 2072 °C. Substance C is very hard, does not conduct electricity, and has a melting point of 3440 °C. Substance D is soft, does not conduct electricity, and has a melting point of 185 °C.

5.6.5.18: S10.5.11

A = metallic; B = ionic; C = covalent network; D = molecular

5.6.5.19: Q10.5.12

Substance A is shiny, conducts electricity well, and melts at 975 °C. Substance A is likely a(n):

a. ionic solid
b. metallic solid
c. molecular solid
d. covalent network solid

5.6.5.20: S10.5.12

(b) metallic solid

5.6.5.21: Q10.5.13

Substance B is hard, does not conduct electricity, and melts at 1200 °C. Substance B is likely a(n):

a. ionic solid
b. metallic solid
c. molecular solid
d. covalent network solid

5.6.5.22: S10.5.13

(d) covalent network solid

5.6.6: 10.6: Lattice Structures

5.6.6.1: Q10.6.1

Describe the crystal structure of iron, which crystallizes with two equivalent metal atoms in a cubic unit cell.

5.6.6.2: S10.6.1

The structure of this low-temperature form of iron (below 910 °C) is body-centered cubic. There is one-eighth atom at each of the eight corners of the cube and one atom in the center of the cube.

5.6.6.3: Q10.6.2

Describe the crystal structure of Pt, which crystallizes with four equivalent metal atoms in a cubic unit cell.

5.6.6.4: Q10.6.3

What is the coordination number of a chromium atom in the body-centered cubic structure of chromium?

5.6.6.5: S10.6.3

eight

5.6.6.6: Q10.6.4

What is the coordination number of an aluminum atom in the face-centered cubic structure of aluminum?

5.6.6.7: Q10.6.5

Cobalt metal crystallizes in a hexagonal closest packed structure. What is the coordination number of a cobalt atom?

5.6.6.8: S10.6.5

12

5.6.6.9: Q10.6.6

Nickel metal crystallizes in a cubic closest packed structure. What is the coordination number of a nickel atom?

5.6.6.10: Q10.6.7

Tungsten crystallizes in a body-centered cubic unit cell with an edge length of 3.165 Å.

a. What is the atomic radius of tungsten in this structure?
b. Calculate the density of tungsten.

5.6.6.11: S10.6.7

(a) 1.370 Å; (b) 19.26 g/cm

5.6.6.12: Q10.6.8

Platinum (atomic radius = 1.38 Å) crystallizes in a cubic closely packed structure. Calculate the edge length of the face-centered cubic unit cell and the density of platinum.

5.6.6.13: Q10.6.9

Barium crystallizes in a body-centered cubic unit cell with an edge length of 5.025 Å

a. What is the atomic radius of barium in this structure?
b. Calculate the density of barium.

5.6.6.14: S10.6.9

(a) 2.176 Å; (b) 3.595 g/cm^3

5.6.6.15: Q10.6.10

Aluminum (atomic radius = 1.43 Å) crystallizes in a cubic closely packed structure. Calculate the edge length of the face-centered cubic unit cell and the density of aluminum.

5.6.6.16: Q10.6.11

The density of aluminum is 2.7 g/cm^3; that of silicon is 2.3 g/cm^3. Explain why Si has the lower density even though it has heavier atoms.

5.6.6.17: S10.6.11

The crystal structure of Si shows that it is less tightly packed (coordination number 4) in the solid than Al (coordination number 12).

5.6.6.18: Q10.6.12

The free space in a metal may be found by subtracting the volume of the atoms in a unit cell from the volume of the cell. Calculate the percentage of free space in each of the three cubic lattices if all atoms in each are of equal size and touch their nearest neighbors. Which of these structures represents the most efficient packing? That is, which packs with the least amount of unused space?

5.6.6.19: Q10.6.13

Cadmium sulfide, sometimes used as a yellow pigment by artists, crystallizes with cadmium, occupying one-half of the tetrahedral holes in a closest packed array of sulfide ions. What is the formula of cadmium sulfide? Explain your answer.

5.6.6.20: S10.6.13

In a closest-packed array, two tetrahedral holes exist for each anion. If only half the tetrahedral holes are occupied, the numbers of anions and cations are equal. The formula for cadmium sulfide is CdS.

5.6.6.21: Q10.6.14

A compound of cadmium, tin, and phosphorus is used in the fabrication of some semiconductors. It crystallizes with cadmium occupying one-fourth of the tetrahedral holes and tin occupying one-fourth of the tetrahedral holes in a closest packed array of phosphide ions. What is the formula of the compound? Explain your answer.

5.6.6.22: Q10.6.15

What is the formula of the magnetic oxide of cobalt, used in recording tapes, that crystallizes with cobalt atoms occupying one-eighth of the tetrahedral holes and one-half of the octahedral holes in a closely packed array of oxide ions?

5.6.6.23: S10.6.15

Co_3O_4

5.6.6.24: Q10.6.16

A compound containing zinc, aluminum, and sulfur crystallizes with a closest-packed array of sulfide ions. Zinc ions are found in one-eighth of the tetrahedral holes and aluminum ions in one-half of the octahedral holes. What is the empirical formula of the compound?

5.6.6.25: Q10.6.17

A compound of thallium and iodine crystallizes in a simple cubic array of iodide ions with thallium ions in all of the cubic holes. What is the formula of this iodide? Explain your answer.

5.6.6.26: S10.6.17

In a simple cubic array, only one cubic hole can be occupied be a cation for each anion in the array. The ratio of thallium to iodide must be 1:1; therefore, the formula for thallium is TlI.

5.6.6.27: Q10.6.18

Which of the following elements reacts with sulfur to form a solid in which the sulfur atoms form a closest-packed array with all of the octahedral holes occupied: Li, Na, Be, Ca, or Al?

5.6.6.28: Q10.6.19

What is the percent by mass of titanium in rutile, a mineral that contains titanium and oxygen, if structure can be described as a closest packed array of oxide ions with titanium ions in one-half of the octahedral holes? What is the oxidation number of titanium?

5.6.6.29: S10.6.19

59.95%; The oxidation number of titanium is +4.

5.6.6.30: Q10.6.20

Explain why the chemically similar alkali metal chlorides NaCl and CsCl have different structures, whereas the chemically different NaCl and MnS have the same structure.

5.6.6.31: Q10.6.21

As minerals were formed from the molten magma, different ions occupied the same cites in the crystals. Lithium often occurs along with magnesium in minerals despite the difference in the charge on their ions. Suggest an explanation.

5.6.6.32: S10.6.21

Both ions are close in size: Mg, 0.65; Li, 0.60. This similarity allows the two to interchange rather easily. The difference in charge is generally compensated by the switch of Si^{4+} for Al^{3+}.

5.6.6.33: Q10.6.22

Rubidium iodide crystallizes with a cubic unit cell that contains iodide ions at the corners and a rubidium ion in the center. What is the formula of the compound?

5.6.6.34: Q10.6.23

One of the various manganese oxides crystallizes with a cubic unit cell that contains manganese ions at the corners and in the center. Oxide ions are located at the center of each edge of the unit cell. What is the formula of the compound?

5.6.6.35: S10.6.23

Mn_2O_3

5.6.6.36: Q10.6.24

NaH crystallizes with the same crystal structure as NaCl. The edge length of the cubic unit cell of NaH is 4.880 Å.

a. Calculate the ionic radius of H^-. (The ionic radius of Li^+ is 0.0.95 Å.)
b. Calculate the density of NaH.

5.6.6.37: Q10.6.25

Thallium(I) iodide crystallizes with the same structure as CsCl. The edge length of the unit cell of TlI is 4.20 Å. Calculate the ionic radius of TI^+. (The ionic radius of I^- is 2.16 Å.)

5.6.6.38: S10.6.25

1.48 Å

5.6.6.39: Q10.6.26

A cubic unit cell contains manganese ions at the corners and fluoride ions at the center of each edge.

a. What is the empirical formula of this compound? Explain your answer.
b. What is the coordination number of the Mn^{3+} ion?
c. Calculate the edge length of the unit cell if the radius of a Mn^{3+} ion is 0.65 A.
d. Calculate the density of the compound.

5.6.6.40: Q10.6.27

What is the spacing between crystal planes that diffract X-rays with a wavelength of 1.541 nm at an angle θ of 15.55° (first order reflection)?

5.6.6.41: S10.6.27

2.874 Å

5.6.6.42: Q10.6.28

A diffractometer using X-rays with a wavelength of 0.2287 nm produced first-order diffraction peak for a crystal angle θ = 16.21°. Determine the spacing between the diffracting planes in this crystal.

5.6.6.43: Q10.6.29

A metal with spacing between planes equal to 0.4164 nm diffracts X-rays with a wavelength of 0.2879 nm. What is the diffraction angle for the first order diffraction peak?

5.6.6.44: S10.6.29

20.2°

5.6.6.45: Q10.6.30

Gold crystallizes in a face-centered cubic unit cell. The second-order reflection (n = 2) of X-rays for the planes that make up the tops and bottoms of the unit cells is at θ = 22.20°. The wavelength of the X-rays is 1.54 Å. What is the density of metallic gold?

5.6.6.46: Q10.6.31

When an electron in an excited molybdenum atom falls from the L to the K shell, an X-ray is emitted. These X-rays are diffracted at an angle of 7.75° by planes with a separation of 2.64 Å. What is the difference in energy between the K shell and the L shell in molybdenum assuming a first-order diffraction?

5.6.6.47: S10.6.31

1.74×10^4 eV

This page titled 5.6: Liquids and Solids (Exercises) is shared under a CC BY license and was authored, remixed, and/or curated by OpenStax.

CHAPTER OVERVIEW

6: Phases and Phase Transitions

6.1: Prelude to Liquids and Solids
6.2: Intermolecular Forces Review
6.3: Properties of Liquids
6.4: Phase Transitions- Overview
6.5: Phase Transitions
6.6: Vaporization and Vapor Pressure
6.7: Sublimation and Fusion
6.8: Heating Curve for Water
6.9: Phase Diagrams
6.10: Water - An Extraordinary Substance

6: Phases and Phase Transitions is shared under a not declared license and was authored, remixed, and/or curated by LibreTexts.

6.1: Prelude to Liquids and Solids

The great distances between atoms and molecules in a gaseous phase, and the corresponding absence of any significant interactions between them, allows for simple descriptions of many physical properties that are the same for all gases, regardless of their chemical identities. As described in the final module of the chapter on gases, this situation changes at high pressures and low temperatures—conditions that permit the atoms and molecules to interact to a much greater extent.



Figure **6.1.1**: Solid carbon dioxide (“dry ice”, left) sublimes vigorously when placed in a liquid (right), cooling the liquid and generating a fog of condensed water vapor above the cylinder. (credit: modification of work by Paul Flowers)

This figure shows pieces of a white substance which appear to be sublimating. To the right of these pieces are three graduated cylinders. Each cylinder holds a different color liquid, and above the liquid, the cylinders are filled with a fog-like substance. This fog-like substance swirls out of the top and around the outside of the cylinders.

In the liquid and solid states, these interactions are of considerable strength and play an important role in determining a number of physical properties that *do* depend on the chemical identity of the substance. In this chapter, the nature of these interactions and their effects on various physical properties of liquid and solid phases will be examined.

This page titled 6.1: Prelude to Liquids and Solids is shared under a CC BY 4.0 license and was authored, remixed, and/or curated by OpenStax via source content that was edited to the style and standards of the LibreTexts platform.

- **10.1: Prelude to Liquids and Solids** by OpenStax is licensed CC BY 4.0. Original source: https://openstax.org/details/books/chemistry-2e.

6.2: Intermolecular Forces Review

Learning Objectives

- Describe the types of intermolecular forces possible between atoms or molecules in condensed phases (dispersion forces, dipole-dipole attractions, and hydrogen bonding)
- Identify the types of intermolecular forces experienced by specific molecules based on their structures
- Explain the relation between the intermolecular forces present within a substance and the temperatures associated with changes in its physical state

As was the case for gaseous substances, the kinetic molecular theory may be used to explain the behavior of solids and liquids. In the following description, the term *particle* will be used to refer to an atom, molecule, or ion. Note that we will use the popular phrase "intermolecular attraction" to refer to attractive forces between the particles of a substance, regardless of whether these particles are molecules, atoms, or ions.

Consider these two aspects of the molecular-level environments in solid, liquid, and gaseous matter:

- Particles in a solid are tightly packed together and often arranged in a regular pattern; in a liquid, they are close together with no regular arrangement; in a gas, they are far apart with no regular arrangement.
- Particles in a solid vibrate about fixed positions and do not generally move in relation to one another; in a liquid, they move past each other but remain in essentially constant contact; in a gas, they move independently of one another except when they collide.

The differences in the properties of a solid, liquid, or gas reflect the strengths of the attractive forces between the atoms, molecules, or ions that make up each phase. The phase in which a substance exists depends on the relative extents of its intermolecular forces (IMFs) and the kinetic energies (KE) of its molecules. IMFs are the various forces of attraction that may exist between the atoms and molecules of a substance due to electrostatic phenomena, as will be detailed in this module. These forces serve to hold particles close together, whereas the particles' KE provides the energy required to overcome the attractive forces and thus increase the distance between particles. Figure 6.2.1 illustrates how changes in physical state may be induced by changing the temperature, hence, the average KE, of a given substance.

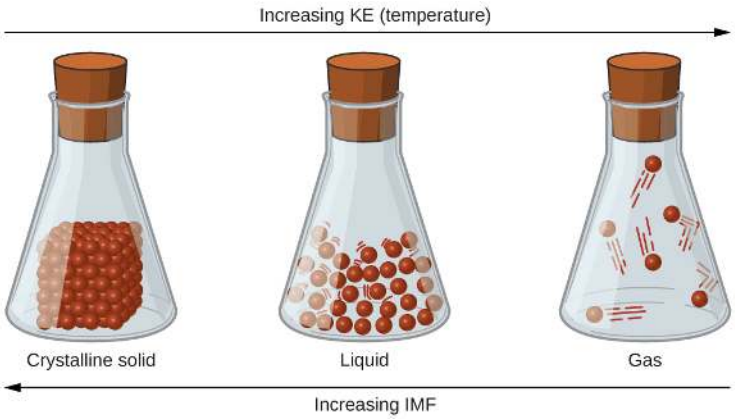


Figure 6.2.1: Transitions between solid, liquid, and gaseous states of a substance occur when conditions of temperature or pressure favor the associated changes in intermolecular forces. (Note: The space between particles in the gas phase is much greater than shown.)

Three sealed flasks are labeled, "Crystalline solid," "Liquid," and "Gas," from left to right. The first flask holds a cube composed of small spheres sitting on the bottom while the second flask shows a lot of small spheres in the bottom that are spaced a small distance apart from one another and have lines around them to indicate motion. The third flask shows a few spheres spread far from one another with larger lines to indicate motion. There is a right-facing arrow that spans the top of all three flasks. The arrow is labeled, "Increasing K E (temperature)." There is a left-facing arrow that spans the bottom of all three flasks. The arrow is labeled, "Increasing I M F."

As an example of the processes depicted in this figure, consider a sample of water. When gaseous water is cooled sufficiently, the attractions between H_2O molecules will be capable of holding them together when they come into contact with each other; the gas

condenses, forming liquid H_2O. For example, liquid water forms on the outside of a cold glass as the water vapor in the air is cooled by the cold glass, as seen in Figure **6.2.2**.



Figure **6.2.2**: Condensation forms when water vapor in the air is cooled enough to form liquid water, such as (a) on the outside of a cold beverage glass or (b) in the form of fog. (credit a: modification of work by Jenny Downing; credit b: modification of work by Cory Zanker)

Image a shows a brown colored beverage in a glass with condensation on the outside. Image b shows a body of water with fog hovering above the surface of the water.

We can also liquefy many gases by compressing them, if the temperature is not too high. The increased pressure brings the molecules of a gas closer together, such that the attractions between the molecules become strong relative to their KE. Consequently, they form liquids. Butane, C_4H_{10}, is the fuel used in disposable lighters and is a gas at standard temperature and pressure. Inside the lighter's fuel compartment, the butane is compressed to a pressure that results in its condensation to the liquid state, as shown in Figure **6.2.3**.



Figure **6.2.3**: Gaseous butane is compressed within the storage compartment of a disposable lighter, resulting in its condensation to the liquid state. (credit: modification of work by "Sam-Cat"/Flickr)

Finally, if the temperature of a liquid becomes sufficiently low, or the pressure on the liquid becomes sufficiently high, the molecules of the liquid no longer have enough KE to overcome the IMF between them, and a solid forms. A more thorough discussion of these and other changes of state, or phase transitions, is provided in a later module of this chapter.

6.2.1: Forces between Molecules

Under appropriate conditions, the attractions between all gas molecules will cause them to form liquids or solids. This is due to intermolecular forces, not *intra*molecular forces. *Intra*molecular forces are those *within* the molecule that keep the molecule

together, for example, the bonds between the atoms. *Inter*molecular forces are the attractions *between* molecules, which determine many of the physical properties of a substance. Figure **6.2.4** illustrates these different molecular forces. The strengths of these attractive forces vary widely, though usually the IMFs between small molecules are weak compared to the intramolecular forces that bond atoms together within a molecule. For example, to overcome the IMFs in one mole of liquid HCl and convert it into gaseous HCl requires only about 17 kilojoules. However, to break the covalent bonds between the hydrogen and chlorine atoms in one mole of HCl requires about 25 times more energy—430 kilojoules.

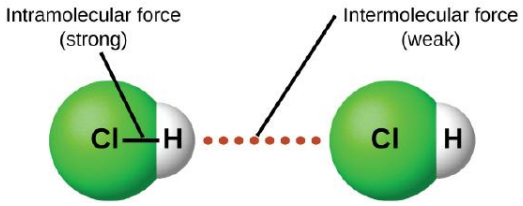


Figure **6.2.4**: Intramolecular forces keep a molecule intact. Intermolecular forces hold multiple molecules together and determine many of a substance's properties.

An image is shown in which two molecules composed of a green sphere labeled "C l" connected on the right to a white sphere labeled "H" are near one another with a dotted line labeled "Intermolecular force (weak)" drawn between them. A line connects the two spheres in each molecule and the line is labeled "Intramolecular force (strong)."

All of the attractive forces between neutral atoms and molecules are known as van der Waals forces, although they are usually referred to more informally as intermolecular attraction. We will consider the various types of IMFs in the next three sections of this module.

6.2.2: Dispersion Forces

One of the three van der Waals forces is present in all condensed phases, regardless of the nature of the atoms or molecules composing the substance. This attractive force is called the London dispersion force in honor of German-born American physicist Fritz London who, in 1928, first explained it. This force is often referred to as simply the dispersion force. Because the electrons of an atom or molecule are in constant motion (or, alternatively, the electron's location is subject to quantum-mechanical variability), at any moment in time, an atom or molecule can develop a temporary, instantaneous dipole if its electrons are distributed asymmetrically. The presence of this dipole can, in turn, distort the electrons of a neighboring atom or molecule, producing an induced dipole. These two rapidly fluctuating, temporary dipoles thus result in a relatively weak electrostatic attraction between the species—a so-called dispersion force like that illustrated in Figure **6.2.5**.

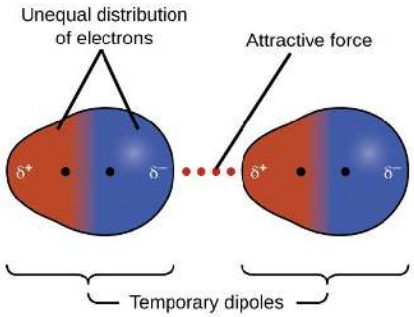


Figure **6.2.5**: Dispersion forces result from the formation of temporary dipoles, as illustrated here for two nonpolar diatomic molecules.

Two pairs of molecules are shown where each molecule has one larger blue side labeled "delta sign, negative sign" and a smaller red side labeled "delta sign, positive sign." Toward the middle of the both molecules, but still on each distinct side, is a black dot. Between the two images is a dotted line labeled, "Attractive force." In the first image, the red and blue sides are labeled, "Unequal distribution of electrons." Below both images are brackets. The brackets are labeled, "Temporary dipoles."

Dispersion forces that develop between atoms in different molecules can attract the two molecules to each other. The forces are relatively weak, however, and become significant only when the molecules are very close. Larger and heavier atoms and molecules exhibit stronger dispersion forces than do smaller and lighter atoms and molecules. F_2 and Cl_2 are gases at room temperature

(reflecting weaker attractive forces); Br_2 is a liquid, and I_2 is a solid (reflecting stronger attractive forces). Trends in observed melting and boiling points for the halogens clearly demonstrate this effect, as seen in Table **6.2.1**.

Table **6.2.1**: Melting and Boiling Points of the Halogens

Halogen	Molar Mass	Atomic Radius	Melting Point	Boiling Point
fluorine, F_2	38 g/mol	72 pm	53 K	85 K
chlorine, Cl_2	71 g/mol	99 pm	172 K	238 K
bromine, Br_2	160 g/mol	114 pm	266 K	332 K
iodine, I_2	254 g/mol	133 pm	387 K	457 K
astatine, At_2	420 g/mol	150 pm	575 K	610 K

The increase in melting and boiling points with increasing atomic/molecular size may be rationalized by considering how the strength of dispersion forces is affected by the electronic structure of the atoms or molecules in the substance. In a larger atom, the valence electrons are, on average, farther from the nuclei than in a smaller atom. Thus, they are less tightly held and can more easily form the temporary dipoles that produce the attraction. The measure of how easy or difficult it is for another electrostatic charge (for example, a nearby ion or polar molecule) to distort a molecule's charge distribution (its electron cloud) is known as polarizability. A molecule that has a charge cloud that is easily distorted is said to be very polarizable and will have large dispersion forces; one with a charge cloud that is difficult to distort is not very polarizable and will have small dispersion forces.

Example **6.2.1**: London Forces and Their Effects

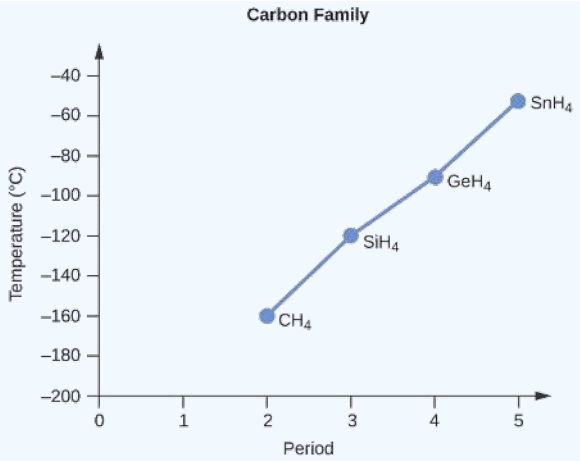
Order the following compounds of a group 14 element and hydrogen from lowest to highest boiling point: CH_4, SiH_4, GeH_4, and SnH_4. Explain your reasoning.

Solution

Applying the skills acquired in the chapter on chemical bonding and molecular geometry, all of these compounds are predicted to be nonpolar, so they may experience only dispersion forces: the smaller the molecule, the less polarizable and the weaker the dispersion forces; the larger the molecule, the larger the dispersion forces. The molar masses of CH_4, SiH_4, GeH_4, and SnH_4 are approximately 16 g/mol, 32 g/mol, 77 g/mol, and 123 g/mol, respectively. Therefore, CH_4 is expected to have the lowest boiling point and SnH_4 the highest boiling point. The ordering from lowest to highest boiling point is expected to be

$$CH_4 < SiH_4 < GeH_4 < SnH_4$$

A graph of the actual boiling points of these compounds versus the period of the group 14 elements shows this prediction to be correct:



A line graph, titled “Carbon Family,” is shown where the y-axis is labeled “Temperature, (degree sign C)” and has values of “negative 200” to “negative 40” from bottom to top in increments of 20. The x-axis is labeled “Period” and has values of “0” to “5” in increments of 1. The first point on the graph is labeled “C H subscript 4” and is at point “2, negative 160.” The second point on the graph is labeled “S i H subscript 4” and is at point “3, negative 120” while the third point on the graph is labeled “G e H subscript 4” and is at point “4, negative 100.” The fourth point on the graph is labeled “S n H subscript 4” and is at point “5, negative 60.”

? Exercise 6.2.1

Order the following hydrocarbons from lowest to highest boiling point: C_2H_6, C_3H_8, and C_4H_{10}.

Answer

All of these compounds are nonpolar and only have London dispersion forces: the larger the molecule, the larger the dispersion forces and the higher the boiling point. The ordering from lowest to highest boiling point is therefore

$$C_2H_6 < C_3H_8 < C_4H_{10}.$$

The shapes of molecules also affect the magnitudes of the dispersion forces between them. For example, boiling points for the isomers *n*-pentane, isopentane, and neopentane (shown in Figure **6.2.6**) are 36 °C, 27 °C, and 9.5 °C, respectively. Even though these compounds are composed of molecules with the same chemical formula, C_5H_{12}, the difference in boiling points suggests that dispersion forces in the liquid phase are different, being greatest for *n*-pentane and least for neopentane. The elongated shape of *n*-pentane provides a greater surface area available for contact between molecules, resulting in correspondingly stronger dispersion forces. The more compact shape of isopentane offers a smaller surface area available for intermolecular contact and, therefore, weaker dispersion forces. Neopentane molecules are the most compact of the three, offering the least available surface area for intermolecular contact and, hence, the weakest dispersion forces. This behavior is analogous to the connections that may be formed between strips of VELCRO brand fasteners: the greater the area of the strip’s contact, the stronger the connection.

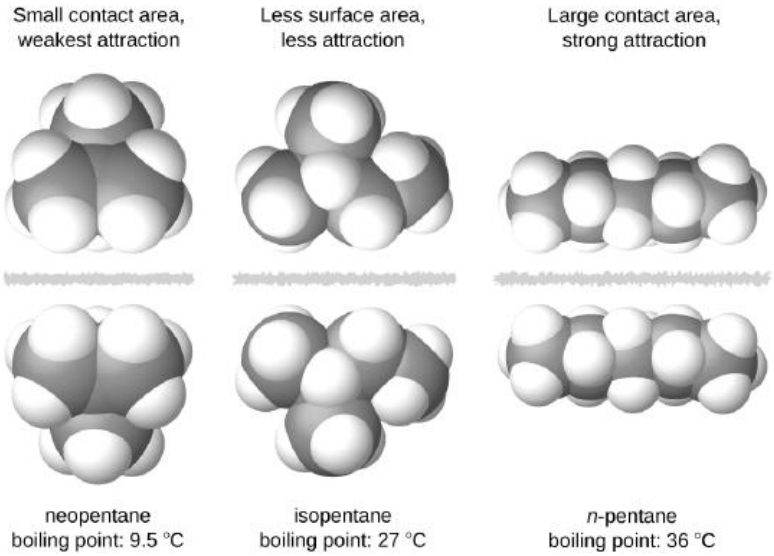


Figure **6.2.6**: The strength of the dispersion forces increases with the contact area between molecules, as demonstrated by the boiling points of these pentane isomers.

Three images of molecules are shown. The first shows a cluster of large, gray spheres each bonded together and to several smaller, white spheres. There is a gray, jagged line and then the mirror image of the first cluster of spheres is shown. Above these two clusters is the label, “Small contact area, weakest attraction,” and below is the label, “neopentane boiling point: 9.5 degrees C.” The second shows a chain of three gray spheres bonded by the middle sphere to a fourth gray sphere. Each gray sphere is bonded to several smaller, white spheres. There is a jagged, gray line and then the mirror image of the first chain appears. Above these two chains is the label, “Less surface area, less attraction,” and below is the label, “isopentane boiling point: 27 degrees C.” The third image shows a chain of five gray spheres bonded together and to several smaller, white spheres. There is a jagged gray line and then the mirror image of the first chain appears. Above these chains is the label, “Large contact area, strong attraction,” and below is the label, “n-pentane boiling point 36 degrees C.”

Applications: Geckos and Intermolecular Forces

Geckos have an amazing ability to adhere to most surfaces. They can quickly run up smooth walls and across ceilings that have no toe-holds, and they do this without having suction cups or a sticky substance on their toes. And while a gecko can lift its feet easily as it walks along a surface, if you attempt to pick it up, it sticks to the surface. How are geckos (as well as spiders and some other insects) able to do this? Although this phenomenon has been investigated for hundreds of years, scientists only recently uncovered the details of the process that allows geckos’ feet to behave this way.

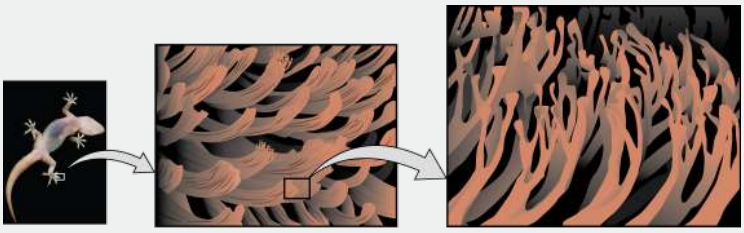


Figure **6.2.7**: Geckos’ toes contain large numbers of tiny hairs (setae), which branch into many triangular tips (spatulae). Geckos adhere to surfaces because of van der Waals attractions between the surface and a gecko’s millions of spatulae. By changing how the spatulae contact the surface, geckos can turn their stickiness “on” and “off.” (credit photo: modification of work by “JC*+A!”/Flickr)

Three figures are shown. The first is a photo of the bottom of a gecko’s foot. The second is bigger version which shows the setae. The third is a bigger version of the setae and shows the spatulae.

Geckos’ toes are covered with hundreds of thousands of tiny hairs known as *setae*, with each seta, in turn, branching into hundreds of tiny, flat, triangular tips called *spatulae*. The huge numbers of spatulae on its setae provide a gecko, shown in Figure **6.2.7**, with a large total surface area for sticking to a surface. In 2000, Kellar Autumn, who leads a multi-institutional gecko research team, found that geckos adhered equally well to both polar silicon dioxide and nonpolar gallium arsenide. This proved that geckos stick to surfaces because of dispersion forces—weak intermolecular attractions arising from temporary,

synchronized charge distributions between adjacent molecules. Although dispersion forces are very weak, the total attraction over millions of spatulae is large enough to support many times the gecko's weight.

In 2014, two scientists developed a model to explain how geckos can rapidly transition from "sticky" to "non-sticky." Alex Greaney and Congcong Hu at Oregon State University described how geckos can achieve this by changing the angle between their spatulae and the surface. Geckos' feet, which are normally nonsticky, become sticky when a small shear force is applied. By curling and uncurling their toes, geckos can alternate between sticking and unsticking from a surface, and thus easily move across it. Further investigations may eventually lead to the development of better adhesives and other applications.



Watch this video to learn more about Kellar Autumn's research that determined that van der Waals forces are responsible for a gecko's ability to cling and climb.

6.2.3: Dipole-Dipole Attractions

Recall from the chapter on chemical bonding and molecular geometry that *polar* molecules have a partial positive charge on one side and a partial negative charge on the other side of the molecule—a separation of charge called a *dipole*. Consider a polar molecule such as hydrogen chloride, HCl. In the HCl molecule, the more electronegative Cl atom bears the partial negative charge, whereas the less electronegative H atom bears the partial positive charge. An attractive force between HCl molecules results from the attraction between the positive end of one HCl molecule and the negative end of another. This attractive force is called a dipole-dipole attraction—the electrostatic force between the partially positive end of one polar molecule and the partially negative end of another, as illustrated in Figure **6.2.8**.

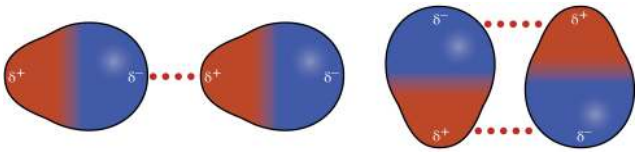


Figure **6.2.8**: This image shows two arrangements of polar molecules, such as HCl, that allow an attraction between the partial negative end of one molecule and the partial positive end of another.

Two pairs of molecules are shown where each molecule has one larger blue side labeled "delta sign, negative sign" and a smaller red side labeled "delta sign, positive sign. In the first pair, the red sides of the two molecules both face to the left and the blue side to the right. A horizontal dotted line lies in between the two. In the second pair, the molecules face up and down, with the red and blue ends aligning. A horizontal dotted line lies between the red and blue ends facing upward and another lies between the red and blue ends facing downward.

The effect of a dipole-dipole attraction is apparent when we compare the properties of HCl molecules to nonpolar F_2 molecules. Both HCl and F_2 consist of the same number of atoms and have approximately the same molecular mass. At a temperature of 150 K, molecules of both substances would have the same average KE. However, the dipole-dipole attractions between HCl molecules are sufficient to cause them to "stick together" to form a liquid, whereas the relatively weaker dispersion forces between nonpolar F_2 molecules are not, and so this substance is gaseous at this temperature. The higher normal boiling point of HCl (188 K) compared to F_2 (85 K) is a reflection of the greater strength of dipole-dipole attractions between HCl molecules, compared to the

attractions between nonpolar F_2 molecules. We will often use values such as boiling or freezing points, or enthalpies of vaporization or fusion, as indicators of the relative strengths of IMFs of attraction present within different substances.

Example 6.2.2: Dipole-Dipole Forces and Their Effects

Predict which will have the higher boiling point: N_2 or CO. Explain your reasoning.

Solution

CO and N_2 are both diatomic molecules with masses of about 28 amu, so they experience similar London dispersion forces. Because CO is a polar molecule, it experiences dipole-dipole attractions. Because N_2 is nonpolar, its molecules cannot exhibit dipole-dipole attractions. The dipole-dipole attractions between CO molecules are comparably stronger than the dispersion forces between nonpolar N_2 molecules, so CO is expected to have the higher boiling point.

A common method for preparing oxygen is the decomposition

Exercise 6.2.2

Predict which will have the higher boiling point: **ICl** or $\mathbf{Br_2}$. Explain your reasoning.

Answer

ICl. ICl and Br_2 have similar masses (~160 amu) and therefore experience similar London dispersion forces. ICl is polar and thus also exhibits dipole-dipole attractions; Br_2 is nonpolar and does not. The relatively stronger dipole-dipole attractions require more energy to overcome, so ICl will have the higher boiling point.

6.2.4: Hydrogen Bonding

Nitrosyl fluoride (ONF, molecular mass 49 amu) is a gas at room temperature. Water (H_2O, molecular mass 18 amu) is a liquid, even though it has a lower molecular mass. We clearly cannot attribute this difference between the two compounds to dispersion forces. Both molecules have about the same shape and ONF is the heavier and larger molecule. It is, therefore, expected to experience more significant dispersion forces. Additionally, we cannot attribute this difference in boiling points to differences in the dipole moments of the molecules. Both molecules are polar and exhibit comparable dipole moments. The large difference between the boiling points is due to a particularly strong dipole-dipole attraction that may occur when a molecule contains a hydrogen atom bonded to a fluorine, oxygen, or nitrogen atom (the three most electronegative elements). The very large difference in electronegativity between the H atom (2.1) and the atom to which it is bonded (4.0 for an F atom, 3.5 for an O atom, or 3.0 for a N atom), combined with the very small size of a H atom and the relatively small sizes of F, O, or N atoms, leads to *highly concentrated partial charges* with these atoms. Molecules with F-H, O-H, or N-H moieties are very strongly attracted to similar moieties in nearby molecules, a particularly strong type of dipole-dipole attraction called hydrogen bonding. Examples of hydrogen bonds include HF···HF, H_2O···HOH, and H_3N···HNH_2, in which the hydrogen bonds are denoted by dots. Figure 6.2.9 illustrates hydrogen bonding between water molecules.

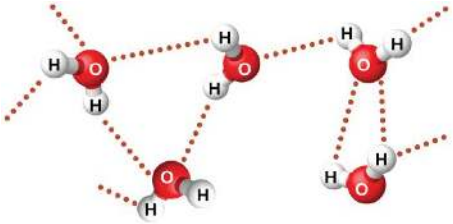


Figure 6.2.9: Water molecules participate in multiple hydrogen-bonding interactions with nearby water molecules.

Five water molecules are shown near one another, but not touching. A dotted line lies between many of the hydrogen atoms on one molecule and the oxygen atom on another molecule.

Despite use of the word “bond,” keep in mind that hydrogen bonds are *intermolecular* attractive forces, not *intramolecular* attractive forces (covalent bonds). Hydrogen bonds are much weaker than covalent bonds, only about 5 to 10% as strong, but are

generally much stronger than other dipole-dipole attractions and dispersion forces.

Hydrogen bonds have a pronounced effect on the properties of condensed phases (liquids and solids). For example, consider the trends in boiling points for the binary hydrides of group 15 (NH_3, PH_3, AsH_3, and SbH_3), group 16 hydrides (H_2O, H_2S, H_2Se, and H_2Te), and group 17 hydrides (HF, HCl, HBr, and HI). The boiling points of the heaviest three hydrides for each group are plotted in Figure **6.2.10**. As we progress down any of these groups, the polarities of the molecules decrease slightly, whereas the sizes of the molecules increase substantially. The effect of increasingly stronger dispersion forces dominates that of increasingly weaker dipole-dipole attractions, and the boiling points are observed to increase steadily. For the group 15, 16, and 17 hydrides, the boiling points for each class of compounds increase with increasing molecular mass for elements in periods 3, 4, and 5.

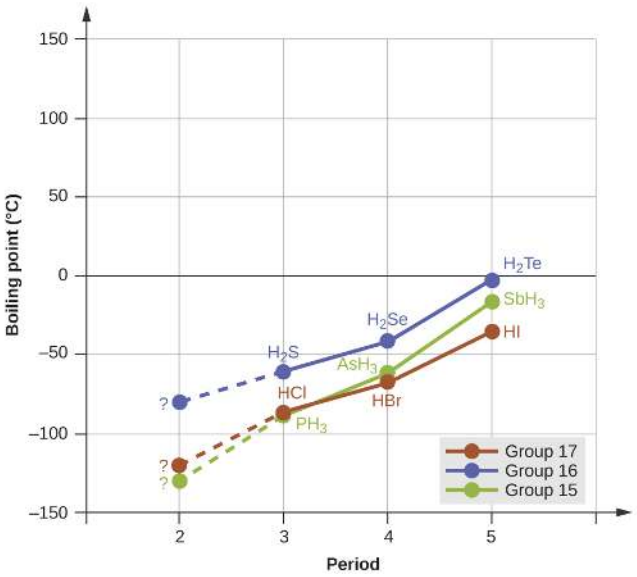


Figure **6.2.10**: In comparison to periods 3−5, the binary hydrides of period 2 elements in groups 17, 16 and 15 (F, O and N, respectively) exhibit anomalously high boiling points due to hydrogen bonding.

A line graph is shown where the y-axis is labeled “Boiling point (, degree sign, C)” and has values of “ negative 150” to “150” from bottom to top in increments of 50. The x-axis is labeled “Period” and has values of “0” to “5” in increments of 1. Three lines are shown on the graph and are labeled in the legend. The red line is labeled as “halogen family,” the blue is “oxygen family” and the green is “nitrogen family.” The first point on the red line is labeled “question mark” and is at point “2, negative 120”. The second point on the line is labeled “H C l” and is at point “3, negative 80” while the third point on the line is labeled “H B r” and is at point “4, negative 60”. The fourth point on the line is labeled “H I” and is at point “5, negative 40.” The first point on the green line is labeled “question mark” and is at point “2, negative 125.” The second point on the line is labeled “P H, subscript 3” and is at point “3, negative 80” while the third point on the line is labeled “A s H, subscript 3” and is at point “4, negative 55.” The fourth point on the line is labeled “S b H, subscript 3” and is at point “5, negative 10.” The first point on the blue line is labeled “question mark” and is at point “2, negative 80.” The second point on the line is labeled “H, subscript 2, S” and is at point “3, negative 55” while the third point on the line is labeled “H, subscript 2, S e” and is at point “4, negative 45.” The fourth point on the line is labeled “H, subscript 2, T e” and is at point “5, negative 3.”

If we use this trend to predict the boiling points for the lightest hydride for each group, we would expect NH_3 to boil at about −120 °C, H_2O to boil at about −80 °C, and HF to boil at about −110 °C. However, when we measure the boiling points for these compounds, we find that they are dramatically higher than the trends would predict, as shown in Figure **6.2.10**. The stark contrast between our naïve predictions and reality provides compelling evidence for the strength of hydrogen bonding.

✔ Example 6.2.3: Effect of Hydrogen Bonding on Boiling Points

Consider the compounds dimethylether (CH_3OCH_3), ethanol (CH_3CH_2OH), and propane ($CH_3CH_2CH_3$). Their boiling points, not necessarily in order, are −42.1 °C, −24.8 °C, and 78.4 °C. Match each compound with its boiling point. Explain your reasoning.

Solution

The VSEPR-predicted shapes of CH_3OCH_3, CH_3CH_2OH, and $CH_3CH_2CH_3$ are similar, as are their molar masses (46 g/mol, 46 g/mol, and 44 g/mol, respectively), so they will exhibit similar dispersion forces. Since $CH_3CH_2CH_3$ is nonpolar, it may

exhibit *only* dispersion forces. Because CH_3OCH_3 is polar, it will also experience dipole-dipole attractions. Finally, CH_3CH_2OH has an −OH group, and so it will experience the uniquely strong dipole-dipole attraction known as hydrogen bonding. So the ordering in terms of strength of IMFs, and thus boiling points, is $CH_3CH_2CH_3 < CH_3OCH_3 < CH_3CH_2OH$. The boiling point of propane is −42.1 °C, the boiling point of dimethylether is −24.8 °C, and the boiling point of ethanol is 78.5 °C.

? Exercise 6.2.3

Ethane (CH_3CH_3) has a melting point of −183 °C and a boiling point of −89 °C. Predict the melting and boiling points for methylamine (CH_3NH_2). Explain your reasoning.

Answer

The melting point and boiling point for methylamine are predicted to be significantly greater than those of ethane. CH_3CH_3 and CH_3NH_2 are similar in size and mass, but methylamine possesses an −NH group and therefore may exhibit hydrogen bonding. This greatly increases its IMFs, and therefore its melting and boiling points. It is difficult to predict values, but the known values are a melting point of −93 °C and a boiling point of −6 °C.

6.2.5: Hydrogen Bonding and DNA

Deoxyribonucleic acid (DNA) is found in every living organism and contains the genetic information that determines the organism's characteristics, provides the blueprint for making the proteins necessary for life, and serves as a template to pass this information on to the organism's offspring. A DNA molecule consists of two (anti-)parallel chains of repeating nucleotides, which form its well-known double helical structure, as shown in Figure **6.2.10**.

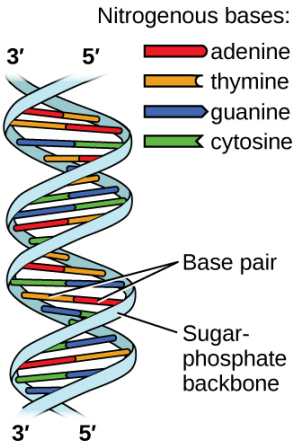


Figure **6.2.11**: Two separate DNA molecules form a double-stranded helix in which the molecules are held together via hydrogen bonding. (credit: modification of work by Jerome Walker, Dennis Myts)

Two images are shown. The first lies on the left side of the page and shows a helical structure like a twisted ladder where the rungs of the ladder, labeled “Base pair” are red, yellow, green and blue paired bars. The red and yellow bars, which are always paired together, are labeled in the legend, which is titled “Nitrogenous bases” as “adenine” and “thymine,” respectively. The blue and green bars, which are always paired together, are labeled in the legend as “guanine” and “cytosine,” respectively. At the top of the helical structure, the left-hand side rail, or “Sugar, dash, phosphate backbone,” is labeled as “3, prime” while the right is labeled as “5, prime.” These labels are reversed at the bottom of the helix. To the right of the page is a large Lewis structure. The top left corner of this structure, labeled “5, prime,” shows a phosphorus atom single bonded to three oxygen atoms, one of which has a superscripted negative charge, and double bonded to a fourth oxygen atom. One of the single bonded oxygen atoms is single bonded to the left corner of a five-membered ring with an oxygen atom at its top point and which is single bonded to an oxygen atom on the bottom left. This oxygen atom is single bonded to a phosphorus atom that is single bonded to two other hydrogen atoms and double bonded to a fourth oxygen atom. The lower left of these oxygen atoms is single bonded to another oxygen atom that is single bonded to a five-membered ring with an oxygen in the upper bonding site. The bottom left of this ring has a hydroxyl group attached to it while the upper right carbon is single bonded to a nitrogen atom that is part of a five-membered ring bonded to a six-membered ring. Both of these rings have points of unsaturation and nitrogen atoms bonded into their structures. On the right side of the six-membered ring are two single bonded amine groups and a double bonded oxygen. Three separate dotted lines extend from these sites to corresponding sites on a second six-membered ring. This ring has points of unsaturation and a nitrogen atom in the bottom right bonding position that is single bonded to a five-membered ring on the right side of the image. This ring is single bonded to a carbon that is single bonded to an oxygen that is single bonded to a phosphorus. The phosphorus is single bonded to two other oxygen atoms and double bonded to a fourth oxygen atom. This group is labeled “5, prime.” The five-membered ring is also bonded on the top side to an oxygen that is bonded to a phosphorus single bonded to two other oxygen atoms and double bonded to a fourth oxygen atom. The upper left oxygen of this group is single bonded to a carbon that is single bonded to a five-membered ring with an oxygen in the bottom bonding position. This ring has a hydroxyl group on its upper right side that is labeled “3, prime” and is bonded on the left side to a nitrogen that is a member of a five-membered ring. This ring is bonded to a six-membered ring and both have points of unsaturation. This ring has a nitrogen on the left side, as well as an amine group, that have two dotted lines leading from them to an oxygen and amine group on a six membered ring. These dotted lines are labeled “Hydrogen bonds.” The six membered ring also has a double bonded oxygen on its lower side and a nitrogen atom on its left side that is single bonded to a five-membered ring. This ring connects to the two phosphate groups mentioned at the start of this to form a large circle. The name “guanine” is written below the lower left side of this image while the name “cytosine” is written on the lower right. The name “thymine” is written above the right side of the image and “adenine” is written on the top right. Three sections are indicated below the images where the left is labeled “Sugar, dash, phosphate backbone,” the middle is labeled “Bases” and the right is labeled “Sugar, dash, phosphate backbone.”

Each nucleotide contains a (deoxyribose) sugar bound to a phosphate group on one side, and one of four nitrogenous bases on the other. Two of the bases, cytosine (C) and thymine (T), are single-ringed structures known as pyrimidines. The other two, adenine (A) and guanine (G), are double-ringed structures called purines. These bases form complementary base pairs consisting of one purine and one pyrimidine, with adenine pairing with thymine, and cytosine with guanine. Each base pair is held together by hydrogen bonding. A and T share two hydrogen bonds, C and G share three, and both pairings have a similar shape and structure Figure **6.2.12**

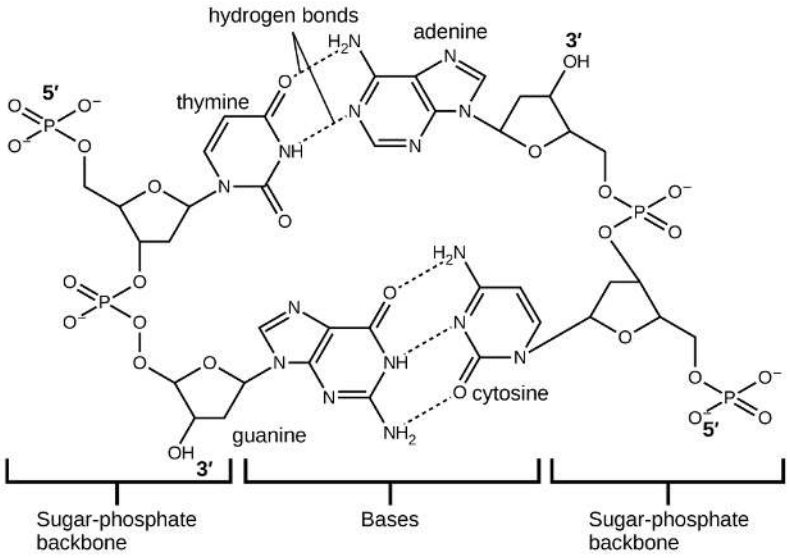


Figure 6.2.12: The geometries of the base molecules result in maximum hydrogen bonding between adenine and thymine (AT) and between guanine and cytosine (GC), so-called “complementary base pairs.”

A large Lewis structure is shown. The top left corner of this structure, labeled “5, prime,” shows a phosphorus atom single bonded to three oxygen atoms, one of which has a superscripted negative charge, and double bonded to a fourth oxygen atom. One of the single bonded oxygen atoms is single bonded to the left corner of a five-membered ring with an oxygen atom at its top point and which is single bonded to an oxygen atom on the bottom left. This oxygen atom is single bonded to a phosphorus atom that is single bonded to two other hydrogen atoms and double bonded to a fourth oxygen atom. The lower left of these oxygen atoms is single bonded to another oxygen atom that is single bonded to a five-membered ring with an oxygen in the upper bonding site. The bottom left of this ring has a hydroxyl group attached to it while the upper right carbon is single bonded to a nitrogen atom that is part of a five-membered ring bonded to a six-membered ring. Both of these rings have points of unsaturation and nitrogen atoms bonded into their structures. On the right side of the six-membered ring are two single bonded amine groups and a double bonded oxygen. Three separate dotted lines extend from these sites to corresponding sites on a second six-membered ring. This ring has points of unsaturation and a nitrogen atom in the bottom right bonding position that is single bonded to a five-membered ring on the right side of the image. This ring is single bonded to a carbon that is single bonded to an oxygen that is single bonded to a phosphorus. The phosphorus is single bonded to two other oxygen atoms and double bonded to a fourth oxygen atom. This group is labeled “5, prime.” The five-membered ring is also bonded on the top side to an oxygen that is bonded to a phosphorus single bonded to two other oxygen atoms and double bonded to a fourth oxygen atom. The upper left oxygen of this group is single bonded to a carbon that is single bonded to a five-membered ring with an oxygen in the bottom bonding position. This ring has a hydroxyl group on its upper right side that is labeled “3, prime” and is bonded on the left side to a nitrogen that is a member of a five-membered ring. This ring is bonded to a six-membered ring and both have points of unsaturation. This ring has a nitrogen on the left side, as well as an amine group, that have two dotted lines leading from them to an oxygen and amine group on a six membered ring. These dotted lines are labeled “Hydrogen bonds.” The six membered ring also has a double bonded oxygen on its lower side and a nitrogen atom on its left side that is single bonded to a five-membered ring. This ring connects to the two phosphate groups mentioned at the start of this to form a large circle. The name “guanine” is written below the lower left side of this image while the name “cytosine” is written on the lower right. The name “thymine” is written above the right side of the image and “adenine” is written on the top right. Three sections are indicated below the images where the left is labeled “Sugar, dash, phosphate backbone,” the middle is labeled “Bases” and the right is labeled “Sugar, dash, phosphate backbone.”

The cumulative effect of millions of hydrogen bonds effectively holds the two strands of DNA together. Importantly, the two strands of DNA can relatively easily “unzip” down the middle since hydrogen bonds are relatively weak compared to the covalent bonds that hold the atoms of the individual DNA molecules together. This allows both strands to function as a template for replication.

Summary

The physical properties of condensed matter (liquids and solids) can be explained in terms of the kinetic molecular theory. In a liquid, intermolecular attractive forces hold the molecules in contact, although they still have sufficient kinetic energy to move past each other. Intermolecular attractive forces, collectively referred to as van der Waals forces, are responsible for the behavior of liquids and solids and are electrostatic in nature. Dipole-dipole attractions result from the electrostatic attraction of the partial negative end of one dipolar molecule for the partial positive end of another. The temporary dipole that results from the motion of the electrons in an atom can induce a dipole in an adjacent atom and give rise to the London dispersion force. London forces

increase with increasing molecular size. Hydrogen bonds are a special type of dipole-dipole attraction that results when hydrogen is bonded to one of the three most electronegative elements: F, O, or N.

Glossary

dipole-dipole attraction
intermolecular attraction between two permanent dipoles

dispersion force
(also, London dispersion force) attraction between two rapidly fluctuating, temporary dipoles; significant only when particles are very close together

hydrogen bonding
occurs when exceptionally strong dipoles attract; bonding that exists when hydrogen is bonded to one of the three most electronegative elements: F, O, or N

induced dipole
temporary dipole formed when the electrons of an atom or molecule are distorted by the instantaneous dipole of a neighboring atom or molecule

instantaneous dipole
temporary dipole that occurs for a brief moment in time when the electrons of an atom or molecule are distributed asymmetrically

intermolecular force
noncovalent attractive force between atoms, molecules, and/or ions

polarizability
measure of the ability of a charge to distort a molecule's charge distribution (electron cloud)

van der Waals force
attractive or repulsive force between molecules, including dipole-dipole, dipole-induced dipole, and London dispersion forces; does not include forces due to covalent or ionic bonding, or the attraction between ions and molecules

---

This page titled 6.2: Intermolecular Forces Review is shared under a CC BY 4.0 license and was authored, remixed, and/or curated by OpenStax via source content that was edited to the style and standards of the LibreTexts platform.

- **10.2: Intermolecular Forces** by OpenStax is licensed CC BY 4.0. Original source: https://openstax.org/details/books/chemistry-2e.

6.3: Properties of Liquids

Learning Objectives

- Distinguish between adhesive and cohesive forces
- Define viscosity, surface tension, and capillary rise
- Describe the roles of intermolecular attractive forces in each of these properties/phenomena

When you pour a glass of water, or fill a car with gasoline, you observe that water and gasoline flow freely. But when you pour syrup on pancakes or add oil to a car engine, you note that syrup and motor oil do not flow as readily. The viscosity of a liquid is a measure of its resistance to flow. Water, gasoline, and other liquids that flow freely have a low viscosity. Honey, syrup, motor oil, and other liquids that do not flow freely, like those shown in Figure **6.3.1**, have higher viscosities. We can measure viscosity by measuring the rate at which a metal ball falls through a liquid (the ball falls more slowly through a more viscous liquid) or by measuring the rate at which a liquid flows through a narrow tube (more viscous liquids flow more slowly).



Figure **6.3.1**: (a) Honey and (b) motor oil are examples of liquids with high viscosities; they flow slowly. (credit a: modification of work by Scott Bauer; credit b: modification of work by David Nagy)

Two photographs are shown and labeled “a” and “b.” Photo a shows a jar of honey with a dipper drizzling it onto a biscuit. More biscuits are shown in a basket in the background. Photo b shows the engine of a car and a person adding motor oil to the engine.

The IMFs between the molecules of a liquid, the size and shape of the molecules, and the temperature determine how easily a liquid flows. As Table **6.3.1** shows, the more structurally complex are the molecules in a liquid and the stronger the IMFs between them, the more difficult it is for them to move past each other and the greater is the viscosity of the liquid. As the temperature increases, the molecules move more rapidly and their kinetic energies are better able to overcome the forces that hold them together; thus, the viscosity of the liquid decreases.

Table **6.3.1**: Viscosities of Common Substances at 25 °C

Substance	Formula	Viscosity (mPa·s)
water	H_2O	0.890
mercury	Hg	1.526
ethanol	C_2H_5OH	1.074
octane	C_8H_{18}	0.508
ethylene glycol	$CH_2(OH)CH_2(OH)$	16.1
honey	variable	~2,000–10,000
motor oil	variable	~50–500

The various IMFs between identical molecules of a substance are examples of cohesive forces. The molecules within a liquid are surrounded by other molecules and are attracted equally in all directions by the cohesive forces within the liquid. However, the molecules on the surface of a liquid are attracted only by about one-half as many molecules. Because of the unbalanced molecular

attractions on the surface molecules, liquids contract to form a shape that minimizes the number of molecules on the surface—that is, the shape with the minimum surface area. A small drop of liquid tends to assume a spherical shape, as shown in Figure **6.3.2**, because in a sphere, the ratio of surface area to volume is at a minimum. Larger drops are more greatly affected by gravity, air resistance, surface interactions, and so on, and as a result, are less spherical.

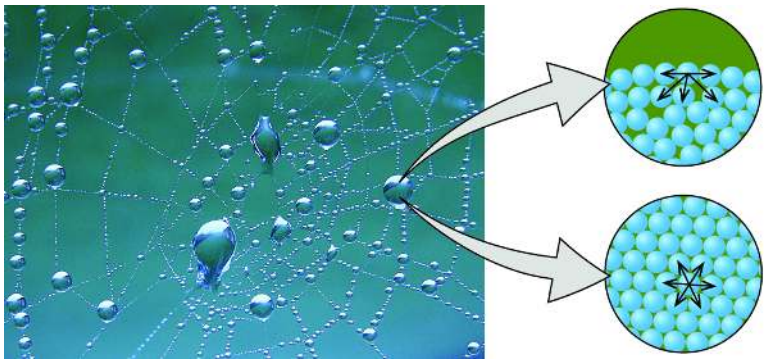


Figure **6.3.2**: Attractive forces result in a spherical water drop that minimizes surface area; cohesive forces hold the sphere together; adhesive forces keep the drop attached to the web. (credit photo: modification of work by "OliBac"/Flickr)

A photo of a spider's web with droplets of water attached to it is shown. Two images are shown the right of the photo and arrows lead from the photo to the images. The upper image shows twenty eight blue spheres stacked one atop the other in the bottom of a circular background. Five arrows are drawn pointing to the sides and downward from the sphere in the top middle of the drawing. The lower image shows another circular background of the same size as the first, but this time the blue spheres fill the image and are packed closely together. A sphere in the middle has six arrows pointing in all directions away from it.

Surface tension is defined as the energy required to increase the surface area of a liquid, or the force required to increase the length of a liquid surface by a given amount. This property results from the cohesive forces between molecules at the surface of a liquid, and it causes the surface of a liquid to behave like a stretched rubber membrane. Surface tensions of several liquids are presented in Table **6.3.2**.

Table **6.3.2**: Surface Tensions of Common Substances at 25 °C

Substance	Formula	Surface Tension (mN/m)
water	H_2O	71.99
mercury	Hg	458.48
ethanol	C_2H_5OH	21.97
octane	C_8H_{18}	21.14
ethylene glycol	$CH_2(OH)CH_2(OH)$	47.99

Among common liquids, water exhibits a distinctly high surface tension due to strong hydrogen bonding between its molecules. As a result of this high surface tension, the surface of water represents a relatively "tough skin" that can withstand considerable force without breaking. A steel needle carefully placed on water will float. Some insects, like the one shown in Figure **6.3.3**, even though they are denser than water, move on its surface because they are supported by the surface tension.

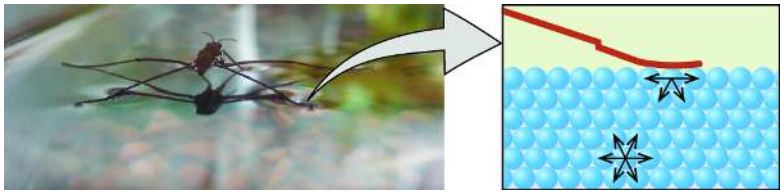


Figure **6.3.3**: Surface tension (right) prevents this insect, a "water strider," from sinking into the water.

A photo and a diagram as shown and a right-facing arrow leads from the photo to the image. The photo shows an insect standing on the surface of a sample of water. The image shows a square background that is two thirds covered in blue spheres that are closely packet together. A brown line starts at the upper left corner of the background and rests on top of the first row of spheres. The sphere directly under this low point of the line has four arrows drawn on it that face to both sides and downward. A sphere in the bottom center of the image has six arrows drawn on it that all face outward in different directions.

The IMFs of attraction between two *different* molecules are called adhesive forces. Consider what happens when water comes into contact with some surface. If the adhesive forces between water molecules and the molecules of the surface are weak compared to the cohesive forces between the water molecules, the water does not "wet" the surface. For example, water does not wet waxed surfaces or many plastics such as polyethylene. Water forms drops on these surfaces because the cohesive forces within the drops are greater than the adhesive forces between the water and the plastic. Water spreads out on glass because the adhesive force between water and glass is greater than the cohesive forces within the water. When water is confined in a glass tube, its meniscus (surface) has a concave shape because the water wets the glass and creeps up the side of the tube. On the other hand, the cohesive forces between mercury atoms are much greater than the adhesive forces between mercury and glass. Mercury therefore does not wet glass, and it forms a convex meniscus when confined in a tube because the cohesive forces within the mercury tend to draw it into a drop (Figure **6.3.4**).

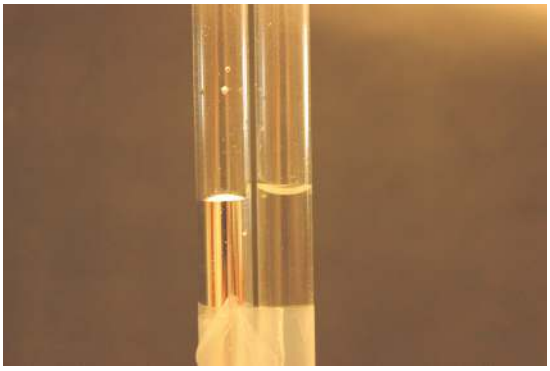


Figure **6.3.4**: Differences in the relative strengths of cohesive and adhesive forces result in different meniscus shapes for mercury (left) and water (right) in glass tubes. (credit: Mark Ott)

This figure shows two test tubes. The test tube on the left contains mercury with a meniscus that rounds up. The test tube on the right contains water with a meniscus that rounds down.

If you place one end of a paper towel in spilled wine, as shown in Figure **6.3.5**, the liquid wicks up the paper towel. A similar process occurs in a cloth towel when you use it to dry off after a shower. These are examples of capillary action—when a liquid flows within a porous material due to the attraction of the liquid molecules to the surface of the material and to other liquid molecules. The adhesive forces between the liquid and the porous material, combined with the cohesive forces within the liquid, may be strong enough to move the liquid upward against gravity.

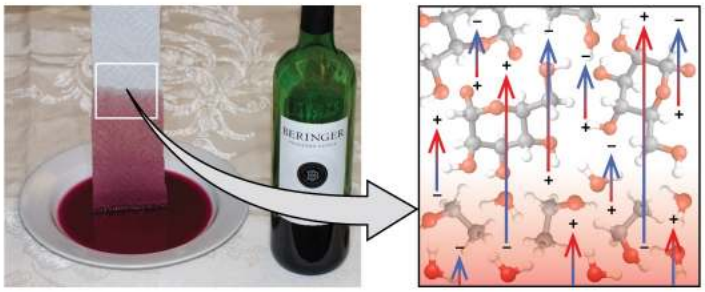


Figure **6.3.5**: Wine wicks up a paper towel (left) because of the strong attractions of water (and ethanol) molecules to the −OH groups on the towel's cellulose fibers and the strong attractions of water molecules to other water (and ethanol) molecules (right). (credit photo: modification of work by Mark Blaser)

A photo and a diagram are shown. In the photo, a paper towel is dipped into a bowl full of a red liquid sitting on a countertop. The red liquid is traveling up the lower part of the paper towel, and this section of the photo has a square drawn around it. A right-facing arrow leads from this square to the image. The image is square and has a background of two types of molecules, mixed together. The first type of molecule is composed of two bonded black spheres, one of which is single bonded to three white spheres and one of which is single bonded to two white spheres and a red sphere that is itself bonded to a white sphere. The other type of molecule is composed of six black spheres bonded together in a row and bonded to other red and white spheres. Six upward-facing arrows are drawn on top of this background. They have positive signs on their lower ends and negative signs on their heads. Four upward-facing arrows are drawn with their signs reversed.

Towels soak up liquids like water because the fibers of a towel are made of molecules that are attracted to water molecules. Most cloth towels are made of cotton, and paper towels are generally made from paper pulp. Both consist of long molecules of cellulose

that contain many −OH groups. Water molecules are attracted to these −OH groups and form hydrogen bonds with them, which draws the H_2O molecules up the cellulose molecules. The water molecules are also attracted to each other, so large amounts of water are drawn up the cellulose fibers.

Capillary action can also occur when one end of a small diameter tube is immersed in a liquid, as illustrated in Figure **6.3.6**. If the liquid molecules are strongly attracted to the tube molecules, the liquid creeps up the inside of the tube until the weight of the liquid and the adhesive forces are in balance. The smaller the diameter of the tube is, the higher the liquid climbs. It is partly by capillary action occurring in plant cells called xylem that water and dissolved nutrients are brought from the soil up through the roots and into a plant. Capillary action is the basis for thin layer chromatography, a laboratory technique commonly used to separate small quantities of mixtures. You depend on a constant supply of tears to keep your eyes lubricated and on capillary action to pump tear fluid away.

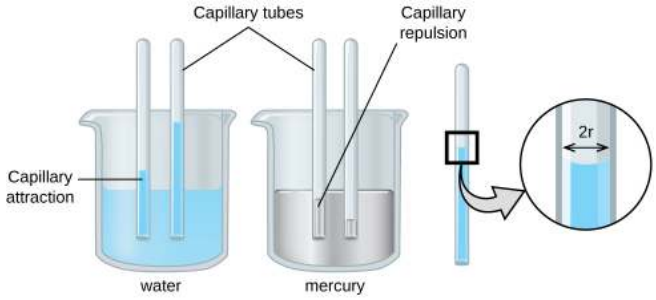


Figure **6.3.6**: Depending upon the relative strengths of adhesive and cohesive forces, a liquid may rise (such as water) or fall (such as mercury) in a glass capillary tube. The extent of the rise (or fall) is directly proportional to the surface tension of the liquid and inversely proportional to the density of the liquid and the radius of the tube.

An image of two beakers and a tube is shown. The first beaker, drawn on the left and labeled “Water,” is drawn half-full of a blue liquid. Two tubes are placed vertically in the beaker and inserted into the liquid. The liquid is shown higher in the tubes than in the beaker and is labeled “Capillary attraction.” The second beaker, drawn in the middle and labeled “Mercury,” is drawn half-full of a gray liquid. Two tubes are placed vertically in the beaker and inserted into the liquid. The liquid is shown lower in the tubes than in the beaker and is labeled “Capillary repulsion.” Lines point to the vertical tubes and label them “Capillary tubes.” A separate drawing of one of the vertical tubes from the first beaker is shown on the right. A right-facing arrow leads from the liquid in the tube to a square call-out box that shows a close-up view of the liquid’s surface. The distance across the tube is labeled “2 r” in this image.

The height to which a liquid will rise in a capillary tube is determined by several factors as shown in the following equation:

$$h = \frac{2T\cos\theta}{r\rho g} \tag{6.3.1}$$

where

- h is the height of the liquid inside the capillary tube relative to the surface of the liquid outside the tube,
- T is the surface tension of the liquid,
- θ is the contact angle between the liquid and the tube,
- r is the radius of the tube, ρ is the density of the liquid, and
- g is the acceleration due to gravity, 9.8 m/s^2.

When the tube is made of a material to which the liquid molecules are strongly attracted, they will spread out completely on the surface, which corresponds to a contact angle of 0°. This is the situation for water rising in a glass tube.

Example **6.3.1**: Capillary Rise

At 25 °C, how high will water rise in a glass capillary tube with an inner diameter of 0.25 mm?

For water, T = 71.99 mN/m and ρ = 1.0 g/cm^3.

Solution

The liquid will rise to a height h given by Equation **6.3.1** :

$$h = \frac{2T\cos\theta}{r\rho g}$$

The Newton is defined as a kg m/s^2, and so the provided surface tension is equivalent to 0.07199 kg/s^2. The provided density must be converted into units that will cancel appropriately: ρ = 1000 kg/m^3. The diameter of the tube in meters is 0.00025 m, so the radius is 0.000125 m. For a glass tube immersed in water, the contact angle is θ = 0°, so cos θ = 1. Finally, acceleration due to gravity on the earth is g = 9.8 m/s^2. Substituting these values into the equation, and cancelling units, we have:

$$h = \frac{2(0.07199\ \text{kg/s}^2)}{(0.000125\ \text{m})(1000\ \text{kg/m}^3)(9.8\ \text{m/s}^2)} = 0.12\ \text{m} = 12\ \text{cm}$$

? Exercise 6.3.1

Water rises in a glass capillary tube to a height of 8.4 cm. What is the diameter of the capillary tube?

Answer

diameter = 0.36 mm

Applications: Capillary Action is Used to Draw Blood

Many medical tests require drawing a small amount of blood, for example to determine the amount of glucose in someone with diabetes or the hematocrit level in an athlete. This procedure can be easily done because of capillary action, the ability of a liquid to flow up a small tube against gravity, as shown in Figure **6.3.7**. When your finger is pricked, a drop of blood forms and holds together due to surface tension—the unbalanced intermolecular attractions at the surface of the drop. Then, when the open end of a narrow-diameter glass tube touches the drop of blood, the adhesive forces between the molecules in the blood and those at the glass surface draw the blood up the tube. How far the blood goes up the tube depends on the diameter of the tube (and the type of fluid). A small tube has a relatively large surface area for a given volume of blood, which results in larger (relative) attractive forces, allowing the blood to be drawn farther up the tube. The liquid itself is held together by its own cohesive forces. When the weight of the liquid in the tube generates a downward force equal to the upward force associated with capillary action, the liquid stops rising.



Figure **6.3.7**:: Blood is collected for medical analysis by capillary action, which draws blood into a small diameter glass tube. (credit: modification of work by Centers for Disease Control and Prevention)

A photograph shows a person's hand being held by a person wearing medical gloves. A thin glass tube is pressed against the persons finger and blood is moving up the tube.

6.3.1: Key Concepts and Summary

The intermolecular forces between molecules in the liquid state vary depending upon their chemical identities and result in corresponding variations in various physical properties. Cohesive forces between like molecules are responsible for a liquid's viscosity (resistance to flow) and surface tension (elasticity of a liquid surface). Adhesive forces between the molecules of a liquid and different molecules composing a surface in contact with the liquid are responsible for phenomena such as surface wetting and capillary rise.

6.3.2: Key Equations

- $h = \frac{2T\cos\theta}{r\rho g}$

Glossary

adhesive force
force of attraction between molecules of different chemical identities

capillary action
flow of liquid within a porous material due to the attraction of the liquid molecules to the surface of the material and to other liquid molecules

cohesive force
force of attraction between identical molecules

surface tension
energy required to increase the area, or length, of a liquid surface by a given amount

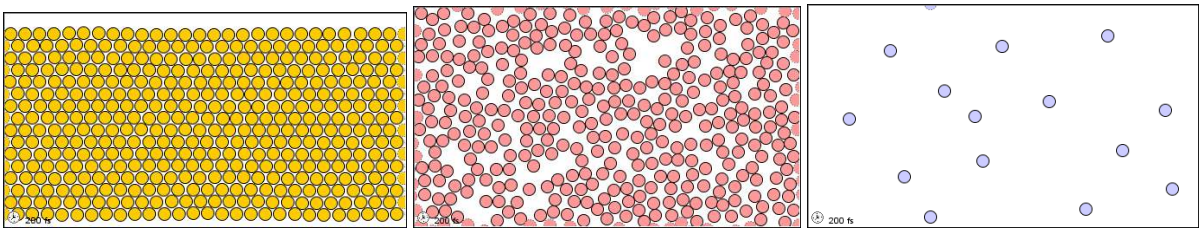
viscosity
measure of a liquid’s resistance to flow

This page titled 6.3: Properties of Liquids is shared under a CC BY 4.0 license and was authored, remixed, and/or curated by OpenStax via source content that was edited to the style and standards of the LibreTexts platform.

- **10.3: Properties of Liquids** by OpenStax is licensed CC BY 4.0. Original source: https://openstax.org/details/books/chemistry-2e.

6.4: Phase Transitions- Overview

We have now looked at the physical properties which chemists use to define the solid, liquid, and gas phases. In a solid, atoms, ions or molecules, are locked into an organized, long range lattice structure, unable to move beyond an average position due to intermolecular forces. In a liquid, this structure breaks down, molecules can slip past each other, but they are still held together by attractive forces. In a gas, these attractive forces are overcome, and the substance expands to fill space, each particle having gained mobility to break free of the others. Below, all 3 phases are shown at the submicroscopic level in animations. Notice how the movement and freedom of molecules steadily increases as attractive forces decrease from solid to liquid to gas phase.



Substances can be transformed from one phase into another. Solids melt into liquids and liquids boil to form vapors at temperatures which depend on their molecular properties, so chemists are interested in these transitions between phases. We are all familiar with the changes in macroscopic properties that accompany these transitions. YouTube has time lapse movies of ice melting on a small scale, or of the more environmentally critical arctic ice melt from 1979 to 2007.

This is a familiar process. As the solid melts, the resulting liquid is able to flow and conforms to the shape of the container. Heat from a flame is needed to bring about this transition. On a microscopic level melting involves breaking the intermolecular interactions between molecules. This requires an increase in the potential energy of the molecules, and the necessary energy is supplied by the Bunsen burner. Melting (or freezing) can, in some cases, be caused by changing just the pressure.

Boiling is equally familiar. Under specific temperature and pressure conditions, liquids start to bubble, and are converted to a gaseous form. A YouTube video "Boiling water with ice" shows that water boils at low temperatures if the pressure is reduced. Heat energy is absorbed when a liquid boils because molecules which are held together by mutual attraction in the liquid are jostled free of each other as the gas is formed. Such a separation requires energy.

In general the energy needed differs from one liquid to another depending on the magnitude of the intermolecular forces. We can thus expect liquids with strong intermolecular forces to boil at higher temperatures. It should be noted as well, that because there is a distribution in the kinetic energies of molecules, an equilibrium between gas and liquid phase is established at temperatures other than the boiling point, and this behavior is another aspect of phase transitions that chemists study.

For phase transitions from solid to liquid, liquid to gas, or solid to gas, energy is required because they involve separation of particles which attract one another. Further, we can predict under which conditions of temperature and pressure such transitions will occur.

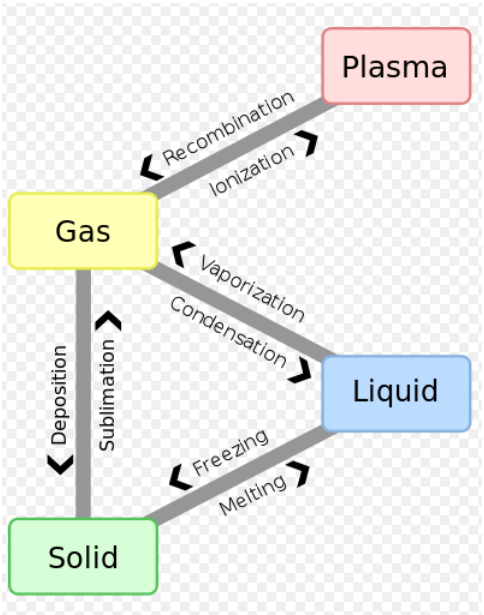


Figure 10.8.1 The figure above shows the transitions between phases and the corresponding names for each transition.

This page titled 6.4: Phase Transitions- Overview is shared under a CC BY-NC-SA 4.0 license and was authored, remixed, and/or curated by Ed Vitz, John W. Moore, Justin Shorb, Xavier Prat-Resina, Tim Wendorff, & Adam Hahn.

- **10.9: Phase Transitions** by Ed Vitz, John W. Moore, Justin Shorb, Xavier Prat-Resina, Tim Wendorff, & Adam Hahn is licensed CC BY-NC-SA 4.0.

6.5: Phase Transitions

Learning Objectives

- Define phase transitions and phase transition temperatures
- Explain the relation between phase transition temperatures and intermolecular attractive forces
- Describe the processes represented by typical heating and cooling curves, and compute heat flows and enthalpy changes accompanying these processes

We witness and utilize changes of physical state, or phase transitions, in a great number of ways. As one example of global significance, consider the evaporation, condensation, freezing, and melting of water. These changes of state are essential aspects of our earth's water cycle as well as many other natural phenomena and technological processes of central importance to our lives. In this module, the essential aspects of phase transitions are explored.

6.5.1: Vaporization and Condensation

When a liquid vaporizes in a closed container, gas molecules cannot escape. As these gas phase molecules move randomly about, they will occasionally collide with the surface of the condensed phase, and in some cases, these collisions will result in the molecules re-entering the condensed phase. The change from the gas phase to the liquid is called condensation. When the rate of condensation becomes equal to the rate of vaporization, neither the amount of the liquid nor the amount of the vapor in the container changes. The vapor in the container is then said to be *in equilibrium* with the liquid. Keep in mind that this is not a static situation, as molecules are continually exchanged between the condensed and gaseous phases. Such is an example of a dynamic equilibrium, the status of a system in which reciprocal processes (for example, vaporization and condensation) occur at equal rates. The pressure exerted by the vapor in equilibrium with a liquid in a closed container at a given temperature is called the liquid's vapor pressure (or equilibrium vapor pressure). The area of the surface of the liquid in contact with a vapor and the size of the vessel have no effect on the vapor pressure, although they do affect the time required for the equilibrium to be reached. We can measure the vapor pressure of a liquid by placing a sample in a closed container, like that illustrated in Figure **6.5.1**, and using a manometer to measure the increase in pressure that is due to the vapor in equilibrium with the condensed phase.

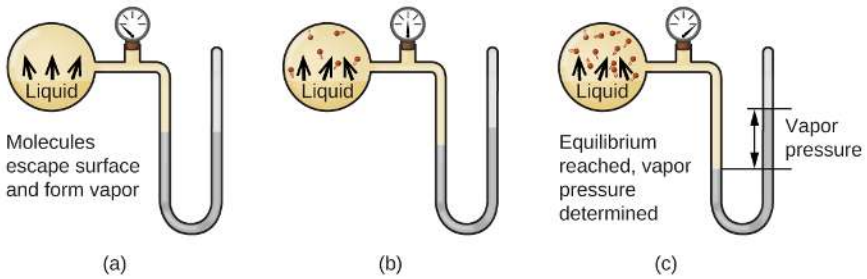


Figure **6.5.1**: In a closed container, dynamic equilibrium is reached when (a) the rate of molecules escaping from the liquid to become the gas (b) increases and eventually (c) equals the rate of gas molecules entering the liquid. When this equilibrium is reached, the vapor pressure of the gas is constant, although the vaporization and condensation processes continue.

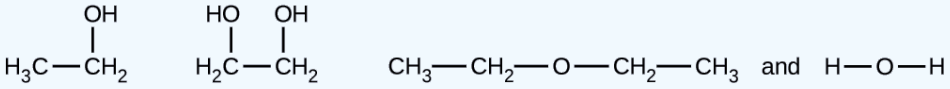
Three images are shown and labeled "a," "b," and "c." Each image shows a round bulb connected on the right to a tube that is horizontal, then is bent vertically, curves, and then is vertical again to make a u-shape. A valve is located in the horizontal portion of the tube. Image a depicts a liquid in the bulb, labeled, "Liquid," and upward-facing arrows leading away from the surface of the liquid. The phrase, "Molecules escape surface and form vapor" is written below the bulb, and a gray liquid in the u-shaped portion of the tube is shown at equal heights on the right and left sides. Image b depicts a liquid in the bulb, labeled, "Liquid," and upward-facing arrows leading away from the surface of the liquid to molecules drawn in the upper portion of the bulb. A gray liquid in the u-shaped portion of the tube is shown slightly higher on the right side than on the left side. Image c depicts a liquid in the bulb, labeled, "Liquid," and upward-facing arrows leading away from the surface of the liquid to molecules drawn in the upper portion of the bulb. There are more molecules present in c than in b. The phrase "Equilibrium reached, vapor pressure determined," is written below the bulb and a gray liquid in the u-shaped portion of the tube is shown higher on the right side. A horizontal line is drawn level with each of these liquid levels and the distance between the lines is labeled with a double-headed arrow. This section is labeled with the phrase, "Vapor pressure."

The chemical identities of the molecules in a liquid determine the types (and strengths) of intermolecular attractions possible; consequently, different substances will exhibit different equilibrium vapor pressures. Relatively strong intermolecular attractive

forces will serve to impede vaporization as well as favoring “recapture” of gas-phase molecules when they collide with the liquid surface, resulting in a relatively low vapor pressure. Weak intermolecular attractions present less of a barrier to vaporization, and a reduced likelihood of gas recapture, yielding relatively high vapor pressures. The following example illustrates this dependence of vapor pressure on intermolecular attractive forces.

Example 6.5.1: Explaining Vapor Pressure in Terms of IMFs

Given the shown structural formulas for these four compounds, explain their relative vapor pressures in terms of types and extents of IMFs:



ethanol ethylene glycol diethyl ether water

Solution

Diethyl ether has a very small dipole and most of its intermolecular attractions are London forces. Although this molecule is the largest of the four under consideration, its IMFs are the weakest and, as a result, its molecules most readily escape from the liquid. It also has the highest vapor pressure. Due to its smaller size, ethanol exhibits weaker dispersion forces than diethyl ether. However, ethanol is capable of hydrogen bonding and, therefore, exhibits stronger overall IMFs, which means that fewer molecules escape from the liquid at any given temperature, and so ethanol has a lower vapor pressure than diethyl ether. Water is much smaller than either of the previous substances and exhibits weaker dispersion forces, but its extensive hydrogen bonding provides stronger intermolecular attractions, fewer molecules escaping the liquid, and a lower vapor pressure than for either diethyl ether or ethanol. Ethylene glycol has two −OH groups, so, like water, it exhibits extensive hydrogen bonding. It is much larger than water and thus experiences larger London forces. Its overall IMFs are the largest of these four substances, which means its vaporization rate will be the slowest and, consequently, its vapor pressure the lowest.

Exercise 6.5.1

At 20 °C, the vapor pressures of several alcohols are given in this table. Explain these vapor pressures in terms of types and extents of IMFs for these alcohols:

At 20 °C, the vapor pressures of several alcohols

Compound	methanol CH_3OH	ethanol C_2H_5OH	propanol C_3H_7OH	butanol C_4H_9OH
Vapor Pressure at 20 °C	11.9 kPa	5.95 kPa	2.67 kPa	0.56 kPa

Answer

All these compounds exhibit hydrogen bonding; these strong IMFs are difficult for the molecules to overcome, so the vapor pressures are relatively low. As the size of molecule increases from methanol to butanol, dispersion forces increase, which means that the vapor pressures decrease as observed:

$$P_{methanol} > P_{ethanol} > P_{propanol} > P_{butanol}$$

As temperature increases, the vapor pressure of a liquid also increases due to the increased average KE of its molecules. Recall that at any given temperature, the molecules of a substance experience a range of kinetic energies, with a certain fraction of molecules having a sufficient energy to overcome IMF and escape the liquid (vaporize). At a higher temperature, a greater fraction of molecules have enough energy to escape from the liquid, as shown in Figure 6.5.2. The escape of more molecules per unit of time and the greater average speed of the molecules that escape both contribute to the higher vapor pressure.

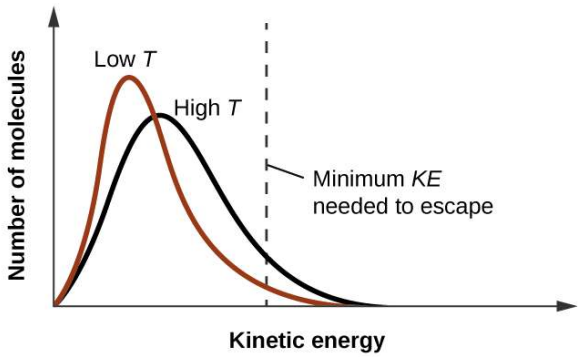


Figure 6.5.2: Temperature affects the distribution of kinetic energies for the molecules in a liquid. At the higher temperature, more molecules have the necessary kinetic energy, KE, to escape from the liquid into the gas phase.

A graph is shown where the y-axis is labeled “Number of molecules” and the x-axis is labeled “Kinetic Energy.” Two lines are graphed and a vertical dotted line, labeled “Minimum K E needed to escape,” is drawn halfway across the x-axis. The first line move sharply upward and has a high peak near the left side of the x-axis. It drops just as steeply and ends about 60 percent of the way across the x-axis. This line is labeled “Low T.” A second line, labeled “High T,” begins at the same point as the first, but does not go to such a high point, is wider, and ends slightly further to the right on the x-axis.

6.5.2: Boiling Points

When the vapor pressure increases enough to equal the external atmospheric pressure, the liquid reaches its boiling point. The boiling point of a liquid is the temperature at which its equilibrium vapor pressure is equal to the pressure exerted on the liquid by its gaseous surroundings. For liquids in open containers, this pressure is that due to the earth’s atmosphere. The normal boiling point of a liquid is defined as its boiling point when surrounding pressure is equal to 1 atm (101.3 kPa). Figure 6.5.3 shows the variation in vapor pressure with temperature for several different substances. Considering the definition of boiling point, these curves may be seen as depicting the dependence of a liquid’s boiling point on surrounding pressure.

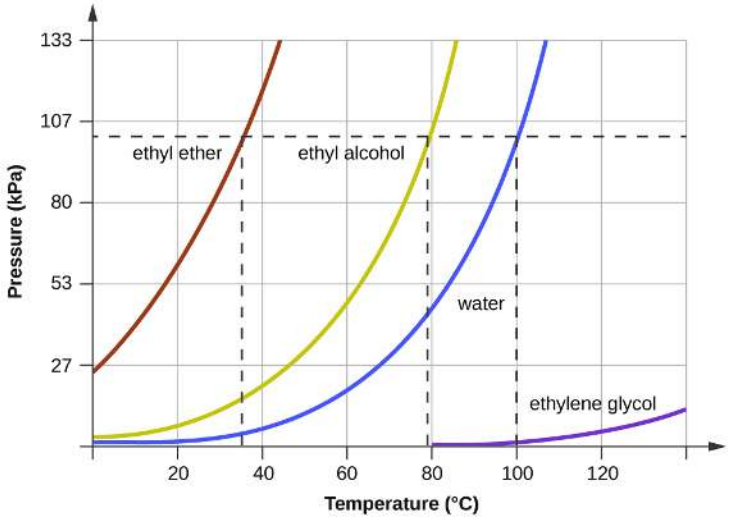


Figure 6.5.3: The boiling points of liquids are the temperatures at which their equilibrium vapor pressures equal the pressure of the surrounding atmosphere. Normal boiling points are those corresponding to a pressure of 1 atm (101.3 kPa.)

A graph is shown where the x-axis is labeled “Temperature (degree sign, C)” and has values of 200 to 1000 in increments of 200 and the y-axis is labeled “Pressure (k P a)” and has values of 20 to 120 in increments of 20. A horizontal dotted line extends across the graph at point 780 on the y-axis while three vertical dotted lines extend from points 35, 78, and 100 to meet the horizontal dotted line. Four lines are graphed. The first line, labeled “ethyl ether,” begins at the point “0 , 200” and extends in a slight curve to point “45, 1000” while the second line, labeled “ethanol”, extends from point “0, 20” to point “88, 1000” in a more extreme curve. The third line, labeled “water,” begins at the point “0, 0” and extends in a curve to point “108, 1000” while the fourth line, labeled “ethylene glycol,” extends from point “80, 0” to point “140, 100” in a very shallow curve.

Example 6.5.2: A Boiling Point at Reduced Pressure

A typical atmospheric pressure in Leadville, Colorado (elevation 10,200 feet) is 68 kPa. Use the graph in Figure **6.5.3** to determine the boiling point of water at this elevation.

Solution

The graph of the vapor pressure of water versus temperature in Figure **6.5.3** indicates that the vapor pressure of water is 68 kPa at about 90 °C. Thus, at about 90 °C, the vapor pressure of water will equal the atmospheric pressure in Leadville, and water will boil.

Exercise 6.5.2

The boiling point of ethyl ether was measured to be 10 °C at a base camp on the slopes of Mount Everest. Use Figure **6.5.3** to determine the approximate atmospheric pressure at the camp.

Answer

Approximately 40 kPa (0.4 atm)

The quantitative relation between a substance's vapor pressure and its temperature is described by the Clausius-Clapeyron equation:

$$P = Ae^{-\Delta H_{vap}/RT} \tag{6.5.1}$$

where

- ΔH_{vap} is the enthalpy of vaporization for the liquid,
- R is the gas constant, and
- $\ln A$ is a constant whose value depends on the chemical identity of the substance.

Equation 6.5.1 is often rearranged into logarithmic form to yield the linear equation:

$$\ln P = -\frac{\Delta H_{vap}}{RT} + \ln A \tag{6.5.2}$$

This linear equation may be expressed in a two-point format that is convenient for use in various computations, as demonstrated in the examples and exercises that follow. If at temperature T_1, the vapor pressure is P_1, and at temperature T_2, the vapor pressure is T_2, the corresponding linear equations are:

$$\ln P_1 = -\frac{\Delta H_{vap}}{RT_1} + \ln A$$

and

$$\ln P_2 = -\frac{\Delta H_{vap}}{RT_2} + \ln A \tag{6.5.3}$$

Since the constant, ln A, is the same, these two equations may be rearranged to isolate $\ln A$ and then set them equal to one another:

$$\ln P_1 + \frac{\Delta H_{vap}}{RT_1} = \ln P_2 + \frac{\Delta H_{vap}}{RT_2}$$

which can be combined into:

$$\ln\left(\frac{P_2}{P_1}\right) = \frac{\Delta H_{vap}}{R}\left(\frac{1}{T_1} - \frac{1}{T_2}\right) \tag{6.5.4}$$

Example 6.5.3: Estimating Enthalpy of Vaporization

Isooctane (2,2,4-trimethylpentane) has an octane rating of 100. It is used as one of the standards for the octane-rating system for gasoline. At 34.0 °C, the vapor pressure of isooctane is 10.0 kPa, and at 98.8 °C, its vapor pressure is 100.0 kPa. Use this information to estimate the enthalpy of vaporization for isooctane.

Solution

The enthalpy of vaporization, ΔH_{vap}, can be determined by using the Clausius-Clapeyron equation (Equation 6.5.4):

$$\ln\left(\frac{P_2}{P_1}\right) = \frac{\Delta H_{\text{vap}}}{R}\left(\frac{1}{T_1} - \frac{1}{T_2}\right)$$

Since we have two vapor pressure-temperature values

- $T_1 = 34.0°C = 307.2\,K$
- $P_1 = 10.0\,kPa$ and
- $T_2 = 98.8°C = 372.0\,K$
- $P_2 = 100\,kPa$

we can substitute them into this equation and solve for ΔH_{vap}. Rearranging the Clausius-Clapeyron equation and solving for ΔH_{vap} yields:

$$\begin{aligned}\Delta H_{\text{vap}} &= \frac{R \cdot \ln\left(\frac{P_2}{P_1}\right)}{\left(\frac{1}{T_1} - \frac{1}{T_2}\right)} \\ &= \frac{(8.3145\,J/mol \cdot K) \cdot \ln\left(\frac{100\,kPa}{10.0\,kPa}\right)}{\left(\frac{1}{307.2\,K} - \frac{1}{372.0\,K}\right)} \\ &= 33,800\,J/mol = 33.8\,kJ/mol\end{aligned}$$

Note that the pressure can be in any units, so long as they agree for both P values, but the temperature must be in kelvin for the Clausius-Clapeyron equation to be valid.

Exercise 6.5.3

At 20.0 °C, the vapor pressure of ethanol is 5.95 kPa, and at 63.5 °C, its vapor pressure is 53.3 kPa. Use this information to estimate the enthalpy of vaporization for ethanol.

Answer

47,782 J/mol = 47.8 kJ/mol

Example 6.5.4: Estimating Temperature (or Vapor Pressure)

For benzene (C_6H_6), the normal boiling point is 80.1 °C and the enthalpy of vaporization is 30.8 kJ/mol. What is the boiling point of benzene in Denver, where atmospheric pressure = 83.4 kPa?

Solution

If the temperature and vapor pressure are known at one point, along with the enthalpy of vaporization, ΔH_{vap}, then the temperature that corresponds to a different vapor pressure (or the vapor pressure that corresponds to a different temperature) can be determined by using the Clausius-Clapeyron equation (Equation 6.5.1) :

$$\ln\left(\frac{P_2}{P_1}\right) = \frac{\Delta H_{\text{vap}}}{R}\left(\frac{1}{T_1} - \frac{1}{T_2}\right)$$

Since the normal boiling point is the temperature at which the vapor pressure equals atmospheric pressure at sea level, we know one vapor pressure-temperature value (T_1 = 80.1 °C = 353.3 K, P_1 = 101.3 kPa, ΔH_{vap} = 30.8 kJ/mol) and want to find the temperature (T_2) that corresponds to vapor pressure P_2 = 83.4 kPa. We can substitute these values into the Clausius-Clapeyron equation and then solve for T_2. Rearranging the Clausius-Clapeyron equation and solving for T_2 yields:

$$T_2 = \left(\frac{-R \cdot \ln\left(\frac{P_2}{P_1}\right)}{\Delta H_{vap}} + \frac{1}{T_1} \right)^{-1}$$

$$= \left(\frac{-(8.3145\ \text{J/mol·K}) \cdot \ln\left(\frac{83.4\ \text{kPa}}{101.3\ \text{kPa}}\right)}{30{,}800\ \text{J/mol}} + \frac{1}{353.3\ \text{K}} \right)^{-1}$$

$$= 346.9\ \text{K or } 73.8°\text{C}$$

Exercise 6.5.4

For acetone $(CH_3)_2CO$, the normal boiling point is 56.5 °C and the enthalpy of vaporization is 31.3 kJ/mol. What is the vapor pressure of acetone at 25.0 °C?

Answer

30.1 kPa

6.5.3: Enthalpy of Vaporization

Vaporization is an endothermic process. The cooling effect can be evident when you leave a swimming pool or a shower. When the water on your skin evaporates, it removes heat from your skin and causes you to feel cold. The energy change associated with the vaporization process is the enthalpy of vaporization, ΔH_{vap}. For example, the vaporization of water at standard temperature is represented by:

$$H_2O(l) \longrightarrow H_2O(g) \quad \Delta H_{vap} = 44.01\ \text{kJ/mol}$$

As described in the chapter on thermochemistry, the reverse of an endothermic process is exothermic. And so, the condensation of a gas releases heat:

$$H_2O(g) \longrightarrow H_2O(l) \quad \Delta H_{con} = -\Delta H_{vap} = -44.01\ \text{kJ/mol}$$

Example 6.5.5: Using Enthalpy of Vaporization

One way our body is cooled is by evaporation of the water in sweat (Figure 6.5.4). In very hot climates, we can lose as much as 1.5 L of sweat per day. Although sweat is not pure water, we can get an approximate value of the amount of heat removed by evaporation by assuming that it is. How much heat is required to evaporate 1.5 L of water (1.5 kg) at T = 37 °C (normal body temperature); $\Delta H_{vap} = 43.46\ kJ/mol$ at 37 °C.



Figure 6.5.4: Evaporation of sweat helps cool the body. (credit: “Kullez”/Flickr)

Solution We start with the known volume of sweat (approximated as just water) and use the given information to convert to the amount of heat needed:

$$1.5\,\cancel{L} \times \frac{1000\,\cancel{g}}{1\,\cancel{L}} \times \frac{1\,\cancel{\text{mol}}}{18\,\cancel{g}} \times \frac{43.46\ \text{kJ}}{1\,\cancel{\text{mol}}} = 3.6 \times 10^3\ \text{kJ}$$

Thus, 3600 kJ of heat are removed by the evaporation of 1.5 L of water.

? Exercise 6.5.5: Boiling Ammonia

How much heat is required to evaporate 100.0 g of liquid ammonia, NH_3, at its boiling point if its enthalpy of vaporization is 4.8 kJ/mol?

Answer

28 kJ

6.5.4: Melting and Freezing

When we heat a crystalline solid, we increase the average energy of its atoms, molecules, or ions and the solid gets hotter. At some point, the added energy becomes large enough to partially overcome the forces holding the molecules or ions of the solid in their fixed positions, and the solid begins the process of transitioning to the liquid state, or melting. At this point, the temperature of the solid stops rising, despite the continual input of heat, and it remains constant until all of the solid is melted. Only after all of the solid has melted will continued heating increase the temperature of the liquid (Figure 6.5.5.



Figure 6.5.5: (a) This beaker of ice has a temperature of −12.0 °C. (b) After 10 minutes the ice has absorbed enough heat from the air to warm to 0 °C. A small amount has melted. (c) Thirty minutes later, the ice has absorbed more heat, but its temperature is still 0 °C. The ice melts without changing its temperature. (d) Only after all the ice has melted does the heat absorbed cause the temperature to increase to 22.2 °C. (credit: modification of work by Mark Ott).

This figure shows four photos each labeled, “a,” “b,” “c,” and, “d.” Each photo shows a beaker with ice and a digital thermometer. The first photo shows ice cubes in the beaker, and the thermometer reads negative 12.0 degrees C. The second photo shows slightly melted ice, and the thermometer reads 0.0 degrees C. The third photo shows more water than ice in the beaker. The thermometer reads 0.0 degrees C. The fourth photo shows the ice completely melted, and the thermometer reads 22.2 degrees C.

If we stop heating during melting and place the mixture of solid and liquid in a perfectly insulated container so no heat can enter or escape, the solid and liquid phases remain in equilibrium. This is almost the situation with a mixture of ice and water in a very good thermos bottle; almost no heat gets in or out, and the mixture of solid ice and liquid water remains for hours. In a mixture of solid and liquid at equilibrium, the reciprocal processes of melting and freezing occur at equal rates, and the quantities of solid and liquid therefore remain constant. The temperature at which the solid and liquid phases of a given substance are in equilibrium is called the melting point of the solid or the freezing point of the liquid. Use of one term or the other is normally dictated by the direction of the phase transition being considered, for example, solid to liquid (melting) or liquid to solid (freezing).

The enthalpy of fusion and the melting point of a crystalline solid depend on the strength of the attractive forces between the units present in the crystal. Molecules with weak attractive forces form crystals with low melting points. Crystals consisting of particles with stronger attractive forces melt at higher temperatures.

The amount of heat required to change one mole of a substance from the solid state to the liquid state is the enthalpy of fusion, ΔHfus of the substance. The enthalpy of fusion of ice is 6.0 kJ/mol at 0 °C. Fusion (melting) is an endothermic process:

$$\mathrm{H_2O_{(s)} \rightarrow H_2O_{(l)} \quad \Delta H_{fus} = 6.01\ kJ/mol} \tag{6.5.5}$$

The reciprocal process, freezing, is an exothermic process whose enthalpy change is −6.0 kJ/mol at 0 °C:

$$\mathrm{H_2O_{(l)} \rightarrow H_2O_{(s)} \quad \Delta H_{frz} = -\Delta H_{fus} = -6.01\ kJ/mol} \tag{6.5.6}$$

6.5.5: Sublimation and Deposition

Some solids can transition directly into the gaseous state, bypassing the liquid state, via a process known as sublimation. At room temperature and standard pressure, a piece of dry ice (solid CO_2) sublimes, appearing to gradually disappear without ever forming any liquid. Snow and ice sublime at temperatures below the melting point of water, a slow process that may be accelerated by winds and the reduced atmospheric pressures at high altitudes. When solid iodine is warmed, the solid sublimes and a vivid purple vapor forms (Figure **6.5.6**). The reverse of sublimation is called deposition, a process in which gaseous substances condense directly into the solid state, bypassing the liquid state. The formation of frost is an example of deposition.



Figure **6.5.6**: Sublimation of solid iodine in the bottom of the tube produces a purple gas that subsequently deposits as solid iodine on the colder part of the tube above. (credit: modification of work by Mark Ott)

This figure shows a test tube. In the bottom is a dark substance which breaks up into a purple gas at the top.

Like vaporization, the process of sublimation requires an input of energy to overcome intermolecular attractions. The enthalpy of sublimation, ΔHsub, is the energy required to convert one mole of a substance from the solid to the gaseous state. For example, the sublimation of carbon dioxide is represented by:

$$\mathrm{CO_2(s) \longrightarrow CO_2(g) \quad \Delta H_{sub} = 26.1\ kJ/mol}$$

Likewise, the enthalpy change for the reverse process of deposition is equal in magnitude but opposite in sign to that for sublimation:

$$\mathrm{CO_2(g) \longrightarrow CO_2(s) \quad \Delta H_{dep} = -\Delta H_{sub} = -26.1\ kJ/mol}$$

Consider the extent to which intermolecular attractions must be overcome to achieve a given phase transition. Converting a solid into a liquid requires that these attractions be only partially overcome; transition to the gaseous state requires that they be completely overcome. As a result, the enthalpy of fusion for a substance is less than its enthalpy of vaporization. This same logic

can be used to derive an approximate relation between the enthalpies of all phase changes for a given substance. Though not an entirely accurate description, sublimation may be conveniently modeled as a sequential two-step process of melting followed by vaporization in order to apply Hess's Law.

$$\begin{aligned} \text{solid} &\longrightarrow \text{liquid} \quad \Delta H_{\text{fus}} \\ \text{liquid} &\longrightarrow \text{gas} \quad \Delta H_{\text{vap}} \\ \hline \text{solid} &\longrightarrow \text{gas} \quad \Delta H_{\text{sub}} = \Delta H_{\text{fus}} + \Delta H_{\text{vap}} \end{aligned}$$

Viewed in this manner, the enthalpy of sublimation for a substance may be estimated as the sum of its enthalpies of fusion and vaporization, as illustrated in Figure 6.5.7. For example:

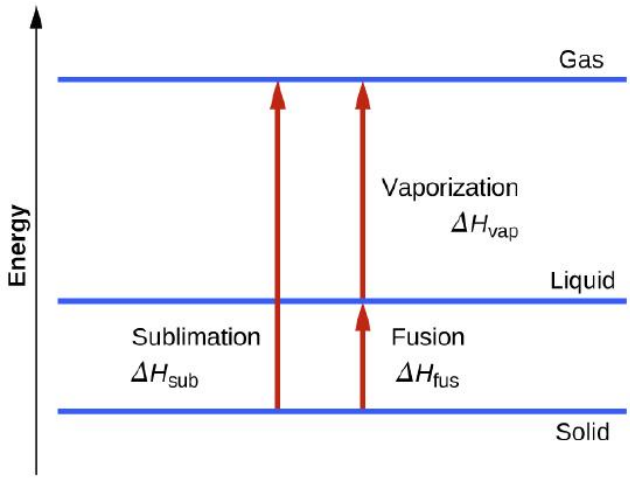


Figure 6.5.7: For a given substance, the sum of its enthalpy of fusion and enthalpy of vaporization is approximately equal to its enthalpy of sublimation.

A diagram is shown with a vertical line drawn on the left side and labeled "Energy" and three horizontal lines drawn near the bottom, lower third and top of the diagram. These three lines are labeled, from bottom to top, "Solid," "Liquid" and "Gas." Near the middle of the diagram, a vertical, upward-facing arrow is drawn from the solid line to the gas line and labeled "Sublimation, delta sign, H, subscript sub." To the right of this arrow is a second vertical, upward-facing arrow that is drawn from the solid line to the liquid line and labeled "Fusion, delta sign, H, subscript fus." Above the second arrow is a third arrow drawn from the liquid line to the gas line and labeled, "Vaporization, delta sign, H, subscript vap."

6.5.6: Heating and Cooling Curves

In the chapter on thermochemistry, the relation between the amount of heat absorbed or related by a substance, q, and its accompanying temperature change, ΔT, was introduced:

$$q = mc\Delta T$$

where m is the mass of the substance and c is its specific heat. The relation applies to matter being heated or cooled, but not undergoing a change in state. When a substance being heated or cooled reaches a temperature corresponding to one of its phase transitions, further gain or loss of heat is a result of diminishing or enhancing intermolecular attractions, instead of increasing or decreasing molecular kinetic energies. While a substance is undergoing a change in state, its temperature remains constant. Figure 6.5.8 shows a typical heating curve.

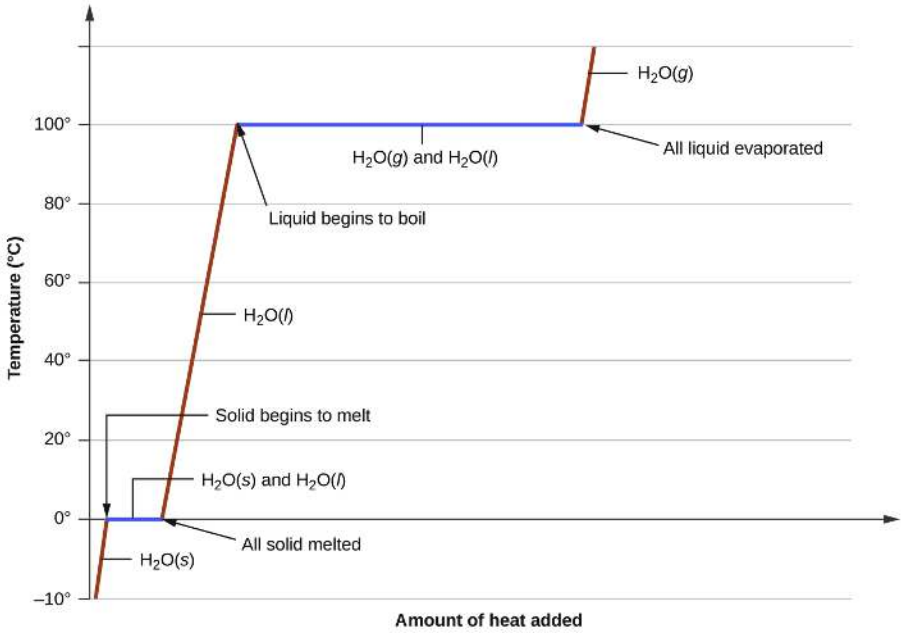


Figure **6.5.8**: A typical heating curve for a substance depicts changes in temperature that result as the substance absorbs increasing amounts of heat. Plateaus in the curve (regions of constant temperature) are exhibited when the substance undergoes phase transitions.

A graph is shown where the x-axis is labeled “Amount of heat added” and the y-axis is labeled “Temperature (degree sign C)” and has values of negative 10 to 100 in increments of 20. A right-facing horizontal arrow extends from point “0, 0” to the right side of the graph. A line graph begins at the lower left of the graph and moves to point “0” on the y-axis. This segment of the line is labeled “H, subscript 2, O (s).” The line then flattens and travels horizontally for a small distance. This segment is labeled “Solid begins to melt” on its left side and “All solid melted” on its right side. The line then goes steeply upward in a linear fashion until it hits point “100” on the y-axis. This segment of the line is labeled “H, subscript 2, O,(l).” The line then flattens and travels horizontally for a moderate distance. This segment is labeled “Liquid begins to boil” on its left side and “All liquid evaporated” on its right side. The line then rises to a point above “100” on the y-axis. This segment of the line is labeled “H, subscript 2, O (g).”

Consider the example of heating a pot of water to boiling. A stove burner will supply heat at a roughly constant rate; initially, this heat serves to increase the water’s temperature. When the water reaches its boiling point, the temperature remains constant despite the continued input of heat from the stove burner. This same temperature is maintained by the water as long as it is boiling. If the burner setting is increased to provide heat at a greater rate, the water temperature does not rise, but instead the boiling becomes more vigorous (rapid). This behavior is observed for other phase transitions as well: For example, temperature remains constant while the change of state is in progress.

✔ Example **6.5.6**: Total Heat Needed to Change Temperature and Phase for a Substance

How much heat is required to convert 135 g of ice at −15 °C into water vapor at 120 °C?

Solution

The transition described involves the following steps:

1. Heat ice from −15 °C to 0 °C
2. Melt ice
3. Heat water from 0 °C to 100 °C
4. Boil water
5. Heat steam from 100 °C to 120 °C

The heat needed to change the temperature of a given substance (with no change in phase) is: $q = m \times c \times \Delta T$ (see previous chapter on thermochemistry). The heat needed to induce a given change in phase is given by $q = n \times \Delta H$.

Using these equations with the appropriate values for specific heat of ice, water, and steam, and enthalpies of fusion and vaporization, we have:

$$q_{\text{total}} = (m \cdot c \cdot \Delta T)_{\text{ice}} + n \cdot \Delta H_{\text{fus}} + (m \cdot c \cdot \Delta T)_{\text{water}} + n \cdot \Delta H_{\text{vap}} + (m \cdot c \cdot \Delta T)_{\text{steam}}$$

$$= (135\ \text{g} \cdot 2.09\ \text{J/g·°C} \cdot 15\text{°C}) + \left(135 \cdot \frac{1\ \text{mol}}{18.02\ \text{g}} \cdot 6.01\ \text{kJ/mol}\right)$$

$$+(135\ \text{g} \cdot 4.18\ \text{J/g·°C} \cdot 100\text{°C}) + \left(135\ \text{g} \cdot \frac{1\ \text{mol}}{18.02\ \text{g}} \cdot 40.67\ \text{kJ/mol}\right)$$

$$+(135\ \text{g} \cdot 1.84\ \text{J/g·°C} \cdot 20\text{°C})$$

$$= 4230\ \text{J} + 45.0\ \text{kJ} + 56,500\ \text{J} + 305\ \text{kJ} + 4970\ \text{J}$$

Converting the quantities in J to kJ permits them to be summed, yielding the total heat required:

$$= 4.23\ \text{kJ} + 45.0\ \text{kJ} + 56.5\ \text{kJ} + 305\ \text{kJ} + 4.97\ \text{kJ} = 416\ \text{kJ}$$

? Exercise 6.5.6

What is the total amount of heat released when 94.0 g water at 80.0 °C cools to form ice at −30.0 °C?

Answer

40.5 kJ

Summary

Phase transitions are processes that convert matter from one physical state into another. There are six phase transitions between the three phases of matter. Melting, vaporization, and sublimation are all endothermic processes, requiring an input of heat to overcome intermolecular attractions. The reciprocal transitions of freezing, condensation, and deposition are all exothermic processes, involving heat as intermolecular attractive forces are established or strengthened. The temperatures at which phase transitions occur are determined by the relative strengths of intermolecular attractions and are, therefore, dependent on the chemical identity of the substance.

6.5.7: Key Equations

- $P = Ae^{-\Delta H_{\text{vap}}/RT}$
- $\ln P = -\dfrac{\Delta H_{\text{vap}}}{RT} + \ln A$
- $\ln\left(\dfrac{P_2}{P_1}\right) = \dfrac{\Delta H_{\text{vap}}}{R}\left(\dfrac{1}{T_1} - \dfrac{1}{T_2}\right)$

Glossary

boiling point
temperature at which the vapor pressure of a liquid equals the pressure of the gas above it

Clausius-Clapeyron equation
mathematical relationship between the temperature, vapor pressure, and enthalpy of vaporization for a substance

condensation
change from a gaseous to a liquid state

deposition
change from a gaseous state directly to a solid state

dynamic equilibrium
state of a system in which reciprocal processes are occurring at equal rates

freezing
change from a liquid state to a solid state

freezing point

temperature at which the solid and liquid phases of a substance are in equilibrium; see also *melting point*

melting

change from a solid state to a liquid state

melting point

temperature at which the solid and liquid phases of a substance are in equilibrium; see also *freezing point*

normal boiling point

temperature at which a liquid's vapor pressure equals 1 atm (760 torr)

sublimation

change from solid state directly to gaseous state

vapor pressure

(also, equilibrium vapor pressure) pressure exerted by a vapor in equilibrium with a solid or a liquid at a given temperature

vaporization

change from liquid state to gaseous state

This page titled 6.5: Phase Transitions is shared under a CC BY 4.0 license and was authored, remixed, and/or curated by OpenStax via source content that was edited to the style and standards of the LibreTexts platform.

- **10.4: Phase Transitions** by OpenStax is licensed CC BY 4.0. Original source: https://openstax.org/details/books/chemistry-2e.

6.6: Vaporization and Vapor Pressure

Learning Objectives

- To know how and why the vapor pressure of a liquid varies with temperature.
- To understand that the equilibrium vapor pressure of a liquid depends on the temperature and the intermolecular forces present.
- To understand that the relationship between pressure, enthalpy of vaporization, and temperature is given by the Clausius-Clapeyron equation.

Nearly all of us have heated a pan of water with the lid in place and shortly thereafter heard the sounds of the lid rattling and hot water spilling onto the stovetop. When a liquid is heated, its molecules obtain sufficient kinetic energy to overcome the forces holding them in the liquid and they escape into the gaseous phase. By doing so, they generate a population of molecules in the vapor phase above the liquid that produces a pressure—the vapor pressure of the liquid. In the situation we described, enough pressure was generated to move the lid, which allowed the vapor to escape. If the vapor is contained in a sealed vessel, however, such as an unvented flask, and the vapor pressure becomes too high, the flask will explode (as many students have unfortunately discovered). In this section, we describe vapor pressure in more detail and explain how to quantitatively determine the vapor pressure of a liquid.

Evaporation and Condensation

Because the molecules of a liquid are in constant motion, we can plot the fraction of molecules with a given kinetic energy (*KE*) against their kinetic energy to obtain the kinetic energy distribution of the molecules in the liquid (Figure **6.6.1**), just as we did for a gas. As for gases, increasing the temperature increases both the average kinetic energy of the particles in a liquid and the range of kinetic energy of the individual molecules. If we assume that a minimum amount of energy (E_0) is needed to overcome the intermolecular attractive forces that hold a liquid together, then some fraction of molecules in the liquid always has a kinetic energy greater than E_0. The fraction of molecules with a kinetic energy greater than this minimum value increases with increasing temperature. Any molecule with a kinetic energy greater than E_0 has enough energy to overcome the forces holding it in the liquid and escape into the vapor phase. Before it can do so, however, a molecule must also be at the surface of the liquid, where it is physically possible for it to leave the liquid surface; that is, only molecules at the surface can undergo evaporation (or vaporization), where molecules gain sufficient energy to enter a gaseous state above a liquid's surface, thereby creating a vapor pressure.

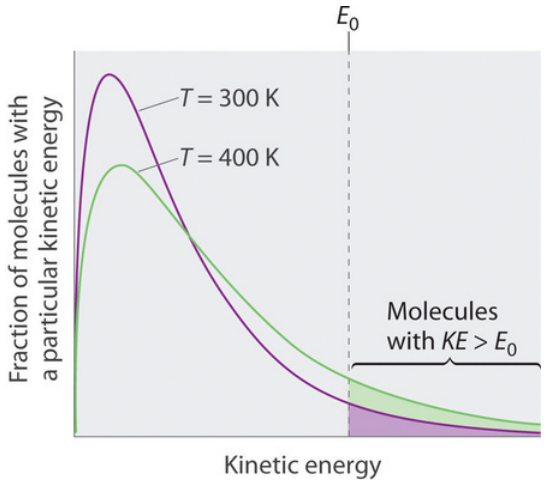


Figure **6.6.1**: The Distribution of the Kinetic Energies of the Molecules of a Liquid at Two Temperatures. Just as with gases, increasing the temperature shifts the peak to a higher energy and broadens the curve. Only molecules with a kinetic energy greater than E_0 can escape from the liquid to enter the vapor phase, and the proportion of molecules with $KE > E_0$ is greater at the higher temperature. (CC BY-SA-NC; Anonymous by request)

Graph of fraction of molecules with a particular kinetic energy against kinetic energy. Green line is temperature at 400 kelvin, purple line is temperature at 300 kelvin.

To understand the causes of vapor pressure, consider the apparatus shown in Figure **6.6.2**. When a liquid is introduced into an evacuated chamber (part (a) in Figure **6.6.2**), the initial pressure above the liquid is approximately zero because there are as yet no molecules in the vapor phase. Some molecules at the surface, however, will have sufficient kinetic energy to escape from the liquid and form a vapor, thus increasing the pressure inside the container. As long as the temperature of the liquid is held constant, the fraction of molecules with $KE > E_0$ will not change, and the rate at which molecules escape from the liquid into the vapor phase will depend only on the surface area of the liquid phase.

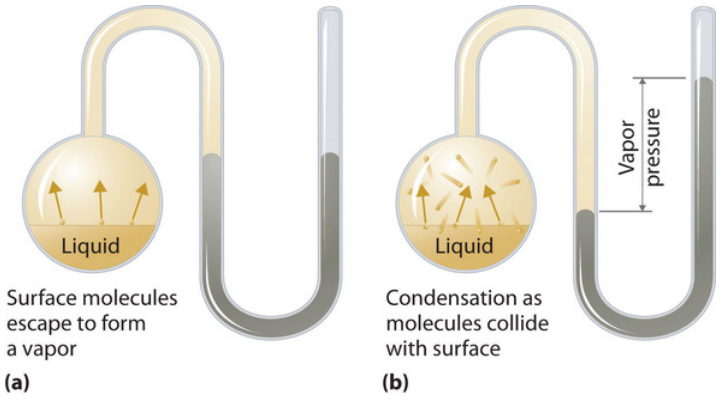


Figure **6.6.2**: Vapor Pressure. (a) When a liquid is introduced into an evacuated chamber, molecules with sufficient kinetic energy escape from the surface and enter the vapor phase, causing the pressure in the chamber to increase. (b) When sufficient molecules are in the vapor phase for a given temperature, the rate of condensation equals the rate of evaporation (a steady state is reached), and the pressure in the container becomes constant. (CC BY-SA-NC; Anonymous by request)

As soon as some vapor has formed, a fraction of the molecules in the vapor phase will collide with the surface of the liquid and reenter the liquid phase in a process known as condensation (part (b) in Figure **6.6.2**). As the number of molecules in the vapor phase increases, the number of collisions between vapor-phase molecules and the surface will also increase. Eventually, a *steady state* will be reached in which exactly as many molecules per unit time leave the surface of the liquid (vaporize) as collide with it (condense). At this point, the pressure over the liquid stops increasing and remains constant at a particular value that is characteristic of the liquid at a given temperature. The rates of evaporation and condensation over time for a system such as this are shown graphically in Figure **6.6.3**.

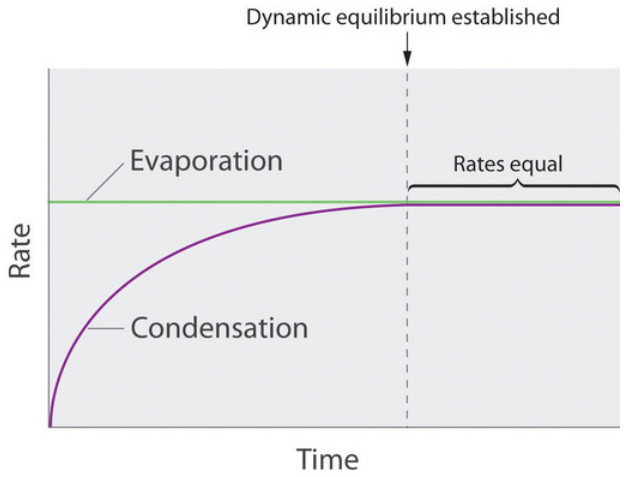


Figure **6.6.3**: The Relative Rates of Evaporation and Condensation as a Function of Time after a Liquid Is Introduced into a Sealed Chamber. The rate of evaporation depends only on the surface area of the liquid and is essentially constant. The rate of condensation depends on the number of molecules in the vapor phase and increases steadily until it equals the rate of evaporation. (CC BY-SA-NC; Anonymous by request)

Graph of rate against time. The green line is evaporation while the pruple line is condensation. Dynamic equilibrium is established when the evaporation and condensation rates are equal.

Equilibrium Vapor Pressure

Two opposing processes (such as evaporation and condensation) that occur at the same rate and thus produce no *net* change in a system, constitute a dynamic equilibrium. In the case of a liquid enclosed in a chamber, the molecules continuously evaporate and condense, but the amounts of liquid and vapor do not change with time. The pressure exerted by a vapor in dynamic equilibrium with a liquid is the equilibrium vapor pressure of the liquid.

If a liquid is in an *open* container, however, most of the molecules that escape into the vapor phase will *not* collide with the surface of the liquid and return to the liquid phase. Instead, they will diffuse through the gas phase away from the container, and an equilibrium will never be established. Under these conditions, the liquid will continue to evaporate until it has "disappeared." The speed with which this occurs depends on the vapor pressure of the liquid and the temperature. Volatile liquids have relatively high vapor pressures and tend to evaporate readily; nonvolatile liquids have low vapor pressures and evaporate more slowly. Although the dividing line between volatile and nonvolatile liquids is not clear-cut, as a general guideline, we can say that substances with vapor pressures greater than that of water (Figure **6.6.4**) are relatively volatile, whereas those with vapor pressures less than that of water are relatively nonvolatile. Thus diethyl ether (ethyl ether), acetone, and gasoline are volatile, but mercury, ethylene glycol, and motor oil are nonvolatile.

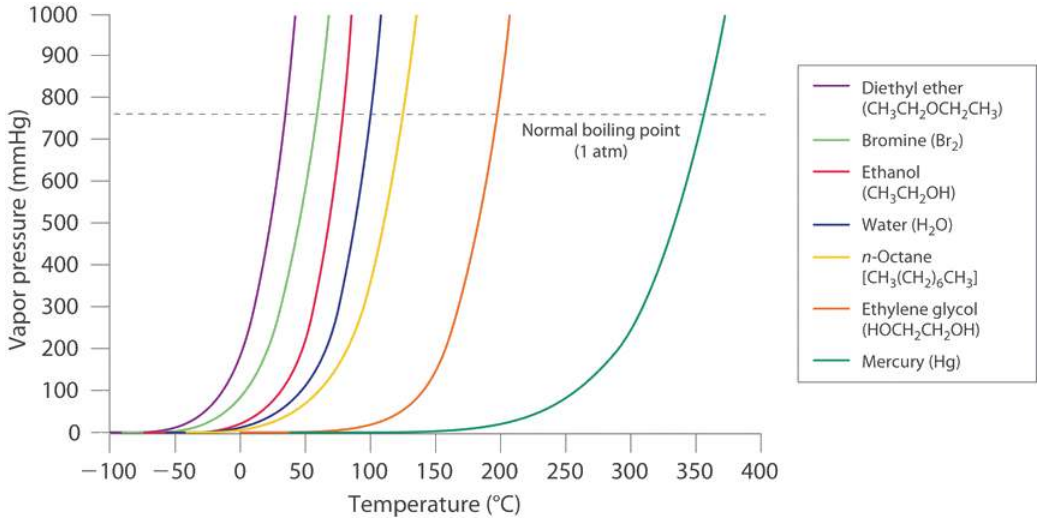


Figure **6.6.4**: The Vapor Pressures of Several Liquids as a Function of Temperature. The point at which the vapor pressure curve crosses the P = 1 atm line (dashed) is the normal boiling point of the liquid. (CC BY-SA-NC; Anonymous by request)

The equilibrium vapor pressure of a substance at a particular temperature is a characteristic of the material, like its molecular mass, melting point, and boiling point. It does *not* depend on the amount of liquid as long as at least a tiny amount of liquid is present in equilibrium with the vapor. The equilibrium vapor pressure does, however, depend very strongly on the temperature and the intermolecular forces present, as shown for several substances in Figure **6.6.4**. Molecules that can hydrogen bond, such as ethylene glycol, have a much lower equilibrium vapor pressure than those that cannot, such as octane. The nonlinear increase in vapor pressure with increasing temperature is *much* steeper than the increase in pressure expected for an ideal gas over the corresponding temperature range. The temperature dependence is so strong because the vapor pressure depends on the fraction of molecules that have a kinetic energy greater than that needed to escape from the liquid, and this fraction increases exponentially with temperature. As a result, sealed containers of volatile liquids are potential bombs if subjected to large increases in temperature. The gas tanks on automobiles are vented, for example, so that a car won't explode when parked in the sun. Similarly, the small cans (1–5 gallons) used to transport gasoline are required by law to have a pop-off pressure release.

> *Volatile substances have low boiling points and relatively weak intermolecular interactions; nonvolatile substances have high boiling points and relatively strong intermolecular interactions.*



A Video Discussing Vapor Pressure and Boiling Points. Video Source: Vapor Pressure & Boiling Point(opens in new window) [youtu.be]

The exponential rise in vapor pressure with increasing temperature in Figure **6.6.4** allows us to use natural logarithms to express the nonlinear relationship as a linear one.

$$\boxed{\ln P = \frac{-\Delta H_{vap}}{R}\left(\frac{1}{T}\right) + C} \tag{6.6.1}$$

where

- $\ln P$ is the natural logarithm of the vapor pressure,
- ΔH_{vap} is the enthalpy of vaporization,
- R is the universal gas constant [8.314 J/(mol•K)],
- T is the temperature in kelvins, and
- C is the y-intercept, which is a constant for any given line.

Plotting $\ln P$ versus the inverse of the absolute temperature ($1/T$) is a straight line with a slope of $-\Delta H_{vap}/R$. Equation 6.6.1, called the Clausius–Clapeyron Equation, can be used to calculate the ΔH_{vap} of a liquid from its measured vapor pressure at two or more temperatures. The simplest way to determine ΔH_{vap} is to measure the vapor pressure of a liquid at **two** temperatures and insert the values of P and T for these points into Equation 6.6.2, which is derived from the Clausius–Clapeyron equation:

$$\ln\left(\frac{P_1}{P_2}\right) = \frac{-\Delta H_{vap}}{R}\left(\frac{1}{T_1} - \frac{1}{T_2}\right) \tag{6.6.2}$$

Conversely, if we know ΔH_{vap} and the vapor pressure P_1 at any temperature T_1, we can use Equation 6.6.2 to calculate the vapor pressure P_2 at any other temperature T_2, as shown in Example **6.6.1**.



A Video Discussing the Clausius-Clapeyron Equation. Video Link: The Clausius-Clapeyron Equation(opens in new window) [youtu.be]

Example 6.6.1: Vapor Pressure of Mercury

The experimentally measured vapor pressures of liquid Hg at four temperatures are listed in the following table:

experimentally measured vapor pressures of liquid Hg at four temperatures

T (°C)	80.0	100	120	140
P (torr)	0.0888	0.2729	0.7457	1.845

From these data, calculate the enthalpy of vaporization (ΔH_{vap}) of mercury and predict the vapor pressure of the liquid at 160°C. (Safety note: mercury is highly toxic; when it is spilled, its vapor pressure generates hazardous levels of mercury vapor.)

Given: vapor pressures at four temperatures

Asked for: ΔH_{vap} of mercury and vapor pressure at 160°C

Strategy:

A. Use Equation 6.6.2 to obtain ΔH_{vap} directly from two pairs of values in the table, making sure to convert all values to the appropriate units.

B. Substitute the calculated value of ΔH_{vap} into Equation 6.6.2 to obtain the unknown pressure (P_2).

Solution:

A The table gives the measured vapor pressures of liquid Hg for four temperatures. Although one way to proceed would be to plot the data using Equation 6.6.1 and find the value of ΔH_{vap} from the slope of the line, an alternative approach is to use Equation 6.6.2 to obtain ΔH_{vap} directly from two pairs of values listed in the table, assuming no errors in our measurement. We therefore select two sets of values from the table and convert the temperatures from degrees Celsius to kelvin because the equation requires absolute temperatures. Substituting the values measured at 80.0°C (T_1) and 120.0°C (T_2) into Equation 6.6.2 gives

$$\ln\left(\frac{0.7457\ \cancel{Torr}}{0.0888\ \cancel{Torr}}\right) = \frac{-\Delta H_{vap}}{8.314\ J/mol \cdot K}\left(\frac{1}{(120+273)\ K} - \frac{1}{(80.0+273)\ K}\right)$$

$$\ln(8.398) = \frac{-\Delta H_{vap}}{8.314\ J/mol \cdot \cancel{K}}\left(-2.88 \times 10^{-4}\ \cancel{K^{-1}}\right)$$

$$2.13 = -\Delta H_{vap}\left(-3.46 \times 10^{-4}\right) J^{-1} \cdot mol$$

$$\Delta H_{vap} = 61,400\ J/mol = 61.4\ kJ/mol$$

B We can now use this value of ΔH_{vap} to calculate the vapor pressure of the liquid (P_2) at 160.0°C (T_2):

$$\ln\left(\frac{P_2}{0.0888\ torr}\right) = \frac{-61,400\ \cancel{J/mol}}{8.314\ \cancel{J/mol}\ K^{-1}}\left(\frac{1}{(160+273)\ K} - \frac{1}{(80.0+273)\ K}\right)$$

Using the relationship $e^{\ln x} = x$, we have

$$\ln\left(\frac{P_2}{0.0888\ Torr}\right) = 3.86$$

$$\frac{P_2}{0.0888\ Torr} = e^{3.86} = 47.5$$

$$P_2 = 4.21 Torr$$

At 160°C, liquid Hg has a vapor pressure of 4.21 torr, substantially greater than the pressure at 80.0°C, as we would expect.

? Exercise 6.6.1: Vapor Pressure of Nickel

The vapor pressure of liquid nickel at 1606°C is 0.100 torr, whereas at 1805°C, its vapor pressure is 1.000 torr. At what temperature does the liquid have a vapor pressure of 2.500 torr?

Answer

1896°C

Boiling Points

As the temperature of a liquid increases, the vapor pressure of the liquid increases until it equals the external pressure, or the atmospheric pressure in the case of an open container. Bubbles of vapor begin to form throughout the liquid, and the liquid begins to boil. The temperature at which a liquid boils at exactly 1 atm pressure is the normal boiling point of the liquid. For water, the normal boiling point is exactly 100°C. The normal boiling points of the other liquids in Figure **6.6.4** are represented by the points at which the vapor pressure curves cross the line corresponding to a pressure of 1 atm. Although we usually cite the normal boiling point of a liquid, the *actual* boiling point depends on the pressure. At a pressure greater than 1 atm, water boils at a temperature greater than 100°C because the increased pressure forces vapor molecules above the surface to condense. Hence the molecules must have greater kinetic energy to escape from the surface. Conversely, at pressures less than 1 atm, water boils below 100°C.

Table **6.6.1**: The Boiling Points of Water at Various Locations on Earth

Place	Altitude above Sea Level (ft)	Atmospheric Pressure (mmHg)	Boiling Point of Water (°C)
Mt. Everest, Nepal/Tibet	29,028	240	70
Bogota, Colombia	11,490	495	88
Denver, Colorado	5280	633	95
Washington, DC	25	759	100
Dead Sea, Israel/Jordan	−1312	799	101.4

Typical variations in atmospheric pressure at sea level are relatively small, causing only minor changes in the boiling point of water. For example, the highest recorded atmospheric pressure at sea level is 813 mmHg, recorded during a Siberian winter; the lowest sea-level pressure ever measured was 658 mmHg in a Pacific typhoon. At these pressures, the boiling point of water changes minimally, to 102°C and 96°C, respectively. At high altitudes, on the other hand, the dependence of the boiling point of water on pressure becomes significant. Table **6.6.1** lists the boiling points of water at several locations with different altitudes. At an elevation of only 5000 ft, for example, the boiling point of water is already lower than the lowest ever recorded at sea level. The lower boiling point of water has major consequences for cooking everything from soft-boiled eggs (a “three-minute egg” may well take four or more minutes in the Rockies and even longer in the Himalayas) to cakes (cake mixes are often sold with separate high-altitude instructions). Conversely, pressure cookers, which have a seal that allows the pressure inside them to exceed 1 atm, are used to cook food more rapidly by raising the boiling point of water and thus the temperature at which the food is being cooked.

> *As pressure increases, the boiling point of a liquid increases and vice versa.*

✓ Example 6.6.2: Boiling Mercury

Use Figure **6.6.4** to estimate the following.

a. the boiling point of water in a pressure cooker operating at 1000 mmHg
b. the pressure required for mercury to boil at 250°C



Mercury boils at 356 °C at room pressure. To see video go to www.youtube.com/watch?v=0iizsbXWYoo

Given: Data in Figure **6.6.4**, pressure, and boiling point

Asked for: corresponding boiling point and pressure

Strategy:

A. To estimate the boiling point of water at 1000 mmHg, refer to Figure **6.6.4** and find the point where the vapor pressure curve of water intersects the line corresponding to a pressure of 1000 mmHg.

B. To estimate the pressure required for mercury to boil at 250°C, find the point where the vapor pressure curve of mercury intersects the line corresponding to a temperature of 250°C.

Solution:

a. **A** The vapor pressure curve of water intersects the P = 1000 mmHg line at about 110°C; this is therefore the boiling point of water at 1000 mmHg.

b. **B** The vertical line corresponding to 250°C intersects the vapor pressure curve of mercury at $P \approx 75$ mmHg. Hence this is the pressure required for mercury to boil at 250°C.

? Exercise 6.6.2: Boiling Ethlyene Glycol

Ethylene glycol is an organic compound primarily used as a raw material in the manufacture of polyester fibers and fabric industry, and polyethylene terephthalate resins (PET) used in bottling. Use the data in Figure **6.6.4** to estimate the following.

a. the normal boiling point of ethylene glycol

b. the pressure required for diethyl ether to boil at 20°C.

Answer a

200°C

Answer b

450 mmHg

Summary

Because the molecules of a liquid are in constant motion and possess a wide range of kinetic energies, at any moment some fraction of them has enough energy to escape from the surface of the liquid to enter the gas or vapor phase. This process, called **vaporization** or **evaporation**, generates a **vapor pressure** above the liquid. Molecules in the gas phase can collide with the liquid surface and reenter the liquid via **condensation**. Eventually, a *steady state* is reached in which the number of molecules evaporating and condensing per unit time is the same, and the system is in a state of **dynamic equilibrium**. Under these conditions, a liquid exhibits a characteristic **equilibrium vapor pressure** that depends only on the temperature. We can express the nonlinear relationship between vapor pressure and temperature as a linear relationship using the **Clausius–Clapeyron equation**. This equation can be used to calculate the enthalpy of vaporization of a liquid from its measured vapor pressure at two or more temperatures. **Volatile liquids** are liquids with high vapor pressures, which tend to evaporate readily from an open container; **nonvolatile liquids** have low vapor pressures. When the vapor pressure equals the external pressure, bubbles of vapor form within the liquid, and it boils. The temperature at which a substance boils at a pressure of 1 atm is its **normal boiling point**.

Contributors and Attributions

- Modified by Joshua Halpern (Howard University)

6.6: Vaporization and Vapor Pressure is shared under a CC BY-NC-SA 4.0 license and was authored, remixed, and/or curated by LibreTexts.

- **11.5: Vapor Pressure** is licensed CC BY-NC-SA 3.0.

6.7: Sublimation and Fusion

Sublimation

Some solids can transition directly into the gaseous state, bypassing the liquid state, via a process known as sublimation. At room temperature and standard pressure, a piece of dry ice (solid CO_2) sublimes, appearing to gradually disappear without ever forming any liquid. Snow and ice sublime at temperatures below the melting point of water, a slow process that may be accelerated by winds and the reduced atmospheric pressures at high altitudes. When solid iodine is warmed, the solid sublimes and a vivid purple vapor forms (Figure **6.7.6**). The reverse of sublimation is called deposition, a process in which gaseous substances condense directly into the solid state, bypassing the liquid state. The formation of frost is an example of deposition.



This figure shows a test tube. In the bottom is a dark substance which breaks up into a purple gas at the top.

Figure **6.7.6**: Sublimation of solid iodine in the bottom of the tube produces a purple gas that subsequently deposits as solid iodine on the colder part of the tube above. (credit: modification of work by Mark Ott)

Like vaporization, the process of sublimation requires an input of energy to overcome intermolecular attractions. The enthalpy of sublimation, ΔHsub, is the energy required to convert one mole of a substance from the solid to the gaseous state. For example, the sublimation of carbon dioxide is represented by:

$$\mathrm{CO_2}(s) \longrightarrow \mathrm{CO_2}(g) \quad \Delta H_{\mathrm{sub}} = 26.1\ \mathrm{kJ/mol} \tag{6.7.1}$$

Likewise, the enthalpy change for the reverse process of deposition is equal in magnitude but opposite in sign to that for sublimation:

$$\mathrm{CO_2}(g) \longrightarrow \mathrm{CO_2}(s) \quad \Delta H_{\mathrm{dep}} = -\Delta H_{\mathrm{sub}} = -26.1\ \mathrm{kJ/mol} \tag{6.7.2}$$

Consider the extent to which intermolecular attractions must be overcome to achieve a given phase transition. Converting a solid into a liquid requires that these attractions be only partially overcome; transition to the gaseous state requires that they be completely overcome. As a result, the enthalpy of fusion for a substance is less than its enthalpy of vaporization. This same logic can be used to derive an approximate relation between the enthalpies of all phase changes for a given substance. Though not an entirely accurate description, sublimation may be conveniently modeled as a sequential two-step process of melting followed by vaporization in order to apply Hess's Law.

$$\begin{array}{l} \mathrm{solid} \longrightarrow \mathrm{liquid} \quad \Delta H_{\mathrm{fus}} \\ \underline{\mathrm{liquid} \longrightarrow \mathrm{gas} \quad \Delta H_{\mathrm{vap}}} \\ \mathrm{solid} \longrightarrow \mathrm{gas} \quad \Delta H_{\mathrm{sub}} = \Delta H_{\mathrm{fus}} + \Delta H_{\mathrm{vap}} \end{array} \tag{6.7.3}$$

Viewed in this manner, the enthalpy of sublimation for a substance may be estimated as the sum of its enthalpies of fusion and vaporization, as illustrated in Figure **6.7.7**. For example:

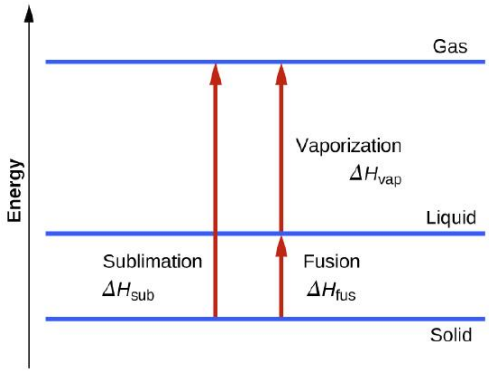


***Figure* 6.7.7**: *For a given substance, the sum of its enthalpy of fusion and enthalpy of vaporization is approximately equal to its enthalpy of sublimation.*

An energy level diagram is shown with three horizontal lines representing states of solid, liquid, and gas in increasing energy levels. The enthalpy of fusion is shown by arrow pointing from solid to liquid. Enthalpy of vaporization is shown with arrow pointing from liquid to gas. The enthalpy of sublimation points from solid to gas and has the same length as the arrows for fusion and vaporization combined.

Fusion

When we heat a crystalline solid, we increase the average energy of its atoms, molecules, or ions and the solid gets hotter. At some point, the added energy becomes large enough to partially overcome the forces holding the molecules or ions of the solid in their fixed positions, and the solid begins the process of transitioning to the liquid state, or melting. At this point, the temperature of the solid stops rising, despite the continual input of heat, and it remains constant until all of the solid is melted. Only after all of the solid has melted will continued heating increase the temperature of the liquid (Figure \(\PageIndex{5}\).

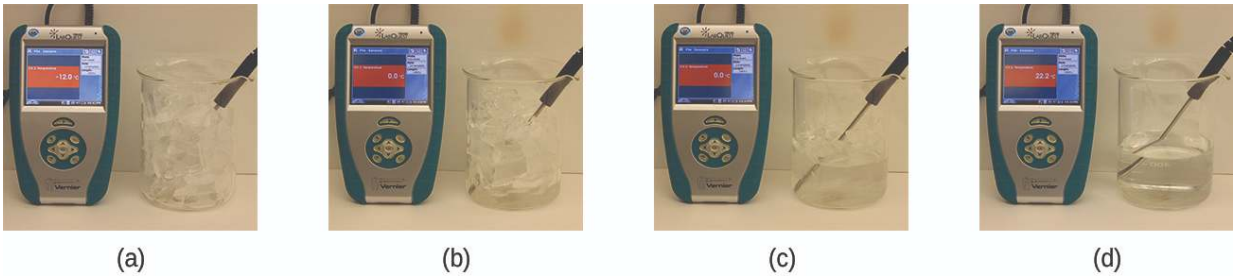


Figure **6.7.5**: (a) This beaker of ice has a temperature of −12.0 °C. (b) After 10 minutes the ice has absorbed enough heat from the air to warm to 0 °C. A small amount has melted. (c) Thirty minutes later, the ice has absorbed more heat, but its temperature is still 0 °C. The ice melts without changing its temperature. (d) Only after all the ice has melted does the heat absorbed cause the temperature to increase to 22.2 °C. (credit: modification of work by Mark Ott).

If we stop heating during melting and place the mixture of solid and liquid in a perfectly insulated container so no heat can enter or escape, the solid and liquid phases remain in equilibrium. This is almost the situation with a mixture of ice and water in a very good thermos bottle; almost no heat gets in or out, and the mixture of solid ice and liquid water remains for hours. In a mixture of solid and liquid at equilibrium, the reciprocal process of melting and freezing occur at equal rates, and the quantities of solid and liquid therefore remain constant. The temperature at which the solid and liquid phases of a given substance are in equilibrium is called the melting point of the solid or the freezing point of the liquid. Use of one term or the other is normally dictated by the direction of the phase transition being considered, for example, solid to liquid (melting) or liquid to solid (freezing).

The enthalpy of fusion and the melting point of a crystalline solid depend on the strength of the attractive forces between the units present in the crystal. Molecules with weak attractive forces form crystals with low melting points. Crystals consisting of particles with stronger attractive forces melt at higher temperatures.

The amount of heat required to change one mole of a substance from the solid state to the liquid state is the enthalpy of fusion, ΔH_{fus} of the substance. The enthalpy of fusion of ice is 6.0 kJ/mol at 0 °C. Fusion (melting) is an endothermic process:

$$H_2O_{(s)} \rightarrow H_2O_{(l)} \quad \Delta H_{fus} = 6.01 \text{ kJ/mol} \tag{6.7.4}$$

The reciprocal process, freezing, is an exothermic process whose enthalpy change is −6.0 kJ/mol at 0 °C:

$$H_2O_{(l)} \rightarrow H_2O_{(s)} \quad \Delta H_{frz} = -\Delta H_{fus} = -6.01 \text{ kJ/mol} \tag{6.7.5}$$

Selected molar enthalpies of fusion are tabulated in Table **6.7.1**. Solids like ice which have strong intermolecular forces have much higher values than those like CH_4 with weak ones. Note that the enthalpies of fusion and vaporization change with temperature.

Table **6.7.1**: Molar Enthalpies of Fusion and Vaporization of Selected Substances.

Substance	Formula	ΔH(fusion) / kJ mol^1	Melting Point / K	ΔH(vaporization) / kJ mol^{-1}	Boiling Point / K	($\Delta H_v/T_b$) / JK^{-1} mol^{-1}
Neon	Ne	0.33	24	1.80	27	67
Oxygen	O_2	0.44	54	6.82	90.2	76
Methane	CH_4	0.94	90.7	8.18	112	73
Ethane	C_2H_6	2.85	90.0	14.72	184	80
Chlorine	Cl_2	6.40	172.2	20.41	239	85
Carbon tetrachloride	CCl_4	2.67	250.0	30.00	350	86
Water*	H_2O	6.00678 at 0°C, 101kPa 6.354 at 81.6 °C, 2.50 MPa	273.1	40.657 at 100 °C, 45.051 at 0 °C, 46.567 at -33 °C	373.1	109
n-Nonane	C_9H_{20}	19.3	353	40.5	491	82
Mercury	Hg	2.30	234	58.6	630	91
Sodium	Na	2.60	371	98	1158	85
Aluminum	Al	10.9	933	284	2600	109
Lead	Pb	4.77	601	178	2022	88

*www1.lsbu.ac.uk/water/data.html

Contributors and Attributions

- Paul Flowers (University of North Carolina - Pembroke), Klaus Theopold (University of Delaware) and Richard Langley (Stephen F. Austin State University) with contributing authors. Textbook content produced by OpenStax College is licensed under a Creative Commons Attribution License 4.0 license. Download for free at http://cnx.org/contents/85abf193-2bd...a7ac8df6@9.110).

This page titled 6.7: Sublimation and Fusion is shared under a CC BY license and was authored, remixed, and/or curated by OpenStax.

6.8: Heating Curve for Water

Freezing, condensation, and deposition, which are the reverse of fusion, sublimation, and vaporization—are exothermic. Thus heat pumps that use refrigerants are essentially air-conditioners running in reverse. Heat from the environment is used to vaporize the refrigerant, which is then condensed to a liquid in coils within a house to provide heat. The energy changes that occur during phase changes can be quantified by using a heating or cooling curve.

Heating Curves

Figure **6.8.3** shows a heating curve, a plot of temperature versus heating time, for a 75 g sample of water. The sample is initially ice at 1 atm and −23°C; as heat is added, the temperature of the ice increases linearly with time. The slope of the line depends on both the mass of the ice and the specific heat (C_s) of ice, which is the number of joules required to raise the temperature of 1 g of ice by 1°C. As the temperature of the ice increases, the water molecules in the ice crystal absorb more and more energy and vibrate more vigorously. At the melting point, they have enough kinetic energy to overcome attractive forces and move with respect to one another. As more heat is added, the temperature of the system does *not* increase further but remains constant at 0°C until all the ice has melted. Once all the ice has been converted to liquid water, the temperature of the water again begins to increase. Now, however, the temperature increases more slowly than before because the specific heat capacity of water is *greater* than that of ice. When the temperature of the water reaches 100°C, the water begins to boil. Here, too, the temperature remains constant at 100°C until all the water has been converted to steam. At this point, the temperature again begins to rise, but at a *faster* rate than seen in the other phases because the heat capacity of steam is *less* than that of ice or water.

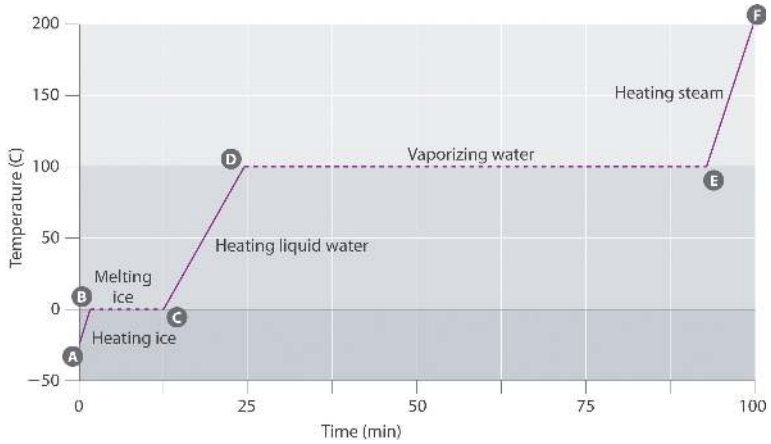


Figure **6.8.1**: A Heating Curve for Water. This plot of temperature shows what happens to a 75 g sample of ice initially at 1 atm and −23°C as heat is added at a constant rate: A–B: heating solid ice; B–C: melting ice; C–D: heating liquid water; D–E: vaporizing water; E–F: heating steam.

Thus *the temperature of a system does not change during a phase change*. In this example, as long as even a tiny amount of ice is present, the temperature of the system remains at 0°C during the melting process, and as long as even a small amount of liquid water is present, the temperature of the system remains at 100°C during the boiling process. The rate at which heat is added does *not* affect the temperature of the ice/water or water/steam mixture because the added heat is being used exclusively to overcome the attractive forces that hold the more condensed phase together. Many cooks think that food will cook faster if the heat is turned up higher so that the water boils more rapidly. Instead, the pot of water will boil to dryness sooner, but the temperature of the water does not depend on how vigorously it boils.

> *The temperature of a sample does not change during a phase change.*

If heat is added at a constant rate, as in Figure **6.8.3**, then the length of the horizontal lines, which represents the time during which the temperature does not change, is directly proportional to the magnitude of the enthalpies associated with the phase changes. In Figure **6.8.3**, the horizontal line at 100°C is much longer than the line at 0°C because the enthalpy of vaporization of water is several times greater than the enthalpy of fusion.

A superheated liquid is a sample of a liquid at the temperature and pressure at which it should be a gas. Superheated liquids are not stable; the liquid will eventually boil, sometimes violently. The phenomenon of superheating causes “bumping” when a liquid is

heated in the laboratory. When a test tube containing water is heated over a Bunsen burner, for example, one portion of the liquid can easily become too hot. When the superheated liquid converts to a gas, it can push or "bump" the rest of the liquid out of the test tube. Placing a stirring rod or a small piece of ceramic (a "boiling chip") in the test tube allows bubbles of vapor to form on the surface of the object so the liquid boils instead of becoming superheated. Superheating is the reason a liquid heated in a smooth cup in a microwave oven may not boil until the cup is moved, when the motion of the cup allows bubbles to form.

Cooling Curves

The cooling curve, a plot of temperature versus cooling time, in Figure **6.8.4** plots temperature versus time as a 75 g sample of steam, initially at 1 atm and 200°C, is cooled. Although we might expect the cooling curve to be the mirror image of the heating curve in Figure **6.8.3**, the cooling curve is *not* an identical mirror image. As heat is removed from the steam, the temperature falls until it reaches 100°C. At this temperature, the steam begins to condense to liquid water. No further temperature change occurs until all the steam is converted to the liquid; then the temperature again decreases as the water is cooled. We might expect to reach another plateau at 0°C, where the water is converted to ice; in reality, however, this does not always occur. Instead, the temperature often drops below the freezing point for some time, as shown by the little dip in the cooling curve below 0°C. This region corresponds to an unstable form of the liquid, a supercooled liquid. If the liquid is allowed to stand, if cooling is continued, or if a small crystal of the solid phase is added (a seed crystal), the supercooled liquid will convert to a solid, sometimes quite suddenly. As the water freezes, the temperature increases slightly due to the heat evolved during the freezing process and then holds constant at the melting point as the rest of the water freezes. Subsequently, the temperature of the ice decreases again as more heat is removed from the system.

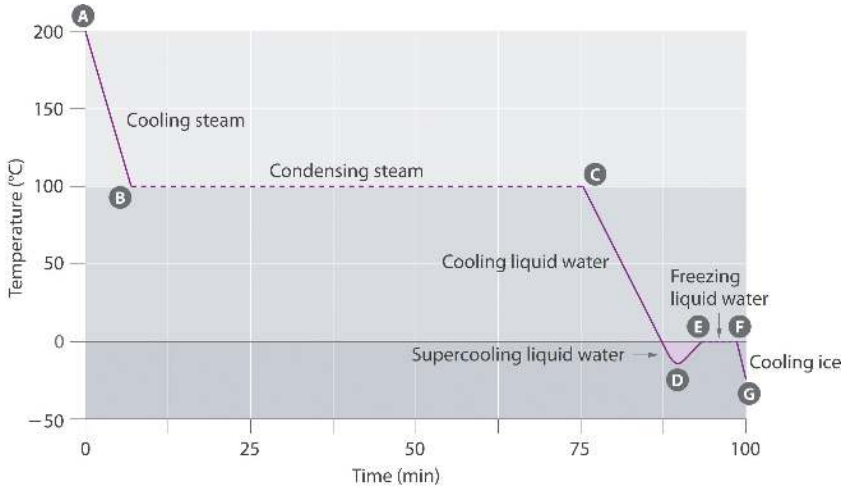


Figure **6.8.2**: A Cooling Curve for Water. This plot of temperature shows what happens to a 75 g sample of steam initially at 1 atm and 200°C as heat is removed at a constant rate: A–B: cooling steam; B–C: condensing steam; C–D: cooling liquid water to give a supercooled liquid; D–E: warming the liquid as it begins to freeze; E–F: freezing liquid water; F–G: cooling ice.

Supercooling effects have a huge impact on Earth's climate. For example, supercooling of water droplets in clouds can prevent the clouds from releasing precipitation over regions that are persistently arid as a result. Clouds consist of tiny droplets of water, which in principle should be dense enough to fall as rain. In fact, however, the droplets must aggregate to reach a certain size before they can fall to the ground. Usually a small particle (a *nucleus*) is required for the droplets to aggregate; the nucleus can be a dust particle, an ice crystal, or a particle of silver iodide dispersed in a cloud during *seeding* (a method of inducing rain). Unfortunately, the small droplets of water generally remain as a supercooled liquid down to about −10°C, rather than freezing into ice crystals that are more suitable nuclei for raindrop formation. One approach to producing rainfall from an existing cloud is to cool the water droplets so that they crystallize to provide nuclei around which raindrops can grow. This is best done by dispersing small granules of solid CO_2 (dry ice) into the cloud from an airplane. Solid CO_2 sublimes directly to the gas at pressures of 1 atm or lower, and the enthalpy of sublimation is substantial (25.3 kJ/mol). As the CO_2 sublimes, it absorbs heat from the cloud, often with the desired results.

Example 6.8.1: Cooling Hot Tea

If a 50.0 g ice cube at 0.0°C is added to 500 mL of tea at 20.0°C, what is the temperature of the tea when the ice cube has just melted? Assume that no heat is transferred to or from the surroundings. The density of water (and iced tea) is 1.00 g/mL over the range 0°C–20°C, the specific heats of liquid water and ice are 4.184 J/(g•°C) and 2.062 J/(g•°C), respectively, and the enthalpy of fusion of ice is 6.01 kJ/mol.

Given: mass, volume, initial temperature, density, specific heats, and ΔH_{fus}

Asked for: final temperature

Strategy:

Substitute the values given into the general equation relating heat gained to heat lost (Equation 5.39) to obtain the final temperature of the mixture.

Solution:

When two substances or objects at different temperatures are brought into contact, heat will flow from the warmer one to the cooler. The amount of heat that flows is given by

$$q = mC_s\Delta T \tag{6.8.1}$$

where q is heat, m is mass, C_s is the specific heat, and ΔT is the temperature change. Eventually, the temperatures of the two substances will become equal at a value somewhere between their initial temperatures. Calculating the temperature of iced tea after adding an ice cube is slightly more complicated. The general equation relating heat gained and heat lost is still valid, but in this case we also have to take into account the amount of heat required to melt the ice cube from ice at 0.0°C to liquid water at 0.0°C.

Exercise 6.8.1: Death by Freezing

Suppose you are overtaken by a blizzard while ski touring and you take refuge in a tent. You are thirsty, but you forgot to bring liquid water. You have a choice of eating a few handfuls of snow (say 400 g) at −5.0°C immediately to quench your thirst or setting up your propane stove, melting the snow, and heating the water to body temperature before drinking it. You recall that the survival guide you leafed through at the hotel said something about not eating snow, but you cannot remember why—after all, it's just frozen water. To understand the guide's recommendation, calculate the amount of heat that your body will have to supply to bring 400 g of snow at −5.0°C to your body's internal temperature of 37°C. Use the data in Example **6.8.1**

Answer

200 kJ (4.1 kJ to bring the ice from −5.0°C to 0.0°C, 133.6 kJ to melt the ice at 0.0°C, and 61.9 kJ to bring the water from 0.0°C to 37°C), which is energy that would not have been expended had you first melted the snow.

6.8: Heating Curve for Water is shared under a CC BY-NC-SA 4.0 license and was authored, remixed, and/or curated by LibreTexts.

6.9: Phase Diagrams

Learning Objectives

- To understand the basics of a one-component phase diagram as a function of temperature and pressure in a closed system.
- To be able to identify the triple point, the critical point, and four regions: solid, liquid, gas, and a supercritical fluid.

The state exhibited by a given sample of matter depends on the identity, temperature, and pressure of the sample. A phase diagram is a graphic summary of the physical state of a substance as a function of temperature and pressure in a closed system.

Introduction

A typical phase diagram consists of discrete regions that represent the different phases exhibited by a substance (Figure **6.9.1**). Each region corresponds to the range of combinations of temperature and pressure over which that phase is stable. The combination of high pressure and low temperature (upper left of Figure **6.9.1**) corresponds to the solid phase, whereas the gas phase is favored at high temperature and low pressure (lower right). The combination of high temperature and high pressure (upper right) corresponds to a supercritical fluid.

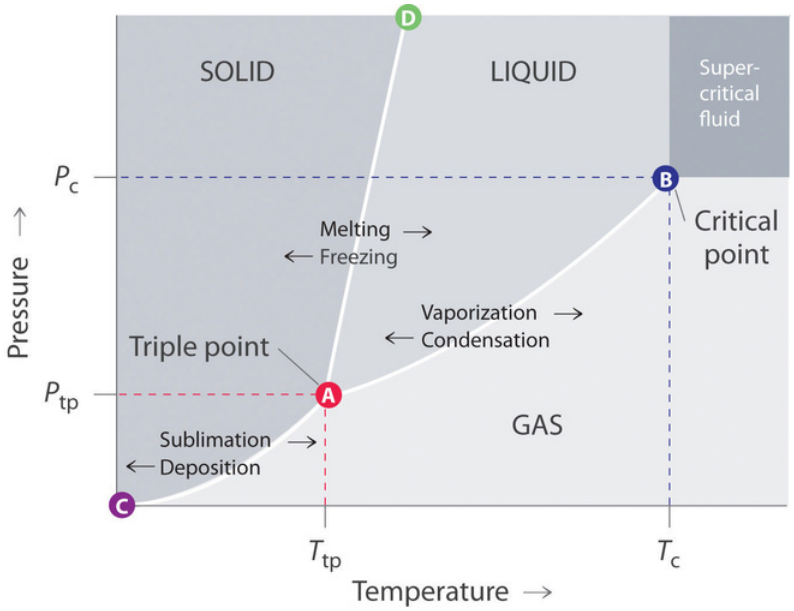


Figure **6.9.1**: A Typical Phase Diagram for a Substance That Exhibits Three Phases—Solid, Liquid, and Gas—and a Supercritical Region

The solid phase is favored at low temperature and high pressure; the gas phase is favored at high temperature and low pressure.

The lines in a phase diagram correspond to the combinations of temperature and pressure at which two phases can coexist in equilibrium. In Figure **6.9.1**, the line that connects points A and D separates the solid and liquid phases and shows how the melting point of a solid varies with pressure. The solid and liquid phases are in equilibrium all along this line; crossing the line horizontally corresponds to melting or freezing. The line that connects points A and B is the vapor pressure curve of the liquid, which we discussed in Section 11.5. It ends at the critical point, beyond which the substance exists as a supercritical fluid. The line that connects points A and C is the vapor pressure curve of the *solid* phase. Along this line, the solid is in equilibrium with the vapor phase through sublimation and deposition. Finally, point A, where the solid/liquid, liquid/gas, and solid/gas lines intersect, is the triple point; it is the *only* combination of temperature and pressure at which all three phases (solid, liquid, and gas) are in equilibrium and can therefore exist simultaneously. Because no more than three phases can ever coexist, a phase diagram can never have more than three lines intersecting at a single point.

Remember that a phase diagram, such as the one in Figure **6.9.1**, is for a single pure substance in a closed system, not for a liquid in an open beaker in contact with air at 1 atm pressure. In practice, however, the conclusions reached about the behavior of a

substance in a closed system can usually be extrapolated to an open system without a great deal of error.

The Phase Diagram of Water

Figure **6.9.2** shows the phase diagram of water and illustrates that the triple point of water occurs at 0.01°C and 0.00604 atm (4.59 mmHg). Far more reproducible than the melting point of ice, which depends on the amount of dissolved air and the atmospheric pressure, the triple point (273.16 K) is used to define the absolute (Kelvin) temperature scale. The triple point also represents the lowest pressure at which a liquid phase can exist in equilibrium with the solid or vapor. At pressures less than 0.00604 atm, therefore, ice does not melt to a liquid as the temperature increases; the solid sublimes directly to water vapor. Sublimation of water at low temperature and pressure can be used to "freeze-dry" foods and beverages. The food or beverage is first cooled to subzero temperatures and placed in a container in which the pressure is maintained below 0.00604 atm. Then, as the temperature is increased, the water sublimes, leaving the dehydrated food (such as that used by backpackers or astronauts) or the powdered beverage (as with freeze-dried coffee).

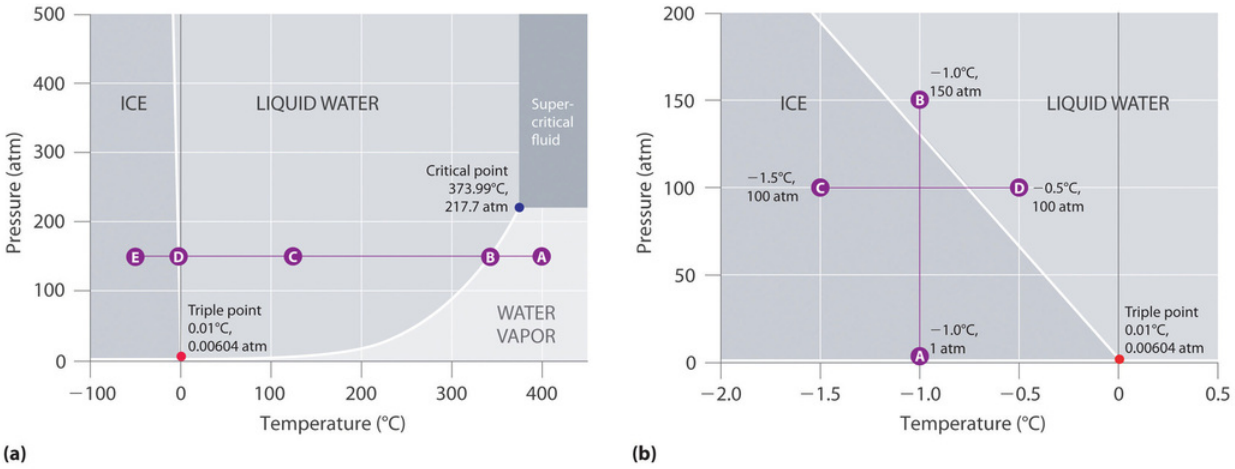


Figure **6.9.2**: Two Versions of the Phase Diagram of Water. (a) In this graph with linear temperature and pressure axes, the boundary between ice and liquid water is almost vertical. (b) This graph with an expanded scale illustrates the decrease in melting point with increasing pressure. (The letters refer to points discussed in Example **6.9.1**).

The phase diagram for water illustrated in Figure **6.9.2***b* shows the boundary between ice and water on an expanded scale. The melting curve of ice slopes up and slightly to the left rather than up and to the right as in Figure **6.9.1**; that is, the melting point of ice *decreases* with increasing pressure; at 100 MPa (987 atm), ice melts at −9°C. Water behaves this way because it is one of the few known substances for which the crystalline solid is *less dense* than the liquid (others include antimony and bismuth). Increasing the pressure of ice that is in equilibrium with water at 0°C and 1 atm tends to push some of the molecules closer together, thus decreasing the volume of the sample. The decrease in volume (and corresponding increase in density) is smaller for a solid or a liquid than for a gas, but it is sufficient to melt some of the ice.

In Figure **6.9.2***b* point A is located at P = 1 atm and T = −1.0°C, within the solid (ice) region of the phase diagram. As the pressure increases to 150 atm while the temperature remains the same, the line from point A crosses the ice/water boundary to point B, which lies in the liquid water region. Consequently, applying a pressure of 150 atm will melt ice at −1.0°C. We have already indicated that the pressure dependence of the melting point of water is of vital importance. If the solid/liquid boundary in the phase diagram of water were to slant up and to the right rather than to the left, ice would be denser than water, ice cubes would sink, water pipes would not burst when they freeze, and antifreeze would be unnecessary in automobile engines.

Ice Skating: An Incorrect Hypothesis of Phase Transitions

Until recently, many textbooks described ice skating as being possible because the pressure generated by the skater's blade is high enough to melt the ice under the blade, thereby creating a lubricating layer of liquid water that enables the blade to slide across the ice. Although this explanation is intuitively satisfying, it is incorrect, as we can show by a simple calculation.



Pressure from ice skates on ice. from wikihow.com.

Recall that pressure (P) is the force (F) applied per unit area (A):

$$P = \frac{F}{A}$$

To calculate the pressure an ice skater exerts on the ice, we need to calculate only the force exerted and the area of the skate blade. If we assume a 75.0 kg (165 lb) skater, then the force exerted by the skater on the ice due to gravity is

$$F = mg$$

where m is the mass and g is the acceleration due to Earth's gravity (9.81 m/s^2). Thus the force is

$$F = (75.0\ kg)(9.81\ m/s^2) = 736\ (kg \bullet m)/s^2 = 736N$$

If we assume that the skate blades are 2.0 mm wide and 25 cm long, then the area of the bottom of each blade is

$$A = (2.0 \times 10^{-3}\ m)(25 \times 10^{-2}\ m) = 5.0 \times 10^{-4} m^2$$

If the skater is gliding on one foot, the pressure exerted on the ice is

$$P = \frac{736\ N}{5.0 \times 10^{-4}\ m^2} = 1.5 \times 10^6\ N/m^2 = 1.5 \times 10^6\ Pa = 15\ atm$$

The pressure is much lower than the pressure needed to decrease the melting point of ice by even 1°C, and experience indicates that it is possible to skate even when the temperature is well below freezing. Thus pressure-induced melting of the ice cannot explain the low friction that enables skaters (and hockey pucks) to glide. Recent research indicates that the surface of ice, where the ordered array of water molecules meets the air, consists of one or more layers of almost liquid water. These layers, together with melting induced by friction as a skater pushes forward, appear to account for both the ease with which a skater glides and the fact that skating becomes more difficult below about −7°C, when the number of lubricating surface water layers decreases.

✔ Example 6.9.1: Water

Referring to the phase diagram of water in Figure **6.9.2**:

a. predict the physical form of a sample of water at 400°C and 150 atm.
b. describe the changes that occur as the sample in part (a) is slowly allowed to cool to −50°C at a constant pressure of 150 atm.

Given: phase diagram, temperature, and pressure

Asked for: physical form and physical changes

Strategy:

A. Identify the region of the phase diagram corresponding to the initial conditions and identify the phase that exists in this region.
B. Draw a line corresponding to the given pressure. Move along that line in the appropriate direction (in this case cooling) and describe the phase changes.

Solution:

a. **A** Locate the starting point on the phase diagram in part (a) in Figure **6.9.2**. The initial conditions correspond to point A, which lies in the region of the phase diagram representing water vapor. Thus water at T = 400°C and P = 150 atm is a gas.

b. **B** Cooling the sample at constant pressure corresponds to moving left along the horizontal line in part (a) in Figure **6.9.2**. At about 340°C (point B), we cross the vapor pressure curve, at which point water vapor will begin to condense and the sample will consist of a mixture of vapor and liquid. When all of the vapor has condensed, the temperature drops further, and we enter the region corresponding to liquid water (indicated by point C). Further cooling brings us to the melting curve, the line that separates the liquid and solid phases at a little below 0°C (point D), at which point the sample will consist of a mixture of liquid and solid water (ice). When all of the water has frozen, cooling the sample to −50°C takes us along the horizontal line to point E, which lies within the region corresponding to solid water. At P = 150 atm and T = −50°C, therefore, the sample is solid ice.

? Exercise 6.9.2

Referring to the phase diagram of water in Figure **6.9.2**, predict the physical form of a sample of water at −0.0050°C as the pressure is gradually increased from 1.0 mmHg to 218 atm.

Answer

The sample is initially a gas, condenses to a solid as the pressure increases, and then melts when the pressure is increased further to give a liquid.

The Phase Diagram of Carbon Dioxide

In contrast to the phase diagram of water, the phase diagram of CO_2 (Figure **6.9.3**) has a more typical melting curve, sloping up and to the right. The triple point is −56.6°C and 5.11 atm, which means that liquid CO_2 cannot exist at pressures lower than 5.11 atm. At 1 atm, therefore, solid CO_2 sublimes directly to the vapor while maintaining a temperature of −78.5°C, the normal sublimation temperature. Solid CO_2 is generally known as dry ice because it is a cold solid with no liquid phase observed when it is warmed.



Dry ice ($CO_2(s)$) sublimed in air under room temperature and pressure. from Wikipedia.

Also notice the critical point at 30.98°C and 72.79 atm. Supercritical carbon dioxide is emerging as a natural refrigerant, making it a low carbon (and thus a more environmentally friendly) solution for domestic heat pumps.

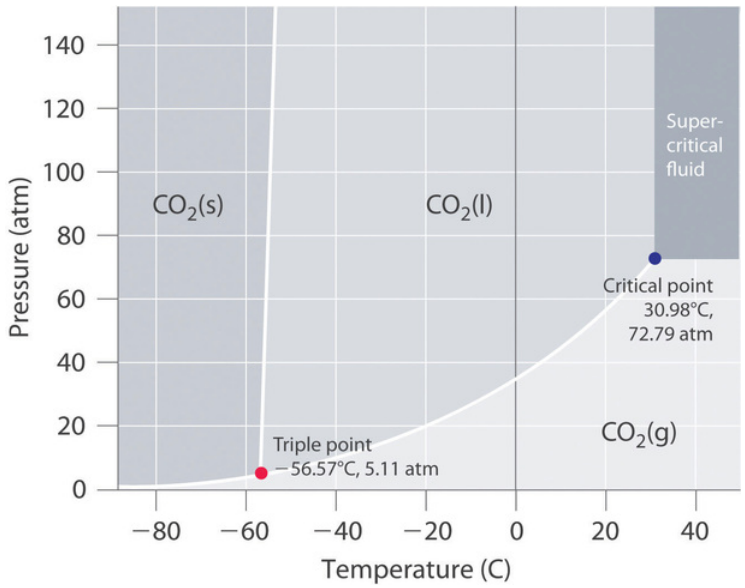


Figure **6.9.3**: The Phase Diagram of Carbon Dioxide. Note the critical point, the triple point, and the normal sublimation temperature in this diagram.

The triple point is at -57.57 degrees C and 5.11 atm. The critical point is at 30.98 degree C and 72.79 atm.

The Critical Point

As the phase diagrams above demonstrate, a combination of high pressure and low temperature allows gases to be liquefied. As we increase the temperature of a gas, liquefaction becomes more and more difficult because higher and higher pressures are required to overcome the increased kinetic energy of the molecules. In fact, for every substance, there is some temperature above which the gas can no longer be liquefied, regardless of pressure. This temperature is the critical temperature (T_c), the highest temperature at which a substance can exist as a liquid. Above the critical temperature, the molecules have too much kinetic energy for the intermolecular attractive forces to hold them together in a separate liquid phase. Instead, the substance forms a single phase that completely occupies the volume of the container. Substances with strong intermolecular forces tend to form a liquid phase over a very large temperature range and therefore have high critical temperatures. Conversely, substances with weak intermolecular interactions have relatively low critical temperatures. Each substance also has a critical pressure (P_c), the minimum pressure needed to liquefy it at the critical temperature. The combination of critical temperature and critical pressure is called the critical point. The critical temperatures and pressures of several common substances are listed in Figure **6.9.1**.

Figure **6.9.1**: Critical Temperatures and Pressures of Some Simple Substances

Substance	T_c (°C)	P_c (atm)
NH_3	132.4	113.5
CO_2	31.0	73.8
CH_3CH_2OH (ethanol)	240.9	61.4
He	−267.96	2.27
Hg	1477	1587
CH_4	−82.6	46.0
N_2	−146.9	33.9
H_2O	374.0	217.7

High-boiling-point, nonvolatile liquids have high critical temperatures and vice versa.



A Video Discussing Phase Diagrams. Video Source: Phase Diagrams(opens in new window) [youtu.be]

6.9: Phase Diagrams is shared under a CC BY-NC-SA 4.0 license and was authored, remixed, and/or curated by LibreTexts.

- **11.6: Phase Diagrams** is licensed CC BY-NC-SA 3.0.

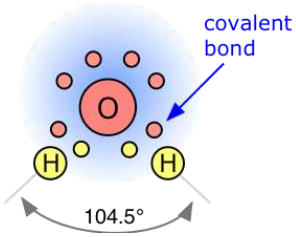
6.10: Water - An Extraordinary Substance

Learning Objectives

- Identify three special properties of water that make it unusual for a molecule of its size, and explain how these result from hydrogen bonding.
- Explain what is meant by hydrogen bonding and the molecular structural features that bring it about.
- Describe the "structure", such as it is, of liquid water.
- Sketch out structural examples of hydrogen bonding in three small molecules other than H_2O.
- Describe the roles of hydrogen bonding in proteins and in DNA.

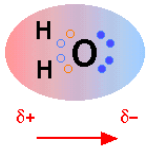
Most students of chemistry quickly learn to relate the structure of a molecule to its general properties. Thus we generally expect small molecules to form gases or liquids, and large ones to exist as solids under ordinary conditions. And then we come to H_2O, and are shocked to find that many of the predictions are way off, and that water (and by implication, life itself) should not even exist on our planet! In this section we will learn why this tiny combination of three nuclei and ten electrons possesses special properties that make it unique among the more than 15 million chemical species we presently know.

In water, each hydrogen nucleus is covalently bound to the central oxygen atom by a pair of electrons that are shared between them. In H_2O, only two of the six outer-shell electrons of oxygen are used for this purpose, leaving four electrons which are organized into two non-bonding pairs. The four electron pairs surrounding the oxygen tend to arrange themselves as far from each other as possible in order to minimize repulsions between these clouds of negative charge. This would ordinarily result in a tetrahedral geometry in which the angle between electron pairs (and therefore the H-O-H *bond angle*) is 109.5°. However, because the two non-bonding pairs remain closer to the oxygen atom, these exert a stronger repulsion against the two covalent bonding pairs, effectively pushing the two hydrogen atoms closer together. The result is a distorted tetrahedral arrangement in which the H—O—H angle is 104.5°.

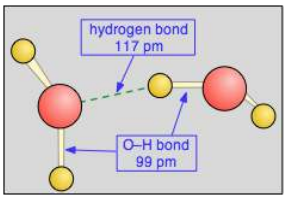


Water's large dipole moment leads to hydrogen bonding

The H_2O molecule is electrically neutral, but the positive and negative charges are not distributed uniformly. This is illustrated by the gradation in color in the schematic diagram here. The electronic (negative) charge is concentrated at the oxygen end of the molecule, owing partly to the nonbonding electrons (solid blue circles), and to oxygen's high nuclear charge which exerts stronger attractions on the electrons. This charge displacement constitutes an *electric dipole*, represented by the arrow at the bottom; you can think of this dipole as the electrical "image" of a water molecule.

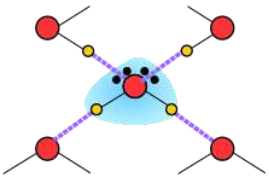


Opposite charges attract, so it is not surprising that the negative end of one water molecule will tend to orient itself so as to be close to the positive end of another molecule that happens to be nearby. The strength of this *dipole-dipole attraction* is less than that of a normal chemical bond, and so it is completely overwhelmed by ordinary thermal motions in the gas phase. However, when the H_2O molecules are crowded together in the liquid, these attractive forces exert a very noticeable effect, which we call (somewhat misleadingly) *hydrogen bonding*. And at temperatures low enough to turn off the disruptive effects of thermal motions, water freezes into ice in which the hydrogen bonds form a rigid and stable network.



Notice that the hydrogen bond (shown by the dashed green line) is somewhat longer than the covalent O—H bond. It is also *much weaker*, about 23 kJ mol^{-1} compared to the O–H covalent bond strength of 492 kJ mol^{-1}.

Water has long been known to exhibit many physical properties that distinguish it from other small molecules of comparable mass. Although chemists refer to these as the "anomalous" properties of water, they are by no means mysterious; all are entirely predictable consequences of the way the size and nuclear charge of the oxygen atom conspire to distort the electronic charge clouds of the atoms of other elements when these are chemically bonded to the oxygen.



The combination of large bond dipoles and short dipole–dipole distances results in very strong dipole–dipole interactions called hydrogen bonds, as shown for ice in Figure **6.10.6**. A hydrogen bond is usually indicated by a dotted line between the hydrogen atom attached to O, N, or F (the *hydrogen bond donor*) and the atom that has the lone pair of electrons (the *hydrogen bond acceptor*). Because each water molecule contains two hydrogen atoms and two lone pairs, a tetrahedral arrangement maximizes the number of hydrogen bonds that can be formed. In the structure of ice, each oxygen atom is surrounded by a distorted tetrahedron of hydrogen atoms that form bridges to the oxygen atoms of adjacent water molecules. The bridging hydrogen atoms are *not* equidistant from the two oxygen atoms they connect, however. Instead, each hydrogen atom is 101 pm from one oxygen and 174 pm from the other. In contrast, each oxygen atom is bonded to two H atoms at the shorter distance and two at the longer distance, corresponding to two O–H covalent bonds and two O···H hydrogen bonds from adjacent water molecules, respectively. The resulting open, cagelike structure of ice means that the solid is actually slightly less dense than the liquid, which explains why ice floats on water rather than sinks.

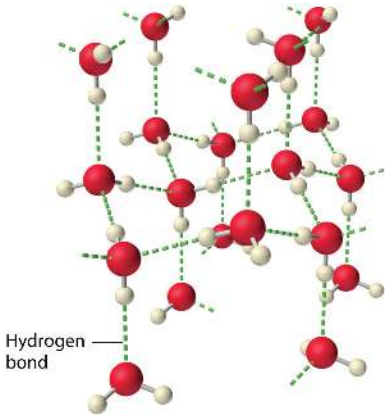


Figure* 6.10.6*: *The Hydrogen-Bonded Structure of Ice.*

Each water molecule accepts two hydrogen bonds from two other water molecules and donates two hydrogen atoms to form hydrogen bonds with two more water molecules, producing an open, cagelike structure. The structure of liquid water is very similar, but in the liquid, the hydrogen bonds are continually broken and formed because of rapid molecular motion.

> *Hydrogen bond formation requires both a hydrogen bond donor and a hydrogen bond acceptor.*

Molecules with hydrogen atoms bonded to electronegative atoms such as O, N, and F (and to a much lesser extent Cl and S) tend to exhibit unusually strong intermolecular interactions. These result in much higher boiling points than are observed for substances in which London dispersion forces dominate, as illustrated for the covalent hydrides of elements of groups 14–17 in Figure **6.10.5**. Methane and its heavier congeners in group 14 form a series whose boiling points increase smoothly with increasing molar mass. This is the expected trend in nonpolar molecules, for which London dispersion forces are the exclusive intermolecular forces. In contrast, the hydrides of the lightest members of groups 15–17 have boiling points that are more than 100°C greater than predicted on the basis of their molar masses. The effect is most dramatic for water: if we extend the straight line connecting the points for H_2Te and H_2Se to the line for period 2, we obtain an estimated boiling point of −130°C for water! Imagine the implications for life on Earth if water boiled at −130°C rather than 100°C.

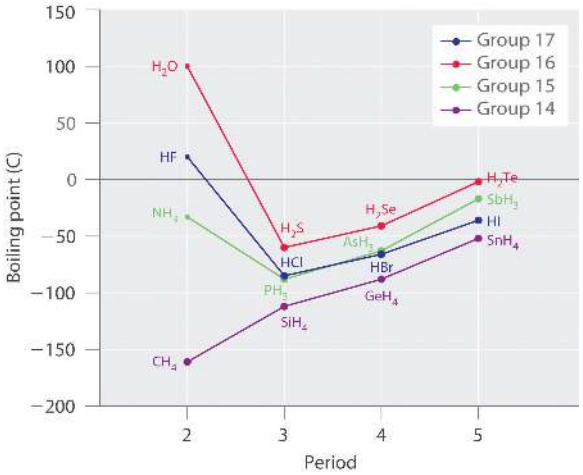
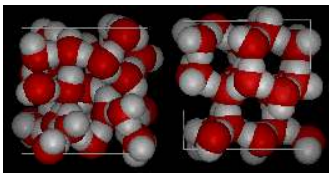


Figure **6.10.5**: The Effects of Hydrogen Bonding on Boiling Points. These plots of the boiling points of the covalent hydrides of the elements of groups 14–17 show that the boiling points of the lightest members of each series for which hydrogen bonding is possible (HF, NH_3, and H_2O) are anomalously high for compounds with such low molecular masses.

Why do strong intermolecular forces produce such anomalously high boiling points and other unusual properties, such as high enthalpies of vaporization and high melting points? The answer lies in the highly polar nature of the bonds between hydrogen and very electronegative elements such as O, N, and F. The large difference in electronegativity results in a large partial positive charge on hydrogen and a correspondingly large partial negative charge on the O, N, or F atom. Consequently, H–O, H–N, and H–F bonds have very large bond dipoles that can interact strongly with one another. Because a hydrogen atom is so small, these dipoles can also approach one another more closely than most other dipoles.

Ice Floats on Water

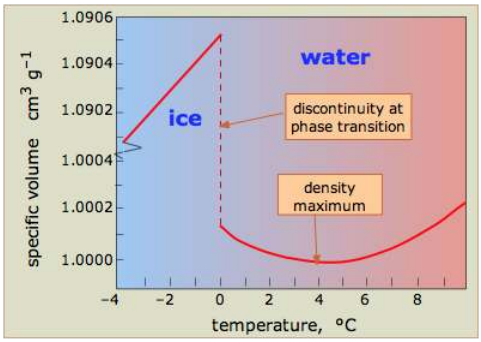
The most energetically favorable configuration of H_2O molecules is one in which each molecule is hydrogen-bonded to four neighboring molecules. Owing to the thermal motions described above, this ideal is never achieved in the liquid, but when water freezes to ice, the molecules settle into exactly this kind of an arrangement in the ice crystal. This arrangement requires that the molecules be somewhat farther apart then would otherwise be the case; as a consequence, ice, in which hydrogen bonding is at its maximum, has a more open structure, and thus a lower density than water.



Here are three-dimensional views of a typical local structure of water (left) and ice (right.) Notice the greater openness of the ice structure which is necessary to ensure the strongest degree of hydrogen bonding in a uniform, extended crystal lattice. The more

crowded and jumbled arrangement in liquid water can be sustained only by the greater amount of thermal energy available above the freezing point.

When ice melts, the more vigorous thermal motion disrupts much of the hydrogen-bonded structure, allowing the molecules to pack more closely. Water is thus one of the very few substances whose solid form has a lower density than the liquid at the freezing point. Localized clusters of hydrogen bonds still remain, however; these are continually breaking and reforming as the thermal motions jiggle and shove the individual molecules. As the temperature of the water is raised above freezing, the extent and lifetimes of these clusters diminish, so the density of the water increases.



At higher temperatures, another effect, common to all substances, begins to dominate: as the temperature increases, so does the amplitude of thermal motions. This more vigorous jostling causes the average distance between the molecules to increase, reducing the density of the liquid; this is ordinary thermal expansion. Because the two competing effects (hydrogen bonding at low temperatures and thermal expansion at higher temperatures) both lead to a decrease in density, it follows that there must be some temperature at which the density of water passes through a maximum. This temperature is 4° C; this is the temperature of the water you will find at the bottom of an ice-covered lake in which this most dense of all water has displaced the colder water and pushed it nearer to the surface.

Because ice is less dense than liquid water, rivers, lakes, and oceans freeze from the top down. In fact, the ice forms a protective surface layer that insulates the rest of the water, allowing fish and other organisms to survive in the lower levels of a frozen lake or sea. If ice were denser than the liquid, the ice formed at the surface in cold weather would sink as fast as it formed. Bodies of water would freeze from the bottom up, which would be lethal for most aquatic creatures. The expansion of water when freezing also explains why automobile or boat engines must be protected by “antifreeze” and why unprotected pipes in houses break if they are allowed to freeze.

Contributors

- Stephen Lower, Professor Emeritus (Simon Fraser U.) Chem1 Virtual Textbook

6.10: Water - An Extraordinary Substance is shared under a CC BY-NC-SA 4.0 license and was authored, remixed, and/or curated by LibreTexts.

CHAPTER OVERVIEW

7: Solutions and their Physical Properties

7.1: Types of Solutions- Some Terminology
7.2: Mixtures of Gases
7.3: Solution Concentration
7.4: Intermolecular Forces and the Solution Process
7.5: Solution Formation and Equilibrium
7.6: Solubilities of Gases
7.7: Vapor Pressures of Solutions
7.8: Osmotic Pressure
7.9: Freezing-Point Depression and Boiling-Point Elevation of Nonelectrolyte Solutions
7.10: Solutions of Electrolytes
7.11: Colloidal Mixtures
7.12: Solubility and Complex-Ion Equilibria
7.12.1: Solubility Product Constant, Ksp
7.12.2: Relationship Between Solubility and Ksp
7.12.3: Common-Ion Effect in Solubility Equilibria
7.12.4: Limitations of the Ksp Concept
7.12.5: Criteria for Precipitation and its Completeness
7.12.6: Fractional Precipitation
7.12.7: Solubility and pH
7.12.8: Equilibria Involving Complex Ions
7.12.9: Qualitative Cation Analysis

7: Solutions and their Physical Properties is shared under a not declared license and was authored, remixed, and/or curated by LibreTexts.

7.1: Types of Solutions- Some Terminology

Learning Objectives

- To understand how enthalpy and entropy changes affect solution formation.
- To use the magnitude of the changes in both enthalpy and entropy to predict whether a given solute–solvent combination will spontaneously form a solution.

In all solutions, whether gaseous, liquid, or solid, the substance present in the greatest amount is the solvent, and the substance or substances present in lesser amounts are the solute(s). The solute does not have to be in the same physical state as the solvent, but the physical state of the solvent usually determines the state of the solution. As long as the solute and solvent combine to give a homogeneous solution, the solute is said to be soluble in the solvent. Table **7.1.1** lists some common examples of gaseous, liquid, and solid solutions and identifies the physical states of the solute and solvent in each.

Table **7.1.1**: Types of Solutions

Solution	Solute	Solvent	Examples
gas	gas	gas	air, natural gas
liquid	gas	liquid	seltzer water (CO_2 gas in water)
liquid	liquid	liquid	alcoholic beverage (ethanol in water), gasoline
liquid	solid	liquid	tea, salt water
solid	gas	solid	H_2 in Pd (used for H_2 storage)
solid	solid	liquid	mercury in silver or gold (amalgam often used in dentistry)

The formation of a solution from a solute and a solvent is a physical process, not a chemical one. That is, both solute and solvent can be recovered in chemically unchanged forms using appropriate separation methods. For example, solid zinc nitrate dissolves in water to form an aqueous solution of zinc nitrate:

$$Zn(NO_3)_2\,(s) + H_2O\,(l) \rightarrow Zn^{2+}\,(aq) + 2\,NO_3^-\,(aq)$$

Because $Zn(NO_3)_2$ can be recovered easily by evaporating the water, this is a physical process. In contrast, metallic zinc appears to dissolve in aqueous hydrochloric acid. In fact, the two substances undergo a chemical reaction to form an aqueous solution of zinc chloride with evolution of hydrogen gas:

$$Zn\,(s) + 2\,H^+\,(aq) + 2\,Cl^-\,(aq) \rightarrow Zn^{2+}\,(aq) + 2\,Cl^-\,(aq) + H_2\,(g)$$

> *Dissolution of a solute in a solvent to form a solution typically does not involve a chemical transformation and largely consist of breaking intermolecular forces rather than covalent bonds.*

When the solution evaporates, we do not recover metallic zinc, so we cannot say that metallic zinc is soluble in aqueous hydrochloric acid because it is chemically transformed when it dissolves. The dissolution of a solute in a solvent to form a solution does not involve a chemical transformation.

Mercury Amalgams: Examples of solid Solutions

An amalgam is an alloy of mercury with another metal. It may be a liquid, a soft paste or a solid, depending upon the proportion of mercury. These alloys are formed through metallic bonding, with the electrostatic attractive force of the

conduction electrons working to bind all the positively charged metal ions together into a crystal lattice structure. Almost all metals can form amalgams with mercury including aluminum (Video **7.1.1**), the notable exceptions being iron, platinum, tungsten, and tantalum. Silver-mercury amalgams are important in dentistry, and gold-mercury amalgam is used in the extraction of gold from ore.



Video **7.1.1**: Aluminum dissolving into Mercury.

Substances that form a single homogeneous phase in all proportions are said to be completely **miscible** in one another. Ethanol and water are miscible, just as mixtures of gases are miscible. If two substances are essentially insoluble in each other, such as oil and water, they are immiscible. Examples of gaseous solutions that we have already discussed include Earth's atmosphere.

7.1: Types of Solutions- Some Terminology is shared under a not declared license and was authored, remixed, and/or curated by LibreTexts.

- **13.1: Types of Solutions - Some Terminology** is licensed CC BY-NC-SA 4.0.

7.2: Mixtures of Gases

Learning Objectives

- To determine the contribution of each component gas to the total pressure of a mixture of gases

In our use of the ideal gas law thus far, we have focused entirely on the properties of pure gases with only a single chemical species. But what happens when two or more gases are mixed? In this section, we describe how to determine the contribution of each gas present to the total pressure of the mixture.

Partial Pressures

The ideal gas law *assumes* that all gases behave identically and that their behavior is independent of attractive and repulsive forces. If volume and temperature are held constant, the ideal gas equation can be rearranged to show that the pressure of a sample of gas is directly proportional to the number of moles of gas present:

$$P = n\left(\frac{RT}{V}\right) = n \times \text{const.} \tag{7.2.1}$$

Nothing in the equation depends on the *nature* of the gas—only the amount.

With this assumption, let's suppose we have a mixture of two ideal gases that are present in equal amounts. What is the total pressure of the mixture? Because the pressure depends on only the total number of particles of gas present, the total pressure of the mixture will simply be twice the pressure of either component. More generally, the total pressure exerted by a mixture of gases at a given temperature and volume is the sum of the pressures exerted by each gas alone. Furthermore, if we know the volume, the temperature, and the number of moles of each gas in a mixture, then we can calculate the pressure exerted by each gas individually, which is its partial pressure, the pressure the gas would exert if it were the only one present (at the same temperature and volume).

To summarize, ***the total pressure exerted by a mixture of gases is the sum of the partial pressures of component gases***. This law was first discovered by John Dalton, the father of the atomic theory of matter. It is now known as *Dalton's law of partial pressures*. We can write it mathematically as

$$P_{tot} = P_1 + P_2 + P_3 + P_4 \ldots = \sum_{i=1}^{n} P_i \tag{7.2.2}$$

where P_{tot} is the total pressure and the other terms are the partial pressures of the individual gases (up to n component gases).

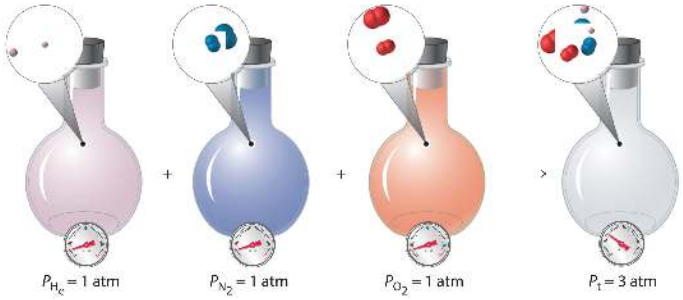


Figure **7.2.1**: Dalton's Law. The total pressure of a mixture of gases is the sum of the partial pressures of the individual gases.

For a mixture of two ideal gases, A and B, we can write an expression for the total pressure:

$$P_{tot} = P_A + P_B = n_A\left(\frac{RT}{V}\right) + n_B\left(\frac{RT}{V}\right) = (n_A + n_B)\left(\frac{RT}{V}\right) \tag{7.2.3}$$

More generally, for a mixture of n component gases, the total pressure is given by

$$P_{tot} = (P_1 + P_2 + P_3 + \cdots + P_n)\left(\frac{RT}{V}\right) \tag{7.2.4}$$

$$P_{tot} = \sum_{i=1}^{n} n_i \left(\frac{RT}{V}\right) \tag{7.2.5}$$

Equation 6.6.4 restates Equation 6.6.3 in a more general form and makes it explicitly clear that, at constant temperature and volume, the pressure exerted by a gas depends on only the total number of moles of gas present, whether the gas is a single chemical species or a mixture of dozens or even hundreds of gaseous species. For Equation 6.6.4 to be valid, the identity of the particles present cannot have an effect. Thus an ideal gas must be one whose properties are not affected by either the size of the particles or their intermolecular interactions because both will vary from one gas to another. The calculation of total and partial pressures for mixtures of gases is illustrated in Example **7.2.1**.

Example 7.2.1

Deep-sea divers must use special gas mixtures in their tanks, rather than compressed air, to avoid serious problems, most notably a condition called "the bends." At depths of about 350 ft, divers are subject to a pressure of approximately 10 atm. A typical gas cylinder used for such depths contains 51.2 g of O_2 and 326.4 g of He and has a volume of 10.0 L. What is the partial pressure of each gas at 20.00°C, and what is the total pressure in the cylinder at this temperature?

Given: masses of components, total volume, and temperature

Asked for: partial pressures and total pressure

Strategy:

A. Calculate the number of moles of He and O_2 present.
B. Use the ideal gas law to calculate the partial pressure of each gas. Then add together the partial pressures to obtain the total pressure of the gaseous mixture.

Solution:

A The number of moles of He is

$$n_{\text{He}} = \frac{326.4\ \text{g}}{4.003\ \text{g/mol}} = 81.54\ \text{mol} \tag{7.2.6}$$

The number of moles of O_2 is

$$n_{\text{O}_2} = \frac{51.2\ \text{g}}{32.00\ \text{g/mol}} = 1.60\ \text{mol} \tag{7.2.7}$$

B We can now use the ideal gas law to calculate the partial pressure of each:

$$P_{\text{He}} = \frac{n_{\text{He}}RT}{V} = \frac{81.54\ \text{mol} \times 0.08206\ \frac{\text{atm} \cdot \text{L}}{\text{mol} \cdot \text{K}} \times 293.15\ \text{K}}{10.0\ \text{L}} = 196.2\ \text{atm} \tag{7.2.8}$$

$$P_{\text{O}_2} = \frac{n_{\text{O}_2}RT}{V} = \frac{1.60\ \text{mol} \times 0.08206\ \frac{\text{atm} \cdot \text{L}}{\text{mol} \cdot \text{K}} \times 293.15\ \text{K}}{10.0\ \text{L}} = 3.85\ \text{atm} \tag{7.2.9}$$

The total pressure is the sum of the two partial pressures:

$$P_{\text{tot}} = P_{\text{He}} + P_{\text{O}_2} = (196.2 + 3.85)\ \text{atm} = 200.1\ \text{atm} \tag{7.2.10}$$

Exercise 7.2.1

A cylinder of compressed natural gas has a volume of 20.0 L and contains 1813 g of methane and 336 g of ethane. Calculate the partial pressure of each gas at 22.0°C and the total pressure in the cylinder.

Answer: $P_{CH_4} = 137\ atm$; $P_{C_2H_6} = 13.4\ atm$; $P_{tot} = 151\ atm$

Mole Fractions of Gas Mixtures

The composition of a gas mixture can be described by the mole fractions of the gases present. The mole fraction (X) of any component of a mixture is the ratio of the number of moles of that component to the total number of moles of all the species present in the mixture (n_{tot}):

$$x_A = \frac{\text{moles of A}}{\text{total moles}} = \frac{n_A}{n_{tot}} = \frac{n_A}{n_A + n_B + \cdots} \tag{7.2.11}$$

The mole fraction is a dimensionless quantity between 0 and 1. If $x_A = 1.0$, then the sample is pure A, not a mixture. If $x_A = 0$, then no A is present in the mixture. The sum of the mole fractions of all the components present must equal 1.

To see how mole fractions can help us understand the properties of gas mixtures, let's evaluate the ratio of the pressure of a gas A to the total pressure of a gas mixture that contains A. We can use the ideal gas law to describe the pressures of both gas A and the mixture: $P_A = n_A RT/V$ and $P_{tot} = n_t RT/V$. The ratio of the two is thus

$$\frac{P_A}{P_{tot}} = \frac{n_A RT/V}{n_{tot} RT/V} = \frac{n_A}{n_{tot}} = x_A \tag{7.2.12}$$

Rearranging this equation gives

$$P_A = x_A P_{tot} \tag{7.2.13}$$

That is, the partial pressure of any gas in a mixture is the total pressure multiplied by the mole fraction of that gas. This conclusion is a direct result of the ideal gas law, which assumes that all gas particles behave ideally. Consequently, the pressure of a gas in a mixture depends on only the percentage of particles in the mixture that are of that type, not their specific physical or chemical properties. By volume, Earth's atmosphere is about 78% N_2, 21% O_2, and 0.9% Ar, with trace amounts of gases such as CO_2, H_2O, and others. This means that 78% of the particles present in the atmosphere are N_2; hence the mole fraction of N_2 is 78%/100% = 0.78. Similarly, the mole fractions of O_2 and Ar are 0.21 and 0.009, respectively. Using Equation 6.6.7, we therefore know that the partial pressure of N_2 is 0.78 atm (assuming an atmospheric pressure of exactly 760 mmHg) and, similarly, the partial pressures of O_2 and Ar are 0.21 and 0.009 atm, respectively.

Example 7.2.2

We have just calculated the partial pressures of the major gases in the air we inhale. Experiments that measure the composition of the air we *exhale* yield different results, however. The following table gives the measured pressures of the major gases in both inhaled and exhaled air. Calculate the mole fractions of the gases in exhaled air.

	Inhaled Air / mmHg	Exhaled Air / mmHg
P_{N_2}	597	568
P_{O_2}	158	116
P_{H_2O}	0.3	28
P_{CO_2}	5	48
P_{Ar}	8	8
P_{tot}	767	767

Given: pressures of gases in inhaled and exhaled air

Asked for: mole fractions of gases in exhaled air

Strategy:

Calculate the mole fraction of each gas using Equation 6.6.7.

Solution:

The mole fraction of any gas A is given by

$$x_A = \frac{P_A}{P_{tot}} \tag{7.2.14}$$

where P_A is the partial pressure of A and P_{tot} is the total pressure. For example, the mole fraction of CO_2 is given as:

$$x_{CO_2} = \frac{48 \text{ mmHg}}{767 \text{ mmHg}} = 0.063 \tag{7.2.15}$$

The following table gives the values of x_A for the gases in the exhaled air.

Gas	Mole Fraction
N_2	0.741
O_2	0.151
H_2O	0.037
CO_2	0.063
Ar	0.010

? Exercise 7.2.2

Venus is an inhospitable place, with a surface temperature of 560°C and a surface pressure of 90 atm. The atmosphere consists of about 96% CO_2 and 3% N_2, with trace amounts of other gases, including water, sulfur dioxide, and sulfuric acid. Calculate the partial pressures of CO_2 and N_2.

Answer

$$P_{CO_2} = 86 \text{ atm}, P_{N_2} = 2.7 \text{ atm}$$



Dalton's Law of Partial Pressures: https://youtu.be/y5-SbspyvBA

Summary

- The partial pressure of each gas in a mixture is proportional to its mole fraction.

The pressure exerted by each gas in a gas mixture (its **partial pressure**) is independent of the pressure exerted by all other gases present. Consequently, the total pressure exerted by a mixture of gases is the sum of the partial pressures of the components (**Dalton's law of partial pressures**). The amount of gas present in a mixture may be described by its partial pressure or its mole fraction. The **mole fraction** of any component of a mixture is the ratio of the number of moles of that substance to the total number of moles of all substances present. In a mixture of gases, the partial pressure of each gas is the product of the total pressure and the mole fraction of that gas.

7.2: Mixtures of Gases is shared under a not declared license and was authored, remixed, and/or curated by LibreTexts.

- **6.6: Mixtures of Gases** is licensed CC BY-NC-SA 4.0.

7.3: Solution Concentration

Learning Objectives

- To describe the concentration of a solution in the way that is most appropriate for a particular problem or application.
- To be familiar with the different units used to express the concentrations of a solution.

There are several different ways to quantitatively describe the concentration of a solution. For example, molarity is a useful way to describe solution concentrations for reactions that are carried out in solution. Mole fractions are used not only to describe gas concentrations but also to determine the vapor pressures of mixtures of similar liquids. Example **7.3.1** reviews the methods for calculating the molarity and mole fraction of a solution when the masses of its components are known.

Example 7.3.1: Molarity and Mole Fraction

Commercial vinegar is essentially a solution of acetic acid in water. A bottle of vinegar has 3.78 g of acetic acid per 100.0 g of solution. Assume that the density of the solution is 1.00 g/mL.

a. What is its molarity?
b. What is its mole fraction?

Given: mass of substance and mass and density of solution

Asked for: molarity and mole fraction

Strategy:

A. Calculate the number of moles of acetic acid in the sample. Then calculate the number of liters of solution from its mass and density. Use these results to determine the molarity of the solution.
B. Determine the mass of the water in the sample and calculate the number of moles of water. Then determine the mole fraction of acetic acid by dividing the number of moles of acetic acid by the total number of moles of substances in the sample.

Solution:

A: The molarity is the number of moles of acetic acid per liter of solution. We can calculate the number of moles of acetic acid as its mass divided by its molar mass.

$$\text{moles } CH_3CO_2H = \frac{3.78 \cancel{\text{ g}}\ CH_3CO_2H}{60.05 \cancel{\text{ g}}/\text{mol}}$$
$$= 0.0629 \text{ mol}$$

The volume of the solution equals its mass divided by its density.

$$\text{volume} = \frac{\text{mass}}{\text{density}}$$
$$= \frac{100.0 \cancel{\text{ g}}\ \text{solution}}{1.00 \cancel{\text{ g}}/\text{mL}} = 100\ mL$$

Then calculate the molarity directly.

$$\text{molarity of } CH_3CO_2H = \frac{\text{moles } CH_3CO_2H}{\text{liter solution}}$$
$$= \frac{0.0629\ mol\ CH_3CO_2H}{(100\ \cancel{mL})(1\ L/1000\ \cancel{mL})} = 0.629\ M\ CH_3CO_2H$$

This result makes intuitive sense. If 100.0 g of aqueous solution (equal to 100 mL) contains 3.78 g of acetic acid, then 1 L of solution will contain 37.8 g of acetic acid, which is a little more than $\frac{1}{2}$ mole. Keep in mind, though, that the mass and volume of a solution are related by its density; concentrated aqueous solutions often have densities greater than 1.00 g/mL.

B: To calculate the mole fraction of acetic acid in the solution, we need to know the number of moles of both acetic acid and water. The number of moles of acetic acid is 0.0629 mol, as calculated in part (a). We know that 100.0 g of vinegar contains 3.78 g of acetic acid; hence the solution also contains (100.0 g − 3.78 g) = 96.2 g of water. We have

$$moles\ H_2O = \frac{96.2\ \cancel{g}\ H_2O}{18.02\ \cancel{g}/mol} = 5.34\ mol\ H_2O$$

The mole fraction χ of acetic acid is the ratio of the number of moles of acetic acid to the total number of moles of substances present:

$$\begin{aligned}\chi_{CH_3CO_2H} &= \frac{moles\ CH_3CO_2H}{moles\ CH_3CO_2H + moles\ H_2O} \\ &= \frac{0.0629\ mol}{0.0629\ mol + 5.34\ mol} \\ &= 0.0116 = 1.16 \times 10^{-2}\end{aligned}$$

This answer makes sense, too. There are approximately 100 times as many moles of water as moles of acetic acid, so the ratio should be approximately 0.01.

? Exercise 7.3.1: Molarity and Mole Fraction

A solution of **HCl** gas dissolved in water (sold commercially as “muriatic acid,” a solution used to clean masonry surfaces) has 20.22 g of **HCl** per 100.0 g of solution, and its density is 1.10 g/mL.

a. What is its molarity?
b. What is its mole fraction?

Answer a

6.10 M HCl

Answer b

$\chi_{HCl} = 0.111$

The concentration of a solution can also be described by its molality (m), the number of moles of solute per kilogram of solvent:

$$\text{molality (m)} = \frac{\text{moles solute}}{\text{kilogram solvent}} \tag{7.3.1}$$

Molality, therefore, has the same numerator as molarity (the number of moles of solute) but a different denominator (kilogram of solvent rather than liter of solution). For dilute aqueous solutions, the molality and molarity are nearly the same because dilute solutions are mostly solvent. Thus because the density of water under standard conditions is very close to 1.0 g/mL, the volume of 1.0 kg of H_2O under these conditions is very close to 1.0 L, and a 0.50 M solution of KBr in water, for example, has approximately the same concentration as a 0.50 m solution.

Another common way of describing concentration is as the ratio of the mass of the solute to the total mass of the solution. The result can be expressed as mass percentage, parts per million (ppm), or parts per billion (ppb):

$$\text{mass percentage} = \frac{\text{mass of solute}}{\text{mass of solution}} \times 100 \tag{7.3.2}$$

$$\text{parts per million (ppm)} = \frac{\text{mass of solute}}{\text{mass of solution}} \times 10^6 \tag{7.3.3}$$

$$\text{parts per billion (ppb)} = \frac{\text{mass of solute}}{\text{mass of solution}} \times 10^9 \tag{7.3.4}$$

In the health sciences, the concentration of a solution is often expressed as parts per thousand (ppt), indicated as a proportion. For example, adrenalin, the hormone produced in high-stress situations, is available in a 1:1000 solution, or one gram of adrenalin per 1000 g of solution.

The labels on bottles of commercial reagents often describe the contents in terms of mass percentage. Sulfuric acid, for example, is sold as a 95% aqueous solution, or 95 g of H_2SO_4 per 100 g of solution. Parts per million and parts per billion are used to describe concentrations of highly dilute solutions. These measurements correspond to milligrams and micrograms of solute per kilogram of solution, respectively. For dilute aqueous solutions, this is equal to milligrams and micrograms of solute per liter of solution (assuming a density of 1.0 g/mL).

Example 7.3.2: Molarity and Mass

Several years ago, millions of bottles of mineral water were contaminated with benzene at ppm levels. This incident received a great deal of attention because the lethal concentration of benzene in rats is 3.8 ppm. A 250 mL sample of mineral water has 12.7 ppm of benzene. Because the contaminated mineral water is a very dilute aqueous solution, we can assume that its density is approximately 1.00 g/mL.

a. What is the molarity of the solution?
b. What is the mass of benzene in the sample?

Given: volume of sample, solute concentration, and density of solution

Asked for: molarity of solute and mass of solute in 250 mL

Strategy:

A. Use the concentration of the solute in parts per million to calculate the molarity.
B. Use the concentration of the solute in parts per million to calculate the mass of the solute in the specified volume of solution.

Solution:

a. A To calculate the molarity of benzene, we need to determine the number of moles of benzene in 1 L of solution. We know that the solution contains 12.7 ppm of benzene. Because 12.7 ppm is equivalent to 12.7 mg/1000 g of solution and the density of the solution is 1.00 g/mL, the solution contains 12.7 mg of benzene per liter (1000 mL). The molarity is therefore

$$\begin{aligned}\text{molarity} &= \frac{\text{moles}}{\text{liter solution}} \\ &= \frac{(12.7\ \cancel{mg})\left(\frac{1\ \cancel{g}}{1000\ \cancel{mg}}\right)\left(\frac{1\ mol}{78.114\ \cancel{g}}\right)}{1.00\ L} \\ &= 1.63 \times 10^{-4} M\end{aligned}$$

b. B We are given that there are 12.7 mg of benzene per 1000 g of solution, which is equal to 12.7 mg/L of solution. Hence the mass of benzene in 250 mL (250 g) of solution is

$$\begin{aligned}\text{mass of benzene} &= \frac{(12.7\ mg\ \text{benzene})(250\ \cancel{mL})}{1000\ \cancel{mL}} \\ &= 3.18\ mg \\ &= 3.18 \times 10^{-3}\ g\ \text{benzene}\end{aligned}$$

Exercise 7.3.2: Molarity of Lead Solution

The maximum allowable concentration of lead in drinking water is 9.0 ppb.

a. What is the molarity of Pb^{2+} in a 9.0 ppb aqueous solution?
b. Use your calculated concentration to determine how many grams of Pb^{2+} are in an 8 oz glass of water.

Answer a

4.3×10^{-8} M

Answer b

2×10^{-6} g

How do chemists decide which units of concentration to use for a particular application? Although molarity is commonly used to express concentrations for reactions in solution or for titrations, it does have one drawback—molarity is the number of moles of solute divided by the volume of the solution, and the volume of a solution depends on its density, which is a function of temperature. Because volumetric glassware is calibrated at a particular temperature, typically 20°C, the molarity may differ from the original value by several percent if a solution is prepared or used at a significantly different temperature, such as 40°C or 0°C. For many applications this may not be a problem, but for precise work these errors can become important. In contrast, mole fraction, molality, and mass percentage depend on only the masses of the solute and solvent, which are independent of temperature.

Mole fraction is not very useful for experiments that involve quantitative reactions, but it is convenient for calculating the partial pressure of gases in mixtures, as discussed previously. Mole fractions are also useful for calculating the vapor pressures of certain types of solutions. Molality is particularly useful for determining how properties such as the freezing or boiling point of a solution vary with solute concentration. Because mass percentage and parts per million or billion are simply different ways of expressing the ratio of the mass of a solute to the mass of the solution, they enable us to express the concentration of a substance even when the molecular mass of the substance is unknown. Units of ppb or ppm are also used to express very low concentrations, such as those of residual impurities in foods or of pollutants in environmental studies.

Table **7.3.1** summarizes the different units of concentration and typical applications for each. When the molar mass of the solute and the density of the solution are known, it becomes relatively easy with practice to convert among the units of concentration we have discussed, as illustrated in Example **7.3.3**.

Table **7.3.1**: Different Units for Expressing the Concentrations of Solutions*

Unit	Definition	Application
molarity (M)	moles of solute/liter of solution (mol/L)	Used for quantitative reactions in solution and titrations; mass and molecular mass of solute and volume of solution are known.
mole fraction (χ)	moles of solute/total moles present (mol/mol)	Used for partial pressures of gases and vapor pressures of some solutions; mass and molecular mass of each component are known.
molality (m)	moles of solute/kg of solvent (mol/kg)	Used in determining how colligative properties vary with solute concentration; masses and molecular mass of solute are known.
mass percentage (%)	[mass of solute (g)/mass of solution (g)] × 100	Useful when masses are known but molecular masses are unknown.
parts per thousand (ppt)	[mass of solute/mass of solution] × 10^3 (g solute/kg solution)	Used in the health sciences, ratio solutions are typically expressed as a proportion, such as 1:1000.
parts per million (ppm)	[mass of solute/mass of solution] × 10^6 (mg solute/kg solution)	Used for trace quantities; masses are known but molecular masses may be unknown.
parts per billion (ppb)	[mass of solute/mass of solution] × 10^9 (µg solute/kg solution)	Used for trace quantities; masses are known but molecular masses may be unknown.

*The molarity of a solution is temperature dependent, but the other units shown in this table are independent of temperature.

Example 7.3.3: Vodka

Vodka is essentially a solution of ethanol in water. Typical vodka is sold as "80 proof," which means that it contains 40.0% ethanol by volume. The density of pure ethanol is 0.789 g/mL at 20°C. If we assume that the volume of the solution is the sum of the volumes of the components (which is not strictly correct), calculate the following for the ethanol in 80-proof vodka.

a. the mass percentage
b. the mole fraction
c. the molarity
d. the molality

Given: volume percent and density

Asked for: mass percentage, mole fraction, molarity, and molality

Strategy:

A. Use the density of the solute to calculate the mass of the solute in 100.0 mL of solution. Calculate the mass of water in 100.0 mL of solution.
B. Determine the mass percentage of solute by dividing the mass of ethanol by the mass of the solution and multiplying by 100.
C. Convert grams of solute and solvent to moles of solute and solvent. Calculate the mole fraction of solute by dividing the moles of solute by the total number of moles of substances present in solution.
D. Calculate the molarity of the solution: moles of solute per liter of solution. Determine the molality of the solution by dividing the number of moles of solute by the kilograms of solvent.

Solution:

The key to this problem is to use the density of pure ethanol to determine the mass of ethanol (CH_3CH_2OH), abbreviated as EtOH, in a given volume of solution. We can then calculate the number of moles of ethanol and the concentration of ethanol in any of the required units. A Because we are given a percentage by volume, we assume that we have 100.0 mL of solution. The volume of ethanol will thus be 40.0% of 100.0 mL, or 40.0 mL of ethanol, and the volume of water will be 60.0% of 100.0 mL, or 60.0 mL of water. The mass of ethanol is obtained from its density:

$$mass\ of\ EtOH = (40.0\ \cancel{mL}) \left(\frac{0.789\ g}{\cancel{mL}} \right) = 31.6\ g\ EtOH$$

If we assume the density of water is 1.00 g/mL, the mass of water is 60.0 g. We now have all the information we need to calculate the concentration of ethanol in the solution.

B The mass percentage of ethanol is the ratio of the mass of ethanol to the total mass of the solution, expressed as a percentage:

$$\begin{aligned} \%EtOH &= \left(\frac{mass\ of\ EtOH}{mass\ of\ solution} \right) (100) \\ &= \left(\frac{31.6\ \cancel{g}\ EtOH}{31.6\ \cancel{g}\ EtOH + 60.0\ \cancel{g}\ H_2O} \right) (100) \\ &= 34.5\% \end{aligned}$$

C The mole fraction of ethanol is the ratio of the number of moles of ethanol to the total number of moles of substances in the solution. Because 40.0 mL of ethanol has a mass of 31.6 g, we can use the molar mass of ethanol (46.07 g/mol) to determine the number of moles of ethanol in 40.0 mL:

$$\begin{aligned} moles\ CH_3CH_2OH &= (31.6\ \cancel{g\ CH_3CH_2OH}) \left(\frac{1\ mol}{46.07\ \cancel{g\ CH_3CH_2OH}} \right) \\ &= 0.686\ mol\ CH_3CH_2OH \end{aligned}$$

Similarly, the number of moles of water is

$$moles\ H_2O = (60.0\ \cancel{g\ H_2O})\left(\frac{1\ mol\ H_2O}{18.02\ \cancel{g\ H_2O}}\right) = 3.33\ mol\ H_2O$$

The mole fraction of ethanol is thus

$$\chi_{CH_3CH_2OH} = \frac{0.686\ \cancel{mol}}{0.686\ \cancel{mol} + 3.33\ \cancel{mol}} = 0.171$$

D The molarity of the solution is the number of moles of ethanol per liter of solution. We already know the number of moles of ethanol per 100.0 mL of solution, so the molarity is

$$M_{CH_3CH_2OH} = \left(\frac{0.686\ mol}{100\ \cancel{mL}}\right)\left(\frac{1000\ \cancel{mL}}{L}\right) = 6.86\ M$$

The molality of the solution is the number of moles of ethanol per kilogram of solvent. Because we know the number of moles of ethanol in 60.0 g of water, the calculation is again straightforward:

$$m_{CH_3CH_2OH} = \left(\frac{0.686\ mol\ EtOH}{60.0\ \cancel{g}\ H_2O}\right)\left(\frac{1000\ \cancel{g}}{kg}\right) = \frac{11.4\ mol\ EtOH}{kg\ H_2O} = 11.4\ m$$

? Exercise 7.3.3: Toluene/Benzene Solution

A solution is prepared by mixing 100.0 mL of toluene with 300.0 mL of benzene. The densities of toluene and benzene are 0.867 g/mL and 0.874 g/mL, respectively. Assume that the volume of the solution is the sum of the volumes of the components. Calculate the following for toluene.

a. mass percentage
b. mole fraction
c. molarity
d. molality

Answer a

mass percentage toluene = 24.8%

Answer b

$\chi_{toluene} = 0.219$

Answer c

2.35 M toluene

Answer d

3.59 m toluene



A Video Discussing Different Measures of Concentration. Video Link: Measures of Concentration, YouTube (opens in new window) [youtu.be]



A Video Discussing how to Convert Measures of Concentration. Video Link: Converting Units of Concentration, YouTube(opens in new window) [youtu.be]

Summary

Different units are used to express the concentrations of a solution depending on the application. The concentration of a solution is the quantity of solute in a given quantity of solution. It can be expressed in several ways: molarity (moles of solute per liter of solution); mole fraction, the ratio of the number of moles of solute to the total number of moles of substances present; mass percentage, the ratio of the mass of the solute to the mass of the solution times 100; parts per thousand (ppt), grams of solute per kilogram of solution; parts per million (ppm), milligrams of solute per kilogram of solution; parts per billion (ppb), micrograms of solute per kilogram of solution; and molality (m), the number of moles of solute per kilogram of solvent.

7.3: Solution Concentration is shared under a not declared license and was authored, remixed, and/or curated by LibreTexts.

- **13.4: Ways of Expressing Concentration** by Anonymous is licensed CC BY-NC-SA 3.0.
- **13.2: Solution Concentration** is licensed CC BY-NC-SA 4.0.

7.4: Intermolecular Forces and the Solution Process

Learning Objectives

- To understand the relationship between solubility and molecular structure.
- To demonstrate how the strength of intramolecular bonding determines the solubility of a solute in a given solvent.

The interactions that determine the solubility of a substance in a liquid depend largely on the chemical nature of the solute (such as whether it is ionic or molecular) rather than on its physical state (solid, liquid, or gas). We will first describe the general case of forming a solution of a molecular species in a liquid solvent and then describe the formation of a solution of an ionic compound.

The Role of Enthalpy in Solution Formation

Energy is required to overcome the intermolecular interactions in a solute, which can be supplied only by the new interactions that occur in the solution, when each solute particle is surrounded by particles of the solvent in a process called **solvation**, or hydration when the solvent is water. Thus all of the solute–solute interactions and many of the solvent–solvent interactions must be disrupted for a solution to form. In this section, we describe the role of enthalpy in this process.

Because enthalpy is a state function, we can use a thermochemical cycle to analyze the energetics of solution formation. The process occurs in three discrete steps, indicated by ΔH1, ΔH_2 , and ΔH_3. in Figure 1 The overall enthalpy change in the formation of the solution $\Delta H_{solution}$ is the sum of the enthalpy changes in the three steps:

$\Delta H_{solution} = \Delta H1 + \Delta H_2 + \Delta H_3$. (Figure 1)

When a solvent is added to a solution, steps 1 and 2 are both endothermic because energy is required to overcome the intermolecular interactions in the solvent ΔH1 and the solute ΔH_2. Because ΔH is positive for both steps 1 and 2, the solute–solvent interactions ΔH_3. must be stronger than the solute–solute and solvent–solvent interactions they replace in order for the dissolution process to be exothermic $\Delta H_{solution} < 0$, When the solute is an ionic solid, ΔH_2 corresponds to the lattice energy that must be overcome to form a solution. The higher the charge of the ions in an ionic solid, the higher the lattice energy. Consequently, solids that have very high lattice energies, such as Lattice Energy for MgO (3791 kJ/mol), are generally insoluble in all solvents.

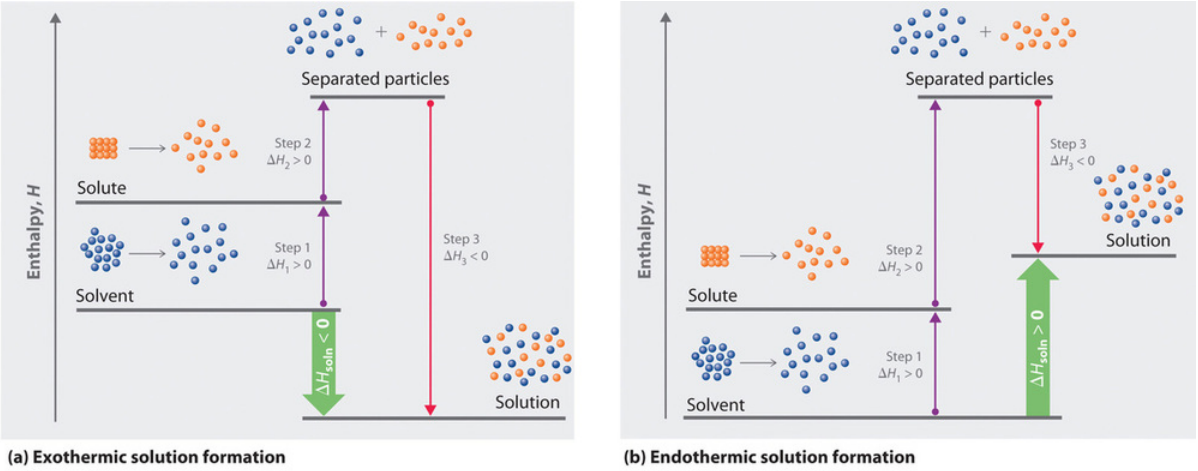


Figure 1. Enthalpy Changes That Accompany the Formation of a Solution. Solvation can be an exothermic or endothermic process depending on the nature of the solute and solvent. In both cases, step 1, separation of the solvent particles, is energetically uphill ($\Delta H_1 > 0$), as is step 2, separation of the solute particles ($\Delta H_2 > 0$). In contrast, energy is released in step 3 ΔH_3. < 0 because of interactions between the solute and solvent. (a) When ΔH_3. is larger in magnitude than the sum of ΔH1 and ΔH_2, the overall process is exothermic $\Delta H_{solution} < 0$, as shown in the thermochemical cycle. (b) When ΔH_3. is smaller in magnitude than the sum of ΔH1 and ΔH_2,, the overall process is endothermic $\Delta H_{solution} > 0$).

A positive value for $\Delta H_{solution}$ does not mean that a solution will not form. Whether a given process, including formation of a solution, occurs spontaneously depends on whether the total energy of the system is lowered as a result. Enthalpy is only one of the contributing factors. A high $\Delta H_{solution}$ is usually an indication that the substance is not very soluble. Instant cold packs used to treat

athletic injuries, for example, take advantage of the large positive $\Delta H_{solution}$ of ammonium nitrate during dissolution (+25.7 kJ/mol), which produces temperatures less than 0°C (Figure 2.)



Figure 2Commercial Cold Packs for Treating Injuries. These packs contain solid ammonium nitrate and water in separate compartments. When the seal between the compartments is broken, the ammonium nitrate dissolves in the water. Because $\Delta H_{solution}$ for ammonium nitrateis much greater than zero, heat is absorbed by the cold pack during the dissolution process, producing local temperatures less than 0°C.

Solutions of Molecular Substances in Liquids

The London dispersion forces, dipole–dipole interactions, and hydrogen bonds that hold molecules to other molecules are generally weak. Even so, energy is required to disrupt these interactions. Unless some of that energy is recovered in the formation of new, favorable solute–solvent interactions, the increase in entropy on solution formation is not enough for a solution to form.

For solutions of gases in liquids, we can safely ignore the energy required to separate the solute molecules ($\Delta H_2 = 0$) because the molecules are already separated. Thus we need to consider only the energy required to separate the solvent molecules (ΔH_1) and the energy released by new solute–solvent interactions (ΔH_3). Nonpolar gases such as N_2, O_2, and Ar have no dipole moment and cannot engage in dipole–dipole interactions or hydrogen bonding. Consequently, the only way they can interact with a solvent is by means of London dispersion forces, which may be weaker than the solvent–solvent interactions in a polar solvent. It is not surprising, then, that nonpolar gases are most soluble in nonpolar solvents. In this case, ΔH_1 and ΔH_3 are both small and of similar magnitude. In contrast, for a solution of a nonpolar gas in a polar solvent, ΔH_1 is far greater than ΔH_3. As a result, nonpolar gases are less soluble in polar solvents than in nonpolar solvents. For example, the concentration of N_2 in a saturated solution of N_2 in water, a polar solvent, is only $7.07 \times 10^{-4}\ M$ compared with $4.5 \times 10^{-3}\ M$ for a saturated solution of N_2 in benzene, a nonpolar solvent.

The solubilities of nonpolar gases in water generally increase as the molecular mass of the gas increases, as shown in Table **7.4.1**. This is precisely the trend expected: as the gas molecules become larger, the strength of the solvent–solute interactions due to London dispersion forces increases, approaching the strength of the solvent–solvent interactions.

Table **7.4.1**: Solubilities of Selected Gases in Water at 20°C and 1 atm Pressure

Gas	Solubility (M) × 10^{-4}
He	3.90
Ne	4.65
Ar	15.2
Kr	27.9
Xe	50.2
H_2	8.06
N_2	7.07
CO	10.6
O_2	13.9
N_2O	281
CH_4	15.5

Virtually all common organic liquids, whether polar or not, are miscible. The strengths of the intermolecular attractions are comparable; thus the enthalpy of solution is expected to be small ($\Delta H_{soln} \approx 0$), and the increase in entropy drives the formation of a solution. If the predominant intermolecular interactions in two liquids are very different from one another, however, they may be immiscible. For example, organic liquids such as benzene, hexane, CCl_4, and CS_2 (S=C=S) are nonpolar and have no ability to act as hydrogen bond donors or acceptors with hydrogen-bonding solvents such as H_2O, HF, and NH_3; hence they are immiscible in these solvents. When shaken with water, they form separate phases or layers separated by an interface (Figure **7.4.3**), the region between the two layers. Just because two liquids are immiscible, however, does not mean that they are completely insoluble in each other. For example, 188 mg of benzene dissolves in 100 mL of water at 23.5°C. Adding more benzene results in the separation of an upper layer consisting of benzene with a small amount of dissolved water (the solubility of water in benzene is only 178 mg/100 mL of benzene).



Figure **7.4.3**: Immiscible Liquids. Separatory funnel demonstrating the separation of oil and colored water. from Wikipedia

The solubilities of simple alcohols in water are given in Table **7.4.2**.

Table **7.4.2**: Solubilities of Straight-Chain Organic Alcohols in Water at 20°C

Alcohol	Solubility (mol/100 g of H_2O)
methanol	completely miscible
ethanol	completely miscible
n-propanol	completely miscible
n-butanol	0.11
n-pentanol	0.030
n-hexanol	0.0058
n-heptanol	0.0008

Only the three lightest alcohols (methanol, ethanol, and n-propanol) are completely miscible with water. As the molecular mass of the alcohol increases, so does the proportion of hydrocarbon in the molecule. Correspondingly, the importance of hydrogen bonding and dipole–dipole interactions in the pure alcohol decreases, while the importance of London dispersion forces increases, which leads to progressively fewer favorable electrostatic interactions with water. Organic liquids such as acetone, ethanol, and tetrahydrofuran are sufficiently polar to be completely miscible with water yet sufficiently nonpolar to be completely miscible with all organic solvents.



Tetrahydrofuran (THF)

The same principles govern the solubilities of molecular solids in liquids. For example, elemental sulfur is a solid consisting of cyclic S_8 molecules that have no dipole moment. Because the S_8 rings in solid sulfur are held to other rings by London dispersion forces, elemental sulfur is insoluble in water. It is, however, soluble in nonpolar solvents that have comparable London dispersion forces, such as CS_2 (23 g/100 mL). In contrast, glucose contains five –OH groups that can form hydrogen bonds. Consequently, glucose is very soluble in water (91 g/120 mL of water) but essentially insoluble in nonpolar solvents such as benzene. The structure of one isomer of glucose is shown here.



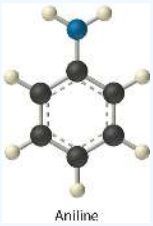
D-Glucose

Low-molecular-mass hydrocarbons with highly electronegative and polarizable halogen atoms, such as chloroform ($CHCl_3$) and methylene chloride (CH_2Cl_2), have both significant dipole moments and relatively strong London dispersion forces. These hydrocarbons are therefore powerful solvents for a wide range of polar and nonpolar compounds. Naphthalene, which is nonpolar, and phenol (C_6H_5OH), which is polar, are very soluble in chloroform. In contrast, the solubility of ionic compounds is largely determined not by the polarity of the solvent but rather by its dielectric constant, a measure of its ability to separate ions in solution, as you will soon see.

Example 7.4.1

Identify the most important solute–solvent interactions in each solution.

a. iodine in benzene
b. aniline ($C_6H_5NH_2$) in dichloromethane (CH_2Cl_2)



c. iodine in water

Given: components of solutions

Asked for: predominant solute–solvent interactions

Strategy:

Identify all possible intermolecular interactions for both the solute and the solvent: London dispersion forces, dipole–dipole interactions, or hydrogen bonding. Determine which is likely to be the most important factor in solution formation.

Solution

a. Benzene and $I2$ are both nonpolar molecules. The only possible attractive forces are London dispersion forces.
b. Aniline is a polar molecule with an $-NH_2$ group, which can act as a hydrogen bond donor. Dichloromethane is also polar, but it has no obvious hydrogen bond acceptor. Therefore, the most important interactions between aniline and CH_2Cl_2 are likely to be London interactions.
c. Water is a highly polar molecule that engages in extensive hydrogen bonding, whereas I_2 is a nonpolar molecule that cannot act as a hydrogen bond donor or acceptor. The slight solubility of I_2 in water ($1.3 \times 10^{-3}\ mol/L$ at 25°C) is due to London dispersion forces.

Exercise 7.4.1

Identify the most important interactions in each solution:

a. ethylene glycol ($HOCH_2CH_2OH$) in acetone
b. acetonitrile ($CH_3C{\equiv}N$) in acetone
c. n-hexane in benzene

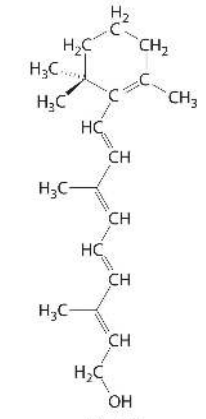
Answer:

a. hydrogen bonding
b. London interactions
c. London dispersion forces

Hydrophilic and Hydrophobic Solutes

A solute can be classified as hydrophilic (literally, “water loving”), meaning that it has an electrostatic attraction to water, or hydrophobic (“water fearing”), meaning that it repels water. A hydrophilic substance is polar and often contains O–H or N–H groups that can form hydrogen bonds to water. For example, glucose with its five O–H groups is hydrophilic. In contrast, a hydrophobic substance may be polar but usually contains C–H bonds that do not interact favorably with water, as is the case with naphthalene and n-octane. Hydrophilic substances tend to be very soluble in water and other strongly polar solvents, whereas hydrophobic substances are essentially insoluble in water and soluble in nonpolar solvents such as benzene and cyclohexane.

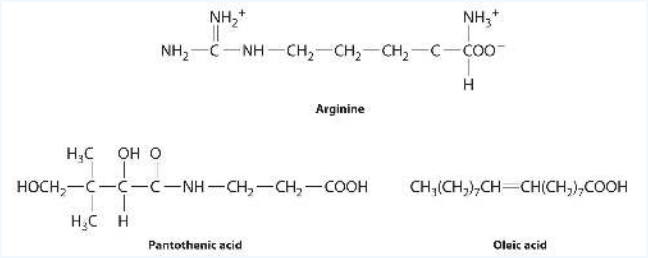
The difference between hydrophilic and hydrophobic substances has substantial consequences in biological systems. For example, vitamins can be classified as either fat soluble or water soluble. Fat-soluble vitamins, such as vitamin A, are mostly nonpolar, hydrophobic molecules. As a result, they tend to be absorbed into fatty tissues and stored there. In contrast, water-soluble vitamins, such as vitamin C, are polar, hydrophilic molecules that circulate in the blood and intracellular fluids, which are primarily aqueous. Water-soluble vitamins are therefore excreted much more rapidly from the body and must be replenished in our daily diet. A comparison of the chemical structures of vitamin A and vitamin C quickly reveals why one is hydrophobic and the other hydrophilic.



Because water-soluble vitamins are rapidly excreted, the risk of consuming them in excess is relatively small. Eating a dozen oranges a day is likely to make you tired of oranges long before you suffer any ill effects due to their high vitamin C content. In contrast, fat-soluble vitamins constitute a significant health hazard when consumed in large amounts. For example, the livers of polar bears and other large animals that live in cold climates contain large amounts of vitamin A, which have occasionally proven fatal to humans who have eaten them.

Example 7.4.2

The following substances are essential components of the human diet:



Using what you know of hydrophilic and hydrophobic solutes, classify each as water soluble or fat soluble and predict which are likely to be required in the diet on a daily basis.

a. arginine
b. pantothenic acid
c. oleic acid

Given: chemical structures

Asked for: classification as water soluble or fat soluble; dietary requirement

Strategy:

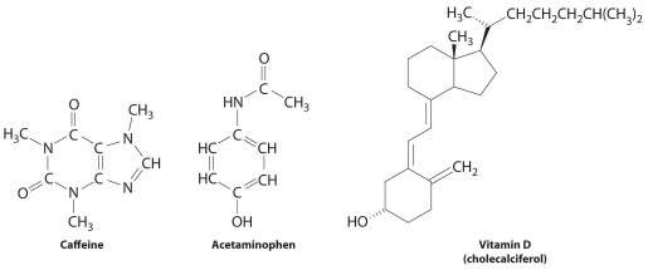
Based on the structure of each compound, decide whether it is hydrophilic or hydrophobic. If it is hydrophilic, it is likely to be required on a daily basis.

Solution:

a. Arginine is a highly polar molecule with two positively charged groups and one negatively charged group, all of which can form hydrogen bonds with water. As a result, it is hydrophilic and required in our daily diet.
b. Although pantothenic acid contains a hydrophobic hydrocarbon portion, it also contains several polar functional groups ($-OH$ and $-CO_2H$) that should interact strongly with water. It is therefore likely to be water soluble and required in the diet. (In fact, pantothenic acid is almost always a component of multiple-vitamin tablets.)
c. Oleic acid is a hydrophobic molecule with a single polar group at one end. It should be fat soluble and not required daily.

Exercise 7.4.2

These compounds are consumed by humans: caffeine, acetaminophen, and vitamin D. Identify each as primarily hydrophilic (water soluble) or hydrophobic (fat soluble), and predict whether each is likely to be excreted from the body rapidly or slowly.



Answer: Caffeine and acetaminophen are water soluble and rapidly excreted, whereas vitamin D is fat soluble and slowly excreted

Solid Solutions

Solutions are not limited to gases and liquids; solid solutions also exist. For example, amalgams, which are usually solids, are solutions of metals in liquid mercury. Because most metals are soluble in mercury, amalgams are used in gold mining, dentistry, and many other applications. A major difficulty when mining gold is separating very small particles of pure gold from tons of crushed rock. One way to accomplish this is to agitate a suspension of the crushed rock with liquid mercury, which dissolves the gold (as well as any metallic silver that might be present). The very dense liquid gold–mercury amalgam is then isolated and the mercury distilled away.

An alloy is a solid or liquid solution that consists of one or more elements in a metallic matrix. A solid alloy has a single homogeneous phase in which the crystal structure of the solvent remains unchanged by the presence of the solute. Thus the microstructure of the alloy is uniform throughout the sample. Examples are substitutional and interstitial alloys such as brass or solder. Liquid alloys include sodium/potassium and gold/mercury. In contrast, a partial alloy solution has two or more phases that can be homogeneous in the distribution of the components, but the microstructures of the two phases are not the same. As a liquid solution of lead and tin is cooled, for example, different crystalline phases form at different cooling temperatures. Alloys usually have properties that differ from those of the component elements.

Network solids such as diamond, graphite, and $ceSiO_2$ are insoluble in all solvents with which they do not react chemically. The covalent bonds that hold the network or lattice together are simply too strong to be broken under normal conditions. They are certainly much stronger than any conceivable combination of intermolecular interactions that might occur in solution. Most metals are insoluble in virtually all solvents for the same reason: the delocalized metallic bonding is much stronger than any favorable metal atom–solvent interactions. Many metals react with solutions such as aqueous acids or bases to produce a solution. However, in these instances the metal undergoes a chemical transformation that cannot be reversed by simply removing the solvent.

Solids with very strong intermolecular bonding tend to be insoluble.

Solubilities of Ionic Substances in Liquids

Ionic substances are generally most soluble in polar solvents; the higher the lattice energy, the more polar the solvent must be to overcome the lattice energy and dissolve the substance. Because of its high polarity, water is the most common solvent for ionic compounds. Many ionic compounds are soluble in other polar solvents, however, such as liquid ammonia, liquid hydrogen fluoride, and methanol. Because all these solvents consist of molecules that have relatively large dipole moments, they can interact favorably with the dissolved ions.

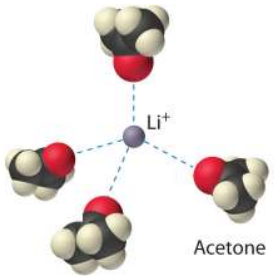


Figure **7.4.4**: Ion–Dipole Interactions in the Solvation of Li+ Ions by Acetone, a Polar Solvent

The interaction of water with Na+ and Cl− ions in an aqueous solution of **NaCl** was illustrated in Figure 4.3. The ion–dipole interactions between Li+ ions and acetone molecules in a solution of LiCl in acetone are shown in Figure **7.4.4**. The energetically favorable Li+–acetone interactions make ΔH_3 in Figure 13.1 sufficiently negative to overcome the positive ΔH_1 and ΔH_2. Because the dipole moment of acetone (2.88 D), and thus its polarity, is actually larger than that of water (1.85 D), one might even expect that LiCl would be more soluble in acetone than in water. In fact, the opposite is true: 83 g of LiCl dissolve in 100 mL of water at 20°C, but only about 4.1 g of LiCl dissolve in 100 mL of acetone. This apparent contradiction arises from the fact that the dipole moment is a property of a single molecule in the gas phase. A more useful measure of the ability of a solvent to dissolve ionic compounds is its dielectric constant (ε), which is the ability of a bulk substance to decrease the electrostatic forces between two charged particles. By definition, the dielectric constant of a vacuum is 1. In essence, a solvent with a high dielectric constant causes the charged particles to behave as if they have been moved farther apart. At 25°C, the dielectric constant of water is 80.1, one of the highest known, and that of acetone is only 21.0. Hence water is better able to decrease the electrostatic attraction between Li+ and Cl− ions, so LiCl is more soluble in water than in acetone. This behavior is in contrast to that of molecular substances, for which polarity is the dominant factor governing solubility.

A solvent's dielectric constant is the most useful measure of its ability to dissolve ionic compounds. A solvent's polarity is the dominant factor in dissolving molecular substances.

Summary

The solubility of a substance is the maximum amount of a solute that can dissolve in a given quantity of solvent; it depends on the chemical nature of both the solute and the solvent and on the temperature and pressure. The solubility of a substance in a liquid is determined by intermolecular interactions, which also determine whether two liquids are miscible. Solutes can be classified as hydrophilic (water loving) or hydrophobic (water fearing). Vitamins with hydrophilic structures are water soluble, whereas those with hydrophobic structures are fat soluble. Many metals dissolve in liquid mercury to form amalgams. Covalent network solids and most metals are insoluble in nearly all solvents. The solubility of ionic compounds is largely determined by the dielectric constant (ε) of the solvent, a measure of its ability to decrease the electrostatic forces between charged particles. Solutions of many ionic compounds in organic solvents can be dissolved using crown ethers, cyclic polyethers large enough to accommodate a metal ion in the center, or cryptands, compounds that completely surround a cation.

This page titled 7.4: Intermolecular Forces and the Solution Process is shared under a CC BY-NC-SA 3.0 license and was authored, remixed, and/or curated by Anonymous.

7.5: Solution Formation and Equilibrium

Learning Objectives

- To understand the relationship among temperature, pressure, and solubility.
- The understand that the solubility of a solid may increase or decrease with increasing temperature,

When a solute dissolves, its individual atoms, molecules, or ions interact with the solvent, become solvated, and are able to diffuse independently throughout the solution (part (a) in Figure **7.5.1**). This is not, however, a unidirectional process. If the molecule or ion happens to collide with the surface of a particle of the undissolved solute, it may adhere to the particle in a process called crystallization. Dissolution and crystallization continue as long as excess solid is present, resulting in a dynamic equilibrium analogous to the equilibrium that maintains the vapor pressure of a liquid. We can represent these opposing processes as follows:

$$\text{solute} + \text{solvent} \underset{\text{dissolution}}{\overset{\text{crystallization}}{\rightleftharpoons}} \text{solution} \tag{7.5.1}$$

Although the terms precipitation and crystallization are both used to describe the separation of solid solute from a solution, crystallization refers to the formation of a solid with a well-defined crystalline structure, whereas precipitation refers to the formation of any solid phase, often one with very small particles.

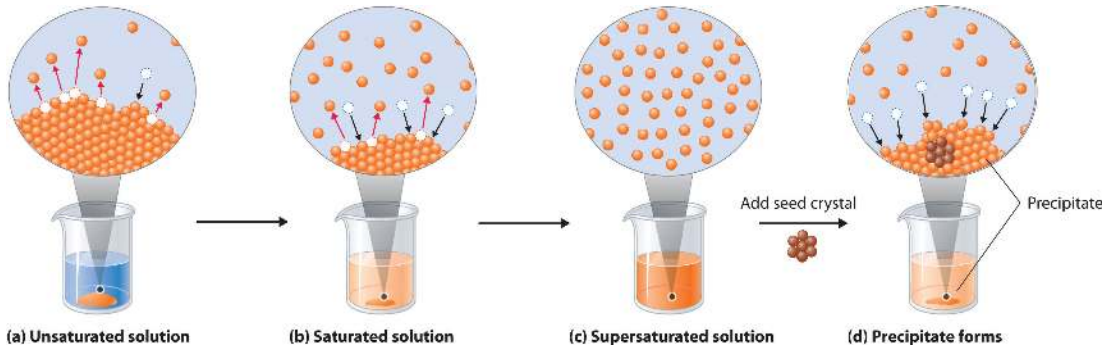


Figure **7.5.1** Dissolution and Precipitation. (a) When a solid is added to a solvent in which it is soluble, solute particles leave the surface of the solid and become solvated by the solvent, initially forming an unsaturated solution. (b) When the maximum possible amount of solute has dissolved, the solution becomes saturated. If excess solute is present, the rate at which solute particles leave the surface of the solid equals the rate at which they return to the surface of the solid. (c) A supersaturated solution can usually be formed from a saturated solution by filtering off the excess solute and lowering the temperature. (d) When a seed crystal of the solute is added to a supersaturated solution, solute particles leave the solution and form a crystalline precipitate. (CC BY-SA-NC 3.0; anonymous)

Solubility as a Function of Temperature

Figure **7.5.2** shows plots of the solubilities of several organic and inorganic compounds in water as a function of temperature. Although the solubility of a solid generally increases with increasing temperature, there is no simple relationship between the structure of a substance and the temperature dependence of its solubility. Many compounds (such as glucose and CH_3CO_2Na) exhibit a dramatic increase in solubility with increasing temperature. Others (such as $NaCl$ and K_2SO_4) exhibit little variation, and still others (such as Li_2SO_4) become less soluble with increasing temperature.

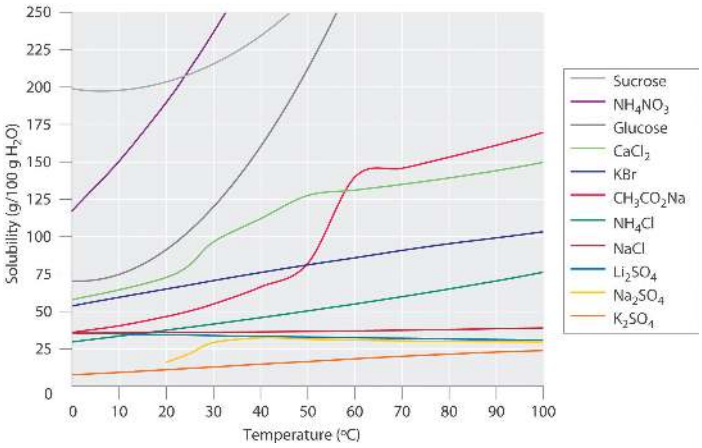


Figure **7.5.2**: Solubilities of Several Inorganic and Organic Solids in Water as a Function of Temperature. Solubility may increase or decrease with temperature; the magnitude of this temperature dependence varies widely among compounds. (CC BY-SA-NC 3.0; anonymous)

Notice in particular the curves for NH_4NO_3 and $CaCl_2$. The dissolution of ammonium nitrate in water is endothermic ($\Delta H_{soln} = +25.7\ kJ/mol$), whereas the dissolution of calcium chloride is exothermic ($\Delta H_{soln} = -68.2\ kJ/mol$), yet Figure **7.5.2** shows that the solubility of both compounds increases sharply with increasing temperature. In fact, the magnitudes of the changes in both enthalpy and entropy for dissolution are temperature dependent. Because the solubility of a compound is ultimately determined by relatively small differences between large numbers, there is generally no good way to predict how the solubility will vary with temperature.

Fractional Crystallization

The variation of solubility with temperature has been measured for a wide range of compounds, and the results are published in many standard reference books. Chemists are often able to use this information to separate the components of a mixture by fractional crystallization, the separation of compounds on the basis of their solubilities in a given solvent (Figure **7.5.3**). For example, if we have a mixture of 150 g of sodium acetate (CH_3CO_2Na) and 50 g of KBr, we can separate the two compounds by dissolving the mixture in 100 g of water at 80°C and then cooling the solution slowly to 0°C. According to the temperature curves in Figure **7.5.2**, both compounds dissolve in water at 80°C, and all 50 g of KBr remains in solution at 0°C. Only about 36 g of CH_3CO_2Na are soluble in 100 g of water at 0°C, however, so approximately 114 g (150 g − 36 g) of CH_3CO_2Na crystallizes out on cooling. The crystals can then be separated by filtration. Thus fractional crystallization allows us to recover about 75% of the original CH_3CO_2Na in essentially pure form in only one step.

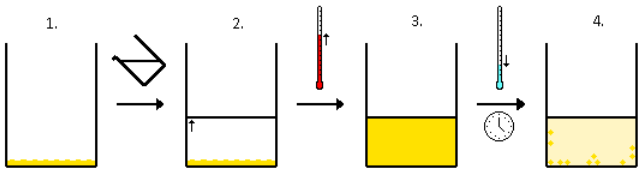


Figure **7.5.3**: Steps in a Fractional crystallization technique: (1 to 2) Solvent added (clear) to compound (orange) (2 to 3) Solvent heated to give saturated compound solution (orange) (3 to 4) Saturated compound solution (orange) allowed to cool over time to give crystals (orange) and a saturated solution (pale-orange). (Public Domain; Quantockgoblin via Wikipedia)

Fractional crystallization is a common technique for purifying compounds as diverse as those shown in Figure **7.5.2** and from antibiotics to enzymes to drugs (Figure **7.5.4**). For the technique to work properly, the compound of interest must be more soluble at high temperature than at low temperature, so that lowering the temperature causes it to crystallize out of solution. In addition, the impurities must be more soluble than the compound of interest (as was KBr in this example) and preferably present in relatively small amounts.



Figure **7.5.4**: Image of a single solvent, slowly cooling ibuprofen salt crystallizing. (CC BY-SA 2.5 Generic; Jacopo Werther via Wikipedia).

Summary

When a solution contains the maximum amount of solute that can dissolve under a given set of conditions, it is a saturated solution. Otherwise, it is unsaturated. Supersaturated solutions, which contain more dissolved solute than allowed under particular conditions, are not stable; the addition of a seed crystal, a small particle of solute, will usually cause the excess solute to crystallize. A system in which crystallization and dissolution occur at the same rate is in dynamic equilibrium. The solubility of most substances depends strongly on the temperature. The solubility of most solid or liquid solutes increases with increasing temperature. The components of a mixture can often be separated using fractional crystallization, which separates compounds according to their solubilities. The solubility of a gas decreases with increasing temperature.

7.5: Solution Formation and Equilibrium is shared under a CC BY-NC-SA 4.0 license and was authored, remixed, and/or curated by LibreTexts.

- **13.4: Solution Formation and Equilibrium** is licensed CC BY-NC-SA 4.0.

7.6: Solubilities of Gases

The chemical structures of the solute and solvent dictate the types of forces possible and, consequently, are important factors in determining solubility. For example, under similar conditions, the water solubility of oxygen is approximately three times greater than that of helium, but 100 times less than the solubility of chloromethane, $CHCl_3$. Considering the role of the solvent's chemical structure, note that the solubility of oxygen in the liquid hydrocarbon hexane, C_6H_{14}, is approximately 20 times greater than it is in water.

Other factors also affect the solubility of a given substance in a given solvent. Temperature is one such factor, with gas solubility typically decreasing as temperature increases (Figure **7.6.1**). This is one of the major impacts resulting from the thermal pollution of natural bodies of water.

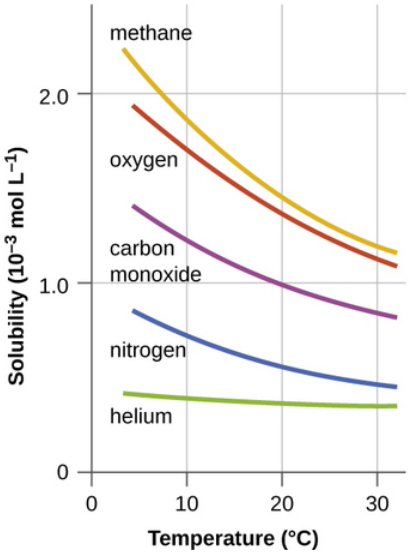


Figure **7.6.1**: The solubilities of these gases in water decrease as the temperature increases. All solubilities were measured with a constant pressure of 101.3 kPa (1 atm) of gas above the solutions.

When the temperature of a river, lake, or stream is raised abnormally high, usually due to the discharge of hot water from some industrial process, the solubility of oxygen in the water is decreased. Decreased levels of dissolved oxygen may have serious consequences for the health of the water's ecosystems and, in severe cases, can result in large-scale fish kills (Figure **7.6.2**).



(a) (b)

Figure **7.6.2**: (a) The small bubbles of air in this glass of chilled water formed when the water warmed to room temperature and the solubility of its dissolved air decreased. (b) The decreased solubility of oxygen in natural waters subjected to thermal pollution can result in large-scale fish kills. (credit a: modification of work by Liz West; credit b: modification of work by U.S. Fish and Wildlife Service)

The solubility of a gaseous solute is also affected by the partial pressure of solute in the gas to which the solution is exposed. Gas solubility increases as the pressure of the gas increases. Carbonated beverages provide a nice illustration of this relationship. The carbonation process involves exposing the beverage to a relatively high pressure of carbon dioxide gas and then sealing the beverage container, thus saturating the beverage with CO_2 at this pressure. When the beverage container is opened, a familiar hiss

is heard as the carbon dioxide gas pressure is released, and some of the dissolved carbon dioxide is typically seen leaving solution in the form of small bubbles (Figure **7.6.3**). At this point, the beverage is *supersaturated* with carbon dioxide and, with time, the dissolved carbon dioxide concentration will decrease to its equilibrium value and the beverage will become "flat."

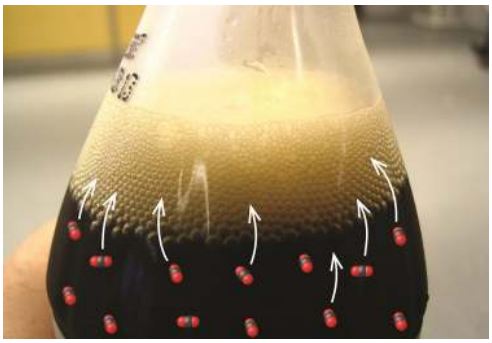


Figure **7.6.3**: Opening the bottle of carbonated beverage reduces the pressure of the gaseous carbon dioxide above the beverage. The solubility of CO_2 is thus lowered, and some dissolved carbon dioxide may be seen leaving the solution as small gas bubbles. (credit: modification of work by Derrick Coetzee)

For many gaseous solutes, the relation between solubility, C_g, and partial pressure, P_g, is a proportional one:

$$C_g = kP_g \tag{7.6.1}$$

where k is a proportionality constant that depends on the identities of the gaseous solute and solvent, and on the solution temperature. This is a mathematical statement of Henry's law: *The quantity of an ideal gas that dissolves in a definite volume of liquid is directly proportional to the pressure of the gas.*

Example **7.6.1**: Application of Henry's Law

At 20 °C, the concentration of dissolved oxygen in water exposed to gaseous oxygen at a partial pressure of 101.3 kPa (760 torr) is 1.38×10^{-3} mol L^{-1}. Use Henry's law to determine the solubility of oxygen when its partial pressure is 20.7 kPa (155 torr), the approximate pressure of oxygen in earth's atmosphere.

Solution

According to Henry's law, for an ideal solution the solubility, C_g, of a gas (1.38×10^{-3} mol L^{-1}, in this case) is directly proportional to the pressure, P_g, of the undissolved gas above the solution (101.3 kPa, or 760 torr, in this case). Because we know both C_g and P_g, we can rearrange this expression to solve for k.

$$\begin{aligned} C_g &= kP_g \\ k &= \frac{C_g}{P_g} \\ &= \frac{1.38 \times 10^{-3}\ \text{mol L}^{-1}}{101.3\ \text{kPa}} \\ &= 1.36 \times 10^{-5}\ \text{mol L}^{-1}\ \text{kPa}^{-1} \\ &\quad (1.82 \times 10^{-6}\ \text{mol L}^{-1}\ \text{torr}^{-1}) \end{aligned}$$

Now we can use k to find the solubility at the lower pressure.

$$C_g = kP_g \tag{7.6.2}$$

$$\begin{aligned} &1.36 \times 10^{-5}\ \text{mol L}^{-1}\ \text{kPa}^{-1} \times 20.7\ \text{kPa} \\ &(\text{or } 1.82 \times 10^{-6}\ \text{mol L}^{-1}\ \text{torr}^{-1} \times 155\ \text{torr}) \\ &= 2.82 \times 10^{-4}\ \text{mol L}^{-1} \end{aligned} \tag{7.6.3}$$

Note that various units may be used to express the quantities involved in these sorts of computations. Any combination of units that yield to the constraints of dimensional analysis are acceptable.

Exercise 7.6.1

Exposing a 100.0 mL sample of water at 0 °C to an atmosphere containing a gaseous solute at 20.26 kPa (152 torr) resulted in the dissolution of 1.45×10^{-3} g of the solute. Use Henry's law to determine the solubility of this gaseous solute when its pressure is 101.3 kPa (760 torr).

Answer

7.25×10^{-3} g in 100.0 mL or 0.0725 g/L

Case Study: Decompression Sickness ("The Bends")

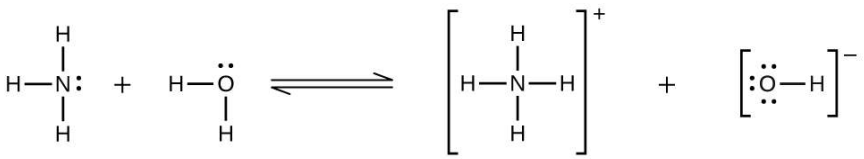
Decompression sickness (DCS), or "the bends," is an effect of the increased pressure of the air inhaled by scuba divers when swimming underwater at considerable depths. In addition to the pressure exerted by the atmosphere, divers are subjected to additional pressure due to the water above them, experiencing an increase of approximately 1 atm for each 10 m of depth. Therefore, the air inhaled by a diver while submerged contains gases at the corresponding higher ambient pressure, and the concentrations of the gases dissolved in the diver's blood are proportionally higher per Henry's law.



Figure **7.6.4**: (a) US Navy divers undergo training in a recompression chamber. (b) Divers receive hyperbaric oxygen therapy.

As the diver ascends to the surface of the water, the ambient pressure decreases and the dissolved gases becomes less soluble. If the ascent is too rapid, the gases escaping from the diver's blood may form bubbles that can cause a variety of symptoms ranging from rashes and joint pain to paralysis and death. To avoid DCS, divers must ascend from depths at relatively slow speeds (10 or 20 m/min) or otherwise make several decompression stops, pausing for several minutes at given depths during the ascent. When these preventive measures are unsuccessful, divers with DCS are often provided hyperbaric oxygen therapy in pressurized vessels called decompression (or recompression) chambers (Figure **7.6.4**).

Deviations from Henry's law are observed when a chemical reaction takes place between the gaseous solute and the solvent. Thus, for example, the solubility of ammonia in water does not increase as rapidly with increasing pressure as predicted by the law because ammonia, being a base, reacts to some extent with water to form ammonium ions and hydroxide ions.



Gases can form supersaturated solutions. If a solution of a gas in a liquid is prepared either at low temperature or under pressure (or both), then as the solution warms or as the gas pressure is reduced, the solution may become supersaturated. In 1986, more than 1700 people in Cameroon were killed when a cloud of gas, almost certainly carbon dioxide, bubbled from Lake Nyos (Figure **7.6.5**), a deep lake in a volcanic crater. The water at the bottom of Lake Nyos is saturated with carbon dioxide by volcanic activity beneath the lake. It is believed that the lake underwent a turnover due to gradual heating from below the lake, and the warmer, less-dense water saturated with carbon dioxide reached the surface. Consequently, tremendous quantities of dissolved CO_2 were released, and the colorless gas, which is denser than air, flowed down the valley below the lake and suffocated humans and animals living in the valley.



(a) (b)

Figure **7.6.5**: (a) It is believed that the 1986 disaster that killed more than 1700 people near Lake Nyos in Cameroon resulted when a large volume of carbon dioxide gas was released from the lake. (b) A CO_2 vent has since been installed to help outgas the lake in a slow, controlled fashion and prevent a similar catastrophe from happening in the future. (credit a: modification of work by Jack Lockwood; credit b: modification of work by Bill Evans)



Henry's Law (The Solubility of Gases in Solvents): https://youtu.be/fiJZCGpArJI

7.6: Solubilities of Gases is shared under a not declared license and was authored, remixed, and/or curated by LibreTexts.

- **11.3: Solubility** by OpenStax is licensed CC BY 4.0. Original source: https://openstax.org/details/books/chemistry-2e.

7.7: Vapor Pressures of Solutions

Learning Objectives

- To describe the relationship between solute concentration and the physical properties of a solution.
- To understand that the total number of nonvolatile solute particles determines the decrease in vapor pressure, increase in boiling point, and decrease in freezing point of a solution versus the pure solvent.

Raoult's Law

Adding a nonvolatile solute, one whose vapor pressure is too low to measure readily, to a volatile solvent decreases the vapor pressure of the solvent. We can understand this phenomenon qualitatively by examining Figure **7.7.1**, which is a schematic diagram of the surface of a solution of glucose in water. In an aqueous solution of glucose, a portion of the surface area is occupied by nonvolatile glucose molecules rather than by volatile water molecules. As a result, fewer water molecules can enter the vapor phase per unit time, even though the surface water molecules have the same kinetic energy distribution as they would in pure water. At the same time, the rate at which water molecules in the vapor phase collide with the surface and reenter the solution is unaffected. The net effect is to shift the dynamic equilibrium between water in the vapor and the liquid phases, decreasing the vapor pressure of the solution compared with the vapor pressure of the pure solvent.

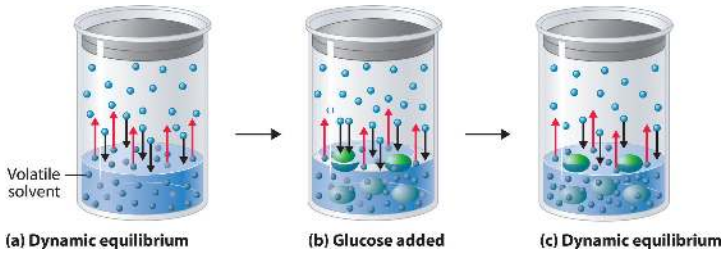


Figure **7.7.1**: A Model Depicting Why the Vapor Pressure of a Solution of Glucose Is Less Than the Vapor Pressure of Pure Water. (a) When water or any volatile solvent is in a closed container, water molecules move into and out of the liquid phase at the same rate in a dynamic equilibrium. (b) If a nonvolatile solute such as glucose is added, some fraction of the surface area is occupied by solvated solute molecules. As a result, the rate at which water molecules evaporate is decreased, although initially their rate of condensation is unchanged. (c) When the glucose solution reaches equilibrium, the concentration of water molecules in the vapor phase, and hence the vapor pressure, is less than that of pure water.

Figure **7.7.2** shows two beakers, one containing pure water and one containing an aqueous glucose solution, in a sealed chamber. We can view the system as having two competing equilibria: water vapor will condense in both beakers at the same rate, but water molecules will evaporate more slowly from the glucose solution because fewer water molecules are at the surface. Eventually all of the water will evaporate from the beaker containing the liquid with the higher vapor pressure (pure water) and condense in the beaker containing the liquid with the lower vapor pressure (the glucose solution). If the system consisted of only a beaker of water inside a sealed container, equilibrium between the liquid and vapor would be achieved rather rapidly, and the amount of liquid water in the beaker would remain constant.

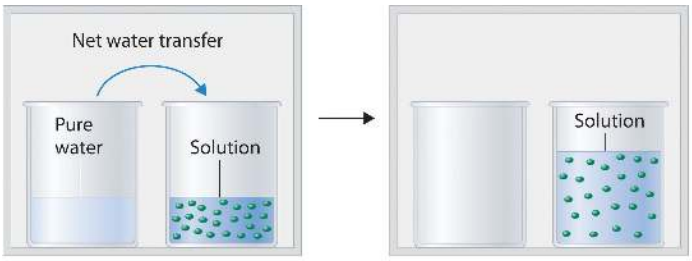


Figure **7.7.2**: Transfer of Water to a Beaker Containing a Glucose Solution. (top) One beaker contains an aqueous solution of glucose, and the other contains pure water. If they are placed in a sealed chamber, the lower vapor pressure of water in the glucose solution results in a net transfer of water from the beaker containing pure water to the beaker containing the glucose solution. (bottom) Eventually, all of the water is transferred to the beaker that has the glucose solution.

If the particles of a solute are essentially the same size as those of the solvent and both solute and solvent have roughly equal probabilities of being at the surface of the solution, then the effect of a solute on the vapor pressure of the solvent is proportional to

the number of sites occupied by solute particles at the surface of the solution. Doubling the concentration of a given solute causes twice as many surface sites to be occupied by solute molecules, resulting in twice the decrease in vapor pressure. The relationship between solution composition and vapor pressure is therefore

$$P_A = X_A P_A^0 \tag{7.7.1}$$

where P_A is the vapor pressure of component A of the solution (in this case the solvent), XA is the mole fraction of A in solution, and P_A^0 is the vapor pressure of pure A. Equation 7.7.1 is known as **Raoult's law**, after the French chemist who developed it. If the solution contains only a single nonvolatile solute (B), then $X_A + X_B = 1$, and we can substitute $X_A = 1 - X_B$ to obtain

$$P_A = (1 - X_B)P_A^0 \tag{7.7.2}$$

$$= P_A^0 - X_B P_A^0 \tag{7.7.3}$$

Rearranging and defining $\Delta P_A = P_A^0 - P_A$, we obtain a relationship between the decrease in vapor pressure and the mole fraction of nonvolatile solute:

$$P_A^0 - P_A = \Delta P_A = X_B P_A^0 \tag{7.7.4}$$

We can solve vapor pressure problems in either of two ways: by using Equation 7.7.1 to calculate the actual vapor pressure above a solution of a nonvolatile solute, or by using Equation 7.7.4 to calculate the decrease in vapor pressure caused by a specified amount of a nonvolatile solute.

Example 7.7.1

Ethylene glycol ($\mathbf{HOCH_2CH_2OH}$), the major ingredient in commercial automotive antifreeze, increases the boiling point of radiator fluid by lowering its vapor pressure. At 100°C, the vapor pressure of pure water is 760 mmHg. Calculate the vapor pressure of an aqueous solution containing 30.2% ethylene glycol by mass, a concentration commonly used in climates that do not get extremely cold in winter.

Given: identity of solute, percentage by mass, and vapor pressure of pure solvent

Asked for: vapor pressure of solution

Strategy:

A. Calculate the number of moles of ethylene glycol in an arbitrary quantity of water, and then calculate the mole fraction of water.
B. Use Raoult's law to calculate the vapor pressure of the solution.

Solution:

A A 30.2% solution of ethylene glycol contains 302 g of ethylene glycol per kilogram of solution; the remainder (698 g) is water. To use Raoult's law to calculate the vapor pressure of the solution, we must know the mole fraction of water. Thus we must first calculate the number of moles of both ethylene glycol (EG) and water present:

$$moles\ EG = (302\ \cancel{g}) \left(\frac{1\ mol}{62.07\ \cancel{g}} \right) = 4.87\ mol\ EG$$

$$moles\ \mathrm{H_2O} = (698\ \cancel{g}) \left(\frac{1\ mol}{18.02\ \cancel{g}} \right) = 38.7\ mol\ H_2O$$

The mole fraction of water is thus

$$X_{\mathrm{H_2O}} = \frac{38.7\ \cancel{mol}\ H_2O}{38.7\ \cancel{mol}\ H_2O + 4.87\ \cancel{mol}\ EG} = 0.888$$

B From Raoult's law (Equation 7.7.1), the vapor pressure of the solution is

$$P_{\mathrm{H_2O}} = (X_{H_2O})(P_{H_2O}^0) = (0.888)(760\ mmHg) = 675\ mmHg$$

Alternatively, we could solve this problem by calculating the mole fraction of ethylene glycol and then using Equation 7.7.4 to calculate the resulting decrease in vapor pressure:

$$X_{EG} = \frac{4.87\ mol\ EG}{4.87\ mol\ EG + 38.7\ mol\ H_2O} = 0.112$$

$$\Delta P_{H_2O} = (X_{EG})(P^0_{H_2O}) = (0.112)(760\ mmHg) = 85.1\ mmHg$$

$$P_{H_2O} = P^0 H_2O - \Delta P_{H_2O} = 760\ mmHg - 85.1\ mmHg = 675\ mmHg$$

The same result is obtained using either method.

? Exercise 7.7.1

Seawater is an approximately 3.0% aqueous solution of $NaCl$ by mass with about 0.5% of other salts by mass. Calculate the decrease in the vapor pressure of water at 25°C caused by this concentration of $NaCl$, remembering that 1 mol of $NaCl$ produces 2 mol of solute particles. The vapor pressure of pure water at 25°C is 23.8 mmHg.

Answer

0.45 mmHg. This may seem like a small amount, but it constitutes about a 2% decrease in the vapor pressure of water and accounts in part for the higher humidity in the north-central United States near the Great Lakes, which are freshwater lakes. The decrease therefore has important implications for climate modeling.



Finding the Vapor Pressure of a Solution (Ionic-Nonvolatile Solute):

https://youtu.be/sRBaRXsql9s

Volatile Solutes

Even when a solute is volatile, meaning that it has a measurable vapor pressure, we can still use Raoult's law. In this case, we calculate the vapor pressure of each component separately. The total vapor pressure of the solution (P_T) is the sum of the vapor pressures of the components:

$$P_T = P_A + P_B \tag{7.7.5}$$

$$= X_A P^0_A + X_B P^0_B \tag{7.7.6}$$

Because $X_B = 1 - X_A$ for a two-component system,

$$P_T = X_A P^0_A + (1 - X_A) P^0_B \tag{7.7.7}$$

Thus we need to specify the mole fraction of only one of the components in a two-component system. Consider, for example, the vapor pressure of solutions of benzene and toluene of various compositions. At 20°C, the vapor pressures of pure benzene and

toluene are 74.7 and 22.3 mmHg, respectively. The vapor pressure of benzene in a benzene–toluene solution is

$$P_{C_6H_6} = X_{C_6H_6}P^0_{C_6H_6} \tag{7.7.8}$$

and the vapor pressure of toluene in the solution is

$$P_{C_6H_5CH_3} = X_{C_6H_5CH_3}P^0_{C_6H_5CH3} \tag{7.7.9}$$

Equations 7.7.8 and 7.7.9 are both in the form of the equation for a straight line: $y = mx + b$, where $b = 0$. Plots of the vapor pressures of both components versus the mole fractions are therefore straight lines that pass through the origin, as shown in Figure Figure **7.7.3**. Furthermore, a plot of the total vapor pressure of the solution versus the mole fraction is a straight line that represents the sum of the vapor pressures of the pure components. Thus the vapor pressure of the solution is always greater than the vapor pressure of either component.

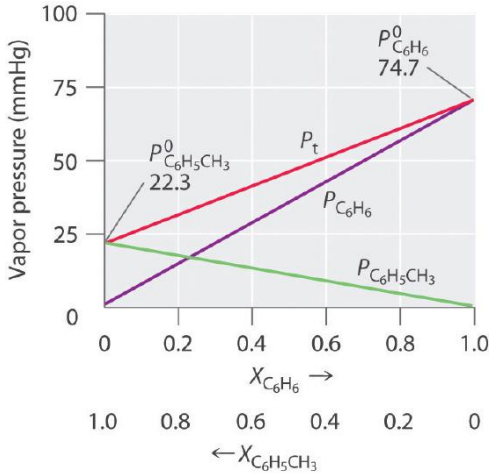


Figure **7.7.3**: Vapor Pressures of Benzene–Toluene Solutions. Plots of the vapor pressures of benzene (C_6H_6) and toluene ($C_6H_5CH_3$) versus the mole fractions at 20°C are straight lines. For a solution like this, which approximates an ideal solution, the total vapor pressure of the solution (Pt) is the sum of the vapor pressures of the components.

A solution of two volatile components that behaves like the solution in Figure **7.7.3**, which is defined as a solution that obeys Raoult's law. Like an ideal gas, an ideal solution is a hypothetical system whose properties can be described in terms of a simple model. Mixtures of benzene and toluene approximate an ideal solution because the intermolecular forces in the two pure liquids are almost identical in both kind and magnitude. Consequently, the change in enthalpy on solution formation is essentially zero ($\Delta H_{soln} \approx 0$), which is one of the defining characteristics of an ideal solution.

> Ideal solutions and ideal gases are both simple models that ignore intermolecular interactions.

Most real solutions, however, do not obey Raoult's law precisely, just as most real gases do not obey the ideal gas law exactly. Real solutions generally deviate from Raoult's law because the intermolecular interactions between the two components A and B differ. We can distinguish between two general kinds of behavior, depending on whether the intermolecular interactions between molecules A and B are stronger or weaker than the A–A and B–B interactions in the pure components. If the A–B interactions are stronger than the A–A and B–B interactions, each component of the solution exhibits a lower vapor pressure than expected for an ideal solution, as does the solution as a whole. The favorable A–B interactions effectively stabilize the solution compared with the vapor. This kind of behavior is called a negative deviation from Raoult's law. Systems stabilized by hydrogen bonding between two molecules, such as acetone and ethanol, exhibit negative deviations from Raoult's law. Conversely, if the A–B interactions are weaker than the A–A and B–B interactions yet the entropy increase is enough to allow the solution to form, both A and B have an increased tendency to escape from the solution into the vapor phase. The result is a higher vapor pressure than expected for an ideal solution, producing a positive deviation from Raoult's law. In a solution of CCl_4 and methanol, for example, the nonpolar CCl_4 molecules interrupt the extensive hydrogen bonding network in methanol, and the lighter methanol molecules have weaker London dispersion forces than the heavier CCl_4 molecules. Consequently, solutions of CCl_4 and methanol exhibit positive deviations from Raoult's law.

Example 7.7.2

For each system, compare the intermolecular interactions in the pure liquids and in the solution to decide whether the vapor pressure will be greater than that predicted by Raoult's law (positive deviation), approximately equal to that predicted by Raoult's law (an ideal solution), or less than the pressure predicted by Raoult's law (negative deviation).

a. cyclohexane and ethanol
b. methanol and acetone
c. n-hexane and isooctane (2,2,4-trimethylpentane)

Given: identity of pure liquids

Asked for: predicted deviation from Raoult's law

Strategy:

Identify whether each liquid is polar or nonpolar, and then predict the type of intermolecular interactions that occur in solution.

Solution:

a. Liquid ethanol contains an extensive hydrogen bonding network, and cyclohexane is nonpolar. Because the cyclohexane molecules cannot interact favorably with the polar ethanol molecules, they will disrupt the hydrogen bonding. Hence the A–B interactions will be weaker than the A–A and B–B interactions, leading to a higher vapor pressure than predicted by Raoult's law (a positive deviation).
b. Methanol contains an extensive hydrogen bonding network, but in this case the polar acetone molecules create A–B interactions that are stronger than the A–A or B–B interactions, leading to a negative enthalpy of solution and a lower vapor pressure than predicted by Raoult's law (a negative deviation).
c. Hexane and isooctane are both nonpolar molecules (isooctane actually has a very small dipole moment, but it is so small that it can be ignored). Hence the predominant intermolecular forces in both liquids are London dispersion forces. We expect the A–B interactions to be comparable in strength to the A–A and B–B interactions, leading to a vapor pressure in good agreement with that predicted by Raoult's law (an ideal solution).

Exercise 7.7.2

For each system, compare the intermolecular interactions in the pure liquids with those in the solution to decide whether the vapor pressure will be greater than that predicted by Raoult's law (positive deviation), approximately equal to that predicted by Raoult's law (an ideal solution), or less than the pressure predicted by Raoult's law (negative deviation):

a. benzene and n-hexane
b. ethylene glycol and CCl_4
c. acetic acid and n-propanol

Answer a

approximately equal

Answer b

positive deviation (vapor pressure greater than predicted)

Answer c

negative deviation (vapor pressure less than predicted)



Finding Vapor Pressure of a Solution (Nonionic-Volatile Solute):

https://youtu.be/s06fzZZtLl0

Summary

- **Henry's law:**

$$C = kP$$

- **Raoult's law**:

$$P_A = X_A P_A^0$$

- **vapor pressure lowering**:

$$P_A^0 - P_A = \Delta P_A = X_B P_A^0$$

- **vapor pressure of a system containing two volatile components**:

$$P_T = X_A P_A^0 + (1 - X_A) P_B^0$$

The vapor pressure of the solution is proportional to the mole fraction of solvent in the solution, a relationship known as **Raoult's law**. Solutions that obey Raoult's law are called ideal solutions. Most real solutions exhibit positive or negative deviations from Raoult's law.

Contributors and Attributions

- Stephen Lower, Professor Emeritus (Simon Fraser U.) Chem1 Virtual Textbook

---

7.7: Vapor Pressures of Solutions is shared under a not declared license and was authored, remixed, and/or curated by LibreTexts.

- **13.6: Vapor Pressures of Solutions** is licensed CC BY-NC-SA 4.0.

7.8: Osmotic Pressure

Learning Objectives

- To describe the relationship between solute concentration and the physical properties of a solution.
- To understand that the total number of nonvolatile solute particles determines the decrease in vapor pressure, increase in boiling point, and decrease in freezing point of a solution versus the pure solvent.

Osmotic pressure is a colligative property of solutions that is observed using a semipermeable membrane, a barrier with pores small enough to allow solvent molecules to pass through but not solute molecules or ions. The net flow of solvent through a semipermeable membrane is called osmosis (from the Greek osmós, meaning “push”). The direction of net solvent flow is always from the side with the lower concentration of solute to the side with the higher concentration.

Osmosis can be demonstrated using a U-tube like the one shown in Figure **7.8.1**, which contains pure water in the left arm and a dilute aqueous solution of glucose in the right arm. A net flow of water through the membrane occurs until the levels in the arms eventually stop changing, which indicates that equilibrium has been reached. The osmotic pressure (**Π**) of the glucose solution is the difference in the pressure between the two sides, in this case the heights of the two columns. Although the semipermeable membrane allows water molecules to flow through in either direction, the rate of flow is not the same in both directions because the concentration of water is not the same in the two arms. The net flow of water through the membrane can be prevented by applying a pressure to the right arm that is equal to the osmotic pressure of the glucose solution.

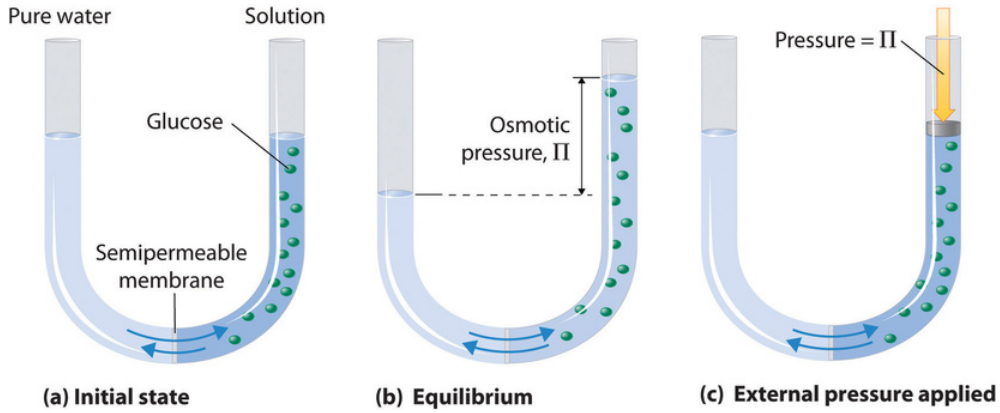


Figure **7.8.1**: Osmotic Pressure. (a) A dilute solution of glucose in water is placed in the right arm of a U-tube, and the left arm is filled to the same height with pure water; a semipermeable membrane separates the two arms. Because the flow of pure solvent through the membrane from left to right (from pure water to the solution) is greater than the flow of solvent in the reverse direction, the level of liquid in the right tube rises. (b) At equilibrium, the pressure differential, equal to the osmotic pressure of the solution (Π_{soln}), *equalizes the flow rate of solvent in both directions. (c) Applying an external pressure equal to the osmotic pressure of the original glucose solution to the liquid in the right arm reverses the flow of solvent and restores the original situation.*

The osmotic pressure of a solution depends on the concentration of dissolved solute particles. Osmotic pressure obeys a law that resembles the ideal gas equation:

$$\Pi = \frac{nRT}{V} = MRT \tag{7.8.1}$$

where

- M is the number of moles of solute per unit volume of solution (i.e., the molarity of the solution),
- R is the ideal gas constant, and
- T is the absolute temperature.

As shown in Example **7.8.1**, osmotic pressures tend to be quite high, even for rather dilute solutions.

Example 7.8.1: Yeast Cells

When placed in a concentrated salt solution, certain yeasts are able to produce high internal concentrations of glycerol to counteract the osmotic pressure of the surrounding medium. Suppose that the yeast cells are placed in an aqueous solution containing 4.0% $NaCl$ by mass; the solution density is 1.02 g/mL at 25°C.

Calculate the osmotic pressure of a 4.0% aqueous $NaCl$ solution at 25°C.

If the normal osmotic pressure inside a yeast cell is 7.3 atm, corresponding to a total concentration of dissolved particles of 0.30 M, what concentration of glycerol must the cells synthesize to exactly balance the external osmotic pressure at 25°C?

Given: concentration, density, and temperature of $NaCl$ solution; internal osmotic pressure of cell

Asked for: osmotic pressure of $NaCl$ solution and concentration of glycerol needed

Strategy:

A. Calculate the molarity of the $NaCl$ solution using the formula mass of the solute and the density of the solution. Then calculate the total concentration of dissolved particles.
B. Use Equation 7.8.1 to calculate the osmotic pressure of the solution.
C. Subtract the normal osmotic pressure of the cells from the osmotic pressure of the salt solution to obtain the additional pressure needed to balance the two. Use Equation 7.8.1 to calculate the molarity of glycerol needed to create this osmotic pressure.

Solution:

A The solution contains 4.0 g of $NaCl$ per 100 g of solution. Using the formula mass of $NaCl$ (58.44 g/mol) and the density of the solution (1.02 g/mL), we can calculate the molarity:

$$\begin{aligned} M_{NaCl} &= \frac{moles\ NaCl}{\text{liter solution}} \\ &= \left(\frac{4.0\ \cancel{g}\ NaCl}{58.44\ \cancel{g}/mol\ NaCl}\right)\left(\frac{1}{100\ \cancel{g\ solution}}\right)\left(\frac{1.02\ \cancel{g\ solution}}{1.00\ \cancel{mL}\ solution}\right)\left(\frac{1000\ \cancel{mL}}{1\ L}\right) \\ &= 0.70\ M\ NaCl \end{aligned}$$

Because 1 mol of $NaCl$ produces 2 mol of particles in solution, the total concentration of dissolved particles in the solution is (2)(0.70 M) = 1.4 M.

B Now we can use Equation 7.8.1 to calculate the osmotic pressure of the solution:

$$\begin{aligned} \Pi &= MRT \\ &= (1.4\ mol/L)\,[0.0821\ (L \cdot atm)/(K \cdot mol)]\,(298\ K) \\ &= 34\ atm \end{aligned}$$

C If the yeast cells are to exactly balance the external osmotic pressure, they must produce enough glycerol to give an additional internal pressure of (34 atm − 7.3 atm) = 27 atm. Glycerol is a nonelectrolyte, so we can solve Equation 7.8.1 for the molarity corresponding to this osmotic pressure:

$$\begin{aligned} M &= \frac{\Pi}{RT} \\ &= \frac{27\ \cancel{atm}}{[0.0821(L \cdot \cancel{atm})/(\cancel{K} \cdot mol)](298\ \cancel{K})} \\ &= 1.1\ M\ glycerol \end{aligned}$$

In solving this problem, we could also have recognized that the only way the osmotic pressures can be the same inside the cells and in the solution is if the concentrations of dissolved particles are the same. We are given that the normal concentration of dissolved particles in the cells is 0.3 M, and we have calculated that the $NaCl$ solution is effectively 1.4 M in dissolved particles. The yeast cells must therefore synthesize enough glycerol to increase the internal concentration of dissolved particles from 0.3 M to 1.4 M—that is, an additional 1.1 M concentration of glycerol.

? Exercise 7.8.1

Assume that the fluids inside a sausage are approximately 0.80 M in dissolved particles due to the salt and sodium nitrite used to prepare them. Calculate the osmotic pressure inside the sausage at 100°C to learn why experienced cooks pierce the semipermeable skin of sausages before boiling them.

Answer: 24 atm

Because of the large magnitude of osmotic pressures, osmosis is extraordinarily important in biochemistry, biology, and medicine. Virtually every barrier that separates an organism or cell from its environment acts like a semipermeable membrane, permitting the flow of water but not solutes. The same is true of the compartments inside an organism or cell. Some specialized barriers, such as those in your kidneys, are slightly more permeable and use a related process called dialysis, which permits both water and small molecules to pass through but not large molecules such as proteins.

The same principle has long been used to preserve fruits and their essential vitamins over the long winter. High concentrations of sugar are used in jams and jellies not for sweetness alone but because they greatly increase the osmotic pressure. Thus any bacteria not killed in the cooking process are dehydrated, which keeps them from multiplying in an otherwise rich medium for bacterial growth. A similar process using salt prevents bacteria from growing in ham, bacon, salt pork, salt cod, and other preserved meats. The effect of osmotic pressure is dramatically illustrated in Figure **7.8.2**, which shows what happens when red blood cells are placed in a solution whose osmotic pressure is much lower or much higher than the internal pressure of the cells.

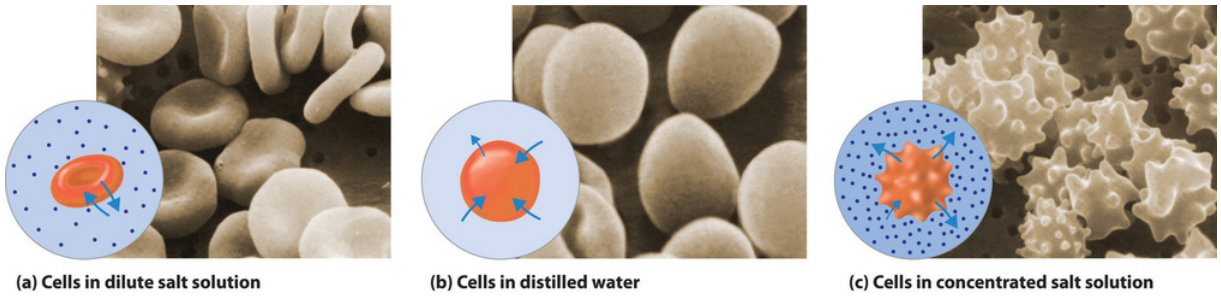


Figure **7.8.2**: Effect on Red Blood Cells of the Surrounding Solution's Osmotic Pressure. (a) When red blood cells are placed in a dilute salt solution having the same osmotic pressure as the intracellular fluid, the rate of flow of water into and out of the cells is the same and their shape does not change. (b) When cells are placed in distilled water whose osmotic pressure is less than that of the intracellular fluid, the rate of flow of water into the cells is greater than the rate of flow out of the cells. The cells swell and eventually burst. (c) When cells are placed in a concentrated salt solution with an osmotic pressure greater than that of the intracellular fluid, the rate of flow of water out of the cells is greater than the rate of flow into the cells. The cells shrivel and become so deformed that they cannot function.

In addition to capillary action, trees use osmotic pressure to transport water and other nutrients from the roots to the upper branches. Evaporation of water from the leaves results in a local increase in the salt concentration, which generates an osmotic pressure that pulls water up the trunk of the tree to the leaves.

Finally, a process called reverse osmosis can be used to produce pure water from seawater. As shown schematically in Figure **7.8.3**, applying high pressure to seawater forces water molecules to flow through a semipermeable membrane that separates pure water from the solution, leaving the dissolved salt behind. Large-scale desalinization plants that can produce hundreds of thousands of gallons of freshwater per day are common in the desert lands of the Middle East, where they supply a large proportion of the freshwater needed by the population. Similar facilities are now being used to supply freshwater in southern California. Small, hand-operated reverse osmosis units can produce approximately 5 L of freshwater per hour, enough to keep 25 people alive, and are now standard equipment on US Navy lifeboats.

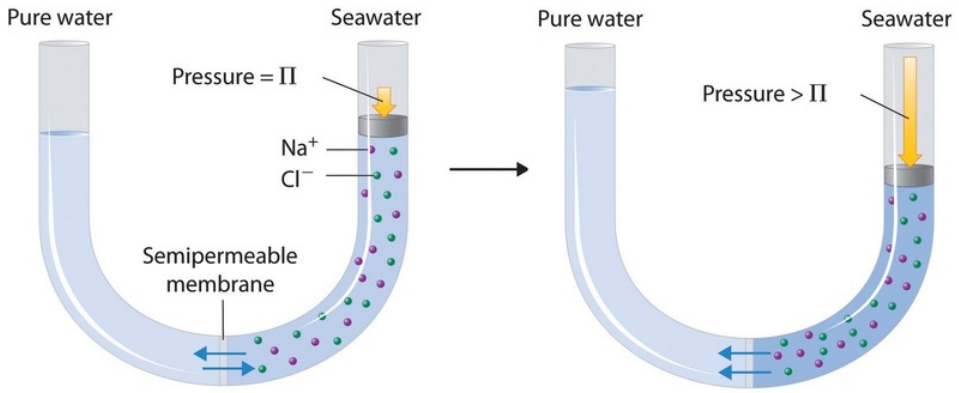


Figure **7.8.3**: Desalinization of Seawater by Reverse Osmosis. (top) When the pressure applied to seawater equals its osmotic pressure (Π_{soln}), *there is no net flow of water across the semipermeable membrane. (bottom) The application of pressure greater than the osmotic pressure of seawater forces water molecules to flow through the membrane, leaving behind a concentrated salt solution. In desalinization plants, seawater is continuously introduced under pressure and pure water is collected, so the process continues indefinitely.*



Osmotic Pressure: https://youtu.be/uYQxI4mi3DA

Summary

When a solution and a pure solvent are separated by a semipermeable membrane, a barrier that allows solvent molecules but not solute molecules to pass through, the flow of solvent in opposing directions is unequal and produces an osmotic pressure, which is the difference in pressure between the two sides of the membrane. Osmosis is the net flow of solvent through such a membrane due to different solute concentrations. Dialysis uses a semipermeable membrane with pores that allow only small solute molecules and solvent molecules to pass through.

7.8: Osmotic Pressure is shared under a not declared license and was authored, remixed, and/or curated by LibreTexts.

- **13.7: Osmotic Pressure** is licensed CC BY-NC-SA 4.0.

7.9: Freezing-Point Depression and Boiling-Point Elevation of Nonelectrolyte Solutions

Learning Objectives

- To describe the relationship between solute concentration and the physical properties of a solution.
- To understand that the total number of nonvolatile solute particles determines the decrease in vapor pressure, increase in boiling point, and decrease in freezing point of a solution versus the pure solvent.

Many of the physical properties of solutions differ significantly from those of the pure substances discussed in earlier chapters, and these differences have important consequences. For example, the limited temperature range of liquid water (0°C–100°C) severely limits its use. Aqueous solutions have both a lower freezing point and a higher boiling point than pure water. Probably one of the most familiar applications of this phenomenon is the addition of ethylene glycol (“antifreeze”) to the water in an automobile radiator. This solute lowers the freezing point of the water, preventing the engine from cracking in very cold weather from the expansion of pure water on freezing. Antifreeze also enables the cooling system to operate at temperatures greater than 100°C without generating enough pressure to explode.

Changes in the freezing point and boiling point of a solution depend primarily on the number of solute particles present rather than the kind of particles. Such properties of solutions are called colligative properties (from the Latin colligatus, meaning “bound together” as in a quantity). As we will see, the vapor pressure and osmotic pressure of solutions are also colligative properties.

When we determine the number of particles in a solution, it is important to remember that not all solutions with the same molarity contain the same concentration of solute particles. Consider, for example, 0.01 M aqueous solutions of sucrose, $NaCl$, and $CaCl_2$. Because sucrose dissolves to give a solution of neutral molecules, the concentration of solute particles in a 0.01 M sucrose solution is 0.01 M. In contrast, both $NaCl$ and $CaCl_2$ are ionic compounds that dissociate in water to yield solvated ions. As a result, a 0.01 M aqueous solution of $NaCl$ contains 0.01 M Na+ ions and 0.01 M Cl^- ions, for a total particle concentration of 0.02 M. Similarly, the $CaCl_2$ solution contains 0.01 M Ca^{2+} ions and 0.02 M Cl^- ions, for a total particle concentration of 0.03 M.These values are correct for dilute solutions, where the dissociation of the compounds to form separately solvated ions is complete. At higher concentrations (typically >1 M), especially with salts of small, highly charged ions (such as Mg^{2+} or Al^{3+}), or in solutions with less polar solvents, dissociation to give separate ions is often incomplete. The sum of the concentrations of the dissolved solute particles dictates the physical properties of a solution. In the following discussion, we must therefore keep the chemical nature of the solute firmly in mind.

Boiling Point Elevation

Recall that the normal boiling point of a substance is the temperature at which the vapor pressure equals 1 atm. If a nonvolatile solute lowers the vapor pressure of a solvent, it must also affect the boiling point. Because the vapor pressure of the solution at a given temperature is less than the vapor pressure of the pure solvent, achieving a vapor pressure of 1 atm for the solution requires a higher temperature than the normal boiling point of the solvent. Thus the boiling point of a solution is always greater than that of the pure solvent. We can see why this must be true by comparing the phase diagram for an aqueous solution with the phase diagram for pure water (Figure **7.9.1**). The vapor pressure of the solution is less than that of pure water at all temperatures. Consequently, the liquid–vapor curve for the solution crosses the horizontal line corresponding to P = 1 atm at a higher temperature than does the curve for pure water.

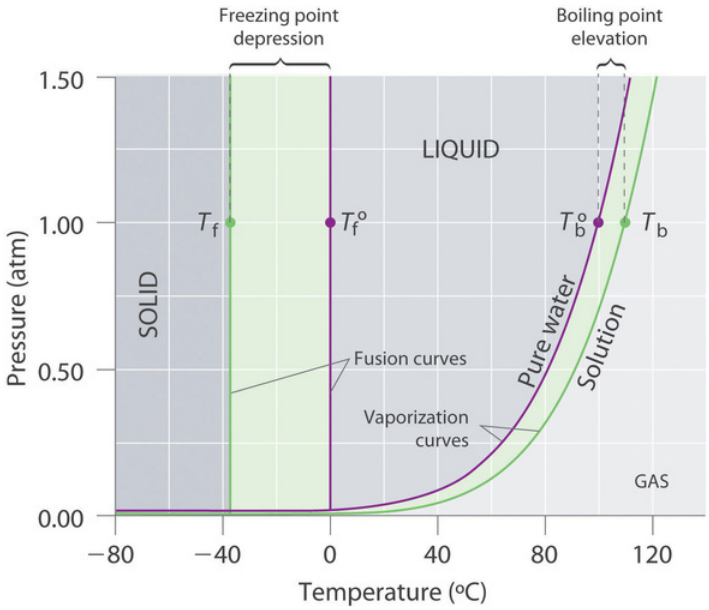


Figure **7.9.1**: Phase Diagrams of Pure Water and an Aqueous Solution of a Nonvolatile Solute. The vaporization curve for the solution lies below the curve for pure water at all temperatures, which results in an increase in the boiling point and a decrease in the freezing point of the solution.

> The boiling point of a solution with a nonvolatile solute is always greater than the boiling point of the pure solvent.

The magnitude of the increase in the boiling point is related to the magnitude of the decrease in the vapor pressure. As we have just discussed, the decrease in the vapor pressure is proportional to the concentration of the solute in the solution. Hence the magnitude of the increase in the boiling point must also be proportional to the concentration of the solute (Figure **7.9.2**). We can define the boiling point elevation (ΔT_b) as the difference between the boiling points of the solution and the pure solvent:

$$\Delta T_b = T_b - T_b^0 \tag{7.9.1}$$

where T_b is the boiling point of the solution and T_b^0 is the boiling point of the pure solvent. We can express the relationship between ΔT_b and concentration as follows

$$\Delta T_b = mK_b \tag{7.9.2}$$

where m is the concentration of the solute expressed in molality, and K_b is the molal boiling point elevation constant of the solvent, which has units of °C/m. Table **7.9.1** lists characteristic Kb values for several commonly used solvents.

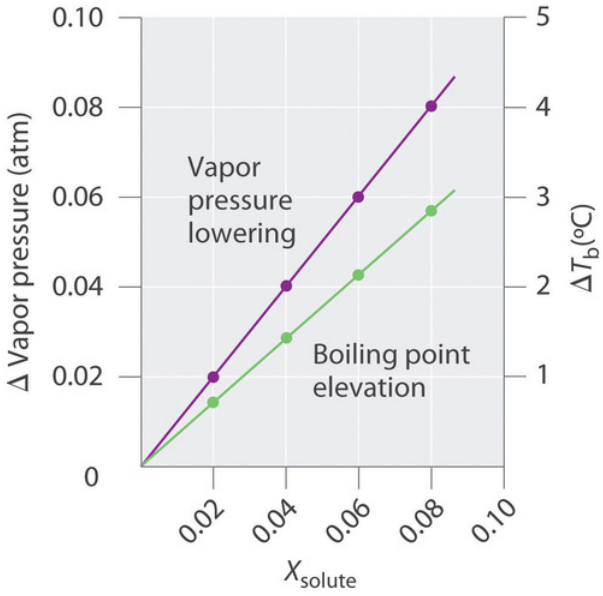


Figure 7.9.2: Vapor Pressure Decrease and Boiling Point Increase as Functions of the Mole Fraction of a Nonvolatile Solute

For relatively dilute solutions, the magnitude of both properties is proportional to the solute concentration.

Table 7.9.1: Boiling Point Elevation Constants (K_b) and Freezing Point Depression Constants (K_f) for Some Solvents

Solvent	Boiling Point (°C)	K_b (°C/m)	Freezing Point (°C)	K_f (°C/m)
acetic acid	117.90	3.22	16.64	3.63
benzene	80.09	2.64	5.49	5.07
d-(+)-camphor	207.4	4.91	178.8	37.8
carbon disulfide	46.2	2.42	−112.1	3.74
carbon tetrachloride	76.8	5.26	−22.62	31.4
chloroform	61.17	3.80	−63.41	4.60
nitrobenzene	210.8	5.24	5.70	6.87
water	100.00	0.51	0.00	1.86

The concentration of the solute is typically expressed as molality rather than mole fraction or molarity for two reasons. First, because the density of a solution changes with temperature, the value of molarity also varies with temperature. If the boiling point depends on the solute concentration, then by definition the system is not maintained at a constant temperature. Second, molality and mole fraction are proportional for relatively dilute solutions, but molality has a larger numerical value (a mole fraction can be only between zero and one). Using molality allows us to eliminate nonsignificant zeros.

According to Table 7.9.1, the molal boiling point elevation constant for water is 0.51°C/m. Thus a 1.00 m aqueous solution of a nonvolatile molecular solute such as glucose or sucrose will have an increase in boiling point of 0.51°C, to give a boiling point of 100.51°C at 1.00 atm. The increase in the boiling point of a 1.00 m aqueous NaCl solution will be approximately twice as large as that of the glucose or sucrose solution because 1 mol of NaCl produces 2 mol of dissolved ions. Hence a 1.00 m NaCl solution will have a boiling point of about 101.02°C.

Example 7.9.3

In Example 7.9.1, we calculated that the vapor pressure of a 30.2% aqueous solution of ethylene glycol at 100°C is 85.1 mmHg less than the vapor pressure of pure water. We stated (without offering proof) that this should result in a higher boiling point for

the solution compared with pure water. Now that we have seen why this assertion is correct, calculate the boiling point of the aqueous ethylene glycol solution.

Given: composition of solution

Asked for: boiling point

Strategy:

Calculate the molality of ethylene glycol in the 30.2% solution. Then use Equation 7.9.2 to calculate the increase in boiling point.

Solution:

From Example 7.9.1, we know that a 30.2% solution of ethylene glycol in water contains 302 g of ethylene glycol (4.87 mol) per 698 g of water. The molality of the solution is thus

$$\text{molality of ethylene glycol} = \left(\frac{4.87\ mol}{698\ \cancel{g}\ H_2O}\right)\left(\frac{1000\ \cancel{g}}{1\ kg}\right) = 6.98m \tag{7.9.3}$$

From Equation 7.9.2, the increase in boiling point is therefore

$$\Delta T_b = mK_b = (6.98\ \cancel{m})(0.51°C/\cancel{m}) = 3.6°C \tag{7.9.4}$$

The boiling point of the solution is thus predicted to be 104°C. With a solute concentration of almost 7 m, however, the assumption of a dilute solution used to obtain Equation 7.9.2 may not be valid.

? Exercise 7.9.3

Assume that a tablespoon (5.00 g) of NaCl is added to 2.00 L of water at 20.0°C, which is then brought to a boil to cook spaghetti. At what temperature will the water boil?

Answer

100.04°C, or 100°C to three significant figures. (Recall that 1 mol of NaCl produces 2 mol of dissolved particles. The small increase in temperature means that adding salt to the water used to cook pasta has essentially no effect on the cooking time.)

Freezing Point Depression

The phase diagram in Figure 7.9.1 shows that dissolving a nonvolatile solute in water not only raises the boiling point of the water but also lowers its freezing point. The solid–liquid curve for the solution crosses the line corresponding to P = 1 atm at a lower temperature than the curve for pure water.

This phenomenon is exploited in “de-icing” schemes that use salt (Figure 7.9.3), calcium chloride, or urea to melt ice on roads and sidewalks, and in the use of ethylene glycol as an “antifreeze” in automobile radiators. Seawater freezes at a lower temperature than fresh water, and so the Arctic and Antarctic oceans remain unfrozen even at temperatures below 0 °C (as do the body fluids of fish and other cold-blooded sea animals that live in these oceans).



Figure 7.9.3: Rock salt (NaCl), calcium chloride ($CaCl_2$), or a mixture of the two are used to melt ice. (credit: modification of work by Eddie Welker)

We can understand this result by imagining that we have a sample of water at the normal freezing point temperature, where there is a dynamic equilibrium between solid and liquid. Water molecules are continuously colliding with the ice surface and entering the solid phase at the same rate that water molecules are leaving the surface of the ice and entering the liquid phase. If we dissolve a nonvolatile solute such as glucose in the liquid, the dissolved glucose molecules will reduce the number of collisions per unit time between water molecules and the ice surface because some of the molecules colliding with the ice will be glucose. Glucose, though, has a very different structure than water, and it cannot fit into the ice lattice. Consequently, the presence of glucose molecules in the solution can only decrease the rate at which water molecules in the liquid collide with the ice surface and solidify. Meanwhile, the rate at which the water molecules leave the surface of the ice and enter the liquid phase is unchanged. The net effect is to cause the ice to melt. The only way to reestablish a dynamic equilibrium between solid and liquid water is to lower the temperature of the system, which decreases the rate at which water molecules leave the surface of the ice crystals until it equals the rate at which water molecules in the solution collide with the ice.

By analogy to our treatment of boiling point elevation,the freezing point depression (ΔT_f) is defined as the difference between the freezing point of the pure solvent and the freezing point of the solution:

$$\Delta T_f = T_f^0 - T_f \tag{7.9.5}$$

where

- T_f^0 is the freezing point of the pure solvent and
- T_f is the freezing point of the solution.

The order of the terms is reversed compared with Equation 7.9.1 to express the freezing point depression as a positive number. The relationship between ΔT_f and the solute concentration is given by an equation analogous to Equation 7.9.2:

$$\Delta T_f = mK_f \tag{7.9.6}$$

where

- m is the molality of the solution and
- K_f is the molal freezing point depression constant for the solvent (in units of °C/m).

Like K_b, each solvent has a characteristic value of K_f (Table 7.9.1). Freezing point depression depends on the total number of dissolved nonvolatile solute particles, just as with boiling point elevation. Thus an aqueous NaCl solution has twice as large a freezing point depression as a glucose solution of the same molality.

People who live in cold climates use freezing point depression to their advantage in many ways. For example, ethylene glycol is added to engine coolant water to prevent an automobile engine from being destroyed, and methanol is added to windshield washer fluid to prevent the fluid from freezing. Heated glycols are often sprayed onto the surface of airplanes prior to takeoff in inclement weather in the winter to remove ice that has already formed and prevent the formation of more ice, which would be particularly dangerous if formed on the control surfaces of the aircraft (Video 7.9.1).



Video 7.9.1: *Freezing point depression is exploited to remove ice from the control surfaces of aircraft.*

The decrease in vapor pressure, increase in boiling point, and decrease in freezing point of a solution versus a pure liquid all depend on the total number of dissolved nonvolatile solute particles.

Example 7.9.4

In colder regions of the United States, $\mathbf{NaCl}$ or $\mathbf{CaCl_2}$ is often sprinkled on icy roads in winter to melt the ice and make driving safer. Use the data in Figure 13.9 to estimate the concentrations of two saturated solutions at 0°C, one of $\mathbf{NaCl}$ and one of $\mathbf{CaCl_2}$, and calculate the freezing points of both solutions to see which salt is likely to be more effective at melting ice.

Given: solubilities of two compounds

Asked for: concentrations and freezing points

Strategy:

A. Estimate the solubility of each salt in 100 g of water from Figure 13.9. Determine the number of moles of each in 100 g and calculate the molalities.
B. Determine the concentrations of the dissolved salts in the solutions. Substitute these values into Equation **7.9.4** to calculate the freezing point depressions of the solutions.

Solution:

A From Figure 13.9, we can estimate the solubilities of $\mathbf{NaCl}$ and $\mathbf{CaCl_2}$ to be about 36 g and 60 g, respectively, per 100 g of water at 0°C. The corresponding concentrations in molality are

$$m_{NaCl} = \left(\frac{36\ \cancel{g\ NaCl}}{100\ \cancel{g}\ H_2O}\right)\left(\frac{1\ mol\ NaCl}{58.44\ \cancel{g\ NaCl}}\right)\left(\frac{1000\ \cancel{g}}{1\ kg}\right) = 6.2\ m \tag{7.9.7}$$

$$m_{CaCl_2} = \left(\frac{60\ \cancel{g\ CaCl_2}}{100\ \cancel{g}\ H_2O}\right)\left(\frac{1\ mol\ CaCl_2}{110.98\ \cancel{g\ CaCl_2}}\right)\left(\frac{1000\ \cancel{g}}{1kg}\right) = 5.4\ m \tag{7.9.8}$$

The lower formula mass of $\mathbf{NaCl}$ more than compensates for its lower solubility, resulting in a saturated solution that has a slightly higher concentration than $\mathbf{CaCl_2}$.

B Because these salts are ionic compounds that dissociate in water to yield two and three ions per formula unit of $\mathbf{NaCl}$ and $\mathbf{CaCl_2}$, respectively, the actual concentrations of the dissolved species in the two saturated solutions are 2 × 6.2 m = 12 m for $\mathbf{NaCl}$ and 3 × 5.4 m = 16 m for $\mathbf{CaCl_2}$. The resulting freezing point depressions can be calculated using Equation **7.9.4**:

$$\mathrm{NaCl}: \Delta T_f = mK_f = (12\ \cancel{m})(1.86°C/\cancel{m}) = 22°C \tag{7.9.9}$$

$$\mathrm{CaCl_2}: \Delta T_f = mK_f = (16\ \cancel{m})(1.86°C/\cancel{m}) = 30°C \tag{7.9.10}$$

Because the freezing point of pure water is 0°C, the actual freezing points of the solutions are −22°C and −30°C, respectively. Note that $\mathbf{CaCl_2}$ is substantially more effective at lowering the freezing point of water because its solutions contain three ions per formula unit. In fact, $\mathbf{CaCl_2}$ is the salt usually sold for home use, and it is also often used on highways.

Because the solubilities of both salts decrease with decreasing temperature, the freezing point can be depressed by only a certain amount, regardless of how much salt is spread on an icy road. If the temperature is significantly below the minimum temperature at which one of these salts will cause ice to melt (say −35°C), there is no point in using salt until it gets warmer

Exercise 7.9.4

Calculate the freezing point of the 30.2% solution of ethylene glycol in water whose vapor pressure and boiling point we calculated in Example **7.9.6**.8 and Example **7.9.6**.10.

Answer

−13.0°C

Example 7.9.5

Arrange these aqueous solutions in order of decreasing freezing points: 0.1 m KCl, 0.1 m glucose, 0.1 m SrCl2, 0.1 m ethylene glycol, 0.1 m benzoic acid, and 0.1 m HCl.

Given: molalities of six solutions

Asked for: relative freezing points

Strategy:

A. Identify each solute as a strong, weak, or nonelectrolyte, and use this information to determine the number of solute particles produced.
B. Multiply this number by the concentration of the solution to obtain the effective concentration of solute particles. The solution with the highest effective concentration of solute particles has the largest freezing point depression.

Solution:

A Because the molal concentrations of all six solutions are the same, we must focus on which of the substances are strong electrolytes, which are weak electrolytes, and which are nonelectrolytes to determine the actual numbers of particles in solution. KCl, $SrCl_2$, and HCl are **strong electrolytes**, producing two, three, and two ions per formula unit, respectively. Benzoic acid is a weak electrolyte (approximately one particle per molecule), and glucose and ethylene glycol are both nonelectrolytes (one particle per molecule).

B The molalities of the solutions in terms of the total particles of solute are: KCl and HCl, 0.2 m; $SrCl_2$, 0.3 m; glucose and ethylene glycol, 0.1 m; and benzoic acid, 0.1–0.2 m. Because the magnitude of the decrease in freezing point is proportional to the concentration of dissolved particles, the order of freezing points of the solutions is: glucose and ethylene glycol (highest freezing point, smallest freezing point depression) > benzoic acid > HCl = KCl > $SrCl_2$.

Exercise 7.9.5

Arrange these aqueous solutions in order of increasing freezing points: 0.2 m $NaCl$, 0.3 m acetic acid, 0.1 m $CaCl_2$, and 0.2 m sucrose.

Answer

0.2 m $NaCl$ (lowest freezing point) < 0.3 m acetic acid ≈ 0.1 m $CaCl_2$ < 0.2 m sucrose (highest freezing point)



Boiling Point Elevation and Freezing Point Depression: https://youtu.be/0MZm1Ay6LhU

Determination of Molar Masses

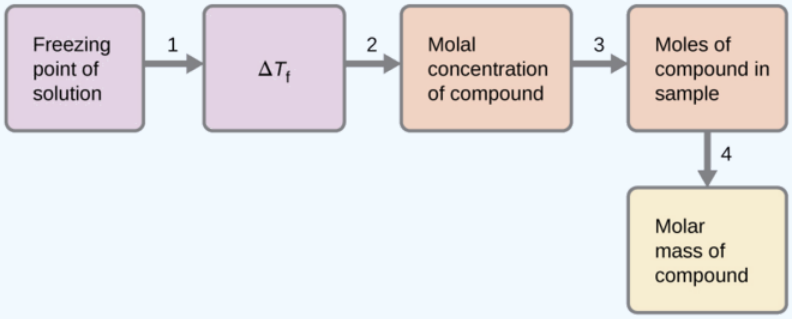
Osmotic pressure and changes in freezing point, boiling point, and vapor pressure are directly proportional to the concentration of solute present. Consequently, we can use a measurement of one of these properties to determine the molar mass of the solute from the measurements.

Determining Molar Mass from Freezing Point Depression

A solution of 4.00 g of a nonelectrolyte dissolved in 55.0 g of benzene is found to freeze at 2.32 °C. What is the molar mass of this compound?

Solution

We can solve this problem using the following steps.



1. *Determine the change in freezing point from the observed freezing point and the freezing point of pure benzene* (Table 7.9.1).

$$\Delta T_f = 5.5\ °C - 2.32\ °C = 3.2\ °C$$

- *Determine the molal concentration from K_f, the freezing point depression constant for benzene* (Table 7.9.1), *and* ΔT_f.

$$\Delta T_f = K_f m$$

$$m = \frac{\Delta T_f}{K_f} = \frac{3.2\ °C}{5.12\ °C m^{-1}} = 0.63\ m$$

- *Determine the number of moles of compound in the solution from the molal concentration and the mass of solvent used to make the solution.*

$$\text{Moles of solute} = \frac{0.62\ \text{mol solute}}{1.00\ \cancel{\text{kg solvent}}} \times 0.0550\ \cancel{\text{kg solvent}} = 0.035\ \text{mol}$$

- *Determine the molar mass from the mass of the solute and the number of moles in that mass.*

$$\text{Molar mass} = \frac{4.00\ \text{g}}{0.034\ \text{mol}} = 1.2 \times 10^2\ \text{g/mol}$$

Exercise 7.9.6

A solution of 35.7 g of a nonelectrolyte in 220.0 g of chloroform has a boiling point of 64.5 °C. What is the molar mass of this compound?

Answer

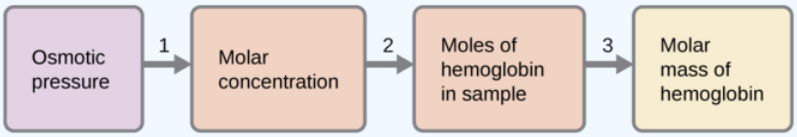
1.8×10^2 g/mol

Determination of a Molar Mass from Osmotic Pressure

A 0.500 L sample of an aqueous solution containing 10.0 g of hemoglobin has an osmotic pressure of 5.9 torr at 22 °C. What is the molar mass of hemoglobin?

Solution

Here is one set of steps that can be used to solve the problem:



1. *Convert the osmotic pressure to atmospheres, then determine the molar concentration from the osmotic pressure.*

$$\Pi = \frac{5.9 \text{ torr} \times 1 \text{ atm}}{760 \text{ torr}} = 7.8 \times 10^{-3} \text{ atm} \tag{7.9.11}$$

$$\Pi = MRT \tag{7.9.12}$$

$$M = \frac{\Pi}{RT} = \frac{7.8 \times 10^{-3} \text{ atm}}{(0.08206 \text{ L atm/mol K})(295 \text{ K})} = 3.2 \times 10^{-4} \text{ M}$$

- *Determine the number of moles of hemoglobin in the solution from the concentration and the volume of the solution.*

$$\text{moles of hemoglobin} = \frac{3.2 \times 10^{-4} \text{ mol}}{1 \cancel{\text{L solution}}} \times 0.500 \cancel{\text{L solution}} = 1.6 \times 10^{-4} \text{ mol}$$

- *Determine the molar mass from the mass of hemoglobin and the number of moles in that mass.*

$$\text{molar mass} = \frac{10.0 \text{ g}}{1.6 \times 10^{-4} \text{ mol}} = 6.2 \times 10^{4} \text{ g/mol}$$

Exercise 7.9.7

What is the molar mass of a protein if a solution of 0.02 g of the protein in 25.0 mL of solution has an osmotic pressure of 0.56 torr at 25 °C?

Answer

2.7×10^4 g/mol



Finding the Molecular Weight of an Unknown using Colligative Properties:

https://youtu.be/faSk2REYy74

Summary

- **vapor pressure lowering**:

$$P_A^0 - P_A = \Delta P_A = X_B P_A^0 \tag{7.9.13}$$

- **vapor pressure of a system containing two volatile components**:

$$P_T = X_A P_A^0 + (1 - X_A) P_B^0 \tag{7.9.14}$$

- **boiling point elevation**:

$$\Delta T_b = m K_b \tag{7.9.15}$$

- **freezing point depression:**

$$\Delta T_f = m K_f \tag{7.9.16}$$

The colligative properties of a solution depend on only the total number of dissolved particles in solution, not on their chemical identity. Colligative properties include vapor pressure, boiling point, freezing point, and osmotic pressure. The addition of a nonvolatile solute (one without a measurable vapor pressure) decreases the vapor pressure of the solvent. The vapor pressure of the solution is proportional to the mole fraction of solvent in the solution, a relationship known as **Raoult's law**. Solutions that obey Raoult's law are called ideal solutions. Most real solutions exhibit positive or negative deviations from Raoult's law. The boiling point elevation (ΔT_b) and freezing point depression (ΔT_f) of a solution are defined as the differences between the boiling and freezing points, respectively, of the solution and the pure solvent. Both are proportional to the molality of the solute.

7.9: Freezing-Point Depression and Boiling-Point Elevation of Nonelectrolyte Solutions is shared under a not declared license and was authored, remixed, and/or curated by LibreTexts.

- **13.8: Freezing-Point Depression and Boiling-Point Elevation of Nonelectrolyte Solutions** is licensed CC BY-NC-SA 4.0.

7.10: Solutions of Electrolytes

Thus far we have assumed that we could simply multiply the molar concentration of a solute by the number of ions per formula unit to obtain the actual concentration of dissolved particles in an electrolyte solution. We have used this simple model to predict such properties as freezing points, melting points, vapor pressure, and osmotic pressure. If this model were perfectly correct, we would expect the freezing point depression of a 0.10 m solution of sodium chloride, with 2 mol of ions per mole of $NaCl$ in solution, to be exactly twice that of a 0.10 m solution of glucose, with only 1 mol of molecules per mole of glucose in solution. In reality, this is not always the case. Instead, the observed change in freezing points for 0.10 m aqueous solutions of $NaCl$ and KCl are significantly less than expected (−0.348°C and −0.344°C, respectively, rather than −0.372°C), which suggests that fewer particles than we expected are present in solution.

The relationship between the actual number of moles of solute added to form a solution and the apparent number as determined by colligative properties is called the van't Hoff factor (i) and is defined as follows:Named for Jacobus Hendricus van't Hoff (1852–1911), a Dutch chemistry professor at the University of Amsterdam who won the first Nobel Prize in Chemistry (1901) for his work on thermodynamics and solutions.

$$i = \frac{\text{apparent number of particles in solution}}{\text{number of moles of solute dissolved}} \tag{7.10.1}$$

> As the solute concentration increases the van't Hoff factor decreases.

The van't Hoff factor is therefore a measure of a deviation from ideal behavior. The lower the van 't Hoff factor, the greater the deviation. As the data in Table **7.10.1** show, the van't Hoff factors for ionic compounds are somewhat lower than expected; that is, their solutions apparently contain fewer particles than predicted by the number of ions per formula unit. As the concentration of the solute increases, the van't Hoff factor decreases because ionic compounds generally do not totally dissociate in aqueous solution.

Table **7.10.1**: van 't Hoff Factors for 0.0500 M Aqueous Solutions of Selected Compounds at 25°C

Compound	i (measured)	i (ideal)
glucose	1.0	1.0
sucrose	1.0	1.0
$NaCl$	1.9	2.0
HCl	1.9	2.0
$MgCl_2$	2.7	3.0
$FeCl_3$	3.4	4.0
$Ca(NO_3)_2$	2.5	3.0
$AlCl_3$	3.2	4.0
$MgSO_4$	1.4	2.0

Instead, some of the ions exist as ion pairs, a cation and an anion that for a brief time are associated with each other without an intervening shell of water molecules (Figure **7.10.1**). Each of these temporary units behaves like a single dissolved particle until it dissociates. Highly charged ions such as Mg^{2+}, Al^{3+}, SO_4^{2-}, and PO_4^{3-} have a greater tendency to form ion pairs because of their strong electrostatic interactions. The actual number of solvated ions present in a solution can be determined by measuring a colligative property at several solute concentrations.

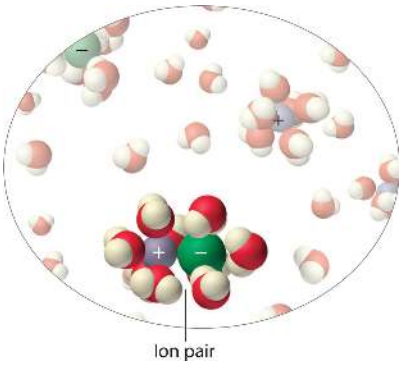


Figure **7.10.1**: Ion Pairs. In concentrated solutions of electrolytes like $NaCl$, some of the ions form neutral ion pairs that are not separated by solvent and diffuse as single particles.

Example 7.10.1: Iron Chloride in Water

A 0.0500 M aqueous solution of $FeCl_3$ has an osmotic pressure of 4.15 atm at 25°C. Calculate the van't Hoff factor i for the solution.

Given: solute concentration, osmotic pressure, and temperature

Asked for: van't Hoff factor

Strategy:

A. Use Equation 13.9.12 to calculate the expected osmotic pressure of the solution based on the effective concentration of dissolved particles in the solvent.
B. Calculate the ratio of the observed osmotic pressure to the expected value. Multiply this number by the number of ions of solute per formula unit, and then use Equation 13.9.1 to calculate the van't Hoff factor.

Solution:

A If $FeCl_3$ dissociated completely in aqueous solution, it would produce four ions per formula unit [Fe3+(aq) plus 3Cl−(aq)] for an effective concentration of dissolved particles of 4 × 0.0500 M = 0.200 M. The osmotic pressure would be

$$\Pi = MRT = (0.200\ mol/L)\,[0.0821\ (L \cdot atm)/(K \cdot mol)]\,(298\ K) = 4.89\ atm \tag{7.10.2}$$

B The observed osmotic pressure is only 4.15 atm, presumably due to ion pair formation. The ratio of the observed osmotic pressure to the calculated value is 4.15 atm/4.89 atm = 0.849, which indicates that the solution contains (0.849)(4) = 3.40 particles per mole of $FeCl_3$ dissolved. Alternatively, we can calculate the observed particle concentration from the osmotic pressure of 4.15 atm:

$$4.15\ atm = M\,[0.0821\ (L \cdot atm)/(K \cdot mol)]\,(298\ K) \tag{7.10.3}$$

$$0.170 mol/L = M \tag{7.10.4}$$

The ratio of this value to the expected value of 0.200 M is 0.170 M/0.200 M = 0.850, which again gives us (0.850)(4) = 3.40 particles per mole of $FeCl_3$ dissolved. From Equation 7.10.1, the van't Hoff factor for the solution is

$$i = \frac{3.40\ \text{particles observed}}{1\ \text{formula unit}\ FeCl_3} = 3.40 \tag{7.10.5}$$

Exercise 7.10.1: Magnesium Chloride in Water

Calculate the van't Hoff factor for a 0.050 m aqueous solution of $MgCl_2$ that has a measured freezing point of −0.25°C.

Answer:

2.7 (versus an ideal value of 3

Key Concepts and Summary

Ionic compounds may not completely dissociate in solution due to **activity** effects, in which case observed colligative effects may be less than predicted.

7.10: Solutions of Electrolytes is shared under a not declared license and was authored, remixed, and/or curated by LibreTexts.

- **13.9: Solutions of Electrolytes** is licensed CC BY-NC-SA 4.0.

7.11: Colloidal Mixtures

A suspension is a heterogeneous mixture of particles of one substance distributed throughout a second phase; the dispersed particles separate from the dispersing phase on standing. In contrast, the particles in a colloid are smaller and do not separate on standing. A colloid can be classified as a sol, a dispersion of solid particles in a liquid or solid; a gel, a semisolid sol in which all of the liquid phase has been absorbed by the solid particles; an aerosol, a dispersion of solid or liquid particles in a gas; or an emulsion, a dispersion of one liquid phase in another. A colloid can be distinguished from a true solution by its ability to scatter a beam of light, known as the Tyndall effect. Hydrophilic colloids contain an outer shell of groups that interact favorably with water, whereas hydrophobic colloids have an outer surface with little affinity for water. Emulsions are prepared by dispersing a hydrophobic liquid in water. In the absence of a dispersed hydrophobic liquid phase, solutions of detergents in water form organized spherical aggregates called micelles. Phospholipids are a class of detergent-like molecules that have two hydrophobic tails attached to a hydrophilic head. A bilayer is a two-dimensional sheet consisting of a double layer of phospholipid molecules arranged tail to tail with a hydrophobic interior and a hydrophilic exterior. Cells are collections of molecules that are surrounded by a phospholipid bilayer called a cell membrane and are able to reproduce themselves.

7.11: Colloidal Mixtures is shared under a not declared license and was authored, remixed, and/or curated by LibreTexts.

- **13.10: Colloidal Mixtures** is licensed CC BY-NC-SA 4.0.

SECTION OVERVIEW

7.12: Solubility and Complex-Ion Equilibria

In an aqueous solution, a complex ion exists in equilibrium with it's components, the central metallic ion and the ligands.

Topic hierarchy

7.12.1: Solubility Product Constant, Ksp

7.12.2: Relationship Between Solubility and Ksp

7.12.3: Common-Ion Effect in Solubility Equilibria

7.12.4: Limitations of the Ksp Concept

7.12.5: Criteria for Precipitation and its Completeness

7.12.6: Fractional Precipitation

7.12.7: Solubility and pH

7.12.8: Equilibria Involving Complex Ions

7.12.9: Qualitative Cation Analysis

7.12: Solubility and Complex-Ion Equilibria is shared under a not declared license and was authored, remixed, and/or curated by LibreTexts.

7.12.1: Solubility Product Constant, Ksp

Learning Objectives

- To calculate the solubility of an ionic compound from its K_{sp}

We begin our discussion of solubility and complexation equilibria—those associated with the formation of complex ions—by developing quantitative methods for describing dissolution and precipitation reactions of ionic compounds in aqueous solution. Just as with acid–base equilibria, we can describe the concentrations of ions in equilibrium with an ionic solid using an equilibrium constant expression.

The Solubility Product

When a slightly soluble ionic compound is added to water, some of it dissolves to form a solution, establishing an equilibrium between the pure solid and a solution of its ions. For the dissolution of calcium phosphate, one of the two main components of kidney stones, the equilibrium can be written as follows, with the solid salt on the left:

$$Ca_3(PO_4)_{2(s)} \rightleftharpoons 3Ca^{2+}_{(aq)} + 2PO^{3-}_{4(aq)} \tag{7.12.1.1}$$

As you will discover in Section 17.4 and in more advanced chemistry courses, basic anions, such as S^{2-}, PO_4^{3-}, and CO_3^{2-}, react with water to produce OH^- and the corresponding protonated anion. Consequently, their calculated molarities, assuming no protonation in aqueous solution, are only approximate.

The equilibrium constant for the dissolution of a sparingly soluble salt is the **solubility product (K_{sp})** of the salt. Because the concentration of a pure solid such as $Ca_3(PO_4)_2$ is a constant, it does not appear explicitly in the equilibrium constant expression. The equilibrium constant expression for the dissolution of calcium phosphate is therefore

$$K = \frac{[Ca^{2+}]^3[PO_4^{3-}]^2}{[Ca_3(PO_4)_2]} \tag{7.12.1.2}$$

$$[Ca_3(PO_4)_2]K = K_{sp} = [Ca^{2+}]^3[PO_4^{3-}]^2 \tag{7.12.1.3}$$

At 25°C and pH 7.00, Ksp for calcium phosphate is 2.07×10^{-33}, indicating that the concentrations of Ca^{2+} and PO_4^{3-} ions in solution that are in equilibrium with solid calcium phosphate are very low. The values of K_{sp} for some common salts are listed in Table **7.12.1.1**, which shows that the magnitude of K_{sp} varies dramatically for different compounds. Although K_{sp} is not a function of pH in Equations 7.12.1.2 and 7.12.1.3, changes in pH can affect the solubility of a compound as discussed later.

> *As with any K, the concentration of a pure solid does not appear explicitly in K_{sp}.*

Table **7.12.1.1**: Solubility Products for Selected Ionic Substances at 25°C

Solid	Color	K_{sp}		Solid	Color	K_{sp}
Acetates				**Iodides**		
$Ca(O_2CCH_3)_2 \cdot 3H_2O$	white	4×10^{-3}		Hg_2I_2*	yellow	5.2×10^{-29}
Bromides				PbI_2	yellow	9.8×10^{-9}
AgBr	off-white	5.35×10^{-13}		**Oxalates**		
Hg_2Br_2*	yellow	6.40×10^{-23}		$Ag_2C_2O_4$	white	5.40×10^{-12}
Carbonates				$MgC_2O_4 \cdot 2H_2O$	white	4.83×10^{-6}
$CaCO_3$	white	3.36×10^{-9}		PbC_2O_4	white	4.8×10^{-10}
$PbCO_3$	white	7.40×10^{-14}		**Phosphates**		
Chlorides				Ag_3PO_4	white	8.89×10^{-17}
AgCl	white	1.77×10^{-10}		$Sr_3(PO_4)_2$	white	4.0×10^{-28}
Hg_2Cl_2*	white	1.43×10^{-18}		$FePO_4 \cdot 2H_2O$	pink	9.91×10^{-16}
$PbCl_2$	white	1.70×10^{-5}		**Sulfates**		
Chromates				Ag_2SO_4	white	1.20×10^{-5}
$CaCrO_4$	yellow	7.1×10^{-4}		$BaSO_4$	white	1.08×10^{-10}
$PbCrO_4$	yellow	2.8×10^{-13}		$PbSO_4$	white	2.53×10^{-8}
Fluorides				**Sulfides**		
BaF_2	white	1.84×10^{-7}		Ag_2S	black	6.3×10^{-50}
PbF_2	white	3.3×10^{-8}		CdS	yellow	8.0×10^{-27}
Hydroxides				PbS	black	8.0×10^{-28}
$Ca(OH)_2$	white	5.02×10^{-6}		ZnS	white	1.6×10^{-24}
$Cu(OH)_2$	pale blue	1×10^{-14}				
$Mn(OH)_2$	light pink	1.9×10^{-13}				
$Cr(OH)_3$	gray-green	6.3×10^{-31}				
$Fe(OH)_3$	rust red	2.79×10^{-39}				

*These contain the Hg_2^{2+} ion.



Definition of a Solubility Product: Definition of a Solubility Product(opens in new window) [youtu.be]

Solubility products are determined experimentally by directly measuring either the concentration of one of the component ions or the solubility of the compound in a given amount of water. However, whereas solubility is usually expressed in terms of mass of solute per 100 mL of solvent, K_{sp}, like K, is defined in terms of the molar concentrations of the component ions.



A color photograph of a kidney stone, 8 mm in length. Kidney stones form from sparingly soluble calcium salts and are largely composed of $Ca(O_2CCO_2)\cdot H_2O$ and $Ca_3(PO_4)_2$. from Wikipedia.

Example 7.12.1.1

Calcium oxalate monohydrate [$Ca(O_2CCO_2)\cdot H_2O$, also written as $CaC_2O_4\cdot H_2O$] is a sparingly soluble salt that is the other major component of kidney stones [along with $Ca_3(PO_4)_2$]. Its solubility in water at 25°C is 7.36×10^{-4} g/100 mL. Calculate its K_{sp}.

Given: solubility in g/100 mL

Asked for: K_{sp}

Strategy:

A. Write the balanced dissolution equilibrium and the corresponding solubility product expression.

B. Convert the solubility of the salt to moles per liter. From the balanced dissolution equilibrium, determine the equilibrium concentrations of the dissolved solute ions. Substitute these values into the solubility product expression to calculate K_{sp}.

Solution

A We need to write the solubility product expression in terms of the concentrations of the component ions. For calcium oxalate monohydrate, the balanced dissolution equilibrium and the solubility product expression (abbreviating oxalate as ox^{2-}) are as follows:

$$Ca(O_2CCO_2)\cdot H_2O(s) \rightleftharpoons Ca^{2+}(aq) + {}^{-}O_2CCO_2^{-}(aq) + H_2O(l) \quad K_{sp} = [Ca^{2+}][ox^{2-}]$$

Neither solid calcium oxalate monohydrate nor water appears in the solubility product expression because their concentrations are essentially constant.

B Next we need to determine [Ca^{2+}] and [ox^{2-}] at equilibrium. We can use the mass of calcium oxalate monohydrate that dissolves in 100 mL of water to calculate the number of moles that dissolve in 100 mL of water. From this we can determine the number of moles that dissolve in 1.00 L of water. For dilute solutions, the density of the solution is nearly the same as that of water, so dissolving the salt in 1.00 L of water gives essentially 1.00 L of solution. Because each 1 mol of dissolved calcium oxalate monohydrate dissociates to produce 1 mol of calcium ions and 1 mol of oxalate ions, we can obtain the equilibrium concentrations that must be inserted into the solubility product expression. The number of moles of calcium oxalate monohydrate that dissolve in 100 mL of water is as follows:

$$\frac{7.36 \times 10^{-4}\ \text{g}}{146.1\ \text{g/mol}} = 5.04 \times 10^{-6}\ \text{mol}\ \text{Ca}(\text{O}_2\text{CCO}_2) \cdot \text{H}_2\text{O}$$

The number of moles of calcium oxalate monohydrate that dissolve in 1.00 L of the saturated solution is as follows:

$$\left(\frac{5.04 \times 10^{-6}\ \text{mol}\ \text{Ca}(\text{O}_2\text{CCO}_2\cdot)\text{H}_2\text{O}}{100\ \text{mL}}\right)\left(\frac{1000\ \text{mL}}{1.00\ \text{L}}\right) = 5.04 \times 10^{-5}\ \text{mol/L} = 5.04 \times 10^{-5}\ \text{M}$$

Because of the stoichiometry of the reaction, the concentration of Ca^{2+} and ox^{2-} ions are both 5.04×10^{-5} M. Inserting these values into the solubility product expression,

$$K_{sp} = [Ca^{2+}][ox^{2-}] = (5.04 \times 10^{-5})(5.04 \times 10^{-5}) = 2.54 \times 10^{-9}$$

In our calculation, we have ignored the reaction of the weakly basic anion with water, which tends to make the actual solubility of many salts greater than the calculated value.

? Exercise 7.12.1.1: Calcite

One crystalline form of calcium carbonate ($CaCO_3$) is "calcite", found as both a mineral and a structural material in many organisms. Calcite is found in the teeth of sea urchins. The urchins create depressions in limestone that they can settle in by grinding the rock with their teeth. Limestone, however, also consists of calcite, so how can the urchins grind the rock without also grinding their teeth? Researchers have discovered that the teeth are shaped like needles and plates and contain magnesium. The concentration of magnesium increases toward the tip, which contributes to the hardness. Moreover, each tooth is composed of two blocks of the polycrystalline calcite matrix that are interleaved near the tip. This creates a corrugated surface that presumably increases grinding efficiency. Toolmakers are particularly interested in this approach to grinding.



A crystal of calcite ($CaCO_3$), illustrating the phenomenon of double refraction. When a transparent crystal of calcite is placed over a page, we see two images of the letters. from Wikipedia

The solubility of calcite in water is 0.67 mg/100 mL. Calcite its K_{sp}.

Answer

4.5×10^{-9}

> *The reaction of weakly basic anions with H_2O tends to make the actual solubility of many salts higher than predicted.*



Finding Ksp from Ion Concentrations: Finding Ksp from Ion Concentrations(opens in new window) [youtu.be]

Tabulated values of K_{sp} can also be used to estimate the solubility of a salt with a procedure that is essentially the reverse of the one used in Example **7.12.1.1**. In this case, we treat the problem as a typical equilibrium problem and set up a table of initial concentrations, changes in concentration, and final concentrations (ICE Tables), remembering that the concentration of the pure solid is essentially constant.

Example 7.12.1.2

We saw that the K_{sp} for $Ca_3(PO_4)_2$ is 2.07×10^{-33} at 25°C. Calculate the aqueous solubility of $Ca_3(PO_4)_2$ in terms of the following:

a. the molarity of ions produced in solution
b. the mass of salt that dissolves in 100 mL of water at 25°C

Given: K_{sp}

Asked for: molar concentration and mass of salt that dissolves in 100 mL of water

Strategy:

A. Write the balanced equilibrium equation for the dissolution reaction and construct a table showing the concentrations of the species produced in solution. Insert the appropriate values into the solubility product expression and calculate the molar solubility at 25°C.
B. Calculate the mass of solute in 100 mL of solution from the molar solubility of the salt. Assume that the volume of the solution is the same as the volume of the solvent.

Solution:

A. **A** The dissolution equilibrium for $Ca_3(PO_4)_2$ (Equation **7.12.1.2**) is shown in the following ICE table. Because we are starting with distilled water, the initial concentration of both calcium and phosphate ions is zero. For every 1 mol of $Ca_3(PO_4)_2$ that dissolves, 3 mol of Ca^{2+} and 2 mol of PO_4^{3-} ions are produced in solution. If we let x equal the solubility of $Ca_3(PO_4)_2$ in moles per liter, then the change in $[Ca^{2+}]$ will be $+3x$, and the change in $[PO_4^{3-}]$ will be $+2x$. We can insert these values into the table.

$$Ca_3(PO_4)_2(s) \rightleftharpoons 3Ca^{2+}(aq) + 2PO_4^{3-}(aq)$$

Solutions to Example 17.4.2

	Ca3(PO4)2	[Ca2+]	$[PO_4^{3-}]$
initial	pure solid	0	0
change	—	$+3x$	$+2x$
final	pure solid	$3x$	$2x$

Although the amount of solid $Ca_3(PO_4)_2$ changes as some of it dissolves, its molar concentration does not change. We now insert the expressions for the equilibrium concentrations of the ions into the solubility product expression (Equation 17.2):

$$K_{sp} = [Ca^{2+}]^3[PO_4^{3-}]^2 = (3x)^3(2x)^2 \quad (7.12.1.4)$$

$$2.07 \times 10^{-33} = 108x^5 \quad (7.12.1.5)$$

$$1.92 \times 10^{-35} = x^5 \quad (7.12.1.6)$$

$$1.14 \times 10^{-7}\ \text{M} = x \quad (7.12.1.7)$$

This is the molar solubility of calcium phosphate at 25°C. However, the molarity of the ions is $2x$ and $3x$, which means that $[PO_4^{3-}] = 2.28 \times 10^{-7}$ and $[Ca^{2+}] = 3.42 \times 10^{-7}$.

b. **B** To find the mass of solute in 100 mL of solution, we assume that the density of this dilute solution is the same as the density of water because of the low solubility of the salt, so that 100 mL of water gives 100 mL of solution. We can then determine the amount of salt that dissolves in 100 mL of water:

$$\left(\frac{1.14 \times 10^{-7}\ \text{mol}}{1\ \text{L}}\right) 100\ \text{mL} \left(\frac{1\ \text{L}}{1000\ \text{mL}}\right) \left(\frac{310.18\ \text{g}\ Ca_3(PO_4)_2}{1\ \text{mol}}\right) = 3.54 \times 10^{-6}\ \text{g}\ Ca_3(PO_4)_2$$

? Exercise 7.12.1.2

The solubility product of silver carbonate (Ag_2CO_3) is 8.46×10^{-12} at 25°C. Calculate the following:

a. the molarity of a saturated solution
b. the mass of silver carbonate that will dissolve in 100 mL of water at this temperature

Answer

a. 1.28×10^{-4} M
b. 3.54 mg



Finding the Solubility of a Salt: Finding the Solubility of a Salt (opens in new window) [youtu.be]

The Ion Product

The **ion product (*Q*)** of a salt is the product of the concentrations of the ions in solution raised to the same powers as in the solubility product expression. It is analogous to the reaction quotient (Q) discussed for gaseous equilibria. Whereas K_{sp} describes equilibrium concentrations, the ion product describes concentrations that are not necessarily equilibrium concentrations.

> *The ion product Q is analogous to the reaction quotient Q for gaseous equilibria.*

As summarized in Figure **7.12.1.1**, there are three possible conditions for an aqueous solution of an ionic solid:

- $Q < K_{sp}$. The solution is unsaturated, and more of the ionic solid, if available, will dissolve.
- $Q = K_{sp}$. The solution is saturated and at equilibrium.

- $Q > K_{sp}$. The solution is supersaturated, and ionic solid will precipitate.

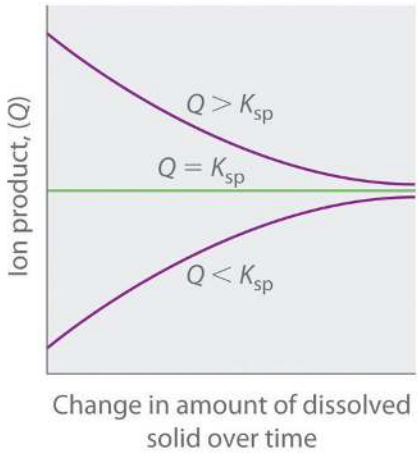


Figure **7.12.1.1**: The Relationship between Q and K_{sp}. If Q is less than K_{sp}, the solution is unsaturated and more solid will dissolve until the system reaches equilibrium ($Q = K_{sp}$). If Q is greater than K_{sp}, the solution is supersaturated and solid will precipitate until $Q = K_{sp}$. If $Q = K_{sp}$, the rate of dissolution is equal to the rate of precipitation; the solution is saturated, and no net change in the amount of dissolved solid will occur.

Graph of ion product against change in amount of dissolved solid over time. The purple curves are when Q is greater or less than Ksp. The green line is when Q is equal to Ksp.

The process of calculating the value of the ion product and comparing it with the magnitude of the solubility product is a straightforward way to determine whether a solution is unsaturated, saturated, or supersaturated. More important, the ion product tells chemists whether a precipitate will form when solutions of two soluble salts are mixed.

Example 7.12.1.3

We mentioned that barium sulfate is used in medical imaging of the gastrointestinal tract. Its solubility product is 1.08×10^{-10} at 25°C, so it is ideally suited for this purpose because of its low solubility when a "barium milkshake" is consumed by a patient. The pathway of the sparingly soluble salt can be easily monitored by x-rays. Will barium sulfate precipitate if 10.0 mL of 0.0020 M Na_2SO_4 is added to 100 mL of 3.2×10^{-4} M $BaCl_2$? Recall that NaCl is highly soluble in water.

Given: K_{sp} and volumes and concentrations of reactants

Asked for: whether precipitate will form

Strategy:

A. Write the balanced equilibrium equation for the precipitation reaction and the expression for K_{sp}.

B. Determine the concentrations of all ions in solution when the solutions are mixed and use them to calculate the ion product (Q).

C. Compare the values of Q and K_{sp} to decide whether a precipitate will form.

Solution

A The only slightly soluble salt that can be formed when these two solutions are mixed is $BaSO_4$ because NaCl is highly soluble. The equation for the precipitation of $BaSO_4$ is as follows:

$$BaSO_{4(s)} \rightleftharpoons Ba^{2+}_{(aq)} + SO^{2-}_{4(aq)}$$

The solubility product expression is as follows:

$$K_{sp} = [Ba^{2+}][SO_4^{2-}] = 1.08 \times 10^{-10}$$

B To solve this problem, we must first calculate the ion product—$Q = [Ba^{2+}][SO_4^{2-}]$—using the concentrations of the ions that are present after the solutions are mixed and before any reaction occurs. The concentration of Ba^{2+} when the solutions are mixed is the total number of moles of Ba^{2+} in the original 100 mL of $BaCl_2$ solution divided by the final volume (100 mL + 10.0 mL = 110 mL):

$$\text{moles } Ba^{2+} = 100 \text{ mL}\left(\frac{1 \text{ L}}{1000 \text{ mL}}\right)\left(\frac{3.2 \times 10^{-4} \text{ mol}}{1 \text{ L}}\right) = 3.2 \times 10^{-5} \text{ mol } Ba^{2+}$$

$$[Ba^{2+}] = \left(\frac{3.2 \times 10^{-5} \text{ mol } Ba^{2+}}{110 \text{ mL}}\right)\left(\frac{1000 \text{ mL}}{1 \text{ L}}\right) = 2.9 \times 10^{-4} \text{ M } Ba^{2+}$$

Similarly, the concentration of SO_4^{2-} after mixing is the total number of moles of SO_4^{2-} in the original 10.0 mL of Na_2SO_4 solution divided by the final volume (110 mL):

$$\text{moles } SO_4^{2-} = 10.0 \text{ mL}\left(\frac{1 \text{ L}}{1000 \text{ mL}}\right)\left(\frac{0.0020 \text{ mol}}{1 \text{ L}}\right) = 2.0 \times 10^{-5} \text{ mol } SO_4^{2-}$$

$$[SO_4^{2-}] = \left(\frac{2.0 \times 10^{-5} \text{ mol } SO_4^{2-}}{110 \text{ mL}}\right)\left(\frac{1000 \text{ mL}}{1 \text{ L}}\right) = 1.8 \times 10^{-4} \text{ M } SO_4^{2-}$$

We can now calculate Q:

$$Q = [Ba^{2+}][SO_4^{2-}] = (2.9\times10^{-4})(1.8\times10^{-4}) = 5.2\times10^{-8}$$

C We now compare Q with the K_{sp}. If $Q > K_{sp}$, then $BaSO_4$ will precipitate, but if $Q < K_{sp}$, it will not. Because $Q > K_{sp}$, we predict that $BaSO_4$ will precipitate when the two solutions are mixed. In fact, $BaSO_4$ will continue to precipitate until the system reaches equilibrium, which occurs when $[Ba^{2+}][SO_4^{2-}] = K_{sp} = 1.08 \times 10^{-10}$.

? Exercise 7.12.1.3

The solubility product of calcium fluoride (CaF_2) is 3.45×10^{-11}. If 2.0 mL of a 0.10 M solution of NaF is added to 128 mL of a 2.0×10^{-5}M solution of $Ca(NO_3)_2$, will CaF_2 precipitate?

Answer

yes ($Q = 4.7 \times 10^{-11} > K_{sp}$)



Determining if a Precipitate forms (The Ion Product): Determining if a Precipitate forms (The Ion Product)(opens in new window) [youtu.be]

The Common Ion Effect and Solubility

The solubility product expression tells us that the equilibrium concentrations of the cation and the anion are inversely related. That is, as the concentration of the anion increases, the maximum concentration of the cation needed for precipitation to occur decreases—and vice versa—so that K_{sp} is constant. Consequently, the solubility of an ionic compound depends on the concentrations of other salts that contain the same ions. Adding a common cation or anion shifts a solubility equilibrium in the direction predicted by Le Chatelier's principle. As a result, the solubility of any sparingly soluble salt is almost always decreased by the presence of a soluble salt that contains a common ion. The exceptions generally involve the formation of complex ions, which is discussed later.

Consider, for example, the effect of adding a soluble salt, such as $CaCl_2$, to a saturated solution of calcium phosphate [$Ca_3(PO_4)_2$]. We have seen that the solubility of $Ca_3(PO_4)_2$ in water at 25°C is 1.14×10^{-7} M ($K_{sp} = 2.07 \times 10^{-33}$). Thus a saturated solution of

$Ca_3(PO_4)_2$ in water contains $3 \times (1.14 \times 10^{-7}\ M) = 3.42 \times 10^{-7}\ M\ Ca^{2+}$ and $2 \times (1.14 \times 10^{-7}\ M) = 2.28 \times 10^{-7}\ M\ PO_4^{3-}$, according to the stoichiometry shown in Equation 7.12.1.1 (neglecting hydrolysis to form HPO_4^{2-} as described in Chapter 16). If $CaCl_2$ is added to a saturated solution of $Ca_3(PO_4)_2$, the Ca^{2+} ion concentration will increase such that $[Ca^{2+}] > 3.42 \times 10^{-7}\ M$, making $Q > K_{sp}$. The only way the system can return to equilibrium is for the reaction in Equation 7.12.1.1 to proceed to the left, resulting in precipitation of $Ca_3(PO_4)_2$. This will decrease the concentration of both Ca^{2+} and PO_4^{3-} until $Q = K_{sp}$.

> *The common ion effect usually **decreases** the solubility of a sparingly soluble salt.*

Example 7.12.1.4

Calculate the solubility of calcium phosphate [$Ca_3(PO_4)_2$] in 0.20 M $CaCl_2$.

Given: concentration of $CaCl_2$ solution

Asked for: solubility of $Ca_3(PO_4)_2$ in $CaCl_2$ solution

Strategy:

A. Write the balanced equilibrium equation for the dissolution of $Ca_3(PO_4)_2$. Tabulate the concentrations of all species produced in solution.

B. Substitute the appropriate values into the expression for the solubility product and calculate the solubility of $Ca_3(PO_4)_2$.

Solution

A The balanced equilibrium equation is given in the following table. If we let x equal the solubility of $Ca_3(PO_4)_2$ in moles per liter, then the change in $[Ca^{2+}]$ is once again $+3x$, and the change in $[PO_4^{3-}]$ is $+2x$. We can insert these values into the ICE table.

$$Ca_3(PO_4)_{2(s)} \rightleftharpoons 3Ca^{2+}_{(aq)} + 2PO^{3-}_{4(aq)}$$

Solutions to Example 17.4.4

	Ca3(PO4)2	$[Ca^{2+}]$	$[PO_4^{3-}]$
initial	pure solid	0.20	0
change	—	$+3x$	$+2x$
final	pure solid	$0.20 + 3x$	$2x$

B The K_{sp} expression is as follows:

$$K_{sp} = [Ca^{2+}]^3[PO_4^{3-}]^2 = (0.20 + 3x)^3(2x)^2 = 2.07 \times 10^{-33}$$

Because $Ca_3(PO_4)_2$ is a sparingly soluble salt, we can reasonably expect that $x << 0.20$. Thus $(0.20 + 3x)$ M is approximately 0.20 M, which simplifies the K_{sp} expression as follows:

$$\begin{aligned} K_{sp} = (0.20)^3(2x)^2 &= 2.07 \times 10^{-33} \\ x^2 &= 6.5 \times 10^{-32} \\ x &= 2.5 \times 10^{-16}\ M \end{aligned}$$

This value is the solubility of $Ca_3(PO_4)_2$ in 0.20 M $CaCl_2$ at 25°C. It is approximately nine orders of magnitude less than its solubility in pure water, as we would expect based on Le Chatelier's principle. With one exception, this example is identical to Example 7.12.1.2—here the initial $[Ca^{2+}]$ was 0.20 M rather than 0.

Exercise 7.12.1.4

Calculate the solubility of silver carbonate in a 0.25 M solution of sodium carbonate. The solubility of silver carbonate in pure water is 8.45×10^{-12} at 25°C.

Answer

2.9×10^{-6} M (versus 1.3×10^{-4} M in pure water)



The Common Ion Effect in Solubility Products: The Common Ion Effect in Solubility Products(opens in new window) [youtu.be]

Summary

The solubility product (K_{sp}) is used to calculate equilibrium concentrations of the ions in solution, whereas the ion product (Q) describes concentrations that are not necessarily at equilibrium. The equilibrium constant for a dissolution reaction, called the solubility product (K_{sp}), is a measure of the solubility of a compound. Whereas solubility is usually expressed in terms of mass of solute per 100 mL of solvent, K_{sp} is defined in terms of the molar concentrations of the component ions. In contrast, the ion product (Q) describes concentrations that are not necessarily equilibrium concentrations. Comparing Q and K_{sp} enables us to determine whether a precipitate will form when solutions of two soluble salts are mixed. Adding a common cation or common anion to a solution of a sparingly soluble salt shifts the solubility equilibrium in the direction predicted by Le Chatelier's principle. The solubility of the salt is almost always decreased by the presence of a common ion.

7.12.1: Solubility Product Constant, Ksp is shared under a not declared license and was authored, remixed, and/or curated by LibreTexts.

- **17.4: Solubility Equilibria** is licensed CC BY-NC-SA 3.0.

7.12.2: Relationship Between Solubility and Ksp

Learning Objectives

- Quantitatively related K_{sp} to solubility

Considering the relation between solubility and K_{sp} is important when describing the solubility of slightly ionic compounds. However, this article discusses ionic compounds that are difficult to dissolve; they are considered "slightly soluble" or "almost insoluble." Solubility product constants (K_{sq}) are given to those solutes, and these constants can be used to find the molar solubility of the compounds that make the solute. This relationship also facilitates finding the K_{sq} of a slightly soluble solute from its solubility.

Introduction

Recall that the definition of *solubility* is the maximum possible concentration of a solute in a solution at a given temperature and pressure. We can determine the solubility product of a slightly soluble solid from that measure of its solubility at a given temperature and pressure, provided that the only significant reaction that occurs when the solid dissolves is its dissociation into solvated ions, that is, the only equilibrium involved is:

$$\mathrm{M_pX_q}(s) \rightleftharpoons p\mathrm{M^{m+}}(aq) + q\mathrm{X^{n-}}(aq) \tag{7.12.2.1}$$

In this case, we calculate the solubility product by taking the solid's solubility expressed in units of moles per liter (mol/L), known as its **molar solubility**.

Calculation of K_{sp} from Equilibrium Concentrations

We began the chapter with an informal discussion of how the mineral fluorite is formed. Fluorite, $\mathrm{CaF_2}$, is a slightly soluble solid that dissolves according to the equation:

$$\mathrm{CaF_2}(s) \rightleftharpoons \mathrm{Ca^{2+}}(aq) + 2\,\mathrm{F^-}(aq)$$

The concentration of Ca^{2+} in a saturated solution of CaF_2 is 2.1×10^{-4} *M*; therefore, that of F^- is 4.2×10^{-4} *M*, that is, twice the concentration of $\mathrm{Ca^{2+}}$. What is the solubility product of fluorite?

Solution

First, write out the K_{sp} expression, then substitute in concentrations and solve for K_{sp}:

$$\mathrm{CaF_2\,(s) \rightleftharpoons Ca^{2+}\,(aq) + 2\,F^-\,(aq)}$$

A saturated solution is a solution at equilibrium with the solid. Thus:

$$\begin{aligned} K_{sp} &= [\mathrm{Ca^{2+}}][\mathrm{F^-}]^2 \\ &= (2.1 \times 10^{-4})(4.2 \times 10^{-4})^2 \\ &= 3.7 \times 10^{-11} \end{aligned}$$

As with other equilibrium constants, we do not include units with K_{sp}.

Exercise 7.12.2.1

In a saturated solution that is in contact with solid $Mg(OH)_2$, the concentration of Mg^{2+} is 3.7×10^{-5} *M*. What is the solubility product for $Mg(OH)_2$?

$$\mathrm{Mg(OH)_2}(s) \rightleftharpoons \mathrm{Mg^{2+}}(aq) + 2\,\mathrm{OH^-}(aq)$$

Answer

2.0×10^{-13}

Determination of Molar Solubility from K_{sp}

The K_{sp} of copper(I) bromide, **CuBr**, is 6.3×10^{-9}. Calculate the molar solubility of copper bromide.

Solution

The solubility product constant of copper(I) bromide is 6.3×10^{-9}.

The reaction is:

$$\mathrm{CuBr}(s) \rightleftharpoons \mathrm{Cu}^{+}(aq) + \mathrm{Br}^{-}(aq)$$

First, write out the solubility product equilibrium constant expression:

$$K_{sp} = [\mathrm{Cu}^{+}][\mathrm{Br}^{-}]$$

Create an ICE table (as introduced in the chapter on fundamental equilibrium concepts), leaving the **CuBr** column empty as it is a solid and does not contribute to the K_{sp}:

	CuBr $\rightleftharpoons$	Cu^+	+ Br^-
Initial concentration (*M*)		0	0
Change (*M*)		*x*	*x*
Equilibrium concentration (*M*)		0 + *x* = *x*	0 + *x* = *x*

At equilibrium:

$$K_{sp} = [\mathrm{Cu}^{+}][\mathrm{Br}^{-}]$$
$$6.3 \times 10^{-9} = (x)(x) = x^2$$
$$x = \sqrt{(6.3 \times 10^{-9})} = 7.9 \times 10^{-5}$$

Therefore, the molar solubility of **CuBr** is 7.9×10^{-5} *M*.



Finding the Solubility of a Salt: https://youtu.be/98BuldrICXM

Summary

Solubility is defined as the maximum amount of solute that can be dissolved in a solvent at equilibrium. Equilibrium is the state at which the concentrations of products and reactant are constant after the reaction has taken place. The solubility product constant (K_{sp}) describes the equilibrium between a solid and its constituent ions in a solution. The value of the constant identifies the degree to which the compound can dissociate in water. The higher the K_{sp}, the more soluble the compound is. K_{sq} is defined in terms of activity rather than concentration because it is a measure of a concentration that depends on certain conditions such as temperature, pressure, and composition. It is influenced by surroundings. K_{sp} is used to describe the saturated solution of ionic compounds. (A saturated solution is in a state of equilibrium between the dissolved, dissociated, undissolved solid, and the ionic compound.)

Contributors and Attributions

- Paul Flowers (University of North Carolina - Pembroke), Klaus Theopold (University of Delaware) and Richard Langley (Stephen F. Austin State University) with contributing authors. Textbook content produced by OpenStax College is licensed under a Creative Commons Attribution License 4.0 license. Download for free at http://cnx.org/contents/85abf193-2bd...a7ac8df6@9.110).

7.12.2: Relationship Between Solubility and Ksp is shared under a not declared license and was authored, remixed, and/or curated by LibreTexts.

- **18.2: Relationship Between Solubility and Ksp** by OpenStax is licensed CC BY 4.0.

7.12.3: Common-Ion Effect in Solubility Equilibria

Learning Objectives

- Recognize common ions from various salts, acids, and bases.
- Calculate concentrations involving common ions.
- Calculate ion concentrations involving chemical equilibrium.

The common-ion effect is used to describe the effect on an equilibrium involving a substance that adds an ion that is a part of the equilibrium.

Introduction

The solubility products K_{sp}'s are equilibrium constants in hetergeneous equilibria (i.e., between two different phases). If several salts are present in a system, they all ionize in the solution. If the salts contain a common cation or anion, these salts contribute to the concentration of the common ion. Contributions from all salts must be included in the calculation of concentration of the common ion. For example, a solution containing sodium chloride and potassium chloride will have the following relationship:

$$[\mathrm{Na^+}] + [\mathrm{K^+}] = [\mathrm{Cl^-}] \tag{7.12.3.1}$$

Consideration of *charge balance* or *mass balance* or both leads to the same conclusion. The solubility product expression tells us that the equilibrium concentrations of the cation and the anion are inversely related. That is, as the concentration of the anion increases, the maximum concentration of the cation needed for precipitation to occur decreases—and vice versa—so that K_{sp} is constant. Consequently, the solubility of an ionic compound depends on the concentrations of other salts that contain the same ions. Adding a common cation or anion shifts a solubility equilibrium in the direction predicted by Le Chatelier's principle. As a result, the solubility of any sparingly soluble salt is almost always decreased by the presence of a soluble salt that contains a common ion. The exceptions generally involve the formation of complex ions, which is discussed later.

Common Ions

When NaCl and KCl are dissolved in the same solution, the $\mathrm{Cl^-}$ ions are *common* to both salts. In a system containing NaCl and KCl, the $\mathrm{Cl^-}$ ions are common ions.

$$\mathrm{NaCl} \rightleftharpoons \mathrm{Na^+} + \mathrm{Cl^-}$$
$$\mathrm{KCl} \rightleftharpoons \mathrm{K^+} + \mathrm{Cl^-}$$
$$\mathrm{CaCl_2} \rightleftharpoons \mathrm{Ca^{2+}} + 2\mathrm{Cl^-}$$
$$\mathrm{AlCl_3} \rightleftharpoons \mathrm{Al^{3+}} + 3\mathrm{Cl^-}$$
$$\mathrm{AgCl} \rightleftharpoons \mathrm{Ag^+} + \mathrm{Cl^-}$$

For example, when AgCl is dissolved into a solution already containing NaCl (actually $\mathrm{Na^+}$ and $\mathrm{Cl^-}$ ions), the $\mathrm{Cl^-}$ ions come from the ionization of both AgCl and NaCl. Thus, $[\mathrm{Cl^-}]$ differs from $[\mathrm{Ag^+}]$. The following examples show how the concentration of the common ion is calculated.

Example 7.12.3.1

What are $[\mathrm{Na^+}]$, $[\mathrm{Cl^-}]$, $[\mathrm{Ca^{2+}}]$, and $[\mathrm{H^+}]$ in a solution containing 0.10 M each of NaCl, $\mathrm{CaCl_2}$, and HCl?

Solution

Due to the conservation of ions, we have

$$[\mathrm{Na^+}] = [\mathrm{Ca^{2+}}] = [\mathrm{H^+}] = 0.10\ \mathrm{M}.$$

but

$$\begin{aligned}[\mathrm{Cl^-}] = &\ 0.10\ (\text{due to NaCl}) \\ &+ 0.20\ (\text{due to } \mathrm{CaCl_2}) \\ &+ 0.10\ (\text{due to HCl}) \\ = &\ 0.40\ \mathrm{M}\end{aligned}$$

? Exercise 7.12.3.1

John poured 10.0 mL of 0.10 M **NaCl**, 10.0 mL of 0.10 M **KOH**, and 5.0 mL of 0.20 M **HCl** solutions together and then he made the total volume to be 100.0 mL. What is $[\mathrm{Cl^-}]$ in the final solution?

$$[\mathrm{Cl^-}] = \frac{0.1\ \mathrm{M} \times 10\ \mathrm{mL} + 0.2\ \mathrm{M} \times 5.0\ \mathrm{mL}}{100.0\ \mathrm{mL}} = 0.020\ \mathrm{M}$$

Le Châtelier's Principle states that if an equilibrium becomes unbalanced, the reaction will shift to restore the balance. If a common ion is added to a weak acid or weak base equilibrium, then the equilibrium will shift towards the reactants, in this case the weak acid or base.

✓ Example 7.12.3.2

Consider the lead(II) ion concentration in this *saturated* solution of $PbCl_2$. The balanced reaction is

$$PbCl_{2(s)} \rightleftharpoons Pb^{2+}_{(aq)} + 2Cl^-_{(aq)}$$

Defining s as the concentration of dissolved lead(II) chloride, then:

$$[Pb^{2+}] = s$$

$$[Cl^-] = 2s$$

These values can be substituted into the solubility product expression, which can be solved for s:

$$\begin{aligned}K_{sp} &= [Pb^{2+}][Cl^-]^2 \\ &= s \times (2s)^2 \\ 1.7 \times 10^{-5} &= 4s^3 \\ s^3 &= \frac{1.7 \times 10^{-5}}{4} \\ &= 4.25 \times 10^{-6} \\ s &= \sqrt[3]{4.25 \times 10^{-6}} \\ &= 1.62 \times 10^{-2}\ mol\ dm^{-3}\end{aligned}$$

The concentration of lead(II) ions in the solution is 1.62 x 10^{-2} M. Consider what happens if sodium chloride is added to this saturated solution. Sodium chloride shares an ion with lead(II) chloride. The chloride ion is **common** to both of them; this is the origin of the term "common ion effect".

Look at the original equilibrium expression again:

$$PbCl_2\ (s) \rightleftharpoons Pb^{2+}\ (aq) + 2Cl^-\ (aq)$$

What happens to that equilibrium if extra chloride ions are added? According to *Le* Châtelier, the position of equilibrium will shift to counter the change, in this case, by removing the chloride ions by making extra solid lead(II) chloride.

Of course, the concentration of lead(II) ions in the solution is so small that only a tiny proportion of the extra chloride ions can be converted into solid lead(II) chloride. The lead(II) chloride becomes even *less soluble*, and the concentration of lead(II) ions in the solution *decreases*. This type of response occurs with any sparingly soluble substance: it is less soluble in a solution which contains any ion which it has in common. This is the common ion effect.

A Simple Example

If an attempt is made to dissolve some lead(II) chloride in some 0.100 M sodium chloride solution instead of in water, what is the equilibrium concentration of the lead(II) ions this time? As before, define s to be the concentration of the lead(II) ions.

$$[Pb^{2+}] = s \tag{7.12.3.2}$$

The calculations are different from before. This time the concentration of the chloride ions is governed by the concentration of the sodium chloride solution. The number of ions coming from the lead(II) chloride is going to be tiny compared with the 0.100 M coming from the sodium chloride solution. In calculations like this, it can be assumed that the concentration of the common ion is entirely due to the other solution. This simplifies the calculation.

So we assume:

$$[Cl^-] = 0.100\ M \tag{7.12.3.3}$$

The rest of the mathematics looks like this:

$$\begin{aligned} K_{sp} &= [Pb^{2+}][Cl^-]^2 \\ &= s \times (0.100)^2 \\ 1.7 \times 10^{-5} &= s \times 0.00100 \end{aligned} \tag{7.12.3.4}$$

therefore:

$$\begin{aligned} s &= \frac{1.7 \times 10^{-5}}{0.0100} \\ &= 1.7 \times 10^{-3}\ \text{M} \end{aligned} \tag{7.12.3.5}$$

Finally, compare that value with the simple saturated solution:

Original solution:

$$[Pb^{2+}] = 0.0162\ M \tag{7.12.3.6}$$

Solution in 0.100 M NaCl solution:

$$[Pb^{2+}] = 0.0017\ M \tag{7.12.3.7}$$

The concentration of the lead(II) ions has decreased by a factor of about 10. If more concentrated solutions of sodium chloride are used, the solubility decreases further.

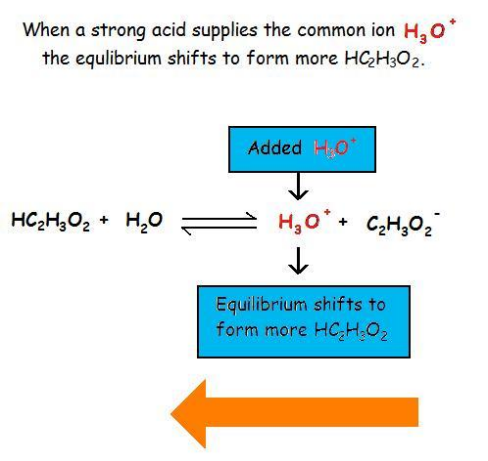
> Adding a common ion to a system at equilibrium affects the equilibrium composition, but **not** the ionization constant.

Common Ion Effect with Weak Acids and Bases

Adding a common ion prevents the weak acid or weak base from ionizing as much as it would without the added common ion. The common ion effect suppresses the ionization of a weak acid by adding more of an ion that is a product of this equilibrium.

Example 7.12.3.3

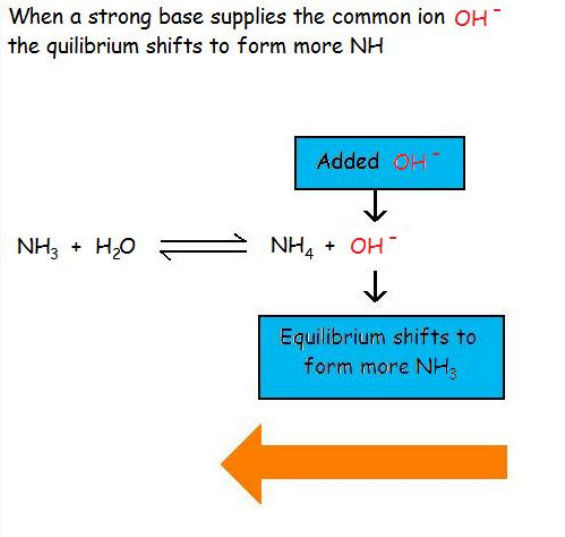
The common ion effect of H_3O^+ on the ionization of acetic acid



The common ion effect suppresses the ionization of a weak base by adding more of an ion that is a product of this equilibrium.

Example 7.12.3.4

Consider the common ion effect of OH^- on the ionization of ammonia



Adding the common ion of hydroxide shifts the reaction towards the left to decrease the stress (in accordance with Le Châtelier's Principle), forming more reactants. This decreases the reaction quotient, because the reaction is being pushed towards the left to reach equilibrium. The equilibrium constant, $K_b = 1.8 \times 10^{-5}$, does not change. The reaction is put out of balance, or equilibrium.

$$Q_a = \frac{[NH_4^+][OH^-]}{[NH_3]}$$

At first, when more hydroxide is added, the quotient is greater than the equilibrium constant. The reaction then shifts right, causing the denominator to increase, decreasing the reaction quotient and pulling towards equilibrium and causing Q to decrease towards K.

Common Ion Effect on Solubility

Consider, for example, the effect of adding a soluble salt, such as $CaCl_2$, to a saturated solution of calcium phosphate [$Ca_3(PO_4)_2$].

$$Ca_3(PO_4)_2(s) \rightleftharpoons 3\,Ca^{2+}(aq) + 2\,PO_4^{3-}(aq) \qquad (7.12.3.8)$$

We have seen that the solubility of $Ca_3(PO_4)_2$ in water at 25°C is 1.14×10^{-7} M ($K_{sp} = 2.07 \times 10^{-33}$). Thus a saturated solution of $Ca_3(PO_4)_2$ in water contains

$$3 \times (1.14 \times 10^{-7}\,M) = 3.42 \times 10^{-7}\,M\,Ca^{2+} \tag{7.12.3.9}$$

and

$$2 \times (1.14 \times 10^{-7}\,M) = 2.28 \times 10^{-7}\,M\,PO_4^{3-} \tag{7.12.3.10}$$

according to the stoichiometry shown in Equation 7.12.3.8 (neglecting hydrolysis to form HPO_4^{2-}). If $CaCl_2$ is added to a saturated solution of $Ca_3(PO_4)_2$, the Ca^{2+} ion concentration will increase such that $[Ca^{2+}] > 3.42 \times 10^{-7}$ M, making $Q > K_{sp}$. The only way the system can return to equilibrium is for the reaction in Equation 7.12.3.8 to proceed to the left, resulting in precipitation of $Ca_3(PO_4)_2$. This will decrease the concentration of both Ca^{2+} and PO_4^{3-} until $Q = K_{sp}$.

> *Adding a common ion decreases solubility, as the reaction shifts toward the left to relieve the stress of the excess product. Adding a common ion to a dissociation reaction causes the equilibrium to shift left, toward the reactants, causing precipitation.*

Example 7.12.3.5

Consider the reaction:

$$PbCl_2(s) \rightleftharpoons Pb^{2+}(aq) + 2Cl^-(aq)$$

What happens to the solubility of $PbCl_2$(s) when 0.1 M NaCl is added?

Solution

$$K_{sp} = 1.7 \times 10^{-5}$$

$$Q_{sp} = 1.8 \times 10^{-5}$$

Identify the common ion: Cl^-

Notice: $Q_{sp} > K_{sp}$ The addition of NaCl has caused the reaction to shift out of equilibrium because there are more dissociated ions. Typically, solving for the molarities requires the assumption that the solubility of $PbCl_2$ is equivalent to the concentration of Pb^{2+} produced because they are in a 1:1 ratio.

Because K_{sp} for the reaction is 1.7×10^{-5}, the overall reaction would be $(s)(2s)^2 = 1.7\times10^{-5}$. Solving the equation for s gives s= 1.62×10^{-2} M. The coefficient on Cl^- is 2, so it is assumed that twice as much Cl^- is produced as Pb^{2+}, hence the '2s.' The solubility equilibrium constant can be used to solve for the molarities of the ions at equilibrium.

The molarity of Cl^- added would be 0.1 M because Na^+ and Cl^- are in a 1:1 ration in the ionic salt, NaCl. Therefore, the overall molarity of Cl^- would be 2s + 0.1, with 2s referring to the contribution of the chloride ion from the dissociation of lead chloride.

$$\begin{aligned} Q_{sp} &= [Pb^{2+}][Cl^-]^2 \\ 1.8 \times 10^{-5} &= (s)(2s + 0.1)^2 \end{aligned} \tag{7.12.3.11}$$

$$\begin{aligned} s &= [Pb^{2+}] \\ &= 1.8 \times 10^{-3} M \\ 2s &= [Cl^-] \\ &\approx 0.1M \end{aligned} \tag{7.12.3.12}$$

Notice that the molarity of Pb^{2+} is lower when NaCl is added. The equilibrium constant remains the same because of the increased concentration of the chloride ion. To simplify the reaction, it can be assumed that $[Cl^-]$ is approximately 0.1M since the formation of the chloride ion from the dissociation of lead chloride is so small. The reaction quotient for $PbCl_2$ is greater than the equilibrium constant because of the added Cl^-. This therefore shift the reaction left towards equilibrium, causing precipitation and lowering the current solubility of the reaction. Overall, the solubility of the reaction decreases with the added sodium chloride.

The common ion effect usually decreases the solubility of a sparingly soluble salt.

Example 7.12.3.6

Calculate the solubility of calcium phosphate [$Ca_3(PO_4)_2$] in 0.20 M $CaCl_2$.

Given: concentration of $CaCl_2$ solution

Asked for: solubility of $Ca_3(PO_4)_2$ in $CaCl_2$ solution

Strategy:

A. Write the balanced equilibrium equation for the dissolution of $Ca_3(PO_4)_2$. Tabulate the concentrations of all species produced in solution.
B. Substitute the appropriate values into the expression for the solubility product and calculate the solubility of $Ca_3(PO_4)_2$.

Solution

A The balanced equilibrium equation is given in the following table. If we let x equal the solubility of $Ca_3(PO_4)_2$ in moles per liter, then the change in [Ca^{2+}] is once again +3x, and the change in [PO_4^{3-}] is +2x. We can insert these values into the ICE table.

$$Ca_3(PO_4)_{2(s)} \rightleftharpoons 3Ca^{2+}_{(aq)} + 2PO^{3-}_{4(aq)} \tag{7.12.3.13}$$

	$Ca_3(PO_4)_2$	[Ca^{2+}]	[PO_4^{3-}]
initial	pure solid	0.20	0
change	—	+3x	+2x
final	pure solid	0.20 + 3x	2x

B The K_{sp} expression is as follows:

$$K_{sp} = [Ca^{2+}]^3[PO_4^{3-}]^2 = (0.20 + 3x)^3(2x)^2 = 2.07\times10^{-33}$$

Because $Ca_3(PO_4)_2$ is a sparingly soluble salt, we can reasonably expect that x << 0.20. Thus (0.20 + 3x) M is approximately 0.20 M, which simplifies the K_{sp} expression as follows:

$$K_{sp} = (0.20)^3(2x)^2 = 2.07 \times 10^{-33}$$
$$x^2 = 6.5 \times 10^{-32}$$
$$x = 2.5 \times 10^{-16}\ \text{M}$$

This value is the solubility of $Ca_3(PO_4)_2$ in 0.20 M $CaCl_2$ at 25°C. It is approximately nine orders of magnitude less than its solubility in pure water, as we would expect based on Le Chatelier's principle. With one exception, this example is identical to Example **7.12.3.2**—here the initial [Ca^{2+}] was 0.20 M rather than 0.

Exercise 7.12.3.4

Calculate the solubility of silver carbonate in a 0.25 M solution of sodium carbonate. The solubility of silver carbonate in pure water is 8.45×10^{-12} at 25°C.

Answer

2.9×10^{-6} M (versus 1.3×10^{-4} M in pure water)



The Common Ion Effect in Solubility Products: https://youtu.be/_P3wozLs0Tc

Summary

Adding a common cation or common anion to a solution of a sparingly soluble salt shifts the solubility equilibrium in the direction predicted by Le Chatelier's principle. The solubility of the salt is almost always **decreased** by the presence of a common ion.

Contributors and Attributions

- Emmellin Tung and Mahtab Danai (UCD)
- Jim Clark (Chemguide.co.uk)
- Chung (Peter) Chieh (Professor Emeritus, Chemistry @ University of Waterloo)

7.12.3: Common-Ion Effect in Solubility Equilibria is shared under a not declared license and was authored, remixed, and/or curated by LibreTexts.

- **18.3: Common-Ion Effect in Solubility Equilibria** is licensed CC BY-NC-SA 4.0.

7.12.4: Limitations of the Ksp Concept

Solubility equilibria defined by a single, simple K_s expression are probably the exception rather than the rule. Such equilibria are often in competition with other reactions with such species as H^+or OH^-, complexing agents, oxidation-reduction, formation of other sparingly soluble species or, in the case of carbonates and sulfites, of gaseous products. The exact treatments of these systems can be extremely complicated, involving the solution of large sets of simultaneous equations. For most practical purposes it is sufficient to recognize the general trends, and to carry out approximate calculations.

The solubility product of an ionic compound describes the concentrations of ions in equilibrium with a solid, but what happens if some of the cations become associated with anions rather than being completely surrounded by solvent? Then predictions of the total solubility of the compound based on the assumption that the solute exists solely as discrete ions would differ substantially from the actual solubility, as would predictions of ionic concentrations. In general, four situations explain why the solubility of a compound may be other than expected: ion pair formation, the incomplete dissociation of molecular solutes, the formation of complex ions, and changes in pH.

The Diverse Ion Effect (The Salt Effect)

A sparingly-soluble salt will be more soluble in a solution that contains non-participating ions. This is just the opposite of the **common ion effect**, and it might at first seem rather counter-intuitive: why would adding more ions of any kind make a salt more likely to dissolve?

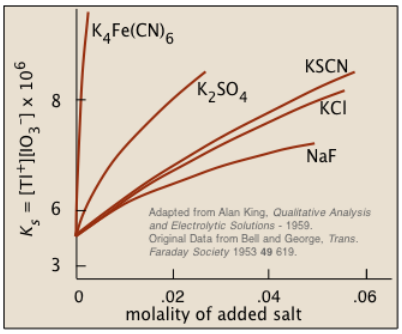


Figure 7.12.4.1: Solubility of thallium iodate in solutions containing dissolved salts

Although the concentrations of ions in equilibrium with a sparingly soluble solid are so low that they are essentially the same as the activities, the presence of other ions at concentrations of about 0.001 M or greater can materially reduce the activities of the dissolution products, permitting the solubilities to be greater than what simple equilibrium calculations would predict.

> *The Diverse Ion Effect typically has the opposite effect on solubility than the common ion effect.*

The higher the charge of the foreign ion, the more pronounced is the salt effect. This tells us that inter-ionic (and thus electrostatic) interactions must play a role. The details are rather complicated, but the general idea is that all ions in solution, besides possessing tightly-held waters of hydration, tend to attract oppositely-charged ions ("*counter-ions*") around them. This "atmosphere" of counterions is always rather diffuse, but much less so (and more tightly bound) when one or both kinds of ions have greater charges. From a distance, these ion-counterion pairs (or ion pairs) bodies appear to be almost electrically neutral, which keeps them from interacting with each other (as to form a precipitate).

Example 7.12.4.1

How does the solubility of $AgCl$ change in absence and presence of $NaNO_3$, given that the molar solubility product of $AgCl$ is 1.76×10^{-10}.

Solution

The Uncommon Ion Effect is a "real" effect and requires the activity definition of K_{sp} to address. The exact definition of the solubility constant is:

$$K_{sp} = a\{Ag^+\} \cdot a\{Cl^-\} = [Ag+]\gamma(Ag^+)[Cl^-]\gamma(Cl^-)$$

Where $a\{Ag^+\}$ and $a\{Cl^-\}$ are the activities of these ions in the presence of the $NaNO_3$. The γ values are the are the corresponding activity coefficients for the ions.

- In dilute solutions (i.e. absence of $NaNO_3$\)

$$\gamma(Ag^+) = \gamma(Cl^-) = 1$$

So, the solubility of $AgCl$ is then

$$[Ag^+] = \sqrt{K_{sp}} = 1.33 \times 10^{-5} \tag{7.12.4.1}$$

- In the presence of $NaNO_3$, the activity coefficients deviate from unity. So

$$[Ag^+] = \frac{\sqrt{K_{sp}}}{\sqrt{\gamma(Ag^+)\gamma(Cl^-)}} \tag{7.12.4.2}$$

. The denominator has to evaluated from an activity table and is 0.769 so \([Ag^+] = \dfrac{\sqrt{K_{sp}}}{0.769} = 1.73 \times 10^{-5}\].

Hence, in the presence of the $NaNO_3$ soluble salt, the molar solubility of the slightly soluble $AgCl$ salt *increases*. An opposite effect is expected if there were a common ions between the two salts.

Incomplete Dissociation of Solutes into Ions

An **ion pair** consists of a cation and an anion that are in intimate contact in solution, rather than separated by solvent (Figure 7.12.4.1). The ions in an ion pair are held together by the same attractive electrostatic force in ionic solids. As a result, the ions in an ion pair migrate as a single unit, whose net charge is the sum of the charges on the ions. In many ways, we can view an ion pair as a species intermediate between the ionic solid (in which each ion participates in many cation–anion interactions that hold the ions in a rigid array) and the completely dissociated ions in solution (where each is fully surrounded by water molecules and free to migrate independently).

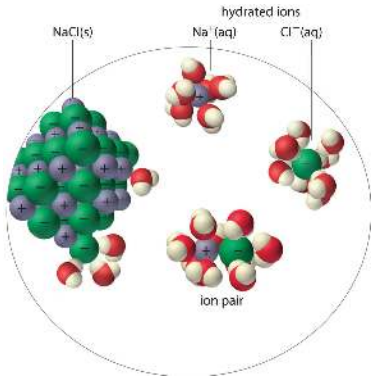


Figure 7.12.4.2: Ion-Pair Formation. In an ion pair, the cation and the anion are in intimate contact in solution and migrate as a single unit. They are not completely dissociated and individually surrounded by solvent molecules, as are the hydrated ions, which are free to migrate independently.

The overall effect is to reduce the concentrations of the less-shielded ions that are available to combine to form a precipitate. We say that the *thermodynamically-effective concentrations* of these ions are less than their "analytical" concentrations. Chemists refer to these effective concentrations as ionic *activities*, and they denote them by curly brackets $\{Ag^+\}$ as opposed to square brackets $[Ag^+]$ which refer to the nominal or analytical concentrations.

As illustrated for calcium sulfate in the following equation, a second equilibrium must be included to describe the solubility of salts that form ion pairs:

$$\underset{\text{ion pair}}{CaSO_4(s) \rightleftharpoons Ca^{2+} \cdot SO_4^{2-}(aq)} \rightleftharpoons Ca^{2+}(aq) + SO_4^{2-}(aq) \tag{7.12.4.3}$$

The ion pair is represented by the symbols of the individual ions separated by a dot, which indicates that they are associated in solution. The formation of an ion pair is a dynamic process, just like any other equilibrium, so a particular ion pair may exist only briefly before dissociating into the free ions, each of which may later associate briefly with other ions.

Ion-pair formation can have a major effect on the measured solubility of a salt. For example, the measured K_{sp} for calcium sulfate is 4.93×10^{-5} at 25°C. The solubility of $CaSO_4$ should be 7.02×10^{-3} M if the only equilibrium involved were as follows:

$$CaSO_{4(s)} \rightleftharpoons Ca^{2+}_{(aq)} + SO^{2-}_{4(aq)} \tag{7.12.4.4}$$

In fact, the experimentally measured solubility of calcium sulfate at 25°C is 1.6×10^{-2} M, almost twice the value predicted from its K_{sp}. The reason for the discrepancy is that the concentration of ion pairs in a saturated $CaSO_4$ solution is almost as high as the concentration of the hydrated ions. Recall that the magnitude of attractive electrostatic interactions is greatest for small, highly charged ions. Hence ion pair formation is most important for salts that contain M^{2+} and M^{3+} ions, such as Ca^{2+} and La^{3+}, and is relatively unimportant for salts that contain monopositive cations, except for the smallest, Li^+. We therefore expect a saturated solution of $CaSO_4$ to contain a high concentration of ion pairs and its solubility to be greater than predicted from its K_{sp}.

Simultaneous Equilibria (Side Reactions)

A molecular solute may also be more soluble than predicted by the measured concentrations of ions in solution due to incomplete dissociation. This is particularly common with weak organic acids. Although strong acids (HA) dissociate completely into their constituent ions (H^+ and A^-) in water, weak acids such as carboxylic acids do not ($K_a = 1.5 \times 10^{-5}$). However, the molecular (undissociated) form of a weak acid (HA) is often quite soluble in water; for example, acetic acid (CH_3CO_2H) is completely miscible with water. Many carboxylic acids, however, have only limited solubility in water, such as benzoic acid ($C_6H_5CO_2H$), with $K_a = 6.25 \times 10^{-5}$. Just as with calcium sulfate, we need to include an additional equilibrium to describe the solubility of benzoic acid:

$$C_6H_5CO_2H_{(s)} \rightleftharpoons C_6H_5CO_2H_{(aq)} \rightleftharpoons C_6H_5CO^-_{2(aq)} + H^+_{(aq)} \tag{7.12.4.5}$$

In a case like this, measuring only the concentration of the ions grossly underestimates the total concentration of the organic acid in solution. In the case of benzoic acid, for example, the pH of a saturated solution at 25°C is 2.85, corresponding to $[H^+] = [C_6H_5CO_2^-] = 1.4 \times 10^{-3}$ M. The total concentration of benzoic acid in the solution, however, is 2.8×10^{-2} M. Thus approximately 95% of the benzoic acid in solution is in the form of hydrated neutral molecules—$C_6H_5CO_2H_{(aq)}$—and only about 5% is present as the dissociated ions (Figure **7.12.4.3**).

> *Incomplete dissociation of a molecular solute that is miscible with water can increase the solubility of the solute.*

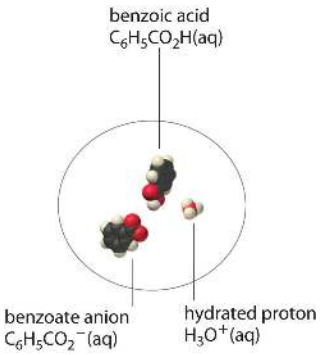


Figure **7.12.4.3**: Incomplete Dissociation of a Molecular Solute. In a saturated solution of benzoic acid in water at 25°C, only about 5% of the dissolved benzoic acid molecules are dissociated to form benzoate anions and hydrated protons. The remaining 95% exists in solution in the form of hydrated neutral molecules. (H_2O molecules are omitted for clarity.)

Although ion pairs, such as $Ca^{2+} \cdot SO_4^{2-}$, and undissociated electrolytes, such as $C_6H_5CO_2H$, are both electrically neutral, there is a major difference in the forces responsible for their formation. Simple electrostatic attractive forces between the cation and the anion hold the ion pair together, whereas a polar covalent O−H bond holds together the undissociated electrolyte.

Example 7.12.4.2: CdI_2 Solubility

The dissolution of cadmium iodide is water is commonly represented as

$$CdI_{2(s)} \rightleftharpoons Cd^{2+} + 2I^- \tag{7.12.4.6}$$

What you were likely taught about the dissociation of salts in water is wrong! To most students (and to most of their teachers!), this would imply that a 0.1$\underline{M}$ solution of this salt would contain 0.1$\underline{M}$ of $Cd^{2+}(aq)$ — and this would be seriously in error because it fails to take into account that the two ions react with each other.

Firstly, they combine to form neutral, largely-covalent molecular species:

$$Cd^{2+}_{(aq)} + 2I^-_{(aq)} \rightarrow CdI_{2(aq)} \tag{7.12.4.7}$$

This non-ionic form accounts for 78% of the Cd present in the solution! In addition, they form a molecular ion $CdI^-_{(aq)}$ according to the following scheme:

Table 7.12.4.1: CdI2 species in solution

$CdI_{2(s)} \rightleftharpoons Cd^{2+} + 2I^-$	$K_1 = 10^{-3.9}$
$Cd^{2+} + I^- \rightleftharpoons CdI^+$	$K_2 = 10^{+2.3}$
$CdI2_{(s)} \rightleftharpoons CdI^+ + I^-$	$K = 10^{-1.6} = 0.023$

As a consequence, the concentration of "free" Cd^{2+}(aq) in an aqueous cadmium iodide solution is only about 2% of the value you would calculate by taking K_1 as the solubility product. The principal component of such as solution is actually [covalently-bound] CdI_2(aq). It turns out that

Many salts, especially those of metals beyond Group 2, are similarly only partially ionized in aqueous solution:

Table 7.12.4.2: Incomplete Dissociation of Select Salts

salt	molarity	% cation	other species
KCl	0.52	95	KCl(aq) 5%
$MgSO_4$	0.04	58	$MgSO_4$(aq) 42%
$CaCl_2$	0.44	70	$CaCl^+$(aq) 30%
$CuSO_4$	0.045	56	$CuSO_4$(aq) 44%
CdI_2	0.50	2	CdI_2(aq) 76%, CdI^-(aq) 22%
$FeCl_3$	0.1	10	$FeCl^{2+}$(aq) 42%, $FeCl_2$(aq) 40%, $FeOH^{2+}$(aq) 6%, $Fe(OH)_2^+$(aq) 2%

The data shown Tables 7.12.4.1 and 7.12.4.2 are taken from the article *Salts are Mostly NOT Ionized* by Stephen Hawkes: 1996 *J Chem Educ.* 73(5) 421-423. This fact was stated by Arrhenius in 1887, but has been largely ignored and is rarely mentioned in standard textbooks.

Summary

The solubility constant, as with all equilibrium constants, are properly defined in terms of *effective concentrations* (activities) and the use of true concentrations to approximate activities in equilibrium constants can often fail. As with all approximations, it is important to understand the conditions that it will fail. three examples are discussed. The salt effect refers to the fact that the presence of a salt which has no ion in common with the solute, has an effect on the ionic strength of the solution and hence on activity coefficients, so that the equilibrium constant, expressed as a concentration quotient, changes.

Contributors and Attributions

- Wikipedia
- Stephen Lower, Professor Emeritus (Simon Fraser U.) Chem1 Virtual Textbook
- Yomen Atassi (via StackExchange)

7.12.4: Limitations of the Ksp Concept is shared under a not declared license and was authored, remixed, and/or curated by LibreTexts.

- **18.4: Limitations of the K_{sp} Concept** is licensed CC BY-NC-SA 4.0.

7.12.5: Criteria for Precipitation and its Completeness

The equation that describes the equilibrium between solid calcium carbonate and its solvated ions is:

$$\mathrm{CaCO_3}(s) \rightleftharpoons \mathrm{Ca^{2+}}(aq) + \mathrm{CO_3^{2-}}(aq) \tag{7.12.5.1}$$

We can establish this equilibrium either by adding solid calcium carbonate to water or by mixing a solution that contains calcium ions with a solution that contains carbonate ions. If we add calcium carbonate to water, the solid will dissolve until the concentrations are such that the value of the reaction quotient ($Q = [\mathrm{Ca^{2+}}][\mathrm{CO_3^{2-}}]$) is equal to the solubility product ($K_{sp} = 4.8 \times 10^{-9}$). If we mix a solution of calcium nitrate, which contains Ca^{2+} ions, with a solution of sodium carbonate, which contains $\mathrm{CO_3^{2-}}$ ions, the slightly soluble ionic solid $CaCO_3$ will precipitate, provided that the concentrations of Ca^{2+} and $\mathrm{CO_3^{2-}}$ ions are such that Q is greater than K_{sp} for the mixture. The reaction shifts to the left and the concentrations of the ions are reduced by formation of the solid until the value of Q equals K_{sp}. A saturated solution in equilibrium with the undissolved solid will result. If the concentrations are such that Q is less than K_{sp}, then the solution is not saturated and no precipitate will form.

We can compare numerical values of Q with K_{sp} to predict whether precipitation will occur, as Example **7.12.5.7** shows. (Note: Since all forms of equilibrium constants are temperature dependent, we will assume a room temperature environment going forward in this chapter unless a different temperature value is explicitly specified.)

The first step in the preparation of magnesium metal is the precipitation of $Mg(OH)_2$ from sea water by the addition of lime, $Ca(OH)_2$, a readily available inexpensive source of OH^- ion:

$$\mathrm{Mg(OH)_2}(s) \rightleftharpoons \mathrm{Mg^{2+}}(aq) + 2\,\mathrm{OH^-}(aq) \quad K_{sp} = 2.1 \times 10^{-13} \tag{7.12.5.2}$$

The concentration of $Mg^{2+}(aq)$ in sea water is 0.0537 *M*. Will $Mg(OH)_2$ precipitate when enough $Ca(OH)_2$ is added to give a $[OH^-]$ of 0.0010 *M*?

Solution

This problem asks whether the reaction:

$$\mathrm{Mg(OH)_2}(s) \rightleftharpoons \mathrm{Mg^{2+}}(aq) + 2\,\mathrm{OH^-}(aq) \tag{7.12.5.3}$$

shifts to the left and forms solid $Mg(OH)_2$ when $[Mg^{2+}] = 0.0537$ *M* and $[OH^-] = 0.0010$ *M*. The reaction shifts to the left if Q is greater than K_{sp}. Calculation of the reaction quotient under these conditions is shown here:

$$Q = [\mathrm{Mg^{2+}}][\mathrm{OH^-}]^2 = (0.0537)(0.0010)^2 = 5.4 \times 10^{-8} \tag{7.12.5.4}$$

Because Q is greater than K_{sp} ($Q = 5.4 \times 10^{-8}$ is larger than $K_{sp} = 2.1 \times 10^{-13}$), we can expect the reaction to shift to the left and form solid magnesium hydroxide. $Mg(OH)_2(s)$ forms until the concentrations of magnesium ion and hydroxide ion are reduced sufficiently so that the value of Q is equal to K_{sp}.

? Exercise 7.12.5.1

Use the solubility products in Appendix J to determine whether $CaHPO_4$ will precipitate from a solution with $[Ca^{2+}] = 0.0001$ *M* and $[\mathrm{HPO_4^{2-}}] = 0.001$ *M*.

Answer

No precipitation of $CaHPO_4$; $Q = 1 \times 10^{-7}$, which is less than K_{sp}

✔ Precipitation of AgCl upon Mixing Solutions

Does silver chloride precipitate when equal volumes of a 2.0×10^{-4}-*M* solution of $AgNO_3$ and a 2.0×10^{-4}-*M* solution of NaCl are mixed?

(Note: The solution also contains Na^+ and $\mathrm{NO_3^-}$ ions, but when referring to solubility rules, one can see that sodium nitrate is very soluble and cannot form a precipitate.)

Solution

The equation for the equilibrium between solid silver chloride, silver ion, and chloride ion is:

$$\mathrm{AgCl}(s) \rightleftharpoons \mathrm{Ag^+}(aq) + \mathrm{Cl^-}(aq)$$

The solubility product is 1.8×10^{-10} (see Appendix J).

AgCl will precipitate if the reaction quotient calculated from the concentrations in the mixture of $AgNO_3$ and NaCl is greater than K_{sp}. The volume doubles when we mix equal volumes of $AgNO_3$ and NaCl solutions, so each concentration is reduced to half its initial value. Consequently, immediately upon mixing, $[Ag^+]$ and $[Cl^-]$ are both equal to:

$$\frac{1}{2}(2.0 \times 10^{-4})\ M = 1.0 \times 10^{-4}\ M$$

The reaction quotient, Q, is *momentarily* greater than K_{sp} for AgCl, so a supersaturated solution is formed:

$$Q = [\mathrm{Ag^+}][\mathrm{Cl^-}] = (1.0 \times 10^{-4})(1.0 \times 10^{-4}) = 1.0 \times 10^{-8} > K_{sp}$$

Since supersaturated solutions are unstable, AgCl will precipitate from the mixture until the solution returns to equilibrium, with Q equal to K_{sp}.

Exercise 7.12.5.2

Will $KClO_4$ precipitate when 20 mL of a 0.050-*M* solution of K^+ is added to 80 mL of a 0.50-*M* solution of ClO_4^-? (Remember to calculate the new concentration of each ion after mixing the solutions before plugging into the reaction quotient expression.)

Answer

No, $Q = 4.0 \times 10^{-3}$, which is less than $K_{sp} = 1.07 \times 10^{-2}$

In the previous two examples, we have seen that $Mg(OH)_2$ or AgCl precipitate when Q is greater than K_{sp}. In general, when a solution of a soluble salt of the M^{m+} ion is mixed with a solution of a soluble salt of the X^{n-} ion, the solid, M_pX_q precipitates if the value of Q for the mixture of M^{m+} and X^{n-} is greater than K_{sp} for M_pX_q. Thus, if we know the concentration of one of the ions of a slightly soluble ionic solid and the value for the solubility product of the solid, then we can calculate the concentration that the other ion must exceed for precipitation to begin. To simplify the calculation, we will assume that precipitation begins when the reaction quotient becomes equal to the solubility product constant.

Precipitation of Calcium Oxalate

Blood will not clot if calcium ions are removed from its plasma. Some blood collection tubes contain salts of the oxalate ion, $C_2O_4^{2-}$, for this purpose (Figure 7.12.5.4). At sufficiently high concentrations, the calcium and oxalate ions form solid, $CaC_2O_4 \cdot H_2O$ (which also contains water bound in the solid). The concentration of Ca^{2+} in a sample of blood serum is 2.2×10^{-3} *M*. What concentration of $C_2O_4^{2-}$ ion must be established before $CaC_2O_4 \cdot H_2O$ begins to precipitate?



Figure 7.12.5.4: Anticoagulants can be added to blood that will combine with the Ca^{2+} ions in blood serum and prevent the blood from clotting. (credit: modification of work by Neeta Lind)

Solution

The equilibrium expression is:

$$\mathrm{CaC_2O_4}(s) \rightleftharpoons \mathrm{Ca^{2+}}(aq) + \mathrm{C_2O_4^{2-}}(aq) \tag{7.12.5.5}$$

For this reaction:

$$K_{sp} = [\mathrm{Ca^{2+}}][\mathrm{C_2O_4^{2-}}] = 2.27 \times 10^{-9} \tag{7.12.5.6}$$

(see Appendix J)

CaC_2O_4 does not appear in this expression because it is a solid. Water does not appear because it is the solvent.

Solid CaC_2O_4 does not begin to form until Q equals K_{sp}. Because we know K_{sp} and $[Ca^{2+}]$, we can solve for the concentration of $\mathrm{C_2O_4^{2-}}$ that is necessary to produce the first trace of solid:

$$\begin{gathered} Q = K_{sp} = [\mathrm{Ca^{2+}}][\mathrm{C_2O_4^{2-}}] = 2.27 \times 10^{-9} \\ (2.2 \times 10^{-3})[\mathrm{C_2O_4^{2-}}] = 2.27 \times 10^{-9} \\ [\mathrm{C_2O_4^{2-}}] = \frac{2.27 \times 10^{-9}}{2.2 \times 10^{-3}} = 1.0 \times 10^{-6} \end{gathered}$$

A concentration of $[\mathrm{C_2O_4^{2-}}] = 1.0 \times 10^{-6}\ M$ is necessary to initiate the precipitation of CaC_2O_4 under these conditions.

Exercise 7.12.5.3

If a solution contains 0.0020 mol of $\mathrm{CrO_4^{2-}}$ per liter, what concentration of Ag^+ ion must be reached by adding solid $AgNO_3$ before Ag_2CrO_4 begins to precipitate? Neglect any increase in volume upon adding the solid silver nitrate.

Answer:

$7.0 \times 10^{-5}\ M$

It is sometimes useful to know the concentration of an ion that remains in solution after precipitation. We can use the solubility product for this calculation too: If we know the value of K_{sp} and the concentration of one ion in solution, we can calculate the concentration of the second ion remaining in solution. The calculation is of the same type as that in Example—calculation of the concentration of a species in an equilibrium mixture from the concentrations of the other species and the equilibrium constant. However, the concentrations are different; we are calculating concentrations after precipitation is complete, rather than at the start of precipitation.

Concentrations Following Precipitation

Clothing washed in water that has a manganese $[Mn^{2+}(aq)]$ concentration exceeding 0.1 mg/L ($1.8 \times 10^{-6}\ M$) may be stained by the manganese upon oxidation, but the amount of Mn^{2+} in the water can be reduced by adding a base. If a person doing laundry wishes to add a buffer to keep the pH high enough to precipitate the manganese as the hydroxide, $Mn(OH)_2$, what pH is required to keep $[Mn^{2+}]$ equal to $1.8 \times 10^{-6}\ M$?

Solution The dissolution of $Mn(OH)_2$ is described by the equation:

$$\mathrm{Mn(OH)_2}(s) \rightleftharpoons \mathrm{Mn^{2+}}(aq) + 2\,\mathrm{OH^-}(aq) \quad K_{sp} = 4.5 \times 10^{-14} \tag{7.12.5.7}$$

We need to calculate the concentration of OH^- when the concentration of Mn^{2+} is $1.8 \times 10^{-6}\ M$. From that, we calculate the pH. At equilibrium:

$$K_{sp} = [\mathrm{Mn^{2+}}][\mathrm{OH^-}]^2 \tag{7.12.5.8}$$

or

$$(1.8 \times 10^{-6})[\mathrm{OH^-}]^2 = 4.5 \times 10^{-14} \tag{7.12.5.9}$$

so

$$[\mathrm{OH^-}] = 1.6 \times 10^{-4}\ M \tag{7.12.5.10}$$

Now we calculate the pH from the pOH:

$$\text{pOH} = -\log[\text{OH}^-] = -\log(1.6 \times 10^{-4}) = 3.80$$
$$\text{pH} = 14.00 - \text{pOH} = 14.00 - 3.80 = 10.20$$

If the person doing laundry adds a base, such as the sodium silicate (Na_4SiO_4) in some detergents, to the wash water until the pH is raised to 10.20, the manganese ion will be reduced to a concentration of 1.8×10^{-6} *M*; at that concentration or less, the ion will not stain clothing.

? Exercise 7.12.5.4

The first step in the preparation of magnesium metal is the precipitation of $Mg(OH)_2$ from sea water by the addition of $Ca(OH)_2$. The concentration of $Mg^{2+}(aq)$ in sea water is 5.37×10^{-2} *M*. Calculate the pH at which $[Mg^{2+}]$ is diminished to 1.0×10^{-5} *M* by the addition of $Ca(OH)_2$.

Answer

11.09

Due to their light sensitivity, mixtures of silver halides are used in fiber optics for medical lasers, in photochromic eyeglass lenses (glass lenses that automatically darken when exposed to sunlight), and—before the advent of digital photography—in photographic film. Even though AgCl ($K_{sp} = 1.6 \times 10^{-10}$), AgBr ($K_{sp} = 7.7 \times 10^{-13}$), and AgI ($K_{sp} = 8.3 \times 10^{-17}$) are each quite insoluble, we cannot prepare a homogeneous solid mixture of them by adding Ag^+ to a solution of Cl^-, Br^-, and I^-; essentially all of the AgI will precipitate before any of the other solid halides form because of its smaller value for K_{sp}. However, we can prepare a homogeneous mixture of the solids by slowly adding a solution of Cl^-, Br^-, and I^- to a solution of Ag^+.

When two anions form slightly soluble compounds with the same cation, or when two cations form slightly soluble compounds with the same anion, the less soluble compound (usually, the compound with the smaller K_{sp}) generally precipitates first when we add a precipitating agent to a solution containing both anions (or both cations). When the K_{sp} values of the two compounds differ by two orders of magnitude or more (e.g., 10^{-2} vs. 10^{-4}), almost all of the less soluble compound precipitates before any of the more soluble one does. This is an example of selective precipitation, where a reagent is added to a solution of dissolved ions causing one of the ions to precipitate out before the rest.



Determining if a Precipitate forms (The Ion Product): https://youtu.be/Naf7PoHPz8Y

Summary

A slightly soluble electrolyte begins to precipitate when the magnitude of the reaction quotient for the dissolution reaction exceeds the magnitude of the solubility product. Precipitation continues until the reaction quotient equals the solubility product. A reagent can be added to a solution of ions to allow one ion to selectively precipitate out of solution. The common ion effect can also play a role in precipitation reactions. In the presence of an ion in common with one of the ions in the solution, Le Chatelier's principle applies and more precipitate comes out of solution so that the molar solubility is reduced.

Glossary

common ion effect

effect on equilibrium when a substance with an ion in common with the dissolved species is added to the solution; causes a decrease in the solubility of an ionic species, or a decrease in the ionization of a weak acid or base

molar solubility

solubility of a compound expressed in units of moles per liter (mol/L)

selective precipitation

process in which ions are separated using differences in their solubility with a given precipitating reagent

solubility product (K_{sp})

equilibrium constant for the dissolution of a slightly soluble electrolyte

Contributors and Attributions

- Paul Flowers (University of North Carolina - Pembroke), Klaus Theopold (University of Delaware) and Richard Langley (Stephen F. Austin State University) with contributing authors. Textbook content produced by OpenStax College is licensed under a Creative Commons Attribution License 4.0 license. Download for free at http://cnx.org/contents/85abf193-2bd...a7ac8df6@9.110).

7.12.5: Criteria for Precipitation and its Completeness is shared under a not declared license and was authored, remixed, and/or curated by LibreTexts.

- **18.5: Criteria for Precipitation and its Completeness** is licensed CC BY-NC-SA 4.0.

7.12.6: Fractional Precipitation

Learning Objectives

- Calculate ion concentrations to maintain a heterogeneous equilibrium.
- Calculate pH required to precipitate a metal hydroxide.
- Design experiments to separate metal ions in a solution of mixtures of metals.

A mixture of metal ions in a solution can be separated by precipitation with anions such as Cl^-, Br^-, SO_4^{2-}, CO_3^{2-}, S^{2-}, $Cr_2O_4^{2-}$, PO_4^{2-}, OH^- etc. When a metal ion or a group of metal ions form insoluble salts with a particular anion, they can be separated from others by precipitation. We can also separate the anions by precipitating them with appropriate metal ions. There are no definite dividing lines between **insoluble salts, sparingly soluble**, and **soluble salts**, but concentrations of their saturated solutions are small, medium, and large. Solubility products are usually listed for insoluble and sparingly soluble salts, but they are not given for soluble salts. Solubility products for soluble salts are very large.

What type of salts are usually soluble, sparingly soluble and insoluble? The following are some general guidelines, but these are not precise laws.

- All nitrates are soluble. The singly charged large NO_3^- ions form salts with high solubilities. So do ClO_4^-, ClO_3^-, NO_2^-, $HCOO^-$, and CH_3COO^-.
- All chlorides, bromides, and iodides are soluble except those of Ag^+, Hg_2^{2+}, and Pb^{2+}. CaF_2, BaF_2, and PbF_2 are also insoluble.
- All sulfates are soluble, except those of Ba^{2+}, Sr^{2+}, and Pb^{2+}. The doubly charged sulfates are usually less soluble than halides and nitrates.
- Most singly charge cations K^+, Na^+, NH_4^+ form soluble salts. However, $K_3Co(NO_2)_6$ and $(NH_4)_3Co(NO_2)_6$ are insoluble.

These are handy rules for us to have if we deal with salts often. On the other hand, solubility is an important physical property of a substance, and these properties are listed in handbooks.

Chemical Separation of Metal Ions

Formation of crystals from a saturated solution is a **heterogeneous equilibrium** phenomenon, and it can be applied to separate various chemicals or ions in a solution. When solubilities of two metal salts are very different, they can be separated by precipitation. The K_{sp} values for various salts are valuable information, and some data are given in Table E3. In the first two examples, we show how barium and strontium can be separated as chromate.

Example 7.12.6.1

The K_{sp} for strontium chromate is 3.6×10^{-5} and the K_{sp} for barium chromate is 1.2×10^{-10}. What concentration of potassium chromate will precipitate the maximum amount of either the barium or the strontium chromate from an equimolar 0.30 M solution of barium and strontium ions without precipitating the other?

Solution

Since the K_{sp} for barium chromate is smaller, we know that $BaCrO_4$ will form a precipitate first as $[CrO_4^{2-}]$ increases so that Q_{sp} for $BaCrO_4$ also increases from zero to K_{sp} of $BaCrO_4$, at which point, $BaCrO_4$ precipitates. As $[CrO_4^{2-}]$ increases, $[Ba^{2+}]$ decreases. Further increase of $[CrO_4^{2-}]$ till Q_{sp} for $SrCrO_4$ increases to K_{sp} of $SrCrO_4$; it then precipitates.

Let us write the equilibrium equations and data down to help us think. Let x be the concentration of chromate to precipitate Sr^{2+}, and y be that to precipitate Ba^{2+}:

$$SrCrO_4(s) \rightarrow Sr^{2+}(aq) + CrO_4^{2-}(aq)$$

According to the definition of K_{sp} we have we have $K_{sp} = (0.30)(x) = 3.6 \times 10^{-5}$. Solving for x gives

$$x = \frac{3.6 \times 10^{-5}}{0.30} = 1.2 \times 10^{-4} M$$

Further, let y be the concentration of chromate to precipitate precipitate Ba^{2+}:

$$BaCrO_4(s) \rightarrow Ba^{2+}(aq) + CrO_4{}^{2-}(aq)$$

with $K_{sp} = (0.30)(y) = 1.2 \times 10^{-10}$. Solving for y gives

$$y = \frac{1.2 \times 10^{-10}}{0.30} = 4.0 \times 10^{-10}\ M$$

The K_{sp}'s for the two salts indicate $BaCrO_4$ to be much less soluble, and it will precipitate before any $SrCrO_4$ precipitates. If chromate concentration is maintained less than $1.2 \times 10^{-4} M$, then all Sr^{2+} ions will remain in the solution.

Discussion

In reality, controling the increase of $[CrO_4{}^{2-}]$ is very difficult.

Example 7.12.6.2

The K_{sp} for strontium chromate is 3.6×10^{-5} and the K_{sp} for barium chromate is 1.2×10^{-10}. Potassium chromate is added a small amount at a time to first precipitate $BaCrO_4$. Calculate $[Ba^{2+}]$ when the first trace of $SrCrO_4$ precipitate starts to form in a solution that contains 0.30 M each of Ba^{2+} and Sr^{2+} ions.

Solution

From the solution given in Example 7.12.6.1, $[CrO_4{}^{2-}] = 3.6 \times 10^{-4}\ M$ when $SrCrO_4$ starts to form. At this concentration, the $[Ba^{2+}]$ is estimated at $3.6 \times 10^{-4} = 1.2 \times 10^{-10}$.

The K_{sp} of $BaCrO_4$.

Thus,

$$[Ba^{2+}] = 3.33 \times 10^{-7}\ M$$

Very small indeed, compared to 0.30. In the fresh precipitate of $SrCrO_4$, the molar ratio of $SrCrO_4$ to $BaCrO_4$ is

$$\frac{0.30}{3.33 \times 10^{-7}} = 9.0 \times 10^{5}.$$

Hence, the amount of Ba^{2+} ion in the solid is only 1×10^{-6} (i.e., 1 ppm) of all metal ions, providing that all the solid was removed when

$$[CrO_4{}^{2-}] = 3.6 \times 10^{-4} M.$$

Discussion

The calculation shown here indicates that the separation of Sr and Ba is pretty good. In practice, an impurity level of 1 ppm is a very small value.

Example 7.12.6.3

What reagent should you use to separate silver and lead ions that are present in a solution? What data or information will be required for this task?

Solution

The K_{sp}'s for salts of silver and lead are required. We list the K_{sp}'s for chlorides and sulfates in a table here. These value are found in the Handbook Menu of our website as Salts K_{sp}.

Solutions to Example 17.6.3

Because the K_{sp}'s $AgCl$ and $PbCl_2$ are very different, chloride, Cl^-, apppears a good choice of negative ions for their separation.

The literature also indicates that $PbCl_2$ is rather soluble in warm water, and by heating the solution to 350 K (80°C), you can keep Pb^{2+} ions in solution and precipitate $AgCl$ as a solid. The solubility of $AgCl$ is very small even at high temperatures.

Discussion

Find more detailed information about the solubility of lead chloride as a function of temperature.

Salt	K_{sp}	Salt	K_{sp}
$AgCl$	1.8×10^{-10}	Ag_2SO_4	1.4×10^{-5}
Hg_2Cl_2	1.3×10^{-18}	$BaSO_4$	1.1×10^{-10}
$PbCl_2$	1.7×10^{-5}	$CaSO_4$	2.4×10^{-5}
		$PbSO_4$	6.3×10^{-7}
		$SrSO_4$	3.2×10^{-7}

Can sulfate be used to separate silver and lead ions? Which one will form a precipitate first as the sulfate ion concentration increases? What is the $[Pb^{2+}]$ when Ag_2SO_4 begins to precipitate in a solution that contains 0.10 M Ag^+?



The Separation of Two Ions by a Difference in Solubility: The Separation of Two Ions by a Difference in Solubility(opens in new window) [youtu.be]

7.12.6: Fractional Precipitation is shared under a not declared license and was authored, remixed, and/or curated by LibreTexts.

- **17.6: Precipitation and Separation of Ions** by Chung (Peter) Chieh is licensed CC BY-NC-SA 3.0.

7.12.7: Solubility and pH

Learning Objectives

- To understand why the solubility of many compounds depends on pH.

The solubility of many compounds depends strongly on the pH of the solution. For example, the anion in many sparingly soluble salts is the conjugate base of a weak acid that may become protonated in solution. In addition, the solubility of simple binary compounds such as oxides and sulfides, both strong bases, is often dependent on pH. In this section, we discuss the relationship between the solubility of these classes of compounds and pH.

The Effect of Acid–Base Equilibria the Solubility of Salts

We begin our discussion by examining the effect of pH on the solubility of a representative salt, $\mathbf{M^+A^-}$, where $\mathbf{A^-}$ is the conjugate base of the weak acid **HA**. When the salt dissolves in water, the following reaction occurs:

$$\mathbf{MA\,(s)} \rightleftharpoons \mathbf{M^+\,(aq) + A^-\,(aq)}$$

with

$$K_{sp} = [\mathrm{M^+}][\mathrm{A^-}]$$

The anion can also react with water in a hydrolysis reaction:

$$\mathbf{A^-\,(aq) + H_2O\,(l)} \rightleftharpoons \mathbf{OH^-\,(aq) + HA\,(aq)} \tag{7.12.7.1}$$

Because of the reaction described in Equation 7.12.7.1, the predicted solubility of a sparingly soluble salt that has a basic anion such as S^{2-}, PO_4^{3-}, or CO_3^{2-} is increased. If instead a strong acid is added to the solution, the added H^+ will react essentially completely with A^- to form HA. This reaction decreases $[A^-]$, which decreases the magnitude of the ion product

$$Q = [\mathrm{M^+}][\mathrm{A^-}] \tag{7.12.7.2}$$

According to Le Chatelier's principle, more MA will dissolve until $Q = K_{sp}$. Hence an acidic pH dramatically increases the solubility of virtually all sparingly soluble salts whose anion is the conjugate base of a weak acid. In contrast, pH has little to no effect on the solubility of salts whose anion is the conjugate base of a stronger weak acid or a strong acid, respectively (e.g., chlorides, bromides, iodides, and sulfates). For example, the hydroxide salt $Mg(OH)_2$ is relatively insoluble in water:

$$Mg(OH)_{2(s)} \rightleftharpoons Mg^{2+}(aq) + 2OH^-(aq) \tag{7.12.7.3}$$

with

$$K_{sp} = 5.61 \times 10^{-12} \tag{7.12.7.4}$$

When acid is added to a saturated solution that contains excess solid $Mg(OH)_2$, the following reaction occurs, removing OH^- from solution:

$$H^+(aq) + OH^-(aq) \rightarrow H_2O(l) \tag{7.12.7.5}$$

The overall equation for the reaction of $Mg(OH)_2$ with acid is thus

$$Mg(OH)_{2(s)} + 2H^+(aq) \rightleftharpoons Mg^{2+}(aq) + 2H_2O(l) \tag{7.12.7.6}$$

As more acid is added to a suspension of $Mg(OH)_2$, the equilibrium shown in Equation 7.12.7.6 is driven to the right, so more $Mg(OH)_2$ dissolves.

Such pH-dependent solubility is not restricted to salts that contain anions derived from water. For example, CaF_2 is a sparingly soluble salt:

$$CaF_{2(s)} \rightleftharpoons Ca^{2+}(aq) + 2F^-(aq) \tag{7.12.7.7}$$

with

$$K_{sp} = 3.45 \times 10^{-11} \tag{7.12.7.8}$$

When strong acid is added to a saturated solution of CaF_2, the following reaction occurs:

$$H^+(aq) + F^-(aq) \rightleftharpoons HF(aq) \tag{7.12.7.9}$$

Because the forward reaction decreases the fluoride ion concentration, more CaF_2 dissolves to relieve the stress on the system. The net reaction of CaF_2 with strong acid is thus

$$CaF_{2(s)} + 2H^+(aq) \rightarrow Ca^{2+}(aq) + 2HF(aq) \tag{7.12.7.10}$$

Example **7.12.7.1** shows how to calculate the solubility effect of adding a strong acid to a solution of a sparingly soluble salt.

> *Sparingly soluble salts derived from weak acids tend to be more soluble in an acidic solution.*

Example 7.12.7.1

Lead oxalate (PbC_2O_4), lead iodide (PbI_2), and lead sulfate ($PbSO_4$) are all rather insoluble, with K_{sp} values of 4.8×10^{-10}, 9.8×10^{-9}, and 2.53×10^{-8}, respectively. What effect does adding a strong acid, such as perchloric acid, have on their relative solubilities?

Given: K_{sp} values for three compounds

Asked for: relative solubilities in acid solution

Strategy:

Write the balanced chemical equation for the dissolution of each salt. Because the strongest conjugate base will be most affected by the addition of strong acid, determine the relative solubilities from the relative basicity of the anions.

Solution

The solubility Equilibria for the three salts are as follows:

$$PbC_2O_{4(s)} \rightleftharpoons Pb^{2+}(aq) + C_2O^{2-}_{4(aq)}$$

$$PbI_{2(s)} \rightleftharpoons Pb^{2+}(aq) + 2I^-(aq)$$

$$PbSO_{4(s)} \rightleftharpoons Pb^{2+}(aq) + SO^{2-}_{4(aq)}$$

The addition of a strong acid will have the greatest effect on the solubility of a salt that contains the conjugate base of a weak acid as the anion. Because HI is a strong acid, we predict that adding a strong acid to a saturated solution of PbI_2 will not greatly affect its solubility; the acid will simply dissociate to form H^+(aq) and the corresponding anion. In contrast, oxalate is the fully deprotonated form of oxalic acid (HO_2CCO_2H), which is a weak diprotic acid (pK_{a1} = 1.23 and pK_{a2} = 4.19). Consequently, the oxalate ion has a significant affinity for one proton and a lower affinity for a second proton. Adding a strong acid to a saturated solution of lead oxalate will result in the following reactions:

$$C_2O^{2-}_{4(aq)} + H^+(aq) \rightarrow HO_2CCO^-_{2(aq)}$$

$$HO_2CCO^-_{2(aq)} + H^+(aq) \rightarrow HO_2CCO_2H(aq)$$

These reactions will decrease $[C_2O_4{}^{2-}]$, causing more lead oxalate to dissolve to relieve the stress on the system. The pK_a of $HSO_4{}^-$ (1.99) is similar in magnitude to the pK_{a1} of oxalic acid, so adding a strong acid to a saturated solution of $PbSO_4$ will result in the following reaction:

$$SO^{2-}_{4(aq)} + H^+(aq) \rightleftharpoons HSO^-_{4(aq)}$$

Because $HSO_4{}^-$ has a pKa of 1.99, this reaction will lie largely to the left as written. Consequently, we predict that the effect of added strong acid on the solubility of $PbSO_4$ will be significantly less than for PbC_2O_4.

? Exercise 7.12.7.1

Which of the following insoluble salts—AgCl, Ag_2CO_3, Ag_3PO_4, and/or AgBr—will be substantially more soluble in 1.0 M HNO_3 than in pure water?

Answer

Ag_2CO_3 and Ag_3PO_4



Solubility Products and pH: https://youtu.be/XJ0s5SATZgQ

Caves and their associated pinnacles and spires of stone provide one of the most impressive examples of pH-dependent solubility Equilbria(part (a) in Figure **7.12.7.1**:). Perhaps the most familiar caves are formed from limestone, such as Carlsbad Caverns in New Mexico, Mammoth Cave in Kentucky, and Luray Caverns in Virginia. The primary reactions that are responsible for the formation of limestone caves are as follows:

$$\mathrm{CO_2\,(aq) + H_2O\,(l) \rightleftharpoons H^+\,(aq) + HCO_3^-\,(aq)} \tag{7.12.7.11}$$

$$\mathrm{HCO_3^-\,(aq) \rightleftharpoons H^+\,(aq) + CO_3^{2-}\,(aq)} \tag{7.12.7.12}$$

$$\mathrm{Ca^{2+}\,(aq) + CO_3^{2-}\,(aq) \rightleftharpoons CaCO_3\,(s)} \tag{7.12.7.13}$$

Limestone deposits that form caves consist primarily of $CaCO_3$ from the remains of living creatures such as clams and corals, which used it for making structures such as shells. When a saturated solution of $CaCO_3$ in CO_2-rich water rises toward Earth's surface or is otherwise heated, CO_2 gas is released as the water warms. $CaCO_3$ then precipitates from the solution according to the following equation (part (b) in Figure **7.12.7.1**:):

$$Ca^{2+}(aq) + 2HCO_{3(aq)}^- \rightleftharpoons CaCO_{3(s)} + CO_{2(g)} + H_2O(l) \tag{7.12.7.14}$$

The forward direction is the same reaction that produces the solid called scale in teapots, coffee makers, water heaters, boilers, and other places where hard water is repeatedly heated.



Figure **7.12.7.1**: The Chemistry of Cave Formation. (a) This cave in Campanet, Mallorca, Spain, and its associated formations are examples of pH-dependent solubility equilibriums. (b) A cave forms when groundwater containing atmospheric CO_2, forming an acidic solution, dissolves limestone ($CaCO_3$) in a process that may take tens of thousands of years. As groundwater seeps into a cave, water evaporates from the solution of $CaCO_3$ in CO_2-rich water, producing a supersaturated solution and a shift in equilibrium that causes precipitation of the $CaCO_3$. The deposited limestone eventually forms stalactites and stalagmites.

When groundwater-containing atmospheric CO_2 (Equations 7.12.7.11 and 7.12.7.12) finds its way into microscopic cracks in the limestone deposits, $CaCO_3$ dissolves in the acidic solution in the reverse direction of Equation 7.12.7.14. The cracks gradually enlarge from 10–50 µm to 5–10 mm, a process that can take as long as 10,000 yr. Eventually, after about another 10,000 yr, a cave forms. Groundwater from the surface seeps into the cave and clings to the ceiling, where the water evaporates and causes the equilibrium in Equation 7.12.7.14 to shift to the right. A circular layer of solid $CaCO_3$ is deposited, which eventually produces a long, hollow spire of limestone called a stalactite that grows down from the ceiling. Below, where the droplets land when they fall from the ceiling, a similar process causes another spire, called a stalagmite, to grow up. The same processes that carve out hollows below ground are also at work above ground, in some cases producing fantastically convoluted landscapes like that of Yunnan Province in China (Figure **7.12.7.2**).

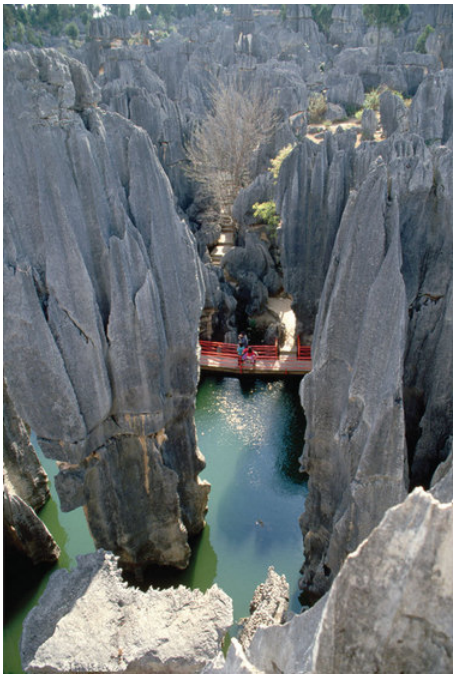


Figure **7.12.7.2**: Solubility Equilbriain the Formation of Karst Landscapes. Landscapes such as the steep limestone pinnacles of the Stone Forest in Yunnan Province, China, are formed from the same process that produces caves and their associated formations.

Acidic, Basic, and Amphoteric Oxides and Hydroxides

One of the earliest classifications of substances was based on their solubility in acidic versus basic solution, which led to the classification of oxides and hydroxides as being either basic or acidic. **Basic oxides** and hydroxides either react with water to produce a basic solution or dissolve readily in aqueous acid. **Acidic oxides** or hydroxides either react with water to produce an acidic solution or are soluble in aqueous base. There is a clear correlation between the acidic or the basic character of an oxide and the position of the element combined with oxygen in the periodic table. Oxides of metallic elements are generally basic oxides, and oxides of nonmetallic elements are acidic oxides. Compare, for example, the reactions of a typical metal oxide, cesium oxide, and a typical nonmetal oxide, sulfur trioxide, with water:

$$Cs_2O(s) + H_2O(l) \rightarrow 2Cs^+(aq) + 2OH^-(aq) \tag{7.12.7.15}$$

$$SO_{3(g)} + H_2O(l) \rightarrow H_2SO_{4(aq)} \tag{7.12.7.16}$$

Cesium oxide reacts with water to produce a basic solution of cesium hydroxide, whereas sulfur trioxide reacts with water to produce a solution of sulfuric acid—very different behaviors indeed

> *Metal oxides generally react with water to produce basic solutions, whereas nonmetal oxides produce acidic solutions.*

The difference in reactivity is due to the difference in bonding in the two kinds of oxides. Because of the low electronegativity of the metals at the far left in the periodic table, their oxides are best viewed as containing discrete M^{n+} cations and O^{2-} anions. At the other end of the spectrum are nonmetal oxides; due to their higher electronegativities, nonmetals form oxides with covalent bonds to oxygen. Because of the high electronegativity of oxygen, however, the covalent bond between oxygen and the other atom, E, is usually polarized: $E^{\delta+}$–$O^{\delta-}$. The atom E in these oxides acts as a Lewis acid that reacts with the oxygen atom of water to produce an oxoacid. Oxides of metals in high oxidation states also tend to be acidic oxides for the same reason: they contain covalent bonds to oxygen. An example of an acidic metal oxide is MoO_3, which is insoluble in both water and acid but dissolves in strong base to give solutions of the molybdate ion (MoO_4^{2-}):

$$MoO_{3(s)} + 2OH^-(aq) \rightarrow MoO^{2-}_{4(aq)} + H_2O(l) \tag{7.12.7.17}$$

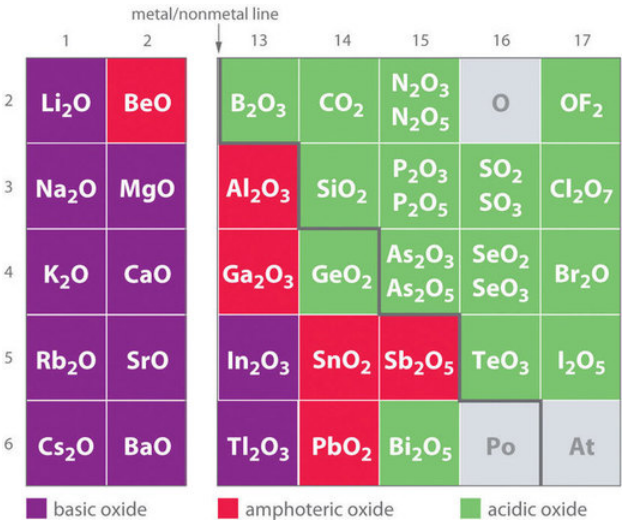


Figure **7.12.7.3**: Classification of the Oxides of the Main Group Elements According to Their Acidic or Basic Character. There is a gradual transition from basic oxides to acidic oxides from the lower left to the upper right in the periodic table. Oxides of metallic elements are generally basic oxides, which either react with water to form a basic solution or dissolve in aqueous acid. In contrast, oxides of nonmetallic elements are acidic oxides, which either react with water to form an acidic solution or are soluble in aqueous base. Oxides of intermediate character, called amphoteric oxides, are located along a diagonal line between the two extremes. Amphoteric oxides either dissolve in acid to produce water or dissolve in base to produce a soluble complex ion. (Radioactive elements are not classified.)

As shown in Figure **7.12.7.3**, there is a gradual transition from basic metal oxides to acidic nonmetal oxides as we go from the lower left to the upper right in the periodic table, with a broad diagonal band of oxides of intermediate character separating the two

extremes. Many of the oxides of the elements in this diagonal region of the periodic table are soluble in both acidic and basic solutions; consequently, they are called **amphoteric oxides** (from the Greek ampho, meaning "both," as in amphiprotic). Amphoteric oxides either dissolve in acid to produce water or dissolve in base to produce a soluble complex. As shown in Video **7.12.7.1**, for example, mixing the amphoteric oxide $Cr(OH)_3$ (also written as $Cr_2O_3•3H_2O$) with water gives a muddy, purple-brown suspension. Adding acid causes the $Cr(OH)_3$ to dissolve to give a bright violet solution of $Cr^{3+}(aq)$, which contains the $[Cr(H_2O)_6]^{3+}$ ion, whereas adding strong base gives a green solution of the $[Cr(OH)_4]^-$ ion. The chemical equations for the reactions are as follows:

$$\mathrm{Cr(OH)_3(s) + 3H^+(aq) \rightarrow \underset{\text{violet}}{Cr^{3+}(aq)} + 3H_2O(l)} \tag{7.12.7.18}$$

$$\mathrm{Cr(OH)_3(s) + OH^-(aq) \rightarrow \underset{\text{green}}{[Cr(OH)_4]^-(aq)}} \tag{7.12.7.19}$$



***Video* 7.12.7.1:** *Chromium(III) Hydroxide [$Cr(OH)_3$ or $Cr_2O_3•3H_2O$] is an Example of an Amphoteric Oxide. All three beakers originally contained a suspension of brownish purple $Cr(OH)_3(s)$ (center). When concentrated acid (6 M H_2SO_4) was added to the beaker on the left, $Cr(OH)_3$ dissolved to produce violet $[Cr(H_2O)_6]^{3+}$ ions and water. The addition of concentrated base (6 M NaOH) to the beaker on the right caused $Cr(OH)_3$ to dissolve, producing green $[Cr(OH)_4]^-$ ions. For a more complete description, see https://www.youtube.com/watch?v=IQNcLH6OZK0*

Example 7.12.7.2

Aluminum hydroxide, written as either $Al(OH)_3$ or $Al_2O_3•3H_2O$, is amphoteric. Write chemical equations to describe the dissolution of aluminum hydroxide in (a) acid and (b) base.

Given: amphoteric compound

Asked for: dissolution reactions in acid and base

Strategy:

Using Equations **7.12.7.18** and **7.12.7.19** as a guide, write the dissolution reactions in acid and base solutions.

Solution

a. An acid donates protons to hydroxide to give water and the hydrated metal ion, so aluminum hydroxide, which contains three OH^- ions per Al, needs three H^+ ions:

$$\mathrm{Al(OH)_{3(s)} + 3H^+(aq) \rightarrow Al^{3+}(aq) + 3H_2O(l)}$$

In aqueous solution, Al^{3+} forms the complex ion $[Al(H_2O)_6]^{3+}$.

b. In basic solution, OH^- is added to the compound to produce a soluble and stable poly(hydroxo) complex:

$$\mathrm{Al(OH)_{3(s)} + OH^-(aq) \rightarrow [Al(OH)_4]^-(aq)}$$

? Exercise 7.12.7.2

Copper(II) hydroxide, written as either $Cu(OH)_2$ or $CuO{\bullet}H_2O$, is *amphoteric*. Write chemical equations that describe the dissolution of cupric hydroxide both in an acid and in a base.

Answer

$$Cu(OH)_{2(s)} + 2H^+(aq) \rightarrow Cu^{2+}(aq) + 2H_2O(l)$$

$$Cu(OH)_{2(s)} + 2OH^-(aq) \rightarrow [Cu(OH)_4]^2_{-(aq)}$$

Selective Precipitation Using pH

Many dissolved metal ions can be separated by the selective precipitation of the cations from solution under specific conditions. In this technique, pH is often used to control the concentration of the anion in solution, which controls which cations precipitate.

> *The concentration of anions in solution can often be controlled by adjusting the pH, thereby allowing the selective precipitation of cations.*

Suppose, for example, we have a solution that contains 1.0 mM Zn^{2+} and 1.0 mM Cd^{2+} and want to separate the two metals by selective precipitation as the insoluble sulfide salts, ZnS and CdS. The relevant solubility equilbria can be written as follows:

$$ZnS(s) \rightleftharpoons Zn^{2+}(aq) + S^{2-}(aq) \tag{7.12.7.20}$$

with

$$K_{sp} = 1.6 \times 10^{-24} \tag{7.12.7.21}$$

and

$$CdS(s) \rightleftharpoons Cd^{2+}(aq) + S^{2-}(aq) \tag{7.12.7.22}$$

with

$$K_{sp} = 8.0 \times 10^{-27} \tag{7.12.7.23}$$

Because the S^{2-} ion is quite basic and reacts extensively with water to give HS^- and OH^-, the solubility equilbria are more accurately written as $MS(s) \rightleftharpoons M^{2+}(aq) + HS^-(aq) + OH^-$ rather than $MS(s) \rightleftharpoons M^{2+}(aq) + S^{2-}(aq)$. Here we use the simpler form involving S^{2-}, which is justified because we take the reaction of S^{2-} with water into account later in the solution, arriving at the same answer using either equilibrium equation.

The sulfide concentrations needed to cause ZnS and CdS to precipitate are as follows:

$$K_{sp} = [Zn^{2+}][S^{2-}] \tag{7.12.7.24}$$

$$1.6 \times 10^{-24} = (0.0010\ M)[S^{2-}] \tag{7.12.7.25}$$

$$1.6 \times 10^{-21}\ M = [S^{2-}] \tag{7.12.7.26}$$

and

$$K_{sp} = [Cd^{2+}][S^{2-}] \tag{7.12.7.27}$$

$$8.0 \times 10^{-27} = (0.0010\ M)[S^{2-}] \tag{7.12.7.28}$$

$$8.0 \times 10^{-24}\ M = [S^{2-}] \tag{7.12.7.29}$$

Thus sulfide concentrations between 1.6×10^{-21} M and 8.0×10^{-24} M will precipitate CdS from solution but not ZnS. How do we obtain such low concentrations of sulfide? A saturated aqueous solution of H_2S contains 0.10 M H_2S at 20°C. The $pK_{a1}$for H_2S is 6.97, and pK_{a2} corresponding to the formation of $[S^{2-}]$ is 12.90. The equations for these reactions are as follows:

$$H_2S(aq) \rightleftharpoons H^+(aq) + HS^-(aq) \tag{7.12.7.30}$$

with

$$pK_{a1} = 6.97 \text{ and hence } K_{a1} = 1.1 \times 10^{-7} \tag{7.12.7.31}$$

$$HS^-(aq) \rightleftharpoons H^+(aq) + S^{2-}(aq) \tag{7.12.7.32}$$

with

$$pK_{a2} = 12.90 \text{ and hence } K_{a2} = 1.3 \times 10^{-13} \tag{7.12.7.33}$$

We can show that the concentration of S^{2-} is 1.3×10^{-13} by comparing K_{a1} and K_{a2} and recognizing that the contribution to $[H^+]$ from the dissociation of HS^- is negligible compared with $[H^+]$ from the dissociation of H_2S. Thus substituting 0.10 M in the equation for K_{a1} for the concentration of H_2S, which is essentially constant regardless of the pH, gives the following:

$$K_{a1} = 1.1 \times 10^{-7} = \frac{[H^+][HS^-]}{[H_2S]} = \frac{x^2}{0.10\ M} \tag{7.12.7.34}$$

$$x = 1.1 \times 10^{-4}\ M = [H^+] = [HS^-]$$

Substituting this value for $[H^+]$ and $[HS^-]$ into the equation for K_{a2},

$$K_{a2} = 1.3 \times 10^{-13} = \frac{[H^+][S^{2-}]}{[HS^-]} = \frac{(1.1 \times 10^{-4}\ M)x}{1.1 \times 10^{-4}\ M} = x = [S^{2-}] \tag{7.12.7.35}$$

Although $[S^{2-}]$ in an H_2S solution is very low (1.3×10^{-13} M), bubbling H_2S through the solution until it is saturated would precipitate both metal ions because the concentration of S^{2-} would then be much greater than 1.6×10^{-21} M. Thus we must adjust $[S^{2-}]$ to stay within the desired range. The most direct way to do this is to adjust $[H^+]$ by adding acid to the H_2S solution (recall Le Chatelier's principle), thereby driving the equilibrium in Equation 7.12.7.33 to the left. The overall equation for the dissociation of H_2S is as follows:

$$H_2S(aq) \rightleftharpoons 2H^+(aq) + S^{2-}(aq) \tag{7.12.7.36}$$

Now we can use the equilibrium constant K for the overall reaction, which is the product of K_{a1} and K_{a2}, and the concentration of H_2S in a saturated solution to calculate the H^+ concentration needed to produce $[S^{2-}]$ of 1.6×10^{-21} M:

$$K = K_{a1}K_{a2} = (1.1 \times 10^{-7})(1.3 \times 10^{-13}) = 1.4 \times 10^{-20} = \frac{[H^+]^2[S^{2-}]}{[H_2S]} \tag{7.12.7.37}$$

$$[H^+]^2 = \frac{K[H_2S]}{[S^{2-}]} = \frac{(1.4 \times 10^{-20})(0.10\ M)}{1.6 \times 10^{-21}\ M} = 0.88 \tag{7.12.7.38}$$

$$[H^+] = 0.94 \tag{7.12.7.39}$$

Thus adding a strong acid such as HCl to make the solution 0.94 M in H^+ will prevent the more soluble ZnS from precipitating while ensuring that the less soluble CdS will precipitate when the solution is saturated with H_2S.

Example 7.12.7.3

A solution contains 0.010 M Ca^{2+} and 0.010 M La^{3+}. What concentration of HCl is needed to precipitate $La_2(C_2O_4)_3 \cdot 9H_2O$ but not $Ca(C_2O_4) \cdot H_2O$ if the concentration of oxalic acid is 1.0 M? K_{sp} values are 2.32×10^{-9} for $Ca(C_2O_4)$ and 2.5×10^{-27} for $La_2(C_2O_4)_3$; $pK_{a1} = 1.25$ and $pK_{a2} = 3.81$ for oxalic acid.

Given: concentrations of cations, K_{sp} values, and concentration and pK_a values for oxalic acid

Asked for: concentration of HCl needed for selective precipitation of $La_2(C_2O_4)_3$

Strategy:

A. Write each solubility product expression and calculate the oxalate concentration needed for precipitation to occur. Determine the concentration range needed for selective precipitation of $La_2(C_2O_4)_3 \cdot 9H_2O$.

B. Add the equations for the first and second dissociations of oxalic acid to get an overall equation for the dissociation of oxalic acid to oxalate. Substitute the $[ox^{2-}]$ needed to precipitate $La_2(C_2O_4)_3 \cdot 9H_2O$ into the overall equation for the dissociation of oxalic acid to calculate the required $[H^+]$.

Solution

A Because the salts have different stoichiometries, we cannot directly compare the magnitudes of the solubility products. Instead, we must use the equilibrium constant expression for each solubility product to calculate the concentration of oxalate needed for precipitation to occur. Using ox^{2-} for oxalate, we write the solubility product expression for calcium oxalate as follows:

$$K_{sp} = [Ca^{2+}][ox^{2-}] = (0.010)[ox^{2-}] = 2.32 \times 10^{-9}$$

$$[ox^{2-}] = 2.32 \times 10^{-7}\ M$$

The expression for lanthanum oxalate is as follows:

$$K_{sp} = [La^{3+}]^2[ox^{2-}]^3 = (0.010)^2[ox^{2-}]^3 = 2.5 \times 10^{-27}$$

$$[ox^{2-}] = 2.9 \times 10^{-8}\ M$$

Thus lanthanum oxalate is less soluble and will selectively precipitate when the oxalate concentration is between $2.9 \times 10^{-8} M$ and $2.32 \times 10^{-7} M$.

B To prevent Ca^{2+} from precipitating as calcium oxalate, we must add enough H^+ to give a maximum oxalate concentration of 2.32×10^{-7} M. We can calculate the required $[H^+]$ by using the overall equation for the dissociation of oxalic acid to oxalate:

$$HO_2CCO_2H(aq) \rightleftharpoons 2H^+(aq) + C_2O^{2-}_{4(aq)} \tag{7.12.7.40}$$

$$K = K_{a1}K_{a2} = (10^{-1.25})(10^{-3.81}) = 10^{-5.06} = 8.7{\times}10^{-6}$$

Substituting the desired oxalate concentration into the equilibrium constant expression,

$$8.7 \times 10^{-6} = \frac{[H^+]^2[ox^{2-}]}{[HO_2CCO_2H]} = \frac{[H^+]^2(2.32 \times 10^{-7})}{1.0} \tag{7.12.7.41}$$

$$[H^+] = 6.1\ M \tag{7.12.7.42}$$

Thus adding enough HCl to give $[H^+]$ = 6.1 M will cause only $La_2(C_2O_4)_3{\bullet}9H_2O$ to precipitate from the solution.

? Exercise 7.12.7.3

A solution contains 0.015 M Fe^{2+} and 0.015 M Pb^{2+}. What concentration of acid is needed to ensure that Pb^{2+} precipitates as PbS in a saturated solution of H_2S, but Fe^{2+} does not precipitate as FeS? K_{sp} values are 6.3×10^{-18} for FeS and 8.0×10^{-28} for PbS.

Answer

0.018 M H^+

Summary

The anion in sparingly soluble salts is often the conjugate base of a weak acid that may become protonated in solution, so the solubility of simple oxides and sulfides, both strong bases, often depends on pH. The anion in many sparingly soluble salts is the conjugate base of a weak acid. At low pH, protonation of the anion can dramatically increase the solubility of the salt. Oxides can be classified as acidic oxides or basic oxides. Acidic oxides either react with water to give an acidic solution or dissolve in strong base; most acidic oxides are nonmetal oxides or oxides of metals in high oxidation states. Basic oxides either react with water to give a basic solution or dissolve in strong acid; most basic oxides are oxides of metallic elements. Oxides or hydroxides that are soluble in both acidic and basic solutions are called amphoteric oxides. Most elements whose oxides exhibit amphoteric behavior are located along the diagonal line separating metals and nonmetals in the periodic table. In solutions that contain mixtures of dissolved metal ions, the pH can be used to control the anion concentration needed to selectively precipitate the desired cation.

Contributors and Attributions

- Anonymous

7.12.7: Solubility and pH is shared under a not declared license and was authored, remixed, and/or curated by LibreTexts.

- **18.7: Solubility and pH** is licensed CC BY-NC-SA 4.0.

7.12.8: Equilibria Involving Complex Ions

Learning Objectives

- To be introduced to complex ions, including ligands.

Previously, you learned that metal ions in aqueous solution are hydrated—that is, surrounded by a shell of usually four or six water molecules. A hydrated ion is one kind of a **complex ion** (or, simply, complex), a species formed between a central metal ion and one or more surrounding **ligands**, molecules or ions that contain at least one lone pair of electrons, such as the $[Al(H_2O)_6]^{3+}$ ion.

A complex ion forms from a metal ion and a ligand because of a Lewis acid–base interaction. The positively charged metal ion acts as a Lewis acid, and the ligand, with one or more lone pairs of electrons, acts as a Lewis base. Small, highly charged metal ions, such as Cu^{2+} or Ru^{3+}, have the greatest tendency to act as Lewis acids, and consequently, they have the greatest tendency to form complex ions.

As an example of the formation of complex ions, consider the addition of ammonia to an aqueous solution of the hydrated Cu^{2+} ion $\{[Cu(H_2O)_6]^{2+}\}$. Because it is a stronger base than H_2O, ammonia replaces the water molecules in the hydrated ion to form the $[Cu(NH_3)_4(H_2O)_2]^{2+}$ ion. Formation of the $[Cu(NH_3)_4(H_2O)_2]^{2+}$ complex is accompanied by a dramatic color change, as shown in Figure **7.12.8.1**. The solution changes from the light blue of $[Cu(H_2O)_6]^{2+}$ to the blue-violet characteristic of the $[Cu(NH_3)_4(H_2O)_2]^{2+}$ ion.



Figure **7.12.8.1**: The Formation of Complex Ions. An aqueous solution of $CuSO_4$ consists of hydrated Cu^{2+} ions in the form of pale blue $[Cu(H_2O)_6]^{2+}$ (left). The addition of aqueous ammonia to the solution results in the formation of the intensely blue-violet $[Cu(NH_3)_4(H_2O)_2]^{2+}$ ions, usually written as $[Cu(NH_3)_4]^{2+}$ ion (right) because ammonia, a stronger base than H_2O, replaces water molecules from the hydrated Cu^{2+} ion. For a more complete description, see https://www.youtube.com/watch?v=IQNcLH6OZK0.

The Formation Constant

The replacement of water molecules from $[Cu(H_2O)_6]^{2+}$ by ammonia occurs in sequential steps. Omitting the water molecules bound to Cu^{2+} for simplicity, we can write the equilibrium reactions as follows:

$$Cu^{2+}(aq) + NH_{3(aq)} \rightleftharpoons [Cu(NH_3)]^{2+}_{(aq)} \quad K_1 \tag{7.12.8.1}$$

$$[Cu(NH_3)]^{2+}_{(aq)} + NH_{3(aq)} \rightleftharpoons [Cu(NH_3)_2]^{2+}_{(aq)} \quad K_2 \tag{7.12.8.2}$$

$$[Cu(NH_3)_2]^{2+}_{(aq)} + NH_{3(aq)} \rightleftharpoons [Cu(NH_3)_3]^{2+}_{(aq)} \quad K_3 \tag{7.12.8.3}$$

$$[Cu(NH_3)_3]^{2+}_{(aq)} + NH_{3(aq)} \rightleftharpoons [Cu(NH_3)_4]^{2+}_{(aq)} \quad K_4 \tag{7.12.8.4}$$

The sum of the stepwise reactions is the overall equation for the formation of the complex ion: The hydrated Cu^{2+} ion contains six H_2O ligands, but the complex ion that is produced contains only four NH_3 ligands, not six.

$$Cu^{2+}_{(aq)} + 4NH_{3(aq)} \rightleftharpoons [Cu(NH_3)_4]^{2+}_{(aq)} \tag{7.12.8.5}$$

The equilibrium constant for the formation of the complex ion from the hydrated ion is called the **formation constant (K_f)**. The equilibrium constant expression for K_f has the same general form as any other equilibrium constant expression. In this case, the expression is as follows:

$$K_f = \frac{[[Cu(NH_3)_4]^{2+}]}{[Cu^{2+}][NH_3]^4} = 2.1 \times 10^{13} = K_1K_2K_3K_4 \tag{7.12.8.6}$$

> *The formation constant (K_f) has the same general form as any other equilibrium constant expression.*

Water, a pure liquid, does not appear explicitly in the equilibrium constant expression, and the hydrated $Cu^{2+}(aq)$ ion is represented as Cu^{2+} for simplicity. As for any equilibrium, the larger the value of the equilibrium constant (in this case, K_f), the more stable the product. With $K_f = 2.1 \times 10^{13}$, the $[Cu(NH_3)_4(H_2O)_2]^{2+}$ complex ion is very stable. The formation constants for some common complex ions are listed in Table **7.12.8.1**.

Table **7.12.8.1**: Formation Constants for Selected Complex Ions in Aqueous Solution*

	Complex Ion	Equilibrium Equation	K_f
Ammonia Complexes	$[Ag(NH_3)_2]^+$	$Ag^+ + 2NH_3 \rightleftharpoons [Ag(NH_3)_2]^+$	1.1×10^7
	$[Cu(NH_3)_4]^{2+}$	$Cu^{2+} + 4NH_3 \rightleftharpoons [Cu(NH_3)_4]^{2+}$	2.1×10^{13}
	$[Ni(NH_3)_6]^{2+}$	$Ni^{2+} + 6NH_3 \rightleftharpoons [Ni(NH_3)_6]^{2+}$	5.5×10^8
Cyanide Complexes	$[Ag(CN)_2]^-$	$Ag^+ + 2CN^- \rightleftharpoons [Ag(CN)_2]^-$	1.1×10^{18}
	$[Ni(CN)_4]^{2-}$	$Ni^{2+} + 4CN^- \rightleftharpoons [Ni(CN)_4]^{2-}$	2.2×10^{31}
	$[Fe(CN)_6]^{3-}$	$Fe^{3+} + 6CN^- \rightleftharpoons [Fe(CN)_6]^{3-}$	1×10^{42}
Hydroxide Complexes	$[Zn(OH)_4]^{2-}$	$Zn^{2+} + 4OH^- \rightleftharpoons [Zn(OH)_4]^{2-}$	4.6×10^{17}
	$[Cr(OH)_4]^-$	$Cr^{3+} + 4OH^- \rightleftharpoons [Cr(OH)_4]^-$	8.0×10^{29}
Halide Complexes	$[HgCl_4]^{2-}$	$Hg^{2+} + 4Cl^- \rightleftharpoons [HgCl_4]^{2-}$	1.2×10^{15}
	$[CdI_4]^{2-}$	$Cd^{2+} + 4I \rightleftharpoons [CdI_4]^{2-}$	2.6×10^5
	$[AlF_6]^{3-}$	$Al^{3+} + 6F^- \rightleftharpoons [AlF_6]^{3-}$	6.9×10^{19}
Other Complexes	$[Ag(S_2O_3)_2]^{3-}$	$Ag^+ + 2S_2O_3^{2-} \rightleftharpoons [Ag(S_2O_3)_2]^{3-}$	2.9×10^{13}
	$[Fe(C_2O_4)_3]^{3-}$	$Fe^{3+} + 3C_2O_4^{2-} \rightleftharpoons [Fe(C_2O_4)_3]^{3-}$	2.0×10^{20}

*Reported values are overall formation constants. Source: Data from *Lange's Handbook of Chemistry*, 15th ed. (1999).

Example 7.12.8.1

If 12.5 g of $Cu(NO_3)_2 \cdot 6H_2O$ is added to 500 mL of 1.00 M aqueous ammonia, what is the equilibrium concentration of $Cu^{2+}(aq)$?

Given: mass of Cu^{2+} salt and volume and concentration of ammonia solution

Asked for: equilibrium concentration of $Cu^{2+}(aq)$

Strategy:

A. Calculate the initial concentration of Cu^{2+} due to the addition of copper(II) nitrate hexahydrate. Use the stoichiometry of the reaction shown in Equation 7.12.8.5 to construct a table showing the initial concentrations, the changes in concentrations, and the final concentrations of all species in solution.

B. Substitute the final concentrations into the expression for the formation constant (Equation 7.12.8.6) to calculate the equilibrium concentration of $Cu^{2+}(aq)$.

Solution

Adding an ionic compound that contains Cu^{2+} to an aqueous ammonia solution will result in the formation of $[Cu(NH_3)_4]^{2+}(aq)$, as shown in Equation 7.12.8.5. We assume that the volume change caused by adding solid copper(II) nitrate to aqueous ammonia is negligible.

A The initial concentration of Cu^{2+} from the amount of added copper nitrate prior to any reaction is as follows:

$$12.5\ \cancel{g}\ Cu(NO_3)_2 \cdot 6H_2O \left(\frac{1\ mol}{295.65\ \cancel{g}}\right)\left(\frac{1}{500\ \cancel{mL}}\right)\left(\frac{1000\ \cancel{mL}}{1\ L}\right) = 0.0846\ M \tag{7.12.8.7}$$

Because the stoichiometry of the reaction is four NH_3 to one Cu^{2+}, the amount of NH_3 required to react completely with the Cu^{2+} is 4(0.0846) = 0.338 M. The concentration of ammonia after complete reaction is 1.00 M − 0.338 M = 0.66 M. These results are summarized in the first two lines of the following table. Because the equilibrium constant for the reaction is large (2.1×10^{13}), the equilibrium will lie far to the right. Thus we will assume that the formation of $[Cu(NH_3)_4]^{2+}$ in the first step is complete and allow some of it to dissociate into Cu^{2+} and NH_3 until equilibrium has been reached. If we define x as the amount of Cu^{2+} produced by the dissociation reaction, then the stoichiometry of the reaction tells us that the change in the concentration of $[Cu(NH_3)_4]^{2+}$ is $-x$, and the change in the concentration of ammonia is $+4x$, as indicated in the table. The final concentrations of all species (in the bottom row of the table) are the sums of the concentrations after complete reaction and the changes in concentrations.

$$Cu^{2+} + 4NH_3 \rightleftharpoons [Cu(NH_3)_4]^{2+}$$

	$[Cu^{2+}]$	$[NH_3]$	$[[Cu(NH_3)_4]^{2+}]$
initial	0.0846	1.00	0
after complete reaction	0	0.66	0.0846
change	$+x$	$+4x$	$-x$
final	x	$0.66 + 4x$	$0.0846 - x$

B Substituting the final concentrations into the expression for the formation constant (Equation 7.12.8.6) and assuming that x << 0.0846, which allows us to remove x from the sum and difference,

$$K_f = \frac{[[Cu(NH_3)_4]^{2+}]}{[Cu^{2+}][NH_3]^4} = \frac{0.0846 - x}{x(0.66 + 4x)^4} \approx \frac{0.0846}{x(0.66)^4} = 2.1 \times 10^{13} \tag{7.12.8.8}$$

$$x = 2.1 \times 10^{-14} \tag{7.12.8.9}$$

The value of x indicates that our assumption was justified. The equilibrium concentration of $Cu^{2+}(aq)$ in a 1.00 M ammonia solution is therefore 2.1×10^{-14} M.

? Exercise 7.12.8.1

The ferrocyanide ion $\{[Fe(CN)_6]^{4-}\}$ is very stable, with a K_f of 1×10^{35}. Calculate the concentration of cyanide ion in equilibrium with a 0.65 M solution of $K_4[Fe(CN)_6]$.

Answer 2×10^{-6} M

The Effect of the Formation of Complex Ions on Solubility

What happens to the solubility of a sparingly soluble salt if a ligand that forms a stable complex ion is added to the solution? One such example occurs in conventional black-and-white photography. Recall that black-and-white photographic film contains light-sensitive microcrystals of AgBr, or mixtures of AgBr and other silver halides. AgBr is a sparingly soluble salt, with a K_{sp} of 5.35×10^{-13} at 25°C. When the shutter of the camera opens, the light from the object being photographed strikes some of the crystals on the film and initiates a photochemical reaction that converts AgBr to black Ag metal. Well-formed, stable negative images appear in tones of gray, corresponding to the number of grains of AgBr converted, with the areas exposed to the most light being darkest. To fix the image and prevent more AgBr crystals from being converted to Ag metal during processing of the film, the unreacted AgBr on the film is removed using a complexation reaction to dissolve the sparingly soluble salt.

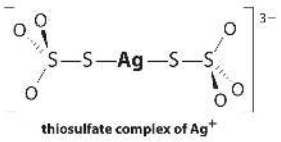
The reaction for the dissolution of silver bromide is as follows:

$$AgBr_{(s)} \rightleftharpoons Ag^+_{(aq)} + Br^-_{(aq)} \tag{7.12.8.10}$$

with

$$K_{sp} = 5.35 \times 10^{-13} \text{ at } 25°C \tag{7.12.8.11}$$

The equilibrium lies far to the left, and the equilibrium concentrations of Ag^+ and Br^- ions are very low (7.31×10^{-7} M). As a result, removing unreacted AgBr from even a single roll of film using pure water would require tens of thousands of liters of water and a great deal of time. Le Chatelier's principle tells us, however, that we can drive the reaction to the right by removing one of the products, which will cause more AgBr to dissolve. Bromide ion is difficult to remove chemically, but silver ion forms a variety of stable two-coordinate complexes with neutral ligands, such as ammonia, or with anionic ligands, such as cyanide or thiosulfate ($S_2O_3^{2-}$). In photographic processing, excess AgBr is dissolved using a concentrated solution of sodium thiosulfate.



thiosulfate complex of Ag^+

The reaction of Ag^+ with thiosulfate is as follows:

$$Ag^+_{(aq)} + 2S_2O^{2-}_{3(aq)} \rightleftharpoons [Ag(S_2O_3)_2]^{3-}_{(aq)} \tag{7.12.8.12}$$

with

$$K_f = 2.9 \times 10^{13} \tag{7.12.8.13}$$

The magnitude of the equilibrium constant indicates that almost all Ag^+ ions in solution will be immediately complexed by thiosulfate to form $[Ag(S_2O_3)_2]^{3-}$. We can see the effect of thiosulfate on the solubility of AgBr by writing the appropriate reactions and adding them together:

$$\mathrm{AgBr(s) \rightleftharpoons Ag^+(aq) + Br^-(aq) \quad K_{sp} = 5.35 \times 10^{-13}} \tag{7.12.8.14}$$

$$\mathrm{Ag^+(aq) + 2S_2O_3^{2-}(aq) \rightleftharpoons [Ag(S_2O_3)_2]^{3-}(aq) \quad K_f = 2.9 \times 10^{13}} \tag{7.12.8.15}$$

$$\mathrm{AgBr(s) + 2S_2O_3^{2-}(aq) \rightleftharpoons [Ag(S_2O_3)_2]^{3-}(aq) + Br^-(aq) \quad K = K_{sp}K_f = 15} \tag{7.12.8.16}$$

Comparing K with K_{sp} shows that the formation of the complex ion increases the solubility of AgBr by approximately 3×10^{13}. The dramatic increase in solubility combined with the low cost and the low toxicity explains why sodium thiosulfate is almost universally used for developing black-and-white film. If desired, the silver can be recovered from the thiosulfate solution using any of several methods and recycled.

> *If a complex ion has a large K_f, the formation of a complex ion can dramatically increase the solubility of sparingly soluble salts.*

Example 7.12.8.2

Due to the common ion effect, we might expect a salt such as AgCl to be much less soluble in a concentrated solution of KCl than in water. Such an assumption would be incorrect, however, because it ignores the fact that silver ion tends to form a two-coordinate complex with chloride ions ($AgCl_2^-$). Calculate the solubility of AgCl in each situation:

a. in pure water
b. in 1.0 M KCl solution, ignoring the formation of any complex ions
c. the same solution as in part (b) except taking the formation of complex ions into account, assuming that $AgCl_2^-$ is the only Ag^+ complex that forms in significant concentrations

At 25°C, $K_{sp} = 1.77 \times 10^{-10}$ for AgCl and $K_f = 1.1 \times 10^5$ for $AgCl_2^-$.

Given: K_{sp} of AgCl, K_f of $AgCl_2^-$, and KCl concentration

Asked for: solubility of AgCl in water and in KCl solution with and without the formation of complex ions

Strategy:

A. Write the solubility product expression for AgCl and calculate the concentration of Ag^+ and Cl^- in water.
B. Calculate the concentration of Ag^+ in the KCl solution.
C. Write balanced chemical equations for the dissolution of AgCl and for the formation of the $AgCl_2^-$ complex. Add the two equations and calculate the equilibrium constant for the overall equilibrium.
D. Write the equilibrium constant expression for the overall reaction. Solve for the concentration of the complex ion.

Solution

a. **A** If we let x equal the solubility of AgCl, then at equilibrium $[Ag+] = [Cl^-] = x$ M. Substituting this value into the solubility product expression,

$$K_{sp} = [Ag^+][Cl^-] = (x)(x) = x^2 = 1.77\times10^{-10}$$
$$x = 1.33\times10^{-5}$$

Thus the solubility of AgCl in pure water at 25°C is 1.33×10^{-5} M.

b. **B** If x equals the solubility of AgCl in the KCl solution, then at equilibrium $[Ag^+] = x$ M and $[Cl^-] = (1.0 + x)$ M. Substituting these values into the solubility product expression and assuming that $x << 1.0$,

$$K_{sp} = [Ag^+][Cl^-] = (x)(1.0 + x) \approx x(1.0) = 1.77\times10^{-10} = x$$

If the common ion effect were the only important factor, we would predict that AgCl is approximately five orders of magnitude less soluble in a 1.0 M KCl solution than in water.

c. **C** To account for the effects of the formation of complex ions, we must first write the equilibrium equations for both the dissolution and the formation of complex ions. Adding the equations corresponding to K_{sp} and K_f gives us an equation that describes the dissolution of AgCl in a KCl solution. The equilibrium constant for the reaction is therefore the product of K_{sp} and K_f:

$$\mathrm{AgCl(s) \rightleftharpoons Ag^+(aq) + Cl^-(aq)} \quad K_{sp} = 1.77 \times 10^{-10} \qquad (7.12.8.17)$$
$$\mathrm{Ag^+(aq) + 2Cl^- \rightleftharpoons [AgCl_2]^-} \quad K_f = 1.1 \times 10^5 \qquad (7.12.8.18)$$
$$\mathrm{AgCl(s) + Cl^- \rightleftharpoons [AgCl_2]^-} \quad K = K_{sp}K_f = 1.9 \times 10^{-5} \qquad (7.12.8.19)$$

D If we let x equal the solubility of AgCl in the KCl solution, then at equilibrium $[AgCl_2^-] = x$ and $[Cl^-] = 1.0 - x$. Substituting these quantities into the equilibrium constant expression for the net reaction and assuming that $x << 1.0$,

$$K = \frac{[\mathrm{AgCl_2^-}]}{[\mathrm{Cl^-}]} = \frac{x}{1.0 - x} \approx 1.9 \times 10^{-5} = x$$

That is, AgCl dissolves in 1.0 M KCl to produce a 1.9×10^{-5} M solution of the $AgCl_2^-$ complex ion. Thus we predict that AgCl has approximately the same solubility in a 1.0 M KCl solution as it does in pure water, which is 10^5 times greater than that predicted based on the common ion effect. (In fact, the measured solubility of AgCl in 1.0 M KCl is almost a factor of 10 greater than that in pure water, largely due to the formation of other chloride-containing complexes.)

? Exercise 7.12.8.2

Calculate the solubility of mercury(II) iodide (HgI_2) in each situation:

a. pure water
b. a 3.0 M solution of NaI, assuming $[HgI_4]^{2-}$ is the only Hg-containing species present in significant amounts

$$K_{sp} = 2.9 \times 10^{-29} \text{ for } HgI_2 \text{ and } K_f = 6.8 \times 10^{29} \text{ for } [HgI_4]^{2-}.$$

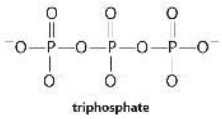
Answer

a. 1.9×10^{-10} M
b. 1.4 M



Solubility of Complex Ions: https://youtu.be/f4pkKDg2XTA

Complexing agents, molecules or ions that increase the solubility of metal salts by forming soluble metal complexes, are common components of laundry detergents. Long-chain carboxylic acids, the major components of soaps, form insoluble salts with Ca^{2+} and Mg^{2+}, which are present in high concentrations in "hard" water. The precipitation of these salts produces a bathtub ring and gives a gray tinge to clothing. Adding a complexing agent such as pyrophosphate ($O_3POPO_3^{4-}$, or $P_2O_7^{4-}$) or triphosphate ($P_3O_{10}^{5-}$) to detergents prevents the magnesium and calcium salts from precipitating because the equilibrium constant for complex-ion formation is large:



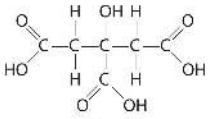
triphosphate

$$Ca^{2+}_{(aq)} + O_3POPO^{4-}_{4(aq)} \rightleftharpoons [Ca(O_3POPO_3)]^{2-}_{(aq)} \tag{7.12.8.20}$$

with

$$K_f = 4 \times 10^4 \tag{7.12.8.21}$$

However, phosphates can cause environmental damage by promoting eutrophication, the growth of excessive amounts of algae in a body of water, which can eventually lead to large decreases in levels of dissolved oxygen that kill fish and other aquatic organisms. Consequently, many states in the United States have banned the use of phosphate-containing detergents, and France has banned their use beginning in 2007. "Phosphate-free" detergents contain different kinds of complexing agents, such as derivatives of acetic acid or other carboxylic acids. The development of phosphate substitutes is an area of intense research.



Citric acid,
a hydroxy polycarboxylic acid

Commercial water softeners also use a complexing agent to treat hard water by passing the water over ion-exchange resins, which are complex sodium salts. When water flows over the resin, sodium ion is dissolved, and insoluble salts precipitate onto the resin surface. Water treated in this way has a saltier taste due to the presence of Na^+, but it contains fewer dissolved minerals.

Another application of complexing agents is found in medicine. Unlike x-rays, magnetic resonance imaging (MRI) can give relatively good images of soft tissues such as internal organs. MRI is based on the magnetic properties of the ^1H nucleus of hydrogen atoms in water, which is a major component of soft tissues. Because the properties of water do not depend very much on whether it is inside a cell or in the blood, it is hard to get detailed images of these tissues that have good contrast. To solve this problem, scientists have developed a class of metal complexes known as "MRI contrast agents." Injecting an MRI contrast agent into a patient selectively affects the magnetic properties of water in cells of normal tissues, in tumors, or in blood vessels and

allows doctors to “see” each of these separately (Figure **7.12.8.2**). One of the most important metal ions for this application is Gd^{3+}, which with seven unpaired electrons is highly paramagnetic. Because $Gd^{3+}(aq)$ is quite toxic, it must be administered as a very stable complex that does not dissociate in the body and can be excreted intact by the kidneys. The complexing agents used for gadolinium are ligands such as $DTPA^{5-}$ (diethylene triamine pentaacetic acid), whose fully protonated form is shown here.

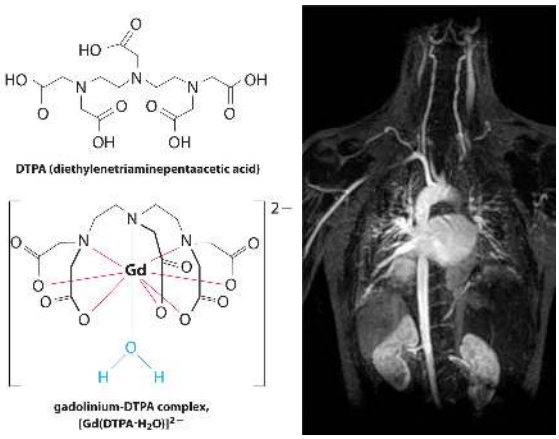


Figure **7.12.8.2**: An MRI Image of the Heart, Arteries, and Veins. When a patient is injected with a paramagnetic metal cation in the form of a stable complex known as an MRI contrast agent, the magnetic properties of water in cells are altered. Because the different environments in different types of cells respond differently, a physician can obtain detailed images of soft tissues.

Summary

The formation of complex ions can substantially increase the solubility of sparingly soluble salts if the complex ion has a large K_f. A complex ion is a species formed between a central metal ion and one or more surrounding ligands, molecules or ions that contain at least one lone pair of electrons. Small, highly charged metal ions have the greatest tendency to act as Lewis acids and form complex ions. The equilibrium constant for the formation of the complex ion is the formation constant (K_f). The formation of a complex ion by adding a complexing agent increases the solubility of a compound.

7.12.8: Equilibria Involving Complex Ions is shared under a not declared license and was authored, remixed, and/or curated by LibreTexts.

- **18.8: Equilibria Involving Complex Ions** is licensed CC BY-NC-SA 4.0.

7.12.9: Qualitative Cation Analysis

Learning Objectives

- To know how to separate metal ions by selective precipitation.
- To understand how several common metal cations can be identified in a solution using selective precipitation.

The composition of relatively complex mixtures of metal ions can be determined using **qualitative analysis**, a procedure for discovering the identity of metal ions present in the mixture (rather than quantitative information about their amounts). The procedure used to separate and identify more than 20 common metal cations from a single solution consists of selectively precipitating only a few kinds of metal ions at a time under given sets of conditions. Consecutive precipitation steps become progressively less selective until almost all of the metal ions are precipitated, as illustrated in Figure **7.12.9.1**.

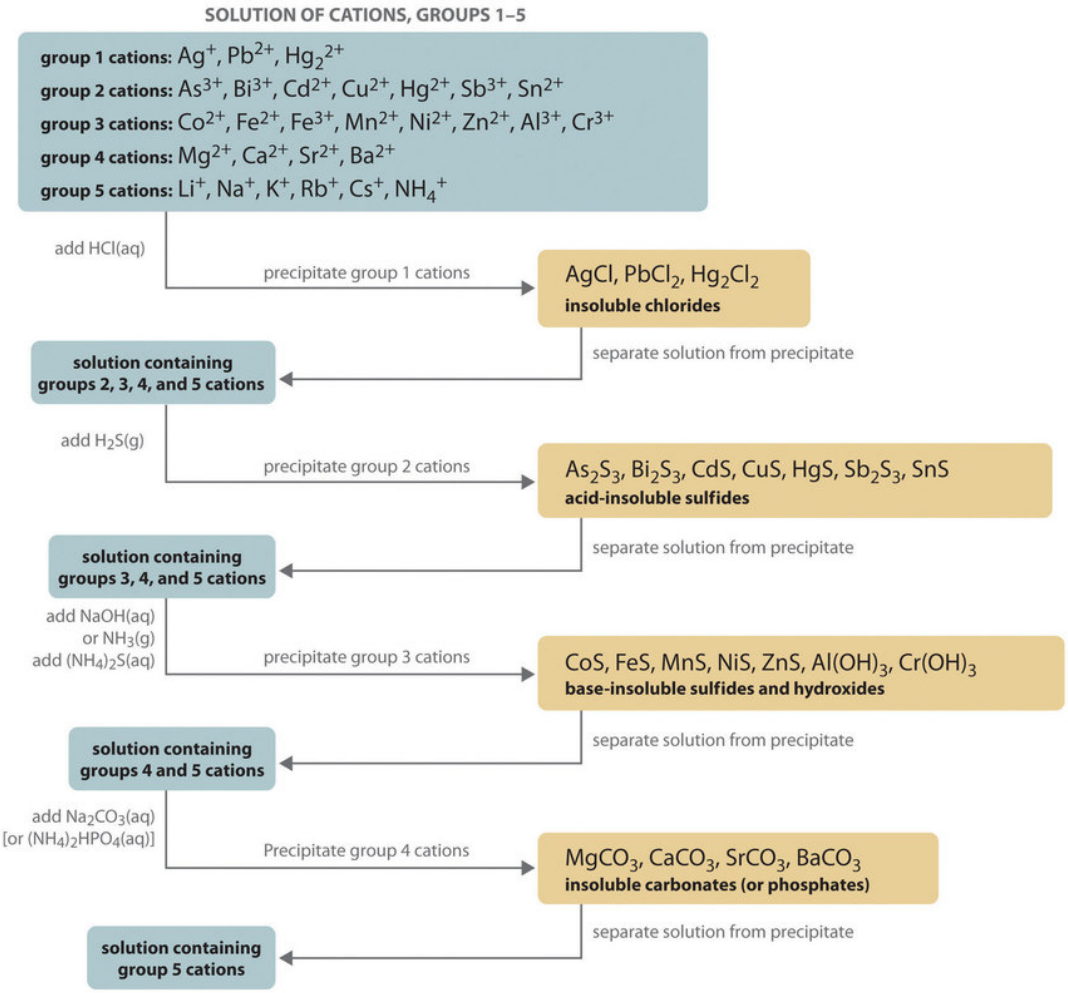


Figure **7.12.9.1**: Steps in a Typical Qualitative Analysis Scheme for a Solution That Contains Several Metal Ions

Group 1: Insoluble Chlorides

Most metal chloride salts are soluble in water; only Ag^+, Pb^{2+}, and Hg_2^{2+} form chlorides that precipitate from water. Thus the first step in a qualitative analysis is to add about 6 M HCl, thereby causing AgCl, $PbCl_2$, and/or Hg_2Cl_2 to precipitate. If no precipitate forms, then these cations are not present in significant amounts. The precipitate can be collected by filtration or centrifugation.

Group 2: Acid-Insoluble Sulfides

Next, the acidic solution is saturated with H_2S gas. Only those metal ions that form very insoluble sulfides, such as As^{3+}, Bi^{3+}, Cd^{2+}, Cu^{2+}, Hg^{2+}, Sb^{3+}, and Sn^{2+}, precipitate as their sulfide salts under these acidic conditions. All others, such as Fe^{2+} and Zn^{2+}, remain in solution. Once again, the precipitates are collected by filtration or centrifugation.

Group 3: Base-Insoluble Sulfides (and Hydroxides)

Ammonia or $NaOH$ is now added to the solution until it is basic, and then $(NH_4)_2S$ is added. This treatment removes any remaining cations that form insoluble hydroxides or sulfides. The divalent metal ions Co^{2+}, Fe^{2+}, Mn^{2+}, Ni^{2+}, and Zn^{2+} precipitate as their sulfides, and the trivalent metal ions Al^{3+} and Cr^{3+} precipitate as their hydroxides: $Al(OH)_3$ and $Cr(OH)_3$. If the mixture contains Fe^{3+}, sulfide reduces the cation to Fe^{2+}, which precipitates as FeS.

Group 4: Insoluble Carbonates or Phosphates

The next metal ions to be removed from solution are those that form insoluble carbonates and phosphates. When Na_2CO_3 is added to the basic solution that remains after the precipitated metal ions are removed, insoluble carbonates precipitate and are collected. Alternatively, adding $(NH_4)_2HPO_4$ causes the same metal ions to precipitate as insoluble phosphates.

Group 5: Alkali Metals

At this point, we have removed all the metal ions that form water-insoluble chlorides, sulfides, carbonates, or phosphates. The only common ions that might remain are any alkali metals (Li^+, Na^+, K^+, Rb^+, and Cs^+) and ammonium (NH_4^+). We now take a second sample from the original solution and add a small amount of $NaOH$ to neutralize the ammonium ion and produce NH_3. (We cannot use the same sample we used for the first four groups because we added ammonium to that sample in earlier steps.) Any ammonia produced can be detected by either its odor or a litmus paper test. A flame test on another original sample is used to detect sodium, which produces a characteristic bright yellow color. The other alkali metal ions also give characteristic colors in flame tests, which allows them to be identified if only one is present.

Metal ions that precipitate together are separated by various additional techniques, such as forming complex ions, changing the pH of the solution, or increasing the temperature to redissolve some of the solids. For example, the precipitated metal chlorides of group 1 cations, containing Ag^+, Pb^{2+}, and Hg_2^{2+}, are all quite insoluble in water. Because $PbCl_2$ is much more soluble in hot water than are the other two chloride salts, however, adding water to the precipitate and heating the resulting slurry will dissolve any $PbCl_2$ present. Isolating the solution and adding a small amount of Na_2CrO_4 solution to it will produce a bright yellow precipitate of $PbCrO_4$ if Pb^{2+} were in the original sample (Figure 7.12.9.2).



Figure 7.12.9.2: When a small amount of Na_2CrO_4 solution is added to a sample containing Pb^{2+} ions in water, a bright yellow precipitate of $PbCrO_4$ forms. (CC BY-SA 3.0 Unported; PRHaney via Wikipedia).

As another example, treating the precipitates from group 1 cations with aqueous ammonia will dissolve any $AgCl$ because Ag^+ forms a stable complex with ammonia: $[Ag(NH_3)_2]^+$. In addition, Hg_2Cl_2 disproportionates in ammonia.

$$2\,Hg_2^{2+} \rightarrow Hg + Hg^{2+}$$

to form a black solid that is a mixture of finely divided metallic mercury and an insoluble mercury(II) compound, which is separated from solution:

$$Hg_2Cl_2\,(s) + 2\,NH_3\,(aq) \rightarrow Hg\,(l) + Hg(NH_2)Cl\,(s) + NH_4^+\,(aq) + Cl^-\,(aq)$$

Any silver ion in the solution is then detected by adding HCl, which reverses the reaction and gives a precipitate of white AgCl that slowly darkens when exposed to light:

$$[\mathrm{Ag(NH_3)_2}]^+(\mathrm{aq}) + 2\,\mathrm{H}^+(\mathrm{aq}) + \mathrm{Cl}^-(\mathrm{aq}) \rightarrow \mathrm{AgCl}(\mathrm{s}) + 2\,\mathrm{NH_4^+}(\mathrm{aq})$$

Similar but slightly more complex reactions are also used to separate and identify the individual components of the other groups.

Summary

In qualitative analysis, the identity, not the amount, of metal ions present in a mixture is determined. The technique consists of selectively precipitating only a few kinds of metal ions at a time under given sets of conditions. Consecutive precipitation steps become progressively less selective until almost all the metal ions are precipitated. Other additional steps are needed to separate metal ions that precipitate together.

7.12.9: Qualitative Cation Analysis is shared under a not declared license and was authored, remixed, and/or curated by LibreTexts.

- **17.7: Qualitative Analysis for Metallic Elements** by Anonymous is licensed CC BY-NC-SA 3.0.

CHAPTER OVERVIEW

8: Acids and Bases

Acids and bases have a multitude of properties and play a large role in the understanding of the formation and breaking of bonds throughout organic and organometallic chemistry. Specifically, aqueous acid and base chemistry has such an important role that it has developed a lot of tools and specific nomenclature for understanding its systems and strengths of the species ionizations/reactions. For this reason, this is broken down into the study of the following two categories:

Acids and Bases in Equilibrium

This studies the properties and equilibrium constants associated with acids, bases, conjugate acid-base pairs, pH, pOH, K_a, K_b, and K_w.

Additional Aspects of Acid-Base Equilibria

This extends the systems from above to specific acid/base interactions such as titrations, buffers, and more complex acid/base systems.

8.1: Acids and Bases at Equilibrium
- 8.1.1: Arrhenius Theory- A Brief Review
- 8.1.2: Brønsted-Lowry Theory of Acids and Bases
- 8.1.3: Self-Ionization of Water and the pH Scale
- 8.1.4: Introduction to Strong Acids and Bases
- 8.1.5: Strong Acids and Strong Bases
- 8.1.6: Weak Acids and Weak Bases
- 8.1.7: Conjugate Acid-Base Pairs and pH
- 8.1.8: Polyprotic Acids
- 8.1.9: Ions as Acids and Bases
- 8.1.10: Molecular Structure and Acid-Base Behavior
- 8.1.11: Lewis Acids and Bases
- 8.1.12: Common-Ion Effect in Acid–Base Equilibria

8.2: Additional Aspects of Acid-Base Equilibria
- 8.2.1: Buffer Solutions
- 8.2.2: Acid–Base Indicators
- 8.2.3: Neutralization Reactions and Titration Curves
- 8.2.4: Solutions of Salts of Polyprotic Acids
- 8.2.5: Acid–Base Equilibrium Calculations- A Summary
- 8.2.6: Exercises on Acids and Bases II
- 8.2.7: E3. Solubility Constants for Compounds at 25°C Data Table
- 8.2.8: pH Calculations for Acid–Base Titrations

8: Acids and Bases is shared under a not declared license and was authored, remixed, and/or curated by LibreTexts.

SECTION OVERVIEW

8.1: Acids and Bases at Equilibrium

Topic hierarchy

8.1.1: Arrhenius Theory- A Brief Review

8.1.2: Brønsted-Lowry Theory of Acids and Bases

8.1.3: Self-Ionization of Water and the pH Scale

8.1.4: Introduction to Strong Acids and Bases

8.1.5: Strong Acids and Strong Bases

8.1.6: Weak Acids and Weak Bases

8.1.7: Conjugate Acid-Base Pairs and pH

8.1.8: Polyprotic Acids

8.1.9: Ions as Acids and Bases

8.1.10: Molecular Structure and Acid-Base Behavior

8.1.11: Lewis Acids and Bases

8.1.12: Common-Ion Effect in Acid–Base Equilibria

8.1: Acids and Bases at Equilibrium is shared under a not declared license and was authored, remixed, and/or curated by LibreTexts.

8.1.1: Arrhenius Theory- A Brief Review

Acids and bases have been known for a long time. When Robert Boyle characterized them in 1680, he noted that acids dissolve many substances, change the color of certain natural dyes (for example, they change litmus from blue to red), and lose these characteristic properties after coming into contact with alkalis (bases). In the eighteenth century, it was recognized that acids have a sour taste, react with limestone to liberate a gaseous substance (now known to be CO_2), and interact with alkalis to form neutral substances. In 1815, Humphry Davy contributed greatly to the development of the modern acid-base concept by demonstrating that hydrogen is the essential constituent of acids. Around that same time, Joseph Louis Gay-Lussac concluded that acids are substances that can neutralize bases and that these two classes of substances can be defined only in terms of each other. The significance of hydrogen was reemphasized in 1884 when Svante Arrhenius defined an acid as a compound that dissolves in water to yield hydrogen cations (now recognized to be hydronium ions) and a base as a compound that dissolves in water to yield hydroxide anions.

Acids and bases are common solutions that exist everywhere. Almost every liquid that we encounter in our daily lives consists of acidic and basic properties, with the exception of water. They have completely different properties and are able to neutralize to form H_2O, which will be discussed later in a subsection. Acids and bases can be defined by their physical and chemical observations (Table 8.1.1.1).

Table **8.1.1.1**: General Properties of Acids and Bases

ACIDS	BASES
produce a piercing pain in a wound.	give a slippery feel.
taste sour.	taste bitter.
are colorless when placed in phenolphthalein (an indicator).	are pink when placed in phenolphthalein (an indicator).
are red on blue litmus paper (a pH indicator).	are blue on red litmus paper (a pH indicator).
have a pH<7.	have a pH>7.
produce hydrogen gas when reacted with metals.	
produce carbon dioxide when reacted with carbonates.	
Common examples: Lemons, oranges, vinegar, urine, sulfuric acid, hydrochloric acid	Common Examples: Soap, toothpaste, bleach, cleaning agents, limewater, ammonia water, sodium hydroxide.

Acids and bases in aqueous solutions will conduct electricity because they contain dissolved ions. Therefore, acids and bases are **electrolytes**. Strong acids and bases will be strong electrolytes. Weak acids and bases will be weak electrolytes. This affects the amount of conductivity.

The Arrhenius Definition of Acids and Bases

In 1884, the Swedish chemist Svante Arrhenius proposed two specific classifications of compounds, termed acids and bases. When dissolved in an aqueous solution, certain ions were released into the solution. The Arrhenius definition of acid-base reactions is a development of the "hydrogen theory of acids". It was used to provide a modern definition of acids and bases, and followed from Arrhenius's work with Friedrich Wilhelm Ostwald in establishing the presence of ions in aqueous solution in 1884. This led to Arrhenius receiving the Nobel Prize in Chemistry in 1903.

An Arrhenius acid is a compound that increases the concentration of H^+ ions that are present when added to water. These H^+ ions form the hydronium ion (H_3O^+) when they combine with water molecules. This process is represented in a chemical equation by adding H_2O to the reactants side.

$$HCl_{(aq)} \rightarrow H^+_{(aq)} + Cl^-_{(aq)}$$

In this reaction, hydrochloric acid (HCl) dissociates into hydrogen (H^+) and chlorine (Cl^-) ions when dissolved in water, thereby releasing H^+ ions into solution. Formation of the hydronium ion equation:

$$HCl_{(aq)} + H_2O_{(l)} \rightarrow H_3O^+_{(aq)} + Cl^-_{(aq)}$$

The Arrhenius definitions of acidity and alkalinity are restricted to aqueous solutions and refer to the concentration of the solvated ions. Under this definition, pure H_2SO_4 or HCl dissolved in toluene are not acidic, despite the fact that both of these acids will donate a proton to toluene. In addition, under the Arrhenius definition, a solution of sodium amide ($NaNH_2$) in liquid ammonia is not alkaline, despite the fact that the amide ion (NH_2^-) will readily deprotonate ammonia. Thus, the Arrhenius definition can only describe acids and bases in an aqueous environment.

Limitation of the Arrhenius Definition of Acids and Bases

The Arrhenius definition can **only** describe acids and bases in an aqueous environment.

In chemistry, acids and bases have been defined differently by three sets of theories: One is the Arrhenius definition defined above, which revolves around the idea that acids are substances that ionize (break off) in an aqueous solution to produce hydrogen (H^+) ions while bases produce hydroxide (OH^-) ions in solution. The other two definitions are discussed in detail alter in the chapter and include the Brønsted-Lowry definition the defines acids as substances that donate protons (H^+) whereas bases are substances that accept protons and the Lewis theory of acids and bases states that acids are electron pair acceptors while bases are electron pair donors.

Contributors and Attributions

- Anonymous

8.1.1: Arrhenius Theory- A Brief Review is shared under a not declared license and was authored, remixed, and/or curated by LibreTexts.

- **16.1: Acids and Bases - A Brief Review** is licensed CC BY-NC-SA 3.0.

8.1.2: Brønsted-Lowry Theory of Acids and Bases

Learning Objectives

- Identify acids, bases, and conjugate acid-base pairs according to the Brønsted-Lowry definition
- Write equations for acid and base ionization reactions
- Use the ion-product constant for water to calculate hydronium and hydroxide ion concentrations
- Describe the acid-base behavior of amphiprotic substances

The Arrhenius definition of an acid as a compound that dissolves in water to yield hydronium ions (H_3O^+) and a base as a compound that dissolves in water to yield hydroxide ions (OH^-). This definition is not wrong; it is simply limited. We extended the definition of an acid or a base using the more general definition proposed in 1923 by the Danish chemist Johannes Brønsted and the English chemist Thomas Lowry. Their definition centers on the proton, H^+. A proton is what remains when a normal hydrogen atom, ${}^1_1H$, loses an electron. A compound that donates a proton to another compound is called a Brønsted-Lowry acid, and a compound that accepts a proton is called a Brønsted-Lowry base. An acid-base reaction is the transfer of a proton from a proton donor (acid) to a proton acceptor (base). In a subsequent chapter of this text we will introduce the most general model of acid-base behavior introduced by the American chemist G. N. Lewis.

Brønsted-Lowry Defintions

- A compound that **donates** a proton to another compound is called a Brønsted-Lowry acid.
- A compound that **accepts** a proton is called a Brønsted-Lowry base.



Definitions of Acids and Bases: https://youtu.be/r8reN0CSIHw

Acids may be compounds such as HCl or H_2SO_4, organic acids like acetic acid (CH_3COOH) or ascorbic acid (vitamin C), or H_2O. Anions (such as HSO_4^-, $H_2PO_4^-$, HS^-, and HCO_3^-) and cations (such as H_3O^+, NH_4^+, and $[Al(H_2O)_6]^{3+}$) may also act as acids. Bases fall into the same three categories. Bases may be neutral molecules (such as H_2O, NH_3, and CH_3NH_2), anions (such as OH^-, HS^-, HCO_3^-, CO_3^{2-}, F^-, and PO_4^{3-}), or cations (such as $[Al(H_2O)_5OH]^{2+}$). The most familiar bases are ionic compounds such as $NaOH$ and $Ca(OH)_2$, which contain the hydroxide ion, OH^-. The hydroxide ion in these compounds accepts a proton from acids to form water:

$$H^+ + OH^- \rightarrow H_2O \tag{8.1.2.1}$$

We call the product that remains after an acid donates a proton the **conjugate base** of the acid. This species is a base because it can accept a proton (to re-form the acid):

$$\text{acid} \rightleftharpoons \text{proton} + \text{conjugate base} \tag{8.1.2.2}$$

$$HF \rightleftharpoons H^+ + F^-$$

$$H_2SO_4 \rightleftharpoons H^+ + HSO_4^-$$

$$H_2O \rightleftharpoons H^+ + OH^-$$

$$HSO_4^- \rightleftharpoons H^+ + SO_4^{2-}$$

$$NH_4^+ \rightleftharpoons H^+ + NH_3$$

We call the product that results when a base accepts a proton the base's **conjugate acid**. This species is an acid because it can give up a proton (and thus re-form the base):

$$\text{base} + \text{proton} \rightleftharpoons \text{conjugate acid} \tag{8.1.2.3}$$

$$OH^- + H^+ \rightleftharpoons H_2O$$

$$H_2O + H^+ \rightleftharpoons H_3O^+$$

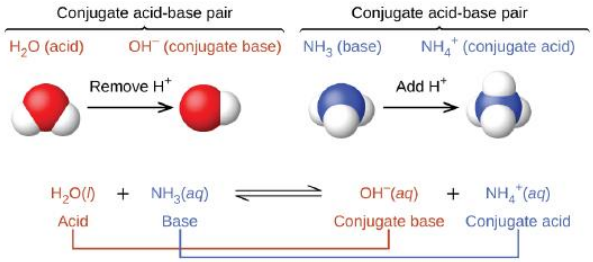
$$NH_3 + H^+ \rightleftharpoons NH_4^+$$

$$S^{2-} + H^+ \rightleftharpoons HS^-$$

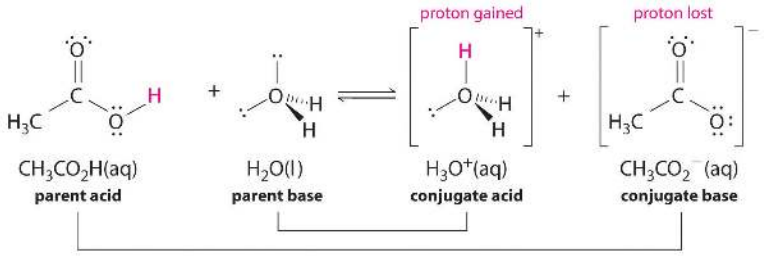
$$CO_3^{2-} + H^+ \rightleftharpoons HCO_3^-$$

$$F^- + H^+ \rightleftharpoons HF$$

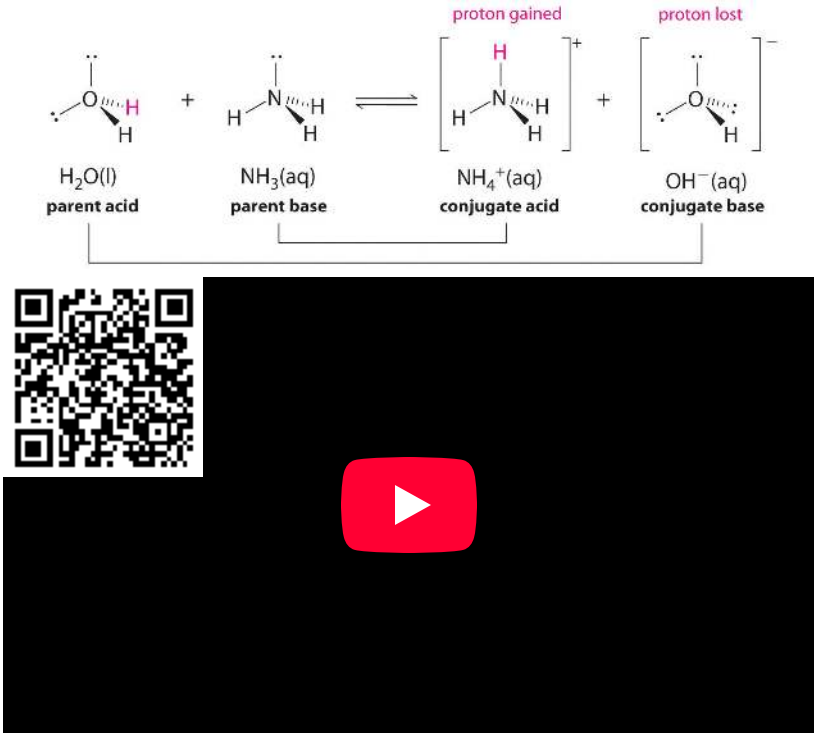
In these two sets of equations, the behaviors of acids as proton donors and bases as proton acceptors are represented in isolation. In reality, all acid-base reactions involve the transfer of protons between acids and bases. For example, consider the acid-base reaction that takes place when ammonia is dissolved in water. A water molecule (functioning as an acid) transfers a proton to an ammonia molecule (functioning as a base), yielding the conjugate base of water, OH^-, and the conjugate acid of ammonia, NH_4^+:



Similarly, in the reaction of acetic acid with water, acetic acid donates a proton to water, which acts as the base. In the reverse reaction, H_3O^+ is the acid that donates a proton to the acetate ion, which acts as the base. Once again, we have two conjugate acid–base pairs: the parent acid and its conjugate base ($CH_3CO_2H/CH_3CO_2^-$) and the parent base and its conjugate acid (H_3O^+/H_2O).



In the reaction of ammonia with water to give ammonium ions and hydroxide ions, ammonia acts as a base by accepting a proton from a water molecule, which in this case means that water is acting as an acid. In the reverse reaction, an ammonium ion acts as an acid by donating a proton to a hydroxide ion, and the hydroxide ion acts as a base. The conjugate acid–base pairs for this reaction are NH_4^+/NH_3 and H_2O/OH^-.



Conjugate Acid-Base Pairs: https://youtu.be/pPrp3xEQef4

Amphiprotic Species

Like water, many molecules and ions may either gain or lose a proton under the appropriate conditions. Such species are said to be amphiprotic. Another term used to describe such species is amphoteric, which is a more general term for a species that may act either as an acid or a base by any definition (not just the Brønsted-Lowry one). Consider for example the bicarbonate ion, which may either donate or accept a proton as shown here:

$$\mathrm{HCO_3^-\,(aq) + H_2O\,(l) \rightleftharpoons CO_3^{2-}\,(aq) + H_3O^+\,(aq)}$$

$$\mathrm{HCO_3^-\,(aq) + H_2O\,(l) \rightleftharpoons H_2CO_3\,(aq) + OH^-\,(aq)}$$

Water is the most important amphiprotic species. It can form both the hydronium ion, $\mathrm{H_3O^+}$, and the hydroxide ion, $\mathrm{OH^-}$ when it undergoes **autoionization**:

$$\mathrm{2\,H_2O_{(l)} \rightleftharpoons H_3O^+(aq) + OH^-(aq)}$$

✔ Example 8.1.2.1: The Acid-Base Behavior of an Amphoteric Substance

Write separate equations representing the reaction of $\mathrm{HSO_3^-}$

a. as an acid with $\mathrm{OH^-}$
b. as a base with HI

Solution

a. $\mathrm{HSO_3^-\,(aq) + OH^-\,(aq) \rightleftharpoons SO_3^{2-}\,(aq) + H_2O\,(l)}$
b. $\mathrm{HSO_3^-\,(aq) + HI\,(aq) \rightleftharpoons H_2SO_3\,(aq) + I^-\,(aq)}$

? Exercise 8.1.2.1

Write separate equations representing the reaction of $\mathrm{H_2PO_4^-}$

a. as a base with HBr

b. as an acid with OH^-

Answer a

$$H_2PO_4^-(aq) + HBr(aq) \rightleftharpoons H_3PO_4(aq) + Br^-(aq)$$

Answer b

$$H_2PO_4^-(aq) + OH^-(aq) \rightleftharpoons HPO_4^{2-}(aq) + H_2O_{(l)}$$

Key Concepts and Summary

A compound that can donate a proton (a hydrogen ion) to another compound is called a Brønsted-Lowry acid. The compound that accepts the proton is called a Brønsted-Lowry base. The species remaining after a Brønsted-Lowry acid has lost a proton is the conjugate base of the acid. The species formed when a Brønsted-Lowry base gains a proton is the conjugate acid of the base. Thus, an acid-base reaction occurs when a proton is transferred from an acid to a base, with formation of the conjugate base of the reactant acid and formation of the conjugate acid of the reactant base. Amphiprotic species can act as both proton donors and proton acceptors. Water is the most important amphiprotic species. It can form both the hydronium ion, H_3O^+, and the hydroxide ion, OH^- when it undergoes autoionization:

$$2\,H_2O_{(l)} \rightleftharpoons H_3O^+(aq) + OH^-(aq)$$

Glossary

acid ionization
reaction involving the transfer of a proton from an acid to water, yielding hydronium ions and the conjugate base of the acid

amphiprotic
species that may either gain or lose a proton in a reaction

amphoteric
species that can act as either an acid or a base

autoionization
reaction between identical species yielding ionic products; for water, this reaction involves transfer of protons to yield hydronium and hydroxide ions

base ionization
reaction involving the transfer of a proton from water to a base, yielding hydroxide ions and the conjugate acid of the base

Brønsted-Lowry acid
proton donor

Brønsted-Lowry base
proton acceptor

conjugate acid
substance formed when a base gains a proton

conjugate base
substance formed when an acid loses a proton

ion-product constant for water (K_w)
equilibrium constant for the autoionization of water

Contributors and Attributions

- Paul Flowers (University of North Carolina - Pembroke), Klaus Theopold (University of Delaware) and Richard Langley (Stephen F. Austin State University) with contributing authors. Textbook content produced by OpenStax College is licensed under a Creative Commons Attribution License 4.0 license. Download for free at http://cnx.org/contents/85abf193-2bd...a7ac8df6@9.110).

8.1.2: Brønsted-Lowry Theory of Acids and Bases is shared under a not declared license and was authored, remixed, and/or curated by LibreTexts.

- **16.2: Brønsted-Lowry Theory of Acids and Bases** is licensed CC BY-NC-SA 4.0.

8.1.3: Self-Ionization of Water and the pH Scale

Learning Objectives

- To understand the autoionization reaction of liquid water.
- To know the relationship among pH, pOH, and pK_w.

Because of its highly polar structure, liquid water can act as either an acid (by donating a proton to a base) or a base (by using a lone pair of electrons to accept a proton). For example, when a strong acid such as HCl dissolves in water, it dissociates into chloride ions (Cl^-) and protons (H^+). The proton, in turn, reacts with a water molecule to form the hydronium ion (H_3O^+):

$$\underset{acid}{HCl\,(aq)} + \underset{base}{H_2O\,(l)} \rightarrow \underset{acid}{H_3O^+\,(aq)} + \underset{base}{Cl^-\,(aq)} \tag{8.1.3.1}$$

In this reaction, HCl is the acid, and water acts as a base by accepting an H^+ ion. The reaction in Equation 8.1.3.1 is often written in a simpler form by removing H_2O from each side:

$$HCl\,(aq) \rightarrow H^+\,(aq) + Cl^-\,(aq) \tag{8.1.3.2}$$

In Equation 8.1.3.2, the hydronium ion is represented by $H^+\,(aq)$, although free H^+ ions do not exist in liquid water as this reaction demonstrates:

$$H^+\,(aq) + H_2O\,(l) \rightarrow H_3O^+\,(aq) \tag{8.1.3.3}$$

Water can also act as an acid, as shown in Equation 8.1.3.4. In this equilibrium reaction, H_2O donates a proton to NH_3, which acts as a base:

$$\underset{acid}{H_2O\,(aq)} + \underset{base}{NH_3\,(aq)} \rightleftharpoons \underset{acid}{NH_4^+\,(aq)} + \underset{base}{OH^-\,(aq)} \tag{8.1.3.4}$$

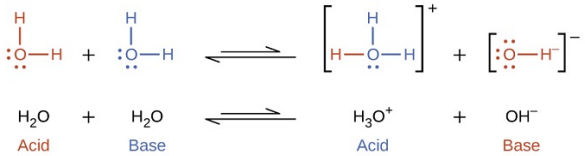
Water is thus termed **amphiprotic**, meaning that it can behave as either an acid or a base, depending on the nature of the other reactant. Notice that Equation 8.1.3.4 is an equilibrium reaction as indicated by the double arrow and hence has an equilibrium constant associated with it.

The Ion-Product Constant of Pure Water

Because water is amphiprotic, one water molecule can react with another to form an OH^- ion and an H_3O^+ ion in an autoionization process:

$$2\,H_2O\,(l) \rightleftharpoons H_3O^+\,(aq) + OH^-\,(aq) \tag{8.1.3.5}$$

In pure water, a very small fraction of water molecules donate protons to other water molecules to form hydronium ions and hydroxide ions:



The equilibrium constant K for this reaction can be written as follows:

$$K_a = \frac{a_{H_3O^+} \cdot a_{OH^-}}{a_{H_2O}^2} \approx \frac{[H_3O^+][HO^-]}{(1)^2} = [H_3O^+][HO^-] \tag{8.1.3.6}$$

where a is the activity of a species. Because water is the solvent, and the solution is assumed to be dilute, the activity of the water is approximated by the activity of pure liquid water, which is defined as having a value of 1. The activity of each solute is approximated by the molarity of the solute.

Note

It is a common error to claim that the molar concentration of the solvent is in some way involved in the equilibrium law. This error is a result of a misunderstanding of solution thermodynamics. For example, it is often claimed that Ka = $K_{eq}[H_2O]$ for aqueous solutions. This equation is incorrect because it is an erroneous interpretation of the correct equation Ka = $K_{eq}(a_{H_2O})$. Because a_{H_2O} = 1 for a dilute solution, $K_a = K_{eq}(1)$, or $K_a = K_{eq}$.

In this reaction, one water molecule acts as an acid and one water molecule acts as a base. Thus, this reaction actually can be designated as the K_a of water and as the K_b of water. It is most common, however, to designate this reaction and the associated law of mass action as the K_w of water:

$$K_w = [H_3O^+][HO^-] \tag{8.1.3.7}$$

When pure liquid water is in equilibrium with hydronium and hydroxide ions at 25 °C, the concentrations of the hydronium ion and the hydroxide ion are equal:

$$[H_3O^+] = [OH^-] = 1.003 \times 10^{-7}\ M \tag{8.1.3.8}$$

Thus the number of dissociated water molecules is very small indeed, approximately 2 ppb.

Substituting the values for $[H_3O^+]$ and $[OH^-]$ at 25°C into this expression

$$K_w = (1.003 \times 10^{-7})(1.003 \times 10^{-7}) = 1.006 \times 10^{-14} \tag{8.1.3.9}$$

The slight ionization of pure water is reflected in the small value of the equilibrium constant; at 25 °C.Thus, to three significant figures, $K_w = 1.01 \times 10^{-14}\ M$ *at room temperature*. Like any other equilibrium constant, K_w varies with temperature, ranging from 1.15×10^{-15} at 0°C to 4.99×10^{-13} at 100°C.

In pure water, the concentrations of the hydronium ion and the hydroxide ion are equal, and the solution is therefore neutral. If $[H_3O^+] > [OH^-]$, however, the solution is acidic, whereas if $[H_3O^+] < [OH^-]$, the solution is basic. For an aqueous solution, the H_3O^+ concentration is a quantitative measure of acidity: the higher the H_3O^+ concentration, the more acidic the solution. Conversely, the higher the OH^- concentration, the more basic the solution. In most situations that you will encounter, the H_3O^+ and OH^- concentrations from the dissociation of water are so small ($1.003 \times 10^{-7} M$) that they can be ignored in calculating the H_3O^+ or OH^- concentrations of solutions of acids and bases, but this is not always the case.

Example 8.1.3.1: Ion Concentrations in Pure Water

What are the hydronium ion concentration and the hydroxide ion concentration in pure water at 25 °C?

Solution

The autoionization of water yields the same number of hydronium and hydroxide ions. Therefore, in pure water, $[H_3O^+] = [OH^-]$. At 25 °C:

$$\begin{aligned} K_w &= [H_3O^+][OH^-] \\ &= [H_3O^+]^2 \\ &= [OH^-]^2 \\ &= 1.0 \times 10^{-14} \end{aligned}$$

So:

$$[H_3O^+] = [OH^-] = \sqrt{1.0 \times 10^{-14}} = 1.0 \times 10^{-7}\ M$$

The hydronium ion concentration and the hydroxide ion concentration are the same, and we find that both equal $1.0 \times 10^{-7}\ M$.

Exercise 8.1.3.1

The ion product of water at 80 °C is 2.4×10^{-13}. What are the concentrations of hydronium and hydroxide ions in pure water at 80 °C?

Answer

$$[H_3O^+] = [OH^-] = 4.9 \times 10^{-7}\ M$$

It is important to realize that the autoionization equilibrium for water is established in all aqueous solutions. Adding an acid or base to water will not change the position of the equilibrium. Example 8.1.3.2 demonstrates the quantitative aspects of this relation between hydronium and hydroxide ion concentrations.

Example 8.1.3.2: The Inverse Proportionality of Hydronium and Hydroxide Concentrations

A solution of carbon dioxide in water has a hydronium ion concentration of $2.0 \times 10^{-6}\ M$. What is the concentration of hydroxide ion at 25 °C?

Solution

We know the value of the ion-product constant for water at 25 °C:

$$2\,H_2O_{(l)} \rightleftharpoons H_3O^+{}_{(aq)} + OH^-{}_{(aq)}$$

and

$$K_w = [H_3O^+][OH^-] = 1.0 \times 10^{-14}$$

Thus, we can calculate the missing equilibrium concentration.

Rearrangement of the k_w expression yields that $[OH^-]$ is directly proportional to the inverse of $[H_3O^+]$:

$$[OH^-] = \frac{K_w}{[H_3O^+]} = \frac{1.0 \times 10^{-14}}{2.0 \times 10^{-6}} = 5.0 \times 10^{-9}$$

The hydroxide ion concentration in water is reduced to $5.0 \times 10^{-9}\ M$ as the hydrogen ion concentration increases to $2.0 \times 10^{-6}\ M$. This is expected from Le Chatelier's principle; the autoionization reaction shifts to the left to reduce the stress of the increased hydronium ion concentration and the $[OH^-]$ is reduced relative to that in pure water.

A check of these concentrations confirms that our arithmetic is correct:

$$K_w = [H_3O^+][OH^-] = (2.0 \times 10^{-6})(5.0 \times 10^{-9}) = 1.0 \times 10^{-14}$$

Exercise 8.1.3.2

What is the hydronium ion concentration in an aqueous solution with a hydroxide ion concentration of 0.001 M at 25 °C?

Answer

$$[H_3O^+] = 1 \times 10^{-11} M$$



Self-Ionization of Water (Kw): https://youtu.be/RMpO0rqUnFg

The Relationship among pH, pOH, and pK_w

The pH scale is a concise way of describing the H_3O^+ concentration and hence the acidity or basicity of a solution. Recall that pH and the H^+ (H_3O^+) concentration are related as follows:

$$pH = -\log_{10}[\mathrm{H^+}] \tag{8.1.3.10}$$

$$[\mathrm{H^+}] = 10^{-pH} \tag{8.1.3.11}$$

Because the scale is logarithmic, a pH difference of 1 between two solutions corresponds to a difference of a factor of 10 in their hydronium ion concentrations. Recall also that the pH of a neutral solution is 7.00 ($[H_3O^+] = 1.0 \times 10^{-7}\ M$), whereas acidic solutions have pH < 7.00 (corresponding to $[\mathrm{H_3O^+}] > 1.0 \times 10^{-7}$) and basic solutions have pH > 7.00 (corresponding to $[\mathrm{H_3O^+}] < 1.0 \times 10^{-7}$).

Similar notation systems are used to describe many other chemical quantities that contain a large negative exponent. For example, chemists use an analogous pOH scale to describe the hydroxide ion concentration of a solution. The pOH and $[\mathrm{OH^-}]$ are related as follows:

$$pOH = -\log_{10}[\mathrm{OH^-}] \tag{8.1.3.12}$$

$$[\mathrm{OH^-}] = 10^{-pOH} \tag{8.1.3.13}$$

The constant K_w can also be expressed using this notation, where $pK_w = -\log\ K_w$.

Because a neutral solution has $[OH^-] = 1.0 \times 10^{-7}$, the pOH of a neutral solution is 7.00. Consequently, the sum of the pH and the pOH for a neutral solution at 25°C is 7.00 + 7.00 = 14.00. We can show that the sum of pH and pOH is equal to 14.00 for any aqueous solution at 25°C by taking the negative logarithm of both sides of Equation ???:

$$-\log K_w = pK_w \tag{8.1.3.14}$$

$$= -\log([H_3O^+][OH^-]) \tag{8.1.3.15}$$

$$= (-\log[H_3O^+]) + (-\log[OH^-]) \tag{8.1.3.16}$$

$$= pH + pOH \tag{8.1.3.17}$$

Thus at any temperature, $pH + pOH = pK_w$, so at 25°C, where $K_w = 1.0 \times 10^{-14}$ and $pH + pOH = 14.00$. More generally, the pH of any neutral solution is half of the pK_w at that temperature. The relationship among pH, pOH, and the acidity or basicity of a solution is summarized graphically in Figure 8.1.3.1 over the common pH range of 0 to 14. Notice the inverse relationship between the pH and pOH scales.

> For any neutral solution, pH + pOH = 14.00 (at 25°C) with pH=pOH=7.

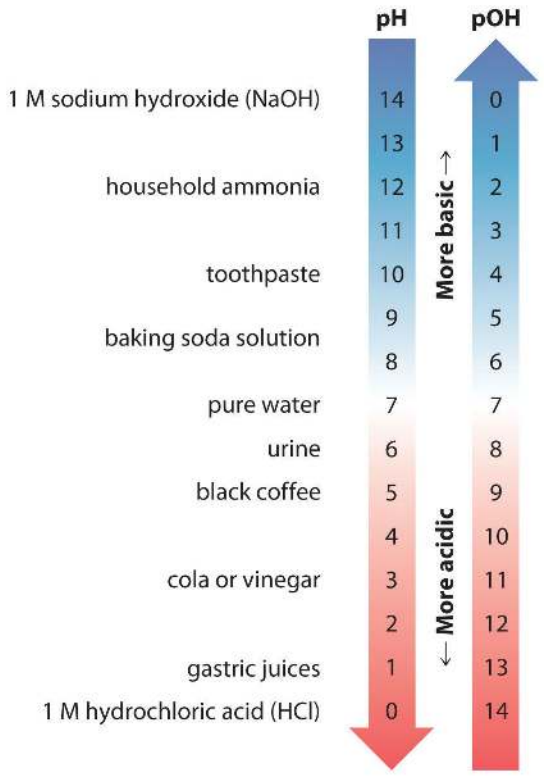


Figure 8.1.3.1: The Inverse Relationship between the pH and pOH Scales. As pH decreases, $[H^+]$ and the acidity increase. As pOH increases, $[OH^-]$ and the basicity decrease. Common substances have pH values that range from extremely acidic to extremely basic. (CC BY; OpenStax)

Example 8.1.3.3

The k_w for water at 100°C is 4.99×10^{-13}. Calculate pK_w for water at this temperature and the pH and the pOH for a neutral aqueous solution at 100°C. Report pH and pOH values to two decimal places.

Given: K_w

Asked for: pK_w, pH, and pOH

Strategy:

A. Calculate pKw by taking the negative logarithm of K_w.

B. For a neutral aqueous solution, $[H_3O^+] = [OH^-]$. Use this relationship and Equation ??? to calculate $[H_3O^+]$ and $[OH^-]$. Then determine the pH and the pOH for the solution.

Solution:

A Because pK_w is the negative logarithm of Kw, we can write

$$pK_w = -\log K_w = -\log(4.99 \times 10^{-13}) = 12.302$$

The answer is reasonable: K_w is between 10^{-13} and 10^{-12}, so pK_w must be between 12 and 13.

B Equation ??? shows that $K_w = [H_3O^+][OH^-]$. Because $[H_3O^+] = [OH^-]$ in a neutral solution, we can let $x = [H_3O^+] = [OH^-]$:

$$\begin{aligned} K_w &= [\mathrm{H_3O^+}][\mathrm{OH^-}] \\ &= (x)(x) \\ &= x^2 \\ x &= \sqrt{K_w} \\ &= \sqrt{4.99 \times 10^{-13}} \\ &= 7.06 \times 10^{-7}\ M \end{aligned}$$

Because x is equal to both $[\mathrm{H_3O^+}]$ and $[\mathrm{OH^-}]$,

$$\begin{aligned} pH = pOH &= -\log(7.06 \times 10^{-7}) \\ &= 6.15 \text{ (to two decimal places)} \end{aligned}$$

We could obtain the same answer more easily (without using logarithms) by using the pK_w. In this case, we know that $pK_w = 12.302$, and from Equation 8.1.3.17, we know that $pK_w = pH + pOH$. Because $pH = pOH$ in a neutral solution, we can use Equation 8.1.3.17 directly, setting $pH = pOH = y$. Solving to two decimal places we obtain the following:

$$pK_w = pH + pOH = y + y = 2y$$

$$y = \frac{pK_w}{2} = \frac{12.302}{2} = 6.15 = pH = pOH$$

? Exercise 8.1.3.3

Humans maintain an internal temperature of about 37°C. At this temperature, $K_w = 3.55 \times 10^{-14}$. Calculate pK_w and the pH and the pOH of a neutral solution at 37°C. Report pH and pOH values to two decimal places.

Answer

$pK_w = 13.45$ and $pH = pOH = 6.73$



Introduction to pH: https://youtu.be/pQOa3bb5YEE

Summary

- For any neutral solution, $pH + pOH = 14.00$ (at 25°C) and $pH = \frac{1}{2}pK_w$.
- Ion-product constant of liquid water:

$$K_w = [H_3O^+][OH^-]$$

- Definition of pH:

$$pH = -\log_{10}[H^+]$$

or

$$[H^+] = 10^{-pH}$$

- Definition of pOH:

$$pOH = -\log_{10}[OH^+]$$

or

$$[OH^-] = 10^{-pOH}$$

- Relationship among pH, pOH, and pK_w:

$$pK_w = pH + pOH$$

Water is amphiprotic: it can act as an acid by donating a proton to a base to form the hydroxide ion, or as a base by accepting a proton from an acid to form the hydronium ion (H_3O^+). The autoionization of liquid water produces OH^- and H_3O^+ ions. The equilibrium constant for this reaction is called the ion-product constant of liquid water (K_w) and is defined as $K_w = [H_3O^+][OH^-]$. At 25°C, K_w is 1.01×10^{-14}; hence $pH + pOH = pK_w = 14.00$. The process is endothermic, and so the extent of ionization and the resulting concentrations of hydronium ion and hydroxide ion **increase with temperature**. For example, at 100 °C, the value for K_w is approximately 5.1×10^{-13}, roughly 100-times larger than the value at 25 °C.

Glossary

acid ionization

reaction involving the transfer of a proton from an acid to water, yielding hydronium ions and the conjugate base of the acid

autoionization

reaction between identical species yielding ionic products; for water, this reaction involves transfer of protons to yield hydronium and hydroxide ions

ion-product constant for water (K_w)

equilibrium constant for the autoionization of water

Contributors and Attributions

- Paul Flowers (University of North Carolina - Pembroke), Klaus Theopold (University of Delaware) and Richard Langley (Stephen F. Austin State University) with contributing authors. Textbook content produced by OpenStax College is licensed under a Creative Commons Attribution License 4.0 license. Download for free at http://cnx.org/contents/85abf193-2bd...a7ac8df6@9.110).

8.1.3: Self-Ionization of Water and the pH Scale is shared under a not declared license and was authored, remixed, and/or curated by LibreTexts.

- **16.3: Self-Ionization of Water and the pH Scale** is licensed CC BY-NC-SA 4.0.
- **16.3: The Autoionization of Water** is licensed CC BY-NC-SA 3.0.

8.1.4: Introduction to Strong Acids and Bases

The most straight-forward examples involving acids and bases deal with *strong* acids and bases. **Strong acids**, like HCl or HNO_3, are such good proton donors that none of their own molecules can remain in aqueous solution. All HCl molecules, for example, transfer their protons to H_2O molecules, and so the solution contains only $H_3O^+(aq)$ and $Cl^-(aq)$ ions. Similarly, the ions of **strong bases**, like BaO or NaH, are such good proton acceptors that they cannot remain in aqueous solution. All O^{2-} ions, for example, are converted to OH^- ions by accepting protons from H_2O molecules, and the H_2O molecules are also converted to OH^-. Therefore a solution of BaO contains only $Ba^{2+}(aq)$ and $OH^-(aq)$ ions.

Table **8.1.4.1** lists molecules and ions which act as strong acids and bases in aqueous solution. In addition to those which react completely with H_2O to form H_3O^+ and OH^-, any compound which itself contains these ions will serve as a strong acid or base. Note that the strength of an acid refers only to its ability to donate protons to H_2O molecules and the strength of a base to its ability to accept protons from H_2O molecules. The acidity or basicity of a solution, on the other hand, depends on the concentration as well as the strength of the dissolved acid or base.

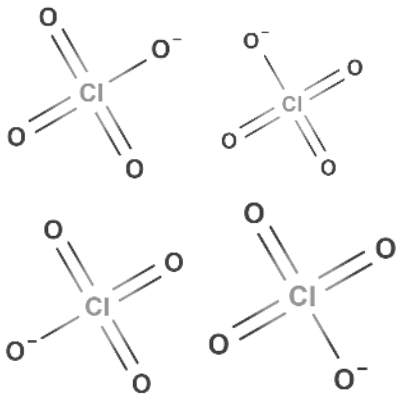
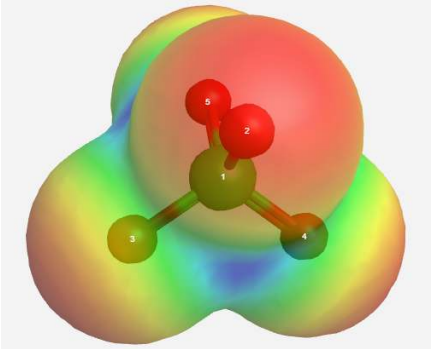
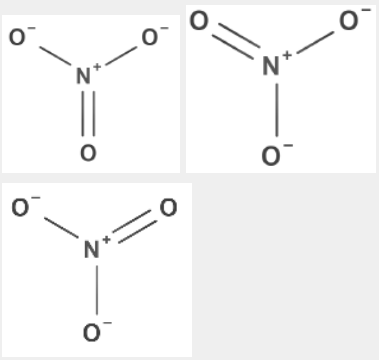
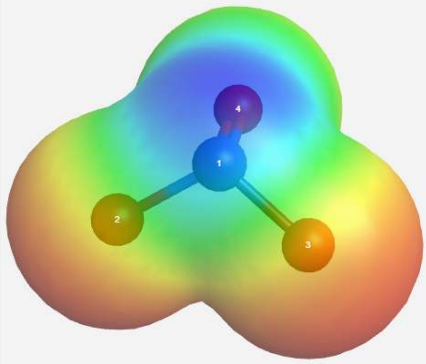
TABLE **8.1.4.1** Species Which Are Strong Acids and Bases in Aqueous Solution.

Strong Acids	Strong Bases
H_3O^+ (Only a few compounds like H_3OCl and H_3ONO_3 are known to contain hydronium ions.)	OH^- [Only LiOH, NaOH, KOH, RbOH, CsOH, $Ca(OH)_2$, $Sr(OH)_2$ and $Ba(OH)_2$ are sufficiently soluble to produce large concentrations of OH^-(aq).]
HCl, HBr, HI $HClO_4$	O^{2-} (Li_2O, Na_2O, K_2O, Rb_2O, Cs_2O, CaO, SrO, and BaO are soluble
HNO_3, H_2SO_4, $HClO_3$	H^-, S^{2-}, NH_2^-, N^{3-}, P^{3-}

Notice that the cations of the strong bases are also soluble in water, as seen in the table from 11.2 on solubility rules. For example, all the Group 1 cations form strong bases and all Group 1 cations are soluble in water. Therefore, you can use your prior understanding of solubility rules to guide your understanding of strong bases. As a general rules, if a cation is soluble in water, it can form a strong base.

As a general rule, strong proton donors are molecules in which a hydrogen is attached to a rather electronegative atom, such as oxygen or a halogen. Considerable electron density is shifted away from hydrogen in such a molecule, making it possible for hydrogen ions to depart without taking along any electrons. The strong acids in Table **8.1.4.1** fit this rule nicely. They are either hydrogen halides (HCl, HBr, HI) or oxyacids (whose general formula is H_nXO_m).

Below are the resonance structures for oxoacids after they donate a proton. The reason for the strength of the following acids is the stability of the anion, which is shown by the number of resonance structures and the distribution of the negative charge amongst all of the oxygen atoms. The distribution of the negative charge can be visualized in the 3D structure, with red being representing negative charge and blue representing positive charge. The 3D structure represents the average of the resonance structures shown to the left.

Name	Lewis Structure (Resonance)	3D Structure
Perchloric Acid		
Nitric Acid		

The Lewis structures indicate a proton bonded to oxygen in each of the oxyacids, hence their general name. Note that for a strong oxyacid the number of oxygens is always larger by two or more than the number of hydrogens. That is, in the general formula H_nXO_m, $m \geq n + 2$.

The strength of a base depends on its ability to attract and hold a proton. Therefore bases often have negative charges, and they invariably have at least one lone pair of electrons which can form a coordinate covalent bond to a proton. The strong bases in Table 1 might be thought of as being derived from neutral molecules by successive removal of protons. For example, OH^- can be obtained by removing H^+ from H_2O, and O^{2-} can be obtained by removing H^+ from OH^-. When the strong bases are considered this way, it is not surprising that they are good proton acceptors.

This page titled 8.1.4: Introduction to Strong Acids and Bases is shared under a CC BY-NC-SA 4.0 license and was authored, remixed, and/or curated by Ed Vitz, John W. Moore, Justin Shorb, Xavier Prat-Resina, Tim Wendorff, & Adam Hahn.

- **11.9: Strong Acids and Bases** by Ed Vitz, John W. Moore, Justin Shorb, Xavier Prat-Resina, Tim Wendorff, & Adam Hahn is licensed CC BY-NC-SA 4.0.

8.1.5: Strong Acids and Strong Bases

Learning Objectives

- Give the names and formulas of some strong acids and bases.
- Explain the pH scale, and convert pH and concentration of hydronium ions.
- Evaluate solution pH and pOH of strong acids or bases.

Acids and bases that are completely ionized when dissolved in water are called **strong acids** and **strong bases** There are only a few strong acids and bases, and everyone should know their names and properties. These acids are often used in industry and everyday life. The concentrations of acids and bases are often expressed in terms of pH, and as an educated person, you should have the skill to convert concentrations into pH and pOH. The pH is an indication of the hydrogen ion concentration, $[H^+]$.

Strong Acids

Strong acids are acids that are completely or nearly 100% ionized in their solutions; Table 8.1.5.1 includes some common strong acids. Hence, the ionization in Equation 8.1.5.1 for a strong acid HA can be represented with a single arrow:

$$HA\,(aq) + H_2O\,(l) \rightarrow H_3O^+\,(aq) + A^-\,(aq) \tag{8.1.5.1}$$

Water is the base that reacts with the acid HA, A^- is the conjugate base of the acid HA, and the hydronium ion is the conjugate acid of water. By definition, a strong acid yields 100% of H_3O^+ and A^- when the acid ionizes in water. Table 8.1.5.1 lists several strong acids.

Table 8.1.5.1: Some of the common strong acids and bases are listed here.

Strong Acids	Strong Bases
perchloric acid ($HClO_4$)	lithium hydroxide ($LiOH$)
hydrochloric acid (HCl)	sodium hydroxide ($NaOH$)
hydrobromic acid (HBr)	potassium hydroxide (KOH)
hydroiodic acid (HI)	calcium hydroxide ($Ca(OH)_2$)
nitric acid (HNO_3)	strontium hydroxide ($Sr(OH)_2$)
sulfuric acid (H_2SO_4)	barium hydroxide ($Ba(OH)_2$)

For a strong acid, $[H^+] = [A^-]$ = concentration of acid if the concentration is much higher than $1 \times 10^{-7}\,M$. However, for a very dilute strong acid solution with concentration less than $1 \times 10^{-7}\,M$, the pH is dominated by the **autoionization of water**

$$H_2O \rightleftharpoons H^+ + OH^- \tag{8.1.5.2}$$

Example 8.1.5.1

Calculate the pH of a solution with $1.2345 \times 10^{-4}\,M HCl$, a strong acid.

Solution

The solution of a strong acid is completely ionized. That is, this equation goes to completion

$$HCl\,(aq) \longrightarrow H\,(aq) + Cl^-\,(aq)$$

Thus, $[H^+] = 1.2345 \times 10^{-4}$.

$$pH = -\log(1.2345 \times 10^{-4}) = 3.90851$$

? Exercise 8.1.5.1

What is the pH for a solution containing 1.234 M [HCl]?

Answer

pH = -0.0913

✓ Example 8.1.5.2

Calculate the pH of a stock HCl solution that is 32% by mass HCl.

Solution

The density of such a solution is needed before we can calculate the pH. Since the density is not on the label, we need to find it from the Material Safety Data Sheet, which gives the specific gravity of 1.150. Thus, the amount of acid in 1.0 L is 1150 g.

$$\begin{aligned}\text{The amount of HCl} &= 1000 \times 1.150 \times 0.32 \\ &= 368\ \text{g}\ \left(\frac{1\ \text{mol}}{36.5\ \text{g}} \leftarrow \text{molar mass of HCl}\right) \\ &= 10.08\ \text{M} \\ &= [\text{H}^+]\end{aligned}$$

$$\text{pH} = -\log(10.08) = -1.003$$

Discussion

Yes, pH have negative values if $[\text{H}^+] > 1.0$

? Exercise 8.1.5.2

Check out the information on nitric acid, a strong acid, and calculate the pH of a stock nitric acid solution.

✓ Example 8.1.5.3

Calculate the pH of a solution containing $1.00 \times 10^{-7}\ M$ of the strong acid HCl.

Solution

$[\text{H}^+] = 1.0 \times 10^{-7}\ M$ from the strong acid, and if x is the amount from the ionization of water, then we have the equilibrium due to the **autoionization** of water. We can model this with an ICE table.

$$H_2O \rightleftharpoons H^+_{(aq)} + OH^-_{(aq)}$$

ICE Table	$H_2O_{(l)}$	$H^+_{(aq)}$	$OH^-_{(aq)}$
Initial	-	1×10^{-7}	0
Change	-	+x	+x
Equilibrium	-	$1 \times 10^{-7} + x$	x

Recall that $K_w = [\text{H}^+]\ [\text{OH}^-\ ] = 1 \times 10^{-14}$, due to the ionization equilibrium of water in the solution:

$$(1.00 \times 10^{-7} + x)x = 1 \times 10^{-14}$$

$$x^2 + 1.00 \times 10^{-7}x - 1.00 \times 10^{-14} = 0$$

Solving this equation for x from the quadratic equation results in

$$x = \frac{-1.00 \times 10^{-7} \pm \sqrt{1.00 \times 10^{-14} + (4)(1)(1.00 \times 10^{-14})}}{2}$$
$$= 0.61 \times 10^{-7}$$

only the additive root is physical (positive concentration); therefore

$$[H^+] = (1.00 + 0.61) \times 10^{-7}\ M$$
$$pH = -\log(1.61 \times 10^{-7})$$
$$= 6.79$$

Discussion

If you require only 1 significant figure, the pH is about 7.

Strong Bases

Strong bases are completely ionized in solution. Table 8.1.5.1 includes some common strong bases. For example, KOH dissolves in water in the reaction

$$KOH \rightarrow K^+ + OH^-$$

Relative to the number of strong acids, there are fewer number of strong bases and most are alkali hydroxides. Calcium hydroxide is considered a strong base, because it is completely, almost completely, ionized. However, the solubility of calcium hydroxide is very low. When $Ca(OH)_2$ dissolves in water, the ionization reaction is as follows:

$$Ca(OH)_2 \rightarrow Ca^{2+} + 2\,OH^-$$

Because of the stoichiometry of calcium hydroxide, upon dissociation, the concentration of OH^- will be twice the concentration of Ca^{2+}:

$$[OH^-] = 2[Ca^{2+}]$$

Example 8.1.5.4

Calculate the pOH of a solution containing $1.2345 \times 10^{-4}\ M$ $Ca(OH)_2$.

Solution

Based on complete ionization of

$$Ca(OH)_2 \rightarrow Ca^{+2} + 2\,OH^-$$
$$[OH^-] = 2 \times 1.2345 \times 10^{-4}$$
$$= 2.4690 \times 10^{-4}\ M$$
$$pOH = -\log(2.4690 \times 10^{-4})$$
$$= 3.6074$$

Exercise 8.1.5.4

The molar solubility of calcium hydroxide is 0.013 M $Ca(OH)_2$. Calculate the pOH.

Answer

pOH = 1.58



Calculating pH in Strong Acid or Strong Base Solutions: https://youtu.be/NNTptn7hV2s

Questions

1. What is the pH of a solution containing 0.01 M $\mathbf{HNO_3}$?
2. What is the pH of a solution containing 0.0220 M $\mathbf{Ba(OH)_2}$? Give 3 significant figures.
3. Exactly 1.00 L solution was made by dissolving 0.80 g of $\mathbf{NaOH}$ in water. What is $[\mathbf{H^+}]$? (Atomic mass: **Na**, 23.0; **O**, 16.0; **H**, 1.0)
4. What is the pH for a solution which is 0.050 M $\mathbf{HCl}$?
5. Which of the following is usually referred to as strong acid in water solution?

$$\mathbf{HF},\ \mathbf{HNO_2},\ \mathbf{H_2CO_3},\ \mathbf{H_2S},\ \mathbf{HSO_4^-},\ \mathbf{Cl^-},\ \mathbf{HNO_3},\ \mathbf{HCN}$$

Solutions

1. ***Answer*** 2

   Hint...

   You do not need a calculator to evaluate $-\log(0.01) = 2$
2. ***Answer*** 12.64

   Hint...

   $\mathbf{Ba(OH)_2} \rightarrow \mathbf{Ba^{2+}} + 2\,\mathbf{OH^-}$
3. ***Answer*** 5.0×10^{-13}

   Hint...

   $[\mathrm{OH^-}] = \dfrac{0.80}{40} = 0.020\ \mathrm{M};\ [H^+] = \dfrac{1.0 \times 10^{-14}}{0.020} = 5 \times 10^{-13} M$. The pH is 12.30.
4. ***Answer*** 1.3

   Hint...

   This solution contains 1.83 g of $\mathbf{HCl}$ per liter. $[\mathbf{H^+}] = 0.050$.
5. ***Answer*** $\mathbf{HNO_3}$

   Consider...

   All others are weak acids

Contributors and Attributions

- Chung (Peter) Chieh (Professor Emeritus, Chemistry @ University of Waterloo)

8.1.5: Strong Acids and Strong Bases is shared under a not declared license and was authored, remixed, and/or curated by LibreTexts.

- **16.4: Strong Acids and Strong Bases** is licensed CC BY-NC-SA 4.0.

8.1.6: Weak Acids and Weak Bases

Learning Objectives

- To know the relationship between acid or base strength and the magnitude of K_a, K_b, pK_a, and pK_b.
- To understand the leveling effect.

The magnitude of the equilibrium constant for an ionization reaction can be used to determine the relative strengths of acids and bases. For example, the general equation for the ionization of a weak acid in water, where HA is the parent acid and A− is its conjugate base, is as follows:

$$HA_{(aq)} + H_2O_{(l)} \rightleftharpoons H_3O^+_{(aq)} + A^-_{(aq)} \tag{8.1.6.1}$$

The equilibrium constant for this dissociation is as follows:

$$K = \frac{[H_3O^+][A^-]}{[H_2O][HA]} \tag{8.1.6.2}$$

As we noted earlier, the concentration of water is essentially constant for all reactions in aqueous solution, so $[H_2O]$ in Equation 8.1.6.2 can be incorporated into a new quantity, the acid ionization constant (K_a), also called the acid dissociation constant:

$$K_a = K[H_2O] = \frac{[H_3O^+][A^-]}{[HA]} \tag{8.1.6.3}$$

Thus the numerical values of K and K_a differ by the concentration of water (55.3 M). Again, for simplicity, H_3O^+ can be written as H^+ in Equation 8.1.6.3. Keep in mind, though, that free H^+ does not exist in aqueous solutions and that a proton is transferred to H_2O in all acid ionization reactions to form H^3O^+. The larger the K_a, the stronger the acid and the higher the H^+ concentration at equilibrium.Like all equilibrium constants, acid–base ionization constants are actually measured in terms of the activities of H^+ or OH^-, thus making them **unitless**. The values of K_a for a number of common acids are given in Table **8.1.6.1**.

Table **8.1.6.1**: Values of K_a, pK_a, K_b, and pK_b for Selected Acids (HA and Their Conjugate Bases (A^-)

Acid	HA	K_a	pK_a	A^-	K_b	pK_b
hydroiodic acid	HI	2×10^{9}	−9.3	I^-	5.5×10^{-24}	23.26
sulfuric acid (1)*	H_2SO_4	1×10^{2}	−2.0	HSO_4^-	1×10^{-16}	16.0
nitric acid	HNO_3	2.3×10^{1}	−1.37	NO_3^-	4.3×10^{-16}	15.37
hydronium ion	H_3O^+	1.0	0.00	H_2O	1.0×10^{-14}	14.00
sulfuric acid (2)*	HSO_4^-	1.0×10^{-2}	1.99	SO_4^{2-}	9.8×10^{-13}	12.01
hydrofluoric acid	HF	6.3×10^{-4}	3.20	F^-	1.6×10^{-11}	10.80
nitrous acid	HNO_2	5.6×10^{-4}	3.25	$NO2^-$	1.8×10^{-11}	10.75
formic acid	HCO_2H	1.78×10^{-4}	3.750	HCO_2-	5.6×10^{-11}	10.25
benzoic acid	$C_6H_5CO_2H$	6.3×10^{-5}	4.20	$C_6H_5CO_2^-$	1.6×10^{-10}	9.80
acetic acid	CH_3CO_2H	1.7×10^{-5}	4.76	$CH_3CO_2^-$	5.8×10^{-10}	9.24
pyridinium ion	$C_5H_5NH^+$	5.9×10^{-6}	5.23	C_5H_5N	1.7×10^{-9}	8.77
hypochlorous acid	$HOCl$	4.0×10^{-8}	7.40	OCl^-	2.5×10^{-7}	6.60
hydrocyanic acid	HCN	6.2×10^{-10}	9.21	CN^-	1.6×10^{-5}	4.79
ammonium ion	NH_4^+	5.6×10^{-10}	9.25	NH_3	1.8×10^{-5}	4.75
water	H_2O	1.0×10^{-14}	14.00	OH^-	1.00	0.00
acetylene	C_2H_2	1×10^{-26}	26.0	HC_2^-	1×10^{12}	−12.0
ammonia	NH_3	1×10^{-35}	35.0	NH_2^-	1×10^{21}	−21.0

*The number in parentheses indicates the ionization step referred to for a polyprotic acid.

Weak bases react with water to produce the hydroxide ion, as shown in the following general equation, where B is the parent base and BH+ is its conjugate acid:

$$\mathrm{B\,(aq) + H_2O\,(l) \rightleftharpoons BH^+\,(aq) + OH^-\,(aq)} \tag{8.1.6.4}$$

The equilibrium constant for this reaction is the **base ionization constant** (K_b), also called the base dissociation constant:

$$K_b = K[H_2O] = \frac{[BH^+][OH^-]}{[B]} \tag{8.1.6.5}$$

Once again, the concentration of water is constant, so it does not appear in the equilibrium constant expression; instead, it is included in the K_b. The larger the K_b, the stronger the base and the higher the OH^- concentration at equilibrium. The values of K_b for a number of common weak bases are given in Table 8.1.6.2.

Table 8.1.6.2: Values of K_b, pK_b, K_a, and pK_a for Selected Weak Bases (B) and Their Conjugate Acids (BH+)

Base	B	K_b	pK_b	BH^+	K_a	pK_a
hydroxide ion	OH^-	1.0	0.00*	H_2O	1.0×10^{-14}	14.00
phosphate ion	PO_4^{3-}	2.1×10^{-2}	1.68	HPO_4^{2-}	4.8×10^{-13}	12.32
dimethylamine	$(CH_3)_2NH$	5.4×10^{-4}	3.27	$(CH_3)_2NH_2^+$	1.9×10^{-11}	10.73
methylamine	CH_3NH_2	4.6×10^{-4}	3.34	$CH_3NH_3^+$	2.2×10^{-11}	10.66
trimethylamine	$(CH_3)_3N$	6.3×10^{-5}	4.20	$(CH_3)_3NH^+$	1.6×10^{-10}	9.80
ammonia	NH_3	1.8×10^{-5}	4.75	NH_4^+	5.6×10^{-10}	9.25
pyridine	C_5H_5N	1.7×10^{-9}	8.77	$C_5H_5NH^+$	5.9×10^{-6}	5.23
aniline	$C_6H_5NH_2$	7.4×10^{-10}	9.13	$C_6H_5NH_3^+$	1.3×10^{-5}	4.87
water	H_2O	1.0×10^{-14}	14.00	H_3O^+	1.0*	0.00

*As in Table 8.1.6.1.

There is a simple relationship between the magnitude of K_a for an acid and K_b for its conjugate base. Consider, for example, the ionization of hydrocyanic acid (HCN) in water to produce an acidic solution, and the reaction of CN^- with water to produce a basic solution:

$$HCN_{(aq)} \rightleftharpoons H^+_{(aq)} + CN^-_{(aq)} \tag{8.1.6.6}$$

$$CN^-_{(aq)} + H_2O_{(l)} \rightleftharpoons OH^-_{(aq)} + HCN_{(aq)} \tag{8.1.6.7}$$

The equilibrium constant expression for the ionization of HCN is as follows:

$$K_a = \frac{[H^+][CN^-]}{[HCN]} \tag{8.1.6.8}$$

The corresponding expression for the reaction of cyanide with water is as follows:

$$K_b = \frac{[OH^-][HCN]}{[CN^-]} \tag{8.1.6.9}$$

If we add Equations 8.1.6.6 and 8.1.6.7, we obtain the following (recall that the equilibrium constant for the sum of two reactions is the product of the equilibrium constants for the individual reactions):

$$\cancel{HCN_{(aq)}} \rightleftharpoons H^+_{(aq)} + \cancel{CN^-_{(aq)}} \quad K_a = [H^+]\,\cancel{[CN^-]} / \cancel{[HCN]} \tag{8.1.6.10}$$

$$\cancel{CN^-_{(aq)}} + H_2O_{(l)} \rightleftharpoons OH^-_{(aq)} + \cancel{HCN_{(aq)}} \quad K_b = [OH^-]\,\cancel{[HCN]} / \cancel{[CN^-]} \tag{8.1.6.11}$$

$$H_2O_{(l)} \rightleftharpoons H^+_{(aq)} + OH^-_{(aq)} \quad K = K_a \times K_b = [H^+][OH^-] \tag{8.1.6.12}$$

In this case, the sum of the reactions described by K_a and K_b is the equation for the autoionization of water, and the product of the two equilibrium constants is K_w:

$$K_aK_b = K_w \tag{8.1.6.13}$$

Thus if we know either K_a for an acid or K_b for its conjugate base, we can calculate the other equilibrium constant for any conjugate acid–base pair.

Just as with pH, pOH, and pK_w, we can use negative logarithms to avoid exponential notation in writing acid and base ionization constants, by defining pK_a as follows:

$$pKa = -\log_{10} K_a \tag{8.1.6.14}$$

$$K_a = 10^{-pK_a} \tag{8.1.6.15}$$

and pK_b as

$$pK_b = -\log_{10} K_b \tag{8.1.6.16}$$

$$K_b = 10^{-pK_b} \tag{8.1.6.17}$$

Similarly, Equation 8.1.6.13, which expresses the relationship between K_a and K_b, can be written in logarithmic form as follows:

$$pK_a + pK_b = pK_w \tag{8.1.6.18}$$

At 25°C, this becomes

$$pK_a + pK_b = 14.00 \tag{8.1.6.19}$$

The values of pK_a and pK_b are given for several common acids and bases in Table 8.1.6.1 and Table 8.1.6.2, respectively, and a more extensive set of data is provided in Tables E1 and E2. Because of the use of negative logarithms, smaller values of pK_a correspond to larger acid ionization constants and hence stronger acids. For example, nitrous acid (HNO_2), with a pK_a of 3.25, is about a 1000 times stronger acid than hydrocyanic acid (HCN), with a pK_a of 9.21. Conversely, smaller values of pK_b correspond to larger base ionization constants and hence stronger bases.

The relative strengths of some common acids and their conjugate bases are shown graphically in Figure 16.5. The conjugate acid–base pairs are listed in order (from top to bottom) of increasing acid strength, which corresponds to decreasing values of pK_a. This order corresponds to decreasing strength of the conjugate base or increasing values of pK_b. At the bottom left of Figure 8.1.6.2 are the common strong acids; at the top right are the most common strong bases. Notice the inverse relationship between the strength of the parent acid and the strength of the conjugate base. Thus the conjugate base of a strong acid is a very weak base, and the conjugate base of a very weak acid is a strong base.

> *The conjugate base of a strong acid is a weak base and vice versa.*

We can use the relative strengths of acids and bases to predict the direction of an acid–base reaction by following a single rule: an acid–base equilibrium always favors the side with the weaker acid and base, as indicated by these arrows:

$$\textbf{stronger acid} + \textbf{stronger base} \rightleftharpoons \textbf{weaker acid} + \textbf{weaker base}$$

In an acid–base reaction, the proton always reacts with the stronger base.

For example, hydrochloric acid is a strong acid that ionizes essentially completely in dilute aqueous solution to produce H_3O^+ and Cl^-; only negligible amounts of HCl molecules remain undissociated. Hence the ionization equilibrium lies virtually all the way to the right, as represented by a single arrow:

$$HCl_{(aq)} + H_2O_{(l)} \rightarrow\rightarrow H_3O^+_{(aq)} + Cl^-_{(aq)} \tag{8.1.6.20}$$

In contrast, acetic acid is a weak acid, and water is a weak base. Consequently, aqueous solutions of acetic acid contain mostly acetic acid molecules in equilibrium with a small concentration of H_3O^+ and acetate ions, and the ionization equilibrium lies far to the left, as represented by these arrows:

$$\mathrm{CH_3CO_2H_{(aq)} + H_2O_{(l)} \rightleftharpoons H_3O^+{}_{(aq)} + CH_3CO_{2(aq)}{}^-}$$

Similarly, in the reaction of ammonia with water, the hydroxide ion is a strong base, and ammonia is a weak base, whereas the ammonium ion is a stronger acid than water. Hence this equilibrium also lies to the left:

$$H_2O_{(l)} + NH_{3(aq)} \rightleftharpoons NH^+_{4(aq)} + OH^-_{(aq)}$$

> *All acid–base equilibria favor the side with the weaker acid and base. Thus the proton is bound to the stronger base.*

Example 8.1.6.1: Butyrate and Dimethylammonium Ions

a. Calculate K_b and pK_b of the butyrate ion ($CH_3CH_2CH_2CO_2^-$). The pK_a of butyric acid at 25°C is 4.83. Butyric acid is responsible for the foul smell of rancid butter.

b. Calculate K_a and pK_a of the dimethylammonium ion ($(CH_3)_2NH_2^+$). The base ionization constant K_b of dimethylamine ($(CH_3)_2NH$) is 5.4×10^{-4} at 25°C.

Given: pK_a and K_b

Asked for: corresponding K_b and pK_b, K_a and pK_a

Strategy:

The constants K_a and K_b are related as shown in Equation 8.1.6.13. The pK_a and pK_b for an acid and its conjugate base are related as shown in Equation 8.1.6.18 and Equation 8.1.6.19. Use the relationships $pK = -\log K$ and $K = 10^{-pK}$ (Equations 8.1.6.14 and 8.1.6.16) to convert between K_a and pK_a or K_b and pK_b.

Solution:

We are given the pK_a for butyric acid and asked to calculate the K_b and the pK_b for its conjugate base, the butyrate ion. Because the pK_a value cited is for a temperature of 25°C, we can use Equation 8.1.6.19: $pK_a + pK_b$ = pKw = 14.00. Substituting the pK_a and solving for the pK_b,

$$\begin{aligned} 4.83 + pK_b &= 14.00 \\ pK_b &= 14.00 - 4.83 \\ &= 9.17 \end{aligned}$$

Because $pK_b = -\log K_b$, K_b is $10^{-9.17} = 6.8 \times 10^{-10}$.

In this case, we are given K_b for a base (dimethylamine) and asked to calculate K_a and pK_a for its conjugate acid, the dimethylammonium ion. Because the initial quantity given is K_b rather than pK_b, we can use Equation 8.1.6.13: $K_aK_b = K_w$. Substituting the values of K_b and K_w at 25°C and solving for K_a,

$$\begin{aligned} K_a(5.4 \times 10^{-4}) &= 1.01 \times 10^{-14} \\ K_a &= 1.9 \times 10^{-11} \end{aligned}$$

Because pK_a = −log K_a, we have $pK_a = -\log(1.9 \times 10^{-11}) = 10.72$. We could also have converted K_b to pK_b to obtain the same answer:

$$\begin{aligned} pK_b &= -\log(5.4 \times 10^{-4}) \\ &= 3.27 \end{aligned}$$

$$\begin{aligned} pKa + pK_b &= 14.00 \\ pK_a &= 10.73 \\ K_a &= 10^{-pK_a} \\ &= 10^{-10.73} \\ &= 1.9 \times 10^{-11} \end{aligned}$$

If we are given any one of these four quantities for an acid or a base (K_a, pK_a, K_b, or pK_b), we can calculate the other three.

Exercise 8.1.6.1: Lactic Acid

Lactic acid ($CH_3CH(OH)CO_2H$) is responsible for the pungent taste and smell of sour milk; it is also thought to produce soreness in fatigued muscles. Its pK_a is 3.86 at 25°C. Calculate K_a for lactic acid and pK_b and K_b for the lactate ion.

Answer

$K_a = 1.4 \times 10^{-4}$ for lactic acid; pK_b = 10.14 and $K_b = 7.2 \times 10^{-11}$ for the lactate ion

Solutions of Strong Acids and Bases: The Leveling Effect

You will notice in Table 8.1.6.1 that acids like H_2SO_4 and HNO_3 lie above the hydronium ion, meaning that they have pK_a values less than zero and are stronger acids than the H_3O^+ ion. Recall that the acidic proton in virtually all oxoacids is bonded to one of the oxygen atoms of the oxoanion. Thus nitric acid should properly be written as $HONO_2$. Unfortunately, however, the formulas of oxoacids are almost always written with hydrogen on the left and oxygen on the right, giving HNO_3 instead. In fact, all six of the common strong acids that we first encountered in Chapter 4 have pK_a values less than zero, which means that they have a greater tendency to lose a proton than does the H_3O^+ ion. Conversely, the conjugate bases of these strong acids are weaker bases than water. Consequently, the proton-transfer equilibria for these strong acids lie far to the right, and adding any of the common strong acids to water results in an essentially stoichiometric reaction of the acid with water to form a solution of the H_3O^+ ion and the conjugate base of the acid.

Although K_a for HI is about 108 greater than K_a for HNO_3, the reaction of either HI or HNO_3 with water gives an essentially stoichiometric solution of H_3O^+ and I− or NO_3^-. In fact, a 0.1 M aqueous solution of any strong acid actually contains 0.1 M H_3O^+, regardless of the identity of the strong acid. This phenomenon is called the leveling effect: any species that is a stronger acid than the conjugate acid of water (H_3O^+) is leveled to the strength of H_3O^+ in aqueous solution because H_3O^+ is the strongest acid that can exist in equilibrium with water. Consequently, it is impossible to distinguish between the strengths of acids such as HI and HNO3 in aqueous solution, and an alternative approach must be used to determine their relative acid strengths.

One method is to use a solvent such as anhydrous acetic acid. Because acetic acid is a stronger acid than water, it must also be a weaker base, with a lesser tendency to accept a proton than H_2O. Measurements of the conductivity of 0.1 M solutions of both HI and HNO_3 in acetic acid show that HI is completely dissociated, but HNO_3 is only partially dissociated and behaves like a weak acid in this solvent. This result clearly tells us that HI is a stronger acid than HNO_3. The relative order of acid strengths and approximate K_a and pK_a values for the strong acids at the top of Table 8.1.6.1 were determined using measurements like this and different nonaqueous solvents.

> **Note: Leveling Effect**
>
> In *aqueous solutions*, H_3O^+ is the strongest acid and OH^- is the strongest base that can exist in equilibrium with H_2O.

The leveling effect applies to solutions of strong bases as well: In aqueous solution, any base stronger than OH^- is leveled to the strength of OH^- because OH^- is the strongest base that can exist in equilibrium with water. Salts such as K_2O, $NaOCH_3$ (sodium methoxide), and $NaNH_2$ (sodamide, or sodium amide), whose anions are the conjugate bases of species that would lie below water in Table 8.1.6.2, are all strong bases that react essentially completely (and often violently) with water, accepting a proton to give a solution of OH^- and the corresponding cation:

$$K_2O(s) + H_2O(l) \longrightarrow 2\,OH^-(aq) + 2\,K^+(aq)$$

$$NaOCH_3(s) + H_2O(l) \longrightarrow OH^-(aq) + Na^+(aq) + CH_3OH(aq)$$

$$NaNH_2(s) + H_2O(l) \longrightarrow OH^-(aq) + Na^+(aq) + NH_3(aq)$$

Other examples that you may encounter are potassium hydride (KH) and organometallic compounds such as methyl lithium (CH_3Li).



Calculating the pH of Weak Acids and Weak Bases: https://youtu.be/zr1V1THJ5P0

Summary

Two species that differ by only a proton constitute a conjugate acid–base pair. The magnitude of the equilibrium constant for an ionization reaction can be used to determine the relative strengths of acids and bases. For an aqueous solution of a weak acid, the dissociation constant is called the acid ionization constant (Ka). Similarly, the equilibrium constant for the reaction of a weak base with water is the base ionization constant (Kb). For any conjugate acid–base pair, $K_aK_b = K_w$. Smaller values of pK_a correspond to larger acid ionization constants and hence stronger acids. Conversely, smaller values of pK_b correspond to larger base ionization constants and hence stronger bases. At 25°C, $pK_a + pK_b = 14.00$. Acid–base reactions always proceed in the direction that produces the weaker acid–base pair. No acid stronger than H_3O^+ and no base stronger than OH^- can exist in aqueous solution, leading to the phenomenon known as the leveling effect.

Key Takeaways

- Acid–base reactions always contain two conjugate acid–base pairs.
- Each acid and each base has an associated ionization constant that corresponds to its acid or base strength.

Key Equations

- Acid ionization constant:

$$K_a = K[H_2O] = \frac{[H_3O^+][A^-]}{[HA]}$$

- Base ionization constant:

$$K_b = K[H_2O] = \frac{[BH^+][OH^-]}{[B]}$$

- Relationship between K_a and K_b of a conjugate acid–base pair:

$$K_aK_b = K_w$$

- Definition of pK_a:

$$pKa = -\log_{10} K_a$$

$$K_a = 10^{-pK_a}$$

- Definition of pK_b:

$$pK_b = -\log_{10} K_b$$

$$K_b = 10^{-pK_b}$$

- Relationship between pK_a and pK_b of a conjugate acid–base pair:

$$pK_a + pK_b = pK_w$$

$$pK_a + pK_b = 14.00 \text{ at } 25°C$$

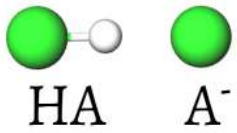
8.1.6: Weak Acids and Weak Bases is shared under a not declared license and was authored, remixed, and/or curated by LibreTexts.

- **16.5: Weak Acids and Weak Bases** by Anonymous is licensed CC BY-NC-SA 3.0.

8.1.7: Conjugate Acid-Base Pairs and pH

One of the more useful aspects of the Brönsted-Lowry definition of acids and bases in helping us deal with the pH of solutions is the concept of the conjugate acid-base pair. We argued qualitatively in the section on conjugate acid-base pairs in aqueous reactions that the strength of an acid and its conjugate base are inversely related. The stronger one is, the weaker the other will be. This relationship can be expressed quantitatively in terms of a very simple mathematical equation involving the appropriate acid and base constants.

Suppose in the general case we have a weak acid HA whose conjugate base is A^-. If either or both of these species are dissolved in H_2O we will have *both* the following equilibria set up simultaneously.



$$\mathrm{HA} + \mathrm{H_2O} \rightleftharpoons \mathrm{H_3O^+} + \mathrm{A^-} \text{ in which HA acts as acid}$$

$$\text{and } \mathrm{A^-} + \mathrm{H_2O} \rightleftharpoons \mathrm{HA} + \mathrm{OH^-} \text{ in which } A^- \text{ acts as base}$$

To the first of these equilibria we can apply the equilibrium constant K_a(HA):

$$K_a(\mathrm{HA}) = \frac{[\mathrm{H_3O^+}][\mathrm{A^-}]}{[\mathrm{HA}]}$$

while to the second we can apply the equilibrium constant $K_b(A^-)$:

$$K_b(\mathrm{A^-}) = \frac{[\mathrm{HA}][\mathrm{OH^-}]}{[\mathrm{A^-}]}$$

Multiplying these two constants together, we obtain a simple relationship between them.

$$K_a(\mathrm{HA}) \times K_b(\mathrm{A^-}) = \frac{[\mathrm{H_3O^+}][\mathrm{A^-}]}{[\mathrm{HA}]} \times \frac{[\mathrm{HA}][\mathrm{OH^-}]}{[\mathrm{A^-}]} \tag{8.1.7.1}$$

$$\tag{8.1.7.2}$$

$$= [\mathrm{H_3O^+}][\mathrm{OH^-}] \tag{8.1.7.3}$$

$$K_a(\mathrm{HA}) \times K_b(\mathrm{A^-}) = K_w \tag{8.1.7.4}$$

If we divide both sides of this equation by the units and take negative logarithms of both sides, we obtain

$$\mathrm{p}K_a = -\log\frac{K_a(\mathrm{HA})}{\mathrm{mol\ L^{-1}}} - \log\frac{K_b(\mathrm{A^-})}{\mathrm{mol\ L^{-1}}} \tag{8.1.7.5}$$

$$\tag{8.1.7.6}$$

$$= -\log\frac{10^{-14}\ \mathrm{mol^2\ L^{-2}}}{\mathrm{mol^2\ L^{-2}}} \tag{8.1.7.7}$$

$$\mathrm{p}K_a(\mathrm{HA}) + \mathrm{p}K_b(\mathrm{A^-}) = \mathrm{p}K_w \tag{8.1.7.8}$$

Thus the product of the acid constant for a weak acid and the base constant for the conjugate base must be K_w, and the sum of pK_a and pK_b for a conjugate acid-base pair is 14.

Equation 8.1.7.4 or 8.1.7.8 enables us to calculate the base constant of a conjugate base from the acid constant of the acid, and vice versa. Given the acid constant for a weak acid like HOCl, for instance, we are able to calculate not only the pH of HOCl solutions but also the pH of solutions of salts like NaOCl or KOCl which are, in effect, solutions of the conjugate base of HOCl, namely, the hypochlorite ion, OCl^-.

Example 8.1.7.1: pH Calculations with K_a

Find the pH of (a) 0.1 *M* HOCl (hypochlorous acid) and (b) 0.1 *M* NaOCl (sodium hypochlorite) from the value for K_a given in the table of K_a values.

Solution

a) For 0.1 *M* HOCl, we find in the usual way that

$$[H_3O^+] = \sqrt{K_a c_a} \tag{8.1.7.9}$$

$$= \sqrt{3.1 \times 10^{-8}\ \text{mol L}^{-1} \times 0.1\ \text{mol}^2\ \text{L}^{-2}} \tag{8.1.7.10}$$

$$= 5.57 \times 10^{-5}\ \text{mol L}^{-1} \tag{8.1.7.11}$$

so that pH = 4.25

b) For 0.1 *M* NaOCl we must first calculate K_b:

$$K_b(OCl^-) = \frac{K_w}{K_a(HOCl)} \tag{8.1.7.12}$$

$$= \frac{1.00 \times 10^{-14}\ \text{mol}^2\ \text{L}^{-2}}{3.1 \times 10^{-8}\ \text{mol L}^{-1}} \tag{8.1.7.13}$$

$$= 3.22 \times 10^{-7}\ \text{mol L}^{-1} \tag{8.1.7.14}$$

Thus

$$[OH^-] = \sqrt{K_b c_b} \tag{8.1.7.15}$$

$$= \sqrt{3.22 \times 10^{-7} \times 0.1\ \text{mol}^2\ \text{L}^{-1}} \tag{8.1.7.16}$$

$$= 1.79 \times 10^{-4}\ \text{mol L}^{-1} \tag{8.1.7.17}$$

From which

pOH = 3.75

and pH = 14.00 – pOH = 10.25

In this, as in all pH problems, it is worth checking that the answers obtained are not wildly unreasonable. A pH of 4 for a weak acid is reasonable, though a little high, but then HOCl is among the weaker acids in table. A pH of 10 corresponds to a mildly basic solution—reasonable enough, for a weak base like OCl^-.

Not only can we use Eq. 8.1.7.4 to find the value of K_b for the base conjugate to a given acid, we can also employ it in the reverse sense to find the value of K_a for the acid conjugate to a given base, as the following example shows.

Example 8.1.7.2: pH Calculation with K_b

Find the pH of 0.05 *M* NH_4Cl (ammonium chloride), using the value $K_b(NH_3) = 1.8 \times 10^{-5}$ mol L^{-1}.

Solution

We regard this solution as a solution of the weak acid NH_4^+ and start by finding K_a for this species:

$$K_a(NH_4^+) = \frac{K_w}{K_b(NH_3)} = \frac{1.00 \times 10^{-14}\ \text{mol}^2\ \text{L}^{-2}}{1.8 \times 10^{-5}\ \text{mol L}^{-1}} \tag{8.1.7.18}$$

$$; = 5.56 \times 10^{-10}\ \text{mol L}^{-1} \tag{8.1.7.19}$$

We can now evaluate the hydronium-ion concentration with the usual approximation:

$$[H_3O^+] = \sqrt{K_a c_a} \tag{8.1.7.20}$$

$$= \sqrt{5.56 \times 10^{-10}\ \text{mol L}^{-1} \times 0.05\ \text{mol L}^{-1}} \tag{8.1.7.21}$$

$$= 5.27 \times 10^{-6}\ \text{mol L}^{-1} \tag{8.1.7.22}$$

whence pH = $-\log(5.27 \times 10^{-6})$ = 5.28

Note

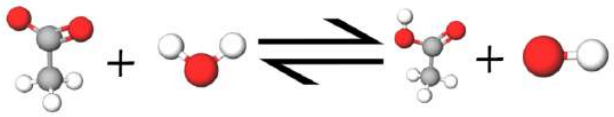
The ammonium ion is a very weak acid (as seen in the Tables of Ka and and Kb values). A solution of NH_4^+ ions will thus not produce a very acidic solution. A pH of 5 is about the same pH as that of black coffee, not very acidic.

Before the Brönsted-Lowry definition of acids and bases and the idea of conjugate acid-base pairs became generally accepted, the interpretation of acid-base behavior revolved very much around the equation

$$\text{Acid + base} \rightarrow \text{salt + water}$$

In consequence the idea prevailed that when an acid reacted with a base, the resultant salt should be neither acidic or basic, but neutral. In order to explain why a solution of sodium acetate was basic or a solution of ammonium chloride was acidic, a special term called **hydrolysis** had to be invoked. Thus, for instance, sodium acetate was said to be hydrolyzed because the acetate ion reacted with water according to the reaction

$$CH_3COO^- + H_2O \rightleftharpoons CH_3COOH + OH^-$$



From the Brönsted-Lowry point of view there is, of course, nothing special about such a hydrolysis. It is a regular proton transfer. Nevertheless you should be aware of the existence of the term hydrolysis since it is still often used in this context.

Because the Brönsted-Lowry definition is so successful at explaining why some salt solutions are acidic and some basic, one must beware of making the mistake of assuming that no salt solutions are neutral. Many are. A good example is 0.10 *M* $NaNO_3$. This solution is neutral because neither the Na^+ ion nor the NO_3^- ion shows any appreciable acidic or basic properties. Since NO_3^- is the conjugate base of HNO_3 we might expect it to produce a basic solution, but NO_3^- is such a weak base that it is almost impossible to detect such an effect. Just how weak a base NO_3^- is can be demonstrated using the value of K_a (HNO_3) = 20 mol L^{-1} obtained from the Tables of Ka and and Kb values.

$$K_b(\text{NO}_3^-) = \frac{K_w}{K_a(\text{HNO}_3)} \tag{8.1.7.23}$$

$$= \frac{1.00 \times 10^{-14}\ \text{mol}^2\ \text{L}^{-2}}{20\ \text{mol L}^{-1}} \tag{8.1.7.24}$$

$$= 5.0 \times 10^{-16}\ \text{mol L}^{-1} \tag{8.1.7.25}$$

If we now apply the conventional formula from equation 4 from the section on the pH of weak base solutions to calculate [OH^-] in 0.10 *M* $NaNO_3$, we obtain

$$[\text{OH}^-] = \sqrt{K_b c_b} \tag{8.1.7.26}$$

$$= \sqrt{5.0 \times 10^{-16} \times 1.0 \times 10^{-1}\ \text{mol L}^{-1}} \tag{8.1.7.27}$$

$$= 7.1 \times 10^{-9}\ \text{mol L}^{-1} \tag{8.1.7.28}$$

But this is less than one-tenth the concentration of OH^- ion which would have been present in pure H_2O, with no added $NaNO_3$. Essentially all the OH^- ions are produced by H_2O, and the pH turns out to be only slightly above 7.00. (Note also that the derivation of equation 4 from the pH of weak base solutions section assumed that the [OH^-] produced by H_2O was negligible. To get an accurate result in this case requires a completely different equation.)

In general all salts in which group I and group II cations are combined with anions which are the conjugate bases of strong acids yield neutral solutions when dissolved in water. Examples are CaI_2, $LiNO_3$, KCl, $Mg(ClO_4)_2$.

There is only one exception to this rule. The hydrated beryllium ion, $Be(H_2O)_4^{2+}$, is a weak acid ($K_a = 3.2 \times 10^{-7}$ mol L^{-1}) so that solutions of beryllium salts are acidic.

Table 8.1.7.1 The Acid-Base Properties of Some Common Ions

	Cations	Anions
Acidic	Cr^{3+}, Fe^{3+}, Al^{3+} Hg^{2+}, Be^{2+} NH_4^+, H_3O^+	HSO_4^-
Neutral	Mg^{2+}, Ca^{2+}, Sr^{2+}, Ba^{2+} Li^+, Na^+, K^+ Ag^+	NO_3^-, ClO_4^- Cl^-, Br^-, I^- SO_4^{2-} (very weakly basic)
Basic	None	PO_4^{3-}, CO_3^{2-}, SO_3^{2-} F^-, CN^-, OH^-, S^{2-} CH_3COO^-, HCO_3^-

The table lists the acid-base properties of some of the more frequently encountered ions and provides a quick reference for deciding whether a given salt will be acidic, basic, or neutral in solution. Note that the table tells us nothing about the strength of any acid or base. If we need to know more about the pH, other than whether it is above, below, or equal to 7, we need information about the actual value of the acid or base constant. The table also lists the SO_4^{2-}ion as neutral, though classifying it as very feebly basic would be more accurate.

Example 8.1.7.3: Acid, Base, or Neutral

Classify the following solutions as acidic, basic, or neutral: (a) 1 *M* KBr; (b) 1 M calcium acetate; (c)1 *M* MgF_2; (d) 1 *M* $Al(NO_3)_3$; (f) 1 *M* $KHSO_4$; (f) 1 *M* NH_4I.

Solution

a. Both cation and anion are neutral: neutral.
b. Cation is neutral but anion basic: basic.
c. Cation is neutral but anion basic: basic.
d. Cation is acidic and anion neutral: acidic.
e. Cation is neutral but anion acidic: acidic.
f. Cation is acidic but anion neutral: acidic.

Example 8.1.7.4: pH Matching

Without actually doing any calculations, match the following solutions and pH values, using the Tables of Ka and and Kb values, and the table on this page.

Aqueous Solution	pH
1 *M* NH_4NO_3	8.0
1 *M* KCN	11.7
1 *M* $Ca(NO_3)_2$	9.4
1 *M* $MgSO_4$	7.0
1 M CH_3COONa(sodium acetate)	1.0
1 *M* $KHSO_4$	4.6

Solution

The pH of 7.0 is easiest to pick. Only one of the salt solutions given has both a neutral anion and a neutral cation. This is $Ca(NO_3)_2$. In the case of $MgSO_4$ the Mg^{2+} ion is neutral but theSO_4^{2-} ion is very feebly basic; this would agree with a pH of 8.0, only slightly basic. The SO_4^{2-} ion is such a feeble base because its conjugate acid, HSO_4^-, is quite a strong acid, certainly the most acidic of all the ions featured. Accordingly we expect 1 *M* $KHSO_4$ to correspond to the lowest pH, namely, 1.0. The only other acidic solution is 4.6, and this must correspond to 1 *M* NH_4NO_3 since NO_4^+ is the only other acidic ion present. Among basic ions the cyanide ion, CN^-, is the strongest. The most basic pH, 11.7, thus corresponds to 1 *M* KCN. Only one solution is left: 1 *M* CH_3COONa. This should be feebly basic and so matches the remaining pH of 9.4 rather well.

This page titled 8.1.7: Conjugate Acid-Base Pairs and pH is shared under a CC BY-NC-SA 4.0 license and was authored, remixed, and/or curated by Ed Vitz, John W. Moore, Justin Shorb, Xavier Prat-Resina, Tim Wendorff, & Adam Hahn.

- **14.7: Conjugate Acid-Base Pairs and pH** by Ed Vitz, John W. Moore, Justin Shorb, Xavier Prat-Resina, Tim Wendorff, & Adam Hahn is licensed CC BY-NC-SA 4.0.

8.1.8: Polyprotic Acids

Learning Objectives

- Extend previously introduced equilibrium concepts to acids and bases that may donate or accept more than one proton

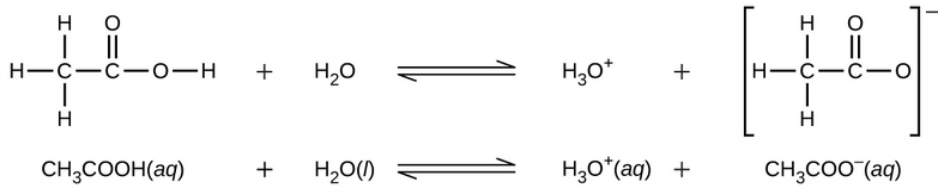
We can classify acids by the number of protons per molecule that they can give up in a reaction. Acids such as $\mathbf{HCl}$, $\mathbf{HNO_3}$, and $\mathbf{HCN}$ that contain one ionizable hydrogen atom in each molecule are called monoprotic acids. Their reactions with water are:

$$\mathbf{HCl}(aq) + \mathbf{H_2O}(l) \longrightarrow \mathbf{H_3O^+}(aq) + \mathbf{Cl^-}(aq)$$

$$\mathbf{HNO_3}(aq) + \mathbf{H_2O}(l) \longrightarrow \mathbf{H_3O^+}(aq) + \mathbf{NO_3^-}(aq)$$

$$\mathbf{HCN}(aq) + \mathbf{H_2O}(l) \longrightarrow \mathbf{H_3O^+}(aq) + \mathbf{CN^-}(aq)$$

Even though it contains four hydrogen atoms, acetic acid, $\mathbf{CH_3CO_2H}$, is also monoprotic because only the hydrogen atom from the carboxyl group ($\mathbf{-COOH}$) reacts with bases:



This image contains two equilibrium reactions. The first shows a C atom bonded to three H atoms and another C atom. The second C atom is double bonded to an O atom and also forms a single bond to another O atom. The second O atom is bonded to an H atom. There is a plus sign and then the molecular formula H subscript 2 O. An equilibrium arrow follows the H subscript 2 O. To the right of the arrow is H subscript 3 O superscript positive sign. There is a plus sign. The final structure shows a C atom bonded the three H atoms and another C atom. This second C atom is double bonded to an O atom and single bonded to another O atom. The entire structure is in brackets and a superscript negative sign appears outside the brackets. The second reaction shows C H subscript 3 C O O H (a q) plus H subscript 2 O (l) equilibrium arrow H subscript 3 O (a q) plus C H subscript 3 C O O superscript negative sign (a q).

Similarly, monoprotic bases are bases that will accept a single proton.

Diprotic Acids

Diprotic acids contain two ionizable hydrogen atoms per molecule; ionization of such acids occurs in two steps. The first ionization always takes place to a greater extent than the second ionization. For example, sulfuric acid, a strong acid, ionizes as follows:

- **The first ionization is**

$$\mathbf{H_2SO_4}(aq) + \mathbf{H_2O}(l) \rightleftharpoons \mathbf{H_3O^+}(aq) + \mathbf{HSO_4^-}(aq)$$

with $K_{a1} > 10^2$; *complete dissociation*.

- **The second ionization is**

$$\mathbf{HSO_4^-}(aq) + \mathbf{H_2O}(l) \rightleftharpoons \mathbf{H_3O^+}(aq) + \mathbf{SO_4^{2-}}(aq)$$

with $K_{a2} = 1.2 \times 10^{-2}$.

This stepwise ionization process occurs for all polyprotic acids. When we make a solution of a weak diprotic acid, we get a solution that contains a mixture of acids. Carbonic acid, $\mathbf{H_2CO_3}$, is an example of a weak diprotic acid. The first ionization of carbonic acid yields hydronium ions and bicarbonate ions in small amounts.

- **First Ionization**

$$\mathbf{H_2CO_3}(aq) + \mathbf{H_2O}(l) \rightleftharpoons \mathbf{H_3O^+}(aq) + \mathbf{HCO_3^-}(aq)$$

with

$$K_{H_2CO_3} = \frac{[H3O+][HCO3-]}{[H2CO3]} = 4.3 \times 10^{-7}$$

The bicarbonate ion can also act as an acid. It ionizes and forms hydronium ions and carbonate ions in even smaller quantities.

- **Second Ionization**

$$HCO_3^-(aq) + H_2O(l) \rightleftharpoons H_3O^+(aq) + CO_3^{2-}(aq)$$

with

$$K_{HCO_3^-} = \frac{[H3O+][CO3^2-]}{[HCO3-]} = 4.7 \times 10^{-11}$$

$K_{H_2CO_3}$ is larger than $K_{HCO_3^-}$ by a factor of 10^4, so H_2CO_3 is the dominant producer of hydronium ion in the solution. This means that little of the HCO_3^- formed by the ionization of H_2CO_3 ionizes to give hydronium ions (and carbonate ions), and the concentrations of H_3O^+ and HCO_3^- are practically equal in a pure aqueous solution of H_2CO_3.

If the first ionization constant of a weak diprotic acid is larger than the second by a factor of at least 20, it is appropriate to treat the first ionization separately and calculate concentrations resulting from it before calculating concentrations of species resulting from subsequent ionization. This can simplify our work considerably because we can determine the concentration of H_3O^+ and the conjugate base from the first ionization, then determine the concentration of the conjugate base of the second ionization in a solution with concentrations determined by the first ionization.

Example 8.1.8.1: Ionization of a Diprotic Acid

When we buy soda water (carbonated water), we are buying a solution of carbon dioxide in water. The solution is acidic because CO_2 reacts with water to form carbonic acid, H_2CO_3. What are $[H_3O^+]$, $[HCO_3^-]$, and $[CO_3^{2-}]$ in a saturated solution of CO_2 with an initial $[H_2CO_3] = 0.033\ M$?

$$H_2CO_3(aq) + H_2O(l) \rightleftharpoons H_3O^+(aq) + HCO_3^-(aq) \quad K_{a1} = 4.3 \times 10^{-7} \qquad \text{(equilibrium step 1)}$$

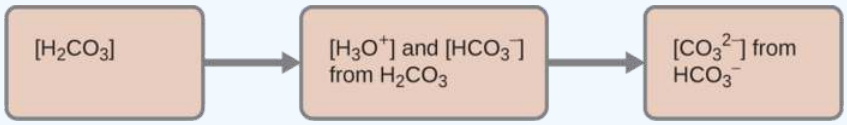
$$HCO_3^-(aq) + H_2O(l) \rightleftharpoons H_3O^+(aq) + CO_3^{2-}(aq) \quad K_{a2} = 4.7 \times 10^{-11} \qquad \text{(equilibrium step 2)}$$

Solution

As indicated by the ionization constants, H_2CO_3 is a much stronger acid than HCO_3^-, so H_2CO_3 is the dominant producer of hydronium ion in solution. Thus there are two parts in the solution of this problem:

1. Using the customary four steps, we determine the concentration of H_3O^+ and HCO_3^- produced by ionization of H_2CO_3.
2. Then we determine the concentration of CO_3^{2-} in a solution with the concentration of H_3O^+ and HCO_3^- determined in (1).

To summarize:



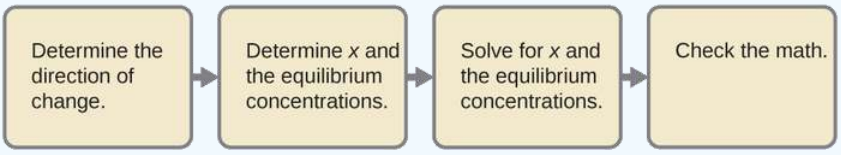
Four tan rectangles are shown that are connected with right pointing arrows. The first is labeled “left bracket H subscript 2 C O subscript 3 right bracket.” The second is labeled “left bracket H subscript 3 O superscript plus right bracket and left bracket H C O subscript 3 superscript negative right bracket from H subscript 2 C O subscript 3.” The third is labeled “left bracket C O subscript 3 superscript 2 negative right bracket from H C O subscript 3 superscript negative.”

1. First Ionization: Determine the concentrations of H_3O^+ *and* HCO_3^-.

Since equilibrium step 1 is has a much bigger $K_{a1} = 4.3 \times 10^{-7}$ than $K_{a2} = 4.7 \times 10^{-11}$ for equilibrium step 2, we can safely ignore the second ionization step and focus only on the first step (but address it in next part of problem).

$$H_2CO_3(aq) + H_2O(l) \rightleftharpoons H_3O^+(aq) + HCO_3^-(aq) \quad K_{a1} = 4.3 \times 10^{-7}$$

As for the ionization of any other weak acid:



Four tan rectangles are shown that are connected with right pointing arrows. The first is labeled “Determine the direction of change.” The second is labeled “Determine x and the equilibrium concentrations.” The third is labeled “Solve for x and the equilibrium concentrations.” The fourth is labeled “Check the math.”

An abbreviated table of changes and concentrations shows:

Abbreviated table of changes and concentrations

ICE Table	$H_2CO_3(aq)$	$H_2O(l)$	$H_3O^+(aq)$	$HCO_3^-(aq)$
Initial (M)	$0.033\ M$	-	0	0
Change (M)	$-x$	-	$+x$	$+x$
Equilibrium (M)	$0.033\ M - x$	-	x	x

Substituting the equilibrium concentrations into the equilibrium constant gives us:

$$K_{H_2CO_3} = \frac{[H3O+][HCO3-]}{[H2CO3]} = \frac{(x)(x)}{0.033 - x} = 4.3 \times 10^{-7}$$

Solving the preceding equation making our standard assumptions gives:

$$x = 1.2 \times 10^{-4}$$

Thus:

$$[H_2CO_3] = 0.033\ M$$

$$[H_3O^+] = [HCO_3^-] = 1.2 \times 10^{-4}\ M$$

2. Second Ionization: Determine the concentration of CO_3^{2-} in a solution at equilibrium.

Since the equilibrium step 1 is has a much bigger K_a than equilibrium step 2, we can the equilibrium conditions calculated from first part of example as the initial conditions for an ICER Table for the equilibrium step 2:

$$HCO_3^-(aq) + H_2O(l) \rightleftharpoons H_3O^+(aq) + CO_3^{2-}(aq)$$

ICER Table for the equilibrium step 2:

ICE Table	$HCO_3^-(aq)$	$H_2O(l)$	$H_3O^+(aq)$	$CO_3^{2-}(aq)$
Initial (M)	$1.2 \times 10^{-4}\ M$	-	$1.2 \times 10^{-4}\ M$	0
Change (M)	$-y$	-	$+y$	$+y$
Equilibrium (M)	$1.2 \times 10^{-4}\ M - y$	-	$1.2 \times 10^{-4}\ M + y$	y

$$K_{HCO_3^-} = \frac{[H3O+][CO3^2-]}{[HCO3-]} = \frac{(1.2 \times 10^{-4}\ M + y)(y)}{(1.2 \times 10^{-4}\ M - y)}$$

To avoid solving a quadratic equation, we can assume $y \ll 1.2 \times 10^{-4}\ M$ so

$$K_{HCO_3^-} = 4.7 \times 10^{-11} \approx \frac{(1.2 \times 10^{-4}\ M)(y)}{(1.2 \times 10^{-4}\ M)}$$

Rearranging to solve for y

$$y \approx \frac{(4.7 \times 10^{-11})(1.2 \times 10^{-4}\ M)}{1.2 \times 10^{-4}\ M}$$

$$[CO_3^{2-}] = y \approx 4.7 \times 10^{-11}$$

To summarize:

In part 1 of this example, we found that the H_2CO_3 in a 0.033-M solution ionizes slightly and at equilibrium $[H_2CO_3] = 0.033\ M$, $[H_3O^+] = 1.2 \times 10^{-4}$, and $[HCO_3^-] = 1.2 \times 10^{-4}\ M$. In part 2, we determined that $[CO_3^{2-}] = 5.6 \times 10^{-11}\ M$.

? Exercise 8.1.8.2: Hydrogen Sulfide

The concentration of H_2S in a saturated aqueous solution at room temperature is approximately 0.1 M. Calculate $[H_3O^+]$, $[HS^-]$, and $[S^{2-}]$ in the solution:

$$H_2S(aq) + H_2O(l) \rightleftharpoons H_3O^+(aq) + HS^-(aq) \quad K_{a1} = 8.9 \times 10^{-8}$$

$$HS^-(aq) + H_2O(l) \rightleftharpoons H_3O^+(aq) + S^{2-}(aq) \quad K_{a2} = 1.0 \times 10^{-19}$$

Answer

$[H_2S] = 0.1M$, $[H_3O^+] = [HS^-] = 0.0001\ M$, $[S^{2-}] = 1 \times 10^{-19}\ M$

We note that the concentration of the sulfide ion is the same as K_{a2}. This is due to the fact that each subsequent dissociation occurs to a lesser degree (as acid gets weaker).

Triprotic Acids

A triprotic acid is an acid that has three dissociable protons that undergo stepwise ionization: Phosphoric acid is a typical example:

- **The first ionization is**

$$H_3PO_4(aq) + H_2O(l) \rightleftharpoons H_3O^+(aq) + H_2PO_4^-(aq)$$

with $K_{a1} = 7.5 \times 10^{-3}$.

- **The second ionization is**

$$H_2PO_4^-(aq) + H_2O(l) \rightleftharpoons H_3O^+(aq) + HPO_4^{2-}(aq)$$

with $K_{a2} = 6.2 \times 10^{-8}$.

- **The third ionization is**

$$HPO_4^{2-}(aq) + H_2O(l) \rightleftharpoons H_3O^+(aq) + PO_4^{3-}(aq)$$

with $K_{a3} = 4.2 \times 10^{-13}$.

As with the diprotic acids, the differences in the ionization constants of these reactions tell us that in each successive step the degree of ionization is significantly weaker. This is a general characteristic of polyprotic acids and successive ionization constants often differ by a factor of about 10^5 to 10^6. This set of three dissociation reactions may appear to make calculations of equilibrium concentrations in a solution of H_3PO_4 complicated. However, because the successive ionization constants differ by a factor of 10^5 to 10^6, the calculations can be broken down into a series of parts similar to those for diprotic acids.

Polyprotic bases can accept more than one hydrogen ion in solution. The carbonate ion is an example of a diprotic base, since it can accept up to two protons. Solutions of alkali metal carbonates are quite alkaline, due to the reactions:

$$H_2O(l) + CO_3^{2-}(aq) \rightleftharpoons HCO_3^-(aq) + OH^-(aq)$$

and

$$\mathrm{H_2O}(l) + \mathrm{HCO_3^-}(aq) \rightleftharpoons \mathrm{H_2CO_3}(aq) + \mathrm{OH^-}(aq)$$

Summary

An acid that contains more than one ionizable proton is a polyprotic acid. The protons of these acids ionize in steps. The differences in the acid ionization constants for the successive ionizations of the protons in a polyprotic acid usually vary by roughly five orders of magnitude. As long as the difference between the successive values of K_a of the acid is greater than about a factor of 20, it is appropriate to break down the calculations of the concentrations of the ions in solution into a series of steps.

Glossary

diprotic acid

acid containing two ionizable hydrogen atoms per molecule. A diprotic acid ionizes in two steps

diprotic base

base capable of accepting two protons. The protons are accepted in two steps

monoprotic acid

acid containing one ionizable hydrogen atom per molecule

stepwise ionization

process in which an acid is ionized by losing protons sequentially

triprotic acid

acid that contains three ionizable hydrogen atoms per molecule; ionization of triprotic acids occurs in three steps

---

8.1.8: Polyprotic Acids is shared under a not declared license and was authored, remixed, and/or curated by LibreTexts.

- **14.5: Polyprotic Acids** by OpenStax is licensed CC BY 4.0. Original source: https://openstax.org/details/books/chemistry-2e.

8.1.9: Ions as Acids and Bases

Learning Objectives

- Extend previously introduced equilibrium concepts to acids and bases that may donate or accept more than one proton

We can also use the relative strengths of conjugate acid–base pairs to understand the acid–base properties of solutions of salts. A neutralization reaction can be defined as the reaction of an acid and a base to produce a salt and water. That is, another cation, such as Na^+, replaces the proton on the acid. An example is the reaction of CH_3CO_2H, a weak acid, with NaOH, a strong base:

$$\underset{acid}{CH_3CO_2H\,(l)} + \underset{base}{NaOH\,(s)} \xrightarrow{H_2O} \underset{salt}{H_2OCH_3CO_2Na\,(aq)} + \underset{water}{H_2O\,(l)} \tag{8.1.9.1}$$

Depending on the acid–base properties of its component ions, however, a salt can dissolve in water to produce a neutral solution, a basic solution, or an acidic solution.

When a salt such as $NaCl$ dissolves in water, it produces $Na^+_{(aq)}$ and $Cl^-_{(aq)}$ ions. Using a Lewis approach, the Na^+ ion can be viewed as an acid because it is an electron pair acceptor, although its low charge and relatively large radius make it a very weak acid. The Cl^- ion is the conjugate base of the strong acid HCl, so it has essentially no basic character. Consequently, dissolving $NaCl$ in water has no effect on the pH of a solution, and the solution remains neutral.

Now let's compare this behavior to the behavior of aqueous solutions of potassium cyanide and sodium acetate. Again, the cations (K^+ and Na^+) have essentially no acidic character, but the anions (CN^- and $CH_3CO_2^-$) are weak bases that can react with water because they are the conjugate bases of the weak acids HCN and acetic acid, respectively.

$$CN^-\,(aq) + H_2O\,(l) \rightleftharpoons HCN\,(aq) + OH^-\,(aq) \tag{8.1.9.2}$$

$$CH_3CO_2^-\,(aq) + H_2O\,(l) \rightleftharpoons CH_3CO_2H\,(aq) + OH^-\,(aq) \tag{8.1.9.3}$$

Neither reaction proceeds very far to the right as written because the formation of the weaker acid–base pair is favored. Both HCN and acetic acid are stronger acids than water, and hydroxide is a stronger base than either acetate or cyanide, so in both cases, the equilibrium lies to the left. Nonetheless, each of these reactions generates enough hydroxide ions to produce a basic solution. For example, the pH of a 0.1 M solution of sodium acetate or potassium cyanide at 25°C is 8.8 or 11.1, respectively. From Table E1 and E2, we can see that CN^- is a stronger base ($pK_b = 4.79$) than acetate ($pK_b = 9.24$), which is consistent with KCN producing a more basic solution than sodium acetate at the same concentration.

In contrast, the conjugate acid of a weak base should be a weak acid. For example, ammonium chloride and pyridinium chloride are salts produced by reacting ammonia and pyridine, respectively, with HCl. As you already know, the chloride ion is such a weak base that it does not react with water. In contrast, the cations of the two salts are weak acids that react with water as follows:

$$NH_4^+\,(aq) + H_2O\,(l) \rightleftharpoons NH_3\,(aq) + H_3O^+\,(aq) \tag{8.1.9.4}$$

$$C_5H_5NH^+\,(aq) + H_2O\,(l) \rightleftharpoons C_5H_5NH\,(aq) + H_3O^+\,(aq) \tag{8.1.9.5}$$

Figure 8.1.9.2 shows that H_3O^+ is a stronger acid than either NH_4^+ or $C_5H_5NH^+$, and conversely, ammonia and pyridine are both stronger bases than water. The equilibrium will therefore lie far to the left in both cases, favoring the weaker acid–base pair. The H_3O^+ concentration produced by the reactions is great enough, however, to decrease the pH of the solution significantly: the pH of a 0.10 M solution of ammonium chloride or pyridinium chloride at 25°C is 5.13 or 3.12, respectively.

What happens with aqueous solutions of a salt such as ammonium acetate, where both the cation and the anion can react separately with water to produce an acid and a base, respectively? According to Figure 16.10, the ammonium ion will lower the pH, while according to Figure 16.9, the acetate ion will raise the pH. This particular case is unusual, in that the cation is as strong an acid as the anion is a base (pKa ≈ pKb). Consequently, the two effects cancel, and the solution remains neutral. With salts in which the cation is a stronger acid than the anion is a base, the final solution has a pH < 7.00. Conversely, if the cation is a weaker acid than the anion is a base, the final solution has a pH > 7.00.



Ions as Acids and Bases: https://youtu.be/XYAGNonPSow

Acidic Metal Ions

Solutions of simple salts of metal ions can also be acidic, even though a metal ion cannot donate a proton directly to water to produce H_3O^+. Instead, a metal ion can act as a Lewis acid and interact with water, a Lewis base, by coordinating to a lone pair of electrons on the oxygen atom to form a hydrated metal ion (Figure 8.1.9.1*a*). A water molecule coordinated to a metal ion is more acidic than a free water molecule for two reasons. First, repulsive electrostatic interactions between the positively charged metal ion and the partially positively charged hydrogen atoms of the coordinated water molecule make it easier for the coordinated water to lose a proton.

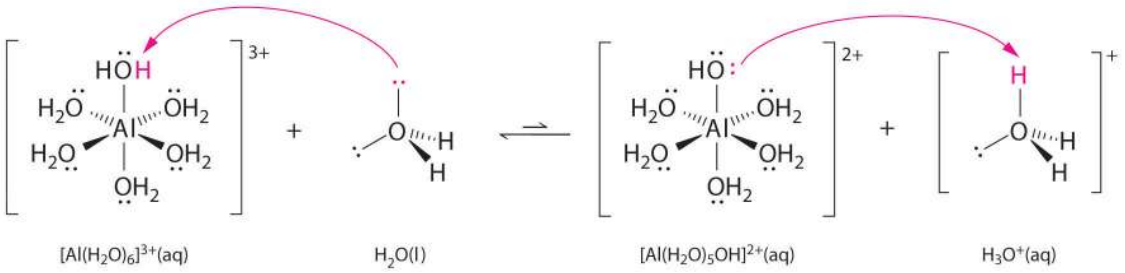
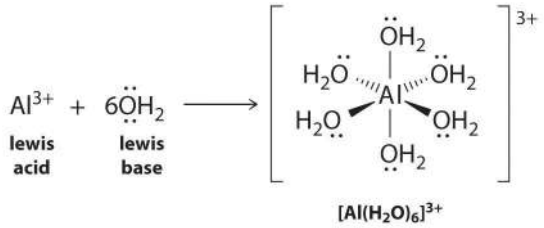
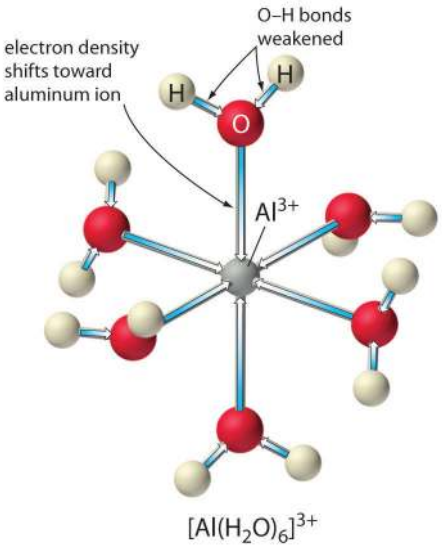


Figure 8.1.9.1

Second, the positive charge on the Al^{3+} ion attracts electron density from the oxygen atoms of the water molecules, which decreases the electron density in the O–H bonds, as shown in Figure 8.1.9.1*b*. With less electron density between the O atoms and the H atoms, the O–H bonds are weaker than in a free H_2O molecule, making it easier to lose a H^+ ion.



(a)



(b)

Figure 8.1.9.2: Effect of a Metal Ion on the Acidity of Water (a) Reaction of the metal ion Al^{3+} with water to form the hydrated metal ion is an example of a Lewis acid–base reaction. (b) The positive charge on the aluminum ion attracts electron density from the oxygen atoms, which shifts electron density away from the O–H bonds. The decrease in electron density weakens the O–H bonds in the water molecules and makes it easier for them to lose a proton.

The magnitude of this effect depends on the following two factors (Figure 8.1.9.3):

1. The charge on the metal ion. A divalent ion (M^{2+}) has approximately twice as strong an effect on the electron density in a coordinated water molecule as a monovalent ion (M^{+}) of the same radius.
2. The radius of the metal ion. For metal ions with the same charge, the smaller the ion, the shorter the internuclear distance to the oxygen atom of the water molecule and the greater the effect of the metal on the electron density distribution in the water molecule.

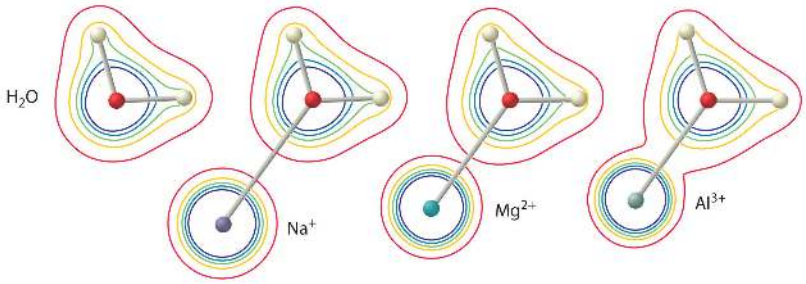


Figure 8.1.9.3: The Effect of the Charge and Radius of a Metal Ion on the Acidity of a Coordinated Water Molecule. The contours show the electron density on the O atoms and the H atoms in both a free water molecule (left) and water molecules coordinated to Na^{+}, Mg^{2+}, and Al^{3+} ions. These contour maps demonstrate that the smallest, most highly charged metal ion (Al^{3+}) causes the greatest decrease in electron density of the O–H bonds of the water molecule. Due to this effect, the acidity of hydrated metal ions increases as the charge on the metal ion increases and its radius decreases.

Thus aqueous solutions of small, highly charged metal ions, such as Al^{3+} and Fe^{3+}, are acidic:

$$[Al(H_2O)_6]^{3+}_{(aq)} \rightleftharpoons [Al(H_2O)_5(OH)]^{2+}_{(aq)} + H^+_{(aq)} \tag{8.1.9.6}$$

The $[Al(H_2O)_6]^{3+}$ ion has a pK_a of 5.0, making it almost as strong an acid as acetic acid. Because of the two factors described previously, the most important parameter for predicting the effect of a metal ion on the acidity of coordinated water molecules is the charge-to-radius ratio of the metal ion. A number of pairs of metal ions that lie on a diagonal line in the periodic table, such as Li^+ and Mg^{2+} or Ca^{2+} and Y^{3+}, have different sizes and charges, but similar charge-to-radius ratios. As a result, these pairs of metal ions have similar effects on the acidity of coordinated water molecules, and they often exhibit other significant similarities in chemistry as well.

Acidic Metal Ions

Solutions of small, highly charged metal ions in water are acidic.

Reactions such as those discussed in this section, in which a salt reacts with water to give an acidic or basic solution, are often called hydrolysis reactions. Using a separate name for this type of reaction is unfortunate because it suggests that they are somehow different. In fact, hydrolysis reactions are just acid–base reactions in which the acid is a cation or the base is an anion; they obey the same principles and rules as all other acid–base reactions.

Hydrolysis

A hydrolysis reaction is an acid–base reaction.

Example 8.1.9.1

Predict whether aqueous solutions of these compounds are acidic, basic, or neutral.

a. KNO_3
b. $CrBr_3 \cdot H_2O$
c. Na_2SO_4

Given: compound

Asked for: acidity or basicity of aqueous solution

Strategy:

A. Assess the acid–base properties of the cation and the anion. If the cation is a weak Lewis acid, it will not affect the pH of the solution. If the cation is the conjugate acid of a weak base or a relatively highly charged metal cation, however, it will react with water to produce an acidic solution.
B. f the anion is the conjugate base of a strong acid, it will not affect the pH of the solution. If, however, the anion is the conjugate base of a weak acid, the solution will be basic.

Solution:

a

A. The K^+ cation has a small positive charge (+1) and a relatively large radius (because it is in the fourth row of the periodic table), so it is a very weak Lewis acid.
B. The NO_3- anion is the conjugate base of a strong acid, so it has essentially no basic character (Table 16.1). Hence neither the cation nor the anion will react with water to produce H^+ or OH^-, and the solution will be neutral.

b.

A. The Cr^{3+} ion is a relatively highly charged metal cation that should behave similarly to the Al^{3+} ion and form the [Cr(H2O)6]3+ complex, which will behave as a weak acid:

$$Cr(H_2O)_6]^{3+}_{(aq)} \rightleftharpoons Cr(H_2O)_5(OH)]^{2+}_{(aq)} + H^+_(aq) \tag{8.1.9.7}$$

B. The Br^- anion is a very weak base (it is the conjugate base of the strong acid HBr), so it does not affect the pH of the solution. Hence the solution will be acidic.

c.

A. The Na^+ ion, like the K^+, is a very weak acid, so it should not affect the acidity of the solution.
B. In contrast, SO_4^{2-} is the conjugate base of HSO_4^-, which is a weak acid. Hence the SO_4^{2-} ion will react with water as shown in Figure 16.6 to give a slightly basic solution.

? Exercise 8.1.9.1

Predict whether aqueous solutions of the following are acidic, basic, or neutral.

a. KI
b. $Mg(ClO_4)_2$
c. $NaHS$

Answer a

neutral

Answer b

acidic

Answer c

basic (due to the reaction of HS^- with water to form H_2S and OH^-)

Summary

A salt can dissolve in water to produce a neutral, a basic, or an acidic solution, depending on whether it contains the conjugate base of a weak acid as the anion (A^-), the conjugate acid of a weak base as the cation (BH^+), or both. Salts that contain small, highly charged metal ions produce acidic solutions in water. The reaction of a salt with water to produce an acidic or a basic solution is called a hydrolysis reaction.

8.1.9: Ions as Acids and Bases is shared under a not declared license and was authored, remixed, and/or curated by LibreTexts.

- **16.7: Ions as Acids and Bases** is licensed CC BY-NC-SA 4.0.

8.1.10: Molecular Structure and Acid-Base Behavior

Learning Objectives

- To understand how molecular structure affects the strength of an acid or base.

We have seen that the strengths of acids and bases vary over many orders of magnitude. In this section, we explore some of the structural and electronic factors that control the acidity or basicity of a molecule.

Bond Strengths

In general, the stronger the $\mathbf{A–H}$ or $\mathbf{B–H^+}$ bond, the less likely the bond is to break to form H^+ ions and thus the less acidic the substance. This effect can be illustrated using the hydrogen halides:

Relative Acid Strength	HF	HCl	HBr	HI
H–X Bond Energy (kJ/mol)	570	432	366	298
pKa	3.20	−6.1	−8.9	−9.3

The trend in bond energies is due to a steady decrease in overlap between the 1s orbital of hydrogen and the valence orbital of the halogen atom as the size of the halogen increases. The larger the atom to which H is bonded, the weaker the bond. Thus the bond between H and a large atom in a given family, such as I or Te, is weaker than the bond between H and a smaller atom in the same family, such as F or O. As a result, acid strengths of binary hydrides increase as we go down a column of the periodic table. For example, the order of acidity for the binary hydrides of Group 16 elements is as follows, with pK_a values in parentheses:

$$H_2O(14.00 = pK_w) < H_2S(7.05) < H_2Se(3.89) < H_2Te(2.6) \tag{8.1.10.1}$$

Stability of the Conjugate Base

Whether we write an acid–base reaction as $AH \rightleftharpoons A^- + H^+$ or as $BH^+ \rightleftharpoons B + H^+$, the conjugate base ($A^-$ or B) contains one more lone pair of electrons than the parent acid (AH or BH^+). Any factor that stabilizes the lone pair on the conjugate base favors dissociation of H^+ and makes the parent acid a stronger acid. Let's see how this explains the relative acidity of the binary hydrides of the elements in the second row of the periodic table. The observed order of increasing acidity is the following, with pKa values in parentheses:

$$CH_4(\ 50) \ll NH_3(\ 36) < H_2O(14.00) < HF(3.20) \tag{8.1.10.2}$$

Consider, for example, the compounds at both ends of this series: methane and hydrogen fluoride. The conjugate base of CH_4 is CH_3^-, and the conjugate base of HF is F^-. Because fluorine is much more electronegative than carbon, fluorine can better stabilize the negative charge in the F^- ion than carbon can stabilize the negative charge in the CH3− ion. Consequently, $\mathbf{HF}$ has a greater tendency to dissociate to form H^+ and F^- than does methane to form H^+ and CH_3^-, making HF a much stronger acid than CH_4.

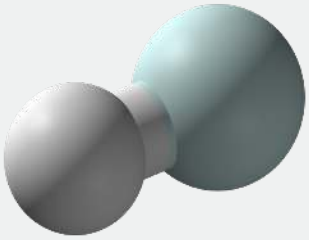
The same trend is predicted by analyzing the properties of the conjugate acids. For a series of compounds of the general formula HE, as the electronegativity of E increases, the E–H bond becomes more polar, favoring dissociation to form E^- and H^+. Due to both the increasing stability of the conjugate base and the increasing polarization of the E–H bond in the conjugate acid, acid strengths of binary hydrides increase as we go from left to right across a row of the periodic table.

Acid strengths of binary hydrides increase as we go down a column or from left to right across a row of the periodic table.

the strongest acid Known: The hydrohelium Cation

The stornger acid, the weaker the covalent bond to a hydrogen atom. So the strongest acid possible is the molecule with the weakest bond. That is the hydrohelium (1+) cation, $\mathbf{HeH^+}$, which is a positively charged ion formed by the reaction of a proton

with a helium atom in the gas phase. It was first produced in the laboratory in 1925 and is isoelectronic with molecular hydrogen (\ce{H2}). It is the strongest known acid, with a proton affinity of 177.8 kJ/mol.



Ball and stick model of the hydrohelium ion. (CC BY-SA 3.0; CCoil).

HeH$^+$ cannot be prepared in a condensed phase, as it would protonate any anion, molecule or atom with which it were associated. However it is possible to estimate a *hypothetical* aqueous acidity using Hess's law:

HHe$^+$(g)	→	H$^+$(g)	+ He(g)	+178 kJ/mol
HHe$^+$(aq)	→	HHe$^+$(g)		+973 kJ/mol
H$^+$(g)	→	H$^+$(aq)		−1530 kJ/mol
He(g)	→	He(aq)		+19 kJ/mol
HHe$^+$(aq)	→	H$^+$(aq)	+ He(aq)	−360 kJ/mol

A free energy change of dissociation of −360 kJ/mol is equivalent to a pK_a of −63.

It has been suggested that **HeH$^+$** should occur naturally in the interstellar medium, but it has not yet been detected.

Inductive Effects

Atoms or groups of atoms in a molecule other than those to which H is bonded can induce a change in the distribution of electrons within the molecule. This is called an inductive effect, and, much like the coordination of water to a metal ion, it can have a major effect on the acidity or basicity of the molecule. For example, the hypohalous acids (general formula HOX, with X representing a halogen) all have a hydrogen atom bonded to an oxygen atom. In aqueous solution, they all produce the following equilibrium:

$$HOX_{(aq)} \rightleftharpoons H^+_{(aq)} + OX^-(aq) \tag{8.1.10.3}$$

The acidities of these acids vary by about three orders of magnitude, however, due to the difference in electronegativity of the halogen atoms:

HOX	Electronegativity of X	pKa
HOCl	3.0	7.40
HOBr	2.8	8.55
HOI	2.5	10.5

As the electronegativity of X increases, the distribution of electron density within the molecule changes: the electrons are drawn more strongly toward the halogen atom and, in turn, away from the H in the O–H bond, thus weakening the O–H bond and allowing dissociation of hydrogen as H^+.

The acidity of oxoacids, with the general formula $HOXO_n$ (with n = 0−3), depends strongly on the number of terminal oxygen atoms attached to the central atom X. As shown in Figure 8.1.10.1, the K_a values of the oxoacids of chlorine increase by a factor of about 10^4 to 10^6 with each oxygen as successive oxygen atoms are added. The increase in acid strength with increasing number of terminal oxygen atoms is due to both an inductive effect and increased stabilization of the conjugate base.

> *Any inductive effect that withdraws electron density from an O–H bond increases the acidity of the compound.*

Because oxygen is the second most electronegative element, adding terminal oxygen atoms causes electrons to be drawn away from the O–H bond, making it weaker and thereby increasing the strength of the acid. The colors in Figure 8.1.10.1 show how the electrostatic potential, a measure of the strength of the interaction of a point charge at any place on the surface of the molecule, changes as the number of terminal oxygen atoms increases. In Figure 8.1.10.1 and Figure 8.1.10.2, blue corresponds to low electron densities, while red corresponds to high electron densities. The oxygen atom in the O–H unit becomes steadily less red from $HClO$ to $HClO_4$ (also written as $HOClO_3$, while the H atom becomes steadily bluer, indicating that the electron density on the O–H unit decreases as the number of terminal oxygen atoms increases. The decrease in electron density in the O–H bond weakens it, making it easier to lose hydrogen as H^+ ions, thereby increasing the strength of the acid.

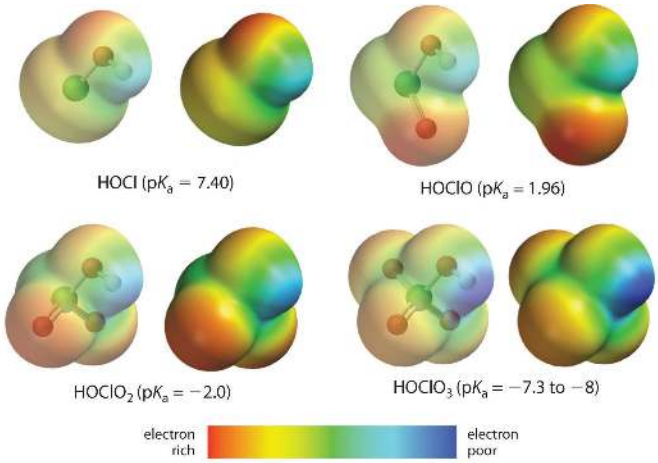
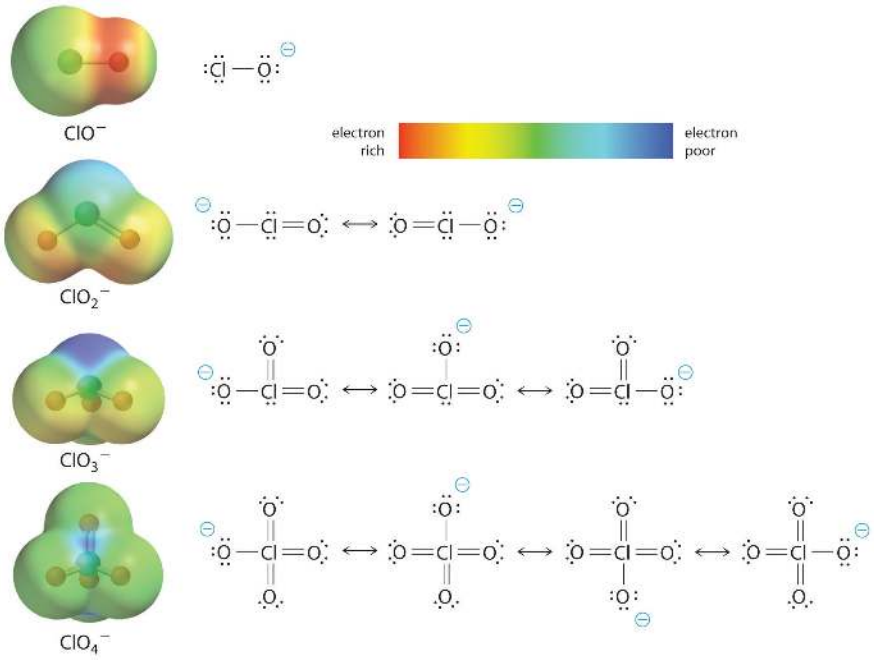


Figure 8.1.10.1: The Relationship between the Acid Strengths of the Oxoacids of Chlorine and the Electron Density on the O–H Unit. These electrostatic potential maps show how the electron density on the O–H unit decreases as the number of terminal oxygen atoms increases. Blue corresponds to low electron densities, whereas red corresponds to high electron densities. Source: Chlorine oxoacids pKa values from J. R. Bowser, Inorganic Chemistry (Pacific Grove, CA: Brooks-Cole,1993).

At least as important, however, is the effect of delocalization of the negative charge in the conjugate base. As shown in Figure 8.1.10.2, the number of resonance structures that can be written for the oxoanions of chlorine increases as the number of terminal oxygen atoms increases, allowing the single negative charge to be delocalized over successively more oxygen atoms.

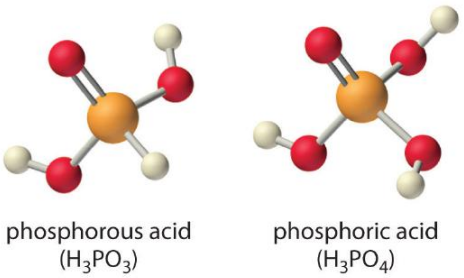
> *Electron delocalization in the conjugate base increases acid strength.*

The electrostatic potential plots in Figure 8.1.10.2 demonstrate that the electron density on the terminal oxygen atoms decreases steadily as their number increases. The oxygen atom in ClO^- is red, indicating that it is electron rich, and the color of oxygen progressively changes to green in ClO_4^+, indicating that the oxygen atoms are becoming steadily less electron rich through the series. For example, in the perchlorate ion (ClO_4^-), the single negative charge is delocalized over all four oxygen atoms, whereas in the hypochlorite ion (OCl^-), the negative charge is largely localized on a single oxygen atom (Figure 8.1.10.2). As a result, the perchlorate ion has no localized negative charge to which a proton can bind. Consequently, the perchlorate anion has a much lower affinity for a proton than does the hypochlorite ion, and perchloric acid is one of the strongest acids known.



As the number of terminal oxygen atoms increases, the number of resonance structures that can be written for the oxoanions of chlorine also increases, and the single negative charge is delocalized over more oxygen atoms. As these electrostatic potential plots demonstrate, the electron density on the terminal oxygen atoms decreases steadily as their number increases. As the electron density on the oxygen atoms decreases, so does their affinity for a proton, making the anion less basic. As a result, the parent oxoacid is more acidic.

Similar inductive effects are also responsible for the trend in the acidities of oxoacids that have the same number of oxygen atoms as we go across a row of the periodic table from left to right. For example, H_3PO_4 is a weak acid, H_2SO_4 is a strong acid, and $HClO_4$ is one of the strongest acids known. The number of terminal oxygen atoms increases steadily across the row, consistent with the observed increase in acidity. In addition, the electronegativity of the central atom increases steadily from P to S to Cl, which causes electrons to be drawn from oxygen to the central atom, weakening the O–H bond and increasing the strength of the oxoacid.



Careful inspection of the data in Table 8.1.10.1 shows two apparent anomalies: carbonic acid and phosphorous acid. If carbonic acid (H_2CO_3) were a discrete molecule with the structure $(HO)_2C{=}O$, it would have a single terminal oxygen atom and should be comparable in acid strength to phosphoric acid (H_3PO_4), for which pKa1 = 2.16. Instead, the tabulated value of pK_{a1} for carbonic acid is 6.35, making it about 10,000 times weaker than expected. As we shall see, however, H_2CO_3 is only a minor component of the aqueous solutions of CO_2 that are referred to as carbonic acid. Similarly, if phosphorous acid (H_3PO_3) actually had the structure $(HO)_3P$, it would have no terminal oxygen atoms attached to phosphorous. It would therefore be expected to be about as strong an acid as $HOCl$ (pKa = 7.40). In fact, the pK_{a1} for phosphorous acid is 1.30, and the structure of phosphorous acid is $(HO)_2P(=O)H$ with one H atom directly bonded to P and one P=O bond. Thus the pKa1 for phosphorous acid is similar to that of other oxoacids with one terminal oxygen atom, such as H_3PO_4. Fortunately, phosphorous acid is the only common oxoacid in which a hydrogen atom is bonded to the central atom rather than oxygen.

Table **8.1.10.1**: Values of pKa for Selected Polyprotic Acids and Bases

Polyprotic Acids	Formula	pK_{a1}	pK_{a2}	pK_{a3}
carbonic acid*	"H_2CO_3"	6.35	10.33	
citric acid	$HO_2CCH_2C(OH)(CO_2H)CH_2CO_2H$	3.13	4.76	6.40
malonic acid	$HO_2CCH_2CO_2H$	2.85	5.70	
oxalic acid	HO_2CCO_2H	1.25	3.81	
phosphoric acid	H_3PO_4	2.16	7.21	12.32
phosphorous acid	H_3PO_3	1.3	6.70	
succinic acid	$HO_2CCH_2CH_2CO_2H$	4.21	5.64	
sulfuric acid	H_2SO_4	−2.0	1.99	
sulfurous acid*	"H_2SO_3"	1.85	7.21	
Polyprotic Bases	**Formula**	pK_{b1}	pK_{b2}	
ethylenediamine	$H_2N(CH_2)_2NH_2$	4.08	7.14	
piperazine	$HN(CH_2CH_2)_2NH$	4.27	8.67	
propylenediamine	$H_2N(CH_2)_3NH_2$	3.45	5.12	

*H_2CO_3 and H_2SO_3 are at best minor components of aqueous solutions of $CO_{2(g)}$ and $SO_{2(g)}$, respectively, but such solutions are commonly referred to as containing carbonic acid and sulfurous acid, respectively.

Inductive effects are also observed in organic molecules that contain electronegative substituents. The magnitude of the electron-withdrawing effect depends on both the nature and the number of halogen substituents, as shown by the pKa values for several acetic acid derivatives:

$$pK_a CH_3CO_2H 4.76 < CH_2ClCO_2H 2.87 < CHCl_2CO_2H 1.35 < CCl_3CO_2H 0.66 < CF_3CO_2H 0.52$$

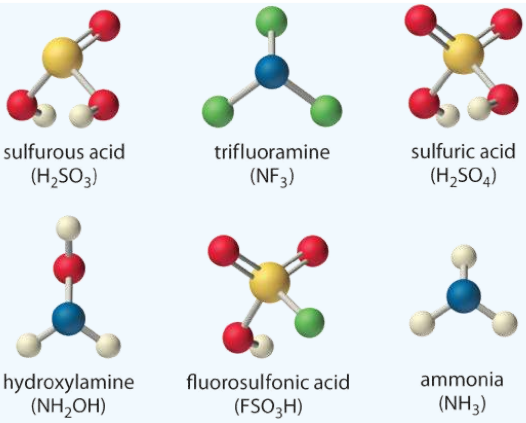
As you might expect, fluorine, which is more electronegative than chlorine, causes a larger effect than chlorine, and the effect of three halogens is greater than the effect of two or one. Notice from these data that inductive effects can be quite large. For instance, replacing the $-CH_3$ group of acetic acid by a $-CF_3$ group results in about a 10,000-fold increase in acidity!

Example 8.1.10.1

Arrange the compounds of each series in order of increasing acid or base strength.

a. sulfuric acid [H_2SO_4, or $(HO)_2SO_2$], fluorosulfonic acid (FSO_3H, or FSO_2OH), and sulfurous acid [H_2SO_3, or $(HO)_2SO$]
b. ammonia (NH_3), trifluoramine (NF_3), and hydroxylamine (NH_2OH)

The structures are shown here.



Given: series of compounds

Asked for: relative acid or base strengths

Strategy:

Use relative bond strengths, the stability of the conjugate base, and inductive effects to arrange the compounds in order of increasing tendency to ionize in aqueous solution.

Solution:

Although both sulfuric acid and sulfurous acid have two –OH groups, the sulfur atom in sulfuric acid is bonded to two terminal oxygen atoms versus one in sulfurous acid. Because oxygen is highly electronegative, sulfuric acid is the stronger acid because the negative charge on the anion is stabilized by the additional oxygen atom. In comparing sulfuric acid and fluorosulfonic acid, we note that fluorine is more electronegative than oxygen. Thus replacing an –OH by –F will remove more electron density from the central S atom, which will, in turn, remove electron density from the S–OH bond and the O–H bond. Because its O–H bond is weaker, FSO_3H is a stronger acid than sulfuric acid. The predicted order of acid strengths given here is confirmed by the measured pKa values for these acids:

$$pKa H_2SO_3 1.85 < H_2SO_4^{-2} < FSO_3H - 10$$

The structures of both trifluoramine and hydroxylamine are similar to that of ammonia. In trifluoramine, all of the hydrogen atoms in NH3 are replaced by fluorine atoms, whereas in hydroxylamine, one hydrogen atom is replaced by OH. Replacing the three hydrogen atoms by fluorine will withdraw electron density from N, making the lone electron pair on N less available to bond to an H^+ ion. Thus NF_3 is predicted to be a much weaker base than NH_3. Similarly, because oxygen is more electronegative than hydrogen, replacing one hydrogen atom in NH_3 by OH will make the amine less basic. Because oxygen is less electronegative than fluorine and only one hydrogen atom is replaced, however, the effect will be smaller. The predicted order of increasing base strength shown here is confirmed by the measured pK_b values:

$$pK_b NF_3 — << NH_2OH 8.06 < NH_3 4.75$$

Trifluoramine is such a weak base that it does not react with aqueous solutions of strong acids. Hence its base ionization constant has never been measured.

? Exercise 8.1.10.1

Arrange the compounds of each series in order of

a. decreasing acid strength: H_3PO_4, $CH_3PO_3H_2$, and $HClO_3$.
b. increasing base strength: CH_3S^-, OH^-, and CF_3S^-.

Answer a

$HClO-3 > CH_3PO_3H_2 > H_3PO_4$

Answer a

$CF_3S^- < CH_3S^- < OH^-$

Summary

Inductive effects and charge delocalization significantly influence the acidity or basicity of a compound. The acid–base strength of a molecule depends strongly on its structure. The weaker the A–H or B–H+ bond, the more likely it is to dissociate to form an H^+ ion. In addition, any factor that stabilizes the lone pair on the conjugate base favors the dissociation of H^+, making the conjugate acid a stronger acid. Atoms or groups of atoms elsewhere in a molecule can also be important in determining acid or base strength through an inductive effect, which can weaken an O–H bond and allow hydrogen to be more easily lost as H^+ ions.

Contributors and Attributions

- Anonymous

8.1.10: Molecular Structure and Acid-Base Behavior is shared under a not declared license and was authored, remixed, and/or curated by LibreTexts.

- **16.8: Molecular Structure and Acid-Base Behavior** is licensed CC BY-NC-SA 4.0.

8.1.11: Lewis Acids and Bases

Learning Objectives

Make sure you thoroughly understand the following essential ideas which have been presented. It is especially important that you know the precise meanings of all the highlighted terms in the context of this topic.

- Write the equation for the proton transfer reaction involving a Brønsted-Lowry acid or base, and show how it can be interpreted as an **electron-pair transfer** reaction, clearly identifying the donor and acceptor.
- Give an example of a **Lewis acid-base reaction** that does not involve protons.
- Write equations illustrating the behavior of a given **non-aqueous acid-base system**.

The Brønsted-Lowry proton donor-acceptor concept has been one of the most successful theories of Chemistry. But as with any such theory, it is fair to ask if this is not just a special case of a more general theory that could encompass an even broader range of chemical science. In 1916, G.N. Lewis of the University of California proposed that the *electron pair* is the dominant actor in acid-base chemistry. The Lewis theory did not become very well known until about 1923 (the same year that Brønsted and Lowry published their work), but since then it has been recognized as a very powerful tool for describing chemical reactions of widely different kinds and is widely used in organic and inorganic chemistry. The Brønsted–Lowry concept of acids and bases defines a base as any species that can accept a proton, and an acid as any substance that can donate a proton. Lewis proposed an alternative definition that focuses on *pairs of electrons* instead. According to Lewis:

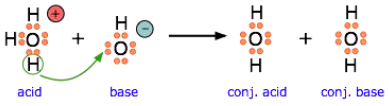
- An *acid* is a substance that **accepts** a pair of electrons, and in doing so, forms a covalent bond with the entity that supplies the electrons.
- A *base* is a substance that **donates** an unshared pair of electrons to a recipient species with which the electrons can be shared.

Note

In modern chemistry, electron donors are often referred to as nucleophiles, while acceptors are electrophiles.

Lewis Acid-Base Neutralization Involving Electron-Pair Transfer

Just as any Arrhenius acid is also a Brønsted acid, any Brønsted acid is also a Lewis acid, so the various acid-base concepts are all "upward compatible". Although we do not really need to think about electron-pair transfers when we deal with ordinary aqueous-solution acid-base reactions, it is important to understand that it is the opportunity for electron-pair sharing that enables proton transfer to take place.

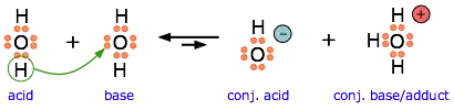


This equation for a simple acid-base neutralization shows how the Brønsted and Lewis definitions are really just different views of the same process. Take special note of the following points:

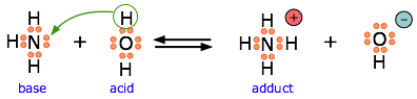
- The arrow shows the movement of a proton from the hydronium ion to the hydroxide ion.
- Note that the electron-pairs themselves do not move; they remain attached to their central atoms. The electron pair on the base is "donated" to the acceptor (the proton) only in the sense that it ends up being *shared* with the acceptor, rather than being the exclusive property of the oxygen atom in the hydroxide ion.
- Although the hydronium ion is the nominal Lewis acid here, it does not itself accept an electron pair, but acts merely as the source of the proton that coordinates with the Lewis base.

The point about the electron-pair remaining on the donor species is especially important to bear in mind. For one thing, it distinguishes a *Lewis acid-base reaction* from an *oxidation-reduction reaction*, in which a physical transfer of one or more electrons from donor to acceptor does occur. The product of a Lewis acid-base reaction is known formally as an "adduct" or "complex", although we do not ordinarily use these terms for simple proton-transfer reactions such as the one in the above

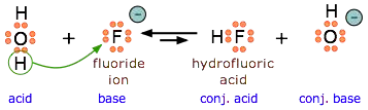
example. Here, the proton combines with the hydroxide ion to form the "adduct" H_2O. The following examples illustrate these points for some other proton-transfer reactions that you should already be familiar with.



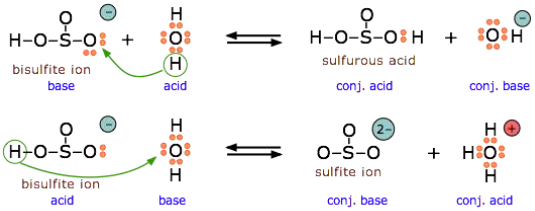
Another example, showing the autoprotolysis of water. Note that the conjugate base is also the adduct.



Ammonia is both a Brønsted and a Lewis base, owing to the unshared electron pair on the nitrogen. The reverse of this reaction represents the *hydrolysis* of the ammonium ion.



Because HF is a weak acid, fluoride salts behave as bases in aqueous solution. As a Lewis base, F^- accepts a proton from water, which is transformed into a hydroxide ion.

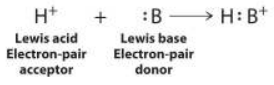


The bisulfite ion is *amphiprotic* and can act as an electron donor or acceptor.

> **Note**
>
> All Brønsted–Lowry bases (proton acceptors), such as OH^-, H_2O, and NH_3, are also electron-pair donors. Thus the Lewis definition of acids and bases does not contradict the Brønsted–Lowry definition. Rather, it expands the definition of acids to include substances other than the H^+ ion.

Lewis Acid-Base Neutralization without Transferring Protons

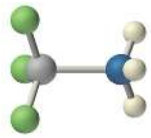
Electron-deficient molecules, such as BCl_3, contain less than an octet of electrons around one atom and have a strong tendency to gain an additional pair of electrons by reacting with substances that possess a lone pair of electrons. Lewis's definition, which is less restrictive than either the Brønsted–Lowry or the Arrhenius definition, grew out of his observation of this tendency. A general Brønsted–Lowry acid–base reaction can be depicted in Lewis electron symbols as follows:



The proton (H^+), which has no valence electrons, is a Lewis acid because it accepts a lone pair of electrons on the base to form a bond. The proton, however, is just one of many electron-deficient species that are known to react with bases. For example, neutral compounds of boron, aluminum, and the other Group 13 elements, which possess only six valence electrons, have a very strong tendency to gain an additional electron pair. Such compounds are therefore potent Lewis acids that react with an electron-pair donor such as ammonia to form an acid–base adduct, a new covalent bond, as shown here for boron trifluoride (BF_3):

$$\underset{\text{Lewis acid}}{BF_3} + \underset{\text{Lewis base}}{:NH_3} \longrightarrow \underset{\text{Acid-base adduct}}{F_3B{:}NH_3}$$

The bond formed between a Lewis acid and a Lewis base is a *coordinate covalent bond* because both electrons are provided by only one of the atoms (N, in the case of $F_3B{:}NH_3$). After it is formed, however, a coordinate covalent bond behaves like any other covalent single bond.



Boron trifluoride-ammonia adduct

Species that are very weak Brønsted–Lowry bases can be relatively strong Lewis bases. For example, many of the group 13 trihalides are highly soluble in ethers (R–O–R′) because the oxygen atom in the ether contains two lone pairs of electrons, just as in H_2O. Hence the predominant species in solutions of electron-deficient trihalides in ether solvents is a Lewis acid–base adduct. A reaction of this type is shown in Figure **8.1.11.1** for boron trichloride and diethyl ether:

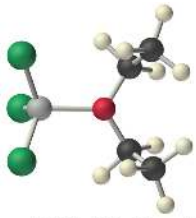
$$\underset{\text{Lewis acid}}{BCl_3} + \underset{\text{Lewis base}}{:\ddot{O}(CH_2CH_3)_2} \longrightarrow \underset{\text{Acid-base adduct}}{Cl_3B{:}\ddot{O}(CH_2CH_3)_2}$$

Figure 8.1.11.1: *Lewis Acid/Base reaction of boron trichloride and diethyl ether reaction*

Note

- Electron-deficient molecules (those with less than an octet of electrons) are Lewis acids.
- The acid-base behavior of many compounds can be explained by their Lewis electron structures.

Many molecules with multiple bonds can act as Lewis acids. In these cases, the Lewis base typically donates a pair of electrons to form a bond to the central atom of the molecule, while a pair of electrons displaced from the multiple bond becomes a lone pair on a terminal atom.



Boron trichloride-diethyl ether adduct

Figure **8.1.11.2**. The highly electronegative oxygen atoms pull electron density away from carbon, so the carbon atom acts as a Lewis acid. Arrows indicate the direction of electron flow.

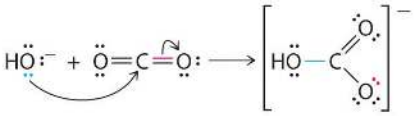


Figure 8.1.11.2: *Lewis Acid/Base reaction of the hydroxide ion with carbon dioxide*

Example 8.1.11.1

Identify the acid and the base in each Lewis acid–base reaction.

a. $BH_3 + (CH_3)_2S \rightarrow H_3B{:}S(CH_3)_2$
b. $CaO + CO_2 \rightarrow CaCO_3$
c. $BeCl_2 + 2\ Cl^- \rightarrow BeCl_4^{2-}$

Given: reactants and products

Asked for: identity of Lewis acid and Lewis base

Strategy:

In each equation, identify the reactant that is electron deficient and the reactant that is an electron-pair donor. The electron-deficient compound is the Lewis acid, whereas the other is the Lewis base.

Solution:

a. In BH_3, boron has only six valence electrons. It is therefore electron deficient and can accept a lone pair. Like oxygen, the sulfur atom in $(CH_3)_2S$ has two lone pairs. Thus $(CH_3)_2S$ donates an electron pair on sulfur to the boron atom of BH_3. The Lewis base is $(CH_3)_2S$, and the Lewis acid is BH_3.
b. As in the reaction shown in Equation 8.21, CO_2 accepts a pair of electrons from the O^{2-} ion in CaO to form the carbonate ion. The oxygen in CaO is an electron-pair donor, so CaO is the Lewis base. Carbon accepts a pair of electrons, so CO_2 is the Lewis acid.
c. The chloride ion contains four lone pairs. In this reaction, each chloride ion donates one lone pair to $BeCl_2$, which has only four electrons around Be. Thus the chloride ions are Lewis bases, and $BeCl_2$ is the Lewis acid.

? Exercise 8.1.11.1

Identify the acid and the base in each Lewis acid–base reaction.

a. $(CH_3)_2O + BF_3 \rightarrow (CH_3)_2O{:}BF_3$
b. $H_2O + SO_3 \rightarrow H_2SO_4$

Answer

a. Lewis base: $(CH_3)_2O$; Lewis acid: BF_3
b. Lewis base: H_2O; Lewis acid: SO_3

? Exercise 8.1.11.2

Here are several more examples of Lewis acid-base reactions that **cannot** be accommodated within the Brønsted or Arrhenius models. Identify the Lewis acid and Lewis base in each reaction.

a. $Al(OH)_3 + OH^- \rightarrow Al(OH)_4^-$
b. $SnS_2 + S^{2-} \rightarrow SnS_3^{2-}$
c. $Cd(CN)_2 + 2CN^- \rightarrow Cd(CN)_4^{2+}$
d. $AgCl + 2NH_3 \rightarrow Ag(NH_3)_2^+ + Cl^-$
e. $Fe^{2+} + NO \rightarrow Fe(NO)^{2+}$
f. $[Ni^{2+} + 6NH_3 \rightarrow Ni(NH_3)_5^{2+}$

Non-Aqueous Acid/Base Systems

We ordinarily think of Brønsted-Lowry acid-base reactions as taking place in aqueous solutions, but this need not always be the case. A more general view encompasses a variety of acid-base *solvent systems*, of which the *water system* is only one (Table **8.1.11.1**). Each of these has as its basis an amphiprotic solvent (one capable of undergoing autoprotolysis), in parallel with the familiar case of water.

The limiting acid in a given solvent is the solvonium ion, such as H_3O^+ (hydronium) ion in water. An acid which has more of a tendency to donate a hydrogen ion than the limiting acid will be a strong acid in the solvent considered, and will exist mostly or entirely in its dissociated form. Likewise, the limiting base in a given solvent is the solvate ion, such as OH^- (hydroxide) ion, in water. A base which has more affinity for protons than the limiting base cannot exist in solution, as it will react with the solvent.

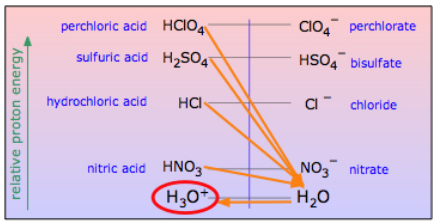


Figure } \PageIndex{3}\): *Use of non-aqueous solvents allows the study of strong acids that are hindered by the "leveling effect" of the solvent.*

The ammonia system is one of the most common non-aqueous system in Chemistry. Liquid ammonia boils at –33° C, and can conveniently be maintained as a liquid by cooling with dry ice (–77° C). It is a good solvent for substances that also dissolve in water, such as ionic salts and organic compounds since it is capable of forming hydrogen bonds. Bases can exist in solution in liquid ammonia which cannot exist in aqueous solution: this is the case for any base which is **stronger** than the hydroxide ion, but **weaker** than the amide ion NH_2^-. The limiting acid in liquid ammonia is the ammonium ion, which has a pK_a value in water of 9.25. The limiting base is the amide ion, NH_2^-. This is a stronger base than the hydroxide ion and so cannot exist in aqueous solution. The pK_a value of ammonia is estimated to be approximately 33. Any acid which is a stronger acid than the ammonium ion will be a strong acid in liquid ammonia. This is the case for acetic acid, which is completely dissociated in liquid ammonia solution. The addition of pure acetic acid and the addition of ammonium acetate have exactly the same effect on a liquid ammonia solution: the increase in its acidity: in practice, the latter is preferred for safety reasons.

Note

As with OH^- and H_3O^+ in water, the strongest acid and base in NH_3 is dictated by the corresponding autoprotolysis reaction of the solvent:

$$2NH_3 \rightleftharpoons NH_4^+ + NH_2^-$$

One use of non-aqueous acid-base systems is to examine the relative strengths of the strong acids and bases, whose strengths are "leveled" by the fact that they are all totally converted into H_3O^+ or OH^- ions in water. By studying them in appropriate non-aqueous solvents which are poorer acceptors or donors of protons, their relative strengths can be determined. Many familiar substances can serve as the basis of protonic solvent systems (Table 8.1.11.1).

Table 8.1.11.1: Popular Solvent systems

solvent	autoprotolysis reaction	pK_a
water	$2H_2O \rightleftharpoons H_3O^+ + OH^-$	14
ammonia	$2NH_3 \rightleftharpoons NH_4^+ + NH_2^-$	33
acetic acid	$2CH_3COOH \rightleftharpoons CH_3COOH_2^+ + CH_3COO^-$	13
ethanol	$2C_2H_5OH \rightleftharpoons C_2H_5OH_2^+ + C_2H_5O^-$	19
hydrogen peroxide	$2HO-OH \rightleftharpoons HO-OH_2^+ + HO-O^-$	13
hydrofluoric acid	$2HF \rightleftharpoons H^2F^+ + F^-$	10
sulfuric acid	$2H_2SO_4 \rightleftharpoons H3SO_4^+ + HSO_4^-$	3.5

The extreme case is a **superacid**, a medium in which the hydrogen ion is only very weakly solvated. The classic example is a mixture of antimony pentafluoride and liquid hydrogen fluoride:

$$SbF_5 + HF \rightleftharpoons H^+ + SbF_6^- \qquad (8.1.11.1)$$

The limiting base, the hexfluoroantimonate anion SbF_6^-, is so weakly attracted to the hydrogen ion that virtually any other base will bind more strongly: hence, this mixture can be used to protonate organic molecules which would not be considered bases in other

solvents. It should noted that pH is undefined in aprotic solvents, which assumes presence of hydronium ions. In other solvents, the concentration of the respective solvonium/solvate ions should be used (e.g., $[NH_4^+]$ and $[NH_2^-]$ in $NH_{3(l)}$.

Contributors and Attributions

- Stephen Lower, Professor Emeritus (Simon Fraser U.) Chem1 Virtual Textbook
- Wikipedia

8.1.11: Lewis Acids and Bases is shared under a not declared license and was authored, remixed, and/or curated by LibreTexts.

- **16.9: Lewis Acids and Bases** is licensed CC BY-NC-SA 4.0.

8.1.12: Common-Ion Effect in Acid–Base Equilibria

Learning Objectives

- Recognize common ions from various salts, acids, and bases.
- Calculate concentrations involving common ions.
- Calculate ion concentrations involving chemical equilibrium.

The common-ion effect is used to describe the effect on an equilibrium involving a substance that adds an ion that is a part of the equilibrium.

Introduction

The solubility products K_{sp}'s are equilibrium constants in heterogeneous equilibria (i.e., between two different phases). If several salts are present in a system, they all ionize in the solution. If the salts contain a common cation or anion, these salts contribute to the concentration of the common ion. Contributions from all salts must be included in the calculation of concentration of the common ion. For example, a solution containing sodium chloride and potassium chloride will have the following relationship:

$$[Na^+] + [K^+] = [Cl^-] \tag{8.1.12.1}$$

Consideration of *charge balance* or *mass balance* or both leads to the same conclusion.

Common Ions

When **NaCl** and **KCl** are dissolved in the same solution, the Cl^- ions are *common* to both salts. In a system containing **NaCl** and **KCl**, the Cl^- ions are common ions.

$$NaCl \rightleftharpoons Na^+ + Cl^-$$

$$KCl \rightleftharpoons K^+ + Cl^-$$

$$CaCl_2 \rightleftharpoons Ca^{2+} + 2Cl^-$$

$$AlCl_3 \rightleftharpoons Al^{3+} + 3Cl^-$$

$$AgCl \rightleftharpoons Ag^+ + Cl^-$$

For example, when **AgCl** is dissolved into a solution already containing **NaCl** (actually Na^+ and Cl^- ions), the Cl^- ions come from the ionization of both **AgCl** and **NaCl**. Thus, $[Cl^-]$ differs from $[Ag^+]$. The following examples show how the concentration of the common ion is calculated.

Example 8.1.12.1

What are $[Na^+]$, $[Cl^-]$, $[Ca^{2+}]$, and $[H^+]$ in a solution containing 0.10 M each of **NaCl**, $CaCl_2$, and **HCl**?

Solution

Due to the conservation of ions, we have

$$[Na^+] = [Ca^{2+}] = [H^+] = 0.10\ M$$

but

$$\begin{aligned}[Cl^-] = &\ 0.10 \text{ (due to NaCl)} \\ &+ 0.20 \text{ (due to } CaCl_2\text{)} \\ &+ 0.10 \text{ (due to HCl)} \\ = &\ 0.40\ M\end{aligned}$$

Exercise 8.1.12.1

John poured 10.0 mL of 0.10 M **NaCl**, 10.0 mL of 0.10 M **KOH**, and 5.0 mL of 0.20 M **HCl** solutions together and then he made the total volume to be 100.0 mL. What is $[Cl^-]$ in the final solution?

Solution

$$[Cl^-] = \frac{0.1\ M \times 10\ mL + 0.2\ M \times 5.0\ mL}{100.0\ mL} = 0.020\ M$$

Le Châtelier's Principle states that if an equilibrium becomes unbalanced, the reaction will shift to restore the balance. If a common ion is added to a weak acid or weak base equilibrium, then the equilibrium will shift towards the reactants, in this case the weak acid or base.

Example 8.1.12.2: Solubility of Lead Chloride

Consider the lead(II) ion concentration in this *saturated* solution of $PbCl_2$. The balanced reaction is

$$PbCl_{2(s)} \rightleftharpoons Pb^{2+}_{(aq)} + 2Cl^-_{(aq)}$$

Defining s as the concentration of dissolved lead(II) chloride, then:

$$[Pb^{2+}] = s$$

$$[Cl^-] = 2s$$

These values can be substituted into the solubility product expression, which can be solved for s:

$$K_{sp} = [Pb^{2+}][Cl^-]^2 \tag{8.1.12.2}$$

$$= s \times (2s)^2 \tag{8.1.12.3}$$

$$1.7 \times 10^{-5} = 4s^3 \tag{8.1.12.4}$$

$$s^3 = \frac{1.7 \times 10^{-5}}{4} \tag{8.1.12.5}$$

$$= 4.25 \times 10^{-6} \tag{8.1.12.6}$$

$$s = \sqrt[3]{4.25 \times 10^{-6}} \tag{8.1.12.7}$$

$$= 1.62 \times 10^{-2}\ mol\ dm^{-3} \tag{8.1.12.8}$$

The concentration of lead(II) ions in the solution is 1.62 x 10^{-2} M. Consider what happens if sodium chloride is added to this saturated solution. Sodium chloride shares an ion with lead(II) chloride. The chloride ion is **common** to both of them; this is the origin of the term "common ion effect".

Look at the original equilibrium expression again:

$$PbCl_2\,(s) \rightleftharpoons Pb^{2+}\,(aq) + 2Cl^-\,(aq)$$

What happens to that equilibrium if extra chloride ions are added? According to *Le* Châtelier, the position of equilibrium will shift to counter the change, in this case, by removing the chloride ions by making extra solid lead(II) chloride.

Of course, the concentration of lead(II) ions in the solution is so small that only a tiny proportion of the extra chloride ions can be converted into solid lead(II) chloride. The lead(II) chloride becomes even *less soluble*, and the concentration of lead(II) ions in the solution *decreases*. This type of response occurs with any sparingly soluble substance: it is less soluble in a solution which contains any ion which it has in common. This is the common ion effect.

Example 8.1.12.3

If an attempt is made to dissolve some lead(II) chloride in some 0.100 M sodium chloride solution instead of in water, what is the equilibrium concentration of the lead(II) ions this time? As before, define s to be the concentration of the lead(II) ions.

$$[Pb^{2+}] = s \tag{8.1.12.9}$$

The calculations are different from before. This time the concentration of the chloride ions is governed by the concentration of the sodium chloride solution. The number of ions coming from the lead(II) chloride is going to be tiny compared with the 0.100 M coming from the sodium chloride solution.

In calculations like this, it can be assumed that the concentration of the common ion is entirely due to the other solution. This simplifies the calculation.

So we assume:

$$[Cl^-] = 0.100\ M \tag{8.1.12.10}$$

The rest of the mathematics looks like this:

$$\begin{aligned} K_{sp} &= [Pb^{2+}][Cl^-]^2 \\ &= s \times (0.100)^2 \\ 1.7 \times 10^{-5} &= s \times 0.00100 \end{aligned}$$

therefore:

$$\begin{aligned} s &= \frac{1.7 \times 10^{-5}}{0.0100} \\ &= 1.7 \times 10^{-3}\,\text{M} \end{aligned} \tag{8.1.12.11}$$

Finally, compare that value with the simple saturated solution:

Original solution:

$$[Pb^{2+}] = 0.0162\ M \tag{8.1.12.12}$$

Solution in 0.100 M NaCl solution:

$$[Pb^{2+}] = 0.0017\ M \tag{8.1.12.13}$$

The concentration of the lead(II) ions has decreased by a factor of about 10. If more concentrated solutions of sodium chloride are used, the solubility decreases further.



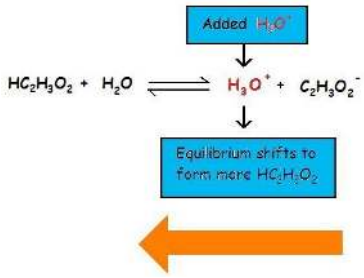
A Video Discussing Finding the Solubility of a Salt: Finding the Solubility of a Salt(opens in new window) [youtu.be]

Common Ion Effect with Weak Acids and Bases

Adding a common ion prevents the weak acid or weak base from ionizing as much as it would without the added common ion. The common ion effect suppresses the ionization of a weak acid by adding more of an ion that is a product of this equilibrium.

> *Adding a common ion to a system at equilibrium affects the equilibrium composition, but not the ionization constant.*

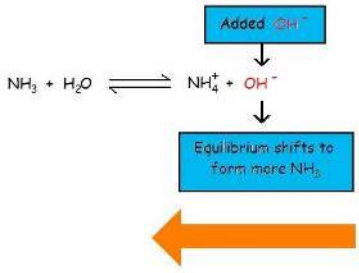
The common ion effect of H_3O^+ on the ionization of acetic acid



HC2H3O2 reactions with H2O to produce H3O plus and C2H3 O2 minus. If more H3O plus is added to the reaction, the equilibrium would shift to form more HC2H3O2.

When a strong acid supplies the common ion $\mathbf{H_3O^+}$ the equilibrium shifts to form more $\mathbf{HC_2H_3O_2}$.

The common ion effect suppresses the ionization of a weak base by adding more of an ion that is a product of this equilibrium. Now consider the common ion effect of $\mathbf{OH^-}$ on the ionization of ammonia



When a strong base supplies the common ion $\mathbf{OH^-}$ the equilibrium shifts to form more $\mathbf{NH_3}$.

NH3 reacts with H2 O to produce NH4 plus and OH minus. If more OH minus is added to the reaction, the equilibrium would shifts to form more NH3.

Adding the common ion of hydroxide shifts the reaction towards the left to decrease the stress (in accordance with Le Chatelier's Principle), forming more reactants. This decreases the reaction quotient, because the reaction is being pushed towards the left to reach equilibrium. The equilibrium constant, $K_b = 1.8 \times 10^{-5}$, does not change. The reaction is put out of balance, or equilibrium.

$$Q_a = \frac{[NH_4^+][OH^-]}{[NH_3]}$$

At first, when more hydroxide is added, the quotient is greater than the equilibrium constant. The reaction then shifts right, causing the denominator to increase, decreasing the reaction quotient and pulling towards equilibrium and causing Q to decrease towards K.

Common Ion Effect on Solubility

When a slightly soluble ionic compound is added to water, some of it dissolves to form a solution, establishing an equilibrium between the pure solid and a solution of its ions. For the dissolution of calcium phosphate, one of the two main components of kidney stones, the equilibrium can be written as follows, with the solid salt on the left:

$$Ca_3(PO_4)_2(s) \rightleftharpoons 3\,Ca^{2+}(aq) + 2\,PO_4^{3-}(aq) \tag{8.1.12.14}$$

As you will discover in more advanced chemistry courses, basic anions, such as S^{2-}, PO_4^{3-}, and CO_3^{2-}, react with water to produce OH^- and the corresponding protonated anion. Consequently, their calculated molarities, assuming no protonation in aqueous solution, are only approximate. The equilibrium constant for the dissolution of a sparingly soluble salt is the **solubility product (K_{sp})** of the salt. Because the concentration of a pure solid such as $Ca_3(PO_4)_2$ is a constant, it does not appear explicitly in the equilibrium constant expression. The equilibrium constant expression for the dissolution of calcium phosphate is therefore

$$K = \frac{[Ca^{2+}]^3[PO_4^{3-}]^2}{[Ca_3(PO_4)_2]} \tag{8.1.12.15}$$

$$[Ca_3(PO_4)_2]K = K_{sp} = [Ca^{2+}]^3[PO_4^{3-}]^2 \tag{8.1.12.16}$$

At 25°C and pH 7.00, K_{sp} for calcium phosphate is 2.07×10^{-33}, indicating that the concentrations of Ca^{2+} and PO_4^{3-} ions in solution that are in equilibrium with solid calcium phosphate are very low. The values of K_{sp} for some common salts vary dramatically for different compounds (Table E3). Although K_{sp} is not a function of pH in Equation 8.1.12.15, changes in pH can affect the solubility of a compound.

The solubility product expression tells us that the equilibrium concentrations of the cation and the anion are inversely related. That is, as the concentration of the anion increases, the maximum concentration of the cation needed for precipitation to occur decreases—and vice versa—so that K_{sp} is constant. **Consequently, the solubility of an ionic compound depends on the concentrations of other salts that contain the same ions.** This dependency is another example of the common ion effect where adding a common cation or anion shifts a solubility equilibrium in the direction predicted by Le Chatelier's principle. As a result, the solubility of any sparingly soluble salt is almost always decreased by the presence of a soluble salt that contains a common ion.

Consider, for example, the effect of adding a soluble salt, such as $CaCl_2$, to a saturated solution of calcium phosphate [$Ca_3(PO_4)_2$]. We have seen that the solubility of $Ca_3(PO_4)_2$ in water at 25°C is 1.14×10^{-7} M ($K_{sp} = 2.07 \times 10^{-33}$). Thus a saturated solution of $Ca_3(PO_4)_2$ in water contains

- $\mathbf{3 \times (1.14 \times 10^{-7}\ M) = 3.42 \times 10^{-7} M\ of\ Ca^{2+}}$
- $\mathbf{2 \times (1.14 \times 10^{-7} M) = 2.28 \times 10^{-7} M\ of\ PO_4^{3-}}$

according to the stoichiometry shown in Equation 8.1.12.15 (neglecting hydrolysis to form HPO_4^{2-}). If $CaCl_2$ is added to a saturated solution of $Ca_3(PO_4)_2$, the Ca^{2+} ion concentration will increase such that $[Ca^{2+}] > 3.42 \times 10^{-7}$ M, making $Q > K_{sp}$. The only way the system can return to equilibrium is for the reaction in Equation 8.1.12.15 to proceed to the left, resulting in precipitation of $Ca_3(PO_4)_2$. This will decrease the concentration of both Ca^{2+} and PO_4^{3-} until $Q = K_{sp}$.

Note

Adding a common ion decreases solubility, as the reaction shifts toward the left to relieve the stress of the excess product. Adding a common ion to a dissociation reaction causes the equilibrium to shift left, toward the reactants, causing precipitation.

Example 8.1.12.5

Consider the reaction:

$$PbCl_2(s) \rightleftharpoons Pb^{2+}(aq) + 2Cl^-(aq)$$

What happens to the solubility of $PbCl_2(s)$ when 0.1 M NaCl is added?

Solution

$$K_{sp} = 1.7 \times 10^{-5}$$

$$Q_{sp} = 1.8 \times 10^{-5}$$

Identify the common ion: Cl^-

Notice: $Q_{sp} > K_{sp}$ The addition of NaCl has caused the reaction to shift out of equilibrium because there are more dissociated ions. Typically, solving for the molarities requires the assumption that the solubility of $PbCl_2$ is equivalent to the concentration of Pb^{2+} produced because they are in a 1:1 ratio.

Because K_{sp} for the reaction is 1.7×10^{-5}, the overall reaction would be $(s)(2s)^2 = 1.7\times10^{-5}$. Solving the equation for s gives $s = 1.62\times10^{-2}$ M. The coefficient on Cl^- is 2, so it is assumed that twice as much Cl^- is produced as Pb^{2+}, hence the '2s.' The solubility equilibrium constant can be used to solve for the molarities of the ions at equilibrium.

The molarity of Cl^- added would be 0.1 M because Na^+ and Cl^- are in a 1:1 ration in the ionic salt, NaCl. Therefore, the overall molarity of Cl^- would be 2s + 0.1, with 2s referring to the contribution of the chloride ion from the dissociation of lead chloride.

$$Q_{sp} = [Pb^{2+}][Cl^-]^2 \quad (8.1.12.17)$$

$$1.8 \times 10^{-5} = (s)(2s + 0.1)^2 \quad (8.1.12.18)$$

$$s = [Pb^{2+}] \quad (8.1.12.19)$$

$$= 1.8 \times 10^{-3} M \quad (8.1.12.20)$$

$$2s = [Cl^-] \quad (8.1.12.21)$$

$$\approx 0.1M \quad (8.1.12.22)$$

Notice that the molarity of Pb^{2+} is lower when NaCl is added. The equilibrium constant remains the same because of the increased concentration of the chloride ion. To simplify the reaction, it can be assumed that $[Cl^-]$ is approximately 0.1M since the formation of the chloride ion from the dissociation of lead chloride is so small. The reaction quotient for $PbCl_2$ is greater than the equilibrium constant because of the added Cl^-. This therefore shift the reaction left towards equilibrium, causing precipitation and lowering the current solubility of the reaction. Overall, the solubility of the reaction decreases with the added sodium chloride.

Exercise 8.1.12.5

Calculate the solubility of silver carbonate in a 0.25 M solution of sodium carbonate. The solubility of silver carbonate in pure water is 8.45×10^{-12} at 25°C.

Answer

2.9×10^{-6} M (versus 1.3×10^{-4} M in pure water)



A Video Discussing the Common Ion Effect in Solubility Products: The Common Ion Effect in Solubility Products (opens in new window) [youtu.be]

References

1. Harwood, William S., F. G. Herring, Jeffry D. Madura, and Ralph H. Petrucci. General Chemistry Principles and Modern Applications. 9th ed. New Jersey: Prentice Hall, 2007.

Contributors and Attributions

- Emmellin Tung, Mahtab Danai (UCD)
- Jim Clark (ChemGuide)
- Chung (Peter) Chieh (Professor Emeritus, Chemistry @ University of Waterloo)

8.1.12: Common-Ion Effect in Acid–Base Equilibria is shared under a not declared license and was authored, remixed, and/or curated by LibreTexts.

- **17.1: The Common-Ion Effect** is licensed CC BY-NC-SA 3.0.



SECTION OVERVIEW

8.2: Additional Aspects of Acid-Base Equilibria

Sections

8.2.1: Buffer Solutions

8.2.2: Acid–Base Indicators

8.2.3: Neutralization Reactions and Titration Curves

8.2.4: Solutions of Salts of Polyprotic Acids

8.2.5: Acid–Base Equilibrium Calculations- A Summary

8.2.6: Exercises on Acids and Bases II

8.2.7: E3. Solubility Constants for Compounds at 25°C Data Table

8.2.8: pH Calculations for Acid–Base Titrations

8.2: Additional Aspects of Acid-Base Equilibria is shared under a CC BY-NC-SA 4.0 license and was authored, remixed, and/or curated by LibreTexts.

8.2.1: Buffer Solutions

Learning Objectives

- To understand how adding a common ion affects the position of an acid–base equilibrium.
- To know how to use the Henderson-Hasselbalch approximation to calculate the pH of a buffer.

Buffers are solutions that maintain a relatively constant pH when an acid or a base is added. They therefore protect, or "buffer," other molecules in solution from the effects of the added acid or base. Buffers contain either a weak acid (HA) and its conjugate base (A^-) or a weak base (B) and its conjugate acid (BH^+), and they are critically important for the proper functioning of biological systems. In fact, every biological fluid is buffered to maintain its physiological pH.

The Common Ion Effect: Weak Acids Combined with Conjugate Bases

To understand how buffers work, let's look first at how the ionization equilibrium of a weak acid is affected by adding either the conjugate base of the acid or a strong acid (a source of H^+). Le Chatelier's principle can be used to predict the effect on the equilibrium position of the solution. A typical buffer used in biochemistry laboratories contains acetic acid and a salt such as sodium acetate. The dissociation reaction of acetic acid is as follows:

$$CH_3COOH(aq) \rightleftharpoons CH_3COO^-(aq) + H^+(aq) \tag{8.2.1.1}$$

and the equilibrium constant expression is as follows:

$$K_a = \frac{[H^+][CH_3COO^-]}{[CH_3CO_2H]} \tag{8.2.1.2}$$

Sodium acetate (CH_3CO_2Na) is a strong electrolyte that ionizes completely in aqueous solution to produce Na^+ and $CH_3CO_2^-$ ions. If sodium acetate is added to a solution of acetic acid, Le Chatelier's principle predicts that the equilibrium in Equation 8.2.1.1 will shift to the left, consuming some of the added CH_3COO^- and some of the H^+ ions originally present in solution.

Because Na^+ is a **spectator ion**, it has no effect on the position of the equilibrium and can be ignored. The addition of sodium acetate produces a new equilibrium composition, in which $[H^+]$ is less than the initial value. Because $[H^+]$ has decreased, the pH will be higher. Thus adding a salt of the conjugate base to a solution of a weak acid increases the pH. This makes sense because sodium acetate is a base, and adding any base to a solution of a weak acid should increase the pH.

If we instead add a strong acid such as HCl to the system, $[H^+]$ increases. Once again the equilibrium is temporarily disturbed, but the excess H^+ ions react with the conjugate base ($CH_3CO_2^-$), whether from the parent acid or sodium acetate, to drive the equilibrium to the left. The net result is a new equilibrium composition that has a lower $[CH_3CO_2^-]$ than before. In both cases, only the equilibrium composition has changed; the ionization constant K_a for acetic acid remains the same. Adding a strong electrolyte that contains one ion in common with a reaction system that is at equilibrium, in this case $CH_3CO_2^-$, will therefore shift the equilibrium in the direction that reduces the concentration of the common ion. The shift in equilibrium is via the common ion effect.

> *Adding a common ion to a system at equilibrium affects the equilibrium composition, but not the ionization constant.*

Example 8.2.1.1

A 0.150 M solution of formic acid at 25°C (pKa = 3.75) has a pH of 2.28 and is 3.5% ionized.

a. Is there a change to the pH of the solution if enough solid sodium formate is added to make the final formate concentration 0.100 M (assume that the formic acid concentration does not change)?
b. What percentage of the formic acid is ionized if 0.200 M HCl is added to the system?

Given: solution concentration and pH, pK_a, and percent ionization of acid; final concentration of conjugate base or strong acid added

Asked for: pH and percent ionization of formic acid

Strategy:

A. Write a balanced equilibrium equation for the ionization equilibrium of formic acid. Tabulate the initial concentrations, the changes, and the final concentrations.
B. Substitute the expressions for the final concentrations into the expression for Ka. Calculate $[H^+]$ and the pH of the solution.
C. Construct a table of concentrations for the dissociation of formic acid. To determine the percent ionization, determine the anion concentration, divide it by the initial concentration of formic acid, and multiply the result by 100.

Solution:

A Because sodium formate is a strong electrolyte, it ionizes completely in solution to give formate and sodium ions. The Na^+ ions are spectator ions, so they can be ignored in the equilibrium equation. Because water is both a much weaker acid than formic acid and a much weaker base than formate, the acid–base properties of the solution are determined solely by the formic acid ionization equilibrium:

$$HCO_2H(aq) \rightleftharpoons HCO_2^-(aq) + H^+(aq)$$

The initial concentrations, the changes in concentration that occur as equilibrium is reached, and the final concentrations can be tabulated.

Final Concentration

ICE	$[HCO_2H(aq)]$	$[H^+(aq)]$	$[HCO_2^-(aq)]$
Initial	0.150	1.00×10^{-7}	0.100
Change	−x	+x	+x
Equilibrium	(0.150 − x)	x	(0.100 + x)

B We substitute the expressions for the final concentrations into the equilibrium constant expression and make our usual simplifying assumptions, so

$$\begin{aligned} K_a = \frac{[H^+][HCO_2^-]}{[HCO_2H]} &= \frac{(x)(0.100+x)}{0.150-x} \\ &\approx \frac{x(0.100)}{0.150} \\ &\approx 10^{-3.75} \\ &\approx 1.8 \times 10^{-4} \end{aligned}$$

Rearranging and solving for x,

$$\begin{aligned} x &= (1.8 \times 10^{-4}) \times \frac{0.150\ M}{0.100\ M} \\ &= 2.7 \times 10^{-4} \\ &= [H^+] \end{aligned}$$

The value of x is small compared with 0.150 or 0.100 M, so our assumption about the extent of ionization is justified. Moreover,

$$K_aC_{HA} = (1.8 \times 10^{-4})(0.150) = 2.7 \times 10^{-5}$$

which is greater than 1.0×10^{-6}, so again, our assumption is justified. The final pH is:

$$pH = -\log(2.7 \times 10^{-4}) = 3.57$$

compared with the initial value of 2.29. Thus adding a salt containing the conjugate base of the acid has increased the pH of the solution, as we expect based on Le Chatelier's principle; the stress on the system has been relieved by the consumption of H^+ ions, driving the equilibrium to the left.

C Because HCl is a strong acid, it ionizes completely, and chloride is a spectator ion that can be neglected. Thus the only relevant acid–base equilibrium is again the dissociation of formic acid, and initially the concentration of formate is zero. We can construct a table of initial concentrations, changes in concentration, and final concentrations.

$$HCO_2H(aq) \leftrightharpoons H^+(aq) + HCO_2^-(aq)$$

initial concentrations, changes in concentration, and final concentrations

	$[HCO_2H(aq)]$	$[H^+(aq)]$	$[HCO_2^-(aq)]$
initial	0.150	0.200	0
change	−x	+x	+x
final	(0.150 − x)	(0.200 + x)	x

To calculate the percentage of formic acid that is ionized under these conditions, we have to determine the final $[HCO_2^-]$. We substitute final concentrations into the equilibrium constant expression and make the usual simplifying assumptions, so

$$K_a = \frac{[H^+][HCO_2^-]}{[HCO_2H]} = \frac{(0.200 + x)(x)}{0.150 - x} \approx \frac{x(0.200)}{0.150} = 1.80 \times 10^{-4}$$

Rearranging and solving for x,

$$x = (1.80 \times 10^{-4}) \times \frac{0.150\ M}{0.200\ M}$$
$$= 1.35 \times 10^{-4} = [HCO_2^-]$$

Once again, our simplifying assumptions are justified. The percent ionization of formic acid is as follows:

$$\text{percent ionization} = \frac{1.35 \times 10^{-4}\ M}{0.150\ M} \times 100\% = 0.0900\%$$

Adding the strong acid to the solution, as shown in the table, decreased the percent ionization of formic acid by a factor of approximately 38 (3.45%/0.0900%). Again, this is consistent with Le Chatelier's principle: adding H^+ ions drives the dissociation equilibrium to the left.

? Exercise 8.2.1.1

A 0.225 M solution of ethylamine ($CH_3CH_2NH_2$ with $pK_b = 3.19$) has a pH of 12.08 and a percent ionization of 5.4% at 20°C. Calculate the following:

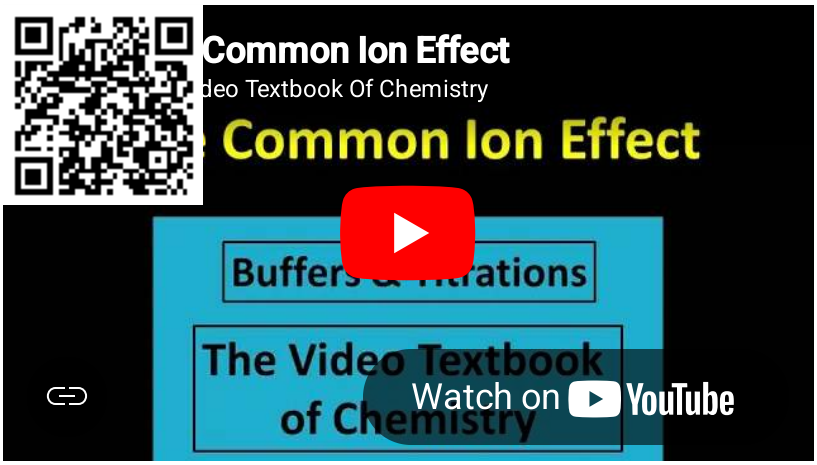
a. the pH of the solution if enough solid ethylamine hydrochloride ($EtNH_3Cl$) is added to make the solution 0.100 M in $EtNH_3^+$
b. the percentage of ethylamine that is ionized if enough solid $NaOH$ is added to the original solution to give a final concentration of 0.050 M $NaOH$

Answer a

11.16

Answer b

1.3%



A Video Discussing the Common Ion Effect: The Common Ion Effecr(opens in new window) [youtu.be]

The Common Ion Effect: Weak Bases Combined with Conjugate Acids

Now let's suppose we have a buffer solution that contains equimolar concentrations of a weak base (B) and its conjugate acid (BH^+). The general equation for the ionization of a weak base is as follows:

$$B(aq) + H_2O(l) \leftrightharpoons BH^+(aq) + OH^-(aq) \tag{8.2.1.3}$$

If the equilibrium constant for the reaction as written in Equation 8.2.1.3 is small, for example $K_b = 10^{-5}$, then the equilibrium constant for the reverse reaction is very large: $K = \frac{1}{K_b} = 10^5$. Adding a strong base such as OH^- to the solution therefore causes the equilibrium in Equation 8.2.1.3 to shift to the left, consuming the added OH^-. As a result, the OH^- ion concentration in solution remains relatively constant, and the pH of the solution changes very little. Le Chatelier's principle predicts the same outcome: when the system is stressed by an increase in the OH^- ion concentration, the reaction will proceed to the left to counteract the stress.

If the pK_b of the base is 5.0, the pK_a of its conjugate acid is

$$pK_a = pK_w - pK_b = 14.0–5.0 = 9.0.$$

Thus the equilibrium constant for ionization of the conjugate acid is even smaller than that for ionization of the base. The ionization reaction for the conjugate acid of a weak base is written as follows:

$$BH^+(aq) + H_2O(l) \leftrightharpoons B(aq) + H_3O^+(aq) \tag{8.2.1.4}$$

Again, the equilibrium constant for the reverse of this reaction is very large: $K = 1/K_a = 10^9$. If a strong acid is added, it is neutralized by reaction with the base as the reaction in Equation 8.2.1.4 shifts to the left. As a result, the H^+ ion concentration does not increase very much, and the pH changes only slightly. In effect, a buffer solution behaves somewhat like a sponge that can absorb H^+ and OH^- ions, thereby preventing large changes in pH when appreciable amounts of strong acid or base are added to a solution.

Buffers are characterized by the pH range over which they can maintain a more or less constant pH and by their buffer capacity, the amount of strong acid or base that can be absorbed before the pH changes significantly. Although the useful pH range of a buffer depends strongly on the chemical properties of the weak acid and weak base used to prepare the buffer (i.e., on K), its buffer capacity depends solely on the concentrations of the species in the buffered solution. The more concentrated the buffer solution, the greater its buffer capacity. As illustrated in Figure 8.2.1.1, when $NaOH$ is added to solutions that contain different concentrations of an acetic acid/sodium acetate buffer, the observed change in the pH of the buffer is inversely proportional to the concentration of the buffer. If the buffer capacity is 10 times larger, then the buffer solution can absorb 10 times more strong acid or base before undergoing a significant change in pH.

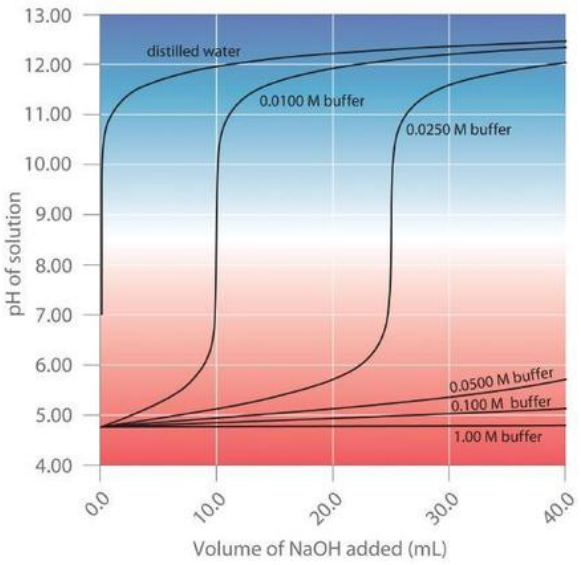


Figure **8.2.1.1**: Effect of Buffer Concentration on the Capacity of a Buffer. (CC BY-SA-NC; Anonymous by request)
Graph of pH of solution against volume of NaOH added. Six different buffer concentrations are plotted.

A buffer maintains a relatively constant pH when acid or base is added to a solution. The addition of even tiny volumes of 0.10 M $NaOH$ to 100.0 mL of distilled water results in a very large change in pH. As the concentration of a 50:50 mixture of sodium acetate/acetic acid buffer in the solution is increased from 0.010 M to 1.00 M, the change in the pH produced by the addition of the same volume of $NaOH$ solution decreases steadily. For buffer concentrations of at least 0.500 M, the addition of even 25 mL of the $NaOH$ solution results in only a relatively small change in pH.

Calculating the pH of a Buffer

The pH of a buffer can be calculated from the concentrations of the weak acid and the weak base used to prepare it, the concentration of the conjugate base and conjugate acid, and the pK_a or pK_b of the weak acid or weak base. The procedure is analogous to that used in Example **8.2.1.1** to calculate the pH of a solution containing known concentrations of formic acid and formate.

An alternative method frequently used to calculate the pH of a buffer solution is based on a rearrangement of the equilibrium equation for the dissociation of a weak acid. The simplified ionization reaction is $HA \leftrightharpoons H^+ + A^-$, for which the equilibrium constant expression is as follows:

$$K_a = \frac{[H^+][A^-]}{[HA]} \tag{8.2.1.5}$$

This equation can be rearranged as follows:

$$[H^+] = K_a \frac{[HA]}{[A^-]} \tag{8.2.1.6}$$

Taking the logarithm of both sides and multiplying both sides by −1,

$$-\log[H^+] = -\log K_a - \log\left(\frac{[HA]}{[A^-]}\right) \tag{8.2.1.7}$$

$$= -\log K_a + \log\left(\frac{[A^-]}{[HA]}\right) \tag{8.2.1.8}$$

Replacing the negative logarithms in Equation 8.2.1.8,

$$pH = pK_a + \log\left(\frac{[A^-]}{[HA]}\right) \tag{8.2.1.9}$$

or, more generally,

$$pH = pK_a + \log\left(\frac{[base]}{[acid]}\right) \tag{8.2.1.10}$$

Equation 8.2.1.9 and Equation 8.2.1.10 are both forms of the Henderson-Hasselbalch approximation, named after the two early 20th-century chemists who first noticed that this rearranged version of the equilibrium constant expression provides an easy way to calculate the pH of a buffer solution. In general, the validity of the Henderson-Hasselbalch approximation may be limited to solutions whose concentrations are at least 100 times greater than their K_a values.

There are three special cases where the Henderson-Hasselbalch approximation is easily interpreted without the need for calculations:

- $[base] = [acid]$: Under these conditions,

  $$\frac{[base]}{[acid]} = 1$$

  in Equation 8.2.1.10. Because $\log 1 = 0$,

  $$pH = pK_a$$

  regardless of the actual concentrations of the acid and base. Recall that this corresponds to the midpoint in the titration of a weak acid or a weak base.
- $[base]/[acid] = 10$: In Equation 8.2.1.10, because $\log 10 = 1$,

  $$pH = pK_a + 1.$$
- $[base]/[acid] = 100$: In Equation 8.2.1.10, because $\log 100 = 2$,

  $$pH = pK_a + 2.$$

Each time we increase the [base]/[acid] ratio by 10, the pH of the solution increases by 1 pH unit. Conversely, if the [base]/[acid] ratio is 0.1, then pH = pK_a − 1. Each additional factor-of-10 decrease in the [base]/[acid] ratio causes the pH to decrease by 1 pH unit.

> If [base] = [acid] for a buffer, then pH = pK_a. Changing this ratio by a factor of 10 either way changes the pH by ±1 unit.

Example 8.2.1.2

What is the pH of a solution that contains

a. 0.135 M HCO_2H and 0.215 M HCO_2Na? (The pK_a of formic acid is 3.75.)
b. 0.0135 M HCO_2H and 0.0215 M HCO_2Na?
c. 0.119 M pyridine and 0.234 M pyridine hydrochloride? (The pK_b of pyridine is 8.77.)

Given: concentration of acid, conjugate base, and pK_a; concentration of base, conjugate acid, and pK_b

Asked for: pH

Strategy:

Substitute values into either form of the Henderson-Hasselbalch approximation (Equations 8.2.1.9 or 8.2.1.10) to calculate the pH.

Solution:

According to the Henderson-Hasselbalch approximation (Equation 8.2.1.9), the pH of a solution that contains both a weak acid and its conjugate base is

$$pH = pK_a + \log([A-]/[HA]).$$

A

Inserting the given values into the equation,

$$pH = 3.75 + \log\left(\frac{0.215}{0.135}\right)$$
$$= 3.75 + \log 1.593$$
$$= 3.95$$

This result makes sense because the $[A^-]/[HA]$ ratio is between 1 and 10, so the pH of the buffer must be between the pK_a (3.75) and $pK_a + 1$, or 4.75.

B

This is identical to part (a), except for the concentrations of the acid and the conjugate base, which are 10 times lower. Inserting the concentrations into the Henderson-Hasselbalch approximation,

$$pH = 3.75 + \log\left(\frac{0.0215}{0.0135}\right)$$
$$= 3.75 + \log 1.593$$
$$= 3.95$$

This result is identical to the result in part (a), which emphasizes the point that the pH of a buffer depends only on the ratio of the concentrations of the conjugate base and the acid, not on the magnitude of the concentrations. Because the $[A^-]/[HA]$ ratio is the same as in part (a), the pH of the buffer must also be the same (3.95).

C

In this case, we have a weak base, pyridine (Py), and its conjugate acid, the pyridinium ion (HPy^+). We will therefore use Equation 8.2.1.10, the more general form of the Henderson-Hasselbalch approximation, in which "base" and "acid" refer to the appropriate species of the conjugate acid–base pair. We are given [base] = [Py] = 0.119 M and $[acid] = [HPy^+] = 0.234\,M$. We also are given $pK_b = 8.77$ for pyridine, but we need pK_a for the pyridinium ion. Recall from Equation 16.23 that the pK_b of a weak base and the pK_a of its conjugate acid are related:

$$pK_a + pK_b = pK_w.$$

Thus pK_a for the pyridinium ion is $pK_w - pK_b = 14.00 - 8.77 = 5.23$. Substituting this pK_a value into the Henderson-Hasselbalch approximation,

$$pH = pK_a + \log\left(\frac{[base]}{[acid]}\right)$$
$$= 5.23 + \log\left(\frac{0.119}{0.234}\right)$$
$$= 5.23 - 0.294$$
$$= 4.94$$

Once again, this result makes sense: the $[B]/[BH^+]$ ratio is about 1/2, which is between 1 and 0.1, so the final pH must be between the pK_a (5.23) and $pK_a - 1$, or 4.23.

? Exercise 8.2.1.2

What is the pH of a solution that contains

a. 0.333 M benzoic acid and 0.252 M sodium benzoate?
b. 0.050 M trimethylamine and 0.066 M trimethylamine hydrochloride?

The pK_a of benzoic acid is 4.20, and the pK_b of trimethylamine is also 4.20.

Answer a

4.08

Answer b

9.68



A Video Discussing Using the Henderson Hasselbalch Equation: Using the Henderson Hasselbalch Equation(opens in new window) [youtu.be] (opens in new window)

The Henderson-Hasselbalch approximation ((Equation 8.2.1.9) can also be used to calculate the pH of a buffer solution after adding a given amount of strong acid or strong base, as demonstrated in Example 8.2.1.3.

Example 8.2.1.3

The buffer solution in Example 8.2.1.2 contained 0.135 M $\mathbf{HCO_2H}$ and 0.215 M $\mathbf{HCO_2Na}$ and had a pH of 3.95.

a. What is the final pH if 5.00 mL of 1.00 M $\mathbf{\mathit{HCl}}$ are added to 100 mL of this solution?
b. What is the final pH if 5.00 mL of 1.00 M $\mathbf{\mathit{NaOH}}$ are added?

Given: composition and pH of buffer; concentration and volume of added acid or base

Asked for: final pH

Strategy:

A. Calculate the amounts of formic acid and formate present in the buffer solution using the procedure from Example 8.2.1.1. Then calculate the amount of acid or base added.
B. Construct a table showing the amounts of all species after the neutralization reaction. Use the final volume of the solution to calculate the concentrations of all species. Finally, substitute the appropriate values into the Henderson-Hasselbalch approximation (Equation 8.2.1.10) to obtain the pH.

Solution:

The added $\mathbf{HCl}$ (a strong acid) or $\mathbf{NaOH}$ (a strong base) will react completely with formate (a weak base) or formic acid (a weak acid), respectively, to give formic acid or formate and water. We must therefore calculate the amounts of formic acid and formate present after the neutralization reaction.

A We begin by calculating the millimoles of formic acid and formate present in 100 mL of the initial pH 3.95 buffer:

$$100\ \cancel{mL}\left(\frac{0.135\ mmol\ HCO_2H}{\cancel{mL}}\right) = 13.5\ mmol\ HCO_2H$$

$$100\ \cancel{mL}\left(\frac{0.215\ mmol\ HCO_2^-}{\cancel{mL}}\right) = 21.5\ mmol\ HCO_2^-$$

The millimoles of H^+ in 5.00 mL of 1.00 M $\mathbf{HCl}$ is as follows:

$$5.00\ \cancel{mL}\left(\frac{1.00\ mmol\ H^+}{\cancel{mL}}\right) = 5\ mmol\ H^+$$

B Next, we construct a table of initial amounts, changes in amounts, and final amounts:

$$\mathrm{HCO^{2-}(aq) + H^+(aq) \rightleftharpoons HCO_2H(aq)}$$

initial amounts, changes in amounts, and final amounts:

	$HCO^{2-}(aq)$	$H^+(aq)$	$HCO_2H(aq)$
Initial	21.5 mmol	5.00 mmol	13.5 mmol
Change	−5.00 mmol	−5.00 mmol	+5.00 mmol
Final	16.5 mmol	~0 mmol	18.5 mmol

The final amount of H^+ in solution is given as "~0 mmol." For the purposes of the stoichiometry calculation, this is essentially true, but remember that the point of the problem is to calculate the final $[H^+]$ and thus the pH. We now have all the information we need to calculate the pH. We can use either the lengthy procedure of Example 8.2.1.1 or the Henderson–Hasselbach approximation. Because we have performed many equilibrium calculations in this chapter, we'll take the latter approach. The Henderson-Hasselbalch approximation requires the concentrations of HCO_2^- and HCO_2H, which can be calculated using the number of millimoles (n) of each and the total volume (VT). Substituting these values into the Henderson-Hasselbalch approximation (Equation 8.2.1.10):

$$\begin{aligned} pH &= pK_a + \log\left(\frac{[HCO_2^-]}{[HCO_2H]}\right) \\ &= pK_a + \log\left(\frac{n_{HCO_2^-}/V_f}{n_{HCO_2H}/V_f}\right) \\ &= pK_a + \log\left(\frac{n_{HCO_2^-}}{n_{HCO_2H}}\right) \end{aligned}$$

Because the total volume appears in both the numerator and denominator, it cancels. We therefore need to use only the ratio of the number of millimoles of the conjugate base to the number of millimoles of the weak acid. So

$$\begin{aligned} pH &= pK_a + \log\left(\frac{n_{HCO_2^-}}{n_{HCO_2H}}\right) \\ &= 3.75 + \log\left(\frac{16.5\ mmol}{18.5\ mmol}\right) \\ &= 3.75\ -0.050 = 3.70 \end{aligned}$$

Once again, this result makes sense on two levels. First, the addition of HClhas decreased the pH from 3.95, as expected. Second, the ratio of HCO_2^- to HCO_2H is slightly less than 1, so the pH should be between the pK_a and pK_a − 1.

A The procedure for solving this part of the problem is exactly the same as that used in part (a). We have already calculated the numbers of millimoles of formic acid and formate in 100 mL of the initial pH 3.95 buffer: 13.5 mmol of HCO_2H and 21.5 mmol of HCO_2^-. The number of millimoles of OH^- in 5.00 mL of 1.00 M $NaOH$ is as follows:

B With this information, we can construct a table of initial amounts, changes in amounts, and final amounts.

$$\mathrm{HCO_2H(aq) + OH^-(aq) \rightleftharpoons HCO_2^-(aq) + H_2O(l)}$$

initial amounts, changes in amounts, and final amounts

	$HCO_2H(aq)$	OH^-	$HCO_2^-(aq)$
Initial	13.5 mmol	5.00 mmol	21.5 mmol
Change	−5.00 mmol	−5.00 mmol	+5.00 mmol
Final	8.5 mmol	~0 mmol	26.5 mmol

The final amount of OH^- in solution is not actually zero; this is only approximately true based on the stoichiometric calculation. We can calculate the final pH by inserting the numbers of millimoles of both HCO_2^- and HCO_2H into the simplified Henderson-Hasselbalch expression used in part (a) because the volume cancels:

$$\begin{aligned} pH &= pK_a + \log\left(\frac{n_{HCO_2^-}}{n_{HCO_2H}}\right) \\ &= 3.75 + \log\left(\frac{26.5\ mmol}{8.5\ mmol}\right) \\ &= 3.75 + 0.494 = 4.24 \end{aligned}$$

Once again, this result makes chemical sense: the pH has increased, as would be expected after adding a strong base, and the final pH is between the pK_a and pK_a + 1, as expected for a solution with a HCO_2^-/HCO_2H ratio between 1 and 10.

? Exercise 8.2.1.3

The buffer solution from Example **8.2.1.2** contained 0.119 M pyridine and 0.234 M pyridine hydrochloride and had a pH of 4.94.

a. What is the final pH if 12.0 mL of 1.5 M **NaOH** are added to 250 mL of this solution?
b. What is the final pH if 12.0 mL of 1.5 M **HCl** are added?

Answer a

5.30

Answer b

4.42

Only the amounts (in moles or millimoles) of the acidic and basic components of the buffer are needed to use the Henderson-Hasselbalch approximation, not their concentrations.



A Video Discussing the Change in pH with the Addition of a Strong Acid to a Buffer: The Change in pH with the Addition of a Strong Acid to a Buffer(opens in new window) [youtu.be]



The Change in pH with the Addition of a Strong Base to a Buffer:

The Change in pH with the Addition of a Strong Base to a Buffer (opens in new window) [youtu.be]

The results obtained in Example **8.2.1.3** and its corresponding exercise demonstrate how little the pH of a well-chosen buffer solution changes despite the addition of a significant quantity of strong acid or strong base. Suppose we had added the same amount of HCl or $NaOH$ solution to 100 mL of an unbuffered solution at pH 3.95 (corresponding to 1.1×10^{-4} M HCl). In this case, adding 5.00 mL of 1.00 M HCl would lower the final pH to 1.32 instead of 3.70, whereas adding 5.00 mL of 1.00 M $NaOH$ would raise the final pH to 12.68 rather than 4.24. (Try verifying these values by doing the calculations yourself.) Thus the presence of a buffer significantly increases the ability of a solution to maintain an almost constant pH.

> *The most effective buffers contain **equal** concentrations of an acid and its conjugate base.*

A buffer that contains approximately equal amounts of a weak acid and its conjugate base in solution is equally effective at neutralizing either added base or added acid. This is shown in Figure **8.2.1.2** for an acetic acid/sodium acetate buffer. Adding a given amount of strong acid shifts the system along the horizontal axis to the left, whereas adding the same amount of strong base shifts the system the same distance to the right. In either case, the change in the ratio of $CH_3CO_2^-$ to CH_3CO_2H from 1:1 reduces the buffer capacity of the solution.

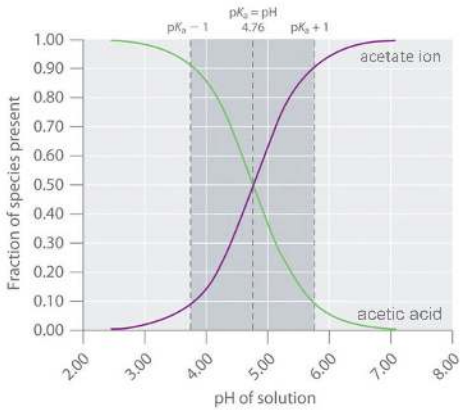


Figure **8.2.1.2**: Distribution Curve Showing the Fraction of Acetic Acid Molecules and Acetate Ions as a Function of pH in a Solution of Acetic Acid. The pH range over which the acetic acid/sodium acetate system is an effective buffer (the darker shaded region) corresponds to the region in which appreciable concentrations of both species are present (pH 3.76–5.76, corresponding to $pH = pK_a \pm 1$). (CC BY-SA-NC; Anonymous by request)

Graph of mole fraction against pH of solution. The green line is acetic acid and the purple line is the acetate ion.



A Video Discussing The Buffer Region: The Buffer Region (opens in new window) [youtu.be]

The Relationship between Titrations and Buffers

There is a strong correlation between the effectiveness of a buffer solution and the titration curves discussed in Section 16.5. Consider the schematic titration curve of a weak acid with a strong base shown in Figure **8.2.1.3**. As indicated by the labels, the region around pK_a corresponds to the midpoint of the titration, when approximately half the weak acid has been neutralized. This portion of the titration curve corresponds to a buffer: it exhibits the smallest change in pH per increment of added strong base, as shown by the nearly horizontal nature of the curve in this region. The nearly flat portion of the curve extends only from approximately a pH value of 1 unit less than the pK_a to approximately a pH value of 1 unit greater than the pK_a, which is why buffer solutions usually have a pH that is within ±1 pH units of the pK_a of the acid component of the buffer.

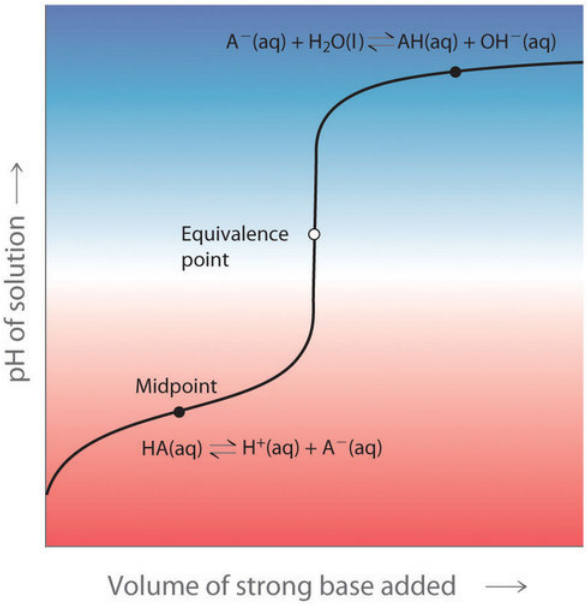


Figure **8.2.1.3**: The Relationship between Titration Curves and Buffers. (CC BY-SA-NC; Anonymous by request)

Titration curves graph pH of solution against volume of strong base added. On the curve we look for the midpoints and equivalence points.

This schematic plot of pH for the titration of a weak acid with a strong base shows the nearly flat region of the titration curve around the midpoint, which corresponds to the formation of a buffer. At the lower left, the pH of the solution is determined by the equilibrium for dissociation of the weak acid; at the upper right, the pH is determined by the equilibrium for reaction of the conjugate base with water.

In the region of the titration curve at the lower left, before the midpoint, the acid–base properties of the solution are dominated by the equilibrium for dissociation of the weak acid, corresponding to K_a. In the region of the titration curve at the upper right, after

the midpoint, the acid–base properties of the solution are dominated by the equilibrium for reaction of the conjugate base of the weak acid with water, corresponding to K_b. However, we can calculate either K_a or K_b from the other because they are related by K_w.

Blood: A Most Important Buffer

Metabolic processes produce large amounts of acids and bases, yet organisms are able to maintain an almost constant internal pH because their fluids contain buffers. This is not to say that the pH is uniform throughout all cells and tissues of a mammal. The internal pH of a red blood cell is about 7.2, but the pH of most other kinds of cells is lower, around 7.0. Even within a single cell, different compartments can have very different pH values. For example, one intracellular compartment in white blood cells has a pH of around 5.0.

Because no single buffer system can effectively maintain a constant pH value over the entire physiological range of approximately pH 5.0 to 7.4, biochemical systems use a set of buffers with overlapping ranges. The most important of these is the CO_2/HCO_3^- system, which dominates the buffering action of blood plasma.

The acid–base equilibrium in the CO_2/HCO_3^- buffer system is usually written as follows:

$$H_2CO_3\,(aq) \rightleftharpoons H^+\,(aq) + HCO_3^-\,(aq) \tag{8.2.1.11}$$

with $K_a = 4.5 \times 10^{-7}$ and $pK_a = 6.35$ at 25°C. In fact, Equation 8.2.1.11 is a grossly oversimplified version of the CO_2/HCO_3^- system because a solution of CO_2 in water contains only rather small amounts of H_2CO_3. Thus Equation 8.2.1.11 does not allow us to understand how blood is actually buffered, particularly at a physiological temperature of 37°C.

As shown in Equation 8.2.1.12, CO_2 is in equilibrium with H_2CO_3, but the equilibrium lies far to the left, with an H_2CO_3/CO_2 ratio less than 0.01 under most conditions:

$$CO_2\,(aq) + H_2O\,(l) \rightleftharpoons H_2CO_3\,(aq) \tag{8.2.1.12}$$

with $K' = 4.0 \times 10^{-3}$ at 37°C. The true pK_a of carbonic acid at 37°C is therefore 3.70, not 6.35, corresponding to a K_a of 2.0×10^{-4}, which makes it a much stronger acid than Equation 8.2.1.11 suggests. Adding Equation 8.2.1.11 and Equation 8.2.1.12 and canceling H_2CO_3 from both sides give the following overall equation for the reaction of CO_2 with water to give a proton and the bicarbonate ion:

$$CO_2\,(aq) + H_2O\,(l) \rightleftharpoons H_2CO_3\,(aq) \tag{8.2.1.13}$$

with $K' = 4.0 \times 10^{-3} (37°C)$

$$H_2CO_3\,(aq) \rightleftharpoons H^+\,(aq) + HCO_3^-\,(aq) \tag{8.2.1.14}$$

with $K_a = 2.0 \times 10^{-4} (37°C)$

$$CO_2\,(aq) + H_2O\,(l) \rightleftharpoons H^+\,(aq) + HCO_3^-\,(aq) \tag{8.2.1.15}$$

with $K = 8.0 \times 10^{-7} (37°C)$

The K value for the reaction in Equation 8.2.1.15 is the product of the true ionization constant for carbonic acid (K_a) and the equilibrium constant (K) for the reaction of $CO_2\,(aq)$ with water to give carbonic acid. The equilibrium equation for the reaction of CO_2 with water to give bicarbonate and a proton is therefore

$$K = \frac{[H^+][HCO_3^-]}{[CO_2]} = 8.0 \times 10^{-7} \tag{8.2.1.16}$$

The presence of a gas in the equilibrium constant expression for a buffer is unusual. According to Henry's law,

$$[CO_2] = kP_{CO_2}$$

where k is the Henry's law constant for CO_2, which is $3.0 \times 10^{-5}\ M/mmHg$ at 37°C. Substituting this expression for $[CO_2]$ in Equation 8.2.1.16,

$$K = \frac{[H^+][HCO_3^-]}{(3.0 \times 10^{-5}\ M/mmHg)(P_{CO_2})}$$

where P_{CO_2} is in mmHg. Taking the negative logarithm of both sides and rearranging,

$$pH = 6.10 + \log\left(\frac{[HCO_3^-]}{(3.0 \times 10^{-5} M/mm\ Hg)\ (P_{CO_2})}\right) \tag{8.2.1.17}$$

Thus the pH of the solution depends on both the CO_2 pressure over the solution and $[HCO_3^-]$. Figure 8.2.1.4 plots the relationship between pH and $[HCO_3^-]$ under physiological conditions for several different values of P_{CO_2}, with normal pH and $[HCO_3^-]$ values indicated by the dashed lines.

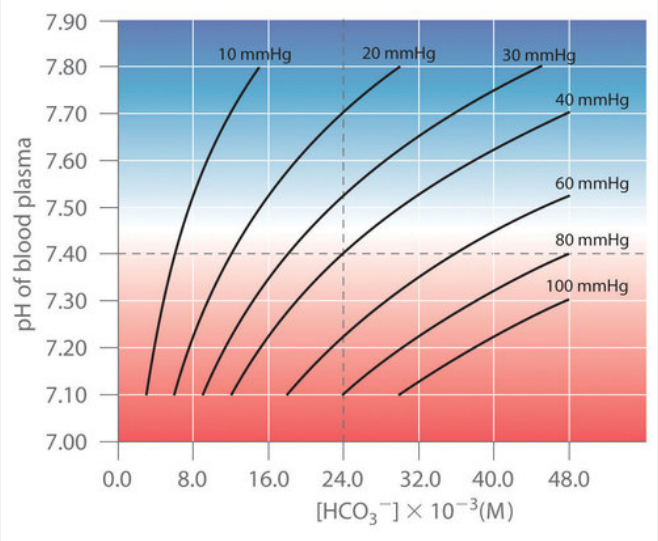


Figure 8.2.1.4: Buffering in Blood: pH versus $[HCO_3^-]$ Curves for Buffers with Different Values of P_{CO_2}. Only those combinations of pH and $[HCO_3^-]$ that lie on a given line are allowed for the particular value of P_{CO_2} indicated. Normal values of blood plasma pH and $[HCO_3^-]$ are indicated by dashed lines. (CC BY-SA-NC; Anonymous by request)

According to Equation 8.2.1.17, adding a strong acid to the CO_2/HCO_3^- system causes $[HCO_3^-]$ to decrease as HCO_3^- is converted to CO_2. Excess CO_2 is released in the lungs and exhaled into the atmosphere, however, so there is essentially no change in P_{CO_2}. Because the change in $[HCO_3^-]/P_{CO_2}$ is small, Equation 8.2.1.17 predicts that the change in pH will also be rather small. Conversely, if a strong base is added, the OH^- reacts with CO_2 to form HCO_3^-, but CO_2 is replenished by the body, again limiting the change in both $[HCO_3^-]/P_{CO_2}$ and pH. The CO_2/HCO_3^- buffer system is an example of an open system, in which the total concentration of the components of the buffer change to keep the pH at a nearly constant value.

If a passenger steps out of an airplane in Denver, Colorado, for example, the lower P_{CO_2} at higher elevations (typically 31 mmHg at an elevation of 2000 m versus 40 mmHg at sea level) causes a shift to a new pH and $[HCO_3^-]$. The increase in pH and decrease in $[HCO_3^-]$ in response to the decrease in P_{CO_2} are responsible for the general malaise that many people experience at high altitudes. If their blood pH does not adjust rapidly, the condition can develop into the life-threatening phenomenon known as altitude sickness.



A Video Summary of the pH Curve for a Strong Acid/Strong Base Titration:

Summary of the pH Curve for a Strong Acid/Strong Base Titration(opens in new window) [youtu.be]

Summary

Buffers are solutions that resist a change in pH after adding an acid or a base. Buffers contain a weak acid (HA) and its conjugate weak base (A^-). Adding a strong electrolyte that contains one ion in common with a reaction system that is at equilibrium shifts the equilibrium in such a way as to reduce the concentration of the common ion. The shift in equilibrium is called the common ion effect. Buffers are characterized by their pH range and buffer capacity. The useful pH range of a buffer depends strongly on the chemical properties of the conjugate weak acid–base pair used to prepare the buffer (the K_a or K_b), whereas its buffer capacity depends solely on the concentrations of the species in the solution. The pH of a buffer can be calculated using the Henderson-Hasselbalch approximation, which is valid for solutions whose concentrations are at least 100 times greater than their K_a values. Because no single buffer system can effectively maintain a constant pH value over the physiological range of approximately 5 to 7.4, biochemical systems use a set of buffers with overlapping ranges. The most important of these is the CO_2/HCO_3^- system, which dominates the buffering action of blood plasma.

8.2.1: Buffer Solutions is shared under a CC BY-NC-SA 4.0 license and was authored, remixed, and/or curated by LibreTexts.

- **17.2: Buffered Solutions** by Anonymous is licensed CC BY-NC-SA 3.0.

8.2.2: Acid–Base Indicators

Learning Objectives

- Explain the function and color changes of acid-base indicators
- Demonstrate how to select the proper indicator for a titration experiment
- Determine the acidic dissociation constants K_a or K_{ai} of indicators.

Certain organic substances change color in dilute solution when the hydronium ion concentration reaches a particular value. For example, phenolphthalein is a colorless substance in any aqueous solution with a hydronium ion concentration greater than 5.0×10^{-9} *M* (pH < 8.3). In more basic solutions where the hydronium ion concentration is less than 5.0×10^{-9} *M* (pH > 8.3), it is red or pink. Substances such as phenolphthalein, which can be used to determine the pH of a solution, are called acid-base indicators. Acid-base indicators are either weak organic acids or weak organic bases.

The equilibrium in a solution of the acid-base indicator methyl orange, a weak acid, can be represented by an equation in which we use HIn as a simple representation for the complex methyl orange molecule:

$$\underbrace{\mathrm{HIn}_{(aq)}}_{\text{red}} + \mathrm{H_2O}_{(l)} \rightleftharpoons \mathrm{H_3O^+}_{(aq)} + \underbrace{\mathrm{In^-}_{(aq)}}_{\text{yellow}} \tag{8.2.2.1}$$

$$K_a = \frac{[H3O+][In-]}{[HIn]} = 4.0 \times 10^{-4} \tag{8.2.2.2}$$

The anion of methyl orange, In^-, is yellow, and the nonionized form, HIn, is red. When we add acid to a solution of methyl orange, the increased hydronium ion concentration shifts the equilibrium toward the nonionized red form, in accordance with Le Chatelier's principle. If we add base, we shift the equilibrium towards the yellow form. This behavior is completely analogous to the action of buffers.

An indicator's color is the visible result of the ratio of the concentrations of the two species In^- and HIn. If most of the indicator (typically about 60−90% or more) is present as In^-, then we see the color of the In^- ion, which would be yellow for methyl orange. If most is present as HIn, then we see the color of the HIn molecule: red for methyl orange. For methyl orange, we can rearrange the equation for K_a and write:

$$\frac{[\mathrm{In^-}]}{[\mathrm{HIn}]} = \frac{[\text{substance with yellow color}]}{[\text{substance with red color}]} = \frac{K_a}{[\mathrm{H_3O^+}]} \tag{8.2.2.3}$$

This shows us how the ratio of $\frac{[In-]}{[HIn]}$ varies with the concentration of hydronium ion. The above expression describing the indicator equilibrium can be rearranged:

$$\frac{[\mathrm{H_3O^+}]}{K_a} = \frac{[\mathrm{HIn}]}{[\mathrm{In^-}]} \tag{8.2.2.4}$$

$$\log\left(\frac{[\mathrm{H_3O^+}]}{K_a}\right) = \log\left(\frac{[\mathrm{HIn}]}{[\mathrm{In^-}]}\right) \tag{8.2.2.5}$$

$$\log([\mathrm{H_3O^+}]) - \log(K_a) = -\log\left(\frac{[\mathrm{In^-}]}{[\mathrm{HIn}]}\right) \tag{8.2.2.6}$$

$$-\mathrm{pH} + \mathrm{p}K_a = -\log\left(\frac{[\mathrm{In^-}]}{[\mathrm{HIn}]}\right) \tag{8.2.2.7}$$

$$\mathrm{pH} = \mathrm{p}K_a + \log\left(\frac{[\mathrm{In^-}]}{[\mathrm{HIn}]}\right) \text{ or } \mathrm{pH} = \mathrm{p}K_a + \log\left(\frac{[\text{base}]}{[\text{acid}]}\right) \tag{8.2.2.8}$$

The last formula is the same as the Henderson-Hasselbalch equation, which can be used to describe the equilibrium of indicators.

When $[H_3O^+]$ has the same numerical value as K_a, the ratio of $[In^-]$ to [HIn] is equal to 1, meaning that 50% of the indicator is present in the red form (HIn) and 50% is in the yellow ionic form (In^-), and the solution appears orange in color. When the

hydronium ion concentration increases to 8×10^{-4} M (a pH of 3.1), the solution turns red. No change in color is visible for any further increase in the hydronium ion concentration (decrease in pH). At a hydronium ion concentration of 4×10^{-5} M (a pH of 4.4), most of the indicator is in the yellow ionic form, and a further decrease in the hydronium ion concentration (increase in pH) does not produce a visible color change. The pH range between 3.1 (red) and 4.4 (yellow) is the color-change interval of methyl orange; the pronounced color change takes place between these pH values.

Many different substances can be used as indicators, depending on the particular reaction to be monitored. For example, red cabbage juice contains a mixture of colored substances that change from deep red at low pH to light blue at intermediate pH to yellow at high pH (Figure **8.2.2.1**). In all cases, though, a good indicator must have the following properties:

- The color change must be easily detected.
- The color change must be rapid.
- The indicator molecule must not react with the substance being titrated.
- To minimize errors, the indicator should have a pKin that is within one pH unit of the expected pH at the equivalence point of the titration.



Figure **8.2.2.1**: Naturally Occurring pH Indicators in Red Cabbage Juice. Image curtesty of Wikipedia.

Red cabbage juice contains a mixture of substances whose color depends on the pH. Each test tube contains a solution of red cabbage juice in water, but the pH of the solutions varies from pH = 2.0 (far left) to pH = 11.0 (far right). At pH = 7.0, the solution is blue.

Synthetic indicators have been developed that meet these criteria and cover virtually the entire pH range. Figure **8.2.2.2** shows the approximate pH range over which some common indicators change color and their change in color. In addition, some indicators (such as thymol blue) are polyprotic acids or bases, which change color twice at widely separated pH values.

Indicator	pK_{in}	Color change
Alizarin yellow R	11.0	yellow to red
Thymolphthalein	9.9	colorless to blue
Phenolphthalein	9.5	colorless to pink
Thymol blue	9.2	yellow to blue
Phenol red	7.4	yellow to red
Bromothymol blue	7.3	yellow to blue
Bromocresol purple	6.4	yellow to purple
Ethyl red	5.4	colorless to red
Resorcin blue	5.3	red to blue
Resazurin	5.1	orange to violet
Methyl red	5.0	red to yellow
Bromophenol blue	4.1	yellow to blue
Thymol blue	1.7	red to yellow
Malachite green	1.3	yellow to turquoise
Methyl violet	0.8	yellow to blue

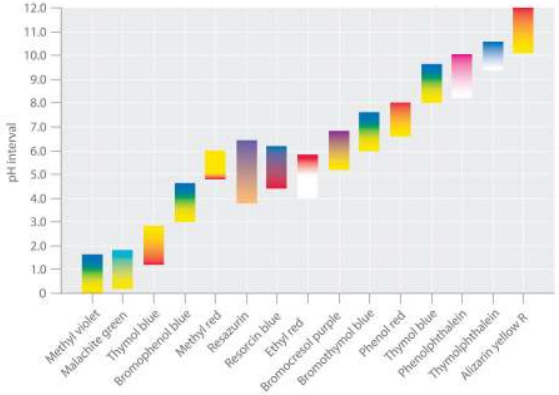


Figure **8.2.2.2**: Some Common Acid–Base Indicators. Approximate colors are shown, along with pKin values and the pH range over which the color changes.

It is important to be aware that an indicator does not change color abruptly at a particular pH value; instead, it actually undergoes a pH titration just like any other acid or base. As the concentration of HIn decreases and the concentration of In^- increases, the color of the solution slowly changes from the characteristic color of HIn to that of In^-. As we will see in Section 16, the $[In^-]/[HIn]$ ratio

changes from 0.1 at a pH one unit below pKin to 10 at a pH one unit above pKin. Thus most indicators change color over a pH range of about two pH units.

We have stated that a good indicator should have a pKin value that is close to the expected pH at the equivalence point. For a strong acid–strong base titration, the choice of the indicator is not especially critical due to the very large change in pH that occurs around the equivalence point. In contrast, using the wrong indicator for a titration of a weak acid or a weak base can result in relatively large errors, as illustrated in Figure **8.2.2.3**. This figure shows plots of pH versus volume of base added for the titration of 50.0 mL of a 0.100 M solution of a strong acid (HCl) and a weak acid (acetic acid) with 0.100 M ***NaOH***. The pH ranges over which two common indicators (methyl red, $pK_{in} = 5.0$, and phenolphthalein, $pK_{in} = 9.5$) change color are also shown. The horizontal bars indicate the pH ranges over which both indicators change color cross the HCl titration curve, where it is almost vertical. Hence both indicators change color when essentially the same volume of ***NaOH*** has been added (about 50 mL), which corresponds to the equivalence point. In contrast, the titration of acetic acid will give very different results depending on whether methyl red or phenolphthalein is used as the indicator. Although the pH range over which phenolphthalein changes color is slightly greater than the pH at the equivalence point of the strong acid titration, the error will be negligible due to the slope of this portion of the titration curve. Just as with the HCl titration, the phenolphthalein indicator will turn pink when about 50 mL of ***NaOH*** has been added to the acetic acid solution. In contrast, methyl red begins to change from red to yellow around pH 5, which is near the midpoint of the acetic acid titration, not the equivalence point. Adding only about 25–30 mL of ***NaOH*** will therefore cause the methyl red indicator to change color, resulting in a huge error.

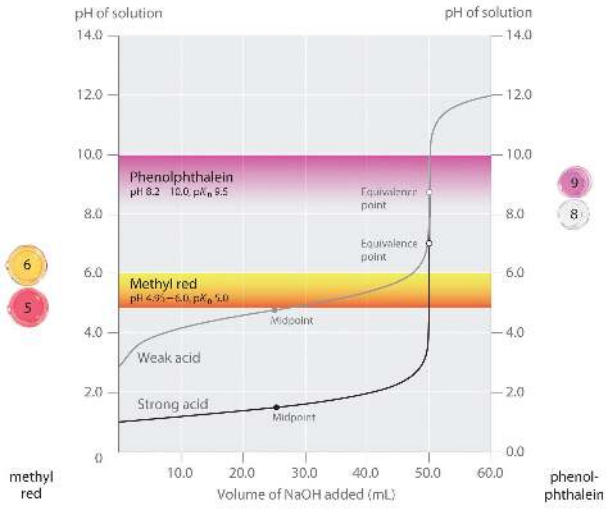


Figure **8.2.2.3**: Choosing the Correct Indicator for an Acid–Base Titration

The graph shows the results obtained using two indicators (methyl red and phenolphthalein) for the titration of 0.100 M solutions of a strong acid (HCl) and a weak acid (acetic acid) with 0.100 M ***NaOH***. Due to the steepness of the titration curve of a strong acid around the equivalence point, either indicator will rapidly change color at the equivalence point for the titration of the strong acid. In contrast, the pKin for methyl red (5.0) is very close to the pKa of acetic acid (4.76); the midpoint of the color change for methyl red occurs near the midpoint of the titration, rather than at the equivalence point.

In general, for titrations of strong acids with strong bases (and vice versa), any indicator with a pK in between about 4.0 and 10.0 will do. For the titration of a weak acid, however, the pH at the equivalence point is greater than 7.0, so an indicator such as phenolphthalein or thymol blue, with pKin > 7.0, should be used. Conversely, for the titration of a weak base, where the pH at the equivalence point is less than 7.0, an indicator such as methyl red or bromocresol blue, with pKin < 7.0, should be used.

✔ Example 8.2.2.1

In the titration of a weak acid with a strong base, which indicator would be the best choice?

a. Methyl Orange
b. Bromocresol Green
c. Phenolphtalein

Solution

The correct answer is C. In the titration of a weak acid with a strong base, the conjugate base of the weak acid will make the pH at the equivalence point greater than 7. Therefore, you would want an indicator to change in that pH range. Both methyl orange and bromocresol green change color in an acidic pH range, while phenolphtalein changes in a basic pH.

The existence of many different indicators with different colors and pKin values also provides a convenient way to estimate the pH of a solution without using an expensive electronic pH meter and a fragile pH electrode. Paper or plastic strips impregnated with combinations of indicators are used as “pH paper,” which allows you to estimate the pH of a solution by simply dipping a piece of pH paper into it and comparing the resulting color with the standards printed on the container (Figure **8.2.2.4**).



Figure **8.2.2.4**: pH Paper. pH paper contains a set of indicators that change color at different pH values. The approximate pH of a solution can be determined by simply dipping a paper strip into the solution and comparing the color to the standards provided.



pH Indicators: https://youtu.be/1IqzUa5lABs

Summary

Acid–base indicators are compounds that change color at a particular pH. They are typically weak acids or bases whose changes in color correspond to deprotonation or protonation of the indicator itself.

Contributors and Attributions

- Paul Flowers (University of North Carolina - Pembroke), Klaus Theopold (University of Delaware) and Richard Langley (Stephen F. Austin State University) with contributing authors. Textbook content produced by OpenStax College is licensed under a Creative Commons Attribution License 4.0 license. Download for free at http://cnx.org/contents/85abf193-2bd...a7ac8df6@9.110).
- {template.ContribBoundless()}}

8.2.2: Acid–Base Indicators is shared under a CC BY-NC-SA 4.0 license and was authored, remixed, and/or curated by LibreTexts.

- **17.3: Acid-Base Indicators** is licensed CC BY-NC-SA 4.0.

8.2.3: Neutralization Reactions and Titration Curves

Learning Objectives

- To calculate the pH at any point in an acid–base titration.

In an acid–base titration, a buret is used to deliver measured volumes of an acid or a base solution of known concentration (the titrant) to a flask that contains a solution of a base or an acid, respectively, of unknown concentration (the unknown). If the concentration of the titrant is known, then the concentration of the unknown can be determined. The following discussion focuses on the pH changes that occur during an acid–base titration. Plotting the pH of the solution in the flask against the amount of acid or base added produces a titration curve. The shape of the curve provides important information about what is occurring in solution during the titration.

Titrations of Strong Acids and Bases

Figure 8.2.3.1*a* shows a plot of the pH as 0.20 M **HCl** is gradually added to 50.00 mL of pure water. The pH of the sample in the flask is initially 7.00 (as expected for pure water), but it drops very rapidly as **HCl** is added. Eventually the pH becomes constant at 0.70—a point well beyond its value of 1.00 with the addition of 50.0 mL of **HCl** (0.70 is the pH of 0.20 M HCl). In contrast, when 0.20 M **NaOH** is added to 50.00 mL of distilled water, the pH (initially 7.00) climbs very rapidly at first but then more gradually, eventually approaching a limit of 13.30 (the pH of 0.20 M NaOH), again well beyond its value of 13.00 with the addition of 50.0 mL of **NaOH** as shown in Figure 8.2.3.1*b*. As you can see from these plots, the titration curve for adding a base is the mirror image of the curve for adding an acid.

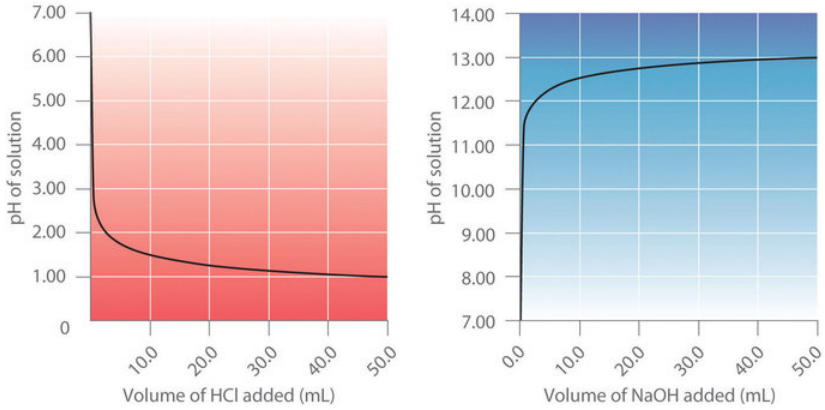


Figure 8.2.3.1: Solution pH as a Function of the Volume of a Strong Acid or a Strong Base Added to Distilled Water. (a) When 0.20 M **HCl** is added to 50.0 mL of distilled water, the pH rapidly decreases until it reaches a minimum at the pH of 0.20 M **HCl**. (b) Conversely, when 0.20 M **NaOH** is added to 50.0 mL of distilled water, the pH rapidly increases until it reaches a maximum at the pH of 0.20 M ***NaOH***. (CC BY-SA-NC; Anonymous by request)

The graphs of water with strong acid added and water with strong base added are inverses of each other.

Suppose that we now add 0.20 M **NaOH** to 50.0 mL of a 0.10 M solution of **HCl**. Because **HCl** is a strong acid that is completely ionized in water, the initial [H^+] is 0.10 M, and the initial pH is 1.00. Adding **NaOH** decreases the concentration of H+ because of the neutralization reaction (Figure 8.2.3.2*a*):

$$OH^- + H^+ \rightleftharpoons H_2O.$$

Thus the pH of the solution increases gradually. Near the equivalence point, however, the point at which the number of moles of base (or acid) added equals the number of moles of acid (or base) originally present in the solution, the pH increases much more rapidly because most of the H^+ ions originally present have been consumed. For the titration of a monoprotic strong acid (**HCl**) with a monobasic strong base (**NaOH**), we can calculate the volume of base needed to reach the equivalence point from the following relationship:

$$moles\ of\ base = (volume)_b(molarity)_b V_b M_b = moles\ of\ acid = (volume)_a(molarity)_a = V_a M_a \tag{8.2.3.1}$$

If 0.20 M **NaOH** is added to 50.0 mL of a 0.10 M solution of **HCl**, we solve for V_b:

$$V_b(0.20 Me) = 0.025 L = 25 mL$$

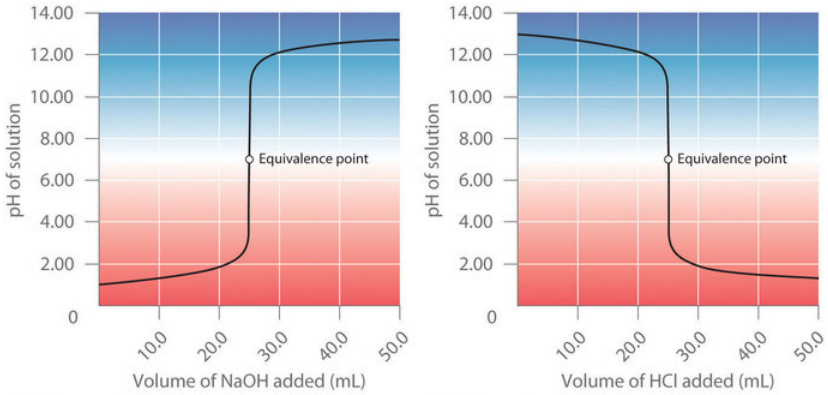


Figure **8.2.3.2**: The Titration of (a) a Strong Acid with a Strong Base and (b) a Strong Base with a Strong Acid(a) As 0.20 M **NaOH** is slowly added to 50.0 mL of 0.10 M HCl, the pH increases slowly at first, then increases very rapidly as the equivalence point is approached, and finally increases slowly once more. (b) Conversely, as 0.20 M **HCl** is slowly added to 50.0 mL of 0.10 M ***NaOH***, the pH decreases slowly at first, then decreases very rapidly as the equivalence point is approached, and finally decreases slowly once more. (CC BY-SA-NC; Anonymous by request)

The titration curves of strong acid titrated with strong base and strong base titrated with strong acid are inverses of each other.

At the equivalence point (when 25.0 mL of **NaOH** solution has been added), the neutralization is complete: only a salt remains in solution (NaCl), and the pH of the solution is 7.00. Adding more **NaOH** produces a rapid increase in pH, but eventually the pH levels off at a value of about 13.30, the pH of 0.20 M ***NaOH***.

As shown in Figure **8.2.3.2*b***, the titration of 50.0 mL of a 0.10 M solution of **NaOH** with 0.20 M **HCl** produces a titration curve that is nearly the mirror image of the titration curve in Figure **8.2.3.2*a***. The pH is initially 13.00, and it slowly decreases as **HCl** is added. As the equivalence point is approached, the pH drops rapidly before leveling off at a value of about 0.70, the pH of 0.20 M **HCl**.

The titration of either a strong acid with a strong base or a strong base with a strong acid produces an S-shaped curve. The curve is somewhat asymmetrical because the steady increase in the volume of the solution during the titration causes the solution to become more dilute. Due to the leveling effect, the shape of the curve for a titration involving a strong acid and a strong base depends on only the concentrations of the acid and base, not their identities.

> The shape of the titration curve involving a strong acid and a strong base depends only on their concentrations, not their identities.

✔ Example 8.2.3.1: Hydrochloric Acid

Calculate the pH of the solution after 24.90 mL of 0.200 M **NaOH** has been added to 50.00 mL of 0.100 M **HCl**.

Given: volumes and concentrations of strong base and acid

Asked for: pH

Strategy:

A. Calculate the number of millimoles of H^+ and OH^- to determine which, if either, is in excess after the neutralization reaction has occurred. If one species is in excess, calculate the amount that remains after the neutralization reaction.
B. Determine the final volume of the solution. Calculate the concentration of the species in excess and convert this value to pH.

Solution

A Because 0.100 mol/L is equivalent to 0.100 mmol/mL, the number of millimoles of $\mathrm{H^+}$ in 50.00 mL of 0.100 M HCl can be calculated as follows:

$$50.00\ \cancel{mL}\left(\frac{0.100\ mmol\ HCl}{\cancel{mL}}\right) = 5.00\ mmol\ HCl = 5.00\ mmol\ H^+$$

The number of millimoles of NaOH added is as follows:

$$24.90\ \cancel{mL}\left(\frac{0.200\ mmol\ NaOH}{\cancel{mL}}\right) = 4.98\ mmol\ NaOH = 4.98\ mmol\ OH^-$$

Thus $\mathrm{H^+}$ is in excess. To completely neutralize the acid requires the addition of 5.00 mmol of $\mathrm{OH^-}$ to the HCl solution. Because only 4.98 mmol of OH^- has been added, the amount of excess $\mathrm{H^+}$ is 5.00 mmol − 4.98 mmol = 0.02 mmol of H^+.

B The final volume of the solution is 50.00 mL + 24.90 mL = 74.90 mL, so the final concentration of $\mathrm{H^+}$ is as follows:

$$[H^+] = \frac{0.02\ mmol\ H^+}{74.90\ mL} = 3 \times 10^{-4}\ M$$

Hence,

$$pH \approx -\log[\mathrm{H^+}] = -\log(3 \times 10^{-4}) = 3.5$$

This is significantly less than the pH of 7.00 for a neutral solution.

? Exercise 8.2.3.1

Calculate the pH of a solution prepared by adding $40.00\ mL$ of $0.237\ M\ HCl$ to $75.00\ mL$ of a $0.133M$ solution of $NaOH$.

Answer

11.6



pH after the addition of 10 ml of Strong Base to a Strong Acid:

https://youtu.be/_cM1_-kdJ20 (opens in new window)



pH at the Equivalence Point in a Strong Acid/Strong Base Titration:

https://youtu.be/7POGDA5Ql2M

Titrations of Weak Acids and Bases

In contrast to strong acids and bases, the shape of the titration curve for a weak acid or a weak base depends dramatically on the identity of the acid or the base and the corresponding K_a or K_b. As we shall see, the pH also changes much more gradually around the equivalence point in the titration of a weak acid or a weak base. As you learned previously, [H^+] of a solution of a weak acid (HA) is not equal to the concentration of the acid but depends on both its pK_a and its concentration. Because only a fraction of a weak acid dissociates, [\(H^+] is less than [HA]. Thus the pH of a solution of a weak acid is greater than the pH of a solution of a strong acid of the same concentration.

Figure 8.2.3.3*a* shows the titration curve for 50.0 mL of a 0.100 M solution of acetic acid with 0.200 M NaOH superimposed on the curve for the titration of 0.100 M HCl shown in part (a) in Figure 8.2.3.2. Below the equivalence point, the two curves are very different. Before any base is added, the pH of the acetic acid solution is greater than the pH of the HCl solution, and the pH changes more rapidly during the first part of the titration. Note also that the pH of the acetic acid solution at the equivalence point is greater than 7.00. That is, at the equivalence point, the solution is basic. In addition, the change in pH around the equivalence point is only about half as large as for the HCl titration; the magnitude of the pH change at the equivalence point depends on the pK_a of the acid being titrated. Above the equivalence point, however, the two curves are identical. Once the acid has been neutralized, the pH of the solution is controlled only by the amount of excess NaOH present, regardless of whether the acid is weak or strong.

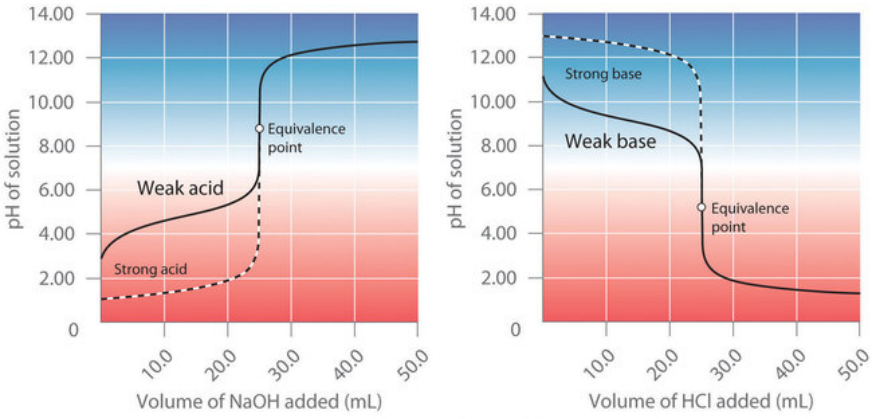


Figure **8.2.3.3**: The Titration of (a) a Weak Acid with a Strong Base and (b) a Weak Base with a Strong Acid. (a) As 0.200 M **NaOH** is slowly added to 50.0 mL of 0.100 M acetic acid, the pH increases slowly at first, then increases rapidly as the equivalence point is approached, and then again increases more slowly. The corresponding curve for the titration of 50.0 mL of 0.100 M **HCl** with 0.200 M **NaOH** is shown as a dashed line. (b) As 0.200 M **HCl** is slowly added to 50.0 mL of 0.100 M NH3, the pH decreases slowly at first, then decreases rapidly as the equivalence point is approached, and then again decreases more slowly. The corresponding curve for the titration of 50.0 mL of 0.100 M **NaOH** with 0.200 M **HCl** is shown as a dashed line. (CC BY-SA-NC; Anonymous by request)

The titration curves of weak acid titrated with strong base and weak base titrated with strong acid are inverse of each other. These curves are shorter than the titration curves with strong acid and strong base.

> The shape of the titration curve of a weak acid or weak base depends heavily on their identities and the K_a or K_b.

The titration curve in Figure **8.2.3.3***a* was created by calculating the starting pH of the acetic acid solution before any **NaOH** is added and then calculating the pH of the solution after adding increasing volumes of $NaOH$. The procedure is illustrated in the following subsection and Example **8.2.3.2** for three points on the titration curve, using the pK_a of acetic acid (4.76 at 25°C; $K_a = 1.7 \times 10^{-5}$.

Calculating the pH of a Solution of a Weak Acid or a Weak Base

As explained discussed, if we know K_a or K_b and the initial concentration of a weak acid or a weak base, we can calculate the pH of a solution of a weak acid or a weak base by setting up a ICE table (i.e, initial concentrations, changes in concentrations, and final concentrations). In this situation, the initial concentration of acetic acid is 0.100 M. If we define x as $[H^+]$ due to the dissociation of the acid, then the table of concentrations for the ionization of 0.100 M acetic acid is as follows:

$$CH_3CO_2H\,(aq) \rightleftharpoons H^+\,(aq) + CH_3CO_2{}^-$$

table of concentrations for the ionization of 0.100 M acetic acid

ICE	$[CH_3CO_2H]$	$[H^+]$	$[CH_3CO_2^-]$
initial	0.100	1.00×10^{-7}	0
change	−x	+x	+x
final	0.100 − x	x	x

In this and all subsequent examples, we will ignore $[H^+]$ and $[OH^-]$ due to the autoionization of water when calculating the final concentration. However, you should use Equation 16.45 and Equation 16.46 to check that this assumption is justified.

Inserting the expressions for the final concentrations into the equilibrium equation (and using approximations),

$$K_a = \frac{[H^+][CH_3CO_2^-]}{[CH_3CO_2H]}$$
$$= \frac{(x)(x)}{0.100 - x}$$
$$\approx \frac{x^2}{0.100}$$
$$\approx 1.74 \times 10^{-5}$$

Solving this equation gives $x = [H^+] = 1.32 \times 10^{-3}\ M$. Thus the pH of a 0.100 M solution of acetic acid is as follows:

$$pH = -\log(1.32 \times 10^{-3}) = 2.879$$



pH at the Start of a Weak Acid/Strong Base Titration: https://youtu.be/AtdBKfrfJNg

Calculating the pH during the Titration of a Weak Acid or a Weak Base

Now consider what happens when we add 5.00 mL of 0.200 M **NaOH** to 50.00 mL of 0.100 M CH_3CO_2H (part (a) in Figure **8.2.3.3**). Because the neutralization reaction proceeds to completion, all of the OH^- ions added will react with the acetic acid to generate acetate ion and water:

$$CH_3CO_2H_{(aq)} + OH^-_{(aq)} \rightarrow CH_3CO^-_{2\ (aq)} + H_2O_{(l)} \tag{8.2.3.2}$$

All problems of this type must be solved in two steps: a stoichiometric calculation followed by an equilibrium calculation. In the first step, we use the stoichiometry of the neutralization reaction to calculate the amounts of acid and conjugate base present in solution after the neutralization reaction has occurred. In the second step, we use the equilibrium equation to determine $[H^+]$ of the resulting solution.

Step 1

To determine the amount of acid and conjugate base in solution after the neutralization reaction, we calculate the amount of CH_3CO_2H in the original solution and the amount of OH^- in the **NaOH** solution that was added. The acetic acid solution contained

$$50.00\ \cancel{mL}\ (0.100\ mmol(CH_3CO_2H)/\cancel{mL}) = 5.00\ mmol(CH_3CO_2H)$$

The **NaOH** solution contained

5.00 mL=1.00 mmol $NaOH$

Comparing the amounts shows that CH_3CO_2H is in excess. Because OH^- reacts with CH_3CO_2H in a 1:1 stoichiometry, the amount of excess CH_3CO_2H is as follows:

5.00 mmol CH_3CO_2H − 1.00 mmol OH^- = 4.00 mmol CH_3CO_2H

Each 1 mmol of OH^- reacts to produce 1 mmol of acetate ion, so the final amount of $CH_3CO_2^-$ is 1.00 mmol.

The stoichiometry of the reaction is summarized in the following ICE table, which shows the numbers of moles of the various species, not their concentrations.

$$CH_3CO_2H\,(aq) + OH^-\,(aq) \rightleftharpoons CH_3CO_2{}^-\,(aq) + H_2O\,(l)$$

ICE table

ICE	$[CH_3CO_2H]$	$[OH^-]$	$[CH_3CO_2{}^-]$
initial	5.00 mmol	1.00 mmol	0 mmol
change	−1.00 mmol	−1.00 mmol	+1.00 mmol
final	4.00 mmol	0 mmol	1.00 mmol

This ICE table gives the initial amount of acetate and the final amount of OH^- ions as 0. Because an aqueous solution of acetic acid always contains at least a small amount of acetate ion in equilibrium with acetic acid, however, the initial acetate concentration is not actually 0. The value can be ignored in this calculation because the amount of $CH_3CO_2^-$ in equilibrium is insignificant compared to the amount of OH^- added. Moreover, due to the autoionization of water, no aqueous solution can contain 0 mmol of OH^-, but the amount of OH^- due to the autoionization of water is insignificant compared to the amount of OH^- added. We use the initial amounts of the reactants to determine the stoichiometry of the reaction and defer a consideration of the equilibrium until the second half of the problem.

Step 2

To calculate $[H^+]$ at equilibrium following the addition of $NaOH$, we must first calculate $[CH_3CO_2H]$ and $[CH_3CO_2{}^-]$ using the number of millimoles of each and the total volume of the solution at this point in the titration:

$$final\ volume = 50.00\ mL + 5.00\ mL = 55.00\ mL$$

$$[CH_3CO_2H] = \frac{4.00\ mmol\ CH_3CO_2H}{55.00\ mL} = 7.27 \times 10^{-2}\ M$$

$$[CH_3CO_2^-] = \frac{1.00\ mmol\ CH_3CO_2^-}{55.00\ mL} = 1.82 \times 10^{-2}\ M$$

Knowing the concentrations of acetic acid and acetate ion at equilibrium and K_a for acetic acid (1.74×10^{-5}), we can calculate $[H^+]$ at equilibrium:

$$K_a = \frac{[CH_3CO_2^-]\,[H^+]}{[CH_3CO_2H]}$$

$$[H^+] = \frac{K_a\,[CH_3CO_2H]}{[CH_3CO_2^-]} = \frac{(1.72 \times 10^{-5})\,(7.27 \times 10^{-2}\ M)}{(1.82 \times 10^{-2})} = 6.95 \times 10^{-5}\ M$$

Calculating $-\log[H^+]$ gives

$$pH = -\log(6.95 \times 10^{-5}) = 4.158.$$

Comparing the titration curves for **HCl** and acetic acid in Figure **8.2.3.3a**, we see that adding the same amount (5.00 mL) of 0.200 M **NaOH** to 50 mL of a 0.100 M solution of both acids causes a much smaller pH change for **HCl** (from 1.00 to 1.14) than for acetic acid (2.88 to 4.16). This is consistent with the qualitative description of the shapes of the titration curves at the beginning of this section. In Example **8.2.3.2**, we calculate another point for constructing the titration curve of acetic acid.



pH Before the Equivalence Point of a Weak Acid/Strong Base Titration:

https://youtu.be/znpwGCsefXc

Example 8.2.3.2

What is the pH of the solution after 25.00 mL of 0.200 M **NaOH** is added to 50.00 mL of 0.100 M acetic acid?

Given: volume and molarity of base and acid

Asked for: pH

Strategy:

A. Write the balanced chemical equation for the reaction. Then calculate the initial numbers of millimoles of OH^- and CH_3CO_2H. Determine which species, if either, is present in excess.

B. Tabulate the results showing initial numbers, changes, and final numbers of millimoles.

C. If excess acetate is present after the reaction with OH^-, write the equation for the reaction of acetate with water. Use a tabular format to obtain the concentrations of all the species present.

D. Calculate K_b using the relationship $K_w = K_aK_b$. Calculate [OH−] and use this to calculate the pH of the solution.

Solution

A Ignoring the spectator ion (Na^+), the equation for this reaction is as follows:

$$CH_3CO_2H_{(aq)} + OH^-(aq) \rightarrow CH_3CO_2^-(aq) + H_2O(l)$$

The initial numbers of millimoles of OH^- and CH_3CO_2H are as follows:

$$25.00 \text{ mL}(0.200 \text{ mmol OH}-\text{mL}=5.00 \text{ mmol } OH-$$

$$50.00\ mL(0.100 CH_3CO_2HL = 5.00 mmol\ CH_3CO_2H$$

The number of millimoles of OH^- equals the number of millimoles of CH_3CO_2H, so neither species is present in excess.

B Because the number of millimoles of OH^- added corresponds to the number of millimoles of acetic acid in solution, this is the equivalence point. The results of the neutralization reaction can be summarized in tabular form.

$$CH_3CO_2H_{(aq)} + OH^-_{(aq)} \rightleftharpoons CH_3CO_2^-(aq) + H_2O(l)$$

results of the neutralization reaction

ICE	$[CH_3CO_2H]$	$[OH^-]$	$[CH_3CO_2^-]$
initial	5.00 mmol	5.00 mmol	0 mmol
change	−5.00 mmol	−5.00 mmol	+5.00 mmol
final	0 mmol	0 mmol	5.00 mmol

C Because the product of the neutralization reaction is a weak base, we must consider the reaction of the weak base with water to calculate [H+] at equilibrium and thus the final pH of the solution. The initial concentration of acetate is obtained from the neutralization reaction:

$$[CH_3CO_2] = \frac{5.00\ mmol\ CH_3CO_2^-}{(50.00 + 25.00)\ mL} = 6.67 \times 10^{-2}\ M$$

The equilibrium reaction of acetate with water is as follows:

$$CH_3CO_2^-\,(aq) + H_2O\,(l) \rightleftharpoons CH_3CO_2H\,(aq) + OH^-\,(aq)$$

The equilibrium constant for this reaction is

$$K_b = \frac{K_w}{K_a} \tag{8.2.3.3}$$

where K_a is the acid ionization constant of acetic acid. We therefore define x as $[OH^-]$ produced by the reaction of acetate with water. Here is the completed table of concentrations:

$$H_2O_{(l)} + CH_3CO_{2(aq)}^- \rightleftharpoons CH_3CO_2H_{(aq)} + OH_{(aq)}^-$$

completed table of concentrations

	$[CH_3CO_2^-]$	$[CH_3CO_2H]$	$[OH^-]$
initial	0.0667	0	1.00 × 10−7
change	−x	+x	+x
final	(0.0667 − x)	x	x

D We can obtain K_b by substituting the known values into Equation 8.2.3.3:

$$K_b = \frac{K_w}{K_a} = \frac{1.01 \times 10^{-14}}{1.74 \times 10^{-5}} = 5.80 \times 10^{-10} \tag{8.2.3.4}$$

Substituting the expressions for the final values from the ICE table into Equation 8.2.3.4 and solving for x:

$$\frac{x^2}{0.0667} = 5.80 \times 10^{-10}$$

$$x = \sqrt{(5.80 \times 10^{-10})(0.0667)}$$

$$= 6.22 \times 10^{-6}$$

Thus $[OH^-] = 6.22 \times 10^{-6}\ M$ and the pH of the final solution is 8.794 (Figure 8.2.3.3*a*). As expected for the titration of a weak acid, the pH at the equivalence point is greater than 7.00 because the product of the titration is a base, the acetate ion, which then reacts with water to produce OH^-.

? Exercise 8.2.3.2

Calculate the pH of a solution prepared by adding 45.0 mL of a 0.213 M HCl solution to 125.0 mL of a 0.150 M solution of ammonia. The pK_b of ammonia is 4.75 at 25°C.

Answer

9.23

As shown in part (b) in Figure 8.2.3.3, the titration curve for NH3, a weak base, is the reverse of the titration curve for acetic acid. In particular, the pH at the equivalence point in the titration of a weak base is less than 7.00 because the titration produces an acid.

The identity of the weak acid or weak base being titrated strongly affects the shape of the titration curve. Figure 8.2.3.4 illustrates the shape of titration curves as a function of the pK_a or the pK_b. As the acid or the base being titrated becomes weaker (its pK_a or pK_b becomes larger), the pH change around the equivalence point decreases significantly. With very dilute solutions, the curve becomes so shallow that it can no longer be used to determine the equivalence point.

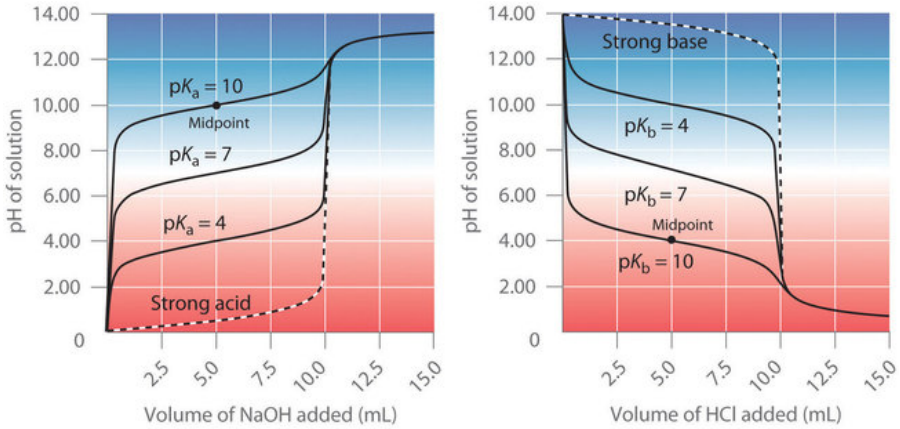


Figure 8.2.3.4: Effect of Acid or Base Strength on the Shape of Titration Curves. Unlike strong acids or bases, the shape of the titration curve for a weak acid or base depends on the pK_a or pK_b of the weak acid or base being titrated. (a) Solution pH as a function of the volume of 1.00 M **NaOH** added to 10.00 mL of 1.00 M solutions of weak acids with the indicated pK_a values. (b) Solution pH as a function of the volume of 1.00 M **HCl** added to 10.00 mL of 1.00 M solutions of weak bases with the indicated pK_b values. The shapes of the two sets of curves are essentially identical, but one is flipped vertically in relation to the other. Midpoints are indicated for the titration curves corresponding to pK_a = 10 and pK_b = 10. (CC BY-SA-NC; Anonymous by request)

The titration curves of weak acids with strong base and weak bases titrated with strong acid are inverses of each other. Three weak acids and three weak bases with pKa and pKb of 4, 7, and 10 are used.

One point in the titration of a weak acid or a weak base is particularly important: the midpoint of a titration is defined as the point at which exactly enough acid (or base) has been added to neutralize one-half of the acid (or the base) originally present and occurs halfway to the equivalence point. The midpoint is indicated in Figures 8.2.3.4*a* and 8.2.3.4*b* for the two shallowest curves. By definition, at the midpoint of the titration of an acid, [HA] = [A−]. Recall that the ionization constant for a weak acid is as follows:

$$K_a = \frac{[H_3O^+][A^-]}{[HA]}$$

If $[HA] = [A^-]$, this reduces to $K_a = [H_3O^+]$. Taking the negative logarithm of both sides,

$$-\log K_a = -\log[H_3O+]$$

From the definitions of pK_a and pH, we see that this is identical to

$$pK_a = pH \tag{8.2.3.5}$$

Thus the pH at the midpoint of the titration of a weak acid is equal to the pK_a of the weak acid, as indicated in part (a) in Figure 8.2.3.4 for the weakest acid where we see that the midpoint for pK_a = 10 occurs at pH = 10. Titration methods can therefore be used to determine both the concentration and the pK_a (or the pK_b) of a weak acid (or a weak base).

The pH at the midpoint of the titration of a weak acid is equal to the pK_a of the weak acid.

Titrations of Polyprotic Acids or Bases

When a strong base is added to a solution of a polyprotic acid, the neutralization reaction occurs in stages. The most acidic group is titrated first, followed by the next most acidic, and so forth. If the pK_a values are separated by at least three pK_a units, then the

overall titration curve shows well-resolved "steps" corresponding to the titration of each proton. A titration of the triprotic acid H_3PO_4 with NaOH is illustrated in Figure 8.2.3.5 and shows two well-defined steps: the first midpoint corresponds to pK_a1, and the second midpoint corresponds to pK_a2. Because HPO_4^{2-} is such a weak acid, pK_a3 has such a high value that the third step cannot be resolved using 0.100 M NaOH as the titrant.

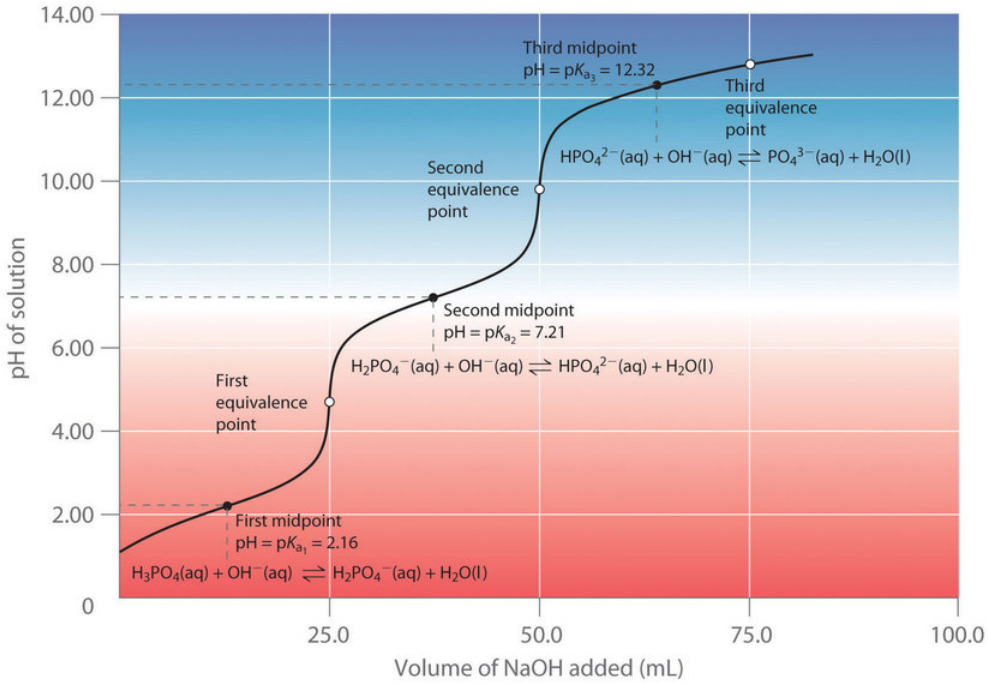
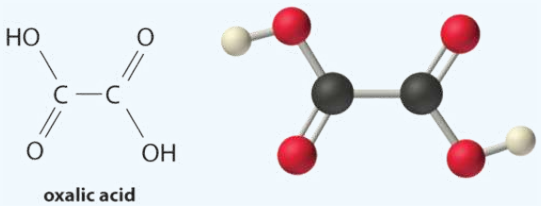


Figure 8.2.3.5: Titration Curve for Phosphoric Acid (H_3PO_4, a Typical Polyprotic Acid. The curve for the titration of 25.0 mL of a 0.100 M H_3PO_4 solution with 0.100 M NaOH along with the species in solution at each Ka is shown. Note the two distinct equivalence points corresponding to deprotonation of H_3PO_4 at pH ≈ 4.6 and $H_2PO_4^{2-}$ at pH ≈ 9.8. Because HPO_4^{2-} is a very weak acid, the third equivalence point, at pH ≈ 13, is not well defined. (CC BY-SA-NC; Anonymous by request)

The titration curve for the reaction of a polyprotic base with a strong acid is the mirror image of the curve shown in Figure 8.2.3.5. The initial pH is high, but as acid is added, the pH decreases in steps if the successive pK_b values are well separated. Table E1 lists the ionization constants and pK_a values for some common polyprotic acids and bases.

Example 8.2.3.3

Calculate the pH of a solution prepared by adding 55.0 mL of a 0.120 M NaOH solution to 100.0 mL of a 0.0510 M solution of oxalic acid (HO_2CCO_2H), a diprotic acid (abbreviated as H_2ox). Oxalic acid, the simplest dicarboxylic acid, is found in rhubarb and many other plants. Rhubarb leaves are toxic because they contain the calcium salt of the fully deprotonated form of oxalic acid, the oxalate ion ($O_2CCO_2^{2-}$, abbreviated ox^{2-}).Oxalate salts are toxic for two reasons. First, oxalate salts of divalent cations such as Ca^{2+} are insoluble at neutral pH but soluble at low pH. As a result, calcium oxalate dissolves in the dilute acid of the stomach, allowing oxalate to be absorbed and transported into cells, where it can react with calcium to form tiny calcium oxalate crystals that damage tissues. Second, oxalate forms stable complexes with metal ions, which can alter the distribution of metal ions in biological fluids.



oxalic acid

Given: volume and concentration of acid and base

Asked for: pH

Strategy:

A. Calculate the initial millimoles of the acid and the base. Use a tabular format to determine the amounts of all the species in solution.
B. Calculate the concentrations of all the species in the final solution. Determine [H+] and convert this value to pH.

Solution:

A Table E5 gives the pK_a values of oxalic acid as 1.25 and 3.81. Again we proceed by determining the millimoles of acid and base initially present:

$$100.00\,\cancel{mL}\left(\frac{0.510\ mmol\ H_2ox}{\cancel{mL}}\right) = 5.10\ mmol\ H_2ox$$

$$55.00\,\cancel{mL}\left(\frac{0.120\ mmol\ NaOH}{\cancel{mL}}\right) = 6.60\ mmol\ NaOH$$

The strongest acid (H_2ox) reacts with the base first. This leaves (6.60 − 5.10) = 1.50 mmol of OH^- to react with Hox−, forming ox^{2-} and H_2O. The reactions can be written as follows:

$$\underset{5.10\ mmol}{H_2ox} + \underset{6.60\ mmol}{OH^-} \rightarrow \underset{5.10\ mmol}{Hox^-} + \underset{5.10\ mmol}{H_2O}$$

$$\underset{5.10\ mmol}{Hox^-} + \underset{1.50\ mmol}{OH^-} \rightarrow \underset{1.50\ mmol}{ox^{2-}} + \underset{1.50\ mmol}{H_2O}$$

In tabular form,

Solutions to Example 17.3.3

	H_2ox	OH^-	Hox^-	ox^{2-}
initial	5.10 mmol	6.60 mmol	0 mmol	0 mmol
change (step 1)	−5.10 mmol	−5.10 mmol	+5.10 mmol	0 mmol
final (step 1)	0 mmol	1.50 mmol	5.10 mmol	0 mmol
change (step 2)	—	−1.50 mmol	−1.50 mmol	+1.50 mmol
final	0 mmol	0 mmol	3.60 mmol	1.50 mmol

B The equilibrium between the weak acid (Hox^-) and its conjugate base (ox^{2-}) in the final solution is determined by the magnitude of the second ionization constant, $K_{a2} = 10^{-3.81} = 1.6 \times 10^{-4}$. To calculate the pH of the solution, we need to know $[H^+]$, which is determined using exactly the same method as in the acetic acid titration in Example 8.2.3.2:

$$\text{final volume of solution} = 100.0\,mL + 55.0\,mL = 155.0\,mL$$

Thus the concentrations of Hox^- and ox^{2-} are as follows:

$$[Hox^-] = \frac{3.60\ mmol\ Hox^-}{155.0\ mL} = 2.32 \times 10^{-2}\ M$$

$$[ox^{2-}] = \frac{1.50\ mmol\ ox^{2-}}{155.0\ mL} = 9.68 \times 10^{-3}\ M$$

We can now calculate [H+] at equilibrium using the following equation:

$$K_{a2} = \frac{[ox^{2-}]\,[H^+]}{[Hox^-]}$$

Rearranging this equation and substituting the values for the concentrations of Hox^- and ox^{2-},

$$[H^+] = \frac{K_{a2}[Hox^-]}{[ox^{2-}]} = \frac{(1.6 \times 10^{-4})(2.32 \times 10^{-2})}{(9.68 \times 10^{-3})} = 3.7 \times 10^{-4}\ M$$

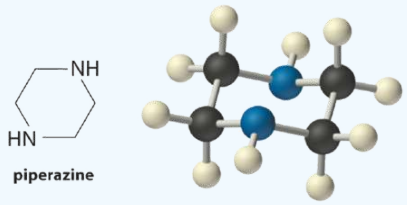
So

$$pH = -\log[H^+] = -\log(3.7 \times 10^{-4}) = 3.43$$

This answer makes chemical sense because the pH is between the first and second pK_a values of oxalic acid, as it must be. We added enough hydroxide ion to completely titrate the first, more acidic proton (which should give us a pH greater than pK_{a1}), but we added only enough to titrate less than half of the second, less acidic proton, with pK_{a2}. If we had added exactly enough hydroxide to completely titrate the first proton plus half of the second, we would be at the midpoint of the second step in the titration, and the pH would be 3.81, equal to pK_{a2}.

? Exercise 8.2.3.3: Piperazine

Piperazine is a diprotic base used to control intestinal parasites ("worms") in pets and humans. A dog is given 500 mg (5.80 mmol) of piperazine (pK_{b1} = 4.27, pK_{b2} = 8.67). If the dog's stomach initially contains 100 mL of 0.10 M HCl (pH = 1.00), calculate the pH of the stomach contents after ingestion of the piperazine.



Answer

pH=4.9

Indicators

In practice, most acid–base titrations are not monitored by recording the pH as a function of the amount of the strong acid or base solution used as the titrant. Instead, an acid–base indicator is often used that, if carefully selected, undergoes a dramatic color change at the pH corresponding to the equivalence point of the titration. Indicators are weak acids or bases that exhibit intense colors that vary with pH. The conjugate acid and conjugate base of a good indicator have very different colors so that they can be distinguished easily. Some indicators are colorless in the conjugate acid form but intensely colored when deprotonated (phenolphthalein, for example), which makes them particularly useful.

We can describe the chemistry of indicators by the following general equation:

$$\mathrm{HIn\,(aq) \rightleftharpoons H^+\,(aq) + In^-\,(aq)}$$

where the protonated form is designated by HIn and the conjugate base by In^-. The ionization constant for the deprotonation of indicator HIn is as follows:

$$K_{In} = \frac{[H^+][In^-]}{[HIn]} \tag{8.2.3.6}$$

The pK_{in} (its pK_a) determines the pH at which the indicator changes color.

Many different substances can be used as indicators, depending on the particular reaction to be monitored. For example, red cabbage juice contains a mixture of colored substances that change from deep red at low pH to light blue at intermediate pH to yellow at high pH. Similarly, *Hydrangea macrophylla* flowers can be blue, red, pink, light purple, or dark purple depending on the soil pH (Figure 8.2.3.6). Acidic soils will produce blue flowers, whereas alkaline soils will produce pinkish flowers.

Irrespective of the origins, a good indicator must have the following properties:

- The color change must be easily detected.

- The color change must be rapid.
- The indicator molecule must not react with the substance being titrated.
- To minimize errors, the indicator should have a pK_{in} that is within one pH unit of the expected pH at the equivalence point of the titration.



Figure 8.2.3.6: Naturally occurring pH indicators can be found in red cabbage and Hydrangea macrophylla flowers. Red Cabbage image (CC BY-SA 3.0; KENPEI via Wikipedia) and Hydrangea macrophylla flowers (pixabay).

Synthetic indicators have been developed that meet these criteria and cover virtually the entire pH range. Figure 8.2.3.7 shows the approximate pH range over which some common indicators change color and their change in color. In addition, some indicators (such as thymol blue) are polyprotic acids or bases, which change color twice at widely separated pH values.

Indicator	pK_{in}	Color change
Alizarin yellow R	11.0	yellow to red
Thymolphthalein	9.9	colorless to blue
Phenolphthalein	9.5	colorless to pink
Thymol blue	9.2	yellow to blue
Phenol red	7.4	yellow to red
Bromothymol blue	7.3	yellow to blue
Bromocresol purple	6.4	yellow to purple
Ethyl red	5.4	colorless to red
Resorcin blue	5.3	red to blue
Resazurin	5.1	orange to violet
Methyl red	5.0	red to yellow
Bromophenol blue	4.1	yellow to blue
Thymol blue	1.7	red to yellow
Malachite green	1.3	yellow to turquoise
Methyl violet	0.8	yellow to blue

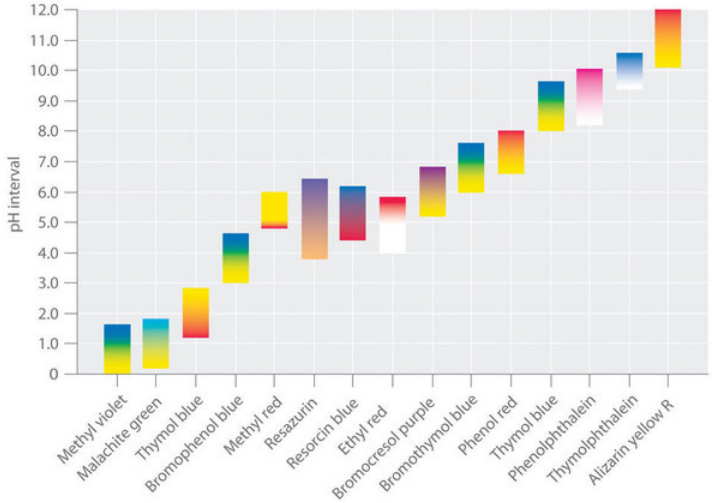


Figure 8.2.3.7: Some Common Acid–Base Indicators. Approximate colors are shown, along with pK_{in} values and the pH range over which the color changes. (CC BY-SA-NC; Anonymous by request)

It is important to be aware that an indicator does not change color abruptly at a particular pH value; instead, it actually undergoes a pH titration just like any other acid or base. As the concentration of HIn decreases and the concentration of In− increases, the color of the solution slowly changes from the characteristic color of HIn to that of In−. As we will see later, the [In−]/[HIn] ratio changes from 0.1 at a pH one unit below pKin to 10 at a pH one unit above pKin. Thus most indicators change color over a pH range of about two pH units.

We have stated that a good indicator should have a pKin value that is close to the expected pH at the equivalence point. For a strong acid–strong base titration, the choice of the indicator is not especially critical due to the very large change in pH that occurs around the equivalence point. In contrast, using the wrong indicator for a titration of a weak acid or a weak base can result in relatively large errors, as illustrated in Figure 8.2.3.8. This figure shows plots of pH versus volume of base added for the titration of 50.0 mL of a 0.100 M solution of a strong acid (HCl) and a weak acid (acetic acid) with 0.100 M $NaOH$. The pH ranges over which two common indicators (methyl red, $pK_{in} = 5.0$, and phenolphthalein, $pK_{in} = 9.5$) change color are also shown. The horizontal bars indicate the pH ranges over which both indicators change color cross the HCl titration curve, where it is almost vertical. Hence both indicators change color when essentially the same volume of NaOH has been added (about 50 mL), which corresponds to the equivalence point. In contrast, the titration of acetic acid will give very different results depending on whether

methyl red or phenolphthalein is used as the indicator. Although the pH range over which phenolphthalein changes color is slightly greater than the pH at the equivalence point of the strong acid titration, the error will be negligible due to the slope of this portion of the titration curve. Just as with the **HCl** titration, the phenolphthalein indicator will turn pink when about 50 mL of **NaOH** has been added to the acetic acid solution. In contrast, methyl red begins to change from red to yellow around pH 5, which is near the midpoint of the acetic acid titration, not the equivalence point. Adding only about 25–30 mL of **NaOH** will therefore cause the methyl red indicator to change color, resulting in a huge error.

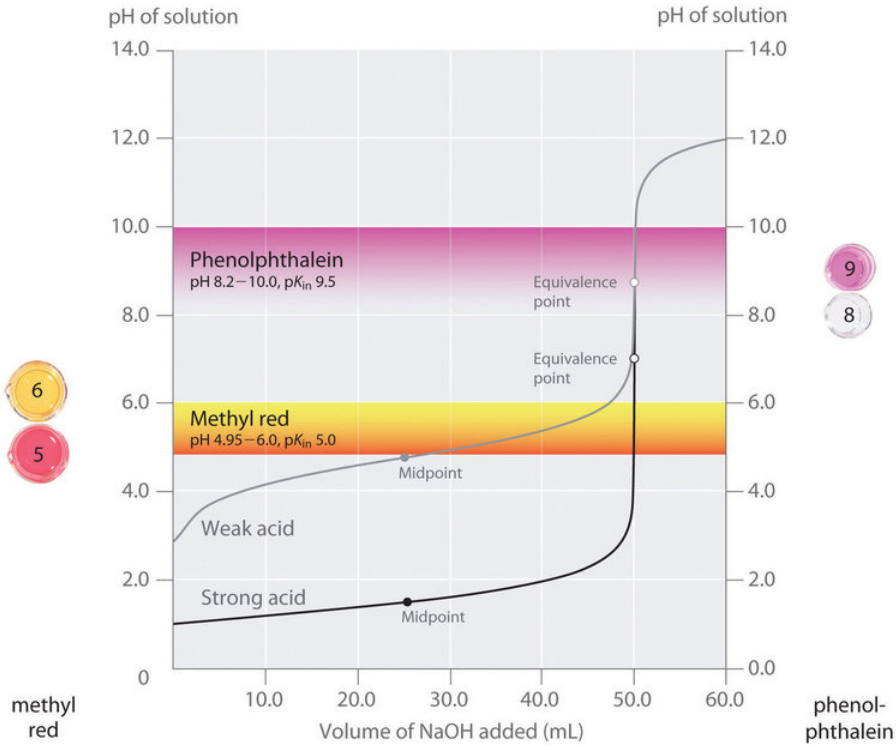


Figure **8.2.3.8**: Choosing the Correct Indicator for an Acid–Base Titration. (CC BY-SA-NC; Anonymous by request)

If the pH of the solution is between 4.95 and 6 then methyl red should be used. If the pH is between 8,2 and 10 then phenolphthalein should be used.

The graph shows the results obtained using two indicators (methyl red and phenolphthalein) for the titration of 0.100 M solutions of a strong acid (HCl) and a weak acid (acetic acid) with 0.100 M ***NaOH***. Due to the steepness of the titration curve of a strong acid around the equivalence point, either indicator will rapidly change color at the equivalence point for the titration of the strong acid. In contrast, the pKin for methyl red (5.0) is very close to the pK_a of acetic acid (4.76); the midpoint of the color change for methyl red occurs near the midpoint of the titration, rather than at the equivalence point.

In general, for titrations of strong acids with strong bases (and vice versa), any indicator with a pKin between about 4.0 and 10.0 will do. For the titration of a weak acid, however, the pH at the equivalence point is greater than 7.0, so an indicator such as phenolphthalein or thymol blue, with pKin > 7.0, should be used. Conversely, for the titration of a weak base, where the pH at the equivalence point is less than 7.0, an indicator such as methyl red or bromocresol blue, with pKin < 7.0, should be used.

The existence of many different indicators with different colors and pKin values also provides a convenient way to estimate the pH of a solution without using an expensive electronic pH meter and a fragile pH electrode. Paper or plastic strips impregnated with combinations of indicators are used as “pH paper,” which allows you to estimate the pH of a solution by simply dipping a piece of pH paper into it and comparing the resulting color with the standards printed on the container (Figure **8.2.3.9**).

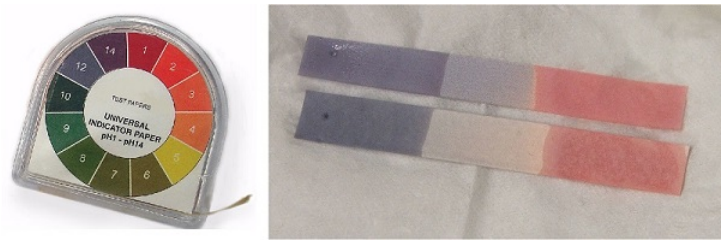


Figure **8.2.3.9**: pH Paper. pH paper contains a set of indicators that change color at different pH values. The approximate pH of a solution can be determined by simply dipping a paper strip into the solution and comparing the color to the standards provided. (CC BY-SA-NC; Anonymous by request)



pH Indicators: pH Indicators(opens in new window) [youtu.be]

Summary and Takeaway

Plots of acid–base titrations generate titration curves that can be used to calculate the pH, the pOH, the pK_a, and the pK_b of the system. The shape of a titration curve, a plot of pH versus the amount of acid or base added, provides important information about what is occurring in solution during a titration. The shapes of titration curves for weak acids and bases depend dramatically on the identity of the compound. The equivalence point of an acid–base titration is the point at which exactly enough acid or base has been added to react completely with the other component. The equivalence point in the titration of a strong acid or a strong base occurs at pH 7.0. In titrations of weak acids or weak bases, however, the pH at the equivalence point is greater or less than 7.0, respectively. The pH tends to change more slowly before the equivalence point is reached in titrations of weak acids and weak bases than in titrations of strong acids and strong bases. The pH at the midpoint, the point halfway on the titration curve to the equivalence point, is equal to the pK_a of the weak acid or the pK_b of the weak base. Thus titration methods can be used to determine both the concentration and the pK_a (or the pK_b) of a weak acid (or a weak base). Acid–base indicators are compounds that change color at a particular pH. They are typically weak acids or bases whose changes in color correspond to deprotonation or protonation of the indicator itself.

8.2.3: Neutralization Reactions and Titration Curves is shared under a CC BY-NC-SA 4.0 license and was authored, remixed, and/or curated by LibreTexts.

- **17.3: Acid-Base Titrations** is licensed CC BY-NC-SA 3.0.

8.2.4: Solutions of Salts of Polyprotic Acids

Learning Objectives

- Predict and calculate the pH of a solution of salts of polyprotic acids

Salts can be thought of as being derived from the neutralization of an acid and a base. A salt formed from a strong acid and a strong base will not hydrolyze (e.g., extract a proton from water). When placed in water, these salts dissociate completely, and their ions remain uncombined in solution (e.g., the NaCl salt is formed from a strong acid (HCl) and a strong base (NaOH).

In discussing the titration of acids and bases, the acid or basic properties of the corresponding salts after a neutralization reaction must be addressed to calculate the final pH of a solution. To calculate the pH of a salt solution one needs to know the concentration of the salt solution, whether the salt is an acidic, basic, or neutral salt, the equation for the interaction of the ion with the water, the equilibrium expression for this interaction and the K_a or K_b value.

Note: The Hydrolysis of Salts

As a quick review, the general rules for the hydrolysis of monoprotic salts are:

1. If neither the cation/anion can affect the pH, the solution is neutral
2. If **only** the cation of the salt is acidic, the solution is acidic
3. If **only** the anion of the salt is basic, the solution will be basic
4. If a salt has a cation that is acidic and an anion that is basic, the pH of the solution is determined by the relative strengths of the acid and base
    - if $K_a = K_b$, then no net effect on pH
    - if $K_a > K_b$, then the solution is slightly acidic
    - if $K_b > K_b$, then the solution is slightly basic

Salts of Polyprotic Acids

Do not be intimidated by the salts of polyprotic acids. Yes they're bigger and "badder" then most other salts, but they can be handled the exact same way as other salts, just with a bit more math.

- All of the rules from above still apply, e.g., the pH of a salt of polyprotic acid will always be greater than 7.
- The same way that polyprotic acids lose H^+ stepwise, salts of polyprotic acids gain H^+ in the same manner, but in reverse order of the polyprotic acid.

Take for example dissociation of carbonic acid (H_2CO_3):

$$H_2CO_{3(aq)} + H_2O_{(l)} \rightleftharpoons H_3O^+_{(aq)} + HCO^-_{3(aq)} \tag{8.2.4.1}$$

with $K_{a1} = 2.5 \times 10^{-4}$

$$HCO^-_{3(aq)} + H_2O_{(l)} \rightleftharpoons H_3O^+_{(aq)} + CO^{2-}_{3(aq)} \tag{8.2.4.2}$$

with $K_{a2} = 5.61 \times 10^{-11}$. This means that when calculating the values for K_b of CO_3^{2-}, The K_b of the first hydrolysis reaction will be $K_{b1} = \frac{K_w}{K_{a2}}$ since it will go in the reverse order.

Example 8.2.4.1: $NaHSO_4$

What is the pH of a 0.100 M $\mathbf{NaHSO_4}$ solution? Sulfuric acid is a strong acid, and the $\mathbf{pK_{a_2}}$ of $\mathbf{HSO_4^-}$ is 1.92.

Solution

First review the ions generates immediate upon dissociation of the salt.

- Na^+ is a non-acidic "spectator ion" that does not affect the acidity or basicity of a solution and can be ignored.

- The HSO_4^- anion will affect the pH

HSO_4^- is part of the dissociation chain of diprotic sulfuric acid (H_2SO_4) with the following steps

$$H_2SO_4 + H_2O \rightarrow H_3O^+ + HSO_4^- \tag{8.2.4.3}$$

Because H_2SO_4 is a strong acid, this step goes to completion and no H_2SO_4 exists in the solution. The HSO_4^- ion is a weak acid and dissociates to a small extent:

$$HSO_4^- + H_2O \rightleftharpoons H_3O^+ + SO_4^{2-} \tag{8.2.4.4}$$

with $K_{a2} = 1.0 \times 10^{-2}$ from Table E1. The equilibrium favors the reactants.

The $NaHSO4$ salt is completely ionized in its solution.

$$\mathrm{NaHSO_{4\,(s)} \rightarrow Na^+_{(sq)} + HSO_4{}^-_{(sq)}} \tag{8.2.4.5}$$

The anion then further ionizes (Equation 8.2.4.4). We can construct an ICE table to solve for the final value of this ionization and hence $[H_3O^+]$

ICE Table	HSO_4^-	H_2O	H_3O^+	SO_4^{2-}
Initial	0.1 M	-	0	0
Change	-x	-	+x	+x
Equilibrium	0.1 M -x	-	x	x

$$K_{a2} = \frac{x^2}{0.100 - x} = 0.0100$$

$$\begin{aligned}[\mathrm{H_3O^+}] &= x \\ &= \frac{-0.120 + \sqrt{0.012^2 + 4 \times 0.00120}}{2} \\ &= 0.0292 \text{ M}\end{aligned}$$

Thus,

$$\mathrm{pH} = -\log\ 0.0292 = 1.54$$

Note that while the dissociation is weak, the quadratic equation cannot be avoided since 0.0292 cannot be ignore when compared to 0.1 M.

? Exercise 8.2.4.1

Which of the following solutions are acidic, basic, or neutral?

a. $\mathrm{Na_2SO_4}$
b. $\mathrm{NaH_2PO_4}$
c. $\mathrm{Na_2HPO_4}$
d. $\mathrm{Na_3PO_4}$
e. $\mathrm{NaNO_3}$

✓ Example 8.2.4.2: Qualitatively Estimating the pH of a Polyprotic Salt Solution

Predict whether the Na_2HPO_4 salt will form an acidic or basic solution when dissolved in water. You will need values from Table E1 to address this.

Solution

First review the ions generates immediate upon dissociation of the salt.

- Na^+ is a non-acidic "spectator ion" that does not affect the acidity or basicity of a solution and can be ignored.
- The HPO_4^{2-} anion will affect the pH and does so via competing hydrolysis steps as discussed below.

From Table E1, the three equilibria values for the three acid/base reactions of the phosphate ion are:

$$H_3PO_{4(sq)} \rightleftharpoons H^+_{(aq)} + H_2PO^{2-}_{4(aq)} \tag{8.2.4.6}$$

with $K_{a1} = 6.9 \times 10^{-3}$

$$H_2PO^-_{4(sq)} \rightleftharpoons H^+_{(aq)} + HPO^{2-}_{4(aq)} \tag{8.2.4.7}$$

with $K_{a2} = 6.2 \times 10^{-8}$

$$HPO^{2-}_{4(sq)} \rightleftharpoons H^+_{(aq)} + PO^{3-}_{4(aq)} \tag{8.2.4.8}$$

with $K_{a3} = 4.8 \times 10^{-11}$

The low K_a value for the deprotonation of $HPO^{2-}_{4(sq)}$ means that it is a poor acid and better functions as a (Brønsted-Lowry) base:

$$HPO^{2-}_{4(aq)} + H_2O_{(l)} \rightleftharpoons H_2PO^-_{4(aq)} + OH^-_{(aq)} \tag{8.2.4.9}$$

The two possible reactions that $HPO^{2-}_{4(aq)}$ undergoes are the acid reaction in Equation 8.2.4.7 and the basic reaction in Equation 8.2.4.9. Whether this ion will cause the solution to be acidic or basic depends on whether the K_a for Equation 8.2.4.7 is bigger than the K_b for Equation 8.2.4.9.

The K_b of this reaction is related to the K_{a2} by

$$K_b = \frac{K_w}{K_a}$$

$$K_b = \frac{1 \times 10^{-14}}{6.2 \times 10^{-8}} = 1.6 \times 10^{-7} \text{ for } HPO_4^{2-}$$

Since $K_b > K_a$, the solution will be **basic**. To determine just how basic requires the use of an ICE table as discussed in Example 8.2.4.3.

Solving the final pH for a Na_2HPO_4 salt solution is more complex than for the $NaHSO_4$, since the latter involves a single equilibrium. Two equilibria must be simultaneously solved for Na_2HPO_4. However, often time (but not always), they can be easily approximated given the relative pk_a describing the reversible reaction.

Example 8.2.4.3: Quantitatively Estimating the pH of a Polyprotic Salt Solution

Calculate the pH of the solution containing 3.875 g of Na_2HPO_4 that has been dissolved in a 250 mL of water.

Solution

First it is best to identify the molarity of Na_2HPO_4 that was initially generated (i.e., before any hydrolysis reactions happens).

$$c = \frac{3.875\ g/\text{molecular mass}}{\text{volume}} = \frac{3.875\ g/141.98\ g/mol}{250\ mL} = 0.11\ M$$

As discussed in Example 8.2.4.1, the low K_a value for the deprotonation of $HPO^{2-}_{4(sq)}$ means that it is a poor acid and instead functions as a base instead. From comparing the ionization constant in Example 8.2.4.1, the Na_2HPO_4 is a far better base than acid. If we ignore the acid properties of the ion and focus on the basic we get the following reaction

$$HPO^{2-}_{4(aq)} + H_2O_{(l)} \rightleftharpoons H_2PO^-_{4(aq)} + OH^-_{(aq)} \tag{8.2.4.10}$$

with a K_b of 1.6×10^{-7}. Now do an ICE table to get the final $[H^+]$ concentration.

ICE Table	$HPO_{4(aq)}^{2-}$	$H_2O_{(l)}$	$H_2PO_{4(aq)}^{-}$	$OH_{(aq)}^{-}$
Initial	0.11 M	-	-	0
Change	-x	-	+x	+x
Equilibrium	0.11 M - x	-	x	x

$$K_b = \frac{[H_2PO_{4(aq)}^{-}][OH_{(aq)}^{-}]}{[HPO_{4(aq)}^{2-}]} = 1.6 \times 10^{-7} \tag{8.2.4.11}$$

$$\frac{x^2}{0.11\ M - x} = 1.6 \times 10^{-7} \tag{8.2.4.12}$$

if $x << 0.11\ M$ then $0.11\ M - x \approx 0.11\ M$ then

$$x = 1.3 \times 10^{-4} = [OH^-] \tag{8.2.4.13}$$

$$pOH = -\log_{10}[OH^-] = 3.8 \tag{8.2.4.14}$$

\[pH = pK_w - pOH]

Assuming that the reaction is at 25°, then $pK_w = 14$ and

$$pH = 14 - 3.8 = 10.2 \tag{8.2.4.15}$$

As expected, the solution is basic.

8.2.4: Solutions of Salts of Polyprotic Acids is shared under a CC BY-NC-SA 4.0 license and was authored, remixed, and/or curated by LibreTexts.

- **17.5: Solutions of Salts of Polyprotic Acids** is licensed CC BY-NC-SA 4.0.

8.2.5: Acid–Base Equilibrium Calculations- A Summary

17.1: The Common-Ion Effect

The common-ion effect argues that the dissociation of a weak electrolyte is decreased by adding a strong electrolyte to the solution that has a **common ion** with the weak electrolyte.

17.2: Buffered Solutions

Buffers are solutions that resist a change in pH

17.2.1 Composition and Action of Buffered Solutions

- buffers have both acidic and basic species to neutralize H^+ and OH^- ions
- acid dissociation equilibrium in buffered solution

$$HX(aq) \rightleftharpoons H^+(aq) + X^-(aq)$$

with

$$K_a = \frac{[H^+][X^-]}{[HX]}$$

or

$$[H^+] = K_a \frac{[HX]}{[X^-]}$$

  - pH determined by: value of K_a and the ratio of $[HX]/[X^-]$
  - if OH^- added:
    - $$OH^-(aq) + HX(aq) \rightleftharpoons H_2O(l) + X^-(aq)$$
      - Therefore [HX] decreases and $[X^-]$ increases
      - if amounts of HX and X^- present are very much larger than the amount of OH^- added, then the ratio of $[HX]/[X^-]$ will not change much, and so the increase in pH due to the added hydroxide ion is rather small
  - when [HX] and $[X^-]$ are about the same, buffers are most effective: i.e., when $[H^+] = K_a$

17.2.2 Buffer Capacity and pH

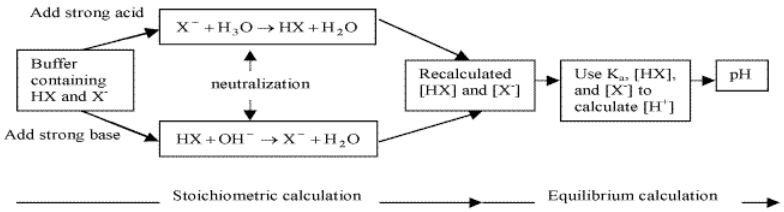
- buffer capacity – amount of acid or base buffer can neutralize before the pH changes considerably
- capacity depends on amount of acid or base in buffer
- pH depends on K_a for acid and relative concentrations of the acid and base
- Henderson-Hasselbalch Approximation:

$$pH = pK_a + \log_{10} \frac{[base]}{[acid]}$$

- [base] and [acid] = concentrations of conjugate acid-base pair
- when [base]=[acid], pH = pK_a
- can use initial concentrations of acid and base components of buffer directly into equation

17.2.3 Addition of Strong Acids or Bases to Buffers

reactions between strong acids and bases go to completion



Buffer contain HX and X minus. Add strong acid or strong bass for neutralization. Recalculate the concentrations. Use Ka to calculate the concentration of H plus and use that to get pH.

Either strong base or acid assumed to be completely consumed by reaction with buffer if buffering capacity is not exceeded

17.3: Acid-Base Titrations

- solution containing a known [base] added to an acid or acid solution added to base
- acid-base indicators used to signal equivalence point
- titration curve – pH vs Volume

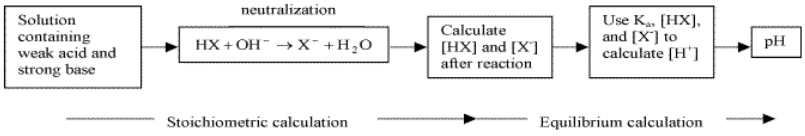
17.3.1 Strong Acid – Strong base Titrations

- pH starts out low ends high
- pH before equivalence point is pH of acid not neutralized by base
- pH at equivalence point is pH of solution
- pH equals 7.00
- for strong base titrations, the pH starts high ends low

17.3.2 The Addition of a Strong Base to a Weak Acid

Reactions between weak acid and strong base goes to completion

- calculating pH before equivalence point
  - stoichiometric calculations: allow strong base to react to completion producing a solution containing a weak acid and its conjugate base



Start with solution contain weak acid and strong base. Go through neutralization. Calculate the concentrations after the reaction. Use Ka to and concentrations to calculate the concentration of H plus. Use H plus to figure out pH.

- equilibrium calculation: use K_a and equilibrium expression to find equilibrium concentrations of the weak acid and its conjugate base, and H^+

17.3.3 Titration Curves for Weak Acids or Weak Bases

Differences between strong acid-strong base titrations

1. solution of weak acid as higher initial pH than solution of a strong acid with same concentration
2. solution of weak acid rises more rapidly in early part of titration and more slowly as it reached the equivalence point
3. pH is not 7.00 at equivalence point

- before equivalence point solution has mixture of weak acid and its salt
- also called the buffer region of curve
- at equivalence point solution contains only salt
- weakly basic due to hydrolysis of anion
- after equivalence point solution has mixture of salt and excess strong base
- pH determined by [base]

17.3.4 Titrations of Polyprotic Acids

- reaction occurs in series of steps
- titration curve shows multiple equivalence points

17.4: Solubility Equilibria

17.4.1 The Solubility-Product Constant, K_{sp}

- saturated solution – dissolved and undissolved solute are at equilibrium
- expressed by g/L
- molar solubility – moles of solute dissolved to form a liter of saturated solution (mol/L)
- K_{sp} equilibrium constant for the equilibrium between an ionic solid and its saturated solution
- Solubility of compound (g/L) à molar solubility of compound (mol/L) à [molar] of ions à K_{sp} of ions

17.5: Factors that Affect Solubility

solubility affected by temperature and presence of other solutes. The solubility of ionic compound affected by:

- the presence of common ions
- pH of solution
- presence of complexing agent

17.5.1 Common-Ion Effect

- solubility of slightly soluble salt decreases when a second solute has a common ion

17.5.2 Solubility and pH

- solubility of any ionic compound affected if solution is acidic or basic
- change only noticeable if both ions are moderately acidic or basic
- solubility of slightly soluble salts containing basic anions increase as $[H^+]$ increases (as pH is lowered)
- the more basic an anion is, the greater the solubility will be affected by pH

17.5.3 Formation of Complex Ions

- metal ions act as Lewis acids in water
- complex ion – metal ion and Lewis base bonded together
- K_f – formation constant, equilibrium expression for formation of a complex ion
- Solubility of metal salts increases in acceptable Lewis bases if metal forms a complex base
- Lewis bases: NH_3, CN^-, OH^-

17.5.4 Amphoterism

- amphoteric substances include hydroxides and oxides of: Al^{3+}, Cr^{2+}, Zn^{2+}, and Sn^{2+}
- dissolve in strongly basic solutions
- formation of complex anions containing, typically four, hydroxides bound to metal ion
- amphoterism also associated with behavior of water molecules that surround and bond to metal ions by Lewis acid-base interactions

17.6: Precipitation and Separation of Ions

Q = ion product

- If $Q > K_{sp}$, precipitation occurs until $Q = K_{sp}$
- If $Q = K_{sp}$, equilibrium exists, have a saturated solution
- If $Q < K_{sp}$, solid dissolves until $Q = K_{sp}$

17.6.1 Selective Precipitation of Ions

- separation of ions in aqueous solution using a reagent that precipitates only with selected ions

17.7: Qualitative Analysis for Metallic Elements

Qualitative analysis: determines presence or absence of a particular metal ion

- ions separated into broad groups on basis of solubility
- ions separated by dissolving selected members in group
- ions identified by specific tests

8.2.5: Acid–Base Equilibrium Calculations- A Summary is shared under a CC BY-NC-SA 4.0 license and was authored, remixed, and/or curated by LibreTexts.

- **17.S: Additional Aspects of Aqueous Equilibria (Summary)** is licensed CC BY-NC-SA 3.0.

8.2.6: Exercises on Acids and Bases II

These are homework exercises to accompany the Textmap created for "General Chemistry: Principles and Modern Applications " by Petrucci et al. Complementary General Chemistry question banks can be found for other Textmaps and can be accessed here. In addition to these publicly available questions, access to private problems bank for use in exams and homework is available to faculty only on an individual basis; please contact Delmar Larsen for an account with access permission.

Q3.1

At room temperature, a solution is made by adding 50mL of 0.325M HF ($Ka = 6.6 \times 10^{-4}$) with 10mL of 0.50M HCl. Calculate the following at equilibrium:

a. $[H_3O^+]$
b. $[OH^-]$
c. $[HF]$
d. $[Cl^-]$

Q3.2 - [Questionable, Please Recheck the question and the answer]

For a solution that is 0.138 M NH_3 ($Ka = 1.9 \times 10^{-5}$) and 0.101 M KN_3 (potassium azide) calculate the following:

a. $[H_3O^+]$
b. $[N_3^-]$
c. $[K^+]$
d. $[OH^-]$

Q3.3

Calculate the change in pH that results from adding

a. 0.150 mol $LiNO_2$ to 1.00 L of 0.150 M $HNO_{2\,(aq)}$
b. 0.150 mol $LiNO_3$ to 1.00 L of 0.150 M $HNO_{3\,(aq)}$

Why are these changes not the same? Explain your answer.

Q3.4

A solution of volume 50.0 mL contains 12.5 mmol $HClO_2$ and 7.25 mmol $KClO_2$.

a. What is the pH of this solution?
b. If 1.00 mmol $Ca(OH)_2$ is added to the solution, what will be the new pH?
c. If 2.00 mL of 6 M HCl is added to the original solution, what will be the new pH?

Q3.5

There are various procedures for preparing buffer solutions. To obtain a $pH = 4.60$, one such way is to mix 18.00 mL of 0.300 M C_5H_5N with 72.00 mL of 0.300 M $C_5H_5NH^+$.

a. Show by calculation that the pH of this solution is 4.60.
b. Would you expect the pH of this solution to remain the same if 100.00 mL of buffer solution were diluted to 500.00 mL? To 1.00 L? Explain.
c. What will be the pH of the original 100.00 mL of buffer solution if 0.40 mL of 1.00 M HBr was added to it?
d. What is the maximum volume of 1.00 M HBr that can be added to the original buffer solution so that the pH does not drop below 4.4?

Q3.6

Use the following data table to answer the following questions

Name	pK_{ind}	Acid Color	pH Range of Color Change	Base Color
Methyl violet		Yellow	0.0 – 1.6	Blue
Thymol blue		Red	1.2 – 2.8	Yellow
Methyl orange	3.7	Red	3.2 – 4.4	Yellow
Bromocresol green		Yellow	3.8 – 5.4	Blue
Methyl red		Red	4.8 – 6.0	Yellow
Litmus	6.5	Red	5.0 – 8.0	Blue
Bromothymol blue	7.9×10^{8}	Yellow	6.0 – 7.6	Blue
Thymol blue		Yellow	8.0 – 9.6	Blue
Phenolphthalein	9.3	Colorless	8.2 – 10.0	Pink
Thymolphthalein	1.0×10^{-10}	Colorless	9.4 – 10.6	Blue
Alizarin yellow R		Yellow	10.1 – 12.0	Red

Identify one indicator (each) that would change color in an acidic solution, a basic solution, and a neutral solution.

Q3.7

What color will a solution with bromphenol blue change to with the following species in solution

a. $Mg(OH)_2$
b. HCl
c. HF

Q3.8

What stoichiometric concentration of the indicated substance is required to obtain an aqueous solution with the pH value: $Na(OH)_2$ for $pH = 10.92$

Q3.9

A solution is prepared with 0.3 M NH_3 and 0.4 M NH_4Cl.

Show that this is a buffer solution.

Calculate the pH of this buffer solution. $K_b = 1.8 \times 10^{-5}$

What is the final pH if 1 L of 0.2 M $NaOH$ is added to 1 L of this buffer solution.

Q3.10

Hydroflouric acid, HF, is a stronger acid than water and when in an aqueous solution, the following reaction occurs.

$$HF + H_2O \rightleftharpoons H_3O^+ + F^- \tag{8.2.6.1}$$

Three experiments were completed to obtain a pKa value for HF at 0^oC. A sample of HF was shaken and separated into two layers, one with 1-pentanol, and the other with water. Assume no ionization or disassociation occurs in the 1-pentanol layer.

- The first experiment showed that the water layer contained 5 times as much HF as the 1-pentanol layer did.
- The 2nd experiment involved adding .5 M $LiOH_{(aq)}$ and 1-pentanol. At equilibrium, the concentration of HF was 0.005 M in the 1-pentanol layer and 0.35 M in the aqueous layer.
- The third experiment showed that when .25 M $LiOH_{(aq)}$ was added, the concentrations in the 1-pentanol layer was .0015 in the 1-pentanol layer and .12 M in the aqueous layer. At 0^oC, $pK_w = 14.94$.

Find pK_a value of HF.

Q3.11

To increase the ionization of H_2S, which of the following compounds should be added to the solution?

a. $NaHSO_4$
b. HCl
c. Acetic acid (CH_3COOH)
d. $NaCN$

Q3.12

For the solution that is 0.330 M CH_3CH_2COOH $K_a = 1.3 \times 10^{-5}$ and 0.010M HI, calculate

(a) [H_3O^+

(b) $[OH^-]$

(c) $[CH_3CH_2COOH]$

(d) $[I^-]$

Q3.13

For a solution that is 0.654 M NH_3 and 0.202 M NH_4Cl, calculate :

(a) $[H_3O^+]$

(b) $[OH^-]$

(c) $[NH_4^+]$

d) $[Cl^-]$

Q3.14

Calculate the change in pH that results from adding (a) 0.300 mol $NaNO_2$ to 1.00 L of 0.200 M $HNO_{2(aq)}$; (b) 0.300 mol $NaNO_3$ to 1.00 L of 0.200M $HNO_{3(aq)}$.

Q3.15

A solution of volume 1L contains 0.500 mol $HCHO_2$ and 0.250 mol $NaHCOO$.

a. What is the pH of this solution?
b. If 0.1 mol $Ba(OH)_2$ is added to to the solution, what will be the new pH?
c. If 10.0 mL of 12 M HCl is added to the original solution what will be the new pH?

Q3.16

To obtain a $pH = 8.00$ you need to mix 35.00 mL of .220 M NH_3 with 65.00 mL of .250 M NH_4Cl.

a. Show the calculation that the pH of this solution is 8.00.
b. Would you expect the pH of this solution to remain at 8.00 if the 100 mL of the buffer were diluted to 1.00 L? 1000L? Explain.
c. What will be the pH of the original solution if 0.20 mL of 1.00 M HCl is added?

Q3.17

Use data from table

Indicator	K_{HIn}	Acid -> Anion
Bromphenol blue	1.4×10^{-4}	yellow -> blue
Bromcresol green	2.1×10^{-5}	yellow -> blue
Bromthymol blue	7.9×10^{-8}	yellow -> blue
2,4 – Dinitrophenol	1.3×10^{-4}	colorless -> yellow
Chlorphenol red	1.0×10^{-6}	yellow -> red
Thymolphthalein	1.0×10^{-10}	colorless -> blue

a) Which of these indicators change color in acidic, basic, or neutral point.

b) What is the approximate pH of a solution if bromocresol green indicator turns green? If chlorphenol red turns orange?

Q3.18

Phenol red indicator changes from yellow to red in pH ranges from 6.6 to 8.0. Without making detailed calculations, state what color the indicator will assume in each of the following solutions.

a. 0.10 M KOH
b. 0.10 M CH_3COOH.
c. 0.10M NH_4NO_3

d. 0.10M HBr
e. 0.10 M $NaCN$
f. 0.10 M CH_3COOH and 0.10 M $NaCH_3COO$.

Q3.19

Two aqueous solutions are mixed. 75 mL of .333 M H_2SO_4 and 25 mLof 0.05 M $NaOH$. What is the pH of the resulting solution?

Q3.20

Explain why the volume of 0.100 M $NaOH$ required to reach the equivalence point in the titration of 30.00 mL of 0.100 M HA is the same regardless of whether HA is a strong or a weak acid, yet the pH at the equivalence point is not the same.

Q3.21

Sketch a titration curve for each of the following three weak acids when titrated with 0.100 M $NaOH$.

a. 10.00 mL of 0.100 M HX; $Ka = 7.0 \times 10^{-3}$
b. 10.00 mL of 0.100 M HY; $Ka = 3.0 \times 10^{-4}$
c. 10.00 mL of 0.100 M HZ; $Ka = 2.0 \times 10^{-8}$

Q3.22

Is 0.20M $Na_2S_{(aq)}$ solution likely to be acidic, basic, or neutral? Explain.

Q3.23

Sodium phosphate, Na_3PO_4, is made by neutralizing phosphoric acid with sodium carbonate to obtain Na_2HPO_4. The Na_2HPO_4 is further neutralized to Na_3PO_4 with $NaOH$.

1. a) Write net ionic equations for these reactions.
2. b) Na_2CO_3 is a much cheaper base than $NaOH$. Why do you suppose that $NaOH$ must be used as well with Na_2CO_3 to produce Na_3PO_4?

Q3.24

The pH of a solution of 19.5 g malonic acid in 0.250 L is 1.47. The pH of a 0.300 M solution of sodium hydrogen malonate is 4.26. What are the values of K_{a1} and K_{a2} for malonic acid?

Q3.25

Using appropriate equilibrium constants but without doing detailed calculations, determine whether a solution can be simultaneously.

a. 0.10 M NH_3 and 0.10 M NH_4Cl, with $pH = 6.07$
b. 0.10 M $NaC_2H_3O_2$ and 0.058 M HI
c. 0.10 M KNO_2 and 0.25 M KNO_3
d. 0.050 M $Ba(OH)_2$ and 0.70 M NH_4Cl
e. 0.018 M C_6H_5COOH and 0.018 M NaC_6H_5COO with $pH = 4.10$

Q3.26

A buffer solution can be prepared by by starting with a weak acid, HA, and converting some of the weak acid to its salt by titration with a strong base. The fraction of the original acid that is converted to the salt is designated F.

1. a) Derive an equation similar to (16.2) but express in terms of F rather than concentrations.
2. b) What is the pH at the point in the titration of phenol, C_6H_5OH, at which $F = 0.27$ (pK_a *of phenol* $= 10.00$)?

Q3.27

Complete the derivation of equation (16.5). Then derive equation (16.6)

Q3.28

A solution is prepared that is 0.200 M CH_3COOH and 0.250M $NaHCOO$.

a. Show that this is a buffer solution
b. Calculate the pH of this solution.

Q3.29

For water at $0°C$, $pK_w = 14.94$. Find the approximate value of K_a for H_2O_2 at $0°C$.

Q3.30

To increase the ionization of formic acid, $HCOOH_{(aq)}$, which of the following should be added to the solution?

a. $NaCl$
b. $NaHCOO$
c. H_2SO_4
d. $NaHCO_3$

Q3.31

For a solution that is 0.345 M hydrosulfuric acid ($K_a = 1.0 \times 10^{-7}$) and a pH of 3.2. Find [H_3O^+].

Q3.32

For a solution that is 0.35 M $HC_2H_3O_2$ and $C_2H_3O_2$ calculate:

a. pH
b. [H_3O^+]

Q3.33

Calculate the pH of the buffer that results from mixing 100.0 ml of .250 M $HCHO_2$ and 10.0 ml of 1 M $NaCHO_2$. $pKa = 3.744$

Q3.34

What is the pH of a 0.07M ammonia solution?

Q3.35

What are the approximate pHs of a solution for the following indicator strips at the specified color change?

a. methyl red indicator strip changes from orange to yellow
b. bromphenol indicator strip changes from yellow to purple
c. thymol blue indicator strip changes from yellow to blue

Q3.36

Azolitman indicator strips change from red to blue in the pH range from 4.5 to 8.3. What color will the indicator be for the following:

a. 0.000014 M HCl
b. 0.00014 M HCl
c. 0.0014 M HCl
d. 0.0000014 M HCl

Q3.37

Why do we usually try to keep the amount of indicator added relatively small when used as acid-base indicators?

Q3.38

Define the equivalence point in a titration curve.

Q3.39

What relationship do the molarity of Base added in a titration and molarity of either strong of weak acid share?

Q3.40

0.205 M $HClO$ reacts with water to form .020 $MClO^-$. The pH of the solution is 4.04. Determine K_a of $HClO$.

Q3.41

Titrate 50mL of 0.200M HNO_3 with 0.100M $NaOH$. Add 150mL $NaOH$. 15mmol HNO_3. And Find pOH and pH.

Q3.42

Is a solution of 0.23 M NaI likely to be acidic, basic, or pH neutral? Explain.

Q3.43

In a strong acid base titration, at what pH does the equivalence point always occur?

Q3.44

Find the pH for HCN at $0°C$ if the pK_b of HCN is 4.8

$$HCN + H_2O \rightleftharpoons H_3O^+ + CN^- \tag{8.2.6.2}$$

Q3.45

Can an aqueous solution of NH_3 and NH_4Cl form a pH of 6 with equal molarity of each added together?

Q3.46

A buffer solution contains 0.50M acetic acid ($Ka = 1.8 \times 10^{-5}$) and 0.50M sodium acetate. Find the pH of the solution.

Q3.47

You need bring the pH of .325 L of .452 M $NaOH$ to 7.00. What volume of which of the following solutions would you use: 5.00 M HBr or 5.00 M Na_2S?

Q3.48

What is the pH of a 0.025 M HCN solution? $K_a = 6.2 \times 10^{-10}$

Q3.49

Define the common Ion Effect and give an example of it.

Q3.50

If a solution contains 50 ml of 0.25M of NH_3 and 75 ml NH_4Cl, calculate the molarity of NH_4Cl.

Q3.51

If given two different solutions, one acid and one base, what is the best method to use to calculate the pH of the solution?

Q3.52

If a mixture of .005 mol $NaOH$ and .008 mol HCl has a volume of 50ml, what is range of pH of the solution?

Q3.53

If an original solution had a pH level of 6.05, in what direction would the pH shift (towards or away from equilibrium) if 50ml of HCl were added

Q3.54

Does Bromecresol Green (2.1×10^{-5}) change color in an acidic or basic solution?

Q3.55

If Chlorphenol Red indicator turns red at $ph = 6.0$, then will it change colors at 0.10 M KOH?

Q3.56

Two aqueous solutions are mixed together, 100 ml of 0.025M H_2SO_4 and a given amount of 0.03M $NaOH$. What is the total volume at equilibrium?

Q3.57

Why is the volume the same if 0.2 M HA in a solution if 0.2 M $NaOH$ is either a weak or strong acid?

Q3.58

Sketch a titration curve of a hypothetical weak acid when .1M of $NaOH$ is added. Assume 100ml at 0.1M of $C_2H_4O_2$.

Q3.59

With the titration of 50ml of 0.1M $NaOH$ with 0.1M HCl, solve for the volume of HCl

Q3.60

Is the solution 0.1M HCl likely to be acidic, basic, or neutral?

Q3.61

Define the term of stoichiometric concentration.

Q3.62

A buffer solution can be made by taking a weak acid and converting a portion to its salt. This is done by titration with what?

Q3.63

If a pH of an unknown substance is set at 5, would a strong acid or a strong base solution be needed for the substance to reach equilibrium?

Q3.64

A solution is made of 0.1M CH_3COOH and 0.1M $NaHCOO$. Calculate the range of pH of this solution.

Q3.65

In a solution of 0.153 M CH_3COOH ($K_a = 1.8 \times 10^{-5}$). Calculate [H_3O^+].

Q3.66

In a Solution of 0.548M HCl ($K_a = 7.2 \times 10^{-4}$) and pure water, calculate pH.

Q3.67

In a 300 mL solution of 0.1 M $HClO_{2(aq)}$ calculate the pH change when adding 10 mL of 0.2 M $HCl_{(aq)}$ to the solution ($K_a = 1.1 \times 10^{-2}$).

Q3.68

A 55 mL solution is made up of 0.45 mmol $HClO_2$ and 6.0 mmol $KClO_2$. Calculate the pH.

Q3.69

In a buffer solution of 50 mL of 0.3 M H_3PO_4 and 25 mL of .3M NaH_2PO_4 with a pH of 1.82 what would the K_a of this solution be?

Q3.70

Between an indicator with a $K_{Hln} = 2 \times 10^{-4}$, an indicator with a $K_{Hln} = 2 \times 10^{-10}$, and an indicator with a $K_{Hln} = 2 \times 10^{-7}$, which would be used in a titration of strong acid and strong base to find the endpoint?

Q3.71

Bromophenol blue changes from yellow to blue-violet in the pH range 3-5. Which of the following titrations would this be best to use in: strong acid-strong base, strong acid-weak base, strong base-weak acid?

Q3.72

When 20mL of 0.05M KOH of is titrated with 0.05M HI, an indicator goes from yellow to red when 10mL of the weak acid is added. What is the pK_{Hln} of the indicator? Does this give the accurate endpoint of titration?

Q3.73

What is the pOH of a solution with 200mL of 0.007M HCl and 300mL of 0.02M $NaOH$?

Q3.74

Which will be greater, the volume of 0.2M $LiOH$ is needed to reach the equivalence point with 20mL of 0.2M HF or with 20mL of 0.2M CH_3COOH? What about their pH at the equivalence point?

Q3.75

Based on K_b, how do titrations curves of strong acids with weak bases differ?

Q3.76

Calculate the pH of the solution in the titration of 0.05M HBr with 40mL of 0.02M $CsOH$ when, 1) 5mL 2)10mL 3) 25mL of HBr is added.

Q3.77

Does 0.05M $NaHSO_4$ produce an acidic, basic, or neutral solution? (given that $pK_{a2} = 1.92$)

Q3.78

How can you obtain Na_3SO_4 from sulfuric acid and sodium carbonate? Write out equations.

Q3.79

Show by calculations that the stoichiometric concentration of CH_3COOH is 0.1 M is required to obtain an aqueous solution with the pH value of about 2.8 .

Q3.80

Determine the pH values of $NaH_2PO_{4\,(aq)}$ and $Na_2HPO_{4\,(aq)}$ when $pK_{a1} = 2.15$, $pK_{a2} = 7.20$, $pK_{a3} = 12.38$. Note that $H_2PO_4^-$ occurs simultaneously.

Q3.81

Define what the term simultaneously means in terms of hydrolysis. Determine whether a solution can be simultaneously (these don't need calculations).

a. 0.20M NH_3 and 0.20 NH_4Cl

b. 0.20 M $NaC_2H_3O_2$ and 0.116 M HI

c. 0.036 M C_6H_5COOH and 0.036 M NaC_6H_5COO

Q3.82

Determine the amount (in mL) of 6.0 M $NaOH$ that is required to adjust the pH of the initial buffer solution to a pH of 7.4.

Note that a student working with this buffer mixes together 400 mL of 1.80 M Na_2HPO_4 and 130 g of NaH_2PO_4.

Q3.83

What is the buffer range for a benzoic acid/ sodium benzoate buffer? [$Ka = 6.3 \times 10^{-5}$].

Q3.84

Define what a common ion effect is when a strong acid supplies the common ion H_3O^+, the equilibrium shifts which way to form more CH_3COOH? When a strong basic supplies the common ion OH^-, the equilibrium shifts which way to form more NH_3?

Q3.85

What is the effect on the pH of adding 0.0060 mol HCl to 0.3 L of a buffer solution that is 0.250 M CH_3COOH and 0.560 M $NaCH_3COO$?

Q3.86 (Questionable – please check question and answer)

Find the pH of 2.0×10^{-8}M HCl. Note that water makes a significant contribution to the $[H_3O^+]$. ($K_w = [H_3O^+][OH^-]$)

Q3.87

Define what ionization energy is and determine which of the following would decrease the ionization of acidic acid, $CH_3COOH_{(aq)}$: $NaCl$, $NaHCOO$, H_2SO_4, and $NaHCO_3$.

Q3.88

0.45M Hypochlorous acid ($HOCl$) with a $K_a = 2.9 \times 10^{-8}$ is mixed with 0.001M HCl.

a) Find $[H_3O^+]$

b) Find $[OH^-]$

c) Find $[OCl^-]$

d) Find $[Cl^-]$

Q3.89

0.3M $C_5O_5H_5N$ with a $K_b = 1.5 \times 10^{-9}$ is mixed with 0.015M C_5H_5NHI

a) Find $[OH^-]$

b) Find $[C_5H_5NH^+]$

c) Find $[I^-]$

d) Find $[H_3O^+]$

Q3.90

A solution of volume 0.25 L contains 0.2 moles of HCN and .004 moles CN^-.

a) What is the pOH?

b) If 0.25M $NaOH$ is added, what is the pH?

c) If .076 L of 3M HNO_3 is added, what is the pH?

Q3.91

A manual says that in order to obtain a buffer with a pH of 7.00 you have to mix 32L of 0.644M $HOCl$ with .7L of 0.406M OCl^-.

a) Show by calculation that the pH of this solution is 7.00

b) Would the pH remain at 7.00 if 1 liter of H_2O was added to the solution?

c) What will the pH be of the original 1.02L solution if 0.15L of 0.8M $NaOH$ is added?

d) What is the maximum volume of 0.8M $NaOH$ that can be added to the 1.02L buffer solution so that the pH does not change above 7.7?

Q3.92

Bromocresol green ($K = 2.1 \times 10^{-5}$), as this indicator change from yellow to blue, the pH ranges from 4-5. Without making detailed calculations, state what color the indicator will assume in each of the following solutions.

a) 0.3M $NaOH$

b) 0.02M $HClO$

c) 0.3M NH_3

d) 0.25M HI

e) 0.4M Na_2CO_2

f) 0.2M HCO_3 and 0.2M \(CO_3^-) (Buffer)

Q3.93

Two liquid solutions are mixed, 25ml of 0.73M HI and 10ml of 0.29M $Ca(OH)_2$. What is the pOH of the resulting solution?

Q3.94

Explain why the volume of 0.25M HCl required to reach the equivalence point in a titration of 50ml of BOH is the same whether it is a strong or a weak base, yet the pOH at the equivalence point is not the same.

Q3.95

Is the solution that is 0.3M Na_3PO_4 likely to be acidic, basic, or pH neutral? Why?

Q3.96

For the solution that is 0.330 M CH_3CH_2COOH that has K_a value to be 1.3×10^{-5} and 0.01M HI, calculate

1. (a) $[H_3O^+]$

2. (b) $[OH^-]$
3. (c) $[CH_3CH_2COO^-]$
4. (d) $[I^-]$

Q3.97

For a solution that is 0.654 M NH_3 and 0.202 M NH_4Cl, calculate $[H_3O^+]$, $[OH^-]$, $[NH_4^+]$ with $K_b = 1.8 \times 10^{-5}$.

Q3.98

Calculate the change in pH that results from adding (a) 0.300 mol $NaNO_2$ to 1.00 L of 0.200 M $HNO_{2(aq)}$; (b) 0.300 mol $NaNO_3$ to 1.00 L of 0.200M $HNO_{3(aq)}$.

Q3.99

A solution of volume 1L contains 0.500 mol $HCHO_2$ and 0.250 mol $NaHCOO$.

a) What is the pH of this solution?

b) If 0.1 mol $Ba(OH)_2$ is added to to the solution, what will be the pH?

c) If 10.0 mL of 12 M HCl is added to the original solution what will be the pH?

Q3.100

To obtain a $pH = 8.00$ you need to mix 35.00 mL of .220 M $NH_3$with 65.00 mL of .250 M NH_4Cl.

a) Show the calculation that the pH of this solution is 8.00.

b) Would you expect the pH of this solution to remain at $pH = 8.00$ if the 100 mL of the buffer were diluted to 1.00 L? 1000L? Explain.

c) What will be the pH of the solution if 0.20 mL of 1.00 M HCl is added?

Q3.101

What stoichiometric concentration of the indicated substance is required to obtain an aqueous solution with the pH value shown?

a) $Ba(OH)_2$ for $pH = 10.00$

b) CH_3COOH in 0.300 M $NaCH_3COO$ for $pH = 4.50$?

Q3.102

You are asked to bring the pH of 1.00 L of 0.500 M $NH_4Cl_{(aq)}$ to 7.00. How many drops (1 drop = 0.05 mL) of which of the following solutions would you use: 10.0 M HCl or 10.0 M NH_3.

Q3.103

A handbook lists various procedures for preparing buffer solutions. To obtain a pH of 9, the handbook says to mix 36.0 mL of 0.200 M NH_3 with 64 mL of 0.200 M NH_4Cl.

a.) Prove that $pH = 9$ is correct

b.) Would the pH remain at 9 if the 100 mL buffer solution was 200 L? Why or why not?

Q3.104

What are the main principal features of a titration curve for the titration of a strong acid with a strong base?

Q3.105

The pH of a solution of 25 g of malonic acid in 0.300 L is 2.68, with a K_{a1} value of 4.5×10^{-12}. What is $[HM^-]$ in the malonic acid solution?

Q3.106

Show the derivation of the Henderson-Hasselbalch equation.

Solutions

S1

$$Moles\ of\ HCl\ added = Moles\ of\ H_3O^+ = 0.01L(0.005M) = 5 \times 10^{-4}\ mol \tag{8.2.6.3}$$

$$Moles\ of\ HF\ added = (0.05L)(0.325M) = 0.01625\ mol \tag{8.2.6.4}$$

$$Total\ Volume = 50mL + 10mL = 60mL = 0.06L \tag{8.2.6.5}$$

$$M_{H_3O^+\ initial} = \frac{5 \times 10^{-4}\ mol}{0.06L} = 0.00833M \tag{8.2.6.6}$$

$$M_{HF} = \frac{0.01625\ mol}{0.06L} = 0.271M \tag{8.2.6.7}$$

$$HF_{(aq)} + H_2O_{(l)} \rightleftharpoons F^-_{(aq)} + H_3O^+_{(aq)} \tag{8.2.6.8}$$

ICE Table	$HF_{(aq)}$	$H_2O_{(l)}$	$F^-_{(aq)}$	$H_3O^+_{(aq)}$
Initial	0.271 M	-	0	0.0083 M
Change	-x	-	+x	+x
Equilibrium	(0.271 –x) M	-	x	(0.00833 +x) M

$$K_a = \frac{[H_3O^+][F^-]}{[HF]} = 6.6 \times 10^{-4} = \frac{x(0.00833 + x)}{0.271 - x} \tag{8.2.6.9}$$

Interpret the equation above we have:

$$6.6 \times 10^{-4}(0.271 - x) = 0.00833x + x^2 \tag{8.2.6.10}$$

$$x^2 + 0.00899x - 1.789 \times 10^{-4} = 0 \tag{8.2.6.11}$$

$$x = 0.009615M \tag{8.2.6.12}$$

a)

$$[H_3O^+] = 0.00833 + x = 0.00833 + 0.009615 = 0.0179M \tag{8.2.6.13}$$

b) At room temperature $pH + pOH = 14$,

$$pH = -log[H_3O^+] = -log(0.0179) = 1.75 \tag{8.2.6.14}$$

$$pOH = -log[OH^-] = 14 - 1.75 = 12.25 \tag{8.2.6.15}$$

Therefore,

$$[OH^-] = 10^{-12.25} = 5.623 \times 10^{-13}M \tag{8.2.6.16}$$

c)

$$[HF] = 0.271 - x = 0.271 - 0.096165 = 0.2614M \tag{8.2.6.17}$$

d)

$$[Cl^-] = [HCl] = 0.00833M \tag{8.2.6.18}$$

S2

$$NH_3 + H_2O \rightleftharpoons H_3O^+ + N_3^- \tag{8.2.6.19}$$

ICE Table	NH_3	H_2O	H_3O^+	N_3^-
Initial	0.138 M	-	0	0.101 M
Change	-x	-	+x	+x
Equilibrium	(0.138-x)	-	x	0.101 +x

$$K_a = \frac{[H_3O^+][[N_3^-]}{[NH_3]} = 1.9 \times 10^{-5} = \frac{x(0.101 + x)}{(0.138 - x)} \approx \frac{0.101x}{0.138} \tag{8.2.6.20}$$

$$x \approx 2.6 \times 10^{-7} \tag{8.2.6.21}$$

The assumption that x<< 0.101 is correct. $[H_3O^+] = 2.6 \times 10^{-7}\ M$

b)

$$[N_3^-] = (0.101 + x) = (0.101 + 2.6 \times 10^{-7)}) \approx 0.101\ M \tag{8.2.6.22}$$

c)

$$[K^+] = [[N_3^-] \approx 0.101\ M \tag{8.2.6.23}$$

d)

$$[OH^-] = \frac{K_w}{[H_3O^+]} = \frac{(1.0 \times 10^{-14})}{(2.6 \times 10^{-7})} = 3.8 \times 10^{-8}\ M \tag{8.2.6.24}$$

S3

a) First, determine the pH of 0.150 M HNO_2.

$$HNO_{2(aq)} + H_2O_{(l)} \rightleftharpoons NO_{2(aq)}^- + H_3O_{(aq)}^+ \tag{8.2.6.25}$$

ICE Table	$HNO_{2(aq)}$	$H_2O_{(l)}$	$NO_{2(aq)}^-$	$H_3O_{(aq)}^+$
Initial	0.150	-	0	0
Change	-x	-	+x	+x
Equilibrium	0.150-x	-	x	x

$$K_a = \frac{[NO_2^-][H_3O^+]}{[HNO_2]} = 7.2 \times 10^{-4} = \frac{x^2}{0.150 - x} \tag{8.2.6.26}$$

Through a successful approximation:

$$x \approx 0.01004\ M = [H_3O^+] \tag{8.2.6.27}$$

Thus $pH \approx -\log(0.01004) = 2.0$

When 0.150 mol $LiNO_2$ is added to 1.00 L of a 0.150 M HNO_2, a solution with $[NO_2^-] = 0.150\ M = [HNO_2]$ is formed. To find the change in the pH we use the Henderson-Hasselbalch approximation at equilibrium

$$pH = pK_a = -\log(7.2 \times 10^{-4}) = 3.14 \tag{8.2.6.28}$$

Thus the addition has caused pH to increase by 1.14

b) $LiNO_3$ contributes nitrate ions to the solution. Since there is no molecular $HNO_{3(aq)}$ in equilibrium with the hydrogen and nitrate ions, there is no equilibrium to be shifted by the addition of the nitrate ions. Thus, the $[H_3O^+]$ and the pH are not affected by the addition of $LiNO_3$ to the solution. The pH changes are not the same because unlike the first solution, the second solution does not have an equilibrium to shift, just a total ionic strength.

S4

a) The pH of the solution can be determined by the Henderson-Hasselbalch equation.

$$pH = pK_a + log\frac{[ClO_2^-]}{[HClO_2]} = -log(1.1 \times 10^{-2}) + log\frac{(\frac{7.25\ mmol}{50.0\ mL})}{(\frac{12.5\ mmol}{50.0\ mL})} \tag{8.2.6.29}$$

$$pH = 1.96 - 0.24 = 1.72 \tag{8.2.6.30}$$

b)

$$Ca(OH)_2 \rightarrow Ca^{2+} + 2OH^- \tag{8.2.6.31}$$

$$Amount\ of\ added\ OH^- = 1.0\ mmol\ Ca(OH)_2 \times \frac{2OH^-}{Ca(OH)_2} = 2.0\ mmol \tag{8.2.6.32}$$

The additional OH^- reacts with the chlorous acid and produces chlorite ion.

$$HClO_2 + OH^- \rightleftharpoons ClO_2^- + H_2O \tag{8.2.6.33}$$

ICE Table	$HClO_2$	OH^-	ClO_2^-	H_2O
Initial	12.5 mmol	2 mmol	7.25 mmol	-
Change	- 2 mmol	- 2 mmol	+ 2 mmol	-
Equilibrium	10.5 mmol	0	9.25 mmol	-

$$pH = pK_a + \log(\frac{[ClO_2^-]}{[HClO_2]}) \tag{8.2.6.34}$$

$$= -log(1.1 \times 10^{-2}) + \log \frac{(\frac{9.25\ mmol}{50.0\ mL})}{(\frac{10.5\ mmol}{50.0\ mL})} \tag{8.2.6.35}$$

$$= 1.96 - 0.055 = 1.90 \tag{8.2.6.36}$$

c)

$$Amount\ of\ added\ H_3O^+ = 2.00\ mL \times (6\ M) = 12\ mmol\ H_3O^+ \tag{8.2.6.37}$$

The additional H_3O^+ reacts with the chlorite ion to produce chlorous acid.

$$ClO_2^- + H_3O^+ \rightleftharpoons HClO_2 + H_2O \tag{8.2.6.38}$$

ICE Table	ClO_2^-	H_3O^+	$HClO_2$	H_2O
Initial	7.25 mmol	12 mmol	12.5 mmol	-
Change	- 7.25 mmol	- 7.25 mmol	+ 7.25 mmol	-
Equilibrium	0	4.25 mmol	19.75 mmol	-

The buffer's capacity has been exceeded. The excess strong acid present determines the pH of the solution.

$$[H_3O^+] = \frac{4.75mmol}{50.0\ mL + 2.0\ mL} = 0.091\ M \tag{8.2.6.39}$$

$$pH = -log\ [H_3O^+] = -log(0.091) = 1.04 \tag{8.2.6.40}$$

S5

a) Use the Henderson-Hasselbalch equation to determine the pH of the solution. The volume of the total solution is

$$18.0\ mL + 72.0\ mL = 100.0\ mL \tag{8.2.6.41}$$

$$pKa = 14 - pKb = 14 - 8.82 = 5.18 \tag{8.2.6.42}$$

$$[C_5H_5N] = \frac{18.0\ mL \times 0.300M\ C_5H_5N}{100.0\ mL} = \frac{5.4\ mmol}{100.0\ mL} = 0.054\ M \tag{8.2.6.43}$$

$$[C_5H_5NH^+] = \frac{72.0\ mL \times 0.300M}{100.0\ mL} = 0.216 \tag{8.2.6.44}$$

$$pH = pKa + log\frac{[C_5H_5N]}{[C_5H_5NH^+]} = 5.18 + log\frac{0.054\ M}{0.216\ M} = 4.57 \approx 4.60 \tag{8.2.6.45}$$

b) The solution has $[OH^-] = 10^{-9.43} = 3.7 \times 10^{-10}\ M$

The Henderson-Hasselbalch equation assumes that:

$$[C_5H_5N] \ll 1.5 \times 10^{-9} \ll [C_5H_5NH^+] \tag{8.2.6.46}$$

If the solution is diluted to 500.00 mL, $[C_5H_5N] = 0.0108\ M$, and $[C_5H_5NH^+] = 4.3 \times 10^{-3}\ M$. Only one of the $[C_5H_5N]$ is consistent with this assumption. So the pH would not remain the same.

If the solution was diluted to 1.00ml, $[C_5H_5N] = 0.0054\ M$, and $[C_5H_5NH^+] = 2.2 \times 10^{-3}\ M$. Again, only the $[C_5H_5N]$ is consistent with the assumption, so in this case as well, the pH would not remain the same.

c) The 0.40 mL of added 1.00 HBr does not significantly change the volume of the solution. However, it does add $0.40\ mL \times 1.00\ M\ HBr = 0.40\ mmol\ H_3O^+$. This added H_3O^+ reacts with C_5H_5N, decreasing its amount from $5.4\ mmol\ C_5H_5N$ to $5.0\ mmol\ C_5H_5N$, and increasing the amount of $C_5H_5NH^+$ from $21.6\ mmol$ to $22\ mmol$.

$$pH = 5.18 + log\frac{(\frac{5.00\ mmol\ C_5H_5N}{100.40\ mL})}{(\frac{22.00\ mmol C_5H_5NH^+}{100.40\ mL})} = 4.54 \tag{8.2.6.47}$$

d) From part c) we see that the total volume of the solution does not affect the pOH of the solution as long as the Henderson-Hasselbalch equation is observed. Let x represent the number of mmols of H_3O^+ added, through $1.00\ M\ HBr$. This increases $C_5H_5NH^+$ and decrease C_5H_5N.

$$pH = 4.4 = 5.18 + log\frac{5.40 - x}{21.6 + x} \tag{8.2.6.48}$$

$$log\frac{5.40 - x}{21.6 + x} = 4.4 - 5.18 = -0.78 \tag{8.2.6.49}$$

By inverting we get:

$$\frac{21.6 + x}{5.40 - x} = 10^{0.78} = 6.03 \tag{8.2.6.50}$$

$$21.6 + x = 6.03(5.4 - x) = 32.6 - 6.03x \tag{8.2.6.51}$$

$$x = \frac{32.6 - 21.6}{1.00 + 6.03} = 1.6\ mmol\ H_3O^+ \tag{8.2.6.52}$$

$$Vol\ 1.00\ M\ HBr = 1.6\ mmol\ H_3O^+ \times \frac{1\ mmol\ HBr}{1\ mmol\ H_3O^+} \times \frac{1\ mL\ soln}{1.00\ mmol\ HBr} = 1.6\ mL\ 1.00\ M\ HBr \tag{8.2.6.53}$$

S6

Solve for the pK_{HIn} using the usual formula; $pK_{HIn} = log(K_{HIn})$

The pH that gives color change is within 1 pH of this value. For example, Bromphenol Blue is an acidic indicator because, since its pK value is 3.9, it has a color change range of between 2.9 and 4.9, all acidic pH values. Furthermore, Bromthymol Blue changes in neutral solutions, and Thymolphthalein changes in basic solutions.

What is the approximate pH of a solution that turns blue in Bromthymol Blue

As we learned from the first problem, the Brothymol Blue is changes in neutral pH range. So, we can safely say that the pH is somewhere between 6.1 and 8.1

S7

a. $Mg(OH)_2$: This solution is basic, so the acidic indicator will show its basic color, which is blue.
b. HCl: This solution is acidic, it will show its acidic color, yellow
c. HF: This is a weak, but will still show the yellow acidic color

S8

$$[Na(OH)_2]\ for\ pH = 10.92 \tag{8.2.6.54}$$

$$pOH = 14 - 10.92 = 3.08 \tag{8.2.6.55}$$

$$[OH^-] = 10^{-3.08} = 8.32 \times 10^{-4} \tag{8.2.6.56}$$

$$[Na(OH)_2] = \frac{8.32 \times 10^{-4}\ mol\ OH^-}{1\ L} \times \frac{1\ mol\ [Na(OH)_2]}{2\ mol\ OH^-} = 4.16 \times 10^{-4} \tag{8.2.6.57}$$

S9

A buffer solution will react with both acids and bases to prevent significant changes in pH. The chlorine is a spectator ion in the ammonium chloride and is therefore irrelevant for the purposes of this question.

$$NH_3 + H_3O^+ \rightleftharpoons NH_4^+ + H_2O \tag{8.2.6.58}$$

$$NH_4^+ + OH^- \rightleftharpoons NH_3 + H_2O \tag{8.2.6.59}$$

This is a buffer solution because based on these reactions that are occur, should either an acid or base be added.

We can use the Henderson-Hasselbach apporximation:

$$pK_a = -log(1.8 \times 10^{-5}) = 4.745 \tag{8.2.6.60}$$

$$pK_b = 14 - pK_a = 9.255 \tag{8.2.6.61}$$

$$pH = 9.255 + log(\frac{0.3}{0.4}) = 9.130 \tag{8.2.6.62}$$

To find the new pH, find the number of moles of each compound using the new volume.

- Moles $NH_3 = 0.3\ M \times 1\ L = 0.3\ mol$
- Moles of $NH_4^+ = 0.4\ M \times 1\ L = 0.4\ mol$
- Moles of $OH^- = 0.2\ M \times 1\ L = 0.2\ mol$

New number of moles using ice table and identifying limiting reactant:

- $0.2\ mol NH_4^+$
- $0\ OH^-$
- $0.1\ mol\ NH_3$

$$pH = 9.255 + \log(\frac{0.1}{0.05}) = 9.556 \tag{8.2.6.63}$$

S10

From experiments 1 and 2:

$$[HF] + [F^-] = 0.35M \tag{8.2.6.64}$$

$$5 \times (.005\ M) + [F^-] = 0.35M \tag{8.2.6.65}$$

$$[F^-] = 0.325M \tag{8.2.6.66}$$

$$[HF] = 0.025M \tag{8.2.6.67}$$

$$[H_3O^+] = 10 - (pK_w - pOH) \tag{8.2.6.68}$$

$$pOH = -log(0.5 - 0.325) = 0.757 \tag{8.2.6.69}$$

$$[H_3O^+] = 10 - (14.94 - .757) = 6.56 \times 10^{-15} \tag{8.2.6.70}$$

$$K_a = \frac{[H_3O^+][F^-]}{[HF]} = 8.52989 \times 10^{-14} \tag{8.2.6.71}$$

$$pK_a = 13.07 \tag{8.2.6.72}$$

S11

The answer is D. Since Na is a spectator ion, CN^- is left to react with the H_3O^+ created from the initial H_2S reaction. This causes the reaction to shift to the right, creating more HS- ions.

S12

Equation	CH_3CH_2COOH	+	$H_2O(l)$	↔	$CH_3CH_2COO^-$	+	H_3O^+
Initial	0.330 M		--		0		0.01M
Change	-x		--		+x		+x
Equilibrium	(0.330 M – x) M		--		x		(0.01 + x) M

$$K_a = \frac{x \times (0.01 + x)}{(0.330\ M – x)} \approx \frac{0.01x}{0.330} \tag{8.2.6.73}$$

$$[CH_3CH_3COO^-] = 4.3 \times 10^{-4}\ M \tag{8.2.6.74}$$

$$[H_3O^+] = [HI^-] = 0.0104\ M \tag{8.2.6.75}$$

$$[OH^-] = \frac{K_w}{[H_3O^+]} \tag{8.2.6.76}$$

$$[OH^-] = 9.6 \times 10^{-13}\ M \tag{8.2.6.77}$$

S13

$$K_b = 1.8 \times 10^{-5} \tag{8.2.6.78}$$

Equation	NH_3	+	$H_2O(l)$	↔	NH_4^+	+	OH^-
Initial	0.654 M		---		0.202 M		0
Change	-x		---		+x		+x
Equilibrium	(0.654 M – x) M		---		(0.202+ x) M		x

$$K_b = x\times \frac{(0.202 + x)}{(0.654\ M – x)}\approx \frac{0.202x}{0.330}$$

$$[OH^-] = 2.9 \times 10^{-5}\ M \tag{8.2.6.79}$$

$$[NH_4^+] = [Cl^-] = 0.202\ M \tag{8.2.6.80}$$

$$[OH^-] = \frac{K_w}{[H_3O^+]} \tag{8.2.6.81}$$

$$[H_3O^+] = 3.4 \times 10^{-10}\ M \tag{8.2.6.82}$$

S14

a)

Equation	HNO_2	+	$H_2O(l)$	↔	HNO_2^-	+	H_3O^+
Initial	0.200 M		--		0		0
Change	-x		--		+x		+x
Equilibrium	(0.200 M – x) M		--		x		x

$$K_a = 7.2 \times 10^{-4} \tag{8.2.6.83}$$

$$K_a = \frac{x^2}{(0.200\ M – x)} \approx \frac{x^2}{0.200} \tag{8.2.6.84}$$

$$x = 0.012\ M \tag{8.2.6.85}$$

$$pH = -log[H_3O^+] \tag{8.2.6.86}$$

$$pH = 1.9 \tag{8.2.6.87}$$

$$pH = pK_a - (-log[M]) \tag{8.2.6.88}$$

$$\delta pH = 1.22 \tag{8.2.6.89}$$

b) Since there is no net change in equilibrium just a shift in ionic strength thus the pH of the second solution will be different.

S15

a)

$$pH = pK_a + log\frac{[base]}{[acid]} \tag{8.2.6.90}$$

$$pH = 3.44 \tag{8.2.6.91}$$

b)

$$OH^- = 0.1\ mol Ba(OH)_2 \times \frac{2\ mol\ OH^-}{1\ mol\ Ba(OH)_2} = 0.2\ mol\ OH^- \tag{8.2.6.92}$$

Equation	$HCHO_2$	+	OH^-	↔	CHO_2^-	+	$H_2O_{(l)}$
Initial	0.5 mols		0.2 mols		0.250 mols		0
Change	-0.2 mols		-0.2 mols		0.2 mols		0
Equilibrium	0.3 mols		0		0.45 mols		0

$$pH = pK_a + log\frac{[base]}{[acid]} \tag{8.2.6.93}$$

$$pH = 3.92 \tag{8.2.6.94}$$

c)

$$H_3O^+ = 0.01L \times 12M\ HCl = 0.12\ mol\ H_3O^+ \tag{8.2.6.95}$$

Equation	CHO_2^-	+	H_3O^+	↔	$HCHO_2$	+	$H_2O_{(l)}$
Initial	0.25 mol				0.50 mol		--
Change	-0.25 mol		-0.25 mol		+0.25 mol		--
Equilibrium	0		0.12 mol		0.75 mol		--

$$H_3O^+ = \frac{0.12\ mol}{(1L + 0.01L)} = 0.119\ M \tag{8.2.6.96}$$

$$pH = 0.92 \tag{8.2.6.97}$$

S16

a)

$$pH = pK_a + log\frac{[base]}{[acid]} \tag{8.2.6.98}$$

$$[NH_3] = 0.035\ L \times \frac{0.220\ M\ NH_3}{0.1\ L} = 0.077\ M \tag{8.2.6.99}$$

$$[NH_4^+] = 0.065 \times \frac{0.250\ M}{0.1\ L} = 0.163M \tag{8.2.6.100}$$

$$pH = 9.00 \tag{8.2.6.101}$$

b) The pH would change since adding more solution will dilute the concentration and thus reduce the pH to something near $pH = 7$.

c) pH should still be 9 since the amount of acid is so insignificant

S17

a)

Indicator	Changes color in
Bromphenol blue	Acidic
Bromcresol green	Acidic
Bromthymol blue	Neutral
2,4 – Dinitrophenol	Acidic
Chlorphenol red	Acidic
Thymolphthalein	Basic

b) Bromcresol green would be green at $pH = 4.7$

Chlorphenol red would be orange at $pH = 6.0$

S18

1. a) red
2. b) yellow
3. c) yellow
4. d) yellow
5. e) red
6. f) yellow

S19

$$Amount\ H_3O^+ = 0.075\ L \times 0.333\ M \times \frac{2\ mol H_3O^+}{1\ mol\ H_2SO_4} = 0.05\ mol \tag{8.2.6.102}$$

$$Amount\ OH^- = 0.025\ L \times 0.05\ M \times \frac{1\ mol}{1\ mol} = 0.0013 mol \tag{8.2.6.103}$$

$$[H_3O^+] = \frac{mole\ H_3O^+}{L\ solution} = 0.487\ mole \tag{8.2.6.104}$$

$$pH = -log[H_3O^+] \tag{8.2.6.105}$$

$$pH = 0.31 \tag{8.2.6.106}$$

S20

Because the molarities of both solutions is the same all of the base will react with the acid. Depending on the strength of the acid at the equivalence point the amount of moles of acid equals the amount of moles of base therefore the volume doesn't change but the pH will depending on the type of acid or base.

S21

$$K_a = \frac{x^2}{0.05} \tag{8.2.6.107}$$

$$x = [H_3O^+] \tag{8.2.6.108}$$

$$K_b = \frac{K_w}{K_a} = \frac{x^2}{0.05} \tag{8.2.6.109}$$

a)

$$[H_3O^+] = 0.019\ M \tag{8.2.6.110}$$

$$pH = 1.7 \tag{8.2.6.111}$$

$$x = [OH^-] = \sqrt{0.05 \times \frac{K_w}{K_a}} = 2.7 \times 10^{-7} \tag{8.2.6.112}$$

$$pOH = 6.57 \tag{8.2.6.113}$$

$$pH = 7.42 \tag{8.2.6.114}$$

b)

$$pH = 8.11 \tag{8.2.6.115}$$

c)

$$pH = 10.2 \tag{8.2.6.116}$$

S22

The solution should be basic due to the hydrolysis of the sulfide anion of a weak acid.

S23

a)

$$H_3PO_{4(aq)} + CO_3^{2-} \rightleftharpoons H_2PO_{4(aq)}^- + HCO_{3(aq)}^- \tag{8.2.6.117}$$

$$H_2PO_{4(aq)}^- + CO_3^{2-} \rightleftharpoons HPO_{4(aq)}^{2-} + HCO_{3(aq)}^- \tag{8.2.6.118}$$

$$HPO_{4(aq)}^{2-} + OH_{(aq)}^- \rightleftharpoons PO_{4(aq)}^{3-} + H_2O_{(l)} \tag{8.2.6.119}$$

b) The inexpensive base is used in the first 2 ionizations and produces the bulk of the products. In the last ionization $NaOH$ must be used because the solution is not strong enough to pull the last hydrogen ion.

S24

$$Malonic\ acid = 104.06 \frac{g}{mol} \tag{8.2.6.120}$$

$$Moles\ malonic\ acid = 19.5g \times \frac{1\ mol}{104.06\ g} = 0.187\ moles \tag{8.2.6.121}$$

$$Concentration = \frac{0.187\ moles}{0.250\ L} = 0.784M \tag{8.2.6.122}$$

Equation	H_2A	+	H_2O	↔	HA^-	+	H_3O^+
Initial	0.784 M		-		0		0
Change	-x		-		+x		+x
Equilibrium	(0.784 – x) M		-		x		x

$$K_a = \frac{x^2}{(0.784 - x)} \tag{8.2.6.123}$$

$$pH = 1.47 \tag{8.2.6.124}$$

$$[H_3O^+] = 10^{-1.47} = 0.034\ M \tag{8.2.6.125}$$

$$K_{a1} = 0.0016 \tag{8.2.6.126}$$

$$K_{a2} = \frac{x^2}{0.300 - x} \tag{8.2.6.127}$$

$$pH = 4.26 \tag{8.2.6.128}$$

$$[H_3O^+] = 10^{-4.26} = 5.5 \times 10^{-5}\ M \tag{8.2.6.129}$$

$$K_{a2} = 1 \times 10^{-8} \tag{8.2.6.130}$$

S25

1. a) No
2. b) No
3. c) Yes
4. d) Yes
5. e) Yes
6. e) No

S26

a)

$$\frac{[conjugatebase]}{[weakacid]} = \frac{(equil.Amountconj.Base)}{(equil.Amountweakacid)} = \frac{(F \times initialAmt.weakacid)}{(1–F) \times initialAmountweakacid} = \frac{F}{1–F} \tag{8.2.6.131}$$

$$pH = pK_a + log\frac{F}{(1–F)} \tag{8.2.6.132}$$

b)

$$pH = 10.00 + log\frac{0.27}{(1–0.23)} = 9.56 \tag{8.2.6.133}$$

S27

a. $for\ \ H_2PO_4^- : pH = \frac{1}{2}(pK_{a1} + pK_{a2})$

a. $for\ \ HPO_4^{2-} : pH = \frac{1}{2}(pK_{a2} + pK_{a3})$

S28

a)

$$CHO^-_{2(aq)} + H_{3(aq)}O^+ \rightleftharpoons HCHO_{2(aq)} + H_2O_{(l)} \tag{8.2.6.134}$$

$$HC_2H_3O_{2(aq)} + OH^-_{(aq)} \rightleftharpoons H_2O_{(l)} + C_2H_3O^-_{2(aq)} \tag{8.2.6.135}$$

Since neither species effects the pH significantly we call this solution a buffer solution.

b)

$$HCHO_{2(aq)} + H_2O_{(l)} \rightleftharpoons CHO^-_{2(aq)} + H_3O^+_{(aq)} \tag{8.2.6.136}$$

$$HC_2H_3O_{2(aq)} + H_2O_{(l)} \rightleftharpoons C_2H_3O^-_{2(aq)} + H_3O^+_{(aq)} \tag{8.2.6.137}$$

$$[Na^+] = 0.250 \tag{8.2.6.138}$$

$$[OH^-] = 0 \tag{8.2.6.139}$$

$$[H_3O^+] = x \tag{8.2.6.140}$$

$$[C_2H_3O_2^-] = y \tag{8.2.6.141}$$

$$[CHO_2^-] = z \tag{8.2.6.142}$$

$$[HC_2H_3O_2] = 0.200–y \tag{8.2.6.143}$$

$$[HCHO_2] = 0.250–z \tag{8.2.6.144}$$

$$K_A = 1.8 \times 10^{-5} = \frac{(xy)}{0.150–y} \tag{8.2.6.145}$$

$$K_F = 1.8 \times 10^{-4} = \frac{xz}{0.250 - z} \tag{8.2.6.146}$$

$$y = \frac{0.150 \times K_A}{K_A + x} \tag{8.2.6.147}$$

$$z = \frac{0.250 \times K_F}{K_F + x} \tag{8.2.6.148}$$

$$[H_3O^+] = 4.0 \times 10^{-5}\ M \tag{8.2.6.149}$$

S29

$$H_2O_{2(aq)} + H_2O_{(l)} \rightleftharpoons H_3O^+_{(aq)} + HO^-_{2(aq)} \tag{8.2.6.150}$$

$$[H_2O_2] + [HO_2^-] = 0.259\ M \tag{8.2.6.151}$$

$$[HO_2^-] = 0.235\ M \tag{8.2.6.152}$$

$$[H_2O_2] = 0.0242\ M \tag{8.2.6.153}$$

$$[H_3O^+] = 10^{-(pK_w - pOH)} = 7.7 \times 10^{-14} \tag{8.2.6.154}$$

$$K_a = \frac{(7.7 \times 10^{-14})(0.235)}{(0.0242)} = 7.4 \times 10^{-13} \tag{8.2.6.155}$$

$$pK_a = 12.14 \tag{8.2.6.156}$$

$$[H_2O_2] + [HO_2^-] = 0.123\ M \tag{8.2.6.157}$$

$$[HO_2^-] = 0.1096\ M \tag{8.2.6.158}$$

$$[H_2O_2] = 0.0134\ M \tag{8.2.6.159}$$

$$[H_3O^+] = 10^{-(pKw - pOH)} = 7.41 \times 10^{-14} \tag{8.2.6.160}$$

$$K_a = \frac{(7.41 \times 10^{-14})(0.1096)}{(0.0134)} = 6.06 \times 10^{-13} \tag{8.2.6.161}$$

$$pK_a = 12.22 \tag{8.2.6.162}$$

$$Average\ pK_a = 12.17 \tag{8.2.6.163}$$

S30

d, because it is a weak base and will shift the formic acid ionization equilibrium to the right.

S31

$$pH = -log[H_3O^+] \tag{8.2.6.164}$$

$$3.2 = -log[H_3O^+] \tag{8.2.6.165}$$

$$[H_3O^+] = 6.31 \times 10^{-4} \tag{8.2.6.166}$$

S32

$$HC_2H_3O_{2(aq)} + H_2O_{(l)} \rightleftharpoons C_2H_3O^-_{2(aq)} + H_3O^+_{(aq)} \tag{8.2.6.167}$$

ICE Table	$HC_2H_3O_{2(aq)}$	$H_2O_{(l)}$	$C_2H_3O^-_{2(aq)}$	$H_3O^+_{(aq)}$
Initial	0.35 M	-	0.62 M	0
Change	-x	-	+x	+x
Equilibrium	0.35-x	-	0.62+x	x

$$K_a = 1.8 \times 10^{-5} = \frac{(0.62 + x)(x)}{(0.35 - x)} \tag{8.2.6.168}$$

Assume: $x << 0.62$

$$K_a = 1.8 \times 10^{-5} = \frac{0.62x}{0.35} \tag{8.2.6.169}$$

$$x = 1.02 \times 10^{-5} = [H_3O^+] \tag{8.2.6.170}$$

Definition of pH

$$pH = -log[H_3O^+] \tag{8.2.6.171}$$

$$pH = -\log(1.02 \times 10^{-5}) = 4.99 \tag{8.2.6.172}$$

S33

$$pH = pKa + log\frac{[base]}{[acid]} \tag{8.2.6.173}$$

Solve for molarities:

$HCHO_2$ is 0.227 and $NaCHO2$ is 0.09 fill in were appropriate in formula and…

$$pH = 4.14 \tag{8.2.6.174}$$

S34

$$K_b = \frac{[NH_4^+][OH^-]}{[NH_3]} = 1.8 \times 10^{-5} \tag{8.2.6.175}$$

Since $NH_3 + H_2O \rightleftharpoons NH_4^+ + OH^-$,

$$[NH_4^+] = [OH^-] \tag{8.2.6.176}$$

$$Let\ x = [OH^-] = [NH_4^+] \tag{8.2.6.177}$$

$$K_b = \frac{(x)(x)}{(7.00 \times 10^{-2} - x)} = 1.8 \times 10^{-5} \tag{8.2.6.178}$$

Solving for x using the quadratic formula,

$$x = 1.11 \times 10^{-3}\ M\ OH^- \tag{8.2.6.179}$$

Hence:

$$pOH = -log[OH^-] = 2.95 \tag{8.2.6.180}$$

$$pH = 14 - pOH = 11.05 \tag{8.2.6.181}$$

So the pH of a 7.00×10^{-2} M solution of ammonia is 11.05

S35

a. $pH = 6.0$
b. $pH = 3.0$
c. $pH = 8.0$

S36

formula: $pH = -log[H_3O^+]$

$$HCl \rightarrow H^+ + Cl^- \tag{8.2.6.182}$$

a)

$[H^+] = [H_3O^+] = 0.000014\ M$

$pH = -log(0.000014) = 4.85$

So the indicator will be blue.

b)

$pH = -log(.00014) = 3.85$

So the indicator will remain red.

c)

$pH = -log(.0014) = 2.85$

So the indicator will remain red.

d)

$pH = -log(.0000014) = 5.85$

So the indicator will turn blue

S37

An indicator is a weak acid and can therefore alter the pH of the mixture if added in excess amounts

S38

A point at which both acid and base have been consumed and neither in excess

S39

Whether strong or weak acid, the necessary amount of HA is the same regardless of a strong or weak acid, but the pH at the equivalence point is not the same

S40

$$4.04 = pK_a + log\frac{0.020}{0.205} \tag{8.2.6.183}$$

$$pK_a = 5.05 \tag{8.2.6.184}$$

$$K_a = 8.90 \times 10^{-6} \tag{8.2.6.185}$$

S41

$$(150ml)(0.100M) = 15\ mmol\ NaOH \tag{8.2.6.186}$$

$$20 - 15 = \frac{5}{50 + 200} = 0.02M = [NaOH] \tag{8.2.6.187}$$

$$pOH = -log(0.02) = 1.70 \tag{8.2.6.188}$$

$$pH = 14 - 1.70 = 12.3 \tag{8.2.6.189}$$

S42

Since sodium ions do not affect the pH of a solution, only the iodine ion needs to be considered. The iodide ion is an anion, meaning in an aqueous solution it will take an H^+ ion from water to form HI and OH^-. Therefore, the solution will be basic.

S43

$pH = 7$

S44

$$pK_a + pK_b = 14 \tag{8.2.6.190}$$

$$pK_a + 4.8 = 14 \tag{8.2.6.191}$$

$$pK_a = 9.2 \tag{8.2.6.192}$$

$$pH = pK_a + log\frac{[conjugate\ base]}{[acid]} \tag{8.2.6.193}$$

$$pH = 9.2 + log(1) \tag{8.2.6.194}$$

$$pHa = 9.2 \tag{8.2.6.195}$$

S45

A solution can be prepared with equal conjugate base and weak acid but would not form the given pH because the buffer ratio would be 1.00 making the $pH = pK_a = 9.26$.

S46

$$HC_2H_3O_{2(aq)} + H_2O_{(l)} \rightleftharpoons C_2H_3O^-_{2(aq)} + H_3O^+_{(aq)} \tag{8.2.6.196}$$

ICE Table	$HC_2H_3O_{2(aq)}$	$H_2O_{(l)}$	$C_2H_3O^-_{2(aq)}$	$H_3O^+_{(aq)}$
Initial	0.50M	-	0.50M	0
Change	-x	-	+x	+x
Equilibrium	0.50-x	-	0.50+x	x

$$1.8 \times 10^{-5} = \frac{(0.50 + x)x}{0.50 - x} \tag{8.2.6.197}$$

$$x = 1.8 \times 10^{-5} \tag{8.2.6.198}$$

$$pH = -\log(1.8 \times 10^{-5}) = 4.74 \tag{8.2.6.199}$$

S47

$NaOH$ is a base, so an acid must be used to neutralize the solution, therefore HBr is the correct substance to use. $NaOH$ and HBr are both strong acids/bases, so the stoichiometric ratio between them is 1:1.

$$Moles\ NaOH = (0.325L)(0.452M) = 0.147\ moles\ NaOH \tag{8.2.6.200}$$

$$Volume\ HBr = \frac{0.147\ mol}{5.00\ M} = 0.0280\ L = 28.0\ mL \tag{8.2.6.201}$$

S48

$$HCN_{(aq)} + H_2O_{(l)} \rightleftharpoons H_3O^+_{(aq)} + CN^-_{(aq)} \tag{8.2.6.202}$$

$$6.2 \times 10^{-10} = \frac{x^2}{(0.025 - x)} \tag{8.2.6.203}$$

assume x<<<0.025, then solve for x

$$x = 3.94 \times 10^{-6}\ M = [H_3O^+] \tag{8.2.6.204}$$

$$pH = -log(3.94 \times 10^{-6}) \tag{8.2.6.205}$$

S49

The effects of a solution that consists the same ions.

$PbCl_{2(s)} \rightleftharpoons Pb^+_{2(aq)} + 2Cl^-_{(aq)}$

S50

0.375 M

S51

Using Ice Table

S52

2< pH < 5

S53

Away from equilibrium

S54

Acidic Solution

S55

Yes

S56

12 L

S57

The molarity is the same therefore the amount does not matter.

S58

Start from bottom and the direction of the curve is going up. The equivalence point is around a pH of 7.

S59

0.05 L

S60

Acidic

S61

The ratio of the concentration of one reaction with another reaction of the same substance.

S62

Strong Base

S63

Strong Base

S64

7.5 < pH < 9.0

S65

$$CH_3COOH_{(aq)} + H_2O_{(l)} \rightleftharpoons H_3O^+_{(aq)} + CH_3COO^-_{(aq)} \tag{8.2.6.206}$$

	CH_3COOH	H_2O	H_3O^+	CH_3COO^-
I	0.153	--	0	0
C	-x	--	+x	+x
E	0.153-x	--	x	x

$$K_a = \frac{[H_3O^+][CH_3COO^-]}{[CH_3COOH]} \tag{8.2.6.207}$$

$$1.8 \times 10^{-5} = \frac{x^2}{(0.153 - x)} \tag{8.2.6.208}$$

$$1.8 \times 10^{-5} \times (0.153 - x) = x^2 \tag{8.2.6.209}$$

$$0 = -x^2 - 1.8 \times 10^{-5}x + 2.754 \times 10^{-6} \tag{8.2.6.210}$$

$$x = [H_3O^+] = 1.65 \times 10^{-3} \tag{8.2.6.211}$$

S66

	$HNO_{2(aq)}$	$H_2O_{(l)}$	$H_3O^+_{(aq)}$	$NO^{2-}_{(aq)}$
I	0.548	--	0	0
C	-x	--	+x	+x
E	0.548-x	--	x	x

$$K_a = \frac{[H_3O^+][Cl^-]}{[HCl]} = 7.2 \times 10^{-4} = \frac{x^2}{0.548 - x} \tag{8.2.6.212}$$

$$x = [H_3O^+] = 0.0198 \tag{8.2.6.213}$$

$$pH = -log[H_3O^+] \tag{8.2.6.214}$$

$$pH = -log(0.0198) \tag{8.2.6.215}$$

$$pH = 1.70 \tag{8.2.6.216}$$

S67

	$HClO_{2(aq)}$	$H_2O_{(l)}$	$H_3O^+_{(aq)}$	$ClO_{2(aq)}$
I	0.10	--	0	0
C	-x	--	+x	+x
E	0.10-x	--	x	x

$$K_a = \frac{[H_3O^+][ClO_2^-]}{[HClO_2]} \tag{8.2.6.217}$$

$$1.1 \times 10^{-2} = \frac{x^2}{(0.1 - x)} \tag{8.2.6.218}$$

$$x = [H_3O^+] = 0.028119 \tag{8.2.6.219}$$

$$pH = -log[H_3O^+] \tag{8.2.6.220}$$

$$pH = 1.55 \tag{8.2.6.221}$$

$$pH = pK_a = -log(1.1 \times 10^{-2}) = 1.95 \tag{8.2.6.222}$$

$$\Delta pH = 1.95 - 1.55 = 0.4 \tag{8.2.6.223}$$

S68

$$pH = pK_a + log\frac{[ClO_2^-]}{[HClO_2]} \tag{8.2.6.224}$$

$$pH = -log(1.1 \times 10^{-2}) + log\frac{(\frac{6mmol}{55mL})}{(\frac{0.45mmol}{55mL})} \tag{8.2.6.225}$$

$$pH = 1.95 + log(13.33) \tag{8.2.6.226}$$

$$pH = 3.08 \tag{8.2.6.227}$$

S69

$$[H_3PO_4] = \frac{(50\ mL \times 0.3\ M)}{75\ mL} = 0.2\ M \tag{8.2.6.228}$$

$$[H_2PO_4^-] = \frac{(25mL \times 0.3M)}{(25mL + 50mL)} = 0.1\ M \tag{8.2.6.229}$$

$$pH = pK_a + log\frac{[H_2PO_4^-]}{[H_3PO^4]} \tag{8.2.6.230}$$

$$1.82 = pK_a + log(\frac{0.1}{0.2}) \tag{8.2.6.231}$$

$$pK_a = 2.12 \tag{8.2.6.232}$$

$$K_a = 10^{-2.12} \tag{8.2.6.233}$$

$$K_a = 7.58 \times 10^{-3} \tag{8.2.6.234}$$

S70

K_{Hln} of 2×10^{-7}. A titration between a strong acid and strong base reach an

endpoint around a neutral pH, therefore the K_{Hln} should be similar to the K_a, 1×10^{-7}. An indicator with a larger K_{Hln}, will be used in acidic solutions. An incidator with a smaller K_{Hln} will be used in basic solutions. Remember, a large K_{Hln} will correspond with a smaller pH, which means more acidic.

S71

Strong acid-weak base. The endpoint is reached in a low pH, because the acid fully dissociated, but the base does not.

S72

$$KOH: \frac{(0.05moles)}{L} \times (0.02L) = 0.001moles \tag{8.2.6.235}$$

$$HI: \frac{(0.05mole)}{L} \times (0.01L) = 0.0005moles \tag{8.2.6.236}$$

$$0.001 - 0.0005 = 0.0005moles\ KOH\ in\ excess \tag{8.2.6.237}$$

$$Strong\ acid,\ fully\ dissociates,\ so\ 0.0005\ moles\ of\ OH^-: \tag{8.2.6.238}$$

$$[OH^-] = \frac{0.0005}{(.01L + 0.02L)} = 0.0166M \tag{8.2.6.239}$$

$$pOH = -log(0.0166) = 1.77 \tag{8.2.6.240}$$

$$pH = 14 - 1.77 = 12.22 \tag{8.2.6.241}$$

$$pK_{Hln} = pH\ (at\ endpoint) = 12.22 \tag{8.2.6.242}$$

This does not give the accurate endpoint of titration, because that should occur around a pH of 7, since it is strong acid-strong base titration.

S73

$$HCl: \frac{(0.007moles)}{L} \times (0.200L) = 0.0014moles \tag{8.2.6.243}$$

$$NaOH: \frac{(0.02moles)}{L} \times (0.300L) = 0.006moles \tag{8.2.6.244}$$

This is strong acid, strong base titration, so they both fully dissociate into ions.

$$0.006 - 0.0014 = 0.0046\ moles\ of\ OH^-\ unreacted \tag{8.2.6.245}$$

$$[OH^-] = \frac{0.0046}{(0.2L + 0.3L)} = 0.0092M \tag{8.2.6.246}$$

$$pOH = -log(0.0092) = 2.036 \tag{8.2.6.247}$$

S74

The volumes will be the same, because they have the same molarity. However, the pH will be different because HF is a stronger acid than CH_3COOH, so its pH will be around or lower 7, while CH_3COOH is a weak acid, so the pH will be greater than 7 (since the strong base, LiOH, has fully dissociated, but the CH_3COOH has not.)

S75

The greater the K_b, the closer the pH will be to 7 at the equivalence point (inflection point of graph), and the steeper the slope will be. However, because it is a weak base, the pH will be lower than 7 no matter what. The lower the K_b, the less steep the slope will be and the lower the pH at the equivalence point will be.

S76

$$CsOH: \frac{(0.02\ moles)}{L} \times (0.04L) = 0.0008\ moles\ CsOH \tag{8.2.6.248}$$

$$\frac{0.05mole}{L} \times (0.005L) = 0.00025\ moles\ HBr \tag{8.2.6.249}$$

$$moles\ OH^- = 0.0008 - 0.00025 = 0.00055 \tag{8.2.6.250}$$

$$[OH^-] = \frac{0.00055}{(0.04L + 0.005L)} = 0.0122 \tag{8.2.6.251}$$

$$pOH = 1.91 \tag{8.2.6.252}$$

$$pH = 14 - 1.91 = 12.09 \tag{8.2.6.253}$$

$$\frac{(0.05mole)}{L} \times (0.01L) = 0.0005\ moles\ HBr \tag{8.2.6.254}$$

$$moles\ OH^- = 0.0008 - 0.0005 = 0.0003 \tag{8.2.6.255}$$

$$[OH^-] = \frac{0.0003}{(0.01L + 0.04L)} = 0.006\ M \tag{8.2.6.256}$$

$$pOH = 2.22 \tag{8.2.6.257}$$

$$pH = 14 - 2.22 = 11.79 \tag{8.2.6.258}$$

$$\frac{(0.05mole)}{L} \times (0.025L) = 0.0013\ moles\ HBr \tag{8.2.6.259}$$

Now more moles of acid than base so,

$$moles\ H^+ = 0.0013 - 0.0008 = 0.0005 \tag{8.2.6.260}$$

$$[H^+] = \frac{0.0005}{(.025 + 0.04)} = 0.0076 \tag{8.2.6.261}$$

$$pH = -log(0.0076) = 2.13 \tag{8.2.6.262}$$

S77

It will be basic. The copper is just a spectator ion. The sulfide ion will form a bond with the H from the water. However, because HS is a weak acid, the concentration of OH^- will be greater than H^+ concentration of the dissociation of HS.

S78

Sulfuric acid can be reduced with sodium carbonate, and then further reduced with $NaOH$.

$$H_2SO_4 + CO_3^{2-} \rightarrow HSO_4^- + HCO_3^- \tag{8.2.6.263}$$

$$HSO_4^- + OH^- \rightarrow SO_4^{2-} + H_2O \tag{8.2.6.264}$$

S79

$$CH_3COOH + H_2O \rightleftharpoons H_3O^+ + CH_3COO^- \tag{8.2.6.265}$$

	CH_3COOH	H_2O	H_3O^+	CH_3COO^-
I	0.1	--	0	0
C	-x	--	+x	+x

E	0.1-x	--	x	x

$$K_a = \frac{[H_3O^+][CH_3COO^-]}{[CH_3COOH]} = 1.8 \times 10^{-5} \tag{8.2.6.266}$$

$$Assume\ x \ll 0.1\ \rightarrow 1.3 \times 10^{-3} = [H_3O^+] \tag{8.2.6.267}$$

$$pH = -log[H_3O^+] = -log[1.3 \times 10^{e-3}] \tag{8.2.6.268}$$

$$pH = 2.89 \tag{8.2.6.269}$$

S80

$for\ H_2PO_4^-\ :\ pH = \frac{1}{2}(pK_{a1} + pK_{a2}) = \frac{1}{2}(2.15 + 7.20) = 4.68$

$forHPO_4^{2-}\ :\ pH = \frac{1}{2}(pK_{a2} + pK_{a3}) = \frac{1}{2}(7.20 + 12.38) = 9.79$

S81

Simultaneously means ionization as an acid and ionization as a base.

a. yes
b. no
c. yes

S82

$K_{a1} = 7.1 \times 10^{-3}$, $K_{a2} = 6.3 \times 10^{-8}$, $K_{a3} = 4.2 \times 10^{-13}$

$$pH = pK_a + log\frac{[base]}{[acid]} \tag{8.2.6.270}$$

$$pK_a = -log(6.3 \times 10^{-8}) \tag{8.2.6.271}$$

$$x = 0.3852\ moles\ NaOH\ needed \tag{8.2.6.272}$$

$$mL = \frac{0.3852\ moles\ NaOH}{6.0M\ NaOH} \times 1000 = 64.2\ mL \tag{8.2.6.273}$$

S83

As a result with buffers;

$$pH = -log[H_3O^+] = -log[K_a] \tag{8.2.6.274}$$

$$pH = -log[6.3 \times 10^{-5}] = 4.2 \tag{8.2.6.275}$$

$$buffer\ range = 4.2 \pm 1 = [3.2, 5.2] \tag{8.2.6.276}$$

S84

The common ion effect is the suppression of the ionization of a weak electrolyte caused by adding more of an ion that is a product of this ionization.

Add $H_3O^+ : CH_3COOH + H_2O \rightleftharpoons H_3O^+ + CH_3COO^- K_a = 1.8 \times 10^{-5}$

Equilibrium shifts to form more CH_3COOH

Add $OH^- : NH_3 + H_2O \rightleftharpoons NH_4^+ + OH^- K_b = 1.8 \times 10^{-5}$

Equilibrium shifts to form more NH_3

S85

$$(0.3\ L)(0.56\ M) = 0.168\ mol\ CH_3COO^- \tag{8.2.6.277}$$

$$(0.3\ L)(0.25\ M) = 0.075\ mol\ CH_3COOH \tag{8.2.6.278}$$

	CH_3COO^-	$H3O^+$	H_2O	CH_3COOH
I	0.168 mol	0.006 mol	--	0.075 mol
C	-0.006 mol	-0.006 mol	--	+0.006 mol
E	0.162 mol	0	--	0.018 mol

$$[CH_3COO^-] = \frac{0.162\ mol}{0.3\ L} = 0.54\ M \tag{8.2.6.279}$$

$$[CH_3COOH] = \frac{0.081\ mol}{0.3\ L} = 0.27\ M \tag{8.2.6.280}$$

$$pH = pK_a + log\frac{[base]}{[acid]} \tag{8.2.6.281}$$

$$pH = 4.74 + log\frac{[0.54M]}{[0.27M]} = 5.04 \tag{8.2.6.282}$$

S86

$$HCl_{(aq)} + H_2O_{(l)} \rightleftharpoons H_3O^+_{(aq)} + Cl^-_{(aq)} \tag{8.2.6.283}$$

$$H_2O_{(l)} + H_2O_{(l)} \rightleftharpoons H_3O^+_{(aq)} + OH^-_{(aq)} \tag{8.2.6.284}$$

	H_2O	H_2O	H_3O^+	OH^-
I	--	--	10^{-8}	0
C	--	--	+x	+x
E	--	--	10^{-8}+x	x

$$K_w = (1 \times 10^{-8} + x)(x) = 1.0 \times 10^{-14} \tag{8.2.6.285}$$

Use the quadratic equation to solve for x;

$$x = 1.1 \times 10^{-7} \tag{8.2.6.286}$$

$$[H_3O^+] = (1 \times 10^{-8} + x) = (1 \times 10^{-8} + 1.1 \times 10^{-7}) = 1.2 \times 10^{-7} \tag{8.2.6.287}$$

$$pH = -log[H_3O^+] = -log[1.2 \times 10^{-7}] = 6.92 \tag{8.2.6.288}$$

S87

Ionization energy is the energy required to completely remove an electron from a gaseous atom or ion. $NaCl$, $NaHCOO$, and $NaHCO_3$ will decrease the ionization of acidic acid.

S88

a)

	HOCl	H_2O	H_3O^+	OCl^-
I	0.45	-	0.001	0
C	- x	-	+ x	+ x
E	0.45 - x	-	0.001 + x	x

$$2.9 \times 10^{-8} = \frac{(0.001 + x)(x)}{(0.45 - x)} \tag{8.2.6.289}$$

$$x = 1.28 \times 10^{-5} \tag{8.2.6.290}$$

$$[H_3O^+] = 0.001 + x = 0.0010128M \tag{8.2.6.291}$$

b)

$$[H_3O^+][OH^-] = K_w \tag{8.2.6.292}$$

$$[OH^-] = 9.9 \times 10^{-14}\ M \tag{8.2.6.293}$$

c)

$$[OCl^-] = x = 1.28 \times 10^{-5}\ M \tag{8.2.6.294}$$

d)

$$[Cl^-] = [H_3O^+] = 0.0010128M \tag{8.2.6.295}$$

S89

a)

	CH_5N	H_2O	OH^-	CH_5NH^+
I	0.3	-	0	0.015
C	-x	-	+x	+x
E	0.3-x	-	x	0.015+x

$$1.5 \times 10^{-9} = \frac{(0.015 + x)(x)}{(0.3 - x)} \tag{8.2.6.296}$$

$$x = 3.0 \times 10^{-8} \tag{8.2.6.297}$$

$$[OH^-] = x = 3.0 \times 10^{-8}\ M \tag{8.2.6.298}$$

b)

$$[C_5H_5NH^+] = 0.015M \tag{8.2.6.299}$$

c)

$$[I^-] = 0.015M \tag{8.2.6.300}$$

d)

$$[H_3O^+][OH^-] = K_w \tag{8.2.6.301}$$

$$[H_3O^+](1.3 \times 10^{-7}) = 1.0 \times 10^{-14} \tag{8.2.6.302}$$

$$[H_3O^+] = 7.69 \times 10^{-8} \tag{8.2.6.303}$$

S90

a)

$$pH = pK_a + log\frac{[B]}{[A]} \tag{8.2.6.304}$$

$$pH = 9.21 + log\frac{0.004}{0.025} \tag{8.2.6.305}$$

$$pH = 7.414 \tag{8.2.6.306}$$

$$pOH = 14 - pH = 6.586 \tag{8.2.6.307}$$

b)

$$pH = pK_a + log\frac{(0.004 + 0.025)}{(0.25 - 0.025)} \tag{8.2.6.308}$$

$$pH = 8.32 \tag{8.2.6.309}$$

$$(3)(0.076) = 0.228\ moles\ HNO_3 \tag{8.2.6.310}$$

$$\frac{(0.228 - 0.004)}{(0.25 + 0.076)} = 0.687\ M \tag{8.2.6.311}$$

$$pH = -log(0.687) = 0.163 \tag{8.2.6.312}$$

S91

a)

$$(0.32L)(0.406M) = 0.13\ moles\ B \tag{8.2.6.313}$$

$$(0.7L)(0.644M) = 0.451\ moles\ A \tag{8.2.6.314}$$

$$pH = pK_a + log\frac{[B]}{[A]} \tag{8.2.6.315}$$

$$pH = 7.54 + log\frac{0.13}{0.451} \tag{8.2.6.316}$$

$$pH = 7 \tag{8.2.6.317}$$

b)

Yes, even if you add 1L of H_2O, the mole ratio will not change

c)

$$(0.15L)(0.8M) = 0.12\ moles\ NaOH \tag{8.2.6.318}$$

$$pH = 7.54 + log\frac{(0.13 + 0.12)}{(0.45 - 0.12)} \tag{8.2.6.319}$$

$$pH = 7.54 \tag{8.2.6.320}$$

d)

$$7.7 = 7.54 + log\frac{(0.13 + x)}{(0.451 - x)} \tag{8.2.6.321}$$

$$x = 0.2135\ moles\ of\ NaOH \tag{8.2.6.322}$$

$$(0.8M)(V) = 0.2135\ mol \tag{8.2.6.323}$$

$$V = 0.2669L\ of\ 0.8M\ NaOH \tag{8.2.6.324}$$

S92

a) blue

b) yellow

c) blue

d) yellow

e) blue

f) blue

S93

$$(0.73M)(0.025L) = 0.01825\ moles\ HI \tag{8.2.6.325}$$

$$2[(0.29M)(0.01L)] = 2(0.0029) = 0.0058\ moles\ Ca(OH)_2 \tag{8.2.6.326}$$

$$0.01825 - 0.0058 = 0.01245\ mol \tag{8.2.6.327}$$

$$[H_3O^+] = \frac{0.01245}{0.035} = 0.3557M \tag{8.2.6.328}$$

$$pH = -log(0.3557) = 0.4489 \tag{8.2.6.329}$$

$$14 - pH = pOH = 13.55 \tag{8.2.6.330}$$

S94

It doesn't matter because the strength of the base doesn't change the number of moles of that base. At the equivalence point, the amount of moles of acid equals the moles of base regardless of strength. The pOH will not be the same however because when titrating a weak base at the equivalence point, there will be a concentration of its conjugate acid which acts acidic in solution.

S95

It will act basic because PO_4^{3-} is a base in solution because it is the conjugate base to HPO_4^{2-}

S96

Equation	CH_3CH_2COOH	+	$H_2O_{(l)}$	↔	$CH_3CH_2COO^-$	+	H_3O^+
Initial	0.330 M		---		0		0.01M
Change	-x		---		+x		+x
Equilibrium	(0.330 M – x) M		---		x		(0.01 + x) M

$$K_a = \frac{x(0.01 + x)}{(0.330\ M - x)} \approx \frac{0.01x}{0.330} \tag{8.2.6.331}$$

$$[CH_3CH_2COO^-] = 4.3 \times 10^{-4}\ M \tag{8.2.6.332}$$

$$[H_3O^+] = [I^-] = 0.0104\ M \tag{8.2.6.333}$$

$$[OH^-] = \frac{K_w}{[H_3O^+]} \tag{8.2.6.334}$$

$$[OH^-] = 9.6 \times 10^{-13}\ M \tag{8.2.6.335}$$

S97

Equation	NH_3	+	$H_2O(l)$	↔	NH_4^+	+	OH^-
Initial	0.654 M		---		0.202 M		0
Change	-x		---		+x		+x
Equilibrium	(0.654 M – x) M		---		(0.202+ x) M		x

$$K_b = \frac{x(0.202 + x)}{(0.654\ M - x)} \approx \frac{0.202x}{0.654} \tag{8.2.6.336}$$

$$[OH^-] = 2.9 \times 10^{-5}\ M \tag{8.2.6.337}$$

$$[NH_4^+] = [Cl^-] = 0.202\ M \tag{8.2.6.338}$$

$$[OH^-] = \frac{K_w}{[H_3O^+]} \tag{8.2.6.339}$$

$$[H_3O^+] = 3.4 \times 10^{-10}\ M \tag{8.2.6.340}$$

S98

Equation	HNO_2	+	$H_2O_{(l)}$	↔	HNO_2^-	+	H_3O^+
Initial	0.200 M		---		0		0
Change	-x		---		+x		+x
Equilibrium	(0.200 M – x)		---		x		x

$$K_a = 7.2 \times 10^{-4} \tag{8.2.6.341}$$

$$K_a = \frac{x^2}{0.200M - x} \approx \frac{x^2}{0.200M} \tag{8.2.6.342}$$

$$x = 0.012\ M \tag{8.2.6.343}$$

$$pH = -log[H_3O^+] \tag{8.2.6.344}$$

$$pH = 1.9 \tag{8.2.6.345}$$

$$pH = pK_a - (-log[M]) \tag{8.2.6.346}$$

$$\Delta pH = 1.22 \tag{8.2.6.347}$$

b) Since there is no net change in equilibrium just a shift in ionic strength thus the pH of the second solution will be different.

S99

a)

$$pH = pK_a + log\frac{[base]}{[acid]} \tag{8.2.6.348}$$

$$pH = 3.44 \tag{8.2.6.349}$$

b)

$$OH^- = 0.1\ mol\ Ba(OH)_2 \times \frac{2\ mol\ OH^-}{1\ mol\ Ba(OH)_2} = 0.2\ mol\ OH^- \tag{8.2.6.350}$$

Equation	$HCHO_2$	+	OH^-	↔	CHO_2^-	+	$H_2O_{(l)}$
Initial	0.5 mols		0.2 mols		0.250 mols		---
Change	-.2 mols		-0.2 mols		+0.2 mols		---
Equilibrium	00.3 mols		0		0.45 mols		---

$$pH = pK_a + log\frac{[base]}{[acid]} \tag{8.2.6.351}$$

$$pH = 3.92 \tag{8.2.6.352}$$

c)

$$H_3O^+ = 0.01L \times 12M\ HCl = 0.12\ mol\ H_3O^+ \tag{8.2.6.353}$$

Equation	CHO_2^-	+	H_3O^+	↔	$HCHO_2$	+	$H_2O_{(l)}$
Initial	0.25 mols		0.37 mols		0.50 mols		---
Change	-0.25 mols		-0.25 mols		+0.25 mols		---
Equilibrium	0		0.12 mols		0.75 mols		---

$$[H_3O^+] = \frac{0.12\ mol}{1L + 0.01\ L} = 0.119\ M \tag{8.2.6.354}$$

$$pH = 0.92 \tag{8.2.6.355}$$

S100

a)

$$pH = pK_a + log\frac{[base]}{[acid]} \tag{8.2.6.356}$$

$$[NH_3] = 0.035\ L \times \frac{0.220\ M\ NH_3}{0.1\ L} = 0.077\ M \tag{8.2.6.357}$$

$$[NH_4^+] = 0.065 \times \frac{0.250\ M}{0.1\ L} = 0.163\ M \tag{8.2.6.358}$$

$$pH = 9.00 \tag{8.2.6.359}$$

b) The pH would change since adding more solution will dilute the concentration and thus reduce the pH to something near $pH = 7$.

c) pH should still be 9 since the amount of acid is so insignificant

S101

a)

$$pOH = 14–10 = 4 \tag{8.2.6.360}$$

$$[OH^-] = \frac{10^{-4}\ moles}{1L} \times \frac{1\ mol\ Ba(OH)_2}{2\ mol\ OH^-} = 0.00005\ M \tag{8.2.6.361}$$

b)

$$pH = pK_a + log\frac{[base]}{[acid]} \tag{8.2.6.362}$$

$$pK_a = 4.74 \tag{8.2.6.363}$$

$$4.5–4.74 = log\frac{[base]}{[acid]} \tag{8.2.6.364}$$

$$10^{-0.24} = \frac{[0.300M]}{[acid]} = 0.52\ M \tag{8.2.6.365}$$

S102

$$K_b = \frac{(0.500M)(1.0 \times 10^{-7}\ M)}{x\ M} = 1.8 \times 10^{-5} \tag{8.2.6.366}$$

$$[NH_3] = 2.8 \times 10^{-3}\ M \tag{8.2.6.367}$$

$$V = 1L \times (2.8 \times 10^{-3}\ M\ NH_3) \times \frac{1\ L}{10.00\ mol\ NH_3} \times \frac{1\ drop}{0.05\ mL} = 3\ drops \tag{8.2.6.368}$$

S103

a)

$$0.2M\ NH_3 = 0.0072\ mol\ NH_3 \tag{8.2.6.369}$$

$$0.2M\ NH_4Cl = 0.0128\ mol\ NH_4Cl \tag{8.2.6.370}$$

$$Moles\ of\ base\ in\ excess = 0.0128 - 0.0072 = 0.0056\ mol \tag{8.2.6.371}$$

$$Total\ volume = 36\ mL + 64\ mL = 100\ mL\ (1L) \tag{8.2.6.372}$$

$$[OH^-] = \frac{0.0056\ mol}{1\ L} = 0.0056\ M \tag{8.2.6.373}$$

$$pOH = -log(0.0056) = 2.25 \tag{8.2.6.374}$$

$$12–2.25 \rightarrow pH = 9.75 \tag{8.2.6.375}$$

b.)

$$[OH^-] = \frac{0.0056\ mol}{200\ L} = 2.8 \times 10^{-5} \tag{8.2.6.376}$$

No, the pH would be different because you are changing the concentration of the base, and thereby change the pH and pOH values.

chemwiki.ucdavis.edu/Physical_Chemistry/Acids_and_Bases/Buffers

S104

1.) The pH starts low. 2.) The pH increases slowly until right before the equivalence point. 3.) At equivalence point, the pH spikes by approximately 6 units for only a couple drops of base. 4.) After equivalence point, the pH rises slowly again. 5.) Any acid-base indicator with color change in a pH range of 4-10 will work.

chemwiki.ucdavis.edu/Analytical_Chemistry/Quantitative_Analysis/Titration/Titration_Of_A_Strong_Acid_With_A_Strong_Base

S105

$$25g\ malonic\ acid\ in\ 0.300\ L = 0.801\ M\ malonic\ acid \tag{8.2.6.377}$$

$$H_2M + H_2O \rightleftharpoons HM^- + H_3O^+ \tag{8.2.6.378}$$

$$K_{a1} = \frac{[HM^-][H_3O^+]}{[H_2M]} \tag{8.2.6.379}$$

$$[H_3O^+] = -log(2.68) = .0021 \tag{8.2.6.380}$$

$$4.5 \times 10^{-12} = \frac{[HM^-](0.0021)}{0.801} \tag{8.2.6.381}$$

$$[HM^-] = 1.72 \times 10^{-9} \tag{8.2.6.382}$$

chemwiki.ucdavis.edu/Physical_Chemistry/Acids_and_Bases/Aqueous_Solutions/The_pH_Scale/Determining_and_Calculating_pH

S106

$$K_a = \frac{[H^+][A^-]}{[HA]} \tag{8.2.6.383}$$

$$log(K_a) = log(\frac{[H^+][A^-]}{[HA]}) \tag{8.2.6.384}$$

$$logK_a = log[H^+] + log(\frac{[A^-]}{[HA]}) \tag{8.2.6.385}$$

$$-pK_a = -pH + log(\frac{[A^-]}{[HA]}) \tag{8.2.6.386}$$

$$pH = pK_a + log(\frac{[A^-]}{[HA]}) \tag{8.2.6.387}$$

chemwiki.ucdavis.edu/Physical_Chemistry/Acids_and_Bases/Buffers/Henderson-Hasselbalch_Approximation

---

8.2.6: Exercises on Acids and Bases II is shared under a CC BY-NC-SA 4.0 license and was authored, remixed, and/or curated by LibreTexts.

8.2.7: E3. Solubility Constants for Compounds at 25°C Data Table

E3. Solubility Constants for Compounds at 25°C

8.2.7: E3. Solubility Constants for Compounds at 25°C Data Table is shared under a CC BY-NC-SA 4.0 license and was authored, remixed, and/or curated by LibreTexts.

8.2.8: pH Calculations for Acid–Base Titrations

Acid–Base Titration Curves

In this section we will learn how to calculate the pH of an analyte solution throughout the titration, and use these values to prepare a titration curve. We also will learn how to sketch a good approximation of any acid–base titration curve using a limited number of simple calculations.

Titrating Strong Acids and Strong Bases

For our first titration curve, let's consider the titration of 50.0 mL of 0.100 M HCl using a titrant of 0.200 M NaOH. When a strong base and a strong acid react the only reaction of importance is

$$H_3O^+(aq) + OH^-(aq) \rightarrow 2H_2O(l) \tag{8.2.8.1}$$

The first task is to calculate the volume of NaOH needed to reach the equivalence point. At the equivalence point we know that

$$moles\ H_3O^+ = moles\ OH^- \tag{8.2.8.2}$$

The volume of NaOH needed to reach the equivalence point is

$$50.0\,mL \times \frac{0.100\,mol\,HCl}{1000\,mL} \times \frac{1\,mol\,NaOH}{1\,mol\,HCl} \times \frac{1000\,mL\,NaOH}{0.200\,mol\,NaOH} = 25\,mL\,NaOH \tag{8.2.8.3}$$

Before the equivalence point, HCl is present in excess and the pH is determined by the concentration of unreacted HCl. At the start of the titration the solution is 0.100 M in HCl, which, because HCl is a strong acid, means the pH is

$$pH = -\log[H_3O^+] = -\log[HCl] = -\log(0.100) = 1.00$$

After adding 10.0 mL of NaOH the concentration of excess HCl is

$$[HCl] = \frac{(\text{mol HCl})_{\text{initial}} - (\text{mol NaOH})_{\text{added}}}{\text{total volume}} = \frac{M_aV_a - M_bV_b}{V_a + V_b}$$

$$[HCl] = \frac{(0.100\text{ M})(50.0\text{ mL}) - (0.200\text{ M})(10.0\text{ mL})}{50.0\text{ mL} + 10.0\text{ mL}} = 0.0500\text{ M}$$

and the pH increases to 1.30.

At the equivalence point the moles of HCl and the moles of NaOH are equal. Since neither the acid nor the base is in excess, the pH is determined by the dissociation of water.

$$K_w = 1.00 \times 10^{-14} = [H_3O^+][OH^-] = [H_3O^+]^2$$
$$[H_3O^+] = 1.00 \times 10^{-7}$$

Thus, the pH at the equivalence point is 7.00.

For volumes of NaOH greater than the equivalence point, the pH is determined by the concentration of excess OH^-. For example, after adding 30.0 mL of titrant the concentration of OH^- is

$$[OH^-] = \frac{(\text{mol NaOH})_{\text{added}} - (\text{mol HCl})_{\text{initial}}}{\text{total volume}} = \frac{M_bV_b - M_aV_a}{V_a + V_b}$$

$$[OH^-] = \frac{(0.200\text{ M})(30.0\text{ mL}) - (0.100\text{ M})(50.0\text{ mL})}{30.0\text{ mL} + 50.0\text{ mL}} = 0.0125\text{ M}$$

To find the concentration of H_3O^+ we use the K_w expression

$$[H_3O^+] = \frac{K_w}{[OH^-]} = \frac{1.00 \times 10^{-14}}{0.0125} = 8.00 \times 10^{-13}\text{ M}$$

to find that the pH is 12.10. Table 6.6.1 and Figure 6.6.1 show additional results for this titration curve. You can use this same approach to calculate the titration curve for the titration of a strong base with a strong acid, except the strong base is in excess

before the equivalence point and the strong acid is in excess after the equivalence point.

Table 6.6.1 . Titration of 50.0 mL of 0.100 M HCl with 0.200 M NaOH

volume of NaOH (mL)	pH	volume of NaOH (mL)	pH
0.00	1.00	26.0	11.42
5.00	1.14	28.0	11.89
10.0	1.30	30.0	12.10
15.0	1.51	35.0	12.37
20.0	1.85	40.0	12.52
22.0	2.08	45.0	12.63
24.0	2.57	50.0	12.70
25.0	7.00		

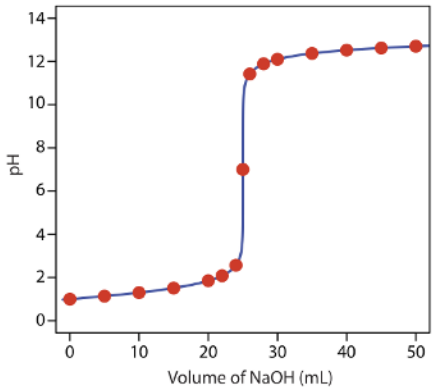


Figure 6.6.1 . Titration curve for the titration of 50.0 mL of 0.100 M HCl with 0.200 M NaOH. The red points correspond to the data in Table 6.6.1 . The blue line shows the complete titration curve.

Exercise 6.6.1

Construct a titration curve for the titration of 25.0 mL of 0.125 M NaOH with 0.0625 M HCl.

Answer

The volume of HCl needed to reach the equivalence point is

$$V_{eq} = V_a = \frac{M_b V_b}{M_a} = \frac{(0.125\ \text{M})(25.0\ \text{mL})}{(0.0625\ \text{M})} = 50.0\ \text{mL}$$

Before the equivalence point, NaOH is present in excess and the pH is determined by the concentration of unreacted OH^-. For example, after adding 10.0 mL of HCl

$$[OH^-] = \frac{(0.125\ \text{M})(25.0\ \text{mL}) - (0.0625\text{M})(10.0\ \text{mL})}{25.0\ \text{mL} + 10.0\ \text{mL}} = 0.0714\ \text{M}$$

$$[H_3O^+] = \frac{K_w}{[OH^-]} = \frac{1.00 \times 10^{-14}}{0.0714\ \text{M}} = 1.40 \times 10^{-13}\ \text{M}$$

the pH is 12.85.

For the titration of a strong base with a strong acid the pH at the equivalence point is 7.00.

For volumes of HCl greater than the equivalence point, the pH is determined by the concentration of excess HCl. For example, after adding 70.0 mL of titrant the concentration of HCl is

$$[\text{HCl}] = \frac{(0.0625\ \text{M})(70.0\ \text{mL}) - (0.125\ \text{M})(25.0\ \text{mL})}{70.0\ \text{mL} + 25.0\ \text{mL}} = 0.0132\ \text{M}$$

giving a pH of 1.88. Some additional results are shown here.

volume of HCl (mL)	pH	volume of HCl (mL)	pH
0	13.10	60	2.13
10	12.85	70	1.88
20	12.62	80	1.75
30	12.36	90	1.66
40	11.98	100	1.60
50	7.00		

Titrating a Weak Acid with a Strong Base

For this example, let's consider the titration of 50.0 mL of 0.100 M acetic acid, CH_3COOH, with 0.200 M NaOH. Again, we start by calculating the volume of NaOH needed to reach the equivalence point; thus

$$\text{mol } CH_3COOH = \text{mol NaOH}$$

$$50.0\ mL\ CH_3COOH \times \frac{0.100\ mol\ CH_3COOH}{1000\ mL} \times \frac{1\ mol\ NaOH}{1\ mol} \times \frac{1000\ mL\ NaOH}{0.200\ mol\ NaOH} = 25.0\ mL\ NaOH \tag{8.2.8.4}$$

Before we begin the titration the pH is that for a solution of 0.100 M acetic acid. Because acetic acid is a weak acid, we calculate the pH using the acid equilibrium constant.

$$CH_3COOH(aq) + H_2O(l) \rightleftharpoons H_3O^+(aq) + CH_3COO^-(aq)$$

$$K_a = \frac{[H_3O^+]\,[CH_3COO^-]}{[CH_3COOH]} = \frac{(x)(x)}{0.100 - x} = 1.75 \times 10^{-5}$$

finding that the pH is 2.88.

Adding NaOH converts a portion of the acetic acid to its conjugate base, CH_3COO^-.

$$CH_3COOH(aq) + OH^-(aq) \longrightarrow H_2O(l) + CH_3COO^-(aq) \tag{8.2.8.5}$$

Because the equilibrium constant for reaction 8.2.8.5 is quite large

$$K = K_a/K_w = 1.75 \times 10^9$$

we can treat the reaction as if it goes to completion.

Any solution that contains comparable amounts of a weak acid, HA, and its conjugate weak base, A^-, is a buffer. We can calculate the pH of a buffer using the Henderson–Hasselbalch equation.

$$\text{pH} = \text{p}K_a + \log\frac{[A^-]}{[HA]}$$

Before the equivalence point the concentration of unreacted acetic acid is

$$[CH_3COOH] = \frac{(\text{mol } CH_3COOH)_{\text{initial}} - (\text{mol NaOH})_{\text{added}}}{\text{total volume}} = \frac{M_aV_a - M_bV_b}{V_a + V_b}$$

and the concentration of acetate is

$$[CH_3COO^-] = \frac{(\text{mol NaOH})_{\text{added}}}{\text{total volume}} = \frac{M_b V_b}{V_a + V_b}$$

For example, after adding 10.0 mL of NaOH the concentrations of CH_3COOH and CH_3COO^- are

$$[CH_3COOH] = \frac{(0.100\text{ M})(50.0\text{ mL}) - (0.200\text{ M})(10.0\text{ mL})}{50.0\text{ mL} + 10.0\text{ mL}} = 0.0500\text{ M}$$

$$[CH_3COO^-] = \frac{(0.200\text{ M})(10.0\text{ mL})}{50.0\text{ mL} + 10.0\text{ mL}} = 0.0333\text{ M}$$

which gives us a pH of

$$\text{pH} = 4.76 + \log\frac{0.0333\text{ M}}{0.0500\text{ M}} = 4.58$$

At the equivalence point the moles of acetic acid initially present and the moles of NaOH added are identical. Because their reaction effectively proceeds to completion, the predominate ion in solution is CH_3COO^-, which is a weak base. To calculate the pH we first determine the concentration of CH_3COO^-

$$[CH_3COO^-] = \frac{(\text{mol NaOH})_{\text{added}}}{\text{total volume}} = \frac{(0.200\text{ M})(25.0\text{ mL})}{50.0\text{ mL} + 25.0\text{ mL}} = 0.0667\text{ M}$$

> Alternatively, we can calculate acetate's concentration using the initial moles of acetic acid; thus
>
> $$[CH_3COO^-] = \frac{(\text{mol } CH_3COOH)_{\text{initial}}}{\text{total volume}} = \frac{(0.100\text{ M})(50.0\text{ mL})}{50.0\text{ mL} + 25.0\text{ mL}} = 0.0667\text{ M}$$

Next, we calculate the pH of the weak base.

$$CH_3COO^-(aq) + H_2O(l) \rightleftharpoons OH^-(aq) + CH_3COOH(aq)$$

$$K_b = \frac{[OH^-]\,[CH_3COOH]}{[CH_3COO^-]} = \frac{(x)(x)}{0.0667 - x} = 5.71 \times 10^{-10}$$

$$x = [OH^-] = 6.17 \times 10^{-6}\text{ M}$$

$$[H_3O^+] = \frac{K_w}{[OH^-]} = \frac{1.00 \times 10^{-14}}{6.17 \times 10^{-6}} = 1.62 \times 10^{-9}\text{ M}$$

finding that the pH at the equivalence point is 8.79.

After the equivalence point, the titrant is in excess and the titration mixture is a dilute solution of NaOH. We can calculate the pH using the same strategy as in the titration of a strong acid with a strong base. For example, after adding 30.0 mL of NaOH the concentration of OH^- is

$$[OH^-] = \frac{(0.200\text{ M})(30.0\text{ mL}) - (0.100\text{ M})(50.0\text{ mL})}{30.0\text{ mL} + 50.0\text{ mL}} = 0.0125\text{ M}$$

$$[H_3O^+] = \frac{K_w}{[OH^-]} = \frac{1.00 \times 10^{-14}}{0.0125} = 8.00 \times 10^{-13}\text{ M}$$

giving a pH of 12.10. Table 6.6.2 and Figure 6.6.2 show additional results for this titration. You can use this same approach to calculate the titration curve for the titration of a weak base with a strong acid, except the initial pH is determined by the weak base, the pH at the equivalence point by its conjugate weak acid, and the pH after the equivalence point by excess strong acid.

Table 6.6.2 . Titration of 50.0 mL of 0.100 M Acetic Acid with 0.200 M NaOH

volume of HCl (mL)	pH	volume of HCl (mL)	pH
0.00	2.88	26.0	11.43
5.00	4.16	28.0	11.89
10.0	4.58	30.0	12.10
15.0	4.94	35.0	12.37
20.0	5.36	40.0	12.52
22.0	5.63	45.0	12.63
24.0	6.14	50.0	12.70
25.0	8.79		

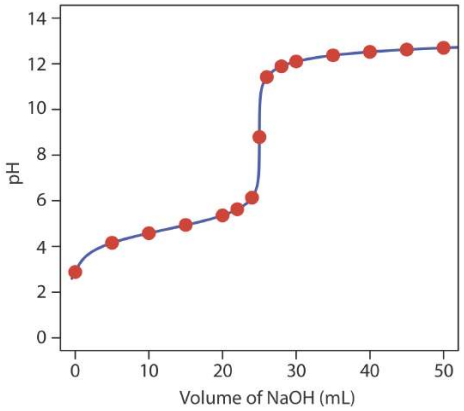


Figure 6.6.2 . Titration curve for the titration of 50.0 mL of 0.100 M CH_3COOH with 0.200 M NaOH. The red points correspond to the data in Table 6.6.2 . The blue line shows the complete titration curve.

Exercise 6.6.2

Construct a titration curve for the titration of 25.0 mL of 0.125 M NH_3 with 0.0625 M HCl.

Answer

The volume of HCl needed to reach the equivalence point is

$$V_{aq} = V_a = \frac{M_b V_b}{M_a} = \frac{(0.125\ \text{M})(25.0\ \text{mL})}{(0.0625\ \text{M})} = 50.0\ \text{mL}$$

Before adding HCl the pH is that for a solution of 0.100 M NH_3.

$$K_b = \frac{[OH^-]\,[NH_4^+]}{[NH_3]} = \frac{(x)(x)}{0.125 - x} = 1.75 \times 10^{-5}$$

$$x = [OH^-] = 1.48 \times 10^{-3}\ \text{M}$$

$$[H_3O^+] = \frac{K_w}{[OH^-]} = \frac{1.00 \times 10^{-14}}{1.48 \times 10^{-3}\ \text{M}} = 6.76 \times 10^{-12}\ \text{M}$$

The pH at the beginning of the titration, therefore, is 11.17.

Before the equivalence point the pH is determined by an NH_3/NH_4^+ buffer. For example, after adding 10.0 mL of HCl

$$[NH_3] = \frac{(0.125\ \text{M})(25.0\ \text{mL}) - (0.0625\ \text{M})(10.0\ \text{mL})}{25.0\ \text{mL} + 10.0\ \text{mL}} = 0.0714\ \text{M}$$

$$[NH_4^+] = \frac{(0.0625\ M)(10.0\ mL)}{25.0\ mL + 10.0\ mL} = 0.0179\ M$$

$$pH = 9.244 + \log \frac{0.0714\ M}{0.0179\ M} = 9.84$$

At the equivalence point the predominate ion in solution is NH_4^+. To calculate the pH we first determine the concentration of NH_4^+

$$[NH_4^+] = \frac{(0.125\ M)(25.0\ mL)}{25.0\ mL + 50.0\ mL} = 0.0417\ M$$

and then calculate the pH

$$K_a = \frac{[H_3O^+]\,[NH_3]}{[NH_4^+]} = \frac{(x)(x)}{0.0417 - x} = 5.70 \times 10^{-10}$$

obtaining a value of 5.31.

After the equivalence point, the pH is determined by the excess HCl. For example, after adding 70.0 mL of HCl

$$[HCl] = \frac{(0.0625\ M)(70.0\ mL) - (0.125\ M)(25.0\ mL)}{70.0\ mL + 25.0\ mL} = 0.0132\ M$$

and the pH is 1.88. Some additional results are shown here.

volume of HCl (mL)	pH	volume of HCl (mL)	pH
0	11.17	60	2.13
10	9.84	70	1.88
20	9.42	80	1.75
30	9.07	90	1.66
40	8.64	100	1.60
50	5.31		

We can extend this approach for calculating a weak acid–strong base titration curve to reactions that involve multiprotic acids or bases, and mixtures of acids or bases. As the complexity of the titration increases, however, the necessary calculations become more time consuming. Not surprisingly, a variety of algebraic and spreadsheet approaches are available to aid in constructing titration curves.

The following papers provide information on algebraic approaches to calculating titration curves: (a) Willis, C. J. *J. Chem. Educ.* **1981**, *58*, 659–663; (b) Nakagawa, K. *J. Chem. Educ.* **1990**, *67*, 673–676; (c) Gordus, A. A. *J. Chem. Educ.* **1991**, *68*, 759–761; (d) de Levie, R. *J. Chem. Educ.* **1993**, *70*, 209–217; (e) Chaston, S. *J. Chem. Educ.* **1993**, *70*, 878–880; (f) de Levie, R. *Anal. Chem.* **1996**, *68*, 585–590.

The following papers provide information on the use of spreadsheets to generate titration curves: (a) Currie, J. O.; Whiteley, R. V. *J. Chem. Educ.* **1991**, *68*, 923–926; (b) Breneman, G. L.; Parker, O. J. *J. Chem. Educ.* **1992**, *69*, 46–47; (c) Carter, D. R.; Frye, M. S.; Mattson, W. A. *J. Chem. Educ.* **1993**, *70*, 67–71; (d) Freiser, H. *Concepts and Calculations in Analytical Chemistry*, CRC Press: Boca Raton, 1992.

Sketching an Acid–Base Titration Curve

To evaluate the relationship between a titration's equivalence point and its end point we need to construct only a reasonable approximation of the exact titration curve. In this section we demonstrate a simple method for sketching an acid–base titration curve. Our goal is to sketch the titration curve quickly, using as few calculations as possible. Let's use the titration of 50.0 mL of

0.100 M CH_3COOH with 0.200 M NaOH to illustrate our approach. This is the same example that we used to develop the calculations for a weak acid–strong base titration curve. You can review the results of that calculation in Table 6.6.2 and in Figure 6.6.2 .

We begin by calculating the titration's equivalence point volume, which, as we determined earlier, is 25.0 mL. Next we draw our axes, placing pH on the *y*-axis and the titrant's volume on the *x*-axis. To indicate the equivalence point volume, we draw a vertical line that intersects the *x*-axis at 25.0 mL of NaOH. Figure 6.6.3 a shows the first step in our sketch.

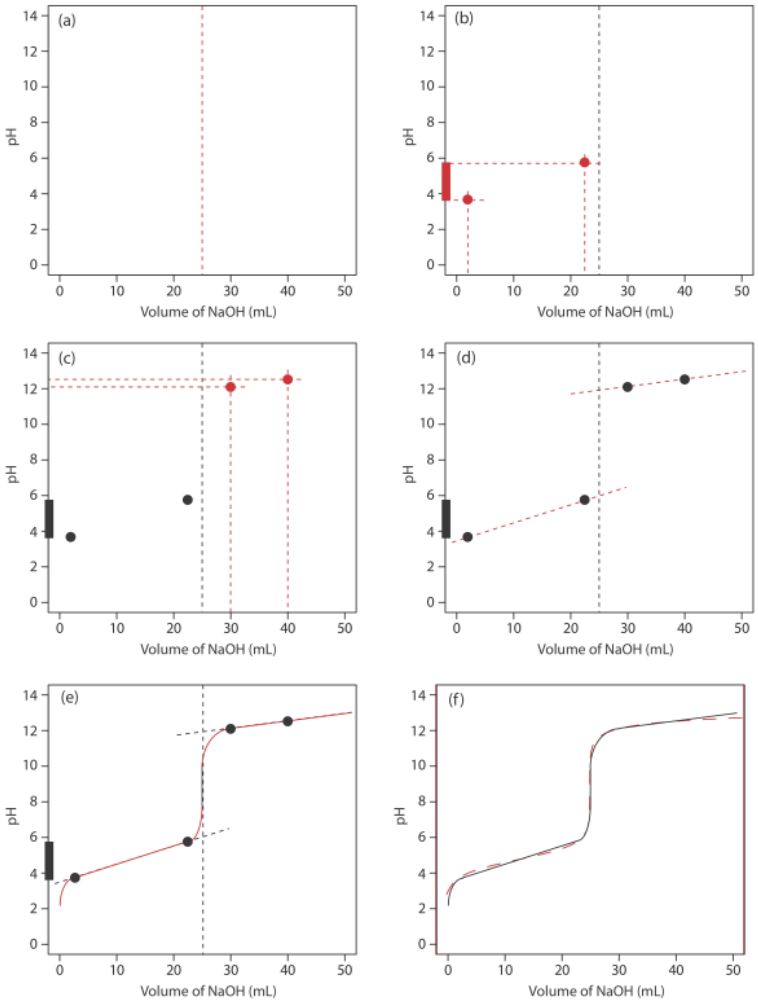


Figure 6.6.3 . Illustrations showing the steps used to sketch an approximate titration curve for the titration of 50.0 mL of 0.100 M CH_3COOH with 0.200 M NaOH: (a) locating the equivalence point volume; (b) plotting two points before the equivalence point; (c) plotting two points after the equivalence point; (d) preliminary approximation of titration curve using straight-lines; (e) final approximation of titration curve using a smooth curve; (f) comparison of approximate titration curve (solid black line) and exact titration curve (dashed red line). See the text for additional details.

Before the equivalence point the titrand's pH is determined by a buffer of acetic acid, CH_3COOH, and acetate, CH_3COO^-. Although we can calculate a buffer's pH using the Henderson–Hasselbalch equation, we can avoid this calculation by making a simple assumption. You may recall from Chapter 6 that a buffer operates over a pH range that extends approximately ±1 pH unit on either side of the weak acid's pK_a value. The pH is at the lower end of this range, pH = pK_a – 1, when the weak acid's concentration is **10×** greater than that of its conjugate weak base. The buffer reaches its upper pH limit, pH = pK_a + 1, when the weak acid's concentration is **10×** smaller than that of its conjugate weak base. When we titrate a weak acid or a weak base, the buffer spans a range of volumes from approximately 10% of the equivalence point volume to approximately 90% of the equivalence point volume.

> The actual values are 9.09% and 90.9%, but for our purpose, using 10% and 90% is more convenient; that is, after all, one advantage of an approximation!

Figure 6.6.3 b shows the second step in our sketch. First, we superimpose acetic acid's ladder diagram on the *y*-axis, including its buffer range, using its pK_a value of 4.76. Next, we add two points, one for the pH at 10% of the equivalence point volume (a pH of 3.76 at 2.5 mL) and one for the pH at 90% of the equivalence point volume (a pH of 5.76 at 22.5 mL).

The third step is to add two points after the equivalence point. The pH after the equivalence point is fixed by the concentration of excess titrant, NaOH. Calculating the pH of a strong base is straightforward, as we saw earlier. Figure 6.6.3 c includes points (see Table 6.6.2) for the pH after adding 30.0 mL and after adding 40.0 mL of NaOH.

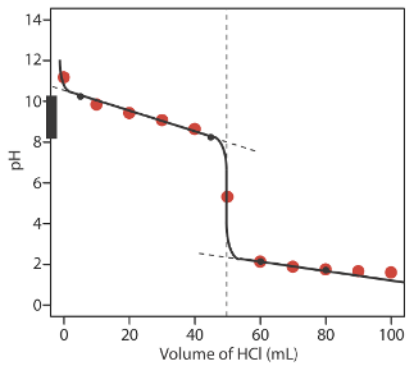
Next, we draw a straight line through each pair of points, extending each line through the vertical line that represents the equivalence point's volume (Figure 6.6.3 d). Finally, we complete our sketch by drawing a smooth curve that connects the three straight-line segments (Figure 6.6.3 e). A comparison of our sketch to the exact titration curve (Figure 6.6.3 f) shows that they are in close agreement.

? Exercise 6.6.3

Sketch a titration curve for the titration of 25.0 mL of 0.125 M NH_3 with 0.0625 M HCl and compare to the result from Exercise 6.6.2 .

Answer

The figure below shows a sketch of the titration curve. The black dots and curve are the approximate sketch of the titration curve. The points in red are the calculations from Exercise 6.6.2 . The two black points before the equivalence point (V_{HCl} = 5 mL, pH = 10.24 and V_{HCl} = 45 mL, pH= 8.24) are plotted using the pK_a of 9.244 for NH_4^+. The two black points after the equivalence point (V_{HCl} = 60 mL, pH = 2.13 and V_{HCl} = 80 mL, pH= 1.75) are from the answer to Exercise 6.6.2 .



As shown in the following example, we can adapt this approach to any acid–base titration, including those where exact calculations are more challenging, including the titration of polyprotic weak acids and bases, and the titration of mixtures of weak acids or weak bases.

✓ Example 6.6.1

Sketch titration curves for the following two systems: (a) the titration of 50.0 mL of 0.050 M H_2A, a diprotic weak acid with a pK_{a1} of 3 and a pK_{a2} of 7; and (b) the titration of a 50.0 mL mixture that contains 0.075 M HA, a weak acid with a pK_a of 3, and 0.025 M HB, a weak acid with a pK_a of 7. For both titrations, assume that the titrant is 0.10 M NaOH.

Solution

Figure 6.6.4 a shows the titration curve for H_2A, including the ladder diagram for H_2A on the *y*-axis, the two equivalence points at 25.0 mL and at 50.0 mL, two points before each equivalence point, two points after the last equivalence point, and the straight-lines used to sketch the final titration curve. Before the first equivalence point the pH is controlled by a buffer of H_2A

and HA^-. An HA^-/A^{2-} buffer controls the pH between the two equivalence points. After the second equivalence point the pH reflects the concentration of excess NaOH.

Figure 6.6.4 b shows the titration curve for the mixture of HA and HB. Again, there are two equivalence points; however, in this case the equivalence points are not equally spaced because the concentration of HA is greater than that for HB. Because HA is the stronger of the two weak acids it reacts first; thus, the pH before the first equivalence point is controlled by a buffer of HA and A^-. Between the two equivalence points the pH reflects the titration of HB and is determined by a buffer of HB and B^-. After the second equivalence point excess NaOH determines the pH.

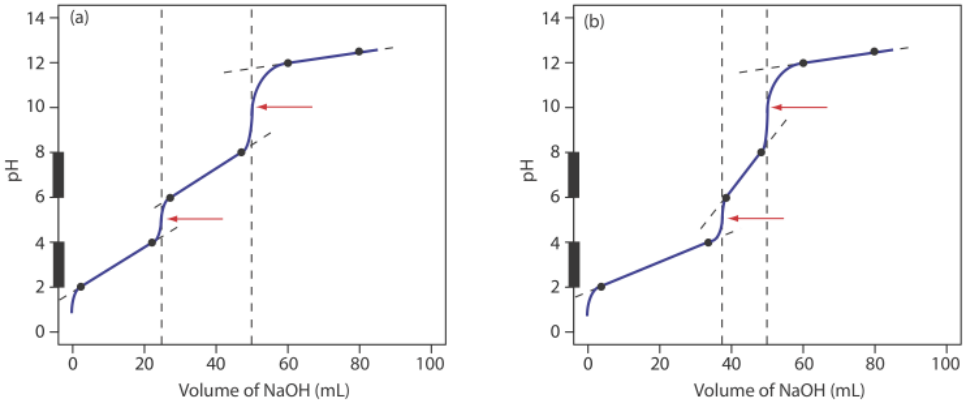


Figure 6.6.4 . Titration curves for Example 6.6.1 . The solid black dots show the points used to sketch the titration curves (shown in blue) and the red arrows show the locations of the equivalence points.

Exercise 6.6.4

Sketch the titration curve for 50.0 mL of 0.050 M H_2A, a diprotic weak acid with a pK_{a1} of 3 and a pK_{a2} of 4, using 0.100 M NaOH as the titrant. The fact that pK_{a2} falls within the buffer range of pK_{a1} presents a challenge that you will need to consider.

Answer

The figure below shows a sketch of the titration curve. The titration curve has two equivalence points, one at 25.0 mL ($\mathbf{H_2A \rightarrow HA^-}$) and one at 50.0 mL ($\mathbf{HA^- \rightarrow A^{2-}}$). In sketching the curve, we plot two points before the first equivalence point using the pK_{a1} of 3 for H_2A

$$\mathbf{V_{HCl} = 2.5\ mL, pH = 2 \text{ and } V_{HCl} = 22.5\ mL, pH = 4}$$

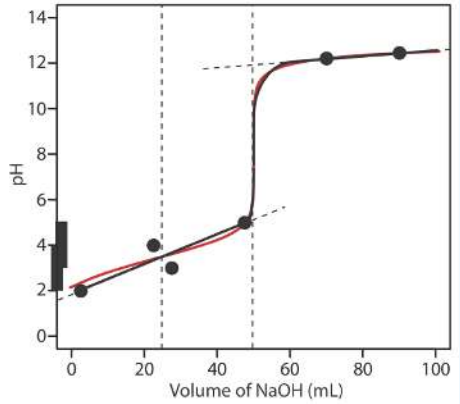
two points between the equivalence points using the pK_{a2} of 5 for HA^-

$$\mathbf{V_{HCl} = 27.5\ mL, pH = 3, \text{ and } V_{HCl} = 47.5\ mL, pH = 5}$$

and two points after the second equivalence point

$$\mathbf{V_{HCl} = 70\ mL, pH = 12.22 \text{ and } V_{HCl} = 90\ mL, pH = 12.46}$$

Drawing a smooth curve through these points presents us with the following dilemma—the pH appears to increase as the titrant's volume approaches the first equivalence point and then appears to decrease as it passes through the first equivalence point. This is, of course, absurd; as we add NaOH the pH cannot decrease. Instead, we model the titration curve before the second equivalence point by drawing a straight line from the first point (V_{HCl} = 2.5 mL, pH = 2) to the fourth point (V_{HCl} = 47.5 mL, pH= 5), ignoring the second and third points. The results is a reasonable approximation of the exact titration curve.



Selecting and Evaluating the End Point

Earlier we made an important distinction between a titration's end point and its equivalence point. The difference between these two terms is important and deserves repeating. An equivalence point, which occurs when we react stoichiometrically equal amounts of the analyte and the titrant, is a theoretical not an experimental value. A titration's end point is an experimental result that represents our best estimate of the equivalence point. Any difference between a titration's equivalence point and its corresponding end point is a source of determinate error.

Where is the Equivalence Point?

Earlier we learned how to calculate the pH at the equivalence point for the titration of a strong acid with a strong base, and for the titration of a weak acid with a strong base. We also learned how to sketch a titration curve with only a minimum of calculations. Can we also locate the equivalence point without performing any calculations. The answer, as you might guess, often is yes!

For most acid–base titrations the inflection point—the point on a titration curve that has the greatest slope—very nearly coincides with the titration's equivalence point. The red arrows in Figure 6.6.4 , for example, identify the equivalence points for the titration curves in Example 6.6.1 . An inflection point actually precedes its corresponding equivalence point by a small amount, with the error approaching 0.1% for weak acids and weak bases with dissociation constants smaller than 10^{-9}, or for very dilute solutions [Meites, L.; Goldman, J. A. *Anal. Chim. Acta* **1963**, *29*, 472–479].

The principal limitation of an inflection point is that it must be present and easy to identify. For some titrations the inflection point is missing or difficult to find. Figure 6.6.5 , for example, demonstrates the affect of a weak acid's dissociation constant, K_a, on the shape of its titration curve. An inflection point is visible, even if barely so, for acid dissociation constants larger than 10^{-9}, but is missing when K_a is 10^{-11}.

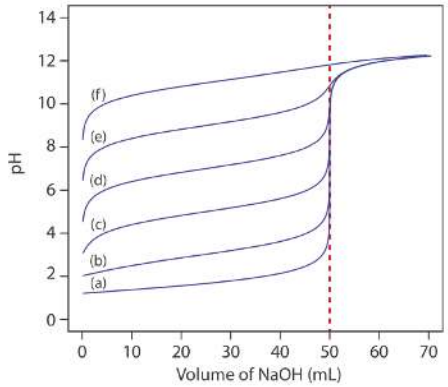


Figure 6.6.5 . Weak acid–strong base titration curves for the titration of 50.0 mL of 0.100 M HA with 0.100 M NaOH. The pK_a values for HA are (a) 1, (b) 3, (c) 5, (d) 7, (e) 9, and (f) 11. The dashed red line shows the equivalence point, which is 50.0 mL for all six analytes.

https://chem.libretexts.org/@go/page/438342

An inflection point also may be missing or difficult to see if the analyte is a multiprotic weak acid or weak base with successive dissociation constants that are similar in magnitude. To appreciate why this is true let's consider the titration of a diprotic weak acid, H_2A, with NaOH. During the titration the following two reactions occur.

$$\mathrm{H_2A}(aq) + \mathrm{OH^-}(aq) \longrightarrow \mathrm{H_2O}(l) + \mathrm{HA^-}(aq) \tag{8.2.8.6}$$

$$\mathrm{HA^-}(aq) + \mathrm{OH^-}(aq) \rightarrow \mathrm{H_2O}(l) + \mathrm{A^{2-}}(aq) \tag{8.2.8.7}$$

To see two distinct inflection points, reaction 8.2.8.6 must essentially be complete before reaction 8.2.8.7 begins.

Figure 6.6.6 shows titration curves for three diprotic weak acids. The titration curve for maleic acid, for which K_{a1} is approximately $20000\times$ larger than K_{a2}, has two distinct inflection points. Malonic acid, on the other hand, has acid dissociation constants that differ by a factor of approximately 690. Although malonic acid's titration curve shows two inflection points, the first is not as distinct as the second. Finally, the titration curve for succinic acid, for which the two K_a values differ by a factor of only $27\times$, has only a single inflection point that corresponds to the neutralization of $\mathrm{HC_2H_4O_4^-}$ to $\mathrm{C_2H_4O_4^{2-}}$. In general, we can detect separate inflection points when successive acid dissociation constants differ by a factor of at least 500 (a ΔK_a of at least 2.7).

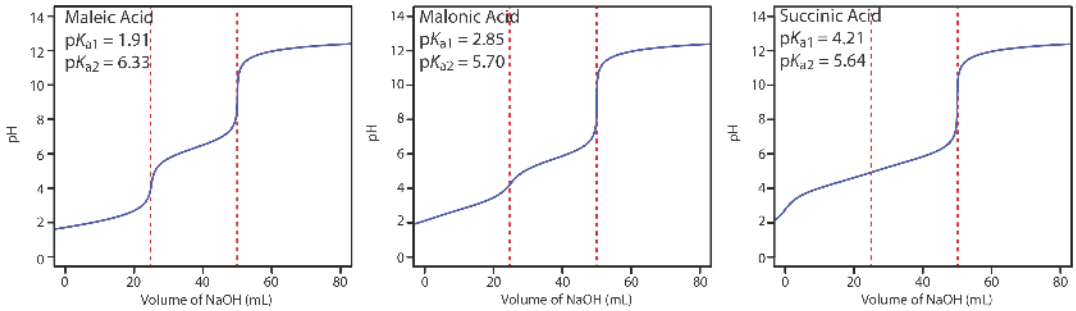


Figure 6.6.6 . Titration curves for the diprotic weak acids maleic acid, malonic acid, and succinic acid. Each titration curve is for 50.0 mL of 0.0500 M weak acid using 0.100 M NaOH as the titrant. Although each titration curve has equivalence points at 25.0 mL and 50.0 mL of NaOH (shown by the dashed red lines), the titration curve for succinic acid shows only one inflection point.

> The same holds true for mixtures of weak acids or mixtures of weak bases. To detect separate inflection points when titrating a mixture of weak acids, their pK_a values must differ by at least a factor of 500.

Finding the End Point with an Indicator

One interesting group of weak acids and weak bases are organic dyes. Because an organic dye has at least one highly colored conjugate acid–base species, its titration results in a change in both its pH and its color. We can use this change in color to indicate the end point of a titration provided that it occurs at or near the titration's equivalence point.

As an example, let's consider an indicator for which the acid form, HIn, is yellow and the base form, In^-, is red. The color of the indicator's solution depends on the relative concentrations of HIn and In^-. To understand the relationship between pH and color we use the indicator's acid dissociation reaction

$$\mathrm{HIn}(aq) + \mathrm{H_2O}(l) \rightleftharpoons \mathrm{H_3O^+}(aq) + \mathrm{In^-}(aq)$$

and its equilibrium constant expression.

$$K_a = \frac{[\mathrm{H_3O^+}]\,[\mathrm{In^-}]}{[\mathrm{HIn}]} \tag{8.2.8.8}$$

Taking the negative log of each side of Equation 8.2.8.8, and rearranging to solve for pH leaves us with a equation that relates the solution's pH to the relative concentrations of HIn and In^-.

$$\mathrm{pH} = \mathrm{p}K_a + \log\frac{[\mathrm{In^-}]}{[\mathrm{HIn}]} \tag{8.2.8.9}$$

If we can detect HIn and In^- with equal ease, then the transition from yellow-to-red (or from red-to-yellow) reaches its midpoint, which is orange, when the concentrations of HIn and In^- are equal, or when the pH is equal to the indicator's pK_a. If the indicator's

pK_a and the pH at the equivalence point are identical, then titrating until the indicator turns orange is a suitable end point. Unfortunately, we rarely know the exact pH at the equivalence point. In addition, determining when the concentrations of HIn and In^- are equal is difficult if the indicator's change in color is subtle.

We can establish the range of pHs over which the average analyst observes a change in the indicator's color by making two assumptions: that the indicator's color is yellow if the concentration of HIn is $10\times$ greater than that of In^- and that its color is red if the concentration of HIn is $10\times$ smaller than that of In^-. Substituting these inequalities into Equation 8.2.8.9

$$\mathrm{pH} = \mathrm{p}K_a + \log\frac{1}{10} = \mathrm{p}K_a - 1$$
$$\mathrm{pH} = \mathrm{p}K_a + \log\frac{10}{1} = \mathrm{p}K_a + 1$$

shows that the indicator changes color over a pH range that extends ±1 unit on either side of its pK_a. As shown in Figure 6.6.7 , the indicator is yel-ow when the pH is less than pK_a – 1 and it is red when the pH is greater than pK_a + 1. For pH values between pK_a – 1 and pK_a + 1 the indicator's color passes through various shades of orange. The properties of several common acid–base indicators are listed in Table 6.6.3 .

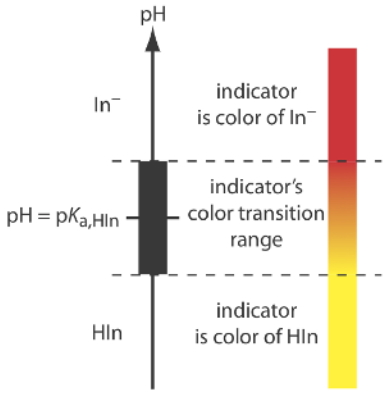


Figure 6.6.7 . Diagram showing the relationship between pH and an indicator's color. The ladder diagram defines pH values where HIn and In^- are the predominate species. The indicator changes color when the pH is between pK_a – 1 and pK_a+1.

Table 6.6.3 . Properties of Selected Acid–Base Indicators

https://chem.libretexts.org/@go/page/438342

indicator	acid color	base color	pH range	pK_a
cresol red	red	yellow	0.2–1.8	—
thymol blue	red	yellow	1.2–2.8	1.7
bromothymol blue	yellow	blue	3.0–4.6	4.1
methyl orange	red	yellow	3.4–4.4	3.7
Congo red	blue	red	3.0–5.0	—
bromocresol green	yellow	blue	3.8–5.4	4.7
methyl red	red	yellow	4.2–6.3	5.0
bromocresol purple	yellow	purple	5.2–6.8	6.1
litmus	red	blue	5.0–8.0	—
bromothymol blue	yellow	blue	6.0–7.6	7.1
phenol red	yellow	blue	6.8–8.4	7.8
cresol red	yellow	red	7.2–8.8	8.2
thymol blue	yellow	red	8.0–9.6	8.9
phenolphthalein	colorless	red	8.3–10.0	9.6
alizarin yellow R	yellow	orange-red	10.1–12.0	—

You may wonder why an indicator's pH range, such as that for phenolphthalein, is not equally distributed around its pK_a value. The explanation is simple. Figure 6.6.7 presents an idealized view in which our sensitivity to the indicator's two colors is equal. For some indicators only the weak acid or the weak base is colored. For other indicators both the weak acid and the weak base are colored, but one form is easier to see. In either case, the indicator's pH range is skewed in the direction of the indicator's less colored form. Thus, phenolphthalein's pH range is skewed in the direction of its colorless form, shifting the pH range to values lower than those suggested by Figure 6.6.7 .

The relatively broad range of pHs over which an indicator changes color places additional limitations on its ability to signal a titration's end point. To minimize a determinate titration error, the indicator's entire pH range must fall within the rapid change in pH near the equivalence point. For example, in Figure 6.6.8 we see that phenolphthalein is an appropriate indicator for the titration of 50.0 mL of 0.050 M acetic acid with 0.10 M NaOH. Bromothymol blue, on the other hand, is an inappropriate indicator because its change in color begins well before the initial sharp rise in pH, and, as a result, spans a relatively large range of volumes. The early change in color increases the probability of obtaining an inaccurate result, and the range of possible end point volumes increases the probability of obtaining imprecise results.

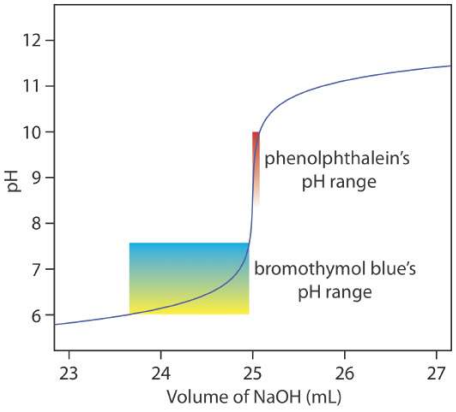


Figure 6.6.8 . Portion of the titration curve for 50.0 mL of 0.050 M CH_3COOH with 0.10 M NaOH, highlighting the region that contains the equivalence point. The end point transitions for the indicators phenolphthalein and bromothymol blue are superimposed on the titration curve.

? Exercise 6.6.5

Suggest a suitable indicator for the titration of 25.0 mL of 0.125 M NH_3 with 0.0625 M NaOH. You constructed a titration curve for this titration in Exercise 6.6.2 and Exercise 6.6.3 .

Answer

The pH at the equivalence point is 5.31 (see Exercise 6.6.2) and the sharp part of the titration curve extends from a pH of approximately 7 to a pH of approximately 4. Of the indicators in Table 6.6.3 , methyl red is the best choice because its pK_a value of 5.0 is closest to the equivalence point's pH and because the pH range of 4.2–6.3 for its change in color will not produce a significant titration error.

This page titled 8.2.8: pH Calculations for Acid–Base Titrations is shared under a CC BY-NC-SA 4.0 license and was authored, remixed, and/or curated by David Harvey.

- **9.2: Acid–Base Titrations** by David Harvey is licensed CC BY-NC-SA 4.0.

CHAPTER OVERVIEW

9: Electrochemistry

Electrochemistry is the study of chemical processes that cause electrons to move. This movement of electrons is called electricity, which can be generated by movements of electrons from one element to another in a reaction known as an oxidation-reduction ("redox") reaction.

9.1: Oxidation-Reduction Reactions
9.2: Balancing Redox Reactions
9.3: Galvanic Cells
9.4: Standard Electrode Potentials
9.5: Strengths of Oxidants and Reductants
9.6: E, ΔG, and K (The Big Triangle of Chemistry)
9.7: Cell Potential as a Function of Concentrations
9.8: Batteries- Producing Electricity Through Chemical Reactions
9.9: Corrosion- Unwanted Voltaic Cells
9.10: Electrolysis- Causing Nonspontaneous Reactions to Occur

---

9: Electrochemistry is shared under a not declared license and was authored, remixed, and/or curated by LibreTexts.

9.1: Oxidation-Reduction Reactions

An oxidation-reduction (redox) reaction is a type of chemical reaction that involves a transfer of electrons between two species. An oxidation-reduction reaction is any chemical reaction in which the oxidation number of a molecule, atom, or ion changes by gaining or losing an electron. Redox reactions are common and vital to some of the basic functions of life, including photosynthesis, respiration, combustion, and corrosion or rusting.

Rules for Assigning Oxidation States

The oxidation state (OS) of an element corresponds to the number of electrons, e^-, that an atom loses, gains, or appears to use when joining with other atoms in compounds. In determining the oxidation state of an atom, there are seven guidelines to follow:

1. The oxidation state of an individual atom is 0.
2. The total oxidation state of all atoms in: a *neutral species* is 0 and in an *ion* is equal to the ion charge.
3. Group 1 metals have an oxidation state of +1 and Group 2 an oxidation state of +2
4. The oxidation state of fluorine is -1 in compounds
5. Hydrogen generally has an oxidation state of +1 in compounds
6. Oxygen generally has an oxidation state of -2 in compounds
7. In binary metal compounds, Group 17 elements have an oxidation state of -1, Group 16 elements of -2, and Group 15 elements of -3.

> *The **sum** of the oxidation states is equal to zero for neutral compounds and equal to the **charge** for polyatomic ion species.*

Example 9.1.1: Assigning Oxidation States

Determine the Oxidation States of each element in the following reactions:

a. $\mathbf{Fe}(s) + \mathbf{O_2}(g) \longrightarrow \mathbf{Fe_2O_3}(g)$
b. $\mathbf{Fe^{2+}}(aq)$
c. $\mathbf{Ag}(s) + \mathbf{H_2S} \longrightarrow \mathbf{Ag_2S}(g) + \mathbf{H_2}(g)$

Solutions

A. **Fe** and $\mathbf{O_2}$ are free elements; therefore, they each have an oxidation state of 0 according to Rule #1. The product has a total oxidation state equal to 0, and following Rule #6, **O** has an oxidation state of -2, which means **Fe** has an oxidation state of +3.
B. The oxidation state of **Fe** ions just corresponds to its charge since it is a single element species; therefore, the oxidation state is +2.
C. **Ag** has an oxidation state of 0, **H** has an oxidation state of +1 according to Rule #5, $\mathbf{H_2}$ has an oxidation state of 0, **S** has an oxidation state of -2 according to Rule #7, and hence **Ag** in $\mathbf{Ag_2S}$ has an oxidation state of +1.

Example 9.1.2: Assigning Oxidation States

Determine the oxidation states of the phosphorus atom bold element in each of the following species:

a. $\mathbf{Na_3PO_3}$
b. $\mathbf{H_2PO_4^-}$

Solutions

a. The oxidation numbers of **Na** and **O** are +1 and -2. Because sodium phosphite is neutral species, the sum of the oxidation numbers must be zero. Letting *x* be the oxidation number of phosphorus, 0= 3(+1) + *x* + 3(-2). *x*=oxidation number of P= +3.

b. Hydrogen and oxygen have oxidation numbers of +1 and -2. The ion has a charge of -1, so the sum of the oxidation numbers must be -1. Letting *y* be the oxidation number of phosphorus, -1= *y* + 2(+1) +4(-2), *y*= oxidation number of P= +5.

Example 9.1.3: Identifying Reduced and Oxidized Elements

Determine which element is oxidized and which element is reduced in the following reactions (be sure to include the oxidation state of each):

a. $\mathrm{Zn + 2\,H^+ \longrightarrow Zn^{2+} + H_2}$
b. $\mathrm{2\,Al + 3\,Cu^{2+} \longrightarrow 2\,Al^{3+} + 3\,Cu}$
c. $\mathrm{CO_3^{2-} + 2\,H^+ \longrightarrow CO_2 + H_2O}$

Solutions

a. Zn is oxidized (Oxidation number: 0 → +2); H^+ is reduced (Oxidation number: +1 → 0)
b. Al is oxidized (Oxidation number: 0 → +3); Cu^{2+} is reduced (+2 → 0)
c. This is not a redox reaction because each element has the same oxidation number in both reactants and products: O= -2, H= +1, C= +4.

An atom is oxidized if its oxidation number increases, the reducing agent, and an atom is reduced if its oxidation number decreases, the oxidizing agent. The atom that is oxidized is the reducing agent, and the atom that is reduced is the oxidizing agent. (Note: the oxidizing and reducing agents can be the same element or compound).

Oxidation-Reduction Reactions

Redox reactions are comprised of two parts, a reduced half and an oxidized half, that *always* occur together. The reduced half gains electrons and the oxidation number decreases, while the oxidized half loses electrons and the oxidation number increases. Simple ways to remember this include the mnemonic devices **OIL RIG,** meaning "*oxidation is loss*" and "*reduction is gain.*" There is no net change in the number of electrons in a redox reaction. Those given off in the oxidation half reaction are taken up by another species in the reduction half reaction.

The two species that exchange electrons in a redox reaction are given special names:

1. The ion or molecule that accepts electrons is called the **oxidizing agent** - by accepting electrons it oxidizes other species.
2. The ion or molecule that donates electrons is called the **reducing agent** - by giving electrons it reduces the other species.

Hence, what is oxidized is the reducing agent and what is reduced is the oxidizing agent. (Note: the oxidizing and reducing agents can be the same element or compound, as in disproportionation reactions discussed below).

A good example of a redox reaction is the thermite reaction, in which iron atoms in ferric oxide lose (or give up) **O** atoms to **Al** atoms, producing $\mathrm{Al_2O_3}$.

$$\mathrm{Fe_2O_3\,(s) + 2\,Al\,(s) \rightarrow Al_2O_3\,(s) + 2\,Fe\,(l)}$$

Example 9.1.4: Identifying Oxidizing and Reducing Agents

Determine what is the oxidizing and reducing agents in the following reaction.

$$\mathrm{Zn + 2\,H^+ \longrightarrow Zn^{2+} + H_2}$$

Solution

The oxidation state of **H** changes from +1 to 0, and the oxidation state of **Zn** changes from 0 to +2. Hence, **Zn** is oxidized and acts as the *reducing agent*. $\mathrm{H^+}$ ion is reduced and acts as the *oxidizing agent*.

Combination Reactions

Combination reactions are among the simplest redox reactions and, as the name suggests, involves "combining" elements to form a chemical compound. As usual, oxidation and reduction occur together. The general equation for a combination reaction is given

below:

$$\mathbf{A + B \longrightarrow AB}$$

Example 9.1.5: Combination Reaction

Consider the combination reaction of hydrogen and oxygen

$$\mathbf{H_2 + O_2 \longrightarrow H_2O}$$

Solution

$$0 + 0 \rightarrow \mathbf{(2)(+1) + (-2) = 0}$$

In this reaction both H_2 and O_2 are free elements; following Rule #1, their oxidation states are 0. The product is H_2O, which has a total oxidation state of 0. According to Rule #6, the oxidation state of oxygen is usually -2. Therefore, the oxidation state of H in H_2O must be +1.

Decomposition Reactions

A **decomposition** reaction is the reverse of a combination reaction, the breakdown of a chemical compound into individual elements:

$$\mathbf{AB \longrightarrow A + B}$$

Example 9.1.6: Decomposition Reaction

Consider the following reaction:

$$\mathbf{H_2O \longrightarrow H_2 + O_2}$$

This follows the definition of the decomposition reaction, where water is "decomposed" into hydrogen and oxygen.

$$(2)(+1) + (-2) = 0 \rightarrow 0 + 0$$

As in the previous example the $\mathbf{H_2O}$ has a total oxidation state of 0; thus, according to Rule #6 the oxidation state of oxygen is usually -2, so the oxidation state of hydrogen in $\mathbf{H_2O}$ must be +1.

Note that the autoionization reaction of water is **not** a redox nor decomposition reaction since the oxidation states do not change for any element:

$$\mathbf{H_2O \longrightarrow H^+ + OH^-}$$

Single Replacement Reactions

A **single replacement** reaction involves the "replacing" of an element in the reactants with another element in the products:

$$\mathbf{A + BC \longrightarrow AB + C}$$

Example 9.1.7: Single Replacement Reaction

Equation:

$$\mathbf{Cl_2 + NaBr \rightarrow NaCl + Br_2}$$

Calculation:

$$(0) + ((+1) + (-1) = 0) \text{ -> } ((+1) + (-1) = 0) + 0$$

In this equation, **Br** is replaced with **Cl**, and the **Cl** atoms in $\mathbf{Cl_2}$ are reduced, while the **Br** ion in **NaBr** is oxidized.

Double Replacement Reactions

A double replacement reaction is similar to a single replacement reaction, but involves "replacing" two elements in the reactants, with two in the products:

$$\mathrm{AB + CD \longrightarrow AD + CB}$$

An example of a double replacement reaction is the reaction of magnesium sulfate with sodium oxalate

$$\mathrm{MgSO_4\,(aq) + Na_2C_2O_4\,(aq) \longrightarrow MgC_2O_4\,(s) + Na_2SO_4\,(aq)}$$

Combustion Reactions

Combustion is the formal terms for "burning" and typically involves a substance reacts with oxygen to transfer energy to the surroundings as light and heat. Hence, combustion reactions are almost always exothermic. For example, internal combustion engines rely on the combustion of organic hydrocarbons $\mathrm{C_xH_y}$ to generate $\mathrm{CO_2}$ and $\mathrm{H_2O}$:

$$\mathrm{C_xH_y + O_2 \longrightarrow CO_2 + H_2O}$$

Although combustion reactions typically involve redox reactions with a chemical being oxidized by oxygen, many chemicals can "burn" in other environments. For example, both titanium and magnesium metals can burn in nitrogen as well:

$$\mathrm{2\,Ti\,(s) + N_2\,(g) \longrightarrow 2\,TiN\,(s)}$$

$$\mathrm{3\,Mg\,(s) + N_2\,(g) \longrightarrow Mg_3N_2\,(s)}$$

Moreover, chemicals can be oxidized by other chemicals than oxygen, such as $\mathrm{Cl_2}$ or $\mathrm{F_2}$; these processes are also considered combustion reactions.

Example 9.1.8: Identifying Combustion Reactions

Which of the following are combustion reactions?

a. $\mathrm{2\,H_2O \longrightarrow 2\,H_2 + O_2}$
b. $\mathrm{4\,Fe + 3\,O_2 \longrightarrow 2\,Fe_2O_3}$
c. $\mathrm{2\,AgNO_3 + H_2S \longrightarrow Ag_2S + 2\,NHO_3}$
d. $\mathrm{2\,Al + N_2 \longrightarrow 2\,AlN_4}$

Solution

Both reaction b and reaction d are combustion reactions, although with different oxidizing agents. Reaction b is the conventional combustion reaction using $\mathrm{O_2}$ and reaction uses $\mathrm{N_2}$ instead.

Disproportionation Reactions

In disproportionation reactions, a single substance can be both oxidized and reduced. These are known as disproportionation reactions, with the following general equation:

$$\mathrm{2\,A \longrightarrow A^{+}_{n} + A^{-}_{n}}$$

where n is the number of electrons transferred. Disproportionation reactions do not need begin with neutral molecules, and can involve more than two species with differing oxidation states (but rarely).

Example 9.1.9: Disproportionation Reaction

Disproportionation reactions have some practical significance in everyday life, including the reaction of hydrogen peroxide, $\mathrm{H_2O_2}$ poured over a cut. This a decomposition reaction of hydrogen peroxide, which produces oxygen and water. Oxygen is present in all parts of the chemical equation and as a result it is both oxidized and reduced. The reaction is as follows:

$$\mathrm{2\,H_2O_2\,(aq) \longrightarrow 2\,H_2O\,(l) + O_2\,(g)}$$

Dicussion

On the reactant side, **H** has an oxidation state of +1 and **O** has an oxidation state of -1, which changes to -2 for the product $\mathbf{H_2O}$ (oxygen is reduced), and 0 in the product $\mathbf{O_2}$ (oxygen is oxidized).

? Exercise 9.1.9

Which element undergoes a bifurcation of oxidation states in this disproportionation reaction:

$$\mathbf{HNO_2 \longrightarrow HNO_3 + NO + H_2O}$$

Answer

The **N** atom undergoes disproportionation. You can confirm that by identifying the oxidation states of each atom in each species.

References

1. Petrucci, et al. *General Chemistry: Principles & Modern Applications*. 9th ed. Upper Saddle River, New Jersey: Pearson/Prentice Hall, 2007.
2. Sadava, et al. *Life: The Science of Biology*. 8th ed. New York, NY. W.H. Freeman and Company, 2007

Contributors and Attributions

- Christopher Spohrer (UCD), Christina Breitenbuecher (UCD), Luvleen Brar (UCD)

9.1: Oxidation-Reduction Reactions is shared under a not declared license and was authored, remixed, and/or curated by LibreTexts.

- **Oxidation-Reduction Reactions** is licensed CC BY-NC-SA 4.0.

9.2: Balancing Redox Reactions

Oxidation-Reduction Reactions, or redox reactions, are reactions in which one reactant is oxidized and one reactant is reduced simultaneously. This module demonstrates how to balance various redox equations.

Identifying Redox Reactions

The first step in balancing any redox reaction is determining whether or not it is even an oxidation-reduction reaction. This requires that one and typically more species changing oxidation states during the reaction. To maintain charge neutrality in the sample, the redox reaction will entail both a reduction component and an oxidation components. These are often separated into independent two hypothetical **half-reactions** to aid in understanding the reaction. This requires identifying which element is oxidized and which element is reduced. For example, consider this reaction:

$$\mathrm{Cu\,(s) + 2\,Ag^{+}\,(aq)\ \rightarrow Cu^{2+}\,(aq) + 2\,Ag\,(s)}$$

The first step in determining whether the reaction is a redox reaction is to split the equation into two hypothetical *half-reactions*. Let's start with the half-reaction involving the copper atoms:

$$\mathrm{Cu\,(s)\ \rightarrow Cu^{2+}\,(aq)}$$

The oxidation state of copper on the left side is 0 because it is an element on its own. The oxidation state of copper on the right hand side of the equation is +2. The copper in this half-reaction is oxidized as the oxidation states increases from 0 in Cu to +2 in $\mathrm{Cu^{2+}}$. Now consider the silver atoms

$$\mathrm{2\,Ag^{+}\,(aq)\ \rightarrow 2\,Ag\,(s)}$$

In this half-reaction, the oxidation state of silver on the left side is a +1. The oxidation state of silver on the right is 0 because it is an pure element. Because the oxidation state of silver decreases from +1 to 0, this is the reduction half-reaction.

Consequently, this reaction is a redox reaction as both reduction and oxidation half-reactions occur (via the transfer of electrons, that are not explicitly shown in equations 2). Once confirmed, it often necessary to balance the reaction (the reaction in equation 1 is balanced already though), which can be accomplished in two ways because the reaction could take place in neutral, acidic or basic conditions.

Balancing Redox Reactions

Balancing redox reactions is slightly more complex than balancing standard reactions, but still follows a relatively simple set of rules. One major difference is the necessity to know the half-reactions of the involved reactants; a half-reaction table is very useful for this. Half-reactions are often useful in that two half reactions can be added to get a total net equation. Although the half-reactions must be known to complete a redox reaction, it is often possible to figure them out without having to use a half-reaction table. This is demonstrated in the acidic and basic solution examples. Besides the general rules for neutral conditions, additional rules must be applied for aqueous reactions in acidic or basic conditions.

One method used to balance redox reactions is called the **Half-Equation Method**. In this method, the equation is separated into two half-equations; one for oxidation and one for reduction.

Half-Equation Method to Balance redox Reactions in **Acidic** Aqueous Solutions

Each reaction is balanced by adjusting coefficients and adding $\mathrm{H_2O}$, $\mathrm{H^{+}}$, and $\mathrm{e^{-}}$ in this order:

1. Balance elements in the equation other than O and H.
2. Balance the oxygen atoms by adding the appropriate number of water ($\mathrm{H_2O}$) molecules to the opposite side of the equation.
3. Balance the hydrogen atoms (including those added in step 2 to balance the oxygen atom) by adding $\mathrm{H^{+}}$ ions to the opposite side of the equation.
4. Add up the charges on each side. Make them equal by adding enough electrons ($\mathrm{e^{-}}$) to the more positive side. (Rule of thumb: $\mathrm{e^{-}}$ and $\mathrm{H^{+}}$ are almost always on the same side.)

5. The e^- on each side must be made equal; if they are not equal, they must be multiplied by appropriate integers (the lowest common multiple) to be made the same.
6. The half-equations are added together, canceling out the electrons to form one balanced equation. Common terms should also be canceled out.

The equation can now be checked to make sure that it is balanced.

Half-Equation Method to Balance redox Reactions in **Basic** Aqueous Solutions

If the reaction is being balanced in a basic solution, the above steps are modified with the the addition of one step between #3 and #4:

3b Add the appropriate number of OH^- to neutralize all H^+ and to convert into water molecules.

The equation can now be checked to make sure that it is balanced.

Neutral Conditions

The first step to balance any redox reaction is to separate the reaction into half-reactions. The substance being reduced will have electrons as reactants, and the oxidized substance will have electrons as products. (Usually all reactions are written as reduction reactions in half-reaction tables. To switch to oxidation, the whole equation is reversed and the voltage is multiplied by -1.) Sometimes it is necessary to determine which half-reaction will be oxidized and which will be reduced. In this case, whichever half-reaction has a higher reduction potential will by reduced and the other oxidized.

Example 9.2.1: Balancing in a Neutral Solution

Balance the following reaction

$$Cu^+(aq) + Fe(s) \rightarrow Fe^{3+}(aq) + Cu(s)$$

Solution

Step 1: Separate the half-reactions. By searching for the reduction potential, one can find two separate reactions:

$$Cu^+(aq) + e^- \rightarrow Cu(s)$$

and

$$Fe^{3+}(aq) + 3e^- \rightarrow Fe(s)$$

The copper reaction has a higher potential and thus is being reduced. Iron is being oxidized so the half-reaction should be flipped. This yields:

$$Cu^+(aq) + e^- \rightarrow Cu(s)$$

and

$$Fe(s) \rightarrow Fe^{3+}(aq) + 3e^-$$

Step 2: Balance the electrons in the equations. In this case, the electrons are simply balanced by multiplying the entire $Cu^+(aq) + e^- \rightarrow Cu(s)$ half-reaction by 3 and leaving the other half reaction as it is. This gives:

$$3Cu^+(aq) + 3e^- \rightarrow 3Cu(s)$$

and

$$Fe(s) \rightarrow Fe^{3+}(aq) + 3e^-$$

Step 3: Adding the equations give:

$$3Cu^+(aq) + 3e^- + Fe(s) \rightarrow 3Cu(s) + Fe^{3+}(aq) + 3e^-$$

The electrons cancel out and the balanced equation is left.

$$3\,Cu^{+}(aq) + Fe(s) \rightarrow 3\,Cu(s) + Fe^{3+}(aq)$$

Acidic Conditions

Acidic conditions usually implies a solution with an excess of H^+ concentration, hence making the solution acidic. The balancing starts by separating the reaction into half-reactions. However, instead of immediately balancing the electrons, balance all the elements in the half-reactions that are not hydrogen and oxygen. Then, add H_2O molecules to balance any oxygen atoms. Next, balance the hydrogen atoms by adding protons (H^+). Now, balance the *charge* by adding electrons and scale the electrons (multiply by the lowest common multiple) so that they will cancel out when added together. Finally, add the two half-reactions and cancel out common terms.

Example 9.2.2: Balancing in a Acid Solution

Balance the following redox reaction in acidic conditions.

$$Cr_2O_7^{2-}(aq) + HNO_2(aq) \rightarrow Cr^{3+}(aq) + NO_3^{-}(aq)$$

Solution

Step 1: Separate the half-reactions. The table provided does not have acidic or basic half-reactions, so just write out what is known.

$$Cr_2O_7^{2-}(aq) \rightarrow Cr^{3+}(aq)$$

$$HNO_2(aq) \rightarrow NO_3^{-}(aq)$$

Step 2: Balance elements other than O and H. In this example, only chromium needs to be balanced. This gives:

$$Cr_2O_7^{2-}(aq) \rightarrow 2\,Cr^{3+}(aq)$$

and

$$HNO_2(aq) \rightarrow NO_3^{-}(aq)$$

Step 3: Add H_2O to balance oxygen. The chromium reaction needs to be balanced by adding 7 H_2O molecules. The other reaction also needs to be balanced by adding one water molecule. This yields:

$$Cr_2O_7^{2-}(aq) \rightarrow 2\,Cr^{3+}(aq) + 7\,H_2O(l)$$

and

$$HNO_2(aq) + H_2O(l) \rightarrow NO_3^{-}(aq)$$

Step 4: Balance hydrogen by adding protons (H^+). 14 protons need to be added to the left side of the chromium reaction to balance the 14 (2 per water molecule * 7 water molecules) hydrogens. 3 protons need to be added to the right side of the other reaction.

$$14\,H^{+}(aq) + Cr_2O_7^{2-}(aq) \rightarrow 2\,Cr^{3+}(aq) + 7\,H_2O(l)$$

and

$$HNO_2(aq) + H_2O(l) \rightarrow 3\,H^{+}(aq) + NO_3^{-}(aq)$$

Step 5: Balance the charge of each equation with electrons. The chromium reaction has (14+) + (2-) = 12+ on the left side and (2 * 3+) = 6+ on the right side. To balance, add 6 electrons (each with a charge of -1) to the left side:

$$6\,e^{-} + 14\,H^{+}(aq) + Cr_2O_7^{2-}(aq) \rightarrow 2\,Cr^{3+}(aq) + 7\,H_2O(l)$$

For the other reaction, there is no charge on the left and a (3+) + (-1) = 2+ charge on the right. So add 2 electrons to the right side:

$$HNO_2(aq) + H_2O(l) \rightarrow 3\,H^{+}(aq) + NO_3^{-}(aq) + 2\,e^{-}$$

Step 6: Scale the reactions so that the electrons are equal. The chromium reaction has $6e^-$ and the other reaction has $2e^-$, so it should be multiplied by 3. This gives:

$$6\,e^- + 14\,H^+(aq) + Cr_2O_7{}^{2-}(aq) \rightarrow 2\,Cr^{3+}(aq) + 7\,H_2O(l)\cdot$$

and

$$3\times\left[HNO_2(aq) + H_2O(l) \rightarrow 3\,H^+(aq) + NO_3{}^-(aq) + 2\,e^-\right]$$
$$3\,HNO_2(aq) + 3\,H_2O(l) \rightarrow 9\,H^+(aq) + 3\,NO_3{}^-(aq) + 6\,e^-$$

Step 7: Add the reactions and cancel out common terms.

$$\begin{aligned} 3\,HNO_2(aq) + 3\,H_2O(l) &\rightarrow 9\,H^+(aq) + 3\,NO_3{}^-(aq) + 6\,e^- \\ 6\,e^- + 14\,H^+(aq) + Cr_2O_7{}^{2-}(aq) &\rightarrow 2\,Cr^{3+}(aq) + 7\,H_2O(l) \\ \hline 3\,HNO_2(aq) + \cancel{3\,H_2O(l)} + \cancel{6e^-} & \\ + 14\,H^+(aq) + Cr_2O_7{}^{2-}(aq) &\rightarrow 9\,H^+(aq) + 3\,NO_3{}^-(aq) + \cancel{6e^-} \\ &\quad + 2\,Cr^{3+}(aq) + \cancel{7}^{4}H_2O(l) \end{aligned}$$

The electrons cancel out as well as 3 water molecules and 9 protons. This leaves the balanced net reaction of:

$$3\,HNO_2(aq) + 5\,H^+(aq) + Cr_2O_7{}^{2-}(aq) \rightarrow 3\,NO_3{}^-(aq) + 2\,Cr^{3+}(aq) + 4\,H_2O(l)$$

Basic Conditions

Bases dissolve into OH^- ions in solution; hence, balancing redox reactions in basic conditions requires OH^-. Follow the same steps as for acidic conditions. The only difference is adding hydroxide ions to each side of the net reaction to balance any H^+. OH^- and H^+ ions on the same side of a reaction should be added together to form water. Again, any common terms can be canceled out.

Example 9.2.1: Balancing in Basic Solution

Balance the following redox reaction in basic conditions.

$$Ag(s) + Zn^{2+}(aq) \rightarrow Ag_2O(aq) + Zn(s)$$

Solution

Go through all the same steps as if it was in acidic conditions.

Step 1: Separate the half-reactions.

$$Ag(s) \rightarrow Ag_2O(aq)$$

$$Zn^{2+}(aq) \rightarrow Zn(s)$$

Step 2: Balance elements other than O and H.

$$2\,Ag(s) \rightarrow Ag_2O(aq)$$

$$Zn^{2+}(aq) \rightarrow Zn(s)$$

Step 3: Add H_2O to balance oxygen.

$$H_2O(l) + 2\,Ag(s) \rightarrow Ag_2O(aq)$$

$$Zn^{2+}(aq) \rightarrow Zn(s)$$

Step 4: Balance hydrogen with protons.

$$H_2O(l) + 2\,Ag(s) \rightarrow Ag_2O(aq) + 2\,H^+(aq)$$

$$Zn^{2+}(aq) \rightarrow Zn(s)$$

Step 5: Balance the charge with e^-.

$$H_2O(l) + 2\,Ag(s) \rightarrow Ag_2O(aq) + 2\,H^+(aq) + 2\,e^-$$

$$Zn^{2+}(aq) + 2\,e^- \rightarrow Zn(s)$$

Step 6: Scale the reactions so that they have an equal amount of electrons. In this case, it is already done.

Step 7: Add the reactions and cancel the electrons.

$$H_2O(l) + 2\,Ag(s) + Zn^{2+}(aq) \rightarrow Zn(s) + Ag_2O(aq) + 2\,H^+(aq)\cdot$$

Step 8: Add OH^- to balance H^+. There are 2 net protons in this equation, so add 2 OH^- ions to each side.

$$H_2O(l) + 2\,Ag(s) + Zn^{2+}(aq) + 2\,OH^-(aq) \rightarrow Zn(s) + Ag_2O(aq) + 2\,H^+(aq) + 2\,OH^-(aq)\cdot$$

Step 9: Combine OH^- ions and H^+ ions that are present on the same side to form water.

$$\cancel{H2O(l)} + 2\,Ag(s) + Zn^{2+}(aq) + 2\,OH^-(aq) \longrightarrow Zn(s) + Ag_2O(aq) + \cancel{2}\,H_2O(l)$$

Step 10: Cancel common terms.

$$2\,Ag(s) + Zn^{2+}(aq) + 2\,OH^-(aq) \rightarrow Zn(s) + Ag_2O(aq) + H_2O(l)$$

References

1. Petrucci, Ralph, William Harwood, Geoffrey Herring, and Jeffry Madura. General Chemistry: Principles & Modern Applications. 9th edition. Upper Saddle River, New Jersey: Pearson Prentince Hall, 2007.
2. Helmenstine, Anne Marie. "How to Balance Redox Reactions - Balancing Redox Reactions." *Balancing Redox Reactions - Half-Reaction Method* (2009): n. pag. Web. 1 Dec 2009. http://chemistry.about.com/od/genera...s/redoxbal.htm
3. Stanitski, Conrad L. "Chemical Equations." *Chemistry Explained Foundations and Applications*. 1st. Chemistry Encyclopedia, 2009. Print.
4. "How to Balance Redox Equations." *Youtube*. Web. 1 Dec 2009.

9.2: Balancing Redox Reactions is shared under a not declared license and was authored, remixed, and/or curated by LibreTexts.

- **Balancing Redox Reactions** by Ann Nguyen, Luvleen Brar is licensed CC BY 4.0.

9.3: Galvanic Cells

Learning Objectives

- To understand the basics of voltaic cells
- To connect voltage from a voltaic cell to underlying redox chemistry

In any electrochemical process, electrons flow from one chemical substance to another, driven by an oxidation–reduction (redox) reaction. A redox reaction occurs when electrons are transferred from a substance that is oxidized to one that is being reduced. The **reductant** is the substance that loses electrons and is oxidized in the process; the **oxidant** is the species that gains electrons and is reduced in the process. The associated potential energy is determined by the potential difference between the valence electrons in atoms of different elements.

Because it is impossible to have a reduction without an oxidation and vice versa, a redox reaction can be described as two **half-reactions**, one representing the oxidation process and one the reduction process. For the reaction of zinc with bromine, the overall chemical reaction is as follows:

$$\mathrm{Zn(s) + Br_2(aq) \rightarrow Zn^{2+}(aq) + 2\,Br^-(aq)}$$

The half-reactions are as follows:

reduction half-reaction:

$$\mathrm{Br_2(aq) + 2\,e^- \rightarrow 2\,Br^-(aq)}$$

oxidation half-reaction:

$$\mathrm{Zn(s) \rightarrow Zn^{2+}(aq) + 2\,e^-}$$

Each half-reaction is written to show what is actually occurring in the system; Zn is the *reductant* in this reaction (it loses electrons), and $\mathrm{Br_2}$ is the *oxidant* (it gains electrons). Adding the two half-reactions gives the overall chemical reaction (Equation 9.3.1). A redox reaction is balanced when the number of electrons lost by the reductant equals the number of electrons gained by the oxidant. Like any balanced chemical equation, the overall process is electrically neutral; that is, the net charge is the same on both sides of the equation.

> *In any redox reaction, the number of electrons lost by the oxidation reaction(s) equals the number of electrons gained by the reduction reaction(s).*

In most of our discussions of chemical reactions, we have assumed that the reactants are in intimate physical contact with one another. Acid–base reactions, for example, are usually carried out with the acid and the base dispersed in a single phase, such as a liquid solution. With redox reactions, however, it is possible to physically separate the oxidation and reduction half-reactions in space, as long as there is a complete circuit, including an external electrical connection, such as a wire, between the two half-reactions. As the reaction progresses, the electrons flow from the reductant to the oxidant over this electrical connection, producing an electric current that can be used to do work. An apparatus that is used to generate electricity from a spontaneous redox reaction or, conversely, that uses electricity to drive a nonspontaneous redox reaction is called an **electrochemical cell**.

There are two types of electrochemical cells: galvanic cells and electrolytic cells. Galvanic cells are named for the Italian physicist and physician Luigi Galvani (1737–1798), who observed that dissected frog leg muscles twitched when a small electric shock was applied, demonstrating the electrical nature of nerve impulses. A **galvanic (voltaic) cell** uses the energy released during a spontaneous redox reaction ($\Delta G < 0$) to generate electricity. This type of electrochemical cell is often called a voltaic cell after its inventor, the Italian physicist Alessandro Volta (1745–1827). In contrast, an **electrolytic cell** consumes electrical energy from an external source, using it to cause a nonspontaneous redox reaction to occur ($\Delta G > 0$). Both types contain two **electrodes**, which are solid metals connected to an external circuit that provides an electrical connection between the two parts of the system (Figure 9.3.1). The oxidation half-reaction occurs at one electrode (the **anode**), and the reduction half-reaction occurs at the other (the **cathode**). When the circuit is closed, electrons flow from the anode to the cathode. The electrodes are also connected by an

electrolyte, an ionic substance or solution that allows ions to transfer between the electrode compartments, thereby maintaining the system's electrical neutrality. In this section, we focus on reactions that occur in galvanic cells.

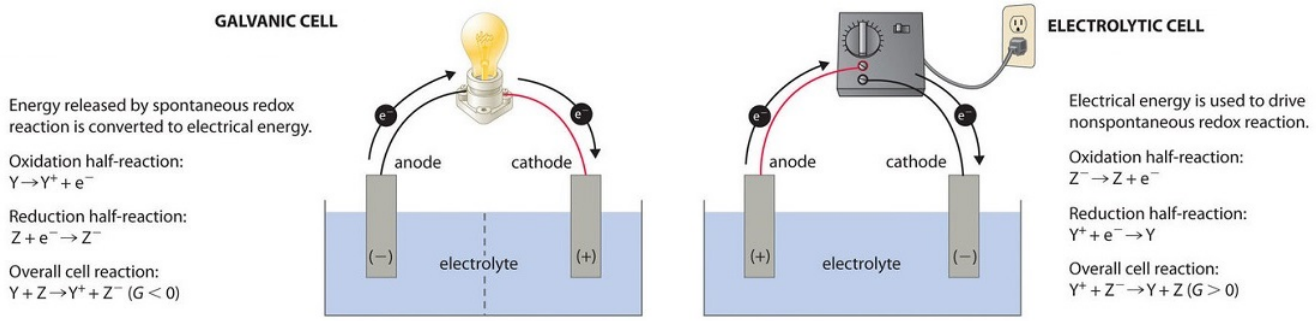


Figure **9.3.1**: Electrochemical Cells. A galvanic cell (left) transforms the energy released by a spontaneous redox reaction into electrical energy that can be used to perform work. The oxidative and reductive half-reactions usually occur in separate compartments that are connected by an external electrical circuit; in addition, a second connection that allows ions to flow between the compartments (shown here as a vertical dashed line to represent a porous barrier) is necessary to maintain electrical neutrality. The potential difference between the electrodes (voltage) causes electrons to flow from the reductant to the oxidant through the external circuit, generating an electric current. In an electrolytic cell (right), an external source of electrical energy is used to generate a potential difference between the electrodes that forces electrons to flow, driving a nonspontaneous redox reaction; only a single compartment is employed in most applications. In both kinds of electrochemical cells, the anode is the electrode at which the oxidation half-reaction occurs, and the cathode is the electrode at which the reduction half-reaction occurs.

Voltaic (Galvanic) Cells

To illustrate the basic principles of a galvanic cell, let's consider the reaction of metallic zinc with cupric ion (Cu^{2+}) to give copper metal and Zn^{2+} ion. The balanced chemical equation is as follows:

$$\mathrm{Zn\,(s) + Cu^{2+}\,(aq) \rightarrow Zn^{2+}\,(aq) + Cu\,(s)} \tag{9.3.1}$$

We can cause this reaction to occur by inserting a zinc rod into an aqueous solution of copper(II) sulfate. As the reaction proceeds, the zinc rod dissolves, and a mass of metallic copper forms. These changes occur spontaneously, but all the energy released is in the form of heat rather than in a form that can be used to do work.



Figure **9.3.2**: The Reaction of Metallic Zinc with Aqueous Copper(II) Ions in a Single Compartment. When a zinc rod is inserted into a beaker that contains an aqueous solution of copper(II) sulfate, a spontaneous redox reaction occurs: the zinc electrode dissolves to give $\mathrm{Zn^{2+}\,(aq)}$ ions, while $\mathrm{Cu^{2+}\,(aq)}$ ions are simultaneously reduced to metallic copper. The reaction occurs so rapidly that the copper is deposited as very fine particles that appear black, rather than the usual reddish color of copper. (youtu.be/2gPRK0HmYu4)

This same reaction can be carried out using the galvanic cell illustrated in Figure **9.3.3***a*. To assemble the cell, a copper strip is inserted into a beaker that contains a 1 M solution of $\mathrm{Cu^{2+}}$ ions, and a zinc strip is inserted into a different beaker that contains a 1 M solution of $\mathrm{Zn^{2+}}$ ions. The two metal strips, which serve as electrodes, are connected by a wire, and the compartments are connected by a **salt bridge**, a U-shaped tube inserted into both solutions that contains a concentrated liquid or gelled electrolyte.

The ions in the salt bridge are selected so that they do not interfere with the electrochemical reaction by being oxidized or reduced themselves or by forming a precipitate or complex; commonly used cations and anions are Na^+ or K^+ and NO_3^- or SO_4^{2-}, respectively. (The ions in the salt bridge do not have to be the same as those in the redox couple in either compartment.) When the circuit is closed, a spontaneous reaction occurs: zinc metal is oxidized to Zn^{2+} ions at the zinc electrode (the anode), and Cu^{2+} ions are reduced to Cu metal at the copper electrode (the cathode). As the reaction progresses, the zinc strip dissolves, and the concentration of Zn^{2+} ions in the solution increases; simultaneously, the copper strip gains mass, and the concentration of Cu^{2+} ions in the solution decreases (Figure 9.3.3*b*). Thus we have carried out the same reaction as we did using a single beaker, but this time the oxidative and reductive half-reactions are physically separated from each other. The electrons that are released at the anode flow through the wire, producing an electric current. Galvanic cells therefore transform chemical energy into electrical energy that can then be used to do work.

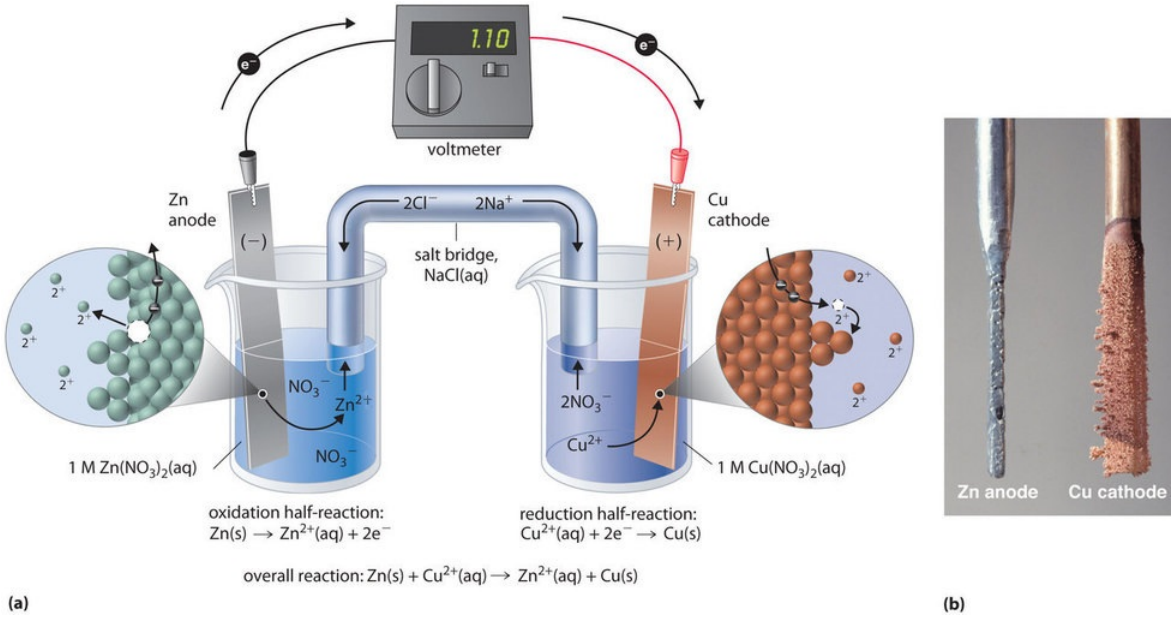


Figure 9.3.3: The Reaction of Metallic Zinc with Aqueous Copper(II) Ions in a Galvanic Cell. (a) A galvanic cell can be constructed by inserting a copper strip into a beaker that contains an aqueous 1 M solution of Cu^{2+} ions and a zinc strip into a different beaker that contains an aqueous 1 M solution of Zn^{2+} ions. The two metal strips are connected by a wire that allows electricity to flow, and the beakers are connected by a salt bridge. When the switch is closed to complete the circuit, the zinc electrode (the anode) is spontaneously oxidized to Zn^{2+} ions in the left compartment, while Cu^{2+} ions are simultaneously reduced to copper metal at the copper electrode (the cathode). (b) As the reaction progresses, the Zn anode loses mass as it dissolves to give Zn^{2+}(aq) ions, while the Cu cathode gains mass as Cu^{2+}(aq) ions are reduced to copper metal that is deposited on the cathode. (CC BY-SA-NC; anonymous)

The electrolyte in the salt bridge serves two purposes: it completes the circuit by carrying electrical charge and maintains electrical neutrality in both solutions by allowing ions to migrate between them. The identity of the salt in a salt bridge is unimportant, as long as the component ions do not react or undergo a redox reaction under the operating conditions of the cell. Without such a connection, the total positive charge in the Zn^{2+} solution would increase as the zinc metal dissolves, and the total positive charge in the Cu^{2+} solution would decrease. The salt bridge allows charges to be neutralized by a flow of anions into the Zn^{2+} solution and a flow of cations into the Cu^{2+} solution. In the absence of a salt bridge or some other similar connection, the reaction would rapidly cease because electrical neutrality could not be maintained.

A voltmeter can be used to measure the difference in electrical potential between the two compartments. Opening the switch that connects the wires to the anode and the cathode prevents a current from flowing, so no chemical reaction occurs. With the switch closed, however, the external circuit is closed, and an electric current can flow from the anode to the cathode. The **potential** (E_{cell}) of the cell, measured in volts, is the difference in electrical potential between the two half-reactions and is related to the energy needed to move a charged particle in an electric field. In the cell we have described, the voltmeter indicates a potential of 1.10 V (Figure 9.3.3*a*). Because electrons from the oxidation half-reaction are released at the anode, the anode in a galvanic cell is negatively charged. The cathode, which attracts electrons, is positively charged.

Not all electrodes undergo a chemical transformation during a redox reaction. The electrode can be made from an inert, highly conducting metal such as platinum to prevent it from reacting during a redox process, where it does not appear in the overall electrochemical reaction. This phenomenon is illustrated in Example **9.3.1**.

> *A galvanic (voltaic) cell converts the energy released by a **spontaneous** chemical reaction to electrical energy. An electrolytic cell consumes electrical energy from an external source to drive a **nonspontaneous** chemical reaction.*

Example 9.3.1

A chemist has constructed a galvanic cell consisting of two beakers. One beaker contains a strip of tin immersed in aqueous sulfuric acid, and the other contains a platinum electrode immersed in aqueous nitric acid. The two solutions are connected by a salt bridge, and the electrodes are connected by a wire. Current begins to flow, and bubbles of a gas appear at the platinum electrode. The spontaneous redox reaction that occurs is described by the following balanced chemical equation:

$$3\,Sn\,(s) + 2\,NO_3^-\,(aq) + 8\,H^+\,(aq) \rightarrow 3\,Sn^{2+}\,(aq) + 2\,NO\,(g) + 4\,H_2O\,(l)$$

For this galvanic cell,

a. write the half-reaction that occurs at each electrode.
b. indicate which electrode is the cathode and which is the anode.
c. indicate which electrode is the positive electrode and which is the negative electrode.

Given: galvanic cell and redox reaction

Asked for: half-reactions, identity of anode and cathode, and electrode assignment as positive or negative

Strategy:

A. Identify the oxidation half-reaction and the reduction half-reaction. Then identify the anode and cathode from the half-reaction that occurs at each electrode.
B. From the direction of electron flow, assign each electrode as either positive or negative.

Solution

A In the reduction half-reaction, nitrate is reduced to nitric oxide. (The nitric oxide would then react with oxygen in the air to form NO_2, with its characteristic red-brown color.) In the oxidation half-reaction, metallic tin is oxidized. The half-reactions corresponding to the actual reactions that occur in the system are as follows:

reduction:

$$NO_3^-\,(aq) + 4\,H^+\,(aq) + 3\,e^- \longrightarrow NO\,(g) + 2\,H_2O\,(l)$$

oxidation:

$$Sn\,(s) \longrightarrow Sn^{2+}\,(aq) + 2\,e^-$$

Thus nitrate is reduced to NO, while the tin electrode is oxidized to Sn^{2+}.

Because the reduction reaction occurs at the Pt electrode, it is the cathode. Conversely, the oxidation reaction occurs at the tin electrode, so it is the anode.

B Electrons flow from the tin electrode through the wire to the platinum electrode, where they transfer to nitrate. The electric circuit is completed by the salt bridge, which permits the diffusion of cations toward the cathode and anions toward the anode. Because electrons flow from the tin electrode, it must be electrically negative. In contrast, electrons flow toward the Pt electrode, so that electrode must be electrically positive.

? Exercise 9.3.1

Consider a simple galvanic cell consisting of two beakers connected by a salt bridge. One beaker contains a solution of MnO_4^- in dilute sulfuric acid and has a Pt electrode. The other beaker contains a solution of Sn^{2+} in dilute sulfuric acid, also with a Pt electrode. When the two electrodes are connected by a wire, current flows and a spontaneous reaction occurs that is described by the following balanced chemical equation:

$$2\,MnO_4^-(aq) + 5\,Sn^{2+}(aq) + 16\,H^+(aq) \rightarrow 2\,Mn^{2+}(aq) + 5\,Sn^{4+}(aq) + 8\,H_2O(l)$$

For this galvanic cell,

a. write the half-reaction that occurs at each electrode.
b. indicate which electrode is the cathode and which is the anode.
c. indicate which electrode is positive and which is negative.

Answer a

$$MnO_4^-(aq) + 8\,H^+(aq) + 5\,e^- \rightarrow Mn^{2+}(aq) + 4\,H_2O(l)$$
$$Sn^{2+}(aq) \rightarrow Sn^{4+}(aq) + 2\,e^-$$

Answer b

The Pt electrode in the permanganate solution is the cathode; the one in the tin solution is the anode.

Answer c

The cathode (electrode in beaker that contains the permanganate solution) is positive, and the anode (electrode in beaker that contains the tin solution) is negative.



Electrochemical Cells: Electrochemical Cells(opens in new window) [youtu.be]

Constructing Cell Diagrams (Cell Notation)

Because it is somewhat cumbersome to describe any given galvanic cell in words, a more convenient notation has been developed. In this line notation, called a cell diagram, the identity of the electrodes and the chemical contents of the compartments are indicated by their chemical formulas, with the anode written on the far left and the cathode on the far right. Phase boundaries are shown by single vertical lines, and the salt bridge, which has two phase boundaries, by a double vertical line. Thus the cell diagram for the Zn/Cu cell shown in Figure 9.3.3*a* is written as follows:

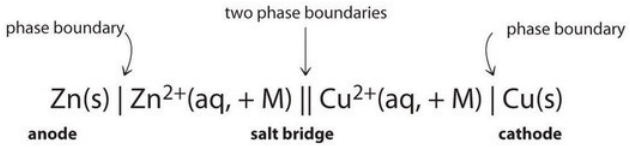


Figure 9.3.4: A cell diagram includes solution concentrations when they are provided. The + M term is meant to indicate the applicable concentration of the species. If the species is a gas, then you substitute the pressure instead.

At the anode is solid zinc. after the phase boundary is aq Zinc two plus and plus M. After the two phase boundary is aq copper two plus and plus M. At the cathode is solid copper.

Galvanic cells can have arrangements other than the examples we have seen so far. For example, the voltage produced by a redox reaction can be measured more accurately using two electrodes immersed in a single beaker containing an electrolyte that completes the circuit. This arrangement reduces errors caused by resistance to the flow of charge at a boundary, called the **junction potential**. One example of this type of galvanic cell is as follows:

$$\mathrm{Pt(s)\ |\ H_2(g)\ |\ HCl(aq,\ 1\,M)\ |\ AgCl(s)\ Ag(s)}$$

This cell diagram does not include a double vertical line representing a salt bridge because there is no salt bridge providing a junction between two dissimilar solutions. Moreover, solution concentrations have not been specified, so they are not included in the cell diagram. The half-reactions and the overall reaction for this cell are as follows:

cathode reaction:

$$\mathrm{AgCl(s) + e^- \rightarrow Ag(s) + Cl^-(aq)}$$

anode reaction:

$$\mathrm{\tfrac{1}{2}\,H_2(g) \longrightarrow H^+(aq) + e^-}$$

overall:

$$\mathrm{AgCl(s) + \tfrac{1}{2}\,H_2(g) \longrightarrow Ag(s) + Cl^- + H^+(aq)}$$

A single-compartment galvanic cell will initially exhibit the same voltage as a galvanic cell constructed using separate compartments, but it will discharge rapidly because of the direct reaction of the reactant at the anode with the oxidized member of the cathodic redox couple. Consequently, cells of this type are not particularly useful for producing electricity.

Example 9.3.2

Draw a cell diagram for the galvanic cell described in Example 9.3.1. The balanced chemical reaction is as follows:

$$\mathrm{3\,Sn(s) + 2\,NO_3^-(aq) + 8\,H^+(aq) \rightarrow 3\,Sn^{2+}(aq) + 2\,NO(g) + 4\,H_2O(l)}$$

Given: galvanic cell and redox reaction

Asked for: cell diagram

Strategy:

Using the symbols described, write the cell diagram beginning with the oxidation half-reaction on the left.

Solution

The anode is the tin strip, and the cathode is the Pt electrode. Beginning on the left with the anode, we indicate the phase boundary between the electrode and the tin solution by a vertical bar. The anode compartment is thus $\mathrm{Sn(s)\,|\,Sn^{2+}(aq)}$. We could include $\mathrm{H_2SO_4(aq)}$ with the contents of the anode compartment, but the sulfate ion (as $\mathrm{HSO_4^-}$) does not participate in the overall reaction, so it does not need to be specifically indicated. The cathode compartment contains aqueous nitric acid, which does participate in the overall reaction, together with the product of the reaction (NO) and the Pt electrode. These are written as $\mathrm{HNO_3(aq)\,|\,NO(g)\,|\,Pt(s)}$, with single vertical bars indicating the phase boundaries. Combining the two compartments and using a double vertical bar to indicate the salt bridge,

$$\mathrm{Sn(s)\ |\,Sn^{2+}(aq)\,||\,HNO_3(aq)\,|\,NO(g)\,|\,Pt_{(s)}}$$

The solution concentrations were not specified, so they are not included in this cell diagram.

Exercise 9.3.2

Draw the cell diagram for the following reaction, assuming the concentration of Ag^+ and Mg^{2+} are each 1 M:

$$Mg(s) + 2\,Ag^+(aq) \rightarrow Mg^{2+}(aq) + 2\,Ag(s)$$

Answer

$$Mg(s)\ \left|Mg^{2+}(aq,\ 1\,M)\right|\left|Ag^+(aq,\ 1\ M)\right|\ Ag(s)$$



Cell Diagrams: Cell Diagrams(opens in new window) [youtu.be]

Summary

A galvanic (voltaic) cell uses the energy released during a spontaneous redox reaction to generate electricity, whereas an electrolytic cell consumes electrical energy from an external source to force a reaction to occur. Electrochemistry is the study of the relationship between electricity and chemical reactions. The oxidation–reduction reaction that occurs during an electrochemical process consists of two half-reactions, one representing the oxidation process and one the reduction process. The sum of the half-reactions gives the overall chemical reaction. The overall redox reaction is balanced when the number of electrons lost by the reductant equals the number of electrons gained by the oxidant. An electric current is produced from the flow of electrons from the reductant to the oxidant. An electrochemical cell can either generate electricity from a spontaneous redox reaction or consume electricity to drive a nonspontaneous reaction. In a galvanic (voltaic) cell, the energy from a spontaneous reaction generates electricity, whereas in an electrolytic cell, electrical energy is consumed to drive a nonspontaneous redox reaction. Both types of cells use two electrodes that provide an electrical connection between systems that are separated in space. The oxidative half-reaction occurs at the anode, and the reductive half-reaction occurs at the cathode. A salt bridge connects the separated solutions, allowing ions to migrate to either solution to ensure the system's electrical neutrality. A voltmeter is a device that measures the flow of electric current between two half-reactions. The potential of a cell, measured in volts, is the energy needed to move a charged particle in an electric field. An electrochemical cell can be described using line notation called a cell diagram, in which vertical lines indicate phase boundaries and the location of the salt bridge. Resistance to the flow of charge at a boundary is called the junction potential.

9.3: Galvanic Cells is shared under a not declared license and was authored, remixed, and/or curated by LibreTexts.

- **20.3: Voltaic Cells** is licensed CC BY-NC-SA 3.0.

9.4: Standard Electrode Potentials

Skills to Develop

- To use redox potentials to predict whether a reaction is spontaneous.
- To balance redox reactions using half-reactions.

In a galvanic cell, current is produced when electrons flow externally through the circuit from the anode to the cathode because of a difference in potential energy between the two electrodes in the electrochemical cell. In the **Zn/Cu** system, the valence electrons in zinc have a substantially higher potential energy than the valence electrons in copper because of shielding of the s electrons of zinc by the electrons in filled d orbitals. Hence electrons flow spontaneously from zinc to copper(II) ions, forming zinc(II) ions and metallic copper. Just like water flowing spontaneously downhill, which can be made to do work by forcing a waterwheel, the flow of electrons from a higher potential energy to a lower one can also be harnessed to perform work.

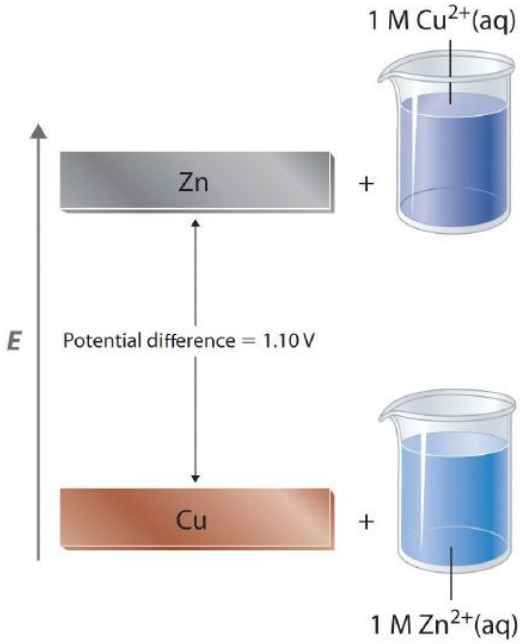


Figure **9.4.1**: Potential Energy Difference in the Zn/Cu System. The potential energy of a system consisting of metallic ***Zn*** and aqueous Cu^{2+} ions is greater than the potential energy of a system consisting of metallic Cu and aqueous Zn^{2+} ions. Much of this potential energy difference is because the valence electrons of metallic Zn are higher in energy than the valence electrons of metallic Cu. Because the Zn(s) + Cu^{2+}(aq) system is higher in energy by 1.10 V than the Cu(s) + Zn^{2+}(aq) system, energy is released when electrons are transferred from Zn to Cu^{2+} to form Cu and Zn^{2+}.

Because the potential energy of valence electrons differs greatly from one substance to another, the voltage of a galvanic cell depends partly on the identity of the reacting substances. If we construct a galvanic cell similar to the one in Figure **9.4.1*a*** but instead of copper use a strip of cobalt metal and 1 M Co^{2+} in the cathode compartment, the measured voltage is not 1.10 V but 0.51 V. Thus we can conclude that the difference in potential energy between the valence electrons of cobalt and zinc is less than the difference between the valence electrons of copper and zinc by 0.59 V.

The measured potential of a cell also depends strongly on the concentrations of the reacting species and the temperature of the system. To develop a scale of relative potentials that will allow us to predict the direction of an electrochemical reaction and the magnitude of the driving force for the reaction, the potentials for oxidations and reductions of different substances must be measured under comparable conditions. To do this, chemists use the **standard cell potential** (E^{o}_{cell}), defined as the potential of a cell measured under standard conditions—that is, with all species in their standard states (1 M for solutions,Concentrated solutions of salts (about 1 M) generally do not exhibit ideal behavior, and the actual standard state corresponds to an activity of 1 rather than a concentration of 1 M. Corrections for nonideal behavior are important for precise quantitative work but not for the more qualitative approach that we are taking here. 1 atm for gases, pure solids or pure liquids for other substances) and at a fixed temperature, usually 25°C.

> *Measured redox potentials depend on the potential energy of valence electrons, the concentrations of the species in the reaction, and the temperature of the system.*

Measuring Standard Electrode Potentials

It is physically impossible to measure the potential of a single electrode: only the difference between the potentials of two electrodes can be measured (this is analogous to measuring **absolute enthalpies** or **free energies** since only differences in enthalpy and free energy can be measured). We can, however, compare the standard cell potentials for two different galvanic cells that have one kind of electrode in common. This allows us to measure the potential difference between two dissimilar electrodes. For example, the measured standard cell potential ($E°$) for the **Zn/Cu** system is 1.10 V, whereas $E°$ for the corresponding **Zn/Co** system is 0.51 V. This implies that the potential difference between the **Co** and **Cu** electrodes is 1.10 V − 0.51 V = 0.59 V. In fact, that is exactly the potential measured under standard conditions if a cell is constructed with the following cell diagram:

$$\mathrm{Co\,(s)\ |\ Co^{2+}\,(aq,\,1\,M)\ ||\ Cu^{2+}\,(aq,\,1\,M)\ |\ Cu\,(s)}\quad E°= 0.59\,V \tag{9.4.1}$$

This cell diagram corresponds to the oxidation of a cobalt anode and the reduction of $\mathrm{Cu^{2+}}$ in solution at the copper cathode.

All tabulated values of standard electrode potentials by convention are listed for a reaction written as a reduction, not as an oxidation, to be able to compare standard potentials for different substances (Table P1). The standard cell potential ($E°_{cell}$) is therefore the difference between the tabulated reduction potentials of the two half-reactions, not their sum:

$$E°_{cell} = E°_{cathode} - E°_{anode} \tag{9.4.2}$$

In contrast, recall that half-reactions are written to show the reduction and oxidation reactions that actually occur in the cell, so the overall cell reaction is written as the sum of the two half-reactions. According to Equation 9.4.2, when we know the standard potential for any single half-reaction, we can obtain the value of the standard potential of many other half-reactions by measuring the standard potential of the corresponding cell.

> The overall cell reaction is the sum of the two half-reactions, but the cell potential is the difference between the reduction potentials:
>
> $$E°_{cell} = E°_{cathode} - E°_{anode}$$

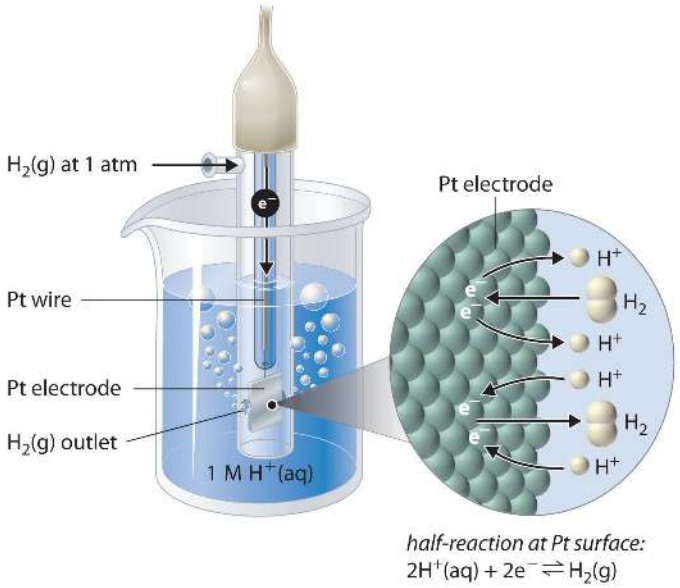


Figure 9.4.2: The Standard Hydrogen Electrode. The SHE consists of platinum wire that is connected to a Pt surface in contact with an aqueous solution containing 1 M H^+ in equilibrium with H_2 gas at a pressure of 1 atm. In the molecular view, the Pt surface catalyzes the oxidation of hydrogen molecules to protons or the reduction of protons to hydrogen gas. (Water is omitted for clarity.) The standard potential of the SHE is arbitrarily assigned a value of 0 V.

Although it is impossible to measure the potential of any electrode directly, we can choose a reference electrode whose potential is defined as 0 V under standard conditions. The **standard hydrogen electrode (SHE)** is universally used for this purpose and is assigned a standard potential of 0 V. It consists of a strip of platinum wire in contact with an aqueous solution containing 1 M $\mathbf{H^+}$ (since it is in standard conditions). The $\mathbf{H^+}$ in solution is in equilibrium with $\mathbf{H_2}$ gas at a pressure of 1 atm at the Pt-solution interface (Figure **9.4.2**). Protons are reduced or hydrogen molecules are oxidized at the **Pt** surface according to the following equation:

$$\mathbf{2\,H^+(aq) + 2\,e^- \rightleftharpoons H_2(g)} \tag{9.4.3}$$

One especially attractive feature of the SHE is that the **Pt** metal electrode is not consumed during the reaction.

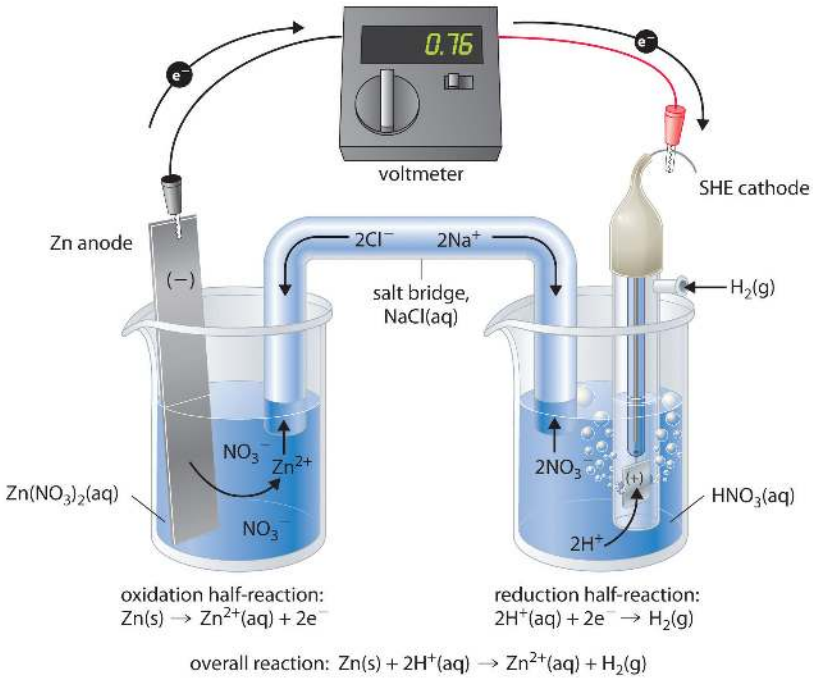


Figure **9.4.3**: Determining a Standard Electrode Potential Using a Standard Hydrogen Electrode. The voltmeter shows that the standard cell potential of a galvanic cell consisting of a SHE and a Zn/Zn^{2+} couple is $E°_{cell}$ = 0.76 V. Because the zinc electrode in this cell dissolves spontaneously to form $Zn^{2+}(aq)$ ions while $H^+(aq)$ ions are reduced to H_2 at the platinum surface, the standard electrode potential of the Zn^{2+}/Zn couple is −0.76 V.

Figure **9.4.3** shows a galvanic cell that consists of a SHE in one beaker and a Zn strip in another beaker containing a solution of Zn^{2+} ions. When the circuit is closed, the voltmeter indicates a potential of 0.76 V. The zinc electrode begins to dissolve to form Zn^{2+}, and H^+ ions are reduced to H_2 in the other compartment. Thus the hydrogen electrode is the cathode, and the zinc electrode is the anode. The diagram for this galvanic cell is as follows:

$$\mathbf{Zn\,(s)\ |\ Zn^{2+}\,(aq)\ ||\ H^+\,(aq,\,1\,M)\ |\ H_2\,(g,\,1\,atm)\ |\ Pt\,(s)}$$

The half-reactions that actually occur in the cell and their corresponding electrode potentials are as follows:

- cathode:

$$\mathbf{2\,H^+\,(aq) + 2\,e^- \longrightarrow H_2\,(g)} \qquad E°_{cathode} = 0\,V$$

- anode:

$$\mathbf{Zn\,(s) \longrightarrow Zn^{2+}\,(aq) + 2\,e^-} \qquad E°_{anode} = -0.76\,V$$

- overall:

$$\mathbf{Zn\,(s) + 2\,H^+\,(aq) \longrightarrow Zn^{2+}\,(aq) + H_2\,(g)}$$

Then via Equation 9.4.2 we can calculate the standard cell potential

$$E^\circ_{cell} = E^\circ_{cathode} - E^\circ_{anode} = 0.76\ V$$

Caution: Watch the Sign

Although the reaction at the anode is an oxidation, by convention its tabulated E^o value is reported as a reduction potential. The potential of a half-reaction measured against the SHE under standard conditions is called the **standard electrode potential** for that half-reaction. In this example, the standard reduction potential for $\mathrm{Zn^{2+}(aq) + 2\,e^- \longrightarrow Zn(s)}$ is −0.76 V, which means that the standard electrode potential for the reaction that occurs at the anode, the oxidation of Zn to $\mathrm{Zn^{2+}}$, often called the $\mathrm{Zn/Zn^{2+}}$ **redox couple**, or the $\mathrm{Zn/Zn^{2+}}$ **couple**, is −(−0.76 V) = 0.76 V.

We must therefore **subtract** E°_{anode} from $E^\circ_{cathode}$ to obtain $E^\circ_{cell} = 0.76\ V$. This is the origin of the negative sign in Equation 9.4.2.

Because electrical potential is the energy needed to move a charged particle in an electric field, standard electrode potentials for half-reactions are intensive properties and do not depend on the amount of substance involved. Consequently, E° values are *independent of the stoichiometric coefficients* for the half-reaction, and, most important, the coefficients used to produce a balanced overall reaction do not affect the value of the cell potential.

> *E° values do NOT depend on the stoichiometric coefficients for a half-reaction, because it is an intensive property.*

Standard Electrode Potentials

To measure the potential of the Cu/Cu^{2+} couple, we can construct a galvanic cell analogous to the one shown in Figure **9.4.3** but containing a Cu/Cu^{2+} couple in the sample compartment instead of Zn/Zn^{2+}. When we close the circuit this time, the measured potential for the cell is negative (−0.34 V) rather than positive. The negative value of E°_{cell} indicates that the direction of spontaneous electron flow is the opposite of that for the Zn/Zn^{2+} couple. Hence the reactions that occur spontaneously, indicated by a positive E°_{cell}, are the reduction of Cu^{2+} to Cu at the copper electrode. The copper electrode gains mass as the reaction proceeds, and H_2 is oxidized to H^+ at the platinum electrode. In this cell, the copper strip is the cathode, and the hydrogen electrode is the anode. The cell diagram therefore is written with the SHE on the left and the Cu^{2+}/Cu couple on the right:

$$\mathrm{Pt(s)\ |\ H_2(g,\ 1\,atm)\ |\ H^+(aq,\ \ 1\ M)\ ||\ Cu^{2+}(aq,\ 1\,M)\ |Cu(s)}$$

The half-cell reactions and potentials of the spontaneous reaction are as follows:

- Cathode:

$$\mathrm{Cu^{2+}(aq) + 2\,e^- \longrightarrow Cu(g)} \qquad E^\circ_{cathode} = 0.34\ V$$

- Anode:

$$\mathrm{H_2(g) \longrightarrow 2\,H^+(aq) + 2\,e^-} \qquad E^\circ_{anode} = 0\ V$$

- Overall:

$$\mathrm{H_2(g) + Cu^{2+}(aq) \longrightarrow 2\,H^+(aq) + Cu(s)}$$

Then via Equation 9.4.2 we can calculate the standard cell potential

$$\begin{aligned} E^\circ_{cell} &= E^\circ_{cathode} - E^\circ_{anode} \\ &= 0.34\ V \end{aligned}$$

Thus the standard electrode potential for the Cu^{2+}/Cu couple is 0.34 V.

Calculating Standard Cell Potentials

The standard cell potential for a redox reaction (E°_{cell}) is a measure of the tendency of reactants in their standard states to form products in their standard states; consequently, it is a measure of the driving force for the reaction, which earlier we called voltage.

We can use the two standard electrode potentials we found earlier to calculate the standard potential for the Zn/Cu cell represented by the following cell diagram:

$$\mathrm{Zn(s)\ |\ Zn^{2+}(aq,\,1\,M)\ ||\ Cu^{2+}(aq,\,1\,M)\ |\ Cu(s)}$$

We know the values of $E°_{anode}$ for the reduction of Zn^{2+} and $E°_{cathode}$ for the reduction of Cu^{2+}, so we can calculate $E°_{cell}$:

- cathode:

$$\mathrm{Cu^{2+}(aq) + 2\,e^- \longrightarrow Cu(s)} \qquad E°_{cathode} = 0.34\ V$$

- anode:

$$\mathrm{Zn(s) \longrightarrow Zn^{2+}(aq,\,1\,M) + 2\,e^-} \qquad E°_{anode} = -0.76\ V$$

- overall:

$$\mathrm{Zn(s) + Cu^{2+}(aq) \longrightarrow Zn^{2+}(aq) + Cu(s)}$$

Then via Equation 9.4.2 we can calculate the standard cell potential

$$\begin{aligned} E°_{cell} &= E°_{cathode} - E°_{anode} \\ &= 1.10\ V \end{aligned}$$

This is the same value that is observed experimentally. If the value of $E°_{cell}$ is positive, the reaction will occur spontaneously as written. If the value of $E°_{cell}$ is negative, then the reaction is not spontaneous, and it will not occur as written under standard conditions; it will, however, proceed spontaneously in the opposite direction. As we shall see in Section 20.9, this does not mean that the reaction cannot be made to occur at all under standard conditions. With a sufficient input of electrical energy, virtually any reaction can be forced to occur. Example 9.4.2 and its corresponding exercise illustrate how we can use measured cell potentials to calculate standard potentials for redox couples.

> *A positive $E°_{cell}$ means that the reaction will occur spontaneously as written. A negative $E°_{cell}$ means that the reaction will proceed spontaneously in the opposite direction.*

Example 9.4.1

A galvanic cell with a measured standard cell potential of 0.27 V is constructed using two beakers connected by a salt bridge. One beaker contains a strip of gallium metal immersed in a 1 M solution of $GaCl_3$, and the other contains a piece of nickel immersed in a 1 M solution of $NiCl_2$. The half-reactions that occur when the compartments are connected are as follows:

- cathode:

$$\mathrm{Ni^{2+}(aq) + 2\,e^- \longrightarrow Ni(s)}$$

- anode:

$$\mathrm{Ga(s) \longrightarrow Ga^{3+}(aq) + 3\,e^-}$$

If the potential for the oxidation of Ga to Ga^{3+} is 0.55 V under standard conditions, what is the potential for the oxidation of Ni to Ni^{2+}?

Given: galvanic cell, half-reactions, standard cell potential, and potential for the oxidation half-reaction under standard conditions

Asked for: standard electrode potential of reaction occurring at the cathode

Strategy:

A. Write the equation for the half-reaction that occurs at the anode along with the value of the standard electrode potential for the half-reaction.

B. Use Equation 9.4.2 to calculate the standard electrode potential for the half-reaction that occurs at the cathode. Then reverse the sign to obtain the potential for the corresponding oxidation half-reaction under standard conditions.

Solution:

A We have been given the potential for the oxidation of Ga to Ga^{3+} under standard conditions, but to report the standard electrode potential, we must reverse the sign. For the reduction reaction $Ga^{3+}(aq) + 3e^- \rightarrow Ga(s)$, $E°_{anode} = -0.55$ V.

B Using the value given for $E°_{cell}$ and the calculated value of $E°_{anode}$, we can calculate the standard potential for the reduction of Ni^{2+} to Ni from Equation 9.4.2:

$$E°_{cell} = E°_{cathode} - E°_{anode}$$
$$0.27\,V = E°_{cathode} - (-0.55V)$$
$$E°_{cathode} = -0.28\,V$$

This is the standard electrode potential for the reaction $Ni^{2+}(aq) + 2e^- \rightarrow Ni(s)$. Because we are asked for the potential for the oxidation of Ni to Ni^{2+} under standard conditions, we must reverse the sign of $E°_{cathode}$. Thus $E° = -(-0.28\text{ V}) = 0.28$ V for the oxidation. With three electrons consumed in the reduction and two produced in the oxidation, the overall reaction is not balanced. Recall, however, that standard potentials are independent of stoichiometry.

Exercise 9.4.1

A galvanic cell is constructed with one compartment that contains a mercury electrode immersed in a 1 M aqueous solution of mercuric acetate $Hg(CH_3CO_2)_2$ and one compartment that contains a strip of magnesium immersed in a 1 M aqueous solution of $MgCl_2$. When the compartments are connected, a potential of 3.22 V is measured and the following half-reactions occur:

- cathode:

$$Hg^{2+}(aq) + 2e^- \longrightarrow Hg(l)$$

- anode:

$$Mg(s) \longrightarrow Mg^{2+}(aq) + 2e^-$$

If the potential for the oxidation of Mg to Mg^{2+} is 2.37 V under standard conditions, what is the standard electrode potential for the reaction that occurs at the cathode?

Answer

0.85 V

Reference Electrodes

When using a galvanic cell to measure the concentration of a substance, we are generally interested in the potential of only one of the electrodes of the cell, the so-called **indicator electrode**, whose potential is related to the concentration of the substance being measured. To ensure that any change in the measured potential of the cell is due to only the substance being analyzed, the potential of the other electrode, the **reference electrode**, must be constant. You are already familiar with one example of a reference electrode: the SHE. The potential of a reference electrode must be unaffected by the properties of the solution, and if possible, it should be physically isolated from the solution of interest. To measure the potential of a solution, we select a reference electrode and an appropriate indicator electrode. Whether reduction or oxidation of the substance being analyzed occurs depends on the potential of the half-reaction for the substance of interest (the sample) and the potential of the reference electrode.

> *The potential of any reference electrode should not be affected by the properties of the solution to be analyzed, and it should also be physically isolated.*

There are many possible choices of reference electrode other than the SHE in Figure 9.4.2. The SHE requires a constant flow of highly flammable hydrogen gas, which makes it inconvenient to use. Consequently, two other electrodes are commonly chosen as reference electrodes. One is the **silver–silver chloride electrode**, which consists of a silver wire coated with a very thin layer of AgCl that is dipped into a chloride ion solution with a fixed concentration. The silver–silver chloride electrode cell diagram is

$$Cl^-(aq) \mid AgCl(s) \mid Ag(s)$$

and corresponding half-reaction is

$$\mathrm{AgCl(s) + e^- \longrightarrow Ag(s) + Cl^-(aq)}.$$

If a saturated solution of KCl is used as the chloride solution, the potential of the silver–silver chloride electrode is 0.197 V versus the SHE. That is, 0.197 V must be subtracted from the measured value to obtain the standard electrode potential measured against the SHE.

A second common reference electrode is the **saturated calomel electrode (SCE)**, which has the same general form as the silver–silver chloride electrode. The SCE consists of a platinum wire inserted into a moist paste of liquid mercury ($\mathrm{Hg_2Cl_2}$; called calomel in the old chemical literature) and KCl. This interior cell is surrounded by an aqueous KCl solution, which acts as a salt bridge between the interior cell and the exterior solution (Figure 9.4.5*a*). Although it sounds and looks complex, this cell is actually easy to prepare and maintain, and its potential is highly reproducible. The SCE cell diagram is

$$\mathrm{Pt(s) \mid Hg_2Cl_2(s) \mid KCl(aq, sat)}$$

and corresponding half-reaction is

$$\mathrm{Hg_2Cl_2(s) + 2\,e^- \longrightarrow 2\,Hg(l) + 2\,Cl^-(aq)}.$$

At 25°C, the potential of the SCE is 0.2415 V versus the SHE, which means that 0.2415 V must be subtracted from the potential versus an SCE to obtain the standard electrode potential.

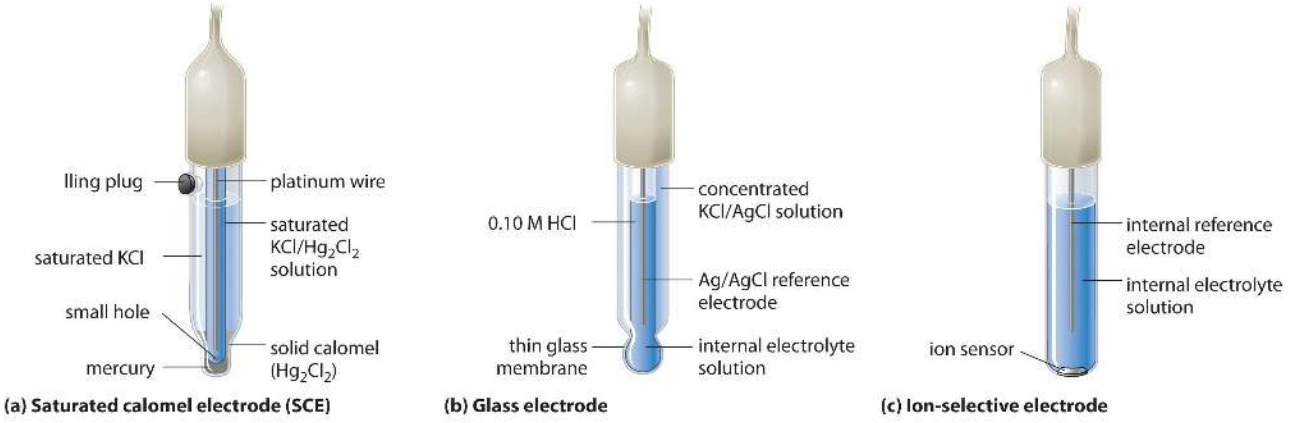


Figure 9.4.5: Three Common Types of Electrodes. (a) The SCE is a reference electrode that consists of a platinum wire inserted into a moist paste of liquid mercury (calomel; $\mathrm{Hg_2Cl_2}$) and KCl. The interior cell is surrounded by an aqueous KCl solution, which acts as a salt bridge between the interior cell and the exterior solution. (b) In a glass electrode, an internal Ag/AgCl electrode is immersed in a 1 M HCl solution that is separated from the sample solution by a very thin glass membrane. The potential of the electrode depends on the H^+ ion concentration of the sample. (c) The potential of an ion-selective electrode depends on the concentration of only a single ionic species in solution.

Using Electrochemistry to Measure Concentrations

One of the most common uses of electrochemistry is to measure the $\mathrm{H^+}$ ion concentration of a solution. A **glass electrode** is generally used for this purpose, in which an internal Ag/AgCl electrode is immersed in a 0.10 M HCl solution that is separated from the solution by a very thin glass membrane (Figure 9.4.5*b*. The glass membrane absorbs protons, which affects the measured potential. The extent of the adsorption on the inner side is fixed because $[\mathrm{H^+}]$ is fixed inside the electrode, but the adsorption of protons on the outer surface depends on the pH of the solution. The potential of the glass electrode depends on $[\mathrm{H^+}]$ as follows (recall that $pH = -\log[\mathrm{H^+}]$):

$$\begin{aligned} E_{glass} &= E' + (0.0591\ V \times \log[H^+]) \\ &= E' - 0.0591\ V \times pH \end{aligned}$$

The voltage E' is a constant that depends on the exact construction of the electrode. Although it can be measured, in practice, a glass electrode is calibrated; that is, it is inserted into a solution of known pH, and the display on the pH meter is adjusted to the

known value (Figure 9.4.7). Once the electrode is properly calibrated, it can be placed in a solution and used to determine an unknown pH.



Figure 9.4.7: A pH meter measures the hydrogen-ion concentration in water-based solutions, indicating its acidity or alkalinity expressed as pH. The pH meter measures the difference in electrical potential between a pH electrode and a reference electrode, and so the pH meter is sometimes referred to as a "potentiometric pH meter". (CC By-SA 2.0 Generic; Sergei Golyshev via Wikipedia)

Ion-selective electrodes are used to measure the concentration of a particular species in solution; they are designed so that their potential depends on only the concentration of the desired species (Figure 9.4.5c). These electrodes usually contain an internal reference electrode that is connected by a solution of an electrolyte to a crystalline inorganic material or a membrane, which acts as the sensor. For example, one type of ion-selective electrode uses a single crystal of Eu-doped LaF_3 as the inorganic material. When fluoride ions in solution diffuse to the surface of the solid, the potential of the electrode changes, resulting in a so-called fluoride electrode. Similar electrodes are used to measure the concentrations of other species in solution. Some of the species whose concentrations can be determined in aqueous solution using ion-selective electrodes and similar devices are listed in Table 9.4.1.

Table 9.4.1: Some Species Whose Aqueous Concentrations Can Be Measured Using Electrochemical Methods

Species	Type of Sample
H^+	laboratory samples, blood, soil, and ground and surface water
NH_3/NH_4^+	wastewater and runoff water
K^+	blood, wine, and soil
CO_2/HCO_3^-	blood and groundwater
F^-	groundwater, drinking water, and soil
Br^-	grains and plant extracts
I^-	milk and pharmaceuticals
NO_3^-	groundwater, drinking water, soil, and fertilizer

Summary

Redox reactions can be balanced using the half-reaction method. The standard cell potential is a measure of the driving force for the reaction.

$$E°_{cell} = E°_{cathode} - E°_{anode}$$

The flow of electrons in an electrochemical cell depends on the identity of the reacting substances, the difference in the potential energy of their valence electrons, and their concentrations. The potential of the cell under standard conditions (1 M for solutions, 1 atm for gases, pure solids or liquids for other substances) and at a fixed temperature (25°C) is called the standard cell potential

($E°_{cell}$). Only the difference between the potentials of two electrodes can be measured. By convention, all tabulated values of standard electrode potentials are listed as standard reduction potentials. The overall cell potential is the reduction potential of the reductive half-reaction minus the reduction potential of the oxidative half-reaction ($E°_{cell} = E°_{cathode} - E°_{anode}$). The potential of the standard hydrogen electrode (SHE) is defined as 0 V under standard conditions. The potential of a half-reaction measured against the SHE under standard conditions is called its standard electrode potential. The standard cell potential is a measure of the driving force for a given redox reaction. All E° values are independent of the stoichiometric coefficients for the half-reaction. Redox reactions can be balanced using the half-reaction method, in which the overall redox reaction is divided into an oxidation half-reaction and a reduction half-reaction, each balanced for mass and charge. The half-reactions selected from tabulated lists must exactly reflect reaction conditions. In an alternative method, the atoms in each half-reaction are balanced, and then the charges are balanced. Whenever a half-reaction is reversed, the sign of E° corresponding to that reaction must also be reversed. If $\boldsymbol{E°_{cell}}$ is positive, the reaction will occur spontaneously under standard conditions. If $\boldsymbol{E°_{cell}}$ is negative, then the reaction is not spontaneous under standard conditions, although it will proceed spontaneously in the opposite direction. The potential of an indicator electrode is related to the concentration of the substance being measured, whereas the potential of the reference electrode is held constant. Whether reduction or oxidation occurs depends on the potential of the sample versus the potential of the reference electrode. In addition to the SHE, other reference electrodes are the silver–silver chloride electrode; the saturated calomel electrode (SCE); the glass electrode, which is commonly used to measure pH; and ion-selective electrodes, which depend on the concentration of a single ionic species in solution. Differences in potential between the SHE and other reference electrodes must be included when calculating values for E°.

9.4: Standard Electrode Potentials is shared under a CC BY-NC-SA 4.0 license and was authored, remixed, and/or curated by LibreTexts.

9.5: Strengths of Oxidants and Reductants

Learning Objectives

- Identify how to view Standard Reduction Potentials from the perspective of viable reducing and oxidizing agents in REDOX reactions.

We can measure the standard potentials for a wide variety of chemical substances, some of which are listed in Table P2. These data allow us to compare the oxidative and reductive strengths of a variety of substances. The half-reaction for the standard hydrogen electrode (SHE) lies more than halfway down the list in Table **9.5.1**. All reactants that lie below the SHE in the table are stronger oxidants than H^+, and all those that lie above the SHE are weaker. The strongest oxidant in the table is F_2, with a standard electrode potential of 2.87 V. This high value is consistent with the high electronegativity of fluorine and tells us that fluorine has a stronger tendency to accept electrons (it is a stronger oxidant) than any other element.

Table **9.5.1**: Standard Potentials for Selected Reduction Half-Reactions at 25°C

Half-Reaction	E° (V)
$Li^+(aq) + e^- \rightleftharpoons Li(s)$	–3.040
$Be^{2+}(aq) + 2e^- \rightleftharpoons Be(s)$	–1.99
$Al^{3+}(aq) + 3e^- \rightleftharpoons Al(s)$	–1.676
$Zn^{2+}(aq) + 2e^- \rightleftharpoons Zn(s)$	–0.7618
$Ag_2S(s) + 2e^- \rightleftharpoons 2Ag(s) + S^{2-}(aq)$	–0.71
$Fe^{2+}(aq) + 2e^- \rightleftharpoons Fe(s)$	–0.44
$Cr^{3+}(aq) + e^- \rightleftharpoons Cr^{2+}(aq)$	–0.424
$Cd^{2+}(aq) + 2e^- \rightleftharpoons Cd(s)$	–0.4030
$PbSO_4(s) + 2e^- \rightleftharpoons Pb(s) + SO_4^{2-}(aq)$	–0.356
$Ni^{2+}(aq) + 2e^- \rightleftharpoons Ni(s)$	–0.257
$2SO_4^{2-}(aq) + 4H^+(aq) + 2e^- \rightleftharpoons S_2O_6^{2-}(aq) + 2H_2O(l)$	–0.25
$Sn^{2+}(aq) + 2e^- \rightleftharpoons Sn(s)$	−0.14
$2H^+(aq) + 2e^- \rightleftharpoons H_2(g)$	0.00
$Sn^{4+}(aq) + 2e^- \rightleftharpoons Sn^{2+}(aq)$	0.154
$Cu^{2+}(aq) + e^- \rightleftharpoons Cu^+(aq)$	0.159
$AgCl(s) + e^- \rightleftharpoons Ag(s) + Cl^-(aq)$	0.2223
$Cu^{2+}(aq) + 2e^- \rightleftharpoons Cu(s)$	0.3419
$O_2(g) + 2H_2O(l) + 4e^- \rightleftharpoons 4OH^-(aq)$	0.401
$H_2SO_3(aq) + 4H^+(aq) + 4e^- \rightleftharpoons S(s) + 3H_2O(l)$	0.45
$I_2(s) + 2e^- \rightleftharpoons 2I^-(aq)$	0.5355
$MnO_4^{2-}(aq) + 2H_2O(l) + 2e^- \rightleftharpoons MnO_2(s) + 4OH^-(aq)$	0.60
$O_2(g) + 2H^+(aq) + 2e^- \rightleftharpoons H_2O_2(aq)$	0.695
$H_2SeO_3(aq) + 4H^+ + 4e^- \rightleftharpoons Se(s) + 3H_2O(l)$	0.74
$Fe^{3+}(aq) + e^- \rightleftharpoons Fe^{2+}(aq)$	0.771
$Ag^+(aq) + e^- \rightleftharpoons Ag(s)$	0.7996
$NO_3^-(aq) + 3H^+(aq) + 2e^- \rightleftharpoons HNO_2(aq) + H_2O(l)$	0.94
$Br_2(aq) + 2e^- \rightleftharpoons 2Br^-(aq)$	1.087
$MnO_2(s) + 4H^+(aq) + 2e^- \rightleftharpoons Mn^{2+}(aq) + 2H_2O(l)$	1.23
$O_2(g) + 4H^+(aq) + 4e^- \rightleftharpoons 2H_2O(l)$	1.229
$Cr_2O_7^{2-}(aq) + 14H^+(aq) + 6e^- \rightleftharpoons 2Cr^{3+}(aq) + 7H_2O(l)$	1.36
$Cl_2(g) + 2e^- \rightleftharpoons 2Cl^-(aq)$	1.396
$Ce^{4+}(aq) + e^- \rightleftharpoons Ce^{3+}(aq)$	1.61
$PbO_2(s) + HSO_4^-(aq) + 3H^+(aq) + 2e^- \rightleftharpoons PbSO_4(s) + 2H_2O(l)$	1.690

Half-Reaction	E° (V)
$H_2O_2(aq) + 2H^+(aq) + 2e^- \rightleftharpoons 2H_2O(l)$	1.763
$F_2(g) + 2e^- \rightleftharpoons 2F^-(aq)$	2.87

Not all oxidizers and reducers are created equal. The standard reduction potentials in Table **9.5.1** can be interpreted as a ranking of substances according to their oxidizing and reducing power. Strong oxidizing agents are typically compounds with elements in high oxidation states or with high electronegativity, which gain electrons in the redox reaction (Figure **9.5.1**). Examples of strong oxidizers include hydrogen peroxide, permanganate, and osmium tetroxide. Reducing agents are typically electropositive elements such as hydrogen, lithium, sodium, iron, and aluminum, which lose electrons in redox reactions. Hydrides (compounds that contain hydrogen in the formal -1 oxidation state), such as sodium hydride, sodium borohydride and lithium aluminum hydride, are often used as reducing agents in organic and organometallic reactions.

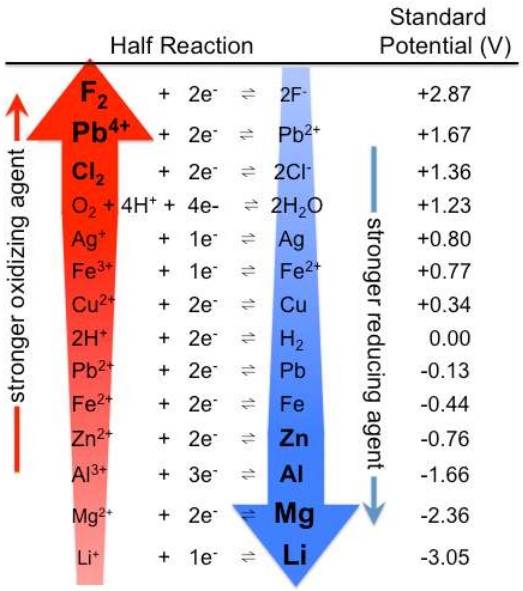


Figure **9.5.1**: Table of standard electrode potentials. **Note that the ranking is the opposite here**, with strong oxidizing agents at the top and strong reducing agents at the bottom, than in Table **9.5.1**. The actual standard potentials are the same of course. (CC BY-SA 3.0; Tem5psu).

Similarly, all species in Table **9.5.1** that lie above H_2 are stronger reductants than H_2, and those that lie below H_2 are weaker. The strongest reductant in the table is thus metallic lithium, with a standard electrode potential of −3.04 V. This fact might be surprising because cesium, not lithium, is the least electronegative element. The apparent anomaly can be explained by the fact that electrode potentials are measured in aqueous solution, where intermolecular interactions are important, whereas ionization potentials and electron affinities are measured in the gas phase. Due to its small size, the Li^+ ion is stabilized in aqueous solution by strong electrostatic interactions with the negative dipole end of water molecules. These interactions result in a significantly greater $\Delta H_{hydration}$ for Li^+ compared with Cs^+. Lithium metal is therefore the strongest reductant (most easily oxidized) of the alkali metals in aqueous solution.

> *The standard reduction potentials can be interpreted as a ranking of substances according to their oxidizing and reducing power. Species in Table* **9.5.1** *that lie above* H_2 *are stronger reducing agents (more easily oxidized) than* H_2*. Species that lie below* $\mathbf{H_2}$ *are stronger oxidizing agents.*

Because the half-reactions shown in Table **9.5.1** are arranged in order of their E° values, we can use the table to quickly predict the relative strengths of various oxidants and reductants. Any species on the left side of a half-reaction will spontaneously oxidize any species on the right side of another half-reaction that lies below it in the table. Conversely, any species on the right side of a half-

reaction will spontaneously reduce any species on the left side of another half-reaction that lies above it in the table. We can use these generalizations to predict the spontaneity of a wide variety of redox reactions ($E°_{cell} > 0$), as illustrated in Example **9.5.1**.

Example 9.5.1: Silver Sulfide

The black tarnish that forms on silver objects is primarily Ag_2S. The half-reaction for reversing the tarnishing process is as follows:

$$Ag_2S(s) + 2e^- \longrightarrow 2Ag(s) + S^{2-}(aq) \qquad E° = -0.69\,V$$

a. Referring to Table **9.5.1**, predict which species—H_2O_2(aq), Zn(s), I^-(aq), Sn^{2+}(aq)—can reduce Ag_2S to Ag under standard conditions.
b. Of these species—H_2O_2(aq), Zn(s), I^-(aq), Sn^{2+}(aq), identify which is the strongest reducing agent in aqueous solution and thus the best candidate for a commercial product.
c. From the data in Table **9.5.1**, suggest an alternative reducing agent that is readily available, inexpensive, and possibly more effective at removing tarnish.



Given: reduction half-reaction, standard electrode potential, and list of possible reductants

Asked for: reductants for Ag_2S, strongest reductant, and potential reducing agent for removing tarnish

Strategy:

A From their positions in Table **9.5.1**, decide which species can reduce Ag_2S. Determine which species is the strongest reductant.

B Use Table **9.5.1** to identify a reductant for Ag_2S that is a common household product.

Solution

We can solve the problem in one of two ways: (1) compare the relative positions of the four possible reductants with that of the Ag_2S/Ag couple in Table **9.5.1** or (2) compare E° for each species with E° for the Ag_2S/Ag couple (−0.69 V).

a. **A** The species in Table **9.5.1** are arranged from top to bottom in order of increasing reducing strength. Of the four species given in the problem, I^-(aq), Sn^{2+}(aq), and H_2O_2(aq) lie above Ag_2S, and one [Zn(s)] lies below it. We can therefore conclude that Zn(s) can reduce Ag_2S(s) under standard conditions, whereas I^-(aq), Sn^{2+}(aq), and H_2O_2(aq) cannot. Sn^{2+}(aq) and H_2O_2(aq) appear twice in the table: on the left side (oxidant) in one half-reaction and on the right side (reductant) in another.
b. The strongest reductant is Zn(s), the species on the right side of the half-reaction that lies closer to the bottom of Table **9.5.1** than the half-reactions involving I^-(aq), Sn^{2+}(aq), and H_2O_2(aq). (Commercial products that use a piece of zinc are often marketed as a “miracle product” for removing tarnish from silver. All that is required is to add warm water and salt for electrical conductivity.)
c. **B** Of the reductants that lie below Zn(s) in Table **9.5.1**, and therefore are stronger reductants, only one is commonly available in household products: Al(s), which is sold as aluminum foil for wrapping foods.

Example 9.5.2

Use the data in Table 9.5.1 to determine whether each reaction is likely to occur spontaneously under standard conditions:

a. $\mathrm{Sn(s) + Be^{2+}(aq) \longrightarrow Sn^{2+}(aq) + Be(s)}$
b. $\mathrm{MnO_2(s) + H_2O_2(aq) + 2H^+(aq) \longrightarrow O_2(g) + Mn^{2+}(aq) + 2H_2O(l)}$

Given: redox reaction and list of standard electrode potentials (Table 9.5.1)

Asked for: reaction spontaneity

Strategy:

A. Identify the half-reactions in each equation. Using Table 9.5.1, determine the standard potentials for the half-reactions in the appropriate direction.
B. Use the $E_{cell} = E^\circ_{srp}(cathode) - E^\circ_{srp}(anode)$ equation to calculate the standard cell potential for the overall reaction. From this value, determine whether the overall reaction is spontaneous.

Solution

a. **A** Metallic tin is oxidized to $\mathrm{Sn^{2+}(aq)}$, and $\mathrm{Be^{2+}(aq)}$ is reduced to elemental beryllium. We can find the standard electrode potentials for the latter (reduction) half-reaction (−1.99 V) and for the former (oxidation) half-reaction (−0.14 V) directly from Table 9.5.1.

B Adding the two half-reactions gives the overall reaction:

$$\begin{aligned} \text{cathode}: \mathrm{Be^{2+}(aq) + 2e^- \rightarrow Be(s)} \\ \text{anode}: \mathrm{Sn(s) \rightarrow Sn^{2+}(s) + 2e^-} \\ \hline \text{overall}: \mathrm{Sn(s) + Be^{2+}(aq) \rightarrow Sn^{2+}(aq) + Be(s)} \end{aligned}$$

with

$$\begin{aligned} E^\circ_{\text{cathode}} &= \text{-1.99 V} \\ E^\circ_{\text{anode}} &= \text{-0.14 V} \\ E^\circ_{\text{cell}} &= E^\circ_{\text{cathode}} - E^\circ_{\text{anode}} \\ &= -1.85 \text{ V} \end{aligned}$$

The standard cell potential is quite negative, so the reaction will not occur spontaneously as written. That is, metallic tin cannot reduce Be^{2+} to beryllium metal under standard conditions. Instead, the reverse process, the reduction of stannous ions (Sn^{2+}) by metallic beryllium, which has a positive value of $E°_{cell}$, will occur spontaneously.

b. **A** $\mathrm{MnO_2}$ is the oxidant ($\mathrm{Mn^{4+}}$ is reduced to $\mathrm{Mn^{2+}}$), while $\mathrm{H_2O_2}$ is the reductant ($\mathrm{O^{2-}}$ is oxidized to $\mathrm{O_2}$). We can obtain the standard electrode potentials for the reduction and oxidation half-reactions directly from Table 9.5.1.

B The two half-reactions and their corresponding potentials are as follows:

$$\begin{aligned} \text{cathode}: \mathrm{MnO_2(s) + 4H^+(aq) + 2e^- \rightarrow Mn^{2+}(aq) + 2H_2O(l)} \\ \text{anode}: \mathrm{H_2O_2(aq) \rightarrow O_2(g) + 2H^+(aq) + 2e^-} \\ \hline \text{overall}: \mathrm{MnO_2(s) + H_2O_2(aq) + 2H^+(aq) \rightarrow O_2(g) + Mn^{2+}(aq) + 2H_2O(l)} \end{aligned}$$

with

$$\begin{aligned} E^\circ_{\text{cathode}} &= 1.23 \text{ V} \\ E^\circ_{\text{anode}} &= 0.70 \text{ V} \\ E^\circ_{\text{cell}} &= E^\circ_{\text{cathode}} - E^\circ_{\text{anode}} \\ &= +0.52 \text{ V} \end{aligned}$$

The standard potential for the reaction is positive, indicating that under standard conditions, it will occur spontaneously as written. Hydrogen peroxide will reduce $\mathrm{MnO_2}$, and oxygen gas will evolve from the solution.

? Exercise 9.5.2

Use the data in Table **9.5.1** to determine whether each reaction is likely to occur spontaneously under standard conditions:

a. $2\,Ce^{4+}(aq) + 2\,Cl^{-}(aq) \longrightarrow 2\,Ce^{3+}(aq) + Cl_2(g)$
b. $4\,MnO_2(s) + 3\,O_2(g) + 4\,OH^{-}(aq) \longrightarrow 4\,MnO_4^{-}(aq) + 2\,H_2O$

Answer a

spontaneous with $E^{o}_{cell} = 1.61\,V - 1.396\,V = 0.214\,V$

Answer b

nonspontaneous with $E^{\circ}_{cell} = -0.20\,V$

Although the sign of E^{o}_{cell} tells us whether a particular redox reaction will occur spontaneously under standard conditions, it does not tell us to what extent the reaction proceeds, and it does not tell us what will happen under nonstandard conditions. To answer these questions requires a more quantitative understanding of the relationship between electrochemical cell potential and chemical thermodynamics.

Summary

The relative strengths of various oxidants and reductants can be predicted using E^{o} values. The oxidative and reductive strengths of a variety of substances can be compared using standard electrode potentials. Apparent anomalies can be explained by the fact that electrode potentials are measured in aqueous solution, which allows for strong intermolecular electrostatic interactions, and not in the gas phase.

Conceptual Problems

1. The order of electrode potentials cannot always be predicted by ionization potentials and electron affinities. Why? Do you expect sodium metal to have a higher or a lower electrode potential than predicted from its ionization potential? What is its approximate electrode potential?
2. Without referring to tabulated data, of Br_2/Br^-, Ca^{2+}/Ca, O_2/OH^-, and Al^{3+}/Al, which would you expect to have the least negative electrode potential and which the most negative? Why?
3. Because of the sulfur-containing amino acids present in egg whites, eating eggs with a silver fork will tarnish the fork. As a chemist, you have all kinds of interesting cleaning products in your cabinet, including a 1 M solution of oxalic acid ($H_2C_2O_4$). Would you choose this solution to clean the fork that you have tarnished from eating scrambled eggs?
4. The electrode potential for the reaction $Cu^{2+}(aq) + 2e^- \rightarrow Cu(s)$ is 0.34 V under standard conditions. Is the potential for the oxidation of 0.5 mol of Cu equal to −0.34/2 V? Explain your answer.
5. Refer to Table **9.5.1** to predict
   A. Which species—$Sn^{4+}(aq)$, $Cl^-(aq)$, $Ag^+(aq)$, $Cr^{3+}(aq)$, and/or $H_2O_2(aq)$—can oxidize $MnO_2(s)$ to MNO_4^- under standard conditions.
   B. Which species—$Sn^{4+}(aq)$, $Cl^-(aq)$, $Ag^+(aq)$, $Cr^{3+}(aq)$, and/or $H_2O_2(aq)$—is the strongest oxidizing agent in aqueous solution.

Conceptual Answer

3. No; E° = −0.691 V for $Ag_2S(s) + 2e^- \rightarrow Ag(s) + S^{2-}(aq)$, which is too negative for Ag_2S to be spontaneously reduced by oxalic acid [E° = 0.49 V for $2CO_2(g) + 2H^+(aq) + 2e^- \rightarrow H_2C_2O_4(aq)$]

5.

A. $Ag^+(aq)$; $H_2O_2(aq)$
B. $H_2O_2(aq)$

9.5: Strengths of Oxidants and Reductants is shared under a not declared license and was authored, remixed, and/or curated by LibreTexts.

- **Comparing Strengths of Oxidants and Reductants** is licensed CC BY-NC-SA 4.0.

9.6: E, ΔG, and K (The Big Triangle of Chemistry)

Learning Objectives

- To understand the relationship between cell potential and the equilibrium constant.
- To use cell potentials to calculate solution concentrations.

Changes in reaction conditions can have a tremendous effect on the course of a redox reaction. For example, under standard conditions, the reaction of $\mathrm{Co(s)}$ with $\mathrm{Ni^{2+}(aq)}$ to form $\mathrm{Ni(s)}$ and $\mathrm{Co^{2+}(aq)}$ occurs spontaneously, but if we reduce the concentration of $\mathrm{Ni^{2+}}$ by a factor of 100, so that $[\mathrm{Ni^{2+}}]$ is 0.01 M, then the reverse reaction occurs spontaneously instead. The relationship between voltage and concentration is one of the factors that must be understood to predict whether a reaction will be spontaneous.

The Relationship between Cell Potential & Gibbs Energy

Electrochemical cells convert chemical energy to electrical energy and vice versa. The total amount of energy produced by an electrochemical cell, and thus the amount of energy available to do electrical work, depends on both the cell potential and the total number of electrons that are transferred from the reductant to the oxidant during the course of a reaction. The resulting electric current is measured in **coulombs (C)**, an SI unit that measures the number of electrons passing a given point in 1 s. A coulomb relates energy (in joules) to electrical potential (in volts). Electric current is measured in **amperes (A)**; 1 A is defined as the flow of 1 C/s past a given point (1 C = 1 A·s):

$$\frac{1\ \mathrm{J}}{1\ \mathrm{V}} = 1\ \mathrm{C} = \mathrm{A \cdot s}$$

In chemical reactions, however, we need to relate the coulomb to the charge on a mole of electrons. Multiplying the charge on the electron by Avogadro's number gives us the charge on 1 mol of electrons, which is called the **faraday (F)**, named after the English physicist and chemist Michael Faraday (1791–1867):

$$\begin{aligned} F &= (1.60218 \times 10^{-19}\ \mathrm{C}) \left(\frac{6.02214 \times 10^{23}\ J}{1\ \mathrm{mol\ e^-}} \right) \\ &= 9.64833212 \times 10^{4}\ \mathrm{C/mol\ e^-} \\ &\simeq 96,485\ J/(\mathrm{V \cdot mol\ e^-}) \end{aligned}$$

The total charge transferred from the reductant to the oxidant is therefore nF, where n is the number of moles of electrons.

Michael Faraday (1791–1867)

Faraday was a British physicist and chemist who was arguably one of the greatest experimental scientists in history. The son of a blacksmith, Faraday was self-educated and became an apprentice bookbinder at age 14 before turning to science. His experiments in electricity and magnetism made electricity a routine tool in science and led to both the electric motor and the electric generator. He discovered the phenomenon of electrolysis and laid the foundations of electrochemistry. In fact, most of the specialized terms introduced in this chapter (electrode, anode, cathode, and so forth) are due to Faraday. In addition, he discovered benzene and invented the system of oxidation state numbers that we use today. Faraday is probably best known for "The Chemical History of a Candle," a series of public lectures on the chemistry and physics of flames.

The maximum amount of work that can be produced by an electrochemical cell (w_{max}) is equal to the product of the cell potential (E°_{cell}) and the total charge transferred during the reaction (nF):

$$w_{max} = nFE_{cell}$$

Work is expressed as a negative number because work is being done by a system (an electrochemical cell with a positive potential) on its surroundings.

The change in free energy (ΔG) is also a measure of the maximum amount of work that can be performed during a chemical process ($\Delta G = w_{max}$). Consequently, there must be a relationship between the potential of an electrochemical cell and ΔG; this relationship is as follows:

$$\Delta G = -nFE_{cell}$$

A spontaneous redox reaction is therefore characterized by a negative value of ΔG and a positive value of E°_{cell}, consistent with our earlier discussions. When both reactants and products are in their standard states, the relationship between ΔG° and E°_{cell} is as follows:

$$\Delta G^\circ = -nFE^\circ_{cell} \tag{9.6.1}$$

A spontaneous redox reaction is characterized by a negative value of ΔG°, which corresponds to a positive value of E°_{cell}.

Example 9.6.1

Suppose you want to prepare elemental bromine from bromide using the dichromate ion as an oxidant. Using the data in Table P2, calculate the free-energy change (ΔG°) for this redox reaction under standard conditions. Is the reaction spontaneous?

Given: redox reaction

Asked for: ΔG^o for the reaction and spontaneity

Strategy:

A. From the relevant half-reactions and the corresponding values of E^o, write the overall reaction and calculate E°_{cell}.

B. Determine the number of electrons transferred in the overall reaction. Then use Equation 9.6.1 to calculate ΔG^o. If ΔG^o is negative, then the reaction is spontaneous.

Solution

A

As always, the first step is to write the relevant half-reactions and use them to obtain the overall reaction and the magnitude of E^o. From Table P2, we can find the reduction and oxidation half-reactions and corresponding E^o values:

cathode:	$Cr_2O_7^{2-}(aq) + 14H^+(aq) + 6e^- \rightarrow 2Cr^{3+}(aq) + 7H_2O(l)$	$E^\circ_{cathode} = 1.36\ V$
anode:	$2Br^-(aq) \rightarrow Br_2(aq) + 2e^-$	$E^\circ_{anode} = 1.09\ V$

To obtain the overall balanced chemical equation, we must multiply both sides of the oxidation half-reaction by 3 to obtain the same number of electrons as in the reduction half-reaction, remembering that the magnitude of E^o is not affected:

cathode:	$Cr_2O_7^{2-}(aq) + 14H^+(aq) + 6e^- \rightarrow 2Cr^{3+}(aq) + 7H_2O(l)$	$E^\circ_{cathode} = 1.36\ V$
anode:	$6Br^-(aq) \rightarrow 3Br_2(aq) + 6e^-$	$E^\circ_{anode} = 1.09\ V$
overall:	$Cr_2O_7^{2-}(aq) + 6Br^-(aq) + 14H^+(aq) \rightarrow 2Cr^{3+}(aq) + 3Br_2(aq) + 7H_2O(l)$	$E^\circ_{cell} = 0.27\ V$

B

We can now calculate ΔG° using Equation 9.6.1. Because six electrons are transferred in the overall reaction, the value of n is 6:

$$\begin{aligned}\Delta G^\circ &= -(n)(F)(E^\circ_{cell}) \\ &= -(6\text{ mole})[96,485\text{ J/(V}\cdot\text{mol)}(0.27\text{ V})] \\ &= -15.6 \times 10^4\text{ J} \\ &= -156\text{ kJ/mol } Cr_2O_7^{2-}\end{aligned}$$

Thus ΔG^o is −168 kJ/mol for the reaction as written, and the reaction is spontaneous.

Exercise 9.6.1

Use the data in Table P2 to calculate ΔG^o for the reduction of ferric ion by iodide:

$$2\,Fe^{3+}(aq) + 2\,I^-(aq) \longrightarrow 2\,Fe^{2+}(aq) + I_2(s)$$

Is the reaction spontaneous?

Answer

−44 kJ/mol I_2; yes

Potentials for the Sums of Half-Reactions

Although Table P2 list several half-reactions, many more are known. When the standard potential for a half-reaction is not available, we can use relationships between standard potentials and free energy to obtain the potential of any other half-reaction that can be written as the sum of two or more half-reactions whose standard potentials are available. For example, the potential for the reduction of $\mathrm{Fe^{3+}(aq)}$ to $\mathrm{Fe(s)}$ is not listed in the table, but two related reductions are given:

$$\mathrm{Fe^{3+}(aq) + e^- \longrightarrow Fe^{2+}(aq)} \quad E^\circ = +0.77V$$

$$\mathrm{Fe^{2+}(aq) + 2\,e^- \longrightarrow Fe(s)} \quad E^\circ = -0.45V$$

Although the sum of these two half-reactions gives the desired half-reaction, we cannot simply add the potentials of two reductive half-reactions to obtain the potential of a third reductive half-reaction because E^o is not a state function. However, because ΔG^o is a state function, the sum of the ΔG^o values for the individual reactions gives us ΔG^o for the overall reaction, which is proportional to both the potential and the number of electrons (n) transferred. To obtain the value of E^o for the overall half-reaction, we first must add the values of $\Delta G^o (= -nFE^o)$ for each individual half-reaction to obtain ΔG^o for the overall half-reaction:

Extra close brace or missing open brace

Solving the last expression for ΔG° for the overall half-reaction,

$$\Delta G^\circ = F[(-0.77V) + (-2)(-0.45V)] = F(0.13V)$$

Three electrons ($n = 3$) are transferred in the overall reaction, so substituting into Equation 9.6.1 and solving for E^o gives the following:

$$\begin{aligned} \Delta G^\circ &= -nFE^\circ_{\text{cell}} \\ F(0.13\text{ V}) &= -(3)(F)(E^\circ_{\text{cell}}) \\ E^\circ &= -\frac{0.13\text{ V}}{3} = -0.043\text{ V} \end{aligned}$$

This value of E^o is very different from the value that is obtained by simply adding the potentials for the two half-reactions (0.32 V) and even has the opposite sign.

> *Values of E^o for half-reactions cannot be added to give E^o for the sum of the half-reactions; only values of $\Delta G^o = -nFE^\circ_{cell}$ for half-reactions can be added.*

The Relationship between Cell Potential & the Equilibrium Constant

We can use the relationship between ΔG° and the equilibrium constant K, to obtain a relationship between E°_{cell} and K. Recall that for a general reaction of the type $aA + bB \rightarrow cC + dD$, the standard free-energy change and the equilibrium constant are related by the following equation:

$$\Delta G^\circ = -RT \ln K$$

Given the relationship between the standard free-energy change and the standard cell potential (Equation 9.6.1), we can write

$$-nFE^\circ_{cell} = -RT \ln K$$

Rearranging this equation,

$$E^\circ_{\text{cell}} = \left(\frac{RT}{nF}\right) \ln K \tag{9.6.2}$$

For $T = 298\,K$, Equation 9.6.2 can be simplified as follows:

$$
\begin{aligned}
E^\circ_{\text{cell}} &= \left(\frac{RT}{nF}\right) \ln K \\
&= \left[\frac{[8.314\ \text{J/(mol}\cdot\text{K)}(298\ \text{K})]}{n[96,485\ \text{J/(V}\cdot\text{mol)}]}\right] 2.303 \log K \\
&= \left(\frac{0.0592\ \text{V}}{n}\right) \log K
\end{aligned} \tag{9.6.3}
$$

Thus E°_{cell} is directly proportional to the logarithm of the equilibrium constant. This means that large equilibrium constants correspond to large positive values of E°_{cell} and vice versa.

Example 9.6.2

Use the data in Table P2 to calculate the equilibrium constant for the reaction of metallic lead with PbO_2 in the presence of sulfate ions to give $PbSO_4$ under standard conditions. (This reaction occurs when a car battery is discharged.) Report your answer to two significant figures.

Given: redox reaction

Asked for: K

Strategy:

A. Write the relevant half-reactions and potentials. From these, obtain the overall reaction and E^o_{cell}.

B. Determine the number of electrons transferred in the overall reaction. Use Equation 9.6.3 to solve for $\log K$ and then K.

Solution

A The relevant half-reactions and potentials from Table P2 are as follows:

cathode:	$PbO_2(s) + SO_4^{2-}(aq) + 4H^+(aq) + 2e^- \rightarrow PbSO_4(s) + 2H_2O(l)$	$E^\circ_{\text{cathode}} = 1.69\ \text{V}$
anode:	$Pb(s) + SO_4^{2-}(aq) \rightarrow PbSO_4(s) + 2e^-$	$E^\circ_{\text{anode}} = -0.36\ \text{V}$
overall:	$Pb(s) + PbO_2(s) + 2SO_4^{2-}(aq) + 4H^+(aq) \rightarrow 2PbSO_4(s) + 2H_2O(l)$	$E^\circ_{\text{cell}} = 2.05\ \text{V}$

B Two electrons are transferred in the overall reaction, so $n = 2$. Solving Equation 9.6.3 for log K and inserting the values of n and E^o,

$$
\log K = \frac{nE^\circ}{0.0591\ \text{V}} = \frac{2(2.05\ \text{V})}{0.0591\ \text{V}} = 69.37
$$

$$
K = 2.3 \times 10^{69}
$$

Thus the equilibrium lies far to the right, favoring a discharged battery (as anyone who has ever tried unsuccessfully to start a car after letting it sit for a long time will know).

Exercise 9.6.2

Use the data in Table P2 to calculate the equilibrium constant for the reaction of $Sn^{2+}(aq)$ with oxygen to produce $Sn^{4+}(aq)$ and water under standard conditions. Report your answer to two significant figures. The reaction is as follows:

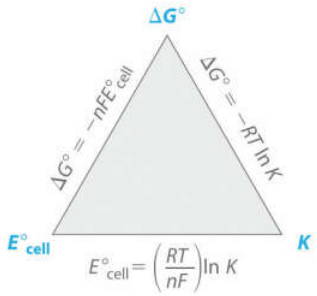
$$
2\,Sn^{2+}(aq) + O_2(g) + 4\,H^+(aq) \rightleftharpoons 2\,Sn^{4+}(aq) + 2\,H_2O(l)
$$

Answer

5.7×10^{72}

Figure 9.6.1 summarizes the relationships that we have developed based on properties of the system—that is, based on the equilibrium constant, standard free-energy change, and standard cell potential—and the criteria for spontaneity ($\Delta G^\circ < 0$). Unfortunately, these criteria apply only to systems in which all reactants and products are present in their standard states, a situation

that is seldom encountered in the real world. A more generally useful relationship between cell potential and reactant and product concentrations, as we are about to see, uses the relationship between ΔG and the reaction quotient Q.



$\Delta G°$	$E°_{cell}$	K	Direction of Reaction
< 0	> 0	> 1	spontaneous in forward direction
> 0	< 0	< 1	spontaneous in reverse direction
0	0	1	no net reaction: system at equilibrium

Figure **9.6.1**: The Relationships among Criteria for Thermodynamic Spontaneity. The three properties of a system that can be used to predict the spontaneity of a redox reaction under standard conditions are K, ΔG°, and $E°_{cell}$. If we know the value of one of these quantities, then these relationships enable us to calculate the value of the other two. The signs of ΔG° and $E°_{cell}$ and the magnitude of K determine the direction of spontaneous reaction under standard conditions. (CC BY-NC-SA; Anonymous by request)

If ΔG is less than zero, E^o is greater than zero and K is greater than 1 then the direction of the reaction is spontaneous in forward direction. If ΔG is greater than zero, E^o is less than zero and K is less than one then the direction of reaction is spontaneous in reverse direction. If ΔG is zero, E is zero and K is one that there is no net reaction and the system is at equilibrium .

Summary

A coulomb (C) relates electrical potential, expressed in volts, and energy, expressed in joules. The current generated from a redox reaction is measured in amperes (A), where 1 A is defined as the flow of 1 C/s past a given point. The faraday (F) is Avogadro's number multiplied by the charge on an electron and corresponds to the charge on 1 mol of electrons. The product of the cell potential and the total charge is the maximum amount of energy available to do work, which is related to the change in free energy that occurs during the chemical process. Adding together the ΔG values for the half-reactions gives ΔG for the overall reaction, which is proportional to both the potential and the number of electrons (n) transferred. Spontaneous redox reactions have a negative ΔG and therefore a positive E_{cell}. Because the equilibrium constant K is related to ΔG, $E°_{cell}$ and K are also related. Large equilibrium constants correspond to large positive values of E°.

9.6: E, ΔG, and K (The Big Triangle of Chemistry) is shared under a not declared license and was authored, remixed, and/or curated by LibreTexts.

- **20.5: Gibbs Energy and Redox Reactions** is licensed CC BY-NC-SA 3.0.

9.7: Cell Potential as a Function of Concentrations

Learning Objectives

- Relate cell potentials to Gibbs energy changes
- Use the Nernst equation to determine cell potentials at nonstandard conditions
- Perform calculations that involve converting between cell potentials, free energy changes, and equilibrium constants

The *Nernst Equation* enables the determination of cell potential under non-standard conditions. It relates the measured cell potential to the reaction quotient and allows the accurate determination of equilibrium constants (including solubility constants).

The Effect of Concentration on Cell Potential: The Nernst Equation

Recall that the actual free-energy change for a reaction under nonstandard conditions, ΔG, is given as follows:

$$\Delta G = \Delta G^\circ + RT \ln Q \tag{9.7.1}$$

We also know that $\Delta G = -nFE_{cell}$ (under non-standard conditions) and $\Delta G^o = -nFE^o_{cell}$ (under standard conditions). Substituting these expressions into Equation 9.7.1, we obtain

$$-nFE_{cell} = -nFE^o_{cell} + RT \ln Q \tag{9.7.2}$$

Dividing both sides of this equation by $-nF$,

$$E_{\text{cell}} = E^\circ_{\text{cell}} - \left(\frac{RT}{nF}\right) \ln Q \tag{9.7.3}$$

Equation 9.7.3 is called the **Nernst equation**, after the German physicist and chemist Walter Nernst (1864–1941), who first derived it. The Nernst equation is arguably the most important relationship in electrochemistry. When a redox reaction is at equilibrium ($\Delta G = 0$), then Equation 9.7.3 reduces to Equation 9.7.4 and 9.7.5 because $Q = K$, and there is no net transfer of electrons (i.e., E_{cell} = 0).

$$E_{\text{cell}} = E^\circ_{\text{cell}} - \left(\frac{RT}{nF}\right) \ln K = 0 \tag{9.7.4}$$

since

$$E^\circ_{\text{cell}} = \left(\frac{RT}{nF}\right) \ln K \tag{9.7.5}$$

Substituting the values of the constants into Equation 9.7.3 with $T = 298\ K$ and converting to base-10 logarithms give the relationship of the actual cell potential (E_{cell}), the standard cell potential ($E°_{cell}$), and the reactant and product concentrations at room temperature (contained in Q):

$$E_{\text{cell}} = E^\circ_{\text{cell}} - \left(\frac{0.0591\ \text{V}}{n}\right) \log Q \tag{9.7.6}$$

The Power of the Nernst Equation

The Nernst Equation (9.7.3) can be used to determine the value of E_{cell}, and thus the direction of spontaneous reaction, for any redox reaction under any conditions.

Equation 9.7.6 allows us to calculate the potential associated with any electrochemical cell at 298 K for any combination of reactant and product concentrations under any conditions. We can therefore determine the spontaneous direction of any redox reaction under any conditions, as long as we have tabulated values for the relevant standard electrode potentials. Notice in Equation 9.7.6 that the cell potential changes by 0.0591/n V for each 10-fold change in the value of Q because log 10 = 1.

Example 9.7.1

The following reaction proceeds spontaneously under standard conditions because $E°_{cell} > 0$ (which means that $\Delta G° < 0$):

$$2\,Ce^{4+}(aq) + 2\,Cl^-(aq) \longrightarrow 2\,Ce^{3+}(aq) + Cl_2(g) \qquad E°_{cell} = 0.25\,V$$

Calculate E_{cell} for this reaction under the following nonstandard conditions and determine whether it will occur spontaneously: $[Ce^{4+}] = 0.013$ M, $[Ce^{3+}] = 0.60$ M, $[Cl^-] = 0.0030$ M, $P_{Cl_2} = 1.0$ atm, and T = 25°C.

Given: balanced redox reaction, standard cell potential, and nonstandard conditions

Asked for: cell potential

Strategy:

Determine the number of electrons transferred during the redox process. Then use the Nernst equation to find the cell potential under the nonstandard conditions.

Solution

We can use the information given and the Nernst equation to calculate E_{cell}. Moreover, because the temperature is 25°C (298 K), we can use Equation 9.7.6 instead of Equation 9.7.3. The overall reaction involves the net transfer of two electrons:

$$2Ce^{4+}_{(aq)} + 2e^- \rightarrow 2Ce^{3+}_{(aq)}$$

$$2Cl^-_{(aq)} \rightarrow Cl_{2(g)} + 2e^-$$

so n = 2. Substituting the concentrations given in the problem, the partial pressure of Cl_2, and the value of $E°_{cell}$ into Equation 9.7.6,

$$\begin{aligned} E_{cell} &= E°_{cell} - \left(\frac{0.0591\ \text{V}}{n}\right)\log Q \\ &= 0.25\ \text{V} - \left(\frac{0.0591\ \text{V}}{2}\right)\log\left(\frac{[Ce^{3+}]^2 P_{Cl_2}}{[Ce^{4+}]^2[Cl^-]^2}\right) \\ &= 0.25\ \text{V} - [(0.0296\ \text{V})(8.37)] = 0.00\ \text{V} \end{aligned}$$

Thus the reaction will not occur spontaneously under these conditions (because E = 0 V and $\Delta G = 0$). The composition specified is that of an equilibrium mixture

Exercise 9.7.1

Molecular oxygen will not oxidize MnO_2 to permanganate via the reaction

$$4\,MnO_2(s) + 3\,O_2(g) + 4\,OH^-(aq) \longrightarrow 4\,MnO_4^-(aq) + 2\,H_2O(l) \quad E°_{cell} = -0.20\,V$$

Calculate E_{cell} for the reaction under the following nonstandard conditions and decide whether the reaction will occur spontaneously: pH 10, P_{O_2} = 0.20 atm, $[MNO_4^-] = 1.0 \times 10^{-4}$ M, and T = 25°C.

Answer

$E_{cell} = -0.22$ V; the reaction will not occur spontaneously.

Applying the Nernst equation to a simple electrochemical cell such as the Zn/Cu cell allows us to see how the cell voltage varies as the reaction progresses and the concentrations of the dissolved ions change. Recall that the overall reaction for this cell is as follows:

$$Zn(s) + Cu^{2+}(aq) \rightarrow Zn^{2+}(aq) + Cu(s) \quad E°cell = 1.10V \tag{9.7.7}$$

The reaction quotient is therefore $Q = [Zn^{2+}]/[Cu^{2+}]$. Suppose that the cell initially contains 1.0 M Cu^{2+} and 1.0×10^{-6} M Zn^{2+}. The initial voltage measured when the cell is connected can then be calculated from Equation 9.7.6:

$$E_{cell} = E^\circ_{cell} - \left(\frac{0.0591\ V}{n}\right) \log \frac{[Zn^{2+}]}{[Cu^{2+}]} \tag{9.7.8}$$

$$= 1.10\ V - \left(\frac{0.0591\ V}{2}\right) \log \left(\frac{1.0 \times 10^{-6}}{1.0}\right) = 1.28\ V \tag{9.7.9}$$

Thus the initial voltage is greater than E° because $Q < 1$. As the reaction proceeds, $[Zn^{2+}]$ in the anode compartment increases as the zinc electrode dissolves, while $[Cu^{2+}]$ in the cathode compartment decreases as metallic copper is deposited on the electrode. During this process, the ratio $Q = [Zn^{2+}]/[Cu^{2+}]$ steadily increases, and the cell voltage therefore steadily decreases. Eventually, $[Zn^{2+}] = [Cu^{2+}]$, so $Q = 1$ and $E_{cell} = E°_{cell}$. Beyond this point, $[Zn^{2+}]$ will continue to increase in the anode compartment, and $[Cu^{2+}]$ will continue to decrease in the cathode compartment. Thus the value of Q will increase further, leading to a further decrease in E_{cell}. When the concentrations in the two compartments are the opposite of the initial concentrations (i.e., 1.0 M Zn^{2+} and 1.0×10^{-6} M Cu^{2+}), $Q = 1.0 \times 10^6$, and the cell potential will be reduced to 0.92 V.

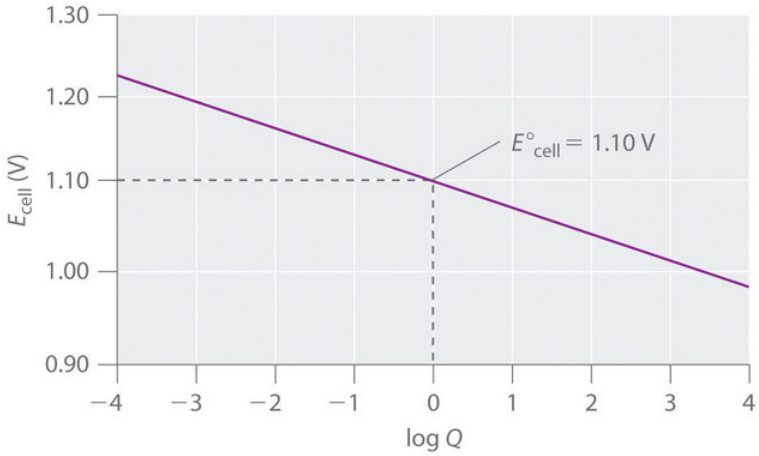


Figure 9.7.1: The Variation of E_{cell} with Log Q for a Zn/Cu Cell. Initially, log Q < 0, and the voltage of the cell is greater than $E°_{cell}$. As the reaction progresses, log Q increases, and E_{cell} decreases. When $[Zn^{2+}] = [Cu^{2+}]$, log Q = 0 and $E_{cell} = E°_{cell} = 1.10$ V. As long as the electrical circuit remains intact, the reaction will continue, and log Q will increase until Q = K and the cell voltage reaches zero. At this point, the system will have reached equilibrium.

The variation of E_{cell} with $\log Q$ over this range is linear with a slope of −0.0591/n, as illustrated in Figure 9.7.1. As the reaction proceeds still further, Q continues to increase, and E_{cell} continues to decrease. If neither of the electrodes dissolves completely, thereby breaking the electrical circuit, the cell voltage will eventually reach zero. This is the situation that occurs when a battery is "dead." The value of Q when $E_{cell} = 0$ is calculated as follows:

$$E_{cell} = E^\circ_{cell} - \left(\frac{0.0591\ V}{n}\right) \log Q = 0 \tag{9.7.10}$$

$$E^\circ = \left(\frac{0.0591\ V}{n}\right) \log Q \tag{9.7.11}$$

$$\log Q = \frac{E°n}{0.0591\ V} = \frac{(1.10\ V)(2)}{0.0591\ V} = 37.23 \tag{9.7.12}$$

$$Q = 10^{37.23} = 1.7 \times 10^{37} \tag{9.7.13}$$

Recall that at equilibrium, $Q = K$. Thus the equilibrium constant for the reaction of Zn metal with Cu^{2+} to give Cu metal and Zn^{2+} is 1.7×10^{37} at 25°C.



The Nernst Equation: The Nernst Equation (opens in new window) [youtu.be]

Concentration Cells

A voltage can also be generated by constructing an electrochemical cell in which each compartment contains the same redox active solution but at different concentrations. The voltage is produced as the concentrations equilibrate. Suppose, for example, we have a cell with 0.010 M $AgNO_3$ in one compartment and 1.0 M $AgNO_3$ in the other. The cell diagram and corresponding half-reactions are as follows:

$$\mathrm{Ag(s)\,|\,Ag^+}(aq, 0.010\ M)\ ||\ \mathrm{Ag^+}(aq, 1.0\ M)\,|\,\mathrm{Ag\,(s)} \tag{9.7.14}$$

cathode:

$$\mathrm{Ag^+}(aq, 1.0\ M) + \mathrm{e^-} \rightarrow \mathrm{Ag\,(s)} \tag{9.7.15}$$

anode:

$$\mathrm{Ag\,(s)} \rightarrow \mathrm{Ag^+}(aq, 0.010\ M) + \mathrm{e^-} \tag{9.7.16}$$

Overall

$$\mathrm{Ag^+}(aq, 1.0\ M) \rightarrow \mathrm{Ag^+}(aq, 0.010\ M) \tag{9.7.17}$$

As the reaction progresses, the concentration of Ag^+ will increase in the left (oxidation) compartment as the silver electrode dissolves, while the Ag^+ concentration in the right (reduction) compartment decreases as the electrode in that compartment gains mass. The total mass of $Ag(s)$ in the cell will remain constant, however. We can calculate the potential of the cell using the Nernst equation, inserting 0 for $E°_{cell}$ because $E°_{cathode} = -E°_{anode}$:

$$\begin{aligned} E_{\text{cell}} &= E°_{\text{cell}} - \left(\frac{0.0591\ \text{V}}{n}\right)\log Q \\ &= 0 - \left(\frac{0.0591\ \text{V}}{1}\right)\log\left(\frac{0.010}{1.0}\right) \\ &= 0.12\ \text{V} \end{aligned}$$

An electrochemical cell of this type, in which the anode and cathode compartments are identical except for the concentration of a reactant, is called a **concentration cell**. As the reaction proceeds, the difference between the concentrations of Ag^+ in the two compartments will decrease, as will E_{cell}. Finally, when the concentration of Ag^+ is the same in both compartments, equilibrium will have been reached, and the measured potential difference between the two compartments will be zero ($E_{cell} = 0$).

✔ Example 9.7.2

Calculate the voltage in a galvanic cell that contains a manganese electrode immersed in a 2.0 M solution of $MnCl_2$ as the cathode, and a manganese electrode immersed in a 5.2×10^{-2} M solution of $MnSO_4$ as the anode (T = 25°C).

Given: galvanic cell, identities of the electrodes, and solution concentrations

Asked for: voltage

Strategy:

A. Write the overall reaction that occurs in the cell.

B. Determine the number of electrons transferred. Substitute this value into the Nernst equation to calculate the voltage.

Solution

A This is a concentration cell, in which the electrode compartments contain the same redox active substance but at different concentrations. The anions (Cl^- and SO_4^{2-}) do not participate in the reaction, so their identity is not important. The overall reaction is as follows:

$$\mathrm{Mn^{2+}}(aq, 2.0\,M) \rightarrow \mathrm{Mn^{2+}}(aq, 5.2 \times 10^{-2}\,M)$$

B For the reduction of Mn^{2+}(aq) to Mn(s), n = 2. We substitute this value and the given Mn^{2+} concentrations into Equation 9.7.6:

$$\begin{aligned} E_{\text{cell}} &= E^\circ_{\text{cell}} - \left(\frac{0.0591\ \text{V}}{n}\right) \log Q \\ &= 0\ \text{V} - \left(\frac{0.0591\ \text{V}}{2}\right) \log\left(\frac{5.2 \times 10^{-2}}{2.0}\right) \\ &= 0.047\ \text{V} \end{aligned}$$

Thus manganese will dissolve from the electrode in the compartment that contains the more dilute solution and will be deposited on the electrode in the compartment that contains the more concentrated solution.

? Exercise 9.7.2

Suppose we construct a galvanic cell by placing two identical platinum electrodes in two beakers that are connected by a salt bridge. One beaker contains 1.0 M HCl, and the other a 0.010 M solution of Na_2SO_4 at pH 7.00. Both cells are in contact with the atmosphere, with P_{O_2} = 0.20 atm. If the relevant electrochemical reaction in both compartments is the four-electron reduction of oxygen to water:

$$\mathrm{O_2\,(g) + 4\,H^+\,(aq) + 4\,e^- \rightarrow 2\,H_2O\,(l)}$$

What will be the potential when the circuit is closed?

Answer

0.41 V

Using Cell Potentials to Measure Solubility Products

Because voltages are relatively easy to measure accurately using a voltmeter, electrochemical methods provide a convenient way to determine the concentrations of very dilute solutions and the solubility products (K_{sp}) of sparingly soluble substances. As you learned previously, solubility products can be very small, with values of less than or equal to 10^{-30}. Equilibrium constants of this magnitude are virtually impossible to measure accurately by direct methods, so we must use alternative methods that are more sensitive, such as electrochemical methods.

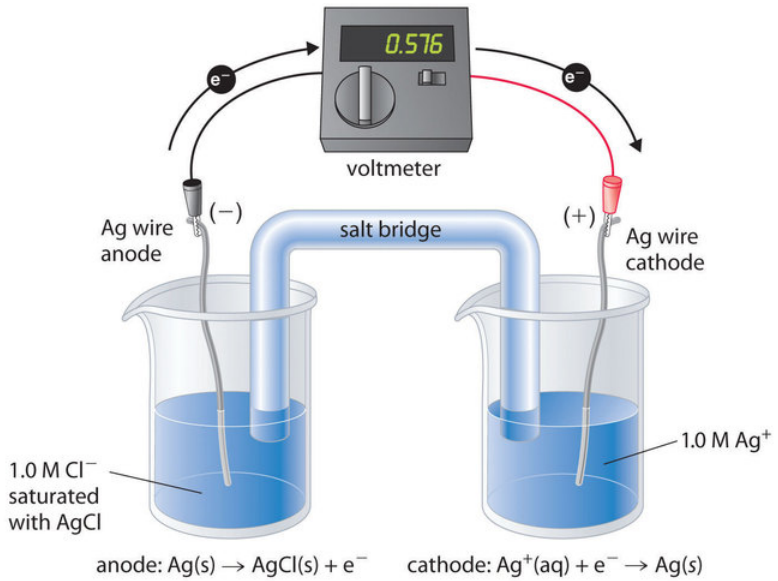


Figure **9.7.1**: A Galvanic ("Concentration") Cell for Measuring the Solubility Product of AgCl. One compartment contains a silver wire inserted into a 1.0 M solution of Ag^+, and the other compartment contains a silver wire inserted into a 1.0 M Cl^- solution saturated with AgCl. The potential due to the difference in $[Ag^+]$ between the two cells can be used to determine K_{sp}. (CC BY-NC-SA; Anonymous by request)

To understand how an electrochemical cell is used to measure a solubility product, consider the cell shown in Figure **9.7.1**, which is designed to measure the solubility product of silver chloride:

$$K_{sp} = [Ag^+][Cl^-].$$

In one compartment, the cell contains a silver wire inserted into a 1.0 M solution of Ag^+; the other compartment contains a silver wire inserted into a 1.0 M Cl^- solution saturated with AgCl. In this system, the Ag^+ ion concentration in the first compartment equals K_{sp}. We can see this by dividing both sides of the equation for K_{sp} by $[Cl^-]$ and substituting:

$$\begin{aligned}[Ag^+] &= \frac{K_{sp}}{[Cl^-]} \\ &= \frac{K_{sp}}{1.0} = K_{sp}.\end{aligned}$$

The overall cell reaction is as follows:

$$Ag^+(aq, \text{concentrated}) \rightarrow Ag^+(aq, \text{dilute})$$

Thus the voltage of the concentration cell due to the difference in $[Ag^+]$ between the two cells is as follows:

$$\begin{aligned}E_{cell} &= 0\ V - \left(\frac{0.0591\ V}{1}\right) \log\left(\frac{[Ag^+]_{dilute}}{[Ag^+]_{concentrated}}\right) \\ &= -0.0591\ V\ \log\left(\frac{K_{sp}}{1.0}\right) \\ &= -0.0591\ V\ \log K_{sp} \qquad (9.7.18)\end{aligned}$$

By closing the circuit, we can measure the potential caused by the difference in [Ag+] in the two cells. In this case, the experimentally measured voltage of the concentration cell at 25°C is 0.580 V. Solving Equation 9.7.18 for K_{sp},

$$\log K_{sp} = \frac{-E_{cell}}{0.0591\ V} = \frac{-0.580\ V}{0.0591\ V} = -9.81$$

$$K_{sp} = 1.5 \times 10^{-10}$$

Thus a single potential measurement can provide the information we need to determine the value of the solubility product of a sparingly soluble salt.

Example 9.7.3: Solubility of lead(II) sulfate

To measure the solubility product of lead(II) sulfate ($PbSO_4$) at 25°C, you construct a galvanic cell like the one shown in Figure 9.7.1, which contains a 1.0 M solution of a very soluble Pb^{2+} salt [lead(II) acetate trihydrate] in one compartment that is connected by a salt bridge to a 1.0 M solution of Na_2SO_4 saturated with $PbSO_4$ in the other. You then insert a Pb electrode into each compartment and close the circuit. Your voltmeter shows a voltage of 230 mV. What is K_{sp} for $PbSO_4$? Report your answer to two significant figures.

Given: galvanic cell, solution concentrations, electrodes, and voltage

Asked for: K_{sp}

Strategy:

A. From the information given, write the equation for K_{sp}. Express this equation in terms of the concentration of Pb^{2+}.

B. Determine the number of electrons transferred in the electrochemical reaction. Substitute the appropriate values into Equation ??? and solve for K_{sp}.

Solution

A You have constructed a concentration cell, with one compartment containing a 1.0 M solution of $\mathbf{Pb^{2+}}$ and the other containing a dilute solution of Pb^{2+} in 1.0 M Na_2SO_4. As for any concentration cell, the voltage between the two compartments can be calculated using the Nernst equation. The first step is to relate the concentration of Pb^{2+} in the dilute solution to K_{sp}:

$$[Pb^{2+}][SO_4^{2-}] = K_{sp}$$

$$[Pb^{2+}] = \frac{K_{sp}}{[SO_4^{2-}]} = \frac{K_{sp}}{1.0\ \text{M}} = K_{sp}$$

B The reduction of Pb^{2+} to Pb is a two-electron process and proceeds according to the following reaction:

$$Pb^{2+}(aq, \text{concentrated}) \rightarrow Pb^{2+}(aq, \text{dilute})$$

so

$$E_{cell} = E^\circ_{cell} - \left(\frac{0.0591}{n}\right) \log Q$$

$$0.230\ \text{V} = 0\ \text{V} - \left(\frac{0.0591\ \text{V}}{2}\right) \log \left(\frac{[Pb^{2+}]_{dilute}}{[Pb^{2+}]_{concentrated}}\right) = -0.0296\ \text{V} \log \left(\frac{K_{sp}}{1.0}\right)$$

$$-7.77 = \log K_{sp}$$

$$1.7 \times 10^{-8} = K_{sp}$$

Exercise 9.7.3

A concentration cell similar to the one described in Example 9.7.3 contains a 1.0 M solution of lanthanum nitrate [$La(NO_3)_3$] in one compartment and a 1.0 M solution of sodium fluoride saturated with LaF_3 in the other. A metallic La strip is inserted into each compartment, and the circuit is closed. The measured potential is 0.32 V. What is the K_{sp} for LaF_3? Report your answer to two significant figures.

Answer

5.7×10^{-17}

Using Cell Potentials to Measure Concentrations

Another use for the Nernst equation is to calculate the concentration of a species given a measured potential and the concentrations of all the other species. We saw an example of this in Example 9.7.3, in which the experimental conditions were defined in such a way that the concentration of the metal ion was equal to K_{sp}. Potential measurements can be used to obtain the concentrations of dissolved species under other conditions as well, which explains the widespread use of electrochemical cells in many analytical devices. Perhaps the most common application is in the determination of $[H^+]$ using a pH meter, as illustrated below.

Example 9.7.4: Measuring pH

Suppose a galvanic cell is constructed with a standard Zn/Zn^{2+} couple in one compartment and a modified hydrogen electrode in the second compartment. The pressure of hydrogen gas is 1.0 atm, but $[H^+]$ in the second compartment is unknown. The cell diagram is as follows:

$$\mathrm{Zn\,(s)\,|Zn^{2+}}(aq, 1.0\,M)\,\|\,\mathrm{H^+}(aq, ?\,M)\,|\,\mathrm{H_2}(g, 1.0\,atm)|Pt(s)$$

What is the pH of the solution in the second compartment if the measured potential in the cell is 0.26 V at 25°C?

Given: galvanic cell, cell diagram, and cell potential

Asked for: pH of the solution

Strategy:

A. Write the overall cell reaction.
B. Substitute appropriate values into the Nernst equation and solve for $-\log[H^+]$ to obtain the pH.

Solution

A Under standard conditions, the overall reaction that occurs is the reduction of protons by zinc to give H_2 (note that Zn lies below H_2 in Table P2):

$$Zn(s) + 2H^{2+}(aq) \rightarrow Zn^{2+}(aq) + H_2(g) \quad E°=0.76\ V$$

B By substituting the given values into the simplified Nernst equation (Equation 9.7.6), we can calculate $[H^+]$ under nonstandard conditions:

$$E_{cell} = E^\circ_{cell} - \left(\frac{0.0591\ V}{n}\right)\log\left(\frac{[Zn^{2+}]P_{H_2}}{[H^+]^2}\right)$$

$$0.26\ V = 0.76\ V - \left(\frac{0.0591\ V}{2}\right)\log\left(\frac{(1.0)(1.0)}{[H^+]^2}\right)$$

$$16.9 = \log\left(\frac{1}{[H^+]^2}\right) = \log[H^+]^{-2} = (-2)\log[H^+]$$

$$8.46 = -\log[H^+]$$

$$8.5 = pH$$

Thus the potential of a galvanic cell can be used to measure the pH of a solution.

Exercise 9.7.4

Suppose you work for an environmental laboratory and you want to use an electrochemical method to measure the concentration of Pb^{2+} in groundwater. You construct a galvanic cell using a standard oxygen electrode in one compartment ($E°_{cathode}$ = 1.23 V). The other compartment contains a strip of lead in a sample of groundwater to which you have added sufficient acetic acid, a weak organic acid, to ensure electrical conductivity. The cell diagram is as follows:

$$Pb_{(s)}\ |\ Pb^{2+}(aq, ?M)\ \|\ H^+(aq), 1.0M\ |\ O_2(g, 1.0atm)\ |\ Pt_{(s)}$$

When the circuit is closed, the cell has a measured potential of 1.62 V. Use Table P2 to determine the concentration of Pb^{2+} in the groundwater.

Answer

$1.2 \times 10^{-9}\ M$

Summary

The Nernst equation can be used to determine the direction of spontaneous reaction for any redox reaction in aqueous solution. The Nernst equation allows us to determine the spontaneous direction of any redox reaction under any reaction conditions from values of the relevant standard electrode potentials. Concentration cells consist of anode and cathode compartments that are identical

except for the concentrations of the reactant. Because $\Delta G = 0$ at equilibrium, the measured potential of a concentration cell is zero at equilibrium (the concentrations are equal). A galvanic cell can also be used to measure the solubility product of a sparingly soluble substance and calculate the concentration of a species given a measured potential and the concentrations of all the other species.

9.7: Cell Potential as a Function of Concentrations is shared under a not declared license and was authored, remixed, and/or curated by LibreTexts.

- **20.6: Cell Potential Under Nonstandard Conditions** is licensed CC BY-NC-SA 3.0.

9.8: Batteries- Producing Electricity Through Chemical Reactions

Because galvanic cells can be self-contained and portable, they can be used as batteries and fuel cells. A **battery (storage cell)** is a galvanic cell (or a series of galvanic cells) that contains all the reactants needed to produce electricity. In contrast, a **fuel cell** is a galvanic cell that requires a constant external supply of one or more reactants to generate electricity. In this section, we describe the chemistry behind some of the more common types of batteries and fuel cells.

Batteries

There are two basic kinds of batteries: disposable, or primary, batteries, in which the electrode reactions are effectively irreversible and which cannot be recharged; and rechargeable, or secondary, batteries, which form an insoluble product that adheres to the electrodes. These batteries can be recharged by applying an electrical potential in the reverse direction. The recharging process temporarily converts a rechargeable battery from a galvanic cell to an electrolytic cell.

Batteries are cleverly engineered devices that are based on the same fundamental laws as galvanic cells. The major difference between batteries and the galvanic cells we have previously described is that commercial batteries use solids or pastes rather than solutions as reactants to maximize the electrical output per unit mass. The use of highly concentrated or solid reactants has another beneficial effect: the concentrations of the reactants and the products do not change greatly as the battery is discharged; consequently, the output voltage remains remarkably constant during the discharge process. This behavior is in contrast to that of the Zn/Cu cell, whose output decreases logarithmically as the reaction proceeds (Figure 9.8.1). When a battery consists of more than one galvanic cell, the cells are usually connected in series—that is, with the positive (+) terminal of one cell connected to the negative (−) terminal of the next, and so forth. The overall voltage of the battery is therefore the sum of the voltages of the individual cells.

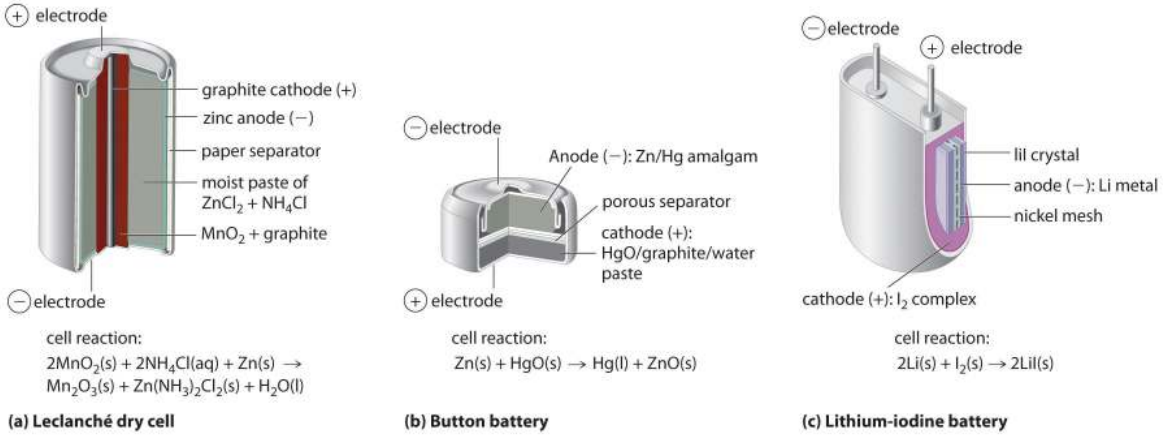


Figure 9.8.1: Three Kinds of Primary (Nonrechargeable) Batteries. (a) A Leclanché dry cell is actually a "wet cell," in which the electrolyte is an acidic water-based paste containing MnO_2, NH_4Cl, $ZnCl_2$, graphite, and starch. Though inexpensive to manufacture, the cell is not very efficient in producing electrical energy and has a limited shelf life. (b) In a button battery, the anode is a zinc–mercury amalgam, and the cathode can be either HgO (shown here) or Ag_2O as the oxidant. Button batteries are reliable and have a high output-to-mass ratio, which allows them to be used in applications such as calculators and watches, where their small size is crucial. (c) A lithium–iodine battery consists of two cells separated by a metallic nickel mesh that collects charge from the anodes. The anode is lithium metal, and the cathode is a solid complex of I_2. The electrolyte is a layer of solid LiI that allows Li^+ ions to diffuse from the cathode to the anode. Although this type of battery produces only a relatively small current, it is highly reliable and long-lived.

> The major difference between batteries and the galvanic cells is that commercial typically batteries use solids or pastes rather than solutions as reactants to maximize the electrical output per unit mass. An obvious exception is the standard car battery which used solution phase chemistry.

Leclanché Dry Cell

The dry cell, by far the most common type of battery, is used in flashlights, electronic devices such as the Walkman and Game Boy, and many other devices. Although the dry cell was patented in 1866 by the French chemist Georges Leclanché and more than 5 billion such cells are sold every year, the details of its electrode chemistry are still not completely understood. In spite of its name, the **Leclanché dry cell** is actually a "wet cell": the electrolyte is an acidic water-based paste containing MnO_2, NH_4Cl, $ZnCl_2$, graphite, and starch (part (a) in Figure 9.8.1). The half-reactions at the anode and the cathode can be summarized as follows:

- cathode (reduction):

$$2\,MnO_2\,(s) + 2\,NH_4^+\,(aq) + 2\,e^- \longrightarrow Mn_2O_3\,(s) + 2\,NH_3\,(aq) + H_2O\,(l)$$

- anode (oxidation):

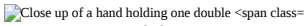
$$Zn\,(s) \longrightarrow Zn^{2+}\,(aq) + 2\,e^-$$

The Zn^{2+} ions formed by the oxidation of $Zn(s)$ at the anode react with NH_3 formed at the cathode and Cl^- ions present in solution, so the overall cell reaction is as follows:

- overall reaction:

$$2\,MnO_2(s) + 2\,NH_4Cl(aq) + Zn(s) \longrightarrow Mn_2O_3(s) + Zn(NH_3)_2Cl_2(s) + H_2O(l) \tag{9.8.1}$$

The dry cell produces about 1.55 V and is inexpensive to manufacture. It is not, however, very efficient in producing electrical energy because only the relatively small fraction of the MnO_2 that is near the cathode is actually reduced and only a small fraction of the zinc cathode is actually consumed as the cell discharges. In addition, dry cells have a limited shelf life because the Zn anode reacts spontaneously with NH_4Cl in the electrolyte, causing the case to corrode and allowing the contents to leak out.



AA

battery" style="width: 287px; height: 215px;" width="287px" height="215px" data-cke-saved-src="/@api/deki/files/16647/battery.jpg" src="/@api/deki/files/16647/battery.jpg" data-quail-id="34">

Source: Photo courtesy of Mitchclanky2008, www.flickr.com/photos/25597837@N05/2422765479/.

The **alkaline battery** is essentially a Leclanché cell adapted to operate under alkaline, or basic, conditions. The half-reactions that occur in an alkaline battery are as follows:

- cathode (reduction)

$$2\,MnO_2(s) + H_2O(l) + 2\,e^- \longrightarrow Mn_2O_3(s) + 2\,OH^-(aq)$$

- anode (oxidation):

$$Zn(s) + 2\,OH^-(aq) \longrightarrow ZnO(s) + H_2O(l) + 2\,e^-$$

- overall reaction:

$$Zn(s) + 2\,MnO_2(s) \longrightarrow ZnO(s) + Mn_2O_3(s)$$

This battery also produces about 1.5 V, but it has a longer shelf life and more constant output voltage as the cell is discharged than the Leclanché dry cell. Although the alkaline battery is more expensive to produce than the Leclanché dry cell, the improved performance makes this battery more cost-effective.

Button Batteries

Although some of the small button batteries used to power watches, calculators, and cameras are miniature alkaline cells, most are based on a completely different chemistry. In these "button" batteries, the anode is a zinc–mercury amalgam rather than pure zinc, and the cathode uses either HgO or Ag_2O as the oxidant rather than MnO_2 in Figure 9.8.1*b*).



Button batteries. (Gerhard H Wrodnigg via Wikipedia)

The cathode, anode and overall reactions and cell output for these two types of button batteries are as follows (two half-reactions occur at the anode, but the overall oxidation half-reaction is shown):

- cathode (mercury battery):

$$HgO(s) + H_2O(l) + 2\,e^- \longrightarrow Hg(l) + 2\,OH^-(aq)$$

- Anode (mercury battery):

$$Zn + 2\,OH^- \longrightarrow ZnO + H_2O + 2\,e^-$$

- overall reaction (mercury battery):

$$Zn(s) + 2\,HgO(s) \longrightarrow 2\,Hg(l) + ZnO(s)$$

with $E_{cell} = 1.35\,V$.

- cathode reaction (silver battery):

$$Ag_2O(s) + H_2O(l) + 2e^- \longrightarrow 2Ag(s) + 2OH^-(aq)$$

- anode (silver battery):

$$Zn + 2OH^- \longrightarrow ZnO + H_2O + 2e^-$$

- Overall reaction (silver battery):

$$Zn(s) + 2Ag_2O(s) \longrightarrow 2Ag(s) + ZnO(s)$$

with $E_{cell} = 1.6\,V$.

The major advantages of the mercury and silver cells are their reliability and their high output-to-mass ratio. These factors make them ideal for applications where small size is crucial, as in cameras and hearing aids. The disadvantages are the expense and the environmental problems caused by the disposal of heavy metals, such as **Hg** and **Ag**.

Lithium–Iodine Battery

None of the batteries described above is actually "dry." They all contain small amounts of liquid water, which adds significant mass and causes potential corrosion problems. Consequently, substantial effort has been expended to develop water-free batteries. One of the few commercially successful water-free batteries is the **lithium–iodine battery**. The anode is lithium metal, and the cathode is a solid complex of I_2. Separating them is a layer of solid LiI, which acts as the electrolyte by allowing the diffusion of Li^+ ions. The electrode reactions are as follows:

- cathode (reduction):

$$I_{2(s)} + 2e^- \rightarrow 2I^-_{(LiI)} \tag{9.8.2}$$

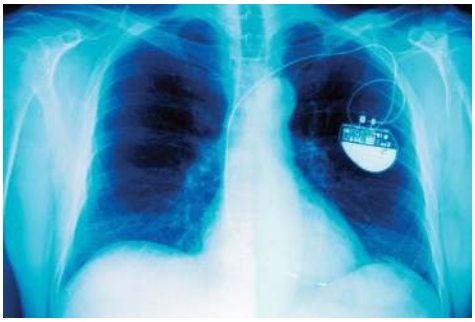
- anode (oxidation):

$$2Li_{(s)} \rightarrow 2Li^+_{(LiI)} + 2e^- \tag{9.8.3}$$

- overall:

$$2Li_{(s)} + I_{2(s)} \rightarrow 2LiI_{(s)} \tag{9.8.4}$$

with $E_{cell} = 3.5\,V$



Cardiac pacemaker: An x-ray of a patient showing the location and size of a pacemaker powered by a lithium–iodine battery.

As shown in part (c) in Figure **9.8.1**, a typical lithium–iodine battery consists of two cells separated by a nickel metal mesh that collects charge from the anode. Because of the high internal resistance caused by the solid electrolyte, only a low current can be drawn. Nonetheless, such batteries have proven to be long-lived (up to 10 yr) and reliable. They are therefore used in applications where frequent replacement is difficult or undesirable, such as in cardiac pacemakers and other medical implants and in computers for memory protection. These batteries are also used in security transmitters and smoke alarms. Other batteries based on lithium anodes and solid electrolytes are under development, using TiS_2, for example, for the cathode.

Dry cells, button batteries, and lithium–iodine batteries are disposable and cannot be recharged once they are discharged. Rechargeable batteries, in contrast, offer significant economic and environmental advantages because they can be recharged and discharged numerous times. As a result, manufacturing and disposal costs drop dramatically for a given number of hours of battery usage. Two common rechargeable batteries are the nickel–cadmium battery and the lead–acid battery, which we describe next.

Nickel–Cadmium (NiCad) Battery

The **nickel–cadmium**, or NiCad, battery is used in small electrical appliances and devices like drills, portable vacuum cleaners, and AM/FM digital tuners. It is a water-based cell with a cadmium anode and a highly oxidized nickel cathode that is usually described as the nickel(III) oxo-hydroxide, NiO(OH). As shown in Figure **9.8.2**, the design maximizes the surface area of the electrodes and minimizes the distance between them, which decreases internal resistance and makes a rather high discharge current possible.

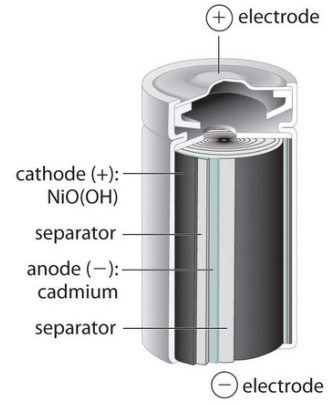


Figure 9.8.2: The Nickel–Cadmium (NiCad) Battery, a Rechargeable Battery. NiCad batteries contain a cadmium anode and a highly oxidized nickel cathode. This design maximizes the surface area of the electrodes and minimizes the distance between them, which gives the battery both a high discharge current and a high capacity.

The electrode reactions during the discharge of a ***NiCad*** battery are as follows:

- cathode (reduction):

$$2NiO(OH)_{(s)} + 2H_2O_{(l)} + 2e^- \rightarrow 2Ni(OH)_{2(s)} + 2OH^-_{(aq)} \tag{9.8.5}$$

- anode (oxidation):

$$Cd_{(s)} + 2OH^-_{(aq)} \rightarrow Cd(OH)_{2(s)} + 2e^- \tag{9.8.6}$$

- overall:

$$Cd_{(s)} + 2NiO(OH)_{(s)} + 2H_2O_{(l)} \rightarrow Cd(OH)_{2(s)} + 2Ni(OH)_{2(s)} \tag{9.8.7}$$

$$E_{cell} = 1.4V$$

Because the products of the discharge half-reactions are solids that adhere to the electrodes [$Cd(OH)_2$ and $2Ni(OH)_2$], the overall reaction is readily reversed when the cell is recharged. Although NiCad cells are lightweight, rechargeable, and high capacity, they have certain disadvantages. For example, they tend to lose capacity quickly if not allowed to discharge fully before recharging, they do not store well for long periods when fully charged, and they present significant environmental and disposal problems because of the toxicity of cadmium.

A variation on the NiCad battery is the nickel–metal hydride battery (NiMH) used in hybrid automobiles, wireless communication devices, and mobile computing. The overall chemical equation for this type of battery is as follows:

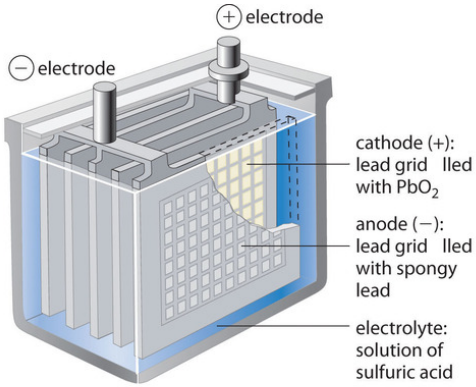
\[NiO(OH)_{(s)} + MH \rightarrow Ni(OH)_{2(s)} + M_{(s)} \label{Eq16} \]

The NiMH battery has a 30%–40% improvement in capacity over the NiCad battery; it is more environmentally friendly so storage, transportation, and disposal are not subject to environmental control; and it is not as sensitive to recharging memory. It is, however, subject to a 50% greater self-discharge rate, a limited service life, and higher maintenance, and it is more expensive than the NiCad battery.

> Directive 2006/66/EC of the European Union prohibits the placing on the market of portable batteries that contain more than 0.002% of cadmium by weight. The aim of this directive was to improve "the environmental performance of batteries and accumulators"

Lead–Acid (Lead Storage) Battery

The **lead–acid battery** is used to provide the starting power in virtually every automobile and marine engine on the market. Marine and car batteries typically consist of multiple cells connected in series. The total voltage generated by the battery is the potential per cell ($E°_{cell}$) times the number of cells.



cell reaction:

$Pb(s) + PbO_2(s) + 2HSO_4^-(aq) + 2H^+(aq) \rightarrow 2PbSO_4(s) + 2H_2O(l)$

Figure **9.8.3**: One Cell of a Lead–Acid Battery. The anodes in each cell of a rechargeable battery are plates or grids of lead containing spongy lead metal, while the cathodes are similar grids containing powdered lead dioxide (PbO_2). The electrolyte is an aqueous solution of sulfuric acid. The value of E° for such a cell is about 2 V. Connecting three such cells in series produces a 6 V battery, whereas a typical 12 V car battery contains six cells in series. When treated properly, this type of high-capacity battery can be discharged and recharged many times over.

As shown in Figure **9.8.3**, the anode of each cell in a lead storage battery is a plate or grid of spongy lead metal, and the cathode is a similar grid containing powdered lead dioxide (***PbO_2***). The electrolyte is usually an approximately 37% solution (by mass) of sulfuric acid in water, with a density of 1.28 g/mL (about 4.5 M ***H_2SO_4***). Because the redox active species are solids, there is no need to separate the electrodes. The electrode reactions in each cell during discharge are as follows:

- cathode (reduction):

\[PbO_{2(s)} + HSO^-_{4(aq)} + 3H^+_{(aq)} + 2e^- \rightarrow PbSO_{4(s)} + 2H_2O_{(l)} \label{Eq17} \]

with $E^\circ_{cathode} = 1.685\ V$

- anode (oxidation):

$$Pb_{(s)} + HSO^-_{4(aq)} \rightarrow PbSO_{4(s)} + H^+_{(aq)} + 2e^- \tag{9.8.8}$$

with $E^\circ_{anode} = -0.356\ V$

- overall:

$$Pb_{(s)} + PbO_{2(s)} + 2HSO^-_{4(aq)} + 2H^+_{(aq)} \rightarrow 2PbSO_{4(s)} + 2H_2O_{(l)} \tag{9.8.9}$$

and $E^\circ_{cell} = 2.041\ V$

As the cell is discharged, a powder of ***$PbSO_4$*** forms on the electrodes. Moreover, sulfuric acid is consumed and water is produced, decreasing the density of the electrolyte and providing a convenient way of monitoring the status of a battery by simply measuring the density of the electrolyte. This is often done with the use of a hydrometer.



A hydrometer can be used to test the specific gravity of each cell as a measure of its state of charge (www.youtube.com/watch?v=SRcOqfL6GqQ).

When an external voltage in excess of 2.04 V per cell is applied to a lead–acid battery, the electrode reactions reverse, and $PbSO_4$ is converted back to metallic lead and PbO_2. If the battery is recharged too vigorously, however, electrolysis of water can occur:

$$2H_2O_{(l)} \rightarrow 2H_{2(g)} + O_{2(g)} \tag{9.8.10}$$

This results in the evolution of potentially explosive hydrogen gas. The gas bubbles formed in this way can dislodge some of the $PbSO_4$ or PbO_2 particles from the grids, allowing them to fall to the bottom of the cell, where they can build up and cause an internal short circuit. Thus the recharging process must be carefully monitored to optimize the life of the battery. With proper care, however, a lead–acid battery can be discharged and recharged thousands of times. In automobiles, the alternator supplies the electric current that causes the discharge reaction to reverse.

Fuel Cells

A fuel cell is a galvanic cell that requires a constant external supply of reactants because the products of the reaction are continuously removed. Unlike a battery, it does not store chemical or electrical energy; a fuel cell allows electrical energy to be extracted directly from a chemical reaction. In principle, this should be a more efficient process than, for example, burning the fuel to drive an internal combustion engine that turns a generator, which is typically less than 40% efficient, and in fact, the efficiency of a fuel cell is generally between 40% and 60%. Unfortunately, significant cost and reliability problems have hindered the wide-scale adoption of fuel cells. In practice, their use has been restricted to applications in which mass may be a significant cost factor, such as US manned space vehicles.

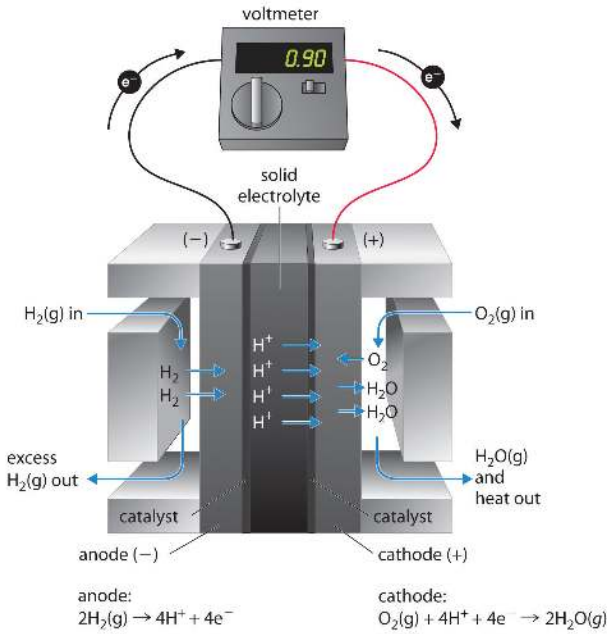


Figure **9.8.4**: A Hydrogen Fuel Cell Produces Electrical Energy Directly from a Chemical Reaction. Hydrogen is oxidized to protons at the anode, and the electrons are transferred through an external circuit to the cathode, where oxygen is reduced and combines with H^+ to form water. A solid electrolyte allows the protons to diffuse from the anode to the cathode. Although fuel cells are an essentially pollution-free means of obtaining electrical energy, their expense and technological complexity have thus far limited their applications.

These space vehicles use a hydrogen/oxygen fuel cell that requires a continuous input of $H_2(g)$ and $O_2(g)$, as illustrated in Figure **9.8.4**. The electrode reactions are as follows:

- cathode (reduction):

$$O_{2(g)} + 4H^+ + 4e^- \rightarrow 2H_2O_{(g)} \tag{9.8.11}$$

- anode (oxidation):

$$2H_{2(g)} \rightarrow 4H^+ + 4e^- \tag{9.8.12}$$

- overall:

$$2H_{2(g)} + O_{2(g)} \rightarrow 2H_2O_{(g)} \tag{9.8.13}$$

The overall reaction represents an essentially pollution-free conversion of hydrogen and oxygen to water, which in space vehicles is then collected and used. Although this type of fuel cell should produce 1.23 V under standard conditions, in practice the device achieves only about 0.9 V. One of the major barriers to achieving greater efficiency is the fact that the four-electron reduction of $O_2(g)$ at the cathode is intrinsically rather slow, which limits current that can be achieved. All major automobile manufacturers have major research programs involving fuel cells: one of the most important goals is the development of a better catalyst for the reduction of $O_2(g)$.

Summary

Commercial batteries are galvanic cells that use solids or pastes as reactants to maximize the electrical output per unit mass. A battery is a contained unit that produces electricity, whereas a fuel cell is a galvanic cell that requires a constant external supply of one or more reactants to generate electricity. One type of battery is the Leclanché dry cell, which contains an electrolyte in an acidic water-based paste. This battery is called an alkaline battery when adapted to operate under alkaline conditions. Button batteries have a high output-to-mass ratio; lithium–iodine batteries consist of a solid electrolyte; the nickel–cadmium (NiCad) battery is rechargeable; and the lead–acid battery, which is also rechargeable, does not require the electrodes to be in separate compartments. A fuel cell requires an external supply of reactants as the products of the reaction are continuously removed. In a fuel cell, energy is not stored; electrical energy is provided by a chemical reaction.

9.8: Batteries- Producing Electricity Through Chemical Reactions is shared under a not declared license and was authored, remixed, and/or curated by LibreTexts.

- **20.7: Batteries and Fuel Cells** is licensed CC BY-NC-SA 3.0.

9.9: Corrosion- Unwanted Voltaic Cells

Learning Objectives

- To understand the process of corrosion.

Corrosion is a galvanic process by which metals deteriorate through oxidation—usually but not always to their oxides. For example, when exposed to air, iron rusts, silver tarnishes, and copper and brass acquire a bluish-green surface called a patina. Of the various metals subject to corrosion, iron is by far the most important commercially. An estimated $100 billion per year is spent in the United States alone to replace iron-containing objects destroyed by corrosion. Consequently, the development of methods for protecting metal surfaces from corrosion constitutes a very active area of industrial research. In this section, we describe some of the chemical and electrochemical processes responsible for corrosion. We also examine the chemical basis for some common methods for preventing corrosion and treating corroded metals.

> *Corrosion is a REDOX process.*

Under ambient conditions, the oxidation of most metals is thermodynamically spontaneous, with the notable exception of gold and platinum. Hence it is actually somewhat surprising that any metals are useful at all in Earth's moist, oxygen-rich atmosphere. Some metals, however, are resistant to corrosion for kinetic reasons. For example, aluminum in soft-drink cans and airplanes is protected by a thin coating of metal oxide that forms on the surface of the metal and acts as an impenetrable barrier that prevents further destruction. Aluminum cans also have a thin plastic layer to prevent reaction of the oxide with acid in the soft drink. Chromium, magnesium, and nickel also form protective oxide films. Stainless steels are remarkably resistant to corrosion because they usually contain a significant proportion of chromium, nickel, or both.

In contrast to these metals, when iron corrodes, it forms a red-brown hydrated metal oxide ($\mathbf{Fe_2O_3 \cdot \mathit{x}\, H_2O}$), commonly known as rust, that does not provide a tight protective film (Figure **9.9.1**). Instead, the rust continually flakes off to expose a fresh metal surface vulnerable to reaction with oxygen and water. Because both oxygen and water are required for rust to form, an iron nail immersed in deoxygenated water will not rust—even over a period of several weeks. Similarly, a nail immersed in an organic solvent such as kerosene or mineral oil will not rust because of the absence of water even if the solvent is saturated with oxygen.

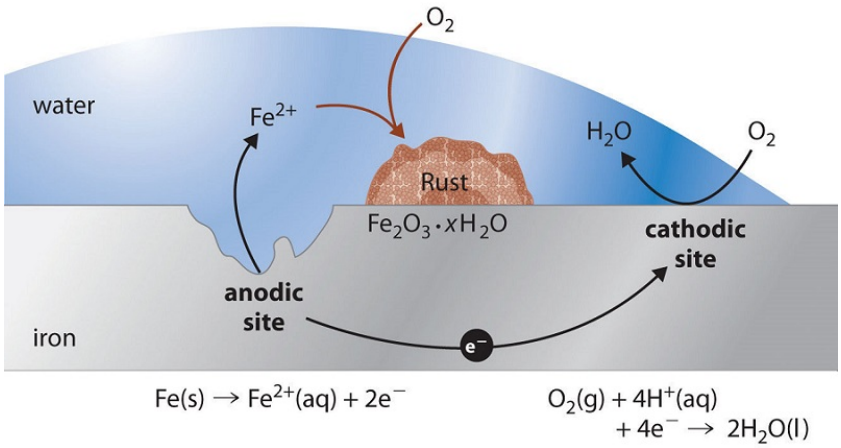


Figure **9.9.1**: Rust, the Result of Corrosion of Metallic Iron. Iron is oxidized to $Fe^{2+}(aq)$ at an anodic site on the surface of the iron, which is often an impurity or a lattice defect. Oxygen is reduced to water at a different site on the surface of the iron, which acts as the cathode. Electrons are transferred from the anode to the cathode through the electrically conductive metal. Water is a solvent for the Fe^{2+} that is produced initially and acts as a salt bridge. Rust (Fe_2O_3•xH_2O) is formed by the subsequent oxidation of Fe^{2+} by atmospheric oxygen. (CC BY-NC-SA; anonymous)

In the corrosion process, iron metal acts as the anode in a galvanic cell and is oxidized to Fe^{2+}; oxygen is reduced to water at the cathode. The relevant reactions are as follows:

- at cathode:

$$\mathbf{O_2\,(g) + 4\,H^+\,(aq) + 4\,e^- \longrightarrow 2\,H_2O\,(l)}$$

with $E^o_{SRP} = 1.23\ V$.

- at anode:

$$\mathrm{Fe(s) \longrightarrow Fe^{2+}(aq) + 2e^-}$$

with $E^o_{SRP} = -0.45\ V$.

- overall:

$$\mathrm{2Fe(s) + O_2(g) + 4H^+(aq) \longrightarrow 2Fe^{2+}(aq) + 2H_2O(l)} \tag{9.9.1}$$

with $E^o_{cell} = 1.68\ V$.

The $\mathrm{Fe^{2+}}$ ions produced in the initial reaction are then oxidized by atmospheric oxygen to produce the insoluble hydrated oxide containing $\mathrm{Fe^{3+}}$, as represented in the following equation:

$$\mathrm{4Fe^{2+}(aq) + O_2(g) + (2 + 4x)H_2O \ \rightarrow 2Fe_2O_3 \cdot xH_2O + 4H^+(aq)} \tag{9.9.2}$$

The sign and magnitude of E^o_{cell} for the corrosion process (Equation 9.9.1) indicate that there is a strong driving force for the oxidation of iron by O_2 under standard conditions (1 M H^+). Under neutral conditions, the driving force is somewhat less but still appreciable (E = 1.25 V at pH 7.0). Normally, the reaction of atmospheric CO_2 with water to form H^+ and HCO_3^- provides a low enough pH to enhance the reaction rate, as does acid rain. Automobile manufacturers spend a great deal of time and money developing paints that adhere tightly to the car's metal surface to prevent oxygenated water, acid, and salt from coming into contact with the underlying metal. Unfortunately, even the best paint is subject to scratching or denting, and the electrochemical nature of the corrosion process means that two scratches relatively remote from each other can operate together as anode and cathode, leading to sudden mechanical failure (Figure 9.9.2).

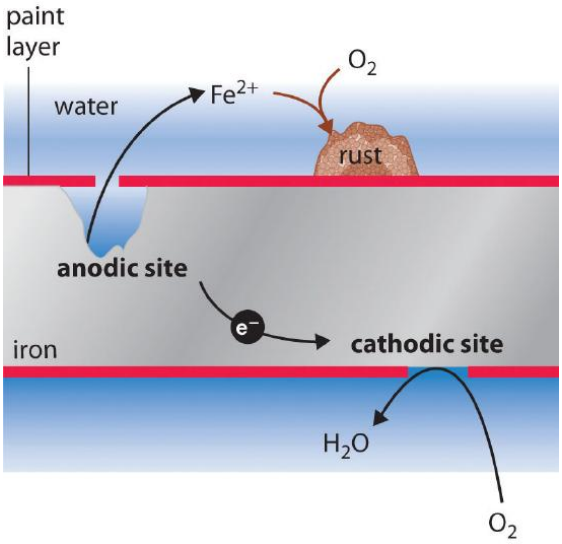


Figure 9.9.2: Small Scratches in a Protective Paint Coating Can Lead to the Rapid Corrosion of Iron. Holes in a protective coating allow oxygen to be reduced at the surface with the greater exposure to air (the cathode), while metallic iron is oxidized to Fe^{2+}(aq) at the less exposed site (the anode). Rust is formed when Fe^{2+}(aq) diffuses to a location where it can react with atmospheric oxygen, which is often remote from the anode. The electrochemical interaction between cathodic and anodic sites can cause a large pit to form under a painted surface, eventually resulting in sudden failure with little visible warning that corrosion has occurred.

Prophylactic Protection

One of the most common techniques used to prevent the corrosion of iron is applying a protective coating of another metal that is more difficult to oxidize. Faucets and some external parts of automobiles, for example, are often coated with a thin layer of chromium using an electrolytic process. With the increased use of polymeric materials in cars, however, the use of chrome-plated steel has diminished in recent years. Similarly, the "tin cans" that hold soups and other foods are actually consist of steel container that is coated with a thin layer of tin. While neither chromium nor tin metals are intrinsically resistant to corrosion, they both form protective oxide coatings that hinder access of oxygen and water to the underlying steel (iron alloy).

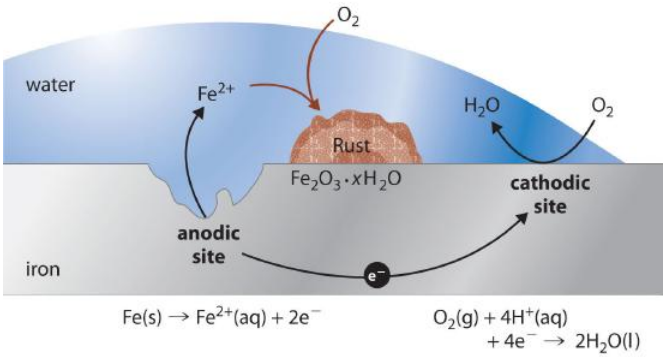


Figure 9.9.3: Galvanic Corrosion. If iron is in contact with a more corrosion-resistant metal such as tin, copper, or lead, the other metal can act as a large cathode that greatly increases the rate of reduction of oxygen. Because the reduction of oxygen is coupled to the oxidation of iron, this can result in a dramatic increase in the rate at which iron is oxidized at the anode. Galvanic corrosion is likely to occur whenever two dissimilar metals are connected directly, allowing electrons to be transferred from one to the other.

As with a protective paint, scratching a protective metal coating will allow corrosion to occur. In this case, however, the presence of the second metal can actually increase the rate of corrosion. The values of the standard electrode potentials for $\mathbf{Sn^{2+}}$ ($E° = -0.14$ V) and Fe^{2+} ($E° = -0.45$ V) in Table P2 show that **Fe** is more easily oxidized than **Sn**. As a result, the more corrosion-resistant metal (in this case, tin) accelerates the corrosion of iron by acting as the cathode and providing a large surface area for the reduction of oxygen (Figure 9.9.3). This process is seen in some older homes where copper and iron pipes have been directly connected to each other. The less easily oxidized copper acts as the cathode, causing iron to dissolve rapidly near the connection and occasionally resulting in a catastrophic plumbing failure.

Cathodic Protection

One way to avoid these problems is to use a more easily oxidized metal to protect iron from corrosion. In this approach, called cathodic protection, a more reactive metal such as **Zn** ($E° = -0.76$ V for $\mathbf{Zn^{2+} + 2\,e^- \longrightarrow Zn}$) becomes the anode, and iron becomes the cathode. This prevents oxidation of the iron and protects the iron object from corrosion. The reactions that occur under these conditions are as follows:

$$\underbrace{O_{2(g)} + 4e^- + 4H^+_{(aq)} \rightarrow 2H_2O_{(l)}}_{\text{reduction at cathode}} \tag{9.9.3}$$

$$\underbrace{Zn_{(s)} \rightarrow Zn^{2+}_{(aq)} + 2e^-}_{\text{oxidation at anode}} \tag{9.9.4}$$

$$\underbrace{2Zn_{(s)} + O_{2(g)} + 4H^+_{(aq)} \rightarrow 2Zn^{2+}_{(aq)} + 2H_2O_{(l)}}_{\text{overall}} \tag{9.9.5}$$

The more reactive metal reacts with oxygen and will eventually dissolve, “sacrificing” itself to protect the iron object. Cathodic protection is the principle underlying galvanized steel, which is steel protected by a thin layer of zinc. Galvanized steel is used in objects ranging from nails to garbage cans.



Crystalline surface of a hot-dip galvanized steel surface. This served both as prophylactic protection (protecting the underlying steel from the oxygen in the air) and cathodic protection (once exposed, the zinc will oxidize before the underlying steel).

In a similar strategy, **sacrificial electrodes** using magnesium, for example, are used to protect underground tanks or pipes (Figure 9.9.4). Replacing the sacrificial electrodes is more cost-effective than replacing the iron objects they are protecting.

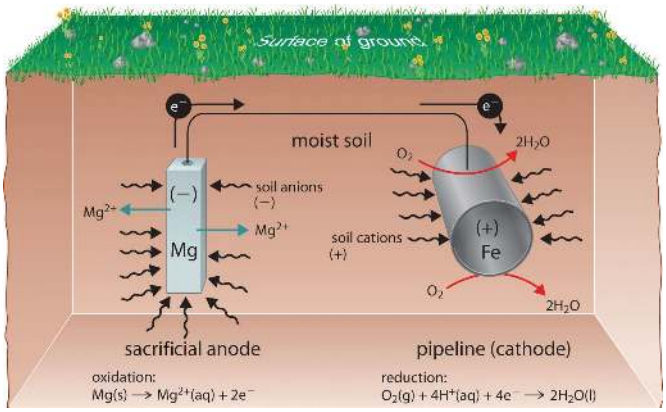


Figure **9.9.4**: The Use of a Sacrificial Electrode to Protect Against Corrosion. Connecting a magnesium rod to an underground steel pipeline protects the pipeline from corrosion. Because magnesium (E° = −2.37 V) is much more easily oxidized than iron (E° = −0.45 V), the Mg rod acts as the anode in a galvanic cell. The pipeline is therefore forced to act as the cathode at which oxygen is reduced. The soil between the anode and the cathode acts as a salt bridge that completes the electrical circuit and maintains electrical neutrality. As Mg(s) is oxidized to Mg^{2+} at the anode, anions in the soil, such as nitrate, diffuse toward the anode to neutralize the positive charge. Simultaneously, cations in the soil, such as H^+ or NH_4^+, diffuse toward the cathode, where they replenish the protons that are consumed as oxygen is reduced. A similar strategy uses many miles of somewhat less reactive zinc wire to protect the Alaska oil pipeline.

Example 9.9.1

Suppose an old wooden sailboat, held together with iron screws, has a bronze propeller (recall that bronze is an alloy of copper containing about 7%–10% tin).

a. If the boat is immersed in seawater, what corrosion reaction will occur? What is $E°°_{cell}$?
b. How could you prevent this corrosion from occurring?

Given: identity of metals

Asked for: corrosion reaction, $E°°_{cell}$, and preventive measures

Strategy:

A. Write the reactions that occur at the anode and the cathode. From these, write the overall cell reaction and calculate $E°°_{cell}$.
B. Based on the relative redox activity of various substances, suggest possible preventive measures.

Solution

a. **A** According to Table P2, both copper and tin are less active metals than iron (i.e., they have higher positive values of $E°°_{cell}$ than iron). Thus if tin or copper is brought into electrical contact by seawater with iron in the presence of oxygen, corrosion will occur. We therefore anticipate that the bronze propeller will act as the cathode at which O_2 is reduced, and the iron screws will act as anodes at which iron dissolves:

cathode:	$O_2(s) + 4H^+(aq) + 4e^- \rightarrow 2H_2O(l)$	$E°_{cathode} = 1.23$ V
anode:	$Fe(s) \rightarrow Fe^{2+} + 2e^-$	$E°_{anode} = -0.45$ V
overall:	$2Fe(s) + O_2(g) + 4H^+(aq) \rightarrow 2Fe^{2+}(aq) + 2H_2O(l)$	$E°_{overall} = 1.68$ V

Over time, the iron screws will dissolve, and the boat will fall apart.

b. **B** Possible ways to prevent corrosion, in order of decreasing cost and inconvenience, are as follows: disassembling the boat and rebuilding it with bronze screws; removing the boat from the water and storing it in a dry place; or attaching an inexpensive piece of zinc metal to the propeller shaft to act as a sacrificial electrode and replacing it once or twice a year. Because zinc is a more active metal than iron, it will act as the sacrificial anode in the electrochemical cell and dissolve (Equation 9.9.5).



Zinc sacrificial anode (rounded object screwed to underside of hull) used to prevent corrosion on the screw in a boat via cathodic protection. Image by Rémi Kaupp and used with permission.

? Exercise 9.9.1

Suppose the water pipes leading into your house are made of lead, while the rest of the plumbing in your house is iron. To eliminate the possibility of lead poisoning, you call a plumber to replace the lead pipes. He quotes you a very low price if he can use up his existing supply of copper pipe to do the job.

a. Do you accept his proposal?
b. What else should you have the plumber do while at your home?

Answer a

Not unless you plan to sell the house very soon because the **Cu/Fe** pipe joints will lead to rapid corrosion.

Answer b

Any existing **Pb/Fe** joints should be examined carefully for corrosion of the iron pipes due to the **Pb—Fe** junction; the less active **Pb** will have served as the cathode for the reduction of O_2, promoting oxidation of the more active **Fe** nearby.

Summary

Corrosion is a galvanic process that can be prevented using cathodic protection. The deterioration of metals through oxidation is a galvanic process called corrosion. Protective coatings consist of a second metal that is more difficult to oxidize than the metal being protected. Alternatively, a more easily oxidized metal can be applied to a metal surface, thus providing cathodic protection of the surface. A thin layer of zinc protects galvanized steel. Sacrificial electrodes can also be attached to an object to protect it.

9.9: Corrosion- Unwanted Voltaic Cells is shared under a not declared license and was authored, remixed, and/or curated by LibreTexts.

- **20.8: Corrosion** is licensed CC BY-NC-SA 3.0.

9.10: Electrolysis- Causing Nonspontaneous Reactions to Occur

Learning Objectives

- To understand electrolysis and describe it quantitatively.

In this chapter, we have described various galvanic cells in which a spontaneous chemical reaction is used to generate electrical energy. In an electrolytic cell, however, the opposite process, called **electrolysis**, occurs: an external voltage is applied to drive a nonspontaneous reaction. In this section, we look at how electrolytic cells are constructed and explore some of their many commercial applications.

Electrolytic Cells

If we construct an electrochemical cell in which one electrode is copper metal immersed in a 1 M Cu^{2+} solution and the other electrode is cadmium metal immersed in a $1\ M\ Cd^{2+}$ solution and then close the circuit, the potential difference between the two compartments will be 0.74 V. The cadmium electrode will begin to dissolve (Cd is oxidized to Cd^{2+}) and is the anode, while metallic copper will be deposited on the copper electrode (Cu^{2+} is reduced to Cu), which is the cathode (Figure **9.10.1***a*).

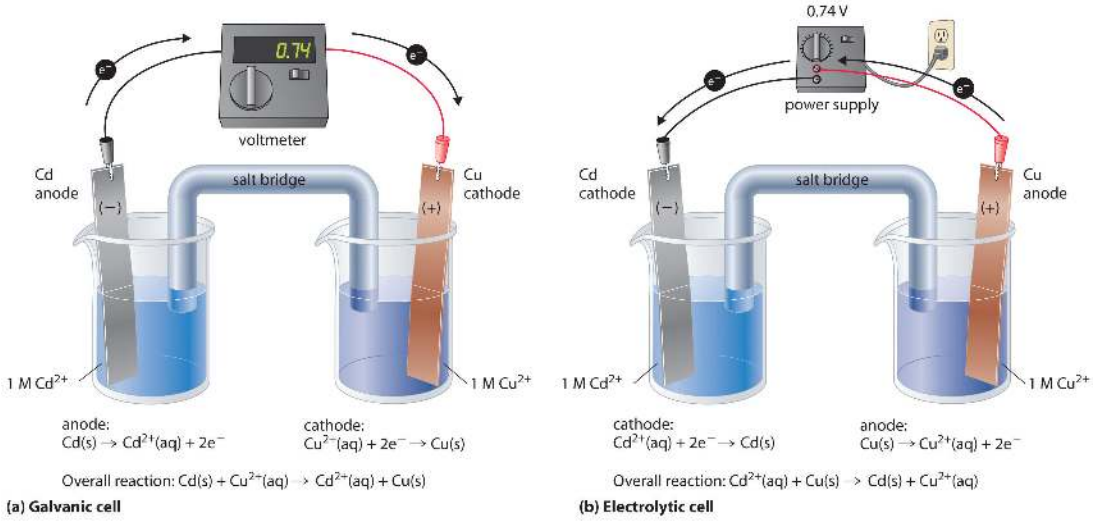


Figure **9.10.1**: An Applied Voltage Can Reverse the Flow of Electrons in a Galvanic Cd/Cu Cell. (a) When compartments that contain a Cd electrode immersed in 1 M Cd^{2+}(aq) and a Cu electrode immersed in 1 M Cu^{2+}(aq) are connected to create a galvanic cell, Cd(s) is spontaneously oxidized to Cd^{2+}(aq) at the anode, and Cu^{2+}(aq) is spontaneously reduced to Cu(s) at the cathode. The potential of the galvanic cell is 0.74 V. (b) Applying an external potential greater than 0.74 V in the reverse direction forces electrons to flow from the Cu electrode [which is now the anode, at which metallic Cu(s) is oxidized to Cu^{2+}(aq)] and into the Cd electrode [which is now the cathode, at which Cd^{2+}(aq) is reduced to Cd(s)]. The anode in an electrolytic cell is positive because electrons are flowing from it, whereas the cathode is negative because electrons are flowing into it. (CC BY-SA-NC; anonymous)

The overall reaction is as follows:

$$\mathrm{Cd\,(s) + Cu^{2+}\,(aq) \rightarrow Cd^{2+}\,(aq) + Cu\,(s)}$$

with $E°_{cell} = 0.74\ V$

This reaction is thermodynamically spontaneous as written ($\Delta G° < 0$):

$$\begin{aligned}\Delta G° &= -nFE°_{\text{cell}} \\ &= -(2\ \text{mol e}^-)[96,485\ \text{J/(V}\cdot\text{mol)}](0.74\ \text{V}) \\ &= -140\ \text{kJ (per mole Cd)}\end{aligned}$$

In this direction, the system is acting as a galvanic cell.

> *In an electrolytic cell, an external voltage is applied to drive a nonspontaneous reaction.*

The reverse reaction, the reduction of Cd^{2+} by Cu, is thermodynamically nonspontaneous and will occur only with an input of 140 kJ. We can force the reaction to proceed in the reverse direction by applying an electrical potential greater than 0.74 V from an external power supply. The applied voltage forces electrons through the circuit in the reverse direction, converting a galvanic cell to an electrolytic cell. Thus the copper electrode is now the anode (Cu is oxidized), and the cadmium electrode is now the cathode (Cd^{2+} is reduced) (Figure **9.10.1***b*). The signs of the cathode and the anode have switched to reflect the flow of electrons in the circuit. The half-reactions that occur at the cathode and the anode are as follows:

- half-reaction at the cathode:

$$\mathrm{Cd^{2+}(aq) + 2\,e^- \rightarrow Cd(s)} \tag{9.10.1}$$

with $E^\circ_{cathode} = -0.40\,V$

- half-reaction at the anode:

$$\mathrm{Cu(s) \rightarrow Cu^{2+}(aq) + 2\,e^-} \tag{9.10.2}$$

with $E^\circ_{anode} = 0.34\,V$

- Overall Reaction:

$$\mathrm{Cd^{2+}(aq) + Cu(s) \rightarrow Cd(s) + Cu^{2+}(aq)} \tag{9.10.3}$$

with $E^\circ_{cell} = -0.74\,V$

Because $E^\circ_{cell} < 0$, the overall reaction—the reduction of Cd^{2+} by Cu—clearly **cannot** occur spontaneously and proceeds only when sufficient electrical energy is applied. The differences between galvanic and electrolytic cells are summarized in Table **9.10.1**.

Table **9.10.1**: Comparison of Galvanic and Electrolytic Cells

Property	Galvanic Cell	Electrolytic Cell
ΔG	< 0	> 0
E_{cell}	> 0	< 0
Electrode Process		
anode	oxidation	oxidation
cathode	reduction	reduction
Sign of Electrode		
anode	−	+
cathode	+	−

Electrolytic Reactions

At sufficiently high temperatures, ionic solids melt to form liquids that conduct electricity extremely well due to the high concentrations of ions. If two inert electrodes are inserted into molten **NaCl**, for example, and an electrical potential is applied, Cl^- is oxidized at the anode, and Na^+ is reduced at the cathode. The overall reaction is as follows:

$$\mathrm{2\,NaCl(l) \rightarrow 2\,Na(l) + Cl_2(g)} \tag{9.10.4}$$

This is the reverse of the formation of **NaCl** from its elements. The product of the reduction reaction is liquid sodium because the melting point of sodium metal is 97.8°C, well below that of **NaCl** (801°C). Approximately 20,000 tons of sodium metal are produced commercially in the United States each year by the electrolysis of molten **NaCl** in a Downs cell (Figure **9.10.2**). In this specialized cell, $CaCl_2$ (melting point = 772°C) is first added to the **NaCl** to lower the melting point of the mixture to about 600°C, thereby lowering operating costs.

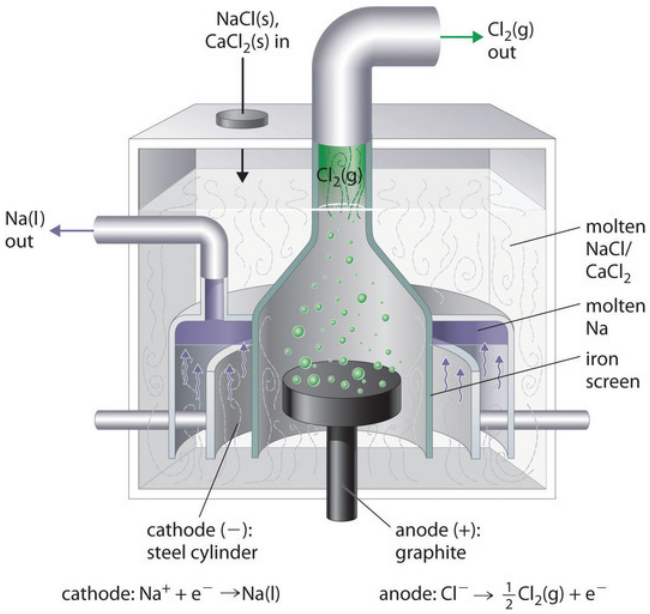


Figure 9.10.2: A Downs Cell for the Electrolysis of Molten NaCl. The electrolysis of a molten mixture of NaCl and $CaCl_2$ results in the formation of elemental sodium and chlorine gas. Because sodium is a liquid under these conditions and liquid sodium is less dense than molten sodium chloride, the sodium floats to the top of the melt and is collected in concentric capped iron cylinders surrounding the cathode. Gaseous chlorine collects in the inverted cone over the anode. An iron screen separating the cathode and anode compartments ensures that the molten sodium and gaseous chlorine do not come into contact. (CC BY-SA-NC; anonymous)

Similarly, in the Hall–Heroult process used to produce aluminum commercially, a molten mixture of about 5% aluminum oxide (Al_2O_3; melting point = 2054°C) and 95% cryolite (Na_3AlF_6; melting point = 1012°C) is electrolyzed at about 1000°C, producing molten aluminum at the cathode and CO_2 gas at the carbon anode. The overall reaction is as follows:

$$2\,Al_2O_3\,(l) + 3\,C\,(s) \longrightarrow 4\,Al\,(l) + 3\,CO_2\,(g) \tag{9.10.5}$$

Oxide ions react with oxidized carbon at the anode, producing CO_2(g).

There are two important points to make about these two commercial processes and about the electrolysis of molten salts in general.

1. The electrode potentials for molten salts are likely to be very different from the standard cell potentials listed in Table P2, which are compiled for the reduction of the hydrated ions in aqueous solutions under standard conditions.
2. Using a mixed salt system means there is a possibility of competition between different electrolytic reactions. When a mixture of NaCl and $CaCl_2$ is electrolyzed, Cl^- is oxidized because it is the only anion present, but either Na^+ or Ca^{2+} can be reduced. Conversely, in the Hall–Heroult process, only one cation is present that can be reduced (Al^{3+}), but there are three species that can be oxidized: C, O^{2-}, and F^-.

In the Hall–Heroult process, C is oxidized instead of O^{2-} or F^- because oxygen and fluorine are more electronegative than carbon, which means that C is a weaker oxidant than either O_2 or F_2. Similarly, in the Downs cell, we might expect electrolysis of a NaCl/$CaCl_2$ mixture to produce calcium rather than sodium because Na is slightly less electronegative than Ca (χ = 0.93 versus 1.00, respectively), making Na easier to oxidize and, conversely, Na^+ more difficult to reduce. In fact, the reduction of Na^+ to Na is the observed reaction. In cases where the electronegativities of two species are similar, other factors, such as the formation of complex ions, become important and may determine the outcome.

✔ Example 9.10.1

If a molten mixture of $MgCl_2$ and KBr is electrolyzed, what products will form at the cathode and the anode, respectively?

Given: identity of salts

Asked for: electrolysis products

Strategy:

A. List all the possible reduction and oxidation products. Based on the electronegativity values shown in Figure 7.5, determine which species will be reduced and which species will be oxidized.

B. Identify the products that will form at each electrode.

Solution

A The possible reduction products are Mg and K, and the possible oxidation products are Cl_2 and Br_2. Because Mg is more electronegative than K (χ = 1.31 versus 0.82), it is likely that Mg will be reduced rather than K. Because Cl is more electronegative than Br (3.16 versus 2.96), Cl_2 is a stronger oxidant than Br_2.

B Electrolysis will therefore produce Br_2 at the anode and Mg at the cathode.

? Exercise 9.10.1

Predict the products if a molten mixture of $AlBr_3$ and LiF is electrolyzed.

Answer

Br_2 and Al

Electrolysis can also be used to drive the thermodynamically nonspontaneous decomposition of water into its constituent elements: H_2 and O_2. However, because pure water is a very poor electrical conductor, a small amount of an ionic solute (such as H_2SO_4 or Na_2SO_4) must first be added to increase its electrical conductivity. Inserting inert electrodes into the solution and applying a voltage between them will result in the rapid evolution of bubbles of H_2 and O_2 (Figure **9.10.3**).

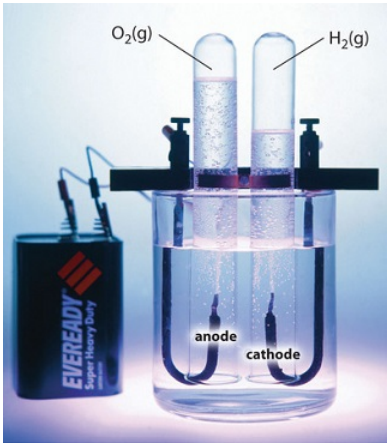


Figure **9.10.3**: The Electrolysis of Water. Applying an external potential of about 1.7–1.9 V to two inert electrodes immersed in an aqueous solution of an electrolyte such as H_2SO_4 or Na_2SO_4 drives the thermodynamically nonspontaneous decomposition of water into H_2 at the cathode and O_2 at the anode. (CC BY-SA-NC; anonymous)

The reactions that occur are as follows:

- cathode:

$$2H^+_{(aq)} + 2e^- \rightarrow H_{2(g)} \qquad E^\circ_{cathode} = 0V \tag{9.10.6}$$

- anode:

$$2H_2O_{(l)} \rightarrow O_{2(g)} + 4H^+_{(aq)} + 4e^- \qquad E^\circ_{anode} = 1.23\ V \tag{9.10.7}$$

- overall:

$$2H_2O_{(l)} \rightarrow O_{2(g)} + 2H_{2(g)} \qquad E^\circ_{cell} = -1.23\ V \tag{9.10.8}$$

For a system that contains an electrolyte such as Na_2SO_4, which has a negligible effect on the ionization equilibrium of liquid water, the pH of the solution will be 7.00 and $[H^+] = [OH^-] = 1.0 \times 10^{-7}$. Assuming that $P_{O_2} = P_{H_2}$ = 1 atm, we can use the standard

potentials to calculate E for the overall reaction:

$$E_{\text{cell}} = E^\circ_{\text{cell}} - \left(\frac{0.0591\ \text{V}}{n}\right)\log(P_{\text{O}_2}P^2_{\text{H}_2}) \tag{9.10.9}$$

$$= -1.23\ \text{V} - \left(\frac{0.0591\ \text{V}}{4}\right)\log(1) = -1.23\ \text{V} \tag{9.10.10}$$

Thus E_{cell} is −1.23 V, which is the value of $E°_{cell}$ if the reaction is carried out in the presence of 1 M H^+ rather than at pH 7.0.

In practice, a voltage about 0.4–0.6 V greater than the calculated value is needed to electrolyze water. This added voltage, called an **overvoltage**, represents the additional driving force required to overcome barriers such as the large activation energy for the formation of a gas at a metal surface. Overvoltages are needed in all electrolytic processes, which explain why, for example, approximately 14 V must be applied to recharge the 12 V battery in your car.

In general, any metal that does not react readily with water to produce hydrogen can be produced by the electrolytic reduction of an aqueous solution that contains the metal cation. The p-block metals and most of the transition metals are in this category, but metals in high oxidation states, which form oxoanions, cannot be reduced to the metal by simple electrolysis. Active metals, such as aluminum and those of groups 1 and 2, react so readily with water that they can be prepared only by the electrolysis of molten salts. Similarly, any nonmetallic element that does not readily oxidize water to O_2 can be prepared by the electrolytic oxidation of an aqueous solution that contains an appropriate anion. In practice, among the nonmetals, only F_2 cannot be prepared using this method. Oxoanions of nonmetals in their highest oxidation states, such as NO_3^-, SO_4^{2-}, PO_4^{3-}, are usually difficult to reduce electrochemically and usually behave like spectator ions that remain in solution during electrolysis.

> *In general, any metal that does not react readily with water to produce hydrogen can be produced by the electrolytic reduction of an aqueous solution that contains the metal cation.*

Electroplating

In a process called **electroplating**, a layer of a second metal is deposited on the metal electrode that acts as the cathode during electrolysis. Electroplating is used to enhance the appearance of metal objects and protect them from corrosion. Examples of electroplating include the chromium layer found on many bathroom fixtures or (in earlier days) on the bumpers and hubcaps of cars, as well as the thin layer of precious metal that coats silver-plated dinnerware or jewelry. In all cases, the basic concept is the same. A schematic view of an apparatus for electroplating silverware and a photograph of a commercial electroplating cell are shown in Figure 9.10.4.

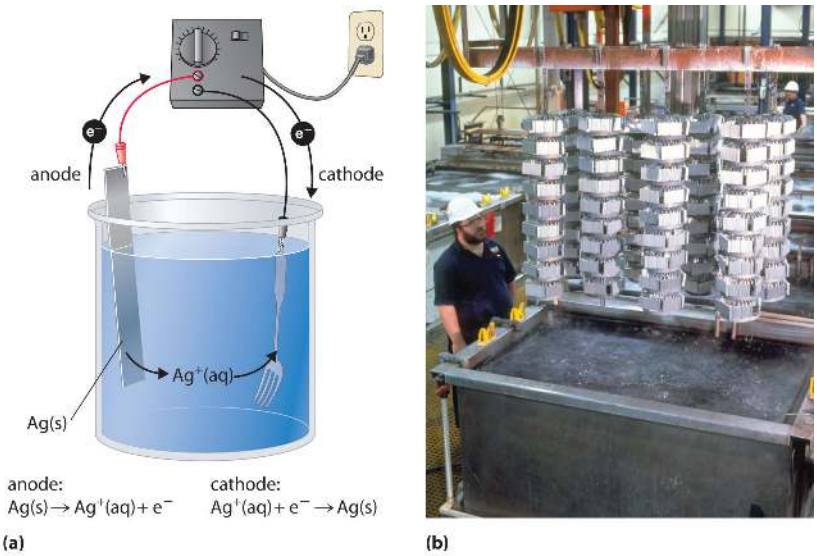


Figure 9.10.3: Electroplating. (a) Electroplating uses an electrolytic cell in which the object to be plated, such as a fork, is immersed in a solution of the metal to be deposited. The object being plated acts as the cathode, on which the desired metal is deposited in a thin layer, while the anode usually consists of the metal that is being deposited (in this case, silver) that maintains the solution concentration as it dissolves. (b) In this commercial electroplating apparatus, a large number of objects can be plated simultaneously by lowering the rack into the Ag^+ solution and applying the correct potential. (CC BY-SA-NC; anonymous)

The half-reactions in electroplating a fork, for example, with silver are as follows:

- cathode (fork):

$$Ag^+(aq) + e^- \longrightarrow Ag(s) \qquad E°_{cathode} = 0.80V$$

- anode (silver bar):

$$Ag(s) \longrightarrow Ag^+(aq) + e^- \qquad E°_{anode} = 0.80V$$

The overall reaction is the transfer of silver metal from one electrode (a silver bar acting as the anode) to another (a fork acting as the cathode). Because $E°_{cell} = 0\,V$, it takes only a small applied voltage to drive the electroplating process. In practice, various other substances may be added to the plating solution to control its electrical conductivity and regulate the concentration of free metal ions, thus ensuring a smooth, even coating.

Quantitative Considerations

If we know the stoichiometry of an electrolysis reaction, the amount of current passed, and the length of time, we can calculate the amount of material consumed or produced in a reaction. Conversely, we can use stoichiometry to determine the combination of current and time needed to produce a given amount of material.

The quantity of material that is oxidized or reduced at an electrode during an electrochemical reaction is determined by the stoichiometry of the reaction and the amount of charge that is transferred. For example, in the reaction

$$Ag^+(aq) + e^- \longrightarrow Ag(s)$$

1 mol of electrons reduces 1 mol of Ag^+ to Ag metal. In contrast, in the reaction

$$Cu^{2+}(aq) + 2\,e^- \longrightarrow Cu(s)$$

1 mol of electrons reduces only 0.5 mol of Cu^{2+} to Cu metal. Recall that the charge on 1 mol of electrons is 1 faraday (1 F), which is equal to 96,485 C. We can therefore calculate the number of moles of electrons transferred when a known current is passed through a cell for a given period of time. The total charge (q in coulombs) transferred is the product of the current (I in amperes) and the time (t, in seconds):

$$q = I \times t \tag{9.10.11}$$

The stoichiometry of the reaction and the total charge transferred enable us to calculate the amount of product formed during an electrolysis reaction or the amount of metal deposited in an electroplating process.

For example, if a current of 0.60 A passes through an aqueous solution of $CuSO_4$ for 6.0 min, the total number of coulombs of charge that passes through the cell is as follows:

$$\begin{aligned} q &= (0.60\ \text{A})(6.0\ \text{min})(60\ \text{s/min}) \\ &= 220\ \text{A} \cdot \text{s} \\ &= 220\ \text{C} \end{aligned}$$

The number of moles of electrons transferred to Cu^{2+} is therefore

$$\begin{aligned} \text{moles e}^- &= \frac{220\ \text{C}}{96{,}485\ \text{C/mol}} \\ &= 2.3 \times 10^{-3}\ \text{mol e}^- \end{aligned}$$

Because two electrons are required to reduce a single Cu^{2+} ion, the total number of moles of Cu produced is half the number of moles of electrons transferred, or 1.2×10^{-3} mol. This corresponds to 76 mg of Cu. In commercial electrorefining processes, much higher currents (greater than or equal to 50,000 A) are used, corresponding to approximately 0.5 F/s, and reaction times are on the order of 3–4 weeks.

Example 9.10.2

A silver-plated spoon typically contains about 2.00 g of Ag. If 12.0 h are required to achieve the desired thickness of the Ag coating, what is the average current per spoon that must flow during the electroplating process, assuming an efficiency of 100%?

Given: mass of metal, time, and efficiency

Asked for: current required

Strategy:

A. Calculate the number of moles of metal corresponding to the given mass transferred.
B. Write the reaction and determine the number of moles of electrons required for the electroplating process.
C. Use the definition of the faraday to calculate the number of coulombs required. Then convert coulombs to current in amperes.

Solution

A We must first determine the number of moles of Ag corresponding to 2.00 g of Ag:

$$\text{moles Ag} = \frac{2.00\ \text{g}}{107.868\ \text{g/mol}} = 1.85 \times 10^{-2}\ \text{mol Ag}$$

B The reduction reaction is $Ag^+(aq) + e^- \rightarrow Ag(s)$, so 1 mol of electrons produces 1 mol of silver.

C Using the definition of the faraday,

$$\text{coulombs} = (1.85 \times 10^{-2}\text{mol e}^-)(96{,}485\ \text{C/mol e}^-) = 1.78 \times 10^3\ \text{C / mole}$$

The current in amperes needed to deliver this amount of charge in 12.0 h is therefore

$$\begin{aligned} \text{amperes} &= \frac{1.78 \times 10^3\ \text{C}}{(12.0\ \text{h})(60\ \text{min/h})(60\ \text{s/min})} \\ &= 4.12 \times 10^{-2}\ \text{C/s} = 4.12 \times 10^{-2}\ \text{A} \end{aligned}$$

Because the electroplating process is usually much less than 100% efficient (typical values are closer to 30%), the actual current necessary is greater than 0.1 A.

? Exercise 9.10.2

A typical aluminum soft-drink can weighs about 29 g. How much time is needed to produce this amount of Al(s) in the Hall–Heroult process, using a current of 15 A to reduce a molten Al_2O_3/Na_3AlF_6 mixture?

Answer

5.8 h



Electroplating: Electroplating(opens in new window) [youtu.be]

Summary

In electrolysis, an external voltage is applied to drive a **nonspontaneous** reaction. The quantity of material oxidized or reduced can be calculated from the stoichiometry of the reaction and the amount of charge transferred. Relationship of charge, current and time:

$$q = I \times t$$

In electrolysis, an external voltage is applied to drive a nonspontaneous reaction. Electrolysis can also be used to produce H_2 and O_2 from water. In practice, an additional voltage, called an overvoltage, must be applied to overcome factors such as a large activation energy and a junction potential. Electroplating is the process by which a second metal is deposited on a metal surface, thereby enhancing an object's appearance or providing protection from corrosion. The amount of material consumed or produced in a reaction can be calculated from the stoichiometry of an electrolysis reaction, the amount of current passed, and the duration of the electrolytic reaction.

9.10: Electrolysis- Causing Nonspontaneous Reactions to Occur is shared under a not declared license and was authored, remixed, and/or curated by LibreTexts.

- **20.9: Electrolysis** is licensed CC BY-NC-SA 3.0.

CHAPTER OVERVIEW

10: Coordination Chemistry

Complexes or **coordination compounds** are molecules that posess a metal center that is bound to ligands (atoms, ions, or molecules that donate electrons to the metal). These complexes can be neutral or charged. When the complex is charged, it is stabilized by neighboring counter-ions.

10.1: Werner’s Theory of Coordination Compounds
10.2: Ligands
10.3: Nomenclature
10.4: Isomerism
10.5: Optical Isomerism in Metal Complexes
10.6: Stability Aspects of Complex-Ion Equilibria
10.7: Chelation
10.8: Bonding in Octahedral Complex Ions- Crystal Field Theory
10.9: Bonding in Non-Octahedral Complex Ions- Crystal Field Theory
10.10: High Spin and Low Spin Complexes
10.11: Magnetic Behavior of Atoms, Molecules, and Materials
10.12: Magnetic Behavior of Complex Ions
10.13: Optical Properties of Coordination Compounds (Color)

10: Coordination Chemistry is shared under a not declared license and was authored, remixed, and/or curated by LibreTexts.

10.1: Werner's Theory of Coordination Compounds

Learning Objectives

- To know the most common structures observed for metal complexes.
- To predict the relative stabilities of metal complexes with different ligands

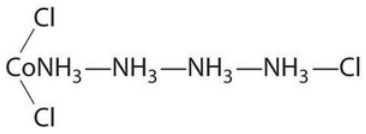
One of the most important properties of metallic elements is their ability to act as Lewis acids that form complexes with a variety of Lewis bases. A metal complex consists of a central metal atom or ion that is bonded to one or more ligands (from the Latin ligare, meaning "to bind"), which are ions or molecules that contain one or more pairs of electrons that can be shared with the metal. Metal complexes can be neutral, such as $Co(NH_3)_3Cl_3$; positively charged, such as $[Nd(H_2O)_9]^{3+}$; or negatively charged, such as $[UF_8]^{4-}$. Electrically charged metal complexes are sometimes called *complex ions*. A *coordination compound* contains one or more metal complexes.

Coordination compounds are important for at least three reasons. First, most of the elements in the periodic table are metals, and almost all metals form complexes, so metal complexes are a feature of the chemistry of more than half the elements. Second, many industrial catalysts are metal complexes, and such catalysts are steadily becoming more important as a way to control reactivity. For example, a mixture of a titanium complex and an organometallic compound of aluminum is the catalyst used to produce most of the polyethylene and polypropylene "plastic" items we use every day. Finally, transition-metal complexes are essential in biochemistry. Examples include hemoglobin, an iron complex that transports oxygen in our blood; cytochromes, iron complexes that transfer electrons in our cells; and complexes of Fe, Zn, Cu, and Mo that are crucial components of certain enzymes, the catalysts for all biological reactions.

History of the Coordination Compounds

Coordination compounds have been known and used since antiquity; probably the oldest is the deep blue pigment called Prussian blue: $\mathbf{KFe_2(CN)_6}$. The chemical nature of these substances, however, was unclear for a number of reasons. For example, many compounds called "double salts" were known, such as $\mathbf{AlF_3 \cdot 3\,KF}$, $\mathbf{Fe(CN)_2 \cdot 4\,KCN}$, and $\mathbf{ZnCl_2 \cdot 2\,CsCl}$, which were combinations of simple salts in fixed and apparently arbitrary ratios. Why should $\mathbf{AlF_3 \cdot 3\,KF}$ exist but not $\mathbf{AlF_3 \cdot 4\,KF}$ or $\mathbf{AlF_3 \cdot 2\,KF}$? And why should a 3:1 KF:AlF3 mixture have different chemical and physical properties than either of its components? Similarly, adducts of metal salts with neutral molecules such as ammonia were also known—for example, $\mathbf{CoCl_3 \cdot 6\,NH_3}$, which was first prepared sometime before 1798. Like the double salts, the compositions of these adducts exhibited fixed and apparently arbitrary ratios of the components. For example, $\mathbf{CoCl_3 \cdot 6\,NH_3}$, $\mathbf{CoCl_3 \cdot 5\,NH_3}$, $\mathbf{CoCl_3 \cdot 4\,NH_3}$, and $\mathbf{CoCl_3 \cdot 3\,NH_3}$ were all known and had very different properties, but despite all attempts, chemists could not prepare $\mathbf{CoCl_3 \cdot 2\,NH_3}$ or $\mathbf{CoCl_3 \cdot NH_3}$.

Although the chemical composition of such compounds was readily established by existing analytical methods, their chemical nature was puzzling and highly controversial. The major problem was that what we now call valence (i.e., the oxidation state) and coordination number were thought to be identical. As a result, highly implausible (to modern eyes at least) structures were proposed for such compounds, including the "Chattanooga choo-choo" model for $CoCl_3 \cdot 4NH_3$ shown here.



$\mathbf{CoCl_3 \cdot 4NH_3}$

The modern theory of coordination chemistry is based largely on the work of Alfred Werner (1866–1919; Nobel Prize in Chemistry in 1913). In a series of careful experiments carried out in the late 1880s and early 1890s, he examined the properties of several series of metal halide complexes with ammonia. For example, five different "adducts" of ammonia with $PtCl_4$ were known at the time: $PtCl_4 \cdot nNH_3$ (n = 2–6). Some of Werner's original data on these compounds are shown in Table **10.1.1**. The electrical conductivity of aqueous solutions of these compounds was roughly proportional to the number of ions formed per mole, while the number of chloride ions that could be precipitated as AgCl after adding $Ag^+(aq)$ was a measure of the number of "free" chloride

ions present. For example, Werner's data on $PtCl_4 \cdot 6NH_3$ in Table **10.1.1** showed that all the chloride ions were present as free chloride. In contrast, $PtCl_4 \cdot 2NH_3$ was a neutral molecule that contained no free chloride ions.

Alfred Werner (1866–1919)

Werner, the son of a factory worker, was born in Alsace. He developed an interest in chemistry at an early age, and he did his first independent research experiments at age 18. While doing his military service in southern Germany, he attended a series of chemistry lectures, and he subsequently received his PhD at the University of Zurich in Switzerland, where he was appointed professor of chemistry at age 29. He won the Nobel Prize in Chemistry in 1913 for his work on coordination compounds, which he performed as a graduate student and first presented at age 26. Apparently, Werner was so obsessed with solving the riddle of the structure of coordination compounds that his brain continued to work on the problem even while he was asleep. In 1891, when he was only 25, he woke up in the middle of the night and, in only a few hours, had laid the foundation for modern coordination chemistry.

Table **10.1.1**: Werner's Data on Complexes of Ammonia with $PtCl_4$

Complex	Conductivity (ohm^{-1})	Number of Ions per Formula Unit	Number of Cl^- Ions Precipitated by Ag^+
$PtCl_4 \cdot 6NH_3$	523	5	4
$PtCl_4 \cdot 5NH_3$	404	4	3
$PtCl_4 \cdot 4NH_3$	299	3	2
$PtCl_4 \cdot 3NH_3$	97	2	1
$PtCl_4 \cdot 2NH_3$	0	0	0

These data led Werner to postulate that metal ions have two different kinds of valence: (1) a primary valence (**oxidation state**) that corresponds to the positive charge on the metal ion and (2) a secondary valence (**coordination number**) that is the total number of ligand-metal bonds bound to the metal ion. If **Pt** had a primary valence of 4 and a secondary valence of 6, Werner could explain the properties of the $\mathbf{PtCl_4 \cdot NH_3}$ adducts by the following reactions, where the metal complex is enclosed in square brackets:

$$[Pt(NH_3)_6]Cl_4 \rightarrow [Pt(NH_3)_6]^{4+}(aq) + 4Cl^-(aq)$$
$$[Pt(NH_3)_5Cl]Cl_3 \rightarrow [Pt(NH_3)_5Cl]^{3+}(aq) + 3Cl^-(aq)$$
$$[Pt(NH_3)_4Cl_2]Cl_2 \rightarrow [Pt(NH_3)_4Cl_2]^{2+}(aq) + 2Cl^-(aq)$$
$$[Pt(NH_3)_3Cl_3]Cl \rightarrow [Pt(NH_3)_3Cl_3]^{+}(aq) + Cl^-(aq)$$
$$[Pt(NH_3)_2Cl_4] \rightarrow [Pt(NH_3)_2Cl_4]^{0}(aq)$$

Further work showed that the two missing members of the series—$[Pt(NH_3)Cl_5]^-$ and $[PtCl_6]^{2-}$—could be prepared as their mono- and dipotassium salts, respectively. Similar studies established coordination numbers of 6 for Co^{3+} and Cr^{3+} and 4 for Pt^{2+} and Pd^{2+}.

Werner's studies on the analogous Co^{3+} complexes also allowed him to propose a structural model for metal complexes with a coordination number of 6. Thus he found that $[Co(NH_3)_6]Cl_3$ (yellow) and $[Co(NH_3)_5Cl]Cl_2$ (purple) were 1:3 and 1:2 electrolytes. Unexpectedly, however, two different $[Co(NH_3)_4Cl_2]Cl$ compounds were known: one was red, and the other was green (Figure **10.1.1*a***). Because both compounds had the same chemical composition and the same number of groups of the same kind attached to the same metal, there had to be something different about the arrangement of the ligands around the metal ion. Werner's key insight was that the six ligands in $[Co(NH_3)_4Cl_2]Cl$ had to be arranged at the vertices of an octahedron because that was the only structure consistent with the existence of two, and only two, arrangements of ligands (Figure **10.1.1*b***. His conclusion was corroborated by the existence of only two different forms of the next compound in the series: $Co(NH_3)_3Cl_3$.

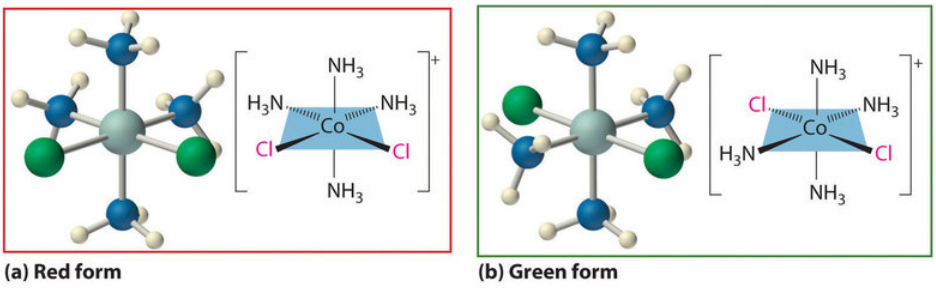


Figure **10.1.1**: Complexes with Different Arrangements of the Same Ligands Have Different Properties. The $[Co(NH_3)_4Cl_2]^+$ ion can have two different arrangements of the ligands, which results in different colors: if the two Cl^- ligands are next to each other, the complex is red (a), but if they are opposite each other, the complex is green (b).

Example 10.1.1

In Werner's time, many complexes of the general formula MA_4B_2 were known, but no more than two different compounds with the same composition had been prepared for any metal. To confirm Werner's reasoning, calculate the maximum number of different structures that are possible for six-coordinate MA_4B_2 complexes with each of the three most symmetrical possible structures: a hexagon, a trigonal prism, and an octahedron. What does the fact that no more than two forms of any MA_4B_2 complex were known tell you about the three-dimensional structures of these complexes?

Given: three possible structures and the number of different forms known for MA_4B_2 complexes

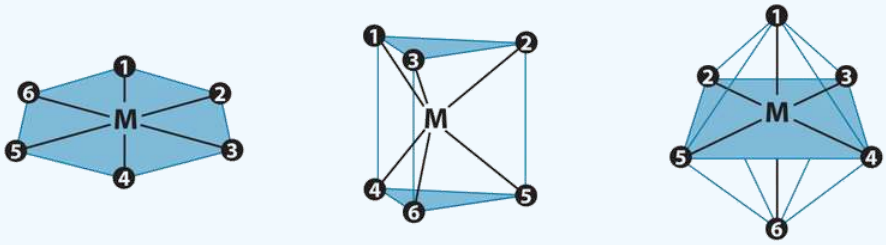
Asked for: number of different arrangements of ligands for MA_4B_2 complex for each structure

Strategy:

Sketch each structure, place a B ligand at one vertex, and see how many different positions are available for the second B ligand.

Solution

The three regular six-coordinate structures are shown here, with each coordination position numbered so that we can keep track of the different arrangements of ligands. For each structure, all vertices are equivalent. We begin with a symmetrical MA_6 complex and simply replace two of the A ligands in each structure to give an MA_4B_2 complex:



For the hexagon, we place the first B ligand at position 1. There are now three possible places for the second B ligand: at position 2 (or 6), position 3 (or 5), or position 4. These are the only possible arrangements. The (1, 2) and (1, 6) arrangements are chemically identical because the two B ligands are adjacent to each other. The (1, 3) and (1, 5) arrangements are also identical because in both cases the two B ligands are separated by an A ligand.

Turning to the trigonal prism, we place the first B ligand at position 1. Again, there are three possible choices for the second B ligand: at position 2 or 3 on the same triangular face, position 4 (on the other triangular face but adjacent to 1), or position 5 or 6 (on the other triangular face but not adjacent to 1). The (1, 2) and (1, 3) arrangements are chemically identical, as are the (1, 5) and (1, 6) arrangements.

In the octahedron, however, if we place the first B ligand at position 1, then we have only two choices for the second B ligand: at position 2 (or 3 or 4 or 5) or position 6. In the latter, the two B ligands are at opposite vertices of the octahedron, with the

metal lying directly between them. Although there are four possible arrangements for the former, they are chemically identical because in all cases the two B ligands are adjacent to each other.

The number of possible MA_4B_2 arrangements for the three geometries is thus: hexagon, 3; trigonal prism, 3; and octahedron, 2. The fact that only two different forms were known for all MA_4B_2 complexes that had been prepared suggested that the correct structure was the octahedron but did not prove it. For some reason one of the three arrangements possible for the other two structures could have been less stable or harder to prepare and had simply not yet been synthesized. When combined with analogous results for other types of complexes (e.g., MA_3B_3), however, the data were best explained by an octahedral structure for six-coordinate metal complexes.

? Exercise 10.1.1

Determine the maximum number of structures that are possible for a four-coordinate MA_2B_2 complex with either a square planar or a tetrahedral symmetrical structure.

Answer

square planar, 2; tetrahedral, 1

Structures of Metal Complexes

The coordination numbers of metal ions in metal complexes can range from 2 to at least 9. In general, the differences in energy between different arrangements of ligands are greatest for complexes with low coordination numbers and decrease as the coordination number increases. Usually only one or two structures are possible for complexes with low coordination numbers, whereas several different energetically equivalent structures are possible for complexes with high coordination numbers (n > 6). The following presents the most commonly encountered structures for coordination numbers 2–9. Many of these structures should be familiar to you from our discussion of the valence-shell electron-pair repulsion (VSEPR) model because they correspond to the lowest-energy arrangements of n electron pairs around a central atom.

> *Compounds with low coordination numbers exhibit the greatest differences in energy between different arrangements of ligands.*

Coordination Number 2

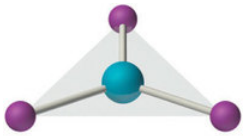
Although it is rare for most metals, this coordination number is surprisingly common for d^{10} metal ions, especially Cu^+, Ag^+, Au^+, and Hg^{2+}. An example is the $[Au(CN)_2]^-$ ion, which is used to extract gold from its ores. As expected based on VSEPR considerations, these complexes have the linear L–M–L structure shown here.



Linear ML_2

Coordination Number 3

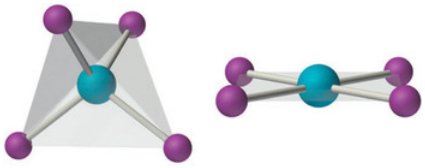
Although it is also rare, this coordination number is encountered with d^{10} metal ions such as Cu^+ and Hg^{2+}. Among the few known examples is the HgI_3^- ion. Three-coordinate complexes almost always have the trigonal planar structure expected from the VSEPR model.



Trigonal planar ML_3

Coordination Number 4

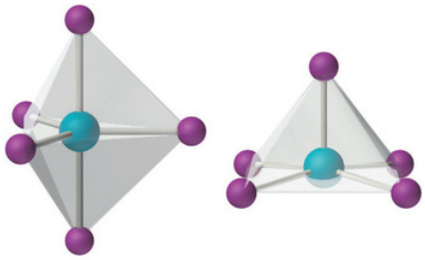
Two common structures are observed for four-coordinate metal complexes: tetrahedral and square planar. The tetrahedral structure is observed for all four-coordinate complexes of nontransition metals, such as $[BeF_4]^{2-}$, and d^{10} ions, such as $[ZnCl_4]^{2-}$. It is also found for four-coordinate complexes of the first-row transition metals, especially those with halide ligands (e.g., $[FeCl_4]^-$ and $[FeCl_4]^{2-}$). In contrast, square planar structures are routinely observed for four-coordinate complexes of second- and third-row transition metals with d^8 electron configurations, such as Rh^+ and Pd^{2+}, and they are also encountered in some complexes of Ni^{2+} and Cu^{2+}.



Tetrahedral and square planar ML_4

Coordination Number 5

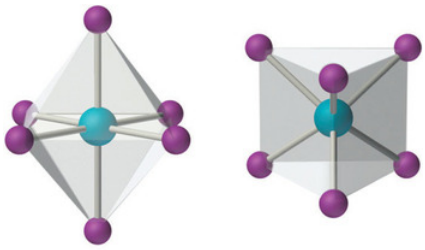
This coordination number is less common than 4 and 6, but it is still found frequently in two different structures: trigonal bipyramidal and square pyramidal. Because the energies of these structures are usually rather similar for most ligands, many five-coordinate complexes have distorted structures that lie somewhere between the two extremes.



Trigonal bipyramidal and square pyramidal ML_5

Coordination Number 6

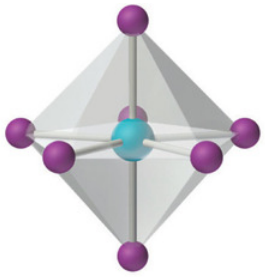
This coordination number is by far the most common. The six ligands are almost always at the vertices of an octahedron or a distorted octahedron. The only other six-coordinate structure is the trigonal prism, which is very uncommon in simple metal complexes.



Octahedral and trigonal prismatic ML_6

Coordination Number 7

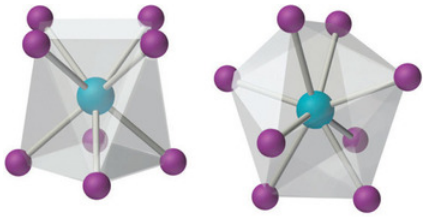
This relatively uncommon coordination number is generally encountered for only large metals (such as the second- and third-row transition metals, lanthanides, and actinides). At least three different structures are known, two of which are derived from an octahedron or a trigonal prism by adding a ligand to one face of the polyhedron to give a “capped” octahedron or trigonal prism. By far the most common, however, is the pentagonal bipyramid.



Pentagonal bipyramidal ML_7

Coordination Number 8

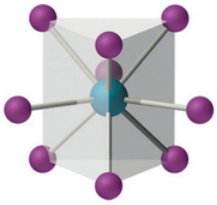
This coordination number is relatively common for larger metal ions. The simplest structure is the cube, which is rare because it does not minimize interligand repulsive interactions. Common structures are the square antiprism and the dodecahedron, both of which can be generated from the cube.



Square antiprismatic and trigonal dodecahedral ML_8

Coordination Number 9

This coordination number is found in larger metal ions, and the most common structure is the tricapped trigonal prism, as in $[Nd(H_2O)_9]^{3+}$.



Tricapped trigonal prismatic ML_9

Key Takeaways

- Coordination compounds are a major feature of the chemistry of over half the elements.
- Coordination compounds have important roles as industrial catalysts in controlling reactivity, and they are essential in biochemical processes.

Summary

Transition metals form metal complexes, polyatomic species in which a metal ion is bound to one or more ligands, which are groups bound to a metal ion. Complex ions are electrically charged metal complexes, and a coordination compound contains one or more metal complexes. Metal complexes with low coordination numbers generally have only one or two possible structures, whereas those with coordination numbers greater than six can have several different structures. Coordination numbers of two and three are common for d^{10} metal ions. Tetrahedral and square planar complexes have a coordination number of four; trigonal bipyramidal and square pyramidal complexes have a coordination number of five; and octahedral complexes have a coordination

number of six. At least three structures are known for a coordination number of seven, which is generally found for only large metal ions. Coordination numbers of eight and nine are also found for larger metal ions.

10.1: Werner's Theory of Coordination Compounds is shared under a not declared license and was authored, remixed, and/or curated by LibreTexts.

- **24.1: Werner's Theory of Coordination Compounds** by Anonymous is licensed CC BY-NC-SA 4.0.

10.2: Ligands

A metal ion in solution does not exist in isolation, but in combination with ligands (such as solvent molecules or simple ions) or chelating groups, giving rise to complex ions or coordination compounds. These complexes contain a central atom or ion, often a transition metal, and a cluster of ions or neutral molecules surrounding it. Ligands are ions or neutral molecules that bond to a central metal atom or ion. Ligands act as Lewis bases (electron pair donors), and the central atom acts as a Lewis acid (electron pair acceptor). Ligands have at least one donor atom with an electron pair used to form covalent bonds with the central atom.

The term ligand come from the latin word *ligare* (which meaning to bind) was first used by Alfred Stock in 1916 in relation to silicon chemistry. Ligands can be anions, cations, or neutral molecules. Ligands can be further characterized as monodentate, bidentate, tridentate etc. where the concept of teeth **(dent)** is introduced, hence the idea of bite angle etc. A monodentate ligand has only one donor atom used to bond to the central metal atom or ion.

Monodentate Ligands

The term "monodentate" can be translated as "one tooth," referring to the ligand binding to the center through only one atom. Some examples of monodentate ligands are: chloride ions (referred to as chloro when it is a ligand), water (referred to as aqua when it is a ligand), hydroxide ions (referred to as hydroxo when it is a ligand), and ammonia (referred to as ammine when it is a ligand).

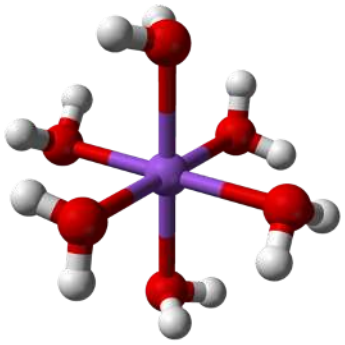


Figure **10.2.1**: Central atom with six monodentate ligands attached. (Image courtesy of Wikimedia Commons.)

Bidentate Ligands

Bidentate ligands have two donor atoms which allow them to bind to a central metal atom or ion at two points. Common examples of bidentate ligands are ethylenediamine (en), and the oxalate ion (ox). Shown below is a diagram of ethylenediamine: the nitrogen (blue) atoms on the edges each have two free electrons that can be used to bond to a central metal atom or ion.

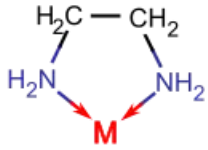


Figure **10.2.2**: Ethylenediamine (en) is an example of a bidentate ligand. (Image courtesy of Wikimedia Commons.). Ethylenediamine (en) is a bidentate ligand that forms a five-membered ring in coordinating to a metal ion M

Polydentate Ligands

Polydentate ligands range in the number of atoms used to bond to a central metal atom or ion. EDTA, a hexadentate ligand, is an example of a polydentate ligand that has six donor atoms with electron pairs that can be used to bond to a central metal atom or ion.

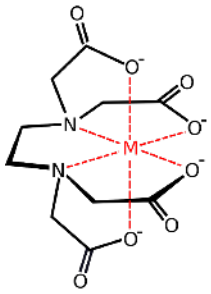
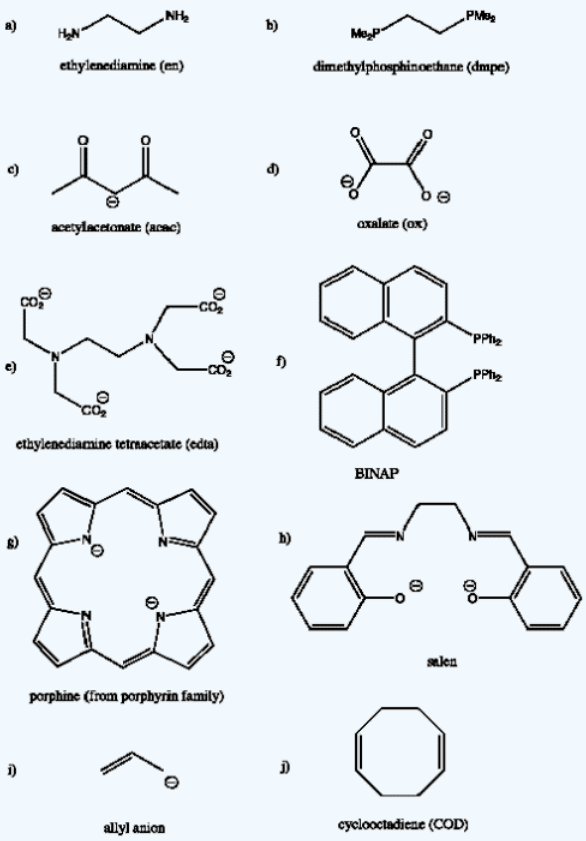


Figure **10.2.3**: Ethylenediaminetetraaceticacid acid (EDTA) is a hexadentate ligand and can bind a Metal via multiple "teeth" (left) Unbound EDTA ion and (right) EDTA bound to a generic transition metal. (Images courtesy of Wikimedia Commons.)

Unlike polydentate ligands, ambidentate ligands can attach to the central atom in two places. A good example of this is thiocyanate, SCN^-, which can attach at either the sulfur atom or the nitrogen atom.

Example 10.2.1

Draw metal complexes using the ligands below and metal ions of your choice.



Chelation

Chelation is a process in which a polydentate ligand bonds to a metal ion, forming a ring. The complex produced by this process is called a chelate, and the polydentate ligand is referred to as a chelating agent. The term chelate was first applied in 1920 by Sir Gilbert T. Morgan and H.D.K. Drew, who stated: "The adjective chelate, derived from the great claw or chela (chely- Greek) of the lobster or other crustaceans, is suggested for the caliperlike groups which function as two associating units and fasten to the central atom so as to produce heterocyclic rings." As the name implies, chelating ligands have high affinity for metal ions relative to ligands with only one binding group (which are called monodentate = "single tooth") ligands. Both Ethylenediamine (Figure **10.2.2**) and Ethylenediaminetetraaceticacid acid (Figure **10.2.3**) are examples of chelating agents, but many others are commonly found in the inorganic laboratory.

The Chelate Effect

The chelate effect is the enhanced affinity of chelating ligands for a metal ion compared to the affinity of a collection of similar nonchelating (monodentate) ligands for the same metal.

The **macrocyclic effect** follows the same principle as the chelate effect, but the effect is further enhanced by the cyclic conformation of the ligand. Macrocyclic ligands are not only multi-dentate, but because they are covalently constrained to their cyclic form, they allow less conformational freedom. The ligand is said to be "pre-organized" for binding, and there is little entropy penalty for wrapping it around the metal ion. For example heme b is a tetradentate cyclic ligand that strongly complexes transition metal ions, including Fe^{+2} in hemogloben (Figure **10.2.4**).

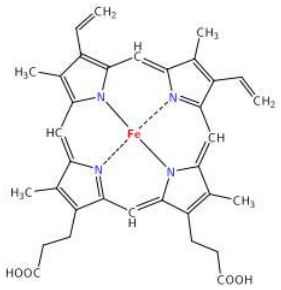
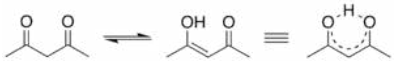


Figure **10.2.4**: Heme b macrocyclic ligand that binds iron in hemoglobin

Some other common chelating and cyclic ligands are shown below:

- **Acetylacetonate** ($acac^-$, top) is an anionic bidentate ligand that coordinates metal ions through two oxygen atoms. $Acac^-$ is a hard base so it prefers hard acid cations. With divalent metal ions, $acac^-$forms neutral, volatile complexes such as $Cu(acac)_2$ and $Mo(acac)_2$ that are useful for chemical vapor deposition (CVD) of metal thin films.



- **2,2'-Bipyridine 2,2'-Bipyridine** (Figure **10.2.5***:* left) and related bidentate ligands such as 1,10-phenanthroline form propeller-shaped complexes with metals such as Ru^{2+}. The $[Ru(bpy)_3]^{2+}$ complex is photoluminescent and can also undergo photoredox reactions, making it an interesting compound for both photocatalysis and artificial photosynthesis.
- **Crown ethers** such as 18-crown-6 **2,2'-Bipyridine** (Figure **10.2.5**: center) are cyclic hard bases that can complex alkali metal cations. Crowns can selectively bind Li^+, Na^+, or K^+ depending on the number of ethylene oxide units in the ring.
- The chelating properties of crown ethers are mimetic of the natural antibiotic **valinomycin** (**2,2'-Bipyridine** (Figure **10.2.5**: right), which selectively transports K^+ ions across bacterial cell membranes, killing the bacterium by dissipating its membrane potential. Like crown ethers, valinomycin is a cyclic hard base.

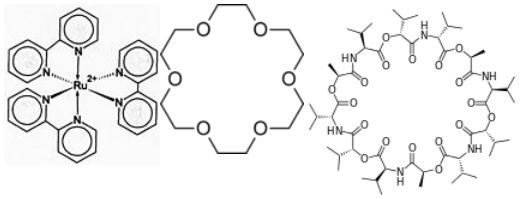


Figure **10.2.5**: (let) 2,2'-Bipyridine, (center) 18-crown-6 2,2'-Bipyridine (right) valinomycin

References

1. Petrucci, Harwood, Herring, Madura. General Chemistry Principles & Modern Applications. Prentice Hall. New Jersey, 2007
2. Cox, Tony. (2004). Instant notes in inorganic chemistry. Oxford, UK: Taylor & Francis.
3. Libraries, Association, Robert Williams, and J. Silva. Bringing chemistry to life. Oxford University Press, USA, 1999. Print.
4. Moeller, Therald, Douville, Judith, & Libraries, Association. (1988). Inorganic Chemistry: A Modern Introduction. Amer Library Assn.

5. Bowker, R., Warmus, Mieczysław, Muzzy, Adrienne, LOCALIZADO, AUTOR, Hopkinson, Barbara, Saur, K, Izod, Irene, Hopkinson, Barbara, Saur, K, Books, K, & Company, K. (1994). Inorganic Chemistry Concepts. K G Saur Verlag Gmbh & Co.
6. Porterfield, William. (1984). Inorganic chemistry. Addison Wesley Publishing Company.

Contributors and Attributions

- Harjeet Bassi (UCD)
- Adapted from the Wikibook constructed by Chemistry 310 students at Penn State University.

10.2: Ligands is shared under a not declared license and was authored, remixed, and/or curated by LibreTexts.

- **24.2: Ligands** is licensed CC BY-SA 4.0.

10.3: Nomenclature

Learning Objectives

- To learn the basis for complex ion and compound nomenclature

Coordination complexes have their own classes of isomers, different magnetic properties and colors, and various applications (photography, cancer treatment, etc), so it makes sense that they would have a naming system as well. Consisting of a metal and ligands, their formulas follow the pattern [Metal ligands]$^{\pm Charge}$, while names are written Prefix Ligands Metal (Oxidation State).

Introduction

According to the Lewis Acid-Base theory, ligands are Lewis bases since they can donate electrons to the central metal atom. The metals, in turn, are Lewis acids since they accept electrons. **Coordination complexes** consist of a ligand and a metal center cation and their charge can be positive, negative, or neutral. **Coordination compounds** are neutral compounds that contain at least one complex ions. Example of coordination complexes and compounds are:

- Complex Cation: $[Co(NH_3)_6]^{3+}$
- Complex Anion: $[CoCl_4(NH_3)_2]^-$
- Neutral Complex: $[CoCl_3(NH_3)_3]$
- Coordination Compound: $K_4[Fe(CN)_6]$

A ligand can be an anion or a neutral molecule that *donates an electron pair* to the complex (NH_3, H_2O, Cl^-). The number of ligands that attach to a metal depends on whether the ligand is **monodentate** or **polydentate**.

Rules to Complex Ion Nomenclature

To begin naming coordination complexes, here are some things to keep in mind.

1. Ligands are named first in alphabetical order.
2. The name of the metal comes next.
3. The oxidation state of the metal follows, noted by a Roman numeral in parentheses (II, IV).

Rule 1: Anionic Ligands

Ligands that act as anions which end in "-ide" are replaced with an ending "-o" (e.g., Chloride → Chloro). Anions ending with "-ite" and "-ate" are replaced with endings "-ito" and "-ato" respectively (e.g., Nitrite → Nitrito, Nitrate → Nitrato).

Table **10.3.1**: Anionic Monodentate Ligands

Molecular Formula	Ligand Name	Molecular Formula	Ligand Name
F^-	Fluoro	OH^-	Hydroxo
Cl^-	Chloro	SO_4^{2-}	Sulfato
Br^-	Bromo	$S_2O_3^{2-}$	Thiosulfato
I^-	Iodo	NO_2^-	Nitrito-N-; Nitro
O^{2-}	Oxo	ONO^-	Nitrito-O-; Nitrito
CN^-	Cyano	SCN^-	Thiocyanato-S-; Thiocyanato
NC^-	Isocyano	NCS^-	Thiocyanato-N-; Isothiocyanato

Rule 2: Neutral Ligands

Most neutral molecules that are ligands carry their normal name. The few exceptions are the first four on the chart: ammine, aqua, carbonyl, and nitrosyl.

Table **10.3.2**: Select Neutral Monodentate Ligands. Note: Ammine is spelled with two m's when referring to a ligand. Amines are a class of organic nitrogen-containing compounds.

Molecular Formula of Ligand	Ligand Name
NH_3	Ammine
H_2O	Aqua
CO	Carbonyl
NO	Nitrosyl
CH_3NH_2	Methylamine
C_5H_5N	Pyridine

Polydentate ligands follow the same rules for anions and neutral molecules.

Table **10.3.3**: Select Polydentate ligands

Short name	Extended name
en	Ethylenediamine
ox^{2-}	Oxalato
$EDTA^{4-}$	Ethylenediaminetetraacetato

Rule 3: Ligand Multiplicity

The number of ligands present in the complex is indicated with the prefixes di, tri, etc. The exceptions are polydentates that have a prefix already in their name (en and $EDTA^{4-}$ are the most common). When indicating how many of these are present in a coordination complex, put the ligand's name in parentheses and use *bis* (for two ligands), *tris* (for three ligands), and *tetrakis* (for four ligands).

Table **10.3.4**: Prefixes for indicating number of ligands in a complex.

Number of Ligands	Monodentate Ligands	Polydentate Ligands
1	mono	-
2	di	bis
3	tri	tris
4	tetra	tetrakis
5	penta	pentakis
6	hexa	hexakis

Prefixes always go before the ligand name; they are not taken into account when putting ligands in alphabetical order. Note that "mono" often is not used. For example, $[FeCl(CO)_2(NH_3)_3]^{2+}$ would be called triamminedicarbonylchloroiron(III) ion. Remember that ligands are always named first, before the metal is.

Example 10.3.1

What is the name of this complex ion: $[CrCl_2(H_2O)_4]^+$?

Solution

Let's start by identifying the ligands. The ligands here are Cl and H_2O. Therefore, we will use the monodentate ligand names of "chloro" and "aqua". Alphabetically, aqua comes before chloro, so this will be their order in the complex's name. There are 4

aqua's and 2 chloro's, so we will add the number prefixes before the names. Since both are monodentate ligands, we will say "tetra[aqua]di[chloro]".

Now that the ligands are named, we will name the metal itself. The metal is Cr, which is chromium. Therefore, this coordination complex is called tetraaquadichlorochromium(III) ion. See the next section for an explanation of the (III).

? Exercise 10.3.1

What is the name of this complex ion: $[CoCl_2(en)_2]^+$?

Answer

We take the same approach. There are two chloro and ethylenediamine ligands. The metal is Co, cobalt. We follow the same steps, except that *en* is a polydentate ligand with a prefix in its name (ethylene**di**amine), so "bis" is used instead of "di", and parentheses are added. Therefore, this coordination complex is called dichlorobis(ethylenediamine)cobalt(III) ion.

Rule 4: The Metals

When naming the metal center, you must know the formal metal name and the oxidation state. To show the oxidation state, we use Roman numerals inside parenthesis. For example, in the problems above, chromium and cobalt have the oxidation state of +3, so that is why they have (III) after them. Copper, with an oxidation state of +2, is denoted as copper(II). If the overall coordination complex is an anion, the ending "-ate" is attached to the metal center. Some metals also change to their Latin names in this situation. Copper +2 will change into cuprate(II). The following change to their Latin names when part of an anion complex:

Table **10.3.5**: Latin terms for Select Metal Ion

Transition Metal	Latin
Iron	Ferrate
Copper	Cuprate
Tin	Stannate
Silver	Argentate
Lead	Plumbate
Gold	Aurate

The rest of the metals simply have -ate added to the end (cobaltate, nickelate, zincate, osmate, cadmate, platinate, mercurate, etc. Note that the -ate tends to replace -um or -ium, if present).

Finally, when a complex has an overall charge, "ion" is written after it. This is not necessary if it is neutral or part of a coordination compound (Example **10.3.3**). Here are some examples with determining oxidation states, naming a metal in an anion complex, and naming coordination compounds.

✓ Example 10.3.2

What is the name of $[Cr(OH)_4]^-$?

Solution

Immediately we know that this complex is an anion. There is only one monodentate ligand, hydroxide. There are four of them, so we will use the name "tetrahydroxo". The metal is chromium, but since the complex is an anion, we will have to use the "-ate" ending, yielding "chromate". The oxidation state of the metal is 3 (x+(-1)4=-1). Write this with Roman numerals and parentheses (III) and place it after the metal to get tetrahydroxochromate(III) ion.

? Exercise 10.3.2

What is the name of $[CuCl_4]^{2-}$?

Answer

tetrachlorocuprate(II) ion

A last little side note: when naming a coordination compound, it is important that you name the cation first, then the anion. You base this on the charge of the ligand. Foe xample, for $NaCl$. The the positive Na cation comes first and the negative Cl^- anion follows.

✓ Example 10.3.3

What is the name of $[Pt(NH_3)_4][Pt(Cl)_4]$?

Solution

NH_3 is neutral, making the first complex positively charged overall. Cl has a -1 charge, making the second complex the anion. Therefore, you will write the complex with NH_3 first, followed by the one with Cl (the same order as the formula). This coordination compound is called tetraammineplatinum(II) tetrachloroplatinate(II).

✓ Exercise 10.3.3: The Nitro/Nitrito Ambidentate Ligand

What is the name of $[CoCl(NO_2)(NH_3)_4]^+$?

Answer

This coordination complex is called tetraamminechloronitrito-N-cobalt(III). N comes before the O in the symbol for the nitrite ligand, so it is called nitrito-N. If an O came first, as in $[CoCl(ONO)(NH_3)_4]^+$, the ligand would be called nitrito-O, yielding the name tetraamminechloronitrito-O-cobalt(III).

Nitro (for NO_2) and nitrito (for ONO) can also be used to describe the nitrite ligand, yielding the names tetraamminechloronitrocobalt(III) and tetraamminechloronitritocobalt(III).

Writing Formulas of Coordination Complexes

While chemistry typically follow the nomenclature rules for naming complexes and compounds, there is disagreement with the rules for constructing formulas of inorganic complexes. For example, the order of ligand names in their formula has been ambiguous with different conventions being used (charged vs neutral, number of each ligand, etc.). In 2005, IUPAC adopted the recommendation that all ligand names in formulas be listed **alphabetically** (in the same way as in the naming convention) irrespective of the charge or number of each ligand type.

However, this rule is not adhered to in many chemistry laboratories. For practice, the order of the ligands in chemical formulas does not matter as long as you write the transition metal first, which is the stance taken here.

✓ Examples 10.3.4

Write the chemical formulas for:

a. Amminetetraaquachromium(II) ion
b. Amminesulfatochromium(II)

Solution

a. Amminetetraaquachromium(II) ion could be written as $[Cr(H_2O)_4(NH_3)]^{+2}$ or $[Cr(NH_3)(H_2O)_4]^{+2}$.
b. Amminesulfatochromium (II) could be written as $[Cr(SO_4)(NH_3)]$ or $[Cr(NH_3)(SO_4)]$.

? Exercise 10.3.4

Write the chemical formulas for

a. Amminetetraaquachromium (II) sulfate
b. Potassium hexacyanoferrate (III)

Answer

a. Amminetetraaquachromium (II) sulfate can be written as $[Cr(H_2O)_4(NH_3)]SO_4$. Although $[Cr(NH_3)(H_2O)_4]SO_4$ is also acceptable.
b. Potassium hexacyanoferrate (III) is be written as $K_3[Fe(CN)_6]$

10.3: Nomenclature is shared under a not declared license and was authored, remixed, and/or curated by LibreTexts.

- **23.3: Nomenclature of Coordination Chemistry** by Justin Hosung Lee, Sophia Muller is licensed CC BY-NC-SA 4.0.

10.4: Isomerism

Learning Objectives

- Explain the differences of Structural and Geometric isomerization in a coordination complexes or complex ions.
- Define Ionization, Linkage, and Coordination Isomerization (structural isomer classes)
- Define cis/tran and mer/fac isomerization (geometric isomer classes)

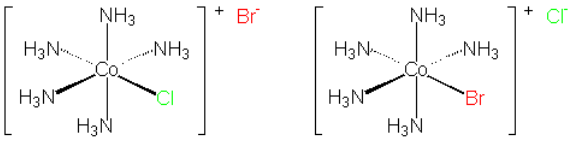
The existence of coordination compounds with the same formula but different arrangements of the ligands was crucial in the development of coordination chemistry. Two or more compounds with the same formula but different arrangements of the atoms are called **isomers**. Because isomers usually have different physical and chemical properties, it is important to know which isomer we are dealing with if more than one isomer is possible. As we will see, coordination compounds exhibit the same types of isomers as organic compounds, as well as several kinds of isomers that are unique. Isomers are compounds with the same molecular formula but different structural formulas and do not necessarily share similar properties. There are many different classes of isomers, like stereoisomers, enantiomers, and geometrical isomers. There are two main forms of isomerism: **structural isomerism** and **stereoisomerism** (spatial isomerism).

Class I: Structural Isomers

Isomers that contain the same number of atoms of each kind but differ in which atoms are bonded to one another are called structural isomers, which differ in structure or bond type. For inorganic complexes, there are three types of structural isomers: *ionization*, *coordination* and *linkage*. Structural isomers, as their name implies, differ in their structure or bonding, which are separate from stereoisomers that differ in the spatial arrangement of the ligands are attached, but still have the bonding properties. The different chemical formulas in structural isomers are caused either by a difference in what ligands are bonded to the central atoms or how the individual ligands are bonded to the central atoms. When determining a structural isomer, you look at (1) the ligands that are bonded to the central metal and (2) which atom of the ligands attach to the central metal.

Ionization Isomerism

Ionization isomers occur when a ligand that is bound to the metal center exchanges places with an anion or neutral molecule that was originally outside the coordination complex. The geometry of the central metal ion and the identity of other ligands are identical. For example, an octahedral isomer will have five ligands that are identical, but the sixth will differ. The non-matching ligand in one compound will be outside of the coordination sphere of the other compound. Because the anion or molecule outside the coordination sphere is different, the chemical properties of these isomers is different. A hydrate isomer is a specific kind of ionization isomer where a water molecule is one of the molecules that exchanges places.



[Co(NH3)5Cl]Br [Co(NH3)5Br]Cl

Figure 10.4.1: Ionization isomerism. The two isomers differ only in which ligands are bound to the center metal and which are counter ions in the second coordination sphere. (left) The chloride ion is bound to the cobalt as a chloro-ligand with the bromide ion as the counter ion. (right) In the other ionization isomer the bromide is acting as a bromo-ligand to the cobalt with the chloride acting as the counter ion. These two isomers are called pentaamminechlorocobalt(II) bromide (left) and pentaamminebromocobalt(II) chloride (right).

The difference between the ionization isomers can be view within the context of the ions generated when each are dissolved in solution. For example, when pentaamminebromocobalt(II) chloride is dissolved in water, $\mathbf{Cl^-}$ ions are generated:

$$\mathbf{CoBr(NH_3)_5Cl\ (s)\ \rightarrow CoBr(NH_3)_5^+\ (aq) + Cl^-\ (aq)} \tag{10.4.1}$$

whereas when pentaamminechlorocobalt(II) bromide is dissolved, $\mathbf{Br^-}$ ions are generated:

$$\mathbf{CoCl(NH_3)_5Br\ (s)\ \rightarrow CoCl(NH_3)_5^+\ (aq) + Br^-\ (aq)} \tag{10.4.2}$$

Notice that both anions are necessary to balance the charge of the complex, and that they differ in that one ion is directly attached to the central metal, but the other is not.

Solvate and Hydrate Isomerism: A special Type of Ionization Isomers

A very similar type of isomerism results from replacement of a coordinated group by a solvent molecule (*Solvate Isomerism*), which in the case of water is called *Hydrate Isomerism*. The best known example of this occurs for chromium chloride ($CrCl_3 \cdot 6H_2O$) which may contain 4, 5, or 6 coordinated water molecules (assuming a coordination number of 6). The dot here is used essentially as an expression of ignorance to indicate that, though the parts of the molecule separated by the dot are bonded to one another in some fashion, the exact structural details of that interaction are not fully expressed in the resulting formula. Alfred Werner's coordination theory indicates that several of the water molecules are actually bonded directly (via coordinate covalent bonds) to the central chromium ion. In fact, there are several possible compounds that use the brackets to signify bonding in the complex and the dots to signify "water molecules that are not bound to the central metal, but are part of the lattice:

- $[CrCl_2(H_2O)_4]Cl \cdot 2H_2O$: bright-green colored
- $[CrCl(H_2O)_5]Cl_2 \cdot H_2O$: grey-green colored
- $[Cr(H_2O)_6]Cl_3$: violet colored

These isomers have very different chemical properties and on reaction with $AgNO_3$ to test for Cl^- ions, would find 1, 2, and 3 Cl^- ions in solution, respectively.

Upon crystallization from water, many compounds incorporate water molecules in their crystalline frameworks. These "waters of crystallization" refers to water that is found in the crystalline framework of a metal complex or a salt, which is **not directly bonded** to the metal cation. In the first two hydrate isomers, there are water molecules that are artifacts of the crystallization and occur inside crystals. These waters of crystallization contribute to the total weight of water in a substance and are mostly present in a definite (stoichiometric) ratio.

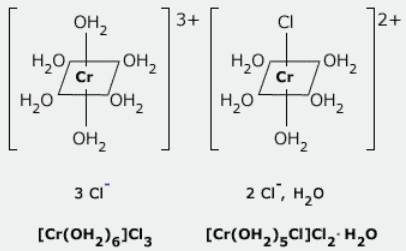


Figure 10.4.2: Hydrate iosomerisim. The $[Cr(H_2O)_6]Cl_3$ hydrate isomer (left) is violet colored and the $[CrCl(H_2O)_5]Cl_2 \cdot H_2O$ hydrate isomer is green-grey colored.

What are "Waters of Crystallization"?

A compound with associated water of crystallization is known as a hydrate. The structure of hydrates can be quite elaborate, because of the existence of hydrogen bonds that define polymeric structures. For example, consider the aquo complex $NiCl_2 \cdot 6H_2O$ that consists of separated *trans*-$[NiCl_2(H_2O)_4]$ molecules linked more weakly to adjacent water molecules. Only four of the six water molecules in the formula are bound to the nickel (II) cation, and the remaining two are waters of crystallization as the crystal structure resolves (Figure 10.4.3).

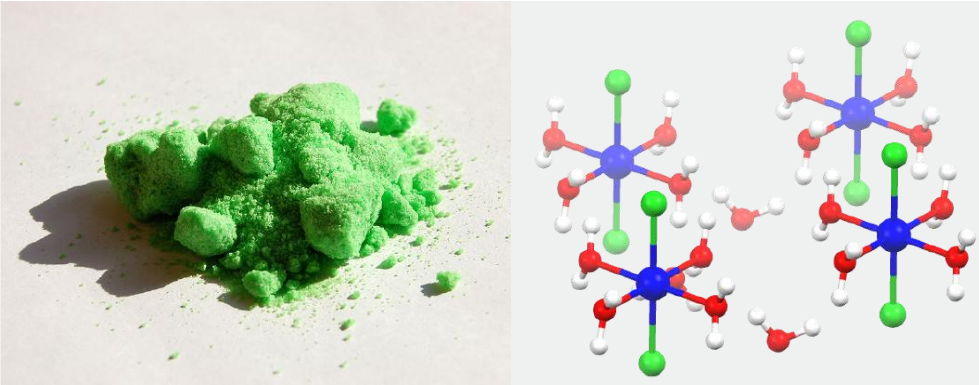


Figure 10.4.3: Water of hydration. (left) Image of $NiCl_2 \cdot 6H_2O$ salt (Public Domain; Benjah-bmm27 via Wikipedia). (right) Crystal Structure of $NiCl_2 \cdot 6H_2O$ with chlorine atoms (green), water molecules (red), and Ni metals (blue) indicated. Note that only four of the waters are bound as ligands to the nickel ions and two are outside of the coordination sphere. (CC BY-SA 4.0; Smokefoot).

Water is particularly common solvent to be found in crystals because it is small and polar. But *all* solvents can be found in some host crystals. Water is noteworthy because it is reactive, whereas other solvents such as benzene are considered to be chemically innocuous.

Coordination Isomerism

Coordination isomerism occurs in compounds containing complex anionic and complex cationic parts and can be viewed as an interchange of some ligands from the cation to the anion. Hence, there are two complex compounds bound together, one with a negative charge and the other with a positive charge. In coordination isomers, the anion and cation complexes of a coordination compound exchange one or more ligands. For example, the $[Zn(NH_3)_4]\,[Cu(Cl_4)]$ and $[Cu(NH_3)_4]\,[Zn(Cl_4)]$ compounds are coordination isomers (Figure 10.4.4).

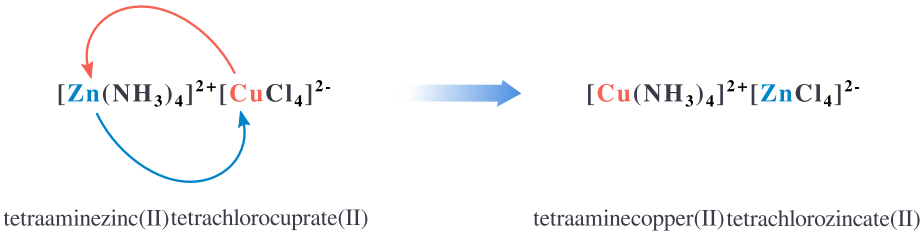


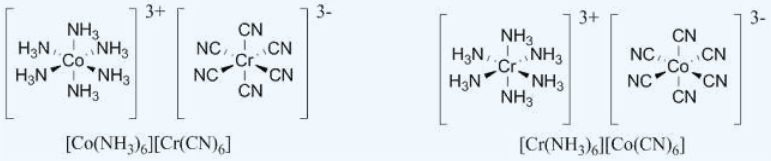
Figure 10.4.4: Coordination Isomerism. (CC BY-NC; Ümit Kaya)

Example 10.4.2: Coordination Isomers

What is the coordination isomer for the $[Co(NH_3)_6]\,[Cr(CN)_6]$ compound?

Solution

Coordination isomerism involves switching the metals between the cation and anion spheres.



Hence the $[Cr(NH_3)_6][Co(CN)_6]$ compound is a coordination isomer of $[Co(NH_3)_6]\,[Cr(CN)_6]$.

Linkage Isomerism

Linkage isomerism occurs with *ambidentate* ligands that are capable of coordinating in more than one way. The best known cases involve the monodentate ligands: SCN^- / NCS^- and NO_2^- / ONO^-. The only difference is what **atoms the molecular ligands bind to the central ion**. The ligand(s) must have more than one donor atom, but bind to ion in only one place. For example, the (NO_2^-) ion is a ligand that can bind to the central atom through the nitrogen or the oxygen atom, but cannot bind to the central atom with both oxygen and nitrogen at once, in which case it would be called a **polydentate ligand** rather than an **ambidentate ligand**.

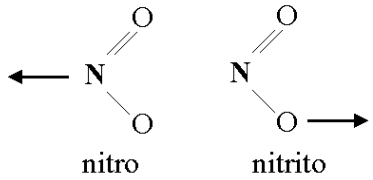


Figure **10.4.5**: Linkage Isomerism in the NO_2 ligand. This occurs when a particular ligand is capable of coordinating to a metal in two different and distinct ways. from Angel C. de Dios.

As with all structural isomers, the formula of the complex is unchanged for each isomer, but the properties may differ. The names used to specify the changed ligands are changed as well. For example, the NO_2^- ion is called *nitro* when it binds with the **N** atom and is called *nitrito* when it binds with the **O** atom.

Example 10.4.3: Linkage Isomerization

The cationic cobalt complex $[Co(NH_3)_5(NO_2)]Cl_2$ exists in two separable linkage isomers of the complex ion: $(NH_3)_5(NO_2)]^{2+}$.

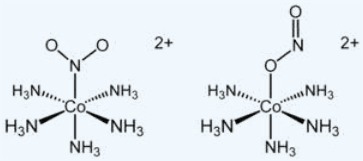


Figure **10.4.6**: Linkage Isomerization. (left) The nitro isomer (Co-NO2) and (right) the nitrito isomer (Co-ONO)

When donation is from nitrogen to a metal center, the complex is known as a *nitro-* complex and when donation is from one oxygen to a metal center, the complex is known as a *nitrito-* complex. An alternative formula structure to emphasize the different coordinate covalent bond for the two isomers

- $[Co(ONO)(NH_3)_5]Cl$: the *nitrito* isomer -O attached
- $[Co(NO_2)(NH_3)_5]Cl$: the *nitro* isomer - N attached.

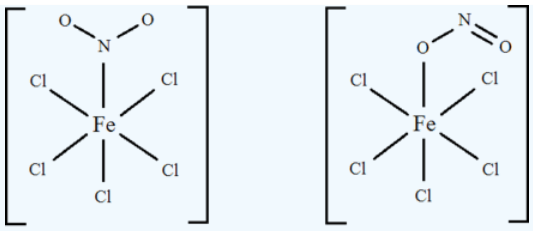
Another example of an ambidentate ligand is thiocyanate, SCN^-, which can attach to the transition metal at either the sulfur atom or the nitrogen atom. Such compounds give rise to linkage isomerism. Other ligands that give rise to linkage isomers include selenocyanate, $SeCN^-$ – isoselenocyanate, $NCSe^-$ and sulfite, SO_3^{2-}.

Exercise 10.4.3

Are $[FeCl_5(NO_2)]^{3-}$ and $[FeCl_5(ONO)]^{3-}$ complex ions linkage isomers of each other?

Answer

Here, the difference is in how the ligand bonds to the metal. In the first isomer, the ligand bonds to the metal through an electron pair on the nitrogen. In the second isomer, the ligand bonds to the metal through an electron pair on one of the oxygen atoms. It's easier to see it:



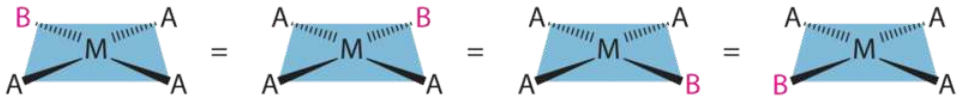
Class 2: Geometric Isomers

The existence of coordination compounds with the same formula but different arrangements of the ligands was crucial in the development of coordination chemistry. Two or more compounds with the same formula but different arrangements of the atoms are called **isomers**. Because isomers usually have different physical and chemical properties, it is important to know which isomer we are dealing with if more than one isomer is possible. Recall that in many cases more than one structure is possible for organic compounds with the same molecular formula; examples discussed previously include n-butane versus isobutane and cis-2-butene versus trans-2-butene. As we will see, coordination compounds exhibit the same types of isomers as organic compounds, as well as several kinds of isomers that are unique.

Planar Isomers

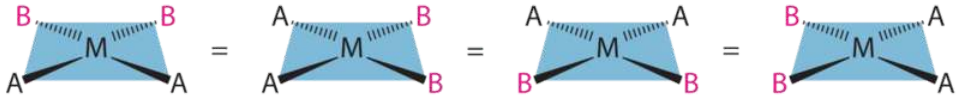
Metal complexes that differ only in which ligands are adjacent to one another (**cis**) or directly across from one another (**trans**) in the coordination sphere of the metal are called geometrical isomers. They are most important for square planar and octahedral complexes.

Because all vertices of a square are equivalent, it does not matter which vertex is occupied by the ligand B in a square planar MA_3B complex; hence only a single geometrical isomer is possible in this case (and in the analogous MAB_3 case). All four structures shown here are chemically identical because they can be superimposed simply by rotating the complex in space:

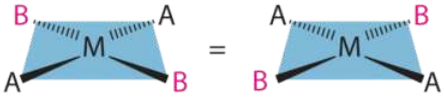


MA_3B square planar complex

For an MA_2B_2 complex, there are two possible isomers: either the A ligands can be adjacent to one another (cis), in which case the B ligands must also be cis, or the A ligands can be across from one another (trans), in which case the B ligands must also be trans. Even though it is possible to draw the cis isomer in four different ways and the trans isomer in two different ways, all members of each set are chemically equivalent:

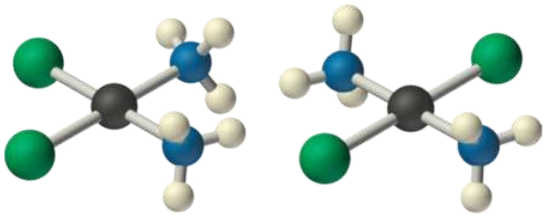


MA_2B_2 square planar complex, *cis* isomer



MA_2B_2 square planar complex, *trans* isomer

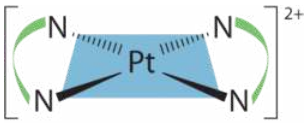
Because there is no way to convert the cis structure to the trans by rotating or flipping the molecule in space, they are fundamentally different arrangements of atoms in space. Probably the best-known examples of cis and trans isomers of an MA_2B_2 square planar complex are cis-$Pt(NH_3)_2Cl_2$, also known as cisplatin, and trans-$Pt(NH_3)_2Cl_2$, which is actually toxic rather than therapeutic.



cis-$Pt(NH_3)_2Cl_2$ *trans*-$Pt(NH_3)_2Cl_2$

The anticancer drug cisplatin and its inactive trans isomer. Cisplatin is especially effective against tumors of the reproductive organs, which primarily affect individuals in their 20s and were notoriously difficult to cure. For example, after being diagnosed with metastasized testicular cancer in 1991 and given only a 50% chance of survival, Lance Armstrong was cured by treatment with cisplatin.

Square planar complexes that contain symmetrical bidentate ligands, such as $[Pt(en)_2]^{2+}$, have only one possible structure, in which curved lines linking the two N atoms indicate the ethylenediamine ligands:



$[Pt(en)_2]^{2+}$

? Exercise 10.4.4

Draw the cis and trans isomers of the following compounds:

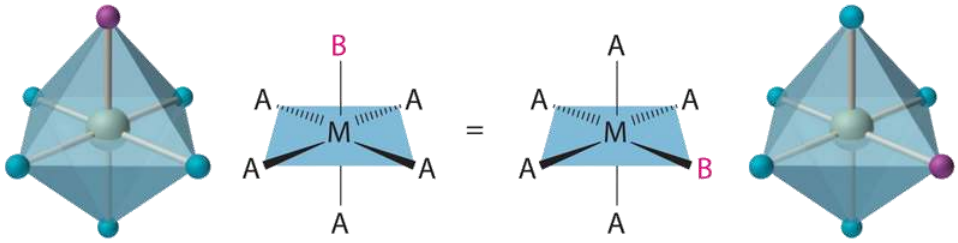
a. $(NH_3)_2IrCl(CO)$
b. $(H_3P)_2PtHBr$
c. $(AsH_3)_2PtH(CO)$

? Exercise 10.4.5

Only one isomer of $(tmeda)PtCl_2$ is possible [tmeda = $(CH_3)_2NCH_2CH_2N(CH_3)_2$; both nitrogens connect to the platinum]. Draw this isomer and explain why the other isomer is not possible.

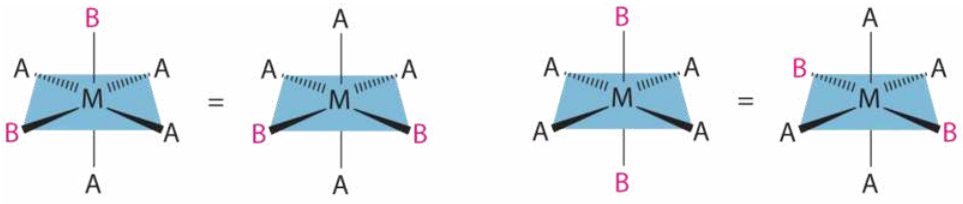
Octahedral Isomers

Octahedral complexes also exhibit cis and trans isomers. Like square planar complexes, only one structure is possible for octahedral complexes in which only one ligand is different from the other five (MA_5B). Even though we usually draw an octahedron in a way that suggests that the four "in-plane" ligands are different from the two "axial" ligands, in fact all six vertices of an octahedron are equivalent. Consequently, no matter how we draw an MA_5B structure, it can be superimposed on any other representation simply by rotating the molecule in space. Two of the many possible orientations of an MA_5B structure are as follows:



MA_5B octahedral complex

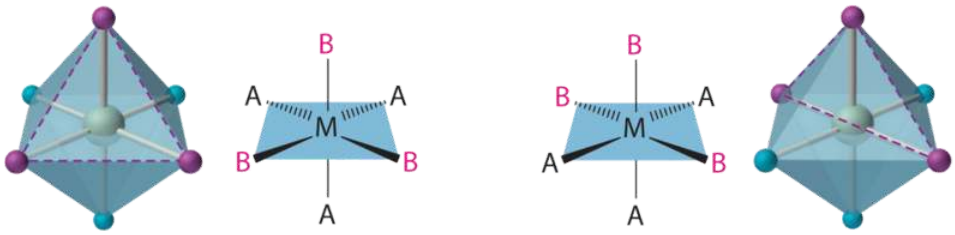
If two ligands in an octahedral complex are different from the other four, giving an MA_4B_2 complex, two isomers are possible. The two B ligands can be cis or trans. Cis- and trans-$[Co(NH_3)_4Cl_2]Cl$ are examples of this type of system:



MA_4B_2 octahedral complex, *cis* isomer

MA_4B_2 octahedral complex, *trans* isomer

Replacing another A ligand by B gives an MA_3B_3 complex for which there are also two possible isomers. In one, the three ligands of each kind occupy opposite triangular faces of the octahedron; this is called the fac isomer (for facial). In the other, the three ligands of each kind lie on what would be the meridian if the complex were viewed as a sphere; this is called the mer isomer (for meridional):



MA_3B_3 octahedral complex, *fac* isomer

MA_3B_3 octahedral complex, *mer* isomer

Example 10.4.4

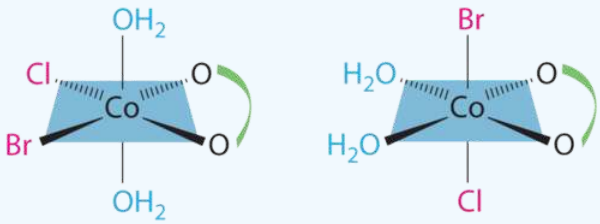
Draw all the possible geometrical isomers for the complex $[Co(H_2O)_2(ox)BrCl]^-$, where ox is $^-O_2CCO_2^-$, which stands for oxalate.

Solution

Given: formula of complex

Asked for: structures of geometrical isomers

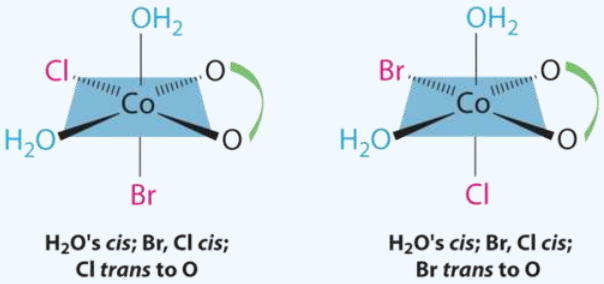
This complex contains one bidentate ligand (oxalate), which can occupy only adjacent (cis) positions, and four monodentate ligands, two of which are identical (H_2O). The easiest way to attack the problem is to go through the various combinations of ligands systematically to determine which ligands can be trans. Thus either the water ligands can be trans to one another or the two halide ligands can be trans to one another, giving the two geometrical isomers shown here:



H_2O's *trans*

Br, Cl *trans*

In addition, two structures are possible in which one of the halides is trans to a water ligand. In the first, the chloride ligand is in the same plane as the oxalate ligand and trans to one of the oxalate oxygens. Exchanging the chloride and bromide ligands gives the other, in which the bromide ligand is in the same plane as the oxalate ligand and trans to one of the oxalate oxygens:

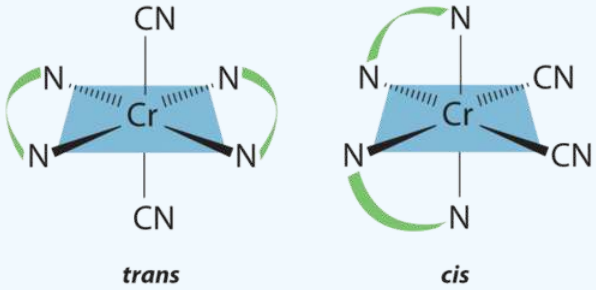


This complex can therefore exist as four different geometrical isomers.

? Exercise 10.4.6

Draw all the possible geometrical isomers for the complex $[Cr(en)_2(CN)_2]^+$.

Answer



Two geometrical isomers are possible: *trans* and *cis*.

Summary

The existence of coordination compounds with the same formula but different arrangements of the ligands was crucial in the development of coordination chemistry. Two or more compounds with the same formula but different arrangements of the atoms are called **isomers**. Many metal complexes form isomers, which are two or more compounds with the same formula but different arrangements of atoms. Structural isomers differ in which atoms are bonded to one another, while geometrical isomers differ only in the arrangement of ligands around the metal ion. Ligands adjacent to one another are cis, while ligands across from one another are trans.

Table **10.4.1** emphasizes the key differences of the three classes of structural isomers discussed below. The highlighted ions are the ions that switch or change somehow to make the type of structural isomer it is.

Table **10.4.1**: Overview of Structural Isomer Classes

Structural Isomer	Examples
Ionization	$[CoBr(H_2O)_5]^+Cl^-$ and $[CoCl(H_2O)_5]^+Br^-$
Coordination	$[Zn(NH_3)_4]^+[CuCl_4]^{2-}$ and $[Cu(NH_3)_4]^+[ZnCl_4]^{2-}$
Linkage	$[Co(NO_2)_6]^{3-}$ and $[Co(ONO)_6]^{3-}$

References

1. Petrucci, Harwood, Herring, and Madura. General Chemistry: Principles and Modern Applications: Ninth Edition. New Jersey: Pearson, 2007.
2. Atkins, Peter, and Loretta Jones. Chemical Principles: The Quest for Insight: Fourth Edition. W. H. Freeman and Company, 2008. Print.

Contributors and Attributions

- Prof. Robert J. Lancashire (The Department of Chemistry, University of the West Indies)
- Chris P Schaller, Ph.D., (College of Saint Benedict / Saint John's University)

10.4: Isomerism is shared under a not declared license and was authored, remixed, and/or curated by LibreTexts.

- **24.4: Isomerism in Coordination Complexes** is licensed CC BY-NC-SA 4.0.

10.5: Optical Isomerism in Metal Complexes

Optical isomers are stereoisomers that are related via non-superimposable mirror images of each other. They differ from geometric stereoisomers in that they rotate the polarization of plane-polarized light. These isomers are referred to as *enantiomers* or *chiral*.

Introduction

Optical activity refers to whether or not a compound has optical isomers. A coordinate compound that is optically active **has** optical isomers and a coordinate compound that is not optically active does **not have** optical isomers. As we will discuss later, optical isomers have the unique property of rotating light. When light is shot through a polarimeter, optical isomers can rotate the light so it comes out in with a different polarization on the other end. Armed with the knowledge of symmetry and mirror images, optical isomers should not be very difficult. There are two ways optical isomers can be determined: using mirror images or using planes of symmetry.

Optical isomers do not exhibit symmetry and do not have identical mirror images. Let's go through a quick review of symmetry and mirror images. A *mirror image* of an object is that object flipped or the way the object would look in front of a mirror. For example, the mirror image of your left hand would be your right hand. Symmetry on the other hand refers to when an object looks exactly the same when sliced in a certain direction with a plane. For example imagine the shape of a square. No matter in what direction it is sliced, the two resulting images will be the same.

What is a Polarimeter?

A polarimeter is a scientific instrument used to measure the angle of rotation caused by passing polarized light through an optically active substance. Some chemical substances are optically active, and polarized (uni-directional) light will rotate either to the left (counter-clockwise) or right (clockwise) when passed through these substances. The amount by which the light is rotated is known as the **angle of rotation**. The polarimeter is made up of a polarizer (#3 on Figure **10.5.1**) and an analyzer (#7 on Figure **10.5.1**). The polarizer allows only those light waves which move in a single plane. This causes the light to become plane polarized. When the analyzer is also placed in a similar position it allows the light waves coming from the polarizer to pass through it. When it is rotated through the right angle no waves can pass through the right angle and the field appears to be dark. If now a glass tube containing an optically active solution is placed between the polarizer and analyzer the light now rotates through the plane of polarization through a certain angle, the analyzer will have to be rotated in same angle.

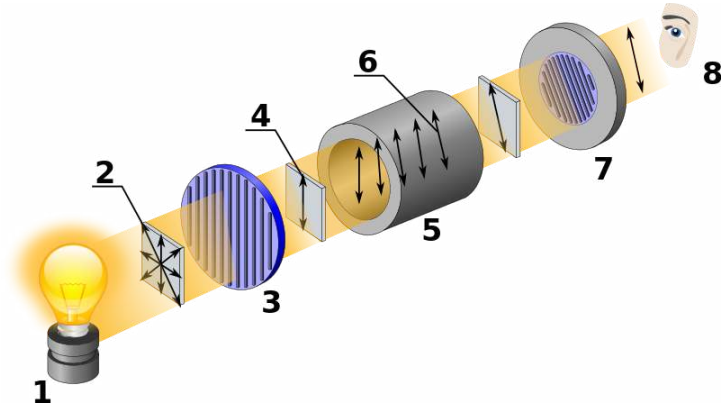


Figure **10.5.1**: Schematic of a polarimeter showing the principles behind it's operation.The plane of polarization of plane polarised light (4) rotates (6) as it passes through an optically active sample (5). This angle is determined with a rotatable polarizing filter (7). (CC BY-SA 3.0; Kaidor via Wikipedia)

Chemists use polarimeters to investigate the influence of compounds (in the sample cell) on plane polarized light. Samples composed only of achiral molecules (e.g. water or hexane), have no effect on the polarized light beam. However, if a single enantiomer is examined (all sample molecules being right-handed, or all being left-handed), the plane of polarization is rotated in either a clockwise (positive) or counter-clockwise (negative) direction, and the analyzer must be turned an appropriate matching angle, **α**, if full light intensity is to reach the detector. In the above illustration, the sample has rotated the polarization plane clockwise by +90º, and the analyzer has been turned this amount to permit maximum light transmission.

The observed rotations (α) of enantiomers are opposite in direction. One enantiomer will rotate polarized light in a clockwise direction, termed **dextrorotatory** or (+), and its mirror-image partner in a counter-clockwise manner, termed **levorotatory** or (–). The prefixes dextro and levo come from the Latin *dexter*, meaning right, and *laevus*, for left, and are abbreviated *d* and *l* respectively. A 50:50 mixture of enantiomers has no observable optical activity. Such mixtures are called **racemates** or **racemic modifications**.

The "Mirror Image Method" to Determine Optical Isomers

Optical isomers do not exhibit symmetry and do not have identical mirror images. Let's go through a quick review of symmetry and mirror images. A *mirror image* of an object is that object flipped or the way the object would look in front of a mirror. For example, the mirror image of your left hand would be your right hand. Symmetry on the other hand refers to when an object looks exactly the same when sliced in a certain direction with a plane. For example imagine the shape of a square. No matter in what direction it is sliced, the two resulting images will be the same.

The **mirror image method** uses a mirror image of the molecule to determine whether optical isomers exist or not. If the mirror image **can** be rotated in such a way that it looks identical to the original molecule, then the molecule is said to be superimposable and has no optical isomers. On the other hand, if the mirror image **cannot** be rotated in any way such that it looks identical to the original molecule, then the molecule is said to be non-superimposable and the molecule has optical isomers. Once again, if the mirror image is superimposable, then no optical isomers, but if the mirror image is non-superimposable, then optical isomers exist.

Non-superimposable means the structure cannot be rotated in a way that one can be put on top of another. This means that no matter how the structure is rotated, it cannot be put on top of another with all points matching. An example of this is your hands. Both left and right hands are identical, but they cannot be put on top of each other with all points matching.

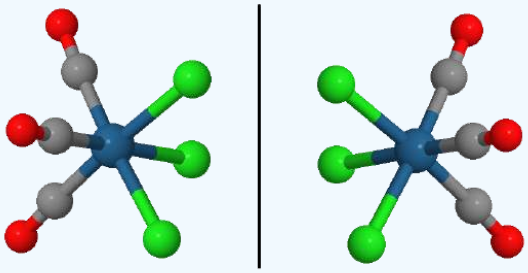
> *Non-superimposable means the structure cannot be rotated in a way that one can be put on top of another.*

Example 10.5.1: The $[OsCl_3(CO)_3]^-$ Ion

Are there enantiomers for the $\boldsymbol{fac}-[OsCl_3(CO)_3]^-$ complex ion?

Solution

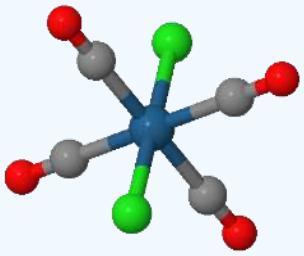
To use mirror image method, we draw the 3D structure for this geometric isomer (not the mer isomer) and then take a mirror image like below.



The left image can be rotated by 180° through a vertical axis to superimpose on the orginal. So the mer-$[OsCl_3(CO)_3]^-$ complex ion is not optically active or we can call it achiral.

Exercise 10.5.1

Use the mirror image method to determine if there are enantiomers for the $\mathbf{mer}-[OsCl_3(CO)_3]^-$ complex ion.



Example 10.5.2

Consider the octahedral complex with six monodentate ligands $\mathbf{MA_2B_2C_2}$ have both cis and trans isomers. However, the cis isomer will also have two optical isomers (Figure **10.5.2**). No matter how one rotates one of the mirror images, they are are **not** superimposable.

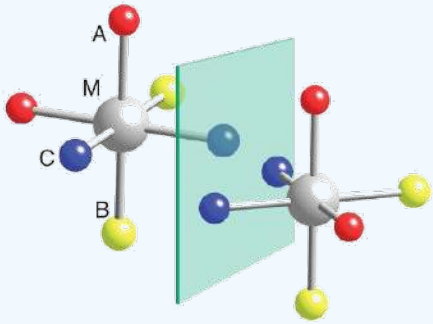


Figure **10.5.2**: Two $\mathbf{MA_2B_2C_2}$ enantiomers. (CC BY-SA-NC 4.0; ChemTube3D via Nick Greeves)

Exercise 10.5.1: $\mathbf{MA_2B_2C_2}$

Confirm to yourself that if two like ligands in $\mathbf{MA_2B_2C_2}$ are *trans* to each other, then the complex will not have an optical isomer.

Answer

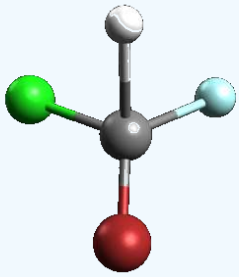
If two like ligands are *trans* then there will be a mirror plane of symmetry normal to the line connecting the ligands that are *trans* to each other. The presence of the mirror plane means this complex will not have an optical isomer.

The "Plane of Symmetry Method" to Determine Optical Isomers

The plane of symmetry method uses symmetry also to identify optical isomers. In this method, one tries to see if such a plane exists which when cut through the coordinate compound produces two exact images. In other words, one looks for the existence of a plane of symmetry within the coordinate compound. If a plane of symmetry exists, then no optical isomers exist for that complex and it is called **achiral**.

Example 10.5.3: A Tetrahedral Complex

Consider the tetrahedral molecule, CHBrClF. Is this molecule optically active?

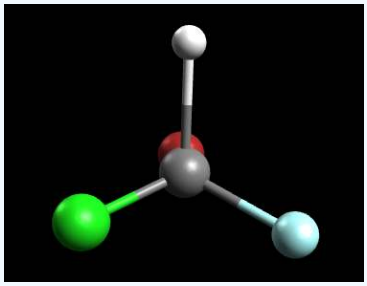


The CHBrClF molecule (note the color scheme: grey=carbon, white=hydrogen, green=chlorine, blue=fluorine, red=bromine)

Solution

- *Mirror-image method*

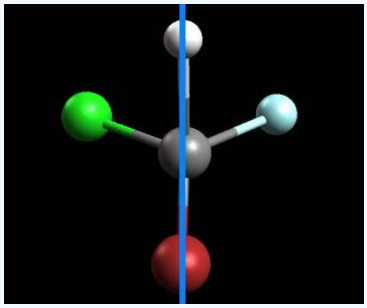
First take the Mirror-image method. The mirror image of the molecule is:



Note that this mirror image is not superimposable. In other words, the mirror image above cannot be rotated in any such way that it looks identical to the original molecule. Remember, if the mirror image is not superimposable, then optical isomers exist. Thus we know that this molecule has optical isomers.

- *Plane of Symmetry Method*

Let's try approaching this problem using the symmetry method. If we take the original molecule and draw an axis or plane of symmetry down the middle, this is what we get:



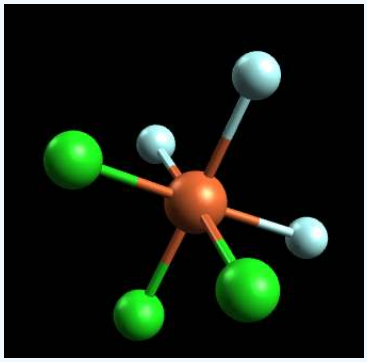
Since the left side is not identical to the right, this molecule does not have a symmetrical center and thus can be called chiral.Additionally, because it does not have a symmetrical center, we can conclude that this molecule has optical isomers. In general, when dealing with a tetrahedral molecule that has 4 different ligands, optical isomers will exist most of the time.

No matter which method you use, the answer will end up being the same.

Optical isomers have no plane of symmetry. For tetrahedral complexes, this is fairly easy to recognize the possibility of this by looking for a center atom with **four** different things attached to it. Unfortunately, this is not quite so easy with more complicated geometries!

Example 10.5.4: An Octahedral Complex

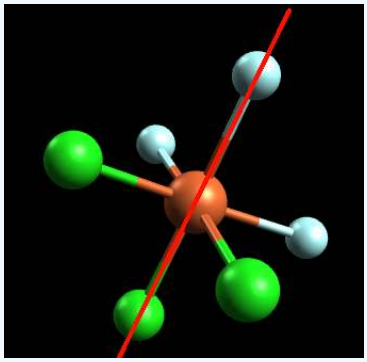
Is the octahedral compound $FeCl_3F_3$ optically active?



(note the color scheme: orange=iron, blue=fluorine, green=chlorine):

Solution

If we try to attempt this problem using the mirror image method, we notice that the mirror image is essentially identical to the original molecule. In other words, the mirror image can be placed on top of the original molecule and is thus superimposable. Since the mirror image is superimposable, this molecule does not have any optical isomers. Let's attempt this same problem using the symmetry method. If we draw an axis or plane of symmetry, this is what we get:



Since the left side is identical to the right side, this molecule has a symmetrical center and is an achiral molecule. Thus, it has no optical isomers.

Enantiomers in Octahedral Complexes with Bidentate Ligands

The examples you are most likely to need occur in octahedral complexes that contain bidentate ligands, e.g., complex ions like $[Ni(NH_2CH_2CH_2NH_2)_3]^{2+}$ or $[Cr(C_2O_4)_3]^{3-}$. In bidentate complexes or chelating complexes, a ligand binds very tightly to the metal because it holds onto the metal via more than one atom. Ethylenediamine is one example of a bidentate ligand.

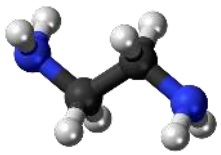
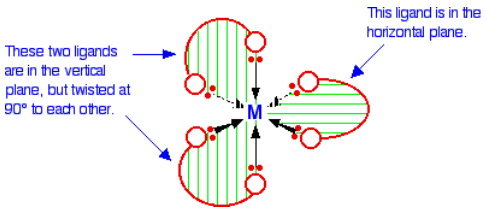


Figure 10.5.3: Ethylenediamine (sometimes abbreviated en) is an example of a bidentate ligand

As you may expect, bidentate ligands bind tightly to metals because they form two bonds with it, rather than just one. It is also important to recognize that in an octahedral complex, the two donor atoms in most bidentate ligand bind *cis* to each other and **cannot** reach all the way around the molecule to bind *trans* to each other (see below). The diagram below shows a simplified view of one of the complex ions with three oxalato ligands (also a bidentate ligand), however, they all have the same shape - all that differs is the nature of the "headphones".



A substance with *no plane of symmetry is going to have optical isomers* - one of which is the mirror image of the other. One of the isomers will rotate the plane of polarization of plane polarized light clockwise; the other rotates it counter-clockwise. In this case, the two isomers are:

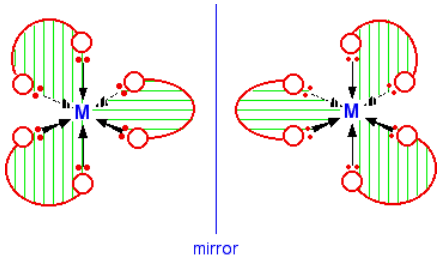
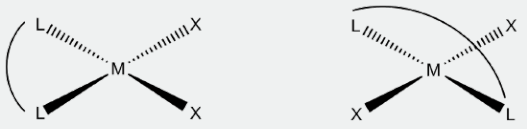


Figure **10.5.4**: A left-handed propeller shape (left) is seen in one optical isomers of the $M(ox)_3^{+}$ octahedral complex. The other optical isomer is a right-handed propeller (right). These shapes are alternatively described as a left-handed screw and a right handed screw. If you can picture turning the shape so that it screws into the page behind it, which direction would you turn the screwdriver? If you would twist the screwdriver clockwise, then you have a right handed screw. If you would twist the screwdriver counter-clockwise, then you have a left handed screw.

Most, but not all, Bidentate Ligands Bind to Metals in the cis Orientation

A wide variety of bidentate ligands bind to metals in the cis fashion, but few can bind in the trans geometry. These are called trans-spanning ligands and required building a bridge between the bonding atoms (e.g. methylene brindges $-CH_2CH_2CH_2CH_2-$).



Trans vs cis ligands in square planar complexes. (CC BY-SA 3.0; via Wikipedia)

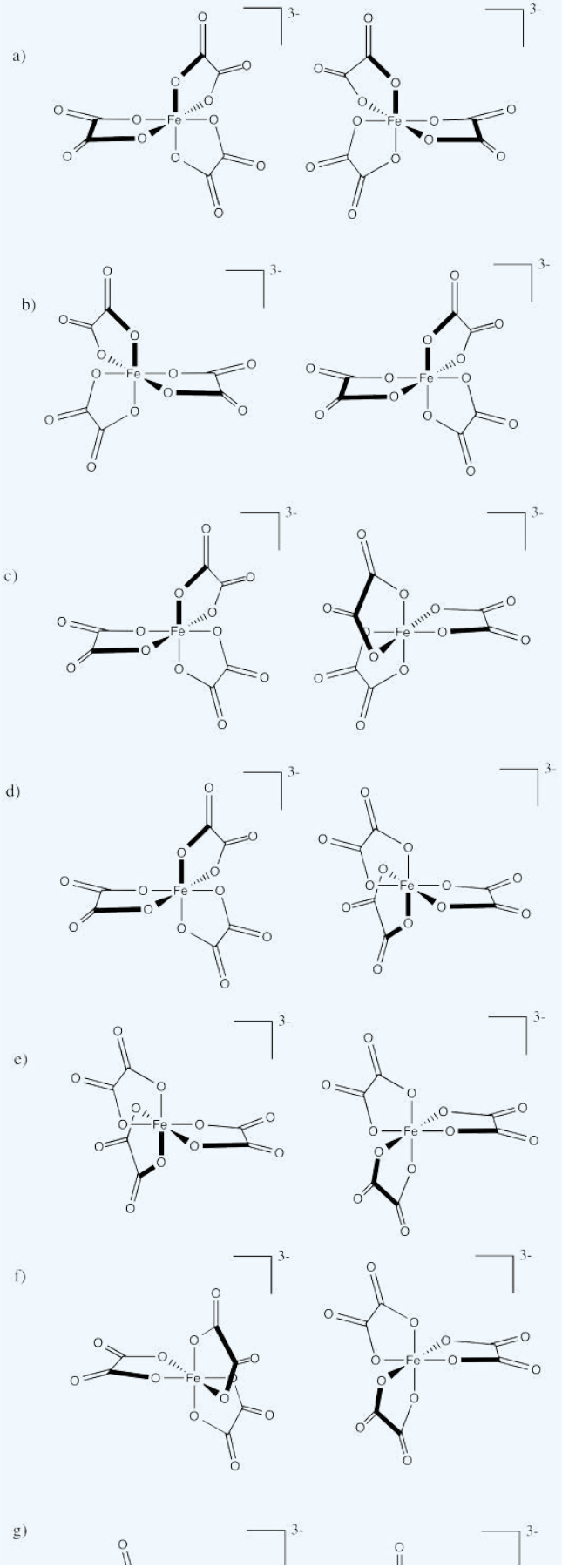
We will not consider any trans-spanning ligands in this text.

A complex containing three bidentate ligands can take on the shape of a left-handed propeller or a right-handed propeller. You may be able to see that there is no way of rotating the second isomer in space so that it looks exactly the same as the first one. As long as you draw the isomers carefully, with the second one a true reflection of the first, the two structures will be different.

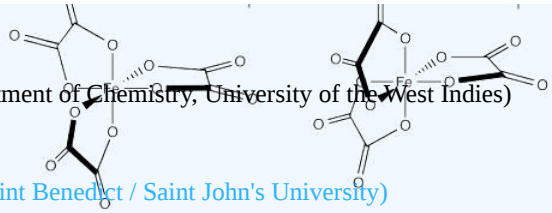
These kinds of complexes were historically important in demonstrating how small molecules and ions bound to metal cations. By showing that some metal complexes were chiral and displayed optical activity, early 20th century workers such as Alfred Werner were able to rule out some competing ideas about the structures of metal compounds. Today, we know that metal complexes play important roles in enzymes in biology, and Werner's work on metal complexes laid the groundwork for how we think about these complexes. In addition, stereochemistry in metal complexes became very important in the late 20th century, especially as pharmaceutical companies looked for catalysts that could aid in the production of one enantiomer of a drug, and not the other, in order to maximize pharmaceutical effectiveness and minimize side effects.

Exercise 10.5.1

Identify the relationships (types of isomers) between the following pairs of iron(III) oxalate ions.


a)
b)
c)
d)
e)
f)
g)
3-

Contributors and Attributions



- Prof. Robert J. Lancashire (The Department of Chemistry, University of the West Indies)
- Jim Clark (Chemguide.co.uk)
- Chris P Schaller, Ph.D., (College of Saint Benedict / Saint John's University)

10.5: Optical Isomerism in Metal Complexes is shared under a not declared license and was authored, remixed, and/or curated by LibreTexts.

10.6: Stability Aspects of Complex-Ion Equilibria

Learning Objectives

- To be introduced to complex ions, including ligands.

Previously, you learned that metal ions in aqueous solution are hydrated—that is, surrounded by a shell of usually four or six water molecules. A hydrated ion is one kind of a complex ion (or, simply, complex), a species formed between a central metal ion and one or more surrounding ligands, molecules or ions that contain at least one lone pair of electrons, such as the $[Al(H_2O)_6]^{3+}$ ion.

A complex ion forms from a metal ion and a ligand because of a Lewis acid–base interaction. The positively charged metal ion acts as a Lewis acid, and the ligand, with one or more lone pairs of electrons, acts as a Lewis base. Small, highly charged metal ions, such as Cu^{2+} or Ru^{3+}, have the greatest tendency to act as Lewis acids, and consequently, they have the greatest tendency to form complex ions.



Figure **10.6.1**: The Formation of Complex Ions. An aqueous solution of $CuSO_4$ consists of hydrated Cu^{2+} ions in the form of pale blue $[Cu(H_2O)_6]^{2+}$ (left). The addition of aqueous ammonia to the solution results in the formation of the intensely blue-violet $[Cu(NH_3)_4(H_2O)_2]^{2+}$ ions, usually written as $[Cu(NH_3)_4]^{2+}$ ion (right) because ammonia, a stronger base than H_2O, replaces water molecules from the hydrated Cu^{2+} ion. For a more complete description, see https://www.youtube.com/watch?v=IQNcLH6OZK0.

As an example of the formation of complex ions, consider the addition of ammonia to an aqueous solution of the hydrated Cu^{2+} ion $\{[Cu(H_2O)_6]^{2+}\}$. Because it is a stronger base than H_2O, ammonia replaces the water molecules in the hydrated ion to form the $[Cu(NH_3)_4(H_2O)_2]^{2+}$ ion. Formation of the $[Cu(NH_3)_4(H_2O)_2]^{2+}$ complex is accompanied by a dramatic color change, as shown in Figure **10.6.1**. The solution changes from the light blue of $[Cu(H_2O)_6]^{2+}$ to the blue-violet characteristic of the $[Cu(NH_3)_4(H_2O)_2]^{2+}$ ion.

The Formation Constant

The replacement of water molecules from $[Cu(H_2O)_6]^{2+}$ by ammonia occurs in sequential steps. Omitting the water molecules bound to Cu^{2+} for simplicity, we can write the equilibrium reactions as follows:

$$Cu^{2+}(aq) + NH_3(aq) \rightleftharpoons [Cu(NH_3)]^{2+}(aq) \quad \text{(step 1)}$$

with

$$K_1 = \frac{[Cu(NH_3)]^{2+}(aq)}{[Cu^{2+}(aq)][NH_3(aq)]}$$

$$[Cu(NH_3)]^{2+}(aq) + NH_3(aq) \rightleftharpoons [Cu(NH_3)_2]^{2+}(aq) \quad \text{(step 2)}$$

with

$$K_2 = \frac{[Cu(NH_3)_2]^{2+}(aq)}{[[Cu(NH_3)]^{2+}(aq)][NH_3(aq)]}$$

$$[Cu(NH_3)_2]^{2+}(aq) + NH_3(aq) \rightleftharpoons [Cu(NH_3)_3]^{2+}(aq) \quad \text{(step 3)}$$

with

$$K_3 = \frac{[Cu(NH_3)_3]^{2+}(aq)}{[[Cu(NH_3)_2]^{2+}(aq)][NH_3(aq)]}$$

$$[Cu(NH_3)_3]^{2+}(aq) + NH_3(aq) \rightleftharpoons [Cu(NH_3)_4]^{2+}(aq) \quad \text{(step 4)}$$

with

$$K_4 = \frac{[Cu(NH_3)_4]^{2+}(aq)}{[[Cu(NH_3)_3]^{2+}(aq)][NH_3(aq)]}$$

The sum of the stepwise reactions is the overall equation for the formation of the complex ion: The hydrated Cu^{2+} ion contains six H_2O ligands, but the complex ion that is produced contains only four NH_3 ligands, not six.

$$Cu^{2+}(aq) + 4\,NH_3(aq) \rightleftharpoons [Cu(NH_3)_4]^{2+}(aq) \quad (10.6.1)$$

The equilibrium constant for the formation of the complex ion from the hydrated ion is called the **formation constant** (K_f). The equilibrium constant expression for K_f has the same general form as any other equilibrium constant expression. In this case, the expression is as follows:

$$\begin{aligned} K_f &= \frac{[Cu(NH_3)_4]^{2+}]}{[Cu^{2+}][NH_3]^4} \\ &= 2.1 \times 10^{13} \\ &= K_1 \times K_2 \times K_3 \times K_4 \end{aligned}$$

> *The formation constant (K_f) has the same general form as any other equilibrium constant expression.*

Water, a pure liquid, does not appear explicitly in the equilibrium constant expression, and the hydrated $Cu^{2+}(aq)$ ion is represented as Cu^{2+} for simplicity. As for any equilibrium, the larger the value of the equilibrium constant (in this case, K_f), the more stable the product. With $K_f = 2.1 \times 10^{13}$, the $[Cu(NH_3)_4(H_2O)_2]^{2+}$ complex ion is very stable. The formation constants for some common complex ions are listed in Table **10.6.1**.

Table **10.6.1**: Formation Constants for Selected Complex Ions in Aqueous Solution*

	Complex Ion	Equilibrium Equation	K_f
Ammonia Complexes	$[Ag(NH_3)_2]^+$	$Ag^+ + 2NH_3 \rightleftharpoons [Ag(NH_3)_2]^+$	1.1×10^7
	$[Cu(NH_3)_4]^{2+}$	$Cu^{2+} + 4NH_3 \rightleftharpoons [Cu(NH_3)_4]^{2+}$	2.1×10^{13}
	$[Ni(NH_3)_6]^{2+}$	$Ni^{2+} + 6NH_3 \rightleftharpoons [Ni(NH_3)_6]^{2+}$	5.5×10^8
Cyanide Complexes	$[Ag(CN)_2]^-$	$Ag^+ + 2CN^- \rightleftharpoons [Ag(CN)_2]^-$	1.1×10^{18}
	$[Ni(CN)_4]^{2-}$	$Ni^{2+} + 4CN^- \rightleftharpoons [Ni(CN)_4]^{2-}$	2.2×10^{31}
	$[Fe(CN)_6]^{3-}$	$Fe^{3+} + 6CN^- \rightleftharpoons [Fe(CN)_6]^{3-}$	1×10^{42}
Hydroxide Complexes	$[Zn(OH)_4]^{2-}$	$Zn^{2+} + 4OH^- \rightleftharpoons [Zn(OH)_4]^{2-}$	4.6×10^{17}
	$[Cr(OH)_4]^-$	$Cr^{3+} + 4OH^- \rightleftharpoons [Cr(OH)_4]^-$	8.0×10^{29}
Halide Complexes	$[HgCl_4]^{2-}$	$Hg^{2+} + 4Cl^- \rightleftharpoons [HgCl_4]^{2-}$	1.2×10^{15}
	$[CdI_4]^{2-}$	$Cd^{2+} + 4I \rightleftharpoons [CdI_4]^{2-}$	2.6×10^5
	$[AlF_6]^{3-}$	$Al^{3+} + 6F^- \rightleftharpoons [AlF_6]^{3-}$	6.9×10^{19}
Other Complexes	$[Ag(S_2O_3)_2]^{3-}$	$Ag^+ + 2S_2O_3^{2-} \rightleftharpoons [Ag(S_2O_3)_2]^{3-}$	2.9×10^{13}
	$[Fe(C_2O_4)_3]^{3-}$	$Fe^{3+} + 3C_2O_4^{2-} \rightleftharpoons [Fe(C_2O_4)_3]^{3-}$	2.0×10^{20}

*Reported values are overall formation constants. Source: Data from *Lange's Handbook of Chemistry*, 15th ed. (1999).

Example 10.6.1

If 12.5 g of $Cu(NO_3)_2 \cdot 6H_2O$ is added to 500 mL of 1.00 M aqueous ammonia, what is the equilibrium concentration of $Cu^{2+}(aq)$?

Given: mass of Cu^{2+} salt and volume and concentration of ammonia solution

Asked for: equilibrium concentration of $Cu^{2+}(aq)$

Strategy:

A. Calculate the initial concentration of $Cu^{2+}(aq)$ due to the addition of copper(II) nitrate hexahydrate. Use the stoichiometry of the reaction shown in Equation 10.6.1 to construct a table showing the initial concentrations, the changes in concentrations, and the final concentrations of all species in solution.

B. Substitute the final concentrations into the expression for the formation constant (K_f) to calculate the equilibrium concentration of $Cu^{2+}(aq)$.

Solution

Adding an ionic compound that contains $Cu^{2+}(aq)$ to an aqueous ammonia solution will result in the formation of $[Cu(NH_3)_4]^{2+}(aq)$, as shown in Equation 10.6.1 We assume that the volume change caused by adding solid copper(II) nitrate to aqueous ammonia is negligible.

A The initial concentration of $Cu^{2+}(aq)$ from the amount of added copper nitrate prior to any reaction is as follows:

$$12.5 \cancel{g}\ Cu(NO_3)_2 \cdot 6H_2O \left(\frac{1\ mol}{295.65 \cancel{g}}\right)\left(\frac{1}{500\ \cancel{mL}}\right)\left(\frac{1000\ \cancel{mL}}{1\ L}\right) = 0.0846\ M$$

Because the stoichiometry of the reaction is four NH_3 to one Cu^{2+}, the amount of NH_3 required to react completely with the Cu^{2+} is 4(0.0846) = 0.338 M. The concentration of ammonia after complete reaction is 1.00 M − 0.338 M = 0.66 M. These results are summarized in the first two lines of the following table. Because the equilibrium constant for the reaction is large (2.1×10^{13}), the equilibrium will lie far to the right. Thus we will assume that the formation of $[Cu(NH_3)_4]^{2+}$ in the first step is complete and allow some of it to dissociate into Cu^{2+} and NH_3 until equilibrium has been reached. If we define x as the amount of Cu^{2+} produced by the dissociation reaction, then the stoichiometry of the reaction tells us that the change in the concentration of $[Cu(NH_3)_4]^{2+}$ is $-x$, and the change in the concentration of ammonia is $+4x$, as indicated in the table. The final concentrations of all species (in the bottom row of the table) are the sums of the concentrations after complete reaction and the changes in concentrations.

$$Cu^{2+} + 4\,NH_3 \rightleftharpoons [Cu(NH_3)_4]^{2+}$$

ICE	$[Cu^{2+}]$	$[NH_3]$	$[[Cu(NH_3)_4]^{2+}]$
initial	0.0846	1.00	0
after complete reaction	0	0.66	0.0846
change	$+x$	$+4x$	$-x$
final	x	$0.66 + 4x$	$0.0846 - x$

B Substituting the final concentrations into the expression for the formation constant (K_f) and assuming that $x \ll 0.0846$, which allows us to remove x from the sum and difference,

$$\begin{aligned} K_f &= \frac{[[Cu(NH_3)_4]^{2+}]}{[Cu^{2+}][NH_3]^4} \\ &= \frac{0.0846 - x}{x(0.66 + 4x)^4} \\ &\approx \frac{0.0846}{x(0.66)^4} = 2.1 \times 10^{13} \\ x &= 2.1 \times 10^{-14} \end{aligned}$$

The value of x indicates that our assumption was justified. The equilibrium concentration of $Cu^{2+}(aq)$ in a 1.00 M ammonia solution is therefore 2.1×10^{-14} M.

? Exercise 10.6.1

The ferrocyanide ion ($[Fe(CN)_6]^{4-}$) is very stable, with a K_f of 1×10^{35}. Calculate the concentration of cyanide ion in equilibrium with a 0.65 M solution of $K_4[Fe(CN)_6]$.

Answer

2×10^{-6} M

The Effect of the Formation of Complex Ions on Solubility

What happens to the solubility of a sparingly soluble salt if a ligand that forms a stable complex ion is added to the solution? One such example occurs in conventional black-and-white photography. Recall that black-and-white photographic film contains light-sensitive microcrystals of AgBr, or mixtures of AgBr and other silver halides. AgBr is a sparingly soluble salt, with a K_{sp} of 5.35×10^{-13} at 25°C. When the shutter of the camera opens, the light from the object being photographed strikes some of the crystals on the film and initiates a photochemical reaction that converts AgBr to black Ag metal. Well-formed, stable negative images appear in tones of gray, corresponding to the number of grains of AgBr converted, with the areas exposed to the most light being darkest. To fix the image and prevent more AgBr crystals from being converted to Ag metal during processing of the film, the unreacted AgBr on the film is removed using a complexation reaction to dissolve the sparingly soluble salt.

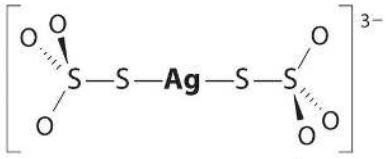
The reaction for the dissolution of silver bromide is as follows:

$$\mathrm{AgBr(s) \rightleftharpoons Ag^+(aq) + Br^-(aq)} \tag{10.6.2}$$

with

$$K_{sp} = 5.35 \times 10^{-13} \text{ at } 25°\mathrm{C} \tag{10.6.3}$$

The equilibrium lies far to the left, and the equilibrium concentrations of Ag^+ and Br^- ions are very low (7.31×10^{-7} M). As a result, removing unreacted AgBr from even a single roll of film using pure water would require tens of thousands of liters of water and a great deal of time. Le Chatelier's principle tells us, however, that we can drive the reaction to the right by removing one of the products, which will cause more AgBr to dissolve. Bromide ion is difficult to remove chemically, but silver ion forms a variety of stable two-coordinate complexes with neutral ligands, such as ammonia, or with anionic ligands, such as cyanide or thiosulfate ($S_2O_3^{2-}$). In photographic processing, excess AgBr is dissolved using a concentrated solution of sodium thiosulfate.



thiosulfate complex of Ag^+

The reaction of Ag^+ with thiosulfate is as follows:

$$Ag^+_{(aq)} + 2S_2O^{2-}_{3(aq)} \rightleftharpoons [Ag(S_2O_3)_2]^{3-}_{(aq)} \tag{10.6.4}$$

with

$$K_f = 2.9 \times 10^{13} \tag{10.6.5}$$

The magnitude of the equilibrium constant indicates that almost all Ag^+ ions in solution will be immediately complexed by thiosulfate to form $[Ag(S_2O_3)_2]^{3-}$. We can see the effect of thiosulfate on the solubility of **AgBr** by writing the appropriate reactions and adding them together:

$$\mathrm{AgBr(s) \rightleftharpoons Ag^+(aq) + Br^-(aq)} \quad K_{sp} = 5.35 \times 10^{-13}$$
$$\mathrm{Ag^+(aq) + 2S_2O_3^{2-}(aq) \rightleftharpoons [Ag(S_2O_3)_2]^{3-}(aq)} \quad K_f = 2.9 \times 10^{13}$$
$$\mathrm{AgBr(s) + 2S_2O_3^{2-}(aq) \rightleftharpoons [Ag(S_2O_3)_2]^{3-}(aq) + Br^-(aq)} \quad K = K_{sp}K_f = 15$$

Comparing K with K_{sp} shows that the formation of the complex ion increases the solubility of **AgBr** by approximately 3×10^{13}. The dramatic increase in solubility combined with the low cost and the low toxicity explains why sodium thiosulfate is almost universally used for developing black-and-white film. If desired, the silver can be recovered from the thiosulfate solution using any of several methods and recycled.

> *If a complex ion has a large K_f, the formation of a complex ion can dramatically increase the solubility of sparingly soluble salts.*

Example 10.6.2: Common Ion Effect in Complexation

Due to the common ion effect, we might expect a salt such as AgCl to be much less soluble in a concentrated solution of KCl than in water. Such an assumption would be incorrect, however, because it ignores the fact that silver ion tends to form a two-coordinate complex with chloride ions ($AgCl_2^-$). Calculate the solubility of AgCl in each situation:

a. in pure water
b. in 1.0 M KCl solution, ignoring the formation of any complex ions
c. the same solution as in part (b) except taking the formation of complex ions into account, assuming that $AgCl_2^-$ is the only Ag^+ complex that forms in significant concentrations

At 25°C, $K_{sp} = 1.77 \times 10^{-10}$ for AgCl and $K_f = 1.1 \times 10^5$ for $AgCl_2^-$.

Given: K_{sp} of AgCl, K_f of $AgCl_2^-$, and KCl concentration

Asked for: solubility of AgCl in water and in KCl solution with and without the formation of complex ions

Strategy:

A. Write the solubility product expression for AgCl and calculate the concentration of Ag^+ and Cl^- in water.
B. Calculate the concentration of Ag^+ in the KCl solution.
C. Write balanced chemical equations for the dissolution of AgCl and for the formation of the $AgCl_2^-$ complex. Add the two equations and calculate the equilibrium constant for the overall equilibrium.
D. Write the equilibrium constant expression for the overall reaction. Solve for the concentration of the complex ion.

Solution

A. If we let x equal the solubility of AgCl, then at equilibrium

$$[Ag^+] = [Cl^-] = x \text{ M}.$$

Substituting this value into the solubility product expression,

$$\begin{aligned} K_{sp} &= [Ag^+][Cl^-] \\ &= (x)(x) \\ &= x^2 \\ &= 1.77 \times 10^{-10} \\ x &= 1.33 \times 10^{-5} \end{aligned}$$

Thus the solubility of **AgCl** in pure water at 25°C is 1.33×10^{-5} M.

B. If x equals the solubility of AgCl in the KCl solution, then at equilibrium $[Ag^+] = x$ M and $[Cl^-] = (1.0 + x)$ M. Substituting these values into the solubility product expression and assuming that $x \le 1.0$:

$$\begin{aligned} K_{sp} &= [Ag^+][Cl^-] \\ &= (x)(1.0 + x) \\ &\approx x(1.0) \\ &= 1.77 \times 10^{-10} = x \end{aligned}$$

If the common ion effect were the only important factor, we would predict that **AgCl** is approximately five orders of magnitude less soluble in a 1.0 M KCl solution than in water.

C. To account for the effects of the formation of complex ions, we must first write the equilibrium equations for both the dissolution and the formation of complex ions. Adding the equations corresponding to K_{sp} and K_f gives us an equation that describes the dissolution of AgCl in a KCl solution. The equilibrium constant for the reaction is therefore the product of K_{sp} and K_f:

$$\begin{aligned} AgCl(s) &\rightleftharpoons Ag^+(aq) + Cl^-(aq) \quad K_{sp} = 1.77 \times 10^{-10} \\ Ag^+aq) + 2Cl^- &\rightleftharpoons [AgCl_2]^- \quad K_f = 1.1 \times 10^5 \\ AgCl(s) + Cl^- &\rightleftharpoons [AgCl_2]^- \quad K = K_{sp}K_f = 1.9 \times 10^{-5} \end{aligned}$$

D. If we let x equal the solubility of AgCl in the KCl solution, then at equilibrium $[AgCl_2^-] = x$ and $[Cl^-] = 1.0 - x$. Substituting these quantities into the equilibrium constant expression for the net reaction and assuming that $x \le 1.0$,

$$\begin{aligned} K &= \frac{[AgCl_2^-]}{[Cl^-]} \\ &= \frac{x}{1.0 - x} \approx 1.9 \times 10^{-5} \\ &= x \end{aligned}$$

That is, AgCl dissolves in 1.0 M KCl to produce a 1.9×10^{-5} M solution of the $AgCl_2^-$ complex ion. Thus we predict that AgCl has approximately the same solubility in a 1.0 M KCl solution as it does in pure water, which is 10^5 times greater than that

predicted based on the common ion effect. (In fact, the measured solubility of AgCl in 1.0 M KCl is almost a factor of 10 greater than that in pure water, largely due to the formation of other chloride-containing complexes.)

? Exercise 10.6.2

Calculate the solubility of mercury(II) iodide ($\mathbf{HgI_2}$) in each situation:

a. pure water
b. a 3.0 M solution of NaI, assuming $[HgI_4]^{2-}$ is the only Hg-containing species present in significant amounts

$$K_{sp} = 2.9 \times 10^{-29} \text{ for } HgI_2 \text{ and } K_f = 6.8 \times 10^{29} \text{ for } [HgI_4]^{2-}.$$

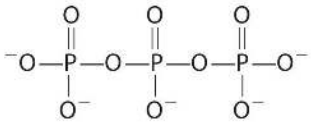
Answer a

1.9×10^{-10} M

Answer b

1.4 M

Complexing agents, molecules or ions that increase the solubility of metal salts by forming soluble metal complexes, are common components of laundry detergents. Long-chain carboxylic acids, the major components of soaps, form insoluble salts with Ca^{2+} and Mg^{2+}, which are present in high concentrations in "hard" water. The precipitation of these salts produces a bathtub ring and gives a gray tinge to clothing.



triphosphate

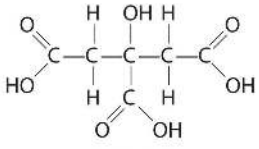
Adding a complexing agent such as pyrophosphate ($O_3POPO_3^{4-}$, or $P_2O_7^{4-}$) or triphosphate ($P_3O_{10}^{5-}$) to detergents prevents the magnesium and calcium salts from precipitating because the equilibrium constant for complex-ion formation is large:

$$\mathbf{Ca^{2+}(aq) + O_3POPO_4^{4-}(aq) \rightleftharpoons [Ca(O_3POPO_3)]^{2-}(aq)}$$

with

$$\mathbf{K_f = 4 \times 10^4}$$

However, phosphates can cause environmental damage by promoting eutrophication, the growth of excessive amounts of algae in a body of water, which can eventually lead to large decreases in levels of dissolved oxygen that kill fish and other aquatic organisms. Consequently, many states in the United States have banned the use of phosphate-containing detergents, and France has banned their use beginning in 2007. "Phosphate-free" detergents contain different kinds of complexing agents, such as derivatives of acetic acid or other carboxylic acids. The development of phosphate substitutes is an area of intense research.



Citric acid,
a hydroxy polycarboxylic acid

Commercial water softeners also use a complexing agent to treat hard water by passing the water over ion-exchange resins, which are complex sodium salts. When water flows over the resin, sodium ion is dissolved, and insoluble salts precipitate onto the resin surface. Water treated in this way has a saltier taste due to the presence of Na^+, but it contains fewer dissolved minerals.

Complexing Agents in MRIs

Another application of complexing agents is found in medicine. Unlike x-rays, magnetic resonance imaging (MRI) can give relatively good images of soft tissues such as internal organs. MRI is based on the magnetic properties of the ^{1}H nucleus of hydrogen atoms in water, which is a major component of soft tissues. Because the properties of water do not depend very much on whether it is inside a cell or in the blood, it is hard to get detailed images of these tissues that have good contrast. To solve this problem, scientists have developed a class of metal complexes known as "MRI contrast agents." Injecting an MRI contrast agent into a patient selectively affects the magnetic properties of water in cells of normal tissues, in tumors, or in blood vessels and allows doctors to "see" each of these separately (Figure **10.6.2**). One of the most important metal ions for this application is Gd^{3+}, which with seven unpaired electrons is highly paramagnetic. Because $Gd^{3+}(aq)$ is quite toxic, it must be administered as a very stable complex that does not dissociate in the body and can be excreted intact by the kidneys. The complexing agents used for gadolinium are ligands such as $DTPA^{5-}$ (diethylene triamine pentaacetic acid), whose fully protonated form is shown in Figure **10.6.2**.

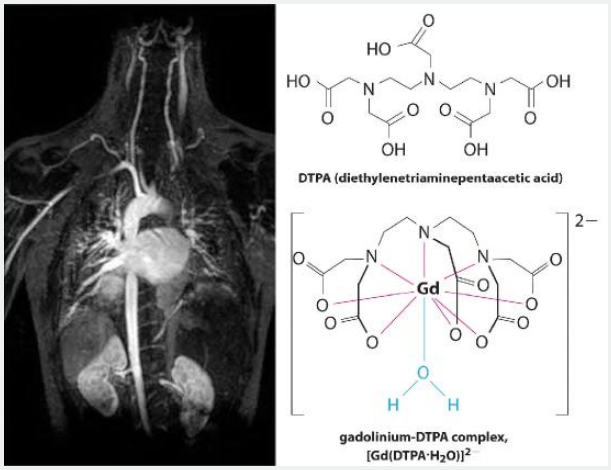


Figure **10.6.2**: An MRI Image of the Heart, Arteries, and Veins. When a patient is injected with a paramagnetic metal cation in the form of a stable complex known as an MRI contrast agent, the magnetic properties of water in cells are altered. Because the different environments in different types of cells respond differently, a physician can obtain detailed images of soft tissues.

Summary

The formation of complex ions can substantially increase the solubility of sparingly soluble salts if the complex ion has a large K_f. A complex ion is a species formed between a central metal ion and one or more surrounding ligands, molecules or ions that contain at least one lone pair of electrons. Small, highly charged metal ions have the greatest tendency to act as Lewis acids and form complex ions. The equilibrium constant for the formation of the complex ion is the formation constant (K_f). The formation of a complex ion by adding a complexing agent increases the solubility of a compound.

10.6: Stability Aspects of Complex-Ion Equilibria is shared under a not declared license and was authored, remixed, and/or curated by LibreTexts.

- **24.8: Aspects of Complex-Ion Equilibria** is licensed CC BY-NC-SA 4.0.

10.7: Chelation

Ligands like chloride, water, and ammonia are said to be monodentate (one-toothed, from the Greek mono, meaning “one,” and the Latin dent-, meaning “tooth”): they are attached to the metal via only a single atom. Ligands can, however, be bidentate (two-toothed, from the Greek di, meaning “two”), tridentate (three-toothed, from the Greek tri, meaning “three”), or, in general, polydentate (many-toothed, from the Greek poly, meaning “many”), indicating that they are attached to the metal at two, three, or several sites, respectively. Ethylenediamine ($H_2NCH_2CH_2NH_2$, often abbreviated as en) and diethylenetriamine ($H_2NCH_2CH_2NHCH_2CH_2NH_2$, often abbreviated as dien) are examples of a bidentate and a tridentate ligand, respectively, because each nitrogen atom has a lone pair that can be shared with a metal ion. When a bidentate ligand such as ethylenediamine binds to a metal such as Ni^{2+}, a five-membered ring is formed. A metal-containing ring like that shown is called a chelate ring (from the Greek chele, meaning “claw”). Correspondingly, a polydentate ligand is a chelating agent, and complexes that contain polydentate ligands are called chelate complexes.



A chelate complex

Experimentally, it is observed that metal complexes of polydentate ligands are significantly more stable than the corresponding complexes of chemically similar monodentate ligands; this increase in stability is called the chelate effect. For example, the complex of Ni^{2+} with three ethylenediamine ligands, $[Ni(en)_3]^{2+}$, should be chemically similar to the Ni^{2+} complex with six ammonia ligands, $[Ni(NH_3)_6]^{2+}$. In fact, the equilibrium constant for the formation of $[Ni(en)_3]^{2+}$ is almost 10 orders of magnitude larger than the equilibrium constant for the formation of $[Ni(NH_3)_6]^{2+}$ (Table E4):

$$[Ni(H_2O)_6]^{2+} + 6NH_3 \rightleftharpoons [Ni(NH_3)_6]^{2+} + 6H_2O(l) \quad K_f = 4 \times 10^8 \tag{10.7.1}$$

$$[Ni(H_2O)_6]^{2+} + 3en \rightleftharpoons [Ni(en)_3]^{2+} + 6H_2O(l) \quad K_f = 2 \times 10^{18} \tag{10.7.2}$$

The formation constants are formulated as ligand exchange reactions with aqua ligands being displaced by new ligands (NH_3 or en) in the examples above.

> *Chelate complexes are more stable than the analogous complexes with monodentate ligands.*

The stability of a chelate complex depends on the size of the chelate rings. For ligands with a flexible organic backbone like ethylenediamine, complexes that contain five-membered chelate rings, which have almost no strain, are significantly more stable than complexes with six-membered chelate rings, which are in turn much more stable than complexes with four- or seven-membered rings. For example, the complex of nickel (II) with three ethylenediamine ligands is about 363,000 times more stable than the corresponding nickel (II) complex with trimethylenediamine ($H_2NCH_2CH_2CH_2NH_2$, abbreviated as tn):

$$[Ni(H_2O)_6]^{2+} + 3en \rightleftharpoons [Ni(en)_3]^{2+} + 6H_2O(l) \quad K_f = 6.76 \times 10^{17} \tag{10.7.3}$$

$$[Ni(H_2O)_6]^{2+} + 3tn \rightleftharpoons [Ni(tn)_3]^{2+} + 6H_2O(l) \quad K_f = 1.86 \times 10^{12} \tag{10.7.4}$$

*The above measurements were done in a solution of ionic strength 0.15 at 25° C.

Example 10.7.1

Arrange $[Cr(en)_3]^{3+}$, $[CrCl_6]^{3-}$, $[CrF_6]^{3-}$, and $[Cr(NH_3)_6]^{3+}$ in order of increasing stability.

Given: four Cr(III) complexes

Asked for: relative stabilities

Strategy:

A Determine the relative basicity of the ligands to identify the most stable complexes.

B Decide whether any complexes are further stabilized by a chelate effect and arrange the complexes in order of increasing stability.

Solution

A The metal ion is the same in each case: Cr^{3+}. Consequently, we must focus on the properties of the ligands to determine the stabilities of the complexes. Because the stability of a metal complex increases as the basicity of the ligands increases, we need to determine the relative basicity of the four ligands. Our earlier discussion of acid–base properties suggests that ammonia and ethylenediamine, with nitrogen donor atoms, are the most basic ligands. The fluoride ion is a stronger base (it has a higher charge-to-radius ratio) than chloride, so the order of stability expected due to ligand basicity is

$$[CrCl_6]^{3-} < [CrF_6]^{3-} < [Cr(NH_3)_6]^{3+} \approx [Cr(en)_3]^{3+}.$$

B Because of the chelate effect, we expect ethylenediamine to form a stronger complex with Cr^{3+} than ammonia. Consequently, the likely order of increasing stability is

$$[CrCl_6]^{3-} < [CrF_6]^{3-} < [Cr(NH_3)_6]^{3+} < [Cr(en)_3]^{3+}.$$

? Exercise 10.7.1

Arrange $[Co(NH_3)_6]^{3+}$, $[CoF_6]^{3-}$, and $[Co(en)_3]^{3+}$ in order of decreasing stability.

Answer: $[Co(en)_3]^{3+} > [Co(NH_3)_6]^{3+} > [CoF_6]^{3-}$

The Chelate Effect

The chelate effect can be seen by comparing the reaction of a chelating ligand and a metal ion with the corresponding reaction involving comparable monodentate ligands. For example, comparison of the binding of 2,2'-bipyridine with pyridine or 1,2-diaminoethane (ethylenediamine=en) with ammonia. It has been known for many years that a comparison of this type always shows that the complex resulting from coordination with the chelating ligand is **much more thermodynamically stable**. This can be seen by looking at the values for adding two monodentates compared with adding one bidentate, or adding four monodentates compared to two bidentates, or adding six monodentates compared to three bidentates.

> *The Chelate Effect is that complexes resulting from coordination with the chelating ligand is much more thermodynamically stable than complexes with non-chelating ligands.*

A number of points should be highlighted from the formation constants in Table E4. In Table **10.7.1**, it can be seen that the ΔH° values for the formation steps are almost identical, that is, heat is evolved to about the same extent whether forming a complex involving monodentate ligands or bidentate ligands. What is seen to vary significantly is the ΔS° term which changes from negative (unfavorable) to positive (favorable). Note as well that there is a dramatic increase in the size of the ΔS° term for adding two compared to adding four monodentate ligands. (-5 to -35 $JK^{-1}mol^{-1}$). What does this imply, if we consider ΔS° to give a measure of disorder?

In the case of complex formation of Ni^{2+} with ammonia or 1,2-diaminoethane, by rewriting the equilibria, the following equations are produced.

$$[Ni(H_2O)_6]^{2+} + 6\,NH_3 \overset{\beta_6}{\Leftrightarrow} [Ni(NH_3)_6]^{2+} \quad \textbf{1f}$$

$$[Ni(NH_3)_6]^{2+} \Leftrightarrow [Ni(H_2O)_6]^{2+} + 6\,NH_3 \quad \textbf{1d}$$

$$[Ni(H_2O)_6]^{2+} + 3\,en \overset{\beta_3}{\Leftrightarrow} [Ni(en)_3]^{2+} \quad \textbf{2f}$$

$$[Ni(NH_3)_6]^{2+} + 3\,en \Leftrightarrow [Ni(en)_3]^{2+} + 6NH_3 \quad \textbf{3}$$

Using the equilibrium constant for the reaction (3 above) where the *three* bidentate ligands replace the *six* monodentateligands, we find that at a temperature of 25° C:

$$\Delta G^\circ = -2.303\,RT\,\log_{10} K$$

$$= -2.303\,RT\,(18.28 - 8.61)$$

$$= -54\ \text{kJ mol}^{-1}$$

Based on measurements made over a range of temperatures, it is possible to break down the $\Delta G°$ term into the enthalpy and entropy components.

$$\Delta G° = \Delta H° - T\Delta S°$$

The result is that: $\Delta H° = -29 kJ mol^{-1}$

$$- T\Delta S° = -25 \text{ kJ mol}^{-1}$$
and at 25C (298K)
$$\Delta S° = +88 \text{ J K}^{-1} \text{ mol}^{-1}$$

For many years, these numbers have been **incorrectly recorded** in textbooks. For example, the third edition of "Basic Inorganic Chemistry" by F.A. Cotton, G. Wilkinson and P.L. Gaus, John Wiley & Sons, Inc, 1995, on page 186 gives the values as:

$$\Delta G° = -67 \text{ kJ mol}^{-1}$$
$$\Delta H° = -12 \text{ kJ mol}^{-1}$$
$$-T\Delta S° = -55 \text{ kJ mol}^{-1}$$

The conclusion they drew from these incorrect numbers was that the chelate effect was essentially an entropy effect, since the $T\Delta S°$ contribution was nearly 5 times bigger than $\Delta H°$.

In fact, the breakdown of the $\Delta G°$ into $\Delta H°$ and $T\Delta S°$ shows that the two terms are nearly equal (-29 and -25 kJ mol^{-1}, respectively) with the $\Delta H°$ term a little bigger! The entropy term found is still much larger than for reactions involving a non-chelating ligand substitution at a metal ion. How can we explain this enhanced contribution from entropy? One explanation is to count the number of species on the left and right hand side of the equation above.

It will be seen that on the left-hand-side there are 4 species, whereas on the right-hand-side there are 7 species, that is a net gain of 3 species occurs as the reaction proceeds. This can account for the increase in entropy since it represents an increase in the disorder of the system. An alternative view comes from trying to understand how the reactions might proceed. To form a complex with 6 monodentates requires 6 separate favorable collisions between the metal ion and the ligand molecules. To form the tris-bidentate metal complex requires an initial collision for the first ligand to attach by one arm but remember that the other arm is always going to be nearby and only requires a rotation of the other end to enable the ligand to form the chelate ring.

If you consider dissociation steps, then when a monodentate group is displaced, it is lost into the bulk of the solution. On the other hand, if one end of a bidentate group is displaced the other arm is still attached and it is only a matter of the arm rotating around and it can be reattached again. **Both** conditions favor the formation of the complex with bidentate groups rather than monodentate groups.

10.7: Chelation is shared under a not declared license and was authored, remixed, and/or curated by LibreTexts.

- **Stability of Metal Complexes and Chelation** by Robert J. Lancashire is licensed CC BY-NC-SA 4.0.

10.8: Bonding in Octahedral Complex Ions- Crystal Field Theory

Learning Objectives

- To understand how crystal field theory explains the electronic structures and colors of metal complexes.

One of the most striking characteristics of transition-metal complexes is the wide range of colors they exhibit. In this section, we describe crystal field theory (CFT), a bonding model that explains many important properties of transition-metal complexes, including their colors, magnetism, structures, stability, and reactivity. The central assumption of CFT is that metal–ligand interactions are purely electrostatic in nature. Even though this assumption is clearly not valid for many complexes, such as those that contain neutral ligands like CO, CFT enables chemists to explain many of the properties of transition-metal complexes with a reasonable degree of accuracy. The Learning Objective of this Module is to understand how crystal field theory explains the electronic structures and colors of metal complexes.

d-Orbital Splittings

CFT focuses on the interaction of the five (n − 1)d orbitals with ligands arranged in a regular array around a transition-metal ion. We will focus on the application of CFT to octahedral complexes, which are by far the most common and the easiest to visualize. Other common structures, such as square planar complexes, can be treated as a distortion of the octahedral model. According to CFT, an octahedral metal complex forms because of the electrostatic interaction of a positively charged metal ion with six negatively charged ligands or with the negative ends of dipoles associated with the six ligands. In addition, the ligands interact with one other electrostatically. As you learned in our discussion of the valence-shell electron-pair repulsion (VSEPR) model, the lowest-energy arrangement of six identical negative charges is an octahedron, which minimizes repulsive interactions between the ligands.

We begin by considering how the energies of the d orbitals of a transition-metal ion are affected by an octahedral arrangement of six negative charges. Recall that the five d orbitals are initially degenerate (have the same energy). If we distribute six negative charges uniformly over the surface of a sphere, the d orbitals remain degenerate, but their energy will be higher due to repulsive electrostatic interactions between the spherical shell of negative charge and electrons in the d orbitals (Figure **10.8.1*a***). Placing the six negative charges at the vertices of an octahedron does not change the average energy of the d orbitals, but it does remove their degeneracy: the five d orbitals split into two groups whose energies depend on their orientations. As shown in Figure **10.8.1*b***, the d_{z^2} and $d_{x^2-y^2}$ orbitals point directly at the six negative charges located on the x, y, and z axes. Consequently, the energy of an electron in these two orbitals (collectively labeled the e_g orbitals) will be greater than it will be for a spherical distribution of negative charge because of increased electrostatic repulsions. In contrast, the other three d orbitals (d_{xy}, d_{xz}, and d_{yz}, collectively called the t_{2g} orbitals) are all oriented at a 45° angle to the coordinate axes, so they point between the six negative charges. The energy of an electron in any of these three orbitals is lower than the energy for a spherical distribution of negative charge.

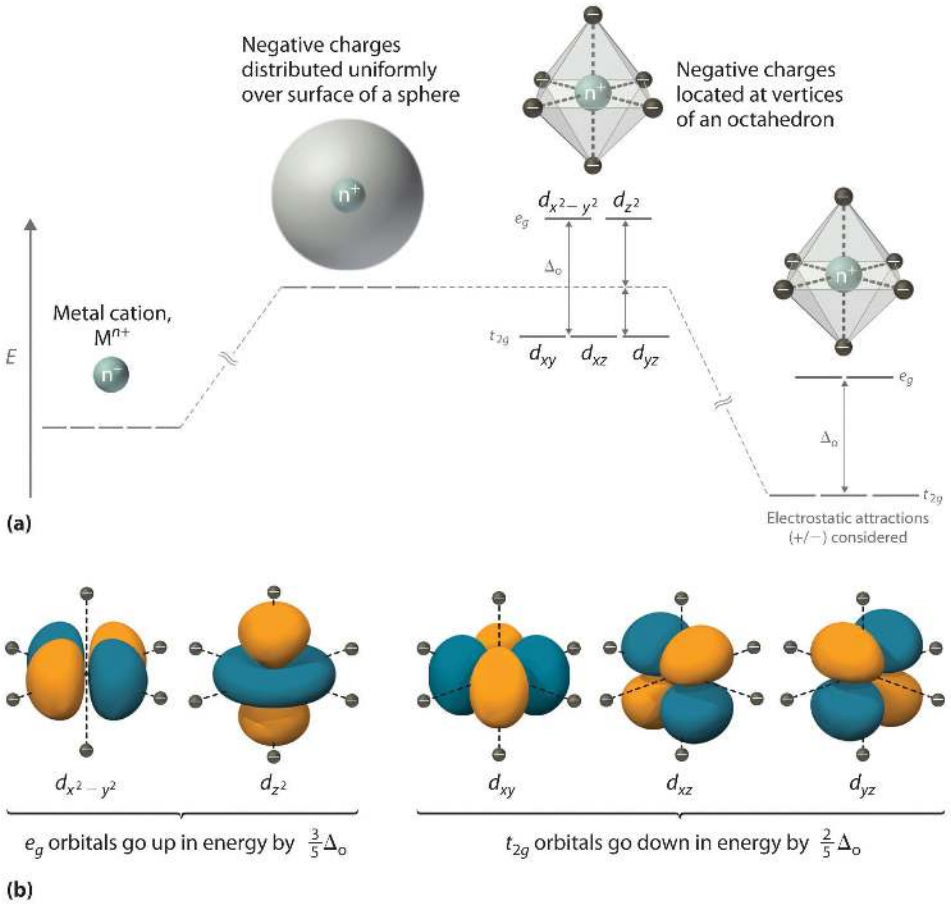


Figure **10.8.1**: An Octahedral Arrangement of Six Negative Charges around a Metal Ion Causes the Five d Orbitals to Split into Two Sets with Different Energies. (a) Distributing a charge of −6 uniformly over a spherical surface surrounding a metal ion causes the energy of all five d orbitals to increase due to electrostatic repulsions, but the five d orbitals remain degenerate. Placing a charge of −1 at each vertex of an octahedron causes the d orbitals to split into two groups with different energies: the $d_{x^2-y^2}$ and d_{z^2} orbitals increase in energy, while the d_{xy}, d_{xz}, and d_{yz} orbitals decrease in energy. The average energy of the five d orbitals is the same as for a spherical distribution of a −6 charge, however. Attractive electrostatic interactions between the negatively charged ligands and the positively charged metal ion (far right) cause all five d orbitals to decrease in energy but does not affect the splittings of the orbitals. (b) The two e_g orbitals (left) point directly at the six negatively charged ligands, which increases their energy compared with a spherical distribution of negative charge. In contrast, the three t_{2g} orbitals (right) point between the negatively charged ligands, which decreases their energy compared with a spherical distribution of charge. (CC BY-SA-NC; anonymous by request)

The difference in energy between the two sets of d orbitals is called the crystal field splitting energy (Δ_o), where the subscript o stands for octahedral. As we shall see, the magnitude of the splitting depends on the charge on the metal ion, the position of the metal in the periodic table, and the nature of the ligands. (Crystal field splitting energy also applies to tetrahedral complexes: Δ_t.) It is important to note that the splitting of the d orbitals in a crystal field does not change the total energy of the five d orbitals: the two e_g orbitals increase in energy by $0.6\Delta_o$, whereas the three t_{2g} orbitals decrease in energy by $0.4\Delta_o$. Thus the total change in energy is

$$2(0.6\Delta_o) + 3(-0.4\Delta_o) = 0. \tag{10.8.1}$$

> *Crystal field splitting does not change the total energy of the d orbitals.*

Thus far, we have considered only the effect of repulsive electrostatic interactions between electrons in the d orbitals and the six negatively charged ligands, which increases the total energy of the system and splits the d orbitals. Interactions between the positively charged metal ion and the ligands results in a net stabilization of the system, which decreases the energy of all five d orbitals without affecting their splitting (as shown at the far right in Figure **10.8.1***a*).

Electronic Structures of Metal Complexes

We can use the d-orbital energy-level diagram in Figure **10.8.1** to predict electronic structures and some of the properties of transition-metal complexes. We start with the Ti^{3+} ion, which contains a single d electron, and proceed across the first row of the transition metals by adding a single electron at a time. We place additional electrons in the lowest-energy orbital available, while keeping their spins parallel as required by Hund's rule. As shown in Figure **10.8.2**, for d^1–d^3 systems—such as $[Ti(H_2O)_6]^{3+}$, $[V(H_2O)_6]^{3+}$, and $[Cr(H_2O)_6]^{3+}$, respectively—the electrons successively occupy the three degenerate t_{2g} orbitals with their spins parallel, giving one, two, and three unpaired electrons, respectively. We can summarize this for the complex $[Cr(H_2O)_6]^{3+}$, for example, by saying that the chromium ion has a d^3 electron configuration or, more succinctly, Cr^{3+} is a d^3 ion.

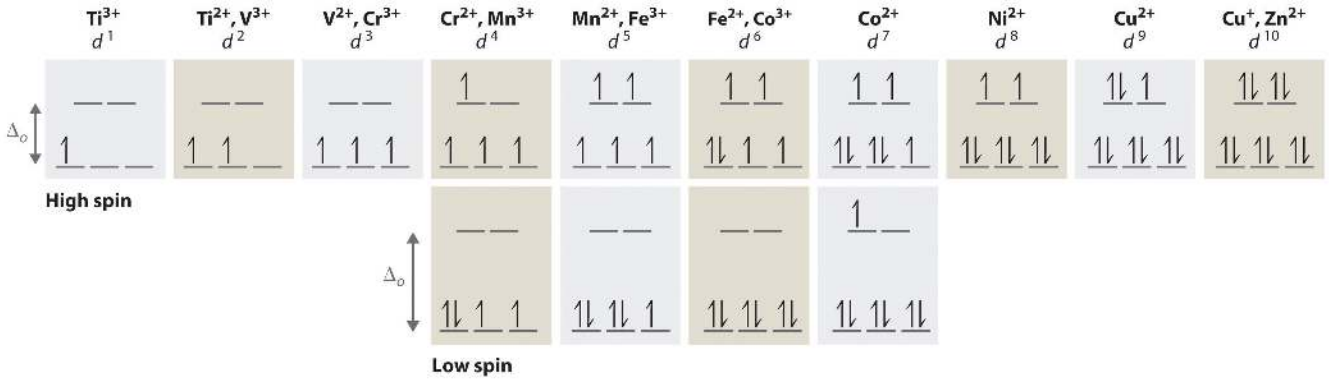


Figure **10.8.2**: The Possible Electron Configurations for Octahedral d^n Transition-Metal Complexes (n = 1–10). Two different configurations are possible for octahedral complexes of metals with d^4, d^5, d^6, and d^7 configurations; the magnitude of Δ_o determines which configuration is observed. (CC BY-SA-NC; anonymous by request)

When we reach the d^4 configuration, there are two possible choices for the fourth electron: it can occupy either one of the empty e_g orbitals or one of the singly occupied t_{2g} orbitals. Recall that placing an electron in an already occupied orbital results in electrostatic repulsions that increase the energy of the system; this increase in energy is called the spin-pairing energy (P). If Δ_o is less than P, then the lowest-energy arrangement has the fourth electron in one of the empty e_g orbitals. Because this arrangement results in four unpaired electrons, it is called a high-spin configuration, and a complex with this electron configuration, such as the $[Cr(H_2O)_6]^{2+}$ ion, is called a high-spin complex. Conversely, if Δ_o is greater than P, then the lowest-energy arrangement has the fourth electron in one of the occupied t_{2g} orbitals. Because this arrangement results in only two unpaired electrons, it is called a low-spin configuration, and a complex with this electron configuration, such as the $[Mn(CN)_6]^{3-}$ ion, is called a low-spin complex. Similarly, metal ions with the d^5, d^6, or d^7 electron configurations can be either high spin or low spin, depending on the magnitude of Δ_o.

In contrast, only one arrangement of d electrons is possible for metal ions with d^8–d^{10} electron configurations. For example, the $[Ni(H_2O)_6]^{2+}$ ion is d^8 with two unpaired electrons, the $[Cu(H_2O)_6]^{2+}$ ion is d^9 with one unpaired electron, and the $[Zn(H_2O)_6]^{2+}$ ion is d^{10} with no unpaired electrons.

> *If Δ_o is less than the spin-pairing energy, a high-spin configuration results. Conversely, if Δ_o is greater, a low-spin configuration forms.*

Factors That Affect the Magnitude of Δ_o

The magnitude of Δ_o dictates whether a complex with four, five, six, or seven d electrons is high spin or low spin, which affects its magnetic properties, structure, and reactivity. Large values of Δ_o (i.e., $\Delta_o > P$) yield a low-spin complex, whereas small values of Δ_o (i.e., $\Delta_o < P$) produce a high-spin complex. As we noted, the magnitude of Δ_o depends on three factors: the charge on the metal ion, the principal quantum number of the metal (and thus its location in the periodic table), and the nature of the ligand. Values of Δ_o for some representative transition-metal complexes are given in Table **10.8.1**.

Table **10.8.1**: Crystal Field Splitting Energies for Some Octahedral (Δ_o)* and Tetrahedral (Δ_t) Transition-Metal Complexes

Octahedral Complexes	Δ_o (cm^{-1})	Octahedral Complexes	Δ_o (cm^{-1})	Tetrahedral Complexes	Δ_t (cm^{-1})
$[Ti(H_2O)_6]^{3+}$	20,300	$[Fe(CN)_6]^{4-}$	32,800	VCl_4	9010
$[V(H_2O)_6]^{2+}$	12,600	$[Fe(CN)_6]^{3-}$	35,000	$[CoCl_4]^{2-}$	3300
$[V(H_2O)_6]^{3+}$	18,900	$[CoF_6]^{3-}$	13,000	$[CoBr_4]^{2-}$	2900
$[CrCl_6]^{3-}$	13,000	$[Co(H_2O)_6]^{2+}$	9300	$[CoI_4]^{2-}$	2700
$[Cr(H_2O)_6]^{2+}$	13,900	$[Co(H_2O)_6]^{3+}$	27,000		
$[Cr(H_2O)_6]^{3+}$	17,400	$[Co(NH_3)_6]^{3+}$	22,900		
$[Cr(NH_3)_6]^{3+}$	21,500	$[Co(CN)_6]^{3-}$	34,800		
$[Cr(CN)_6]^{3-}$	26,600	$[Ni(H_2O)_6]^{2+}$	8500		
$Cr(CO)_6$	34,150	$[Ni(NH_3)_6]^{2+}$	10,800		
$[MnCl_6]^{4-}$	7500	$[RhCl_6]^{3-}$	20,400		
$[Mn(H_2O)_6]^{2+}$	8500	$[Rh(H_2O)_6]^{3+}$	27,000		
$[MnCl_6]^{3-}$	20,000	$[Rh(NH_3)_6]^{3+}$	34,000		
$[Mn(H_2O)_6]^{3+}$	21,000	$[Rh(CN)_6]^{3-}$	45,500		
$[Fe(H_2O)_6]^{2+}$	10,400	$[IrCl_6]^{3-}$	25,000		
$[Fe(H_2O)_6]^{3+}$	14,300	$[Ir(NH_3)_6]^{3+}$	41,000		

*Energies obtained by spectroscopic measurements are often given in units of wave numbers (cm^{-1}); the wave number is the reciprocal of the wavelength of the corresponding electromagnetic radiation expressed in centimeters: 1 cm^{-1} = 11.96 J/mol.

Source of data: Duward F. Shriver, Peter W. Atkins, and Cooper H. Langford, Inorganic Chemistry, 2nd ed. (New York: W. H. Freeman and Company, 1994).

Factor 1: Charge on the Metal Ion

Increasing the charge on a metal ion has two effects: the radius of the metal ion decreases, and negatively charged ligands are more strongly attracted to it. Both factors decrease the metal–ligand distance, which in turn causes the negatively charged ligands to interact more strongly with the d orbitals. Consequently, the magnitude of Δ_o increases as the charge on the metal ion increases. Typically, Δ_o for a tripositive ion is about 50% greater than for the dipositive ion of the same metal; for example, for $[V(H_2O)_6]^{2+}$, Δ_o = 11,800 cm^{-1}; for $[V(H_2O)_6]^{3+}$, Δ_o = 17,850 cm^{-1}.

Factor 2: Principal Quantum Number of the Metal

For a series of complexes of metals from the same group in the periodic table with the same charge and the same ligands, the magnitude of Δ_o increases with increasing principal quantum number: Δ_o (3d) < Δ_o (4d) < Δ_o (5d). The data for hexaammine complexes of the trivalent Group 9 metals illustrate this point:

$$[Co(NH_3)_6]^{3+}: \Delta_o = 22{,}900\ cm^{-1}$$

$$[Rh(NH_3)_6]^{3+}: \Delta_o = 34{,}100\ cm^{-1}$$

$$[Ir(NH_3)_6]^{3+}: \Delta_o = 40{,}000\ cm^{-1}$$

The increase in Δ_o with increasing principal quantum number is due to the larger radius of valence orbitals down a column. In addition, repulsive ligand–ligand interactions are most important for smaller metal ions. Relatively speaking, this results in shorter M–L distances and stronger d orbital–ligand interactions.

Factor 3: The Nature of the Ligands

Experimentally, it is found that the Δ_o observed for a series of complexes of the same metal ion depends strongly on the nature of the ligands. For a series of chemically similar ligands, the magnitude of Δ_o decreases as the size of the donor atom increases. For example, Δ_o values for halide complexes generally decrease in the order $F^- > Cl^- > Br^- > I-$ because smaller, more localized charges, such as we see for F^-, interact more strongly with the d orbitals of the metal ion. In addition, a small neutral ligand with a highly localized lone pair, such as NH_3, results in significantly larger Δ_o values than might be expected. Because the lone pair points directly at the metal ion, the electron density along the M–L axis is greater than for a spherical anion such as F^-. The experimentally observed order of the crystal field splitting energies produced by different ligands is called the spectrochemical series, shown here in order of decreasing Δ_o:

$$\underset{\text{strong-field ligands}}{CO \approx CN^- > NO_2^-} > en > NH_3 > \underset{\text{intermediate-field ligands}}{SCN^- > H_2O > oxalate^{2-} > OH^- > F} > acetate^- > \underset{\text{weak-field ligands}}{Cl^- > Br^- > I^-}$$

The values of Δ_o listed in Table **10.8.1** illustrate the effects of the charge on the metal ion, the principal quantum number of the metal, and the nature of the ligand.

> *The largest Δ_o splittings are found in complexes of metal ions from the third row of the transition metals with charges of at least +3 and ligands with localized lone pairs of electrons.*

Example 10.8.1

For each complex, predict its structure, whether it is high spin or low spin, and the number of unpaired electrons present.

a. $[CoF_6]^{3-}$
b. $[Rh(CO)_2Cl_2]^-$

Given: complexes

Asked for: structure, high spin versus low spin, and the number of unpaired electrons

Strategy:

a. From the number of ligands, determine the coordination number of the compound.
b. Classify the ligands as either strong field or weak field and determine the electron configuration of the metal ion.
c. Predict the relative magnitude of Δ_o and decide whether the compound is high spin or low spin.
d. Place the appropriate number of electrons in the d orbitals and determine the number of unpaired electrons.

Solution

a. A With six ligands, we expect this complex to be octahedral.

B The fluoride ion is a small anion with a concentrated negative charge, but compared with ligands with localized lone pairs of electrons, it is weak field. The charge on the metal ion is +3, giving a d^6 electron configuration.

C Because of the weak-field ligands, we expect a relatively small Δ_o, making the compound high spin.

D In a high-spin octahedral d^6 complex, the first five electrons are placed individually in each of the d orbitals with their spins parallel, and the sixth electron is paired in one of the t_{2g} orbitals, giving four unpaired electrons.

b. A This complex has four ligands, so it is either square planar or tetrahedral.

B C Because rhodium is a second-row transition metal ion with a d^8 electron configuration and CO is a strong-field ligand, the complex is likely to be square planar with a large Δ_o, making it low spin. Because the strongest d-orbital interactions are along the x and y axes, the orbital energies increase in the order $d_{z^2}d_{yz}$, and d_{xz} (these are degenerate); d_{xy}; and $d_{x^2-y^2}$.

D The eight electrons occupy the first four of these orbitals, leaving the $d_{x^2-y^2}$. orbital empty. Thus there are no unpaired electrons.

? Exercise 10.8.1

For each complex, predict its structure, whether it is high spin or low spin, and the number of unpaired electrons present.

a. $[Mn(H_2O)_6]^{2+}$
b. $[PtCl_4]^{2-}$

Answer a

octahedral; high spin; five

Answer b

square planar; low spin; no unpaired electrons

Crystal Field Stabilization Energies

Recall that stable molecules contain more electrons in the lower-energy (bonding) molecular orbitals in a molecular orbital diagram than in the higher-energy (antibonding) molecular orbitals. If the lower-energy set of d orbitals (the t_{2g} orbitals) is selectively populated by electrons, then the stability of the complex increases. For example, the single d electron in a d^1 complex such as $[Ti(H_2O)_6]^{3+}$ is located in one of the t_{2g} orbitals. Consequently, this complex will be more stable than expected on purely electrostatic grounds by $0.4\Delta_o$. The additional stabilization of a metal complex by selective population of the lower-energy d orbitals is called its crystal field stabilization energy (CFSE). The CFSE of a complex can be calculated by multiplying the number of electrons in t_{2g} orbitals by the energy of those orbitals ($-0.4\Delta_o$), multiplying the number of electrons in e_g orbitals by the energy of those orbitals ($+0.6\Delta_o$), and summing the two. Table **10.8.2** gives CFSE values for octahedral complexes with different d electron configurations. The CFSE is highest for low-spin d^6 complexes, which accounts in part for the extraordinarily large number of Co(III) complexes known. The other low-spin configurations also have high CFSEs, as does the d^3 configuration.

Table **10.8.2**: CFSEs for Octahedral Complexes with Different Electron Configurations (in Units of Δo)

	High Spin		CFSE (Δ_o)	Low Spin		CFSE (Δ_o)
	t_{2g}	e_g		t_{2g}	e_g	
d^0			0			
d^1	↑		0.4			
d^2	↑ ↑		0.8			
d^3	↑ ↑ ↑		1.2			
d^4	↑ ↑ ↑	↑	0.6	↑↓ ↑ ↑		1.6
d^5	↑ ↑ ↑	↑ ↑	0.0	↑↓ ↑↓ ↑		2.0
d^6	↑↓ ↑ ↑	↑ ↑	0.4	↑↓ ↑↓ ↑↓		2.4
d^7	↑↓ ↑↓ ↑	↑ ↑	0.8	↑↓ ↑↓ ↑↓	↑	1.8
d^8	↑↓ ↑↓ ↑↓	↑ ↑	1.2			
d^9	↑↓ ↑↓ ↑↓	↑↓ ↑	0.6			
d^{10}	↑↓ ↑↓ ↑↓	↑↓ ↑↓	0.0			

CFSEs are important for two reasons. First, the existence of CFSE nicely accounts for the difference between experimentally measured values for bond energies in metal complexes and values calculated based solely on electrostatic interactions. Second, CFSEs represent relatively large amounts of energy (up to several hundred kilojoules per mole), which has important chemical consequences.

> *Octahedral d^3 and d^8 complexes and low-spin d^6, d^5, d^7, and d^4 complexes exhibit large CFSEs.*

Summary

Crystal field theory, which assumes that metal–ligand interactions are only electrostatic in nature, explains many important properties of transition-metal complexes, including their colors, magnetism, structures, stability, and reactivity. Crystal field theory (CFT) is a bonding model that explains many properties of transition metals that cannot be explained using valence bond theory. In CFT, complex formation is assumed to be due to electrostatic interactions between a central metal ion and a set of negatively charged ligands or ligand dipoles arranged around the metal ion. Depending on the arrangement of the ligands, the d orbitals split into sets of orbitals with different energies. The difference between the energy levels in an octahedral complex is called the crystal field splitting energy (Δ_o), whose magnitude depends on the charge on the metal ion, the position of the metal in the periodic table, and the nature of the ligands. The spin-pairing energy (P) is the increase in energy that occurs when an electron is added to an already occupied orbital. A high-spin configuration occurs when the Δ_o is less than P, which produces complexes with the maximum number of unpaired electrons possible. Conversely, a low-spin configuration occurs when the Δ_o is greater than P, which produces complexes with the minimum number of unpaired electrons possible. Strong-field ligands interact strongly with the d orbitals of the metal ions and give a large Δ_o, whereas weak-field ligands interact more weakly and give a smaller Δ_o. The colors of transition-metal complexes depend on the environment of the metal ion and can be explained by CFT.

10.8: Bonding in Octahedral Complex Ions- Crystal Field Theory is shared under a not declared license and was authored, remixed, and/or curated by LibreTexts.

- **24.5: Bonding in Complex Ions: Crystal Field Theory** is licensed CC BY-NC-SA 4.0.

10.9: Bonding in Non-Octahedral Complex Ions- Crystal Field Theory

Learning Objectives

- Understand the d-orbital degeneracies of square planar and tetrahedral metal complexes.

Tetragonal and Square Planar Complexes

If two *trans*- ligands in an octahedral complex are either chemically different from the other four (as in *trans*-$[Co(NH_3)_4Cl_2]^+$), or at a different distance from the metal than the other four, the result is a tetragonally distorted octahedral complex. The electronic structures of such complexes are best viewed as the result of distorting an octahedral complex. Consider, for example, an octahedral complex such as $[Co(NH_3)_6]^{3+}$: two *trans*- NH_3 molecules are slowly removed from the metal along the ±z axes, as shown in the top half of Figure **10.9.1**. As the two axial Co–N distances increase simultaneously, the d-orbitals that interact most strongly with the two axial ligands decrease in energy due to a decrease in electrostatic repulsions between the electrons in these orbitals and the negative ends of the ligand dipoles. The affected d orbitals are those with a component along the ±z axes—d_{z^2}, d_{xz}, and d_{yz}. These orbitals are not affected equally, however: because the d_{z^2} orbital points directly at the two ligands being removed, its energy will decrease much more rapidly than the degenerate energies of the d_{xz} and d_{yz}, as shown in the bottom half of Figure **10.9.1**. In addition, the effective positive charge on the metal increases somewhat as the axial ligands are removed, increasing the attraction between the four remaining ligands and the metal. This increases the extent of their interactions with the other two d orbitals and increases their energies. Again, the two d orbitals are not affected equally: because the $d_{x^2-y^2}$ orbital points directly at the four in-plane ligands, its energy increases to a greater extent than the energy of the d_{xy} orbital, which points between the in-plane ligands. If the two axial ligands are moved infinitely far away from the metal, a square planar complex is formed. The energy of the d_{xy} orbital actually surpasses that of the d_{z^2} orbital in the process. The largest orbital splitting in a square planar complex, between the $d_{x^2-y^2}$ and d_{xy} energy levels, is identical in magnitude to Δ_o.

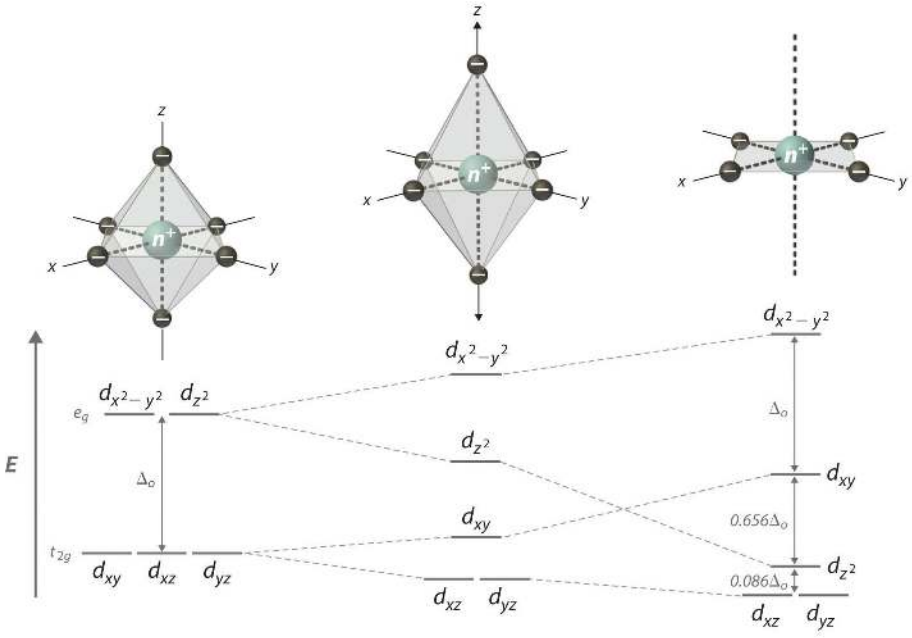


Figure **10.9.1** d-Orbital Splittings for Tetragonal and Square Planar Complexes. (CC BY-SA-NC; anonymous by request)

Moving the two axial ligands away from the metal ion along the z axis initially generates an elongated octahedral complex (the center compound of Figure **10.9.1**) and eventually produces a square planar complex (right). As shown below the structures, an axial elongation causes the d_{z^2} d_{xz} and d_{yz} orbitals to decrease in energy and the $\boldsymbol{d_{x^2-y^2}}$ and $\boldsymbol{d_{xy}}$ orbitals to increase in energy. The change in energy is not the same for all five d orbitals. The d_{z^2} orbital has a smaller xy component than does the d_{xy} orbital, so it reaches a lower energy level; thus, the order of these orbitals is reversed.

Tetrahedral Complexes

In a tetrahedral arrangement of four ligands around a metal ion, none of the ligands lies on any of the three coordinate axes (illustrated in part (a) in Figure **10.9.2**); consequently, none of the five d orbitals points directly at the ligands. Nonetheless, the d_{xy}, d_{xz}, and d_{yz} orbitals interact more strongly with the ligands than do $d_{x^2-y^2}$ and d_{z^2}; this again results in a splitting of the five d orbitals into two groups. The splitting of the energies of the orbitals in a tetrahedral complex (Δ_t) is much smaller than that for an octahedral complex (Δ_o), however, for two reasons: first, the d orbitals interact less strongly with the ligands in a tetrahedral arrangement; second, there are only four negatively-charged regions rather than six, which decreases the electrostatic interactions by one-third if all other factors are equal. It can be shown that for complexes of the same metal ion with the same charge, the same ligands, and the same M–L distance, $\Delta_t = \frac{4}{9}\Delta_o$. The relationship between the splitting of the five d orbitals in octahedral and tetrahedral crystal fields imposed by the same ligands is shown schematically in part (b) in Figure **10.9.2**.

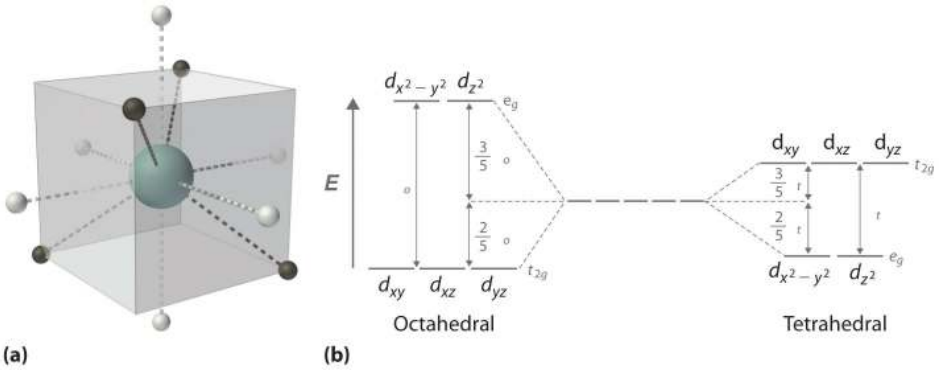


Figure **10.9.2**: d-Orbital Splittings for a Tetrahedral Complex. (a) In a tetrahedral complex, none of the five d orbitals points directly at or between the ligands. (b) Because the d_{xy}, d_{xz}, and d_{yz}orbitals (the t_{2g} orbitals) interact more strongly with the ligands than do the $d_{x^2-y^2}$ and d_{z^2} orbitals (the e_g orbitals), the order of orbital energies in a tetrahedral complex is the opposite of the order in an octahedral complex. (CC BY-SA-NC; anonymous by request)

> *$\Delta_t < \Delta_o$ because of weaker d-orbital–ligand interactions and decreased electrostatic interactions.*

Example **10.9.1**: Predicting Structure

For each complex, predict its structure, whether it is high spin or low spin, and the number of unpaired electrons present.

1. $[Cu(NH_3)_4]^{2+}$
2. $[Ni(CN)_4]^{2-}$

Solution

Because Δ_o is so large for the second- and third-row transition metals, all four-coordinate complexes of these metals are square planar due to the much higher crystal field stabilization energy (CFSE) for square planar versus tetrahedral structures. The only exception is for d^{10} metal ions such as Cd^{2+}, which have zero CFSE and are therefore tetrahedral as predicted by the VSEPR model. Four-coordinate complexes of the first-row transition metals can be either square planar or tetrahedral; the former is favored by strong-field ligands, whereas the latter is favored by weak-field ligands. For example, the $[Ni(CN)_4]^{2-}$ ion is square planar, while the $[NiCl_4]^{2-}$ ion is tetrahedral.

1.

The copper in this complex is a d^9 ion and it has a coordination number of 4. So it is probably either square planar or tetrahedral. To estimate which, we need to fill in the CFT splitting diagrams for each with 9 electrons and ask which has a lower energy. Comparing the square planer (Figure **10.9.1**) splitting diagram with tetrahedral (Figure **10.9.2**), suggests that 9 electrons will have a net lower total energy for square planar (since the $d_{x^2-y^2}$ orbital is high in energy, the others are lower).

For the square planar structure, neither high nor low spin states are possible (only one state) with a single unpaired electron.

2.

The nickle in this complex is a d^8 ion and it has a coordination number of 4. So it is probably either square planar or tetrahedral. To estimate which, we need to fill in the CFT splitting diagrams for each with 8 electrons and ask which has a lower energy. Comparing the square planer (Figure **10.9.1**) splitting diagram with tetrahedral (Figure **10.9.2**), suggests that 8 electrons will have a net lower total energy for square planar (since the $d_{x^2-y^2}$ orbital is high in energy, the others are lower).

For the square planar structure, it is a low spin complex since a high spin requires a lot of energy to promote to the $d_{x^2-y^2}$ orbital. Hence, there are no unpaired electrons

? Exercise 10.9.1

What are the geometries of the following two complexes?

1. $[AlCl_4]^-$
2. $[Ag(NH_3)_2]^+$

Answer 1

tetrahedral

Answer 2

linear

Summary

Distorting an octahedral complex by moving opposite ligands away from the metal produces a tetragonal or square planar arrangement, in which interactions with equatorial ligands become stronger. Because none of the d orbitals points directly at the ligands in a tetrahedral complex, these complexes have smaller values of the crystal field splitting energy Δ_t. In tetrahedral molecular geometry, a central atom is located at the center of four substituents, which form the corners of a tetrahedron. Tetrahedral geometry is common for complexes where the metal has d^0 or d^{10} electron configuration. The CFT diagram for tetrahedral complexes has $d_{x^2-y^2}$ and d_{z^2} orbitals equally low in energy because they are between the ligand axis and experience little repulsion. In square planar molecular geometry, a central atom is surrounded by constituent atoms, which form the corners of a square on the same plane. The square planar geometry is prevalent for transition metal complexes with d^8 configuration. The CFT diagram for square planar complexes can be derived from octahedral complexes yet the $d_{x^2-y^2}$ level is the most destabilized and is left unfilled.

10.9: Bonding in Non-Octahedral Complex Ions- Crystal Field Theory is shared under a not declared license and was authored, remixed, and/or curated by LibreTexts.

- **Non-octahedral Complexes** by Anonymous is licensed CC BY-NC-SA 4.0.

10.10: High Spin and Low Spin Complexes

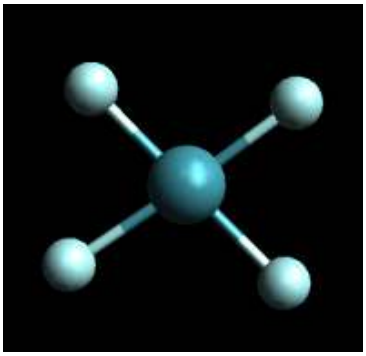
High spin and low spin are two possible classifications of spin states that occur in coordination compounds. These classifications come from either the ligand field theory, which accounts for the energy differences between the orbitals for each respective geometry, or the crystal field theory, which accounts for the breaking of degenerate orbital states, compared to the pairing energy.

Introduction

To understand the ligand field theory, one must understand molecular geometries. The three molecular geometries relevant to this module are: square planar, tetrahedral, and octahedral. Besides geometry, electrons and the rules governing the filling of the orbitals are also reviewed below.

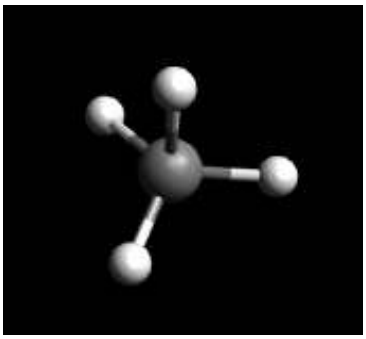
Square Planar Geometry

Square planar is the geometry where the molecule looks like a square plane. Additionally, the bond angles between the ligands (the ions or molecules bounded to the central atom) are 90°. This compound has a coordination number of 4 because it has 4 ligands bound to the central atom. An example of the square planar molecule XeF_4 is provided below.



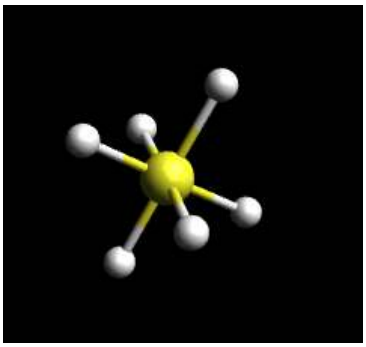
Tetrahedral Geometry

Tetrahedral geometry is a bit harder to visualize than square planar geometry. Tetrahedral geometry is analogous to a pyramid, where each of corners of the pyramid corresponds to a ligand, and the central molecule is in the middle of the pyramid. This geometry also has a coordination number of 4 because it has 4 ligands bound to it. Finally, the bond angle between the ligands is 109.5^o. An example of the tetrahedral molecule CH_4, or methane, is provided below.



Octahedral Geometry

Octahedral geometry is still harder to visualize because of how many ligands it contains. Octahedral geometry can be visualized in two ways: it can be thought of as two pyramids stuck together on their bases (one pyramid is upright and the other pyramid is glued to the first pyramid's base in an upside down manner) or it can be thought of as a molecule with square planar geometry except it has one ligand sticking out on top of the central molecule and another ligand sticking out under the central molecule (like a jack). Finally, the bond angle between the ligands is 90°. An example of the octahedral molecule SF_6 is provided below.



Electrons and Orbitals

When placing electrons in orbital diagrams, electrons are represented by arrows. An arrow pointing up corresponds a spin of +1/2 and an arrow pointing corresponds to a spin of -1/2. Electrons in different singly occupied orbitals of the same sub-shell have the same spins (or parallel spins, which are arrows pointing in the same direction). The sub-shell relates to the s, p, d, and f blocks that the electrons of an observed element are located. The s sub-shell has one orbital, the p sub-shell has three orbitals, the d sub-shell has five orbitals, and the f sub-shell has seven orbitals.

When filling orbitals with electrons, a couple of rules must be followed. According to the Aufbau principle, orbitals with the lower energy must be filled before the orbitals with the higher energy. Hunds rule states that all orbitals must be filled with one electron before electron pairing begins. Finally, the Pauli exclusion principle states that an orbital cannot have two electrons with the same spin. The ligand field theory and the splitting of the orbitals helps further explain which orbitals have higher energy and in which order the orbitals should be filled.

Ligand Field Theory

The ligand field theory is the main theory used to explain the splitting of the orbitals and the orbital energies in square planar, tetrahderal, and octahedral geometry. The ligand field theory states that electron-electron repulsion causes the energy splitting between orbitals. It states that the ligand fields may come in contact with the electron orbitals of the central atom, and those orbitals that come in direct contact with the ligand fields have higher energy than the orbitals that come in indirect contact with the ligand fields. This is because when the orbital of the central atom comes in direct contact with the ligand field, a lot of electron-electron repulsion is present as both the ligand field and the orbital contain electrons. Remember, opposites attract and likes repel. Thus, due to the strong repelling force between the ligand field and the orbital, certain orbitals have higher energies than others. One thing to keep in mind is that this energy splitting is different for each molecular geometry because each molecular geometry can hold a different number of ligands and has a different shape to its orbitals.

Spin

A complex can be classified as high spin or low spin. When talking about all the molecular geometries, we compare the crystal field splitting energy (Δ) and the pairing energy (P). Normally, these two quantities determine whether a certain field is low spin or high spin.

When the crystal field splitting energy is greater than the pairing energy, electrons will fill up all the lower energy orbitals first and only then pair with electrons in these orbitals before moving to the higher energy orbitals. Electrons tend to fall in the lowest possible energy state, and since the pairing energy is lower than the crystal field splitting energy, it is more energetically favorable for the electrons to pair up and completely fill up the low energy orbitals until there is no room left at all, and only then begin to fill the high energy orbitals. On the other hand, when the pairing energy is greater than the crystal field energy, the electrons will occupy all the orbitals first and then pair up, without regard to the energy of the orbitals. If every orbital of a lower energy had one electron, and the orbitals of the hext higher energy had none, an electron in this case would occupy the higher energy orbital. This follows Hund's rule that says all orbitals must be occupied before pairing begins. Remember, this situation only occurs when the pairing energy is greater than the crystal field energy. These phenomena occur because of the electron's tendency to fall into the lowest available energy state.

Another method to determine the spin of a complex is to look at its field strength and the wavelength of color it absorbs. If the field is strong, it will have few unpaired electrons and thus low spin. If the field is weak, it will have more unpaired electrons and thus high spin. In terms of wavelength, a field that absorbs high energy photons (in other words, low wavelength light) has low spin and a field that absorbs low energy photons (high wavelength light) has high spin.

Once again, whether a complex is high spin or low spin depends on two main factors: the crystal field splitting energy and the pairing energy. The electrons will take the path of least resistance--the path that requires the least amount of energy. If the paring energy is greater than Δ, then electrons will move to a higher energy orbital because it takes less energy. If the pairing energy is less than Δ, then the electrons will pair up rather than moving singly to a higher energy orbital. Below, tips and examples are given to help figure out whether a certain molecule is high spin or low spin.

Example 1

Is the $[Co(H_2O)_6]^{3+}$ complex ion expected to be high or low spin?

Solution

What do we know?

- The complex has an octahedral shape
- The aqua ligand (H_2O) is typically regarded as weak-field ligand
- The d electron configuration for Co is d^6
- The splitting energy is small

Therefore, the complex is expected to be high spin.

Example 2

Do you expect the $[Ni(CN)_4]^{2-}$ complex ion to be high or low spin?

Solution

What do we know?

- The complex has a square planar shape
- CN^- is a strong-field ligand
- The d electron configuration for Ni is d^8
- The splitting energy is large

Therefore, the complex is low spin.

Example 3

Do you expect the $[CoF_6]^{3-}$ complex ion to be high or low spin?

Solution

What do we know?

- The complex has an octahedral shape
- F^- is a weak-field ligand
- The d electron configuration for Co is d^6
- The splitting energy is small

Therefore, the complex is high spin.

Spectrochemical Series

Another tool used often in calculations or problems regarding spin is called the spectrochemical series. The spectrochemical series is a list that orders ligands on the basis of their field strength. Ligands that have a low field strength, and thus high spin, are listed first and are followed by ligands of higher field strength, and thus low spin. This trend also corresponds to the ligands abilities to split d orbital energy levels. The ones at the beginning, such as I^-, produce weak splitting (small Δ) and are thus weak field ligands. The ligands toward the end of the series, such as CN^-, will produce strong splitting (large Δ) and thus are strong field ligands. A picture of the spectrochemical series is provided below.

(weak) $I^- < Br^- < S^{2-} < SCN^- < Cl^- < NO_3^- < N_3^- < F^- < OH^- < C_2O_4^{2-} \approx H_2O <$

$NCS^- < CH_3CN < py < NH_3 < en < bipy < phen < NO_2^- < PPh_3 < CN^- \approx CO$ *(strong)*

Octahedral Complexes

Octahedral complexes have a coordination number of 6, meaning that there are six places around the metal center where ligands can bind. Interactions between the electrons of the ligands and those of the metal center produce a crystal field splitting where the dz^2 and dx^2-y^2 orbitals raise in energy, while the other three orbitals of dxz, dxy, and dyz, are lower in energy. This results from the interaction between the orbitals and the ligand field. The ligand field runs almost right into the dz^2 and dx^2-y^2 orbitals, thus having direct contact with these two orbitals. Due to this direct contact, a lot of electron-electron repulsion occurs between the ligand fields and the dz^2 and dx^2-y^2 orbitals, which results in the dz^2 and dx^2-y^2 orbitals having high energy, as the repulsion has to be manifested somewhere. The ligand field only brushes through the other three dxz, dxy, and dyz orbitals. Since the ligand field does not have such direct contact with these orbitals and since there is not as much resulting electron-electron repulsion, the dxz, dxy, and dyz orbitals have lesser energy than the dz^2 and dx^2-y^2 orbitals. It is this difference in energy between the dz^2 and dx^2-y^2 orbitals and the dxz, dxy, and dyz orbitals that is known as crystal field splitting.

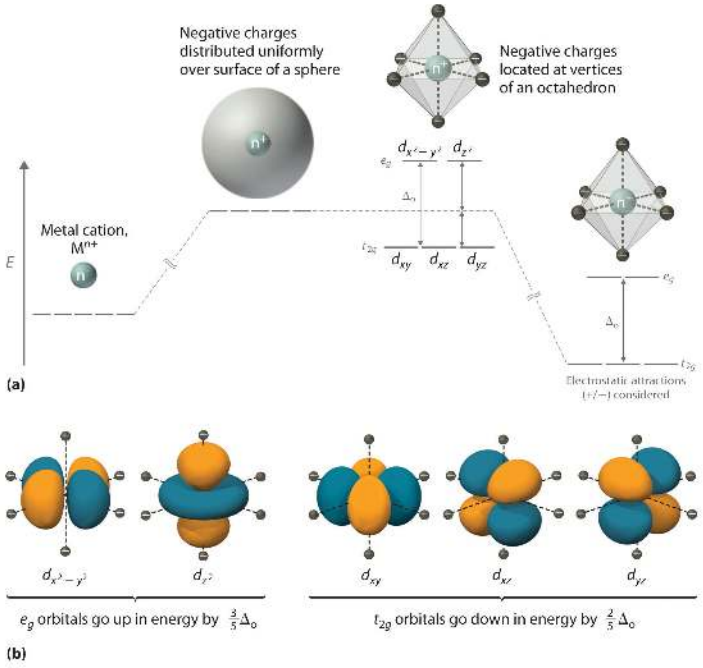


***Figure 1**: Octahedral Complex Splitting:*

In an octahedral complex, when Δ is large (strong field ligand), the electrons will first fill the lower energy d orbitals before any electrons are placed on the higher energy d orbitals. It is then classified as low spin because there is a minimal amount of unpaired electrons. When Δ is small, the pairing energy exceeds the splitting energy, and the electrons will fill the d orbitals as if they were degenerate; this is classified as high spin.

The oxidation state of the metal also determines how small or large Δ is. The higher the oxidation state of the metal, the stronger the ligand field that is created. In the event that there are two metals with the same d electron configuration, the one with the higher

oxidation state is more likely to be low spin than the one with the lower oxidation state.

Usually, the field strength of the ligand, which is also determined by large or small Δ, determines whether an octahedral complex is high or low spin. This is where we use the spectrochemical series to determine ligand strength. Strong-field ligands, like CN^- and NO_2^-, increase Δ which results in low spin. While weak-field ligands, like I^- and Cl^-, decrease the Δ which results in high spin.

Tetrahedral Complexes

The splitting of tetrahedral complexes is directly opposite that of the splitting of the octahedral complexes. Recall that in octahedral complexes, the d_{z^2} and $d_{x^2-y^2}$ orbitals have higher energy than the d_{xz}, d_{xy}, and d_{yz} orbitals. In tetrahedral complexes, the opposite occurs because the d_{xz}, d_{xy}, and d_{yz} orbitals have higher energy than the dz^2 and dx^2-y^2 orbitals. This is once again because the contact between the ligands and the orbitals is reverse that of octahedral complexes. Unlike octahedral complexes, the ligands of tetrahedral complexes come in direct contact with the d_{xz}, d_{xy}, and d_{yz} orbitals. Thus, these orbitals have high electron-electron repulsion, due to the direct contact, and thus higher energy. The d_{z^2} and $d_{x^2-y^2}$ orbitals do not have as direct contact as the ligands kind of squeeze past or slide by these orbitals, thus lowering the electron-electron repulsion and the energy of the orbital.

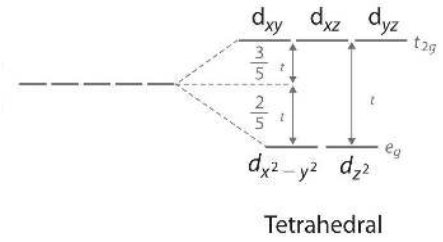
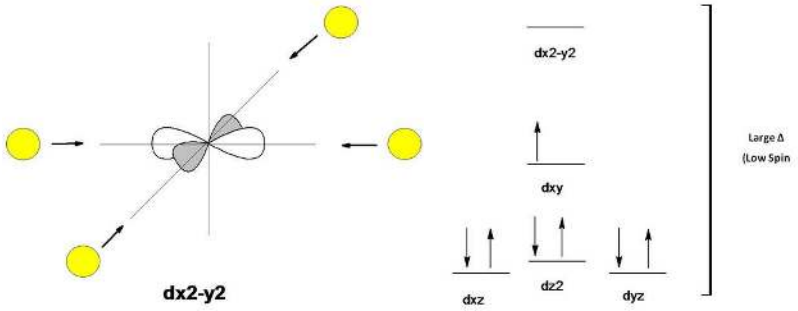


***Figure** 2: Tetrahedral Complex Splitting:*

In a tetrahedral complex, Δ_t is relatively small even with strong-field ligands as there are fewer ligands to bond with. It is rare for the Δ_t of tetrahedral complexes to exceed the pairing energy. Usually, electrons will move up to the higher energy orbitals rather than pair. Because of this, most tetrahedral complexes are high spin.

Square Planar Complexes

A square planar complex also has a coordination number of 4. The structure of the complex differs from tetrahedral because the ligands form a simple square on the x and y axes. Because of this, the crystal field splitting is also different. Since there are no ligands along the z-axis in a square planar complex, the repulsion of electrons in the d_{xz}, d_{yz}, and the d_{z^2} orbitals are considerably lower than that of the octahedral complex (the dz^2 is slightly higher in energy to the "doughnut" that lies on the x,y axis). The dx^2-y^2 orbital has the most energy, followed by the dxy orbital, which is followed by the remaining orbtails (although dz^2 has slightly more energy than the dxz and dyz orbital). This pattern of orbital splitting remains constant throughout all geometries. Whichever orbitals come in direct contact with the ligand fields will have higher energies than orbitals that slide past the ligand field and have more of indirect contact with the ligand fields. So when confused about which geometry leads to which splitting, think about the way the ligand fields interact with the electron orbitals of the central atom.



In square planar complexes Δ will almost always be large, even with a weak-field ligand. Electrons tend to be paired rather than unpaired because paring energy is usually much less than Δ. Therefore, square planar complexes are usually low spin.

Tips For Determining High Spin or Low Spin Configurations

1. Determine the shape of the complex (i.e. octahedral, tetrahedral, square planar)
2. Determine the oxidation state of the metal center
3. Determine the d electron configuration of the metal center
4. Draw the crystal field diagram of the complex with regards to its geometry
5. Determine whether the splitting energy is greater than the pairing energy
6. Determine the strength of the ligand (i.e. spectrochemical series)

Crystal Field Splitting Electron Count

In order to make a crystal field diagram of a particular coordination compound, one must consider the number of electrons. This can be done simply by recognizing the ground state configuration of the electron and then adjusting the number of electrons with respect to the charge of the metal. For example, one can consider the following chemical compounds. These four examples demonstrate how the number of electrons are determined and used in making Crystal Field Diagrams.

Example 4

What is the number of electrons of the metal in this complex: $[CoF_6]^{3-}$?

Solution

This coordination compound has Cobalt as the central transition metal and 6 Fluoro monodentate ligands. However, in this example as well as most other examples, we will focus on the central transition metal. We must determine the oxidation state of Cobalt in this example. Fluorine has a charge of -1 and the overall molecule has a charge of -3. Since there are six fluorines, the overall charge of fluorine is -6. The charge of Cobalt will add to this -6, so that the charge of the overall molecule is -3. Thus, we know that Cobalt must have a charge of +3 (see below). The electron configuration of Cobalt is $[Ar]4s^23d^7$. When observing Cobalt 3+, we know that Cobalt must lose three electrons. The first two to go are from the 4s orbital and Cobalt becomes:$[Ar]4s^03d^7$. Then, the next electron leaves the 3d orbital and the configuration becomes: $[Ar]4s^03d^6$. Thus, we can see that there are six electrons that need to be apportioned to Crystal Field Diagrams. The pairing of these electrons depends on the ligand. Since Fluorine is a weak field, it will be a high spin complex.

Cobalt charge Fluorine charge Overall charge

$x + -1(6) = -3$

$x + -6 = -3$

$x=-3+6$

$x=+3$

Example 5

What is the number of electrons of the metal in this complex: $[Co(NH_3)_6]^{3+}$?

Solution

This coordination compound has Cobalt as the central Transition Metal and 6 Ammonias as Monodentate Ligands. We must determine the oxidation state of Cobalt in this example. Ammonia has a charge of 0 and the overall molecule has a charge of +3. Since there are six Ammonias the overall charge of of it is 0. The charge of Cobalt will add to this 0, so that the charge of the overall molecule is +3. Thus, we know that Cobalt must have a charge of +3 (see below). In order to find the number of electrons, we must focus on the central Transition Metal. The electron configuration of Cobalt is $[Ar]4s^23d^7$. When observing Cobalt 3+, we know that Cobalt must lose three electrons. The first two to go are from the 4s orbital and Cobalt becomes: $[Ar]4s^03d^7$. Then, the next electron leaves the 3d orbital and the configuration becomes: $[Ar]4s^03d^6$. Thus, we can see that there are six electrons that need to be apportioned to Crystal Field Diagrams. The pairing of these electrons depends on the ligand. Since Ammonia is a strong field ligand, it will be a low spin complex.

Cobalt charge Ammonia charge Overall charge

x + 0(6) = +3

x + 0 = +3

x=+3

Example 6

What is the number of electrons of the metal in this complex: $[Fe(CN)_6]^{3-}$?

Solution

This coordination compound has Iron as the central Transition Metal and 6 Cyanides as Monodentate Ligands. We must determine the oxidation state of Iron in this example. Cyanide has a charge of -1 and the overall molecule has a charge of -3. Since there are six Cyanides the overall charge of of it is -6. The charge of Iron will add to this -6, so that the charge of the overall molecule is -3. Thus, we know that Iron must have a charge of +3 (see below). In order to find the number of electrons, we must focus on the central Transition Metal. The electron configuration of Iron is $[Ar]4s^23d^6$. When observing Iron 3+, we know that Iron must lose three electrons. The first two to go are from the 4s orbital and Iron becomes:$[Ar]4s^03d^6$. Then, the next electron leaves the 3d orbital and the configuration becomes: $[Ar]4s^03d^5$. Thus, we can see that there are five electrons that need to be apportioned to Crystal Field Diagrams. The pairing of these electrons depends on the ligand. Since Cyanide is a strong field ligand, it will be a low spin complex.

Iron charge Cyanide charge Overall charge

x + -1(6) = -3

x + -6 = -3

x=-3+6

x=+3

Example 7

$[Ni(CN)_4]^{2-}$

Solution

This coordination compound has Nickel as the central Transition Metal and 4 Cyanides as Monodentate Ligands. We must determine the oxidation state of Nickel in this example. Cyanide has a charge of -1 and the overall molecule has a charge of -2. Since there are four Cyanides, the overall charge of it is -4. The charge of Nickel will add to this -4, so that the charge of the overall molecule is -2. Thus, we know that Nickel must have a charge of +2 (see below). In order to find the number of electrons, we must focus on the central transition metal. The electron configuration of Nickel is $[Ar]4s^23d^8$. When observing Nickel 3+, we know that Nickel must lose two electrons. The two to go are from the 4s orbital and Nickel becomes:$[Ar]4s^03d^8$. Thus, we can see that there are eight electrons that need to be apportioned to Crystal Field Diagrams. The pairing of these electrons depends on the ligand. Since Cyanide is a strong field ligand, it will be a low spin complex.

Nickel charge Cyanide charge Overall charge

x + -1(4) = -2

x + -4 = -2

x=-2+4

x=+2

Applications

Magnetism

The crystal field splitting can also be used to figure out the magnetism of a certain coordination compound. Recall, that diamagnetism is where all the electrons are paired and paramagnetism is where one or more electron is unpaired. This property can be used to determine the magnetism and in some cases the filling of the orbitals. For example, given a high spin octahedral molecule, one just has to fill in all the orbitals and check for unpaired electrons. If no unpaired electrons exist, then the molecule is diamagnetic but if unpaired molecules do exist, the molecule is paramagnetic. These properties of magnetism can also be used to predict how the orbitals will be filled, an alternate method to relying on spin to predict the filling of orbitals. For example, if a given molecule is diamagnetic, the pairing must be done in such a way that no unpaired electrons exist. On the other hand, if the given molecule is paramagnetic, the pairing must be done in such a way that unpaired molecules do exist. Examples of these properties and applications of magnetism are provided below.

Color

Crystal field splitting can be used to account for the different colors of the coordinate compounds. *Low spin* complexes with *strong field* ligands absorb light at *shorter wavelengths* (higher energy) and *high spin* complexes with *weak field* ligands absorb light at *longer wavelengths* (lower energy). Based on the ligands involved in the coordination compound, the color of that coordination compound can be estimated using the strength the ligand field. See Tanabe-Sugano Diagrams for more advanced applications.

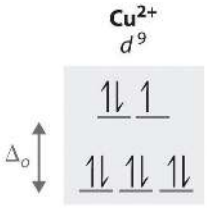
Sample Problems

Questions

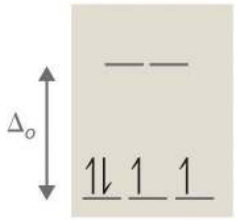
1. Is square planar usually low spin or high spin?
2. Draw the crystal field energy diagram of $[Cu(Cl)_6]^{-4}$.
3. What is the spectrochemical series?
4. Draw the crystal field energy diagram of $[Mn(CN)_4]^{-1}$.
5. What causes the energy difference between the orbitals in an octahedral field?
6. Classify the spin of $[FeBr_4]^{-2}$.

Answers

1. Due to the high crystal field splitting energy, square planar complexes are usually low spin.
2. By doing some simple algebra and using the -1 oxidation state of chloro ligand and the overall charge of -4, we can figure out that the oxidation state of copper is +2 charge. In its non-ionized state, copper has the following electron distribution: $[Ar]4s^1 3d^{10}$. +2 means that copper will loose two electrons and will thus have a configuration of $[Ar]3d^9$. Using the spectrochemical series, we can figure out that the chloro ligand is a weak field and induces low spin complex. How this is meaningless this problem since the appropriate crystal field energy diagram shows that only one configuration is possible irrespective of the strength of the ligand field:



3. The spectrochemical series is a series that orders ligands based on their field strength. It is often used in problems to determine the strength and spin of a ligand field so that the electrons can be distributed appropriately.
4. Just like problem 2, the first thing to do is to figure out the charge of Mn. Since we know the CN has a charge of -1, and there are four of them, and since the overall molecule has a charge of -1, manganese has a oxidation state of +3. In its ground state, manganese has the following electron distribution: $[Ar]4s^2 3d^5$. The +3 oxidation state means that manganese will loose three electrons and will thus have a configuration of $[Ar]3d^4$. Using the spectrochemical series, we can figure out the strength of the CN ligand field, which is a strong field ligand and induces low spin complexes. The appropriate crystal field energy diagram would look like:



Low spin

5. The negative-negative repulsion between the electrons of the central atom and between the ligand field causes certain orbitals, namely the dz^2 and dx^2-y^2 orbitals, to have higher energy than the d_{xz}, d_{xy}, and d_{yz} orbitals.
6. Since the bromo ligand is a weak field ligand (as per the spectrochemical series), this molecule is high spin.

External Links

1. Orbitals and electron configuration review part one of two. http://www.youtube.com/watch?v=M7fgT-hI6jk
2. Orbitals and electron configuration review part two of two. http://www.youtube.com/watch?v=9frZH1UsY_s&feature=related
3. Electronic structure of coordination complexes. http://www.youtube.com/watch?v=mAPFhZpnV58

Resources

1. Petrucci, Ralph H. General Chemistry Principles and Modern Applications. 9th ed. Upper Saddle River: Pearson Prentice Hall, 2002, Chapter 24
2. Rodgers, Glen E. Descriptive Inorganic, Coordination, and Solid-State Chemistry. 2nd ed. McGraw-Hill: New York, 1994, Chapter

Contributors and Attributions

- Angad Oberoi (UCD), Justin Nuckles (UCD)

10.10: High Spin and Low Spin Complexes is shared under a CC BY-NC-SA 4.0 license and was authored, remixed, and/or curated by LibreTexts.

10.11: Magnetic Behavior of Atoms, Molecules, and Materials

Learning Objectives

- To understand the difference between Ferromagnetism, paramagnetism and diamagnetism
- To identify if a chemical will be paramagnetic or diamagnetic when exposed to an external magnetic field

The magnetic moment of a system measures the strength and the direction of its magnetism. The term itself usually refers to the magnetic dipole moment. Anything that is magnetic, like a bar magnet or a loop of electric current, has a magnetic moment. A magnetic moment is a vector quantity, with a magnitude and a direction. An electron has an electron magnetic dipole moment, generated by the electron's intrinsic spin property, making it an electric charge in motion. There are many different magnetic behavior including paramagnetism, diamagnetism, and ferromagnetism.

An interesting characteristic of transition metals is their ability to form magnets. Metal complexes that have unpaired electrons are magnetic. Since the last electrons reside in the d orbitals, this magnetism must be due to having unpaired d electrons. The spin of a single electron is denoted by the quantum number m_s as +(1/2) or –(1/2). This spin is negated when the electron is paired with another, but creates a weak magnetic field when the electron is unpaired. More unpaired electrons increase the paramagnetic effects. The electron configuration of a transition metal (d-block) changes in a coordination compound; this is due to the repulsive forces between electrons in the ligands and electrons in the compound. Depending on the strength of the ligand, the compound may be paramagnetic or diamagnetic.

Ferromagnetism (Permanent Magnet)

Ferromagnetism is the basic mechanism by which certain materials (such as iron) form **permanent magnets**. This means the compound shows permanent magnetic properties rather than exhibiting them only in the presence of an external magnetic field (Figure 10.11.1). In a ferromagnetic element, electrons of atoms are grouped into domains in which each domain has the same charge. In the presence of a magnetic field, these domains line up so that charges are parallel throughout the entire compound. Whether a compound can be ferromagnetic or not depends on its number of unpaired electrons and on its atomic size.

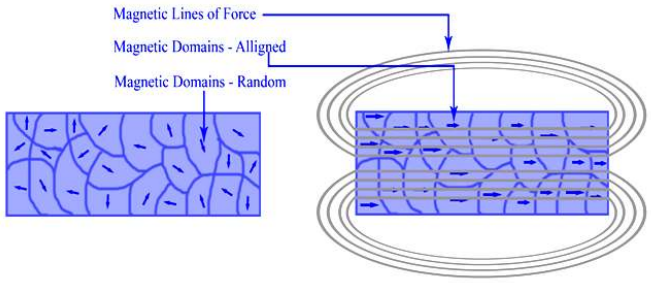


Figure 10.11.1: Ferromagnetism (a) nonmagnatized material and (2) Magnetized material with corresponding magnetic fields shown.

Ferromagnetism, the permanent magnetism associated with nickel, cobalt, and iron, is a common occurrence in everyday life. Examples of the knowledge and application of ferromagnetism include Aristotle's discussion in 625 BC, the use of the compass in 1187, and the modern-day refrigerator. Einstein demonstrated that electricity and magnetism are inextricably linked in his theory of special relativity.

Paramagnetism (Attracted to Magnetic Field)

Paramagnetism refers to the magnetic state of an atom with one or more unpaired electrons. The unpaired electrons are attracted by a magnetic field due to the electrons' magnetic dipole moments. Hund's Rule states that electrons must occupy every orbital singly before any orbital is doubly occupied. This may leave the atom with many unpaired electrons. Because unpaired electrons can spin in either direction, they display magnetic moments in any direction. This capability allows paramagnetic atoms to be attracted to magnetic fields. Diatomic oxygen, O_2 is a good example of paramagnetism (described via molecular orbital theory). The following video shows liquid oxygen attracted into a magnetic field created by a strong magnet:



Video 10.11.1: Paramagnetism of Liquid Oxygen

Diamagnetism (Repelled by Magnetic Field)

As shown in the video, molecular oxygen (O_2) is paramagnetic and is attracted to the magnet. In contrast, molecular nitrogen (N_2) has no unpaired electrons and is diamagnetic; it is unaffected by the magnet. Diamagnetic substances are characterized by paired electrons, e.g., no unpaired electrons. According to the Pauli Exclusion Principle which states that no two electrons may occupy the same quantum state at the same time, the electron spins are oriented in opposite directions. This causes the magnetic fields of the electrons to cancel out; thus there is no net magnetic moment, and the atom cannot be attracted into a magnetic field. In fact, diamagnetic substances are weakly ***repelled*** by a magnetic field as demonstrated with the pyrolytic carbon sheet in Figure 10.11.2.

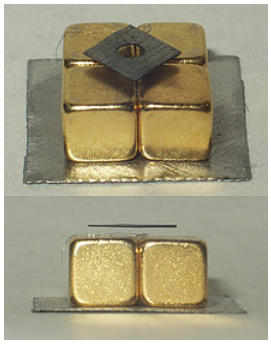


Figure 10.11.2: Levitating pyrolytic carbon: A small (~6 mm) piece of pyrolytic graphite levitating over a permanent neodymium magnet array (5 mm cubes on a piece of steel). Note that the poles of the magnets are aligned vertically and alternate (two with north facing up, and two with south facing up, diagonally). (Public Domain; Splarka via Wikipedia).

How to Tell if a Substance is Paramagnetic or Diamagnetic

The magnetic properties of a substance can be determined by examining its electron configuration: If it has unpaired electrons, then the substance is paramagnetic and if all electrons are paired, the substance is then diamagnetic. This process can be broken into three steps:

1. Write down the electron configuration
2. Draw the valence orbitals
3. Identify if unpaired electrons exist
4. Determine whether the substance is paramagnetic or diamagnetic

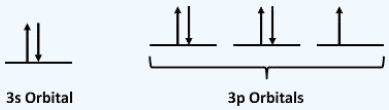
Example 10.11.1: Chlorine Atoms

Step 1: Find the electron configuration

For Cl atoms, the electron configuration is $3s^2 3p^5$

Step 2: Draw the valence orbitals

Ignore the core electrons and focus on the valence electrons only.



Step 3: Look for unpaired electrons

There is one unpaired electron.

Step 4: Determine whether the substance is paramagnetic or diamagnetic

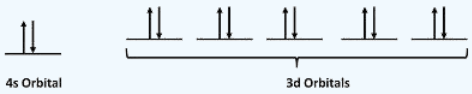
Since there is an unpaired electron, **Cl** atoms are paramagnetic (albeit, weakly).

Example 10.11.2: Zinc Atoms

Step 1: Find the electron configuration

For Zn atoms, the electron configuration is $4s^2 3d^{10}$

Step 2: Draw the valence orbitals



Step 3: Look for unpaired electrons

There are no unpaired electrons.

Step 4: Determine whether the substance is paramagnetic or diamagnetic

Because there are no unpaired electrons, **Zn** atoms are diamagnetic.

Exercise 10.11.1

a. How many unpaired electrons are found in oxygen atoms ?
b. How many unpaired electrons are found in bromine atoms?
c. Indicate whether boron atoms are paramagnetic or diamagnetic.
d. Indicate whether $\mathbf{F^-}$ ions are paramagnetic or diamagnetic.
e. Indicate whether $\mathbf{Fe^{2+}}$ ions are paramagnetic or diamagnetic.

Answer a

The O atom has $2s^2 2p^4$ as the electron configuration. Therefore, O has 2 unpaired electrons.

Answer b

The Br atom has $4s^2 3d^{10} 4p^5$ as the electron configuration. Therefore, Br has 1 unpaired electron.

Answer c

The B atom has $2s^2 2p^1$ as the electron configuration. Because it has one unpaired electron, it is paramagnetic.

Answer d

The $\mathbf{F^-}$ ion has $2s^2 2p^6$ as the electron configuration. Because it has no unpaired electrons, it is diamagnetic.

Answer e

The Fe^{2+} ion has $3d^6$ as the electron configuration. Because it has 4 unpaired electrons, it is paramagnetic.

References

1. Pettrucci, Ralph H. General Chemistry: Principles and Modern Applications. 9th. Upper Saddle River: Pearson Prentice Hall, 2007
2. Sherman, Alan, Sharon J. Sherman, and Leonard Russikoff. Basic Concepts of Chemistry Fifth Edition. Boston, MA: Houghton Mifflin Company, 1992. Print.

Contributors and Attributions

- Jim Clark (Chemguide.co.uk)
- Dr. Richard Spinney (The Ohio State University)

10.11: Magnetic Behavior of Atoms, Molecules, and Materials is shared under a not declared license and was authored, remixed, and/or curated by LibreTexts.

10.12: Magnetic Behavior of Complex Ions

Learning Objectives

- Discuss the correlation between the electronic structure of a coordination complex and its magnetic properties

Experimental evidence of magnetic measurements supports the theory of high- and low-spin complexes. Remember that molecules such as O_2 that contain unpaired electrons are paramagnetic. Paramagnetic substances are attracted to magnetic fields. Many transition metal complexes have unpaired electrons and hence are paramagnetic. Molecules such as N_2 and ions such as Na^+ and $[Fe(CN)_6]^{4-}$ that contain no unpaired electrons are **diamagnetic**. Diamagnetic substances have a slight tendency to be **repelled** by magnetic fields.

When an electron in an atom or ion is unpaired, the magnetic moment due to its spin makes the entire atom or ion **paramagnetic**. The size of the magnetic moment of a system containing unpaired electrons is related directly to the number of such electrons: the greater the number of unpaired electrons, the larger the magnetic moment. Magnetic susceptibility measures the force experienced by a substance in a magnetic field. When we compare the weight of a sample to the weight measured in a magnetic field (Figure 10.12.1), paramagnetic samples that are attracted to the magnet will appear heavier because of the force exerted by the magnetic field. We can calculate the number of unpaired electrons based on the increase in weight.

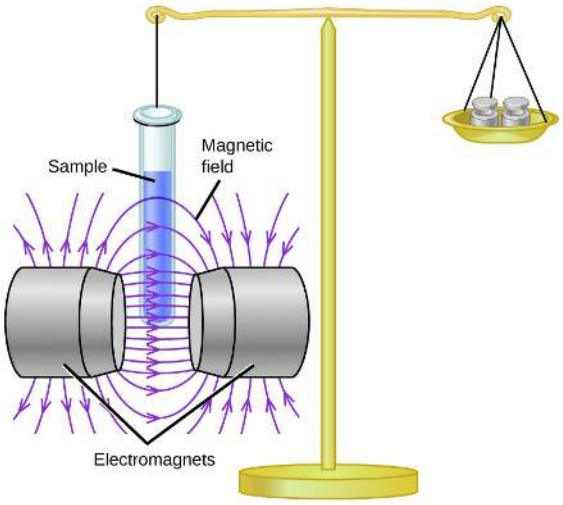


Figure 10.12.1: A Gouy balance compares the mass of a sample in the presence of a magnetic field with the mass with the electromagnet turned off to determine the number of unpaired electrons in a sample. (CC BY-SA 3.0; OpenStax).

From this experiment, the measured magnetic moment of low-spin d^6 $[Fe(CN)_6]4-$ ion confirms that iron is diamagnetic, whereas the high-spin d^6 $[Fe(H_2O)_6]^{2+}$ complex has four unpaired electrons with a magnetic moment that confirms this arrangement. Therefore, the observed magnetic moment is used to determine the number of unpaired electrons present.

Magnetic Properties of Coordination Compounds

An interesting characteristic of transition metals is their ability to form magnets. Metal complexes that have unpaired electrons are magnetic. Since the last electrons reside in the d orbitals, this magnetism must be due to having unpaired d electrons. Considering only monometallic complexes, unpaired electrons arise because the complex has an odd number of electrons or because electron pairing is destabilized. For example, the Ti(III) ion has one d electron and must be (weakly) paramagnetic, regardless of the geometry or the nature of the ligands. However, the Ti(II) ion with two d-electrons, sometimes forms complexes with two unpaired electrons and sometimes forms complexes with no unpaired electrons.

As an example, Fe prefers to exist as Fe^{3+} and is known to have a coordination number of six. Since the configuration of Fe^{3+} has five d electrons, we would expect to see five unpaired spins in complexes with Fe. This is true for $[FeF_6]^{3-}$; however, $[Fe(CN)_6]^{3-}$ only has one unpaired electron, making it a weaker magnet. This trend can be explained based on the properties of the ligands.

Based off the spectrochemical series, we expect CN^- ligands to have a stronger electric field than that of F^- ligands, so the energy differences in the d-orbitals should be greater for the cyanide complex.

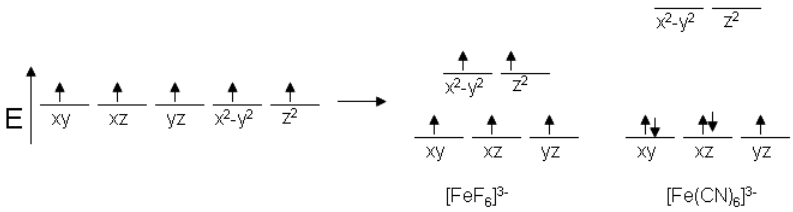


Figure 10.12.2: Crystal field theory splitting diagram. Example of influence of ligand electronic properties on d orbital splitting. This shows the comparison of low-spin versus high-spin electrons.

For this to make sense, there must be some sort of energy benefit to having paired spins for our cyanide complex (the spin pairing energy). That is, the energy level difference must be more than the repulsive energy of pairing electrons together. Since systems strive to achieve the lowest energy possible, the electrons will pair up before they will move to the higher orbitals. This is referred to as low spin, and an electron moving up before pairing is known as high spin.

Exercise 10.12.1

Which ligand is most likely to form a high-spin complexes when bound to transition metals: en, F^- , or CN^-?

Answer

F^- are more likely to form high spin complexes, since is a weak-field ligand on the spectrochemical series.

Tetrahedral complexes have naturally weaker splitting because none of the ligands lie within the plane of the orbitals. As a result, they have either have too many or too few d electrons to warrant consideration about high or low spin configurations. Square planar compounds, on the other hand, stem solely from transition metals with eight d electrons. For example, $[Ni(CN)_4]^{2-}$, $[Pt(NH_3)_3Cl]^+$, and $[PtCl_4]^{2-}$ are all diamagnetic. Since this encompasses the full spectrum of ligand strength, we can conclude that square planar compounds are always low spin and therefore are weakly magnetic.

Example 10.12.2

Which one of the following coordination compounds would you expect to be paramagnetic?

a. $[Zn(NH_3)_4]Cl_2$
b. $K[FeCl_4]$ (low spin, tetrahedral)
c. $[Cd(H_2O)_6]SO_4$

Solution

Let's consider each compound individually. Since each compound has only one complex ion, we only need to consider how the d electrons are distributed in the ligand field of that ion. We can ignore the other parts (the counter ions) of the compound.

a. The zinc ion in $[Zn(NH_3)_4]Cl_2$ has a +2 oxidation state, so it is a d^{10} ion since the zinc atom loses two 4s electrons and no 3d electrons to form the ion. We do not need to fill ion the electrons in the corresponding tetrahedral d-orbital diagram, since we know they will all be paired up. This is a diamagnetic compound.
b. The iron ion in $K[FeCl_4]$ (low spin, tetrahedral) has a 3+ oxidation state so it is a d^5 ion since the iron atom loses two 4s electrons and one 3d electron. Adding 5 electrons to the tetrahedral d-orbital diagram identifies that one electron will be unpaired. This compound will be paramagnetic (but weakly since only on electron is unpaired).
c. The cadmium ion in $[Cd(H_2O)_6]SO_4$ has a +2 oxidation state, so it is a d^{10} ion since the cadmium atom loses two 5s electrons and no 4d electrons to form the ion. We do not need to fill ion the electrons in the corresponding octahedral d-orbital diagram, since we know they will all be paired up. This is a diamagnetic compound.

Exercise 10.12.2

Predict the number of unpaired electrons for each of the following complex ions

a. $[Fe(CN)_6]^{4-}$
b. $[Ru(NH_3)_6]^{3+}$
c. $[Cr(NH_3)_6]^{2+}$
d. $[EuCl_6]^{4-}$

Answer a

Fe^{2+} is $3d^6$ ion and has 0 unpaired electron in low spin complexes

Answer b

Ru^{3+} is $4d^5$ ion and has 1 unpaired electron in low spin complexes

Answer c

Cr^{2+} is $4d^4$ ion and has 4 and 2 unpaired electrons in high spin and low spin complexes, respectively, depending on spin pairing energy

Answer d

Eu^{2+} is $4f^7$ ion and has 7 unpaired electrons in high spin complexes

In bi- and polymetallic complexes, in which the individual centers have an odd number of electrons or electrons are high-spin, the situation is more complicated. If there is interaction between the two (or more) metal centers, the electrons may couple, resulting in a weak magnet, or they may enhance each other. When there is no interaction, the two (or more) individual metal centers behave as if in two separate molecules.

Summary

- Unpaired electrons exist when the complex has an odd number of electrons or because electron pairing is destabilized.
- The more unpaired electrons, the stronger the magnetic property.
- Tetrahedral complexes have weaker splitting because none of the ligands lie within the plane of the orbitals.
- Square planar compounds are always low-spin and therefore are weakly magnetic.
- In bi- and polymetallic complexes, the electrons may couple through the ligands, resulting in a weak magnet, or they may enhance each other.

Contributors and Attributions

- Source: Boundless. "Magnetic Properties." *Boundless Chemistry* Boundless, 26 May. 2016. Retrieved 4 May. 2017 from www.boundless.com/chemistry/...ties-616-6882/.

10.12: Magnetic Behavior of Complex Ions is shared under a not declared license and was authored, remixed, and/or curated by LibreTexts.

10.13: Optical Properties of Coordination Compounds (Color)

The human eye perceives a mixture of all the colors, in the proportions present in sunlight, as white light. Complementary colors, those located across from each other on a color wheel, are also used in color vision. The eye perceives a mixture of two complementary colors, in the proper proportions, as white light. Likewise, when a color is missing from white light, the eye sees its complement. For example, when red photons are absorbed from white light, the eyes see the color green. When violet photons are removed from white light, the eyes see lemon yellow (Figure **10.13.1**).

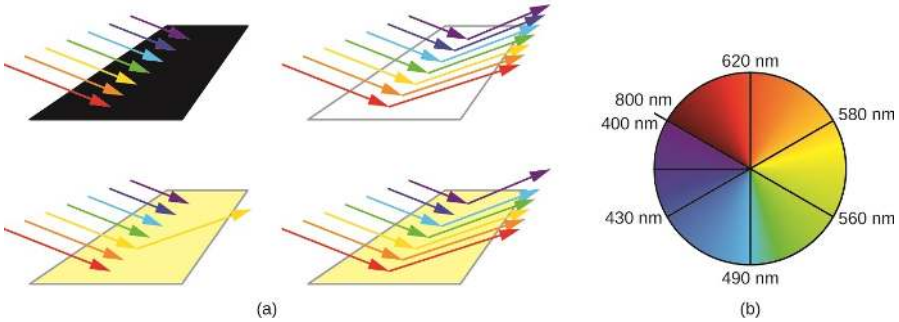


Figure **10.13.1**: (a) An object is black if it absorbs all colors of light. If it reflects all colors of light, it is white. An object has a color if it absorbs all colors except one, such as this yellow strip. The strip also appears yellow if it absorbs the complementary color from white light (in this case, indigo). (b) Complementary colors are located directly across from one another on the color wheel. (CC BY 4.0; OpenStax)

The blue color of the $[Cu(NH_3)_4]^{2+}$ ion results because this ion absorbs orange and red light, leaving the complementary colors of blue and green (Figure **10.13.2**). If white light (ordinary sunlight, for example) passes through $[Cu(NH_3)_4]SO_4$ solution, some wavelengths in the light are absorbed by the solution. The $[Cu(NH_3)_4]^{2+}$ ions in solution absorb light in the red region of the spectrum. The light which passes through the solution and out the other side will have all the colors in it except for the red. We see this mixture of wavelengths as pale blue (cyan). The diagram gives an impression of what happens if you pass white light through a $[Cu(NH_3)_4]SO_4$ solution.

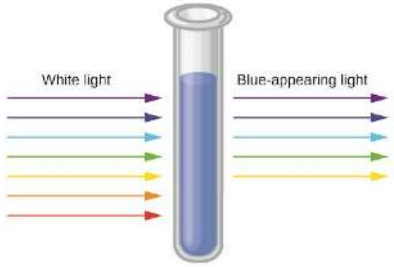


Figure **10.13.2**: A solution of $[Cu(NH_3)_4]^{2+}$ ions absorbs red and orange light, so the transmitted light appears as the complementary color, blue. (CC BY 4.0; OpenStax)

Working out what color you will see is not easy if you try to do it by imagining "mixing up" the remaining colors. You would not have thought that all the other colors apart from some red would look cyan, for example. Sometimes what you actually see is quite unexpected. Mixing different wavelengths of light doesn't give you the same result as mixing paints or other pigments. You can, however, sometimes get some estimate of the color you would see using the idea of complementary colors.

Recall that the color we observe when we look at an object or a compound is due to light that is transmitted or reflected, not light that is absorbed, and that reflected or transmitted light is complementary in color to the light that is absorbed. Thus a green compound absorbs light in the red portion of the visible spectrum and vice versa, as indicated by the complementary color wheel.



Figure **10.13.3**: The partially filled d orbitals of the stable ions $Cr^{3+}(aq)$, $Fe^{3+}(aq)$, and $Co^{2+}(aq)$ (left, center and right, respectively) give rise to various colors. (credit: Sahar Atwa)

The striking colors exhibited by transition-metal complexes are caused by excitation of an electron from a lower-energy d orbital to a higher-energy d orbital, which is called a **d–d transition** (Figure **10.13.4**). For a photon to effect such a transition, its energy must be equal to the difference in energy between the two d orbitals, which depends on the magnitude of Δ_o.

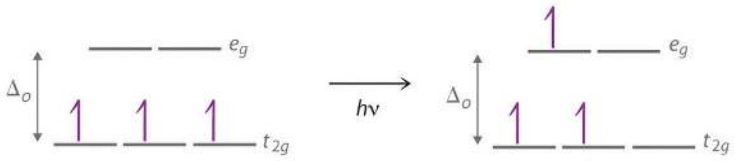


Figure **10.13.4**: In a d–d transition of an octahedral complex, an electron in one of the t_{2g} orbitals of an octahedral complex such as the $[Cr(H_2O)_6]^{3+}$ ion absorbs a photon of light with energy equal to Δ_o, which causes the electron to move to an empty or singly occupied e_g orbital.

Example 10.13.1: Colors of Complexes

The octahedral complex $[Ti(H_2O)_6]^{3+}$ has a single *d* electron. To excite this electron from the ground state t_{2g} orbital to the e_g orbital, this complex absorbs light from 450 to 600 nm. The maximum absorbance corresponds to Δ_o and occurs at 499 nm. Calculate the value of Δ_o in Joules and predict what color the solution will appear.

Solution

We can convert wavelength to frequency:

$$\nu = \frac{c}{\lambda}$$

$$= \frac{3.00 \times 10^8\, m/s}{(499\ \cancel{nm}) \times \left(\frac{1\, m}{10^9\ \cancel{nm}}\right)}$$

$$= 6.01 \times 10^{14} s^{-1} = 6.01 \times 10^{14}\, Hz$$

And then using Planck's equation that related the frequency of light to energy

$$E = h\nu$$

so

$$E = (6.63 \times 10^{-34} \text{J·s}) \times (6.01 \times 10^{14}\, Hz)$$

$$= 3.99 \times 10^{-19}\, J$$

Because the complex absorbs 600 nm (orange) through 450 (blue), the indigo, violet, and red wavelengths will be transmitted, and the complex will appear purple.

Note: This is the energy for one transition (i.e., in one complex). If you want to calculate the energy in J/mol, then you have to multiply this by Avogadro's number (N_A).

Exercise 10.13.1

A complex that appears green, absorbs photons of what wavelengths?

Answer

red, 620–800 nm

Color Depends on Oxidation State

Small changes in the relative energies of the orbitals that electrons are transitioning between can lead to drastic shifts in the color of light absorbed. Therefore, the colors of coordination compounds depend on many factors. As shown in Figure **10.13.4**, different aqueous metal ions can have different colors. In addition, different oxidation states of one metal can produce different colors, as shown for the vanadium complexes in the link below.



Watch this video of the reduction of vanadium complexes to observe the colorful effect of changing oxidation states.

Color Depends on Ligand Field

The specific ligands coordinated to the metal center also influence the color of coordination complexes. Because the energy of a photon of light is inversely proportional to its wavelength, the color of a complex depends on the magnitude of Δ_o, which depends on the structure of the complex. For example, the complex $[Cr(NH_3)_6]^{3+}$ has strong-field ligands and a relatively large Δ_o. Consequently, it absorbs relatively high-energy photons, corresponding to blue-violet light, which gives it a yellow color. A related complex with weak-field ligands, the $[Cr(H_2O)_6]^{3+}$ ion, absorbs lower-energy photons corresponding to the yellow-green portion of the visible spectrum, giving it a deep violet color. For example, the iron(II) complex $[Fe(H_2O)_6]SO_4$ appears blue-green because the high-spin complex absorbs photons in the red wavelengths (Figure **10.13.5**). In contrast, the low-spin iron(II) complex $K_4[Fe(CN)_6]$ appears pale yellow because it absorbs higher-energy violet photons.



Figure **10.13.5**: Both (a) hexaaquairon(II) sulfate and (b) potassium hexacyanoferrate(II) contain d^6 iron(II) octahedral metal centers, but they absorb photons in different ranges of the visible spectrum. (CC BY 4.0; OpenStax)

In general, strong-field ligands cause a large split in the energies of *d* orbitals of the central metal atom (large Δ_{oct}). Transition metal coordination compounds with these ligands are yellow, orange, or red because they absorb higher-energy violet or blue light. On the other hand, coordination compounds of transition metals with weak-field ligands are often blue-green, blue, or indigo because they absorb lower-energy yellow, orange, or red light.

> *Strong-field ligands cause a large split in the energies of d orbitals of the central metal atom and transition metal coordination compounds with these ligands are typically yellow, orange, or red because they absorb higher-energy violet or blue light. Coordination compounds of transition metals with weak-field ligands are often blue-green, blue, or indigo because they absorb lower-energy yellow, orange, or red light.*

Example **10.13.2**: Matching Colors to Ligand Fields

Identify the color (either blue, green, yellow, or orange) for the following complex ions formed with Co^{3+}:

a. $[Co(CN)_6]^{-2}_3$

b. $[Co(NH_3)_6]^{3+}_3$
c. $[CoF_6]^{-4}_3$
d. $[Co(H_2O)_6]^{3+}$

Solution

Each of these complex ions has the same metal with the same oxidation state, so the ligand field is the relevant factors. Each of the complex ions also has an octahedral ligand field, so we only need to compare the strength of the ligands in determining Δ_o, which is determined by the spectrochemical series.

The ligands for each complex ions are: (a) CN^-, (b) NH_3, (c) F^- and (d) H_2O, which are ranked in increasing Δ_o magnitude:

$$F^- < H_2O < NH_3 < CN^- \tag{10.13.1}$$

The relationship between the Δ_o and the energy of the photons are absorbed in the d-d transition of Co^{3+} is given by equating Planck's equation to the crystal field splitting parameter:

$$E = h\nu = \frac{hc}{\lambda} = \Delta_o \tag{10.13.2}$$

Now, we need to get a relative correlation between observed color (to the eye) and the wavelength of the light that is absorbed. From the complementary color wheel in Figure **10.13.1** we get the following relationships (arranged from highest energy absorbed to lowest):

- 400-nm Violet light absorbed → Green-yellow observed
- 430-nm Blue light absorbed → Orange observed
- 450-nm Blue light absorbed → Yellow observed
- 490-nm Blue-green light absorbed → Red observed
- 570-nm Yellow-green light absorbed → Violet observed
- 580-nm Yellow light absorbed → Dark blue observed
- 600-nm Orange light absorbed → Blue observed
- 650-nm Red light absorbed → Green observed

Of the four possible colors given in the problem (blue, green, yellow, and orange), the corresponding colors that are absorbed are (600 nm, 650 nm, 450 nm, and 430, respectively). From Equation 10.13.2, the smaller λ of absorbed light corresponds to the higher energy photons, so we would correlate the four wavelengths of absorbing photons in terms of increasing energy to observed color:

$$\underbrace{650\,nm}_{green} < \underbrace{600\,nm}_{blue} < \underbrace{450\,nm}_{yellow} < \underbrace{430\,nm}_{orange} \tag{10.13.3}$$

Now, just correlate the ranking in Equation 10.13.3 to the ranking in Equation 10.13.1:

$$\underbrace{F^-}_{green} < \underbrace{H_2O}_{blue} < \underbrace{NH_3}_{yellow} < \underbrace{CN^-}_{orange}$$

and more specifically in terms of the original question

$$\underbrace{[CoF_6]^{-4}_3}_{green} < \underbrace{[Co(H_2O)_6]^{3+}}_{blue} < \underbrace{[Co(NH_3)_6]^{3+}_3}_{yellow} < \underbrace{[Co(CN)_6]^{-2}_3}_{orange}$$

? Exercise 10.13.1

If a complex ion $[M(NH_3)_6]^{2+}$ is red in solution, which of the following ligands, after a ligand exchange reaction to substitute for the ammine ligands, may shift the solution to be orange? More than one answer is possible.

$$Cl^-, CN^-, CO, F^- H_2O, I^-, en, NO_2^-, OH^-, SCN^-$$

Answer

Shifting from red to orange is an increase in Δ_o, so those ligands that are stronger field ligands than NH_3 in the list (deterimined via the spectrochemical series) are CN^-, CO, en, and NO_2^-.

A coordination compound of the Cu^+ ion has a d^{10} configuration, and all the e_g orbitals are filled. To excite an electron to a higher level, such as the 4*p* orbital, photons of very high energy are necessary. This energy corresponds to very short wavelengths in the ultraviolet region of the spectrum. No visible light is absorbed, so the eye sees no change, and the compound appears white or colorless. A solution containing $[Cu(CN)_2]^-$, for example, is colorless. On the other hand, octahedral Cu^{2+} complexes have a vacancy in the e_g orbitals, and electrons can be excited to this level. The wavelength (energy) of the light absorbed corresponds to the visible part of the spectrum, and Cu^{2+} complexes are almost always colored—blue,

blue-green violet, or yellow (Figure **10.13.6**). Although CFT successfully describes many properties of coordination complexes, molecular orbital explanations (beyond the introductory scope provided here) are required to understand fully the behavior of coordination complexes.



Figure **10.13.6**: (a) Copper(I) complexes with d^{10} configurations such as CuI tend to be colorless, whereas (b) d^9 copper(II) complexes such as $Cu(NO_3)_2{\cdot}5H_2O$ are brightly colored. (CC BY 4.0; OpenStax)

Gems

A ruby is a pink to blood-red colored gemstone that consist of trace amounts of chromium in the mineral corundum $\boldsymbol{Al_2O_3}$. In contrast, emeralds are colored green by trace amounts of chromium within a $Be_3Al_2Si_6O_{18}$ matrix. We can now understand why emeralds and rubies have such different colors, even though both contain Cr^{3+} in an octahedral environment provided by six oxide ions. Although the chemical identity of the six ligands is the same in both cases, the Cr–O distances are different because the compositions of the host lattices are different (Al_2O_3 in rubies and $Be_3Al_2Si_6O_{18}$ in emeralds). In ruby, the Cr–O distances are relatively short because of the constraints of the host lattice, which increases the d orbital–ligand interactions and makes Δ_o relatively large. Consequently, rubies absorb green light and the transmitted or reflected light is red, which gives the gem its characteristic color. In emerald, the Cr–O distances are longer due to relatively large $[Si_6O_{18}]^{12-}$ silicate rings; this results in decreased d orbital–ligand interactions and a smaller Δ_o. Consequently, emeralds absorb light of a longer wavelength (red), which gives the gem its characteristic green color. It is clear that the environment of the transition-metal ion, which is determined by the host lattice, dramatically affects the spectroscopic properties of a metal ion.



Gem-quality crystals of ruby and emerald. The colors of both minerals are due to the presence of small amounts of Cr^{3+} impurities in octahedral sites in an otherwise colorless metal oxide lattice.

The absorbance spectrum of a ruby is shown Figure **10.13.7**;. The number and positions of the peaks in the spectrum is determined by the electronic structure of the compound, which in this case depends upon the identity of the metal and the identities, number, and geometry of the surrounding ions. Crystal field theory may be used to predict the electronic structure and thus the absorbance spectrum. If white light is shown on the gem, the absorbance spectrum indicates which wavelengths of light are removed. In this case, there are strong bands centered at 414 and 561 nm. These wavelengths correspond with blue and yellow-green light, respectively. For the most part, these colors are not present in the light reaching ones eyes. An alternative way to express this concept is to recognize that the spectrum of light reaching the eye is the product of the spectrum of the incident light (white light) and the **transmittance spectrum**. For this ruby, the transmittance spectrum has a peak at 481 nm and a broad plateau past 620 nm. (Note that there is significant attenuation of the light across the entire spectrum.) Thus only light with wavelengths near 481 nm (cyan) and greater than 620 nm (red) reach the eye.

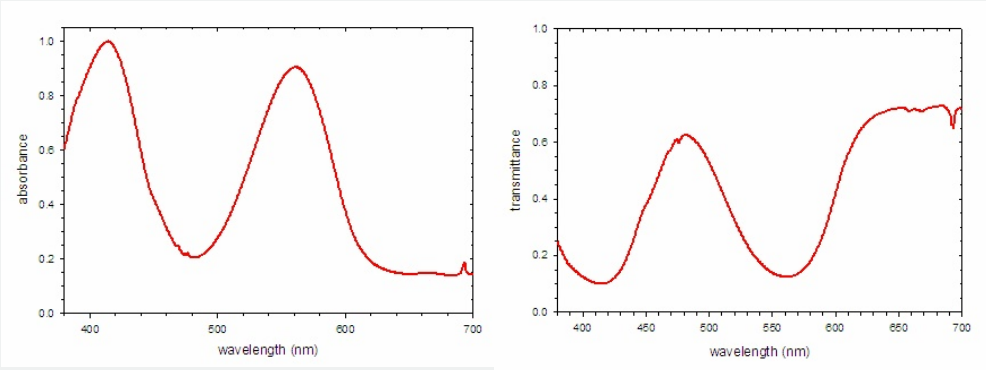
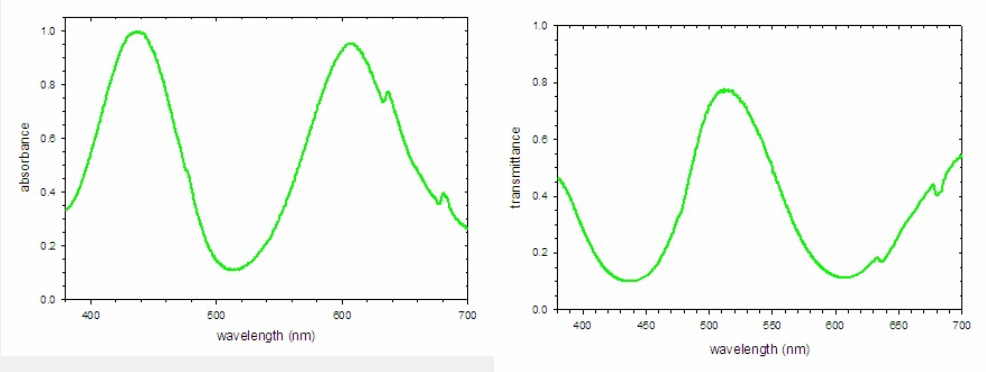


Figure **10.13.7**: (left) Absorbance spectrum of a ruby from Chanthaburi, Thailand. (right) corresponding Transmittance spectrum of a ruby from Chanthaburi, Thailand. Data obtained from the Caltech Mineral Spectroscopy Server

A similar analysis of the spectrum of an emerald is possible. The absorbance spectrum (Figure **10.13.8;**) shows strong bands at 438 and 606 nm, which remove blue and orange light, respectively. The light that is not absorbed is shown by the transmittance spectrum, which indicates the dominant band of light reaching the eye is centered at 512 nm (green light) with smaller contributions from the far blue and red portions of the spectrum. This combination of wavelengths produces a deep green color.



(left) Absorbance spectrum of an emerald from Malyshevo, Ural, Russia. (right) Corresponding transmittance spectrum of the emerald from Malyshevo, Ural, Russia. Data obtained from the Caltech Mineral Spectroscopy Server

Summary

When atoms or molecules absorb light at the proper frequency, their electrons are excited to higher-energy orbitals. For many main group atoms and molecules, the absorbed photons are in the ultraviolet range of the electromagnetic spectrum, which cannot be detected by the human eye. For coordination compounds, the energy difference between the *d* orbitals often allows photons in the visible range to be absorbed.

Contributors and Attributions

- Paul Flowers (University of North Carolina - Pembroke), Klaus Theopold (University of Delaware) and Richard Langley (Stephen F. Austin State University) with contributing authors. Textbook content produced by OpenStax College is licensed under a Creative Commons Attribution License 4.0 license. Download for free at http://cnx.org/contents/85abf193-2bd...a7ac8df6@9.110).
- Prof. David Blauch (Davidson College)

10.13: Optical Properties of Coordination Compounds (Color) is shared under a not declared license and was authored, remixed, and/or curated by LibreTexts.

- **24.7: Color and the Colors of Complexes** by OpenStax is licensed CC BY 4.0.

11: Applications in Polymer and Biological Chemistry

11: Applications in Polymer and Biological Chemistry is shared under a not declared license and was authored, remixed, and/or curated by LibreTexts.

SECTION OVERVIEW

11.1: Bioinorganic Chemistry

Introduction to Bioinorganic Chemistry

What is bioinorganic chemistry? To answer this question, we should probably define what the other fields of chemistry are first...

You probably know that "**biochemistry**" is the study of the chemistry of biology - or life. The term "**organic chemistry**" literally means the *chemistry of life*. Organic chemistry is the study of carbon-based molecules because the first molecules that were isolated from living organisms contained carbon. On the other hand, the first minerals and other non-living things seemed to be made of other elements. For quite some time scientists naively assumed that all living things were made of carbon-based molecules, while non-living things did not contain carbon. "Organic chemistry" was the study of the carbon-based molecules of life, while "**inorganic chemistry**" was the study of "non-living" and "non-carbon" molecules.

Do these these historic definitions still hold true? To answer that question, let's look at one of the most important reactions in *your* life, shown below.

$$O_2 + 4e^- + 4H^+ \rightleftharpoons H_2O \tag{11.1.1}$$

Is this reaction *carbon-based*? Is it *living*? Well, take a deep breath! When you breath, you inhale mostly nitrogen gas (N_2), but also some oxygen gas (O_2). The oxygen gas that you inhale is critical for energy production in every one of your cells. During aerobic metabolism, O_2 accepts 4 electrons and 4 hydrogen ions to become two molecules of water. This reaction provides the driving force for phosphorylation of ATP that is required to fuel countless other essential reactions that keep you alive. This reaction is responsible for all aerobic life. And, it's *inorganic*! This simple example shows how the historic names of organic and inorganic chemistry should not be taken literally.

There are additional inorganic components required for this reaction too! For example, most of the proteins of the electron transport chain (the proteins that catalyze reduction of oxygen in the mitochondria of your cells) require metal cofactors and metal active sites. Please watch the video below to see some examples. Articles about the individual proteins from the video are provided below.



Links to articles about proteins discussed in this video:

- Cytochrome C Oxidase
- Ribozyme (has not been written yet!)
- Hemocyanin (has not been written yet!)
- Urease (has not been written yet!)

Sources

1. Franz, Katherine J., The Periodic Table of Life, Core Concepts in Chemistry, a free course on iTunes U from Duke University.

11.1.1: A Molecular Depot- Human Serum Albumin Carries Essential Cu and Zn in Serum

11.1.2: Iron acquisition in bacteria- Siderophores

11.1.3: Fe Wars- Lactoferrin

11.1.4: Iron Storage- Ferritin

11.1.5: Antioxidant- Cu/Zn Superoxide dismutase (SOD1)

11.1.6: Keep Cu Safe- Intracellular Copper Chaperones

11.1.7: Cytochrome C

11.1.8: Cytochrome Oxidase

11.1.9: Potassium Channels

11.1.10: Chemotherapy- Pt anticancer agents

11.1: Bioinorganic Chemistry is shared under a not declared license and was authored, remixed, and/or curated by LibreTexts.

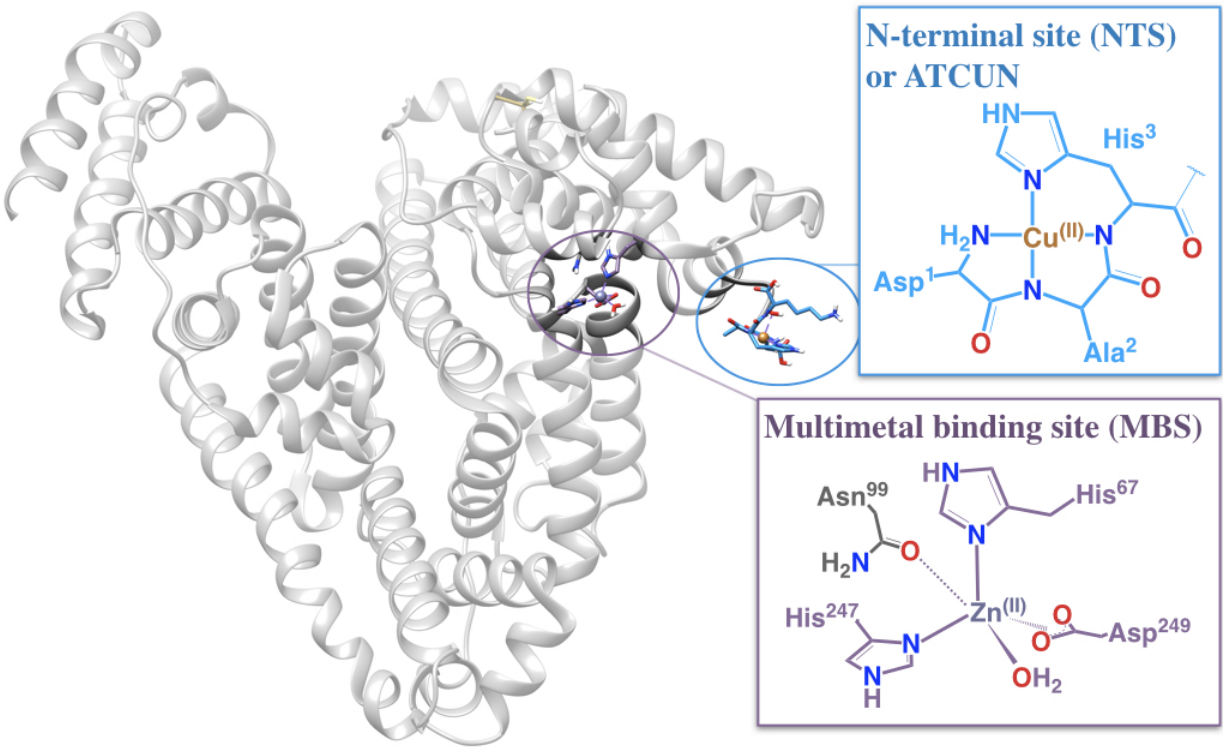
11.1.1: A Molecular Depot- Human Serum Albumin Carries Essential Cu and Zn in Serum

Human Serum Albumin

Human serum albumin (HSA) is a 66.5 kD protein found in human blood plasma and cerebrospinal fluid. In fact, it is the most abundant protein in human blood, constituting over half of plasma protein with a concentration of 0.6 mM under normal physiological conditions.[1]

HSA is a heart-shaped molecule comprised of three homologous domains (referred to as I, II, and III). Each domain contains two helical subdomains (referred to as A and B) connected by a random coil.[2] The structural arrangement of HSA engenders it's extraordinary ligand binding capacity. Various classes of ligands, including fatty acids (ie. myristate), drugs (ie. ibuprofen or warfarin), hormones (ie. thyroxine), and metal ions are bound and transported by albumin.[3-5] Thus, HSA is commonly referred to as a "molecular depot."

Metal binding to HSA has been extensively explored in various contexts. For example, HSA is an important transporter of essential metal ions, like Cu(II) and Zn(II), but it can also bind toxic metals, such as Ni(II) and Cd(II). Furthermore, HSA-metal binding has been exploited in the development of anticancer drugs due to its ability to bind soft Pt(IV) and Au(I).[6] For a comprehensive review of metal ion interactions with HSA, see reference 6. In this lesson, we will focus on only the interactions between HSA and two metals which are key components in many biological processes: copper and zinc (see figure below).



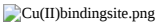
This is a ribbon diagram of human serum albumin with both Cu(II) and Zn(II) bound in their high-affinity binding sites. This structure was created by merging the protein crystal structure of HSA bound to Zn(II) at pH 9.0 (PDB 5IJF) and the small molecule crystal structure of the DAKH model peptide bound to Cu(II) (CCDC-809109). You can print or download a 3D model of this image on the Bioinorganic 3D Shapeways workshop.

Copper

Copper is an essential metal ion involved in a variety of metabolic processes, including mitochondrial respiration, melanin synthesis, cross-linking of collagen, quenching of reactive oxygen species, neurotransmitter development, and more.[7] Its utility in these various systems is oftentimes attributed to its unique ability to cycle between the Cu(I) and Cu(II) oxidation states. Thus, it can act as an electron donor or acceptor as redox cycling occurs.

As copper is absorbed by our digestive system, it enters the bloodstream bound by copper carrying proteins such as ceruloplasmin or HSA. The majority of serum copper (70-95%) is bound to ceruloplasmin; however, this copper is not readily exchangeable. HSA, on the other hand, is capable of exchanging copper with cellular copper acquisition proteins, such as the human copper transporter, Ctr1. Once the exchange occurs, Ctr1 can transport Cu(I) across the plasma membrane, for its involvement in intracellular metabolic processes, like the ones mentioned above.

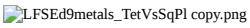
Cu(II) binding to HSA involves the well-characterized ATCUN (amino terminal copper and nickel) binding site, made up of its first three amino acids, Asp-Ala-His. (Figure below) Characteristic of this site are four donor atoms coming from a free -NH_2 terminus, a Histidine in the third position (XXH), and two contributing peptide backbone nitrogens. In aqueous environments, the far coordination sphere also includes an axial water molecule as a fifth ligand, which is oftentimes ignored due to its lability and rather long distance from the Cu center. This water molecule is usually undetectable by spectroscopic techniques other than crystallography. The multidentate characteristic of this binding site contributes to highly stable complexes with Cu(II).



The HSA's Cu(II) binding "ATCUN" site from crystal structure CCDC-809109: Made of the first three amino acids DAH, this site coordinates Cu(II) and Ni(II) in a square-planar 4-N coordination geometry. Axial coordination of a labile H_2O molecule is shown, however is often not considered as part of the stable coordination geometry.

According to Ligand Field Theory (LFT), all of the backbone nitrogen donor atoms at the Cu(II) binding site are classified as sigma donors, which means they are capable of sigma bonding with the metal. The N-terminal amine, and backbone amides are also pi donors, which means they are capable of forming pi bonds with the metal. Pi donors are weak field ligands and favor small Δ. The deporotonated amides are especially strong bases that stabilize the bonding interaction despite that they are weak field ligands. The imidazole nitrogen is both a sigma donor and a pi acceptor, due to its double bonded pi system. This means that the imidazole donor is capable of accepting electrons from the metal ion into its pi* orbitals. Pi-acceptors are strong field ligands and favor large Δ. Therefore, the ATCUN site contains both pi-donor that are strong bases and a pi-acceptor. The presence of both types of ligands helps in making this complex more stable.

LFT predicts that the N-ligands are coordinated around the Cu(II) center with square planar geometry. With four ligands (ignoring the axial H_2O), geometry is typically square planar or tetrahedral. A d^9 metal, like Cu(II) prefers square planar arrangements due to LFSE. A comparison of tetrahedral and square planar splitting diagrams for d^9 metals is shown below.

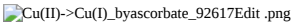


Comparison of LFSE for d^9 metals with 4 coordinating ligands. In the case of d^9, the square planar arrangement, with a more negative LFSE is more energetically favorable.

Shown above is a comparison of the d-orbital splitting diagrams of two possible geometries for 4 donor groups around a metal center, as we see in the ATCUN site of HSA. From LFSE calculations, it is clear that in this case, the square planar arrangement is more energetically favorable. (LFSE calculations are shown with an energy scale relative to Δ_o.) Because Cu(II) is a d^9 metal and will always have one unpaired electron, it does not have distinct high or low spin states. However, it should be noted that all square planar complexes favor low spin, because of the large Δ that is a consequence of square planar geometry.

In the presence of ascorbate, a biological reductant, HSA can facilitate Cu reduction from Cu(II)-->Cu(I) oxidation state (Figure below). The precise location of HSA's Cu(I) binding site is currently unknown, but details of its coordination environment have been elucidated through X-ray absorption spectroscopy.[15] This protein's bidentate Cu(I) binding site is comprised of two Histidine residues, oriented 180° apart approximately 1.89 Å from the Cu center. Although two-coordinate geometry are not usually observed for other first-row transition metal ions, it a common geometry observed when Cu(I) is bound to polypeptides. Since Cu(I) is a d^{10}

metal with no LFSE, it can be oriented in any coordination geometry. Because Cu(I) has a relatively low charge, two ligands can apparently be enough to satisfy it electrostatically.



Reduction of Cu(II) bound to HSA: Scheme of Cu(II) reduction to Cu(I) in the presence of electron donor, Vitamin C (ascorbic acid or ascorbate). The Cu(II) complex at the NTS has Jahn-Teller distorted square planar geometry, and the Cu(I) complex has linear geometry. The Cu(II) complex has a measurable d-d transition, while the Cu(I) complex does not.

In the reaction shown in the figure above, Cu(II) gains an electron via the weak reducing agent, Vitamin C. UV-vis spectroscopic techniques are oftentimes employed to monitor Cu(II)-->Cu(I) reduction such as this. This is possible because as a d^9 metal, Cu(II) has a d-d transition which absorbs radiation in the UV-vis range. This transition yields a measurable signal. Cu(I), on the other hand, does not have any d-d transitions because all d orbitals are filled, and it is therefore spectroscopically silent. During experimentation, Cu(I) presence is measured by the disappearance of a signal given by Cu(II)'s d-d transitions.

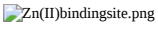
In terms of kinetics, Cu(II) exchanges ligands faster than Cu(I), but Cu(I) is still labile. Both oxidation states allow for little or no LFSE, and both oxidation states have d electrons occupying antibonding molecular orbitals. Both of these factors contribute to increased ligand exchange rate.

Zinc

Zinc is the second-most abundant transition metal in living systems (iron is the most abundant but does not bind significantly to HSA; rather Fe binds tightly to transferrin in serum).[11] Because Zn(II) is effectively a Lewis acid, it serves as a cofactor in many enzymatic reactions. For example, Zn(II) is found at the active site of carbonic anhydrase, which regulates CO_2 balance in blood and other tissues.[12] Moreover, Zn(II) provides structure to some proteins, as in the case of "zinc fingers." Zinc fingers are part of transcription factors, which recognize and bind a specific DNA sequence during DNA transcription and replication. Zn also functions in the brain, playing a role in synaptic plasticity and learning. However, it has also been recognized as a neurotoxin in high concentrations; thus, Zn homeostasis is important in sustaining life.[11]

HSA is involved in Zn homeostasis, and is the primary Zn transport protein in the human circulatory system.[8] In many cases, HSA acts as a "zinc buffer," controlling the amount of free Zn(II) that is available for cellular uptake.[10] Interestingly, HSA-Zn binding and HSA-fatty acid binding is interdependent. Upon fatty acid binding, HSA undergoes a conformational change which disturbs the preformed Zn(II) binding site. Therefore, researchers suggest that HSA might facilitate the interplay between extracellular Zn speciation and energy metabolism.[14]

Zn(II) binds to HSA at what is referred to as the multi-metal binding site, or MBS. This site gets its name for its ability to coordinate a variety of metals including Cu(II), Ni(II), Zn(II) and Cd(II). Thorough spectroscopic investigation of Zn(II) binding to the MBS indicates that the first ligand shell includes two imidazole N's of His 67 and 247, two carbonyl oxygens of Asn 99 and Asp 249 and a third oxygen from a coordinating water molecule at pH 7.4.[9] However, crystal structure data collected at pH 9.0 and representing HSA with a bound Zn ion does not show coordination of Asn 99. (Figure below, pdb.5IJF) Differences in pH are known to result in conformational changes to HSA and could explain the discrepancy in coordinating atoms observed in the crystal structure and in spectroscopic data.



Structure of Zn(II) bound to HSA from PDB 5IJF: Close up of HSA's Zn(II) binding site at pH 9.0, located at the interface of domains I and II. Other spectroscopic data (collected at pH close to 7) indicates coordination through His 67, His 247, Asp 249, Asn 99, and H_2O. In PDB entry 51JF, above, binding is similar, though not involving Asn 99.

The HSAB character of Zn(II) and its coordinating ligands can explain this site's metal preference. Imidazole nitrogens are borderline bases, and carbonyl groups are hard bases. Zn(II) is typically considered a borderline acid, so it makes sense for these ligands to prefer Zn(II) over a softer acids such as Cu(I) or Cd(II).

Because Zn(II) is a d^{10} metal, it has zero LFSE. Therefore, LFSE is not a contributing factor when determining the geometry of this binding site. Instead, geometry is determined by the most sterically favorable arrangement of ligands. In the case of 4 coordinate

ligand arrangements, tetrahedral geometry, with bond angles of 109.5°, is more sterically favorable than square planar geometry, with bond angles of 90°. It is worth noting that steric factors may also include the structural constraints of the protein itself due to folding or otherwise. Another consequence of zero LFSE is increased lability or rate of ligand exchange, which is essential considering the biological implications of HSA-Zn binding.

As mentioned previously, metal binding to HSA is not only relevant for normal physiological processes, but also in pharmaceuticals. HSA is a target for a variety of metallodrugs, including some for the treatment of cancer.[13] Such metal binding occurs at the Cys-34 residue, which is the only Cysteine out of 35 in the protein that is not involved in disulfide bridging.[6] Therefore it provides a S-donor that can attract metallodrugs, especially those containing soft metals like Au(I) and Pt(II). Unlike the other metal binding sites, this one is not stabilized by the chelate effect, and binds metals via a single metal-sulfur bond.

Sources:

1. (1) Carter, D. C.; Ho, J. X., Structure of Serum Albumin. Advances in Protein Chemistry 1994, 45, 153-203.
2. (2) He, X. M.; Carter, D. C. Atomic Structure and Chemistry of Human Serum Albumin. Nature 1992, 358 (6383), 209–215.
3. (3) Bhattacharya, A. A.; Grüne, T.; Curry, S. Crystallographic Analysis Reveals Common Modes of Binding of Medium and Long-Chain Fatty Acids to Human Serum albumin11Edited by R. Huber. Journal of Molecular Biology 2000, 303 (5), 721–732.
4. (4) Sudlow, G.; Birkett, D. J.; Wade, D. N. The Characterization of Two Specific Drug Binding Sites on Human Serum Albumin. Mol Pharmacol 1975, 11 (6), 824–832.
5. (5a) Fasano, M.; Curry, S.; Terreno, E.; Galliano, M.; Fanali, G.; Narciso, P.; Notari, S.; Ascenzi, P. The Extraordinary Ligand Binding Properties of Human Serum Albumin. IUBMB Life 2005, 57 (12), 787–796.
6. (5b) Petitpas, I.; Petersen, C. E.; Ha, C.-E.; Bhattacharya, A. A.; Zunszain, P. A.; Ghuman, J.; Bhagavan, N. V.; Curry, S. Structural Basis of Albumin–thyroxine Interactions and Familial Dysalbuminemic Hyperthyroxinemia. PNAS 2003, 100 (11), 6440–6445.
7. (6) Bal, W.; Sokolowska, M.; Kurowska, E.; Faller, P. Binding of Transition Metal Ions to Albumin: Sites, Affinities and Rates. Biochim. Biophys. Acta-Gen. Subj. 2013, 1830 (12), 5444–5455.
8. (7) Stern, B. R.; Solioz, M.; Krewski, D.; Aggett, P.; Aw, T.-C.; Baker, S.; Crump, K.; Dourson, M.; Haber, L.; Hertzberg, R.; Keen, C.; Meek, B.; Rudenko, L.; Schoeny, R.; Slob, W.; Starr, T. Copper and Human Health: Biochemistry, Genetics, and Strategies for Modeling Dose-Response Relationships. Journal of Toxicology and Environmental Health, Part B 2007, 10 (3), 157–222.
9. (8) Stewart, A. J.; Blindauer, C. A.; Berezenko, S.; Sleep, D.; Sadler, P. J. Interdomain Zinc Site on Human Albumin. PNAS 2003, 100 (7), 3701–3706.
10. (9) Blindauer, C. A.; Harvey, I.; Bunyan, K. E.; Stewart, A. J.; Sleep, D.; Harrison, D. J.; Berezenko, S.; Sadler, P. J. Structure, Properties, and Engineering of the Major Zinc Binding Site on Human Albumin. J. Biol. Chem. 2009, 284 (34), 23116–23124.
11. (10) Lu, J.; Stewart, A. J.; Sadler, P. J.; Pinheiro, T. J. T.; Blindauer, C. A. Albumin as a Zinc Carrier: Properties of Its High-Affinity Zinc-Binding Site. Biochemical Society Transactions 2008, 36 (6), 1317–1321.
12. (11) Frassinetti, S.; Bronzetti, G. L.; Caltavuturo, L.; Cini, M.; Croce, C. D. The Role of Zinc in Life: A Review. JEP(T) 2006, 25 (3).
13. (12) Keilin, D.; Mann, T. Carbonic Anhydrase. Purification and Nature of the Enzyme. Biochem J 1940, 34 (8-9), 1163–1176.
14. (13) Espósito, B. P.; Najjar, R. Interactions of Antitumoral Platinum-Group Metallodrugs with Albumin. Coordination Chemistry Reviews 2002, 232 (1), 137–149.
15. (14) Barnett, J. P.; Blindauer, C. A.; Kassaar, O.; Khazaipoul, S.; Martin, E. M.; Sadler, P. J.; Stewart, A. J. Allosteric Modulation of Zinc Speciation by Fatty Acids. Biochimica et Biophysica Acta (BBA) - General Subjects 2013, 1830 (12), 5456–5464.
16. (15) Sendzik, M.; Pushie, M. J.; Stefaniak, E.; Haas, K. L., The Structure and Affinity of Cu(I) Bound to Human Serum Albumin. Inorg. Chem. Manuscript ID: ic-2017-02397f. Submitted Sept 18, 2017

Contributed by

*This work was originally written by **Madison Sendzik**, Fall 2017: Madison is currently (as of 2017) a senior chemistry major at Saint Mary's College in Notre Dame, IN. She is the first author on Reference 15 and plans to pursue her Ph.D. in chemistry beginning in Fall 2018.*

11.1.1: A Molecular Depot- Human Serum Albumin Carries Essential Cu and Zn in Serum is shared under a not declared license and was authored, remixed, and/or curated by LibreTexts.

11.1.2: Iron acquisition in bacteria- Siderophores

Siderophores

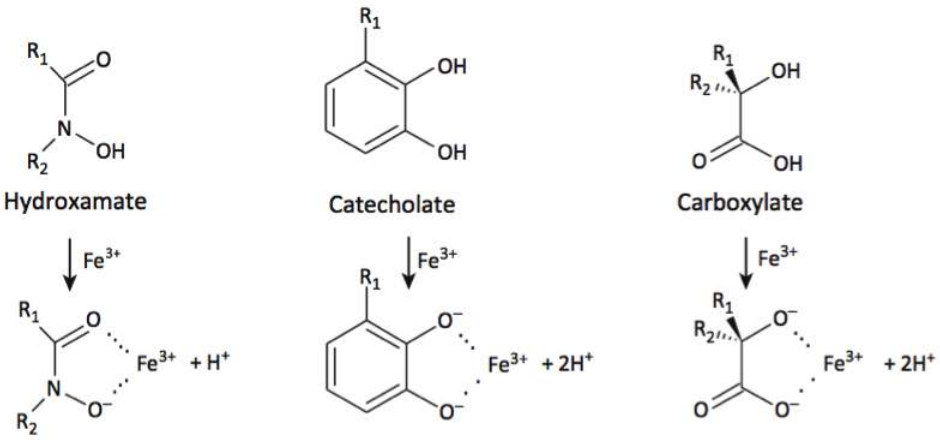
This is a video introduction to siderophores: the small molecules produced and secreted by bacteria to acquire precious iron from their environment.



Most all living organisms require iron for crucial processes that allow for the life and growth of cells. Animals receive this nutrient from diet, but plants and single-celled organisms must utilize different strategies.[1] There are two main mechanisms by which cells acquire iron. The simpler of the two, is iron diffusion across cellular membranes.[2] This mechanism is more difficult, despite the prominence of iron in the atmosphere. This is due to the aerobic nature of the environment, which causes iron to be present in the highly insoluble form, $Fe(OH)_3$. The insolubility means there is a low Fe(III) concentration (10^{-18} M) of available iron; too low to provide sustenance to microorganisms, which require a minimum concentration of 10^{-8} M to live and grow.[3, 4] To circumvent the lacking bioavailability of iron, these organisms synthesize and secrete siderophores. Siderophores are low molecular weight compounds that chelate iron and transport it into cells under low iron environments.[5] Siderophores have the highest specificity and affinity for Fe(III), but are capable of forming complexes with other metallic ions, like Fe^{2+}, Zn^{2+}, Ga^{3+}, and Cr^{3+}.[2]

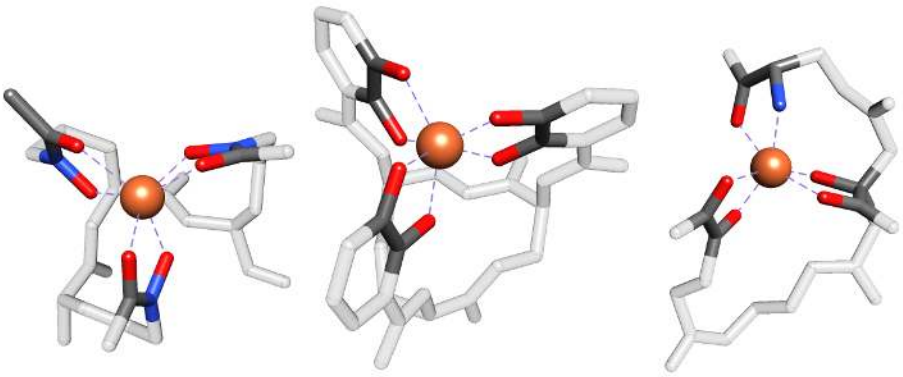
Siderophores are an incredibly diverse group of biocompounds, with hundreds of different types categorized. The most common siderophores fall into three main categories: hydroxamates, catecholates, and carboxylates.[2] The functional groups of these structures that are the main component in iron chelation are shown below, in Figure 1.

Figure 1[2]: Functional groups of siderophores and the complexes that form upon binding to Fe(III). R-groups represent the variable groups.



These bidentate functional groups interact with iron through two negatively-charged oxygen atoms, but this is not a steadfast rule. Some distortions can occur and other atoms like nitrogen or sulfur can be substituted as one of the interacting atoms (although this has a tendency to reduce Fe(III) affinity).[6] The functional groups act as bidentate ligands, but naturally occurring siderophores can arrange multiples of these groups through the variable R-groups into a higher chelating structure. Hexadentate and tetradentate structures are the most common. Hexadentate siderophores tend to bind to Fe(III) more so than tetradentate or bidentate siderophores, due to the chelate effect. The resulting hexadentate complexes are also more stable and less labile, which makes sense, since one iron-bound ligand–instead of two or three–increases the entropy.[3] Examples of hexadentate siderophores are in Figure 2.

Figure 2: Examples of the three types of siderophores in a hexadentate formation. The colored portions highlight the iron and siderophore functional groups. The light gray represents the variable groups. (A) A ferrichrome ligand, a type of hydroxamate from an Esherichia coli cell.[7] (B) An enterobactin ligand, a type of catecholate from a Bacillus subtilis cell.[8] (C) A staphyloferrin ligand, a type of carboxylate from a Staphylococci.[9]

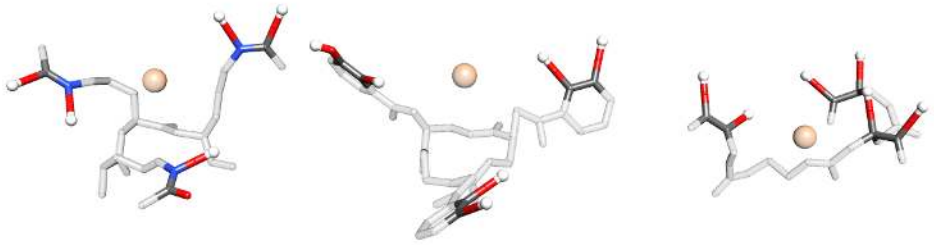


Fe(III) is typically found in an environment with an aqueous solution, meaning the naturally-occurring complex is the octahedral $Fe(H_2O)_6^{3+}$. Siderophores surround this complex, usually in a hexadentate manner that results in octahedral geometry. Typically, the water is replaced completely by siderophore in an entropically-favorable way. In this new complex, Fe(III) is in a d^5 electron configuration. As previously mentioned, siderophores donate multiple oxygen atoms to form a complex with iron. The donation of oxygen atoms means these ligands are σ and π donors, which are weak field ligands and support a high spin configuration. The combination of the complex's geometry and the metal center's high spin configuration means that there is no ligand field stabilization energy.

Without bound Fe(III), siderophore are not rigid compounds (Figure 3). The metal-ligand bond is what stabilizes their structure. Complex stability and the siderophores' high affinity for iron comes from the aforementioned ligand denticity as well as the multiple hard acid and hard base interactions. Fe(III) is a hard acid and the oxygen atoms on the siderophore are all hard bases.[10] The affinity for iron increases with higher negative charges on siderophores.[6] More negatively-charged siderophores are harder bases, which form tighter interaction to Fe(III). As shown in Figure 1, catecholates and carboxylates usually have two negatively-charged oxygen atoms per functional group, while hydroxamates have one. This alludes to the idea that the former groups have higher iron affinity.

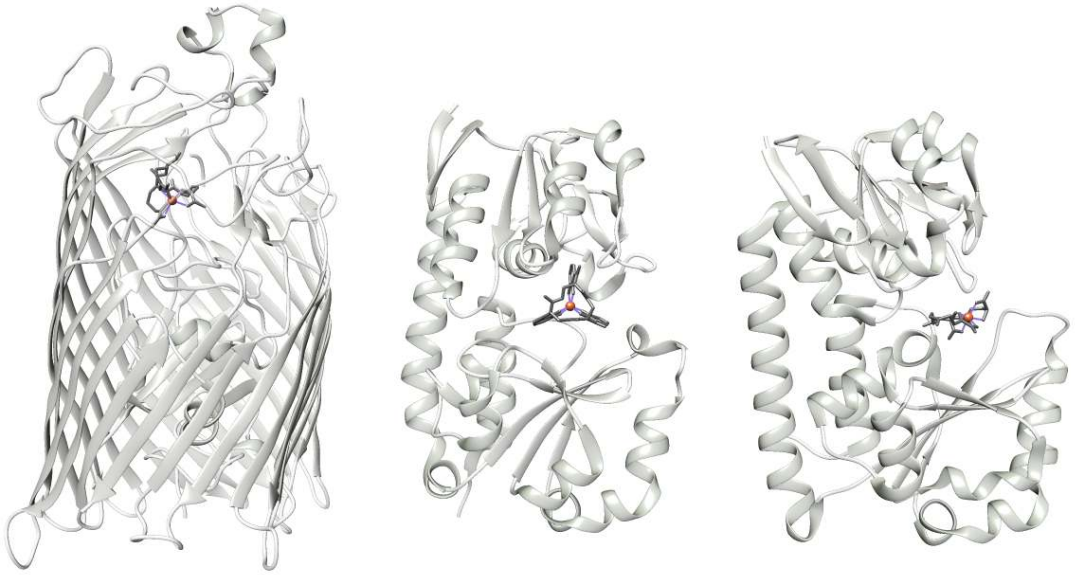
Fe(III)-siderophore complexation is sensitive to pH values. Free iron and protons (hydrogen atoms) compete for the unbound siderophores.[11] In low pH environments, there is a high concentration of solvated hydrogen atoms, resulting in higher competition for the siderophores (Figure 3). A low pKa value relates to a strong acid that is able to donate protons. In Figure 1 above, both the catecholate and carboxylate groups donate two hydrogen atoms (protons), as opposed to the hydroxamate group, which donates one. The former two will have lower pKa, and thus a higher negative charge density, which means a higher iron affinity.[6]

Figure 3[7, 8, 9]: Siderophores unbound to Fe(III). The octahedral geometry is not held without the metal. Here, hydrogens have bound to the siderophores, replacing the Fe(III) bonds.



Once the Fe(III)-siderophore complex has formed, it is introduced into the cells by complex, energy-dependent transportation mechanisms.[12] The introduction usually begins when the complex binds to a receptor protein on the cellular outer membrane, which have high affinity for the complexes. The binding changes the protein conformationally as the Fe(III)-siderophore complex is shuttled through and released into the periplasm. Once there, it binds to another high affinity proton and then taken directly or passed through a chain of transport proteins until it reaches its final destination.[13] Examples of some membrane-bound transport proteins are in Figure 4.

Figure 4: Examples of the three types of siderophores in a hexadentate formation. The dark gray and colored portions highlight the Fe(III)-siderophore complexes. The light gray represents the membrane proteins. **(A)** An FhuA protein bound to a ferrichrome ligand.[7, 12] **(B)** An FeuA protein bound to an enterobactin ligand.[8, 14] **(C)** A SirA protein bound to a staphylococci ligand.[9, 15]



The function of a siderophore is to bring insoluble iron from the environment into the cell. All siderophore perform this task uniformly. However, there are multiple mechanisms for iron release into the cell. There are two common mechanisms utilized by the majority siderophores. The first involves a reduction of Fe(III) to Fe(II), which results in a lowered iron affinity and looser bond to the siderophore. This is energetically favorable as it does not degrade the siderophore in any way, so it can be reused in iron

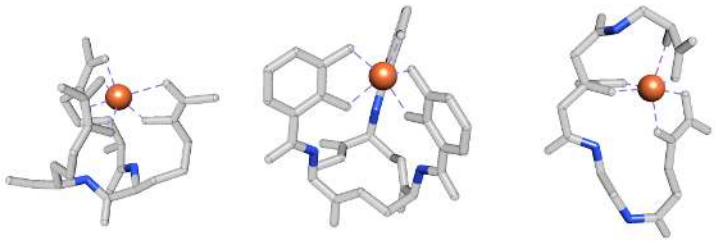
acquisition.[16] Less frequently, the backbone of a siderophore undergoes a hydrolysis reaction. These have a tendency to yield a siderophore product that is useless for re-secretion into the environment.[16, 17]

Reduction to Fe(II) produces a weaker bond to the siderophore and, overall, a less stable complex. Stability constants for the reduced iron form are on average 20 orders of magnitude lower. Contributing to this, is the fact that Fe(II) is a softer acid, which has weaker interactions with the strongly basic oxygen-donor groups. What's more, it's not as effective at outcompeting solvated hydrogens to bind these groups. This weaker metal-ligand interaction means Fe(II) is more labile and likely to dissociate.[3]

The stability of the Fe(III)-siderophore complexes make it difficult for reduction to occur, but various facilitators help the reaction along. There are certain chelators and reductive enzymes that directly catalyze the reduction reaction, but the surrounding environment plays multiple roles as well.[6] Hydrophobic regions and low pH mediums stimulate reduction. In acidic conditions, H^+ ions can partially dechelate the iron-siderophore complex. This reduced ligand denticity results in a less stable complex, which makes reduction more likely.[3]

Reduced denticity is the main theory behind the second release mechanism. Here chelation is decreased through hydrolysis of the siderophore backbone instead of through protonation of the donor groups. This reaction effectively breaks the siderophore, but significantly decreases iron affinity. The disposal of a siderophore is not energetically favorable, which is one reason this mechanism is not as popular of a strategy. What's more, siderophore hydrolysis requires a siderophore with hydrolyzable groups embedded into its backbone (Figure 5), which leaves a limited selection of siderophores.[3]

Figure 5[7, 8, 9]: Hydrolyzable portions of siderophore backbones shown in blue.



Although siderophores are bacterial structures, they're helpful to humans using the above chemistry to chelate iron and either acquire the metal or sequester it away. Medicinally, siderophores act as sneaky antibiotics through a "Trojan-Horse" strategy. These drugs kill toxic bacterial cells by covalently linking an antibiotic agent to the backbone of a siderophore. The modified siderophore still binds to Fe(III) and the bacterial cell–which is unable to sense the new cytotoxic agent–allows the complex inside.[10] Siderophores also help with iron excess diseases (hemochromatosis, iron poisoning) and malaria by chelating Fe(III). In the case of the former, this helps remove iron buildup; in the latter, Fe(III) is sequestered away from cells inside the parasite (which leads to death).[5]

Sources:

[1]Hider, R.C., Bickar, D., Morrison, I.E.G., Silver, J. Siderophore iron-release mechanisms. *J. Am. Chem Soc.*, **1984**, *106*: 6983-6987.

[2]Górska, A., Sloderbach, A., Marszałł, M.P. Siderophore–drug complexes: potential medicinal applications of the 'Trojan horse' strategy. *Trends in Pharm. Sci.* **2014**, *35*: 442-449.

[3]Dhungana, S., Crumbliss, A. L. Coordination chemistry and redox processes in siderophore-mediated iron transport. *Geomicrobiol. J.* **2005**, *22*: 87-98.

[4]Stintzi, A., Barnes, C., Xu, J., Raymond, K. N. Microbial iron transport via a siderophore shuttle: A membrane ion transport paradigm. *PNAS*. **2000**, *97*: 10691-10696.

[5]Ali, S. S.; Vidhale, N. N. Bacterial siderophore and their application: A review. *Int. J. Curr. Microbiol. App. Sci* **2013**, *2*, 303–312.

[6]Hider, R.C., Kong, X. Chemistry and biology of siderophores. *Nat. Prod. Rep*. **2010**, *27*: 637-657.

[7]Image of 1BY5 (Locher, K.P., Rees, B., Koebnik, R., Mitschler, A., Moulinier, L., Rosenbusch, J.P., Moras, D. Transmembrane signaling across the ligand-gated FhuA receptor: crystal structures of free and ferrichrome-bound states reveal allosteric changes. *Cell*. **1998**, *95*: 771-778) created with Chimera (Pettersen E.F., Goddard T.D., Huang C.C., Couch G.S., Greenblatt D.M., Meng E.C., Ferrin T.E. UCSF Chimera–a visualization system for exploratory research and analysis. *J. Comput. Chem.* **2004**, *25*: 1605-1612).

[8]Image of 2XUZ (Peuckert, F., Ramos-Vega, A.L., Miethke, M., Schwoerer, C.J., Albrecht, A.G., Oberthuer, M., Marahiel, M.A. The siderophore binding protein FeuA shows limited promiscuity toward exogenous triscatecholates. *Chem. Biol*. **2011**, *18*: 907-191) created with Chimera (Pettersen E.F., Goddard T.D., Huang C.C., Couch G.S., Greenblatt D.M., Meng E.C., Ferrin T.E. UCSF Chimera–a visualization system for exploratory research and analysis. *J. Comput. Chem.* **2004**, *25*: 1605-1612).

[9]Image of 3MWF (Grigg, J.C., Cheung, J., Heinricks, D.E., Murphy, M.E. Staphylococcus aureus SirA specificity for staphyloferrin B is driven by localized conformational change) created with Chimera (Pettersen E.F., Goddard T.D., Huang C.C., Couch G.S., Greenblatt D.M., Meng E.C., Ferrin T.E. UCSF Chimera–a visualization system for exploratory research and analysis. *J. Comput. Chem.* **2004**, *25*: 1605-1612).

[10]Miethke, M., Marahiel, M.A. Siderophore-based iron acquisition and pathogen control. *Microbiol. Molec. Biol. Rev.* **2007**, *71*: 413-451.

[11]Ahmed, E. Holmström, S.J.M. Minireview: Siderophores in environmental research: roles and applications. *Microbial Biotech.* **2014**, *7*: 196-208.

[12]Eisenhauer, H.A., Shames, S., Pawelek, P.D., Coulton, J.W. Siderophore transport through *Escherichia coli* outer membrane receptor FhuA with disulfide-tethered cork and barrel domains. *J. Biol. Chem.* **2005**, *280*: 30574-30580.

[13]Bertini, I., Gray, H.B., Stiefel, E.I., Valentine, J.S. (2006). Siderophores. In Stiefel, J. (Ed.), *Biological inorganic chemistry: Structure and reactivity* (151-160). Sausalito, California: University Science Books.

[14]Peuckert, F., Ramos-Vega, A.L., Miethke, M., Schwoerer, C.J., Albrecht, A.G., Oberthuer, M., Marahiel, M.A. The siderophore binding protein FeuA shows limited promiscuity toward exogenous triscatecholates. *Chem. Biol*. **2011**, *18*: 907-191

[15]Grigg, J.C., Cheung, J., Heinricks, D.E., Murphy, M.E. Specificity of Staphyloferrin B recognition by the SirA receptor from *Staphylococcus aureus*. *J. Biol. Chem.* **2010**, *285*: 34579-34588.

[16]Cooper, S.R., McArdle, J.V., Raymond, K.N. Siderophore electrochemistry: Relation to intracellular iron release mechanism. *Proc. Natl. Acad. Sci. USA.* **1978**, *75*: 3551-3554.

[17]Lippard, S.J., Berg, J.M. (1994). Bioavailability of metal ions. In Kelly, A. (Ed.), *Principles of Bioinorganic Chemistry* (105-139). Mill Valley, California: University Science Books.

Contributed By:

This work was originally written by ***Emma Bridgman****, Fall 2016: Emma is currently (as of 2016) a senior chemistry major at Saint Mary's College in Notre Dame, IN.*

This work was originally edited by Dr. Kathryn Haas, Assistant Professor at Saint Mary's College.

11.1.2: Iron acquisition in bacteria- Siderophores is shared under a not declared license and was authored, remixed, and/or curated by LibreTexts.

11.1.3: Fe Wars- Lactoferrin

Iron Wars

Wars can be started over metals like gold or silver, but the human body wages an internal war against pathogens on a daily basis over a seemingly insignificant metal: iron (see figure 1). While largely known for its rusting abilities, iron is also the catalyst for numerous metabolic processes, a binding agent in molecules like hemoglobin, and is even speculated to be a contributing ion to the early formation of macromolecules that eventually led to life forms.[1] However, humans aren't the only organisms that need this ion as a nutrient source; bacterial species depend on ions like iron to survive.[1] As a result of this mutual need, iron wars break out between bacteria and the human body, and each side has used scientific methods to more efficiently acquire this resource.

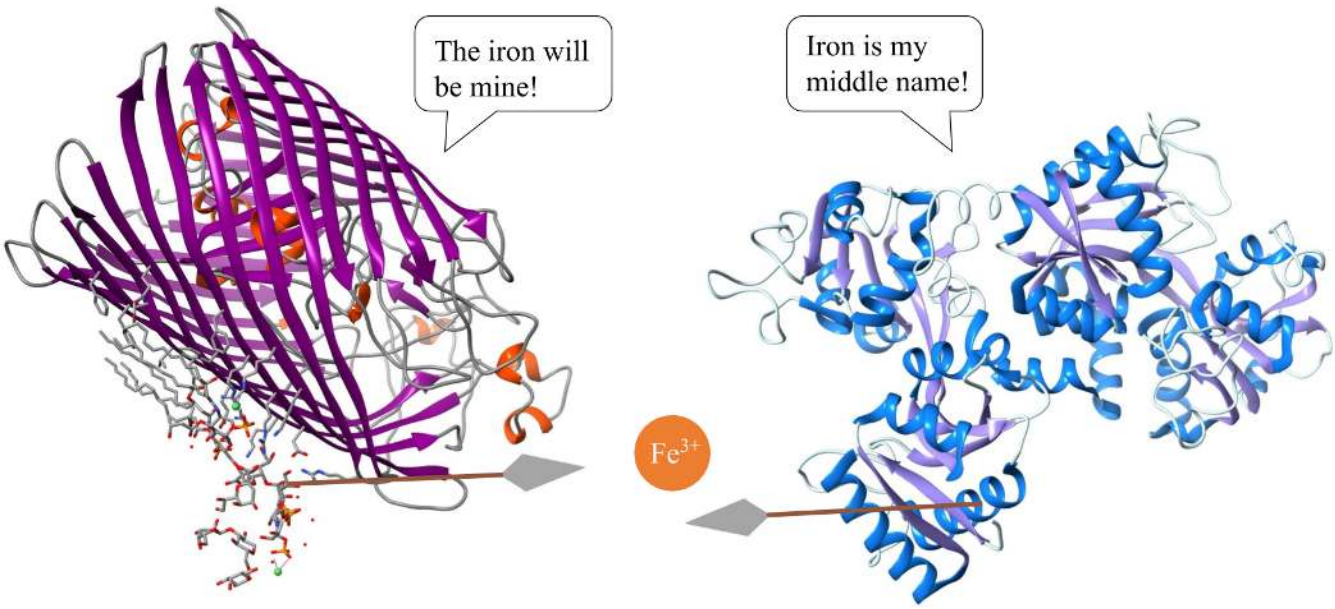


Figure 1: Cartoon depicting the "iron wars" between human and bacterial iron-sequestering proteins. Right: *E. Faecalis* siderophore, ferric hydroxamate. Left: human protein, lactoferrin.

Enter to the scene lactoferrin, a iron-chelating protein that has an extremely high binding affinity for iron (III).[2] Lactoferrin is a member of the transferrin family, a group of proteins that bind specifically to iron and perform various functions in the body (see figure 2).[2] Transferrin, while in some cases able to prevent bacterial infection, is used more efficiently as an iron transport protein. Transferrin has a lower binding affinity to iron than lactoferrin does, and a slight dip below biological pH can trigger the protein to release its ion.[3] On the other hand, lactoferrin binds to iron with a much higher affinity, and the ion is not known to be released until pH drops to around 2-3.[4] A pH of this acidity can be found in the body in places such as inflammation sites, cellular vesicles, or the stomach.[4] The ability for lactoferrin to retain iron in a pH far below the biological level of 7.4 makes lactoferrin a more effective tool in the war over iron than transferrin, but less effective as an iron source for the body itself.

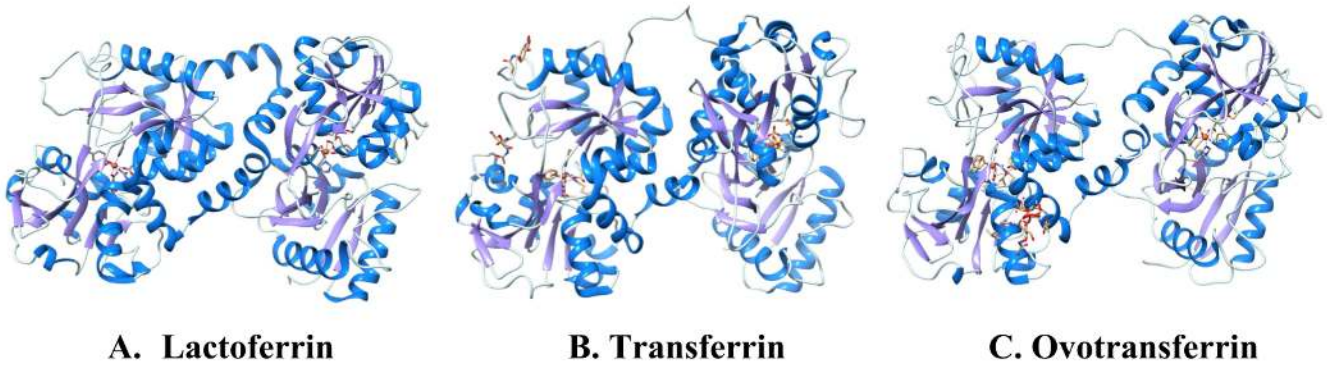


Figure 2: Comparison of the structures of three iron chelating proteins in the transferrin family: Lactoferrin, transferrin, and ovotransferrin. All transferrin proteins bind with high affinity to iron (III) ions, but lactoferrin has the highest binding affinity ($K_D \sim 10^{-20}$ M compared with $K_D \sim 10^{-9}$ M for transferrin). [6,10]

In addition to its antibacterial defenses, lactoferrin performs other functions in the body. The overall structure includes a unique cationic region on its N-terminal (See figure 3).[2] This basic region has been found to bind to lipopolysaccharides and glycosaminoglycans.[2] This binding feature allows lactoferrin to more directly attack bacteria because lipopolysaccharides and glycosaminoglycans are commonly found in the cell membrane of bacteria, and lactoferrin has been found to bind to the surfaces of bacteria and prevent iron uptake.[2] Additionally, this cationic region can bind to DNA, and thus serves as a defense against viruses by binding to viral DNA and preventing its spread through the body.[2] Recent research has taken particular interest in using lactoferrin as an oral cancer treatment, because when it is digested in the stomach, it is broken down to the peptide lactoferricin and absorbed into the bloodstream.[2] Lactoferricin has been found to prevent cellular growth by inhibiting the function of proteins involved in cellular reproduction.[5]

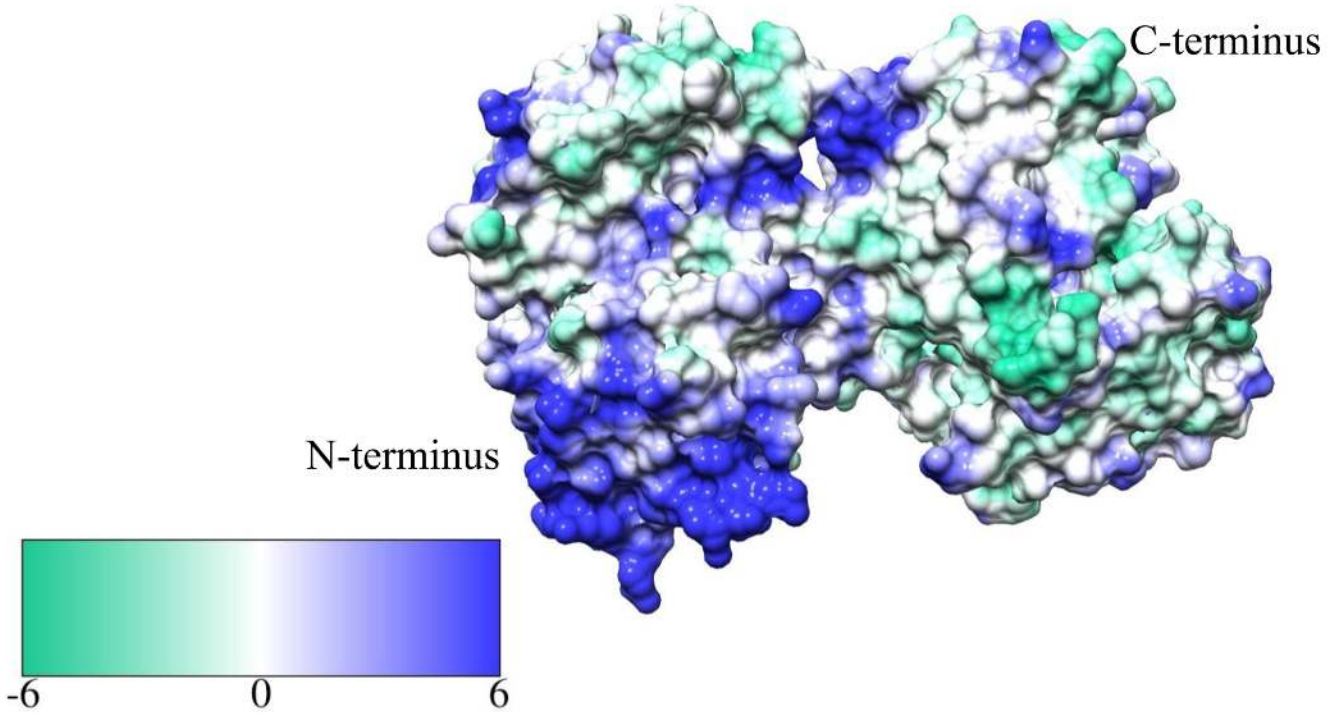


Figure 3: The cationic region of lactoferrin is highlighted in blue. This site on the N-terminus provides lactoferrin with unique properties that aid in its antimicrobial defense system.[2,5] It is able to bind directly to the surfaces of bacteria, the free DNA of viruses, and even inhibit overproduction of cancer cells.[2,5]

The structure of lactoferrin is essential for its high binding affinity. Lactoferrin has two hemispheres; the N-terminal, and the C-terminal, which are connected by an alpha helix (see figure 4a).[2] Each terminal is divided into two lobes, with a “cleft” between them where the metal binding site is located.[6] The amino acids found at the binding site are the same in all transferrin proteins, and consists of two phenolate oxygens from two tyrosines, a histidine, an aspartic acid, and a carbonate ion bound to an arginine (see figure 4b).[2,4]

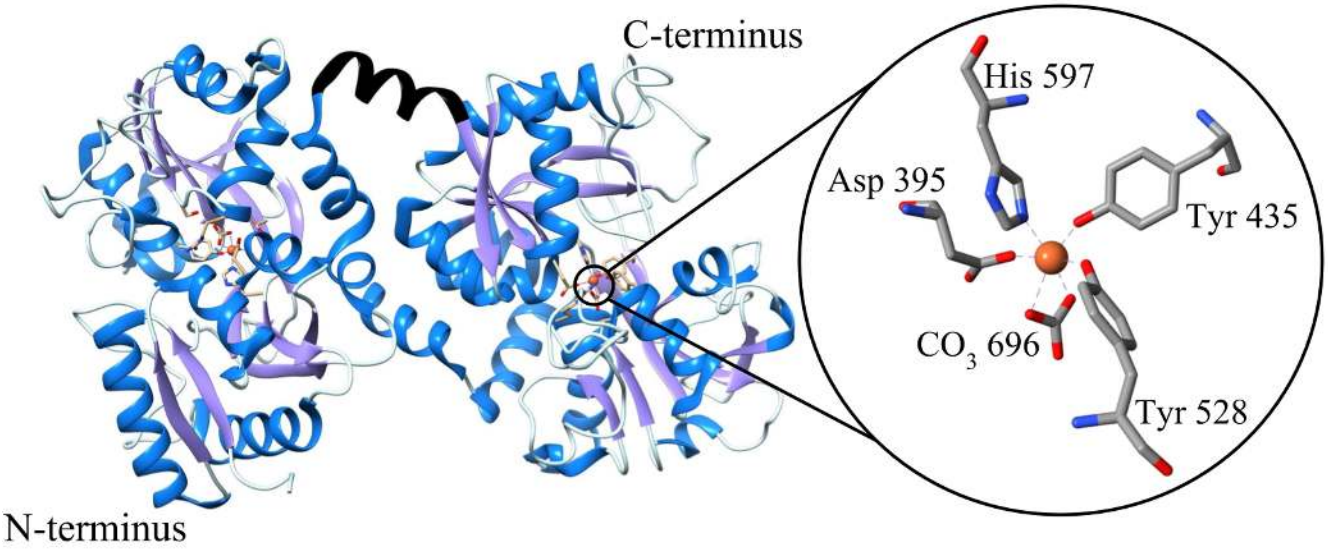


Figure 4 a-b: a) Molecule lactoferrin pictured, the alpha helix connecting N-terminal to C-terminal is pictured in black. In other transferrin proteins, this connection is a flexible beta sheet. It is predicted that this rigid helix contributes to the conformational changes experienced by lactoferrin that allow it to retain iron ions at a lower pH.[6] b) The active binding site of lactoferrin on the C-terminus, but identical amino acids are on the N-terminal. Consists of four amino acids, and a carbonate ion with an iron (III) ion in the center.

It is predicted that the carbonate is the first to bind to the iron ion, followed by the tyrosine groups.[6] Then lactoferrin undergoes a conformational change, wherein the N-terminus closes like a hinge, to lock the iron into place.[6] The resulting structure brings the iron closer to the histidine and the aspartic acid found at the binding site, and the resulting complex displays an octahedral coordination geometry (see figure 5).[6] This final structure is very stable and allows the lactoferrin protein to retain the iron ions in a pH as low as 2-3.[2]

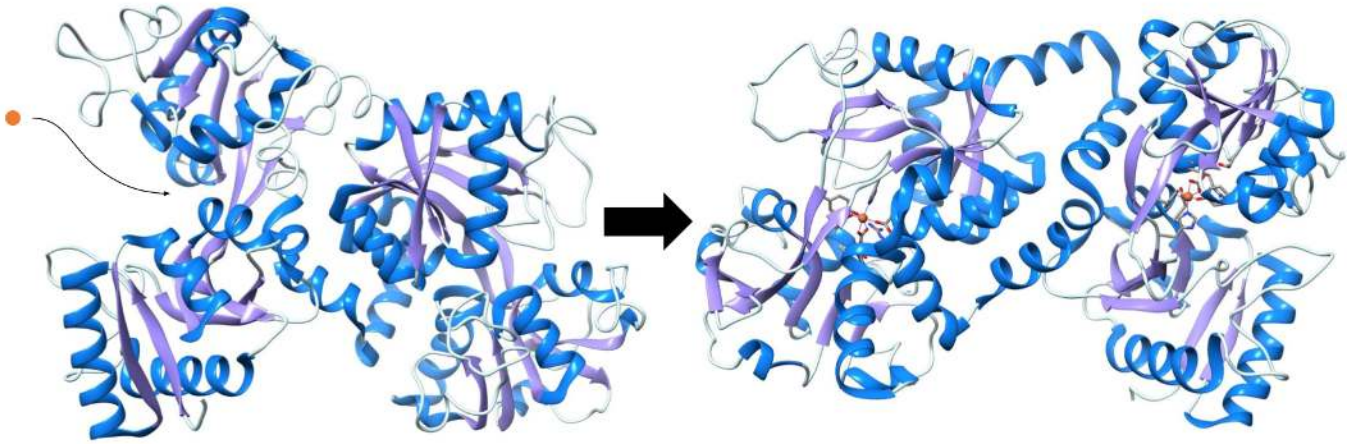


Figure 5: The apo-form of lactoferrin (left) undergoes a conformational change upon binding to iron (III) on the N-terminal side. The lobe closes like a hinge around the binding site, which locks the iron into place and creates an extremely stable complex.

Lactoferrin has high specificity for iron (III) ions. This is likely due to the combination of several different factors, some of which contribute to general stability of the metal complex, and some that lead to the iron (III) preference.

The chelate effect is a thermodynamic factor that contributes to general metal complex stability, because it explains that stability increases as entropy increases. That is to say that as the number of individual molecules in a system increases, so does the stability of a complex. For example, when an ion (M^{n+}) is not bound to a system or protein in the body, it is likely bound to six water molecules, since this complex is more stable than a charged ion, and there is plenty of water in the body. So, when that ion binds to a single complex with multiple binding atoms, the chelate effect contributes to high stability of the metal-protein complex, because the number of free molecules goes from two to seven (see figure 6). For this reason, it is entropically favorable for iron to form a bond with lactoferrin because it replaces six individual molecules with a multidentate ligand.

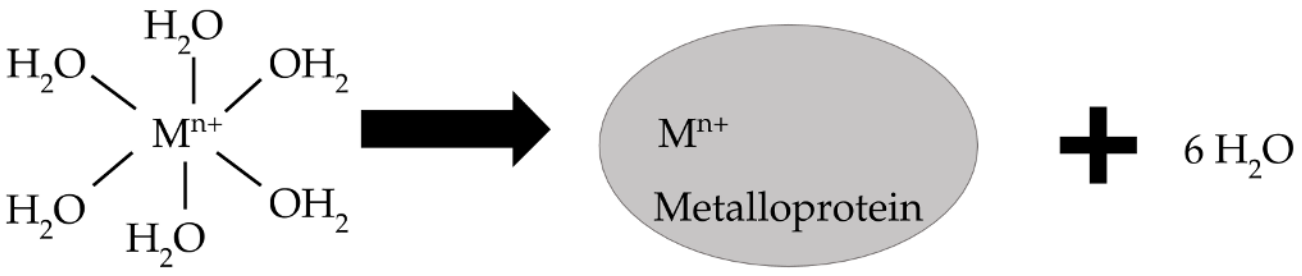


Figure 6: When an iron (III) is “free” in the human body, it usually forms bonds to water molecules. The chelate effect explains that increasing the number of free individual molecules is a favorable reaction, so when that ion binds to a protein with multiple binding atoms, it forms a single metal-protein complex and six free water molecules. Thus, the total number of molecules in a system goes from two to seven, which increases the entropy, or chaos.

The chelate effect is a thermodynamic explanation for the stability of the formation of a metalloprotein complex. Hard soft acid-base (HSAB) theory contributes to the iron selectivity of lactoferrin. HSAB theory is a thermodynamic concept that can predict the stability of metal-ligand interactions. Metals are acids, ligands are bases, and generally hard acids interact with hard bases, and soft acids interact with soft bases. Factors such as charge density and characteristics of an interaction (electrostatic vs covalent) contribute to whether a metal or ligand is considered hard or soft. All of the amino acids found in the binding site, with the exception of histidine, prefer hard acids. Since like binds with like, and iron (III) is a hard acid, the site is favorable for iron. However, several other metals are hard acids as well, including magnesium (II), chromium (III), and calcium (II). These other metals are also known to be able to bind to lactoferrin, but are not nearly as common as iron (III), and don’t usually remain bound lower than a pH of 4-5.[7]

Once lactoferrin has bound to the metal ion, the iron(III)-protein complex that forms is extremely stable, as it is with all transferrin proteins. An important factor in this stability is the geometry of the binding site. The d-orbitals of metals have a large influence on geometry. When a metal binds to a ligand, it can form bonding and antibonding orbitals for electrons to occupy. The difference between the orbitals can influence electron spin and configuration (see figure 7). The energy difference between these d-orbitals can be called the field splitting ($\triangle_O$). When $\triangle_O$ is small, the system is said to have a weak field and the electrons are high spin, which means they will occupy the higher energy orbitals before pairing up. On the other hand, when $\triangle_O$ is large, the system has a strong field and are low spin, so they will pair up before occupying a higher orbital.

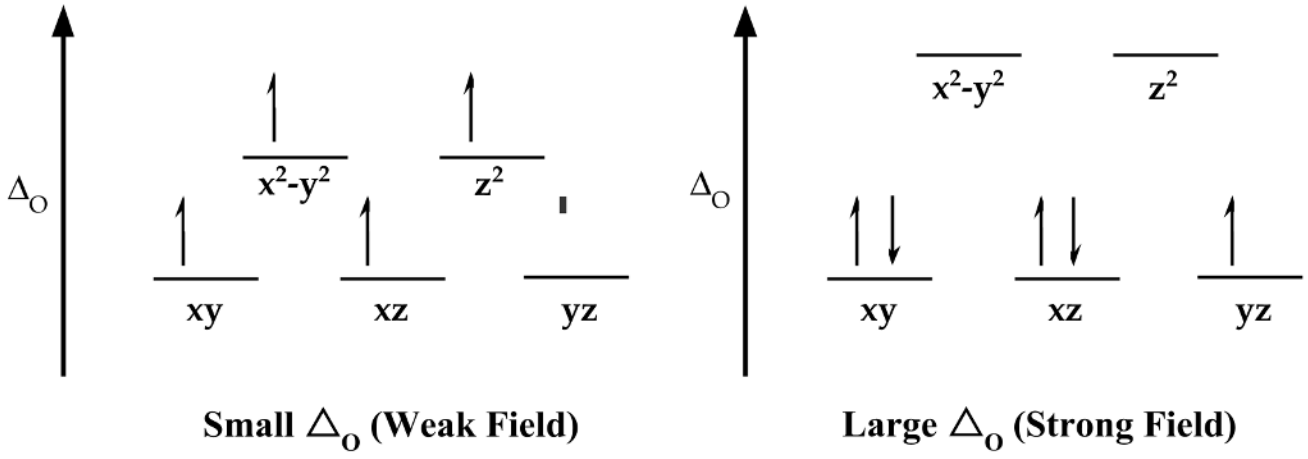


Figure 7: The difference between d-orbitals in metal ions is $\triangle_o$, which influences their electron spin. If $\triangle_o$ is small, then it requires less energy for the electrons to move up into a higher energy orbital than it does to pair up, but when $\triangle_o$ is large, the jump into the next orbital would be too high. Note that this only impacts d_4-d_7 electrons.

Some of the factors that contribute to $\triangle_O$ include the formal charge of the ion, the location of the ion on the periodic table, and the types of ligands in the system. All of the donor atoms in the binding site of lactoferrin (except histidine) are sigma and pi donors. Sigma and pi donors are typically involved in weak field interactions, which is a smaller distance between d-orbitals ($\triangle_O$). In addition, iron (III) has a location in the fourth row of the periodic table, and $\triangle_O$ decreases going up the periodic table. These factors indicate that iron (III) in lactoferrin has a weak field. Since Iron (III) is a d^5 electron, a weak field means that iron's d-electrons will occupy the higher energy orbitals, and won't pair up.

Ligand field stabilization energy (LFSE) can suggest the preferred geometry of an ion. The LFSE is calculated using the equation LFSE = -0.4x + 0.6y, where x is equal to the number of electrons in lower energy orbitals, and y is equal to the number of electrons in higher energy orbitals. Iron (III) has a LFSE of zero, which means there is no other ligand position that would provide a lower LFSE, and so iron is able to form stable bonds in any geometry configuration. Usually d^5 metal ions form an octahedral complex when bound to six ligands (See figure 8). However, in the case of lactoferrin, the carbonate ion causes a slight change in the geometry which results in a distorted octahedral configuration.

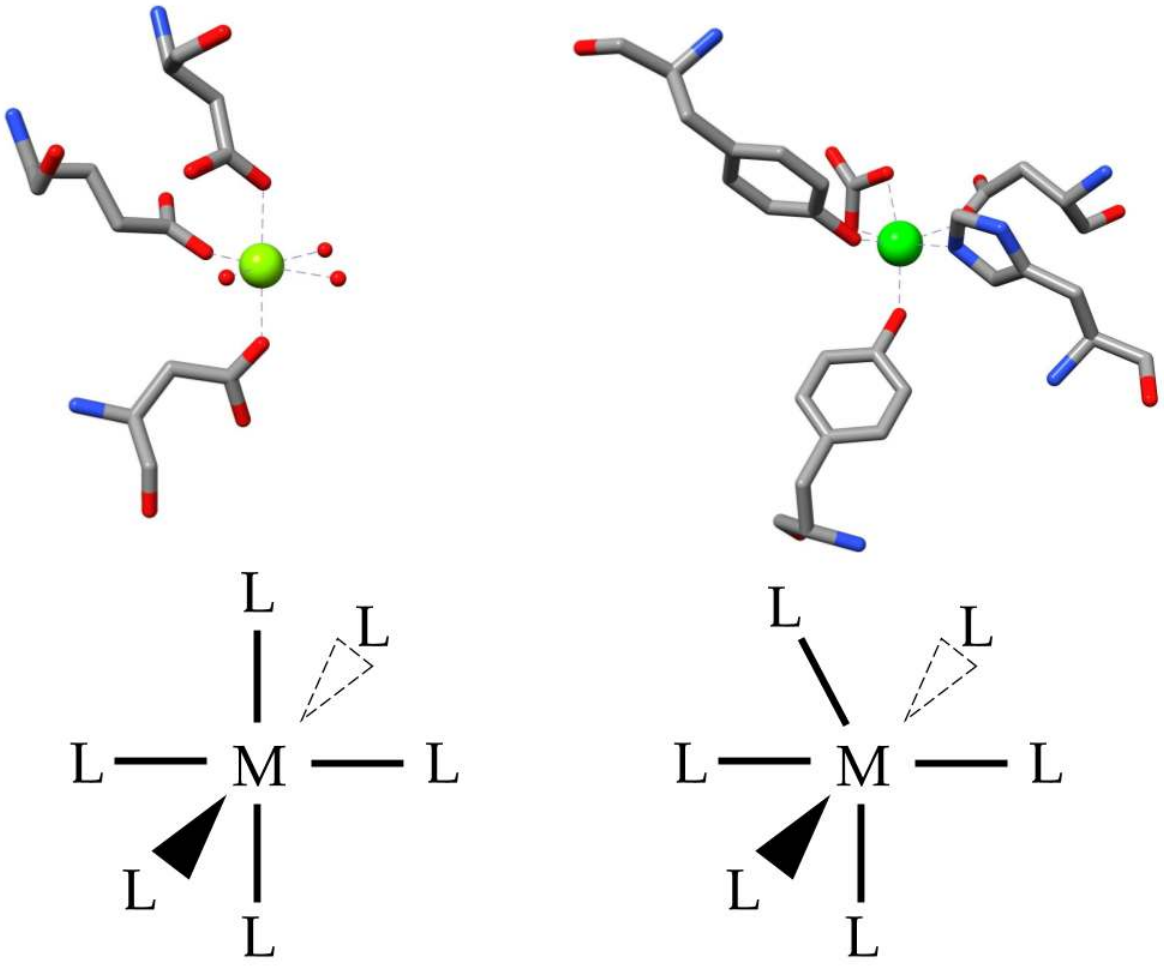


Figure 8: Comparison of the molecular geometries of a standard octahedron and the distorted octahedron of lactoferrin. The carbonate ion found in the binding site of lactoferrin causes the ligand position to shift.

Understanding this concept of crystal field theory provides some insight to how scientists are able to "see" when iron is bound to lactoferrin. The size of $\triangle_O$ can be indicative of whether an ion will undergo a d-d transition or a charge transfer transition. When light waves hit a metal ion and the electrons are excited into a higher d-orbital, the ion is undergoing a d-d transition. Charge transfer, on the other hand, can occur with an exchange of electrons from either the metal to the ligand (MLCT) or from the ligand to the metal (LMCT). In the case of lactoferrin, the majority of the ligands are pi-donors, which is indicative of a ligand to metal charge transfer because the ligand has remaining pi-electrons in its orbitals. The lightwaves excite these electrons into a higher binding orbital of the metal, which produce vibrant colors and strong spectroscopic bands.

Research found the extinction coefficient for the system to be rather large, around 2,500 M^{-1} at a wavelength of 464 nm, which is highly indicative of a charge transfer transition. In addition, the light absorption for lactoferrin is found to be λ=465 nm, which corresponds to the wavelength of blue light. Since colors appear in color as the opposite of the wavelength they absorb (see figure 9), lactoferrin appears as a red-orange color, which is in conjunction with observations initially made of lactoferrin describing it as a red substance found in milk.[2,8]

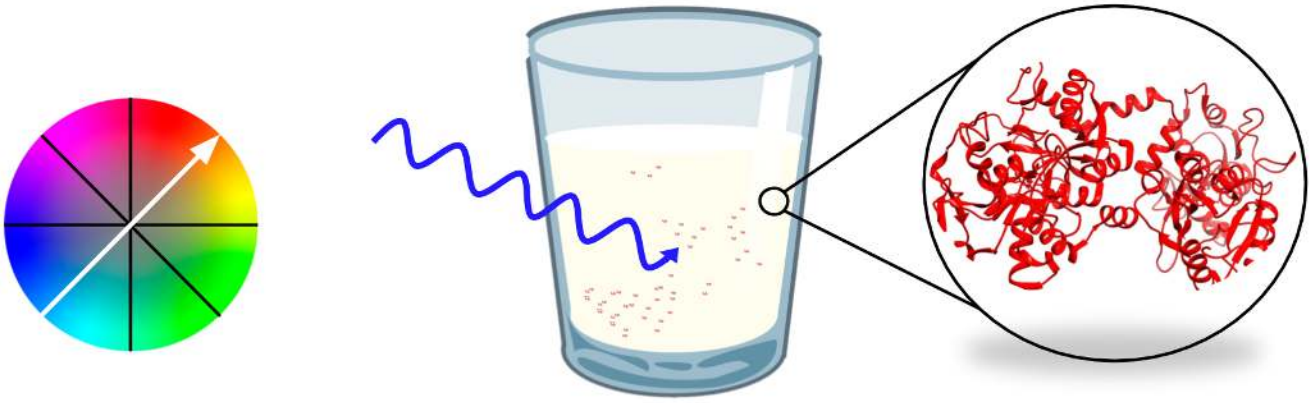


Figure 9: When using spectroscopy, light waves are used to excite electrons in molecular orbitals, and the resulting visible wavelength is the opposite color on a color wheel. In the case of lactoferrin, a wavelength of 465 nm is used to excite the electrons which corresponds to an aqua blue light, and the resulting visible color is red.

Lactoferrin's ability to sequester iron from its environment makes it useful as a defense protein in the innate immune system. After both lobes have taken up an iron ion, it can take a pH as low as 2-3 to remove it. Since bacteria are often not this acidic, but still require iron to perform biological functions, lactoferrin essentially starves bacteria from their nutrition source. Most bacteria are defeated by this tactic, with some notable exceptions.

Some bacteria, such as enterococci, have developed tactics to fight against iron sequestering proteins, including lactoferrin.[9] These tactics include the use of siderophores, ferric reduction, and proteases that can cleave lactoferrin. Siderophores are essentially bacteria's version of lactoferrin, and are also able to bind to iron (III) with high affinity by using the chelate effect the same way lactoferrin does. The method of iron reduction, on the other hand, utilizes HSAB theory, and changes the hard acid iron (III) into an intermediate, which would make the ion less stable in its environment. Finally, proteases that can cleave proteins like lactoferrin are able to change the binding site, which ultimately impacts the ligands bound to the iron. This would cause a change in the geometry of the binding site and cause the iron to "pop out" of place.[9]

While bacteria use these defenses to regain some iron ions, these methods might shed some light on how the human body regains iron ions from lactoferrin. To date, this remains elusive, and it is unclear exactly how the body removes ferric iron from lactoferrin. Unlike transferrin, which has a role that involves sequestering iron ions as well as transporting them for further use,[10] lactoferrin exists almost exclusively in secreted fluids, and is not known to be used for any other reasons than lowering iron concentration. Since transferrin needs to be able to both obtain and release iron fairly easily, it makes sense that iron ions are released around a pH of 5.5, and even a slight dip in pH has been known to trigger the release mechanism.[6,3, 10] However, since lactoferrin is used far more efficiently as an antibacterial agent, then its ability to remain bound to iron in a much lower pH is better at preventing bacteria from obtaining the iron, but makes it a poor source of iron for the body. It is known that lactoferrin can be a source of iron for infants under six months,[11] and it is speculated that lactoferrin must undergo a conformational change to release bound ions. However, further research is needed to understand what this change entails.[6] Since lactoferrin is largely found in secreted fluids, it could be a possibility that it is not intended to release iron ions, since the body is disposing of the protein.

Sources

1. Rosa, L.; Cutone, A.; Lepanto, M.; Paesano, R.; Valenti, P. Lactoferrin: A Natural Glycoprotein Involved In Iron And Inflammatory Homeostasis. *International Journal of Molecular Sciences* 2017, *18*, 1985.

2. Vogel, H. Lactoferrin, A Bird'S Eye View. *Biochemistry and Cell Biology* 2012, *90*, 233-244.

3.Carmona, F.; González, A.; Sánchez, M.; Gálvez, N.; Cuesta, R.; Capdevila, M.; Dominguez-Vera, J. Varying Iron Release From Transferrin And Lactoferrin Proteins. A Laboratory Experiment. *Biochemistry and Molecular Biology Education* 2017, *45*, 521-527.

4. Sill, C.; Biehl, R.; Hoffmann, B.; Radulescu, A.; Appavou, M.; Farago, B.; Merkel, R.; Richter, D. Structure And Domain Dynamics Of Human Lactoferrin In Solution And The Influence Of Fe(III)-Ion Ligand Binding. *BMC Biophysics* 2016, *9*.

5. Gibbons, J. Lactoferrin And Cancer In Different Cancer Models. *Frontiers in Bioscience* 2011, *S3*, 1080.

6. Baker, H.; Baker, E. Lactoferrin And Iron: Structural And Dynamic Aspects Of Binding And Release. *BioMetals* 2004, *17*, 209-216.

7. Ainscough, E.; Brodie, A.; Plowman, J. The Chromium, Manganese, Cobalt, And Copper Complexes Of Human Lactoferrin. *Inorganica Chimica Acta* 1979, *37*, 282.

8. Carmona, F.; Muñoz-Robles, V.; Cuesta, R.; Gálvez, N.; Capdevila, M.; Maréchal, J.; Dominguez-Vera, J. Monitoring Lactoferrin Iron Levels By Fluorescence Resonance Energy Transfer: A Combined Chemical And Computational Study. *JBIC Journal of Biological Inorganic Chemistry* 2014, *19*, 439-447.

9. Lisiecki, P. Transferrin And Lactoferrin – Human Iron Sources For Enterococci. *Polish Journal of Microbiology* 2017, *66*, 419-425.

10. Dautry-Varsat, A.; Ciechanover, A.; Lodish, H. Ph And The Recycling Of Transferrin During Receptor-Mediated Endocytosis. *Proceedings of the National Academy of Sciences*1983, *80*, 2258-2262.

11. Lönnerdal, B. Nutritional Roles Of Lactoferrin. *Current Opinion in Clinical Nutrition and Metabolic Care* 2009, *12*, 293-297.

Contributed by

*This work was originally written by **Chloe Griggs**, Spring 2018: Chloe is currently (as of 2018) a sophomore chemistry major at Saint Mary's College in Notre Dame, IN.*

This work was originally edited by Dr. Kathryn Haas (Assistant Professor), Madison Sendzik (Teaching and Research Assistant), and Dr. Dorothy Feigl (Professor) at Saint Mary's College.

11.1.3: Fe Wars- Lactoferrin is shared under a not declared license and was authored, remixed, and/or curated by LibreTexts.

11.1.4: Iron Storage- Ferritin

Iron is necessary for life. It is an essential nutrient and living organisms use it frequently and in large amounts. Iron is necessary in the active sites of enzymes that play roles in respiration, electron transfer reactions, energy metabolism, DNA synthesis, and gene regulation.[1] Iron is also necessary for oxygen transport and oxygen storage in the proteins hemoglobin and myoglobin.[2]

Despite the importance of iron for life, excess iron can be toxic.[3] Unregulated free iron can catalyze the production of harmful reactive oxygen species (ROS) and free radicals, most commonly via Fenton chemistry. The Fenton reaction (below) is the reaction between iron(II) ions and hydrogen peroxide to produce the extremely reactive and harmful hydroxyl radical (**$^{\bullet}$OH**).[1]

$$Fe^{2+} + H_2O_2 \rightarrow Fe^{3+} + OH^- + {}^{\bullet}OH$$

ROS are strong oxidizing agents and can cause permanent cell damage, organ failure, and death.[4] Furthermore, iron ions have notoriously low solubility. The issues of solubility particularly apply to iron(III) ions which have a solubility of 10^{-18} M at physiological conditions.[1] In environments where oxygen is present, like the bloodstream, iron can form insoluble aggregates, similar to rust.[5,6] For example, dying red blood cells produce ~0.54 mmol of iron per day. If that iron is left free in its aerobic environment, it will react with oxygen and form insoluble rust-like compounds. It's been estimated that a human would have to drink 10^{13} liters of water every day to avoid "rusty" kidneys.[1] Additionally, pathogens need iron to replicate and to survive. Thus, excess iron in an organism could be used both to nourish the organism itself and to nourish infection and disease-causing organisms.[4] Due to the biological necessity of iron, the storage and collection of excess iron in a nontoxic form is vital.

The cell's answer to these obstacles is ferritin. Ferritin is the universal iron storage protein found throughout nature—both in prokaryotic and eukaryotic organisms.[4,7] It is found in plants, animals, and bacteria and is necessary for all living things. In fact, deletion of the ferritin gene is lethal.[8] Ferritin functions both intracellularly and extracellularly.[5] Intracellularly, human ferritin is found in the cytoplasm of the cell.[3,4] Extracellularly, human ferritin has been found in serum. It is currently unknown where this extracellular ferritin comes from and how it leaves the cell, but its concentration in blood is used as a common clinical test for iron levels.[5] The measurement of serum ferritin is considered as one of the most specific and sensitive blood tests for diagnosing iron deficiency.[5]

Ferritin solves the previously discussed obstacles of excess iron in the body. Considering the poor solubility of Fe^{3+} ions, human ferritin is actually rather soluble and gathers excess iron ions without creating insoluble clusters of iron in the body.[6] The transport protein transferrin brings excess iron ions to ferritin as Fe^{2+}. The ferritin protein surrounds the collected iron ions to prevent the Fe^{3+} ions from aggregating in the cytoplasm of the cell or in the bloodstream and to protect them against reaction with any other species present, thus avoiding the production of ROS.[6] Any other ligands in the cell that might bind to iron are blocked out and the iron is stored in a stable form.[2] Ferritin stores excess iron until iron is needed for one of the many processes in which it plays a part. Iron stored in ferritin can comprise almost 10% of total iron in the body.[2]

Structurally, ferritin is a hollow cage and the sequestered iron is stored as an iron(III) mineral within the protein shell (Figure 1).[2,3]

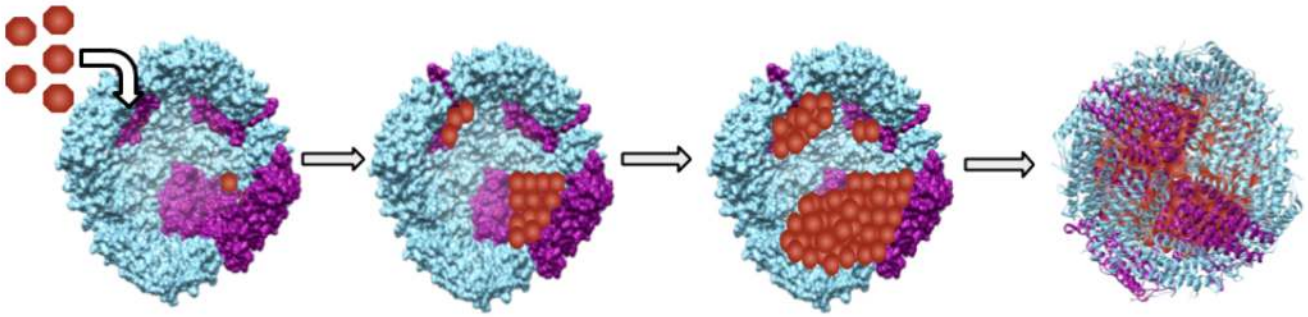


Figure 1. A cartoon diagram of sequestration of iron, which has been crystallized and is stored as an iron/oxy mineral in the hollow cage of ferritin. From left to right, the diagram depicts the cross section of the ferritin protein cage and the growing nucleation in the hollow center of ferritin. Each red shape represents some crystalline, mineral combination of iron, oxygen, and hydrogen (FeOOHcore). Nucleation begins on the purple surfaces of ferritin, which will be discussed in detail later, but is otherwise random. The final image in the diagram on the far right is the spherical ribbon structure of full iron-containing ferritin protein with the cartoon depiction of iron/oxy mineral (red shapes) within the center. While this diagram depicts ferritin being filled to capacity with iron, in reality, ferritin can be filled as much or as little with iron, as needed. Thus, this figure can also be interpreted as different ferritin proteins in environments of different iron concentrations and so storing different amounts of iron. N.B. This diagram is not biologically or chemically representative of the process of iron storage, but is included to provide the reader with a visual of the storage of iron/oxy mineral within the hollow cage of ferritin. The actual process of storage is discussed later.

Ferritin is made of subunits. Each subunit has four polypeptide α-helices or spirals.[2] Structures of ferritin differ based on the organism which produces it. Most ferritin is made of 24 of these subunits.[6] Human ferritin is a 24-subunit, 480 kDa, 12 nm globular protein with a hollow center cavity (cavity diameter of 8 nm).[2] One 24-subunit ferritin protein can store up to 4500 iron ions in its hollow center.[2] Ferritin is a very good space-saving model for the cell because of its high iron to protein ratio (4500 iron ions/8 nm cavity).[2,9] This iron to protein ratio is 200 times that of hemoglobin.[9] Up to 24% of ferritin's weight could be stored iron ions. Meanwhile, bacterial ferritin can be either a 12- or 24-subunit globular protein.[6] However, it is thought that the 12-subunit ferritin's may play an additional role in protecting DNA from oxidative damage, while the 24-subunit bacterial ferritin may control bacterial iron metabolism.[3]

The subunits of human ferritin are classified as the heavy subunit or "H-chain" and the light subunit or "L-chain" (Figure 2).[6] The two subunits, however, are not extremely different in molecular weight or amino acid sequence. The H-chain is made of 178 amino acids with a molecular weight of 21 kDa and the L-chain is made 171 amino acids and weighs 18 kDa.[4] The two types of subunits have ~53% protein sequence identity.[4] The designations of heavy and light are actually a modern recasting of designations that originally reflected the organs from which the two forms were isolated, "H" for heart and "L" for liver.[8]

The two types of subunits combine in different ratios to form the 24-subunit protein shell in humans (Figure 2).[6] This ratio is dependent on the tissue where the ferritin is synthesized.[6] The H subunit is responsible for catalyzing the oxidation of iron(II).[8] The L subunit hosts the site of nucleation and storage of iron.[8] The ratio of H:L will be higher in tissues where iron oxidation activity is high and iron detoxification is needed, such as the heart or the brain.[1,4] Tissues, like those in the spleen, are used more for storage and will have a lower H:L ratio. The human liver produces ferritin that is 50% H and 50% L.

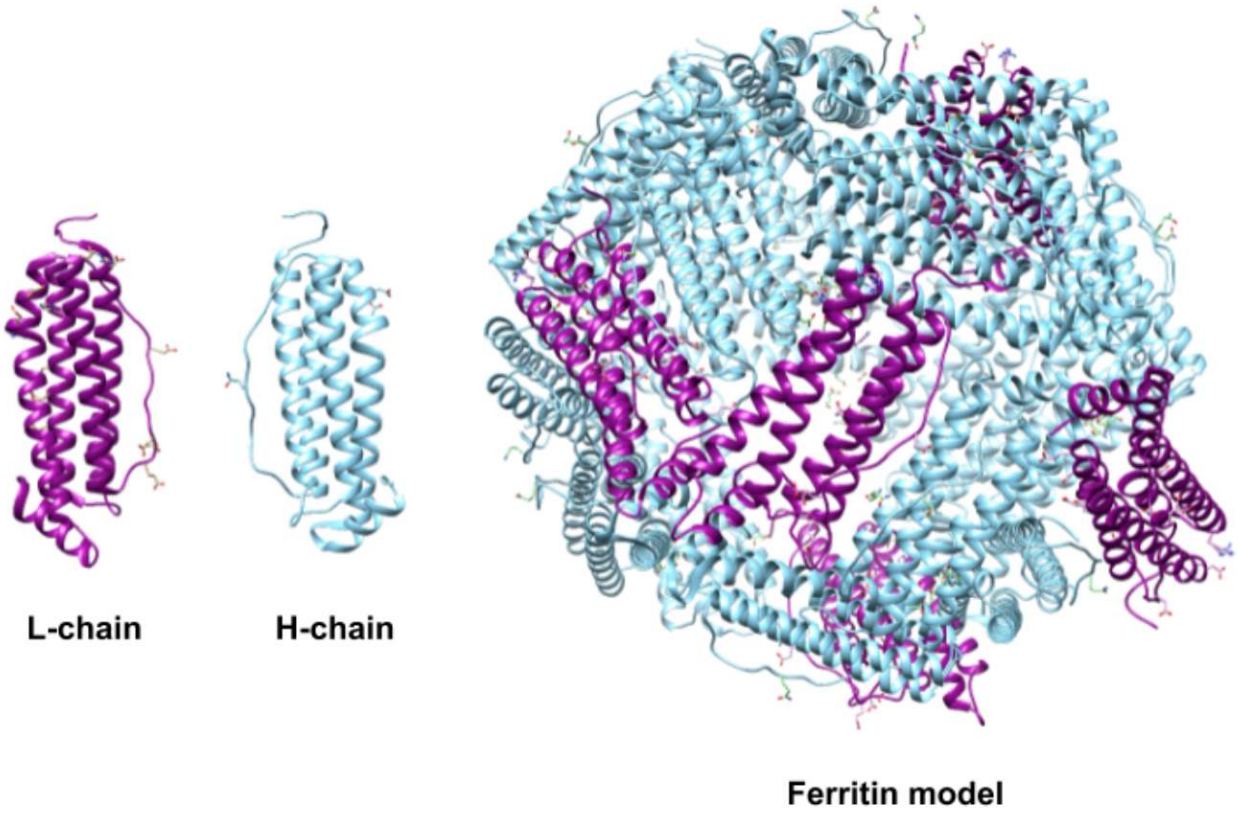


Figure 2. Light (L) (PDB 2FFX) and heavy (H) (PDB 2FHA) human ferritin subunit chains combine to form the human ferritin shell in specific ratios. The H:L ratio is dependent on the tissue where the protein is synthesized. The model seen here was created from the crystal structures of individual subunits, not a biologically obtained structure. However, it is approximately 30% L-type subunit and 70% H-type subunit and would be of a similar ratio to the ferritin found in the brain.[1]

In bacterial ferritin, the H-chain is the only subunit present in the either 12- or 24-subunit shell.[2] Amphibious or fish ferritin can be made up of two to three different types of subunits ("H-","L-", and middle "M-chains").[7] The H and M subunits share similar functions of oxidizing iron.[12] This report will focus on the H and L subunits of human ferritin.

While iron storage has been determined as an important function, it is unknown if this is the only or even primary function of ferritin.[6] Other proposed functions fall mainly under the umbrella of ferritin's role as an antioxidant. It has been proposed that the main role of ferritin could be in reducing oxidative stress and preventing harmful production of ROS from reactions between iron and oxygen or hydrogen peroxide. The exact mechanism of how ferritin works as an antioxidant is unclear, but its characteristic functions can all contribute.[6] For example, the ability to remove O_2 or ROS through reaction with Fe^{2+} and to remove excess Fe^{2+} from the environment both directly reduce oxidative stress; however, if ferritin is produced by the cell for this purpose has yet to be determined.[6]

Entrance: Ferritin's Selectivity for Iron

Fe^{2+} ions are brought to ferritin for storage by the transport protein transferrin. The ions are believed to enter through one of the eight symmetric 3-fold channels or one of the six symmetric 4-fold channels formed by the subunits in the ferritin structure highlighted in Figure 3.[6]

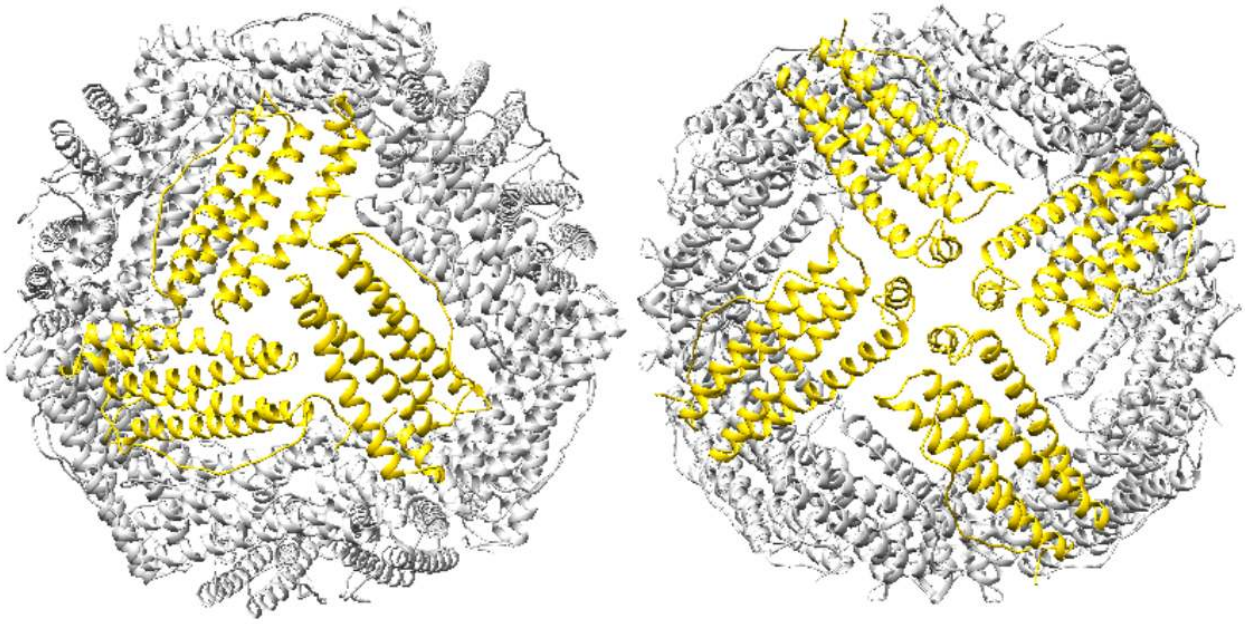


Figure 3. Symmetric channels of entry and exit in Ferritin (PDB: 1FHA). The 3-fold channel on the left appears eight times in the 24 subunit ferritin protein. The 3-fold channel is formed by three subunits. The 4-fold channel on the right appears six times in the 24 subunit ferritin protein. The 4-fold channel is formed by four subunits.

The 3-fold channels are lined with the polar side chains aspartate and glutamate and make the channel hydrophilic.[2] The hydrophilicity of the channel allows for the transport of water, metal cations, and hydrophilic molecules of an appropriate size into and and out of the ferritin center.[4] Most studies indicate that the 3-fold channel is the main channel for Fe^{2+} ions both into and out of the cell.[1,3]

The 4-fold channels are lined with the non-polar side chain leucine and make the channel hydrophobic. It is widely thought that the 4-fold channels are involved with the diffusion of oxygen and hydrogen peroxide into and out of the ferritin center.[1]

Iron(II) ions are oxidized at the “ferroxidase site” on the H-chain subunits (Figure 4). After conversion to Fe^{3+}, the iron is stored as a crystalline iron/oxy mineral.[2] The mineral accumulates on the L-chain (Figure 5).[8]

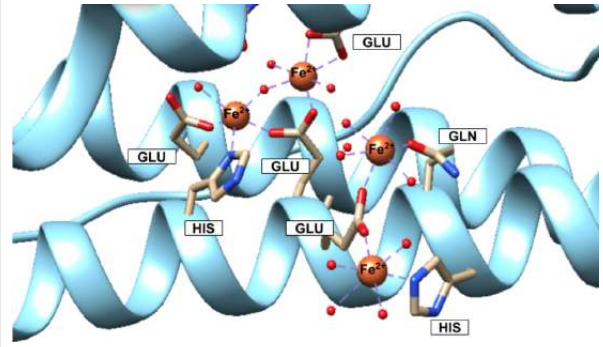


Figure 4. Human Ferritin H-chain (PDB 4YKH). Fe^{2+} ions are both shown traveling on their way to the ferroxidase site and at the ferroxidase site, to be covered in detail later. Fe^{2+} ions can be seen binding to water molecules, oxidizing agents and residues glutamic acid (Glu or GLU), glutamine (Gln or GLN), and histidine (His or HIS). The smaller red balls connecting to the Fe^{2+} ions via a purple dashed line are the oxidizing agents—oxygen molecules, hydrogen peroxide, or water molecules.

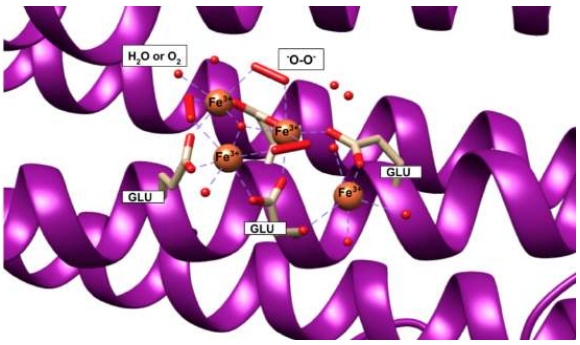


Figure 5. Human Ferritin L-chain (PDB 5LG8). Fe^{3+} ions can be seen binding to water and oxygen molecules (small red balls), peroxo groups (long red cylinders), and residues of glutamic acid (Glu or GLU) from the L-chain. Fe^{3+} is stored as an iron/oxy mineral on the L-chain. This is the beginning of nucleation within the ferritin cavity.

Figures 4 and 5 show iron(II) at the ferroxidase site and iron/oxy mineral at the nucleation site, according to the available crystal structures. The structure of the entire iron mineral core, however, is actually inconsistent throughout the whole mineral and differs even between identical ferritin shells.

Traditionally, it was believed that the iron(III)/oxy mineral that makes up the core was similar to ferrihydrite and ideally structured as 20% tetrahedral and 80% octahedral; however, as more evidence has become available this model has been replaced by a "polyphasic" or heterogeneous model of the iron core that is thought to be more accurate.[2,4] According to the polyphasic model, the mineral structure is heterogeneous in its chemical content and geometric structure.[4] X-ray absorption fine structure (EXAFS) studies concluded that the iron core of ferritin was made of iron ions that are surrounded by six or seven oxygen atoms, surrounded by another shell of iron ions.[2] This inconsistency leads to the conclusion that the mineral is a heterogeneous, hydrated iron(III)/oxy.[3] In other words, the iron core itself is not packed regularly or in a pattern within ferritin.[6]

The composition of the protein shell does not affect the composition of the iron/oxy mineral, however.[6] In fact, two ferritin proteins that are identical in protein makeup (with same H:L ratio) are likely to have a different make-up of their iron cores. The H:L ratio is suspected to affect the geometry of the crystal, due to their inherently different properties. Because the H-chain hosts the ferroxidase site and L-chain hosts the nucleation site, the rate at which the iron is accumulated and the mineral core is formed varies as the ratio does.[6] Studies on the crystal structure of the mineral core have found some cores to be more highly ordered and crystalline and other less ordered and more amorphous; these observations are thought to be the result of, or at least correlate to, different H:L ratios.[6]

Selectivity of iron(II) by ferritin can be explained through hard-soft acid base (HSAB) theory. HSAB theory characterizes metal ions and ligands as either hard, soft, or borderline acids and bases based on the Lewis definition. Characterization, however, should be noted to be a gradient scale for all ions and ligands.HSAB theory states that similarly characterized acids and bases will be more likely to bind with one another; that is, a hard acid will be more likely to bind to a hard base over a soft or borderline base and vice versa. Borderline acids or bases prefer to bind to borderline bases or acids, respectively; however, borderline is more intermediate in character and more flexible in binding. It isn't uncommon for a borderline acid or base to be more slightly more hard or soft in character.

Ferritin binds an Fe^{2+} ion for oxidation. Fe^{2+} is categorized as a borderline acid. The binding sites on the H-chain are glutamic acid (Glu), histidine (His), and glutamine (Gln) residues (Figure 4).[6] Glu and Gln are categorized as hard bases, while His is categorized as borderline base. The oxidizing agents—oxygen molecules, hydrogen peroxide, or water molecules all have hard character. Fe^{2+} as a borderline acid binds well with the binding site of mixed hard and borderline character. HSAB theory supports the selection of Fe^{2+} as the metal ion for the ligand. The selection of Fe^{2+} in ferritin is further supported by experimental work where metals like zinc (which also exists in the body) were also shown to have binding abilities to ferritin.[5] But, zinc, although it is also borderline, has softer character than Fe^{2+} and so would not be as stable or favorable with the hard Glu and Gln ligands.[10]

Because of the initial selection of Fe^{2+} by the H-chain and the crystalline nature of the iron(III) core, the binding of Fe^{3+} by the protein is not as key. However, Fe^{3+} is characterized as a hard acid and the Glu residues on the L-chain and the oxide species in the mineral are also hard, so binding remains preferable.

Selectivity of Fe^{2+} is further supported by the chelate effect. The chelate effect is an entropic effect where a ligand has multiple donor groups for a metal ion. The entropy increases favorably when a chelator is used to bind because there is one molecule binding to the metal ion through multiple donor atoms, rather than multiple individual ligands. The Fe^{2+} binding site of ferritin is a chelator. At the ferroxidase site on the H-chain subunit, the binding site of the Fe^{2+} ions are shown in Figure 6.

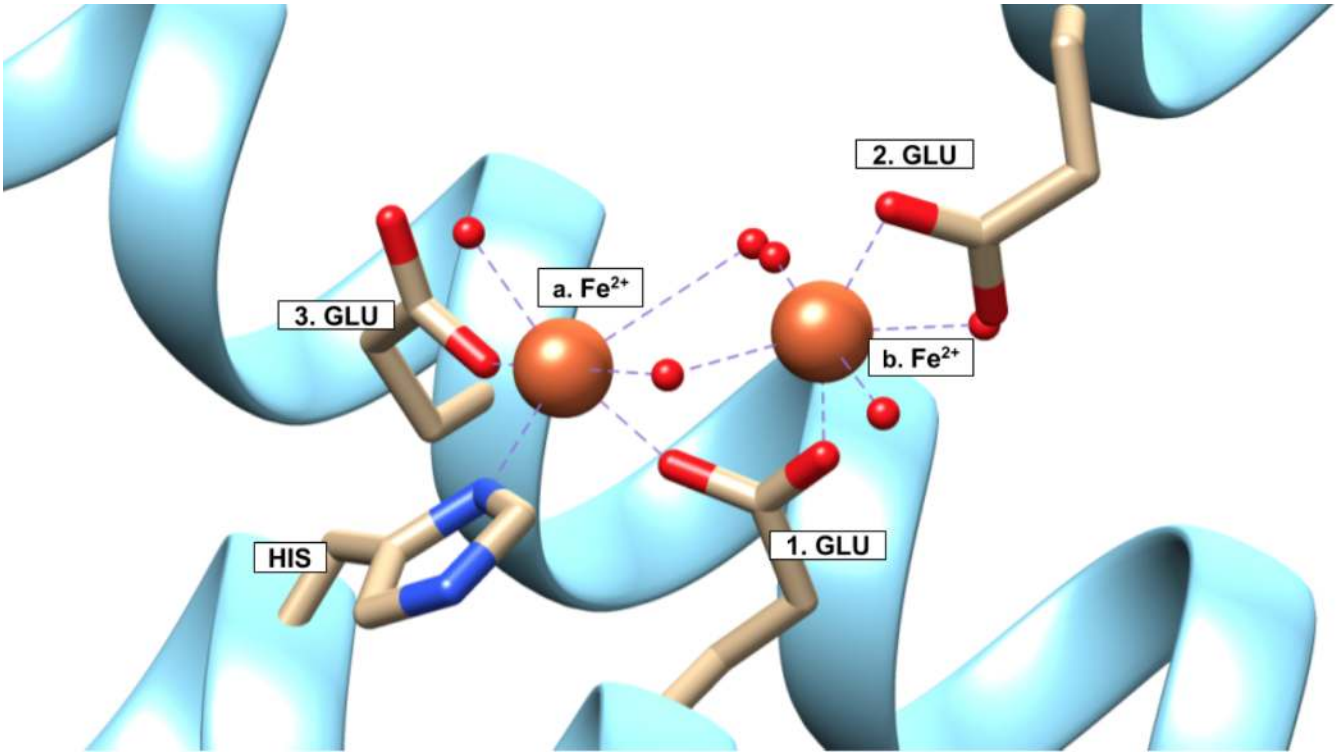


Figure 6. The ferritin protein acts as multidentate chelator for Fe^{2+} at the ferroxidase site. All residues are a part of the same protein. Ferritin binds to a. Fe^{2+} on the left through three different donor atoms, 1. Glu, 3. Glu, and His. Ferritin binds to b. Fe^{2+} on the right through two different donor atoms, 1. Glu and 2. Glu.

According to the crystal structure in Figure 6, the Fe^{2+} binds to a His residue and three different Glu residues all from the same protein. Ferritin can thus be considered a multidentate chelator for Fe^{2+}. The ability for ferritin to perform as a chelator serves ferritin well. Because ferritin stores iron at such high volumes (up to 4500 iron ions), ferritin needs to be able to bind a lot of iron favorably. Based on the increase in entropy from binding, the chelate effect lets ferritin bind iron favorably. That ferritin can bind more than one metal ion to the same molecule creates an even greater increase in entropy and favorability.

Binding at the Ferroxidase Site

The human H-chain has two binding sites for iron(II) called site A and site B. Both sites are occupied by an iron ion, but site A has shown a higher affinity for iron(II).[11] The mechanism for binding at the ferroxidase site is currently unknown. At the present moment, there are two common proposals: the stepwise mechanism and pairwise mechanism.[1] The stepwise mechanism is shown in Figure 7. The mechanism proposes that the two binding sites are occupied one iron at a time.

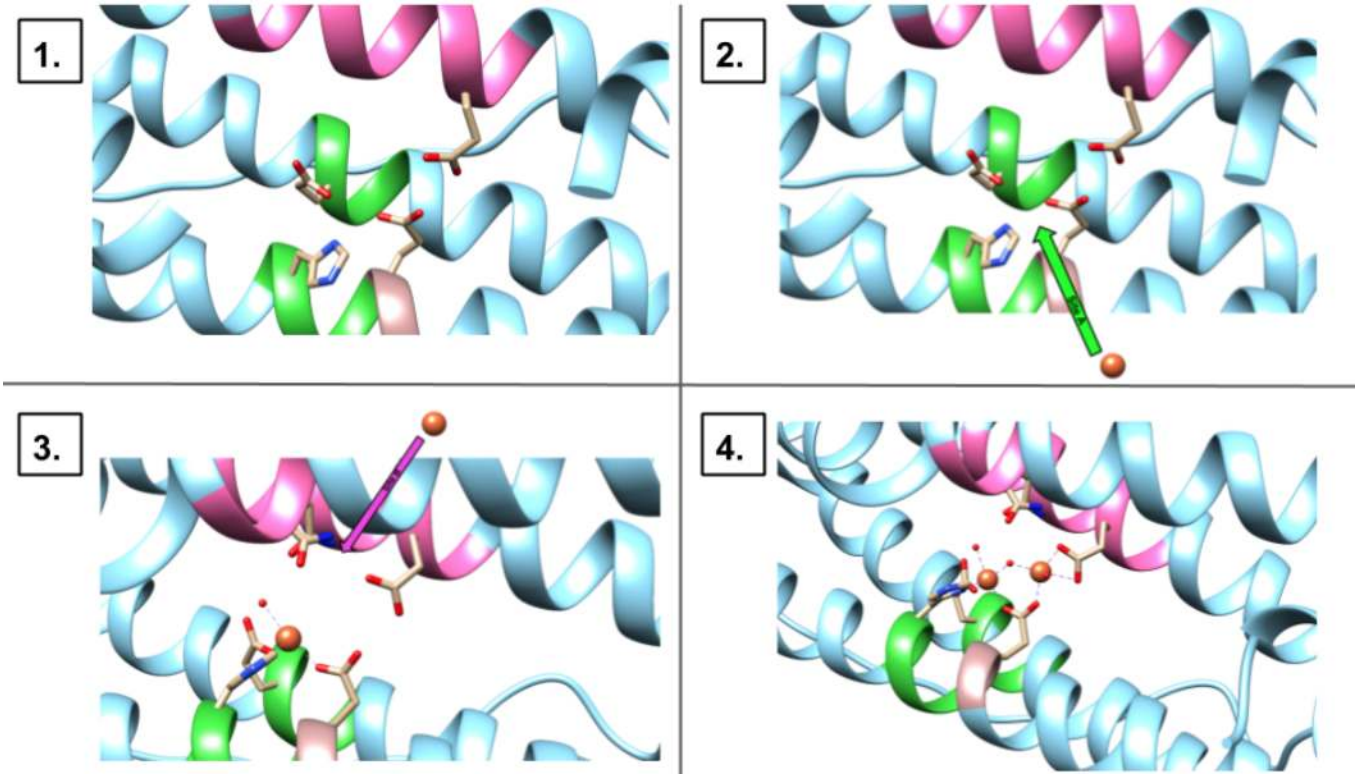


Figure 7. The proposed stepwise binding mechanism states that because site A in green has a higher affinity for Fe (orange spheres) it will be bound before site B in pink is bound by Fe ion. 1. The empty binding site on the H-chain subunit of human ferritin. Site A is in green and on the bottom helix and site B is in pink on the top helix. 2. One Fe^{2+} ion binds to site A. The green arrow denotes where the Fe ion will bind. 3. After site A is bound by iron, a second Fe^{2+} ion binds to site B. The pink arrow denotes where the second Fe^{2+} ion will bind. 4. The di-iron binding site has two iron ions bound. One is bound at site A and one is bound at site B. An oxidizing agent (small red sphere) binds the two metal ions together.

First, one Fe^{2+} binds to site A, then, a second Fe^{2+} will bind to site B. The pairwise mechanism shown in Figure 8 proposes that two Fe^{2+} ions enter site A and site B, in a concerted fashion.

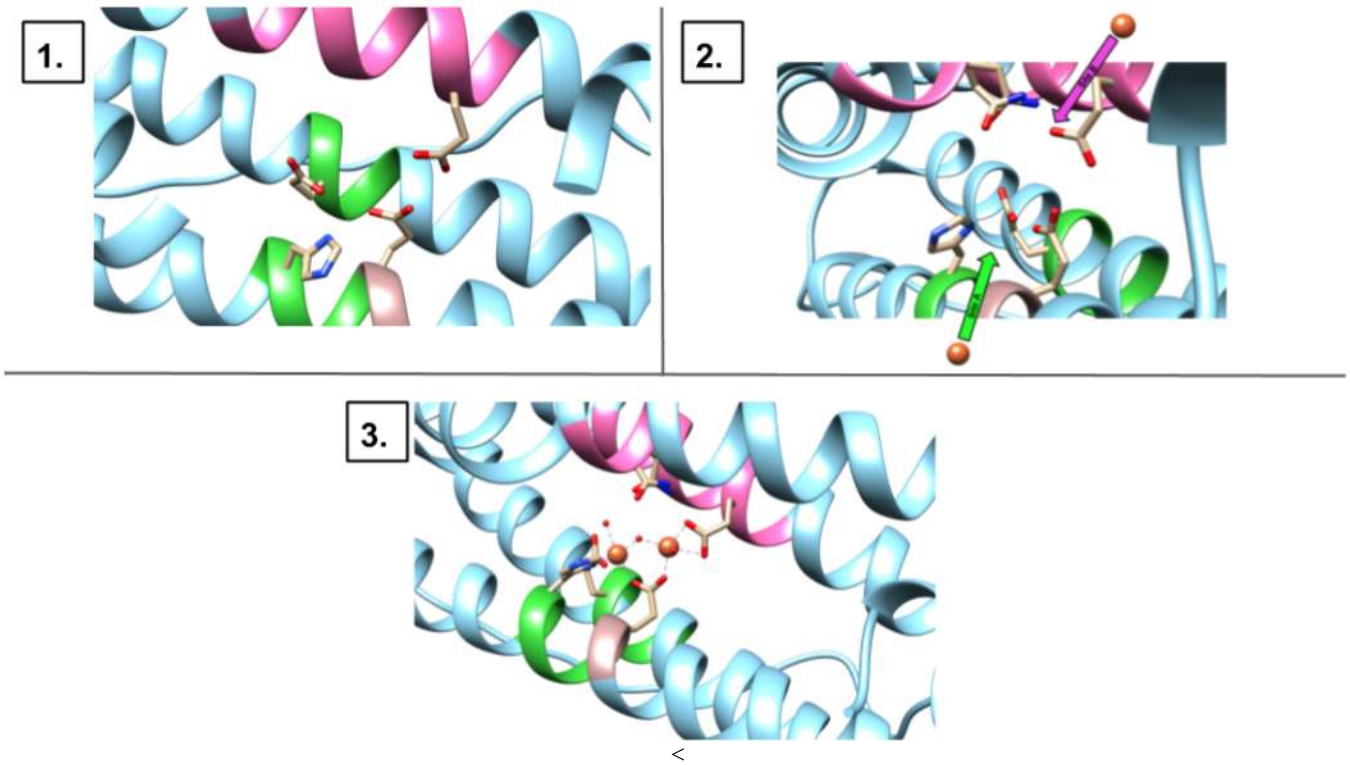


Figure 8. The proposed pairwise binding mechanism states that two Fe^{2+} ions (orange spheres) bind simultaneously to sites A and B. 1. The empty binding site on the H-chain subunit of human ferritin. Site A is in green and on the bottom helix and site B is in pink on the top helix. 2. Two Fe^{2+} ions bind to sites A and B. The green arrow denotes where the Fe^{2+} ion will bind on site A. The pink arrow denotes where the second Fe^{2+} ion will bind on site B. 3. The di-iron binding site has two iron ions bound. One is bound at site A and one is bound at site B. An oxidizing agent (small red sphere) binds the two metal ions together.

There has been evidence, however, that one site, site A, can be occupied by one Fe^{2+} while site B remains unoccupied. This result supports the stepwise mechanism (Figure 7) for binding at the ferroxidase site on the H-chain.[1]

After the iron ions bind to ferritin, a single molecule of some oxidizing agent binds to both ions. The binding of both ions by one molecule is referred to as bridging because the iron ions at sites A and B are bridged by the oxidizing agent.

Redox and Iron Mineralization

Iron(II) is oxidized at the ferroxidase site on the H-chain (sites A and B) by some oxidizing agent, most probably O_2 and H_2O_2.[1] Three reactions/models for Fe^{2+} oxidation and mineralization have been observed. There is a ferroxidation reaction or protein catalysis model (Reactions **1 and 1a-1c**), a mineralization reaction or crystal growth model (Reaction **2**), and a detoxification reaction of Fe^{2+} + H_2O_2 (Reaction **3**).[1] The ferroxidation reaction occurs at the ferroxidase site on the H-chain of ferritin. The ferroxidation reaction for the protein catalysis model of ferritin oxidation can be written as:

$2\ Fe^{2+} + O_2 + 4\ H_2O \rightarrow [Fe^{3+}\text{-O-O-}Fe^{3+}]^{2+}$ (**1a.**)

$[Fe^{3+}\text{-O-O-}Fe^{3+}]^{2+} \rightarrow [Fe_2O\text{-}(OH)_2]^{2+}$ (**1b.**)

$[Fe_2O(OH)_2]^{2+} \rightarrow 2FeOOH_{core} + H_2O_2 + 4\ H^+$ (**1c.**)

Net: $2Fe^{2+} + O_2 + 4\ H_2O \rightarrow 2FeOOH_{core} + H_2O_2 + 4\ H^+$ (**1.**).[1]

The net mineralization reaction for the crystal growth model of ferritin oxidation is written as:

$4\ Fe^{2+} + O_2 + 6\ H_2O \rightarrow 4\ FeOOH_{core} + 8\ H^+$ (**2.**).[1]

The most recently identified of the oxidation and mineralization reactions, the Fe^{2+} + H_2O_2 detoxification reaction is written as:

$2\ Fe^{2+} + H_2O_2 + 2\ H_2O \rightarrow 2\ FeOOH_{core} + 4\ H^+$ (**3.**).[1]

The ferroxidation reaction involves the ferritin molecule most directly. Reaction **1** occurs on the H-chain at the ferroxidase site and has been the reaction focused on up to this point. The two schemes for this reaction that are most frequently proposed are a 2-electron oxidation scheme or a two successive 1-electron oxidation scheme.

The first intermediate produced in reaction **1a** ($[Fe^{3+}\text{-O-O-}Fe^{3+}]^{2+}$) is a μ-peroxo di-iron(III) complex (μ = number of metal ions bridged by a ligand, and μ_2 is often shortened to just "μ"). Raman and Mössbauer spectroscopy, stopped-flow kinetics, and EXAFS have confirmed the existence of the complex. The complex is formed within the first 25-100 ms of the reaction and decays within 150 ms.[1] The μ-peroxo di-iron(III) complex intermediate has been the focus of various studies for its blue coloring and appearance not only in human ferritin, but also other eukaryotic, archaeal, and bacterial ferritin.[12] The blue intermediate from human H-chain ferritin has a UV-vis absorbance of 650 nm and an extinction coefficient measured at 850-1000 $M^{-1}\ cm^{-1}$ per the dimer of $[Fe^{3+}\text{-O-O-}Fe^{3+}]^{2+}$.[1,12] The extinction coefficient (ε < 1000) suggests that this complex is absorbing d-d transitions.

The second intermediate is produced in reaction **1b** ($[Fe_2O\text{-}(OH)_2]^{2+}$) from the decay of the first intermediate is a μ-oxo(hydroxo)-bridged di-iron(III) intermediate.[1] A distance of 3.00 Å has been observed between the two iron ions.[11] Less data is available on this intermediate. While studies have provided strong evidence of the decay of the blue intermediate, the decay product is still in debate and the possibility of a variety of products has been noted.[1]

Oxidation of iron ions for storage in ferritin also proceeds through reactions **2** and **3**. Studies suggest that the primary method and reaction of oxidizing iron for storage in ferritin depends on the flux of iron into ferritin at that time. For example, at a low flux of ≤ 50 Fe^{2+}/ferritin, the iron is oxidized mainly by reaction **1** at the ferroxidase site.[1] However, as more H_2O_2 is produced as a byproduct of reaction **1**, the detoxification reaction (**3**) takes over as the primary reaction. Iron flux of about 100-500 Fe^{2+}/ferritin will cause this switch.[1] Once the iron flux reaches ~800 Fe^{2+}/ferritin, reaction **2** becomes dominant.

Reaction **2** is based on the crystal growth model of ferritin oxidation. At high iron(II) flux into ferritin and after a minimum of 200 Fe^{2+}/ferritin have already formed an iron/oxy mineral core in the center of ferritin, the crystal growth model appears to begin.[1] In this model, iron(II) ions are entering at high rates. Rather than oxidizing every new iron(II) ion at the ferroxidase site or by the detoxification reaction, the iron(II) ions can be oxidized directly by the already-forming iron/oxy mineral core and can be deposited directly onto the mineral.[1] As can be seen in reaction **2**, stoichiometrically, iron(II) ions can be oxidized and directly deposited onto the mineral at 4 Fe^{2+}/O_2, while reaction **1** catalyzed by ferritin can only oxidize 2 Fe^{2+}/O_2.

It has not been determined if both Fe^{2+} ions are required to be bound at the ferroxidase site in order for oxidation to take place. However, unlike binding where there is evidence of a single Fe^{2+} ion being bound at site A, oxidation has never been observed without both Fe^{2+} ions, one at site A and one at site B and bridged by the oxidizing agent, present.[1]

As previously mentioned, nucleation starts on the L-chain subunit of ferritin. However, it is important to note that the majority of the actual iron/oxy mineral formed by the reactions above and held in the center of ferritin does not actually bind to the protein.[8] Instead, the solid mineral core is stabilized by the protein surrounding it.[8]

Metal Center Geometries

The ligands for the ferroxidase site are His and Glu residues as well as a variety of oxygen-containing oxidants, such as O_2 or H_2O_2 molecules.[1,7] Ligand Field Theory (LFT) helps to predict the geometry of metal-ligand complexes. Complexes are classified as high spin or low spin based on the energy field splitting or Δ_o between the non-bonding t_{2g} and the antibonding e_g. High spin complexes will prefer to keep electrons unpaired in the t_{2g}, but low spin complexes will prefer to pair electrons in the t_{2g}. The ligands of LFT encourage strong fields (low spin, large Δ_o) or weak fields (high spin, small Δ_o) based on their categorization as a σ donor, π donor, or π acceptor.

The iron binding sites of ferritin, however, are not simple metal-ligand complexes. As discussed above, when binding to the ferroxidase, two ions of iron(II) bind to the site and are bridged by the oxidizing agent, most commonly O_2. The bridging ligand makes this one binding site and one complex, not two separate single metal or mononuclear complexes. The ferroxidase site is considered to have a di-iron center and to be a dinuclear binding site or dinuclear complex.[1] Because there are two metals in the metal center, molecular orbital interactions in dinuclear complexes are different than those in the one metal center. This difference

is especially noticed in bridged metal complexes, as is present in ferritin, because the orbitals of the two metal ions can overlap.[13] Due to this overlap, electron filling and pairing does not always occur as one would expect with a single metal center.

These dinuclear bridged complexes with iron(II) and iron(III) are not unique to ferritin, but have been seen in methane monooxygenase (MMO), ribonucleotide reductase (RNR), and fatty acid desaturase.[8,12] Comparisons with these other proteins with ferritin have been attempted, but iron's special role as a substrate in ferritin rather than an enzyme cofactor in the others sets it apart and makes ferritin more difficult to discern.[12] Furthermore, the comparisons with these other proteins is not completely correct based on the lability of the di-iron complexes in ferritin. The di-iron(II) binding site complex and the di-iron(III) intermediates of oxidation are labile as they react, degrade, and move toward the center of ferritin. In contrast, the di-iron complexes of MMO are stable cofactors.

For ease, ferritin's ferroxidase binding site will be analyzed according to LFT without consideration of the overlapping of molecular orbitals. Note though that the following analysis does not entirely capture the complexity of the metal-ligand-metal interactions.

According to LFT, His residue is a π acceptor and a weak field ligand. This ligand increases Δ_o and encourages low spin complexes. All oxygen ligands, including water, OH^-, O^{2-}, and Glu residues are π donors and weak field ligands, which decrease Δ_o and encourage high spin complexes. A close-up of the binding sites at the ferroxidase site, such as in Figure 7, shows that the majority of the ligands for both a. Fe^{2+} and b. Fe^{2+} are water or the like and Glu residues, the high spin complex-favoring ligands. Fe^{2+} is a $3d^6$ transition metal with a charge of +2 and thus can be high or low spin. However, when bound to H_2O, Fe^{2+} is high spin with an electron filling diagram shown in Figure 9.

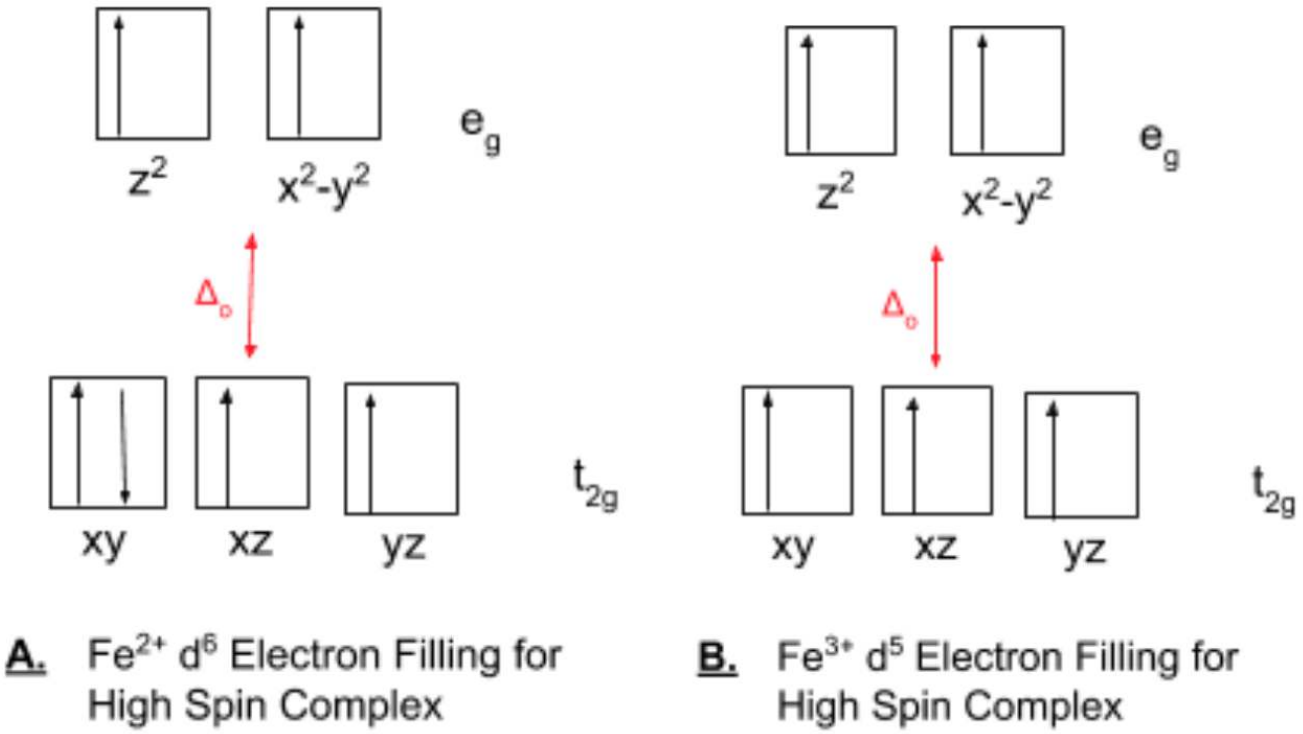


Figure 9. A. LFSE splitting diagram for a high spin single Fe^{2+} metal center. Electrons occupy e_g before pairing up. Δ_o is small. B. LFSE splitting diagram for a high spin single Fe^{3+}. Electrons occupy e_g before pairing up. Δ_o is small.

The complex is thus, overall, high spin and has been described in the literature as initially binding in a high-spin state with octahedral geometry shown in Figure 10.[11,14]

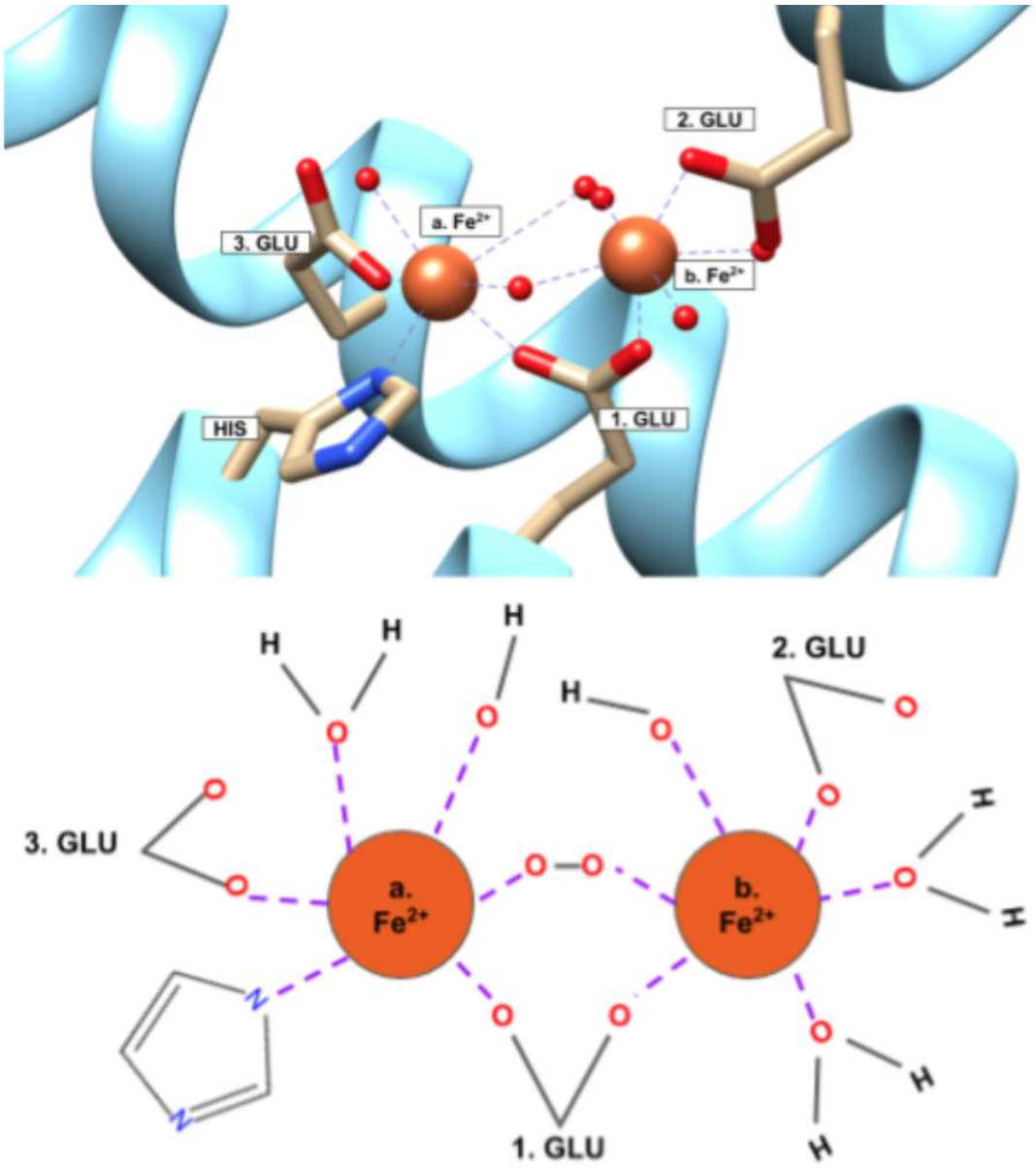


Figure 10. The octahedral geometry can be seen in the crystal structure and in the cartoon diagram extracted from the crystal structure to show the six ligand coordination more clearly. Adapted from Bou-Abdallah, et al.

The ligands for the iron oxide mineral are primarily H_2O, OH^-, or O^{2-}. These use the oxygen as the donor atom. These are all high spin ligands that contribute to the weak field. These ligands will favor a smaller Δ_o and keeping electrons unpaired. Fe^{3+} is a $3d^5$ transition metal with a +3 charge and is more likely to be low spin based on recorded, however, known values of Δ_o for Fe^{3+} and literature on the Fe^{3+} intermediates categorize these Fe^{3+}-O-Fe^{3+} groups as high spin (see electron filling diagram in Figure 9 for a single metal center high spin diagram). $\Delta_o$will thus be smaller and weak field ligands such as the oxygen ligands will be favored.

To highlight the complexity of the dinuclear metal-ligand complex, studies on the magnetic susceptibility (the ratio of magnetic moment per unit volume to the applied magnetizing field intensity) of the Fe^{3+}-O-Fe^{3+} groups suggest that the high spin iron complexes have about one unpaired electron per group.[14] This calculation is clearly in conflict with the molecular orbital diagram in Figure 9, yet the complex is still known to be on average octahedral and high spin.[14] The calculation magnetic moment itself has been a controversial pursuit among scientists.[9]

Iron Release

When cells require iron, for enzyme synthesis, after blood loss, or during embryonic development, the iron stored in ferritin must be released rapidly, on demand, and under control.[8] Although, as with many aspects of ferritin function, the mechanism of iron release to the cell from ferritin is unknown. What is known inherently about the process is that over its course it must essentially reverse mineralization: the iron(III)/oxy mineral must be dissolved from its solid state to aqueous ions and the iron(III) ions must be reduced to iron(II).

Proposed models for ferritin iron release include (1) an equilibrium between the iron stored in ferritin and the iron in the cytoplasm of the cell, (2) ferritin protein degradation, (3) spontaneous, direct dissolution of iron(III) from the mineral core from scavenging by iron(III) binding proteins, and (4) the reduction of the iron(III) mineral which is then complexed iron(II) by a chelating agent and transported out of ferritin.[4,12] The last model (4) lacks confirmation, yet is considered by many to be the physiological mechanism. This model is the most efficient method and the presence of reducing agents under physiological conditions.[4]

Except the second model (2), the physiological relevance of all above models is still to be seen.[12] The ferritin degradation model (2) is the only mechanism to have been observed under physiological conditions. However, since this model would require iron release to be dependent of the turnover and synthesis of ferritin, another model is suspected to be necessary.[12]

However iron is released from ferritin, studies indicate that the physical exit of the iron from ferritin takes place via the 3-fold channels. One proposal for exit based on observations in bacterial ferritin is the localized folding/unfolding of ferritin.[4] The ferritin channels can be unfolded without affecting the overall function or structure of the protein. Unfolding the channels and thus, widening the opening, would allow for quick release of demineralized iron. The channels become highly disordered when this occurs to the effect that they do not appear in crystal structures.[8]

Much remains to be determined about human ferritin. Other functions of ferritin in the body, and the mechanisms for how Fe^{2+} enters and binds to ferritin, how Fe^{2+} is oxidized to Fe^{3+} for storage, and how iron is released remain undetermined, among others, are thought to be non-universal—even within the same organism.[3,6]

While much of the chemistry behind ferritin is, as of now, unexplained, ferritin is still an important protein for all life. Wherever iron is noted as an essential nutrient, ferritin must also be present for management and storage. The elucidation of ferritin can lead to advancements in iron metabolism and neurological disorders and new uses of ferritin chemistry in nanochemistry and catalytic industrial applications.[3,4]

Sources

[1] Bou-Abdallah, F. The Iron Redox and Hydrolysis Chemistry of the Ferritins. *Biochimica et Biophysica Acta (BBA) - General Subjects* **2010**, *1800* (8), 719–731.

[2] Crabb, E.; Moore, E. *Metals and life*; Royal Society of chemistry: Cambridge, **2010**.

[3] Theil, E. C.; Tosha, T.; Behera, R. K. Solving Biology's Iron Chemistry Problem with Ferritin Protein Nanocages. *Accounts of Chemical Research* **2016**, *49* (5), 784–791.

[4] Carmona, F.; Palacios, Ò.; Gálvez, N.; Cuesta, R.; Atrian, S.; Capdevila, M.; Domínguez-Vera, J. M. Ferritin Iron Uptake and Release in the Presence of Metals and Metalloproteins: Chemical Implications in the Brain. *Coordination Chemistry Reviews* **2013**, *257* (19–20), 2752–2764.

[5] Knovich, M. A.; Storey, J. A.; Coffman, L. G.; Torti, S. V. Ferritin for the Clinician. *Blood Rev* **2009**, *23* (3), 95–104.

[6] Bradley, J. M.; Le Brun, N. E.; Moore, G. R. Ferritins: Furnishing Proteins with Iron. *JBIC Journal of Biological Inorganic Chemistry* **2016**, *21* (1), 13–28.

[7] Watt, G. D.; Jacobs, D.; Frankel, R. B. Redox Reactivity of Bacterial and Mammalian Ferritin: Is Reductant Entry into the Ferritin Interior a Necessary Step for Iron Release? *Proceedings of the National Academy of Sciences* **1988**, *85* (20), 7457–7461.

[8] Bertini, I. *Biological Inorganic Chemistry: Structure and Reactivity*; University Science Books, **2007**.

[9] Chasteen, N. D.; Harrison, P. M. Mineralization in Ferritin: An Efficient Means of Iron Storage. *Journal of Structural Biology* **1999**, *126* (3), 182–194.

[10] Joshi, J. G.; Sczekan, S. R.; Fleming, J. T. Ferritin—A General Metal Detoxicant. *Biol Trace Elem Res* **1989**, *21* (1), 105.

[11] Bertini, I.; Lalli, D.; Mangani, S.; Pozzi, C.; Rosa, C.; Theil, E. C.; Turano, P. Structural Insights into the Ferroxidase Site of Ferritins from Higher Eukaryotes. *Journal of the American Chemical Society* **2012**, *134*(14), 6169–6176.

[12] Honarmand Ebrahimi, K.; Hagedoorn, P.-L.; Hagen, W. R. Unity in the Biochemistry of the Iron-Storage Proteins Ferritin and Bacterioferritin. *Chemical Reviews* **2015**, *115* (1), 295–326.

[13] H. Rodriguez, J.; Mccusker, J. Density Functional Theory of Spin-Coupled Models for Diiron-Oxo Proteins: Effects of Oxo and Hydroxo Bridging on Geometry, Electronic Structure, and Magnetism. *Journal of Chemical Physics* **2002**, *116*.

[14] Bertini, I., *Bioinorganic Chemistry*; Ed.; University Science Books: Mill Valley, Calif, **1994**.

Contributed By

*This work was originally written by **Anna Shadid,** Spring 2018: Anna is currently (as of 2018) a junior chemistry major at Saint Mary's College in Notre Dame, IN.*

This work was originally edited by Dr. Kathryn Haas, Associate Professor, and Madison Sendzik, Teaching and Research Assistant, of Saint Mary's College.

11.1.4: Iron Storage- Ferritin is shared under a not declared license and was authored, remixed, and/or curated by LibreTexts.

11.1.5: Antioxidant- Cu/Zn Superoxide dismutase (SOD1)

This is a video introduction to the Cu,Zn superoxide dismutase (SOD1), which acts as an antioxidant in the cytoplasm of mammalian cells. (PDB 1sxz)



The role of the copper-zinc superoxide dismutase system (SOD1) is to catalyze the conversion of the potentially toxic superoxide anion, $O_2^{\cdot-}$, to the less toxic substance hydrogen peroxide, H_2O_2. Dioxygen, O_2, is also a product of this reaction.[1] Superoxide is produced in aerobes as a product of metabolism. The superoxide anion can be an intermediate or a byproduct of metabolic processes such as respiration or photosynthesis.[2] Superoxide, $O_2^{\cdot-}$, is toxic when in the protonated form, $HO_2^{\cdot}$, and can cause damage to the cells.[1] Superoxide is involved in the oxidative damage phenomena also known as *oxidative stress*.[2] Oxidative stress is harmful and it is caused by radicals, such as superoxide, that can attack lipids, proteins, and DNA within the body. Oxidative stress is linked to many human diseases including hypertension, diabetes mellitus, ischemic diseases, and malignancies.[3] Cells use superoxide dismutase in order to prevent oxidative damage by removing superoxide free radicals.[2]

Superoxide dismutase participates in a dismutation reaction in order to convert superoxide into the less toxic substances of hydrogen peroxide and dioxygen. A dismutation reaction is a reaction in which one substance is oxidized and the other is reduced simultaneously.[5] There are two redox reactions that occur in the copper zinc superoxide dismutase system, and copper catalyzes these reactions. In one reaction Cu^{2+} is reduced to Cu^{1+}, while the superoxide molecule, O_2^-, is oxidized to O_2. In the second step Cu^{1+} is oxidized to Cu^{2+}, while a second superoxide molecule is reduced to hydrogen peroxide, H_2O_2.[7] A simplified catalytic cycle can be seen in the Figure below.

The overall reduction potential of the overall reaction is dependent on the half reactions which are:

$$O_2 \rightarrow e^- + O_2^- \tag{11.1.5.1}$$

with E = -0.16 V

$$O_2 + e^- \rightarrow 2H^+ + H_2O_2 \tag{11.1.5.2}$$

with E = +0.89 V

Therefore, the overall reduction potential of this reaction must be within -0.16V and 0.89V.[6]

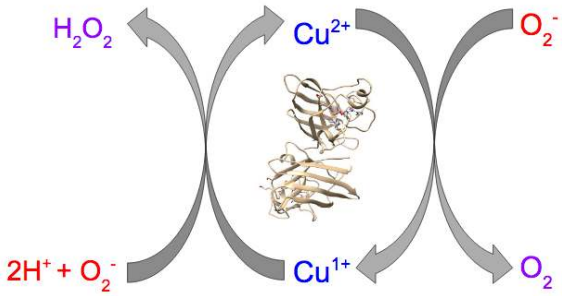
> ***The overall reaction catalyzed by superoxide dismutase enzymes is shown below. When catalyzed by Cu,Zn Superoxide Dismuase (SOD1), the reaction happens in two steps: In one step, Cu^{+2} at the enzyme active site is reduced to Cu^{+1} as superoxide is oxidized to dioxygen. (see right of simplified reaction cycle shown below) In another step, Cu^{+1} is oxidized to Cu^{+2} as superoxide is reduced to hydrogen peroxide. This step also requires two hydrogen ions (see left of simplified reaction cycle shown below).***

Overall Reaction:

$$2\,O_2^{\bullet -} + 2H^+ \rightleftharpoons H_2O_2 + O_2$$

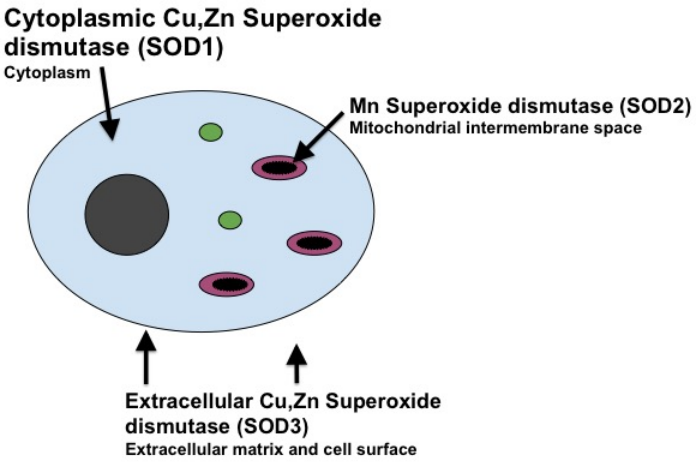
superoxide — hydrogen peroxide and dioxygen

Simplified Catalytic Cycle:



There are three different types of superoxide dismutase that are found in mammals. The primary form of superoxide dismutase is Cu,Zn superoxide dismutase, which is referred to as SOD1. SOD1 is primarily found in the cytoplasm of cells but a small portion is found in the intermembrane space of the mitochondria. A key feature of SOD1 is that is possesses a copper cofactor, which is used to catalyze the superoxide dismutation reaction. A second type of superoxide dismutase is manganese superoxide dismutase, which is referred to as SOD2. Manganese superoxide dismutase is found in the mitochondrial matrix of the cell. SOD2 is produced in the cytoplasm and then transported to the mitochondrial matrix. Manganese (Mn) is the metal cofactor used to catalyze the conversion of superoxide in SOD2. A third type of mammalian superoxide dismutase is the extracellular Cu,Zn superoxide dismutase, referred to as SOD3. SOD3 is primarily found in tissues on the extracellular matrix and on cell surfaces. There is a small amount of SOD3 that is found in plasma and extracellular fluids. SOD3 is similar to SOD1 in that it poseses copper at its active site.[4] This page focuses specifically on SOD1.

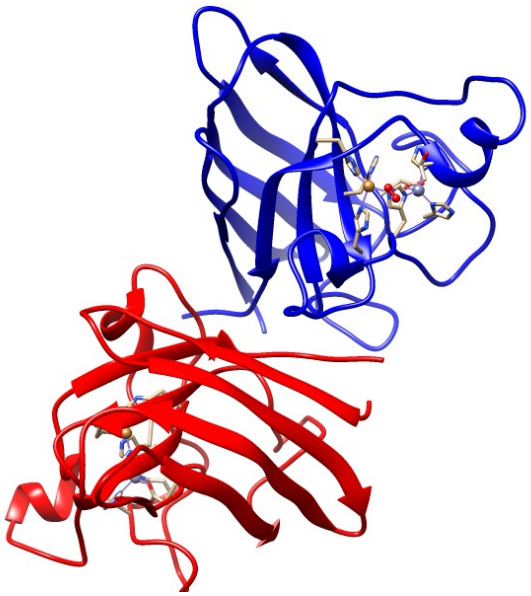
This figure illustrates the three types of SOD found in mammals, and their primary localization in reference to the cell.



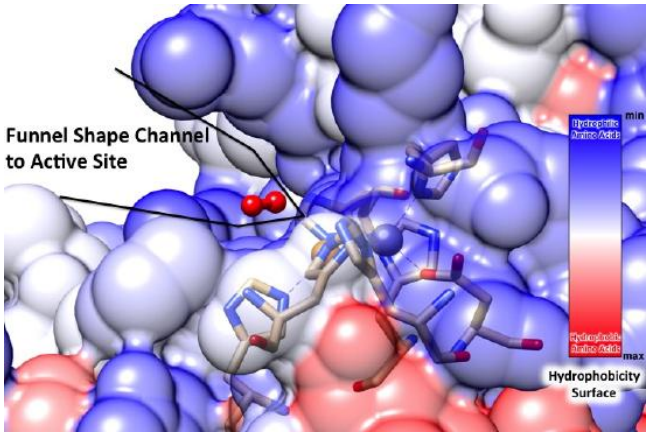
Amyotrophic lateral sclerosis (ALS), the disease commonly referred to as Lou Gehrig's disease, can be caused by a genetic mutation in SOD1. About one tenth of all cases of ALS are hereditary, and in these hereditary cases of ALS there are mutations in the SOD1 gene. Much research has been aimed at understanding how this mutation in SOD1 causes ALS, with hopes of developing better treatments or a potential cure for this disease.[5]

The SOD1 protein is a dimer composed of two identical subunits (homodimer). The two subunits are differentiated in red and blue in the Figure below. The two subunits are oriented so the two active sites are facing away from each other. Each subunit is composed of 151 amino acid residues. These amino acids are arranged in eight β-sheets and three exterior loops. Each subunit contains a copper ion and a zinc ion at the active site. The copper ion acts as an electron transfer center in this catalyst, while the zinc ion serves as a structural scaffold and a contributes to the positive charge of the active site, which attracts the negatively charged superoxide anion.

Ribbon diagram of the reduced form of Cu,Zn SOD with two subunits differentiated in blue and red. Active site side chains and metal cofactors are shown with superoxide bound. (Modified from PDB 1sxz). [6]



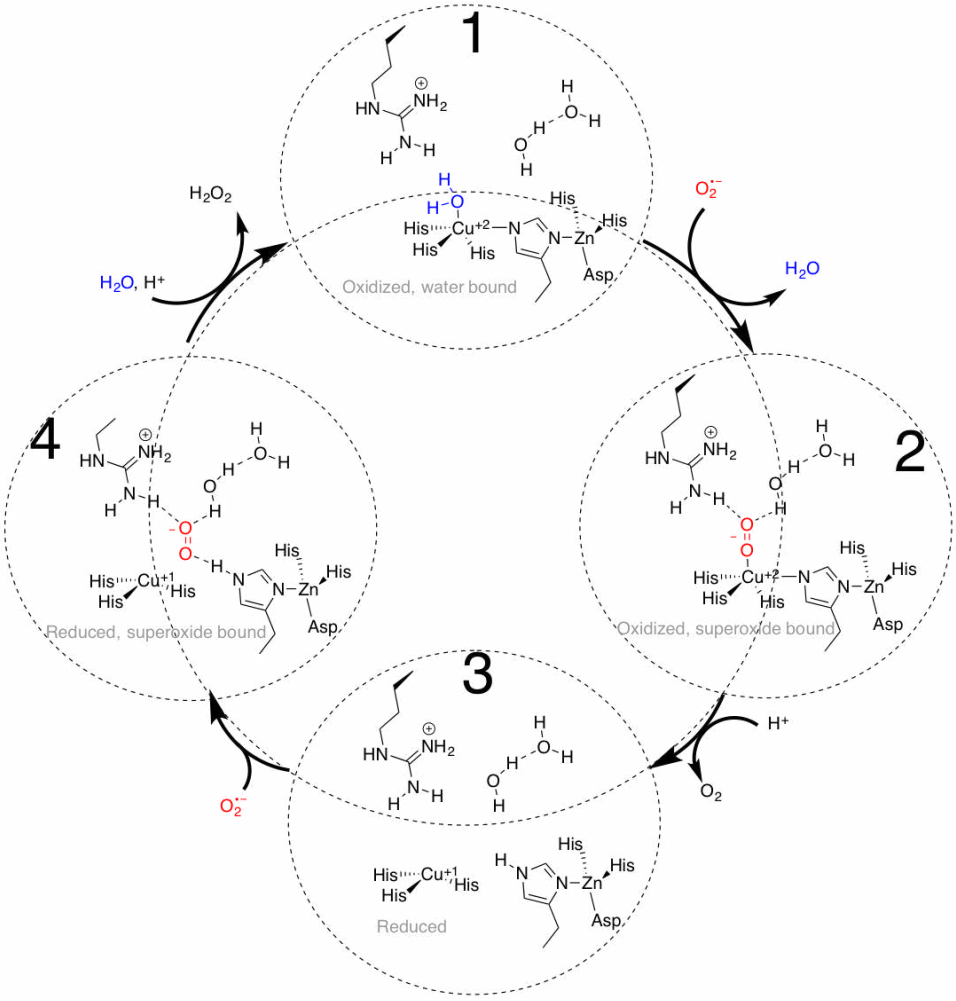
The placement of the active site of this complex as well as the geometry surrounding the copper metal centers are critical for this reaction to occur. The active site of this complex is at the bottom of a channel. The copper ion is exposed at the bottom of this channel to allow binding of superoxide to the copper ion, while the zinc ion is buried within the protein.[8] This funnel shape leading to the active site is very important to the superoxide dismutase function.[9] Superoxide dismutase has a very small active site compared to the entire size of the enzyme. The small funnel shape is selective towards small molecules such as superoxide, as seen in the Figure below. In the funnel shaped channel are copper and zinc cations as well as two positively charged hydrophilic amino acids, histidine and arginine. The strong positive charge provided by these amino acids and metal ions attracts the negatively charged superoxide to the active site where the superoxide can be converted into less toxic substances.[5]



At the active site of Cu,Zn superoxide dismutase, copper provides a redox-active binding site for the superoxide anion, while zinc provides structural support and positve charge.[1] **There are several histidine amino acids that surround the copper and zinc metal centers**. The copper ion is bound to either three or four histidine side chains, and may also be bound to either water or superoxide, depending on the copper oxidation state and the step in the catalytic cycle (see Figure below). The zinc coordination is more static, and zinc is consistently bound to three hisidine and one aspartate side chain (see Figure below).

The four steps of the detailed catalysts cycle are shown below. This catalytic cycle alternates between electron counts of 19 and 16. Structure 1 below is of the copper(II) metal center with a four histidine ligands and a water ligand. This five coordinate system yields an electron count of 19. Then the water molecule is displaced as the superoxide molecule binds to copper(II). This is a ligand substitution reaction and once again the structure that is formed, seen as the structure on the right of Figure 13, has 19 electrons. When copper(II) is reduced to copper(I), there are only three histidine ligands that are attached. This copper(I) structure in a trigonal planar geometry is illustrated below as tStructure 3. This copper(I) structure with three ligands attached yields an electron count of 16. Then superoxide binds near copper in the active site, and the copper(I) is oxidized to copper(II), while the superoxide molecule is reduced to hydrogen peroxide. A water binds to the oxidixed Cu^{+2}, to return to structure 1 with an electron count of 19. This continuous cycle converts the superoxide molecule to hydrogen peroxide and dioxygen.[9,10]

The detailed catalytic cycle at the active site of SOD1. Adapted from reference 9.



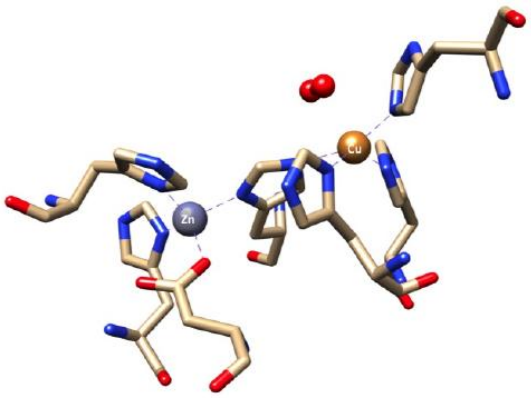
Hard-soft acid-base (HSAB) theory predicts that "like" classes of acids and bases prefer to interact (ex: hard acid + hard base is better than hard + soft), thus this binding site of primarily borderline bases is ideal for their borderline metal cations. The aspartate, which is bound to zinc and is a hard donor atom, may provide charge balance.According to Ligand Field Theory (LFT), histidine amino acids are strong σ donors and are π acceptors. Thus, histidine is a relatively strong field ligand ,compared to water and other

amino acid side chain ligands, and would encourage a relatively large Δ. The aspartate is both a σ donor and π donor, and is a weak field ligand.

Ligand field theory would predict the geometry surrounding the copper(II) metal center as Jahn-Teller distorted octahedron. This would create either a square pyramid or square plane geometry. The geometry that surrounds the copper(II) metal center, however, is a distorted square pyramid when ether water or superoxide is bound (see structures 1 and 2 in the figure above).[1] This distorted from the ideal geometry for a d^9 metal center such as copper(II). However, this causes a slight destabilization of the copper(II) metal center, which helps promote copper into its d^{10}, monovalent oxidation state. In other words, the destabilization of Cu(II) allows redox cycling to occur more easily (this is also related to Marcus theory, and this article should be elaborated to describe application of Marcus Theory). If the geometry was a perfect square pyramid, the Cu^{2+} would be more stable, and it would be more difficult to reduce to Cu^{+1}. In the redox reaction, the copper(II) metal center oxidizes the superoxide molecule to dioxygen, while the copper(II) metal center is reduced to copper(I). This step (from 2 to 3 in the figure above) occurs via an **inner sphere electron transfer** as the superoxide molecule is bound directly to the copper(II) metal center.[8] Upon reduction of copper, the dioxygen product is immediately released (structure 3, figure above). According to hard-soft acid-base theory, hard acids are attracted to hard bases and soft acids are attracted to soft bases. The superoxide molecule is a hard base and copper(II) is a borderline acid. Thus the binding of superoxide directly to the copper(II) metal is not surpising based on their close hard-soft acid-base character.

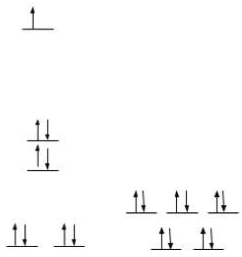
Ligand field theory cannot predict a preferred geometry surrounding the copper(I) metal center, as Cu^{+1} is a d^{10} metal, and there is no ligand-field stabilization energy. The geometry that surrounds the copper(I) metal center in SOD1 is a distorted trigonal plane (structures 3 and 4, figure above).[1] In conversion from structure structure 3 to 4 in the figure above, superoxide binds in the active site through H-bonding and electrostatic attraction, however does not directly coordinate to the copper center. In conversion of structure 4 to 1, the copper(I) metal center reduces the superoxide molecule to hydrogen peroxide, while copper(I) is oxidized to copper(II).[9] The fact that superoxide binds directly to copper(II) in the first part of the cycle (structure 1 to 2 above), but does not bind directly to copper(I) in the second part of the cycle (structure 3 to 4 above) is not surprising based on hard-soft acid-base principles. According to hard-soft acid-base theory, the soft copper(I) ion is not a preferred acid for the hard superoxide base.

A "snapshot" of the Cu,Zn SOD active site, adapted from PDB structure 1SXZ, is shown below. In the PDB structure, 1SXZ, azide is bound to the reduced copper center. We have converted azide to superoxide.



The active site of SOD1 has a zinc metal center that is present for structural support and stabilization. Ligand field theory does not play a role in the determination of the geometry surrounding the zinc metal center since zinc is a d^{10} metal and does not have ligand field stabilization energy. Instead. the geometry is determined by steric preference of ligands and structural constraints imposed by the protein. For example, the tetrahedral geometry, with bond angels of 109.5° is preferred in terns of sterics compared to a square plane, with smaller bond angles of 90°. Thus, the geometry that surrounds the zinc metal center is distorted tetrahedron which is the favored geometry due to sterics and structural constraints imposed by the polypeptide.[1]

The crystal field splitting diagrams for the copper metal center is a distorted square pyramid geometry and the zinc metal center in a tetrahedron geometry are shown below.



Cu^{2+} is a d^9 metal; therefore, there is an empty orbital for an electron to move up in energy as seen in Figure 11. Therefore, d-d transitions can occur in this molecule when superoxide dismutase is in its reduced form, Cu^{2+}. However, when superoxide dismutase is in its oxidized form, Cu^{1+}, d-d transitions cannot occur. This is because Cu^{1+} is a d^{10} metal. Therefore, all of the orbitals will be filled. Figure 12 is the crystal field splitting diagram of Zn^{2+} in a tetrahedral geometry. Zn^{2+} is a d^{10} metal; therefore, all of the orbitals are filled so d-d transitions cannot occur here. The square pyramidal crystal field splitting diagram indicates that there are electrons in the anti-bonding orbitals, therefore, weakening the bonds. This makes the molecule more labile and more reactive, making the reaction more likely to occur.

The copper-zinc superoxide dismutase system is a necessary molecule in the body that converts the toxic superoxide molecule into the less toxic substances of hydrogen peroxide and dioxygen. The superoxide molecule can cause oxidative damage in the body. There has recently been discovered a connection between a mutation in SOD1 and a hereditary form of Lou Gehrig's disease. This molecule catalyzes the dismutation reaction of the conversion of superoxide. This reaction occurs due to the destabilization of the copper(II) metal center due to the distorted square pyramid geometry and the lability of copper. The zinc metal center is a structural scaffold for this molecule. The copper, zinc superoxide dismutase system is a necessary for the body in order to prevent oxidative damage that can affect lipids, proteins, and DNA.

Sources:

[1]Miessler, G.L.; Tarr, D.A.; *Inorganic Chemistry.* **2010.** 644-647.

[2]Pelmenschikov, V.; Siegbahn, P. Copper-zinc superoxide dismutase: theoretical insights into the catalytic mechanism. *Inorg. Chem.* **2005,** *44*, 3311-3320.

[3]Yoshikawa, T.; Naito, Y. What is oxidative stress? *JMAJ.* **2002,** *45*, 271-276.

[4]Fukai, T.; Ushio-Fukai, M. Superoxide dismutases: role in redox signaling, vascular function, and diseases. *Antioxid Redox Signal.* **2011,** *15*, 1583-1606.

[5]Goodsell, D. Superoxide dismutase. *Protein Data Bank.* **2007.**

https://pdb101.rcsb.org/motm/94.

[6]Ferraroni, M.; Rypniewski, W.; Bruni, B.; Orioli, P.; Mangani, S. Crystallographic determination of reduced bovine superoxide dismutase at pH 5.0 and of anion binding to its active stie. *J. Biol. Inorg. Chem.* **1998,** *3*, 411-422.

[7]Azab, H.A.; Banci, L.; Borsari, M.; Luchinat, C.; Sola, M.; Viezzoli, M.S. Redox chemistry of superoxide dismutase. Cyclic voltammetry of wild-type enzymes and mutants on functionally relevant residues. *Inorg. Chem.* **1992,** *31*, 4649-4655.

[8]Tainer, J.A.; Getzoff, E.D.; Richardson, J.S.; Richardson, D.C. Structure and mechanism of copper, zinc superoxide dismutase. *Nature.* **1983,** *306*, 284-287.

[9]Gray, H.B.; Stiefel, E. I.; Valentine, J.S.; Bertini, I. *Biological Inorganic Chemistry: Structure and Reactivity.* **2007.** 331-337.

[10]Rakhit, R; Charkrabartty, A. Structure, folding, and misfolding of Cu, Zn superoxide dismutase in amyotrophic lateral sclerosis. *Biochimica et Biophysica Acta.* **2006.** 1762: 1025-1037.

Contributed by:

*This work was originally written by **Margaret Mraz**, Fall 2016: Margaret is currently (as of 2016) a senior chemistry major at Saint Mary's College in Notre Dame, IN.*

This work was originally edited by Dr. Kathryn Haas, Assistant Professor at Saint Mary's College.

11.1.5: Antioxidant- Cu/Zn Superoxide dismutase (SOD1) is shared under a not declared license and was authored, remixed, and/or curated by LibreTexts.

11.1.6: Keep Cu Safe- Intracellular Copper Chaperones

Copper Chaperone Atx1

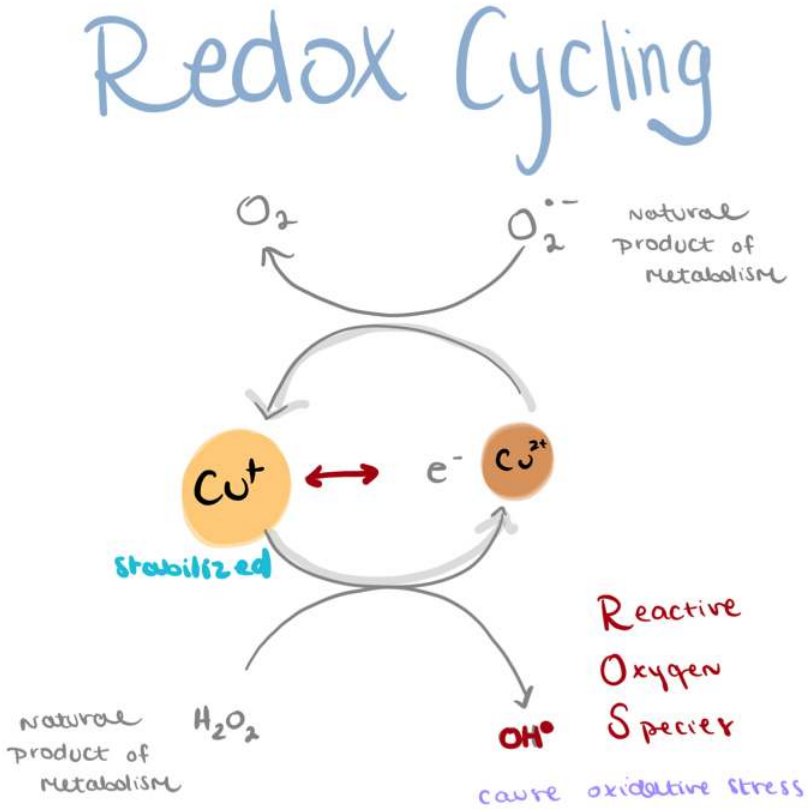
Copper chaperones are intracellular proteins that protect Cu along the pathway from Cu entry into the cell, through the cytoplasm, to its intracellular targets. This page focuses on the yeast Cu chaperone Atx1. Intracellular Cu chaperones, like Atx1, are well-conserved throughout eukaryotic species. The analogous protein in mammalian cells is Atox1.

This is a video introduction to the intracellular yeast Cu chaperone protein Atx1 (or Atox1 in mammals).



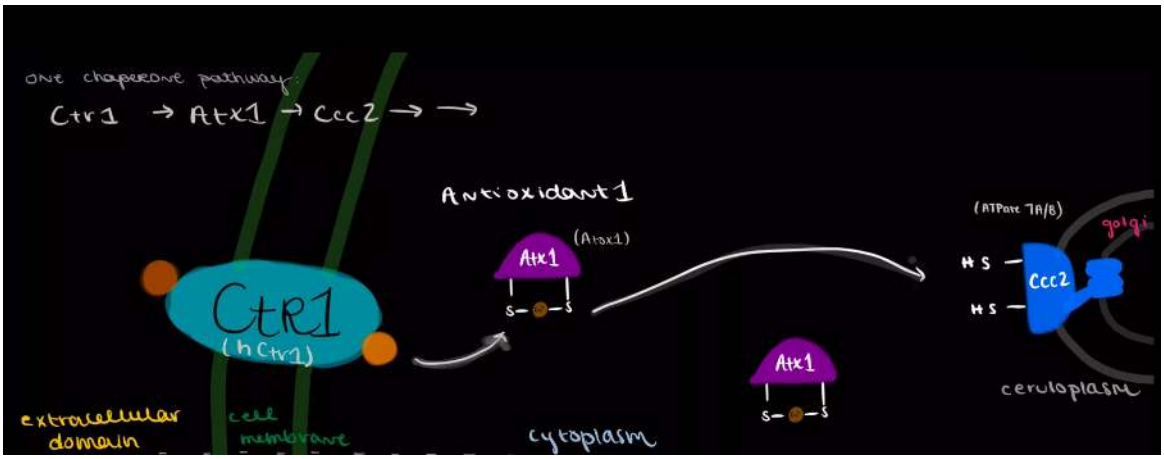
A copper chaperone is protein which binds intracellular copper and delivers it safely to essential intracellular locations. The primary function of a copper chaperone protein is to prevent unwanted, and dangerous, oxidizing reactions of copper as it travels through the cytoplasm. Unwanted redox cycling of copper causes a chain of aberrant chemical reactions that occur in the cell when unregulated Cu(I) interacts with oxidative species and then produces Cu(II) and reactive oxygen species, or ROS.[1] The reactive oxygen species, such as $HO^{\bullet -}$, are hazardous to the health of the cell because the potential impact of oxidative stress when they interact with proteins and surfaces within the cell, overall leading to the aging and potential death of the cell. Figure 1 below provides a scheme for redox cycling in the cell. This reaction is continually harmful because the Cu(II) may be reduced to Cu(I) and the cycle continues to cause cell damage as long as the metal remains free. If copper chaperones do not properly transport and protect intracellular copper, the reactive products of redox cycling will irreversibly damage the cell. In order to prevent redox cycling, the copper chaperone stabilizes one oxidative state of copper; the Cu(I) oxidation state is selected because the cell is a reducing environment and prefers this case already.[1]

Redox cycling occurs when reactive products of metabolism meet free copper to produce oxidative species that may cause damages to the cell. (Original artwork by Adrienne Bruggeman)



This page focuses on the yeast copper chaperone, **Antioxidant1, or Atx1** in shorthand. Copper chaperone Atox1 is the homologous chaperone present in mammalian (human) cells.[2] Yeast (*Saccharomyces cerevisiae*) is a model system that is simpler to study than mammalian cells. Most of what we know about the copper transport pathways of mammalian cells is derived from yeast model studies. Atx1 in yeast is assumed to be identical in its function to the human protein, Atox1.[2] These proteins are part of an elaborate system dedicated to safe copper transport through the cellular cytoplasm. This system protects the cell by relaying copper from the plasma membrane protein Copper Transporter 1 (Ctr1), to Atx1, to the ATP-dependent Cross-Complements Ca^{2+} protein, abbreviated Ccc2, which takes Cu into the golgi.[3] In short, the Atx1 is a member of a team of proteins dedicated to copper transport, protection, and usage through the cell. In mammalian cells, the copper chaperone Atox1 accepts copper from hCtr1 and delivers to proteins ATP7A and ATP7B. Atx1 and all copper chaperones are integral features of copper transport within the cell, most importantly stabilizing the Cu(I) oxidation state in order to prevent the harm caused by redox cycling.

The figure below illustrates one of the yeast intracellular Cu pathways which is mediated by the Cu Chaperone Atx1 (or Atox1 in mammals). Atx1 shuttles Cu from its cellular entry point at Ctr1 to the golgi, where it can be incorporated into enzymes destined for outside the cell. Ctr1 is the plasma membrane Cu transporter that is responsible for transporting Cu from the extracellular environment to the cytoplasm (hCtr1 in human). Ccc2 is the ATP-dependant protein that recieves Cu from Atx1 and transports Cu into the golgi. ATPase7A and ATPase7B are the human analogs to yeast Ccc2. (Original artwork by Adrienne Bruggeman)

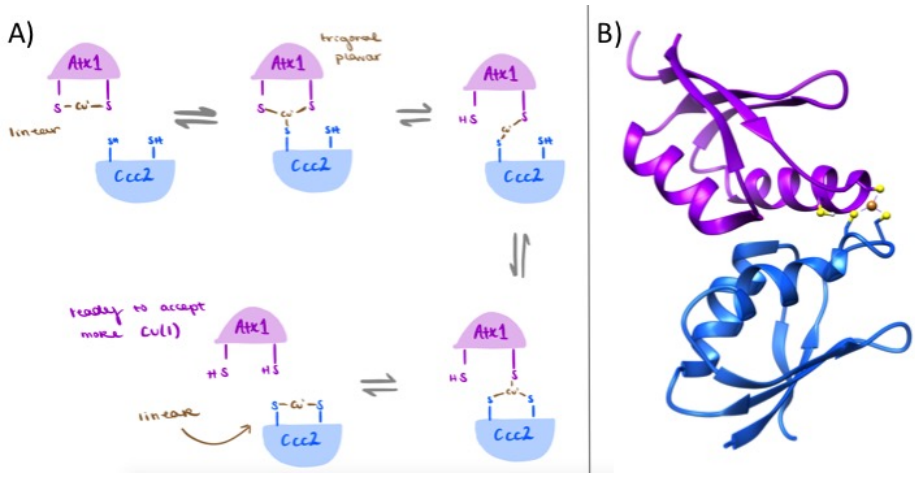


Hard soft acid base (HSAB) theory can be applied to explain how the chaperone's donor atoms help to stabilize Cu(I) over Cu(II) to prevent redox cycling. The theory of HSAB categorizes acids and bases according to ionic radius, charge/ion balance, and charge of ions to predict the binding capacity between an acid and a base.[4] The HSAB theory follows the convention that soft acids and bases prefer to interact while hard acids and bases prefer to interact compared to a hard-soft mixed interaction. According to this theory, the thiolate (S^-) ligand of a deprotonated cysteine is a soft base due to its large ionic radius and small charge. Similarly due to radius and charge, Cu(I) is characterized as a soft acid, while Cu(II) is characterized as a borderline acid. Thus, the soft binding site of Atx1 prefers to bind with the soft Cu(I) rather than the borderline Cu(II), and in the presence of both, the sulfur will prefer the Cu(I) and not the Cu(II). This strong preference for Cu(I) over Cu(II) increases the stability of Cu(I) in the cell, and helps prevent it from being oxidized to Cu(II). This stabilization of Cu(I) discourages undesirable redox cycling.

Ligand Field Theory (LFT) is another principle of coordination chemistry that can be applied to explain how Atx1 stabilizes the Cu(I) oxidation state. The d^{10} electron filling of Cu(I) results in a ligand field stabilization energy (LFSE) of zero.[5] The value of zero comes from the balance of a full set of electrons in higher energy orbitals and in lower energy orbitals. A zero LFSE indicates that there is no stabilization energy for any particular geometry, and thus gives the Cu(I) freedom to bind in any geometry.[2] When bound to Atx1, Cu(I) takes a linear geometry between two cysteine residues. Cu(II) is a d^9 metal with a LFSE of -0.6Δ. This negative stabilization energy indicates that the Cu(II) will have geometric preference for octahedral-type geometry, and thus would disfavor 2-coordinate binding geometries.[5] Thus the geometry of the Atx1 binding site is disfavorable to Cu(II), further stabilizing the preference of Cu(I) in the cell.

The zero LFSE of Cu(I) also assists in the transfer mechanism from the copper chaperone to another protein, such as Ccc2. During the docking and transfer process to Ccc2, copper bound to Atx1 forms an additional bond with an adjacent cysteine residue of the docked Ccc2 protein before breaking any initial bonds with Atx1.[3] Part A of the figure below provides an illustration of the transfer mechanism from Atx1 to Ccc2. Note that the geometry transitions from linear to trigonal planar before breaking the bonds with Atx1 and returning to a linear geometry at the Ccc2 site.[3] The two-coordinate linear and three-coordinate trigonal planar complexes are both favorable to the Cu(I) over Cu(II) due to the LFSE preference. This mechanism again promotes stability of Cu(I) and disfavors Cu(II).

A) The cartoon diagram of the Atx1 transfer of copper to Ccc2. The complex begins as 2-coordinate, becomes 3-coordinate twice during the transfer and ends as 2-coordinate again. (Original artwork by Adrienne Bruggeman) B) A ribbon diagram of the three-coordinate complex of Atx1 (purple) to Ccc2 (blue).



C) Below is an animation of the transfer mechanism illustrated above.



The Cu chaperone transfer mechanism also makes sense in terms of electron counting (think 18-electron rule). As previously mentioned, Cu(I) is a full shell d^{10} metal and is bound to two sulfurs of the Atx1 chaperone. Each of the sulfur ligands will donate two electrons to the copper. Thus the total electron count of the metal binding site is 14. A metal's capacity for electrons is 18, and since the copper does not yet have 18, it is able to accept electrons until it reaches this capacity. This ability to accept electrons is relevant to the copper chaperone system because at its binding step, which docks the copper to Ccc2, the copper accepts an additional sulfur bond before breaking either of the preexisting cysteine bonds with Atx1. Cu(I)'s ability to accept an additional ligand from Ccc2 while it is still coordinated to Atx1 means that that the metal will not be released as a free ion into the cell.[3] Thus Cu is always "protected" by Atx1 and/or Ccc2 coordination, preventing redox cycling.

The LFSE and geometry-fluidity of Cu(I) not only impacts the transfer mechanism towards greater stability of Cu(I) over Cu(II), but also reduces the thermodynamic energy cost during the transfer of Cu between Atx1 and Ccc2. Through the geometry-fluidity of Cu(I), the metal will bind to the chaperone reversibly and easily change its geometry when necessary. Thus at the end of the mechanism, an unbound Atx1 is produced.[6] If Cu(I) tended to bind with a specific preferred geometry, it would be more difficult to change out of that geometry. Thus the zero LFSE allows the Cu(I) to change geometry with low thermodynamic cost.

Finally, the lability of the Cu(I) reduces the energy cost of the transport from Atx1 to Ccc2. When a metal ion is labile, this means that it reacts at a high kinetic rate and may readily replace ligands in coordination complexes.[7] Copper, both as Cu(II) and as Cu(I) is especially labile. This lability comes as a result of the presence of d-electrons in the complex's high energy antibonding orbitals. When these electrons are present in the high energy orbitals, they contribute to high lability (the complex exchanges ligands at a high rate). When the Cu(I) enters the cell through Ctr1, the copper chaperone complex binds and transports the copper through the cell to the metal's next binding site. The copper's high lability is necessary so that the metal is able to change ligands readily, thus encouraging the ongoing binding and transport of the metal between chaperones and target proteins.[7]

The protective function of the copper chaperone is realized by the application of many chemical principles towards the prevention of redox cycling in the cell. In order to best prevent redox cycling, Atx1 stabilizes one oxidation state of copper. Because the cell is a reducing environment, it prefers Cu(I) over Cu(II), and because Ctr1 delivers copper in this form into the cell, the copper chaperone Atx1 is best suited to stabilize Cu(I). According to HSAB Theory and Ligand Field Theory, the binding site of Atx1, composed of two linear cysteines, stabilizes Cu(I) over Cu(II). Similarly, the mechanism of copper transfer from Atx1 to Ccc2 is used to further stabilize Cu(I) over Cu(II) in the cell and to prevent the exposure of free copper to the cell. Through coordination geometries only accessible to Cu(I) and the high lability of copper, the copper chaperone is able to transfer copper stably and with low energy costs. The ability for Atx1 and any copper chaperone to bind stably with copper not only successfully transports biologically needed metal ions, but also proactively reduces the damaging effects of free copper, redox cycling, and oxidative stress to the cell.

Sources

1. Rodriguez-Montelongo, L.; de la Cruz-Rodriguez, L. C.; Farías, R. N.; Massa, E. M. Membrane-Associated Redox Cycling of Copper Mediates Hydroperoxide Toxicity in Escherichia Coli. Biochimica et Biophysica Acta (BBA) - Bioenergetics 1993, 1144 (1), 77–84.
2. Rosenzweig, A. C.; O'Halloran, T. V. Structure and Chemistry of the Copper Chaperone Proteins. Curr Opin Chem Biol 2000, 4 (2), 140–147.
3. Finney, L. A.; O'Halloran, T. V. Transition Metal Speciation in the Cell: Insights from the Chemistry of Metal Ion Receptors. Science 2003, 300 (5621), 931–936.
4. Gray, H.B.; Stiefel, E. I.; Valentine, J.S.; Bertini, I. *Biological Inorganic Chemistry: Structure and Reactivity.* **2007.** 331-337.
5. Schaller, C. P. Ligand Field Theory http://chem.libretexts.org/LibreTexts/Saint_Mary's_College%2C_Notre_Dame%2C_IN/CHEM_342%3A_Bio-inorganic_Chemistry/Chapters/Chapter_3%3A_Introduction_to_Advanced_Bonding_Theories/3.2_Ligand_Field_Theory/B._Ligand_Field_Theory/B.1_Ligand_Field_Theory (accessed Oct 11, 2016).
6. O'Halloran, T. V.; Culotta, V. C. Metallochaperones, an Intracellular Shuttle Service for Metal Ions. J. Biol. Chem. 2000, 275 (33), 25057–25060.
7. Pope, C. R.; De Feo, C. J.; Unger, V. M. Cellular Distribution of Copper to Superoxide Dismutase Involves Scaffolding by Membranes. Proc. Natl. Acad. Sci. U.S.A. 2013, 110 (51), 20491–20496.

Contributed by:

*This work was originally written by **Adrienne Bruggeman**, Fall 2016: Adrienne is currently (as of 2016) a senior chemistry major at Saint Mary's College in Notre Dame, IN.*

This work was originally edited by Dr. Kathryn Haas, Assistant Professor at Saint Mary's College.

11.1.6: Keep Cu Safe- Intracellular Copper Chaperones is shared under a not declared license and was authored, remixed, and/or curated by LibreTexts.

11.1.7: Cytochrome C

All cells require energy in the form of ATP, Adenosine Triphosphate, to drive essential metabolic processes for survival. When an aerobic organism digests its food, glucose ($C_6H_{12}O_6$) is broken down into two molecules of pyruvate in the process of glycolysis. The reduced electron carriers, NADH and $FADH_2$ are produced as a byproduct of this reaction.

NAD^+ gains two electrons ($2e^-$) and a hydrogen ion (H^+) to form NADH. Similarly, FAD accepts two hydrogen ions ($2H^+$) and two electrons ($2e^-$) to form $FADH_2$. These electrons from NADH and $FADH_2$ then enter the complexes of the Electron Transport Chain. The Electron Transport Chain (ETC) is a series of electron transport proteins located in the inner membrane of the mitochondria--the powerhouse of the cell (Figure 1). Embedded in the mitochondrial membrane is a series of redox-active proteins, which act like a wire by shuttling electrons through the ETC. Through a series of redox reactions, these proteins pump protons (H^+) from the mitochondrial matrix to the intermembrane space. The accumulation of protons in the intermembrane space generates an electrochemical gradient which powers the synthesis of ATP by the enzyme ATP Synthase. The Electron Transport Chain produces a total of 34 molecules of ATP which the cell can use to carry out its metabolic processes for survival. [1]

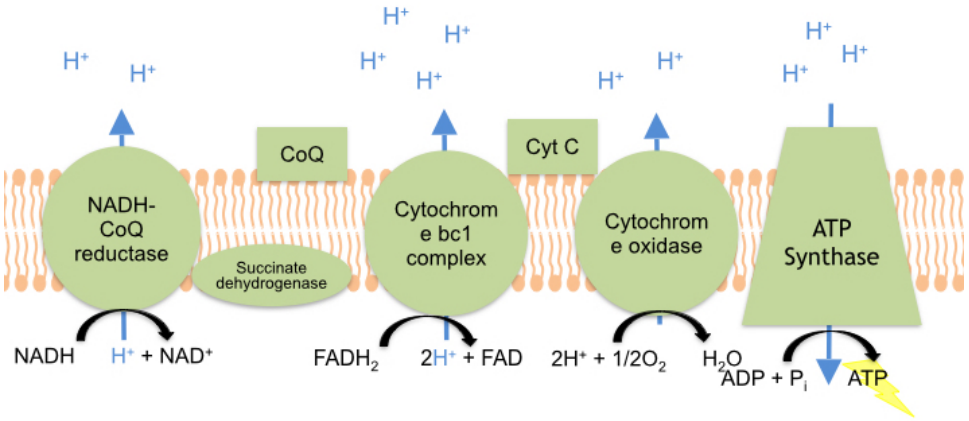


Figure 1. The Electron Transport Chain

This is a general overview of The Electron Transport Chain (ETC). The ETC is a series of four protein complexes: NADH dehydrogenase, succinate dehydrogenase, cytochrome bc_1, and cytochrome c oxidase, embedded in the inner membrane of the mitochondria. As electrons are transferred through these protein complexes, a proton (H^+) gradient accumulates in the intermembrane space of the mitochondria. ATP Synthase uses this proton gradient established by the ETC to synthesize energy in the form of ATP.

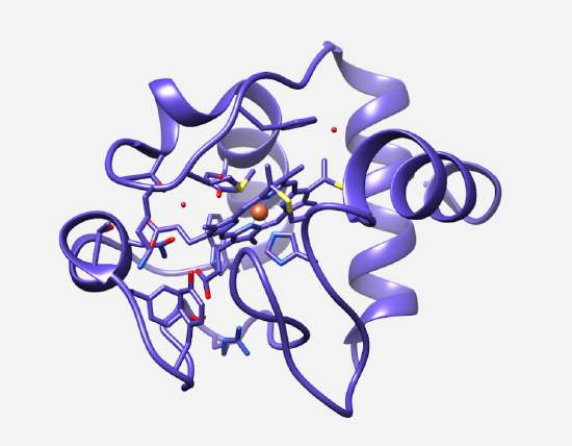


Figure 2. Full Length Ribbon Structure of Cytochrome C (PDB 3cyt).[3] This is the biological assembly of one cytochrome c monomer. Within the central heme is an iron ion shown in orange. The heme is covalently bonded to the protein via disulfide bonds made possible by the recurring Cys-X-Y-Cys-His motif found in cytochromes.

Cytochrome c is an important component of the Electron Transport Chain for the synthesis of ATP (Figure 2). Cytochrome c is a water soluble electron transport protein that is loosely associated with the mitochondrial inner membrane. In the Electron Transport Chain, cytochrome c transfers one electron at a time via its heme group from the third complex of the electron transport chain, cytochrome bc_1, to the fourth complex of the electron transport chain, cytochrome c oxidase.[2]

Cytochrome c contains a heme iron metal center that is essential to its function. During the electron transport process, this heme iron interconverts between the Fe^{3+} and Fe^{2+} oxidation states, which allows for electrons to be accepted and donated.[4] When cytochrome c is in its oxidized form, an electron is transferred from the cytochrome bc_1 complex to the heme Fe^{3+}, reducing it to Fe^{2+}. Finally, cytochrome c releases the electron to the final electron carrier of the ETC, cytochrome c oxidase. At this point, the iron center will return to its Fe^{3+}oxidation state.

The iron metal center of cytochrome c represents an octahedral geometry due to the coordination of six ligands around the central iron ion (Figure 3). An octahedral geometry is preferred for cytochrome c because each of the 6 electron rich ligands contribute to stabilizing the positively charged metal iron ion. The heme iron shown in orange is coordinated by four nitrogen atoms of a rigid square planar porphyrin ring and two axial ligands: the sulfur atom of a methionine residue and a nitrogen atom of a histidine imidazole ring. The porphyrin ring of cytochrome c is considered to be a tetradentate chelating ligand because the four nitrogen atoms of the porphyrin ring bind to the central iron, forming a stable organometallic complex. Based on the chelate effect, this tetradentate ligand binding site is more entropically favorable compared to the affinity of a monodentate ligand for the same metal ion. [5]

The ligands of cytochrome c are appropriate based on Hard Soft Acid Base Theory. (HSAB). HSAB categorizes acids and bases as hard, soft, or borderline. Soft acids and bases are larger and easily polarizable while hard acids and bases are smaller and less polarizable. Species that lie in between hard and soft are considered borderline. [6] Based on HSAB, it is logical that the borderline iron coordinates with the nitrogen of the histidine imidazole ring (a borderline base), the nitrogen atoms provided by the porphyrin ring (borderline bases), and the sulfur of the methionine (a soft base).

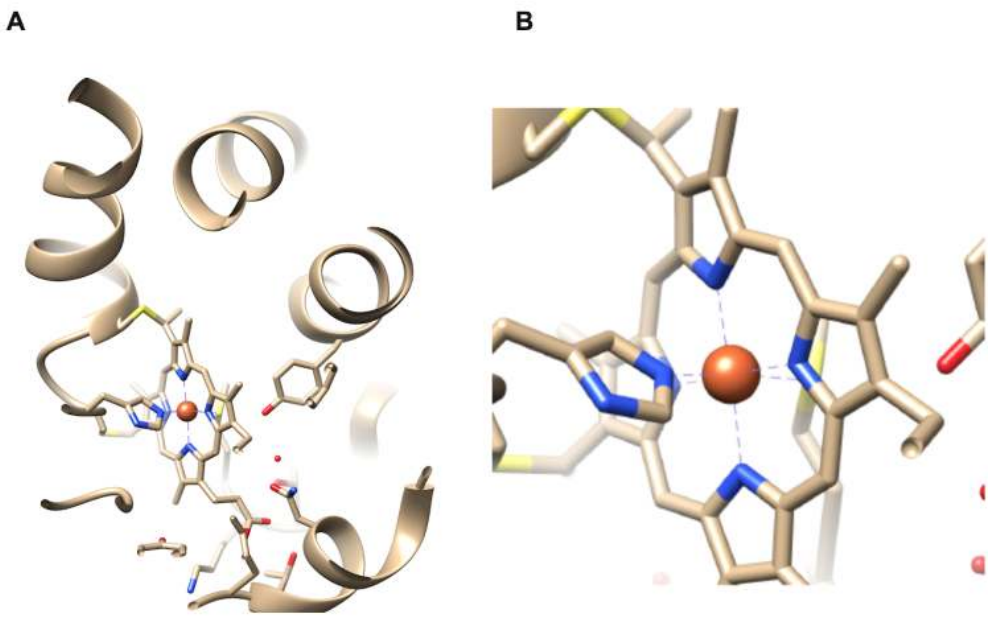


Figure 3. Iron Metal Center of Cytochrome C[3]

Figure 3A shows the entire structure of cytochrome c while Figure 3B is a magnified inset of the heme iron metal center essential to the electron transport function of cytochrome c. The heme iron shown in orange is coordinated by four nitrogen atoms of a rigid square planar porphyrin ring (blue) as well as two axial ligands: a sulfur atom of a methionine residue (yellow) and a nitrogen atom of a histidine imidazole ring (blue).

The iron metal center of cytochrome c represents an octahedral geometry due to the coordination of six ligands around the central iron ion (Figure 3). An octahedral geometry is preferred for cytochrome c because each of the 6 electron rich ligands contribute to stabilizing the positively charged metal iron ion. The heme iron shown in orange is coordinated by four nitrogen atoms of a rigid square planar porphyrin ring and two axial ligands: the sulfur atom of a methionine residue and a nitrogen atom of a histidine imidazole ring. The porphyrin ring of cytochrome c is considered to be a tetradentate chelating ligand because the four nitrogen atoms of the porphyrin ring bind to the central iron, forming a stable organometallic complex. Based on the chelate effect, this tetradentate ligand binding site is more entropically favorable compared to the affinity of a monodentate ligand for the same metal ion.[5]

The ligands of cytochrome c are appropriate based on Hard Soft Acid Base Theory. (HSAB). HSAB categorizes acids and bases as hard, soft, or borderline. Soft acids and bases are larger and easily polarizable while hard acids and bases are smaller and less polarizable. Species that lie in between hard and soft are considered borderline. [6] Based on HSAB, it is logical that the borderline iron coordinates with the nitrogen of the histidine imidazole ring (a borderline base), the nitrogen atoms provided by the porphyrin ring (borderline bases), and the sulfur of the methionine (a soft base).

Although the heme iron metal center changes oxidation state during the electron transport proces, cytochrome c always adopts an octahedral, low spin geometry regardless of the oxidation state on the iron. [7] This geometry is preferred based on Ligand Field Stabilization Energy (LFSE). LFSE is the total energy of the d-electrons of a metal complex relative to the theoretical barycenter. The formula for determining LFSE is shown in Equation 1 below, where x= number of d-electrons in the low energy t_{2g} orbitals and y= the number of d-electrons in the high energy e_g orbitals.

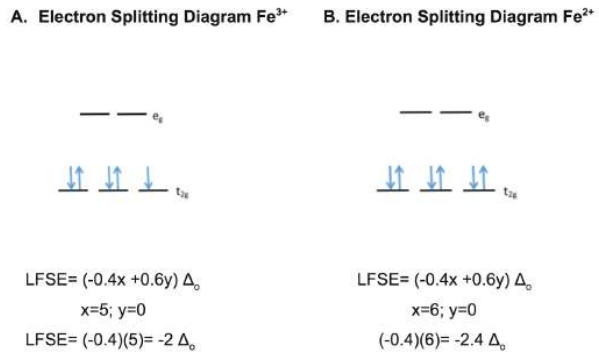


Figure 4. LFSE Splitting Diagram of Low Spin Fe^{3+} and Fe^{2+}

The electron splitting diagrams and calculations for low spin Fe^{3+} and Fe^{2+} are shown in figures A and B, respectively. The more negative LFSE values for low spin iron compared to high spin iron indicate that this low spin conformation is more energetically favorable and is therefore the configuration that the complex will adopt.

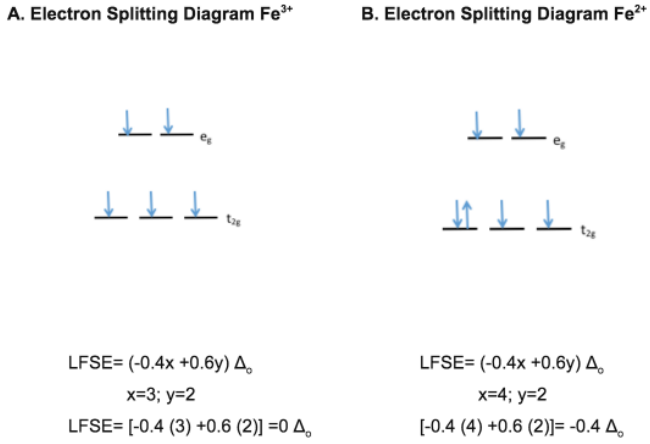


Figure 5. LFSE Splitting Diagrams of high spin Fe^{3+} and Fe^{2+}

The theoretical electron splitting diagrams and calculations for high spin Fe^{3+} and Fe^{2+} are shown in figures A and B, respectively. However, the LFSE values are more negative for low spin iron than for high spin iron, regardless of the oxidation state. Therefore, the heme iron metal center of cytochrome c will always adopt a low spin octahedral geometry regardless of the oxidation state on the iron.

In the low spin state, the d-electrons pair in the low energy t_{2g} orbitals before occupying the higher energy e_g orbitals, which increases stability. In the high spin state, the d-electrons singly occupy both the t_{2g} and e_g orbitals, without regard to the energy of the orbitals, and then pair up. The more negative the LFSE, the more stable the complex. The LFSE values for low spin iron are more negative than the LFSE values for high spin iron, regardless of the oxidation state present on the iron. Thus, the iron metal center of cytochrome c will always adopt the more energetically favorable low spin conformation.

During the electron transport process, the heme iron of cytochrome c cycles between the +2 and +3 oxidation states. As cytochrome c accepts an electron from the third complex of the electron transport chain, cytochrome bc_1, the Fe^{3+} iron metal center is reduced to Fe^{2+}. When cytochrome c releases this electron to the final complex of the electron transport chain, cytochrome c oxidase, the Fe^{3+}oxidation state is restored. However, despite this change in the oxidation state of the iron, the heme coordination does not change; the iron ion is “locked in place” and undergoes minimum reorganization.

Reduction potential also facilitates the electron transport function of cytochrome c in the ETC. Reduction potential (E°’) is the tendency for a chemical species to acquire electrons and therefore be reduced. The more positive the reduction potential, the greater the tendency for that chemical species to accept an electron and to be reduced. The reduction potential for cytochrome bc_1 (complex III of the ETC) is 0.194 V. Cytochrome bc_1 donates one electron to the oxidized form of cytochrome c (Fe^{3+}), reducing the iron of cytochrome c by one oxidation state to become Fe^{2+}. The reduction potential for cytochrome c is 0.254 V. The reduction potential for cytochrome c oxidase (Complex IV of the ETC) is 0.562 V. [8] Cytochrome C Oxidase accepts an electron from the reduced cytochrome c (Fe^{2+}) returning cytochrome c to its oxidized form (Fe^{3+}). The complexes of the Electron Transport Chain are arranged in order of increasing redox potential (each complex has higher affinity for electrons than the previous), which drives the flow of electrons towards the final complex of the Electron Transport Chain, Cytochrome C Oxidase.

E°’donor < E°’ electron transfer protein/center < E°’acceptor: Must be true for reaction to be spontaneous!

In conclusion, cytochrome c is an essential electron transfer protein which shuttles electrons between complexes III and IV of the ETC. The heme iron metal center readily interconverts between the Fe^{3+} and Fe^{2+} which allows for electrons to be accepted and donated. If this electron transfer did not occur, the ATP required to power many metabolic processes such as muscle movement, DNA synthesis, and active transport would not be produced. Therefore, cytochrome c is an important component in facilitating the production of this ATP through its electron transfer to Cytochrome C Oxidase, which provides cells the energy they need to carry out these vital processes necessary for survival.[9]

Sources

1. Alberts, B.; Johnson, A.; Lewis, J, et al. *Molecular Biology of the Cell*. 4th ed.; New York. Garland Science; 2002. Electron Transport Chains and Their Protein Pumps. Available from: https://www.ncbi.nlm.nih.gov/books/NBK26904/
2. Lehninger, A.L.; Nelson, D.L.; Cox, M.M. *Lehninger Principles of Biochemistry*; Macmillan Higher Education: Houndmills, 2017.
3. Takano, T.; Dickerson, R.E. *Redox conformation changes in refined tuna cytochrome c*. Proc. Natl. Acad. Sci. USA. **1980.** 77, 6371-6375.
4. Roat-Malone, R.M. *Bioinorganic Chemistry- a short course;* Wiley & Sons: Hoboken, NJ, 2007.
5. Xinshan, K. & Carey, J. (1999). Role of Heme in Structural Organization of Cytochrome c Probed by Semisynthesis. *Biochemistry, 38* (48), 15944-15951.
6. Chemistry LibreTexts: Hard and Soft Acids and Bases
7. Silva, J.J.R.; Williams, R.J.P. *The biological chemistry of the elements: the inorganic chemistry of life;* Oxford University Press: Oxford, 2001.
8. Bertini, I. *Biological inorganic chemistry: structure and reactivity*; University Science Books: Sausalito, CA, 2007.
9. Erecińska, M.; Silver, I.A. ATP and Brain Function. *Journal of Cerebral Blood Flow and Metabolism.* **1989**, 9, 2-19.

Contributed By

- *This work was originally written by **Hannah Voss**, Spring 2018: Hannah is currently (as of 2018) a junior biology major at Saint Mary's College in Notre Dame, IN.*
- *This work was originally edited by Dr. Kathryn Haas (Assistant Professor) and Madison Sendzik (Teaching and Research Assistant) at Saint Mary's College.*

11.1.7: Cytochrome C is shared under a not declared license and was authored, remixed, and/or curated by LibreTexts.

11.1.8: Cytochrome Oxidase

The electron transport system (ETS) is an energy production system for aerobic organisms found in the mitochondria of cells. It is the third and final step in cellular respiration, which is the process by which the cell produces energy. When an organism takes in carbohydrate nutrients, they are converted to glucose which can be further broken down through a set of chemical reactions to pyruvate through glycolysis. After glycolysis, this pyruvate molecule is oxidized in the Kreb's cycle which in turn produces ATP and high energy molecules, NADH, and $FADH_2$. Only a few ATP are produced directly from the Kreb's cycle; however the NADH and $FADH_2$ are transported to the ETS where they can be oxidized to produce more ATP (Figure 1).[1]

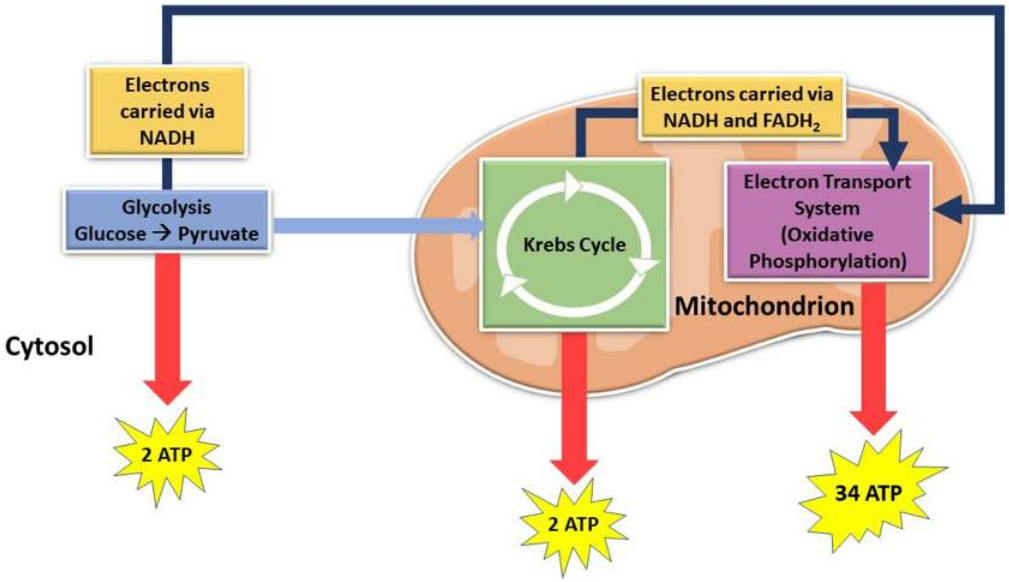


Figure 1. The Process of Cellular Respiration. Cellular respiration is the process used by aerobic organisms to break down sugars to produce energy. The process begins with glycolysis where glucose is broken down into pyruvate producing 2 ATP. Next, the pyruvate moves into the Kreb's cycle in the mitochondria and goes through a series of reactions producing 2 ATP and high energy molecules, NADH and $FADH_2$. These high energy molecules are then transferred to the electron transport system where they are oxidized and start a series of reactions that will ultimately produce 34 ATP.

After the NADH and $FADH_2$ are oxidized to NAD^+ and FAD, the electrons that are removed from NADH and $FADH_2$ and are transported through the four electron transport complexes of the ETS. The movement of electrons provides energy to pump hydrogen ions (H^+) across the inner mitochondrial membrane into the intermembrane space through four complexes.1 The four complexes are NADH-CoQ (ubiquinone reductase), succinate dehydrogenase, cytochrome bc1, and cytochrome oxidase (Figure 2).[2]

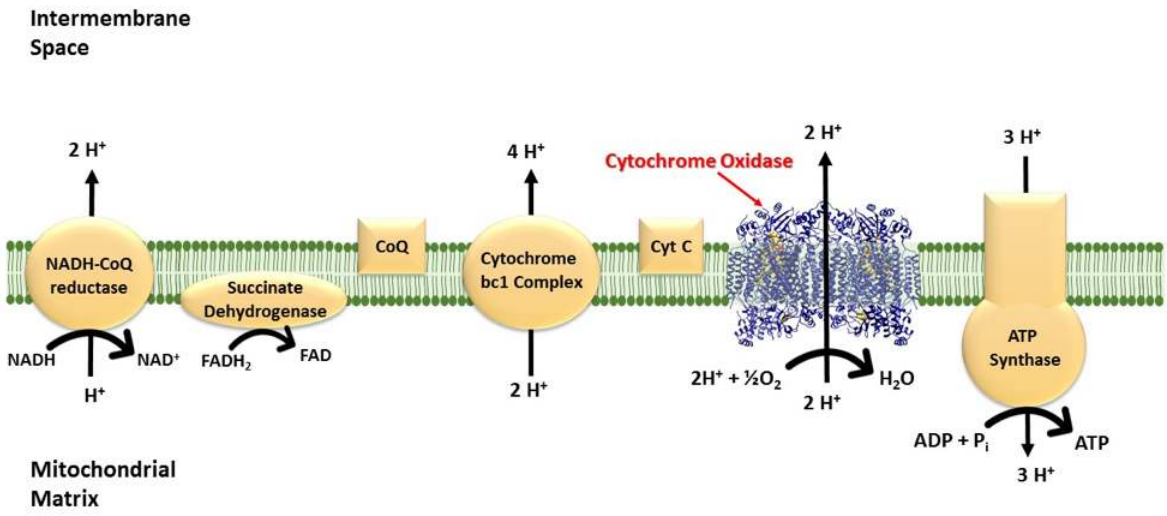


Figure 2. The electron transport system (ETS). The ETS is involved in energy production and occurs in the inner mitochondrial membrane of the mitochondrial matrix. NADH and $FADH_2$ are oxidized allowing electrons to travel through the membrane to the four complexes, NADH-CoQ reductase, succinate dehydrogenase, cytochrome bc1, and cytochrome oxidase (shown in ribbon depiction, PDB 1OCC), pumping H^+ ions across the membrane. The H^+ concentration in the intermembrane space increases and H^+ ions travel through the ATP Synthase to the mitochondrial matrix providing energy to convert ADP to ATP.

The pumping of hydrogen ions through the four complexes stores potential energy by creating a concentration gradient, with higher hydrogen ion concentration in the intermembrane space. This energy is captured as hydrogen ions cross back over to the matrix of the mitochondria, via the ATP synthase, producing energy for the cell in the form of ATP.[1] The hydrogen ion concentration will then increase in the mitochondrial matrix and travel through the three complexes again when another NADH and $FADH_2$ are introduced to the ETS. This process will continue to cycle and produce high numbers of ATP for the cell to use as energy (Figure 2).[1]

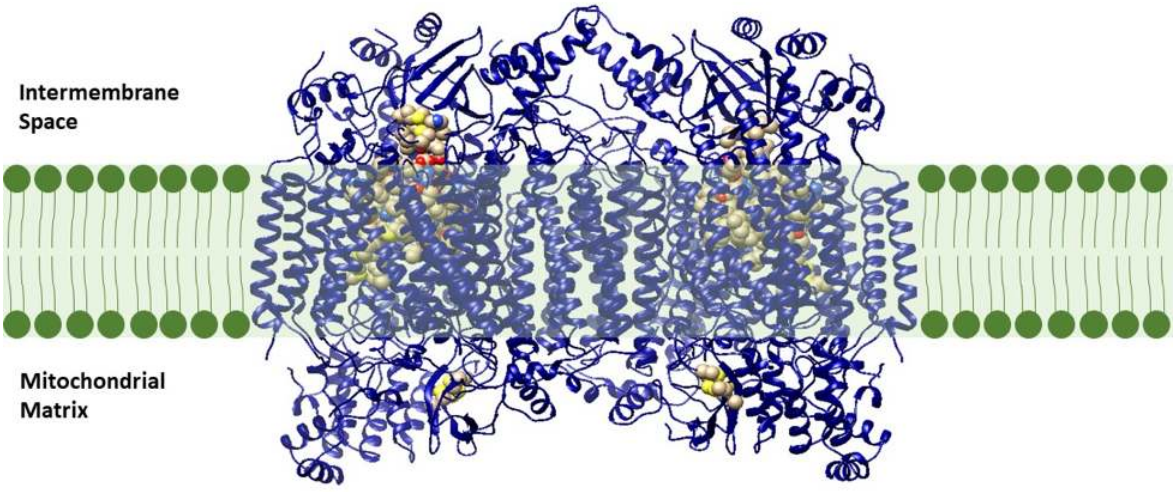


Figure 3. Structure of cytochrome oxidase (1OCC) in the inner mitochondrial membrane. Cytochrome oxidase is a transmembrane protein in the inner mitochondrial membrane. It is a dimer with two identical chemical units containing two hemes,

three coppers, magnesium and a zinc.[2] The protein is shown in ribbon depiction, with atoms of the metal-containing electron transport centers shown in spheres.

Cytochrome oxidase, also known as complex IV, is the terminal, or final, enzyme of the electron transport system (this does not include ATP synthase). Cytochrome oxidase is a transmembrane molecule found in the mitochondria of eukaryotes and in the cellular space of aerobic prokaryotes. This molecule is a proton pump that plays a vital role in producing energy, in the form of ATP, via the ETS (Figure 3). In the last steps of the energy production process, cytochrome oxidase oxidizes the waste products from the end of the energy making process, converting reactive species, H^+ and dioxygen (O_2), to a more stable molecule, water (H_2O). In the absence of cytochrome oxidase, this energetically favorable reaction could be explosive and no energy production would occur.[2] Cytochrome oxidase allows this reaction to occur safely while harnessing energy to form the H^+ ion gradient. This energy produced from the reaction is used to pump H^+ ions from the matrix to the intermembrane space of the mitochondria (Figure 2).[1]

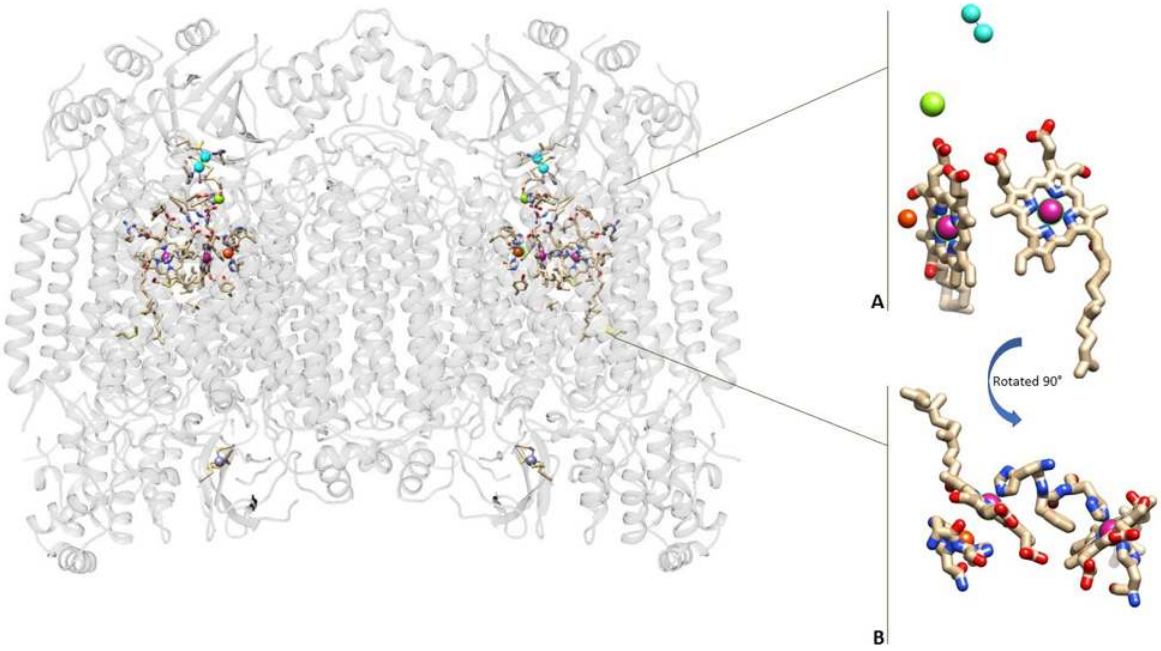


Figure 4. The structure of the metals and their ligands in cytochrome oxidase. This figure shows the two hemes and their irons (purple), two Cu_A (light blue), Cu_B (orange), one magnesium (light green), and one zinc (blue). Cytochrome oxidase is a dimer with its two sets of Cu_A, $heme_a$, $heme_{a3}$, Cu_B, and zinc. The metal complex dimer mirrors one another. Inset A shows a detailed view of Cu_A, magnesium, $heme_a$ (right), $heme_{a3}$ (left), and Cu_B and their spatial relation to one another. Inset B shows $heme_a$ bound to two imidazoles, and $heme_{a3}$ bound to an imidazole. $heme_{a3}$ and Cu_B are close to one another, but do not bind. This space between $heme_{a3}$ and Cu_B is where the oxygen then can bind to the iron. Cu_B is bound to three imidazoles. From PDB 1OCC.

Cytochrome oxidase is a dimer meaning it is made up of two identical proteins. The two proteins in cytochrome oxidase mirror one another. The system uses multiple metals to complete its function including the two irons in the two hemes, three coppers, one magnesium, and one zinc (Figure 4). The irons in the two hemes and the three copper molecules are vital to the success of the enzyme in aerobic respiration.[1]

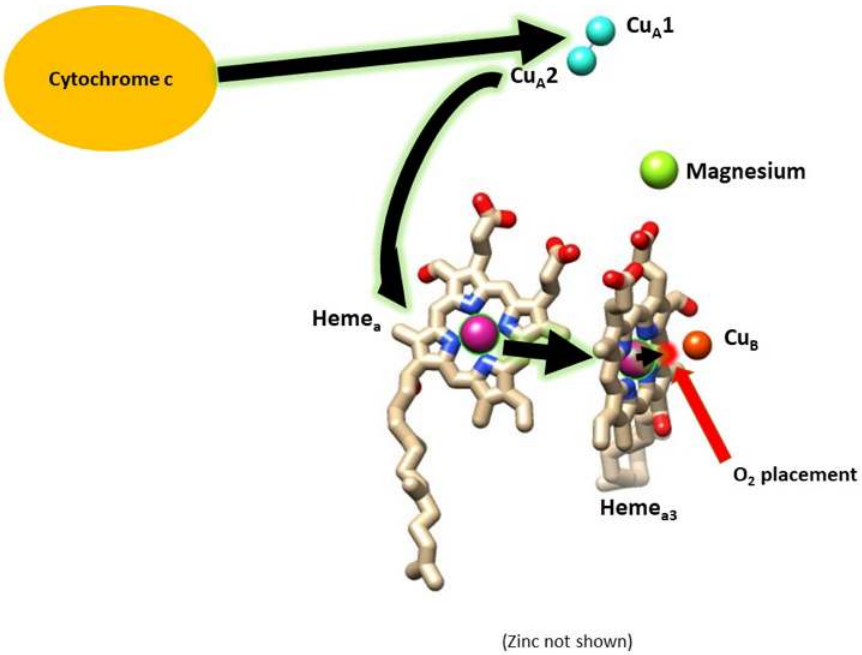


Figure 5. The transfer of electrons from cytochrome c to cytochrome oxidase. This figure shows the transfer of electrons the cytochrome c to the two Cu_A (light blue), to $heme_a$ (purple, left) to $heme_{a3}$ (purple, right), to finally to the oxygen molecule (red sphere). From PDB 1OCC.

---

2 Cu_A molecules function in allowing the electrons to enter the enzyme from cytochrome c.2,3 The electrons travel from the Cu_A molecules to the first heme, also known as $heme_a$. $heme_a$ functions in allowing the electrons to be transferred from Cu_A to the second heme, $heme_{a3}$. The iron in $heme_{a3}$ functions in binding oxygen, with the help of Cu_B. The energy production system selects a heme iron group to bind the oxygen along with the other copper atom and is the location of oxygen reduction (Figure 5).3 The function of magnesium and zinc remains unknown.[4]

$$4e^- + 8H^+ + O_2 \rightarrow 4e^- + 4H^+ + 2H_2O.^{9} \text{ (1)}$$

The overall reduction that occurs in cytochrome oxidase is shown above (Reaction 1). The electron transfers from the electron donor, cytochrome c, to Cu_A to $heme_a$ to $heme_{a3}$ and finally to the electron acceptor, oxygen, are carried out mostly by redox reactions (Figure 5).[3]

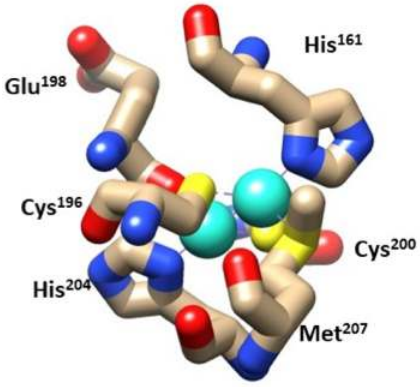


Figure 6. Cu_{A1} and Cu_{A2} with their ligands. This figure shows the two Cu_A (light blue) with their ligands. Cu_{A1} is bound by His^{204}, Cys^{200}, Cys^{196}, and Glu^{198}. Cu_{A2} is bound by His^{161}, Cys^{200}, Cys^{196}, and Met^{207}. From PDB 1OCC.

The electrons travel from cytochrome c to the two Cu_A molecules in the intermembrane space at a fast rate of 70,000 s^{-1} and with an E°' value of 0.27 V.[3,5,6] The Eo', or standard reduction potential, is a value indicating the likelihood a chemical species will be reduced, with a more positive value meaning it is more likely to be reduced. Literature has shown that Cu_A has a mixed oxidation state of I and II (or 1.5 each). Because of this mixed oxidation state when the electrons enter the cytochrome oxidase the charge is shared between the two Cu_A. Only a single electron is transferred from the cytochrome c to the Cu_A.[6] In the cell the environment is different than laboratory conditions, therefore the E°' value would be about +0.05 V.[3]

The two Cu_A molecules are what bring the electrons from the cytochrome c to $heme_a$. They both have tetradentate ligands with a tetrahedron shape.[7] Cu_{A1} is bound by His^{204}, Cys^{200}, Cys^{196}, and Glutamic $acid^{198}$. Cu_{A2} is bound by His^{161}, Cys^{200}, Cys^{196}, and Met^{207}. Both Coppers are bound by Cys^{196} and Cys^{200}, this chelating effect helps stabilize the molecule (Figure 6). The Hard Soft Acid Base (HSAB) theory helps explain the stability of the hemes. HSAB theory characterizes metals as hard, borderline, or soft acids and bases based upon their charge density. HSAB shows that chemical species like to bind with similar species, for example hard acids like to pair with hard bases and borderline acids like to pair with borderline bases. Cu_A applies to the HSAB theory as the copper binds to the imidazole residue on histidine which is borderline for HSAB. The two cysteine and glutamic acid residues that bind with Cu (I) or (II) are soft and hard bases, respectively, for HSAB and may still bind as they are next to borderline. Therefore HSAB may still be a selective method for the Cys and Glu ligands.[3]

As Cu (II) is a d^{10} metal its d orbital is full of electrons. As the d orbital is full the LFSE (ligand field stabilization energy) would be zero. The LFSE is a number that defines the energy of the electrons compared to the average energy of the orbitals. A more negative LFSE indicates lower energy and a more stable complex. As Cu(II) has an LFSE of zero this indicates that the geometry of the metal and its ligands it likely dependent upon sterics. Therefore the tetrahedral geometries of the Cu_{A1} and Cu_{A2} is a result of reducing steric hindrance between the ligands. Cu_{A1} and Cu_{A2} would have an electron count of 17-18. Both coppers each have four ligands with no charge thus having 8 ligand electrons. Copper can have an oxidation state of (I or II), and therefore will have 9-10 d electrons bringing the electron count to 17-18.3

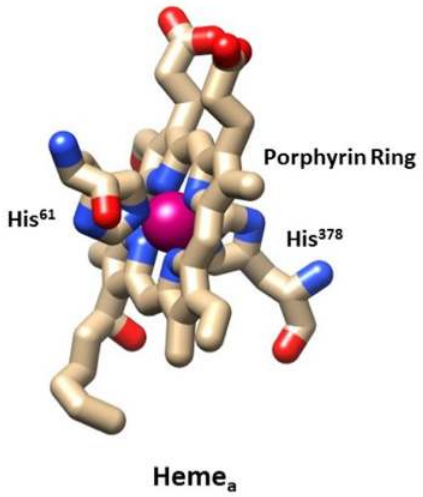


Figure 7. The structure of $heme_a$ and its ligands in cytochrome oxidase. This figure shows the $heme_a$ (purple) in the porphyrin ring and bound by the two histidine ligands, His61 and His378.

After the electrons have entered the cytochrome oxidase from the cytochrome c to the Cu_A molecules they will then transfer to $heme_a$ (Figure 7). This transfer is made possible by 14 covalent bonds and 2 hydrogen bonds spanning 19.5 Å and taking about 20,000 s-1.3 The iron transfers the electrons one at a time and changes from Fe (III) to Fe (II). However, literature shows that the iron only changes its charge about 10-15% as the change in charge is spread over the porphyrin ring decreasing the amount of energy needed.6

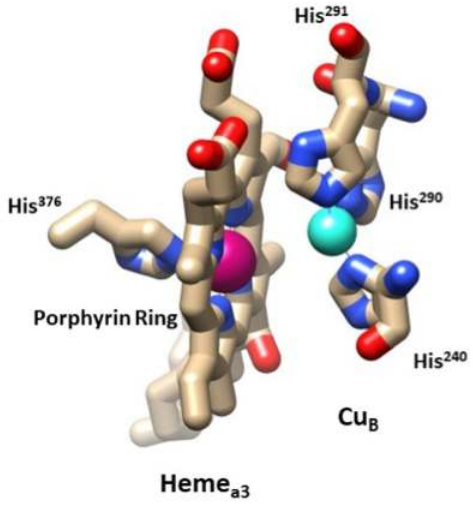


Figure 8. The structure of the heme$_{a3}$ and Cu$_B$ and their ligands in cytochrome oxidase. This figure shows the heme$_{a3}$ (purple) in the porphyrin ring with its histidine ligand and Cu$_B$ (light blue) with its three histidine ligands. Oxygen placement occurs between the heme$_{a3}$ and the Cu$_B$.

Next, the electrons transfer from heme$_a$ to heme$_{a3}$ (Figure 8). The hemes are perpendicular to one another and the edges are located 7 Å apart.[8] How the transfer of electrons from heme$_a$ to heme$_{a3}$ occurs is still not fully understood. Literature shows that electron tunneling stops at heme$_a$, and from heme$_a$ to heme$_{a3}$ the electrons are transferred from the edges of the heme and propelled by protons pumping to the intermembrane space.[6]

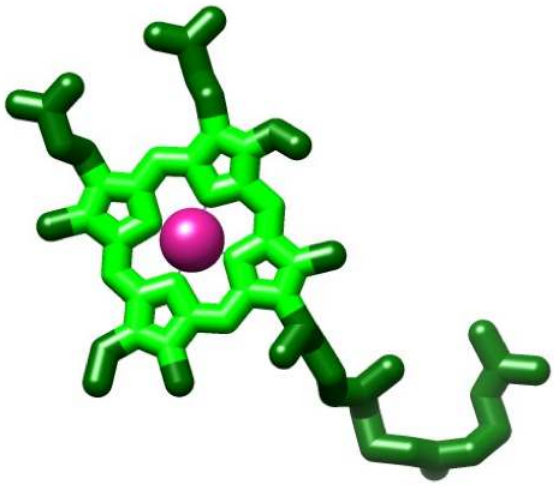


Figure 9. The structure of a porphyrin ring. This figure shows the structure of a porphyrin ring (light green) with its four pyrrole rings and planar geometry. The iron (purple) is in the center of the porphyrin ring and the side groups (dark green) vary depending on the type of heme.

The structure of the heme molecule is a porphyrin ring that is tetradentate chelating of an iron molecule with four nitrogens. Iron can form up to six bonds due to steric constraints that cost the molecule energy by not having enough space for the electrons which repel one another. A porphyrin ring is the building block for heme and is a planar structure composed of four pyrrole rings (Figure 9). Four of the bonds are with the nitrogens of the porphyrin ring, as previously stated, while the fifth coordination site is occupied by an imidazole in histidine, and the sixth coordination site is occupied by another imidazole for heme$_a$, or O_2 for heme$_{a3}$ (Figure 10). Both irons have a planar shape with the heme molecules, but with the addition of their ligands (two imidazole residues for heme$_a$ or an imidazole and an oxygen for heme$_{a3}$) they becomes an octahedral shape.3 The geometry of the hemes can be attributed

to LFSE as the the LFSE equals -0.4 for Fe(II) and -2.0 for Fe(III). This indicates that the geometry of the molecule may be a result of the high stability due to the lower energy of the electrons and their orbitals.[8]

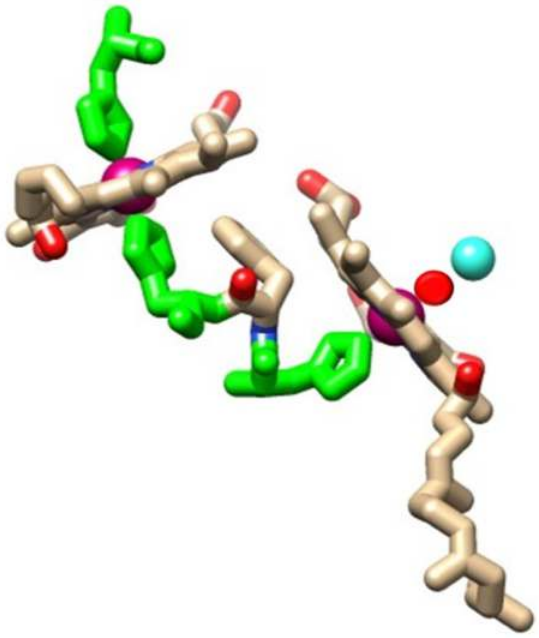


Figure 10. The structure of the metals and their ligands in cytochrome oxidase. This figure shows the two hemes in cytochrome oxidase, $heme_a$ (left) and $heme_{a3}$ (right). $heme_a$ is bound by two imidazoles from Histidines (light green) and $heme_{a3}$ is bound by an imidazole (light green) and an oxygen molecule (red).

Thermodynamic theories are important for ML binding as they provide ideas about the energy needed for breaking bonds and the stability of a molecule. The two hemes in cytochrome oxidase both maintain their stability largely due to their macrocyclic porphyrin ring. This porphyrin ring is made up of 4 pyrroles that bind their nitrogens to the iron. In cytochrome oxidase the iron never needs to leave the hemes and the stability of the porphyrin ring may help the iron stay in its place to properly transfer electrons to oxygen (Figure 10).[9]

The iron does not leave the porphyrin ring for either hemes and the ligands of $heme_a$ remain bound as well. The heme molecules are very stable due to the chelating effect of the porphyrin ring and is relatively inert meaning it holds its metal ion and maintains its planar geometry. The iron in $heme_{a3}$ has an imidazole ligand that remains bound to the iron, but also has a position for oxygen. The oxygen iron bond is broken when electrons are transferred to the oxygen and bound to two H^+ ions.[3] The high lability, or ability of the metal-ligand bond (Fe (II) and O_2) to be broken, is necessary for the water to be released from $heme_{a3}$ and for the cytochrome oxidase to reset for the next set of electrons. The high lability of the Fe (II) is likely a result of the low LFSE value of -0.4. The rate constant is unknown for the iron bound to oxygen. The HSAB theory applies to the iron and the porphyrin ring as Fe (II) and N (in the pyrrole ring) are both classified as having borderline acid character. Like prefers like, indicating that Fe (II) may be using this to select the right ligand to help it bind oxygen, which is hard base for the HSAB theory. The nitrogen in the pyrrole ring is likely a borderline base as it is in a ring structure like pyrimidine and imidazole which are borderline nitrogen containing ring structures as well.[8]

The iron in $heme_a$ transitions between two oxidation states, Fe (III) and Fe (II). The iron $heme_{a3}$ transitions from Fe (II, III, and IV).[10] The two irons in the heme a and a3 both have an electron count of 16-18, as the oxidation state changes. Both irons are bound by four nitrogens from a porphyrin ring, an imidazole nitrogen from His and an O_2 molecule. All of the nitrogen donor atoms are neutral. With six ligands bound to the Fe there would be a total of 12 ligand electrons (6e- x 2=12e-). Knowing that the iron may be missing 2-4 electrons, based on its oxidation state, there remains 4-6 d-electrons giving a total electron count of 16-18 (12 ligand e^- + 4-6 d e^- = 16-18 e^-) (Figure 11). Literature has shown that the iron in $heme_a$ is low spin as it is a 3d metal with a 3+ charge and because it has imidazole ligands that are pi acceptors which are strong field. While the other iron metal center in $heme_{a3}$ is high spin as it is a 3d metal with a 2+ charge.[10,11]

Lastly, the electrons transfer from heme$_{a3}$ to O_2. This transfer is made possible by the iron on the heme$_{a3}$, Cu_B, and a tyrosine. These set of molecules are also known as the bionuclear center (BNC).[3] Once the electron reaches the heme$_{a3}$, Fe(III) becomes Fe (II) and the oxygen binds to the Fe (II). The H^+ ion from the tyrosine ligand of Cu_B transfers to the oxygen bound to Cu_B (I) changing it to Cu_B (II). During this state the Fe (II) double bonds to the oxygen and becomes Fe (IV). The first H^+ and e^- enter the BNC and the H^+ binds to the oxygen on the Cu_B (II). During this step, while the electron places on the tyrosine oxygen the tyrosine oxygen moves to the Cu_B(II) oxygen. Next, the second H^+ and e- set enter with the new H^+ replacing an H^+ on the Cu_B(II) site and the e- placing on the Fe (IV) changing it to Fe (III). The replaced H^+ moves to the Fe (IV). The third set of H^+ and e^- move in with the third H^+ going on the tyrosine oxygen and the electron going on the Cu_B (II) causing it to become Cu_B (I). The final H^+ and e- enter the BNC and place on the Fe (III) causing it to become Fe(II). This stage is also where the two water molecules bound to Fe (III) and Cu_B(I) fall off. The cycle then restarts when oxygen binds to the Fe (II) (Figure 11).[12]

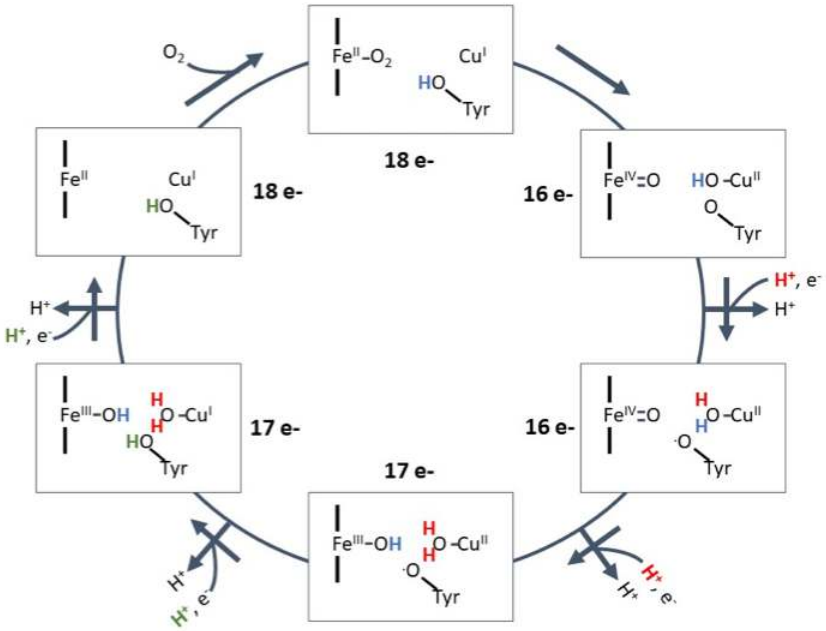


Figure 11. The catalytic cycle of the reaction of O_2 to H_2O in cytochrome oxidase. This figure shows the catalytic cycle that occurs when the oxygen in bound to the Fe (II). The electrons transferred in cytochrome oxidase are brought to the Fe (II) and used to react O_2 and H^+ ions to form water.

Cu_B is vital to the reaction of cytochrome oxidase and has tridentate ligands. All three ligands are imidazole side chains (His^{240}, His^{290}, and His^{291}). With the three imidazole ligands, Cu_B forms a trigonal planar shape and is stabilized by the chelating His^{290} and His^{291} ligands (Figure 8).[3] Similar to the Cu_A ions, Cu_B has an LFSE of 0 and has a trigonal planar geometry due to steric hindrance of the three His ligands. Copper can have an oxidation state of (I) or (II).[10] Cu_B would have an electron count of 14-16. This copper has three imidazole ligands with no charge therefore it has 6 ligand electrons. The HSAB theory also applies to the Cu (II) (Cu_B) center and the 3 imidazole ligands as both are considered borderline acids and bases, respectively, for HSAB and like attracts like, indicating that Cu (II) may be using this to select the right ligands. Cu (I) also occurs and may still be using HSAB to select the imidazole groups as it is close to borderline. Copper can have an oxidation state of +I, or +II, and therefore will have 9-10 d electrons bringing the electron count to 15-16. Cu_B takes on an oxygen and releases it after two H^+ ions are bound to it producing one molecule of water (Figure 11). The rate constant of the O-Cu_B bond is 3.5 x 108 $M^{-1}s^{-1}$ showing that the breaking of the bond is quick as and that it is a weak bond. As previously mentioned, the Cu_B has an LFSE of 0 indicating it is highly labile which correlates with the Cu_B's ability to react quickly with the oxygen.[3]

The reduction potential of the cytochrome oxidase reaction (Reaction 1) is +0.82 V. Beginning with the initial electron donor, cytochrome c, and ending with the final electron acceptor, O_2, we see that the reduction potential went from +0.27 V to +0.82 V. This increase in reduction potential from the electron donor to the electron acceptor makes the overall reactions of cytochrome oxidase spontaneous.[6]

Cytochrome oxidase is a colored protein. Cu_A has absorption bands at about 480 nm, 530 nm, and even one in the infrared spectrum at about 830 nm.[12] Literature has shown that although these absorbances reflect a blue/purple color in the lab, in an intact cytochrome oxidase the hemes hide the Cu_A absorbances with their own absorbances. Cu_A absorptions are charge transfer absorptions as ε>1000 cm-1 (ε=2000 cm^{-1}).[12]

$Heme_a$ has been found to have absorbances at 446 nm and 605 nm. $heme_{a3}$ has absorbances at 441 nm, 611 nm, and 656 nm.[12] The absorbances for both hemes mean the reflected light gives the hemes a reddish/purple color. The absorbances and colors of both hemes have been to found to be likely a result of charge transfers; however no ε value was found in the literature. Cu_B is not colored as it does not have any absorbances in the visual spectrum.[12]

Cytochrome oxidase is a key molecule in aerobic respiration and without a properly functioning enzyme can lead to cell death. The primary disorder associated with cytochrome oxidase is cytochrome oxidase deficiency which is a relatively rare, autosomal recessive disorder.[13] Leigh's Syndrome is a human disease caused by cytochrome oxidase deficiency and its symptoms include poor muscle tone and muscle movement, mental impairment, and lack of growth. These symptoms begin to manifest in infancy and the disorder usually results in death within two to three years of life. Although there is no cure for Leigh's Syndrome, treatment with Vitamin B1 has been shown to help prolong the patient's life. Therefore, cytochrome oxidase is very important to humans and all other aerobic organisms as it is the primary reason we breathe oxygen and is what helps our bodies produce energy to keep us alive.[14]

References

1. Alberts B, Johnson A, Lewis J, et al. 2002. *Molecular Biology of the Cell.*, 4th edition. New York: Garland Science.
2. Goodsell, D. 2000. Cytochrome c Oxidase. *Protein Database* (PDB). (accessed Jan. 23, 2018).
3. Michel, H., Behr, J., Harrenga, A. Kannt, A. 1998. Cytochrome c oxidase: structure and spectroscopy. *Annu. Rev. Biophys. Biomol. Struct.*, 27.
4. Florens L. et al. 1999. The Role of Magnesium and Its Associated Water Channel in Activity and Regulation of Cytochrome *c* Oxidase. *The Phototrophic Prokaryotes*. Springer, Boston, MA.
5. Ludwig, B., Bender, E., Arnold,S., Hüttemann, M., Lee, I., and Kadenbach, B. 1999. Cytochrome c Oxidase and the Regulation of Oxidative Phosphorylation. *Biochemistry*, 38 (46): 15129–15140.
6. Kaila, V. R. I., Verkhovsky, M. I., and Wikstrom, M. 2010. Proton-Coupled Electron Transfer in Cytochrome Oxidase. *Chem. Rev.*, 110: 7062–7081.
7. Youfen Li, Jeong-Soon Park, Jian-Hong Deng, and Yidong Bai. (2006). Cytochrome c oxidase subunit IV is essential for assembly and respiratory function of the enzyme complex. *J Bioenerg Biomembr*, 38 (5-6): 283–291.
8. Carter, K. Palmer, G. 1982. Models of the Two Heme Centers in Cytochrome Oxidase. *The Journal of Biological Chemistry*, 257(22): 13507-13514.
9. Crofts, A. 1994. Cytochrome oxidase: Complex IV. University of Illinois at Urbana-Champaign. Accessed 4 April 2018.
10. Tsukihara, Tomitake, et al. 1996. Structures of metal sites of oxidized bovine heart cytochrome c oxidase at 2.8 angstroms. *Science*, 269: 1136-1144.
11. Kepp, K. 2017. Heme: From quantum spin crossover to oxygen manager of life. *Coordination Chemistry Reviews*, 344: 363-374.
12. Hellwig, P., Soulimane, T., Buse, G., and Mantele, W. 1999. Electrochemical, FTIR, and UV/VIS Spectroscopic Properties of the ba3 Oxidase from *Thermus thermophilus*. *Biochemistry*, 38: 9648-9658.
13. Shoubridge, E. A. 2001. Cytochrome c oxidase deficiency. *American Journal of Medical Genetics*, 106 (1): 46-52.
14. U.S. National Library of Medicine: Genetics Home Reference. (2018, March 6). Leigh Syndrome. Retrieved from https://ghr.nlm.nih.gov/condition/leigh-syndrome.

Contributed by

*This work was originally written by **Allyson Slusser**, Spring 2018: Allyson is currently (as of 2018) a senior biology major at Saint Mary's College in Notre Dame, IN.*

This work was originally edited by Dr. Kathryn Haas (Assistant Professor) and Madison Sendzik (Teaching and Research Assistant) at Saint Mary's College.

11.1.8: Cytochrome Oxidase is shared under a not declared license and was authored, remixed, and/or curated by LibreTexts.

11.1.9: Potassium Channels

K+ Channels

Ion channels are large membrane-spanning proteins that allow selective transport of an ion. This can occur for ions like potassium, calcium, and sodium.[1] These channels are responsible for the electrical conduction in nervous systems to allow nerve and muscle cells to function properly. Neuron plasma membranes contain ion channels that have the ability to open and close based on these electric signals received from neuron activity. Electrical activity of neurons that send signals to the plasma membrane include conduction, transmission, and receiving of electric signals.[2] When there is an unequal distribution of charge across a membrane, ions will spontaneously diffuse across the membrane to equalize the charge (Figure 1).[1] Transport of ions across a membrane can be either active or passive depending on if energy is required. Ion channels are passive, or otherwise known as spontaneous, which allows the flow of ions to be transported across the a membrane based on when the signals are received.[1-2] The flow of the ions goes from the cytoplasm to the extracellular solution, and thus depolarizing the cell. Potassium channels are one of many different types of ion channels. Main cellular functions include cell volume regulation and electrical impulse formation.[3]

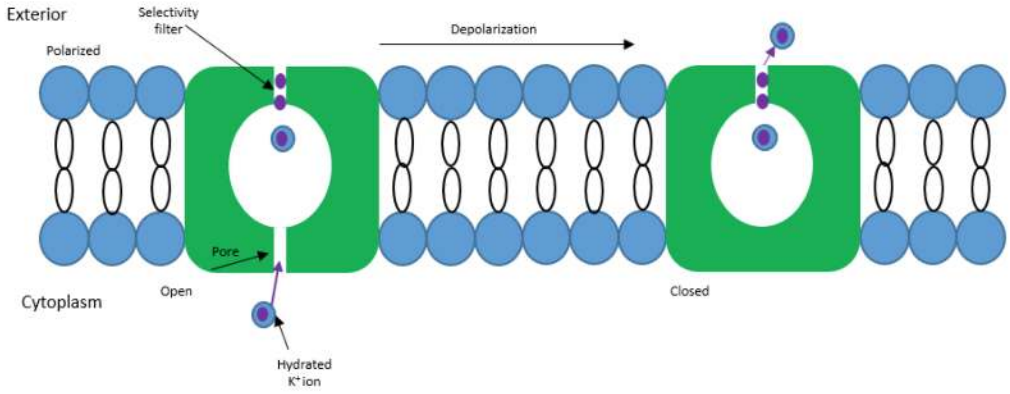


Figure 1. Schematic of how the membrane potential is diffused across the membrane. *This shows how the mechanism occurs. First, the potential difference across the membrane is sensed and signal is received causing the pore to open. Ions lose their water molecules before entering the selectivity filter. The pore then closes to allow for control of diffusion across the membrane once potassium ions are flowing the the filter.*[1]

There are many types of ion channels, but this paper will be focusing on potassium channels.The human genome contains over 90 genes that encode for potassium channels.[3] Dysfunction of potassium channels have been shown to link an individual to diseases such as the hyper-and hypokalemic periodic paralysis, myotonia, and epilepsy.[4] Potassium channels specifically allow potassium ions to penetrate the membrane when there is a response to a change in the membrane potential. This “specificity” means that no other ions can pass through this channel including sodium, which is very similar to potassium in regards to charge and size.[3] This selection is completed at rates that approach the diffusion limit. There are four main types of potassium channels which are as followed: calcium activated, inwardly rectifying, tandem pore domain, and voltage-gated. The differences between these types are mainly with how the gate receives its signal, whereas the structure of these channels is similar. A general structure for potassium channels can be seen below in Figure 2.[3]

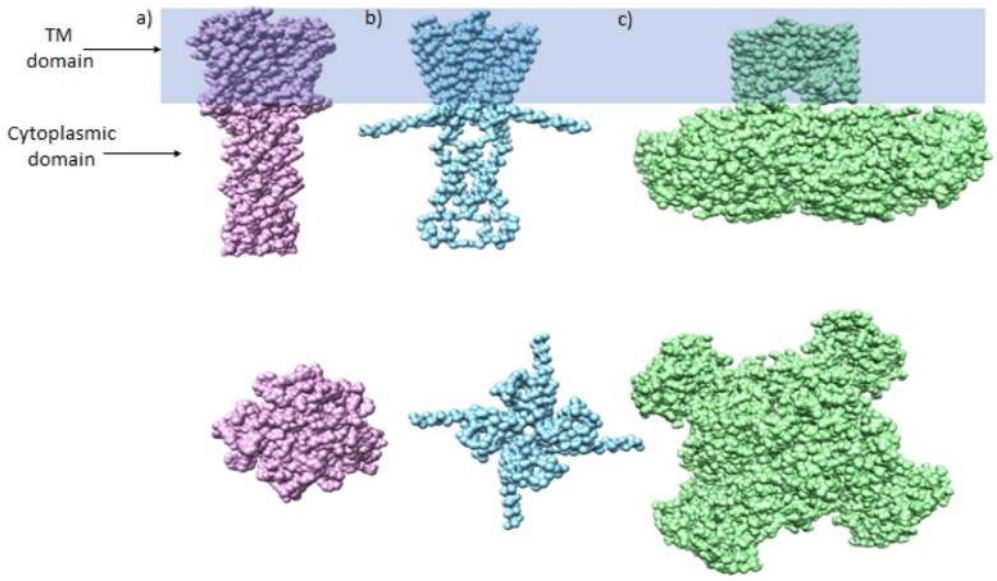


Figure 2. General structure of potassium channels showing the two conformations of the closed state (a and b) of KcsA vs. the open state of MthK. *Also, the transmembrane (TM) domain and the cytoplasmic domain of highlighted here. The gray rectangle represents the molecule would be located in the membrane. All three molecules are from bacteria, but have different gating dependence. KcsA is pH dependent, whereas MthK is voltage dependent. PDB 3EFF,* 1K4C, and 1LNQ.[3]

Potassium

Potassium is an alkali metal with a valence electron configuration of *n*s1 and contributes only one element to the molecular orbital band. There are some common trends that can be found from the periodic table, and there are specific ones that are for alkali metals. Alkali metals contain low first ionization energies and will want to form M^+ metals increasingly down the group. Potassium's thermodynamic tendency to become K^+ is due to the large and negative standard potentials that occur. Oxidation becomes more favorable going down the group because the enthalpies of sublimation and ionization decrease. Group 1 element ions are hard Lewis acids and mainly form complexes with hard donors like O and N.[1]

KcsA Channel: Structure

This paper will be focusing on KcsA, a potassium channel from *Streptomyces lividans*, which contains two domains. The first being the transmembrane portion, which contains 120 residues. This will be discussed in detail below. The second domain is a cytoplasmic domain that contains about 40 residues. The cytoplasmic domain contributes to the stability of the closed state. This is concluded based on data that shows a decrease in efficiency of channel folding and assembly and thermal stability being affect when the cytoplasmic domain is removed from the crystal structure.[5] As seen in Figure 2, the water filled C-terminal cytoplasmic domain is 4-helix bundle structure that extends linearly towards the cytoplasm.[5-6] It has been shown by electron paramagnetic resonance, EPR, data produced by Uysal, that the C-terminal has a stretch that bulges out where the C-terminal domain meets the transmembrane domain.[5] This stretch of helix that connects the two has a higher degree of flexibility than the other parts that potentially plays a role during the opening of the channel.[5] There is still much research that needs to be conducted to fully understand the functionality of the C-terminal domain. A suggested function of the domain is that it may serve as a receptor for an unidentified plasmic activator protein or ligand, but others argue that there is no significant effect on the permeation path for the ion. The structure does not yet contain orientation of any side chains, but the arrangement of the helices suggest electrostatic interactions in the subunit.[6] Figure 3, demonstrates how the cytoplasmic domain compares between an open channel vs. a closed channel with two bacteria channels.[7] The rest of the paper will be focusing on the transmembrane domain that selects for potassium.

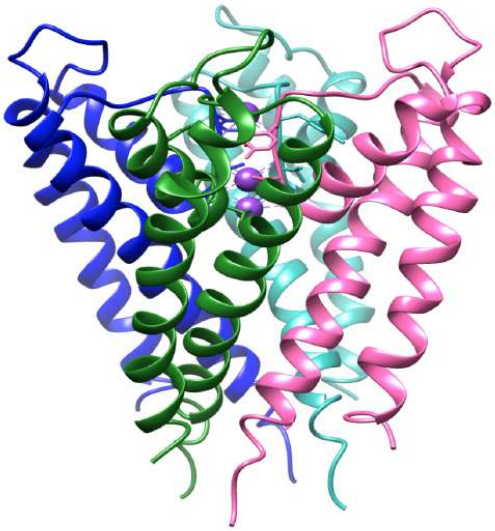


Figure 3. The transmembrane domain. *Each subunit is colored differently and the potassium ions are purple. PDB 1BL8.*

The selectivity for potassium ions relies heavily on the structure of the potassium channel selectivity filter. The coordination environment of the channel has selective ligands that bind specifically to potassium ions.[8] The potassium channel protein is a tetramer, that contains four identical subunits that form a central pore.[8-9] The ions flow into a pore that opens and closes, directing the ions to the central cavity. The subunits contain two alpha helices where one faces the central pore, inner helix, and one faces the lipid membrane, otherwise known as the outer helix.[3] Along with the inner and outer helices, each subunit includes a pore helix.[3,8] The subunits are tilted, as seen in Figure 3, where the selectivity filter is near the extracellular surface of the membrane. The four inner helices are structured in a way where they come together near the intracellular surface. Both the intra- and extracellular entryways are negatively charged by acidic amino acids. This allows for a higher concentration of cations near the membrane and less anions because of the opposing charges.[8]

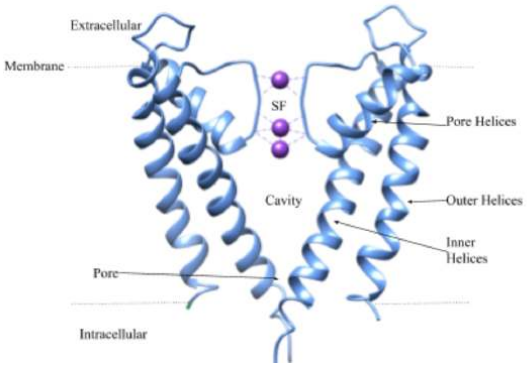


Figure 4. Potassium channel (KcsA structure from *Streptomyces lividans*) with key structural components labeled. *The main aspects to note are the pore, cavity, and selectivity filter (SF). These are the parts of the channel where potassium ions travel through. First, the ion flows through the pore and enters the cavity hydrated when the pore is open. Then a potassium ion is dehydrated and selected to travel through the SF where it will then enter the cell. Note that only two subunits are shown in this image for easier visualization. PBD 1K4C.*

The pore region was first identified with pore-blocking scorpion toxins. They interact with amino acids at the entrance of the pore causing blocking and dysfunction. The pore is where the potassium ion enters, where then it is transferred to the central cavity, as seen in Figure 4. During this time the potassium ion stays hydrated.[8] The intracellular pore is the feature of the channel that allows potassium ions to enter the cell when it is open, or be blocked from entering when closed. The channels opens when there is a change in membrane potential, allowing a influx of potassium ions into the cavity filter. Once selective binding occurs in the

selectivity filter, the potential drops across the membrane, thus closing the pore.[1] The pore and the cavity are hydrophobically lined, allowing the ability to lower electrostatic barrier. There needs to be a lower electrostatic barrier so the energetic cost of dehydration is compensated due to the large energy barrier for ion permeation (dielectric barrier). Thus, the water filled cavity allows for an energetically favourable environment.[3,8,10,11]

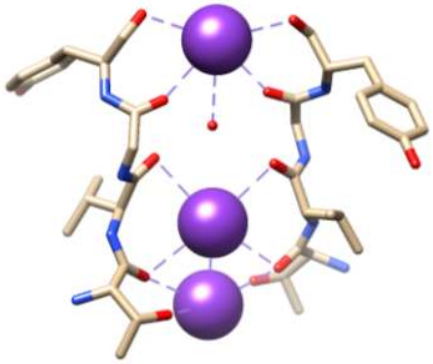


Figure 5. Binding of potassium ions (purple) to specific ligands by the backbone O's of Thr 75, Val 76, Gly 77, and Tyr 78. The full coordination is not shown here for easier visualization. *Reproduced from Samsom.*[11]

Next, the ions need to be selected into the selectivity filter (SF), which is lined with polar main chain atoms that belong to amino acids. The SF is so narrow that the ions must first be dehydrated before entering it. There are two essential features in the SF. First, the main chain atoms create suitable dimensions for coordinating a dehydrated potassium ion by stacking, thus making sequential oxygen rings. This creates a very small distance that the potassium ion must travel to reach each site while traveling through the filter. This forms a sequence of four cubic eightfold coordination sites, as seen in Figure 6.[3,8] At any time, these sites are occupied by two K^+ ions and two water molecules in an alternating sequence The second feature is the protein packing around the SF, which follows a sequence of T-V-G-Y-G, shown in Figure 5.[9] Conduction can then occur when two potassium ions enter the SF, causing a balance between attractive force that occurs from the SF to the ion with the repulsive force that occurs between the two potassium ions.[8] This repulsion helps potassium ions overcome its intrinsic affinity for binding tightly to the binding sites.[3] Further discussion of the selection mechanism will be discussed below.

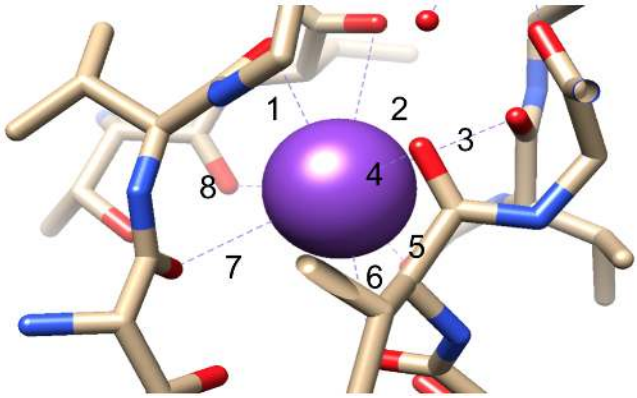


Figure 6. One example of a potassium ion (purple) in an eightfold coordination site. *Binding numbered for easier visualization.*

K+ Selectivity

The SF consists of four sites (S1-S4) that are formed by oxygen molecules, as seen in Figure 7.[11] The selectivity of potassium channels is of functional importance due to the fact that if sodium ions were to be selected, membrane repolarization would not

occur. Even though sodium ions are smaller than potassium, ~.95 Å and ~1.33 Å respectively, they are not able to penetrate the membrane.[12-13] This selection of potassium ions occurs by a factor of more than 1000 compared to sodium ions. Much research has been conducted to elucidate the mechanistic nature of how exactly potassium channels select for potassium ions, in which conclusions can vary by the type of potassium channel. This description will be based on KcsA..[9, 12, 13]

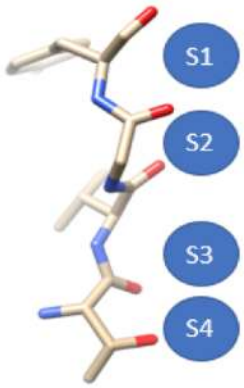


Figure 7. Showing one subunit demonstrating where the binding sites are in the selectivity filter. *Each site (S1, S2, S3, and S4) represents where an ion would be placed in the filter. PDB 1BL8.*

Selectivity of potassium ions has been attributed to the sequence motif TVGYG in positions 75-78 of each monomer. As stated above, potassium channels bind to ligands through an eight coordinate, octahedral coordination environment.[11] These are optimally placed to allow for the interaction with potassium ions, making the transfer of energy from the central cavity to the SF extremely low because the environment is not drastically changing.[8,11] When a potassium ion binds to the SF, eight water molecules are released from a hydrated potassium ion. The ion is then bound to eight carbonyl oxygens at each of the four sites in the SF. At the last site, the ion binds to four of the carbonyl oxygens as well as four water molecules, keeping the eightfold coordination number. Once the ion has completely diffused through the channel, the ion becomes rehydrated once again in the extracellular matrix.[3,8] This mechanism can be viewed in Figure 8.

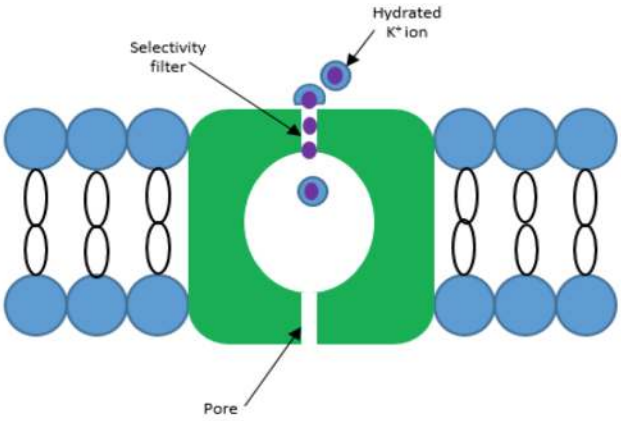


Figure 8. Mechanism of the diffusion of potassium ions through the channel, emphasizing when the potassium channel is hydrated. *The ion first goes through the pore where it resides in the central cavity. At this point the ion is still hydrated. When the ion is selected, it then moves to through the selectivity filter, where it becomes dehydrated. Following, the ion enters the extracellular matrix hydrated where it is hydrated once more.*

This simple reaction is favorable because of low energy cost to lose the water molecules and bind the to the selectivity filter. Potassium ions are normally surrounded by eight water molecules, which are stripped before entering the filter. The filter is designed to have similar dimensions that mimic the shell of water that encloses potassium by lining the pore with eight oxygen

atoms, as stated above. These are optimally placed to allow for the interaction with potassium ions. This makes the transfer of energy from the central cavity to the selectivity filter extremely low because the environment is not drastically changing.This static environment completely compensates for the energetic cost of K^+ ion dehydration when it enters the cavity.[9] The selection of the right metal allows for the ability for potassium channels to function correctly.

Atomic Radii: Na^+ vs. K^+

Sodium is a metal that is very similar in charge and size, as stated above, but sodium ions are not selected. This is due to the size of the ions.[3,8,11] Sodium ions are smaller in ionic radius. As seen in Figure 9, sodium ions have a smaller ion radius resulting in the inability to coordinate with the all eight oxygens at the first site. This demonstrates why sodium ions are not selected to go through the channel, even though the ions are smaller than potassium ions. This results in sodium ions favoring the shell of water.[9,12,13]



Figure 9. Comparison of potassium and sodium ion binding to a site in the selectivity filter. *The sodium ion has too small of an ionic radius to be fully coordinated to all the carboxylic groups in the filter. It should be noted that the figure for easier visualization only shows only four of the eight potential carbonyl oxygens available at each site. The red represents the amino acid.*

Additional Bio-inorganic Properties to Explain K+ Binding/Release

HSAB Theory

The potassium ion binds to carbonyl oxygens which are hard bases.[14] Hard Soft Acid Base theory characterizes metals as either “hard” or “soft”. This is dependent on the charge density, polarizability, and the type of bonding interactions. For example, hard metals tend to have higher charge density and/or form more electrostatic interactions, while soft metals tend to have lower charge density and/or more covalent bonding. Since potassium is characterized as a hard metal due to its electrostatic interactions, it would most likely bind to ligands that are hard. This theory helps explain why potassium binds to Thr 75, Val 76, Gly 77, and Tyr 78, which are mainly hard ligands.[11,14]

Lability

Lability refers to the ability for a metal-ligand bond to break. When a compound has bonds that are easily broken between the metal-ligand, then that metal is referred to as labile. A common trend that occurs is that alkali metals tend to be more labile compared to other metals that have higher charges. When metals have higher charges, they tend to be stronger Lewis acids. This would allow the metal to bind the ligands more tightly, resulting in harder bonds to break. Another trend that has been observed is that metals that have no d electrons tend to be more labile because of there are no electrons in the way for a new ligand to donate its electrons. Potassium channels are extremely labile because it has a $^+1$ charge, as well as a 0 ligand field stabilization energy (contains zero d electrons). Potassium being labile is extremely important since its diffusion rate is so high that the ion needs to be able to go from one site to the next. If the metal was not labile, the channel would not be able to flow potassium ions as quickly as it can because the metal-ligand complexes would not be as easily breakable.

Conclusions

Potassium channels are necessary for cellular function, especially assisting in neuronal signaling. There are many features that make up the channel, but the key feature is the selectivity filter. The SF is what keeps the channel functioning by specifically

selecting potassium ions. Overall, this selectivity for potassium over other ions can be attributed to the size of the ion and HSAB theory. The SF is the the correct fit to allow an eightfold coordination environment with potassium ions. The specific ligands assist with the binding of the potassium channels because the HSAB theory suggest that like binds to like and both the ligands and metals are characterized as hard. To conclude, there are many features of potassium channels, and this paper only began to touch on the functionality of the channels.

Sources

1. Shriver, D F, P W. Atkins, and Cooper H. Langford. Inorganic Chemistry. Oxford: Oxford University Press, 1994. Print.
2. Lodish, Harvey, et al. The Action Potential and Conduction of Electric Impulses. 2000. www.ncbi.nlm.nih.gov, https://www.ncbi.nlm.nih.gov/books/NBK21668/.
3. MacKinnon, R. Potassium Channels. FEBS Letters 2003, 555 (1), 62–65.
4. Dworakowska, B.; Dołowy, K. Ion Channels-Related Diseases. Acta Biochim. Pol. 2000, 47 (3), 685–703.
5. Uysal, S.; Vásquez, V.; Tereshko, V.; Esaki, K.; Fellouse, F. A.; Sidhu, S. S.; Koide, S.; Perozo, E.; Kossiakoff, A. Crystal Structure of Full-Length KcsA in Its Closed Conformation. *Proc Natl Acad Sci U S A* **2009**, *106* (16), 6644–6649.
6. Cortes, D. M.; Cuello, L. G.; Perozo, E. Molecular Architecture of Full-Length KcsA. *J Gen Physiol* **2001**, *117* (2), 165–180.
7. Goodsell, D. S. Potassium Channels. *RCSB Protein Data Bank* **2003**.
8. Doyle, D. A.; Morais Cabral, J.; Pfuetzner, R. A.; Kuo, A.; Gulbis, J. M.; Cohen, S. L.; Chait, B. T.; MacKinnon, R. The Structure of the Potassium Channel: Molecular Basis of K+ Conduction and Selectivity. *Science* **1998**, *280* (5360), 69–77.
9. Kuang, Q.; Purhonen, P.; Hebert, H. Structure of Potassium Channels. Cell Mol Life Sci 2015, 72, 3677–3693.
10. Roux, B. The Cavity and Pore Helices in the KcsA K+ Channel: Electrostatic Stabilization of Monovalent Cations. Science 1999, 285 (5424), 100–102.
11. Sansom, M. S. P.; Shrivastava, I. H.; Bright, J. N.; Tate, J.; Capener, C. E.; Biggin, P. C. Potassium Channels: Structures, Models, Simulations. Biochimica et Biophysica Acta (BBA) - Biomembranes 2002, 1565 (2), 294–307.
12. Nimigean, C. M.; Allen, T. W. Origins of Ion Selectivity in Potassium Channels from the Perspective of Channel Block. The Journal of General Physiology 2011, 137 (5), 405–413.
13. Thompson, A. N.; Kim, I.; Panosian, T. D.; Iverson, T. M.; Allen, T. W.; Nimigean, C. M. Mechanism of Potassium Channel Selectivity Revealed by Na+ and Li+ Binding Sites within the KcsA Pore. Nat Struct Mol Biol 2009, 16 (12), 1317–1324.
14. Noskov, S. Y.; Berneche, S.; Roux, B. Control of Ion Selectivity in Potassium Channels by Electrostatic and Dynamic Properties of Carbonyl Ligands. Nature 2004, 431 (7010), 830.

Contributed By:

*This work was originally written by **Courtney Weston**, Spring 2018; Courtney recently (as of May 2018) received her B.S. in Chemistry from Saint Mary's College (Notre Dame, IN) and will finish her second degree in Environmental Engineering next Spring.*

This work was originally edited by Dr. Kathryn Haas (Assistant Professor), Madison Sendzik (Teaching and Research Assistant).

11.1.9: Potassium Channels is shared under a not declared license and was authored, remixed, and/or curated by LibreTexts.

11.1.10: Chemotherapy- Pt anticancer agents

Platinum complex drugs commonly used in chemotherapy as anticancer agents. Pt chemotherapeutics make up roughly 50% of all chemotherapeutic drug regimens. Platinum drugs are used in both Pt (II) and Pt(IV) oxidation states. Pt antitumor complexes have at least three components in common:

1. They are electrostatically neutral Pt coordination complexes.
2. They are either square planar Pt(II) compounds or octahedral Pt(IV) compounds with two donor groups that are either primary or secondary amines. These amine ligands are either two *cis* monodentate ligands or one bidentate chelating ligand.
3. They all have two donors groups that act as leaving groups. These donors are either Cl or O, and can be either two monodentate or one bidentate ligand.

Specific examples of both Pt(II) and Pt(IV) drugs will be discussed. Platinum itself is a soft metal, which based on the Hard Soft Acid Base (HSAB) Theory, has a higher affinity to softer ligands which is important in biological systems. It has been hypothesized that Pt drugs use copper transport systems including members of the Ctr family to enter and exit cells.[2] The exact mechanism of this process is still highly debated. Studies have shown that Pt drugs have an affinity towards methionine-rich Ctr1 motifs, which may suggest that Pt(II) has a similar affinity for the sulfur of methionine to that of Cu(I),[2] which is typically transported within the cell by the Ctr family. Pt ions within the drug complex are capable of binding to sulfur on amino acids because Pt is a soft acid and sulfur is a soft base. Pt(IV) complexes do not have the same level of affinity to bind to cysteine and methionine in biological systems as Pt (II) complexes.

Pt(II) Complexes

Common Pt (II) complexes are depicted in the figure below. Cisplatin and oxaliplatin are the most common and effective complexes in chemotherapy. These complexes are all in square planar d^8 configuration. These complexes only have four ligands, which limit the geometries to either square planar or tetrahedral, their splitting diagram is depicted below. Complexes in the square planar position tend to have more Ligand Field Stabilization Energy (LFSE) than those in tetrahedral due to their Δ values which separate their antibonding orbitals from the nonbonding. The Δ value is much higher for d8 complexes in the square planar geometry than those in tetrahedral, which affects the the complex's LFSE. Figures 2 and 3 below depict splitting diagrams for d8 Pt(II), in possible square planar and tetrahedral geometries, respectively. If this system is in a tetrahedral geometry, spin would be an irrelevant factor because Pt(II) is a d8 metal and its electrons must be in the anti-bonding orbitals because the first four electrons occupy the nonbonding orbitals. However, spin is a relevant factor for this system in the case of square planar geometry. In this configuration, the no electrons reside in the x2-y2 anti-bonding orbital because of high LFSE and large Δ value. This stabilizes the complex, which explains the affinity of Pt(II) complexes for square planar geometry. On cisplatin, the two Pt-NH3 bonds are kinetically inert and thermodynamically stable, while the Pt-Cl bonds are semi-labile and can act as leaving groups for nucleophiles. Lability refers to the rate at which the ligands can be replaced with other molecules. Because the Pt-Cl are considered labile, they have a greater ability to act as leaving groups and react with other molecules than non-labile bonds. In cisplatin, the NH3-Pt bonds are not as labile as the Pt-Cl bonds and therefore will not leave the metal complex at the same rate as the Pt-Cl bond would to react with other molecules. This is counterintuitive based on electrostatic theory. The Cl- ligands have a negative charge, which influences the overall charge of the complex. However the -NH3 ligands are neutrally charged and are more inert than the neighboring -Cl- ligands. Typically, this would cause the NH3 ligands to be more labile. But, ligand field theory (LFT) explains that Cl- is both a sigma and pi donor ligand, while NH3 is only a sigma donor ligand. Because Cl- is a sigma and pi donor, its electrons also fill antibonding orbitals when binding to Pt. Since NH3 is only a sigma donor, its electrons do not fill the antibonding orbitals when binding to Pt. Due to the presence of electrons in the antibonding orbitals, the Pt-Cl bonds are not as strong as the Pt-NH3 the Cl- ligands are more labile than NH3. During cisplatin's mechanism of action, the chloride ligands are substituted by water molecules, acting as nucleophiles through a process called aquation, which is important in the drug's efficacy3,4,5.

Cisplatin

Cisplatin $[Pt(II)Cl_2(NH_3)_2]^{2-}$ is one of the most widely used anticancer drugs used especially for testicular and ovarian cancers treatments. This was first discovered in 1965 by biophysicist, Barnett Rosenberg while attempting to investigate effects of electric

fields on cell division with Pt electrodes in a cell growth medium. Instead of the cells dividing properly, they formed filaments while undergoing electrolysis and undergoing subsequent reactions of Pt ions[1].

$$\text{Pt (electrode)} \xrightarrow{\text{electrolysis}} [\text{Pt(IV) Cl}_6]^{2-} \longrightarrow \text{NH}_4{}^{+} \xrightarrow{h\nu} [\text{Pt(IV) Cl}_4\ (\text{NH}_3)_2] \qquad (11.1.10.1)$$

The initial product of electrolysis is bacteriostatic and therefore does not promote filamentous growth. Pt in oxidation state (IV) is kinetically inert, low-spin 5d6 and very slow while undergoing reactions. Because of this, Pt(II) was thought to be more effective. Cisplatin, the cis isomer of [Pt(II)Cl2(NH3)2]2- was not bacteriostatic and promoted filamentous growth among the cells, which then in turn, prevented further growth of cancer cells.

Cisplatin in unstable in water, so it is immersed in saline solution to prevent aquation within the body. Saline is a combination of NaCl and water which controls the water levels within the body. If aquation would occur, the water ligands would make the Pt(II) complex very acidic, with pKa values ranging from 5-8. Hydroxyl (-OH) ligands bind and are less reactive because they are more of a strong field ligand than a weak field, like Cl- , the previous ligands. This makes the complex more stable.

The cis conformation of cisplatin affects the distance of the chloro ligands and its drug efficacy as compared to transplatin. The two chloro ligands, the reactive sites, are further apart in transplatin (4.64 A) than cisplatin (3.29 A). This affects how Pt(II) cross-links at DNA sites, which affects its efficacy. Because the Pt ion binds to DNA to stop DNA production, if the Pt ion in transplatin cannot cross-link into DNA because of its ligands, it will not stop DNA production of the cancer cells, or at least not as well as cisplatin. Transplatin reacts very slowly because of the new trans oxygen ligand at its second aquation1.

To promote anticancer activity, the goal is that the Pt ion from the original cisplatin molecule binds to DNA, preventing replication of the cancer cells. After undergoing aquation, the hydroxyl groups leave the Pt ion allowing it to bind to N7 of guanine (G), DNA's major Pt- binding site. The N7 of guanine is one of DNA's major binding site because complexes can easily access this area via the major groove in DNA's B-form6, the most common DNA form. While this is the prefered binding site, cisplatin and other Pt(II) drugs can also bind to N7 of adenine and N3 of cytosine. During cisplatin treatment, cancer cell DNA undergoes 1,2 intrastrand cross-linking of two guanines and sometimes guanine and adenine. The second chloro group undergoes aquation and binds to the second guanine on the DNA strand creating a chelating effect. This cross-linking induced by Cisplatin causes DNA to bend or kink which then causes neighboring proteins to bind to the kinked DNA because they now recognize them as high mobility groups. When this occurs, these newly bound proteins often block these kinks from repair, which halts replication and causes cell apoptosis7. Unfortunately, cisplatin also affects healthy cells as well as cancer cells. Fortunately, healthy cells recognize the damage caused by the kink, where cancer cells do not. This allows enzymes to repair the DNA damage in healthy cells, so they do not undergo apoptosis7. in Figure 4 below shows a Chimera image of a DNA strand within DNA polymerase (ribbons) with the Pt ion, shown in purple, binding to guanine in the DNA strand. The blue atoms bound to the Pt represent the NH3 ligands. Figure 6 shows the same Chimera image, but focused on the binding site between Pt and guanine. The atoms are labeled.

Pt (IV) Complexes

Pt (IV) complexes, commonly referred to as Pt(IV) pro-drugs, are also used as chemotherapeutic agents. These complexes have some benefits over Pt(II) drugs including, they are stable enough to administered orally versus IV, their stability may diminish the side effects caused by Pt(II) drugs, and they may have higher affinity to structural modification via their axial ligands which can enhance their pharmacological properties. Some common Pt(IV) complex drugs are depicted to the right. Pt(IV) complexes differ from Pt(II) complexes in that they have a d6 octahedral geometry with monodentate ligand, except tetraplatin which has one bidentate ligand in addition to the other monodentate ligands. Pt resides in the 5d row of the transition metals. Typically, metals belonging in the 4d and 5d rows of the transition metals have a larger Δ value than those of the 3d metals. This is due to the increase in subshell and size of atoms going down the periodic table. As subshell increases, so does Δ. Another trend to mention is as positive charge on the metal increases, as does Δ. Since the charge on Pt in this system is +4 and it is in the 5d row of the transition metals, I speculate that this system will have a low spin based on the metal ion alone. The splitting diagram of Pt(IV) is depicted below. This image shows the effects of LFSE on the metal. Pt (IV) is low spin with a large Δ value and all electrons residing in the lower energy t2g orbital. This indicates high LFSE which also explains increased bond strength and overall stability of the complex. An increase in LFSE also increases inertness of the system, which decreases lability. The ligands of Pt(IV) will not be as labile as some of Pt(II) due to the difference in LFSE. Pt(II) do not have as much LFSE, therefore, their ligands are more labile and reactive.

Pt(IV) complexes in an octahedral geometry are said to be **substitution-inert**, which makes their interactions and reactions with biological nucleophiles such as cysteine and methionine, very slow. Pt(IV) complexes are considered pro-drugs because they are activated intracellularly in vivo by reduction that makes them act as their square-planar counterparts with the eliminations of their axial ligands.Figure 8 below shows the reduction process. The Pt(IV) complex begins as a Pt(II) complex during synthesis with four ligands in a square planar geometry. The Pt(IV) octahedral configuration is established with the addition of two axial ligands either during a chlorination reaction or an addition reaction with hydrogen peroxide and possible further reactions. When administered orally, Pt(IV) is reduced back to Pt(II) square-planar configuration intracellularly8. Because these complexes can only act as Pt(II) complexes within the cell, where they bind to DNA, they travel throughout the rest of the body as inert Pt(IV) complexes, they may reduce toxicity8.

References

1. Bertini, Ivano; Gray, Harry B.; Stiefel, Edward I.; Valentine, Joan Selverstone. Biological Inorganic Chemistry: Structure and Reactivity, Fifth Edition, W.H. Freeman and Co., New York, 2010.
2. Aresano, Fabio; Losacco, Maurizio; Natile, Giovanni. An Updated View of Cisplatin Transport. 2013. European Journal of Inorganic Chemistry.
3. Johnstone, Timothy C.; Park, Ga Young; Lippard, Stephen J. Understanding Platinum Anticancer Drugs- Phenanthriplatin. Anticancer Res. 34(1): 471-476 Jan 2014.
4. Johnstone, Timothy C.; Lippard, Stephen J. The Chiral Potential of Phenanthriplatin and its Influence On Guanine Binding. Journal of American Chemistry Society. 2014. 136 (5): 2126-2134.
5. Lovejoy, Katherine S.; Serova, Maria; Bieche, Ivan; Emami, Shahin; D'Incalci, Maurizio; Broggini, Massimo; Erba, Eugenio; Gespach, Christain; Cvitkovic, Esteban; Faivre,Sandrine; Raymond, Eric; Lippard, Stephen J. Anticancer Activity of Pyriplatin, a Monofunctional Cationic Platinum (II) Compound, In Human Cancer Cells. Mol Cancer Ther. 2011. 10 (9): 1709-1719.
6. Monaco, PR. A novel major groove binding site in B-form DNA for ethidium cation. J Biomol Struct Dyn. 2007. 25(5):119-25.
7. Reedijk, Jan. Increased understanding of platinum anticancer chemistry. Pure Appl. Chem. 2011. 83 (9): 1709-1719.
8. Wexselblatt, Ezequiel; Gibson, Dan. What do we know about the reduction of Pt(IV) pro-drugs?. Journal of Biochemistry 29 February 2012.

11.1.10: Chemotherapy- Pt anticancer agents is shared under a not declared license and was authored, remixed, and/or curated by LibreTexts.

TABLE OF CONTENTS

This text covers material that could be included in a one-quarter or one-semester course in bioinorganic chemistry for graduate students and advanced undergraduate students in chemistry or biochemistry. The authors believe that such a course should provide students with the background required to follow the research literature in the field. The topics were chosen to represent those areas of bioinorganic chemistry that are mature enough for textbook presentation. Although each chapter presents material at a more advanced level than that of bioinorganic textbooks published previously, the chapters are not specialized review articles.

Licensing

Preface

11.2.1: Transition-Metal Storage, Transport, and Biomineralization

- 11.2.1.1: Biological Significance of Iron, Zinc, Copper, Molybdenum, Cobalt, Chromium, Vanadium, and Nickel
- 11.2.1.2: Biological Systems of Metal Storage
- 11.2.1.3: Chemical Properties Relative to Storage and Transport
- 11.2.1.4: Iron Biomineralization
- 11.2.1.5: Transport of Iron
- 11.2.1.6: Transport of Zinc, Copper, Vanadium, Chromium, Molybdenum, and Cobalt

11.2.2: The Reaction Pathways of Zinc Enzymes and Related Biological Catalysts

- 11.2.2.1: About Carbonic Anhydrase
- 11.2.2.2: Acid-base Equilibria
- 11.2.2.3: Catalytic Mechanism
- 11.2.2.4: Coordinated Water and NMR
- 11.2.2.5: Coordination Geometries
- 11.2.2.6: Ester Hydrolysis and Phosphoryl Transfer
- 11.2.2.7: Group Transfer and Vitamin B-12
- 11.2.2.8: Metal Substitution
- 11.2.2.9: Model Chemistry
- 11.2.2.10: Nucleophilic Addition of \(OH^{-}\) and \(H^{-}\)
- 11.2.2.11: Peptide Hydrolysis
- 11.2.2.12: pH Dependence of Inhibitor Binding
- 11.2.2.13: Selecting Zinc
- 11.2.2.14: Steady-State and Equilibrium Kinetics of Carbonic Anhydrase-Catalyzed \(CO_{2}/HCO_{3}^{-}\) Interconversion
- 11.2.2.15: Strategies for the Investigation of Zinc Enzymes
- 11.2.2.16: The Natural Catalysts
- 11.2.2.17: What Do We Learn?

11.2.3: Calcium in Biological Systems

- 11.2.3.1: Ca^{2+}-binding Proteins in Microorganisms- The Search for a Prokaryotic Calmodulin
- 11.2.3.2: Basic Facts About Calcium- Its Compounds and Reactions
- 11.2.3.3: Calcium in Mineralized Tissues
- 11.2.3.4: Calmodulin
- 11.2.3.5: Extracellular Calcium Ion-binding Proteins

11.2.3.6: Inositol Trisphosphate and the Calcium Ion Messenger System
11.2.3.7: Intracellular Calcium Ion Transport
11.2.3.8: Measurements of "Free" Calcium Concentrations
11.2.3.9: Measurements of Total Calcium Concentrations
11.2.3.10: Mitochondrial Calcium Ion Transport
11.2.3.11: Molecular Aspects of Calcium Ion-Regulated Intracellular Processes (Part 1)
11.2.3.12: Molecular Aspects of Calcium Ion-regulated Intracellular Processes (Part 2)
11.2.3.13: Paravalbumin and Calbindins \(D_{9K}\) and \(D_{28K}\)
11.2.3.14: The Transport and Regulation of Ca^{2+} Ions in Higher Organisms
11.2.3.15: Troponin C

11.2.4: Biological and Synthetic Dioxygen Carriers

11.2.4.1: Biological Dioxygen Transport Systems
11.2.4.2: Biological Oxygen Carriers
11.2.4.3: Detailed Structures of Hemoglobins and Model Systems
11.2.4.4: Dioxygen Carriers and Bioinorganic Chemistry
11.2.4.5: General Aspects of the Chemistry of Cobalt
11.2.4.6: General Aspects of the Chemistry of Copper
11.2.4.7: General Aspects of the Chemistry of Dioxygen
11.2.4.8: General Aspects of the Chemistry of Iron
11.2.4.9: General Structural Features that Modulate Ligand Activity
11.2.4.10: Hazards of Life with Dioxygen
11.2.4.11: Nature of the Metal-Dioxygen Linkage in Biological Systems
11.2.4.12: Other Ligands for Biological Oxygen Carriers
11.2.4.13: Requirements for a Model System for Hemoglobin
11.2.4.14: Requirements for Effective Oxygen Carriers
11.2.4.15: Role of the Protein in Effecting Biological Oxygen Transport
11.2.4.16: Selected Chemistry of Dioxygen, Iron, Copper, and Cobalt
11.2.4.17: Stereochemical Changes Upon Ligation
11.2.4.18: Structural Basis of Ligand Affinities of Oxygen Carriers
11.2.4.19: Structures Relevant to Liganded Hemoglobins
11.2.4.20: Thermodynamic Factors
11.2.4.21: Ch. 4 References and Abbreviations

11.2.5: Dioxygen Reactions

11.2.5.1: Catalase and Peroxidase
11.2.5.2: Chemistry of Dioxygen
11.2.5.3: Copper-zinc Superoxide Dismutase
11.2.5.4: Cytochrome c Oxidase
11.2.5.5: Dioxygen Toxicity
11.2.5.6: Monooxygenases
11.2.5.7: Oxygenases

11.2.6: Electron Transfer

11.2.6.1: Biological Redox Components
11.2.6.2: Coupling Electron Transfers and Substrate Activation
11.2.6.3: Electron-transfer Rates
11.2.6.4: Electron-Transfer Theory
11.2.6.5: Energy Storage and Release
11.2.6.6: Long-range Electron Transfer in Proteins (Part 1)
11.2.6.7: Long-range Electron Transfer in Proteins (Part 2)
11.2.6.8: Marcus Theory

11.2.7: Ferrodoxins, Hydrogenases, and Nitrogenases - Metal-Sulfide Proteins

11.2.7.1: Iron-sulfur Proteins and Models
11.2.7.2: Iron-sulfur Proteins and Models (Part 2)
11.2.7.3: Iron-sulfur Proteins and Models (Part 3)
11.2.7.4: Iron-sulfur Proteins and Models (Part 4)
11.2.7.5: Multisite Redox Enzymes
11.2.7.6: Multisite Redox Enzymes (Part 2)
11.2.7.7: Multisite Redox Enzymes (Part 3)
11.2.7.8: Multisite Redox Enzymes (Part 4)
11.2.7.9: Multisite Redox Enzymes (Part 5)
11.2.7.10: Multisite Redox Enzymes (Part 6)
11.2.7.11: Report on the Nitrogenase Crystal Structure\(\;^{378-381}\)
11.2.7.12: Rubredoxin- A Single-Fe Tetrathiolate Protein

11.2.8: Metal/Nucleic Acid Interactions

11.2.8.1: The Basics
11.2.8.2: The Basics (Part 2)
11.2.8.3: A Case Study- Tris(phenanthroline) Metal Complexes
11.2.8.4: Applications of Different Metal Complexes that Bind Nucleic Acids
11.2.8.5: Applications of Different Metal Complexes that Bind Nucleic Acids (Part 2)
11.2.8.6: Nature's Use of Metal/Nucleic-acid Interactions

11.2.9: Metals in Medicine

11.2.9.1: Metal Deficiency and Disease
11.2.9.2: Toxic Effects of Metals
11.2.9.3: Aspects of Platinum Binding to DNA
11.2.9.4: Survey of Metals Used for Diagnosis and Chemotherapy
11.2.9.5: Platinum Anticancer Drugs- A Case Study
11.2.9.6: Mapping the Major Adducts of cis- and trans-DDP on DNA; Sequence Specificity
11.2.9.7: Structure of Platinum-DNA Complexes
11.2.9.8: Site-specifically Platinated DNA \(\;^{154}\)
11.2.9.9: Bioinorganic Chemistry of Platinum Anticancer Drugs- How Might They Work?
11.2.9.10: Bioinorganic Chemistry of Platinum Anticancer Drugs; How Might They Work? (Part 2)
11.2.9.11: Design of New Inorganic Anticancer Drugs

Detailed Licensing

Thumbnail: The ball-and-stick model of diisobutylaluminium hydride, showing aluminium as pink, carbon as black, and hydrogen as white. Image used with permission (Public Domain; Benjah-bmm27).

Contributors and Attributions

- Bertini, Ivano and Gray, Harry B. and Lippard, Stephen J. and Valentine, Joan Selverstone (1994) *Bioinorganic Chemistry.* University Science Books , Mill Valley, CA. ISBN 0-935702-57-1. http://resolver.caltech.edu/CaltechBOOK:1994.002

11.2: Bioinorganic Chemistry (Bertini et al.) is shared under a CC BY-NC-SA 4.0 license and was authored, remixed, and/or curated by LibreTexts.

CHAPTER OVERVIEW

Front Matter

Licensing
Preface

Licensing

*A detailed breakdown of this resource's licensing can be found in **Back Matter/Detailed Licensing**.*

Preface

This text covers material that could be included in a one-quarter or one-semester course in bioinorganic chemistry for graduate students and advanced undergraduate students in chemistry or biochemistry. We (Bertini, Gray, Lippard, and Valentine) believe that such a course should provide students with the background required to follow the research literature in the field. The topics were chosen to represent those areas of bioinorganic chemistry that are mature enough for textbook presentation. Although each chapter presents material at a more advanced level than that of bioinorganic textbooks published previously, the chapters are not specialized review articles. What we have attempted to do in each chapter is to teach the underlying principles of bioinorganic chemistry as well as outlining the state of knowledge in selected areas. We have chosen not to include abbreviated summaries of the inorganic chemistry, biochemistry, and spectroscopy that students may need as background in order to master the material presented. We instead assume that the instructor using this book will assign reading from relevant sources that is appropriate to the background of the students taking the course. For the convenience of the instructors, students, and other readers of this book, we have included an appendix that lists references to reviews of the research literature that we have found to be particularly useful in our courses on bioinorganic chemistry.

The idea of preparing a bioinorganic chemistry textbook was conceived by one of us (IB) at a "Metals in Biology" Gordon Conference in January, 1986. The contributing authors were recruited to the project shortly thereafter. The project evolved as a group effort, with substantial communication among the authors at all stages of planning and execution. Both first and revised drafts of the book were class-tested at UCLA, Caltech, and the University of Wisconsin and modified in response to the reviews of students and teachers. Particularly valuable suggestions were made by Professor Judith N. Burstyn (University of Wisconsin); Ken Addess, Raymond Ro, Kathy Kinnear, Clinton Nishida, Roger Pak, Marlene Sisemore (UCLA); and Deborah Wuttke (Caltech) during the review process. We thank them for their contributions. Even with all this help, the book would never have seen the light of day had it not been for the dedication and hard work of Debbie Wuttke. With RBG, Debbie checked every line through four rounds of galleys and pages. Grazie mille, Debbie!

11.2.1: Transition-Metal Storage, Transport, and Biomineralization

Living organisms store and transport transition metals both to provide appropriate concentrations of them for use in metalloproteins or cofactors and to protect themselves against the toxic effects of metal excesses; metalloproteins and metal cofactors are found in plants, animals, and microorganisms. The normal concentration range for each metal in biological systems is narrow, with both deficiencies and excesses causing pathological changes. In multicellular organisms, composed of a variety of specialized cell types, the storage of transition metals and the synthesis of the transporter molecules are not carried out by all types of cells, but rather by specific cells that specialize in these tasks. The form of the metals is always ionic, but the oxidation state can vary, depending on biological needs. Transition metals for which biological storage and transport are significant are, in order of decreasing abundance in living organisms: iron, zinc, copper, molybdenum, cobalt, chromium, vanadium, and nickel. Although zinc is not strictly a transition metal, it shares many bioinorganic properties with transition metals and is considered with them in this chapter. Knowledge of iron storage and transport is more complete than for any other metal in the group.

I. General Principles

A. Biological Significance of Iron, Zinc, Copper, Molybdenum, Cobalt, Chromium, Vanadium, and Nickel

B. Chemical Properties Relative to Storage and Transport

1. Iron
2. Zinc, Copper, Vanadium, Chromium, Molybdenum, and Cobalt

II. Biological Systems of Metal Storage, Transport, and Mineralization

A. Storage

1. Iron
2. Zinc, Copper, Vanadium, Chromium, Molybdenum, Cobalt, Nickel, and Manganese

B. Transport

1. Iron
2. Zinc, Copper, Vanadium, Chromium, Molybdenum, and Cobalt

C. Iron Biomineralization

III. Summary

Transition metals (Fe, Cu, Mo, Cr, Co, Mn, V) play key roles in such biological processes as cell division (Fe, Co), respiration (Fe, Cu), nitrogen fixation (Fe, Mo, V), and photosynthesis (Mn, Fe). Zn participates in many hydrolytic reactions and in the control of gene activity by proteins with "zinc fingers." Among transition metals, Fe predominates in terrestial abundance; since Fe is involved in a vast number of biologically important reactions, its storage and transport have been studied extensively. Two types of Fe carriers are known: specific proteins and low-molecular-weight complexes. In higher animals, the transport protein transferrin binds two Fe atoms with high affinity; in microorganisms, iron is transported into cells complexed with catecholates or hydroxamates called siderophores; and in plants, small molecules such as citrate, and possibly plant siderophores, carry Fe. Iron complexes enter cells through complicated paths involving specific membrane sites (receptor proteins). A problem yet to be solved is the form of iron transported in the cell after release from transferrin or siderophores but before incorporation into Fe-proteins.

Iron is stored in the protein ferritin. The protein coat of ferritin is a hollow sphere of 24 polypeptide chains through which Fe^{2+} passes, is oxidized, and mineralizes inside in various forms of hydrated Fe_2O_3. Control of the formation and dissolution of the mineral core by the protein and control of protein synthesis by Fe are subjects of current study.

Biomineralization occurs in the ocean (e.g., Ca in shells, Si in coral reefs) and on land in both plants (e.g., Si in grasses) and animals (e.g., Ca in bone, Fe in ferritin, Fe in magnetic particles). Specific organic surfaces or matrices of protein and/or lipid allow living organisms to produce minerals of defined shape and composition, often in thermodynamically unstable states.

IV. References

1. (a) J. H. Martin and R. M. Gordon, *Deep Sea Research* **35** (1988), 177; (b) F. Egami, *J. Mol. Evol.* **4** (1974), 113.
2. J. F. Sullivan *et al.*, *J. Nutr.* **109** (1979), 1432.
3. M. D. McNeely *et al.*, *Clin. Chem.* **17** (1971), 1123
4. A. R. Byrne and L. Kosta, *Sci. Total Env.* **10** (1978), 17
5. A. S. Prasad, *Trace Elements and Iron in Human Metabolism*, Plenum Medical Book Company, 1978.
6. E. C. Theil, *Adv. Inorg. Biochem.* **5** (1983), 1.
7. E. C. Theil and P. Aisen, in D. van der Helm, J. Neilands, and G. Winkelmann, eds., *Iron Transport in Microbes, Plants, and Animals*, VCH, 1987, p. 421.
8. C. F. Mills, ed., *Zinc in Human Biology*, Springer-Verlag, 1989.
9. B. L. Vallee and D. S. Auld, *Biochemistry* **29** (1990), 5647.
10. J. Miller, A. D. McLachlan, and A. Klug, *EMBO J.* **4** (1985), 1609.
11. J. M. Berg, *J. Biol. Chem.* **265** (1990), 6513.
12. C. Sennett, L. E. G. Rosenberg, and I. S. Millman, *Annu. Rev. Biochem.* **50** (1981), 1053.
13. J. J. G. Moura *et al.*, in A. V. Xavier, ed., *Frontiers in Biochemistry*, VCH, 1986, p. 1.
14. C. T. Walsh and W. H. Orme-Johnson, *Biochemistry* **26** (1987), 4901.
15. H. Kim and R. J. Maier, *J. Biol. Chem.* **265** (1990), 18729.
16. Reference 5, p. 5.
17. V. L. Schramm and F. C. Wedler, eds., *Manganese in Metabolism and Enzyme Function*, Academic Press, 1986.
18. (a) D. W. Boyd and K. Kustin, *Adv. Inorg. Biochem.* **6** (1984), 312; (b) R. C. Bruening *et al.*, *J. Nat. Products* **49** (1986), 193.
19. T. G. Spiro, ed., *Molybdenum Biochemistry*, Wiley, 1985.
20. L. L. Fox, *Geochim. Cosmochim. Acta* **52** (1988), 771.
21. M. E. Farago, in A. V. Xavier, ed., *Frontiers in Bioinorganic Chemistry*, VCH, 1986, p. 106.
22. I. G. Macara, G. C. McCloud, and K. Kustin, *Biochem. J.* **181** (1979), 457.
23. R. C. Bruening *et al.*, *J. Am. Chem. Soc.* **107** (1985), 5298.
24. E. Bayer and H. H. Kneifel, *Z. Naturforsch.* **27B** (1972), 207.
25. E. Bayer and H. H. Kneifel, in A. V. Xavier, ed., *Frontiers in Bioinorganic Chemistry*, VCH, 1986, p. 98.
26. J. Felcman, J. J. R. Frausto da Silva, and M. M. Candida Vaz, *Inorg. Chim. Acta* **93** (1984), 101.
27. W. Mertz, *Nutr. Rev.* **3** (1975), 129.
28. E. C. Theil, *J. Biol. Chem.* **265** (1990), 4771; *Biofactors* **4** (1993), 87.
29. J. S. Rohrer *et al.*, *Biochemistry* **29** (1990), 259.
30. P. H. Connett and K. Wetterhahn, *Struct. Bonding* **54** (1983), 94.
31. E. C. Theil, *Ann. Rev. Biochem.* **56** (1987), 289; *Adv. Enzymol.* **63** (1990), 421.
32. G. C. Ford *et al.*, *Philos. Trans. Roy. Soc. Land. B*, **304** (1984),551.
33. G. D. Watt, R. B. Frankel, and G. C. Papaefthymiou, *Proc. Natl. Acad. Sci. USA* 82 (1985), 3640.
34. (a) J. S. Rohrer *et al.*, *J. Biol. Chem.* **262** (1987), 13385; (b) J. S. Rohrer *et al.*, *Inorg. Chem.* **28** (1989), 3393.
35. D. H. Hamer, *Ann. Rev. Biochem.* **55** (1986), 913.
36. A. H. Robbins, D. E. McRee, M. Williamson, S. A. Collett, N. H. Xuong, W. F. Furey, B. C. Want, and C. D. Stout, *J. Mol. Biol.* **221** (1991), 1269.
37. N. D. Chasteen, *Adv. Inorg. Biochem.* **5** (1983), 201.
38. P. Aisen and I. Listowsky, *Annu. Rev. Biochem.* **49** (1980), 357.
39. B. T. Anderson *et al.*, *Proc. Natl. Acad. Sci. USA* **84** (1987), 1768; E. N. Baker, B. F. Anderson, and H. M. Baker, *Int. J. Biol. Macromol.* **13** (1991), 122.
40. S. Bailey *et al.*, *Biochemistry* **27** (1988), 5804.
41. M. Ragland *et al.*, *J. BioI. Chem.* **263** (1990), 18339.
42. B. F. Matzanke, G. Muller, and K. N. Raymond, in T. M. Loehr, ed., *Iron Carriers and Iron Proteins*, VCH, 1989, pp. 1-121.
43. L. Stryer, *Biochemistry*, Freeman, 1981, pp. 110-116.
44. D. J. Ecker *et al.*, *J. Am. Chem. Soc.* **110** (1988), 2457.
45. Y. Sugiura and K. Nomoto, *Struct. Bonding* **58** (1984), 107.

46. S. Mann, *Struct. Bonding* **54** (1986), 125.
47. A. R. Bulls *et al.*, *J. Am. Chern. Soc.* **112** (1990), 2627.
48. J. Webb, in P. Westbroek and E. W. de Jong, eds., *Biomineralization and Biological Metal Accumulation*, Reidel, 1983, pp. 413-422.
49. K. Kustin *et al.*, *Struct. Bonding* **53** (1983), 139.
50. R. B. Frankel and R. P. Blakemore, *Philos. Trans. Roy. Soc. Lond. B* **304** (1984), 567.
51. S. J. Lippard, *Angew. Chemie* **22** (1988), 344.
52. K. E. Wieghardt, *Angew. Chemie* **28** (1989), 1153.
53. E. C. Theil, in R. B. Frankel, ed., *Iron Biomineralization*, Plenum Press, 1990.
54. S. Maun, J. P. Harrington, and R. J. P. Williams, *Nature* **234** (1986), 565.
55. W. H. Armstrong and S. J. Lippard, *J. Am. Chern. Soc.* **107** (1985), 3730.
56. L. Que, Jr. and R. C. Scarrow, in L. Que, ed., *Metal Clusters in Proteins*, ACS Symposium Series 372, American Chemical Society, Washington, DC, 1988, p. 152 and references therein.
57. S. M. Gorun aud S. J. Lippard, *J. Am. Chem. Soc.* **107** (1985), 4570.
58. S. M. Gorun *et al.*, *J. Am. Chern. Soc.* **109** (1987), 3337.
59. Q. Islam *et al.*, *J. Inorg. Biochem.* **36** (1989), 51.
60. C.-Y. Yang *et al.*, *J. Inorg. Biochem.* **28** (1986), 393.
61. A. N. Mansour *et aI.*, *J. Biol. Chern.* **260** (1985), 7975.
62. D. C. Hams and P. Aisen, in T. M. Loehr, ed., *Iron Carriers and Iron Proteins*, VCH, 1989, pp. 239-352.
63. P. M. Harrison and T. M. Lilley, in Reference 62, pp. 123-238.
64. G. S. Waldo *et al. Science* **259** (1993), 796.
65. J. Trikha, G. S. Waldo, F. A. Lewandowski, Y. Ha, E. C. Theil, P. C. Weber, and N. M. Allewell, *Protein* **18** (1994), issue #2, in press.

These references contain general reviews of the subjects indicated:

- Chromium: 27, 30
- Cobalt: 12
- Copper: 8
- Iron
  - Biochemistry; 7, 31, 37, 42
  - Biomineralization polynuclear models: 6, 42, 56, 57, 58
  - Siderophores: 42
  - Structure of storage and transport proteins: 32, 62, 63
- Manganese: 17
- Molybdenum: 19
- Nickel: 13, 14
- Vanadium: 18
- Zinc: 8, 9, 11, 35

Contributors and Attributions

- Elizabeth C. Theil (North Carolina State University, Department of Biochemistry)
- Kenneth N. Raymond (University of California at Berkeley, Department of Chemistry)

11.2.1: Transition-Metal Storage, Transport, and Biomineralization is shared under a CC BY-NC-SA 4.0 license and was authored, remixed, and/or curated by LibreTexts.

11.2.1.1: Biological Significance of Iron, Zinc, Copper, Molybdenum, Cobalt, Chromium, Vanadium, and Nickel

The transition metals and zinc are among the least abundant metal ions in the sea water from which contemporary organisms are thought to have evolved (Table 1.1).[1-5] For many of the metals, the concentration in human blood plasma greatly exceeds that in sea water. Such data indicate the importance of mechanisms for accumulation, storage, and transport of transition metals and zinc in living organisms.

Table 1.1: Concentrations of transition metals and zinc in sea water and human plasma.a*Data from References 1 - 5 and 12

Element	Sea Water (M) x 10^8	Human Plasma (M) x 10^8
Fe	0.005 - 2	2230
Zn	8.0	1720
Cu	1.0	1650
Mo	10.0	1000
Co	0.7	0.0025
Cr	0.4	5.5
V	4.0	17.7
Mn	0.7	10.9
Ni	0.5	4.4

The metals are generally found either bound directly to proteins or in cofactors such as porphyrins or cobalamins, or in clusters that are in turn bound by the protein; the ligands are usually O, N, S, or C. Proteins with which transition metals and zinc are most commonly associated catalyze the intramolecular or intermolecular rearrangement of electrons. Although the redox properties of the metals are important in many of the reactions, in others the metal appears to contribute to the structure of the active state, e.g., zinc in the Cu-Zn dismutases and some of the iron in the photosynthetic reaction center. Sometimes equivalent reactions are catalyzed by proteins with different metal centers; the metal binding sites and proteins have evolved separately for each type of metal center.

Iron is the most common transition metal in biology.[6,7] Its use has created a dependence that has survived the appearance of dioxygen in the atmosphere ca. 2.5 billion years ago, and the concomitant conversion of ferrous ion to ferric ion and insoluble rust (Figure 1.1 See color plate section, page C-1.). All plants, animals, and bacteria use iron, except for a lactobacillus that appears to maintain high concentrations of manganese instead of iron. The processes and reactions in which iron participates are crucial to the survival of terrestrial organisms, and include ribonucleotide reduction (DNA synthesis), energy production (respiration), energy conversion (photosynthesis), nitrogen reduction, oxygen transport (respiration, muscle contraction), and oxygenation (e.g., steroid synthesis, solubilization and detoxification of aromatic compounds). Among the transition metals used in living organisms, iron is the most abundant in the environment. Whether this fact alone explains the biological predominance of iron or whether specific features of iron chemistry contribute is not clear.

Many of the other transition metals participate in reactions equivalent to those involving iron, and can sometimes substitute for iron, albeit less effectively, in natural Fe-proteins. Additional biological reactions are unique to nonferrous transition metals.

Zinc is relatively abundant in biological materials.[8,9] The major location of zinc in the body is metallothionein, which also binds copper, chromium, mercury, and other metals. Among the other well-characterized zinc proteins are the Cu-Zn superoxide dismutases (other forms have Fe or Mn), carbonic anhydrase (an abundant protein in red blood cells responsible for maintaining the pH of the blood), alcohol dehydrogenase, and a variety of hydrolases involved in the metabolism of sugars, proteins, and nucleic acids. Zinc is a common element in nucleic-acid polymerases and transcription factors, where its role is considered to be structural rather than catalytic. Interestingly, zinc enhances the stereoselectivity of the polymerization of nucleotides under reaction

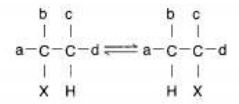
conditions designed to simulate the environment for prebiotic reactions. Recently a group of nucleic-acid binding proteins, with a repeated sequence containing the amino acids cysteine and histidine, were shown to bind as many as eleven zinc atoms necessary for protein function (transcribing DNA to RNA).[10] Zinc plays a structural role, forming the peptide into multiple domains or "zinc fingers" by means of coordination to cysteine and histidine (Figure 1.2A See color plate section, page C-l.). A survey of the sequences of many nucleic-acid binding proteins shows that many of them have the common motif required to form zinc fingers. Other zinc-finger proteins called steroid receptors bind both steroids such as progesterone and the progesterone gene DNA (Chapter 8). Much of the zinc in animals and plants has no known function, but it may be maintaining the structures of proteins that activate and deactivate genes.[11]

Copper and iron proteins participate in many of the same biological reactions:

1. reversible binding of dioxygen, e.g., hemocyanin (Cu), hemerythrin (Fe), and hemoglobin (Fe);
2. activation of dioxygen, e.g., dopamine hydroxylase (Cu) (important in the synthesis of the hormone epinephrine), tyrosinases (Cu), and catechol dioxygenases (Fe);
3. electron transfer, e.g., plastocyanins (Cu), ferredoxins, and c-type cytochromes (Fe);
4. dismutation of superoxide by Cu or Fe as the redox-active metal (superoxide dismutases).

The two metal ions also function in concert in proteins such as cytochrome oxidase, which catalyzes the transfer of four electrons to dioxygen to form water during respiration. Whether any types of biological reactions are unique to copper proteins is not clear. However, use of stored iron is reduced by copper deficiency, which suggests that iron metabolism may depend on copper proteins, such as the serum protein ceruloplasmin, which can function as a ferroxidase, and the cellular protein ascorbic acid oxidase, which also is a ferrireductase.

Cobalt is found in vitamin B_{12} , its only apparent biological site.[12] The vitamin is a cyano complex, but a methyl or methylene group replaces CN in native enzymes. Vitamin-B_{12} deficiency causes the severe disease of pernicious anemia in humans, which indicates the critical role of cobalt. The most common type of reaction in which cobalamin enzymes participate results in the reciprocal exchange of hydrogen atoms if they are on adjacent carbon atoms, yet not with hydrogen in solvent water:



(An important exception is the ribonucleotide reductase from some bacteria and lower plants, which converts ribonucleotides to the DNA precursors, deoxyribonucleotides, a reaction in which a sugar -OH is replaced by -H. Note that ribonucleotide reductases catalyzing the same reaction in higher organisms and viruses are proteins with an oxo-bridged dimeric iron center.) The cobalt in vitamin B_{12} is coordinated to five N atoms, four contributed by a tetrapyrrole (corrin); the sixth ligand is C, provided either by C5 of deoxyadenosine in enzymes such as methylmalonyl-CoA mutase (fatty acid metabolism) or by a methyl group in the enzyme that synthesizes the amino acid methionine in bacteria.

Nickel is a component of a hydrolase (urease), of hydrogenase, of CO dehydrogenase, and of S-methyl CoM reductase, which catalyzes the terminal step in methane production by methanogenic bacteria. All the Ni-proteins known to date are from plants or bacteria.[13,14] However, about 50 years elapsed between the crystallization of jack-bean urease in 1925 and the identification of the nickel component in the plant protein. Thus it is premature to exclude the possibility of Ni-proteins in animals. Despite the small number of characterized Ni-proteins, it is clear that many different environments exist, from apparently direct coordination to protein ligands (urease) to the tetrapyrrole F430 in methylreductase and the multiple metal sites of Ni and Fe-S in a hydrogenase from the bacterium *Desulfovibrio gigas*. Specific environments for nickel are also indicated for nucleic acids (or nucleic acid-binding proteins), since nickel activates the gene for hydrogenase.[15]

Manganese plays a critical role in oxygen evolution catalyzed by the proteins of the photosynthetic reaction center. The superoxide dismutase of bacteria and mitochondria, as well as pyruvate carboxylase in mammals, are also manganese proteins.[16,17] How the multiple manganese atoms of the photosynthetic reaction center participate in the removal of four electrons and protons from water is the subject of intense investigation by spectroscopists, synthetic inorganic chemists, and molecular biologists.[17]

Vanadium and chromium have several features in common, from a bioinorganic viewpoint.[18a] First, both metals are present in only small amounts in most organisms. Second, the biological roles of each remain largely unknown.[18] Finally, each has served as a

probe to characterize the sites of other metals, such as iron and zinc. Vanadium is required for normal health, and could act *in vivo* either as a metal cation or as a phosphate analogue, depending on the oxidation state, V(lV) or V(V), respectively. Vanadium in a sea squirt (tunicate), a primitive vertebrate (Figure 1.2B), is concentrated in blood cells, apparently as the major cellular transition metal, but whether it participates in the transport of dioxygen (as iron and copper do) is not known. In proteins, vanadium is a cofactor in an algal bromoperoxidase and in certain prokaryotic nitrogenases. Chromium imbalance affects sugar metabolism and has been associated with the glucose tolerance factor in animals. But little is known about the structure of the factor or of any other specific chromium complexes from plants, animals, or bacteria.

Molybdenum proteins catalyze the reduction of nitrogen and nitrate, as well as the oxidation of aldehydes, purines, and sulfite.[19] Few Mo-proteins are known compared to those involving other transition metals. Nitrogenases, which also contain iron, have been the focus of intense investigations by bioinorganic chemists and biologists; the iron is found in a cluster with molybdenum (the iron-molybdenum cofactor, or FeMoCo) and in an iron-sulfur center (Chapter 7). Interestingly, certain bacteria (*Azotobacter*) have alternative nitrogenases, which are produced when molybdenum is deficient and which contain vanadium and iron or only iron. All other known Mo-proteins are also Fe-proteins with iron centers, such as tetrapyrroles (heme and chlorins), Fe-sulfur clusters, and, apparently, non-heme/non-sulfur iron. Some Mo-proteins contain additional cofactors such as the Havins, e.g., in xanthine oxidase and aldehyde oxidase. The number of redox centers in some Mo-proteins exceeds the number of electrons transferred; reasons for this are unknown currently.

11.2.1.1: Biological Significance of Iron, Zinc, Copper, Molybdenum, Cobalt, Chromium, Vanadium, and Nickel is shared under a CC BY-NC-SA 4.0 license and was authored, remixed, and/or curated by LibreTexts.

11.2.1.2: Biological Systems of Metal Storage

Iron

Three properties of iron can account for its extensive use in terrestrial biological reactions:

a. facile redox reactions of iron ions;
b. an extensive repertoire of redox potentials available by ligand substitution or modification (Table 1.4);
c. abundance and availability (Table 1.1) under conditions apparently extant when terrestrial life began (see Section I.B.).

Ferrous ion appears to have been the environmentally stable form during prebiotic times. The combination of the reactivity of ferrous ion and the relatively large amounts of iron used by cells may have necessitated the storage of ferrous ion; recent results suggest that ferrous ion may be stabilized inside ferritin long enough to be used in some types of cells. As primitive organisms began to proliferate, the successful photosynthetic cells, which trapped solar energy by reducing CO_2 to make carbohydrates $(CH_2O)_n$ and produce O_2, exhausted from the environment the reductants from H_2 or H_2S or NH_3. The ability of primitive organisms to switch to the use of H_2O as a reductant, with the concomitant production of dioxygen, probably produced the worst case of environmental pollution in terrestrial history. As a result, the composition of the atmosphere, the course of biological evolution, and the oxidation state of environmental iron all changed profoundly. Paleogeologists and meteorologists estimate that there was a lag of about 200 - 300 million years between the first dioxygen production and the appearance of significant dioxygen concentrations in the atmosphere, because the dioxygen produced at first was consumed by the oxidation of ferrous ions in the oceans. The transition in the atmosphere, which occurred about 2.5 billion years ago, caused the bioavailability of iron to plummet and the need for iron storage to increase. Comparison of the solubility of Fe^{3+} at physiological conditions (about 10^{-18} M) to the iron content of cells (equivalent to 10^{-5} to 10^{-8} M) emphasizes the difficulty of acquiring sufficient iron.

Iron is stored mainly in the ferritins, a family* of proteins composed of a protein coat and an iron core of hydrous ferric oxide $[Fe_2O_3(H_2O)_n]$ with various amounts of phosphate.[6,7] As many as 4,500 iron atoms can be reversibly stored inside the protein coat in a complex that is soluble; iron concentrations equivalent to 0.25 M [about 10^{16}-fold more concentrated than Fe(III) ions] can be easily achieved *in vitro* (Figure 1.1). Ferritin is found in animals, plants, and even in bacteria; the role of the stored iron varies, and includes intracellular use for Fe-proteins or mineralization, long-term iron storage for other cells, and detoxification of excess iron. Iron regulates the synthesis of ferritin, with large amounts of ferritin associated with iron excess, small or undetectable amounts associated with iron deficiency. [Interestingly, the template (mRNA) for ferritin synthesis is itself stored in cells and is recruited by intracellular iron or a derivative for efficient translation into protein.[31] Iron does not appear to interact directly with ferritin mRNA nor with a ferritin mRNA-specific regulatory (binding) protein; however, the specific, mRNA regulatory (binding) protein has sequence homology to aconitase, and formation of an iron-sulfate cluster prevents RNA binding.] Because iron itself determines in part the amount of ferritin in an organism, the environmental concentration of iron needs to be considered before one can conclude that an organism or cell does not have ferritin.

Ferritin is thought to be the precursor of several forms of iron in living organisms, including hemosiderin, a form of storage iron found mainly in animals. The iron in hemosiderin is in a form very similar to that in ferritin, but the complex with protein is insoluble, and is usually located within an intracellular membrane (lysosomes). Magnetite (Fe_3O_4) is another form of biological iron derived, apparently, from the iron in ferritin. Magnetite plays a role in the behavior of magnetic bacteria, bees, and homing pigeons (see Section II.C).

The structure of ferritin is the most complete paradigm for bioinorganic chemistry because of three features: the protein coat, the iron-protein interface, and the iron core.[6,7]

---

* A family of proteins is a group of related but distinct proteins produced in a single organism and usually encoded by multiple, related genes.

Protein Coat

Twenty-four peptide chains (with about 175 amino acids each), folded into ellipsoids, pack to form the protein coat,* which is a hollow sphere about 100 Å in diameter; the organic surface is about 10 Å thick (Figure 1.9). Channels which occur in the protein coat at the trimer interfaces may be involved in the movement of iron in and out of the protein.[62,63,65] Since the protein coat is

stable with or without iron, the center of the hollow sphere may be filled with solvent, with $Fe_2O_3 \cdot H_2O$, or, more commonly, with both small aggregates of iron and solvent. Very similar amino-acid sequences are found in ferritin from animals and plants. Sorting out which amino acids are needed to form the shape of the protein coat and the ligands for iron core formation requires the continued dedication of bioinorganic chemists; identification of tyrosine as an Fe(III)-ligand adds a new perspective.[64]

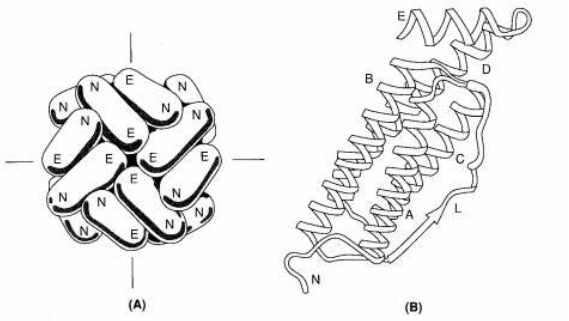


Figure 1.9 - (A) The protein coat of horse spleen apoferritin deduced from x-ray diffraction of crystals of the protein.[32] The outer surface of the protein coat shows the arrangement of the 24 ellipsoidal polypeptide subunits. N refers to the N-terminus of each polypeptide and E to the E-helix (see B). Note the channels that form at the four-fold axes where the E-helices interact, and at the threefold axes near the N-termini of the subunits. (B) A ribbon model of a subunit showing the packing of the four main alpha-helices (A, B, C, and D), the connecting L-loop and the E-helix.

* Some ferritin subunits, notably in ferritin from bacteria, bind heme in a ratio of less than one heme per two subunits. A possible role of such heme in the oxidation and reduction of iron in the core is being investigated.

Iron-Protein Interface

Formation of the iron core appears to be initiated at an Fe-protein interface where Fe(II)-O-Fe(Ill) dimers and small clusters of Fe(Ill) atoms have been detected attached to the protein and bridged to each other by oxo/hydroxo bridges. Evidence for multiple nucleation sites has been obtained from electron microscopy of individual ferritin molecules (multiple core crystallites were observed) and by measuring the stoichiometry of binding of metal ions, which compete with binding of monoatomic iron, e.g., VO(IV) and Tb(III) (about eight sites per molecule). EXAFS (*E*xtended *X*-ray *A*bsorption *F*ine *S*tructure) and Mössbauer spectroscopies suggest coordination of Fe to the protein by carboxyl groups from glutamic (Glu) and aspartic (Asp) acids. Although groups of Glu or Asp are conserved in all animal and plant ferritins, the ones that bind iron are not known. Tyrosine is an Fe(III)-ligand conserved in rapid mineralizing ferritins identified by Uv-vis and resonance Raman spectroscopy.[64]

Iron Core

Only a small fraction of the iron atoms in ferritin bind directly to the protein. The core contains the bulk of the iron in a polynuclear aggregate with properties similar to ferrihydrite, a mineral found in nature and formed experimentally by heating neutral aqueous solutions of $Fe(III)(NO_3)_3$. X-ray diffraction data from ferritin cores are best fit by a model with hexagonal close-packed layers of oxygen that are interrupted by irregularly incomplete layers of octahedrally coordinated Fe(III) atoms. The octahedral coordination is confirmed by Mössbauer spectroscopy and by EXAFS, which also shows that the average Fe(III) atom is surrounded by six oxygen atoms at a distance of 1.95 Å and six iron atoms at distances of 3.0 to 3.3 Å.

Until recently, all ferritin cores were thought to be microcrystalline and to be the same. However, x-ray absorption spectroscopy, Mössbauer spectroscopy, and high-resolution electron microscopy of ferritin from different sources have revealed variations in the degree of structural and magnetic ordering and/or the level of hydration. Structural differences in the iron core have been associated with variations in the anions present, e.g., phosphate[29] or sulfate, and with the electrochemical properties of iron. Anion concentrations in turn could reflect both the solvent composition and the properties of the protein coat. To understand iron storage, we need to define in more detail the relationship of the ferritin protein coat and the environment to the redox properties of iron in the ferritin core.

Experimental studies of ferritin formation show that Fe(II) and dioxygen are needed, at least in the early stages of core formation. Oxidation to Fe(III) and hydrolysis produce one electron and an average of 2.5 protons for iron atoms incorporated into the ferritin iron core. Thus, formation of a full iron core of 4,500 iron atoms would produce a total of 4,500 electrons and 11,250 protons. After

core formation by such a mechanism inside the protein coat, the pH would drop to 0.4 if all the protons were retained. It is known that protons are released and electrons are transferred to dioxygen. However, the relative rates of proton release, oxo-bridge formation, and electron transfer have not been studied in detail. Moreover, recent data indicate migration of iron atoms during the early stages of core formation and the possible persistence of Fe^{2+} for periods of time up to 24 hours. When large numbers of Fe(II) atoms are added, the protein coat appears to stabilize the encapsulated Fe(III).[34a,b] Formation of the iron core of ferritin has analogies to surface corrosion, in which electrochemical gradients are known to occur. Whether such gradients occur during ferritin formation and how different protein coats might influence proton release or alter the structure of the core are subjects only beginning to be examined.

Zinc, Copper, Vanadium, Chromium, Molybdenum, Cobalt, Nickel, and Manganese

Ions of nonferrous transition metals require a much less complex biological storage system, because the solubilities are much higher ($\geq 10^{-8}$ M) than those for Fe^{3+}. As a result, the storage of nonferrous transition metals is less obvious, and information is more limited. In addition, investigations are more difficult than for iron, because the amounts in biological systems are so small. Essentially nothing is known yet about the storage of vanadium, chromium, molybdenum, cobalt, nickel, and manganese, with the possible exception of accumulations of vanadium in the blood cells of tunicates.

Zinc and copper, which are used in the highest concentrations of any of the non-ferrous transition metals, are specifically bound by the protein metallothionein[35,36] (see Figure 1.10). Like the ferritins, the metallothioneins are a family of proteins, widespread in nature and regulated by the metals they bind. In contrast to ferritin, the amounts of metal stored in metallothioneins are smaller (up to twelve atoms per molecule), the amount of protein in cells is less, and the template (mRNA) is not stored. Because the cellular concentrations of the metallothioneins are relatively low and the amount of metal needed is relatively small, it has been difficult to study the biological fate of copper and zinc in living organisms, and to discover the natural role of metallothioneins. However, the regulation of metallothionein synthesis by metals, hormones, and growth factors attests to the biological importance of the proteins. The unusual metal environments of metallothioneins have attracted the attention of bioinorganic chemists.

Metallothioneins, especially in higher animals, are small proteins[35,36] rich in cysteine (20 per molecule) and devoid of the aromatic amino acids phenylalanine and tyrosine. The cysteine residues are distributed throughout the peptide chain. However, in the native form of the protein (Figure 1.10), the peptide chains fold to produce two clusters of -SH, which bind either three or four atoms of zinc, cadmium, cobalt, mercury, lead, or nickel. Copper binding is distinct from zinc, with 12 sites per molecule.

In summary, iron is stored in iron cores of a complicated protein. Ferritin, composed of a hollow protein coat, iron-protein interface, and an inorganic core, overcomes the problems of redox and hydrolysis by directing the formation of the quasi-stable mineral hydrous ferric oxide inside the protein coat. The outer surface of the protein is generally hydrophilic, making the complex highly soluble; equivalent concentrations of iron are ≤ 0.25 M. By contrast to iron, storage of zinc, copper, chromium, manganese, vanadium, and molybdenum is relatively simple, because solubility is high and abundance is lower. Little is known about the molecules that store these metals, with the possible exception of metallothionein, which binds small clusters of zinc or copper.

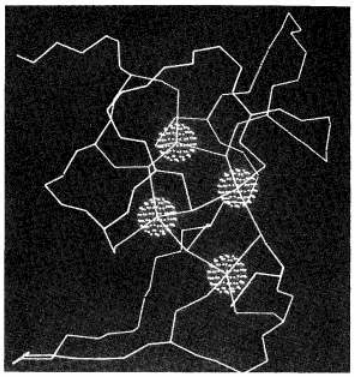


Figure 1.10 - The three-dimensional structure of the a domain from rat cd_7 metallothionein-2, determined by NMR in solution (Reference 36a), based on data in Reference 36b. The four metal atoms, bonded to the sulfur of cysteine side chains, are indicated as spherical collections of small dots. A recent description of the structure of the cd_5Zn_2 protein, determined from x-ray diffraction of crystals, agrees with the structure determined by NMR (Reference 36c).

11.2.1.2: Biological Systems of Metal Storage is shared under a CC BY-NC-SA 4.0 license and was authored, remixed, and/or curated by LibreTexts.

11.2.1.3: Chemical Properties Relative to Storage and Transport

Iron

Iron is the most abundant transition element in the Earth's crust and, in general, in all life forms. An outline of the distribution of iron in the Earth's crust[20,21] is shown in Table 1.2. As can be seen, approximately one-third of the Earth's mass is estimated to be iron. Of course, only the Earth's crust is relevant for life forms, but even there it is the most abundant transition element. Its concentration is relatively high in most crustal rocks (lowest in limestone, which is more or less pure calcium carbonate). In the oceans, which constitute 70 percent of the Earth's surface, the concentration of iron is low but increases with depth, since this iron exists as suspended particulate matter rather than as a soluble species. Iron is a limiting factor in plankton growth, and the rich fisheries associated with strong up-welling of ocean depths result at least in part from the biological growth allowed by these iron supplies. Properties that dominate the transport behavior of most transition metal ions are: (l) redox chemistry, (2) hydrolysis, and (3) the solubility of the metal ions in various complexes, particularly the hydroxides.

Table 1.2 - Iron: its terrestrial distribution.[a]

a) Data from References 1a and 20

One third of Earth's mass, most abundant element by weight

- Distribution in crustal rocks (weight %):
  - igneous 5.6
  - shale 4.7
  - sandstone 1.0
  - limestone 0.4
- Ocean (70% of Earth's surface):
  - 0.003 - 0.1 ppb, increasing with depth; limiting factor in plankton growth
- Rivers:
  - 0.07 - 7 ppm
- K_{sp} for $Fe(OH)_3$ is approximately 10^{-39}, hence at pH 7 $[Fe^{3+}]$ 10^{-18} M

As an example of the effects of solubility, consider the enormous variation in the concentration of iron in rivers, depending on whether the water is from a clear mountain stream running over rock or a muddy river carrying large amounts of sediment. However, the amount of dissolved iron in the form of free ferric ion or its hydrolysis products, whatever the source of water, is extremely low. As can be seen from the solubility of hydrated Fe(III) ($K_s \sim 10^{-18}$ M) (Table 1.2), the concentration of free ferric ion is extraordinarily low at neutral pH; so significant concentrations of soluble iron species can be attained only by strong complex formation.

One example of the versatility of iron as a function of its environment is how the ligand field can strongly alter the structural and ligand exchange properties of the metal ion (Figure 1.3). The ligand field can also alter the redox properties. For high-spin ferric ion, as found in the aquo complex or in many other complexes (including the class of microbial iron-transport agents called siderophores, to be discussed later), the coordination geometry is octahedral or pseudo-octahedral. In the relatively weak ligand field (high-spin ground state), the complex is highly labile. In a strong ligand field, such as an axially ligated porphyrin complex of ferric ion, or the simple example of the ferrocyanide anion, the low-spin complex is exchange-inert. Similarly, the high-spin octahedral ferrous complexes are exchange-labile, but the corresponding axially ligated porphyrin complexes, or the ferrocyanide complexes, are spin-paired (diamagnetic) and ligand exchange-inert. Large, bulky ligands or constrained ligands, such as those provided by metalloprotein and enzyme sites, can cause a tetrahedral environment, in which both ferrous ion and ferric ion form high-spin complexes.

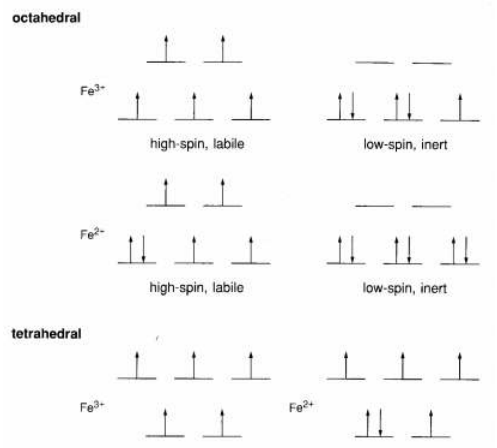


Figure 1.3 - Versatility of Fe coordination complexes.

The distribution of specific iron complexes in living organisms depends strongly on function. For example, although there are many different iron complexes in the average human, the relative amounts of each type differ more than 650-fold (Table 1.3). The total amount of iron in humans is quite large, averaging more than three and up to five grams for a healthy adult. Most of the iron is present as hemoglobin, the plasma oxygen-transport protein, where the function of the iron is to deliver oxygen for respiration. A much smaller amount of iron is present in myoglobin, a muscle oxygen-storage protein. For transport, the most important of these iron-containing proteins is transferrin, the plasma iron-transport protein that transfers iron from storage sites in the body to locations where cells synthesizing iron proteins reside; the major consumers of iron in vertebrates are the red blood cells. However, at any given time relatively little of the iron in the body is present in transferrin, in much the same way that at any given time in a large city only a small fraction of the population will be found in buses or taxis. Other examples of iron-containing proteins and their functions are included in Table 1.3 for comparison.

Table 1.3 - Average human Fe distribution

Protein	Function	Oxidation State of Fe	Amount of Fe (g)	Percent of Total
Hemoglobin	Plasma O_2 transport	2	2.6	65
Myoglobin	Muscle O_2 storage	2	0.13	6
Transferrin	Plasma Fe transport	3	0.007	0.2
Ferritin	Cell Fe storage	3	0.52	13
Hemosiderin	Cell Fe storage	3	0.48	12
Catalase	H_2O_2 metabolism	2	0.004	0.1
Cytochrome *c*	Electron transport	$\frac{2}{3}$ (11.2.1.3.1)	0.004	0.1
Other	Oxidases, other enzymes, etc.		0.14	3.6

An example of different iron-coordination environments, which alter the chemical properties of iron, is the difference in the redox potentials of hydrated Fe^{3+} and the electron-transport protein cytochrome *c* (Table 1.4). The coordination environment of iron in cytochrome *c* is illustrated in Figure 1.4. For example, the standard reduction potential for ferric ion in acid solution is 0.77 volts; so here ferric ion is quite a good oxidant. In contrast, cytochrome *c* has a redox potential of 0.25 volts. A wide range of redox potentials for iron is achieved in biology by subtle differences in protein structure, as listed in Table 1.4. Notice the large difference in the potential of cytochrome *c* and rubredoxin (Figure 1.5), 0.25 volts vs. -0.06 volts, respectively. In polynuclear ferredoxins, in

which each iron is tetrahedrally coordinated by sulfur, reduction potentials are near -0.4 volts. Thus, the entire range of redox potentials, as illustrated in Table 1.4, is more than one volt.

Table 1.4 - Fe redox potentials

Complex	Coord. no., type	Fe^{3+}/Fe^{2+} E^o (mV)
$Fe(OH_2)_6^{3+}$	6, aquo complex	770
Cytochrome a_3	6, heme	390
HIPIP	4, $Fe_4S_4(SR)_4^-$	350
Cytrochrome *c*	6, heme	250
Rubredoxin	4, $Fe(SR)_4$	-60
Ferredoxins	4, $Fe_4S_4(SR)_4^{2-}$	-400

Zinc, Copper, Vanadium, Chromium, Molybdenum, and Cobalt

The chemical properties of the other essential transition elements simplify their transport properties. For zinc there is only the +2 oxidation state, and the hydrolysis of this ion is not a limiting feature of its solubility or transport. Zinc is an essential element for both animals and plants.[8,9,20,21] In general, metal ion uptake into the roots of plants is an extremely complex phenomenon. A cross-sectional diagram of a root is shown in Figure 1.6. It is said that both diffusion and mass flow of the soil solution are of significance in the movement of metal ions to roots. Chelation and surface adsorption, which are pH dependent, also affect the availability of nutrient metal ions. Acid soil conditions in general retard uptake of essential divalent metal ions but increase the availability (sometimes with toxic results) of manganese, iron, and aluminum, all of which are normally of very limited availability because of hydrolysis of the trivalent ions.

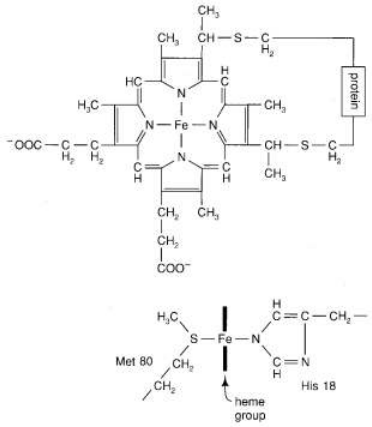


Figure 1.4 - Heme group and iron coordination in cytochrome c.

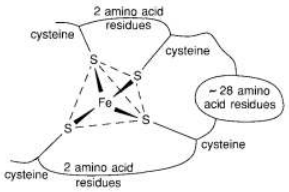


Figure 1.5 - $Fe^{3+/2+}$ coordination in rubredoxin.

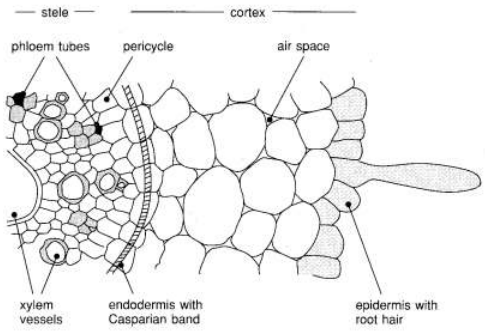


Figure 1.6 - Transverse section of a typical root.[20] The complex features of the root hair surface that regulate reductase and other activities in metal uptake are only beginning to be understood.

Vanadium is often taken up as vanadate, in a pathway parallel to phosphate.[18] However, its oxidation state within organisms seems to be highly variable. Unusually high concentrations of vanadium occur in certain ascidians (the specific transport behavior of which will be dealt with later). The workers who first characterized the vanadium-containing compound of the tunicate, *Ascidia nigra*, coined the name tunichrome.[22] The characterization of the compound as a dicatecholate has been reported.[23]

Quite a different chemical environment is found in the vanadium-containing material isolated from the mushroom *Amanita muscaria*. Bayer and Kneifel, who named and first described amavadine,[24] also suggested the structure shown in Figure 1.7.[25] Recently the preparation, proof of ligand structure, and (by implication) proof of the complex structure shown in Figure 1.7 have been established.[26] Although the exact role of the vanadium complex in the mushroom remains unclear, the fact that it is a vanadyl complex is now certain, although it may take a different oxidation state *in vivo*.

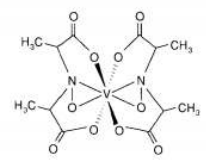


Figure 1.7 - A structure proposed for amavadine.[27]

The role of chromium in biology remains even more mysterious. In human beings the isolation of "glucose tolerance factor" and the discovery that it contains chromium goes back some time. This has been well reviewed by Mertz, who has played a major role in discovering what is known about this elusive and apparently quite labile compound.[27] It is well established that chromium is taken up as chromic ion, predominantly via foodstuffs, such as unrefined sugar, which presumably contain complexes of chromium, perhaps involving sugar hydroxyl groups. Although generally little chromium is taken up when it is administered as inorganic salts, such as chromic chloride, glucose tolerance in many adults and elderly people has been reported to be improved after supplementation with 150 - 250 mg of chromium per day in the form of chromic chloride. Similar results have been found in malnourished children in some studies in Third World countries. Studies using radioactively labeled chromium have shown that, although inorganic salts of chromium are relatively unavailable to mammals, brewer's yeast can convert the chromium into a usable form; so brewer's yeast is today the principal source in the isolation of glucose tolerance factor and has been used as a diet supplement.

Although chromium is essential in milligram amounts for human beings as the trivalent ion, as chromate it is quite toxic and a recognized carcinogen.[30] The uptake-reduction model for chromate carcinogenicity as suggested by Connett and Wetterhahn is shown in Figure 1.8. Chromate is mutagenic in bacterial and mammalian cell systems, and it has been hypothesized that the difference between chromium in the +6 and +3 oxidation states is explained by the "uptake-reduction" model. Chromium(III), like the ferric ion discussed above, is readily hydrolyzed at neutral pH and extremely insoluble. Unlike Fe^{3+}, it undergoes extremely slow ligand exchange. For both reasons, transport of chromium(III) into cells can be expected to be extremely slow unless it is present as specific complexes; for example, chromium(III) transport into bacterial cells has been reported to be rapid when iron is replaced by chromium in the siderophore iron-uptake mediators. However, chromate readily crosses cell membranes and enters cells, much as sulfate does. Because of its high oxidizing power, chromate can undergo reduction inside organelles to give chromium(m), which binds to small molecules, protein, and DNA, damaging these cellular components.

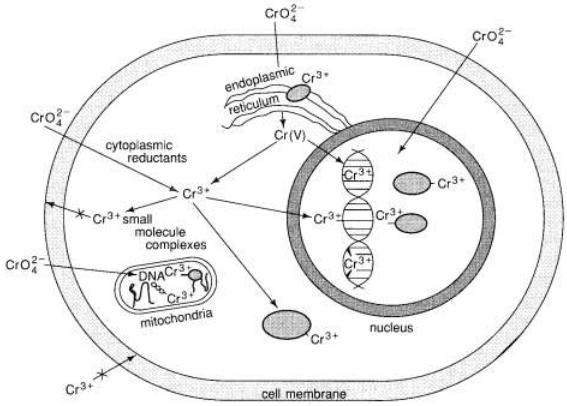


Figure 1.8 - The uptake-reduction model for chromate carcinogenicity. Possible sites for reduction of chromate include the cytoplasm, endoplasmic reticulum, mitochondria, and the nucleus.[27]

In marked contrast to its congener, molybdenum is very different from chromium in both its role in biology and its transport behavior, again because of fundamental differences in oxidation and coordination chemistry properties. In contrast to chromium, the higher oxidation states of molybdenum dominate its chemistry, and molybdate is a relatively poor oxidant. Molybdenum is an essential element in many enzymes, including xanthine oxidase, aldehyde reductase, and nitrate reductase.[19] The range of oxidation states and coordination geometries of molybdenum makes its bioinorganic chemistry particularly interesting and challenging.

The chemistry of iron storage and transport is dominated by high concentrations, redox chemistry (and production of toxic-acting oxygen species), hydrolysis (pK_a is about 3, far below physiological pH), and insolubility. High-affinity chelators or proteins are required for transport of iron and high-capacity sequestering protein for storage. By comparison to iron, storage and transport of the other metals are simple. Zinc, copper, vanadium, chromium, manganese, and molybdenum appear to be transported as simple salts or loosely bound protein complexes. In vanadium or molybdenum, the stable anion, vanadate or molybdate, appears to dominate transport. Little is known about biological storage of any metal except iron, which is stored in ferritin. However, zinc and copper are bound to metallothionein in a form that may participate in storage.

11.2.1.3: Chemical Properties Relative to Storage and Transport is shared under a CC BY-NC-SA 4.0 license and was authored, remixed, and/or curated by LibreTexts.

11.2.1.4: Iron Biomineralization

Many structures formed by living organisms are minerals. Examples include apatite [$Ca_2(OH)PO_4$] in bone and teeth, calcite or aragonite ($CaCO_3$) in the shells of marine organisms and in the otoconia (gravity device) of the mammalian ear, silica (SiO_2) in grasses and in the shells of small invertebrates such as radiolara, and iron oxides, such as magnetite (Fe_3O_4) in birds and bacteria (navigational devices) and ferrihydrite FeO(OH) in ferritin of mammals, plants, and bacteria. Biomineralization is the formation of such minerals by the influence of organic macromolecules, e.g., proteins, carbohydrates, and lipids, on the precipitation of amorphous phases, on the initiation of nucleation, on the growth of crystalline phases, and on the volume of the inorganic material.

Iron oxides, as one of the best-studied classes of biominerals containing transition metals, provide good examples for discussion. One of the most remarkable recent characterizations of such processes is the continual deposition of single-crystal ferric oxide in the teeth of chiton.[48] Teeth of chiton form on what is essentially a continually moving belt, in which new teeth are being grown and moved forward to replace mature teeth that have been abraded. However, the study of the mechanisms of biomineralization in general is relatively recent; a great deal of the information currently available, whether about iron in ferritin or about calcium in bone, is somewhat descriptive.

Three different forms of biological iron oxides appear to have distinct relationships to the proteins, lipids, or carbohydrates associated with their formation and with the degree of crystallinity.[49] Magnetite, on the one hand, often forms almost perfect crystals inside lipid vesicles of magneto-bacteria.[50] Ferrihydrite, on the other hand, exists as large single crystals, or collections of small crystals, inside the protein coat of ferritin; however, iron oxides in some ferritins that have large amounts of phosphate are very disordered. Finally, goethite [α-FeO(OH)] and lepidocrocite [γ-FeO(OH)] form as small single crystals in a complex matrix of carbohydrate and protein in the teeth of some shellfish (limpets and chitons); magnetite is also found in the lepidocrocite-containing teeth. The differences in the iron-oxide structures reflect differences in some or all of the following conditions during formation of the mineral: nature of co-precipitating ions, organic substrates or organic boundaries, surface defects, inhibitors, pH, and temperature. Magnetite can form in both lipid and protein/carbohydrate environments, and can sometimes be derived from amorphous or semicrystalline ferrihydrite-like material (ferritin). However, the precise relationship between the structure of the organic phase and that of the inorganic phase has yet to be discovered. When the goal of understanding how the shape and structure of biominerals is achieved, both intellectual satisfaction and practical commercial and medical information will be provided.

Synthetic iron complexes have provided models for two stages of ferritin iron storage and biomineralization:[51-59]

1. the early stages, when small numbers of clustered iron atoms are bound to the ferritin protein coat, and
2. the final stages, where the bulk iron is a mineral with relatively few contacts to the protein coat. In addition, models have begun to be examined for the microenvironment inside the protein coat.[54]

Among the models for the early or nucleation stage of iron-core formation are the binuclear Fe(III) complexes with $[Fe_2O(O_2CR_2)]^{2+}$ cores;[55,56] the three other Fe(III) ligands are N. The μ-oxo complexes, which are particularly accurate models for the binuclear iron centers in hemerythrin, purple acid phosphatases, and, possibly, ribonucleotide reductases, may also serve as models for ferritin, since an apparently transient Fe(II)-O-Fe(III) complex was detected during the reconstitution of ferritin from protein coats and Fe(II). The facile exchange of (O_2CR) for (O_2PR) in the binuclear complex is particularly significant as a model for ferritin, because the structure of ferritin cores varies with the phosphate content. An asymmetric trinuclear $(Fe_3O)^{7+}$ complex[57] and an $(FeO)_{11}$ complex (Figure 1.21) have been prepared; these appear to serve as models for later stages of core nucleation (or growth).[59]

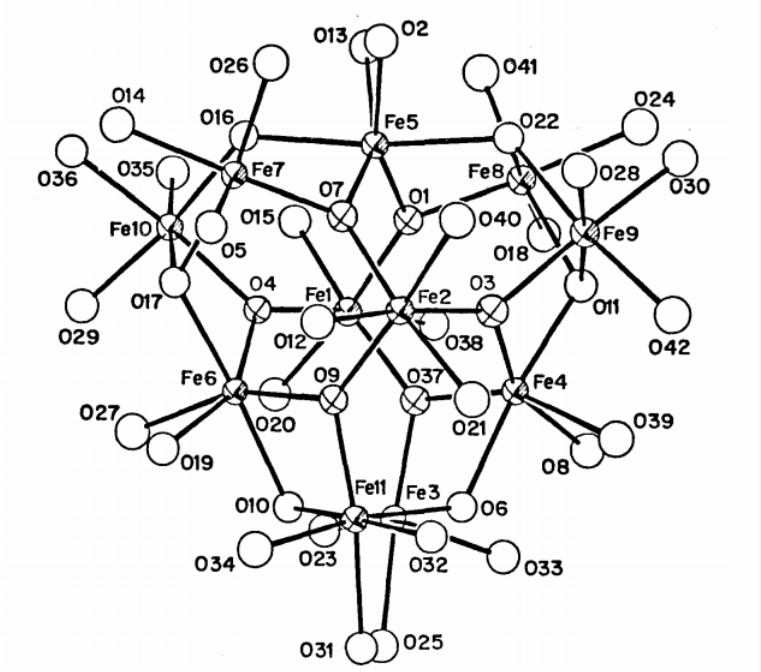


Figure 1.21 - The structure of a model for a possible intermediate in the formation of the ferritin iron core. The complex consists of 11 Fe(III) atoms with internal oxo-bridges and a coat of benzoate ligands; the Fe atoms define a twisted, pentacapped trigonal prism. See Reference 53.

Models for the full iron core of ferritin include ferrihydrite, which matches the ordered regions of ferritin cores that have little phosphate; however, the site vacancies in the lattice structure of ferrihydrite [FeO(OH)] appear to be more regular than in crystalline regions of ferritin cores. A polynuclear complex of iron and microbial dextran $(\alpha\text{-}1,4\text{-D-glucose})_n$ has spectroscopic (Mössbauer, EXAFS) properties very similar to those of mammalian ferritin, presumably because the organic ligands are similar to those of the protein (-OH, -COOH). In contrast, a polynuclear complex of iron and mammalian chondroitin sulfate $(\alpha\text{-}1,4\text{-}[\alpha\text{-}1,3\text{-D-glucuronic acid-N-acetyl-D-galactosamine-4-sulfate}]_n)$ contains two types of domains: one like mammalian ferritin [FeO(OH)] and one like hematite ($\alpha\text{-}Fe_2O_3$), which was apparently nucleated by the sulfate, emphasizing the importance of anions in the structure of iron cores.[60] Finally, a model for iron cores high in phosphate, such as those from bacteria, is Fe-ATP (4:1), in which the phosphate is distributed throughout the polynuclear iron complex, providing an average of 1 or 2 of the 6 oxygen ligands for iron.[61]

The microenvironment inside the protein coat of ferritin has recently been modeled by encapsulating ferrous ion inside phosphatidylcholine vesicles and studying the oxidation of iron as the pH is raised. The efficacy of such a model is indicated by the observation of relatively stable mixtures of Fe(II)/Fe(III) inside the vesicles, as have also been observed in ferritin reconstituted experimentally from protein coats and ferrous ion.[43,54]

Models for iron in ferritin must address both the features of traditional metalprotein interactions and the bulk properties of materials. Although such modeling may be more difficult than other types of bioinorganic modeling, the difficulties are balanced by the availability of vast amounts of information on Fe-protein interactions, corrosion, and mineralization. Furthermore, powerful tools such as x-ray absorption, Mössbauer and solid state NMR spectroscopy, scanning electron and proton microscopy, and transmission electron microscopy reduce the number of problems encountered in modeling the ferritin ion core.

Construction of models for biomineralization is clearly an extension of modeling for the bulk phase of iron in ferritin, since the major differences between the iron core of ferritin and that of other iron-biominerals are the size of the final structure, the generally higher degree of crystallinity, and, at this time, the more poorly defined organic phases. A model for magnetite formation has been provided by studying the coulometric reduction of half the Fe^{3+} atoms in the iron core of ferritin itself. Although the conditions for producing magnetite have .yet to be discovered, the unexpected observation of retention of the Fe^{2+} by the protein coat has provided lessons for understanding the iron core of ferritin. Phosphatidyl choline vesicles encapsulating Fe^{2+} appear to serve as models for both ferritin and magnetite; only further investigation will allow us to understand the unique features that convert Fe^{2+} to [FeO(OH)], on the one hand, and Fe_3O_4, on the other.

11.2.1.4: Iron Biomineralization is shared under a CC BY-NC-SA 4.0 license and was authored, remixed, and/or curated by LibreTexts.

11.2.1.5: Transport of Iron

The storage of iron in humans and other mammals has been dealt with in the previous section. Only a small fraction of the body's inventory of iron is in transit at any moment. The transport of iron from storage sites in cellular ferritin or hemosiderin occurs via the serum-transport protein transferrin. The transferrins are a class of proteins that are bilobal, with each lobe reversibly (and essentially independently) binding ferric ion.[37-39] This complexation of the metal cation occurs via prior complexation of a synergistic anion that *in vivo* is bicarbonate (or carbonate). Serum transferrin is a monomeric glycoprotein of molecular weight 80 kDa. The crystal structure of the related protein, lactoferrin,[39] has been reported, and recently the structure of a mammalian transferrin[40] has been deduced.

Ferritin is apparently a very ancient protein and is found in higher animals, plants, and even microbes; in plants and animals a common ferritin progenitor is indicated by sequence conservation.[41] In contrast, transferrin has been in existence only relatively recently, since it is only found ia the phylum Chordata. Although the two iron-binding sites of transferrin are sufficiently different to be distinguishable by kinetic and a few other studies, their coordination environments have been known for some time to be quite similar. This was first discovered by various spectroscopies, and most recently was confirmed by crystal-structure analysis, which shows that the environment involves two phenolate oxygens from tyrosine, two oxygens from the synergistic, bidentate bicarbonate anion, nitrogen from histidine, and (a surprise at the time of crystal-structure analysis) an oxygen from a carboxylate group of an aspartate.[39]

The transferrins are all glycoproteins, and human serum transferrin contains about 6 percent carbohydrate. These carbohydrate groups are linked to the protein, and apparently strongly affect the recognition and conformation of the native protein.

Although transferrins have a high molecular weight and bind only two iron atoms, transferrin is relatively efficient, because it is used in many cycles of iron transport in its interaction with the tissues to which it delivers iron. Transferrin releases iron *in vivo* by binding to the cell surface and forming a vesicle inside the cell (endosome) containing a piece of the membrane with transferrin and iron still complexed. The release of the iron from transferrin occurs in the relatively low pH of the endosome, and apoprotein is returned to the outside of the cell for delivery of another pair of iron atoms. This process in active reticulocytes (immature red blood cells active in iron uptake) can turn over roughly a million atoms of iron per cell per minute.[38] A schematic structure of the protein, deduced from crystal-structure analysis, is shown in Figure 1.11.

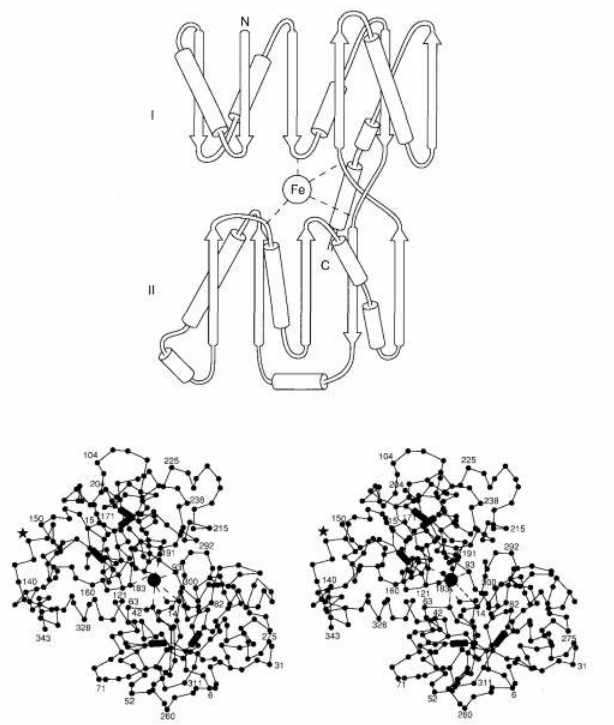


Figure 1.11: Three-dimensional structure of lactotransferrin. Top: schematic representation of the folding pattern of each lactoferrin lobe; Domain 1 is based on a beta-sheet of four parallel and two antiparallel domains; Domain II is formed from four parallel and one antiparallel strand. Bottom: stereo Ca diagram of the N lobe of lactoferrin; (●) *iron atom between domain 1 (residues 6 - 90+) and domain II (residues 91 - 251);* (⬛) *disulfide bridges;* (★) *carbohydrate attachment site. See Reference 39.*

Transferrin is an ellipsoidal protein with two subdomains or lobes, each of which binds iron. The two halves of each subunit are more or less identical, and are connected by a relatively small hinge. In human lactoferrin, the coordination site of the iron is the same as the closely related serotransferrin site. A major question that remains about the mechanism of iron binding and release is how the protein structure changes in the intracellular compartment of low pH to release the iron when it forms a specific complex with cell receptors (transferrin binding proteins) and whether the receptor protein is active or passive in the process. Recent studies suggest that the cell binding site for transferrin (a membrane, glycoprotein called the transferrin receptor) itself influences the stability of the iron-transferrin complex. The path of iron from the endosome to Feproteins has not been established; and the form of transported intracellular iron is not known.

Another major type of biological iron transport occurs at the biological opposite of the higher organisms. Although almost all microorganisms have iron as an essential element, bacteria, fungi, and other microorganisms (unlike humans and other higher organisms) cannot afford to make high-molecular-weight protein-complexing agents for this essential element when those complexing agents would be operating extracellularly and hence most of the time would be lost to the organism. As described earlier, the first life forms on the surface of the Earth grew in a reducing atmosphere, in which the iron was substantially more available because it was present as ferrous-containing compounds. In contrast to the profoundly insoluble ferric hydroxide, ferrous hydroxide is relatively soluble at near neutral pH. It has been proposed that this availability of iron in the ferrous state was one of the factors that led to its early incorporation in so many metabolic processes of the earliest chemistry of life.[6,38] In an oxidizing environment, microorganisms were forced to deal with the insolubility of ferric hydroxide and hence when facing iron deficiency secrete high-affinity iron-binding compounds called siderophores (from the Greek for iron carrier). More than 200 naturally occurring siderophores have been isolated and characterized to date.[42]

Most siderophore-mediated iron-uptake studies in microorganisms have been performed by using cells obtained under iron-deficient aerobic growth conditions. However, uptake studies in *E. coli* grown under anaerobic conditions have also established the presence of siderophore-specific mechanisms. In both cases, uptake of the siderophore-iron complex is both a receptor- and an energy-dependent process. In some studies the dependence of siderophore uptake rates on the concentration of the iron-siderophore complex has been found to conform to kinetics characteristic of protein catalysts, i.e., Michaelis-Menten kinetics. For example,

saturable processes with very low apparent dissociation constants of under one micromolar (1 μM) have been observed for ferric-enterobactin transport in *E. coli* (a bacterium), as shown in Figure 1.12.

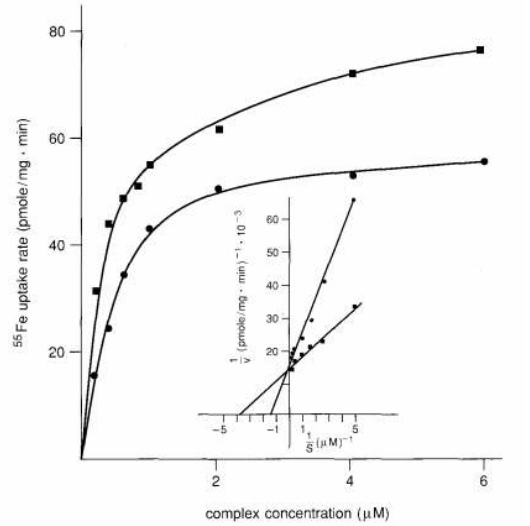


Figure 1.12 - Effect of MECAM analogues on iron uptake from E. coli. Iron transport by 2 μM ferric enterobactin is inhibited by ferric MECAM.

Similarly, in a very different microorganism, the yeast *Rhodoturala pilimanae*, Michaelis-Menten kinetics were seen again with a dissociation constant of approximately 6 μM for the ferric complex of rhodotoroulic acid; diagrams of some representative siderophores are shown in Figure 1.13. The siderophore used by the fungus *Neurospora crassa* was found to have a dissociation constant of about 5 μM and, again, saturable uptake kinetics.

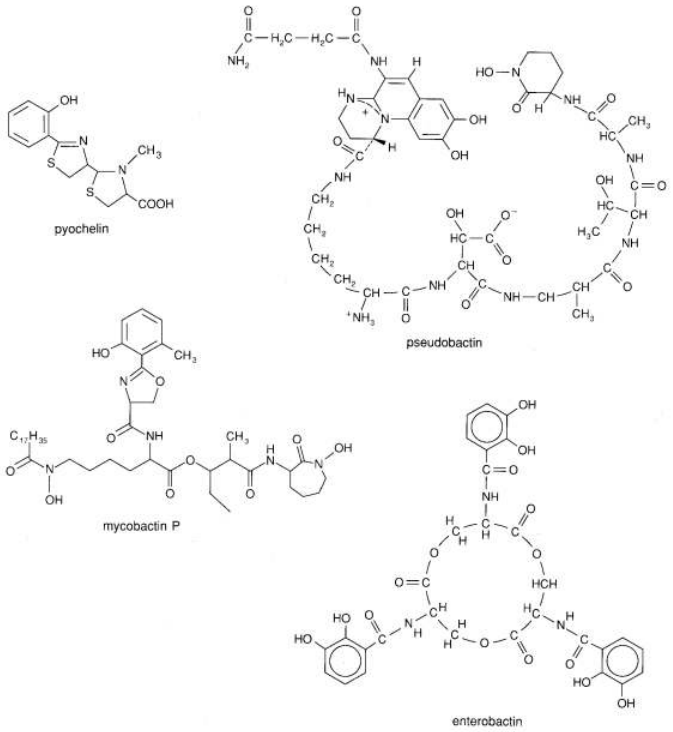


Figure 1.13 - Examples of bacterial siderophores. See Reference 42.

Although the behavior just described seems relatively simple, transport mechanisms in living cells probably have several more kinetically distinct steps than those assumed for the simple enzyme-substrate reactions underlying the Michaelis-Menten mechanism. For example, as ferric enterobactin is accumulated in *E. coli*, it has to pass through the outer membrane, the periplasm,

and the cytoplasm membrane, and is probably subjected to reduction of the metal in a low-pH compartment or to ligand destruction.

A sketch of a cell of E. coli and some aspects of its transport behavior are shown in Figure 1.14. Enterobactin-mediated iron uptake in *E. coli* is one of the best-characterized of the siderophore-mediated iron-uptake processes in microorganisms, and can be studied as a model. After this very potent iron-sequestering agent complexes iron, the ferric-enterobactin complex interacts with a specific receptor in the outer cell membrane (Figure 1.14), and the complex is taken into the cell by active transport. The ferric complexes of some synthetic analogs of enterobactin can act as growth agents in supplying iron to *E. coli*. Such a feature could be used to discover which parts of the molecule are involved in the sites of structural recognition of the ferric-enterobactin complex. Earlier results suggested that the metal-binding part of the molecule is recognized by the receptor, whereas the ligand platform (the triserine lactone ring; see Figure 1.13) is not specifically recognized.

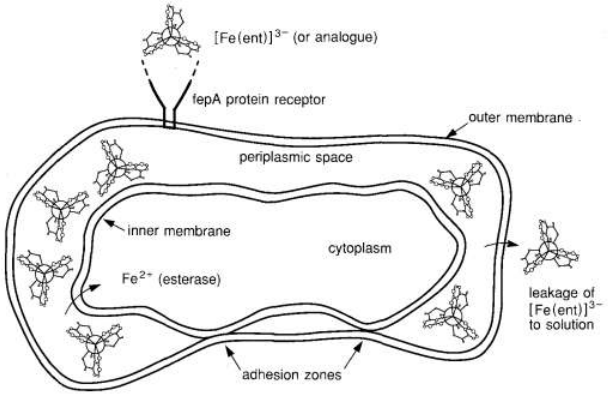


Figure 1.14 - Model for enterobactin-mediated Fe uptake in E. coli.

To find out which domains of enterobactin are required for iron uptake and recognition, rhodium complexes were prepared with various domains of enterobactin (Figure 1.15) as ligands to use as competitors for ferric enterobactin.[44] The goal was to find out if the amide groups (labeled Domain II in Figure 1.15), which linked the metal-binding catechol groups (Domain III, Figure 1.15) to the central ligand backbone (Domain I, Figure 1.15), are necessary for recognition by the receptor protein. In addition, synthetic ligands were prepared that differed from enterobactin by small changes at or near the catecholate ring. Finally, various labile trivalent metal cations, analogous to iron, were studied to see how varying the central metal ion would affect the ability of metal enterobactin complexes to inhibit competitively the uptake of ferric enterobactin by the organism. For example, if rhodium MECAM (Figure 1.16) is recognized by the receptor for ferric enterobactin on living microbial cells, a large excess of rhodium MECAM will block the uptake of radioactive iron added as ferric enterobactin. In fact, the rhodium complex completely inhibited ferric-enterobactin uptake, proving that Domain I is not required for recognition of ferric enterobactin.

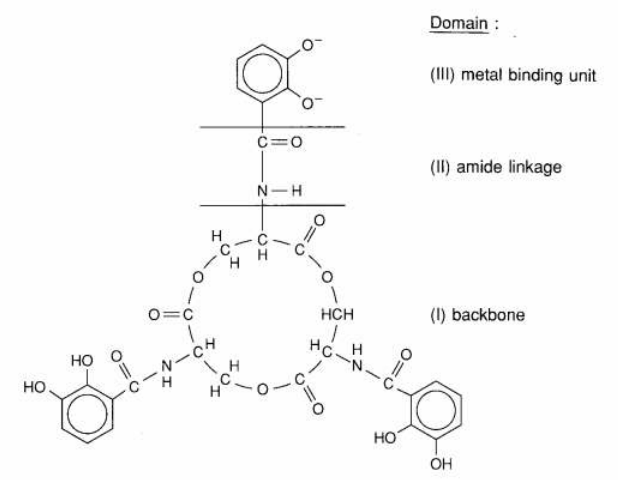


Figure 1.15 - Definition of recognition domains in enterobactin.

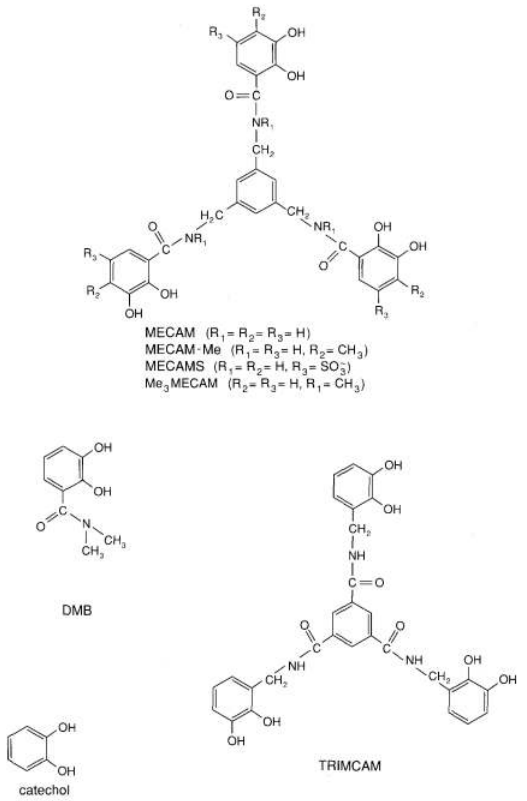


Figure 1.16 - MECAM and related enterobactin analogues.

However, if only Domain III is important in recognition, it would be expected that the simple tris(catecholato)-rhodium(III) complex would be an equally good inhibitor. In fact, even at concentrations in which the rhodium-catechol complex was in very large excess, no inhibition of iron uptake was observed, suggesting that Domain II is important in the recognition process.

The role of Domain II in the recognition process was probed by using a rhodium dimethyl amide of 2,3-dihydroxybenzene (DMB) as a catechol ligand, with one more carbonyl ligand than in the tris(catecholato)-rhodium(III) complex. Remarkably, this molecule shows substantially the same inhibition of enterobactin-mediated iron uptake in *E. coli* as does rhodium MECAM itself. Thus, in addition to the iron-catechol portion of the molecule, the carbonyl groups (Domain II) adjacent to the catechol-binding subunits of enterobactin and synthetic analogs are required for recognition by the ferric-enterobactin receptor. In contrast, when a methyl group was attached to the "top" of the rhodium MECAM complex, essentially no recognition occurred.

In summary, although the structure of the outer-membrane protein receptor of *E. coli* is not yet known, the composite of the results just described gives a sketch of what the ferric-enterobactin binding site must look like: a relatively rigid pocket for receiving the ferric-catecholate portion of the complex, and proton donor groups around this pocket positioned to hydrogen bond to the carbonyl oxygens of the ferric amide groups. The mechanisms of iron release from enterobactin, though followed phenomenologically, are still not known in detail.

11.2.1.5: Transport of Iron is shared under a CC BY-NC-SA 4.0 license and was authored, remixed, and/or curated by LibreTexts.

11.2.1.6: Transport of Zinc, Copper, Vanadium, Chromium, Molybdenum, and Cobalt

As described in an earlier section, transport problems posed by the six elements listed in the heading are somewhat simpler (with the exception of chromium) than those for iron. One very interesting recent development has been the characterization of sequestering agents produced by plants which complex a number of metal ions, not just ferric ions. A key compound, now well-characterized, is mugeneic acid (Figure 1.17).[45] The structural and chemical similarities of mugeneic acid to ethylenediaminetetraacetic acid (EDTA) have been noted. Like EDTA, mugeneic acid forms an extremely strong complex with ferric ion, but also forms quite strong complexes with copper, zinc, and other transition-metal ions. The structure of the cobalt complex (almost certainly essentially identical with that of the iron complex) is shown in Figure 1.18. Like the siderophores produced by microorganisms, the coordination environment accommodated by mugeneic acid is essentially octahedral. Although the coordination properties of this ligand are well laid out, and it has been shown that divalent metal cations, such as copper, competitively inhibit iron uptake by this ligand, the detailed process of metal-ion delivery by mugeneic acid and related compounds has not been elucidated.

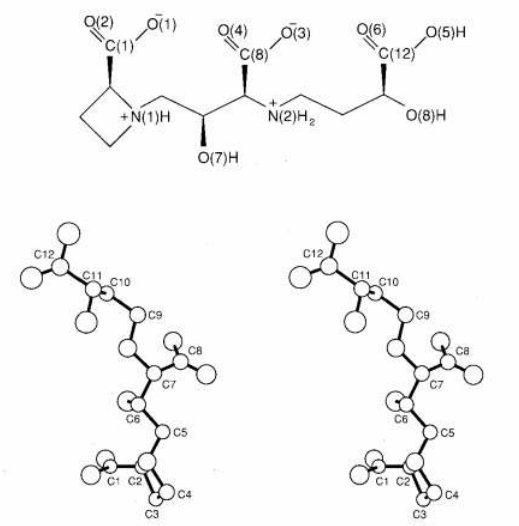


Figure 1.17 - Structure and a stereo view of mugeneic acid. See Reference 42.

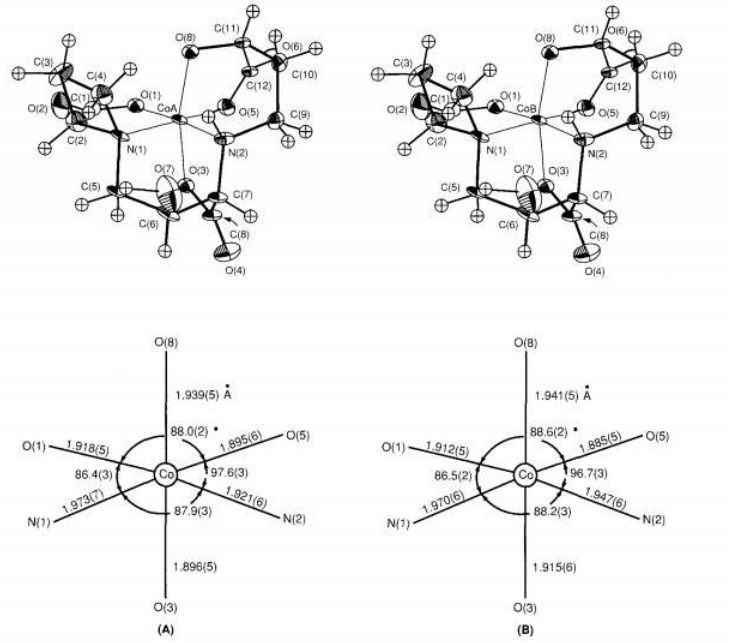


Figure 1.18 - Molecular structures of the complexes (molecules A and B) and coordination about the cobalt ion in molecules A and B of the mugeneic acid-Co(III) complex. Bond lengths in Å; angles in degrees. See Reference 42.

As noted in an earlier section, the biochemistry of vanadium potentially involves four oxidation states that are relatively stable in aqueous solution. These are V^{2+}, V^{3+}, VO^{2+} , and VO^{2+} (the oxidation states 2, 3, 4, and 5, respectively). Since even without added sequestering agents, V^{2+} slowly reduces water to hydrogen gas, it presumably has no biological significance. Examples of the remaining three oxidation states of vanadium have all been reported in various living systems. One of the most extensively investigated examples of transition-metal-ion accumulation in living organisms is the concentration of vanadium in sea squirts (tunicates), which is reported to be variable; many species have vanadium levels that are not exceptionally high. Others such as *Ascidia nigra* show exceptionally high vanadium concentrations.[46]

In addition to showing a remarkable concentration of a relatively exotic transition-metal ion, tunicates are a good laboratory model for uptake experiments, since they are relatively simple organisms. They possess a circulation system with a one-chambered heart, and a digestive system that is essentially a pump and an inlet and outlet valve connected by a digestive tract. The organism can absorb dissolved vanadium directly from sea water as it passes through the animal. The influx of vanadate into the blood cells of *A. nigra* has been studied by means of radioisotopes. The corresponding influx of phosphate, sulfate, and chromate (and the inhibition of vanadate uptake by these structurally similar oxoanions) has been measured. In the absence of inhibitors, the influx of vanadate is relatively rapid (a half-life on the order of a minute near 0 ºC) and the uptake process shows saturation behavior as the vanadate concentration is increased. The uptake process (in contrast to iron delivery in microorganisms, for example, and to many other uptake processes in microorganisms or higher animals) is *not* energy-dependent. Neither inhibitors of glycolysis nor decouplers of respiration-dependent energy processes show any significant effect on the rate of vanadate influx.

Phosphate, which is also readily taken up by the cells, is an inhibitor of vanadate influx. Neither sulfate nor chromate is taken up significantly, nor do they act as significant inhibitors for the vanadate uptake. Agents that inhibit transport of anions, in contrast, were found to inhibit uptake of vanadate into the organism. These results have led to the model proposed in Figure 1.19:

1. vanadate enters the cell through anionic channels; this process eliminates positively charged metal ion or metal-ion complexes present in sea water;
2. vanadate is reduced to vanadium(III); since the product is a cation, and so cannot be transported through the anionic channels by which vanadate entered the cell, the vanadium(III) is trapped inside the cell-the net result is an accumulation of vanadium. [It has been proposed that the tunichrome could act either as a reducing agent (as the complex) or (as the ligand) to stabilize the general vanadium(III); however, this seems inconsistent with its electrochemical properties (see below).]

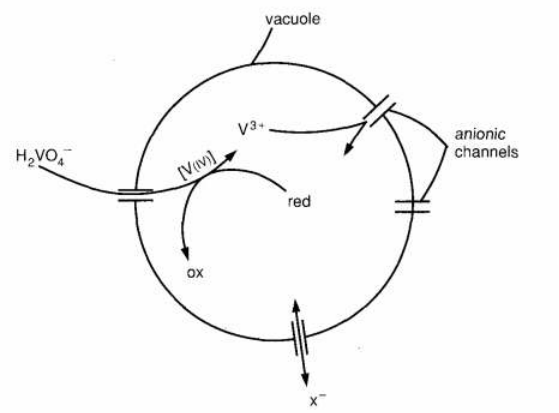


Figure 1.19 - Diagram of a vanadium accumulation mechanism. Vanadium enters the vacuole within the vanadocyte as mononegative $H_2VO_4^-$, although it may be possible for the dinegative anion, HVO_4^{2-}, to enter this channel as well (X^- stands for any negative ion such as Cl^- , $H_2PO_4^-$, etc., that may exchange across the membrane through the anionic channel). Reduction to V^{3+} takes place in two steps, via a V(IV) intermediate. The resulting cations may be trapped as tightly bound complexes, or as free ions that the anionic channel will not accept for transport. The nature of the reducing species is unknown.

Synthetic models of tunichrome b-1 (Figure 1.20) have been prepared. Tunichrome is a derivative of pyrogallol whose structure precludes the formation of an octahedral complex of vanadium as a simple 1:1 metal:ligand complex. The close analogue, described as 3,4,5-TRENPAMH$_9$, also cannot form a simple octahedral 1:1 complex. In contrast, the synthetic ligands TRENCAM and 2,3,4-TRENPAM can form pseudo-octahedral complexes. The structure of the vanadium TRENCAM complex shows that it is indeed a simple pseudo-octahedral tris-catechol complex.[47] The electrochemical behavior of these complexes is similar, with vanadium(IV/III) potentials of about -0.5 to -0.6 volts versus NHE. These results indicate that tunichrome b-1 complexes of

vanadium(IV/III) would show similar differences in their redox couples at high pH. At neutral pH, in the presence of excess pyrogallol groups, vanadium(IV) can be expected to form the intensely colored tris-catechol species. However, comparison of the EPR properties reported for vanadium-tunichrome preparations with model vanadium(lV)-complexes would indicate predominantly bis(catechol) vanadyl coordination. In any case, the vanadium(III) complexes must remain very highly reducing. It has been pointed out that the standard potential of pyrogallol is 0.79 V and decreases 60 mV per pH unit (up to about pH 9), so that at pH 7 the potential is about 0.4 V. The potentials of the vanadium couples for the tunichrome analogs are about -0.4 V. It has been concluded, therefore, that tunichrome or similar ligands cannot reduce the vanadium(IV) complex; so the highly reducing vanadium(III) complex of tunichrome must be generated in some other way.[47]

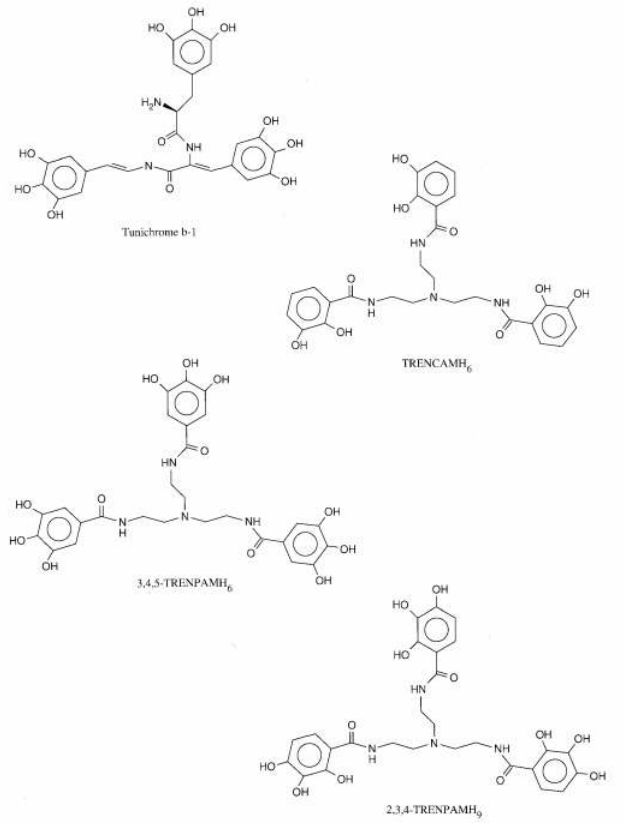


Figure 1.20 - Structures of tunichrome b-1 and synthetic analogues.[43]

Although a detailed presentation of examples of the known transport properties of essential transition-metal ions into various biological systems could be the subject of a large book, the examples that we have given show how the underlying inorganic chemistry of the elements is used in the biological transport systems that are specific for them. The regulation of metal-ion concentrations, including their specific concentration when necessary from relatively low concentrations of surrounding solution, is probably one of the first biochemical problems that was solved in the course of the evolution of life.

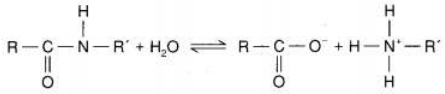
Iron is transported in forms in which it is tightly complexed to small chelators called siderophores (microorganisms) or to proteins called transferrins (animals) or to citrate or mugeneic acid (plants). The problem of how the iron is released in a controlled fashion is largely unresolved. The process of mineral formation, called biomineralization, is a subject of active investigation. Vanadium and molybdenum are transported as stable anions. Zinc and copper appear to be transported loosely associated with peptides or proteins (plants) and possibly mugeneic acid in plants. Much remains to be learned about the biological transport of nonferrous metal ions.

11.2.1.6: Transport of Zinc, Copper, Vanadium, Chromium, Molybdenum, and Cobalt is shared under a CC BY-NC-SA 4.0 license and was authored, remixed, and/or curated by LibreTexts.

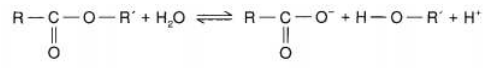
11.2.2: The Reaction Pathways of Zinc Enzymes and Related Biological Catalysts

I. Introduction

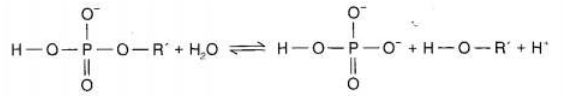
This chapter deals with metalloenzymes wherein the metal acts mainly as a Lewis acid; i.e., the metal does not change its oxidation state nor, generally, its protein ligands. Changes in the coordination sphere may occur on the side exposed to solvent. The substrate interacts with protein residues inside the active cavity and/or with the metal ion in order to be activated, so that the reaction can occur. Under these circumstances the catalyzed reactions involve, as central steps with often complex reaction pathways, the following bond-breaking and/or formation processes:



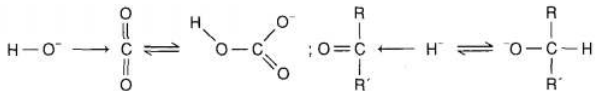
Peptide Hydrolysis



Carboxylic Ester Hydrolysis

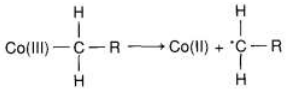


Phosphoric Ester Hydrolysis



Nucleophilic Addition of OH^- and H^-

Scheme (2.3) also pertains to the reactions which need ATP hydrolysis to promote endoenergetic reactions. We will also briefly deal with coenzyme B_{12}; this is a cobalt(III) complex that, by interacting with a number of proteins, produces an R-CH_2 radical by homolytic breaking of the Co-C bond as follows:



After an R-CH_2 radical is formed, it initiates a radical reaction. This is the only system we treat in which the oxidation state changes.

II. The Natural Catalysts

III. Strategies for the Investigation of Zinc Enzymes

A. Why Zinc?

1. The Groups to Which Zinc(II) is Bound
2. The Reactivity of Zinc(II) in Cavities
3. The Investigation of Zinc Enzymes

B. Metal Substitution

IV. Elucidation of Structure-Function Relationships: Carbonic Anhydrase as an Example

A. About the Enzyme

B. Steady-State and Equilibrium Kinetics of Carbonic Anhydrase-Catalyzed CO_2/HCO_3^- Interconversion

C. What Do We Learn from Cobalt Substitution?

1. Acid-base Equilibria
2. Coordination Geometries
3. Coordinated Water and NMR
4. pH Dependence of Inhibitor Binding

D. What Do We Learn from Copper Substitution?

E. What Do We Learn from Manganese and Cadmium Substitution?

F. Catalytic Mechanism

G. Model Chemistry

V. Other Enzymatic Mechanisms and Model Chemistry

A. Peptide Hydrolysis

B. Ester Hydrolysis and Phosphoryl Transfer

C. Nucleophilic Addition of OH^- and H^-

D. Group Transfer and Vitamin B_{12}

1. Group Transfer Enzymes
2. The B_{12}-dependent Enzymes

VI. Perspectives

Although a great deal is known about the biophysical characteristics of the various enzyme derivatives mentioned in this chapter, we are still far from a clear understanding of their mechanisms of action, especially if we take into consideration the role of each amino-acid residue inside the active-site cavity. Although we can successfully discuss why certain metal ions are used in certain biological reactions, we still do not know why nickel(II), for example, is involved in the enzymatic hydrolysis of urea.[199,200] If we are content with the explanations given in Sections III.A or V.D, we would need model compounds that are good catalysts and perform the job in several steps. This latter requirement would make the various models much more interesting, and would represent a new objective in the investigation of the structure-function relationship of catalytically active molecules. Indeed, the synthesis of large polypeptides may in principle provide such models. In this respect we need to know more about protein folding, for which emerging techniques like protein computer graphics and molecular dynamics are very promising.

Chemical modifications of proteins like the alkylation of carboxylate[124,201] or histidine[202] residues have been performed for a long time. A newer approach toward modeling the function of a protein, and understanding the role of the active site, involves cleaving part of a naturally occurring protein through enzymatic or chemical procedures, and then replacing it with a synthetic polypeptide. The use of modem techniques of molecular genetics has allowed site-directed mutagenesis to become in principle a very powerful technique for changing a single residue in a cavity. Site-directed mutagenesis is a very popular approach, and its principal limitation with respect to the synthetic polypeptide route is that only natural amino acids can be used (aside from the technical difficulties in both approaches). Small quantities of site-directed mutants have been obtained for CPA[125-127] and AP,[203] whereas the expression of CA[204,205] is now satisfactory.

Predictions of the changes in structure needed to affect the reaction pathway can nowadays be made with the aid of computers. The occurrence of the predicted change can be checked through x-ray analysis and NMR. The latter spectroscopy is today well-

recognized as being able to provide structural information on small (≲20 kDa) proteins through 2- or 3-dimensional techniques.[206-208] These techniques are increasingly being applied to paramagnetic metalloproteins such as many of those discussed here.[208,209] The advantage of handling a paramagnetic metalloprotein is that we can analyze signals shifted far away from their diamagnetic positions, which correspond to protons close to the metal ion,[69] even for larger proteins. It is possible to monitor the distances between two or more protons under various conditions, such as after the addition of inhibitors or pseudosubstrates, chemical modification, or substitution of a specific amino acid.

VII. References

1. H. Sigel and A. Sigel, eds., *Metal Ions in Biological Systems*, Dekker, **26** (1990).
2. R. K. Andrews, R. L. Blakeley, and B. Zemer, in Reference 1, **23** (1988).
3. K. Doi, B. C. Antanaitis, and P. Aisen, *Struct. Bonding* **70** (1988), I.
4. M. M. Werst, M. C. Kennedy, H. Beinert, and B. M. Hoffman, *Biochemistry* **29** (1990), 10526, and references therein.
5. A. G. Orpen *et al.*, *J. Chem. Soc., Dalton Trans.* **S1** (1989).
6. F. H. Westheimer, *Spec. Publ. Chem. Soc.* **8** (1957), I.
7. F. Basolo and R. G. Pearson, *Mechanisms of Inorganic Reactions*, Wiley, 2d ed., 1967.
8. L. G. Sillen and A. E. Martell, *Stability Constants of Metal-Ion Complexes*, Spec. Publ. Chern. Soc., London, **25**, 1971.
9. E. J. Billo, *Inorg. Nucl. Chem. Lett.* **11** (1975), 491.
10. I. Bertini, G. Canti, C. Luchinat, and F. Mani, *Inorg. Chem.* **20** (1981), 1670.
11. S. Burki, Ph.D. Thesis, Univ. Basel, 1977.
12. P. Wolley, *Nature* **258** (1975), 677.
13. J. T. Groves and R. R. Chambers, *J. Am. Chem. Soc.* **106** (1984), 630.
14. J. T. Groves and J. R. Olson, *Inorg. Chem.* **24** (1985), 2717.
15. L. J. Zompa, *Inorg. Chem.* **17** (1978), 2531.
16. E. Kimura, T. Koike, and K. Toriumi, *Inorg. Chem.* **27** (1988), 3687; E. Kimura *et al.*, *J. Am. Chem. Soc.* **112** (1990), 5805.
17. R. S. Brown *et al.*, *J. Am. Chem. Soc.* **104** (1982), 3188.
18. I. Bertini *et al.*, *Inorg. Chem* **29** (1990), 1460.
19. R. J. P. Williams, *Coord. Chem. Rev.* **100** (1990), 573.
20. D. W. Christianson, *Adv. Prot. Chem.* **42** (1991), 281.
21. I. Bertini, C. Luchinat, and M. S. Viezzoli, in I. Bertini *et al.*, eds., *Zinc Enzymes*, Birkhauser, 1986, p.27.
22. D. S. Auld and B. L. Vallee, in Reference 21, p. 167.
23. G. Formicka-Kozlowska, W. Maret, and M. Zeppezauer, in Reference 21, p. 579.
24. I. Bertini and C. Luchinat, in Reference 30, p. 101.
25. I. Bertini and C. Luchinat, *Adv. Inorg. Biochem.* **6** (1984), 71.
26. H. Sigel, ed., *Metal Ions in Biological Systems*, Dekker, **12** (1981).
27. T. G. Spiro, ed., *Copper Proteins*, Wiley, 1981.
28. J. E. Coleman and P. Gettins, in Reference 21, p. 77.
29. J. E. Coleman and D. P. Giedroc, in Reference 1, **25** (1989).
30. H. Sigel, ed., *Metal Ions in Biological Systems*, Dekker, **15** (1983).
31. N. U. Meldrum and F. J. W. Roughton, *J. Physiol.* **75** (1932), 4.
32. D. Keilin and T. Mann, *Biochem. J.* **34** (1940), 1163.
33. S. Lindskog, in T. G. Spiro, ed., *Zinc Enzymes: Metal Ions in Biology*, Wiley, **5** (1983), 78; D. N. Silverman and S. Lindskog, *Acc. Chem. Res.* **21** (1988), 30.
34. J.-Y. Liang and W. N. Lipscomb, *J. Am. Chem. Soc.* **108** (1986), 5051.
35. K. M. Merz, *J. Am. Chem. Soc.* **112** (1990), 7973.
36. (a) G. Sanyal, *Ann. N. Y. Acad. Sci.* **429** (1984), 165; (b) G. Sanyal and T. H. Maren, *J. Biol. Chem.* **256** (1981), 608.
37. T. Kararli and D. N. Silverman, *J. Biol. Chem.* **260** (1985), 3484.
38. A. Liljas *et al.*, *Nature* **235** (1972), 131.
39. K. K. Kannan *et al.*, *Proc. Natl. Acad. Sci. USA*, **72** (1975), 51.
40. E. A. Eriksson *et al.*, in Reference 21, p. 317.
41. S. Lindskog in Reference 21, p. 307.

42. E. Clementi *et al.*, *FEBS Lett.* **100** (1979), 313.
43. B. P. N. Ko *et al.*, *Biochemistry* **16** (1977), 1720.
44. A. Ikai, S. Tanaka, and H. Noda, *Arch. Biochem. Biophys.* **190** (1978), 39.
45. I. Bertini, C. Luchinat, and A. Scozzafava, *Struct. Bonding* **48** (1982), 45.
46. A useful review by W. W. Cleland on pH-dependent kinetics can be found in *Methods Enzymol.*, 1987, 390.
47. Y. Pocker and S. Sarkanen, *Adv. Enzymol.* **47** (1978), 149.
48. I. Bertini and C. Luchinat, *Acc. Chern. Res.* **16** (1983), 272.
49. S. Lindskog and I. Simonsson, *Eur. J. Biochem.* **123** (1982), 29.
50. B.-H. Jonsson, H. Steiner, and S. Lindskog, *FEBS Lett.* **64** (1976), 310.
51. H. Steiner, B.-H. Jonsson, and S. Lindskog, *Eur. J. Biochem.* **59** (1975), 253.
52. D. N. Silverman *et al.*, *J. Am. Chem. Soc.* **101** (1979), 6734.
53. S. H. Koenig *et al.*, *Pure Appl. Chem.* **40** (1974), 103.
54. I. Simonsson, B.-H. Jonsson, and S. Lindskog, *Eur. J. Biochem.* **93** (1979), 4.
55. T. J. Williams and R. W. Henkens, *Biochemistry* **24** (1985), 2459.
56. I. Bertini, C. Luchinat, and M. Monnanni, in Reference 99, p. 139.
57. I. Bertini *et al.*, in Reference 21, p. 371.
58. I. Bertini *et al.*, *Inorg. Chem.* **24** (1985), 301.
59. I. Bertini *et al.*, *J. Am. Chem. Soc.* **100** (1978), 4873.
60. R. C. Rosenberg, C. A. Root, and H. B. Gray, *J. Am. Chem. Soc.* **97** (1975), 21.
61. B. Holmquist, T. A. Kaden, and B. L. Vallee, *Biochemistry* **14** (1975), 1454, and references therein.
62. M. W. Makinen and G. B. Wells, in H. Sigel, ed., *Metal Ions in Biological Systems*, Dekker, **22** (1987).
63. M. W. Makinen *et al.*, *J. Am. Chem. Soc.* **107** (1985), 5245.
64. A. E. Eriksson, Uppsala Dissertation, Faculty of Science, n. 164, 1988.
65. A. E. Eriksson, A. T. Jones, and A. Liljas, *Proteins* **4** (1989), 274.
66. A. E. Eriksson *et al.*, *Proteins* **4** (1989), 283.
67. I. Bertini *et al.*, *Inorg. Chem.*, **31** (1992), 3975.
68. P. H. Haffner and J. E. Coleman, *J. Biol. Chem.* **248** (1973), 6630.
69. I. Bertini and C. Luchinat, *NMR of Paramagnetic Molecules in Biological Systems*, Benjamin/Cummings, 1986.
70. R. D. Brown III, C. F. Brewer, and S. H. Koenig, *Biochemistry* **16** (1977), 3883.
71. I. Bertini, C. Luchinat, and M. Messori, in Reference 62, vol. 21.
72. I. Solomon, *Phys. Rev.* **99** (1955), 559.
73. I. Bertini *et al.*, *J. Magn. Reson.* **59** (1984), 213.
74. L. Banci, I. Bertini, and C. Luchinat, *Magn. Res. Rev.*, **11** (1986), 1.
75. I. Bertini *et al.*, *J. Am. Chem. Soc.*, **103** (1981), 7784.
76. T. H. Maren, A. L. Parcell, and M. N. Malik, *J. Pharmacol. Exp. Theor.* **130** (1960), 389.
77. J. E. Coleman, *J. Biol. Chem.* **243** (1968), 4574.
78. S. Lindskog, *Adv. Inorg. Biochem.* **4** (1982), 115.
79. G. Alberti *et al.*, *Biochim. Biophys. Acta* **16** (1981), 668.
80. J. I. Rogers, J. Mukherjee, and R. G. Khalifah, *Biochemistry* **26** (1987), 5672.
81. C. Luchinat, R. Monnanni, and M. Sola, *Inorg. Chim. Acta* **177** (1990), 133.
82. L. Morpurgo *et al.*, *Arch. Biochem. Biophys.* **170** (1975),360.
83. I. Bertini and C. Luchinat, in K. D. Karlin and J. Zubieta, eds., *Biological and Inorganic Copper Chemistry,* vol. 1, Adenine Press, 1986.
84. I. Bertini *et al.*, *J. Chem. Soc., Dalton Trans.* (1978), 1269.
85. P. H. Haffner and J. E. Coleman, *J. Biol. Chem.* **250** (1975), 996.
86. I. Bertini *et al.*, *J. Inorg. Biochem.* **18** (1983), 221.
87. I. Bertini, E. Borghi, and C. Luchinat, *J. Am. Chem. Soc.* **102** (1979), 7069.
88. I. Bertini *et al.*, *J. Am. Chem. Soc.* **109** (1987), 7855.
89. P. Yeagle, Y. Lochmtiller, and R. W. Henkens, *Proc. Natl. Acad. Sci. USA* **48** (1975), 1728.
90. P. J. Stein, S. T. Merrill, and R. W. Henkens, *J. Am. Chem. Soc.* **99** (1977), 3194.

91. P. S. Hubbard, *Proc. Roy. Soc. London* **291** (1966), 537.
92. A. Lanir and G. Navon, *Biochemistry* **11** (1972), 3536.
93. J. J. Led and E. Neesgard, *Biochemistry* **26** (1987), 183.
94. N. B.-H. Johnsson *et al.*, *Proc. Natl. Acad. Sci. USA* **77** (1980), 3269.
95. J. L. Evelhoch, D. F. Bocian, and J. L. Sudmeier, *Biochemistry* **20** (1981), 4951.
96. J.-Y. Liang and W. N. Lipscomb, *Proc. Natl. Acad. Sci. USA* **87** (1990), 3675.
97. K. M. Merz, *J. Mol. Biol.* **214** (1990), 799.
98. C. A. Fierke, T. L. Calderone, and J. F. Krebs, *Biochemistry* **30** (1991) 11054.
99. M. Aresta and G. Forti, eds., *Carbon Dioxide as a Source of Carbon*, Reidel, 1987.
100. M. Aresta and J. V. Schloss, eds., *Enzymatic and Model Carboxylation and Reduction Reactions for Carbon Dioxide Utilization*, Kluwer, 1990.
101. C. K. Tu and D. N. Silverman, *J. Am. Chem. Soc.* **108** (1986), 6065.
102. E. Chaffee, T. P. Dasgupta, and J. M. Harris, *J. Am. Chem. Soc.* **95** (1973), 4169.
103. J. B. Hunt, A. C. Rutenberg, and H. Taube, *J. Am. Chem. Soc.* **74** (1983), 268.
104. R. S. Brown, N. J. Curtis, and J. Huguet, *J. Am. Chem. Soc.* **103** (1981), 6953.
105. I. Tabushi and Y. Kuroda, *J. Am. Chem. Soc.* **106** (1984), 4580.
106. I. Bertini *et al.*, *Gazz. Chim. Ital.* **118** (1988), 777.
107. L. Meriwether and F. H. Westheimer, *J. Am. Chem. Soc.* **78** (1956), 5119.
108. D. A. Buckingham, D. M. Foster, and A. M. Sargeson, *J. Am. Chem. Soc.* 92 (1970), 6151.
109. M. L. Bender, R. J. Bergeron, and M. Komiyama, *The Bioorganic Chemistry of Enzymatic Catalysis*, Wiley, 1984.
110. B. Anderson *et al.*, *J. Am. Chem. Soc.* **99** (1977), 2652.
111. M. L. Bender and B. W. Tumquest, *J. Am. Chem. Soc.* **77** (1955), 4271.
112. D. L. Miller and F. H. Westheimer, *J. Am. Chem. Soc.* **88** (1966), 1514.
113. H. Kroll, *J. Am. Chem. Soc.* **74** (1952), 2036.
114. D. A. Buckingham, D. M. Foster, and A. M. Sargeson, *J. Am. Chem. Soc.* **90** (1968), 6032.
115. R. Breslow, in R. F. Gould, ed., *Bioinorganic Chemistry (Advances in Chemistry Series*, vol. **100**), American Chemical Society, 1971; Chapter 2.
116. A. Schepartz and R. Breslow, *J. Am. Chem. Soc.* **109** (1987), 1814.
117. J. T. Groves and R. R. Chambers, Jr., *J. Am. Chem. Soc.* **106** (1984), 630.
118. M. A. Wells and T. C. Bruice, *J. Am. Chem. Soc.* **99** (1977), 5341.
119. H. Sigel, ed., *Metal Ions in Biological Systems*, Dekker, **5** (1976).
120. N. E. Dixon and A. M. Sargeson, in Reference 33.
121. R. W. Hay, G. Wilkinson, R. D. Gillard, and J. A. McCleverty, eds., in *Comprehensive Coordination Chemistry*, Pergamon Press, 1987.
122. D. C. Rees, M. Lewis, and W. N. Lipscomb, *J. Mol. Biol.* **168** (1983), 367.
123. D. C. Rees *et al.*, in Reference 21, p. 155.
124. D. S. Auld, K. Larson, and B. L. Vallee, in Reference 21, p. 133.
125. W. J. Rutter, personal communication.
126. D. Hilvert et al., *J. Am. Chem. Soc.* **108** (1986), 5298.
127. S. J. Gardell *et al.*, *J. Biol. Chem.* **262** (1987), 576.
128. D. S. Auld *et al.*, *Biochemistry*, **31** (1992), 3840; W. L. Mock and J. T. Tsay, *J. Biol. Chem.* **263** (1988), 8635.
129. G. Shoham, D. C. Rees, and W. N. Lipscomb, *Proc. Natl. Acad. Sci. USA* **81** (1984), 7767.
130. K. F. Geoghegan *et al.*, *Biochemistry* **22** (1983), 1847.
131. I. Bertini *et al.*, *J. Inorg. Biochem.* **32** (1988), 13.
132. C. Luchinat *et al.*, *J. Inorg. Biochem.* **32** (1988), 1.
133. R. Bicknell *et al.*, *Biochemistry* **27** (1988), 1050.
134. I. Bertini *et al.*, *Biochemistry* **27** (1988), 8318.
135. M. E. Sander and H. Witzel, in Reference 21, p. 207.
136. M. W. Makinen, in Reference 21, p. 215.
137. D. W. Christianson and W. N. Lipscomb, *Acc. Chem. Res.* **22** (1989), 62.

138. D. W. Christianson *et al.*, *J. Biol. Chem.* **264** (1989), 12849.
139. B. W. Matthews, *Acc. Chem. Res.* **21** (1988), 333, and references therein.
140. B. S. Cooperman, in Reference 119.
141. D. M. Blow, J. J. Birktoft, and B. S. Hartley, *Nature* **221** (1969), 337.
142. R. C. Nordlie, in P. D. Boyer, ed., *T he Enzymes*, Academic Press, 3d ed., **4** (1975), 543.
143. R. Breslow *et al.*, *Proc. Natl. Acad. Sci. USA* **80** (1983), 4585.
144. H. W. Wyckoff *et al.*, *Adv. Enzymol.* **55** (1983), 453.
145. E. E. Kim and H. W. Wyckoff, *J. Mol. Biol.* **218** (1991), 449.
146. L. Banci *et aI.*, *J. Inorg. Biochem.* **30** (1987), 77.
147. P. Gettins and J. E. Coleman, *J. Biol. Chem.* **259** (1984), 11036.
148. I. Bertini *et al.*, *Inorg. Chem.* **28** (1989), 352.
149. A. Chaidaroglou *et al.*, *Biochemistry* **27** (1988), 8338.
150. E. C. Dinovo and P. D. Boyer, *J. Biol. Chem.* **246** (1971), 4586.
151. H. Dutler, A. Ambar, and J. Donatsch, in Reference 21, p. 471.
152. H. Eklund and C.-I. Bränden, in *Biological Macromolecules and Assemblies*, Wiley, 1985.
153. C.-I. Branden *et al.*, *The Enzymes* **11** (1975), 104.
154. E. S. Cedergren-Zeppezauer, in Reference 21, p. 393.
155. H. Theorell, *Feder. Proc.* **20** (1961), 967.
156. M. W. Makinen and W. Maret, in Reference 21, p. 465.
157. J. Kvassman and G. Pettersson, *Eur. J. Biochem.* **103** (1980), 565.
158. P. F. Cook and W. W. Cleland, *Biochemistry* **20** (1981),1805.
159. I. Bertini *et al.*, *J. Am. Chem. Soc.* **106** (1984), 1826.
160. W. Maret *et al.*, *J. Inorg. Biochem.* **12** (1980), 241.
161. H. B. Gray and E. I. Solomon, in Reference 27, p. 1.
162. J. S. Valentine and M. W. Pantoliano, in Reference 27, p. 291.
163. M. F. Dunn, A. K. H. MacGibbon, and K. Pease, in Reference 21, p. 486.
164. I. Bertini *et al.*, *Eur. Biophys. J.* **14** (1987), 431.
165. W. Maret and M. Zeppezauer, *Biochemistry* **25** (1986), 1584.
166. C. Sartorius, M. Zeppezauer, and M. F. Dunn, *Rev. Port. Quim.* **27** (1985), 256; C. Sartorius *et al.*, *Biochemistry* **26** (1987), 871.
167. G. Pettersson, in Reference 21, p. 451.
168. E. Garces and W. W. Cleland, *Biochemistry* **8** (1969), 633.
169. B. Edlund *et al.*, *Eur. J. Biochem.* **9** (1969), 451.
170. R. K. Crane, in M. Horkin and E. H. Stotz, eds., *Comprehensive Biochemistry*, Elsevier, **15** (1964), 200.
171. B. M. Babior and J. S. Krouwer, *CRC Crit. Rev. Biochem.* **6** (1979), 35.
172. C. Brink-Shoemaker *et al.*, *Proc. Roy. Soc. London, Ser. A* **278** (1964), 1.
173. B. T. Golding and P. J. Sellars, *Nature* (1983), p. 204.
174. D. Lexa and J. M. Saveant, *Acc. Chem. Res.* **16** (1983), 235.
175. R. A. Firth *et al.*, *Chem. Commun.* (1967), 1013.
176. G. N. Schrauzer and L. P. Lee, *J. Am. Chem. Soc.* **90** (1968), 6541.
177. R. A. Firth *et al.*, *Biochemistry* **6** (1968), 2178.
178. V. B. Koppenhagen and J. J. Pfiffner, *J. Biol. Chem.* **245** (1970), 5865.
179. H. A. O. Hill, in G. L. Eichhorn, ed., *Inorganic Biochemistry*, Elsevier, **2** (1973), 1067.
180. J. Halpern, *Pure. Appl. Chem.* **55** (1983), 1059.
181. J. Halpern, S. H. Kim, and T. W. Leung, *J. Am. Chem. Soc.* **106** (1984), 8317.
182. R. G. Finke and B. P. Hay, *Inorg. Chem.* **23** (1984), 3041; B. P. Hay and R. G. Finke, *Polyhedron* **4** (1988), 1469; R. G. Finke, in C. Bleasdale and B. T. Golding, eds., *Molecular Mechanisms in Bioorganic Processes*, The Royal Society of Chemistry; Cambridge, England (1990).
183. B. P. Hay and R. G. Finke, *J. Am. Chem. Soc.* **108** (1986), 4820.
184. B. P. Hay and R. G. Finke, *J. Am. Chem. Soc.* **109** (1987), 8012.
185. J. M. Pratt, *Quart. Rev.* (1984), 161.

186. J. Halpern, *Science* **227** (1985), 869.
187. B. M. Babier, *Acc. Chem. Res.* **8** (1975), 376.
188. B. T. Golding, in D. Dolphin, ed., B_{12} , Wiley, **2** (1982), 543.
189. N. Bresciani-Pahor *et al.*, *Coord. Chem. Rev.* **63** (1985), 1.
190. J. M. Pratt, *J. Mol. Cat.* **23** (1984), 187.
191. S. M. Chennaly and J. M. Pratt, *J. Chem. Soc., Dalton Trans.* (1980), 2259.
192. *Ibid*., p. 2267.
193. *Ibid*., p. 2274.
194. L. G. Marzilli *et al.*, *J. Am. Chem. Soc.* **101** (1979), 6754.
195. J. Glusker, in Reference 188, **1** (1982), 23.
196. G. De Alti *et al.*, *Inorg. Chim. Acta* **3** (1969), 533.
197. K. Geno and J. Halpern, *J. Am. Chem. Soc.* **109** (1987), 1238.
198. C. Mealli, M. Sabat, and L. G. Marzilli, *J. Am. Chem. Soc.* **109** (1987), 1593.
199. *Nickel and its Role in Biology*, vol. 23 of Reference 62.
200. C. T. Walsh and W. H. Orme-Johnson, *Biochemistry* **26** (1987), 4901.
201. J. F. Riordan and H. Hayashida, *Biochem. Biophys. Res. Commun.* **41** (1970), 122.
202. R. G. Khalifah, J. I. Rogers, and J. Mukherjee, in Reference 21, p. 357.
203. A. Chaidaroglou *et al.*, *Biochemistry* **27** (1988), 8338.
204. C. Forsman *et al.*, *FEBS Lett.* **229** (1988), 360; S. Lindskog *et al.*, in *Carbonic Anhydrase*, F. Botre, G. Gros, and B. T. Storey, eds., VCH, 1991.
205. C. A. Fierke, J. F. Krebs, and R. A. Venters, in *Carbonic Anhydrase*, F. Botre, G. Gros, and B. T. Storey, eds., VCH, 1991.
206. K. Wüthrich, *NMR in Biological Research*, Elsevier-North Holland, 1976.
207. K. Wüthrich, *NMR of Proteins and Nucleic Acids*, Wiley, 1986.
208. I. Bertini, H. Molinari, and N. Niccolai, eds., *NMR and Biomolecular Structure*, Verlag Chemie, 1991.
209. J. T. J. LeComte, R. D. Johnson, and G. N. La Mar, *Biochim. Biophys. Acta* **829** (1985), 268.
210. Recently, ^{67}Zn has been used as a relaxing probe to monitor the binding of ^{13}C-enriched cyanide to zinc in carbonic anhydrase (see Section IV.C).
211. Recent work on HCA II has improved the resolution to 1.54 Å (K. Hakan *et al.*, *J. Mol. Biol.* **227** (1993), 1192). Mutants at positions 143 (R. S. Alexander, S. K. Nair, and D. W. Christianson, *Biochemistry* **30** (1991), 11064) and 200 (1. F. Krebs et al., Biochemistry 30 (1991),9153; Y. Xue *et al.*, *Proteins* **15** (1993), 80) also have been characterized by x-ray methods.
212. An x-ray study of the cyanate and cyanide derivatives of the native enzyme has shown that the anions sit in the cavity without binding to the metal ion (M. Lindahl, L.A. Svensson, and A. Liljas, *Proteins* **15** (1993), 177). Since NCO^- has been shown to interact with the paramagnetic cobalt(II) center, and ^{13}C-enriched cyanide has been shown to interact with ^{67}Zn-substituted CA (see Reference 67), it appears that the structures in the solid state and solution are strikingly different.
213. Recent x-ray data on the adduct of 1,2,4-triazole with HCA II confirm H-bonding with Thr-200 (S. Mangani and A. Liljas, *J. Mol. Biol.* **232** (1993), 9).
214. An HCO_3^--complex of the His-200 mutant of HCA II has been studied by x-ray methods. The data are consistent with the coordinated oxygen being protonated and H-bonded to Thr-199 (Y. Xue *et al.*, *Proteins* **15** (1993), 80).

Contributors and Attributions

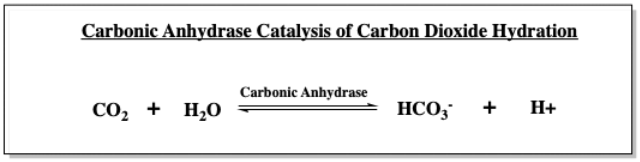
- Ivano Bertini (University of Florence, Department of Chemistry)
- Claudio Luchinat (University of Bologna, Institute of Agricultural Chemistry)

11.2.2: The Reaction Pathways of Zinc Enzymes and Related Biological Catalysts is shared under a CC BY-NC-SA 4.0 license and was authored, remixed, and/or curated by LibreTexts.

11.2.2.1: About Carbonic Anhydrase

Introduction

Carbon-dioxide (CO2) hydration and its mechanism in living systems are of fundamental importance for bioinorganic chemistry. In 1932 the existence of an enzyme catalyzing CO2 hydration in red blood cells was established,31 The enzyme was named carbonic anhydrase (abbreviated CA). In 1939 the enzyme was recognized to contain zinc (Zn).32 Because CO2 is either the starting point for photosynthesis or the endpoint of substrate oxidation, carbonic anhydrases are now known to be ubiquitous, occurring in animals, plants, bacteria, and fungi. Different enzymes from different sources, catalyzing the same reaction and usually having homologous structures, are termed isoenzymes. Thus far, a total of 7 distinct classes of CAs have been identified based upon organism: alpha, beta, gamma, delta, zeta, eta, and theta. Each class may contain multiple isoenzymes. Sometimes the same organism has more than one isoenzyme for a particular function, as is true for human carbonic anhydrase. Humans have 15 CAs that belong to the alpha class; these isozymes vary by location in the body and by catalytic activity. CA is a classic example of a hydrolytic enzyme, one that catalyzes addition or removal of water to a substrate molecule. More specifically, CA catalyzes the reversible conversion of carbon dioxide (CO2) to bicarbonate (HCO3-), also referred to as carbonic acid.



Although hydration of CO2 is spontaneous in water at pH 7, the reaction is kinetically slow (k = 10-1 s-1), too slow to convert all CO2 produced in respiration. Only above pH 9 does the uncatalyzed reaction become fast, owing to direct attack of OH-, which is a much better nucleophile than H2O (k = 104 M-1 s-1, where M-1 refers to the OH- concentration). The figure below compares nucleophilic attack of water versus hydroxide (OH-) on CO2.

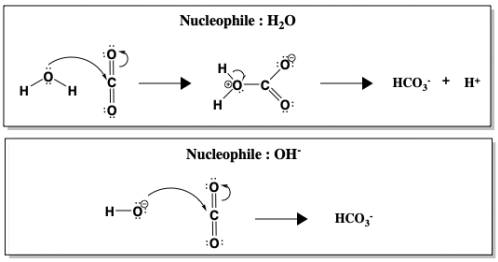


Figure: This figure depicts nucleophilic attack on carbon in carbon dioxide (CO2) in the formation of bicarbonate (HCO3-). In the top panel, H2O is the nucleophile. The bottom panel shows the reaction with hydroxide (OH-) as the nucleophile. Since the OH- is a stronger nucleophile, HCO3- formation is faster when OH- is the nucleophile.

Between H2O and OH-, formation of HCO3- occurs faster when OH- is the nucleophile. A faster reaction at higher pH, when more OH- ions are present, suggests OH- is involved in the rate determining step. However, realistically, the pH of human blood cannot be changed to speed up hydration of CO2. Instead, humans use carbonic anhydrase to catalyse the reaction. When CA is present, the reaction is sped up to a rate of k = 106 s-1.

The ubiquity of CA in different organisms reflects the importance of these enzymes in sustaining life. The speed of CA-catalyzed CO2 hydration is essential to meet the needs of living cells. Some physiological CA functions include pH regulation, electrolyte secretion, ion transport, and CO2 homeostasis. In the digestive tract, CAs plays a role in the secretion of acid and keep saliva neutral by modulating pH.G,H Among these functions, CA most notably plays a role in transport of CO2 and HCO3- related to respiration, the process of atmospheric oxygen and carbon dioxide exchange that occurs when humans inhale oxygen and exhale carbon dioxide. With low solubility, CO2 must be converted to a more soluble form, HCO3-, for transport throughout the body. Bicarbonate ion (HCO3-) eventually reaches the lungs, gets converted back to CO2, and exits the body through exhalation.C

Medical research revolving around CA focuses on the Zn-containing active site as a therapeutic target for various disease treatments; both CA inhibitors and activators are incorporated in drug design. CA inhibitors are used as treatment for epilepsy, ulcers, cancer, obesity, and other neurological disorders. In the eye, CA produces hydrogen ions that maintain optic pressure.

However, too much pressure in the eye can damage the optic nerve and cause glaucoma. CA activity can create a concentration gradient that drives the transport of water to the optical nerve. When too much water is around the optical nerve, pressure around the nerve increases causing damage. Inhibition of CA has become a key treatment of glaucoma.

Beyond pharmaceutical applications, CA has also been investigated for its utility in carbon capture and carbon sensor applications. Carbon capture and storage happens as CAs convert CO2 to bicarbonate. Increased availability of bicarbonate in the presence of calcium ions (Ca2+) causes precipitation of calcite (CaCO3). This process, called bio-mineralization, may be a viable mode of long term storage of CO2 in calcite to mitigate CO2 emissions.

Details about the structure and function of CA's Zn-containing active site have been elucidated over 80 years of research. The current article delves into the metalloenzyme active site using bioinorganic concepts.

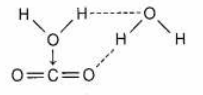
Old Text Below ----------

Carbon-dioxide hydration and its mechanism in living systems are of fundamental importance for bioinorganic chemistry. In 1932 the existence of an enzyme catalyzing CO_2 hydration in red blood cells was established,[31] The enzyme was named carbonic anhydrase (abbreviated CA). In 1939 the enzyme was recognized to contain zinc.[32] Because CO_2 is either the starting point for photosynthesis or the endpoint of substrate oxidation, carbonic anhydrases are now known to be ubiquitous, occurring in animals, plants, and several bacteria. Different enzymes from different sources, catalyzing the same reaction and usually having homologous structures, are termed isoenzymes. Sometimes the same organism has more than one isoenzyme for a particular function, as is true for human carbonic anhydrase.

CO_2 gas is relatively soluble in water (3×10^{-2} M at room temperature under p_{CO2} = 1 atm), equilibrating with hydrogen carbonate at pK_a 6.1:

$$CO_2 + H_2O \rightleftharpoons HCO_3^- + H^- \quad (2.6)$$

The uncatalyzed reaction is kinetically slow around physiological pH ($k \simeq 10^{-1}\ s^{-1}$), whereas, in the presence of the most efficient isoenzyme of CA, the maximal CO_2 turnover number (i.e., the number of substrate molecules transformed per unit time by each molecule of enzyme)[33] is $\simeq 10^6\ s^{-1}$. The uncatalyzed attack by water on CO_2 may be facilitated by two hydrogen-bonded water molecules, one of which activates the carbon by means of a hydrogen bond to a terminal CO_2 oxygen, the other of which binds the carbon atom via oxygen: [34,35]



Only above pH 9 does the uncatalyzed reaction become fast, owing to direct attack of OH^-, which is a much better nucleophile than H_2O ($k \simeq 10^4\ M^{-1}s^{-1}$, where M^{-1} refers to the OH^- concentration):

$$CO_2 + OH^- \rightleftharpoons HCO_3^- \quad (2.8)$$

On the other hand, the rate constant in the presence of the enzyme, called k_{cat}, is pH-independent above pH 8 in every CA isoenzyme (Figure 2.2).[33,36]

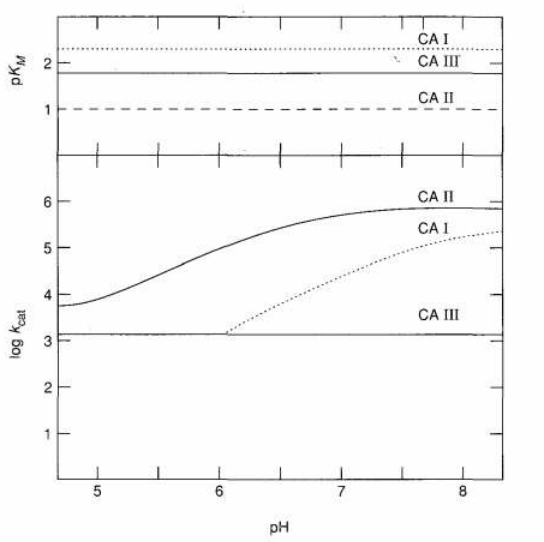


Figure 2.2 - pH dependence of k_{cat} and K_m values for CO_2 hydration catalyzed by carbonic anhydrase I, II, and III isoenzymes.[33,36]

In vitro, carbonic anhydrase is quite versatile, catalyzing several reactions that involve both OH^- and H^+, such as the hydrolysis of esters and the hydration of aldehydes. The various isoenzymes have been characterized to different degrees of sophistication. High-activity forms are labeled II ($k_{cat} \simeq 10^6\ s^{-1}$ at 25 °C); low-activity forms I ($k_{cat} \simeq 10^5\ s^{-1}$), and the very-low-activity forms III ($k_{cat} \simeq 10^3\ s^{-1}$).[37] X-ray structural information at nominal 2 Å resolution is available for HCA I[38] and HCA II,[39] where H indicates human. The structure of HCA II has been refined recently.[40] High-resolution structures of mutants and of their substrate and inhibitor derivatives are being reported.[211] All isoenzymes are single-chain polypeptides, with M.W. about 30 kDa and one zinc ion per molecule. They have the shape of a rugby ball with a crevice 16 Å deep running through the south pole (Figure 2.3 See color plate section, page C-2.). At the bottom of the crevice, the zinc ion is anchored to the protein by three histidine nitrogen atoms and is exposed to solvent. Two histidines (His-94 and His-96, HCA I numbering) are bound to zinc via their Nϵ2 atoms, whereas one (His-119) is bound via its Nδ1 atom (Figure 2.4). It is quite general that histidines bind zinc equally well by either of the two histidine nitrogens, the preference being probably dictated by the steric constraints imposed by the protein folding. The three histidine NH protons are all engaged in H-bonding (Figure 2.4). Histidine-119 is involved in H-bonding with a glutamate residue. As mentioned, this could be a way of controlling the basicity of the metal ligands. A solvent molecule bound to zinc is involved in an H-bond with Thr-199, which in turn is H-bonded to Glu-106. This H-bonding network is important for understanding the subtle structural changes that occur with pH changes; these could, in principle, account for the pH-dependent properties. Although the structure of crystals grown at pH 8 in sulfate-containing buffer gives some indication of a single solvent molecule bound to zinc (Figures 2.3 and 2.5 See color plate section, pages C2, C3.), theoretical studies indicate that two water molecules can be at bonding distances.[42] Such a finding is consistent with spectroscopic studies on other derivatives and with the concept that attachment and detachment of substrates occur through five coordination.

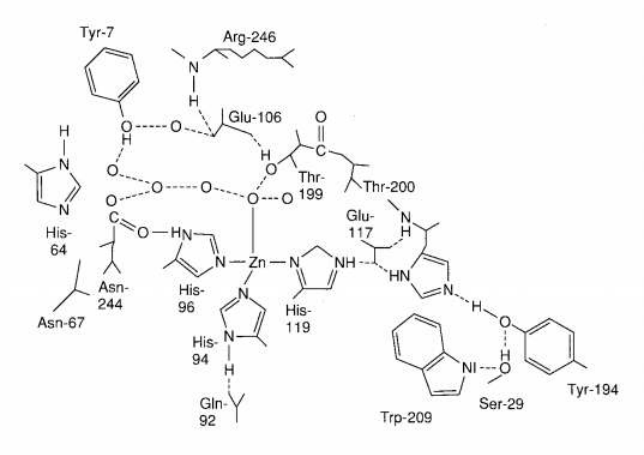


Figure 2.4 - Schematic representation of the active site of human carbonic anhydrase II. Hydrogen bonds (---) and ordered water molecules (o) are indicated.[41]

Just as is true for every zinc enzyme in which zinc is at the catalytic site, activity is lost if the metal is removed, and is restored by zinc uptake. The tertiary structure of carbonic anhydrase is maintained in the absence of zinc; even the denatured apoprotein can refold spontaneously from a random coil to a native-like conformation. Although such a process is accelerated by zinc,[43,44] the presence of the metal does not seem to be an absolute requirement for the correct folding of CA, whereas it is an absolute requirement for several other metalloproteins.[23,29,30]

Anions are attracted in the metal cavity by the positive $Zn(N_3OH_2)^{2+}$ moiety, and are believed to bind to zinc in carbonic anhydrase very effectively; so their use should be avoided as much as possible if the goal is to study the enzyme as it is. When the protein is dialyzed against freshly doubly distilled or carefully deionized water under an inert atmosphere, the pH of the sample approaches the isoelectric point, which is below 6 for HCA I and bovine (BCA II) enzymes. The pH can then be adjusted by appropriate additions of NaOH. All the measurements reported in the literature performed in acetate, phosphate, imidazole, or tris sulfate buffers are affected by the interference of the anion with the metal ion. However, buffer species containing large anions like Hepes (4[(2-hydroxyethyl)-l-piperazinyl]ethanesulfonic acid) can be used,[45] since these anions do not enter the cavity.

There are many indications that zinc in the high-pH form of CA is four-coordinate with an OH group in the fourth coordination site. At low pH the enzyme exists in a form that contains coordinated water; the coordination number can be four (one water molecule) or five (two water molecules). Of course, the occurrence of the low-pH species depends on the pK_a's of the complex acid-base equilibria.

11.2.2.1: About Carbonic Anhydrase is shared under a CC BY-NC-SA 4.0 license and was authored, remixed, and/or curated by LibreTexts.

11.2.2.2: Acid-base Equilibria

It is convenient to discuss the cobalt-substituted carbonic anhydrase enzyme, since its electronic spectra are markedly pH-dependent and easy to measure (Figures 2.7 and 2.8).[56,57] The spectra are well-shaped, and a sharp absorption at 640 nm is present at high pH and absent at low pH. Whereas CoHCA I is almost entirely in the low-pH form at pH 5.7, this is not true for the CoBCA II isoenzyme. The acid-base equilibrium for Co-substituted carbonic anhydrase (deprotonation of the metal-coordinated water) involves three species:

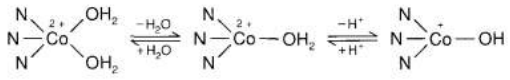


Figure 2.8).

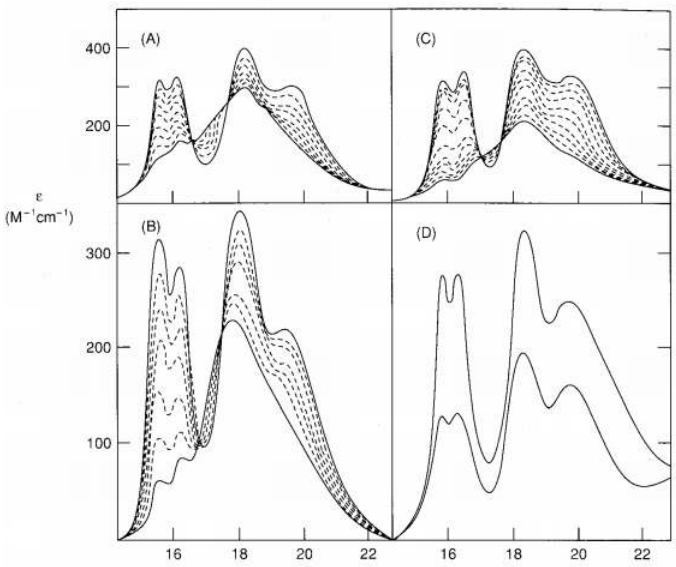


Figure 2.7 - pH-variation of the electronic spectra of cobalt(II)-substituted BCA II (A), HCA II (B), HCA I (C), and BCA III (D). The pH values, in order of increasing $\epsilon_{15\cdot6}$, are (A) 5.8, 6.0, 6.3, 6.7, 7.3, 7.7, 7.9, 8.2, 8.8; (B) 6.1, 6.6, 7.1, 7.8, 8.3, 8.6, 9.5; (C) 5.3, 6.1, 6.6, 7.0, 7.3, 7.5, 7.9, 8.4, 8.6, 9.1, 9.6.[56]

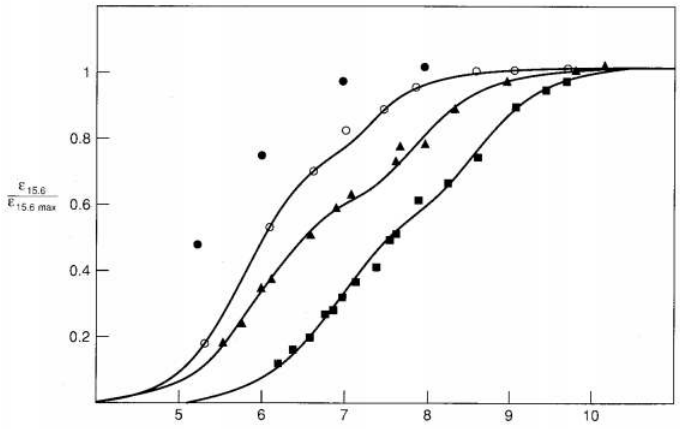


Figure 2.8 - pH dependence of $\epsilon_{15\cdot6}$ for cobalt(II)-substituted BCA III (●), *HCA II (o), BCA II* (▲), *and HCA I* (■) *isoenzymes. The high pH limit value of* $\epsilon_{15\cdot6}$ *is normalized to I for each isoenzyme.*[57]

* An isosbestic point is a value of frequency where the two species in an A ⇌ B equilibrium have the same absorption. As a consequence, all mixtures of A and B also show the same absorption at that frequency, and all the spectra along, e.g., a pH titration from A to B, plotted one on top of the other, cross at the isosbestic point. The presence of isosbestic points thus indicates the presence of only two species in equilibrium.

These kinds of isoenzymes contain at least another histidine in the cavity, which represents another acidic group, with a pK_a of about 6.5 in its free state. The interaction between such an acidic group and metal-coordinated water, for example, via a network of hydrogen bonds, provides a physical picture that can account for the observed experimental data.[49] Two apparent acid dissociation constants K_a can be obtained from the fitting of the curves of Figure 2.8. They are called apparent, because they do not represent actual acid dissociations at the microscopic level. When there are two acidic groups interacting with each other, the system must be described in terms of four constants, also called microconstants, because the dissociation of each of the two groups is described by two different pK_a's, depending on the ionization state of the other group (Figure 2.9); so the two apparent constants can be expressed in terms of four microconstants describing two interacting acidic groups.

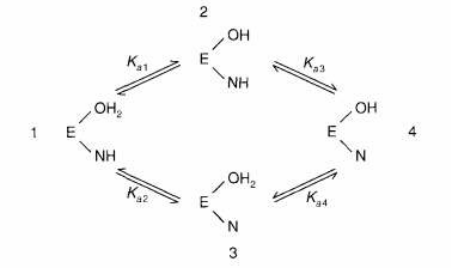


Figure 2.9 - General scheme for two coupled acid-base equilibria applied to carbonic anhydrase. The two acid-base groups are the metal-coordinated water molecule and a histidine residue present in the active-site cavity.[58]

It is again a general feature of these systems that the four microconstants can be obtained only by making some assumptions. In one analysis the molar absorbances of species (1) and (3), and of species (2) and (4), were assumed to be equal.[58] In other words, it is assumed that the changes in the electronic spectra of cobalt(II) (Figure 2.7) are due entirely to the ionization of the coordinated water, not at all to the ionization state of the other group. This assumption accounts for the observation of approximate isosbestic points, even though there is an equilibrium between more than two species. With this assumption the four microconstants could be obtained (Table 2.5).

Table 2.5 - Values of microconstants associated with acid-base equilibria[a] in cobalt(II)-substituted carbonic anhydrases.[58]

a) As defined in Figure 2.9

	pK_{a1}	pK_{a2}	pK_{a3}	pK_{a4}
CoHCA I	7.14	7.21	8.45	8.38
CoHCA II	5.95	562	6.62	6.95
CoBCA II	6.12	6.28	7.75	7.59

Recall that the activity and spectroscopic profiles follow one another (see Figure 2.2 and Section IV.B). Furthermore, similar microconstant values had been obtained on ZnHCA II by analyzing the pH dependence of the maximum velocity of the hydration reaction, V_{max}, assuming that the two hydroxo-containing species had the same activity.[49] The present analysis implies that species (2) and (3) of Figure 2.9 are distinguishable, although their interconversion may be fast.

Metal coordination lowers the pK_a of coordinated water. Factors affecting the acidity of the coordinated water are many, and their effects are probably overlapping, making the analysis quite complex (see also Section III.A). Nonetheless, the following factors probably contribute to the lowering of the pK_a:

1. the charge of the chromophore, which in this case is 2+, although it may be somewhat lowered by the H-bonding between a coordinated histidine and a negative glutamate residue;
2. the coordination number (which is four), since a higher value leads to a larger electron density on the metal ion ligands;
3. the presence of other acidic groups with which the coordinated water interacts;
4. the presence of positively charged residues inside the metal binding cavity that favors the removal of a proton from the cavity.

This last factor is presumably operating for CA III, which contains several arginine residues in the cavity; the same factor may also induce changes in the microscopic properties of the solvent inside the active cavity. These considerations account for the

observation that most model complexes have a significantly higher pK_a value than the protein itself.

11.2.2.2: Acid-base Equilibria is shared under a CC BY-NC-SA 4.0 license and was authored, remixed, and/or curated by LibreTexts.

11.2.2.3: Catalytic Mechanism

All the above structural and kinetic information obtained under a variety of conditions with different metal ions can be used to propose a catalytic cycle for carbonic anhydrase (Figure 2.21), As shown by studies on the pH-dependent properties of native and metal-substituted CAs, both type-I and type-II proteins have two acidic groups, the zinc-coordinated water and a free histidine. At physiological pH the enzyme is essentially in the Zn—OH form (step A in Figure 2.21). A Zn—OH moiety is a relatively good nucleophile, poised for nucleophilic attack on carbon dioxide. It is possible that the hydrogen bond with Thr-199, which seems to be consistent with an sp^3 oxygen, orients the OH for attack at the substrate CO_2 . Studies of the copper derivative indicated that the concentration of CO_2 in the cavity is higher than in bulk solution (step B).

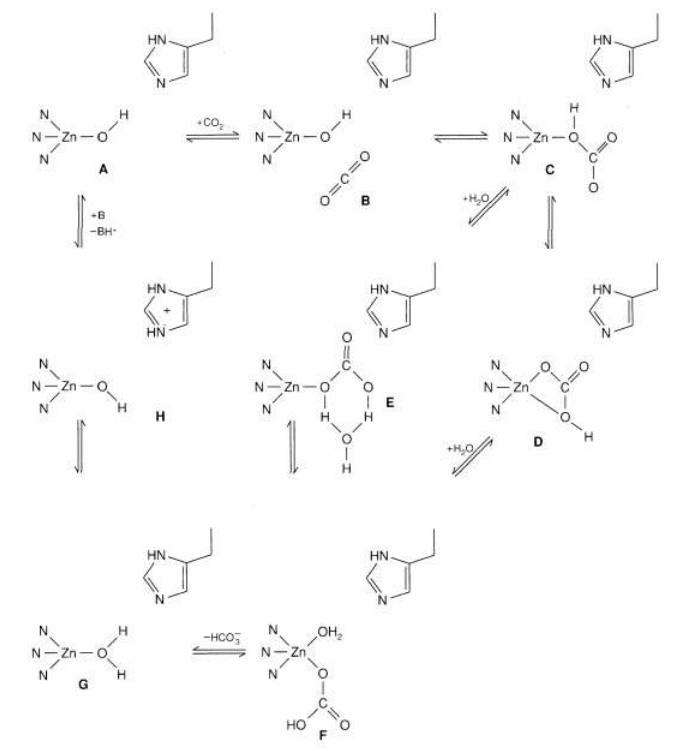


Figure 2.21 - Proposed catalytic cycle of CA.

Molecular dynamics calculations have shown that there are either three[96] or two[97] potential wells for CO_2 in the hydrophobic pocket. It was shown[98] that when Val-143 is replaced by the much larger Phe, the activity decreases by a factor of 10^3. Apparently the large Phe residue does not leave space within the cavity to accomodate CO_2.

It would also be nice if the enzyme were able to activate CO_2. There is no evidence that it does, even though the positive charge around zinc and the NH of Thr-199 would represent two electrostatic attraction points that could activate CO_2. It is well-known that CO_2's interactions with positive charges activate the carbon for nucleophilic attack.[99,100] The positioning of CO_2 between zinc and the peptide NH of Thr-199 would be ideal for the OH attack. Merz[97] locates it as shown in Figure 2.22.

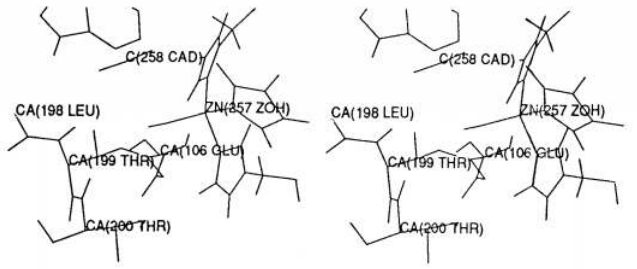


Figure 2.22 - Stereo view of the site of activation of CO_2 in the cavity of CA as proposed by Merz.[97]

It was believed that, once bicarbonate is formed (C), the proton has to transfer to a terminal oxygen atom, either via an intermediate in which bicarbonate is bidentate (D) or via a hydrogen-bond network (E). Indeed, in model compounds one would expect HCO_3^- to bind through a nonprotonated oxygen. However, the possibility of restoring the hydrogen bond with Thr-199 as in sulfonamide adducts could justify the presence of the hydrogen on the coordinating oxygen.[214] The bicarbonate derivative is presumably in equilibrium between four- and five-coordinate species (F), as shown by the electronic spectra of the cobalt derivative.[59] The five-coordinate species provides a low barrier for the substrate detachment step via an associative mechanism involving coordination of a water molecule (G). A possible five-coordinate species would contain bicarbonate in the B site and water in the C site (Figure 2.12). It is reasonable that the measured K_m for the reaction of bicarbonate dehydration is the thermodynamic dissociation constant of the M—HCO_3^- species. Anionic or neutral inhibitors are competitive with bicarbonate because they tend to bind at the same site. At this stage the second substrate, which is H^+, has to be released (H). It is reasonable that the water proton transfers to a group inside the cavity, e.g. , the free histidine mentioned above, and subsequently to the solvent. In the absence of buffers the latter step is rate-limiting for the high-activity isoenzymes, since the diffusion rate cannot exceed the product of the concentration times the diffusion coefficient, i.e., 10^{-7} M x 10^{11} $M^{-1}s^{-1}$. Such a limit is then 10^4 s^{-1}, whereas the turnover rate is 10^6 s^{-1}. The presence of buffer can assist in proton transfer at this stage, in such a way that the rate-limiting step becomes the internal proton transfer. The release of H^+ from the Zn—OH_2 moiety is also the rate-limiting step for the low-activity CA III, as nicely shown by the electronic spectra of CoCA III. These spectra change from the basic form at the beginning of the reaction to the acidic form upon CO_2 addition (Figure 2.23).[101] After the interconversion of CO_2 into bicarbonate, there is an accumulation of the $CoOH_2$ species, the deprotonation of which is slower than the release of HCO_3^-.

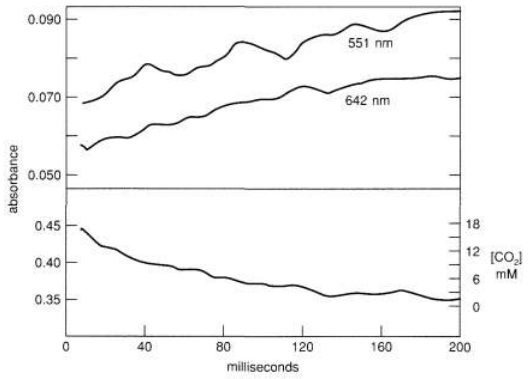


Figure 2.23 - Time dependence of $\epsilon_{15.6}$ and $\epsilon_{18\cdot1}$ of cobalt(II)-substituted CA III after addition of CO_2 to a buffered enzyme solution at pH 8. The initial drop of absorbance reflects the accumulation of a $CoOH_2$ intermediate.[101]

11.2.2.3: Catalytic Mechanism is shared under a CC BY-NC-SA 4.0 license and was authored, remixed, and/or curated by LibreTexts.

11.2.2.4: Coordinated Water and NMR

It is quite relevant to know whether a water molecule is coordinated to the metal ion in a metalloenzyme, and whether it is still coordinated in the presence of substrates and inhibitors. The presence or absence of H_2O coordinated to a paramagnetic center can in principle be monitored by solvent water ^{1}H NMR,[69] by exploiting the occurrence of a magnetic interaction between the magnetic moments of the unpaired electrons and the nuclear magnetic moments of the water protons. When this interaction fluctuates with time, it causes a shortening of the water-proton relaxation times.*

* The nuclear longitudinal relaxation time, T_1 can be defined as the rate constant by which the populations of the $M_I = \frac{1}{2}$ and $M_I = -\frac{1}{2}$ (for protons) levels reach their equilibrium value after an external perturbation (e.g., a radiofrequency pulse in an NMR experiment). The transverse relaxation time, T_2, can be defined as the average lifetime of a hydrogen nucleus in a given spin state. The NMR linewidth is inversely proportional to T_2. The relation $T_2 \leq T_1$, always holds.

The longitudinal relaxation rate values, T_1^{-1}, of all the solvent water protons increase when even a single water molecule interacts with a paramagnetic center, provided that this bound water exchanges rapidly with free water molecules. To obtain the necessary experimental data, a methodology has been developed based on the measurement of water ^{1}H T_1^{-1} values at various magnetic fields (Nuclear Magnetic Relaxation Dispersion, NMRD).[69-71] The experimental data contain information on the correlation time, i.e., the time constant for the dynamic process that causes the proton-unpaired electron interaction to fluctuate with time; furthermore, under certain conditions, they may provide quantitative information on the number of interacting protons and their distance to the metal. The enhancement of T_1^{-1}, called T_{1p}^{-1}, is caused by the paramagnetic effect on bound water molecules and by the exchange time τ_m, according to the relationship

$$(T_{1p})^{-1} = f_M(T_{1M} + \tau_M)^{-1} \tag{2.11}$$

where f_M is the molar fraction of bound water and T_{1M} is the relaxation time of a bound water proton. Therefore we measure the water ^{1}H T_1^{-1}, subtract the diamagnetic effect (i.e., the water-proton relaxation rate measured in a solution of a diamagnetic analogue), obtain T_{1p}^{-1}, then check that τ_m is negligible with respect to T_{1M} For high-spin cobalt(II), T_{1M} is of the order of 10^{-3} s, whereas τ_m is about 10^{-5} s. Then the experimental T_{1p} can be safely related to T_{1M}. It is now important, in order to proceed with the analysis, to define the correlation time for the interaction between proton nuclei and unpaired electrons, τ_c. Its definition is important in order to obtain a physical picture of the system, and to quantitatively analyze the obtained T_{1M} values.[69] τ_c is defined by

$$\tau_c^{-1} = \tau_r^{-1} + \tau_s^{-1} + \tau_m^{-1} \tag{2.12}$$

where $(\tau)_r$ is the rotational correlation time, $(\tau)_s$ is the electronic relaxation time, and $(\tau)_m$has been previously defined. $(\tau)_r$ depends on the size of the molecule, which can be calculated rigorously if the molecule is spherical, or approximately if it is not. The appropriate expression is

$$\tau_r = \frac{4\pi\eta a^3}{3k_BT} \tag{2.13}$$

where η is the microviscosity of the solution, a is the radius (or approximate radius) of the molecule, k_B is the Boltzmann constant, and T is the absolute temperature. For CA, τ_r can be safely calculated to be $\simeq 10^{-8}$ s at room temperature. Since the correlation time τ_c in high-spin cobalt proteins varies between 10^{-11} and 10^{-12} s, it must therefore be determined by the electronic relaxation time.

Water ^{1}H NMRD profiles are often analyzed by using the classical dipolar interaction approach, as first described by Solomon:[72]

$$T_{1M}^{-1} = \frac{2}{15}\left(\frac{\mu_0}{4\pi}\right)^2 \frac{\gamma_I^2 g_e^2 \mu_B^2 S(S+1)}{r^6}\left(\frac{7\tau_c}{1+\omega_S^2\tau_c^2} + \frac{3\tau_c}{1+\omega_I^2\tau_c^2}\right) \tag{2.14}$$

where μ_0 is the permeability of vacuum, γ_I is the nuclear magnetogyric ratio, g_e is the electron g-factor, S is the electron spin quantum number, r is the electron-nucleus distance, and ω_S and ω_I are the electron and nuclear Larmor frequencies, respectively. This equation describes the dipolar interaction between the magnetic moment of nucleus $I(\hbar\gamma_I\sqrt{I(I+1)})$ and the magnetic moment of the electrons $S(g_e\mu_B\sqrt{S(S+1)})$as a function of the correlation time (τ_c) and of the magnetic field (expressed as $(\omega)_I$ and ω

s). Neglect of the zero-field splitting of the S = $\frac{3}{2}$ manifold may introduce an error in the quantitative estimates within a factor of two. [73]

Fitting of the data for pseudotetrahedral complexes shows that they have τ_s of 10^{-11} s, whereas five-coordinate complexes have a shorter τ_s, on the order of 10^{-12} s. The latter derivatives also have exchangeable protons that could correspond to a water molecule in the coordination sphere, whereas the former do not.[25] The τ_s values are thus proposed as indicators of the coordination number in low-symmetry, four- and five-coordinate cobalt complexes. The shorter electronic relaxation times are related to low-lying excited states, which, independently of the particular mechanism, favor electron relaxation.[74]

Short electronic relaxation times in paramagnetic compounds cause only minor broadening of ^{1}H NMR lines, whereas the isotropic shifts (i.e., the shifts due to the presence of unpaired electron(s), usually very large) are independent of the value of the electronic relaxation times. For cobalt-substituted carbonic anhydrase, the ^{1}H NMR spectra have been recorded for several derivatives, and the proton signals of histidines coordinated to the metal were found to be shifted well outside the diamagnetic region (Figure 2.14).[75] Five-coordinate species give sharper signals than four-coordinate ones. The spectra in D_2O for both kinds of derivatives show three fewer isotropically shifted signals than in H_2O. These signals are assigned to histidine NH protons, which are replaced by deuterons in D_2O. Five-coordinate species provide ^{1}H NMR spectra with many signals slightly shifted from the diamagnetic position. It is believed that such complexes have relatively large magnetic anisotropy, which, summed up to the external magnetic field, provides further differentiation in shifts of the protons. Such shift contributions are called pseudocontact shifts. These shifts depend on the third power of the distance from the metal and on the position of the proton with respect to the molecular axes. These signals belong to protons of noncoordinated residues from 5 to 10 Å from the metal. Their assignment in principle provides further information on the structure in the vicinity of the metal ion. The ^{1}H NMR spectra of cobalt(II) enzymes thus afford a powerful method for monitoring structure and reactivity of the metal-bound residues. This is one task for future investigations of the enzyme.

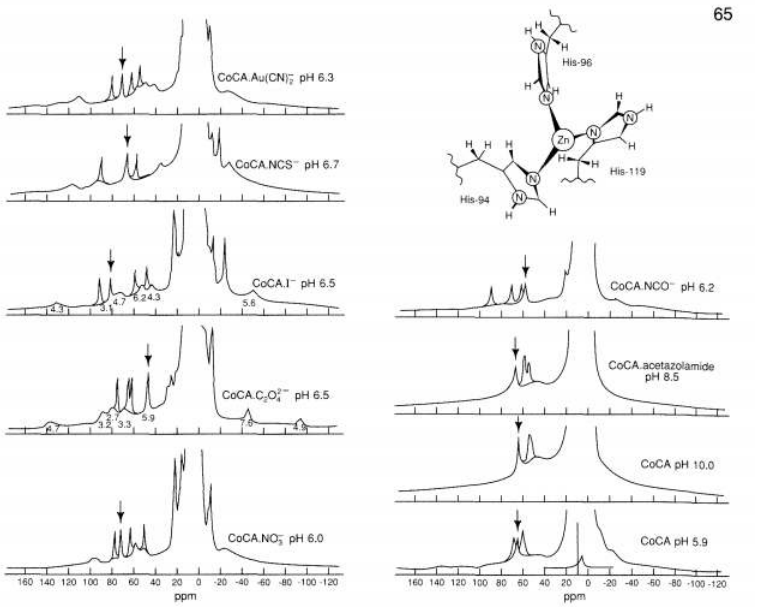


Figure 2.14 - ^{1}H NMR spectra of cobalt(II)-substituted bovine carbonic anhydrase II and some inhibitor derivatives. The three sharp downfield signals in each spectrum disappear in D_2O and are assigned to the exchangeable ring NH protons of the three coordinated histidines. The sharp signal labeled with an arrow is assigned to the Hδ2 proton of His-119, which is the only non-exchangeable ring proton in a meta-like rather than in an ortho-like position with respect to the coordinating nitrogen. The T_1 values (ms) of the signals for the I^- and $C_2O_4^{2-}$ derivatives are also shown.[25,75]

11.2.2.4: Coordinated Water and NMR is shared under a CC BY-NC-SA 4.0 license and was authored, remixed, and/or curated by LibreTexts.

11.2.2.5: Coordination Geometries

The binding of inhibitors is also pH-dependent. It is possible, however, to obtain fully inhibited systems by adjusting the inhibitor concentration and pH. In this manner the so-called limit spectra of CoCA derivatives are obtained. Many systems have been characterized, providing a variety of spectral characteristics[59] (Figure 2.10).

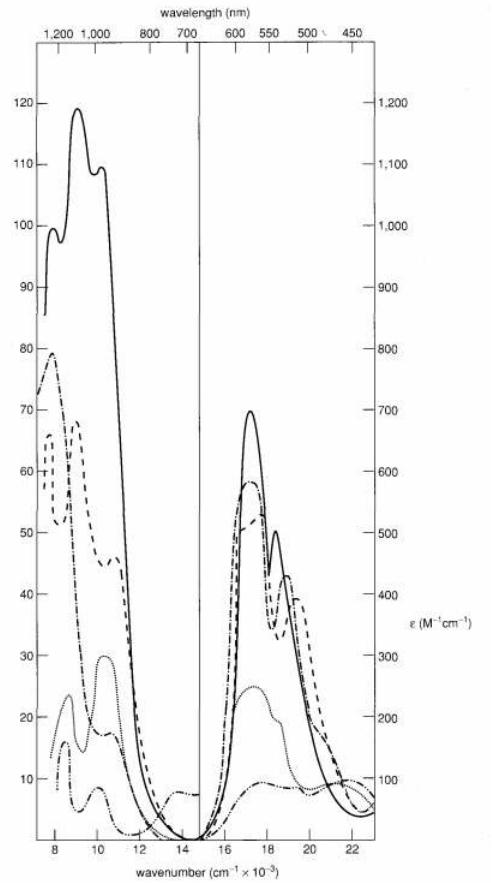


Figure 2.10 - Electronic spectra of cyanide (---), *cyanate* (-•-•-), *acetazolamide* (---), *azide* (• • • • •), *and thiocyanate* (-••-) *adducts of cobalt(II)-substituted bovine carbonic anhydrase II.*[59]

The differences in molar absorbance are larger than expected for changing only one coordinated atom. A rationalization of the experimental data came by applying a criterion, first suggested by Gray,[60] according to which four-coordinate species have larger maximal absorption than five-coordinate species. This property theoretically arises from greater mixing of p and d metal orbitals in the four-coordinate case, which makes the d-d transitions partially allowed, neglecting other factors such as the covalency of the coordination bond, nephelauxetic effects,* or vicinity of charge transfer bands. Subsequent extension of the measurements to the near-infrared region was instructive:[59] the low-intensity spectra exhibited a weak absorption between 13,000 and 15,000 cm^{-1}. The latter band was assigned to the highest in energy of the F → F transitions, which increases in energy with the coordination number. † Therefore both the low intensity of the bands (ϵ_{max} < 200 $M^{-1}cm^{-1}$) and the presence of the F → F transition at high energy were taken as evidence for five coordination. Spectra showing high maximal absorption (ϵ_{max} > 300 $M^{-1}cm^{-1}$) were assigned as arising from four-coordinate species. The corresponding chromophores are $CoN_3In(OH_2)$ and CoN_3In, where In denotes inhibitor. Intermediate maximal absorptions may indicate an equilibrium between four- and five-coordinate species. In Table 2.6 some inhibitors are classified according to their behavior. Bicarbonate, which is a substrate of the enzyme, gives rise to an equilibrium between four- and five-coordinate species.[48,59]

Table 2.6 - Classification of inhibitors of bovine carbonic anhydrase II according to the electronic spectral properties of the adducts with cobalt(II) derivatives. [a 48,59]

*Donor sets in parentheses

Four-coordinate	Equilibria between four- and five-coordinate species	Five-coordinate
Sulphonamides (N_4)	Bicarbonate (N_3O—N_3O_2)	Carboxylates (N_3O_2)
Cyanide (N_3C)	Chloride (N_3Cl—N_3OCl)	Thiocyanate (N_4O)
Cyanate (N_4)	Bromide (N_3Br—N_3OBr)	Nitrate (N_3O_2)
Aniline (N_4)	Azide (N_4—N_4O)	Iodide (N_3OI)
Phenol (N_3O)		
Chlorate (N_3O)		

* Nephelauxetic (literally, cloud-expanding) effects are due to partial donation of electrons by the ligand to the metal, and are stronger for less electronegative and more reducing ligands

† By F → F transition we mean here a transition between two electronic states originating from the same F term (the ground term) in the free ion and split by the ligand field; the stronger the ligand field, the larger the splitting. For high-spin cobalt(II), the free-ion ground state ^4F (quartet F) is split in octahedral symmetry into $^4T_{2g}$, $^4T_{1g}$, and $^4A_{2g}$ states, the $^4T_{2g}$ lying lowest; in lower symmetries the T states are further split. The highest F → F transition is, therefore, that from the ground state $^4T_{2g}$, or the lowest of its substates in low symmetry, to the $^4A_{2g}$ state. For the same type of ligands, e.g., nitrogens or oxygens, the ligand field strength, and therefore the energy of the F → F transition, increases with the number of ligands.

The differences in the electronic spectra outlined above also have been detected in both CD and MCD spectra. In the latter, pseudotetrahedral species give a sizably positive band in the high-energy region, whereas five-coordinate species show a much weaker positive band and six-coordinate complexes have only weak negative bands (Figure 2.11).[21,61] This additional empirical criterion may be helpful in assigning the coordination number. A further criterion is based on how much of the splitting of the S = $\frac{3}{2}$ ground state is caused by spin-orbit coupling (zero-field splitting). This splitting can be indirectly measured from the temperature dependence of the electronic relaxation times of the cobalt complexes, in turn estimated from their ability to saturate the EPR lines of the complexes at low temperatures.[62] There are theoretical reasons to predict that the above splitting increases in the order four coordination < five coordination < six coordination.[63]

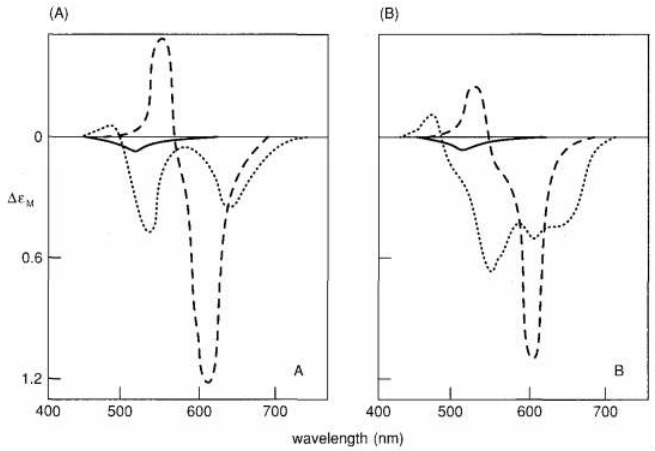


Figure 2.11 - (A) MCD spectra of model six-coordinate ($Co(Gly\text{-}Gly)_2$, ——), *five-coordinate* ($(CoMe_6tren)Br_2$, ...), *and four-coordinate* ($Co(py)_2Br_2$, ---) *cobalt(II) complexes and (B) MCD spectra of the cobalt(II) derivatives of pyruvate kinase* (——), *alkaline phosphatase* (• • • • •), *and carbonic anhydrase in the presence of acetazolamide* (---).[21,61]

https://chem.libretexts.org/@go/page/437996

Three binding sites have been identified in the cavity of CA[40,64-66] (Figure 2.12). The OH^- binding site, which provides a tetrahedral structure around the metal ion, is called the A site. The hydrogen interacts via hydrogen bonding with the oxygen of Thr-199. Thr-199 and Thr-200, together with their protein backbone, identify a hydrophilic region that probably plays a fundamental role in the energetic balance of ligand binding. On the back of the cavity there is a hydrophobic region formed by Val-143, Leu-198, and Trp-209. Although this cavity is hydrophobic, the x-ray structure shows evidence of a water molecule, H-bonded to the coordinated water. Ligands with a hydrophobic end could easily be located in this binding position, which is called B. The coordinated water molecule would change its position in order to make reasonable angles between coordinated groups. The new position is labeled C. The x-ray structure of the thiocyanate derivative of HCA II[40,64] illustrates the latter case (see Figure 2.5). The NCS^- ion is in van der Waals contact with Val-143, Leu-198, and Trp- 209. The water interacts with the hydroxyl group of Thr-199. The geometry of the five-coordinate derivative can be roughly described as a distorted square pyramid with His-94 in the apical position (Figure 2.13A). This could be a typical structure for those derivatives that have spectra typical of five-coordinate adducts, like the carboxylate derivatives.

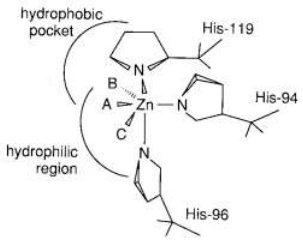


Figure 2.12 - Schematic drawing of the active cavity of HCA II showing the three possible ligand binding sites.[64- 66] Site A is the site of the OH^- ligand in the active form; site B is the binding site of NCS^- , which gives rise to a five-coordinate adduct with a water molecule in the C site.[64-66]

In aromatic sulfonamide ($Ar—SO_2—NH_2$) derivatives, which probably bind as anions (see Section IV.C.4), the NH^- group binds zinc in the A position,[64--66] giving rise to an H-bond with Thr-199. The oxygens do not interact with the metal; one of them sits in the hydrophobic pocket. The chromophore around zinc is pseudotetrahedral (Figure 2.13B). The energy involved in the coordination includes the coordination bond, the hydrophobic interactions of the aromatic sulfonamide ring, and the maintainance of the Zn-X-H-Thr-199 hydrogen bonding (X=N,O). It is interesting to note that cyanate, according to spectroscopic studies,[48,59] gives rise to tetrahedral derivatives, probably because the terminal oxygen can enter into H-bonds with the hydrophilic region of the cavity. ^{13}C NMR data on $N^{13}CO^-$ interacting with CoBCA indicate that the anion interacts directly with the metal ion.[67] We do not have direct information on where it binds.[212]

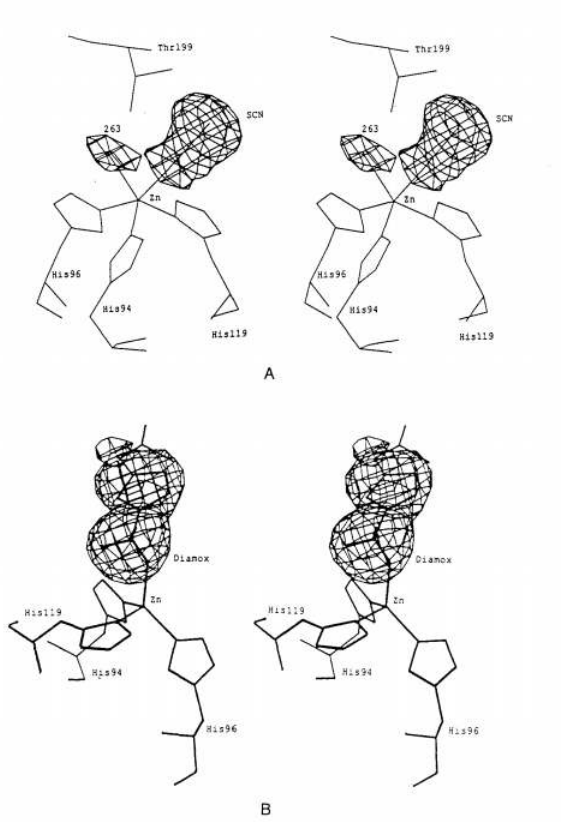


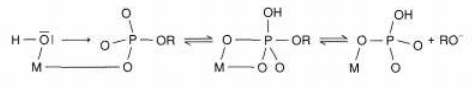
Figure 2.13 - Stereo views of the NCS^- (A) and acetazolamide (B) adducts of HC II.[40]

The fine balance between hydrophobic and hydrophilic interactions, as well as major steric requirements, play important roles in the binding of inhibitors. Cyanide is the only ligand that may bind in a 2:1 ratio.[68] It is likely that the bis-cyanide adduct has the same arrangement as the NCS^-—H_2O derivative. The spin state of the bis-cyanide adduct is $S = \frac{1}{2}$.[68]

11.2.2.5: Coordination Geometries is shared under a CC BY-NC-SA 4.0 license and was authored, remixed, and/or curated by LibreTexts.

11.2.2.6: Ester Hydrolysis and Phosphoryl Transfer

Hydrolysis of carboxylic and phosphoric esters is also a slow process at neutral pH, and is catalyzed by acids and bases by mechanisms similar to those involved in amide and peptide hydrolysis. Metal ions are also good catalysts of both carboxylic and phosphoric ester hydrolysis, typically with rate increases much higher than those observed for hydrolysis of amides or peptides (Table 2.8). The ability of metal ions to coordinate to the carbonyl oxygen—which is higher in amides than in esters—is inversely correlated with their catalytic properties, perhaps because the main role of the metal ion is not in polarizing the carbonyl group, but in providing a metal-coordinated hydroxide as the attacking nucleophile.[108] For the hydrolysis of phosphate esters, it is difficult to draw conclusions based on experience with carboxylic esters, because, although the coordinating ability of the phosphoric oxygen may be higher, thus favoring the polarizing role of the metal, the nucleophilic attack is also likely to be easier, because the energy of the trigonal bipyramidal intermediate is probably rather low. Base-catalyzed hydrolysis of phosphate esters occurs with inversion of configuration, and this supports the existence of a trigonal bipyramidal intermediate.[140] The metal acts both as activator of substrate through binding and as Lewis acid to provide the OH moiety for the nucleophilic attack:



As with peptide hydrolysis, several enzyme systems exist that catalyze carboxylic and phosphoric ester hydrolysis without the need for a metal ion. They generally involve a serine residue as the nucleophile; in turn, serine may be activated by hydrogen-bond formation—or even proton abstraction—by other acid-base groups in the active site. The reaction proceeds to form an acyl- or phosphoryl-enzyme intermediate, which is then hydrolyzed with readdition of a proton to the serine oxygen. Mechanisms of this type have been proposed for chymotrypsin.[141] In glucose-6-phosphatase the nuc1eophile has been proposed to be a histidine residue.[142]

Again by analogy with peptide hydrolysis, metalloenzymes catalyzing ester hydrolysis may take advantage of additional chemical features provided by amino-acid residues present in the active-site cavity. This situation occurs with carboxypeptidase,[143] which shows esterase activity *in vitro*. Although the rate-limiting steps for carboxylic esters and peptides may differ, several features, such as the pH dependences of k_{cat} and K_m and the presence of two spectroscopically observable intermediates, point to substantially similar mechanisms. On the other hand, carboxylic ester hydrolysis catalyzed by carbonic anhydrase seems to rely on fewer additional features of the active-site cavity, perhaps only on the presence of a metal-coordinated hydroxide that can perform the nucleophilic attack on the carbonyl carbon atom.[47]

Metalloenzyme-catalyzed phosphoric ester hydrolysis can be illustrated by alkaline phosphatase, by far the most-investigated enzyme of this class. The protein is a dimer of 94 kDa containing two zinc(II) and one magnesium(II) ions per monomer, and catalyzes, rather unspecifically, the hydrolysis of a variety of phosphate monoesters as well as transphosphorylation reactions. The x-ray structure at 2.8 Å resolution obtained on a derivative in which all the native metal ions were replaced by cadmium(II) reveals three metals in each subunit, all located in a single binding region (Figure 2.32). In the native enzyme M_1 and M_2 sites are occupied by zinc and M_3 by magnesium.[144] M_1 was first reported to be coordinated to three histidine residues (His-331, 372, and 412 in Figure 2.32). Further refinement indicated that Asp-327 could be a ligand to M_1, in the place of His-372.[145] ^{1}H NMR spectroscopy of the enzyme with cobalt substituted in the M_1 site shows that there are three exchangeable protons sensing the paramagnetic metal ion.[146] They could come from three histidine NHs, or from two histidine NHs and another group containing the exchangeable proton very close to the metal ion, like an arginine. Protein ligands to M_2 are Asp-369, His-370, and Asp-51, the latter probably bridging M_2 to M_3 with the other carboxyl oxygen. M_3 is coordinated, in addition, to Asp-51, to Asp-153, to Thr- 155, and to Glu-322. Several spectroscopic pieces of evidence on the native and metal-substituted derivatives indicate that M_1 is five-coordinate, but M_2 and M_3 are six-coordinate, probably with water molecules completing the coordination spheres.[28]

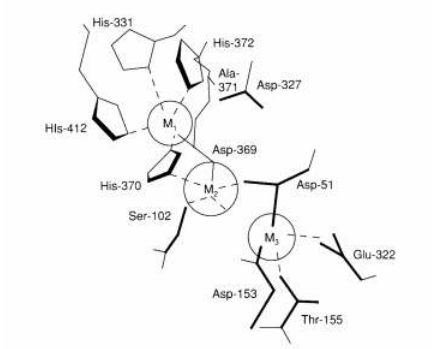


Figure 2.32 - Schematic drawing of the active-site cavity of a subunit of alkaline phosphatase.[28,144,145] The catalytic metal is labeled M_1. The M_1-M_2 distance is = 4 Å, the M_2-M_3 distance is = 5 Å, and the M_1-M_3 distance is = 7 Å.[144,145]

M_1 is essential for activity, but full catalytic efficiency is reached only when all metal ions are present. These data suggest that maximum activity is the result of fine-tuning several chemical properties of the active site as a whole, including the nature of the M_1 metal, which can be only zinc or cobalt (Table 2.4).

A further key feature of the active site is the presence of a serine residue (Ser-102), the oxygen atom of which is close to the M_1 - M_2 pair (especially to M_2), although not at direct binding distance according to the crystal structure. There is ample and direct evidence that Ser-102 is reversibly phosphorylated during the course of the catalytic reaction, and that M_1 is able to coordinate a phosphate ion.[28]

Another crucial piece of information obtained by physico-chemical techniques is that the lability of the phosphoseryl intermediate and the catalytic activity increase with pH, depending on the state of ionization of an active-site group, which is most likely a water molecule coordinated to M_1.[147] Thus the active form of the enzyme is again a metal-hydroxide species. Furthermore, an inactive derivative with copper ions in the M_1 and M_2 sites shows evidence of magnetic coupling between the metal ions, of the magnitude expected if the two metals shared a common donor atom.[148] Likely candidates are a bridging hydroxide ion or Ser-102, which thus might be somewhat mobile relative to the position occupied in the x-ray structure, and demonstrate its potential ability to be activated for the nucleophilic attack by coordination to a metal ion. Such a mechanism would be an "inorganic" version of the type of activation postulated for chymotrypsin and other hydroIases.

A possible mechanism for alkaline phosphatase-catalyzed phosphoric ester hydrolysis could involve the following steps (Figure 2.33):

1. Binding of the phosphate group to M_1—in the place of a water molecule—by one of the nonprotonated oxygens, and subsequent activation of the phosphorus atom for nucleophilic attack. The binding of the substrate may be strengthened by interaction with the positively charged Arg-166 residue[149] (not shown). The steric alteration in the active site could cause movement of Ser-102 toward M_2, with deprotonation upon binding.
2. Nucleophilic attack on phosphorus by the coordinated serine alkoxide, cleaving the ester bond and liberating the alcohol product.
3. Formation of the phosphoseryl intermediate with cleavage of the M_1- phosphate bond, decreasing the pK_a of the second coordinated water molecule, the proton of which could be taken up by the leaving alcohol.
4. Attack by the metal-coordinated hydroxide on the phosphoryl derivative, possibly with M_2 again polarizing the seryl oxygen, yielding a free phosphate ion coordinated to M_1. A further water molecule could aid in the liberation of phosphate via an associative mechanism.

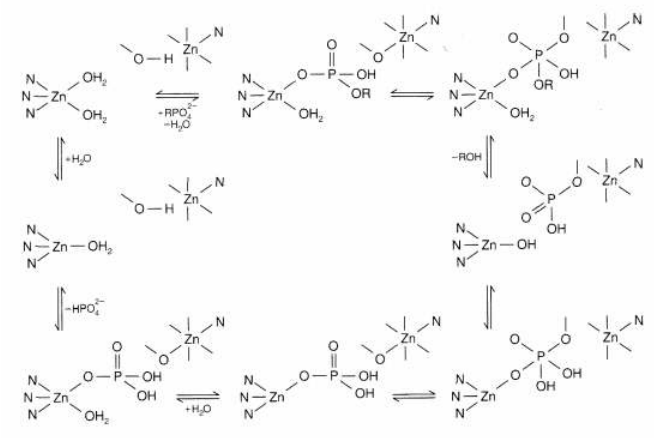


Figure 2.33 - Possible catalytic cycle of AP.

In the presence of alcohols, alkaline phosphatase displays transphosphorylation activity, i.e., hydrolysis of the starting ester and esterification of the phosphate group with a different alcohol. This ability is easily understood if one keeps in mind that the reaction depicted above is reversible, and that a different alcohol may be involved in the formation of the ester bond. Most group-transfer reactions catalyzed by metalloenzymes are likely to proceed through the same elementary steps proposed for hydrolytic reactions.

11.2.2.6: Ester Hydrolysis and Phosphoryl Transfer is shared under a CC BY-NC-SA 4.0 license and was authored, remixed, and/or curated by LibreTexts.

11.2.2.7: Group Transfer and Vitamin B-12

Group Transfer Enzymes

The phosphodiester bond in ATP and in related molecules is a high-energy bond whose hydrolysis liberates a large quantity of energy:

$$ATP + H_2O \rightleftharpoons ADP + P_i + 30 - 50\ kJ\ mol^{-1} \tag{2.25}$$

In many systems, typically the ATPases, the terminal phosphoryl group is transferred to another acidic group of the enzyme, e.g., a carboxylate group, to form another high-energy bond whose energy of hydrolysis is needed later for some endoenergetic transformation. Therefore the first step of the reaction is the phosphoryl transfer to a group of the enzyme.

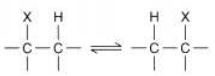
Kinases, a subset of the class of transferases, constitute a large group of enzymes that phosphorylate organic substrates:

$$ATP_{4-} + HX \rightleftharpoons ADP^{3-} + PX^{2-} + H^+ \tag{2.26}$$

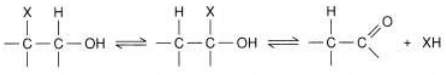
In some kinases, such as nucleoside diphosphate kinase,[168,169] an intermediate step is the phosphoryl transfer to a group belonging to the enzyme, as happens in ATPase and as was discussed in detail for alkaline phosphatase (Section V.B). In other kinases the phosphoryl transfer occurs directly from the donor to the acceptor in a ternary complex of the enzyme with the two substrates.[170] Often metal ions like magnesium or manganese are needed. These ions interact with the terminal oxygen of the ATP molecule, thus facilitating the nucleophilic attack by the acceptor. The metal ion is often associated with the enzyme. For mechanistic schemes, see the proposed mechanism of action of alkaline phosphatase, especially when a phosphoryl enzyme intermediate is involved.

The B_{12}-dependent Enzymes

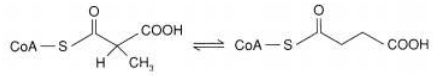
There are many enzymes that need a cobalt complex as cofactor in order to carry out vicinal 1,2 interchange:



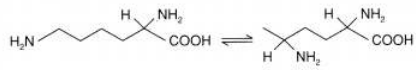
or



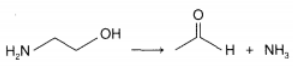
For the former type of reactions, X can be a group containing either C or N. Typical reactions[171] include insertion of a secondary methyl group into a main chain



isomerization of an amino group from a primary to a secondary carbon



and deamination reactions



A list of coenzyme-B_{12}-dependent enzymes is given in Table 2.10.

Table 2.10 - Some coenzyme-B_{12}-dependent enzymes.

MethylmalonylCoA mutase
Glutamate mutase
α-Methylene-glutarate mutase
Dioldehydrase
Glyceroldehydrase
Ethanoldeaminase
L-β-lysine mutase
D-α-Iysine mutase
Ribonucleotide reductase
Methionine synthetase
Methane synthetase
Methyl transferase
Acetate synthetase

In coenzyme-B_{12}, cobalt is bound to a tetraazamacrocyclic ligand[172] (Figure 2.40). The cobalt atom lies approximately in the plane of the corrin ligand (shown in bold). Note that rings A and D are directly linked. The conjugation therefore extends over only 13 atoms, excluding the cobalt, and involves 14 π electrons. Complexes that possess the α-D-ribofuranose-3-phosphate and the terminal 5,6-dimethylbenzimidazole as an axial ligand are called cobalamins. The name cobamides applies to complexes that lack or have different heterocyclic groups. Finally, the upper or β position is occupied by another ligand, which may be water, OH^-, CN^-, an alkyl group, etc. The cyano derivative (ii) is vitamin B_{12}. 5'-deoxyadenosylcobalamin (i) is called coenzyme B_{12}. The cobalt atom in these complexes is a diamagnetic cobalt(III) system (d^6).

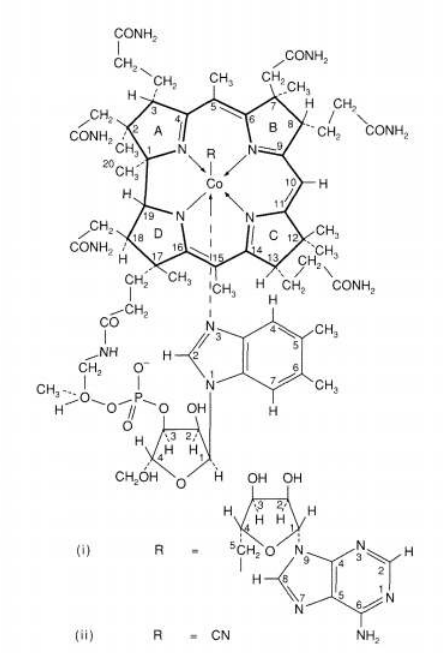


Figure 2.40 - Structure of (i) coenzyme B_{12}, 5'-deoxyadenosylcobalamin, and (ii) vitamin B_{12}, cyanocobalamin.[172]

The aquo complex has a pK_a of 7.8, which compares with that of 5.7 for the aquopentaamminecobalt(III) complex at 298 K.[173] The difference has been mainly ascribed to the difference in solvation of the two complexes, although the corrin ligand bears a negative charge, which reduces the positive charge and therefore the Lewis acidity of the metal ion. The standard reduction potential

between pH 2.9 and 7.8 is -0.04 V vs. SCE, featuring the conversion from aquocobalamin with bound benzimidazole (base on) to base-on cob(II)alamin.[174] The potential decreases with pH above pH 7.8 down to -0.3 V. The reduced form is five-coordinate, without the water molecule above pH 2.9, and lowspin.[175,176] The system can be further reduced at a potential of -0.85 V to obtain cob(I)alamin, in which the metal ion is four-coordinate and low-spin (d^8). The standard reduction potential for the hexaaquocobalt(III) complex is 1.95 V, which is lowered to 0.10 for the hexaammine complex, to -0.13 for the tris-ethylenediamine complex, and to -0.80 for the hexacyanocobaltate(III) ion.[173] After reduction to cobalt(II), the model complexes are reduced to the metal.

The electronic spectrum of the metal-free corrin resembles that of metal derivatives; it seems therefore that the bands are essentially π-π^* transitions modified by the central atom and by the axial ligands.[177,178] The cob(III)alamins are red, whereas the cob(II)alamins, which are brown, show an additional band at 600 nm.[179] The latter have an EPR spectrum typical of an unpaired electron in the d_z^2 orbital with some 4s mixing: the cob(II)alamin at pH 7 has $g_{\|}$ = 2.004, $g_{\perp}$ = 2.32, $A_{\|}$(Co) = 0.0100, $A_{\perp}$ (Co) = 0.0027 cm^{-1}, and $A_{\|}$ (N) = 0.00173 cm^{-1}.

Both cobalt(I) and cobalt(II)-containing cobalamins readily react with alkyl derivatives to give alkylcob(III)alamins:

$$Cob(II)alamin + CH_3I \rightarrow CH_3 - Cob(III)alamin + \frac{1}{2}I_2 \tag{2.32}$$

$$Cob(I)alamin + CH_3I \rightarrow CH_3 - Cob(III)alamin + I^- \tag{2.33}$$

These can formally be regarded as complexes of cobalt(III) with a carbanion. These are rare examples of naturally occurring organometallic compounds. The Co—C bond in alkylcobalamins is relatively weak (bond dissociation energy = 100 kJ mol^{-1}, though higher values are reported in the literature[182,183]) and can be broken thermally (by heating the complex above 100 °C)[182-184] or photochemically, even in daylight exposure.[180,181] The energy of the Co—C bond is about 17 kJ mol^{-1} greater when the transaxial base is absent.[184]

The cobalamin coenzyme is bound by the apoenzyme with no significant change in the absorption spectrum.[185] This suggests that no major change occurs in the coordination of cobalt(III). The first step of the reaction involves homolytic fission of the Co—C bond:[182-184, 186-188]

$$B - CO^{III} - R \rightarrow B - CO^{II\cdot} + R\cdot \tag{2.34}$$

where Band R are the ligands at the α and β apical positions. The 5'-deoxyadenosyl radical probably reacts with the substrate, generically indicated as SubH, to give the Sub· radical and RH. Then the rearrangement reaction proceeds along a not-well-established pathway. It is the protein-substrate binding that controls the subsequent chemistry. In the absence of protein the Co—C bond is kinetically stable; in the presence of protein and substrate the rate of labilization of the Co—C bond increases by a factor of 10^{11}-10^{12}.[182-185] By generating the radical in the coenzyme without the protein by means of photolysis or thermolysis, we enable the coenzyme to catalyze some rearrangement reactions without the protein. It may therefore be that the protein plays a major role in inducing the homolytic fission, but a relatively minor role in the subsequent steps, perhaps confined to preventing the various species from diffusing away from each other.

Studies on protein-free corrinoids and model complexes have shown that increasing the steric bulkiness around the coordinated Cα atom can cause a dramatic labilization of the Co—C bond.[189] The protein-coenzyme adduct might contain the coenzyme in a resting state and the protein in a strained state; the substrate would then switch the system into a strained coenzyme and a relaxed enzyme with little thermodynamic barrier. The strained form of the coenzyme is then in labile equilibrium with base-on cobalt(II) and the free radical.[190] This hypothesis, that conformational changes in cobalamin can switch chemical reactions on and off, is closely analogous with the known aspects of hemoglobin function.

It has been suggested that the radical formation in the coenzyme is triggered by a steric perturbation involving an enzyme-induced conformational distortion of the corrin ring toward the deoxyadenosyl group, thereby weakening the cobalt-carbon bond.[187,190-194] Structural studies of different corrinoid complexes reveal highly puckered and variable conformations of the corrin ring, attesting to its flexibility.[195] For the dimethylglyoxime models, it has been shown that increasing the size of the axial ligand B does induce Co—C bond lengthening and weakening because of conformational distortion of the equatorial ligand away from B and toward the R group.[196] It has been proposed that the flexibility of the corrin ligand is the reason why Nature does not use the porphyrin ligand in

vitamin B_{12}.[197] In an alternative explanation, the weakening of the Co—C bond would be an electronic effect associated with the labilization of the Co—N bond.[198]

11.2.2.7: Group Transfer and Vitamin B-12 is shared under a CC BY-NC-SA 4.0 license and was authored, remixed, and/or curated by LibreTexts.

11.2.2.8: Metal Substitution

With zinc enzymes, metallosubstitution is a convenient tool for monitoring the protein and its function by means of spectroscopic techniques. Furthermore, it is interesting to learn how reactivity depends on the nature of the metal ion and its coordination properties, because much of it depends on the protein structure, which seemingly remains constant. As discussed, zinc enzymes can be studied by replacing zinc with other spectroscopically useful metal ions, whose activities have been checked, and by transferring the information obtained to the native enzyme. The strategy of metal substitution is not limited to zinc enzymes, since it has been used for magnesium-activated enzymes and, occasionally, other metalloenzymes as well.

By dialyzing a protein solution against chelating agents, such as EDTA, 1,10-phenanthroline, or 2,6-dipicolinic acid at moderately acidic pH, or by reversibly unfolding the protein with denaturing agents (as has been done with alkaline phosphatase), one can cause zinc proteins to release their metal ions, giving rise to the corresponding but inactive apoprotein. Sometimes (e.g., by using alcohol dehydrogenase) dialysis against chelating agents can be applied to a suspension of protein microcrystals. In this way the chelating agent is still able to reach and remove the active site metal by slowly diffusing in the crystals through the hydration water, while the apoprotein is maintained in the native conformation by the crystal packing forces and denaturation is avoided. After the chelating agent is dialyzed out, often against a high-salt (e.g., ClO_4^-) buffer to reduce nonspecific binding, a new metalloprotein can obtained by addition of the appropriate metal salt.[23]

Cobalt(II)-substituted zinc proteins often show about as much activity as the native zinc enzymes (Table 2.4). This is a general characteristic of the cobalt-substituted zinc enzymes,[24] since the coordination chemistry of cobalt(II) is very similar to that of zinc(II). The two ions also show virtually identical ionic radii. Cobalt(II) derivatives generally display useful electronic spectra. High-spin cobalt(II) ions are paramagnetic, containing three unpaired electrons ($S = \frac{3}{2}$); thus they can also give rise to EPR spectra. The electronic relaxation times, i.e., the average lifetimes of the unpaired electrons in a given spin state of the S manifold ($-\frac{3}{2}$, $-\frac{1}{2}$, $\frac{1}{2}$, $\frac{3}{2}$), are very short (10^{-11} to 10^{-12} s) at room temperature. In order to detect EPR spectra, the sample temperature is usually decreased, often down to liquid helium temperature, to increase the electronic relaxation times and sharpen the EPR linewidths. On the other hand, as the paramagnetic broadening of the NMR lines in such systems is inversely proportional to the electronic relaxation times (see Section IV.C.3), room-temperature ^1H NMR spectra of cobalt(II) complexes can be easily detected, even in the absence of chemical exchange. Therefore cobalt(II) is an exceptional probe to monitor the structure and reactivity of zinc enzymes. Of course, the transfer of information from the artificial to the native enzyme must be done with caution. However, if we can understand the functioning of the cobalt enzyme, we then have a reference frame by which to understand the kinetic properties of the native enzyme. The spectroscopic properties of cobalt(Il) in cobalt-substituted proteins have been reviewed.[25]

Copper(Il)-substituted zinc proteins are generally inactive with respect to the natural and most artificial substrates (Table 2.4). In model compounds copper(Il) is often principally four-coordinate, with at most two more ligands present at metal-ligand distances that are longer than normal coordination bonds. As a consequence, the ability of zinc to switch between four- and five-coordinate species without any appreciable barrier and with usual metal-donor distances is not mimicked by copper. Furthermore, binding at the four principal coordination positions is generally stronger for copper than for zinc. It follows that substrates may have slow detachment kinetics. These properties are unfavorable for catalysis.

Copper(II) can be easily and meaningfully studied by means of electronic spectroscopy. Moreover, the EPR spectra can be recorded even at room temperature because of the long electronic relaxation times, which are of the order of 10^{-9} s. Because a protein is a macromolecule, it rotates slowly, and the EPR spectra in solution at room temperature look like those of crystalline powders or frozen solutions (powder-like spectra). ENDOR spectra are also easily obtained for copper proteins at low temperatures, because at low temperature the electronic relaxation times are even longer, and saturation of the EPR lines (which is a requirement to obtain ENDOR spectra) is easy to accomplish. The long electronic relaxation times make the broadening effects on the NMR lines of nuclei sensing the metal ion too severe; so these lines, unlike those of cobalt(Il) complexes, generally escape detection. However, if the nucleus under investigation is in fast exchange between a free species in large excess and a bound species, the line may be observed, because the broadening effects are scaled down by a factor equal to the molar fraction of bound species. The nuclear relaxation parameters contain precious structural and/or dynamic information (see Section IV.C.3). The spectroscopic properties of copper(II) in proteins have been extensively reviewed.[26,27]

Cadmium-substituted zinc proteins may also be active (Table 2.4), although usually at higher pH. This observation is readily explained in terms of the pK_a of a coordinated water, which is expected to be higher than that of analogous zinc complexes because

the cadmium ion is larger and polarizes the Cd-OH_2 bond less.

^{113}Cd and ^{111}Cd are nuclei with relatively high sensitivity for NMR spectroscopic study. The ^{113}Cd chemical shift spans from -200 to 800 ppm relative to $CdSO_4$ in H_2O, depending on the number and nature of donor atoms.[24,28] Sulfur donor atoms cause larger downfield shifts than oxygens or nitrogens, and the downfield shift increases with decreasing number of donor atoms. Therefore, ^{113}Cd NMR probes have been used extensively to study zinc enzymes, metal-storage proteins like thioneins, and other proteins with cysteine ligands, and chemical shifts in various cadmium proteins, together with the proposed ligand donor set, have been obtained (Figure 2.1).

Manganese(II)-containing proteins give rise to detectable EPR signals; however, their interpretation in terms of structure and dynamics is not always informative. The electronic relaxation times of Mn^{2+} are the longest among metal ions, of the order of 10^{-8} s at room temperature and at the magnetic fields of interest. This property and the large S = $\frac{5}{2}$ value account for a large NMR linewidth, even larger than in copper(II) systems. Manganese(II)- and nickel(II)- substituted zinc proteins have often been reported to have fractional activity (Table 2.4).[24] Several efforts have been devoted to Mn(II) derivatives, especially by studying the NMR signals of nuclei in molecules that exchange rapidly with the metalloprotein.

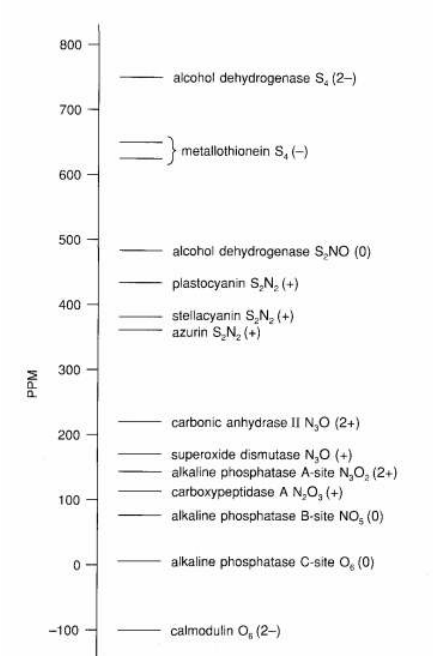


Figure 2.1 - ^{113}Cd chemical shifts in cadmium(II)-substituted metalloproteins. [24,28] Donor sets and overall charges (in parentheses) of the complexes are indicated.

Finally, several other metal-substituted zinc metalloprotein derivatives have been prepared, including those of VO^{2+} , Fe(II), Co(III), Pt(II), and $HgCl_2$. Although these systems add little directly to our understanding of the relationship between structure and function of the enzymes, nonetheless they represent new bioinorganic compounds and are of interest in themselves, or can add information on the coordinating capabilities, and reactivity in general, of the residues present in the active cavity.

Under the heading *zinc enzymes* there are several enzymes in which zinc is essential for the biological function, but is not present in the catalytic site. Among the most-studied enzymes, zinc has a structural role in superoxide dismutase, where the ligands are three histidines and one aspartate. In alcohol dehydrogenase there is a zinc ion that has a structural role, besides the catalytically active one. The former zinc has four cysteine ligands. Cysteine ligands are also present in zinc thioneins, which are zinc-storage proteins. The recently discovered class of genetic factors containing "zinc fingers" are zinc proteins in which the metal has an essentially structural role.[29] Such a role may consist of lowering the folding enthalpy of a protein to induce an active conformation or to stabilize a particular quaternary structure.

Zinc may also have a regulatory role; i.e., it does not participate in the various catalytic steps, but its presence increases the catalytic rate. This is a rather loose but common definition. Typically, zinc in the B site of alkaline phosphatase (Section V.B) has such a role, and the ligands are histidines, aspartates, and water molecules.

The enzymes in which zinc plays a structural or regulatory role will not be further discussed here, because they do not participate in the catalytic mechanisms; see the broader review articles.[23] ,[29,30] Rather, we will describe in some detail the enzyme carbonic anhydrase, in order to show how researchers have investigated such complicated systems as enzymes. We will discover as we look at the details of the structures and mechanisms of enzymes that there are large differences between reactivities in solution and in enzymatic cavities. The fundamental properties underlying these differences are still not fully understood.

11.2.2.8: Metal Substitution is shared under a CC BY-NC-SA 4.0 license and was authored, remixed, and/or curated by LibreTexts.

11.2.2.9: Model Chemistry

Some efforts have been reported in the literature to simulate the activity of CA and therefore to obtain further information on the mechanism. The pK_a of Zn—OH_2 moieties in various complexes has been studied as discussed in Section III.A. The electronic spectra of some cobalt analogues have been found to be similar. One such example is shown in Figure 2.24; the complex $Co(TPyMA)OH_2^{2+}$ (Table 2.3) [10] provides a five-coordinate adduct with a weakly bound axial nitrogen (Figure 2.25A).

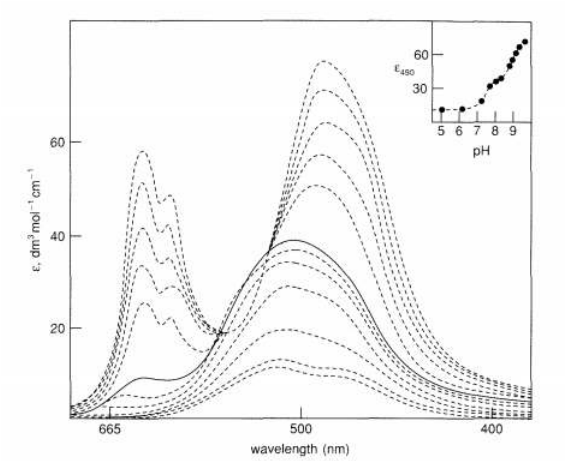


Figure 2.7.[56]

The interconversion between $Co(TPyMA)OH_2^{2+}$ and $Co(TPyMA)OH^{+}$ was studied by electronic spectroscopy (Figure 2.24). Despite the difference in the number of coordinated nitrogens, the difference between the high- and low-pH forms resembles that of the cobalt enzyme (cf. Figure 2.7).[10]

Table 2.3 shows that only one compound, with zinc(II) as the metal ion, seems to have three nitrogens and a water, whereas all the other models have a higher coordination number[15-17] The simple $[Co^{III}(NH_3)_5OH]^{2+}$ complex has been shown to accelerate the formation of bicarbonate ($k = 2 \times 10^2\ M^{-1}s^{-1}$), but, of course, bicarbonate remains coordinated to the metal because of the kinetic inertness of cobalt(III).[102,103] Some relatively ill-defined systems have been reported to have some kind of activity. The ligand shown in Figure 2.25B, with zinc(II) as the metal ion in H_2O, accelerates the attainment of the equilibrium[104]

$$CO_2 + H_2O \underset{k_{-1}}{\overset{k_1}{\rightleftharpoons}} HCO_3^- + H^+ \qquad (2.17)$$

with $k_{obs} = k_1 + k_{-1} \simeq 10^3\ M^{-1}s^{-1}$. The system in Figure 2.25C, with Zn^{2+} and excess imidazole, promotes CO_2 hydration, though not the back reaction.[105] The cobalt(II) analogue shows no activity.[106]

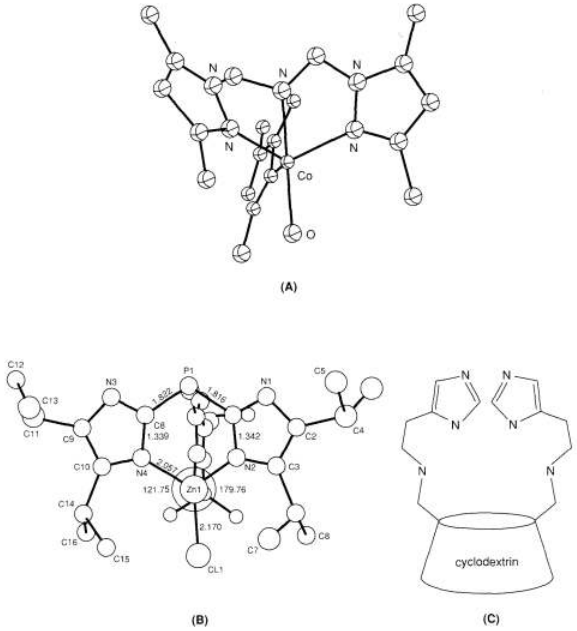


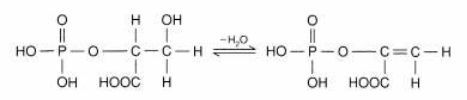
Figure 2.25 - Some multidentate ligands as models of CA: (A) tris-(3,5-dimethyl-l-pyrazolylmethyl) amine[4] (cobalt[II] complex); (8) tris (4,5- diisopropylimidozal-2yl)phosphine[104] (zinc[II] complex); (C) bis(histamino) β-cyclodextrin.

It can be concluded that the M—OH group can indeed be involved in one step of the enzymatic pathway. The sophistication of the whole enzymatic function has not yet been fully achieved with the present generation of models, even though the functionalization of both hydrophilic and hydrophobic molecules like cyclodextrins (Figure 2.25C) has also been used.[105]

11.2.2.9: Model Chemistry is shared under a CC BY-NC-SA 4.0 license and was authored, remixed, and/or curated by LibreTexts.

11.2.2.10: Nucleophilic Addition of $O\ \ H^-$ and H^-

Nucleophilic addition of OH^- ions as a step in enzymatic pathways is not restricted to hydrolytic processes; it often occurs in lyases, the class of enzymes catalyzing removal (or incorporation in the reverse reaction) of neutral molecules such as H_2O—but also NH_3, CO_2, etc.—from a substrate. It is outside the scope of this section to review all other mechanisms involved in lyase reactions, especially because they are not reducible to common steps and because several of them do not require the presence of a metal ion. We restrict ourselves to H_{2O} removal (or incorporation), a widespread feature of which seems to be the splitting of water into the constituents H^+ and OH^- ions at some step of the mechanism. As an example, the dehydration of 2-phospho-D-glycerate to phosphoenolpyruvate catalyzed by enolase, a Mg-activated enzyme,

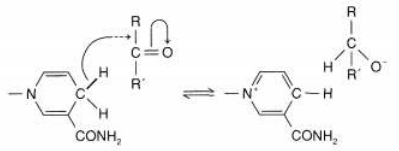


has been shown by kinetic isotope-effect studies[150] to proceed via fast H^+ removal from substrate followed by slow release of the product, and finally by release of OH^-. The role of a metal ion like magnesium might be to activate the substrate by coordinating the phosphate group, rather than by providing a coordinated hydroxide for nucleophilic attack.

Other lyases, however, contain transition metal ions [often iron(II)], and their main role might well be that of lowering the pK_a of water. None of them, however, is yet known well enough to allow a detailed discussion of the molecular mechanism. A striking exception is carbonic anhydrase, which has been so extensively and successfully studied that it is ideal as a case study (Section IV).

Hydride transfer is another elementary process encountered in many enzymatic reactions. Although hydride transfer implies a redox reaction, it also involves nucleophilic attack on substrate as in the foregoing examples. Unlike OH^-, hydride ions do not exist in aqueous solutions as free ions. In biological systems hydride is always directly transferred from one organic moiety to another by simultaneous breakage and formation of covalent bonds. The activation energy for this process is much higher than, for example, that of H^+ transfer via the formation of hydrogen bonds. Moreover, unlike hydrogen-bonded species, there is no intermediate in the process that can be stabilized by the catalyst. Instead, reacting species can be destabilized in order to lower the activation energy barrier. The role of the enzyme, and of the metal ion when present, is to provide binding sites for both substrates. The enzyme achieves this both geometrically, by allowing for proper orientation of the groups, and electronically, by providing energy to overcome the activation barrier.

These general concepts can be exemplified by liver alcohol dehydrogenases (LADH), dimeric zinc enzymes of 80 kDa that catalyze the following class of reactions using the $NADH/NAD^+$ system as coenzyme (or, really, as cosubstrate):



In particular, LADHs catalyze the reversible dehydrogenation of primary and secondary alcohols to aldehydes and ketones, respectively. Other enzymatic activities of LADHs are aldehyde dismutation and aldehyde oxidation.[151] The physiological role, although surely related to the metabolism of the above species, is not definitely settled. Much effort is being devoted to understanding the mechanism of action of this class of enzymes, which have obvious implications for the social problem of alcoholism.

Each monomer unit of LADH contains two zinc ions: one coordinated to four cysteine sulfurs, the other coordinated to two cysteine sulfurs, one histidine nitrogen, and a water molecule. The former has no apparent role in catalysis; the latter is essential for catalytic activity. The x-ray structure of the metal-depleted enzyme from horse liver has been solved at 2.4 Å resolution, and that of the holoenzyme at 2.9 Å resolution (Figure 2.34 See color plate section, page C-6.). Many crystal structures are also available for binary complexes with substrates, pseudosubstrates, or coenzymes, as well as for ternary complexes with coenzyme and substrates.[152] The very detailed picture emerging from such structural information has helped us understand how LADH functions. As will be evident from the following discussion, elucidation of this mechanism also reveals some important fundamental chemistry.

A key property of the enzyme, established by x-ray data, is the existence of two protein domains in each monomer that are relatively free to rotate relative to each other. The apo- and holo-enzymes exist in the so-called open form, whereas binding of NADH coenzyme induces rotation of one domain, resulting in the so-called closed form[153,154] (Figures 2.34 and 2.35). Closure brings the catalytic zinc ion into an ideal position to bind the aldehyde substrate in such a way that the reactive CH_2 group of the nicotinamide ring of NADH points toward the carbonyl carbon (Figure 2.35).

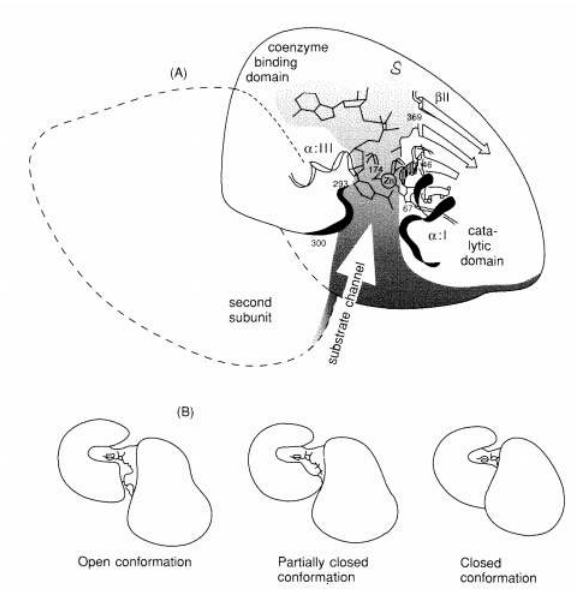
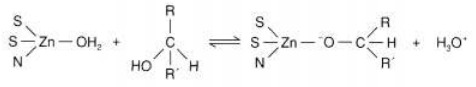


Figure 2.35 - Schematic drawing of (A) the LADH dimer and (B) the domains constituting the active site of a subunit.[154]

The main functions of the metal are thus to orient the substrate geometrically and to polarize the carbon-oxygen bond. Although the latter makes obvious chemical sense for the aldehyde reduction reaction, since polarization of the C=O bond facilitates nucleophilic attack of hydride at the carbonyl carbon, coordination of an alcohol to a metal is expected to decrease the alcohol's tendency to transfer hydride to NAD^+, unless the hydroxyl proton is released upon coordination.[155]



Formation of an alkoxide ion as an intermediate has often been questioned, because the pK_a of the alcohol would have to be reduced by about 10 units upon coordination.[156] The possibility that hydride transfer from alcohol to NAD^+ and hydroxyl proton release could occur simultaneously is attractive, but careful experiments have shown that the two steps must be kinetically separate.[157] We summarize here the key information that leads to a full, although circumstantial, rationalization of the chemical behavior of the enzyme.

1. The activity versus pH profiles[156,158] are bell-shaped, with k_{cat} increasing with a pK_a below 7, reaching a plateau, and decreasing with a pK_a above 11, and K_m increasing with a pK_a of about 9.
2. X-ray data show that the zinc ion is accessible to solvent in the open conformation, much less so in the closed conformation when the reduced coenzyme is bound, and inaccessible when the substrate is coordinated to the metal in the ternary complex, extruding all the water molecules from the active site.[152] None of the complexes has a coordinated water molecule as a fifth ligand when substrates or inhibitors are bound to the metal. The metal ion is always four coordinate and pseudotetrahedral. Computer graphics reveal beyond any doubt that there is no room for a fifth ligand in the active site, at least in the closed form.
3. Many (although not all) spectroscopic data on metal-substituted derivatives and their binary and ternary complexes have also been interpreted as indicative of a four-coordinate metal.[159] Even nickel(II) and copper(II), which have little tendency to adapt to a pseudotetrahedral ligand environment, do so in LADH, the electronic structure of the latter resembling that of blue proteins (Figure 2.36).[160]

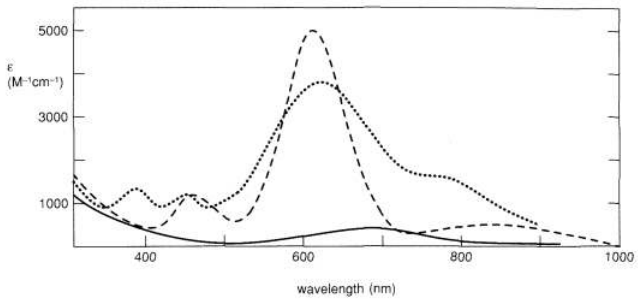
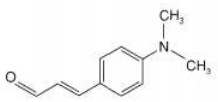


Figure 2.36 - Electronic spectra of liver alcohol dehydrogenase substituted with copper at the catalytic site (• • • • •),[160] *together with the spectra of blue (stellacyanin, ---)*[161] *and non-blue (superoxide dismutase, ———)*[162] *copper proteins.*

4. The substrate binding site is actually "created" by the closure of the protein (Figure 2.34). The reactive species are thus trapped in an absolutely anhydrous environment. The chromophoric aldehyde DACA has been extensively used as an "indicator" of the polarity of the binding site. Large red shifts of the ligand π-π^* transition upon binding indicate the polarity of the site to be much higher than in water; there is a further sizeable increase in polarity when NAD^+ instead of NADH is bound in the ternary complex.[163]



5. The electronic spectra of the cobalt-substituted derivative are characteristically different when different anions are bound to the metal (Figure 2.37).[164] A catalytically competent ternary complex intermediate displays the electronic absorption pattern typical of anion adducts.[166]

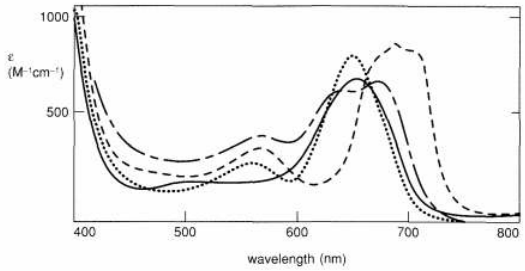


Figure 2.37 - Electronic spectra of liver alcohol dehydrogenase substituted with cobalt at the catalytic site. Binary complex with NAD^+ (———);[165] *ternary complex with* NAD^+ *and* Cl^-(---);[165] *binary complex with acetate* (• • • • •);[164] *intermediate in the oxidation of benzyl alcohol with* NAD^+ (— — — —).[166]

6. From extended kinetics measurements a protonation scheme (Figure 2.38) has been proposed that accounts for the many pK_a values observed under different conditions.[167] This scheme again requires formation of a coordinated alkoxide intermediate, but has the advantage of rationalizing in a simple way a complex pattern. In essence, the only relevant acid-base group supplied by the enzyme is the metal-coordinated water, which has a pK_a of 9.2 in the free enzyme (open form). Upon binding of NADH the pK_a increases to 11.2. Since NADH dissociation is the last and rate-limiting step of the alcohol oxidation reaction, the decrease in k_{cat} with this pK_a is accounted for by a decrease in dissociation rate of NADH from the hydroxo form. On the other hand, the pK_a of water is decreased to 7.6 upon binding of NAD^+. These rather large changes in both directions are best explained by a marked sensitivity of the coordinated water molecule to the polarity of the environment, which, with the possible exception of the unligated form that has a more or less "regular" pK_a value of 9.2, can be almost completely anhydrous and much different from that of bulk water. The nonpolar nicotinamide ring of NADH decreases the overall electrostatic interactions of the water molecule, whereas the positive charge of NAD^+ drastically increases them. In this scheme, the association rates of both coenzymes are predicted to (and, in fact, do) decrease with a pK_a of 9.2, the dissociation rate of NAD^+ is predicted to (and does) decrease with a pK_a of 7.6, and the dissociation rate of NADH is predicted to decrease with a pK_a of 11.2 (and, indeed, it is pH-independent up to and above pH 10).

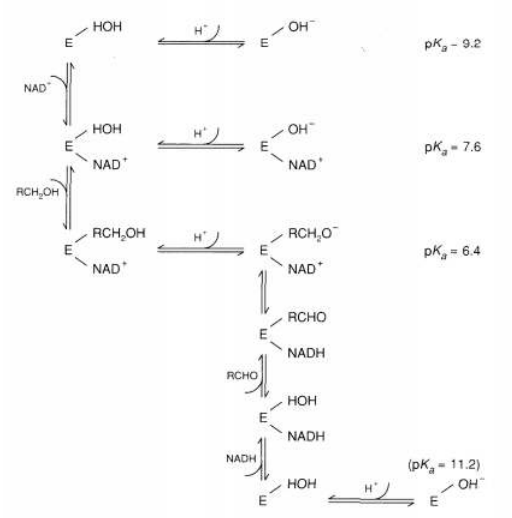


Figure 2.38 - Protonation scheme for LADH and its adducts with coenzymes and substrates.[157,167]

The decrease of k_{cat} at low pH depends on an ionization that in turn depends on the substrate. This pK_a must be that of the coordinated alcohol; at too Iowa pH, deprotonation of the coordinated alcohol becomes the rate-limiting step. The pK_a values observed for this process range from 6.4 for ethanol to 4.3 for triftuoroethanol. What is surprising for aqueous-solution chemistry—that the pK_a of a coordinated alcohol is lower than the pK_a of a coordinated water molecule—can now be explained in terms of the different polarity of the two adducts in LADH. In the binary complex with NAD^+ (pK_a = 7.6), the water molecule is still free to interact through H-bonding with the solvent and partially dissipate the electrostatic charge. In the ternary complex with any alcohol, the R group may prevent access of the solvent to the cavity, decreasing the dielectric constant of the medium. As a consequence, the polarity of the environment is increased. It is interesting to speculate that Nature could have chosen a stronger Lewis acid than a zinc ion coordinated to two negatively charged residues to decrease the pK_a of a coordinated alkoxide, but then the pK_a of the coordinated water would have simultaneously undergone a parallel and possibly even stronger decrease. Instead, LADH provides a self-regulating environment that is tailored to decrease the pK_a of a coordinated alcohol, once properly positioned, more than that of a coordinated water. The full catalytic cycle for the dehydrogenation reaction at pH around 7 can be summarized as follows (Figure 2.39):

1. NAD^+ binds to the open, water-containing form of the enzyme with a maximal on-rate. The pK_a of water is decreased to 7.6, but water is still mostly unionized.
2. A neutral alcohol molecule enters the crevice between the two domains, and coordinates the zinc ion by displacing the water molecule. The protein is still in the open form.
3. Domain rotation brings the protein into the closed form, excluding all the residual water molecules from the active site; the combined effect of the metal positive charge and of the unshielded positive charge of the nicotinamide ring lowers the pK_a of the coordinated alcohol below 7. A proton is expelled from the cavity, possibly via a hydrogen-bond network of protein residues.
4. Direct hydride transfer takes place from the alcohol CH to the 4-position of the properly oriented nicotinamide ring. The resulting ternary complex is an NADH-aldehyde adduct. The polarity of the active site dramatically drops.
5. The aldehyde product leaves and is replaced by a neutral water molecule (its pK_a now being 11.2). Additional water molecules can now enter the crevice, favoring the partial opening of the structure.
6. The loss of contacts between the two halves of the channel favors a complete opening and then the release of NADH, whose dissociation rate is maximal and pH-independent.

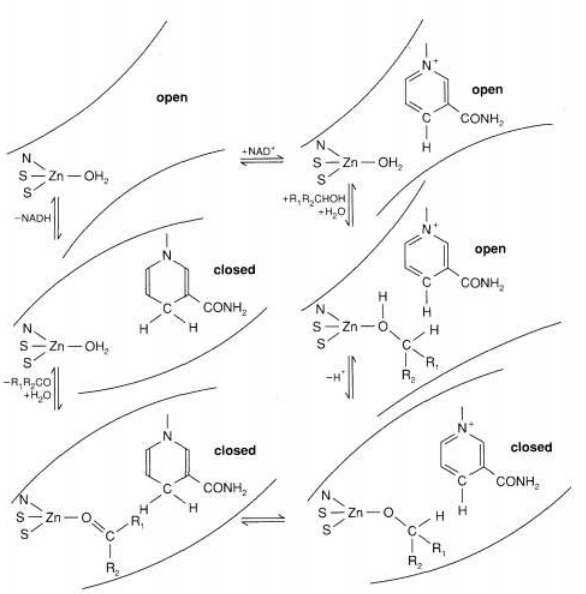


Figure 2.39 - Possible catalytic cycle of LADH.

11.2.2.10: Nucleophilic Addition of OH^- and H^- is shared under a CC BY-NC-SA 4.0 license and was authored, remixed, and/or curated by LibreTexts.

11.2.2.11: Peptide Hydrolysis

At neutral pH the uncatalyzed hydrolysis of amides or peptides

$$R-CO-NH-R'+H_2O \rightleftharpoons R-COO^- + R'-NH_3^+ \quad (2.18)$$

is a slow process, with rate constants as low as $10^{-11}s^{-1}$. Peptide hydrolysis catalyzed by carboxypeptidase or thermolysin can attain k_{cat} values of 10^4 s^{-1}. Organic chemistry teaches us that amide hydrolysis is relatively efficiently catalyzed by acids and bases. The general mechanisms involve protonation of the carbonyl oxygen (or amide nitrogen), and addition of OH^- (or of a general nucleophile) to the carbonyl carbon atom. Several organic and inorganic bases have been found to be reasonably efficient catalysts. On the other hand, transition metal aqua-ions or small metal-ion complexes also display catalytic efficiency (Table 2.8).[107-114] A metal ion is a Lewis acid, capable of effectively polarizing the carbonyl bond by metal-oxygen coordination. Furthermore, the metal ion can coordinate a hydroxide group in such a way that there is a high OH^- concentration at neutral or slightly alkaline pH. It is thus conceivable that a metalloenzyme may combine some or all of these features and provide a very efficient catalyst.

Table 2.8 - Rate constants for amide and ester hydrolysis catalyzed by acids, bases, or metal ions. * autohydrolysis

Compound	Catalyst and Conditions	Rate Constant	Reference
Glycine amide	pH 9.35 Cu^{2+}, pH 9.35	1.9×10^{-5} s^{-1} 2.6×10^{-3} $M^{-1}s^{-1}$	107 107
$[Co(en)_2(glycine\ amide)]^{3+}$	pH 9.0[a]	2.6×10^{-4} s^{-1}	108
D,L-phenylalanine ethylester	pH 7.3 Cu^{2+}, pH 7.3	5.8×10^{-9} s^{-1} 3.4×10^{-2} $M^{-1}s^{-1}$	109 109
$(tn)_2O_3PO—C_6H_4NO_2$	OH^-	5.1 $M^{-1}s^{-1}$	110
$Co^{III}—(tn)_2O_3PO—C_6H_4NO_2$	—[a]	7×10^{-5} s^{-1}	110
Ethyl-β-phenylpropionate	H^+ OH^-	5×10^{-3} M^{-1} s^{--1} 1.3×10^{-6} $M^{-1}s^{-1}$	111 111
Adenosine triphosphate	pH 5.3 Cu^{2+}, pH 5.3	5.6×10^{-6} s^{-1} 1.1×10^{-2} $M^{-1}s^{-1}$	112 112
Glycine methylester	Co^{2+}(1:1), pH 7.9 Cu^{2+}(1:1), pH 7.3	1.6×10^{-2} s^{-1} 4.2×10^{-2} s^{-1}	113 113
Glycine propylester	Co^{3+}(1:1), pH 0 Co^{3+}(1:1), pH 8.5	1.1×10^{-3} s^{-1} $>1 \times 10^{-2}$ s^{-1}	114 114

Much experimental work has been done on mimicking ester and especially peptide hydrolysis with model coordination compounds. Most of the work carried out has involved[108,110,115,116] cobalt(III), Although such an ion may not be the best conceivable model for zinc-promoted hydrolytic reactions (see Section IV.G), it has the great advantage of being substitutionally inert, thus removing mechanistic ambiguities due to equilibration among isomeric structures in the course of the reaction, Interesting amide hydrolysis reactions also have been described using complexes with other metal ions, such as copper(Il)[117] and zinc(Il)[118] itself. In recent years efforts have focused on the construction of bifunctional catalysts to better mimic or test the enzymatic function. For instance, phenolic and carboxylic groups can be placed within reach of Co(III)-chelated amides in peptidase models.[116] The presence of the phenolic group clearly accelerates amide hydrolysis, but carboxyl groups are ineffective. This model chemistry is too simple to provide insights into the actual enzymatic mechanism, which must start with recognizing the substrate through several steps, orienting it, activating it, performing the reaction, and finally releasing the products. See the more specialized reviews dealing with nonenzymatic reactivity.[119-121]

From basic knowledge of the chemistry of hydrolytic reactions, the x-ray structures of carboxypeptidase A and a variety of its derivatives with inhibitors as substrate analogues, product analogues, and transition-state analogues have revealed several features of the active site that are potentially relevant for the catalytic mechanism (Figures 2.26-2.28 See color plate section, pages C4,

C5.).[122] The metal ion is coordinated to two histidine residues (His-69 and His-196), to a glutamate residue that acts as a bidentate ligand (Glu-72), and to a water molecule. The metal is thus solvent-accessible and, as such, can activate the deprotonation of a water molecule to form a hydroxide ion, or polarize the carbonyl oxygen of the substrate by coordinating it in the place of the solvent molecule, or both, if some flexibility of the coordination sphere is allowed. Another glutamic-acid residue (Glu-270) is in close proximity to the metal center. If the role of the metal were mainly to polarize the carbonyl carbon, Glu-270 in its deprotonated form could be positioned to perform a nucleophilic attack on the carbonyl carbon, yielding an anhydride intermediate. Alternatively, the metal could mainly serve to provide a coordinated hydroxide ion that, in turn, could attack the carbonyl carbon; here Glu-270 would help form ZnOH by transferring the proton to the carboxylate group:

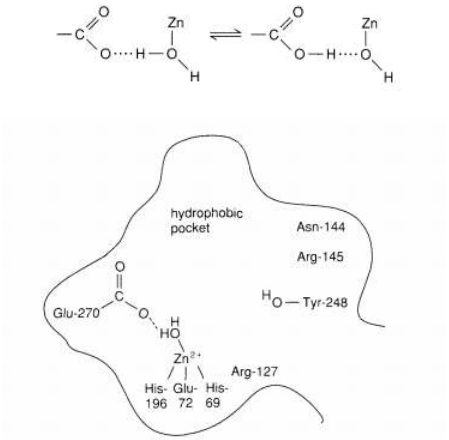


Figure 2.26 - Schematic drawing of the active-site cavity of carboxypeptidase A.[122] Only the residues believed to playa role in the catalytic mechanism are shown.

On the opposite side of the cavity is a tyrosine residue that has been shown to be quite mobile and therefore able to approach the site where the catalytic events occur. The cavity has a hydrophobic pocket that can accommodate the residue, R, of nonpolar C-terminal amino acids of the peptide undergoing hydrolysis (Figures 2.26 and 2.28), thereby accounting for the higher efficiency with which hydrophobic C-terminal peptides are cleaved. Finally, an Asn and three Arg residues are distributed in the peptide-binding domain; Asn-144 and Arg-145 can interact via hydrogen bonds with the terminal carboxyl group. Arg-127 can hydrogen-bond the carbonyl oxygen of the substrate.

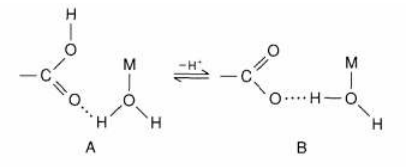
All these features have enabled detailed interpretation of many chemical and physico-chemical data at the molecular level. The essential data are as follows:

1. *Metal substitution*. Table 2.9 lists the divalent metals that have been substituted for zinc(II) in CPA, together with their relative peptidase (and esterase) activities.[22] For some of them, the available x-ray data show[123] that the active-site structure is essentially maintained. Even the copper derivative is slightly active. The apoenzyme is completely inactive, however.

Table 2.9 - Catalytic activities of metal-substituted carboxypeptidases.[a 22] a) Activities are relative to the native enzyme, taken as 100%. b) Some activity toward both peptides and esters has recently been observed. [22]

	Peptidase	Esterase
Apo	0	0
Cobalt	200	110
Nickel	50	40
Manganese	30	160
Cadmium	5	140
Mercury	0	90
Rhodium	0	70
Lead	0	60
Copper	—[b]	—[b]

2. *Active-site modifications*. Chemical modification and site-directed mutagenesis experiments suggest that Glu-270 is essential for catalysis.[124,125] Tyr-248,[126] Tyr-198,[127] and one or more of the arginines[124] are involved but not essential.
3. *Kinetics*. k_{cat}/K_m pH profiles are bell-shaped, characterized by an acid pK_a, limb around 6 and an alkaline pK_a limb around 9: k_{cat} increases with the pK_a of 6 and then levels off, and K_m increases with a pK_a of 9. Several lines of evidence suggest that the $pK_a \approx 6$ corresponds to the ionization of the Glu-270-coordinated H_2O moiety:



   Site-directed mutagenesis has ruled out Tyr-248 as the group with the pK_a of 9 in the rat enzyme.[125,126] Unfortunately, in this enzyme the pK_a of 9 is observed in k_{cat} rather than K_m; so the situation for the most studied bovine enzyme is still unclear. Tyr-248 favors substrate binding three to five times more than the mutagenized Phe-248 derivative.[126] The three possible candidates for this pK_a, are the coordinated water, Tyr-248, and the metal-coordinated His-196, whose ring NH is not hydrogen-bonded to any protein residue.[128] The x-ray data at different pH values show a shortening of the Zn—O bond upon increasing pH.[129] This favors the ZnOH hypothesis.

4. *Anion binding*. The metal binds anionic ligands only below pH 6, i.e., when Glu-270 is protonated, when Glu-270 is chemically[130] or genetically[125] modified, or when aromatic amino acids or related molecules are bound in the C-terminal binding domain (Arg-145 + hydrophobic pocket).[131-134]
5. *Intermediates*. An anhydride intermediate involving Glu-270 for a slowly hydrolyzed substrate may have been identified.[135] Some other intermediates have been observed spectroscopically at subzero temperatures with the cobalt(II) derivative.[22,136] Peptides bind in a fast step without altering the spectroscopic properties of cobalt(II), following which a metal adduct forms and accumulates.[22] Thus, if an anhydride intermediate is formed, it is further along the catalytic path.

On the basis of these data, and many related experiments, a detailed mechanism can be formulated (Figure 2.29). The incoming peptide interacts with arginine residues through its terminal carboxylate group. The interaction could initially involve Arg-71 (not shown); then the peptide would smoothly slide to its final docking position at Arg-145, while the R residue, if hydrophobic, moves to the hydrophobic pocket (Figure 2.29B). The carbonyl oxygen forms a strong hydrogen bond with Arg-127. Additional stabilization could come from hydrogen bonding of Tyr-248 to the penultimate peptide NH. This adduct might be the first intermediate suggested by cryospectroscopy [22,136] (Figure 2.24).

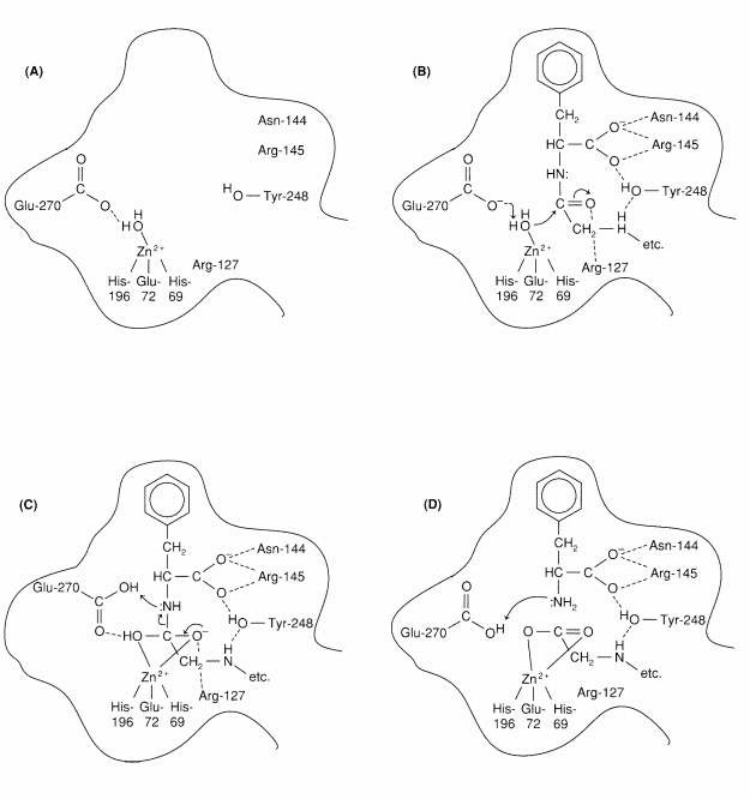


Figure 2.29 - Possible catalytic cycle of CPA.

At this point the metal-bound hydroxide, whose formation is assisted by Glu-270, could perform a nucleophilic attack on the carbonyl carbon activated by Arg-127 and possibly, but not necessarily, by a further electrostatic interaction of the carbonyl oxygen with the metal ion. The structure of the substrate analogue α-R-β-phenylpropionate shows that the carbonyl binds in a bidentate fashion:

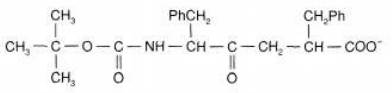


Figure 2.29C).

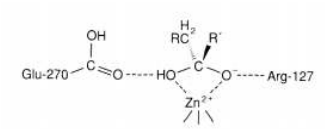


Figure 2.30 - Binding mode of α-R-β-phenylpropionate to the zinc(II) ion in CPA.[137]

The system then evolves toward breaking of the C—N bond, caused by addition of a proton to the amino nitrogen. This proton could come from Glu-270, which thereby returns to the ionized state. The breaking of the peptide bond could be the rate-limiting step.[22] The second proton required to transform the amino nitrogen into an NH_3^+ group could come from the coordinated carboxylic group of the substrate, which now bears one excess proton, again through Glu-270 (Figure 2.29D). The system shown in Figure 2.29D can, in fact, be seen as a ternary complex with a carboxylate ligand and an amino-acid zwitterion, bound synergistically.[131-134] Finally, the metal moves back to regain a bidentate Glu-72 ligand, and the cleaved peptide leaves, while a further water molecule adds to the metal ion and shares its proton with the free carboxylate group of Glu-270.

Once the hydrolysis has been performed, the cleaved amino acid still interacts with Arg-145 and with the hydrophobic pocket, whereas the amino group interacts with Glu-270. The carboxylate group of the new terminal amino acid interacts with zinc. This picture, which is a reasonable subsequent step in the catalytic mechanism, finds support from the interaction of L- and D-phenylalanine with carboxypeptidase.[131-134,138]

This mechanism, essentially based on the recent proposal by Christianson and Lipscomb,[137] underlines the role of the Zn—OH moiety in performing the nucleophilic attack much as carbonic anhydrase does. This mechanism can apply with slight changes to thermolysin[139] and other proteases. Thermolysin cleaves peptidic bonds somewhere in the peptidic chain. The mechanism could be very similar, involving zinc bound to two histidines and Glu-166 (Figure 2.31).[139] Glu-166 is monodentate. The role of Glu-270 in CPA is played by Glu-143 and the role of Arg-127 is played by His-231.

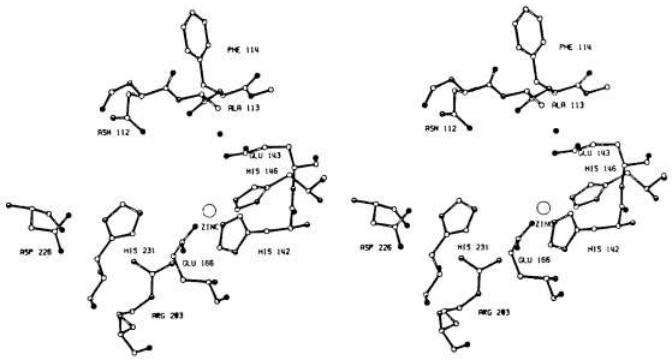


Figure 2.31 - Stereo view of the active site of thermolysin.[139]

11.2.2.11: Peptide Hydrolysis is shared under a CC BY-NC-SA 4.0 license and was authored, remixed, and/or curated by LibreTexts.

11.2.2.12: pH Dependence of Inhibitor Binding

The ease with which electronic spectra can be obtained provides a simple way of determining the affinity constants of inhibitors for the cobalt-substituted enzymes. An aliquot of enzyme is diluted in a spectrophotometric cell up to a fixed volume, and the spectrum is measured. Then the spectra are remeasured on samples containing the same amount of enzyme plus increasing amounts of inhibitor in the same cell volume. The pH is rigorously controlled. If solutions of enzyme and inhibitor have the same pH, the pH should be verified after the spectral measurements, in order to avoid contamination from the electrode salt medium. Both absolute values and pH dependences of affinity constants obtained from electronic spectra are the same as those obtained from inhibition measurements, where known, and are comparable to those obtained on the native enzyme.

Although affinity constant values reported in the literature were measured under different experimental conditions of, e.g., pH, buffer type, and buffer concentration, several pH-dependent trends are apparent. According to such dependences, three classes of inhibitors can be identified[48] (Figure 2.15).

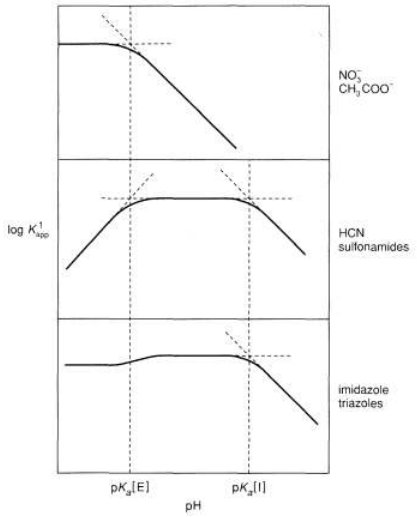


Figure 2.15 - Types of pH dependences observed for the affinity constants of inhibitors for cobalt(II)-substituted carbonic anhydrases. pK_a[E] represents the main pK_a value of the enzyme, pK_a[I] that of the inhibitor, if present.[48]

In the first class, the affinity constant, expressed as log K, decreases linearly with increasing pH. Anions that are weak Lewis bases (Cl^-,N_3^-,CH_3COO^-, NO_3^-, etc.) behave in this manner, as do neutral ligands like CH_3OH and aniline. An example is shown in Figure 2.16. A qualitative fit to such curves can be obtained using a single pK_a. This behavior could be accounted for by assuming that the ligand binds only the low-pH form of the enzyme, in a simplified scheme in which only one pK_a value determines the species distribution in CA. We know, however, that the picture is more complex.

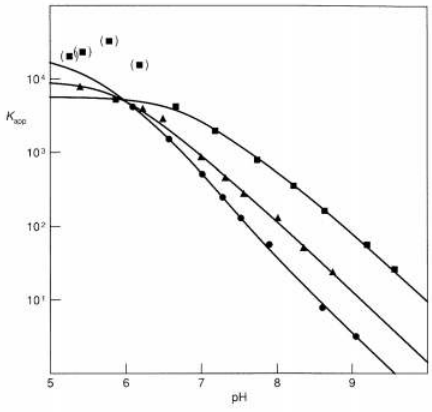


Figure 2.16: *pH dependence of the apparent affinity constants of nitrate for human I* ■, *bovine II* (▲), *and human II* (•) *carbonic anhydrases. The curves are best-fit curves obtained assuming non-zero affinity of the anion for species I and 3 of Figure 2.9. The*

best-fit parameters are reported in Table 2.6. Points in parentheses for HCA I reflect possible binding of a second nitrate ion and have been excluded from the fit.[57]

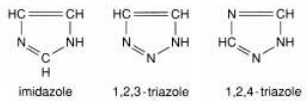
If the species distribution calculated according to the scheme of Figure 2.9 is assumed to hold, and if it is assumed that only the two water-containing species (1) and (3) can be bound by the ligand, then actual affinity constants can be evaluated for both species (1) and (3)[57] (see Table 2.7). Such constants are similar for the three isoenzymes, whereas the apparent affinity constants at pH 7, for example, mainly depend on the pK_a's of the coordinated water according to the values of Table 2.5. Therefore, the low-activity species CA I has larger affinity for anions like nitrate (and bicarbonate) than do the high-activity forms at pH 7.

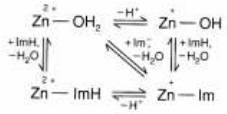
Table 2.7: Affinity constants of nitrate for species 1 and 3a of cobalt(II)-substituted carbonic anhydrases.[57] * As defined in Figure 2.9

	HCA I	BCA II	HCA II
log K_1	3.74 ± 0.04	4.01 ± 0.02	4.34 ± 0.04
log K_3	2.62 ± 0.06	2.56 ± 0.04	2.61 ± 0.05

A second type of behavior occurs for weak acids like HCN, H_2S, and aromatic sulfonamides ($ArSO_2NH_2$).[76,77] Assuming that the anions (conjugated bases) bind the low-pH species of the enzyme, the bell-shaped plot of log K versus pH (Figure 2.15) can be accounted for. In fact, at low pH, the inhibitors are in the protonated form, which is not suitable for metal binding. At high pH the concentration of the low-pH species of the enzyme decreases. The maximal apparent affinity is experimentally halfway between the pK_a of the inhibitor and the "pK_a" of the enzyme, treated as if it were only one. The same type of curve is also expected if the high-pH species of the enzyme binds the weak acid. Indeed, kinetic measurements seem to favor this hypothesis for sulfonamides.[78]

A third type of behavior obtains for inhibitors like imidazole and triazoles, which bind the enzyme with similar affinities over a large range of pH (Figure 2.15),[79,80] because both the imidazolate anion and the neutral imidazole can bind to the aquo forms of the enzyme with essentially the same affinity,[48,80,81] and the reaction of imidazole with the Zn—OH species cannot be distinguished thermodynamically from the reaction of imidazolate with the aquo forms:





It is possible that the noncoordinated nitrogen can interact with a group in the protein via a hydrogen bond. A candidate could be the NH group of His-200 in HCA I or the hydroxyl group of Thr-200 in HCA II. Indeed, only imidazole and triazoles, which have two nitrogens in 1,3-positions, seem to have this ability.[213]

In summary, from cobalt substitution we have learned:

1. the coordination geometry of the high- and low-pH forms by means of electronic spectroscopy;
2. the values of the pK_a's from the pH dependence of the electronic spectra;
3. the four and five coordination of the various derivatives with exogenous ligands;
4. the affinity constants of exogenous ligands and their pH dependence;
5. a fingerprint in the ^1H NMR spectra that can be used to monitor structural variations.

Most of these conclusions can be safely transferred to the native zinc enzyme, although minor differences can occur, for example, in the position of the equilibrium between four- and five-coordinate species.

11.2.2.12: pH Dependence of Inhibitor Binding is shared under a CC BY-NC-SA 4.0 license and was authored, remixed, and/or curated by LibreTexts.

11.2.2.13: Selecting Zinc

Zinc has a specific role in bioinorganic processes because of the peculiar properties of the coordination compounds of the zinc(II) ion.

(1) Zinc(II) can easily be four-, five-, or six-coordinate, without a marked preference for six coordination. The electronic configuration of zinc(II) is $3d^{10}$ with two electrons per orbital. In coordination compounds, there is no ligand-field stabilization energy, and the coordination number is determined by a balance between bonding energies and repulsions among the ligands. Tetrahedral four-coordinate complexes have shorter metal-donor distances than five-coordinate complexes, and the latter have shorter ones than six-coordinate complexes (Table 2.2), whereas the ligand repulsion increases in the same order.

Table 2.2 - Average zinc(II)-donor atom distances (A) for some common zinc(II) ligands in four-, five-, and six-coordinate complexes.5

Ligand	Coordination Number		
	4	5	6
H_2O	2.00	2.08	2.10
R-COO^-	1.95	2.02	2.07
Imidazole	2.02	—	2.08
Pyridine	2.06	2.12	2.11
R-NH_2	—	2.06	2.15
R, R'NH	2.19	2.27	—

The repulsion can be both steric and electronic. In enzymes, zinc(II) usually has coordination numbers smaller than six, so that they have available binding sites in their coordination spheres. Substrate can in principle bind to zinc by substituting for a coordinated water or by increasing the coordination number. This behavior would be typical of Lewis acids, and, indeed, zinc is the most common Lewis acid in bioinorganic chemistry. Zinc could thus substitute for protons in the task of polarizing a substrate bond, e.g., the carbonyl C-O bond of peptides and esters, by accepting a substrate atom (oxygen) as a ligand. This has been shown to be possible in model systems. Relative to the proton, a metal ion with an available coordination position has the advantage of being a "superacid," 6 in the sense that it can exist at pH values where the H_3O^+ concentration is extremely low. Also, relative to the proton, the double positive charge partly compensates for the smaller electrophilicity due to the smaller charge density.

(2) As a catalyst, zinc in zinc enzymes is exposed to solvent, which for enzymes is almost always water. A coordinated water molecule exchanges rapidly, because ligands in zinc complexes are kinetically labile. This, again, can be accounted for by zinc's lack of preference for a given coordination number. A six-coordinate complex can experience ligand dissociation, giving rise to a five-coordinate complex with little energy loss and then little energetic barrier. On the other side, four-coordinate complexes can add a fifth ligand with little energetic barrier and then another ligand dissociates.[7] The coordinated water has a pK_a sizably lower than free water. Suitable models have been synthesized and characterized in which a solvent water molecule coordinated to various dipositive metal ions has pKa values as low as 7 (Table 2.3).

Table 2.3 - The pK_a values of coordinated water in some metal complexes.

a) dacoda = 1,4-diaza-cyciooctane-1 ,4-diacetate.

b) TPyMA = tris(3,5-dimethyl-1-pyrazolylmethyl)amine.

c) TMC = 1,4,8,11-tetramethyl-1,4,8,11-tetraaza-cyclotetradecane.

d) CR = Schiff base between 2,6-diacetylpyridine and bis(3-aminopropyl)amine.

e) DMAM-PMHD = 1-[(6(dimethylamino)methyl)-2-pyridyl)methyl]hexahydro-1,4-diazepin-5-one.

f) C-PMHD = 1[(6-carboxy)-2-pyridyl)methyl]hexa-hydro-1,4-diazepin-5-one.

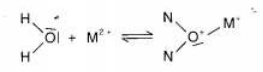
g) [12]aneN$_3$ = 1,5,9-triaza-cyclododecane.

h) HP[12]aneN$_3$ = 2-(2-hydroxyphenylate)-1,5,9-triaza-cyclododecane.

i)TImMP = tris(4,5-dimethyl-2-imidazolylmethyl)phosphinoxide.

Complex	Note	Donor Set	pK$_a$	Reference
$Ca(NO_3)_2(OH_2)_4^{2+}$		O_6	10.3	8
$Cr(OH_2)_6^{3+}$		O_6	4.2	8
$Cr(NH_2)_5OH_2^{3+}$		N_5O	5.1	8
$Mn(OH_2)_6^{2+}$		O_6	10.5	8
$Fe(OH_2)_6^{3+}$		O_6	1.4	8
$Co(OH_2)_6^{2+}$		O_6	9.8	8
$Co(dacoda)OH_2^{2+}$	(a)	N_2O_3	9.4	9
$Co(TPyMA)OH_2^{2+}$	(b)	N_4O	9.0	10
$Co(TMC)OH_2^{2+}$	(c)	N_4O	8.4	11
$Co(CR)OH_2^{2+}$	(d)	N_4O	8.0	12
$Co(NH_3)_5OH_2^{3+}$		N_5O	6.2	8
$Ni(OH_2)_6^{2+}$		O_6	10.0	8
$Cu(OH_2)_6^{2+}$		O_6	7.3	8
$Cu(DMAM\text{-}PMHD)OH_2^{2+}$	(e)	N_3O_2	7.1	13
$Cu(C\text{-}PMHD)OH_2^{+}$	(f)	N_2O_3	6.6	14
$Zn(OH_2)_6^{2+}$		O_6	9.0	8
$Zn(DMAM\text{-}PMHD)OH_2^{2+}$	(e)	N_3O	9.2	13
$Zn(C\text{-}PMHD)OH_2^{+}$	(f)	N_3O_2	7.1	14
$Zn(CR)OH_2^{2+}$	(d)	N_4O	8.7	12
$ZN([12]aneN_3)OH_2^{2+}$	(g)	N_3O	7.3	15, 16
$Zn(HP[12]aneN_3)OH_2^{+}$	(h)	N_3O_2	10.7	16
$Zn(TImMP)OH_2^{2+}$	(i)	N_3O	< 7	17
$Co(TImMP)OH_2^{2+}$	(i)	N_3O	7.8	17

This is the result of the formation of the coordination bond. The oxygen atom donates two electrons to the metal ion and formally becomes positively charged:

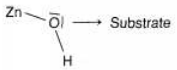


Under these conditions a proton is easily released. The nucleophilicity of coordinated water is, of course, decreased with respect to free water, owing to the decreased electronic charge on the oxygen atom, but a significant concentration of M-OH species may

exist in neutral solution. In turn, the coordinated hydroxide is a slightly poorer nucleophile than the free OH^- ion, but better than water. On the basis of recent MO calculations,[18] the order of nucleophilicity for solvent-derived species can be summarized as follows:

$$H_3O^+ < H_2O - M^{2+} \simeq H_2O < HO - M^+ \simeq HO^- \quad (11.2.2.13.1)$$

Therefore, at neutral or slightly alkaline pH, the small decrease in efficiency of coordinated vs. free hydroxide ions is more than compensated for by the higher concentration of reactive species available (i.e., HO-M^+ vs. HO^-). Another common role for zinc enzymes is thus to provide a binding site at which the substrate can be attacked by the metal-coordinated hydroxide:



The pK_a of coordinated water in zinc complexes is controlled by the coordination number and by the total charge of the complex, in the sense that it decreases with decreasing coordination number and with increasing positive charge, because a zinc ion, bearing in effect a more positive charge, will have greater attraction for the oxygen lone pair, thus lowering the pKa. Charged ligands affect water pK_a's more than does the number of ligands.[18] The pK_a in metalloproteins is further controlled by the presence of charged groups from protein side chains inside the cavity or by the binding of charged cofactors. The coordinated water may have a pK_a as low as 6, as in carbonic anhydrase (see later). On the other hand, the pK_a of the coordinated water is 7.6 in liver alcohol dehydrogenase (LADH) when NAD^+ is bound, 9.2 in the coenzyme-free enzyme, and 11.2 in the presence of NADH (see Section V.C).

(3) As mentioned before, Zn complexes show facile four- to five-coordinate interconversion. The low barrier between these coordination geometries is quite important, because the substrate may add to the coordination sphere in order to replace the solvent or to be coordinated together with the solvent. If the interconversion between four- and five-coordination is fast, catalysis is also fast.

Thus, to summarize, zinc is a good Lewis acid, especially in complexes with lower coordination numbers; it lowers the pK_a of coordinated water and is kinetically labile, and the interconversion among its four-, five-, and six-coordinate states is fast. All of these properties make zinc quite suitable for biological catalysis.[19]

11.2.2.13: Selecting Zinc is shared under a CC BY-NC-SA 4.0 license and was authored, remixed, and/or curated by LibreTexts.

11.2.2.14: Steady-State and Equilibrium Kinetics of Carbonic Anhydrase-Catalyzed CO_2/HCO_3^- Interconversion

The $CO_2 \rightleftharpoons HCO_3^-$ interconversion catalyzed by CA is extremely fast. The usual kinetic parameters describing an enzymatic reaction are the turnover number or kinetic constant for the reaction, k_{cat}, and the Michaelis constant K_m. In the simple catalytic scheme

$$E + S \underset{k_{-1}}{\overset{k_1}{\rightleftharpoons}} ES \xrightarrow{k_2} E + P, \tag{11.2.2.14.1}$$

where E stands for enzyme, S for substrate, and P for product, K_m^{-1} is given by $k_1/(k_{-1} + k_2)$. If k_2 is small, $k_{cat} = k_2$ and $K_m^{-1} = k_1/k_{-1}$, the latter corresponding to the thermodynamic affinity constant of the substrate for the enzyme. The pH dependences[46] of k_{cat} and K_m for CO_2 hydration for the high- and low-activity isoenzymes have been determined (Figure 2.2).[33,36] It appears that K_m is pH-independent, whereas k_{cat} increases with pH, reaching a plateau above pH 8. For bicarbonate dehydration (the reverse of Equation 2.6), H^+ is a cosubstrate of the enzyme. The pH dependence of k_{cat}/K_m for HCO_3^- dehydration is also mainly due to k_{cat}, which shows the same pH profile as that for CO_2 if the experimental kinetic data are divided by the available concentration of the H^+ cosubstrate.[47,48] Further measurements have shown that the pH dependence of k_{cat} reflects at least two ionizations if the measurements are performed in the absence of anions.[49] The value of k_{cat} reaches its maximum at alkaline pH only when buffer concentrations exceed 10^{-2} M.[50] In other words, the exchange of the proton with the solvent is the rate-limiting step along the catalytic pathway if relatively high concentrations of proton acceptors and proton donors are not provided by a buffer system. This limit results from the high turnover of the enzyme, which functions at the limit imposed by the diffusion rate of the H^+ cosubstrate. At high buffer concentration, k_{cat} shows an isotope effect consistent with the occurrence of an internal proton transfer as the new rate-limiting step.[51]

Measurements of the catalyzed reaction performed at chemical equilibrium starting from mixtures of ^{12}C-^{18}O-labeled HCO_3^- and ^{13}C-^{16}O-labeled CO_2 have shown the transient formation of ^{13}C-^{18}O-labeled species (both CO_2 and HCO_3^-) before ^{18}O-labeled water appears in solution.[52] These experiments provided evidence that, at chemical equilibrium, an oxygen atom can pass from HCO_3^- to CO_2 and vice versa several times before being released to water. Furthermore, maximal exchange rates are observed even in the absence of buffers.

Under chemical equilibrium conditions, ^{13}C NMR spectroscopy is particularly useful in investigating substrate interconversion rates, since the rates pass from a slow-exchange regime in the absence of enzyme to fast exchange at sufficient enzyme concentration. In the absence of enzyme two ^{13}C signals are observed, one for CO_2 and the other for HCO_3^-. In the presence of enzyme only one averaged signal is observed (Figure 2.6). Starting from the slow exchange situation, in the absence of enzyme, the increase in linewidth ($\Delta\nu$) of the substrate (A) and product (B) signals (caused by exchange broadening that is caused in turn by the presence of a small amount of catalyst) depends on the exchange rate and on the concentration of each species, according to the following relation:

$$\Delta\nu_A[A] = \Delta\nu_B[B] = \tau_{esch}^{-1} \tag{2.9}$$

Therefore, the exchange rate τ_{esch}^{-1} can be calculated.[53] The appearance of the NMR spectrum for different τ_{esch}^{-1} values is illustrated in Figure 2.6 under the condition [A] = [B]. For the high-activity enzyme it was found that the maximal exchange rates are larger than the maximal turnover rates under steady-state conditions; the ratio between k_{exch} of the high-activity (type II) and low-activity (type I) forms is 50, i.e., larger than the ratio in k_{cat}[49,54] This result is consistent with the idea that the rate-limiting step in the steady-state process is an intramolecular proton transfer in the presence of buffer for type II enzymes, whereas it may not be so for the type I enzymes. The exchange is pH-independent in the pH range 5.7 - 8, and does not show a proton-deuteron isotope effect. The apparent substrate binding (HCO_3^-) is weaker than steady-state K_m values, indicating that these values are not true dissociation constants. Chloride is a competitive inhibitor of the exchange.[49]

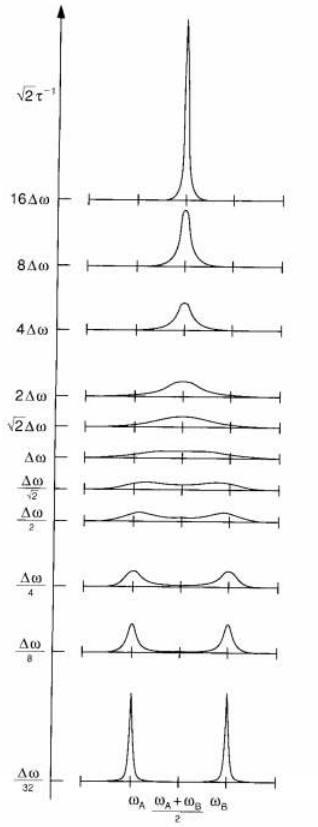


Figure 2.6 - Calculated lineshape for the NMR signals of nuclei equally distributed between two sites ([A] = [B]), as a function of the exchange rate τ^{-1}. $\Delta\omega$ is the peak separation in rad s^{-1}.

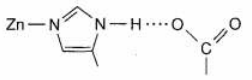
A similar investigation was conducted for type I CoHCA at pH 6.3, where the concentrations of CO_2 and HCO_3^- are equal.[55] The two lines for the two substrates were found to have different linewidths but equal T_1 values. Measurements at two magnetic fields indicate that the line broadening of the HCO_3^- resonance is caused by substrate exchange and by a paramagnetic contribution due to bonding. The temperature dependence of the linewidth shows that the latter is determined by the dissociation rate. Such a value is only about 2.5 times larger than the overall $CO_2 \rightleftharpoons HCO_3^-$ exchange-rate constant. Therefore the exchange rate between bound and free HCO_3^- is close to the threshold for the rate-limiting step. Such an exchange rate is related to the higher affinity of the substrate and anions in general for type I isoenzymes than for type II isoenzymes. This behavior can be accounted for in terms of the pK_a of coordinated water (see Section C).

11.2.2.14: Steady-State and Equilibrium Kinetics of Carbonic Anhydrase-Catalyzed CO_2/HCO_3^- Interconversion is shared under a CC BY-NC-SA 4.0 license and was authored, remixed, and/or curated by LibreTexts.

11.2.2.15: Strategies for the Investigation of Zinc Enzymes

The Groups to which Zinc(II) is Bound

Zinc(II) is an ion of borderline hardness and displays high affinity for nitrogen and oxygen donor atoms as well as for sulfur. It is therefore found to be bound to histidines, glutamates or aspartates, and cysteines. When zinc has a catalytic role, it is exposed to solvent, and generally one water molecule completes the coordination, in which case the dominating ligands are histidines. It has been noted[20] recently that coordinated histidines are often hydrogen-bonded to carboxylates:



It is possible that the increase in free energy for the situation in which the hydrogen is covalently bound to the carboxylate oxygen and H-bonded to the histidine nitrogen is not large compared to k_BT. Under these circumstances the protein could determine the degree of imidazolate character of the ligand and therefore affect the charge on the metal.

The binding of zinc(II) (like that of other metal ions) is often determined by entropic factors. Water molecules are released when zinc(II) enters its binding position, thus providing a large entropy increase. Most commonly zinc is bound to three or four protein ligands. Large entropy increases are not observed, however, when zinc(II) binds to small polypeptides like the recently discovered zinc fingers, for here the binding site is not preformed (see Section III.B), and zinc(II) must be present for the protein to fold properly into the biologically active conformation.

The Reactivity of Zinc(II) in Cavities

In the preceding section we discussed the properties of zinc(II) as an ion. These properties are, of course, important in understanding its role in biological catalysis, but it would be too simplistic to believe that reactivity can be understood solely on this basis. Catalysis occurs in cavities whose surfaces are constituted by protein residues. Catalytic zinc is bound to a water molecule, which often is H-bonded to other residues in the cavity and/or to other water molecules. The structure of the water molecules in the cavity cannot be the same as the structure of bulk water. Furthermore, the substrate interacts with the cavity residues through either hydrophilic (H-bonds or electric charges) or hydrophobic (London dispersive forces) interactions. As a result, the overall thermodynamics of the reaction pathway is quite different from that expected in bulk solutions. Examples of the importance of the above interactions will be given in this chapter.

The Investigation of Zinc Enzymes

Direct spectroscopic investigation of zinc enzymes is difficult, because zinc(II) is colorless and diamagnetic; so it cannot be studied by means of electronic or EPR spectroscopy. Its NMR-active isotope, ^{67}Zn, the natural abundance of which is 4.11%, has a small magnetic moment, and cannot (with present techniques) be examined by means of NMR spectroscopy at concentrations as low as 10^{-3} M. The enzymes could be reconstituted with ^{67}Zn. However, ^{67}Zn has a nuclear quadrupolar moment, which provides efficient relaxation times, especially in slow-rotating proteins and low-symmetry chromophores, making the line very broad.[210] Of course, ^{1}H NMR can be useful for the investigation of the native enzymes. However, often the molecular weight is such that the proteins are too large for full signal assignment given the current state of the art. At the moment the major source of information comes from x-ray data. Once the structure is resolved, it is possible to obtain reliable structural information on various derivatives by the so-called Fourier difference map. The new structure is obtained by comparing the Fourier maps of the native and of the derivative under investigation. Many x-ray data are now available on carboxypeptidase (Section V.A) and alcohol dehydrogenase (Section V.C).

The zinc ion can be replaced by other ions, and sometimes the enzymatic activity is retained fully or partially (Table 2.4). These new systems have attracted the interest of researchers who want to learn about the role of the metal and of the residues in the cavity, and to characterize the new systems per se. Spectroscopic techniques can be appropriate for the new metal ions; so it is possible to quickly monitor properties of the new derivative that may be relevant for the investigation of the zinc enzyme.

Table 2.4 - Representative metal-substituted zinc enzymes. Percent activities with respect to the native zinc enzyme in parentheses.[a]

Enzyme	Substituted Metals
Alcohol dehydrogenase	Co(II)(70), Cu(II)(1), Cu(I)(8), Cd(II)(30), Ni(II)(12)
Superoxide dismutase	Co(II)(90), Hg(II)(90), Cd(II)(70), Cu(II)(100)
Aspartate transcarbamylase	Cd(II)(100), Mn(II)(100), Ni(II)(100)
Transcarboxylase	Co(II)(100), Cu(II)(0)
RNA polymerase	Co(II)(100)
Carboxypeptidase A	Mn(II)(30), Fe(II)(30), Co(II)(200), Ni(II)(50), Cu(II)(0),[b] Cd(II)(5), Hg(II)(0), Co(III)(0), Rh(II)(0), Pb(II)(0)
Thermolysin	Co(Il)(200), Mn(II)(10), Fe(II)(60), Mg(II)(2), Cr(II)(2), Ni(II)(2), Cu(II)(2), Mo(II)(2), Pb(II)(2), Cd(II)(2), Nd(III)(2), Pr(III)(2)
Alkaline phosphatase	Co(II)(30), Cd(II)(1), Mn(II)(1), Ni(II)(0), Cu(II)(0), Hg(II)(0)
β-Lactamase II	Mn(II)(3), Co(II)(11), Ni(II)(0), Cu(II)(0), Cd(II)(11), Hg(II)(4)
Carbonic anhydrase[c]	Cd(II)(2), Hg(II)(0), Cu(II)(0), Ni(II)(2), Co(II)(50), Co(III)(0), Mn(II)(18), V(IV)O^{2+}(0)
Aldolase	Mn(II)(15), Fe(II)(67), Co(II)(85), Ni(II)(11), Cu(II)(0), Cd(II)(0), Hg(II)(0)
Pyruvate carboxylase	Co(II)(100)
Glyoxalase	Mg(II)(50), Mn(II)(50), Co(II)(50)

a) Taken from Reference 21. b) Recent data indicate nonnegligible catalytic activity.[22] c) BCA II, except the value for Cd(II) obtained with HCA II

11.2.2.15: Strategies for the Investigation of Zinc Enzymes is shared under a CC BY-NC-SA 4.0 license and was authored, remixed, and/or curated by LibreTexts.

11.2.2.16: The Natural Catalysts

Table 2.1 lists metalloenzymes that catalyze hydrolytic and related reactions. According to the above guidelines the hydrolysis of peptide bonds is catalyzed by enzymes called peptidases that belong to the class of hydrolases (according to the official enzyme classification). Two peptidases (carboxypeptidase and thermolysin) are known in great detail, because their structures have been elucidated by high-resolution x-ray crystallography. They share many features; e.g., their metal ions coordinate to the same kind of protein residues. A discussion of the possible mechanism of carboxypeptidase A will be given in Section V.A. Metallopeptidases are zinc enzymes: generally they are single polypeptide chains with molecular weights in the range 30 to 40 kDa. Metallohydrolases of carboxylic and phosphoric esters are also often zinc enzymes. Alkaline phosphatase will be described in Section V.B as a representative of this class. Magnesium is sometimes involved in hydrolytic reactions. This is common when phosphate groups are involved, probably because the affinity of Mg^{2+} for phosphate groups is high.[1] However, hydrolytic reactions can be performed by other systems (not treated here) like urease, which contains nickel(II),[2] or acid phosphatase, which contains two iron ions,[3] or aconitase, which contains an Fe_4S_4 cluster.[4]

Table 2.1 - Representative metalloenzymes catalyzing hydrolytic and related reactions

Enzyme	Metal(s)	Function
Carboxypeptidase	Zn^{2+}	Hydrolysis of C-terminal peptide residues
Leucine aminopeptidases	Zn^{2+}	Hydrolysis of leucine N-terminal peptide residues
Dipeptidase	Zn^{2+}	Hydrolysis of dipeptides
Neutral protease	Zn^{2+}, Ca^{2+}	Hydrolysis of peptides
Collagenase	Zn^{2+}	Hydrolysis of collagen
Phospholipase C	Zn^{2+}	Hydrolysis of phospholipids
β-Lactamase II	Zn^{2+}	Hydrolysis of β-lactam ring
Thermolysin	Zn^{2+}, Ca^{2+}	Hydrolysis of peptides
Alkaline phosphatase	Zn^{2+}, Mg^{2+}	Hydrolysis of phosphate esters
Carbonic anhydrase	Zn^{2+}	Hydration of CO_2
α-Amylase	Ca^{2+}, Zn^{2+}	Hydrolysis of glucosides
Phospholipase A_2	Ca^{2+}	Hydrolysis of phospholipids
Inorganic pyrophosphatase	Mg^{2+}	Hydrolysis of pyrophosphate
ATPase	Mg^{2+}	Hydrolysis of ATP
Na^+ - K^+ - ATPase	Na^+, K^+	Hydrolysis of ATP with transport of cations
Mg^{2+} - Ca^{2+} - ATPase	Mg^{2+}, Ca^{2+}	Hydrolysis of ATP with transport of cations
Phosphatases	Mg^{2+}, Zn^{2+}	Hydrolysis of phosphate esters
Creatine kinase	M^{2+}	Phosphorylation of creatine
Pyruvate kinase	M^+, M^{2+}	Dephosphorylation of phosphoenolpyruvate
Phosphoglucomutase	Mg^{2+}	Phosphate transfer converting glucose-I-phosphate to glucose-6-phosphate
DNA polymerase	Mg^{2+} (Mn^{2+})	Polymerization of DNA with formation of phosphate esters
Alcohol dehydrogenase	Zn^{2+}	Hydride transfer from alcohols to NAD^+

Examples of enzymes catalyzing nucleophilic addition of OH^- (other than hydrolysis) and H^- are carbonic anhydrase and alcohol dehydrogenase. Both are zinc enzymes. In the official biochemical classification of enzymes, carbonic anhydrase belongs to the class of lyases. Lyases are enzymes that cleave C-C, C-O, C-N, or other bonds by elimination, leaving double bonds, or conversely add groups to double bonds. Carbonic anhydrase has a molecular weight around 30 kDa, and is among the most-studied metalloenzymes. It catalyzes the deceivingly simple CO_2 hydration reaction. The subtleties of its biological function, unraveled by a combination of techniques, make it an ideal example for bioinorganic chemistry. Section IV is fully dedicated to this enzyme. Alcohol dehydrogenase is a 90-kDa enzyme that catalyzes the reversible transfer of a hydride ion from alcohols to NAD^+. Although it is a redox enzyme (in fact, classified as an oxidoreductase) and not a hydrolytic one, it will illustrate a different use that Nature makes of zinc to catalyze nucleophilic attack at carbon (Section V.C). Finally, the enzymatic transfer of organic radicals by enzymes involving coenzyme B_{12} will be briefly considered.

11.2.2.16: The Natural Catalysts is shared under a CC BY-NC-SA 4.0 license and was authored, remixed, and/or curated by LibreTexts.

11.2.2.17: What Do We Learn?

From Copper Substitution

The coordination chemistry of CuCA is not yet fully understood, since the electronic spectra are not very pH-sensitive. Nevertheless, the affinity of anions is pH-dependent, as it is for CoCA.[82] As could be anticipated from Section III.B, the affinity of anions, including HCO_3^-, is higher than that of CoCA. Water is usually present in the coordination sphere, along with the anion, as checked by water ^1H NMRD.[83,84] The steric requirements of the three histidines and of the cavity allow the anion and the water molecule to arrange in an essentially square pyramidal geometry (Figure 2.17).

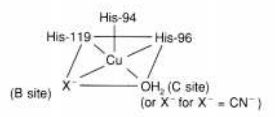


Figure 2.17 - Schematic representation of the suggested coordination geometry for the anion adducts of CuCA.

This is consistent with the electronic and EPR spectra. In particular, the EPR spectra are all axial, with g-values decreasing from 2.31 in the nonligated enzyme to 2.24 in the various anion adducts.[84] The water molecule would be in the C site or hydrophilic binding site, and the anion would be in the B site or hydrophobic pocket. His-94 would be in the apical position of the square pyramid. It has been shown by EPR spectroscopy that at low temperature two cyanide anions bind to copper. The donor atoms are two cyanide carbon and two histidine nitrogen atoms in the basal plane, and the third histidine nitrogen in the axial position.[85] The hyperfine splitting is observed only with nuclei in the basal plane. It is observed both with ^{13}C nuclei of ^{13}C-enriched CN^- and with the two ^{14}N of two histidines. The second cyanide may thus displace the coordinated water (Figure 2.17). Oxalate and sulfonamides displace water from the coordination sphere.[85,86] For the oxalate ion this may occur through bidentate behavior. Coordination to an oxygen of the sulfonamide cannot be ruled out, although the electronic and EPR spectra of the sulfonamide complex are more consistent with a pseudotetrahedral chromophore. The SO_2 moiety would in any case point toward the B binding site. It is likely that sulfonamides bind as in ZnCA. Bicarbonate also shows less water relaxivity than other monodentate anions.[83,84.86]

^{13}C NMR spectroscopy has been used to investigate the location of the two substrates, CO_2 and HCO_3 ,with respect to the metal ion in CuCA.[86-88] As was pointed out in Section IV.B, the interconversion between the two species is slow on the NMR timescale in the absence of catalysts. Therefore, two signals are observed (Figures 2.6 and 2.18). In the presence of the catalytically active CoCA, only one signal is observed at suitable enzyme concentrations, and individual information on CO2 binding cannot be obtained.[89,90] In the presence of inactive CuCA, two signals are again observed, which are broadened to different extents.

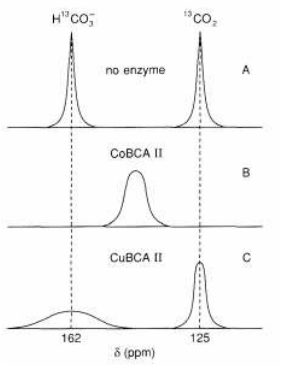


Figure 2.18 - Schematic representation of the ^{13}C NMR spectra of the CO_2/HCO_3^- system (A) in pure water, (B) in the presence of CoCA, and (C) in the presence of CuCA.[56]

For the HCO_3^- signal the T_2^{-1} values as estimated from the linewidth are much larger than T_1^{-1}. Since the equation for T_2^{-1}, analogous to Equation (2.14), would predict similar T_1 and T_2 values,[69,72] a sizeable broadening due to chemical exchange must be present. Indeed, unlike T_{1p}^{-1} (Equation 2.1l), T_{2p}^{-1} may be a complicated function of the exchange time τ_M and of the isotropic shift, $\Delta\omega_M$,

$$T_{2p}^{-1} = \frac{f_M}{\tau_M} \frac{T_{2M}^{-2} + T_{2M}^{-1}\tau_M^{-1} + (\Delta\omega_M)^2}{(T_{2M}^{-1} + \tau_M^{-1})^2 + (\Delta\omega_M)^2} \tag{2.15}$$

In the slow-exchange region, i.e., when two separate signals are observed and the broadening is due to exchange, $T_{2p}^{-1} = f_M \tau_M^{-1}$. This region is characterized by a marked increase in linewidth with increasing temperature, as confirmed by measurements at 4 and 25 °C. Therefore, T_{2p} gives a direct measure of τ_M.[56] The ^{13}C T_1^{-1} values of HCO_3^- are consistent with bicarbonate bound to the metal. The Cu—C distance would be 2.5 Å if the unpaired electron were completely on the copper ion, as estimated by using Equation (2.1) and a value of $\tau_c = 2.1 \times 10^{-9}$ s independently obtained from water ^1H NMRD.[83] This distance is much too short for a coordinated bicarbonate; however, electron delocalization on the bicarbonate ligand may account for such a short calculated distance; the possibility of a bidentate type of ligation cannot be discarded. The dissociation rate, which is very low, by itself accounts for the lack of activity of the derivative.

For CO_2, a carbon-copper distance could be calculated if the affinity constants of the substrate for the protein were known. When the binding site, if any, starts being saturated, fast exchange with excess ligand (in this case, CO_2) decreases the observed paramagnetic effect. From this behavior, the affinity constant may be estimated. For CO_2 the paramagnetic effect remained constant up to 1 M CO_2; i.e., the affinity constant is smaller than 1 M^{-1}. This means that practically there is no affinity for copper; yet the paramagnetic effect is paradoxically high.[88]

Another picture comes by analyzing the NMR data in terms of a pure diffusive model.[88] Here Hubbard's equation[91] has been used:

$$T_{2p}^{-1} = N_M \left(\frac{\mu_0}{4\pi}\right)^2 \frac{8\pi}{225} \frac{\gamma_I^2 n_e^2 \mu_B^2 S(S+1)}{d(D_N + D_M)} \left(13 f(\omega_S, \tau_D) + 3 f(\omega_S, \tau_D)\right) \tag{2.16}$$

where

$$f(\omega, \tau_D) = \frac{15}{2} I(u) \tag{11.2.2.17.1}$$

$$u = [\omega \tau_D]^{1/2} \tag{11.2.2.17.2}$$

$$I(u) = u^{-5}\{u^2 - 2 + e^{-u}[(u^2 - 2)\sin u + (u^2 + 4u + 2)\cos u]\} \tag{11.2.2.17.3}$$

d is the distance of closest approach, D_N and D_M are the diffusion coefficients of the molecules containing the nucleus under investigation, and $\tau_D = 2d^2/(D_N + D_M)$. The experimental paramagnetic effect can be reproduced with a CO_2 concentration inside the cavity much larger than the one in the bulk solution. This result indicates that substrate does not bind to a specific site, but probably binds in the hydrophobic region. Note that CO_2 is more soluble in organic solvents than in water.

The effect of the cavity is to attract CO_2 by interaction either with the metal ion or with a hydrophobic part of the cavity itself. But the affinity constant is in any case lower than expected from the Michaelis constant (see Section IV.B) measured under steady-state conditions, indicating that the latter does not represent the dissociation constant of the enzyme-CO_2 system.

In summary, the main information concerning the catalytic cycle obtained from the copper derivative is the structural and kinetic characterization of both CO_2 and HCO_3^- species when they are not interconverting but present within the cavity. In this way we have further proof that HCO_3^- is bound to the metal and that CO_2 is attracted inside the cavity either by hydrophobic interactions or by the metal ion or both. The data obtained on the geometry around copper are consistent with those obtained on cobalt.

From Manganese and Cadmium Substitutions

Several studies have been performed on MnCA. Although CA is not the protein for which Mn(II) has been most extensively used as a paramagnetic probe to map substrates and inhibitors within the metal cavity, by measuring the T_{2M}^{-1} values of protons of the inhibitor N-acetyl-sulfanilamide, and by assuming that dipolar contributions are dominant, researchers have mapped the orientation of the inhibitor inside the active cavity (Figure 2.19).[92] This orientation is consistent with x-ray data on stronger binding sulfonamides.[64-66] MnCA is not completely inactive. ^{13}C NMR studies of the $CO_2 \rightleftharpoons HCO_3^-$ interconversion at pH 8.5 showed that the interconversion rate is about 4 percent that of the native enzyme.[93] The T_1^{-1} and T_2^{-1} values of $H^{13}CO_3^-$ suggest that bicarbonate might be bidentate in the central step of the catalytic cycle.[93]

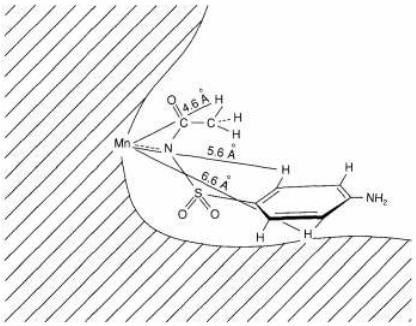


Figure 2.19 - Schematic drawing of the geometric arrangement of the inhibitor N-acetyl-sulfanilamide in the active cavity of manganese(II)-substituted CA, as revealed by ^{1}H NMR spectroscopy.[92]

Data from ^{113}Cd studies that have been performed on CdBCA II and CdHCA I are consistent with the general picture presented here.[94] The ^{113}Cd chemical shifts are indeed consistent with a donor set of three nitrogens and two oxygens. The cadmium(II) derivative could thus be five-coordinate with two water molecules, in agreement with the expectation based on its ionic radius being larger than that of zinc(II). The ^{113}Cd signal of CdBCA II in the presence of benzene-sulfonamide enriched in ^{15}N is split into a doublet because of the nitrogen-cadmium coupling (Figure 2.20).[95] This result provides direct evidence for metal-nitrogen bonding in sulfonamides, which has been confirmed by x-ray data.[65]

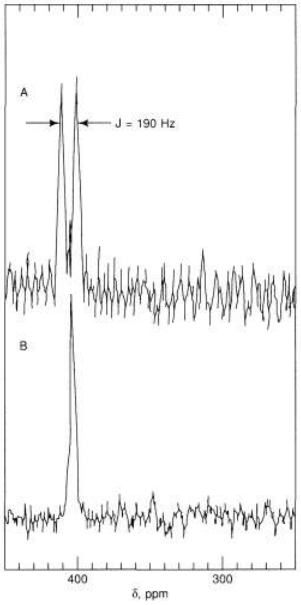


Figure 2.20 - ^{113}Cd NMR spectra of Cd-substituted bovine carbonic anhydrase II in the presence of ^{15}N-enriched (A) or ^{14}N-enriched (B) benzenesulfonamide inhibitor.[95]

11.2.2.17: What Do We Learn? is shared under a CC BY-NC-SA 4.0 license and was authored, remixed, and/or curated by LibreTexts.

11.2.3: Calcium in Biological Systems

Calcium, like many other "inorganic elements" in biological systems, has during the last decade become the subject of much attention both by scientists and by the general public.[1] The presence and central role of calcium in mammalian bones and other mineralized tissues were recognized soon after its discovery as an element by Davy in 1808. Much later, the insight arrived that Ca^{2+} ions could play an important role in other tissues as well. Experiments of great historical influence were performed by the British physiologist Sidney Ringer a little over a century ago.[2] He was interested in the effects of various cations on frog-heart muscle and somewhat serendipitously discovered that Ca^{2+} ions, everpresent in the tap water distributed in central London, in millimolar concentrations were necessary for muscle contraction and tissue survival.

Today it is widely recognized that Ca^{2+} ions are central to a complex intracellular messenger system that is mediating a wide range of biological processes: muscle contraction, secretion, **glycolysis** and **gluconeogenesis**, ion transport, cell division and growth (for definitions of terms in boldface, see Appendix A in Section IX). The detailed organization of this messenger system is presently the subject of considerable scientific activity, and some details are already known. One of the links in the system is a class of highly homologous Ca^{2+}-binding proteins, to be discussed later on in this chapter, that undergo Ca^{2+}-dependent conformational changes and respond to transitory increases in intracellular Ca^{2+}-ion concentrations. A prerequisite for the proper function of the calcium messenger system in higher organisms is that the **cytosolic** Ca^{2+} concentration in a "resting" cell be kept very low, on the order of 100 to 200 nM. Transitory increases in the Ca^{2+} concentration that may result from hormonal action on a membrane receptor must rapidly be reduced. Several transport proteins, driven either by ATP hydrolysis or by gradients of some other ion like Na^{+}, are involved in this activity.

Ca^{2+} ions are also known to play various roles outside cells. In the plant kingdom Ca^{2+} ions often form links between individual cells and are required for maintaining the rigidity of whole plants; some seaweeds are typical examples. In the blood plasma of mammals, in which the Ca^{2+} concentration exceeds the intracellular by a factor of about 10^4, Ca^{2+} ions are instrumental in joining certain proteins in the blood-clotting system with membrane surfaces of circulating cells. Many extracellular enzymes also contain Ca^{2+} ions, sometimes at the active site but most often at other locations. It is generally believed that Ca^{2+} ions confer on proteins an increased thermal stability, and indeed proteins in heat-tolerant microorganisms often hold many such ions.

Vertebrates require much calcium in their food; in the USA the recommended daily allowance (RDA) for adult humans is 800 mg, and most other countries have comparable recommendations. During gestation in mammals, calcium must be transported across the placenta into the fetus, in particular during those phases of pregnancy when bone formation is most rapid. Interestingly, there appear to be some parallels between intestinal and placental transport that will be discussed further below. The role of calcium in biominerals is a vast subject that we can treat only superficially in this chapter.

To provide a background to the more biologically oriented sections that follow, we begin with a brief recapitulation of some basic facts about calcium. Then we continue with an outline of calcium distribution in biological tissues and organelles, and of the methods that can be used to obtain this information. After this follows a brief section on Ca^{2+} transport, and an account of the mechanism of intracellular Ca^{2+} release as it is presently understood. A discussion of some selected Ca^{2+}-binding proteins of general interest, both intracellular and extracellular, then follows. Before we conclude the chapter, we will summarize some recent observations on Ca^{2+}-binding proteins in prokaryotes.

II. Basic Facts About Calcium: Its Compounds and Reactions

A. Basic Facts

B. Essentials of Ca^{2+} Chemistry

III. Calcium In Living Cells: Methods For Determining Concentrations And Spatial Distributions

A. Measurements of "Free" Calcium Concentrations

1. Ca^{2+}-selective microelectrodes
2. Bioluminescence
3. Complexing Agents with Ca^{2+}-dependent Light Absorption or Fluorescence
4. Complexing Agents with Ca^{2+}-dependent NMR Spectra

B. Measurements of Total Calcium Concentrations
1. Electron Probe and Electron Energy-loss Techniques
2. Proton-induced X-ray Emisssion (PIXE)
3. Ion Microscopy

C. Summary

Much of our present knowledge about the biological role of Ca^{2+} rests on detailed measurements of the concentration, distribution, and chemical nature of Ca^{2+} and its complexes. Concentrations of uncomplexed, or "free," Ca^{2+} can be measured by Ca^{2+}-selective microelectrodes, bioluminescence and complexing agents with Ca^{2+}-dependent light absorption, fluorescence, or NMR spectra. An outcome of such studies is that the "free" Ca^{2+} concentration in resting **eukaryotic** cells generally is very low, on the order of 100 to 200 nM. Total Ca^{2+} concentrations, uncomplexed and complexed, can be measured by a variety of physical techniques. Some techniques, like atomic absorption, are sensitive but give poor spatial resolution. Others involve the bombardment of the sample with electrons or charged atoms, and can yield spatial resolutions of the order of a few nm; however, there is a trade-off between detectability and resolution

IV. The Transport and Regulation of Ca^{2+} Ions in Higher Organisms

A. Ca^{2+} Uptake and Secretion

B. Intracellular Ca^{2+} Transport
1. The Ca^{2+}-ATPases
2. The Na^+/Ca^{2+} Exchanger of the Plasma Membrane
3. Mitochondrial Ca^{2+} Transport: Influx
4. Mitochondrial Ca^{2+} Transport: Efflux
5. Ca^{2+} Efflux from Non-mitochondrial Stores
6. Other Voltage-gated or Receptor-activated Ca^{2+} Channels

C. Inositol Trisphosphate and the Ca^{2+} Messenger System

D. Summary

The fluxes of Ca^{2+} ions and their regulation in higher organisms, as well as in microorganisms, depend on several transport proteins in addition to vesicular and gated processes. An important class of transport proteins are the Ca^{2+}-ATPases, which are particularly abundant in muscle cells. These proteins translocate Ca^{2+} ions against large activity (or concentration) gradients through the expenditure of ATP. Transport of Ca^{2+} ions against activity gradients across membranes may also be accomplished by coupled transport of other ions, like Na^+, with a gradient in the opposite direction.

As a result of some external stimulus—the action of a hormone, for example—the "free" Ca^{2+}-ion concentrations in the cytoplasm of many cell types may transiently increase several orders of magnitude. This increase largely results from the release of Ca^{2+} from intracellular stores (ER, SR) in response to the initial formation of a new type of messenger, 1,4,5-IP_3. The activity of Ca^{2+}-transport proteins eventually restores the Ca^{2+} concentration levels to resting levels. This sequence of events forms the basis for Ca^{2+}'s role in the regulation of a wide variety of cellular activities (see Section V).

V. Molecular Aspects of Ca^{2+}-regulated Intracellular Processes

A. Calmodulin

B. Troponin C

C. Parvalbumin and Calbindins D_{9K} and D_{28K}

D. Sarcoplasmic Calcium-Binding Protein from *Nereis diversicolor*

E. Membrane Cytoskeleton and Phospholipid Binding Proteins

F. Ca^{2+}-dependent Proteases

G. Protein Kinase C

H. Summary

Many different biological processes in eukaryotic cells are regulated by intracellular Ca^{2+} concentration levels. Examples of such processes are muscle contraction, transport processes, cell division and growth, enzyme activities, and metabolic processes. A link in this regulatory chain is a number of intracellular Ca^{2+} receptors with Ca^{2+} affinities such that their binding sites are largely unoccupied at resting Ca^{2+} concentration levels, but are occupied at Ca^{2+} levels reached as a result of some external stimulus. This class of Ca^{2+} receptors is often called the "calmodulin superfamily" and includes the well-known members troponin C (regulating muscle contraction in striated muscle) and calmodulin (playing an important role in the regulation of many cellular processes). Amino-acid sequence determinations as well as x-ray and 2D ^1H NMR studies have revealed a strong homology between the regulatory Ca^{2+}-binding proteins. The Ca^{2+}-binding sites are located in a loop flanked by two helices, and the Ca^{2+} ions are ligated with approximately octahedral or pentagonal bipyramidal symmetry. The ligands are six or seven oxygen atoms that are furnished by side-chain carboxylate or hydroxyl groups, backbone carbonyls, and water molecules. Pairs of these Ca^{2+} sites, rather than individual sites, appear to be the functional unit, and a common consequence of their arrangement is cooperative Ca^{2+} binding. Ca^{2+} binding to the intracellular receptor proteins is accompanied by structural changes that expose hydrophobic patches on their surfaces, thereby enabling them to bind to their target proteins.

VI. Extracellular Ca^{2+}-binding Proteins

A. Ca^{2+}-binding in Some Extracellular Enzymes

B. Summary

In higher organisms, the Ca^{2+} concentration in extracellular fluids generally is considerably higher than the intracellular concentrations. In mammalian body fluids, the Ca^{2+} concentration is typically on the order of a few mM. The extracellular concentration levels are highly regulated and undergo only minor variations. A consequence of these high levels of Ca^{2+} in extracellular fluids is that the binding constant need be only 10^3 to 10^4 M^{-1} in order for a protein site to be highly occupied by Ca^{2+}. Several extracellular enzymes and enzyme activators have one or more Ca^{2+} ions as integral parts of their structures. Some Ca^{2+} ions are bound at, or near, the active cleft and may take part in the enzymatic reactions (e.g., phospholipase A_2, α-amylase). In other molecules, for example, serine proteases like trypsin and chymotrypsin, the Ca^{2+} ion is not essential for enzymatic activity, and may play more of a structural role. Ca^{2+} ions are involved in the cascade of enzymatic events that results in blood clotting in mammals. Several of the proteins in this system contain two new amino acids, γ-carboxyglutamic acid (Gla) and β-hydroxyaspartic acid (Hya), which are strongly suspected to be involved as ligands in Ca^{2+} binding. In the presence of Ca^{2+} ions, prothrombin and other Gla-containing proteins will bind to cell membranes containing acidic phospholipids, in particular, the platelet membrane. It appears likely that Ca^{2+} ions form a link between the protein and the membrane surface.

VII. Calcium in Mineralized Tissues

Summary

Calcium is, along with iron, silicon, and the alkaline earth metals, an important constituent of mineralized biological tissues. Some Ca^{2+}-based biominerals, like bone or mother-of-pearl, can be regarded as complex composites with microscopic crystallites embedded in a protein matrix. The formation of calcified biominerals is a highly regulated process, and human bone, for instance, is constantly being dissolved and rebuilt. When the rates of these two counteracting processes are not in balance, the result may be decalcification, or *osteoporosis*, which seriously reduces the strength of the bone.

VIII. Ca^{2+}-binding Proteins in Microorganisms: The Search for a Prokaryotic Calmodulin

Summary

The role of Ca^{2+} ions in the regulation of biological activities of procaryotic organisms is still largely unsettled. Over the last decade, however, evidence has gradually accumulated that calcium ions are involved in diverse bacterial activities, such as chemotaxis and substrate transport, sporulation, initiation of DNA replication, phospholipid synthesis, and protein phosphorylation.[168] An important landmark is the recent demonstration that the intracellular Ca^{2+} concentration in *E. coli* is tightly regulated to about 100 nM, a level similar to that typical of resting eukaryotic cells.[169] Furthermore, increasing numbers of calcium-binding proteins, some of which also have putative EF-hand Ca^{2+} sites characteristic of the calmodulin superfamily of intracellular regulatory proteins, have been isolated in bacteria.[168]

IX. Appendixes

Antiport	A transport protein that carries two ions or molecules in opposite directions across a membrane.
Basal lateral membrane	The membrane in intestinal epithelial cells that is located on the base of the cells, opposite the microvilli that face the intestinal lumen.
Cytosol	The unstructured portion of the interior of a cell—the cell nucleus excluded—in which the organelles are bathed.
Electrogenic	A biological process driven by electric field gradients.
Endocytosis	The process by which eukaryotic cells take up solutes and/or particles by enclosure in a portion of the plasma membrane to (temporarily) form cytoplasmic vesicles.
Endoplasmic reticulum (ER)	Sheets of folded membranes, within the cytoplasm of eukaryotic cells, that are the sites for protein synthesis and transport.
Epithelial cells	Cells that form the surface layer of most, if not all, body cavities (blood vessels, intestine, urinary bladder, mouth, etc.).
Erythrocytes	Red-blood corpuscles.
Eukaryotic cells	Cells with a well-definied nucleus.
Exocytosis	The process by which eukaryotic cells release packets of molecules (e.g., neurotransmitters) to the environment by fusing vesicles formed in the cytoplasm with the plasma membrane.
Gluconeogenesis	Metabolic synthesis of glucose.
Glycolysis	Metabolic degradation of glucose.
Hydropathy	A measure of the relative hydrophobic or hydrophilic character of an amino acid or amino-acid side chain.
Lamina propria mucosae	The layer of connective tissue underlying the epithelium of a mucous membrane.
Mitrochondrion	A double-membrane organelle in eukaryotic cells that is the center for aerobic oxidation processes leading to the formation of energy-rich ATP.
Organelle	A structurally distinct region of the cell that contains specific enzymes or other proteins that perform particular biological functions.
Osteoporosis	Brittle-bond disease.
Phorbol esters	Polycyclic organic molecules that act as analogues to diacylglycerol and therefore are strong activators of protein kinase C.
Prokaryotic cells	Cells lacking a well-defined nucleus.
Sarcoplasmic reticulum	The ER of muscle cells.
Trophoblasts	The cells between the maternal and fetal circulation systems.

Tryptic digest	Fragmentation of proteins as a result of treatment with the proteolytic enzyme trypsin.
Uniporter	A transport protein that carries a particular ion or molecule in one direction across a membrane.

B. One-Letter Code for Amino-Acid Residues

A—alanine, C—cysteine, D—aspartate, E—glutamate, F—phenylalanine, G—glycine, H—histidine, I—isoleucine, K—Iysine, L—Ieucine, M—methionine, N—asparagine, P—proline, Q—glutamine, R—arginine, S—serine, T—threonine, V—valine, W—tryptophan, Y—tyrosine.

C. The Activity of a Transport Protein

This is usually described in terms of the classical Michaelis-Menten scheme:

$$V(=transport\ rate) = V_{max} \cdot \frac{[S]}{[S] + K_m}, \tag{11.2.3.1}$$

where [S] is the concentration of the solute to be transported and $K_m = (k_{-1}+k_2)/k_1$ is the Michaelis constant (dimension "concentration") for the reaction

$$E + S \underset{k_{-1}}{\overset{k_1}{\rightleftharpoons}} ES \xrightarrow{k_2} R. \tag{11.2.3.2}$$

Approximated as the reciprocal ratio between on- and off-rate constants relevant to the solute-protein complex, $1/K_m = k_1/k_{-1}$ may be taken as a lower limit of the affinity of the protein for the solute.

X. References

1. See, for example, "Going Crazy over Calcium" in the Health and Fitness section of *Time*, February 23, 1987, p. 49, or C. Garland *et al.*, *The Calcium Diet*, Penguin Books, 1990.
2. S. Ringer, *J. Physiol.* **3** (1883), 195.
3. *Handbook of Chemistry and Physics*, 64th ed., CRC Press, 1984.
4. R. D. Shannon, *Acta Cryst.* A, **32** (1976), 751.
5. R. J. P. Williams, in *Calcium in Biological Systems*, Cambridge Univ. Press, 1976, p. 1.
6. B. A. Levine and R. J. P. Williams, in L. J. Anghileri and A. M. T. Anghileri, eds., *Role of Calcium in Biological Systems*, CRC Press, 1982, pp. 3-26.
7. A. K. Campbell, *Intracellular Calcium: Its Universal Role as Regulator*, Wiley, 1983.
8. A. P. Somlyo, M. Bond, and A. V. Somlyo, *Nature* **314** (1985), 622.
9. T. B. Johansson, R. Akselsson, and S. A. E. Johansson, *Nucl. Inst. Methods* **84** (1970), 141.
10. R. B. Martin, in H. Sigel, ed., *Metal Ions in Biological Systems*, Dekker, **17** (1984), I.
11. H. Einspahr and C. E. Bugg, in *ibid.*, pp. 52-97.
12. L. G. Sillen and A. E. Martell, eds., Stability *Constants of Metal Ion Complexes*, Chemical Soc., London, 1964.
13. A. E. Martell and R. M. Smith, eds., *Critical Stability Constants*, Plenum Press, **1**, 1975.
14. J. D. Potter and J. Gergely, *J. Biol. Chem.* **250** (1975), 4628.
15. W. Marki, M. Oppliger, and R. Schwyzer, *Helvetica Chemica Acta* **60** (1977), 807.
16. C. M. Frey and J. Stuehr, in H. Sigel, ed., *Metal Ions in Biological Systems*, Dekker, **1** (1974), 51.
17. W. J. Moore, *Physical Chemistry*, Longman, 5th ed., 1972, Chapter 10.
18. M. V. Thomas, *Techniques in Calcium Research*, Academic Press, London, 1982.
19. T. J. Rink, *Pure Appl. Chem.* **55** (1988), 1977.
20. W. Simon *et al.*, *Ann. N.Y. Acad. Sci.* **307** (1987), 5269.
21. R. C. Thomas, *Ion-Sensitive Intracellular Microelectrodes*, Academic Press, London, 1987.
22. J. R. Blinks *et al.*, *Prog. Biophys. Mol. Biol.* **4** (1983), I.
23. R. Y. Tsien, *Biochemistry* **19** (1980), 2396.
24. G. Grynkiewicz, M. Poenie, and R. Y. Tsien, *J. Biol. Chem.* **260** (1985), 3440.

25. A. Minta, J. P. Y. Kao, and R. Y. Tsien, *J. Biol. Chem* **264** (1989), 8171.
26. R. Y. Tsien and M. Poenie, *Trends Biochem. Sci.* **11** (1986), 450.
27. E. Chiancone *et al.*, *J. Biol. Chem.* 26 (1986), 16306.
28. G. A. Smith *et al.*, *Proc. Natl. Acad. Sci. USA* **80** (1983), 7178.
29. J. C. Metcalfe, T. R. Hesketh, and G. A. Smith, *Cell Calcium* **6** (1985), 183.
30. A. P. Somlyo, *Cell Calcium* **6** (1985), 197.
31. G. W. Grime *et al.*, *Trends Biochem. Sci.* **10** (1985), 6.
32. G. H. Morrison and G. Slodzian, *Anal. Chem.* **47** (1975), 932A.
33. S. Chandra and G. H. Morrison, *Science* **228** (1985), 1543.
34. E. Murphy *et al.*, *Circulation Research* **68** (1991), 1250.
35. R. H. Wasserman and C.S. Fullmer, in W. Y. Cheung, ed., *Calcium and Cell Function*, Academic Press, **2** (1982), 176.
36. H. Rasmussen, O. Fontaine, and T. Matsumoto, *Ann. N. Y. Acad. Sci.* **77** (1981), 518.
37. S. Linse *et al.*, *Biochemistry* **26** (1987), 6723.
38. D. T. W. Bryant and P. Andrews, *Biochem. J.* **219** (1984), 287.
39. R. H. Kretsinger, J. E. Mann, and J. G. Simmonds, in A. W. Norman *et al.*, eds., *Vitamin D, Chemical, Biochemical, and Clinical Endocrinology of Calcium Metabolism*, W. de Gruyter, pp. 232-248.
40. J. J. Feher, *Am. J. Physiol.* **244** (1983), 303.
41. I. Nemere, V. Leathers, and A. W. Norman, *J. Biol. Chem.* **261** (1986), 16106.
42. G. E. Lester. *Feder. Proc.* **45** (1986), 2524.
43. P. Marche, C. LeGuern, and P. Cassier, *Cell Tissue Res.* **197** (1979), 69.
44. M. Warembourg, C. Perret, and M. Thomasset, *Endocrinol.* **119** (1986), 176.
45. H. J. Schatzman, *Experientia* **22** (1966), 364.
46. V. Niggli, J. T. Penniston, and E. Carafoli, *J. Biol. Chem.* **254** (1979), 9955.
47. E. Carafoli, M. Zurini, and G. Benaim, in *Calcium and the Cell*, CIBA Foundation Symposium no. 122, Wiley, 1986, pp. 58~65.
48. D. MacLennan, J. Biol. Chem. 245 (1970), 4508.
49. N. M. Green *et al.*, in Reference 47, pp. 93.
50. D. M. Clarke *et aI.*, *Nature* **339** (1989), 476.
51. G. Inesi, *Annu. Rev. Physiol.* **47** (1985), 573.
52. R. J. P. Williams, *Eur. J. Biochem.* **150** (1985), 231.
53. C. Tanford, *Proc. Natl. Acad. Sci. USA* **79** (1982), 6527.
54. D. H. MacLennan, K. P. Campbell, and R. A. Reithmeier, in Reference 35, pp. 151-173.
55. A. Maurer *et al.*, *Proc. Natl. Acad. Sci. USA* **82** (1985), 4036.
56. M. P. Blaustein and M. T. Nelson, in E. Carafoli, ed., *Membrane Transport of Calcium*, Academic Press, 1982, pp. 217-236.
57. P. F. Baker, in Reference 47, pp. 73-84.
58. E. Carafoli, G. Inesi, and B. P. Rosen, in Reference 10, pp. 140-143.
59. G. Fiskum, in Reference 10, pp. 187-214.
60. A. L. Lehninger *et al.*, in F. Bronner and M. Peterlik, eds., *Calcium and Phosphate Transport Across Membranes*, Academic Press, 1981, pp. 73-78.
61. E. Carafoli, in Reference 56, pp. 109-139.
62. M. J. Berridge, in Reference 47, pp. 39-49.
63. R. F. Irvine, *Brit. Med. Bull.* **42** (1986), 369.
64. E. W. McCleskey *et al.*, *J. Exp. BioI.* **124** (1986), 177.
65. D. J. Adams, T. Dwyer, and B. Hille, *J. Gen. Physiol.* **75** (1980), 493.
66. A. B. MacDermott *et al.*, *Nature* **321** (1986), 519.
67. R. J. Miller, *Science* **235** (1987), 46.
68. R. W. Tsien, *Annu. Rev. Physiol.* **45** (1983), 341.
69. E. W. Sutherland, *Science* **177** (1972), 401.
70. M. J. Berridge and R. F. Irvine, *Nature* **312** (1984), 315.
71. M. J. Berridge, *Biochem. J.* **212** (1983), 849.

72. M. J. Berridge, *J. Exp. Biol.* **124** (1986), 323.
73. C. C. Chadwick, A. Saito, and S. Fleischer, *Proc. Natl. Acad. Sci. USA* **87** (1990), 2132.
74. A. R. Hughes and J. W. Putney, *Envir. Health Perspec.* **84** (1990), 141.
75. A. S. Manalan and C. B. Klee, in *Adv. Cycl. Nucl. Prot. Phospho Res.* (1984), 227.
76. J. D. Potter and J. D. Johnson, in Reference 35, pp. 145.
77. (a) R. H. Kretsinger, *Cold Spring Harbor Symp. Quant. Biol.* **52** (1987), 499; (b) C. W. Heizmann and K. Braun, *Trends in Neurosciences* **15** (1992), 259.
78. A. Marks *et al.*, *J. Neurochem.* **41** (1983), 107.
79. P. B. Moore and J. R. Dedman, in H. Hidaka and P. J. Hartshorne, eds., *Calmodulin Antagonists and Cellular Physiology*, Academic Press, 1985, pp. 483-494.
80. Y. Nishizuka, *Phil. Trans. Roy. Soc. Lond.* (B) **302** (1983), 101.
81. M. J. Geisow, *FEBS Lett.* **203** (1986) 99.
82. M. J. Crumpton and J. R. Dedman, *Nature* **345** (1990), 212.
83. Y. S. Babu, C. E. Bugg, and W. J. Cook, *J. Mol. Biol.* **204** (1988), 191.
84. R. H. Kretsinger and C. E. Nockolds, *J. Biol. Chem.* **248** (1973), 3313.
85. S. Forsén, H. J. Vogel, and T. Drakenberg, in Reference 35, **6** (1986) 113.
86. M. D. Tsai *et aI.*, *Biochemistry* **26** (1987), 3635.
87. S. R. Martin *et al.*, *Eur. J. Biochem.* **151** (1985), 543.
88. A. Teleman, T. Drakenberg, and S. Forsén, *Biochim. Biophys. Acta* 873, (1986), 204.
89. L. Sjölin, *Acta Cryst.* **B46** (1990), 209.
90. S. R. Martin and P. M. Bayley, *Biochem. J.* **238** (1986), 485.
91. D. B. Heidorn and J. Trewhella, *Biochemistry* **27** (1988), 909.
92. D. K. Blumenthal *et al.*, *Proc. Natl. Acad. Sci. USA* **82** (1985), 3187.
93. R. E. KIevit *et al.*, *Biochemistry* **24** (1985), 8152.
94. S. Linse, T. Drakenberg, and S. Forsén, *FEBS Lett.* **199** (1986), 28.
95. S. H. Seeholzer *et al.*, *Proc. Natl. Acad. Sci. USA* **83** (1986), 3634.
96. A. Persechini and R. H. Kretsinger, *J. Cardiovasc. Pharm.* **12** (suppl. 5, 1988), S1.
97. G. Barbato *et al.*, *Biochemistry*, in press.
98. M. Ikura *et al.*, *Biochemistry* **30** (1991), 5498.
99. C. H. Keller *et al.*, *Biochemistry* **21** (1982), 156.
100. O. Herzberg and M. N. G. James, *Nature* **313** (1985), 653.
101. K. A. Satyshur *et al.*, *J. Biol. Chem.* **263** (1988), 1628.
102. E. D. McCubbin and C. M. Kay, *Ace. Chem. Res.* **13** (1980), 185.
103. M. T. Hincke, W. D. McCubbin, and C. M. Kay, *Can. J. Biochem.* **56** (1978), 384.
104. P. C. Leavis *et al.*, *J. BioI. Chem.* **253** (1978), 5452.
105. O. Teleman *et al.*, *Eur. J. Biochem.* **134** (1983), 453.
106. H. J. Vogel and S. Forsén, in L. J. Berliner and J. Reuben, eds., *Biological Magnetic Resonance*, Plenum Press, **7** (1987), 247.
107. S. Forsén *et al.*, in B. de Bernard *et al.*, eds., *Calcium Binding Proteins 1983*, Elsevier, 1984, pp. 121-131.
108. T. Drakenberg *et al.*, *J. Biol. Chem.* **262** (1987), 672.
109. K. B. Seamon and R. H. Kretsinger, in T. G. Spiro, ed., *Calcium in Biology*, Wiley, 6 (1983), 1; review of the literature.
110. B. A. Levine and D. C. Dalgamo, *Biochim. Biophys. Acta* **726** (1983), 187.
111. O. Herzberg, J. Moult, and M. N. G. James, *J. Biol. Chem.* **261** (1986), 2638.
112. W. Chazin *et al.*, personal communication.
113. M. L. Greaser and J. Gergely, *J. Biol. Chem.* **246** (1971), 4226.
114. W. Wnuk, J. A. Cox, and E. A. Stein, in Reference 35, pp. 243-278.
115. C. W. Heizmann, in Reference 109, pp. 61-63.
116. R. H. Kretsinger, *CRC Crit. Rev. Biochem.* **8** (1980), 119; R. H. Kretsinger and C. D. Barry, *Biochim. Biophys. Acta* **405** (1975), 4051.
117. W. Hunziker, *Proc. Natl. Acad. Sci. USA* **83** (1986), 7578.
118. A. L. Swain, R. H. Kretsinger, and E. L. Arnma, *J. Biol. Chem.* **264** (1988), 16620.

119. M. F. Summers, *Coord. Chem. Rev.* **86** (1988), 43; review of the literature.
120. J. M. Gillis *et al.*, *J. Muscl. Res. Cell. Mot.* **3** (1982), 377.
121. D. M. E. Szebenyi and K. Moffat, *J. Biol. Chem.* **261** (1986), 8761.
122. M. Akke, T. Drakenberg, and W. J. Chazin, *Biochemistry* **31** (1992), 1011.
123. S. Linse *et al.*, *Biochemistry* **30** (1991), 154.
124. S. Linse *et al.*, *Nature* **335** (1988), 651.
125. M. Akke and S. Forsén, *Proteins* **8** (1990), 23.
126. W. Chazin *et al.*, *Proc. Natl. Acad. Sci. USA* **86** (1989), 2195.
127. W. Wnuk, J. A. Cox, and E. A. Stein, in Reference 35, pp. 243-278.
128. W. J. Cook *et al.*, *J. Biol. Chem.* **266** (1991), 652.
129. J. J. Geisow and H. H. Walker, *Trends Biochem. Sci.* **11** (1986), 420.
130. R. H. Kretsinger and C. E. Creutz, *Nature* **320** (1986), 573.
131. M. R. Crompton, S. E. Moss, and M. J. Crumpton, *Cell* **55**(1988), 1.
132. J. Kay in A. Heidland and W. H. Horl, eds., *Protease Role in Health and Disease*, 1984, pp. 519- 570.
133. S. Ohno *et al.*, *Nature* **312** (1984), 566.
134. D. E. Croall and G. N. DeMartino, *Physiol. Rev.* **71** (1991), 813.
135. D. Carpenter, T. Jackson, and M. J. Hanley, *Nature* **325** (1987), 107.
136. S. Ohno *et al.*, *Nature* **325** (1987), 161.
137. J. F. Harper *et al.*, *Science* **252** (1991), 951.
138. H. Rasmussen, *Am. J. Med.* **50** (1971), 567.
139. W. Bode and P. Schwager, *J. Mol. Biol.* **98** (1975), 693.
140. E. Chiancone *et al.*, *J. Mol. Biol.* **185** (1985), 201.
141. B. W. Dijkstra *et al.*, *J. Mol. Biol.* **147** (1983), 97.
142. D. L. Scott *et al.*, *Science* **250** (1990), 1541.
143. T. Drakenberg *et al.*, *Biochemistry* **23** (1984), 2387.
144. R. J. P. Williams, in Reference 47, pp. 144-159.
145. D. I. Stuart *et al.*, *Nature* **324** (1986), 84.
146. G. L. Nelsestuen, in Reference 10, pp. 354-380.
147. M. Soriano-Garcia *et al.*, *Biochemistry* **28** (1989), 6805.
148. D. W. Deerfield *et al.*, *J. Biol. Chem.* **262** (1987), 4017.
149. K. Harlos *et al.*, *Nature* **330** (1987), 82.
150. J. Lawler and R. O. Hynes, *J. Cell. Biol.* 103 (1986), 1635.
151. V. M. Dixit *et aI.*, *J. Biol. Chem.* **261** (1986), 1962.
152. J. M. K. Slane, D. F. Mosher, and C.-S. Lai, *FEBS Lett.* **229** (1988), 363.
153. R. E. Wuthier, in Reference 10, pp. 411-472.
154. F. G. E. Pautard and R. J. P. Williams, in *Chemistry in Britain*, pp. 188-193 (1982).
155. W. E. Brown and L. C. Chow, *Annu. Rev. Material Sci.* **6** (1976), 213.
156. O. R. Bowen, *Publ. Health Reports Suppl.* Sept.-Oct. 1989, pp. 11-13.
157. B. Alberts *et al.*, *Molecular Biology of the Cell*, Garland, 1983, pp. 933-938.
158. T. N. Davis *et al.*, *Cell* **47** (1986), 423.
159. S. Inouye, T. T. Franceschini, and M. Inouye, *Proc. Natl. Acad. Sci. USA* **80** (1983), 6829.
160. G. Wistow, L. Summers, and T. L. Blundell, *Nature* **315** (1985), 771.
161. P. F. Leadlay, G. Roberts, and J. E. Walker, FEBS Lett. 178 (1984), 157; D. G. Swan *et al.*, *Nature* **329** (1987), 84.
162. N. Bylsma *et al.*, *FEBS Lett.* **299** (1992), 44.
163. J. A. Cox and A. Bairoch, *Nature* **331** (1988), 491.
164. M. A. Stevenson and S. K. Calderwood, *Mol. Cell Biol.* **10** (1990), 1234.
165. K. T. O'Neil and W. F. DeGrado, *Trends Biochem. Sci.* **170** (1990), 59.
166. V. Norris *et al.*, *Mol. Microbiol.* **5** (1991), 775.
167. M. R. Knight *et al.*, *FEBS Lett.* **282** (1991), 405.
168. S. Supattapone *et al.*, *J. Biol. Chem.* **263** (1988), 1530.

169. C. D. Ferris *et al.*, *Nature* **342** (1989), 87.
170. R. Huber *et al.*, *J. Mol. Biol.* **223** (1992), 683.
171. (a) M. Ikura *et al.*, *Science* **256** (1992), 632; (b) W. E. Meador, A. R. Means, and F. A. Quiocho, *Science* **257** (1992), 1251.
172. M. R. Knight *et al.*, *FEBS Lett.* **282** (1991), 405.
173. R. W. Tsieu and R. Y. Tsien, *Annu. Rev. Cell Biol.* **6** (1990), 715.
174. T. E. Gunter and D. R. Pfeiffer, *Am. J. Physiol.* **258** (1990), c755.
175. The authors would like to express their warm gratitude to the many students, colleagues, and coworkers who, during the preparation of this chapter, have supplied helpful comments, preprints of unpublished work, background material for figures, etc. Their encouragement is much appreciated. Special thanks are due to Drs. R. J. P. Williams and G. B. Jameson, who critically read and commented on an early version of the chapter.

Contributors and Attributions

- Sture Forsén (University of Lund, Chemical Centre, Physical Chemistry 2)
- Johan Kördel (University of Lund, Chemical Centre, Physical Chemistry 2)

11.2.3: Calcium in Biological Systems is shared under a CC BY-NC-SA 4.0 license and was authored, remixed, and/or curated by LibreTexts.

11.2.3.1: Ca^{2+}-binding Proteins in Microorganisms- The Search for a Prokaryotic Calmodulin

Since Ca^{2+} ions evidently play an important role in regulating a variety of cellular responses in animals and higher organisms, one may ask whether this use of Ca^{2+} is a recent discovery of Nature, or if it was invented early in evolution. It now appears well-established that the key intracellular "Ca^{2+}- receptor" protein calmodulin (CaM; see Section V.A) is present in all eukaryotic cells. Even in a unicellular eukaryote like common yeast (*Saccharomyces cerevisiae*), Ca^{2+} has an important regulatory role, and recently yeast CaM, as well as the single-gene encoding for it, was isolated.[160]

The amino-acid sequence of the yeast CaM (147 a.a.; M_r = 16.1 kDa) is 60 percent identical with the sequences of all other CaMs known. In fact, if generally accepted conservative amino-acid replacements are allowed, the homology increases to 80 percent or more, the most highly conserved portions being the four putative Ca^{2+}-binding sites. Sites I and III match the EF-hand test sequence (see Figure 3.24) very well; in site a His occurs after the "z"- ligand instead of the archetypal Gly; and in site IV there is no amino acid between the residues that usually make up ligands "x" and "y." The effect of these alterations on the Ca^{2+} affinity of yeast CaM is not yet known.

That CaM is essential for the growth of yeast cells was shown by deletion or disruption of the gene. This constitutes, in fact, the first demonstration in any organism that CaM is an essential protein. (Deletions of genes in mammals are ethically questionable research procedures!)

In the biochemically less sophiscated (than eukaryotes) **prokaryotic** cells, a regulatory role of Ca^{2+} is not well-established. What is known is that calcium is massively accumulated during sporulation in many bacteria, for example, in strains of *Bacillus*, *Streptomyces*, and *Myxococcus*. In *Myxococcus xanthus* a development-specific protein called protein S assembles at the surface of myxospores in the presence of Ca^{2+}. The DNA sequence of the gene that encodes this protein has been deciphered.[161] The primary sequence of protein S (175 a.a., M_r = 19.2 kDa) turns out to closely resemble mammalian CaM. It has four internally homologous regions with putative Ca^{2+} sites. At least two of these are partly similar to the typical EF-hand, but uncharacteristically there are many more prolines in the *M. xanthus* protein than in bovine CaM (12 versus 2); so it is questionable if the bacterial protein really has the repeated helix-loop-helix structure found in mammalian CaM.[162]

One candidate for a prokaryotic CaM was reported by Leadlay *et al.*[163] in *Streptomyces erythreaus*, the bacterium that produces the well-known antibiotic "erythromycin." The amino-acid sequence of a low-molecular-weight Ca^{2+}- binding protein, as determined from the gene encoding it, revealed a high homology with mammalian CaM. The protein is made up of 177 amino acids (M_r = 20.1 kDa), and has four regions that are predicted to have the helix-loop-helix secondary structure typical of EF-hand proteins. The aligned sequences of the 12 residues in each of the four potential calcium-binding loops in the *S. erythreaus* protein are compared with those of human calmodulin in Table 3.6.

Table 3.6 - Aligned EF-hand sequences for the prokaryotic and human calmodulins

Ligands	1		3		5		7		9			12
S. erythraeus protein I	D	F	D	G	N	G	A	L	E	R	A	D
S. erythraeus protein II	G	V	G	S	D	G	S	L	T	E	E	Q
S. erythraeus protein III	D	K	N	A	D	G	Q	I	N	A	D	E
S. erythraeus protein IV	D	T	N	G	N	G	E	L	S	L	D	E
Human calmodulin I	D	K	D	G	D	G	T	I	T	T	K	E
Human calmodulin II	D	A	D	G	N	G	T	I	D	F	P	E
Human calmodulin III	D	K	D	G	N	G	Y	I	S	A	A	E
Human calmodulin IV	D	I	D	G	D	G	Q	V	N	Y	E	E

The pattern of residues in the *S. erythraeus* protein is typical of an EF-hand at least in sites I, III, and IV. Site II is unusual in having Gly at both positions 1 and 3. ^{113}Cd NMR studies show that the bacterial protein binds three metal ions strongly ($K \gtrsim 10^5\ M^{-1}$) with chemical shifts close to those expected for EF-hands, and ^{1}H NMR studies show that it undergoes a Ca^{2+}- dependent conformational change.[164]

Although the *S. erythraeus* protein has a homology with eukaryotic CaM, it has been pointed out that the protein has an even higher homology with a group of eukaryotic sarcoplasmic Ca^{2+}-binding proteins[165] (see Section V.D). The search for a prokaryotic CaM analogue continues, and the prospect of success has been improved after recent reports of a 21-amino-acid-Iong polypeptide from an *E. coli* heat-shock protein[166] that shows the typical structural features of CaM-binding domains in other eukaryotic proteins.[167]

11.2.3.1: Ca^{2+}-binding Proteins in Microorganisms- The Search for a Prokaryotic Calmodulin is shared under a CC BY-NC-SA 4.0 license and was authored, remixed, and/or curated by LibreTexts.

https://chem.libretexts.org/@go/page/438010

11.2.3.2: Basic Facts About Calcium- Its Compounds and Reactions

Basic Facts

Calcium was first recognized as an element in 1808 by Humphry Davy, and the name was given after the Latin for lime: *calx*. Several isotopes of calcium are known. The stable isotopes are, in order of decreasing natural abundance, ^{40}Ca (96.94%), ^{44}Ca (2.1%), ^{42}Ca (0.64%), and ^{43}Ca (0.145%). ^{43}Ca is the only isotope with a nuclear spin (I = $\frac{7}{2}$) different from zero, which makes it amenable to NMR studies. ^{45}Ca is a radioactive isotope of some importance (β^- decay; 8.8 min half life).[3] It has been used in studies of calcium localization and transport in biological systems.

Calcium constitutes about 3 percent by weight of the Earth's crust, mostly in the form of sedimentary rocks of biological origin dating back some three billion years. In sea water the total concentration of calcium ranges from 5 to 50 times higher than in fresh water, which, in turn, has a calcium concentration ten times that of rain water (see Table 3.1). This explains the pleasant feeling when ordinary soaps are used in rain water. The calcium concentration in ordinary tap water varies with location; calcium is usually added to water in distributing networks in order to prevent corrosion of iron pipes. Tap water with a calcium concentration above 1.5 mM is usually classified as "hard." Interestingly, the taste of beer seems related to the calcium concentration, and it is claimed that "good" beer should have a concentration higher than that of "hard" tap water.

In the body fluids of higher organisms the total calcium concentration is usually on the order of a few millimolar (see Table 3.1). In adult human serum, the concentration is observed to be, within narrow limits, 2.45 mM.

Table 3.1 - Ca^{2+} concentrations in fluids and tissues.[6-9]

Specimen	Units are mM if not otherwise stated
Sea water	10
Fresh water	0.02 - 2
Rain water	0.002 - 0.02
"Hard" tap water	1.5
"Good" beer	4
Adult human serum	2.45 ± 0.05
Serum of other vertebrates	1.5 - 5
Nematote body fluids	6
Molluscan serum - marine	9 - 15
Molluscan serum - fresh water	1.5 - 7.8
Molluscan serum - land	3.3 - 12.3
Milk	70
Bone	0.8 - 1.0
Mitochondria from rat liver	0.8 ± 0.1 mmol/kg
Endoplasmatic reticulum	8 - 10 mmol/kg
Cytoplasm of a resting mammalian cell	0.0001
Cytoplasm of *E. coli*	0.0001

Essentials of Ca^{2+} Chemistry

Since the Ca^{2+} ion accomplishes its biological tasks in an environment with 1 to 3 mM Mg^{2+}, it is of particular interest to compare the properties of these two ions in order to understand how a discrimination is made in biological systems. In addition, the coordination chemistry of Ca^{2+} is closely related to that of Mg^{2+} (as well as Cd^{2+}), though there are several obvious differences. First of all, the ionic radius of a Ca^{2+} ion with a given coordination number (CN) is always higher than that of an Mg^{2+} or Cd^{2+} ion with the same CN. At CN = 6, the ionic radii of Ca^{2+}, Cd^{2+}, and Mg^{2+} are 1.00, 0.95, and 0.72 Å, respectively, whereas at CN = 8 they are 1.12, 1.10, and 0.89 Å, respectively.[4]

Ligand preferences of Ca^{2+} depend on the fact that it is a hard metal ion. Thus Ca^{2+} strongly prefers oxygen ligands over nitrogen or sulfur ligands; Ca^{2+}••••N bonds are about 0.25—0.3 Å longer than Ca^{2+}••••O bonds.[5,6,10] Large differences in coordination number and geometry have been observed for Ca^{2+} complexes. In a study of 170 x-ray structures of Ca^{2+} complexes involving carboxylate groups,[11] binding was found to be either (i) unidentate, in which the Ca^{2+} ion interacts with only one of the two carboxylate oxygens, (ii) bidentate, in which the Ca^{2+} ion is chelated by both carboxylate oxygens, or (iii) mixed ("α-mode") in which the Ca^{2+} ion is chelated by one of the carboxylate oxygens and another ligand attached to the α-carbon (see Figure 3.1). The Ca^{2+}- oxygen distances span a range from 2.30 to 2.50 Å, with the average distance being 2.38 Å in the unidentate and 2.53 Å in the bidentate mode, respectively.[11] Observed coordination numbers follow the order 8 > 7 > 6 > 9. By contrast, Mg^{2+} nearly always occupies the center of an octahedron of oxygen atoms (CN = 6) at a fixed Mg^{2+}-oxygen distance of 2.05 ± 0.05 Å.

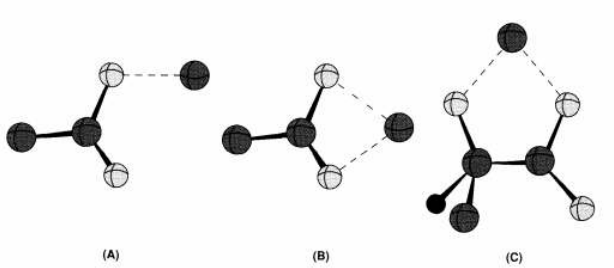


Figure 3.1 - The three commonly observed modes of calcium carboxylate ligation. (A) The unidentate mode, in which the calcium ion interacts with only one of the two carboxylate oxygens. (B) The bidentate mode, in which the calcium ion is chelated by both oxygen atoms. (C) The α-mode, in which the calcium ion is chelated by one carboxylate oxygen, and another ligand is attached to the a-carbon. Adapted from Reference II.

In Table 3.2, stability constants for the binding of Ca^{2+} and Mg^{2+} to various ligands are collected. We may note that selectivity of Ca 2+ over Mg^{2+} is not very great for simple carboxylate ligands, but that it tends to increase for large multidentate ligands, such as EDTA and in particular EGTA. The Ca^{2+} sites in many intracellular proteins with "EF-hand" binding sites (see Section V. C) bind Ca^{2+} about 10^4 times more strongly than Mg^{2+}.

Table 3.2 - Ca^{2+} and Mg^{2+} (where available) stability constants (log K) for different organic and biochemical ligands. Most values are at ionic strength 0.1 and 25 °C.[5,6,12-15]

a) EGTA: ethylenebis(oxyethylenenitrilo)tetraacetate

b) EDTA: ethylenedinitrilotetraacetate

Ligand	Ca^{2+}	Mg^{2+}
Acetate	0.5	0.5
Lactate	1.1	0.9
Malonate	1.5	2.1
Aspartate	1.6	2.4
Citrate	3.5	3.4
Nitrilotriacetate	6.4	5.5
EGTA[a]	10.9	5.3
EDTA[b]	10.6	8.8
Glycine (Gly)	1.4	3.4
γ-Carboxyglutamic acid (Gla)	1.3	
Gly-Gly dipeptide	1.2	
Gla-Gla dipeptide	3.2	
Macrobicyclic amino cryptate [2.2.2]	4.5	
Fluo-3	6.2	2.0
Fura-2	6.9	2.0
BAPTA	7.0	1.8
Quin-2	7.1	2.7
Phospholipase A2	3.6	
Thrombin fragment 1	3.7	3.0
Trypsinogen	3.8	
Chymotrypsinogen	3.9	
Chymotrypsin	4.1	
Calmodulin, N-terminal	4.5	3.3
Trypsin	4.6	
Calmodulin, C-terminal	5.3	
Protein kinase C	~7	
α-Lactabumin	~7	
Rabbit skeletal muscle		
Troponin C, Ca^{2+}/Mg^{2+} sites	7.3	3.6
Carp parvalbumin	~8.5	4.2
Bovine calbindin D_{9K}	8.8	~4.3

Another difference in ligand-binding properties of Mg^{2+} and Ca^{2+} can be seen by comparing the rates of substitution of water molecules in the inner hydration sphere by simple ligands, according to

$$M(H_2O)_n^{2+} + L \xrightarrow{k} ML(H_2O)_{n-1}^{2+} + H_2O \qquad (11.2.3.2.1)$$

This rate (log k, with k in s^{-1}) has been determined to be 8.4 for Ca^{2+} and 5.2 for Mg^{2+}.[16]

The formation of biominerals is a complex phenomenon. In order to obtain a feeling for the conditions under which inorganic solid phases in biological systems are stable, it is of some interest to look at solubility products. Solubility products, K_{sp}^{o}, have a meaning only if the composition of the solid phase is specified. For a solid compound with the general composition $(A)_k(B)_l(C)_m$ the solubility product is defined as

$$K_{sp}^{o} = [A]^k[B]^l[C]^m \qquad (3.1)$$

where [A], [B], etc., denote activities of the respective species, usually ionic, in equilibrium with the solid. Activities are concentrations multiplied by an activity coefficient, γ, nearly always less than unity. Activity coefficients for ions in real solutions can be estimated from Debye-Hückel theory[17] if the ionic strength of the solution is known. In human blood plasma, the ionic strength, I, is about 0.16, and the activity coefficient for Ca^{2+} at 37 °C is 0.34. In many discussions it may be sufficient to equate concentrations with activities.

The solid phase involved is essentially assumed to be an infinitely large, defect- and impurity-free crystal with a well-defined structure. Microscopic crystals have higher solubilities than large crystals, a well-known phenomenon that leads to "aging" of precipitates, in which larger crystals grow at the expense of smaller ones.

Many anionic species appearing in the solubility products may also be involved in protonation equilibria in solution, such as those of phosphoric acid: $H_2PO_4^- \rightleftharpoons H^+ + HPO_4^{2-}$; $HPO_4^{2-} \rightleftharpoons PO_4^{3-} + H^+$; etc. When the prospects for the formation of a solid phase under certain solution conditions are investigated, the activity, or concentration, of the particular anionic species specified in the solubility product must be known, not only "total phosphate" or "total calcium," etc. The data in Table 3.3 show that, at pH > 5, the most stable (i.e., insoluble) solid calcium phosphate is hydroxyapatite.

Table 3.3 - Solubility products, at pH 5 and 25 °C, for solid calcium phosphates

Solid Phase	-log K_{sp}^{o}	-log K_{sp}^{o} of corresponding Mg^{2+} compound where applicable
$CaSO_4 \cdot 2H_2O$ (sulfate, "gypsum")	5.1	< 1.0
$Ca(OH)_2$ (hydroxide)	5.3	10.7
$CaHPO_4 \cdot 2H_2O$ (hydrogen phosphate)	6.6	—
$CaCO_3$ (carbonate, "calcite," "aragonite")	8.5	7.5
$CaC_2O_4 \cdot H_2O$ (oxalate, "whewellite")	10.5	5.0
β-$Ca_3(PO_4)_2$ (β-phosphate)	29	—
$Ca_5(PO_4)_3OH$ (hydroxyapatite)	58	—

11.2.3.2: Basic Facts About Calcium- Its Compounds and Reactions is shared under a CC BY-NC-SA 4.0 license and was authored, remixed, and/or curated by LibreTexts.

11.2.3.3: Calcium in Mineralized Tissues

The formation of calcified tissue—shells, bone, and teeth—is a very complex process that is under strict regulatory control. Despite the obvious importance of this field, relatively little research has been directed toward elucidation of the underlying mechanisms, perhaps because the field spans a broad range of subjects, from inorganic solution and solid-state chemistry to cellular physiology.[155]

Historically, it was long held that formation of biological minerals such as bone was simply the nucleation and growth of calcium hydroxyapatite within an extracellular matrix of collagen. Many proteins other than collagen have now been discovered in appreciable quantities in bone and other biological minerals. It is also apparent that the pattern of calcification differs in shells, bone, teeth, and other mineralized tissues; so it is not likely that there is only one underlying mechanism. Considering the immensity of the subject, we will here only make a few brief comments, mainly about bone and teeth.

As was briefly mentioned earlier in this chapter, the inorganic matter of bone and teeth in many ways resembles apatite minerals ($Ca_5(OH)(PO_4)_3$). Table 3.5 summarizes inorganic solid components of other biominerals.

Table 3.5 - A summary of the main inorganic solid component[8] of the most-common biominerals in living systems.[148]

a) Most real biominerals are actually nonstoichiometric, and contain a number of additional cations (e. g., Mg^{2+}) or anions (e.g., F^-). In addition, the inorganic phase may be interpenetrated by a biopolymer.

Anion	Formula	Crystal Form	Occurrence	Main Function
Carbonate	$CaCO_3$	Calcite Aragonite Valerite	Sea corals, molluscs, and many animals and plants	Exoskeleton; Ca-store; eye lens
Oxalate	$Ca(COO)_2•H_2O$ $Ca(COO)_2•2H_2O$	Whewellite Weddelite	Insect eggs; vertebrate stones	Deterrent; cytoskeleton; Ca store
Phosphate	$(Ca)_{10}(PO_4)_6(OH)_2$ (unit cell comp.)	Hydroxyapatite	Bones; teeth; shells; intracellular in some bacteria	Skeletal; Ca storage; pressure-transducer (piezo-electric)
Sulfate	$CaSO_4•H_2O$	Gypsum	Jelly fish; plants	Gravity device; S and Ca store

A detailed analysis[156] shows that, apart from Ca^{2+} and PO_4^{3-}, many other cations and anions occur in bone, e.g., Mg^{2+}, Na^+, K^+, Sr^{2+}, CO_3^{2-}, F^-, Cl^-, and citrate. X-ray diffraction patterns and electron-microscope pictures of bone show that the inorganic phase is made up of many very small and imperfect crystals. By contrast, dental enamel is made up of much larger and uniform thin crystals. Although the solubility product of calcium hydroxyapatite (see Section II) is such that the equilibrium Ca^{2+} concentration should be in the low micromolar range, bone mineral appears to be in equilibrium with much higher Ca^{2+} concentrations (0.8-1.0 mM).[157] This discussion brings us to the question of how the inorganic crystallites are formed. Obviously both Ca^{2+} and PO_4^{3-} ions must be concentrated in cells or organelles bordering on the regions where mineralization is to take place. Fresh layers of bone matrix are formed by a continuously replenished layer of cells called *osteoblasts* (Figure 3.32A), which, in addition to apatite crystallites, also secrete collagen, and large specific proteins called *osteonectin*, *osteocalcin* (a Gla protein), proteoglycans, and phosphoproteins. In tissues undergoing rapid mineral deposition, the crystallites appear to be formed in vesicles that may have peeled off from the adjacent cell layers. These vesicles seem able to concentrate calcium and phosphate in a manner not well understood.

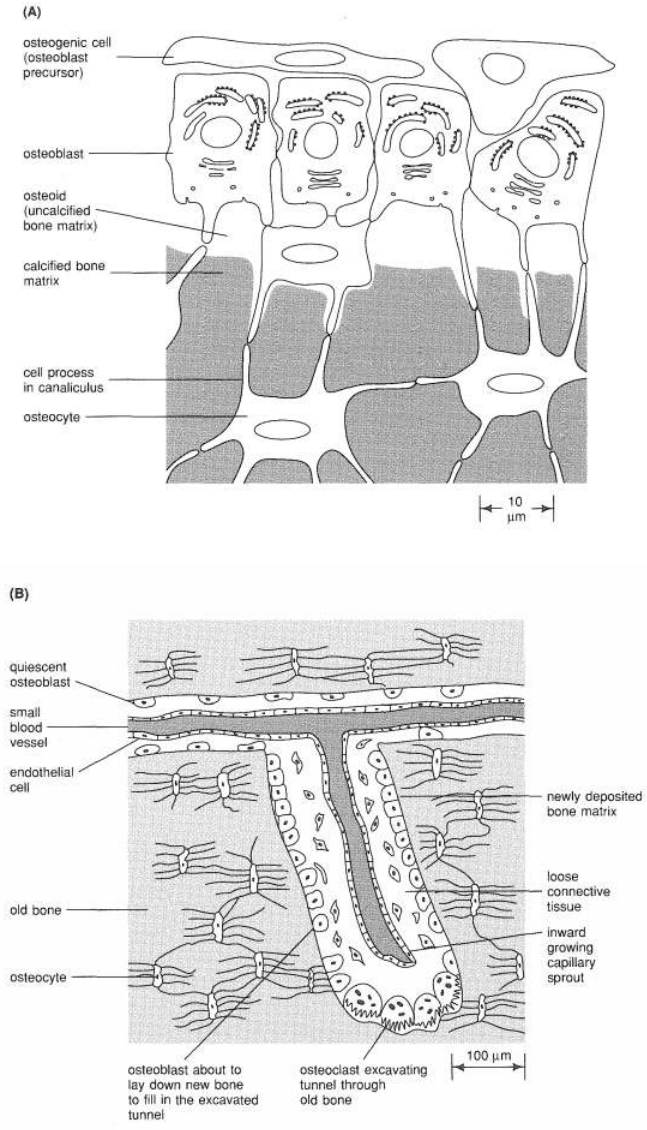


Figure 3.32 - Schematic diagram depicting the roles of the most important cell types in bone formation. (A) The osteoblast cells line the bone surface and secrete the inorganic and organic components (collagen, etc.) that will form new bone. Some osteoblast cells gradually become embedded in their own secretion. A particular secreted bone-specific protein, osteonectin, forms strong links between calcium hydroxyapatite and collagen. The bone-forming cells that become trapped in the bone matrix are now called osteocytes. (B) The osteoclast cells function to remodel compact bone. A group of cells acting together excavate a tunnel through old bone at a rate of about 50 μm per day. Behind the advancing osteoclasts follow a contingent of osteoblasts that line the wall of the tunnel and start to form new bone. Concurrently a capillary vessel is formed along the center of the tunnel and provides the cells with nutrients. Eventually the tunnel will become filled with concentric layers of new bone with only a narrow canal remaining. It is apparent that bone is far from a dull inorganic deposit, and very much a site of continuous activity. It is estimated that 5 to 10 percent of the bone in an adult mammal is replaced per year. Adapted from Reference 159.

Bone, unlike diamond, is not forever. It can be remodeled and dissolved. A serious medical problem, which affects some women after menopause, is **osteoporosis**, i.e., the decalcification of bone. This loss of bone mass, which occurs with increasing age, makes bones more susceptible to breaking under stress. About 50 percent of American women, and 25 percent of American men, over 45 years of age are affected by osteoporosis.[158] Whereas osteoblast cells handle bone formation, another type of cells, *osteoclasts*, can erode it (Figure 3.32B). These macrophage-like cells can form deep tunnels in a bone matrix, and the cavities left behind are rapidly invaded by other cells forming blood vessels and new layers of osteoblasts. The *modus operandi* of osteoclast cells is not well understood at present. They may secrete calcium-chelating organic anions, such as citrate, to assist in the solubilization of the bones, as well as extracellular proteases that degrade the organic part of the matrix.

11.2.3.3: Calcium in Mineralized Tissues is shared under a CC BY-NC-SA 4.0 license and was authored, remixed, and/or curated by LibreTexts.

https://chem.libretexts.org/@go/page/438012

11.2.3.4: Calmodulin

Calmodulin is a small acidic protein ($M_r \approx 16{,}700$), the amino-acid sequence of which has been remarkably preserved during evolution. Early on, an analysis of its amino-acid sequence indicated that it should have four Ca^{2+}-binding sites, a deduction that proved to be correct. The three-dimensional x-ray structure of bovine brain calmodulin[85] has been solved to a resolution of 2.2 Å. A space-filling model is shown in Figure 3.17. (See color plate section, page C-9.) The molecule has a dumbbell-like shape, with two globular domains connected by an eight-turn α-helix—an unusual structural feature. In the crystal structure, there are no direct contacts between the two globular domains, each of which contains two Ca^{2+}-binding sites. The Ca^{2+}sites are all constructed in the same way: two α-helices separated by a calcium-binding loop, 12 amino acids long, and wrapped around the Ca^{2+} ion. This structural arrangement is nearly identical with that first observed in the x-ray structure of carp parvalbumin, and is colloquially termed "*the EF-hand*."[86] This structural unit is also observed in all available x-ray structures of proteins of the calmodulin superfamily (see Sections V.B and V.C). The Ca^{2+} ligands are all oxygen atoms, located approximately at the vertices of a pentagonal bipyramid.

The binding of Ca^{2+} and other cations to CaM has been extensively investigated.[87] The first two Ca^{2+} ions are bound in a cooperative manner, with an average binding constant of about 2×10^5 M^{-1} in 150 mM KCl and 1 mM Mg^{2+}. The third and fourth Ca^{2+} ions are bound with binding constants of about 3×10^4 M^{-1} under the same conditions. Spectroscopic evidence has shown that the first two Ca^{2+}-ions are bound in the C-terminal domain. Mg^{2+} has been shown to bind primarily to the N-terminal domain (see Table 3.2).[88]

The rates of dissociation of Ca $^{2+}$ from the $(Ca^{2+})_4$ CaM complex have been studied by both stopped-flow and NMR techniques.[89,90] Fast and slow processes are observed, both corresponding to the release of two Ca^{2+} ions. At an ionic strength I = 0.1 and 25 °C, the rates for the two processes differ by a factor of 30 (see Table 3.4).

Table 3.4 - Rates of Ca^{2+}-dissociation and -association of some enzymes and proenzymes.

	k_{off} [s^{-1}]	k_{on} [M^{-1} s^{-1}]
Macrobicyclic amino cryptate [2.2.2]	0.3	10^4
Phospholipase A2	1.1×10^3	4×10^6
sTroponin C: Ca^{2+} sites	300	
sTroponin C: Ca^{2+}-Mg^{2+} sites	5	
Trypsin	3	1.1×10^5
Trypsinogen	≤ 10	6×10^4
Chymotrypsin	70	$\sim 10^6$
Chymotrypsinogen	350	2.8×10^5
Calmodulin: N-terminal	300-500	10^7
Calmodulin: C-terminal	10-20	

A body of biophysical measurements, mostly made before the advent of x-ray structures, indicated that CaM is constructed from two largely independent domains.[87] This conclusion emanated from studies of the two tryptic fragments, TR_1C and TR_2C. The major site of cleavage is between Lys-77 and Asp-78 of the central helix, and results in N-terminal and C-terminal fragments of nearly equal size. To a good approximation, the biophysical properties of the intact CaM molecule—NMR, UV and CD spectra, kinetic properties, thermochemical data, etc.—are the sum of the same properties of the fragments TR_1C and TR_2C. This means that we may assign the slow dissociation process, k_{off}^f, to the C-terminal domain, and the fast, k;ff' to the N-terminal domain of CaM. Combining binding constants and off-rates, we may calculate that the rates of Ca^{2+} binding to CaM are on the order of 10^7 M^{-1} s^{-1} at high ionic strength, and 10^8 M^{-1} s^{-1} or higher at low ionic strength. Recently the x-ray structure of the C-terminal fragment TR_2C was solved, and indeed showed a structure nearly identical with C-terminal domain of intact CaM.[91]

The structural changes occurring in CaM as Ca^{2+} ions are bound are associated with pronounced changes in ^1H NMR, UV, fluorescence, and CD spectra.[87] The observed changes in CD and fluorescence spectra in the presence of Mg^{2+} are only about 20 to 25 percent of those induced by Ca^{2+}. A comparison of the CD spectra of CaM and its **tryptic** fragments indicates that the structural changes induced by Ca^{2+} are substantially greater in the C-terminal than in the N-terminal half.[92] By and large, few structural details of the conformation changes have as yet been obtained. However, one aspect of the Ca^{2+}-induced conformation change is that *hydrophobic sites*, probably one on each domain of the molecule, become exposed. In the presence of excess Ca^{2+}, CaM will bind to other hydrophobic molecules, e.g., phenyl-Sepharose, a variety of drugs, many small peptides, and—last but not least—its target proteins. This brings us to the question of how CaM recognizes and interacts with the latter. We may suspect that the hydrophobic sites on each domain are somehow involved, but the role played by the central helix is still not clear. To explain small-angle x-ray scattering data, the interconnecting helix needs to be kinked, bringing the intact globular domains closer.[93]

A putative CaM-binding segment (27 amino acids long) of myosin light-chain kinase (MLCK), an enzyme activated by CaM, has been identified.[94] The interaction between the segment peptide ("M13") and CaM has been studied[95] by CD spectroscopy and ^1H NMR. From these studies it appears that a unique 1:1 complex is formed, and that secondary and tertiary structural changes occur not only in the peptide M13 but also in both halves of the CaM molecule. Further NMR studies 96,97 of the interaction between CaM and naturally occurring peptides (mellitin and mastoparan) that share some structural features of M13—clusters of basic residues, hydrophobic residues adjacent to the basic residues, and a predicted high α-helical content—show very much the same results. Based on these results, a model, shown in Figure 3.18, for the interaction between CaM and M13 has been proposed. In this model the central helix is kinked at position[81], allowing the two domains to wrap around the assumed α-helical M13. Preliminary structure calculations of calcium-loaded CaM, based on NMR data, indicate that the central helix in solution indeed is kinked and very flexible,[99] and comparisons[100] of chemical shifts in calmodulin with and without M13 complexed supports the model in Figure 3.18. Recent structural studies using NMR spectroscopy and x-ray diffraction have essentially confirmed the general features of this model, although the orientation of the peptide is found to be reversed.[173]

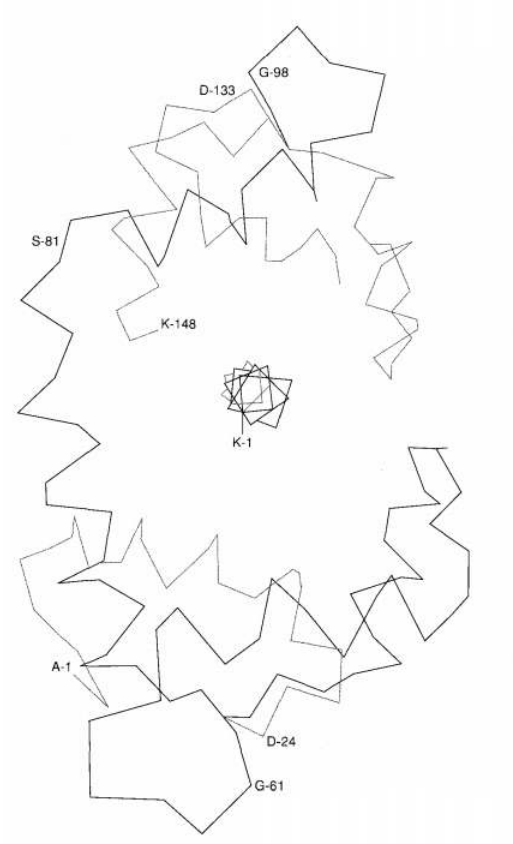


Figure kindly provided by R. Kretsinger; see also Reference 98.

In conclusion, two important features of the protein should be recognized.

i. The binding of Ca^{2+} to CaM (and to its complex with the target protein) is quite likely *cooperative*, meaning that the switch from inactive to active conformation may occur over a much more narrow Ca^{2+}-concentration interval than otherwise.

ii. The effective Ca^{2+} affinity will be different in the presence of the target proteins. To illustrate this second point, consider the standard free energies in the minimum scheme depicted in Figure 3.19. If the affinity of the Ca^{2+}-calmodulin complex ($CaM(Ca)_4$) for the target protein (P) is greater than that of Ca^{2+}-free calmodulin (CaM)—i.e., $|\Delta G_{III}| > |\Delta G_{II}|$—it follows that the Ca^{2+} affinity of the complex between P and CaM (P•CaM) must be higher than in CaM itself. This effect is also found experimentally in model systems.[101]

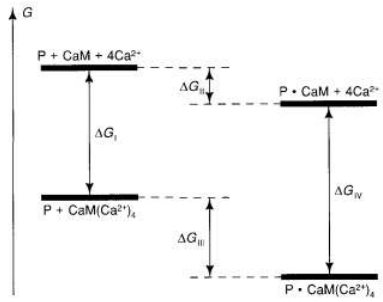


Figure 3.19 - Scheme depicting the standard free energies of different states in a system consisting of Ca^{2+}, calmodulin (CaM), and a target protein (P). P•CaM denotes a complex between calcium-free CaM and P, P•$CaM(Ca^{2+})_4$ denotes a complex with Ca^{2+}-loaded CaM. If the affinity of the Ca^{2+}-loaded CaM with the target protein P is higher than that of the Ca^{2+}-free form—i.e., $|\Delta G_{III}| > |\Delta G_{II}|$—it follows that the Ca^{2+} affinity of the complex p. CaM is higher than that of CaM itself.

11.2.3.4: Calmodulin is shared under a CC BY-NC-SA 4.0 license and was authored, remixed, and/or curated by LibreTexts.

11.2.3.5: Extracellular Calcium Ion-binding Proteins

The Ca^{2+} concentration in extracellular fluids is usually orders of magnitude higher than intracellular concentrations. In mammalian body fluids, the "free" Ca^{2+} concentration is estimated to be 1.25 mM (total Ca^{2+} is ~2.45 mM) with only minor variations.[140] We would thus expect that Ca^{2+} ions in extracellular fluids playa very different role from that inside cells. To ensure Ca^{2+} binding the macromolecular binding sites need have only a modest Ca^{2+} affinity ($K_B^{Ca2+} \approx 10^3$ to 10^4 M^{-1}), and since extracellular Ca^{2+} does not seem to have a signaling function, the rates of Ca^{2+} association or dissociation in protein-binding sites need not be very high.

One particularly important aspect of Ca^{2+} in mammals is its role in the blood coagulation system. Here we will meet a new type of amino acid, γ-carboxyglutamic acid ("Gla")-see Figure 3.29, that seems to have been designed by Nature as a Ca^{2+} ligand with rather special functions. Gla-containing proteins are also encountered in some mineralized tissues. The formation of bone, teeth, and other calcified hard structures is an intriguingly complicated phenomenon that will be dealt with in Section VII. We start, however, with a brief discussion of the role of Ca^{2+} in some extracellular enzymes.

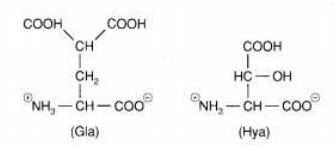


Figure 3.29 - Chemical structures of two novel amino acids believed to bind calcium in, e.g., blood-clotting proteins.

Ca^{2+}-binding in Some Extracellular Enzymes

Several extracellular enzymes have one or more Ca^{2+} ions as integral parts of their structure. In a very few of them the Ca^{2+} ion is bound at or near the active cleft, and appears necessary for maintaining the catalytic activity (phospholipase A_2 , α-amylase, nucleases), whereas other enzymes show catalytic activity even in the absence of Ca^{2+} (trypsin and other serine proteases). In the latter proteins, the Ca^{2+} ion is usually ascribed a "structural" role, although its function may be rather more related to "dynamics" and so be more subtle and complex.

Trypsin has one Ca^{2+}-binding site with four ligands (two side-chain and two backbone oxygens) donated by the protein (Glu-70, Asn-72 , Val-75, and Glu-80) and two ligating water molecules, making the site roughly octahedral.[141] The binding constant of Ca^{2+} to trypsin and its inactive precursor "proenzyme," *trypsinogen*, has been measured (see Table 3.2). The binding constant is slightly smaller for the precursor, as is also true for *chymotrypsin* and *chymotrypsinogen*.[142] The Ca^{2+} affinities of the serine proteases and their proenzymes are such that their Ca^{2+} sites will be largely occupied in extracellular fluids, but would be unoccupied inside a cell. It has been suggested that this phenomenon constitutes a safeguard against unwanted conversion of the proenzymes into the active enzymes as long as they still are inside the cells where they are synthesized.

The rates of Ca^{2+} dissociation of the above enzymes and proenzymes have been measured by ^{43}Ca NMR and stopped-flow techniques,[142] and are collected in Table 3.4. We note that the values of k_{on} and k_{off} are generally much smaller than in the intracellular regulatory EF-hand proteins discussed in Section VI. Whereas the latter have dynamic and equilibrium properties similar to those of flexible low-molecular- weight chelators such as EDTA and EGTA, the serine proteases are more similar to the more-rigid cryptates, such as the macrobicyclic amino cryptate [2.2.2] (see Tables 3.2 and 3.4).

As mentioned above, there are a few enzymes in which a Ca^{2+} ion is present in the active cleft and essential for activity. Pancreatic *phospholipase* A_2 ($M_r \approx 14$ kDa) is an enzyme of this type. The x-ray structure is known to high resolution, and a single Ca^{2+} ion is found to be surrounded by six ligands, four presented by the protein (Tyr-28, Glu-30, Glu-32, and Asp-49) and two water molecules.[143] A mechanism for the action of phospholipase A_2 has been proposed[144] and is shown in Figure 3.30.

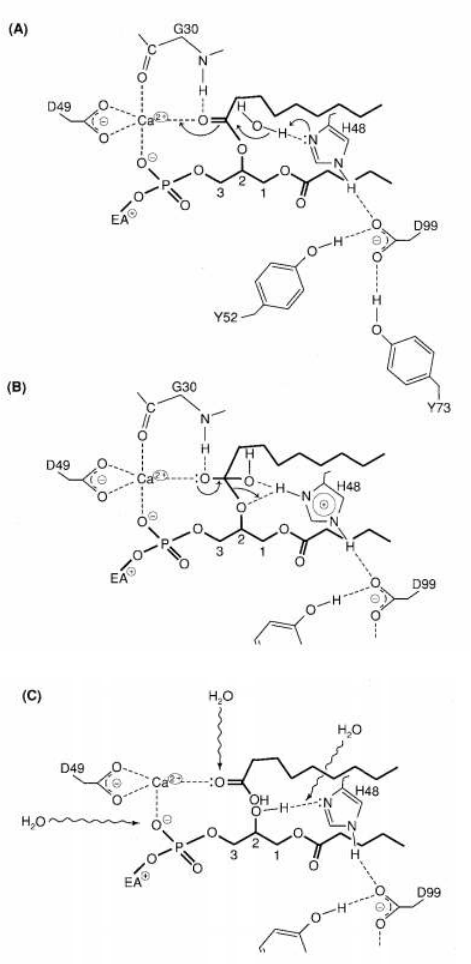


Figure kindly provided by P. B. Sigler.

This mechanism is based on three high-resolution x-ray crystal structures of phospholipase A_2 with and without transition-state analogues bound. The binding constant for Ca^{2+} together with the rate of dissociation found from variable-temperature ^{43}Ca NMR studies[145] can be used to calculate $k_{on} \approx 4 \times 10^6\ M^{-1}s^{-1}$, again lower than in EF-hand proteins. Recent ^1H NMR studies indicate that the global structure of the lipase is very much the same in the Ca^{2+}-free and the Ca^{2+}-bound forms. Structural changes upon Ca^{2+} binding appear primarily located in the region of the binding site.[112,146]

The mammary glands produce, among other substances, a Ca^{2+}-binding enzyme activator, *α-lactalbumin*, that has about 40 percent sequence identity with lysozyme. This protein, which is involved in the conversion of glucose into lactose, is secreted in large quantities, and in human milk constitutes some 15 percent of total protein. The Ca^{2+}-binding constant of bovine or human α-lactalbumin is on the order of $10^7\ M^{-1}$ under physiological conditions. In addition to Ca^{2+}, the enzyme also binds Zn^{2+}. It appears that Ca^{2+}-ion binding affects enzymatic activity, and somehow controls the secretion process, but the biological role of metal-ion binding to a-lactalbumin needs to be studied further. The x-ray structure of a-lactalbumin from baboon milk ($M_r \approx 15$ kDa) has been determined[147] to a high resolution (~1.7 Å). The Ca^{2+}-binding site has an interesting structure. The ion is surrounded by seven oxygen ligands, three from the carboxylate groups of aspartyl residues (82, 87, and 88), two carbonyl oxygens (79 and 84), and two water molecules. The spatial arrangement is that of a slightly distorted pentagonal bipyramid with the carbonyl oxygens at the apices, and the five ligands donated by the proteins are part of a tight "elbow"-like turn. The α-lactalbumin site has a superficial structural similarity to an "EF-hand," although the enzyme presumably has no evolutionary relationship with the intracellular Ca^{2+}-binding regulatory proteins.

Blood clotting proceeds in a complicated cascade of linked events involving many enzymes and proenzymes. About a decade ago it was shown that several of these proteins contained a previously unknown amino acid, γ-carboxyglutamic acid (Gla), and more recently yet another new amino acid, β-hydroxyaspartie acid (Hya), has been discovered (see Figure 3.29). The former is formed postribosomally by a vitamin-K-dependent process in the liver.[148] Presently the most-studied Gla protein in the blood-clotting

system is *prothrombin* ($M_r \approx 66$ kDa). Ten Gla residues are clustered pairwise in the N-terminal region, essentially lining one edge of the molecule, forming a highly negatively charged region.[149] A small (48 residues) proteolytic fragment (F1) that contains all ten Gla amino acids can be prepared. Prothrombin can bind about 10 Ca^{2+} ions, but F1 binds only 7. Binding studies to F1 show that the Ca^{2+} ions bind at three high-affinity cooperative sites and four noninteracting sites,[150] and that this binding takes places in conjunction with a spectroscopically detectable conformational change (see Table 3.1).

In the presence of Ca^{2+} ions, prothrombin and other vitamin-K-dependent proteins in the blood-coagulation system will bind to cell membranes containing acidic phospholipids, in particular, the platelet membrane, which is rich in phosphatidylserine. A proposed model for the prothrombin-membrane interaction is shown in Figure 3.31.

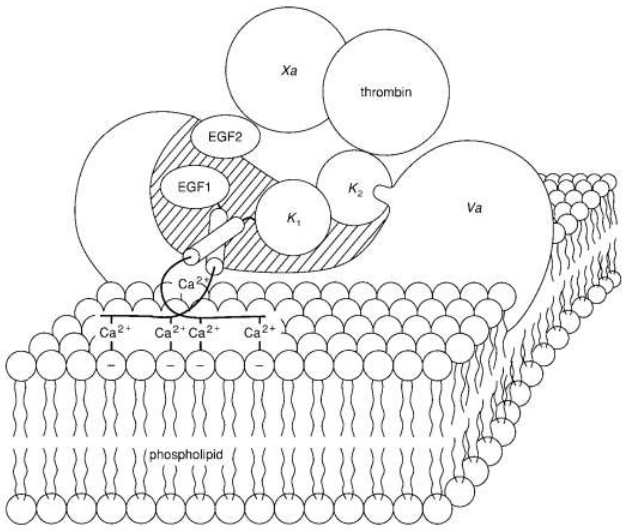


Figure kindly provided by C. C. F. Blake

It has long been known that calcium ions are involved in cell-to-cell and cell-to-extracellular matrix interactions, but the molecular details largely remain to be unraveled. In the late 1980s a large, adhesive, calcium-binding matrix glycoprotein ($M_r \sim 420$ kDa) named thrombospondin was characterized. This multifunctional adhesion molecule is composed of three polypeptide chains, each with 38 amino-acid-Iong repeats that are homologous with the calcium-binding helix-loop-helix sites of the calmodulin superfamily.[152] Each thrombospondin molecule is reported to bind 12 calcium ions with an affinity of about 10^4 M^{-1}, and the removal of calcium is accompanied by a conformational change.[153,154]

11.2.3.5: Extracellular Calcium Ion-binding Proteins is shared under a CC BY-NC-SA 4.0 license and was authored, remixed, and/or curated by LibreTexts.

11.2.3.6: Inositol Trisphosphate and the Calcium Ion Messenger System

A "second" messenger is an entity that inside a cell mediates the action of some hormone at the plasma membrane, the hormone being considered the "first" messenger. The first such second messenger to be discovered—in fact, the very molecule that led to the formulation of the whole concept—was cyclic AMP.[69] During the decade following the discovery of cAMP, it was gradually realized that intracellular release of Ca^{2+} ions also accompanied hormonal stimuli, and the Ca^{2+} ion slowly became regarded as a second messenger. This idea was first clearly enunciated by Rasmussen[70] as early as 1970, and gained general acceptance when the ubiquitous intracellular Ca^{2+}-binding protein calmodulin (see Section V.A) was discovered. In the mid-1970s this protein was shown to be a Ca^{2+}-dependent regulator of a large number of Ca^{2+}-dependent enzymes, transport proteins, etc., establishing a molecular basis for Ca^{2+} action in cells.

There were some puzzling facts, however. Although a transitory increase in intracellular Ca^{2+} concentration in response to the binding of a hormone or transmitter substance to a surface receptor could result from extracellular Ca^{2+} being released into the cytoplasm, there was compelling evidence for muscle cells that the main Ca^{2+} source was the sarcoplasmic reticulum (SR). This result led to the hypothesis of "Ca^{2+}-induced Ca^{2+} release," i.e., that upon stimulation of the cell, a small amount of Ca^{2+} entered into the cytoplasm and triggered the release of greater amounts of Ca^{2+} from the SR. For some cell types it could, however, be shown that transient increases in intracellular Ca^{2+} could occur even when extracellular Ca^{2+} was removed, although *prolonged* responses required the presence of extracellular Ca^{2+}. Although some specialized cells have gated plasma-membrane Ca^{2+} channels, release of Ca^{2+} into the cytoplasm from intracellular stores appears to be of at least equal importance. Furthermore, there is now overwhelming evidence[63,70-72] that intracellular Ca^{2+} is released in response to the formation of a new type of intracellular messenger: 1,4,5-IP_3. Receptors for this messenger have recently been found in the membranes of intracellular organelles, and binding of 1,4,5-IP_3 to these receptors results in the release of Ca^{2+} ions.[73]

1,4,5-IP_3 is formed as a product in the hydrolysis of a special phospholipid present in the cell membrane: phosphatidyl-inositol-4,5-bisphosphate. This reaction, then, is the initial receptor-stimulated event. The newly formed 1,4,5-IP_3 is assumed to diffuse into the cytoplasm, and eventually reach intracellular 1,4,5-IP_3 receptors on the ER, thereby triggering the release of Ca^{2+}. A simplified reaction scheme is shown in Figure 3.15.

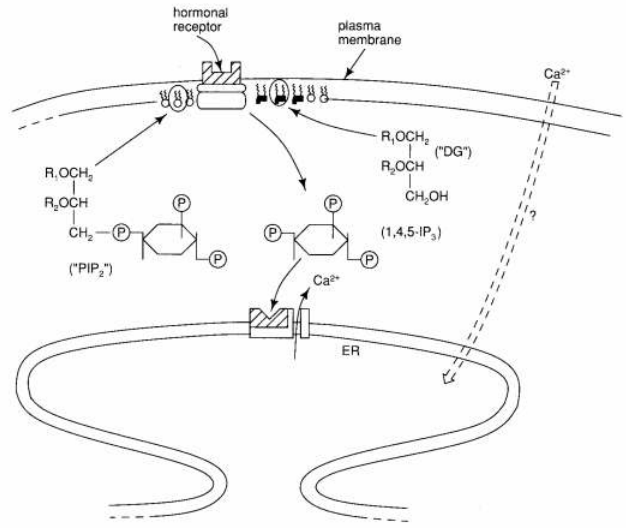


Figure 3.9) and also by a direct influx of Ca^{2+} from the extracellular medium.[70,81]

A diacylglycerol (DG) is also formed in the hydrolysis step. DG can also act as an intracellular messenger, and stimulates the activity of a membrane-bound protein kinase, known as *protein kinase C* (PKC). As a result, PKC may phosphorylate certain key proteins and influence their activity. Protein kinase C is also activated by Ca^{2+} ions, a fact that illustrates Nature's knack in designing regulatory networks! 1,4,5-IP_3 is either directly degraded in a series of enzymatic steps back to inositol, which is then used to resynthesize the phospholipid, or it may be further phosphorylated to inositol-1,3,4,5,-tetraphosphate (1,3,4,5-IP_4), which may undergo dephosphorylation to form inositol-1,3,4-trisphosphate (1,3,4-IP_3). The biological functions of the latter compounds are now being investigated.

The intracellular levels of Ca^{2+} are restored back to the normal low resting values (100 to 200 nM) via transport back into the SR, and/or into mitochondria, or out through the plasma membrane by the pumping mechanisms discussed in Section IV.B. As was briefly mentioned above, depriving a cell of extracellular Ca^{2+} will eventually make the cell incapable of prolonged responses to external stimuli. It appears that the intracellular Ca^{2+} stores may become depleted if not replenished. It has been suggested that the intracellular ER Ca^{2+} pool has a direct route of access to the extracellular pool, a route that is closed when the ER pool is full.[74]

In a sense, then, Ca^{2+} seems to have been downgraded by the inositolphosphates from a "second" to a "third" messenger; however, the pivotal role of Ca^{2+} as a regulator of cellular activities remains undisputed.

11.2.3.6: Inositol Trisphosphate and the Calcium Ion Messenger System is shared under a CC BY-NC-SA 4.0 license and was authored, remixed, and/or curated by LibreTexts.

11.2.3.7: Intracellular Calcium Ion Transport

In order to provide a better understanding of the role of Ca^{2+} as an almost universal regulator of cellular function, we need to take a brief look at the many ways by which Ca^{2+} ions can be transported in or out of eukaryotic cells. Although various transport pathways have been elucidated, the present picture is probably not complete, since the molecular structures and properties of the transport proteins are only partially known. The major pathways for Ca^{2+} transport across cellular membranes involve three membrane systems: the plasma membrane, the inner mitochondrial membrane, and the membrane of the endoplasmic reticulum (ER) (or, in striated muscle cells, a specialized form of ER called the sarcoplasmic reticulum (SR): (Figure 3.9). Two of the membrane-bound transport systems are Ca^{2+}-ATPases, since they derive their main energy from the hydrolysis of ATP (1 and 2 in Figure 3.9). Their properties do, however, differ in many other respects, as we will see.

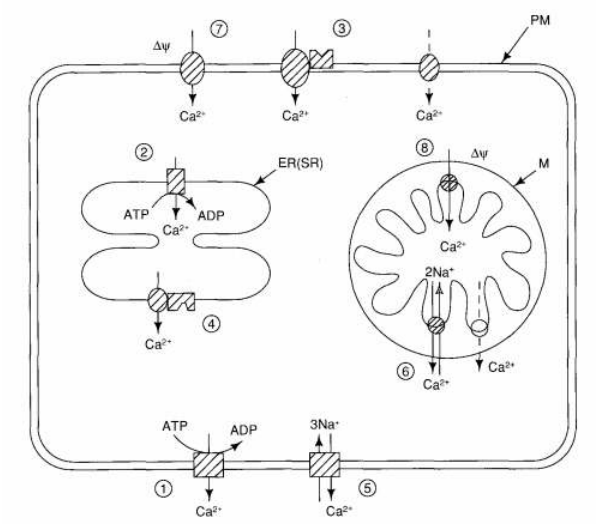


Figure 3.9 - Schematic representation of the major pathways for the transport of Ca^{2+} across cellular membranes. PM, plasma membrane; ER(SR), endoplasmic reticulum (sarcoplasmic reticulum); M, mitochondria; **ΔΨ**, difference in membrane potential. The transport proteins shown are: 1 and 2, PM and ER(SR) Ca^{2+}-ATPases; 3 and 4, PM and ER(SR) receptor-mediated Ca^{2+} channels; 5 and 6, PM and M (inner-membrane) Na^{+}/Ca^{2+} exchangers; 7 and 8, PM and M voltage-sensitive Ca^{2+} channels. In addition, some not-well-defined "passive" transport pathways are indicated by dashed arrows.

The Ca^{2+}-ATPases

The plasma membrane Ca^{2+}-ATPase (PM Ca^{2+}-ATPase) of **erythrocytes**—first recognized by Schatzmann in 1966[45]—was isolated in pure form by Niggli *et al.* in 1979, using an affinity column with an ATP-ase binding protein, calmodulin (see Section V.A), coupled to the gel.[46] Ca^{2+}-ATPases purified from other types of plasma membranes appear to be very similar. The schematic structure of the erythrocyte membrane Ca^{2+}-ATPase is presented in Figure 3.10.[47] The sarcroplasmic reticulum in muscle cells is abundant in Ca^{2+}- ATPase. It is estimated that this protein constitutes more than 80 percent of the integral membrane proteins, and covers a third of the surface area.

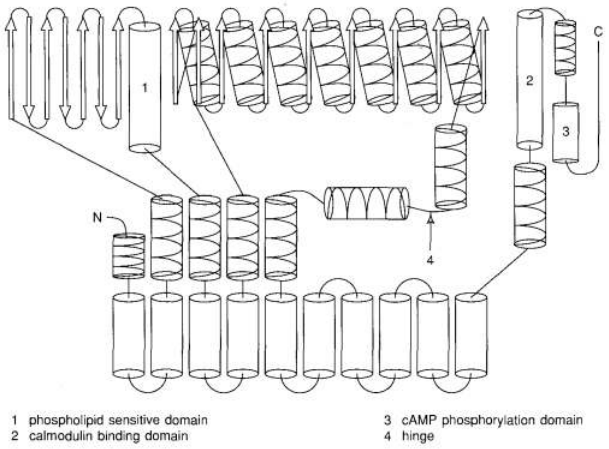


Figure kindly provided by R. Moser and E. Carafoli.

The sarcoplasmic reticulum Ca^{2+}-ATPase (SR Ca^{2+}-ATPase) was first purified by MacLennan in 1970.[48] Presently it is the best characterized Ca^{2+}-ATPase. A schematic model and a summary of some properties are given in Figure 3.11.[49] Ten hydrophobic segments of about 20 amino-acid residues each are revealed by **hydropathy** plots, and these segments are assumed to span the membrane as α-helices. (For the one-letter codes for amino acids, see Appendix B in Section IX.) The phosphorylation site has been identified as Asp-351, and the nucleotide binding domain is following the phosphorylation domain. The Ca^{2+}-binding sites are located within the predicted trans-membrane domains (see Figure 3.11). This was shown through a series of site-directed mutations in which likely Ca^{2+}-liganding residues like Asp, GIu, and Thr were mutated into residues lacking possible side-chain ligands (e.g., Asn, GIn, and Ala).[50]

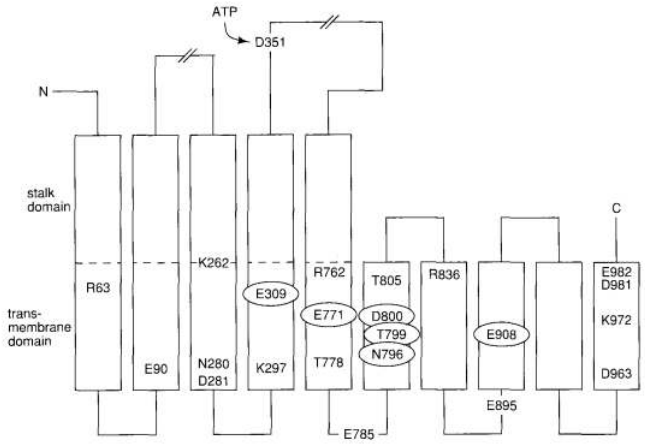


Figure 3.11 - Schematic structure of the Ca^{2+}-ATPase of sarcoplasmic reticulum. Some molecular characteristics are: M_r = 110,000; K_m < 1 μM (two Ca^{2+} sites on cytoplasmic side in high-affinity form); Ca^{2+}/ATP ratio, 2; Mg^{2+} required for activity. The amino-acid residues labeled were mutated to a residue lacking side chains capable of binding Ca^{2+}. Mutations at the circled positions resulted in complete loss of Ca^{2+} transport activity, suggesting that the circled residues participate in Ca^{2+} binding. Adapted from Reference 50.

The presently accepted reaction cycle involves two main alternative conformations, E_1 and E_2, the former with two high-affinity sites ($K_m \lesssim 1$ μM)[4] on the cytoplasmic side, which in E_2 are open to the luminal side with $K_m \sim 1$ mM.[49,51] The mechanism suggested for Ca^{2+} transport (Figure 3.12) has many features similar to that suggested by Williams for H^+ translocation in the mitochondrial ATPase.[52]

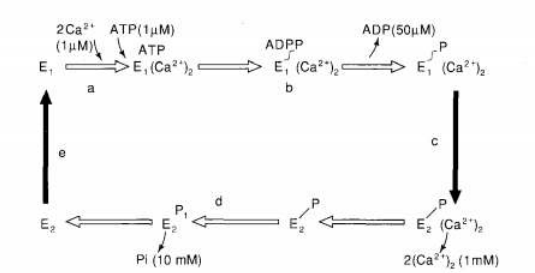


Figure 3.12 - Simplified schematic reaction cycle of the Ca^{2+}-ATPase of sarcoplasmic reticulum (SR).[49,51] The transport protein is assumed to be in either of two states, E_1 on the cytoplasmic side, or E_2 on the side of the SR lumen. Starting from E_1 in the upper left comer, the reactions steps shown are: (a) binding of Ca^{2+} and ATP (approximate dissociation constants within parentheses); (b) rapid phosphorylation of Asp-351 of the protein (E_1-P) and release of ADP; (c) transformation from an energy-rich, high-Ca^{2+}-affinity conformation (E_1-P) $(Ca^{2+})_2$ to a low-energy, low-affinity conformation (E_2-P)$(Ca^{2+})_2$; (d) hydrolysis of the phosphorylated protein and release of the phosphate into the lumen; (e) return to the original state.

It is instructive to consider briefly the thermodynamic limits of the transport. (The discussions about the thermodynamics behind Ca^{2+}/Na^+ transport pertain to Na^+/K^+ gradients in excitable tissues as well). Let us define an "inside" and an "outside" separated by a membrane, as shown in Figure 3.13, where $[Ca^{2+}]$ and ψ denote activities and membrane potentials, respectively. The difference in electrochemical potential, $\Delta\mu$, across the membrane for a Ca^{2+} ion is given by

$$\Delta\mu_{Ca^{2+}} = +RTln\frac{[Ca^{2+}]_o}{[Ca^{2+}]_i} + 2F\Delta\psi \qquad (3.4)$$

where F is Faraday's constant, T the temperature, and R the gas constant. If we assume $\Delta\Psi = 0$, which appears reasonable for the SR membrane according to experimental evidence, we may calculate the free-energy change, ΔG, at 25 °C for transferring Δn moles of Ca^{2+} across the membrane. This becomes $\Delta G = -\Delta n \times \Delta\mu_{Ca^{2+}} = \Delta n \times 4.1$ kcal/mol if $[Ca^{2+}]_o/[Ca^{2+}]_j = 10^{-3}$ and $\Delta G = \Delta n \times 5.4$ kcal/mol if $[Ca^{2+}]_o/[Ca^{2+}]_j = 10^{-4}$. Under the pertinent cellular conditions, the free-energy change associated with ATP hydrolysis to ADP and P_i has been calculated by Tanford to be $\Delta G = -13$ to -14 kcal/mol.[53] In the absence of a membrane potential, it is thus possible to transport two Ca^{2+} ions for every ATP molecule hydrolyzed against a concentration (or activity) gradient of 10^4 or more. This treatment says nothing, of course, about the molecular details of this transport. A more detailed model for the transport cycle has been proposed by Tanford.[53]

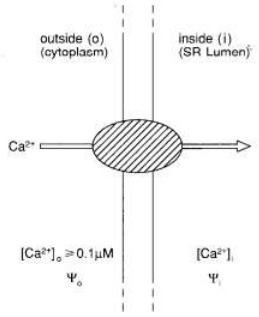


Figure 3.13 - Schematic representation of Ca^{2+} transport through a membrane by a Ca^{2+}-ATPase molecule. Ψ denotes membrane potentials.

In the specialized cells of muscle tissue, the sarcoplasmic reticulum may contain much calcium, and if all were "free" Ca^{2+}, the concentration could be as high as 30 mM.[54] This value would cause an osmotic pressure difference across the membrane, as well as put a high demand on the SR Ca^{2+}-ATPase. A lowering of the free Ca^{2+} concentration inside the SR would clearly be beneficial. In the presence of oxalate or phosphate ions in the external medium, calcium oxalate or phosphate may precipitate inside the sarcoplasmic reticulum, but under normal circumstances it appears that Ca^{2+} ions inside the SR are bound to a very acidic protein, *calsequestrin*.[54] Each molecule ($M_r \approx 40$ kDa) is able to bind 40 to 50 Ca^{2+} ions with an effective dissociation constant of about 1 mM (at I = 0.1). The protein has a low cation specificity and behaves in many respects like a negatively charged polyelectrolyte. It has been crystallized[55] and we may soon have access to its x-ray structure.

The Na^+/Ca^{2+} Exchanger of the Plasma Membrane

Presently available information on the Na^+/Ca^{2+} exchanger has mainly been obtained from studies of the large cells of the giant squid axon and of plasma-membrane vesicles from various other tissues.[56,57] In heart plasma-membrane vesicles, the exchanger has the following characteristics: K_m = 1.5-5 μM for Ca^{2+} and ~20 nM for Na^+; $V_{max} \approx$ 20 nmol Ca^{2+}/mg protein.[58] The stoichiometry is at least 3:1 Na^+/Ca^{2+}. Very few molecular details of the exchanger are available at present. We may again briefly consider the thermodynamic framework for an Na^+/Ca^{2+} exchanger (Figure 3. 14). The difference in electrochemical potential for Na and Ca^{2+} across the membrane is:

$$\Delta\mu_{Ca^{2+}} = RTln\frac{[Ca^{2+}]_o}{[Ca^{2+}]_i} + 2F\Delta\Psi, \tag{3.5}$$

$$\Delta\mu_{Na^+} = RTln\frac{[Na^+]_o}{[Na^+]_i} + F\Delta\Psi. \tag{3.6}$$

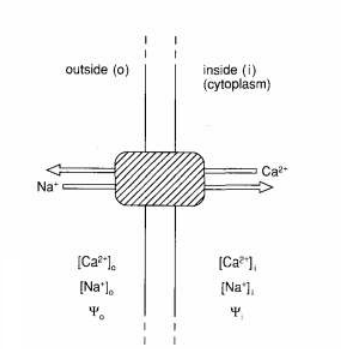


Figure 3.14 - Schematic representation of the Ca^{2+}/Na^+ exchanger of the plasma membrane. Ψ denotes membrane potentials.

The free-energy change, ΔG_t^{Ca2+}, associated with a transfer of $\Delta n_{Ca^{2+}}$ moles of Ca^{2+} from the inside to the outside is $\Delta G_t^{Ca2+} = \Delta n_{Ca^{2+}} \times \Delta\mu_{Ca^{2+}}$, and the corresponding change associated with the movement of Δn_{Na^+} moles of Na^+ from the outside in is $\Delta G_t^{Na+} = -\Delta n_{Na^+} \times \Delta\mu_{Na^+}$. If these free-energy changes are coupled via the exchanger, there will be a net flux of Ca^{2+} as long as the free-energy difference,

$$\Delta\Delta G = \Delta G_t^{Ca^{2+}} - \Delta G_t^{Na^+} = \Delta n_{Ca^{2+}} \times \Delta\mu_{Ca^{2+}} - \Delta n_{Na^+} \times \Delta\mu_{Na^+}, \tag{3.7}$$

is less than zero. We can write $\Delta\Delta G$ for the transport of 1 mol Ca^{2+} as

$$\Delta\Delta G = 2.303RT\left[log\frac{[Ca^{2+}]_o}{[Ca^{2+}]_i} - \Delta n_{Na^+} \times log\frac{[Na^+]_o}{[Na^+]_i}\right] + (2 - \Delta n_{Na^+}) \times F\Delta\Psi. \tag{3.8}$$

Equating ion activities with concentrations, we note that in a typical mammalian cell $[Na^+]_o \approx$ 110-145 mM, and $[Na^+]_i \approx$ 7-15 mM, or $[Na^+]_o/[Na^+]_i \approx 10$. In the absence of a membrane potential difference ($\Delta\Psi = 0$), Equation (3.8) can thus be simplified to

$$\Delta\Delta G = 2.3RT\left[log\frac{[Ca^{2+}]_o}{[Ca^{2+}]_i} - \Delta n_{Na^+}\right]. \tag{3.9}$$

To pump one Ca^{2+} ion out of a cell against a concentration gradient of about 10^3 (1 μM $\rightarrow$ 1 mM) requires that at least 3 Na^+ ions pass in the opposite direction, thus maintaining $\Delta\Delta G < O$. What then will be the effect of a membrane potential difference? Most animal cells, particularly excitable cells such as nerve and muscle cells, have resting potential differences, $\Delta\Psi$, over the plasma membrane of 30 to 90 mV (cytoplasm negative). For this value we find the change in free energy, $\Delta\Delta G$, for the transport of one mol Ca^{2+} to be

$$\Delta\Delta G = 2.3RT\left[log\frac{[Ca^{2+}]_o}{[Ca^{2+}]_i} - \Delta n_{Na^+}\right] + (2 - \Delta n_{Na^+})0.1F. \tag{3.10}$$

Thus for $\Delta n_{Na^+} > 2$, we have $\Delta\Delta G < 0$, and the transport of Ca^{2+} against a concentration gradient of about 10^3 will be promoted. This is another good reason for having a Na^+/Ca^{2+} exchange stoichiometry of 3:1.

11.2.3.7: Intracellular Calcium Ion Transport is shared under a CC BY-NC-SA 4.0 license and was authored, remixed, and/or curated by LibreTexts.

11.2.3.8: Measurements of "Free" Calcium Concentrations

Much of our present knowledge of the biological role of Ca^{2+} ions in the regulation and modulation of cellular activities rests on the development of analytical techniques in three different areas: our ability to measure the low concentration levels in the cytoplasm of resting cells, follow the concentration changes, both temporally and spatially, that may occur as a result of an external stimulus, and measure the distribution of Ca^{2+} in various compartments of a cell. The last decade has seen the emergence of many such new techniques, and the improvement of old ones, which has had a major impact on our understanding of the detailed molecular mechanisms and dynamics of the Ca^{2+} messenger system. In this section, we will survey some of the most important techniques and results obtained using these. Broadly speaking there are two main groups of experimental techniques: those that aim at measuring the concentration of "*free*" (or uncomplexed) *Ca^{2+}-ion concentrations* (or activities), and those that measure *total calcium*.

Ca^{2+}-selective Microelectrodes

Ion-selective electrodes can be made from a micropipette (external diameter 0.1-1\(\mu\)m) with an ion-selective membrane at the tip.[18,19] For Ca^{2+} the membrane can be made of a polyvinyl chloride gel containing a suitable Ca^{2+}-selective complexing agent soluble in the polymer gel. A commonly used complexing agent is "ETH 1001" (see Figure 3.2A). An additional "indifferent" reference electrode is needed. For measurements inside cells, the reference electrode can also be made from a micropipette filled with an electrolyte gel. Often the ion-selective and reference electrodes are connected in a double-barrelled combination microelectrode.[21] The whole assembly can then be inserted, using a micromanipulator, into a single cell typically 30-50 \(\mu\)m across. The arrangement is depicted in Figure 3.2B. With proper care, Ca^{2+} microelectrodes can be used to measure Ca^{2+}-ion concentrations down to 10^{-8} M.[19,21] One limitation of the technique is that the response time is usually in seconds or even minutes, making rapid concentration transients difficult to follow.

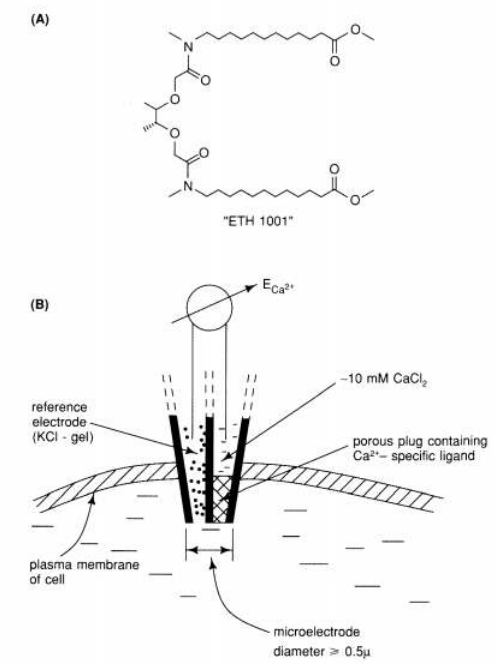


Figure 3.2 - (A) Structure of a commonly used neutral Ca^{2+} chelator in Ca^{2+}-selective electrodes, "ETH 1001" (N,N'-di[11-(ethoxycarbonyl) undecul]-N,N'-4,S-tetramethyl-3,6-dioxaoctan-1 ,8-diamide).[20] (B) Schematic arrangement for the measurement of the activity (or concentration) of Ca^{2+} ions in cells using a Ca^{2+}-selective double-barreled microelectrode. Frequently the microelectrode is supplemented by a third, indifferent, electrode inserted into the bathing medium surrounding the cell.[21]

Bioluminescence

Several living oganisms are able to emit light. The light-emitting system in the jellyfish (Aequorea) is a protein called aequorin (M_r \(\simeq\) 20 kDa). The light is emitted when a high-energy state involving a prosthetic group (coelenterazine) returns to the ground state in a chemical reaction that is promoted by Ca^{2+} ions. At Ca^{2+} concentrations below ~0.3 \(\mu M\) the emission is

weak, but in the range 0.5-10 \(\mu M\) the emission is a very steep function of the concentration (roughly as $[Ca^{2+}]^{2.5}$).[18,19,22] The response to a Ca^{2+}-concentration transient is rapid ($\tau_{1/2}$ = 10 ms at room temperature), and the light emitted can be accurately measured even at very low light levels by means of image intensifiers and/or photon counting. For measurements of Ca^{2+} concentrations inside cells, aequorin has usually been introduced either through microinjection or through some other means. A novel idea, however, is to utilize recombinant aequorin reconstituted within the cells of interest, thus circumventing the often difficult injection step.[174]

Complexing Agents with Ca^{2+}-dependent Light Absorption or Fluorescence

An important advance in the field of Ca^{2+}-ion detennination was made by R. Y. Tsien, who in 1980 described[23] the synthesis and spectroscopic properties of several new tetracarboxylate indicator dyes that had high affinity and reasonable selectivity for Ca^{2+}. All these dye molecules have a high UV absorbance that is dependent on whether Ca^{2+} is bound or not; a few also show a Ca^{2+}-dependent fluorescence. Tsien has also demonstrated that these anionic chelators can be taken up by cells as tetraesters, which, once inside the cells, are rapidly enzymatically hydrolyzed to give back the Ca^{2+}-binding anionic forms. Fluorescent tetracarboxylate chelators with somewhat improved Ca^{2+} selectivity such as "BAPTA," "Quin-2," and "Fura-2" (Figure 3.3) were later described.[24] These chelators are very suitable for measurement of Ca^{2+}-ion concentrations in the range 1 \(\mu\)M to 10 nM in the presence of 1 mM Mg^{2+} and 100 mM Na^+ and/or K^+—i.e., conditions typically prevailing in animal cells. Recently a new set of chelators that are more suitable for measurements of calcium concentrations above 1 \(\mu\)M was presented.[25] The most interesting of these is "Fluo-3," with a calcium-binding constant of 1.7 x 10^6.

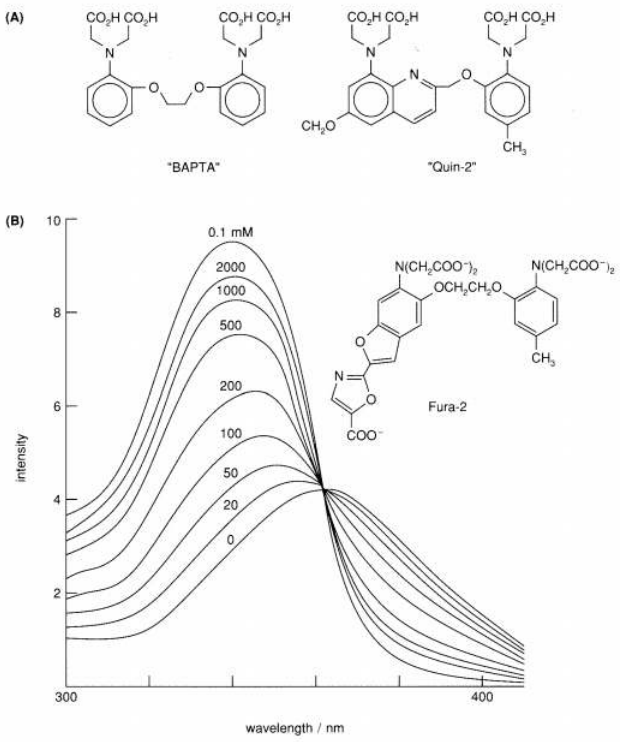


Figure 3.3 - Molecular structure of three chelators frequently used in measurements of "free" Ca^{2+}-ion concentrations. They may all be regarded as aromatic analogues of the classical chelator "EDTA"; their optical spectroscopic properties change upon binding Ca^{2+} ions. (A) For "BAPTA" the spectral changes are confined to the absorption spectrum, whereas "Quin-2" and the "Fura-2" in (B) show Ca^{2+}-dependent changes in their fluorescence spectra.[23, 24] (B) The relative fluorescence intensity of "Fura-2" at 505 nm as a function of the wavelength of the excitation light at different Ca^{2+} concentrations. The data[26] refer to a solution containing 115 mM KCI, 20 mM NaCl, and 1 mM Mg^{2+} at 37 °C and pH 7.05. At increasing Ca^{2+} concentration, the excitation efficiency at ~350 nm is increased, but that at ~385 nm is decreased. In order to eliminate (as much as possible) variations in fluorescence intensity in biological samples due to slight variations in dye concentrations and/or cell thickness, it is often advantageous to measure the intensity ratio at 345 and 385 nm excitation wavelengths.

Whereas the emission spectrum for Fura-2 (Figure 3.3B), which peaks at 505-510 nm, hardly shifts wavelength when Ca^{2+} is bound, the absorption spectrum shifts toward shorter wavelengths. In studies of free Ca^{2+} concentrations where internal referencing

is necessary, for example, in studies of single cells, it is therefore advantageous to excite alternately at \(\sim\)350 and 385 nm, and to measure the ratio of fluorescence intensity at \(\sim\)510 nm.

The use of fluorescent chelators has recently permitted studies in single cells of rapid fluctuations or oscillations of free Ca^{2+} and the formation of Ca^{2+} concentration gradients. Using a fluorescence microscope coupled to a low-light-level television camera feeding a digital image processor, Tsien *et al.*[26] have been able to reach a time resolution of about 1 s in single-cell studies. The results of some highly informative studies made using this instrument are shown in Figure 3.4. (See color plate section, page C-7.) The concentration of free Ca^{2+} is presented in pseudocolor, and the Fura-2 concentration inside cells is 50-200 \(\mu\)M, as indicated in the figures. We see a Ca^{2+} gradient diffusing through an entire sea-urchin egg (~120 \(\mu\) across) in 30 s. The free Ca^{2+} concentration of the resting egg (~100 nM) is increased to about 2 \(\mu\)M as Ca^{2+} diffuses through the egg. The mechanism of propagation is believed to be a positive feedback loop with inositol trisphosphate releasing Ca^{2+} and vice versa (see Section V).

A pertinent question concerning the uses of intracellular Ca^{2+} chelators is whether or not the chelator significantly perturbs the cell. The chelator will obviously act as a Ca^{2+} buffer in addition to all other Ca^{2+}-binding biomolecules in the cell. The buffer effect is probably not of any major consequence, since the cell may adjust to the new situation by an increase in total Ca^{2+}, especially if the chelator concentration is in the \(\mu\)M range. The chelators could, however, interact with and inhibit intracellular enzymes or other molecules, an effect that could result in aberrant cellular behavior. It is not unlikely that BAPTA will bind to certain proteins.[27]

Complexing Agents with Ca^{2+}-dependent NMR Spectra

A series of symmetrically substituted fluorine derivatives of BAPTA (see Figure 3.3A) has been synthesized.[28,29] One of these chelators is 5F-BAPTA (Figure 3.5A), which has a binding constant for Ca^{2+}, K_B^{Ca}, of 1.4 x 10^6 M^{-1} and a ^{19}F NMR chemical shift, \(\delta\), that in the free ligand is different from that in the complex with Ca^{2+} ($\Delta\delta)_{Ca^{2+}} \approx 6$ ppm). The rate of Ca^{2+} dissociation, k_{off}, is 5.7 x 10^2 s^{-1}, which gives the rate of association, k_{on}, as 8 x 10^8 $M^{-1}s^{-1}$ according to

$$K_B = k_{on} / k_{off} \tag{3.2}$$

This exchange rate means that we are approaching the slow exchange limit in ^{19}F NMR, and in subsaturating concentrations of Ca^{2+} two ^{19}F signals are seen (see Figure 3.5B).

Since the areas of the NMR signals from the bound (B) and free (F) forms of the ligand are proportional to their concentration, the free Ca^{2+} concentration is obtained simply as

$$[Ca^{2+}]_{free} = \frac{B}{F} \cdotp \frac{1}{K_B}\ldotp \tag{3.3}$$

An additional beneficial property of 5F-BAPTA and other fluorinated analogues of BAPTA is that they will also bind other metal ions with a ^{19}F chemical shift of the complex that is characteristic of the metal ion.[29] Under favorable circumstances, it is thus possible to measure simultaneously the concentrations of several cations.

For 5F-BAPTA the selectivity for Ca^{2+} over Mg^{2+} is very good ($K_B^{Mg2+} \approx 1$ M^{-1}). In applications of 5F-BAPTA to intracellular studies, the same protocol is used as with the parent compound and its fluorescent derivatives: some esterified derivative, e.g., the acetoxymethyl ester, is taken up by the cells and allowed to hydrolyze in the cytoplasm. The intracellular concentrations of 5F-BAPTA needed to get good ^{19}F NMR signals depend on the density of cells in the sample tube and the number of spectra accumulated. With accumulation times on the order of ten minutes (thus precluding the observation of concentration transients shorter than this time), Ca^{2+} concentrations of the order of 1 \(\mu\)M have been studied in perfused rat hearts using 5F-BAPTA concentrations of about 20 \(\mu\)M.[34]

11.2.3.8: Measurements of "Free" Calcium Concentrations is shared under a CC BY-NC-SA 4.0 license and was authored, remixed, and/or curated by LibreTexts.

11.2.3.9: Measurements of Total Calcium Concentrations

The measurement of total calcium in a biological sample can be made by any method sensitive only to the element and not to its particular chemical form. Atomic absorption spectroscopy is excellent as such a method. Obviously, the spatial resolution that can be obtained with this method is limited, and it is hard to imagine its application to elemental mapping of single cells. The techniques discussed in this subsection have been limited to those that permit a spatial resolution of at least 1 μm on samples usually prepared by sectioning the frozen biological specimens.

Electron Probe and Electron Energy-loss Techniques

When the electron beam in an electron microscope hits a thin sample, some atoms in the sample will be excited or ionized, and returning to their ground state will emit characteristic x-rays. The x-ray emission at different wavelengths may then be measured by a photon-energy-sensitive detector. This is the basis of electron probe x-ray microanalysis (EPMA). The electrons that pass through the sample, and that give the transmission image in electron microscopy, will suffer energy losses that depend on the nature (to some extent also, the chemical state) and distribution of different elements. The outcome of these phenomena forms the basis of electron energy-loss spectroscopy (EELS; see Figure 3.6).

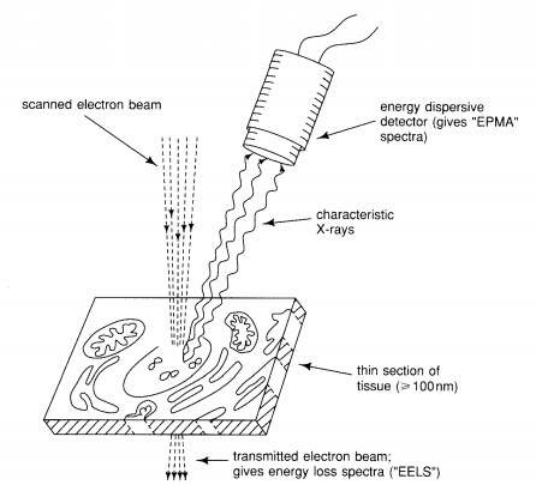


Figure 3.6 - Principles of electron probe microanalysis ("EPMA") and electron energy loss spectroscopy ("EELS"). A thin slice of a freeze-dried sample is exposed to a collimated beam of electrons that may be scanned across the sample. Atoms ionized by electron collisions will emit x-radiation at wavelengths characteristic of their nuclear charge (i.e., characteristic of each element). With the use of an energy dispersive x-ray detector, signals from different elements can be differentiated. Apart from the characteristic x-rays, a broad-spectrum background x-ray emission is also present because of inelastic scattering of the incident electrons. Some of the electrons that pass through the sample will have lost energy because of ionization of atoms in the sample. The energy loss is again characteristic for each element, and if the energy distribution of the transmitted electrons is analyzed, this will have "peaks" at certain characteristic energies. If the energy resolution is pushed far enough < 1 eV), the loss peaks even become sensitive to the chemical state of the element.

The EPMA technique as applied to calcium has been improved by Somlyo in particular.[30] Typically samples are rapidly frozen and sectioned at low temperatures (-130 °C) to preserve the *in vivo* localization of diffusible ions and molecules. Spatial resolutions of 10 nm or better have been attained on ≳100 nm thick freeze-dried cryosections. The minimal detectable concentration, which requires some signal averaging, is approximately 0.3 mmol Ca per kg dry specimen (i.e., 10 ppm). The calcium content of **mitochondria** and **endoplasmic reticulum** in rat liver cells has been studied by EPMA (see Table 3.1).[8]

The high calcium content of endoplasmic reticulum (ER) is consistent with the view that this organelle is the major source of intracellular Ca^{2+} released through the messenger inositol trisphosphate (see Section IV.C). Other EPMA studies have shown mitochondria to have a large capacity for massive calcium accumulation in cells where cytoplasmic Ca^{2+} concentrations have been abnormally high, for example, as a result of damage of the cell membrane.[30]

EELS is presently less well-developed than EPMA. Two of the major difficulties in the use of EELS for quantitative analysis of calcium and other elements are (i) large background, since it is a difference technique, and (ii) sensitivity to specimen thickness.

The major advantage of EELS is that the spatial resolution is potentially much better than in EPMA, and can be 1 to 2.5 nm in favorable specimens.

Proton-induced X-ray Emission (PIXE)

A specimen exposed to a beam of high-energy (1 to 4 MeV) protons will also emit characteristic x-rays just as in EPMA. The advantage of using protons instead of electrons is that protons are more likely to collide with an atom, thus producing excited atoms emitting x-rays. The sensitivity in detecting a particular element is therefore much higher in PIXE than in EPMA or EELS. The PIXE technique, which was developed at the University of Lund, Sweden, in the late 1960s, was originally used mainly for studies of fairly large objects.[9]

In 1980 a group at Oxford University succeeded in focusing the proton beam to a diameter of 1 μm with sufficient energy (4 MeV) and beam intensity (100 pA/μm^2) to allow elemental mapping at ppm concentrations.[31] Similar beam performances (~0.5 μm diameter) are now also available at the University of Lund and other laboratories. Beam diameters of 0.1 μm are likely to be achieved in the near future. Like EPMA, the PIXE method allows the simultaneous observation of several elements in the same sample. The biological applications of the microbeam PIXE technique are limited, but it is clear that its potential is great. Some representative results obtained with the Oxford microbeam are shown in Figure 3.7. (See color plate section, page C-8.)

Ion Microscopy

Ion microscopy is another technique capable of detecting all elements at the ppm level. The basic idea is to expose a freeze-fixed, cryofractured, and freeze-dried sample, which has been put onto a conducting substrate in a vacuum chamber, to a beam of ions (e.g., D_2^+ or Ar^+). These ions will remove the top two or three atomic layers of the sample surface by sputtering. A certain fraction of the removed atoms will leave as ions. This secondary ion beam is accelerated into a double-focusing mass spectrometer, where the ions are separated according to their mass-to-charge ratio. The ion optics are designed to preserve the spatial distribution of the emitted secondary ions, and an element image of the sample can thus be produced with a spatial resolution of ~0.5 μm.[32] The ion-microscope technique can form images of a particular isotope of an element. In principle, then, one could perform isotope labeling or "isotope chase" studies and follow, say, the fate of isotope-enriched ^{43}Ca externally applied to a cell. The ion-microscope technique has not yet come into widespread use, but the quality of element (or ion) images obtained on single cells is impressive.[33]

11.2.3.9: Measurements of Total Calcium Concentrations is shared under a CC BY-NC-SA 4.0 license and was authored, remixed, and/or curated by LibreTexts.

11.2.3.10: Mitochondrial Calcium Ion Transport

Influx

Mitochondria isolated from various types of animal cells—but, interestingly, not those from plant cells—can rapidly accumulate exogenous Ca^{2+}.[59] The transporter is located in the inner membrane and the driving force behind the Ca^{2+} transport appears to be merely the high potential difference across this membrane ($\Delta\Psi \approx$ 150 to 180 mV, negative in the inner matrix). This potential difference is fairly closely maintained by the pumping out of H^+ from the matrix by cell respiration. For the transport of 1 mol Ca^{2+} from the "outside" (= cytoplasm) to the "inside" (= inner mitchondrial matrix), we may deduce from Equation (3.4) that the free-energy change ΔG may be written ($\Delta n_{Ca^{2+}} = -1$)

$$\Delta G = -RT \cdot ln \frac{[Ca^{2+}]_o}{[Ca^{2+}]_i} - 2F\Delta\Psi. \tag{3.11}$$

From this analysis it may be inferred that the limiting Ca^{2+} concentration (or activity) ratio that can be achieved by this **electrogenic** pump (i.e., $\Delta G = 0$) is

$$\frac{[Ca^{2+}]_o}{[Ca^{2+}]_i} = e^{\frac{-2F\Delta\Psi}{RT}} \tag{3.12}$$

With $\Delta\Psi$ = 150 mV, this ratio is calculated to be 8.4 x 10^{-6} at 25 °C. It is evident that, as long as the Ca^{2+} influx would not lower the membrane potential difference, the Ca^{2+} **uniporter** has a very high pumping potential. Measured values of the pumping rate, V_{max}, are indeed high (>10 nmol/mg protein[59]) and probably limited only by the rate of electron transport and H^+ extrusion in the mitochondria.

Mitochondria may accumulate large quantities of Ca^{2+}, probably to maintain electroneutrality. To prevent the buildup of high concentrations of free Ca^{2+} (and of osmotic pressure), phosphate ions are also transported into the inner matrix, where an amorphous calcium phosphate—or possibly a phosphocitrate[60]—is formed. The equilibrium concentration of free Ca^{2+} in the mitochondrial matrix may as a result be comparatively low, on the order of 1 μM.

The molecular nature of the mitochondrial Ca^{2+} uniporter continues to be elusive, and needs to be studied further.

Efflux

Mitochondria, as well as SR, release Ca^{2+} ions by mechanisms other than "back leakage" through the pumps. In mitochondria from excitable cells, the efflux occurs mainly through an antiport, where 2 Na^+ ions are transported inward for every Ca^{2+} ion departing for the cytosolic compartment.[61] In other cells there is evidence for the dominance of a $2H^+$-Ca^{2+} antiport.[59] In all likelihood the Ca^{2+} efflux is regulated, possibly by the redox state of pyridine nucleotides in the mitochondria. As with the Ca^{2+} uniporter, few details on the molecular nature of the antiporters are presently available.

Ca^{2+} Efflux from Non-mitrochondrial Stores

Release of Ca^{2+} from ER and SR presently appears to be the prime effect of the new intracellular messenger 1,4,5-triphosphoinositol (1,4,5-IP_3) released into the cytoplasm as a result of an external hormonal stimulus (see Section IV.C). It seems that receptors for 1,4,5-IP_3 have been established on ER, and that the binding of 1,4,5-IP_3 causes a release of Ca^{2+} stored in this organelle.[62,63,170,171] In addition to the receptor-controlled Ca^{2+} efflux, there may be other pathways for Ca^{2+} release, and Ca^{2+} mobilization may be regulated by other intracellular entities, the Ca^{2+} ions themselves included.

Other Voltage-gated or Receptor-activated Ca^{2+} Channels

In addition to the transport pathways already discussed, some cells seem to have Ca^{2+} channels in the plasma membrane that can be opened by the action of an agonist on a receptor or that are gated in response to changes in membrane potential.[64] For example, Ca^{2+} channels can be opened by nicotinic cholinergic agonists[65] or by the excitatory amino acid N-methyl-D-aspartate (NMDA).[66] Endochrine cells and also some muscle and neuronal cells have voltage-sensitive Ca^{2+} channels.[67,68] We will not discuss these further, but merely point to their existence. We finally note that during the last few years knowledge about the mechanisms of Ca^{2+}

entry and release to and from extracellular and intracellular pools has increased dramatically, and we refer the reader to recent reviews of the field.[175,176]

11.2.3.10: Mitochondrial Calcium Ion Transport is shared under a CC BY-NC-SA 4.0 license and was authored, remixed, and/or curated by LibreTexts.

11.2.3.11: Molecular Aspects of Calcium Ion-Regulated Intracellular Processes (Part 1)

So far we have mainly discussed the routes and means by which the concentration of Ca^{2+} ions in the cytoplasm can be transiently increased and brought back to resting levels. But changing the cytoplasmic Ca^{2+} concentration is not enough. In order to influence the cellular machinery, the Ca^{2+} ions must interact with different proteins, *intracellular Ca^{2+} receptors* if you like. These intracellular Ca^{2+}-receptor proteins must have certain properties in order to function.

i. Their Ca^{2+}-affinity must be such that their Ca^{2+}-binding sites are essentially unoccupied at resting levels of free Ca^{2+} ($\sim 10^{-7}$ M) and occupied at levels reached upon stimulus (generally assumed to be 10^{-5} to 10^{-6} M). This means that the binding constants K_B^{Ca2+} should be $\sim 10^6$ M^{-1}.
ii. We should also remember that Ca^{2+} must exert its function in the presence of a number of other ions; in mammalian cells the intracellular concentration of "free" Mg^{2+} ions is around 1 mM, and that of K^+ ions around 100 to 150 mM. The receptors must therefore have an adequate selectivity for Ca^{2+}.
iii. In response to Ca^{2+} binding, a Ca^{2+} receptor must undergo some kind of conformation change that either alters its interaction with other molecules or changes its activity if it is an enzyme.
iv. Finally, there are *kinetic* considerations. In many cells a rapid response is essential, and therefore the receptors must be able to interact swiftly—within milliseconds—with incoming Ca^{2+} ions, and the ions must also be able to depart almost as rapidly.

A few proteins have been discovered that qualify as intracellular Ca^{2+} receptors. The best known of these is *calmodulin* (CaM), which appears to be present in all eukaryotic cells. Most of the cellular responses elicited by Ca^{2+} appear to result from interactions between the Ca^{2+}-calmodulin complex and various other target enzymes and proteins.[75] Another important Ca^{2+}-receptor protein is *troponin C* (TnC), which occurs in muscle cells and is instrumental in mediating muscle contraction.[76] These two types of proteins are highly homologous, as we shall see, and may be considered members of a superfamily of closely related intracellular Ca^{2+}-binding proteins. This superfamily has been given the name "the calmodulin superfamily," and close to 200 distinct family members are presently known.[77] Not all members of the superfamily may qualify as Ca^{2+} receptors; some like *parvalbumins* and *calbindins* (see Section IV.A) appear to have a role in intracellular transport and/or Ca^{2+}-buffering. For others, such as the *S-100* proteins[78] found predominantly in brain tissue, and *calcimedins*,[79] isolated from smooth muscle, the biological function is still unclear.

One Ca^{2+} receptor with enzymatic activity is *protein kinase C*. Its activity is markedly increased in the presence of Ca^{2+}, and it has a high calcium-binding constant (see Table 3.2) in the presence of diacylglycerol or **phorbol esters**.[80]

During recent years, groups interested in the role of Ca^{2+} in secretion and in the control of membrane cytoskeleton have identified some intracellular Ca^{2+}/phospholipid-binding proteins that appear to be distinct from the calmodulin superfamily; these include *lipocortin*, *endonexin*, *calelectrin*, *p36*, and *calpactin*.[81-83] These membrane-binding proteins are collectively called *annexins*,[84] and contain repeated domains distinct from EF-hands. The Ca^{2+} sites are very similar to that observed in phospholipase A_2, as shown by the recently determined x-ray structure of annexin V.[172] A condensed overview of the interaction of Ca^{2+} with intracellular proteins is shown in Figure 3.16. We will now go on to discuss the molecular properties of some of the proteins mentioned above, starting with calmodulin.

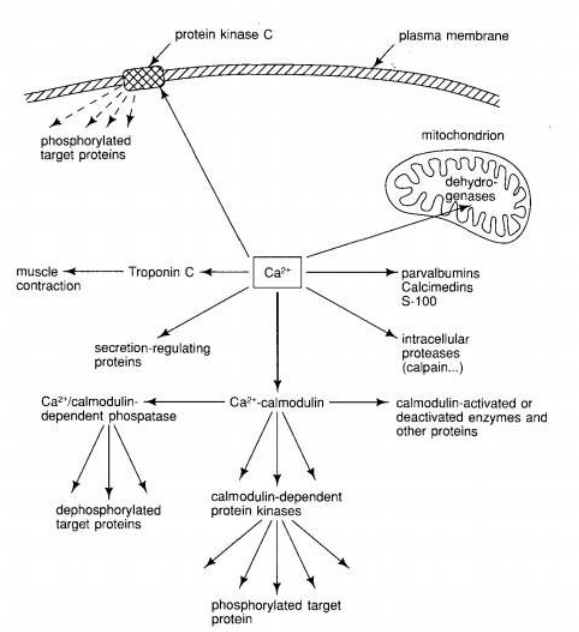


Figure 3.16 - Condensed overview of the interaction of Ca^{2+} with intracellular proteins.

11.2.3.11: Molecular Aspects of Calcium Ion-Regulated Intracellular Processes (Part 1) is shared under a CC BY-NC-SA 4.0 license and was authored, remixed, and/or curated by LibreTexts.

11.2.3.12: Molecular Aspects of Calcium Ion-regulated Intracellular Processes (Part 2)

Sarcoplasmic Calcium-binding Protein from *Nereis diversicolor*

The calmodulin superfamily of proteins also includes' *sarcoplasmic Ca^{2+}-binding proteins* (SCPs) that can be found in both vertebrate and invertebrate muscle.[129] The function of SCPs is not yet known, but their sequence homology with Ca^{2+}-binding proteins of known tertiary structure suggests that they originally contained four helix-loop-helix Ca^{2+}-binding domains. Ca^{2+} binding has been preserved in the first and third domains of all known SCPs, but only one, if any, of domains II and IV is functional. The three-dimensional crystal structure of an SCP from the sandworm *Nereis diversicolor* analyzed at 3.0 Å resolution[130] can be seen in Figure 3.26. (See color plate section, page C-11.) The C-terminal half (domains III and IV) of the molecule contains two Ca^{2+}- binding EF-hands (green and red in Figure 3.26) similar to calbindin D_{9k} and the globular domains of troponin C and calmodulin. The N-terminal half is, on the contrary, markedly different from the normal helix-loop-helix geometry. Domain I binds Ca^{2+} with a novel helix-loop-helix conformation, whereas domain H lacks calcium-binding capacity. The two halves are packed closely together, and are not, as in troponin C or calmodulin, connected by a solvent-exposed α-helix.

Membrane Cytoskeleton and Phospholipid Binding Proteins

It has long been suspected that Ca^{2+} ions are somehow involved in exocytosis. Recently several groups[131] have isolated intracellular proteins that associate with membranes, and/or membrane cytoskeleton proteins, in a Ca^{2+}-dependent manner, and that seem able to mediate vesicle fusion or aggregation at Ca^{2+} concentrations above 200 μM. These proteins—endonexin, calelectrin, p36, and pII—have stretches of consensus amino-acid sequences that are also found in a phospholipase A_2 inhibitor protein, lipocortin.[132] It appears that further studies of this new class of proteins, known as annexins, will lead to new insights into cell-signaling pathways. Multiple functions have been proposed for the annexins, but no cellular role has yet been defined.[133] The first crystal structure of an annexin, human annexin V—which *in vitro* will form voltage-gated Ca^{2+} channels—has been determined recently.[172] In annexin, the three Ca^{2+}-binding sites are located on the side of the molecule that is involved in membrane binding.

Ca^{2+}-dependent Proteases

An interesting Ca^{2+}-activated intracellular protease, sometimes called *calpain*, was discovered during the last decade.[134] The ending -pain refers to its relation with other proteolytic enzymes like papain. It may seem dangerous to have a proteolytic enzyme loose inside a cell, and it must have rather specialized functions and be under strict control. The complete primary structure of the calcium protease ($M_r \approx 80{,}000$) in chicken tissues has recently been deduced from the nucleotide sequence of cloned DNA.[135,136] The findings are quite unexpected.

The protein contains four distinct domains. The first and third domains have no clear sequence homologies with known protein sequences, but the second domain has a high homology with the proteolytic enzyme papain, and the fourth domain is highly homologous to calmodulin. This fourth domain thus has four EF-hand-type Ca^{2+}-binding sites, although the third site has a somewhat unusual loop sequence. Here we apparently are faced with an unusual invention by Nature: by fusing the gene for a protease with that of the canonical Ca^{2+} receptor, she has created a molecule in which a regulatory protein is covalently linked to its target enzyme!

Protein Kinase C

Before we leave our brief survey of intracellular Ca^{2+}-binding proteins, we must write a few lines about an important Ca^{2+}-regulated kinase (a phosphorylating enzyme), i.e., *protein kinase C* (PKC). The activity of this enzyme, or rather family of enzymes,[137] appears to be regulated by three factors: phospholipids, in particular phosphatidylserine; diacyl-glycerols, one of the products of inositol lipid breakdown; and Ca^{2+} ions. The high-activity form of PKC, which appears responsible for much of the phosphorylation activity of many cells, is presumably membrane-bound, whereas the low-activity form may be partly cytosolic (Figure 3.27). The schematic structure of rabbit PKC ($M_r \approx 77$ kDa) according to Ohno *et al.*[138] is shown in Figure 3.28. The Ca^{2+} site(s) are presumably in the regulatory domain. No typical "EF-hand" pattern has been found in the amino-acid sequence. A protein kinase that requires Ca^{2+} but not phospholipids nor calmodulin for activity has been purified from soybean. From the amino-acid sequence the protein appears to have a calmodulin-like Ca^{2+}-binding domain, very much as in calpain.[139]

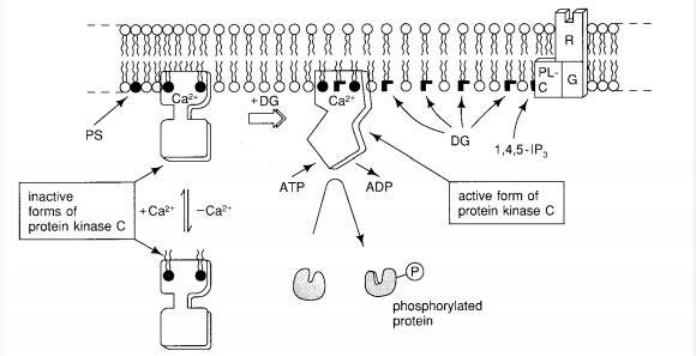


Figure 3.27 - Outline of the cellular events that result in the activation of protein kinase C (PKC). The enzyme apparently exists in at least two states. Recent sequence work indicates that it has a Ca^{2+}-binding site of the EF-hand type. When no Ca^{2+} ion is bound, and when the "concentration" of diacylglycerol (DG) in the inner layer of the plasma membrane is low, the kinase exists in a low-activity form, possibly dissociated from the membrane. When a hormone binds to a plasmamembrane receptor (R), cleavage of phosphoinositol into 1,4,5-IP_3 and DG is induced. The latter lipid may bind to and activate the calcium-loaded form of PKC. The active form of protein kinase C will now phosphorylate other cytoplasmic proteins, and in this way modify their biochemical properties. R = receptor; PL-C = phospholipase C; G = a GTP-binding protein that is assumed to act as an intermediary between the receptor and the membrane bound PL-C.

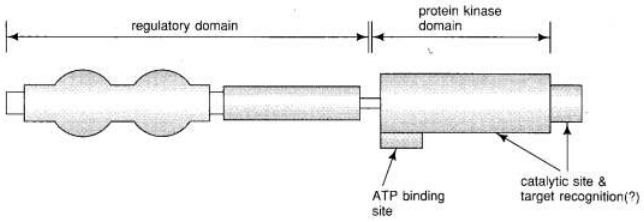


Figure 3.28 - Schematic representation of the structure of rabbit protein kinase C.[138] Three highly homologous protein kinases C were actually identified with $M_r \approx 76{,}800$. The kinase region shows clear similarity with other kinases. The regulatory domain should contain binding sites for Ca^{2+}, phosphatidyl serine (PS), and diacylglycerol (DG).

11.2.3.12: Molecular Aspects of Calcium Ion-regulated Intracellular Processes (Part 2) is shared under a CC BY-NC-SA 4.0 license and was authored, remixed, and/or curated by LibreTexts.

11.2.3.13: Paravalbumin and Calbindins D 9 K and D 28 K

A few intracellular Ca^{2+}-binding proteins have been discovered that by sequence homology clearly belong to the CaM-TnC family with Ca^{2+} sites of the "EF-hand"-type, but that do not appear to exert a direct regulatory function. Parvalbumins ($M_r \approx 12$ kDa), calbindin D_{9K} ($M_r \approx 8.7$ kDa) and calbindin D_{28K} ($M_r \approx 28$ kDa) belong to this group. *Parvalbumin(s)* exist in two main types, α and β, found in large quantities in the white muscle of fish, amphibia, and reptiles, but also in different mammalian tissues,[116,117] including neurons of the central and peripheral nervous system. The molecule has two fairly strong Ca^{2+}- binding sites (see Table 3.2). The x-ray structure of carp parvalbumin was solved in 1973 by Kretsinger *et al.*,[118] and for a decade provided the basis for all discussions on intracellular Ca^{2+}-binding proteins. The concept of the canonical "EF-hand" Ca^{2+}-binding site originated from the parvalbumin work, and the name "EF" derives from the labeling of the two helices that flank the second of the two Ca^{2+} sites in parvalbumin, as shown in Figure 3.23.

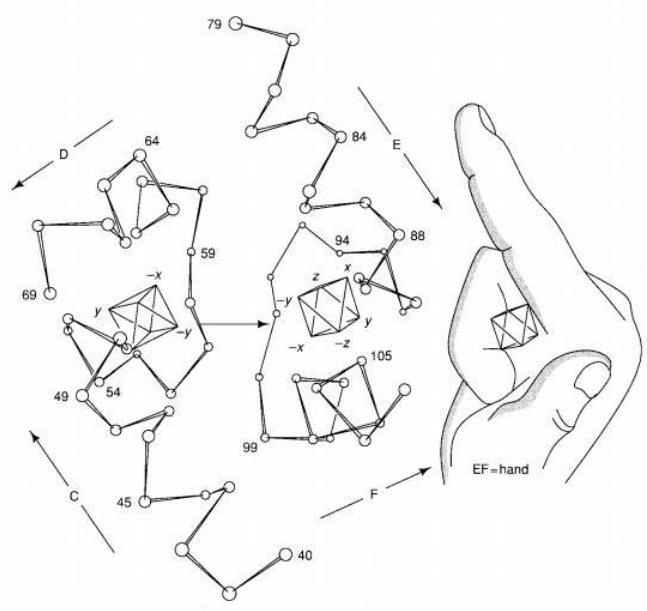


Figure 3.23 - Structure of the Ca^{2+}-binding sites of carp parvalbumin. The Ca^{2+} ions are depicted as regular octahedra making six ligand contacts with oxygen atoms at each vertex, labeled x, y, z, -x, -y, -z. The helix-loop-helix structure that forms a Ca^{2+}-binding site can be regarded as a hand with the forefinger representing one helix (e.g., the E-helix) in the plane of the figure, the thumb oriented perpendicular to the plane representing the second helix (the F-helix), and the remaining fingers make up the Ca^{2+}-binding loop. After Kretsinger and Barry.[118]

If the first Ca^{2+} ligand in the approximately octahedral coordination sphere is given number 1 (or "x") the others come in the order 3("y"), 5("z"), 7("-y"), 9("-x"), and 12("-z"). In the second site of parvalbumin, "-x" is actually a H_2O molecule, but in the first site it is the carboxylate of a Glu. Studies[118] of putative Ca^{2+}-binding sites in other proteins with known primary sequences led to the generalized EF-hand structure—including residues in the flanking α-helices—shown in Figure 3.24.

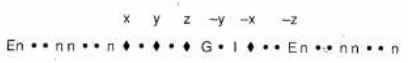


Figure 3.24 - One consensus EF-hand sequence including residues in the flanking α-helices; x, y, z, -x, -y, - z denote positions in the octahedral Ca^{2+} coordination sphere. E—glutamic acid residue, G—glycine residues, I—isoleucine residue, n—nonpolar residue, ♦—a residue with a nonaromatic oxygen-containing side chain (i.e., Glu, Gin, Asp, Asn, Ser, or Thr), and •—nonspecific residue.

This sequence, with minor modifications, has been widely used in searching for "EF-hands" in libraries of amino-acid (or DNA) sequences of new proteins with unknown properties. In this way, *calbindin* D_{28k} a protein with unknown function, initially discovered in chicken intestine, but later found also in brain, testes, and other tissue, has been shown to have four EF-hand sites.[119]

Recently two structures of carp parvalbumin, both with a resolution of 1.6 Å, were published.[120] One of these structures is the native calcium-loaded form of the protein; the second is the structure of parvalbumin in which Ca^{2+} has been replaced by Cd^{2+}. No significant differences are observed upon replacement of calcium by cadmium. ^{113}Cd has a nuclear spin of I = $\frac{1}{2}$, making it much

more amenable to NMR studies than the quadrupolar ^{43}Ca (I = $\frac{7}{2}$), This study supports the use of ^{113}Cd NMR as a tool for the study of calcium-binding proteins.[121]

The function of parvalbumin has long been assumed to be that of buffering Ca^{2+} in muscle cells, i.e., taking up Ca^{2+} ions released from Ca^{2+}-troponin complexes, thereby ensuring that the cytoplasmic levels of free Ca^{2+} are always kept very low, even during short bursts of muscle activity,[122] The widespread occurrence of parvalbumin in non-muscle tissue indicates that it probably has other roles as well.

Calbindin D_{9k} ($M_r \approx 8.7$ kDa) is another intracellular Ca^{2+}-binding protein with unknown function. It was briefly mentioned in connection with Ca^{2+} uptake and transport in the intestine and placenta (Section IV.A). Like the avian calbindin D_{28k} the D_{9k} calbindin has been observed in many types of tissue. The homology between the D_{9k} and D_{28k} calbindins is much less than the name suggests; both their syntheses are, however, regulated by vitamin D. The x-ray structure of bovine calbindin D_{9k} has been determined[123] and refined to a resolution of 2.3 Å, and a three-dimensional *solution* structure of porcine calbindin D_{9k} is also available.[124] The average solution structure calculated from NMR data is shown in Figure 3.25 (See color plate section, page C-10.)

The protein has four main α-helices and two Ca^{2+}-binding loops (I and II). The interior of the molecule shows a loose clustering of several hydrophobic side chains; in particular, three phenylalanine rings come very close in space. The Ca^{2+}-binding loops constitute the least-mobile parts of the molecule. The crystallographic temperature factors have pronounced minima in these regions, with the lowest overall B-factor observed in loop II. Both Ca^{2+} ions are roughly octahedrally coordinated with protein oxygen atoms. There are some striking differences between the two sites, however. Whereas the C-terminal site (II) has a general structure very similar to the archetypal "EF-hand," as observed in CaM, sTnC, and parvalbumin, the N-terminal site (I) has an extra amino-acid residue inserted between vertices x and y, and z and -y (see Figure 3.24). As a consequence, the peptide fold in site I is different from that in site II. Three carboxylate groups are ligands in site II, but in site I there is only one.

Despite this marked difference in charge and peptide fold, the Ca^{2+} affinity of both Ca^{2+} sites is remarkably similar, as has been shown in a study in which site-directed mutagenesis was combined with different biophysical measurements.[37] Cooperative Ca^{2+} binding in the native calbindin D_{9k} (the "wild type") was first demonstrated at low ionic strength by means of the values of the two stoichiometric Ca^{2+}-binding constants, K_1 and K_2, which could be measured with good accuracy ($K_1 = 4.4 \times 10^8\ M^{-1}$ and $K_2 = 7.4 \times 10^8\ M^{-1}$). The effects of amino-acid substitutions in Ca^{2+} site I were primarily localized to this site, with virtually no effects on the structure or other biophysical properties pertinent to site II. The appearance of sequential Ca^{2+} binding in some of the calbindin mutants did allow the identification of ^1H NMR resonances that respond primarily to binding of Ca^{2+} to either one of the sites. This result in tum permitted an estimate of the ratio between the site-binding constants (K_A and K_B) in the wild-type protein and in one of the mutant proteins (Tyr-13 → Phe). In this way the reseachers[125] could assess, to within narrow limits, the free energy of interaction, $\Delta\Delta G$, between the two Ca^{2+} sites as 7.7 kJ/mol at low ionic strength and 4.6 kJ/mol in the presence of 0.15 M KCl. How this site-site interaction is transmitted on a molecular level is still unknown.

Through a combination of site-specific mutations and biophysical measurements, it has recently been demonstrated that carboxylate groups at the surface of the protein, but not directly ligated to the bound Ca^{2+} ions, have a profound effect on the Ca^{2+} affinity.[126] Neutralization of the surface charges reduces affinity and increases the stability of the protein toward unfolding by urea.[127]

A surprising discovery about the structure of bovine calbindin D_{9k} in solution has also been made recently.[128] Detailed analysis of the 2D ^1H NMR spectrum of wild-type calbindin has revealed that it exists as a 3:1 equilibrium mixture of two forms, corresponding to a *trans* and *cis* conformation around the Gly-42-Pro-43 peptide bond. The global fold appears essentially the same in the two forms, and structural differences are primarily located in the inter-domain loop in which Pro-43 is located.

11.2.3.13: Paravalbumin and Calbindins D_{9K} and D_{28K} is shared under a CC BY-NC-SA 4.0 license and was authored, remixed, and/or curated by LibreTexts.

11.2.3.14: The Transport and Regulation of Ca^{2+} Ions in Higher Organisms

All living organisms need calcium, which must be taken up from the environment. Thus, Ca^{2+} ions have to be distributed throughout the organism and made available where needed. In higher organisms, such as humans, the blood-plasma level of total calcium is kept constant (≈2.45 mM) within narrow limits, and there must be a mechanism for regulating this concentration. On a cellular level we have already seen in the preceding section that the basal cytoplasmic Ca^{2+} concentration, at least in eucaryotic cells, is very low, on the order of 100 nM. At the same time the concentrations of Ca^{2+} in certain organelles, such as endoplasmic (or sarcoplasmic) reticulum or mitochondria, may be considerably higher. If Ca^{2+} ions are to be useful as intracellular "messengers," as all present evidence has it, Ca^{2+} levels in the cytoplasm would have to be raised transitorily as a result of some stimulus. Ca^{2+} ions may enter the cytoplasm either from the extracellular pool or from the Ca^{2+}-rich organelles inside the cell (or both). We could imagine Ca^{2+} channels being regulated by chemical signaling, perhaps by a hormone acting directly on the channel, or by a small molecule released intracellularly when a hormone is attached to a membrane-bound receptor. Some channels may be switched on by voltage gradients, and both these mechanisms may operate concurrently.

Increased intracellular Ca^{2+} levels must eventually be brought back to the basal levels, in some cells very quickly. The ions could be transported out of the cell or back into the Ca^{2+}-rich organelles. This transport will be against an electrochemical potential gradient, and thus requires energy. There are many possibilities for different forms of Ca^{2+} transport and regulation in living systems, and we still know fairly little about the whole picture. Detailed studies are also complicated by the fact that, in higher organisms, cells are differentiated. Nature is multifarious, and what is valid for one type of cell may not be relevant for another. With these words of caution we will start out on a macroscopic level and continue on toward molecular levels.

Ca^{2+} Uptake and Secretion

The uptake of Ca^{2+} from food has mostly been studied in typical laboratory animals, such as rats, hamsters, chickens, and humans. In humans, uptake occurs in the small intestine, and transport is regulated by a metabolite of vitamin D, calcitriol (1,25-dihydroxy vitamin D_3).[34] The uptake process is not without loss; roughly 50 percent of the calcium content in an average diet is not absorbed. To maintain homeostasis and keep the calcium level in blood plasma constant, excess Ca^{2+} is excreted through the kidney. The main factor controlling this phenomenon in vertebrates is the level of the parathyroid hormone that acts on kidney (increases Ca^{2+} resorption), on bone, and, indirectly, via stimulated production of calcitriol, on the intestinal tract (increases Ca^{2+} uptake). Calcium enters the cells from the outside world, i.e., the intestinal lumen, by traveling through the brush-border membrane of the intestinal **epithelial cells**, through the cytosolic interior of these cells, and into the body fluids through the **basal lateral membranes** of the same cells. The molecular events involved need to be studied further. Figure 3.8 outlines the Ca^{2+} transport processes known or thought to occur.

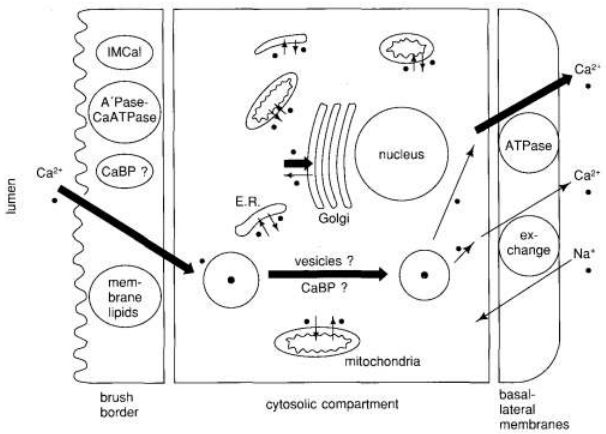


Figure 3.8 - A scheme representing some of the known and hypothetical molecular participants in the transport of Ca^{2+} across intestinal epithelial cells. Transport across the brush-border membrane is generally assumed to be passive or to be facilitated by a carrier (IM Cal), and is also influenced by vitamin D. Transport through the cell may be in vesicles and/or in association with Ca^{2+}-binding proteins (CaBP), notably calbindins D_{9k} (mammals) or D_{28k} (avians). Temporary storage or buffering of Ca^{2+} may be through cytosolic CaBPs, mitochondria, endoplasmic reticula (ER), or other organelles. Transport of Ca^{2+} out of the cell through the basal-lateral membranes is energetically uphill, and appears primarily accomplished by a Ca^{2+}-ATPase and possibly to some extent by a Na^{2+}-Ca^{2+} antiport. Adapted from Reference 35.

Transfer through the brush-border membrane is assumed to be "passive" although indirectly facilitated by calcitriol. The calcitriol effect may be due to synthesis of a carrier protein,[35] but could also be an effect of altered membrane lipid composition. [36] The fate of Ca^{2+} ions, once inside the epithelial cell, is a much-debated subject. What appears clear is that the Ca^{2+} ions entering through the brush-border membrane do not cause an increase of the low cytosolic Ca^{2+} concentration. It is thus quite likely that the Ca^{2+} ions are carried through the cell but the means of transportation is unknown. One plausible carrier is the intracellular low-molecular-weight Ca^{2+}-binding protein calbindin D_{9K} ($M_r \approx 9$ kDa) formerly known as ICaBP (see Section V.C).[35] Its synthesis is induced by vitamin D, and it is mainly found in mammalian intestines. The porcine and bovine calbindin D_{9K} has a Ca^{2+} binding constant of $K_B \approx 3 \times 10^8\ M^{-1}$ in low ionic strength media[37] and $K_B = 2 \times 10^6\ M^{-1}$ in the presence of 1 mM Mg^{2+} and 150 mM K^+.[38] The concentration of calbindin D_{9K} in epithelial cells can reach millimolar levels,[35] which could allow it to facilitate Ca^{2+} diffusion across the cytosol. This was first suggested by Williams, subsequently elaborated by Kretsinger *et aI.* in 1982,[39] and later demonstrated in a model cell by Feher.[40] The basic idea is that, although the diffusion rate of Ca^{2+} ions ($\sim 10^{-5}\ cm^2\ s^{-1}$) is higher than for the $(Ca^{2+})_2$ calbindin complex ($\sim 0.2 \times 10^{-5}\ cm^2\ s^{-1}$), the fact that the concentration of the latter complex may be about 10^3 times higher than that of free Ca^{2+} will result in an increased net calcium transport rate. Calbindin would, in fact, act very much like myoglobin in facilitating oxygen transport through muscle tissue.

Plausible as the above mechanism may seem, it may, however, not be the whole truth. An alternative mechanism is vesicular transport. In chicken intestine it has been shown that the only epithelial organelles that increased in Ca^{2+} content as a result of calcitriol treatment were the lysosomes.[41] The result lends support to a transport mechanism involving Ca^{2+} uptake across the brush-border membrane by **endocytic vesicles**, fusion of these vesicles with lysosomes, and possibly also delivery of Ca^{2+} to the basal lateral membrane of the epithelial cell by **exocytosis**. This process would also explain the vitamin-D-induced alterations in brush-border-membrane lipid compositions as a consequences of preferential incorporation of certain types of lipids into the vesicles. Interestingly, the lysosomes in the chicken studies also contained high levels of calbindin D_{28k}—a type of vitamin-D-induced Ca^{2+}-binding protein found in avian intestines—making it conceivable that this protein acts as a "receptor" for Ca^{2+} at the brush-border membrane and upon Ca^{2+} binding could become internalized in endocytic vesicles.[41]

The basal lateral plasma membrane contains at least two types of Ca^{2+} pumps that also may play a role in Ca^{2+} uptake, one ATP-driven, one driven by a concurrent flow of Na^+ ions into the cytoplasm (i.e., a Na^+-Ca^{2+} **antiport**; see Figure 3.8). We discuss these types of transporting proteins in the next subsection.

There are some apparent analogies between intestinal Ca^{2+} transport and that occurring in the placenta. Transplacental movements of Ca^{2+} increase dramatically during the last trimester of gestation.[42] In mammalian placental **trophoblasts**, high concentrations of calbindin D_{9K} are found.[43,44] The protein synthesis also in this tissue appears to be under calcitriol regulation. Ca^{2+} ions have to be supplied by mammalian females, not only to the fetus during pregnancy, but also to the newborn child through the mother's milk. The molecular details of Ca^{2+} transport in the mammalian glands have not been extensively studied. In milk, Ca^{2+} is bound mainly to micelles of casein, and the average Ca^{2+} content is reported to be 2.5 g/liter (see Table 3.1).

11.2.3.14: The Transport and Regulation of Ca^{2+} Ions in Higher Organisms is shared under a CC BY-NC-SA 4.0 license and was authored, remixed, and/or curated by LibreTexts.

11.2.3.15: Troponin C

The contraction of striated muscle is triggered by Ca^{2+} ions. Muscle cells are highly specialized, and contain two types of filaments that may slide past each other in an energy-consuming process. One of the filaments, the thin filament, is built up by actin molecules ($M_r \approx 42$ kDa) polymerized end-to-end in a double helix. In the grooves of this helix runs a long rod-like molecule, tropomyosin; and located on this molecule at every seventh actin, is a complex of three proteins, *troponin*. The three proteins in the troponin complex are *troponin I* (TnI), *troponin T* (TnT), and *troponin C* (TnC). A schematic picture of the organization of the thin filament is shown in Figure 3.20.

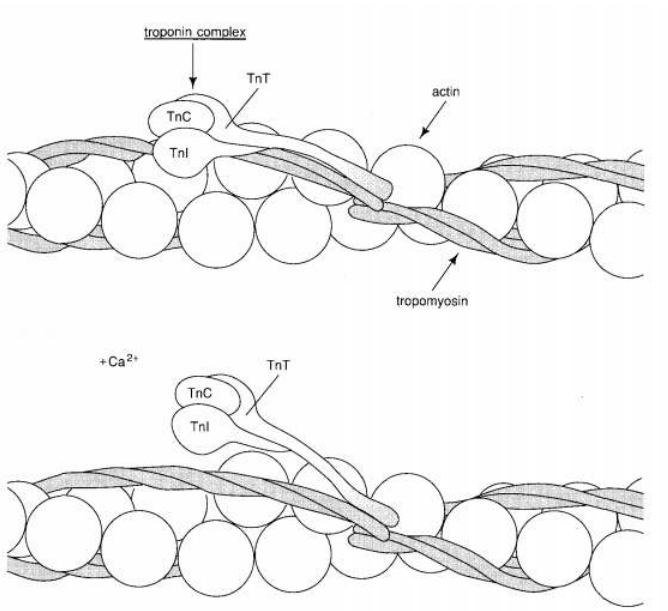


Figure 3.20 - Schematic diagram of the organization of skeletal muscle thin filament, showing the position of tropo-myosin and the troponin complex on the actin filament. The binding of Ca^{2+} to TnC, the calcium-binding subunit of the troponin complex, removes TnI, the inhibitory subunit, from actin and thus permits an interaction with a specialized protein, myosin, on neighboring thick muscle filaments (not shown). An ATP-driven conformation change in the myosin head group makes the thick and thin filaments move relative to one another, so that muscle contraction occurs.

Troponin C is the Ca^2 -binding subunit of troponin, and it is structurally highly homologous to calmodulin. Skeletal-muscle troponin C (sTnC; $M_r \approx 18$ kDa) can bind four Ca^{2+} ions, but cardiac-muscle troponin C (cTnC) has one of the four calcium sites modified, so that it binds only three Ca^{2+} ions. The x-ray structures of sTnC from turkey and chicken skeletal muscle have been determined to resolutions of 2.8 and 3.0 Å, respectively.[102,103] The structure of turkey sTnC is shown in Figure 3.21.

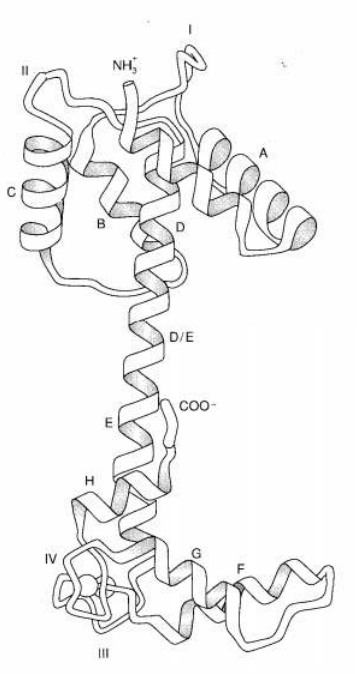


Figure 3.17).

The similarity between the structures of CaM (Figure 3.17) and sTnC is obvious. In sTnC we again find two domains, each with two potential Ca^{2+} sites, separated by a 9-turn α-helix. The crystals were grown in the presence of Ca^{2+} at a low pH (pH = 5), and only two Ca^{2+} ions are found in the C-terminal domain. The two Ca^{2+}-binding sites in this domain have the same helix-loop-helix motif that is found in CaM, and they both conform to the archetypal EF-hand structure. The interhelix angles between helices E and F and between G and H are close to 110°. By contrast, the helices in the N-terminal domain, where no Ca^{2+} ions are bound, are closer to being antiparallel, with interhelix angles of 133° (helices A and B) and 151° (helices C and D).

Both sTnC and cTnC have two high-affinity Ca^{2+}-binding sites (see Table 3.2) that also bind Mg^{2+} ions competitively, although with a much lower affinity. These two sites are usually called "*the Ca^{2+}-Mg^{2+} sites*." *76,104* In sTnC there are also two (in cTnC, only one) Ca^{2+}-binding sites of lower affinity ($K_B^{Ca2+} \approx 105\ M^{-1}$) that bind Mg^{2+} weakly and therefore have been called "*the Ca^{2+}-specific sites*." Since Ca^{2+} binding to the latter sites is assumed to be the crucial step in the contractile event, they are often referred to as "*the regulatory sites*" (see below). The existence of additional weak Mg^{2+} sites ($K_B \approx 300\ M^{-1}$) on sTnC, not in direct competition with Ca^{2+}, has also been inferred.[76,104,105] Spectroscopic studies have shown that the two strong Ca^{2+}- Mg^{2+} sites are located in the C-terminal domain, and the weaker Ca^{2+}-specific sites in the N-terminal domain of sTnC.[106] This pattern is similar to that observed with CaM. NMR spectroscopic studies strongly suggest that binding of Ca^{2+} to both sTnC and cTnC is cooperative.[107] In sTnC the C-terminal domain binds Mg^{2+} much more strongly than the N-terminal domain, by contrast to CaM, where the reverse is true.

The rates of dissociation of Ca^{2+} and Mg^{2+} from sTnC have been measured by both stopped-flow and ^{43}Ca NMR techniques.[76,108] As with CaM, the actual numbers depend on the solution conditions, ionic strength, presence of Mg^{2+}, etc. (see Table 3.4). On the rate of Mg^{2+} dissociation from the Ca^{2+}- Mg^{2+} sites, quite different results have been obtained by stopped-flow studies[76] of fluorescence-labeled sTnC ($k_{off}^{Mg2+} \approx 8\ s^{-1}$) and by ^{25}Mg NMR ($k_{off}^{Mg2+} \simeq 800\text{-}1000\ s^{-1}$).[109] This apparent discrepancy seems to have been resolved by the observation that both binding and release of Mg^{2+} ions to the Ca^{2+}-Mg^{2+} sites occur *stepwise*, with $k_{off}^{Mg2+} < 20\ s^{-1}$ for one of the ions, and $k_{off}^{Mg2+} \geq 800\ s^{-1}$ for the other.[110] The rates of dissociation of the Mg^{2+} ions are important, since under physiological conditions the Ca^{2+}-Mg^{2+} sites of sTnC are likely to be predominantly occupied by Mg^{2+} ions, release of which determines the rate at which Ca^{2+} can enter into these sites.

Spectroscopic and biochemical data[111] indicate that upon binding Ca^{2+}, sTnC and cTnC undergo significant conformation changes. Comparisons of NMR spectroscopic changes on Ca^{2+} binding to intact sTnC, as well as to the two fragments produced by tryptic cleavage (essentially the N-terminal and C-terminal halves of the molecule, just as was the case with CaM), have shown that the conformation changes induced are mainly localized within the domain that is binding added ions.[110,112] Thus the central α-helix

connecting the domains seems unable to propagate structural changes from one domain to the other. It has been suggested that the structural differences found in the x-ray structure of turkey sTnC between the C-terminal domain, which in the crystal contains two bound Ca^{2+} ions, and the N-terminal domain, in which no Ca^{2+} ions were found, may represent these conformational changes.[113] This rather substantial conformational change is schematically depicted in Figure 3.22.

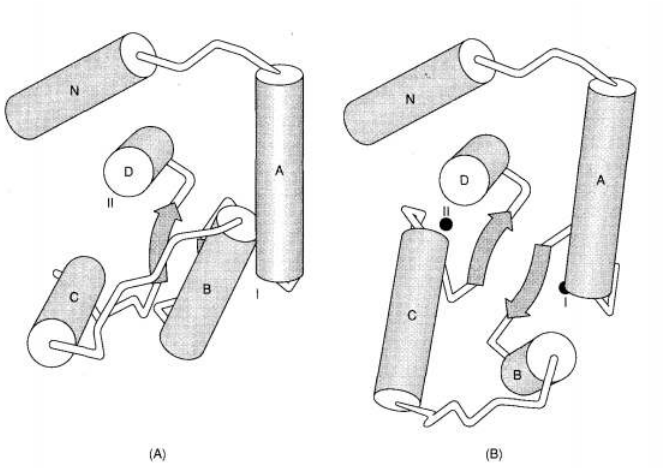


Figure kindly provided by N. C. J. Strynadka and M. N. G. James.

However, preliminary structure calculations[114] of the calcium-saturated and calcium-free forms of calbindin D_{9k} indicate that much more subtle conformational changes take place upon binding Ca^{2+} in calbindin D_{9k}. Interestingly, ^{1}H NMR spectroscopy has provided evidence for the concept that the structural change induced by Mg^{2+} binding to the C-terminal domain of sTnC must be very similar to that induced by Ca^{2+} ions. Another result obtained by ^{113}Cd NMR studies[108] is that the cadmium-loaded N-terminal domain of sTnC in solution undergoes a rapid interchange between two or more conformations, with an exchange rate on the order of 10^{3}-10^{4} s^{-1}.

Just as CaM exerts its biological function in complexes with other proteins, TnC participates in the three-protein troponin complex. It presently appears that TnC and TnI form a primary complex that is anchored by TnT to a binding site on tropomyosin.[115] In the troponin complex the Ca^{2+} affinity is increased by a factor of about ten over that in isolated sTnC, both at the Ca^{2+}-Mg^{2+} sites and at the Ca^{2+}-specific sites. A similar increase in affinity is found for Mg^{2+}. Given the amounts of "free" Mg^{2+} inside muscle cells (1 to 3 mM), it seems likely that the Ca^{2+}-Mg^{2+} sites in the resting state of troponin are filled with Mg^{2+}, so that a transitory release of Ca^{2+} leads primarily to rapid Ca^{2+} binding to the Ca^{2+}-specific sites, and subsequently to conformation change and contraction.

11.2.3.15: Troponin C is shared under a CC BY-NC-SA 4.0 license and was authored, remixed, and/or curated by LibreTexts.

11.2.4: Biological and Synthetic Dioxygen Carriers

I. Introduction

A. Requirements for Effective Oxygen Carriers
1. Thermodynamic Factors[19-20]
2. Kinetic Factors
3. Dioxygen Reactions

B. Biological Oxygen Carriers
1. The Hemoglobin Family
2. The Hemocyanin Family
3. The Hemerythrin Family

C. Hazards of Life with Dioxygen

II. Selected Chemistry of Dioxygen, Iron, Copper, and Cobalt

A. General Aspects of the Chemistry of Dioxygen
1. Redox Chemistry of Free Molecular Dioxygen
2. Geometry and Electronic Structure of Coordinated Dioxygen

B. General Aspects of the Chemistry of Iron
1. Irreversible Oxidation
2. Spectroscopy of the Fe^{III}—O—Fe^{III} Moiety
3. Oxidation and Spin States of Iron Porphyrins

C. General Aspects of the Chemistry of Copper

D. General Aspects of the Chemistry of Cobalt

E. Other Ligands for Biological Oxygen Carriers
1. Carbon Monoxide
2. Nitric Oxide
3. Isocyanide and Nitroso Species

F. Nature of the Metal-Dioxygen Linkage in Biological Systems
1. Oxyhemocyanin and Oxyhemerythrin
2. Oxyhemoglobin
3. A Simple Model for the Electronic Structure of Liganded Hemoglobins

G. Role of the Protein in Effecting Biological Oxygen Transport
1. Provision of Ligands to the Metal
2. Protection of the Metal-dioxygen Moiety
3. Modulation of Ligand-binding Properties

H. Requirements for a Model System for Hemoglobin

III. Structural Basis of Ligand Affinities of Oxygen Carriers

A. Ligand Affinities in Hemoglobins and Their Models

B. General Structural Features that Modulate Ligand Affinity
1. Proximal Effects
2. Distal Effects
3. Approximate Contribution of Proximal and Distal Effects to Ligand Affinity

C. Detailed Structures of Hemoglobins and Model Systems
1. Structures Relevant to Deoxy Hemoglobins
2. Structures Relevant to Liganded Hemoglobins

D. Stereochemical Changes Upon Ligation
1. Structural Changes in Normal-affinity Systems
2. Structural Changes in Low-affinity Systems
3. Structural Changes in High-affinity Systems

IV. Dioxygen Carriers and Bioinorganic Chemistry

V. References

VI. Abbreviations

Contributors and Attributions

- Geoffrey B. Jameson (Georgetown University, Department of Chemistry)
- James A. Ibers (Northwestern University, Department of Chemistry)

11.2.4: Biological and Synthetic Dioxygen Carriers is shared under a CC BY-NC-SA 4.0 license and was authored, remixed, and/or curated by LibreTexts.

11.2.4.1: Biological Dioxygen Transport Systems

Most organisms require molecular oxygen in order to survive. The dioxygen is used in a host of biochemical transformations, although most is consumed in the reaction

$$O_2 + 4H^+ + 4e^- \rightarrow 2H_2O \tag{4.1}$$

that is the terminal (or primary) step of oxidative phosphorylation (Chapters 5 and 6). For some small animals and for plants, where the surface-to-volume ratio is large, an adequate supply of dioxygen can be obtained from simple diffusion across cell membranes. The dioxygen may be extracted from air or water; for plants that produce dioxygen in photosynthesis, it is also available endogenously. For other organisms, particularly those with non-passive lifestyles, from scorpions to whales, diffusion does not supply sufficient dioxygen for respiration.

An elegant three-component system has evolved to transport dioxygen from regions of high abundance—water (at least if free of pollutant reductants) and air—to regions of relatively low abundance and high demand—the interior cells of the organism. This process is illustrated in Figure 4.1.[1-3]

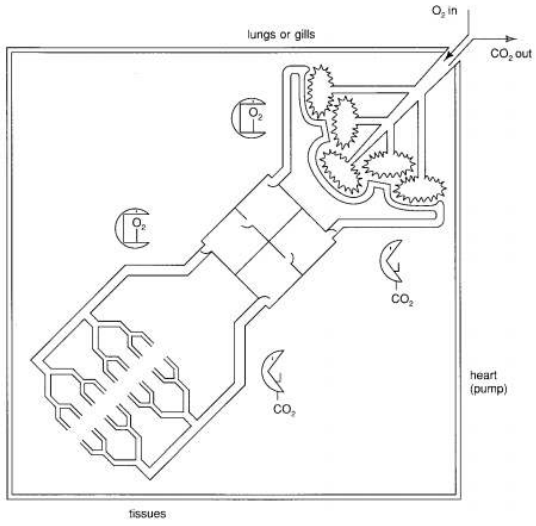


Figure 4.1: Oxygen sequestration and transport in the generalized organism Squarus squorur. The surface area of lungs or gills is typically 1-2 orders of magnitude greater than the external surface area of the organism.

The central component is a dioxygen-carrier protein. In the three chemically distinct carriers that have evolved and are found today, the dioxygen-binding site in the protein, that is, the so-called "active site," is a complex either of copper or of iron.[4-6] For hemoglobins, the most widely distributed family of dioxygen carriers, the active site has long been known to consist of an iron porphyrin (heme) group embedded in the protein. Almost all hemoglobins share the basic structure illustrated in Figure 4.2.[7-12] Hemocyanin[13-15] and hemerythrin,[16-18] the other two biological dioxygen carriers, feature pairs of copper atoms and iron atoms, respectively, at the active sites.* Some basic properties of these metalloproteins are summarized in Table 4.1.[4-6]



(A) Fe^{II} protoporphyrin IX (heme b) [hemoglobins and erythrocruorins]

(B) Chloroheme [chlorocruorin]

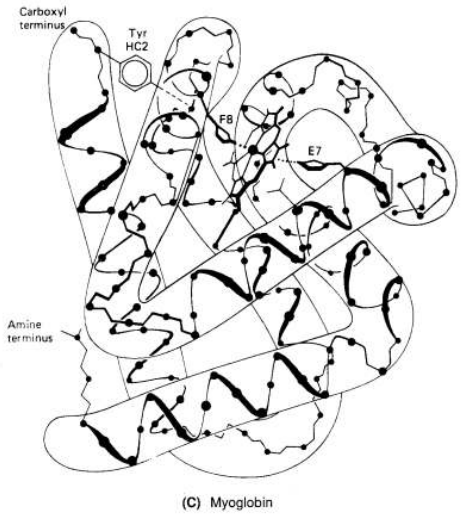


Figure 4.2: Heme groups used in hemoglobin: (A) Protoporphyrin IX (heme b), (hemoglobins and erythrocruorins); (B) Chloroheme (chlorocruorin); (C) The encapsulation of the heme molecule in myoglobin.[11a] Reproduced with permission from M. F. Perutz, Nature **228** (1970), 726-737.

Table 4.1: General Features of Dioxygen-carrier Proteins

https://chem.libretexts.org/@go/page/438026

Metalloprotein	Active Site of deoxy
Hemoglobins	
Vertebrate	
Human A	heme Fe^{II}
Invertebrate	
Erythrocruroin (*Lumbricus terrestris*, earthworm)	heme Fe^{II}
Chlorocruorn *(Eudistylia vancouveri)*	chloroheme Fe^{II}

		green
Hemocyanins		
Mollusc (*Helix pomatia*-α, edible snail)	$Cu^{I} \ldots Cu^{I}$	colorless/blue
Arthropod (*Cancer magister*, crab)	$Cu^{I} \ldots Cu^{I}$	colorless/blue
Hemerythrins (*Phascolopsis* syn. *golfingia gouldii*)	$Fe^{II} \ldots Fe^{II}$	b

urgundy

* The use of the prefix *hem-* is confusing. In this context *hem* connotes blood. Thus, since hemocyanin and hemerythrin lack a heme group [an iron(II) porphyrin], they are nonheme metalloproteins.

The second component of the dioxygen-transport system facilitates the sequestration of dioxygen by the dioxygen-carrier protein. Specialized organs, such as lungs in air-breathing creatures or gills in fish, offer a very large surface area to the outside environment in order to facilitate diffusion. The third component is the delivery system. The oxygen carrier is dissolved or suspended in a fluid, called blood plasma or hemolymph, that is pumped throughout the animal by another specialized organ, the heart, through a network of tubes, the blood vessels. In many organisms an additional dioxygen-binding protein, which stores dioxygen, is located in tissues that are subject to sudden and high dioxygen demand, such as muscles. These dioxygen-storage proteins are prefixed *myo-* (from the Greek root *mys* for muscle). Thus for the dioxygen-transport protein hemerythrin there exists a chemically similar dioxygen-storage protein myohemerythrin. For the hemoglobin family the corresponding storage protein is called myoglobin. Interestingly, some organisms that use hemocyanin as the dioxygen-*transport* protein use myoglobin as the dioxygen-*storage* protein.

At the center of biological dioxygen transport are transition-metal complexes of iron or copper. To model such systems, chemists have prepared several synthetic oxygen carriers, especially of iron and cobalt porphyrins. In this chapter the structures and properties of biological and nonbiological oxygen carriers are described, with particular attention to the hemoglobin family. This family has been studied in more detail than any other group of proteins, and as a result a deeper understanding of the relationships among structure, properties, and biological function (i.e., physiology) exists. The central focus of this chapter is to delineate chemical features that determine the affinity of an active site, especially an iron porphyrin, for molecular oxygen. In order to develop this theme, macroscopic (thermodynamic and kinetic) factors associated with dioxygen binding and release are summarized first. The nonbiological chemistry of iron and copper in the presence of dioxygen is described briefly to elucidate the key role that the protein plays in supporting oxygen transport by preventing irreversible oxidation of the binding site or of its ligands. The macroscopic behavior of the biological systems is related to the microscopic picture that has been developed over the last 30 years from x-ray crystallographic studies and a miscellany of spectroscopic probes of the oxygen-binding site. Relationships between the geometry and charge distribution in the metal-dioxygen moiety and the nature of the interactions between this moiety and its surroundings are examined. Nonbiological dioxygen carriers have proved particularly useful in providing precise and accurate structural information as well as thermodynamic and kinetic data against which the corresponding data from biological oxygen carriers can be contrasted.

The bioinorganic chemistry of the hemoglobin family of oxygen binders is particularly amenable to study by means of small-molecule model systems: four of the five ligands that make up the active site are provided by a square-planar tetradentate ligand, the protoporphyrin IX dianion (Figure 4.2). One axial ligand in hemoglobin, imidazole from a histidine residue, is provided by the protein, and the remaining sixth coordination site is available for the exogenous ligand, e.g., dioxygen or carbon monoxide. Thus a model system that approximates the stereochemistry of the active site in hemoglobin may be assembled from an iron(II) porphyrin and a ligand, such as imidazole or pyridine. On the other hand, in hemocyanin and hemerythrin most of the ligands are supplied by the protein. Thus the assembly of a model system that provides appropriate ligands correctly disposed around the pair of metal atoms poses a major synthetic challenge, especially for hemocyanin, where details on the number, type, and arrangement of ligands have been difficult to establish. Many aspects of the physical, inorganic, and structural chemistry underlying biological oxygen transport and utilization (Chapter 5) have been clarified through model systems.

11.2.4.1: Biological Dioxygen Transport Systems is shared under a CC BY-NC-SA 4.0 license and was authored, remixed, and/or curated by LibreTexts.

11.2.4.2: Biological Oxygen Carriers

As noted earlier, three solutions to the problem of dioxygen transport have evolved: hemoglobin (Hb), hemocyanin (Hc), and hemerythrin (Hr). Their remarkable distribution over plant and animal kingdoms is shown in Figure 4.8.[15]

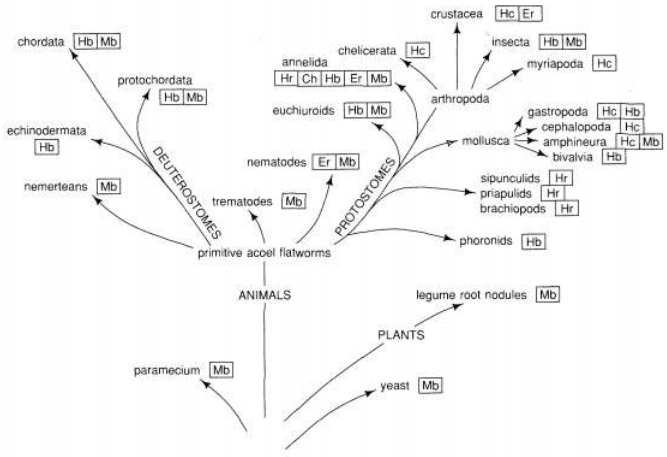


Figure 4.8 - Phylogenetic distribution of oxygen-carrier proteins: Hb, hemoglobin; Mb, myoglobin; Er, erythrocruorin; Ch, chlorocruorin; He, hemocyanin; Hr, hemerythrin.[15a] Reproduced with permission from K. E. van Holde and K. I. Miller, Quart. Rev. Biophys. **15** (1982), 1-129.

The hemoglobins and myoglobins found in plants, snails, and vertebrates all appear to share a common, very ancient ancestor. There is some evidence now for a common ancestral hemocyanin.[42c] The appearance of hemerythrin in a few annelid worms is an evolutionary curiosity. These few words and the diagram will suffice to give some hints about how respiratory proteins evolved, a subject that is outside the scope of this book.

The Hemoglobin Family

Hemoglobins are the most evolutionarily diverse family of dioxygen carriers. They are found in some plants (e.g., leghemoglobin in the nitrogen-fixing nodules of legumes), many invertebrates (including some insect larvae), crustaceans, molluscs (especially bivalves and snails), almost all annelid worms, and in *all* vertebrates with one possible exception, the Antarctic fish *Cyclostomata*.

With few exceptions the monomeric and oligomeric hemoglobins all share a basically similar building block: a single heme group is embedded in a folded polypeptide with a molecular weight of about 16 kDa (see Figure 4.2), and is anchored to the protein by coordination of the iron center to an imidazole ligand from a histidine residue. Mammalian myoglobin is often taken as the archetypical myoglobin (see Table 4.1). Sperm whale, bovine, or equine myoglobin are specific examples; the muscle tissue from which they may be extracted is more available than that from *Homo sapiens*. The archetypical oligomeric hemoglobin that shows cooperative binding of O_2 is the tetrameric hemoglobin A. It is readily available from the blood of human donors.* In some invertebrate hemoglobins, especially those of annelids, aggregates may contain as many as 192 binding sites, to give a molecular weight of about 3 x 10^6 Dalton. These and other high-molecular-weight hemoglobins of arthropods are often referred to as erythrocruorins (Er). In a few annelid worms, the otherwise ubiquitous heme b or protoheme is replaced by chloroheme (see Figure 4.2) to give chlorocruorins (Ch), which tum green upon oxygenation (*chloros*, Greek for green). Some organisms, for example the clam *Scapharca equivalvis*, feature a dimeric hemoglobin.

The only known anomalous hemoglobin is Hb *Ascaris*, which comes from a parasitic nematode found in the guts of pigs. It has a molecular weight of about 39 kDa per heme; this value is not a multiple of the myoglobin building block.[31] Moreover, presumably in response to the low availability of O_2 in pigs' guts, Hb *Ascaris* has an extraordinarily high affinity for dioxygen, in large part owing to an extremely slow rate of dioxygen release.[32] Leghemoglobin is another carrier with a high affinity for dioxygen, in this case because of a high rate of O_2 binding. Since O_2 is a poison for the nitrogenase enzyme, yet the nodules also require dioxygen, diffusion of O_2 is facilitated, but the concentration of free dioxygen in the vicinity of nitrogen-fixing sites is minimized.[33]

Kinetic and thermodynamic data for dioxygen binding and release from a variety of hemoglobins are summarized in Table 4.2.[9,10,31,34-36] Notice that for the hemoglobin tetramer, which comprises two pairs of slightly dissimilar subunits, the α and β

chains bind O_2 with significantly different affinities and rate constants, especially in the T state. Isolated chains behave like monomeric vertebrate hemoglobins, such as whale myoglobin, which have affinities close to those of R-state hemoglobin. The chlorocruorins have a low affinity compared to other erythrocruorins. Especially for proteins that bind O_2 cooperatively, a range of values is specified, since affinities and rates are sensitive to pH, ionic strength, specific anions and cations (allosteric effectors), and laboratory. For example, as we noted above, the O_2 affinity of hemoglobin A is sensitive to the concentration of 2,3-DPG and to pH (Bohr effect). Trout hemoglobin I is insensitive to these species, whereas a second component of trout blood, trout hemoglobin IV, is so sensitive to pH (Root effect) that at pH < 7 trout hemoglobin IV is only partially saturated at $P(O_2)$ = 160 Torr.[4] Note that O_2 affinities span five orders of magnitude. Since heme catabolism produces carbon monoxide, and since in some environments CO is readily available exogenously, selected data for CO binding are also presented.

---

* Blood from human donors is also a source for a variety of abnormal hemoglobins, the most famous of which is HbS, the hemoglobin giving rise to sickle-cell anemia, It was Pauling and coworkers[30] who first found that HbS differs from HbA through the *single* substitution of valine for glutamic acid in each of two of the four subunits comprising Hb, Sickle-cell anemia was the first condition to be denoted a "molecular disease."

The Hemocyanin Family

Hemocyanins (Hc), the copper-containing dioxygen carriers, are distributed erratically in two large phyla, *Mollusca* (for example, octopi and snails) and *Arthropoda* (for example, lobsters and scorpions). The functional form of hemocyanin consists of large assemblies of subunits.[14,15,37] In the mollusc family the subunit has a molecular weight of about 50 kDa and contains two copper atoms. From electron-microscopic observations, hemocyanin molecules are cylindrical assemblies about 190 or 380 Å long and 350 Å in diameter comprising 10 or 20 subunits, respectively, for a molecular weight as high as 9×10^6 Dalton. In the arthropod family, the subunit has a molecular weight of about 70 kDa with two copper atoms. Molecular aggregates are composed of 6, 12, 24, or 48 subunits. Upon oxygenation the colorless protein becomes blue (hence cyanin from *cyanos*, Greek for blue). Spectral changes upon oxygenation, oxygen affinities, kinetics of oxygen binding (Table 4.2),[4.5,14,15,38] anion binding, and other chemical reactions show that the active site in the phylum *Arthropoda* and that in *Mollusca*, although both containing a pair of copper atoms, are not identical.[4,14]

No monomeric hemocyanins, analogous to myoglobin and myohemerythrin (next section), are known. For some hemocyanins the binding of dioxygen is highly cooperative, if calcium or magnesium ions are present, with Hill coefficients as high as n ~ 9. However, the free energy of interaction per subunit can be small in comparison with that for tetrameric hemoglobin; 0.9 to 2.5 kcal/mol compared to 3.0 kcal/mol. Allosteric effects, at least for a 24-subunit tarantula hemocyanin, can be separated into those within a dodecamer (12 subunits)—the major contributor to overall allostery—and those between dodecamers.[39c] This has been termed *nested allostery*. In contrast to the hemoglobin family, isolated chains have affinities typical of the T-state conformation for hemocyanin. The binding of CO, which binds to only one copper atom, is at best weakly cooperative.[39]

As alluded to above, the distribution of hemocyanins is striking, Among the molluscs exclusive use of hemocyanin as the respiratory protein occurs only with the cephalopods (squid, octopi, and cuttlefish), and in the arthropods only among the decapod (ten-footed) crustaceans (lobsters, shrimp, and crabs). The bivalve molluscs (for example, oysters and scallops) all use small dimeric or octameric hemoglobins. The edible gastropod (snail) *Helix p*omatia uses hemocyanin, whereas the apparently closely related fresh-water snail *Planorbis* uses a high-oligomer hemoglobin. Both use a myoglobin as the oxygen-storage protein. The structure of the active site has been extensively probed by EXAFS methods,[40,41] and the x-ray crystal structure of a hexameric deoxyhemocyanin is known.[42] Each copper atom is coordinated to three imidazole groups from histidine residues. The pinwheel arrangement of the six subunits, the domain structure of a single subunit, and the domain containing the active site are shown in Figure 4.9.

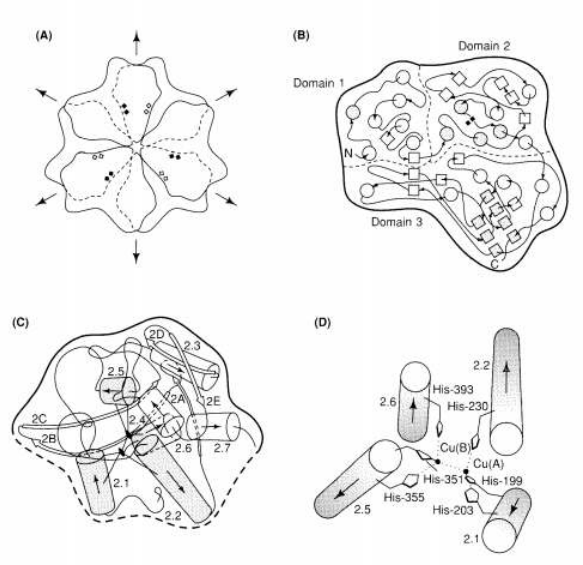


Figure 4.9 - Diagram of the structure of deoxyhemocyanin from Panulirus interruptus at 3.2 Å resolution:[42c] (A) The hexameric arrangement of subunits; (B) The domain structure of one subunit; (C) The tertiary structure of domain 2, which contains the pair of copper atoms: α-helices are represented by cylinders; β-strands by arrows, and copper atoms by diamonds; (D) The active site and its histidine ligands. Reproduced with permission from B. Linzen, Science **229** (1985), 519-524.

The Hemerythrin Family

The biological occurrence of hemerythrins (Hr in Figure 4.8), the third class of dioxygen carriers, is relatively rare, being restricted to the sipunculid family (nonsegmented worms), a few members of the annelid (segmented worm) family, a couple of brachiopods (shrimps), and a couple of priapulids. The oxygen-binding site contains, like hemocyanin, a pair of metal atoms, in this case, iron. Upon oxygenation the colorless protein becomes purple-red. Monomeric (myohemerythrin), trimeric, and octameric forms of hemerythrin are known; all appear to be based on a similar subunit of about 13.5 kDa. When hemerythrin is extracted from the organism, its oxygen binding is at best only weakly cooperative, with Hill coefficients in the range 1.1 to 2.1.[18] In coelomic cells (the tissue between the inner membrane lining the digestive tract and the outer membrane of the worm—analogous to flesh in vertebrates), oxygen apparently binds with higher cooperativity (n ~ 2.5).[43] Perchlorate ions have been observed to induce cooperativity: since ClO_4^- has no biological role, it appears that in protein purifications the biological allosteric effector is lost. No Bohr effect occurs. Dioxygen binding data are accumulated in Table 4.2.[36,44]

The structure of hemerythrin in a variety of derivatives (oxy, azido, met, and deoxy) is now well-characterized. With three bridging ligands, a distinctive cofacial bioctahedral stereochemistry is seen (Figure 4.10).[45-48]

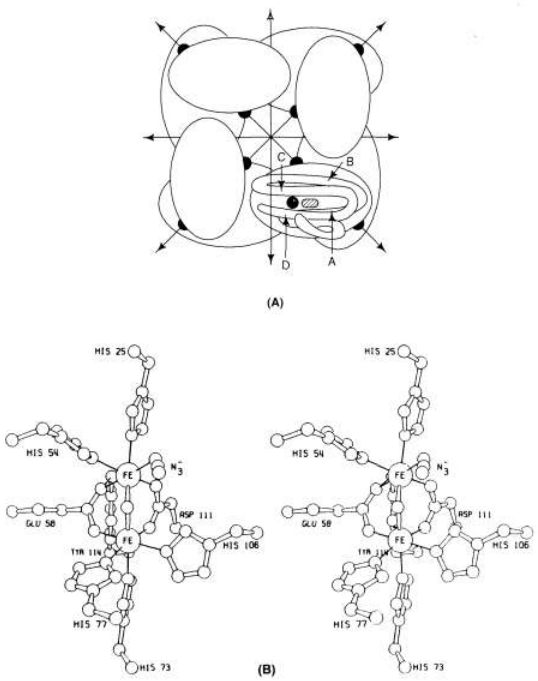


Figure 4.10 - Structure of hemerythrin: (A) The tertiary structure of octameric hemerythrin[46b] with four (α-helices (A, B, C, D) of one of the eight subunits. The filled half-circles denote anion binding sites (e.g., ClO_4^-); the filled circle the Fe_2 site; and the cross-hatched oval the N_3^- and SCN^- binding sites $(Fe^{III})_2$ and the O_2 binding sites $(Fe^{II})_2$. Reproduced with permission from R. E. Stenkamp, L. C. Sieker, and L. H. Jensen, J. Mol. Biol. **126** (1978), 457-466. (B) The structure of the active site of metazidomyohemerythrin,[48] showing the cofacial bioctahedral stereochemistry. The structure of oxyhemerythrin is very similar, including the orientations of the $(H)O_2{}^{II}$Iigand.[45] Reproduced with permission from S. Sheriff, W. A. Hendrickson, and J. L. Smith, J. Mol. Biol. **197** (1987), 273-296.

Table 4.2 - Thermodynamics and kinetics of ligand binding to biological oxygen carriers (at 20-25 °C and buffered at pH 6.5-8.5).

Solubility of O2 in water: 1.86×10^{6} M/Torr

Solubility of CO in water: 1.36×10^{-6} M/Torr

a) 10 mM Ca^{2+} added: necessary for cooperativity

b) CO binding at pH 9.6.

Carrier	Dioxygen binding					Carbon Monoxide Binding				
	$P_{1/2}(O_2)$ Torr	∇H kcal/mol	∇S eu	k_{on} $\hbar M^{-1}s^{-1}$	k_{off} s^{-1}	$P_{1/2}(O_2)$ Torr	∇H kcal/mol	∇S eu	k_{on} $\hbar M^{-1}s^{-1}$	k_{off} s^{-1}
Hemoglobins										
Hb *Ascaris*	0.0047	—	—	1.5	0.0041	0.063	—	—	0.21	0.018
Leg Hb	0.047	-18.9	—	156.	1.	0.00074	—	—	13.5	0.012
whale Mb	0.51	-14.9	—	14.	12.	0.018	-13.5	—	0.51	0.019
Whale Mb	—	—	—	140.	1600.	—	—	—	—	—
HbA isolated chains - α	0.74	-142	-21.	50.	28.	0.0025	—	—	4.0	0.013
HbA isolated chains - β	0.42	-16.9	-29	60.	16.	0.0016	—	—	4.5	0.008
HbA R α chain	0.15-1.5	-18.	-30.	29.	10.	0.001-0.004	—	—	3.2	0.005
HbA R β chain	0.15-1.5	-18.	-30.	100.	21.	0.001-0.004	—	—	9.8	0.009
HbA R α E7His→Gly				220.	620.				19.	0.007
HbA R β E7His→Gly				100.	3.				5.0	0.0013
HbA T α chain	9-160	-12	-35	2.9	183.	0.10-2.8	—	—	0.099	0.09
HbA T β chain	9-160	-12	-35	11.8	2500.	0.10-2.8	—	—	0.099	0.09
Chironimus Mb	0.40	—	—	300.	218.	0.0019	—	—	27.	0.095
Glycera Mb	5.2	—	—	190.	1800.	0.00089	—	—	27.	0.042
Aplysia Mb	2.7	-13.6	—	15.	70.	0.013	—	—	0.49	0.02
Spriographis chlorocruorin	16-78	-4.5	—	—	—	—	—	—	—	—
Hemocyanins[a]										

Carrier	$P_{1/2}(O_2)$ Torr	∇H kcal/mol	Dioxygen ∇S eu	binding k_{on} $M^{-1}s^{-1}$	k_{off} s^{-1}	$P_{1/2}(O_2)$ Torr	Carbon ∇H kcal/mol	Monoxide ∇S eu	Binding k_{on} $M^{-1}s^{-1}$	k_{off} s^{-1}
Mollusca n Hc										
Helix pomatia R	2.7	-11.5	-12.6	3.8	10.	10.	-13.5	-24	0.66	70.
Helix pomatia T	55.	-15.4	-31.1	1.3	300.	CO	binding	noncoope rative	since not	measurea ble
Levantina hierosohimia R	3.8	-7.5	-1.8	—	—	—	—	—	—	—
Levantina hierosohimia T	18.	+3.1	+31.	—	—	—	—	—	—	—
Arthropo d Hc										
Panulirus interruptus R[b]	1.0	—	—	31.	60.	720.	-6.0 CO	-2.7 binding	4.1 noncoope rative	8100.
P. interruptus monomer	9.3	—	—	57.	100.	—	—	—	—	—
Leirus quinquestris R	1.7	-7.4	0.	—	—	—	—	—	—	—
Leirus quinquestris T	117.	+3.1	+27.	—	—	—	—	—	—	—
Hemeryt hrins										
Phascolopsis gouldii	2.0	-12.4	-18	7.4	56	not	known	to	bind	CO
Themiste zostericola 8-mer	6.0	—	—	7.5	82					
T. zostericol	2.2	—	—	78.	315.					

Carrier	$P_{1/2}(O_2)$ Torr	ΔH kcal/mol	Dioxygen ΔS eu	binding k_{on} $\mu M^{-1}s^{-1}$	k_{off} s^{-1}	$P_{1/2}(O_2)$ Torr	Carbon ΔH kcal/mol	Monoxide ΔS eu	Binding k_{on} $\mu M^{-1}s^{-1}$	k_{off} s^{-1}
a monomer										

11.2.4.2: Biological Oxygen Carriers is shared under a CC BY-NC-SA 4.0 license and was authored, remixed, and/or curated by LibreTexts.

11.2.4.3: Detailed Structures of Hemoglobins and Model Systems

With thermodynamic background and general structural features relevant to ligand affinity enumerated, attention may now be turned to the detailed structural aspects of the active site and its surroundings. As was shown crudely in Figure 4.3, the ligand affinity of an iron porphyrin may be perturbed either by modulating the structure of the deoxy material or by modulating the structure and surroundings of the liganded material or both. The model systems provide the reference points against which the protein structures may be compared.

Structures Relevant to Deoxy Hemoglobins

The structure of the picket-fence porphyrin compound, Fe(PF)(2-MeIm), is shown in Figure 4.28.[172] Minus the pickets, it is essentially a magnified view of the active site of deoxymyoglobin, shown in Figure 4.29.[181] Some metrical details of these structures, of a very similar unsubstituted tetraphenylporphyrin,[110] and of several other deoxyhemoglobins[11c,182-185] are listed in Table 4.7. In general they are all similar, but important differences exist.

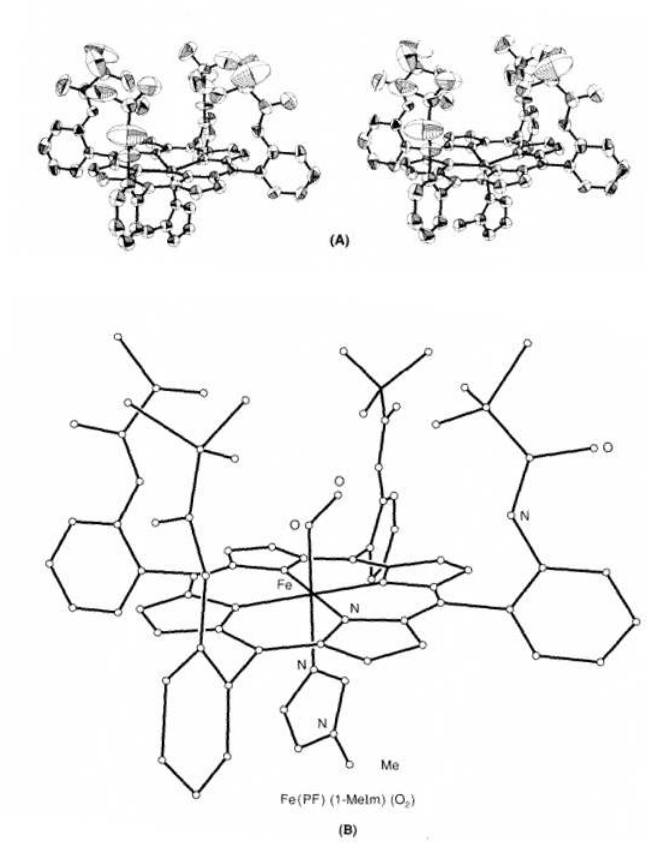


Figure 4.28 - (A) Stereodiagram of the structure of Fe(PF)(2-MeIm).[172] (B) Structure of Fe(PF)(1-MeIm)(O_2).[187]

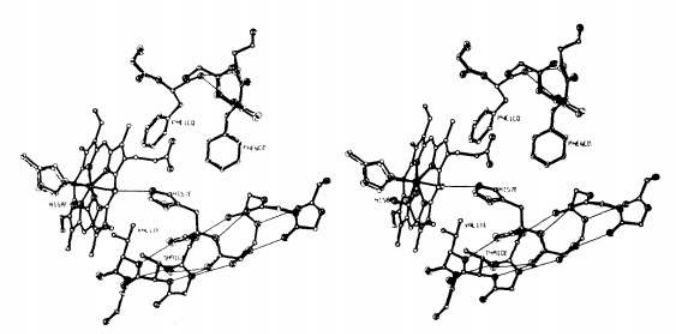


Figure 4.29 - Structure of metmyoglobin and deoxymyoglobin at 2.0 Å resolution near the heme.[181a] Solid bonds are for metmyoglobin; open bonds for deoxymyoglobin. Note the water molecule coordinated to the iron center and hydrogen bonded to the distal imidazole group in metmyoglobin. Reproduced with permission from T. Takano, J. Mol. Biol. **110** (1977), 569-584.

Table 4.7 - Metrical detalis of deoxyhemoglobins and their models[a]

a) See Figure 4.25 for definition of symbols.

b) From a difference refinement of CoHb vs. Hb, where the difference in metal-to-porphyrin-plane separation was 0.24(2) Å and the difference in M-N_{Im} was 0.13(4) Å. Doming is similar to Hb.

Compound	Resol. (Å)	Fe-N_p (Å)	Fe • • • Porp (Å)	Doming (Å)	Fe—N_{Im} (Å)	ϕ (deg)	Tilt (deg)
Fe(PF)(2-Melm)	—	2.072(5)	0.43	0.03	2.095(6)	22.8	9.6
Fe(TPP)(2-Melm)	—	2.086(6)	0.40	0.13	2.161(5)	7.4	10.3
Mb	1.4	2.03(10)	0.42	0.08	2.22	19	11
Er • • • H_2O	1.4	2.02	0.17	-0.06	2.25	7	3
HbA (α • • • H_2O)	1.74	2.08(3)	0.40(5)	0.16(6)	2.16(6)	18(1)	12(2)
HbA (β • • • H_2O)	1.74	2.05(3)	0.36(5)	0.10(6)	2.09(6)	24(1)	11(2)
CoHb[b]	2.5	—	0.14(5)	0.13	2.24(6)	—	—
Co(TPP)(1-MeIm)	—	1.977(6)	0.13	0.01	2.157(3)	3.8	0
Co(TPP)(1,2-Me_2Im)	—	1.985(3)	0.15	0.05	2.216(2)	10	—

In all structures, except deoxyerythrocruorin,[183] the iron atom is displaced about 0.4 to 0.5 Å from the plane of the porphyrin toward the axial base. For deoxyerythrocruorin the displacement is less than half this, perhaps because the water molecule is weakly coordinated to the iron center.

An imidazole group from a histidine residue—the distal histidine E7 in position 7 on helix labeled E—hovers over the binding site for most vertebrate hemoglobins, except for genetically engineered mutants of human hemoglobin (βE7His → Gly), pathological mutant hemoglobins, such as hemoglobin Zürich (βE7His → Arg), and some others, such as elephant hemoglobin. Long believed to be noncoordinating, this distal histidine may, in fact, coordinate weakly to the Fe center at low temperature.[159] In the α chains of human deoxyhemoglobin, hemoglobin A, a water molecule is found in the binding cavity.[182] For many years the binding cavity has been referred to as the hydrophobic pocket—literally, water-hating. Although many hydrophobic groups, such as valine, leucine, isoleucine, and phenylalanine are positioned over the porphyrin, the immediate environment around the binding site is, in fact, polar, with the distal histidine and associated water molecules, as well as the heme group itself. As will be shown in the next

section, the label "hydrophobic pocket" becomes more misleading when the interaction of coordinated ligands with distal groups is examined.

The orientation of the axial base, angle ϕ_1, is similar for Fe(PF)(2-MeIm) and for several vertebrate deoxyhemoglobins. On the other hand, Fe(TPP)(2- Melm) and deoxyerythrocruorin have a similar eclipsed axial-base orientation. At least for five-coordinate species, where the iron center is substantially out of the porphyrin plane, orientation of the axial base does not invariably induce structural perturbations, e.g., doming, in the porphyrin skeleton.

The conformation of the protein chain is such that the proximal histidine in deoxyhemoglobin coordinates in a slightly tilted manner,[182,186] comparable to the tilt that the sterically active 2-methyl substituent induces in the synthetic systems.[172] Clearly, coordination of the histidine to the heme in a symmetric manner, as would be expected in the absence of the protein constraints, does *not* produce the conformation of lowest free energy for the *whole* molecule.

11.2.4.3: Detailed Structures of Hemoglobins and Model Systems is shared under a CC BY-NC-SA 4.0 license and was authored, remixed, and/or curated by LibreTexts.

11.2.4.4: Dioxygen Carriers and Bioinorganic Chemistry

To the student the subject of biological and synthetic molecular-oxygen carriers offers unusual insights into how bioinorganic chemistry works and what its aims and uses are. First, consider another bioinorganic problem, that of the nature of the blue copper proteins. When bioinorganic chemists entered the scene, the nature, function, and structure of copper blues were largely unknown. To take a Cu(lI) solution, add a nitrogen base, and obtain a spectrum that "resembled" that of the proteins was not a contribution to the solution of the biological puzzle, although it was the activity of some bioinorganic chemists. The difficulty here was that too little was known about the protein system. But the challenge did not diminish once the structure of a blue copper protein was known, for that structure allowed definition of the active site, one that contained (in the oxidized form) a Cu(lI) center surrounded by two imidazole, one cysteine, and one methionine residue. Now the bioinorganic chemist was faced with the formidable (and still incompletely solved) synthetic problem of designing a tetradentate ligand that (i) would present two N atoms, one thiolate S atom, and one thioether SR_2 group to a Cu(lI) center and (ii) would remain intact if the Cu(lI) center were reduced to Cu(I). If we could prepare such complexes, we would be in a position to examine in some detail the effects on physical properties, such as redox potentials or spectra, of chemical substitution. In other words, we could learn about structure-function relationships in the copper blues. But the risks involved included the possibility that the specially designed ligand, even if it could be synthesized, might not bind Cu(Il) or Cu(l) in the desired manner.

Contrast such a situation with that of the oxygen carriers. Hemoglobin[208] and myoglobin[209] were the first crystallized proteins to have their structures determined. Their functions were well-known. They had been studied by a wide variety of physical techniques, in part because their structures were known, and even before that because of their role in human health. The central tetradentate ligand of the heme group, namely, the porphyrin, was well-defined and much porphyrin chemistry was known. The structural puzzles that intrigued chemists and biologists were not answered in the initial, early structural studies of the proteins; for example, how is O_2 bound and why is CO not bound more firmly? Model chemistry in this area looked as though it would be easy; after all, the metalloporphyrins were readily synthesized, and all one needed was an axial base, some spectroscopic equipment, perhaps some single crystals, and then the structure-function relationships in the biological oxygen carriers would be understood! Indeed, as often happens, the situation was more complicated than it appeared. The irreversible oxidation of iron porphyrins was a major stumbling block to simple modeling. This obstacle was overcome in solution studies through the use of low temperatures and aprotic solvents; some very useful measurements of O_2 and CO binding were made on model systems in such solutions. But in order to isolate oxygen complexes so that they could be studied by diffraction methods, another approach, that of synthesizing elaborated porphyrins, such as those in Figure 4.23, was necessary. This task entailed difficult organic chemistry that ultimately led to successful models that proved to be stable under ambient conditions. From such models we have learned much about local stereochemistry and, through spectroscopic congruence, about the biological systems. In short, bioinorganic chemistry has made a major contribution to the understanding of biological molecular-oxygen carriers, primarily because knowledge of the biological systems was advanced, the systems "self-assemble," and the goals of the studies were well-defined.

The complementarity of the two approaches continues. There are several unanswered questions, including:

1. What is the structural basis for cooperativity? Indeed, is there a structural basis at all, or is the ~6 kcallmol that represents the effect spread over many interactions, so that there is no obvious structural effect to be modeled?
2. Can one design a model where hydrogen bonding to the bound O_2 molecule can be demonstrated by diffraction experiments? How will the oxygen uptake properties depend on the strength of the hydrogen bond?
3. Can one design a "high-affinity" model system? What will this tell us about the largely ill-defined high-affinity systems that are found in Nature?

There remain many intriguing questions about biological molecular-oxygen carriers, questions that will be answered by complementary studies on the biological and model systems. To make and study such model systems is an example of the challenge and excitement of this aspect of bioinorganic chemistry.

11.2.4.4: Dioxygen Carriers and Bioinorganic Chemistry is shared under a CC BY-NC-SA 4.0 license and was authored, remixed, and/or curated by LibreTexts.

11.2.4.5: General Aspects of the Chemistry of Cobalt

Many parallels exist between the chemistry of Fe^{II}- and Co^{II}-porphyrinato systems. Dioxygen binds to many Co^{II} complexes to give mononuclear 1:1 $Co:O_2$ complexes with a bent geometry



and dinuclear 2:1 $Co:O_2$ complexes,[64,66] analogous to those described for Fe^{II} systems in Reactions (4.29a) and (4.29b). Indeed, these dinuclear systems were the first nonbiological oxygen carriers to be isolated. The geometry of the dioxygen moiety, spanning two metals, may be *cis* or *trans*:



However, whereas these dinuclear cobalt species are invariably octahedral, dinuclear copper-peroxo species are tetrahedral or distorted square pyramidal.[40,41]

In the late 1960s, 1:1 $Co:O_2$ species were first isolated by use of a combination of low temperatures and specific Schiff-base ligands.[104] It was found that cobalt corrins, such as vitamin B_{12}, also formed 1:1 dioxygen adducts,[105] although this chemistry is not known to be utilized by living systems.[103] Cobalt(Il) porphyrins also form 1:1 adducts but with low O_2 affinity, especially in nonpolar, aprotic solvents. Thus hemoglobin and myoglobin may be reconstituted from a cobaltoheme with preservation not only of dioxygen-binding capabilities but also of cooperativity.[106] The synthetic 1:1 $Co:O_2$ complexes have proven to be very useful in increasing our understanding of factors that determine oxygen affinity for cobalt systems and by extrapolation for iron systems. Two important differences make Co^{II} systems more accessible. First, in contrast to iron systems, the cleavage reaction (4.29c) and redimerization to a μ-oxo species (Reaction 4.29d) do not occur (see Figure 4.15). Thus Co^{II} complexes of O_2 are stable in solution at room temperature without the need for protection illustrated in Figure 4.14. Second, for Co^{II}-porphyrinato systems, the equilibrium constant for the addition of a second axial base, such as pyridine or 1-methylimidazole, is small. Thus the disproportionation to four-coordinate and six-coordinate species that occurs for corresponding Fe^{II} systems (Reaction 4.33) does not occur. This difference simplifies the interpretation of spectral changes that are used to obtain thermodynamic and kinetic parameters of which there are now voluminous examples.[66]

Moreover, the 1:1 Co-O_2 complexes are paramagnetic. From the small ^{59}Co hyperfine splitting, it is deduced that the single unpaired electron resides primarily on the dioxygen moiety.[104a,105] From other experiments[107] it is apparent that net transfer of electron density from the metal onto the dioxygen varies considerably, from about $0.1e^-$ to about $0.8e^-$. For example, it is found for a given Co^{II} Schiff base, Co(bzacen), that the redox potential of the cobalt-Schiffbase center LCo, measured by cyclic voltammetry, $E_{1/2}$,

$$B_2LCo^{III} + e^- \rightleftharpoons B_2LCo^{II} \tag{4.39}$$

$$B = substituted\ pyridine \tag{11.2.4.5.1}$$

is a linear function of log $K(O_2)$ as the axial base B is varied. The more easily the Co^{II} center may be oxidized, the higher is the O_2 affinity,[103] as illustrated in Figure 4.18A. The dioxygen affinity also increases as the basicity of the axial nitrogenous ligand increases.[104a] This effect is illustrated in Figure 4.18B. Because of differing steric requirements, dimethylformamide (DMF), substituted imidazole, and piperidine (pip) ligands do not fall on the correlation defined by the series of substituted pyridine species. Note the synergistic nature of dioxygen binding: in general, the more electron density that is pumped onto the metal by the axial base, the more electron density is available for donation into the π^* orbitals of the dioxygen ligand. $E_{1/2}$ and log $K(O_2)$ are also correlated, although more weakly, for a number of hemoglobins (Figure 4.18C).[108] Here the porphyrin and axial base remain constant, but presumably the surroundings of the heme group and O_2 binding site vary in a manner that is less well-defined than in the model systems of Figure 4.18A and B. Notwithstanding these various perturbations to the metal center, the O—O stretch occurs at about 1140 cm^{-1}, placing all 1:1 cobalt and iron-dioxygen complexes of nitrogenous and other hard ligands into the superoxo class.*

Cobalt(II) porphyrins and their adducts with diamagnetic molecules invariably have spin S = $\frac{1}{2}$. (See Figure 4.16, but add one electron.) Thus the structural changes are less pronounced than for corresponding iron(II) systems.[110,111] From the similarities in

geometries and differences in electronic structures between cobalt- substituted and native hemoglobins and their models, many insights have been gained about the factors that determine oxygen affinity as well as how cooperativity might, or might not, work at the molecular level.[112,113] The mechanism of cooperativity has also been probed by the substitution of other metalloporphyrins into the globin: for example, zinc porphyrins have been used for their excited triplet-state properties,[114] manganese porphyrins for their EPR activity,[115] and ruthenium porphyrins as a member of the iron triad.[116]

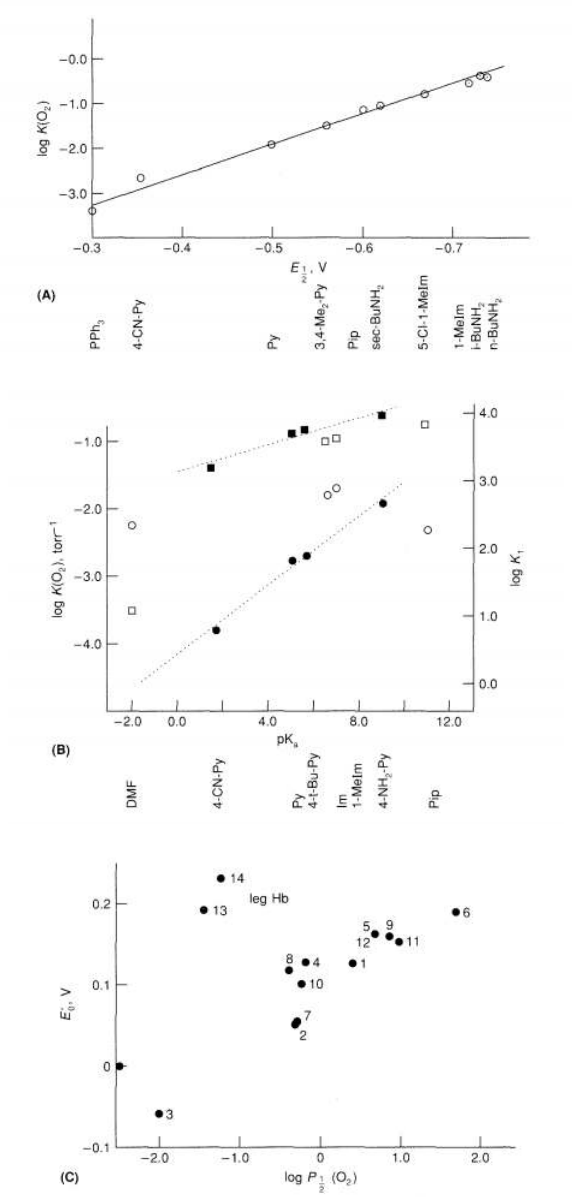


Figure 4.18 - Linear free-energy relationships: (A) Correlation of the O_2 affinity at -21 °C of Co(bzacen)L with the $CO^{III} \rightleftharpoons CO^{II}$ cyclic voltammetric wave of Co(bzacen)L_2 species,[104a] (B) Correlation of ligand affinity with pK_a. Squares (□) *pertain to the binding of L to Co(PPIX) at 23 °C. Circles (◯) pertain to the O_2 affinity at -45 °C of Co(PPIX)L species, Filled shapes pertain to substituted pyridines; the least-squares lines shown are calculated from these data only,*[104a] *(C) Correlation of E°′ (from cyclic voltammetry) with affinity for a miscellany of hemoglobins:*[108] *1, Aphysia limacina Mb; 2, Physeter macrocephalus Mb; 3, Candida mycoderma Hb; 4, Chironomus thummi Hb; 5, Hb_M-Hyde Park; 6, Hb_M-Iwate; 7, Hb α chain; 8, Hb β chain; 9, Hb F; 10, Hb γ chain; 11, HbA; 12, Glycera dibranchiata; 13, IegHb-a; 14, IegHb-c, Reproduced with permission from A, W. Addison and S. Burman, Biochim. Biophys. Acta* ***828*** *(1985), 362-368.*

* Because the O—O stretch may be coupled with other ligand modes,[109] its value should not be used to estimate superoxo character, although in a series of μ-superoxo and μ-peroxo complexes of carefully controlled stereochemistry, small changes in ν(O—O) have been correlated with the pK_a of the suite of ligands.[66]

11.2.4.5: General Aspects of the Chemistry of Cobalt is shared under a CC BY-NC-SA 4.0 license and was authored, remixed, and/or curated by LibreTexts.

11.2.4.6: General Aspects of the Chemistry of Copper

The chemistry of copper in biological systems is limited to oxidation states I and II. The Cu^{I} state has electronic configuration d^{10}. Unless there are ligand bands or strong ligand-to-copper charge-transfer bands, diamagnetic Cu^{I} species are colorless. Complexes of Cu^{II} (d^{9}) are often blue in color. The single unpaired electron makes Cu^{II} amenable to electron paramagnetic resonance (EPR) techniques, at least if the electron spins of Cu^{II} centers are independent of one another. In oxyhemocyanin the spins are so strongly coupled ($-J > 600\ cm^{-1}$) that at room temperature and below the system is effectively diamagnetic and the pair of Cu^{II} ions is EPR silent.[14]

In aqueous solutions the Cu^{I} ion is unstable with respect to disproportionation to Cu metal and Cu^{II} ion:[62]

$$Cu^{II} + 2e^{-} \rightleftharpoons Cu \qquad E^{o} = 0.3402V \tag{11.2.4.6.1}$$

$$Cu^{+} + e^{-} \rightleftharpoons Cu \qquad E^{o} = 0.522V \tag{4.35}$$

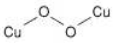
$$2Cu^{+} \rightleftharpoons Cu + Cu^{II-} \qquad E^{o} = 0.182V \tag{11.2.4.6.2}$$

The Cu^{I} state may be stabilized by ligands, especially sulfur-containing ones, or by immobilization as afforded by a protein matrix, or in nonaqueous solvents, such as acetonitrile, in the absence of dioxygen. Whereas Cu^{I} thiolate species are stable, Cu^{II} thiolate species usually are unstable with respect to the disproportionation:[101]

$$2Cu^{II}\text{—}SR \rightarrow 2Cu^{I} + R\text{—}S\text{—}S\text{—}R \tag{4.36}$$

Again, immobilization may give kinetic stability to Cu^{II} thiolate species, as occurs in the blue-copper family of electron-transport proteins.

Copper(l) complexes are often two-coordinate with a linear arrangement of ligands. Three-, four-, and possibly five-coordinate complexes are known.

In the presence of O_2, nonbiological copper(l) [and iron(II)] complexes are often susceptible to ligand degradation, which may give the illusion of O_2 binding.[102] The mechanisms by which this reaction occurs remain essentially unknown. Iron-porphyrin systems are rather more robust. Nonetheless, there are now several well-characterized copper(l) systems that reversibly bind dioxygen,[15b,103] at least at low temperature. One that has been structurally characterized features a 

dicopper(II)-peroxo moiety,[103f] while a second, with more properties in common with oxyhemocyanin, features a 

moiety.[103g]

11.2.4.6: General Aspects of the Chemistry of Copper is shared under a CC BY-NC-SA 4.0 license and was authored, remixed, and/or curated by LibreTexts.

11.2.4.7: General Aspects of the Chemistry of Dioxygen

Redox Chemistry of Free Molecular Dioxygen

Dioxygen has a rich redox chemistry that is not explicitly exploited in the oxygen carriers, but which is central to enzymes that coordinate and activate dioxygen for subsequent reaction with a substrate. On reduction of dioxygen by one electron, the superoxide anion radical $O_2^{-\bullet}$ is formed. Concomitant with a reduction in bond order from 2.0 to 1.5 is an increase in bond length from 1.21 to 1. 30 Å. A second reduction step produces the peroxide anion 0_2^{2-}; the bond order is one, and the O—O separation is 1.49 Å. Each of these reduced species, $O_2^{-\bullet}$ and O_2^{2-}, has a characteristic O—O stretching vibration in the infrared region. The free-energy changes and electrochemical potentials for the reduction of dioxygen at unit activity, pH = 1 (E°), are different from those at pH 7.0 (E°'), as shown in Figure 4.11.[58,62] The values at pH 7.0 are more relevant to physiological conditions. Note that the superoxide anion may function as either an oxidant or a reductant.

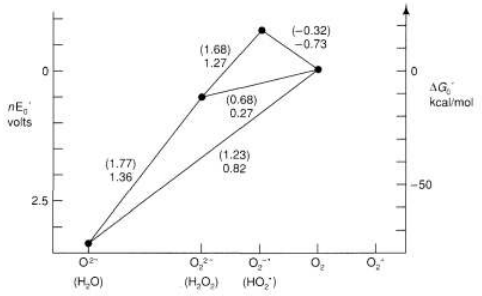


Figure 4.11 - Free-energy changes in the aqueous redox chemistry of dioxygen. Standard state $P(O_2) = 1$. Electrode potentials are at pH 7; those in parentheses are at unit activity.

Geometry and Electronic Structure of Coordinated Dioxygen

In coordinating to metals, dioxygen shows a great variety of geometries and two formal oxidation states. Many complexes have *v*(O—O) values in the range 740 to 930 cm^{-1}, and, where known, an O—O separation in the range 1.40 to 1.50 Å. By analogy with the peroxide anion, these species are designated peroxo, O_2^{II-}. Similarly, the designation superoxo O_2^{I-} is applied to those complexes where *v*(O—O) values are in the range 1075 to 1200 cm^{-1}, and the O—O separation is around 1.30 Å.[63] Although such O—O separations and vibrations are consistent with coordinated peroxide or superoxide moieties, the net amount of charge transferred onto the dioxygen ligand from the metal and its other ligands is difficult to measure experimentally and is probably variable. Thus the oxidation state of the dioxygen ligand and that of the metal are best considered in a formal sense rather than literally—hence the use of the terminology O_2^{I-} to indicate oxidation state I- for the O_2 moiety as a unit (not each O atom). Because of the high degree of covalency in the M—O bond, a more sensible comparison, at least for the peroxo class of compounds, is with organic peroxides, ROOH or ROOR. The clear separation of coordinated dioxygen into either the superoxo or the peroxo class is shown in Figure 4.12.[63-66] *Only* those compounds for which both stretching frequencies (*v*(O—O)) and O—O separations (*r*(O—O)) are available are shown; for the purpose of the plot, non-coordinated anions and cations, replacement of ethylenendiamine by two ammonia ligands, and replacement of triphenylphosphine by alkylphenylphosphines are assumed not to perturb significantly *v*(O—O) or *r*(O—O).

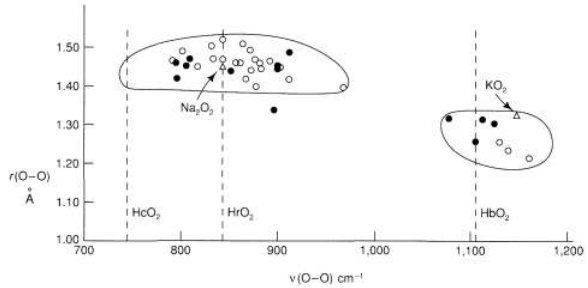
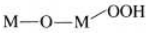


Figure 4.12 - Scatter diagram showing the distribution of O—O stretching frequencies and separations in ionic superoxides and peroxides (△) and in coordination compounds. An open circle denotes O_2 coordinated to one metal; a filled circle denotes O_2 bridging two metals. The O—O stretching frequencies of oxyhemoglobin, oxyhemocyanin, and oxyhemerythrin are marked by dashed lines.

At least seven different geometries have been observed for the coordination of dioxygen (Figure 4.13),[63-66] only three or four of which are currently known to be biologically relevant—the superoxo  (for oxyhemoglobin), the peroxo  or  (for oxyhemocyanin), and the hydroperoxo  (for oxyhemerythrin).

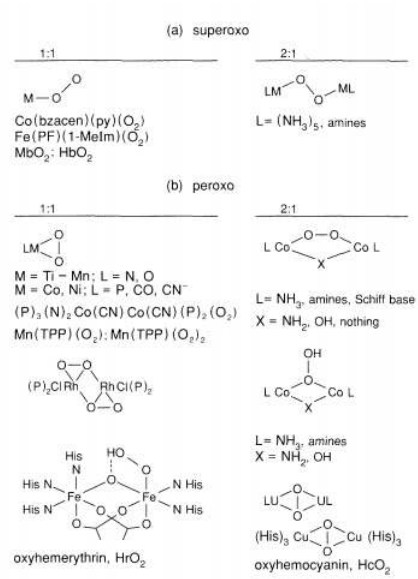
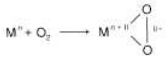


Figure 4.13 - Modes of attachment of O_2 to metals. P, N, and O denote phosphine, amine, and oxygen ligands, respectively.

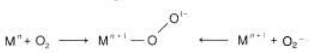
The geometry is a function of the metal, its oxidation state, and its ligands. For the late transition metals of the cobalt and nickel triads, with soft π-acid ligands, such as phosphines and carbonyls, and with an initially low oxidation state of the metal, triangular coordination of a peroxo species with covalent M-O_2 bonds is common.[63] Concomitant with the formal reduction of dioxygen, the metal center undergoes a formal two-electron oxidation:



In this example, where the metal has undergone, at least formally, a two-electron oxidation, the UV-visible properties of the metal-dioxygen complex tend to resemble those of bona fide M^{n+II} rather than M^n species.

Early transition metals (Ti, V, Cr triads) often coordinate several peroxo species, leaving the metal in formally a very high oxidation state (e.g., $Cr(O_2)_4^{3-}$, a Cr^V ion).[63] The M—O_2 links have more ionic character, with the η-peroxo groups acting as bidentate ligands. Titanium and molybdenum(II) porphyrins bind, respectively, one and two dioxygen molecules in this manner.[65]

With harder σ-donor ligand systems, such as those containing nitrogen and oxygen donors, and the metal center in a normal oxidation state, a formal one-electron reduction to an end-on coordinated superoxo species occurs with a bent  bond. Metal-dioxygen species can also be formed by adding the superoxide anion to the oxidized species:[64]



In the absence of steric constraints, dimerization to a (bridging) μ-peroxo species frequently occurs, especially for cobalt-dioxygen complexes:



Figure 4.12 is one such example.

These dicobalt species (right-hand side of Equation 4.28) may be oxidized by one electron to give a μ-superoxo moiety. A clear shortening of the O—O bond and concomitant increase in the value of ν(O—O) are observed in several superoxo-peroxo pairs. These and other modes of O_2 attachment are illustrated in Figure 4.13. Some geometries are represented by only one or two examples, and some geometries, for example, a linear M—O—O species, have never been observed.

In binding to metals, O_2 effectively functions both as a π acid, accepting into its π^* orbitals electron density from the filled d orbitals of the metal, and as a σ donor, donating electron density into an empty metal d orbital. Thus other σ donor or π acceptor ligands, such as nitric oxide (NO), alkyl isocyanides (R—NC), alkyl nitroso (R—NO), and carbon monoxide (CO), are often observed to bind to the same metal complexes that bind O_2. The nature of the metal-dioxygen linkage in biological oxygen carriers and their models will be examined in more detail later.

11.2.4.7: General Aspects of the Chemistry of Dioxygen is shared under a CC BY-NC-SA 4.0 license and was authored, remixed, and/or curated by LibreTexts.

11.2.4.8: General Aspects of the Chemistry of Iron

Irreversible Oxidation

In the presence of dioxygen, iron(II) species are readily oxidized to iron(III) species. In the presence of water, iron(III) species frequently associate into μ-oxodiiron(III) dimers. For iron(II)-porphyrin complexes this process may take only milliseconds at room temperature. The following mechanism was proposed in 1968 for the irreversible oxidation of iron(II)-porphyrinato species;[67,68] subsequent work has largely confirmed it.[69-71]

$$Fe^{II} + O_2 \rightleftharpoons Fe^{III}—O_2^{I-} \tag{4.29a}$$

$$Fe^{III}—O_2^{I-} + Fe^{II} \rightleftharpoons Fe^{III}—O_2^{II-}—Fe^{III} \tag{4.29b}$$

$$Fe^{III}—O_2^{II-}—Fe^{III} \rightarrow 2Fe^{IV} = O \tag{4.29c}$$

$$Fe^{IV} = O + Fe^{II} \rightarrow Fe^{III}—O—Fe^{III} \tag{4.29d}$$

In particular, the dimerization reaction (4.29b) may be rendered less favorable by low temperatures (< -40 °C) or by sterically preventing the bimolecular contact of an Fe^{III}-O_2^{I-} moiety with an Fe^{II} moiety. In the latter case, sterically bulky substituents on the equatorial ligand surround the coordinated O_2 ligand and the other axial position, trans to the coordinated dioxygen ligand, is protected with a nitrogenous base, such as imidazole, or with additional bulky substituents on the equatorial ligand (Figure 4.14).[72] The protein effectively provides such protection and thus plays a key role in preventing the bimolecular contact of two hemes. The first observation of reversible binding of dioxygen to an iron(II)-porphyrin in the absence of protein was made in 1958.[73] In that pioneering study, a heme group was immobilized on a polymer support specially modified to contain imidazole functions. The structurally characterizable hemoglobin or myoglobin species was replaced by a noncrystalline structurally uncharacterized polymer.

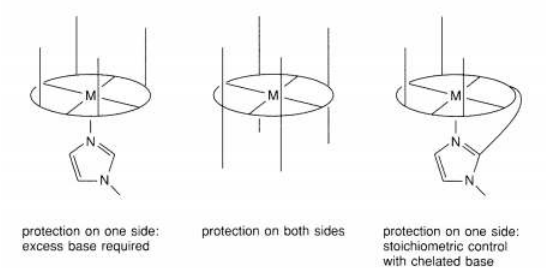


Figure 4.14 - Stylized representation of steric hindrances preventing irreversible oxidation.

Why does this irreversible oxidation not occur analogously for cobalt systems? Step (4.29c) involves cleavage of the O—O bond, which in H_2O_2 has a bond energy of 34.3 kcal/mol or in Na_2O_2 of 48.4 kcal/mol. By way of comparison, for O_2 the bond energy is 117.2 and for HO_2• it is 55.5 kcal/mol.[64] A simple molecular orbital picture gives insight into why an Fe^{IV}=O species is stabilized relative to the analogous Co^{IV}=O species.[74] From Figure 4.15 we see that for metals with electronic configuration d^n, where $n \leq 5$, no electrons occupy the antibonding orbital π^* for Fe^{III}-$O^{I-\bullet}$ or Fe^{IV}=O moieties. For Co^{III} (d^6) the extra electron goes into the antibonding orbital π^*. As predicted by the model, Mn^{III} is observed indeed to behave like Fe^{III}.

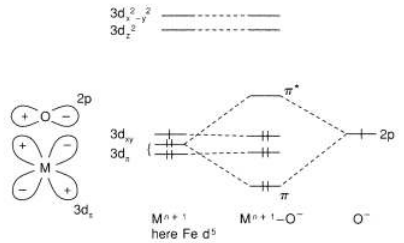


Figure 4.15 - Orbital scheme showing the differing stabilities of M—O species, M = Co(d^6), Fe(d^5); σ-bonding of $2p_z$ with $3d_{z^2}$ not shown.[74]

A second oxidation pathway does not require the bimolecular contact of two iron(II)-porphyrins. Coordinated dioxygen may be released not as O_2, as in normal dioxygen transport, but, as noted in Section I.C, as a superoxide radical anion $O_2^{-\bullet}$ in a process called *autoxidation*:

$$Fe^{III}—O_2^{I-} \rightleftharpoons Fe^{III} + O_2 \tag{4.30}$$

This process is assisted by the presence of other nucleophiles that are stronger than the superoxide anion, such as chloride, and by protons that stabilize the $O_2^{-\bullet}$ anion as $HO_2^{\bullet}$:

$$Fe_{III} + Cl^- \rightleftharpoons Fe^{III}—Cl^- \tag{4.31}$$

The formation of methemoglobin occurs *in vivo*, probably by the above mechanism, at the rate of ~ 3 percent of total hemoglobin per day.

If exogenous reductants are present, then further reduction of dioxygen can occur:

$$2H^+ + Fe^{III}—O_2^{I-} + e^- \rightarrow Fe^V = O + H_2O \tag{4.32}$$

Such processes are important, for example, in the cytochrome P-450 system. With suitably small reductants, oxygenase activity also has been observed for hemoglobin A. This has led to the characterization of hemoglobin as a "frustrated oxidase."[75] Note the formal similarity between this process (Equation 4.32) and the bimolecular irreversible oxidation of iron(II) porphyrins: the second Fe(II) complex in Reaction (4.29b) functions like the electron in Reaction (4.32).

Spectroscopy of the Fe^{III}—O—Fe^{III} moiety

The end products of the irreversible bimolecular oxidation of Fe^{II} species contain the Fe^{III}—O—Fe^{III} fragment. Given the facile formation of μ-oxodiiron(III) species, it is not surprising that the Fe—O—Fe motif is incorporated into a variety of metalloproteins, including the oxygen-carrier hemerythrin (Figure 4.10),[16-18] the hydrolase purple acid phosphatase,[76] the oxidoreductases ribonucleotide reductase[77] and methane monoxygenase,[78] an iron-sulfur protein rubrerythrin,[79a] and the iron-transport protein ferritin.[79b] In ferritin higher-order oligomers are formed.

This μ-oxodiiron(III) moiety has a distinctive fingerprint that has made it easy to identify this motif in proteins.[80] Regardless of the number (4, 5, 6, or 7), geometry (tetrahedral, square pyramidal, tetragonally distorted octahedral, or pentagonal bipyramidal), and type of ligands (halide, RO^-, $RCOO^-$, aliphatic N, or aromatic N) around the iron center, and of the Fe—O—Fe angle, the magnetic susceptibility at room temperature lies in the range 1.5 to 2.0 Bohr magnetons per Fe^{III}—O—Fe^{III} group, equivalent to about one unpaired electron. [81,82] In other words, the high-spin ($S = \frac{5}{2}$) iron centers are strongly antiferromagnetically coupled. Other bridging groups, such as OH^-, Cl^-, carboxylate, alkoxide, or phenoxide, give very weak coupling.[83-86]

The asymmetric Fe—O stretch, ν_{as}(Fe—O), lies in the range 730 to 880 cm^{-1}; in multiply bridged complexes this mode is weak in the infrared region. The symmetric vibration, ν_s(Fe—O), forbidden in the infrared region for linear, symmetric Fe—O—Fe groups, occurs in the range 360 to 545 cm^{-1}. The symmetric mode is usually,[87a] but not always,[87b] observed by resonance Raman techniques upon irradiating on the low-energy side of the Fe—O chargetransfer band that occurs at about 350 nm.

Few dinuclear iron(II) complexes are known where the ligands approximately resemble those believed or known to occur in the family of μ-oxodiiron(III) proteins.[88] The dioxygen-binding process in hemerythrin has no close nonbiological analogue. Although spectroscopically similar to oxyhemerythrin, the unstable monomeric purple peroxo complex formed by the addition of hydrogen peroxide to basic aqueous Fe^{III}(EDTA) solutions remains structurally uncharacterized.[89,90]

Oxidation and Spin State of Iron Porphyrins

Iron porphyrins, the active sites of the hemoglobin family, have a rich magnetochemistry.[91] Iron porphyrins may be octahedral (two axial ligands), square pyramidal (one axial ligand), or square planar (no axial ligand). The metal d orbitals, now having partial porphyrin π^* character, are split, as shown in Figure 4.16. The radius of the metal atom is much greater when it is high spin (S = 2 for Fe^{II}, S = $\frac{5}{2}$ for Fe^{III}) than when it is low spin (S = 0 for Fe^{II}, S = $\frac{1}{2}$ for Fe^{III}). This difference influences Fe—N_{porph} separations, porphyrin conformation, and the displacement of the iron center with respect to the porphyrin plane. For iron(II)-porphyrins, two strong-field axial ligands, such as a pair of imidazoles or an imidazole and carbon monoxide, lead to diamagnetic complexes (S =

0) with the six 3d electrons occupying those orbitals of approximate t_{2g} symmetry. In a classic experiment in 1936, Pauling and Coryell proved that oxyhemoglobin and carbonmonoxyhemoglobin are diamagnetic.[92]*

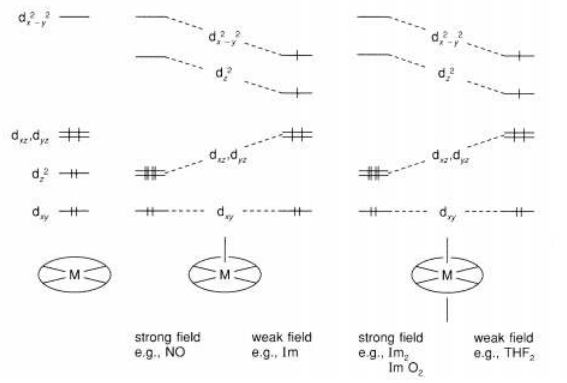


Figure 4.16 - d-Orbital splitting in metalloporphyrins as a function of number and ligand-field strength of ligands.[91] Orbital occupancy is illustrated for a d^6 species (Fe^{II} or CO^{III}).

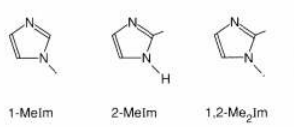
---

* There was a considerable flurry of interest when an Italian group, using a SQUID (Superconducting Quantum Mechanical Interference Device), reported that at room temperature oxyhemoglobin was significantly paramagnetic.[93] Not surprisingly, several theoretical papers followed that "proved" the existence of low-lying triplet and quintet excited states[94-96] Subsequently, the residual paramagnetism was doubted[97] and shown to arise from incomplete saturation of hemoglobin by O_2; in other words, small amounts of deoxy hemoglobin remained[98] Since oxygen affinity increases with decreased temperature, the concentration of paramagnetic impurity decreased with decreasing temperature.

No axial ligands at all may lead to a spin state of S = 1, with unpaired electrons in the d_{xy} and d_{z2} orbitals. Five-coordinate iron(II)-porphyrinato complexes are commonly high spin, S = 2, although strong σ-donor π-acceptor ligands, such as phosphines, carbon monoxide, nitric oxide, and benzyl isocyanide,[99] enforce a low-spin state. Five-coordinate iron(II)-porphyrinato complexes with aromatic nitrogenous axial ligands, such as pyridine or 1-methylimidazole, bind a second such axial ligand 10 to 30 times more avidly than the first to give the thermodynamically and kinetically (d^6, S = 0) stable hemochrome species, a process that is avoided by hemoglobins. That is, the equilibrium constant for the following disproportionation reaction is greater than unity,

$$Fe—N + Fe—N \rightleftharpoons N—Fe—N + Fe \tag{4.33}$$

except for bulky ligand N, such as 2-methylimidazole and 1,2-dimethylimidazole, for which the five-coordinate species predominates at room temperature even with a mild excess of ligand:[100]



For iron(III)-porphyrinato complexes, strong-field ligands lead to low-spin ($S = \frac{1}{2}$) complexes. A pair of identical weak-field ligands, such as tetrahydrofuran, leads to intermediate-spin ($S = \frac{3}{2}$) species. Five-coordinate species are, with few exceptions, high-spin ($S = \frac{5}{2}$), with all five 3d electrons in separate orbitals. Spin equilibria $S = \frac{1}{2} \rightleftharpoons S = \frac{5}{2}$ and $S = \frac{3}{2} \rightleftharpoons S = \frac{5}{2}$ are not unusual. Specific examples of these spin systems are given in Table 4.4.[65,91] Higher oxidation states are found in some other hemoproteins. Fe(V)-porphyrin systems actually occur as Fe(IV)-porphyrin cation radical species, and Fe(I)-porphyrin systems exist as Fe(II)-porphyrin anion radical species.

Substantial structural changes occur upon the addition of ligands and upon changes in spin state. In one mechanism of cooperativity these changes are the "trigger" (metrical details are deferred until the next section). Spectral changes in the UV-visible region are observed also (Figure 4.17)[10] and may be monitored conveniently to evaluate the kinetic and thermodynamic parameters of ligand binding to hemoglobin.

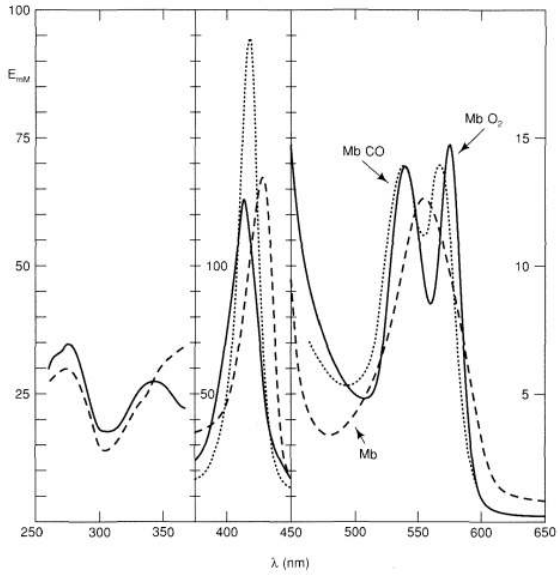


Figure 4.17 - Spectral changes accompanying the oxygenation and carbonylation of myoglobin.[10] Reproduced with permission from E. Antonini and M. Brunori, Hemoglobin and Myoglobin in Their Reactions with Ligands, North Holland, 1971.

Table 4.4 - Oxidation and spin states of iron porphyrins and their biological occurrences

a) Could be placed in Fe^{III} column

b) Could be placed in Fe^{III} column with spin = 0.

c) Non-linear Fe—NCS moiety.

State	Fe^{II}		Fe^{III}	
High spin	Fe(PF)(2-MeIm)	5-coord	Fe(TPP)Cl	5-coord
	Hb		Cytochrome P-450(ox)	
Fe^{II} $S = 2(d^6)$	Fe (TPP)$(THF)_2$	6-coord	$[Fe(TPP)(H_2O)_2]^+$	6-coord
Fe^{III} $S = \frac{5}{2}(d^5)$	Hb(H_2O)?		$[Fe(OEP)(3\text{-}ClPy)_2]^+$ (293 K)	
			Fe(OEP)(Py)(NCS)	
			MetHb(H_2O)	
Intermediate spin	Fe(TPP)	4-coord	$[Fe(TPP)(C(CN)_3)]_n$	
Fe^{II} $S = 1$ (d^6)	no biol. occurrence		Fe(TPP)$(OClO_3)$ $(S = \frac{3}{2}, \frac{5}{2})$	
Fe^{III} $S = \frac{3}{2}(d^5)$			cytochrome c'	
Low spin	Fe(TPP)(NO)	[a] 5-coord	[Fe(TPP)(Ph)]	5-coord
Fe^{II} $S = 0(d^6)$	Hb(NO)·DPG(T)			
Fe^{III} $S = \frac{1}{2}(d^5)$	Fe(PF)(2-MeIm)(O_2) [b]	6-coord	$[Fe(TPP)(Im)_2]^+$	6-coord
$(S = \frac{1}{2}$, Fe—NO adducts)	Fe(TPP)(1-MeIm)(NO)		$[Fe(OEP)(3\text{-}Cl\text{-}Py)_2]^+$ (98 K)	
	Fe(TPP)(Py)(CO)		Fe(TPP)(Py)(CN)	
	Fe(TPP)$(1\text{-}MeIm)_2$		Fe(TPP)(Py)(NCS)[c]	
	Hb(CO), Hb(NO),[a] Hb(O_2) [b]		cytochrome b_5, c, c_3	
	cytochrome b_5, c, c_3		metHb (CN)	

11.2.4.8: General Aspects of the Chemistry of Iron is shared under a CC BY-NC-SA 4.0 license and was authored, remixed, and/or curated by LibreTexts.

11.2.4.9: General Structural Features that Modulate Ligand Activity

There are many ways in which ligand affinity may be perturbed (Figure 4.25). It is convenient to divide these into two groups, referred to as distal and proximal effects.[163] *Proximal* effects are associated with the stereochemistry of the metalloporphyrinato moiety and the coordination of the axial base, and thus their influence on O_2 and CO affinity is indirect. *Distal* effects pertain to noncovalent interactions of the metal-porphyrinato skeleton and the sixth ligand (O_2, CO, etc.) with neighboring solvent molecules, with substituents, such as pickets or caps, on the porphyrin, and with the surrounding protein chain. The distal groups that hover over the O_2-binding site engender the most important distal effects. For convenience, the effects of crystal packing and the protein matrix on porphyrin conformation will be discussed among the proximal effects, although as nonbonded interactions they properly are distal effects.

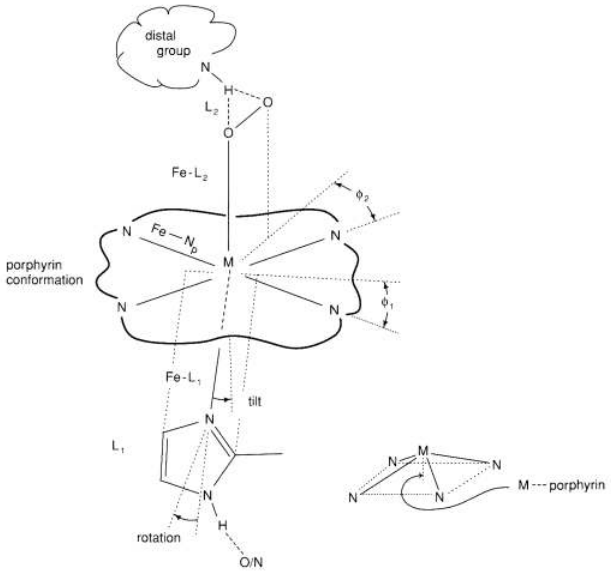


Figure 4.25 - Structural parameters and features that determine the affinity of oxygen carriers.

To a first approximation, the effects of substituents on the porphyrin ring, as transmitted through bonds to the metal center, do not perturb the ligand binding properties as much as do distal effects.[170] Thus substituents, such as vinyl and propionic-acid groups on protoporphyrin IX and o-pivalamidophenyl pickets, are ignored; one porphyrin is much like another. At the end of this subsection the various ways ligand affinity may be modulated will be summarized in an augmented version of Figure 4.3.

Proximal Effects

Few molecules have had their conformational properties characterized as exhaustively as have metalloporphyrins.

a. Porphyrin Conformation and M-N_p Separations

The cyclic aromatic 24-atom porphyrinato skeleton offers a tightly constrained metal-binding site. The conformation of least strain is planar, and the radius of the hole of the dianion is close to 2.00 Å,[110] leading to metal-porphyrinato nitrogen-atom separations, M-N_p, of 2.00 Å if the metal is centered in the square plane defined by the four porphyrinato nitrogen atoms. Small deviations from planarity are generally observed and attributed to crystal packing effects; large deviations may be induced by bulky substituents on the porphyrin skeleton, especially at the *meso* positions, by the crystal matrix,[65] or by the highly anisotropic protein matrix. The 2.00 Å radius hole neatly accommodates low-spin (S = 0) and intermediatespin (S = 1) iron(II), low-spin (S = $\frac{1}{2}$) iron(III), and cobalt(II) and cobalt(III) ions.[91]* With few exceptions the metal is centered in or above the central hole for mononuclear porphyrin species; only rarely do M-N_p bonds show a significant (though still small) scatter about their mean value.

* In order to accommodate smaller ions, such as nickel(II), the porphyrin skeleton may contract by ruffling, with little loss of aromaticity; like a pleated skirt the pyrrole rings rotate alternately clockwise and counterclockwise about their respective M-N_p vectors. This distortion leaves the four porphyrinato nitrogen atoms, N_p, still coplanar. Alternatively, the porphyrin skeleton may buckle to give a saddle conformation; the N_p atoms may acquire a small tetrahedral distortion in this process. M-N_p bonds as short

as 1.92 Å have been observed. Metals with one or two electrons in their $3d_{x^2-y^2}$ orbital have a radius larger than 2.00 Å. In order to accommodate them in the plane of the porphyrin, the porphyrin skeleton expands. M-N_p separations as long as 2.07 Å may occur with the metal still centered in the plane of the N_p atoms.[110]

b. M • • • Porph Displacement

For five-coordinate complexes the magnitude of the displacement of the metal from the plane of the four nitrogen atoms, M • • • porph, is a consequence of the electronic configuration of ML_5 complexes. Of course, the effect is augmented if the $3d_{x^2-y^2}$ orbital (directed along M-N_p bonds, Figure 4.16) is occupied. Compare a displacement of 0.14 Å for Co(TPP)(1,2-Me_2Im) (no $3d_{x^2-y^2}$ occupancy)[111] with 0.43 Å for Fe(PF)(2-MeIm) ($3d_{x^2-y^2}$ occupied).[169] For six-coordinate complexes where the two axial ligands, L_1 and L_2, are different, the M • • • porph displacement usually reflects relative *trans* influences.

Generally, displacement of the metal from the plane of the porphyrinatonitrogen atoms is within 0.04 Å of the displacement from the 24-atom mean plane of the entire porphyrin skeleton. On occasions this second displacement may be much larger, for example in Fe(TPP)(2-MeIm), where it is 0.15 Å larger[110] than it is for Fe(PF)(2-MeIm). This effect is called *doming*, and it is usually attributed to crystal packing forces. Interaction of the porphyrin with protein side chains leads to considerable doming or folding of the heme in vertebrate hemoglobins.

c. M-L Separations

The metal-axial ligand separations, M-L (when more than one, L_1 denotes the heterocyclic axial base), are dependent on the nature of the ligand, L. When L_1 and L_2 are different, the M-L separations are sensitive to the relative *trans* influences of L_1 and L_2 as well as to steric factors. For example, for Fe(TPP)(1-Melm)$_2$, the Fe—N_{Im} bond length is 2.016(5) Å,[110] whereas for Fe(TPP)(1-Melm)(NO) it is 2.180(4) Å.[111]For sterically active ligands, such as 2-methylimidazole compared to 1-methylimidazole (4.34), the longer Co—N_{Im} bond occurs for the 2-Melm ligand because of steric clash between the 2-methyl group and the porphyrin.[111]It is possible that combinations of intrinsic bonding and steric factors may give rise to a double minimum and two accessible axial ligand conformations (Figure 4.26). This situation seems to occur in the solid state for Fe(PF)(2-Melm)(O_2)•EtOH, where a short Fe—N_{Im} and a long Fe—O bond are observed both from the structure revealed by single-crystal x-ray diffraction methods and by EXAFS data. On the other hand, for solvate-free Fe(PF)(2-MeIm)(O_2) and for Fe(PF)(1,2-Me_2Im)(O_2), the EXAFS patterns are interpreted in terms of a short Fe—O and long Fe—Im bond.[171]

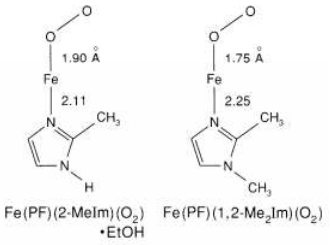


Figure 4.26 - Two arrangements of axial ligands. The right-hand side features a short L_2 and long L_1; the left-hand side the opposite.

d. The Angle ϕ

This parameter is the minimum angle that the plane of the axial base (e.g., pyridine, substituted imidazole, etc.) makes with a plane defined by the N_p, M, and L_1 atoms (Figure 4.25).[65] If there are two axial ligands, e.g., 1-methylimidazole and O_2, then, as before, the angle the axial base makes is denoted ϕ_1 and the other angle ϕ_2. For a linear CO ligand bound perpendicularly to the porphyrin plane, ϕ_2 is undefined. Note that the orientation of the second ligand is influenced by distal effects.

When ϕ = 0, the axial base eclipses a pair of M-N_p bonds; contacts with the porphyrin are maximized. When ϕ = 45°, contacts are minimized. Unless the axial base has a 2-substituent, however, the contacts are not excessively close for any value of ϕ. With a 2-methyl substituent, the contacts are sufficiently severe that the M-N_{L1} vector is no longer perpendicular to the porphyrin plane, and the imidazole group is rotated so that the M-N_{L1} vector no longer approximately bisects the imidazole C—N—C bond angle, as illustrated Figure 4.25.[110,172]

Distal Effects

Distal effects arise from noncovalent interactions of the coordinated dioxygen, carbon monoxide, or other ligand with its surroundings. The protein matrix, the pickets, and the caps are functionally equivalent to an anisotropic solvent matrix that contains a variety of solutes. The limits of this simplification are illustrated in the following example. The electronically similar cobalt meso-, deutero-, and protoporphyrin IX complexes bind dioxygen with similar affinities under identical solvent conditions. When they are embedded in globin, larger differences in affinity and changes in cooperativity are observed.[170] These effects are attributed to the slightly different nestling of the porphyrin molecules in the cleft in hemoglobin or, in the generalization introduced, to slightly different solvation effects.

Interaction of the coordinated O_2 or CO molecule with solvent molecules or with the protein has a profound influence on kinetics and thermodynamics (see Figure 4.24, and Tables 4.2 and 4.5). As discussed earlier, there is accumulation of negative charge on the dioxygen ligand. The possibility then arises for stabilization of coordination through hydrogen bonding or dipolar interactions with solute molecules,[175] porphyrin substituents (such as amide groups in the picket-fence porphyrins[176] and some species of strapped porphyrins[161]), or with protein residues* (such as histidine).[167,177-179]

Destabilization of coordinated ligands and lowered affinity can result if the coordinated ligand is unable, through steric clash, to achieve its optimum stereochemistry or if the closest neighboring groups are electronegative, as are the ether and ester linkages on capped porphyrins.[31,180] We will describe in detail in the next subsection (III.C) the fascinating variety of means by which ligand binding is modulated by distal amino-acid residues.

---

* For *Glycera* $CoMbO_2$ no change in EPR parameters occurs on substituting D_2O for H_2O.[168] No hydrogen bond between O_2 and a distal group comparable in strength to that in whale $CoMbO_2$ was inferred.

Approximate Contribution of Proximal and Distal Effects to Ligand Affinity

Dissimilar systems may show similar affinities for a ligand as a result of a different mix of the proximal and distal effects enumerated above. These effects are not all of equal magnitude, and an attempt is made here to show the increment in free energy that occurs if the effect is manifest in the deoxy or liganded state of Figure 4.3. Increasing the free energy of the deoxy state while holding that of the liganded state constant leads to an increase in affinity. The reference state is gaseous Fe(TPP)(1-MeIm). The magnitude and sign of these effects are shown in Figure 4.27. For the coordination of alkylisocyanide molecules to hemoglobin, the steric effects of different alkyl groups have been quantified.[35] Lowered affinity occurs with increasing alkyl chain length, with the exception of methyl isocyanide.

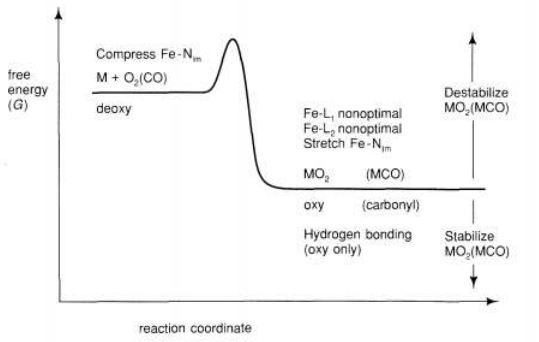


Figure 4.27 - Proximal and distal effects on the ligand affinities.

11.2.4.9: General Structural Features that Modulate Ligand Activity is shared under a CC BY-NC-SA 4.0 license and was authored, remixed, and/or curated by LibreTexts.

11.2.4.10: Hazards of Life with Dioxygen

The binding of dioxygen is normally a reversible process:

$$M + O_2 \rightleftharpoons MO_2 \tag{4.22}$$

Under some circumstances, such as in the presence of added nucleophiles and protons, coordinated dioxygen is displaced as the superoxide anion radical, O_2^-, leaving the metal center oxidized by one electron and unreactive to dioxygen:[49,50]

$$MO_2 \rightleftharpoons M^+ + O_2^- \tag{4.23}$$

For hemoglobin there exists a flavoprotein reductase system, comprising a reduced pyridine nucleotide (e.g., NADH), cytochrome b_5 reductase, and cytochrome b_5 , that reduces the ferric iron back to the ferrous state, so that it may coordinate dioxygen again.[1,51] In addition, all aerobically respiring organisms and many air-tolerant anaerobes contain a protein, superoxide dismutase, that very efficiently catalyzes the dismutation of superoxide ion to dioxygen and hydrogen peroxide:[52-54]

$$2O_2^- + 2H^+ \rightarrow O_2 + H_2O_2 \tag{4.24}$$

However, the physiological effects of the superoxide moiety remain controversial.[53,54] Finally, there is a third enzyme, the hemoprotein catalase, that converts the toxic hydrogen peroxide into water and dioxygen:[1]

$$2H_2O_2 \rightarrow O_2 + 2H_2O \tag{4.25}$$

This topic is discussed further in Chapter 5.

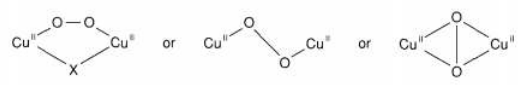
11.2.4.10: Hazards of Life with Dioxygen is shared under a CC BY-NC-SA 4.0 license and was authored, remixed, and/or curated by LibreTexts.

11.2.4.11: Nature of the Metal-Dioxygen Linkage in Biological Systems

Many techniques have been used to probe the geometry and electronic structure of the metal-dioxygen moiety in biological systems and in synthetic models. The results form the basis of any understanding of the factors that determine and modulate oxygen affinity.

Oxyhemocyanin and Oxyhemerythrin

By resonance Raman techniques, the O—O stretch is observed at 744 cm^{-1} in oxyhemocycanin and at 844 cm^{-1} in oxyhemerythrin.[140-142] Dioxygen is therefore coordinated as peroxo species. By use of unsymmetrically labeled dioxygen, $^{18}O—^{16}O$, it was established that dioxygen coordinates symmetrically:[141]



Carbon monoxide binds to only one of the Cu^{I} centers in deoxyhemocyanin, through the C atom,* apparently blocking the second Cu^{I} site.[15] Similar behavior is also seen for the nitrosyl adduct.

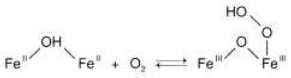
---

* A report[143] that CO binds to the copper center through the O atom, an unprecedented mode, has been challenged.[144]

On the other hand, in an experiment parallel to that just described for hemocyanin, dioxygen was found to bind asymmetrically in oxyhemerythrin:[142]



Figure 4.13).[45] This mode of dioxygen coordination remains unobserved to date in small-molecule synthetic systems. The O_2-binding process is formally very similar to the combinations of Reactions (4.29a) and (4.29b), except that dioxygen attaches to only one Fe center (bridging carboxylato groups omitted in Reaction 4.45):



The existence and location of the proton, which cannot be proven in the crystal structure of deoxyhemerythrin or of oxyhemerythrin, are inferred from a model system for the former that contains a hydroxo group bridging two high-spin, weakly antiferromagnetically coupled Fe^{II} centers ($J = -10\ cm^{-1}$).[88] For oxyhemerythrin (and for one conformation of methydroxohemerythrin), a small change in the position of the symmetric Fe—O—Fe mode is observed when H_2O is replaced by D_2O.[146] The strong antiferromagnetic coupling observed for methemerythrin and oxyhemerythrin ($-J \sim 100\ cm^{-1}$)[147] is uniquely consistent with a bridging oxo moiety between a pair of Fe^{III} centers.[80] Finally, a Bohr effect (release or uptake of protons) is absent in oxygen binding to hemerythrin.[16,18] These observations are consistent with a μ-oxo group slightly perturbed by hydrogen bonding to a coordinated hydroperoxo species. An important role for the protein in hemerythrin is to assemble an asymmetric diiron(II) species. Only a few of the myriad of known μ-oxodiiron(III) complexes are asymmetric,[81] and the synthesis of realistic asymmetric models remains a challenge.

Deoxyhemocyanin (Cu^{I} d^{10}) and deoxyhemerythrin (Fe^{II} d^{6}) are colorless. In the oxygenated derivatives there is considerable charge transfer between the coordinated peroxo groups and the metal centers. This phenomenon makes the essentially d-d metal transitions more intense than those for the simple aquated Fe^{3+} or Cu^{2+} ions, and permits facile measurement of oxygen-binding curves. The spectral changes accompanying oxygenation are shown in Figures 4.20 and 4.21.[5]

Nitric oxide binds to deoxyhemocyanin, to deoxyhemerythrin, and to the mixed valence $Fe^{III} \cdots Fe^{II}$ semimethemerythrin.[148] Carbon monoxide binds to neither form of hemerythrin: apparently the other ligands have insufficiently strong fields to stabilize the low-spin state for which electron density would be available for back donation into the CO π^* orbitals.

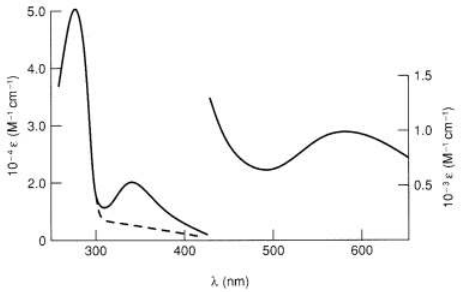


Figure 4.20 - Spectral changes accompanying oxygenation of hemocyanin: deoxyhemocyanin (- - -); oxyhemocyanin (——).[5] Reproduced with permission from A. G. Sykes, in A. G. Sykes, ed., Advances in Irorganic and Bioinorganic Mechanisms, Academic Press, **1** (1985), 121-178.

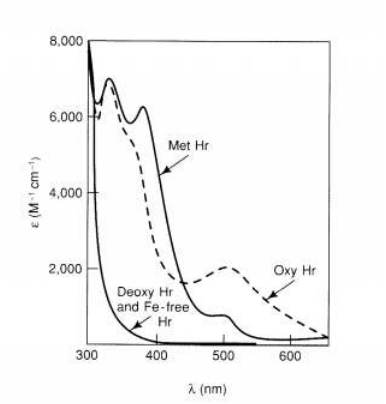


Figure 4.21 - Spectral ehanges accompanying oxygenation of hemerythrin.[5] Reprodueed with permission from A. G. Sykes, in A. G. Sykes, ed., Advances in Inorganic and Bioinorganic Mechanisms, Academic Press, **1** (1985), 121-178.

Oxyhemoglobin

The O—O stretch that is observed by difference infrared techniques at around 1105 cm^{-1} for oxyhemoglobin and oxymyoglobin[149] clearly categorizes the dioxygen moiety as a superoxo species; that is, the order of the O—O bond is about 1.5. Considerable ink has been spilled about the nature of the Fe—O_2 fragment since Pauling's original suggestion[150] in 1948 that dioxygen binds to iron in an end-on bent fashion:



He subsequently reaffirmed this geometry, and proposed that hydrogen bonding between the coordinated dioxygen and the distal imidazole H—N group was important in stabilizing the Fe—O_2 species.[137] In an alternative model Weiss proposed that a low-spin Fe^{III} center ($S = \frac{1}{2}$) was very strongly antiferromagnetically coupled to a superoxide anion radical ($S = \frac{1}{2}$).[151] A triangular peroxo mode has also been advanced.[152,153] The problem has been how to resolve the observed diamagnetism of oxyhemoglobin[92,98] with UV-visible, x-ray absorption, and resonance Raman spectroscopic characteristics[154] that are distinctly different from those of Fe^{II} systems (such as carbonmonoxyhemoglobin and low-spin six-coordinated hemochromes, such as Fe(Porph)$(Py)_2$) and from unambiguously Fe^{III} systems (such as chloromethemoglobin or cyanomethemoglobin).

Any adequate theoretical treatment must also explain how iron-porphyrin systems can bind not only O_2, but also CO, NO, alkyl isocyanides, and alkyl-nitroso moieties. A simple qualitative model presented by Wayland and coworkers[129,155] conveniently summarizes ligand-binding geometries of cobalt and iron porphyrins. Although a reasonable quantitative theoretical consensus exists for 1:1 cobalt-dioxygen species, the same cannot be said yet for irondioxygen systems.

A Simple Model for the Electronic Structure of Liganded Hemoglobins

Why does dioxygen bind to iron and cobalt porphyrins in an end-on bentbond fashion as in (4.37) and (4.46)? Why does carbon monoxide bind in a linear manner (Equation 4.40)? Why are six-coordinate dioxygen and carbonmonoxide adducts more stable

than five-coordinate ones? A unified picture of ligand binding that addresses these questions is important in understanding properly the specific case of dioxygen binding to hemoglobin and related systems.

The splitting of the metal d orbitals for a four-coordinate metalloporphyrin is shown in the center of Figure 4.22. These orbitals contain some porphyrin character and are antibonding with respect to metal-porphyrin bonds. As shown in Figure 4.16, the primary effect of a single σ-donor axial ligand, such as pyridine or 1-methylimidazole, is to elevate the energy of the antibonding d_{z^2} and lower the energy of the $d_{x^2-y^2}$ orbital and hence lead to a high-spin species in place of the intermediate-spin four-coordinate one. Thus, for simplicity in highlighting interaction of the metal center with the diatomic σ-donor: π-acid ligands CO, NO, and O_2, the perturbations wrought by primarily σ-donor ligands, such as 1-methylimidazole, are omitted. For the corresponding cobalt(II) compound, there is an additional electron. The diatomic ligands of interest share a qualitatively similar molecular orbital scheme. The filling of orbitals for CO is shown on the left-hand side. Dioxygen, which is shown on the right-hand side, has two more electrons than CO; these occupy the doubly degenerate π^* orbitals. Quantitative calculations show that the energy of the π^* orbitals decreases monotonically from CO to NO to O_2, indicating increasing ease of reduction of the coordinated molecule, a feature that has not been included in the diagram. Only those interactions of molecular orbitals that have appropriate symmetry and energy to interact significantly with the metal d orbitals are shown.

Two extremes are shown in Figure 4.22 for the interaction of a diatomic molecule A-B with the metal center: a linear geometry on the left and a bent geometry on the right. A side-on geometry is omitted for the binding of O_2 to a Co^{II} or Fe^{II} porphyrin, since this would lead to either an M^{III} side-on superoxo or an M^{IV} peroxo species; both these modes of coordination to these metals are currently without precedent.

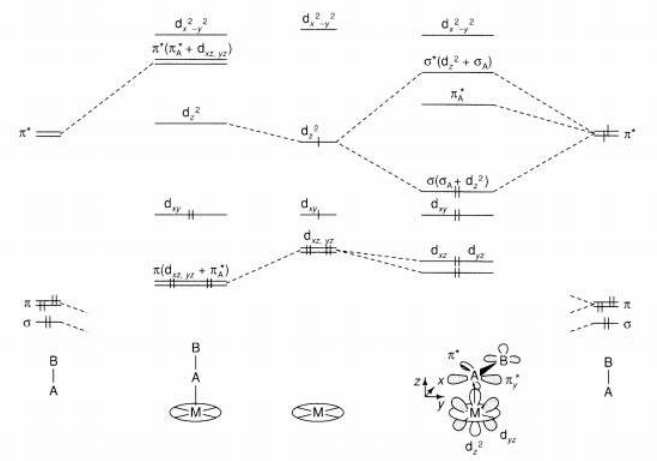


Figure 4.22 - A simple general model for ligand binding to metalloporphyrins:[129] AB = CO(π^{*0}), NO (π^{*1}), O_2(π^{*2}); M=Co ^{II}(d^7), Fe^{II}(d^6).

Linear diatomic metal bonding maximizes the metal-d_π to ligand-p_{π^*} bonding. When a ligand coordinates in a bent manner, axial symmetry is destroyed, and the degeneracy of the ligand p_{π^*} orbitals is lifted. One p_{π^*} orbital is now oriented to combine with the metal d_{z^2} orbital to form a σ bond, and the other is oriented to combine with d_{xz} and d_{yz} orbitals to form a π bond. A bent geometry for the diatomic molecule will result when either or both of the metal d_{z^2} or the ligand p_{π^*} orbitals are occupied, since this geometry stabilizes the occupied d_{z^2} orbital in the five-coordinate complex. Thus O_2 binds in a strongly bent manner to Co^{II} and Fe^{II} porphyrins; NO binds in a strongly bent manner to Co^{II} porphyrins; CO binds in a linear fashion to Fe^{II} porphyrins.

The interaction of NO with Fe^{II} porphyrins and CO with Co^{II} porphyrins—the resultant species are formally isoelectronic—is more complicated. The degree of bending seen in Fe^{II}(TPP)(NO) is midway between the two extremes.[111]For CO the higher-energy p_{π^*} orbitals lead to a greater mismatch in energy between the d_{z^2} and p_{π^*} orbitals, and less effective σ bonding. In EPR experiments the odd electron is found to be localized in a molecular orbital with about 0.87 metal d_{z^2} character for the five-coordinate Co—CO adduct, as expected for a nearly linear geometry.[129] On the other hand, for the Fe—NO adduct the metal d_{z^2} character of the odd electron is about 0.4 to 0.5;[155] a somewhat bent geometry (140°) is observed in the crystal structure of Fe(TPP)(NO). Because the CO ligand is a very weak σ donor, the Co—CO species exists only at low temperatures.

Only qualitative deductions can be made from this model about the extent of electron transfer, if any, from the metal onto the diatomic ligand, especially for dioxygen. The higher in energy the metal d_{z^2} orbital is with respect to the dioxygen p_{π^*} orbitals, the closer the superoxo ligand comes to being effectively a coordinated superoxide anion. With an additional electron, the dioxygen ligand in Co—O_2 complexes can acquire greater electron density than it can in Fe—O_2 complexes.

From the diagram it may be inferred that a ligand with very strong π-acceptor properties will lower the energy of the d_{xz} and d_{yz} orbitals through strong (d_{xz}, d_{yz})-π^* interaction. The resultant energy gap between these two orbitals and the other three metal d orbitals may be sufficient to overcome the energy involved in spin-pairing, and hence lead to five-coordinate low-spin species, as happens for complexes containing phosphines and carbon monosulfide.[99,132]

11.2.4.11: Nature of the Metal-Dioxygen Linkage in Biological Systems is shared under a CC BY-NC-SA 4.0 license and was authored, remixed, and/or curated by LibreTexts.

11.2.4.12: Other Ligands for Biological Oxygen Carriers

As noted above, a variety of other α-donor or π-acceptor ligands will bind to the active sites of biological oxygen carriers.

Carbon Monoxide

As documented in Table 4.2, carbon monoxide (CO) generally binds more strongly to hemoglobin than does dioxygen, hence causing carbon-monoxide poisoning. In addition to being readily available from car exhausts and tobacco smoke to convert oxyhemoglobin to carbonmonoxyhemoglobin, CO is produced in the catabolism of heme molecules.[117] Thus under even the most favorable of conditions, about 3 percent of human hemoglobin is in the carbonmonoxy form. When CO binds to a single metal atom in nonbiological systems, *without exception* it does so through the carbon atom and in a linear manner:[56]

$$Fe—C=O \leftarrow Fe^{II} + {}^{-}C=O^{+} \tag{4.40}$$

Model systems for carbonmonoxy (also called carbonyl) hemoglobin show a geometry similar to that of the Fe—C≡O group, linear or nearly so and essentially perpendicular to the porphyrin plane.[110,118-121] The biochemical literature is littered with reports that this is *not* the geometry adopted by CO in binding to hemoglobins.[122-128] We will return to this topic later in this chapter, since the physiological consequences are potentially important.

Carbon monoxide binds weakly as a σ-donor ligand to four-coordinate cobalt(II) systems.[129] Despite a bout of artifactual excitement,[130] CO has never been observed to bind significantly to five-coordinate Co^{II} systems with a nitrogenous axial base to yield octahedral six-coordinate species.[131] The sulfur analogue thiocarbonyl (CS), although not stable as a free entity, binds very strongly to iron-porphyrin species in a linear manner.[132]

Nitric Oxide

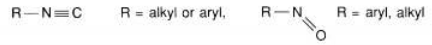
Nitric oxide (NO) binds to hemes even more strongly than CO (and hence O_2),[10] so strongly, in fact, that the Fe—N_{1m} bond is very weak and easily ruptured.[11,111,133] Attachment to the metal is via the nitrogen atom; however, the geometry of attachment is sensitive to the π basicity of the metalloporphyrin, and ranges from linear to strongly bent. In binding to Co^{II} the NO ligand is effectively reduced to NO^{-}, with concomitant oxidation of Co^{II} to Co^{III}.[111]



In much the same way that cobalt-dioxygen systems are paramagnetic ($S = \frac{1}{2}$) and amenable to EPR studies, iron-nitric oxide (also called iron nitrosyl) species are also paramagnetic and isoelectronic with cobalt-dioxygen species. The unpaired spin is localized mostly on the NO group.

Isocyanide and Nitroso Species

In contrast to the dioxygen, carbon-monoxide, and nitric-oxide ligands, the isocyanide and nitroso functions bear an organic tail. Moreover, nitroso ligands are isoelectronic with dioxygen.



Thus, in principle, not only may the steric bulk of the ligand be varied, in order to probe the dimensions[35] of the dioxygen-binding pocket,* but also the σ-donor/π-acceptor properties of the ligands may be varied by appropriate substituents on the aryl ring.

Isocyanide groups may bind to metals in a variety of ways. For 1:1 adducts (Figure 4.19), the isocyanide group is approximately linear, although some flexibility seems to exist in a bis(t-butylisocyanide)iron(Il)tetraphenylporphyrinato complex.[135] For zerovalent metals with much electron density available for donation into ligand π^* orbitals, the isocyanide ligand has been observed to bend at the N atom.[136] One prediction exists that an isocyanide ligand binds in this manner to hemoglobin.[137]

For 1:1 adducts of nitroso ligands, side-on,[138] O-, and N-ligated modes are possible (Figure 4.19). No O-nitroso complexes have been definitively characterized by diffraction methods. For hemoglobin the N-nitroso mode is likely, since this is the mode found

for the nitrosoalkane in Fe(TPP)(amine)(RNO).[139]

To date isocyanide ligands have not achieved their potential as probes of the geometry of the ligand-binding pocket in hemoglobin, partly because we lack structural data on the preferred geometry of attachment of these ligands in a sterically uncongested environment.

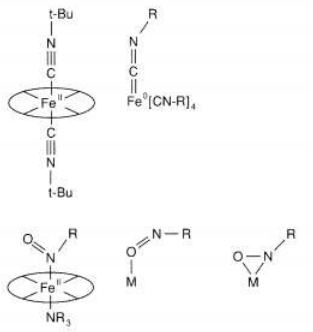


Figure 4.19 - Modes of coordination of isocyanide and nitroso species.

* In fact, this classic experiment of St. George and Pauling established, for the first time and before any crystallographic data were available, that the heme group and the ligand-binding site in hemoglobin reside at least partway inside the protein, rather than on the surface.[134]

11.2.4.12: Other Ligands for Biological Oxygen Carriers is shared under a CC BY-NC-SA 4.0 license and was authored, remixed, and/or curated by LibreTexts.

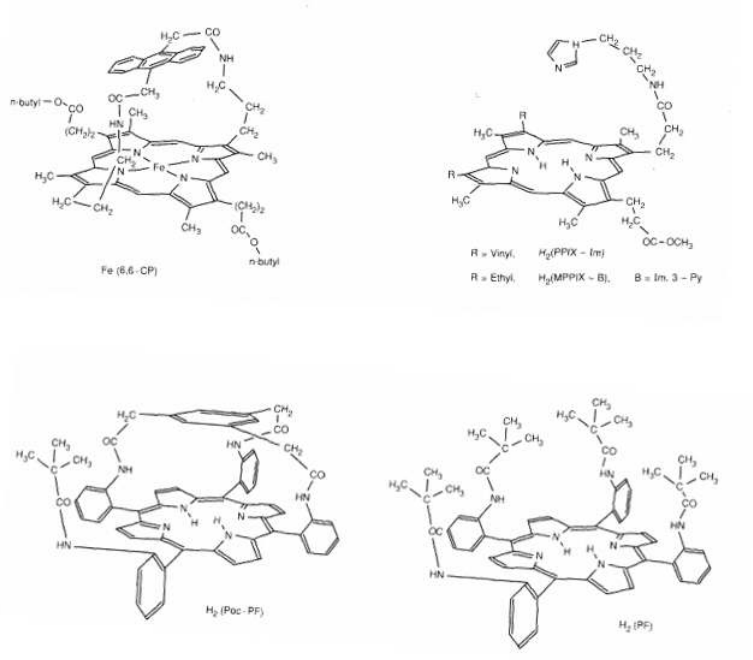
11.2.4.13: Requirements for a Model System for Hemoglobin

For hemoglobin, the majority of ligands around the iron center are provided by a fairly rigid macrocycle, the protoporphyrin IX dianion (Figure 4.1), that by itself enforces a square-planar stereochemistry. Thus, the task of assembling synthetic analogues of the active site in hemoglobin is simplified. Essentially, any square-planar, tetradentate ligand containing at least a couple of nitrogen atoms will suffice: to this end a variety of other porphyrins have been used, as well as Schiff-base and non-porphyrinato nitrogen-containing macrocycles that serve to delineate the role of the porphyrin in dioxygen binding. Tetraphenylporphyrin, in place of the naturally occurring porphyrins, has served as the basis of numerous model systems. It is easily synthesized and derivatized (see below). Its fourfold symmetry precludes formation of chemical isomers that may arise if substitution on the asymmetric, naturally occurring porphyrins is attempted. Moreover, its derivatives can be crystallized. Finally, with the porphyrin *meso* positions occupied by phenyl groups, the molecule is less susceptible to photoinduced oxidation.

In order to obtain five-coordinate species, putative models for a deoxy hemoglobin, access to one side of the porphyrin must be blocked to the coordination of a second axial base (Reaction 4.33), but still must be accessible for the binding of small molecules (O_2, NO, CO, etc). Or second, an axial base may be attached covalently to the porphyrin, to give so-called "tail-under" or "chelated" porphyrins. Here the chelate effect ensures an effectively 100 percent five-coordinate complex with only a 1:1 stoichiometric ratio of axial base to porphyrin. These two approaches are illustrated in Figure 4.14. A third means is to incorporate a sterically bulky substituent in the 2-position of the base, such as a methyl group, to give 2-methylimidazole (4.34). The formation of the hemochrome Fe(porph)(2-MeIm)$_2$, where the iron atom is in the center of the porphyrin ring, is strongly disfavored relative to the 1-methylimidazole analogue, because the 2-methyl substituents clash with the porphyrin ring. The axial base needs to be a strong σ donor, such as imidazole or pyridine, in order to increase affinity at the iron (or cobalt) center for dioxygen (Figure 4.18).

Steric hindrance on one side, or on both, provides a pocket for small molecules to bind and, for O_2, prevents the bimolecular contact of two iron(II)-porphyrinato species that would lead to irreversible oxidation (Reaction 4.29). A picturesque collection of substituted porphyrins has been synthesized. Some of these are illustrated in Figure 4.23.[31,72,160-164] The only system that has led to crystalline dioxygen complexes stable at room temperature is the "picket-fence" porphyrin.[72]* A derivative of this, the "pocket" porphyrin,[165] and various "capped" porphyrins,[166] provide binding sites with steric hindrance even to small diatomic molecules.

In the next section the structures of various derivatives of hemoglobin and its models are presented, and the relationship of structure to ligand-binding properties is examined. Although there is now a wealth of thermodynamic data available from model systems, attention is focused primarily on those for which structural data are also available.



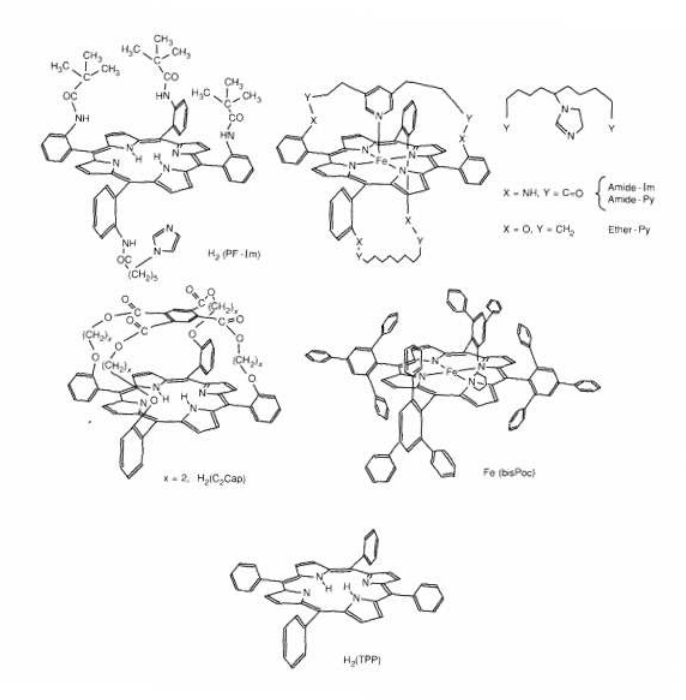


Figure 4.23 - A selection of synthetic porphyrins used to probe the dioxygen-binding process.

* The pivalamido pickets (—NH—CO—$C(CH_3)_3$) of the picket-fence porphyrin are sufficiently bulky that their free rotation is sterically hindered. Thus the various *atropisomers*-$\alpha\alpha\alpha\alpha$, $\alpha\alpha\alpha\beta$, $\alpha\beta\alpha\alpha$, $\alpha\alpha\beta\beta$, where α denotes picket "up" and β denotes picket "down"—can be separated chromatographically on the basis of their different polarities. The tail-under picket-fence porphyrin is derived from the $\alpha\alpha\alpha\beta$ atropisomer.[72]

11.2.4.13: Requirements for a Model System for Hemoglobin is shared under a CC BY-NC-SA 4.0 license and was authored, remixed, and/or curated by LibreTexts.

11.2.4.14: Requirements for Effective Oxygen Carriers

In order for dioxygen transport to be more efficient than simple diffusion through cell membranes and fluids, it is not sufficient that a metalloprotein merely binds dioxygen. Not only is there an optimal affinity of the carrier for dioxygen, but also, and more importantly, the carrier must bind and release dioxygen at a rapid rate. These thermodynamic and kinetic aspects are illustrated in Figure 4.3, a general diagram of energy vs. reaction coordinate for the process

$$M + O_2 \underset{k_{-1}}{\overset{k_1}{\rightleftharpoons}} MO_2 \tag{4.2}$$

where M is an oxygen carrier, for example hemocyanin or a simple nonbiological metal complex. Thermodynamic or equilibrium aspects are summarized by ΔG in Figure 4.3. As illustrated there, ΔG is negative, and thus the forward reaction, dioxygen binding, is spontaneous. The equilibrium constant (K) is given by

$$K = \frac{a(MO_2)}{a(M)a(O_2)}, \tag{4.3}$$

where a is the activity (i.e., effective concentration) of the component. The equilibrium constant is related to the change in free energy by

$$\Delta G^o = -RT \ln K. \tag{4.4}$$

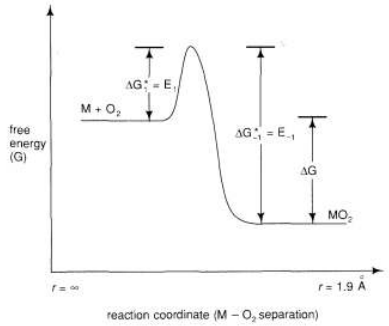


Figure 4.3: Schematic diagram of energy changes in dioxygen binding.

The rate of the forward reaction (k_1) is related to ΔG_1^*; the rate of the reverse reaction (k_{-1}) is related to ΔG_{-1}^*. Provided that oxygen binding is effectively a single-step process, then

$$K = \frac{k_1}{k_{-1}}. \tag{4.5}$$

Usually the rates of the forward and reverse reactions are related by the empirical Arrhenius expression to quantities termed the activation energies (E_1 and E_{-1}) of the reactions, where

$$k_1 = A_1^{\frac{-E_1}{RT}} \; and \; k_{-1} = A_{-1}^{\frac{-E_{-1}}{RT}}. \tag{4.6}$$

These quantities are experimentally accessible through the change in rate as a function of temperature.

Kinetic Factors

It is of little benefit to the organism if its dioxygen carrier, such as hemoglobin, binds and releases O_2 at such slow rates that O_2 is not delivered faster than it would be by simple diffusive processes. Thus, a binding rate within a couple of orders of magnitude of the rate of diffusion, together with the high carrying capacity of O_2 that high concentrations of oxygen carrier enable (noted earlier), and a pumping system ensure adequate O_2 supplies under all but the most physiologically stressful conditions.

Whereas measurements of equilibrium give little or no molecular information, rather more molecular information may be inferred from kinetic data. The processes of binding and release can be examined by a variety of techniques, with timescales down to the picosecond range. The temperature behavior of the rates gives information on the heights of energy barriers that are encountered as dioxygen molecules arrive at or depart from the binding site. The quantitative interpretation of kinetic data generally requires a

molecular model of some sort. It is because of this multibarrier pathway that the equilibrium constant measured as k_1/k_{-1} (Equation 4.5) may differ substantially from the thermodynamically measured value (Equation 4.3).

The simple Adair scheme outlined above is readily adapted to cater to kinetic data.

Dioxygen Reactions

Most biological conversions involving dioxygen require enzymatic catalysis. It is reasonable then that metals found in the proteins involved in the transport and storage of O_2 also frequently appear, with minor modification of ligands, in enzymes that incorporate oxygen from dioxygen into some substrate. Dioxygen, in this case, is not only coordinated, but also activated and made available to the substrate. In the family of proteins with heme groups, hemoglobin is a dioxygen carrier and cytochrome P-450 is an oxygenase. A similar differentiation in function is also found for hemocyanin and tyrosinase from the family of proteins with a dinuclear copper complex at the active site. Note that not all enzymes that mediate the incorporation of oxygen from O_2 into some substrate coordinate and activate dioxygen. For example, lipoxygenase probably catalyzes the conversion of a 1,4-diene to a 1,3-diene-4-hydroxyperoxy species by activation of the organic substrate. The active site does not resemble that of any known oxygen-carrier protein. This topic is discussed more fully in Chapter 5.

11.2.4.14: Requirements for Effective Oxygen Carriers is shared under a CC BY-NC-SA 4.0 license and was authored, remixed, and/or curated by LibreTexts.

11.2.4.15: Role of the Protein in Effecting Biological Oxygen Transport

In our survey of the dioxygen chemistry of iron and copper species in earlier subsections, three general functions for the protein matrix became apparent: provision of ligand(s) in an appropriate stereochemistry; protection of the metal-dioxygen moiety from oxidation and competitive ligands; and modulation of dioxygen affinity through nonbonded interactions with distal groups.

Provision of Ligands to the Metal

In the hemoglobin family the heme group is anchored in a cleft in the globin chain by an imidazole ligand from a histidine residue (the proximal histidine). The other (distal) side of the heme plane is more or less open to accommodate a small sixth ligand (see Figure 4.2).

For hemerythrin and hemocyanin the requirements of the protein chain are more severe. In contrast to the hemoglobin family, all but two of the ligands are provided by the protein chain, and in addition the metal ions are encapsulated as a pair. The exogenous ligands for hemerythrin are a μ-(hydr)oxo moiety and dioxygen or anions (depending on oxidation state); for hemocyanin, the identity of the second exogenous ligand, if there is one at all, is still unclear. Although hemerythrin has a distinctive cofacial bioctahedral structure (Figure 4.10)[46-48] that would appear to be very difficult to assemble in the absence of the protein, it turns out that with a variety of tridentate ligands the (μ-oxo)bis(μ-carboxylato)diiron(III) core may be assembled rather easily.[82,156,157] Thus, this core appears to be a thermodynamically very stable structural motif. Such a synthesis has been termed "self-assembly" and appears to be a common phenomenon in biological systems.[158] The low-temperature assembly of bis-copper(II)-μ-peroxo complexes (models for oxyhemocyanin) from mononuclear copper(l) compounds provides other examples of this phenomenon.[103f,g]

Protection of the Metal-Dioxygen Moiety

The immobilization of the heme group inside the protein prevents (i) the bimolecular contact of an FeO_2 species with an Fe^{ll} species (Reaction 4.29b), the key step in the irreversible oxidation of Fe^{II} porphyrins; (ii) the facile access of nucleophiles that would cause autoxidation (Reactions 4.30 and 4.31); (iii) the oxygenase activity (Reaction 4.32) that is the normal function of other hemoproteins, such as cytochrome P-450, horseradish peroxidase, catalase, etc.; and (iv) the self-oxygenase activity that has been observed in some iron(II) systems that bind dioxygen, activating it for destruction of the ligand itself. Avoiding these last two fates also appears to be very important in the active site of hemocyanin. Finally (v), the globin chain serves to restrain the binding of the distal histidine to give a six-coordinate hemochrome (Reaction 4.33), at least at room temperature.[159] Thus, unoxygenated hemoglobin is held in a five-coordinate state, allowing a rapid rate of oxygen binding and greater oxygen affinity—hemochromes such as $Fe(TPP)(Py)_2$ are impervious to oxygenation and subsequent oxidation.

Modulation of Ligand-binding Properties

The protein chain in hemoglobin may place restraints on the iron-to-proximal histidine bond. On the other side of the heme, the distal histidine and occluded water molecules may hydrogen-bond to the coordinated dioxygen and force ligands to adopt geometries that are different from those observed in the absence of steric hindrances. The conformation of the porphyrin skeleton may also be perturbed by the protein chain. Clearly, it is the protein chain that bestows the property of cooperativity on oligomeric oxygen carriers.

11.2.4.15: Role of the Protein in Effecting Biological Oxygen Transport is shared under a CC BY-NC-SA 4.0 license and was authored, remixed, and/or curated by LibreTexts.

11.2.4.16: Selected Chemistry of Dioxygen, Iron, Copper, and Cobalt

Dioxygen is a powerful oxidant, capable of oxidizing all but the noble metals and of converting many low-valent metal complexes to higher-valent states. As will be detailed in this section, the binding of dioxygen to metals is most usefully considered as an oxidative addition process. The nature of the interaction is determined by the metal, its oxidation state, and its ligands that modulate the redox properties of the metal center. In biological and nonbiological oxygen carriers, several factors allow reversible binding of O_2 to occur, even though this process is metastable with respect to (irreversible) oxidation of the metal, or its ligands, or other species that may be present. Later in this section the bioinorganic chemistry of iron, copper, and cobalt is described. For a wider perspective on the coordination chemistry of these metals, see comprehensive texts on inorganic chemistry.[56-58]

Many techniques have been used to probe the metal-dioxygen moiety. A summary of these techniques, key concepts, and results is presented in Table 4.3.[59-61] UV-visible spectroscopy usually characterizes the oxidation state of the metal and in favorable cases the number, geometry, and ligand field strength of ligands. The O—O and M—O stretching modes may be investigated with infrared spectroscopy, provided that the complex is not a centrosymmetric dimer, for then the O—O stretch for the μ-dioxygen species is infrared-inactive. Resonance Raman techniques complement infrared spectroscopy. Not only are the selection rules different in Raman spectroscopy, but a suitable choice of the irradiating wavelength (to coincide approximately with an M-L electronic transition) can amplify those vibrational modes that are coupled, or in resonance, with the electronic transition. This technique is particularly suited as a probe of the metal-ligand environment of metalloproteins, since the many solely protein vibrational modes disappear into background noise. Geometric information on the orientation of the CO moiety with respect to the heme normal has been obtained by examining polarization behavior of infrared bands following photolysis of the Fe—CO bond by linearly polarized light.

Spin and oxidation states of mononuclear iron-porphyrin systems may be assigned directly from magnetic susceptibility measurements and indirectly from Mössbauer spectroscopy. Variable temperature susceptibility measurements are particularly useful for detecting dinuclear systems that share at least one ligand in common if there is antiferromagnetic (or ferromagnetic) coupling of the electron spin of one metal center with that of a second.

Definitive characterization of the stereochemistry is usually provided by x-ray diffraction data when single crystals are available. In general, the level of resolution and precision available from protein crystal structures leads to tantalizing uncertainties over the geometry of the M—O_2 species and of the structural changes occurring on oxygenation that are the origin of cooperativity. Precise structural data are more readily obtained from small-molecule model systems. The relevance of these to biological systems is established through congruence of spectroscopic and functional properties. X-ray diffraction techniques also provide important information on the environment beyond the immediate surroundings of the metal center: this information is usually unobtainable from other techniques, although recent developments in two-dimensional NMR spectroscopy can provide this information for diamagnetic systems. Limited information may be obtained with the use of spin labels or, if the metal center is paramagnetic, with EPR techniques.

Two other techniques that selectively probe the immediate environment of the metal center are EXAFS (Extended X-ray Absorption Fine Structure)[60] and XANES (X-ray Absorption Near-Edge Structure).[61] The former may yield information on the number and type of bonded atoms and their radial separation from the metal center. The latter technique may reveal the oxidation state and, in principle, may yield geometric information, although in its present state of development some interpretations are contentious. Both techniques have the advantage of not requiring crystalline material. The structural information is more reliable if definitive model systems are available for comparison.

X-ray (and, less frequently, neutron) diffraction techniques on single crystals give absolute structural information* and thus provide the basis for interpretation of data obtained from these other techniques that yield relative structural information.

---

* In favorable situations, sophisticated NMR techniques have been applied successfully to detennine the polypeptide folding (e.g., in metallothionein).[55]

Table 4.3: Techniques used to probe the active sites of oxygen carriers

Technique	Abbrev.	Description of Technique	Description of Results
Nuclear Magnetic Resonance	NMR	Quantized orientation of nuclear spin in a magnetic field. Energy separations sampled with radio-frequency radiation.	Identification of histidine by deuterium exchange (N—H vs. N—D) at or near metal, especially if paramagnetic.
Electron Paramagnetic Resonance	EPR	Quantized orientation of electron spin in a magnetic field. Energy separations samples with X- or Q-band microwave radiation.	Location of unpaired electron density from hyperfine splitting by metals or atoms with nuclear spin.
Magnetic Susceptibility		Strength of interaction of sample with magnetic field. Solid state or solution state by Evans' NMR method.	Identification of spin state, spin-equilibria, and spin coupling (ferro- or antiferromagnetic); identificaiton of Fe^{III}—O—Fe^{III} moiety.
Infrared Spectroscopy	IR	Vibrational modes involving change in dipole moment.	Classificaiton of O—O moiety (superoxo vs. peroxo). Identification of *v*(M—O) and *v*(M—O—M) modes, etc.
Raman and Resonance Raman	R, RR	Vibrational modes involving a change in polarizability. For RR enchancement of modes coupled with electronic transition excited by laser light source.	Complementary to *v*(O—O) and *v*(M—O) especially in metalloproteins. In porphyrins, oxidation and spin state.
UV-visible spectroscopy	UV-Vis	Valence electron transition	Electronic state of metal from d-d transitions. Identification of unusual ligands, e.g., CU(II)—SR, FE^{III}—OPh, Fe^{III}—O—Fe^{III}. Single crystals and polarized light give geometrical information.
X-ray Photoelectron Spectroscopy	XPS (ESCA)	Inner-shell electron transitions.	Oxidation state of metal.
Mössbauer Spectroscopy		Excitation of nuclear spin by γ rays.	Oxidation and spin state. Antiferromagnetic coupling (Fe only).
X-ray Single-crystal Diffraction		Fourier transform of diffraction data reveals location of electron density.	Precise three-dimensional structure, bond distances and angles for small molecules. Lower resolution and precision for proteins.
Extended X-ray Absorption Fine Structure	EXAFS	Backscattering of x-rays produces interference fringes on absorption curve at energies just greater than metal absorption edge (Kβ transition)	Number, type, and radial distance of ligand donor atoms bonded to the metal.

Technique	Abbrev.	Description of Technique	Description of Results
X-ray Absorption Near-edge Structure	XANES	Similar to EXAFS except that absorption is monitored at energies near and below the absorption edge.	As for EXAFS. May give geometric information

11.2.4.16: Selected Chemistry of Dioxygen, Iron, Copper, and Cobalt is shared under a CC BY-NC-SA 4.0 license and was authored, remixed, and/or curated by LibreTexts.

11.2.4.17: Stereochemical Changes Upon Ligation

Upon binding a second axial ligand, the iron center together with the axial base move toward the plane of the porphyrin, initiating a change in spin state from high-spin to low-spin when the sixth ligand is O_2 or CO or any other strong ligand with an even number of valence electrons. Given these general features, what are the structural differences between systems that bind O_2 with high affinity and those that bind O_2 with low affinity? The answers to this question are relevant to understanding at the molecular level the mechanism of cooperativity, where a low-affinity conformation, the T state, and a high-affinity conformation, the R state, are in dynamic equilibrium in one tetrameric molecule. In looking at crystallographic data one sees a particular conformation frozen in the crystal, usually the one of lowest free energy among many in equilibrium in the solution state. The R $\rightleftharpoons$ T equilibrium for hemoglobin is moderately rapid, at 4×10^3 s^{-1}; hemocyanin also switches quaternary conformations with a similar rate constant.[4]

Human hemoglobins are a heterogeneous group. Many mutants are known, and several have been structurally characterized. A structural alteration that affects the equilibrium between R and T states has a marked effect on ligand affinity and cooperativity in hemoglobin. If a specific amino-acid substitution destabilizes the T state, then the transition to the R state will occur earlier in the ligation process, and the hemoglobin will have an increased oxygen affinity. Hemoglobin Kempsey is an example. In this mutant an aspartic acid on the β chain is replaced by asparagine. Conversely, if the R state is destabilized, then the hemoglobin will have a lowered oxygen affinity. Hemoglobin Kansas is an example. Here an asparagine on the β chain has been replaced by threonine.[9]

Structural Changes in Normal-affinity Systems

It was proposed earlier that the molecule Fe(PF)(1-MeIm)(O_2) in the solid or solution state was a fair approximation to the reference gas-phase molecule. The axial base, although not oriented for minimization of contacts with the porphyrin (i.e., $\phi = 45°$), is well-removed from an eclipsing orientation where $\phi = 0 \pm 10°$; the Fe atom is centered in the plane of a highly planar porphyrin; the O_2 ligand is oriented for minimization of contacts with the porphyrin, and its geometry is largely unconstrained by distal groups (the pickets); no groups are hydrogen-bonded to the axial base. The major difference from the reference state is that there is a significant attractive interaction between the electronegative dioxygen moiety and the amide groups on the pickets, and a smaller repulsive interaction with the picket t-butyl groups.[176]

For the CO adduct, contacts with the pickets are all at ideal van der Waals' separations and the Fe—CO moiety is free to assume its normal linear geometry. For CO binding the reference molecule is again the carbonyl adduct of the iron picket-fence porphyrinato molecule. In contrast to O_2 binding, there are no specific distal effects, such as hydrogen bonding, by which CO affinity may be increased; there remain many ways, as with O_2 binding, by which CO affinities may be reduced. Thus, the CO binder with highest affinity is the iron picket-fence porphyrin.

The O_2 affinities of myoglobin, R-state hemoglobin, and the Fe(PF)(1-MeIm) system are similar. However, the means by which this is achieved are different, and this difference is reflected most clearly in the kinetics of binding and release of O_2, which for Mb are much slower. The similarities and differences are summarized in Table 4.9, which is culled from Tables 4.2, 4.4, and 4.5.

Table 4.9 - Comparison of the picket-fence porphyrin system with Mb.

a) Solution state studies on Fe(PF-Im). Structural details on Fe(PF)(1-Melm)(O_2) and Fe(PF)(2-Melm).

Characteristic	Mb	Fe(PF-Im)[a] Fe(PF)(1-MeIm)	Fe(Poc-PF) (1-MeIm)
$P_{1/2}(O_2)$, Torr	0.7	0.58	0.36
$P_{1/2}(CO)$, Torr	0.018	0.000022	0.0015
$k_{on}(O_2)$, $\mu M^{-1}s^{-1}$	15	430	2.2
$k_{off}(O_2)$, s^{-1}	10	2,900	9
$k_{on}(CO)$, $\mu M^{-1}s^{-1}$	0.50	36	0.58
$k_{off}(CO)$, s^{-1}	0.015	0.0078	0.0086
Solvent	H_2O/PO_4^{3-}	toulene	toulene
Local Environment	His (H_2O) polar, protic	H-N(amide) polar, aprotic	H-N (amide) phenyl
O_2 • • • distal, Å	2.97(18)	NH 4.06(5) CH_3 2.67(6)	
CO • • • distal, Å (calc.)	2.7	NH 5.0 CH_3 3.3	
Fe-N_{Im}(deoxy), Å	2.22	2.095(6)	
Fe-N_{Im}(oxy), Å	2.07(6)	2.07(2)	
Fe-O, Å	1.83(6)	1.75(2)	
ϕ_{Im} (deoxy), deg	19°	22.8°	
ϕ_{Im} (oxy), deg	1°	20°	
ϕ_{O2}, deg	~0°	45°	
Fe • • • porph(deoxy), Å	0.42	0.43	
Fe • • • porph(oxy), Å	0.18	-0.03	

For the cobalt-dioxygen derivative, the putative hydrogen bonding between the dioxygen and the amide groups of the pickets assumes greater importance because the coordinated dioxygen is substantially more negative. Again the picket-fence porphyrin, being structurally characterized, is the reference system. Although no Co picket-fence porphyrin structures have been determined, the structures may be predicted with confidence from the iron analogues together with related structures of Co^{II} and Co^{III} tetraphenylporphyrinato systems.*

* For $CoHbO_2$, single-crystal EPR spectra have been interpreted in terms of a nearly triangularly coordinated O_2,[197] although a crystal structure of $CoMbO_2$ shows a bent CoOO group.[198] There is no precedent for this triangular arrangement in any Co^{III}-superoxo (O_2^{1-}) system, whereas there are many for angularly coordinated O_2 in electronically not dissimilar square-planar Schiff-base systems.[66] Regardless of geometry, the picket amide • • • O_2 contacts do not change substantially.

Structural Changes in Low-affinity Systems

The 2-methyl substituent on 2-methylimidazole is not sterically active in the five-coordinate structures Fe(PF)(2-MeIm) and Fe(TPP)(2-MeIm), since the iron atom is displaced from the plane of the porphyrin by the expected amount and the Fe—N_{Im} bond is unstretched and similar to that in deoxyhemoglobin (low O_2 affinity) and deoxyMb (higher O_2 affinity). Moreover, resonance Raman measurements also indicate little strain† in this bond.[200] In other words, there is no "tension at the heme," a key concept in early discussions of cooperativity before structures on model systems and high-resolution, refined protein structures became

available.[11a] On moving into the plane of the porphyrin upon oxygenation, the 2-methyl substituent prevents the Fe-imidazole group from achieving its optimum geometry with the iron at the center of the porphyrin hole, as seen in the structure of Fe(PF)(1-MeIm)(O_2). Thus, the sterically active 2-methyl substituent leads to lowered O_2 (and CO) affinity relative to the 1-methyl analogue. In metrical terms the lowered affinity is reflected in an increase in the sum of the axial bond lengths from 1.75 + 2.07 = 3.82 Å to 1.90 + 2.11 = 4.01 Å.

In the crystal structure of Fe(C_2Cap)(1-MeIm)(CO) the cap is about 5.6 Å from the porphryin plane.[121d] Hence, in the crystal structures of the free base H2(C_2Cap)[201a] and FeCI(C_2Cap)[201b] species, in which the cap is screwed down to approximately 4.0 Å from the porphyrin plane, considerable conformational rearrangement of the cap and the four chains attaching it to the porphyrin is needed to provide room for a small ligand such as CO. This is even more pronounced in a Co(C_3Cap) complex where the cap is only 3.49 Å from the mean porphyrin plane.[202] Thus not only is affinity for CO lowered, but some additional discrimination against it is induced, since a linear, perpendicular coordination creates considerable strain energy elsewhere in the molecule.

For the pocket porphyrin (Figure 4.23), structural data are available on the carbonyl adduct.[121b]The CO ligand is unable to achieve the linear perpendicular geometry seen in the high-affinity picket-fence porphyrin derivative, Fe(PF)(1-MeIm)(CO),[110]and distortion of the porphyrin core is greater. In the pocket-porphyrin system, O_2 affinity is unaffected, but CO affinity is lowered.

The crystal structure of partially oxygenated hemoglobin, $[\alpha\text{-}FeO_2]_2[\beta\text{-}Fe]_2$,[191a] reveals that the quaternary structure, except in the immediate vicinity of the α hemes, which have O_2 coordinated, resembles that of T-state deoxyhemoglobin rather than R-state liganded hemoglobin. In accord with the low affinity of T-state hemoglobin, the Fe—N_{Im} bonds for the six-coordinate α-hemes at 2.37 Å are significantly longer than those in fully oxygenated R-state oxyhemoglobin, $[\alpha\text{-}FeO_2]_2[\beta\text{-}FeO_2]_2$ in the notation above, (1.94 (α-hemes) and 2.06 Å (β hemes)) and that found in oxymyoglobin (2.07 Å). In contrast to the R-state structure and oxyMb, the a-hemes are folded as seen in the deoxy parent, leaving the Fe still substantially displaced (0.2 Å) from the plane of the four pyrrole nitrogen atoms. The deoxyhemoglobin T-state quaternary structure also has been observed in two other partially liganded hybrid hemoglobins, $[\alpha\text{-}FeCO]_2[\beta\text{-}Mn(II)]_2$[203] and $[\alpha\text{-}Ni]_2[\beta\text{-}FeCO]_2$.[191d] Again, structural changes upon coordination do not propagate beyond the immediate vicinity of the liganded heme to the critical $\alpha_1\beta_2$ interfaces.

Note that although the crystal structure of hemoglobin A reveals that access to the binding site for the β chains is blocked by groups at the entrance to the cavity above the iron center, this does not prevent facile access to the binding site; the rate of O_2 binding is slowed by a factor of only five. A similar situation occurs also for vertebrate myoglobins.

The large structural differences that exist between deoxy (T) and oxy (R) hemoglobin and the much smaller differences between deoxy (T) and partially liganded (T) hybrid hemoglobin are shown in Figure 4.32.[203]

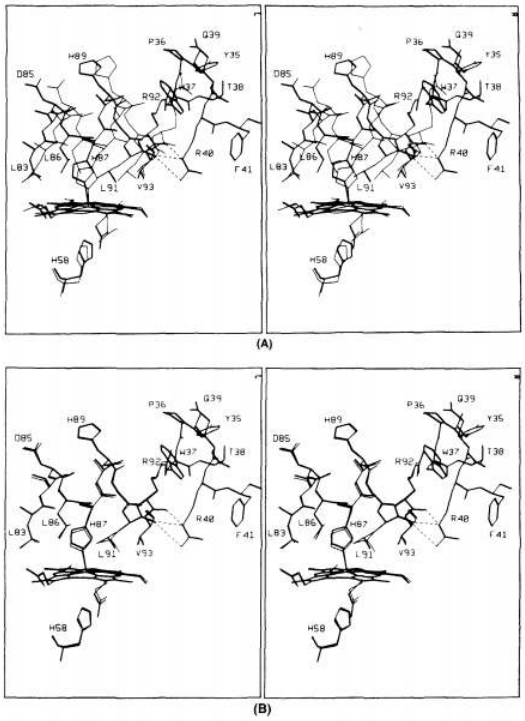


Figure 4.32 - The effects of changes in ligation and in quaternary structure on stereochemistry in the vicinity of α hemes:[203] (A) Stereodiagram of the large structural differences between deoxy T-state (heavy lines) and oxy R-state hemoglobin (light lines). (B) Stereodiagram of the small structural differences between deoxy T-state (heavy lines) and partially liganded T-state [α-FeCO]$_2$[β-Mn]$_2$ hemoglobin (light lines). Reproduced with permission from A. Arnone et al., J. Mol. Biol. **188** (1986), 693-706.

Because of the steric hindrance afforded by the distal histidine, all biological systems have low affinity for CO relative to the picket-fence porphyrins, with the exception of mutants where the distal histidine has been replaced by glycine. Thus low affinity to CO is associated primarily with the inability of the Fe-CO group to achieve its preferred linear geometry perpendicular to the porphyrin.

Low-affinity O_2 binding in the hemoglobins appears to be associated with the inability of the Fe-proximal histidine unit to move into the plane of the porphyrin and less so to distal effects, such as a cavity too small to accommodate the coordinated ligand. The blocked access to the site affects the kinetics but not necessarily the thermodynamics of ligand binding, as evidenced by the structure of T-state [α-FeNi]$_2$[β-FeCO]$_2$[191d] Some similarities between the structures and properties of partially oxygenated (T-state) [α-FeO$_2$]$_2$[β-Fe]$_2$ hemoglobin and Fe(PF)(2-MeIm)(O_2) are provided in Table 4.10. In the synthetic systems low O_2 affinity can be induced by 2-methyl substituents—a restraint on the movement of the Fe-imidazole moiety analogous to that provided by the protein chain. A second means is by distal effects, such as caps and straps.

Table 4.10 - Comparison of the low-affinity picket-fence porphyrin system with low-affinity (T-state) partially liganded hemoglobin.

a) Ligand binding to Fe(PF)(1,2-Me$_2$Im)

Characteristic	HbA^T $[\alpha\text{-}FeO_2]_2[\beta\text{-}Fe]_2$	Fe(PF)(2-MeIm) Fe(PF)(1,22-Me_2Im)[a]
$P_{1/2}(O_2)$, Torr	46, first O_2	38
$P_{1/2}$(CO), Torr	~0.7, 1st CO	0.0089
$k_{on}(O_2)$, $\mu M^{-1}s^{-1}$	2.9(α)	106
$k_{off}(O_2)$, s^{-1}	183(β)	46,000
k_{on}(CO), $\mu M^{-1}s^{-1}$	0.099	1.4
k_{off}(CO), s^{-1}	0.09	0.14
Solvent	Tris buffer, pH 7, no 2,3-DPG	toluene
Local Environment	histidine polar	H-N(amide) polar, aprotic
O_2 • • • distal, Å	?	NH 3.88 CH_3 2.77(3)
CO • • • distal, Å (calc.)		NH 4.9 CH_3 3.5
Fe-N_{Im}(deoxy), Å	2.13(6) (average of α and β	2.095(6)
Fe-N_{Im}(oxy), Å	2.24(10)	2.107(4)
Fe-O, Å	1.82(4)	1.898(7)
ϕ_{Im} (deoxy), deg	21(3) (average of α and β	22.8
ϕ_{Im} (oxy), deg	~6	22.2
ϕ_{O2}, deg	?	45
Fe • • • porph(deoxy), Å	0.38(5) (average of α and β	0.43
Fe • • • porph(oxy), Å	0.19(5)	0.09

† Shortly (10^{-9}-10^{-12} s) after a ligand dissociates, a large difference in ν(Fe—N_{Im}) between R and T structures is observed, prior to relaxation to the equilibrium R and T conformations.[199]

Structural Changes in High-affinity Systems

Few structural data are available for high-affinity oxygen carriers. The crystal structures of two leghemoglobin derivatives, a monomeric myoglobin-like oxygen carrier found in the nitrogen-fixing nodules of legumes, are known at 2.0 and 3.3 Å.[204,205] The binding pocket appears more open, perhaps allowing H_2O to enter and partake in stronger hydrogen bonding than that offered by the distal imidazole. Consistent with this notion is the more rapid rate of autoxidation observed for oxyleghemoglobin. *Aplysia* oxymyoglobin, which lacks a distal histidine, also autoxidizes rapidly,[204] although a distal arginine further along the helix E, E10Arg, fulfills the role of the distal histidine by hydrogen bonding to the sixth ligand, at least in the fluoride derivative, met-MbF.

Although no structural data are available, a tenfold increase in O_2 affinity was observed between an ester-strapped porphyrin, offering no hydrogen-bonding possibilities, and its conformationally very similar amide analogue. O_2 • • • amide hydrogen bonding was demonstrated by means of NMR shift data (Zn and Fe—CO complexes vs. the Fe—O_2 complex) and from infrared spectroscopy, which showed shifted amide N—H absorptions.[166]

The *specific* structural features that lead to the extraordinarily high affinity for O_2 and low affinity for CO in hemoglobin *Ascaris* remain unidentified. This high affinity is due to an *extremely* slow dissociation rate of O_2 of only $0.1s^{-1}$; in most hemoglobins the

rate is about 10 to 2,500 s^{-1} (Table 4.2). Dioxygen binding is thus close to irreversible. Figure 4.27 shows that hydrogen bonding to the coordinated dioxygen ligand, unrestrained motion of the Fe-proximal histidine group into the plane of the porphyrin, hydrogen bonding to the proximal histidine, and, in the deoxy form, compression of the Fe—N_{Im} bond and decrease in the out-of-plane displacement of the Fe atom will all increase O_2 affinity over that of a system where these effects are absent.

When hydrogen bonding is impossible, as in various synthetic systems (Table 4.5) as well as hemoglobin *Glycera* and Mb(E7His → Gly), O_2 affinity is much lower than when hydrogen bonding can occur (see Table 4.6), especially for the cobalt analogues. But caution is needed in the absence of complete structural information: the lowered affinity of *Aplysia* hemoglobin had been attributed to the lack of a distal histidine and its attendant hydrogen-bonding capabilities. However, the crystal structure reveals that an arginine residue, normally directed out into the solution, is capable of folding back into the ligand-binding pocket and of hydrogen bonding to ligands at the sixth site. In oxyhemerythrin the hydrogen bonding of the coordinated hydroperoxy group to the oxo bridge linking the two iron atoms (Figure 4.10B), described in Section II.F.1, may not only increase the stability of oxyhemerythrin,[146] but also facilitate electron transfer that occurs in dioxygen binding.[205]

11.2.4.17: Stereochemical Changes Upon Ligation is shared under a CC BY-NC-SA 4.0 license and was authored, remixed, and/or curated by LibreTexts.

11.2.4.18: Structural Basis of Ligand Affinities of Oxygen Carriers

The interaction of ligands, such as dioxygen, with metal complexes, such as iron-porphyrinato systems, and the means by which this interaction is characterized, have been covered in broad outline in the previous sections. As noted earlier, the affinities of hemoglobins for carbon monoxide and dioxygen span a wide range (see Table 4.2 and Figure 4.24). In this section the active site is examined in much finer detail than before in order to develop relationships between perturbations in structure and affinity (and hence function)—so called structure-function relationships. The reference point is the somewhat hypothetical situation where the dioxygen binder is in the gas phase and independent of interactions with solvent molecules, solute molecules, and itself, and where dioxygen, carbon monoxide, and other small molecules may bind without steric constraints—in other words, a state where intrinsic affinity is measured. In this section attention is focused exclusively on the hemoglobin family and on iron- and cobalt-porphyrinato systems. In recent years structural data on hemoglobin, myoglobin, and their derivatives have become available with a precision that permits meaningful comparison with the more precisely determined model or synthetic systems. In addition, the various hemoglobins and myoglobins, and especially the naturally occurring mutants of hemoglobin A (human Hb), have provided a sort of poor man's site-directed mutagenesis. Now the techniques of molecular biology permit the site of mutation to be selected, the altered gene to be inserted into *E. coli*, and the mutant protein to be expressed in large (mg) quantities. With the conditions for crystallization of hemoglobins now well-established, we can discover quite rapidly what structural perturbations are caused by the substitution of one amino acid for another, and can relate these to the perturbations in properties, such as cooperativity, dioxygen affinity, and kinetics of ligand binding.

The principles enunciated here are applicable generally to hemerythrin and hemocyanin; however, we currently lack the thermodynamic and especially structural data we would like to have for these systems.

Ligand Affinities in Hemoglobins and Their Models

The O2 affinities in biological carriers span five orders of magnitude, which at room temperature corresponds to a difference in the free energy of oxygen binding

$$\delta\Delta G = -RTln(K_{max}/K_{min}) = -RTln(P_{1/2min}/P_{1/2max}) \tag{4.47}$$

of about 6.0 kcal/mol. This wide range of O_2 and CO affinities has not yet been paralleled in synthetic systems; the values for O_2 affinity do not exceed those for R-state human hemoglobin. A selection of values from model systems is given in Table 4.5.[23,31,160-165] For the flat-open porphyrin system (Figure 4.23) the dioxygen ostensibly binds in an unconstrained manner, but is actually subject to solvent influences. In order to obtain thermodynamic constants on these "unhindered" systems, one must gather data at several low temperatures and then extrapolate to room temperature, or obtain them from kinetic measurements, $K = k_{on}/k_{off}$, at room temperature.

For the picket-fence porphyrins, dioxygen binds in a protected pocket that is deep enough to accommodate it and to prevent the dimerization that leads to irreversible oxidation, provided that there is a slight excess of base to ensure full saturation of the coordination sites on the unprotected face of the porphyrin.[72] Thus the picket-fence, the capped, and the bis-pocket porphyrins reversibly bind dioxygen at room temperature with little oxidation over many cycles. This stability facilitated isolation of crystals of a synthetic iron-dioxygen species of the picket-fence porphyrin. The capped porphyrin offers a more highly protected site. The low affinity these latter systems have for dioxygen indicates that the binding cavity is so small that repulsive steric interactions between coordinated dioxygen and the cap are unavoidable. The left-hand side of Figure 4.24 depicts on a logarithmic scale the range of O_2 affinities. Each power of 10 corresponds to around 1.2 kcal/mol at 25 °C.

The right-hand side of Figure 4.24 illustrates the range of affinities for CO binding. For many synthetic systems the CO affinities are orders of magnitude greater than in the biological systems that have an O_2 affinity similar to the synthetic; for example, see the entries for the picket-fence porphyrin. Comparison of the left- and right-hand sides of Figure 4.24 reveals that the strongest O_2 binder, hemoglobin *Ascaris*, is one of the weakest CO binders. The O_2 affinity of the picket-fence porphyrins is very similar to that of myoglobin, but, as will be detailed shortly, one cannot infer from this that the binding sites are strictly comparable. Indeed, similar affinities have been observed with a non-porphyrin iron complex.[121,162] Moreover, if the CO affinity of myoglobin paralleled that of the picket-fence porphyrins, some 20 percent of myoglobin (and hemoglobin) would be in the carbonmonoxy form (in contrast to the approximately 3 percent that occurs naturally), a level that could render reading this section while chewing gum physically taxing.[117]

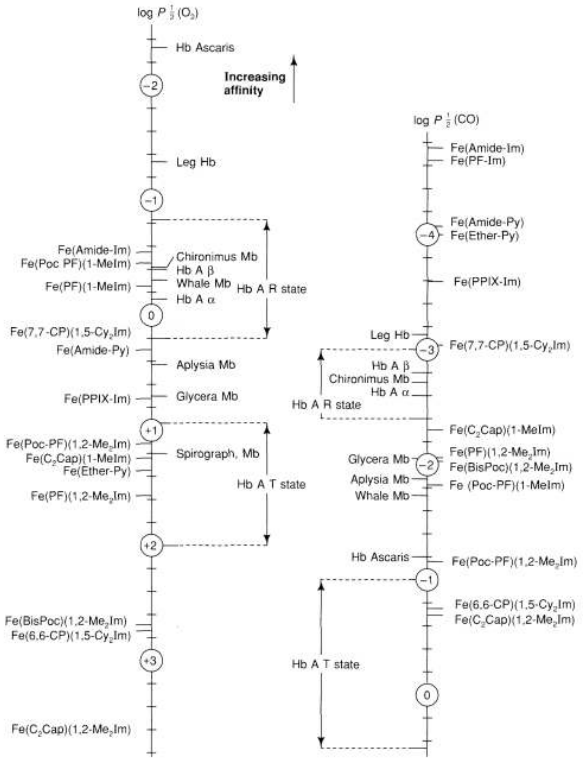


Figure 4.24 - CO and O_2 affinities of a selection of hemoglobins and model systems. Affinities are given as $P_{1/2}$, and the scale is logarithmic. One order of magnitude corresponds to 1.2 kcal/mol at 25 °C.

Table 4.5 - Thermodynamics and kinetics of ligand binding to synthetic oxygen carriers at 20-25 ºC

a) When available $P_{1/2}$ are from thermodynamic measurements, otherwise from k_{on}/k_{off}, where solubility of O_2 in toluene is 1.02×10^5 M/Torr and of CO in toluene is 1.05×10^{-2}; solubilities in benzene are very similar.

b) Some k_{off} are calculated from $K(O_2)$, $k_{on}(CO)$, and M.

Carrier	Dioxygen			Binding		Carbon	Monoxide		Binding	
	$P_{1/2}(O_2)$ Torr	∇H kcal/mol	∇S eu	k_{on} $M^{-1}s^{-1}$	k_{off} s^{-1}	$P_{1/2}(CO)$ Torr	∇H kcal/mol	∇S eu	k_{on} $M^{-1}s^{-1}$	k_{off} s^{-1}
Toluene/ benzene solvent										
Picket fence, pocket										
Fe(PF-Im)	0.58	-16.3	-40	430	2,900	0.000022	—	—	36	0.0078
Fe(PF)(1,2-Me_2Im)	38	-14.3	-42	106	46,000	0.0089	—	—	1.4	0.14
Fe(Poc-PF)(1-MeIm)	0.36	—	—	2.2	9	0.0015	—	—	0.58	0.0086
Fe(Poc-PF) (1, 2-Me_2lm)	12.6	-13.9	-28	1.9	280	0.067	—	—	0.098	0.055
Fe(Bis-Poc) (1, 2-Me_2Im)	508	-14.4	-47	—	—	0.0091	—	—	—	—
Cap										
Fe(C_2Cap) (1-MeIm)	23	-10.5	-28	—	—	0.0054	—	—	0.95	0.05
Fe(C_2Cap) (1, 2-Me_2Im)	4,000	-9.7	-36	—	—	0.20	—	—	—	—
Strapped										
Fe(7, 7-CP) (1, 5-Cy_2Im)	1.4	—	—	65	1,000	0.00091	—	—	6	0.05
Fe(6, 6-CP) (1, 5-Cy_2Im)	700	—	—	0.1	800	0.17	—	—	0.03	0.05
Flat open										
Fe(PPIX-Im)	5.6	—	—	62	4,200	0.00025	—	—	11	0.025
Bis-strapped										

Carrier	Dioxygen Binding					Carbon Monoxide Binding				
	$P_{1/2}(O_2)$ Torr	ΔH kcal/mol	ΔS eu	k_{on} $\mu M^{-1}s^{-1}$	k_{off} s^{-1}	$P_{1/2}(CO)$ Torr	ΔH kcal/mol	ΔS eu	k_{on} $\mu M^{-1}s^{-1}$	k_{off} s^{-1}
Fe(Amide-Im)	0.29	—	—	310	620	0.000017	—	—	40	0.067
Fe(Amide-Py)	2.0	—	—	360	5,000	0.00009	—	—	35	0.03
Fe(Ether-Py)	18	—	—	300	40,000	0.0001	—	—	68	0.069
H_2O, alkylammonium micelles, pH 7.3										
Fe(PPIX-Im)	1.0	-14.0	-3.5	26	4.7	0.002	-17.5	-34	3.6	0.009
Fe(MPIX-Im)	0.57	—	—	22	23	0.0013	—	—	11	0.019
Fe(MPIX-Py)	12.2	—	—	1	380	0.0021	—	—	12	0.035

There is a convenient index to summarize the extent to which CO (or O_2) binding is discriminated against for a given iron-porphyrin system. M is defined as the ratio of O_2 affinity (as $P_{1/2}$) to CO affinity for a particular system and experimental conditions:

$$M = \frac{P_{1/2}(O_2)}{P_{1/2}(CO)} \tag{4.48}$$

From Figure 4.24 and from Tables 4.2 and 4.5 the M values calculated may be somewhat arbitrarily divided into three classes: those where $M > 2 \times 10^4$ (good CO binder); those where $2 \times 10^2 < M < 2 \times 10^4$; and those where $M < 2 \times 10^2$ (good O_2 binder). An analogous parameter, N, may be defined to summarize the differences in the O_2 affinity between an iron-porphyrin system and its cobalt analogue:

$$M = \frac{P_{1/2}(O_2—Co)}{P_{1/2}(O_2—Fe)}. \tag{4.49}$$

For the picket-fence porphyrins and for vertebrate hemoglobins N is in the range 10 to 250, whereas for the flat-open porphyrins and for some hemoglobins that lack a distal histidine (e.g., hemoglobin *Glycera* and hemoglobin *Aplysia*), N is at least an order of magnitude larger, indicating for these latter species that the cobalt analogue binds O_2 relatively poorly[167,168] (see Table 4.6).

Note that whereas the O_2 binding of the picket-fence porphyrins is similar to that for myoglobin, the kinetics of the process are very different; the synthetic system is more than an order of magnitude faster in k_1 and k_{-1} (often also referred to as k_{on} and k_{off}). On the other hand, O_2 binding to the pocket porphyrin is similar to that for the biological system. The factors by which ligand affinities are modulated, generally to the benefit of the organism, are subtle and varied, and their elucidation requires the *precise* structural information that is currently available only from x-ray diffraction experiments. Figure 4.25 shows the structural features of interest that will be elaborated upon in the next subsections.[110,169]

Table 4.6 - Relative affinities (M) of iron-porphyrinato systems for O_2 and CO, and relative affinities (N) for O_2 of iron and cobalt-porphyrinato systems.

Compound	$P_{1/2}(Fe—CO)$ Torr	$P_{1/2}(Fe—O_2)$ Torr	$M = P_{1/2}(Fe—O_2)/P_{1/2}(Fe—CO)$	$N = P_{1/2}(Co—O_2)/P_{1/2}(Fe—O_2)$
H_2O, pH 7				
Whale Mb	0.018	0.51	28	1,200
Whale Mb (E7H	0.0049	6.2	1,300	1

is → Gly)			
Aplysia Mb	0.013	2.7	5×10^{-8}
Glycera Mb	0.00089	5.2	5×10^{-8}
Fe(PPIX-Im)	0.002	1.0	500
Toluene/Benzene			

ne			
Fe(PF-Im)/Co(PF)(1-MeIm)	0.000022	0.58	27,400
M(PF)(1,2-Me$_2$Im)	0.0089	38	49,200
M(Bis-Poc	0.0091	508	55,800

)-(1,2-Me$_2$Im)			
Fe(PPIX-Im)/Co(PPIX)(1-MeIm)	0.00025	5.6	2,3,2,0,0,0,0
M(C$_2$-Cap)(1	0.0054	23	4,4,0,0,0,0

- M e l m)	

11.2.4.18: Structural Basis of Ligand Affinities of Oxygen Carriers is shared under a CC BY-NC-SA 4.0 license and was authored, remixed, and/or curated by LibreTexts.

11.2.4.19: Structures Relevant to Liganded Hemoglobins

Stereochemistry of the Active Site

Before the advent of techniques that enabled the preparation and stabilization of oxyhemoglobin crystals, key information on the probable structure of oxyhemoglobin and thence on the mechanism of cooperativity was extrapolated from structures of methemoglobin derivatives[11] and from various five- and six-coordinate cobalt-porphyrinato complexes.[110,112,113] The structures of these met derivatives have proved to be similar to that of oxyhemoglobin, at least in the stereochemistry of the metalloporphyrinato species and for the protein tertiary and quaternary structure as well.

Two synthetic iron-dioxygen adducts built from the picket-fence porphyrins have been structurally characterized.[172,187] The high, effectively fourfold symmetry of the binding pocket in these systems results in fourfold disorder of the angularly coordinated dioxygen molecule, and precludes the precise and accurate measurements of the Fe—O—O angle and O—O separation that are grist to the theoretical mills.* Figure 4.28B illustrates the stereochemistry for one conformer. Subsequently, the structures of several dioxygen adducts of biological oxygen carriers have been determined.[183,188-191] Although the dioxygen moiety is usually ordered, the precision is tantalizingly just less than that needed to decide whether the apparently more-linear geometry seen for oxyerythrocruorin[183] and oxyhemoglobin[190] is significantly different from that for oxymyoglobin[188] and therefore attributable to the water molecule or imidazole that is hydrogenbonded to the coordinated dioxygen ligand. Nonetheless, several interesting differences emerge.

The axial base in oxymyoglobin and oxyhemoglobin is almost eclipsed; that is, $\phi_1 \approx 0°$. The axial base has moved from a tilted position in deoxyhemoglobin to a symmetric one in oxyhemoglobin. In the absence of steric constraints, the iron atom is essentially in the center of the porphyrin plane for Fe(PF)(1-MeIm)(O_2), oxymyoglobin, and oxyhemoglobin. For the 2-methyl analogue, Fe(PF)(2-MeIm)(O_2), the iron remains significantly out of the plane, as also appears to occur for oxyerythrocruorin.

In the structure of Fe(TPP)(Py)(CO), Figure 4.30, a model for carbonyl hemoglobins, the iron atom is in the plane and the Fe—C≡O bond is linear and perpendicular, as expected.[118] Not so for carbonyl hemoglobins, where the blob of electron density that is identified with the coordinated carbon monoxide lies substantially off the normal to the porphyrin. We return to this point shortly. In general, with the exception of the coordinated ligand, the structures of sixcoordinate low-spin hemoglobins, whether Fe^{II} or Fe^{III}, are similar. Indeed, the refined structures of oxy- and carbonmonoxyhemoglobin are superimposable within experimental uncertainties, except in the immediate vicinity of the diatomic ligand. Some metrical details are given in Table 4.8.[11c,118,121,172,183,187,188,190-192]

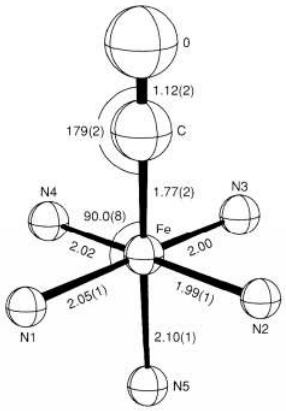


Figure 4.30: Molecular structure of Fe(TPP)(py)(CO), a model for unhindered coordination of CO.[118]

Table 4.8 - Metrical details of selected liganded hemoglobins and their modelsa a) See Figure 4.25 for definition of symbols. b) Alternative interpretation of EXAFS data.

Compound	Resol. Å	Fe-N_p Å	Fe-porph Å	Doming Å	Fe-L_1 Å	Fe-L_2 Å	Fe-XY deg.	∅ deg.	∅ deg.	Tilt deg.
Dioxygen Adducts										
Fe(PF)(1-MeIm)(O_2)	—	1.98(1)	-0.03	0.02	2.07(2)	1.75(2)	131(2)	20	45	0
Fe(PF)(2-MeIm)(O_2)	—	1.996(4)	0.09	0.02	2.107(4)	1.898(7)	129(1)	22	45	7
MbO_2	1.6	1.95(6)	0.18(3)	0.01	2.07(6)	1.83(6)	115(4)	1	~0	4
	EXAFS	2.02(2)	—	—	2.06(2)	1.80(2)	123(4) 148(8)[b]	—	—	—
ErO_2	1.4	2.04	0.38	-0.08	2.1	1.8	150	7	3	—
HbO_2 α	2.1	1.99(5)	0.12(8)	0.04	1.94(9)	1.66(8)	153(7)	11	0	3
HbO_2 β		1.96(6)	-0.11(8)	0.11	2.07(9)	1.87(3)	159(12)	27	45	5
	EXAFS	1.99(2)		—	2.05(2)	1.82(2)	122(4) 143(8)[b]	—	—	—
[α-FeO_2]$_2$[β-Fe]$_2$ α	2.1	2.04(4)	0.19(5)	0.17(5)	2.24(10)	1.82(4)	153(4)	6	—	11
[α-FeO_2]$_2$[β-Fe]$_2$ β			0.3	—	2.2	—	—	—		
Carbonmonoxy Adducts										
MbCO	1.5	1.97(3)	0.00	0.03	2.2	1.9	140	—	30	—
	EXAFS	2.01(2)	—	—	2.20(2)	1.93(2)	127(4) 145(8)[b]	—	—	—
ErCO	1.4	2.01	-0.11	-0.10	2.1	2.2	161(9)	7	—	1
HbCO α	2.2	2.02	-0.10	—	1.95	1.83	175(15)	—	—	—
HbCO β		2.03	-0.10	—	2.20	1.70	171(15)	—	—	—
[α-Ni][β-FeCo] α	2.6	—	—	—	—	—	—	—	—	—
[α-Ni][β-FeCo] β			0.15	0.12	2.23(5)	—	—	—	—	—
Fe(TPP)(Py)(CO)		2.02(3)	-0.02	-0.02	2.10(2)	1.77(2)	179(2)	45	—	~0
	EXAFS	2.02(2)	—	—	2.09(2)	1.81(2)	138(6)	—	—	—

Compound	Resol. Å	Fe-N_p Å	Fe-porph Å	Doming Å	Fe-L_1 Å	Fe-L_2 Å	Fe-XY deg.	$\varnothing_1$ deg.	$\varnothing_2$ deg.	Tilt deg.
							180(11)[b]			
Fe(poc)(1,2-Melm)(CO)		1.973(8)	0.001	—	2.079(5)	1.768(7)	172.5(6)	—	—	—
Fe(C_2Cap)(1-Melm)(CO)		1.990(7) 1.988(13)	0.01 0.02	—	2.043(6) 2.041(5)	1.742(7) 1.748(7)	172.9(6) 175.9(6)	—	—	—

Interactions of Coordinated Ligands with Distal Groups

Without exception to date (but see footnote 1 in Reference 168), in structurally characterized oxyhemoglobins, the coordinated dioxygen ligand is hydrogen-bonded to the distal histidine or to a water molecule—even though theoretical calculations show that hydrogen bonding would destabilize M—O_2 moieties.[192] This universal observation of hydrogen bonding in these biological systems is consistent with notions that electron density accumulates on the dioxygen molecule upon coordination. Given the errors associated with atomic positions (at best, ±0.20 Å) the x-ray crystallographic evidence could be equivocal, since hydrogen atoms on the distal imidazole are not observed. There are at least three lines of evidence that support the existence of a specific $O_2 \bullet \bullet \bullet$ HN interaction. First, the EPR spectrum of cobalt oxyhemoglobin indicates that the coordinated dioxygen is hydrogen-bonded to something.[177-179] Second, and more directly, in the neutron-diffraction structure of oxymyoglobin,[189] where hydrogen and especially deuterium nuclides scatter strongly, the imino hydrogen or deuteron was located on the nitrogen atom closest to the coordinated dioxygen, as illustrated in Figure 4.31A. In contrast, in the neutron-diffraction structure of carbonmonoxymyoglobin, the alternative imidazole tautomer was observed (Figure 4.3IB).[125,189] The absence of hydrogen bonding of the distal imidazole residue with the coordinated CO molecule is consistent with other lines of evidence that there is little accumulation of electron density on the carbonyl ligand. Third, but less directly, genetically engineered mutants have been produced in which the distal histidine has been replaced by glycine—sperm whale Mb E7His → Gly, and HbαE7His → Gly and HbA βE7His → Gly.[35b,192] For the myoglobin mutant, the O_2 binding rate constant at room temperature increases by an order of magnitude, but the dissociation rate constant increases by two orders of magnitude, leading to a decrease in affinity of more than an order of magnitude, as derived from k_{on}/k_{off}. This leads to an estimate of the free energy associated with hydrogen bonding of

$$\Delta G = -RTlog\left[\frac{P_{1/2}(O_2)\cdot Native}{P_{1/2}(O_2)\cdot Mutant}\right] = 1.5kcal/mol. \qquad (11.2.4.19.1)$$

In addition, this mutant myoglobin autooxidizes rapidly compared to the native one. On the other hand, the affinity for CO is greatly increased, leading to a value of M for the mutant of 1300, compared to 16 for the native. Thus the distal histidine stabilizes a coordinated O_2 ligand by hydrogen bonding and destabilizes a coordinated CO ligand by steric clash.

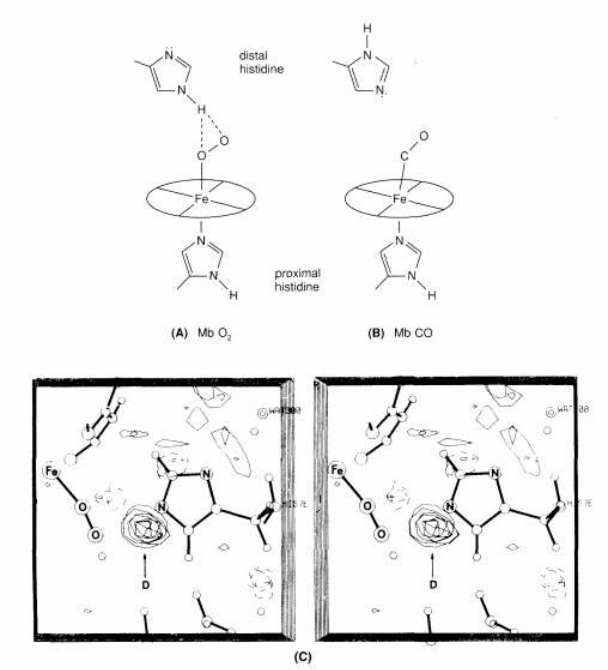
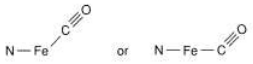


Figure 4.31 - (A) The hydrogen bonding interaction between coordinated dioxygen and the distal histidine. (B) The interaction of coordinated carbon monoxide and the distal histidine, showing the absence of hydrogen bonding. (C) Stereodiagram of a neutron-difference density map for oxymyoglobin. The refined structure showing the FeO_2 and distal histidine moieties is superimposed. The imidazole deuterium atom is arrowed.[189] Reproduced with permission from S. E. V. Phillips and B. P. Schoenborn, Nature **292** (1981), 81-82.

A similar discrimination is seen for the α chains of the hemoglobin mutant in the binding of the fourth O_2 or CO molecule. For the β chains little difference is seen relative to the native protein: hydrogen bonding between the distal histidine and the coordinated dioxygen ligand appears to be much weaker in β chains, as evidenced by longer N(H) • • • O separations than those seen in the α chains. Comparison of the crystal structures of the native and mutant $\alpha_2(\beta E7His \rightarrow Gly)_2$ structures reveals negligible changes in the distal environment, except for that occasioned by the replacement of $—CH_2—C_3N_2H_3$ (histidine side chain) by —H (glycine side chain).

Studies of hemoglobin mutants where the nonpolar distal residue βValE11 ($—CH(CH_3)_2$) is replaced by alanine ($—CH_3$), isoleucine ($—CH(CH_3)CH_2CH_3$), and leucine ($—CH_2CH(CH_3)_2$) reveal that this valine offers steric hindrance to oxygen binding in the T state.

Whereas the angularly coordinated O_2 ligand fits comfortably around the distal histidine, a perpendicular and linear CO moiety cannot. Either the distal histidine rotates out of the way, or the CO tilts off axis, or the Fe—C≡O group bends, or some combination of these occurs. Notwithstanding the absence of bent M—CO moieties in the inorganic literature, reports of strongly bent M—CO groups appear in the biochemical literature.[122-127] The controversy is illustrative of the synergistic interplay of data from models and proteins, and the importance of examining a problem with a miscellany of techniques. The molecular orbital model of ligand-metal interactions presented in Figure 4.22 does not preclude a bent M—C≡O moiety on symmetry grounds. Groups related to CO can bend; the normally linearly coordinated SCN^- moiety has been observed[194] to become strongly bent under severe steric stress, with an Fe—N—CS of 140°. Unfortunately, the resolution in protein crystal structures is not sufficient to distinguish unequivocally a linear tilted stereochemistry from a bent one or from a combination of tilt and bend. Studies by the XANES technique have been interpreted in terms of a bent Fe—C≡O moiety (150°)



both in MbCO[127] and in the CO adduct of a chelated heme in micelles, the latter being an especially surprising result. From EXAFS data on a number of carbonyl adducts, *two* interpretations were offered: linear or moderately bent (150°) FeCO moieties for unhindered model systems, and moderately bent or strongly bent (130°) FeCO moieties for hindered synthetic and biological systems.[195] In the crystal structure of MbCO at 1.5 Å resolution,[122] the CO group is disordered, and Fe—C≡O angles of 120° and

140° were proposed, although the alternative model of tilted, nearly linear Fe—C≡O stereochemistry could not be eliminated, and is indeed far more likely to account for the off-axis nature of the oxygen position. Vibrational spectroscopy confirms the existence of two major configurations, and indicates a third minor configuration of the Fe—C≡O moiety in MbCO.[196] An elegant infrared study of the polarization of reattached carbon-monoxide molecules following photolysis of MbCO by linearly polarized light at 10 K gave tilt angles of the CO vector with respect to the heme normal of 15(3)°, 28(2)°, and 33(4)° for the three conformational substates;[196b] the former two values were confirmed in a similar study at room temperature.[196c] Note that these studies do not yield the tilt of the Fe—C bond to the heme normal.

In three synthetic compounds with severe steric hindrance, the extent of bending and tilting of the Fe—CO moiety is small. In one nonporphyrinic system the Fe—C≡O group is bent by 9.4(5)° and tilted by 4.2°.[121a] In Fe(PocPF)(1,2-Me_2Im)(CO) the Fe—C≡O angle is 172.5(6)° and modest tilting of the Fe—CO group and substantial buckling of the porphyrin ring are apparent.[121b] In Fe(C_2Cap)(1-MeIm)(CO) the two independent Fe—C≡O angles are 172.9(6)° and 175.9(6)° and modest tilting of the Fe—CO group is again apparent.[121d]

From a detailed analysis of the force constants describing the vibrational spectroscopy for the Fe—CO moiety, values of 171° for the Fe—CO angle, 9.5° for the tilt, and 11° for porphyrin buckling were calculated for MbCO.[121c] These results are particularly important, for in a model complex very closely related to Fe(Poc-PF)(1,2-Me_2Im)(CO), just mentioned, an EXAFS study[195] suggested an Fe—C≡O bond angle of 127(4)°; that same study ascribed an Fe—C≡O bond angle of around 130° to MbCO. The structure of carbonmonoxyhemoglobin, $Hb(CO)_4$, now is interpreted in terms of a nearly linear tilted geometry.[192] Clearly the geometry of attachment of CO to hemoglobins is perturbed by the surroundings of the ligand-binding site and hence the affinity of hemoglobins for CO is also perturbed. Unfortunately, a clear resolution of the geometry of the Fe—CO moiety in MbCO does not exist yet.

11.2.4.19: Structures Relevant to Liganded Hemoglobins is shared under a CC BY-NC-SA 4.0 license and was authored, remixed, and/or curated by LibreTexts.

11.2.4.20: Thermodynamic Factors

The equilibrium constant K was defined in Equation (4.3) in terms of the activity a_i of component i. The a_i may be expressed as a function of concentration as

$$a_i = \gamma_i[i], \tag{4.7}$$

where for species i, γ_i is its activity coefficient and [i] is its concentration (strictly molality, but usually as molarity in mol L^{-1}). At infinite dilution $\gamma_i = 1$. Provided that the charge and size of species M and MO_2 are similar and that O_2 forms an ideal solution, then the activities of Equation (4.3) may be approximated by concentrations to give the expression

$$K_c = \frac{[MO_2]}{[M][O_2]}. \tag{4.8}$$

However, Equation (4.8) does not permit a direct comparison of the oxygen-binding behavior of one species in some solvent with that of a second in some other solvent. First, for a given partial pressure of dioxygen, the concentration of O_2 in the solution varies considerably with temperature and from one solvent to another. Second, reliable measurements of oxygen solubilities are not always available, and it is only relatively recently that oxygen electrodes have been developed to measure directly oxygen concentrations (strictly, activities). However, oxygen-binding measurements are normally made with a solution of M in equilibrium with gaseous dioxygen. At equilibrium the molar Gibbs' free energies (chemical potentials) of the dissolved and gaseous dioxygen are identical—if they are not, gaseous O_2 would dissolve, or dissolved O_2 would be released. Thus the solvent-dependent quantity $[O_2]$ in Equation (4.8) may be replaced by the solvent-independent quantity $P(O_2)$, the partial pressure of dioxygen. Under almost all experimental conditions the quantity $P(O_2)$ is a very good approximation to the gas-phase activity (fugacity) of dioxygen; hence we obtain for the equilibrium constant*

$$K_p = \frac{[MO_2]}{[M]P(O_2)}. \tag{4.9}$$

* There has been considerable discussion as to whether K_c (4.8) or K_p (4.9) should be used to compare dioxygen binding under different solvent conditions[21-23] We believe that the latter is more appropriate, since for a system al equilibrium, the chemical potential of gaseous O_2 must be identical with that of dissolved O_2[19] On the other hand, the concentration of O_2 varies from one solvent to another.

It is very convenient to express the affinity as the partial pressure of dioxygen required for half-saturation of the species M, $P_{1/2}(O_2)$. Under such conditions, [M] = $[MO_2]$, one obtains

$$P_{1/2}(O_2) = 1/K_p, \tag{4.10}$$

where $P_{1/2}(O_2)$ is usually given in Torr or mm Hg.* As will be detailed shortly, values for $P_{1/2}(O_2)$ are typically in the range 0.5 to 40 Torr.

The dioxygen affinity is composed of enthalpic (ΔH) and entropic (ΔS) components, with

$$\Delta G^o = -RTlnK = \Delta H^o - T\Delta S^o. \tag{4.11}$$

Within a family of oxygen carriers the values of ΔS^o and ΔH° are usually similar. Large deviations (such as a change of sign) are therefore indicative of a change in the nature of the oxygen-binding process.

* Many authors use the symbol P_{50} (corresponding to 50% saturation) for $P_{1/2}$.

a. Non-cooperative Dioxygen Binding

If the oxygen-binding sites M are mutually independent and noninteracting, as in moderately dilute solutions of monomeric molecules, then the concentration of species MO_2 as a function of the partial pressure of O_2 is generally well fit by a Langmuir isotherm.[20] Here a plot of the fractional saturation of dioxygen binding sites, θ, where

$$\theta = \frac{[MO_2]}{[M] + [MO_2]} = \frac{K_pP(O_2)}{1 + K_pP(O_2)} \tag{4.12}$$

versus $P(O_2)$ gives the hyberbolic curve labeled "non-cooperative" in Figure 4.4A.[9] Alternatively,[24] a plot of log (θ/(1 - θ)) versus log ($P(O_2)$), the so-called "Hill plot," gives a straight line with a slope of unity and an intercept of -log $P_{1/2}(O_2)$ (Figure 4.4B). A differential form is shown as the dotted line in Figure 4.4C. Such binding, where the dioxygen sites are independent of each other, is termed *non-cooperative*.

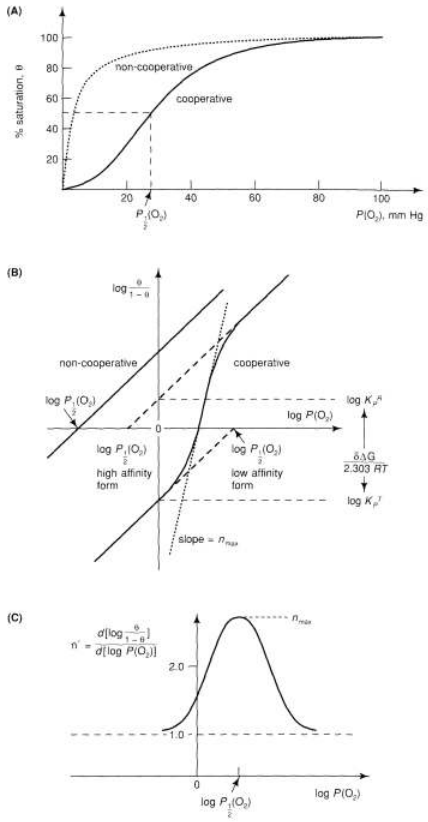


Figure 4.4 - Cooperative and non-cooperative binding of dioxygen:[9] (A) Binding curves; (B) Hill plot of binding curves; (C) First derivative (slope) of the Hill plots.

b. Cooperative Dioxygen Binding

Many dioxygen-binding proteins are not independent monomers, with only one dioxygen-binding site, but oligomeric species with the protein comprising two or more similar subunits. The subunits may be held together by van der Waals' forces or by stronger interactions, such as hydrogen bonds or salt bridges, or even by covalent bonds. For example, most mammalian hemoglobins are tetramers, consisting of two pairs $[\alpha\beta]_2$ of myoglobin-like subunits denoted as α and β. Either none, one, two, three, or all four sites may be occupied by dioxygen. This situation is illustrated schematically in Figure 4.5, which also shows the statistical weighting of each level of saturation, treating the α and β subunits as identical. Thus the binding or release of dioxygen at one site *may* affect the affinity and kinetics of ligand binding and release at a neighboring site. As a result, the saturation curve becomes sigmoidal in shape, as illustrated in Figure 4.4A. The dioxygen binding is *cooperative*. When cooperativity is positive, the affinity of a vacant site is increased by occupancy of an adjacent one.

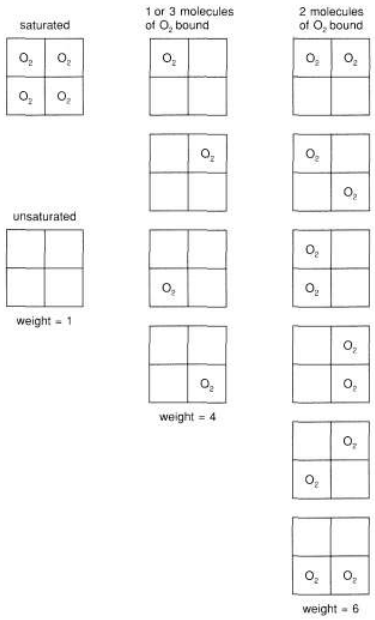


Figure 4.5 - Diagram of tetrameric hemoglobin, showing statistical weights of different saturations (see text).

This behavior, where the binding of one molecule influences the binding of successive molecules *of the same kind*, is referred to as a *homotropic allosteric* interaction. A *heterotropic allosteric* interaction occurs when the interaction with the protein of a second *unlike* molecule, for instance, an organic polyphosphate for human hemoglobins, influences the binding of the first molecule (e.g., dioxygen). Such molecules are often termed *allosteric effectors*. A commonly observed heterotropic allosteric interaction is the Bohr effect, named after the biologist Christian Bohr, father of physicist Niels Bohr. This effect, which relates the change in partial pressure of O_2 to a change in pH at constant saturation of binding sites (θ), is related thermodynamically to the Haldane effect, which relates the number of protons released ($\#H^+$) with a change in θ at constant pH (Equation 4.13). A very large Bohr effect, where O_2 affinity decreases sharply with pH, is often called the Root effect.[25a] It is physiologically important for fish such as trout, probably in maintaining buoyancy, but its molecular basis in trout hemoglobin IV remains to be discovered.[25b]

$$\left[\frac{\partial(\#H^+)}{\partial\theta}\right]_{pH} = \left[\frac{\partial(logP(O_2))}{\partial pH}\right]_{\theta} \tag{4.13}$$

The degree of cooperativity can be characterized in a number of ways. By means of a Hill plot of log (θ/(1 - θ)) versus log ($P(O_2)$), the limiting slopes (which should be unity) at high O_2 pressure and low O_2 pressure may be extrapolated as shown in Figure 4.4B to log (θ/(1 - θ)) = 0, where θ = 0.5. Two limiting values for $P_{1/2}(O_2)$ are obtained, one characterizing the regime of high partial pressure of dioxygen, where the O_2 affinity is high (for the case illustrated of positive cooperativity). The other $P_{1/2}(O_2)$ value characterizes the regime of low partial pressure of dioxygen, where affinity is relatively low. This difference in affinities can be converted into a difference between the free-energy change upon O_2 binding in the low-affinity state (K_p^T) and the high-affinity state (K_p^R) [the designations T and R will be described in subsection d]:

$$\delta\Delta G^o = -RTln\left(\frac{K_p^T}{K_p^R}\right). \tag{4.14}$$

A second way to characterize cooperativity involves fitting the oxygen-binding data at intermediate saturation ($0.2 < \theta < 0.8$)—that is, about the inflection point in a Hill plot—to the Hill equation

$$\frac{\theta}{1-\theta} = K_p P^n(O_2) \tag{11.2.4.20.1}$$

or

$$log\left(\frac{\theta}{1-\theta}\right) = -log(P_{1/2}(O_2)) + nlog(P(O_2)). \tag{4.15}$$

The Hill coefficient (n) is an empirical coefficient that has a value of unity for non-cooperative binding, where Equation (4.15) reduces to the Langmuir isotherm, Equation (4.12). Any number greater than unity indicates positive cooperativity. If O_2 binding is an all-or-nothing affair, where dioxygen binding sites are either all occupied or all vacant, n equals the number of subunits in the molecule. The fit is only approximate, since the Hill plot is only approximately linear about the inflection point, as may be seen in Figure 4.4B. A more precise value of n may be obtained by plotting the slope in the Hill plot (n') as a function

$$n' = \frac{d\left[log\left(\frac{\theta}{1-\theta}\right)\right]}{d[log(P(O_2))]} \tag{4.16}$$

of log ($P(O_2)$) (Figure 4.4C). The maximum value of n' is taken as the Hill coefficient n.[9] Note that the maximum in this first-derivative plot of the binding curve will occur at $P_{1/2}(O_2)$ only if the Hill plot is symmetric about its inflection point. For tetrameric hemoglobins, a maximum Hill coefficient of around 3.0 is seen, and for hemocyanins n may be as high as 9. These values, like $P_{1/2}(O_2)$ values, are sensitive to the nature and concentrations of allosteric effectors.

c. Benefits of Cooperative Ligand Binding

In general, oxygen-carrier proteins, being oligomeric, coordinate dioxygen cooperatively, whereas oxygen-storage proteins, being monomeric, do not. Oligomerization and cooperative binding confer enormous physiological benefits to an organism. The first benefit derives directly from oligomerization. Oxygen carriers either form small oligomers that are encapsulated into cells or erythrocytes (such hemoglobins are referred to as intracellular hemoglobins) or associate into large oligomers of 100 or more subunits. Such encapsulation and association reduce by orders of magnitude the number of independent particles in the blood, with consequent reductions in the osmotic pressure of the solution and in strain on vascular membranes.

The second benefit derives from cooperative binding of ligands and the abilities of heterotropic allosteric effectors to optimize exquisitely the oxygen-binding behavior in response to the external and internal environment. The situation is illustrated in general terms in Figure 4.6.[9] Most organisms that require O_2 live in an environment where the activity of O_2 corresponds to about 21 percent of an atmosphere, that is, to about 160 Torr, although usually the effective availability, because of incomplete exchange of gases in the lungs, for example, is around 100 Torr. The concentration of O_2 in vertebrate tissues at rest is equivalent to a partial pressure of about 35-40 Torr dioxygen; lower values obtain at times of exertion. Now consider a noncooperative oxygen binder with an affinity expressed as $P_{1/2}(O_2)$ of 60 Torr (Figure 4.6, curve a). Then, at 100 Torr the fractional saturation θ is 0.625. In other words, in a realm of high O_2 availability, only 62.5 percent of the oxygen-binding capacity is used, which is not particularly efficient if the organism wished to climb Mt. Everest, where the partial pressure of O_2 is less than half that at sea level. In the tissues, where $P(O_2)$ = 40 Torr, the fractional saturation is about 40 percent. Thus, only about one third of the coordinated dioxygen is released to the tissues, and total effciency is only 22.5 percent. Consider now a noncooperative oxygen carrier with a much higher affinity, $P_{1/2}(O_2)$ = 1.0 Torr (Figure 4.6, curve b). If we assume the same ambient pressure of O_2 in the tissues, the fractional saturation is 97.6 percent. Note that at 100 Torr of O_2 the carrier is 99.0 percent saturated. In other words, only about 1.4 percent of the available oxygen is delivered.

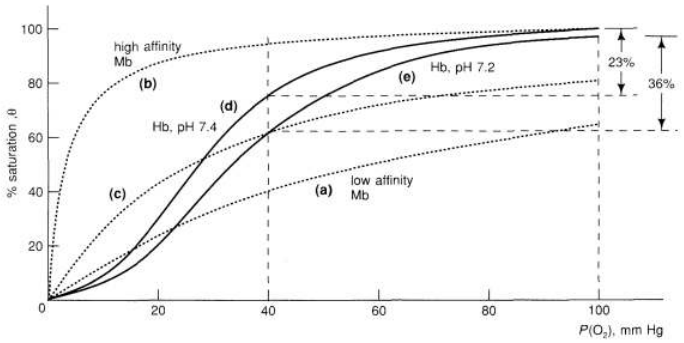


Figure 4.6 - Physiological benefits of cooperativity and heterotropic allosteric effectors.[9]

With an oligomeric protein that binds dioxygen cooperatively, the problem of inefficient and inflexible oxygen delivery disappears. For example, the tetrameric protein hemoglobin has a mean affinity for O_2 of $P_{1/2}(O_2) \approx 26$ Torr at 37 °C and pH 7.4. If hemoglobin bound O_2 noncooperatively, then the hyberbolic binding curve (c) in Figure 4.6 would represent the O_2 binding.

Instead, the observed binding follows curve (d). Since the partial pressure of dioxygen in the lungs and arterial blood of vertebrates is around 100 Torr, but in the tissues and venous blood it is around 40 Torr, then at these pressures a typical myoglobin ($P_{1/2}(O_2)$ = 1 Torr) remains effectively saturated. On the other hand, about 25 percent of the available dioxygen can be delivered, even in the absence of myoglobin. With venous blood remaining 75 percent oxygenated, hemoglobin has substantial capacity to deliver more O_2 at times of exertion or stress when $P(O_2)$ in the tissues falls below 40 Torr.

The net result is that whole blood, which contains about 15 g of hemoglobin per 100 mL, can carry the equivalent of 20 mL of O_2 (at 760 Torr) per 100 mL, whereas blood plasma (no hemoglobin) has a carrying capacity of only 0.3 mL of O_2 per 100 mL.[9]

Oxygen binding *in vivo* is modulated by allosteric effectors that through interaction with the protein change the affinity and degree of cooperativity. For hemoglobin A (adult human hemoglobin), naturally occurring allosteric effectors include the proton, carbon dioxide, and 2,3-diphosphoglycerate (2,3-DPG). Increasing concentrations of these species progressively lower the affinity of free hemoglobin A, thereby enhancing the release of coordinated O_2 (Figure 4.6, curve e). For example, 2,3-DPG is part of a subtle mechanism by which dioxygen is transferred from mother to fetus across the placenta. The subunits comprising fetal hemoglobin and adult hemoglobin are slightly different. In the absence of allosteric effectors (referred to as stripped hemoglobin), the oxygen-binding curves are identical. However, 2,3-DPG binds less strongly to fetal hemoglobin than to adult hemoglobin. Thus fetal hemoglobin has a slightly higher affinity for dioxygen, thereby enabling dioxygen to be transferred. The proton and carbon dioxide are part of a short-term feedback mechanism. When O_2 consumption outpaces O_2 delivery, glucose is incompletely oxidized to lactic acid (instead of CO_2). The lactic acid produced lowers the pH, and O_2 release from oxyhemoglobin is stimulated (Figure 4.6, curve e). The CO_2 produced in respiration forms carbamates with the amino terminals, preferentially of deoxy hemoglobin.

$$R-NH_2+CO_2 \rightleftharpoons R-NH-COO^-+H^+ \tag{11.2.4.20.2}$$

Thus hemoglobin not only delivers O_2 but also facilitates removal of CO_2 to the lungs or gills, where CO_2 is exhaled.

d. Models for Cooperativity

The binding of Oz to hemoglobin can be described as four successive equilibria:

$$Hb+O_2 \overset{K^{(1)}}{\rightleftharpoons} Hb(O_2) \qquad P_{1/2}^{(1)}(O_2)=123[46]Torr \tag{11.2.4.20.3}$$

$$Hb(O_2)_1+O_2 \overset{K^{(2)}}{\rightleftharpoons} Hb(O_2)_2 \qquad P_{1/2}^{(2)}(O_2)=30[16]Torr \tag{4.17}$$

$$Hb(O_2)_2+O_2 \overset{K^{(3)}}{\rightleftharpoons} Hb(O_2)_3 \qquad P_{1/2}^{(3)}(O_2)=33[3.3]Torr \tag{11.2.4.20.4}$$

$$Hb(O_2)_3+O_2 \overset{K^{(4)}}{\rightleftharpoons} Hb(O_2)_4 \qquad P_{1/2}^{(4)}(O_2)=0.26[0.29]Torr \tag{11.2.4.20.5}$$

(0.6 mM hemoglobin A, bis(Tris) buffer, pH 7.4, 0.1 M Cl^-, 2 mM 2,3-DPG, 25 °C. The values in square brackets are affinities in Torr measured in the absence of 2,3- DPG.)

This simple scheme proposed by Adair[26] assumes that each of the four binding sites is identical. The $P_{1/2}(O_2)$ values given come from fitting the binding curve to this scheme.[27] When 2,3-DPG is removed, the affinity of hemoglobin for the first three molecules of Oz is substantially increased, and the degree of cooperativity is lowered (values in square parentheses). For progressively stronger binding, the following inequalities, reflecting the proper statistical weighting illustrated in Figure 4.5, should hold:

$$\frac{1}{4}K^{(1)} > \frac{4}{6}K^{(2)} > \frac{6}{4}K^{(3)} > \frac{4}{1}K^{(4)} \tag{4.18}$$

The $\frac{6}{4}$ ratio, for example, reflects the six equivalent forms of the doubly and the four equivalent forms of the triply ligated species. In other words, relative to a noncooperative system, at low O_2 availability dioxygen *release* is facilitated; at high O_2 availability dioxygen *binding* is facilitated. The scheme is readily extended to higher orders of oligomerization.

A simple model for analyzing cooperative ligand binding was proposed by Monod, Wyman, and Changeux in 1965, and is usually referred to as the MWC two-state concerted model.[28] Molecules are assumed to be in equilibrium between two conformations or quaternary structures, one that has a low ligand affinity and a second that has a high ligand affinity. The low-affinity conformation

is often designated the T or tense state, and the high-affinity conformation the R or relaxed state. The equilibrium between the two conformations is characterized by the allosteric constant

$$L_0 = \frac{[R_0]}{[T_0]} \tag{4.19}$$

where the subscript denotes the unliganded Rand T states. The free-energy change upon binding a ligand to the R state, irrespective of saturation, is assumed to be a constant, and the associated equilibrium constant is designated K_R; a third constant, K_T, characterizes binding to the T state. Figure 4.7 illustrates this model, and introduces the terminology conventionally used.

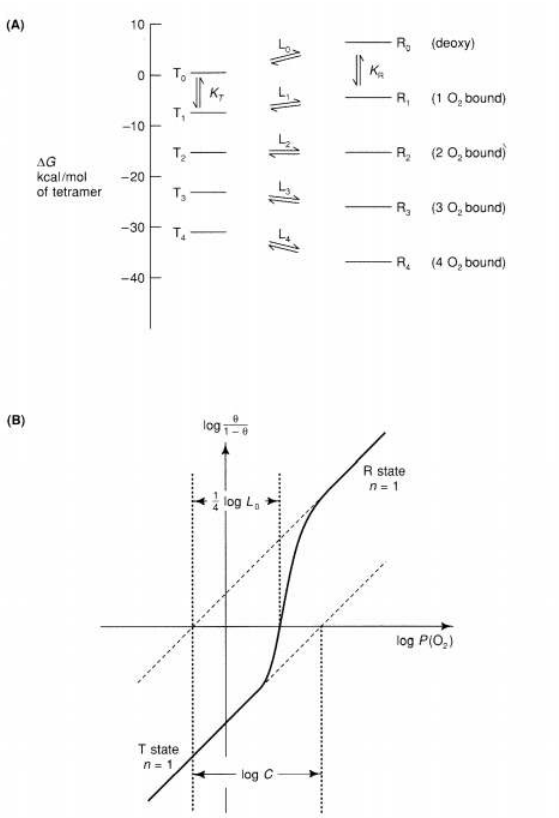


Figure 4.7 - The MWC two-state model for cooperative ligand binding:[4] (A) Free-energy relationships among R and T states; (B) Calculation of the allosteric constants from the binding curve.

To a reasonable approximation, the cooperative binding of dioxygen can be summarized by these three parameters, L_0, K_R, and K_T. The Adair constants may be expressed in terms of these parameters:

$$K^{(1)} = \frac{(1 + L_0 C)K_T}{1 + L_0}, \qquad K^{(2)} = \frac{(1 + L_0 C^2)K_T}{1 + L_0}, \tag{4.20}$$

$$K^{(3)} = \frac{(1 + L_0 C^3)K_T}{1 + L_0 C^2}, \qquad K^{(4)} = \frac{(1 + L_0 C^4)K_T}{1 + L_0 C^3}, \tag{11.2.4.20.6}$$

where $C = K_R/K_T$. The fractional saturation is given as

$$\theta = \frac{\alpha(1+\alpha)^3 + L_0 \alpha C(1 + \alpha C)^3}{(1+\alpha)^4 + L_0 \alpha C(1 + \alpha C)^4}, \tag{4.21}$$

where $a = K_T[X]$, and [X] is the concentration of the free ligand (e.g., O_2) in the same units (M or Torr) in which K_T is expressed. Figure 4.7B illustrates how the allosteric parameters, $C = K_R/K_T$ and $L_0 = [R_0]/[T_0]$, are extracted from a plot of saturation (as log [θ/(1 - θ)]) versus partial pressure of dioxygen (as log [$P(O_2)$]). Notice how the two-state model (Figure 4.7B) matches very closely the form of the binding curve for hemoglobin (Figure 4.4B). Equations (4.20) and (4.21) may be generalized to an oligomer with n subunits. In the case of hemoglobin, Perutz and coworkers,[11] through the determination of the crystal structures of a variety of

hemoglobin derivatives, have given subsequently a sound structural basis to the MWC model of two basic quaternary states (see below).

A more exact treatment of ligand-binding data would allow for different affinities for different binding sites (called subunit heterogeneity) and different intrinsic affinities for ligand binding to the R-state conformation compared with the T-state conformation, for each level of ligand saturation—that is, for tertiary structure change within subunits upon ligation. This more exact treatment requires 25 separate equilibrium constants. Statistical thermodynamical approaches exist.[29] These explicitly incorporate the different types of subunit interactions that structural studies have revealed, and give improved fits to oxygen-binding data and to the Bohr effect. The key element of two basic quaternary states is preserved, at least for dioxygen binding.[29b]

For some modified hemoglobins, for example $[\alpha\text{-Fe(II)}_2[\beta\text{-Mn(III)}]_2$, where in the β subunits the heme iron is replaced by Mn(III), there is now strong evidence for three quaternary states,[29c] with the singly and several of the doubly ligated species having an energy state intermediate between the T (unliganded) and R (fully, triply, and the other doubly liganded) states.

11.2.4.20: Thermodynamic Factors is shared under a CC BY-NC-SA 4.0 license and was authored, remixed, and/or curated by LibreTexts.

11.2.4.21: Ch. 4 References and Abbreviations

References

1. C. K. Mathews and K. E. van Holde, *Biochemistry*, Benjamin/Cummings, 1990.
2. a) M. Nikinmaa, *Vertebrate Red Blood Cells: Adaptations of Function to Respiratory Requirements*, Springer-Verlag, 1990. b) D. Hershey, ed., *Blood Oxygenation*, Plenum, 1970. c) D. W. Lübbers, H. Acker, E. Leniger-Follert, and T. K. Goldstick, eds., *Oxygen Transport to Tissues V*, Plenum, 1984. d) F. Kreuzer, S. M. Cain, Z. Turek, and T. K. Goldstick, eds., *Oxygen Transport to Tissues VII*, Plenum, 1984.
3. a) P. Astrup and M. Rørth, eds., Oxygen *Affinity of Hemoglobin and Red Cell Acid Base Status*, Munksgaard, 1972. b) G. L. Eichhorn, ed., *Inorganic Biochemistry*, Elsevier, 2 vols., 1973.
4. M. Brunori, A. Coletta, and B. Giardina, in P. M. Harrison, ed., *Topics in Molecular and Structural Biology*, Verlag Chemie, **7**, Part 2 (1985), 263-331.
5. A. G. Sykes, in A. G. Sykes, ed., *Advances in Inorganic and Bioinorganic Mechanisms*, Academic Press, **1** (1985), 121-178.
6. M. Brunori, B. Giardina, and H. A. Kuiper, in H. A. O. Hill, ed., *Inorganic Biochemistry*, Royal Society of Chemistry **3** (1982), 126-182.
7. R. E. Dickerson and I. Geis, *Hemoglobin: Structure, Function, Evolution, and Pathology*, Benjamin/ Cummings, 1983.
8. H. F. Bunn, B. G. Forget, and H. M. Ranney, *Human Hemoglobins*, Saunders, 1977.
9. K. Imai, *Allosteric Effects in Haemoglobin*, Cambridge University Press, 1982.
10. E. Antonini and M. Brunori, *Hemoglobin and Myoglobin in Their Reactions with Ligands*, North Holland, 1971.
11. a) M. F. Perutz, *Nature* **228** (1970), 726-739. b) M. F. Perutz, Annu. *Rev. Biochem.* **48** (1979), 327-386. c) M. F. Perutz *et al.*, *Acc. Chem. Res.* **20** (1987), 309-321.
12. M. C. M. Chung and H. D. Ellerton, *Prog. Biophys. Mol. Biol.* **35** (1979), 53-102.
13. J. Lamy and J. Lamy, eds., *Invertebrate Oxygen-Binding Proteins: Structure, Active Site and Function*, Dekker, 1981.
14. H. D. Ellerton, N. F. Ellerton, and H. A. Robinson, *Prog. Biophys. Mol. Biol.* **41** (1983), 143-248.
15. a) K. E. van Holde and K. I. Miller, *Quart. Rev. Biophys.* **15** (1982), 1-129. b) K. D. Karlin and J. Zubieta, eds., *Biological and Inorganic Chemistry of Copper*, Academic Press, 2 vols., 1986.
16. P. C. Wilkins and R. G. Wilkins, *Coord. Chem. Rev.* 79 (1987), 195-214; in this see references to the original literature.
17. I. M. Klotz and D. M. Kurtz, Jr., *Acc. Chem. Res.* **17** (1984), 16-22.
18. J. Sanders Loehr and T. M. Loehr, *Adv. Inorg. Blochem.* **1** (1979), 235-252.
19. K. Denbigh, *The Principles of Chemical Equilibrium*, Cambridge University Press, 4th ed., 1981.
20. P. W. Atkins, *Physical Chemistry*, Freeman, 3d ed., 1986.
21. J. P. Collman, J. I. Brauman, and K. M. Doxsee, *Proc. Natl. Acad. Sci. USA* **76** (1979), 6035-6039.
22. D. Lexa *et al.*, *Inorg. Chem.* **25** (1986), 4857-4865.
23. K. S. Suslick, M. M. Fox, and T. J. Reinert, *J. Am. Chem. Soc.* **106** (1984), 4522-4525.
24. A. V. Hill, *J. Physiol.* 40 (1910), iv-vii.
25. a) R. W. Root, *Biol. Bull.* (Woods Hole, Mass.) **61** (1931), 427-456. b) G. G. Dodson *et al.*, *J. Mol. Biol.* **211** (1990), 691-692.
26. G. S. Adair, *J. Biol. Chem.* **63** (1925), 529-545.
27. Reference 9, 114.
28. J. Monod, J. Wyman, and J.-P. Changeux, *J. Mol. Biol.* **12** (1965), 88-118.
29. a) M. L. Johnson, B. W. Turner, and G. K. Ackers, *Proc. Natl. Acad. Sci. USA* **81** (1984), 1093-1097. b) M. Straume and M. L. Johnson, *Biochemistry* **27** (1988), 1302-1310. c) G. K. Ackers and F. R. Smith, *Annu. Rev. Biophys. Chem.* **16** (1987), 583-609.
30. L. Pauling *et al.*, *Science*, **110** (1949), 543-548.
31. G. B. Jameson and J. A. Ibers, *Comments Inorg. Chem.* **2** (1983), 97-126; in this see references to the original literature.
32. Q. H. Gibson and M. H. Smith, *Proc. Roy. Soc., Ser. B, Biol. Sci.* **163** (1965), 206-214.
33. a) T. Imamura, A. Riggs, and Q. H. Gibson, *J. Biol. Chem.* **247** (1972), 521-526. b) J. B. Wittenberg, C. A. Appleby, and B. A. Wittenberg, *J. Biol. Chem.* **247** (1972), 527-531.
34. L. J. Parkhurst, *Annu. Rev. Phys. Chem.* **30** (1979), 503-546; in this see references to the original literature.
35. a) M. P. Mims *et al.*, *J. Biol. Chem.* **258** (1983), 14219-14232; in this see references to the original literature. b) J. S. Olson *et al.*, *Nature* **336** (1988), 265-266.

36. G. D. Armstrong and A. G. Sykes, *Inorg. Chem.* **25** (1986), 3135-3139.
37. R. Lontie and R. Winters, in H. Sigel, ed., *Metal Ions in Biological Systems*, Dekker, **13** (1981), 229-258.
38. a) M. Brunori *et al.*, in Reference 13, 693-701. b) E. Antonini *et al.*, *Biophys. Chem.* **18** (1983), 117-124.
39. a. B. Richey, H. Decker, and S. J. Gill, *Biochemistry* **24** (1985), 109-117. b) M. Brunori *et al.*, *J. Mol. Biol.* **153** (1981), 1111-1123. c) H. Decker *et al.*, *Biochemistry* **27** (1988), 6901-6908.
40. a) G. L. Woolery *et al.*, *J. Am. Chem. Soc.* **106** (1984), 86-92. b) J. M. Brown *et al.*, *J. Am. Chem. Soc.* **102** (1980), 4210-4216.
41. M. S. Co. *et al.*, *J. Am. Chem. Soc.* **103** (1981), 984-986.
42. a) W. P. J. Gaykema *et aI.*, *Nature* **309** (1984),23-29. b) W. P. J. Gaykema, A. Volbeda, and W. G. J. Hol, *J. Mol. BioI.* 187 (1985), 255-275. c) B. Linzen *et al.*, *Science* **229** (1985), 519-524.
43. a) H. A. DePhillips, Jr., *Arch. Biochem. Biophys.* **144** (1971), 122-126. b) D. E. Richardson, R. C. Reem, and E. I. Solomon, *J. Am. Chem. Soc.* **105** (1982), 7780-7781.
44. D. J. A. de Waal and R. G. Wilkins, *J. BioI. Chem.* **251** (1976), 2339-2343.
45. R. E. Stenkamp *et al.*, *Proc. Natl. Acad. Sci. USA* **82** (1985), 713-716.
46. a) R. E. Stenkamp, L. C. Sieker, and L. H. Jensen, *J. Am. Chem. Soc.* **106** (1984), 618-622. b) Ibid., *J. Mol. Biol.* 126 (1978), 457-466.
47. S. Sheriff *et al.*, *Proc. Natl. Acad. Sci. USA* **82** (1985), 1104-1107.
48. S. Sheriff, W. A. Hendrickson, and J. L. Smith, *J. Mol. Biol.* **197** (1987), 273-296.
49. H. P. Misra and I. Fridovich, *J. Biol. Chem.* **247** (1972), 6960-6962.
50. W. J. Wallace, J. C. Maxwell, and W. S. Caughey, *FEBS Lett.* 43 (1974),33-36; *Biochem. Biophys. Res. Comm.* **57** (1974), 1104-1110.
51. a) D. E. Hultquist, L. J. Sannes, and D. A. Juckett, *Curr. Top. Cell. Regul.* **24** (1984), 287-300. b) M. R. Mauk and A. G. Mauk, *Biochemistry* **21** (1982), 4730-4734.
52. I. Fridovich, *Acc. Chem. Res.* **5** (1972), 321-326.
53. D. T. Sawyer and J. S. Valentine, *Acc. Chem. Res.* **14** (1981), 393-400.
54. I. Fridovich vs. D. T. Sawyer and J. S. Valentine, *Acc. Chem. Res.* **15** (1982), 200 (correspondence).
55. W. Braun *et al.*, *J. Mol. Biol.* **187** (1986), 125-129.
56. F. A. Cotton and G. Wilkinson, *Advanced Inorganic Chemistry: A Comprehensive Text*, Wiley, 4th ed., 1980.
57. A. F. Wells, *Structural Inorganic Chemistry*, Oxford University Press, 5th ed., 1984.
58. J. E. Huheey, *Inorganic Chemistry: Principles of Structure and Reactivity*, Harper and Row, 3rd ed., 1983.
59. S. A. Fairhurst and L. H. Sutcliffe, *Prog. Biophys. Mol. Biol.* **34** (1978), 1-79.
60. B. K. Teo, *EXAFS: Basic Principles and Data Analysis*, Springer-Verlag, 1986.
61. A. Bianconi *et al.*, *Phys. Rev. B* **26** (1982), 6502-6508.
62. *Handbook of Chemistry and Physics*, CRC Press, 68th ed., 1987-88, D151-D155.
63. L. Vaska, *Acc. Chem. Res.* **9** (1976), 175-183; in this see references to the original literature.
64. R. D. Jones, D. A. Summerville, and F. Basolo, *Chem. Rev.* **79** (1979), 139-179; in this see references to the original literature.
65. W. R. Scheidt and Y. J. Lee, *Structure and Bonding* **64** (1987), 1-70; in this see references to the original literature.
66. E. C. Niederhoffer, J. H. Timmons, and A. E. Martell, *Chem. Rev.* **84** (1984), 137-203; in this see references to the original literature.
67. J. O. Alben *et al.*, *Biochemistry* **7** (1968), 624-635.
68. G. S. Hammond and C.-S. Wu, *Adv. Chem. Ser.* **77** (1968), 186-207.
69. D.-H. Chin *et al.*, *J. Am. Chem. Soc.* **99** (1977), 5486-5488.
70. J. E. Penner-Hahn *et al.*, *J. Am. Chem. Soc.* **108** (1986), 7819-7825.
71. A. L. Balch *et al.*, *J. Am. Chem. Soc.* **106** (1984), 7779-7785.
72. J. P. Collman, *Acc. Chem. Res.* **10** (1977), 265-272.
73. J. H. Wang, *J. Am. Chem. Soc.* **80** (1958), 3168-3169.
74. E.-I. Ochiai, *Inorg. Nucl. Chem. Lett.* **10** (1974), 453-457.
75. C. C. Winterbourn and J. K. French, *Biochem. Soc. Trans.* **5** (1977), 1480-1481; J. K. French, C. C. Winterbourn, and R. W. Carrell, *Biochem. J.* **173** (1978), 19-26.
76. B. C. Antanaitis and P. Aisen, *Adv. Inorg. Biochem.* **5** (1983), 111-136.
77. B.-M. Sjöberg and S. A. Graslund, *Adv. Inorg. Biochem.* **5** (1983), 87-110.

78. a) H. Toftlund *et al.*, *J. Chem. Soc. Chem. Comm.* (1986), 191-192. b) M. P. Woodland and H. Dalton, *J. Biol. Chem.* **259** (1984), 53-59.
79. a) J. LeGall *et al.*, *Biochemistry* **27** (1988), 1636-1642. b) E. C. Theil, *Adv. Inorg. Biochem.* **5** (1983), 1-38.
80. K. S. Murray, *Coord. Chem. Rev.* **12** (1974), 1-35.
81. P. Gomez-Romero, G. C. DeFotis, and G. B. Jameson, *J. Am. Chem. Soc.* **108** (1986), 851-853.
82. W. H. Armstrong *et al.*, *J. Am. Chem. Soc.* **106** (1984), 3653-3667.
83. C. C. Ou *et al.*, *J. Am. Chem. Soc.* **100** (1978), 2053-2057.
84. W. M. Reiff, G. J. Long, and W. A. Baker, Jr., *J. Am. Chem. Soc.* **90** (1968), 6347-6351.
85. J. A. Bertrand and P. G. Eller, *Inorg. Chem.* **13** (1974), 927-934.
86. B. F. Anderson *et al.*, *Nature* **262** (1976), 722-724.
87. a) R. S. Czernuszewicz, J. E. Sheats, and T. G. Spiro, *Inorg. Chem.* **26** (1987), 2063-2067. b) B. A. Averill *et al.*, *J. Am. Chem. Soc.* **109** (1987), 3760-3767.
88. a). P. Chaudhuri *et al.*, *Angew. Chem. Intl. Ed. Engl.* **24** (1985), 778-779. b) J. A. R. Hartman *et al.*, *J. Am. Chem. Soc.* **109** (1987), 7387-7396.
89. C. Bull, G. J. McClune, and J. A. Fee, *J. Am. Chem. Soc.* **105** (1983), 5290-5300.
90. a) R. E. Hester and E. M. Nour, *J. Raman Spectrosc.* **11** (1981), 35-38. b) S. Ahmad *et al.*, *Inorg. Chem.* **27** (1988), 2230-2233.
91. W. R. Scheidt and C. A. Reed, *Chem. Rev.* **81** (1981), 543-555; in this see references to the original literature.
92. L. Pauling and C. D. Coryell, *Proc. Natl. Acad. Sci. USA* **22** (1936), 210-216.
93. M. Cerdonio *et al.*, *Proc. Natl. Acad. Sci. USA* **74** (1977), 398-400.
94. Z. S. Herman and G. H. Loew, *J. Am. Chem. Soc.* **102** (1980), 1815-1821.
95. A. Dedieu, M.-M. Rohmer, and A. Veillard, in B. Pullman and N. Goldblum, eds., *Metal Ligand Interactions in Organic Chemistry and Biochemistry*, Part 2, Reidel, 1977, 101-130.
96. W. A. Goddard III and B. D. Olafson, *Ann. N. Y. Acad. Sci.* **367** (1981), 419-433.
97. B. Boso *et al.*, *Biochim. Biophys. Acta* **791** (1984), 244-251.
98. J. P. Savicki, G. Lang, and M. Ikeda-Saito, *Proc. Natl. Acad. Sci. USA* **81** (1984), 5417-5419.
99. P. E. Ellis, Jr., R. D. Jones, and F. Basolo, *J. Chem. Soc. Chem. Comm.* (1980), 54-55.
100. M. Rougee and D. Brault, *Biochemistry* **14** (1975), 4100-4106.
101. J. S. Thompson, T. J. Marks, and J. A. Ibers, *J. Am. Chem. Soc.* **101** (1979), 4180-4192.
102. M. G. Burnett *et al.*, *J. Chem. Soc. Chem. Comm.* (1980), 829-831; M.G. Burnett, V. McKee, and S. M. Nelson, *loc. cit.* (1980), 599-601.
103. a). J. S. Thompson, *J. Am. Chem. Soc.* **106** (1984), 8308-8309. b) C. L. Merrill *et al.*, *J. Chem. Soc., Dalton Trans.* (1984), 2207-2221. c) L. Casella, M. S. Silver, and J. A. Ibers, *Inorg. Chem.* **23** (1984), 1409-1418. d) Y. Nishida *et al.*, *Inorg. Chim. Acta* **54** (1981), L103-L104. e) K. D. Karlin *et al.*, *J. Am. Chem. Soc.* **110** (1988), 1196-1207. f) R. R. Jacobson *et al.*, *J. Am. Chem. Soc.* **110** (1988), 3690-3692. g) N. Kitajima *et al.*, *J. Am. Chem. Soc.* **114** (1992), 1277-1291.
104. a) F. Basolo, B. M. Hoffman, and J. A. Ibers, *Acc. Chem. Res.* **8** (1975), 384-392; in this see references to the original literature. b) G. A. Rodley and W. T. Robinson, *Nature* **235** (1972), 438-439.
105. T. D. Smith and J. R. Pilbrow, *Coord. Chem. Rev.* **39** (1981), 295-383; in this see references to the original literature, and a critical reanalysis of results in References 107a and 197.
106. B. M. Hoffman and D. H. Petering, *Proc. Natl. Acad. Sci. USA* **67** (1970), 637-643.
107. a) B. S. Tovrog, D. J. Kitko, and R. S. Drago, *J. Am. Chem. Soc.* **98** (1976), 5144-5153. b) R. S. Drago and B. B. Corden, *Acc. Chem. Res.* **13** (1980), 353-360.
108. A. W. Addison and S. Burman, *Biochim. Biophys. Acta* **828** (1985), 362-368.
109. L. M. Proniewicz, K. Nakamoto, and J. R. Kincaid, *J. Am. Chem. Soc.* **110** (1988), 4541-4545.
110. J. L. Hoard, in K. M. Smith, ed., *Porphyrins and Metalloporphyrins*, Elsevier, 1975, 317-380.
111. W. R. Scheidt, *Acc. Chem. Res.* **10** (1977), 339-345.
112. R. G. Little and J. A. Ibers, *J. Am. Chem. Soc.* **96** (1974), 4452-4463.
113. J. L. Hoard and W. R. Scheidt, *Proc. Natl. Acad. Sci. USA* **70** (1973), 3919-3922, and **71** (1974), 1578.
114. S. E. Peterson-Kennedy *et al.*, *J. Am. Chem. Soc.* **108** (1986), 1739-1746.
115. N. V. Blough and B. M. Hoffman, *J. Am. Chem. Soc.* **104** (1982), 4247-4250.
116. a) D. R. Paulson *et al.*, *J. Biol. Chem.* **254** (1979), 7002-7006. b) T. S. Srivastava, *Biochim. Biophys. Acta* **491** (1977), 599-604.

117. R. B. Frydman and B. Frydman, *Acc. Chem. Res.* **20** (1987), 250-256.
118. S.-M. Peng and J. A. Ibers, *J. Am. Chem. Soc.* **98** (1976), 8032-8036.
119. V. L. Goedken and S.-M. Peng, *J. Am. Chem. Soc.* **96** (1974), 7826-7827.
120. V. L. Goedken *et al.*, *J. Am. Chem. Soc.* **98** (1976), 8391-8400.
121. a) D. H. Busch *et al.*, *Proc. Natl. Acad. Sci. USA* **78** (1981), 5919-5923. b) K. Kim *et al.*, *J. Am. Chem. Soc.* **111** (1989), 403-405. c) X.-Y. Li and T. G. Spiro, *J. Am. Chem. Soc.* **110** (1988), 6024-6033. d) K. Kim and J. A. Ibers, *J. Am. Chem. Soc.* **113** (1991), 6077-6081.
122. J. Kuriyan *et al.*, *J. Mol. Biol.* **192** (1986), 133-154.
123. J. M. Baldwin, *J. Mol. Biol.* **136** (1980), 103-128.
124. E. J. Heidner, R. C. Ladner, and M. F. Perutz, *J. Mol. Biol.* **104** (1976), 707-722.
125. a) J. C. Norvell, A. C. Nunes, and B. P. Schoenborn, *Science* **190** (1975), 568-570. b) J. C. Hanson and B. P. Schoenborn, *J. Mol. Biol.* **153** (1981), 117-146.
126. E. A. Padlan and W. E. Love, *J. Biol. Chem.* **249** (1974), 4067-4078.
127. A. Bianconi *et al.*, *Nature* **318** (1985), 685-687.
128. A. Bianconi *et al.*, *Biochim. Biophys. Acta* **831** (1985), 114-119.
129. B. B. Wayland, J. V. Minkiewicz, and M. E. Abd-Elmageed, *J. Am. Chem. Soc.* **96** (1974),2795- 2801.
130. B. S. Tovrog and R. S. Drago, *J. Am. Chem. Soc.* **96** (1974), 6765-6766.
131. B. M. Hoffman, T. Szymanski, and F. Basolo, *J. Am. Chem. Soc.* **97** (1975), 673-674.
132. W. R. Scheidt and D. K. Geiger, *lnorg. Chem.* **21** (1982), 1208-1211.
133. J. C. Maxwell and W. S. Caughey, *Biochemistry* **15** (1976), 388-396.
134. R. C. C. St. George and L. Pauling, *Science* **114** (1951), 629-634.
135. G. B. Jameson and J. A. Ibers, *lnorg. Chem.* **18** (1979), 1200-1208.
136. J.-M. Bassett *et al.*, *J. Chem. Soc. Chem. Comm.* (1977), 853-854.
137. L. Pauling, *Nature* **203** (1964), 182-183.
138. L. S. Liebeskind *et al.*, *J. Am. Chem. Soc.* **100** (1978), 7061-7063.
139. D. Mansuy *et al.*, *J. Am. Chem. Soc.* **105** (1983), 455-463.
140. T. B. Freedman, J. S. Loehr, and T. M. Loehr, *J. Am. Chem. Soc.* **98** (1976), 2809-2815.
141. T. J. Thamann, J. S. Loehr, and T. M. Loehr, *J. Am. Chem. Soc.* **99** (1977), 4187-4189.
142. D. M. Kurtz, Jr., D. F. Shriver, and J. M. Klotz, *J. Am. Chem. Soc.* **98** (1976), 5033-5035.
143. L. Y. Fager and J. O. Alben, *Biochemistry* **11** (1972), 4786-4792.
144. M. Munakata, S. Kitagawa, and K. Goto, *J. lnorg. Biochem.* **16** (1982), 319-322.
145. R. R. Gay and E. I. Solomon, *J. Am. Chem. Soc.* **100** (1978), 1972-1973.
146. A. K. Shiernke, T. M. Loehr, and J. Sanders-Loehr, *J. Am. Chem. Soc.* **108** (1986), 2437-2443.
147. a) J. W. Dawson *et al.*, *Biochemistry* **11** (1972), 461-465. b) M. J. Maroney *et al.*, *J. Am Chem. Soc.* **108** (1986), 6871-6879.
148. J. M. Nocek *et al.*, *J. Am. Chem. Soc.* **107** (1985), 3382-3384.
149. C. H. Barlow *et al.*, *Biochem. Biophys. Res. Comm.* **55** (1973), 91-95.
150. L. Pauling, *Stanford Med. Bull.* **6** (1948), 215-222.
151. J. J. Weiss, *Nature* **202** (1964), 83-84.
152. J. S. Griffith, *Proc. Roy. Soc. A* **235** (1956), 23-36.
153. H. B. Gray, *Adv. Chem. Ser.* **100** (1971), 365-389.
154. T. G. Spiro, in A. B. P. Lever and H. B. Gray, eds., *Iron Porphyrins*, Addison-Wesley (1983), Part II, 89-159.
155. B. B. Wayland and L. W. Olson, *J. Am Chem. Soc.* **96** (1974), 6037-6041.
156. K. Wieghardt, K. Pohl, and W. Gebert, *Angew. Chem. Intl. Ed. Engl.* **22** (1983), 727.
157. P. Gomez-Romero *et al.*, *J. Am. Chem. Soc.* **110** (1988), 1988-1990.
158. J. A. Ibers and R. H. Holm, *Science* **209** (1980), 223-235.
159. A. Levy and J. M. Rifkind, *Biochemistry* **24** (1985), 6050-6054.
160. K. S. Suslick and M. M. Fox, *J. Am. Chem. Soc.* **105** (1983), 3507-3510.
161. a) M. Momenteau *et al.*, *J. Chem. Soc. Chem. Comm.* (1983), 962-964. b) J. Mispelter *et al.*, *J. Am. Chem. Soc.* **105** (1983), 5165-5166.
162. N. Herron *et al.*, *J. Am. Chem. Soc.* **105** (1983), 6585-6596.

163. T. G. Traylor, *Acc. Chem. Res.* **14** (1981), 102-109.
164. T. G. Traylor, N. Koga, and L. A. Deardurff, *J. Am Chem. Soc.* **107** (1985), 6504-6510.
165. J. P. Collman *et al.*, *J. Am. Chem. Soc.* **105** (1983), 3052-3064.
166. J. Almog *et al.*, *J. Am. Chem. Soc.* **97** (1975), 226-227.
167. M. Ikeda-Saito M. Brunori, and T. Yonetani, *Biochim. Biophys. Acta* **533** (1978), 173-180.
168. M. Ikeda-Saito *et al.*, *J. Biol. Chem.* **252** (1977), 4882-4887.
169. G. B. Jameson, W. T. Robinson, and J. A. Ibers, in C. Ho, ed., *Hemoglobin and Oxygen Binding*, Elsevier, 1982, 25-35.
170. T. Yonetani, H. Yamamoto, and G. V. Woodrow III, *J. Biol. Chem.* **249** (1974), 682-690.
171. G. L. Woolery *et al.*, *J. Am. Chem. Soc.* **107** (1985), 2370-2373.
172. G. B. Jameson *et al.*, *J. Am. Chem. Soc.* **102** (1980), 3224-3237.
173. W. Byers *et al.*, *Inorg. Chem.* **25** (1986), 4767-4774.
174. M. M. Doeff, D. A. Sweigart, and P. O'Brien, *Inorg. Chem.* **22** (1983), 851-852.
175. R. S. Drago, J. P. Cannady, and K. A. Leslie, *J. Am. Chem. Soc.* **102** (1980), 6014-6019.
176. G. B. Jameson and R. S. Drago, *J. Am. Chem. Soc.* **107** (1985), 3017-3020.
177. F. A. Walker and J. Bowen, *J. Am. Chem. Soc.* **107** (1985), 7632-7635.
178. T. Yonetani, H. Yamamoto, and T. lizuka, *J. Biol. Chem.* **249** (1974), 2168-2174.
179. T. Kitagawa *et al.*, *Nature* **298** (1982), 869-871.
180. J. E. Linard *et al.*. *J. Am. Chem. Soc.* **102** (1980), 1896-1904.
181. a) T. Takano, *J. Mol. Biol.* **110** (1977), 569-584. b) Deoxymyoglobin at 1.6 Å resolution has been determined (S. E. V. Phillips). See Reference 182.
182. G. Fermi *et al.*, *J. Mol. Biol.* **175** (1984), 159-174.
183. W. Steigemann and E. Weber, *J. Mol. Biol.* **127** (1979), 309-338.
184. G. Fermi *et al.*, *J. Mol. Biol.* **155** (1982), 495-505.
185. E. A. Padlan, W. A. Eaton, and T. Yonetani, *J. Biol. Chem.* **250** (1975), 7069-7073.
186. J. Baldwin and C. Chothia, *J. Mol. Biol.* **129** (1979), 175-220.
187. G. B. Jameson *et al.*, *Inorg. Chem.* **17** (1978), 850-857.
188. S. E. V. Phillips, *J. Mol. Biol.* **142** (1980), 531-554.
189. S. E. V. Phillips and B. P. Schoenborn, *Nature* **292** (1981), 81-82.
190. B. Shaanan, *J. Mol. Biol.* **171** (1983), 31-59.
191. a) A. Brzozowski *et al.*, *Nature* **307** (1984), 74-76. b) Z. Derewenda *et al.*, *J. Mol. Biol.* **211** (1990), 515-519. c) R. Liddington *et al.*, *Nature* **331** (1988), 725-728. d) B. Luisi *et al.*, *J. Mol. Biol.* **214** (1990), 7-14.
192. K. Nagai *et al.*, *Nature* **329** (1987), 858-860.
193. A. Dedieu *et al.*, *J. Am. Chem. Soc.* **98** (1976), 3717-3718.
194. a) J. C. Stevens *et al.*, *J. Am. Chem. Soc.* **102** (1980), 3283-3285. b) P. J. Jackson *et al.*, *Inorg. Chem.* **25** (1986), 4015-4020.
195. L. Powers *et al.*, *Biochemistry* **23** (1984), 5519-5523.
196. a) D. Braunstein *et al.*, *Proc. Natl. Acad. Sci. USA* **85** (1988), 8497-8501. b) P. Ormos *et al.*, *Proc. Natl. Acad. Sci. USA* **85** (1988), 8492-8496. c) J. N. Moore, P. A. Hansen, and R. M. Hochstrasser, *Proc. Natl. Acad. Sci. USA* 85 (1988), 5062- 5066.
197. J. C. W. Chien and L. C. Dickinson, *Proc. Natl. Acad. Sci. USA* **69** (1972), 2783-2787; L. C. Dickinson and J. C. W. Chien, *Proc. Natl. Acad. Sci. USA* **77** (1980), 1235-1239.
198. G. A. Petsko *et al.*, in P. L. Dutton, J. S. Leigh, and A. Scarpa, eds., *Frontiers in Bioenergetics*, Academic Press, 1978, 1011-1017.
199. E. W. Findsen *et al.*, *Science* **229** (1985), 661-665.
200. K. Nagai and T. Kitagawa, *Proc. Natl. Acad. Sci. USA* **77** (1980), 2033-2037.
201. a) G. B. Jameson and J. A. Ibers, *J. Am. Chem. Soc.* **102** (1980), 2823-2831. b) M. Sabat and J. A. Ibers, *J. Am. Chem. Soc.* **104** (1982), 3715-3721.
202. J. W. Sparapany *et al.*, *J. Am. Chem. Soc.* **110** (1988), 4559-4564.
203. A. Arnone *et al.*, *J. Mol. Biol.* **188** (1986),693-706.
204. É. G. Arutyunyan *et al.*, *Sov. Phys. Crystallogr.* **25** (1980), 43-58.
205. D. L. Ollis *et al.*, *Austral. J. Chem.* **36** (1983), 451-468.
206. a) K. Shikama and A. Matsuoka, *Biochemistry* **25** (1986), 3898-3903. b) M. Bolognesi *et al.*, *J. Mol. Biol.* **213** (1990), 621-625.

207. S. J. Lippard, *Angew. Chem. Intl. Ed. Engl.* **27** (1988), 344-361.
208. M. F. Perutz and F. S. Mathews, *J. Mol. Biol.* **21** (1966), 199-202.
209. J. C. Kendrew *et al.*, *Nature* **185** (1960), 422-427.
210. GBJ gratefully acknowledges support from the National Institutes of Health (DK 37702) and sabbatical-leave support from the Department of Chemistry and Biochemistry, Massey University, Palmerston North, New Zealand. JAI is pleased to acknowledge the support of the National Institutes of Health (HL 13157).

Abbreviations

1-MeIm	1-methylimidazole
1,2-Me_2Im	1, 2-dimethylimidazole
2-MeIm	2-methylimidazole
2,3-DPG	2,3-diphosphoglycerate
3,4-Me_2-Py	3,4-dimethylpyridine
4-t-Bu-Py	4-t-butylpyridine
4-CN-Py	4-cyanopyridine
4-NH_2-Py	4-aminopyridine
a_i	activity of component i
Arg	arginine
B	general axial base ligand that binds to a metalloporphyrin
Ch	chlorocruorin
E_1, E_{-1}	activation energy
EDTA	ethylenediaminetetraacetic acid
E°	electrochemical potential at unit activity and fugacity
E°′	electrochemical potential at physiological pH (7.4) and unit pressure (1 atm = 760 Torr)
Er	ertythrocruorin
EtOH	ethanol
EXAFS	extended x-ray absorption fine structure
G	Gibbs free energy
H	enthalpy
H_2(6,6-CP)	cyclophane-strapped porphyrin (see Figure 4.23)
H_2(Poc-PF)	pocket picket-fence porphyrin
H_2Amide-Im	basket-handle porphyrin: imidazole base covalently attached to porphyrin with amide straps; amide straps on other side of porphyrin (see Figure 4.23)
H_2Bis-Poc	meso-tetrakis (2,4,6-triphenylphenyl) porphyrin
H_2bzacen	N,N-ethylenebis (benzoylacetoninime)
H_2C_2Cap	capped porphyrin; see Figure 4.23
H_2Ether-Py	basket-handle porphyrin: as for H_2Amide-Im except ether straps and pyridine base (see Figure 4.23)
H_2MPIX-Im	mesoporphyrin IX dimethylester with imidazole covalently attached to porphyrin (see Figure 4.23)
H_2PF	picket fence porphyrin, meso-tetrakis ($\alpha,\alpha,\alpha,\alpha$-o-

	pivalamidephenyl) porphyrin (see Figure 4.23)
H_2PPIX	protoporphyrin IX dimethylester
H_2PPIX-Im	protoporphyrin IX dimethylester with imidazole covalently attached to porphyrin (see Figure 4.23)
Hb	hemoglobin
HbA	human adult hemoglobin
HbF	human fetal hemoglobin
Hc	hemocyanin
His	histidine
His^{203}	position on polypeptide chain (203) of a histidine residue
Hr	hemerythrin
Im	imidazole
k	rate constant
K_p, K_c	equilibrium constant: concentration of gas expressed in terms of pressure (P) and molarity (M), respectively
L_i	allosteric constant: equilibrium constant for conformational change of protein with i ligands bound
M	general metalloprophyrinato species
M	molarity, moles/L
M	general metal complex
Mb	myoglobin
Me	methyl group
met	oxidized (e.g. met Hb)
OEP	2,3,7,8,12,13,17,18-octaethylporphyrinato
P	pressure, usually in Torr or mm Hg
THF	tetrahydrofuran
TPP	5,10,15,20-tetraphenylporphyrinato

11.2.4.21: Ch. 4 References and Abbreviations is shared under a CC BY-NC-SA 4.0 license and was authored, remixed, and/or curated by LibreTexts.

11.2.5: Dioxygen Reactions

I. Introduction[1]

The major pathway of dioxygen use in aerobic organisms is four-electron reduction to give two molecules of water per dioxygen molecule:[2]

$$O_2 + 4H^+ + 4e^- \rightarrow 2H_2O \qquad E^o = +0.815V \tag{5.1}$$

This reaction represents the major source of energy in aerobic organisms when coupled with the oxidation of electron-rich organic foodstuffs, such as glucose. Biological oxidation of this type is called respiration, and has been estimated to account for 90 percent or more of the dioxygen consumed in the biosphere. It is carried out by means of a series of enzyme-catalyzed reactions that are coupled to ATP synthesis, and the ATP produced is the major source of energy for the organism. The actual site of the reduction of dioxygen in many organisms is the enzyme cytochrome c oxidase.[2]

Another use of dioxygen in aerobic organisms is to function as a source of oxygen atoms in the biosynthesis of various molecules in metabolic pathways, or in conversions of lipid-soluble molecules to water-soluble forms for purposes of excretion. These reactions are also enzyme-catalyzed, and the enzymes involved are either monooxygenase or dioxygenase enzymes, depending on whether one or both of the oxygen atoms from dioxygen are incorporated in the final organic product. Many of these enzymes are metalloenzymes.[2-4]

The advantages of life in air are considerable for an aerobic organism as compared to an anaerobic organism, mainly because the powerful oxidizing power of dioxygen can be controlled and efficiently converted to a form that can be stored and subsequently used.[5] But aerobic metabolism has its disadvantages as well. The interior of a living cell is a reducing environment, and many of the components of the cell are fully capable thermodynamically of reacting directly with dioxygen, thus bypassing the enzymes that control and direct the beneficial reactions of dioxygen.[6] Luckily, for reasons that are discussed below, these reactions generally are slow, and therefore represent minor pathways of biological dioxygen consumption. Otherwise, the cell would just burn up, and aerobic life as we know it would be impossible. Nevertheless, there are small but significant amounts of products formed from nonenzymatic and enzymatic reactions of dioxygen that produce partially reduced forms of dioxygen, i.e., superoxide, O_2^-, and hydrogen peroxide, H_2O_2 , in aerobic cells. These forms of reduced dioxygen or species derived from them could carry out deleterious reactions, and enzymes have been identified that appear to protect against such hazards. These enzymes are, for superoxide, the superoxide dismutase enzymes, and, for peroxide, catalase and the peroxidase enzymes. All of these enzymes are metalloenzymes.[2-4]

Much of the fascination of the subject of biological reactions of dioxygen stems from the fact that the mechanisms of the biological, enzyme-catalyzed reactions are clearly quite different from those of the uncatalyzed reactions of dioxygen or even those of dioxygen reactions catalyzed by a wide variety of nonbiological metal-containing catalysts.[7] Investigators believe, optimistically, that once they truly understand the biological reactions, they will be able to design synthetic catalysts that mimic the biological catalysts, at least in reproducing the reaction types, even if these new catalysts do not match the enzymes in rate and specificity. To introduce this topic, therefore, we first consider the factors that determine the characteristics of nonbiological reactions of dioxygen.

II. Chemistry of Dioxygen

A. Thermodynamics

B. Kinetics

C. Free-Radical Autoxidation

D. How Do Enzymes Overcome These Kinetic Barriers?

III. Dioxygen Toxicity

A. Background

B. Biological Targets

C. Defense and Repair Systems
1. Nonenzymatic Oxidant Scavengers
2. Detoxification Enzymes
3. Systems for Sequestration of Redox-active Metal Ions
4. Systems for the Repair or Replacement of Damaged Materials

D. Molecular Mechanisms of Dioxygen Toxicity

E. Summary of Dioxygen Toxicity

IV. Cytochrome c Oxidase

A. Background

B. Spectroscopic Characterization
1. Models
2. Spectroscopy of the Enzyme

C. Mechanism of Dioxygen Reduction
1. Models
2. Mechanistic Studies of the Enzyme

V. Oxygenases

A. Background

B. Dioxygenases
1. Intradiol Catechol Dioxygenases

C. Monoxygenases
1. Cytochrome P-450
2. Other Metal-containing Monoxygenase Enzymes

VI. Catalase and Peroxidase

A. Description of the Enzymes

B. Mechanism

C. Comparisons of Catalase, Peroxidase, and Cytochrome P-450

VII. Copper-zinc Superoxide Dismutase

A. Background

B. Enzymatic Activity

C. Structure

D. Enzymatic Activity and Mechanism

E. Anions as Inhibitors

F. Metal-Ion Substitutions

1. SOD activity
2. Spectroscopy

VIII. References

1. The references in this chapter cite recent review articles or books when available; these are indicated by (R) or (B), respectively, in the citation, and the titles of review articles are given. Students should consult these sources if they want more detailed information about a particular topic or references to the original literature.
2. B. G. Malmström, "Enzymology of Oxygen" (R), *Annu. Rev. Biochem*. **51** (1982), 21-59.
3. L. L. Ingraham and D. L. Meyer, *Biochemistry of Dioxygen* (B), Plenum, 1985.
4. O. Hayaishi, ed., *Molecular Mechanisms of Oxygen Activation* (B), Academic Press, 1974, pp. 405- 451.
5. P. George, "The Fitness of Oxygen" (R), in T. E. King, H. S. Mason, and M. Morrison, eds., *Oxidases and Related Redox Systems*, Wiley, **1** (1965), 3-36.
6. B. Halliwell and J. M. C. Gutteridge, *Free Radicals in Biology and Medicine* (B), Clarendon Press, 1989.
7. R. A. Sheldon and J. K. Kochi, *Metal-Catalyzed Oxidations of Organic Compounds* (B), Academic Press, 1981.
8. D. T. Sawyer, "The Chemistry and Activation of Dioxygen Species (O_2, $O_2^{\bullet-}$, and HOOH) in Biology" (R), in A. E. Martell and D. T. Sawyer, eds., *Oxygen Complexes and Oxygen Activation by Transition Metals*, Plenum, 1988, pp. 131-148.
9. P. M. Wood, *Trends in Biochem. Sci.* **12** (1987), 250-251.
10. R. H. Holm, "Metal-Centered Oxygen Atom Transfer Reactions" (R), *Chem. Rev*. **87** (1987), 1401- 1449.
11. Calculated from data in D. D. Wagman *et al.*, *Selected Values of Chemical Thermodynamic Properties*, Institute for Basic Standards, NBS, 1968.
12. Calculated from data in M. Bertholon *et al.*, *Bull. Soc. Chim. Fr.* **9** (1971), 3180-3187.
13. Calculated from data in A. Finch, P. J. Gardner, and D. Wu, *Thermochim. Acta* **66** (1983), 333-342.
14. L. Shaofeng and G. Pilcher, *J. Chem. Thermodynamics* **20** (1988), 463-465.
15. G. A. Hamilton, "Chemical Models and Mechanisms for Oxygenases" (R), in Reference 4, pp. 405- 451.
16. H. Taube, "Mechanisms of Oxidation with Oxygen" (R), *J. Gen. Physiol.* **49**, part 2 (1965), 29-52.
17. J. G. Calvert and J. N. Pitts, *Photochemistry*, Wiley, 1966.
18. H. H. Wasserman and R. W. Murray, eds., *Singlet Oxygen* (B), Academic Press, 1979.
19. A. A. Frimer, ed., *Singlet* O_2 (B), CRC Press, 1985.
20. T. C. Bruice, "Chemical Studies and the Mechanism of Flavin Mixed Function Oxidase Enzymes (R), in J. F. Liebman and A. Greenberg, eds., Mechanistic *Principles of Enzyme Activity*, VCH Publishers, 1988, pp. 315-352.
21. Reference 7, p. 18.
22. Reference 7, p. 316.
23. Reference 3, p. 16.
24. N. A. Porter *et al.*, *J. Am. Chem. Soc.* **103** (1981), 6447-6455.
25. W. Day, *Genesis on Planet Earth: The Search for Life's Beginning*, Yale University Press, 2d ed., 1984.
26. D. L. Gilbert, ed., *Oxygen and Living Processes: An Interdisciplinary Approach* (B), Springer-Verlag, 1981.
27. B. Quebedeaux *et al.*, Plant Physiol. **56** (1975), 761-764.
28. O. R. Brown and F. Yein, *Biochem. Biophys. Res. Commun.* **85** (1978), 1219-1224.
29. L. J. Machlin and A. Bendich, *FASEB J.* **1** (1987), 441-445.
30. D. S. Tarbell, in N. Kharasch, ed., *Organic Sulfur Compounds*, Pergamon, **1** (1961), 97-102.
31. C. Walling, *Acc. Chem. Res*. **8** (1975), 125-132.
32. D. C. Harris and P. Aisen, in T. M. Loehr, ed., *Iron Carriers and Iron Proteins*, VCH Publishers, 1989, pp. 239-371.
33. G. Storz, L. A. Tartaglia, and B. N. Ames, *Science* **248** (1990), 189-194, and references therein.
34. T. Keng and L. Guarente, *Proc. Natl. Acad. Sci. USA* **84** (1987), 9113-9117, and references therein.

35. R. Gerschman *et al.*, *Science* **119** (1954), 623-626.
36. J. M. McCord and J. Fridovich, *J. Biol. Chem.* **244** (1969), 6049-6055.
37. D. T. Sawyer and J. S. Valentine, "How Super is Superoxide?" (R), *Acc. Chem. Res.* **14** (1981), 393- 400.
38. L. W. Oberley, ed., *Superoxide Dismutase*, CRC Press, 2 vols., 1982, vol. 3, 1985.
39. J. A. Fee, "Is Superoxide Important in Oxygen Poisoning?" (R), *Trends Biochem. Sci.* **7** (1982), 84- 86, and references therein.
40. P. Korbashi *et al.*, *J. Biol. Chem.* **264** (1989), 8479-8482.
41. E. R. Stadtman, "Metal Ion-Catalyzed Oxidation of Proteins: Biochemical Mechanism and Biological Consequences" (R), *Free Radicals in Biology & Medicine* **9** (1990), 315-325.
42. D. O. Natvig *et al.*, *J. BioI. Chem.* **262** (1987), 14697-14701.
43. C. Bowler *et al.*, *J. Bacteriol.* **172** (1990), 1539-1546.
44. M. Wikstrom and G. T. Babcock, *Nature* **348** (1990), 16-17.
45. G. Palmer, "Cytochrome Oxidase: a Perspective" (R), *Pure Appl. Chem.* **59** (1987), 749-758.
46. T. Vanngard, ed., *Biophysical Chemistry of Dioxygen Reactions in Respiration and Photosynthesis, Chemica Scripta* **28A** (B), Cambridge University Press, 1988.
47. W. R. Scheidt and C. A. Reed, "Spin-State/Stereochemical Relationships in Iron Porphyrins: Implications for the Hemoproteins" (R), *Chem. Rev.* **81** (1981), 543-555.
48. F. S. Mathews, M. Levine, and P. Argos, *J. Mol. Biol.* **64** (1972), 449-464.
49. W. E. Blumberg and J. Peisach, *Adv. Chem. Ser.* **100** (1971), 271-291.
50. J. Peisach, W. E. Blumberg, and A. Adler, *Ann. N.Y. Acad. Sci.* **206** (1973), 310-327.
51. J. P. Collman, T. R. Halbert, and K. S. Suslick, "O_2 Binding to Heme Proteins and Their Synthetic Analogues" (R), in T. G. Spiro, ed., *Metal-Ion Activation of Dioxygen*, Wiley, 1980, pp. 1-72.
52. R. Quinn, M. Nappa, and J. S. Valentine, *J. Am. Chem. Soc.* **104** (1982), 2588-2595.
53. F. A. Cotton and G. Wilkinson, *Advanced Inorganic Chemistry*, Wiley, 5th ed., 1988, pp. 755-775.
54. T. H. Stevens *et al.*, *J. Biol. Chem.* **257** (1982), 12106-12113.
55. W. B. Mims *et al.*, *J. Biol. Chem.* **255** (1980), 6843-6846.
56. T. H. Stevens *et al.*, *Proc. Natl. Acad. Sci USA* **76** (1979), 3320-3324.
57. T. A. Kent *et al.*, *J. Biol. Chem.* **258** (1983), 8543-8546.
58. J. Cline *et al.*, *J. Biol. Chem.* **258** (1983), 5124-5128.
59. T. H. Stevens and S. I. Chan, *J. Biol. Chem.* **256** (1981), 1069-1071.
60. D. H. Chin, G. N. La Mar, and A. Balch, *J. Am. Chem. Soc.* **102** (1980), 4344-4350.
61. A. L. Balch *et al.*, *J. Am. Chem. Soc.* **106** (1984), 7779-7785.
62. K. D. Karlin and Y. Gultneh, "Binding and Activation of Molecular Oxygen by Copper Complexes" (R), *Prog. Inorg. Chem.* **35** (1987), 219-327.
63. R. R. Jacobson *et al.*, *J. Am. Chem. Soc.* **110** (1988), 3690-3692.
64. N. Kitajima, K. Fujisawa, and Y. Moro-oka, *J. Am. Chem. Soc.* **111** (1989), 8975-8976.
65. S. Han, Y.-C. Chin, and D. L. Rousseau, *Nature* **348** (1990), 89-90.
66. L. Que, Jr., "The Catechol Dioxygenases" (R), in Reference 32, pp. 467-524.
67. L. Que, Jr., "Spectroscopic Studies of the Catechol Dioxygenases" (R), *J. Chem. Ed.* **62** (1985), 938- 943.
68. J. W. Whittaker *et al.*, *J. Biol. Chem.* **259** (1984), 4466-4475.
69. Y. Tomimatsu, S. Kint, and J. R. Scherer, *Biochemistry* **15** (1976), 4918-4924.
70. D. H. Ohlendorf, J. D. Lipscomb, and P. C. Weber, *Nature* **336** (1988), 403-405.
71. D. D. Cox and L. Que, Jr., *J. Am. Chem. Soc.* **110** (1988), 8085-8092.
72. Y. Sawaki and C. S. Foote, *J. Am. Chem. Soc.* **105** (1983), 5035-5040.
73. P. R. Ortiz de Montellano, ed., *Cytochrome P-450: Structure, Mechanism, and Biochemistry* (B), Plenum, 1986.
74. K. Lerch, "Copper Monooxygenases: Tyrosinase and Dopamine β-Monooxygenase" (R), *Metal Ions Biol. Syst.* **13** (1981), 143-186.
75. J. Green and H. Dalton, *J. Biol. Chem.* **264** (1989), 17698-17703, and references therein.
76. A. Ericson *et al.*, *J. Am. Chem. Soc.* **110** (1988), 2330-2332.
77. J. E. Colbert, A. G. Katopodis, and S. W. May, *J. Am. Chem. Soc.* **112** (1990), 3993-3996, and references therein.

78. L. C. Stewart and J. P. Klinman, "Dopamine β-Hydroxylase of Adrenal Chromaffin Granules: Structure and Function" (R), *Annu. Rev. Biochem.* **57** (1988), 551-592.
79. T. A. Dix and S. J. Benkovic, "Mechanism of Oxygen Activation by Pteridine-Dependent Monooxygenases" (R), *Acc. Chem. Res.* **21** (1988), 101-107.
80. T. L. Poulos, "The Crystal Structure of Cytochrome P-450$_{cam}$" (R), in Reference 73, pp. 505-523.
81. T. J. McMurry and J. T. Groves, "Metalloporphyrin Models for Cytochrome P-450" (R), in Reference 73, pp. 1-28.
82. J. T. Groves, T. E. Nemo, and R. S. Myers, *J. Am. Chem. Soc.* **101** (1979), 1032-1033.
83. . J. T. Groves, "Key Elements of the Chemistry of Cytochrome P-450: The Oxygen Rebound Mechanism" (R), *J. Chem. Ed.* **62** (1985), 928-931.
84. D. Dolphin *et al.*, *Ann. N.Y. Acad. Sci.* **206** (1973),177-200.
85. E. McCandlish *et al.*, *J. Am. Chem. Soc.* **102** (1980), 4268-4271.
86. J. N. Burstyn *et al.*, *J. Am. Chem. Soc.* **110** (1988), 1382-1388.
87. J. S. Valentine, J. N. Burstyn, and L. D. Margerum, "Mechanisms of Dioxygen Activation in Metal-Containing Monooxygenases: Enzymes and Model Systems" (R), in Reference 8, pp. 175-187.
88. T. C. Bruice, "Chemical Studies Related to Iron Protoporphyrin-IX Mixed Function Oxidases" (R), in Reference 20, pp. 227-277.
89. T. G. Traylor, W.-P. Fann, and D. Bandyopadhyay, *J. Am. Chem. Soc.* **111** (1989), 8009-8010.
90. R. Raag and T. L. Poulos, *Biochemistry* **28** (1989), 7586-7592, and references therein.
91. P. R. Ortiz de Montellano, "Oxygen Activation and Transfer" (R), in Reference 73, pp. 217-271.
92. K. Murata *et al.*, *J. Am. Chem. Soc.* **112** (1990), 6072-6083, and references therein.
93. T. G. Traylor and J. P. Ciccone, *J. Am. Chem. Soc.* **111** (1989), 8413-8420, and references therein.
94. J. Everse, K. E. Everse, and M. B. Grisham, eds., *Peroxidases in Chemistry and Biology* (B), CRC Press, 1991.
95. H. B. Dunford, "Peroxidases" (R), *Adv. Inorg. Biochem.* **4** (1982), 41-68.
96. T. L. Poulos and J. Kraut, *J. Biol. Chem.* **225** (1980), 8199-8205.
97. M. Morrison and G. R. Schonbaum, *Annu. Rev. Biochem.* **45** (1976), 861-888.
98. R. Quinn *et al.*, *J. Am. Chem. Soc.* **106** (1984), 4136-4144.
99. P. R. Ortiz de Montellano *et al.*, *J. Biol. Chem.* **262** (1987), 11641-11646.
100. J. S. Valentine and M. W. Pantoliano, "Protein-Metal Ion Interactions in Cuprozinc Protein (Superoxide Dismutase)" (R), in T. G. Spiro, ed., *Copper Proteins*, 1981, pp. 291-358.
101. J. S. Valentine and D. Mota de Freitas, *J. Chem. Ed.* **62** (1985), 990-997.
102. J. V. Bannister, W. H. Bannister, and G. Rotilio, "Aspects of the Structure, Function, and Applications of Superoxide Dismutase" (R), *CRC Crit. Rev. Biochem.* **22** (1987), 111-180.
103. See Reference 38.
104. S. B. Farr, R. D'Ari, and D. Touati, *Proc. Natl. Acad. Sci. USA* **83** (1986), 8268-8272.
105. O. Bermingham-McDonogh, E. B. Gralla, and J. S. Valentine, *Proc. Natl. Acad. Sci. USA* **85** (1988), 4789-4793.
106. J. S. Valentine and A. B. Curtis, *J. Am. Chem. Soc.* **97** (1975), 224-226.
107. M. Nappa *et al.*, *J. Am. Chem. Soc.* **101** (1979), 7744-7746.
108. G. J. McClune *et al.*, *J. Am. Chem. Soc.* **99** (1977), 5220-5222.
109. P. Natarajan and N. V. Raghavan, *J. Am. Chem. Soc.* **102** (1980), 4518-4519.
110. M. W. Pantoliano *et al.*, *J. Inorg. Biochem.* **17** (1982), 325-341.
111. J. A. Roe *et al.*, *Biochemistry* **27** (1988), 950-958.
112. J. A. Tainer *et al.*, *Nature* **306** (1983),284-289.
113. J. A. Fee and C. Bull, *J. Biol. Chem.* **261** (1986), 13000-13005.
114. I. Bertini *et al.*, *J. Am. Chem. Soc.* **111** (1989), 714-719.
115. L. Banci *et al.*, *Inorg. Chem.* **27** (1988), 107-109.
116. D. Mota de Freitas *et al.*, *Inorg. Chem.* **26** (1987), 2788-2791.
117. L.-J. Ming and J. S. Valentine, *J. Am. Chem. Soc.* **109** (1987), 4426-4428.
118. I. Bertini *et al.*, *J. Am. Chem. Soc.* **107** (1985), 4391-4396.
119. L.-J. Ming *et al.*, *Inorg. Chem.* **27** (1988), 4458-4463.
120. L. Banci *et al.*, *Inorg. Chem.* **29** (1990), 2398-2403, and references therein.

121. J. A. Imlay and I. Fridovich, *J. Biol. Chem.* **266** (1991), 6957-6965.
122. P. R. Gardner and I. Fridovich, *J. BioI. Chem.* **266** (1991), 19328-19333.
123. J. S. Beckman *et al.*, *Proc. Natl. Acad. Sci. USA* **87** (1990), 1620-1624.
124. P. R. Ortiz de Montellano, *Annu. Rev. Pharmacol.* **32** (1992),89-107.
125. The author gratefully acknowledges research support from the National Science Foundation and the National Institutes of Health while this chapter was being written, editoral assistance from Dr. Bertram Selverstone, and patience and support from Dr. Andrew J. Clark.
126. It has been suggested recently that the Cu_A site in cytochrome c oxidase may contain two copper ions. See P. M. Kroneck *et aI.*, *FEBS Lett.* **268** (1990), 274-276.
127. An excellent review relevant to this chapter has recently appeared. K. D. Karlin, *Science* **261** (1993), 701-708.

Contributors and Attributions

- Joan Selverstone Valentine (University of California, Los Angeles, Department of Chemistry and Biochemistry)

11.2.5: Dioxygen Reactions is shared under a CC BY-NC-SA 4.0 license and was authored, remixed, and/or curated by LibreTexts.

11.2.5.1: Catalase and Peroxidase

Description of the Enzymes

Catalase and peroxidase are heme enzymes that catalyze reactions of hydrogen peroxide.[94,95] In catalase, the enzymatic reaction is the disproportionation of hydrogen peroxide (Reaction 5.82) and the function of the enzyme appears to be prevention of any buildup of that potentially dangerous oxidant (see the discussion of dioxygen toxicity in Section III).

$$2H_2O_2 \xrightarrow{catalase} 2H_2O + O_2 \tag{5.82}$$

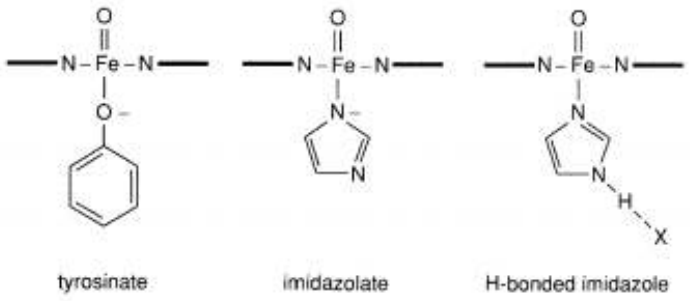
Peroxidase reacts by mechanisms similar to catalase, but the reaction catalyzed is the oxidation of a wide variety of organic and inorganic substrates by hydrogen peroxide (Reaction 5.83).

$$H_2O_2 + AH_2 \xrightarrow{peroxidase} 2H_2O + A \tag{5.83}$$

(The catalase reaction can be seen to be a special case of Reaction 5.83 in which the substrate, AH_2, is hydrogen peroxide.) Some examples of peroxidases that have been characterized are horseradish peroxidase, cytochrome c peroxidase, glutathione peroxidase, and myeloperoxidase.[94,95]

X-ray crystal structures have been determined for beef-liver catalase[80] and for horseradish peroxidase[96] in the resting, high-spin ferric state. In both, there is a single heme b group at the active site. In catalase, the axial ligands are a phenolate from a tyrosyl residue, bound to the heme on the side away from the active-site cavity, and water, bound to heme within the cavity and presumably replaced by hydrogen peroxide in the catalytic reaction. In horseradish peroxidase, the axial ligand is an imidazole from a histidyl residue. Also within the active-site cavity are histidine and aspartate or asparagine side chains that appear to be ideally situated to interact with hydrogen peroxide when it is bound to the iron. These residues are believed to play an important part in the mechanism by facilitating O—O bond cleavage (see Section VI.B below).

Three other forms of catalase and peroxidase can be generated, which are referred to as compounds I, II, and III. Compound I is generated by reaction of the ferric state of the enzymes with hydrogen peroxide. Compound I is green and has spectral characteristics very similar to the $Fe^{IV}(P^{\bullet-})(O)^+$ complex prepared at low temperatures by reaction of ferric porphyrins with single-oxygenatom donors (see Section V.C.1.a). Titrations with reducing agents indicate that it is oxidized by two equivalents above the ferric form. It has been proposed (see 5.84) that the anionic nature of the tyrosinate axial ligand in catalase may serve to stabilize the highly oxidized iron center in compound I of that enzyme,[80] and furthermore that the histidyl imidazole ligand in peroxidase may deprotonate, forming imidazolate,[52,97] or may be strongly hydrogen bonded,[98] thus serving a similar stabilizing function for compound I in that enzyme.



Reduction of compound I by one electron produces compound II, which has the characteristics of a normal ferryl-porphyrin complex, analogous to **2**, i.e., (L)Fe^{IV}(P)(O). Reaction of compound II with hydrogen peroxide produces compound III, which can also be prepared by reaction of the ferrous enzyme with dioxygen. It is an oxy form, analogous to oxymyoglobin, and does not appear to have a physiological function. The reactions producing these three forms and their proposed formulations are summarized in Reactions (5.85) to (5.88).

$$Fe^{III}(P)^+ + H_2O_2 \rightarrow Fe^{IV}(P^-)(O)^+ + H_2O \tag{5.85}$$

$$\underset{ferric\ form}{} \qquad \underset{Compound\ I}{} \tag{11.2.5.1.1}$$

$$Fe^{IV}(P^{\cdot-})(O)^{+} + e^{-} \rightarrow Fe^{IV}(P)(O) \tag{5.86}$$

$$\underset{Compound\ I}{} \qquad \underset{Compound\ II}{} \tag{11.2.5.1.2}$$

$$Fe^{IV}(P)(O) + H_2O_2 \rightarrow Fe(P)O_2 + H_2O \tag{5.87}$$

$$\underset{Compound\ II}{} \qquad \underset{Compound\ III}{} \tag{11.2.5.1.3}$$

$$FeII(P) + O_2 \rightarrow Fe(P)O_2 \tag{5.88}$$

$$\underset{ferrous\ form}{} \qquad \underset{Compound\ III}{} \tag{11.2.5.1.4}$$

Mechanism

The accepted mechanisms for catalase and peroxidase are described in Reactions (5.89) to (5.94).

$$Fe^{III}(P)^{+} + H_2O_2 \rightarrow Fe^{III}(P)(H_2O_2)^{+} \rightarrow Fe^{IV}(P^{\cdot-})(O)^{+} + H_2O \tag{5.89}$$

$$\underset{Compound\ I}{} \tag{11.2.5.1.5}$$

catalase:

$$Fe^{IV}(P^{\cdot-})(O)^{+} + H_2O_2 \rightarrow Fe^{III}(P)^{+} + H_2O + O_2 \tag{5.90}$$

$$\underset{Compound\ I}{} \tag{11.2.5.1.6}$$

peroxidase:

$$Fe^{IV}(P^{\cdot-})(O)^{+} + AH_2 \rightarrow Fe^{IV}(P)(O) + HA^{\cdot} + H^{+} \tag{5.91}$$

$$\underset{Compound\ I}{} \qquad \underset{Compound\ II}{} \tag{11.2.5.1.7}$$

$$Fe^{IV}(P)(O) + AH_2 \rightarrow Fe^{III}(P)^{+} + HA^{\cdot} + OH^{-} \tag{5.92}$$

$$\underset{Compound\ II}{} \tag{11.2.5.1.8}$$

$$2HA^{\cdot} \rightarrow A + AH_2 \tag{5.93}$$

or

$$2HA^{\cdot} \rightarrow HA - AH \tag{5.94}$$

In the catalase reaction, it has been established by use of $H_2{}^{18}O_2$ that the dioxygen formed is derived from hydrogen peroxide, i.e., that O—O bond cleavage does not occur in Reaction (5.90), which is therefore a two-electron reduction of compound I by hydrogen peroxide, with the oxo ligand of the former being released as water. For the peroxidase reaction under physiological conditions, it is believed that the oxidation proceeds in one-electron steps (Reactions 5.91 and 5.92), with the final formation of product occurring by disproportionation (Reaction 5.93) or coupling (Reaction 5.94) of the one-electron oxidized intermediate.[94,95]

Comparisons of Catalase, Peroxidase, and Cytochrome P-450

The proposal that these three enzymes all go through a similar high-valent oxo intermediate, i.e., **3** or compound I, raises two interesting questions. The first of these is why the same high-valent metal-oxo intermediate gives two very different types of reactions, i.e., oxygen-atom transfer with cytochrome P-450 and electron transfer with catalase and peroxidase. The answer is that, although the high-valent metal-oxo heme cores of these intermediates are in fact very similar, the substrate-binding cavities seem to differ substantially in how much access the substrate has to the iron center. With cytochrome P-450, the substrate is jammed right up against the location where the oxo ligand must reside in the high-valent oxo intermediate. But the same location in the peroxidase enzymes is blocked by the protein structure so that substrates can interact only with the heme edge. Thus oxidation of the substrate by electron transfer is possible for catalase and peroxidase, but the substrate is too far away from the oxo ligand for oxygen-atom transfer.[99,124]

The second question is about how the the high-valent oxo intermediate forms in both enzymes. For catalase and peroxidase, the evidence indicates that hydrogen peroxide binds to the ferric center and then undergoes heterolysis at the O—O bond. Heterolytic cleavage requires a significant separation of positive and negative charge in the transition state. In catalase and peroxidase, analysis of the crystal structure indicates strongly that amino-acid side chains are situated to aid in the cleavage by stabilizing a charge-separated transition state (Figure 5.14).

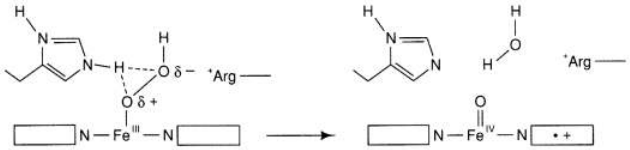


Figure 5.14 - Schematic representation of the mechanism for heterolytic O—O bond cleavage to form Compound I in peroxidase, as proposed in Reference 96. The histidyl imidazole aids in transfer of a proton from the oxygen atom of hydrogen peroxide that is bound to the iron to the departing oxygen atom, while the positive charge of the arginyl side chain stabilizes the developing negative charge on the departing oxygen, thus facilitating heterolytic O—O bond cleavage.

In cytochrome P-450, as mentioned in Section V.C.1, no such groups are found in the hydrophobic substrate-binding cavity. It is possible that the cysteinyl axial ligand in cytochrome P-450 plays an important role in O—O bond cleavage, and that the interactions found in catalase and peroxidase that appear to facilitate such cleavage are therefore not necessary.

11.2.5.1: Catalase and Peroxidase is shared under a CC BY-NC-SA 4.0 license and was authored, remixed, and/or curated by LibreTexts.

11.2.5.2: Chemistry of Dioxygen

Thermodynamics

The reduction potential for the four-electron reduction of dioxygen (Reaction 5.1) is a measure of the great oxidizing power of the dioxygen molecule.[8] However, the reaction involves the transfer of four electrons, a process that rarely, if ever, occurs in one concerted step, as shown in Reaction (5.2).

$$O_2 \xrightarrow{e^-} O_2^- \xrightarrow{e^-,2H^+} H_2O_2 \xrightarrow{e^-,H^+} H_2O + OH \xrightarrow{e^-,H^+} 2H_2O \tag{5.2}$$

$$\begin{aligned} dioxygen \xrightarrow{e^-} superoxide \xrightarrow{e^-,2H^+} hydrogen\ peroxide \xrightarrow{e^-,H^+} water \\ + hyrdoxyl\ radical \xrightarrow{e^-,H^+} water \end{aligned} \tag{11.2.5.2.1}$$

Since most reducing agents can transfer at most one or two electrons at a time to an oxidizing agent, the thermodynamics of the one- and two-electron reductions of dioxygen must be considered in order to understand the overall mechanism.

In aqueous solution, the most common pathway for dioxygen reduction in the absence of any catalyst is one-electron reduction to give superoxide. But this is the least favorable of the reaction steps that make up the full four-electron reduction (see Table 5.1) and requires a moderately strong reducing agent. Thus if only one-electron pathways are available for dioxygen reduction, the low reduction potential for one-electron reduction of O_2 to O_2^- presents a barrier that protects vulnerable species from the full oxidizing power of dioxygen that comes from the subsequent steps. If superoxide is formed (Reaction 5.3), however, it disproportionates quite rapidly in aqueous solution (except at very high pH) to give hydrogen peroxide and dioxygen (Reaction 5.4). The stoichiometry of the overall reaction is therefore that of a net two-electron reduction (Reaction 5.5). It is thus impossible under normal conditions to distinguish one-electron and two-electron reaction pathways for the reduction of dioxygen in aqueous solution on the basis of stoichiometry alone.

$$2O_2 + 2e^- \rightarrow 2O_2^- \tag{5.3}$$

$$2O_2^- + 2H^+ \rightarrow H_2O_2 + O_2 \tag{5.4}$$

$$O_2 + 2e^- + 2H^+ \rightarrow H_2O_2 \tag{5.5}$$

Table 5.1: Standard reduction potentials for dioxygen species in water. a) The standard state used here is unit pressure. If unit activity is used for the standard state of O_2, the redox potentials for reactions of that species must be adjusted by +0.17 V.[8,9]

Reaction		E°, V vs. NHE, pH 7, 25 °C
$O_2 + e^- \rightarrow O_2^-$	(11.2.5.2.2)	-0.33[a]
$O_2^- + e^- + 2H^+ \rightarrow H_2O_2$	(11.2.5.2.3)	+0.89
$H_2O_2 + e^- + H^+ \rightarrow H_2O + OH$	(11.2.5.2.4)	+0.38
$OH + e^- + H^+ \rightarrow H_2O$	(11.2.5.2.5)	+2.31
$O_2 + 2e^- + 2H^+ \rightarrow H_2O_2$	(11.2.5.2.6)	+0.281[a]
$H_2O_2 + 2e^- + 2H^+ \rightarrow 2H_2O$	(11.2.5.2.7)	+1.349
$O_2 + 4H^+ + 4e^- \rightarrow 2H_2O$	(11.2.5.2.8)	+0.815[a]

The thermodynamics of dioxygen reactions with organic substrates is also of importance in understanding dioxygen reactivity. The types of reactions that are of particular interest to us here are hydroxylation of aliphatic and aromatic C—H bonds and epoxidation of olefins, since these typical reactions of oxygenase enzymes are ones that investigators are trying to mimic using synthetic reagents. Some of the simpler examples of such reactions (plus the reaction of H_2 for comparison) are given in the reactions in Table 5.2. It is apparent that all these reactions of dioxygen with various organic substrates in Table 5.2 are thermodynamically favorable. However, *direct* reactions of dioxygen with organic substrates in the absence of a catalyst are generally very slow, unless the substrate is a particularly good reducing agent. To understand the sluggishness of dioxygen reactions with organic substrates, we must consider the kinetic barriers to these reactions.

Table 5.2: Examples of hydroxylation and epoxidation reactions.

Reaction	ΔH in kcal/mol	Reference
$CH_{4(g)} + \frac{1}{2}O_{2(g)} \rightarrow CH_3OH_{(g)}$ (11.2.5.2.9)	-30	10
$C_6H_{6(g)} + \frac{1}{2}O_{2(g)} \rightarrow C_6H_5OH_{(g)}$ (11.2.5.2.10)	-43	11,12
$C_6H_5OH_{(g)} + \frac{1}{2}O_{2(g)} \rightarrow C_6H_5(OH)_{2(g)}$ (11.2.5.2.11)	-42	12,13
$C_2H_{4(g)} + \frac{1}{2}O_{2(g)} \rightarrow C_2H_4O_{(g)}$ (11.2.5.2.12)	-25	10
$C_5H_5N_{(g)} + \frac{1}{2}O_{2(g)} \rightarrow C_5H_5NO_{(g)}$ (11.2.5.2.13)	-13	14
$H_{2(g)} + \frac{1}{2}O_{2(g)} \rightarrow H_2O_{(g)}$ (11.2.5.2.14)	-58	10

Kinetics

The principal kinetic barrier to direct reaction of dioxygen with an organic substrate arises from the fact that the ground state of the dioxygen molecule is triplet, i.e., contains two unpaired electrons.[15,16] Typical organic molecules that are representative of biological substrates have singlet ground states, i.e., contain no unpaired electrons, and the products resulting from their oxygenation also have singlet ground states. Reactions between molecules occur in shorter times than the time required for

conversions from triplet to singlet spin. Therefore the number of unpaired electrons must remain the same before and after each elementary step of a chemical reaction. For these reasons, we know that it is impossible for Reaction (5.6) to go in one fast, concerted step.

$$\frac{1}{2}\,{}^3O_2 + {}^1X \rightarrow {}^1XO \tag{5.6}$$

$$\uparrow\uparrow \quad \downarrow\uparrow \quad \downarrow\uparrow \tag{11.2.5.2.15}$$

The arrows represent electron spins: ↓↑ represents a singlet molecule with all electron spins paired; ↑↑ represents a triplet molecule with two unpaired electrons; and ↑ (which we will see in Reaction 5.13) represents a doublet molecule, also referred to as a free radical, with one unpaired electron. The pathways that do not violate the spin restriction are all costly in energy, resulting in high activation barriers. For example, the reaction of ground-state triplet dioxygen, i.e.,$^3O_2$, with a singlet substrate to give the excited triplet state of the oxygenated product (Reaction 5.7) is spin-allowed, and one could imagine a mechanism in which this process is followed by a slow spin conversion to a singlet product (Reaction 5.8).

$$\frac{1}{2}\,{}^3O_2 + {}^1X \rightarrow {}^3XO \tag{5.7}$$

$$\uparrow\uparrow \quad \downarrow\uparrow \quad \uparrow\uparrow \tag{11.2.5.2.16}$$

$${}^3XO \xrightarrow{slow} {}^1XO \tag{5.38}$$

$$\uparrow\uparrow \quad \downarrow\uparrow \tag{11.2.5.2.17}$$

But such a reaction pathway would give a high activation barrier, because the excited triplet states of even unsaturated molecules are typically 40-70 kcal/mol less stable than the ground state, and those of saturated hydrocarbons are much higher.[17] Likewise, a pathway in which O_2 is excited to a singlet state that then reacts with the substrate would be spin-allowed (Reactions 5.9 and 5.10). The high reactivity of singlet dioxygen, generated by photochemical or chemical means, is well-documented.[18,19] However, such a pathway for a reaction of dioxygen, which is initially in its ground triplet state, would also require a high activation energy, since the lowest-energy singlet excited state of dioxygen is 22.5 kcal/mol higher in energy than ground-state triplet dioxygen.[15,16]

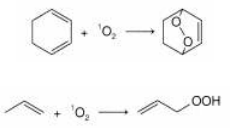
$${}^3O_2 + 22.5\ kcal/mol \rightarrow {}^1O_2 \tag{5.9}$$

$$\uparrow\uparrow \quad \downarrow\uparrow \tag{11.2.5.2.18}$$

$$\frac{1}{2}\,{}^1O_2 + {}^1X \rightarrow {}^1XO \tag{5.10}$$

$$\downarrow\uparrow \quad \downarrow\uparrow \quad \downarrow\uparrow \tag{11.2.5.2.19}$$

Moreover, the products of typical reactions of singlet-state dioxygen with organic substrates (Reactions 5.11 and 5.12, for example) are quite different in character from the reactions of dioxygen with organic substrates catalyzed by oxygenase enzymes (see Section V):



One pathway for a direct reaction of triplet ground-state dioxygen with a singlet ground-state organic substrate that can occur readily without a catalyst begins with the one-electron oxidation of the substrate by dioxygen. The products of such a reaction would be two doublets, i.e., superoxide and the oneelectron oxidized substrate, each having one unpaired electron (Reaction 5.13). These free radicals can diffuse apart and then recombine with their spins paired (Reaction 5. 14).

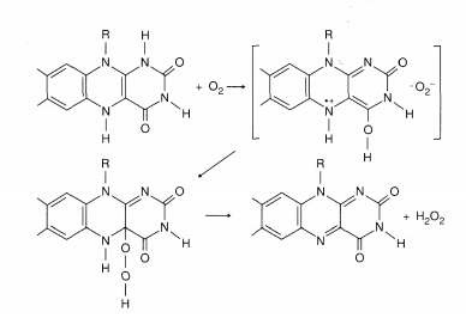
$${}^3O_2 + {}^1X \rightarrow {}^2O_2^- + {}^2X^+ \tag{5.13}$$

$$\uparrow\uparrow \quad \downarrow\uparrow \quad \uparrow \quad \uparrow \tag{11.2.5.2.20}$$

$${}^2O_2^- + {}^2X^+ \rightarrow {}^2O_2^- + 2X^+ \rightarrow {}^1XO_2 \tag{5.14}$$

↑ ↑ ↑ ↓ ↓↑ (11.2.5.2.21)

Such a mechanism has been shown to occur for the reaction of dioxygen with reduced flavins shown in Reaction (5.15).[20]



However, this pathway requires that the substrate be able to reduce dioxygen to superoxide, a reaction that requires an unusually strong reducing agent (such as a reduced flavin), since dioxygen is not a particularly strong one-electron oxidizing agent (see Table 5.1 and discussion above). Typical organic substrates in enzymatic and nonenzymatic oxygenation reactions usually are not sufficiently strong reducing agents to reduce dioxygen to superoxide; so this pathway is not commonly observed.

The result of these kinetic barriers to dioxygen reactions with most organic molecules is that uncatalyzed reactions of this type are usually quite slow. An exception to this rule is an oxidation pathway known as free-radical autoxidation.

Free-Radical Autoxidation

The term free-radical autoxidation describes a reaction pathway in which dioxygen reacts with an organic substrate to give an oxygenated product in a free-radical chain process that requires an initiator in order to get the chain reaction started.[21] (A free-radical initiator is a compound that yields free radicals readily upon thermal or photochemical decomposition.) The mechanism of free radical autoxidation is as shown in Reactions (5.16) to (5.21).

Initiation: $$X_{2} \rightarrow 2X \cdotp \tag{5.16}$$

$$X\cdot + RH \rightarrow XH + R\cdot \tag{5.17}$$

Propagation: $$R \cdotp + O_{2} \rightarrow ROO \cdotp \tag{5.18}$$

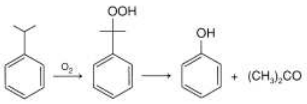
↓ ↑↑ ↑ (11.2.5.2.22)

$$ROO\cdot + RH \rightarrow ROOH + R\cdot \tag{5.19}$$

Termination: $$R \cdotp + ROO \cdotp \rightarrow ROOR \tag{5.20}$$

$$2ROO\cdot \rightarrow ROOOOR \rightarrow O_2 + ROOR \tag{5.21}$$

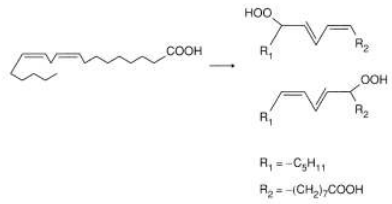
(plus other oxidized products, such as ROOH, ROH, RC(O)R, RC(O)H). This reaction pathway results in oxygenation of a variety of organic substrates, and is not impeded by the spin restriction, because triplet ground-state dioxygen can react with the free radical R• to give a free-radical product ROO•, in a spin-allowed process (Reaction 5.18). It is a chain reaction, since R• is regenerated in Reaction (5.19), and it frequently occurs with long chain lengths prior to the termination steps, resulting in a very efficient pathway for oxygenation of some organic substrates, such as, for example, the oxidation of cumene to give phenol and acetone (Reaction 5.22).[22]



When free-radical autoxidation is used for synthetic purposes, initiators are intentionally added. Common initiators are peroxides and other compounds capable of fragmenting readily into free radicals. Free-radical autoxidation reactions are also frequently observed when no initiator has been intentionally added, because organic substrates frequently contain peroxidic impurities that may act as initiators. Investigators have sometimes been deceived into assuming that a metal-complex catalyzed reaction of

dioxygen with an organic substrate occurred by a nonradical mechanism. In such instances, the reactions later proved, upon further study, to be free-radical autoxidations, the role of the metal complex having been to generate the initiating free radicals.

Although often useful for synthesis of oxygenated derivatives of relatively simple hydrocarbons, free-radical autoxidation lacks selectivity and therefore, with more complex substrates, tends to give multiple products. In considering possible mechanisms for biological oxidation reactions used *in vivo* for biosynthesis or energy production, free-radical autoxidation is not an attractive possibility, because such a mechanism requires diffusion of highly reactive free radicals. Such radicals, produced in the cell, will react indiscriminately with vulnerable sites on enzymes, substrates, and other cell components, causing serious damage.[6] In fact, free-radical autoxidation is believed to cause certain deleterious reactions of dioxygen in biological systems, for example the oxidation of lipids in membranes. It is also the process that causes fats and oils to become rancid (Reaction 5.23).[23,24]



How do Enzymes Overcome These Kinetic Barriers?

We see then the reasons that uncatalyzed reactions of dioxygen are usually either slow or unselective. The functions of the metalloenzymes for which dioxygen is a substrate are, therefore, to overcome the kinetic barriers imposed by spin restrictions or unfavorable one-electron reduction pathways, and, for the oxygenase enzymes, to direct the reactions and make them highly specific. It is instructive to consider (1) how these metalloenzymes function to lower the kinetic barriers to dioxygen reactivity, and (2) how the oxygenase enzymes redirect the reactions along different pathways so that very different products are obtained. The first example given below is cytochrome c oxidase. This enzyme catalyzes the four-electron reduction of dioxygen. It overcomes the kinetic barriers to dioxygen reduction by binding dioxygen to two paramagnetic metal ions at the dioxygen binding site, thus overcoming the spin restriction, and by reducing dioxygen in a two-electron step to peroxide, thus bypassing the unfavorable one-electron reduction to form free superoxide. The reaction occurs in a very controlled fashion, so that the energy released by dioxygen reduction can be used to produce ATP. A second example is provided by the catechol dioxygenases, which appear to represent substrate rather than dioxygen activation, and in which dioxygen seems to react with the substrate while it is complexed to the paramagnetic iron center. Another example given below is the monooxygenase enzyme cytochrome PASO, which catalyzes the reaction of dioxygen with organic substrates. It binds dioxygen at the paramagnetic metal ion at its active site, thus overcoming the spin restriction, and then carries out what can be formally described as a multielectron reduction of dioxygen to give a highly reactive high-valent metal-oxo species that has reactivity like that of the hydroxyl radical. Unlike a free hydroxyl radical, however, which would be highly reactive but nonselective, the reaction that occurs at the active site of cytochrome P-450 can be highly selective and stereospecific, because the highly reactive metal-oxo moiety is generated close to a substrate that is bound to the enzyme in such a way that it directs the reactive oxygen atom to the correct position. Thus, metalloenzymes have evolved to bind dioxygen and to increase while controlling its reactivity.

11.2.5.2: Chemistry of Dioxygen is shared under a CC BY-NC-SA 4.0 license and was authored, remixed, and/or curated by LibreTexts.

11.2.5.3: Copper-zinc Superoxide Dismutase

Background

Two families of metalloproteins are excellent catalysts for the disproportionation of superoxide (Reaction 5.95).

$$2O_2^- + 2H^+ \xrightarrow{SOD} O_2 + H_2O_2 \tag{5.95}$$

These are (1) the copper-zinc superoxide dismutases, CuZnSOD,[100-102] found in almost all eukaryotic cells and a very few prokaryotes, and (2) the manganese and iron superoxide dismutases, MnSOD and FeSOD, the former found in the mitochondria of eukaryotic cells, and both found in many prokaryotes.[103] Recent studies of bacterial[104] and yeast[105] mutants that were engineered to contain no superoxide dismutases demonstrated that the cells were unusually sensitive to dioxygen and that the sensitivity to dioxygen was relieved when an SOD gene was reintroduced into the cells. These results indicate that the superoxide dismutase enzymes playa critical role in dioxygen metabolism, but they do not define the chemical agent responsible for dioxygen toxicity (see Section III).

Enzymatic Activity

Several transition-metal complexes have been observed to catalyze superoxide disproportionation; in fact, aqueous copper ion, Cu^{2+}, is an excellent SOD catalyst, comparable in activity to CuZnSOD itself![37] Free aqueous Cu^{2+} would not itself be suitable for use as an SOD *in vivo*, however, because it is too toxic (see Section III) and because it binds too strongly to a large variety of cellular components and thus would not be present as the free ion. (Most forms of complexed cupric ion show much less superoxide dismutase activity than the free ion.) Aside from aqueous copper ion, few other complexes are as effective as the SOD enzymes.

Two mechanisms (Reactions 5.96 to 5.99) have been proposed for catalysis of superoxide disproportionation by metal complexes and metalloenzymes.[37]

Mechanism I: $$M^{n+} + O_{2}^{-} \rightarrow M^{(n-1)+} + O_{2} \tag{5.96}$$

$$M^{(n-1)+} + O_2^- \rightarrow M^{n+}(O_2^{2-}) \xrightarrow{2H^+} M^{n+} + H_2O_2 \tag{5.97}$$

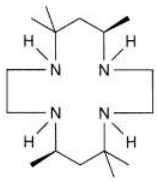
Mechanism II: $$M^{n+} + O_{2}^{-} \rightarrow M^{n+} (O_{2}^{-}) \tag{5.98}$$

$$M^{n+}(O_2^-) + O_2^- \rightarrow M^{n+}(O_2^{2-}) \xrightarrow{2H^+} M^n + H_2O_2 \tag{5.99}$$

$$+O_2 \tag{11.2.5.3.1}$$

In Mechanism I, which is favored for the SOD enzymes and most redox-active metal complexes with SOD activity, superoxide reduces the metal ion in the first step, and then the reduced metal ion is reoxidized by another superoxide, presumably via a metal-peroxo complex intermediate. In Mechanism II, which is proposed for nonredox metal complexes but may be operating in other situations as well, the metal ion is never reduced, but instead forms a superoxo complex, which is reduced to a peroxo complex by a second superoxide ion. In both mechanisms, the peroxo ligands are protonated and dissociate to give hydrogen peroxide.

Analogues for each of the separate steps of Reactions (5.96) to (5.99) have been observed in reactions of superoxide with transition-metal complexes, thereby establishing the feasibility of both mechanisms. For example, superoxide was shown to reduce $Cu^{II}(phen)_2^{2+}$ to give $Cu^{I}(phen)_2^{+}$ (phen = 1,10-phenanthroline),[106] a reaction analogous to Reaction (5.96). On the other hand, superoxide reacts with Cu^{II}(tet b)$^{2+}$ to form a superoxo complex[107] (a reaction analogous to Reaction 5.98), presumably because Cu^{II}(tet b)$^{2+}$ is not easily reduced to the cuprous state, because the ligand cannot adjust to the tetrahedral geometry that Cu^{I} prefers.[53]



tet b

Reaction of superoxide with a reduced metal-ion complex to give oxidation of the complex and release of hydrogen peroxide (analogous to Reaction 5.97) has been observed in the reaction of Fe^{II}EDTA with superoxide.[108] Reduction of a Co^{III} superoxo complex by free superoxide to give a peroxo complex (analogous to Reaction 5.99) has also been observed.[109]

If a metal complex can be reduced by superoxide and if its reduced form can be oxidized by superoxide, both at rates competitive with superoxide disproportionation, the complex can probably act as an SOD by Mechanism I. Mechanism II has been proposed to account for the apparent catalysis of superoxide disproportionation by Lewis acidic nonredox-active metal ions under certain conditions.[37] However, this mechanism should probably be considered possible for redox metal ions and the SOD enzymes as well. It is difficult to distinguish the two mechanisms for redox-active metal ions and the SOD enzymes unless the reduced form of the catalyst is observed directly as an intermediate in the reaction. So far it has not been possible to observe this intermediate in the SOD enzymes or the metal complexes.

Structure

The x-ray crystal structure of the oxidized form of CuZnSOD from bovine erythrocytes shows a protein consisting of two identical subunits held together almost entirely by hydrophobic interactions.[100-102] Each subunit consists of a flattened cylindrical barrel of β -pleated sheet from which three external loops of irregular structure extend (Figure 5.15). The metal-binding region of the protein binds Cu^{II} and Zn^{II} in close proximity to each other, bridged by the imidazolate ring of a histidyI side chain. Figure 5.16 represents the metal-binding region. The Cu^{II} ion is coordinated to four histidyl imidazoles and a water in a highly distorted square-pyramidal geometry with water at the apical position. The Zn^{II} ion is coordinated to three histidyl imidazoles (including the one shared with copper) and an aspartyl carboxylate group, forming a distorted tetrahedral geometry around the metal ion.

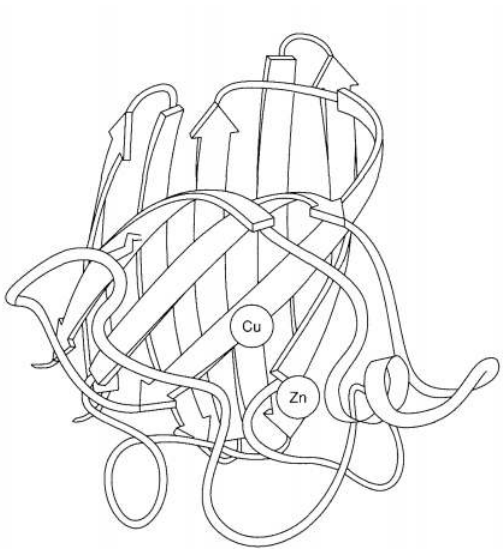


Figure 5.15 - Schematic drawing of the polypeptide backbone of one of the two subunits of bovine CuZnSOD. The strands of the β structure are shown as arrows. The active-site channel provides access to the copper site from the direction of the viewer. (From J. A. Tainer et al., J. Mol. Biol. **160** (1982), 181-217.)

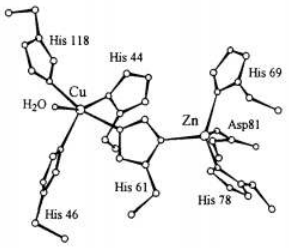
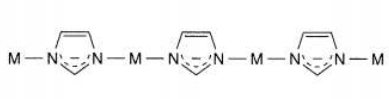


Figure 5.16 - Representation of the metal-binding region of bovine CuZnSOD.

One of the most unusual aspects of the structure of this enzyme is the occurrence of the bridging imidazolate ligand, which holds the copper and zinc ions 6 Å apart. Such a configuration is not unusual for imidazole complexes of metal ions, which sometimes form long polymeric imidazolate-bridged structures.



However, no other imidazolate-bridged bi- or polymetallic metalloprotein has yet been identified.

The role of the zinc ion in CuZnSOD appears to be primarily structural. There is no evidence that water, anions, or other potential ligands can bind to the zinc, so it is highly unlikely that superoxide could interact with that site. Moreover, removal of zinc under conditions where the copper ion remains bound to the copper site does not significantly diminish the SOD activity of the enzyme.[110] However, such removal does result in a diminished thermal stability, i.e., the zinc-depleted protein denatures at a lower temperature than the native protein, supporting the hypothesis that the role of the zinc is primarily structural in nature.[111]

The copper site is clearly the site of primary interaction of superoxide with the protein. The x-ray structure shows that the copper ion lies at the bottom of a narrow channel that is large enough to admit only water, small anions, and similarly small ligands (Figure 5.17). In the lining of the channel is the positively charged side chain of an arginine residue, 5 Å away from the copper ion and situated in such a position that it could interact with superoxide and other anions when they bind to copper. Near the mouth of the channel, at the surface of the protein, are two positively charged lysine residues, which are believed to play a role in attracting anions and guiding them into the channel.[112] Chemical modification of these lysine or arginine residues substantially diminishes the SOD activity, supporting their role in the mechanism of reaction with superoxide.[100-102]

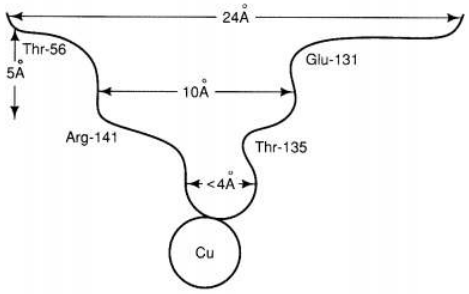


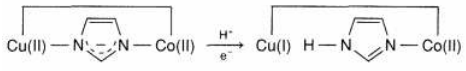
Figure 5.17 - Schematic diagram of a cross section of the active-site channel in CuZnSOD. The diameter of the channel narrows as the Cu^{II} center is approached, and only small ligands can actually reach that site. In addition to the positively charged Cu^{II} ion at the bottom of the channel, the positively charged side chain of Arg-141 is part of the walls of the channel. Two positively charged lysine side chains, not shown in this diagram, are close to the mouth of the channel. (From E. D. Getzoff, R. A. Hallewell, and J. A. Tainer, in M. Inouye, ed., Protein Engineering: Applications in Science, Industry, and Medicine, Academic Press, 1986, pp. 41-69.)

The x-ray structural results described above apply only to the oxidized form of the protein, i.e., the form containing Cu^{II}. The reduced form of the enzyme containing Cu^{I} is also stable and fully active as an SOD. If, as is likely, the mechanism of CuZnSOD-catalyzed superoxide disproportionation is Mechanism I (Reactions 5.96-5.97), the structure of the reduced form is of critical importance in understanding the enzymatic mechanism. Unfortunately, that structure is not yet available.

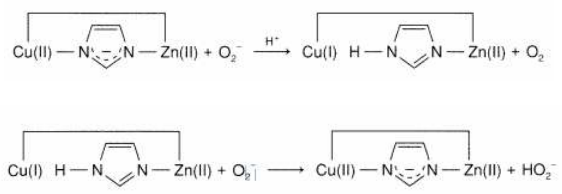
Enzymatic Activity and Mechanism

The mechanism of superoxide disproportionation catalyzed by CuZnSOD is generally believed to go by Mechanism I (Reactions 5.96-5.97), i.e., reduction of Cu^{II} to Cu^{I} by superoxide with the release of dioxygen, followed by reoxidation of Cu^{I} to Cu^{II} by a second superoxide with the release of HO_2^- or H_2O_2. The protonation of peroxide dianion, O_2^{2-}, prior to its release from the enzyme is required, because peroxide dianion is highly basic and thus too unstable to be released in its unprotonated form. The source of the proton that protonates peroxide in the enzymatic mechanism is the subject of some interest.

Reduction of the oxidized protein has been shown to be accompanied by the uptake of one proton per subunit. That proton is believed to protonate the bridging imidazolate in association with the breaking of the bridge upon reduction of the copper. Derivatives with Co^{II} substituted for Zn^{II} at the native zinc site have been used to follow the process of reduction of the oxidized Cu^{II} form to the reduced Cu^{I} form. The Co^{II} in the zinc site does not change oxidation state, but acts instead as a spectroscopic probe of changes occurring at the native zinc-binding site. Upon reduction (Reaction 5.102), the visible absorption band due to Co^{II} shifts in a manner consistent with a change occurring in the ligand environment of Co^{II}. The resulting spectrum of the derivative containing Cu^{I} in the copper site and Co^{II} in the zinc site is very similar to the spectrum of the derivative in which the copper site is empty and the zinc site contains Co^{II}. This result suggests strongly that the imidazolate bridge is cleaved and protonated and that the resulting imidazole ligand is retained in the coordination sphere of Co^{II} (Reaction 5.102).[101]



The same proton is thus an attractive possibility for protonation of peroxide as it is formed in the enzymatic mechanism (Reactions 5.103 and 5.104).



Attractive as this picture appears, there are several uncertainties about it. For example, the turnover of the enzyme may be too fast for protonation and deprotonation of the bridging histidine to occur.[113] Moreover, the mechanism proposed would require the presence of a metal ion at the zinc site to hold the imidazole in place and to regulate the pK_a of the proton being transferred. The observation that removal of zinc gives a derivative with almost full SOD activity is thus surprising and may also cast some doubt on this mechanism. Other criticisms of this mechanism have been recently summarized.[102]

Studies of CuZnSOD derivatives prepared by site-directed mutagenesis are also providing interesting results concerning the SOD mechanism. For example, it has been shown that mutagenized derivatives of human CuZnSOD with major differences in copper-site geometry relative to the wild-type enzyme may nonetheless remain fully active.[114] Studies of these and similar derivatives should provide considerable insight into the mechanism of reaction of CuZnSOD with superoxide.

Anions as Inhibitors

Studies of the interaction of CuZnSOD and its metal-substituted derivatives with anions have been useful in predicting the behavior of the protein in its reactions with its substrate, the superoxide anion, $O_2^{-\cdot}$.[101,102] Cyanide, azide, cyanate, and thiocyanate bind to the copper ion, causing dissociation of a histidyl ligand and the water ligand from the copper.[115] Phosphate also binds to the enzyme at a position close to the Cu^{II} center, but it apparently does not bind directly to it as a ligand. Chemical modification of Arg-141 with phenylglyoxal blocks the interaction of phosphate with the enzyme, suggesting that this positively charged residue is the site of interaction with phosphate.[116]

Electrostatic calculations of the charges on the CuZnSOD protein suggest that superoxide and other anions entering into the vicinity of the protein will be drawn toward and into the channel leading down to the copper site by the distribution of positive charges on the surface of the protein, the positively charged lysines at the mouth of the active-site cavity, and the positively charged arginine and copper ion within the active-site region.[112] Some of the anions studied, e.g., CN^-, F^-, N_3^-,and phosphate, have been

shown to inhibit the SOD activity of the enzyme. The source of the inhibition is generally assumed to be competition with superoxide for binding to the copper, but it may sometimes result from a shift in the redox potential of copper, which is known to occur sometimes when an anion binds to copper.[100,101]

Metal-ion Substitutions

1. SOD Activity

In the example described above, studies of a metal-substituted derivative helped in the evaluation of mechanistic possibilities for the enzymatic reaction. In addition, studies of such derivatives have provided useful information about the environment of the metal-ion binding sites. For example, metal-ion-substituted derivatives of CuZnSOD have been prepared with Cu^{II}, Cu^{I}, Zn^{II}, Ag^{I}, Ni^{II}, or Co^{II} bound to the native copper site, and with Zn^{II}, Cu^{II}, Cu^{I}, Co^{II}, Hg^{II}, Cd^{II}, Ni^{II}, or Ag^{I} bound to the native zinc site.[100,101,117] The SOD activities of these derivatives are interesting; only those derivatives with copper in the copper site have a high degree of SOD activity, whereas the nature of the metal ion in the zinc site or even its absence has little or no effect.[100,101]

2. Spectroscopy

Derivatives of CuZnSOD are known with Cu^{II} ion bound either to the native copper site or to the native zinc site. The electronic absorption spectra of these derivatives indicate that the ligand environments of the two sites are very different. Copper(II) is a d^9 transition-metal ion, and its d-d transitions are usually found in the visible and near-IR regions of the spectrum.[53] Copper(II) complexes with coordinated nitrogen ligands are generally found to have an absorption band between 500 and 700 nm, with an extinction coefficient below 100 $M^{-1}cm^{-1}$. Bands in the absorption spectra of complexes with geometries that are distorted away from square planar tend to be red-shifted because of a smaller d-d splitting, and to have higher extinction coefficients because of the loss of centrosymmetry. Thus the optical spectrum of CuZnSOD with an absorption band with a maximum at 680 nm (14,700 cm^{-1}; see Figure 5.18A) and an extinction coefficient of 155 $M^{-1}cm^{-1}$ per Cu is consistent with the crystal structural results that indicate that copper(II) is bound to four imidazole nitrogens and a water molecule in a distorted square-pyramidal geometry. Metal-substituted derivatives with Cu^{II} at the native copper site but with Co^{II}, Cd^{II}, Hg^{II}, or Ni^{II} substituted for Zn^{II} at the native zinc site all have a band at 680 nm, suggesting that the substitution of another metal ion for zinc perturbs the copper site very little, despite the proximity of the two metal sites. The absorption spectra of native CuZnSOD and these CuMSOD derivatives also have a shoulder at 417 nm (24,000 cm^{-1}; see Figure 5.18A), which is at lower energy than normal imidazole-to-Cu^{II} charge-transfer transitions, and has been assigned to an imidazolate-to-Cu^{II} charge transfer, indicating that the imidazolate bridge between Cu^{II} and the metal ion in the native zinc site is present, as observed in the crystal structure of CuZnSOD. Derivatives with the zinc site empty, which therefore cannot have an imidazolate bridge, are lacking this 417 nm shoulder.

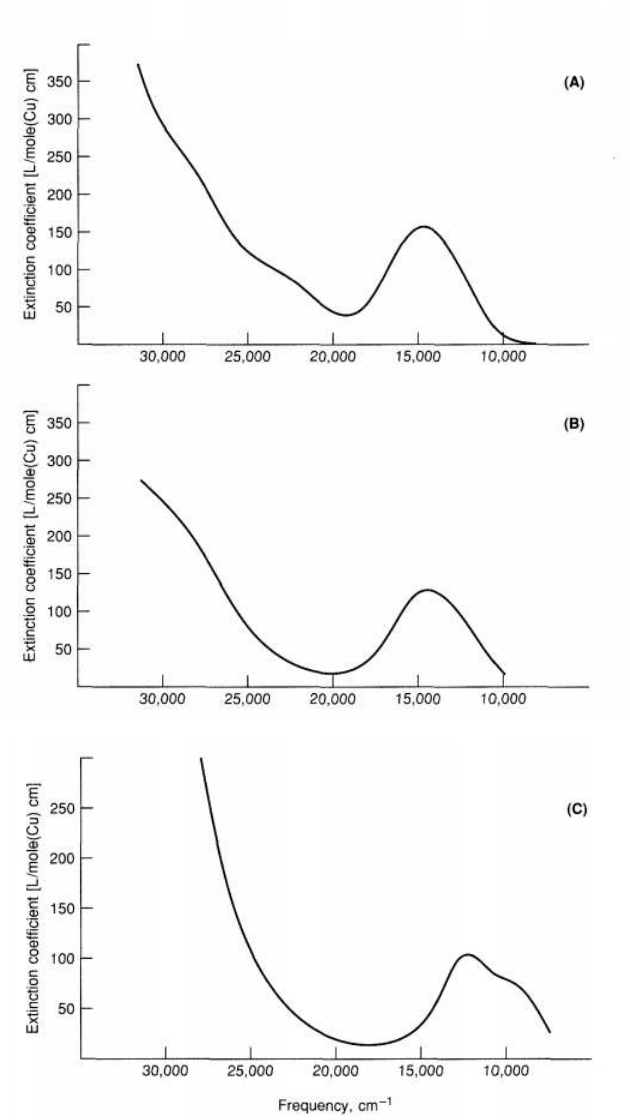


Figure 5.18 - Vis-UV spectra of (A) CuZnSOD, (B) copper-only SOD (zinc site empty), and (C) $Ag^{I}CuSOD$, In all three spectra, the low-energy band is the Cu^{II} d-d transition. Note that the spectrum of CuZnSOD contains a shoulder at 24,000 cm^{-1} (417 nm) that is assigned to the imidazolate-to-copper(II) charge-transfer transition. This shoulder is not present in the copper-only derivative. For $Ag^{I}CuSOD$, the d-d transition is red-shifted because of the change in the ligand geometry when Cu^{II} is moved from the copper site to the zinc site (see text), (From M. W. Pantoliano, L. A. Nafie, and J. S. Valentine, J. Am. Chem. Soc. **104** (1982), 6310-6317.)

Small but significant changes in the absorption spectrum are seen when the metal ion is removed from the zinc site, e.g., in copper-only SOD (Figure 5.18B). The visible absorption band shifts to 700 nm (14,300 cm^{-1}), presumably due to a change in ligand field strength upon protonation of the bridging imidazolate. In addition, the shoulder at 417 nm has disappeared, again due to the absence of the imidazolate ligand.

The spectroscopic properties due to copper in the native zinc site are best observed in the derivative $Ag^{I}CuSOD$, which has Ag^{I} in the copper site and Cu^{II} in the zinc site (see Figure 5.18C), since the d^{10} Ag^{I} ion is spectroscopically silent. In this derivative, the d-d transition is markedly red-shifted from the visible region of the spectrum into the near-IR, indicating that the ligand environment of Cu^{II} in that site is either tetrahedral or five coordinate. The EPR properties of Cu^{II} in this derivative are particularly interesting (as discussed below).

The derivative with Cu^{II} bound at both sites, CuCuSOD, has a visible-near IR spectrum that is nearly a superposition of the spectra of CuZnSOD and $Ag^{I}CuSOD$ (see Figure 5.19), indicating that the geometry of Cu^{II} in each of these sites is little affected by the nature of the metal ion in the other site.

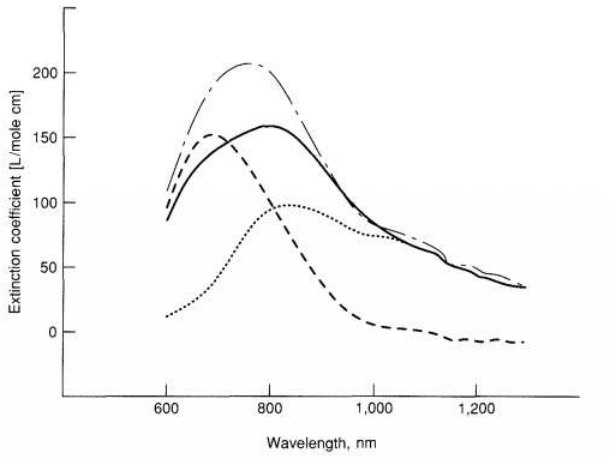


Figure 5.19 - Comparison of the visible absorption spectrum of CuCuSOD, --------, *with that of CuZnSOD,* ———, *and of* $Ag^{I}CuSOD$, • • • • • • • • • •, *A digital addition of the spectra of CuZnSOD and of* $Ag^{I}CuSOD$ *generated the other spectrum,* -•-•-•-•. *Note that the spectrum of CuCuSOD, which has* Cu^{II} *ions in both the copper and the zinc sites, closely resembles a superposition of the spectra of CuZnSOD, which has* Cu^{II} *in the copper site, and* $Ag^{I}CuSOD$, *which has* Cu^{II} *in the zinc site. (From M. W. Pantoliano, L. A. Nafie, and J. S. Valentine, J. Am. Chem. Soc.* ***104*** *(1982), 6310-6317.)*

EPR spectroscopy has also proven to be particularly valuable in characterizing the metal environments in CuZnSOD and derivatives. The EPR spectrum of native CuZnSOD is shown in Figure 5.20A. The $g_{\|}$ resonance is split by the hyperfine coupling between the unpaired electron on Cu^{II} and the I = $\frac{3}{2}$ nuclear spin of copper. The $A_{\|}$ value, 130 G, is intermediate between the larger $A_{\|}$ typical of square-planar Cu^{II} complexes with four nitrogen donor ligands and the lower $A_{\|}$ observed in blue copper proteins (see Chapter 6). The large linewidth seen in the $g_{\perp}$ region indicates that the copper ion is in a rhombic (i.e., distorted) environment. Thus, the EPR spectrum is entirely consistent with the distorted square-pyramidal geometry observed in the x-ray structure.

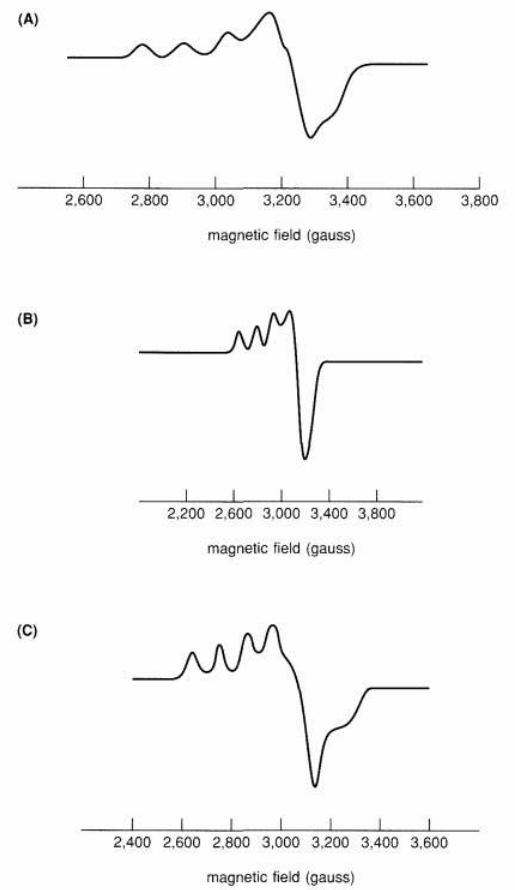


Figure 5.20 - Frozen solution EPR spectra of (A) CuZnSOD, (B) copper-only SOD (zinc site empty), and (C) $Ag^{I}CuSOD$. See text for discussion. (Adapted from References 100 and 101.)

Removal of zinc from the native protein to give copper-only SOD results in a perturbed EPR spectrum, with a narrower $g_{\perp}$ resonance and a larger $A_{\parallel}$ value (142 G) more nearly typical of Cu^{II} in an axial N_4 environment (Figure 5.20B). Apparently the removal of zinc relaxes some constraints imposed on the geometry of the active-site ligands, allowing the copper to adopt to a geometry closer to its preferred tetragonal arrangement.

The EPR spectrum due to Cu^{II} in the native Zn^{II} site in the $Ag^{I}CuSOD$ derivative indicates that Cu^{II} is in a very different environment than when it is in the native copper site (Figure 5.20C). The spectrum is strongly rhombic, with a low value of $A_{\parallel}$ (97 G), supporting the conclusion based on the visible spectrum that copper is bound in a tetrahedral or five-coordinate environment. This type of site is unusual either for copper coordination complexes or for copper proteins in general, but does resemble the Cu^{II} EPR signal seen when either laccase or cytochrome c oxidase is partially reduced (see Figure 5.21).

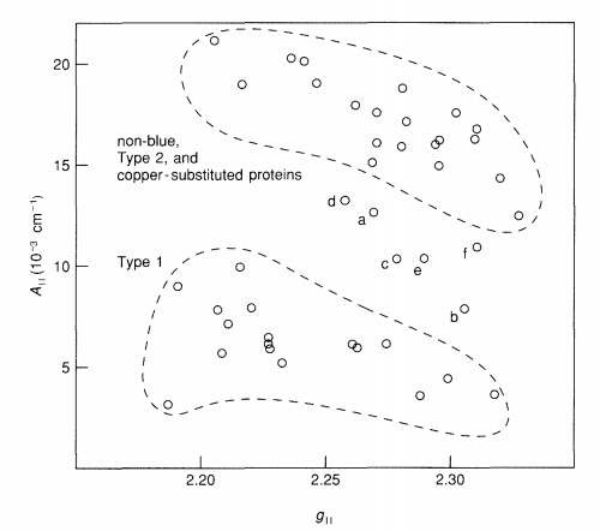


Figure 5.21 - Relationship between $g_{\parallel}$ and $A_{\parallel}$ for naturally occurring copper proteins and copper-substituted metalloproteins. Points labeled a-f are for laccases (a and b), cytochrome c oxidase (c), CuZnSOD (d), $Ag^{I}CuSOD$ (e), and $Cu^{I}Cu^{II}SOD$ (f). See text for discussion. (From M. W. Pantoliana, L. A. Nafie, and J. S. Valentine, J. Am. Chem. Soc. **104** (1982), 6310-6317.)

Partial reduction disrupts the magnetic coupling between these Cu^{II} centers that makes them EPR-silent in the fully oxidized protein.

The EPR spectrum of CuCuSOD is very different from that of any of the other copper-containing derivatives (Figure 5.22) because the unpaired spins on the two copper centers interact and magnetically couple across the imidazolate bridge, resulting in a triplet EPR spectrum. This spectrum is virtually identical with that of model imidazolate-bridged binuclear copper complexes.[101]

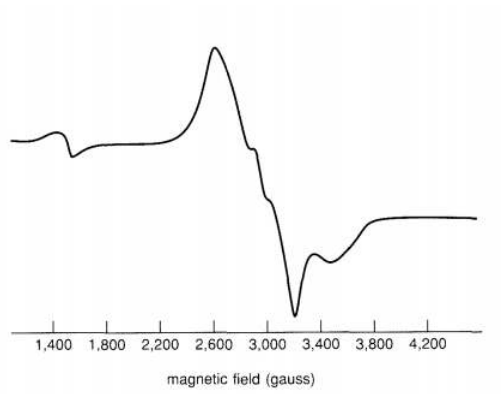


Figure 5.20. These differences are due to the fact that the two Cu^{II} centers are magnetically coupled across the imidazolate bridge.[100]

Electronic absorption and EPR studies of derivatives of CuZnSOD containing Cu^{II} have provided useful information concerning the nature of the metal binding sites of those derivatives. ^{1}H NMR spectra of those derivatives are generally not useful, however, because the relatively slowly relaxing paramagnetic Cu^{II} center causes the nearby proton resonances to be extremely broad. This difficulty has been overcome in two derivatives, CuCoSOD and CuNiSOD, in which the fast-relaxing paramagnetic Co^{II} and Ni^{II} centers at the zinc site interact across the imidazolate bridge and increase the relaxation rate of the Cu^{II} center, such that well-resolved paramagnetically shifted ^{1}H NMR spectra of the region of the proteins near the two paramagnetic metal centers in the protein can be obtained and the resonances assigned.[118,119]

The use of ^{1}H NMR to study CuCoSOD derivatives of CuZnSOD in combination with electronic absorption and EPR spectroscopies has enabled investigators to compare active-site structures of a variety of wild-type and mutant CuZnSOD proteins in order to find out if large changes in active-site structure have resulted from replacement of nearby amino-acid residues.[120]

11.2.5.3: Copper-zinc Superoxide Dismutase is shared under a CC BY-NC-SA 4.0 license and was authored, remixed, and/or curated by LibreTexts.

11.2.5.4: Cytochrome c Oxidase

Most of the O_2 consumed by aerobic organisms is used to produce energy in a process referred to as "oxidative phosphorylation," a series of reactions in which electron transport is coupled to the synthesis of ATP and in which the driving force for the reaction is provided by the four-electron oxidizing power of O_2 (Reaction 5.1). (This subject is described in any standard text on biochemistry and will not be discussed in detail here.) The next to the last step in the electrontransport chain produces reduced cytochrome c, a water-soluble electron-transfer protein. Cytochrome c then transfers electrons to cytochrome c oxidase, where they are ultimately transferred to O_2. (Electron-transfer reactions are discussed in Chapter 6.)

Cytochrome c oxidase is the terminal member of the respiratory chain in all animals and plants, aerobic yeasts, and some bacteria.[44-46] This enzyme is always found associated with a membrane: the inner mitochondrial membrane in higher organisms or the cell membrane in bacteria. It is a large, complex, multisubunit enzyme whose characterization has been complicated by its size, by the fact that it is membrane-bound, and by the diversity of the four redox metal sites, i.e., two copper ions and two heme iron units, each of which is found in a different type of environment within the protein. Because of the complexity of this system and the absence of detailed structural information, spectroscopic studies of this enzyme and comparisons of spectral properties with O_2-binding proteins and with model iron-porphyrin and copper complexes have been invaluable in its characterization.

Spectroscopic Characterization

1. Models

Iron-porphyrin complexes of imidazole are a logical starting point in the search for appropriate spectroscopic models for heme centers in metalloproteins, since the histidyl imidazole side chain is the most common axial ligand bound to iron in such enzymes. Iron-porphyrin complexes with two axial imidazole ligands are known for both the ferrous and ferric oxidation states.[47]

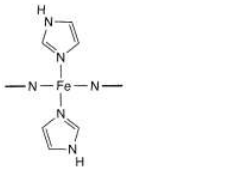


Figure 5.2.

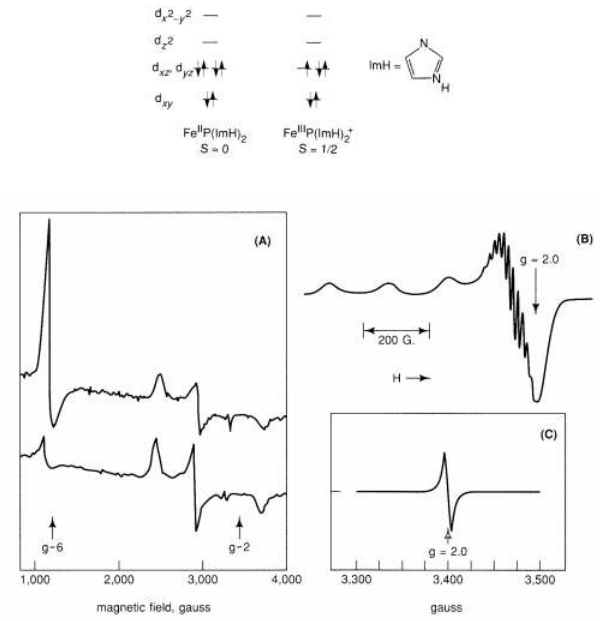


Figure 5.20). (C) Simulated EPR spectrum of a typical organic free radical with no hyperfine interaction. Note the narrow linewidth and a g value close to 2.00, i.e., near the g value for a free electron.

Monoimidazole complexes of iron porphyrins are also known for both the ferrous and the ferric oxidation states. The design of these model complexes has been more challenging than for six-coordinate complexes because of the high affinity of the five-coordinate complexes for a sixth ligand. In the ferrous complex, five coordination has been achieved by use of 2-methylimidazole ligands, as described in Chapter 4. The ferrous porphyrin binds a single 2-methylimidazole ligand, and, because the Fe^{ll} center is raised out of the plane of the porphyrin ring, the 2-methyl substituent suffers minimal steric interactions with the porphyrin. However, the affinity of the five-coordinate complex for another 2-methylimidazole ligand is substantially lower, because the Fe^{II} must drop down into the plane of the porphyrin to form the six-coordinate complexes, in which case the 2-methyl substitutents on both axial ligands suffer severe steric interactions with the porphyrin.[51] Using this approach, five-coordinate monoimidazole complexes can be prepared. They are coordinatively unsaturated, and will bind a second axial ligand, such as O_2 and CO. They have been extensively studied as models for O_2-binding heme proteins such as hemoglobin and myoglobin. Monoimidazole ferrous porphyrins thus designed are high-spin d6 with four unpaired electrons. They are even-spin systems and EPR spectra have not been observed.

Five-coordinate monoimidazole ferric-porphyrin complexes have also been prepared in solution[52] by starting with a ferric porphyrin complex with a very poorly coordinating anion, e.g., $Fe^{III}P(SbF_6)$. Addition of one equivalent of imidazole results in formation of the five-coordinate monoimidazole complex (Reaction 5.33).

$$Fe^{III}(TPP)(SbF_6) + ImH \rightarrow [Fe^{III}(TPP)(ImH)]^+ + SbF_6^- \tag{5.33}$$

When imidazole is added to ferric-porphyrin complexes of other anionic ligands, e.g., Cl^-, several equivalents of imidazole are required to displace the more strongly bound anionic ligand; consequently, only six-coordinate complexes are observed (Reaction 5.34).

$$FE^{III}(TPP)Cl + 2ImH \rightarrow [Fe^{III}(TPP)(ImH)_2]^+ + Cl^- \tag{5.34}$$

Monoimidazole ferric porphyrins are coordinatively unsaturated, readily bind a second axial ligand, and thus are appropriate models for methemoglobin or metmyoglobin. The five-coordinate complexes are high-spin d^5, but usually become low-spin upon binding another axial ligand to become six-coordinate.

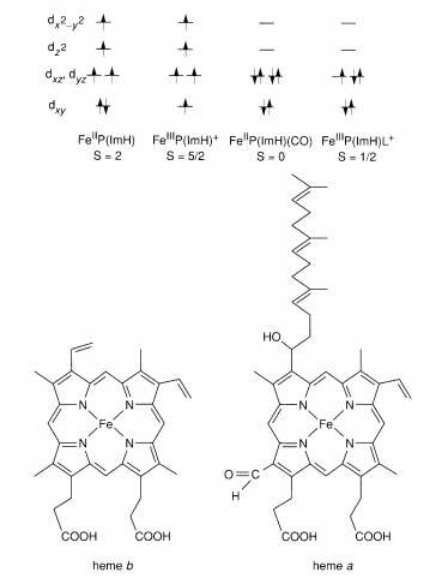


Figure 5.2).

2. Spectroscopy of the Enzyme

The oxidized form of cytochrome c oxidase contains two Cu^{II} and two Fe^{III} heme centers. It can be fully reduced to give a form of the enzyme containing two Cu^{I} and two Fe^{II} heme centers.[44-46] The heme found in cytochrome c oxidase is different from that found in other heme proteins. It is heme a, closely related to heme b, which is found in hemoglobin, myoglobin, and cytochrome P-

450, but has one of the vinyl groups replaced by a farnesyl substituent and one of the methyl groups replaced by a formyl substituent (see 5.35).

Each of the four metal centers has a different coordination environment appropriate to its function. Cytochrome a and Cu_A appear solely to carry out an electron-transfer function without interacting directly with dioxygen. Cytochrome a_3 and Cu_B appear to be part of a binuclear center that acts as the site for dioxygen binding and reduction. A schematic describing the probable nature of these four metal sites within cytochrome oxidase is given in Figure 5.3 and a description of the evidence supporting the formulation of each center then follows.

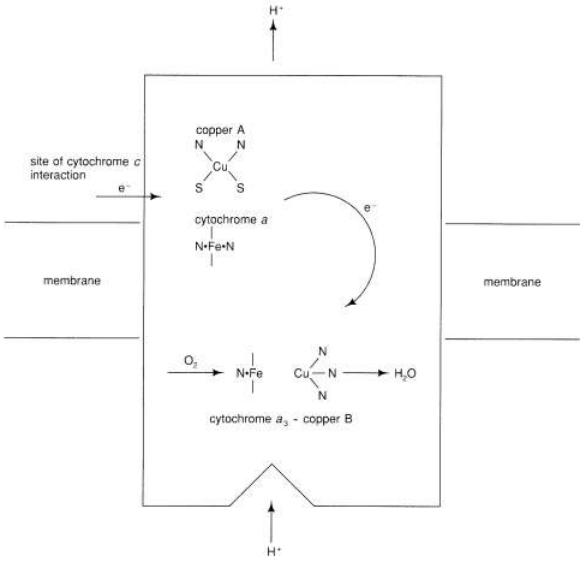


Figure 5.3 - Schematic representation of the metal centers in cytrochrome c oxidase.

Cytochrome a in both oxidation states has spectral characteristics that are entirely consistent with a low-spin ferric heme center with two axial imidazole ligands. In its oxidized form, it gives an EPR spectrum with g values[44-46] similar to those obtained with model ferric-porphyrin complexes with two axial imidazole ligands [49,50] (see above, Section IV.B.1). Moreover, addition of cyanide anion to the oxidized enzyme or CO to the reduced enzyme does not perturb this center, indicating that cyanide does not bind to the heme, again consistent with a six-coordinate heme. The absence of ligand binding is characteristic of six-coordinate heme sites found in electron-transfer proteins and suggests strongly that cytochrome a functions as an electron-transfer center within cytochrome c oxidase.

Cu_A is also believed to act as an electron-transfer site. It has quite remarkable EPR spectroscopic characteristics, with g values at g = 2.18, 2.03, and 1.99, and no hyperfine splitting,[44-46] resembling more an organic free radical than a typical Cu^{II} center (see Figures 5.2 and 5.4A). ENDOR studies of yeast cytochrome c oxidase containing ^{2}H-cysteine or ^{15}N-histidine (from yeast grown with the isotopically substituted amino acids) showed shifts relative to the unsubstituted enzyme, indicating that both of these ligands are bound to Cu_A.[54] But the linear electric-field effect of Cu_A did not give the patterns characteristic of Cu^{II}-histidine complexes, indicating that the unpaired electron is not on the copper ion.[55] The current hypothesis about this center is that copper is bonded in a highly covalent fashion to one, or more likely two, sulfur ligands, and that the unpaired electron density is principally on sulfur, i.e., $[Cu^{II}\text{-}^{-}SR \leftrightarrow Cu^{I}\text{-} \bullet SR]$. Copper-thiolate model complexes with spectroscopic properties similar to Cu_A have never been synthesized, presumably because such complexes are unstable with respect to disulfide bond formation, i.e, 2 RS• → RS-SR. In the enzyme, RS• radicals are presumably constrained in such a way that they cannot couple to form disulfide bonds.

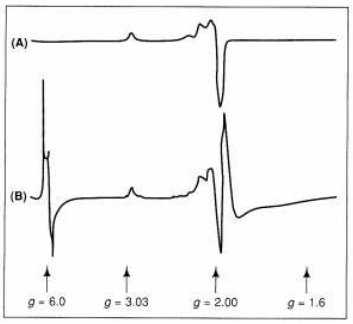


Figure 5.4 - (A) EPR spectrum of oxidized cytochrome c oxidase. The signal at g = 2 is assigned to Cu_A^{II} and the signal at g = 3 is assigned to cytochrome a in the low-spin ferric state. No signals attributable to the other two metal centers, i.e., cytochrome a_3 and Cu_B, are observed (see text). (B) Spectrum obtained after addition of NO. Binding of NO to CUBII decouples the two metal ions, and thereby allows the high-spin ferric heme signal of cytochrome a_3 at g = 6 to be observed. (From M. Brunori et at., Adv. lnorg. Biochem. **7** (1988), 93-153, adapted from Reference 56.)

The other heme center, cytochrome a_3, does bind ligands such as cyanide to the Fe^{III} form and carbon monoxide to the Fe^{II} form, indicating that it is either five-coordinate or that it has a readily displaceable ligand. Reaction with CO, for example, produces spectral changes characteristic of a five-coordinate ferrous heme binding CO to give the six-coordinate carbonmonoxy product analogous to MbCO. The cytochrome a_3 site is therefore an excellent candidate for O_2 binding within cytochrome oxidase.

The EPR spectrum of fully oxidized cytochrome c oxidase might be expected to give signals corresponding to two Cu^{II} centers and two ferric heme centers. In fact, all that is observed in the EPR spectrum of the oxidized enzyme is the typical low-spin six-coordinate ferric heme spectrum due to cytochrome G and the EPR signal attributed to Cu_A (see Figure 5.4A). The fact that signals attributable to cytochrome a_3 and Cu_B are not observed in the EPR spectrum led to the suggestion that these two metal centers are antiferromagnetically coupled.[44-46] The measured magnetic susceptibility for the isolated enzyme was found to be consistent with this hypothesis, suggesting that these two metal centers consist of an S = $\frac{1}{2}$ Cu^{II} antiferromagnetically coupled through a bridging ligand to a high-spin S = $\frac{5}{2}$ Fe^{III} to give an S = 2 binuclear unit.[45] EXAFS measurements indicating a copper-iron separation of 3-4 Å as well as the strength of the magnetic coupling suggest that the metal ions are linked by a single-atom ligand bridge, but there is no general agreement as to the identity of this bridge.[45,46]

The cytochrome a_3-Cu_B coupling can be disrupted by reduction of the individual metal centers. In this fashion, a g = 6 ESR signal can be seen for cytochrome a_3 or g = 2.053, 2.109, and 2.278 signals for Cu_B. Nitric-oxide binding to Cu_B also decouples the metals, allowing the g = 6 signal to be seen[56] (see Figure 5.4B). Mössbauer spectroscopy also indicates that cytochrome a_3 is high-spin in the oxidized as well as the reduced state.[57] ENDOR studies suggest that Cu_B has three nitrogens from imidazoles bound to it with water or hydroxide as a fourth ligand.[58] Studies using ^{15}N-labeled histidine in yeast have demonstrated that histidine is a ligand to cytochrome a_3.[59] All of these features have been incorporated into Figure 5.3.

Mechanism of Dioxygen Reduction

1. Models

Before we consider the reactions of cytochrome c oxidase with dioxygen, it is instructive to review the reactions of dioxygen with iron porphyrins and copper complexes. Dioxygen reacts with ferrous-porphyrin complexes to make mononuclear dioxygen complexes (Reaction 5.36; see preceding chapter for discussion of this important reaction). Such dioxygen complexes react rapidly with another ferrous porphyrin, unless sterically prevented from doing so, to form binuclear peroxo-bridged complexes[60,61] (Reaction 5.37). These peroxo complexes are stable at low temperature, but, when the temperature is raised, the O—O bond cleaves and two equivalents of an iron(IV) oxo complex are formed (Reaction 5.38). Subsequent reactions between the peroxo-bridged complex and the Fe^{IV} oxo complex produce theμ-oxo dimer (see Reactions 5.39-5.40).

$$3Fe^{II}(P) + 3O_2 \rightarrow 3Fe(P)(O_2) \tag{5.36}$$

$$3Fe(P)(O_2) + 3Fe^{II}(P) \rightarrow 3(P)Fe^{III}\text{—}O\text{—}O\text{—}Fe^{III}(P) \tag{5.37}$$

$$(P)Fe^{III}\text{—}O\text{—}O\text{—}Fe^{III}(P) \rightarrow 2Fe^{IV}(P)(O) \tag{5.38}$$

$$2Fe^{IV}(P)(O) + 2(P)Fe^{III}—O—O—Fe^{III}(P) \rightarrow 2(P)Fe^{III}—O—Fe^{III}(P) + 2Fe(P)(O_2) \tag{5.39}$$

$$2Fe(P)(O_2) \rightarrow 2Fe^{II}(P) + 2O_2 \tag{5.40}$$

$$4Fe^{II}(P) + O_2 \rightarrow 2(P)Fe^{III}—O—Fe^{III}(P) \tag{5.41}$$

The reaction sequence (5.36) to (5.40) thus describes a four-electron reduction of O_2 in which the final products, two oxide, O^{2-}, ligands act as bridging ligands in binuclear ferric-porphyrin complexes (Reaction 5.41).

Copper(l) complexes similarly react with dioxygen to form peroxo-bridged binuclear complexes.[62] Such complexes do not readily undergo O—O bond cleavage, apparently because the copper(III) oxidation state is not as readily attainable as the Fe(IV) oxidation state in an iron-porphyrin complex. Nevertheless, stable peroxo complexes of copper(II) have been difficult to obtain, because, as soon as it is formed, the peroxo complex either is protonated to give free hydrogen peroxide or is itself reduced by more copper(l) (Reactions 5.42 to 5.46).

$$2Cu^{I} + O_2 \rightarrow Cu^{II}—O—O—Cu^{II} \tag{5.42}$$

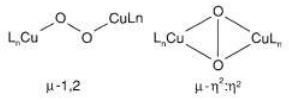
$$Cu^{II}—O—O—Cu^{II} + 2H^{+} \rightarrow 2Cu^{II} + H_2O_2 \tag{5.43}$$

$$2Cu^{I} + H_2O_2 + 2H^{+} \rightarrow 2Cu^{II} + 2H_2O \tag{5.44}$$

or $$Cu^{II}—O—O—Cu^{II} + 2 Cu^{I} + 4 H^{+} \rightarrow 4 Cu^{II} + 2 H_{2}O \tag{5.45}\]

$$4Cu^{I} + O_2 + 4H^{+} \rightarrow 4Cu^{II} + 2H_2O \tag{5.46}$$

Recently, however, examples of the long-sought stable binuclear copper(II) peroxo complex have been successfully synthesized and characterized, and interestingly enough, two entirely different structural types have been identified, i.e., μ-1,2 and μ-η^2:η^2 dioxygen complexes[63,64] (see 5.47)



2. Mechanistic Studies of the Enzyme

A single turnover in the reaction of cytochrome c oxidase involves (1) reduction of the four metal centers by four equivalents of reduced cytochrome c, (2) binding of dioxygen to the partially or fully reduced enzyme, (3) transfer of four electrons to dioxygen, coupled with (4) protonation by four equivalents of protons to produce two equivalents of water, all without the leakage of any substantial amount of potentially harmful partially reduced dioxygen byproducts such as superoxide or hydrogen peroxide.[44-46] At low temperatures, the reaction can be slowed down, so that the individual steps in the dioxygen reduction can be observed. Such experiments are carried out using the fully reduced enzyme to which CO has been bound. Binding of CO to the Fe^{II} heme center in reduced cytochrome c oxidase inhibits the enzyme and makes it unreactive to dioxygen. The CO-inhibited derivative can then be mixed with dioxygen and the mixture cooled. Photolysis of metal-CO complexes almost always leads to dissociation of CO, and CO-inhibited cytochrome c oxidase is no exception. Photolytic dissociation of CO frees the Fe^{II} heme, thereby initiating the reaction with dioxygen, which can then be followed spectroscopically.[44-46] Dioxygen reacts very rapidly with the fully reduced enzyme to produce a species that appears to be the dioxygen adduct of cytochrome a_3 (Reaction 5.48). Such a species is presumed to be similar to other mononuclear oxyheme derivatives. The dioxygen ligand in this species is then rapidly reduced to peroxide by the nearby Cu_B, forming what is believed to be a binuclear μ-peroxo species (Reaction 5.49). These steps represent a two-electron reduction of dioxygen to the peroxide level, and are entirely analogous to the model reactions discussed above (Reactions 5.36 to 5.46), except that the binuclear intermediates contain one copper and one heme iron. The μ-peroxo Fe^{III} - (O_2^{2-}) - Cu^{II} species is then reduced by a third electron, resulting in cleavage of the O—O bond (Reaction 5.50). One of the oxygen atoms remains with iron in the form of a ferryl complex, i. e., an Fe^{IV} oxo, and the other is protonated and bound to copper in the form of a Cu^{II} aquo complex.[65] Reduction by another electron leads to hydroxo complexes of both the Fe^{III} heme and the Cu^{II} centers (Reaction 5.51).[65] Protonation then causes dissociation of two water molecules from the oxidized cytochrome a_3-Cu_B center (Reaction 5.52).

$$(cyt\ a_3)\overbrace{Fe^{II}\quad Cu_B^I}+O_2 \rightarrow (cyt\ a_3)\overbrace{Fe^{III}(O_2^-)\quad Cu_B^I} \tag{5.48}$$

$$(cyt\ a_3)\overbrace{Fe^{III}(O_2^-)\quad Cu_B^I} \rightarrow (cyt\ a_3)\overbrace{Fe^{III}-(O_2^{2-})\quad Cu_B^{II}} \tag{5.49}$$

$$(cyt\ a_3)\overbrace{Fe^{III}-(O_2^{2-})-Cu_B^{II}}+e^-+2H^+ \rightarrow (cyt\ a_3)\overbrace{Fe^{IV}=O\quad H_2O-Cu_B^{II}} \tag{5.50}$$

$$(cyt\ a_3)\overbrace{Fe^{IV}=O\quad H_2O-Cu_B^{II}}+e^- \rightarrow (cyt\ a_3)\overbrace{Fe^{III}-(OH^-)\quad (HO^-)-Cu_B^{II}} \tag{5.51}$$

$$(cyt\ a_3)\overbrace{Fe^{III}-(OH^-)\quad (HO^-)-Cu_B^{II}}+2H^+ \rightarrow (cyt\ a_3)\overbrace{Fe^{III}\quad Cu_B^{II}}+2H_2O \tag{5.52}$$

Several important questions remain to be resolved in cytochrome c oxidase research. One is the nature of the ligand bridge that links cytochrome a_3 and Cu_B in the oxidized enzyme. Several hypotheses have been advanced (imidazolate, thiolate sulfur, and various oxygen ligands), but then discarded or disputed, and there is consequently no general agreement concerning its identity. However, EXAFS measurements of metal-metal separation and the strength of the magnetic coupling between the two metal centers provide evidence that a single atom bridges the two metals.[45,46] Another issue, which is of great importance, is to find out how the energy released in the reduction of dioxygen is coupled to the synthesis of ATP. It is known that this occurs by coupling the electron-transfer steps to a proton-pumping process, but the molecular mechanism is unknown.[46] Future research should provide some interesting insights into the mechanism of this still mysterious process.

11.2.5.4: Cytochrome c Oxidase is shared under a CC BY-NC-SA 4.0 license and was authored, remixed, and/or curated by LibreTexts.

11.2.5.5: Dioxygen Toxicity

Background

Before we consider the enzymatically controlled reactions of dioxygen in living systems, it is instructive to consider the uncontrolled and deleterious reactions that must also occur in aerobic organisms. Life originally appeared on Earth at a time when the atmosphere contained only low concentrations of dioxygen, and was reducing rather than oxidizing, as it is today. With the appearance of photosynthetic organisms approximately 2.5 billion years ago, however, the conversion to an aerobic, oxidizing atmosphere exposed the existing anaerobic organisms to a gradually increasing level of oxidative stress.[25,26] Modern-day anaerobic bacteria, the descendants of the original primitive anaerobic organisms, evolved in ways that enabled them to avoid contact with normal atmospheric concentrations of dioxygen. Modern-day aerobic organisms, by contrast, evolved by developing aerobic metabolism to harness the oxidizing power of dioxygen and thus to obtain usable metabolic energy. This remarkably successful adaptation enabled life to survive and flourish as the atmosphere became aerobic, and also allowed larger, multicellular organisms to evolve. An important aspect of dioxygen chemistry that enabled the development of aerobic metabolism is the relatively slow rate of dioxygen reactions in the absence of catalysts. Thus, enzymes could be used to direct and control the oxidation of substrates either for energy generation or for biosynthesis. Nevertheless, the balance achieved between constructive and destructive oxidation is a delicate one, maintained in aerobic organisms by several means, e.g.: compartmentalization of oxidative reactions in mitochondria, peroxisomes, and chloroplasts; scavenging or detoxification of toxic byproducts of dioxygen reactions; repair of some types of oxidatively damaged species; and degradation and replacement of other species.[6]

The classification "anaerobic" actually includes organisms with varying degrees of tolerance for dioxygen: strict anaerobes, for which even small concentrations of O_2 are toxic; moderate anaerobes, which can tolerate low levels of dioxygen; and microaerophiles, which require low concentrations of O_2 for growth, but cannot tolerate normal atmospheric concentrations, i.e., 21 percent O_2, 1 atm pressure. Anaerobic organisms thrive in places protected from the atmosphere, for example, in rotting organic material, decaying teeth, the colon, and gangrenous wounds. Dioxygen appears to be toxic to anaerobic organisms largely because it depletes the reducing equivalents in the cell that are needed for normal biosynthetic reactions.[6]

Aerobic organisms can, of course, live in environments in which they are exposed to normal atmospheric concentrations of O_2. Nevertheless, there is much evidence that O_2 is toxic to these organisms as well. For example, plants grown in varying concentrations of O_2 have been observed to grow faster in lower than normal concentrations of O_2.[27] *E. coli* grown under 5 atm of O_2 ceased to grow unless the growth medium was supplemented with branched-chain amino acids or precursors. High concentrations of O_2 damaged the enzyme dihydroxy acid dehydratase, an important component in the biosynthetic pathway for those amino acids.[28] In mammals, elevated levels of O_2 are clearly toxic, leading first to coughing and soreness of the throat, and then to convulsions when the level of 5 atm of 100 percent O_2 is reached. Eventually, elevated concentrations of O_2 lead to pulmonary edema and irreversible lung damage, with obvious damage to other tissues as well.[6] The effects of high concentrations of O_2 on humans is of some medical interest, since dioxygen is used therapeutically for patients experiencing difficulty breathing, or for those suffering from infection by anaerobic organisms.[6]

Biological Targets

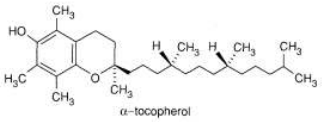
The major biochemical targets of O_2 toxicity appear to be lipids, DNA, and proteins. The chemical reactions accounting for the damage to each type of target are probably different, not only because of the different reactivities of these three classes of molecules, but also because of the different environment for each one inside the cell. Lipids, for example, are essential components of membranes and are extremely hydrophobic. The oxidative damage that is observed is due to free-radical autoxidation (see Reactions 5.16 to 5.21), and the products observed are lipid hydroperoxides (see Reaction 5.23). The introduction of the hydroperoxide group into the interior of the lipid bilayer apparently causes that structure to be disrupted, as the configuration of the lipid rearranges in order to bring that polar group out of the hydrophobic membrane interior and up to the membrane-water interface.[6] DNA, by contrast, is in the interior of the cell, and its exposed portions are surrounded by an aqueous medium. It is particularly vulnerable to oxidative attack at the base or at the sugar, and multiple products are formed when samples are exposed to oxidants *in vitro*.[6] Since oxidation of DNA *in vivo* may lead to mutations, this type of damage is potentially very serious. Proteins also suffer oxidative damage, with amino-acid side chains, particularly the sulfur-containing residues cysteine and methionine, appearing to be the most vulnerable sites.[6]

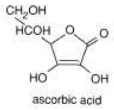
Defense and Repair Systems

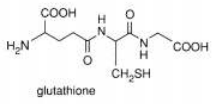
The biological defense systems protecting against oxidative damage and its consequences are summarized below.

1. Nonenzymatic Oxidant Scavengers

Some examples of small-molecule antioxidants are α-tocopherol (vitamin E; 5.24), which is found dissolved in cell membranes and protects them against lipid peroxidation, and ascorbate (vitamin C; 5.25) and glutathione (5.26), which are found in the cytosol of many cells. Several others are known as well.[6,29]







2. Detoxification Enzymes

The enzymatic antioxidants are (a) catalase and the various peroxidases, whose presence lowers the concentration of hydrogen peroxide, thereby preventing it from entering into potentially damaging reactions with various cell components (see Section VI and Reactions 5.82 and 5.83), and (b) the superoxide dismutases, whose presence provides protection against dioxygen toxicity that is believed to be mediated by the superoxide anion, O_2^- (see Section VII and Reaction 5.95).

Some of the enzymatic and nonenzymatic antioxidants in the cell are illustrated in Figure 5.1.

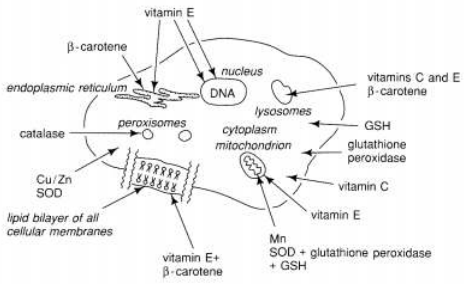


Figure 5.1 - Cartoon showing some of the antioxidant agents inside the cell.[29]

3. Systems for Sequestration of Redox-active Metal Ions

Redox-active metal ions are present in the cell in their free, uncomplexed state only in extremely low concentrations. They are instead sequestered by metal-ion storage and transport proteins, such as ferritin and transferrin for iron (see Chapter 1) and ceruloplasmin for copper. This arrangement prevents such metal ions from catalyzing deleterious oxidative reactions, but makes them available for incorporation into metalloenzymes as they are needed.

In vitro experiments have shown quite clearly that redox-active metal ions such as $Fe^{2+/3+}$ or $Cu^{+/2+}$ are extremely good catalysts for oxidation of sulfhydryl groups by O_2 (Reaction 5.27).[30]

$$4RSH + O_2 \xrightarrow{M^{n+}} 2RSSR + 2H_2O \qquad (5.27)$$

In addition, in the reducing environment of the cell, redox-active metal ions catalyze a very efficient one-electron reduction of hydrogen peroxide to produce hydroxyl radical, one of the most potent and reactive oxidants known (Reactions 5.28 to 5.30).[31]

$$M^{n+} + Red^{-} \rightarrow M^{(n-1)+} + Red \tag{5.28}$$

$$M^{(n-1)+} + H_2O_2 \rightarrow M^{n+} + OH^{-} + HO\cdot \tag{5.29}$$

$$Red^{-} + H_2O_2 \rightarrow Red + OH^{-} + HO\cdot \tag{5.30}$$

$$(Red^{-} = reducing\ agent) \tag{11.2.5.5.1}$$

Binding those metal ions in a metalloprotein usually prevents them from entering into these types of reactions. For example, transferrin, the iron-transport enzyme in serum, is normally only 30 percent saturated with iron. Under conditions of increasing iron overload, the empty iron-binding sites on transferrin are observed to fill, and symptoms of iron poisoning are not observed *in vivo* until after transferrin has been totally saturated with iron.[32] Ceruloplasmin and metallothionein may playa similar role in preventing copper toxicity.[6] It is very likely that both iron and copper toxicity are largely due to catalysis of oxidation reactions by those metal ions.

4. Systems for the Repair or Replacement of Damaged Materials

Repair of oxidative damage must go on constantly, even under normal conditions of aerobic metabolism. For lipids, repair of peroxidized fatty-acid chains is catalyzed by phospholipase A_2, which recognizes the structural changes at the lipid-water interface caused by the fatty-acid hydroperoxide, and catalyzes removal of the fatty acid at that site. The repair is then completed by enzymatic reacylation.[6] Although some oxidatively damaged proteins are repaired, more commonly such proteins are recognized, degraded at accelerated rates, and then replaced.[6] For DNA, several multi-enzyme systems exist whose function is to repair oxidatively damaged DNA.[6] For example, one such system catalyzes recognition and removal of damaged bases, removal of the damaged part of the strand, synthesis of new DNA to fill in the gaps, and religation to restore the DNA to its original, undamaged state. Mutant organisms that lack these repair enzymes are found to be hypersensitive to O_2, H_2O_2, or other oxidants.[6]

One particularly interesting aspect of oxidant stress is that most aerobic organisms can survive in the presence of normally lethal levels of oxidants if they have first been exposed to lower, nontoxic levels of oxidants. This phenomenon has been observed in animals, plants, yeast, and bacteria, and suggests that low levels of oxidants cause antioxidant systems to be induced *in vivo*. In certain bacteria, the mechanism of this induction is at least partially understood. A DNA-binding regulatory protein named OxyR that exists in two redox states has been identified in these systems.[33] Increased oxidant stress presumably increases concentration of the oxidized form, which then acts to turn on the transcription of the genes for some of the antioxidant enzymes. A related phenomenon may occur when bacteria and yeast switch from anaerobic to aerobic metabolism. When dioxygen is absent, these microorganisms live by fermentation, and do not waste energy by synthesizing the enzymes and other proteins needed for aerobic metabolism. However, when they are exposed to dioxygen, the synthesis of the respiratory apparatus is turned on. The details of this induction are not known completely, but some steps at least depend on the presence of heme, the prosthetic group of hemoglobin and other heme proteins, whose synthesis requires the presence of dioxygen.[34]

Molecular Mechanisms of Dioxygen Toxicity

What has been left out of the preceding discussion is the identification of the species responsible for oxidative damage, i.e., the agents that directly attack the various vulnerable targets in the cell. They were left out because the details of the chemistry responsible for dioxygen toxicity are largely unknown. In 1954, Rebeca Gerschman formulated the "free-radical theory of oxygen toxicity" after noting that tissues subjected to ionizing radiation resemble those exposed to elevated levels of dioxygen.[35] Fourteen years later, Irwin Fridovich proposed that the free radical responsible for dioxygen toxicity was superoxide, O_2^{-}, based on his identification of the first of the superoxide dismutase enzymes.[36] Today it is still not known if superoxide is the principal agent of dioxygen toxicity, and, if so, what the chemistry responsible for that toxicity is.[6]

There is no question that superoxide is formed during the normal course of aerobic metabolism,[121] although it is difficult to obtain estimates of the amount under varying conditions, because, even in the absence of a catalyst, superoxide disproportionates quite rapidly to dioxygen and hydrogen peroxide (Reaction 5.4) and therefore never accumulates to any great extent in the cell under normal conditions of pH.[37]

One major problem in this area is that a satisfactory chemical explanation for the purported toxicity of superoxide has never been found, despite much indirect evidence from *in vitro* experiments that the presence of superoxide can lead to undesirable oxidation

of various cell components and that such oxidation can be inhibited by superoxide dismutase.[38] The mechanism most commonly proposed is production of hydroxyl radicals via Reactions (5.28) to (5.30) with $Red^- = O_2^-$, which is referred to as the "Metal-Catalyzed Haber-Weiss Reaction". The role of superoxide in this mechanism is to reduce oxidized metal ions, such as Cu^{2+} or Fe^{3+}, present in the cell in trace amounts, to a lower oxidation state.[37] Hydroxyl radical is an extremely powerful and indiscriminate oxidant. It can abstract hydrogen atoms from organic substrates, and oxidize most reducing agents very rapidly. It is also a very effective initiator of free-radical autoxidation reactions (see Section II.C above). Therefore, reactions that produce hydroxyl radical in a living cell will probably be very deleterious.[6]

The problem with this explanation for superoxide toxicity is that the only role played by superoxide here is that of a reducing agent of trace metal ions. The interior of a cell is a highly reducing environment, however, and other reducing agents naturally present in the cell such as, for example, ascorbate anion can also act as Red^- in Reaction (5.28), and the resulting oxidation reactions due to hydroxyl radical are therefore no longer inhibitable by SOD.[39]

Other possible explanations for superoxide toxicity exist, of course, but none has ever been demonstrated experimentally. Superoxide might bind to a specific enzyme and inhibit it, much as cytochrome oxidase is inhibited by cyanide or hemoglobin by carbon monoxide. Certain enzymes may be extraordinarily sensitive to direct oxidation by superoxide, as has been suggested for the enzyme aconitase, an iron-sulfur enzyme that contains an exposed iron atom.[122] Another possibility is that the protonated and therefore neutral form of superoxide, HO_2, dissolves in membranes and acts as an initiator of lipid peroxidation. It has also been suggested that superoxide may react with nitric oxide, NO, in the cell producing peroxynitrite, a very potent oxidant.[123] One particularly appealing mechanism for superoxide toxicity that has gained favor in recent years is the "Site-Specific Haber-Weiss Mechanism."[40,41] The idea here is that traces of redox-active metal ions such as copper and iron are bound to macromolecules under normal conditions in the cell. Most reducing agents in the cell are too bulky to come into close proximity to these sequestered metal ions. Superoxide, however, in addition to being an excellent reducing agent, is very small, and could penetrate to these metal ions and reduce them. The reduced metal ions could then react with hydrogen peroxide, generating hydroxyl radical, which would immediately attack at a site near the location of the bound metal ion. This mechanism is very similar to that of the metal complexes that cause DNA cleavage; by reacting with hydrogen peroxide while bound to DNA, they generate powerful oxidants that react with DNA with high efficiency because of their proximity to it (see Chapter 8).

Although we are unsure what specific chemical reactions superoxide might undergo inside of the cell, there nevertheless does exist strong evidence that the superoxide dismutases play an important role in protection against dioxygen-induced damage. Mutant strains of bacteria and yeast that lack superoxide dismutases are killed by elevated concentrations of dioxygen that have no effect on the wild-type cells. This extreme sensitivity to dioxygen is alleviated when the gene coding for a superoxide dismutase is reinserted into the cell, even if the new SOD is of another type and from a different organism.[42,43]

Summary of Dioxygen Toxicity

In summary, we know a great deal about the sites that are vulnerable to oxidative damage in biological systems, about the agents that protect against such damage, and about the mechanisms that repair such damage. Metal ions are involved in all this chemistry, both as catalysts of deleterious oxidative reactions and as cofactors in the enzymes that protect against and repair such damage. What we still do not know at this time, however, is how dioxygen initiates the sequence of chemical reactions that produce the agents that attack the vulnerable biological targets *in vivo*.

11.2.5.5: Dioxygen Toxicity is shared under a CC BY-NC-SA 4.0 license and was authored, remixed, and/or curated by LibreTexts.

11.2.5.6: Monooxygenases

Metal-containing monooxygenase enzymes are known that contain heme iron, nonheme iron, or copper at their active sites.[2] For most of these enzymes, there is only limited information about the nature of the active site and the mode of interaction with dioxygen or substrates. But there are three monooxygenase enzymes that strongly resemble well-characterized reversible dioxygen-carrying proteins (see preceding chapter), suggesting that dioxygen binding to the metalloenzyme in its reduced state is an essential first step in the enzymatic mechanisms, presumably followed by other steps that result in oxygenation of substrates. The enzymes are:

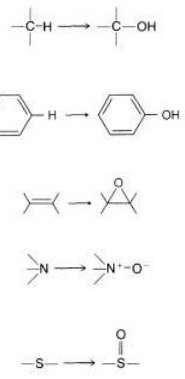
1. cytochrome P-450,[73] a heme-containing protein whose active site resembles the dioxygen-binding sites of myoglobin or hemoglobin in many respects, except that the axial ligand to iron is a thiolate side chain from cysteine rather than an imidazole side chain from histidine;
2. tyrosinase,[74] which contains two copper ions in close proximity in its active site and which has deoxy, oxy, and met states that closely resemble comparable states of hemocyanin in their spectroscopic properties; and
3. methane monooxygenase,[75,76] which contains two nonheme iron ions in close proximity and which resembles hemerythrin in many of its spectroscopic properties.

In addition to these three, there are also monooxygenase enzymes containing single nonheme iron[77] or copper ions,[78] or nonheme iron plus an organic cofactor such as a reduced pterin at their active sites.[79] Just as with the dioxygenase enzymes, we do not know how similar the mechanisms of the different metal-containing monooxygenase enzymes are to one another. The enzyme for which we have the most information is cytochrome P-450, and we will therefore focus our discussion on that system. Speculations about the mechanisms for the other systems are discussed at the end of this section.

1. Cytochrome P-450

Cytochrome P-450 enzymes are a group of monooxygenase enzymes that oxygenate a wide variety of substrates.[73] Examples of such reactions are:

1. hydroxylation of aliphatic compounds (Reaction 5.59);
2. hydroxylation of aromatic rings (Reaction 5.60);
3. epoxidation of olefins (Reaction 5.61);
4. amine oxidation to amine oxides (Reaction 5.62);
5. sulfide oxidation to sulfoxides (Reaction 5.63); and
6. oxidative dealkylation of heteroatoms (for example, Reaction 5.64).



$$Ph\text{—}O-CH_3 \longrightarrow Ph\text{—}OH + HCHO \tag{5.64}$$

Some of these reactions have great physiological significance, because they represent key transformations in metabolism, as in lipid metabolism and biosynthesis of corticosteroids, for example.[73] Cytochrome P-450 is also known to catalyze the transformation of certain precarcinogens such as benzpyrene into their carcinogenic forms.[73]

Many of the P-450 enzymes have been difficult to characterize, because they are membrane-bound and consequently relatively insoluble in aqueous solution. However, cytochrome $P\text{-}450_{cam}$, which is a component of the camphor 5-monooxygenase system

isolated from the bacterium *Pseudomonas putida*, is soluble and has been particularly useful as the subject of numerous spectroscopic and mechanistic studies, as well as several x-ray crystallographic structure determinations.[80] This enzyme consists of a single polypeptide chain, mainly α-helical, with a heme b group (Fe-protoporphyrin IX) sandwiched in between two helices, with no covalent attachments between the porphyrin ring and the protein. One axial ligand complexed to iron is a cysteinyl thiolate. In the resting state, the iron is predominantly low-spin Fe^{III}, probably with a water as the other axial ligand. When substrate binds to the resting enzyme, the spin state changes to high-spin, and the non-cysteine axial ligand is displaced. The enzyme can be reduced to an Fe^{II} state, which is high-spin, and resembles deoxyhemoglobin or myoglobin in many of its spectroscopic properties. This ferrous form binds dioxygen to make an oxy form or carbon monoxide to make a carbonyl form. The CO derivative has a Soret band (high-energy π-π* transition of the porphyrin ring) at 450 nm, unusually low energy for a carbonyl derivative of a heme protein because of the presence of the axial thiolate ligand. This spectroscopic feature aids in the isolation of the enzyme and is responsible for its name.

a. "Active Oxygen"

Camphor 5-monooxygenase is a three-component system, consisting of cytochrome $P\text{-}450_{cam}$ and two electron-transfer proteins, a flavoprotein, and an iron-sulfur protein (see Chapters 6 and 7). The role of the electron-transfer proteins is to deliver electrons to the P-450 enzyme, but these may be replaced *in vitro* by other reducing agents. The reaction sequence is in Figure 5.10.

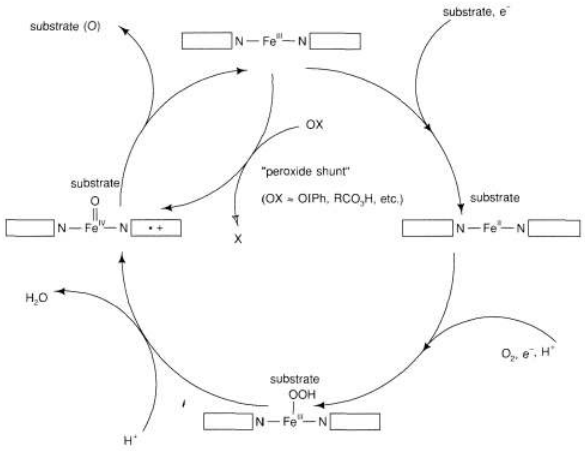


Figure 5.10 - Proposed mechanism for cytochrome P-450. The resting enzyme is shown at the top of the cycle. Substrate binds to the enzyme at a position close to the iron center, but it is not directly coordinated to the metal ion. The enzyme-substrate complex is then reduced to the ferrous form. Dioxygen then binds to form an oxy complex (not shown). The oxy complex is then reduced by another electron and protonated, giving a ferric-hydroperoxy complex shown at the bottom of the cycle. The ligand bound here to the Fe^{III} center is HO_2^-, i.e. deprotonated hydrogen peroxide. The ferric hydroperoxy form of the enzyme-substrate complex then undergoes heterolytic O—O bond cleavage, giving a high-valent Fe^{IV} oxo center, with the porphyrin ligand oxidized by one equivalent (see text). This species then transfers a neutral oxygen atom to the bound substrate, which is then released, giving the oxygenated product and regenerating the resting form of the enzyme. The "peroxide shunt" refers to the mechanism proposed for the cytochrome P450-catalyzed oxygenation of substrates by single-oxygen-atom donors (see text). It is believed that the same high-valent iron-oxo intermediate is generated in these types of reactions as well.

For cytochrome P-450, the question that is possibly of greatest current interest to the bioinorganic chemist is just what mechanism enables activation of dioxygen and its reaction with substrate. It seems clear that dioxygen binds to the ferrous state of the enzyme-substrate complex, and that the resulting oxy ligand, which presumably is similar to the oxy ligand in oxyhemoglobin and oxymyoglobin, is not sufficiently reactive to attack the bound substrate. The oxy form is then reduced and the active oxidant is generated, but the nature of the active oxidant has not been deduced from studies of the enzyme itself, nor has it been possible to observe and characterize intermediates that occur between the time of the reduction and the release of product. Three species are potential candidates for "active oxygen," the oxygen-containing species that attacks the substrate, in cytochrome P-450. They are:

1. a ferric peroxo, **1a**, or hydroperoxo complex, **1b**, formed from one-electron reduction of the oxy complex (Reaction 5.65);
2. an iron(IV) oxo complex, **2**, formed by homolytic O—O bond cleavage of a ferric hydroperoxo complex (Reaction 5.66); and
3. a complex at the oxidation level of an iron(V) oxo complex, **3**, formed by heterolytic O—O bond cleavage of a ferric hydroperoxo complex (Reaction 5.67).

The hydroxyl radical, HO•, although highly reactive and capable of attacking P-450 substrates, is considered to be an unlikely candidate for "active oxygen" because of the indiscriminate character of its reactivity.

$$Fe^{II}P + O_2 \rightarrow FePO_2 \xrightarrow{e^-} [Fe^{III}P(O_2^{2-})]^- \xrightarrow{H^+} Fe^{III}P(O_2H^-) \quad (5.65)$$

$$\mathbf{1a} \qquad\qquad \mathbf{1b} \quad (11.2.5.6.1)$$

$$Fe^{III}P(O_2H^-) \rightarrow Fe^{IV}P(O) + HO\cdot \quad (5.66)$$

$$\mathbf{1b} \qquad \mathbf{2} \quad (11.2.5.6.2)$$

$$Fe^{III}P(O_2H^-) \rightarrow [Fe^{V}(P^{2-})(O)^+ \leftrightarrow Fe^{IV}(P^-)(O)^+] + HO^- \quad (5.67)$$

$$\mathbf{1b} \qquad\qquad \mathbf{3} \quad (11.2.5.6.3)$$

(P^{2-} = porphyrin ligand; P^- = one-electron oxidized porphyrin ligand)

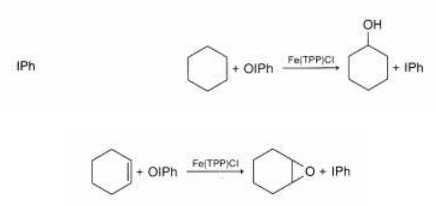
An iron(V) oxo complex (or a related species at the same oxidation level), **3**, formed via Reaction (5.67), is the favored candidate for "active oxygen" in cytochrome P-450.[81] This conclusion was initially drawn from studies of reactions of the enzyme with alkylhydroperoxides and single-oxygen-atom donors. Single-oxygen-atom donors are reagents such as iodosylbenzene, OIPh, and periodate, IO_4^-,capable of donating a neutral oxygen atom to an acceptor, forming a stable product in the process (here, iodobenzene, IPh, and iodate, IO_3^-). It was discovered that ferric cytochrome P-450 could catalyze oxygenation reactions using organic peroxides or single-oxygen-atom donors in place of dioxygen and reducing agents. Usually the same substrates would give the identical oxygenated product. This reaction pathway was referred to as the "peroxide shunt" (see Figure 5.10). The implication of this discovery was that the same form of "active oxygen" was generated in each reaction, and the fact that single-oxygen-atom donors could drive this reaction implied that this species contained only one oxygen atom, i.e., was generated subsequent to O—O bond cleavage. The mechanism suggested for this reaction was Reactions (5.68) and (5.69).

$$Fe(III)P^+ + OX \rightarrow \mathbf{3} + X \quad (5.68)$$

$$\mathbf{3} + substrate \rightarrow Fe(III)P^+ + substrate(O) \quad (5.69)$$

b. Metalloporphyrin Model Systems

Studies of the reactivities of synthetic metalloporphyrin complexes in oxygen-transfer reactions and characterization of intermediate species observed during the course of such reactions have been invaluable in evaluating potential intermediates and reaction pathways for cytochrome P-450. Logically, it would be most desirable if one could mimic the enzymatic oxygenation reactions of substrates using iron porphyrins, dioxygen, and reducing agents. However, studies of such iron-porphyrin-catalyzed reactions have failed to produce meaningful results that could be related back to the P-450 mechanism. This is perhaps not surprising, since the enzyme system is designed to funnel electrons into the iron-dioxygen-substrate complex, and thus to generate the active oxidant within the confines of the enzyme active site in the immediate proximity of the bound substrate. Without the constraints imposed by the enzyme, however, iron porphyrins generally will either (1) catalyze the oxidation of the reducing agent by dioxygen, leaving the substrate untouched, or (2) initiate free-radical autoxidation reactions (see Section II.C). A different approach was suggested by the observation of the peroxide shunt reaction (Reactions 5.68 and 5.69) using organic peroxides or single-oxygen-atom donors, and the earliest successful studies demonstrated that Fe(TPP)Cl (TPP = tetraphenylporphyrin) would catalyze the epoxidation of olefins and the hydroxylation of aliphatic hydrocarbons by iodosylbenzene[81](Reactions 5.70 and 5.71).



Reactions (5.70) and (5.71) were postulated to occur via an iron-bound oxidant such as **3** in Reaction (5.67). This hypothesis was tested by studying the reaction of dioctyl Fe(PPIX)CI with iodosylbenzene, which resulted in 60 percent hydroxylation at positions 4 and 5 on the hydrocarbon tail (see 5.72), positions for which there is no reason to expect increased reactivity except for the fact

that those particular locations are predicted from molecular models to come closest to the iron center when the tail wraps around the porphyrin molecule.[82]

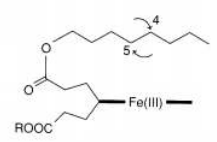


Figure 5.11).[83]

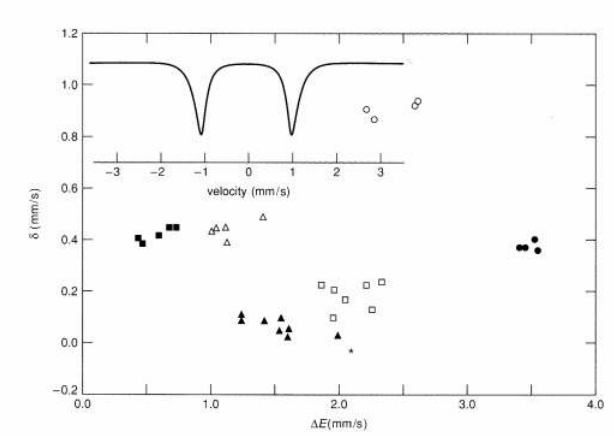
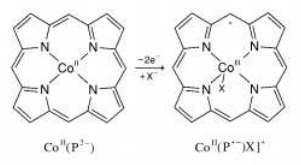


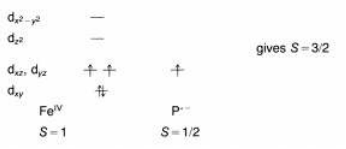
Figure 5.11 - Comparative Mössbauer data for iron-porphyrin complexes: ■ *high-spin* Fe^{III} , □ *low-spin* Fe^{III} , ● *intermediate-spin (admixed)* Fe^{III} , ◯ *high-spin* Fe^{II}, △ *low-spin* Fe^{II}, ▲ *oxo- and imido-*Fe^{IV}, * *dimethoxyiron(IV)TMP. Insert shows the zero-field Mössbauer spectrum of* ^{57}*Fe-dimethoxyiron(IV)TMP at 4.2 K. (From Reference 83.)*

Visible absorption spectra of porphyrin complexes are due largely to π-π* transitions of the porphyrin ligand. The bright green color is unusual for iron-porphyrin complexes, which are usually red or purple. (However, this green color has been seen for compound I of catalase and peroxidases; see Section VI below.) The unusually long-wavelength visible absorption bands that account for the green color result from the fact that the porphyrin ring has been oxidized by one electron. Similar visible absorption bands can be seen, for example, in other oxidized porphyrin complexes, such as $Co^{III}(P^{\bullet-})^{+}$, formed by two-electron oxidation of $Co^{II}(P^{2-})$(see 5.73).[84]



Oxidized porphyrin ligands also give characteristic proton NMR spectra, which are seen for the green porphyrin complex as well.[81,83]

Magnetic measurements indicate that the green porphyrin complex contains three unpaired electrons. Detailed analysis of the Mössbauer spectra has indicated that the two unpaired electrons on the Fe^{IV} ion are strongly ferromagnetically coupled to the unpaired electron on the porphyrin, accounting for the resulting S = $\frac{5}{3}$ state.[81,83]



Studies of the reactions of this species with P-450-type substrates demonstrate that this species is reactive enough to make it an attractive candidate for" active oxygen" in the enzymatic mechanism.[81,83]

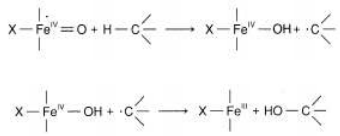
Synthetic analogues for two of the other candidates for "active oxygen" have also been synthesized and their reactivities assessed. For example, Fe^{III} and Mn^{III}-porphyrin peroxo complexes analogous to **1a** in Reaction (5.65) have been synthesized. The x-ray crystal structure of the Mn complex shows that the peroxo ligand is bound to the metal in a triangular, side-on fashion (see 5.75). The Fe complex is believed to have a similar structure.[85,86]



Studies of this species indicate that **1a** in Reaction (5.65) would not have the requisite reactivity to be a candidate for "active oxygen" in the cytochrome P-450 mechanism, since it will not even oxidize triphenylphosphine, PPh_3, to triphenylphosphine oxide, $OPPh_3$, one of the more facile oxygenation reactions known.[87] Attempts to examine the protonated form, **1b** in Reaction (5.65), however, indicate that it is highly unstable, and its reactivity has not yet been thoroughly examined.[87] Fe^{IV}-oxo-porphyrin complexes analogous to **2** in Reaction (5.66) have also been prepared in solution and characterized by NMR.[60,61] Such complexes will react with PPh_3 to give $OPPh_3$, but are relatively unreactive with olefins and totally unreactive with saturated hydrocarbons. Thus **2** is also ruled out as a candidate for "active oxygen" in P-450 mechanisms.

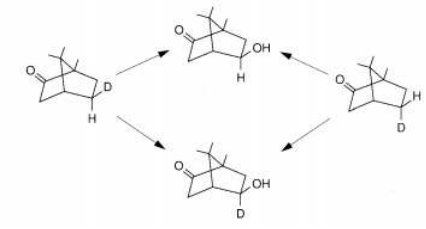
These reactivity studies, and the observation of the peroxide shunt described above, indicate that $Fe^{V}(P^{2-})(O)^{+}$ or $Fe^{IV}(P^{-})(O)^{+}$ is the most likely candidate for "active oxygen." These two formulations are, of course, isoelectronic, and it is tempting to conclude that the latter is the more likely formulation of the enzymatic intermediate. However, it is important to remember that the model systems lack the axial cysteinylligand present in cytochrome P-450. The effect of the relatively easily oxidized sulfur ligand on the electron distribution within that intermediate is not known, since model systems for high-valent iron-oxo complexes containing axial thiolate ligands have not been synthesized.

The mechanism of reactions of the high-valent oxo complex **3** in Reaction (5.67) with a variety of substrates is an area of active interest.[81,88] Such studies are generally carried out by generation of the species *in situ* from the reaction of a ferric porphyrin with a single-oxygen-atom donor, such as a peracid or iodosylbenzene.[89] In hydroxylation reactions of aliphatic hydrocarbons, the initial step appears to be abstraction of a hydrogen atom from the substrate to form a substrate radical and an Fe^{IV} hydroxide complex held together in a cage created by the enzyme active site so that they cannot diffuse away from each other (Reaction 5.76). This step is then followed by recombination of the OH fragment with the substrate radical to make the hydroxylated product (Reaction 5.77). This mechanism is referred to as the "oxygen rebound mechanism."[83]



The radical character of the intermediates formed in this reaction is supported by the observation that such reactions carried out using synthetic porphyrins and single-oxygen-atom donors in the presence of $BrCCl_3$ give substantial amounts of alkyl bromides as products, a result that is consistent with radical intermediates and inconsistent with either carbanion or carbonium-ion intermediates.[83]

In the enzymatic reactions themselves, there is also strong evidence to support a stepwise mechanism involving free-radical intermediates. For example, cytochrome $P\text{-}450_{cam}$ gives hydroxylation of d-camphor only in the 5-*exo* position, but deuterium-labeling studies show that either the 5-*exo* or the 5-*endo* hydrogen is lost (Reaction 5.78).[88]



Such results are obviously inconsistent with a concerted mechanism in which the oxygen atom would be inserted into the 5-*exo* C—H bond in one step; so there would be no chance for the hydrogens in the two positions to exchange. (Remember that alcohol protons exchange rapidly with water and therefore are not expected to remain deuterated when the reaction is carried out in H_2O.)

The crystal structure of reduced cytochrome P-450_{cam} with CO bound to the iron and the substrate camphor bound[90] adjacent to it has been examined and compared with the crystal structure of the oxidized enzyme with camphor bound. The former is expected to be similar in structure to the less-stable oxy complex. The comparison shows that the substrate camphor is closer to the iron center in the oxidized enzyme. It is therefore possible that a similar movement of the substrate occurs during the catalytic reaction after either a 5-*exo* or a 5-*endo* hydrogen is abstracted, and that the new position of the camphor molecule then restricts the hydroxylation step to the 5-*exo* position. It is interesting to note that the 5-*exo* position on the camphor that is hydroxylated is held in very close proximity to the Fe^{III} center, and therefore to the presumed location of the oxo ligand in the high-valent oxo intermediate in the structure of the ferric enzyme plus camphor derivative (Figure 5.12). Crystal structures of the ferric form of cytochrome P-450_{cam} with norcamphor and adamantanone bound in place of camphor have also been determined.[90] These alternative substrates are smaller than camphor, and appear to fit more loosely than camphor. It is therefore reasonable to assume that they "rattle around" to a certain extent in the substrate binding site, which probably accounts for the less-specific pattern of hydroxylation observed for these alternative substrates.

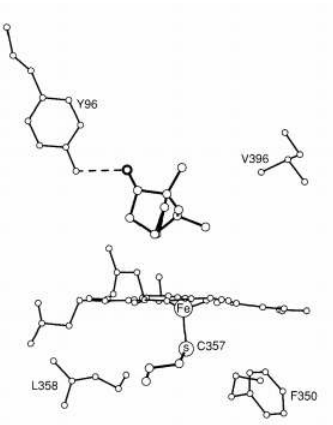


Figure 5.12 - Edge-on view of the P-450 active-site region with the substrate camphor molecule bound.[80] The substrate camphor is located in a hydrophobic pocket directly above the heme and is oriented by a hydrogen bond between the carbonyl oxygen of the camphor and Tyr-96. The position that is hydroxylated in the oxygenation reaction, i.e., the 5-exo position, is the closest point of approach of the substrate to the expected position of the oxygen atom bound to iron in the highvalent iron-oxo intermediate.

Mechanisms for olefin epoxidations catalyzed either by the enzyme or by model porphyrin complexes are not as well understood as those for hydroxylation of aliphatic hydrocarbons. Some of the possibilities that have been proposed[88,91] are represented schematically in Figure 5.13.

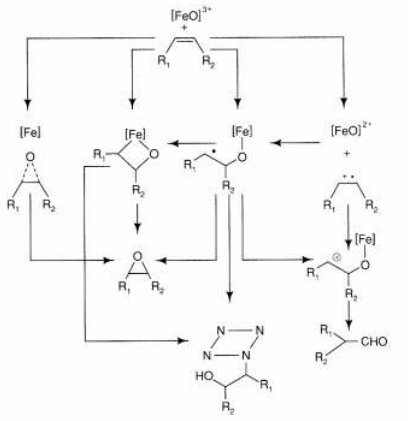


Figure 5.13 - Schematic representation of possible mechanistic pathways for olefin epoxidation by **3**. The mechanisms described are, from right to left, concerted addition of oxygen to the double bond, reaction via a metallocylic intermediate, reaction via a ring-opened radical intermediate, and reaction proceeding via an initial electron-transfer step.[91]

c. O—O Bond Cleavage

The evidence is persuasive that the "active oxygen" species that attacks substrate in cytochrome P-450 is a high-valent iron-oxo complex. However, the mechanism of formation of that species in the catalytic reaction with dioxygen is less well-understood. Heterolytic O—O bond cleavage of a ferric porphyrin hydroperoxide complex, **1b** (Reaction 5.67), is the logical and anticipated route, but it has not yet been unequivocally demonstrated in a model complex.[92,93] The catalase and peroxidase enzymes catalyze heterolytic O—O bond cleavage in reactions of hydrogen peroxide, but in them the active sites contain amino-acid side chains situated to facilitate the developing charge separation that occurs in heterolytic cleavage (see Section VI). The crystal structure of cytochrome $P\text{-}450_{cam}$ shows no such groups in the activesite cavity, nor does it give any clue to the source of a proton to protonate the peroxide ligand when it is produced.[80] Also, we have little experimental evidence concerning possible roles that the cysteinyl sulfur axial ligand might play in facilitating O—O bond cleavage. These issues remain areas of active interest for researchers interested in cytochrome P-450 mechanisms.

Other Metal-containing Monooxygenase Enzymes

As mentioned above, much less is known about the structural characteristics and mechanisms of the nonheme metal-containing monooxygenase enzymes. From the similarities of the overall stoichiometries of the reactions and the resemblance of some of the enzymes to dioxygen-binding proteins, it is likely that the initial steps are the same as those for cytochrome P-450, i.e., dioxygen binding followed by reduction to form metal-peroxide or hydroperoxide complexes. It is not obvious that the next step is the same, however (i.e., O—O bond cleavage to form a high-valent metal-oxo complex prior to attack on substrate). The problem is that such a mechanism would generate metal-oxo complexes that appear to contain metal ions in chemically unreasonable high-oxidation states, e.g., Fe^{V}, Cu^{III}, or Cu^{IV} (Reactions 5.79-5.81).

$$(Fe^{III}-OOH)^{2+} \rightarrow (Fe^{V}O)^{3+} + OH^{-} \tag{5.79}$$

$$(Cu^{II}-OOH)^{+} \rightarrow (Cu^{IV}O)^{2+} + OH^{-} \tag{5.80}$$

$$(Cu^{II}-OO-Cu^{II})^{2+} \rightarrow 2(Cu^{III}O)^{+} \tag{5.81}$$

An alternative mechanism is for the peroxide or hydroperoxide ligand to attack the substrate directly; i.e., O—O bond cleavage could be concerted with attack on substrate. Another possibility is that the oxygen atom is inserted in a metalligand bond prior to transfer to the substrate. Neither of these alternative mechanisms has been demonstrated experimentally. These various possibilities remain to be considered as more information about the monooxygenase enzymes becomes available.

11.2.5.6: Monooxygenases is shared under a CC BY-NC-SA 4.0 license and was authored, remixed, and/or curated by LibreTexts.

11.2.5.7: Oxygenases

Background

The oxygenase enzymes catalyze reactions of dioxygen with organic substrates in which oxygen atoms from dioxygen are incorporated into the final oxidized product.[2-4] These enzymes can be divided into dioxygenases, which direct both atoms of oxygen into the product (Reaction 5.53), and monooxygenases, where one atom of oxygen from dioxygen is found in the product and the other has been reduced to water (Reaction 5.54):

$$Dioxygenase: \ substrate + {}^*O_2 \rightarrow substrate({}^*O)_2 \tag{5.53}$$

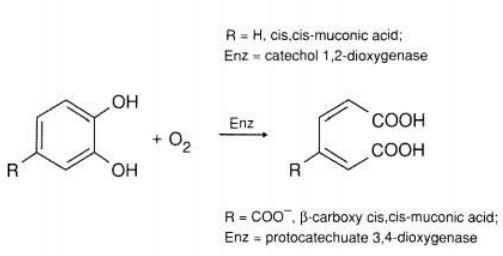
$$Monoxygenase: \ substrate + {}^*O_2 + 2H^+ + 2e^- \rightarrow substrate({}^*O) + H_2{}^*O \tag{5.54}$$

Dioxygenases

Dioxygenase enzymes are known that contain heme iron, nonheme iron, copper, or manganese.[66,67] The substrates whose oxygenations are catalyzed by these enzymes are very diverse, as are the metal-binding sites; so probably several, possibly unrelated, mechanisms operate in these different systems, For many of these enzymes, there is not yet much detailed mechanistic information. However, some of the intradiol catechol dioxygenases isolated from bacterial sources have been studied in great detail, and both structural and mechanistic information is available.[66,67] These are the systems that will be described here.

1. Intradiol Catechol Dioxygenases

The role of these nonheme iron-containing enzymes is to catalyze the degradation of catechol derivatives to give muconic acids (Reaction 5.55, for example). The enzymes are induced when the only carbon sources available to the bacteria are aromatic molecules. The two best-characterized members of this class are catechol 1,2-dioxygenase (CTD) and protocatechuate 3,4-dioxygenase (PCD).



a. Characterization of the Active Sites

Even before the x-ray crystal structure of PCD was obtained, a picture of the active site had been constructed by detailed spectroscopic work using a variety of methods. The success of the spectroscopic analyses of these enzymes is a particularly good example of the importance and usefulness of such methods in the characterization of metalloproteins. The two enzymes referred to in Reaction (5.55) have different molecular weights and subunit compositions,[66] but apparently contain very similar active-site structures and function by very similar mechanisms. In both, the resting state of the enzyme contains one Fe^{III} ion bound at the active site. EPR spectra show a resonance at g = 4.3, characteristic of high-spin Fe^{III} in a so-called rhombic (low symmetry) environment,[66] and the Mössbauer parameters are also characteristic of high-spin ferric.[66-68] Reactions with substrate analogues (see below) cause spectral shifts of the iron chromophore, suggesting strongly that the substrate binds directly to the iron center in the course of the enzymatic reaction.

It is straightforward to rule out the presence of heme in these enzymes, because the heme chromophore has characteristic electronic-absorption bands in the visible and ultraviolet regions with high extinction coefficients, which are not observed for these proteins. Likewise, the spectral features characteristic of other known cofactors or iron-sulfur centers are not observed. Instead, the dominant feature in the visible absorption spectrum is a band with a maximum near 460 nm and a molar extinction coefficient of 3000 to 4000 $M^{-1}cm^{-1}$ per iron (see Figure 5.5).

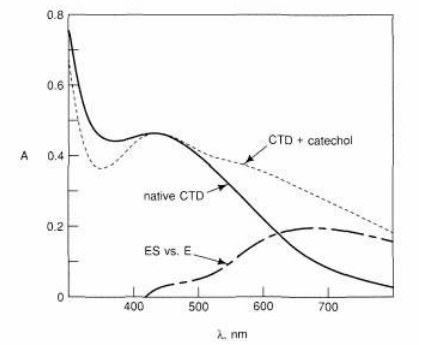


Figure 5.5 - Visible absorption spectra of catechol 1,2-dioxygenase and its substrate complex: E, native enzyme; ES, enzyme-substrate complex.[66]

This type of electronic absorption spectrum is characteristic of a class of proteins, sometimes referred to as iron-tyrosinate proteins, that contain tyrosine ligands bound to iron(III) in their active sites, and which consequently show the characteristic visible absorption spectrum due to phenolate-to-iron(III) charge-transfer transitions. This assignment can be definitively proven by examination of the resonance Raman spectrum, which shows enhancement of the characteristic tyrosine vibrational modes (typically ~1170, 1270, 1500, and 1600 cm^{-1}) when the sample is irradiated in the charge-transfer band described above. Ferric complexes of phenolate ligands may be seen to give almost identical resonance Raman spectra (see Figure 5.6).

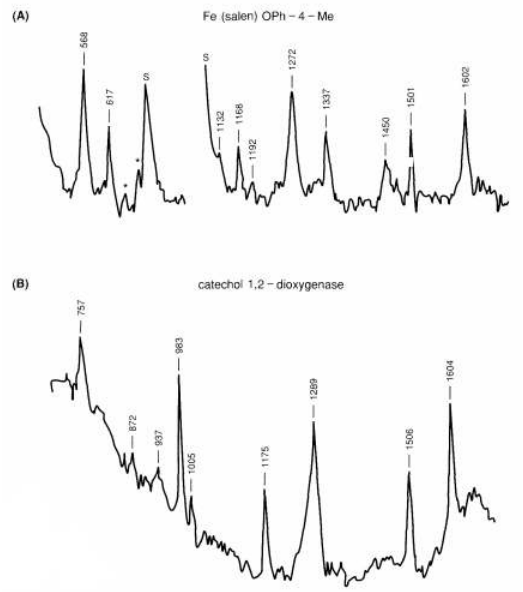


Figure 5.6 - Resonance Raman specta of (A) Fe^{III}(salen)(O - C_6H_4 -4 - CH_3) and (B) catechol 1,2-dioxygenase.[66]

These bands have been assigned as a C—H bending vibration and a C—O and two C—C stretching vibrations of the phenolate ligand.[69] In addition, NMR studies of the relaxation rates of the proton spins of water indicate that water interacts with the paramagnetic Fe^{III} center in the enzyme. This conclusion is supported by the broadening of the Fe^{III} EPR signal in the presence of $H_2{}^{17}O$, due to interaction with the I = $\frac{5}{2}$ nuclear spin of ^{17}O. Thus numerous spectroscopic studies of the catechol dioxygenases led to the prediction that the high-spin ferric ion was bound to tyrosine ligands and water. In addition, EXAFS data, as well as the resemblance of the spectral properties to another, better characterized iron-tyrosinate protein, i.e., transferrin (see Chapter 1), suggested that histidines would also be found as ligands to iron in these proteins.[66,67]

Preliminary x-ray crystallographic results on protocatechuate 3,4-dioxygenase completely support the earlier predictions based on spectroscopic studies.[70] The Fe^{III} center is bound to two histidine and two tyrosine ligands and a water, the five ligands being arranged in a trigonal bipyramidal arrangement, with a tyrosine and a histidine located in axial positions, and with the equatorial water or hydroxide ligand facing toward a cavity assumed to be the substrate-binding cavity. The cavity also contains the positively charged guanidinium group of an arginine side chain, in the correct position to interact with the negatively charged carboxylate group on the protocatechuate substrate (see Figure 5.7).

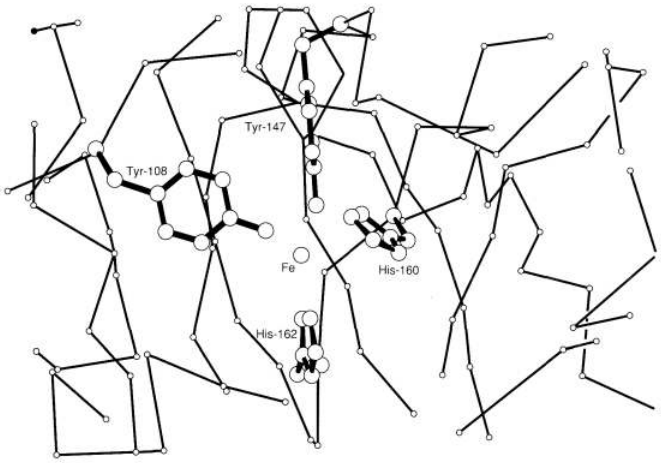
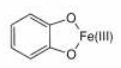


Figure 5.7 - A view of the active site of protocatechuate 3,4-dioxygenase based on the results of the x-ray crystal structure.[70] The Fe^{III} center is approximately trigonal bipyramidal, with Tyr-147 and His-162 as axial ligands, and Tyr-108 and His-160 in the equatorial plane along with a solvent molecule (not shown) in the foreground.[66]

b. Mechanistic Studies

As mentioned above, substrates and inhibitors that are substrate analogues bind to these enzymes and cause distinct changes in the spectral properties, suggesting strongly that they interact directly with the Fe^{III} center. Nevertheless, the spectra remain characteristic of the Fe^{III} oxidation state, indicating that the ferric center has not been reduced. Catecholates are excellent ligands for Fe^{III} (see, for example, the catecholate siderophores, Chapter 1) and it might therefore be assumed that the catechol substrate would bind to iron using both oxygen atoms (see 5.56).



However, the observation that phenolic inhibitors p-X-C_6H_4-OH bind strongly to the enzymes suggested the possibility that the substrate binds to the iron center through only one oxygen atom (see 5.57).

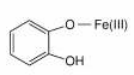
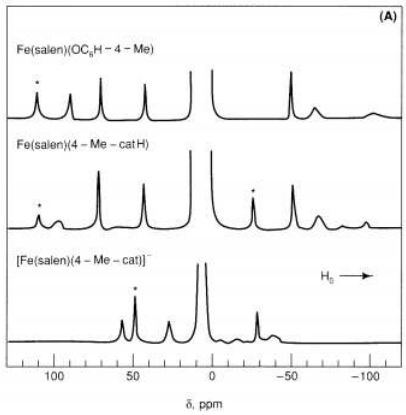


Figure 5.8).



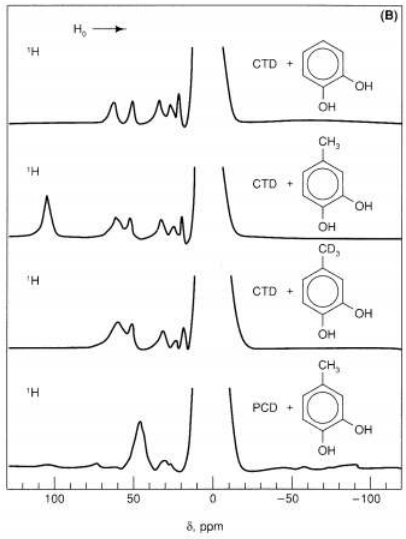


Figure 5.8 - (A) Paramagnetically shifted ^{1}H-NMR spectra of Fe(salen) complexes with 4-methylphenolate and 4-methylcatecholate ligands. Starred resonances are assigned to methyl groups. The top spectrum is of the ferric-salen complex of the monodentate 4-methylphenolate ligand. The middle spectrum is of the ferric-salen complex of the monoprotonated 4-methylcatecholate ligand. Note that two isomers are present, because the two oxygen atoms on the ligand are inequivalent, and either may be used to make the monodentate complex. The bottom spectrum is of the ferric-salen complex of the fully deprotonated 4-methylcatecholate ligand, which binds to the iron in a bidentate fashion. Note the smaller span of isotropic shifts, which has been demonstrated to be diagnostic of bidentate coordination. (B) Paramagnetically shifted ^{1}H-NMR spectra of enzyme-substrate complexes of the dioxygenase enzymes catechol 1,2-dioxygenase (CTD) and protocatecholate 3,4-dioxygenase (PCD). Note the resemblance between the position of the methyl resonance in the complex of 4-methylcatechol with CTD and that of one of the methyl resonances in the middle spectrum in (A), indicating that 4-methylcatechol binds to the ferric center in CTD in a monodentate fashion through the O-1 oxygen only. By contrast, the spectrum of 4-methylcatechol with PCD resembles the bottom spectrum in (A), indicating that here the 4-methylcatecholate ligand is bidentate.[66]

These results contradict an early hypothesis that the mode of substrate binding, i.e., monodentate versus bidentate, might be a crucial factor in activating the substrate for reaction with dioxygen.[67]

Spectroscopic observations of the enzymes during reactions with substrates and substrate analogues have enabled investigators to observe several intermediates along the catalytic pathway. Such studies have led to the conclusion that the iron center remains high-spin Fe^{III} throughout the entire course of the reaction. This conclusion immediately presents a problem in understanding the nature of the interaction of dioxygen with the enzyme, since dioxygen does not in general interact with highly oxidized metal ions such as Fe^{III}. The solution seems to be that this reaction represents an example of *substrate* rather than *dioxygen* activation.

Studies of the oxidation of ferric catecholate coordination complexes have been useful in exploring mechanistic possibilities for these enzymes.[71] A series of ferric complexes of 3,5-di-t-butyl-catechol with different ligands L have been found to react with O_2 to give oxidation of the catechol ligand (Reaction 5.58)

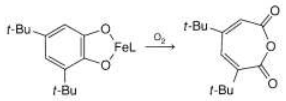


Figure 5.9) and that complexes of ligands that are poor donors tend to favor electron donation from catechol to Fe III, thus increasing the relative amount of minor form B. It should be noted that the spectroscopic characteristics of these complexes are nevertheless dominated by the major resonance form A, regardless of the nature of L.

All these studies of the enzymes and their model complexes have led to the mechanism summarized in Figure 5.9.[66] In this proposed mechanism, the catechol substrate coordinates to the ferric center in either a monodentate or a bidentate fashion, presumably displacing the water or hydroxide ligand. The resulting catechol complex then reacts with dioxygen to give a peroxy derivative of the substrate, which remains coordinated to Fe^{III}. The subsequent rearrangement of this peroxy species to give an anhydride intermediate is analogous to well-characterized reactions that occur when catechols are reacted with alkaline hydrogen peroxide.[72] The observation that both atoms of oxygen derived from O_2 are incorporated into the product requires that the ferric

oxide or hydroxide complex formed in the step that produces the anhydride does not exchange with external water prior to reacting with the anhydride to open it up to the product diacid.

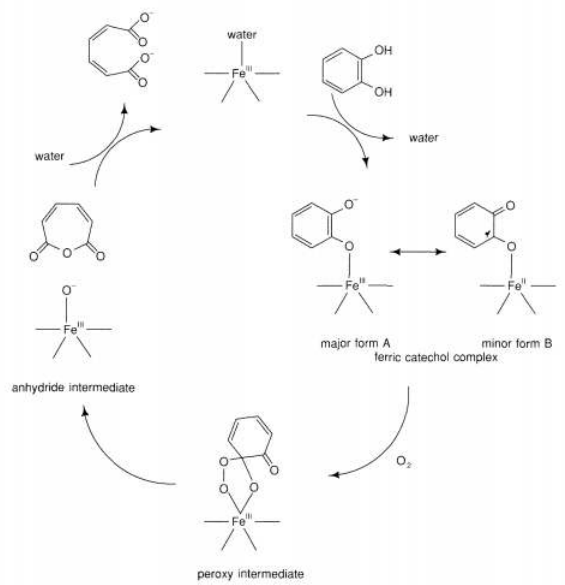


Figure 5.9 - Proposed mechanism for catechol dioxygenases (modified from Reference 45). The major form A is shown here with the catechol bound in a monodentate fashion. It may sometimes be bound in a bidentate fashion as well (see text).

It is interesting to consider how the intradiol dioxygenase enzymes overcome the kinetic barriers to oxidations by dioxygen, and why this particular mechanism is unlikely to be applicable to the monooxygenase enzymes. The first point is that the ferric catechol intermediate is paramagnetic, with resonance forms that put unpaired electron density onto the carbon that reacts with dioxygen. The spin restriction is therefore not a problem. In addition, the catechol ligand is a very good reducing agent, much more so than the typical substrates of the monooxygenase enzymes (see next section). It is possible, therefore, that the reaction of dioxygen with the ferric catechol complex results in a concerted two-electron transfer to give a peroxy intermediate, thus bypassing the relatively unfavorable one-electron reduction of O_2.

11.2.5.7: Oxygenases is shared under a CC BY-NC-SA 4.0 license and was authored, remixed, and/or curated by LibreTexts.

11.2.6: Electron Transfer

I. Electron Transfers in Biology

A. Biological Redox Components

B. Energy Storage and Release

C. Coupling Electron Transfers and Substrate Activation

II. Electron-transfer Rates

A. Overview

B. Self-exchange and Cross Reactions

III. Electron-transfer Theory

A. Basic Concepts

B. Marcus Theory

1. Cross Reactions of Blue Copper Proteins

IV. Long-range Electron Transfer in Proteins

A. Electronic Coupling

1. Binding Sites on the Plastocyanin Molecular Surface

B. Modified Metalloproteins

1. Ruthenium-modified Myoglobin

C. Protein-protein Complexes

1. Cytochrome b_5-cytochrome c
2. Hybrid Hemoglobins

D. Cytochrome c

1. Ruthenium-modified Cytochrome c

E. Bacterial Photosynthetic Reaction Centers

V. References

1. R. C. Prince, *Trends Biochem. Sci.* **13** (1988), 286-288.
2. R. C. Prince and G. N. George, *Trends Biochem. Sci.* **15** (1990), 170-172.
3. E. T. Adman, *Biochim. Biophys. Acta* **549** (1979), 107-144.
4. H. B. Gray and B. G. Malmström, *Comments Inorg. Chem.* **2** (1983), 203-209.
5. T. E. Meyer and M. A. Cusanovich, *Biochim. Biophys. Acta* **975** (1989), 1-28.
6. R. P. Simondsen and G. Tollin, *Mol. Cellular Biochem.* **33** (1980), 13-24.
7. C. T. W. Moonen and F. Müller, *Biochemistry* **21** (1982), 408-414.

8. H. B. Gray and E. I. Solomon, in T. G. Spiro, ed., *Copper Proteins*, Wiley, 1981, pp. 1-39.
9. E. T. Adman, in P. Harrison, ed., *Metalloproteins*, Macmillan, 1985, Part I, pp. 1-42.
10. O. Farver and I. Pecht, in R. Lontie, ed., *Copper Proteins and Copper Enzymes*, CRC Press, 1984, vol. I, pp. 183-214.
11. G. E. Norris, B. F. Anderson, and E. N. Baker, *J. Am. Chem. Soc.* **108** (1986), 2784-2785.
12. E. W. Ainscough *et al.*, *Biochemistry* **26** (1987), 71-82.
13. W. Lovenberg, ed., *Iron-Sulfur Proteins*, Academic Press, 1973-1977, 3 vols.
14. T. G. Spiro, ed., *Iron-Sulfur Proteins*, Wiley, 1982.
15. K. Fukuyama *et al.*, *Nature* **286** (1980), 522-524.
16. J. Rawlings, O. Siiman, and H. B. Gray, *Proc. Natl. Acad. Sci. USA* **71** (1974), 125-127.
17. C. W. Carter *et al.*, *Proc. Natl. Acad. Sci. USA* **69** (1972), 3526-3529.
18. G. R. Moore, G. W. Pettigrew, and N. K. Rogers, *Proc. Natl. Acad. Sci. USA* **83** (1986), 4998-4999.
19. T. E. Meyer and M. D. Kamen, *Adv. Protein Chem.* **35** (1982), 105-212.
20. G. R. Moore and G. W. Pettigrew, *Cytochromes c*, Springer-Verlag, 1984.
21. R. E. Dickerson, *Sci. Amer.* **242** (1980), 137-153.
22. F. S. Mathews, *Prog. Biophys. Mol. Biol.* **45** (1985), 1-56.
23. R. P. Ambler, in A. B. Robinson and N. D. Kaplan, eds., *From Cyclotrons to Cytochromes*, Academic Press, 1980, pp. 263-279.
24. K. Kimura *et al.*, *J. Chem. Phys.* **70** (1979), 3317-3323.
25. D. Keilin, *Proc. Roy. Soc. (London)* **898** (1925), 312-339.
26. Y. Hatefi, *Annu. Rev. Biochem.* **54** (1985), 1015-1069.
27. B. P. S. N. Dixit and J. M. Vanderkooi, *Curr. Top. Bioenergetics* **13** (1984), 159-202.
28. C. W. Jones, *Biological Energy Conservation*, Chapman and Hall, 2d ed., 1981.
29. C. R. Hackenbrock, *Trends Biochem. Sci.* **6** (1981), 151-154.
30. S. Gupte *et al.*, *Proc. Natl. Acad. Sci. USA* **81** (1984), 2606-2610.
31. R. K. Clayton, *Photosynthesis: Physical Mechanisms and Chemical Patterns*, Cambridge Univ. Press, 1980.
32. F. K. Fong, ed., *Light Reaction Path of Photosynthesis*, Springer-Verlag, 1982.
33. R. K. Clayton and W. R. Sistrom, eds., *The Photosynthetic Bacteria*, Plenum, 1978.
34. *Photosynthesis, Vol. I: Energy Conversion by Plants and Bacteria*, Academic Press, 1982.
35. B. W. Matthews and R. E. Fenna, *Acc. Chem. Res.* **13** (1980), 309-317.
36. J. Deisenhofer *et al.*, *J. Mol. Biol.* **180** (1984), 385-398.
37. R. Hille and V. Massey, in T. G. Spiro, ed., *Molybdenum Enzymes*, Wiley, 1985, pp. 443-518.
38. R. Hille, W. R. Hagen, and W. R. Dunham, *J. Biol. Chem.* **260** (1985), 10569-10575.
39. A. Bhattacharyya *et al.*, *Biochemistry* **22** (1983), 5270-5279.
40. J. Stubbe, *Adv. Enzymology* **63** (1990), 349-419.
41. P. Nordlund, B.-M. Sjöberg, and H. Eklund, *Nature* **345** (1990), 593-598.
42. R. E. White and M. J. Coon, *Annu. Rev. Biochem.* **49** (1980), 315-356.
43. S. G. Sligar and R. I. Murray, in P. R. Ortiz de Montellano, ed., *Cytochrome P-450: Structure, Mechanism, and Biochemistry*, Plenum, 1986, pp. 429-503.
44. C. B. Brewer and J. A. Peterson, *J. Biol. Chem.* **263** (1988), 791-798.
45. F. A. Annstrong, H. A. O. Hill, and N. J. Walton, *Quart. Rev. Biophys.* **18** (1986), 261-322.
46. G. D. Hitchens, *Trends Biochem. Sci.* **14** (1989), 152-155.
47. F. A. Annstrong, *Structure and Bonding* **72** (1989), 137-221; A. Heller, *J. Phys. Chem.* **96** (1992), 3579-3587.
48. H. A. O. Hill *et al.*, *J. Chem. Soc. Chem. Commun.* (1985), 1469-1471.
49. H. Taube, *Angew. Chem. Int. Ed. Engl.* **23** (1984), 329-334.
50. R. D. Cannon, *Electron-Transfer Reactions*, Butterworths, 1980.
51. *Prog. Inorg. Chem.* **30** (1983).
52. S. L. Mayo *et al.*, *Science* **233** (1986), 948-952.
53. A. G. Sykes, *Chem. Brit.* **24** (1988), 551-554.
54. M. Faraggi, M. R. De Felippis, and M. H. Klapper, *J. Am. Chem. Soc.* **111** (1989), 5141-5145.
55. G. McLendon, *Acc. Chem. Res.* **21** (1988), 160-167.
56. O. Farver and I. Pecht, *Proc. Natl. Acad. Sci. USA* **86** (1989), 6968-6972.

57. S. E. Peterson-Kennedy *et al.*, *Coord. Chem. Rev.* **64** (1985), 125-133.
58. D. E. Richardson, *Comments Inorg. Chem.* **3** (1985), 367-384.
59. S. Dahlin, B. Reinhammar, and M. T. Wilson, *Biochem. J.* **218** (1984), 609-614.
60. R. A. Marcus, *Annu. Rev. Phys. Chem.* **15** (1964), 155-196.
61. W. L. Reynolds and R. W. Lumry, *Mechanisms of Electron Transfer*, Ronald Press, 1966.
62. J. Ulstrup, *Charge Transfer Process in Condensed Media*, Springer-Verlag, 1979.
63. N. Sutin, *Acc. Chem. Res.* **15** (1982), 275-282.
64. M. D. Newton and N. Sutin, *Annu. Rev. Phys. Chem.* **35** (1984), 437-480.
65. P. Bertrand, *Biochimie* **68** (1986), 619-628.
66. J. V. McArdle *et al.*, *J. Am. Chem. Soc.* **99** (1977), 2483-2489.
67. S. Wherland *et al.*, *J. Am. Chem. Soc.* **97** (1975), 5260-5262.
68. A. G. Mauk, R. A. Scott, and H. B. Gray, *J. Am. Chem. Soc.* **102** (1980), 4360-4363.
69. S. Wherland and I. Pecht, *Biochemistry* **17** (1978), 2585-2591.
70. B. S. Brunschwig and N. Sutin, *Comments Inorg. Chem.* **6** (1987), 209-235.
71. N. Sutin, in J. J. Zuckerman, ed., *Inorganic Reactions and Methods*, VCH Publishers, 1986, **XV**, 23- 24.
72. R. A. Marcus and N. Sutin, *Biochim. Biophys. Acta* **811** (1985), 265-322.
73. J. R. Winkler and H. B. Gray, *Chem. Rev.* **92** (1992), 369-379.
74. H. B. Gray and J. R. Winkler, *Pure Appl. Chem.* **64** (1992), 1257-1262.
75. J. Jortner and M. Bixon, *J. Chem. Phys.* **88** (1988), 167-170.
76. J. J. Hopfield, *Proc. Natl. Acad. Sci. USA* **71** (1974), 3640-3644.
77. G. L. Closs and J. R. Miller, *Science* **240** (1988), 440-447.
78. H. Oevering *et al.*, *J. Am. Chem. Soc.* **109** (1987), 3258-3269.
79. C. C. Moser *et al.*, *Nature* **355** (1992), 796-802.
80. C. C. Moser and P. L. Dutton, *Biochim. Biophys. Acta* **1101** (1992), 171-176.
81. H. E. M. Christensen *et al.*, *Inorg. Chem.* **29** (1990), 2808-2816.
82. M. A. Ratner, *J. Phys. Chem.* **94** (1990), 4877-4883.
83. S. Larsson, *Chem. Scripta* **28A** (1988), 15-20.
84. D. N. Beratan and J. N. Onuchic, *Photosynthesis Res.* **22** (1989), 173-186.
85. D. N. Beratan *et al.*, *J. Am. Chem. Soc.* **112** (1990), 7915-7921.
86. J. N. Onuchic *et al.*, *Annu. Rev. Biophys. Biomol. Struct.* **21** (1992), 349-377.
87. A. G. Sykes, *Chem. Soc. Rev.* **14** (1985), 283-315.
88. H. C. Freeman, in J. L. Laurent, ed., *Coordination Chemistry-21*, Pergamon Press, 1981, pp. 29-51.
89. D. Boulter *et al.*, in D. H. Northcote, ed., *Plant Biochemistry*, Univ. Park Press, 1977, **II**, 1-40.
90. J. M. Guss *et al.*, *J. Mol. Biol.* **192** (1986), 361-387.
91. J. McGinnis *et al.*, *Inorg. Chem.* **27** (1988), 2306-2312.
92. O. Farver and I. Pecht, *Proc. Natl. Acad. Sci. USA* **78** (1981), 4190-4193.
93. O. Farver, Y. Shahak, and I. Pecht, *Biochemistry* **21** (1982), 1885-1890.
94. B. S. Brunschwig *et al.*, *Inorg. Chem.* **24** (1985), 3743-3749.
95. S. K. Chapman *et al.*, in M. Chisholm, ed., *Inorganic Chemistry: Toward the Twenty-first Century*, American Chemical Society, 1983, pp. 177-197.
96. H. B. Gray, *Chem. Soc. Rev.* **15** (1986), 17-30.
97. D. W. Conrad and R. A. Scott, *J. Am. Chem. Soc.* **111** (1989), 3461-3463.
98. L. P. Pan *et al.*, *Biochemistry* **27** (1988), 7180-7184.
99. C. M. Lieber, J. L. Karas, and H. B. Gray, *J. Am. Chem. Soc.* **109** (1987), 3778-3779.
100. J. L. Karas, C. M. Lieber, and H. B. Gray, *J. Am. Chem. Soc.* **110** (1988), 599-600.
101. J. A. Cowan *et al.*, *Ann. N.Y. Acad. Sci.* **550** (1988), 68-84.
102. T. Takano, *J. Mol. Biol.* **110** (1977), 537-568 and 559-584.
103. K. Tsukahara, *J. Am. Chem. Soc.* **111** (1989), 2040-2044.
104. E. T. Kaiser and D. S. Lawrence, *Science* **226** (1984), 505-511.
105. R. E. Offord, *Protein Eng.* **1** (1987), 151-157.

106. E. T. Kaiser, *Angew. Chem. Int. Ed. Engl.* **27** (1988), 913-922.
107. T. Kokubo, S. Sassa, and E. T. Kaiser, *J. Am. Chem. Soc.* **109** (1987), 606-607; J. Kuriyan *et al.*, *J. Am. Chem. Soc.* **110** (1988), 6261-6263.
108. C. Chothia and J. Janin, *Nature* **256** (1975), 705-708.
109. A. G. Amit *et al.*, *Science* **233** (1986), 747-753.
110. H. M. Geysen *et al.*, *Science* **235** (1987), 1184-1190.
111. F. R. Salemme, *J. Mol. Biol.* **102** (1976), 563-568.
112. J. J. Wendoloski *et al.*, *Science* **238** (1987), 794-797.
113. G. L. McLendon *et al.*, *J. Am. Chem. Soc.* **107** (1985), 739-740.
114. M. R. Mauk, L. S. Reid, and A. G. Mauk, *Biochemistry* **21** (1982),1843-1846.
115. J. A. Komblatt *et al.*, *J. Am. Chem. Soc.* **110** (1988), 5909-5911.
116. S. Ng *et al.*, *Biochemistry* **16** (1977), 4975-4978.
117. M. R. Mauk *et al.*, *Biochemistry* **25** (1986), 7085-7091.
118. P. W. Holloway and H. H. Mantsch, *Biochemistry* **27** (1988), 7991-7993.
119. A. M. Burch *et al.*, *Science* **247** (1990), 831-833; K. K. Rodgers and S. G. Sligar, *J. Mol. Biol.* **221** (1991), 1453-1460.
120. J. Stonehuemer, J. B. Williams, and F. Millett, *Biochemistry* **18** (1979), 5422-5427; L. D. Eltis *et al.*, *Biochemistry* **30** (1991), 3663-3674.
121. K. T. Conklin and G. McLendon, *Inorg. Chem.* **25** (1986), 4806-4807.
122. N. Liang *et al.*, *Science* **240** (1988) 311-313.
123. J. L. McGourty *et al.*, *Biochemistry* **26** (1987), 8302-8312.
124. S. E. Peterson-Kennedy *et al.*, *J. Am. Chem. Soc.* **108** (1986), 1739-1746.
125. D. J. Gingrich *et al.*, *J. Am. Chem. Soc.* **109** (1987), 7533-7534.
126. J. Jortner, *J. Chem. Phys.* **64** (1976), 4860-4867.
127. P. Siders and R. A. Marcus, *J. Am. Chem. Soc.* **103** (1981), 741-747.
128. F. R. Salemme, *Annu. Rev. Biochem.* **46** (1977), 299-329.
129. S. Ferguson-Miller, D. L. Brautigan, and E. Margoliash, in D. Dolphin, ed., *The Porphyrins*, Academic Press, 1979, **VII**, 149-240.
130. R. Timkovich, in Reference 129, pp. 241-294.
131. G. Williams, G. R. Moore, and R. J. P. Williams, *Comments Inorg. Chem*. **4** (1985), 55-98.
132. G. R. Moore, C. G. S. Eley, and G. Williams, *Adv. Inorg. and Bioinorg. Mech.* **3** (1984), 1-96.
133. E. Margoliash and H. R. Bosshard, *Trends Biochem. Sci.* **8** (1983), 316-320.
134. T. Takano and R. E. Dickerson, *J. Mol. Biol.* **153** (1981), 79-94 and 95-115.
135. G. Williams *et al.*, *J. Mol. Biol.* **183** (1985), 447-460.
136. Y. Feng, H. Roder, and S. W. Englander, *Biochemistry* **29** (1990), 3494-3504.
137. Y. Feng and S. W. Englander, *Biochemistry* **29** (1990), 3505-3509.
138. F. K. Rodkey and E. G. Ball, *J. Biol. Chem.* **182** (1950), 17-20.
139. J. B. Wooten *et al.*, *Biochemistry* **20** (1981), 5394-5402.
140. G. R. Moore and R. J. P. Williams, *Eur. J. Biochem.* **103** (1980), 513-521.
141. I. Pecht and M. Faraggi, *Proc. Natl. Acad. Sci. USA* **69** (1972), 902-906.
142. R. J. Kassner, *Proc. Natl. Acad. Sci. USA* **69** (1972), 2263-2267.
143. A. K. Churg and A. Warshel, *Biochemistry* **25** (1986), 1675-1681.
144. A. L. Raphael and H. B. Gray, *Proteins* **6** (1989), 338-340.
145. C. J. A. Wallace *et al.*, *J. Biol. Chem.* **264** (1989), 15199-15209.
146. H. A. Harbury *et al.*, *Proc. Natl. Acad. Sci. USA* **54** (1965), 1658-1664.
147. T. N. Sorrell, P. K. Martin, and E. F. Bowden, *J. Am. Chem. Soc.* **111** (1989), 766-767.
148. R. L. Cutler *et al.*, *Biochemistry* **28** (1989), 3188-3197.
149. A. L. Raphael and H. B. Gray, *J. Am. Chem. Soc.* **113** (1991), 1038-1040.
150. J. Butler *et al.*, *J. Am. Chem. Soc.* **103** (1981), 469-471.
151. G. D. Armstrong *et al.*, *Biochemistry* **25** (1986), 6947-6951.
152. W. H. Koppenol and E. Margoliash, *J. Biol. Chem.* **257** (1982), 4426-4437.

153. P. Nicholls, *Biochim. Biophys. Acta* **346** (1974), 261-310.
154. P. C. Weber and G. Tollin, *J. Biol. Chem.* **260** (1985), 5568-5573.
155. (a) T. L. Poulos and J. Kraut, *J. Biol. Chem.* **255** (1980), 10322-10330; (b) H. Pelletier and J. Kraut, *Science* **258** (1992), 1748-1755; D. N. Beratan *et al.*, *Science* **258** (1992), 1740-1741.
156. S. H. Northrup *et al.*, *J. Am. Chem. Soc.* **108** (1986), 8162-8170.
157. B. W. König *et al.*, *FEBS Lett.* **111** (1980), 395-398.
158. K. S. Schmitz and J. M. Schurr, *J. Phys. Chem.* **76** (1972), 534-545.
159. B. Michel *et al.*, *Biochemistry* **28** (1989), 456-462.
160. A. K. Churg *et al.*, *J. Phys. Chem.* **87** (1983), 1683-1694.
161. I.-J. Chang, H. B. Gray, and J. R. Winkler, *J. Am. Chem. Soc.* **113** (1991), 7056-7057.
162. D. S. Wuttke *et al.*, *Science* **256** (1992), 1007-1009.
163. D. S. Wuttke *et aI.*, *Biochim. Biophys. Acta* **1101** (1992), 168-170.
164. A. Kuki, *Structure and Bonding* **75** (1991), 49-83.
165. P. Siddarth and R. A. Marcus, *J. Phys. Chem.* **94** (1990), 8430-8434; **96** (1992), 3213-3217.
166. A. Brao and S. Larsson, *J. Phys. Chem.* **95** (1991), 4925-4928.
167. C. Liang and M. D. Newton, *J. Phys. Chem.* **96** (1992), 2855-2866.
168. H. Sigel and A. Sigel, eds., *Metal Ions in Biological Systems*, Dekker, 1991, vol 27.
169. D. N. Beratan, J. N. Betts, and J. N. Onuchic, *J. Phys. Chem.* **96** (1992), 2852-2855; *Science* **252** (1991), 1285-1288.
170. J. N. Betts, D. N. Beratan, and J. N. Onuchic, *J. Am. Chem. Soc.* **114** (1992), 4043-4046.
171. J. R. Norris and M. Schiffer, *Chem. Eng. News* **68** (July 30, 1990), 22-35.
172. G. Feher *et al.*, *Nature* **339** (1989), 111-116.
173. J. Deisenhofer and H. Michel, *Annu. Rev. Biophys. Biophys. Chem* **20** (1991), 247-266.
174. S. Kartha, R. Das, and J. R. Norris, *Metal Ions Biol. Syst.* **27** (1991), 323-359.
175. M. R. Wasielewski, *Metal Ions BioI. Syst.* **27** (1991), 361-430.
176. S. G. Boxer, *Annu. Rev. Biophys. Biophys. Chem.* **19** (1990), 267-299.
177. J. P. Allen *et al.*, *Proc. Natl. Acad. Sci. USA* **84** (1987), 5730-5734 and 6162-6166.
178. T. O. Yeates *et al.*, *Proc. Natl. Acad. Sci. USA* **84** (1987), 6438-6442.
179. R. J. Debus, G. Feher, and M. Y. Okamura, *Biochemistry* **25** (1986), 2276-2287.
180. S. G. Boxer *et aI.*, *J. Phys. Chem.* **93** (1989), 8280-8294.
181. C.-K. Chan *et al.*, *Proc. Natl. Acad. Sci. USA* **88** (1991), 11202-11206.
182. M. Nonella and K. Schulten, *J. Phys. Chem.* **95** (1991), 2059-2067.
183. K. Schulten and M. Tesch, *Chem. Phys.* **158** (1991), 421-446.
184. The authors thank Deborah Wuttke for invaluable assistance with the preparation of the final draft of the manuscript and for many helpful discussions. We acknowledge the National Science Foundation, the National Institutes of Health, and the Arnold and Mabel Beckman Foundation for support of our work on biological electron-transfer reactions.

Contributors and Attributions

- Harry B. Gray (California Institute of Technology, Beckman Institute)
- Walther R. Ellis, Jr. (University of Utah, Department of Chemistry)

11.2.6: Electron Transfer is shared under a CC BY-NC-SA 4.0 license and was authored, remixed, and/or curated by LibreTexts.

11.2.6.1: Biological Redox Components

Three types of oxidation-reduction (redox) centers are found in biology: protein side chains, small molecules, and redox cofactors. The first class is frequently overlooked by mechanistic enzymologists. The sulfhydryl group of cysteine is easily oxidized to produce a dimer, known as cystine:

$$2R-SH \xrightarrow[-2H^+]{-2e^-} R-S-S-R \tag{6.1}$$

This type of interconversion is known to occur in several redox proteins, including xanthine oxidase, mercuric ion reductase, and thioredoxin. Other enzyme systems display spectral evidence pointing to the presence of a protein-based radical in at least one intermediate. EPR spectroscopy provides a powerful tool in studying such systems; the observation of a g = 2.0 signal that cannot be attributed to impurities or an organic redox cofactor is generally taken to be evidence for a protein-based radical. Radicals localized on tyrosine (e.g., in photosystem II and the B2 subunit of ribonucleotide reductase[1]) and tryptophan (e.g., in yeast cytochrome c peroxidase[2]) have been unambiguously identified using EPR techniques together with protein samples containing isotopically labeled amino acids (e.g., perdeuterated Tyr) or single amino-acid mutations (e.g., Trp → Phe).

A variety of small molecules, both organic and inorganic, can function as redox reagents in biological systems. Of these, only the nicotinamide and quinone coenzymes are found throughout the biosphere. Nicotinamide adenine dinucleotide (NAD) and nicotinamide adenine dinucleotide phosphate (NADP) participate in a wide variety of biological redox reactions. The 4-position of the pyridine ring is the reactive portion of both molecules (Figure 6.1). Both typically function as 2-electron redox reagents.

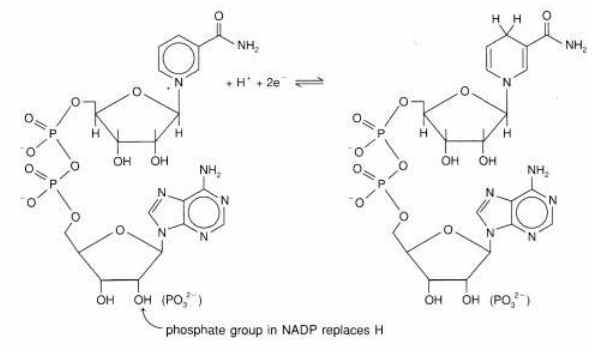


Figure 6.1 - Reduction of NAD^+ to NADH.

In contrast, quinones may function as either 1- or 2-electron carriers:

$$Q \overset{e^-,H^+}{\rightleftharpoons} QH\cdot \overset{e^-,H^+}{\rightleftharpoons} QH_2 \tag{6.2}$$

Free-radical semiquinone (QH•) intermediates have been detected by EPR spectroscopy in some electron transfers. Coenzyme Q, also called ubiquinone because it occurs in virtually all cells, contains a long isoprenoid tail that enables it to diffuse through membranes rapidly. This quinone derivative, which occurs in both free and protein-bound forms, is called ubiquinol when reduced (Figure 6.2). Other types of quinones are less frequently found in cells.

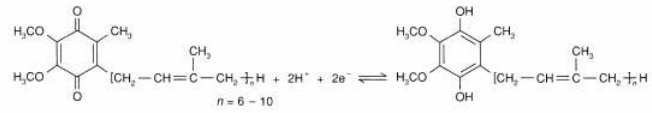


Figure 6.2 - Reduction of coenzyme Q (ubiquinone) to ubiquinol.

Metalloproteins containing a single type of redox cofactor can be divided into two general classes: electron carriers and proteins involved in the transport or activation of small molecules. Adman[3] has identified some of the factors that seem to be characteristic of electron-transfer proteins (these proteins are sometimes called "electron transferases"): (a) possession of a suitable cofactor to act as an electron sink; (b) placement of the cofactor close enough to the protein surface to allow electrons to move in and out; (c) existence of a hydrophobic shell adjacent to, but not always entirely surrounding, the cofactor; (d) small structural changes accompanying electron transfer; and (e) an architecture that permits slight expansion or contraction in preferred directions upon electron transfer.

Proteins that function as electron transferases typically place their prosthetic groups in a hydrophobic environment and may provide hydrogen bonds (in addition to ligands) to assist in stabilizing both the oxidized and the reduced forms of the cofactor. Metal-ligand bonds remain intact upon electron transfer to minimize inner-sphere reorganization[4] (discussed in Section III). Many of the complex multisite metalloenzymes (e.g., cytochrome c oxidase, xanthine oxidase, the nitrogenase FeMo protein) contain redox centers that function as intramolecular electron transferases, shuttling electrons to/from other metal centers that bind exogenous ligands during enzymatic turnover.

There are four classes[3,5] of electron transferases, each of which contains many members that exhibit important structural differences: flavodoxins, blue copper proteins, iron-sulfur proteins, and cytochromes.

The flavodoxins[6] are atypical in that they contain an organic redox cofactor, flavin mononucleotide (FMN; see Figure 6.3). These proteins have molecular weights in the 8-13 kDa range, and are found in many species of bacteria and algae. The FMN cofactor is found at one end of the protein, near the molecular surface, but only the dimethylbenzene portion of FMN is significantly exposed to the solvent (Figure 6.4). FMN can act as either a 1- or a 2-electron redox center. In solution, the semiquinone form of free FMN is unstable, and disproportionates to the quinone (oxidized) and hydroquinone (reduced) forms. Hence, free FMN functions in effect as a 2-electron reagent. FMN in flavodoxins, on the other hand, can function as a single-electron carrier. This is easily discerned by comparing reduction potentials for free and protein-bound FMN (Table 6.1). Clearly, the protein medium is responsible for this drastic alteration in oxidation-state stability. From an NMR study[7] of the *M. elsdenii* flavodoxin quinone/semiquinone and semiquinone/hydroquinone electron self-exchange rates, it was concluded that the latter is approximately 300 times faster than the former, in keeping with the view that the physiologically relevant redox couple is semiquinone/hydroquinone.

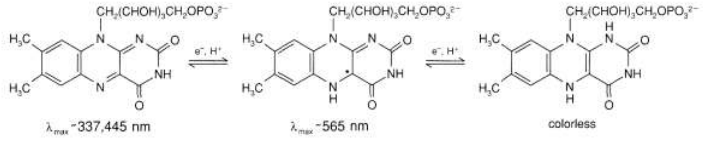


Figure 6.3 - Reduction of FMN.

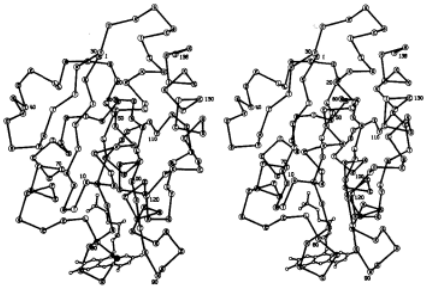


Figure kindly provided by M. L. Ludwig.

Table 6.1 - Reduction potentials of FMN couples.

Abbreviations: Q, quinone; SQ, semiquinone; HQ, hydroquinone.

	E°Q/SQ	E°SQ/HQ
Free FMN	-238 mV	-172 mV
C.M.P. flavodoxin	-92 mV	-399 mV

The blue copper proteins are characterized by intense S(Cys) → Cu chargetransfer absorption near 600 nm, an axial EPR spectrum displaying an unusually small hyperfine coupling constant, and a relatively high reduction potential.[4,8-10] With few exceptions (e.g., photosynthetic organisms), their precise roles in bacterial and plant physiology remain obscure. X-ray structures of several blue copper proteins indicate that the geometry of the copper site is approximately trigonal planar, as illustrated by the *Alcaligenes denitrificans* azurin structure (Figure 6.5).[11,12] In all these proteins, three ligands (one Cys, two His) bind tightly to the copper in a trigonal arrangement. Differences in interactions between the copper center and the axially disposed ligands may significantly

contribute to variations in reduction potential that are observed[12] for the blue copper electron transferases. For example, E°' = 276 mV for *A. denitrificans* azurin, whereas that of *P. vulgaris* plastocyanin is 360 mV. In *A. denitrificans* azurin, the Cu-S(Met) bond is 0.2 Å longer than in poplar plastocyanin, and there is a carbonyl oxygen 3.1 Å from the copper center, compared with 3.8 Å in plastocyanin. These differences in bond lengths are expected to stabilize Cu^{II} in azurin to a greater extent than in plastocyanin, and result in a lower E°' value for azurin.

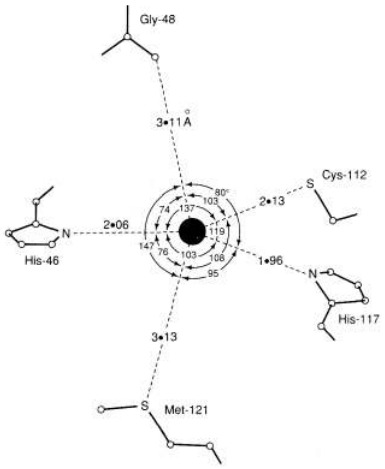


Figure 6.5 - Structure of the blue copper center in azurin.[11]

The iron-sulfur proteins play important roles[13,14] as electron carriers in virtually all living organisms, and participate in plant photosynthesis, nitrogen fixation, steroid metabolism, and oxidative phosphorylation, as well as many other processes (Chapter 7). The optical spectra of all iron-sulfur proteins are very broad and almost featureless, due to numerous overlapping charge-transfer transitions that impart red-brown-black colors to these proteins. On the other hand, the EPR spectra of iron-sulfur clusters are quite distinctive, and they are of great value in the study of the redox chemistry of these proteins.

The simplest iron-sulfur proteins, known as rubredoxins, are primarily found in anaerobic bacteria, where their function is unknown. Rubredoxins are small proteins (6 kDa) and contain iron ligated to four Cys sulfurs in a distorted tetrahedral arrangement. The E°' value for the $Fe^{III/II}$ couple in water is 770 mV; that of *C. pasteurianum* rubredoxin is -57 mV. The reduction potentials of iron-sulfur proteins are typically quite negative, indicating a stabilization of the oxidized form of the redox couple as a result of negatively charged sulfur ligands.

The [2Fe-2S] ferredoxins (10-20 kDa) are found in plant chloroplasts and mammalian tissue. The structure of *Spirulina platensis* ferredoxin[15] confirmed earlier suggestions, based on EPR and Mössbauer studies, that the iron atoms are present in a spin-coupled [2Fe-2S] cluster structure. One-electron reduction (E°' ~ -420 mV) of the protein results in a mixed-valence dimer (Equation 6.3):

$$[Fe_2S_2(SR)_4]^{2-} \underset{-e^-}{\overset{+e^-}{\rightleftharpoons}} [Fe_2S_2(SR)_4]^{3-} \tag{6.3}$$

$$Fd_{ox} \qquad Fd_{red} \tag{11.2.6.1.1}$$

$$2Fe(III) \qquad Fe(II) + Fe(III) \tag{11.2.6.1.2}$$

The additional electron in Fd_{red} is associated with only one of the iron sites, resulting in a so-called trapped-valence structure.[16] The $[Fe_2S_2(SR)_4]^{4-}$ cluster oxidation state, containing two ferrous ions, can be produced *in vitro* when strong reductants are used.

Four-iron clusters [4Fe-4S] are found in many strains of bacteria. In most of these bacterial iron-sulfur proteins, also termed ferredoxins, two such clusters are present in the protein. These proteins have reduction potentials in the -400 mV range and are rather small (6-10 kDa). Each of the clusters contains four iron centers and four sulfides at alternate comers of a distorted cube. Each iron is coordinated to three sulfides and one cysteine thiolate. The irons are strongly exchange-coupled, and the [4Fe-4S] cluster in bacterial ferredoxins is paramagnetic when reduced by one electron. The so-called "high-potential ironsulfur proteins" (HiPIPs) are found in photosynthetic bacteria, and exhibit anomalously high (~350 mV) reduction potentials. The *C. vinosum* HiPIP (10 kDa) structure demonstrates that HiPIPs are distinct from the [4Fe-4S] ferredoxins, and that the reduced HiPIP cluster

structure is significantly distorted, as is also observed for the structure of the oxidized *P. aerogenes* ferredoxin. In addition, oxidized HiPIP is paramagnetic, whereas the reduced protein is EPR-silent.

This bewildering set of experimental observations can be rationalized in terms of a "three-state" hypothesis (i.e., $[4Fe\text{-}4S(SR)_4]^{n-}$ clusters exist in three physiological oxidation states).[17] This hypothesis nicely explains the differences in magnetic behavior and redox properties observed for these iron-sulfur proteins (Equation 6.4):

$$[4Fe-4S(SR)_4]^{-} \underset{-e^-}{\overset{+e^-}{\rightleftharpoons}} [4Fe-4S(SR)_4]^{2-} \underset{-e^-}{\overset{+e^-}{\rightleftharpoons}} [4Fe-4S(SR)_4]^{3-} \quad (6.4)$$

$$HiPIP_{ox} \qquad HiPIP_{red} \qquad Ferredoxin_{red} \quad (11.2.6.1.3)$$

$$Ferredoxing_{ox} \quad (11.2.6.1.4)$$

The bacterial ferredoxins and HiPIPs all possess tetracubane clusters containing thiolate ligands, yet the former utilize the -2/-3 cluster redox couple, whereas the latter utilize the -1/-2 cluster redox couple.

The protein environment thus exerts a powerful influence over the cluster reduction potentials. This observation applies to *all* classes of electron transferases—the factors that are critical determinants of cofactor reduction potentials are poorly understood at present but are thought[18] to include the low dielectric constants of protein interiors (~4 for proteins vs. ~78 for H_2O), electrostatic effects due to nearby charged amino-acid residues, hydrogen bonding, and geometric constraints imposed by the protein.

As a class, the cytochromes[19-22] are the most thoroughly characterized of the electron transferases. By definition, a cytochrome contains one or more heme cofactors. These proteins were among the first to be identified in cellular extracts because of their distinctive optical properties, particularly an intense absorption in the 410-430 nm region (called the Soret band). Cytochromes are typically classified on the basis of heme type. Figure 6.6 displays the three most commonly encountered types of heme: heme a possesses a long phytyl "tail" and is found in cytochrome c oxidase; heme b is found in b-type cytochromes and globins; heme c is covalently bound to c-type cytochromes via two thioether linkages. Cytochrome nomenclature presents a real challenge! Some cytochromes are designated according to the historical order of discovery, e.g., cytochrome c_2 in bacterial photosynthesis. Others are designated according to the λ_{max} of the α band in the absorption spectrum of the reduced protein (e.g., cytochrome c_{551}).

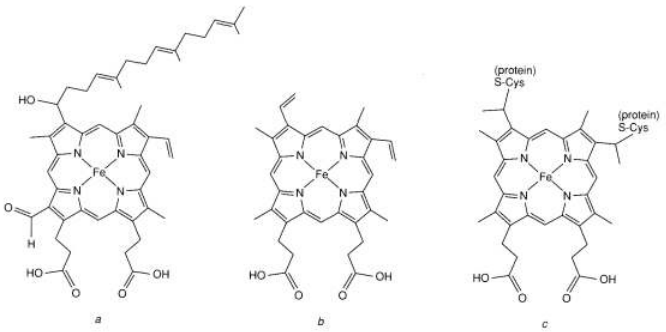


Figure 6.6 - Structures of hemes a, b, and c.

Cytochromes c are widespread in nature. Ambler[23] divided these electron carriers into three classes on structural grounds. The Class I cytochromes c contain axial His and Met ligands, with the heme located near the N-terrninus of the protein. These proteins are globular, as indicated by the ribbon drawing of tuna cytochrome c (Figure 6.7). X-ray structures of Class I cytochromes c from a variety of eukaryotes and prokaryotes clearly show an evolutionarily conserved "cytochrome fold," with the edge of the heme solvent-exposed. The reduction potentials of these cytochromes are quite positive (200 to 320 mV). Mammalian cytochrome c, because of its distinctive role in the mitochondrial electron-transfer chain, will be discussed later.

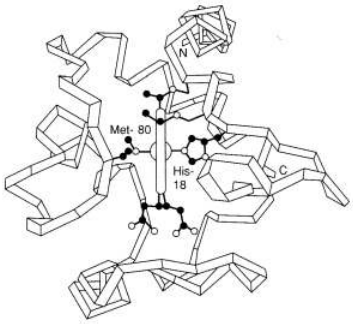


Figure 6. - Structure of tuna cytochrome c.

Class II cytochromes c ($E°' \sim -100$ mV) are found in photosynthetic bacteria, where they serve an unknown function. Unlike their Class I cousins, these c-type cytochromes are high-spin: the iron is five-coordinate, with an axial His ligand. These proteins, generally referred to as cytochromes c' , are four-α-helix bundles (Figure 6.8). The vacant axial coordination site is buried in the protein interior.

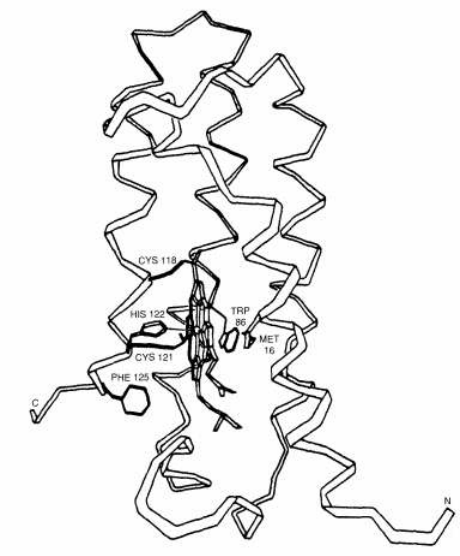


Figure 6.8 - Structure of cytochrome c'.

Finally, Class III cytochromes c, also called cytochromes c_3, contain four hemes, each ligated by two axial histidines. These proteins are found in a restricted class of sulfate-reducing bacteria and may be associated with the cytoplasmic membrane. The low molecular weights of cytochromes c_3 (~14. 7 kDa) require that the four hemes be much more exposed to the solvent than the hemes of other cytochromes (see Figure 6.9), which may be in part responsible for their unusually negative (-200 to -350 mV) reduction potentials. These proteins possess many aromatic residues and short heme-heme distances, two properties that could be responsible for their anomalously large solid-state electrical conductivity.[24]

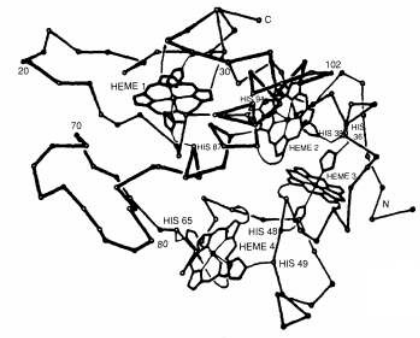


Figure 6.9 - Structure of cytochrome c_3.

11.2.6.1: Biological Redox Components is shared under a CC BY-NC-SA 4.0 license and was authored, remixed, and/or curated by LibreTexts.

11.2.6.2: Coupling Electron Transfers and Substrate Activation

Electron transfers are key steps in many enzymatic reactions involving the oxidation or reduction of a bound substrate. Relevant examples include cytochrome c oxidase ($O_2 \rightarrow 2H_2O$) and nitrogenase ($N_2 \rightarrow 2NH_3$). To reinforce the claim that electron-transfer steps are of widespread importance, several other redox systems, representative of diverse metabolic processes, will be mentioned here.

Xanthine oxidase (275 kDa; α_2 dimer) catalyzes the two-electron oxidation[37-39] of xanthine to uric acid (Equation 6.7).

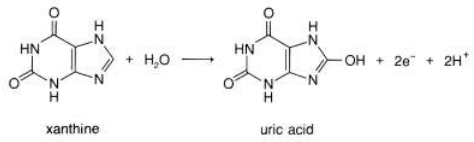


Figure 6.17 displays the cofactors in a subunit: a Mo-pterin, termed MoCo; two [2Fe-2S] centers; and one FAD. The binuclear iron-sulfur sites serve to shuttle electrons between the reduced substrate (XH) and O_2.

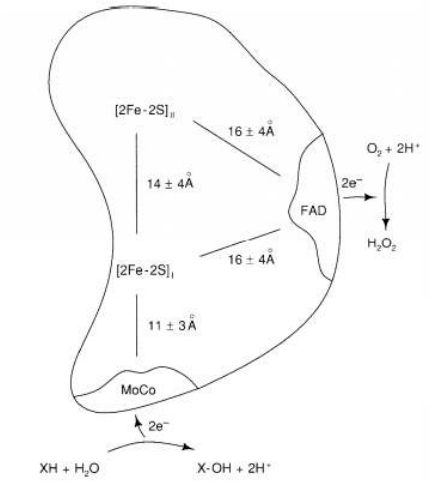
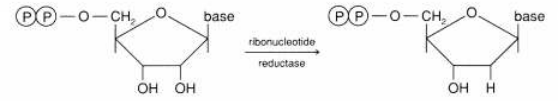


Figure 6.17 - Representation of the cofactors in one subunit of xanthine oxidase.

The first step in the biosynthesis of DNA involves the reduction of ribonucleotides (Equation 6.8) catalyzed by ribonucleotide reductase.[40] The *E. coli* enzyme is an $\alpha_2\beta_2$ tetramer composed of a B1 protein (160 kDa) and a B2 protein (78 kDa). The B1 protein (a dimer) contains redox-active dithiol groups, binding sites for ribonucleotide substrates, and regulatory binding sites for nucleotide diphosphates. Protein B2, also a dimer, possesses a phenolate radical (Tyr-122) that is stabilized by an antiferromagnetically coupled binuclear iron center (Figure 6.18). This radical is essential for enzyme activity, and is ~10 Å from the protein-B1/protein-B2 interface. Hence it cannot directly participate in an H-atom abstraction from the substrate (bound to protein B1). Instead, the x-ray structure of the B2 protein[41] suggests that a long-range electron transfer from the Tyr radical to a residue (perhaps Trp-48) on the B1 protein is operative during enzyme turnover.



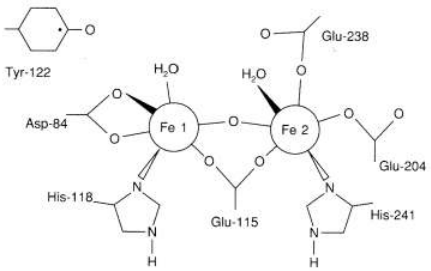
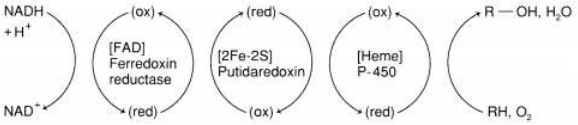


Figure 6.18 - Schematic of the binuclear iron center and Tyr-122 radical in the B2 protein of E. coli ribonucleotide reductase.[41]

Most of the presently known metal-containing mono- and dioxygenases are multicomponent, requiring the involvement of additional proteins (electron transferases) to shuttle electrons from a common biological reductant (usually NADH or NADPH) to the metallooxygenase. Cytochrome P-450, whose substrate oxidation chemistry was discussed in detail in Chapter 5, serves as an excellent example. Figure 5.10 presented a catalytic cycle for cytochrome P-450-dependent hydroxylations[42] that begins with substrate (RH) binding to the ferric enzyme (RH is camphor for *Pseudomonas putida* cytochrome P-450). To hydroxylate the camphor substrate, the monooxygenase must be reduced via the electron-transport chain in Equation (6.9).



The ferredoxin reductase receives two electrons from NADH and passes them on, one at at time, to putidaredoxin, a [2Fe-2S] iron-sulfur protein. Thus, two single-electron-transfer steps from reduced putidaredoxin to cytochrome P-450 are required to complete one enzyme turnover.

The activity of the enzyme appears to be regulated at the first reduction step.[43] In a 1:1 putidaredoxin-cytochrome P-450 complex, the reduction potential of putidaredoxin is -196 mV, but that of cytochrome P-450 is -340 mV in the absence of camphor; reduction of the cytochrome P-450 is thus thermodynamically unfavorable ($k \sim 0.22\ s^{-1}$). Upon binding camphor, the reduction potential of cytochrome P-450 shifts to -173 mV, and the electron-transfer rate in the protein complex accordingly increases to $41\ s^{-1}$. "Costly" reducing equivalents are not wasted, and there are no appreciable amounts of noxious oxygen-reduction products when substrate is not present.

In the third step, molecular oxygen binds to the camphor adduct of ferrous cytochrome P-450. This species, in the presence of reduced putidaredoxin, accepts a second electron, and catalyzes the hydroxylation of the bound camphor substrate. The turnover rate for the entire catalytic cycle is 10-20 s^{-1}, and the second electron-transfer step appears to be rate-determining.[44]

The bulk of the interest in electron-transfer reactions of redox proteins has been directed toward questions dealing with long-range electron transfer and the nature of protein-protein complexes whose structures are optimized for rapid intramolecular electron transfer. Before we undertake a discussion of these issues, it is worth noting that studies of the reactions of redox proteins at electrodes are attracting increasing attention.[45-47] Direct electron transfer between a variety of redox proteins and electrode surfaces has been achieved. Potential applications include the design of substrate-specific biosensors, the development of biofuel cells, and electrochemical syntheses. An interesting application of bioelectrochemical technology is the oxidation of p-cresol to p-hydroxybenzaldehyde (Figure 6.19).[48]

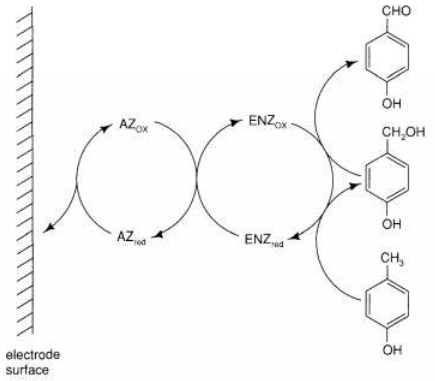


Figure 6.19 - Enzyme-catalyzed electrochemical oxidation of p-cresol to p-hydroxybenzaldehyde. AZ is azurin, and ENZ is p-cresol methylhydroxylase.[48]

11.2.6.2: Coupling Electron Transfers and Substrate Activation is shared under a CC BY-NC-SA 4.0 license and was authored, remixed, and/or curated by LibreTexts.

11.2.6.3: Electron-transfer Rates

Overview

Measurements of the rates of oxidation-reduction reactions began in the late 1940s. A great deal of the early experimental work was carried out by inorganic chemists, and by the 1970s the reactivity patterns of many complexes had been uncovered.[49-51] Chemists studying the mechanisms of metalloprotein electrontransfer reactions frequently seek parallels with the redox behavior of less-complicated inorganic complexes.

In examining biological electron transfers, it is important to remember that metalloproteins are more than just metal ions in disguise. Virtually every property of a protein (excluding its amino-acid sequence) depends on the solution pH. Redox proteins are very large polyelectrolytes whose redox prosthetic groups are typically buried in the protein interior. One important distinction between redox reactions of proteins and redox reactions of small transition-metal complexes is the magnitude of the electron donor-to-acceptor distance. The relevant distance for small molecules, unlike redox proteins, is generally taken to be van der Waals contact. Within the last ten years, it has been convincingly demonstrated that electrons can "tunnel" at significant rates across distances of 15 Å or more in protein interiors.[52-58]

Experimental investigation of the factors that control the rates of biological redox reactions has not come as far as the study of the electron transfers of metal complexes, because many more variables must be dealt with (e.g., asymmetric surface charge, nonspherical shape, uncertain details of structures of proteins complexed with small molecules or other proteins). Many experimental approaches have been pursued, including the covalent attachment of redox reagents to the surfaces of metalloproteins.

Self-exchange and Cross Reactions

The simplest reactions in solution chemistry are electron self-exchange reactions (Equation 6.10), in which the reactants and products are the same (the asterisk is used to identify a specific isotope).

$$ {}^{*}A_{ox} + A_{red} \rightarrow {}^{*}A_{red} + A_{ox} \tag{6.10} $$

The only way to establish chemically that a reaction has taken place is to introduce an isotopic label. There is no change in the free energy ($\Delta G° = 0$) for this type of reaction. As will become evident later on, the reason why these types of reactions are studied is because self-exchange rates and activation parameters are needed to interpret redox reactions in which a net chemical change occurs. The experimental measurement[58] of self-exchange rates is tedious and usually only results in an order-of-magnitude estimate of the rate constant (as inferred from the experimental timescale; see Table 6.2). Most of the protein self-exchange rates reported to date have been measured by NMR line-broadening studies. Other potentially useful methods, such as Mössbauer spectroscopy and EPR, have not been widely used.

Table 6.2 - Experimental timescales in seconds

Laser Flash Photolysis	$\geq 10^{-14}$	(11.2.6.3.1)
Pulse Radiolysis	$\sim 10^{-9}$	(11.2.6.3.2)
Mössbauer Spectroscopy (^{57}Fe)	$10^{-9} - 10^{-6}$	(11.2.6.3.3)
EPR (transition metals)	$10^{-9} - 10^{-8}$	(11.2.6.3.4)
Temperature-jump Spectrometry	$\geq 10^{-8}$	(11.2.6.3.5)
NMR (^{1}H)	$\sim 10^{-5}$	(11.2.6.3.6)
Chemical Mixing	$\geq 10^{-3}$	(11.2.6.3.7)

An elegant example of the measurement of an electron self-exchange rate of a redox protein was reported by Dahlin *et al.*[59] The copper ion of stellacyanin was removed and then replaced with either ^{63}Cu or ^{65}Cu. Oxidized [^{63}Cu] stellacyanin was allowed to react with reduced [^{65}Cu] stellacyanin for various times (10 ms to 7 min) at 20 °C, after which the reaction was quenched by lowering the solution temperature to -120°C using a rapid-freeze apparatus:

$$^{63}Cu^{2+} + {}^{65}Cu^{+} \rightarrow {}^{63}Cu^{+} + {}^{65}Cu^{2+} \tag{6.11}$$

Subtle differences in the EPR spectra (Figure 6.20) of the two isotopic forms of stellacyanin (due to a small difference in the nuclear magnetic moments of the two isotopes) were used to monitor the progress of the reaction, yielding a rate constant of 1.2 x 10^5 $M^{-1}s^{-1}$.

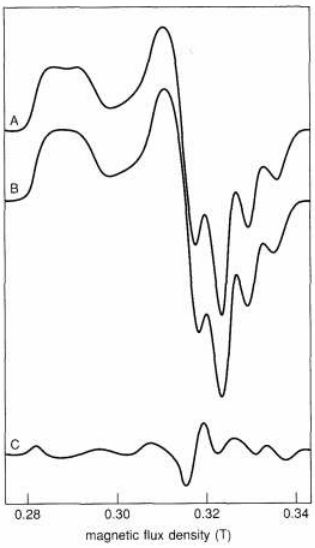


Figure 6.20 - Frozen-solution EPR spectra of stellacyanin (20 K, 9.25 GHz): (A) ^{65}Cu; (B) ^{63}Cu; (C) Difference spectrum (A - B).[59]

Much more common are cross reactions (Equation 6.12), where A_{ox} is the oxidized reactant, B_{red} is the reduced reactant, A_{red} is the reduced product, and B_{ox} is the oxidized product.

$$A_{ox} + B_{red} \rightarrow A_{red} + B_{ox} \tag{6.12}$$

For these reactions, $\Delta G° \neq 0$. The experimental measurement of cross-reaction rates is generally more straightforward than the measurement of self-exchange rates. Either the reactants are simply mixed together, or a thermodynamically unstable system is generated rapidly (via pulse radiolysis, flash photolysis, or temperature-jump relaxation) to initiate the redox reaction. Absorption spectroscopy has almost always been used to monitor the progress of protein cross reactions. The primary goal of theory, as will become evident, is to provide a relationship between $\Delta G°$ and $\Delta G^{‡}$ for cross reactions.

Both self-exchange and cross reactions can be broadly classified as inner-sphere or outer-sphere reactions. In an inner-sphere reaction, a ligand is shared between the oxidant and reductant in the transition state. An outer-sphere reaction, on the other hand, is one in which the inner coordination shells of both the oxidant and the reductant remain intact in the transition state. There is no bond breaking or bond making, and no shared ligands between redox centers. Long-range electron transfers in biology are all of the outer-sphere type.

11.2.6.3: Electron-transfer Rates is shared under a CC BY-NC-SA 4.0 license and was authored, remixed, and/or curated by LibreTexts.

11.2.6.4: Electron-Transfer Theory

The simplest electron transfer occurs in an outer-sphere reaction. The changes in oxidation states of the donor and acceptor centers result in a change in their equilibrium nuclear configurations. This process involves geometric changes, the magnitudes of which vary from system to system. In addition, changes in the interactions of the donor and acceptor with the surrounding solvent molecules will occur. The Franck-Condon principle governs the coupling of the electron transfer to these changes in nuclear geometry: during an electronic transition, the electronic motion is so rapid that the nuclei (including metal ligands and solvent molecules) do not have time to move. Hence, electron transfer occurs at a fixed nuclear configuration. In a self-exchange reaction, the energies of the donor and acceptor orbitals (hence, the bond lengths and bond angles of the donor and acceptor) must be the same before efficient electron transfer can take place.

The incorporation of the Franck-Condon restriction leads to the partitioning[60-65] of an electron-transfer reaction into reactant (precursor complex) and product (successor complex) configurations. The steps in Equations 11.2.6.4.1 to 11.2.6.4.3 go from reactants to products: K is the equilibrium constant for the formation of the precursor complex [A_{ox}, B_{red}], and k_{et} is the forward electron transfer rate to produce the successor complex [A_{red}, B_{ox}].

$$A_{ox} + B_{red} \overset{K}{\rightleftharpoons} [A_{ox},\ B_{red}] \tag{11.2.6.4.1}$$

$$[A_{ox},\ B_{red}] \xrightarrow{k_{et}} [A_{red},\ B_{ox}] \tag{11.2.6.4.2}$$

$$[A_{red},\ B_{ox}] \xrightarrow{fast} A_{red} + B_{ox} \tag{11.2.6.4.3}$$

Marcus pioneered the use of potential energy diagrams as an aid in describing electron-transfer processes.[60] For the sake of simplicity, the donor and acceptor are assumed to behave like collections of harmonic oscillators. Instead of two separate potential energy surfaces being used for the reactants, they are combined into a single surface that describes the potential energy of the precursor complex as a function of its nuclear configuration (i.e., the sum of the translational, rotational, and vibrational degrees of freedom of the reactant molecules and the molecules in the surrounding solvent-3N coordinates, where N is the number of nuclei present). Similarly, a single potential energy (3N-dimensional) surface is used to describe the potential energy of the successor complex as a function of its nuclear configuration. It has become conventional to simplify such potential energy diagrams by using one-dimensional slices through the reactant and product surfaces in order to visualize the progress of a reaction, as illustrated in Figure 6.21.

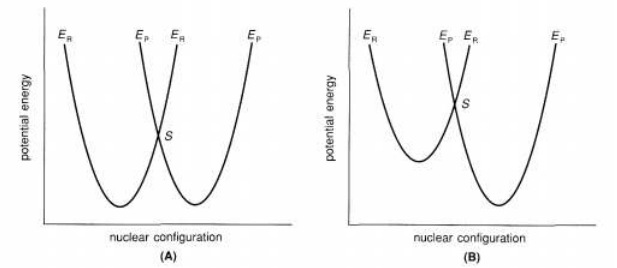


Figure 6.21 - Potential energy diagrams: (A) self-exchange reaction; (B) cross reaction. Point S represents the activated complex. E_R and E_P are the reactant and product surfaces, respectively.

The intersection of the reactant and product surfaces (point S) represents the transition state (or "activated complex"), and is characterized by a loss of one degree of freedom relative to the reactants or products. The actual electron-transfer event occurs when the reactants reach the transition-state geometry. For bimolecular reactions, the reactants must diffuse through the solvent, collide, and form a precursor complex prior to electron transfer. Hence, disentangling the effects of precursor complex formation from the observed reaction rate can pose a serious challenge to the experimentalist; unless this is gone, the factors that determine the kinetic activation barrier for the electron-transfer step cannot be identified with certainty.

The surfaces depicted in Figure 6.21 presume that the electrons remain localized on the donor and acceptor; as long as this situation prevails, no electron transfer is possible. Thus some degree of electronic interaction, or coupling, is required if the redox system is to pass from the precursor to the successor complex. This coupling removes the degeneracy of the reactant and product states at the intersection of their respective zero-order surfaces (points S in Figure 6.21) and leads to a splitting in the region of the intersection

of the reactant and product surfaces (Figure 6.22). If the degree of electronic interaction is sufficiently small, first-order perturbation theory can be used to obtain the energies of the new first-order surfaces, which do not cross. The splitting at the intersection is equal to $2H_{AB}$, where H_{AB} is the electronic-coupling matrix element.

The magnitude of H_{AB} determines the behavior of the reactants once the intersection region is reached. Two cases can be distinguished. First, H_{AB} is very small; for these so-called "nonadiabatic" reactions, there is a high probability that the reactants will "jump" to the upper first-order potential energy surface, leading to very little product formation. If the electronic interaction is sufficiently large, as it is for "adiabatic" reactions, the reactants will remain on the lower first-order potential energy surface upon passage through the transition-state region.

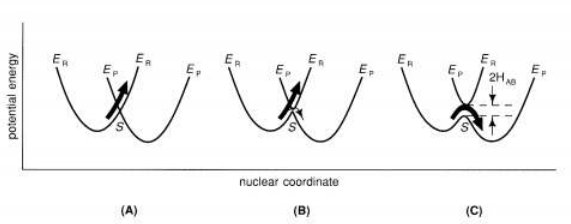


Figure 6.22 - Potential energy diagrams: (A) $H_{AB} = 0$, $\kappa = 0$ (no transfer); (B) H_{AB} small, $\kappa \ll 1$ (nonadiabatic transfer); (C) H_{AB} large, $\kappa = 1$ (adiabatic transfer). The arrows indicate the relative probability of crossing to the product surface (E_R to E_P).

The term adiabatic (Greek: *a-dia-bainein*, not able to go through) is used in both thermodynamics and quantum mechanics, and the uses are analogous. In the former, it indicates that there is no heat flow in or out of the system. In the latter, it indicates that a change occurs such that the system makes no transition to other states. Hence, for an adiabatic reaction, the system remains on the same (i.e., lower) first-order electronic surface for the entire reaction. The probability of electron transfer occurring when the reactants reach the transition state is unity. The degree of adiabaticity of the reaction is given by a transmission coefficient, κ, whose value ranges from zero to one. For systems whose H_{AB} is sufficiently large ($>k_BT$, where k_B is the Boltzmann constant), $\kappa = 1$. This situation occurs when the reacting centers are close together, the orbital symmetries are favorable, and no substantial changes in geometry are involved. The transmission coefficient is generally very small ($\kappa < 1$) for electron-transfer reactions of metalloproteins, owing to the long distances involved.

11.2.6.4: Electron-Transfer Theory is shared under a CC BY-NC-SA 4.0 license and was authored, remixed, and/or curated by LibreTexts.

11.2.6.5: Energy Storage and Release

Electron-transfer reactions play key roles in a great many biological processes, including collagen synthesis, steroid metabolism, the immune response, drug activation, neurotransmitter metabolism, nitrogen fixation, respiration, and photosynthesis. The latter two processes are of fundamental significance-they provide most of the energy that is required for the maintenance of life. From the point of view of global bioenergetics, aerobic respiration and photosynthesis are complementary processes (Figure 6.10). The oxygen that is evolved by photosynthetic organisms is consumed by aerobic microbes and animals. Similarly, the end products of aerobic respiratory metabolism (CO_2 and H_2O) are the major nutritional requirements of photosynthetic organisms. The global C, H, and O cycles are thus largely due to aerobic respiration and photosynthesis.

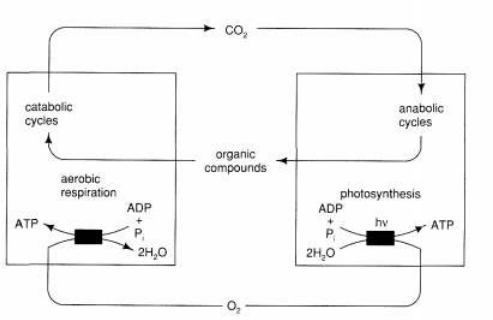


Figure 6.10 - Aerobic respiration and photosynthesis.

The extraction of energy from organic compounds, carried out by several catabolic pathways (e.g., the citric-acid cycle), involves the oxidation of these compounds to CO_2 and H_2O with the concomitant production of water-soluble reductants (NADH and succinate). These reductants donate electrons to components of the mitochondrial electron-transfer chain, resulting in the reduction of oxygen to water:

$$\frac{1}{2}O_2 + NADH + H^+ \rightarrow H_2O + NAD^+ \tag{6.5}$$

In aerobic organisms, the terminal oxidant is, of course, oxygen. However, some species of bacteria respire anaerobically and are able to use inorganic oxyanions (nitrate or sulfate) as terminal oxidants. The translocation of protons across the inner mitochondrial membrane accompanies the electron transfers that ultimately lead to the reduction of O_2; these protons, in turn, activate ATP synthase, which catalyzes the phosphorylation of ADP to ATP (a process known as oxidative phosphorylation). Because the hydrolysis of ATP is very exoergonic (i.e., $\Delta G < 0$), the newly synthesized ATP is used as a molecular energy source to drive thermodynamically unfavorable reactions to completion.

The rediscovery of cytochromes by Keilin[25] in 1925 led him to propose that the reduction of O_2 is linked to the oxidation of reduced substrates by a series of redox reactions, carried out by cellular components collectively referred to as the respiratory electron-transport chain. Progress toward a molecular understanding of these redox reactions has been painfully slow. Most of the components are multisubunit proteins that reside in the inner mitochondrial membrane (Figure 6.11). These proteins (Complexes I-IV) are quite difficult to purify with retention of *in vivo* properties, and they do not crystallize well.

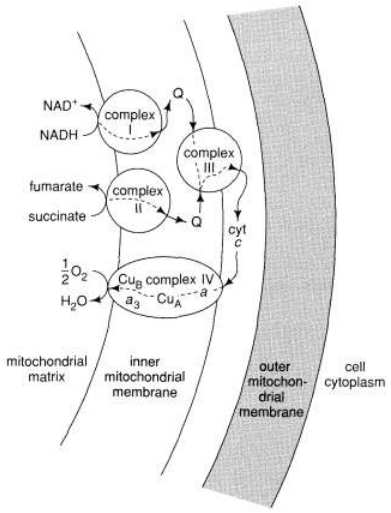


Figure 6.11 - Redox components in mitochondria.

The components[26-28] of the respiratory chain contain a variety of redox cofactors. Complex I (NADH-Q reductase; > 600 kDa) contains five iron-sulfur clusters and FMN. Complex II (succinate-Q reductase; 150 kDa) contains several iron-sulfur clusters, FAD (flavin adenine dinucleotide), and cytochrome b_{568}. Complex III (ubiquinol-cytochrome C reductase; 250 kDa) contains a [2Fe-2S] iron-sulfur center and cytochromes b_{562}, b_{566}, and c_1. Complex IV (cytochrome C oxidase; 200 kDa) contains at least two copper ions and cytochromes a and a_3; Q denotes coenzyme Q, which may be bound to hydrophobic subunits of Complexes I, II, and/or III *in vivo*. Cytochrome c (cyt c in Figure 6.11) is a water-soluble protein (12.4 kDa) that is only peripherally associated with the inner mitochondrial membrane; it has been so thoroughly studied that it is generally regarded as the prime example of an electron transferase.

More than 20 redox centers are involved in the electron-transport chain. Figure 6.12 depicts a simplified view of the flow of electrons from NADH to O_2 via this series of electron carriers. Electron flow through Complexes I, III, and IV is associated with the release of relatively large amounts of energy, which is coupled to proton translocation by these complexes (and therefore ATP production). The redox potentials of the electron carriers thus appear to playa role in determining the pathway of electron flow through the electron-transport chain.

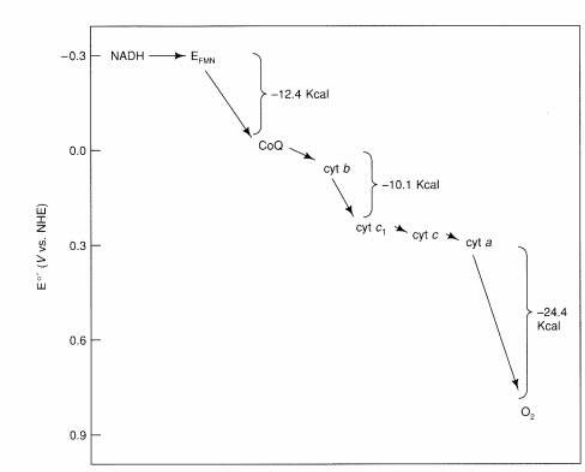


Figure 6.12 - Electron flow from NADH to O_2 in the mitochondrial electron-transport chain.

Approximately 50 percent of the surface area of the inner mitochondrial membrane is lipid bilayer that is unoccupied by membrane proteins and through which these proteins, in principle, are free to diffuse laterally. Kinetic (laser photobleaching and fluorescence recovery) and ultrastructural (freeze-fracture electron microscopy) studies[29,30] indicate that Complexes I-IV diffuse independently and laterally over the inner membrane, whereas cytochrome c diffuses in three dimensions (i.e., through the intramembrane space). Respiratory electron transport has been shown to be a diffusion-coupled kinetic process.[29,30] The term "electron-transport chain" is

thus somewhat misleading, because it implies a degree of structural order that does not exist beyond the level of a given protein complex.

In view of these observations, why are all of the electron transfers associated with mitochondrial respiration required? For example, why is cytochrome c needed to shuttle electrons in Figures 6.11 and 6.12 when the cofactor reduction potentials of Complex III are more negative than those of Complex IV? Evidently, factors other than $\Delta G°$ are of importance—these will be discussed in Sections III and IV.

Photosynthesis could be viewed as the most fundamental bioenergetic process. Biological reactions are driven by an energy flux, with sunlight serving as the energy source. Photosynthesis[31-36] is the process by which radiant solar energy is converted into chemical energy in the form of ATP and NADPH, which are then used in a series of enzymatic reactions to convert CO_2 into organic compounds. The photosynthetic algae that appeared on Earth two million years ago released oxygen into the atmosphere and changed the environment from a reducing to an oxidizing one, setting the stage for the appearance of aerobically respiring organisms.

Photosynthesis is initiated by the capture of solar energy, usually referred to as "light harvesting." A large number of organic pigments, including chlorophylls, carotenoids, phycoerythrin, and phycocyanin (in green plants and algae) are clustered together in pigment-protein complexes called photosystems. These pigments collectively absorb most of the sunlight reaching the Earth—their absorption spectra are displayed in Figure 6.13.

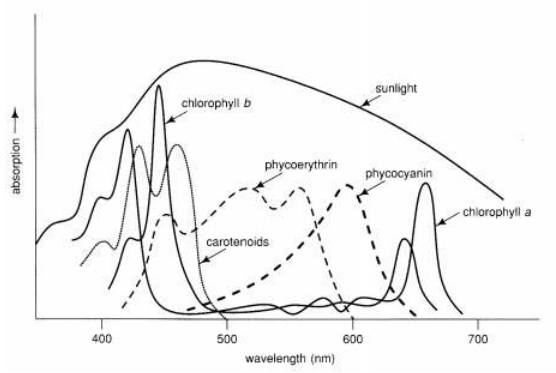


Figure 6.13 - Absorption spectra of the photosystem pigments.

Light is transformed into chemical energy in pigment-protein complexes called reaction centers. The concentration of reaction centers within a photosynthetic cell is too small to offer a suitable absorption cross section for sunlight. Hence, hundreds of these lightharvesting pigments function as molecular antennas; an x-ray structure[35] of one subunit of a bacteriochlorophyll-protein complex is displayed in Figure 6.14.

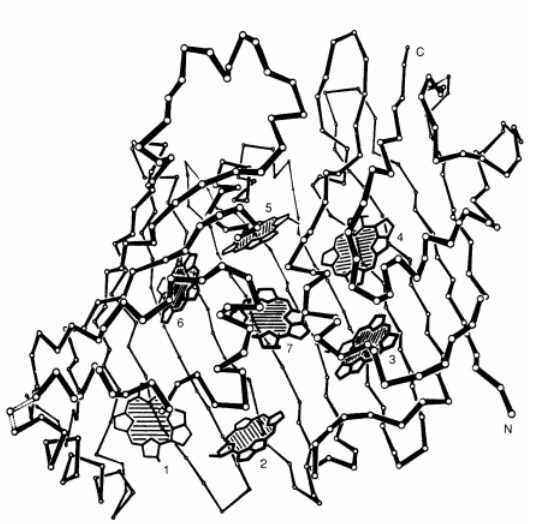


Figure 6.14 - Structure of a subunit of a bacteriochlorophyll-protein complex. Reproduced with permission from Reference 35.

Absorption of a photon by an antenna pigment promotes the pigment into an electronically excited state, which can return to the ground state by a variety of relaxation processes, including fluorescence or resonance transfer of excitation energy to a nearby pigment at picosecond rates. As much as 100 ps may elapse between the photon absorption and the arrival of the light energy at a reaction center. During this time, the energy may "migrate" in a random-walk fashion among hundreds of pigments.

The energy of the excited state is converted into electrochemical potential energy at the reaction center, which contains a primary electron donor P that transfers an electron to a nearby acceptor Al within the same protein (and P becomes oxidized to P^+):

$$PA_1A_2A_3\cdots \xrightarrow{h\nu} P^*A_1A_2A_3\cdots \rightarrow P^+A_1^-A_2A_3\cdots \tag{6.5}$$

This *charge separation* is of paramount importance. The key problem is maintaining the charge separation, which involves minimization of the energy-wasting back reaction. Reaction centers contain an ordered array of secondary electron acceptors (A_1, A_2, A3•••) that optimize the $\Delta G°$ that occurs at each step:

$$P^+A_1^-A_2A_3\cdots \rightarrow P^+A_1A_2^-A_3\cdots \rightarrow P^+A_1A_2A_3^-\cdots \tag{6.6}$$

Thus, the back reaction is circumvented by optimizing forward electron transfers that rapidly remove electrons from A_1^-. As the acceptors are separated by greater and greater distances from P^+, the probability of the back electron transfer to P^+ decreases. Put another way, the overlap of P^+ and each acceptor orbital decreases in the order $P^+/A_1^- > P^+/A_2^- > P^+/A_3^-$.

Photosynthetic bacteria contain only one type of reaction center (l00 kDa). The solution of the x-ray structure (at 2.9 Å resolution) of the *Rps. viridis* reaction center was reported[36] in 1984, providing conclusive proof that electrons can "tunnel" over 10-20 Å distances through protein interiors. The reaction-center protein contains many cofactors (Figure 6.15): two bacteriochlorophylls (BChl) in close proximity (the so-called "special pair"), two further bacteriochlorophylls that are spectroscopically identical, two bacteriopheophytins (BPh), two quinones (Q_A and Q_B), and one iron center. (Q_B was lost during isolation of the *Rps. viridis* reaction center and thus does not appear in Figure 6.15.) The reaction center contains an approximate two-fold rotation axis. Despite this strikingly high symmetry in the reaction center, one pathway of electron flow predominates, as the cartoon in Figure 6.16 indicates.

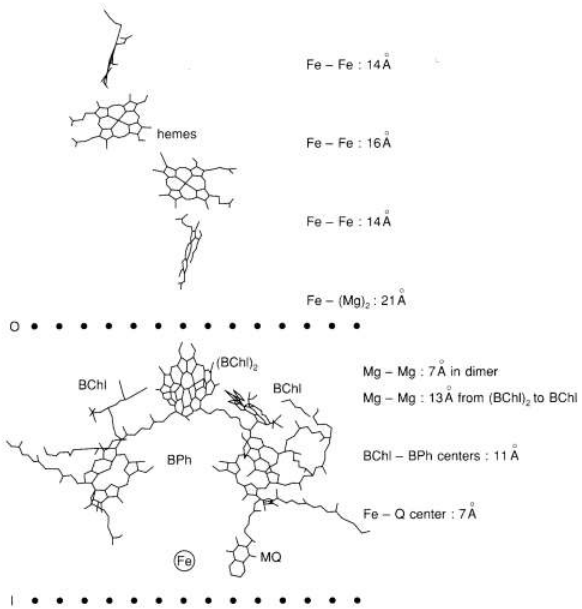


Figure 6.15 - Structure of the Rps. viridis photosynthetic reaction-center cofactors. The black dots delineate the outward (O)- and inward (I)-facing portions of the membrane. Adapted from Reference 36.

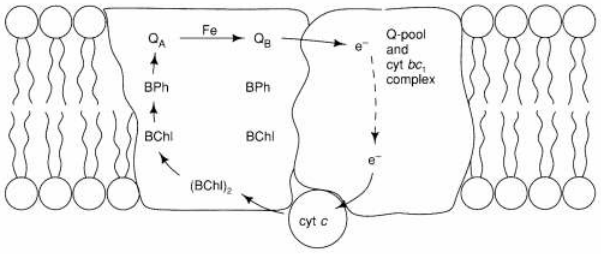


Figure 6.16 - Electron flow in the bacterial photosynthetic reaction center.

11.2.6.5: Energy Storage and Release is shared under a CC BY-NC-SA 4.0 license and was authored, remixed, and/or curated by LibreTexts.

11.2.6.6: Long-range Electron Transfer in Proteins (Part 1)

Electronic Coupling

The electron-transfer reactions that occur within and between proteins typically involve prosthetic groups separated by distances that are often greater than 10 Å. When we consider these distant electron transfers, an explicit expression for the electronic factor is required. In the nonadiabatic limit, the rate constant for reaction between a donor and acceptor held at fixed distance and orientation is:[70-73]

$$k_{et} = \left[\frac{H_{AB}{}^2}{\hbar}\left(\frac{\pi}{\lambda RT}\right)^{1/2}\right]^{\frac{-(\lambda+\Delta G^{o})^2}{4\lambda RT}}. \tag{6.27}$$

The electronic (or tunneling) matrix element H_{AB} is a measure of the electronic coupling between the reactants and the products at the transition state. The magnitude of H_{AB} depends upon donor-acceptor separation, orientation, and the nature of the intervening medium. Various approaches have been used to test the validity of Equation (6.27) and to extract the parameters H_{AB} and λ. Driving-force studies have proven to be a reliable approach, and such studies have been emphasized by many workers.[73,74]

In the nonadiabatic limit, the probability is quite low that reactants will cross over to products at the transition-state configuration.[72] This probability depends upon the electronic hopping frequency (determined by H_{AB}) and upon the frequency of motion along the reaction coordinate.[75] In simple models, the electronic-coupling strength is predicted to decay exponentially with increasing donor-acceptor separation (Equation 6.28):[72,76]

$$H_{AB} = (H^{o}_{AB})^{\frac{-\beta}{2}(\mathbf{d}-\mathbf{d}^{o})} \tag{6.28}$$

In Equation (6.28), $H_{AB}°$ is the electronic coupling at close contact ($\mathbf{d}°$), and β is the rate of decay of coupling with distance ($\mathbf{d}$). Studies of the distance dependence of electron-transfer rates in donor-acceptor complexes, and of randomly oriented donors and acceptors in rigid matrices, have suggested $0.8 \leq \beta \leq 1.2$ Å^{-1}.[73,74,77,78]

Analysis of a large number of intramolecular electron-transfer rates has suggested a β value of 1.4 Å^{-1} for protein reactions (Figure 6.24).[79,80] Assigning a single protein β implies that the intervening medium is homogenous. At best this is a rough approximation, because the medium separating two redox sites in a protein is a heterogenous array of bonded and nonbonded interactions.[81-86] Beratan and Onuchic have developed a formalism that describes the medium in terms of "unit blocks" connected together to form a tunneling pathway.[84-86] A unit block may be a covalent bond, a hydrogen bond, or a through-space jump, each with a corresponding decay factor. Dominant tunneling pathways in proteins are largely composed of bonded groups (e.g., peptide bonds), with less favorable through-space interactions becoming important when a through-bond pathway is prohibitively long (Figure 6.25).[84] The tunneling pathway model has been used successfully in an analysis of the electron-transfer rates in modified cytochromes c (Section IV.D.1).

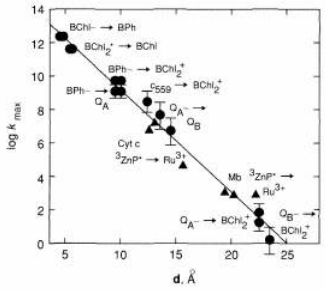


Figure 6.24 - Maximum electron-transfer rate (k_{max}) vs. edge-to-edge distance ($\mathbf{d}$) for proteins. Photosynthetic reaction center rates are shown as circles and ^{3}ZnP* to Ru^{3+} rates in modified myoglobins and cytochromes c are shown as triangles. Adapted from Reference 80.

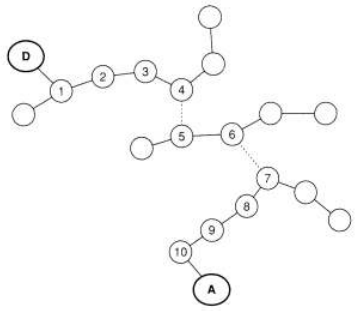


Figure 6.25 - Example of a tunneling pathway.[79] The donor is coupled to the bonded pathway through bond 1 and the acceptor through bond 10. There are three bonded segments and two through-space jumps (between orbitals 4 and 5 and between orbitals 6 and 7).

1. Binding Sites on the Plastocyanin Molecular Surface

Plastocyanin cycles between the Cu^{II} and Cu^{I} oxidation states, and transfers electrons from cytochrome f to the P_{700} component of photosystem I in the chloroplasts of higher plants and algae.[87-89] The low molecular weight (10.5 kDa) and availability of detailed structural information[90] have made this protein an attractive candidate for mechanistic studies, which, when taken together,[87,91-94] point to two distinct surface binding sites (i.e., regions on the plastocyanin molecular surface at which electron transfer with a redox partner occurs). The first of these, the solvent-exposed edge of the Cu ligand His-87 (the adjacent site A in Figure 6.26), is ~6 Å from the copper atom and rather nonpolar. The second site (the remote site R in Figure 6.26) surrounds Tyr-83, and is much farther (~15 Å) from the copper center. Negatively charged carboxylates at positions 42-45 and 59-61 make this latter site an attractive one for positively charged redox reagents.

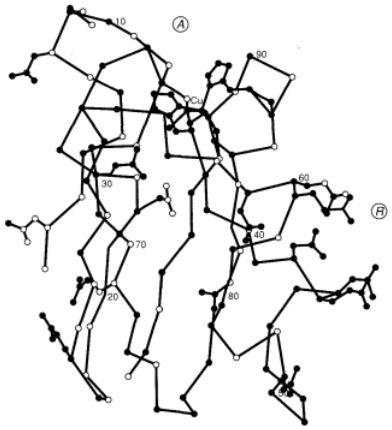
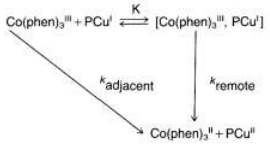


Figure 6.26 - Structure of poplar plastocyanin illustrating the adjacent (A) and remote (R) surface binding sites.

Bimolecular electron-transfer reactions are typically run under pseudo-first-order conditions (e.g., with an inorganic redox reagent present in ~15-fold excess):

$$Rate = k[plastocyanin][complex] = k_{obs}[plastocyanin]. \quad (6.29)$$

For some reactions [e.g., $Co(phen)_3^{3+}$ oxidation of plastocyanin (Cu^{I})] the expected linear plot of k_{obs} vs. [complex] is not observed. Instead, the rate is observed to saturate (Figure 6.27).[95] A "minimal" model used to explain this behavior involves the two pathways for electron transfer shown in Equation (6.30).



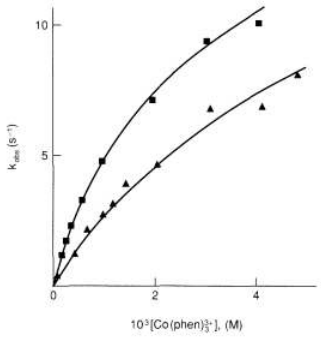


Figure 6.27 - Dependence of first-order rate constants kobs (25 °C) on $[Co(phen)_3^{3+}]$ for the oxidation of plastocyanin PCu^I at pH 7.5. Key: ■, *spinach; and* ▲, *parsley.*[95]

Surprisingly, the rate ratio $k_{remote}/k_{adjacent}$ is 7.

Calculations[81] indicate that, despite the significant differences in distances, H_{AB} for the remote site is ~15 percent of H_{AB} for the adjacent site. This figure is much higher than would be expected from distance alone, suggesting that the value of the decay parameter β in Equation (6.28) depends strongly on the structure of the intervening medium.

Modified Metalloproteins

Chemical modification of structurally characterized metalloproteins by transition-metal redox reagents has been employed[52,53,96-98] to investigate the factors that control long-range electron-transfer reactions. In these semisynthetic multisite redox systems, the distance is fixed, and tunneling pathways between the donor and acceptor sites can be examined.

1. Ruthenium-modified Myoglobin

Sperm-whale myoglobin can be reacted with $(NH_3)_5Ru(OH_2)^{2+}$ and then oxidized to produce a variety of ruthenated products,[52,99-101] including a His-48 derivative whose Ru ↔ Fe tunneling pathway is depicted in Figure 6.28.

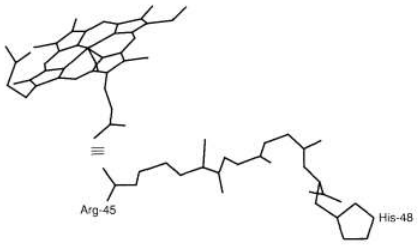


Figure 6.28 - Electron-tunneling pathway for myoglobin modified at His-48. The pathway moves along the protein backbone from His-48 to Arg-45, and then to the heme via an H-bond (=) to the heme propionate. The His-48 to heme edge-edge distance is 12.7 Å.[101]

Electrochemical data (Table 6.5) indicate that the $(NH_3)_5Ru^{3+}$ group does not significantly perturb the heme center, and that equilibrium (i.e., $k_{obs} = k_1 + k_{-1}$) should be approached when a mixed-valent intermediate is produced by flash-photolysis techniques:

$$(NH_3)_5Ru^{3+} - Mb(Fe^{3+}) \xrightarrow[e^-]{fast} (NH_3)_5Ru^{2+} - Mb(Fe^{3+}) \underset{k_{-1}}{\overset{k_1}{\rightleftharpoons}} (NH_3)_5Ru^{3+} - Mb(Fe^{2+}) \tag{6.31}$$

This kinetic behavior was observed,[52] and both the forward (k_1) and reverse (k_{-1}) reactions were found to be markedly temperature-dependent: $k_1 = 0.019\ s^{-1}$ (25 °C), $\Delta H_1^{\ddagger} = 7.4$ kcal/mol, $k_{-1} = 0.041\ s^{-1}$) (25°C), $\Delta H_1^{\ddagger} = 19.5$ kcal/mol. X-ray crystallographic studies[102] indicate that the axial water ligand dissociates upon reduction of the protein. This conformational change does not control the rates, since identical results were obtained when a second flash-photolysis technique[99] was used to generate $(NH_3)_5Ru^{3+}$-Mb(Fe^{2+}) in order to approach the equilibrium from the other direction.

Table 6.5 - Thermodynamic parameters for the reduction of $(NH_3)_5Ru^{3+}$ and the heme site in native and modified myoglobin (Mb).[a]

a) pH 7.0 μ = 0.1 M phosphate buffer.

Thermodynamic Parameter	Native Mb $Fe^{3+/2+}$	Modified Mb	
		$Fe^{3+/2+}$	$(NH_3)_5Ru^{3+/2+}$
E°, mV vs. NHE (25 °C)	58.8 ± 2	65.4 ± 2	85.8 ± 2
Δ G°, kcal mol^{-1} (25 °C)	-1.26 ± 0.05	-1.51 ± 0.05	-1.98 ± 0.05
ΔS°, e.u.	-39.2 ± 1.2	-37.6 ± 1.2	4.2 ± 1.2
ΔH°, kcal mol^{-1} (25 °C)	-13.0 ± 0.4	-12.7 ± 0.4	-0.7 ± 0.4

Cyanogen bromide has been used[103] to modify the six-coordinate metmyoglobin heme site, causing the coordinated water ligand to dissociate. The CNBr-modified myoglobin heme site is thus five-coordinate in *both* oxidation states. As expected, the self-exchange rate increased from ~1 $M^{-1}s^{-1}$ to ~10^4 $M^{-1}s^{-1}$.

Recent efforts in modeling biological electron transfers using chemically modified redox proteins[104-106] point the way toward the design of semisynthetic redox enzymes for catalytic applications. An intriguing example, termed flavohemoglobin, was produced by reaction of hemoglobin with a flavin reagent designed to react with Cys-93 of the β-chain (i.e., the hemoglobin molecule was modified by two flavin moieties).[107] The resulting derivative, unlike native hemoglobin, accepts electrons directly from NADPH and catalyzes the *para*-hydroxylation of aniline in the presence of O_2 and NADPH.

Protein-protein Complexes

In physiologically relevant precursor complexes, both redox centers are frequently buried in protein matrices. Characterization of such protein-protein complexes is clearly important, and several issues figure prominently:

1. What are the "rules" that govern complex formation? How important are protein-dipole/protein-dipole interactions, intermolecular hydrogen bonding, and hydrophobic interactions?
2. Are the water (and small solute) molecules associated with protein surfaces "squeezed" out of the interfacial region upon complex formation?
3. Within a given complex, is there a high degree of structural order, or do the proteins retain some independent mobility?

Most of our knowledge about the structures of protein-protein complexes comes from crystallographic studies[108-110] of antigen-antibody complexes and multisubunit proteins; such systems generally exhibit a high degree of thermodynamic stability. On the other hand, complexes formed as a result of bimolecular collisions generally are much less stable, and tend to resist attempts to grow x-ray-quality crystals; the high salt conditions typically used in protein crystallizations often lead to dissociation of such complexes.

1. Cytochrome b_5-cytochrome c

One of the most widely studied protein-protein complexes is that formed between mammalian cytochrome b_5 and cytochrome c. Using the known x-ray structures of both proteins, Salemme[111]generated a static computer graphics model of this electron-transfer complex by docking the x-ray structures of the individual proteins. Two features of this model and its revision[112] by molecular dynamics simulations (Figure 6.29 See color plate section, page C-12.) are noteworthy: (1) several Lys residues on cytochrome c and carboxylate-containing groups on cytochrome b_5 form "salt bridges" (i.e., intermolecular hydrogen bonds); and (2) the hemes are nearly coplanar and are ~17 Å (Fe-Fe) apart. This distance was confirmed by an energy-transfer experiment[113] in which the fluorescence of Zn-substituted cytochrome c was quenched by cytochrome b_5. Spectroscopic studies[114,115] have verified the suggestion that these proteins form a 1:1 complex at low ionic strength (Figure 6.30). In addition, chemical modification[116] and spectroscopic analyses[117-119] are all in agreement with the suggestion[111,112] that the complex is primarily stabilized by electrostatic interactions of the ($-NH_3^+$ ••• ^-O_2C—) type. The effect of ionic strength on the reduction of cytochrome c by cytochrome b_5 is also in accord with this picture:[120] lowering the ionic strength increases the reaction rate, as expected for oppositely charged molecules.

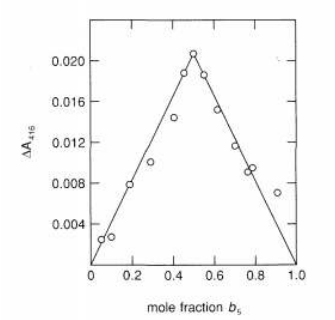
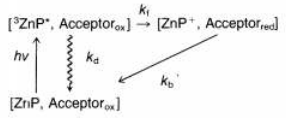


Figure 6.30 - Job plot of the ehange in absorbance at 416 nm due to complex formation between cytochrome b_5 and cytochrome c (25 °C, pH 7.0 (phosphate), μ = 1 mM, 10.54 μM total protein concentration).[114]

2. Hybrid Hemoglobins

A common[52,55,57,121,122] experimental strategy for studying electron transfers *between* proteins uses a metal-substituted heme protein as one of the reactants. In particular, the substitution of zinc for iron in one of the porphyrin redox centers allows facile initiation of electron transfer through photoexcitation of the zinc porphyrin (ZnP). The excited zinc porphyrin, ^{3}ZnP* in Equation (6.32), may decay back ($k_d \sim 10^2$ s^{-1}) to the ground state or transfer an electron to an acceptor.



The ZnP^+ cation radical produced in the k_f step is a powerful oxidant; back electron transfer (k_b) will thus occur and regenerate the starting material.

The reactions shown in Equation (6.32) have been investigated in mixedmetal [Zn, Fe] hemoglobins.[123-125] A hemoglobin molecule can be viewed as two independent electron-transfer complexes, each consisting of an α_1-β_2 subunit pair (Figure 6.31), since the α_1-α_2, (\beta_{1}\)-(\beta_{2}\), and α_1-(\beta_{1}\) distances are prohibitively long (> 30 Å).

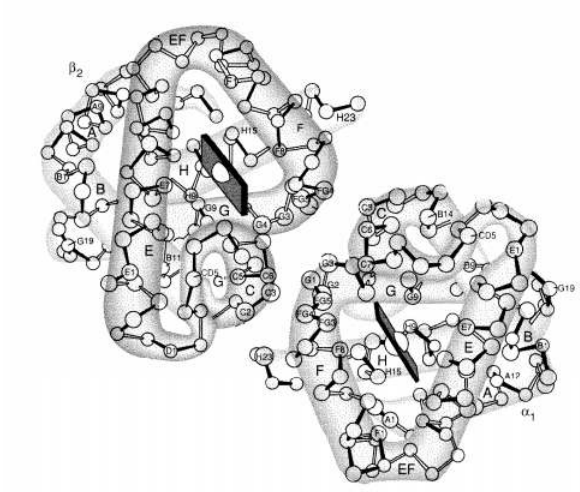


Figure 6.31 - Structure of the α_1 and β_2 subunits of hemoglobin. The edge-edge separation of the two hemes is 20 Å.

Both [α(Zn), β(Fe)] and [α(Fe), β(Zn)] hybrids have been studied. The ZnP and FeP are nearly parallel, as in the cytochrome b_5-cytochrome c model complex. Long-range electron transfer (^{3}ZnP* → Fe^{3+}) between the α_1 and β_2 subunits has been observed (the heme-edge/heme-edge distance is ~20 Å). The driving force for the forward electron-transfer step is ~0.8 eV, and k_f (see Equation 6.32) is ~100 s^{-1} at room temperature, but decreases to ~9 s^{-1} in the low-temperature region (Figure 6.32). Below 140-160 K the vibrations that induce electron transfer "freeze out"; nuclear tunneling is usually associated with such slow, temperature-independent rates. A complete analysis of the full temperature dependence of the rate requires a quantum-mechanical

treatment[126,127] of λ_i rather than that employed in the Marcus theory. It is interesting to note that the heme b vinyl groups (see Figure 6.6) for a given [α_1(Fe), β_2Zn)] hybrid point toward each other and appear[125] to facilitate electron transfer.

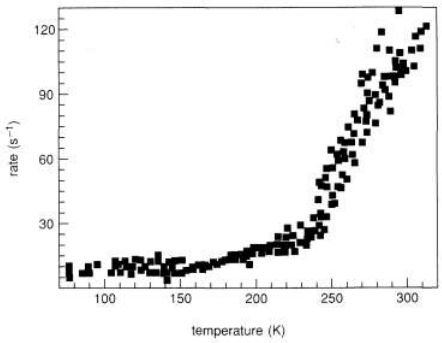


Figure 6.32 - Temperature dependence of the forward electron-transfer rate, k_f, for [α(Zn), β($Fe^{III}H_2O$)]; adapted from Reference 124.

11.2.6.6: Long-range Electron Transfer in Proteins (Part 1) is shared under a CC BY-NC-SA 4.0 license and was authored, remixed, and/or curated by LibreTexts.

11.2.6.7: Long-range Electron Transfer in Proteins (Part 2)

Cytochrome c

Cytochrome c occupies a prominent place in the mitochondrial electron-transport chain. Its water solubility, low molecular weight (12.4 kDa), stability, and ease of purification have allowed many experiments, which, when taken together, present a detailed picture of the structure and biological function of this electron carrier.[128-133]

X-ray structures[134] of oxidized and reduced tuna cytochrome c are very similar; most of the differences are confined to changes in the orientations of the side chains of some surface-exposed amino acids and sub-Ångström adjustments of some groups in the protein interior. Upon reduction, the heme active site becomes slightly more ordered (Figure 6.33). Two-dimensional NMR studies[135-137] confirm this interpretation of the x-ray data, and further establish that the crystal and solution structures of cytochrome c differ in only minor respects.

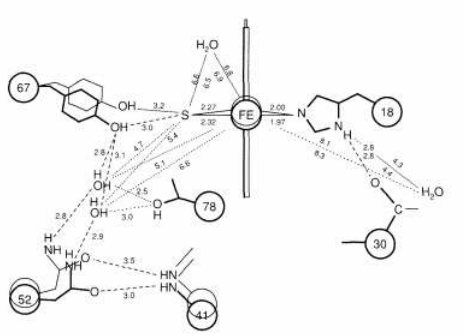


Figure 6.33: Side-chain motion in the vicinity of the heme of cytochrome c. Heavy lines indicate the reduced molecule, and light lines the oxidized molecule.[134]

Cytochrome c exhibits several pH-dependent conformational states. In particular, an alkaline transition with a pK_a ~ 9.1 has been observed for ferricytochrome c. This transition is believed to be associated with the dissociation of Met-80; the reduction potential decreases dramatically,[138] and the 695-nm absorption band, associated with a sulfur → iron charge-transfer transition, disappears. The ^2H NMR resonance due to (^2H_3C-) Met-80 in deuterium-enriched ferricytochrome c disappears from its hyperfine-shifted upfield position without line broadening, and reappears coincident with the (^2H_3C-)Met-65 resonance.[139] In contrast, ferrocytochrome c maintains an ordered structure over the pH range 4 to 11.[140] The heme iron in ferricytochrome c remains low-spin throughout this transition, and a new strong-field ligand must therefore replace Met-80. It has been suggested that an e-amino nitrogen of a nearby Lys provides the new donor atom, but this has not been confirmed. However, it is clear that reduction of ferricytochrome c at alkaline pH values below 11 causes a drastic conformational change at the heme site. The unknown sixth ligand must be displaced by Met-80 in order for the reduced protein to assume a structure similar to the one at neutral pH. This structural change is accompanied by a decrease in the rate of reduction of ferricytochrome c by hydrated electrons,[141] as expected.

How does the protein control the reduction potential of the iron center in cytochrome c? Factors that appear to play a role include the nature of the axial ligands, the stability and solvent accessibility of the heme crevice, and the hydrophobicities of the amino acids that line the heme crevice. These issues have been addressed theoretically[142,143] and experimentally[144-149] using cytochrome c variants engineered by protein semisynthesis or site-directed mutagenesis. Results for horse heart cytochrome c are set out in Table 6.6. Point mutations at either of positions 78 or 83 do not significantly alter E°'; however, the double mutant (Thr-78 → Asn-78; Tyr-83 → Phe-83) exhibits a substantially lower redox potential. Evidently, the results of such changes are not necessarily additive; great care must be taken in drawing conclusions about structure-function relations in engineered proteins. Finally, the ~310 mV difference between the values for the heme octapeptide and the native protein (the axial ligands are the same in both) provides a dramatic illustration of protein environmental effects on the redox potential: shielding the heme from the solvent is expected to stabilize Fe^{II} and therefore result in an increase in E°'.

Table 6.6: Reduction potentialsa of horse heart cytochrome c. a) pH 7.0, 25 °C. b) In 2M N-acetyl-DL-methionine.

Cytochrome	E°' (mV vs. NHE)	Reference
Native	262	138
Met-80 → His-80	41	144
Tyr-67 → Phe-67	225	145
Thr-78 → Asn-78	264	145
Tyr-83 → Pro-83	266	145
Thr-78, Tyr-83 → Asn-78, Pro-83	235	145
Heme octapeptide[b]	-50	146

During the last fifteen years, much has been learned about the interaction of cytochrome c with its redox partners.[128-133] Cytochrome c is a highly basic protein (pI = 10.05); lysine residues constitute most of the cationic amino acids. Despite the indication from the x-ray structures that only ~1 percent of the heme surface is solvent-exposed, the asymmetric distribution of surface charges, particularly a highly conserved ring of Lys residues surrounding the exposed edge of the heme crevice, led to the suggestion that electron-transfer reactions of cytochrome c (and other Class I cytochromes as well) occur via the exposed heme edge.

Chemical modification of the surface Lys residues of cytochrome c has afforded opportunities to alter the properties of the surface ε-amino groups suspected to be involved in precursor complex formation. Margoliash and coworkers[133,150,151] used a 4-carboxy-2,6-dinitrophenol (CDNP) modification of the Lys residues to map out the cytochrome c interaction domains with various transition-metal redox reagents and proteins. These experiments have shown that cytochrome c interacts with inorganic redox partners near the exposed heme edge.

Numerous studies[129,152,153] of cytochrome c with physiological reaction partners are in accord with electrostatic interactions featured in the model cytochrome c/cytochrome b_5 complex discussed earlier. Similar types of interactions have been proposed for cytochrome c/flavodoxin[154] and cytochrome c/cytochrome c peroxidase complexes.[155] (Recent x-ray crystal structure work[155b] has shed new light on this problem.) Theoretical work[156] additionally suggests that electrostatic forces exert torques on diffusing protein reactants that "steer" the proteins into a favorable docking geometry. However, the domains on cytochrome c for interaction with physiological redox partners are not identical, as Figure 6.34 illustrates.

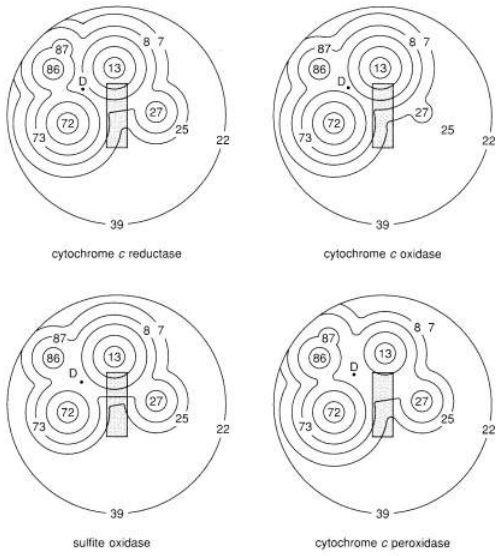


Figure 6.34: Domains on cytochrome c for interaction with physiological redox partners. The heme edge is represented by the shaded rectangle. The number of circles around a given Lys residue is proportional to the percentage of the observed inhibition in redox assays when the corresponding CDNP-modified cytochrome c is used.[151]

Reactions between cytochrome c and its physiological redox partners at low ionic strength generally are very fast, ~10^8 $M^{-1}s^{-1}$, even though the thermodynamic driving force may be as low as 20 mV, as it is for the reduction of cytochrome a in cytochrome c oxidase. Such rates are probably at the diffusioncontrolled limit for such protein-protein reactions.[157,158] A more detailed understanding of these reactions will require studies that focus on the dynamical (rather than static) features of complexes of cytochrome c with other proteins. For example, there is evidence[159] that a cytochrome c conformational change in the vicinity of the heme edge accompanies the formation of the complex with cytochrome c oxidase. Studies of the influence of geometry changes on activation energies[52,60,160] are of particular importance in elucidating the mechanisms of protein-protein reactions.

1. Ruthenium-modified Cytochrome c

Intramolecular electron transfer in cytochrome c has been investigated by attaching photoactive Ru complexes to the protein surface.[98,161] $Ru(bpy)_2(CO_3)$ (bpy = 2,2'-bipyridine) has been shown to react with surface His residues to yield, after addition of excess imidazole (im), $Ru(bpy)_2(im)(His)^{2+}$. The protein-bound Ru complexes are luminescent, but the excited states ($*Ru^{2+}$) are rather short lived ($\tau \leq 100$ ns). When direct electron transfer from $*Ru^{2+}$ to the heme cannot compete with excited-state decay, electron-transfer quenchers (e.g., $Ru(NH_3)_6^{3+}$) are added to the solution to intercept a small fraction (1-10%) of the excited molecules, yielding (with oxidative quenchers) Ru^{3+}. If, before laser excitation of the Ru site, the heme is reduced, then the Fe^{2+} to Ru^{3+} reaction (k_{et}) can be monitored by transient absorption spectroscopy. The k_{et} values for five different modified cytochromes have been reported: (Ru(His- 33), 2.6(3) x 10^6; Ru(His-39), 3.2(4) x 10^6; Ru(His-62), 1.0(2) x 10^4; Ru(His- 72), 9.0(3) x 10^5; and Ru(His-79), > 10^8 s^{-1}).[162,163]

According to Equation (6.27), rates become activationless when the reaction driving force (- $\Delta G°$) equals the reorganization energy (A), The driving force (0.74 eV) is approximately equal to the reorganization energy (0.8 eV) estimated for the $Ru(bpy)_2(im)(His)$-cyt c reactions.[161] The activationless (maximum) rates (k_{max}) are limited by H_{AB}^2, where H_{AB} is the electronic matrix element that couples the reactants and products at the transition state. Values of k_{max} and H_{AB} for the Fe^{2+} to Ru^{3+} reactions are given in Table 6.7.

Table 6.7: Electron-transfer parameters163 for Ru(bpy)2(im)(His-X)-cytochromes c.a) C = covalent bond, H = hydrogen bond, S = space jump.

X	k_{max} (s^{-1})	H_{AB} (cm^{-1}) [Fe^{2+}—Ru^{3+}]	**d** (Å)	n_{eff}[a]	σ 1(Å)
79	> 1.0 x 10^8	> 0.6	4.5	8 (8C)	11.2
39	3.3 x 10^6	0.11	12.3	14.0 (11C) (1H)	19.6
33	2.7 x 10^6	0.097	11.1	13.9 (11C) (1H)	19.5
72	9.4 x 10^5	0.057	8.4	17.6 (7C) (1S)	24.6
62	1.0 x 10^4	0.006	14.8	20.6 (16C) (2H)	28.8

Calculations that explicitly include the structure of the intervening medium[81- 86,164-169] have been particularly helpful in developing an understanding of distant electronic couplings. As discussed in Section IV.A, the couplings in proteins can be interpreted in terms of pathways comprised of covalent, H-bond, and through-space contacts. An algorithm has been developed[85,170] that searches a protein structure for the best pathways coupling two redox sites (the pathways between the histidines (33, 39, 62, 72, 79) and the heme are shown in Figure 6.35). A given coupling pathway consisting of covalent bonds, H-bonds, and through-space jumps can be described in terms of an equivalent covalent pathway with an effective number of covalent bonds (n_{eff}). Multiplying the effective number of bonds by 1.4 Å/bond gives a-tunneling lengths (σ1) for the five pathways (Table 6.7) that correlate well with the maximum rates (one-bond limit set at 3 x 10^{12} s^{-1}; slope of 0.71 $Å^{-1}$) (Figure 6.35). The 0.71 $Å^{-1}$ decay accords closely with related distance dependences for covalently coupled donor-acceptor molecules.[73,77]

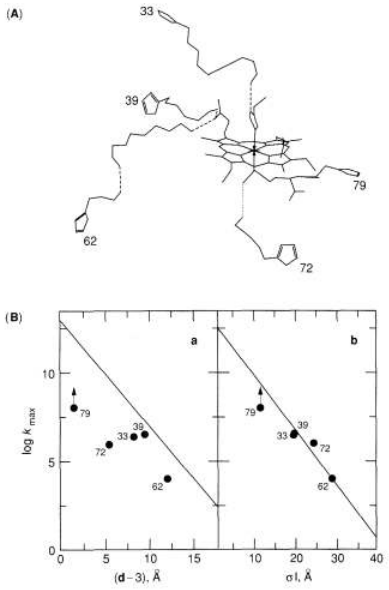


Figure 6.35 - (A) Electronic coupling pathways to the heme from Ru-modified residues in native (His-33 horse heart, His-39 yeast), genetically engineered (His-62 yeast), and semisynthetic (His-72, His-79 horse heart) cytochromes c. Solid lines are covalent bonds; dashed lines are hydrogen bonds; and the dotted line (His-72 pathway) is a space jump. (B) The left half of the diagram (a) shows maximum electron-transfer rate vs. **d** minus 3 Å (van der Waals contact). Exponential-decay line with 1 x 10^{13} s^{-1} intercept and 1.4 $Å^{-1}$ slope. The right half of the diagram (b) shows maximum rate vs. σ1: 0.71 $Å^{-1}$ slope; 3 x 10^{12} s^{-1} intercept. Adapted from References 162 and 163.

Bacterial Photosynthetic Reaction Centers

Photosynthetic bacteria produce only one type of reaction center, unlike green plants (which produce two different kinds linked together in series), and are therefore the organisms of choice in photosynthetic electon-transfer research.[171- 176] As indicated in Section I.B, the original reaction center structure (Figure 6.15) lacked a quinone (Q_B). Subsequent structures for reaction centers from other photosynthetic bacteria[177,178] contain this quinone (Figure 6.36 See color plate section, page C-13.). The *Rps. sphaeroides* reaction center contains ten cofactors and three protein subunits. (Note that the *Rps. viridis* structure contains a cytochrome subunit as well.) The cofactors are arrayed so that they nearly span the 40-Å-thick membrane (Figure 6.37 See color plate section, page C-13.). The iron atom is indicated by the red dot near the cytoplasmic side of the membrane (bottom). In spite of the near two-fold axis of symmetry, electron transfer proceeds along a pathway that is determined by the A branch. In particular, $BChl_B$ and $BPhe_B$ do not appear to play an important role in the electron transfers.

It was demonstrated long ago that $(BChl)_2$ is the primary electron donor and that ubiquinone (or metaquinone) is the ultimate electron acceptor. Transient flash photolysis experiments indicate that several electron-transfer steps occur in order to translocate the charge across the membrane (Figure 6.38). Curiously, the high-spin ferrous iron appears to play no functional role in the Q_A to Q_B electron transfer.[179] In addition, the part played by $BChl_A$ is not understood—it may act to promote reduction of $BPhe_A$ via a superexchange mechanism.[180,181] Cytochromes supply the reducing equivalents to reduce the special pair $(BChl)_2^+$.

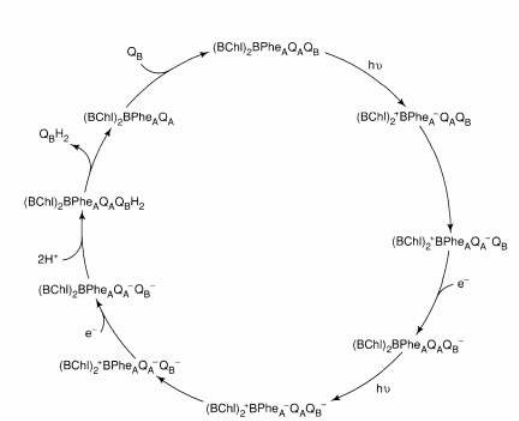


Figure 6.38 - Forward electron transfer through the reaction center. Note that two charge translocations must occur in order for the (labile) quinol Q_BH_2 to be produced. Once Q_BH_2 dissociates from the RC and is replaced by another, oxidized, Q_B, the cycle can begin anew.

Estimated rate constants for the various electron-transfer steps, together with approximate reduction potentials, are displayed in Figure 6.39. For each step, the forward rate is orders of magnitude faster than the reverse reaction. The rapid rates suggest that attempts to obtain x-ray structures of intermediates (especially the early ones!) will not be successful. However, molecular dynamics methods are being explored in computer simulations of the structures of various intermediates.[182,183] Within a few years we may begin to understand why the initial steps are so fast.

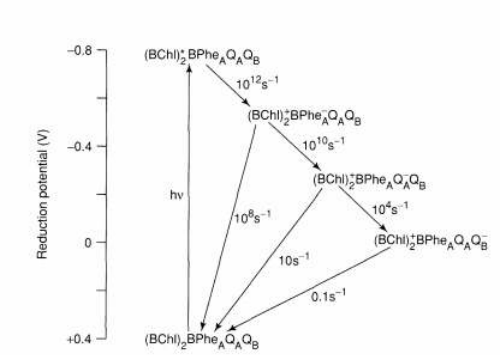


Figure 6.39 - Electron-transfer rates (for forward and reverse reactions) and reduction potentials for RC intermediates.

11.2.6.7: Long-range Electron Transfer in Proteins (Part 2) is shared under a CC BY-NC-SA 4.0 license and was authored, remixed, and/or curated by LibreTexts.

11.2.6.8: Marcus Theory

In classical transition-state theory, the expression for the rate constant of a bimolecular reaction in solution is

$$k = (\kappa \nu_n)^{\frac{-\Delta G^*}{RT}}, \tag{6.16}$$

where ν_n, the nuclear frequency factor, is approximately 10^{11} $M^{-1}s^{-1}$ for small molecules, and ΔG^* is the Gibbs-free-energy difference between the activated complex and the precursor complex. This theoretical framework provides the starting point for classical electron-transfer theory. Usually the transmission coefficient κ is initially assumed to be unity. Thus, the problem of calculating the rate constant involves the calculation of ΔG^*, which Marcus partitioned into several parameters:

$$\Delta G^* = w^r + \left(\frac{\lambda}{4}\right)\left(1+\frac{\Delta G^{o\prime}}{\lambda}\right)^2, \tag{6.17}$$

$$\Delta G^{o\prime} = \Delta G^o + w^p - w^r. \tag{6.18}$$

Here w^r is the electrostatic work involved in bringing the reactants to the mean reactant separation distance in the activated complex, and w^p is the analogous work term for dissociation of the products. These terms vanish in situations where one of the reactants (or products) is uncharged. $\Delta G°$ is the Gibbs-free-energy change when the two reactants and products are an infinite distance apart, and $\Delta G°'$ is the free energy of the reaction when the reactants are a distance r apart in the medium; $\Delta G°$ is the standard free energy of the reaction, obtainable from electrochemical measurements (the quantity - $\Delta G°$ is called the *driving force* of the reaction).

The reorganization energy λ is a parameter that contains both inner-sphere (λ_i) and outer-sphere (λ_o) components; $\lambda = \lambda_i + \lambda_o$. The inner-sphere reorganization energy is the free-energy change associated with changes in the bond lengths and angles of the reactants. The λ_i term can be evaluated within the simple harmonic-oscillator approximation:

$$\lambda_i = \left(\frac{1}{2}\right)\sum_j k_j(\Delta x_j)^2, \tag{6.19}$$

where k_j values are normal-mode force constants, and the Δx_j values are differences in equilibrium bond lengths between the reduced and oxidized forms of a redox center.

The outer-sphere reorganization energy reflects changes in the polarization of solvent molecules during electron transfer:

$$\lambda_o = e^2\left[\left(\frac{1}{2r_A}\right)+\left(\frac{1}{2r_B}\right)-\left(\frac{1}{d}\right)\right]\left[\left(\frac{1}{D_{op}}\right)-\left(\frac{1}{D_s}\right)\right]; \tag{6.20}$$

d is the distance between centers in the activated complex, generally taken to be the sum of the reactant radii r_A and r_B; D_{op} is the optical dielectric constant of the medium (or, equivalently, the square of the refractive index); and D_s is the static dielectric constant. This simple model for the effect of solvent reorganization assumes that the reactants are spherical, and that the solvent behaves as a dielectric continuum. (Sometimes the latter approximation is so rough that there is no correspondence between theory and experiment.)

Variations in λ can have enormous effects on electron-transfer rates, Some of the possible variations are apparent from inspection of Equation (6.20). First, λ_o decreases with increasing reactant size. Second, the dependence of the reaction rate on separation distance attributable to $\lambda_o$occurs via the $\frac{1}{d}$ term. Third, λ_o decreases markedly as the solvent polarity decreases. For nonpolar solvents, $D_s \simeq D_{op} \simeq 1.5$ to 4.0. It is significant to note that protein interiors are estimated to have $D_s \simeq 4$, whereas, $D_s \simeq 78$ for water. An important conclusion is that metalloproteins that contain buried redox cofactors need not experience large outer-sphere reorganization energies.

The key result of Marcus theory is that the free energy of activation displays a quadratic dependence on $\Delta G°$ and λ (ignoring work terms). Hence, the reaction rate may be written as

$$k_{et} = (\nu_n \kappa)^{\frac{-(\lambda+\Delta G^o)^2}{4\lambda RT}}. \tag{6.21}$$

For intramolecular reactions, the nuclear frequency factor (ν_n) is ~10^{13} s^{-1}. One of the most striking predictions of Marcus theory follows from this equation: as the driving force of the reaction increases, the reaction rate increases, reaching a maximum at - $\Delta G°$

= λ; when - ΔG° is greater than λ, the rate decreases as the driving force increases (Figure 6.23).

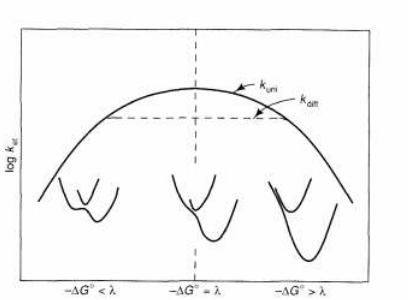


Figure 6.23 - Plot of log k_{et} as a function of increasing driving force (- ΔG°). Three ΔG° regions are indicated: normal (- ΔG° < λ); activationless (- ΔG° = λ); and inverted (- ΔG° > λ). The corresponding two-well (E_R, E_P), diagrams also are shown. The dashed curve (k_{diff}) is for a bimolecular reaction. The predicted behavior of a unimolecular reaction (k_{uni}) is given by the solid curve; here the rate could be as high as 10^{13} s^{-1}, because it is not masked by diffusional processes.

Two free-energy regions, depending on the relative magnitudes of - ΔG° and λ, are thus distinguished. The normal free-energy region is defined by - ΔG° < λA. In this region, ΔG* decreases if - ΔG° increases or if λ decreases. If - ΔG° = λ, there is no free-energy barrier to the reaction. In the inverted region, defined by - ΔG° > λ, ΔG* increases if λ decreases or if - ΔG° increases. Another widely used result of Marcus theory deals with the extraction of useful kinetic relationships for cross reactions from parameters for self-exchange reactions. Consider the cross reaction, Equation (6.22), for which the rate

$$A_1(ox) + A_2(red) \rightarrow A_1(red) + A_2(ox) \tag{6.22}$$

and equilibrium constants are k_{12} and K_{12}, respectively. Two self-exchange reactions are pertinent here:

$$A_1(ox) + A_1(red) \rightarrow A_1(red) + A_1(ox) \tag{6.23a}$$

$$A_2(ox) + A_2(red) \rightarrow A_2(red) + A_2(ox) \tag{6.23b}$$

These reactions are characterized by rate constants k_{11} and k_{22}, respectively. The reorganization energy ($\lambda_{12}$for the cross reaction can be approximated as the mean of the reorganization energies for the relevant self-exchange reactions:

$$\lambda_{12} = \frac{1}{2}(\lambda_{11} + \lambda_{22}) \tag{6.24}$$

Substitution of Equation (6.24) into Equation (6.17) leads to the relation

$$\Delta G^*_{12} = \frac{1}{2}(\Delta G^*_{11} + \Delta G^*_{22}) + \frac{1}{2}\Delta G^*_{12}(1+\alpha), \tag{6.25a}$$

where

$$\alpha = \frac{\Delta G^*_{12}}{4(\Delta G^*_{11} + \Delta G^*_{22})}. \tag{6.25b}$$

When the self-exchange rates k_{11} are corrected for work terms or when the latter nearly cancel, the cross-reaction rate k_{12} is given by the **Marcus cross relation**,

$$k_{12} = (k_{11}k_{22}K_{12}f_{12})^{\frac{1}{2}}, \tag{6.26a}$$

where

$$ln f_{12} = \frac{(ln K_{12})^2}{4\ ln\left(\frac{k_{11}k_{22}}{\nu_n^2}\right)}. \tag{6.26b}$$

This relation has been used to predict and interpret both self-exchange and cross-reaction rates (or even K_{12}, depending on which of the quantities have been measured experimentally. Alternatively, one could study a series of closely related electron-transfer reactions (to maintain a nearly constant λ_{12}) as a function of ΔG_{12}; a plot of In k_{12} vs. In K_{12} is predicted to be linear, with slope

0.5 and intercept 0.5 In ($k_{11}k_{22}$). The Marcus prediction (for the normal free-energy region) amounts to a linear free-energy relation (LFER) for outer-sphere electron transfer.

Cross Reactions of Blue Copper Proteins

Given the measured self-exchange rate constant for stellacyanin (k_{11} 1.2 x 10^5 M $^1s^{-1}$), the Marcus cross relation (Equation 6.26a) can be used to calculate the reaction rates for the reduction of Cu^{II}-stellacyanin by $Fe(EDTA)^{2-}$ and the oxidation of Cu^{I}-stellacyanin by $Co(phen)_3^{3+}$. E°($Cu^{2+/+}$) for stellacyanin is 0.18 V vs. NHE, and the reduction potentials and self-exchange rate constants for the inorganic reagents are given in Table 6.3.[66,67] For relatively small $\Delta E°$ values, f_{12} is ~1; here a convenient form of the Marcus cross relation is log k_{12} = 0.5[log k_{11} + log k_{22} + 16.9$\Delta E_{12}°$]' Calculations with k_{11}, k_{22}, and $\Delta E_{12}°$ from experiments give k_{12} values that accord quite closely with the measured rate constants.

$$Cu^{II}St + Fe(EDTA)^{2-} \rightarrow Cu^{I}St + Fe(EDTA)^{-} \quad (11.2.6.8.1)$$

$$k_{12}(calc.) = 2.9 \times 10^5 M^{-1}s^{-1} \qquad (\Delta E_{12}^o = 0.06V) \quad (11.2.6.8.2)$$

$$k_{12}(obs.) = 4.3 \times 10^5 M^{-1}s^{-1} \quad (11.2.6.8.3)$$

$$Cu^{I}St + Co(phen)_3^{3+} \rightarrow Cu^{II}St + Co(phen)_3^{2+} \quad (11.2.6.8.4)$$

$$k_{12}(calc.) = 1.4 \times 10^5 M^{-1}s^{-1} \qquad (\Delta E_{12}^o = 0.19V) \quad (11.2.6.8.5)$$

$$k_{12}(obs.) = 1.8 \times 10^5 M^{-1}s^{-1} \quad (11.2.6.8.6)$$

Table 6.3 - Reduction potentials and self-exchange rate constants for inorganic reagents.

Reagent	E°(V vs. NHE)	k_{22} ($M^{-1}s^{-1}$)
$Fe(EDTA)^{-/2-}$	0.12	6.9 x 10^4
$Co(phen)_3^{3+/2+}$	0.37	9.8 x 10^1

The success of the Marcus cross relation with stellacyanin indicates that the copper site in the protein is accessible to inorganic reagents. The rate constants for the reactions of other blue copper proteins with inorganic redox agents show deviations from cross-relation predictions (Table 6.4).[68] These deviations suggest the following order of surface accessibilities of blue copper sites: stellacyanin > plastocyanin > azurin. Rate constants for protein-protein electron transfers also have been subjected to cross-relation analysis.[69]

Table 6.4 - Reactions of blue copper proteins with inorganic reagents.

a) $M^{-1}s^{-1}$

Protein	Reagent	k_{12} (obs.)[a]	$\Delta E_{12}°$	k_{11} (obs.)[a]	k_{11} (calc.)[a]
Stellacyanin	$Fe(EDTA)^{2-}$	4.3 x 10^5	0.064	1.2 x 10^5	2.3 x 10^5
	$Co(phen)_3^{3+}$	1.8 x 10^5	0.186	1.2 x 10^5	1.6 x 10^5
	$Ru(NH_3)_5py^{3+}$	1.94 x 10^5	0.069	1.2 x 10^5	3.3 x 10^5
Plastocyanin	$Fe(EDTA)^{2-}$	1.72 x 10^5	0.235	~10^3 - 10^4	7.3 x 10^1
	$Co(phen)_3^{3+}$	1.2 x 10^3	0.009	~10^3 - 10^4	1.1 x 10^4
	$Ru(NH_3)_5py^{3+}$	3.88 x 10^3	-0.100	~10^3 - 10^4	4.9 x 10^4
Azurin	$Fe(EDTA)^{2-}$	1.39 x 10^3	0.184	2.4 x 10^6	2.8 x 10^{-2}
	$Co(phen)_3^{3+}$	2.82 x 10^3	0.064	2.4 x 10^6	7.0 x 10^3
	$Ru(NH_3)_5py^{3+}$	1.36 x 10^3	-0.058	2.4 x 10^6	1.1 x 10^3

11.2.6.8: Marcus Theory is shared under a CC BY-NC-SA 4.0 license and was authored, remixed, and/or curated by LibreTexts.

11.2.7: Ferrodoxins, Hydrogenases, and Nitrogenases - Metal-Sulfide Proteins

Transition-metal/sulfide sites, especially those containing iron, are present in all forms of life and are found at the active centers of a wide variety of redox and catalytic proteins. These proteins include simple soluble electron-transfer agents (the ferredoxins), membrane-bound components of electron-transfer chains, and some of the most complex metalloenzymes, such as nitrogenase, hydrogenase, and xanthine oxidase. In this chapter we first review the chemistry of the Fe-S sites that occur in relatively simple rubredoxins and ferredoxins, and make note of the ubiquity of these sites in other metalloenzymes. We use these relatively simple systems to show the usefulness of spectroscopy and model-system studies for deducing bioinorganic structure and reactivity. We then direct our attention to the hydrogenase and nitrogenase enzyme systems, both of which use transition-metalsulfur clusters to activate and evolve molecular hydrogen.

I. Iron-sulfur Proteins and Models

A. Rubredoxin: A Singe-Fe Tetrathiolate Protein

B. Rubredoxin Model Systems

C. Fe_2S_2 Ferredoxins

D. Rieske Centers

E. Fe_2S_2 Models

F. Fe_4S_4 Ferredoxins (including HiPIPs)

G. Fe_4S_4 Models

H. Core Extrusion/Cluster Displacement Reactions

I. Fe_3S_4 Centers

J. Fe_3 Model Systems

K. Fe-S Chemistry: Comments and New Structures

L. Detection of Fe-S Sites

M. Redox Behavior

II. Multisite Redox Enzymes

A. Hydrogenase and Nitrogenase

B. Hydrogenases

1. Physiological Significance
2. Dihydrogen: The Molecule
3. Iron Hydrogenases
4. Nickel-iron Hydrogenases
5. Insights from Inorganic Chemistry

C. Nitrogenases

1. The Scope of Biological Nitrogen Fixation
2. Dinitrogen: The Molecule and Its Reduced Intermediates
3. The Dominant Hypothesis for Molybdenum Nitrogenase[239,240,242,243]
4. Protein Purity and Active Sites
5. FeMoco
6. The P-clusters
7. EPR, ENDOR, and ESEEM studies
8. Mössbauer Studies

9. X-ray Absorption Studies
10. Substrate Reactions
11. The Role of ATP

D. The Alternative Nitrogenases
1. Vanadium Nitrogenase
2. The All-iron Nirogenase[322]
3. Model Systems

E. N_2 and Related Complexes

F. Insights from Relevant Inorganic Reactivity

III. Report on the Nitrogenase Crystal Structure[378-381]

IV. References

1. F. Armstrong, in A. G. Sykes, ed., *Advances in Inorganic and Bioinorganic Mechanisms*, Vol. **I**, Academic Press, 1982.
2. H. Beinert and S. P. J. Albracht, *Biochim. Biophys. Acta* **683** (1982), 245.
3. A. V. Xavier, J. J. G. Moura, and I. Moura, in J. B. Goodenough *et al.*, eds., *Structure and Bonding*, Springer-Verlag, **43** (1981), 187-213.
4. D. C. Yoch and R. P. Carithers, *Microbiol. Rev*. **43** (1979), 384.
5. H. B. Dunford *et aI.*, eds., *The Biological Chemistry of Iron: A Look at the Metabolism of Iron and Its Subsequent Uses in Living Organisms*, Reidel, 1981.
6. R. K. Thauer and P. Schönheit, in Reference 8, p. 329.
7. A. Bezkorovainy, *Biochemistry of Nonheme Iron*, Plenum, 1980, pp. 343-393.
8. T. G. Spiro, ed., *Iron-Sulfur Proteins*, Wiley-Interscience, 1985.
9. W. Lovenberg, ed., *Iron-Sulfur Proteins*, Vol. I, Academic Press, 1973.
10. Reference 9, Vol. II, Academic Press, 1973.
11. Reference 10, Vol. III, Academic Press, 1977.
12. Nomenclature, *Eur. J. Biochem.* **93** (1979), 427.
13. Nomenclature, *Biochim. Biophys. Acta* 549 (1979), 101.
14. C. F. Yocum, J. N. Sadow, and A. San Pietro, in Reference 9, p. 112.
15. B. B. Buchanan, in Reference 9, p. 129.
16. T. P. Singer and R. R. Ramsay, in A. N. Martonosi, ed., *The Enzymes of Biological Membranes*, Plenum, 1985, pp. 301-332.
17. T. Yagi, H. Inokuchi, and K. Kimura, *Acc. Chem. Res.* **16** (1983), 2; Y. Higuchi *et al.*, *J. Mol. Biol.* **172** (1984), 109.
18. R. Lemberg and J. Barrett, *Cytochromes*, Academic Press, 1973.
19. H. Beinert, in Reference 9, p. 1.
20. K. K. Rao and D. O. Hall, in G. V. Leigh, ed., *Evolution of Metalloenzymes, Metalloproteins, and Related Materials*, 1977, p. 39.
21. D. O. Hall, R. Cammack, and K. K. Rao, *Nature* **233** (1977), 136.
22. T. Ohnishi and J. C. Salerno, in Reference 8, p. 285.
23. F. A. Cotton and G. Wilkinson, *Advanced Inorganic Chemistry*, Wiley, 1980.
24. D. E. McRee *et al.*, *J. Biol. Chem.* **261** (1986), 10277.
25. S. J. N. Burgmayer and E. I. Stiefel, *J. Chem. Educ.* **62** (1985), 943.
26. W. Lovenberg and B. E. Sobel, *Proc. Natl. Acad. Sci. USA* **54** (1965), 193.
27. E. T. Lode and M. J. Coon, in Reference 9, pp. 173-191.
28. I. C. Gunsalus and J. D. Lipscomb, in Reference 11, p. 151.
29. R. W. Estabrook *et al*., in Reference 9.
30. I. Moura *et al*., *Biochem. Biophys. Res. Commun*. **75** (1977), 1037.

31. I. Moura *et al*., *J. Biol. Chem.* **255** (1980), 2493. a) J. LeGall *et al*., *Biochemistry* **27** (1988), 1636.
32. K. D. Watenpaugh, L. C. Sieker, and L. H. Jensen, *J. Mol. Biol*. **138** (1980), 615.
33. E. T. Adman *et al*., *J. Mol. Biol.* **112** (1977), 113. a) C. D. Stout, in Reference 8, p. 97.
34. K. D. Watenpaugh *et al*., *Acta Cryst*. **B29** (1973), 943.
35. R. G. Shulman *et al*., *Proc. Natl. Acad. Sci. USA* **72** (1975), 4003.
36. R. G. Shulman *et al*., *J. Mol. Biol.* **124** (1978), 305.
37. W. D. Phillips *et al*., *Nature* **227** (1970), 574.
38. J. C. Rivoal *et aI*., *Biochim. Biophys. Acta* **493** (1977), 122.
39. D. E. Bennett and M. K. Johnson, *Biochim. Biophys. Acta* **911** (1987), 71. a) M. S. Gebhard *et al*.,*J. Am. Chem. Soc*. **112** (1990), 2217. b) K. D. Butcher, M. S. Gebhard, and E. I. Solomon, *Inorg. Chem*. **29** (1990), 2067.
40. M. C. W. Evans, in Reference 8, p. 249.
41. W. A. Eaton and W. J. Lovenberg, *J. Am. Chem. Soc*. **92** (1970), 7195.
42. M. K. Johnson, A. E. Robinson, and A. J. Thomson, in Reference 8, p. 367.
43. P. J. Stephens *et aI*., *Proc. Natl. Acad. Sci. USA* **75** (1978), 5273.
44. J. Peisach *et al*., *J. Biol. Chem.* 246 (1971), 5877.
45. P. M. Champion and A. J. Siever, *J. Chem. Phys.* **66** (1977), 1819; D. Coucouvanis *et al*., *J. Am. Chem Soc.* **101** (1979), 3392.
46. R. Cammack, D. S. Patil, and V. M. Fernandez, *Biochem. Soc. Trans.* **13** (1985), 572.
47. B. L. Trumpower, *Biochim. Biophys. Acta* **639** (1981), 129.
48. H. Beinert, *Biochem. Soc. Trans.* **13** (1985), 542.
49. G. Palmer, *Biochem. Soc. Trans.* **13** (1985), 548.
50. R. Malkin and A. J. Bearden, *Biochim. Biophys. Acta* **505** (1978), 147.
51. C. E. Johnson, *J. Inorg. Biochem.* **28** (1986), 207.
52. E. Münck and T. A. Kent, *Hyperfine Interactions* **27** (1986), 161.
53. K. K. Rao *et al*., *Biochem. J.* **129** (1972), 1063.
54. I. Bertini and C. Luchinat, eds., *NMR of Paramagnetic Molecules in Biological Systems*, Benjamin/ Cummings, 1986.
55. G. N. La Mar, W. D. Horrocks, Jr., and R. H. Holm, NMR *of Paramagnetic Molecules*, Academic Press, 1973.
56. M. T. Werth *et al*., *J. Am. Chem. Soc.* **109** (1987), 273.
57. T. G. Spiro *et al*., in Reference 8, p. 407. a) T. V. Long and T. M. Loehr, *J. Am. Chem. Soc.* **92** (1970), 6384.
58. G. Christou, B. Ridge, and H. N. Rydon, *J. Chem. Soc. Chem. Commun.* (1979), 20.
59. S. W. May and J.-Y. Kuo, *Biochemistry* **17** (1978), 3333.
60. S. W. May *et al*., *Biochemistry* **23** (1984), 2187.
61. P. Saint-Martin *et al*., *Proc. Natl. Acad. Sci. USA* **85** (1988), 9378.
62. R. W. Lane *et al*., *Proc. Natl. Acad. Sci. USA* **72** (1975), 2868.
63. R. W. Lane *et al*., *J. Am. Chem. Soc.* **99** (1977), 84.
64. D. G. Holah and D. Coucouvanis, *J. Am. Chem. Soc.* **97** (1975), 6917.
65. D. Coucouvanis *et al*., *J. Am. Chem. Soc.* **93** (1976), 5721.
66. M. Millar *et al*., *lnorg. Chem.* **21** (1982), 4105.
67. S. A. Koch and L. E. Madia, *J. Am. Chem. Soc.* **105** (1983), 5944.
68. M. Millar, S. A. Koch, and R. Fikar, *lnorg. Chim. Acta* **88** (1984), L15.
69. J. C. Deaton *et al*., *J. Am. Chem. Soc.* **110** (1988), 6241.
70. D. B. Knaff, *Trends Biochem. Sci.* **13** (1988), 461. a) T. Tsukihara *et al*., *J. Biochem.* **90** (1981), 1763.
71. D. R. Ort and N. E. Good, *Trends Biochem. Sci.* **13** (1988), 467.
72. V. Massey, in Reference 9, p. 301.
73. M. K. Johnson *et al*., *J. Biol. Chem.* **260** (1985), 7368.
74. J. C. Salerno *et al*., *J. Biol. Chem.* **254** (1979), 4828.
75. T. P. Singer, M. Gutman, and V. Massey, in Reference 9, p. 225.
76. H. Twilfer, F.-H. Bernhardt, and K. Gersonde, *Eur. J. Biochem.* **119** (1981), 595.
77. L. Petersson, R. Cammack, and K. Krishna Rao, *Biochim. Biophys. Acta* **622** (1980), 18.
78. B.-K. Teo and R. G. Shulman, in Reference 8, p. 343.

79. T. Tsukihara *et al.*, in K. Kimura, ed., *Molecular Evolution, Protein Polymorphism and the Neutral Theory*, Japan Scientific Societies Press and Springer-Verlag, 1982, p. 299.
80. T. Tsukihara *et al.*, *BioSystems* **15** (1982), 243.
81. D. Petering and G. Palmer, *Arch. Biochem. Biophys*. **141** (1970), 456.
82. J. F. Gibson *et aI.*, *Proc. Natl. Acad. Sci. USA* **56** (1966), 987.
83. W. A. Eaton *et al.*, *Proc. Natl. Acad. Soc. USA* **68** (1971), 3015. a) L. B. Dugad *et al.*, *Biochemistry* **29** (1990), 2663.
84. J. Rawlings, O. Siiman, and H. B. Gray, *Proc. Natl. Acad. Sci. USA* **71** (1974), 125.
85. I. Salmeen and G. Palmer, *Arch. Biochem. Biophys.* **150** (1972), 767.
86. J. J. Mayerle *et al.*, *Proc. Natl. Acad. Sci. USA* **70** (1973), 2429.
87. J. L. Markley *et al.*, *Science* **240** (1988), 908. a) L. Banci, I. Bertini, and C. Luchinat, *Structure and Bonding* **72** (1990), 113.
88. V. K. Yachandra *et al.*, *J. Am. Chem. Soc.* **105** (1983), 6462.
89. S. Hwa, R. S. Czernuszewicz, and T. G. Spiro, *J. Am. Chem. Soc*. **111** (1989), 3496.
90. S. Hwa *et al.*, *J. Am. Chem. Soc.* **111** (1989), 3505.
91. J. R. Rieske, D. H. MacLennan, and R. Coleman, *Biochem. Biophys. Res. Commun.* **15** (1964), 338.
92. W. D. Bonner, Jr., and R. C. Prince, *FEBS Lett.* **177** (1984), 47.
93. J. F. Cline *et al.*, *J. Biol. Chem.* **260** (1985), 3251.
94. H.-T. Tsang *et al.*, *Biochemistry* **28** (1989), 7233.
95. R. C. Prince, S. J. G. Linkletter, and P. L. Dutton, *Biochem. Biophys. Acta* **635** (1981), 132.
96. J. G. Reynolds and R. H. Holm, *lnorg. Chem.* **19** (1980), 3257; **20** (1981), 1873. a) J. J. Mayerle *et al., J. Am. Chem. Soc.* **97** (1977), 1032. b) Y. Do, E. D. Simhon, and R. H. Holm, *lnorg. Chem.* **22** (1983), 3809. c) S. Han, R. Czernuszewicz, and T. G. Spiro, *lnorg. Chem.* **25** (1986), 2276. d) H. Strasdeit, B. Krebs, and G. Henkel, *lnorg. Chim. Acta* **89** (1989), LII.
97. P. K. Mascharak *et al.*, *J. Am. Chem. Soc.* **103** (1981), 6110.
98. P. Beardwood *et al.*, *J. Chem. Soc.* Dalton Trans. (1982), 2015.
99. D. Coucouvanis *et al.*, *J. Am. Chem. Soc.* **106** (1984), 6081.
100. P. Beardwood and J. F. Gibson, *J. Chem. Soc. Chem. Commun.* **102** (1985), 490 and 1345.
101. L. C. Sieker, E. Adman, and L. H. Jensen, *Nature* **235** (1971), 40.
102. J. M. Berg, K. O. Hodgson, and R. H. Holm, *J. Am. Chem. Soc.* **101** (1970), 4586.
103. P. J. Stephens *et al.*, *Proc. Natl. Acad. Sci. USA* **82** (1985), 5661.
104. M. W. W. Adams and L. E. Mortenson, in Reference 235a.
105. L. W. Lim *et al.*, *J. Biol. Chem.* **261** (1986), 15 and 140.
106. J. C. Salerno *et al.*, *Biochem. Biophys. Res. Commun.* **73** (1976), 833.
107. G. Strahs and J. Kraut, *J. Mol. Biol.* **35** (1968), 503.
108. C. W. Carter, Jr., *et al.*, *Proc. Natl. Acad. Sci. USA* **69** (1972), 3526.
109. C. W. Carter, Jr., *et al.*, *J. Biol. Chem.* **249** (1974), 4212.
110. K. Fukuyama, *J. Mol. Biol.* 199 (1988), 183. a) K. Fukuyama *et al.*, *J. Mol. Biol.* **210** (1989), 383.
111. G. H. Stout *et al.*, *Proc. Natl. Acad. Sci. USA* **85** (1988), 1020.
112. C. D. Stout, *J. Biol. Chem.* **263** (1988), 9256.
113. A. H. Robbins and C. D. Stout, *Proc. Natl. Acad. Sci. USA* **86** (1989), 3639.
114. E. T. Adman, L. C. Sieker, and L. H. Jensen, *J. Biol. Chem.* **248** (1973), 3987.
115. R. C. Prince and M. W. W. Adams, *J. Biol. Chem.* **262** (1987), 5125.
116. L. E. Mortenson, R. C. Valentine, and J. E. Carnahan, *Biochem. Biophys. Res. Commun.* **7** (1962), 448.
117. W. Lovenberg, B. B. Buchanan, and J. C. Rabinowitz, *J. Biol. Chem.* **254** (1979), 4499.
118. R. Mathews *et al.*, *J. Biol. Chem.* **249** (1974), 4326.
119. A. J. Thomson, in P. M. Harrison, ed., *Metalloproteins, Part I: Metal Proteins with Redox Roles*, Verlag Chemie, 1985, pp. 79-120.
120. R. Cammack, *Biochem. Biophys. Res. Commun.* **54** (1973), 548.
121. M. J. Carney *et al.*, *Inorg. Chem.* **27** (1988), 346.
122. M. J. Carney *et al.*, *J. Am. Chem. Soc.* **110** (1988), 6084.
123. L. Noodleman, D. A. Case, and A. Aizman, *J. Am. Chem. Soc.* **110** (1988), 1001.
124. L. Noodleman, *Inorg. Chem.* 27 (1988), 3677.

125. J.-M. Moulis, J. Meyer, and M. Lutz, *Biochemistry* **23** (1984), 6605. a) W. D. Phillips and M. Poe, in Reference 10, p. 255. b) E. L. Packer *et al.*, *J. Biol. Chem.* **252** (1977), 2245. c) J. Bertini *et al.*, *Inorg. Chem.* **29** (1990), 1874. d) B.-K. Teo *et al.*, *J. Am. Chem. Soc.* **101** (1979), 5624.
126. T. Herskovitz *et al.*, *Proc. Natl. Acad. Sci. USA* **69** (1972), 2437.
127. B. A. Averill *et al.*, *J. Am. Chem. Soc.* **95** (1973), 3523.
128. J. M. Berg and R. H. Holm, in Reference 8, p. I.
129. G. B. Wang, M. A. Bobrick, and R. H. Holm, *Inorg. Chem.* **17** (1978), 578.
130. D. Coucouvanis *et al.*, *J. Am. Chem. Soc.* **104** (1982), 1874.
131. A. Müller and N. Schladerbeck, *Chimia* **39** (1985), 23.
132. A. Müller, N. Schladerbeck, and H. Bagge, *Chimia* **39** (1985), 24.
133. S. Rutchik, S. Kim, and M. A. Walters, *Inorg. Chem.* **27** (1988), 1513.
134. W. E. Cleland *et al.*, *J. Am. Chem. Soc.* **105** (1983), 6021.
135. M. G. Kanatzidis *et al.*, *J. Am. Chem. Soc.* **106** (1984), 4500.
136. M. G. Kanatzidis *et al.*, *Inorg. Chem.* **22** (1983), 179.
137. R. E. Johnson *et al.*, *J. Am. Chem. Soc.* **105** (1983), 7280.
138. M. G. Kanatzidis *et al.*, *J. Am. Chem. Soc.* **107** (1985), 4925. a) K. S. Hagen, J. G. Reynolds, and R. H. Holm, *J. Am. Chem. Soc.* **103** (1981), 4054. b) G. Christou and C. D. Gamer, *J. Chem. Soc. Dalton Trans.* (1979), 1093. c) M. J. Carney *et al.*, *Inorg. Chem.* **27** (1988), 346. d) P. Barbaro *et al.*, *J. Am. Chem. Soc.* **112** (1990), 7238.
139. E. J. Laskowski *et al.*, *J. Am. Chem. Soc.* **100** (1978), 5322.
140. E.1. Laskowski *et al.*, *J. Am. Chem. Soc.* **101** (1979), 6562.
141. T. O'Sullivan and M. Millar, *J. Am. Chem. Soc.* **107** (1985), 4096.
142. M. Millar, private communication.
143. T. D. P. Stack and R. H. Holm, *J. Am. Chem. Soc.* **110** (1989), 2484. a) T. D. P. Stack, M. J. Carney, and R. H. Holm, *J. Am. Chem. Soc.* **111** (1989), 1670. b) S. Ciurli *et al.*, *J. Am. Chem. Soc.* **112** (1990), 2654. c) P. R. Challen *et al.*, *J. Am. Chem. Soc.* **112** (1990), 2455.
144. L. Que, Jr., R. H. Holm, and L. E. Mortenson, *J. Am. Chem. Soc.* **97** (1975), 463.
145. N. R. Bastian *et al.*, in Reference 10, p. 227.
146. H. Beinert and A. J. Thomson, *Arch. Biochem. Biophys.* **222** (1983), 333.
147. M. H. Emptage *et al.*, *J. Biol. Chem.* **255** (1980), 1793.
148. W. W. Sweeney, J. C. Rabinowitz, and D. C. Yoch, *J. Biol. Chem.* **250** (1985), 7842.
149. B. A. Averill, J. R. Bal, and W. H. Orme-Johnson, *J. Am. Chem. Soc.* **100** (1978), 3034.
150. C. D. Stout, *Nature* **279** (1979), 83.
151. D. Ghosh *et al.*, *J. Biol. Chem.* **256** (1981), 4185.
152. D. Ghosh *et al.*, *J. Mol. Biol.* **158** (1982), 73.
153. M. K. Johnson *et al.*, *J. Am. Chem. Soc.* **105** (1983), 6671.
154. H. Beinert and A. J. Thomson, *Arch. Biochem. Biophys.* **222** (1983), 333.
155. M. R. Antonio *et al.*, *J. Biol. Chem.* **257** (1982), 6646.
156. E. Miinck, in Reference 8, p. 147.
157. C. E. Johnson, *J. Inorg. Biochem.* **207** (1986), 28.
158. B. H. Huynh *et al.*, *J. Biol. Chem.* **255** (1980), 3242.
159. J. J. G. Moura *et al.*, *J. Biol. Chem.* **257** (1982), 6259. a) H. Beinert and M. C. Kennedy, *Eur. J. Biochem.* **186** (1989), 1865.
160. C. R. Kissinger *et al.*, *J. Am. Chem. Soc.* **110** (1988), 8721. a) S. Ciurli and R. H. Holm, *Inorg. Chem.* **28** (1989), 1685.
161. T. A. Kent *et al.*, *J. Biol. Chem.* **260** (1985), 6871.
162. A. H. Robbins and C. D. Stout, *J. Biol. Chem.* **260** (1985), 2328.
163. M. K. Johnson *et al.*, *J. Biol. Chem.* **258** (1983), 12771.
164. M. C. Kennedy *et al.*, *J. Biol. Chem.* **258** (1983), 11098.
165. J. TeIser *et al.*, *J. Biol. Chem.* **261** (1986), 4840.
166. D. H. Flint, M. H. Emptage, and J. R. Guest, *J. Inorg. Biochem.* **36** (1989), 306. a) R. L. Switzer, *BioFactors* **2** (1989), 77.
167. H. Beinert *et al.*, *Proc. Natl. Acad. Sci. USA* **80** (1983), 393.
168. M. K. Johnson *et al.*, *J. Biol. Chem.* **256** (1981), 9806.

169. T. R. Halbert *et al.*, *J. Am. Chem. Soc.* **106** (1984),1849.
170. G. N. George and S. J. George, *Trends Biochem. Sci.* **13** (1988), 369. a) I. Moura *et al.*, *J. Am. Chem. Soc.* **108** (1986), 349. b) K. K. Surerus *et al.*, *J. Am. Chem. Soc.* **109** (1987), 3805. c) R. C. Conover *et al.*, *J. Am. Chem. Soc.* **112** (1990), 4562. d) J. K. Money, J. C. Huffman, and G. Christou, *Inorg. Chem.* **27** (1988), 507.
171. B. H. Huynh *et al.*, *Proc. Natl. Acad. Sci. USA* **81** (1984), 3728.
172. T. R. Hawkes and B. E. Smith, *Biochem. J.* 223 (1984), 783.
173. M. A. Whitener *et al.*, *J. Am. Chem. Soc.* **108** (1986), 5607.
174. K. S. Hagen and R. H. Holm, *J. Am. Chem. Soc.* **104** (1982), 5496.
175. K. S. Hagen, A. D. Watson, and R. H. Holm, *J. Am. Chem. Soc.* **105** (1983), 3905. a) J.-J. Girard *et al.*, *J. Am. Chem. Soc.* **106** (1984), 5941.
176. M. C. Kennedy *et al.*, *J. Biol. Chem.* 259 (1984), 14463. a) H. Strasdeit, B. Krebs, and G. Henkel, *Inorg. Chem.* **23** (1983), 1816.
177. M. G. Kanatzidis *et al.*, *J. Chem. Soc. Chem. Commun.* (1984), 356.
178. M. G. Kanatzidis, A. Salifoglou, and D. Coucouvanis, *J. Am. Chem. Soc.* **107** (1985), 3358; *Inorg. Chem.* **25** (1986), 2460.
179. S. Pohl and W. Saak, *Angew. Chem. Int. Ed. Engl.* **23** (1984), 907. a) S. A. AI-Ahmand *et al.*, *Inorg. Chem.* **29** (1990), 927.
180. F. Cecconi, C. A. Ghilardi, and S. Midolini, *J. Chem. Soc. Chem. Commun.* (1981), 640.
181. A. Agresti *et al.*, *Inorg. Chem.* **24** (1985), 689.
182. K. S. Hagen, J. M. Berg, and R. H. Holm, *Inorg. Chim. Acta* **45** (1980), L17. a) B. S. Snyder and R. H. Holm, *Inorg. Chem.* **27** (1988), 1816. b) B. S. Synder *et al.*, *Inorg. Chem.* **27** (1988), 595. c) M. S. Reynolds and R. H. Holm, *Inorg. Chem.* **27** (1988), 4494. d) B. S. Snyder and R. H. Holm, *Inorg. Chem.* **29** (1990), 274.
183. I. Noda, B. S. Snyder, and R. H. Holm, *Inorg. Chem.* **25** (1986), 3851. a) J.-F. You, B. S. Snyder, and R. H. Holm, *J. Am. Chem. Soc.* **110** (1988), 6589. b) J.-F. You *et al.*, *J. Am. Chem. Soc.* **112** (1990), 1067. c) W. R. Hagen, A. J. Pierik, and C. Veeger, *J. Chem. Soc., Faraday Trans. I* **85** (1989), 4083.
184. E. I. Stiefel *et al.*, *Adv. Chem. Ser.* **162** (1977), 353. a) I. Moura and J. J. G. Moura, in Reference 5, p. 179. b) J. R. Lancaster, Jr., ed., *The Bioinorganic Chemistry of Nickel*, VCH Publishers, 1988. c) H. J. Grande *et al.*, in Reference 5, p. 193. d M. W. W. Adams, L. E. Mortenson, and J.-S. Chen, *Biochim. Biophys. Acta* **594** (1981), 105. e) J. LeGall and H. D. Peck, Jr., in Reference 5, p. 207. f) J. LeGall *et al.*, in Reference 8, p. 177. g) S. P. Ballantine and D. H. Boxer, *Eur. J. Biochem.* **156** (1986), 276. h) W. H. Onne-Johnson and N. R. Onne-Johnson, in Reference 8, p. 67.
185. B. Bowien and H. G. Schlegel, *Annu. Rev. Microbiol.* **35** (1981), 401.
186. C. R. Bowers and D. P. Weitekamp, *J. Am. Chem. Soc.* **109** (1987), 5541.
187. T. C. Eisenschmid *et al.*, *J. Am. Chem. Soc.* **109** (1987), 8089.
188. M. W. W. Adams *et al.*, *Biochimie* **68** (1986), 35.
189. R. Cammack, V. M. Fernandez, and K. Schneider, in Reference 184b, p. 167. 189a. M. W. W. Adams, *Biochem. Biophys. Acta* **1020** (1990),115.
190. H. J. Grande *et al.*, *Eur. J. Biochem.* **136** (1983), 201.
191. M. W. W. Adams and L. E. Mortenson, *J. Biol. Chem.* **259** (1984), 7045.
192. S. W. Ragsdale and L. G. L. Ljungdahl, *Arch. Microbial*. **139** (1984), 361.
193. C. R. Woese, *Microbial. Rev.* **81** (1987), 221.
194. M. W. W. Adams, E. Eccleston, and J. B. Howard, *Proc. Natl. Acad. Sci. USA* **86** (1989), 4932.
195. D. S. Patil *et al.*, *J. Am. Chem. Soc.* **110** (1988), 8533.
196. A. T. Kowal, M. W. W. Adams, and M. K. Johnson, *J. Biol. Chem.* **264** (1989), 4342.
197. W. R. Hagen *et al.*, *FEBS Lett.* **203** (1986), 59.
198. I. C. Zambrano *et al.*, *J. Biol. Chem.* **264** (1989), 20974.
199. M. W. W. Adams, *J. Biol. Chem.* **262** (1987), 15054.
200. T. V. Morgan, R. C. Prince, and L. E. Mortenson, *FEBS Lett*. **206** (1986), 4.
201. W. R. Hagen *et al.*, *FEBS Lett*. **201** (1986), 158.
202. F. M. Rusnak *et al.*, *J. Biol. Chem.* **262** (1987), 38.
203. G. Wang *et al.*, *J. Biol. Chem.* **259** (1984), 14328.
204. J. Telser *et al.*, *J. Biol. Chem.* **262** (1987), 6589.
205. J. Telser *et al.*, *J. Biol. Chem.* **261** (1986), 15536.

206. H. Thomann, M. Bernardo, and M. W. W. Adams, *J. Am. Chem. Soc.* **113** (1991), 7044.
207. A. J. Thomson *et al.*, *Biochem. J.* **227** (1985), 333.
208. K. A. Macor *et al.*, *J. Biol. Chem.* **282** (1987), 9945.
209. G. N. George *et al.*, *Biochem. J.* **259** (1989), 597.
210. R. Cammack, *Adv. Inorg. Chem.* **32** (1988), 297.
211. J. J. G. Moura *et al.*, in Reference 5, p. 191.
212. J. R. Lancaster, *FEBS Lett.* **115** (1980), 285.
213. M. Teixeira *et al.*, *J. Biol. Chem.* **260** (1985), 8942.
214. J. W. Van der Zwaan *et al.*, *FEBS Lett.* **179** (1985), 271.
215. M. K. Eidsness, R. J. Sullivan, and R. A. Scott, in Reference 184b, p. 73.
216. M. K. Eidsness *et al.*, *Proc. Natl. Acad. Sci. USA* **86** (1989), 147.
217. P. A. Lindahl *et al.*, *J. Am. Chem. Soc.* **106** (1984), 3062.
218. R. A. Scott *et al.*, *J. Am. Chem. Soc.* **106** (1984), 6864.
219. S. P. J. Albracht *et al.*, *Biochim. Biophys. Acta* **874** (1986), 116.
220. A. Chapman *et al.*, *FEBS Lett.* **242** (1988), 134.
221. S. L. Tau *et al.*, *J. Am. Chem. Soc.* **106** (1984), 3064.
222. G. J. Kubas *et al.*, *J. Am. Chem. Soc.* **106** (1984), 451.
223. G. J. Kubas and R. R. Ryan, *Polyhedron* **5** (1986), 473.
224. G. J. Kubas *et al.*, *J. Am. Chem. Soc.* **108** (1986), 7000.
225. M. Rakowski DuBois *et al.*, *J. Am. Chem. Soc.* **102** (1980), 7456.
226. C. Bianchini *et al.*, *Inorg. Chem.* **25** (1986), 4617.
227. W. Tremel *et al.*, *Inorg. Chem.* **27** (1988), 3886.
228. W. Tremel and G. Henkel, *Inorg. Chem.* **27** (1988), 3896.
229. I. Dance, *Polyhedron* **5** (1986), 1037; P. J. Blower and J. R. Dilworth, *Coord. Chem. Rev.* **76** (1987), 121.
230. C. L. Coyle and E. I. Stiefel, in Reference 184b, p. 1.
231. M. Kumar *et al.*, *J. Am Chem. Soc.* **111** (1989), 5974.
232. M. Kumar *et al.*, *J. Am. Chem. Soc.* **111** (1989), 8323.
233. T. H. Blackburn, in W. E. Krumbein, ed., *Microbial Geochemistry*, Blackwell Scientific, 1983, p. 63.
234. J. R. Postgate, *Fundamentals of Nitrogen Fixation*, Cambridge University Press, 1982.
235. R. W. F. Hardy, *Treatise on Dinitrogen Fixation*, Wiley, 1979, Section I. a) T. G. Spiro, ed., *Molybdenum Enzymes*, Wiley-Interscience, 1985.
236. W. J. Brill, *NATO Adv. Sci. Inst., Ser. A* **63** (1983), 231.
237. R. Haselkorn, *Annu. Rev. Microbial.* **40** (1986), 525.
238. A. C. Robinson, D. R. Dean, and B. K. Burgess, *J. Biol. Chem.* **262** (1987), 14327.
239. P. J. Stephens, in Reference 235a, p. 117.
240. A. H. Gibson and W. E. Newton, eds., Current *Perspectives in Nitrogen Fixation*, Australian Academy of Science, 1981.
241. E. I. Stiefel, in W. E. Newton and C. Rodriquez-Barrucco, eds., in *Recent Progress in Nitrogen Fixation*, Academic Press, 1977, p. 69.
242. C. Veeger and W. E. Newton, eds., *Advances in Nitrogen Fixation Research*, Nijhoff/Junk, 1984.
243. H. J. Evans, P. J. Bottomley, and W. E. Newton, eds., *Nitrogen Fixation Research Progress*, Martinus Nijhoff, 1985. a) A. Braaksma *et al.*, in Reference 5, p. 223. b) B. H. Huynh, E. Münck, and W. H. Orme-Johnson, in Reference 5, p. 241.
244. E. I. Stiefel, in Reference 240, p. 55.
245. R. V. Hageman and R. H. Burris, *Proc. Natl. Acad. Sci. USA* **75** (1978), 2699.
246. V. Sundaresan and F. M. Ausubel, *J. Biol. Chem.* **256** (1981), 2808. a) R. P. Hausinger and J. B. Howard, *J. Biol. Chem.* **258** (1983), 13486. b) M. M. Georgiadis, P. Chakrabarti, and D. C. Rees, *SSRL Annual Report* (1989), p. 94.
247. L. E. Mortenson, M. N. Walker, and G. A. Walker, in W. E. Newton and C. J. Nyman, eds., *Proceedings of the First International Conference on Nitrogen Fixation*, Washington State University Press (1976), p. 117.
248. W. H. Orme-Johnson et al., in W. E. Newton, J. R. Postgate, and C. Rodriguez Barrucco, eds., *Recent Developments in Nitrogen Fixation*, Academic Press, 1977, p. 131.
249. G. D. Watt and J. W. McDonald, *Biochemistry* **24** (1985), 7226.

250. W. R. Hagen *et al.*, *FEBS Lett.* **189** (1986), 250.
251. L. Noodleman *et al.*, *J. Am. Chem. Soc.* **107** (1985), 3418.
252. G. D. Watt, Z.-C. Wang, and R. R. Knotts, *Biochemistry* **25** (1986),8156; J. Cordewener *et al.*, *Eur. J. Biochem.* **148** (1985), 499.
253. L. E. Mortenson and R. N. F. Thorneley, *Annu. Rev. Biochem.* **48** (1979), 387.
254. A. V. Kulikov *et al.*, *Dokl. Akad. Nauk SSR* **262** (1981), 1177.
255. R. N. F. Thorneley and D. J. Lowe, in Reference 235, p. 221. a) F. A. Schultz, S. F. Gheller, and W. E. Newton, Proc. *Int. Symp. Redox Mech. Interfacial Prop. Mol. Biol. Importance* **3** (1988), 203.
256. B. K. Burgess and W. E. Newton, in A. Müller and W. E. Newton, eds., *Nitrogen Fixation: The Chemical-Biochemical-Genetic Interface*, Plenum, 1983, p. 83.
257. E. I. Stiefel and S. P. Cramer, in Reference 235, p. 88.
258. V. Shah and W. J. Brill, *Proc. Natl. Acad. Sci. USA* **74** (1977), 3249.
259. S. D. Conradson *et al.*, *J. Am. Chem. Soc.* **109** (1987), 7507. a) P. A. McLean *et al.*, *Biochemistry* **28** (1989), 9402. b) D. A. Wink *et al.*, *Biochemistry* **28** (1989), 9407.
260. M. A. Walters, S. K. Chapman, and W. H. Orme-Johnson, *Polyhedron* **5** (1986), 561.
261. P. A. McLean and R. A. Dixon, *Nature* **292** (1981), 655.
262. P. A. McLean and B. E. Smith, *Biochem. J.* **211** (1983), 589.
263. T. R. Hawkes, P. A. McLean, and B. E. Smith, *Biochem. J.* **217** (1984), 317.
264. T. R. Hoover *et al.*, *Biochemistry* **27** (1988), 3647.
265. T. R. Hoover *et al.*, *Biochemistry* **28** (1989), 2768. a) J. Liang *et al.*, *Biochemistry* **29** (1990), 8377. b) M. S. Madden *et al.*, *Proc. Natl. Acad. Sci. USA* **87** (1990), 6517.
266. A. C. Robinson, D. Dean, and B. K. Burgess, *J. Biol. Chem.* **262** (1989), 14327. a) A. C. Robinson *et al.*, *J. Biol. Chem.* **264** (1989), 10088. b) D. J. Scott *et al.*, *Nature* **343** (1990), 188. c) H. M. Kent *et al.*, *Biochem. J.* **264** (1989), 257.
267. W. R. Hagen *et al.*, *Eur. J. Biochem*. **169** (1987), 457.
268. P. A. McLean *et al.*, *J. Biol. Chem.* **262** (1987), 12900.
269. P. A. Lindahl *et al.*, *J. Biol. Chem.* **263** (1988), 19442.
270. G. D. Watt, A. Burns, and D. L. Tennent, *Biochemistry* **20** (1981), 7272; G. D. Watt and Z. C. Wang, *Biochemistry* **25** (1986), 5196.
271. R. Zimmermann *et al.*, *Biochim. Biophys. Acta.* **537** (1978), 185.
272. D. M. Kurtz *et al.*, *Proc. Natl. Acad. Sci. USA* **76** (1979), 4986.
273. R. A. Venters *et al.*, *J. Am. Chem. Soc*. **108** (1986), 3487. a) J. Bolin, in P. M. Gresshoff, L. E. Roth, G. Stacey, and W. E. Newton, eds., *Nitrogen Fixation: Achievements and Objectives*, Chapman and Hall, 1990, p. 111.
274. B. M. Hoffman, J. E. Roberts, and W. H. Orme-Johnson, *J. Am. Chern. Soc.* **104** (1982), 860.
275. A. E. True *et al.*, *J. Am. Chem. Soc.* **110** (1988), 1935. a) A. E. True *et al.*, *J. Am. Chem. Soc.* **112** (1990), 651.
276. G. N. George *et aI.*, *Biochem. J.* **262** (1989), 349.
277. W. B. Mims and J. Peisach, in R. G. Shulman, ed., *Biological Applications of Magnetic Resonance*, Academic Press, 1980, p. 221.
278. W. H. Orme-Johnson *et al.*, in Reference 8, p. 79.
279. H. Thomann *et al.*, *J. Am. Chem. Soc.* **109** (1987), 7913.
280. H. Thomann *et al.*, *Proc. Natl. Acad. Sci. USA*, **88** (1991), 6620.
281. B. H. Huynh, E. Munck, and W. H. Orme-Johnson, *Biochim. Biophys. Acta* **527** (1979), 192.
282. B. H. Huynh *et aI.*, *Biochim. Biophys. Acta* **623** (1980), 124.
283. E. Münck *et al.*, *Biochim. Biophys. Acta* **400** (1975), 32. a) W. E. Newton *et al.*, *Biochem. Biophys. Res. Commun*. **162** (1989), 882.
284. S. D. Conradson, B. K. Burgess, and R. H. Holm, *J. Biol. Chem*. **263** (1988), 13743.
285. W. R. Dunham *et aI.*, *Eur. J. Biochem.* **146** (1985), 497.
286. S. P. Cramer *et al.*, *J. Am. Chem. Soc*. **100** (1978), 3398.
287. M. K. Eidsness *et al.*, *J. Am. Chem. Soc*. **108** (1986), 2746.
288. S. D. Conradson *et aI.*, *J. Am. Chem. Soc.* **107** (1985), 7935; Reference 259.
289. B. Hedman *et al.*, *J. Am. Chem. Soc*. **110** (1988), 3798.

290. M. R. Antonio *et al.*, *J. Am. Chem. Soc.* **104** (1982), 4703.
291. J. M. Arber *et al.*, *Biochem. J.* **252** (1988), 421.
292. M. S. Weininger and L. E. Mortenson, *Proc. Natl. Acad. Sci. USA* **79** (1982), 378.
293. N. I. Sosfenov *et al.*, *Dokl. Akad. Nauk. SSSR* **291** (1986), 1123.
294. T. Yamane *et al.*, *J. Biol. Chem.* **257** (1982), 1221.
295. A. M. Flank *et aI.*, *J. Am. Chem. Soc.* **108** (1986), 1049.
296. J. F. Rubinson *et aI.*, *Biochemistry* **24** (1985), 273.
297. E. I. Stiefel, *Proc. Natl. Acad. Sci. USA* **70** (1973), 988.
298. K. L. Hadfield and W. A. Bulen, *Biochemistry* **8** (1969), 5103.
299. F. B. Simpson and R. Burris, *Science* **224** (1984), 1095.
300. B. K. Burgess *et al.*, *Biochemistry* **20** (1981), 5140.
301. S. Wherland *et aI.*, *Biochemistry* **20** (1981), 5132.
302. J. H. Guth and R. H. Burris, *Biochemistry* **22** (1983), 5111.
303. Z.-c. Wang and G. D. Watt, *Proc. Natl. Acad. Sci. USA* **81** (1984), 376.
304. B. E. Smith *et al.*, *Phil. Trans. Roy. Soc. London* **B317** (1987), 131.
305. R. N. F. Thorneley, R. R. Eady, and D. J. Lowe, *Nature* **272** (1978), 557.
306. S. Wherland *et al.*, *Biochemistry* **20** (1981), 5132.
307. B. K. Burgess *et al.*, *Biochemistry* **20** (1981), 5140.
308. H. Bortels, *Arch. Mikrobiol.* **1** (1930), 333.
309. R. C. Bray, *Quart. Rev. Biophys.* **21** (1988), 299.
310. H. Bortels, *Zentbl. Bakt. Parasiten Abt. II* **95** (1935), 193.
311. C. E. McKenna, J. R. Benemann, and T. G. Traylor, *Biochem. Biophys. Res. Commun.* **41** (1970), 1501.
312. R. C. Burns, W. H. Fuchsman, and R. W. F. Hardy, *Biochem. Biophys. Res. Commun.* **42** (1971), 353.
313. J. R. Benemann *et al.*, *Biochim. Biophys. Acta* **264** (1972), 25.
314. P. E. Bishop, D. M. L. Jarlenski, and D. R. Hetherington, *Proc. Natl. Acad. Sci. USA* **77** (1980), 7342.
315. P. E. Bishop *et al.*, *Science* **232** (1986), 92.
316. B. J. Hales, D. J. Langosch, and E. E. Case, *J. Biol. Chem.* **261** (1986), 15301.
317. B. J. Hales *et al.*, *Biochemistry* **26** (1987), 1795.
318. J. Morningstar *et al.*, *Biochemistry* **26** (1987), 1795.
319. R. L. Robson *et al.*, *Nature* **322** (1986), 388.
320. R. R. Eady *et al.*, *Biochem. J.* **244** (1987), 197.
321. M. J. Dilworth *et al.*, *Nature* **327** (1987), 167.
322. R. N. Pau, *Trends Biochem. Res.* **14** (1989), 186; P. E. Bishop and R. D. Joerger, *Annu. Rev. Plant Physiol. Plant Mol. Biol.* **41** (1990), 109.
323. J. E. Morningstar and B. J. Hales, *J. Am. Chem. Soc.* **109** (1987), 6854.
324. J. M. Arber *et al.*, *Nature* **372** (1987), 325.
325. G. N. George *et al.*, *J: Am. Chem. Soc.* **110** (1988), 4057.
326. R. R. Eady *et al.*, *Recueil des Travaus Chim. des Pays-Bas* **106** (1987), 175.
327. M. J. Carney *et al.*, *J. Am. Chem. Soc.* **108** (1986), 3519.
328. R. H. Holm, *Chem. Soc. Rev.* (1981), 455.
329. G. Christou and C. D. Gamer, *J. Chem. Soc. Dalton Trans.* (1980), 2354.
330. C. D. Gamer *et al.*, *Phil. Trans. Roy. Soc. Land.* **A308** (1982), 159. a). R. H. Holm and E. D. Simhon, in Reference 235a, p. 1.
331. W. H. Armstrong, P. K. Mascharak, and R. H. Holm, *Inorg. Chem.* **21** (1982),1699.
332. R. E. Palermo and R. H. Holm, *J. Am. Chem. Soc.* **105** (1983), 4310. a) D. Coucouvanis, E. D. Simhon, and N. C. Baenziger, *J. Am. Chem. Soc.* **102** (1980), 6644. b) G. D. Friesen *et al.*, *Inorg. Chem.* **22** (1983), 2203. c) P. Stremple, N. C. Baenziger, and D. Coucouvanis, *J. Am. Chem. Soc.* **103** (1981), 4601. d) D. Coucouvanis *et al.*, *J. Am. Chem. Soc.* **102** (1980), 1732. e) A. Müller *et al.*, *Inorg. Chim. Acta* **148** (1988), 11. f) A. Müller *et al.*, *Angew. Chem. Int. Ed. Engl.* **21** (1982), 860. g) D. Coucouvanis *et al.*, *Inorg. Chem.* **27** (1988), 4066. h) P. A. Eldridge *et al.*, *J. Am. Chem. Soc.* **110** (1988), 5573. i) K. S. Bose *et al.*, *J. Am. Chem. Soc.* **111** (1989), 8953. j) J. A. Kovacs, J. K. Bashkin, and R. H. Holm, *Polyhedron* **6** (1987), 1445.
333. R. D. Sanner *et al.*, *J. Am. Chem. Soc.* **98** (1972), 8351. a) M. B. O'Regan *et al.*, *J. Am. Chem. Soc.* **112** (1990), 4331.

334. G. Pez, P. Apgar, and R. K. Crissey, *J. Am. Chem. Soc.* **104** (1982), 462.
335. K. Jones *et al.*, *J. Am. Chem. Soc.* **98** (1976), 74.
336. G. J. Leigh, *J. Mol. Catal*. **47** (1988), 363.
337. R. A. Henderson, G. J. Leigh, and C. J. Pickett, *Adv. Inorg. Chem. Radiochem*. **27** (1984), 198. a) M. Hidai and Y. Mizobe, in P. S. Braterman, ed., *Reactions of Coordinated Ligands*, Plenum, **2** (1989),53. b) T. Yoshida *et al.*, *J. Am. Chem. Soc.* **110** (1988), 4872. c) T. Yoshida, T. Adachi, and T. Ueda, *Pure Appl. Chem*. **62** (1990), 1127.
338. D. Sellmann *et al.*, *Angew. Chem. Int. Ed. Engl.* **28** (1989), 1271.
339. A. E. Shilov, in M. Gratzel, ed., *Energy Resources through Chemistry and Catalysis*, Academic Press, 1983, p. 533.
340. W. E. Newton *et al.*, *Inorg. Chem.* **19** (1980), 1997.
341. T. R. Halbert, W.-H. Pan, and E. I. Stiefel, *J. Am. Chem. Soc.* **105** (1983), 5476.
342. M. Rakowski DuBois *et al.*, *J. Am. Chem. Soc.* **101** (1979), 5245.
343. R. H. Crabtree, *Inorg. Chim. Acta* **125** (1986), 27.
344. W. B. Mims and J. Peisach, in J. Berliner and J. Reuben, eds., *Biological Magnetic Resonance*, Plenum, **3** (1981), 213.
345. T. Yamane *et al.*, *J. Biol. Chem.* **257** (1982), 1221.
346. D. C. Rees and J. B. Howard, *J. Biol. Chem.* **2587** (1983), 12733.
347. R. B. Frankel *et al.*, *J. de Physique* **37** (1976), C6.
348. C. E. Johnson, *J. Appl. Phys.* **42** (1971), 1325.
349. P. Middleton *et al.*, *Eur. J. Biochem.* **88** (1978), 135.
350. K. Tagawa and D. I. Amon, *Biochim. Biophys. Acta* **153** (1968), 602.
351. G. Palmer, R. H. Sands, and L. E. Mortenson, *Biochim. Biophys. Acta* **23** (1966), 357.
352. R. H. Sands and W. R. Dunham, *Quart. Rev. Biophys*. **4** (1975), 443.
353. R. Cammack, in M. J. Allen and P. N. R. Usherwood, eds., *Charge and Field Effects in Biosystems*, Abacus Press, 1984, p. 41.
354. J. Cardenas, L. E. Mortenson, and D. C. Yoch, *Biochim. Biophys. Acta* **434** (1976), 244.
355. R. Cammack, M. J. Barber, and R. C. Bray, *Biochem. J.* **157** (1976), 469.
356. R. C. Bray, in *The Enzymes*, 3d ed., **12** (1975), 299.
357. J. A. Fee *et al.*, *J. Biol. Chem.* **259** (1984), 124.
358. R. N. Mullinger *et al.*, *Biochem. J.* **151** (1975), 75.
359. R. Cammack *et al.*, *Biochim. Biophys. Acta* **490** (1977), 311.
360. F. A. Armstrong *et al.*, *FEBS Lett.* **234** (1988), 107.
361. W. R. Hagen *et al.*, *Biochim. Biophys. Acta* **828** (1985), 369.
362. E. deGryse, N. Glandsdorff, and A. Piérard, *Arch. Microbiol.* **117** (1978), 189.
363. V. M. Fernandez, E. C. Hatchikian, and R. Cammack, *Biochim. Biophys. Acta* **832** (1985), 69.
364. V. Niviére, *Biochem. Biophys. Res. Commun.* **139** (1986), 658.
365. M. Teixeira *et al.*, *Biochimie* **68** (1986), 75.
366. D. J. Lowe, B. E. Smith, and R. R. Eady, in N. S. Subba Rao, ed., *Recent Advances in Biological Nitrogen Fixation*, Arnold, 1980, p. 34.
367. R. C. Bums, R. D. Holsten, and R. W. F. Hardy, *Biochem. Biophys. Res. Commun*. **39** (1970), 90.
368. M. G. Yates and K. Planque, *Eur. J. Biochem.* **60** (1975), 467.
369. T. C. Huang, W. G. Zumft, and L. E. Mortenson, *J. Bact.* **113** (1973), 884.
370. P. C. Hallenback, P. J. Kostel, and J. R. Benemann, *Eur. J. Biochem.* **98** (1979), 275.
371. S. Norlund, U. Erikson, and H. Baltscheffsky, *Biochim. Biophys. Acta* **504** (1978), 248.
372. B. K. Burgess *et al.*, in Reference 242.
373. S. D. Conradson *et aI.*, *J. Am. Chem. Soc.* **109** (1987), 7507.
374. S. A. Vaughn and B. K. Burgess, *Biochemistry* **28** (1989), 419.
375. R. W. Miller and R. R. Eady, *Biochim. Biophys. Acta* **952** (1988), 290.
376. B. K. Burgess, in Reference 235a, p. 161.
377. B. J. Hales *et al.*, *Biochemistry* **25** (1986), 7251.
378. M. M. Georgiadis *et al.*, *Science* **257** (1992), 1653.
379. J. T. Bolin *et al.*, in P. M. Greshoff et al., eds., *Nitrogen Fixation: Achievements and Objectives*, Chapman and Hall, 1990, p. 117.

380. J. Kim and D. C. Rees, *Science* **257** (1992), 1677.
381. J. Kim and D. C. Rees, *Nature* **360** (1992), 553.
382. For allowing us to see and quote their work prior to publication, we are grateful to Prof. M. W. W. Adams, Prof. B. K. Burgess, Dr. R. Cammack, Prof. D. Coucouvanis, Prof. S. P. Cramer, Dr. S. J. George, Prof. J. N. Enemark, Prof. J. Lancaster, Dr. Michelle Millar, Prof. M. Maroney, Prof. W. E. Newton, Prof. D. C. Rees, Prof. Dieter Sellman, Prof. A. E. Shilov, Dr. Barry E. Smith, Dr. R. N. F. Thorneley, and Prof. G. D. Watt. We thank Pat Deuel for her superb efforts under difficult circumstances in the preparation of this manuscript.

Contributors and Attributions

- Edward I. Stiefel (Exxon Research and Engineering Company)
- Graham N. George (Exxon Research and Engineering Company)

11.2.7: Ferrodoxins, Hydrogenases, and Nitrogenases - Metal-Sulfide Proteins is shared under a CC BY-NC-SA 4.0 license and was authored, remixed, and/or curated by LibreTexts.

11.2.7.1: Iron-sulfur Proteins and Models

Iron sulfide proteins involved in electron transfer are called *ferredoxins* and *rubredoxins*.* The ferredoxins were discovered first, and were originally classified as bacterial (containing Fe_4S_4 clusters) and plant (containing Fe_2S_2 clusters) ferredoxins. This classification is now recognized as being not generally useful, since both Fe_2S_2 and Fe_4S_4 ferredoxins are found in plants,[14,15] animals,[2,6,16] and bacteria.[4] Ferredoxins are distinguished from rubredoxins by their possession of acid-labile sulfide; i.e., an inorganic S^{2-} ion that forms H_2S gas upon denaturation at low pH. Rubredoxins have no acid-labile sulfide, and generally have a single iron in a more or less isolated site. Despite their lack of acid-labile sulfide, rubredoxins are included in this chapter because they have sequences much like those of the ferredoxins, and because their simple mononuclear Fe^{2+} and Fe^{3+} sites provide convenient illustrations of key structural and spectroscopic features.

In most ferredoxins, and in all rubredoxins, the protein ligands are cysteines, which provide four thiolate donors to the 1Fe, 2Fe, or 4Fe center. Additionally, the existence of 3Fe centers and of Fe-S sites that contain a second metal (i.e., heteronuclear clusters) make the Fe-S class a broad and multifunctional one.

Simple cytochromes and simple iron-sulfide proteins are similar, in that both can undergo one-electron transfer processes that are generally uncoupled from proton-, atom-, or group-transfer processes. Some of these proteins, such as cytochrome c_3 from *Desulfovibrio* with four hemes[17] or ferredoxin from *Clostridium pasteurianum* with two Fe_4S_4 centers,[6] can transfer more than one electron, because they have multiple copies of a one-electron transfer group. The cytochromes were discovered in 1886 by McMunn,[18] and their role in metabolism was discovered in the 1920s by Keilin (Chapter 6). The intense optical absorbance of these heme-containing proteins contributed singularly to their discovery and biochemical characterization. In contrast, the iron-sulfur proteins, although red to red-brown, absorb far more weakly in the visible region than do the cytochromes. Their presence is sometimes obscured by the cytochromes, and their frequent air instability made their initial recognition and isolation more difficult. It was not until the early 1960s that discoveries by several research groups[19] led to the isolation, recognition, and characterization of the ferredoxins. The use of EPR spectroscopy and its application to biological systems had a profoundly stimulating effect on the field (see below).

Although cytochromes were discovered first, the ferredoxins are likely to be the older proteins from an evolutionary perspective.[20] Ferredoxins have relatively low-molecular-weight polypeptide chains, require no organic prosthetic group, and often lack the more complex amino acids. In fact, the amino-acid composition in clostridial ferredoxin is close to that found in certain meteorites.[21]

The various Fe-S sites found in electron-transfer proteins (ferredoxins) are also found in many enzymes,[6,11,22.23] where these centers are involved in intraor interprotein electron transfer. For example, sulfite reductase contains a siroheme and an Fe_4S_4 center,[24] which are strongly coupled and involved in the sixelectron reduction of SO_3^{2-} to H_2S. Xanthine oxidase (see Figure 7.1) has two identical subunits, each containing two different Fe_2S_2 sites plus molybdenum and FAD sites. In xanthine oxidase, the Mo(VI) site carries out the two-electron oxidation of xanthine to uric acid, being reduced to Mo(IV) in the process.[25] The Mo(VI) site is regenerated by transferring electrons, one at a time, to the Fe_2S_2 and flavin sites, thereby readying the Mo site for the next equivalent of xanthine. Although the Fe_2S_2 sites do not directly participate in substrate reactions, they are essential to the overall functioning of the enzyme system. The Fe_2S_2 centers in xanthine oxidase play the same simple electron-transfer role as the Fe_2S_2 ferredoxins play in photosynthesis.

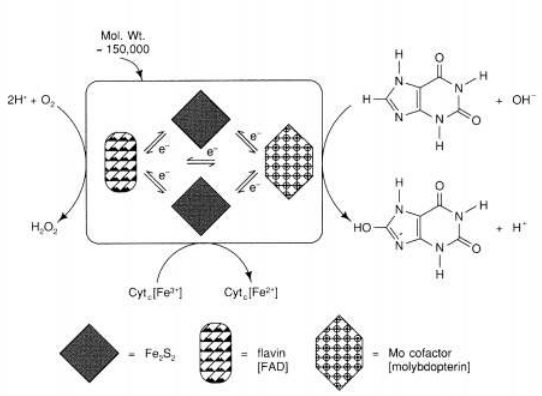


Figure 7.1 - A schematic drawing of xanthine oxidase illustrating the Mo, flavin, and Fe_2S_2 sites and interaction of the enzyme with substrate and oxidant(s).

Structurally, all the iron-sulfur sites characterized to date are built up of (approximately) tetrahedral iron units (see Figure 7.2). In rubredoxins the single iron atom is bound in tetrahedral coordination by four thiolate ligands provided by cysteine side chains. In two-iron ferredoxins the Fe_2S_2 site consists of two tetrahedra doubly bridged through a pair of sulfide ions, i.e., $Fe_2(\mu_2\text{-}S)_2$, with the tetrahedral coordination of each Fe completed by two cysteine thiolates. In four-iron or eight-iron ferredoxins, the 'thiocubane' Fe_4S_4 cluster consists of four tetrahedra sharing edges with triply bridging S^{2-} ions, i.e., $Fe_4(\mu_3\text{-}S)_4$, with each Fe completing its tetrahedron by binding to a single cysteine thiolate. Finally, for Fe_3S_4 clusters, which are now being found in more and more proteins, the well-established structure has one triply bridging and three doubly bridging sulfide ions, $Fe_3(\mu_3\text{-}S)(\mu_2S)_3$. The Fe_3S_4 unit can be thought of as derived from the 'thiocubane' Fe_4S_4 unit by the removal of a single iron atom.

In what follows we will introduce these structures in the order 1Fe, 2Fe, 4Fe, and 3Fe. For each, we will first discuss the physiological role(s) of the particular proteins, then the structural features, followed by the spectroscopic properties and model systems.

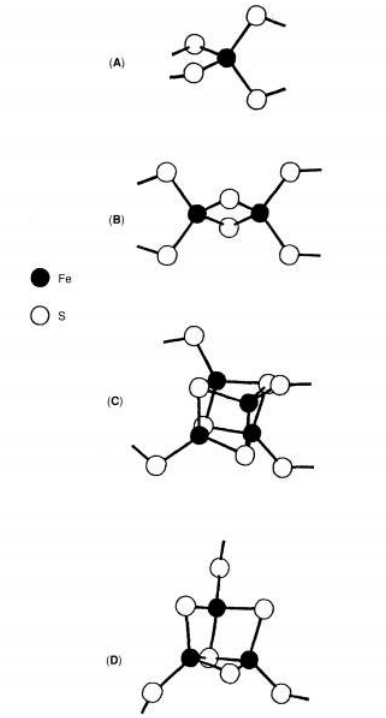


Figure 7.2 - Structural systematics of Fe-S units found in proteins: (A) rubredoxin single Fe center; (B) Fe_2S_2 unit; (C) Fe_4S_4 unit; (d) Fe_3S_4 unit.

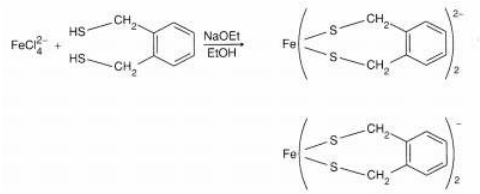
* For review articles, see References 1-11. For a discussion of nomenclature, see References 12 and 13.

11.2.7.1: Iron-sulfur Proteins and Models is shared under a CC BY-NC-SA 4.0 license and was authored, remixed, and/or curated by LibreTexts.

11.2.7.2: Iron-sulfur Proteins and Models (Part 2)

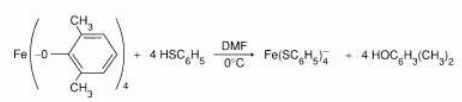
Rubredoxin Model Systems

The simple mononuclear tetrahedral site of Rd has been chemically modeled in both its reduced and its oxidized forms. The bidentate o-xylyl-α,α'-dithiolate ligand forms bis complexes of Fe(II) and Fe(III) that have spectroscopic features quite similar to those of the protein.[62,63] The preparative procedure is relatively straightforward (Equation 7.1).



The UV-visible-NIR spectra, Mössbauer spectra, and magnetic susceptibility differ only slightly from those of oxidized and reduced rubredoxins.

The monodentate benzenethiolate (thiophenolate) ligand, $C_6H_5S^-$, similarly forms the ferrous $Fe(SC_6H_5)_4^{2-}$ complex.[64,65] Although for some time it was felt that the oxidized form, $Fe(SC_6H_5)_4^-$, was inherently unstable, the sterically hindered monothiolate ligand 2,3,5,6-tetramethylbenzenethiolate was found to form[66-68] a stable, quite symmetric Fe(III) tetrathiolate anion. Armed with this information, the preparation of the tetrakis(benzenethiolate) Fe(III) complex was reinvestigated, and the complex successfully synthesized[67] (Equation 7.2).



The Fe(III) and Fe(II) tetrathiolate species now serve as excellent structural models for the Fe sites of both oxidized and reduced Rd.[69]

The structural parameters for the oxidized rubredoxin analogues are very similar to those of the oxidized Rd iron site. The reduced complexes reveal a lengthening of the average Fe-S bond from 2.27 to 2.36 Å, consistent with the change in oxidation state from ferric to ferrous. The addition of an electron has a more profound structural effect in this single-iron center than in some of the multiiron clusters, where electrons are more delocalized.

Clearly, for the single-Fe sites, the dominant structural feature is their near-tetrahedral tetrathiolate coordination. The dominant electronic structural feature is the presence of high-spin Fe^{3+} and Fe^{2+} sites. The important mode of chemical reactivity is a simple one-electron transfer. Each of these features carries over to the 2Fe, 4Fe, and 3Fe sites discussed below.

Fe_2S_2 Ferredoxins

The simple 2Fe-2S proteins are sometimes referred to as "plant" or "plant-type" ferredoxins. The protein from spinach, which serves as an electron acceptor in the photosynthetic apparatus,[14,15,50,70] was among the first to be wellcharacterized and widely studied, and could be considered the prototypical 2Fe-2S ferredoxin, However, 2Fe-2S proteins are also well-known in bacteria.[4] The protein from the cyanobacterium (blue-green alga) *Spirulina platensis* has been structurally elucidated by x-ray crystallography.[47] Putidaredoxin, from *Pseudomonas putida*, which serves as a donor to the P-450 camphor monooxygenase system, has been extensively studied.[28] Fe_2S_2 centers are also well-established in mammalian proteins. Adrenodoxin[29] serves as the electron donor to the P-450 monooxygenase system that carries out the 11-β-hydroxylation of steroids, The so-called "Rieske proteins" are found in the bc_1 complex of mitochondria[47] as well as in the bd complex of the photosynthetic apparatus of plants.[71] In addition, Fe_2S_2 centers are well-known constituents of such redox proteins as xanthine oxidase,[25,72] CO oxidase,[25] succinate dehydrogenase,[73-75] and putidamonooxin.[76] Table 7.1 lists some of the Fe_2S_2 proteins and their properties.

The x-ray crystal structure of only the single 2Fe-2S protein mentioned above has been determined;[70a] the 2Fe-2S ferredoxin from the blue-green alga Spirulina platensis[6,22,47,77,78] shows significant sequence identity with chloroplast ferredoxins typical of higher plants.[79,80] As Figure 7.8 shows, the Fe_2S_2 unit in this 11-kDa protein is bound by Cys-41, Cys-46, Cys-49, and Cys-79, The

binuclear iron cluster is found in a largely hydrophobic region of the protein, but is within 5 Å of the protein surface.[6] The sulfur atoms of the cluster, both inorganic and cysteinyl, are hydrogen-bonded to six peptide NH groups and one serine OH group, which presumably stabilize the cluster/protein complex, The serine involved in the H-bonding, Ser-40, is conserved in all plant and algal 2Fe-2S ferredoxins sequenced, which implies that it plays a crucial structural or functional role.

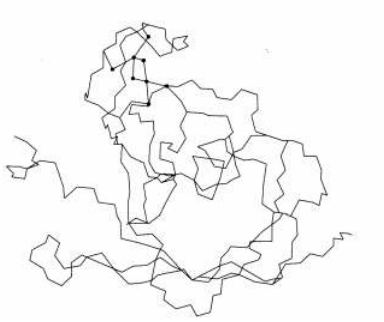


Figure 7.8 - The x-ray crystal structure of the Fe_2S_2 ferredoxin from Spirulina platensis.[70a]

The structure of the 2Fe-2S core in Figure 7.2 reveals a tetrahedron of S ligands surrounding each Fe atom. The two tetrahedra share an edge defined by the two bridging sulfide ions, and the core structure is designated $Fe_2(\mu_2\text{-}S)_2$. Fe-S distances and angles cannot be measured accurately in the structure at the present 2.5-Å resolution;[70a] so we will later discuss these details in terms of model compounds.

The Fe_2S_2 center shows nicely how spectroscopy can be used to deduce the structure of an active site. Indeed, in this case the now well-established active-site structure was deduced by a combination of chemical, spectroscopic, and magnetic methods, and the site was successfully modeled long before the first protein crystallographic study was reported. The presence of acid-labile, inorganic sulfide is a key feature of both the Fe_2S_2 and the Fe_4S_4 centers. The 1:1 stoichiometry between iron and acid-labile sulfide was eventually established analytically for Fe_2S_2 centers.[9-11] Care must be taken to ensure that both the protein and its active-site complement are homogeneous. Although protein homogeneity is usually established by electrophoretic methods, these methods may not distinguish between pure proteins and those with absent or incomplete active centers. Fortunately, absorption at 420 nm is due solely to the Fe_2S_2 cluster, whereas the 275-nm absorption is dominated by the protein. Therefore a good criterion for active-site saturation and homogeneity is the ratio of the absorbances at 420 and 275 nm, $A_{420\ nm}/A_{275\ nm}$, which is ~0.48 for pure spinach ferredoxin.[81] Once homogeneous protein is obtained, the Fe_2S_2 composition of the "plant" ferredoxins can be correctly deduced analytically.

The Fe_2S_2 center displays two redox states that differ by a single electron. The potential range for the couple is -250 to -420 mV, revealing the highly reducing nature of the ferredoxin. The correct structure of the Fe_2S_2 center was first proposed in 1966 based on EPR studies.[82] The reduced state of the cluster shows a rhombic EPR signal with g values of 1.88, 1.94, and 2.04 (Figure 7.6B) characteristic of an $S = \frac{1}{2}$ center. The oxidized state is EPR-silent. The weakness of the sulfur ligand field causes the iron atoms to be high-spin. But how can two sulfur-ligated iron atoms, each with a tendency to be high-spin, produce a state with a single unpaired electron?

The individual Fe atoms in the Fe_2S_2 cluster resemble those in rubredoxin quite closely. The two redox states of the Fe_2S_2 protein correspond to an Fe^{3+}-Fe^{3+} and an Fe^{3+}-Fe^{2+} pair, respectively, as shown in Figure 7.9. In the all-ferric oxidized state, the two Fe^{3+} sites are antiferromagnetically coupled; i.e., the spins of the five d electrons on the two iron atoms are oppositely aligned, such that their pairing produces an effective S = 0, diamagnetic ground state. In the reduced form, a single unpaired electron is present, because the $S = \frac{5}{2}$ Fe^{3+} and S = 2 Fe^{2+} sites are antiferromagnetically coupled, leaving one net unpaired spin and an $S = \frac{1}{2}$ ground state. The profound difference between the electronic properties of rubredoxin and Fe_2S_2 ferredoxin arises because the latter has two Fe atoms in close proximity, which allows for their magnetic coupling.

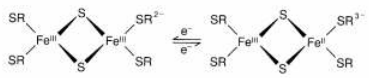


Figure 7.9 - Redox states of Fe_2S_2 proteins: (A) reduced; (B) oxidized.

Strong support for the spin-coupling model in Fe_2S_2 ferredoxins comes from a detailed analysis of their absorption and circular dichroism spectra.[83] As with rubredoxin (see Figure 7.5), we expect no low-energy spin-allowed d-d bands for the ferric site in either the oxidized or the reduced state. Indeed, the oxidized state containing all Fe^{3+} shows no low-energy bands; the reduced state containing a single Fe^{2+} displays low-energy, low-intensity bands in the region 4,000-9,000 cm^{-1}, in close analogy to the situation in reduced rubredoxin. The combined EPR and optical spectra leave little doubt about the structural assignment: two coupled high-spin ferric ions in the oxidized state, and coupled high-spin ferric and ferrous ions in the reduced state. Moreover, the spectra are consistent only with a localized model, i.e., one in which the Fe(II) site is associated with a single iron.[83,83a] The Fe_2S_2 site is inherently asymmetric, and inequivalence of the Fe(llI) sites is spectroscopically detectable in the all-ferric oxidized form.[84] In fact, the localized valence trapping is present in reduced model compounds that contain no ligand asymmetry.

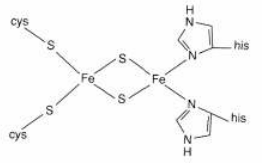
Mössbauer spectra provide additional and striking confirmation of the structural assignment. The spectrum of the oxidized ferredoxin (Figure 7.7) resembles strongly that of oxidized rubredoxin, indicating the presence of high-spin Fe^{3+}, even though the net spin is zero. In the reduced form, the Mössbauer spectrum involves the superposition of signals from a high-spin Fe^{2+} and a high-spin Fe^{3+}, i.e., a reduced and an oxidized rubredoxin, respectively. Clearly, the simplest interpretation of this result consistent with the S = $\frac{1}{2}$ spin state required by the EPR is the localized Fe^{2+}-Fe^{3+} antiferromagnetic coupling model discussed above.

NMR studies of oxidized Fe_2S_2 proteins reveal broad isotropically shifted resonances for the CH_2 protons of the cysteine ligands.[85] Despite the coupling of the irons, the net magnetism at room temperature is sufficient to lead to large contact shifts (-30 to -40 ppm downfield from TMS). The assignment of the resonance was confirmed with the synthesis and spectroscopic analysis of model compounds.[86] Extensive NMR studies of the Fe_2S_2 proteins have been reported.[87,87a]

Resonance Raman spectra of Fe_2S_2 sites[88,89,90] reveal many bands attributable to Fe-S stretching. Detailed assignments have been presented for the four bridging and four terminal Fe-S modes. A strong band at 390 cm^{-1}, which shifts on ^{34}S sulfide labeling, is assigned to the A_{1g} "breathing" mode; another band at 275 cm^{-1} is assigned to B_{3u} symmetry in point group D_{2h}.[57,88] Spectroscopic differences in the terminal, Fe-S(Cys) stretches between plant ferredoxins and adrenodoxin (which also differ somewhat in redox potential) seem to reflect different conformations of the cysteine ligands in the two classes. Evidence for asymmetry of the iron atoms is found in the intensity of the resonance enhancement of certain modes.

Rieske Centers

Within the class of Fe_2S_2 ferredoxins there is a subclass called the Rieske proteins, or the Rieske centers.[47,91,92] The Rieske iron-sulfur centers are found in proteins isolated from mitochondria and related redox chains.[47,92] In addition, the phthalate dioxygenase system from *Pseudomonas cepacia*[93,94] contains one Fe_2S_2 Rieske center as well as one additional nonheme Fe atom. Although the Rieske centers appear to contain an Fe_2S_2 core, there is extensive evidence for nonsulfur ligands coordinated to at least one of the Fe atoms. The proposed model in Scheme (7.3) has two imidazole ligands bound to one Fe atom. The nitrogen atoms are seen in ENDOR (Electron Nuclear Double Resonance) experiments,[93] and are manifest in EXAFS spectra, which are consistent with the presence of a low-Z (atomic number) ligand bound to iron.[94] The potentials for the Rieske proteins range from +350 to -150 mV,[47] in contrast to the plant-type Fe_2S_2 centers, which range from -250 to -450 mV. The strong dependence of redox potential on pH[95] suggests a possible role in coupling protonand electron-transfer processes.



Fe_2S_2 Models

Although spectroscopic studies led to the correct deduction of the structure of the Fe_2S_2 core, the synthesis of model compounds containing this core provided unequivocal confirmation. The model compounds allowed detailed structural analysis unavailable for the proteins. Moreover, by using a uniform set of peripheral ligands, properties inherent to the Fe_2S_2 core could be discerned.

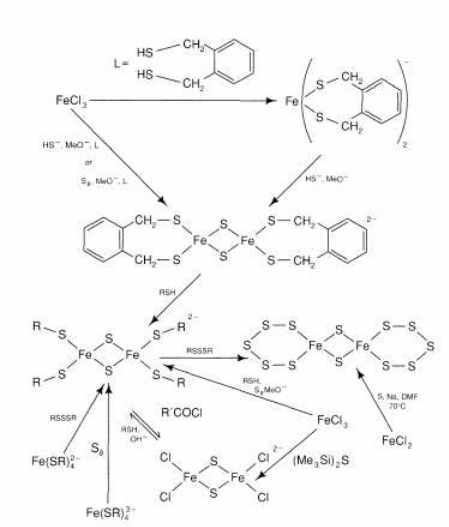


Figure 7.10: Preparative schemes leading to complexes containing the Fe_2S_2 core.[128]

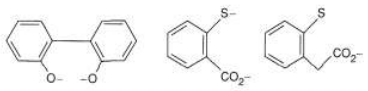
The Fe_2S_2 core has been synthesized by several routes[86,96a,b,c,d] (see Figure 7.10). For example, the reaction of $Fe(SR)_4^{2-}$, the ferrous rubredoxin model, with elemental sulfur produces the complex $Fe_2S_2(SR)_4^{2-}$. In this reaction the sulfur presumably oxidizes the Fe^{2+} to Fe^{3+}, being reduced to sulfide in the process. The Fe_2S_2 core has been prepared with a variety of peripheral S-donor ligands. Metrical details for $Fe_2S_2(SC_6H_4\text{-}p\text{-}CH_3)_4^{2-}$ are given in Table 7.3. Notable distances are the Fe-S (bridging) distance of 2.20 Å, the Fe-S (terminal) distance of 2.31 Å, and the Fe-Fe distance of 2.69 Å.

Table 7.3: Structural parameters for $Fe_2S_2(SC_6H_4-p-CH_3)_4^{2-}$. a) Data from Reference 211.

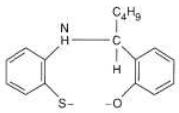
Atoms[a]	Distance Å	Atoms[a]	Angle[a]
Fe-Fe	2.691 (1)	Fe-S-Fe	75.3
Fe-S1 (bridge)	2.200 (1)	S-Fe-S	104.6
Fe-S2 (bridge)	2.202 (1)	S-Fe-S	115.1
Fe-S3	2.312 (1)	S-Fe-S	105.4

To date, all analogue systems structurally characterized contain the Fe^{3+}-Fe^{3+} fully oxidized form. Attempts to isolate the Fe^{3+}-Fe^{2+} form have so far failed. However, the mixed-valence Fe_2S_2 form can be generated and trapped by freezing for spectroscopic examination.[97,98] Mössbauer spectroscopy reveals the presence of distinct Fe^{2+} and Fe^{3+} ions, as found in the proteins, clearly showing that "trapped" valence states are an inherent characteristic of the $Fe_2S_2^{2+}$ core and are *not* enforced by the protein.[97,98]

The existence of noncysteine-bound Fe_2S_2 cores in Rieske-type proteins has led to attempts to synthesize complexes with oxygen and nitrogen ligands.[99-101] Characterized species include $Fe_2S_2(OC_6H_5)_4^{2-}$, $Fe_2S_2(OC_6H_4\text{-}p\text{-}CH_3)_4^{2-}$, $Fe_2S_2(C_4H_4N)_4^{2-}$, and $Fe_2S_2(L)_2^{2-}$, where L is a bidentate ligand.



The potentially tridentate ligand



acts in a bidentate fashion, binding through S and O but not N.

No Fe_2S_2 complexes containing mixed S,N terminal ligands, such as those suggested for the Rieske site, have been prepared. The Se^{2-} bridged analogue has been prepared for some of the complexes.[102,103]

11.2.7.2: Iron-sulfur Proteins and Models (Part 2) is shared under a CC BY-NC-SA 4.0 license and was authored, remixed, and/or curated by LibreTexts.

11.2.7.3: Iron-sulfur Proteins and Models (Part 3)

Fe_4S_4 Ferredoxins (including HiPIPs)

We now turn our attention to proteins containing the Fe_4S_4 center. Historically, within this class a strong distinction was made between the "ferredoxins," which are low-potential (as low as -600 mV in chloroplasts) iron-sulfur proteins, and the "HiPIPs" = High Potential Iron Proteins, which have positive redox potentials (as high as +350 mV in photosynthetic bacteria). Although the HiPIP designation is still useful, proteins of both high and low potential are considered ferredoxins, whose key defining feature is the presence of iron and acid-labile sulfide.[13]

The Fe_4S_4 proteins participate in numerous electron-transfer functions in bacteria, and in some organisms (such as *Clostridium*) are the immediate electron donors for the nitrogenase and/or hydrogenase enzymes. The function of the HiPIPs seems obscure at present. In addition, Fe_4S_4 centers have been shown or postulated to occur in numerous microbial, plant, and mammalian redox enzymes, including nitrate reductase,[104] sulfite reductase,[24] trimethylamine dehydrogenase,[105] succinate dehydrogenase,[73,106] hydrogenase, and, possibly, in altered forms, nitrogenase. Table 7.1 lists some of the Fe_4S_4 ferredoxins and their properties.

In the Fe_2S_2 ferredoxins, combined spectroscopic, analytical, and model-system work led to an unequivocal assignment of the structural nature of the active site long before the crystallography was done. In contrast, for Fe_4S_4 systems and in particular the 8Fe-8S = $2Fe_4S_4$ systems from bacteria, the initial chemical suggestions were fallacious, and even the number and stoichiometry of the clusters were in doubt. In these cases, crystallography provided the definitive structural information.

The first indication of the presence of the "thiocubane" structure came in 1968, when a 4-Å resolution study[107] indicated a compact cluster of potentially tetrahedral Fe_4 shape in the HiPIP from *Chromatium vinosum*. This finding did not lead to much excitement, since it was not yet appreciated that HiPIPs and ferredoxins were structurally similar. In 1972, the high-resolution structure solution of both *Chromatium* HiPIP[108] and the 8Fe ferredoxin from *Peptococcus aerogenes* (formerly *Microbacter aerogenes*)[101] confirmed the presence of virtually identical thiocubane clusters in the two proteins.[108] Moreover, the structures for both oxidized and reduced HiPIP were deduced, and these revealed that the Fe_4S_4 cluster remained intact during the redox interconversion.[109] Subsequently, four-iron clusters have been crystallographically confirmed in an Fe_4S_4 ferredoxin from *Bacillus thermoproteolyticus*,[110,110a] in *Azotobacter vinelandii* ferredoxin I (also previously called Shethna Fe-S protein II), which also contains a 3Fe-4S cluster,[111,112] in the active form of aconitase,[113] and in sulfite reductase, where the cluster is probably bridged by cysteine sulfur to a siroheme.

In all the proteins characterized to date, the Fe_4S_4 clusters adopt the thiocubane structure,[108] which is discussed at greater length in the section on models. The clusters are usually bound to their proteins by four cysteine residues. As shown in Figure 7.11, in the *P. aerogenes* protein the two Fe_4S_4 clusters are bound by cysteines numbered 8, 11, 14, 18, 35, 38, 41, and 45.[101,114] The presence of the Cys-x-x-Cys unit is again apparent. However, this sequence seems prominent in all Fe-S proteins, and so is not specific for a particular Fe-S site. At first glance one might expect one cluster to be bound by cysteines 8,11,14, and 18, the other by cysteines 35, 38, 41, and 45. Actually, one cluster is bound by cysteines 8, 11, 14, and 45, the other by cysteines 35, 38, 41, and 18. The binding of a given cluster by cysteine residues from different portions of the polypeptide chain apparently helps stabilize the tertiary structure of the protein and brings the two clusters into relatively close proximity, the center-center distance being 12 Å.[114]

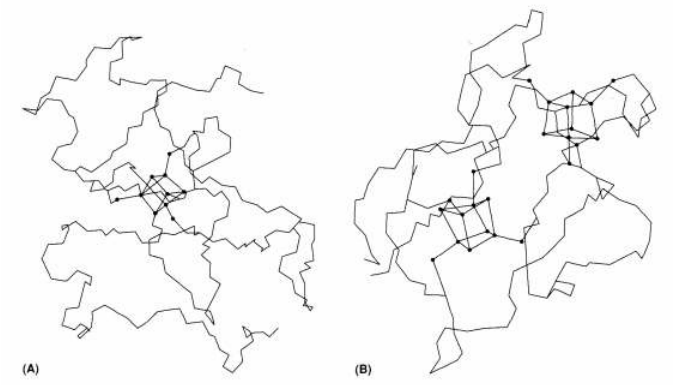


Figure 7.11 - The x-ray crystal structures of (A) *Chromatium vinosum* HiPIP[108] and (B) the 8Fe-8S ferredoxin from *Peptococcus aerogenes*.[101]

The *C. pasteurianum* protein displays weak magnetic coupling, which leads to an unusual EPR spectrum[115] consistent with the 12-Å cluster-cluster separation. However, the redox potentials for the two sites seem virtually identical at -412 mV, thus allowing the 8Fe ferredoxin to deliver two electrons at this low redox potential.[115] Significant sequence identity indicates the likelihood that other 8Fe ferredoxins, such as the well-studied one from *C. pasteurianum*,[116-118] have quite similar structures.

The thiocubane unit of Fe_4S_4 proteins can exist in proteins in at least three stable oxidation states. This so-called three-state model[74,109,119,120] contrasts dramatically with the situation for Rd(1Fe), Fe_2S_2, and Fe_3S_4 systems, in which only two oxidation states are accessible through simple electron transfer for each center. For the thiocubane structure, the three accessible states can be designated $Fe_4S_4^{3+}$, $Fe_4S_4^{2+}$, and $Fe_4S_4^{+}$, corresponding to $[Fe(III)_2Fe(II)]$, $[Fe(III)_2Fe(II)_2]$, and $[Fe(III)Fe(II)_3]$ valence-state combinations, respectively. It is crucial to note that, in sharp contrast to the Fe_2S_2 and Fe_3S_4 sites, the oxidation states are not localized in the Fe_4S_4 clusters. In most cases, each Fe atom behaves as if it had the same average oxidation level as the other Fe atoms in the cluster. The redox interconversion of the Fe4S4 sites is shown in Figure 7.12. The $Fe_4S_4^{3+} \rightleftharpoons Fe_4S_4^{2+}$ couple is the high-potential redox couple characteristic of HiPIPs; the $Fe_4S_4^{2+} \rightleftharpoons Fe_4S_4^{+}$ couple is responsible for the low-potential process characteristic of the classical ferredoxins. In any given protein under physiological conditions, only one of the two redox couples appears to be accessible and functional.

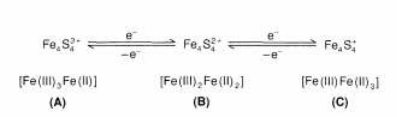


Figure 7.12 - The redox interconversions of Fe_4S_4 sites illustrating the three-state model. The states are found in (A) oxidized HiPIP; (B) reduced HiPIP and oxidized ferredoxin; (C) reduced ferredoxin.

Both the $Fe_4S_4^{+}$ and the $Fe_4S_4^{3+}$ states of the thiocubane cluster are paramagnetic and display characteristic EPR spectra (Figure 7.6C,D). The $Fe_4S_4^{3+}$ site in reduced ferredoxins[46,48,49,119] displays a rhombic EPR signal (Figure 7.6C) with g = 1.88, 1.92, and 2.06. The oxidized form of low-potential ferredoxins is EPR-silent, and attempts to "superoxidize" it to achieve the $Fe_4S_4^{3+}$ state invariably lead to irreversible cluster decomposition, probably through a 3Fe-4S structure. The $Fe_4S_4^{3+}$ signal is usually referred to as the HiPIP signal (Figure 7.6D) and shows distinct g values at 2.04($g_\perp$) and 2.10($g_\parallel$); it is present in oxidized HiPIP but absent in reduced HiPIP.[46,119] Reduction of HiPIP to a "super-reduced" state apparently occurs under partially denaturing conditions in aqueous DMSO.[108] The observed axial EPR signal with g = 1.94 and 2.05 is assigned to the $Fe_4S_4^{+}$ state characteristic of reduced ferredoxins. This result[108] is consistent with structural and spectroscopic identity of the HiPIP and Fd sites, as required by the three-state model of the Fe_4S_4 proteins (Figure 7.12).

In Fe_4S_4 centers at each level of oxidation, electronic transitions give rise to characteristic visible and UV spectra, although the delocalized nature of the electronic states makes detailed assignment difficult. MCD spectra of clusters in the three states of oxidation are clearly distinguishable from each other and from MCD of Fe_2S_2 clusters.[43,119] MCD, magnetic susceptibility, and Mössbauer spectra provide evidence that the S = $\frac{1}{2}$ state, whose EPR signal is so distinct in reduced ferredoxins, may coexist at higher T with S = $\frac{3}{2}$ and perhaps even higher spin states. Indeed, recent studies with model systems[121,122] and theoretical treatments[123,124] clearly support the ability of the Fe_4S_4 cluster to display a number of spin states that are in labile equilibria, which are influenced, perhaps quite subtly, by local structural conditions. The iron protein of nitrogenase also displays this behavior.

The Mössbauer spectra of Fe_4S_4 centers of ferredoxins reveal the equivalence of the Fe sites, and quadrupole splittings and isomer shifts at averaged values for the particular combination of oxidation states present.[3,51,52] Representative spectra are shown in Figure 7.7. Magnetic coupling is seen for the paramagnetic states.

Resonance Raman spectra (and IR spectra) have been extensively investigated in *C. pasteurianum* ferredoxin and in model compounds.[57,125] Selective labeling of either thiolate sulfur or sulfide sulfur with ^{34}S allows modes associated with the Fe_4S_4 core to be distinguished from modes associated with the FeSR ligands. The band at 351 cm^{-1} is assigned to Fe-SR stretching, and Fe_4S_4 modes occur at 248 and 334 cm^{-1} in reduced ferredoxin from *C. pasteurianum.* There is little difference between the oxidized and reduced spectra, although an extra band at 277 cm^{-1} seems present in the oxidized protein. The Fe_4Se_4 substituted protein has also been studied.[125]

As in the 1Fe and 2Fe proteins, ^1H NMR spectra reveal resonances from contact-shifted-CH_2-groups of cysteinyl residues.[125a] However, unlike the other proteins, where all states are at least weakly magnetic, only the reduced ferredoxin and the oxidized HiPIP states show contact shifts.[87a,125a,b,c]

EXAFS studies on proteins and on model compounds clearly identify the Fe-S distance of ~2.35 Å and an Fe-Fe distance of 2.7 Å. These distances, as expected, vary only slightly with state of oxidation.[125d]

Fe_4S_4 Models

Judging from the ease with which models of Fe_4S_4 are prepared under a variety of conditions and their relative stability, the $Fe_4S_4^{2+}$ core structure seems to be a relatively stable entity, a local thermodynamic minimum in the multitude of possible iron-sulfide-thiolate complexes. The initial preparation and structural characterization[126,127] of the models showed that synthetic chemistry can duplicate the biological centers in far-simpler chemical systems, which can be more easily studied in great detail.

The general synthetic scheme for Fe-S clusters is shown in Figure 7.13. Many different synthetic procedures can be used to obtain complexes with the Fe_4S_4 core.[126-138,138a,b] The multitude of preparative procedures is consistent with the notion that the $Fe_4S_4^{2+}$ core is the most stable entity present and "spontaneously self-assembles" when not limited by stoichiometric constraints.

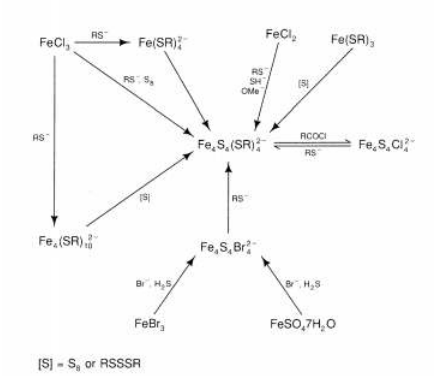


Figure 7.13 - Preparative schemes leading to complexes containing the Fe_4S_4 core.[128]

The thiocubane structure can be viewed as two interpenetrating tetrahedra of 4Fe and 4S atoms. The 4S tetrahedra are the larger, since the S-S distance is ~3.5 Å, compared with the Fe-Fe distance of ~2.7 Å. The S_4 tetrahedron encloses ~2.3 times as much volume as does the Fe_4 tetrahedron.[128] Key distances and angles for $Fe_4S_4(SCH_2C_6H_5)_4^{2-}$ given in Table 7.4 are extremely similar to those found in oxidized ferredoxin and reduced HiPIP centers in proteins.[127]

Table 7.4 - Structural parameters for $Fe_4S_4(SCH_2C_6H_5)_4^{2-}$.

a) Data from References 126 and 127.

Atoms[a]	Average Distances	Number of Bonds	Type
Fe(1)-S(3)	2.310 (3)	8	Sulfide
Fe(1)-S(2)	2.239 (4)	4	Sulfide
Fe(1)-S(5)	2.251 (3)	4	Thiolate
Fe(1)-Fe(2)	2.776 (10)	2	
Fe-Fe(other)	2.732 (5)	4	

Atoms[a]	Average Distances	Number of Bonds	Type
Fe-S-Fe	73.8 (3)	12	
S-Fe-S	104.1 (2)	12	Sulfide-Fe-Sulfide
S-Fe-S	111.7-117.3	12	Sulfide-Fe-Thiolate

The idealized symmetry of $Fe_4S_4^{2+}$ model systems is that of a regular tetrahedron, i.e., T_d. Though the distortion of the cube is quite pronounced, all known examples of the Fe_4S^{2+} core show distortion, which lowers the symmetry at least to D_{2d}. In most Fe_4S^{2+} core structures, this distortion involves a tetragonal compression, which leaves four short and eight long Fe-S bonds.

Complexes with non-S-donor peripheral ligands have been prepared and studied. The halide complexes $Fe_4S_4X_4^{2-}$ (X = Cl^-, Br^-, I^-) have been prepared, and serve as useful starting points for further syntheses.[129-133] The complex $Fe_4S_4(OC_6H_5)_4^{2-}$ can be prepared[134] from the tetrachloride (or tetrathiolate) thiocubane by reaction with $NaOC_6H_5$ (or HOC_6H_5). There are a few examples of synthetic $Fe_4S_4^{2+}$ cores in which the peripheral ligands are not identical. For example, $Fe_4S_4Cl_2(OC_6H_5)_2^{2-}$ and $Fe_4S_4Cl_2(SC_6H_5)_2^{2-}$ have structures characterized by D_{2d} symmetry.[135] The complexes $Fe_4S_4(SC_6H_5)_2[S_2CN(C_2H_5)_2]^{2-}$ and $Fe_4S_4(SC_6H_4OH)_4^{2-}$ are similarly asymmetric, containing both four- and five-coordinate iron.[136-138] The presence of five-coordinate iron in the Fe_4S_4 cluster is notable, since it offers a possible mode of reactivity for the cluster wherever it plays a catalytic role (such as in aconitase). Complexes with Fe_4Se^{2+} and $Fe_4Te_4^{2+}$ cores have also been prepared.[138c,d]

One structural analysis of $Fe_4S_4(SC_6H_5)_4^{3-}$, which contains the reduced $Fe_4S_4^+$ core, revealed a tetragonal elongation[139] in the solid state. In contrast, analysis of $Fe_4S_4(SCH_2C_6H_5)_4^{3-}$ revealed a distorted structure possessing C_{2v} symmetry.[102] It would appear that the $Fe_4S_4^+$ clusters maintain the thiocubane structure, but are nevertheless highly deformable. Interestingly, when the solidstate C_{2v} structure, $Fe_4S_4(SCH_2C_6H_5)_4^{3-}$, is investigated in solution, its spectroscopic and magnetic behavior change to resemble closely those of the $Fe_4S_4(SC_6H_5)_4^{3-}$ cluster,[140] which does not change on dissolution. The simplest interpretation assigns the elongated tetragonal structure as the preferred form for $Fe_4S_4^+$ cores with deformation of sufficiently low energy that crystal packing (or, by inference, protein binding forces) could control the nature of the distortions in specific compounds.[128] The elongated tetragonal structure has four long and eight short bonds in the core structure. The terminal (thiolate) ligands are 0.03-0.05 Å longer in the reduced structure, consistent with the presence of 3Fe(ll) and 1Fe(III) in the reduced form, compared to 2Fe(II) and 2Fe(III) in the oxidized form. There is no evidence for any valence localization.[128]

The oxidized $Fe_4S_4^{3+}$ core defied isolation and crystallization in a molecular complex prior to the use of sterically hindered thiolate ligands. With 2,4,6 tris(isopropyl)phenylthiolate, the $Fe_4S_4L_4^-$ complex could be isolated and characterized.[141] The structure is a tetragonally compressed thiocubane with average Fe-S and Fe-SR distances 0.02 and 0.04 Å shorter than the corresponding distances in the $Fe_4S_4L_4^{2-}$ complex. Again, there is no evidence for Fe inequivalence or more profound structural distortion in this 3Fe(III)-1Fe(II) cluster. Clearly, the Fe_4S_4 clusters have highly delocalized bonding.

Evidence from model systems using sterically hindered thiolate ligands indicates the existence of an $Fe_4S_4^{4+}$, i.e., all-ferric fully oxidized cube.[142] The existence of the complete series $Fe_4S_4[(Cy)_3C_6H_2S]_4^n$ (Cy =cyclohexyl; n = 0, -1, -2, -3) is implied by reversible electrochemical measurements. Clearly, five different states of the Fe_4S_4 core—including the (at least) transient fully oxidized state and the all-ferrous fully reduced state—may have stable existence. Although only the central three states have been shown to exist in biological contexts, one must not rule out the possible existence of the others under certain circumstances.

Recently, specifically designed tridentate ligands have been synthesized that bind tightly to three of the four Fe atoms in the thiocubane structure.[143,143a,b] The remaining Fe atom can then be treated with a range of reagents to produce a series of subsite-differentiated derivatives and variously bridged double-cubane units. These derivatives illustrate the potential to synthesize complexes that mimic the more unusual features of Fe_4S_4 centers that are bound specifically and asymmetrically to protein sites. The recently synthesized complex ion $[(Cl_3Fe_4S_4)_2S]^{4-}$, containing two Fe_4S_4 units bridged by a single S^{2-} ligand, illustrates the potential coupling of known clusters into larger aggregates.[143c]

The model-system work has made an important contribution to our understanding of the Fe_4S_4 centers. The existence of three states, the exchange of ligands, the redox properties, the metrical details of the basic Fe_4S_4 unit, and the subtleties of structural distortion can each be addressed through the study of models in comparison with the native proteins.

11.2.7.3: Iron-sulfur Proteins and Models (Part 3) is shared under a CC BY-NC-SA 4.0 license and was authored, remixed, and/or curated by LibreTexts.

11.2.7.4: Iron-sulfur Proteins and Models (Part 4)

Core Extrusion/Cluster Displacement Reactions

Synthetic model-system work led to the realization that the cluster cores can exist outside the protein and undergo relatively facile ligand-exchange reactions.[128] This behavior of the purely inorganic complexes allowed core extrusion reactions[128,144] to be developed. The basic assumption behind these reactions is that the cluster core retains its integrity when it is substituted by low-MW thiolates, especially aryl thiolates, which replace the cysteinyl ligands that bind it to the protein. In order to free the cluster from the protein, one must at least partially denature the protein, usually by using ~80 percent aqueous solution of a polar aprotic solvent, such as DMSO or HMPA. The resulting inorganic clusters can be identified and quantified by measurement of their characteristic electronic absorption or NMR spectra. An alternative approach involves transferal of the unknown cluster in question to an apoprotein that binds a cluster of known type.[145]

Since the 1Fe, 2Fe, and 4Fe sites are each usually bound to the protein by four cysteine residues, it is perhaps not surprising that there have been reports[58] of interconversion of cluster types bound to a given protein. Specifically, in 90 percent aqueous DMSO, the single Fe site in rubredoxin from *C. pasteurianum* is converted to an Fe_4S_4 cluster by the addition of sodium sulfide, ferrous chloride, and ferric chloride in ratio 4:2:1. Presumably the spacing and geometric disposition of the cysteines are suitable to bind a single Fe or the Fe_4S_4 cluster, which is readily formed under the reaction conditions. Another example of cluster rearrangement involves the three-iron center discussed below that does *not* extrude as an Fe_3S_4 center. Rather, at least under *certain* conditions, the Fe_{3Sx} center rearranges to form Fe_2S_2 centers.[146] The facile interconversion of the Fe clusters demonstrated the lability of Fe-S systems, and indicates that caution must be exercised in interpreting the results of cluster-displacement reactions.

Fe_3S_4 Centers

Three-iron centers are a comparatively recent finding,[119,146] and the full scope of their distribution is not yet known. Although they have now been confirmed in dozens of proteins, it often remains uncertain what physiological role these centers play. Indeed, since Fe_3S_4 centers can be produced as an artifact upon oxidation of Fe_4S_4 centers, it has been suggested that 3Fe centers may not be truly physiological, and could be side products of aerobic protein isolation. This caveat notwithstanding, the 3Fe sites are being found in more and more proteins and enzymes. Their physiological *raison d' être* may be more subtle than that of their 1, 2, and 4Fe cousins; we should certainly try to find out more about them. Some proteins containing Fe_3S_4 centers are listed in Table 7.1.

The 3Fe center was first recognized[147] in the protein ferredoxin I from the anaerobic nitrogen-fixing bacterium *Azotobacter vinelandii*. The protein is called *Av* FdI for short. It is instructive to sketch historically the evolution of our understanding of this protein. *Av* ferredoxin I was reported to have 6 to 8 Fe atoms and was first thought to resemble the clostridial 8Fe ferredoxins. However, unlike the clostridial protein, the *Av* FdI clusters appeared to have two quite different redox couples at +320 and -420 mV. Although it might have been thought that this protein contained one HiPIP-type and one Fd- or "ferredoxin"-type Fe_4S_4 cluster, the protein as isolated had an EPR signal with g = 2.01, which differed significantly (Figure 7.6) from that of an oxidized HiPIP or a reduced Fd.[148] Cluster extrusion reactions also seemed to indicate the presence of an unusual cluster type.[149]

Fortunately, the protein was crystallized, and could be studied by x-ray diffraction. Unfortunately, the initial conclusions[150] and subsequent revisions[151,152] of the crystal-structure analysis have proven to be wrong, teaching us in the process that protein x-ray crystallography, taken alone, does not always provide definitive results. Specifically, the first crystallographic report suggested the presence of a conventional Fe_4S_4 cluster and a smaller packet of electron density that was assigned as a 2Fe-2S center.[150] However, upon further refinement, and following the formulation of the 3Fe center by Mössbauer spectroscopy,[147] a 3Fe-3S center was identified and refined.[151,152] The "refined" Fe_3S_3 center was a six-membered alternating iron-sulfide ring with an open, almost flat, twistedboat conformation (Figure 7. 14). The Fe-Fe separation of 4.1 Å and the structural type was unprecedented, and did not agree with the results of resonance Raman spectroscopy,[153] with x-ray absorption spectroscopy on the native protein or on samples from which the Fe_4S_4 center was removed,[103] or even with stoichiometry, which eventually led to the reformulation[154] of the cluster as Fe_3S_4. The x-ray absorption studies (EXAFS) clearly led to the assignment of a 2.7-Å Fe-Fe distance for the 3Fe cluster.[103]

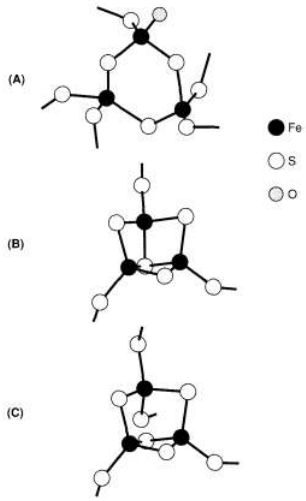


Figure 7.14 - Fe_3S_n structures: (A) open Fe_3S_3 structure proposed from initial x-ray studies (now shown to be in error); (B) the thiocubane fragment structure believed present in most Fe_3S_4 proteins; (C) open Fe_3S_4 structure (not found to date).

In parallel with the studies on *Av* FdI, two additional proteins played key roles in the resolution of the nature of the Fe_3 cluster. These are FdII from *Desulfovibrio gigas* and aconitase from beef heart. Each contains (under certain conditions) only Fe_3S_4 sites, thus enabling more definitive structural, stoichiometric, and spectral information to be acquired. Studies on these proteins using EXAFS,[155] Mössbauer,[52,156,157] EPR,[146] and resonance Raman (to which we will return briefly) clearly favor the closed structure shown in Figure 7.14C. Indeed, x-ray crystallography on aconitase by the same group that did the initial x-ray work on *Av* FdII revealed the compact structure in agreement with the spectroscopy.[20]

In 1988 the structural error in the crystallography of *Av* FdI was found by two groups, and a new refinement in a corrected space group led to a structure in agreement with the spectroscopy.[111,112] The Fe_3S_4 cluster has the apoFe thiocubane structure, with each iron atom bound to the protein by a single cysteinyl thiolate. Clearly, even x-ray crystallography is potentially fallible, and its findings must be critically integrated with the data from other techniques in arriving at full structural definition of metalloenzyme sites.

The studies on the ferredoxins from *D. gigas* present an interesting lesson on the lability of the Fe-S cluster systems. Two distinct proteins from *D. gigas*, FdI and FdII, contain the same polypeptide chain (6 kDa) in different states of aggregation,[158,159] Whereas FdI is a trimer containing three Fe_4S_4 clusters, FdII is a tetramer that contains four Fe_3S_4 clusters. The ferredoxins differ in their redox potentials and appear to have different metabolic functions in *D. gigas*. The oxidation of *D. gigas* FdI with $Fe(CN)_6^{3-}$ leads to FdII, and treatment of FdII with iron salts leads to FdI. The *D. gigas* system reveals the lability and interconvertibility of Fe-S clusters. The recently reported[160] crystal structure of *D. gigas* FdII shown in Figure 7.15 confirms the partial (apoFe) thiocubane Fe_3S_4 center. The iron atoms are ligated by three cysteinyl residues from protein side chains. The cube missing an iron is now firmly established as a viable structural type.

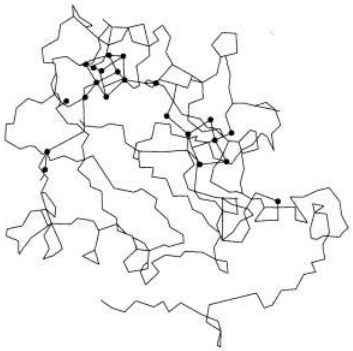
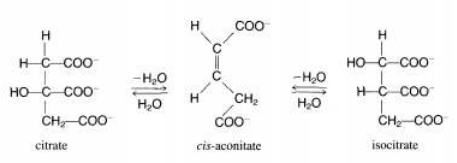


Figure 7.15 - The x-ray crystal structure of D.gigas FdII, illustrating the Fe_4S_4 and Fe_3S_4 centers in this protein.[160]

The aconitase system presents yet another fascinating story.[159a] Aconitase is a key enzyme in the Krebs cycle, catalyzing the conversion of citrate and isocitrate through the intermediacy of cis-aconitate, as shown in Equation (7.6).



This is a hydrolytic nonredox process, and for some time it was thought that aconitase was a simple Fe^{2+} protein wherein the ferrous iron was involved in the Lewis-acid function of facilitating the hydrolytic reaction. Indeed, aconitase is inactive when isolated from mitochondria, and requires the addition of Fe^{2+} to achieve activity.

Surprisingly, the isolated aconitase was found by analysis and Mossbauer spectroscopy to possess an Fe_3S_4 site in its inactive form.[161] Low-resolution crystallographic study supports the presence of an apo-Fe thiocubane, Fe_3S_4 structure in aconitase.[162] Resonance Raman[163] and EXAFS[103,155] studies clearly fingerprint the Fe_3S_4 cluster. The current hypothesis for aconitase activation involves the Fe_3S_4 thiocubane fragment reacting with Fe^{2+} to complete the cube, which is the active form of the enzyme.[164] Recent crystallographic studies[113] confirm the presence of a complete cube in the activated aconitase. The dimensions and positioning of the Fe_3S_4 and Fe_4S_4 centers in the cube are virtually identical. The added Fe^{2+} iron atom is ligated by a water (or hydroxide) ligand, consistent with the absence of any cysteine residues near the exchangeable iron. Since this water (or a hydroxide) is also present in the Fe_3S_4 system, one wonders whether a small ion such as Na^+ might be present in the Fe_3S_4 aconitase system.

Questions of detailed mechanism for aconitase remain open. ENDOR spectroscopy[165] shows that both substrate and water (or OH^-) can bind at the cluster. Does one of its Fe-atom vertices play the Lewis-acid role necessary for aconitase activity? Is the $Fe_3S_4 \rightleftharpoons Fe_4S_4$ conversion a redox- or iron-activated switch, which works as a control system for the activity of aconitase? These and other questions will continue to be asked. If aconitase is indeed an Fe-S enzyme with an iron-triggered control mechanism, it may be representative of a large class of Fe_3/Fe_4 proteins. Other hydrolytic enzymes containing similar Fe-S centers have recently been reported.[166,166a]

Spectroscopically, the Fe_3S_4 center is distinct and clearly distinguishable from 1Fe, 2Fe, and 4Fe centers. The center is EPR-active in its oxidized form, displaying a signal (Figure 7.6) with g = 1.97, 2.00, and 2.06 (*D. gigas* FdII).[158] The Mössbauer spectrum (Figure 7.7) shows a single quadrupole doublet with ΔQ = 0.53 nm/s and isomer shift of 0.27 nm, suggesting the now familiar highspin iron electronic structure.[158,159] In its reduced form, the center becomes EPR-silent, but the Mössbauer spectrum now reveals two quadrupole doublets of intensity ratio 2:1. The suggestion of the presence of a 3Fe center was first made based on this observation.[147] The picture of the reduced Fe_3S_4 state that has emerged involves a coupled, delocalized Fe^{2+}/Fe^{3+} unit responsible for the outer doublet, with a single Fe^{3+} unit responsible for the inner doublet of half the intensity. The oxidized state contains all Fe^{3+} ions, which are coupled in the trinuclear center.

EXAFS studies were consistent and unequivocal in finding an Fe-Fe distance of ~2.7 Å in all putative Fe_3S_4 proteins.[103,155,167] Resonance Raman spectra compared with those of other proteins and of model compounds with known structures[168,169] for other metals also favored the structure of Figure 7.14B. Clearly, what has been termed the spectroscopic imperative[170] has been crucial in the successful elucidation of the 3Fe structure. An interesting excursion has led to isolation of what are presumed to be $ZnFe_3S_4$, $CoFe_3S_4$, and $NiFe_3S_4$ thiocubane structures by adding Zn^{2+}, Co^{2+}, or Ni^{2+}, respectively, to proteins containing reduced Fe_3S_4 cores.[170a,b,c] These modified proteins provide interesting electronic structural insights and, potentially, new catalytic capabilities.

Fe_3 Model Systems

To date, the Fe_3S_4 center is the only structurally characterized biological iron-sulfide center that does not have an analogue in synthetic Fe chemistry. In fact, the closest structural analogue[21,170d] is found in the $Mo_3S_4^{4+}$ or $V_3S_4^{3+}$ core in clusters such as $Mo_3S_4(SCH_2CH_2S)_3^{2-}$, whose structure is shown in Figure 7.16.

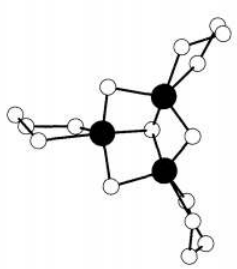


Figure 7.16 - The x-ray crystal structure of $Mo_3S_4(SCH_2CH_2S)_3^{2-}$. (From Reference 10a.)

The resonance Raman spectrum[169] of this complex bears a close resemblance to that of the *D. gigas* ferredoxin II. Since the vibrational bands responsible for the resonance Raman spectrum are not strongly dependent on the electronic properties, it is not surprising that an analogue with a different metal can be identified using this technique.

In synthetic Fe chemistry, although there is no precise structural analogue, it is instructive to consider three types of trinuclear and one hexanuclear center in relation to the three-iron biocenter.

The trinuclear cluster $Fe_3S[(SCH_2)C_6H_4]_3^{2-}$ is prepared[171,172] by the reaction of $FeCI_3$, $C_6H_4(CH_2SH)_2$, $Na^+OCH_3^-$, and p-CH_3-C_6H_4-SH in CH_3OH. As shown in Figure 7.17A, this cluster has, like the biocluster, a single triply bridging sulfide ion but, unlike the biocluster, it uses the sulfur atoms of the ethane 1,2-dithiolate as doubly bridging, as well as terminal, groups. The inorganic ring $Fe_3(SR)_3S_6^{3-}$ (X = CI, Br) has a planar $Fe_3(SR)_3$ core, which resembles the now-discredited structure for *Av* FdI[173] (Figure 7. 14A).

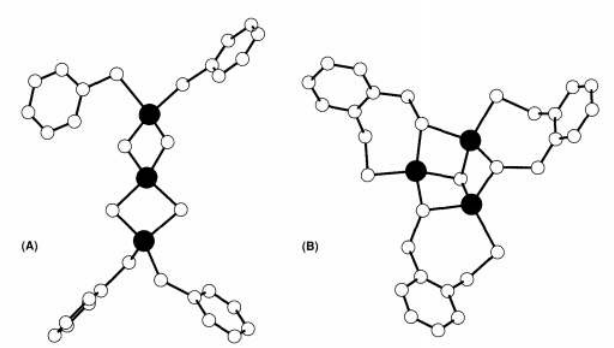


Figure 7.17 - The x-ray crystal structures of trinuclear Fe complexes: (A) $Fe_3S_4(SR)_4^{3-}$; (B) $Fe_3S[(SCH_2)_2C_6H_4]_3^{2-}$. (Data from References 171, 172, 174, 175.)

The complex $Fe_3S_4(SR)_4^{3-}$ is prepared[174,175] by reaction of $Fe(SR)_4^{2-}$ with sulfur. The x-ray-determined structure reveals two tetrahedra sharing a vertex with the linear Fe-Fe-Fe array shown in Figure 7.17B. This complex has distinctive EPR, Mössbauer, and NMR spectra that allow it to be readily identified[174,175,175a] Interestingly, after the complex was reported, a study of (denatured) aconitase at high pH (>9.5) revealed that the thiocubane fragment Fe_3S_4 site in that enzyme rearranged to adopt a structure that was spectroscopically almost identical with that of the linear complex.[176] Although the state may not have any physiological significance, it does show that Fe-S clusters different from the common (conventional) ones already discussed could be important in proteins under certain physiological conditions or in certain organisms; i.e., iron centers first identified synthetically may yet prove to be present in biological systems.

A synthetic cluster that displays features related to the biological Fe_3S_4 cluster is the hexanuclear cluster $Fe_6S_9(SR)_2^{4-}$ shown in Figure 7.18. This cluster contains two Fe_3S_4 units bridged through their diiron edges by a unique quadruply bridging S^{2-} ion (μ_4-S^{2-}) and by two additional μ_2S^{2-} bridges. The inability of synthetic chemists to isolate an Fe_3S_4 analogue may indicate that in proteins this unit requires strong binding. Significant sequestration by the protein may be needed to stabilize the Fe_3S_4 unit against oligomerization through sulfide bridges or, alternatively, rearrangement to the stable Fe_4S_4 center.

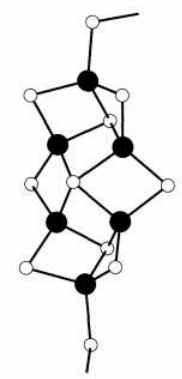


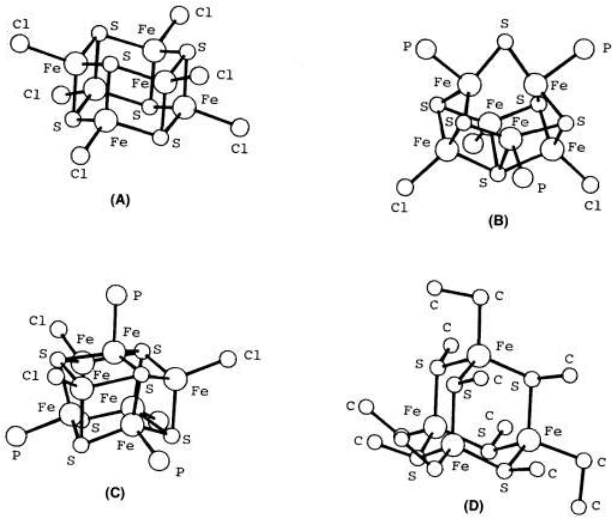
Figure 7.18 - The x-ray crystal structure[176a,b] of $Fe_6S_9(SR)_2^{4-}$.

Fe-S Chemistry: Comments and New Structures

The first successful model system for an iron-sulfur protein was an analogue of the Fe_4S_4 system, i.e., the system with the largest presently established biological Fe cluster. The reactions used to synthesize the cluster shown in Figure 7.13 are said to involve self-assembly, meaning that starting materials are simply mixed together, and thermodynamic control causes the cluster to assemble in its stable form. Interestingly, the Fe_4S_4-containing proteins, such as those of *C. pasteurianum*, are considered to be among the most ancient of proteins. Perhaps on the anaerobic primordial Earth, Fe-S clusters self-assembled in the presence of protein ligands to form the progenitors of the modem ferredoxins.

Much progress has been made in synthetic chemistry, and it is clear that both understanding and control of Fe-S chemistry are continuing to grow. New preparations for known clusters continue to be found, and new clusters continue to be synthesized, Although many of the new clusters appear to be abiological, we should not ignore them or their potential. They add to our understanding of Fe-S chemistry in general, and serve as starting points in the study of heteronuclear clusters, There is also the distinct possibility that one or more of these synthetic clusters represent an existing biological site that has not yet been identified in an isolated system.

Among the "nonbiological" structures that have been synthesized are complexes with $Fe_6S_6^{3+/2+}$ cores[177,178] including the thioprismanes,[108,109,177-179] the octahedron/cube $Fe_6S_8^{3+}$ cores,[180,181] the $Fe_6S_9^{2-}$ cores[176a,b] discussed above, the adamantane-like $Fe_6(SR)_{10}^{4-}$ complexes related to Zn and Cu structures in metallothioneins,[182] basket $Fe_6S_6^{2+}/Fe_6S_6^{+}$ cores,[182a,b,c,d] monocapped prismatic $Fe_7S_6^{3+}$ cores,[183] the cube/octahedron $Fe_8S_6^{5+}$ cores,[179] and the circular Na^+-binding $Fe_{18}S_{30}^{10-}$ unit.[183a,b] Representative ions are shown in Figure 7.19. Some of these cores are stabilized by distinctly nonbiological phosphine ligands. Nevertheless, one should not *a priori* eliminate any of these structures from a possible biological presence. Indeed, recently a novel, apparently six-iron protein from *Desulfovibio gigas* has been suggested[183c] to have the thioprismane core structure first found in model compounds.



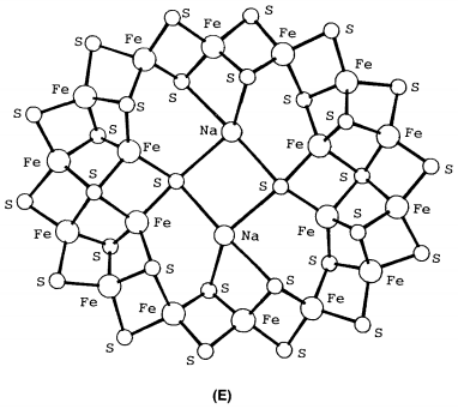


Figure 7.19 - Structures of "to date nonbiological" Fe-S clusters: (A) the thioprismane structure;[177] (B) basket-handle structure;[182a] (C) monocapped prismatic structure;[183] (D) adamantane structure;[182] (E) circular $Fe_{18}S_{30}^{10-}$ core unit.[183a,b]

Detection of Fe-S Sites

Several recent reviews have concentrated on the ways in which the various Fe-S centers can be identified in newly isolated proteins.[5,6,184] It is instructive to summarize the central techniques used in the identification of active sites. Optical spectra are usually quite distinctive, but they are broad and of relatively low intensity, and can be obscured or uninterpretable in complex systems. MCD spectra can give useful electronic information, especially when the temperature dependence is measured. EPR spectra, when they are observed, are distinctive, and are usually sufficiently sharp to be useful even in complex systems. Mössbauer and resonance Raman spectroscopies have each been applied with good effect when they can be deconvoluted, and NMR and magnetic susceptibility have given important information in some simple, lower-MW protein systems. X-ray absorption spectra, especially EXAFS, give accurate Fe-S and Fe-Fe distances when a single type of Fe atom is present. Analytical and extrusion data complement the spectroscopic and magnetic information. Extrusion data must be viewed with considerable caution, because of possible cluster-rearrangement reactions. Even x-ray crystallography has led to incorrect or poorly refined structures. In general, no one technique can unequivocally identify a site except in the very simplest systems, and there is continued need for synergistic and collaborative application of complementary techniques to a given system.

Redox Behavior

Figure 7.20 shows the ranges of redox behavior known for Fe-S centers. Clearly, the Fe-S systems can carry out low-potential processes. The rubredoxins cover the mid-potential range, and the HiPIPs are active in the high-potential region. The lack of extensive Fe-S proteins in the positive potential region may reflect their instability under oxidizing conditions and their preemption by Mn, Cu, or heme-iron sites (such as in cytochrome c), which function in this region.

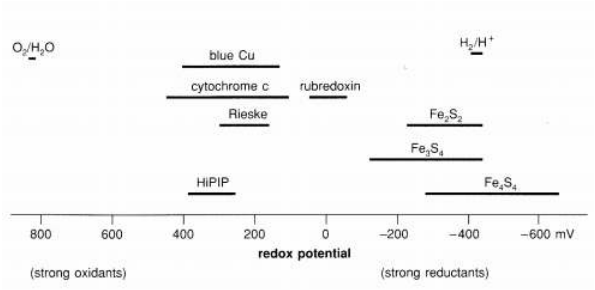


Figure 7.20 - A schematic diagram of the redox potential of the various FeS centers in comparison with other known redox centers.

11.2.7.4: Iron-sulfur Proteins and Models (Part 4) is shared under a CC BY-NC-SA 4.0 license and was authored, remixed, and/or curated by LibreTexts.

11.2.7.5: Multisite Redox Enzymes

In making the transition from the relatively simple electron-transfer proteins to the far more complex Fe-S-containing enzymes, we must recognize that the difference in our degree of understanding is enormous. Not only are the catalytic proteins ten to twenty times larger than the redox proteins, but they often also have several subunits and multiple copies of prosthetic groups. Moreover, very few crystal structures are known for the redox enzymes, and none is known at high resolution. In the absence of three-dimensional protein structural information, we do not know the arrangement, relative separation, or orientation of the prosthetic groups. Finally, studies on model systems have not yet approached the sophisticated state that they have for the structurally known centers.

In general, multicomponent redox enzyme systems appear to be organized in two distinct ways to effect their substrate reactions. In the first mode, the enzyme is designed to bring the oxidant and reductant together so that they may directly interact. For example, oxygenases bring O_2 and an organic molecule together, and activate one or both of these reactants to cause them to react directly with each other. This mode can be called *proximation*, as the reactants are brought near each other by the enzyme catalyst.

In contrast to proximation, many redox enzymes keep the oxidant and reductant well-separated, and use rapid (usually long-distance) internal electron transfer to bring electrons from the reductant to the oxidant. We can term their mode of action *electrochemical*. The oxidant and reductant are separated spatially. The enzyme provides the "anode" site to interact with the reductant, the "cathode" site to interact with the oxidant, and the wire to allow electronic flow between the "anode" and "cathode" sites. Hydrogenases and nitrogenases adopt the electrochemical mode of redox activation. In hydrogenases, the electron acceptor, even if it must formally take up hydrogen (e.g., $NAD^+ \rightarrow NADH$), does not interact at the same site as the H_2. There is no direct transfer of H^- from H_2 to NAD^+. Rather, H_2 reduces the enzyme at one site, and NAD^+ or other acceptors, such as methylene blue, retrieve the electrons at other sites following internal electron transfer. For nitrogenase, the redox partners are even more removed, as a separate protein, the Fe protein, delivers electrons to the FeMo protein, that eventually end up at the FeMoco site ready to reduce N_2 to NH_3. These enzymes work much like electrochemical cells.

Hydrogenase and Nitrogenase

Hydrogenase is the enzyme responsible for the uptake or evolution of H_2. Nitrogenase is the enzyme that catalyzes the ATP-dependent reduction of N_2 to NH_3, with concomitant evolution of H_2.

The relationship between H_2 and N_2 in biology is intricate.[184] Metabolically, H_2 use and N_2 use are tightly coupled in many nitrogen-fixing organisms, with H_2 serving indirectly as the reductant for N_2. Moreover, H_2 and N_2 react in related ways with various transition-metal complexes, which are at present the closest (albeit quite imperfect) models of the enzyme active sites. The biological fixation of molecular nitrogen is dependent on iron-sulfide proteins that also contain molybdenum or vanadium. The biological production or uptake of H_2 depends on the presence of iron-sulfide proteins, which often also contain nickel and sometimes selenium. Spectroscopic and model-system studies, which have played such a key role in advancing the understanding of simple Fe-S sites, are now helping to foster an understanding of these more complex enzyme sites, although we have much yet to learn about structure and mechanism in these enzymes. The remainder of this chapter seeks to convey the state of our rapidly evolving knowledge.

Hydrogenases

1. Physiological Significance

Molecular hydrogen, H_2, is evolved by certain organisms and taken up by others. For either process, the enzyme responsible is called hydrogenase. The raison *d' être* for hydrogenases in particular organisms depends on the metabolic needs of the organism. Properties of some representative hydrogenases are given in Table 7.5.[184,184a-g]

Hydrogenases are found in a wide variety of anaerobic bacteria, such as the eubacterial *C. pasteurianum* and *Acetobacterium woodii* and the archaebacterial *Methanosarcina barkerii*. Interestingly, *C. pasteurianum* sometimes evolves H_2 during its growth on sugars. This H_2 evolution is required for continued metabolism, since it allows the organism to recycle (reoxidize) cofactors that are reduced in the oxidation of sugars (or their metabolic descendants, lactate or ethanol). In effect, H^+ is acting as the terminal oxidant in clostridial metabolism, and H_2 is the product of its reduction. In contrast, methanogens such as methanosarcina take up H_2 and in effect use it to reduce CO_2 to CH_4 and other carbon products. Clearly, either H_2 uptake or H_2 evolution may be important

in particular anaerobic metabolic contexts. The hydrogenases of the anaerobic sulfate-reducing bacteria of the genus *Desulfovibrio* have been particularly well-studied (see Table 7.5).

Table 7.5 - Properties of some representative hydrogenases.

Organism (designation)	MW (subunits)	Approximate Composition	Reference
Clostridium pasteurianum (Hydrogenase I)	60,000 (1)	12Fe 22Fe	191 194
Clostridium pasteurianum (Hydrogenase II)	53,000 (1)	8Fe 17Fe	191 194
Acetobacterium woodii	15,000	Fe	192
Megasphaera elsdenii	50,000 (1)	12Fe	188
Desulfovibrio vulgaris (periplasmic)	56,000 (2)	12Fe	171
Desulfovibrio gigas	89,000 (2)	11Fe, 1Ni	363
Desulfovibrio africanus	92,000	11Fe, 1Ni	364
Methanobacterium thermoautotrophicum	200,000	Fe, 1Ni	145
Methanosarcina barkeri	60,000	8-10Fe, 1Ni	77
Methanococcus vanielli	3400,000	Fe, Ni, 1Se, FAD	365
Desulfovibrio baculatus	85,000 (2)	12Fe, 1Ni, 1Se	365

In nitrogen-fixing organisms, H_2 is evolved during the nitrogen-fixation process, and hydrogenase is present to recapture the reducing equivalents, which can then be recycled to fix more nitrogen. In N_2-fixing organisms, such "uptake" hydrogenases can make an important contribution to the overall efficiency of the nitrogen-fixation process. In fact, certain species of rhizobia lacking the hydrogen-uptake system (*hup*$^-$ strains) can be made more efficient by genetically engineering the hup activity into them.

Aerobic bacteria such as *Azotobacter vinelandii*, *Alcaligenes eutrophus*, and *Nocardia opaca*, and facultative anaerobes, such as *Escherichia coli* and various species of *Rhizobium* and *Bradyrhizobium* (the symbionts of leguminous plants), also contain hydrogenase, as do photosynthetic bacteria such as *Chromatium vinosum*, *Rhodobacter capsulatus* (formerly *Rhodopseudomonas capsulata*), and *Anabaena variabilis* (a filamentous cyanobacterium). The thermophilic hydrogen oxidizer *Hydrogenobacter thermophilus*, which grows in alkaline hot springs above 70 °C, obviously has a critical requirement for hydrogenase.

In certain aerobic organisms, such as hydrogenomonas, H_2 and O_2 are caused to react (but not directly) according to the Knallgas reaction[185]

$$2H_2 + O_2 \rightarrow 2H_2O \qquad \Delta G^o = -54.6 kcal/mol \tag{7.7}$$

These organisms break up this thermodynamically highly favorable redox process by using intermediate carriers, thereby allowing the large negative free-energy change to be captured in biosynthetic capacity.

Hydrogenases seem to be especially prevalent in anaerobic, nitrogen-fixing, and photosynthetic organisms. However, although hydrogenases are obviously found widely among prokaryotes, unlike nitrogenase, their domain is not restricted to prokaryotes. Eukaryotic green algae such as *Chlorella fusca* and *Chlamydomonas reinhardtii* possess hydrogenase. The anaerobic protozoan *Trichomonas vaginalis*, which lacks typical aerobic organelles, such as mitochondria and peroxisomes, has an organelle called a hydrogenosome, whose function is to oxidize pyruvate to acetate, producing H_2, via hydrogenase, in the process.

The various hydrogenase enzymes are all transition-metal sulfide proteins. However, before we discuss these enzymes, we turn briefly to the dihydrogen molecule and its physical and chemical properties.

2. Dihydrogen: The Molecule

Diatomic H_2 has a single H—H bond formed by overlap of the two 1s orbitals of the two hydrogen atoms. In molecular orbital terms, this overlap forms bonding σ and antibonding σ^* orbitals, shown in the energy-level diagram in Figure 7.21A and displayed spatially in Figure 7.21B. The H-H distance is 0.74 Å, and the bond dissociation energy is 103.7 kcal/mole. The isotopes of hydrogen $^1H_1$, $^2H_1$ = $^2D_1$, $^3H_1$ = $^3T_1$ are called protium (a designation seldom used), deuterium, and tritium, respectively. Deuterium, at natural abundance of 0.015 percent, is a stable isotope with nuclear spin I = 1, whereas both ^1H and ^3T have nuclear spin I = $\frac{1}{2}$. NMR has been fruitfully applied to all the hydrogen isotopes, including tritium. Tritium is radioactive, decaying to $^3He_2$ by β^- emission with a half-life of 12 years. The nuclear properties of deuterium and tritium make them useful as labels to probe structure and mechanism in hydrogen-containing compounds. "Exchange" reactions involving the formation of HD or HT have played a significant role in mechanistic studies of both hydrogenase and nitrogenase.

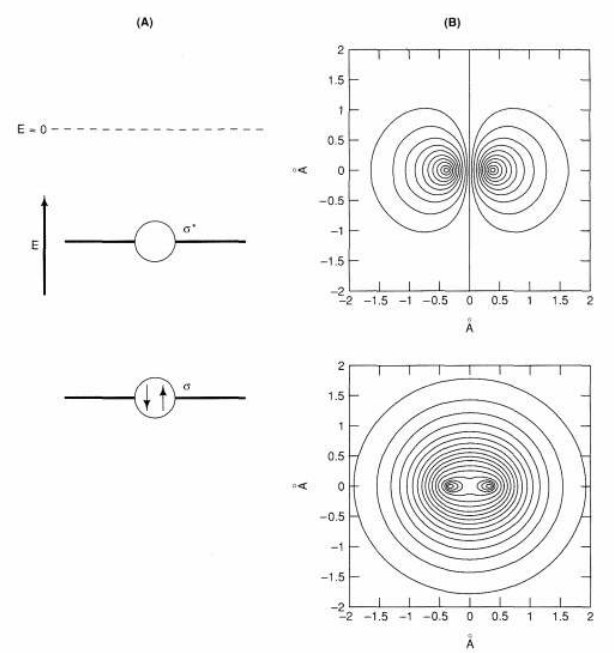


Figure 7.21 - Molecular orbital scheme for binding in H_2: (A) energy-level diagram; (B) bonding and antibonding orbitals.

In molecular hydrogen, the existence of nuclear-spin energy levels is responsible for the distinction between *ortho* and *para* hydrogen, which correspond to the triplet and singlet (i.e., parallel and antiparallel) orientations, respectively, of the two nuclei in H_2. Because of the coupling of the rotational and spin levels, *ortho* and *para* hydrogen differ in specific heat and certain other properties. The correlated orientation of the nuclear spins in *para* H_2 has recently been shown to constitute a powerful mechanistic probe, wherein NMR may be used to trace the relative fate of the two H nuclei in the original molecule.[186,187] Although this technique has not yet been applied to any enzyme systems, hydrogenase is known to catalyze the interconversion of the *ortho* and *para* forms of H_2 (as does the hydrogenase analogue Pd).

Dihydrogen is a reducing agent. The H_2/H^+ couple at $[H^+]$ = 1 M defines the zero of the potential scale. At pH = 7 the hydrogen half-reaction

$$H_2 \rightarrow 2H^+ + 2e^- \qquad (7.8)$$

has E_o' = -420 mV. Dihydrogen is therefore one of the strongest biological reductants.

Although many hydrogenases are reversible, some "specialize" in the uptake of H_2. One hydrogenase has been reported[188] to specialize in the evolution of H_2. This "specialization" seems curious, since it appears to contradict the notion of microscopic reversibility, and seems to violate the rule that catalysts increase the speed of both forward and backward reactions without changing the course (direction) of a reaction. In fact, there is no contradiction or violation, since the overall reactions catalyzed by the various types of hydrogenases are fundamentally different. The electron acceptor in uptake hydrogenases *differs* from the electron donor/acceptor in the reversible hydrogenases. The difference involves structure and, more importantly, redox potential.

The reaction catalyzed by the uptake hydrogenase involves an acceptor of such high positive redox potential that its reaction with H_2 is essentially irreversible. The enzyme appears to be designed so that it can transfer electrons only to the high potential acceptor.

A selection of hydrogenases from various organisms is given in Table 7.5. All hydrogenases contain Fe-S centers. The hydrogenases from more than 20 organisms[189] have been found to contain Ni by analysis and/or spectroscopy. Many more Ni hydrogenases are likely to be found, given the nutritional requirements[189] for hydrogenase synthesis or growth on H_2. Hydrogenases may be cytoplasmic (as in *C. pasteurianum*), membrane-bound (as in *E. coli*), or located in the periplasmic space (as in *Desulfovibrio v*ulgaris). The isolation of hydrogenases is sometimes complicated by their air sensitivity or membranebound nature. Many hydrogenases have now been isolated and studied in detail; they can be divided into two categories, the iron hydrogenases and the nickeliron hydrogenases.

11.2.7.5: Multisite Redox Enzymes is shared under a CC BY-NC-SA 4.0 license and was authored, remixed, and/or curated by LibreTexts.

11.2.7.6: Multisite Redox Enzymes (Part 2)

3. Iron Hydrogenases

The iron hydrogenases[189a] generally have higher activities than the NiFe enzymes, with turnover numbers approaching 10^6 min^{-1}. Iron hydrogenases from four genera of anaerobic bacteria have been isolated: *Desulfovibrio*,[190] *Megasphaera*,[188] *Clostridium*,[191] and *Acetobacterium*.[192] Of these, the enzymes from *Desulfovibrio vulgaris*, *Megasphaera elsdenii*, *Clostridium pasteurianum* (which contains two different hydrogenases), and *Acetobacterium woodii*[192] have been well-characterized (especially the *D. vulgaris* and *C. pasteurianum* enzymes). Although *Acetobacterium* and *Clostridium* are closely related, the other organisms are only distant cousins.[193] Nevertheless, their hydrogenases display significant similarities; all contain two different types of iron-sulfur cluster, called F and H clusters,[194] and carbon monoxide is a potent inhibitor (although this has not been reported for the *M. elsdenii* enzyme). The F clusters are thought to be of the $Fe_4S_4^{+/2+}$ thiocubane type, and give S = $\frac{1}{2}$ EPR signals when the enzyme is in the reduced form. On the other hand, the H cluster, which is thought to be the hydrogen-activating site, gives an EPR signal only when the enzyme is in the oxidized form. The H-cluster EPR signals of all the enzymes are quite similar (g = 2.09, 2.04, 2.00), and are quite unlike the signals from other oxidized iron-sulfide clusters (such as Fe_3S_4 clusters and HiPIPs), in that they are observable at relatively high temperatures (> 100 K). Inhibition of the *D. vulgaris* and both *C. pasteurianum* enzymes by carbon-monoxide yields a photosensitive species that has a modified H-cluster EPR signal.[195,196]

The two different hydrogenases of *C. pasteurianum*, called hydrogenase I and II, have both been quite extensively studied, and can be regarded as prototypical iron-only hydrogenases. Hydrogenase I is active in catalyzing both H_2 oxidation and H_2 evolution, whereas hydrogenase II preferentially catalyzes H_2 oxidation.[188] The two enzymes differ in their iron contents: hydrogenase I contains about 20 iron atoms, 16 of which are thought to be involved in four F clusters,[194] while the remainder presumably constitute the H cluster, which may contain six Fe atoms.[194] Hydrogenase II contains about 14 iron atoms as two F clusters and one H cluster.[194] These estimates of iron content result from a recent reappraisal of the metal contents (based on amino-acid analysis) that indicated a rather higher Fe content than previously realized.[188,194] It is important to note that much of the spectroscopic work, which will be discussed below, was initially interpreted on the basis of the earlier, erroneous, iron analysis. Of particular interest is the possibility (first suggested[197] for the *D. vulgaris* enzyme) that the H cluster contains six iron atoms.

Carbon-monoxide treatment of the *D. vulgaris* and both *C. pasteurianum* enzymes yields a photosensitive species that has a modified H cluster EPR signal.[195,196] Interestingly, the *C. pasteurianum* enzymes also form complexes with O_2, in a process that is distinguishable from the deactivation of hydrogenase by O_2, which results from a much more prolonged exposure to O_2 than that required to form the O_2 complex. The O_2 complexes have (photosensitive) EPR signals much like those of the CO complex.[196] It is important to note that although CO, when in excess, is a potent inhibitor of the enzymes, the hydrogenase I-CO complex is actually quite active.[196] With hydrogenase II, the CO complex is dissociated on exposure to H_2, restoring the "active" enzyme.[196] The EPR spectrum of reduced hydrogenase I is typical of (interacting) $Fe_4S_4^+$ clusters, and integrates to 3 or 4 spins/protein.[194,198] Electrochemical studies[199] show that these clusters possess indistinguishable reduction potentials. Recently, MCD and EPR spectroscopies have been used to demonstrate the presence of significant quantities of an S = $\frac{3}{2}$ species in reduced hydrogenase I. This signal apparently integrates to about one spin per molecule, and probably originates from an S = $\frac{3}{2}$ state of an Fe_4S_4 cluster.[198] No information is yet available on the reduction potential of the S = $\frac{3}{2}$ species. However, based on analogy with the nitrogenase iron protein,[200] we might expect the S = $\frac{3}{2}$ form to have electrochemistry indistinguishable from the S = $\frac{1}{2}$ form. EPR signals with high g values (g = 6.1 and 5.0) have also been observed in *C. pasteurianum* hydrogenase I, and in the *D. vulgaris* enzyme.[198,201] Since there is some uncertainty about the nature and origin of these signals,[198] we will not discuss them further. The F clusters of hydrogenase II, on the other hand, give two different EPR signals that integrate to one spin each per protein molecule, and that correspond to sites with different redox potentials.[194,198,199] This suggests that hydrogenase II contains two different F clusters, called F and F' (note that the presence of F' was in fact first suggested by Mössbauer spectroscopy[202]). The EPR spectrum from the F' cluster is unusually broad. The H-cluster EPR signals of active hydrogenase I and II are quite similar and have essentially identical redox potentials.[199]

The redox behavior of the F and H centers in hydrogenases I and II is nicely consistent with their respective modes of function. As shown in Figure 7.22, the F clusters are presumed to transfer electrons intermolecularly with the external electron carrier and intramolecularly with the H center. In the reversible hydrogenase I, the F and H centers have the same redox potentials (about -400 mV at pH 8), similar to that of the hydrogen electrode (-480 mV at pH 8). Thus, electrons may flow in either direction when a

mediator such as methyl viologen ($E^{\circ\prime}$ = -440 mV at pH 8) is used as the external electron acceptor (methyl viologen is the 4,4'-bipyridinium ion). On the other hand, for hydrogenase II, the F clusters have $E^{\circ\prime}$ (pH 8) = -180 mV and $E^{\circ\prime}$ > -300 mV for F and F', respectively. In hydrogenase II, therefore, electrons can only move favorably from H_2 to the H cluster, through F' and F, and then to a lower-potential acceptor, such as methylene blue [for which $E^{\circ\prime}$ (pH 8) = 11 mV].

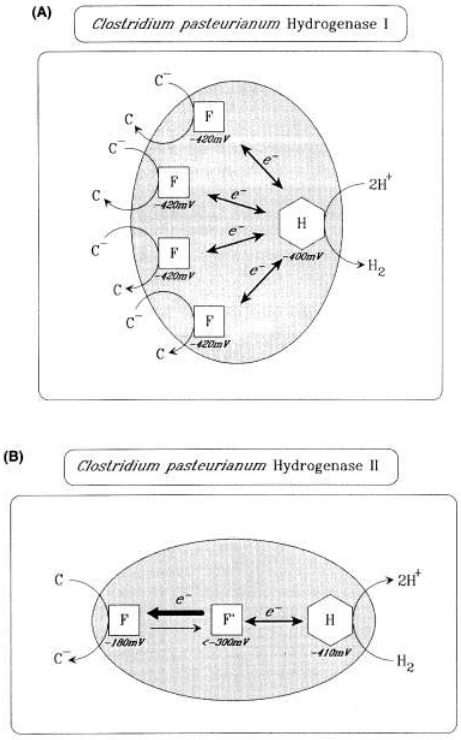


Figure 7.22 - Redox schemes illustrating proposed action of Fe hydrogenases: (A) Clostridium pasteurianum hydrogenase I; (B) Clostridium pasteurianum hydrogenase II.[189a,199]

Mössbauer spectroscopic studies of both hydrogenase I and II have been reported.[202,203] Our discussion focuses primarily on the H cluster. The results are similar for the two enzymes, but better defined for hydrogenase II because of the smaller number of clusters. The H cluster apparently contains only two types of iron, in the ratio of 2:1, with quadrupole splittings reminiscent of Fe_3S_4 clusters. The oxidized cluster is confirmed to be an S = $\frac{1}{2}$ system, also reminiscent of Fe_3S_4 clusters, and the reduced H cluster is an S = 0 system; this contrasts with reduced Fe_3S_4 clusters, which have S = 2. In agreement with the Mössbauer studies, ENDOR spectroscopy of ^{57}Fe-enriched protein indicates at least two different types of iron in the H cluster, with metal hyperfine couplings of about 18 and 7 MHz in hydrogenase II. Rather-less-intense ENDOR features were also observed at frequencies corresponding to couplings of about 11 and 15 MHz.[204] The H-cluster EPR signals of hydrogenase II and hydrogenase I change on binding carbon monoxide. Although the signals of the uncomplexed enzymes are quite similar, the signals of the CO-bound species are very different (note, however, that *C. pasteurianum* CO-bound hydrogenase I has EPR similar to that of the CO-bound *D. vulgaris* enzyme), When produced with ^{13}C-enriched CO, the EPR signal of hydrogenase II shows resolved ^{13}C hyperfine coupling (A_{av} = 33 MHz) to a single ^{13}C nucleus, indicating that only a single CO is bound, presumably as a metal carbonyl. A slightly smaller coupling of 20 MHz was obtained using ENDOR spectroscopy for the corresponding species of hydrogenase I.[205]

Recent ESEEM spectroscopy of hydrogenase I indicates the presence of a nearby nitrogen, which may be a nitrogen ligand to the H-cluster. This nitrogen possesses an unusually large nuclear electric quadrupole coupling and a rather novel structure, involving an amide amino-acid side chain connected to an H-cluster sulfide via a bridging proton ligand, has been suggested for it.[206] Although the nitrogen in question must come from a chemically novel species, the proposed proton bridge might be expected to be exchangeable with solvent water. The ENDOR-derived result[205] that there are no strongly coupled exchangeable protons in the oxidized H cluster may argue against such a structure.

Rather weak MCD[198,207] and resonance Raman spectra[208] have also been reported for iron hydrogenases. The lack of an intense MCD spectrum[198,207] contrasts markedly with results for other biological FeS clusters. The resonance Raman spectra of

hydrogenase I resemble, in some respects, spectra from Fe_2S_2 sites.[208] These results further emphasize that the hydrogenase H clusters are a unique class of iron-sulfur clusters. Perhaps most tantalizing of all are the recent EXAFS results on hydrogenase II.[209] It is important to remember that for enzymes with multiple sites, the EXAFS represents the sum of all sites present (i.e., the iron of the F, F', and H clusters). Despite this complication, useful information is often forthcoming from these experiments. The EXAFS of oxidized hydrogenase I showed both iron-sulfur and iron-iron interactions; the latter, at about 2.7 Å, is at a distance typical of Fe_2S_2, Fe_3S_4, and Fe_4S_4 clusters, and thus is not unexpected. The reduced enzyme, however, gave an additional, long Fe-Fe interaction at 3.3 Å. This Fe-Fe separation is not found in any of the FeS model compounds reported to date.[209] The appearance of the 3.3-Å interaction indicates a change in structure on reduction of the H cluster, again revealing a cluster of unique structure and reactivity. The large structural change of this H cluster on H_2 reduction is likely to have significant mechanistic implications.

4. Nickel-iron Hydrogenases

The presence of nickel in hydrogenases has only been recognized relatively recently. Purified preparations of the active enzymes were the subject of quite intensive studies for years before the Ni content was discovered by nutritional studies (see Reference 189 for a history). Some workers even tried (in vain) to purify out "impurity" EPR signals that were later found to be from the Ni. In contrast to the Fe hydrogenases discussed in the previous section, the Ni enzymes possess a variety of compositions, molecular weights, activation behavior, and redox potentials.[189,210,211] As Table 7.5 shows, some of the Ni hydrogenases contain selenium, likely in the form of selenocysteine, some contain flavin (FMN or FAD), and all contain iron-sulfur centers, but in amounts ranging from 4 to 14 iron atoms per Ni atom.

Among the different Ni hydrogenases there is a common pattern of protein composition, to which many, but not all, seem to conform (especially those enzymes originating from purple eubacteria). There are two protein subunits, of approximate molecular masses 30 and 60 kDa, with the nickel probably residing in the latter subunit. The hydrogenase of the sulfate-reducing bacterium *Desulfovibrio gigas* is among the best investigated, and we will concentrate primarily on this enzyme. *D. gigas* hydrogenase contains a single Ni, two Fe_4S_4 clusters, and one Fe_3S_4 cluster. Of primary interest is the Ni site, which is thought to be the site of H_2 activation.[189,210,211]

EPR signals attributable to mononuclear Ni [as shown by enrichment with ^{61}Ni ($I = \frac{3}{2}$)] have been used in numerous investigations of the role of Ni in hydrogenases.[189,210,211] Three major Ni EPR signals are known, which are called Ni-A, Ni-B, and Ni-C. The principal g values of these signals are: 2.32, 2.24, and 2.01 for Ni-A; 2.35, 2.16, and 2.01 for Ni-B; and 2.19, 2.15, and 2.01 for Ni-C. Of these, Ni-C is thought to be associated with the most active form of the enzyme (called active); the other two are thought to originate from less-active enzyme forms.[189,210]

In the enzyme as prepared (aerobically) the Ni-A EPR is characteristically observed. On hydrogen reduction the Ni-A EPR signal disappears, and the enzyme is converted into a higher-activity form (Ni-B arises from reoxidation of this form). Further progressive reduction of the enzyme gives rise to the Ni-C EPR signal, which also finally disappears. These redox properties show that Ni-C arises from an intermediate enzyme oxidation state. Although the Ni-A and Ni-B EPR signals[189,210-212] almost certainly originate from low-spin Ni(III), the formal oxidation state of Ni-C is rather less certain. Both an Ni(I) site[189,210] and an Ni(III) hydride[213] have been suggested, with the former alternative currently favored because of the apparent absence of the strong proton hyperfine coupling expected for the latter. In the fully reduced enzyme, Ni-C is converted to an EPR-silent species. This has variously been suggested to be Ni(0), Ni(II), or an Ni(II) hydride.[214] One possible reaction cycle[189,210] is shown in Figure 7.23.

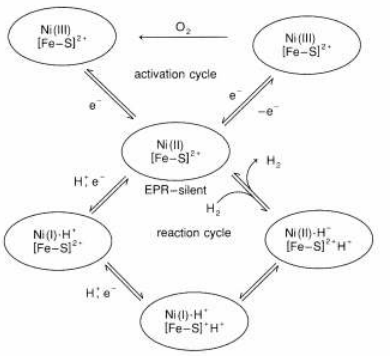


Figure 7.23 - Proposed activation/reactivity scheme for Ni hydrogenases.[189]

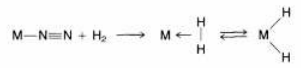
Information on the coordination environment of the nickel has been obtained from both x-ray absorption spectroscopy and EPR spectroscopy. The Ni K-edge EXAFS of several different hydrogenases,[215-218] and EPR spectroscopy of ^{33}S enriched *Wolinella succinogenes* hydrogenase,[219] clearly indicate the presence of sulfur coordination to nickel. A recent x-ray absorption spectroscopic investigation of the selenium-containing *D. baculatus* hydrogenase, using both Ni and Se EXAFS, suggests seienocysteine coordination to Ni.[216]

ESEEM spectroscopy of the Ni-A and Ni-C EPR signals[220,221] indicate the presence of ^{14}N coupling, which probably arises from a histidine ligand to Ni. Interestingly, Ni-C, but not Ni-A, shows coupling to a proton that is exchangeable with solvent water. Although this coupling is too small to suggest a nickel-hydride (consistent with conclusions drawn from EPR), the proton involved could be close enough to the Ni to playa mechanistic role.

Despite the extensive studies reported to date, there are still many unanswered questions about the mechanism of the NiFe hydrogenases, which remain as exciting topics for future research. Despite our lack of detailed knowledge of enzyme mechanism, it is nevertheless not premature to seek guidance from inorganic chemistry.

5. Insights from Inorganic Chemistry

Recent years have brought insights into the way dihydrogen can be bound at a transition-metal site. Unexpectedly, it has been shown that molecular H_2 forms simple complexes with many kinds of transition-metal sites.[222-224] This finding contrasts with the classical situation, in which H_2 interacts with a transition-metal site by oxidative addition to form a dihydride complex.[23]The H—H bond is largely maintained in the new/nonclassical structures. The dihydrogen and dihydride complexes can exist in simple equilibrium,[224] as in Equation (7.9).



The bonding of dihydrogen to a metal occurs via the σ^b orbital of the H—H bond acting as a donor, with the σ^* level of H_2 acting as a weak acceptor. If the back donation is too strong, sufficient electron density will build up in the *sigma** level to cause cleavage of the H—H bond, leading to the formation of a dihydride. Dihydrogen complexes therefore require a delicate balance, in which the metal coordination sphere facilitates some back-bonding, but not too much.

The proclivity of a metal center to form H_2 complexes can be judged by the stretching frequency of the corresponding N_2 complexes: N_2 can usually displace H_2 from the H_2 complex to form an N_2 complex without changing the remainder of the coordination sphere. If $\nu(N{\equiv}N)$ is between 2060 and 2160 cm^{-1}, H_2 complexes form upon replacement of N_2. If $\nu(N{\equiv}N)$ is less than 2060 cm^{-1}, indicative of electron back-donation from the metal center, a dihydride complex should form. For example, $\nu(N{\equiv}N)$ = 1950 cm^{-1} in $MoN_2(PCy_3)_5$ and $MoH_2(PCy_3)_5$ is a dihydride complex, but $\nu(N{\equiv}N)$ = 2090 cm^{-1} in $Mo(Ph_2PCH_2CH_2PPh_2)CO(N_2)$ and $Mo(Ph_2PCH_2CH_2PPh_2)H_2(CO)_2$ is a dihydrogen complex. By comparison, $Mo(Et_2PCH_2CH_2PEt_2)_2(CO)(N_2)$ has $\nu(N{\equiv}N)$ = 2050 cm^{-1} and forms a dihydride complex, $Mo(Et_2PCH_2CH_2PEt_2)_2H_2(CO)$. The correlation between $\nu(N{\equiv}N)$ and the type of hydrogen complex formed seems quite useful.

Since Fe-S and Ni-S sites are implied for hydrogenase, the reactivity of transition-metal/sulfide systems with H_2 may also be relevant. Interestingly, H_2 can react with metal-sulfide systems at S instead of at the metal site. For example,[225] $(Cp')_2Mo_2S_4$ reacts with H_2 to form $(Cp')_2Mo_2(SH)_4$. Here the dihydrogen is cleaved without any evidence for direct interaction with the metal center, and the resulting complex contains bridging SH groups and no direct metal-H bonding.[225] In recent work,[226] the binuclear rhodium-sulfur complex $\{RhS[P(C_6H_5)_2CH_2CH_2]_3CH\}_2$ was reported to react with two equivalents of dihydrogen to yield the complex $\{Rh(H)(SH)[P(C_6H_5)_2CH_2CH_2]_3CH\}_2$, in which two SH groups bridge the two Rh centers, each of which contains a single hydrido ligand. Figure 7.24 illustrates the possibilities for hydrogen activation. Each of these types of reactivity must be considered as possibilities for the hydrogen activation process of hydrogenase.

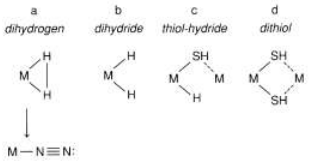


Figure 7.24 - Possible modes of H_2/H bonding at a transition-metal sulfide site.

Recently, a great deal of attention has been given to the chemistry of nickel-sulfur systems, inspired in part by the results showing that many hydrogenases are nickel-sulfur proteins.[227-230] A particularly interesting finding is that Ni thiolates can react with O_2 to produce sulfinate complexes.[231,232] The oxygenated thiolate can be regenerated, thus providing a potential model for the O_2 inactivation of Ni hydrogenases.

11.2.7.6: Multisite Redox Enzymes (Part 2) is shared under a CC BY-NC-SA 4.0 license and was authored, remixed, and/or curated by LibreTexts.

11.2.7.7: Multisite Redox Enzymes (Part 3)

Nitrogenases

Nitrogen fixation is a key reaction of the biological nitrogen cycle.[233] Fixed nitrogen, in which N is in molecules other than N_2, is frequently the limiting factor in plant growth.[234] Since natural systems often cannot provide enough fixed nitrogen for agriculture or animal husbandry, industrial processes have been developed to "fix nitrogen" chemically. The major process in use, often referred to as ammonia synthesis, is the Haber-Bosch process, in which N_2 and H_2 are reacted at temperatures between 300-500°C and pressures of more than 300 atm, using catalysts (usually) based on metallic iron. 235 Hundreds of massive chemical plants are located throughout the world, some producing more than 1,000 tons of NH_3/day. In contrast, in the biological process, N_2 is reduced locally as needed at room temperature and ~0.8 atm by the enzyme system called nitrogenase (variously pronounced with the accent on its first or second syllable).

1. The Scope of Biological Nitrogen Fixation

Biological nitrogen fixation occurs naturally only in certain prokaryotic organisms (sometimes called diazotrophs). Although the majority of bacterial species are not nitrogen fixers, the process of nitrogen fixation has been confirmed in at least some members of many important phylogenetic groups. Nitrogen fixation occurs in strict anaerobes such as *Clostridium pasteurianum*, in strict aerobes such as *Azotobacter vinelandii*, and in facultative aerobes such as *Klebsiella pneumoniae*. Much of the established biochemistry of N_2 reduction has been gleaned from studies of these three species. However, nitrogen fixation has a far broader range, occurring in archaebacterial methanogens such as *Methanobacillus omelianskii*, which produce methane, and eubacterial methanotrophs such as *Methylococcus capsulatus*, which oxidize methane. Photosynthetic organisms ranging from the purple bacterium *Rhodobacter capsulatus* (formerly *Rhodopseudomonas capsulata*) to the cyanobacterium (blue-green alga) *Anabaena cylindrica* fix nitrogen. Nitrogen fixation occurs mostly in mesophilic bacteria (existing between 15 and 40 °C), but has been found in the thermophilic archaebacterial methanogen *Methanococcus thermolithotrophicus* at 64 °C.

Many organisms fix N_2 in nature only symbiotically. Here the most studied systems are species of *Rhizobium* and *Bradyrhizobium*, which fix nitrogen in the red root nodules of leguminous plants such as soybeans, peas, alfalfa, and peanuts. The red color inside the nodules is due to leghemoglobin, a plant O_2-binding protein analogous to animal myoglobins and hemoglobins (Chapter 4). Other symbioses include that of blue-green algae such as *Anabaena azollae* with *Azola* (a water fern); actinomycetes such as *Frankia* with trees such as alder; and *Citrobacter freundii*, living in the anaerobic hind gut of termites. The distribution of nitrogenase clearly points to its adaptability as a metabolic option for species occupying widespread ecological niches.

The absence of nitrogen fixation in eukaryotes therefore seems somewhat puzzling. There would appear to be no fundamental limitation to the existence of nitrogen fixation in higher organisms. Indeed, *nif* genes have been transferred to yeast, where they work effectively under anaerobic conditions. Furthermore, the problem of the simultaneous presence of nitrogen fixation and aerobiosis has been solved effectively by aerobic bacteria such as *Azotobacter*, *Gleocapsa*, and *Anabaena*. Indeed, the lack of a fundamental limitation has encouraged researchers to propose the construction of nonsymbiotic nitrogen-fixing plants (whose niche to date is limited to the grant proposal).

Due to the mild conditions under which it occurs, the biological nitrogen-fixation process may seem inherently simpler than the industrial one. However, it is not; the biological process displays a complexity[235,235a] that belies the simplicity of the chemical conversion of $N_2 \rightarrow 2NH_3$. Genetic analysis reveals that *at least* twenty genes are required for nitrogen fixation in the bacterium *Klebsiella pneumoniae*.[236,237] These *nif* genes (illustrated in Figure 7.25) specify proteins that are involved in regulation (*nif* A and L), pyruvate oxidation/flavin reduction (*nif* J), electron transfer (*nif* F for flavodoxin), the subunits of the structural proteins of the nitrogenase (*nif* H, D, K), Fe-S cluster assembly (*nif* M) and biosynthesis of the iron-molybdenum cofactor, FeMoco (*nif* N, B, E, Q, V, H).[238] The last two functions specify proteins that are responsible for the incorporation of unusual transition-metal sulfide clusters into the nitrogenase proteins. These clusters have allowed nitrogenase to be studied by biophysical and bioinorganic chemists to establish aspects of its structure and mechanism of action.

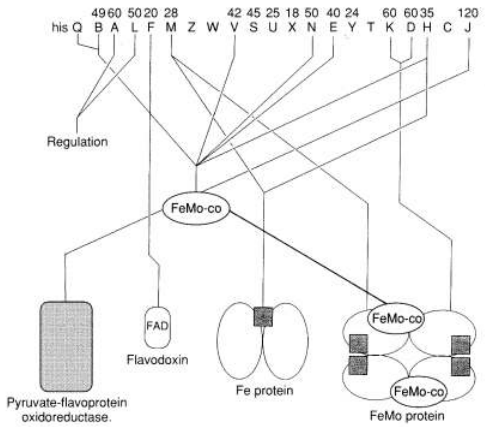


Figure 7.25 - Nif genes required for nitrogen fixation as arranged in Klebsiella pneumoniae, and their respective gene products. The numbers on the top are the molecular weights in kilodaltons of the respective gene products.

We will first discuss the N_2 molecule and focus on its reduction products, which are the presumed intermediates or final product of nitrogen fixation. We then present what has been called[239,240] the "Dominant Hypothesis" for the composition, organization, and function of molybdenum-based nitrogenases. Until 1980, it was thought that molybdenum was essential for nitrogen fixation. However, work starting in 1980 led finally in 1986 to the confirmation of vanadiumbased nitrogen fixation. The newly discovered vanadium-based nitrogenases differ in reactivity from the Mo-based enzyme in having "alternative" substrate specificity. The distinct reaction properties of the different nitrogenases point to the importance of the study of alternative substrate reactions in probing the mechanism of nitrogen fixation.

2. Dinitrogen: The Molecule and Its Reduced Intermediates

The N_2 molecule has a triple bond with energy 225 kcal/mole, a ν(N≡N) stretch of 2331 cm^{-1}, and an N≡N distance of 1.098 Å. The stable isotopes of nitrogen are ^{14}N(I = 1) with natural abundance of 99.64 percent and ^{15}N(I = $\frac{1}{3}$) with an abundance of 0.36 percent.

The challenge to which nitrogenase rises is to break and reduce at a reasonable rate the extremely strong N≡N triple bond. The kinetic inertness of N_2 is highlighted by the fact that carrying out reactions "under nitrogen" is considered equivalent to doing the chemistry in an inert atmosphere. Despite this kinetic inertness, thermodynamically the reduction of N_2 by H_2 is a favorable process,

$$N_2 + 3H_2 \rightarrow 2NH_3 \qquad \Delta G^o = -3.97 kcal/mole \tag{7.10}$$

and at pH = 7 the reaction

$$N_2 + 8H^+ + 6e^- \rightarrow 2NH_4^+ \qquad E^{o\,\prime} = -280 mV \tag{7.11}$$

has an E°' value that makes it easily accessible to biological reductants such as the low-potential ferredoxins discussed earlier in this chapter.

What, then, is the cause of the kinetic inertness of the N_2 molecule? The thermodynamically favorable reduction of N_2 to $2NH_3$ is a six-electron process. Unless a concerted $6e^-$, $6H^+$ process can be effected, intermediates between N_2 and NH_3 must be formed. However, all the intermediates on the pathway between N_2 and NH_3 are higher in energy than either the reactants or the products. The EO' values for the formation of N_2H_2 (= diimine, diazene, diamide) or N_2H_4 (hydrazine) are estimated[241] as

$$N_2 + 2H^+ + 2e^- \rightarrow N_2H_2 \qquad E^{o\,\prime} \sim -1000 to -1500 mV \tag{7.12}$$

$$\$\$N_2 + 5H^+ + 4e^- \rightarrow N_2H_5^+ \qquad E^{o\,\prime} = -695 mV \tag{7.13}$$

Clearly, these potentials are sufficiently negative that the normal biological reductants cannot effect the reaction. The difficulty of reaching these intermediates is indicated in Figure 7.26.

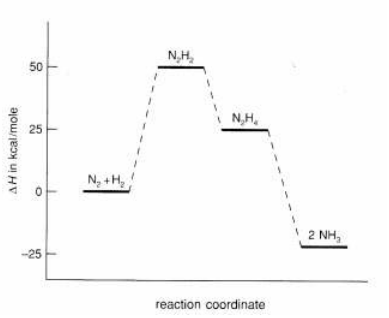


Figure 7.26 - Energetics of N_2, NH_3, and some potential intermediates along the reaction pathway for their interconversion.

Several factors may allow this barrier to be overcome. First, the six-electron reduction might be carried out in a concerted or near-concerted manner to avoid the intermediates completely. Alternatively, the intermediates could be compIexed at metal centers to stabilize them to a greater extent than either the reactants or products. Finally, the formation reaction for the unfavorable intermediate could be coupled with ATP hydrolysis or with the evolution of dihydrogen, each a favorable process, so that the overall process is favorable. Which of the above strategies is used by nitrogenase is unknown, but it seems likely that some combination of the last two of these is used to effect the difficult reduction of N_2 to NH_3. To probe the possibilities, a variety of complexes of N_2, diazenes, and hydrazines has been prepared and chemically characterized, and these are discussed toward the end of this section.

3. The Dominant Hypothesis for Molybdenum Nitrogenase[239,240,242,243]

The action of the Mo-nitrogenase enzyme involves the functioning of two separately isolatable component proteins, as sketched in Figure 7.27A. The larger of the two proteins, sometimes incorrectly[244] designated[245] dinitrogenase has, in the past, been called molybdoferredoxin, azofermo, or component I. More often this protein is called the MoFe or FeMo protein ([MoFe] or [FeMo]). The smaller protein, formerly called azoferredoxin or component II, is sometimes incorrectly[244] referred to[245] as dinitrogenase reductase.* This protein is properly called the Fe protein or [Fe]. A useful nomenclature for discussions of kinetics and comparative biochemistry designates the FeMo protein as *Xyl*, where X and y are the first letters of the first and second name of the bacterial source, respectively. For example, *Cpl* is the FeMo protein from *Clostridium pasteurianum*. Similarly, for the Fe protein the designation *Xy2* is given; for example, the Fe protein of *Azotobacter vinelandii* is called *Av2*. This system will be used where appropriate to distinguish the protein source. Properties of representative Mo nitrogenases are given in Table 7.6.

Table 7.6: Properties of some representative nitrogenases.

Organism	Component	MW	Metal Content	Reference
Azotobacter vinelandii	[MoFe] [Fe]	234,000 64,000	2Mo, 34-38Fe, 26-28S 3.4Fe, 2.8S	366, 367
Azotobacter chrococcum	[MoFe] [Fe]	227,000 65,400	2Mo, 22Fe, 20S 4Fe, 3.9S	366, 368
Clostridium pasteurianum	[MoFe] [Fe]	221,800 55,000	2Mo, 24Fe, 24S 4Fe, 4S	366, 369
Klebsiella pneumoniae	[MoFe] [Fe]	229,000 66,800	2Mo, 20Fe, 20S	366
Anabaena cylindrica	[MoFe] [Fe]	223,000 60,000	2Mo, 20Fe, 20S	370
Rhodospirillum rubrum	[MoFe] [Fe]	215,000 60,000	2Mo, 25-30Fe, 19-22S	371

The schematic diagram in Figure 7.27 shows some of the compositional and functional relationships of the nitrogenase proteins. The iron protein contains two identical subunits of MW ~ 30 kDa. The subunits are products of the *nif* H gene.[246] A single Fe_4S_4

center is present in the protein and appears to be bound between the subunits.[246a] A recent x-ray structure[246b] of the iron protein confirms this picture. As shown in Figure 7.27A, the single Fe_4S_4 center is located at one end of the molecule, in the only region of significant contact between the two subunits. *In vivo*, the Fe protein is reducible by ftavodoxin or ferredoxin. *In vitro*, artificial reductants such as dithionite or viologens are generally used. The single Fe_4S_4 center undergoes a single one-electron redox process, wherein the reduced form is EPR-active and the oxidized form is diamagnetic. As such, this center resembles four-iron-cluster-containing ferredoxins. Its redox potential is dependent on the ATP or ADP level in the solution. For example, *Cp2* (the Fe protein from *Clostridium pasteurianum*) shows E°' = -294 mV in the absence and -400 mV in the presence of MgATP.[247] Two equivalents of MgATP and MgADP each bind to [Fe].

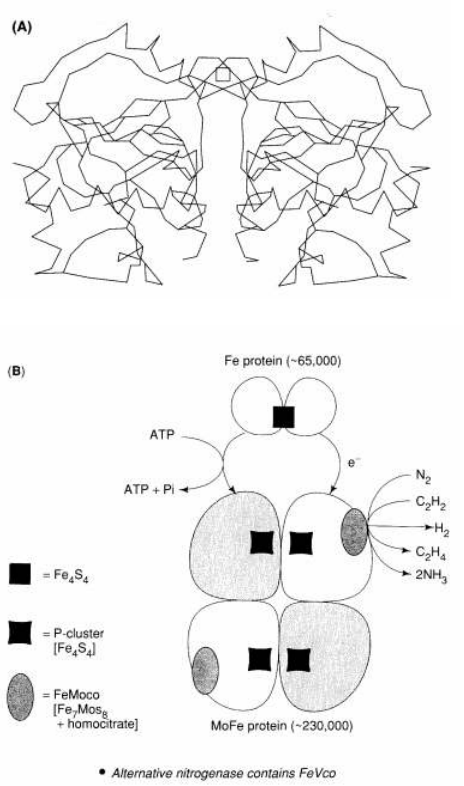


Figure 7.27 - (A) Preliminary x-ray crystal structure of the Azotobacter vinelandii nitrogenase Fe protein.[246b] (B) Schematic of the nitrogenase proteins illustrating their composition and mode of action.

Until recently there was a major mystery over the number of Fe_4S_4 centers in [Fe] as deduced by EPR quantitation of the Fe_4S_4 centers compared to the number derived analytically or by extrusion experiments.[239,248] However, it has now[9,200,249,250] been clearly established that the single Fe_4S_4 center can exist in this protein in two spin states, $S = \frac{1}{2}$ and $S = \frac{3}{2}$ Only that part of the EPR signal corresponding to the $S = \frac{1}{2}$ form, with its g values near 2, was considered in earlier spin quantitations. When the $S = \frac{3}{2}$ center, with g values between 4 and 6, is included, the EPR spin integration shows one paramagnetic site per Fe_4S_4 unit. Model systems[121,122] and theoretical studies[123,124,251] strongly support the ability of Fe_4S_4 to exist in various spin states. During enzyme turnover, the single Fe_4S_4 of the Fe-protein center transfers electrons to the FeMo protein in one-electron steps. There is no evidence for any difference in redox behavior between the $S = \frac{1}{2}$ and $S = \frac{3}{2}$ states of the protein.[200]

The Fe protein binds two molecules of MgATP.[252] The recent structure[246b,378] suggests that a cleft between the two subunits may serve as the ATP binding site. As the enzyme system turns over, a minimum of two molecules of MgATP are hydrolyzed to MgADP and phosphate in conjunction with the transfer of each electron to the FeMo protein.[253] The ATP/$2e^-$ ratio is generally accepted to have a minimum value of 4. Higher numbers represent decreased efficiency, often attributed to "futile cycling," where back electron transfer from [FeMo] to [Fe] raises the effective ratio.[248,253] Except for an as-yet-unconfirmed report of reduction by thermalized electrons produced by pulse radiolysis,[254] there is no evidence that the FeMo protein can be reduced to a catalytically active form without the Fe protein present.

Even though [Fe] must be present for catalysis to take place, the Dominant Hypothesis[239] designates [FeMo] as the protein immediately responsible for substrate reduction, and genetic/biochemical evidence supports this view. The FeMo protein contains an ($\alpha_2\beta_2$ subunit structure, where α and β are coded by the *nif* D and *nif* K genes,[15,229] respectively. The overall molecular weight of about 230 kDa reflects the 50- to 60-kDa MW of each of its four subunits. In addition to protein, a total of 30 Fe, 2 Mo, and 30 S^{2-}, all presumed to be in the form of transition-metal sulfide clusters, add relatively little to the molecular weight, but are presumed to be major parts of the active centers of the protein. Figure 7.27, which is highly schematic, displays the cluster types in accord with the Dominant Hypothesis.

---

* The nomenclature proposal[245] that [FeMo] be designated as dinitrogenase and [Fe] as dinitrogenase reductase, although sometimes used in the literature, is incorrect or, at best, premature.[244] The suggested nomenclature implies that both [FeMo] and [Fe] are enzymes. However, neither protein can function catalytically in the absence of the other. [FeMo] will not reduce N_2 or C_2H_2 or evolve H_2 in the absence of [Fe]. The iron protein will not hydrolyze MgATP in the absence of [FeMo]. Nitrogen fixation requires the simultaneous presence of both proteins. Although mechanistic considerations[255] point to [FeMo] as the substrate binding and reducing protein, and [Fe] as the ATP binding locus, catalytic reactions characteristic of this enzyme system have never been consumated by one protein in the absence of the other (but see later for the uptake of H_2). In this chapter, we use the [FeMo] and [Fe] designations in accord with most workers in the field.

4. Protein Purity and Active Sites

It has been almost 20 years since the first relatively pure preparations of nitrogenase became available. Indeed, homogeneous preparations are a *sine qua non* for progress in our understanding of the chemical nature and reactivity of any active site. In metalloproteins, there are two levels of homogeneity. The first involves purity with respect to the protein/subunit composition. This type of purity is achieved by conventional protein-purification techniques, and can be monitored by gel electrophoresis under native and denaturing conditions. In the language of polymer science, the macromolecular portion of the protein can be said to be monodisperse, corresponding to a single molecular weight for the polypeptide chain(s). However, even if the protein is homogeneous by this criterion, it may be inactive or only partially active because it does not have a full complement of active metal sites. The metal sites may be empty, filled with the wrong metals, or otherwise imperfect. Often the apo or inactive enzyme has chromatographic, electrophoretic, and centrifugal behavior very much like that of the holo protein, and therefore copurifies with it. Therefore, purification to electrophoretic homogeneity is only the first step. It is then necessary to ensure the chemical homogeneity of the active site. Very often activity is the major criterion for the approach toward such purity; i.e., the most homogeneous preparations are usually those in which the activity is highest. Several studies done on preparations that lacked active-site homogeneity were, as a result, not meaningful.

The two types of centers present in the nitrogenase FeMo protein are designated P clusters and FeMoco (or M) centers. Both types of centers display unique spectroscopic properties, but only FeMoco continues to display most of those properties when it is extracted from the protein.

5. FeMoco

The presence of the FeMo cofactor within the FeMo protein of nitrogenase, i.e., the M center, is revealed through spectroscopic and redox studies.[239] In the resting state of [FeMo], as isolated in the presence of dithionite, the M center has a distinct S = $\frac{3}{2}$ EPR signal, which is discussed below (see Figure 7.28).

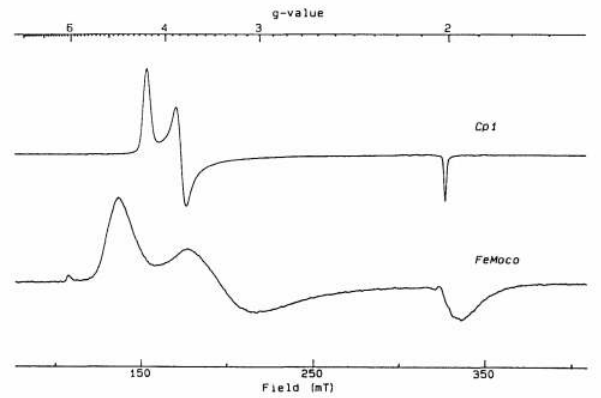


Figure 7.28: EPR spectra: (A) the S = $\frac{3}{2}$ M center in Clostridium pasteurianum nitrogenase FeMo protein; and (B) the FeMoco extracted into NMF from the protein. (Spectra courtesy of R. Bare and G. N. George.)

When the enzyme is turning over the EPR signal essentially disappears, leaving an EPR-silent state in which the FeMoco site is super-reduced to what is presumed to be its catalytically active form. In addition, a third state in which the S = $\frac{3}{2}$ EPR signal disappears is produced upon oxidation under non-turnover conditions. Thus the M center within the protein shows three states of oxidation, and these appear to have been reproduced in the FeMoco extracted from the protein:[255a]

$$FeMoco\ (oxidized) \xrightarrow{e^-} FeMoco\ (reduced) \xrightarrow{e^-} FeMoco\ (super-reduced) \tag{7.14}$$

The detailed characterization of the FeMoco site has involved parallel studies of the site within the protein and in its extracted form. The authentication of the extracted FeMoco involves the production and use of mutant organisms that make an inactive FeMo protein that contains all subunits and P clusters, but lacks the FeMoco sites.[172,256] A mutant of *Azotobacter vinelandii* called UW-45 (UW = University of Wisconsin) was first used to assay for isolated FeMoco.[257] Since several genes are involved in specifying FeMoco biosynthesis, mutants lacking these genes produce FeMo protein either lacking FeMoco or having a defective version of FeMoco. Mutants such as *Nif* B^- of *Klebsiella pneumoniae*[172] lack cofactor, and an inactive "apo" protein can be isolated from them.

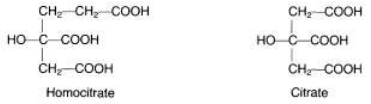
The breakthrough in this field[257] came in 1976, when FeMoco was extracted from [FeMo] into N-methylformamide[258] after the protein was acidified and then neutralized, The acidification removes most of the acid-labile P clusters, and partially denatures the protein. Reneutralization precipitates the protein (near its isoelectric point) and the precipitated denatured protein can then be extracted.

It has been shown that FeMoco can be extracted into many organic solvents,[10,257,259-259b] provided proper combinations of cations and anions[259a] are present in the solvent. The role of the cation is to balance the charge of the negatively charged cofactor. The role of the anion is to displace the cofactor from anion-exchange columns, such as DEAE cellulose or TEAE cellulose, to which the cofactor and/or its protein source had been adsorbed. The ability to dissolve cofactor in such solvents as CH_3CN, acetone, THF, and even benzene should facilitate attempts at further characterization and crystallization.[259,259a]

The biochemical authenticity of FeMoco has been assayed by its ability to activate the FeMo protein from the cofactor-less mutant organism.[258] The stoichiometry of the cofactor is $MoFe_{6\text{-}8}S_{7\text{-}10}$, with the variability likely due to sample inhomogeneity. The extracted cofactor resembles the M-center unit spectroscopically and structurally as shown in Table 7.7, The differences are presumed to result from differences in the peripheral ligands of the metal-sulfide center between the protein and the organic solvent.[260]

Strong evidence to support FeMoco as the site of substrate binding and reduction comes from the study of *nif* V mutants.[261-263] (The V designation is somewhat unfortunate, as *nif* V has nothing to do with vanadium.) The *Nif* V mutants do not fix nitrogen *in vivo*, and have altered substrate specificity *in vitro.* Dihydrogen evolution by isolated *nif* V nitrogenase is inhibited by CO, in contrast to the wild type, where H_2 evolution is insensitive to CO. FeMoco can be extracted from the *nif* V protein and used to reactivate the FeMoco-deficient mutants, such as *nif* B or UW-45. Remarkably, the reconstituted FeMo protein has CO-sensitive H_2 evolution, which is characteristic of *nif* V; i.e., the *nif* V phenotype is a property of FeMoco and not of the protein.[263] This result clearly implicates the FeMoco site as an important part of the substrate reactions of the nitrogenase enzyme complex.

Recently, a heat-stable factor called the V-factor has been discovered that restores the wild-type phenotype when added to *nif* V mutants during *in vitro* FeMoco assembly reactions.[264] The V-factor has been shown to be homocitrate (see Scheme 7.15) and ^{14}C labeling strongly suggests that homocitrate (or a part of it) is a component of the cofactor center. Interestingly, the far more metabolically common citrate appears to be present in the *nif* V mutant.[265a] Replacement of homocitrate by analogues that differ in structure or stereochemistry yields modified FeMoco sites that have altered substrate specificities.[265b] Thus, as is true for many cofactors (e.g., heme = porphyrin + iron; B_{12} = corrin + cobalt; F430 = corphin + nickel; Moco, the molybdenum cofactor = Mo +molybdopterin), both inorganic and organic components are present in FeMoco.



The biosynthesis of the cofactor and its insertion into [FeMo] apparently requires the presence of [Fe] and ATP in A. vinelandii.[266,266a] Whether this involves redox or conformational change in [FeMo] induced by [Fe] is unknown, but the fact that inactive versions of [Fe] are effective would seem to favor the nonredox mechanism. An attractive idea[266] is that [Fe]•MgATP binds to [FeMo], producing a state that is conformationally accessible for cofactor insertion.

Recently, site-directed mutagenesis studies[266b,c] have shown that cysteine residues are involved in binding FeMoco to the subunits of [FeMo]. Moreover, these studies again implicate FeMoco in the substrate-reducing site.

6. The P-clusters

Evidence has been presented[229] for the presence of four Fe_4S_4-like clusters (designated as P-clusters) in [FeMo]. The P-clusters are, however, by no means ordinary Fe_4S_4 clusters, and may not be Fe_4S_4 clusters at all. P-clusters are manifest[239,248] in electronic absorption and, especially, MCD and Mössbauer spectra of [FeMo]. These spectra are clearly not conventional; i.e., they are not like those found in ferredoxins and have not yet been seen in model compounds. In their oxidized forms, the P-clusters are high-spin, probably S = $t\frac{7}{2}$ according to EPR studies.[267] Mössbauer spectra reveal decidedly inequivalent Fe populations,[268,269] indicating that the putative Fe_4S_4 clusters are highly distorted or asymmetric. The four P-clusters do not appear to behave identically under many circumstances, and it is clear that they form at least two subsets. There is open disagreement over the redox behavior of these sets.[239,270,271] Furthermore, an additional Mössbauer signal sometimes designated as S may also be part of the P-cluster signal.[268]

Although spectroscopic studies of the P-clusters do not unequivocally reveal their structural nature, extrusion of these clusters from the protein leads to the clear identification of three or four Fe_4S_4 clusters.[248,272] As discussed previously, the extrusion technique has inherent uncertainties, because it may be accompanied by cluster rearrangement. Nevertheless, the experimental result does support the Dominant Hypothesis, which designates the P centers as highly unusual Fe_4S_4 clusters.* The P-clusters are thought to be involved in electron storage and transfer, and presumably provide a reservoir of low-potential electrons to be used by the M center (FeMoco) in substrate reduction. Attractive as it may seem, there is no direct evidence to support this notion.

Table 7.7 - Comparison of the FeMo protein and isolated FeMoco.[a]

a) Distance in Å with number of atoms in parentheses.
b) From 287; earlier study reported in 286.
c) Data from 373; earlier study reported in 372.
d) Data from 290.
e) Data from 291.
f) Data from 288, 289.

https://chem.libretexts.org/@go/page/438071

	FeMo protein (M center)	FeMoco (in NMF)
EPR		
g' values	4.27	4.8
	3.79	3.3
	2.01	2.0
EXAFS[a]		
Mo-S	2.36 (4)[b]	2.37 (3.1)[c]
Mo-Fe	2.69 (3)[b]	2.70 (2.6)[c]
Mo-O or N	2.18 (1)[b]	2.10 (3.1)[c]
Fe-S		2.25 (3.4)[d] 2.20 (3.0)[e]
Fe-Fe		2.66 (2.3)[d] 2.64 (2.2)[e] 2.66 (2.3)[d] 3.68 (0.8)[e]
Fe-Mo		2.76 (0.4)[d] 2.70 (0.8)[e]
Fe-O or N		1.81 (1.2)[d]
XANES MoO_3S_3 fits best[f]		

* Recent x-ray crystallographic results show that, if Fe_4S_4 clusters are present, they are very close together in two pairs,[379,380] which may account for their unusual properties.

11.2.7.7: Multisite Redox Enzymes (Part 3) is shared under a CC BY-NC-SA 4.0 license and was authored, remixed, and/or curated by LibreTexts.

11.2.7.8: Multisite Redox Enzymes (Part 4)

7. EPR, ENDOR, and ESEEM Studies

The FeMoco or M center has been identified spectroscopically within the FeMo protein;[239,248,273] it has a distinctive EPR signal with effective g values of 4.3, 3.7, and 2.01, and originates from an S = $\frac{3}{2}$ state of the M center. The signal arises from transitions within the $\pm\frac{1}{2}$ ground-state Kramers doublet of the S = $\frac{3}{2}$ system (D = +5.1 cm^{-1}, E/D = 0.04). The isolated cofactor (FeMoco) gives a similar EPR signal, but with a rather larger rhombicity (E/D = 0.12). Spectra from the *C. pasteurianum* nitrogenase and cofactor are shown in Figure 7.28, and comparative data are given in Table 7.7. The M-center EPR signal has proved useful in characterizing the nature of the site, especially when more sophisticated magnetic resonance techniques, such as ENDOR or ESEEM, are used.

Extensive ENDOR investigations[274,275,275a] have been reported using protein samples enriched with the stable magnetic isotopes ^{2}H, ^{33}S, ^{57}Fe, ^{95}Mo, and ^{97}Mo. The ^{57}Fe couplings have been investigated in the most detail. Individual hyperfine tensors of five coupled ^{57}Fe nuclei are discernible, and were evaluated by simulation of the polycrystalline ENDOR spectrum.[275] The data from ^{33}S and ^{95}Mo were analyzed in less detail; ^{33}S gave a complex ENDOR spectrum, evidently with quite large hyperfine couplings, although no quantification was attempted because of the complexity of the spectrum.[274] On the other hand, ^{95}Mo was shown to possess a small hyperfine coupling, indicating that the molybdenum possesses very little spin density (although the quantitative aspects of the conclusions of the ^{95}Mo ENDOR study have recently been shown to be in error[276]).

Although no nitrogen splittings were reported in any of the ENDOR studies, evidence for involvement of nitrogen as a cluster component has been forthcoming from ESEEM spectroscopy.[277-279] ^{14}N modulations are observed in the ESEEM of the M center. The observed ^{14}N is not from the substrate (N_2), or from an intermediate or product of nitrogen fixation, because enzyme turnover using ^{15}N as a substrate does not change the ESEEM spectrum. The isolated cofactor (FeMoco) does not show the modulation frequencies observed for the M center in the protein. These experiments suggest that the M-center ^{14}N ESEEM arises from a nitrogen atom that is associated with the M center, and probably from an amino-acid side chain (most likely a histidine) ligated to the cluster.[279] Recent evidence from site-directed mutagenesis of the *Azotobacter vinelandii* protein[280] provides strong support for the presence of histidine ligation, and points specifically to His-195 of the α subunit as the N ligand.

8. Mössbauer Studies

Extensive Mossbauer investigations of nitrogenase[271,281-283] and FeMoco[283a] have been reported. Unlike EPR and EPR-based spectroscopies, which can be used to investigate only the EPR-active S = $\frac{3}{2}$ oxidation state, all three available M-center oxidation states are accessible to Mössbauer spectroscopy. The fully reduced site was found to be diamagnetic with S = 0 (but see Reference 284), whereas the oxidized site was found to have $S \geq 1$. The zero-field spectrum of reduced *C. pasteurianum* nitrogenase is shown in Figure 7.29; the spectrum is comprised of four quadrupole doublets, one of which was concluded to originate from the M site.[282] Mössbauer spectra taken in the presence of applied magnetic fields were used to deduce the presence of four types of ^{57}Fe hyperfine coupling; these were called sites A1, A2, and A3, which have negative hyperfine couplings, and B sites, which have positive hyperfine couplings. The A sites were quantitated as a single Fe each; the B sites were estimated to contain three irons. These conclusions were largely confirmed and extended by later ENDOR investigations,[274] although the B sites were resolved as two inequivalent, rather than three equivalent, sites. ENDOR is rather more sensitive to the nature of the hyperfine couplings than Mössbauer, although it cannot usually be used to count numbers of exactly equivalent sites. Thus the number of iron atoms in the M center is minimally five, although larger numbers cannot be excluded. Note also that some of the quantitative aspects of the earlier Mossbauer investigations have been criticized.[285]

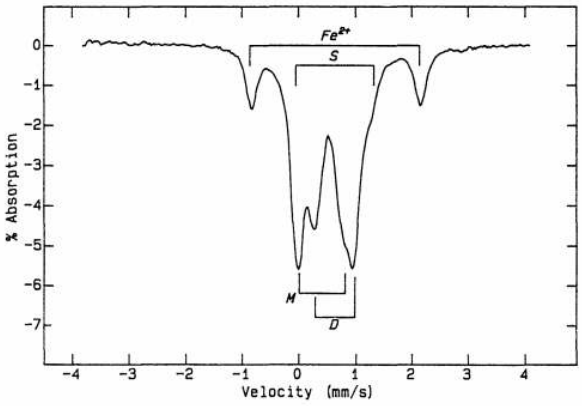
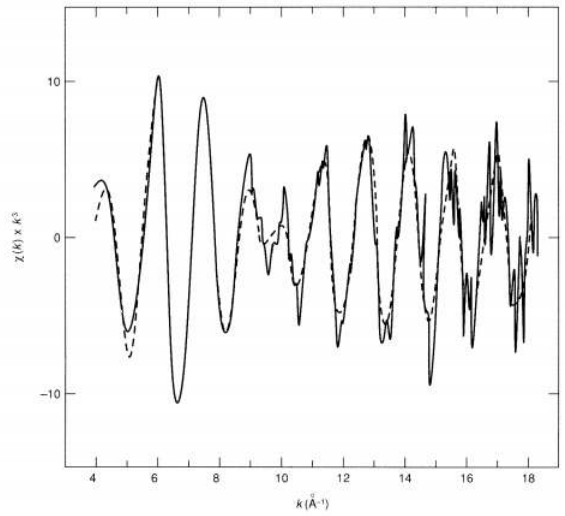


Figure 7.29 - Mössbauer spectrum of C. pasteurianum nitrogenase FeMo protein,[282] indicating the various components (quadrupole doublets) and their assignments. The doublet labeled M is the cofactor signal; those labeled D, S, and Fe^{2+} are attributed to the P-clusters.

9. X-ray Absorption Studies

One of the early triumphs of biological x-ray absorption spectroscopy was the deduction that the nitrogenase M center is an Mo-Fe-S cluster.[286] (It is also worth noting that nitrogenase was the first *enzyme* to be studied by x-ray absorption spectroscopy.) Early work on lyophilized protein samples indicated the presence of two major contributions to the Mo K-edge EXAFS, which were attributed to Mo-S ligands, plus a more distant Mo-Fe contribution.[286] Subsequently, these conclusions have been confirmed and extended, using samples in solution and with much more sensitive detection systems.

Most EXAFS studies to date have been on the molybdenum K-edge of the protein or of FeMoco, and indicate a very similar Mo environment in both (Table 7.7, Figure 7.30). A consensus of the best available analyses[287] indicates that Mo is coordinated by three or four sulfur atoms at 2.4 Å, one to three oxygens or nitrogens at 2.2 Å, with approximately three nearby iron atoms at 2.7 Å. Of these, the EXAFS evidence for the oxygen/nitrogen contribution is weakest. However, comparison of Mo K-edge[288] and Mo L-edge XANES[289] spectra with model compounds indicates strong similarities with $MoFe_3S_4$ thiocubane model compounds possessing MoS_3O_3 coordination, and provides some support for the presence of O/N ligands.



https://chem.libretexts.org/@go/page/438072

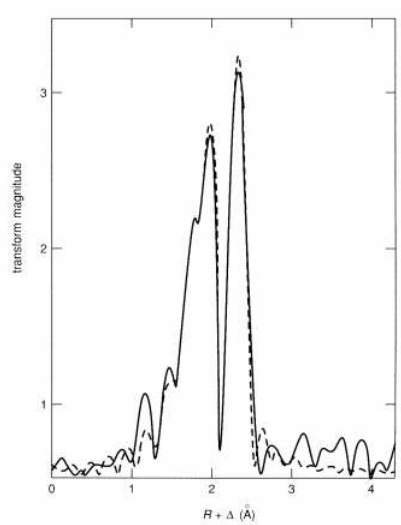


Figure 7.30 - Mo K-edge EXAFS spectrum (left panel) and EXAFS Fourier transform (right panel) of Klebsiella pneumoniae nitrogenase MoFe protein. The solid line is the processed experimental spectrum and the dashed line a calculated one. [287]

The iron EXAFS of FeMoco has been independently examined by two groups.[290,291] Both groups agree that the iron is coordinated largely to sulfur at about 2.2 Å, with more distant Fe-Fe interactions at about 2.6 Å. They differ, however, concerning the presence of short (1.8 Å) Fe-O interactions. Such interactions were apparently observed in the earlier study,[290] but not in the later study.[291] One possible explanation for this discrepancy is that the short Fe-O interactions of the earlier study were due to extraneous iron coordinated to solvent, contaminating the FeMoco preparation.[291] A final resolution of this discord must, however, await the results of further experiments. Interestingly, a long Fe-Fe interaction at 3.7 Å was also observed in the later study.[291]

Largely on the basis of the Mo K-edge EXAFS results and model studies discussed below, several proposals for the structure of the M center have been put forward. These are illustrated in Figure 7.31.

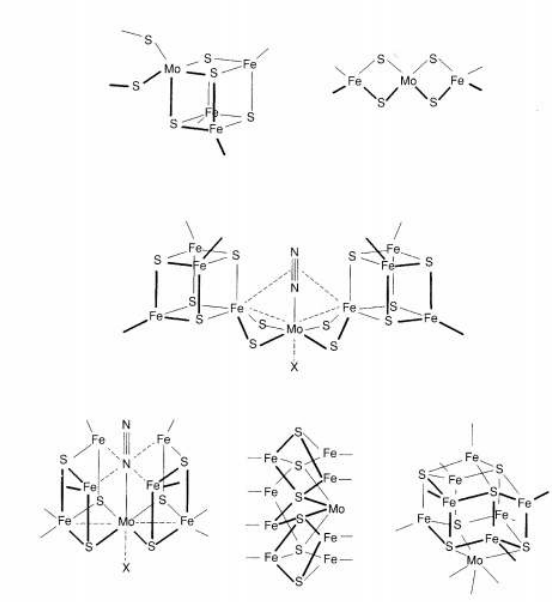


Figure 7.31 - Proposed models for FeMoco. (Compare with the recent model from the x-ray structure on page 444.)

The MoFe proteins from *Clostridium pasteurianum*[292] and from *Azotobacter vinelandii*[293] have been crystallized. For the former protein, crystals of space group $P2_1$ are obtained, with two molecules per unit cell of dimensions 70 x 151 x 122 Å. There is good evidence for a molecular two-fold axis, which presumably relates equivalent sites in the two $\alpha\beta$ dimers that make up the protein molecule.[294] Preliminary refinement reveals that the two FeMoco units per protein are about 70 Å apart and the four P clusters are grouped in two pairs.

Single crystal EXAFS studies[295] have provided important structural information on the molybdenum site. For different crystal orientations (relative to the polarized x-ray beam), the amplitude of the Mo-Fe EXAFS changes by a factor of 2.5, but the Mo-S EXAFS changes only slightly. Analysis of the anisotropy of the Mo-Fe EXAFS using the available crystallographic information[294] is consistent with either a tetrahedral $MoFe_3$ geometry such as that found in thiocubanes (Figure 7.32) or a square-based pyramidal $MoFe_4$ arrangement of metals. This interpretation tends to rule out some of the structural proposals shown in Figure 7.33. The observed orientation-dependence of the iron amplitudes is too small for clusters containing a linear or planar arrangement of iron and molybdenum (e.g., Figure 7.33B,C), and too large for arrangements that involve regular disposition of iron about molybdenum. Moreover, the lack of anisotropy of the sulfur EXAFS (which was apparently not considered in the original interpretation[295]) argues against an MoS_3 $(O/N)_3$ model that has molybdenum coordinated by sulfur atoms that bridge only to Fe atoms disposed to one side of the molybdenum. Significant anisotropy for the Mo-S EXAFS (of opposite polarization, and smaller than that for Mo-Fe) would be expected for such an arrangement of sulfur atoms. However, the cubane model of Figure 7.33, which provides the best model of both geometric and electronic structure, remains viable if one of the nonbridging ligands to molybdenum is a sulfur atom (rather than oxygen or nitrogen) with a bond length similar to that of the bridging sulfides.

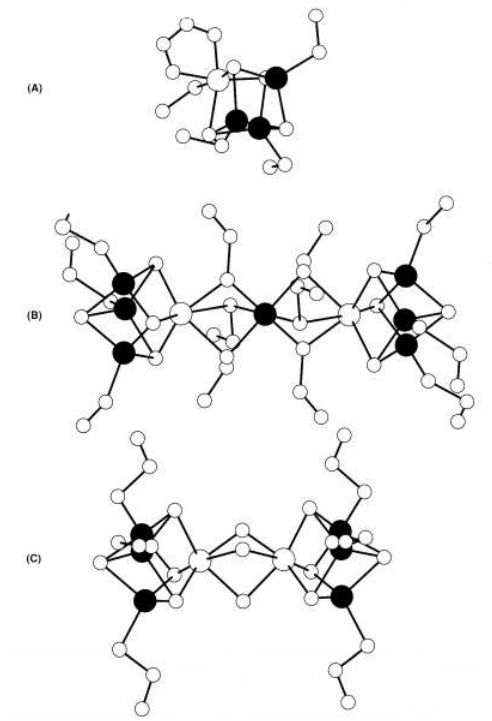


Figure 7.32 - Structures of thiocubanes that display Mo-S and Mo-Fe distances similar to FeMoco: (A) $(Fe_3MoS_4)_2(SR)_9^{3-}$; (B) $(MoFe_3S_4)_2Fe(SR)_{12}^{3-/4-}$; (C) $MoFe_3S_4(SEt)_3(cat)CN^{3-}$. (Data on A and B from References 328, 330a; data on C from References 331, 332.)

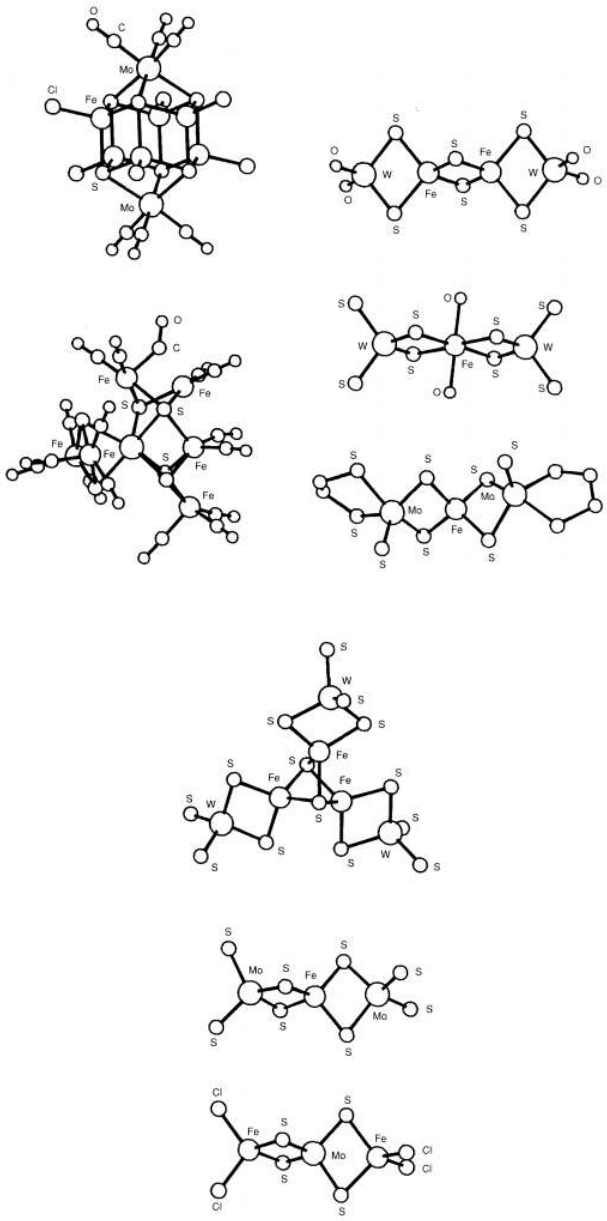


Figure 7.33 - FeMoS and FeWS structures of potential interest with respect to nitrogenase.[331,332,332a-j]

10. Substrate Reactions

The two-component Mo-nitrogenase enzyme catalyzes the reduction of N_2 to $2NH_4^+$ as its physiological reaction. Concomitant with the reduction of N_2, H_2 evolution occurs, with electrons supplied by the same reductants that reduce N_2. The limiting stoichiometry appears to be

$$N_2 + 10H^+ + 8E^- \rightarrow 2NH_4^+ + H_2 \quad (7.16)$$

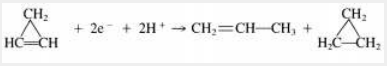
If N_2 is omitted from the assay, all the electrons go to H_2 evolution. Indeed, to a first approximation the rate of electron flow through nitrogenase is independent of whether the enzyme is producing only H_2, producing both NH_4^+ and H_2, or reducing most of the alternative substrates. As displayed in Table 7.8, many alternative substrates are known for this enzyme.[240,243,296] The most important of these from a practical perspective is acetylene, C_2H_2, which is reduced by the Mo nitrogenase exclusively to ethylene, C_2H_4. Acetylene can completely eliminate H_2 evolution by nitrogenase. Many of the substrates in Table 7.8 have a triple bond. Indeed, the only triple-bonded molecule not reduced by nitrogenase is CO, which nevertheless inhibits all substrate reactions, but not H_2 evolution (in the wild type). Triple-bonded molecules such as acetylene (H—C≡C—H) are useful probe molecules for

related reactivity as discussed below for simple inorganic systems. *All* substrate reductions involve the transfer of two electrons or multiples thereof (i.e., 4,6,8 . . .). Multielectron substrate reductions may involve the stepwise execution by the enzyme of two-electron processes. Further, about as many protons as electrons are usually transferred to the substrate. One way of viewing the nitrogenase active site is that it can add the elementary particles (H^+ and e^-) of H_2 to the substrate. This may have mechanistic implications.[297]

It is potentially fruitful to pursue the intimate connection between H_2 and the N_2 binding site in nitrogenase. It has been shown unequivocally[298,299] that one H_2 is evolved for each N_2 "fixed" even at 50 atm of N_2, a pressure of N_2 well above full saturation. Moreover, H_2 is a potent inhibitor of N_2 fixation, and under D_2, HD is formed, but only in the presence of N_2. These complex relationships between N_2 and $H_2(D_2)$ have elicited a variety of interpretations.[255,300-302]

Recently, it has been demonstrated that the FeMo protein alone acts as an uptake hydrogenase.[303] Dihydrogen in the presence of [FeMo] causes the reduction of oxidizing dyes such as methylene blue or dichlorophenolindophenol *in the absence of Fe protein*. This is the only known catalytic reaction displayed by the FeMo protein alone. The hydrogen evolution and uptake by [FeMo] suggest that understanding hydrogen interaction with transition-metal/sulfur centers may be crucial to understanding the mechanism of nitrogenase action.

Table 7.8 - Table 7.8 Nitrogenase substrate reactions.[296,374-376]

Two-electron Reductions	
$$2e^{-} + 2H^{+} \rightarrow H_{2}	
$$C_2H_2 + 2e^- + 2H^+ \rightarrow C_2H_4$$	(11.2.7.8.1)
$$N_3^- + 2e^- + 3H^+ \rightarrow NH_3 + N_2$$	(11.2.7.8.2)
$$N_2O + 2e^- + 2H^+ \rightarrow H_2O + N_2$$	(11.2.7.8.3)
	
Four-electron Reductions	
$$HCN + 4e^- + 4H^+ \rightarrow CH_3NH_2$$	(11.2.7.8.4)
$$RNC + 4e^- + 4H^+ \rightarrow RNHCH_3$$	(11.2.7.8.5)
Six-electron Reductions	
$$N_2 + 6e^- + 6H^+ \rightarrow 2NH_3$$	(11.2.7.8.6)
$$HCN + 6e^- + 6H^+ \rightarrow CH_4 + NH_3$$	(11.2.7.8.7)
$$HN_3 + 6e^- + 6H^+ \rightarrow NH_3 + N_2H_4$$	(11.2.7.8.8)
$$RNC + 6e^- + 6H^+ \rightarrow RNH_2 + CH_4$$	(11.2.7.8.9)
$$RCN + 6e^- + 6H^+ \rightarrow RCH_3 + NH_3$$	(11.2.7.8.10)
$$NCNH_2 + 6e^- + 6H^+ \rightarrow CH_3NH_2 + 2NH_3$$	(11.2.7.8.11)
$$NO_2^- + 6e^- + 6H^+ \rightarrow NH_3$$	(11.2.7.8.12)
Multielectron Reductions	
$$RNC \rightarrow (C_2H_6, C_3H_6, C_3H_8) + RNH_2$$	(11.2.7.8.13)
$$NCNH_2 + 8e^- + 8H^+ \rightarrow CH_4 + 2NH_3$$	(11.2.7.8.14)

11. The Role of ATP

ATP hydrolysis appears to be mandatory, and occurs during electron transfer from [Fe] to [FeMo]. Dissociation of [Fe] and [FeMo] following electron transfer is probably the rate-limiting step in the overall turnover of the enzyme.[255] The fact that reductant and substrate levels do not affect turnover rates is consistent with this finding.

The role of ATP on a molecular level remains one of the great mysteries of the mechanism of nitrogen fixation. As discussed above, the overall thermodynamics of N_2 reduction to NH_3 by H_2 or by its redox surrogate flavodoxin or ferredoxin is favorable. The requirement for ATP hydrolysis must therefore arise from a kinetic necessity. This requirement is fundamentally different from the

need for ATP in other biosynthetic or active transport processes, wherein the free energy of hydrolysis of ATP is needed to overcome a thermodynamic limitation.

What is the basis for the kinetic requirement of ATP hydrolysis in nitrogen fixation? To answer this question, we again look at the potential reduction products of the N_2 molecule. Of these, only N_2H_2 (diimide, three potential isomers), N_2H_4 (hydrazine and its mono and dications), and NH_3 (and its protonated form, NH_4^+) are isolable products. (In the gas phase, other species such as N_2H, N_2H_3, or NH_2 also have a "stable" existence.) In the presence of H_2, only the formation of ammonia is thermodynamically favored (Figure 7.26). Clearly, the formation of the intermediate species in the free state cannot occur to any reasonable extent. However, this does not mean that nitrogenase must form NH_3 directly without the formation of intermediates. It is possible for these reactive intermediates to be significantly stabilized by binding to a metal-sulfur center or centers.

Detailed kinetic studies[255,304] have suggested a scheme in which intermediates with bound and probably reduced nitrogen are likely to be present. Rapid quenching experiments in acid solution lead to the detection of hydrazine during nitrogenase turnover.[305] Likewise, studies of inhibition of N_2 fixation by H_2 and the formation of HD under D_2 have been interpreted in terms of a bound diimide intermediate.[306,307] Although a bound "dinitrogen hydride" is likely to be present, its detailed structure remains unknown.

11.2.7.8: Multisite Redox Enzymes (Part 4) is shared under a CC BY-NC-SA 4.0 license and was authored, remixed, and/or curated by LibreTexts.

11.2.7.9: Multisite Redox Enzymes (Part 5)

The Alternative Nitrogenases

1. Vanadium Nitrogenase

The "essentiality" of molybdenum for nitrogen fixation was first reported by Bortels in 1930.[308] This finding led ultimately to the characterization of the molybdenum nitrogenases discussed in the preceding section. Bortels' work has been cited many times, and is often referred to without citation. Following this seminal work, many other Mo-containing enzymes were subsequently sought and found.[25,309] At present more than a dozen distinct Mo enzymes are known, and new ones are continually being discovered.

In addition to the classic 1930 paper, Bortels[310] reported in 1935 that vanadium stimulated nitrogen fixation. In contrast to the 1930 paper, the 1935 paper languished in obscurity. Then, starting in the 1970s, attempts were made to isolate a vanadium nitrogenase. In 1971, two groups reported isolating a vanadium-containing nitrogenase from *A. vinelandii*.[311,312] The interesting notion at this time was that V might substitute for Mo in nitrogenase, *not* that there was a separate system. The isolated enzyme was reported to be similar to the Mo enzyme, but had a lower activity and an altered substrate specificity. One of the groups carefully reinvestigated their preparation, and found small amounts of molybdenum, which were presumed to be sufficient to account for the low activity, although the altered selectivity was not addressed.[313] The vanadium was suggested to play a stabilizing role for [FeMo], allowing the small amount of active Mo-containing protein to be effectively isolated. Apparently the possibility was not considered that a truly alternative nitrogenase system existed, whose protein and metal centers both differed from that of the Mo nitrogenase.

The unique essentiality of molybdenum for nitrogenase fixation went unchallenged until 1980, when it was demonstrated[314] that an alternative nitrogenfixation system could be observed in *A. vinelandii* when this organism was starved for molybdenum.[315] Despite skepticism from the nitrogenase research community, it was eventually shown that even in a mutant from which the structural genes for the Mo nitrogenase proteins (*nif* H, D, and K) had been deleted, the alternative system was elicited upon Mo starvation. In 1986, two groups[316-321] isolated the alternative nitrogenase component proteins from different species of *Azotobacter*, and demonstrated unequivocally that one component contained vanadium and that neither component contained molybdenum.

One of the two components of the V-nitrogenase system is extremely similar to the Fe protein of nitrogenase. This similarity is evident in the isolated proteins from *A. vinelandii*[316] and in the genetic homology between *nif* H (the gene coding for the subunit of the Fe protein in the Mo-nitrogenase system) and *nif* H* (the corresponding gene in the V-based system). Both Fe proteins have an α_2 subunit structure, and contain a single Fe_4S_4 cluster that is EPR-active in its reduced state.

The FeV proteins from *Azotobacter vinelandii* and *Azotobacter chroococcum* each have an $\alpha_2\beta_2\delta_2$ subunit structure.[322] Metal composition and spectroscopic comparisons between the FeMo and FeV proteins are shown in Table 7.9. Although there is the major difference involving the presence of V instead of Mo in the FeV protein and in the probable presence of the small δ subunits (13 kDa), the two nitrogenase systems are otherwise quite similar.[322] In each, a system of two highly oxygen-sensitive proteins carries out an ATP-dependent N_2 reduction with concomitant H_2 evolution. The Fe proteins have the same subunit structure and cluster content, and are spectroscopically very similar. The V versions of the larger protein have somewhat lower molecular weights than their Mo analogues, and by MCD spectroscopy seem to contain P-like clusters.[318] The FeV site still may be an S = $\frac{3}{2}$ center (by EPR, although its EPR differs significantly from that of the FeMo center).[323] The V-S and V-Fe distances as measured by EXAFS[324,325] are similar to those in thiocubane VFe_3S_4 clusters and to Mo-S and Mo-Fe distances like those in [FeMo], which are in turn similar to those in $MoFe_3S_4$ thiocubanes. Likewise, XANES[324,325] indicates VS_3O_3 type coordination in [FeV] nitrogenase similar to the MoS_3O_3 coordination suggested by XANES for FeMoco. The "FeV cofactor" is extractable into NMF, and can reconstitute the *nif* B^-, FeMoco-deficient mutant of the Mo system.[326] Despite the substitution of V for Mo, the proteins and their respective M-Fe-S sites do not differ drastically. However, the compositional changes do correlate with altered substrate reactivity.

A major difference between the V and Mo enzymes lies in substrate specificity and product formation.[321] As is clearly shown in Table 7.9, the FeV nitrogenase has a much lower reactivity toward acetylene than does the Mo system. Furthermore, whereas the FeMo system exclusively produces ethylene from acetylene, the FeV system yields significant amounts of the four-electron reduction product, ethane.[321] The detection of ethane in the acetylene assay may prove a powerful technique for detecting the presence of the V nitrogenase in natural systems.[322] Moreover, this reactivity pattern is found in the *nif* B^- mutant reconstituted with FeVco, indicating that the pattern is characteristic of the cofactor and not the protein.[326] The reactivity change upon going from Mo

to V in otherwise similar protein systems clearly adds weight to the implication of the M-Fe-S center (M = V or Mo) in substrate reduction.

Table 7.9 - Comparison of alternative nitrogenase proteins[a]

a) Av1 is the FeMo protein of *Azotobacter vinelandii*, Av1* is the FeV protein of *A. vinelandii* and Ac1* is the FeV protein of *A. chroococcum*. Data from References 317,377, and 319, respectively.
b) Atoms per molecule.
c) nmol product/min/mg of protein.

Property	Av1[47]	Av1*[47]	Ac1*[50]
Molecular Weight	240,000	200,000	210,000
Molybdenum[b]	2	< 0.05	< 0.06
Vanadium[b]	—	0.7	2
Iron[b]	30-32	9.3	23
Activity[c]			
H^+	2200	1400	1350
C_2H_2	2000	220	608
N_2	520	330	350
EPR g values	4.3	5.31	5.6
	3.7	4.34	4.35
	2.01	2.04	3.77
		1.93	1.93

2. The All-iron Nitrogenase[322]

The first sign that there is yet another alternative nitrogenase again came from genetic studies. A mutant of *A. vinelandii* was constructed with deletions in both *nif* HDK and *nif* H*D*K*, i.e., the structural genes for the Mo and V nitrogenases, respectively. Despite lacking the ability to make the two known nitrogenases, the mutant strain nevertheless was able to fix nitrogen, albeit poorly. Moreover, this mutant strain's nitrogenase activity was clearly inhibited when either Mo or V was present in the culture medium. Preliminary studies indicate that the nitrogenase proteins produced by this organism are closely related to those previously isolated. A 4Fe-4S Fe-protein *nif* $H^\dagger$ and a protein due to *nif* $D^\dagger$ was produced. The latter appeared to contain no stoichiometric metal other than iron. Symmetry of nomenclature would suggest calling this the FeFe protein and its cofactor FeFeco. Interestingly, this nitrogenase seems to be the poorest of the set in reducing N_2 and makes ethane from ethylene. The finding of the all-iron nitrogenase, if fully confirmed, will add significantly to the comparative biochemistry of nitrogen fixation. Speculatively, one might suggest that the concomitant absence of V and Mo suggests that nitrogen fixation need not directly involve the noniron heterometal in the cofactor cluster. This result may explain the lack of direct implication of Mo in the nitrogen fixation mechanism, despite many years of intense effort by workers in the field. (The above discussion should be taken *cum grana salis* until the existence of the all-iron nitrogenase is confirmed.)

3. Model Systems

Three types of model systems for nitrogenase may be considered. First, there are transition-metal sulfide clusters that resemble the FeMoco or FeVco centers of the active proteins. Although there has been significant progress, there are not yet any definitive models (as there are for Fe_2S_2 and Fe_4S_4). A second approach uses the reactions of N_2 and related substrates or intermediates with metal centers in order to gain insights into the way in which transition-metal systems bind N_2 and activate it toward reduction. Here to date the most reactive systems bear little direct chemical resemblance to the nitrogenase active sites. Nevertheless, these systems carry out *bona fide* nitrogen fixation from which one may learn the various ways in which N_2 can be activated. Finally, there are

other inorganic systems that display some of the structural and possibly some of the reactivity characteristics of the nitrogenase active sites without binding or reducing N_2 or precisely mimicking the active center. We may nevertheless be able to learn effectively about nitrogenase reactivity from these interesting chemical systems.

a. Transition-metal Sulfide Models for Nitrogenase Sites

Although there has been great activity in synthetic Fe-S cluster chemistry, there is to date no example of a spectroscopic model for the P-cluster sites in nitrogenase. If the P-clusters are indeed asymmetrically bound high-spin Fe_4S_4 clusters, then the recent work on high-spin versions of Fe_4S_4 clusters[327] and site-selectively derivatized Fe_4S_4 centers[143] may hint that appropriate model systems are forthcoming.

b. Fe-M-S Cluster Models for FeMoco

Despite the importance of P-clusters, the modeling of the FeMoco center has properly received the most attention. The significant structural parameters that any model must duplicate are the Mo-S and Mo-Fe distances detennined by EXAFS. Spectroscopically, the S = $\frac{3}{2}$ EPR signal provides a stringent feature that model systems should aspire to mimic.

Many FeMoS clusters have been prepared in the quest to duplicate the FeMoco center, but *none* of the chemically synthesized clusters can reactivate the (UW-45 or *Nif* B^-) cofactor-less mutants, perhaps because of their lack of homocitrate, which only recently has been discovered as a key component of FeMoco. Undoubtedly, new FeMoS clusters containing homocitrate will be prepared, and perhaps these will activate the mutant proteins, thereby revealing a close or full identity with FeMoco.

Despite the absence of homocitrate, some interesting model systems have been investigated. It is beyond the scope of this chapter to give a comprehensive account of FeMoS chemistry. We concentrate on the so-called "thiocubane" model systems. Heterothiocubane models were first synthesized using self-assembly approaches analogous to those used for the simpler Fe-S model systems. The reaction[328-330a]

$$MoS_4^{2-} + Fe^{3-} + SR^- \rightarrow (MoFe_3S_4)_2(SR)_9^{3-} \; and \; (MoFe_3S_4)_2Fe(SR)_{12}^{3-,4-} \tag{7.17}$$

uses tetrathiomolybdate, MoS_4^{2-},as the source of Mo, and leads to the double cubane structures shown in Figure 7.32A,B. The $Fe_7Mo_2S_8$ structure proved particularly interesting, since it was possible to complex the central ferric iron atom with substituted catecholate ligands[331,332] and eventually isolate a single thiocubane unit (Figure 7.32C). Significantly, the single unit has S = $\frac{3}{2}$ and Mo-S and Mo-Fe distances that match precisely those found by EXAFS for the M center of nitrogenase. Single cubes with VMo_3S_4 cores have also been prepared.[160,160a] Although the single thiocubanes display spectroscopic similarity and distance identity with FeMoco, they are not complete models. They are stoichiometrically Fe and S deficient, lack homocitrate, and most importantly, fail to activate the UW-45 and *Nif* B^- mutants.

Other interesting FeMoS (and FeWS) clusters with structurally distinct properties are shown in Figure 7.33. These include the "linear" $(MoS_4)_2Fe^{3-}$ ion, the linear $(WS_4)_2Fe[HCON(CH_3)_2]_2^{2-}$ ion, the linear $Cl_2FeS_2MS_2Fe_2CI_2^{2-}$ (M = Mo, W), the "linear" $(MoS_4)_2Fe_2S_2^{4-}$ ion, the trigonal $(WS_4)_3Fe_3S_2^{4-}$, the capped thioprismane $Fe_6S_6X_6[M(CO)_3]_2^{3-}$ (X = CI, Br, I; M = Mo, W), and the organometallic clusters $MoFe_6S_6(CO)_{16}^{2-}$, $MoFe_3S_6(CO)_6(PEt_3)3$, and $MoFe_3S_6(CO)_6^{2-}$. Structures suggested for FeMoco based on these and other chemically synthesized transition metal sulfides and on spectroscopic studies of the enzyme are shown in Figure 7.31.

11.2.7.9: Multisite Redox Enzymes (Part 5) is shared under a CC BY-NC-SA 4.0 license and was authored, remixed, and/or curated by LibreTexts.

11.2.7.10: Multisite Redox Enzymes (Part 6)

N_2 and Related Complexes

The triple bond of N_2 has one σ and two πcomponents. Each nitrogen atom has a lone pair oriented along the N-N direction. The two lone pairs allow N_2 to bind in an end-on fashion in either a terminal or a bridging mode. Both modes of binding are illustrated in the binuclear zirconium complex[333] shown in Figure 7.34. In this and in many other N_2 complexes, the N-N bond is not significantly lengthened and is therefore presumed to be insignificantly weakened in the complex. Interestingly, the complex in Figure 7.34, despite not having long N-N distances, forms hydrazine quantitatively upon protonation. Only one of the three N_2 molecules is reduced, and all four electrons required come from the two Zr(III) by presumed internal electron transfer. The related \(\mu])-N_2 complex [W(η^5-C_5Me_5)Me_2($SC_6H_2Me_3$)]$_2$(μ-N_2) is one of the few dinitrogen complexes to contain an S donor ligand.[333a]

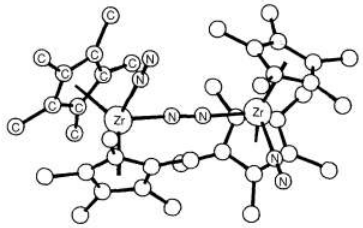


Figure 7.34 - The x-ray crystal structure[333] of (Cp')$_2$Zr(N_2)(μ_2-N_2)Zr(N_2)(Cp')$_2$.

In addition to the N lone pairs, the π components of the N≡N triple bond can serve as donor-acceptor orbitals in the Dewar-Chatt-Duncanson (olefin binding) manner. This less-common mode of N_2 binding is illustrated by the structure of the Ti complex[334] shown in Figure 7.35. Here, as in the few other known side-on bound N_2 complexes,[335] the N-N bond is significantly lengthened. The lengthened bond at 1.30 Å is presumed to be sufficiently weakened [ν(N-N) = 1280 cm^{-1}] that it is susceptible to further lengthening and reduction. As the N-N distance lengthens, it is more appropriate to consider the ligand as a deprotonated diimide or hydrazine.

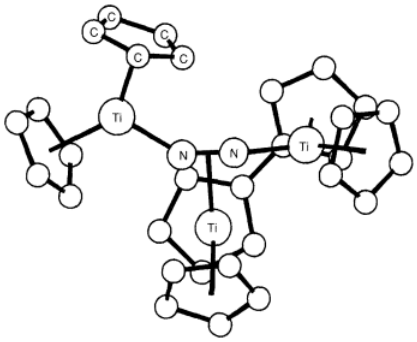


Figure 7.35 - The structure of a multiply bound dinitrogen titanium compound.[334]

Complexes that have proven particularly useful are bis(dinitrogen)phosphines of Mo(0) and W(0) such as M(N_2)$_2$($Ph_2PCH_2CH_2PPh_2$)$_2$ and M(N_2)$_2$(PPh_2Me)$_4$. As shown in Figure 7.36, treatment of the complexes[336-337a] with acid leads to the formation of the diazenido(-H) and hydrazido(-2H) complexes, and sometimes to the production of ammonia. The finding of a bound $N_2H_2^{2-}$ species is consistent with the proposed presence of similar bound species in nitrogenase. The complexes of reduced dinitrogen intermediates are stabilized by multiple M-N binding. Further protonation of these intermediates or treatment of the original complex with strong acid leads to the formation of NH_3 from the bound nitrogen. Here the Mo(0) starting complex has enough electrons [six from the Mo(0) → Mo(VI) conversion] to reduce one N_2 molecule in conjunction with its protonation from the external solution.

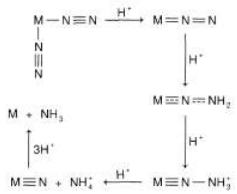


Figure 7.36 - Structure and reactions of $M(N_2)_2(Ph_2PCH_2CH_2PPh_2)_2$ (M = Mo, W) and related complexes. Not all of the intermediates in this scheme have been isolated in anyone particular system.[336,337,337a] The phosphine ligands are not shown.

In a general sense this reaction may be telling us something about nitrogenase. The enzyme may be able to deliver six reducing equivalents to N_2, and protonation, perhaps carefully orchestrated by neighboring amino-acid or homocitrate groupings, may facilitate the process. However, it is virtually certain that the Mo in nitrogenase is not able to change its oxidation state by six units. In the enzyme the multimetal, multisulfur FeMoco site may serve the equivalent function, by providing multiple sites at which reduced intermediates can simultaneously bind.

Only a few of the known N_2 complexes contain S-donor ligands. One of these, $Mo(N_2)_2(S(CH_2C(CH_3)_2CH_2S)_3)$, shown in Figure 7.37, has four thioether S-donor atoms bound to Mo(0). This Mo(0) complex shows reactivity reminiscent of the related phosphine complexes.[337a] A remarkable complex (Figure 7.38) has been isolated[338] in which two lone pairs of *trans*-diimide bind to two Fe, concomitantly with H-binding of the two diimide hydrogen atoms to coordinated sulfur atoms. The ability of an Fe-S system to stabilize the very reactive trans-N_2H_2 grouping adds support to the notion that similar metal-sulfide sites of nitrogenase may stabilize related intermediates along the $N_2 \rightarrow 2NH_3$ reaction path.

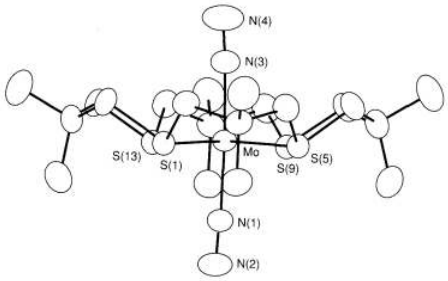


Figure 7.37 - The structure of $Mo(N_2)_2L$ (L is a tetrathiacyclohexadecane)[337b,c]

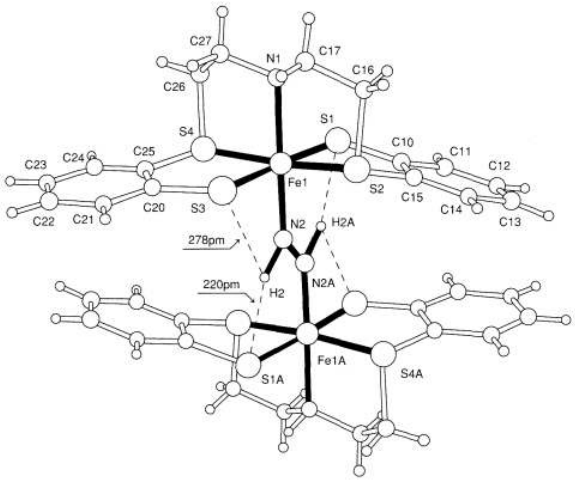


Figure 738 - The structure[338] of $FeL(N_2H_2)FeL$ ($L = SC_6H_4SCH_2CH_2SCHCH_2SC_6H_4S$).

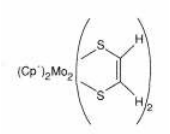
Most of the model systems involving N_2 do not lead to NH_3 formation. Moreover, many systems that do form NH_3 are not catalytic. However, certain V-based and Mo-based systems can catalytically reduce N_2 to N_2H_4 or NH_3 using strong reducing agents.[339] Although kinetic studies indicate the possibility of intermediates, little structural information is available at present on these interesting systems.

Insights from Relevant Inorganic Reactivity

Certain studies on inorganic systems that do not model the nitrogen-fixation process can nevertheless potentially give insight into nitrogenase action. Two categories of relevant chemistry are acetylene binding/reactivity and dihydrogen binding/activation. Modes of dihydrogen activation on sulfide systems have previously been discussed in the section on hydrogenase.

Acetylene has long been known to bind to metal centers using its $\pi$and π^* orbitals as, respectively, σ-donor and \(\pi)-acceptor orbitals. Even when the metal is predominantly sulfur-coordinated,[340,341] such side-on bonding of RC_2R is well known[340,341] as in $MoO(S_2CNR_2)_2(RC{\equiv}CR)$ and $Mo(S_2CNR_2)_2(RC{\equiv}CR)_2$. The direct interaction of acetylene with the metal center must be considered as a potential binding mode for nitrogenase substrates.

A totally different, sulfur-based mode of acetylene binding is now also well established. For example, $(Cp')_2Mo_2S_4$ reacts with acetylene[342,225] to produce



containing a bridging ethylene-1,2-dithiolate (dithiolene). The acetylene binds directly to the sulfur atoms by forming S—C bonds. Acetylenes or substituted (activated) acetylenes are able to displace ethylene from bridging or terminal 1,2-dithiolate ligands[225,341] to produce the 1,2-dithiolenes. In these reactions the sulfur rather than the metal sites of the cluster are reactive toward these small unsaturated molecules. Clearly, for nitrogenase, where we do not know the mode of binding, sulfur coordination might be a viable possibility. The $(Cp')_2Mo_2S_4$ systems that bind H_2 and C_2H_2, wherein bound C_2H_2 can be reduced to C_2H_4 and displaced by C_2H_2, are potential models for substrate reduction by nitrogenase.[225,342]

The versatility of transition-metal sulfur systems is further illustrated by the observation that activated acetylene can insert into a metal-sulfur bond in $Mo_2O_2S_2(S_2)_2^{2-}$, forming a vinyl-disulfide-chelating ligand

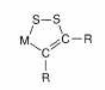


Figure 7.39 shows three possible modes of C_2H_2 binding, each of which is possible for the nitrogenase system.

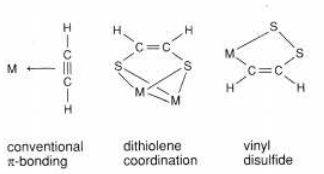


Figure 7.39 - Possible modes of acetylene binding to metal-sulfur sites.

It has recently been suggested[343] that the presence of a dihydrogen complex is required for H_2 to be displaced by N_2 to form a dinitrogen complex. This reaction would explain the required stoichiometry of N_2 reduction and H_2 evolution. Such an explanation had been suggested previously with dihydride complexes acting as the N_2-binding and N_2-displacing site.[182] Clearly, this new suggestion is an interesting embellishment of potential N_2/H_2 relationships.

At present, the activation process that is at work in the enzyme is unknown. We need greater structural definition of the active site, which should be forthcoming through the continued application of sophisticated diffraction and spectroscopic probes. Diffraction alone, however, will be incapable of locating protons and possibly other low-molecular-weight ligands. Therefore, spectroscopic probes such as ENDOR[10] and ESEEM,[277-Z79,344] which are based on EPR spectroscopy, and x-ray-based techniques, such as EXAFS and XANES, will remain crucial in elucidating mechanistically significant structural details.

11.2.7.10: Multisite Redox Enzymes (Part 6) is shared under a CC BY-NC-SA 4.0 license and was authored, remixed, and/or curated by LibreTexts.

11.2.7.11: Report on the Nitrogenase Crystal Structure 378 − 381

A significant breakthrough has occurred in the crystallographic analysis of the iron-molybdenum protein of nitrogenase. The overall distribution of the metal clusters in the protein is shown in Figure 7.40. The distance between the two FeMoco units is fully consistent with each cofactor acting as an independent active site. On the other hand, the closeness of the P cluster and FeMoco centers in each unit is indicative of their likely cooperation in the N_2 fixation reaction.

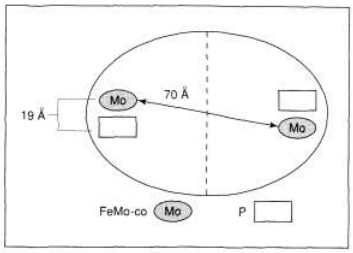


Figure 7.40 - A schematic representation of the spatial arrangement of the metal sulfur clusters bound to Cpl as determined by the x-ray anomalous scattering studies described in the text. The representation of the large, "8-Fe" cluster with a P symbol indicates only that it must contain the Fe atoms normally assigned to P-clusters.

The proposed structure of the P cluster, shown in Figure 7.41, involves a doubly bridged, double cubane unit consisting of one normally bound Fe_4S_4 cluster with all cysteine ligands and one Fe_4S_4 cluster that contains an unusual cysteine/serine (S/O) ligand pair on one of its two nonbridged Fe positions. Such five-coordinate iron in an Fe_4S_4 cluster is not unprecedented.[138] The two Fe_4S_4 clusters are disposed to produce a face-sharing arrangement with two cysteine ligands bridging the two sets of Fe atoms. An interesting feature of the structure is a disulfide unit linking the two clusters; this unit potentially could be redox-active during nitrogenase turnover.

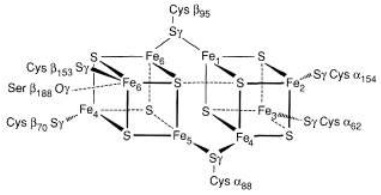


Figure 7.41 - Proposed P-cluster pair in A. vinelandii FeMo protein.

Most striking of the new results is the proposed structure of FeMoco shown in Figure 7.42. The cluster core of composition Fe_7MoS_8 can be viewed as two halves bridged by two S^{2-} ions and an unknown ligand (designated Y in the figure). The $MoFe_3S_3$ half of the core is in the shape of a thiocubane fragment missing one μ_3-S^{2-} ion. The Mo is six coordinate; the ligands are three μ_2-S^{2-} ions, which bridge to the three Fe ions, an α-His-442 nitrogen, and two oxygen donors (the hydroxyl and central carboxylate) of the homocitrate ligand. Interestingly, the second half of FeMoco is a similar thiocubane fragment, Fe_4S_3, also missing a μ_3-S^{2-} ion. This unit has a single noncore ligand, α-Cys-275, which is bound to the terminal Fe atom of the cluster. The two thiocubane fragments ($MoFe_3S_3$ and Fe_4S_3) are bridged by three ligands in a face-sharing mode with the two Fe_3 faces eclipsed with respect to each other. The eight metal ions display a bis(end-capped) trigonal prismatic arrangement with three bridges on the edges of the prism, which connect the two thiocubane fragments. The two sulfide bridges between the thiocubane halves are clearly defined in the structure, but the third bridge is not, suggesting the possibility that this is in fact part of the N_2-binding site. Interestingly, α-His-195, identified as essential for N_2 fixation by mutagenesis and ESEEM studies, does not appear to be covalently bound, although it is close to the FeMoco unit.

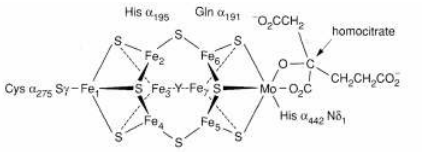


Figure 7.42 - Proposed cofactor cluster in A. vinelandii FeMo protein.

Clearly, this structure is not the same as any of those previously proposed (Figure 7.31), although it does possess many features that were identified in model studies. While it is tempting to speculate that the central bridge of the cluster (the Y ligand) is the site of

N_2 reduction, this is in no way established at present. The structural definition of the nitrogenase proteins is now progressing at a rapid rate. Many of the physical measurements will have to be reexamined in light of the new data. Through further experimentation involving physical methods, mutagenesis, and kinetic/mechanistic studies, much more information about the role of ATP, the activation of hydrogen, and the binding, activation, and reduction of N_2 and other nitrogenase substrates should be obtained.

11.2.7.11: Report on the Nitrogenase Crystal Structure [378–381] is shared under a CC BY-NC-SA 4.0 license and was authored, remixed, and/or curated by LibreTexts.

11.2.7.12: Rubredoxin- A Single-Fe Tetrathiolate Protein

The physiological role of rubredoxins (sometimes abbreviated as Rd) is not always known with certainty. In particular, although rubredoxin was first identified[26] in the anaerobe *Clostridium pasteurianum*, its role in anaerobic metabolism remains obscure. Some rubredoxins, such as that from the aerobe *Pseudomonas oleovorans*, participate in fatty acid ω-hydroxylation, i.e., hydroxylation at the end of the hydrocarbon chain farthest from the carboxylic acid.[27] Like the Fe_2S_2 proteins putidaredoxin[28] and adrenodoxin,[29] the rubredoxin provides electrons to the hydroxylase, which acts as a monooxygenase forming the w-alcohol product and water (see Figure 7.3). In a reaction catalyzed by rubredoxin reductase, rubredoxin is reduced by NADH to the ferrous state and reoxidized by the w-hydroxylase to the ferric form during the catalytic cycle.

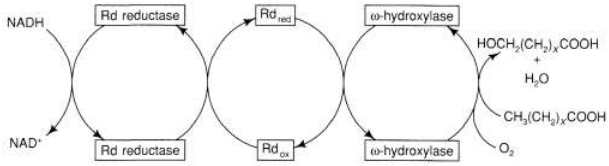


Figure 7.3 - Diagram illustrating the redox changes that occur in the rubredoxin-dependent ω-hydroxylase of Pseudomonas oleovorans.[27]

Most rubredoxins contain a single Fe atom, which can exist in the ferrous or ferric state. For the rubredoxin from Clostridium pasteurianum,[26] the $E^{o'}$ value is -57 mV, which is much more positive than that of ferredoxins from the same organism (see below). The 6-kDa clostridial protein has only 54 amino acids in its polypeptide chain, and has a very low isoelectric point of 2.93. The rubredoxin from *P. oleovorans*[27] has one or two iron atoms in a single polypeptide chain of MW ~ 20 kDa. Its redox potential is -37 mV for the $Fe^{3+/2+}$ couple. Rubredoxins as a class show considerable sequence identity, and the larger 2Fe members of the class show evidence, involving internal-sequence homology, that they may have. evolved through gene duplication.

A protein from *Desulfovibrio gigas*, called desulforedoxin,[30,31] appears to resemble rubredoxins in some respects, but the two Fe atoms in the 7.6-kDa protein appear to be spectroscopically and structurally distinct from the Fe atoms in rubredoxins.[31] A protein from *Desulfovibrio vulgaris* called ruberythrin has a single rubredoxin site as well as a strongly coupled 2Fe site resembling that of hemerythrin. Its physiological function is unknown. Table 7.1 lists some of the known rubredoxins and their properties.

Table 7.1 - Properties of some iron-sulfur proteins.

a) g'-tensors for $\pm \frac{1}{2}$ and $\pm\frac{3}{2}$ Kramers doublets, respectively, of the S = $\frac{5}{2}$ system. The values of 0.9 and 1.25 are calculated (not observed)[44]

b) The fully reduced protein has a complex spectrum due to magnetic coupling between the two identical Fe_4S_4 clusters. The g-values are those for partly reduced samples, and represent a magnetically isolated cluster.

c) The reported spectrum is complex because of magnetic interaction with the reduced Fe_3S_4 cluster.

d) Recent evidence suggests that *Thermus thermophilus* and *Thermus aquaticus* are actually the same species.[362] EPR parameters of the homologous *Thermus thermophilus* ferredoxin estimated from computer simulations.[361] In this protein a signal originating from the Fe_3S_4 cluster at g' $\simeq$ 12, attributable to $\Delta M_s = \pm 4$ transitions, is observed for the reduced (S = 2) cluster.

Protein Source	Molecular Weight (subunits)	Fe-S Composition	Redox Potention mV (pH)	EPR g values			References
Rubredoxins							
Clostridium pasteurianum	6,000	Fe	-58 (7)	9.3	4.3		26
Pseudomonas oleovorans	6,000	Fe		9.42 4.02	0.9 4.77	1.25[a] 4.31	44
Fe_2S_2 Proteins							
Spinach ferredoxin	11,000	[2Fe-2S]	-420 (7.0)	2.05	1.96	1.89	350, 351
Parsley ferredoxin	11,000	[2Fe-2S]		2.05	1.96	1.90	352
Euglena ferredoxin	11,000	[2Fe-2S]		2.06	1.96	1.89	352
Adrenal cortex ferredoxin (pig) [Adrenodoxin]	16,000	[2Fe-2S]	-270 (7.0)	2.02	1.93	1.93	352, 353
Pseudomonas putida ferredoxin [Putidaredoxin]	12,500	[2Fe-2S]	-240 (7.0)	2.02	1.93	1.93	352, 353
Clostridium pasteurianum	25,000	[2Fe-2S]	-300 (7.5)	2.00	1.96	1.94	354
Xanthine Oxidase	280,000 (2)	2 x [2Fe-2S] I II	-343 (8.2) -303 (8.2)	2.02 2.12	1.94 2.01	1.90 1.91	355, 356
Thermus thermophilus Rieske	20,000	2 x [2Fe-2S]	+150 (7.8)	2.02	1.90	1.80	93, 357
Fe_4S_4 Proteins							
Clostridium pasteurianum	6,000	2 x [4Fe-4S]	-420 (8.2)	2.06	1.92	1.89[b]	115
Bacillus stearothermophilus	9,100	[4Fe-4S]	-280 (8.0)	2.06	1.92	1.89	358
Desulfovibrio gigas	18,000 (3)	[4Fe-4S]	-455 (8.0)	2.07	1.94	1.92	359

Protein Source	Molecular Weight (subunits)	Fe-S Composition	Redox Potention mV (pH)	EPR g values			References
ferredoxin I							
Aconitase (beef heart) [active]	81,000	[4Fe-4S]		2.06	1.93	1.86	
Chromatium vinosum HiPIP	10,000	[4Fe-4S]	+356 (7.0)	2.12	2.04	2.04	353
Paracoccus sp.	10,000	[4Fe-4S]	+282 (7.0)				353
Azotobacter vinlandii Fd I	14,500	[3Fe-4S] [4Fe-4S]	-645 (8.3)	2.06	1.93	1.89[c]	360
Thermus aquaticus	10,500	[3Fe-4S] [4Fe-4S]	-550 (9.0)	2.06	1.93	1.92[c]	353, 361
Fe_3S_4 Proteins							
Desulfovibrio gigas Fd II	6,000 (4)	[3Fe-4S]	-130 (8.0)	2.02			359
Azotobacter vinlandii Fd I	14,500	[3Fe-4S] [4Fe-4S]	-450 (8.3)	2.01			360
Thermus aquaticus	10,500	[3Fe-4S] [4Fe-4S]	-260 (9.0)	2.02	1.99	1.94[d]	353, 361
Aconitase (beef heart) [inactive]	81,000	[3Fe-4S]		2.01			

The x-ray crystal structures of the rubredoxins from *C. pasteurianum*[32] and *D. vulgaris*[33] have been determined.[33a] The *C. pasteurianum* protein structure is known to a resolution of 1.2 Å, placing it among the metalloproteins whose structures are known with greatest precision. The individual Fe and S atoms are clearly resolvable. As shown in Figure 7.4, the single iron is coordinated by four S ligands provided by Cys-6, Cys-9, Cys-39, and Cys-42. The sequence Cys-x-y-Cys is a common one in Fe-S proteins, because it allows both cysteine residues to bind to the same metal site or cluster. The Fe-S distances and angles in the clostridial rubredoxin are shown in Table 7.2. The range of distances and angles reveals a slightly distorted tetrahedral structure.

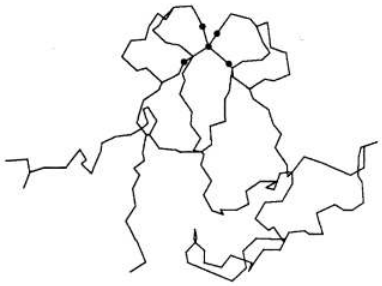


Figure 7.4 - The x-ray crystal structure of rubredoxin from Clostridium pasteurianum.[32]

Table 7.2 - Bond distances and bond angles around Fe in rubredoxin from *Clostridium pasteurianum* (W1).[32]

	Distance (Å)
Fe-S[Cys(6)]	2.33(11)
Fe-S[Cys(9)]	2.288(15)
Fe-S[Cys(39)]	2.300(15)
Fe-S[Cys(42)]	2.235(12)
	Angle (°)
S-Fe-S[Cys(6)-Fe-Cys(9)]	113.8 (4)
S-Fe-S[Cys(6)-Fe-Cys(39)]	109.0 (4)
S-Fe-S[Cys(6)-Fe-Cys(42)]	103.8 (4)
S-Fe-S[Cys(9)-Fe-Cys(39)]	103.7 (4)
S-Fe-S[Cys(9)-Fe-Cys(42)]	114.3 (5)
S-Fe-S[Cys(39)-Fe-Cys(42)]	112.4 (5)

The initial structural results on *C. pasteurianum* rubredoxin were reported at a slightly lower resolution than those displayed in Table 7.2. In fact, the early study[34] reported a range of Fe-S distances from 2.05 to 2.34 Å. Prior to the higher-resolution refinement, a synchrotron-radiation x-ray-absorption spectroscopy study of the iron-absorption edge of rubredoxin was reported.[35,36] Using the technique of Extended X-ray Absorption Fine Structure,* EXAFS, the average Fe-S distance was found [35,36] to be 2.26 Å, in agreement with the average distance from the x-ray crystallographic study. However, the EXAFS indicated a much narrower permissible range of Fe-S distances than did the early crystallographic study. The later, more highly refined crystallographic treatment[32] agreed nicely with the EXAFS result, illustrating the importance of applying more than one technique to the elucidation of key parameters. Here, as with the 3Fe proteins we will discuss later, EXAFS proved a useful complementary technique to x-ray crystallography.

---

* X-ray absorption spectroscopy is most commonly (and conveniently) used with the K-edges of transition-metal ions, such as Fe or Mo. It can be split up into two distinct types; X-ray Absorption Near-Edge Structure (or XANES), and Extended X-ray Absorption Fine Structure (or EXAFS) spectroscopy. The former consists of features near the absorption edge itself, which are due to transitions of the photoelectron to bound states and also to other, more complex, phenomena (e.g., the so-called shape resonances). Although the spectra are highly dependent on the nature of the site, they are quite difficult to interpret, and most analyses are based upon simple comparisons with spectra from model compounds. The EXAFS are oscillations of the absorption coefficient at rather higher x-ray energies, and arise from scattering of the emitted photoelectron by surrounding atoms. In contrast to the XANES, EXAFS spectra are relatively simple to interpret in a quantitative manner, yielding a local radial structure. With proper interpretation of the spectra, very accurate interatomic distances (e.g., to ± 0.02 Å), plus more approximate ligand coordination numbers and atomic numbers can be obtained.

The tetrahedral iron sites in rubredoxins offer an interesting glimpse of ligand-field theory in action, and illustrate the use of various physical methods in deducing electronic structure and coordination geometry. The four sulfur ligands are expected to split the iron 3d orbitals into e and t_2 sets, with the e set lower as shown in Figure 7.5. The small tetrahedral splitting causes the $3d^5$ Fe^{3+} ion to have five unpaired electrons, $(e)^2(t^2)^3$, $^6A_1$. Consistent with this configuration, the magnetic susceptibility of rubredoxin gives a μ_{eff} of 5.85 Bohr magnetons.[37] No spin-allowed ligand-field transitions are expected, and the red color is caused by S → Fe charge-transfer transitions in the visible region.[38,39]

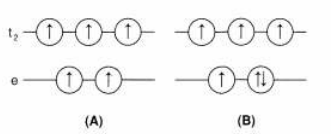
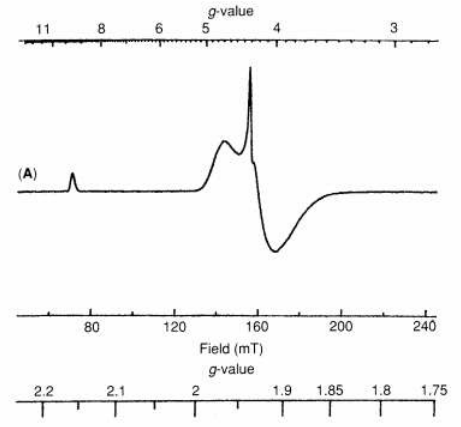


Figure 7.5 - Splitting of the 3d orbitals of Fe by the tetrahedral ligand field of four coordinated cysteine residues: (A) Fe^{3+}; (B) Fe^{2+}.

In contrast, the $3d^6$ Fe^{2+} state, with one additional electron, has four unpaired electrons, as confirmed by its magnetic moment of 5.05 Bohr magnetons. In exact tetrahedral symmetry, a single, low-energy, low-intensity d-d absorption of designation $^5E \rightarrow {}^5T$ $[(e)^3(t_2)^3 \rightarrow (e)^2(t_2)^4]$ is expected for the high-spin ferrous site (Figure 7.5). Indeed, reduced rubredoxin displays a band in the near-infrared region at 6,250 cm^{-1} that arises as a component of the $^5E \rightarrow {}^5T_2$ transition.[40] This band stands out particularly vividly in the low-energy circular dichroism (CD) spectrum of reduced rubredoxin.[41] Moreover, magnetic circular dichroism (MCD) has proven valuable in dissecting electronic transitions in several rubredoxins and metal-sulfide proteins.[38,39,42,43]

The EPR spectrum of oxidized rubredoxin (Figure 7.6) shows characteristic peaks at g = 4.31 and 9.42 (*P. oleovorans*), which have been assigned[44] to transitions within excited and ground-state Kramers doublets, respectively, of a nearly completely rhombic $S = \frac{5}{2}$ site, with D = 1.8 and E = 0.5 cm^{-1}. These values for the mononuclear Fe^{3+} ion stand in sharp contrast to those for other iron-sulfur proteins, which are usually $S = \frac{1}{2}$ (when reduced) and have g values close to 2. The even-electron Fe^{2+} state (S = 2) in reduced rubredoxin has no detectable EPR when conventional instruments are used.*



https://chem.libretexts.org/@go/page/438076

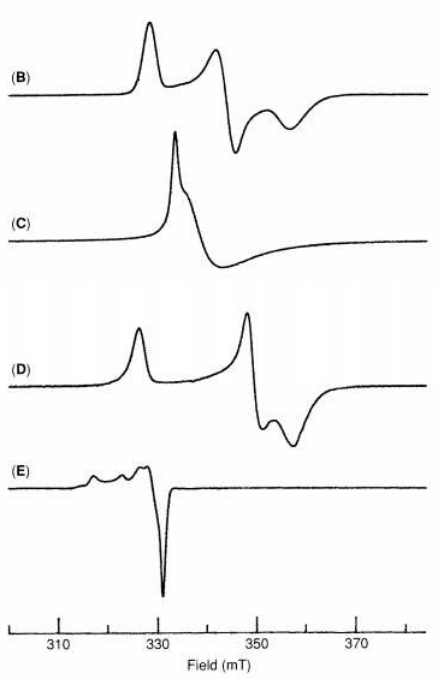


Figure 7.6 - EPR spectra of various Fe-S proteins: (A) oxidized Desulfovibrio gigas rubredoxin; (B) reduced spinach ferredoxin $[Fe_2S_2]^+$; (C) reduced Bacillus stearothermophilus ferredoxin $[Fe_4S_4]^+$; (D) oxidized Thermus aquaticus ferredoxin $[Fe_3S_4]^+$; (E) oxidized Chromatium vinosum HiPIP $[Fe_4S_4]^+$. (Spectra courtesy of S. J. George.)

Mössbauer spectroscopy has proven to be a particularly powerful complementary tool to EPR in probing the iron sites in Fe-S proteins.[3,37,51,52] It is a nuclear spectroscopy that can give valuable information not available from other techniques.† Unlike EPR, where only *paramagnetic* centers are "seen," every ^{57}Fe atom in the sample will contribute to the Mössbauer spectrum. For rubredoxin, the high-spin nature of the ferric and ferrous sites are clearly seen in the Mössbauer spectra.[53] The high-spin Fe^{3+} sites show a small quadrupole splitting of roughly 0.7-0.8 mm/s due to the almost spherical distribution of the five d electrons in the five d orbitals (Figure 7,7A). In contrast, the high-spin Fe^{2+} ion with an additional d electron has a significant asymmetry, and thus displays large and quite characteristic quadrupole splitting of 3.1-3.4 mm/s (Figure 7.7B). The isotope shift also distinguishes between Fe^{2+} and Fe^{3+}, although not as dramatically.[37] Finally, the observation[53] of magnetic hyperfine interaction in the Mössbauer spectrum at low temperature in the Fe^{3+} state directly reveals the presence of unpaired electrons, i.e., magnetic coupling with a hyperfine field of 370 ± 3 kG. Although in rubredoxins with a single Fe atom, this observation of magnetic coupling does not reveal any new information, similar magnetic coupling is particularly useful in unraveling the Fe sites in more complex multiiron proteins.

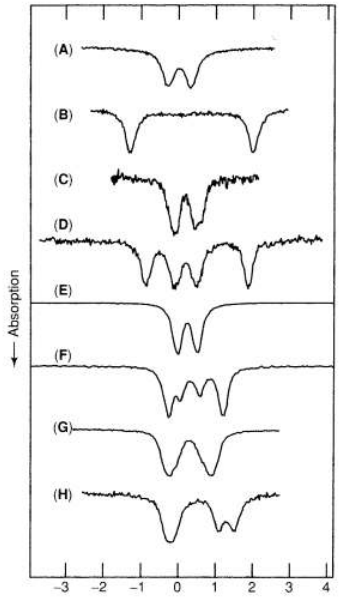


Figure 7.7 - Mössbauer spectra of various Fe-S sites: (A) oxidized and (B) reduced $Fe(SR)_4$ (Fe^{3+} and Fe^{2+}, respectively) rubredoxin models (data from Reference 347); (C) oxidized and (D) reduced Scenedesmus Fe_2S_2 ferredoxin ($2Fe^{3+}$ and [Fe^{3+}, Fe^{2+}], respectively, data from Reference 348); (E) oxidized and (F) reduced Desulfovibrio gigas Fe_3S_4 ferredoxin II ($3Fe^{3+}$ and [$2Fe^{3+}$, Fe^{2+}], respectively, data from Reference 158); (G) oxidized and (H) reduced Bacillus sterothermophilus Fe_4S_4 ferredoxin (data from Reference 349).

* But see Reference 45. EPR spectroscopy uses magnetic fields to split the electron spin states into levels that differ by energy in the microwave region of the spectrum. For an S = $\frac{1}{2}$ system, the g value (and its anisotropy) and the a values (hyperfine splitting from various nuclei and their anisotropy) are the major parameters reported. EPR spectroscopy has played a role in the development of Fe-S biochemistry akin to the role played by optical spectroscopy in the development of the biochemistry of the cytochromes,[46-49] particularly for mitochondria[47] and chloroplasts,[50] where the g = 1.9 EPR signal has facilitated the monitoring of electron flow through these redox systems. Although EPR has been a powerful tool, it does have some important limitations. A necessary but not sufficient condition for EPR is that the center to be observed must be in a paramagnetic state. Fortunately, this condition is met for at least one member of each one-electron redox couple, i.e., the odd-electron species. However. even when the even-electron species is paramagnetic, it is usually not observed in the EPR, because of the presence of large zero-field splittings. Moreover, relaxation effects and/or the population of excited states often cause the EPR of proteins to be unobservable at room temperature. necessitating the use of liquid N_2 or liquid He temperatures to observe the signals in the frozen state. The need to freeze samples prior to observation can lead to artifacts involving the observation of nonphysiological states and processes. On the positive side, the low temperature increases the signal intensity by altering the Boltzmann distribution of the spin population, and allows various quenching techniques to be used with EPR to evaluate kinetic and electrochemical parameters. Nevertheless, one cannot usually observe real-time kinetics or be certain that one is observing a physiologically relevant state. Despite these caveats, EPR has proven a valuable and, in some cases, indispensable tool for identification and monitoring of Fe-S sites. Recently, the advanced EPR techniques ENDOR (Electron Nuclear Double Resonance) and ESEEM (Electron Spin Echo Envelope Modulation) have allowed the extraction of additional information from the EPR signal.

† Mossbauer spectroscopy measures nuclear absorption of light at γ-ray energies, and can be used to probe nuclear energy levels (usually of ^{57}Fe). The splitting of these levels is influenced by the (s) electron density at the nucleus, and by the electric-field gradient that is set up by nearby atoms. These factors affect the isomer shift and the quadrupole splitting of the Mössbauer spectrum, respectively. Information on nuclear hyperfine couplings is also available when experiments are conducted in the presence of an external (usually applied) magnetic field. Fortunately, the nucleus most commonly (and easily) studied by this technique is present in all the proteins discussed in this chapter, although the level of ^{57}Fe (2 percent natural abundance) must be increased by isotopic enrichment to achieve a high-enough signal-to-noise ratio. For spectra containing one type of site, the spectra are relatively straightforward to interpret. For multisite systems deconvolution is required to get data on individual centers. When possible, selective labeling of sites with ^{57}Fe is extremely helpful in the deconvolution process.

NMR studies on both the oxidized and the reduced states of rubredoxins have been reported. The strongly paramagnetic iron atoms have a profound effect on the NMR spectra of protons in the vicinity of the iron. The iron drastically affects the relaxation behavior of such protons, causing line-broadening, sometimes so much that the protons become nonobservable. If observed, the protons are shifted far from the values found in diamagnetic proteins by combinations of Fermi contact (through overlap/through bond) and pseudo-contact (through space/dipolar) coupling.[54,55] In the rubredoxins, the reduced state shows resolved spectra,[37,56] which can be assigned[56] with the help of data from model systems.*

Resonance Raman spectroscopy provides information involving molecular vibrations that is not dependent on either nuclear or magnetic properties. Electronic excitation of bands involving S → Fe charge transfer often leads to resonance enhancement of Fe-S stretching modes. In rubredoxin,[57,57a] the Fe-S stretching vibrations are located between 300-400 cm^{-1}. Deviations of the expected two-band tetrahedral pattern (T_2 and A_1 modes) are attributable to coupling of the Fe-S vibrations with S-C-C bending modes. This coupling makes for greater variability, and the detailed vibrational assignment is thus more difficult for bands involving the cysteinyl sulfur atoms. In contrast, for sites containing inorganic S^{2-}, the Fe-S vibrations involving the inorganic core are less variable and therefore more characteristic of the core type.[57]

In theory, each of the spectroscopic techniques applied to rubredoxins can give useful information about the other iron-sulfur proteins. In practice, some techniques have proven more useful than others in particular situations, and combined use of several techniques is necessary to draw meaningful conclusions.

Chemical studies of rubredoxins have led to the replacement of the Fe^{2+} with an Fe_4S_4 center,[58] with Co^{2+}, and with Ni^{2+}. The Co^{2+} replacement of Fe^{2+}, in *P. oleovorans* rubredoxin, leads to a stable protein that displays reduced (but not trivial) reactivity in the ω-hydroxylation reaction.[59,60] The spectral properties of the cobalt(II) site show the expected changes in d-d bands and the expected shifts in charge-transfer transitions.[59] Interestingly, when Ni^{2+} is substituted into rubredoxins from desulfovibrio species, the resultant proteins show hydrogenase activity.[61]

---

* NMR is a technique whose great utility in the study of low-molecular-weight proteins and model systems has not (yet) carried over to the study of larger proteins. Slower tumbling rates, rapid electronic relaxation, multiple paramagnetic sites, large numbers of protons, and more dilute solutions conspire to make the observation and/or interpretation of NMR spectra a daunting task in multisite redox proteins of > 50 kDa.

11.2.7.12: Rubredoxin- A Single-Fe Tetrathiolate Protein is shared under a CC BY-NC-SA 4.0 license and was authored, remixed, and/or curated by LibreTexts.

11.2.8: Metal/Nucleic Acid Interactions

I. Introduction

The interest of the bioinorganic community in the field of metal/nucleic-acid interactions has burgeoned in the last decade. This interest and the resulting progress have come about primarily because of the tremendous advances that have occurred in nucleic-acid technology. We can now isolate, manipulate, and even synthesize nucleic acids of defined sequence and structure, as we would other molecules that chemists commonly explore. Furthermore, as may be evident already in other chapters of this book, bioinorganic chemistry has itself been evolving from a field focused on delineating metal centers in biology to one that includes also the application of inorganic chemistry *to probe* biological structures and function. In the past decades it has become clear that nucleic acids, structurally, functionally and even remarkably in terms of catalysis, play active and diverse roles in Nature. Transition-metal chemistry, both in the cell and in the chemist's test tube, provides a valuable tool both to accomplish and to explore these processes.

There are also many practical motivations behind the study of how metal ions and complexes interact with nucleic acids. Heavy-metal toxicity in our environment arises in part from the covalent interactions of heavy-metal ions with nucleic acids. In addition, these heavy metals interfere with metalloregulatory proteins and in so doing disrupt gene expression. We need to understand the functioning of the natural metalloregulators of gene expression and we need to design new metal-specific ligands, which, like the proteins themselves, capture heavy metals before their damage is done. Heavy-metal interactions with nucleic acids indeed have provided the basis also for the successful application of cisplatin and its derivatives as anticancer chemotherapeutic agents (see Chapter 9). The design of new pharmaceuticals like cisplatin requires a detailed understanding of how platinum and other metal ions interact with nucleic acids and nucleic-acid processing. Furthermore, we are finding that metal complexes can be uniquely useful in developing spectroscopic and reactive probes of nucleic acids, and hence may become valuable in developing new diagnostic agents. Finally, Nature itself takes advantage of metal/nucleic-acidchemistry, from the biosynthesis of natural products such as bleomycin, which chelates redox-active metal ions to target and damage foreign DNA, to the development of basic structural motifs for eukaryotic regulatory proteins, the zinc-finger proteins, which bind to DNA and regulate transcription. In all these endeavors, we need first to develop an understanding of how transition-metal ions and complexes interact with nucleic acids and how this chemistry may best be exploited.

In this chapter we first summarize the "basics" needed to consider the interactions of metal ions and complexes with nucleic acids. What are the structures of nucleic acids? What is the basic repertoire of modes of association and chemical reactions that occur between coordination complexes and polynucleotides? We then consider in some detail the interaction of a simple family of coordination complexes, the tris(phenanthroline) metal complexes, with DNA and RNA to illustrate the techniques, questions, and applications of metal/nucleic-acid chemistry that are currently being explored. In this section, the focus on tris(phenanthroline) complexes serves as a springboard to compare and contrast studies of other, more intricately designed transition-metal complexes (in the next section) with nucleic acids. Last we consider how Nature uses metal ions and complexes in carrying out nucleic-acid chemistry. Here the principles, techniques, and fundamental coordination chemistry of metals with nucleic acids provide the foundation for our current understanding of how these fascinating and complex bioinorganic systems may function.

II. The Basics

A. Nucleic-acid Structures[1]

B. Fundamental Interactions with Nucleic Acids
   1. Coordination
   2. Interecalation and Hydrogen Bonding

C. Fundamental Reactions with Nucleic Acids
   1. Redox Chemistry
   2. Hydrolytic Chemistry

III. A Case Study: Tris(phenanthroline) Metal Complexes

A. Binding Interactions with DNA

B. Techniques to Monitor Binding

IV. Applications of Different Metal Complexes that Bind Nucleic Acids

A. Spectroscopic Probes

B. Metallofootprinting Reagents

C. Conformational Probes

1. Nonspecific Reactions of Transition-metal Complexes
2. Transition-metal Complexes as Shape-selective Probes

D. Other Novel Techniques

V. Nature's Use of Metal/Nucleic-acid Interactions

A. A Structural Role

B. A Regulatory Role

C. A Pharmaceutical Role

D. A Catalytic Role

VI. References

1. W. Saenger, *Principles of Nucleic Acid Structure*, Springer-Verlag, 1984; J. K. Barton, *Chem. Eng. News* **66** (Sept. 26, 1988), 30.
2. M. McCall, T. Brown, and O. Kennard, *J. Mol. Biol.* 183 (1985), 385.
3. R. Wing *et al.*, *Nature* **287** (1980), 755.
4. A. H.-J. Wang *et al.*, *Nature* **282** (1979), 680.
5. S. H. Kim *et al.*, *Proc. Natl. Acad. Sci. USA* **71** (1974), 4970.
6. E. N. Trifonov and J. L. Sussman, *Proc. Natl. Acad. Sci USA* **77** (1980), 3816; J. C. Marini *et al.*, *Proc. Natl. Acad. Sci. USA* **79** (1982), 7664; H.-S. Koo, H.-M. Wu, and D. M. Crothers, *Nature* **320** (1986), 501.
7. M. Gellert *et al.*, *Cold Spring Harbor Symps. Quant. Biol*. **43** (1979), 35; D. M. J. Lilley, *Proc. Natl. Acad. Sci. USA* **77** (1980), 6468.
8. J. S. Lee *et al.*, *Nucleic Acids Res.* **12** (1984), 6603; V. I. Lyamichev, *J. Biomol. Struct. Dyn*. **3** (1986), 667; H. Htun and J. E. Dahlberg, *Science* **241** (1988), 1791.
9. R. D. Kornberg, *Annu. Rev. Biochem*. **46** (1977), 931; A. Klug *et al.*, *Nature* **287** (1980), 509.
10. T. R. Cech, *Science* **236** (1987), 1532.
11. (a) J. K. Barton and S. J. Lippard, *Metal Ions in Biol*. **1** (1980), 31; (b) A. M. Pyle and J. K. Barton, *Prog. Inorg. Chem.* **38** (1990), 413; (c) C. S. Chow and J. K. Barton, *Meth. Enzym.* **212** (1992), 219.
12. S. E. Sherman *et al.*, *Science* **230** (1985), 412.
13. D. Hodgson, *Prog. Inorg. Chem.* **23** (1977), 211.
14. G. L. Eichhorn and Y. A. Shin, *J. Am. Chem. Soc.* **90** (1968), 7323.
15. L. G. Marzilli, *Prog. Inorg. Chem.* **23** (1977), 255.
16. C. H. Chang, M. Beer, and L. G. Marzilli, *Biochemistry* **16** (1977), 33; G. C. Glikin *et al.*, *Nucleic Acids Res*. **12** (1984), 1725.
17. M. B. Fleisher, H. Y. Mei, and J. K. Barton, *Nucleic Acids and Mol. Biol.* **2** (1988), 65.
18. S. J. Lippard, *Acc. Chem. Res.* **11** (1978), 211.
19. R. V. Gessner *et al.*, *Biochemistry* **24** (1985), 237.

20. (a) K. W. Jennette *et al.*, *Proc. Natl. Acad. Sci. USA* **71** (1974), 3839; (b) A. H. Wang et al., *Nature* **276** (1978), 471.
21. H. Sigel, in T. D. Tullius, ed., *Metal-DNA Chemistry, ACS Symposium* **402** (1989), 159.
22. R. P. Hertzberg and P. B. Dervan, *J. Am. Chem. Soc.* **104** (1982), 313; R. P. Hertzberg and P. B. Dervan, *Biochemistry* **23** (1984), 3934.
23. J. A. Latham and T. R. Cech, *Science* **245** (1989), 276.
24. P. B. Dervan, *Science* **232** (1986), 464.
25. S. M. Hecht, ed., *Bleomycin*, Springer-Verlag, 1979.
26. D. S. Sigman, *Acc. Chem. Res.* **19** (1986), 180; S. Goldstein and G. Czapski, *J. Am. Chem. Soc.* **108** (1986), 2244.
27. For other examples of metal-mediated redox cleavage of DNA, see also: N. Grover and H. H. Thorp, *J. Am. Chem. Soc.* **113** (1991), 7030; X. Chen, S. E. Rokita, and C. J. Burrows, *J. Am. Chem. Soc.* **113** (1991), 5884.
28. H. Y. Mei and J. K. Barton, *J. Am. Chem. Soc.* **108** (1986), 7414.
29. H. Y. Mei and J. K. Barton, *Proc. Natl. Acad. Sci. USA* **85** (1988), 1339.
30. A. M. Pyle, E. C. Long, and J. K. Barton, *J. Am. Chem. Soc.* **111** (1989), 4520.
31. A. Sitlani *et al.*, *J. Am. Chem. Soc.* **114** (1992), 2303.
32. M. D. Purugganan *et al.*, *Science* **241** (1988), 1645.
33. L. A. Basile and J. K. Barton, *Metal Ions Biol. Syst.*, **25** (1989), 31; J. K. Barton, in *Frontiers of Chemistry: Biotechnology,* Chem. Abstr. Serv., **5** (1989).
34. D. R. Jones, L. F. Lindoy, and A. M. Sargeson, *J. Am. Chem. Soc.* **106** (1984), 7807.
35. S. H. Gellman, R. Petter, and R. Breslow, *J. Am. Chem. Soc.* **108** (1986), 2388; J. Chin and X. Zhou, *J. Am. Chem. Soc.* **110** (1988), 223; J. R. Morrow and W. C. Trogler, *Inorg. Chem.* **27** (1988), 3387.
36. L. A. Basile, A. L. Raphael, and J. K. Barton, *J. Am. Chem. Soc.* **109** (1987), 7550.
37. G. L. Eichhorn and Y. A. Shin, *J. Am. Chem. Soc.* **90** (1968), 7322.
38. R. S. Brown, J. C. Dewan, and A. Klug, *Biochemistry* **24** (1985), 4785.
39. L. Behlen *et al.*, *Biochemistry* **29** (1990), 2515.
40. J. K. Barton, *Science* **233** (1986), 727.
41. J. K. Barton *et al.*, *J. Am. Chem. Soc.* **108** (1986), 2081.
42. A. M. Pyle *et al.*, *J. Am. Chem. Soc.* **111** (1989), 3051.
43. C. V. Kumar, J. K. Barton, and N. J. Turro, *J. Am. Chem. Soc.* **107** (1985), 5518.
44. S. J. Lippard *et al.*, *Science* **194** (1976), 726.
45. J. K. Barton, J. J. Dannenberg, and A. L. Raphael, *J. Am. Chem. Soc.* **104** (1982), 4967.
46. J. K. Barton, A. T. Danishefsky, and J. M. Goldberg, *J. Am. Chem. Soc.* **106** (1984), 2172.
47. R. F. Pasternack, E. J. Gibbs, and J. J. Villafranca, *Biochemistry* **22** (1983), 2406; R. F. Pasternack and E. J. Gibbs in T. D. Tullius, ed., *Metal-DNA Chemistry*, *ACS Symposium* **402** (1989), 59.
48. J. K. Barton and E. Lolis, *J. Am. Chem. Soc.* **107** (1985), 708.
49. R. E. Mahnken *et al.*, *Photochem. Photobiol.* **49** (1989), 519.
50. J. P. Rehmann and J. K. Barton, *Biochemistry* **29** (1990), 1701.
51. J. C. Caradonna *et al.*, *J. Am. Chem. Soc.* **104** (1982), 5793.
52. J. P. Rehmann and J. K. Barton, *Biochemisty* **29** (1990), 1710.
53. A. Jack et al., *J. Mol. Biol.* **111** (1977), 315.
54. M. T. Carter and A. J. Bard, *J. Am. Chem. Soc.* **109** (1987), 7528.
55. J. K. Barton and A. L. Raphael, *J. Am. Chem. Soc.* **106** (1984), 2466.
56. M. B. Fleisher *et al.*, *Inorg. Chem.* **25** (1986), 3549.
57. M. W. van Dyke, R. P. Hertzberg, and P. B. Dervan, *Proc. Natl. Acad. Sci. USA* **79** (1982), 5470; M. W. van Dyke and P. B. Dervan, *Nucleic Acids Res.* **11** (1983), 5555.
58. J. K. Barton *et al.*, *Proc. Natl. Acad. Sci. USA* **81** (1984), 1961; A. E. Friedman *et al.*, *Nucleic Acids. Res.* **19** (1991), 2595.
59. A. E. Friedman et al., *J. Am. Chem. Soc.* **112** (1990), 4960; R. Hartshorn and J. K. Barton, *J. Am. Chem. Soc.* 114 (1992), 5919.
60. W. deHorrocks and S. Klakamp, *Biopolymers* **30** (1990), 33.
61. R. Tamilarasan, S. Ropertz, and D. R. McMillin, *Inorg. Chem.* **27** (1988), 4082.
62. D. J. Galas and A. Schmitz, *Nucleic Acids Res.* **5** (1978), 3157.
63. T. D. Tullius *et al.*, *Methods in Enzym.* **155** (1987), 537.

64. R. Law *et al.*, *Proc. Natl. Acad. Sci. USA* **84** (1987), 9160; C. L. Peterson and K. L. Calane, *Mol. Cell Biol.* **7** (1987), 4194.
65. J. C. Dabrowiak, B. Ward, and J. Goodisman, *Biochemistry* **28** (1989), 3314.
66. P. E. Nielsen, C. Jeppesen, and O. Buchardt, *FEBS Lett.* **235** (1988), 122; C. Jeppesen and P. E. Nielsen, *Nucleic Acids Res.* **17** (1989), 4947.
67. K. Uchida *et al.*, *Nucleic Acids Res.* **17** (1989), 10259.
68. A. M. Burkhoff and T. D. Tullius, *Cell* **48** (1987), 935; A. M. Burkhoff and T. D. Tullius, *Nature* **331** (1988), 455.
69. B. H. Johnston and A. Rich, *Cell* **42** (1985), 713; E. Palacek, E. Rasovka, and P. Boublikova, *Biochem. Biophys. Res. Comm.* **150** (1988), 731.
70. J. K. Barton and A. L. Raphael, *Proc. Natl. Acad. Sci. USA* **82** (1985), 6460.
71. B. C. Muller, A. L. Raphael, and J. K. Barton, *Proc. Natl. Acad. Sci. USA* **84** (1987), 1764; I. Lee and J. K. Barton, *Biochemistry* **32** (1993), 6121.
72. M. R. Kirshenbaum, R. Tribolet, and J. K. Barton, *Nucleic Acids Res.* **16** (1988), 7948.
73. A. M. Pyle, T. Morii, and J. K. Barton, *J. Am. Chem. Soc.* **112** (1990), 9432.
74. J. M. Kean, S. A. White, and D. E. Draper, *Biochemistry* **24** (1985), 5062.
75. G. J. Murakawa *et al.*, *Nucleic Acids Res.* **17** (1989), 5361
76. C. S. Chow and J. K. Barton, *J. Am. Chem. Soc.* **112** (1990), 2839; C. S. Chow et al., *Biochemistry* **31** (1992), 972.
77. H. E. Moser and P. B. Dervan, *Science* **238** (1987), 645.
78. C. B. Chen and D. S. Sigman, *Science* **237** (1987), 1197.
79. J. P. Sluka *et al.*, *Science* **238** (1987), 1129.
80. D. P. Mack, B. L. Iverson, and P. B. Dervan, *J. Am. Chem. Soc.* **110** (1988), 7572.
81. J. S. Heras *et al.*, *J. Biol. Chem.* **258** (1983), 14120.
82. J. Miller, A. D. McLachlan, and A. Klug, *EMBO* **4** (1985), 1609.
83. J. M. Berg, *Science* **232** (1986), 485.
84. A. Klug and D. Rhodes, *Trends Biochem. Sci.* **12** (1987), 464; R. M. Evans and S. M. Hollenberg, *Cell* **52** (1988), 1.
85. J. M. Berg, *Proc. Natl. Acad. Sci. USA* **85** (1988), 99.
86. M. S. Lee *et al.*, *Science* **245** (1989), 635; G. Parraga *et al.*, *Science* **241** (1988), 1489.
87. N. P. Pavletich and C. O. Pabo, *Science* **252** (1991), 809.
88. (a) T. Pan and J. E. Coleman, *Proc. Natl. Acad. Sci. USA* **86** (1989), 3145; (b) R. Marmorstein *et al.*, *Nature* **356** (1992), 408.
89. B. F. Luisi *et al.*, *Nature* **352** (1991), 497.
90. (a) T. V. O'Halloran, *Metal Ions Biol. Syst.* **25** (1989), 105; (b) C. T. Walsh *et al.*, *FASEB* **2** (1988), 124; T. V. O'Halloran and C. T. Walsh, *Science* **235** (1987), 211.
91. J. D. HeImann, B. T. Ballard, and C. T. Walsh, *Science* **248** (1990), 946.
92. J. E. Penner-Hahn *et al.*, *Physica B* **158** (1989), 117.
93. J. H. Griffin and P. B. Dervan, *J. Am. Chem. Soc.* **109** (1987), 6840.
94. A. Bagg and J. B. Neilands, *Microbiol. Rev.* **51** (1987), 509.
95. P. Furst *et al.*, *Cell* **55** (1988), 705; C. Buchman *et al.*, *Mol. Cell Biol.* **9** (1989).
96. J. Stubbe and J. W. Kozarich, *Chem. Rev.* **87** (1987), 1107.
97. E. A. Sausville, J. Peisach, and S. B. Horwitz, *Biochem. Biophys. Res. Comm.* **73** (1976), 814.
98. Y. Iitaka *et al.*, *J. Antibiot.* **31** (1978), 1070.
99. S. M. Hecht, *Acc. Chem. Res.* **19** (1986), 383.
100. C. W. Wu, F. Y. Wu, and D. C. Speckhard, *Biochemistry* **16** (1977), 5449.
101. D. P. Giedroc and J. E. Coleman, *Biochemistry* **25** (1986), 4946.
102. J. E. Coleman and D. P. Giedroc, *Metal Ions Biol. Syst.* **25** (1989), 171.
103. A. S. Mildvan and E. H. Serpersu, *Metal Ions Biol. Syst.* **25** (1989), 309.
104. D. Suck and C. Oefner, *Nature* **321** (1986), 620.
105. J. E. Coleman, *Metal Ions in Biol.* **5** (1983), 219.
106. H. Asahara *et al.*, *Biochemistry* **28** (1989), 4444.
107. I am grateful to my students and coworkers for their scientific contributions to some of the work described in this chapter and for their critical review of the manuscript. I also thank in particular Dr. Sheila David for preparation of the figures.

Contributors and Attributions

- Jacqueline K. Barton (California Institute of Technology, Division of Chemistry and Chemical Engineering)

11.2.8: Metal/Nucleic Acid Interactions is shared under a CC BY-NC-SA 4.0 license and was authored, remixed, and/or curated by LibreTexts.

11.2.8.1: The Basics

Nucleic-acid Structures[1]

Figure 8.1 displays a single deoxyribonucleotide and the four different nucleic-acid bases. As may be evident, each mononucleotide along a nucleic-acid polymer contains a variety of sites for interactions with metal ions, from electrostatic interactions with the anionic phosphate backbone to soft nucleophilic interactions with the purine heterocycles. The different nucleic-acid bases furthermore offer a range of steric and electronic factors to exploit. Coordination of a metal complex to the N7 nitrogen atom of a purine, for example, would position other coordinated ligands on the metal center for close hydrogen bonding to the O6 oxygen atom of guanine, but would lead to clashes with the amine hydrogen atoms of adenine.

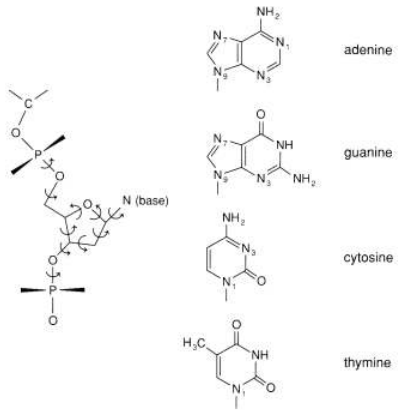


Figure 8.1 - Illustration of a mononucleotide unit. Arrows indicate the various torsional angles within each unit that together generate the wide range of conformations available in the polymer. Also shown are the individual bases as well as the commonly employed numbering scheme.

The monomeric units strung together in a polynucleotide furthermore provide an array of polymeric conformers. Figure 8.2A (See color plate section, pages C-14, C-15.) shows three crystallographically characterized structures of double-helical DNA oligonucleotides,[2-4] Figure 8.2B a schematic illustration of other conformations of DNA, and Figure 8.2C the crystal structure[5] of yeast $tRNA^{Phe}$. In double-helical DNA,[1] the two antiparallel polynucleotide strands are intertwined in a helix, stabilized through Watson-Crick hydrogen bonding between purines and pyrimidines, and through $\pi - \pi$ stacking interactions among the bases arranged in the helical column. There are electrostatic repulsions between the anionic phosphate backbones of the polymer, causing a stiffening; each double-helical step has two formal negative charges. An atmosphere of metal ions condensed along the sugar-phosphate backbone serves partially to neutralize these electrostatic interactions. In the B-DNA conformation, the bases are stacked essentially perpendicular to the helical axis, and the sugars are puckered in general, with a C2'-endo geometry (the C2' carbon is to the same side as the C5' position relative to a plane in the sugar ring defined by the C1', C4', and O atoms). This conformer yields a right-handed helix with two distinct, well-defined grooves, termed the major and minor. The A-form helix, while still right-handed, is distinctly different in structure. The sugar rings are puckered generally in the C3'-endo conformation, causing the bases to be pushed out from the center of the helix toward the minor groove, and tilted relative to the helix perpendicular by almost 20°. What results is a shorter and fatter helix than the B-form; the helical pitch is 28.2 Å in A-DNA for an 11-residue helix and 33.8 Å for a 10-residue helix in B-DNA. The A-form helical shape is best characterized by the very shallow minor groove surface; what was the major groove in the B-form has been pulled deeply into the interior of the A-conformer and is really not accessible to binding by small molecules in solution. Transitions to the A-conformation are promoted by hydrophobic solvents or solutions of high ionic strength. The Z-conformation is perhaps most distinctive, owing to its left-handed helicity.[4] The conformer was dubbed Z-DNA because of the zig-zag in the helix. Alternations both in sugar puckering, between C2'-endo and C3'-endo, and in the rotation of the base about the glycosidic bond, anti or syn relative to the sugar, are evident, and lead to a dinucleoside repeating unit versus a mononucleoside repeat in the A- and B-helices. Alternating purinepyrimidine sequences have the highest propensity to undergo transitions into the Z-form. It is actually this syn conformation of purines that leads to the lefthanded helicity of the polymer. But it is not only its left-handedness that distinguishes the Z-conformation. The polymer is long and slender (the pitch is 45 Å for a 12-

residue helix), and the major groove is a shallow and wide, almost convex, surface, whereas the minor groove is narrowed into a sharp and small crevice.

These crystal structures, shown in Figure 8.2A (see color plate section, page C-15), in fact each represent a family of conformations. The bases in a base pair often do not lie in the same plane, but are instead propeller-twisted with respect to one another. The local unwinding of the helix and tilting of the base pairs furthermore tend to vary with the local nucleic-acid sequence so as to maximize stacking or hydrogen-bonding interactions among the bases. Hence there is a variety of structures within each conformational family. Our understanding of these structural variations as a function of solution conditions and importantly of local sequence is still quite poor. But surely these structural variations affect and are affected by the binding of metal ions and complexes.

Even less defined structurally are other conformations of DNA, some of which are illustrated schematically in Figure 8.2B (see color plate section, page C-15). Double-helical DNA can bend,[6] form loops and cruciforms,[7] and fold back on itself into intramolecular triple helices, termed H-DNA.[8] At the ends of chromosomes, four strands may even come together in a unique conformation. These structures, characterized thus far by means of biochemical techniques, arise because of sequence and local torsional stress, or supercoiling. Many of these structures are stabilized by the binding of highly charged metal ions, probably because the highly charged metal center in a small volume can neutralize the electrostatic repulsions between polyanionic strands that are bundled together. Metal complexes can furthermore be extremely useful in targeting and characterizing these structures, as we will see. In chromosomes the DNA is packaged by histone proteins into even tighter bundles, with helical segments wrapped about the basic proteins to form superhelical nucleosomal units which are then arranged like beads on a string of more loosely packed DNA.[9]

This complexity in DNA structure is in fact small compared to that of RNA. Figure 8.2C (see color plate section, page C-15) shows the first crystallographically characterized structure[5] of an RNA polymer, yeast $tRNA^{Phe}$. Ostensibly single-stranded RNAs do not exist as random coils, but instead fold up into well-defined three-dimensional structures, much like proteins. The structural variety, of course, bears some resemblance to that found in DNAs. Double-helical regions in the tRNA are A-like in conformation; helices fold together as one might imagine to occur in cruciforms, and even triple-helical segments are evident where three strands fold together in the polymer. But overall our ability to characterize structures of RNA thus far is lower than that with DNAs. RNAs are less stable in solution than is DNA, and fewer chemical as well as enzymatic tools are available for structural characterization. Yet the recent discovery of ribozymes,[10] the finding that RNAs can indeed catalyze nucleolytic reactions, makes our need to understand these structures even greater. Again transition-metal chemistry may participate in stabilizing, promoting, and probing these structures.

Fundamental Interactions with Nucleic Acids

Metal ions and complexes associate with DNA and RNA in a variety of ways, as illustrated in Figure 8.3. Both strong covalent interactions and weak noncovalent complexes are observed.[11] Each may yield a significant perturbation in the nucleic acid and/or may be exploited to obtain a site-specific response. Clearly there are some general guidelines, based on principles of coordination chemistry, that may be helpful in sorting out these interactions.

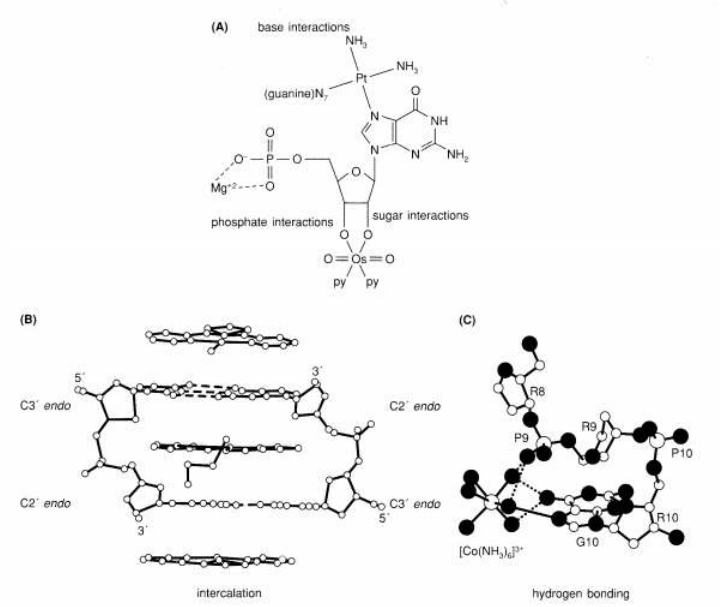


Figure 8.3 - Covalent and noncovalent binding modes of metal complexes with DNA. (A) Representative covalent interactions. Shown schematically are examples of coordination to the DNA base, sugar, and phosphate moieties given by the covalent binding of cis-(diammine)platinum to the N7 nitrogen atom of neighboring guanine residues, the formation of an osmate ester with ribose hydroxyl groups, and the primarily electrostatic association between $Mg(H_2O)_6^{2+}$ and the guanosine phosphate, respectively. (B) Noncovalent intercalative stacking of a metal complex. Shown is the crystal structure[20b] of (terpyridyl)(2-hydroxyethanethiolate)platinum(II) intercalated and stacked above and below the base-paired dinucleotide d(CpG). (C) An illustration of hydrogen bonding of coordinated ligands. Shown is a partial view of the crystal structure[19] of Z-form $d(CG)_3$ with $Co(NH_3)_6^{3+}$ hydrogen-bonded both to the guanine base (G10) and phosphate backbone (P9).

1. Coordination

Most prevalent among covalent complexes with DNA are those involving coordination between soft metal ions and nucleophilic positions on the bases. The structure[12] of *cis*-$(NH_3)_2$Pt-dGpG is an example: its platinum center coordinates to the N7 position of the guanine bases. In terms of interactions with the full polynucleotide, it is likely that the *cis*-diammineplatinum center, with two coordination sites available, would yield an intrastrand crosslink between neighboring guanine residues on a strand (see Chapter 9). Other nucleophilic sites targeted by soft metal ions on the bases include the N7 position of adenine, the N3 position on cytosine, and the deprotonated N3 position on thymine and uracil.[12,13] Some additional covalent binding to the N1 positions of the purines has also been observed. Indeed, coordination by the metal to one site on the heterocyclic base lowers the pK_a and increases the metal-binding affinity to secondary sites. It is noteworthy, however, that in base-paired double-helical DNA only the N7 positions on the purines are easily accessible in the major groove of the helix. Base binding at the purine N7 position is, of course, not limited to soft metal ions such as Pt(II), Pd(II), and Ru(II). Coordination at these sites has been evident also with first-row transition-metal ions such as Cu(II) and Zn(II).[13] For these, as is consistent with basic coordination chemistry, the lability of complexes formed is higher.

Transition-metal ions with decreasing softness are capable of coordinating also to the phosphate oxygen atoms. The ionic versus covalent character of these complexes clearly depends on the metal ions involved. In a classic study, examining the melting temperature of double-helical DNA in the presence of different metal ions and as a function of their concentration, Eichhorn and coworkers established the preference of the metal ions for base versus phosphate binding (Figure 8.4).[14] The preference for phosphate over base association was found to decrease in the order Mg(II) > Co(II) > Ni(II) > Mn(II) > Zn(II) > Cd(II) > Cu(II). This series arises from examination of DNA helix-melting temperatures, since base interactions in general should destabilize the helical form [except where interstrand crosslinking occurs, as may happen with Ag(I)], whereas phosphate coordination and neutralization would increase the helix stability and hence the melting temperature.

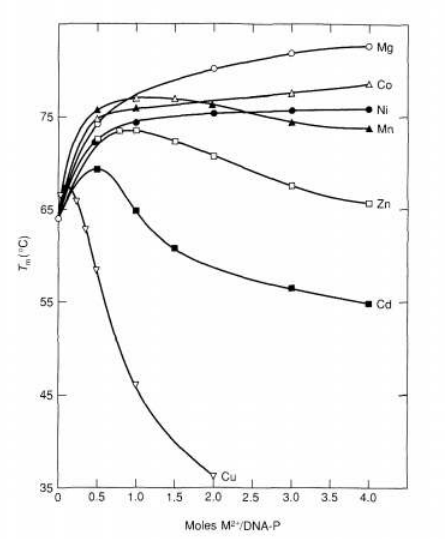


Figure 8.4 - The effects of various metal ions on the melting temperature (T_m) of calf thymus DNA.[14] Reproduced with permission from Reference 14.

Also of interest, but less common, are covalent interactions with the sugar moiety.[15,16] Although the pentose ring in general provides a poor ligand for metal ions, osmate esters can form quite easily across the C2'-C3' positions in ribose rings. This particular interaction has been suggested as a basis for heavymetal staining of RNA. In fact, OsO_4 is not restricted in its reactivity with the sugar positions. Cisoid osmate esters form as well upon reaction of OsO_4 across the electron-rich C5-C6 double bonds of accessible pyrimidines on DNA.

11.2.8.1: The Basics is shared under a CC BY-NC-SA 4.0 license and was authored, remixed, and/or curated by LibreTexts.

11.2.8.2: The Basics (Part 2)

2. Intercalation and Hydrogen Bonding

But important interactions of metal complexes with polynucleotides are not restricted to those involving direct coordination of the metal center to the polymer. Instead, an abundance of highly selective interactions arise from an ensemble of weaker noncovalent interactions between the ligands of coordinatively saturated metal complexes and the nucleic acid. Two primary examples of noncovalent association are given by metallointercalation and hydrogen-bonding interactions of coordinated ligands.[17,18] Planar aromatic heterocyclic ligands such as phenanthroline and terpyridine can stack in between the DNA base pairs, stabilized through dipole-dipole interactions. Here, depending on the complex and its extent of overlap with the base pairs, the free energy of stabilization can vary from ~2 to 10 kcal. Nonintercalative hydrophobic interactions of coordinated ligands in the DNA grooves also can occur, as we will see. Hydrogenbonding interactions of coordinated ligands with the polynucleotide are quite common, and arise in particular with the phosphate oxygen atoms on the backbone. With cobalt hexaammine, for example, hydrogen bonding to an oligonucleotide occurs between the ammine hydrogens and both phosphate oxygen atoms and purine bases.[19]

A mix of covalent and noncovalent interactions is also possible. With *cis*-diammineplatinum(II) coordinated to the guanine N7 position, the ammine ligands are well-poised for hydrogen-bonding interactions with the phosphate backbone.[12] The steric constraints on the molecule must be considered, however. With $Pt(terpy)CI^{+}$, both intercalation of the terpy ligand and direct coordination of the platinum center (after dissociation of the coordinated chloride) are available, but not simultaneously; coordination of the platinum to the base would likely position the terpyridyl ligand away from the base stack in the DNA major groove, precluding intercalation.[20] Sigel and coworkers[21] have studied the thermodynamics of noncovalent interactions coupled to direct coordination of simple first-row transition-metal complexes with mononucleotides, and these results illustrate well the interplay of weak noncovalent interactions and direct coordination in generating geometric specificity in complex formation.

Fundamental Reactions with Nucleic Acids

The reactions of transition-metal complexes with polynucleotides generally fall into two categories: (i) those involving a redox reaction of the metal complex that mediates oxidation of the nucleic acid; and (ii) those involving coordination of the metal center to the sugar-phosphate backbone so as to mediate hydrolysis of the polymer. Both redox and hydrolytic reactions of metal complexes with nucleic acids have been exploited with much success in the development of tools for molecular biology.

1. Redox Chemistry

The simplest redox reaction with polynucleotides one might consider as an illustration is the Fenton reaction, which indirectly promotes DNA strand scission through radical reactions on the sugar ring. The reaction with $Fe(EDTA)^{2-}$ is shown in Figure 8.5A. As do other redox-active divalent metal ions, ferrous ion, in the presence of hydrogen peroxide, generates hydroxyl radicals, and in the presence of a reductant such as mercaptoethanol, the hydroxyl radical production can be made catalytic. Although ferrous ion itself does not appear to interact appreciably with a nucleic acid, especially when chelated in an anionic EDTA complex and repelled by the nucleic-acid polyanion, the hydroxyl radicals, produced in appreciable quantities catalytically, attack different sites on the sugar ring, indirectly yielding scission of the sugar-phosphate backbone. One such reaction that has been characterized in some detail is that involving hydroxyl radical reaction at the C4' position, the position most accessible to the diffusible radical in the minor groove of the helix.[22] As illustrated in Figure 8.5B, the products of this reaction include a 5'-phosphate, a mixture of 3'-phosphate and phosphoglycolates, and a mixture of free bases and base propenalso Reactions of the hydroxyl radical at other sites on the sugar ring are now being identified as well by isotope-labeling studies. Comparable reactions with RNA have also been described.[23]

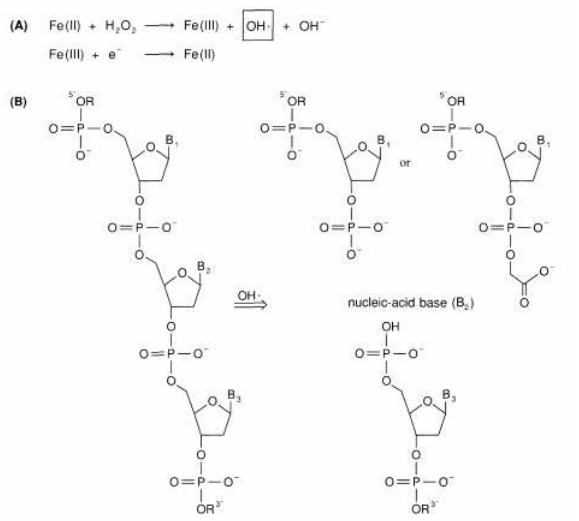


Figure 8.5 - An illustration of DNA strand cleavage mediated by hydroxyl radicals produced by the Fenton reaction (A) of $Fe(EDTA)^{2-}$ with hydrogen peroxide. The cleavage scheme (B) shows the products obtained as a result of initial C4'-H abstraction by the hydroxyl radicals.

The application of this Fenton chemistry to promote site-specific or sequence-neutral cleavage of DNA was first demonstrated[24] by Dervan and coworkers, and has provided the basis for the design of a tremendous range of new and valuable DNA cleavage agents. The development of this chemistry was originally based on modeling Fe-bleomycin, a natural product with antitumor and antibiotic activity, which binds and cleaves DNA.[25] The chemistry mediated by Fe-bleomycin, as we will discuss later, is likely to be far more complex, however, involving direct reaction of an intimately bound ferryI intermediate species with the nucleic acid, rather than net oxidation of the sugar mediated by a diffusing hydroxyl radical. Other metal ions such as Cu(Il) can also promote redox-mediated cleavage of DNA[26,27] through reactions on the sugar ring; whether the oxidizing radical is still coordinated to the metal or is a dissociated and diffusing species is a topic of much debate.[26]

Metal ions can also be used to generate other oxidizing intermediates in aerated aqueous solution, such as superoxide ion and singlet oxygen. DNA strand-cleavage reactions mediated by superoxide have not thus far been demonstrated, however. Singlet oxygen may be produced by photosensitization of $Ru(phen)_3^{2+}$, and indeed photolysis of $Ru(phen)_3^{2+}$ bound to DNA yields oxygen-dependent, alkaline-sensitive strand cleavage.[28,29] For singlet oxygen, the oxidation occurs on the nucleic-acid base rather than on the sugar ring. As such, the reaction varies with base composition; guanine residues are most reactive. Furthermore, since the primary lesion is that of a base modification, piperidine treatment, or other weakly basic conditions, are needed to convert the base lesion into a strand-scission event.

Another scheme for oxidative cleavage of DNA mediated by metal complexes involves formation of a coordinated ligand radical bound to the helix that directly abstracts a hydrogen atom from the sugar ring. The photoreaction of $Rh(phen)_2phi^{3+}$ (phi = 9,10-phenanthrenequinone diimine) exemplifies this strategy.[30] Here photolysis promotes a ligand-to-metal charge transfer with formation of a phi-centered radical. Isotope-labeling studies and product analysis have shown that this phi radical bound intercalatively in the major groove of DNA directly abstracts the C3'-H (which sits in the major groove of the helix);[31] subsequent hydroxylation or dioxygen addition at this position promotes DNA strand scission without base treatment. Some potent photooxidants can also produce outer-sphere electron transfer from the DNA. Here it is the guanine bases, likely those stacked with neighboring purines, that are most easily oxidized and hence most susceptible to attack. Again, this base modification requires alkaline treatment to convert the lesion to a strand breakage.[11b,17]The DNA double helix can furthermore also mediate electron-transfer reactions between bound metal complexes. The DNA polymer has, for example, been shown to catalyze photoinduced electron-transfer reactions between $Ru(phen)_3^{2+}$ and $Co(phen)_3^{3+}$ bound along the DNA strand.[32] Table 8.1 summarizes different redox reactions of metal complexes bound to DNA.

Table 8.1 - Examples of metal complexes that cleave DNA through redox chemistry.

a) DNA may be modified by attack either at the sugar or at the nucleotide base position.

b) The reactive species involved in DNA cleavage, if known.

c) Some reactive species are diffusible, producing broad patterns of DNA damage along the strand. Others are nondiffusible, resulting in cuts at single discrete sites.
d) The site of metal complex binding to DNA, if known.
e) The sites cleaved by the metal complex.
f) Not known.
* Indicates an excited-state reaction requiring photoactivation.

Complex	Target[a]	Chemistry[b]	Diffusibility[c]	DNA Binding[d]	Site Selectivity[e]
$Fe(EDTA)^{2-}$	sugar	OH•, Fenton	diffusible	none	none
MPE-Fe(II)	sugar (C4'-H)	OH•, Fenton	diffusible	sequence-neutral	none
$Co(NH_3)_6^{3+}$*	base	phtoelectron transfer	[f]	hydrogen-bonding	5'-G-pur-3'
$Cu(phen)_2$*	sugar	Cu^{2+}-OH•	slight	AT-rich	AT-rich
Mn-Porphyrin	sugar	M=O	none	AT-rich	At-rich
$U(O_2)(NO_3)_2$*	[f]	[f]	diffusible	[f]	none
$Ru(TMP)_3^{2+}$*	base	$^1O_2$	diffusible	A-form	A-form, G
$Ru(phen)_3^{2+}$*	base	$^1O_2$	diffusible	sequence-neutral	G
$Co(DIP)_3^{3+}$*	sugar	ligand radical	none	Z-form (non-B)	Z-form (non-B)
$Rh(DIP)_3^{3+}$*	sugar	ligand radical	none	Z, cruciforms	Z, cruciforms
$Rh(phen)_2phi^{3+}$*	sugar (C3'-H)	ligand radical	none	open major groove	5'-pyr-pyr-pur-3'
$Rh(phi)_2bpy^{3+}$*	sugar (C3'-H)	ligand radical	none	sequence-neutral	none

2. Hydrolytic Chemistry

Hydrolysis reactions of nucleic acids mediated by metal ions are important elements in natural enzymatic reactions; chemists would like to exploit them in the design of artificial restriction endonucleases.[33] Hydrolysis reactions of the phosphodiester linkage of polynucleotides appear preferable to redox-mediated cleavage reactions, since in the hydrolytic reaction all information is preserved. In redox cleavage by sugar oxidation, for example, both a sugar fragment and free nucleic-acid base are released from the polymer, and, in contrast to hydrolytic chemistry, the direct religation of the fragments becomes practically impossible.

Metal ions can be effective in promoting hydrolysis of the phosphodiester, since they can function as Lewis acids, polarizing the phosphorus-oxygen bond to facilitate bond breakage, and can also deliver the coordinated nucleophile to form the pentacoordinate phosphate intermediate. Figure 8.6 illustrates one crystallographically characterized model system developed by Sargeson and coworkers, where hydrolysis of a model phosphodiester was enhanced dramatically by taking advantage of both the acidic and the nucleophilic characteristics of the bound cobalt(III) species.[34] A whole series of model systems utilizing both cobalt and zinc ions has been designed to explore the hydrolytic reactions of simple phosphodiesters.[35] This strategy coupled to a DNA binding functionality has also been exploited, albeit inefficiently, in the hydrolytic cleavage of doublehelical DNA by $Ru(DIP)_2$Macro with Zn^{2+}, Cd^{2+}, or Pb^{2+} added *in situ*.[36] In this complex (see Figure 8.6), the central portion of the molecule, held together by the ruthenium(II), is responsible for DNA binding. Tethered onto the coordinatively saturated ruthenium complex are two diethylenetriamine functionalities (in the Macro ligand), however, and these serve to coordinate hydrolytically active metal ions such as Zn(II) and Co(II), which promote DNA hydrolysis once delivered to the sugar-phosphate backbone by the DNA-binding domain.

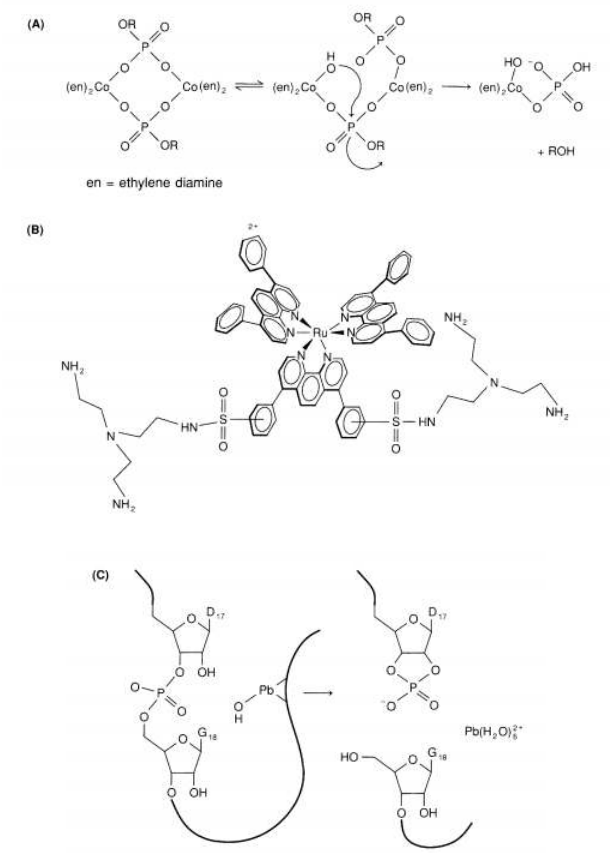


Figure 8.6 - Hydrolysis reactions catalyzed by metal ions and complexes. (A) Illustration of a phosphate ester hydrolysis in a binuclear model complex catalyzed by coordinated cobaltic ions, with one metal ion functioning as a Lewis acid and the other functioning to deliver the coordinated hydroxide.[34] (B) $Ru(DIP)_2Macro$, a metal complex constructed to contain a central DNA-binding domain ($Ru(DIP)_3^{2+}$) with two tethered amine arms to chelate additional metal ions (Zn^{2+}) to deliver to the sugar-phosphate backbone and promote hydrolytic strand cleavage.[36] (C) RNA site-specificially hydrolyzed by lead ion. Diagram of the proposed mechanism of sugar-phosphate backbone cleavage between residue D_{17} and G_{18} in yeast RNA^{Phe}.[38]

Perhaps simpler and certainly better understood are the hydrolytic reactions of RNAs mediated by metal ions. More than twenty years ago Eichhorn and coworkers showed that simple metal ions such as Zn(II) and Pb(II) promote the hydrolysis of RNA.[37] Figure 8.6 illustrates also the crystallographically characterized site-specific hydrolyis in tRNA by plumbous ion.[38] In tRNA, Pb(II) occupies three quite specific high-affinity binding sites, and at one of these sites, the metal ion becomes poised to promote strand cleavage. The crystal structure with bound Pb^{2+} suggests that the lead-coordinated hydroxide ion deprotonates the 2'-hydroxyl of one residue, so that the resulting 2'-oxygen nucleophile may attack the phosphate to give a pentavalent intermediate that decays to form the 2',3'-cyclic phosphate and, after reprotonation, the 5'-hydroxide. This very specific cleavage reaction is already being used by biologists as a tool in probing structures of mutant tRNAs, since the reaction is exquisitely sensitive to the stereochemical alignment of the nucleic-acid residues, phosphate backbone, and associated metal ion. In hydrolytic reactions on RNA, it is commonly considered, though certainly not established, that the job of the metal ion may be simpler than with DNA, since the ribose provides a nearby nucleophile already in the 2'-hydroxide. The reaction of tRNA with Pb(II) nonetheless illustrates how a metal ion may be utilized in promoting highly specific chemistry on a nucleic-acid polymer.

Last, it must be mentioned that metal coordination to the purine N7 position can also indirectly promote strand cleavage, although not through direct hydrolytic reaction on the sugar-phosphate backbone. Metal ions such as Pd^{2+} and Cu^{2+}, through coordination at N7, promote depurination. The depurinated site then becomes easily susceptible to hydrolysis upon treatment with mild base.

11.2.8.2: The Basics (Part 2) is shared under a CC BY-NC-SA 4.0 license and was authored, remixed, and/or curated by LibreTexts.

11.2.8.3: A Case Study- Tris(phenanthroline) Metal Complexes

Now we may examine in detail the interaction of one class of metal complexes with nucleic acids, how these complexes bind to polynucleotides, the techniques used to explore these binding interactions, and various applications of the complexes to probe biological structure and function. Tris(phenanthroline) metal complexes represent quite simple, well-defined examples of coordination complexes that associate with nucleic acids. Their examination should offer a useful illustration of the range of binding modes, reactivity, techniques for study, and applications that are currently being exploited and explored. In addition, we may contrast these interactions with those of other transition-metal complexes, both derivatives of the tris(phenanthroline) family and also some complexes that differ substantially in structure or reactivity.

Binding Interactions with DNA

Tris(phenanthroline) complexes of ruthenium(II), cobalt(III), and rhodium(III) are octahedral, substitutionally inert complexes, and as a result of this coordinative saturation the complexes bind to double-helical DNA through a mixture of noncovalent interactions. Tris(phenanthroline) metal complexes bind to the double helix both by intercalation in the major groove and through hydrophobic association in the minor groove.[11b,40] Intercalation and minor groove-binding are, in fact, the two most common modes of noncovalent association of small molecules with nucleic acids. In addition, as with other small molecules, a nonspecific electrostatic interaction between the cationic complexes and the DNA polyanion serves to stabilize association. Overall binding of the tris(phenanthroline) complexes to DNA is moderate (log K = 4).[41]

The extent of intercalative versus groove binding is seen to depend upon environmental conditions, such as temperature and ionic strength, the charge of the metal center, and the DNA base sequence; groove binding is favored at AT-rich sequences.[41] Second-generation mixed-ligand derivatives of the tris(phenanthroline) series have been prepared, and their interactions with DNA have provided useful insight into the factors important for promoting either intercalation or groove binding.[42] Aromatic heterocyclic ligands with increased surface areas that are planar bind DNA with increasing avidity through intercalation, irrespective of the charge on the metal center. Intercalative binding constants greater than 10^7 M^{-1} can be easily achieved with planar heterocyclic ligands that jut out from the metal center. Not surprisingly, complexes containing ligands of increasing hydrophobicity that are not planar favor minor-groove binding.[28]

Critically important as well in determining the binding mode is the chirality of the metal complex.[40] Intercalation into the right-handed helix favors the **Δ**-isomer, whereas groove binding favors the **Λ**-isomer. Figure 8.7 illustrates these symmetry-selective interactions. In intercalation, we consider that one phenanthroline inserts and stacks in between the base pairs, essentially perpendicular to the helix axis. For the **Δ**-isomer, once intercalated, the ancillary non-intercalated ligands are aligned along the right-handed groove of the helix. For the **Λ**-isomer, in contrast, with one ligand intercalated, the ancillary ligands are aligned in opposition to the right-handed groove, and steric interactions become evident between the phenanthroline hydrogen atoms and the phosphate oxygen atoms. Increasing the steric bulk on these phenanthrolines furthermore increases the enantioselective preference for intercalation of the **Δ**-isomer.[40,43] *For intercalation*, then, *the chiral discrimination depends on matching the symmetry of the metal complex to that of the DNA helix. For groove binding*, where the metal complex is thought to bind *against* the helix, instead *it is a complementary symmetry that is required*. In our model for groove binding of the tris(phenanthroline) metal complex, two phenanthroline ligands are likely bound against the right-handed helical groove, stabilized through hydrophobic association. For the **Λ**-isomer, bound in this fashion, the ligands lie against and complement the right-handed groove; with the **Δ**-isomer, the ligands oppose the groove, and no close surface contacts are made.

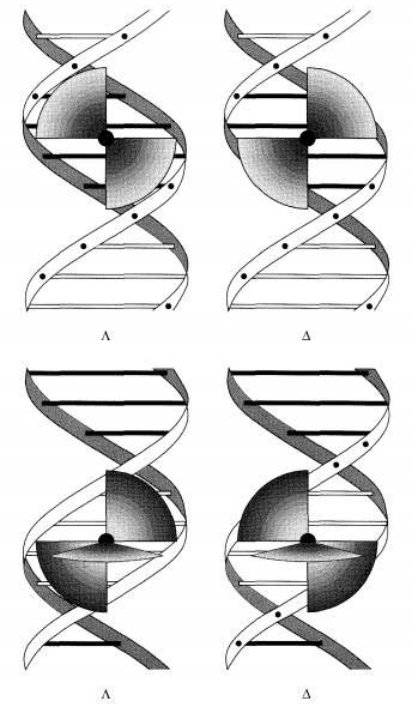


Figure 8.7 - Enantiomeric discrimination in binding to DNA. Shown above is the basis for the preference for **Δ**-Ru(phen)$_3^{2+}$ upon intercalation and **Λ**-Ru(phen)$_3^{2+}$ for surface binding against a right-handed helix. With intercalation (top) the symmetry of the metal complex matches the symmetry of the helix; steric interactions preclude a close association of the **Λ**-isomer. With groove binding (bottom), where the metal complex binds against the minor-groove helical surface, complementary symmetries are required, and it is the **Λ**-isomer that is preferred.

Intercalation of metal complexes in DNA is not uncommon. Lippard and coworkers first established metallointercalation by Pt(II) complexes in the 1970s.[18,20] Square-planar platinum(II) complexes containing the terpyridyl ligand were shown to intercalate into DNA. In an elegant series of x-ray diffraction experiments on DNA fibers, Lippard illustrated the requirement for planarity in the complex.[18,44] Although (phen)Pt(en)$^{2+}$ and (bpy)pt(en)$^{2+}$ were shown to intercalate into the helix, (pyr)$_2$Pt(en)$^{2+}$, with pyridine ligands rotated out of the coordination plane, could not. Complex planarity is in itself insufficient to promote intercalation, however. *Cis*-(NH$_3$)$_2$PtCI$_2$ or even *cis*-(NH$_3$)Pt(en)$^{2+}$ does not appear to intercalate into a helix, despite full planarity. Instead, aromatic heterocyclic ligands must be included in order to promote dipole-dipole interactions with the heterocyclic bases stacked in the helix. Indeed, planarity of the full complex is not required. Intercalation is not restricted to coordination complexes that are square planar. The tris(phenanthroline) complexes represented the first examples of "three-dimensional intercalators" and illustrated that octahedral metal complexes could also intercalate into the helix.[40,45,46] Here one can consider the partial intercalation of one ligand into the helix, providing the remaining ligands on the complex an opportunity to enhance specificity or reactivity at a given site.

Curiously, one unique and apparently general characteristic of metallointercalators is their preference for intercalation from the *major groove* of the helix. Most small molecules associate with DNA from the minor groove, but metallointercalators, both those that are square planar, such as (terpyridyl)platinum(II) complexes, and those that are octahedral, such as the tris(phenanthroline) metal complexes, appear to intercalate into the major groove. This then mimics quite well the association of much larger DNA-binding proteins with the helix; DNA regulatory proteins generally appear to target the major groove. The reason why metallointercalators favor major groove association is still unclear.

Transition-metal complexes with aromatic ligands also generally associate by minor-groove binding or through the mix of intercalative and groove-bound interactions. Cu(phen)$_2^+$, a tetrahedral complex, appears to favor minor-groove binding over intercalation.[26] Perhaps the tetrahedral coordination does not permit appreciable overlap of the phenanthroline ring with the bases in an intercalative mode. Metalloporphyrins, despite their large expanse and the presence commonly of nonplanar substituents, appear to bind to double-helical DNA both by intercalation and by minor-groove binding at AT-rich sequences.[47] Occupation of the porphyrins by transition-metal ions, such as Cu(II), which bind axial ligands, leads to the favoring of groove binding over intercalation. Figure 8.8 illustrates some of the complexes that bind DNA noncovalently.

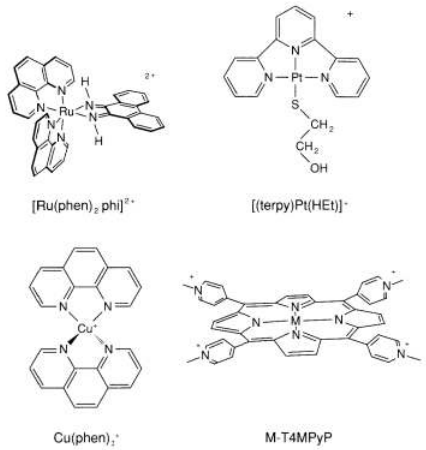


Figure 8.8 - Some metal complexes that bind DNA noncovalently primarily through intercalation (top) or binding in the minor groove (bottom). Some metalloporphyrins also primarily associate via intercalation.

The tris(phenanthroline) metal complexes themselves do not offer an illustration of hydrogen-bonding interactions with the helix, since these ligands lack hydrogen-bonding donors and acceptors, but as mentioned already, hydrogen bonding of coordinated ligands to the helix can add some measure of stabilization, comparable to, but likely no greater in magnitude than, that provided by intercalative stacking, hydrophobic, or dispersive interactions. Indeed, mixed-ligand derivatives of the phenanthroline complexes have been prepared that include hydrogen-bonding groups (amides, hydroxyls, and nitro substituents) on the ancillary phenanthroline ligands, and these have shown no greater avidity for double-helical DNA than their counterparts with hydrophobic substituents.[42] A large number of weak hydrogen-bonding interactions to DNA by one complex can be stabilizing, however, as with, for example, hexaamminecobalt(III) or hexaaquoterbium(III).

Tris(phenanthroline) metal complexes also do not offer an opportunity to explore covalent binding interactions with the helix in greater detail, but these interactions are, in fact, a major focus of Chapter 9, concerned with the mode of action of cisplatin. One derivative of the tris(phenanthroline) series, $Ru(phen)_2Cl_2$, has been shown to bind to DNA covalently.[48] In aqueous solution the dichlororuthenium(II) complex undergoes hydrolysis to form an equilibrium mixture of bis(phenanthroline) diaquo and chloroaquo species. These species bind covalently to DNA, with preferential reactivity at guanine sites. It is interesting that the same structural deformations in the DNA evident upon binding *cis*-diammineplatinum units become apparent upon coordination of bis(phenanthroline)ruthenium(II). It is also noteworthy that the chiral preference in coordination is for the **Λ**-isomer. As with groove binding, direct coordination to base positions requires a complementary symmetry, with the the **Λ**-isomer binding *against* the right-handed groove. This preference for the **Λ**-isomer reaffirms that, rather than noncovalent intercalation (which would favor the **Δ**-isomer), covalent binding dominates the interaction. The energetic stabilization in direct coordination of the ruthenium(II) center is certainly more substantial than the weaker stabilization derived from intercalation. $Rh(phen)_2Cl_2^+$ and its derivatives have also been shown to bind covalently to DNA but only upon photoactivation, since light is needed to promote dissociation of the coordinated chloride and substitution of the nucleic acid base as a ligand.[49]

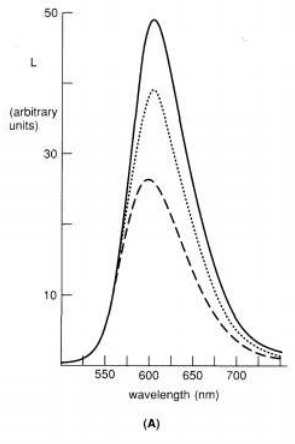
Techniques to Monitor Binding

Many of the same techniques employed in studying the basic chemistry of coordination complexes can be be used in following the binding of transition-metal complexes to nucleic acids, but biochemical methods, with their often exquisite sensitivity, become valuable aids as well in delineating specific binding interactions. Tris(phenanthroline) metal complexes are particularly useful to illustrate this point, since here the metal center in the complex is selected in terms of the technique used for examination.

Coordination complexes are often visibly colored, and these colorations provide a useful and sensitive spectroscopic handle in following fundamental reactions. This notion holds as well with tris(phenanthroline) metal complexes in their interactions with nucleic acids. $Ru(phen)_3^{2+}$ and its derivatives are highly colored because of an intense metal-to-ligand charge-transfer band (λ_{max} = 447 nm, ϵ = 1.9 x 10^4 $M^{-1}cm^{-1}$). Furthermore, the complexes are highly photoluminescent (λ_{em} = 610 nm, τ = 0.6 μs in aerated aqueous solution). On binding to nucleic acids these transitions are perturbed. Hypochromism is observed in the charge-transfer band, and intercalation leads to an increase in lifetime of the charge-transfer excited state.[43,46] Indeed, single-photon counting

experiments show a biexponential decay in emission from $Ru(phen)_3^{2+}$ bound to double-helical DNA. The longer-lived component (τ = 2 μs) has been assigned as the intercalated component and the shorter-lived 0.6 μs component has been attributed to a mixture of free and groove-bound species. These spectroscopic perturbations permit one to define equilibrium-binding affinities for the different components of the interaction as a function of metal-center chirality and under different solution conditions.[41] One can also follow the polarization of emitted light from the complexes after excitation with polarized light, and these studies have been helpful in describing the dynamics of association of the complexes on the helix.[41,43] Mixed-ligand complexes of ruthenium(II) show similar spectroscopic perturbations, and these have been used to characterize binding affinities and chiral preferences, as well as the extent of intercalation versus groove binding as a function of ligand substitution on the metal center.[42] The spectroscopic handle of the metal center therefore affords a range of experiments to monitor and characterize the binding of the metal complexes to polynucleotides.

Binding interactions of metal complexes with oligonucleotides can also be followed by NMR, and here as well the metal center offers some useful characteristics to exploit. As with organic DNA-binding molecules, shifts in the ^{1}H-NMR resonances of both the DNA-binding molecule and the oligonucleotide become apparent as a function of increased association with the helix. These shift variations can be used empirically to watch the dynamics of association and to gain some structural insights into the binding modes of the complexes on the helix. These kinds of experiments have been performed with tris(phenanthroline) complexes of ruthenium(II) and rhodium(III), where it was observed that the double-helical oligonucleotide is an exceedingly good chiralshift reagent to separate resonances in an enantiomeric mixture of the tris(phenanthroline) complexes.[50] For covalent binding molecules, such as *cis*-diammineplatinum(II), furthermore, the lowering of the pK_a of purine positions and therefore shifting of resonances as a function of coordination to an alternate site has been helpful as well in assigning the sites of covalent binding on the oligonucleotide.[51] But also in NMR experiments, special advantage can be taken of the metal center. For tris(phenanthroline) metal complexes, ^{1}H-NMR experiments[52] were performed on the paramagnetic analogues, $Ni(phen)_3^{2+}$ and $Cr(phen)_3^{3+}$. It was reasonable to assume the binding characteristics would be identical with their respective diamagnetic analogues, Ru(II) and Rh(III); yet paramagnetic broadening by the metal complexes of nearby resonances on the oligonucleotide would allow one to deduce where along the helix the complexes associate. Using this method the groove-binding interaction of the complexes was identified as occurring in the minor groove of the helix. Figure 8.9 illustrates the monitoring of DNA binding by tris(phenanthroline) metal complexes using both the luminescence characteristics of ruthenium(II) complexes and the paramagnetic characteristics of nickel(II).



https://chem.libretexts.org/@go/page/438080

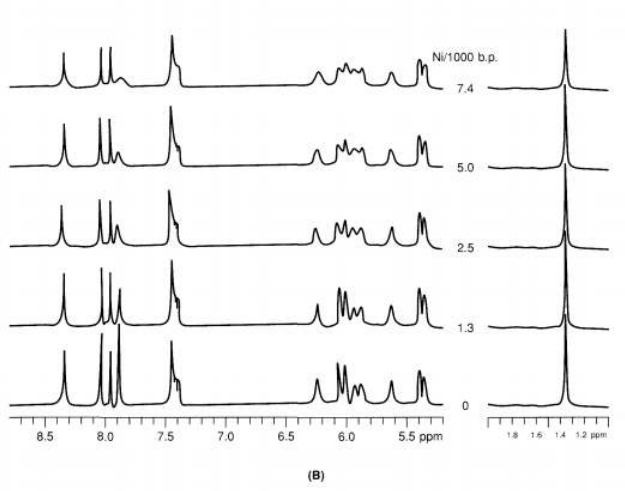


Figure 8.9 - An illustration of two spectroscopic techniques used to probe DNA. (A) The variation in luminescence characteristics of $Ru(phen)_3^{2+}$ with DNA binding. Shown is the emission spectrum of free $Ru(phen)_3^{2+}$ (----), *Λ-$Ru(phen)_3^{2+}$ in the presence of DNA* (• • • • •), *and* **Δ**-*$Ru(phen)_3^{2+}$ in the presence of DNA* (——) *illustrating the spectroscopic perturbation with DNA binding as well as the associated enantioselectivity in binding of the complexes to the helix. As is evident from the greater luminescence of the* **Δ** *isomer on binding, it is this* **Δ**-*isomer that intercalates preferentially into the right-handed helix. (B) An application of paramagnetic broadening by metal complexes in NMR experiments to obtain structural information on their association with nucleic acids. Shown is the ^{1}H-NMR spectrum of $d(GTGCAC)_2$ with increasing amounts of Λ-$Ni(phen)_3^{2+}$. Note the preferential broadening of the adenine AH2 resonance (7.8 ppm), indicating the association of this enantiomer in the minor groove of the helix.*

There are numerous other classic techniques of inorganic chemistry that have been or could be applied in studying the binding of metal complexes to nucleic acids. Coordination complexes have invariably been used in x-ray diffraction experiments because of the high electron density of the metal center. The tris(phenanthroline) metal complexes have not yet been applied in this context, but, as mentioned already, platinum metallointercalators were examined by fiber diffraction to delineate intercalation requirements. In fact, many nucleic-acid crystal structures have required specific metal ion additions for isomorphous heavy-metal derivatives to solve the structure. Such has certainly been true for the crystal structure of $tRNA^{Phe}$, where heavy-metal ions such as platinum, osmium, and mercury were targeted to specific base positions, and lanthanide ions were used to label phosphate positions around the periphery of the molecule.[53] Other techniques can also be exploited to monitor and characterize binding. A recent novel illustration is one from electrochemistry, which has been applied in monitoring the binding of $Co(phen)_3^{3+}$ to DNA.[54] Surely other techniques, from EXAFS to scanning tunneling microscopy, will be exploited in the future.

Biochemistry also provides very sensitive techniques that have been invaluable in characterizing interactions of metal complexes with nucleic acids. First are simply gel electrophoresis experiments, which permit an assessment of changes in the nucleic-acid conformation, through its changes in gel mobility, as a function of metal binding. A classic illustration is that of the unwinding of superhelical DNA as a function of intercalation. Closed circular DNA has much the same topological constraints on it as does a rope or a telephone cord; the DNA helices can wind up in coils. We define the duplex turning in a double helix as the secondary helical turns, and turns of the helices about one another as the supercoils or tertiary turns. As long as a DNA double helix is closed in a circle (form I), the total winding, that is, the total number of secondary and tertiary turns, is fixed. Molecules with differing extents of winding have different superhelical densities. In a circular molecule with one strand scission, what we call form II (nicked) DNA, the topological constraints are relaxed, and no supercoils are apparent. The same, by analogy, can be said of a telephone cord off the phone receiver, which can turn about itself to relax its many supercoils. Now let us consider a DNA unwinding experiment, monitored by gel electrophoresis. Supercoiled form I DNA can be distinguished from nicked DNA (form II) in an agarose gel because of their differing mobilities; the wound-up supercoiled molecule moves easily through the gelatinous matrix to the positive pole, whereas the nicked species is more floppy and thus is inhibited in its travels down the gel. A closed circular molecule with no net supercoils (form I_0) comigrates with the nicked species. Consider now the supercoiled molecule in the presence of an intercalator. Since the intercalator unwinds the DNA base pairs, the number of secondary helical turns in the DNA is reduced. In a negatively supercoiled, closed circular DNA molecule, the number of supercoils must be increased in a compensatory fashion (the total winding is fixed); hence the total number of negative supercoils is reduced, and the molecule runs with slower mobility through the gel. As the intercalator concentration is increased still further, the mobility of the supercoiled species decreases until no supercoils are left, and the species comigrates with the nicked form II DNA. Increasing the bound

intercalator concentration still further leads to the positive supercoiling of the DNA and an increase in mobility. Figure 8.10 illustrates the experiment with tris(phenanthroline)ruthenium(II) isomers.[46] This kind of unwinding experiment is an example of the sensitivity with which DNA structural changes can be monitored using biochemical methods; only low quantities (< μg) of materials are needed to observe these effects.

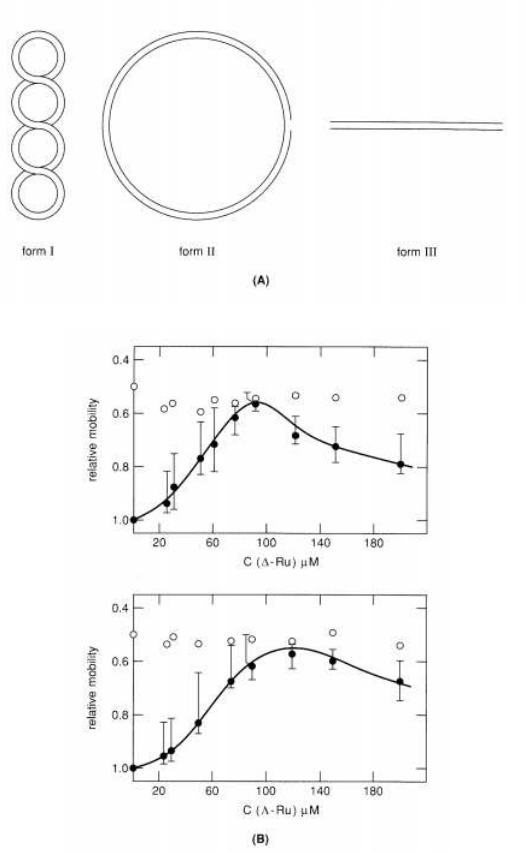


Figure 8.10 - The application of DNA supercoiling to probe metal-complex interactions with DNA. (A) A schematic representation of supercoiled DNA (form I), nicked DNA (form II) that, as a result of the single-strand scission, relaxes to a circular form lacking supercoils, and linear (form III) DNA. (B) Plots of the relative electrophoretic mobilities of form I (●) *and form II* (◯) *DNA as a function of increasing concentration of* **Δ**-*(top) and* **Λ**-*(bottom)* $Ru(phen)_3^{2+}$ *in the gel.*[46] *Increasing concentrations of bound intercalator unwind the negatively supercoiled DNA. Given the higher intercalative binding affinity of the* **Δ**-*isomer, slightly lower concentrations of this isomer are needed to unwind the plasmid to a totally relaxed state (where form I and II comigrate).*

DNA strand scission can also be sensitively monitored, and even more importantly the specific nucleotide position cleaved can be pinpointed by biochemical methods. This methodology has been applied successfully in monitoring both the efficiency of DNA strand scission by metal complexes and the specific sites cleaved, and hence where the complexes are specifically bound on the helical strand.

Relative extents of cleavage of DNA by different metal complexes can be easily assayed in an experiment that is an extension of the unwinding experiment described above. One simply measures the conversion of supercoiled form I DNA to nicked form II species. One strand cleavage on the DNA circle releases the topological constraints on the circular molecule and relaxes the supercoils. Two cleavage events within 12 base pairs on opposite strands will convert the DNA to a linear form (III), which also has a distinguishable gel mobility. Photoactivated cleavage of DNA by tris(phenanthroline) complexes of cobalt(lIl) and rhodium(III) was first demonstrated using this assay.[55,56] Given the high sensitivity of this assay, redox-mediated cleavage of DNA by a wide range of metal complexes can be easily demonstrated. However, other techniques are required to analyze whether appreciable and significant cleavage results, and, if so, what products are obtained. Since the assay can monitor, in a short time using little sample, a single nick in a full 4,000-base-pair plasmid, reactions of very low, almost insignificant yield can be detected. The assay provides, however, a simple scheme to assess *relative* extents of cleavage by different metal complexes, as well as a first indication that a cleavage reaction by a given metal complex occurs at all.

More informative are experiments on ^{32}P-labeled DNA fragments using high-resolution polyacrylamide gel electrophoresis, since these experiments allow one to find the exact nucleotide where the complexes break the sugar-phosphate backbone. Consider a cleavage reaction by a given metal complex on a DNA fragment of 100 base pairs in length that has been labeled enzymatically with ^{32}P on one end of one strand. If the metal complex cleaves the DNA at several different sites, then one can arrive at conditions where full cleavage is not obtained, but instead a population of molecules is generated where single cleavage events per strand are obtained, and cleavage at each of the sites is represented. After denaturation of the fragment, electrophoresis through a high-density polyacrylamide gel, and autoradiography, only fragments that are radioactively end-labeled are detected, and hence the population of sites cleaved is determined. The denatured cleaved fragments move through the gel according to their molecular weight. By measuring their length, using molecular-weight markers, one can find the specific position cleaved relative to the end of the fragment. By this route the specific sites cleaved by a molecule that binds and cleaves DNA, or end-labeled RNA, at unique positions may be identified. In a complementary experiment, using footprinting, where a molecule cleaves DNA nonspecifically at all sites along a fragment, one can find the binding positions of other molecules such as DNA-binding proteins. In this experiment, cleavage with the sequence-neutral cleaving reagent is carried out both in the presence and in the absence of the other binding molecule. In the absence of the protein, cleavage ideally occurs at all sites; hence a ladder of cleaved fragments is apparent on the autoradiograph. If cleavage is carried out in the presence of the protein, however, those sites that are bound by the protein are protected from cleavage by steric considerations, producing a shadow or footprint of the protein-binding site on the gel. Both the site-specific and footprinting experiments are illustrated schematically in Figure 8.11. This very powerful technology was first applied by Dervan and coworkers in demonstrating the application of methidium-propyl-FeEDTA (MPE-Fe) as a chemical footprinting reagent.[22,57] Tris(phenanthroline) metal complexes have been shown to cleave DNA nonspecifically, and their derivatives have been applied either as sensitive photofootprinting reagents, or as site-specific cleaving molecules, as we will see.

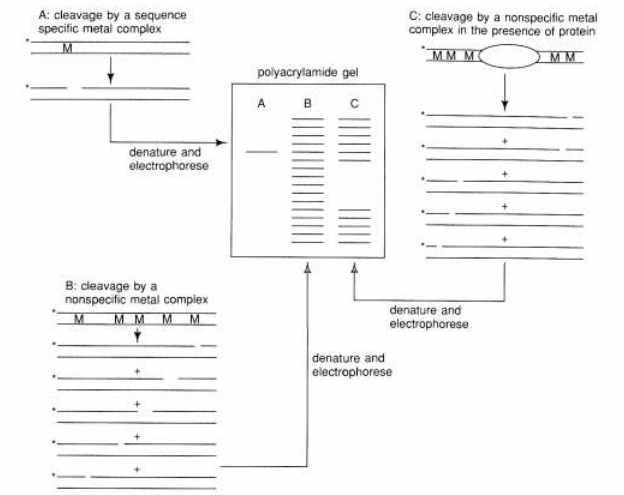


Figure 8.11 - DNA cleavage by metal complexes. Shown schematically is the method used with single-base resolution to discover the sites where metal complexes are bound on double helical DNA. After the metal complex is bound to several sites on a radioactively end-labeled (*) DNA fragment and activated to permit strand cleavage at the binding sites, the nicked DNA is denatured and electrophoresed on a high-resolution polyacrylamide gel, and the gel submitted to autoradiography. From the molecular weights of the end-labeled denatured fragments, the positions of cleavage and therefore binding by the metal complex may be deduced. The results in lane A show the cleavage pattern observed for a metal complex that binds to a specific site. The results in lane B show cleavage observed for a nonspecifically bound metal complex that binds and therefore cleaves at every base site. Lane C illustrates a footprinting experiment. When protein is bound to DNA at a specific site, it protects the DNA from cleavage by the metal complex at its binding site, thus producing a "footprint" in the gel: the absence of end-labeled fragments of those lengths that are protected from cleavage as a result of protein binding.

11.2.8.3: A Case Study- Tris(phenanthroline) Metal Complexes is shared under a CC BY-NC-SA 4.0 license and was authored, remixed, and/or curated by LibreTexts.

11.2.8.4: Applications of Different Metal Complexes that Bind Nucleic Acids

Both the spectroscopy and the chemical reactivity of transition-metal complexes, coupled to biochemical assays, can therefore be exploited to obtain a wide range of useful reagents to probe nucleic acids. Here some specific applications are described.

Spectroscopic Probes

As discussed previously, the tris(phenanthroline)ruthenium(II) complexes offer a novel spectroscopic probe of nucleic acids, since their luminescence is increased upon intercalation into the double helix. As a result the complexes provide a simple luminescent stain for DNA in fluorescent microscopy experiments. More interesting, perhaps, is the conformational selectivity of derivatives of tris(phenanthroline)ruthenium. $Ru(DIP)_3^{2+}$ (DIP = 4,7-diphenyl-1,10-phenanthroline) shows enantiospecificity in binding to B-form DNA.[40] Because of the steric bulk of the phenyl rings, detectable binding is seen only with the **Δ**-isomer in a righthanded helix; no binding is evident with the **Λ**-isomer. But with the left-handed Z-form helix, both isomers bind avidly.[40,58] The shallow left-handed major groove can accomodate the two enantiomers., A left-handed but more B-like helix shows selectivity instead for the **Λ**-isomer. Spectroscopic experiments that measure the chiral selectivity of $Ru(DIP)_3^{2+}$ isomers in binding to a given DNA then provide a novel probe for helical handedness. Indeed, **Λ**-$Ru(DIP)_3^{2+}$ was the first spectroscopic probe for Z-DNA (or other alternate conformations that are sufficiently unwound to permit binding by the bulky left-handed isomer).[58]

Another set of derivatives of the tris(phenanthroline) metal complexes that may become exceedingly useful as spectroscopic probes are $Ru(bpy)_2dppz^{2+}$ and $Ru(phen)_2dppz^{2+}$ (dppz = dipyridophenazine).[59] In these complexes the metal-to-ligand charge transfer is preferentially to the electron-accepting dppz ligand. In nonaqueous solutions, the complexes luminesce. However, in aqueous solution at pH 7, no luminescence is observed, likely because hydrogen bonding by water to the phenazine nitrogen atoms quenches the charge-transfer excited state. But the dppz ligand is also an expansive, aromatic heterocyclic ligand, and as a result both $Ru(bpy)_2dppz^{2+}$ and $Ru(phen)_2dppz^{2+}$ bind avidly to DNA by intercalation. Once intercalated, the phenazine ligand is protected from water. Therefore these complexes are luminescent when intercalated into DNA, whereas no luminescence is apparent from the complexes in the absence of DNA in aqueous solution. The enhancement factor is > 10^4 with DNA. One might consider the ruthenium complexes as true "molecular light switches" for DNA.

Both simpler bipyridyl and phenanthroline derivatives as well as dppz complexes of ruthenium are currently being tethered onto other DNA binding moieties, in particular onto oligonucleotides, so as to develop new, nonradioactive luminescent probes for DNA sequences. These transition-metal complexes may provide the basis for the development of new families of DNA diagnostic agents, and many industrial laboratories are currently exploring routes to accomplish these goals. Figure 8.12 illustrates **Λ**-$Ru(DIP)3^{2+}$ and $Ru(bpy)_2dppz^{2+}$, two complexes whose luminescence properties can be employed to probe nucleic acids.

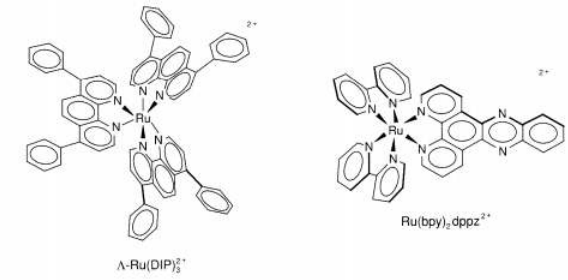


Figure 8.12 - Two spectroscopic probes of nucleic acids: **Λ**-$Ru(DIP)_3^{2+}$ and $Ru(bpy)_2dppz^{2+}$.

Other transition-metal complexes besides those of ruthenium have shown some promise in spectroscopic applications with nucleic acids. Lanthanide ions have been applied both in NMR experiments and in luminescence experiments to probe tRNAs, and more recently with synthetic DNAs of differing sequence and structure.[60] Lanthanide ions have been exceedingly useful in probing Ca^{2+} binding sites in proteins, and one would hope that a parallel utility would be achieved with nucleic acids. Their poor absorptivity have made luminescent experiments difficult, however, requiring relatively high concentrations of material. Nonetheless, the sensitivity of luminescent lifetimes to coordination and indeed solvation is providing a novel spectroscopic handle to explore binding sites and structures of the macromolecules. Another quite novel luminescent handle has been phenanthroline and diphenylphenanthroline complexes of copper(I).[61] These complexes are extremely valuable cleavage probes, as we will see later; to characterize better their interactions with the helix, luminescence experiments are being explored. A problem here has been the

nonphysiological conditions necessary to achieve detectable luminescence. Nonetheless, studies with the copper complexes demonstrate how the whole range of transition-metal chemistry and spectroscopy is beginning to be applied in sorting through nucleic-acid interactions.

Metallofootprinting Reagents

Probably the most widespread application of metal nucleic-acid chemistry in the biology community has been the utilization of metal complexes for chemical footprinting. The footprinting technique (Figure 8.11) was developed by biologists[62] as a means of locating protein-binding sites on DNA. ^{32}P-end-labeled double-stranded DNA fragments could be digested with a nuclease, such as DNAse, in the presence or absence of DNA-binding protein. After electrophoresis of the denatured digests and autoradiography, one would find a "footprint," that is, the inhibition of cleavage by DNAse, at the spot bound by protein, in comparison to a randomly cleaved pattern found on the DNA in the absence of binding protein. Although DNAse is still widely used, this footprinting reagent has some disadvantages: (i) the nuclease is not sequence-neutral in its cleavage, resulting in lots of noise in the footprinting background; and (ii) since the nuclease is itself a large protein, its ability to provide high-resolution footprinting patterns of smaller molecules is quite limited.

Several metal complexes now serve as high-resolution, sequence-neutral chemical footprinting reagents. Some of these reagents are shown in Figure 8.13. The first, as mentioned previously, was MPE-Fe(II).[57] The complex cotains a sequence-neutral DNA binding moiety, the intercalator methidium, and a tethered DNA redox cleaving moiety, Fe(EDTA). The methidium, in binding nonspecifically to DNA, delivers the hydroxyl radicals, generated via Fenton chemistry at the Fe(II) center in the presence of peroxide and a reducing agent, to the DNA backbone in a random manner. Since the complex is small, high resolution can be achieved. Indeed, MPE-Fe(II) has been shown to footprint small natural products that bind to DNA, in addition to footprinting much larger DNA-binding peptides and proteins.

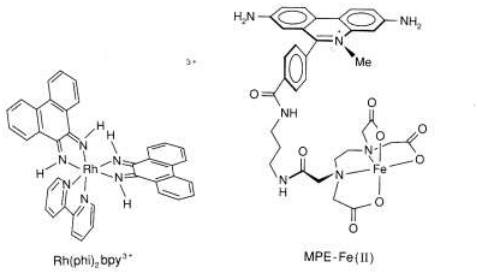


Figure 8.13 - Examples of metallofootprinting reagents. $Rh(phi)_2bpy^{3+}$, a photofootprinting intercalator, and MPE-Fe(II), a sequence-neutral intercalating agent.

Perhaps simpler still and now very widely used as a footprinting reagent is $Fe(EDTA)^{2-}$ itself.[63] The concept here is that $Fe(EDTA)^{2-}$, as a dianion, is unlikely to associate at all with the DNA polyanion. Hence hydroxyl radicals, generated via Fenton chemistry at a distance from the helix, would likely diffuse to the helix with a uniform concentration along the helix and provide a completely sequence-neutral pattern of cleavage. Tullius and coworkers have demonstrated[63] this to be the case. The resolution is furthermore extremely high since the hydroxyl radical is sufficiently small that it can even diffuse within the DNA-binding protein to delineate binding domains. Some difficulties are found, however, with the high concentrations of activating reagents needed to activate a cleavage reagent that *does not* bind to the helix, and problems of course arise in trying to footprint metalloproteins. Nonetheless, $Fe(EDTA)^{2-}$, a reagent easily found on the biologist's shelf, is now finding great utility in labs as a chemical substitute for DNAse.

Other transition-metal complexes are also finding applications in chemical footprinting. Both $Cu(phen)_2^+$ and manganese porphyrins have been used to footprint DNA-binding proteins.[64,65] These complexes likely cleave DNA through either Fenton chemistry or direct reaction of a coordinated metal-oxo intermediate with the sugar-phosphate backbone. The complexes, however, appear to bind DNA predominantly along the surface of the DNA minor groove, and with some preference for AT-rich regions. The patterns obtained are actually quite similar to those found with DNAse, and thus the lack of high sequence neutrality is somewhat limiting. Furthermore, the complexes are most sensitive to binding moieties in the minor groove, rather than those in the major groove, where proteins bind. Intercalators such as MPE-Fe(II) can sense binding species in both grooves. $Cu(phen)_2^+$ has nonetheless proved to be quite effective in detecting hyperreactivities in the minor groove, owing to DNA structural perturbations

that arise from protein binding in the major groove. Whether this sensitivity emanates from the intimate interaction of $Cu(phen)_2^+$ in the minor groove of the helix, or because of the characteristics of the reactive radical formed, is not known.

Inorganic photochemistry has also been applied in developing metal complexes as photofootprinting reagents. Uranyl acetate, for example, at high concentrations, upon photolysis, promotes DNA cleavage.[66] It is thought that the ions interact with the phosphates, generating some excited-state radical chemistry, although no detailed characterization of this chemistry has been undertaken. The cleavage reaction is nonetheless remarkably sequence-neutral and therefore shows some promise for photofootprinting applications. In fact, the applicability of uranyl acetate typifies how simple coordination chemistry and now even photochemistry may be helpful in the design of a variety of reagents that interact and cleave DNA, both nonspecifically and specifically. The biochemical techniques used to monitor such processes are sufficiently sensitive that even quite inefficient reactions in solution can be harnessed in developing useful reagents. The better our understanding of the chemistry of the coordination complex, the more effectively it may be utilized.

The best derivative of a tris(phenanthroline) metal complex currently being applied in footprinting experiments is $Rh(phi)_2bpy^{3+}$, a second-generation derivative of the tris(phenanthroline) series[67] that binds DNA avidly by intercalation and in the presence of light promotes direct strand cleavage by hydrogenatom abstraction at the C3'-position on the sugar.[31] Since no diffusing intermediate is involved in this photocleavage reaction, the resolution of the footprinting pattern is to a single nucleotide. Here the excited-state transition-metal chemistry involves a ligand-to-metal charge transfer, producing a phi cation radical that directly abstracts the hydrogen from the sugar at the intercalated site. The high efficiency of this photoreaction and high sequence-neutral binding of the complex to double-stranded DNA add to the utility of this reagent in footprinting studies. Indeed, both DNA-binding proteins, bound in the major groove, and small natural products, associated with the minor groove, have been footprinted with $Rh(phi)_2bpy^{3+}$ to precisely that size expected based upon crystallographic results. One may hope that this and other photofootprinting reagents will soon find applications for footprinting experiments *in vivo*.

11.2.8.4: Applications of Different Metal Complexes that Bind Nucleic Acids is shared under a CC BY-NC-SA 4.0 license and was authored, remixed, and/or curated by LibreTexts.

11.2.8.5: Applications of Different Metal Complexes that Bind Nucleic Acids (Part 2)

Conformational Probes

Metal complexes are also finding wide application in probing the local variations in conformation that arise along nucleic-acid polymers. X-ray crystallography has been critical in establishing the basic conformational families of double-helical DNA, and to some extent how conformations might vary as a function of nucleic-acid sequence. Yet many conformations have still not been described to high resolution, and only a few oligonucleotides have been crystallized. Other techniques are therefore required to bridge the small set of oligonucleotide crystal structures that point to plausible structures and the large array of structures that arise as a function of sequence on long helical polymers. Furthermore, only a very small number of RNA polymers has been characterized crystallographically; hence other chemical methods have been needed to describe the folding patterns in these important biopolymers. Metal complexes, mainly through specific noncovalent interactions, appear to be uniquely useful in probing the structural variations in nucleic acids.

1. Nonspecific Reactions of Transition-metal Complexes

Hydroxyl radical cleavage with $Fe(EDTA)^{2-}$ illustrates again how simple metal complexes can be used in characterizing nucleic acids. One example involves efforts to describe the local structural variations in "bent" DNA. Biochemists had found that DNA fragments containing runs of adenines, such as in the tract dAAAAAA, possessed unusual gel-electrophoretic mobilities. Indeed, kinetoplast DNA isolated from mitochondria of trypanosomes showed a remarkable lacework pattern of structure, with loops and circles of DNA; these structures were found to be governed by the placement of these $d(A)_6$ tracts. By constructing a series of oligonucleotides with adenine runs positioned either in or out of phase relative to one another, researchers found that the adenine tracts caused a local bending of the DNA toward the minor groove.[6] But what were the detailed characteristics of these bent sites? Using hydroxyl radical cleavage of DNA, generated with $Fe(EDTA)^{2-}$, Tullius and coworkers found a distinctive pattern of cleavage across the adenine tracts, consistent with a locally perturbed structure.[68]Here the notion again was that $Fe(EDTA)^{2-}$ in the presence of peroxide would generate hydroxyl radicals at a distance from the helix, and thus careful densitometric analysis of the cleavage across ^{32}P-end-Iabeled DNA fragments would reveal any differential accessibility of sugar residues to cleavage mediated by the radicals caused by the bending. The cleavage patterns suggested a smooth bending of the DNA across the tract and indicated furthermore an asymmetry in structure from the 5'- to 3'-end of the adenine run.

The reactivities of other transition-metal reagents have also been used advantageously in probing nucleic-acid structures. As described in Section II, OsO_4 reacts across the 5,6 position of accessible pyrimidines to form a *cis*-osmate ester. Upon treatment with piperidine, this base modification can yield scission of the sugar-phosphate backbone. Hence DNAs containing unusual local conformations with prominent solvent-accessible pyrimidines can be probed with OsO_4. The junction regions of Z-DNA, the single-stranded loops in cruciform structures, and a segment of the dangling third strand in H-DNA, have all been probed by means of the differential reactivity of osmium tetroxide with DNA sites dependent upon their accessibility.[7,8,16,69] Surely other transition-metal chemistry will become similarly applicable.

2. Transition-metal Complexes as Shape-selective Probes

Transition-metal complexes have also been designed with three-dimensional structures that target complementary structures along the helical polymer. This recognition of DNA sites, based upon *shape selection*, has proved to be extremely useful both in demarcating and in characterizing structural variations along the polymer and in developing an understanding of those factors important to the recognition of specific polynucleotide sites. Complexes, basically derivatives of the tris(phenanthroline) metal series, have been designed that specifically target A- and Z-form helices, cruciforms, and even subtle variations such as differential propeller twisting within B-form DNA.[11c] By appropriate substitution of the metal at the center of the coordinatively saturated complex, complexes that cleave the DNA at the binding site are obtained. Figure 8.14 shows some of these shape-selective conformational probes.

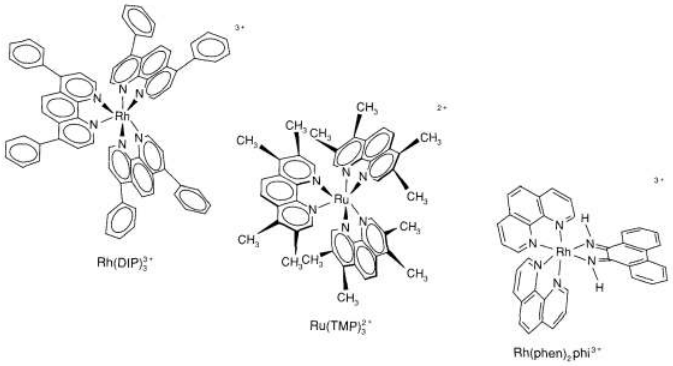


Figure 8.14 - Shape-selective probes that target local DNA conformations. Rh(DIP)$_2^{3+}$, which with photoactivation promotes double-stranded cleavage at cruciform sites; Ru(TMP)$_3^{2+}$, a photoactivated probe for A-like conformations; and Rh(phen)$_2$phi^{3+}, which targets openings in the DNA major groove.

One example of this shape-selective cleavage is apparent in reactions of Ru(TMP)$_3^{2+}$ (TMP = 3,4,7,8-tetramethylphenanthroline), a probe of the A-conformation.[28,29] The complex was designed by incorporating methyl groups about the periphery of each phenanthroline ligand to preclude intercalative binding of the complex to the helix, owing to the bulkiness of the methyl groups, and at the same time to promote hydrophobic groove binding, Importantly, however, this hydrophobic groove binding could not occur against the minor groove of B-DNA, given the width and depth of the groove versus the size of the complex. Instead, the shape of the complex was matched well to the shallow minor-groove surface of an A-form helix. Binding studies with synthetic polynucleotides of A, B, and Z-form were consistent with this scheme. Photolysis of the ruthenium complex, furthermore, as with Ru(phen)$_3^{2+}$, leads to the sensitization of singlet oxygen, and hence, after treatment with piperidine, to strand cleavage. Thus, photocleavage reactions with Ru(TMP)$_3^{2+}$ could be used to delineate A-like regions, with more shallow minor grooves, along a helical polymer. At such sites, Ru(TMP)$_3^{2+}$ would bind preferentially, and upon photolysis, generate *locally* higher concentrations of singlet oxygen to mediate cleavage of the sugar-phosphate backbone. This scheme revealed that homopyrirnidine stretches along the helix adopt a more A-like conformation.[29]

The targeting of altered conformations such as Z-DNA has been described earlier[58] in the context of a spectroscopic probe, A-Ru(DIP)$_3^{2+}$. Substitution of a photoredox-active metal into the core of the tris(diphenylphenanthroline) unit leads also to a complex that both binds and, with photoactivation, cleaves at the altered conformation.[55] Both Co(III) polypyridyl and Rh(III) polypyridyl complexes have been shown to be potent photooxidants. Coupled to site-specific DNA binding, these metal complexes, with photoactivation, become conformationally selective DNA cleavage agents. Co(DIP)$_3^{3+}$, for example, has been shown to cleave specifically at Z-form segments inserted into DNA plasmids.[55,70] Perhaps even more interesting, on both natural plasmids and viral DNAs, the various sites cleaved by Co(DIP)$_3^{3+}$, corresponding both to Z-form sites and to other locally altered non-B-conformations, coincide with functionally important regions of the genome, e.g., regulatory sites, gene termination sites, and intron-exon joints.[70,71] The altered structures recognized by the metal complexes, therefore, appear to mark biologically important sites, those presumably recognized also by cellular proteins. Cleavage studies with these metal complexes, therefore, are providing some insight also into how Nature specifically targets and accesses the sequence information encoded along the DNA polymer, sequence information encoded indirectly through local structure.

The most striking example of the specificity to be derived from shape-selective targeting has been given by the double-stranded cleavage induced by Rh(DIP)$_3^{3+}$ at cruciforms.[72] Rh(DIP)$_3^{3+}$, like its Co(III) and Ru(II) congeners, binds to locally unwound, non-B-conformations such as Z-DNA, but interestingly this potent photooxidant yields the specific cleavage of *both* DNA strands at cruciform sites. Lacking any crystallographic information, our understanding of the local structure of a cruciform is poor. In these palindromic sites, a torsionally strained DNA extrudes two intrastrand hydrogen-bonded helices from the main helix (see Figure 8.2B). Clearly the structure is grossly altered and locally unwound. Rh(DIP)$_3^{3+}$ appears to bind into a pocket generated by the folding of the extruded helix onto the main helix. The recognition is of this intricately folded structure, not of the sequence used to generate the cruciform. Studies with the transition-metal complex on different cruciforms should be useful in helping to characterize this interesting tertiary DNA structure.

Shape-selective transition-metal probes have also been useful in delineating more subtle variations in structure, such as the propeller twisting and tilting evident in B-form DNA.[30,73] Rh(phen)$_2$phi^{3+} was found to target preferentially sites in the major

groove where the DNA base pairs are more open; this preferential recognition arises from the steric constraints at more-closed intercalation sites because of the bulkiness of the ancillary phenanthroline ligands above and below the intercalation plane. Two straightforward structural perturbations that lead to an opening of the major groove involve the propeller twisting of bases with respect to one another and the tilting of base pairs along the helix. Chiral discrimination in cleavage by $Rh(phen)_2phi^{3+}$ is now being used quantitatively to discriminate among these structural parameters. The goal in these studies is to use cleavage results with the shape-selective metal complexes to describe the three-dimensional structure of a long double-helical DNA sequence in solution. Probing structurally well-defined sequences with a whole family of shape-selective metal complexes may provide a route to this goal.

As mentioned above, describing the three-dimensional structures of RNAs is an even more complicated task than it is for double-stranded DNAs. Only a few tRNAs have been characterized crystallographically to high resolution, and for other larger RNA structures, such as 5S RNA, or any of the catalytic intervening-sequence RNAs, little is known about their folding characteristics. To understand the regulation and catalytic functions of these biopolymers, we need to develop chemical tools to explore these structures. Figure 8.15 shows the results of cleavage studies using the variety of transition-metal probes on $tRNA^{Phe}$. Hydroxyl-radical cleavage mediated by $Fe(EDTA)^{2-}$ reveals the protection of solvent-inaccessible regions, the "inside" of the molecule.[23] MPE-Fe(II) appears to demarcate the double-helical regions,[74] $Cu(phen)_2^{+}$ shows the loopedout single-stranded segments,[75] and $Rh(phen)_2phi^{3+}$ seems to delineate those regions involved in triple-base interactions, the sites of tertiary folding.[76] Taken together, the full structure of the tRNA can be described based upon cleavage data with transition-metal complexes. It therefore seems as if this full family of coordination complexes might be generally useful in delineating RNA structures. Still more work is needed quantitatively to compare the patterns obtained with the few well-characterized structures. Nonetheless, an important role for these and possibly other transition-metal reagents is indicated.

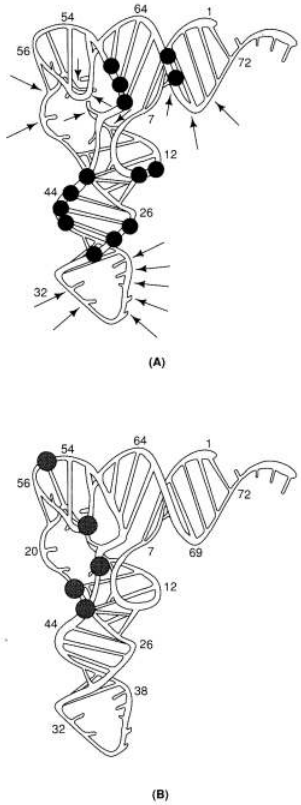


Figure 8.15 - The diversity of cleavage sites for metal complexes on $tRNA^{Phe}$. In (A) is shown cleavage by probes that primarily detect features of RNA secondary structure. $Cu(phen)_2^{+}$ (arrows), detecting single-stranded regions and MPE-Fe(II) (black dots), detecting double-helical segments. In (B) are shown probes that detect protected or more complex structures on tRNA. Inaccessible sites protected from OH• after treatment with $Fe(EDTA)^{2-}$ are shown as shaded portions of the molecule, and specific cleavage by $Rh(phen)_2(phi)^{3+}$ at tertiary folds is indicated by the circles.[11b]

Other Novel Techniques

Transition-metal ions can also be used advantageously tethered onto peptides, proteins, oligonucleotides, and other natural products, to provide a chemical probe for their binding interactions with nucleic acids. This strategy, termed *affinity cleavage*, was developed by Dervan and coworkers in preparing and characterizing distamycin-Fe(II)EDTA.[24] Distamycin is a known natural product that binds in the minor groove of DNA at AT-rich sequences. By tethering Fe(II)EDTA onto distamycin, the researchers converted the DNA-binding moiety into a DNA-cleaving moiety, since, as with MPE-Fe(1I), in the presence of peroxide and a reductant, hydroxyl radical chemistry would be delivered to the distamycin binding site. Unlike MPE-Fe(II), however, the distamycin moiety shows preferential binding at some sites along the polymer, and hence only at those sites would the local hydroxyl-radical concentration be increased and cleavage be obtained. As a result the tethered $Fe(EDTA)^{2-}$ could be used as a cleavage probe, marking sites of specific binding.

Affinity cleaving has been generalized so that now $Fe(EDTA)^{2-}$ can be tethered onto both oligonucleotides and peptides to follow their interactions with nucleic acids. The sequence-specific binding of oligonucleotides to double-helical DNA through triple-helix formation is but one of many examples where the tethering of $Fe(EDTA)^{2-}$ has been applied advantageously.[77]

Other redox-active metals can be incorporated into DNA-binding moieties as well. Schemes have been developed to functionalize accessible lysine residues on DNA-binding repressor proteins with phenanthrolines, so that in the presence of copper ion, peroxide, and a reductant, the phenanthroline-bound copper on the protein would induce DNA strand cleavage. Through this scheme, again the conversion of a DNA-binding moiety into a cleaving moiety by incorporation of a redox-active metal, the specific binding sites of repressor proteins can be readily identified (far more quickly on large DNA than through footprinting).[78]

Another scheme, which perhaps takes advantage more directly of bioinorganic chemistry, involves engineering redox metal-binding sites into DNA-binding proteins and peptides. The DNA-binding domain of the protein Hin recombinase was synthesized chemically, and first, to examine the folding of the peptide on the DNA helix, EDTA was tethered onto the peptide for Fe(II) cleavage experiments.[79] But as is illustrated repeatedly in these chapters, Nature has already provided amino-acid residues for the chelation of metal ions into proteins. Thus the DNA-binding domain of Hin recombinase was synthesized again, now including at its terminus the residues Gly-Gly-His, a known chelating moiety for copper(II).[80] This chemically synthesized peptide, with now both DNA-binding and DNA-cleaving domains, as illustrated in Figure 8.16, specifically promotes cleavage at the Hin recombinase binding site in the presence of bound copper and ascorbate. Interestingly, the addition of nickel(II) also leads to specific strand cleavage, without diffusible intermediates. Using this approach, taking advantage of the chelating abilities of amino acids and the cleaving abilities of different metal ions, one may prepare new synthetic, functional metalloproteins that bind and react with DNA.

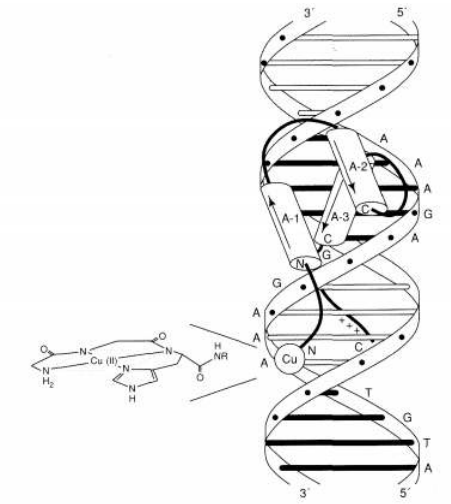


Figure 8.16 - A schematic of a synthetic DNA-cleaving peptide bound to DNA that was constructed by synthesis of the DNA-binding domain of Hin Recombinase with Gly-Gly-His at the N-terminus to coordinate copper.[80] Reproduced with permission from Reference 80.

11.2.8.5: Applications of Different Metal Complexes that Bind Nucleic Acids (Part 2) is shared under a CC BY-NC-SA 4.0 license and was authored, remixed, and/or curated by LibreTexts.

https://chem.libretexts.org/@go/page/438082

11.2.8.6: Nature's Use of Metal/Nucleic-acid Interactions

In the context of what we understand about the fundamental interactions and reactions of metal ions and complexes with nucleic acids, and also in comparison to how chemists have been exploiting these interactions in probing nucleic acids, we can also consider how Nature has taken advantage of metal ions in the construction of metalloproteins, nucleic-acid assemblies, and smaller natural products containing metal ions that interact with DNA and RNA.

A Structural Role

One of the chief functions attributed to metal ions in biological systems is their ability to provide a structural center to direct the folding of a protein. Just as shape-selective recognition has been helpful in targeting metal complexes to specific sites on DNA, it appears that one element of the recognition of sites by DNA regulatory proteins may also involve the recognition of complementary shapes. Furthermore, metal ions appear to be used in these proteins to define the shape or folding pattern of the peptide domain that interacts specifically with the nucleic acid.

The DNA-binding metalloproteins that have received the greatest attention recently have been the "zinc-finger" regulatory proteins. It was discovered in 1983 that zinc ions played a role in the functioning of the nucleic acid-binding transcription factor IlIA (TFIIIA) from *Xenopus laevis*, which binds specifically both DNA, the internal control region of the 5S rRNA gene, and RNA, the 5S RNA itself.[81] The protein (actually the 7S storage particle) was found to contain two to three equivalents of zinc ion. Dialysis removed both the associated zinc ions and the nucleic-acid-binding ability of the protein. Importantly, treatment with zinc ion, or in later studies with higher concentrations of Co^{2+}, restored the specific binding ability. Hence, zinc ion was shown to be functionally important in these eukaryotic regulatory proteins.

The notion of a "zinc-finger structural domain" was first provided by Klug and coworkers, after examination of the amino-acid sequence in TFIIIA.[82] It was found that TFIIIA contained nine imperfect repeats of a sequence of approximately 30 amino acids, and furthermore that each repeat contained two cysteine residues, two histidine residues, and three hydrophobic residues, in conserved positions. In addition, subsequent metal analyses were revealing higher zinc contents (7 to 11 equivalents) associated with the protein, and protein-digestion experiments indicated that several repeated structural domains existed in the protein. The two cysteine thiolates and two histidine imidazoles in each repeated domain could certainly serve to coordinate a zinc ion. Thus it was proposed that each peptide repeat formed an independent nucleic-acid-binding domain, stabilized in its folded structure through coordination of a zinc ion. The peptide unit was termed a "zinc finger," which is illustrated schematically in Figure 8.17. TFIIIA was therefore proposed to contain nine zinc fingers, which would cooperatively bind in the internal control region of the 5S RNA gene.

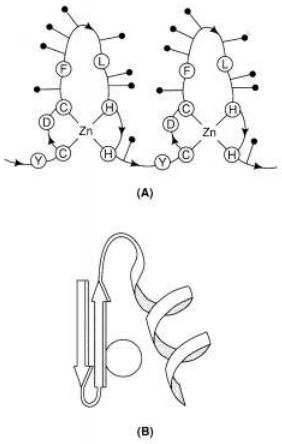


Figure 8.17 - (A) A schematic of a zinc-finger peptide domain.[82] (B) The proposed schematic structure of a zinc-finger domain based on comparisons to other structurally characterized metalloproteins.[85]

An enormous number of gene sequences from a variety of eukaryotic regulatory proteins was then found to encode strikingly similar amino-acid sequences,[83] and many were dubbed zinc-finger proteins. The bioinorganic chemist, however, should be aware that chemical analyses supporting such assignments are first required. Nonetheless, several legitimate examples of eukaryotic

nucleic-acid-binding zinc-finger proteins containing multiple zinc-binding peptide domains have emerged since the first study of TFIIIA, including the proteins Xfin from *Xenopus*, the Kruppel protein from *Drosophila*, the Sp1 transcription factor, and human testes-determining factor. It has therefore become clear that *the zinc-finger domain represents a ubiquitous structural motif for eukaryotic DNA-binding proteins.*[84]

What is the structure of a zinc finger, and how is this structure important for binding a specific nucleic-acid site? Based on a search of crystallographic databases for metalloproteins and an examination of the consensus sequence emerging for zinc fingers (that is, which residues were truly conserved and common to the different putative zinc fingers), Berg proposed a three-dimensional structure for a zinc finger, shown schematically in Figure 8.17.[85] The proposed structure included the tetrahedral coordination of zinc by the two cysteine and histidine residues at the base of the finger and an α-helical region running almost the length of the domain. EXAFS studies also supported the tetrahedral zinc site. Since this proposal, two detailed two-dimensional NMR studies have been reported that are consistent with the tetrahedral zinc coordination and the a-helical segment.[86] More recently, a crystal structure of a three-finger binding domain associated with an oligonucleotide was determined.[87] The zinc fingers lie in the major groove of DNA, the α-helical region being within the groove. Not surprisingly, given basic coordination chemistry, the zinc does not interact directly with the nucleic acid. Instead, the zinc ion must serve a structural role, defining the folding and three-dimensional structure of the protein scaffolding about it. This structure, defined by the metal at its center, like other coordination complexes, is able to recognize its complementary structure on the nucleicacid polymer.

It should also be noted that this zinc-finger structural motif is not the only metal-containing or even zinc-containing structural motif important in nucleic-acid-binding proteins.[88] A clearly different domain is evident in the protein GAL4, a transcription factor required for galactose utilization in *S. cerevisiae*.[88a] A recent crystal structure of the protein bound to an oligonucleotide shows the protein to bind to DNA as a dimer; each monomer contains a binuclear zinc cluster with two zinc ions tetrahedrally coordinated by six cysteines (two cysteines are bridging), not dissimilar from proposed structures in metallothionein. Still another structural motif is found in the glucocorticoid receptor DNA-binding domain. Crystallography[89] has revealed that this domain also binds DNA as a dimer; here each monomer contains two zinc-nucleated substructures of distinct conformation. The zinc ions are each tetrahedrally coordinated to four cysteine residues. Likely this too represents another structural motif for proteins that bind nucleic acids, and one again in which the metal serves a structural role.

Lastly, one might consider why zinc ion has been used by Nature in these nucleic-acid binding proteins. Certainly, the natural abundance of zinc is an important criterion. But also important is the absence of any redox activity associated with the metal ion, activity that could promote DNA damage [as with Fe(II) or Cu(II), for example]. In addition, other softer, heavier metal ions might bind preferentially to the DNA bases, promoting sequence-specific covalent interactions. Zinc ion, therefore, is clearly well-chosen for the structural center of these various nucleic-acid-binding proteins.

A Regulatory Role

Metalloregulatory proteins, like the transcription factors described above, affect the expression of genetic information through structural interactions that depend upon the metal ions, but unlike the zinc-finger proteins, metalloregulatory proteins act as triggers, repressing or activating transcription given the presence or absence of metal ion. In some respects, even more than zinc fingers, these systems resemble the Ca^{2+}-activated proteins described in Chapter 3.

Consider the biological system that must respond to changing intracellular metal concentrations. At high concentrations many metal ions become toxic to the cell; hence, a full system of proteins must be synthesized that will chelate and detoxify the bound-metal-ion pool. In order to actively engage these proteins, the genes that encode them must be rapidly transcribed. But at the same time, the DNA itself must be protected from the high concentrations of metal ion. Hence the need for these metalloregulatory proteins, which bind DNA in the absence of metal ion, usually repressing transcription, but in the presence of metal ion bind the metal ion tightly and specifically, and as a consequence amplify transcription.

Perhaps the best-characterized metalloregulatory system thus far is the MerR system, regulating mercury resistance in bacteria.[90] An inducible set of genes arranged in a single operon is under the control of the metal-sensing MerR protein, and it is this system that mediates mercury resistance. Mercury resistance depends upon the expression of these genes to import toxic Hg(lI), reduce Hg(II) to the volatile Hg(0) by NADPH, and often additionally to cleave organomercurials to their corresponding hydrocarbon and Hg(II) species. The MerR protein regulates mercury resistance both negatively and positively. As illustrated in Figure 8.18, MerR in the absence of Hg(II) binds tightly and sequence-specifically to the promoter. In so doing, MerR inhibits binding to the promoter

by RNA polymerase. When Hg^{2+} is added at low concentrations, the metal ion binds specifically and with high affinity to the DNA-bound MerR, and causes a DNA conformational change detectable by using other metal reagents as conformational probes. This conformational change now facilitates the binding of RNA polymerase and hence activates expression of the gene family.

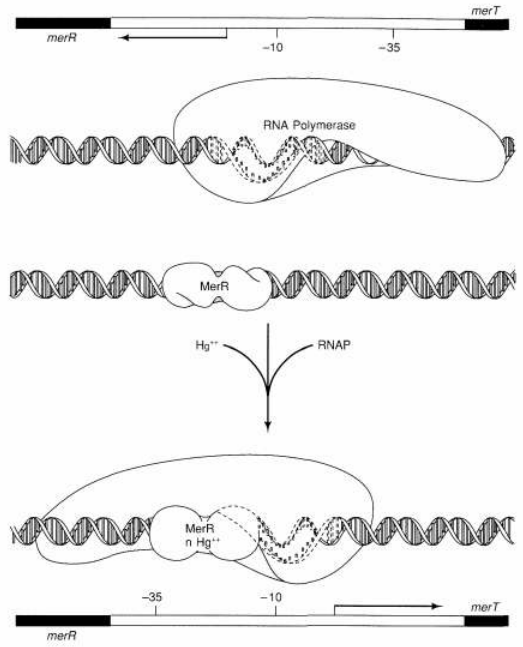


Figure 8.18 - A model for MerR metalloregulation.[90a] In the absence of MerR, RNA polymerase binds and transcribes the MerR promoter. In the presence of MerR, the preferential binding of MerR to the promoter is observed that inhibits transcription by the polymerase. The addition of Hg^{2+} then leads to a conformational change that promotes binding of the polymerase, substantially increasing transcription. Reproduced with permission from Reference 90a.

What are the structural requirements in the metal-binding site? Certainly one requirement is Hg(II) specificity, so that other metal ions will not also trigger transcriptional activation. Another is high metal-binding affinity to protect the DNA from direct coordination of the Hg(lI). The MerR protein is dimeric, and contains four cysteine residues per monomer. Site-directed mutagenesis studies[91] have indicated that three of these four cysteine residues are needed for Hg(II) binding, and EXAFS studies[92] have been consistent with tricoordinate ligation, clearly a well-designed system for Hg(II) specificity. Perhaps even more interesting, the site-directed mutagenesis studies[91] on heterodimers (a mixture of mutant and wild-type monomers) have indicated that the coordinated Hg(II) bridges the dimer, ligating two cysteines of one monomer and one cysteine of the other. This scheme may provide the basis also for the kinetic lability needed in a rapidly responsive cellular system.

Model systems are also being constructed to explore metal modulation of DNA binding. One system involves the assembly of two dipeptides linked by a central acyclic metal-binding polyether ligand, with $Fe(EDTA)^{2-}$ tethered to one end to mark site-specific binding.[93] In the presence of alkaline earth cations, which induce a conformational change that generates a central macrocycle, the linked peptides become oriented to promote sequence-specific binding in the minor groove. In the absence of the alkaline earth ion, no site-specific binding, or cleavage of DNA, is evident. One might consider this system as a simple, first-order synthetic model for the metalloregulatory proteins.

MerR is clearly only one natural metalloregulatory system. Other metal ions bind regulatory factors to mediate the regulation of gene expression in a metalspecific manner. Two examples include the Fe(II)-binding Fur protein from enteric bacteria[94] and the copper-binding protein ACE1/CUP2 from *S. cerevisiae*.[95] Both copper and iron are essential trace elements for which high concentrations are toxic; for nucleic acids this toxicity is certainly the result of redox-mediated strand damage. Other metal-specific regulatory systems are surely present as well. Both the MerR and the synthetic system may exemplify how these various systems function, how Nature might construct a ligand system to facilitate toxicmetal-specific binding in the presence of DNA that then alters or triggers how other moieties bind and access the nucleic acid.

A Pharmaceutical Role

With the exception of cisplatin (see Chapter 9), most pharmaceuticals currently being used as DNA-binding agents were first isolated as natural products from bacteria, fungi, plants, or other organisms. For the most part they represent complex organic moieties, including peptide and/or saccharide functionalities, and often a unique functionality, such as the ene-diyne in calichimycin. These natural products bind DNA quite avidly, through intercalation, groove binding, or a mixture thereof. Often the efficacy of these antitumor antibiotics stems from subsequent alkylation or DNA strand-cleavage reactions that damage the DNA.

Among the various natural products used clinically as antitumor antibiotics are bleomycins, a family of glycopeptide-derived species isolated from cultures of *Streptomyces*.[25,96] The structure of bleomycin A_2 is shown schematically in Figure 8.19. The molecular mode of action of these species clearly involves binding to DNA and the promotion of single-stranded cleavage at GT and GC sequences. Importantly, as demonstrated by Horwitz, Peisach, and coworkers, this DNA cleavage requires the presence of Fe(II) and oxygen.[97] Thus, one might consider Fe-bleomycin as a naturally occurring inorganic pharmaceutical.

What is the role of the metal ion in these reactions? As one might imagine, based upon our earlier discussions of metal-promoted DNA cleavage, the iron center is essential for the oxidative cleavage of the strand through reaction with the sugar moiety. The reaction of Fe(II)-bleomycin can, however, clearly be distinguished from the $Fe(EDTA)^{2-}$ reactions discussed earlier in that here no diffusible intermediate appears to be involved. Instead of generating hydroxyl radicals, the Fe center must be positioned near the sugar-phosphate backbone and activated in some fashion to promote strand scission *directly*.

Despite extensive studies, in fact little is known about how Fe(II)-bleomycin is oriented on the DNA. Indeed, the coordination about the metal is the subject of some debate. The structure of Cu(II)-P-3A,[98] a metallobleomycin derivative, is also shown in Figure 8.19. On the basis of this structure and substantive spectroscopic studies on Fe-bleomycin itself, it is likely that, as with Cu(II), in the Fe(II)-bleomycin complex the metal coordinates the β-hydroxyimidazole nitrogen, the secondary amine of β-aminoalanine, and the N1 nitrogen of the pyrimidine. Whether in addition the primary amines of the amino alanine and of the histidine coordinate the metal is still not settled. Possibly bithiazole coordination or some coordination of the sugar moieties is involved. Nonetheless, given five different coordination sites to the bleomycin, the sixth axial site is available for direct coordination of dioxygen. How is this Fe—O_2 complex oriented on the DNA? It is likely that at least in part the complex binds against the minor groove of the helix. There is some evidence that suggests that the bithiazole moiety intercalates in the helix. It is now becoming clear, however, that the structure of the metal complex itself, its three-dimensional shape, rather than simply the tethered bithiazole or saccharide, is needed for the sequence selectivity associated with its mode of action.

Although the coordination and orientation of the metal complex are still not understood, extensive studies have been conducted concerning the remarkable chemistry of this species.[96,99] The overall mechanism of action is described in Figure 8.19. In the presence of oxygen, the Fe(Il) O_2 species is formed and is likely rapidly converted to a ferric superoxide species. The one-electron reduction of this species, using either an organic reductant or another equivalent of Fe(II)-bleomycin, leads formally to an Fe(III)-peroxide, which then undergoes O—O bond scission to form what has been termed "activated bleomycin." This species might be best described as Fe(V)=O (or $[Fe\ O]^{3+}$). This species is comparable in many respects to activated cytochrome P-450 or perhaps even more closely to the Fe center in chloroperoxidase (see Chapter 5). Like these systems, activated bleomycin can also epoxidize olefins and can generally function as an oxo transferase. In contrast to these systems, Fe-bleomycin clearly lacks a heme. How this species can easily shuttle electrons in and out, forming and reacting through a high-valent intermediate, without either the porphyrin sink or another metal linked in some fashion, is difficult to understand. In fact, understanding this process, even independently of our fascination with how the reaction is exploited on a DNA helix, forms the focus of a substantial effort of bioinorganic chemists today.

What has been elucidated in great detail is the reaction of activated bleomycin with DNA. It has been established that the activated species promotes hydrogen abstraction of the C4'-H atom, which is positioned in the minor groove of the helix (Figure 8.19). Addition of another equivalent of dioxgen to this C4'-radical leads to degradation of the sugar to form a 5'-phosphate, a 3'-phosphoglycolate, and free base propenal. Alternatively, oxidation of the C4'-radical followed by hydroxylation in the absence of oxygen yields, after treatment with base, a 5'-phosphate, an oxidized sugar phosphate, and free base.

Other metals such as copper and cobalt can also activate bleomycins, although their mechanistic pathways for strand scission are clearly different from that of Fe(II)-bleomycin. Whether other natural products that bind DNA also chelate metal ions and exploit them for oxidative strand cleavage is not known, but several systems provide hints that they do. Furthermore, such a fact would not

be surprising given our understanding of the utility of metal ions in promoting this chemistry. An even more detailed understanding of this chemistry might lead to the development of second-generation synthetic transition-metal pharmaceuticals that specifically and efficiently target and cleave DNA sites.

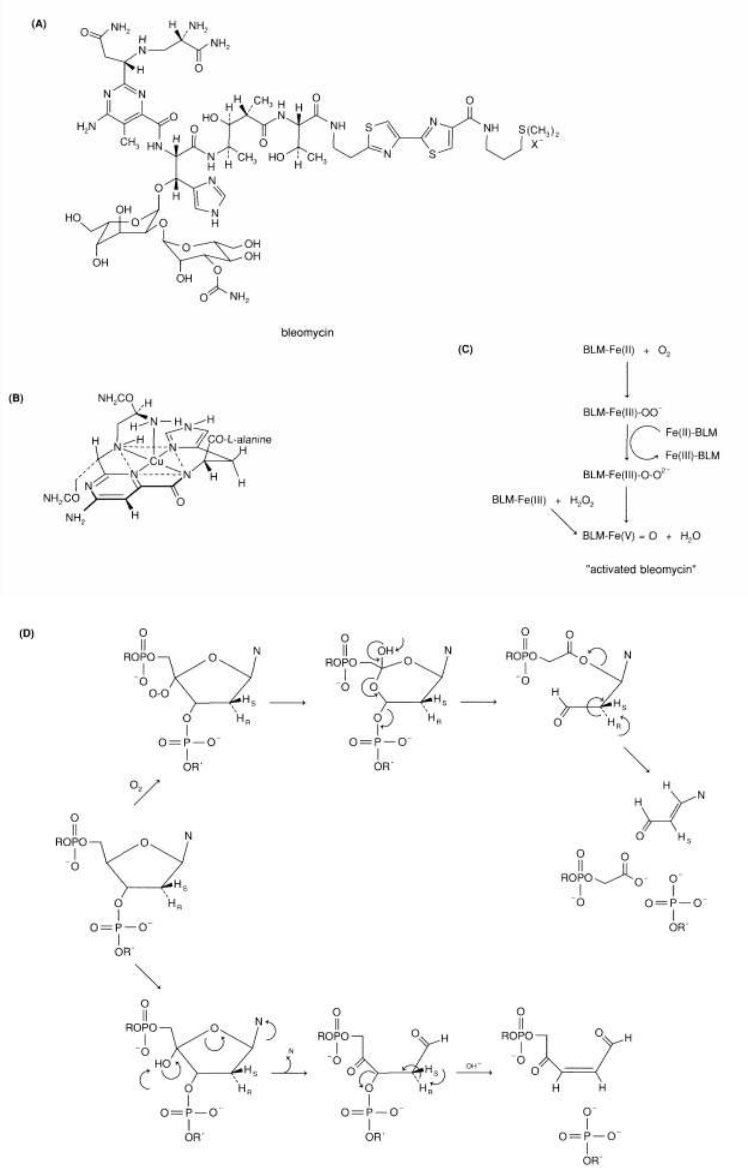


Figure 8.19 - (A) The structure of bleomycin A_2. (B) The crystallographically determined structure[98] of a copper derivative of bleomycin, P3A. (C) A scheme to generate "activated bleomycin." (D) The proposed mechanism of action of activated Fe-bleomycin.

A Catalytic Role

In addition to serving structural and modulating roles in proteins which bind nucleic acids, metal ions also appear to be essential to the functioning of various complex enzymes that act on nucleic acids. At this stage our understanding of the participation of the metal ion in the catalytic chemistry of these enzymes is somewhat sketchy, and we are relying more on our current understanding of the possible roles where metal ions may prove advantageous. These remain areas of biochemical focus where the inorganic chemist could make a major contribution.

For example, zinc ion appears to be essential to the functioning of both RNA polymerases and DNA topoisomerases.[100-102] These multisubunit enzymes perform quite complex tasks. RNA polymerase must bind site-specifically to its DNA template, bind its nucleotide and primer substrates, and form a new phosphodiester bond in elongating the growing RNA. Two zinc ions appear to be involved. One may be involved in orienting the nucleotide substrate, and the other structurally in template recognition. It would not

be surprising, however—indeed, it might be advantageous—if one or both metal ions also participated in the polymerization step. Our mechanistic understanding of how topoisomerases function is even more cursory. These complex enzymes bind supercoiled DNA, sequentially break one strand through hydrolytic chemistry, move the strand around the other (releasing one tertiary turn), and religate the strand. Again, the zinc ion might participate in the hydrolytic chemistry, the ligation step, or both; alternatively, the metal might again serve a structural role in recognition of the site of reaction.

We do have some understanding of the role of metal ions in several endonucleases and exonucleases. As discussed in Section II.C, metal ions may effectively promote phosphodiester hydrolysis either by serving as a Lewis acid or by delivering a coordinated nucleophile. Staphylococcal nuclease[103] is an extracellular nuclease of *Staphylococcus aureus* that can hydrolyze both DNA and RNA in the presence of Ca^{2+}. The preference of the enzyme is for single-stranded DNA, in which it attacks the 5'-position of the phosphodiester linkage, cleaving the 5'-P-O bond to yield a 5'-hydroxyl and 3'-phosphate terminus. Ca^{2+} ions are added as cofactors and are strictly required for activity. The structure of staphylococcal nuclease, determined by x-ray crystallography and crystallized in the presence of Ca^{2+} and the enzyme competitive inhibitor pdTp, as well as subsequent NMR and EPR studies on mutant enzymes using Mn^{2+} as a substitute for the Ca^{2+} ion, have provided the basis for a detailed structural analysis of the mechanism of this enzyme. In this phosphodiester hydrolysis, the metal ion appears to function primarily as an electrophilic catalyst, polarizing the P-O bond, and stabilizing through its positive charge the evolving negative charge on the phosphorus in the transition state. The base is thought here not to be directly coordinated to the metal; instead, action of a general base is invoked.

Metal ions also participate in the functioning of other nucleases, although the structural details of their participation are not nearly as established as those for staphylococcal nuclease. DNAse I also requires Ca^{2+} for its catalytic activity.[104] S1 endonuclease, mung bean nuclease, and *Physarum polycephalem* nuclease require zinc ion either as cofactors or intrinsically for nuclease activity, and the restriction enzyme EcoRI may also require intrinsically bound zinc ion.[33] In terms of how the zinc ion might function in these enzymes, one can look both to staphylococcal nuclease and to bacterial alkaline phosphatase[105] for some illustrations. One would expect that this metal ion could serve both as an electrophilic catalyst and also in the delivery of a zinc-coordinated hydroxide, as it does in alkaline phosphatase, directly attacking the phosphate ester. More work needs to be done to establish the mechanisms by which zinc ion promotes phosphodiester hydrolysis in these enzymatic systems.

Probably most intriguing and mysterious at this stage is the metal participation in the very complex DNA-repair enzyme endonuclease III from *E. coli* (similar enzymes have also been isolated from eukaryotic sources). This enzyme is involved in the repair of DNA damaged by oxidizing agents and UV irradiation, and acts through an N-glycosylase activity to remove the damaged base, and through an apurinic/apyrimidinic endonuclease activity to cleave the phosphodiester bond adjacent to the damaged site. Although more complex in terms of recognition characteristics, this enzyme functions in hydrolyzing the DNA phosphodiester backbone. What is so intriguing about this enzyme is that it contains a 4Fe-4S cluster (see Chapter 7) that is essential for its activity![106] We think generally that Fe-S clusters best serve as electron-transfer agents. In the context of this repair enzyme, the cluster may be carrying out both an oxidation and a reduction, to effect hydrolysis, or alternatively perhaps a completely new function for this metal cluster will emerge. (Fe-S clusters may represent yet another structural motif for DNA-binding proteins and one which has the potential for regulation by iron concentration.) Currently the basic biochemical and spectroscopic characterization of the enzyme is being carried out. Understanding this very novel interaction of a metal center and nucleic acid will require some new ideas, and certainly represents one new challenge for the bioinorganic chemist.

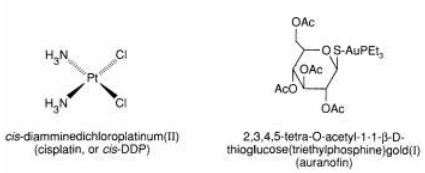
11.2.8.6: Nature's Use of Metal/Nucleic-acid Interactions is shared under a CC BY-NC-SA 4.0 license and was authored, remixed, and/or curated by LibreTexts.

11.2.9: Metals in Medicine

Metal ions are required for many critical functions in humans. Scarcity of some metal ions can lead to disease. Well-known examples include pernicious anemia resulting from iron deficiency, growth retardation arising from insufficient dietary zinc, and heart disease in infants owing to copper deficiency. The ability to recognize, to understand at the molecular level, and to treat diseases caused by inadequate metal-ion function constitutes an important aspect of medicinal bioinorganic chemistry.

Metal ions can also induce toxicity in humans, classic examples being heavy-metal poisons such as mercury and lead. Even essential metal ions can be toxic when present in excess; iron is a common household poison in the United States as a result of accidental ingestion, usually by children, of the dietary supplement ferrous sulfate. Understanding the biochemistry and molecular biology of natural detoxification mechanisms, and designing and applying ion-specific chelating agents to treat metal overloads, are two components of a second major aspect of the new science that is evolving at the interface of bioinorganic chemistry and medicine.

Less well known than the fact that metal ions are required in biology is their role as pharmaceuticals. Two major drugs based on metals that have no known natural biological function, Pt (cisplatin) and Au (auranofin), are widely used for the treatment of genitourinary and head and neck tumors and of rheumatoid arthritis, respectively. In addition, compounds of radioactive metal ions such as ^{99m}Tc and complexes of paramagnetic metals such as Gd(III) are now in widespread use as imaging agents for the diagnosis of disease. Many patients admitted overnight to a hospital in the U.S. will receive an injection of a ^{99m}Tc compound for radiodiagnostic purposes. Yet, despite the obvious success of metal complexes as diagnostic and chemotherapeutic agents, few pharmaceutical or chemical companies have serious in-house research programs that address these important bioinorganic aspects of medicine.



This chapter introduces three broad aspects of metals in medicine: nutritional requirements and diseases related thereto; the toxic effects of metals; and the use of metals for diagnosis and chemotherapy. Each area is discussed in survey form, with attention drawn to those problems for which substantial chemical information exists. Since there is only a primitive understanding at the molecular level of the underlying biochemical mechanisms for most of the topics, this field is an important frontier area of bioinorganic chemistry. The major focus of this chapter is on the platinum anticancer drug cisplatin, which is presented as a case study exemplifying the scope of the problem, the array of methodologies employed, and the progress that can be made in understanding the molecular basis of a single, if spectacular, metal complex used in medicine today.

II. Metal Deficiency and Disease[1]

A. Essential Metals

B. Anemia and Iron[2]

C. Causes and Consequences of Zinc Deficiency[4-6]

D. Copper Deficiency[7]

E. Summary

III. Toxic Effects of Metals

A. Two Classes of Toxic Metal Compounds

B. Copper Overload and Wilson's Disease[8]

C. Iron Toxicity[9]

D. Toxic Effects of Other Essential Metals[10,11]

E. Plutonium: A Consequence of the Nuclear Age[12]

F. Mercury Toxicity[13] and Bacterial Resistance[14-17]

G. Cadmium and Lead Toxicity[18]

H. Metals as Carcinogens[19,20]

I. Summary

IV. Survey of Metals Used for Diagnosis and Chemotherapy

A. Radiodiagnostic Agents[21,22]

B. Magnetic Resonance Imaging (MRI)[27]

C. Lithium and Mental Health[28-31]

D. Gold and Rheumatoid Arthritis[23,32,33]

E. Anticancer Drugs

1. Platinum Ammine Halides[34,35]
2. Metallocenes and Their Halides: Ti, V, Fe[36,37]
3. Gold and Other Metal Phosphines[39]
4. Other Main Group and Transition-Metal Compounds[36,40,41]

F. Miscellaneous Metals in Medicine

G. Summary and Prospectus

V. Platinum Anticancer Drugs: A Case Study

A. History of Discovery[47]

B. Principles that Underlie Drug Development

1. Strategic Considerations
2. Pre-clinical and Clinical Trials[49]
3. Mechanism of Action Studies

C. Clinical Picture for Cisplatin and Carboplatin[49,52]

1. Responsive Tumors and Combination Chemotherapy
2. Dose-limiting Problems; Toxicology
3. Pharmacology[49,52]

D. Bioinorganic Chemistry of Platinum Anticancer Drugs; How Might They Work?

1. Reactions of *cis*-DDP and Related Compounds in Aqueous, Biological, and Other Media
2. Evidence that DNA is the Target
3. Aspects of Platinum Binding to DNA
4. Mapping the Major Adducts of *cis*- and *trans*-DDP on DNA; Sequence Specificity

5. Structure of Platinum-DNA Complexes
6. Effects of DNA Structure on Platinum Binding
7. Speculations About the Molecular Mechanism
8. Site-Specifically Platinated DNA[154]

E. Design of New Inorganic Anticancer Drugs

1. Objectives
2. Strategies for Drug Development
3. Second- and Third-generation Platinum Anticancer Drugs
4. Nonplatinum Antitumor Metal Complexes

VI. Restrospective

The topics discussed in this chapter are helping to expand bioinorganic chemistry from a subject that arose chiefly from spectroscopic analysis of metal centers in proteins, because they were uniquely convenient functional groups, to a discipline where fundamental knowledge about metal functions and the application of metals as diagnostic and chemotherapeutic agents are making important contributions to medicine. As the case study of cisplatin is intended to demonstrate, progress in understanding how metals function in chemotherapy can be made only by the combined efforts of many disciplines, including synthetic and physical inorganic and organic chemistry, molecular and cell biology, immunology, pharmacology, toxicology, and clinical medicine. Although we have not yet reached the day where chemotherapeutic agents can be rationally designed from knowledge of a molecular mechanism, such a concept does not seem that farfetched. If nothing else, knowledge of fundamental bioinorganic processes related to metal-macromolecule interactions will continue to grow enormously through efforts to achieve this ultimate goal.

VII. References

1. H. Sigel, ed., *Metal Ions in Biological Systems*, Dekker, vol. 14, 1982.
2. D. A. Brown, *Metal Ions Biol. Syst.* **14** (1982), 125.
3. A. D. Young and R. W. Noble, *Methods Enzymol*. **76** (1981), 792.
4. D. A. Phipps, *Metals and Metabolism*, Oxford University Press, 1976, p. 63.
5. G. J. Brewer, *Metal Ions Biol. Syst*. **14** (1982), 57.
6. A. S. Prasad, *Metal Ions Biol. Syst.* **14** (1982), 37.
7. J. R. J. Sorenson, *Metal Ions Biol. Syst.* 14 (1982), 77.
8. D. R. Williams, *An Introduction to Bioinorganic Chemistry*, C. C. Thomas, 1976, p. 327.
9. Reference 8, p. 371.
10. Reference 4, p. 56.
11. Reference 8, p. 372.
12. K. N. Raymond and W. L. Smith, *Struct. Bonding* **43** (1981), 159.
13. Reference 8, p. 366.
14. C. T. Walsh *et al*., *FASEB* **2** (1988), 124.
15. J. G. Wright *et al.*, *Prog. Inorg. Chem*. **38** (1990), 323.
16. J. D. HeImann, L. M. Shewshuck, and C. T. Walsh, *Adv. Inorg. Biochem.* **8** (1990), 331.
17. M. J. Moore *et al*., *Acc. Chem. Res*. **23** (1990), 301.
18. Reference 8, p. 363.
19. Reference I, vol. 10, 1980.
20. K. E. Wetterhahn. *J. Am. Coll. Toxicol.* **8** (1989), 1275.
21. C. J. Mathias *et al.*, *Nucl. Med. Biol.* **15** (1988), 69.
22. A. Yokoyama and H. Saji, *Metal Ions Biol. Syst.* **10** (1980), 313.
23. R. C. Elder and M. K. Eidness, *Chem. Rev*. **87** (1987), 1027.
24. J. C. Dabrowiak, *Adv. lnorg. Chem*. **4** (1982), 70.
25. J. Stubbe and J. W. Kozarich, *Chem. Rev*. **87** (1987), 1107.
26. C. F. Meares and T. G. Wensel, *Acc. Chem. Res*. **17** (1984), 202.

27. R. B. Laufer, *Chem. Rev*. **87** (1987), 901.
28. N. J. Birch, *Metal Ions Biol. Syst.* **14** (1982),257.
29. S. Avissar *et al*., *Nature* **331** (1988), 440.
30. M. C. Espanol and D. Mota de Freitas, *Inorg. Chem*. **26** (1987), 4356.
31. P. F. Worley *et al*., *Science* **239** (1988), 1428.
32. B. M. Sutton, in Reference 159, p. 355.
33. K. C. Dash and H. Schmidbauer, *Metal Ions Biol. Syst.* **14** (1982), 179.
34. M. J. Cleare and J. D. Hoeschele, *Bioinorg. Chem.* **2** (1973), 187.
35. B. Rosenberg *et al*., *Nature* **222** (1969), 385.
36. P. Köpf-Maier and H. Köpf, *Chem. Rev.* **87** (1987), 1137.
37. P. Köpf-Maier and H. Köpf, *Struct. Bonding* **70** (1988), 105.
38. J. H. Toney, C. P. Brock, and T. J. Marks, *J. Am. Chem. Soc.* **108** (1986), 7263.
39. S. J. Bemers-Price and P. J. Sadler, in Reference 41, p. 527.
40. Reference 1, vol. 11, 1980.
41. M. Nicolini, ed., *Platinum and Other Metal Coordination Compounds in Cancer Chemotherapy*, Nijhoff, 1988.
42. Reference 8, p. 316.
43. Reference 4, p. 60.
44. C. C. Hinckley *et aI.*, in Reference 159, p. 421.
45. D. D. Perrin and H. Stiinzi, *Metal Ions Biol. Syst.* **14** (1982), 207.
46. C. Hill, M. Weeks, and R. F. Sehinazi, *J. Med. Chem.* **33** (1990), 2767.
47. B. Rosenberg, *Metal Ions in Biol.* **1** (1980), 1.
48. S. J. Lippard, *Science* **218** (1982), 1075.
49. B. Rosenberg, *Metal Ions Biol. Syst*. **11** (1980), 127.
50. J. M. Paseoe and J. J. Roberts, *Biochem. Pharmacol*. **23** (1974), 1345.
51. J. K. Barton and S. J. Lippard, *Metal Ions in Biol.* **1** (1980), 31.
52. P. J. Loehrer and L. H. Einhorn, *Ann. Intern. Med*. **100** (1984), 704.
53. R. F. Boreh, in Reference 41, p. 216.
54. L. R. Kelland *et al*., *Cancer Res*. **52** (1992), 822.
55. M. E. Howe-Grant and S. J. Lippard, *Metal Ions Biol. Syst.* **11** (1980), 63.
56. R. Faggiani *et al*., *J. Am. Chem. Soc*. **99** (1977), 777.
57. R. Faggiani *et al*., *Inorg. Chem*. **16** (1977), 1192.
58. T. G. Appleton, 1. R. Hall, and S. F. Ralph, in Reference 41, p. 634.
59. M. C. Lim and R. B. Martin, *J. Inorg. Nucl. Chem.* **38** (1976), 1911.
60. S. K. Mauldin *et al*., *Cancer Res*. **48** (1988), 5136.
61. W. I. Sundquist *et al*., *Inorg. Chem*. **26** (1987), 1524.
62. H. C. Harder and B. Rosenberg, *Int. J. Cancer* **6** (1970), 207.
63. J. H. Howle and G. R. Gale, *Biochem. Pharmacol*. **19** (1970), 2757.
64. S. Reslova, *Chem.-Biol. Interact*. **4** (1971), 66.
65. S. Reslova-Vasilukova, in T. A. Connors and J. J. Roberts, eds., *Recent Results in Cancer Research*, Springer, 1974, p. 105.
66. J. J. Roberts and A. J. Thomson, *Prog. Nucl. Acids Res. Mol. Biol*. **22** (1979), 71.
67. D. P. Bancroft, C. A. Lepre, and S. J. Lippard, *J. Am. Chem. Soc*. **112** (1990), 6860.
68. J.-P. Macquet, J.-L. Butour, and N. P. Johnson, in Reference 159, p. 75.
69. N. P. Johnson *et al*., *J. Am. Chem. Soc.* **107** (1985), 6376.
70. R. B. Ciccarelli, unpublished results.
71. J. C. Caradonna and S. J. Lippard, *Inorg. C*hem. **27** (1988), 1454.
72. K. Inagaki and Y. Kidani, *J. Inorg. Biochem.* **11** (1979), 39.
73. B. K. Teo *et al*., *J. Am. Chem. Soc.* **100** (1978), 3225.
74. H. M. Ushay, Ph.D. Dissertation, Columbia University, 1984.
75. A. B. Robins and M. O. Leach, *Cancer Treat. Rep*. **67** (1983), 245.
76. P. Bedford *et al*., *Cancer Res*. **48** (1988), 3019.

77. W. Bauer *et al.*, *Biochemistry* **17** (1978), 1060.
78. J. Filipski *et al.*, *Science* **204** (1979), 181.
79. K. M. Comess, C. E. Costello, and S. J. Lippard, *Biochemistry* **29** (1990), 2102.
80. W. A. Rembers, in *Antineoplastic Agents*, Wiley, 1984; p. 83.
81. S. E. Sherman and S. J. Lippard, *Chem. Rev.* **87** (1987), 1153.
82. J.-P. Macquet and T. Theophanides, *Bioinorg. Chem.* **5** (1975), 59.
83. D. M. L. Goodgame *et al.*, *Biochim. Biophys. Acta* **378** (1975), 153.
84. L. A. Zwelling *et al.*, *Cancer Res.* **38** (1978), 1762.
85. R. B. Ciccarelli *et al.*, *Biochemistry* **24** (1985), 7533.
86. S. J. Lippard and J. D. Hoeschele, *Proc. Natl. Acad. Sci. USA* **76** (1979), 6091.
87. G. L. Cohen *et al.*, *Science* **203** (1979), 1014.
88. S. J. Lippard, *Acc. Chem. Res.* **11** (1978), 211.
89. M. Howe-Grant *et al.*, *Biochemistry* **15** (1976), 4339.
90. J.-L. Butour and J.-P. Macquet, *Eur. J. Biochemistry* **78** (1977), 455.
91. J.-P Macquet and J.-L. Butour, *Biochimie* **60** (1978), 901.
92. S. F. Bellon and S. J. Lippard, *Biophys. Chem.* **35** (1990), 179.
93. J. A. Rice *et aI.*, *Proc. Natl. Acad. Sci. USA* **85** (1988), 4158.
94. H.-M. Wu and D. M. Crothers, *Nature* **308** (1984), 509.
95. S. F. Bellon, J. H. Coleman, and S. J. Lippard, *Biochemistry* **30** (1991), 8026.
96. W. Heiger-Bernays, J. M. Essigmann, and S. J. Lippard, *Biochemistry* **29** (1990), 8461.
97. J. J. Roberts *et al.*, in Reference 41, p. 16.
98. M. F. Pera, C. J. Rawlings, and J. J. Roberts, *Chem.-Biol. Interact.* **37** (1981), 245.
99. A. M. J. Fichtinger-Schepman *et al.*, in Reference 41, p. 32.
100. D. J. Beck *et al.*, *Nucleic Acids Res.* **13** (1985), 7395.
101. J. D. Page *et al.*, *Biochemistry* **29** (1990), 1016.
102. G. A. Curt, N. J. Clendeninn, and B. A. Chabner, *Cancer Treat. Rep.* **68** (1984), 87.
103. W. H. DeJong *et al.*, *Cancer Res.* **43** (1983), 4927.
104. A. Eastman and N. Schulte, *Biochemistry* **27** (1988), 4730.
105. A. Eastman *et al.*, in Reference 41, p. 178.
106. V. M. Richon, N. Schulte, and A. Eastman, *Cancer Res.* **47** (1987), 2056.
107. B. A. Donahue *et al.*, *Biochemistry* **29** (1990), 5872.
108. P. J. Stone, A. D. Kelman, and F. M. Sinex, *J. Mol. Biol.* **104** (1976), 793.
109. P. J. Stone, A. D. Kelman, and F. M. Sinex, *Nature* **251** (1974), 736.
110. H. M. Ushay, T. D. Tullius, and S. J. Lippard, *Biochemistry* **20** (1981), 3744.
111. T. D. Tullius and S. J. Lippard, *J. Am. Chem. Soc.* **103** (1981), 4620.
112. B. Royer-Pokora, L. K. Gordon, and W. A. Haseltine, *Nucleic Acids Res.* **9** (1981), 4595.
113. M. C. Poirier *et al.*, *Proc. Natl. Acad. Sci USA* **79** (1982), 6443.
114. S. J. Lippard *et al.*, *Biochemistry* **22** (1983), 5165.
115. E. Reed *et al.*, *J. Clin. Invest.* **77** (1986), 545.
116. M. C. Poirier *et al.*, *Environ. Health Persp.* **62** (1985), 49.
117. W. L Sundquist, S. J. Lippard, and B. D. Stollar, *Proc. Natl. Acad. Sci. USA* **84** (1987), 8225.
118. A. Eastman, *Biochemistry* **25** (1986), 3912.
119. A. M. J. Fichtinger-Schepman *et al.*, *Biochemistry* **24** (1985), 707.
120. A. M. J. Fichtinger-Schepman *et al.*, *Chem.-Biol. Interact.* **55** (1975), 275.
121. A. C. M. Plooyetal., *Carcinogenesis* **6** (1985), 561.
122. A. M. J. Fichtinger-Schepman *et al.*, *Cancer Res.* 47 (1987), 3000.
123. J. C. Dewan, *J. Am. Chem. Soc.* **106** (1984), 7239.
124. T. W. Hambly, *J. Chem. Soc. Chem. Comm.* (1988), 221.
125. J. H. J. den Hartog *et al.*, *J. Biomol. Struct. Dynam.* **2** (1985), 1137.
126. B. van Hemelryck *et al.*, *Biochem. Biophys. Res. Comm.* **138** (1986), 758.

127. L. S. Hollis *et al.*, in Reference 41, p. 538.
128. R. M. Wing *et al.*, *EMBO* **3** (1984), 1201.
129. J. R. Rubin, M. Sabat, and M. Sundaralingam, *Nucleic Acids Res.* **11** (1983), 6571.
130. S. E. Sherman *et al.*, *Science* **230** (1985), 412.
131. G. Admiraal *et al.*, *J. Am. Chem. Soc.* **109** (1987), 592.
132. S. F. Bellon, T. Takahara, and S. J. Lippard, unpublished results.
133. J. Kozelka *et al.*, *Biopolymers* **26** (1987), 1245.
134. B. Lippert, Prog, Inorg. Chem. 37 (1989), 1.
135. A. L. Pinto and S. J. Lippard, *Proc. Natl. Acad. Sci. USA* **82** (1985), 4616.
136. C. A. Lepre, K. G. Strothkamp, and S. J. Lippard, *Biochemistry* **26** (1987), 5651.
137. D. Gibson and S. J. Lippard, *Inorg. Chem.* **26** (1987), 2275.
138. J. L. van der Veer *et al.*, *J. Am. Chem. Soc.* **108** (1986), 3860.
139. C. A. Lepre *et al.*, unpublished results.
140. W. Saenger, *Principles of Nucleic Acid Structure*, Springer, 1984.
141. B. Malfoy, B. Hartman, and M. Leng, *Nucleic Acids Res.* **9** (1981), 5659.
142. T. D. Tullius and S. J. Lippard, *Proc. Natl. Acad. Sci. USA* **79** (1982), 3489.
143. B. E. Bowler and S. J. Lippard, *Biochemistry* **25** (1986), 3031.
144. B. E. Bowler, Ph.D. Dissertation, Massachusetts Institute of Technology, 1987.
145. J.-M Malinge, A. Schwartz, and M. Leng, *Nucleic Acids Res.* **15** (1987), 1779.
146. W. I. Sundquist *et al.*, *J. Am. Chem. Soc.* **112** (1990), 1590.
147. W. I. Sundquist *et al.*, *J. Am. Chem. Soc.* **110** (1988),8559.
148. D. P. Bancroft *et al.*, *J. Am. Chem. Soc.*, in press.
149. K. M. Comess, *Biochemistry* **25** (1992), 3975.
150. S. L. Bruhn, J. H. Toney, and S. J. Lippard, *Prog. Inorg. Chem.* **38** (1990), 477.
151. A. Sancar and G. B. Sancar, *Annu. Rev. Biochem.* **57** (1988), 29.
152. J. H. Toney *et al.*, *Proc. Natl. Acad. Sci. USA* **86** (1990), 8328; S. L. Bruhn *et al.*, *Proc. Natl. Acad. Sci. USA* **89** (1992), 2307; P. M. Pil and S. J. Lippard, *Science* **256** (1992), 234.
153. S. J. Brown, P. J. Kellett, and S. J. Lippard, *Science* **261** (1993), 603.
154. L. J. Naser *et al.*, *Biochemistry* **27** (1988), 4357.
155. S. E. Sherman *et al.*, *J. Am. Chem. Soc.* **107** (1988), 7368.
156. E. Rotondo *et al.*, *Tumori* **69** (1983), 31.
157. V. Brabec, O. Vrana, and V. Kleinwachter, *Studia Biophys.* **114** (1986), 199.
158. G. E. Plum and V. A. Bloomfield, *Biopolymers* **27** (1988), 1045.
159. J. K. Barton, *Chem. Eng. News* **66** (Sept. 26, 1988), 30.
160. S. J. Lippard, *Platinum, Gold. and Other Metal Chemotherapeutic Agents*, American Chemical Socicty, 1983.
161. W. I. Sundquist and S. J. Lippard, *Coord. Chem. Rev.* **100** (1990), 293.
162. I am grateful to the Alexander von Humboldt Foundation for a U.S. Senior Scientist Award, Massachusetts Institute of Technology for sabbatical leave time, and Prof. Drs. W. Herrmann and K. Wieghardt for their kind hospitality, all of which were essential for the preparation of the first draft of this chapter during the spring of 1988. I very much appreciate help from the following individuals: A. Davison, for providing Figure 9.2, and D. L. Bancroft, S. F. Bellon, S. L. Bruhn, J. N. Burstyn, K. M. Comess, G. B. Jameson, C. A. Lepre, and J. T. Toney for commenting critically on the manuscript. I also thank M. Mason for typing the first draft.

Contributors and Attributions

- Stephen J. Lippard (Massachusetts Institute of Technology, Department of Chemistry)

Thumbnail: Cisplatin, $PtCl_2(NH_3)_2$ A platinum atom with four ligands. Image used with permission (Public Domain; Benjah-bmm27).

11.2.9: Metals in Medicine is shared under a CC BY-NC-SA 4.0 license and was authored, remixed, and/or curated by LibreTexts.

11.2.9.1: Metal Deficiency and Disease

Essential Metals

Four main group (Na, K, Mg, and Ca) and ten transition (V, Cr, Mn, Fe, Co, Ni, Cu, Zn, Mo, and Cd) metals are currently known or thought to be required for normal biological functions in humans. Table 9.1 lists these elements, their relative abundances, and the medical consequences of insufficient quantities where known. The nutritional requirements for selected members of the essential metals are discussed in the following sections.

Table 9.1 - Essential metals and medical consequences resulting from their deficiency.[a]

a) Data taken from E.-i. Ochiai, *Bioinorganic Chemistry*, Allyn & Bacon, 1977, p. 6

Metal	Abundance	Abundance	Diseases Resulting from Metal Deficiency
	Sea Water mg/1 (ppm)	Earth's Crust mg/1 (ppm)	
Na	1.05×10^{4}	2.83×10^{4}	
K	380	2.59×10^{4}	
M-	1.35×10^{4}	2.09×10^{4}	
Ca	400	3.63×10^{4}	bone deterioration
V	2×10^{-3}	135	
Cr	5×10^{-3}	100	glucose tolerance (?)
Mn	2×10^{-5}	950	
Fe	1×10^{-2}	5.00×10^{4}	anemia
Co	1×10^{-4}	25	anemia
Ni	2×10^{-4}	75	
Cu	3×10^{-3}	55	brain disease, anemia, heart disease
Zn	1×10^{-2}	70	growth retardation, skin changes
Mo	1×10^{-2}	1.5	
Cd	1.1×10^{-4}	0.2	

Anemia and Iron[2]

Anemia results from insufficient oxygen supply, often because of a decrease in hemoglobin (Hb) blood levels. Approximately 65 to 70 percent of total body iron resides in Hb. In the U.S., many foods, especially those derived from flour, are enriched in iron. In third-world countries, however, scarcity of dietary iron is a major contributor to anemia. This information illustrates one important fact about disease that results from metal deficiency, namely, the need for an adequate supply of essential metals in food. A related aspect, one of greater interest for bioinorganic chemistry, is the requirement that metals be adequately absorbed by cells, appropriately stored, and ultimately inserted into the proper environment to carry out the requisite biological function. For iron, these tasks, among others, are performed by specific iron-chelating agents, the storage protein ferritin and the transport protein transferrin, the bioinorganic chemistry of which is extensively discussed in Chapter 1.

Another cause of anemia exists in individuals who have a mutant variety of hemoglobin, HbS, in which valine has been substituted for glutamic acid in the sixth position of the β subunits.[3] Interestingly, extensive studies have shown that this phenomenon, which

leads to sickling of the red blood cells, does not result from failure of the protein to bind heme or from changes in the O_2 binding constant of the iron atom. Rather, deoxy HbS polymerizes into soluble, ordered fibrous structures that lower the ability of blood to carry oxygen effectively to the tissues. These results illustrate the importance of structural features remote from the metal-binding domain in determining the functional characteristics of a metalloprotein.

Causes and Consequences of Zinc Deficiency[4-6]

The average adult contains ~ 2 g of zinc and requires a daily intake of 15 to 20 mg, only half of which is absorbed, to maintain this level. Although food in many technologically advanced societies contains sufficient zinc to afford this balance, zinc deficiencies occur in certain populations where there is either an unbalanced diet or food that inhibits zinc absorption. An especially interesting example of the latter phenomenon is found in certain villages in the Middle East where phytates, organic phosphates present in unleavened bread, chelate zinc ion and render it inaccessible. Zinc deficiency produces growth retardation, testicular atrophy, skin lesions, poor appetite, and loss of body hair. Little is known about the biochemical events that give rise to these varied consequences, although the three most affected enzymes are alkaline phosphatase, carboxypeptidase, and thymidine kinase. About 30 percent of zinc in adults occurs in skin and bones, which are also likely to be affected by an insufficient supply of the element. Zinc deficiency is readily reversed by dietary supplements such as $ZnSO_4$, but high doses (>200 mg) cannot be given without inducing secondary effects of copper, iron, and calcium deficiency.

Copper Deficiency[7]

More copper is found in the brain and heart than in any other tissue except for liver, where it is stored as copper thionein and released as ceruloplasmin or in the form of a complex with serum albumin. The high metabolic rate of the heart and brain requires relatively large amounts of copper metalloenzymes including tyrosinase, cytochrome c oxidase, dopamine-β-hydroxylase, pyridoxal-requiring monamine oxidases, and Cu-Zn superoxide dismutase. Copper deficiency, which can occur for reasons analogous to those discussed above for Fe and Zn, leads to brain disease in infants, anemia (since cytochrome oxidase is required for blood formation), and heart disease. Few details are known about the molecular basis for copper uptake from foods.

Summary

From the above anecdotal cases, for which similar examples may be found for the other metals in Table 9.1, the biological consequences of metal deficiency are seen to result from a breakdown in one or more of the following steps: adequate supply in ingestible form in foodstuffs; absorption and circulation in the body; uptake into cells; insertion into critical proteins and enzymes requiring the element; adequate storage to supply needed metal in case of stress; and an appropriate mechanism to trigger release of the needed element under such circumstances. Only for iron, and to a lesser extent copper and zinc, is there a reasonably satisfying picture of the molecular processes involved in this chain of events. The elucidation of the detailed mechanisms of these phenomena, for example, the insertion of iron into ferritin, remains an exciting challenge for the bioinorganic chemist (see Chapter 1).

11.2.9.1: Metal Deficiency and Disease is shared under a CC BY-NC-SA 4.0 license and was authored, remixed, and/or curated by LibreTexts.

11.2.9.2: Toxic Effects of Metals

Two Classes of Toxic Metal Compounds

As intimated in the previous section, the presence of excess quantities of an essential metal can be as deleterious as insufficient amounts. This situation can arise from accidental ingestion of the element or from metabolic disorders leading to the incapacitation of normal biochemical mechanisms that control uptake and distribution phenomena. These possibilities constitute one major class of metal toxicity. The other broad class results from entry of nonessential metals into the cell through food, skin absorption, or respiration. The toxicities associated with this latter class have received much recent attention because of the public health risks of chemical and radioisotopic environmental pollutants.

In this section, we survey examples of both categories, and discuss ways in which bioinorganic chemistry can contribute to the removal of toxic metals and restoration of normal function. One way involves chelation therapy, in which metal-specific chelating agents are administered as drugs to complex and facilitate excretion of the unwanted excess element. The use of desferrioxamine to treat iron poisoning is one example of this approach. A second role of bioinorganic chemistry is to identify fundamental biological mechanisms that regulate metal detoxification, and to apply the principles that emerge to help control the toxic effects of metal ions in the environment. Recent studies of mercury resistance and detoxification in bacteria provide an elegant example of the way in which biochemistry and molecular biology can be used to elucidate events at the molecular level. This work, which has uncovered the existence of metalloregulatory proteins, is described in some detail in Section III.F below. It represents a benchmark by which other investigations into the mechanisms of metal-detoxification phenomena may be evaluated.

Copper Overload and Wilson's Disease[8]

Wilson's disease results from a genetically inherited metabolic defect in which copper can no longer be tolerated at normal levels. The clinical manifestations are liver disease, neurological damage, and brown or green (Kayser-Fleischer) rings in the cornea of the eyes. Patients suffering from Wilson's disease have low levels of the copper-storage protein ceruloplasmin; the gene and gene products responsible for the altered metabolism have not yet been identified. Chelation therapy, using $K_2Ca(EDTA)$, the Ca^{2+} ion being added to replenish body calcium stores depleted by EDTA coordination, 2,3-dimercaptopropan-1-ol (BAL, British Anti-Lewisite), or d-penicillamine to remove excess copper, causes the symptoms to disappear. The sulfhydryl groups of the latter two compounds presumably effect removal of copper as Cu(I) thiolate complexes. Wilson's disease offers an excellent opportunity for modem methodologies to isolate and clone the gene responsible for this altered Cu metabolism, ultimately providing a rational basis for treatment.

Iron Toxicity[9]

Chelation therapy is also used to treat iron overload. Acute iron poisoning, such as that resulting from accidental ingestion of $FeSO_4$ tablets, results in corrosion of the gastrointestinal tract. Chronic iron poisoning, or hemochromatosis, arises from digestion of excess iron usually supplied by vessels used for cooking. A classic case of the latter is siderosis induced in members of the Bantu tribe in South Africa, who consume large quantities of beer brewed in iron pots and who suffer from deposits of iron in liver, kidney, and heart, causing failure of these organs. The chelating agent of choice for iron toxicity is the siderophore desferrioxamine, a polypeptide having a very high affinity for Fe(III) but not for other metals. Ferrioxamine chelates occur naturally in bacteria as iron-transport agents. Attempts to mimic and improve upon the natural systems to provide better ligands for chelation therapy constitutes an active area of bioinorganic research (see Chapter 1).

Toxic Effects of Other Essential Metals[10,11]

When present in concentrations above their normal cellular levels, most of the other metals listed in Table 9.1 are toxic. Calcium levels in the body are controlled by vitamin D and parathyroid hormones. Failure to regulate Ca^{2+} leads to calcification of tissue, the formation of stones and cataracts, a complex process about which little is understood (see Chapter 3). Chronic manganese poisoning, which can occur following ingestion of metal-oxide dust, e.g., among miners in Chile, produces neurological symptoms similar to Parkinson's disease. Neuron damage has been demonstrated. Although Zn toxicity is rare, it can lead to deficiencies in other essential metals, notably calcium, iron, and copper. Cobalt poisoning leads to gastrointestinal distress and heart failure. Metal poisoning by those elements has been treated by chelating agents, most frequently CaNaiEDTA), but the selectivity offered by the

ferrioxamine class of ligands available for iron has not even been approached. Fortunately, there are few cases involving these metals.

Plutonium: A Consequence of the Nuclear Age[12]

Some of the chelating agents developed to treat iron toxicity have found application as therapeutics for plutonium poisoning. Diethylenetriaminepentaacetic acid (DTPA) salts and siderophores are especially effective. Some improvement over the naturally occurring chelates has been made by tailoring the ligand to encapsulate completely the eight-coordinate Pu(IV) center. Although few individuals have been affected, ingestion of ^{239}Pu, for example, as small particles of PuO_2, at nuclear-reactor sites can have dire consequences. ^{239}Pu emits high energy ex particles, leading to malignancies of bone, liver, lung and lymph nodes, to which tissues it is transported by transferrin. With a maximum tolerated dose of only 1.5 μg, plutonium is among the most toxic metals known. We turn now to other, more classic examples of such industrial pollutants.

Mercuy Toxicity[13] and Bacterial Resistance[14-17]

Mercury is released into the environment as Hg(II) ions through weathering of its most common ore, HgS, red cinnabar. Organomercurials of general formula RHgX used in agriculture have also entered the environment as toxic waste. Both RHgX and HgX_2 compounds bind avidly to sulfhydryl groups in proteins, which can lead to neurological disease and kidney failure. Metallothionein is a favored protein target, which may help to limit mercury toxicity. A highly publicized case occurred in 1953 at Minimata, Japan, where 52 people died after eating mercury-contaminated fish and crustaceans near a factory waste outlet. The volatile, elemental form of mercury, Hg(0), is reportedly nontoxic, but its conversion to alkylmercury compounds by anaerobic microorganisms utilizing a vitamin B-12 biosynthetic pathway constitutes a serious health hazard.

Because of the high affinity of mercury for sulfur-donor ligands, mercury poisoning is treated by BAL; N-acetylpenicillamine has also been proposed. Recently, a very interesting natural detoxification system has been discovered in bacteria resistant to mercury; this system, when fully elucidated, might provide important strategies for treating heavy-metal poisoning in humans.

Presumably under environmental pressure, bacteria have developed mechanisms of resistance to HgX_2 and RHgX compounds in which mercury is recycled back to Hg(0). At least five gene products are involved in the bacterial mercury-resistance mechanism. MerT and MerP mediate the specific uptake of mercury compounds. MerB, organomercury lyase, and MerA, mercuric reductase, catalyze two of the reactions, given in Equations (9.1) and (9.2). Plasmids encoding the genes for these two proteins have been isolated. A typical arrangement of genes in the *mer* operon

$$RHgX + H^+ + X^- \xrightarrow[lyase]{organomercury} HgX_2 + RH \tag{9.1}$$

$$Hg(SR)_2 + NADPH + H^+ \xrightarrow[reductase]{mercuric} Hg(0) + NADP^+ + 2RSH \tag{9.2}$$

region of these plasmids is shown in Figure 9.1. The most thoroughly studied gene product is MerR, a metalloregulatory protein that controls transcription of the *mer* genes. In the absence of Hg(II) the MerR protein binds to DNA as a repressor, preventing transcription of the *merT, P, A*, and *B* genes (Figure 9.1) and negatively autoregulating its own synthesis. When Hg(II) is present, transcription of these genes is turned on. Interestingly, the MerR protein remains bound to the same site on DNA whether acting as an activator in the presence of Hg(II) or as a repressor in its absence. Random and site-specific mutagenesis studies implicate several cysteine residues in the carboxyl terminal region of the protein as candidates for the mercury-binding site.

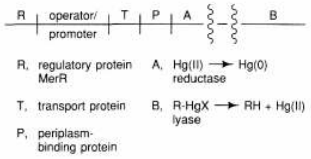
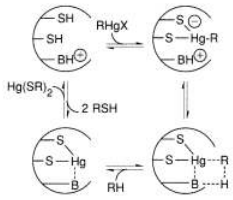


Figure 1, Reference 14).

Organomercury lyase, encoded by the *merB* gene, achieves the remarkable enzymatic step of breaking Hg-C bonds (Equation 9.1). It is a 22-kDa protein with no metals or cofactors. Two cysteine-sulfhydryl groups on the protein have been postulated to effect this chemistry, as depicted in Equation (9.3). Stereochemical studies of the Hg-C bond cleavage revealed retention of configuration, indicating that cleavage of the Hg-C bond probably does not proceed by a radical pathway. A novel concerted S_E2 mechanism has

been suggested. The enzyme turnover numbers, ranging from 1 min^{-1} for CH_3HgCl to 240 min^{-1} for butenylmercuric chloride, although slow, are ~10^5-10^8-fold faster than the nonenzymatic rate.



Mercuric ion reductase, the FAD-containing *merA* gene product, has several pairs of conserved cysteines. From site-specific mutagenesis studies, cysteine residues in the sequence 134-Thr-Cys-Val-Asn-Val-Gly-Cys-140 are known to comprise a redox-active disulfide group; in addition, a redox-inactive pair of cysteines near the carboxyl terminus is also required for the selective reduction of Hg(II). Exactly how the enzyme achieves the chemistry shown in Equation (9.2) is currently uncertain, but the redox activities of the flavin and disulfide/ thiol centers are undoubtedly involved. This enzyme serves both to detoxify mercury supplied directly from the environment as Hg(II) salts and to complete clearance of Hg^{2+} generated by the MerB protein from RHgX compounds. Clearly, Nature has invented a remarkable system to detoxify mercury in this fascinating class of Hg-resistant bacteria.

Cadmium and Lead Toxicity[18]

Gastrointestinal, neurological, and kidney toxicity are among the symptoms experienced by acute or chronic exposure to these heavy metals. The use of unleaded gasoline and the removal of lead-containing pigments from paint have substantially diminished the quantity of this element released to the environment each year. Cadmium sources include alkaline batteries, pigments, and plating. Lead poisoning can be treated by chelation therapy using $CaNa_2$(EDTA) (acute) or penicillamine (chronic). Although both Cd(II) and Pb(II) bind to sulfhydryl groups in thionein, we have little information at the molecular level on the mechanisms by which these elements induce toxicity.

Metals as Carcinogens[19,20]

Although most metal ions have been reported to be carcinogenic, the three most effective cancer-causing metals are Ni, Cr, and, to a lesser extent, Cd. Nickel subsulfide, Ni_2S_3, found in many nickel-containing ores, has been extensively studied and shown to be carcinogenic in humans and other animals. In short-term bioassays including mutagenesis, enhanced infidelity of gene replication *in vitro* and altered bacterial DNA repair were observed. Chromium is most carcinogenic as chromate ion (CrO_4^{2-}), which enters cells by the sulfate uptake pathway and is ultimately reduced to Cr(III) via a Cr(V)-glutathione intermediate species. The latter complex binds to DNA to produce a kinetically inert and potentially damaging lesion. Despite the fact that much information is available about metal-DNA interactions, molecular mechanisms of metal-induced carcinogenesis have not been elucidated. Two aspects of the problem are tumor initiation and tumor development, which are likely to involve different pathways. As new methods become available for studying the molecular events responsible for cancer (oncogenesis), it should be possible for bioinorganic chemists to unravel details of how metals act as carcinogens and as mutagens. Since cancer has genetic origins, metal/nucleic-acid chemistry is likely to be prominent in such mechanisms. As discussed later, metal-DNA interactions are an important aspect of the antitumor drug mechanism of *cis*-$[Pt(NH_3)_2Cl_2]$.

Summary

Toxicity can arise from excessive quantities of either an essential metal, possibly the result of a metabolic deficiency, or a nonessential metal. Both acute and chronic exposure can be treated by chelation therapy, in which hard-soft acid-base relationships are useful in the choice of chelating agent. Since chelates can also remove essential metals not present in toxic amounts, ligands with high specificity are greatly desired. The design and synthesis of such ligands for chelation therapy remains an important objective for the medicinal bioinorganic chemist. Until recently, studies of the toxic effects of metals and their removal, sometimes categorized under "environmental chemistry," have been empirical, with little insight at the molecular level. Application of the new tools of molecular biology to these problems has the potential to change this situation, as illustrated by rapid progress made in cloning the genes and studying the gene products of the mercury-resistance phenotype in bacteria. The discovery of such resistance

phenomena in mammalian cells, and even the remote prospect of transferring Hg-resistant genes from bacteria to humans, are exciting possibilities for the future.

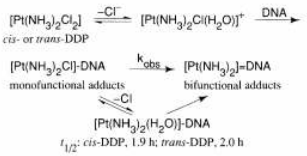
11.2.9.2: Toxic Effects of Metals is shared under a CC BY-NC-SA 4.0 license and was authored, remixed, and/or curated by LibreTexts.

11.2.9.3: Aspects of Platinum Binding to DNA

Given that DNA is a major target of platinum binding in cells, it is incumbent upon the bioinorganic chemist to investigate the nature of these interactions and their biological consequences. Of all the ligands studied in coordination chemistry, DNA is surely among the most complex. In the ensuing discussion, we first present experiments that delineate the chemical steps involved in *cis*- and *trans*-DDP binding to DNA as well as the chemical consequences of the adducts formed. We next describe the physical changes in the double helix that accompany platinum binding, and then we discuss the biological consequences that attend the platination of DNA. Subsequent sections describe the major adducts formed, in other words the regiospecificity of the drug, the three-dimensional structures of the adducts, and the way in which different structures within DNA can modulate platinum binding. Finally, we consider the response of the cell to Pt-DNA adducts, including studies with site-specifically modified DNA, and speculate about how this chemistry might relate to the antitumor drug mechanism.

a. Kinetics of Platinum Binding to DNA

The binding of *cis*- and *trans*-DDP to DNA has been studied[67] by ^{195}Pt NMR spectroscopy with the use of isotopically enriched ^{195}Pt, which has a nuclear spin I = $\frac{1}{2}$. The DNA used in this experiment was obtained from chicken red blood cell chromosomes that had been enzymatically degraded to relatively small pieces ranging from 20 to 60 base pairs in length (molecular-weight range 13 to 30 kDa). Since the ^{195}Pt chemical shifts are very sensitive to chemical environment, this NMR study provided important details about the kinetics and mechanism of platinum binding to the biopolymer. The rate-determining step in platination of the DNA is loss of chloride ion (Equation 9.5) to form the monoaqua complex, which rapidly coordinates to a nitrogen donor on the nucleic acid. The identification of the coordinating atom as nitrogen was possible because the ^{195}Pt chemical shift is characteristic of species having one chloride and three nitrogen ligands bound to Pt(II).[67] The spectroscopic changes that accompany the formation of the family of monofunctional adducts are shown in Figure 9.8. Subsequent hydrolysis of the second chloride ion leads to the formation of a second bond with DNA. This sequence of events affords bifunctional adducts and is similarly accompanied by discrete ^{195}Pt spectral changes (Figure 9.8). From the ^{195}Pt chemical-shift range of the final products, it was apparent that the *cis*-$\{Pt(NH_3)_2\}^{2+}$ moiety is bound primarily to two nitrogen donors on the nucleic acid. This chemistry is summarized in Equation (9.10), together with the half-lives for the mono-functional adducts. The half-lives were calculated from a kinetic analysis of the time-dependence of the ^{195}Pt spectral changes. As can be seen, the rates of closure of mono- to bifunctional adducts for the two isomers are quite similar, suggesting that their different biological properties are not a consequence of the kinetics of binding to DNA.



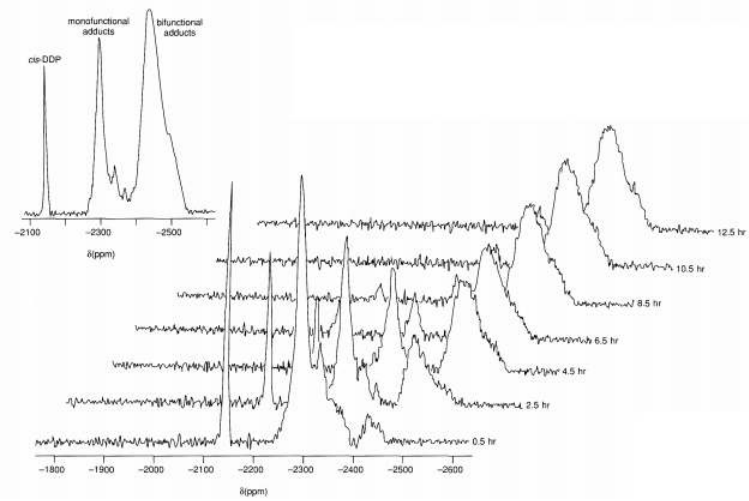


Figure 9.8 - Time course of the reaction between double-stranded chicken erythrocyte DNA and cis-$[Pt(NH_3)_2(H_2O)Cl]^+$ at a D/N = 0.07, in 3 mM NaCl and 1 mM NaH_2PO_4, 37 °C, pH 6.5. Each spectrum consists of 200,000 transients. The inset shows the sum of the individual spectra (reproduced by permission from Reference 67).

The next logical question to address is what donor atoms on DNA are coordinating to platinum in the mono- and bifunctional adducts. This important issue is discussed in considerable detail in Sections V.D.4 and V.D.5. As will be shown, the N7 atoms of the purine bases adenine and guanine are the principal binding sites. Alkylation of DNA at these positions facilitates depurination. Platinum binding to N7 atoms of purines (Figure 9.9), however, stabilizes the glycosidic (N9-C1') linkage.[68-70] Presumably the positive charge is better distributed over the platinum atom and its ligands in the adduct than over a purine alkylated at N7. On the other hand, platinum binding to N7 of guanine does perturb the charge distribution in the purine ring, as evidenced by the lowering of the pK_a of N1 by ≈ 2 units from its value in the unplatinated nucleotide (usually from $pK_a \approx 10$ to $pK_a \approx 8$).[71,72] This effect has been used to assign platinum binding sites in DNA fragments, as discussed below.

https://chem.libretexts.org/@go/page/438087

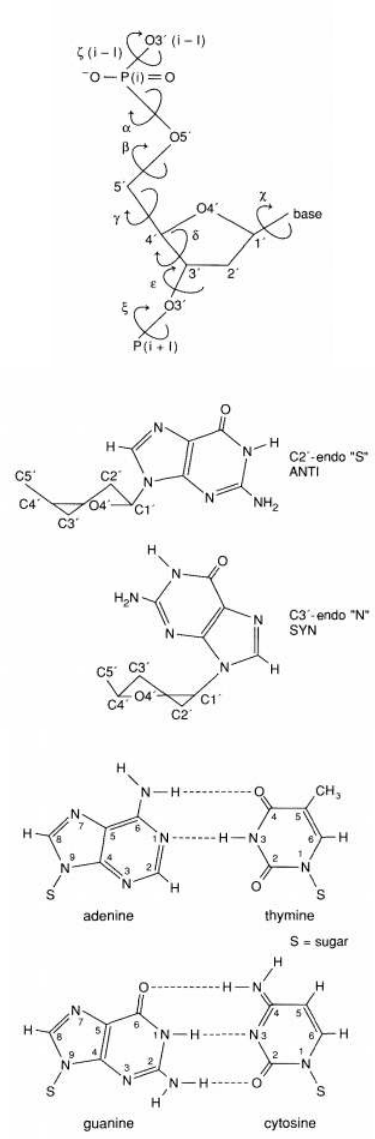


Figure 9.9 - Structural components of DNA. The left panel shows a schematic of the DNA backbone, including the deoxyribose ring numbering scheme and torsion angles. The center panel gives the two main classes of sugar pucker and base orientations. The right panel gives the bases in their Watson-Crick, A-T, and G-C pairs and the base numbering scheme, viewed down the helix axis, with the major grooves pointing toward the top of the figure and the minor grooves toward the bottom.

What are the chemical changes at the platinum center when *cis*-DDP binds to DNA? Both chloride ions are lost from the coordination sphere, as already indicated. Platinum EXAFS studies of calf-thymus DNA modified with *cis*-DDP revealed no chlorine backscattering features characteristic of Pt-CI bonds.[73] The spectra were consistent with the presence of four Pt-N/O linkages, since the technique is unable to distinguish between the two low-Z elements oxygen and nitrogen. Various studies reveal that, under most circumstances, the NH_3 ligands are not lost from DNA upon the binding of platinum ammine halides. For example, when ^{14}C-Iabeled *cis*-[$Pt(NH_2CH_3)_2Cl_2$] was allowed to bind to T7 (47 percent GC content) or *M. luteus* (73 percent GC content) DNA, no loss of radiolabel was found to accompany platinum binding.[74] *In vivo*, however, loss of amine ligands has been observed. Injection of ^{195m}Pt and ^{14}C doubly labeled [Pt(en)CI_2] into tumor-bearing mice resulted in unequal distribution of the two labels in various biochemical fractions, but there is no reason to believe that this result is relevant to the antitumor mechanism.[75] Metabolic inactivation of the drug could occur in a variety of ways unrelated to anticancer activity. The best evidence that ammine loss does not occur at the critical biological target of cisplatin is the finding, by using antibodies specific for *cis*-$\{Pt(NH_3)_2\}^{2+}$ nucleotide complexes (see Section V.D.4.c), that DNA, extracted from cells in culture or from human cancer patients treated with *cis*-DDP and subsequently degraded, contains intact Pt-NH_3 Iinkages.[76]

Once bonds are made between Pt and its targets on DNA, they are relatively inert kinetically. Platinum-DNA complexes can be subjected to various physical methods of separation and purification, including gel electrophoresis, ethanol precipitation, centrifugation, and chromatography, as well as to enzymatic and even chemical degradation procedures that digest the DNA, without releasing the platinum. Platinum can be removed, however, either by use of cyanide ion, to form the very stable ($K \sim 10^{41}$) $[Pt(CN)_4]^{2-}$ complex, or by excess thiourea.[77,78] These properties have proved to be extremely valuable in facilitating localization and characterization of the major *cis*- and *trans*-DDP binding sites on DNA.

Although Pt-DNA linkages are, generally speaking, kinetically inert, sometimes a particular adduct will rearrange into a more stable linkage isomer. One interesting example is the product of the reaction of *trans*-DDP with the dodecanucleotide 5'-d(TCTACGCGTTCT).[79] Initially the platinum coordinates to the two guanosine residues, forming a *trans*-$[Pt(NH_3)_2\{d(GCG)\}]$ 1,3-intrastrand crosslink. This complex rearranges to a more stable trans-$[Pt(NH_3)_2\{d(CGCG)\}]$ 1,4-intrastrand crosslink with a half-life of 129 h at 30 °C or 3.6 h at 62 °C. In this rearrangement product the platinum is coordinated to a cytosine and a guanosine residue.

As just described, the binding of bifunctional platinum complexes to DNA proceeds in a stepwise fashion. The second step is sufficiently slow (a few hours), however, that various reagents such as NH_3, nucleobases, and low concentrations of thiourea can coordinate to the fourth site and trap the monoadducts. Generally speaking, however, given sufficient time both *cis*- and *trans*-DDP will bind DNA in a bifunctional manner. As such, they bear some resemblance to organic alkylating agents, such as the nitrogen mustards, which have been employed as anticancer agents.[80]

b. Crosslinking Reactions of Platinum Complexes

There are three broad classes of DNA adducts that can be made by bifunctional platinum complexes. As illustrated for *cis*-DDP in Figure 9.10, they are DNA-protein crosslinks, interstrand DNA-DNA crosslinks, and intrastrand crosslinks,[81] A fourth possibility for platinum complexes is bidentate chelate ring formation utilizing two donor atoms on a nucleotide. For many years, a favored such postulated mode of binding was chelation by the N7-O6 positions of the guanine base (Figure 9.9), since this structure could be formed only by *cis*- and not by *trans*-DDP.[82,83]

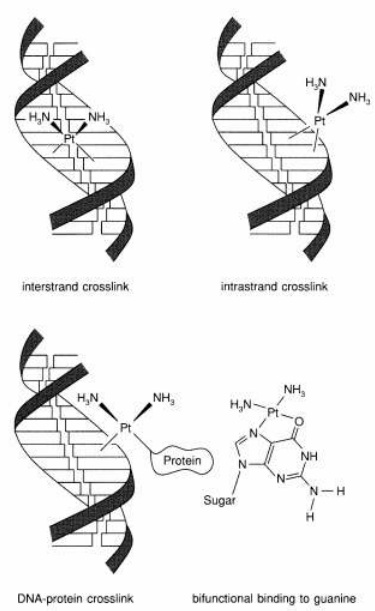


Figure 9.10 - Possible bifunctional binding modes of cis-DDP with DNA (reproduced by permission from Reference 81).

Such a structure has never been observed for *cis*-DDP binding to DNA, however. DNA-protein and interstrand crosslinks formed by platinum complexes have been the focus of many attempts to explain cytotoxicity and antitumor behavior.[84] The technique of alkaline elution, in which crosslinked DNA-DNA strands or DNA-protein molecules bind to filter paper following denaturation under basic conditions, sensitively and easily reveals such adducts. *trans*-DDP forms such adducts more rapidly than the *cis* isomer, perhaps because of its faster chloride-ion hydrolysis rates (see above) and a more favorable geometry, but they also seem to be repaired more rapidly in cells. As will be shown, interstrand and DNA-protein crosslinks are a small minority of adducts formed by

cisplatin, and their contribution to the cytotoxic and anticancer properties of the drug remains to be established. In studies of SV40 replication *in vivo*, DNA-protein crosslinking by *cis*- and *trans*-DDP was shown not to be correlated with the inhibition of DNA replication.[85]

What proteins form crosslinks to DNA? One possibility is the histones that make up the spools around which DNA is wound when packaged into chromatin in the nucleus. Studies[86] of *cis*- and *trans*-DDP binding to nucleosome core particles (each particle made up of eight histone proteins; around each particle is wound a 146-bp piece of DNA in a shallow superhelix of 1.75 turns) revealed the DNA binding to be little affected by the protein core. Both DNA-protein and specific histone crosslinked species were observed; from the latter it was suggested that DDP complexes might be useful crosslinking probes of biological structures. Other proteins likely to form crosslinks to DNA in the presence of platinum complexes are DNA-processing enzymes, or enzymes requiring a DNA template for normal function. In the *in vivo* SV40 study, for example, T antigen was one of the proteins found to be crosslinked to SV40 DNA by cisplatin.[85] Other nuclear proteins such as the high-mobility group (HMG) class are also crosslinked to DNA in the presence of *cis*-DDP. In all cases so far, DNA-protein crosslinking has occurred when platinum was added to cells. There is as yet no evidence that transfection of platinated DNA into cells results in such crosslinking or that crosslinks form during *in vitro* enzymatic digestions of platinated DNAs.

c. Physical Effects of Platinum-DNA Binding

(i). Unwinding, Shortening, and Bending of the Double Helix

Early studies of *cis*- and *trans*-DDP binding to DNA employed closed and nicked circular plasmids.[87] As was described in more detail in Chapter 8, closed circular DNAs are topologically constrained such that any change in the number of helical turns must result in an equal and opposite number of superhelical turns. Any reagent that unwinds the double helix reduces the number of helical turns. Consider, for example, a stretch of DNA that is 360 base pairs (bp) long. Normal B-DNA has ≈ 10.5 bp per turn or a helical winding angle of ≈ 34.3° per bp. Suppose the DNA is unwound, so that there are now 12 bp per turn or a winding angle of ≈ 30°. Instead of 34.3 helical turns (360 ÷ 10.5), the DNA now has only 30 (360 ÷ 12). If this DNA molecule were in the form of a covalently closed circle, the helical unwinding of -4.3 turns would be accompanied by a superhelical winding of +4.3 turns.

Planar organic dyes such as ethidium bromide (EtdBr) and inorganic complexes such as $[Pt(terpy)(HET)]^+$ (Figure 9.11) bind to DNA by intercalation, inserting between the base pairs and unwinding the double helix by ~ 26° per molecule bound (Figure 9.12).[88] This unwinding can be measured by monitoring changes in the superhelicity of closed circular DNA. This kind of DNA is subjected to certain topological constraints that lead to the formation of supercoils and superhelical winding that dramatically alter the hydrodynamic properties of the DNA. Either gel electrophoresis or analytical ultracentrifugation can be used to measure this phenomenon. The platinum complexes *cis*- and *trans*-DDP also produce changes in the superhelix density when bound to closed circular DNA.[87] As shown in Figure 9.13, increasing concentrations of platinum bound per nucleotide on the DNA first retard its mobility and then increase its mobility through the gel. These interesting alterations in gel mobility occur because the negatively coiled superhelix unwinds first into an open, or untwisted, form and then into a positively supercoiled form. The conformational changes, which are depicted in Figure 9.14, are directly proportional to the drug-per-nucleotide, or $(D/N)_b$, ratio. In addition to superhelical winding, both platinum complexes increase the mobility of nicked circular DNA in the gels (Figure 9.13). Nicked DNA has one or more breaks in the sugar-phosphate backbone, which relieve the topological constraint and prohibit the DNA from twisting into superhelical structures.

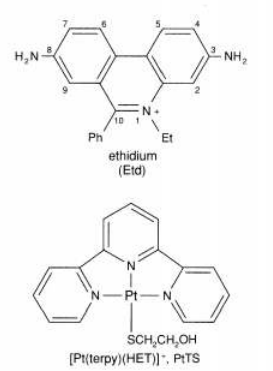


Figure 9.11 - Organic (top) and inorganic (bottom) intercalators.

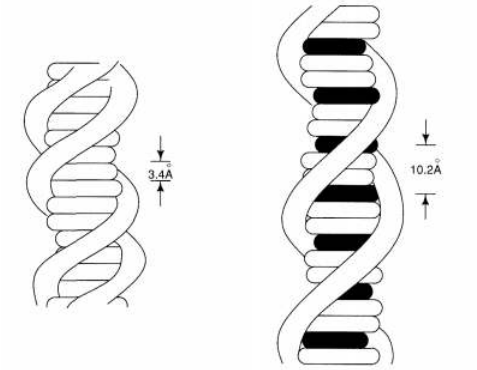


Figure 9.12 - Schematic representation of double-stranded DNA without (left) and with (shaded area, right) a bound intercalator (reproduced with permission from Reference 51).

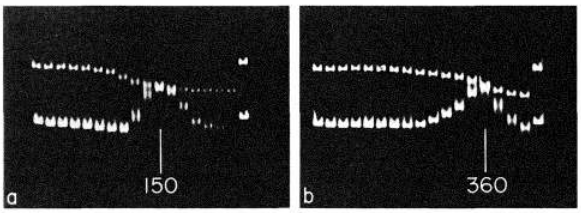


Figure 9.13 - Electrophoresis in 1 percent agarose gels of nicked and closed circular PSMI DNA incubated with (a) cis- and (b) trans-$[Pt(NH_3)_2Cl_2]$ as function of time. After electrophoresis, gels were stained with ethidium bromide. Reproduced with permission from Reference 51.

https://chem.libretexts.org/@go/page/438087

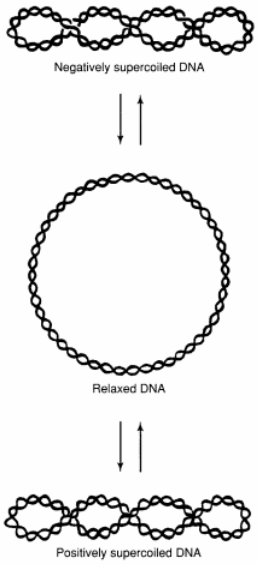


Figure 9.14 - Topological forms of closed circular DNA.

What could be the cause of these physical changes in the DNA structure upon *cis*- or *trans*-DDP binding? Intercalation can be excluded, not only because the compounds do not have the aromatic character normally associated with intercalators (Figure 9.11), but also through studies of the manner by which these and other platinum complexes inhibit the intercalative binding of EtdBr to DNA.[89,90] Platinum metallointercalators such as $[Pt(terpy)(HET)]^+$ are competitive inhibitors of EtdBr binding, as measured by fluorescence Scatchard plots, whereas the non-intercalators *cis*- and *trans*-DDP are not. Moreover, intercalation tends to lengthen and stiffen the double helix, whereas the mobility changes of nicked circular DNAs upon binding of *cis*- or *trans*-DDP were shown by electron microscopy experiments to arise from a pronounced shortening of the DNA with increased Pt binding.

One manner by which *cis*- or *trans*-DDP might produce these physical alterations in DNA structure is by kinking the double helix at or near the binding site. Such an effect could be produced by the bidentate attachment of platinum; the monofunctional $[Pt(dien)Cl]^+$ complex does not have these pronounced effects on DNA secondary structure.[91] Recently, it has been demonstrated that *cis*-DDP binding to DNA does indeed produce a pronounced bend in the helix axis.[92,93] The proof employed a gel-electrophoretic method of analysis that had previously been used to study DNA bending at naturally occurring specific sequences called A-tracts, consisting of five or six adenosine nucleosides in a row followed by about the same number of thymidine residues.[94] When these $d(A_5T_5)_2$ sequences are positioned in the center of a DNA restriction fragment of, say, 150 bp, the mobility of the DNA through polyacrylamide electrophoresis gels is greatly retarded compared to that of a similar DNA fragment where the A-tract is at the end. For the former fragment, the bent molecules presumably cannot snake their way through the pores of the polyacrylamide as well as the molecules whose bends are at the ends and have little effect on the linear structure. It was further shown that A-tracts bend the duplex toward the minor groove of the DNA. Moreover, in a DNA containing multiple A-tracts, the bends must be separated by integral numbers of helical turns (~ 10.5 bp) or else the effect will cancel and the gel mobility will be that of normal DNA of similar length. This latter phenomenon has been referred to as phasing.

With this background information in mind, we can now discuss the experiments with *cis*-DDP that demonstrated bending.[92,93] By methods described in Section V.D.8, a 22-bp oligonucleotide (22-mer) containing self-complementary overhanging ends ("sticky ends") was synthesized with a single *cis*-diammineplatinum(II) moiety linking adjacent guanosine residues (Figure 9.15A). A 22-mer was chosen since it has approximately two helical turns, accounting for some platinum-induced unwinding, and will thus have phased bends when polymerized. This platinated DNA was then labeled with ^{32}P and treated with the enzyme DNA ligase, which seals the ends, producing oligomers of the 22-mer having lengths 22, 44, 66, 88, 110, etc., bp. In these oligomers, the platinum atoms are spaced apart approximately by integral numbers of helical turns. As shown in Figure 9.15, studies of this family of oligomers by gel electrophoresis revealed a pronounced retardation compared to the mobility of unplatinated DNA oligomers of comparable size (line P22 in Figure 9.15B). The plots in this figure show the relative mobilities (R_L) of the different length multimers, compared to a control in which the top strand is not platinated, as a function of the length in base pairs. From the resulting curves may be extracted the extent of cooperative bending. When oligomers of a platinated DNA fragment in which the

metal atoms were spaced apart by 27 bp were examined, their relative mobilities were found to be nearly the same as unplatinated control molecules (line P27 in Figure 9.15B). These experiments unequivocally established that platinum kinks the double helix. As with A-tract-induced bends, the platinum atoms must be phased in order to induce cooperative bending. Comparison of the magnitudes of the gel mobility changes made it evident that *cis*-$\{Pt(NH_3)_2\}^{2+}$ binding produces a bend comparable to that of two A-tracts, ≈ 34°.

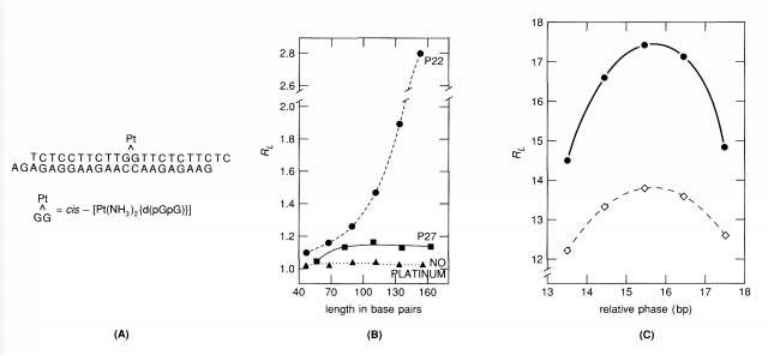


Figure 9.15 - Experiment to demonstrate that cis-$[Pt(NH_3)_2\{d(pGpG)\}]$ intrastrand crosslinks bend duplex DNA by ≈ 34°. Panel A shows the platinated 22-mer sequence, panel B the effect of platination on the gel-electrophoresis mobility of the 22-mer (P22) and a control 27-mer (P27) oligomers, and panel C the mobility of copolymerized DNAs containing cis-DDP and A-tract induced bends (●), 128-bp Pt + A-tract DNA; ♢ , 96-bp Pt + A-tract DNA) that maximize at approximately halfintegral helical turns corresponding to their phasing. For more detail consult Reference 93.

In a related series of experiments,[93] the platinated 22-mer was copolymerized with various A-tract-containing Il-mers to produce ladders of oligomers in which the phasing of Pt with respect to the center of the A-tract was varied, but the Pt atoms were always in phase. The results of these studies showed that maximum gel-mobility retardation occurred when the Pt and A-tract center were spaced apart by half-integral numbers of helical turns (Figure 9.15C). Since A-tracts bend the DNA into the minor groove, this result implies that platinum bends the DNA into the major groove. Only when phased by n/2 (n = integer) turns will copolymers of species situated alternatively in the major and minor grooves of DNA exhibit such cooperative bending. It will be shown later that helix bending of *cis*-DDP-DNA adducts into the major groove is in accord with their known structures.

The ability to prepare site-specifically platinated oligonucleotides (see Section V.D.8) has provided a means for measuring the extent to which *cis*-DDP produces local unwinding of the double helix.[95] When the platinum atoms are positioned with respect to one another, or phased, by exactly integral numbers of helical turns, the retardation of the DNA multimers in the gel is maximized. This phenomenon is illustrated in Figure 9.16, where the R_L values are plotted as a function of the interplatinum spacing for oligonucleotides containing the *cis*-$\{Pt(NH_3)_2d(GpG)\}$ intrastrand crosslink. When the resulting curve was analyzed, the maximum was found to occur at 21.38 bp. Since normal B-DNA has a helical repeat of 10.5 bp, one can compute the effect of platination from the expression [(21.38 - 2(10.5)] bp = 0.38 bp. From the fact that one helical turn of DNA comprises 360° and 10.5 bp, the unwinding of the DNA double helix due to the presence of a single *cis*-$\{Pt(NH_3)_2d(GpG)\}$ intrastrand crosslink can be calculated as

$$\left(\frac{0.38}{10.5}\right) \times 360 = 13^{o}. \qquad (11.2.9.3.1)$$

Similar studies of DNA platinated with *trans*-DDP have been carried out. In these, oligonucleotides containing the 1,3-*trans*-{Pt(NH3hd(GpNpG)} intrastrand crosslink were examined. The electrophoresis gels of polymerized 15-mers and 22-mers containing this adduct showed cooperative bending. This result indicates that bends at the sites of platination by *trans*-DDP are not phase sensitive, and has been interpreted to imply the formation of a "hinge joint" at these positions.[92,95] The directed bends and local unwinding of DNA produced by cisplatin could be an important structural element that triggers a response by cellular proteins. This subject is discussed in greater detail in Section V.D.7.d.

d. Biological Consequences of Platinum-DNA Binding

(i). Inhibition of Replication

Binding of *cis*-DDP to DNA inhibits replication both *in vivo* and *in vitro*, as shown by a variety of assays. Inhibition of replication of SV40 viral DNA in African green monkey cells as a function of the concentration of added *cis*-DDP is shown in Figure 9.17.

When SV40 virus infects monkey cells, it does not integrate its DNA into the genome of the host. Instead, it forms its own chromosomes in the cell nucleus. These so-called mini-chromosomes consist of ≈ 20 nucleosomes, fundamental chromosome building blocks. SV40 has its own life cycle, using virally encoded and cellular proteins to replicate and, ultimately, reassemble virus particles before lysing the cell and departing to infect neighboring cells.

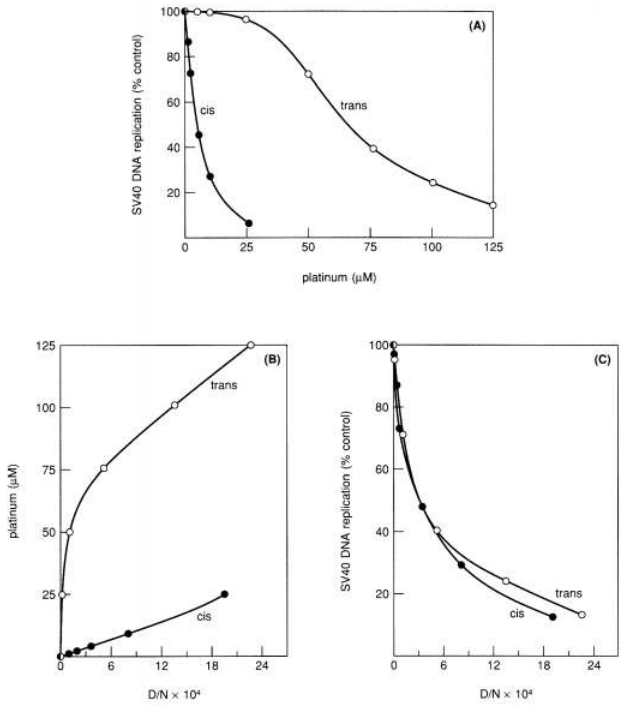


Figure 9.17 - SV40 DNA replication in CV-1 cells as a function of platinum concentration in the medium (panel A) or D/N (panel C). In panel B, DIN is plotted as a function of platinum concentration in the medium. SV40-infected cells were treated with cis-DDP (●) *or trans-DDP* (o) *at the indicated concentrations for 40 h. SV40 DNA replication relative to control (untreated) cells was measured by incorporation of [^{3}H]thymidine, added after the first 24 h of platinum treatment, and Pt in isolated SV40 chromosomes was measured by AAS. The data shown are from a representative experiment. Experiments were carried out in quadruplicate. Reproduced by permission from Reference 85.*

In the experiment shown in Figure 9.17, the SV40-infected cells were treated with cisplatin. After 24 h, [^{3}H]thymidine was added and, after 24 more hours, the cells were harvested, and SV40 DNA was isolated; the amount of DNA synthesis was recorded by comparing incorporated radiolabel with results from control experiments where no platinum was present. The data show that, when 25 μM platinum was present, SV40 DNA replication was reduced to about 5 percent of control. Quantitation reveals that, at ≈ 2 platinum atoms bound per thousand nucleotides (drug-per-nucleotide, or $(D/N)_b$, = 0.002), synthesis is only 10 percent that of control.

Recently, a related series of experiments has been carried out that can monitor DNA synthesis from templates platinated *in vitro*.[96] In this work, DNA plasmids containing the SV40 origin of replication are added to cellular extracts prepared from human kidney cells previously infected with adenovirus. In the presence of large T antigen, a virally encoded protein required for replication, SV40 DNA is synthesized from the plasmid templates. Synthesis can be conveniently monitored by [^{32}P]dATP incorporation. At a $(D/N)_b$ ratio of only 1.7 x 10^{-3}, DNA synthesis is about 5 percent of control, in agreement with the results of the *in vivo* study.

The binding of *cis*-DDP to DNA has also been measured for normal and tumor cells implanted in nude mice and in cells obtained from the ascites fluid of patients with ovarian carcinoma 24 h after their last dose.[97] The data for mouse bone marrow and a human pancreatic tumor xenograft show that, at a dose of 10 mg/kg, (D/Nh platinum binding levels of 3.3 x 10^{-6} and 1.82 x 10^{-6} reduce survival to 20 and 10 percent of control, respectively. These ratios are in good accord with platinum levels required to inhibit DNA synthesis in mammalian cells, as revealed by various studies, but substantially less than that needed for replication inhibition in the SV40 experiments described above. The difference can be readily explained, illustrating an important point. The SV40 genome, like most other DNAs of viral or plasmid origin, consists of only 15,000 nucleotides whereas the nuclear DNA of mammals has about 10^9 nucleotides. Thus, $(D/N)_b$ levels of ~ 10^{-6} would leave 99 out of 100 SV40 DNA molecules with no platinum at all, and

replication would hardly be affected. For the mammalian genome, $(D/N)_b$ values of 10^{-6} place 10^3 platinum atoms on each DNA genome, sufficient to inhibit replication and reduce cell survival. Platinum-DNA binding levels of this magnitude are found for ovarian ascites cells taken from patients receiving cisplatin chemotherapy.[97]

(ii). Mutagenesis and Repair

Apart from inhibition of DNA synthesis, what are the other biological consequences of cisplatin binding to DNA? One such consequence is mutagenesis, in which a normal base in the sequence is replaced by a different base. This phenomenon has been demonstrated for *cis*-DDP-treated cells in a variety of studies. What brings about such mutagenesis? There are several possibilities. One is that errors are introduced in DNA strands during attempts of the replication apparatus to synthesize past a platinum lesion. Another is that the platinum-damaged DNA is recognized by cellular repair systems that, in attempting to eliminate the platinated stretch of DNA, incorporate one or more incorrect nucleotides. Platinum-induced mutagenesis can lead to deleterious long-term health problems in patients treated with cisplatin. It is therefore important to understand the mechanism by which cellular DNA becomes mutated following platination, and to devise strategies for minimizing or eliminating this mutagenesis.

The foregoing considerations bring up another biological consequence of *cis*-DDP binding, namely, DNA repair. Removal of platinum from DNA by cellular repair mechanisms has been demonstrated by several groups. For example, in studying cis-DDP-treated human fibroblast cells in culture, it was found that the amount of bound platinum per nucleotide decreased according to first-order kinetics, from $(D/N)_b$ of 2.3×10^{-5} to 3.3×10^{-6} over a six-day period. Since Pt-DNA adducts are stable with respect to dissociation from DNA under physiological conditions (see above discussion), loss of platinum was attributed to DNA repair.[98]

How does the cell remove platinum from DNA? One mechanism is by a process known as excision repair, whereby the sugar-phosphate backbone on the platinated strand is hydrolyzed ("nicked") on either side of the damage and the remaining, unplatinated strand is used as a template for new DNA synthesis. The platinated oligonucleotide is displaced and the resulting gap filled in. In support of this picture is the fact that, in xeroderma pigmentosum (XP) human fibroblast cells, known to be deficient in excision repair, there is very little removal of platinum during post-treatment incubation.[99] Recent studies of *in vitro* repair of cisplatin-DNA adducts by a defined enzyme system, the ABC excision nuclease of *E. coli*, have provided some details at the molecular level about the process.[100,101] [^{32}P]-Labeled double-stranded DNA fragments containing $\{Pt(NH_3)_2\}^{2+}$ or $\{Pt(en)\}^{2+}$ adducts at random or defined sites were incubated with the enzyme. Cleavage of the platinated strand occurred at the 8th phosphodiester bond 5', and the 4th phosphodiester bond 3', to the GG or AG intrastrand crosslink. Further details about the identification and construction of such specific crosslinks will be given later in this chapter.

(iii). Drug Resistance

Another biological consequence of DNA-platinum interactions, probably related to the repair phenomenon, is resistance. Resistance of a cell to a chemotherapeutic agent, which can be inherent or acquired, is a phenotypical ability of the cell to tolerate doses of a drug that would be toxic to normal, or parent, cells.[102] Resistance is often acquired by prolonged exposure of cells in culture to the drug or, in patients, to repeated doses of drug therapy. There is not yet any direct proof that platinum-DNA interactions are responsible for acquired resistance to cisplatin. Studies of sensitive and resistant tumors in rats have shown, however, that after intravenous injection of 10 mg/kg of the drug, the platinum levels were the same after an hour, but after 24 hours a larger proportion of adducts had been removed in the resistant cells.[103] Similar results have been found for studies of Pt-DNA adducts in cultured L1210 cells of varying levels of resistance to cisplatin where, in the 18 h following a 6-hour incubation with the drug, the resistant cells had up to fourfold more platinum removed than the sensitive cells.[104]

Experiments have also been carried out showing that *cis*-DDP binding to DNA inhibits transcription, the formation of RNA from a gene, and that this phenomenon is less efficiently reversed for parent versus resistant L1210 cells in culture.[105] The assay involves transfection (the process whereby free or viral DNA or RNA is taken into a cell) of pRSVcat plasmid DNA into L1210 cells. The plasmid contains the bacterial *cat* gene in a position that permits its expression in mammalian cells. The *cat* gene encodes the enzyme chloroamphenicol acyltransferase (CAT), an activity readily measured following lysis of the cells. Transfection of the *cis*-DDP-damaged plasmid into resistant L1210 cells showed that up to eight times the amount of platinum was required in the resistant versus sensitive cells to produce a mean lethal hit (63 percent reduction in activity). This result is consistent with greater repair of platinum-DNA adducts in the resistant cells.

These results should not be construed to mean that DNA repair is the only mechanism of cisplatin resistance. There is evidence that relative amounts of glutathione are increased in cisplatin-resistant cells.[106] Glutathione presumably uses its thiol moiety to

coordinate platinum and diminish the amount that can bind to DNA. Reduced influx or increased efflux of a drug constitutes additional mechanisms by which cells become resistant. Further studies are required to ascertain which of these possibilities is most important for the cisplatin resistance phenomenon.

The discovery that cells can become resistant to cisplatin by repairing DNA lesions suggests a way to explain the selectivity of the drug for certain tumor tissue, and even the selective cytotoxicity of the drug for tumor versus normal cells of the same tissue. Tumor cells that cannot repair platinum-DNA adducts would be most affected by *cis*-DDP. This idea forms one of the central hypotheses about the molecular mechanism of action of *cis*-DDP, details of which can be probed by bioinorganic chemists. Specifically, it is important to inquire what DNA adducts formed by *cis*-DDP are both cytotoxic and repairable, what enzymes are responsible for such repair in mammalian cells, by what mechanisms these enzymes operate, and how this knowledge can be used to design better metal-based antitumor drugs and chemotherapeutic protocols.

(iv). DNA-protein Interactions

Most of the phenomena discussed in this section, inhibition of replication, DNA repair, drug resistance, and mutagenesis, probably involve interaction of a protein or group of proteins with platinated DNA. These interactions are clearly important in determining the biological consequences of DNA templates containing bound platinum. Very recent experiments have uncovered the existence of proteins from a variety of mammalian sources that bind specifically to DNA platinated with *cis*- but not *trans*-DDP.[107] Identifying the nature and function of these factors may provide important clues about the mechanisms of antitumor activity, drug resistance, or repair. Study of protein-DNA-drug interactions is an essential feature of the bioinorganic chemistry of platinum chemotherapeutic agents.

11.2.9.3: Aspects of Platinum Binding to DNA is shared under a CC BY-NC-SA 4.0 license and was authored, remixed, and/or curated by LibreTexts.

11.2.9.4: Survey of Metals Used for Diagnosis and Chemotherapy

Radiodiagnostic Agents[21,22]

Metal complexes having radioactive nuclei find many applications in medicine, such as in organ, and tissue imaging, Early detection of cancer, for example, by selective and imaging of the tumor using a radioactive metal compound can facilitate surgical removal or chemotherapeutic treatment before the disease reaches an advanced stage. radioisotopes used for diagnostic purposes be emit low-energy γ and no α or β particles. Table 9.2 lists the radionuclides most commonly employed for purpose in nuclear medicine. Among these, ^{99m}Tc is perhaps the most desirable,[23] for it gives off a 140-keV γ ray that is detected scintillation cameras and produces clear images. radionuclide is prepared from an alumina column loaded with $^{99}MoO_4^{2-}$, which decays to form $^{99m}TcO_4^-$, which in turn may be selectively eluted from the column with saline owing to its lower charge. treatment with a reducing agent in the presence of the appropriate ligands produces radiopharmaceuticals with desired water stability, and properties. Such complexes may be injected at concentrations of 10^{-6}-10^{-8} M. For example, isocyanide complexes such as $[Tc(CNR)_6]^+$= t-Bu, $CH_2CO_2Bu^t$, etc.) have been found to be taken up selectively into heart tissue and thus have the potential to be used as heart-imaging agents. Figure 9.2 displays bone as imaged a ^{99m}Tc bone agent. The dark correspond to surface areas of metabolic which can be used to diagnose or disease. One goal of research in this field is to images of myocardial infarcts or clogged arteries for physicians who can watch the patient's heart on a video surgery. Although chemical details responsible for the selective tissue of Tc isocyanide, and other complexes are largely synthetic modifications are and have many new compounds for evaluation.

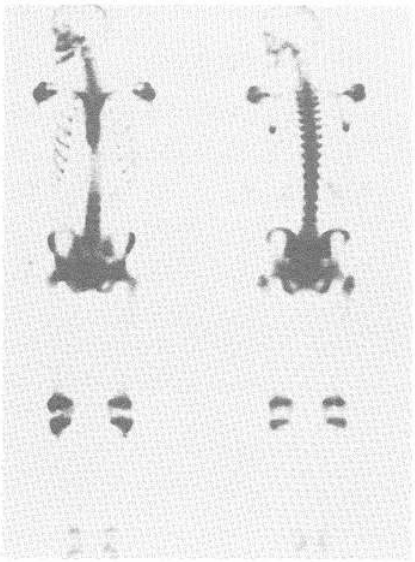


Figure 9.2 - Human skeleton (bone) imaged with ^{99m}Tc. Both anterior (left) and posterior (right) views are shown.

Table 9.2 - Radionuclides most commonly employed in diagnostic nuclear medicine.[a]

a) Data are from Table of the Isotopes in D. R. Lide, ed., *CRC Handbook of Chemistry and Physics*, CRC Press, 71 st ed., 1990-91, pp. 11-33 ff.

Radionuclide	Half-Life	Energy (keV)
^{57}Co	271 d	836
^{67}Ga	78 h	1,001
^{99m}Tc	6 h	140
^{111}In	67 h	172, 247
^{113m}In	104 m	392
^{123}I	13 h	1,230
^{169}Yb	32 d	207
^{197}Hg	64 h	159
^{201}Tl	72 h	135, 167

Among the few known to be absorbed selectively tumor cells is the antitumor antibiotic bleomycin (BLM),[24,25] the structure of which is portrayed in Figure 9.3. binds most radioactive metal ions, but the $^{57}Co(III)$ complex has the best tumor-to-blood ratio. Unfortunately, the long ^{57}Co (Table 9.2) has limited its clinical utility. Attempts to prepare ^{99m}Tc complexes of BLM with selective uptake properties approaching that of the cobalt have not yet been successful, although the target molecule would be a most valuable radiodiagnostic agent. One imaginative solution[26] to this problem was achieved by covalent attachment of an EDTA moiety to the terminal thiazole ring of BLM (Figure 9.3). The resulting Co(III) BLM-EDTA molecule was radiolabeled with $^{111}In^{3+}$ and found to be useful for diagnosis of cancer in humans. Also used for tumor imaging are ^{99m}Tc and ^{67}Ga citrate complexes, the latter being the agent of choice for many applications. Again, there is little known at the molecular level about the mechanism of tumor-cell specificity

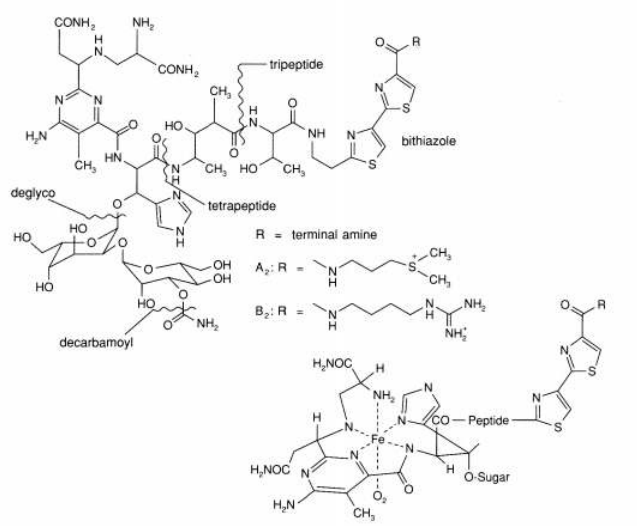


Figure 9.3 - Structure of bleomycin and its proposed iron complex (reproduced by permission from Reference 25).

An alternative approach to radionuclide-based tumor-imaging agents for diagnosis of disease is to modify, with metal chelating agents, antibodies raised against a biological substance, such as a tumor-cell antigen, hormone, or other target. Antibodies are proteins that are synthesized by specialized cells of the immune system in response to an external stimulant, or antigen. The high specificity and affinity of antibodies for the antigen can be used to target the antibody to a particular biological site, such as a site on the membrane of a particular cell type. Chelating agents are now routinely attached to antibodies and used to bind radioactive metal ions. The resulting radionuclide-labeled products are currently under extensive study in diagnostic medicine.[26]

Magnetic Resonance Imaging (MRI)[27]

Nuclear magnetic resonance (NMR) spectroscopy can be used to image specific tissues of biological specimens because of differences in the relaxation times of water proton resonances, usually brought about by paramagnetic metal ions. An early, pioneering example was the demonstration that Mn(lI) salts localize in normal heart-muscle tissue in dogs rather than in regions affected by blocked coronary arteries. Since the paramagnetism of the d^5 Mn(lI) ions alters the relaxation rate of nearby water protons, the normal and diseased tissue could be distinguished. Of the various metal ions surveyed in attempts to provide clinically useful NMR images in humans, Gd(III), Fe(III) , and Mn(lI) were found to give the best proton-relaxation enhancements. The gadolinium complex $[Gd(DTPA)(H_2O)]^{2-}$,an agent currently used in the clinic, has been successfully employed to image brain tumors. Ferric chloride improves gastrointestinal tract images in humans and, as already mentioned, manganous salts can be used for heart imaging. NMR imaging methodologies have advanced to the stage where increases as small as 10 to 20 percent in T_1^{-1}, the inverse nuclear-spin relaxation time, can be detected. As with radionuclide labeling, the complexes must be soluble and stable in biological fluids and relatively nontoxic, and are of greatest value when able to target a specific tissue. Even more important than targeting, however, is that proton relaxivity be maximally enhanced, an objective that depends not only upon the local binding constant but also upon large magnetic moments, long electron-spin relaxation (T_{le}) values, access to and the residence lifetime in the inner and outer coordination spheres by water molecules, and the rotational correlation time of the complex at its binding site. An obvious advantage of paramagnetic NMR over radioisotopic imaging agents is that there is no possibility of radiation damage; on the other hand, the need for 10-100 μM concentrations at the site of imaging is a distinct drawback. Both methods are likely to continue to be used in the future, and both will benefit from the design of new stable chelates that are selectively absorbed by the tissue to be diagnosed.

Lithium and Mental Health[28-31]

One in every 1,000 people in the United States currently receives lithium, as Li_2CO_3, for the treatment and prophylaxis of manic-depressive behavior. Doses of 250 mg to 2 g per day are administered in order to maintain a 0.5 to 2.0 mM concentration window, outside of which the drug is either toxic or ineffective. The detailed molecular mechanism by which Li^+ ion brings about its remarkable chemotherapeutic effects is largely unknown, but there are various theories. One theory proposes that lithium binds to inositol phosphates, inhibiting their breakdown to inositol, and so reducing inositol-containing phospholipids. A consequence of this chain of events would be disruption of the neurotransmission pathway based on inositol 1,4,5-triphosphate and 1,2-diacylglycerol, reducing neuronal communication, which is most likely hyperactivated in the manic state. This theory does not account for the antidepressive action of the drug, however. An alternative explanation is that lithium inhibits cyclic adenosine monophosphate (AMP) formation, again interfering with neurotransmission by intercepting this key intracellular signaling molecule. Recent experiments indicate that lithium affects the activation of G-proteins, a class of guanosine triphosphate (GTP)-binding proteins involved in information transduction. Possibly these effects result from displacement by Li^+ of Mg^{2+} from GTP and/or from protein-binding sites normally required for activation. Use of ^{7}Li NMR spectroscopy to study lithium transport in human erythrocytes suggests that it might be possible to apply this method to unravel details of the bioinorganic chemistry of lithium associated with the management of manic depression.

Gold and Rheumatoid Arthritis[23,32,33]

Gold compounds have been used in medicine for centuries, an application known as chrysotherapy. Since 1940, however, complexes of gold have been used most successfully to treat arthritic disorders in humans and other animals. Au(I) compounds are currently the only class of pharmaceuticals known to halt the progression of rheumatoid arthritis.

Until recently, gold compounds used to treat arthritis were painfully administered as intramuscular injections. Included were colloidal gold metal, colloidal gold sulfides, $Na_3[Au(S_2O_3)_2]$ (Sanocrysin), gold thiomalate and its sodium and calcium salts (Myochrisin), and polymeric gold thioglucose (Solganol, approved by the FDA). It was discovered, however, that triethylphosphinegold(l) tetra-O-acetylthioglucose (auranofin, Figure 9.4, approved by the FDA) was equally effective against rheumatoid arthritis and could be orally administered. The availability of this compound has sparked many studies of its biodistribution, stability, and possible metabolism that lead to antiarthritic activity. The mode of action of antiarthritic gold drugs is largely unknown, but it may involve binding of Au(I) to protein thiol groups, a process that inhibits the formation of disulfide bonds, and could lead to denaturation and subsequent formation of macroglobulins.

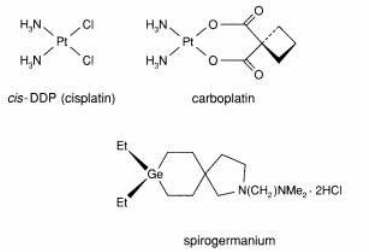


Figure 9.4 - Structures and trivial names of metal-based antitumor drugs.

Anticancer Drugs

1. Platinum Ammine Halides[34,35]

The discovery that *cis*-diamminedichloroplatinum(Il), *cis*-DDP or cisplatin (Figure 9.4), has anticancer activity in mice, and its subsequent clinical success in the treatment of genitourinary and head and neck tumors in humans, constitutes the most impressive contribution to the use of metals in medicine. Given in combination chemotherapy as an intravenous injection together with large amounts of saline solution to limit kidney toxicity, cisplatin treatment results in long-term (>5 yr) survival for more than 90 percent of testicular cancer patients. In a typical course, ~ 5 mg/kg body weight of the drug is administered once a week for four weeks. Extensive studies of platinum ammine halide analogues led to a series of empirical rules governing their chemotherapeutic potential. Specifically, it was concluded that active compounds should:

1. be neutral, presumably to facilitate passive diffusion into cells;
2. have two leaving groups in a *cis* configuration;
3. contain nonleaving groups with poor trans-Iabilizing ability, similar to that of NH_3 or organic amines;
4. have leaving groups with a "window of lability" centered on chloride.

These early structure-activity relationships have had to be modified somewhat, however, since chelating dicarboxylate ligands such as 1,1-dicarboxylatocyclobutane can replace the two chloride ions, and since cationic complexes with only one labile ligand, specifically, *cis*-$[Pt(NH_3)_2CI(4\text{-}X\text{-}py)]^+$, where X = H, Br, CH_3, etc., showed activity in some tumor screens. The two compounds shown in Figure 9.4, cisplatin and carboplatin (Figure 9.4), were the first to be approved for clinical use. Of particular interest to the bioinorganic chemist is that complexes having a *trans* disposition of leaving groups are inactive *in vivo*. This difference suggests the presence of a specific cellular receptor that, when identified, should facilitate the design of new, metal-based anticancer drugs. Present evidence strongly points to DNA as being the relevant cellular target molecule. Section V of this chapter expands on this topic in considerable detail.

2. Metallocenes and Their Halides: Ti, V, Fe[36,37]

Several compounds in this category, including $[(C_5H_5)_2TiX_2]$ (X = CI, Br, O_2CCl_3), $[(C_5H_5)_2VCl_2]$, $[(C_5H_5)_2NbCl_2]$, $[(C_5H_5)_2MoCl_2]$, and $[(C_5H_5)_2Fe]^+$ salts, exhibit significant activity against experimental animal tumors. Higher quantities (200 mg/kg) of these compounds than of *cis*-DDP can be tolerated with fewer toxic side effects, but their failure in two mouse leukemia screens commonly used to predict the success of platinum anticancer agents appears to have delayed their introduction into human clinical trials. Studies of Ehrlich ascites tumor cells treated with $[(C_5H_5)_2VCl_2]$ *in vitro* revealed selective inhibition of incorporation of radiolabeled thymidine, versus uridine or leucine, indicating that the complex blocks DNA replication. Unlike cisplatin, however, metallocene halides undergo rapid hydrolysis reactions in aqueous media, forming oxobridged and aqua complexes that may have a higher affinity for phosphate oxygen atoms than the heterocyclic nitrogen atoms of the bases in DNA.[38] Exactly how the ferrocenium ion might bind to DNA is even more obscure, although partial metallointercalation and groove binding are more likely than covalent attachment of the chemically unmodified cation. From the limited information available, metallocenes and their halides appear to behave fundamentally differently from platinum antitumor compounds. As a class, they provide a promising new opportunity to expand the scope of metal complexes used in cancer chemotherapy.

3. Gold and Other Metal Phosphines[39]

Following the successful entry of the soluble gold-phosphine complex auranofin (Figure 9.4) into the metal-based pharmaceuticals industry, several gold-phosphine complexes were examined for possible anticancer activity. Although auranofin itself was active in only a small fraction of the mouse tumor models tested, biological activity approaching that of cisplatin was discovered for many

analogues, most notably the diphosphine bridged complex [ClAu($PPh_2CH_2CH_2$ PPh_2)AuCI]. Attempts to replace the phosphine with As or S donor ligands, to increase or decrease the length of the 2-carbon bridge, or to replace the phenyl with alkyl groups all led to diminished activity. Most noteworthy is that the diphosphine ligands themselves have activity very similar to that of their gold complexes, and that Ag(I) and Cu(I) analogues are also effective. These results strongly imply that the phosphine ligands are the chemical agents responsible for the anticancer properties of these compounds. Coordination to a metal presumably serves to protect phosphines against oxidation to the phosphine oxides, which independent investigations have proved to be ineffective. A possible role for the metal in the cytotoxicity of the compounds cannot be ruled out, however.

4. Other Main Group and Transition-metal Compounds[36,40,41]

Several main group metal complexes exhibit anticancer activity. Gallium(III) nitrate is active against human lymphomas, but with dose-limiting side effects on the kidneys and gastrointestinal tract. Tin complexes of general formula $R_2L_2SnX_2$, where R = alkyl or phenyl, L_2 = py_2, bpy, or phen, and X_2 = two *cis*-oriented halide or pseudohalide leaving groups, are active against the mouse P388 leukemia tumor. The *cis* disposition of the leaving groups suggests a possible mechanism analogous to that of cisplatin (see below). Organo-gennanium compounds are also active, notably the derivative spirogermanium shown in Figure 9.4. Nothing is known about the mechanism of action of any of these compounds.

Following the discovery of activity for cisplatin, several thousand platinum and nearly 100 other transition-metal complexes have been screened in various tumor model systems in the hope of achieving better activity against a broader range of tumors. Among the classes of nonplatinum compounds showing some activity are ruthenium complexes *cis*-[$RuCl_2(DMSO)_4$], [$Ru(NH_3)_5$(Asc)] (CF_3SO_3), where Asc is ascorbate dianion, and *fac*-[$Ru(NH_3)_2Cl_4$] , all of which are believed to bind to DNA; binuclear rhodium complexes [$Rh_2(O_2CR)_4L_2$]; octahedral Pd(IV) complexes such as *cis*-[$Pd(NH_3)_2CI_4$]; and such miscellaneous molecules as the iron(II) complex of 2-formylpyridine thiosemicarbazone, the site of action of which is thought to be ribonucleotide reductase. These examples illustrate the broad scope encompassed by this field, which has a potential for developing fundamental infonnation about metal-biomolecule interactions as well as novel anticancer drugs. Much remains to be explored.

Miscellaneous Metals in Medicine

Numerous other anecdotal and some fairly elaborate studies have been reported for metal complexes as medicinal agents. The use of zinc applied topically to promote the healing of wounds dates back to around 1500 B.C., and silver is now commonly applied to prevent infection in bum patients.[42,43] Osmium carbohydrate polymers have been reported to have antiarthritic activity.[44] Transition-metal complexes have a long history of use as antibacterial and antiviral agents; for example, Zn^{2+} is used to treat herpes, possibly by inhibiting the viral DNA polymerase.[45] Early transition-metal (e.g., tungsten) polyoxoanions have been employed to treat AIDS patients.[46] Numerous reports have appeared detailing the anti-inflammatory, antiulcer, and analgesic activities of copper carboxylate complexes.[7] As in the previous section, these reports and others like them require more serious attention from bioinorganic chemists to elucidate the molecular events responsible for such a fascinating menu of biologically active metal complexes.

Summary and Prospectus

The clinical successes of platinum anticancer and gold antiarthritic drugs have changed the attitudes of many who doubted that heavy-metal compounds, notorious for their deleterious effects on human health, would ever playa serious role in chemotherapy. Indeed, we have seen that Hg^{2+}, Pb^{2+}, and Cd^{2+} are toxic elements. Even essential metals can be highly toxic if present in excess, either because of chronic or acute poisoning or because of metabolic defects that deregulate their control in the cell. An important common theme running throughout this discussion is selectivity. For a drug to be effective, it must be selectively toxic to diseased tissue while leaving nonnal tissue alone; or it must selectively kill harmful microorganisms at levels where it fails to deplete helpful ones. For a chelating agent to be useful in the toxic effects of metals, it must bind as selectively as possible to the deleterious ion while coordinating only weakly, if all, to others. For a diagnostic metal complex to be it must be taken up (or excluded) selectively from diseased cells relative to normal ones, or to one tissue type versus another. Rarely has such selectivity been designed in advance of the discovery of a useful metal-based pharmaceutical, although spectacular advances in biology, such as monoclonal antibodies, may be hastening the day when such an objective be common. Interestingly, the successes of such unlikely as *cis*-[$Pt(NH_3)_2Cl_2$] and [(Et_3P)Au(OAc_4-thioglucose)] in chemotherapy were driven by the personal involvement of individuals like B. Rosenberg for the former and B. Sutton for the latter. Like Hollywood producers, these men mustered every conceivable resource

to promote the compounds for testing, introduction into human clinical trials, and eventually approval by the FDA. Such zeal requires years, usually more than a decade, of sustained personal effort, and may be the reason why other metal complexes, such as those mentioned above, have not had the impact of a cisplatin or an auranofin. On average, only one of 7,000 such compounds makes it from the laboratory bench to the patient, at an average cost of 250 million dollars and a time interval of 13 years.

Another component of the evolving field of metals in medicine, however, is that, once a has proved its in the clinic, how does it work? This question is deceptively for coordination chemistry *in vivo*, and the of cells to respond to unnatural external stimuli such as metal complexes, are matters about which we are beginning to learn. As progress is made in this latter area, it should become possible to design drugs in a rational way to achieve the required selectivity.

The remainder of this chapter focuses on a case study where some progress in unraveling the molecular mechanism of a metal-based drug, cisplatin being made. If nothing else, this discussion will elucidate strategic guidelines that may be employed to attack similar questions about other chemotherapeutic metal compounds discussed earlier in this section. Unfortunately, there is very little information available about the molecular mechanisms of these other complexes. At this transition in our discussion, we move from general considerations to a specific, analysis. The reader must here take time to become familiar with the biological aspects of the new material.

11.2.9.4: Survey of Metals Used for Diagnosis and Chemotherapy is shared under a CC BY-NC-SA 4.0 license and was authored, remixed, and/or curated by LibreTexts.

11.2.9.5: Platinum Anticancer Drugs- A Case Study

History of the Discovery[47]

cis-[Pt(NH3hCh], a molecule known since the mid-19th century, has been a subject of considerable importance in the of inorganic stereochemistry and substitution reaction kinetics.[48] Its biological was discovered by accident. In the mid-1960s, biophysicist Barnett Rosenberg, at Michigan State University, was studying the effects of electric fields on the growth of *Escherichia coli* cells in culture. They had hypothesized that, during cell division, the orientation of the mitotic be affected by local electric which they hoped to perturb. Instead, they observed growth without cell division, the result being elongated, spaghetti-like bacterial filaments approaching 1 cm in length. After much detective work, they realized that small amounts of platinum from the electrodes used to apply the electric fields had reacted with NH_4CI in their buffer to produce various platinum ammine halide compounds. Two of these, *cis*-$[Pt(NH_3)_2Cl_2]$ and *cis*-$[Pt(NH_3)_2CI_4]$, were capable of inducing filamentous growth in the absence of any electric field. Since chemicals that produce filamentation in bacteria had been known to exhibit antitumor activity, Rosenberg was eager to have his platinum compounds tested. Unable to convince existing agencies like the National Cancer Institute (who to their credit later spearheaded the development of cisplatin) that a heavy-metal complex could actually be beneficial to animals, the Michigan State group set up their own animal-tumor screens. The results were nothing short of spectacular. Injection of *cis*-DDP directly into the abdominal cavity of mice into which a solid Sarcoma-180 tumor had been implanted led within a few days to a blackening (necrosis), reduction in size, and eventual disappearance of the tumor (Figure 9.5). The cured mouse enjoyed a normal lifespan. From these and other animal studies, physicians became convinced that administering platinum compounds to cancer patients might be worthwile, and a new field involving bioinorganic chemistry and cancer chemotherapy was born. The drug, marketed as Platinol with the generic name cisplatin, received FDA approval in 1979 and is today one of the leading anticancer agents.

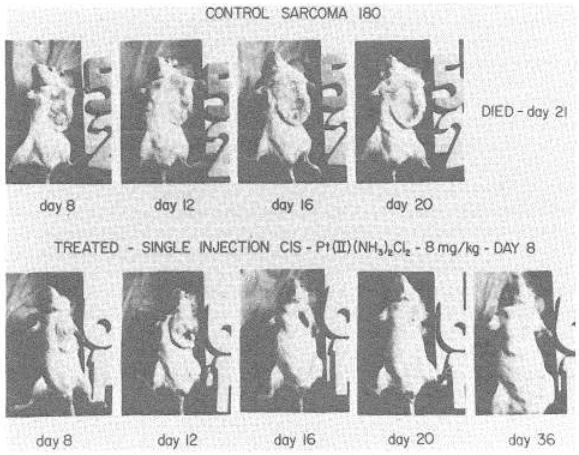


Figure 9.5 - Photographic demonstration of the dramatic ability of cisplatin to cure a Sarcoma-180murine tumor (reproduced by permission from Reference 47).

Principles that Underlie Drug Development

1. Strategic Considerations

There are two general routes to the development of inorganic complexes, and indeed most chemical compounds, as drugs. One, illustrated by cisplatin, arises from an empirical observation of biological activity followed by attempts to optimize the efficacy through investigations of structure-activity relationships (SAR). The goals are to minimize toxicity, to develop cell culture and animal screens for testing related compounds, and ultimately to elucidate the molecular mechanism. Knowledge of the molecular mechanism might evenlead to a rational strategy for designing better drugs.

The second general approach to drug design begins with known biochemistry. For example, ribonucleotide reductase is required in the first committed step in the biosynthesis of DNA, the conversion of ribo- to deoxyribonucleoside dir)hclsphat.es. The mammalian enzyme contains a binuclear non-heme iron center required for activity. Compounds that would selectively inhibit this enzyme by destroying this center are potentially useful as antiviral or antitumor agents. Another example is the enzyme reverse Iranscriptase, encoded by the HIV (AIDS) virus and required for its integration into the genome of the host cell. Compounds like

3'-azidothymidine (AZT) are accepted by the enzyme as substrates but, when added to the growing DNA chain, cannot be linked to the next nucleotide. Chain termination therefore occurs and the replication process becomes permanently interrupted. Attempts to find organic molecules or inorganic complexes that are more effective chain terminators than AZT constitute a rational strategy for developing new anti-AIDS drugs.

In the remainder of this chapter we describe research that has evolved following the discovery of biological activity for cisplatin. Although the initial breakthrough was serendipitous, subsequent studies have revealed many aspects of the molecular mechanism. From this known biochemistry we may one day be in a position to design more effective anticancer drugs and therapies based upon the fundamental bioinorganic chemistry of cisplatin.

2. Pre-clinical and Clinical Trials[49]

Predicting the chemotherapeutic potential of an inorganic compound such as *cis*-DDP prior to its introduction into human cancer patients is an important objective. Compounds are most easily tested for their cytotoxic effects on bacterial or mammalian cells in culture. Shown in Figure 9.6 are results for the survival of cultured L1210 cells in the presence of increasing amounts of *cis*- or *trans*-DDP.[50,51] The data reveal the markedly greater toxicity of the *cis* isomer, which is a much better anticancer agent than its stereoisomer. Unfortunately, no single assay has yet been found that can predict the chemotherapeutic potential of platinum compounds in humans. The best that can be obtained are results relative to those for *cis*-DDP, in which case toxicity at low dose is usually scored positive.

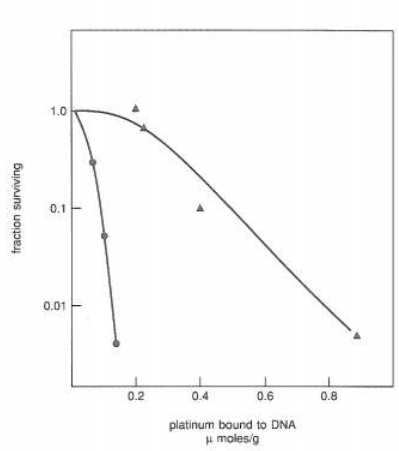


Figure 9.6 - Differential toxicity of cis- (●) and trans-DDP (▲) on HeLa cells growing in culture (reproduced by permission from Reference 51).

The next level of testing, often employed directly without first examining cell-culture results, involves animal (usually mammals, excluding human) screens.[49] Among the most popular measures of the chemotherapeutic activity of platinum compounds has been their ability to prolong the survival of mice bearing the L1210 or P388 leukemia. A suspension of cells is inoculated intraperitoneally (i.p., in the abdominal cavity), producing a leukemia that eventually progresses to the generalized disease. In one commonly used protocol, platinum compounds are dissolved in physiological saline (0.85 percent NaCl) or sterile H_2O and injected i.p. 24 h, 5, 9, and 13 days after inoculation of the leukemia cells. Several indices of antitumor activity and toxicity have been defined. The percent I.L.S., or increased lifespan measures the mean survival of treated versus control animals that were given no platinum drug. A related index is the median survival, percent T/C (Test/Control), which is 100 + percent I.L.S. The LD_{50} value measures toxicity as mean lethal dose,the amount of drug (usually in mg/kg body weight) required to kill half the animals. Potency is defined by lD_{90}, the inhibiting dose at which 90 percent of the tumor cells are killed. From these values, a therapeutic index (TI) = LD_{50}/lD_{90} is sometimes defined, which should be substantially greater than one. Typical values for *cis*-DDP are 85 percent I.L.S. at 8 mg/kg for the L1210 tumor, 13.0 mg/kg LD_{50}, and 1.6 mg/kg lD_{90} resulting in a TI of 8.1.

In addition to being tested in mice, cisplatin and related compounds have been screened in other mammals, specifically dogs and monkeys, mainly to look for possible dose-limiting side effects. Severe vomiting, once thought to be an insurmountable obstacle, was monitored by using ferrets. None of the animal screens can substitute for the ultimate test, however, which is human clinical trials. In 1972, such trials were initiated using terminally ill cancer patients. It was determined that intravenous (i.v.) injection,

rather than i.p. or oral administration, was the preferred method for giving the drug. Further details of the clinical development of cisplatin are discussed in a later section.

From the animal screens emerged the set of structure-activity relationships enumerated earlier (Section IV.E.1). Both cisplatin and carboplatin conform to these rules, and to date no compounds with demonstrably better antitumor activity have been tested in humans. The decision to move an experimental drug into the clinic is a difficult one, however, and it may be that molecules such as cis- $[Pt(NH_3)_2(4\text{-Br-py})Cl]Cl$ (see Section V.D.7.c) would be effective for tumors that are refractive to cisplatin chemotherapy. In any case, the foregoing chain of events, from studying the effects of a compound on cells in culture through animal screens and eventually to humans, constitutes the principal route for introducing a new anticancer drug. The process can take more than a decade.

3. Mechanism of Action Atudies

Once a class of compounds has been identified as biologically active, studies to elucidate the molecular mechanism of action can be undertaken. A first step is to identify the major cellular target or targets responsible for the chemotherapeutic properties of the drug. These investigations must also focus on chemical transformations that might take place in the solutions being administered and in the biological fluids that transport the drug to its ultimate target site. The next major step is to characterize the adduct or family of adducts made with the biological target molecule. The structure and kinetic lifetime of these adducts need to be investigated. Once this information is in hand, the effect of the adducts on the structure, stability, and function of the biological target molecule must be studied. Here many powerful new methodologies of modern molecular biology, genetics, and immunology can be brought to bear on the problem. The ultimate goals are to translate the molecular events elucidated into a realistic mechanism for how the drug molecule brings about its toxic effects selectively at the sites responsible for the disease and to use this information to design even better drugs.

Having progressed this far, we next need to bridge the gap between fundamental knowledge gained in studies of the mechanism of action and the SAR gleaned through pre-clinical and clinical trials. Whether such a happy situation can be reached for cisplatin remains to be seen, but there are encouraging signs, as we hope to demonstrate in the following discussion.

Clinical Picture for Cisplatin and Carboplatin[49,52]

1. Responsive Tumors and Combination Chemotherapy

It was an early observation that the best responses to cisplatin occurred in patients with genitourinary tumors. For testicular cancer, once a leading cause of death for males of age 20-40, cisplatin cures nearly all patients with stage A (testes alone) or B (metastasis or retroperitoneal lymph nodes) carcinomas. Platinum is usually given in combination with other drugs, commonly vinblastine and bleomycin for testicular cancer. This combination chemotherapy, as it is known, has several objectives. Some tumors have a natural or acquired resistance to one class of drugs and, by applying several, it is hoped that an effective reduction in tumor mass can be achieved. In addition, various drugs are known to affect different phases of the cell cycle, so several are applied simultaneously to allow for this possibility. Finally, synergism, where the response is greater than expected from simple additive effects, can occur, although it is rare. In addition to testicular cancer, platinum chemotherapy has produced responses in patients with ovarian carcinomas (>90 percent), head and neck cancers, non-small-cell lung cancer, and cervical cancer. Cisplatin is also effective when combined with radiation therapy.

2. Dose-limiting Problems; Toxicology

An early and quite worrisome adverse side effect of cisplatin was kidney toxicity. This problem, not commonly encountered with the older cancer drugs, nearly prevented its widespread use and eventual FDA approval. The major breakthrough here was made by E. Cvitkovic, who, while working at Sloan-Kettering Memorial Hospital in New York, administered large quantities of water by intravenous injection to patients, together with an osmotic diuretic agent such as D-mannitol. The rationale was that such hydration could ameliorate kidney toxicity by flushing out the heavy-metal complex. This simple idea worked, and the dose of the platinum compound could be increased threefold without accompanying nephrotoxicity. Hydration therapy is now commonly employed when cisplatin is administered. Among the other toxic effects encountered in cisplatin chemotherapy are nausea and vomiting, but this problem has also been controlled by use of antiemetic agents. Patients have also been known to experience bone-marrow suppression, a ringing in the ears, and occasional allergic reactions.

More recently, attempts have been made to extend cisplatin treatment to other broad classes of tumors by raising the dose above the ~5 mg/kg body weight levels given by i.v. injection every few weeks. Direct injection into the peritoneal cavity has been employed for refractory ovarian tumors. These more aggressive therapeutic protocols have been frustrated by drug resistance, a phenomenon by which cells learn to tolerate a toxic agent and for which many mechanisms exist, and by the return of the usual cisplatin side effects, most notably kidney toxicity and neurotoxicity. In order to combat toxic effects to the kidneys, chemoprotector drugs have been introduced. Based on the known affinity of platinum(II) complexes for sulfur-donor ligands, sodium diethyldithiocarbamate (DDTC) has been given both to experimental animals and to humans by i.v. infusion over about an hour following cisplatin administration.[53] DDTC inhibits many of the toxic side effects, particularly to the kidneys and bone marrow, without itself producing long-term side effects or apparently inhibiting the antitumor properties of *cis*-DDP. Similar efforts have been made to reduce the toxic effects of cisplatin with other sulfur-containing compounds including thiosulfate and the naturally occurring biomolecules glutathione, cysteine, and methionine. The relative amounts of the latter three molecules can be controlled by drugs that affect their normal cellular concentrations.

Another approach to reducing cisplatin toxicity is to develop new classes of platinum drugs or different routes of their administration. Carboplatin (Figure 9.4) is one result of these efforts. The bidentate chelating dicarboxylate leaving group in carboplatin presumably retards the rates of reactions leading to toxicity, but does not adversely interfere with the chemistry required for antitumor activity. Recently, promising platinum compounds for oral administration have been developed.[54] In Pt(IV) complexes of the kind *cis*, *trans*, *cis*-$[Pt(NH_3)(C_6H_{11}NH_2)\bullet(O_2CCH_3)_2Cl_2]$, where $C_6H_{11}NH_2$ is cyclohexylamine, have been found to be effective in preclinical screens. The greater kinetic inertness of these complexes apparently renders them sufficiently stable to the chemically harsh environment of the gastrointestinal tract. Once absorbed into the bloodstream, these compounds are metabolized to the Pt(II) analogues, *cis*-$[Pt(NH_3)(C_6H_{11}NH_2)Cl_2]$, which are presumed to be the active form of the drug. The Pt(IV) compound has recently entered clinical trials.

Although impressive inroads have been made in the management of human tumors by platinum chemotherapy, the fact remains that, apart from testicular and to a lesser extent ovarian cancer, the median survival times are measured in months. Clearly, there is much room for improvement.

3. Pharmacology[49,52]

Solutions of cisplatin are usually given in physiological saline (NaCl), since hydrolysis reactions occur that can modify the nature of the compound and its reactions *in vivo* (see below). Cisplatin is rapidly cleared from the plasma after injection, 70-90 percent of the platinum being removed within the first 15 minutes. It has been found that more than half the platinum binds to serum proteins and is excreted. Most of the platinum exits the body via the urine within a few days. These results account for the use of multiple-dose chemotherapy at intervals of several weeks. Animal studies employing *cis*-DDP labeled with ^{195m}Pt, a 99 keV γ-emitter with a 4.1-day half-life, reveal retention half-times in various tissues of 8.4 (kidney), 6.0 (ileum), 4.1 (liver), 2.8 (tumor), and 1.9 (serum) days following a single dose. Platinum distributes widely to all tissue, with kidney, uterus, liver, and skin having the most, and muscles, testes, and brain the least amount of the compound. There is no evidence for selective uptake into normal versus tumor cells.

11.2.9.5: Platinum Anticancer Drugs- A Case Study is shared under a CC BY-NC-SA 4.0 license and was authored, remixed, and/or curated by LibreTexts.

11.2.9.6: Mapping the Major Adducts of cis- and trans-DDP on DNA; Sequence Specificity

As we have seen, the antitumor activity of cisplatin is most likely the result of its DNA-binding properties. But what are the adducts? The human genome has more than a billion nucleotides. Does platinum recognize any special regions of the DNA or any particular sequences? In other words, is binding simply random or is there at least a regioselectivity? In this section, we discuss the best strategies for answering these questions, strategies that evolved in pursuit of learning how *cis*-DDP binds to DNA. We also illustrate their power in elucidating the DNA-binding properties of other metal complexes of interest to bioinorganic chemists.

a. Early Strategic Approaches

The first experiments to imply the sequence preferences of *cis*-DDP binding to DNA employed synthetic polymers.[108,109] Specifically, the buoyant density of poly(dG)•poly(dC), poly(dG•dC), and their *cis*-DDP adducts was studied in the analytical ultracentrifuge. The greatest shift in buoyant density was seen for the platinum adducts of poly(dG)•poly(dC), from which it was concluded that platinum forms an intrastrand crosslink between two neighboring guanosine nucleosides on the same strand. This interpretation was suggested by the known preference of metal ions, and especially platinum, for binding at the N7 position on the guanine base (Figure 9.9), information available from model studies of metal-nucleobase chemistry. Although other interpretations of the buoyant-density shift were possible, especially since the amount of platinum bound was not quantitated, the conclusion proved to be correct, as confirmed by later investigations. Interestingly, *trans*-DDP did not selectively increase the buoyant density of poly(dG)•poly(dC).

Following these initial experiments, the regioselectivity of *cis*-DDP binding was investigated by studying the inhibition of enzymatic digestion of platinated DNA. For example, the platinum complex inhibits the cleavage of DNA by restriction enzymes that recognize specific sequences and cut both strands of the double helix.[110] The resulting fragments are readily identified on electrophoresis gels. One such restriction enzyme is Bam HI. As shown by the arrows in Scheme (9.11), Bam HI cleaves a six-bp palindromic sequence at the phosphodiester bonds between two guanosine nucleosides. Formation of an intrastrand crosslink between the two adjacent guanosine nucleosides inhibits digestion by the enzyme. Another method, termed exonuclease mapping, involves digestion of the strands of duplex DNA from its 3'-ends.[111,112] When the enzyme encounters a bound platinum atom, it is unable to proceed further. Analysis of the digestion products by gel electrophoresis reveals the presence of discrete bands caused by the inhibition of digestion by bound platinum at specific sequences. Results from experiments of this kind were the most definitive at this time in demonstrating the profound regioselectivity of cisplatin for adjacent guanosines, and strongly supported the earlier conclusion that the drug was making an intrastrand d(GpG) crosslink.



Figure 9.18. Platinum is first bound to a single-stranded DNA template, in this example from bacteriophage M13mp18, to which is next annealed a short, complementary oligonucleotide termed a "primer" for DNA synthesis. Addition of the large (Klenow) fragment of *E. coli* DNA polymerase I and deoxynucleoside triphosphates, one of which bears a ^{32}P label, [α-^{32}P]dATP, initiates replication. When the enzyme encounters a platinum adduct, the chain is terminated. By running out the newly synthesized DNA strands on a sequencing gel, the sites of platinum binding can be detected by comparing the positions of the radiolabeled fragments with those obtained from sequencing ladders. The results of this procedure, which has been termed "replication mapping," confirmed that *cis*-DDP binds selectively to $(dG)_n$ ($n \geq 2$) sequences. In addition, they showed that *trans*-DDP blocks replication, in a much less regioselective manner, in the vicinity of sequences of the kind d(GpNpG), where N is an intervening nucleotide. These data afforded the first clear insight into the sequence preferences for *trans*-DDP on DNA. A control experiment run with DNA platinated by the monofunctional complex $[Pt(dien)CI]^+$ gave the interesting result that DNA synthesis was virtually unaffected.

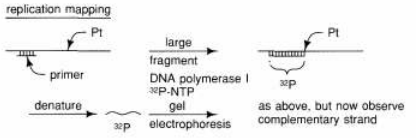


Figure 9.18 - Diagram illustrating the replication mapping experiment. To a single-stranded, platinated template is annealed a short primer for DNA synthesis using DNA polymerase I (Klenow fragment) and radiolabeled nucleotides. Sites of platinum binding are revealed as bands on gel electrophoresis where chain termination occurs (see text for details).

In yet another approach to the problem, DNA containing *cis*- or *trans*-DDP adducts was electrostatically coupled to bovine serum albumin, to enhance its antigenicity, and injected into rabbits.[113,114] The resulting antisera and antibodies were then studied for their ability to recognize and bind specifically to platinated DNAs having defined sequences, such as poly(dG)•poly(dC) and poly[d(GC)]•poly[d(GC)].

From experiments of this kind, the major *cis*-DDP adduct recognized by the antibody was found to be *cis*-[$Pt(NH_3)_2${d(GpG)}], in accord with the findings of the enzymatic mapping experiments. Unplatinated DNA was not recognized, nor was DNA platinated with *trans*-DDP. On the other hand, the antibody recognized DNA platinated with antitumor-active compounds [$Pt(en)Cl_2$] and [Pt(DACH)(CP)], where DACH = 1,2-diaminocyclohexane and CP = 4-carboxyphthalate. This result revealed that the antibody recognized the structural change in DNA that accompanies formation of d(GpG) intrastrand crosslinks, irrespective of the diamine ligand in the coordination sphere of the platinum atom. The antibody is also capable of distinguishing adducts formed by active versus inactive platinum complexes. Most importantly, DNA isolated from the cells of mice bearing the L1210 tumor five hours after cisplatin injection, was recognized.[113,115] Subsequent studies[116] revealed that these antibodies could detect cisplatin-DNA adducts formed in the white blood cells of patients receiving platinum chemotherapy. Thus, the antibody work linked the regiospecificity of platination chemistry *in vitro* with that occurring *in vivo* and in a clinically relevant manner.

Additional studies with monoclonal antibodies generated using DNA platinated with *cis*- or *trans*-DDP further confirmed and extended these results.[117] This later work indicated that intrastrand crosslinked d(ApG) and d(GpG) sequences possess a common structural determinant produced by *cis*-DDP platination, and that carboplatin is also capable of inducing the same DNA structure. For *trans*-DDP-platinated DNA, a monoclonal antibody was obtained that appeared to have the intrastrand d(GpTpG) adduct as its major recognition site. In all these studies, the primary structural determinant appears to be DNA duplex opposite the site of platination, since fairly major stereochemical changes could be made in the amine ligands with no appreciable effect on antibody binding.

b. Degradation, Chromatographic Separation, and Quantitation of DNA Adducts

Experiments in which DNA platinated with *cis*-DDP is degraded to chromatographically separable, well-defined adducts have been invaluable in revealing the spectrum of products formed. In a typical experiment, platinated DNA is digested with DNAse I, nuclease P1, and alkaline phosphatase. These enzymatic digestions degrade DNA into nucleosides that can be readily separated by high-performance liquid chromatography (HPLC). Detection of the adducts can be accomplished by the UV absorption of the nucleoside bases at 260 nm or, for platinum complexes containing a radioactively labeled ligand such as [^{14}C]ethylenediamine,[118] by monitoring counts. In addition to peaks corresponding to dA, dC, dG, and dT, the chromatographic trace contains additional peaks corresponding to specific platinum nucleobase adducts such as *cis*-[$Pt(NH_3)_2(dG)_2$]. The precise nature of these adducts was established by comparison with chemically synthesized compounds structurally characterized by NMR spectroscopy.[118-121] An alternative method for identifying the adducts employed antibodies raised against specific platinum-nucleobase complexes.[122]

This approach has revealed the relative amounts of various adducts formed by a variety of platinum complexes; selected results are summarized in Table 9.4. Usually, for cisplatin, the relative amounts of the various adducts formed varies according to the series *cis*-[$Pt(NH_3)_2${d(pGpG)}] > *cis*-[$Pt(NH_3)_2${d(pApG)}] > *cis*-[$Pt(NH_3)_2${d(GMP)}$_2$] > monofunctional adducts. Only when the total incubation time was short, less than an hour, were the monofunctional adducts more prevalent, as expected from the kinetic studies of *cis*-DDP binding to DNA discussed previously. It is noteworthy that no d(pGpA) adducts were detected. This result, which is consistent with information obtained by enzymatic mapping, can be understood on stereochemical grounds.[123] If the guanosine nucleoside N7 position is the most-preferred binding site on DNA, closure to make an N7,N7 intrastrand crosslink between two adjacent purine nucleotides is more feasible in the 5' direction along the helix backbone (N7•••N7 distance of ≈ 3 Å) than in the 3' direction (N7•••N7 distance ≈ 5 Å). In addition, molecular-mechanics modeling studies[124] indicate that a highly unfavorable steric

clash occurs between the 6-amino group of the 3'-adenosine residue in a d(pGpA) crosslink and the platinum ammine ligand, whereas in the platinated d(pApG) sequence, the 6-oxo group forms a stabilizing hydrogen bond to this ligand. A 28 kJ mol^{-1} preference of *cis*-DDP for binding d(pApG) over d(pGpA) was calculated.

Table 9.4 - Geometric features of the platinum coordination spheres of *cis*- [$Pt(NH_3)_2${d(pGpG)}].

a) Bond distances are in Angstroms and angles are in degrees.

b) Conventions used for assigning Base/Base and Base/PtN4 dihedral angles can be found in J. D. Orbell, L. G. Marzilli, and T. J. Kistenmacher, *J. Am. Chem. Soc.* **103** (l981), 5126. The numbers in square brackets refer to the corresponding N(ammine)•••O6 distance, in Å (see text).

Bond Distances and Angles[a]	Molecule 1	Molecule 2	Molecule 3	Molecule 4
Pt-N1	2.03(2)	2.01(2)	2.08(2)	2.08(2)
Pt-N2	2.03(3)	2.09(2)	2.04(3)	2.06(3)
Pt-N7A	2.01(2)	2.02(2)	1.91(3)	1.93(3)
Pt-N7B	2.05(2)	1.95(3)	2.00(3)	2.06(3)
N7A-Pt-N1	88.6(9)	90.3(9)	91.0(1)	88.4(9)
N7A-Pt-N2	179(1)	173.3(8)	178(1)	177(1)
N7A-Pt-N7B	89.1(9)	90.0(1)	85(1)	89(1)
N1-Pt-N2	92(9)	90.8(9)	91(1)	93(1)
qN1-Pt-N7B	176.5(9)	179.0(1)	173(1)	175(1)
N2-Pt-N7B	90.3(9)	89.0(1)	93(1)	89(1)

Dihedral Angles[b] Molecule	3'-Gua/5'-Gua	5'-Gua/PtN_4	3'-Gua/PtN_4
1	76.2(5)	110.6(5) [3.30(3)]	86.1(5)
2	81.0(5)	110.8(5) [3.49(3)]	95.5(5)
3	86.8(6)	81.0(6)	58.0(6) [3.11(4)]
4	80.6(5)	76.6(6)	59.6(6) [3.18(4)]

There are two likely sources of *cis*-[$Pt(NH_3)_2${d(GMP)}$_2$] in the spectrum of adducts. This species could arise from long-range intrastrand crosslinks, where the two coordinated guanosines are separated by one or more nucleotides. In support of this possibility is the fact that digestion of chemically synthesized *cis*-[$Pt(NH_3)_2${d(GpNpG)}], where N = C or A, led to *cis*-[$Pt(NH_3)_2${d(Gua)}-{d(GMP)}] and mononucleotides.[118,119,121] The other source of this product is interstrand crosslinked DNA, known to occur from the alkaline elution studies.

As indicated in Table 9.4, in all the experiments there was platinum that was unaccounted for in the quantitation procedures, which employed either antibodies, platinum atomic absorption spectroscopy, or a radiolabeled ethylenediamine ligand. Some of this material was assigned to oligonucleotides having high platinum content, resistant to enzymatic degradation.

Two important points emerge from the quantitation of adducts by this method. One is that intrastrand d(GpG) and d(ApG) crosslinks constitute the major adducts (>90 percent of total platination) made by cisplatin on DNA *in vivo*. Because they were identified by an antibody specific for their structures, no chemical change brought about by cellular metabolism has occurred. Secondly, the preponderance of these adducts far exceeds the frequency of adjacent guanosine or guanosine/adenosine nucleosides in DNA. This latter result implies a kinetic preference for, or recognition of, d(pGpG)- and d(pApG)-containing sequences by cisplatin.

c. Postscript: A Comment on Methodologies

With few exceptions, none of the experimental studies described in this section could have been carried out in 1969, when Rosenberg first demonstrated the anticancer activity of *cis*-DDP. The techniques of DNA sequencing, monoclonal antibody formation, oligonucleotide synthesis, HPLC, FPLC, and many of the higher resolution gel electrophoresis methodologies employed were the result of later developments driven by rapid advances in the fields of molecular biology and immunology. Future progress in elucidating the molecular mechanisms of action of cisplatin and other inorganic pharmaceuticals will no doubt benefit from new technological discoveries and inventions of this kind yet to come.

11.2.9.6: Mapping the Major Adducts of cis- and trans-DDP on DNA; Sequence Specificity is shared under a CC BY-NC-SA 4.0 license and was authored, remixed, and/or curated by LibreTexts.

11.2.9.7: Structure of Platinum-DNA Complexes

a. NMR Studies of Platinated Oligonucleotides

Once the major spectrum of adducts formed by *cis*- and *trans*-DDP with DNA began to emerge, it was of immediate interest to learn to what positions on the nucleobases the platinum atom was coordinated. Proton NMR spectroscopy soon proved to be an invaluable tool for obtaining this information.[71,125,126] Several ribo- and deoxyribooligonucleotides containing GG, AG, or GNG sequences were synthesized, and allowed to react with *cis*-DDP or its hydrolysis products, and the resulting complexes were purified by chromatography. All GG-containing oligomers formed intrastrand crosslinks with the $\{Pt(NH_3)_2\}^{2+}$ moiety coordinated to the N7 atoms. This structure was deduced from several criteria. Most frequently studied were the nonexchangeable base protons H8 and H2 of adenine, H6 of thymine, H8 of guanine, and H5 and H6 of cytosine (Figure 9.9). Coordination of platinum to N7 of guanine causes a downfield shift of the H8 proton resonance. More importantly, however, it also lowers the pK_a of the N1 proton by ~ 2 units, because platination adds positive charge to the base. Thus, titration of the platinated oligonucleotide over a pH range, and comparison of the results to those obtained for the unplatinated oligomer, reveals a difference in the midpoint of the transition in chemical shift of the H8 proton by 2 pH units if coordination occurs at N7. This effect is illustrated in Figure 9. 19 for the adduct *cis*- $[Pt(NH_3)_2\{d(ApGpGpCpCpT)\}N7\text{-}G(2),N7\text{-}G(3)]$, where the pK_a of N1 is seen to shift from ~ 10 to ~ 8 upon platination.[71] The pH titration in this example also reveals the pH-dependent chemical shift of the cytosine ^1H resonances at a pH of ~ 4.5, corresponding to protonation of the N3 atoms. The protonation of adenine N7 (pK_a ~ 4) is also frequently observed in these studies. These results conclusively demonstrate platinum coordination at N7 of the two guanosine nucleosides.

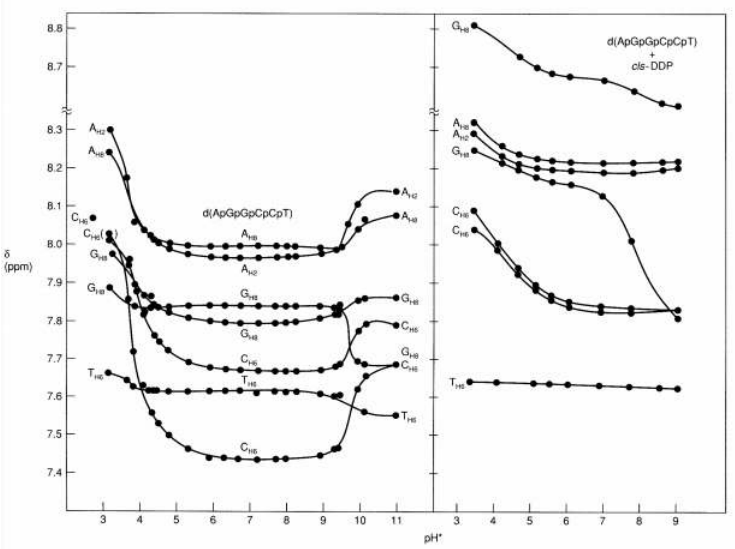


Figure 9.19 - Chemical shift (***δ***) vs. pH* of the nonexchangeable base protons of D_2O solutions of $[d(ApGpGpCpCpT)]_2$ (3.5 mM, 35 °C) and its cis-DDP adduct (2.5 mM, 70 °C). The pyrimidine resonances of the latter sample show no chemical shift changes with temperature over the range 35 < T < 70 °C while the purine resonances show a slight temperature-dependent chemical shift change of up to 0.1 ppm. Tetramethylammonium chloride was used as the internal standard (***δ*** 3.180). Reproduced by permission from J. C. Caradonna, S. J. Lippard, M. J. Gait, and M. Singh, J. Am. Chem. Soc. **104** (1982), 5793.

Although several of the oligonucleotides studied have self-complementary sequences, such that they can form a double helix when unplatinated, in no such case was a duplex observed for their platinated forms. The presence of the platinum-induced crosslink presumably decreases the stability of the doublestranded form of the oligonucleotide. Another interesting result is that all intrastrand $\{Pt(NH_3)_2\}^{2+}$ adducts of d(GpG) or d(ApG) have an altered deoxyribosesugar ring conformation. In normal, unplatinated form, these single-stranded or duplex oligonucleotides have a C2'-endo sugar pucker (Figure 9.9). Upon platination, the 5'-nucleotide switches to C3'-endo. This change is readily monitored by the ring proton-coupling constants $J_{H1'\text{-}H2'}$ and $J_{H1'\text{-}H2''}$. These protons constitute an ABX spin system such that the sum, $\Sigma^3J = {}^3J_{1'2'} + {}^3J_{1'2'}$, is most easily measured as the separation between the outermost peaks in the multiplet. For the C2'-endo conformation, a pseudotriplet occurs with Σ^3J = 13.6 Hz, and for C3'-endo, Σ^3J = 7.5 Hz. The 3'-guanosines in the adducts show greater conformational flexibility, having ~ 70 to 80 percent C2'-endo sugar puckers, depending upon the temperature.

Another conformational feature that could be deduced from ^{1}H NMR studies of all *cis*-DDP-platinated oligonucleotides containing an embedded d(GpG) sequence is that both guanosine nucleosides retain the anti orientation of the base around the C1'-N9 glycosidic linkage (Figure 9.9). This result was deduced from the lack of a pronounced nuclear Overhauser effect (NOE) between H8 and the H1' protons, such as would occur in the syn conformation. An NOE between H8 resonances on the two coordinated nucleosides was observed for adducts of d(ApTpGpG) and d(CpGpG), indicating that the two bases are in a head-to-head orientation with respect to the platinum coordination plane. In other words, both O6 atoms lie on the same side of that plane. Two oligonucleotides containing *cis*-$[Pt(NH_3)_2(ApG)]$ adducts have been examined; their structural properties closely resemble those of the (GpG) adducts, with platinum coordinated to N7 of both purine bases.

In order to study double-stranded DNAs platinated on one strand, it was necessary to adopt a special strategy. First, the desired oligonucleotide is synthesized. It is preferable that the DNA strands not be self-complementary, since the affinity of such an oligomer for itself is so much greater than that for its platinated form that the desired, singly platinated duplex will not form. After the platinated single strand is synthesized and purified, the complementary strand is added. Several duplex oligonucleotide-containing *cis*-$[Pt(NH_3)_2\{d(pGpG)\}]$-embedded adducts prepared in this manner have been studied by ^{1}H NMR spectroscopy. With the use of two-dimensional and temperature-dependent techniques, both the nonexchangeable base and sugar protons as well as the exchangeable (guanine N1 and thymine N3) N-H (imino) proton resonances were examined. The last are useful, since they give some measure of the extent to which the double helix remains intact. When not base-paired to their complements in the other strand, these protons exchange more rapidly with solvent (water) protons, leading at moderate exchange rates to broadening of the resonances and, at high exchange rates ($>10^{7}$ s^{-1}), disappearance of the signals. Several interesting results were obtained in these studies. In all of them, platination of the d(GpG) sequence brought about the same C2'-endo → C3'-endo sugar-ring pucker switch for the 5'-guanosine as seen in the single-stranded adducts. Head-to-head, anti conformations were also observed. At low temperatures, below the melting transition temperature, above which the duplex becomes single-stranded, the imino proton resonances were observed. This result was interpreted to mean that normal, Watson-Crick base pairs can still exist between the *cis*-DDP d(GpG) adduct and the d(CpC) sequence on the complementary strand. In the case of [d(TpCpTpCpG*pG*pTpCpTpC)]•[d(GpApGpApCpCpGpApGpA)], where the asterisks refer to the sites of platination, the imino proton resonances were assigned with the assistance of NOE experiments.[125] Temperature-dependent studies showed that, in the range - 4° < T < 46 °C, the imino resonances of the coordinated guanosine nucleosides broadened first with increasing temperature. Apparently the base pairs of the intrastrand crosslinked, platinated duplex DNA are disrupted, or "melted," outward from the point of platination as well as from the ends. Since the amino hydrogen atoms involved in base pairing were not observed in this study, a completely definitive structural analysis was not possible. Nevertheless, the authors proposed that the duplex would be kinked by an angle of ~ 60° at the *cis*-DDP binding site in order to preserve full duplex character.

Another useful NMR nucleus for monitoring *cis*-DDP-DNA interactions is ^{195}Pt, which is 34 percent abundant with I = $\frac{1}{2}$. When used in conjunction with ^{15}N (I = $\frac{1}{2}$) enriched NH_3 ligands, ^{195}Pt NMR resonances provide a powerful means for characterizing complexes in solution. The ^{195}Pt and ^{15}N chemical shifts are both sensitive to the ligand trans to the NH_3 group, as is the ^{195}Pt-^{15}N coupling constant.[127] ^{195}Pt NMR studies of *cis*-DDP binding have been carried out using nucleobases, small oligonucleotides, and even double-stranded fragments of 20 to 40 bp in length, as previously described (Section V.D.l). The major contribution of this method is to show whether platinum coordinates to a nitrogen or an oxygen donor atom on the DNA, since the ^{195}Pt chemical shift is sensitive to this difference in ligation.

b. X-ray Structural Studies

In recent years several oligonucleotide duplexes have been crystallized and characterized by x-ray diffraction methods. The probability of forming suitable single crystals of DNA fragments is disappointingly low, however, with only 1 in 10 such attempts being successful. Correspondingly, it has been difficult to crystallize platinated oligonucleotides. An alternative approach has been to soak nucleic-acid crystals of known structure with the platinum reagent in the hope of forming an isomorphous derivative, the structure of which could be obtained by using the changes in phases from the native material. In attempts to characterize a *cis*-DDP nucleic acid adduct, crystals of $tRNA^{Phe}$ and the self-complementary dodecamer d(CpGpCpGpApApTpTpCpGpCpG) were soaked with cisplatin solutions in the hope of obtaining useful metric information.[123,128,129] These efforts have thus far failed to produce a high-resolution structure, although they confirm the predilection for platinum to coordinate to the N7 position of purine rings. Addition of *cis*-DDP tends to disorder the crystal, with platinum going to several sites of partial occupancy.

A more fruitful approach has been to crystallize a purified oligonucleotide containing the coordinated *cis*-$\{Pt(NH_3)_2\}^{2+}$ moiety. The first x-ray structure to be deciphered through such a strategy was that of *cis*-$[Pt(NH_3)_2\{d(pGpG)\}]$.[130] This compound crystallizes with water solvent and glycine buffer molecules in the lattice. The crystals were grown at pH 3.8, where the terminal phosphate is monoprotonated in order to provide a neutral complex of diminished solubility. Two crystalline forms have been obtained, and both structures solved, one to 0.94 Å resolution. The latter contains four crystallographically independent molecules, which, although complicating the structure solution, afforded four independent views of the major adduct formed by *cis*-DDP with DNA. The four molecules form an aggregate, held together by hydrogen bonding and intermolecular base-base stacking interactions (Figure 9.20). There are two conformationally distinct classes that comprise molecules 1 and 2, and molecules 3 and 4; within each class, the molecules are related by an approximate C_2 symmetry axis.

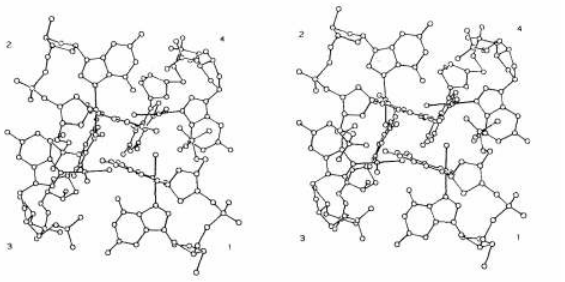


Figure 9.20 - Stereoview of aggregate of four cis-$[Pt(NH_3)_2\{d(pGpG)\}]$ molecules (reproduced by permission from Reference 130).

The molecular structure of molecule 1 is displayed in Figure 9.21; geometric information about all four molecules is contained in Table 9.4. As expected from the NMR studies, platinum coordinates to N7 atoms of the guanine bases, which are completely destacked (dihedral angles range from 76.2 to 86.7°), to form a square-planar geometry. The bases have a head-to-head configuration and conformational angles χ (Table 9.4 and Figure 9.9) that fall in the anti range. The sugar puckers of the 5'-deoxyribose rings for all four molecules have a C3'-endo conformation, and some of the 3'-sugar carbon atoms exhibit large thermal parameters suggestive of a less well-ordered structure. These results further demonstrate the similarity of the structure as detected in the solid state by x-ray diffraction and in the solution state by NMR spectroscopy.

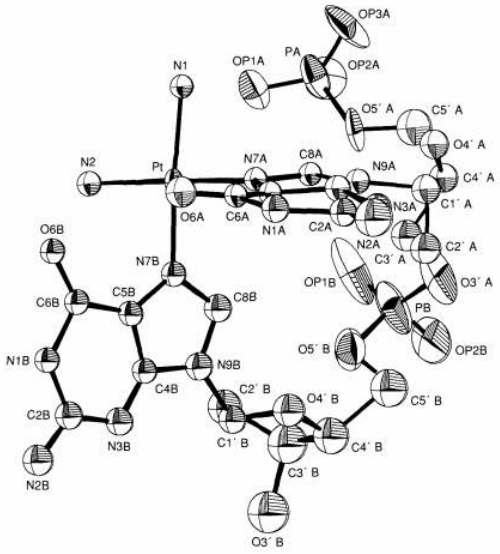


Figure 9.21 Molecular structure of cis-$[Pt(NH_3)_2d(pGpG)\}]$.

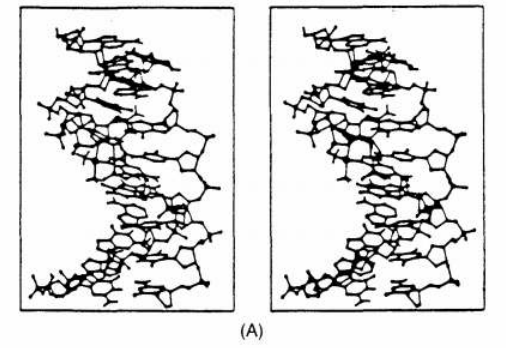
An interesting additional feature of the *cis*-$[Pt(NH_3)_2\{d(pGpG)\}]$ crystal structure is a hydrogen bonding interaction between an ammine ligand and the oxygen atom of the terminal phosphate group (OP1A•••N1, Figure 9.21). This intramolecular hydrogen bond is prominent in three of the four molecules in the asymmetric unit. Although the relevance of this hydrogen bonding interaction to the solution structure and molecular mechanism of cisplatin is presently unknown, it is interesting to note that the antitumor activity of platinum amine halide complexes is reduced when protons on coordinated NH_3 are replaced by alkyl groups.[34]

A second *cis*-DDP-oligonucleotide adduct characterized by x-ray crystallography is the neutral molecule *cis*-[$Pt(NH_3)_2${d(CpGpG)}].[131] Here again, there are several (three) molecules in the asymmetric unit. Although determined at lower resolution, the structure is similar in most respects to that of *cis*-[$Pt(NH_3)_2${d(pGpG)}] except for the presence of some weak NH_3•••O6(guanosine) intramolecular hydrogen bonding interactions and a few unusual sugar-phosphate backbone torsional angles. Also, no NH_3(H)••• phosphate(O) hydrogen bonds were observed.

From the foregoing discussion, it is apparent that adequate x-ray structure information is available for the *cis*-$\{Pt(NH_3)_2\}^{2+}$/d(pGpG) intrastrand crosslink. What is needed now are structures of the minor adducts and, most importantly, of adducts in double-stranded DNA. Very recently, dodecanucleotide duplexes containing *cis*-$\{Pt(NH_3)_2\}^{2+}$/d(pGpG) adducts have been crystallized, the structures of which are currently being investigated.[132]

c. Molecular Mechanics Calculations on Platinated Duplexes

As a supplement to x-ray structural information on double-stranded oligonucleotides containing an embedded *cis*-[$Pt(NH_3)_2${d(pGpG)}] adduct, several models have been constructed by using a molecular mechanics approach.[133] In this work, a set of coordinates was first obtained by amalgamation of structural information about standard double-helical DNAs and the platinated d(pGpG) fragment. Various starting structures were assumed, both linear and bent. The models were then refined according to various charge and stereochemical constraints built into the calculation. The results, which can reveal only what is feasible and not necessarily what actually happens, for both linear and bent structures are depicted in Figure 9.22 for two of the duplex sequences studied. In the linear model, the 5'-coordinated guanosine is rotated out of the stack, and its hydrogen bonding to the cytosine on the complementary strand is seriously disrupted. The imino N-H group is still involved in H-bonding, however; so this structure is not inconsistent with the NMR results. Two classes of kinked platinated duplex structures were encountered, with bending angles of 61 and 50°. In one of these, all Watson-Crick hydrogen bonds remain intact. These kinked structures are supported most strongly by the gel-electrophoresis experiments discussed in Section V.D.3.b.v.



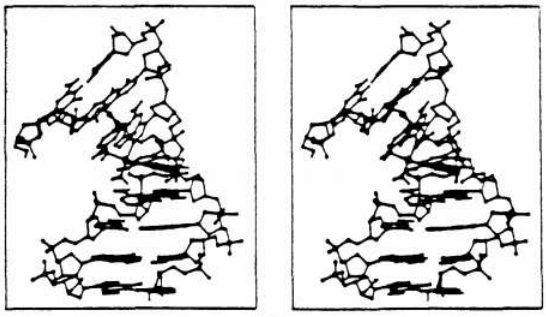


Figure 9.22 - (A) Stereoscopic view of the unkinked, platinated model of duplex d(TpCpTpCpG*pG*pTpCpTpC) from molecular-mechanics calculations. Counter ions used to stabilize the negative charge of the phosphates are not shown. (B) Stereoscopic view of the "high-salt" kinked, platinated model of duplex d(GpGpCpCpG*pG*pCpC) from molecular-mechanics calculations. Counter-ions are not depicted, with the exception of the bridging ion. (C) Stereoscopic view of the "low-salt" kinked, platinated model of duplex d(GpGpCpCpG*pG*pCpC). Counter-ions are not depicted. Reproduced with permission from Reference 133.

Molecular mechanics and the related molecular dynamics calculations are a potentially valuable tool for the bioinorganic chemist interested in how metal complexes might perturb the structures of biopolymers. Analysis of the results for cisplatin-DNA binding reveals that, compared with the sum of all contributions from the biopolymer, the Pt-DNA interactions constitute a small part of the overall energy. For the most accurate results, it is important to know the charge distributions on the metal and its ligands as well as the effects of solvent interactions. Much work needs to be done in these areas before the results of molecular mechanics and dynamics calculations can be used reliably to predict or analyze structures. At present, however, they are far superior to examination of space-filling molecular models, for example, and produce quantitatively revealing structural diagrams.

d. Platinum-Nucleobase Model Complexes

Several studies have been carried out of the *cis*-diammineplatinum(II) moiety coordinated to nucleobases in which the N9 (purine) or N3 (pyrimidine) positions either have been alkylated, to simulate the glycosidic linkages, or in which the actual nucleotide (AMP, dGMP, etc.) is employed.[134] These investigations are in many respects analogous to the synthesis and characterization by bioinorganic chemists of model complexes for the active site of a metalloenzyme. Their purpose is to simplify the problem, revealing kinetic, thennodynamic, and structural preferences of the primary building blocks involved in the metallodrug-biopolymer interaction, without the profound stereochemical constraints of the latter. Early studies of *cis*- and *trans*-DDP adducts with nucleobases (i) revealed the kinetic preferences for platinum binding to GMP and AMP, (ii) mapped out the preferred sites of platination (N7 of A and G; N1 of A; N3 of C; no N7-O6 chelate; no ribose or deoxyribose binding; only rare binding to phosphate oxygen atoms), (iii) demonstrated that Pt-N7 binding to G lowered the pK_a of N1-H by ~ 2 units, and (iv) led to the discovery of interesting new classes of coordination complexes such as the *cis*-diammineplatinum pyrimidine blues and metal-metal bonded diplatinum(III) complexes.

Attempts to model the intrastrand d(GpG) crosslink with nucleobases have met with only moderate success. Usually the O6 atoms of the two guanosine rings are on opposite sides of the platinum coordination plane ("head-to-tail" isomer). Only for *cis*-$[Pt(NH_3)_2(9\text{-EtG})_2]^{2+}$ was the correct isomer obtained. Nucleobase complexes of the *cis*-diammineplatinum(II) moiety have been valuable for testing the controversial proposal of N7,O6 chelate formation, which to date has not been observed. Several interesting discoveries of metal-nucleobase chemistry are that metal binding can stabilize rare tautomers, for example, the 4-imino, 2-oxo form of cytosine, through N4 binding, that coordination of platinum often produces unusual base pairing, and that metal migration from one donor site to another on an isolated nucleobase can occur. These model studies will continue to provide valuable insights into the possible chemistry of platinum antitumor drugs with DNA.

e. trans-DDP-DNA Adducts

Because *trans*-DDP is biologically inactive, it has received less attention than the *cis* isomer. Nevertheless, knowledge of its binding to DNA is important to have as a reference point for mechanistic comparison with the active compounds. Shortly after replication mapping experiments established that *trans*-DDP binds preferentially to d(GpNpG) and d(ApNpG) sequences,[135] several synthetic oligonucleotides containing such sequences were prepared and used to investigate reactions with the *trans* isomer.[136-138] Kinetic studies of *trans*-DDP with d(GpCpG) and d(ApGpGpCpCpT) revealed the presence of, presumably

monofunctional, intermediates that closed to form both intra- and interstrand products. In the reaction with d(GpCpG), the 1,3-intrastrand G-G chelate accounted for 70 percent of the product, and 21 percent of the remaining material was unreacted oligonucleotide. Proton NMR studies of purified *trans*-[$Pt(NH_3)_2${d(GpCpG)}] as well as the d(GpTpG) analog established platinum binding to N7 positions of the two trans guanosine nucleosides. As with the *cis*-[$Pt(NH_3)_2${d(pGpG)}] adducts, the 5'-guanosine residue no longer retained the normal B-DNA type conformation; instead, the sugar ring pucker switched to C3'-endo. A fairly detailed ^1H NMR characterization of *trans*- [$Pt(NH_3)_2${d(ApGpGpCpCpT)-N7-A(1),N7-G(3)}] revealed very similar features. This example nicely illustrates the different stereoselectivity of *cis*- and *trans*-DDP binding to DNA. The *cis* isomer forms exclusively an intrastrand d(GpG) crosslink, whereas the *trans* isomer makes a 1,3-d(A*pGpG*) adduct. A schematic depiction of the *trans*-$\{Pt(NH_3)_2\}^{2+}$ adduct is shown in Figure 9.23. As can be seen, the two purine rings enclose a large, 23-membered ring, the central guanosine residue is "bulged out," and the 5'-residue has a C3'-endo sugar pucker. This structure may be compared with that of *cis*-[$Pt(NH_3)_2${d(pGpG)}] (Figure 9.21), where the platinum is part of a smaller, 17-membered ring. Both space-filling model building studies and molecular mechanics calculations reveal that it would be stereochemically very unfavorable for the *trans*-$\{Pt(NH_3)_2\}^{2+}$ fragment to replace the *cis* analogue in an intrastrand crosslinked d(GpG) structure of the kind shown in Figure 9.21. Thus, for bidentate adducts, it seems clear that the important difference between *cis*- and *trans*-DDP binding to single-stranded DNA is revealed by the structures shown in Figures 9.21 and 9.23, respectively.

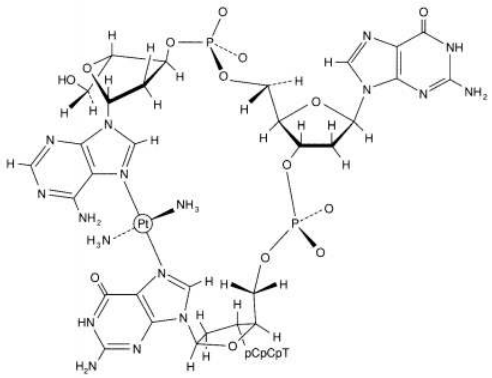


Figure 9.23 - Structure of the intrastrand 1,3-d(A*pGpG*) crosslink formed in the reaction of trans-DDP with d(ApGpGpCpCpT). Reproduced by permission from Reference 136.

Information about *trans*-DDP binding to double-stranded DNA is scanty, but very recent studies indicate that the *trans*-[$Pt(NH_3)_2${d(GpApG)-N7-G(1),N7-G(3)}] intrastrand crosslinked fragment can be embedded in duplex dodecamers.[139] Interestingly, for one sequence the melting temperature (T_M) of this duplex is not reduced over that of the unplatinated DNA fragment, in contrast to results for *cis*-DDP intrastrand d(GpG) adducts. This intriguing result, which agrees with earlier T_M studies of DNA platinated by *trans*-DDP, does not yet have a structural rationale. It is possibly relevant to the processing of bifunctional *trans*-DDP-DNA adducts *in vivo*.

f. Effects of Platination on DNA Structure

It is valuable to summarize at this stage all that has been learned concerning the changes in DNA structure that occur upon *cis*- or *trans*-DDP binding. *cis*-DDP intrastrand crosslinks result in unstacking of neighboring bases and a switch in the sugar pucker of the 5'-nucleoside from C2'-endo, the standard B-DNA conformation, to C3'-endo, a conformation encountered in A-DNA. These various forms of DNA have already been introduced in the previous chapter. Watson-Crick base pairing, although weakened, is probably maintained. Evidence that base pairing is altered comes from studies with antinucleoside antibodies that bind appreciably better to DNA platinated with *cis*-DDP than to unmodified DNA. These antibodies recognize the nucleobases much better in platinated than in unplatinated DNA, presumably because platination disrupts the double helix. Additional support for base-pair disruption comes from gradient gel-denaturation experiments using sitespecifically platinated DNA (see Section V.D.8.b). Intrastrand crosslinking by *cis*-DDP also bends the helix by about 34° and unwinds the duplex by 13°. When *trans*-DDP forms 1,3-intrastrand crosslinks, the nucleotides situated between the platinated residues may be bulged out; consistent with this picture is the fact that they present an especially good target for antinucleoside antibodies. In 1,3-intrastrand d(GpNpG) or d(ApNpG) adducts, the 5'-nucleoside sugar pucker is altered to C3 I-endo. Intrastrand crosslink formation by *trans*-DDP also leads to DNA bending,

but the platinum serves as the locus for a hinge joint and not for cooperative bending. These different effects of platination on DNA structure brought about by the two isomers are likely to be related to their different biological activities.

11.2.9.7: Structure of Platinum-DNA Complexes is shared under a CC BY-NC-SA 4.0 license and was authored, remixed, and/or curated by LibreTexts.

11.2.9.8: Site-specifically Platinated DNA 154

a. The Problem

Much of the information obtained about the mechanism of action of cisplatin has been derived from experiments where Pt-DNA binding has occurred *in vivo* or *in vitro*, with the use of random-sequence DNA having all available targets for the drug. In these studies, platination is controlled by the inorganic chemistry of *cis*-DDP in the medium and the accessibility of target sites on the DNA, as already discussed in considerable detail. As such, this situation best represents drug action as it actually occurs in the tumor cell. On the other hand, the resultant spectrum of DNA adducts makes it difficult, if not impossible, to understand the structural and functional consequences of any specific adduct. In order to address this problem, a methodology has been developed in which a single platinum adduct is built into a unique position in the genome. This approach is powerful and has the potential to be extended to the study of many other metal-based drugs. In this section, we discuss the strategy used to construct such site-specifically platinated DNA molecules and the information obtained thus far from their study. Some uses have already been discussed.

b. Synthesis and Characterization

Figure 9.29 displays the map of a genome constructed by insertion of platinated or unplatinated dodecanucleotide duplexes d(pTpCpTpApGpGpCpCpTpTpCpT)•d(pApGpApApGpGpCpCpTpApGpA) into DNA from bacteriophage M13mp18. This genome was constructed in the following manner.[154] Double-stranded DNA from M13mp18 was first digested with Hinc II, a restriction enzyme that recognizes a unique six-base-pair sequence in the DNA and cleaves the double helix there, leaving a blunt-ended (no overhanging bases) cleavage site. The unplatinated dodecamer duplex was next ligated into the Hinc II site, and the DNA amplified *in vivo*. The dodecamer can insert into the genome in two different orientations, the desired one of which, termed M13-12A-Stu I, was identified by DNA sequencing. The presence of the insert in the new DNA was checked by its sensitivity to the restriction enzyme Stu I, which cleaves at the d(AGGCCT) sequence uniquely situated in the dodecamer insert, and the absence of cleavage by Hinc II the site for which was destroyed. Next, Hinc II-linearized M13mp18 replicative form (RF) DNA was allowed to form a heteroduplex with excess viral DNA (which has only the + strand in the presence of the denaturant formamide which was dialyzed away during the experiment. The resulting circular DNA has a gap in the minus strand into which the platinated d(TCTAG*G*CCTTCT) was ligated (Figure 9.30). The latter material was prepared by the methods described in Section V.D.5.a and characterized by ^{1}H NMR spectroscopy. The resulting site-specifically platinated DNA contains a single *cis*-[$Pt(NH_3)_2${d(pGpG)}] intrastrand crosslink built into a unique position. The methodology is general, and has been used to create other known platinum-DNA adducts site-specifically in M13mp18.

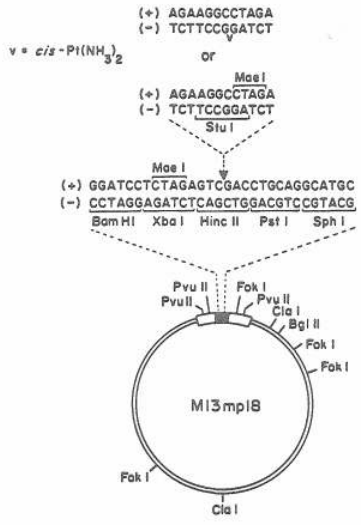


Figure 9.29 - Map of the genome created by insertion of cis-DDP platinated or unplatinated d(TpCpTpApGpGpCpCpTpTpCpT)-d(ApGpApApGpGpCpCpTpApGpA) into the Hinc II restriction site of bacteriophage M13mp18 DNA.

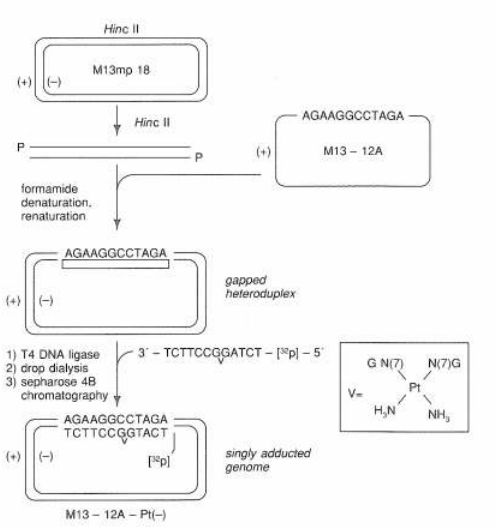


Figure 9.30 - Scheme for constructing site-specifically platinated genomes via gapped heteroduplex synthesis (reproduced by permission from Reference 154).

The chemical properties of the platinated DNA, termed M13-12A-Pt(-)-Stu I, were investigated by enzymatic, digestion and gel electrophoresis experiments. Platinum completely inhibits cleavage of the DNA by Stu I, as expected from the earlier restriction enzyme mapping studies. In addition, the *cis*- [$Pt(NH_3)_2${d(pGpG)}] and *cis*-[$Pt(NH_3)_2${d(pApG)}] intrastrand crosslinks were found to inhibit a variety of DNA polymerases, with only a small amount of bypass of the platinum lesion.[149] These results indicate that the most abundant adducts of cisplatin on DNA are able to block replication efficiently.

c. Biological Properties

When M13-12A-Pt(-)-Stu I DNA was introduced into *E. coli* cells by transformation, DNA synthesis was uninterrupted, because the cell can both repair the damage and use the unmodified (+) strand for synthesis. Consequently, a slightly different strategy was used to construct single-stranded M13-12A-Pt(+)-Stu I DNA, the details of which are available elsewhere.[154] This platinated template, in which the damage can neither be repaired nor bypassed by known mechanisms *in vivo*, was then transformed into *E. coli* cells co-plated with GW5100 cells. Under these conditions, viral DNA replication is detected by the expression of the *β*-galactosidase gene, which, in the presence of appropriate reagents in the medium, leads to formation of blue plaques on a clear background. The results clearly indicate that many fewer plaques appear when M13-12A-Pt(+) is introduced into the cells than when M13-12A-u(+) was employed, where u stands for unmodified DNA. In three repeats of this experiment, survival of DNA containing only a single *cis*-[Pt(NH3h{d(pGpG)}] crosslink was only 11 ± 1 percent.

These data provide unambiguous proof that the most frequent DNA adduct formed by cisplatin is toxic, capable of inhibiting replication when only a single such lesion is present on a natural DNA template of 7,167 nucleotides. The fact that as many as 10 percent of the transformed cells can bypass or repair the lesion is also of interest, and parallels the results found *in vitro*. In related work, it was found that the *cis*-[$Pt(NH_3)_2${d(pGpG)}] intrastrand crosslink is not very mutagenic, but that *cis*-[$Pt(NH_3)_2${d(pApG)}] intrastrand adducts are considerably more so. This finding is important, since mutations could lead to long-term secondary tumor production in patients treated with cisplatin. The methodology affords a way to screen new compounds that one would like to be equally effective at inhibiting replication but less mutagenic. In addition, by using repairdeficient mutant cell lines, as well as cisplatin resistant cells, one can study the effects of varying the properties of the host cells. Incorporation of site-specifically platinated DNA sequences into appropriate shuttle vectors will also facilitate investigation of toxicity, repair, and resistance in mammalian cells.

d. Prospectus

The foregoing discussion illustrates the power of site-specifically platinated DNAs as a probe of the molecular mechanism of the drug. We recall that similar strategies were employed to obtain uniquely modified DNA in the bending[92,93] and unwinding[95] experiments discussed previously. In principle, this technique can be applied to examine other aspects of the molecular mechanism of other metallochemotherapeutic agents. The requirements are a synthetic route to the uniquely modified genome, for which both

the inorganic coordination chemistry and molecular biology must be amenable, an adduct stable to the biological conditions for DNA synthesis, and a method (usually genetic) for scoring the biological effects being investigated. Site-specifically platinated DNAs allow the bioinorganic chemist to have maximal control over the genetics and should continue to provide valuable information about the molecular mechanism of action of cisplatin.

11.2.9.8: Site-specifically Platinated DNA [154] is shared under a CC BY-NC-SA 4.0 license and was authored, remixed, and/or curated by LibreTexts.

11.2.9.9: Bioinorganic Chemistry of Platinum Anticancer Drugs- How Might They Work?

The material in this section constitutes the major portion of this chapter. One important goal of the discussion is to illustrate, by means of an in-depth analysis of a single case history, the questions that must be addressed to elucidate the molecular mechanism of an inorganic pharmaceutical. Another is to introduce the techniques that are required to answer these questions, at least for the chosen case. The inorganic chemist reading this material with little or no biological background may find the experience challenging, although an attempt has been made to explain unfamiliar terms as much as possible. It is strongly advised that material in Chapter 8 be read before this section. Toward the end of this section, the results obtained are used to speculate about a molecular mechanism to account for the biological activity of the drug. Experiments directed toward evaluating the various hypotheses are delineated. Once the mechanism or mechanisms are known, it should be possible to design new and better antitumor drugs which, if successful, would be the ultimate proof of the validity of the hypotheses. This topic is discussed in the next and final section of the chapter. Such an analysis could, in principle, be applied to probe the molecular mechanisms of the other metals used in medicine described previously. In fact, it is hoped that the approach will prove valuable to students and researchers in these other areas, where much less information is currently available at the molecular level.

The material in this section has been organized in the following manner. First we discuss the relevant inorganic chemistry of platinum complexes in biological media. Next we summarize the evidence that DNA is a major target of cisplatin in the cancer cell, responsible for its antitumor activity. The chemical, physical, and biological consequences of damaging DNA by the drug are then described, followed by a presentation of the methodologies used to map its binding sites on DNA. The detailed structures of the DNA adducts of both active and inactive platinum complexes are then discussed, together with the way in which the tertiary structure of the double helix can modulate these structures. Finally, the response of cellular proteins to cisplatin-damaged DNA is presented, leading eventually to hypotheses about how tumor cells are selectively destroyed by the drug. Together these events constitute our knowledge of the' 'molecular mechanism," at least as it is currently understood.

1. Reactions of *cis*-DDP and Related Compounds in Aqueous, Biological, and Other Media

cis-Diamminedichloroplatinum(II) is a square-planar d^8 complex. As such, it belongs to a class of compounds extensively investigated by coordination chemists.[55] Typically, such compounds are relatively inert kinetically, do not usually expand their coordination numbers, and undergo ligand substitution reactions by two independent pathways with the rate law as given by Equation (9.4). The rate constants k_1 and k_2 correspond to first-order (solvent-assisted) and second-order (bimolecular) pathways;

$$Rate = (k_1 + k_2[Y])[complex] \tag{9.4}$$

[Y] is the concentration of the incoming ligand. Usually, $k_1 << k_2$ by several orders of magnitude. In biological fluids, however, the concentration of a potential target molecule could be ~10^{-6} M, in which case $k_1 \simeq k_2$[Y]. Substitution of ligands in *cis*-DDP, required for binding to a cellular target molecule, is therefore likely to proceed by the solvent-assisted pathway. Such a pathway is assumed in the ensuing discussion.

For the hydrolysis of the first chloride ion from *cis*- or *trans*-DDP,

$$[Pt(NH_3)_2Cl_2] + H_2O \rightleftharpoons [Pt(NH_3)_2Cl(OH_2)]^+ + Cl^- \tag{9.5}$$

the k_1 values at 25 °C are 2.5 x 10^{-5} and 9.8 x 10^{-5} s^{-1}, respectively.[55] These hydrolyzed complexes can undergo further equilibrium reactions, summarized by Equations (9.6) to (9.9).

$$[Pt(NH_3)_2Cl(OH_2)]^+ \rightleftharpoons [Pt(NH_3)_2Cl(OH)] + H^+ \tag{9.6}$$

$$[Pt(NH_3)_2Cl(OH_2)]^+ + H_2O \rightleftharpoons [Pt(NH_3)_2(OH_2)_2]^{2+} + Cl^- \tag{9.7}$$

$$[Pt(NH_3)_2(OH_2)_2]^{2+} \rightleftharpoons [Pt(NH_3)_2(OH_2)(OH)]^+ + H^+ \tag{9.8}$$

$$[Pt(NH_3)_2(OH_2)(OH)]^+ \rightleftharpoons [Pt(NH_3)_2(OH)_2] + H^+ \tag{9.9}$$

The formation of dimers such as $[Pt(NH_3)_2(OH)]_2^{2+}$ and higher oligomers can also occur,[56,57] but such reactions are unlikely to be important at the low platinum concentrations encountered in biological media, Reactions (9.5) to (9.9), which depend on pH and

the chloride-ion concentrations, have been followed by ^{195}Pt (I = $\frac{1}{2}$, 34.4 percent abundance) and ^{15}N (using enriched compounds) NMR spectroscopy. The latter method has revealed for the *cis*-diammine complexes pK_a values of 6.70 ± 0.10 at 25 °C for Reaction (9.6) and of 5.95 ± 0.1 and 7.85 ± 0.1 at 5 °C for Reactions (9.8) and (9.9), respectively.[58]

The effects of pH and Cl^- ion concentration on the species distribution of platinum compounds have been used to fashion the following plausible argument for the chemistry of *cis*-DDP *in vivo*.[59] With the use of thermodynamic data for the ethylenediamine (en) analogue [Pt(en)Cl_2] the relative concentrations of hydrolyzed species at pH 7.4 were estimated (see Table 9.3) for blood plasma and cytoplasm (Figure 9.7). The higher chloride ion concentration in plasma preserves the complex as the neutral molecule cis-DDP, which passively diffuses across cell membranes. The lower intracellular chloride ion concentration facilitates hydrolysis reactions such as Equations (9.5) to (9.9), thereby activating the drug for binding to its biological target molecules. There is, of course, a reasonable probability that *cis*-DDP and species derived from it will encounter small molecules and macromolecules *in vivo* that divert it from this route to the target. We have already seen such cases; cisplatin binds to serum proteins, and there is good evidence that intracellular thiols react with the drug.[60] Glutathione, for example, is present in millimolar concentrations in cells. How, one might ask, does cisplatin swim through such a sea of sulfur donors to find its target in the tumor cell? Is it possible that a modified form of the drug, in which a Pt-CI bond has been displaced by thiolate to fonn a Pt-S bond, is the actual species responsible for its activity? Although these questions have not yet been satisfactorily answered, there is reason to believe that such reactions are not directly involved in the molecular mechanism of action. As evident from structure-activity relationship studies, the most active compounds have two labile ligands in *cis* positions. If Pt-S bonds were required, then compounds already having such linkages would be expected to exhibit activity and they do not. Rather, it seems most likely that the antitumor activity of cisplatin results from surviving species of the kind written in Equations (9.5) to (9.9) that find their way to the target molecule, and that the induced toxicity must arise from a significantly disruptive structural consequence of drug binding. Since only *cis* complexes are active, it is reasonable for the coordination chemist to infer that the stereochemistry of this interaction is of fundamental importance.

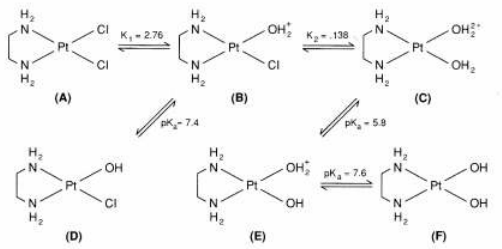


Figure 9.7 - Hydrolysis reactions of antitumor platinum complexes and an estimate of the species present in plasma and cytoplasm (reproduced by permission from Reference 51).

Table 9.3 - Distribution of various adducts formed between *cis*-DDP or [^{3}H][Pt(en)Cl_2][a] and DNA *in vitro* and *in vivo*.[118-122]

a) A radiolabeled analogue of *cis*-DDP, [^{3}H]dichloroethylenediamineplatinum(II).

b) A_2 represents either $(NH_3)_2$ or ethylenediamine.

c) By difference.

d) Percentage of adducts based on total amount of platinum eluted from the separation column.

e) Percentage of adducts based on total amount of radioactivity eluted from the separation column.

f) Not given.

g) Chinese hamster ovary cells treated with 83 μM *cis*-DDP.

h) Results from ELISA.

i) Results from AAS. Where the signal was too weak for reliable quantitation, the maximal amount possible is given. Adapted from Table 1 in Reference 81.

D/N Ratio	Total Incubation Time	Adducts Formed			Mono-functional Adducts	Remaining Platinum[c]
		cis-[PtA_2{d(pGpGl}][b]	*cis*-[PtA_2{d(pApG}][b]	*cis*-[PtA_2{d(GMP)}$_2$][b]		
In vitro						
0.055[c]	5 h (50 °C)	47-50%	23-28%	8-10%	2-3%	10%
0.022[d]	5 h (50 °C)	60-65%	20%	~4%	~2%	9-14%
0.01[e]	16 h (37 °C)	62%	21%	7%	—	10%
[ef]	30 m (37 °C)	36%	3%	8%	40%	13%
[ef]	2 h (37 °C)	54%	9%	9%	14%	14%
[ef]	3 h (37 °C)	57%	15%	9%	4%	15%
In vivo						
[dg]	1 h (37 °C)	35.9 ± 4.7%[h]	<34%[i]	3.1 ± 1.6%[h]	38.5%[i]	~22%
[dg]	25 h (37 °C)	46.6 ± 6.8%[h]	<48%[i]	3.0 ± 0.9%[h]	<14.5%[i]	~50%

Reactions of platinum compounds with components in media used to dissolve them can give and undoubtedly have given rise to misleading results, both in fundamental mechanistic work and in screening studies. A particularly noteworthy example is dimethylsulfoxide (DMSO), which even recently has been used to dissolve platinum compounds, presumably owing to their greater solubility in DMSO compared to water. As demonstrated by ^{195}Pt NMR spectroscopy, both *cis*- and *trans*-DDP react rapidly ($t_{1/2}$ = 60 and 8 min at 37 °C, respectively) to form $[Pt(NH_3)_2CI(DMSO)]^+$ complexes with chemical and biological reactivity different from those of the parent ammine halides.[61]

2. Evidence that DNA is the Target

Two early sets of experiments pointed to interactions of cisplatin with DNA, rather than the many other possible cellular receptors, as an essential target responsible for cytotoxicity and antitumor properties.[62,63] Monitoring the uptake of radiolabeled precursors for synthesizing DNA, RNA, and proteins, showed that [^{3}H]thymidine incorporation was most affected by therapeutic levels of cisplatin for both cells in culture and Ehrlich ascites cells in mice. Since independent studies showed that *cis*-DDP binding to DNA polymerase does not alter its ability to synthesize DNA, it was concluded that platination of the template and not the enzyme was responsible for the inhibition of replication.

In a second kind of experiment demonstrating that DNA is a target of cisplatin, hydrolyzed forms of the drug in low concentrations were added to a strain of *E. coli* K12 cells containing a sex-specific factor F.[64,65] After free platinum was removed, these F^+ cells were conjugated with a strain of *E. coli* K12 cells lacking this factor that had previously been infected with lambda bacteriophage. Addition of *cis*-DDP, but not *trans*-DDP, directly to the latter infected F^- cells had been shown in a separate study to accelerate cell lysis. Conjugation with the platinum-treated F^+ cells produced the same effect, strongly suggesting that Pt had been transferred from the F^+ to the F^- cells. Since only DNA is passed between the F^+ and F^- strains, it was concluded that Pt was attached to the DNA and that this modification was essential for the observed lysis of the cell. Further studies showed a good correlation between cell lysis by platinum compounds and their antitumor properties.

Various other observations are consistent with the notion that platinum binding to DNA in the cell is an event of biological consequence.[66] The filamentous bacterial growth observed in the original Rosenberg experiment is one such piece of evidence, since other known DNA-damaging agents, for example, alkylating drugs and x-irradiation, also elicit this response. Another is the greater sensitivity toward *cis*-DDP of cells deficient in their ability to repair DNA. Finally, quantitation of the amount of platinum bound to DNA, RNA, and proteins revealed that, although more Pt was bound to RNA per gram biomolecule, much more Pt was on the DNA when expressed as a per-molecule basis. In the absence of any selective interaction of Pt with a specific molecule, only

one out of every 1,500 protein molecules (average M.W. ~60 kDa) in a cell will contain a single bound platinum atom, whereas hundreds or thousands of Pt atoms are coordinated to DNA (M.W. ~10^{11}). If the replication apparatus cannot bypass these lesions, then cell division will not occur, and tumor growth is inhibited.

Although these and other results all point to DNA as an important cellular target of cisplatin, most likely responsible for its anticancer activity, this information does not explain why tumor cells are more affected by *cis*-DDP than non-tumor cells of the same tissue. Moreover, why is *trans*-DDP, which also enters cells, binds DNA, and inhibits replication, albeit at much higher doses (see discussion below), not an active anticancer drug? What causes cisplatin to kill cells and not merely to arrest tumor growth? The latter can be explained by DNA synthesis inhibition, but not necessarily the former. Very recent studies have begun to address these questions using powerful new methodologies of molecular and cell biology, as described in subsequent sections of this chapter. The results, although preliminary, continue to point to DNA as the most important cellular target of cisplatin.

11.2.9.9: Bioinorganic Chemistry of Platinum Anticancer Drugs- How Might They Work? is shared under a CC BY-NC-SA 4.0 license and was authored, remixed, and/or curated by LibreTexts.

11.2.9.10: Bioinorganic Chemistry of Platinum Anticancer Drugs; How Might They Work? (Part 2)

6. Effects of DNA Structure on Platinum Binding

a. A-, B-, and Z-DNA[140]

As discussed in more detail in Chapter 8, double-helical DNA can adopt different polymorphic forms depending on the conditions in solution or polycrystalline fiber. Even within a given DNA molecule, there can be sequence-dependent local secondary and tertiary structural differences that constitute important signals for cellular DNA binding and processing molecules. An example already discussed is the recognition of palindromic sequences by type II restriction endonucleases. As shown in Figure 9.24, three such DNA polymorphs are the right-handed A- and B- and the left-handed Z-forms. Most commonly encountered in solution is B-DNA, characterized by well-classified major and minor grooves designated by arrows in Figure 9.24. The targets of platinum binding, guanine N7 atoms, are situated in the major groove.

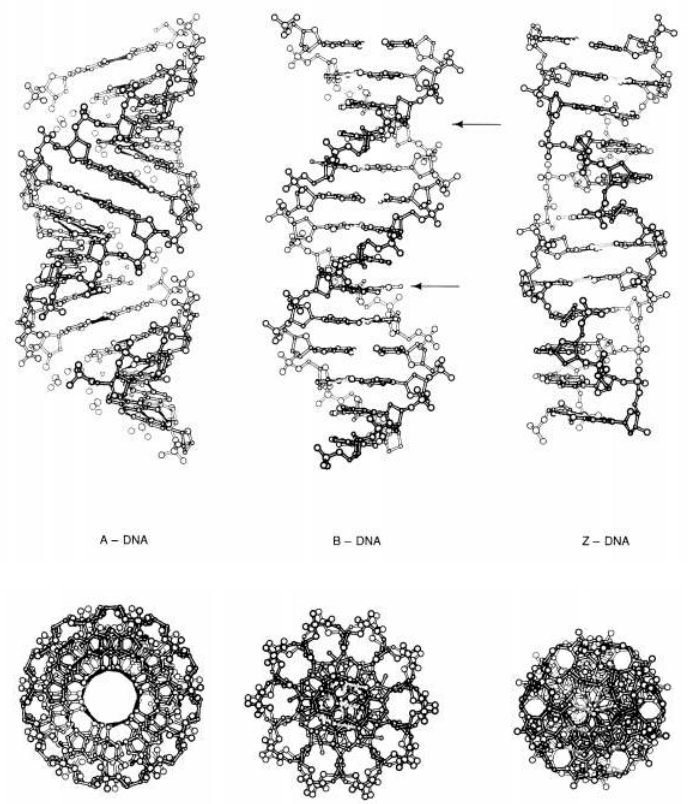


Figure 9.24 - Representations of side (above) and top (below) views of three major classes of double-stranded DNA. For B-DNA, arrows near the top and bottom of the helix designate the minor and major grooves, respectively. Reproduced with permission from Reference 140.

To what extent do sequence-dependent local structural modulations affect platinum binding? Although no general answer to this question can be given, there are several interesting anecdotal pieces of information worth mentioning. Z-DNA, a form favored by alternating purine-pyrimidine sequences such as in poly d(GC), does not constitute a particularly good target for *cis*-DDP binding. For one thing, it lacks the preferred d(GpG) or d(ApG) sequences. The monofunctional $[Pt(dien)Cl]^{+}$ complex, however, facilitates the B-DNA → Z-DNA conformational transition, as demonstrated by circular dichroism and ^{31}P NMR spectroscopic data.[141] In Z-DNA, the guanosine nucleoside adopts the syn conformation (Figure 9.9), which is presumably favored by placing a bulky $\{Pt(dien)\}^{2+}$ moiety on N7. Moreover, the local charge density on DNA is greater in Z- than B-DNA, owing to the closer proximity of the phosphate groups, and the former is presumably stabilized by the +2 charge on the platinum complex.

b. Effects of Local Sequence and of Free and Linked Intercalators on Platinum Binding

Of more interest perhaps to anticancer drug-DNA interactions is the fact that some d(GpG), d(ApG), and even d(GpA) targets for *cis*-DDP binding are very sensitive to the sequences in which they are embedded. This phenomenon was first discovered during exonuclease III mapping studies of cisplatin binding to a 165-bp restriction fragment from pBR322 DNA.[142] Although *cis*-DDP binding stops the enzyme at G_3, G_5, and GAGGGAG sequences, at a $(D/N)_b$ ratio of 0.05 there is little evidence for coordination to an apparently favored G_6CG_2 sequence (Figure. 9.25, lane 8). When platination was carried out in the presence of the DNA intercalator EtdBr (Figure 9.11), however, the G_6CG_2 sequence became a Pt binding site (Figure 9.25, lanes 9-12). A more extensive exonuclease III mapping study of this phenomenon suggested that d(CGG)-containing sequences in general are less well platinated by *cis*-DDP.[143,144] Moreover, only EtdBr, and not other acridine or phenanthridinium type intercalators, was able to promote an enzyme-detectable *cis*-DDP binding to these sequences. A suggested explanation for these results is that local d(purCGG) sequences might have an A-DNA-type structure (Figure 9.24) in which the major groove is narrow, inhibiting access of platinum to N7 of guanosine nucleosides. In the presence of the intercalator EtdBr, the local DNA structure might be altered in such a manner as to permit binding.[143,144]

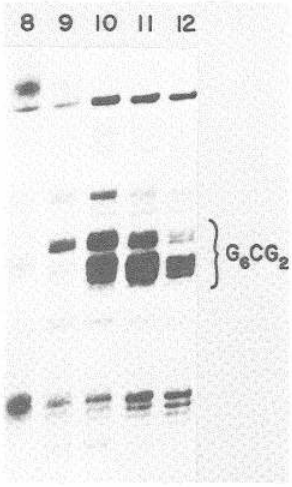


Figure 9.25 - Autoradiograph of Exo III mapping results for cis-DDP binding to a 165-bp DNA restriction fragment. The Pt/nucleotide ratio is 0.05. Lanes 8-12 contain DNA platinated in the presence of 0, 0.012, 0.057, 0.12, and 0.23 Etd/nucleotide, respectively. For more details, see Reference 142.

In accord with this interpretation, and further to delineate a possible reason why acridines and deaminated ethidium cations do not promote cisplatin binding to d(purCGG) sequences, NMR studies were performed that revealed the mean residence time of EtdBr on DNA to be 6 to 21 times longer than that of any of the other intercalators examined.[144] Thus, for these latter intercalators, the local DNA structure presumably can relax back to one unfavored for cisplatin binding before it can diffuse to the site. Moreover, when acridine orange (AO), one of the five intercalators studied that does not promote cisplatin binding to excluded sites, was covalently attached to dichloroethylenediamineplatinum(ll) (Figure 9.26) via a hexamethylene linker chain, the resulting AO-Pt molecule was able to bind to all d(CpGpG) sites, as determined by exonuclease III mapping. In the tethered molecule, the high local concentration near the intercalator binding site facilitates attachment of the $\{Pt(en)\}^{2+}$ moiety to DNA before the acridine orange fragment can diffuse away and the structure can relax to reform the excluded site.

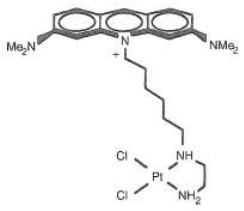


Figure 9.26 - Structure of AO-Pt in which the $\{Pt(en)C_{12}\}$ moiety is linked by a hexamethylene chain to acridine orange.

Subsequently, the excluded site phenomenon was found for *cis*-DDP binding, as assayed by the 3'-5'-exonuclease activity of T4 DNA polymerase.[145] Enzyme stopping sites were observed at all d(GpG) sequences, but only weakly when at a d(GTGGTC) site.

Similarly, d(ApG) was not modltled when embedded in pyGAGCpy and pyGAGCA sequences. Although most d(GpA) sequences were not platinated, as detected by T4 mapping, a few were. These results further underscore the importance of local sequence modulation of cisbinding to DNA.

c. DNA-Promoted Reaction Chemistry

In the EtdBr-enhanced binding of *cis*-DDP to DNA, a small fraction (< 5 percent) of the intercalator is strongly bound and can be dialyzed out only very slowly.[145] The detailed structure of this DNA-cisplatin-EtdBr ternary complex has been established, and involves *cis*-$\{Pt(NH_3)_2\}^{2+}$ binding to the exocyclic amino groups of ethidium as well as to donor sites on DNA.[146] This assignment was proved by synthesizing *cis*- $[Pt(NH_3)_2CEtd)CI]^{2+}$ complexes in dimethylformamide solution and then allowing them to react with DNA. The optical spectra of the resulting adducts were identical to that of the ternary complex. The reaction of *cis*-DDP, and DNA to form the ternary complex is promoted by the favorable orientation of the exocyclic amino group of intercalated Etd with respect to the coordination plane of bound to the double helix. The N-8 exocyclic amino group of ethidium, bound intercalatively at a site adjacent to a purine N-7 coordinated *cis*-$\{Pt(NH_3)_2CI\}^{+}$ moiety, is positioned above the platinum atom in a structure resembling the transition state for a square-planar substitution reaction. The structure of this transition state has been modeled in a molecular mechanics calculation (Figure 9.27 See color plate section, page C-16.),[147] and evidence has been obtained that indicates selective binding of platinum to the Etd N-8 amino position.[148]

Since cisplatin is usually administered in combination chemotherapy with other drugs, many of which contain intercalating functionalities, strong covalent, DNA-promoted interactions between drug molecules at a target site must be considered as possibly relevant to the molecular mechanism of action. In such a situation, there must be a strong binding preference for both drug molecules for the same target sequences, since on probability grounds alone it is unlikely that both would migrate to the same site by random diffusion at the low concentrations found *in vivo*.

d. Effects of DNA Function on Platinum Binding

Although there is yet little known about this topic for cisplatin, it is worth pointing out that other DNA-targeted drugs, such as bifunctional alkylating agents, bind preferentially to actively transcribed genes. It is therefore possible that platinum exhibits such preferences, for example, to single-stranded DNA at or beyond the transcription fork, compared to duplex DNA in chromatin structures. Or, perhaps, it too binds selectively to actively transcribed DNA. Investigation of these possibilities seems worthwhile.

7. Speculations About the Molecular Mechanism

a. Is There a Single Mechanism?

Most investigators now agree that DNA is the cytotoxic target of cisplatin. We have seen that the drug inhibits DNA replication by binding to the template and halting the processive action of DNA polymerase. Less well-studied is the inhibition of transcription by platinum-DNA adducts, but recent evidence clearly indicates that they can do so. Studies of the effects of platinum on cells growing in culture reveal that DNA replication and cell growth can continue without cell division in the presence of low levels (1 μ g/mL) of *cis*-DDP cells are arrested at the G2 phase, the stage of cell growth just preceding division.[105] G2 arrest was reversible, but at higher cisplatin levels (8 μg/mL), cell death occurred. These observations led to the speculation that, perhaps, post-replication DNA repair can handle the toxicity associated with a platinum-damaged template, at least for DNA synthesis, but that there is no known pathway by which transcription can circumvent Pt-DNA lesions. Possibly, inhibition of transcription is ultimately a more lethal event than inhibition of replication. This idea is inconsistent with the well-established fact that thymidine incorporation into DNA is more affected by low levels of cisplatin than is uridine incorporation into RNA. Might there be more than one biochemical pathway by which cisplatin manifests its anticancer activity? Further work is necessary to address this intriguing question.

b. Is There a "Critical Lesion"?

We now have an excellent understanding of the major DNA adducts made by *cis*-DDP, their structures, and the corresponding DNA distortions. Information about adducts made by the inactive *trans* isomer, though not as complete, is also substantial. During the period when this knowledge was being accumulated, it was of interest to learn whether a "critical lesion," a specific DNA adduct with a unique molecular structure might be responsible for the antitumor activity of the drug. At present, it appears that all bidentate adducts made by *cis*- and *trans*-DDP can inhibit replication, although they may not be equally efficient at doing so.[149]

Even monofunctional adducts of the kind formed by *cis*-$[Pt(NH_3)_2(4\text{-Br-py})Cl]^+$ can block replication.[96] Thus, it be better to think about the concept of "critical lesion" in a functional sense, where the rates of adduct formation, removal, and enzyme inhibition together determine which family of adducts will exhibit antitumor activity and which will not. Here the biochemistry of the host cell will also be an important determinant. Clearly, more studies are required to delineate these possibilities.

c. Replication and Repair in the Tumor Cell[150]

If the anticancer activity of cisplatin arises from damaged DNA templates, then the drug could be selectively toxic to cancer versus normal cells of the same tissue if repair of DNA damage occurred more efficiently in the latter. The best way to study this phenomenon would be to measure the platinum-DNA levels and list the spetrum of adducts formed in tumor versus normal biopsy tissue obtained from patients undergoing cisplatin chemotherapy. As described previously, methodologies are now reaching the point where such experiments can be carried out in order to test the key hypotheses about the mechanism of action of cisplatin. In addition, powerful new methods have recently been developed to screen for DNA bmdlnlg proteins. If one could identify proteins that bind selectively to *cis*-DDP-platinated DNA and determine function, further insights into cellular replication and repair phenomena would be forthcoming. Such cellular factors that bind selectively to DNA containing cisplatin adducts have, in fact, recently been discovered.[107] The experiments that led to this finding and their possible implications for the molecular mechanism of cisplatin are described in the next section.

d. Structure-Specific (or Damage) Recognition Proteins[150]

If selective repair of platinum-DNA adducts in cells of different origin is an integral part of the anticancer mechanism of *cis*-DDP, then it is important to identify the cullular factors associated this phenomenon. In bacteria, *cis*-DDP adducts on DNA are removed by excision repair, a process in which the lesion is first identified and then excised by the uvrABC excinuclease system.[151] In this process, the uvrA protein first binds to the adducted DNA. Subsequently, the uvrB and C proteins excise the damaged strand, which additional cellular proteins rebuild by copying the genetic information from the remaining strand.

The repair of *cis*-DDP intrastrand crosslinks in mammalian cells is much less well understood. Under the assumption that an analogue of the uvrA protein might exist in such cells, experiments were carried out to try to isolate and clone the gene for such a protein. In particular, the mobility of platinated DNA restriction fragments of defined length was found to be substantially retarded in electrophoresis gels following incubation extracts from human HeLa cells.[107] This gel-mobility shift was attributed to the binding of factors termed "damage recognition proteins" (or DRPs). Subsequent studies with site-specifically platinated oligonucleotides (see V.D.8) revealed that the cisplatin DRP binds specifically to DNA containing the intrastrand *cis*-$[Pt(NH_3)_2\{d(pGpG)\}]$ or *cis*-$[Pt(NH_3)_2\{d(pApG)\}]$ crosslink. In parallel work, the gene encoding for a DRP was cloned[152] and used to demonstrate the occurrence of such a in nearly all eukaryotic cells. Since binding of the DRP to platinated DNA is not specific for the ammine ligands opposite the crosslinked nucleobases, the interaction is thougllt to involve recognition of local changes in the twist and bending of the double helix. Figure 9.28 depicts one possible structure for the complex formed between *cis*-DDP platinated DNA and a DRP. More recently, the cloned proteins were found to contain a high mobility group (HMG) protein box, and even HMG 1 itself binds to cisplatin-modified DNA.[152] The class of proteins was renamed "structure-specific recognition proteins" (SSRPs).

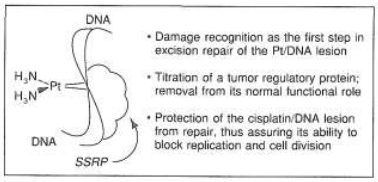


Figure 9.28 - Model depicting the binding of an SSRP to cisplatin-damaged DNA and several hypotheses for its role in the molecular mechanism.

The discovery of SSRPs that bind specifically to cisplatin-modified DNA raises several questions that are the subjects of current study. The first is to determine whether the proteins are an integral component in the mechanism of action of the drug. Although it has not yet been possible to induce the proteins by treating cells with cisplatin, nor have elevated or suppressed levels been found in platinum-resistant cells, deletion of an SSRP gene in yeast has re(~enltlv afforded a mutant strain less sensitive to cisplatin than wild-type cells.[153] This result links a yeast SSRP with cellular sensitization to the drug. Such a protein could contribute to the molecular mechanism in one of several ways (Figure 9.28). It might be the analogue of uvrA, which, as mentioned above,

recognizes damage and signals the cell to perform excision repair. If so, then one would like to depress the levels of the protein in cancer cells to make them more sensitive to the drug. A second possibility is that the true role of the SSRP is to serve as a tumor-cell activator, and that cisplatin lesions titrate it away from its functionally active sites on the DNA. Alternatively, binding of the protein could protect cisplatin adducts from repair, preserving their lethality at the time of cell division and leading to the arrest of tumor growth. This last hypothesis would require more of the SSRP in cells sensitive to the drug. Studies are currently in progress to delineate these three and other hypotheses, and to learn whether the discovery of the SSRPs has heralded the final chapter in the quest for the molecular mechanism of cisplatin or merely been an entertaining sidelight.

e. Drug Resistance: What Do We Know?[150]

Perhaps the most serious problem for successful chemotherapy of tumors is drug resistance.[102] In most tumors there exists a subpopulation of cells that are naturally resistant to a given drug; as the sensitive cells are killed, these refractory clones take over. In addition, resistance can be acquired by tumor cells following repeated application of the drug. Attempts to identify mechanisms responsible for cisplatin resistance have therefore been the subjects of considerable research activity. Other DNA-damaging agents sometimes amplify genes as a mechanism of drug resistance. An example is the multidrug resistance phenomenon, in which a gene encoded for a P-glycoprotein is amplified in cells resistant to agents such as daunomycin. This protein is believed to increase efflux of the drug through the cell membrane by an ATP-dependent, energy-driven pump. There is currently an intensive search underway to see whether the cisplatin resistance phenomenon has a genetic origin. If a cisplatin resistance gene could be cloned and its phenotype identified, a powerful new avenue would be opened to overcome drug resistance.

11.2.9.10: Bioinorganic Chemistry of Platinum Anticancer Drugs; How Might They Work? (Part 2) is shared under a CC BY-NC-SA 4.0 license and was authored, remixed, and/or curated by LibreTexts.

11.2.9.11: Design of New Inorganic Anticancer Drugs

1. Objectives

Although chemotherapy has made significant contributions to cancer treatment, the effect of cisplatin on testicular cancer being a showcase example, early detection and surgical removal of all neoplastic tissue still remain the preferred means of combating most forms of the disease. What steps need to be taken to devise better chemotherapeutic agents? One answer is to understand the biochemical mechanisms that underlie the transformation of normal into neoplastic cells and to attack the disease on the basis of that knowledge. The value of this approach is indisputable, but it need not be the only one. We have seen that *cis*-$[Pt(NH_3)_2Cl_2]$, a simple third-row transition-metal complex containing no carbon atoms, can contribute significantly to cancer chemotherapy. This example alone should lead us to search for improved inorganic drugs based on the evolving knowledge of the mechanism of action of *cis*-DDP. What then should our objectives be? Three answers are immediately apparent. First, we need to find compounds that are active against resistant cells. Such compounds are termed "second-generation" platinum drugs, and are the focus of much activity in the pharmaceutical industry. Their development will be facilitated by understanding the fundamental biochemistry of cisplatin drug resistance, designing complexes to circumvent the cellular resistance mechanisms. Second, there needs to be an improved spectrum of activity, to be provided by the so-called "third-generation" compounds. The major cancers of the colon, breast, and lung are not effectively diminished by cisplatin chemotherapy. Finally, cisplatin toxicity is often dose-limiting, and there is a need for agents with a greater chemotherapeutic index-to-toxicity ratio. Some of these objectives may ultimately be met by modifying the mode of delivery of cisplatin, for example, by encapsulating the drug in a tumor-seeking liposome or attaching it to a tissue-specific monoclonal antibody. A major step in alternative delivery has recently been taken with the development of a class of oral platinum complexes that have just entered clinical trials.[54] These complexes are platinum(IV) cycloalkylamine species of the kind *cis*, *trans*, *cis*-$[Pt(NH_3)(C_6H_5NH_2)(O_2CCH_3)_2Cl_2]$. The prospects are reasonably good that new platinum and other metal anticancer drugs can be designed in a bioinorganic chemical approach to the problem.

2. Strategies for Drug Development

a. Can We Build on Our Knowledge About Cisplatin?

If we consider what is known about the molecular mechanism of cisplatin, what properties are desirable in the design of new metal complexes for testing? The molecules should be reasonably stable kinetrically and soluble in biological fluids, cross the cell membrane, bind covalently to DNA, and inhibit gene function. As described previously in this section of the chapter, powerful methods are now available to screen compounds for these properties in a relatively short time. But there are additional factors required for metallodrug anticancer activity, above and beyond these criteria; *trans*-DDP, after all, has all five of the above properties and is not active. Probably one should add to the list the requirement that the complex have two substitutionally labile *cis* sites for intrastrand crosslinking of adjacent DNA nucleotides; such a criterion would, of course, rule out molecules like *trans*-DDP. Recall, however, that *cis*-$[Pt(NH_3)_2(4\text{-X-py})CI]^+$ complexes (X = Br, Me) are active. These cations have the five properties listed above, but, as far as is currently known, bind only monofunctionally to DNA. The pyridine ring moiety of a covalently attached platinum atom could possibly intercalate into a neighboring interbase pair site on the DNA, making a pseudointrastrand crosslinked adduct structurally similar to the *cis*-DDP-d(pGpG) structure. Further information is required about these active, monofunctional cations before any firm conclusions can be drawn. Nevertheless, it is useful to remember that if the requirement of two substitutionally labile *cis* ligands had been rigorously followed, this new class of monofunctional platinum complexes would not have been discovered.

Another rationale for designing new platinum or other metal antitumor drugs could emerge with a better understanding of the SSRPs in the mechanism of action of cisplatin. For example, if they serve to protect cisplatin lesions on DNA from repair, one would want to design complexes that form adducts that bind even more strongly to the purified protein. The strength of this binding interaction, having been a serendipitous discovery, surely cannot have been maximized. A tighter SSRP-platinated DNA complex would require the use of less platinum, and thus afford lower toxicities.

b. Is Platinum Uniquely Suited?

Given the above criteria, platinum is the only metal to be chosen for further drug development? The answer to this question is "probably not" but a few points need to be kept in mind. Given the assumption that the geometry of the *cis*-$[Pt(NH_3)_2\{d(GpG)\}]$

intrastrand crosslink was important for the antitumor activity of cisplatin, computer graphics methods were employed to probe the stereochemical consequences of modifying this structure.[155] Addition of axial chloride or water ligands in fifth and sixth coordination positions to form pseudo-octahedral adducts, for example, introduces several steric clashes with the guanosine O6 atoms. An octahedral complex, for example *cis*,*cis*,*cis*-$[Pt(NH_3)_2Cl_2(OH)_2]$, bifunctionally coordinated to DNA either would not form an intrastrand d(GpG) crosslink or would form an adduct structurally different from that made by *cis*-DDP. This octahedral complex Pt(IV), known as "tetraplatin" in the pharmaceutical industry, is active, but is believed to be reduced *in vivo* to platinum(II) before coordinating to DNA.[156,157] These considerations might imply that the best strategy for inorganic drug development would be to employ square-planar d^8 complexes. Clearly there are as yet no definitive answers. Nevertheless, the criteria derived from the mechanism of action studies of cisplatin represent an excellent starting point for designing new antitumor metallodrugs.

c. How Important are Amine Ligands?

Here again, the answer is not unequivocal, but amines (including NH_3) are probably ideally suited ligands for covalent DNA-binding metal complexes. Even completely inert complexes such as $[Co(NH_3)_6]^{3+}$ show sequence and DNA polymorph binding preferences,[158] suggesting that the N-H bonds orient toward the phosphate and heterocyclic nitrogen atoms in the major groove, forming hydrogen-bonding interactions. This chemistry is analogous to the binding and recognition of organic amines and polyamines, such as spermine and spermidine, by nucleic acids. Apart from amines, hydrophobic groove-binding and/or intercalating ligands such as o-phenanthroline and its derivatives should be considered. Molecules such as $[Rh(DIP)_3]^{3+}$, where DIP = 4,7-diphenyl-1,10penanthroline, bind to DNA and have proved to be useful structural probes (Chapter 8). Recent work has shown that $[Rh(DIP)_2Cl_2]^+$ binds preferentially to d(GpG) sequences, like cisplatin, although its antitumor properties have not yet been investigated.[159]

3. Second and Third-generation Platinum Anticancer Drugs

Improvements over cisplatin have been made, most notably the molecule carboplatin (Figure 9.4), which is less nephrotoxic and has been reported to be effective in some patients where cisplatin chemotherapy has failed. These properties come solely from the dicarboxylate leaving group, which is kinetically more inert to substitution. Studies with monoclonal antibodies have shown the DNA adducts of carboplatin to be identical with those formed by *cis*-DDP.[117]Other platinum compounds that have undergone clinical trials are close analogues of *cis*-$[PtA_2X_2]$, or tetraplatin, *cis*,*cis*,*cis*-$[PtA_2X_2Y_2]$, that obey the classic structure-activity relationships. The activity of cationic triamines, *cis*-$[Pt(NH_3)_2LCI]CI$, where L is pyridine, a substituted pyridine, pyrimidine, or purine, against S180 ascites and L1210 tumors in mice opens a new vista of possible structures to be tried. The intercalator-linked complex AO-Pt (Figure 9.26) has also been found to show activity in the S180 ascites system, suggesting a further class of complexes that could be studied. The oral compounds, *cis*,*trans*,*cis*-$[Pt(NH_3)(C_6H_5NH_2)(O_2CCH_3)_2Cl_2]$, survive the digestive tract, are taken across the gastrointestinal mucosa, and metabolize to *cis*-$[Pt(NH_3)(C_6H_5NH_2)Cl_2]$, a cisplatin analogue.[54] As such they are effective pro-drugs that could become the major platinum agent in clinical use. Until these recent advances, there was a general impression that, by chance, the best compound discovered was the first one, cisplatin. There is now sufficient reason to expect that innovative experimentation will lead to improved drugs, bearing in mind the comment made earlier (Section IV.G.) that sustained individual effort for up to a decade can be required to move a compound from the laboratory bench into the clinic.

4. Nonplatinum Antitumor Metal Complexes

a. Soft Metals

As mentioned in Section IV.E., some compounds of Pd(II), Au(I), Rh(II), and Ru(II or III) have been screened for antitumor activity, but much more work needs to be done in this arena. The higher metal-ligand exchange rates of Pd(II), ~10^5 faster than those of Pt(Il), make these complexes potentially more toxic, as some preliminary animal studies have shown. By use of chelating or organometallic complexes, however, this problem might be avoided. The properties of Ru, Rh, and to a lesser extent Au amine and polypyridine complexes would seem to make them attractive candidates, and indeed there appears to be renewed interest in these molecules.[160] Inorganic chemists interested in pursuing drug development with these metals need to forge alliances with biological colleagues equipped to do the necessary animal screening and to develop in-house expertise for cell culture and related biochemical work. The techniques are not all that difficult and it is actually fun to undertake studies of the biological consequences of metallodrug chemistry.

b. Metallocenes and Metallocene Dihalides[36-37]

Although complexes such as $[(C_5H_5)_2TiCl_2]$ are superficially analogous to *cis*-DDP, in being potentially bifunctional DNA crosslinking agents, their hydrolytic reactions are sufficiently different to cast doubt on the value of this comparison. The fact that antitumor activity has been found for this very different class of inorganic compound, however, suggests that perhaps bioinorganic chemists have explored only a very small sample of possible metallodrugs.

11.2.9.11: Design of New Inorganic Anticancer Drugs is shared under a CC BY-NC-SA 4.0 license and was authored, remixed, and/or curated by LibreTexts.

CHAPTER OVERVIEW

Back Matter

Detailed Licensing

https://chem.libretexts.org/@go/page/438096

Detailed Licensing

Overview

Title: 11.2: Bioinorganic Chemistry (Bertini et al.)

Webpages: 118

Applicable Restrictions: Noncommercial

All licenses found:

- CC BY-NC-SA 4.0: 97.5% (115 pages)
- Undeclared: 2.5% (3 pages)

By Page

- 11.2: Bioinorganic Chemistry (Bertini et al.) - *CC BY-NC-SA 4.0*
  - Front Matter - *CC BY-NC-SA 4.0*
    - Licensing - *Undeclared*
    - Preface - *Undeclared*
  - 11.2.1: Transition-Metal Storage, Transport, and Biomineralization - *CC BY-NC-SA 4.0*
    - 11.2.1.1: Biological Significance of Iron, Zinc, Copper, Molybdenum, Cobalt, Chromium, Vanadium, and Nickel - *CC BY-NC-SA 4.0*
    - 11.2.1.2: Biological Systems of Metal Storage - *CC BY-NC-SA 4.0*
    - 11.2.1.3: Chemical Properties Relative to Storage and Transport - *CC BY-NC-SA 4.0*
    - 11.2.1.4: Iron Biomineralization - *CC BY-NC-SA 4.0*
    - 11.2.1.5: Transport of Iron - *CC BY-NC-SA 4.0*
    - 11.2.1.6: Transport of Zinc, Copper, Vanadium, Chromium, Molybdenum, and Cobalt - *CC BY-NC-SA 4.0*
  - 11.2.2: The Reaction Pathways of Zinc Enzymes and Related Biological Catalysts - *CC BY-NC-SA 4.0*
    - 11.2.2.1: About Carbonic Anhydrase - *CC BY-NC-SA 4.0*
    - 11.2.2.2: Acid-base Equilibria - *CC BY-NC-SA 4.0*
    - 11.2.2.3: Catalytic Mechanism - *CC BY-NC-SA 4.0*
    - 11.2.2.4: Coordinated Water and NMR - *CC BY-NC-SA 4.0*
    - 11.2.2.5: Coordination Geometries - *CC BY-NC-SA 4.0*
    - 11.2.2.6: Ester Hydrolysis and Phosphoryl Transfer - *CC BY-NC-SA 4.0*
    - 11.2.2.7: Group Transfer and Vitamin B-12 - *CC BY-NC-SA 4.0*
    - 11.2.2.8: Metal Substitution - *CC BY-NC-SA 4.0*
    - 11.2.2.9: Model Chemistry - *CC BY-NC-SA 4.0*
    - 11.2.2.10: Nucleophilic Addition of \(OH^{-}\) and \(H^{-}\) - *CC BY-NC-SA 4.0*
    - 11.2.2.11: Peptide Hydrolysis - *CC BY-NC-SA 4.0*
    - 11.2.2.12: pH Dependence of Inhibitor Binding - *CC BY-NC-SA 4.0*
    - 11.2.2.13: Selecting Zinc - *CC BY-NC-SA 4.0*
    - 11.2.2.14: Steady-State and Equilibrium Kinetics of Carbonic Anhydrase-Catalyzed \(CO_{2}/HCO_{3}^{-}\) Interconversion - *CC BY-NC-SA 4.0*
    - 11.2.2.15: Strategies for the Investigation of Zinc Enzymes - *CC BY-NC-SA 4.0*
    - 11.2.2.16: The Natural Catalysts - *CC BY-NC-SA 4.0*
    - 11.2.2.17: What Do We Learn? - *CC BY-NC-SA 4.0*
  - 11.2.3: Calcium in Biological Systems - *CC BY-NC-SA 4.0*
    - 11.2.3.1: Ca^{2+}-binding Proteins in Microorganisms-The Search for a Prokaryotic Calmodulin - *CC BY-NC-SA 4.0*
    - 11.2.3.2: Basic Facts About Calcium- Its Compounds and Reactions - *CC BY-NC-SA 4.0*
    - 11.2.3.3: Calcium in Mineralized Tissues - *CC BY-NC-SA 4.0*
    - 11.2.3.4: Calmodulin - *CC BY-NC-SA 4.0*
    - 11.2.3.5: Extracellular Calcium Ion-binding Proteins - *CC BY-NC-SA 4.0*
    - 11.2.3.6: Inositol Trisphosphate and the Calcium Ion Messenger System - *CC BY-NC-SA 4.0*
    - 11.2.3.7: Intracellular Calcium Ion Transport - *CC BY-NC-SA 4.0*
    - 11.2.3.8: Measurements of "Free" Calcium Concentrations - *CC BY-NC-SA 4.0*
    - 11.2.3.9: Measurements of Total Calcium Concentrations - *CC BY-NC-SA 4.0*
    - 11.2.3.10: Mitochondrial Calcium Ion Transport - *CC BY-NC-SA 4.0*

- 11.2.3.11: Molecular Aspects of Calcium Ion-Regulated Intracellular Processes (Part 1) - *CC BY-NC-SA 4.0*
- 11.2.3.12: Molecular Aspects of Calcium Ion-regulated Intracellular Processes (Part 2) - *CC BY-NC-SA 4.0*
- 11.2.3.13: Paravalbumin and Calbindins \(D_{9K}\) and \(D_{28K}\) - *CC BY-NC-SA 4.0*
- 11.2.3.14: The Transport and Regulation of Ca^{2+} Ions in Higher Organisms - *CC BY-NC-SA 4.0*
- 11.2.3.15: Troponin C - *CC BY-NC-SA 4.0*

11.2.4: Biological and Synthetic Dioxygen Carriers - *CC BY-NC-SA 4.0*

- 11.2.4.1: Biological Dioxygen Transport Systems - *CC BY-NC-SA 4.0*
- 11.2.4.2: Biological Oxygen Carriers - *CC BY-NC-SA 4.0*
- 11.2.4.3: Detailed Structures of Hemoglobins and Model Systems - *CC BY-NC-SA 4.0*
- 11.2.4.4: Dioxygen Carriers and Bioinorganic Chemistry - *CC BY-NC-SA 4.0*
- 11.2.4.5: General Aspects of the Chemistry of Cobalt - *CC BY-NC-SA 4.0*
- 11.2.4.6: General Aspects of the Chemistry of Copper - *CC BY-NC-SA 4.0*
- 11.2.4.7: General Aspects of the Chemistry of Dioxygen - *CC BY-NC-SA 4.0*
- 11.2.4.8: General Aspects of the Chemistry of Iron - *CC BY-NC-SA 4.0*
- 11.2.4.9: General Structural Features that Modulate Ligand Activity - *CC BY-NC-SA 4.0*
- 11.2.4.10: Hazards of Life with Dioxygen - *CC BY-NC-SA 4.0*
- 11.2.4.11: Nature of the Metal-Dioxygen Linkage in Biological Systems - *CC BY-NC-SA 4.0*
- 11.2.4.12: Other Ligands for Biological Oxygen Carriers - *CC BY-NC-SA 4.0*
- 11.2.4.13: Requirements for a Model System for Hemoglobin - *CC BY-NC-SA 4.0*
- 11.2.4.14: Requirements for Effective Oxygen Carriers - *CC BY-NC-SA 4.0*
- 11.2.4.15: Role of the Protein in Effecting Biological Oxygen Transport - *CC BY-NC-SA 4.0*
- 11.2.4.16: Selected Chemistry of Dioxygen, Iron, Copper, and Cobalt - *CC BY-NC-SA 4.0*
- 11.2.4.17: Stereochemical Changes Upon Ligation - *CC BY-NC-SA 4.0*
- 11.2.4.18: Structural Basis of Ligand Affinities of Oxygen Carriers - *CC BY-NC-SA 4.0*
- 11.2.4.19: Structures Relevant to Liganded Hemoglobins - *CC BY-NC-SA 4.0*
- 11.2.4.20: Thermodynamic Factors - *CC BY-NC-SA 4.0*
- 11.2.4.21: Ch. 4 References and Abbreviations - *CC BY-NC-SA 4.0*

11.2.5: Dioxygen Reactions - *CC BY-NC-SA 4.0*

- 11.2.5.1: Catalase and Peroxidase - *CC BY-NC-SA 4.0*
- 11.2.5.2: Chemistry of Dioxygen - *CC BY-NC-SA 4.0*
- 11.2.5.3: Copper-zinc Superoxide Dismutase - *CC BY-NC-SA 4.0*
- 11.2.5.4: Cytochrome c Oxidase - *CC BY-NC-SA 4.0*
- 11.2.5.5: Dioxygen Toxicity - *CC BY-NC-SA 4.0*
- 11.2.5.6: Monooxygenases - *CC BY-NC-SA 4.0*
- 11.2.5.7: Oxygenases - *CC BY-NC-SA 4.0*

11.2.6: Electron Transfer - *CC BY-NC-SA 4.0*

- 11.2.6.1: Biological Redox Components - *CC BY-NC-SA 4.0*
- 11.2.6.2: Coupling Electron Transfers and Substrate Activation - *CC BY-NC-SA 4.0*
- 11.2.6.3: Electron-transfer Rates - *CC BY-NC-SA 4.0*
- 11.2.6.4: Electron-Transfer Theory - *CC BY-NC-SA 4.0*
- 11.2.6.5: Energy Storage and Release - *CC BY-NC-SA 4.0*
- 11.2.6.6: Long-range Electron Transfer in Proteins (Part 1) - *CC BY-NC-SA 4.0*
- 11.2.6.7: Long-range Electron Transfer in Proteins (Part 2) - *CC BY-NC-SA 4.0*
- 11.2.6.8: Marcus Theory - *CC BY-NC-SA 4.0*

11.2.7: Ferrodoxins, Hydrogenases, and Nitrogenases - Metal-Sulfide Proteins - *CC BY-NC-SA 4.0*

- 11.2.7.1: Iron-sulfur Proteins and Models - *CC BY-NC-SA 4.0*
- 11.2.7.2: Iron-sulfur Proteins and Models (Part 2) - *CC BY-NC-SA 4.0*
- 11.2.7.3: Iron-sulfur Proteins and Models (Part 3) - *CC BY-NC-SA 4.0*
- 11.2.7.4: Iron-sulfur Proteins and Models (Part 4) - *CC BY-NC-SA 4.0*
- 11.2.7.5: Multisite Redox Enzymes - *CC BY-NC-SA 4.0*
- 11.2.7.6: Multisite Redox Enzymes (Part 2) - *CC BY-NC-SA 4.0*
- 11.2.7.7: Multisite Redox Enzymes (Part 3) - *CC BY-NC-SA 4.0*
- 11.2.7.8: Multisite Redox Enzymes (Part 4) - *CC BY-NC-SA 4.0*

- 11.2.7.9: Multisite Redox Enzymes (Part 5) - *CC BY-NC-SA 4.0*
- 11.2.7.10: Multisite Redox Enzymes (Part 6) - *CC BY-NC-SA 4.0*
- 11.2.7.11: Report on the Nitrogenase Crystal Structure\(\;^{378-381}\) - *CC BY-NC-SA 4.0*
- 11.2.7.12: Rubredoxin- A Single-Fe Tetrathiolate Protein - *CC BY-NC-SA 4.0*

- 11.2.8: Metal/Nucleic Acid Interactions - *CC BY-NC-SA 4.0*
  - 11.2.8.1: The Basics - *CC BY-NC-SA 4.0*
  - 11.2.8.2: The Basics (Part 2) - *CC BY-NC-SA 4.0*
  - 11.2.8.3: A Case Study- Tris(phenanthroline) Metal Complexes - *CC BY-NC-SA 4.0*
  - 11.2.8.4: Applications of Different Metal Complexes that Bind Nucleic Acids - *CC BY-NC-SA 4.0*
  - 11.2.8.5: Applications of Different Metal Complexes that Bind Nucleic Acids (Part 2) - *CC BY-NC-SA 4.0*
  - 11.2.8.6: Nature's Use of Metal/Nucleic-acid Interactions - *CC BY-NC-SA 4.0*
- 11.2.9: Metals in Medicine - *CC BY-NC-SA 4.0*
  - 11.2.9.1: Metal Deficiency and Disease - *CC BY-NC-SA 4.0*
  - 11.2.9.2: Toxic Effects of Metals - *CC BY-NC-SA 4.0*
  - 11.2.9.3: Aspects of Platinum Binding to DNA - *CC BY-NC-SA 4.0*
  - 11.2.9.4: Survey of Metals Used for Diagnosis and Chemotherapy - *CC BY-NC-SA 4.0*
  - 11.2.9.5: Platinum Anticancer Drugs- A Case Study - *CC BY-NC-SA 4.0*
  - 11.2.9.6: Mapping the Major Adducts of cis- and trans-DDP on DNA; Sequence Specificity - *CC BY-NC-SA 4.0*
  - 11.2.9.7: Structure of Platinum-DNA Complexes - *CC BY-NC-SA 4.0*
  - 11.2.9.8: Site-specifically Platinated DNA \(\;^{154}\) - *CC BY-NC-SA 4.0*
  - 11.2.9.9: Bioinorganic Chemistry of Platinum Anticancer Drugs- How Might They Work? - *CC BY-NC-SA 4.0*
  - 11.2.9.10: Bioinorganic Chemistry of Platinum Anticancer Drugs; How Might They Work? (Part 2) - *CC BY-NC-SA 4.0*
  - 11.2.9.11: Design of New Inorganic Anticancer Drugs - *CC BY-NC-SA 4.0*
- Back Matter - *CC BY-NC-SA 4.0*
  - Detailed Licensing - *Undeclared*

SECTION OVERVIEW

11.3: Cisplatin - The Invention of an Anticancer Drug

We begin our story with an experiment designed to elucidate the effect of electric fields on the bacterial growth of E. coli. The serendipitous result of this experiment was that it was not the electric fields that inhibited bacterial growth but rather a platinum containing complex that later came to be known as **cisplatin**. Cisplatin chemotherapy now recognized for dramatic lengthening of survival for some common types of lung cancer. Read through this unit for a description of cisplatin science. Sometimes the principles of chemistry are embedded in another science. Sometimes it is not obvious that chemistry is at the heart of invention. The story of the invention of the anticancer drug cisplatin is a story of chemistry hidden in the science of biology. A group of researchers at Michigan State University subsequently found that cisplatin could also be used to inhibit the growth of cancer cells. For the past twenty years, cisplatin has proven to be highly effective for the treatment of various cancers, particularly testicular cancer. Unfortunately, toxicity and drug resistance have become serious concerns, and research efforts continue in the hope of improving this drug.

11.3.1: Cisplatin 1. Study of the Effect of Electric Fields on E. coli

11.3.2: Cisplatin 2. Control Experiments for the Effect of Electric Fields on E. coli

11.3.3: Cisplatin 3. Redox Chemistry

11.3.4: Cisplatin 4. Electrochemistry

11.3.5: Cisplatin 5. The Role of Platinum Electrodes

11.3.6: Cisplatin 6. Transition Metal Chemistry

11.3.7: Cisplatin 7. Bioinorganic Chemistry

11.3.8: Cisplatin 8. Discovery of Cisplatin

11.3.9: Cisplatin 9. The Discovery - One Scientist's Story

11.3.10: Cisplatin 10. Research as a Career

11.3.11: Cisplatin 11. Cisplatin as an Anticancer Drug

11.3.12: Cisplatin 12. Modes of Action of Cisplatin

11.3.13: Cisplatin 13. Further Studies/Recent Developments

11.3.14: Cisplatin 14. DNA

11.3.15: Cisplatin 15. FDA Drug Approval Process

11.3.16: Cisplatin 16. Profits from Cisplatin

11.3.17: Cisplatin 17. Drug Resistance

11.3.18: Cisplatin 18. Toxicity

11.3.19: Cisplatin 19. Cancer

11.3.20: Cisplatin 20. Other Treatments for Cancer

Template:HideTOC

This page titled 11.3: Cisplatin - The Invention of an Anticancer Drug is shared under a CC BY-NC-SA 4.0 license and was authored, remixed, and/or curated by ChemCases.

11.3.1: Cisplatin 1. Study of the Effect of Electric Fields on E. coli

Our story begins in 1961 when a young physics professor named Barnett Rosenberg left his position at New York University to help found a new department of biophysics at Michigan State University. As a physicist, he had long been intrigued by microphotographs depicting the process of cell division, called mitosis. These photographs reminded him of a natural physical phenomenon: the magnetic dipole field created when one places iron filings over a bar magnet. The field lines created by magnets have the same shape as those created by electricity between two equal and opposite point charges.

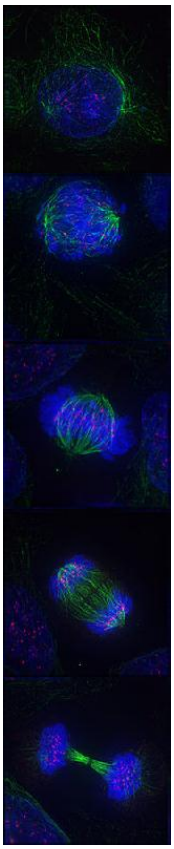


Figure 1: Mitotic cells can be visualized microscopically by staining them with fluorescent antibodies and dyes. (left to tright): prophase, prometaphase , Metaphase, Anaphase and Telophase. Images used with permission from Wikipedia (Public Domain: credit Roy van Heesbeen)

His observation of the similarities between the shape of cells as they are undergoing mitosis and the shape of electrical and magnetic field lines presented him with a perfect avenue for shifting his research focus more toward biology. He and others hypothesized that this similarity in shape was perhaps not an accident, but of nature that such a dipole might be involved in cell division. His idea was that if the mitotic dipole was exposed to electromagnetic radiation of a resonant frequency, the dipole might absorb some energy. His goal, then, was to see how the cell was affected by the absorption of this energy.[3] As is often the case in scientific research, particularly in interdisciplinary fields, Rosenberg decided that it would be a good idea to have a collaborator who had been trained in biology.

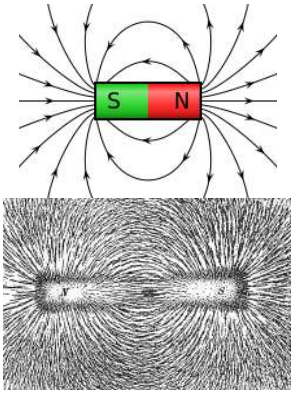


Figure 2: Magnetic field lines: Magnetic field of an ideal cylindrical magnet with its axis of symmetry inside the image plane. The magnetic field is represented by magnetic field lines, which show the direction of the field at different points. (a) magnetic field patterns surrounding a bar magnet as displayed with iron filings; (b)The direction of magnetic field lines represented by the alignment of iron filings sprinkled on paper placed above a bar magnet. Images used with permission from Wikipedia.

Therefore, he hired a biologist and together they set up a specially designed continuous culture apparatus for the cells they were planning to study. Their plan was to use mammalian cells, which are known to undergo mitosis. They decided to test the apparatus first, however, by using Escherichia coli bacterial cells, which (along with other prokaryotes) do not form the mitotic figures in cell division, as shown above. For their experiments, they chose a medium commonly used for studying the growth of E. coli bacteria; this medium was enriched with glucose and magnesium chloride. The culture chamber was kept at a constant temperature of 37° C, and compressed air was bubbled into the chamber through a glass frit bubbler. Two strains of *E. coli* were used to inoculate the chamber: *E. coli* B and *E. coli* K-12. After about 24 hours, the bacterial population reached a steady state, as determined by turbidity measurements. These measurements showed that the steady state was maintained for 10 to 14 days longer. Therefore, all experiments were performed within 10 days of inoculation.4 To study the effect of electric fields on growth processes in bacteria, an audio oscillator was used to supply sinusoidal voltages of 50 to 100,000 cycles/second (c/s). These signals were amplified by a conventional audio power amplifier and then sent to a pair of platinum electrodes in the chamber. (Platinum was chosen as the material for the electrodes because of its well-known chemical inertness.) The impedance of the chamber was approximately 6 ohms and was perfectly matched to the output impedance of the amplifier, allowing for the most efficient transfer of power. In the first experiment, the electric field was turned on to 1,000 c/s, 2 amp (peak to peak) through the chamber. After 1 hour, the turbidity began to decrease, meaning that cell growth was slowing down. After 2 hours, the bacterial population was almost completely washed out, and the voltage was turned off. After 8 more hours, the population density of the bacteria returned to its previous value. This process could be repeated.

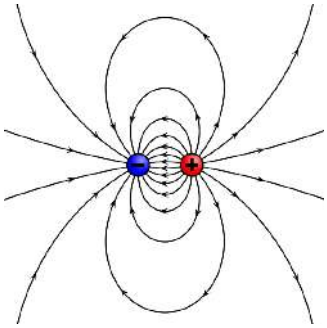


Figure 3: Electric field lines: The magnetic pole model: two opposing poles, North (+) and South (−), separated by a distance d produce a magnetic field (lines). from WIkipedia (CC-SA-3.0 Credit Geek3)

Rosenberg and his colleague found a surprising and unexpected phenomenon at this point. The researchers observed that the bacterial cells stopped dividing 1 to 2 hours after the voltage had been applied and that the cells started to elongate in that time, forming long filaments. For 1 to 2 hours after the voltage was removed, the cells continued to increase in length, but after 2 hours had elapsed, cell division started to occur again.[4] These effects were tested over a range of applied voltages. When the frequency of the applied voltage was between 500 to 6,000 c/s, **bacterial growth was affected and filamentous growth of the bacteria occurred**. Filamentous growth occurs when cell division is inhibited, but cell growth is not. During filamentous growth, E. coli are still able to grow, but since they cannot divide, they form long filaments, as shown in Figure 4, part (b). Under normal conditions,

E. coli form short rods, as shown in Figure 4, part (a). The extent of filamentous growth varied over the 500 to 6,000 c/s frequency range: At 500 c/s, filamentous growth was at a maximum, whereas at 6,000 c/s, no filaments could be seen. Moreover, at frequencies above 6,000 c/s (i.e., from 6,000 to 100,000 c/s), no effects were observed in 24-hour trials.4

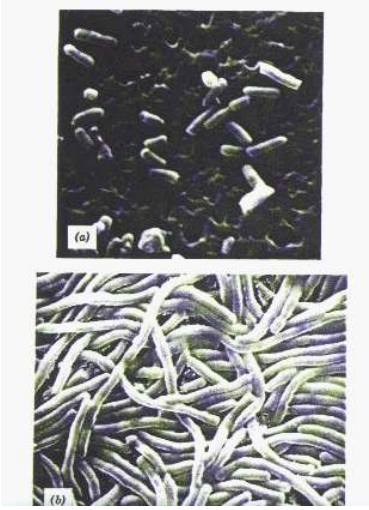


Figure 4. Normal and elongated E. coli: (a) scanning electron microphotograph of normal E. coli (Gram-negative rods); (b) scanning electron microphotograph of E. coli grown in medium containing a few parts per million of cis-diamminedichloroplatinum(II). Same magnification in both pictures. The platinum drug has inhibited cell division, but not growth, leading to long filaments. (Courtesy of D. Beck) Reprinted with permission.

Along with variations in frequency, the presence of oxygen was an important factor in causing filamentous growth in E. coli cells. Filamentous growth occurred at the frequencies mentioned above only when oxygen was present. If another gas, such as nitrogen or helium, were bubbled through the cell, no effect was observed. Having observed the unexpected result that electric fields indeed seemed to affect bacterial cell division, Rosenberg and his coworkers conducted more experiments to try to determine the exact cause of this effect. In their subsequent experiments, they varied one experimental parameter at a time in an effort to determine exactly why filamentous growth of bacterial cells occurred under their experimental conditions. Such control experiments are essential in scientific research. As we will see, negative control experiments can often give as much information as positive ones.

References

1. Alberts, B., Bray, D., Lewis, J., Raff, M., Roberts, K., Watson, J. D. Molecular Biology of the Cell, 3rd ed. Garland Publishing, Inc.: New York, 1994, pp. 919, 925.
2. Serway, R. A. Principles of Physics, 2nd ed. Harcourt Brace & Company: Fort Worth, 1998, p. 639.
3. Rosenberg, B. In Nucleic Acid-Metal Ion Interactions, T. G. Spiro, Ed., John Wiley & Sons, Inc.: New York, 1980, Vol. 1, pp. 1-29.
4. Rosenberg, B., VanCamp, L., Krigas, T. Nature, 1965, 205, pp. 698-699.

This page titled 11.3.1: Cisplatin 1. Study of the Effect of Electric Fields on E. coli is shared under a CC BY-NC-SA 4.0 license and was authored, remixed, and/or curated by ChemCases.

- **Cisplatin 1. Study of the Effect of Electric Fields on E. coli** by ChemCases is licensed CC BY-NC-SA 4.0.

11.3.2: Cisplatin 2. Control Experiments for the Effect of Electric Fields on E. coli

With the result that application of an electric field apparently halted bacterial cell division and led to filamentous growth, Barnett Rosenberg's group sought to understand better the cause of this phenomenon. (Recall that filamentous growth occurs when cell division—but not cell growth—is inhibited.) For this reason, the researchers conducted a variety of control experiments in which they varied one experimental parameter at a time. They knew that the filamentous growth they had observed in *E. coli* bacterial cells could be caused by several known physical and chemical agents such as the following:

- dyes such as methylene blue and penicillin,
- transfer to an unaccustomed medium,
- osmotic pressure changes,
- near ultraviolet irradiation,
- and magnesium deficiency or excess.

Based on the experimental conditions, Rosenberg and his colleagues were able to rule out the first three possibilities. They then conducted a variety of tests and ruled out not only the last two possibilities but also several others:

- ultraviolet light,
- temperature,
- pH.

They also found that adaptive mechanisms and mutation effects in the bacteria did not play a role in filamentous growth.[1] **The researchers then considered the possibility that the application of an electric field to the bacterial medium might have led to an electrolysis reaction and that the chemical products of this reaction might have affected bacterial cell division**. For this reason, they conducted more control experiments. In one experiment, they decided to separate the electrodes from the E. coli bacteria. Their new apparatus had two chambers: an electrolysis chamber containing the electrodes but no bacteria, and a bacterial chamber containing E. coli cells but no electrodes. In the experiment, the nutrient was pumped into the electrolysis chamber and a voltage was applied to the electrodes. The nutrient was then pumped from the electrolysis chamber into the bacterial chamber. The idea was that if a new chemical species was produced in the electrolysis chamber, and if it was relatively stable (meaning long-lived), then it would be pumped into the bacterial chamber along with the nutrient. Such a new chemical species might be the cause of the observed filamentous growth (also called elongation) of the bacterial cells. The researchers found that under this new set of experimental conditions, they again observed that the bacterial cells formed long filaments.

From the results of this experiment, they concluded that the application of the electric current (voltage) was not itself responsible for the observed effects on bacterial growth, but rather that the electric current led to the formation of a new chemical species that affected bacterial elongation. Furthermore, they again observed that oxygen had to be present in the electrolysis chamber for bacterial elongation to occur.1 This result led them to consider the possibility that electrolysis was generating an oxidizing agent, which might be contributing to the observed effects on bacterial growth. They then conducted another control experiment to look for the presence of an oxidizing agent. One test commonly used to detect the presence of an oxidizing agent is the potassium iodide-starch test. For example, if the putative oxidizing agent is a metal ion with a +2 charge (represented here as M^{2+}), the metal ion gains two electrons to form the neutral, elemental metal (M0) and is therefore reduced. The two electrons come from two iodide ions (I^-), each of which gives up one electron, producing a molecule of elemental iodine (I_2). When elemental iodine exists in the presence of excess iodide ion, an acid-base reaction occurs in which elemental iodine acts as a Lewis acid and iodide ion acts as a Lewis base to produce a triiodide ion, I_3^-. Triiodide ion is a linear species and forms a blue complex with starch. Therefore, the potassium iodide-starch test is able to detect the presence of an oxidizing agent, here M^{2+}. For more information on oxidations and reductions (i.e., redox chemistry), go to the redox chemistry and electrochemistry modules.

$$M^{2+} + 2I^- \rightarrow M^0 + I_2 \qquad \text{(redox reaction)}$$

$$I^- + I_2 \rightarrow I_3^- \qquad \text{(acid-base reaction)}$$

$$+ \quad \text{———————————}$$

$$M^{2+} + 3I^- \rightarrow M^0 + I_3^- \qquad \text{(net reaction)}$$

The researchers used the potassium iodide-starch test to see whether any oxidizing agents were present in the medium they were using to grow bacterial cells. They found that the ordinary medium gave no reaction with potassium iodide and starch but that the electrolyzed medium gave a positive test, in which a blue color developed after 5 minutes. From this result, they concluded that **an oxidizing agent was indeed present in the medium**. Furthermore, they found that the appearance of the blue color indicating the presence of oxidizing agent **coincided with the elongation of the bacterial cells**. And finally, they observed that the **intensity of the blue color corresponded to the frequency of the applied voltage**. When the frequency was 500 c/s, the blue color was most intense, indicating that the concentration of the oxidizing agent was highest at this frequency; when the frequency was 6,000 c/s, the blue color was not detectable (recall that in the electric fields module, we learned that when the applied voltage was 500 c/s, filamentous growth was at a maximum, whereas at 6,000 c/s, no filaments were observed). These last two results strongly suggested that a new chemical species, an oxidizing agent, was causing the changes in bacterial cell growth.[1] The next step for the researchers was to determine the **identity of this mystery oxidizing agent**. To do this, they ran another set of control experiments. They deduced that several possible oxidizing agents could be created from the medium during electrolysis:

- hypochlorite ion (ClO^-),
- chlorite ion (ClO_2^-),
- chlorate ion (ClO_3^-),
- perchlorate ion (ClO_4^-),
- hydrogen peroxide (H_2O_2),
- hydroxylamine (NH_2OH),
- and persulfate ion ($S_2O_8^{2-}$).

Sensitive qualitative tests showed that none of these ions existed in the medium. In a separate set of control experiments, each component of the medium was made up in the appropriate concentration and electrolyzed for 6 amp-h. Following electrolysis, each solution was subjected to the potassium iodide-starch test. A mixture of negative and positive results were obtained. Negative tests resulted in the following cases, meaning that no oxidizing agents were found in these electrolyzed solutions: phosphate ion (PO_4^{3-}); sulfate ion (SO_4^{2-}); phosphate ion + glucose; phosphate ion + sulfate ion + glucose; sodium sulfate (Na_2SO_4); and sodium carbonate (Na_2CO_3). However, oxidizing agents were found in the following cases, as evidenced by positive tests: ammonium sulfate ($(NH_4)_2SO_4$); ammonium carbonate ($(NH_4)_2CO_3$); ammonium chloride (NH_4Cl); and other chlorides. Sodium chloride (NaCl) gave a faint positive response.[1] To learn the conclusions that Rosenberg and his coworkers reached as a result of this set of control experiments, go to the module on the role of platinum electrodes.

References

1. Rosenberg, B., Camp, L. V., Krigas, T. Nature ,1965, 205, pp. 698-699.

This page titled 11.3.2: Cisplatin 2. Control Experiments for the Effect of Electric Fields on E. coli is shared under a CC BY-NC-SA 4.0 license and was authored, remixed, and/or curated by ChemCases.

- **Cisplatin 2. Control Experiments for the Effect of Electric Fields on E. coli** by ChemCases is licensed CC BY-NC-SA 4.0.

11.3.3: Cisplatin 3. Redox Chemistry

The transfer of electrons from one species to another is called oxidation-reduction chemistry, or redox chemistry. Oxidation refers to a loss of electrons, whereas reduction refers to a gain of electrons. When discussing redox chemistry, it is useful to assign oxidation numbers to elements undergoing a transfer of electrons. The use of oxidation numbers is a bookkeeping method that chemists use to keep track of electrons. The oxidation number is defined so that oxidation corresponds to an increase in oxidation number, and reduction corresponds to a decrease in oxidation number. Another way to think about redox chemistry and oxidation numbers is that in redox chemistry we exaggerate the ionic character of bonds; in other words, redox chemistry is based on a representation in which the atoms are pictured as ions. Assigning oxidation numbers requires following three rules:

1. 1. **The oxidation number of an element in its elemental form is 0**. (For example, the oxidation number of Na is 0, and the oxidation number of Cl_2 is also 0.).
2. **The oxidation number of an element when it exists as a monatomic ion is the same as its charge**. (For example, the oxidation number of Na+ is +1, and the oxidation number of Cl^- is -1).
3. **The sum of the oxidation numbers of all the atoms in a species is equal to its total charge**. (For example, the sum of the oxidation numbers in SO_4^{2-} is -2.)

In addition, there are a few elements that have specific values for their oxidation numbers:

- **The oxidation number of hydrogen is +1 when bonded to a nonmetal and -1 when bonded to a metal.** The reason for this is that hydrogen is less electronegative than nonmetals. When we treat a hydrogen-nonmetal bond as an *ionic* bond, hydrogen donates its electron to the nonmetal, resulting in a +1 oxidation number for H. For example, in a molecule of water, two hydrogen atoms are bonded to an oxygen atom (a nonmetal that is *more* electronegative than hydrogen). H has an oxidation number of +1, and O has an oxidation number of -2. (To restate rule #3 above: the sum of the oxidation numbers in a neutral molecule is 0.) The oxidation number of hydrogen atoms in metal-hydrogen bonds can also be explained by the electronegativity differences between H and M. Hydrogen is more electronegative than metals. Therefore, in an ionic treatment of a metal-hydrogen bond, the metal atom donates an electron to the hydrogen atom, resulting in a -1 oxidation number for H. For example, in sodium hydride (NaH), sodium has an oxidation state of +1, whereas hydrogen has an oxidation state of -1.
- **The oxidation number of oxygen is almost always -2.** This can also be explained on the basis of electronegativity. Oxygen is the second most electronegative element—after fluorine. Therefore, in an ionic treatment of a bond containing oxygen and another element—with the exception of fluorine—oxygen will accept two electrons and take on a -2 oxidation number. For example, in sulfate ion (SO42-), each oxygen has an oxidation number of -2, whereas sulfur has an oxidation number of +6. (Again, see rule #3 above: total charge on ion = -2 = 4 x [oxid. no. of O] + [oxid. no. of S].)
- **The oxidation number of fluorine is always -1.** The oxidation of the other halogens is -1 unless the halogen is bonded to oxygen or another halogen higher in the group. Again, these values can be explained based on electronegativity differences. Fluorine is the most electronegative element of all. Using an ionic model, fluorine always accepts an electron from an atom it is bonded to, giving fluorine both a -1 charge and a -1 oxidation number. Other halogen atoms will also have a -1 oxidation state *unless* they are bonded to a more electronegative atom, such as oxygen or another halogen higher in the group, such as fluorine. For example, in the molecule FI, fluorine has a -1 oxidation number, whereas iodine has a +1 oxidation state.

The species that causes oxidation is called the **oxidizing agent**. It does this by accepting electron(s) from the species being oxidized. In other words, the oxidizing agent is reduced. According to our bookkeeping method of calculating oxidation numbers, the oxidizing agent contains an atom that undergoes a decrease in oxidation number. Likewise, the species that causes reduction is called the **reducing agent**. The reducing agent donates electron(s) to the species being reduced. Therefore, the reducing agent is itself oxidized and undergoes an increase in oxidation number. For example, in the following redox reaction—which occurs during the potassium iodide-starch test described in the control

experiments module—a metal with an oxidation state of +2 reacts with iodide ion. Let us say that the metal is platinum, and let's write the oxidation numbers below each reactant and product:

$$Pt^{2+} + 2I^{-} \rightarrow Pt^{0} + I_2$$

+2 2 x -1 0 0

In this case, Pt^{2+} (also called Pt(II)) reacts with iodide ion to form Pt^{0} (or Pt(0)) and iodine. Using our oxidation number bookkeeping method, we see that the oxidation number of platinum decreases by 2; therefore, platinum undergoes a two electron reduction. Pt(II) acts as the oxidizing agent by oxidizing iodide ion to iodine. Two iodide ions each undergo a one electron oxidation to give one molecule of I2, resulting in a two electron oxidation overall. Likewise, the two iodide ions act as the reducing agents because they reduce Pt(II) to Pt(0). Just as with all other chemical reactions, redox equations must balance. There are two rules to keep in mind when balancing redox equations:

1. **Atoms must balance.** (In the example above, there is one Pt atom and two I atoms on each side of the reaction; therefore the atoms balance.)
2. **Total charge on each side must balance.** (In the example above, the charge on the left is equal to [+2 + 2(-1)], or 0 overall. Likewise, the charge on the right is equal to [0 + 0], or 0 overall. Therefore, the equation is also balanced with respect to charge.)

References

1. Atkins, P. W., Jones, L. L. Chemistry: Molecules, Matter, and Change; 3rd ed. W. H. Freeman and Company: New York, 1997, Chapter 3: Sections 3.12 to 3.15.

This page titled 11.3.3: Cisplatin 3. Redox Chemistry is shared under a CC BY-NC-SA 4.0 license and was authored, remixed, and/or curated by ChemCases.

- **Cisplatin 3. Redox Chemistry** by ChemCases is licensed CC BY-NC-SA 4.0.

11.3.4: Cisplatin 4. Electrochemistry

Electrochemistry, which is the study of the interaction of electricity and chemical reactions, is a central theme in the story of the discovery of cisplatin. In the redox chemistry module, we saw how electrons are transferred from one species to another in a chemical reaction, and we also learned some of the formalisms for describing these types of reactions. Now we will take these concepts a step further and discuss how various chemical species vary in their ability to "pull" electrons—that is, to be reduced. The implications of the different pulling powers of various species are far reaching. As a result of this phenomenon, we are able to power batteries, produce aluminum, extract metals from their salts, and protect metals through electroplating. We can also gain a more complete understanding of the serendipitous discovery of cisplatin.

In the modules on control experiments and the role of platinum electrodes (as well as the discovery of cisplatin), we saw that platinum-containing electrolysis products were responsible for causing both elongation of bacterial cells and regression of murine tumors. We now discuss the origin of these electrolysis products. **Electrolysis** occurs when an electric current from an external source is used to bring about a nonspontaneous chemical reaction. The researchers found that when they applied an electric current through platinum electrodes in a continuous culture chamber containing *E. coli* bacteria, a reaction occurred in which the supposedly inert platinum metal (Pt^0) of the electrodes was oxidized to form both platinum(II) (Pt^{2+}) and platinum(IV) (Pt^{4+}). Complexes containing oxidized forms of platinum—particularly Pt^{2+}—were found to be the causative agents in bacterial elongation. Let us now examine the oxidation reaction in which Pt^0 is converted into Pt^{2+}:

$$Pt^0_{(s)} \rightarrow Pt^{2+}_{(aq)} + 2e^-$$

Chemists can determine whether this oxidation reaction is spontaneous and if so, how much energy is released. Likewise, they can determine whether the reaction is nonspontaneous and how much energy is required to make the reaction proceed. Knowing the amount of energy released or required for various oxidation and reduction reactions gives us an idea of the ability these reactions (called cell reactions) have to push or pull electrons through a circuit; the measure of this ability is called the **cell potential**. The cell potential is a useful value when it can be compared to other cell potentials obtained under the same standard set of conditions—that is, when all participating gases exist at a pressure of 1 atm, and all ions are present in a concentration of 1 mol L^{-1}.

A cell potential under standard conditions is called a **standard cell potential**, or a standard electrode potential, $E°$. Standard cell potentials are reported only for reduction reactions; for this reason, they are also called standard reduction potentials. Standard electrode potentials are all measured in reference to the hydrogen electrode's standard potential, which is arbitrarily set at zero. If another species oxidizes a molecule of H^2 to H^+ ions, the other species is itself reduced and has a positive standard reduction potential. On the other hand, if H^+ ions oxidize another species, that species has a negative standard reduction potential. Most general chemistry textbooks have tables of standard cell potential values. When we look up the standard cell potential for the reduction of Pt^{2+} to Pt^0 (the opposite of the oxidation reaction written above), we see that this reaction has a positive value for $E°$, meaning that Pt^{2+} oxidizes H^2 to H^+ under standard conditions.

$$Pt^{2+}_{(aq)} + 2e^- \rightarrow Pt^0_{(s)} \quad E^o = +1.20\ V$$

As stated above, we are really more interested in the reverse reaction, the oxidation of Pt^0 to Pt^{2+}. The standard cell potential for the oxidation reaction has the same value but the opposite sign as that for the reduction reaction:

$$Pt^0_{(s)} \rightarrow Pt^{2+}_{(aq)} + 2e^- \quad E^o = -1.20\ V$$

Now let's take a look at what these cell potential values mean. We will see that the cell potential is related both to the reaction free energy, which tells us whether or not the reaction is spontaneous, and to the equilibrium constant for the reaction, which tells us the extent of the reaction at equilibrium. The standard cell potential is related to the standard reaction free energy through the following equation:

$$\Delta G^o = -nFE^o$$

Here, *n* is the number of moles of electrons participating in the reaction. *F* is the Faraday constant, which is the magnitude of charge per mole of electrons, and is equal to 9.6485 x 10^4 C mol-1. We can now calculate the standard free energy for the oxidation reaction written above:

$$\Delta G^o = -nFE^o = -2 \times (9.6485 \times 10^4\, C\, mol^{-1}) \times (-1.20\ V)$$

$$= +231,564\ C \cdot V\ mol^{-1}$$

$$= +231,564\ J\ mol^{-1}$$

$$= +232\ kJ\ mol^{-1}$$

When the reaction free energy is positive (and the cell potential is negative), the reaction is nonspontaneous in the direction written. Therefore, the oxidation of Pt^0 to Pt^{2+} is nonspontaneous; energy must be supplied in order for the reaction to proceed. The energy required for the oxidation of Pt^0 (from the platinum electrodes) can be supplied in the form of an electric current; such a current was applied to the continuous culture chamber containing *E. coli* bacteria. The standard cell potential is also related to the equilibrium constant, K, for the redox reaction:

$$\Delta G^o = -RT \ln K$$

Here, *R* is the gas constant, 8.31451 J K-1 mol-1, and *T* is the temperature. Given this expression and the relationship above between reaction free energy and cell potential, we can relate the cell potential directly to the equilibrium constant:

$$\Delta G^o = -RT\ lnK = -nFE^o$$

$$\ln K = \frac{nFE^o}{RT}$$

$$K = e^{(\frac{nFE^o}{RT})}$$

Therefore, at 25° C (298.15 K), the equilibrium constant for the oxidation of Pt^0 to Pt^{2+} is calculated to be the following:

$$K = e^{(\frac{nFE^o}{RT})} = e^{-93.41}$$

$$= 2.70 \times 10^{-41}$$

As this calculation shows, when Pt^0 is oxidized to Pt^{2+}, the reaction strongly favors the reactants—unless energy is supplied to the reaction. Now that we have seen how Pt^{2+} can be generated under the reaction conditions described in the electric fields module, we can understand the control experiment in which the potassium iodide-starch test was used as a way to detect the presence of an oxidizing agent. We saw in the control experiments and redox chemistry modules that in this test, an oxidizing agent (here, Pt^{2+}) reacts with iodide ions to form the reduced, neutral metal and elemental iodine:

$$Pt^{2+}_{(aq)} + 2I^-_{(aq)} \rightarrow Pt^0_{(s)} + I^2_{(s)}$$

One way to see the electron transfer more clearly is to break this redox reaction into two **half-reactions**:

$$2I^-_{(aq)} \rightarrow I^2_{(s)} + 2e^-$$

$$Pt^{2+}_{(aq)} + 2e^- \rightarrow Pt^0_{(s)}$$

The two iodide ions are each losing one electron—in a net two-electron oxidation. As we learned in the redox chemistry module, I- is the reducing agent. Likewise, Pt^{2+} is gaining two electrons and is reduced, so Pt^{2+} is the oxidizing agent. Using half-reactions is a convenient way to keep track what is going on in a redox reaction. However, it is important to realize that the electrons are not ever actually free in solution, as the half-reactions suggest; rather, they are in transit between the reducing agent and the oxidizing agent. Now, if we add these two half-reactions together, we see that we

obtain the original balanced redox equation. Rules for balancing simple redox equations are given in the redox chemistry module.

$2\ I^-(aq) \rightarrow I^2(s) + 2\ e^-$

$Pt^{2+}((aq) + 2\ e^- \rightarrow Pt^0(s)$

$Pt^{2+}(aq) + 2\ I^-(aq) \rightarrow Pt^0(S) + I^2(s)$

Just as we added together the two half-reactions to obtain a balanced redox equation, we can add together the two standard cell potentials to obtain the net potential.

$2\ I^-(aq) \rightarrow I^2(s) + 2\ e^-$ $E°$ = -0.54 V

$Pt^{2+}(aq) + 2\ e^- \rightarrow Pt^0(s)$ $E°$ = +1.20 V

$Pt^{2+}(aq) + 2$ I-(aq) $\rightarrow Pt^0(S) + I^2(s)$ $E°$ = + 0.66 V

We see that the net potential for the redox reaction occurring in the potassium iodide-starch test is a positive number; this will lead to a negative value for the reaction free energy, meaning that the reaction is spontaneous as written. This means that Pt^{2+} is a strong enough oxidizing agent to effect the oxidation of iodide ions, explaining why Pt^{2+}gives a positive result in the potassium iodide-starch test. In summary, we have seen how Pt^{2+} is generated when an electric current is applied to the platinum electrodes in the continuous culture chamber. We have also seen how the presence of Pt^{2+} gives a positive result when subjected to the potassium iodide-starch test. We now have the pieces of the puzzle to understand how platinum-containing complexes such as cisplatin are generated under the reaction conditions. We will do this in the transition metal chemistry module.

References

1. Atkins, P. W., Jones, L. L. *Chemistry: Molecules, Matter, and Change,* 3rd ed. W. H. Freeman and Company: New York, 1997, Chapter 17.

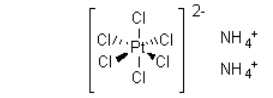
This page titled 11.3.4: Cisplatin 4. Electrochemistry is shared under a CC BY-NC-SA 4.0 license and was authored, remixed, and/or curated by ChemCases.

- **Cisplatin 4. Electrochemistry** by ChemCases is licensed CC BY-NC-SA 4.0.

11.3.5: Cisplatin 5. The Role of Platinum Electrodes

As we saw in the module on control experiments, Barnett Rosenberg and his coworkers wanted to find out if any oxidizing agents were generated in the nutrient medium used for growing E. coli bacterial cells following electrolysis. They isolated various components of the medium, subjected them to electrolysis, and then tested them for the presence of an oxidizing agent with the potassium iodide-starch test (described in the control experiments module).

The researchers found that many solutions containing either ammonium ion or chloride ion or both gave a positive test. Specifically, the following ionic compounds present in the nutrient medium formed oxidizing agents after electrolysis with platinum electrodes: ammonium sulfate ($(NH_4)_2SO_4$); ammonium carbonate ($(NH_4)_2CO_3$); ammonium chloride (NH_4Cl); and other chlorides. Sodium chloride (NaCl) gave a faint positive response.1 The researchers had finally found an oxidizing agent formed during electrolysis, and they believed that this new compound (or compounds) might be responsible for inhibiting cell division in E. coli bacteria. Their quest now was to determine the identity of this new compound. They knew that platinum electrodes could be attacked by an acidified chloride solution during electrolysis, generating platinum hexachloride, $PtCl_6^{2-}$, and they hypothesized that a soluble platinum salt was the reactive compound. That platinum, a supposedly chemically inert material, might actually be reacting to form the causative agent in inhibiting bacterial cell division was an unexpected result indeed. To test the notion that a soluble platinum salt might be responsible for halting mitosis in E. coli, an inorganic chemist in Rosenberg's group made up a solution of the ammonium salt of platinum hexachloride ($(NH_4)_2PtCl_6$), in which platinum existed in its +4 oxidation state. The positively charged ammonium ions acted as counterions to the negatively charged platinum hexachloride ion.



platinum hexachloride, ammonium salt

When (NH4)2PtCl6 was subjected to the potassium iodide-starch test, the results were identical to those obtained when the nutrient medium was electrolyzed, as long as there was a sufficient concentration of platinum present (>100 p.p.m.)—meaning that $(NH_4)_2PtCl_6$ could be an oxidizing agent. This new result suggested that a soluble platinum salt, generated from the platinum electrodes during electrolysis, in combination with the ions present in the nutrient medium, might be the active agent in inhibiting cell division and leading to filamentous growth. Indeed, when this soluble platinum salt ($(NH_4)_2PtCl_6$) was used to inoculate the culture chamber used in the original experiments (see the electric fields module), the E. coli bacterial cells formed filaments![1]

[Note: A later account suggests that $(NH_4)_2PtCl_6$ at first caused cell death—then later, after standing on a laboratory shelf for a few weeks, produced a small number of filaments. This will be discussed more in the discovery of cisplatin module.]

The researchers did not stop there: they wanted to know whether other transition metals in group VIIIB, meaning those in groups 8, 9, and 10 (see the transition metal chemistry module), would have a similar effect on E. coli bacterial cells. For this reason, they made and tested many more compounds containing various transition metals, including cobalt (Co), iridium (Ir), nickel (Ni), osmium (Os), palladium (Pd), rhodium (Rh), and ruthenium (Ru), as well as several other platinum-containing compounds. As it turned out, several of the transition metal compounds tested were toxic to bacterial cells; these are listed in column A of Table 1. Another group of compounds caused no change to the bacterial cells; these are listed in column B. Finally, several transition metal compounds caused elongation of the bacterial cells, just as (NH4)2PtCl6 did. Many of these compounds contained platinum, but others contained rhodium or ruthenium.

Table 1. *Effects of group VIIIB transition metal compounds on bacterial growth. (Concentrations of metal ions maintained for 2 h at 8 p.p.m. in the continuous culture chamber.)*[1]

A. Caused bacterial death	B. Caused no change	C. Caused elongation
$CoCl_2$	$[Co(NH_3)_6]Cl_2$	K^+,NH_4^+,H^+—$[PtCl_6]^{2-}$
$(NH4)_2IrCl_6$	$K_2Ir(NO_2)_6$	$(NH_4)_2PtBr_6$
$NiCl_2$	$[Ni(NH3)6]Cl_2$	$(NH4)_2PtI_6$
$(NH4)_2OsCl_6$		$[Pt(en)_3]Cl_4$
$(NH4)_2PdCl_4$	cis $[Rh(en)_2Cl_2]NO_3$	$RhCl_3$
$[Rh(NH_3)5Cl]Cl_2$	trans$[Rh(en)_2Cl_2]NO_3$	$(NH_4)_3RhCl_6$
$PdCl_2$		$[Ru(NH_3)_4ClOH]Cl$

Although the researchers found several compounds that inhibited cell division of E. coli without interfering with cell growth, they were not yet able to define the roles played by either the metal oxidation states or the ligands. Having found the answers to many of the questions that came up during their study of the effect of electromagnetic fields on cell division in E. coli, Rosenberg and his coworkers found that many new questions arose. Indeed, a well-designed experiment often leads to answers as well as new questions. They posed some of these questions at the end of their first publication on this topic:

- "What is the mechanism of action of these metal ions?
- Where is the locus of action in the bacterial cell?
- How does the effect of these metal ions relate to the actions of the other causative agents of filamentous growth—is there a weak link that all operate on?
- Can these metal ions inhibit cell division in other bacteria, or cells?"[1]

We will see that subsequent studies, conducted by both Rosenberg's group and by other research groups, provided answers to these new questions.

References

1. Rosenberg, B., Van Camp, L., Krigas, T. Nature , 1965, 205, pp. 698-699.

This page titled 11.3.5: Cisplatin 5. The Role of Platinum Electrodes is shared under a CC BY-NC-SA 4.0 license and was authored, remixed, and/or curated by ChemCases.

- **Cisplatin 5. The Role of Platinum Electrodes** by ChemCases is licensed CC BY-NC-SA 4.0.

11.3.6: Cisplatin 6. Transition Metal Chemistry

The transition metals, also called the d-block elements, are found in groups 3-12 of the periodic table. These elements make the transition between the representative metals in groups 1 and 2 and the metalloids, representative metals, and nonmetals in groups 13-18. Moreover, it is in this block of elements in the periodic table that the d-orbitals are being filled with electrons. For example, elements in the first group of the d-block (group 3 of the periodic table: scandium, yttrium, lanthanum, and actinium) each have one d-electron. Likewise, elements in the eighth group of the d-block (group 10 of the periodic table: nickel, palladium, and platinum) each have eight d-electrons when in the +2 oxidation state

The transition metals have several features in common: unlike representative metals, most transition metals have variable valence, meaning that they have more than one possible oxidation—or valence—state. For example, platinum exists most commonly in the +2 and +4 oxidation states, but it can also be found in the +5 and +6 oxidation states.

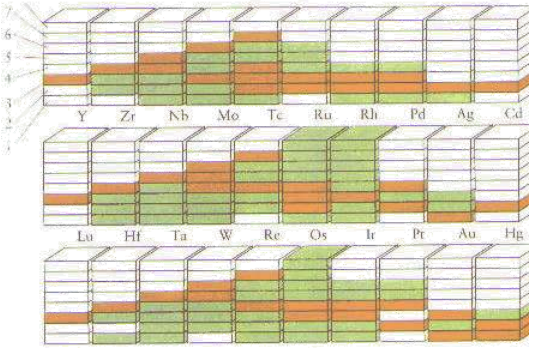


Figure 1. The oxidation (valence) states of the d-block elements. The orange blocks mark the common oxidation numbers for each element; the green blocks mark the other known states. Reprinted with permission.1

Another common feature of the transition metals is their size. To understand why the d-metals are roughly the same size, we need to examine two competing effects: nuclear charge and electron-electron repulsions. As one moves across the periodic table, the size (that is, the atomic radius) of elements generally decreases due to increasing nuclear charge. The increasing nuclear charge is usually more significant than the electron-electron repulsions resulting from the addition of electrons as one moves across a period. In keeping with this trend, transition metals also generally decrease in size as one moves from left to right across the d-block. Here, the exceptionally weak shielding offered by the d-electrons causes these electrons to experience a greater nuclear charge and be pulled more strongly toward the nucleus. The last few elements in each row of the d-block are slightly larger than those preceding them; here, electron-electron repulsions outweigh increasing nuclear charge as the d-orbitals are filled. The trend of decreasing size is most pronounced in row 6 of the periodic table (the third row of the d-block, in which the 5d-orbitals are being filled). The third row of the d-block is interrupted by the lanthanide elements, in which the 4f-orbital is being filled. Like d-electrons, electrons in f-orbitals are also ineffective at shielding nuclear charge; the increased nuclear charge in the third row transition metals causes them to be smaller than expected and virtually identical in size to the second row transition metals.

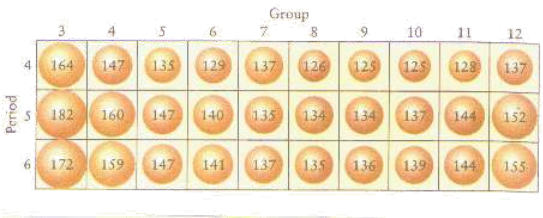


Figure 2. The atomic radii of the d-block elements (in picometers). Notice the similarity of all the values, and in particular the close similarity between the second and third rows as a result of the lanthanide contraction. Reprinted with permission.1

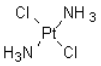
In addition to making the third row transition metals smaller, the lanthanide contraction also makes them less reactive because the valence electrons are relatively close to the nucleus and not available for chemical reactions. In short, several generalizations may be made about the transition metals, or d-metals: most transition metals have a number of possible oxidation states. Also, the d-

metals are all roughly the same size. This is particularly noticeable when comparing the second and third row d-metals. Due to the lanthanide contraction, the third row d-metals are approximately the same size as the second row d-metals; the lanthanide contraction also causes the third row d-metals to be relatively inert. The inertness of the third row transition metals has many benefits. For example, these metals—particularly gold and platinum—are often used in jewelry. Furthermore, these metals—specifically, platinum—should be able to conduct an electric current but not react with their surroundings. For this reason, Barnett Rosenberg and his coworkers chose platinum as an electrode material in their original experiments to study the effect of electric fields on E. coli. However, as we have seen in the module on the role of platinum electrodes, even though their choice was based on sound chemical principles, they obtained unexpected results, which led to the serendipitous discovery of cisplatin.

Transition Metal Complexes[1] Transition metals are excellent Lewis acids and accept electron density from many molecules or ions that act as Lewis bases; when a Lewis base donates its electron pair to a Lewis acid, it is said to coordinate to the Lewis acid and form a coordinate covalent bond. When Lewis bases coordinate to metals acting as Lewis acids and form an integral structural unit, a coordination compound is formed. In this type of compound, or complex, the Lewis bases are called ligands. One of the first known coordination compounds was Peyrone's Chloride (also known as cis-diamminedichloroplatinum(II), or cis-DDP), first reported in 1845. This compound was not fully understood until 1893, when Alfred Werner deduced its structure and described cis-DDP and its trans isomer in a landmark paper.



Peyrone's Chloride
cis-diamminedichloroplatinum(II)
cis-DDP



trans-diamminedichloroplatinum(II)
trans-DDP

The two isomers of diamminedichloroplatinum(II) have the same connectivity of atoms, meaning that platinum is the central atom and is bonded to four ligands—two chlorine atoms and two amino groups—in a square planar arrangement. However, the ligands are arranged differently in the *cis* and *trans* isomers: In *cis*-DDP, the ammonia molecules are on the same side of the DDP molecule, but in *trans*-DDP, the ammonia molecules are on opposite sides of the DDP molecule. These types of isomers are called geometrical isomers. Crystal Field Theory[1-3] It is possible to imagine several ways that four ligands can be arranged around a central metal atom. Werner deduced that the ligands in *cis*- and *trans*-DDP were placed at the corners of a square, with the platinum atom at the center of the square; this is called square planar geometry. Another way that four ligands could have been arranged around the central platinum atom would have been at the corners of a tetrahedron; this is referred to as tetrahedral geometry (and is the geometry adopted by carbon atoms having four substituents in organic compounds). In tetrahedral geometry, however, no isomers are possible, whereas with square planar geometry, two isomers are possible and can be identified, as shown above. To understand why different four-coordinate complexes (that is, those having four ligands around a central metal atom) adopt different geometries, we use the concepts described by crystal field theory (CFT), first proposed in 1929 by Hans Bethe. CFT uses an electrostatic model to explain all metal ion-ligand interactions. (A subsequent theory—called ligand field theory—builds on the principles of CFT and allows for some covalency, as well. CFT, however, will suffice to explain the geometries of various four-coordinate complexes.) Because CFT bases all interactions on electrostatics, each ligand is represented by a negative point charge. The way these point charges interact with the *d*-orbitals of a metal atom explains the geometries adopted by various transition metal complexes. In the absence of ligands (meaning in the absence of a crystal field), all *d*-orbitals in a particular metal have the same energy and are said to be degenerate. When ligands coordinate to the metal, however, the ligands (treated as point charges) cause the *d*-orbitals to be either stabilized or destabilized. A stabilizing effect from a ligand lowers the energy of the interacting *d*-orbital, whereas a destabilizing effect raises the energy of the *d*-orbital. Before we address the question of different four-coordinate geometries, it is useful to examine a very common geometry in transition metal complexes: the six-coordinate, octahedral geometry. In an octahedral complex, six ligands are placed symmetrically along the axes of a Cartesian coordinate system (the *x*-, *y*-, and *z*-axes in three-dimensional space), with the metal at the origin. Knowing the shapes of the five *d*-orbitals is essential in understanding octahedral geometry. As shown in Figure 3(a), there are two *d*-orbitals that point directly along Cartesian axes: the dz^2 orbital, which points along the *z*-axis, and the dx^2-y^2 orbital, which has lobes on both the *x*- and *y*-axes. The interaction of six ligands with the dz^2 and the dx^2-y^2 orbitals

raises the energy of these two *d*-orbitals through repulsive interactions. Moreover, the energy of these two orbitals is increased by the same amount, so the dz^2 and the dx^2-y^2 orbitals are degenerate. In the nomenclature of crystal field theory, these orbitals are called the *e* orbitals. The other three *d*-orbitals, the *dxy*, *dzx*, and *dyz* orbitals, which all have lobes in between the Cartesian axes, are repelled less by the ligands and are in effect stabilized to a lower energy. The *dxy*, *dzx*, and *dyz* orbitals are also degenerate; collectively, they are called the *t* orbitals. (See Figure 3(b).)

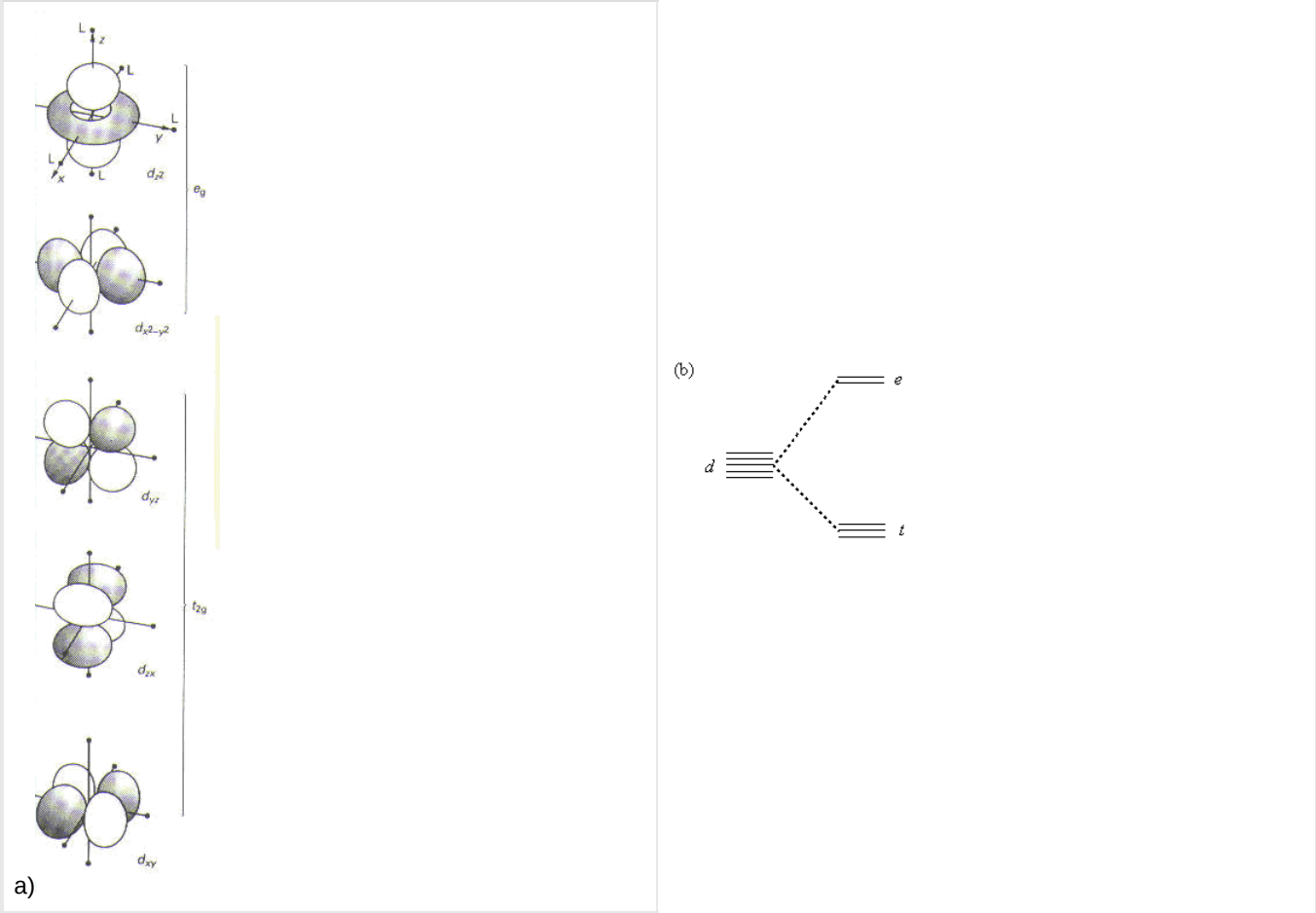


Figure 3. (a) The orientation of the five d-orbitals with respect to the ligands of an octahedral complex: the degenerate e pair, and the degenerate t triplet. Reprinted with permission.[3] (b) Splitting of the five d-orbitals by an octahedral field.

We use similar logic to explain the crystal field splitting of the *d*-orbitals in a four-coordinate, tetrahedral complex. One way to represent a tetrahedral species is to show four ligands (treated as point charges in crystal field theory) on alternating corners of a cube. In a tetrahedral complex, the ligands do not point directly at any of the five *d*-orbitals, but they come close to the *dxy*, *dzx*, and *dyz* orbitals, which are directed toward the edges of the cube, as shown in Figure 4(a); these orbitals are raised in energy and are degenerate. The dz^2 and the dx^2-y^2 orbitals point toward the sides of the cube and are therefore directed away from the attached ligands; these two orbitals are lowered in energy and are

degenerate. The relative energies (and crystal field splitting) of the five *d*-orbitals in a tetrahedral complex are shown in Figure 4(b).

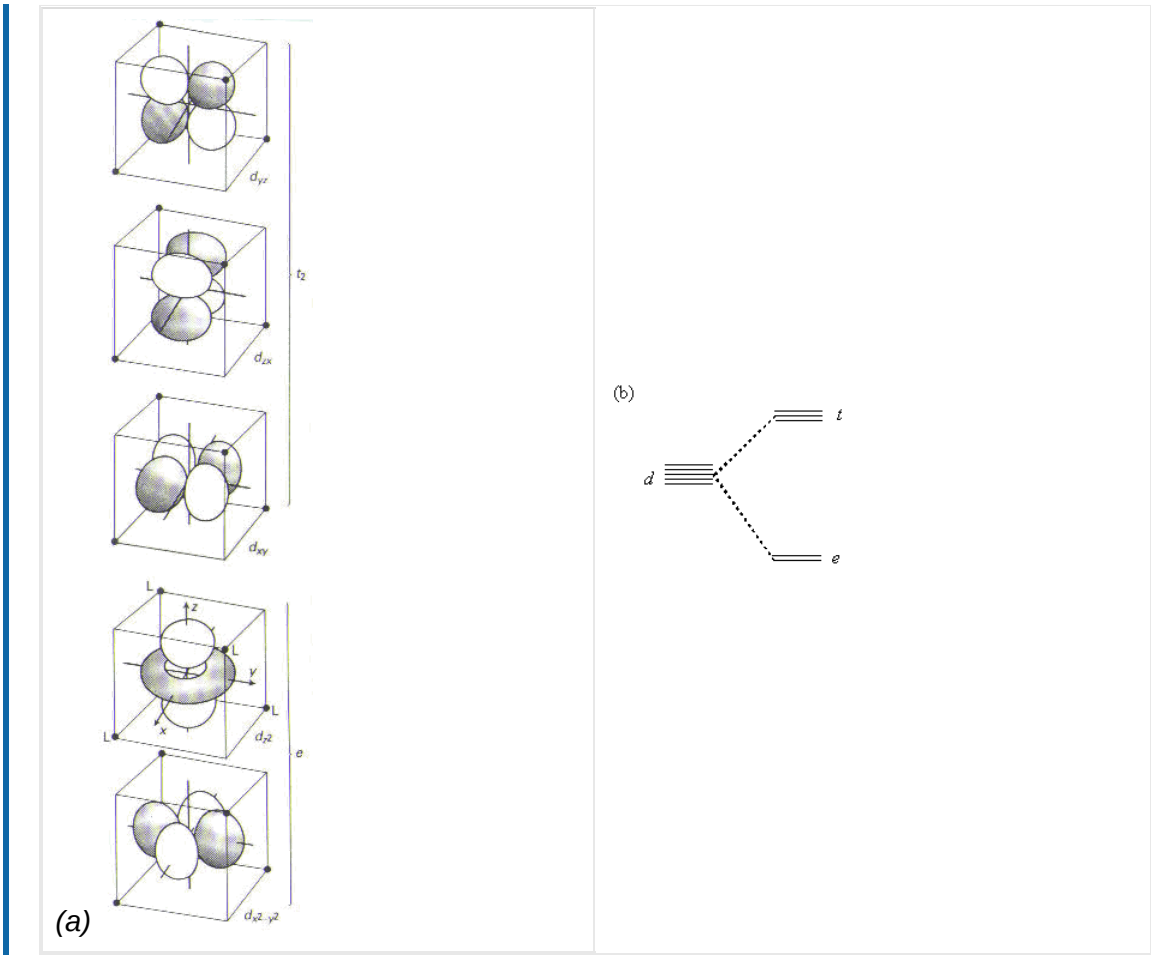


Figure 4. *(a) The effect of a tetrahedral crystal field on a set of d-orbitals is to split them into two sets; the e pair (which point less directly at the ligands) lie lower in energy than the t triplet. Reprinted with permission.*[3] *(b) Splitting of the five d-orbitals by a tetrahedral field.*

Crystal field theory also explains the four-coordinate, square planar geometry. In this case, we imagine an octahedral complex in which the ligands on the *z*-axis (that is, those interacting most directly with the dz^2 orbital) are removed. The dz^2 orbital is therefore lowered in energy. Furthermore, the other *d*-orbitals having *z*-character—specifically, the *dzx* and *dyz* orbitals—also decrease in energy. However, since the ligands are all now in the *xy* plane, both *d*-orbitals having *x*- and *y*-character—namely, the dx^2-y^2 and the *dxy* orbitals—are raised in energy. The crystal field splitting pattern of a square planar complex is shown in Figure 5.

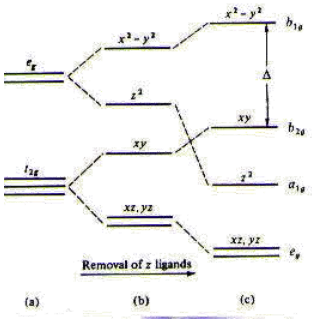
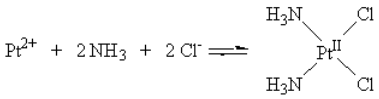


Figure 5. (a) An octahedral complex that (b) undergoes z-axis elongation such that it becomes distorted and (c) finally reaches the square planar limit. Reprinted with permission.2

What determines whether a four-coordinate transition metal complex is tetrahedral or square planar? The answer lies in the number of *d*-electrons in the central transition metal. If the metal has eight *d*-electrons, as is the case for Pt^{2+}, it is energetically advantageous for the complex to adopt a square planar geometry. In this case, the eight *d*-electrons will achieve some stabilization in energy by occupying the *dzx*, *dyz*, *dz²*, and *dxy* orbitals. < **face="Arial">Formation of Cisplatin under the Experimental Conditions** Now that we have some background in transition metal chemistry, particularly transition metal complexes, we can understand how cisplatin, or *cis*-diamminedichloroplatinum(II), was generated under the original reaction conditions in which elongation of *E. coli* bacterial cells was observed. As we saw in the electrochemistry module, a divalent platinum ion (Pt^{2+}) could be generated when an electric current was supplied to the supposedly inert platinum electrodes in the continuous culture chamber. Moreover, as we saw in the control experiments module, solutions containing either ammonium ion or chloride ion or both tested positive for the presence of an oxidizing agent using the potassium iodide–starch test. One of the oxidizing agents present—namely, *cis*-diamminedichloroplatinum(II)—was responsible for bacterial elongation. How does *cis*-PtII(NH3)2Cl2 form from Pt^{2+}, NH^{4+}, and Cl- ions? Remember that in an aqueous solution, ammonium ion (NH^{4+}) is in equilibrium with its conjugate base, ammonia (NH3):

Missing superscript or subscript argument

Assuming that sufficient concentrations of Pt^{2+}, NH3, and Cl- ions exist in solution, the square planar cisplatin molecule will be formed:



< face="Arial">Speaking the Language of Transition Metal Chemistry—Vocabulary

- **Coordinate:** Use of a lone pair to form a coordinate covalent bond **Coordinate covalent bond:** A bond formed between a Lewis base and a Lewis acid by sharing an electron pair originally belonging to the Lewis base
- **Coordination compound:** A compound in which a metal ion or atom is bonded to one or more molecules or anions so as to define an integral structural unit
- **Ligand:** A group attached to a central metal ion in a complex
- **Isomer:** One of two or more compounds that contain the same number of the same atoms in different arrangements **Stereoisomers:** Isomers that have the same connectivity of atoms but differ in the arrangement of their parts in space (identical atom-to-atom bonding but different arrangements of the atoms in space)
- **Geometrical isomers**: Stereoisomers that differ in the spatial arrangement of the atoms
- **Crystal field:** The electrostatic influence of the ligands (modeled as negative point charges) on the central ion of a complex
- **Degenerate:** Having the same energy, as in orbitals
- **Octahedral complex:** A complex in which six ligands are arranged at the corners of a regular octahedron with the metal atom at the center

- **Tetrahedral complex:** A complex in which four ligands lie at the corners of a regular tetrahedron with the metal atom at the center
- **Square planar complex:** A complex in which four ligands lie at the corners of a square with the metal atom at the center.

References

1. Atkins, P. W., Jones, L. L. Chemistry: Molecules, Matter, and Change, 3rd ed. W. H. Freeman and Company: New York, 1997, Chapter 21.
2. Huheey, J. E., Keiter, E. A., Keiter, R. L. Inorganic Chemistry: Principles of Structure and Reactivity, 4th ed. HarperCollins College Publishers: New York, 1993, Chapter 11.
3. Shriver, D. F., Atkins, P., Langford, C. H. Inorganic Chemistry, 2nd ed. W. H. Freeman and Company: New York, 1994, Chapter 6.

This page titled 11.3.6: Cisplatin 6. Transition Metal Chemistry is shared under a CC BY-NC-SA 4.0 license and was authored, remixed, and/or curated by ChemCases.

- **Cisplatin 6. Transition Metal Chemistry** by ChemCases is licensed CC BY-NC-SA 4.0.

11.3.7: Cisplatin 7. Bioinorganic Chemistry

Heavy metals, such as platinum, have long been considered toxic to the human body. The discovery of cisplatin (in which the central atom is platinum) as an effective antitumor agent therefore came as a surprise to the medical community. As it turns out, a great many metals are vitally important in biology. The study of metals in biological systems is called bioinorganic chemistry. Biologically significant metals can be split into two classes: naturally occurring metals in biological systems and metals that are used for probes or drugs in biological systems.[1] (See Figure 1.)

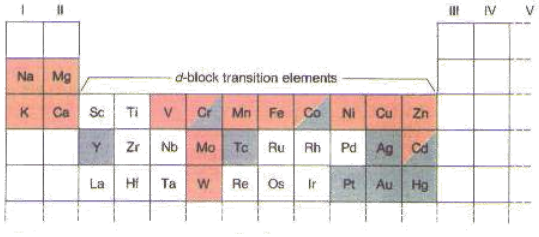


Figure 1. Selected elements important in bioinorganic chemistry. Naturally occurring elements are show in color; those used as probes or drugs are depicted in gray. Reprinted with permission.1

An astounding number of metals occur naturally in biological systems and are, in fact, required for biological function. For example, magnesium is found in chlorophyll, which is necessary for photosynthesis; both chlorophyll and iron-containing heme groups are found in the photosynthetic reaction center. Cobalt is found in coenzyme B12, which is essential for the transfer of alkyl groups from one molecule to another in biological systems, as well as the reduction of the ribose ring in ribonucleotides that make up RNA to the deoxyribose ring in deoxyribonucleotides that make up DNA. Nickel is found in factor F430, which is required for methanogenesis, a process used by the archaeobacteria in which the simple gases, such as H2, CO, and CO_2, are used to provide both energy and a carbon source. Iron is found in a variety of iron-sulfur clusters, which are necessary for nitrogen fixation, as well as in heme groups, found in hemoglobin, which is used for dioxygen transport and storage in the body.[1,2] (See Figure 2.)

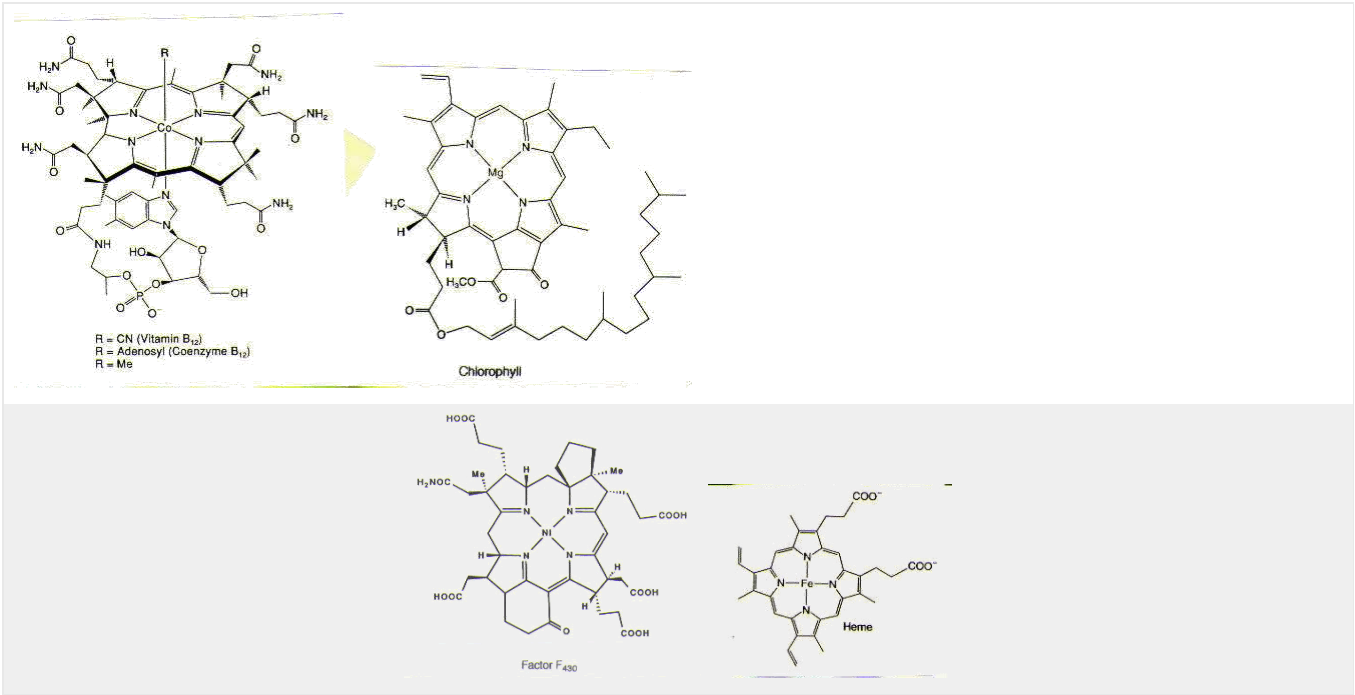


Figure 2. Metals in biological systems: magnesium in chlorophyll, which is found in the photosynthetic reaction center; cobalt in coenzyme B12; nickel in factor F430; and iron in heme, which is found in hemoglobin. Reprinted with permission.1,2

Metals have also been introduced into biological systems to probe structure and function of those systems. For example, heavy metals such as mercury and platinum are employed to help determine the structure of macromolecules by x-ray crystallography and electron microscopy. Furthermore, metal-containing compounds are used to diagnose a variety of conditions. For example, a technetium radiopharmaceutical, called cardiolyte, supplies 99mTc, which is selectively taken up by myocardial tissue (the muscle tissue found in the heart) and used to image the heart. Finally, metals are found in drugs used to treat a variety of diseases and ailments. Among them is a gold-containing agent called Auranofin used to treat rheumatoid arthritis; unlike other antiarthritic gold agents, this one can be taken orally. Also, as we have seen, a platinum-containing compound called cisplatin is used as a chemotherapeutic agent in the treatment of testicular, ovarian, and head and neck tumors.1(See Figure 3.)

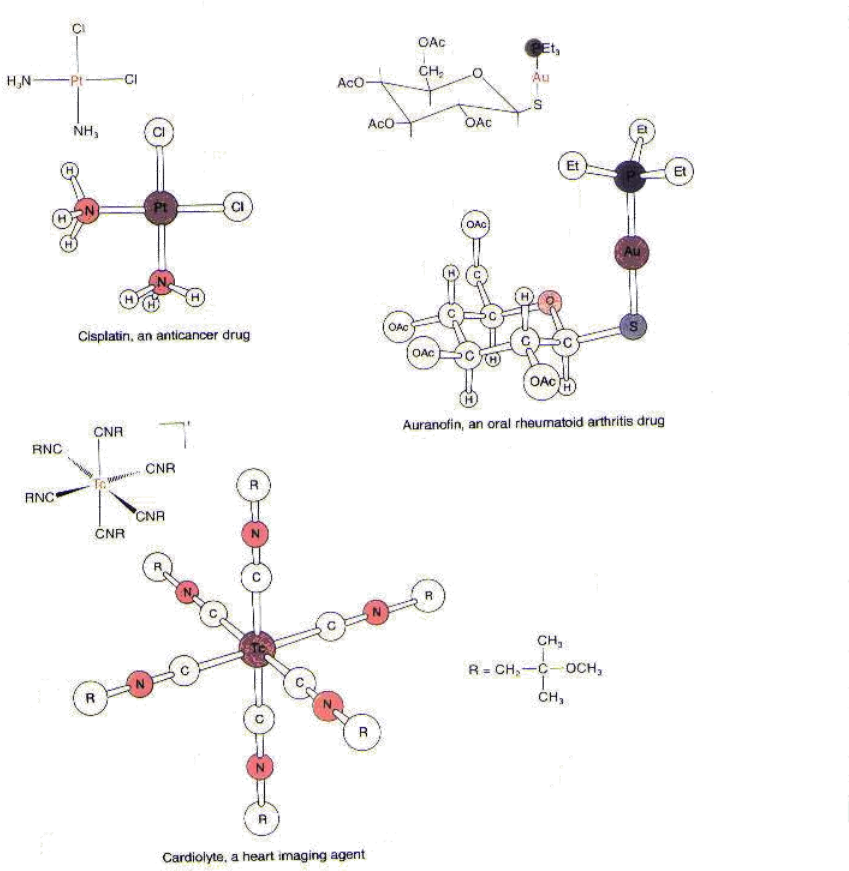


Figure 3. Structures of three inorganic compounds used in modern medicine. Reprinted with permission.1

In short, many metals play an extremely important role in biology. Some metals are essential for biological function and are found in enzymes and cofactors required for various processes. In addition, some metals have been used to explore biological systems; still others have been used to treat a variety of diseases and conditions.

References

1. Lippard, S. J., Berg, J. M. Principles of Bioinorganic Chemistry. University Science Books: Mill Valley, CA, 1994.
2. Crabtree, R. H. The Organometallic Chemistry of the Transition Metals. John Wiley & Sons, Inc.: New York, 1988.

This page titled 11.3.7: Cisplatin 7. Bioinorganic Chemistry is shared under a CC BY-NC-SA 4.0 license and was authored, remixed, and/or curated by ChemCases.

- **Cisplatin 7. Bioinorganic Chemistry** by ChemCases is licensed CC BY-NC-SA 4.0.

11.3.8: Cisplatin 8. Discovery of Cisplatin

As we saw in the role of platinum electrodes module, the researchers found that certain transition metal complexes—specifically, soluble metal salts—caused elongation of E. coli bacterial cells. Among them was the ammonium salt of platinum hexachloride ($(NH_4)_2PtCl_6$), in which platinum existed in its +4 oxidation state. Upon closer examination, however, the researchers realized that light was necessary for the filamentous growth of the bacteria to occur. In fact, exposure of this soluble platinum salt to ultraviolet light produced a new, neutral species:

$$(NH_4)_2Pt(IV)Cl_6 + \text{uv light} \rightarrow Pt(IV)(NH_3)_2Cl_4$$

This neutral product was chemically identical to the electrolytically formed agent and was shown to cause bacterial elongation. However, when one of the chemists in the group did a control experiment in which he synthesized this new, neutral species, diamminetetrachloroplatinum(IV) ($PtIV(NH_3)_2Cl_4$), by known chemical techniques, he found that no bacterial elongation occurred!1 In order to explain this surprising result, the researchers thought more carefully about the compounds and realized that there were, in fact, two possible structures with the molecular formula $PtIV(NH_3)_2Cl_4$, as shown in Figure 1.

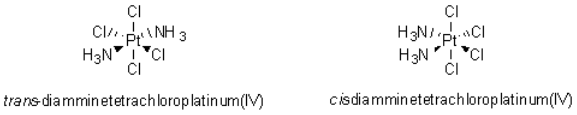


Figure 1. Two possible structures for $PtIV(NH_3)_2Cl_4$.

In the structure on the left, the two amino (NH3) groups are on opposite sides of the central platinum(IV) atom; we say that the amino groups are trans to each other. In the structure on the right, the two amino groups are on the same side of the molecule, or cis to each other. (see the transition metal chemistry module) The trans configuration is more thermodynamically stable than the cis conformation, and the trans molecule was the one that the researchers first synthesized and studied. When they made the compound on the right, with the cis configuration, they achieved complete success.1 Along with different possible geometries of transition metal complexes, the central transition metals can have different possible oxidation states. (See the redox chemistry module.) For example, platinum has two dominant oxidation states, +2 and +4. The studies described above were done with platinum complexes in which platinum was in the +4 oxidation state; such complexes are octahedral, as can be seen above with the trans- and cis-diamminetetrachloroplatinum(IV) complexes. On the other hand, when platinum is in the +2 oxidation state, it forms square planar complexes. The researchers decided to synthesize and test a variety of neutral platinum complexes, having platinum with either the +2 or +4 oxidation state. Among others, they made the following four compounds: (1) cis-$PtIV(NH_3)_2Cl_4$; (2) cis-$PtII(NH_3)_2Cl_2$; (3) $PtII(NH_2CH_2CH_2NH_2)Cl_2$; and (4) $PtIV(NH_2CH_2CH_2NH_2)Cl_4$, as shown in Figure 2.

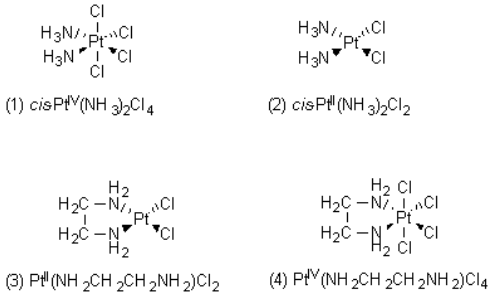


Figure 2. Platinum-containing complexes that were tested for antitumor activity in mice.

Having shown that these four compounds inhibited bacterial cell division without being toxic to these cells, the researchers also wanted to see how these compounds would affect cell division in mammalian cells. They thought that perhaps the platinum-containing compounds would stop cell division in tumor cells without being extremely toxic to the host animal. For this reason they turned their attention to two murine (mouse) cancer cell lines, Sarcoma 180 and Leukemia L1210.1,2 First, the researchers had to determine safe dose levels for mice. One of the biologists found that the dose that killed half of the animals (LD50, meaning "lethal dose, 50%") was about 13 mg of the drug per kilogram of animal body weight (in other words, LD50 = 13 mg/kg). A nonlethal dose for mice was 8 mg/kg.1 The next step was to see whether these compounds could be used to treat murine tumors without killing the mouse. At this point, another biologist implanted a standard transplantable animal tumor (solid Sarcoma 180) beneath the skin under one armpit of each mouse. Tumor growth was determined by cutting out the tumor and weighing it; this could be

done because the tumor was nonmetastatic, meaning that it remained localized under the armpit of the mouse. After 10 days, the tumor had increased to 100 times its original mass.1 Different conditions were used for the experiments that followed. The first set of experiments followed the standard protocol of the National Cancer Institute. After implantation of the tumor on day 0, the drug was injected on day 1, and the animals were sacrificed on day 8. The efficacy of the drug was determined by finding the ratio of the tumor size in the treated group to that in the control group (T/C). When this ratio was less than 0.5, the drug was considered to be effective in treating the tumor. The biologist conducted many experiments on the mice, dosing them with different nonlethal amounts of the platinum-containing compounds shown above. The results showed that all of these drugs reduced the size of the tumors and that their T/C ratios were all well below 0.5. Compound 2 (cis-PtII(NH_3)$_2$$Cl_2$, or cis-diamminedichloroplatinum(II)) was the most effective of all the compounds in reducing the size of the tumors, as it had the lowest T/C ratios.1,2 In another set of experiments, the tumors were implanted into the mice on day 0, and instead of injecting the drugs on day 1, the tumors were allowed to grow for 8 days until they reached the mass of a gram; this was a fairly sizable tumor, considering that the mice only weighed about 20 grams each (see photo, Figure 3). On day 8 the test group of mice was injected with one of the platinum-containing compounds. Again, compound 2 (cis-PtII(NH_3)$_2$$Cl_2$, or cis-diamminedichloroplatinum(II)) gave dramatic results, as shown in Figure 3.

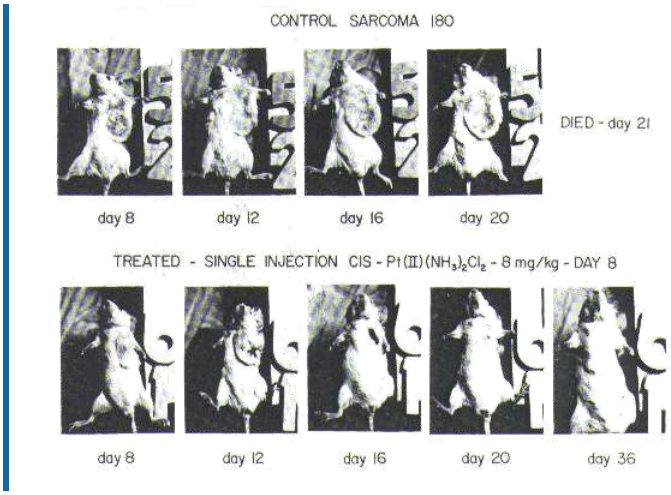


Figure 3. Time sequence photographs of two mice with solid Sarcoma 180 tumors. The mouse at the top was an untreated negative control. She died on day 21 when the tumor weighed about 3 g. The bottom mouse was in the group treated on day 8 with an intraperitoneal injection of cis-diamminedichloroplatinum(II). Her tumor was completely regressed six days after treatment, and she died of age-related causes almost 3 years later. Reprinted with permission.[1]

References

1. Rosenberg, B. In Nucleic Acid-Metal Ion Interactions. T. G. Spiro, Ed. John Wiley & Sons, Inc.: New York, 1980, Vol. 1, pp. 1-29.
2. Rosenberg, B., VanCamp, L., Trosko, J. E., Mansour, V. H. Nature,1969, 222, pp. 385-386.

This page titled 11.3.8: Cisplatin 8. Discovery of Cisplatin is shared under a CC BY-NC-SA 4.0 license and was authored, remixed, and/or curated by ChemCases.

- **Cisplatin 8. Discovery of Cisplatin** by ChemCases is licensed CC BY-NC-SA 4.0.

11.3.9: Cisplatin 9. The Discovery - One Scientist's Story

"God didn’t make anything so complicated that it can’t be worked out." These are the words of one of the key scientists involved in the discovery of cisplatin.

When the research on the effect of electric fields on E. coli was begun in 1962, it was essential that a biologist -- specifically, a microbiologist -- contribute to the project. She does not want her name used because she did not become a scientific researcher for fame, but rather for the challenge of putting pieces of a scientific puzzle together.



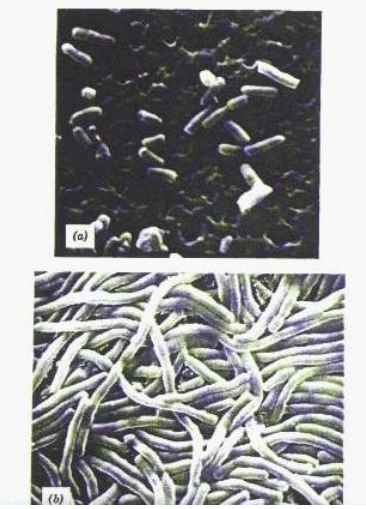
Marie Curie, who won two Nobel prizes: physics in 1903, chemistry in 1911.

As a girl, she was inspired by the work of great scientists: she read the story of the cure of malaria in the Panama Canal; she also read a biography of Madame Curie. These accounts inspired her to pursue a career in scientific research. After high school, she worked for the Michigan Department of Health, where she did research in biology and microbiology. There, her colleagues saw her talent and encouraged her to pursue science as a career. She went on to earn a bachelor’s degree from Michigan State University in 1948 in medical technology, a field encompassing microbiology, pathology, and chemistry.

When she began working at Michigan State in the early 1960s, she was balancing the demands of scientific research with the needs of her family. At that time both of her children were in school. She would work in the lab in the morning while they were at school, go home to see them at lunch, return to the lab for the afternoon, go home for dinner, and return to the lab in the evening, if necessary.

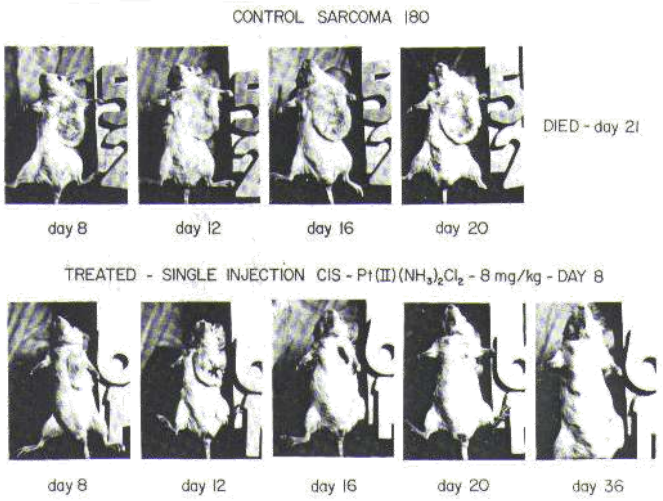
At that time, there were fewer women scientists working than there are today, but she encountered several in her career. At the Michigan Department of Health, many of her colleagues were women and, consequently, she did not feel isolated because of her gender—nor did she feel that she was treated differently because she was a woman.

While working at Michigan State, she also felt that she was treated with respect by her peers. Her colleagues, among them veterinarians and Ph.D. chemists, all treated her as an equal. On the whole, she believes that there is not a great deal of difference between men and women in science.



The enthusiasm is still present in her voice when she describes the work she did more than 30 years ago leading to the discovery of cisplatin. After the initial experiment, which showed that the E. coli bacterial cells elongated when an electric current was applied to the continuous culture chamber, it took some time to establish that electrolysis products from the platinum electrodes were responsible because many control experiments had to be run (see modules on electric fields and control experiments). However, when she saw that the cells elongated to 50 to 60 times their normal length and then returned to normal after the electric current was removed, she realized that the experimental conditions weren't doing any permanent damage to the bacterial cells.

Later, when the focus of the project shifted from studying bacterial cells to studying mammalian cells, she conducted a critical experiment in which she implanted tumors into mice and then treated one group of the mice with cisplatin. (A second group of mice was not treated; this was the control group.) When she administered cisplatin to the mice, she did not know what to expect. She knew that cisplatin caused bacterial elongation and wondered whether the mice might also elongate!



However, cisplatin caused the tumors in the test group of mice to vanish entirely, and the mice were completely cured (see the module on the discovery of cisplatin). At this point, she knew that she and her colleagues were onto something.



She describes a typical day in the lab as one in which she worked long hours. When setting up experiments, many adjustments had to be made; also, many control experiments had to be run to verify the results of their tests. For example, she and her colleagues had to check the line voltage when they were applying electric currents. Also, when they were trying to determine the most effective dose schedules for curing mouse tumors, they had to divide the injections they gave to the mice. If they wanted to dose the mice with 8 mg total of cisplatin, they might administer 1 mg per hour over an 8-hour period. Alternatively, they might give the mice 4 mg per hour over 2 hours

Finally, in order to monitor the fate of cisplatin in the mice, they ran several radioactive experiments, in which they used one of two radioactive isotopes of platinum (either 191Pt or 195Pt). They had to make sure that the injections were timed appropriately to take advantage of the short (4-day) half-life of the radioactive isotopes. In other words, there was a lot of "programming" to be done—so that the results from the experiments would be credible.

New Drug Testing on Animals

Animal rights activists question the necessity of testing drugs on animals before they are tested on humans. When asked whether she thought there was any way that the initial tests on cisplatin and related drugs could have been done without using animals (mice, dogs, monkeys), she responded in the negative. She said that without animal studies, the only other option would be to test the drug on people. Animal studies allow the researcher to figure out the limitations and the side effects of drugs before they are tested on people.Scientists are careful to include animal testing only as necessary as a part of drug development.

Good scientists look for clues to potential medical uses by combining their basic knowledge and keen observation of laboratory phenomena. The discoverers of cisplatin observed an unexpected cell phenomenon, then they evaluated what they saw and came to an exciting hypothesis that something was changing cell behavior in a way that might be useful medically. But the first proofs must often come through prudent tests on animals as a necessary step on the way to use in humans

Following the initial discovery, she continued to study cisplatin in an effort to understand its mechanism of action in the body. She was still doing research on cisplatin when it was approved as an anticancer drug in 1978 by the Food and Drug Administration. She has two friends whose mothers were successfully treated with cisplatin (probably in combination with other drugs); these women are now in remission. She is proud to have been a part of their cure. She realizes, however, that more work needs to be done to find a cure for all types of cancer: her mother had breast cancer, and her husband had leukemia. Neither was treated with cisplatin. Even though cisplatin is used successfully to treat ovarian, bladder and testicular cancers, it is not a panacea.

She has continued to do research on cisplatin. Today, at age 73, she is supporting research on finding cisplatin’s cellular target, which is currently believed to be DNA. However, this is the subject of some controversy, and the cellular target may in fact be something else. This work is being conducted by another research group at Michigan State. With her vast research experience on cisplatin, she serves an invaluable role as a consultant to that group.

An unanticipated bonus for all her hard work has been that she has received royalties from the sale of cisplatin and related drugs (see module on profits). She views this as a mixed blessing. While she is glad to have the freedom to do what she wants, she finds that she also receives unwanted attention from organizations and individuals seeking donations or loans. She has continued to give money to the place where it all started, Michigan State University.

She has thoroughly enjoyed her career in scientific research and would recommend it to anyone. She enjoys reading mystery stories and finds that doing research is like solving a mystery. Her advice for people interested in pursuing a career in research is that they must be honest and that they must be willing to work hard. Often, it is necessary to run five control experiments to verify just one test result. She also stresses that when conducting research, it is important to keep your mind clear. She doesn't have any advanced degrees, and she sees this as an advantage. Because she has an open mind, there is no place [scientifically] that she can't go. When running the initial experiments that led to the discovery of cisplatin, she ran all possible experiments. As Louis Pasteur said, "In the fields of observation, chance favors only the mind that is prepared." By leaving herself open to all possibilities, she was prepared for any result.

Template:HideTOC

This page titled 11.3.9: Cisplatin 9. The Discovery - One Scientist's Story is shared under a CC BY-NC-SA 4.0 license and was authored, remixed, and/or curated by ChemCases.

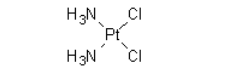
- **Cisplatin 9. The Discovery - One Scientist's Story** by ChemCases is licensed CC BY-NC-SA 4.0.

11.3.10: Cisplatin 10. Research as a Career

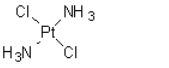
The field of chemistry presents an abundance of career opportunities. Certainly, research propels chemistry (and science in general) forward and gives us a greater understanding of the world around us. The history of cisplatin is an excellent example of the circuitous path scientific research can take in furthering our understanding of the natural world.

American Chemical Society: The society consists of more than 140,000 chemists and other scientists worldwide. It provides meetings, publications and other forums about chemistry by chemists. I made the contacts that led to my preparation of this curriculum unit at a National meeting of the society.

Let's discuss the progress of chemical research that led to the discovery of cisplatin. In a 19th century research laboratory (in 1845, to be exact), Peyrone first synthesized cis-diamminedichloroplatinum(II), also called cis-DDP, and the compound came to be known as Peyrone's Chloride. It took nearly 50 years before its structure was deduced by Alfred Werner. In a paper published in 1893, Werner discussed both the cis and trans isomers of diamminedichloroplatinum(II). This discussion laid the foundation for coordination chemistry (see module on transition metal chemistry).



cis-diamminedichloroplatinum(II)
*cis*DDP



trans-diamminedichloroplatinum(II)
trans-DDP

Moreover, knowledge of these compounds was invaluable 70 years later when scientists working in Barnett Rosenberg's laboratory at Michigan State discovered that the bacterial elongation they were observing was caused by electrolysis products generated from the platinum electrodes they were using—and that the identity of one of these electrolysis products was cis-diamminedichloroplatinum(II). Not only does the discovery of cisplatin show that scientific research can take many unexpected turns, but it also demonstrates that knowledge of many disciplines of science—including chemistry—may be needed to gain a complete understanding of a given problem. Rosenberg, trained as a physicist, needed the expertise of many other scientists to carry out the research program that eventually led to the use of cisplatin as one of the leading chemotherapeutic agents for the treatment of cancer today. When he first wanted to study the effect of electric fields on cell division in E. coli, he hired a microbiologist to work with him. Later, when it became evident that something else was halting bacterial cell division, he added an inorganic chemist who was instrumental in solving the mystery that transition metal complexes were involved. In addition to microbiology and coordination chemistry, the cisplatin project required tapping the expertise of scientists in the fields of molecular biology, biochemistry, biophysics, physiology, pathology, pharmacology, and electron microscopy.1 In fact, Rosenberg commented about his collaborations with medical doctors on this research project in an account he wrote 15 years after the first paper on this topic was published:

> ***I recall two strict admonitions from my major professor when I informed him of my growing interest in biophysics. These were, not to work with medical doctors untrained in research and to avoid cancer research, since many had tarnished their reputations from a malignant neglect of scientific objectivity in their desire to do something useful. I have broken both injunctions, but I cannot say that I am sorry. With a very few exceptions, all connected with the network impressed me as dedicated, selfless, humane scientists. The expected ego clashes and political infighting that characterize so much of science seems to have been muted by the urgency of the problem at hand.1***

Interdisciplinary research occurs in many environments. As we are seeing from the cisplatin example, this type of research occurs in academia—in this case, at Michigan State University. This type of research also occurs at pharmaceutical companies such as Merck, where chemists and biologists work together to discover potential drug candidates. In some cases, a natural product is found to have pharmaceutical applications. Often biologists find these natural products, conduct tests on them to see whether they have any useful properties, such as antibacterial, antifungal, or antitumor activity. If the desired activity is found, an analytical chemist then uses various techniques to determine the structure of the compound. At this point, biologists, biochemists, and pharmacologists conduct further studies on the compound to determine how the compound can best be administered (for example, intravenously or orally), how the compound acts in the body, what the appropriate dose levels are, and what potential side effects

might occur. While these studies are being conducted, a team of medicinal chemists tries to synthesize the compound in the lab; if the compound may be obtained synthetically—rather than from natural sources only—it can be made more widely available, and it can help more people. Another role medicinal chemists play is to try to make analogs of the compound. Analogs, which are structurally related compounds, are synthesized for several reasons. Sometimes a natural product will cause undesirable or even toxic side effects; an analog may be just as efficacious as the original compound—if not more so—and produce few or no side effects. Furthermore, it may only be possible to administer the original natural product intravenously. Because it is usually more convenient if the drug can be taken orally, an analog may make this possible. (go to the case discussion on the need for funding in pharmaceutical research) In short, interdisciplinary research occurs in many places—including both academia and industry. Finally, chemists are employed in many other areas besides research: business, chemical information, computer-related careers, conservation of art and historic works, consulting, education, entrepreneurial ventures, finance, government work, human resources, law (particularly patent law; see the ChemCase on Gatorade), medicine, professional trade associations, quality assurance and control, regulatory work, science writing, technical sales and marketing, technical service, and technology transfer (see module on profits).2

1. Rosenberg, B. In *Nucleic Acid-Metal Ion Interactions*. T. G. Spiro, Ed. John Wiley & Sons, Inc.: New York, 1980, Vol. 1, pp. 1-29.
2. Owens, F. Uhler, R. Marasco, C. *Careers for Chemists: A World Outside the Lab*. American Chemical Society: Washington, DC, 1997.

This page titled 11.3.10: Cisplatin 10. Research as a Career is shared under a CC BY-NC-SA 4.0 license and was authored, remixed, and/or curated by ChemCases.

- **Cisplatin 10. Research as a Career** by ChemCases is licensed CC BY-NC-SA 4.0.

11.3.11: Cisplatin 11. Cisplatin as an Anticancer Drug

NEWS: June 22, 2005 Cisplatin and Lung Cancer: Cisplatin chemotherapy now recognized for dramatic lengthening of survival for some common types of lung cancer. Read through this unit for a description of cisplatin science

"Testicular cancer went from a disease that normally killed about 80% of the patients, to one which is close to 95% curable. This is probably the most exciting development in the treatment of cancers that we have had in the past 20 years. It is now the treatment of first choice in ovarian, bladder, and osteogenic sarcoma [bone] cancers as well."

—Barnett Rosenberg, who led the research group that discovered cisplatin, commenting on the impact of cisplatin in cancer chemotherapy1

The success of cis-diamminedichloroplatinum(II), or cisplatin, in curing tumors in mice, along with the toxicity information gained from studies on dogs and monkeys, suggested that this compound might be effective as an antitumor agent in people with cancer. Before any new drug candidate can be approved for use in the United States, it must undergo extensive testing—in several phases—according to the guidelines set by the Food and Drug Administration (see module on the FDA drug approval process). In the first phase of clinical trials, a new potential anticancer drug is tested on terminally ill patients with cancer who no longer respond to current therapies. After these people have signed an informed consent agreement, they may be treated with new drugs. Unfortunately, the majority of these people are not cured of cancer. At this stage, they are already very ill, and their strength has been sapped by the disease and by other treatments they may have received. However, people who participate in phase I clinical trials serve an invaluable service in that they provide information about side effects and appropriate dosage levels and schedules. For example, it was at this point in cisplatin studies that researchers became aware of the side effect of hearing loss—something that could not have easily been determined from animal studies (see module on toxic side effects).[2]

Despite the poor prognosis for many cancer patients at this stage, some patients did benefit from treatment with cisplatin: roughly 20% of the patients experienced partial or complete remissions. In particular, cisplatin produced responses in approximately 80% of patients with testicular cancers, greater than 90% of patients with ovarian carcinomas, roughly 40% of patients with head and neck cancers, and also around 40% of patients with some lymphomas. Sadly, colon carcinoma, a type of cancer that is very resistant to drugs, did not respond to cisplatin at all. The success of cisplatin in treating a fairly wide variety of cancers, however, showed the promise of this new drug. Later, as one clinician put it, " . . . [cisplatin] appears to be too good a therapeutic agent to abandon, yet too toxic for general use."[2] This clinician was referring to newly discovered kidney toxicity, for which treatments have now been developed, as described in the module on toxic side effects. In the second phase of clinical trials, cisplatin was used in a crossover pattern with other anticancer drugs to treat recently diagnosed cancer patients. A patient was first treated with one drug, and if s/he did not respond to that drug, s/he was treated with a second drug and vice versa. Cisplatin produced higher response rates in phase II clinical trials than it did in phase I, a fairly common result.

> ***In fact, combination therapies to treat cancer are quite common. The hope is that the drugs will work together, producing a synergistic—or at least an additive—effect to cure the cancer, while not producing an additive effect for dose limiting side effects. Cisplatin is often used in combination with one, two, three, or even four other drugs, with good results. One striking example of this is the combination of cisplatin with 5-fluorouracil to treat terminally ill colon carcinoma patients. In a study done at the University of Wisconsin, the tumors in three of nine such patients decreased in size by more than 50% for varying lengths of time. This was an encouraging result, particularly since cisplatin alone showed no effect on colon cancers in phase I clinical trials.[2]***

Following the encouraging results of these studies, cisplatin was approved by the Food and Drug Administration at the end of 1978 for the treatment of genitourinary tumors. Today it is one of the most widely used and successful drugs for the treatment of cancer.[3]

1. Katz, L.G., Paul Treichel, J. Chemistry and Chemical Reactivity, 4th ed. Saunders College Publishing: Philadelphia, 1999.

1. Bolz, J. C., Paul Fletcher, J. Chemistry and Chemical Reactivity, 4th ed. Saunders College Publishing: Philadelphia, 1999.
2. Rosenberg, B. In Nucleic Acid-Metal Ion Interactions, T. G. Spiro, Ed. John Wiley & Sons, Inc.: New York, 1980, Vol. 1, pp. 1-29.
3. Pil, P. Lippard, S. J. In Encyclopedia of Cancer, J. R. Bertino, Ed. Academic Press: San Diego, CA, 1997, Vol. 1, pp. 392-410.

This page titled 11.3.11: Cisplatin 11. Cisplatin as an Anticancer Drug is shared under a CC BY-NC-SA 4.0 license and was authored, remixed, and/or curated by ChemCases.

- **Cisplatin 11. Cisplatin as an Anticancer Drug** by ChemCases is licensed CC BY-NC-SA 4.0.

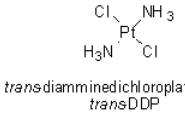
11.3.12: Cisplatin 12. Modes of Action of Cisplatin

The discovery of cisplatin (cis-diamminedichloroplatinum, or cis-DDP) in the early 1960s generated a tremendous amount of research activity as scientists strove to understand how the drug worked in the human body to destroy cancer cells. We now believe that cisplatin coordinates to DNA and that this coordination complex not only inhibits replication and transcription of DNA, but also leads to programmed cell death (called apoptosis).

As it turns out, however, formation of **any** platinated coordination complex with DNA is not sufficient for cytotoxic (that is, cell-killing) activity. The corresponding trans isomer of cisplatin (namely, trans-DDP) also forms a coordination complex with DNA but unlike cisplatin, trans-DDP is not an effective chemotherapeutic agent.



cisplatin
*cis*diamminedichloroplatinum(II)
*cis*DDP

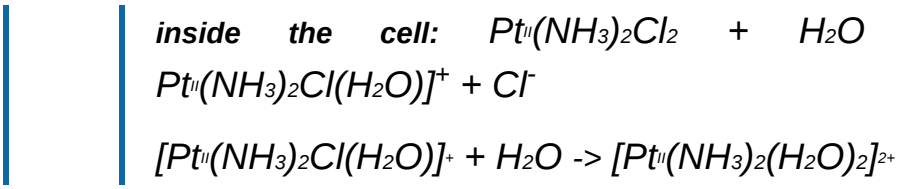


*trans*diamminedichloroplatinum(II)
*trans*DDP

Due to the difference in geometry between cis- and trans-DDP, the types of coordination complexes formed by the two compounds with DNA are not the same. It appears that these differences are critically important in determining the efficacy of a particular compound for the treatment of cancer. For this reason, a great deal of effort has been placed on discovering the specific cellular proteins that recognize cisplatin-DNA complexes and then examining how the interaction of these proteins with the complexes might lead to programmed cell death of cancer cells.[1]

Cellular Uptake of Cisplatin

Before we describe the interactions of cisplatin in the cell, we need to understand how it gets there. Cisplatin is administered to cancer patients intravenously as a sterile saline solution (that is, containing salt—specifically, sodium chloride). Once cisplatin is in the bloodstream, it remains intact due the relatively high concentration of chloride ions (~100 mM). The neutral compound then enters the cell by either passive diffusion or active uptake by the cell. Inside the cell, the neutral cisplatin molecule undergoes hydrolysis, in which a chlorine ligand is replaced by a molecule of water, generating a positively charged species, as shown below and in Figure 1. Hydrolysis occurs inside the cell due to a much lower concentration of chloride ion (~3-20 mM)—and therefore a higher concentration of water.



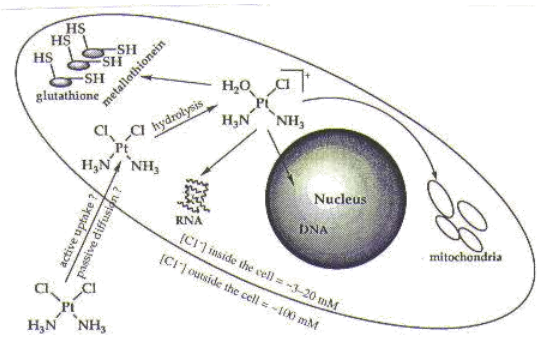


Figure 1. The cellular uptake of cisplatin and its targets. Reprinted with permission.1

As seen in Figure 1, once inside the cell, cisplatin has a number of possible targets: DNA; RNA; sulfur-containing enzymes such as metallothionein and glutathione; and mitochondria. The effects of DNA on mitochondria are not well understood, but it is possible that damage to mitochondrial DNA resulting from cisplatin treatment contributes to cell death. The interaction of cisplatin with sulfur-containing enzymes is better understood and is believed to be involved in

resistance of cells to cisplatin (as discussed in the drug resistance module). The effects of cisplatin on RNA and DNA have been studied extensively. We will briefly discuss the interaction of cisplatin with RNA. We will also describe the interaction of cisplatin with DNA in some detail and discuss why DNA is the target of cisplatin that is believed to be responsible for cell death.1

Interaction of Cisplatin with RNA

Although cisplatin can coordinate to RNA, this interaction is not believed to play an important role in cisplatin's mechanism of action in the body for two reasons. First, a single damaged RNA molecule can be replaced by newly synthesized material; studies have revealed that cisplatin does not affect RNA synthesis (but that it does affect DNA synthesis). Second, when cisplatin was administered in vitro at its lethal dose to a strain of cancer cells, only a small fraction (1% to 10%) of RNA molecules were damaged.[1]

Interaction of Cisplatin with DNA

Cisplatin coordinates to DNA mainly through certain nitrogen atoms of the DNA base pairs; these nitrogen atoms (specifically, the N7 atoms of purines) are free to coordinate to cisplatin because they do not form hydrogen bonds with any other DNA bases, as shown in Figure 2. (Also see the module on DNA.)

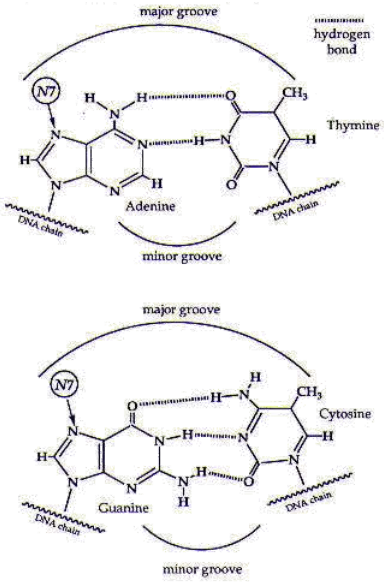


Figure 2. *The DNA base pairs. Cisplatin coordinates to the N7 atoms of the purine (guanine and adenine) bases. Reprinted with permission.1*

Many types of cisplatin–DNA coordination complexes, or adducts, can be formed. The most important of these appear to be the ones in which the two chlorine ligands of cisplatin are replaced by purine nitrogen atoms on adjacent bases on the same strand of DNA; these complexes are referred to 1,2-intrastrand adducts. The purine bases most commonly involved in these adducts are guanines; however, adducts involving one guanine and one adenine are also found. The formation of these adducts causes the purines to become destacked and the DNA helix to become kinked, as shown in Figure 3.

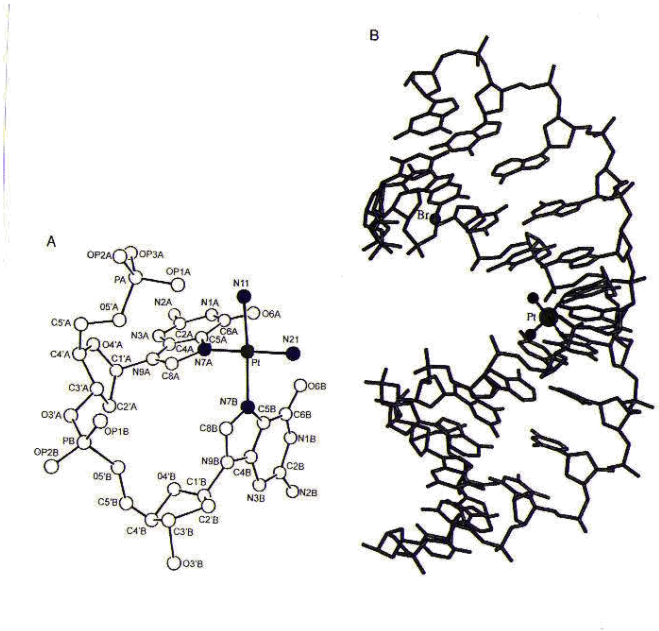


Figure 3. *(a) The structure of cisplatin (with platinum shown in green and nitrogen ligands shown in blue) coordinated to a dinucleotide containing two guanines. Notice the destacking of guanine bases, which would normally be parallel to one another. (b) The structure of cisplatin coordinated to two guanines in a DNA duplex. Reprinted with permission.1*

Due to its geometry, *trans*-DDP cannot form 1,2-intrastrand adducts with DNA. Since *trans*-DDP is inactive in killing cancer cells, it is believed that the 1,2-intrastrand adducts formed between cisplatin and DNA are important for the anticancer activity of cisplatin.1

We have seen how cisplatin binds DNA, and now we want to understand how the binding of cisplatin to DNA leads to programmed cell death. Researchers have found that this binding affects both replication and transcription of DNA, as well as mechanisms of DNA repair. The effects of both cisplatin and *trans*-DDP on DNA replication were studied both *in vitro* (using cell extracts outside the host organism) and *in vivo* (inside the host organism). *In vitro* studies on both prokaryotic (bacterial) and eukaryotic (mammalian) cells revealed that DNA adducts of both cisplatin and *trans*-DDP blocked the action of DNA polymerase, an enzyme necessary for replication. In particular, 1,2-intrastrand adducts of cisplatin with DNA all stopped polymerases from doing their job. Likewise, *in vivo* studies showed that cisplatin and *trans*-DDP inhibited replication equally well. Since other studies have shown that cisplatin is an effective antitumor agent but *trans*-DDP is not, these results suggest that DNA replication is not the only factor important for the clinical activity of cisplatin in destroying cancer cells.1 The effects of cisplatin and *trans*-DDP on DNA transcription are harder to interpret than the effects on replication. However, cisplatin does not appear to inhibit transcription, possibly leading to programmed cell death.1

Cisplatin and DNA Repair

The cytotoxic activity of cisplatin may arise from the cell's inability to repair DNA damage caused by cisplatin. Indeed, in vitro studies on cell extracts suggest that the most common cisplatin–DNA adducts (that is, 1,2-intrastrand adducts) are not readily repaired by the excision repair system (see DNA module). It is dangerous to draw too many conclusions from these studies, however, because there may be mechanisms of repair present in the organism that are not apparent from studies on cell extracts alone.1

Interactions of Cellular Proteins with Cisplatin-Damaged

DNA Researchers have conducted further studies to address the possibility that cisplatin's cytotoxic activity may result from a failure of the excision repair system. In this repair system before the damaged portion of DNA is even excised from the rest of the strand, it must be recognized by the cell. The cell detects DNA damage by the action of damage recognition proteins. Therefore, as

a first step in studying the excision repair system, researchers looked for evidence of proteins attached to cisplatin–DNA adducts. Several types of assays can differentiate between DNA that is bound to a protein and free DNA; researchers have been able to use these assays to isolate several proteins that bind to cisplatin–DNA adducts. These proteins all contain a common portion (that is, similar or even identical sequences of amino acids, which are the building blocks of proteins) called a high mobility group (HMG); proteins in this class are called HMG-domain proteins. The tests described above have shown that HMG-domain proteins bind cisplatin–DNA adducts in vitro . In vivo assays on yeast have also provided evidence that HMG-domain proteins are important for the activity of cisplatin: cells lacking the gene that codes for HMG-domain proteins are less sensitive to cisplatin than cells containing the gene, meaning that cisplatin is less effective in killing these cells. This result suggests that HMG-domain proteins play an important role in cisplatin's activity in killing cells; these effects may also be in operation in mammalian cells.1 Two theories explain the possible role of HMG-domain proteins in cisplatin's cytotoxic activity. Many HMG-domain proteins are transcription factors, meaning that they are required for the synthesis of RNA from a DNA template. One theory asserts that if HMG-domain-containing transcription factors bind preferentially to the cisplatin–DNA adducts, they could wreak havoc with the transcriptional machinery, possibly leading to cell death. A second theory suggests that when HMG-domain proteins bind to the cisplatin–DNA adducts, the adducts would not be recognized by the repair machinery.2 DNA repair would then be slower than normal, as shown in Figure 4.

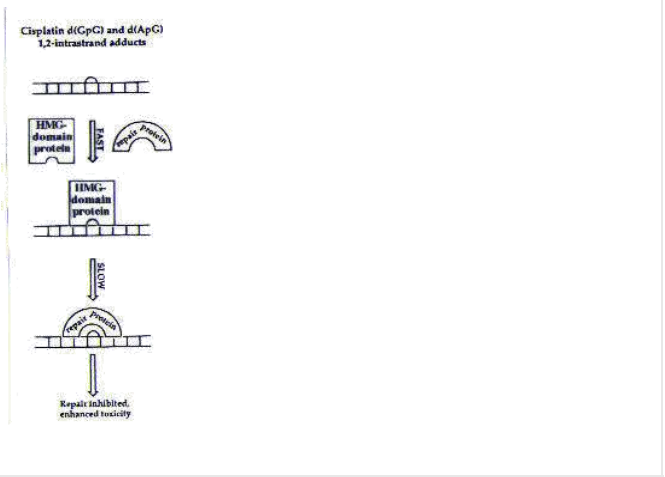


Figure 4. Model for the inhibition of cisplatin adduct repair in the presence of HMG-domain proteins. Reprinted with permission.1

The cisplatin–DNA adducts would then be more persistent than they would in the absence of HMG-domain proteins, and DNA repair would be slower. This could interfere with the normal functions of the cell (among them, replication and transcription) and possibly trigger cell death.2

For some recent developments in this area, go to the module on further studies.

References

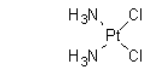
1. Pil, P., Lippard, S. J. In Encyclopedia of Cancer, J. R. Bertino, Ed. Academic Press: San Diego, CA, 1997, Vol. 1, pp. 392-410.
2. Marla, S., Personal communication, 1999.

This page titled 11.3.12: Cisplatin 12. Modes of Action of Cisplatin is shared under a CC BY-NC-SA 4.0 license and was authored, remixed, and/or curated by ChemCases.

- **Cisplatin 12. Modes of Action of Cisplatin** by ChemCases is licensed CC BY-NC-SA 4.0.

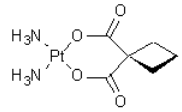
11.3.13: Cisplatin 13. Further Studies/Recent Developments

The publication of the original papers in the 1960s describing the ability of certain platinum-containing compounds—specifically, cisplatin—to kill cancer cells has generated a tremendous amount of research. It would be impossible to describe all of that research here, so we will focus on just two areas of continuing study: the development of second- and third-generation drugs in the cisplatin family, and the research on the cellular target of cisplatin.

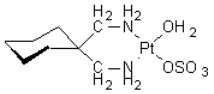


cisplatin
cis-diamminedichloroplatinum(II)

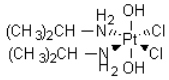
Second- and Third-Generation Drugs Once a successful drug has been discovered for the treatment of a particular disease or condition, researchers will often try to improve on that drug by synthesizing and studying related compounds, referred to as analogs or second-generation drugs. There are several reasons for making such analogs. First, the analogs may be able to improve on the efficacy of the original drug, meaning that lower doses are able to produce the same beneficial effects. Second, the toxicity profile of the analogs may be better than that of the original drug; in other words, the analogs may have fewer toxic side effects than the original drug. Third, the analogs may be able to be used to treat cases that have become resistant to the original drug. Finally, if the original drug can only be administered intravenously, the analogs may be able to be taken orally. After the efficacy and toxicity profiles of second-generation analogs are obtained, more analogs can be synthesized and studied; these analogs are called third-generation drugs. Many second-generation analogs of cisplatin have been made; some have been found to produce the same therapeutic effects as cisplatin—but with lower required doses and reduced side effects. Three of these analogs are carboplatin, spiroplatin, and iproplatin, shown below.



carboplatin
cis-diammine(1,1-cyclobutane-dicarboxylato)platinum(II)

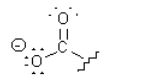


spiroplatin
aqua-1,1-bis(aminomethyl)-cyclohexanesulfatoplatinum(II)

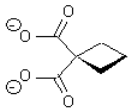


iproplatin
cis-dichlorobis(isopropylamine)-*trans*-dihydroxoplatinum(IV)

Carboplatin has proven to be the most useful of these three analogs, and was approved by the FDA for the treatment of ovarian cancers in 1989. Carboplatin and cisplatin have been shown to form an identical type of adduct with DNA and have similar activities against ovarian and lung tumors; however, carboplatin is less toxic to the peripheral nervous system and the kidneys. The lower toxicity of carboplatin compared to cisplatin is believed to be due to the structure of carboplatin. The presence of the bidentate dicarboxylate ligand (shown in Figure 1) in carboplatin slows down the degradation of carboplatin into potentially damaging derivatives.



a carboxylate group



a dicarboxylate group

> ***Figure 1. A carboxylate and a dicarboxylate group. Note that for simplicity, in the drawing of the dicarboxylate group, the electrons are not included, and the carbon atoms are not drawn out explicitly but rather are represented by the vertices in the structure. The dicarboxylate group is a bidentate ligand, meaning that it can bind a metal ion in two places.***

Indeed, at 98.6 °F (37 °C) the retention half-life of carboplatin in blood plasma is 30 hours, whereas that for cisplatin is only 1.5-3.6 hours. In addition to the lower toxicity of carboplatin, it has been shown to work in some cases when cisplatin has failed.1,2 The decreased toxicity of carboplatin and the activity of carboplatin against cisplatin-resistant tumors have led to greater use of carboplatin which has resulted in carboplatin becoming the greater money-maker of the two drugs. (see module on profits) In

addition to carboplatin and other second-generation cisplatin analogs, several third-generation drugs have been synthesized and tested. One broad class of these drugs, having the general structure shown in Figure 2, can be taken orally—a significant improvement over cisplatin, which must be administered intravenously.

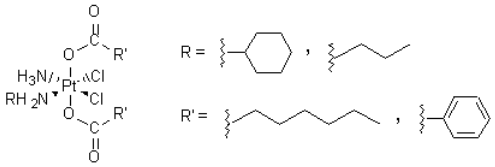


Figure 2. The general structure of ammine/amine platinum(IV) dicarboxylates. Many different R and R' groups were tried; two examples for each are shown here.

These complexes are stable enough to survive passage down the digestive tract. They are then transported across the gastrointestinal mucosa into the bloodstream. After absorption into the bloodstream, these compounds are metabolized to form four-coordinate, platinum(II) cisplatin analogs. These new four-coordinate complexes are assumed to be the active forms of the drug.1,3 A variety of six-coordinate platinum(IV) complexes were tested in cell culture using six human ovarian cancer cell lines. Researchers found that as the ring size of ligand R increased, the complexes became increasingly more effective than cisplatin at killing cancer cells. Moreover, like carboplatin, these complexes were also toxic to certain cancer cell lines that were resistant to cisplatin. Researchers believe that these third-generation drugs are more effective than cisplatin because they are taken up into the cell in greater concentrations than cisplatin.3 Cellular Target of Cisplatin The cellular target of cisplatin has long been believed to be DNA (see modules on mode of action and DNA). Cisplatin has been shown to bind DNA and cause the DNA duplex to bend and unwind. For many years, however, researchers have been trying to determine precisely how the cisplatin–DNA complex leads to cell death. A recent crystal structure4 provides some clues about what may be occurring on a subcellular level. The research group of Stephen Lippard at the Massachusetts Institute of Technology has crystallized a ternary complex (that is, one having three components) comprising cisplatin, DNA, and a cellular protein called a high mobility group (HMG) protein. This protein inserts a phenyl group protruding from its backbone5 into the notch created when cisplatin forms a complex with DNA and causes it to bend, as shown in Figure 3. A mutant protein lacking this phenyl group does not form a complex with cisplatin and DNA, suggesting that the phenyl group is crucial for complex formation. The interaction of an HMG-protein with the cisplatin–DNA complex may shield DNA from intracellular repair; the inability of DNA to repair itself may cause cancer cells to die. (See module on mode of action) Knowledge of this ternary complex should aid in the development of future anticancer strategies. Scientists may now use the information about HMG-proteins to design proteins that will bind the cisplatin–DNA complex even more tightly. In addition, they may use the knowledge gained from this research to continue to look for cisplatin analogs that will form even better drug–DNA–protein complexes.6

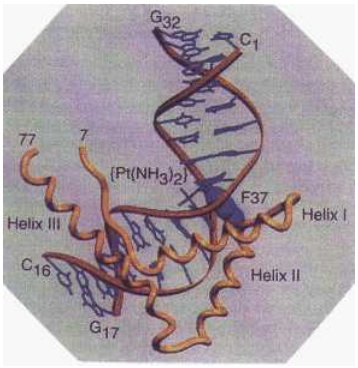
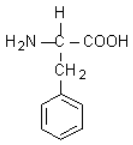


Figure 3. A ternary complex comprising cisplatin (green), DNA (red and dark blue), and an HMG-protein (yellow). The phenyl group (light blue spheres, labeled F37), which is a part of the HMG-protein, is inserted into the notch created by the formation of a platinated DNA complex. Reprinted with permission.6



phenylalanine

1. Bertini, I., Gray, H. B., Lippard, S. J., Valentine, J. S. Bioinorganic Chemistry. University Science Books: Sausalito, CA, 1994.
2. Kaim, W., Schwederski, B. Bioinorganic Chemistry: Inorganic Elements in the Chemistry of Life. John Wiley & Sons Ltd: Chichester, England, 1994.
3. Kelland, L. R., Murrer, B. A., Abel, G., Giandomenico, C. M., Mistry, P., Harrap, K. R. Cancer Research ,1992, 52, pp. 822-828.
4. A crystal structure shows the three-dimensional arrangement of atoms in a molecule and is obtained from the diffraction pattern of x-rays passing through a crystal of the molecule.
5. The phenyl group is the side chain of phenylalanine, which is an amino acid contained in the backbone of the HMG-protein. There are 20 naturally occurring amino acids; these are the building blocks of proteins.
6. Ohndorf, U.-M., Rould, M. A., He, Q., Pabo, C. O., Lippard, S. J. Nature, 1999, 399, pp. 708-712.

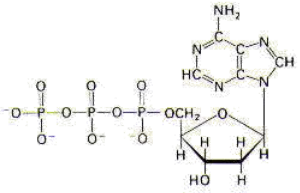
This page titled 11.3.13: Cisplatin 13. Further Studies/Recent Developments is shared under a CC BY-NC-SA 4.0 license and was authored, remixed, and/or curated by ChemCases.

- **Cisplatin 13. Further Studies/Recent Developments** by ChemCases is licensed CC BY-NC-SA 4.0.

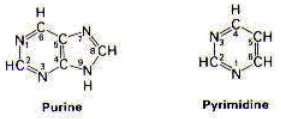
11.3.14: Cisplatin 14. DNA

Deoxyribonucleic acid, or DNA, stores all of our genetic information. It makes up the genes of all cells (animal and plant) as well as many viruses. In this module, we will examine the structure of DNA so that we can better understand its interaction with cisplatin. We will also examine replication and transcription, which are the processes by which genetic information is expressed. Finally, we will describe one mechanism by which damaged DNA is repaired in the cell.

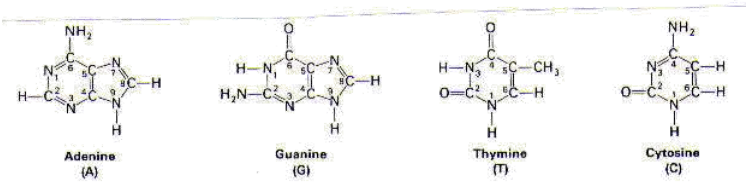
< face="Arial">**Structure**1 DNA is a remarkably long, threadlike macromolecule. DNA varies in length, depending on the organism. Certain viral DNA is 1.7 ᵐm, whereas human DNA is nearly a meter in length. DNA is made up of many **deoxyribonucleotide** subunits. A **nucleotide** comprises a **nitrogenous base**, a **sugar**, and one or more **phosphate** groups, as shown below.



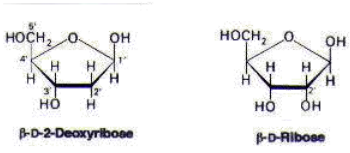
The **nitrogenous base** is a derivative of either **purine** or **pyrimidine**.



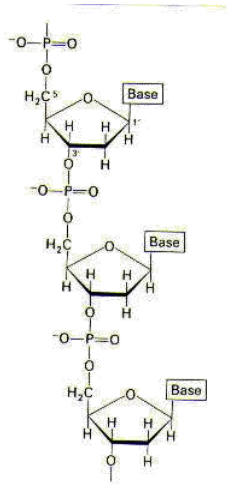
In DNA, the **purines** are **adenine (A)** and **guanine (G)**, and the **pyrimidines** are **thymine (T)** and **cytosine (C)**.



The **sugar** present in a deoxyribonucleotide is **deoxyribose**, which lacks an oxygen that is present in its parent compound, ribose.



The sugars and phosphate groups make up the backbone of DNA and therefore provide DNA's structure; the backbone of DNA does not vary. The sequence of the bases does vary, however, and this is how genetic information is carried. The structure of part of a DNA chain is shown below.



The three-dimensional structure of DNA was deduced in 1953 by James Watson and Francis Crick. Their model of DNA had five important features: 1. Two helical chains of polynucleotides are coiled around a common axis; the chains run in opposite directions, as shown in Figure 1.

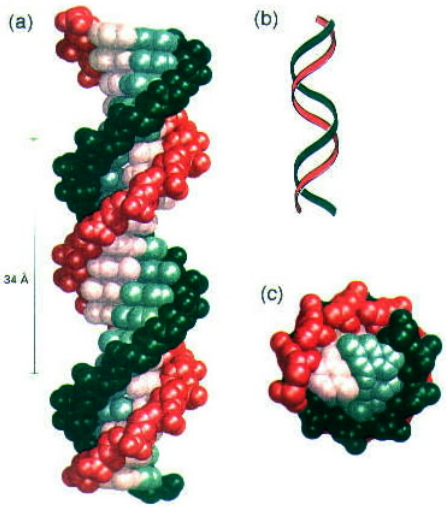


Figure 1. Model of a double-helical DNA. One chain is shown in green and the other in red. The purine and pyrimidine bases are shown in lighter colors than the sugar-phosphate backbone. (a) Axial view. The structure repeats along the helix axis (vertical) at intervals of 34 Å, which corresponds to 10 residues on each chain. (b) A schematic "ribbon" representation of an axial view of DNA. (Courtesy of M. Meselson and F. W. Stahl) (c) Radial view, looking down the helix axis. Reprinted with permission.[1]

2. The bases are on the inside of the helix, whereas the backbone (the sugars and phosphates) are on the outside. The bases are perpendicular to the helix axis and are said to stack (as plates are stacked when they are stored). The sugars are nearly parallel to the helix axis. See Figure 2.

14axial.gif (19203 bytes)

> ***Figure 2. Diagram of one of the strands of a DNA double helix, viewed down the helix axis. the bases (all pyrimidines here) are inside, whereas the sugar-phosphate backbone is outside. The bases are shown in blue and the sugars in red. Reprinted with permission.[1]***

3. The diameter of the helix is 20 Å. The helical structure repeats after ten deoxyribonucleotide units on each chain (at intervals of 34 Å), as shown in Figure 1. 4. The two chains are held together by hydrogen bonds between pairs of bases. Adenine and thymine are always paired (and are joined by two hydrogen bonds); guanine and cytosine are always paired (and are joined by three hydrogen bonds), as shown in Figure 3.



> ***Figure 3. Hydrogen bonding interactions (a) between adenine and thymine, and (b) between guanine and cytosine. Reprinted with permission.[1]***

5. There are no restrictions on the sequence of bases along a polynucleotide chain, however, the precise sequence of bases carries the genetic information. < **face="Arial">Replication**[1]DNA duplicates itself by a process called replication. In replication, a strand from the original DNA molecule acts as a template for the formation of a new strand. The template can be either single- or double-stranded DNA; single-stranded DNA is formed when the hydrogen bonds between base pairs are broken. More than 20 proteins are required for the process of DNA replication. One of these is DNA polymerase I, which catalyzes the step-by-step addition of activated deoxyribonucleotide units to a DNA chain; the activated deoxyribonucleotide units for adenine, guanine, thymine, and cytosine are represented as dATP, dGTP, dTTP, and dCTP, respectively. Divalent magnesium (Mg^{2+}) is also required for replication to occur. A schematic representation of DNA replication is shown in Figure 4.

> ***Figure 4. A schematic representation of DNA replication, showing the addition of a guanine residue first, and then a thymine residue. Reprinted with permission.[1]***

In short, replication describes the process by which genetic information is stored and transmitted. < **face="Arial">Transcription**< face="Arial">[1] Genetic information is expressed through the processes of transcription, in which RNA (ribonucleic acid) is synthesized from a DNA template strand, and translation, in which proteins are synthesized from RNA—specifically, messenger RNA—templates. We will briefly discuss transcription here. Like DNA, RNA is made up of a sugar-phosphate backbone having four possible nitrogenous bases. Unlike DNA, however, ribose (shown below)—not deoxyribose—is found in RNA. The four nitrogenous bases in RNA are adenine, guanine, cytosine, and uracil (instead of thymine), as shown below.

An enzyme called RNA polymerase catalyzes the initiation and elongation of RNA chains, in which one activated ribonucleotide unit (represented by ATP, GTP, UTP, and CTP) is added at a time. The preferred template for transcription is double-stranded DNA. A divalent metal ion—either Mg^{2+} or Mn^{2+}—is required for transcription. In short, transcription describes the first step in the expression of the genetic information stored by DNA. < **face="Arial">Repair**< face="Arial">[1,2] DNA is damaged in a variety of ways, and all cells have mechanisms by which to repair the damage. DNA repair is possible because genetic information is stored in *both* strands of the double helix; therefore, information lost from one strand can be retrieved from the other. One way in which DNA becomes damaged is by the covalent cross-linking of DNA bases; cross-links can be formed from bases on either the same strand of the helix (intrastrand cross-linking) or opposite strands of the helix (interstrand cross-linking). Covalent intrastrand cross-links can be formed by chemical agents, such as cisplatin, or by ultraviolet light, leading to the formation of a pyrimidine dimer, as shown in Figure 5.

Figure 5. A thymine dimer, which is an example of a pyrimidine dimer. Reprinted with permission.[1]

Such a pyrimidine dimer cannot fit into the double helix, so the normal functions of the cell (such as replication and transcription) are blocked until the dimer is removed. The removal, or excision, of the dimer and the subsequent repair of the damaged DNA strand is referred to as the excision repair system and requires the action of several enzymes, three of which are described here and shown in Figure 6. After recognition of DNA damage by a damage recognition protein, the DNA strand containing the dimer is cut at two sites by an **excinuclease**. Then, the cut DNA strand is regenerated by **DNA polymerase I**. Finally, the newly replicated portion of the DNA strand is joined to the undamaged part of the DNA strand by **DNA ligase**.

Figure 6. Repair of a region of DNA containing a thymine dimer by the sequential action of a specific excinuclease, a DNA polymerase, and a DNA ligase. The thymine dimer is

> ***shown in blue, and the new region of DNA in red. (Courtesy of P. C. Hanawalt) Reprinted with permission.[1]***

As we have seen from studies into the **mode of action** of cisplatin, covalent intrastrand cross-links can also be formed by chemical agents, such as cisplatin. A similar mechanism is believed to repair damage done to cancer cells by cisplatin, as we will see when we discuss drug resistance.

1. (1) Stryer, L. *Biochemistry,* 4th ed. W. H. Freeman and Company: New York, 1995, Chapters 4, 5, and 31.
2. (2) Pil, P., Lippard, S. J. In *Encyclopedia of Cancer*, J. R. Bertino, Ed. Academic Press: San Diego, CA, 1997, Vol. 1, pp. 392-410.

This page titled 11.3.14: Cisplatin 14. DNA is shared under a CC BY-NC-SA 4.0 license and was authored, remixed, and/or curated by ChemCases.

11.3.15: Cisplatin 15. FDA Drug Approval Process

As we saw in the module on cisplatin as an anticancer drug, cisplatin went through several phases of testing before it was approved by the Food and Drug Administration (FDA) for use in the United States. In this module we give a brief outline of the steps required for approval of a drug by the FDA; much more information can be found on the FDA's home page, particularly the sites describing the role of the Center for Drug Evaluation and Research (CDER) on the new drug development policy.

Before an investigational new drug (IND) can even be tested on humans, extensive pre-clinical research must be conducted. This includes first identifying potential drug candidates:

- Sometimes a drug is discovered purely by serendipity, as was the case with cisplatin.
- Other times natural products produced by microorganisms are screened for antifungal, antibiotic, antiviral, or antitumor activity.
- Another approach is to use computer modeling to design drugs that will interact effectively with a particular receptor in the body—for example, DNA or a specific enzyme.
- Once an active compound or a target has been identified, many new compounds—hundreds, even thousands—are synthesized. These hundreds or thousands of compounds are then usually screened *in vitro* (generally, using cell cultures in a Petri dish—that is, outside the living organism). The most active compounds are then screened *in vivo* (using animal assays). The drug candidate is tested on at least two different species of animals (one rodent and one non-rodent) because drugs do not always affect different species the same way. (For example, cisplatin was tested on both mice and dogs.) Both short- and long-term testing is conducted on animals. Short-term testing lasts from 2 weeks to 3 months and is designed to examine the metabolism and toxicity of the drug candidate. Long-term testing lasts from a few weeks to several years and is done to see whether long-term use of the drug will lead to cancer or birth defects.

After the completion of pre-clinical research, the FDA meets with the sponsor of the drug (usually a pharmaceutical company—in the case of cisplatin, Bristol-Myers), and the sponsor submits data demonstrating that the drug candidate is both biologically active and safe for administration to humans. After these meetings, the sponsor submits the drug candidate as an IND, and clinical testing can begin. The purpose of clinical research is to determine the safety and efficacy of the IND for the treatment of a particular disease or condition in humans. Clinical research is divided into three phases in the normal course of testing. (Certain drugs are placed in an accelerated development and review process; this will not be discussed here, but is described more fully on the FDA website on the new drug development process

< face="Arial">**Courtesy FDA**

- Phase 1 clinical studies represent the first time that an IND is tested on humans—generally, healthy volunteers, but sometimes patients (the latter was the case with phase 1 clinical studies of cisplatin). The purpose of these studies is to determine the metabolism, structure-reactivity relationships, mechanism of action, and side effects of the drug in humans. If possible, phase 1 studies are used to ascertain the efficacy of the drug. Phase 1 studies are usually conducted on 20 to 80 subjects.
- The purpose of phase 2 clinical trials is to determine the efficacy of a drug to treat patients with a specific disease or condition, as well as common short-term side effects or risks. These studies are conducted on a larger scale than phase 1 studies and typically involve several hundred patients.
- Phase 3 clinical trials provide more information about the efficacy and safety of the drug and allow scientists to extrapolate the results of clinical studies to the general population. Phase 3 studies generally involve several hundred to several thousand people.

There are several checks and balances in the process of clinical trials; among them is the use of institutional review boards (IRBs) and advisory committees. IRBs are designed to protect the rights and welfare of people participating in clinical trials both before and during the trials. IRBs comprise at least five experts and lay people with a variety of backgrounds to provide a complete review of clinical proceedings. In addition, the CDER uses advisory committees comprising various experts in order to obtain outside opinions and advice about a new drug, a new indication for a previously approved drug, labeling information about a drug, guidelines for developing particular kinds of drugs, or the adequacy of safety and efficacy data. The sponsor of a drug makes a formal application to the FDA to approve a new drug for use in the United States by submitting a new drug application (NDA). An NDA must include results and analyses from tests of the drug on both animals and humans, as well as a description of how the drug was manufactured. The NDA must provide enough information for FDA reviewers to make several critical decisions, including whether the drug is safe and efficacious and whether its benefits outweigh its risks, whether the drug's labeling information is appropriate, and whether the manufacturing methods used to obtain the drug are adequate for ensuring the purity and integrity of the drug. The process of developing and testing a new drug is a lengthy one. The FDA estimates that it takes a little over 8 years to test a drug—including early laboratory and animal testing—before the final approval for use by the general public.

Inside the FDA—Vocabulary CDER: Center for Drug Evaluation and Research FDA: Food and Drug Administration IND: Investigational New Drug IRB: Institutional Review Board NDA: New Drug Application

---

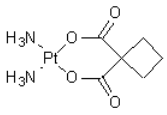
This page titled 11.3.15: Cisplatin 15. FDA Drug Approval Process is shared under a CC BY-NC-SA 4.0 license and was authored, remixed, and/or curated by ChemCases.

11.3.16: Cisplatin 16. Profits from Cisplatin

Following the discovery by Barnett Rosenberg and coworkers at Michigan State University (see modules on electric fields, platinum electrodes, one scientist's story) that certain platinum-containing compounds inhibited cell division and cured solid tumors resulting from cancer, cisplatin was approved by the Food and Drug Administration for the treatment of genitourinary tumors in 1978.1 Since then, Michigan State has collected over $160 million in royalties from cisplatin and a related drug, carboplatin, which was approved by the FDA in 1989 for the treatment of ovarian cancers.



cisplatin
(*cis*-diamminedichloroplatinum(II))



carboplatin

The distribution of the profits from these drugs has generated a great deal of controversy, resulting in two (unrelated) lawsuits. Let's provide some background, as well as some detail about these two lawsuits because they illustrate difficulties that can arise when universities and businesses cooperate.

After cisplatin was discovered by researchers at Michigan State, members of the university made an agreement with a pharmaceutical company, Bristol-Myers, to develop and produce the drug. This agreement was made possible with the help of a technology-licensing organization known today as Research Corporation Technology (RCT). RCT is a daughter company of Research Corporation, a charitable foundation founded in 1912, whose stated mission is to promote "the advancement and extension of technical and scientific investigation, research, experimentation, and education" by making grants.

In 1950, well before Barnett Rosenberg and his coworkers discovered the medical uses of cisplatin, Michigan State University and Research Corporation signed an agreement that stated that for any discoveries patented at Michigan State, the inventors would receive the first 15 percent of all royalties, and the remaining royalties would then be split evenly between the university and Research Corporation.2 In 1987, Research Corporation decided that investing and business activities related to "technology transfer" (such as the licensing agreements between universities where discoveries were made and companies where these inventions could be developed and marketed) could not be carried out by a charitable organization such as itself. For this reason, Research Corporation created a new daughter company to handle all its rights to patents and licenses. This new company was called Research Corporation Technology (RCT), an independent, nonprofit company that pays taxes and has no shareholders; the formation of this new company was made possible by the Tax Reform Act of 1986. Unlike its parent company, the new company (RCT) does not make grants; rather, revenues from RCT are used to finance licensing activities, patent litigation, and creation of new companies to commercialize inventions. RCT has agreements—like the one with Michigan State—with over 100 universities.2

In 1995, Michigan State University attempted to terminate its contract with RCT by suing them. There were several reasons that the university wanted to become independent of RCT. First, representatives for Michigan State accused RCT of using its share of the profits of cisplatin and carboplatin to "unconscionably" enrich itself—particularly because RCT was not using these profits to promote scientific research at universities; rather, RCT was using the funds to give salary bonuses to high-ranking officials at the corporation. In short, Michigan State contended that RCT was acting in a manner that was inconsistent with the charitable mission of its parent company, Research Corporation. Michigan State hoped to rectify the wrongs by seeking damages of $50 million each from Research Corporation and RCT. Second, representatives for the university stated that the services provided by RCT were no longer needed because there was enough in-house expertise at Michigan State. Finally, along with the damages sought by the university, there was a significant financial incentive for Michigan State to end its relationship with RCT.

Under the original agreement, the university and RCT evenly split the profits remaining after the inventors received their share. Under a termination clause in the original agreement, however, the university would be entitled to 70 percent of the remaining profits if its agreement with RCT ended. Both Michigan State and RCT profit handsomely from the royalty income generated by cisplatin and carboplatin: Nearly all of the university's royalty income comes from cisplatin and carboplatin, and nearly 20 percent of RCT revenues comes from the two drugs.2 Because of this monetary component to the lawsuit, many people—including officials at other universities having contracts with RCT, as well as Barnett Rosenberg, whose research group discovered cisplatin and carboplatin—perceived that greed, not moral principle, was the primary driving force for the lawsuit. One official at another

midwestern university having a similar agreement with RCT stated that "a contract is a contract" and that "it was good enough when they signed up." Likewise, Barnett Rosenberg, who has retired from Michigan State and now conducts research at a private research institute in Michigan, said that he didn't think that he "would have acted the way the university did." He is proud of his role in the development of these important anticancer drugs but has stated that his efforts have "led to the creation of a lot of selfish, money-hungry university personnel." He said that he puts most of the money he receives from royalties of the drugs toward research projects at the Barros Institute in Lansing Michigan of which he is president.2 Now, a settlement has been reached between Michigan State and Research Corporation Technology.

Exact details of the settlement are not available; however, it is known that RCT will continue to manage the patents and licensing for cisplatin and carboplatin—but under new terms. Furthermore, the allocation of royalty income from the two drugs has changed: Michigan State will now receive more of the royalties from carboplatin, which now earns nearly six times more money in royalties than cisplatin. (See Figure 1.)

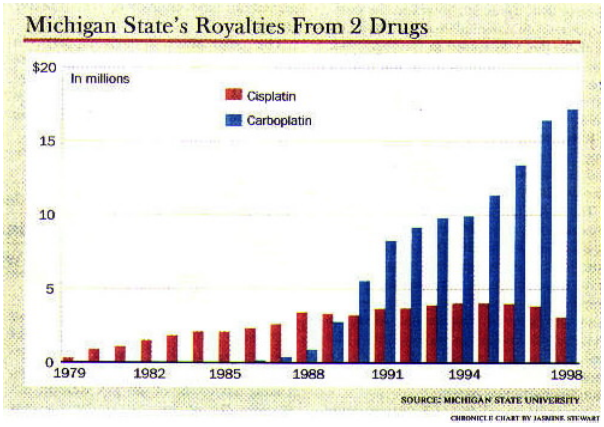


Figure 1. After FDA approval of carboplatin for the treatment of ovarian cancers in 1989, it outpaced cisplatin in earning royalties. Reprinted with permission. 3

Finally, RCT will pay Michigan State an additional $4.5 million over the next 2 years. Neither Michigan State University nor Research Corporation Technology commented extensively on the settlement, but each organization issued written statements that it had resolved its differences with the other.2 An additional benefit of the settlement for Michigan State is that the university will be represented by RCT in a second lawsuit arising from disagreements about profits from the anticancer drugs. In October 1996, a new patent was issued that allowed Michigan State to continue to receive royalties after the original cisplatin patent (issued in 1979) expired in 1996. In addition, Bristol-Myers Squibb will retain exclusive rights to the drug, as well as the obligation to pay royalties to Michigan State, until 2012. The second lawsuit has been brought by four generic-drug companies that want to manufacture their own, presumably less expensive, versions of cisplatin. Manufacture of these generic drugs would not require royalty payments to Michigan State. Lawyers for the four generic-drug companies contend that the 1996 patent should never have been issued because its fundamental claim is nearly the same as that made in the original patents. Double patenting is illegal. Because of their recent settlement with RCT, Michigan State will not be directly involved in this lawsuit because RCT is responsible for protecting the cisplatin patent.2

In short, cisplatin has produced not only physical, but also monetary, side effects. In the past few years, there have been two lawsuits contesting how the profits of cisplatin should be distributed.

1. Pil, P., Lippard, S. J. In Encyclopedia of Cancer, J. R. Bertino, Ed. Academic Press: San Diego, CA, 1997, Vol. 1, pp. 392-410.
2. Blumenstyk, G. In The Chronicle of Higher Education, 12 Feb 1999, pp. A39-A40.
3. Stewart, J. In The Chronicle of Higher Education; 12 Feb 1999, p. A39.

This page titled 11.3.16: Cisplatin 16. Profits from Cisplatin is shared under a CC BY-NC-SA 4.0 license and was authored, remixed, and/or curated by ChemCases.

- **Cisplatin 16. Profits from Cisplatin** by ChemCases is licensed CC BY-NC-SA 4.0.

https://chem.libretexts.org/@go/page/438114

11.3.17: Cisplatin 17. Drug Resistance

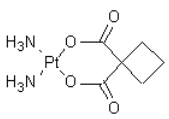
Even though cisplatin has proven to be a highly effective chemotherapeutic agent for treating various types of cancers, it has encountered the same fate as many other drugs used in cancer chemotherapy—namely, drug resistance. Resistance occurs when cells once destroyed by a particular drug no longer respond to treatment with that drug. Drug resistance is a major complication in cancer chemotherapy and accounts for the failure of chemotherapy to cure the majority of cancer patients.1 Drug resistance has been described as "the single most common reason for discontinuation of a drug."[2]

Indeed, drug resistance has significant clinical implications. When cells become resistant to cisplatin, the doses must be increased; a large dose escalation can lead to severe multiorgan toxicities (such as failures of the kidneys and bone marrow), intractable vomiting, and deafness.[3] (See module on toxic side effects.) Drug resistance exists in two forms: acquired resistance, in which a drug is initially beneficial but becomes ineffective over time and intrinsic resistance, in which the drug is ineffective from the outset. Drug resistance can operate by a number of mechanisms, none of which is fully understood. Postulated mechanisms of cisplatin drug resistance include decreased intracellular accumulation of cisplatin, increased intracellular levels of certain sulfur-containing macromolecules, and increased DNA repair.[1,3]

- **Decreased Intracellular Accumulation** If cisplatin cannot accumulate in the cell, it cannot reach the DNA found inside the cell, bind the DNA, and cause cell death. Therefore, it is beneficial for the cancer cell to develop mechanisms either to keep cisplatin out of the cell or to remove cisplatin from the cell; indeed, reducing cisplatin accumulation by cancer cells seems to be a major form of acquired resistance. The mechanism of decreased intracellular accumulation of cisplatin is not well understood, but it appears that the cell has some control over whether cisplatin enters the cell. This suggests that cisplatin does not enter the cell by passive diffusion alone but that there is some active transport system involved. Furthermore, additional experiments have shown that decreased cellular accumulation of cisplatin is not due to increased efflux of cisplatin.[1,3]
- **Sulfur-Containing Macromolecules** Once inside the cell, cisplatin can interact with a variety of other molecules besides DNA—including two sulfur-containing macromolecules, metallothionein and glutathione, that sequester cisplatin and remove it from the cell. Metallothionein (MT) is believed to be involved with the detoxification of heavy metal ions in the cell. Production of MT is triggered by the presence of heavy metal ions, glucocorticoids (which are steroid hormones that promote the formation of both glucose from noncarbohydrate sources and glycogen, enhance the degradation of fat and protein, and enable animals to respond to stress), interferon (which is a signaling molecule in the immune system that greatly enhances antiviral responses), and stress. Both cisplatin and trans-DDP bind to MT, with 10 platinum atoms per molecule of MT. MT may contribute to cisplatin resistance, but the results are inconclusive. In some cases, the levels of MT are higher in cisplatin-resistant cells, but in other cases, the MT levels are unaffected.1,3 Like metallothionein, glutathione (GSH) is also involved in detoxification. GSH reacts with hydrogen peroxide and organic peroxides, the harmful byproducts of aerobic life. GSH is also essential for maintaining the normal structure of red blood cells.4 In the presence of cisplatin, GSH forms a 2:1 (GSH:platinum) complex that is then eliminated from the cell. Again, like MT, levels of GSH are increased in some—but not all—cisplatin-resistant cells, suggesting that there are other mechanisms of cellular resistance.[3]
- **Increased DNA Repair** Another way that cells can become resistant to cisplatin is to have an enhanced ability to remove cisplatin-DNA adducts and to repair cisplatin-induced lesions in DNA. Such an ability might result from the presence of certain DNA repair proteins. One example of a DNA repair protein that has been shown to repair cisplatin lesions is a nuclear protein called XPE-BF (xeroderma pigmentosum group E binding factor). Levels of XPE-BF were found to increase early in the development of cisplatin resistance. Another example of a DNA repair protein that may be involved in the recognition of cisplatin damage is ERCC1, most likely a DNA-binding protein. The gene encoding for ERCC1 is expressed at higher levels in cisplatin-resistant cells than in cells that are sensitive to cisplatin. Furthermore, in one case, a patient was treated with carboplatin, a close relative of cisplatin (see below); carboplatin was initially effective in treating the patient's tumor, but resistance to this drug eventually occurred. As the tumor cells became resistant to carboplatin, the level of ERCC1 expression was found to increase.[3]



cisplatin



carboplatin

As with other mechanisms of cisplatin resistance, it appears that DNA repair is one of several possible mechanisms. Studies showing an increase in levels of DNA repair proteins as tumor cells become less sensitive—and therefore more resistant—to treatment with cisplatin have suggested that DNA repair seems to be the mechanism activated first in cisplatin resistance. As time goes on, other mechanisms, such as decreased intracellular accumulation and sequestration of cisplatin by sulfur-containing macromolecules, may also become significant.3

1. Pil, P., Lippard, S. J. In Encyclopedia of Cancer, J. R. Bertino, Ed. Academic Press: San Diego, CA, 1997, Vol. 1, pp. 392-410.
2. Zamble, D. B. Lippard, S. J. Trends in Biochemical Sciences, 1995, 20, pp. 435-439.
3. Chu, G. Journal of Biological Chemistry,1994, 269, pp. 787-790.
4. Stryer, L. Biochemistry, 4th ed. W. H. Freeman and Company: New York, 1995.

This page titled 11.3.17: Cisplatin 17. Drug Resistance is shared under a CC BY-NC-SA 4.0 license and was authored, remixed, and/or curated by ChemCases.

- **Cisplatin 17. Drug Resistance** by ChemCases is licensed CC BY-NC-SA 4.0.

11.3.18: Cisplatin 18. Toxicity

"Certainly Dr. Cohn was kind to my mother. She always came downstairs to visit during her chemotherapy, took her hand, and talked with her quietly about her symptoms as the chemicals did their methodical drip-drip dance. "There's platinum in this stuff, Ellen," my mother said, smiling, during the second round, "just like in my wedding ring. That's why my mouth tastes like tin." "Is it working?" I said. "I can't say how well it's working yet," Dr. Cohn said. "I'll be doing some tests and I'd like to hear how well you felt, Kate, after the first time." "She threw up the entire next day. Everything. Every bit of food she ate. And when that was gone she had the dry heaves. Plus her hair is starting to come out all over her pillow." Dr. Cohn's smile was so faint that it was little more than a pucker at the corners of her mouth. "Those aren't unexpected side effects. But I'd like to hear from Kate about how she's feeling." "It's not too bad. I do hate the tinny taste. I'm losing weight, although I never thought I'd see that as a problem. And my hair looks pretty awful." My mother ran her fingers through her thinning red curls. excerpted from One True Thing (pp. 59-60) by Anna Quindlen1

Since cancer is a disease in which tumor cells divide rapidly (see cancer), many chemotherapeutic agents used to treat cancer target rapidly dividing cells. Unfortunately, most chemotherapeutic agents are nonselective and attack other types of rapidly dividing cells in the body. Such cells can be found in the gastrointestinal tract, in hair follicles, and in bone marrow. For this reason, some of the common adverse side effects of drugs used in cancer chemotherapy are nausea, alopecia (hair loss), and myelosuppression (a reduction of activity in the bone marrow—in particular, toxicity to the blood forming elements).

Indeed, nearly all people who are treated with cisplatin (which is marketed by Bristol-Myers Squibb under the name of Platinol) experience gastrointestinal problems—specifically, intense nausea and vomiting. Nausea and vomiting usually begin within 1 to 4 hours after treatment and can last up to 24 hours.2 However, in the case of cisplatin, it is believed that the nausea and vomiting result from an effect on the central nervous system rather than from gastrointestinal damage.3

Some people who are given cisplatin treatments also experience alopecia. 2 Furthermore, myelosuppression occurs in 25 to 30 percent of people who undergo treatments with cisplatin. The levels of platelets and white blood cells (or leukocytes) associated with myelosuppression are generally lowest about 3 weeks after treatment and returns to normal a little more than 2 weeks after that. The loss of platelets (called thrombocytopenia) and the loss of leukocytes (called leukopenia) are more pronounced when higher doses of cisplatin are given. In addition to a loss of platelets and white blood cells, the use of cisplatin can also cause a decrease in the number of red blood cells (anemia). Anemia occurs with the same frequency and with the same timing as thrombocytopenia and leukopenia. 2 In addition to the adverse side effects listed above, use of cisplatin has been linked with nephrotoxicity (renal, or kidney, toxicity). In fact, renal insufficiency is the major and most severe form of toxicity associated with use of cisplatin as a chemotherapeutic agent. Renal toxicity can result both from doses that are higher than recommended and from an accumulation of cisplatin in the body. 2 Researchers at Memorial Sloan-Kettering Cancer Center in New York have discovered one solution to this problem: that is, administering an osmotic diuretic agent such as D-mannitol, while making sure that the patient is properly hydrated. 3 Some people receiving cisplatin treatments also experience hearing difficulties (also called ototoxicity). Ototoxicity has been observed in up to a third of the people treated with cisplatin and can be manifested in the form of tinnitus (a buzzing, ringing, or whistling in the ears) or hearing loss in the high frequency range,2 and in a few cases, total deafness. This hearing loss results from damage to the sound detecting hair cells in the inner ear. 3 Several other negative side effects are sometimes associated with the use of cisplatin: serum electrolyte disturbances—particularly those involving low levels of magnesium, calcium, sodium, potassium, and phosphates—have been reported and are probably related to renal tubular damage (see nephrotoxicity above). Hyperuricemia (an increase in uric acid) has also been reported. In addition, neurotoxicity (abnormalities with the nervous system) can be a complication; symptoms include muscle cramps, seizures, and a loss of taste. Cases of ocular toxicity, including inflammation of the optic nerve and cerebral blindness, have been reported in rare cases even when cisplatin is administered in the recommended doses. Anaphylactic-like reactions have occasionally been reported in conjunction with the use of cisplatin and can be controlled by injection of epinephrine with corticosteroids and/or antihistamines. Finally, hepatotoxicity, in which liver enzymes are elevated, has also been reported.[2]

1. Quindlen, A. One True Thing; Random House: New York, 1994.
2. Physician's Desk Reference, 50th ed.; Arky, R., Ed. Medical Economics Company: Montvale, NJ, 1996. (3) Rosenberg, B. In Nucleic Acid-Metal Ion Interactions, T. G. Spiro, Ed. John Wiley & Sons, Inc.: New York, 1980, Vol. 1, pp. 1-29.

This page titled 11.3.18: Cisplatin 18. Toxicity is shared under a CC BY-NC-SA 4.0 license and was authored, remixed, and/or curated by ChemCases.

- **Cisplatin 18. Toxicity** by ChemCases is licensed CC BY-NC-SA 4.0.

11.3.19: Cisplatin 19. Cancer

Cancer, a group of diseases in which cell growth spirals out of control, is a killer that moves across race and class lines and has a devastating effect on its victims and their families. While much work remains to be done to understand all the causes of cancer, recent research has shed some light on how cancer develops.

< **face="Arial">Types of Cancer** One of the reasons that the cure for cancer has been so elusive is that cancer is not a single disease but rather a complex set of diseases. One way to classify different types of cancer is to describe the type of affected tissue:

> • ***Carcinomas*** *are the most common cancers (80-90% of cases) and originate in epithelial tissue, which includes the skin and the covering and lining of the organs and internal passageways. Some examples of carcinomas are breast cancer, lung cancer, and colon cancer.*
>
> • ***Sarcomas*** *begin in connective tissue such as bones, tendons, cartilage, muscle, and fat.*
>
> • ***Leukemias*** *encompass all the other types of cancers that do not fit into either of the above two broad categories. Leukemias develop in the bone marrow and lymph systems, which make blood.*[1,2]

< face="Arial">Causes of Cancer Cancer can be either genetic or inherited or both. A genetic disease results from faulty DNA (see the module on DNA). Mutations can occur in genes, causing normal cells to become cancerous. More specifically, a defective gene leading to increased cellular proliferation in one cell can be passed down to a daughter cell; the accumulation of mutations in subsequent generations of daughter cells can cause cells to proliferate even more rapidly and eventually undergo structural changes to become malignant. An inherited disease is caused by a defective gene that is passed from parent to child.[3] Cancer cells are believed to result from at least two genetic mutations, or "hits," to a normal cell. This explains why people with a family history of cancer do not necessarily get cancer themselves. These people may inherit a defective gene through the sperm or egg of their parents, but a second mutation must occur if cancer is to develop. This theory also explains why people with no family history of cancer can get the disease: As long as least two genetic defects occur (from a variety of possible causes), cancer can result. Figure 1 shows how a series of genetic mutations, known as clonal evolution, results in the formation of cancer cells.[3]

> *19fig1.jpg (93893 bytes)*
>
> ***Figure 1. Emergence of a cancer cell from mutations of a normal cell through the process known as clonal evolution. First, one daughter cell (pink) either inherits or acquires a cancer-promoting mutation; this defect is passed on to subsequent generations. Later on, a descendant acquires a second mutation (red), and a later descendant acquires a third (green). Once a cell accumulates enough mutations (purple), the cell can become malignant and cancer can occur. Reprinted with permission.[3]***

When researchers realized that cancer cells were merely normal cells with altered genes, they sought to understand which type of mutations led to cancer. They realized that certain genes are quiescent most of the time but capable of causing cancer if activated; such genes are called **proto-oncogenes**. Activation of proto-oncogenes can occur when certain viruses (called DNA tumor viruses) invade a normal cell. Once the correct mutation has occurred to convert a proto-oncogene into a carcinogenic form (called an **oncogene**), cancer results.[3] Along with activation of normally quiescent proto-oncogenes, cancer can develop as a result of a different type of genetic damage. Sometimes genes

coding for proteins that inhibit cell replication are damaged; the result is that the cell no longer knows when to stop reproducing itself, and cell replication proceeds unchecked. Since these genes halt cell growth, they are known as **tumor suppressors** (see Figure 2).[3]

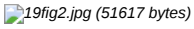


Figure 2. The reproduction of a normal cell occurs in response to stimulation by external growth factors (green). Reproduction is halted by the action of growth-inhibiting factors (red). Abnormal activation of growth factors or inactivation or loss of growth-inhibiting factors can lead to cancer. Reprinted with permission.[3]

Activation of proto-oncogenes to form oncogenes and damage to tumor suppressors are two ways that cancer disrupts the normal cycle of the cell. To understand more fully how cancer operates through the cell cycle, we will examine the cell cycle by looking at their different phases, as well as the regulation of these phases. We will then discuss some of the ways that normal cell growth can go awry and lead to cancer. We will see some specific instances of both oncogenes and tumor suppressors within the cell cycle. The cell cycle (shown in Figure 3) consists of two overall phases: division and interphase. Division comprises both nuclear division (mitosis, or **M**) and cell fission (cytokinesis). Before cell division can occur, the cell must double its mass and duplicate all its contents. This period of growth in the cell cycle is referred to as interphase. Interphase typically makes up 90 percent or more of the total cell cycle time and comprises three phases of the cell cycle: a gap phase (**G1**), in which the cells resume the biosynthetic activity which has been dormant during mitosis; a synthesis phase (**S**), in which the DNA content of the cell is doubled and the chromosomes are replicated; and a second gap phase (**G2**).[2,4,5]

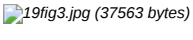


Figure 3. The cell cycle, whose two overall phases are division (including mitosis, or M phase) and interphase (including DNA synthesis, or S phase, as well as two gap phases, G1 and G2). Reprinted with permission.[2]

The levels of certain enzyme proteins regulating the cell cycle rise and fall over the course of the cell cycle; these proteins are called **cyclins**. Cyclins activate proteins called **kinases** (also known as cyclin-dependent protein kinases, or **Cdk proteins**). Cdk proteins must be complexed with their corresponding cyclins in order to act. Cyclins and Cdk proteins work together to help control the progression from one stage of the cell cycle to the next (Figure 4).

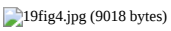


Figure 4. Two key components of the cell cycle. Together they form a complex that causes the cell to progress through its normal cell cycle. Reprinted with permission. [2]

There are two main classes of cyclins: Mitotic cyclins are required for mitosis and bind to Cdk proteins during G2 phase. G1 cyclins bind to Cdk proteins during G1 phase and are required for entry into S phase (see Figure 5).[2] There is mounting evidence that certain cyclins and kinases are directly involved in cancer. Some of the most compelling evidence suggests that cyclin D1, which is a G1 cyclin, is an oncogene. The cyclin D1 gene has been found to cause both benign tumors of the parathyroid gland and B cell lymphoma. In addition, overexpression of the gene for cyclin D1 may contribute to more common cancers, such as cancers of the breast and esophagus. Indeed, studies conducted on cancer patients have shown amplification of the cyclin D1 gene and elevated levels of the cyclin D1 protein in up to a third of cases of esophageal and breast cancer. Experiments done on cell culture have shown that overexpression of the cyclin D1 gene can contribute to tumor production. Furthermore, the cyclin D1 gene has been shown to cooperate

with another oncogene, the *ras* oncogene, to transform normal cells into cancer cells; this result is consistent with the growing body of evidence that several genetic changes are necessary for cancer to occur. In short, the D cyclins are active during a crucial part of the cell cycle, and they signal the cell to enter its synthesis phase. Once a cell has committed to DNA synthesis, it must carry on with the rest of the cell cycle. Cell division can then occur without any external stimulus—one of the hallmarks of cancer.[5] In addition to the D cyclins, cyclins E and A may also play a role in the development of cancer. Cyclin E, another G1 cyclin, is overexpressed in breast cancer cell lines grown in culture, as well as in primary human breast tumors. Moreover, cancer cells have been shown to contain three different varieties of cyclin E protein, whereas normal cells contain only one. Finally, the overexpression of the gene for cyclin A, also a G1 cyclin, allows cells to grow without being anchored to a surface—another classic feature of cancer cells.[5]

> ***Figure 5. The role of specific cyclins and Cdk proteins in the cell cycle. Reprinted with permission.*** [5]

The cell-cycle control system triggers a cascade of events that take time and must be completed before the cell can proceed to the next phase of the cell cycle. If this series of events is not allowed to occur as intended, the cell may mutate or die. To counteract these negative consequences, several feedback controls exist in the cell. An example of a feedback control is a protein called ***p53***, which accumulates in the cell in response to DNA damage and halts the cell cycle in the G1 phase until the damage has been repaired.[2] p53 is believed to act within the cell cycle by blocking the activity of certain kinases—specifically, Cdk2, as well as other Cdks; in this way p53 acts as a tumor suppressor. When the DNA damage has been repaired, p53 no longer exerts its effect, and Cdk2 can again work in conjunction with its cyclin to cause the cell cycle to progress.[5] Mutations in the gene that codes for the p53 protein represent the most common genetic malfunction in human cancers and are present in more than half of all cases of the disease. Apparently, these genetic mutations disable the feedback control and allow the cell cycle to progress with damaged DNA.[2] Cancer appears in many different types of tissue in the body and results from a variety of factors. In general, cancer is a genetic disease; either defective genes are passed from parent to child (in these cases, cancer is inherited as well as genetic), or a mutation occurs as the result of the action of an oncogene. However, more than one mutation is necessary for cancer to develop. Genetic mutations can lead to malfunctioning proteins that wreak havoc on the cell cycle machinery. For example, if proteins necessary for cell division are activated at the wrong time, the cell may start to grow uncontrollably and become cancerous. Furthermore, if proteins that normally tell the cell to stop dividing are inactivated or lost, cell growth may continue beyond what is normal. As more research is done on cancer and its causes are better understood, more methods of treatment can be developed. (see module on other treatments)

1. (1) Murphy, G. P., Morris, L. B., Lange, D. *Informed Decisions: The Complete Book of Cancer Diagnosis, Treatment, and Recovery*. Viking Penguin: New York, 1997.
2. (2) Alberts, B., Bray, D., Lewis, J., Raff, M., Roberts, K., Watson, J. D. *Molecular Biology of the Cell*, 3rd ed.; Garland Publishing, Inc.: New York, 1994.
3. (3) Cavenee, W. K., White, R. L. *Scientific American* ,1995, March, pp. 72-79.
4. (4) Stryer, L. *Biochemistry*, 4th ed. W. H. Freeman and Company: New York, 1995.
5. (5) Marx, J. *Science*, 1994, 263, pp. 319-321.

This page titled 11.3.19: Cisplatin 19. Cancer is shared under a CC BY-NC-SA 4.0 license and was authored, remixed, and/or curated by ChemCases.

11.3.20: Cisplatin 20. Other Treatments for Cancer

Chemotherapy is one of three forms of treatment conventionally used to combat cancer. Surgery and radiation are two other options. In the majority of cases, a combination of at least two of these three types of therapy is used to treat cancer, either as the primary therapy (when cancer first occurs) or as therapy for a recurrent tumor. Combination therapies have been shown to be effective in attaining the three main goals of cancer treatment: removing all of the known tumor, preventing its recurrence, and minimizing negative side effects.[1]

Surgery is used to diagnose or treat most people with cancer. Surgery is a local treatment, meaning that it only affects one part of the body. When surgery is used as a diagnostic aid, a biopsy is done. A biopsy is the removal of a suspicious piece of tissue for microscopic examination. (Biopsies need not involve surgery, but for tumors deep within the body, surgical biopsies give the most definitive results. Biopsies may also be carried out using a needle or an endoscope, which is a lighted, cylinder-shaped magnifying instrument that is narrow enough to pass through one of the body's natural openings.) When surgery is used to treat cancer, the tumor and possibly some of the surrounding tissue is removed. Removal of the tumor at an early stage in the cancer often results in a complete cure.[1]

Radiation is also a local treatment for cancer, and is used to treat 60 percent of cancer patients. Radiation uses x-rays, electron beams, or radioactive isotopes (from naturally occurring radioactive elements such as radium, or from artificially produced radioactive isotopes of nonradioactive elements such as cesium) to shrink tumors either by destroying cancer cells or by damaging them so much that they can no longer multiply. Radiation is an extremely useful cancer treatment because it kills cancer cells while causing only minimal damage to normal cells. (If exposed to radiation, normal tissue is usually able to recover with little or no permanent damage; nonetheless, healthy tissue is shielded from radiation as well as possible.) Radiation works by ionizing atoms in cells, usually atoms in DNA; once a cancer cell's DNA is destroyed, it can no longer undergo replication (see module on DNA), and the cell dies. Radiation is most effective when the cancer cell is actually dividing, that is, when the cancer cell is in the **M** (mitosis) phase of its cell cycle (see module on cancer). Cancers with rapidly dividing cells, such as leukemia (cancer of the blood cells) and lymphoma (cancer of the lymph nodes) are more sensitive to radiation than cancers in which the cells divide more slowly. The effectiveness of radiation is enhanced when it is used in combination with either surgery or chemotherapy. For example, radiation may be used before surgery to shrink the tumor so that it can be more easily removed. Alternatively, radiation may be used after surgery to kill any remaining cancer cells.[1]

Chemotherapy, unlike surgery and radiation, is a systemic treatment because the chemotherapeutic agents enter the bloodstream and are distributed throughout the body; chemotherapy drugs can therefore attack cancer cells wherever they are in the body.

Most people with cancer receive one or more of some 50 available anticancer drugs (among them, cisplatin) during the course of their treatment. Chemotherapy drugs are designed to disrupt the cell cycle of rapidly dividing cells; some drugs target cancer cells when they are dividing, or in the **M** phase of the cell cycle, and other drugs destroy both resting and dividing cells. Unfortunately, chemotherapy drugs also affect rapidly dividing cells of certain normal tissues, such as those found in hair follicles, bone marrow, and the lining of the gastrointestinal tract. Such drug treatment can lead to problems during cancer chemotherapy, such as alopecia (hair loss), myelosuppression (suppression of the bone marrow), and nausea. (See module on toxic side effects). To minimize the occurrence of toxic side effects, two or more chemotherapeutic agents are often used in combination. Again, like radiation, chemotherapy works best on cancers having a high proportion of dividing cells, such as leukemias and lymphomas. Chemotherapy is less effective on cancers characterized by a low proportion of dividing cells, such as solid tumors found in the colon, rectum, lung, and breast. Malignant tumors of the latter type, the solid tumors, are more common and are unfortunately much harder to treat by drugs alone. For this reason, chemotherapy is used in conjunction with either radiation or surgery. When used in combination with radiation, chemotherapy can either render cancer cells more sensitive to radiation or kill cells independently.

Chemotherapy can also be used either before or after surgery; the more common case is to administer chemotherapy drugs after a tumor has been surgically removed in order to destroy cancer cells that may remain near the tumor or that have spread to other parts of the body.[1] In addition to the three conventional approaches to cancer treatment described above, there are a number of new treatments—some that are still being developed and others that are currently undergoing clinical trials.

Two examples of these newer types are therapy are immunotherapy and bone marrow transplants. In **immunotherapy**, which is also referred to as biological therapy or biotherapy, the body's own immune system is used to recognize, attack, and destroy cancer cells. At first, the immune system does not fight cancer cells because the cancer cells are "self" cells and are not recognized as foreign. Activating the immune system to combat cancer requires the use of any of a number of biological response modifiers. Immunotherapy is appealing because the body's own immune system is used to combat cancer. Unfortunately, this form of treatment has many temporary side effects, including fatigue, fever, rashes, and diarrhea. Furthermore, biological therapy does not replace the more conventional forms of treatment, but it is often used in conjunction with surgery and chemotherapy.[1] **Bone marrow transplants**, once used only to treat leukemia and lymphoma, are now used to help people who are undergoing chemotherapy or radiation for other types of cancers, such as breast cancer. Bone marrow transplants are used in two ways: in some cases, the bone marrow of a cancer patient is removed before he or she undergoes chemotherapy or radiation and is replaced after the other treatments are complete. In other cases, bone marrow from a healthy donor is used to replace the depleted bone marrow of a cancer patient. Bone marrow is essential to life because bone marrow tissue (which is found within the cavities of bones) constantly replenishes the blood supply. However, like cancer cells, cells of the bone marrow divide rapidly and are consequently targeted by chemotherapeutic agents. Suppression of the bone marrow (called myelosuppression) is a major side effect of cancer chemotherapy. Furthermore, the amount of radiation needed to kill cancer cells also destroys bone marrow. For these reasons, replacing the bone marrow with healthy cells is critically important for cancer patients undergoing other forms of treatment. Complications of bone marrow transplants include increased chance of infection, veno-occlusive disease (a very serious disease of the liver), rejection of the donor's bone marrow by the recipient, graft versus host disease (in which the white blood cells in the newly transplanted bone marrow recognize the recipient as foreign and attack the recipient's own cells), and pneumonia. Modern medicine can counteract many of these problems, but they do remain risks nonetheless.[1] Finally, several new classes of drugs with novel mechanisms of action also hold promise for the treatment of cancer. Among these are telomerase inhibitors, angiogenic inhibitors, and pro-apoptotic compounds. Telomerase is an enzyme found in cancer cells that allows them to keep growing indefinitely. Telomerase restores short sequences of DNA to the tips of DNA, as shown in Figure 1; these short sequences, or telomeres, are required for DNA replication, which is necessary before cell division can occur. Each time a cell divides, its telomeres shorten. When telomeres get down to a minimum length, the cell stops dividing. The telomerase gene is present in all cells but lies dormant in normal cells, meaning that normal cells will eventually stop proliferating. On the other hand, telomerase is active in cancer cells and allows them to grow indefinitely. The development of **telomerase inhibitors**—compounds that bind to telomerase and halt DNA replication and cell division—should be an effective treatment for cancer and could be used in conjunction with the existing conventional therapies.[2-4]

> ***Figure 1. Telomere replication. This figure shows how telomeres, the repeating G-rich sequences (red) that make up the ends of chromosomes, are formed. Telomere replication requires the action of telomerase (light green), which is a protein–RNA complex that carries an RNA strand (blue) that serves as a template for the formation of the G-rich telomere DNA sequence. After telomere replication, DNA synthesis can continue, and a new DNA strand (dark green) formed. Reprinted with permission.[4]***

Angiogenesis is the process by which a new blood capillary forms by sprouting from an existing small vessel, as shown in Figure 2. When the new capillary encounters and connects with another capillary, blood can circulate. Angiogenesis is important in tumor growth, which is limited by its blood supply. Indeed, if a tumor does not have a direct blood supply, it must depend on the diffusion of nutrients from its surroundings and even then will not grow very big. Thus, it is beneficial for tumors to induce the formation of a capillary network so that nutrients can be supplied directly to the tumor; in this way, tumor cells are said to parasitize the blood vessels of normal cells. Inhibition of this form of angiogenesis should limit tumor growth, and the search for **anti-angiogenic drugs** is an active area in cancer research. Two proteins, angiostatin and endostatin, have been shown to possess anti-angiogenic activity. Converting proteins into effective drugs is challenging, and scientists are now trying to use their knowledge about the way these proteins work to design marketable anti-angiogenic drugs.[2,4]

> ***Figure 2. Angiogenesis. A new blood capillary forms by the sprouting of an endothelial cell from the wall of an existing small vessel; endothelial cells line all blood vessels. (Courtesy of C.C. Speidel) Reprinted with permission.[4]***

Apoptosis, or programmed cell death, is the body's way of ridding itself of old or unnecessary cells, as shown in Figure 3. Normal cells undergo apoptosis in an orderly fashion when the cell shrinks and is absorbed by neighboring cells; in this way, cells are believed to commit suicide. Research has shown that programmed cell death works in a similar way in worms and humans, suggesting that apoptosis is a fundamental property of animal cells. Unlike normal cells, however, cancer cells do not undergo apoptosis but continue to grow unchecked. Drugs able to induce cell suicide, or **proapoptotic compounds**, would be a valuable addition to the arsenal of anticancer agents. There are two possible ways that pro-apoptotic compounds induce cell death: by attacking the cell's main energy source, the

mitochondria, or by destroying the cell's DNA. Researchers in Sweden have found that one of the most abundant proteins in human breast milk, a-lactalbumin, induces apoptosis in cancer cells; they are now trying to understand exactly how this occurs.[2,4,5]

> ***Figure 3. Apoptosis. Normal cell deaths are believed to be suicides that occur in response to signals from within the cell itself. This picture represents apoptotic cell death in the nematode worm C. elegans. Reprinted with permission.[4]***

1. 1) Murphy, G. P., Morris, L. B., Lange, D. *Informed Decisions: The Complete Book of Cancer Diagnosis, Treatment, and Recovery*. Viking Penguin: New York, 1997.
2. (2) Weinberg, R. In an interview on Fresh Air with Terry Gross, National Public Radio, 1999.
3. (3) Menon, S. *Discover*, 1999, 20, pp. 33-34. (4) Alberts, B., Bray, D., Lewis, J., Raff, M., Roberts, K., Watson, J. D. *Molecular Biology of the Cell*, 3rd ed. Garland Publishing, Inc.: New York, 1994. (5) Radetsky, P. *Discover*, 1999, 20, pp. 68-75.

This page titled 11.3.20: Cisplatin 20. Other Treatments for Cancer is shared under a CC BY-NC-SA 4.0 license and was authored, remixed, and/or curated by ChemCases.

SECTION OVERVIEW

11.4: Polymeric Materials and Soft Condensed Matter

An General Chemistry Libretexts Textmap organized around the textbook

Principles of Modern Chemistry

by Oxtoby, Gillis, and Campion

I II III IV V VI VII VIII IX X XI XII XIII XIV XV XVI
XVII XVIII XIX XX XXI XXII XXIII • **Homework Exercises**

Template:HideTOC

A polymer is a large molecule, or macromolecule, composed of many repeated subunits. Because of their broad range of properties, both synthetic and natural polymers play essential and ubiquitous roles in everyday life. Polymers range from familiar synthetic plastics such as polystyrene to natural biopolymers such as DNA and proteins that are fundamental to biological structure and function.

11.4.1: Polymerization Reactions for Synthetic Polymers

11.4.2: Natural Polymers

11.4: Polymeric Materials and Soft Condensed Matter is shared under a CC BY-NC-SA 4.0 license and was authored, remixed, and/or curated by LibreTexts.

11.4.1: Polymerization Reactions for Synthetic Polymers

Prior to the early 1920's, chemists doubted the existence of molecules having molecular weights greater than a few thousand. This limiting view was challenged by Hermann Staudinger, a German chemist with experience in studying natural compounds such as rubber and cellulose. In contrast to the prevailing rationalization of these substances as aggregates of small molecules, Staudinger proposed they were made up of **macromolecules** composed of 10,000 or more atoms. He formulated a **polymeric** structure for rubber, based on a repeating isoprene unit (referred to as a monomer). For his contributions to chemistry, Staudinger received the 1953 Nobel Prize. The terms **polymer** and **monomer** were derived from the Greek roots poly (many), mono (one) and meros (part).

Recognition that polymeric macromolecules make up many important natural materials was followed by the creation of synthetic analogs having a variety of properties. Indeed, applications of these materials as fibers, flexible films, adhesives, resistant paints and tough but light solids have transformed modern society. Some important examples of these substances are discussed in the following sections.

Contributors and Attributions

- William Reusch, Professor Emeritus (Michigan State U.), Virtual Textbook of Organic Chemistry

11.4.1: Polymerization Reactions for Synthetic Polymers is shared under a CC BY-NC-SA 4.0 license and was authored, remixed, and/or curated by LibreTexts.

SECTION OVERVIEW

11.4.2: Natural Polymers

Polymers are long chain, giant organic molecules are assembled from many smaller molecules called monomers. Polymers consist of many repeating monomer units in long chains, sometimes with *branching* or *cross-linking* between the chains.

Template:HideTOC

11.4.2: Natural Polymers is shared under a CC BY-NC-SA 4.0 license and was authored, remixed, and/or curated by LibreTexts.

TABLE OF CONTENTS

Licensing

11.5.1: Monomers and Polymers

- 11.5.1.1: Difunctional Carboxyloids
- 11.5.1.2: Cyclic Carboxyloids
- 11.5.1.3: Olefins
- 11.5.1.4: Cyclic Olefins
- 11.5.1.5: Coordination Polymers
- 11.5.1.6: Supramolecular Assemblies
- 11.5.1.7: Other Polymers
- 11.5.1.8: Polymer Topology
- 11.5.1.E: Solutions for Selected Problems

11.5.2: Synthetic Methods in Polymer Chemistry

- 11.5.2.1: Ziegler-Natta Polymerization
- 11.5.2.2: Solutions to Selected Problems
- 11.5.2.3: Step Growth and Chain Growth
- 11.5.2.4: Cationic Polymerization
- 11.5.2.5: Living Cationic Polymerization
- 11.5.2.6: Anionic Polymerization
- 11.5.2.7: Living Anionic Polymerization
- 11.5.2.8: Ring-Opening Polymerization
- 11.5.2.9: Radical Polymerization
- 11.5.2.10: Living Radical Polymerization- RAFT
- 11.5.2.11: Living Radical Polymerization- ATRP

11.5.3: Kinetics and Thermodynamics of Polymerization

- 11.5.3.1: Thermodynamics of Polymerization
- 11.5.3.2: Kinetics of Step-Growth Polymerization
- 11.5.3.3: Kinetics of Chain Polymerization
- 11.5.3.4: Kinetics of Catalytic Polymerization
- 11.5.3.5: Solutions to Selected Problems

11.5.4: Polymer Properties

- 11.5.4.1: Molecular Weight of Polymers
- 11.5.4.2: Viscosity of Polymers
- 11.5.4.3: Rheology
- 11.5.4.4: Glass Transition
- 11.5.4.5: Crystallinity in Polymers
- 11.5.4.6: Microphase Separation
- 11.5.4.7: Stress-Strain Relationships
- 11.5.4.8: Storage and Loss Modulus

11.5.4.9: Modulus, Temperature, Time
11.5.4.10: Chapter Solutions

Detailed Licensing

Thumbnail: Space-filling model of a section of the polyethylene terephthalate polymer, also known as PET and PETE, a polyester used in most plastic bottles. Color code: Carbon, C (black), Hydrogen, H (white), and Oxygen, O (red). (Public Domain; Jynto).

This page titled 11.5: Polymer Chemistry (Schaller) is shared under a CC BY-NC 3.0 license and was authored, remixed, and/or curated by Chris Schaller via source content that was edited to the style and standards of the LibreTexts platform.

CHAPTER OVERVIEW

Front Matter

Licensing

Licensing

*A detailed breakdown of this resource's licensing can be found in **Back Matter/Detailed Licensing**.*

SECTION OVERVIEW

11.5.1: Monomers and Polymers

11.5.1.1: Difunctional Carboxyloids

11.5.1.2: Cyclic Carboxyloids

11.5.1.3: Olefins

11.5.1.4: Cyclic Olefins

11.5.1.5: Coordination Polymers

11.5.1.6: Supramolecular Assemblies

11.5.1.7: Other Polymers

11.5.1.8: Polymer Topology

11.5.1.E: Solutions for Selected Problems

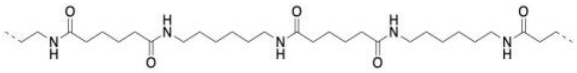
Template:HideTOC

Thumbnail: Space-filling model of a section of the polyethylene terephthalate polymer, also known as PET and PETE, a polyester used in most plastic bottles. Color code: Carbon, C (black), Hydrogen, H (white), and Oxygen, O (red). (Public Domain; Jynto).

This page titled 11.5.1: Monomers and Polymers is shared under a CC BY-NC 3.0 license and was authored, remixed, and/or curated by Chris Schaller via source content that was edited to the style and standards of the LibreTexts platform.

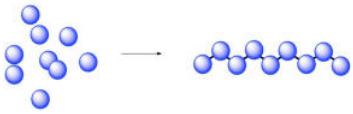
11.5.1.1: Difunctional Carboxyloids

The first synthetic polymer to really seize the public's consciousness -- the first one to change the course of world events -- was nylon. Not long after its discovery in the 1930s, it had supplanted silk as the material of choice for stockings, having transformed a luxury item into a widely available commodity. Nylon came just in time for the Second World War. Soon, parachutes, too, went from being made of silk to being fabricated from nylon.

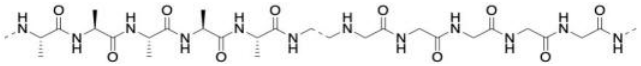


The development of nylon took place at Du Pont's Experimental Research Station in Delaware. For much of the twentieth century, Du Pont and other large companies relied on the pursuit of basic science as an engine of future development. Knowledge was the infrastructure that made future products possible, and so scientists were asked to explore the unknown; the applications of this work would follow naturally.

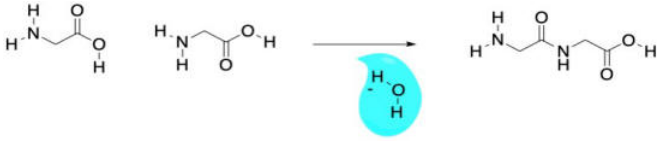
When Wallace Carrothers of Du Pont developed nylon, he had been trying to explore some ideas proposed by Hermann Staudinger at ETH Zurich. These ideas, initially controversial, held that many materials around us, including things like cotton and spider silk, are made of small molecular units covalently bonded to each other. These little molecules, *monomers*, bind together to form immensely long chains. In so doing, the monomers lose their individual identities and simply become repeating units in a long chain. They come together to form *polymers*.



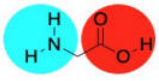
Nylon, in particular, is an example of a *polyamide*. It is composed of very long chains that contain regularly repeating amide bonds, N-C=O. That's the same motif found in proteins in biology, and it's the same pattern found in spider's silk, which is composed of protein.



Conceptually, we are taught in biology class that proteins are made of amino acids. An amide bond (or peptide bond) occurs when the nitrogen of an amine is brought together with the carbon of a carboxylic acid. A molecule of water is lost, and the nitrogen takes the place of the oxygen on the carboxylic acid, forming an amide, instead. The loss of water leads to the term "condensation reaction" because early studies of these reactions led to water forming droplets on laboratory glassware as it bubbled out of the reaction. In practice, industrial nylon production is really no more complicated than that.

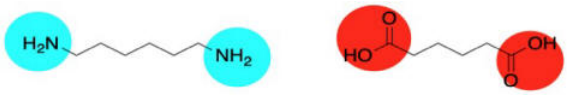


Of course, not just any old amide can become a protein. What makes amino acids special is the fact that they are *difunctional*. They contain not just one functional group (an amine, say, or a carboxylic acid), but two. So, when the amine group of an amino acid bonds with the carbonyl of a neighbour, the carboxyl group can bond to the amine of a different neighbour. It's like it has two hands; it can hold onto a friend with each hand, and each of those friends can hold onto another, and so on, forming a chain.

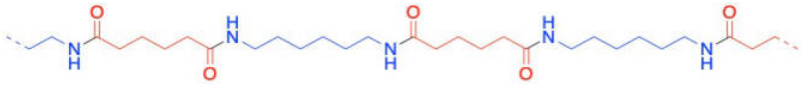


This *functionality* is a key part of how polymers can form. Because difunctional molecules can form bonds in two directions, a simple coupling reaction (an amine plus a carboxylic acid making an amide, two small molecules making another small molecule) becomes a polymerization (many small molecules forming an enormous molecule).

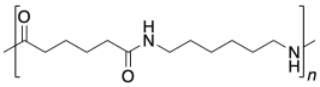
Well, nylon isn't made from an amino acid, although the coupling reaction is similar. Instead, it is made from two different molecules, both of which are difunctional: a diamine and a dicarboxylic acid. The diamine bonds to a neighbouring carbonyl through each end and the dicarboxylic acid bonds to a neighbouring amine through each end. For the most common material, each of the two reactants is six carbons long, giving rise to the term "nylon 66".



Nylon 66 is an example of something called an *alternating co-polymer*. It isn't just one unit repeating over and over along a chain, but two. The two monomers make the polymer together. We sometimes say that the monomers are *enchained* when they become part of a polymer. And of course, they have to alternate along the chain, so that one can bind to the complementary other.



In the drawings above, the dashed lines are meant to suggest continuity: the pattern shown in the drawing keeps repeating to the right and to the left. More commonly, polymers are drawn using parenthetical notation. Below, the part shown in the parentheses is what keeps repeating. If we could make a stamp of that picture, we could construct the polymer chain by simply stamping that image over and over across a sheet of paper.

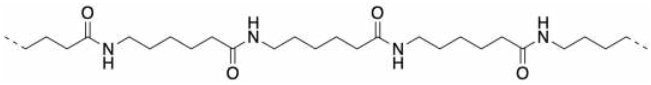


This page titled 11.5.1.1: Difunctional Carboxyloids is shared under a CC BY-NC 3.0 license and was authored, remixed, and/or curated by Chris Schaller via source content that was edited to the style and standards of the LibreTexts platform.

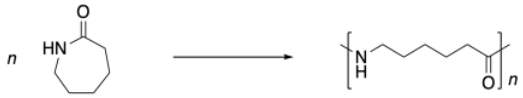
- **1.1: Difunctional Carboxyloids** by Chris Schaller is licensed CC BY-NC 3.0. Original source: https://employees.csbsju.edu/cschaller/Advanced/Polymers/Polycontents.htm.

11.5.1.2: Cyclic Carboxyloids

Carrothers' development of nylon at Du Pont led indirectly to a very similar polymer that was made in a very different way. Across the Atlantic Ocean, Paul Schlack at IG Farben in Germany was looking for a way to make a similar material that would not be subject to Du Pont's patent. His efforts led to a material called perlon, sometimes referred to as nylon 6.



Nylon 6 is not an alternating co-polymer like nylon 66. It's just a polymer. And it isn't made from a difunctional monomer like nylon 66 or proteins. Instead, it's made from a cyclic amide, sometimes called a lactam. To polymerize, the lactam has to break open into a linear form, and the lactam monomers end up enchained head-to-tail. This process is called *ring-opening polymerization*.

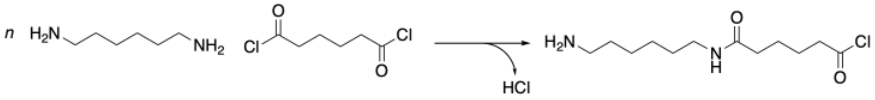


There are a number of things that are different about these two ways of making nylon. One of them turns on the whole concept of synthesis. Synthesis is the act of making things. It's a little like cooking. You gather the ingredients. You take the right amount of this and the right amount of that. You mix them together and you get something wonderful. But that's the difference here: in making nylon 66, Carrothers mixed two different compounds together. He poured one compound out of one bottle and another compound out of another bottle. He mixed them together and he got a polymer.

In contrast, Schlack didn't mix anything together, at least as far as we have seen so far. It all came out of one bottle. So why wasn't it already nylon 6 in the bottle? If the monomers just react with themselves, couldn't they have just gone ahead and done that in the bottle?

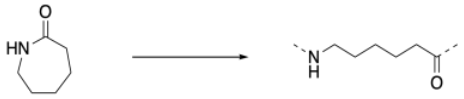
Ring-opening polymerization, at least in this context, is an example of a chain reaction. Chain reactions don't just happen by themselves; they need a jump start.

To understand why, you have to appreciate that these two materials come about through two very different classes of polymerization reactions. Nylon 66 is the product of a condensation reaction. An amine is mixed with a carboxylic acid, water is released, and an amide bond is formed. Even if the pair of reactants is chosen to be more synthetically efficient -- say, an amine and an acid chloride instead of a carboxylic acid -- a condensation reaction still results, in this case releasing hydrogen chloride.



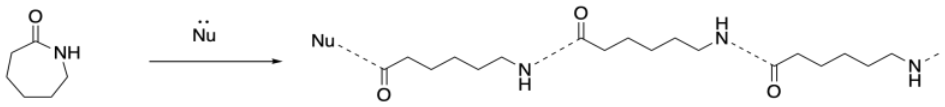
Nylon 6, on the other hand, is not the product of a condensation reaction -- at least at first glance. Look carefully at the monomer and the polymer. Count the atoms. There's nothing missing. No molecule of water or hydrogen chloride or anything else was released. The nitrogen at one end of the chain simply attaches to the carbonyl of the next.

But if you walk down to the end of that chain, until you reach the very last carbonyl, what do you find there? There's no nitrogen attached. That nitrogen was the nucleophile that bound to the carbonyl in the next monomer. There has to be something, though, because the carbon cannot be sitting there with only three bonds. So there must have been some nucleophile that added to that carbonyl, springing loose the amine that added to the next carbonyl, springing the next amine, and so on. There had to be an original nucleophile.

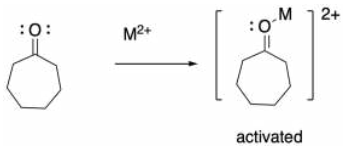


This is the jump start that the chain reaction needed. A nucleophile had to be added to get things going. Once it reacted with the first monomer, the amine became the nucleophile for the next monomer, and that ring-opening produced another amine nucleophile, and so on. Because there is always a new nucleophile produced when the next ring opens, the reaction just keeps

going. That first nucleophile, the one that got everything started, is called an *initiator*. The need for an initiator is a hallmark of chain reactions.



In addition to the initiator, ring-opening polymerizations frequently employ catalysts to accelerate the reaction, just as in some condensation polymerizations. The catalyst may be a Lewis acid that activates the carbonyl or an "organocatalyst" that does the same thing via hydrogen bonding. Both catalytic approaches can also make use of nucleophilic catalysis. In that case, the nucleophilicity of the nucleophile may be enhanced, or else a temporary nucleophile may add to the carbonyl until it is replaced by the nucleophilic group resulting in enchainment.



Other polyamides can also be made by ring-opening cyclic amides. The same approach is also used to prepare polyesters from cyclic esters, also called lactones. In that case, the reaction is sometimes called *ring-opening trans-esterification polymerization*, or *ROTEP* for short.

This page titled 11.5.1.2: Cyclic Carboxyloids is shared under a CC BY-NC 3.0 license and was authored, remixed, and/or curated by Chris Schaller via source content that was edited to the style and standards of the LibreTexts platform.

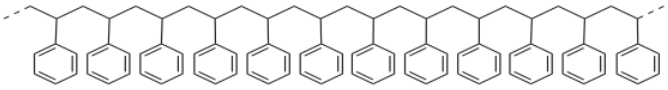
- **1.2: Cyclic Carboxyloids** by Chris Schaller is licensed CC BY-NC 3.0. Original source: https://employees.csbsju.edu/cschaller/Advanced/Polymers/Polycontents.htm.

11.5.1.3: Olefins

Polyolefins are made from "olefins", which you may know as alkenes. Olefin is an older term for an alkene that is still commonly used in the industry.

These compounds make up a significant fraction of commercially-used polymers today. If you think of the common recyclable plastics, polyethylene (#2 and #4, depending on how the material is made), poly(vinyl chloride) (#3), polypropylene (#5) and polystyrene (#6) are all examples of polyolefins.

Polyolefins have been known for some time, although it took about a century from the time that they were first documented until they were recognized as polymers. German chemists in the mid-1800s were aware that certain tree resins gave rise to hard materials over time, and these materials included polystyrene.



If you compare the repeating structure of polystyrene to the structure of styrene, you can imagine that polystyrene is made from a series of styrene molecules that have been strung together. Essentially, the double bond of styrene has moved to attach to the next molecule, and the double bond there has done the same thing, and so on.



Polyolefins are formed in the same way from a wide variety of alkenes, leading to an array of different materials with properties that are suited to unique applications.

Note that, like ring-opening polymerization, olefin polymerization depends on molecules reacting with other molecules that are just like them. That isn't likely to happen; they will need something to come along and induce reaction between them. Olefin polymerization is thus another case in which monomers are tied together through a chain reaction. The reaction will require an initiator to get things started. That initiator is likely to become an end group, hanging from one end of the polymer chain or the other.

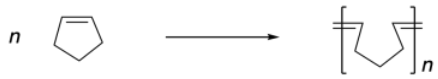
This page titled 11.5.1.3: Olefins is shared under a CC BY-NC 3.0 license and was authored, remixed, and/or curated by Chris Schaller via source content that was edited to the style and standards of the LibreTexts platform.

- **1.3: Olefins** by Chris Schaller is licensed CC BY-NC 3.0. Original source: https://employees.csbsju.edu/cschaller/Advanced/Polymers/Polycontents.htm.

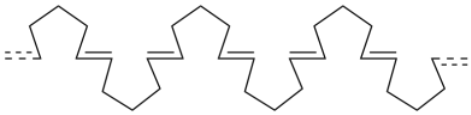
11.5.1.4: Cyclic Olefins

Polyolefins are usually made from olefins by tethering one alkene unit to the next, trading in a pi bond within a monomer for a single bond between two repeat units. However, there is another approach that converts cyclic alkenes into polymers. This approach is reminiscent of the ring-opening of cyclic esters and amides.

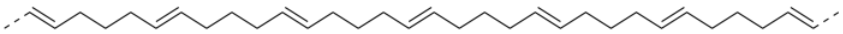
For example, imagine a cyclopentene ring opening up at the double bond and reaching out to join with other rings on either side of it.



A series of cyclopentene rings that joined together in a row would look something like this:



We would probably draw it in the usual zig-zag conformation.



This act of taking a cyclic alkene, splitting open its double bond, and knitting it together with other such alkenes in a long chain is called *ring-opening metathesis polymerization*. Sometimes it is called *ROMP* for short. It has some things in common with other ring-opening polymerizations, such as ROTEP. In both ROTEP and ROMP, like molecules react together to form a polymer. In ROTEP, it would be two cyclic esters. In ROMP, it would be two cyclic alkenes. That was different from condensation polymerization, which required two complementary molecules, such as a difunctional amine and a difunctional acid chloride.

Partly as a consequence of like molecules reacting together, ROTEP and ROMP are both chain reactions. In order to get the molecules to react with themselves, they need an initiator. The initiator jump-starts the reaction.

Other olefin polymerizations followed this pattern as well. Alkenes don't normally react together (there are some circumstances when they will, but we needn't get into that now, as those events don't usually have anything to do with polymerization). Olefin polymerizations, in general, go through chain reactions that require an initiator to get started.

Despite these similarities, ROTEP and ROMP reactions are actually quite different in how they occur, as are regular olefin polymerizations, and the conditions required to initiate polymerization are unique to each case. ROMP requires something called an olefin metathesis catalyst. An olefin metathesis catalyst is a transition metal compound that is capable of splitting the double bond of an alkene in half and putting the two pieces together with other alkenes. The key part of an olefin metathesis catalyst is a metal-carbon double bond. That is the group that is capable of switching the ends of alkenes around with different partners.

This page titled 11.5.1.4: Cyclic Olefins is shared under a CC BY-NC 3.0 license and was authored, remixed, and/or curated by Chris Schaller via source content that was edited to the style and standards of the LibreTexts platform.

- **1.4: Cyclic Olefins** by Chris Schaller is licensed CC BY-NC 3.0. Original source: https://employees.csbsju.edu/cschaller/Advanced/Polymers/Polycontents.htm.

11.5.1.5: Coordination Polymers

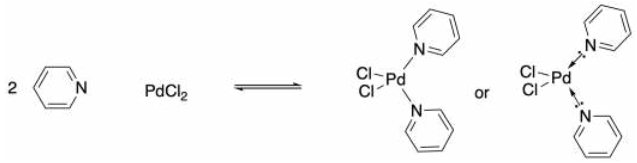
Polymers are long-chain molecules formed from individual molecular building blocks. Typically, the building blocks are organic molecules held together via covalent bonds. What other kinds of building blocks are available?

The formation of coordination compounds is one of many important aspects of inorganic chemistry. In a coordination compound, an electron pair donor, called a ligand, shares its electron pair with a metal atom. Frequently, the metal atom is a transition metal, and very commonly it is a transition metal ion, but there are other examples as well.

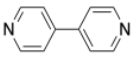
For example, the nitrogen in a pyridine ring has a lone pair. Pyridine can act as a ligand if its lone pair is shared with a metal center, such as the vanadium in trichloro(oxo)vanadium. The lone pair becomes a nitrogen-vanadium bond. Sometimes, this bond is drawn as a short arrow from the lone pair to the vanadium, emphasizing its origin, but more often it is simply drawn as a line, like any other bond.



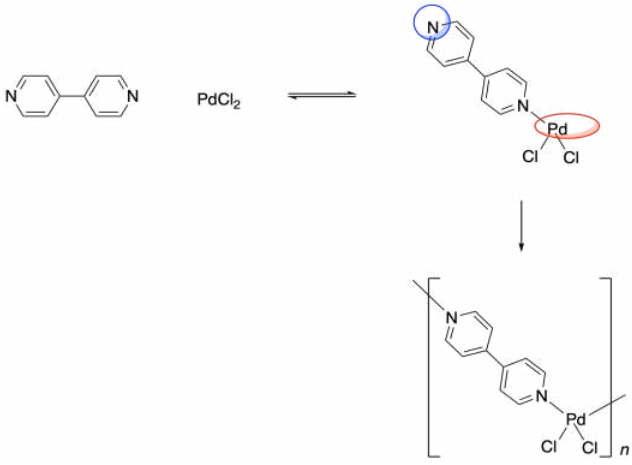
One of the interesting things about metal atoms is their capacity to form variable numbers of bonds. Although palladium dichloride could form a coordination complex by binding with one pyridine ligand, it can also do so with two pyridines. In the former case, it would form a three-coordinate complex, but the latter case would lead to a four-coordinate palladium compound.



Remember, the ability to bond with two neighbouring groups, rather than just one, is an important feature that can allow a small molecule to become enchained in a polymer. The palladium here is a link in a chain that is three units long. What if the ligand also had this capacity to bind to two things? What if, instead of pyridine, the ligand were 4,4'-bipyridine?



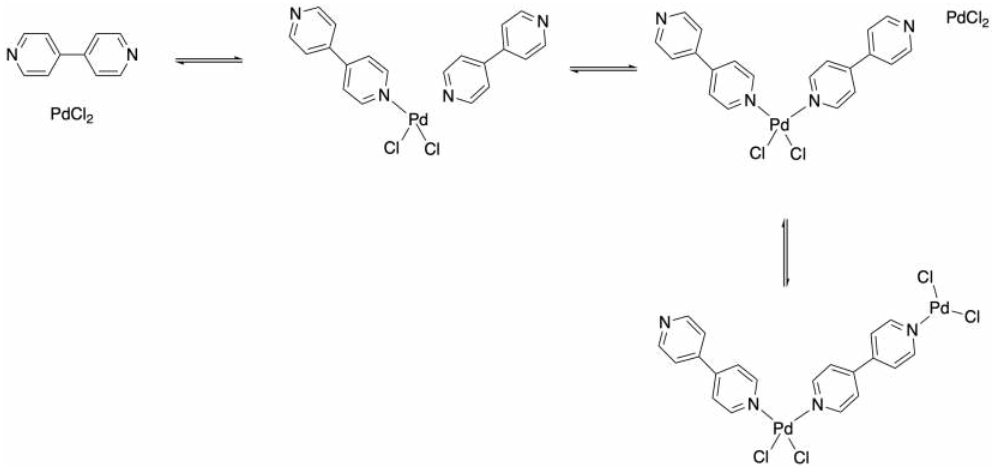
That molecule could bind a palladium atom on either end. Once a bpy (that's an abbreviation for bipyridine, pronounced "bippy") bound to a palladium atom, it would still have a second nitrogen lone pair that it could use to bind another. The palladium, too, would be free to bind a second bpy. As a result, these two monomeric units are able to form an alternating chain.



Why would people want to do that? The general idea is to exploit the properties of these metal atoms in new ways. What are metals good at? They are good at conducting electricity, and sometimes they hold useful magnetic properties. If these properties can be

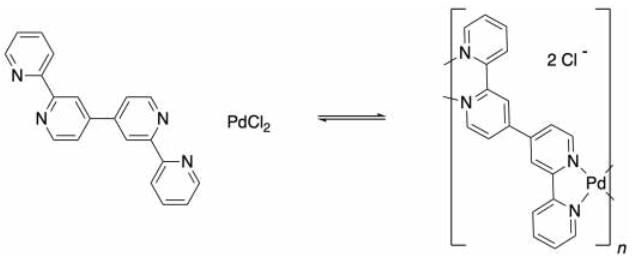
incorporated into a material that is more like organic polymers, which tend to be inexpensive and very lightweight, then maybe they can be used to make materials that will have all sorts of applications in everyday life. Metals are also very good catalysts for a wide range of reactions. A coordination polymer serves to space metal atoms out evenly within a structure that has a lot of surface area, which could promote catalytic efficiency. All of these potential uses have driven a great deal of research into coordination polymers in recent years (as well as related "metal-organic frameworks").

Now, can all of the bonds along this metal-ligand chain really hold together to form a polymer? One key difference between the covalent bonds you have seen in organic polymers and the dative bonds here is that dative bonds are reversible. There is always an equilibrium between the metal-ligand complex and the free metal and ligand. Of course, this bond might be very strong, in which case the equilibrium lies toward the metal-ligand complex. In other words, a large fraction of the material would form the metal-ligand complex. How large a fraction? The real value isn't that important at the moment. For our purposes, let's just say we put a metal and a ligand together and 90% of the molecules form a complex. And suppose that's also true in the next step, bringing another ligand into the picture to bind to the metal, and in the step after that, bringing another metal in to bind to the other end of one of the ligands, and so on. So, suppose each of these events leads to 90% product formation.



Just getting to that four-unit chain relies on three different equilibria. If, as we say, each step proceeds about 90% of the way (which sounds pretty good; you would be happy with a 90% yield on a reaction in the lab), then the entire three-step process would yield 0.90 x 0.90 x 0.90 = 0.73, or 73% product. Not bad. But useful polymer chains might be a thousand units long or more, in which case the amount of polymer actually formed of the proper chain length would be about $(0.90)^{999}$ = 1.94 x 10^{-46} or 1.94 x 10^{-44} %, and that's a ridiculously small amount.

Now, a real calculation of the equilibrium concentration is of course more sophisticated than that, but this quick exercise underscores an important point: in order to form a stable coordination polymer of an appreciable length, the metal must bind the ligand very tightly. For that reason, many approaches to coordination polymers have employed multidentate ligands, which of course bind more tightly than monodentate ligands. For example, the polymer formed using the bidentate binding shown below would be much more stable with respect to depolymerization (i.e. falling apart into monomers again) than the monodentate example shown earlier.



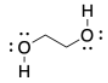
This page titled 11.5.1.5: Coordination Polymers is shared under a CC BY-NC 3.0 license and was authored, remixed, and/or curated by Chris Schaller via source content that was edited to the style and standards of the LibreTexts platform.

- **1.5: Coordination Polymers** by Chris Schaller is licensed CC BY-NC 3.0. Original source: https://employees.csbsju.edu/cschaller/Advanced/Polymers/Polycontents.htm.

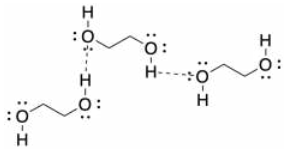
11.5.1.6: Supramolecular Assemblies

So far, we have seen how covalent bonds can be used to bind monomers together into longer chains, forming polymers. There has also been a great deal of interest recently in using intermolecular attractions to make similar structures. Of course, intermolecular attractions are very important in forming large, organized structures in biology. Think about the twin helices held together in DNA, or the secondary and higher-order structures in proteins. Clearly, intermolecular attractions can be used to form large, stable structures.

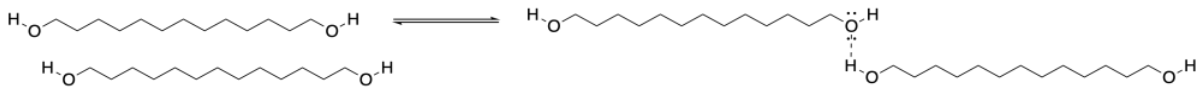
If the goal is to form a chain, analogous to the chains of monomers we have seen in other polymers, then it would be useful to have two sites within a monomer that can interact with other monomers. Such a molecule would be able to hold hands with two other partners, so to speak. If we take hydrogen bonding as an example of a strong intermolecular force, then we can look at a molecule such as ethylene glycol (also called 1,2-dihydroxyethane).



Ethylene glycol looks kind of like ethanol (CH_3CH_2OH) with an extra OH group. A physical sample of ethylene glycol is a colorless liquid, just like ethanol, but there are noticeable differences between the two. The boiling point of ethylene glycol is around 198°C, which is over a hundred degrees higher than that of ethanol. Furthermore, ethanol isn't very viscous; it pours quite easily, but if you tried to stir or pour ethylene glycol you would notice that it seems much thicker. Something is holding those ethylene glycol molecules very tightly together. It isn't hard to imagine the formation of chain structures involving groups of these molecules.

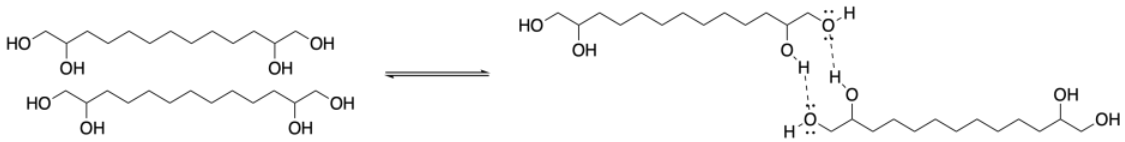


If we look at diols containing longer carbon chains, it's even easier to imagine something that looks kind of like a polymer, with monomers enchained together via hydrogen bonding interactions.



Hydrogen bonds are strong, but they are still just intermolecular attractions, rather than true covalent bonds. They are readily reversible, so any chains that formed via interaction between these diols could depolymerize very easily. Individual diols could readily fall of the end of the chain, and diol chains could just as easily break somewhere in the middle.

What about a tetraol? If there were two hydroxy groups at either end of the chain, then the chain would be much less likely to come apart. Even if one hydrogen bond broke at one of the linkages, there would still be a second one holding two neighbors together. A molecule like that could form a much more stable supramolecular assembly.



The dynamic nature of supramolecular assemblies is part of what makes them so interesting to researchers. Stable structures that can easily form under one set of circumstances, but gently come apart under another, could have lots of applications. For example, some researchers are interested in developing novel materials, such as liquid crystals, that might be converted from one form into another using different stimuli. Others are trying to develop materials that have useful medicinal and therapeutic applications.

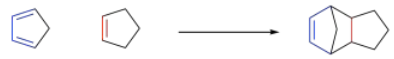
This page titled 11.5.1.6: Supramolecular Assemblies is shared under a CC BY-NC 3.0 license and was authored, remixed, and/or curated by Chris Schaller via source content that was edited to the style and standards of the LibreTexts platform.

- **1.6: Supramolecular Assemblies** by Chris Schaller is licensed CC BY-NC 3.0. Original source: https://employees.csbsju.edu/cschaller/Advanced/Polymers/Polycontents.htm.

11.5.1.7: Other Polymers

The principle of functionality means that almost any type of organic reaction could potentially be used to make polymers. For instance, if a compound has two functional groups of the same kind, it could undergo reaction at two different sites, forming new bonds with two neighbors. The compound thereby becomes enchained in a trio of formerly independent molecules. If the neighboring molecules are also difunctional, then this pattern can repeat, forming a polymer.

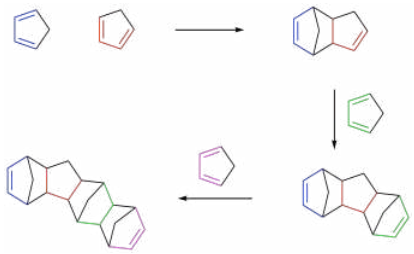
Take the Diels Alder reaction as an illustrative example. On paper, the reaction is fairly straightforward, even if it isn't all that common. A molecule with a pair of conjugated alkenes, the diene, cyclizes with another alkene, the dienophile, to form a new six-membered ring, a cyclohexene.



The diene needs two double bonds but the dienophile only needs one. Nevertheless, what happens if the dienophile has an extra double bond? The Diels Alder adduct that forms would end up with two double bonds: one formed from the original diene, as always, and the other leftover from the dienophile.



The resulting compound is a difunctional alkene. Each end of this molecule could potentially undergo another Diels Alder reaction with an additional diene. Each time that reaction occurs, a new alkene is left behind where the diene used to be, preserving that difunctionality for another step. That difunctionality forms the basis for potential polymer chemistry.



In fact, Diels Alder reactions have been exploited by researchers in a number of ways to make materials with useful properties. The fact that six-membered rings are introduced along the backbone, rather than a chain of single bonds, means that these materials display varying levels of conformational rigidity, resulting in some unique properties.

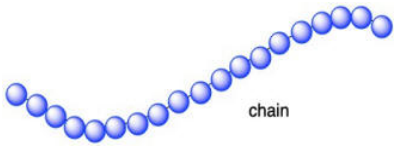
This page titled 11.5.1.7: Other Polymers is shared under a CC BY-NC 3.0 license and was authored, remixed, and/or curated by Chris Schaller via source content that was edited to the style and standards of the LibreTexts platform.

- **1.7: Other Polymers** by Chris Schaller is licensed CC BY-NC 3.0. Original source: https://employees.csbsju.edu/cschaller/Advanced/Polymers/Polycontents.htm.

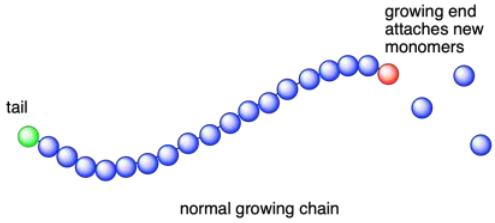
11.5.1.8: Polymer Topology

Polymers are very large molecules made from smaller ones. How those smaller units are arranged within the polymer is an issue we haven't addressed very closely yet. Topology is the study of three-dimensional shapes and relationships, or of how individual parts are arranged within a whole. Let's take a look at the topology of polymers.

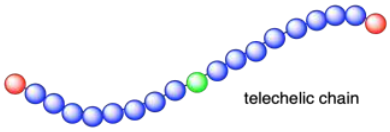
At the simplest level, we have been thinking of polymers as chains of monomers strung together like beads on a string. We even use the verb "enchain" to describe the act of taking a monomer and tying it into a larger polymer. The chain is the most basic of polymer structures. This topology is often referred to simply as a chain or, to underscore the structure, a linear polymer.



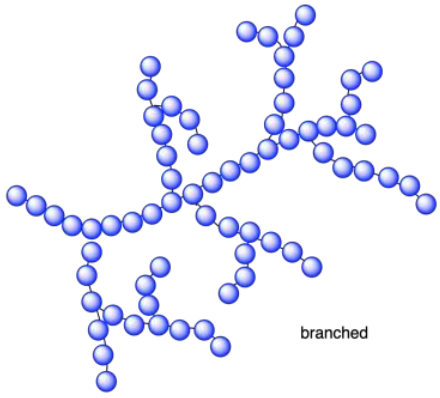
Even a simple chain, in this context, can have additional structural features worth considering. These features are connected to how a polymer chain grows up from individual monomers. If the polymer results from a chain reaction, typically used for the polymerization of alkenes, then the growing chain usually has two distinct ends. One end, sometimes called the tail, is the site of the first monomer to be incorporated into the polymer, as well as some remnant of the initiator to begin the polymerization process. The other end, sometimes called the head but more commonly just the growing end, is the active site, the place where new monomers are about to be enchained into the polymer.



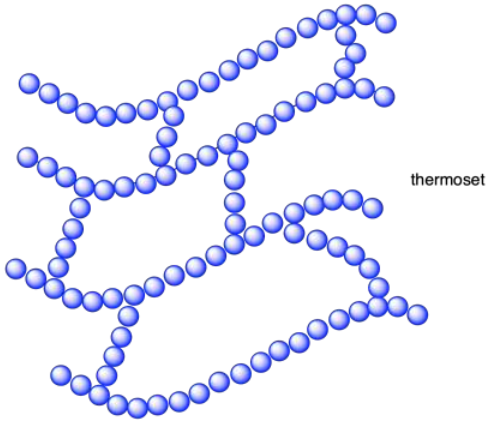
That's what happens in most cases when the initiator is capable of reacting with one monomer and starting the chain reaction. However, sometimes initiators are difunctional. Difunctional initiators are capable of getting two monomers to start growing a polymer chain: one in each direction. In that case, the initiator fragment is left behind in the middle of this new growing chain, which grows outward from the middles. Both ends of the chain are growing ends. In this type of growth, the chain is referred to as "telechelic".



Sometimes, polymer chains do not have simple, linear structures. Instead, their chains branch out here and there. This topology is called "branched". Instead of looking like a snake or a piece of spaghetti, this structure looks more like a length of seaweed. Branching is sometimes an artifact of how the polymer was made, and so sometimes the same monomers may lead to a more linear polymer or a more branched one. The prime example if polyethylene, which can form high-density polyethylene (HDPE) or low-density polyethylene (LDPE) depending on the conditions under which the ethylene is enchained.



In a branched polymer, smaller chains grow out like limbs along a tree trunk or leaves along a stem. We can take that arrangement a step further into something that looks more like a net. In what we call a crosslinked structure, branches connect one main chain to the next, tying them together into one big piece. Sometimes, this type of structure is called a thermoset.



The word "thermoset" is really a description of a physical property of a polymer, in contrast to "thermoplastic". A thermoplastic is a polymer that can be melted and reformed into new shapes after polymerization. In contrast, once a thermoset has been polymerized, it retains its shape even when heated; it doesn't melt. These terms have connotations about the topology of the material, nonetheless.

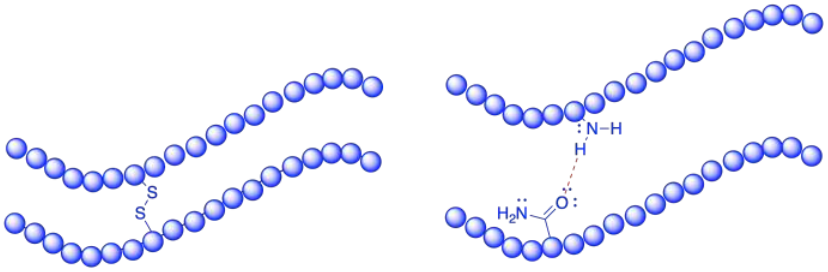
The reason thermoplastics can be melted and formed into new shapes is that they are made of separate molecules. The molecules may be very long, and they may even be branched, but at high enough temperatures these molecules can move completely independently of each other. They can melt and so the material that is comprised of these separate molecules take on new shapes.

In a thermoset, crosslinks connect the different chains in the material, forming bridges that span from chain to chain to chain, essentially uniting the material into one big molecule. If it is one big molecule, the chains can never move completely independently of each other, and the material cannot form a new shape. Looked at in another way, those crosslinks tie the main chains in place. They may be able to move around some, but they can never get very far. If the amount of crosslinking is sufficient, they will always hold the material in the same basic shape.

Of course, just a little bit of crosslinking may not have the same effect. You may have two or three chains tied together to form one big molecule, but they behave more like highly branched chains than like extended nets.

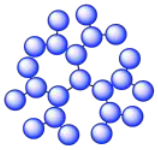
It's also worth noting that the term "crosslink" can actually mean different things when used in different ways. Sometimes, crosslinks refer to true covalent bonds connecting two chains together. These connections are called "chemical crosslinks"; the word chemical refers to the covalent bonds. Alternatively, chains can be connected to each other through strong intermolecular forces. That's not at all the same thing, of course, because these intermolecular forces can be overcome with sufficient energy, and so at some point, the chains may no longer be tied together. These connections are called "physical crosslinks" to distinguish them from permanent bonds.

To use a biology analogy, sulfide bonds in proteins would be an example of chemical crosslinks; they hold the protein firmly in one shape, and a chemical reaction is required to break that connection. The ordinary hydrogen bonds that are so prevalent in the protein are physical crosslinks. Because they can be overcome by adding heat, proteins are very sensitive to temperature.



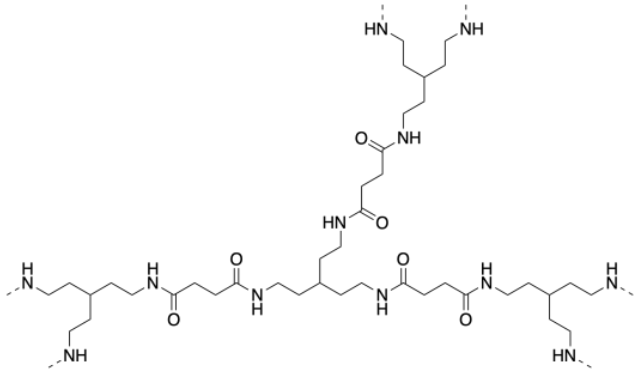
chemical crosslink physical crosslink

Dendrimers are another type of branched structure; the term comes from the Greek *dendron* or tree. Dendrimers differ from regular branched polymers in that they have a much more regular branching pattern. A dendrimer will actually grow outward from the center, branching out at regular intervals.

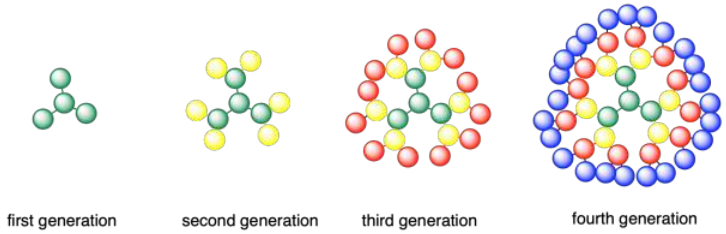


dendrimer

Many dendrimers are polyamides, although there are other types as well. Generally, at least one of the monomers is trifunctional, which introduces the branching in a predictable way.



As dendrimers grow outward, layer by layer, they are often described in terms of generations. Suppose you start with a trifunctional monomer in the middle. That's generation 0. If the monomer is polymerized outward until there is another set of trifunctional monomers attached on the edge, we have a first generation dendrimer. If we keep going and add another layer of trifunctional monomers, we have a second generation dendrimer, and so on.

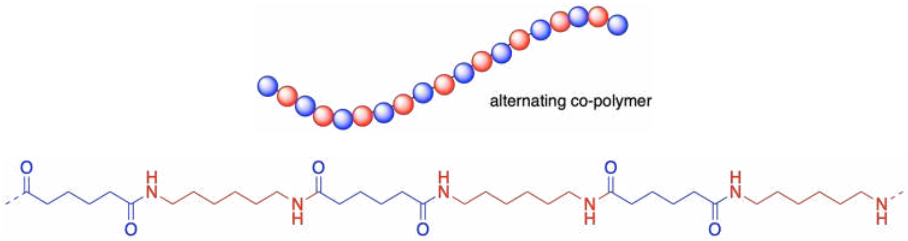


first generation second generation third generation fourth generation

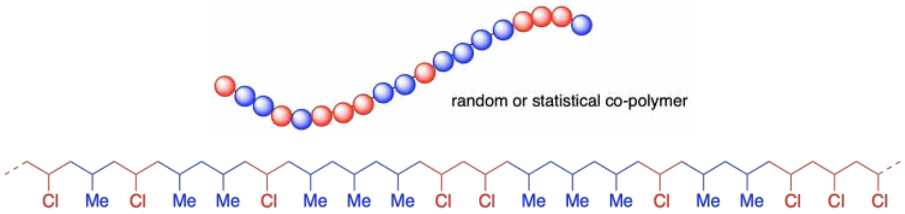
These dendrimers start to look circular on paper, like pancakes, but steric interactions between the groups forces things into three dimensions. As a result, dendrimers are roughly spherical in shape.

In some of the examples of polymers we have seen, the chain is actually composed of two different monomers. That's true in the case of polyamides such as nylon-6,6. In that example, the chain is composed of difunctional amines alternating with difunctional

carboxyloids (such as carboxylic acids or acid chlorides). We can think of a polymer like that as being composed of two different monomers. Of course, because of their complementary reactivity they have to alternate: an amine and then a carboxyloid, to form an amide, and so on. We can think of these polymers as "co-polymers", meaning they are formed from more than one kind of monomer. We can go further and say that they are "alternating co-polymers" because the two different monomers alternate with each other along the chain.

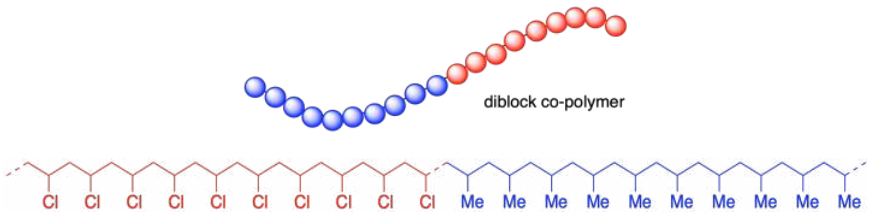


In some cases, there is no need for the two different monomers to alternate the way they do in nylon-6,6. If you take a mixture of alkenes that are capable of forming polymers and you polymerize them together, you may well get them randomly enchained into a growing polymer. This arrangement is called a "random co-polymer" or sometimes a "statistical co-polymer". For example, maybe you manage to get a random sequence of propene and vinyl chloride units along with the polymer.



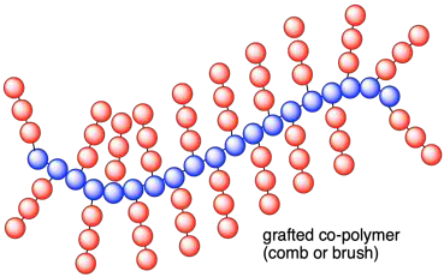
Notice that in the above example we still have the same zig-zag main chain in the polymer; all that changes between one monomer and the other is the group attached to that main chain. It is sometimes useful to think about this main chain or "backbone" separately from the attached or "pendant groups". In this case, we have what looks like a polyethylene backbone with pendant chlorides or methyls randomly attached.

A random arrangement isn't the only possibility. Maybe all of the vinyl chlorides polymerized in a row, and then all of the propenes were incorporated after them. The result would be a diblock co-polymer; there is a solid block of poly(vinyl chloride) at one end of the chain and a solid block of polypropylene at the other end.



There are a couple of ways that could happen. Maybe you waited until all of the vinyl chlorides were enchained before adding any propene so that all of the vinyl chlorides were enchained at the tail end and the propenes were added at the growing end later. Alternatively, maybe you added them all at once but the vinyl chlorides just underwent polymerization a whole lot faster than the propenes; the vinyl chlorides all became enchained before the propenes had a chance.

Those possibilities assume that the monomers are all enchained linearly. There are other possibilities. Maybe one set of monomers form the polymer backbone and the other set form pendant branches along the chain. That arrangement is called a "graft co-polymer", as though we have little apple trees grafted onto the trunk of another breed.

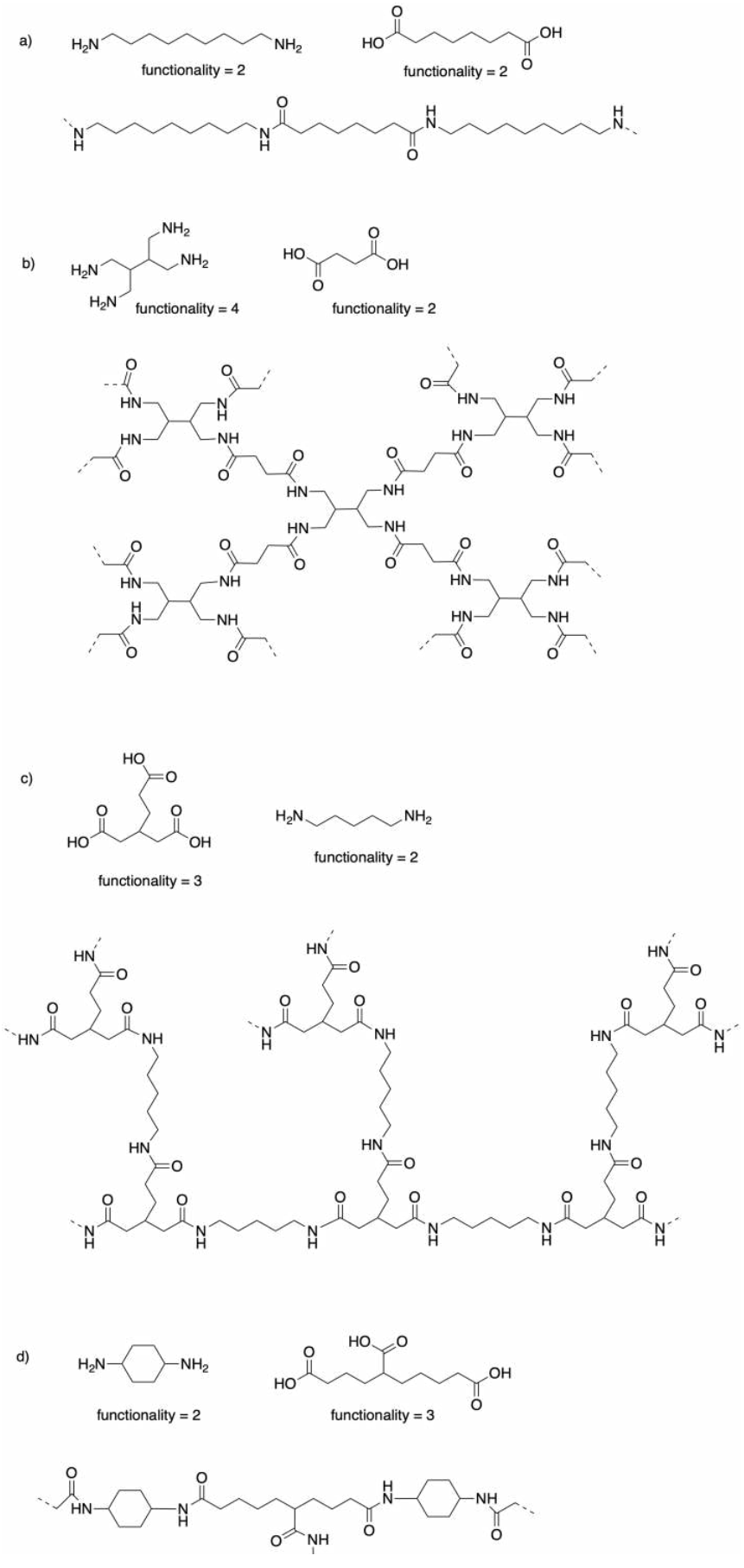


This page titled 11.5.1.8: Polymer Topology is shared under a CC BY-NC 3.0 license and was authored, remixed, and/or curated by Chris Schaller via source content that was edited to the style and standards of the LibreTexts platform.

- **1.8: Polymer Topology** by Chris Schaller is licensed CC BY-NC 3.0. Original source: https://employees.csbsju.edu/cschaller/Advanced/Polymers/Polycontents.htm.

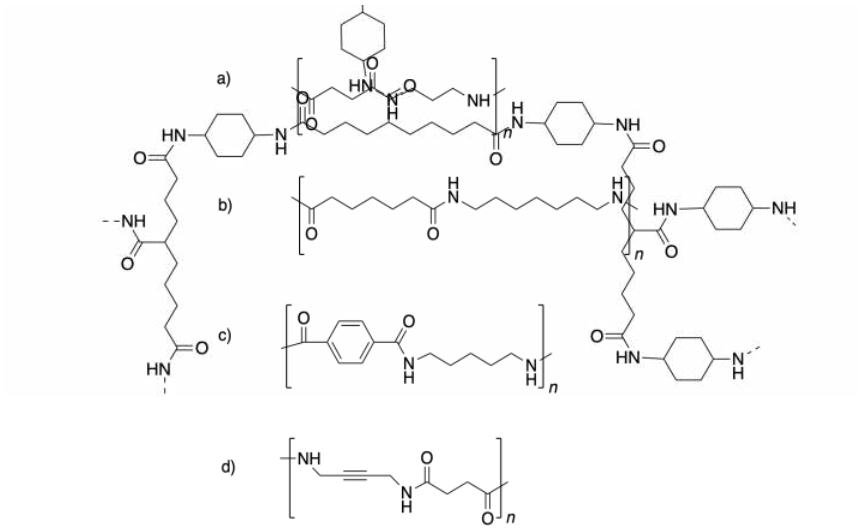
11.5.1.E: Solutions for Selected Problems

Problem MP1.1.

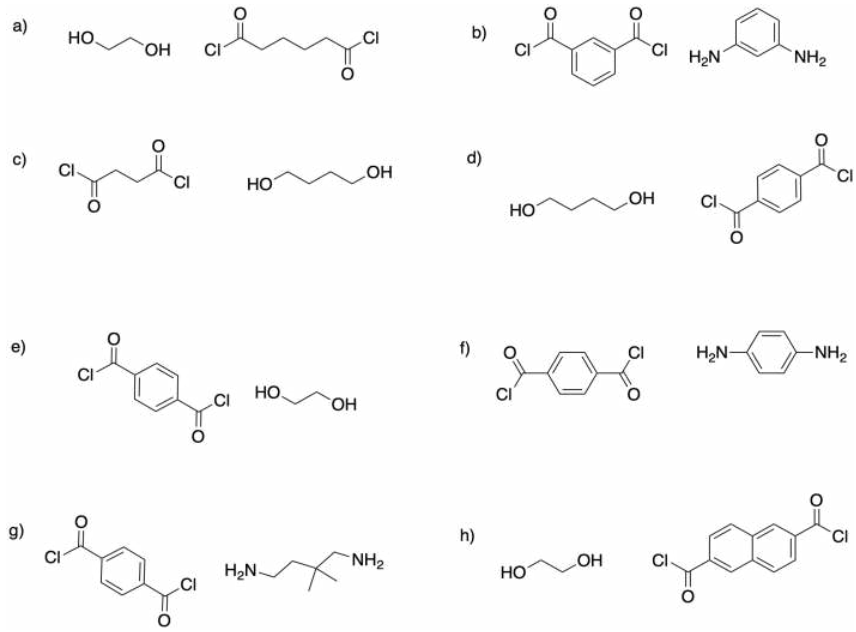


https://chem.libretexts.org/@go/page/438134

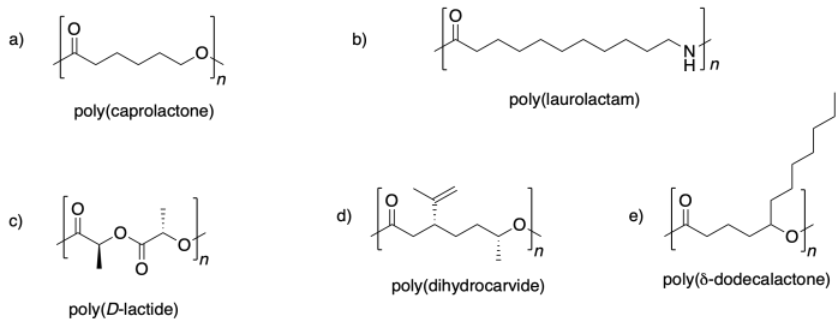
Problem MP1.2.



Problem MP1.3.

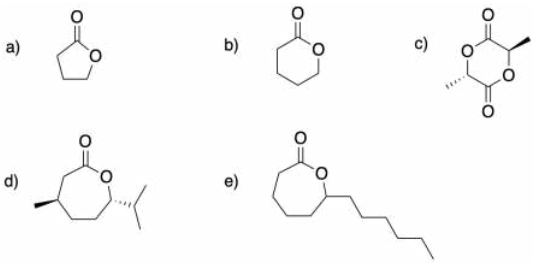


Problem MP2.1.

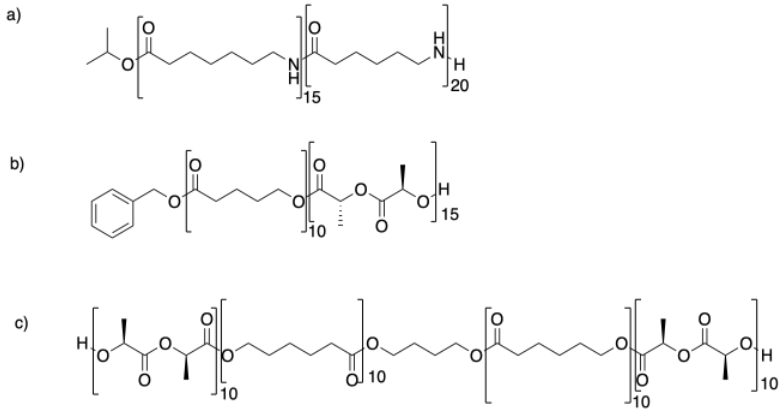


Problem MP2.2.

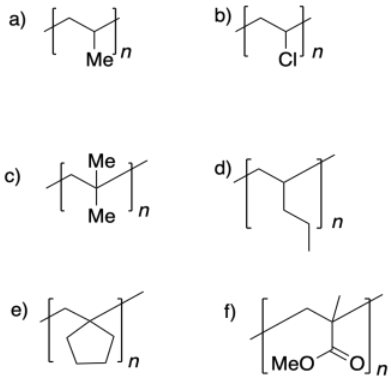
https://chem.libretexts.org/@go/page/438134



Problem MP2.3.



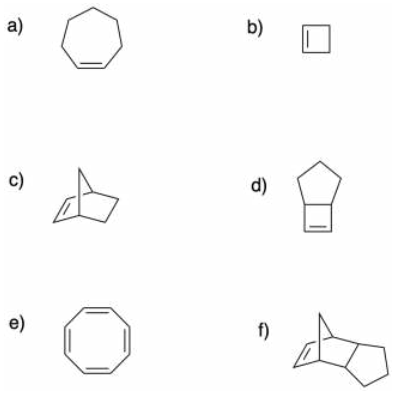
Problem MP3.1.



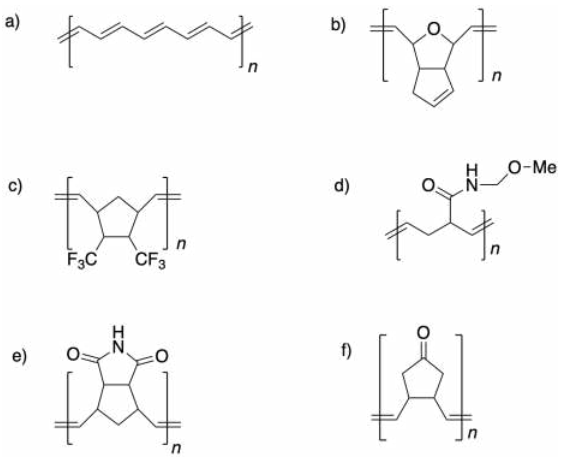
Problem MP3.2.



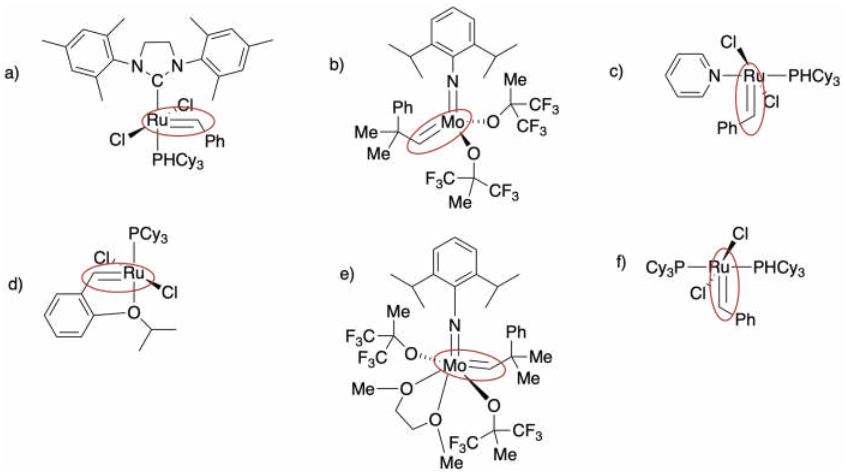
Problem MP4.1.



Problem MP4.2.

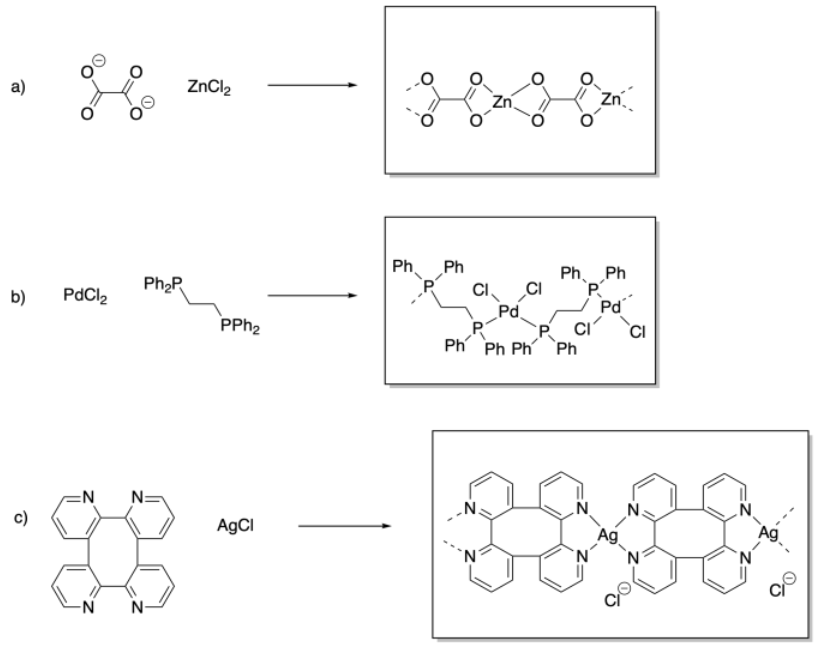


Problem MP4.3.

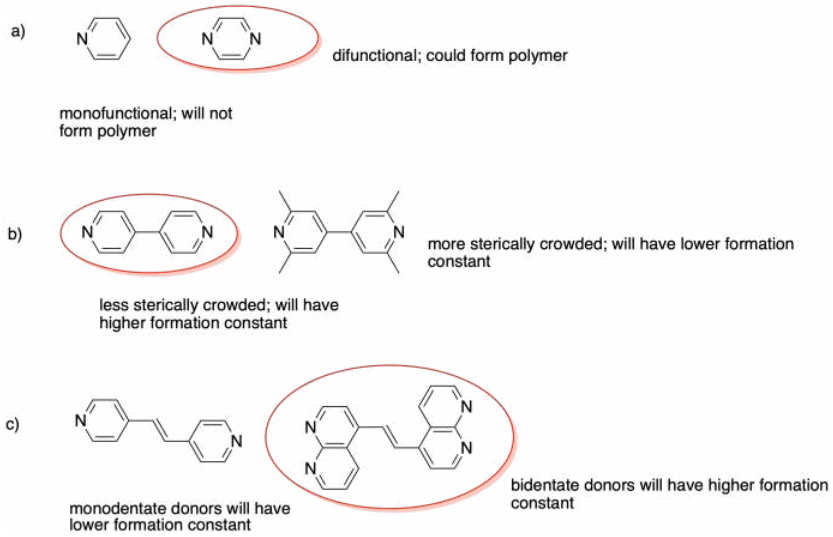


Problem MP5.1.

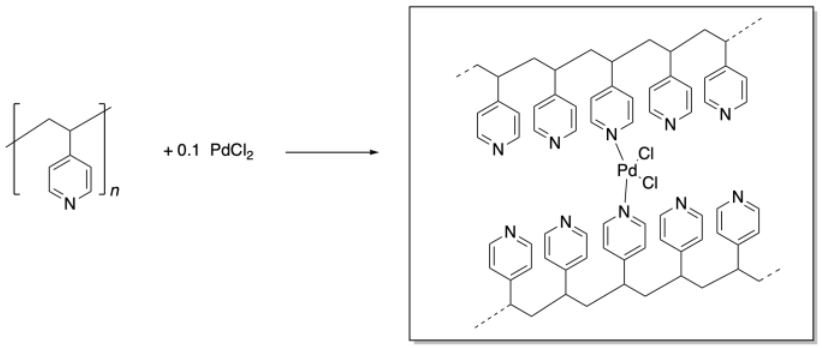
https://chem.libretexts.org/@go/page/438134



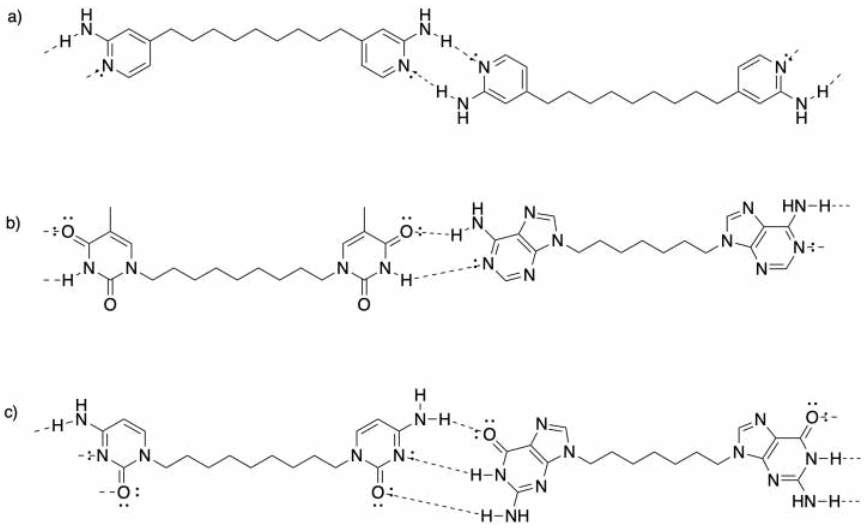
Problem MP5.2.



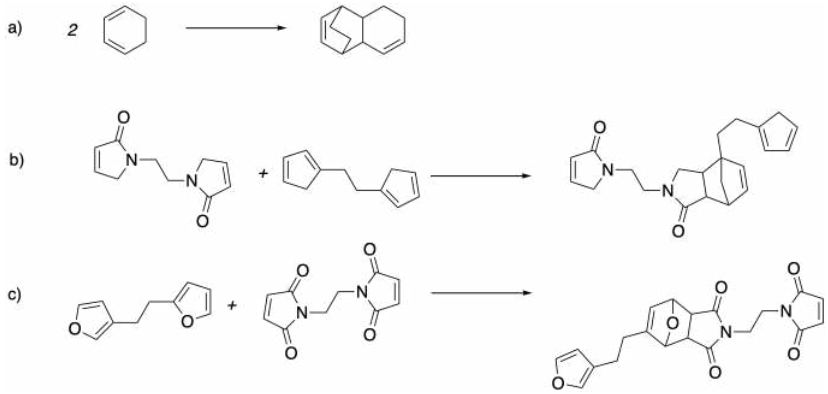
Problem MP5.3.



Problem MP6.1.

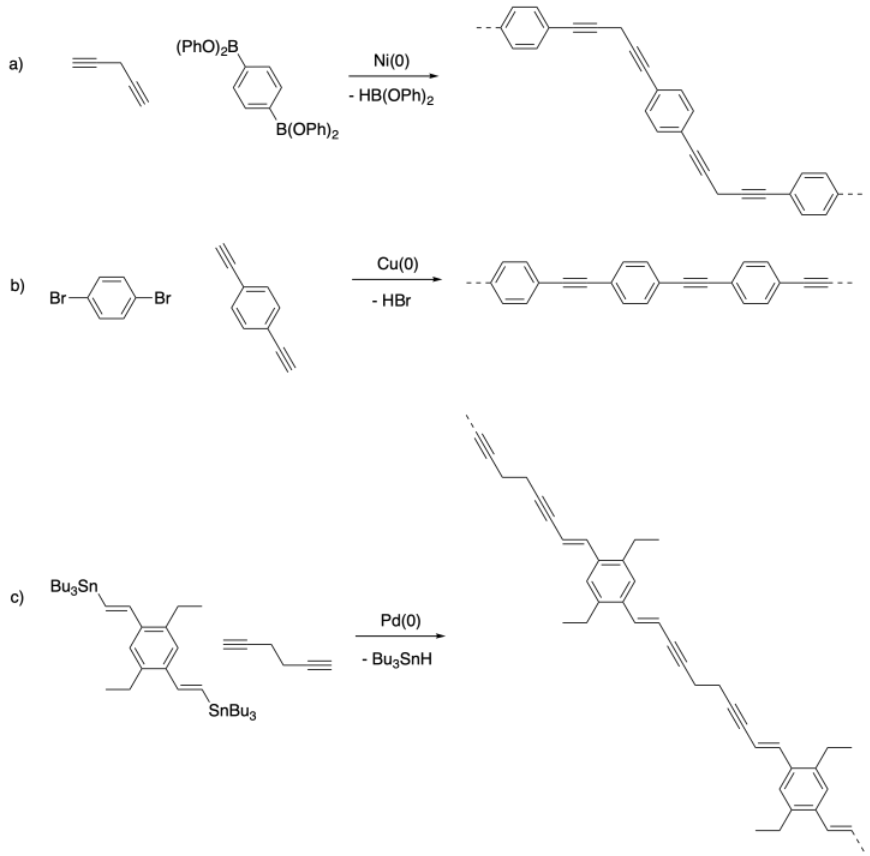


Problem MP7.1.



Problem MP7.2.

https://chem.libretexts.org/@go/page/438134



This page titled 11.5.1.E: Solutions for Selected Problems is shared under a CC BY-NC 3.0 license and was authored, remixed, and/or curated by Chris Schaller via source content that was edited to the style and standards of the LibreTexts platform.

- **1.E: Solutions for Selected Problems** by Chris Schaller is licensed CC BY-NC 3.0. Original source: https://employees.csbsju.edu/cschaller/Advanced/Polymers/Polycontents.htm.

SECTION OVERVIEW

11.5.2: Synthetic Methods in Polymer Chemistry

11.5.2.1: Ziegler-Natta Polymerization

11.5.2.2: Solutions to Selected Problems

11.5.2.3: Step Growth and Chain Growth

11.5.2.4: Cationic Polymerization

11.5.2.5: Living Cationic Polymerization

11.5.2.6: Anionic Polymerization

11.5.2.7: Living Anionic Polymerization

11.5.2.8: Ring-Opening Polymerization

11.5.2.9: Radical Polymerization

11.5.2.10: Living Radical Polymerization- RAFT

11.5.2.11: Living Radical Polymerization- ATRP

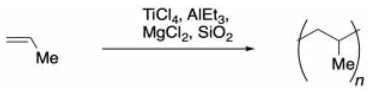
This page titled 11.5.2: Synthetic Methods in Polymer Chemistry is shared under a CC BY-NC 3.0 license and was authored, remixed, and/or curated by Chris Schaller via source content that was edited to the style and standards of the LibreTexts platform.

11.5.2.1: Ziegler-Natta Polymerization

There are alkenes that do not give rise to cations stable enough for cationic polymerization, and don't form stable enough anions for anionic polymerization, either. The two most prominent examples are ethene and propene. Nevertheless, ethene and propene are the most common feedstocks for polymers, with about 100 millions tons of global polyethylene production annually, and around 50 million of polypropylene. So, how do we make such huge quantities of polyethylene and polypropylene?

These monomers are instead polymerized via an organometallic cycle of alkene associations and 1,2-insertions, so that the last alkene becomes part of a metal alkyl group ready to undergo insertion with the next alkene that binds the metal. This process was developed in 1952 by Karl Ziegler at the Max Planck Institute for Coal Research in Mulheim, Germany. The method was later improved by Giulio Natta at Milan Polytechnic.

Commonly used industrial conditions for Ziegler-Natta polymerization employ a multi-component system. There is always an early transition metal catalyst, from the left-hand side of the d-block of the periodic table. Typically this catalyst is $TiCl_4$ or $TiCl_3$; under the reaction conditions, $TiCl_4$ is probably reduced to $TiCl_3$ anyway. This catalyst is supported on other metal halides such as $MgCl_2$. In heterogeneous catalysis, a support is a layer which strongly interacts with the catalyst, tuning its properties; exactly how that works is somewhat complicated. The catalyst and support are deposited on a solid carrier, such as silica, SiO_2, which distributes the catalyst, increasing the usable surface area. In addition, the carrier may modify the three-dimensional space around the catalyst, providing a binding pocket for the catalyst and the substrate, for example. Finally, the system needs an activator, which is a p-block metal alkyl such as triethylaluminum. This compound transfers a starting alkyl group to the catalyst and may also reduce the transition metal species.



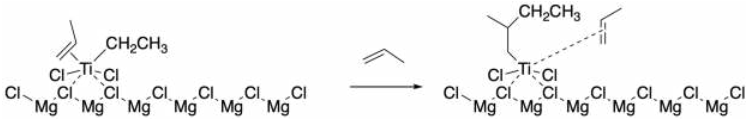
A Ti(III) rather than Ti(IV) catalyst has the advantage of being better able to bind the alkene substrate. Ti(IV) is a d^0 species, and d^0 metals are typically incapable of binding alkenes. The relatively weak π-bond donation to a metal is normally augmented by back donation from an occupied metal d orbital into the alkene π* orbital.

Exercise 2.1.1

Let's take a look at some alternative Ziegler-Natta reagents. Identify each component as a possible catalyst, support, carrier or activator.

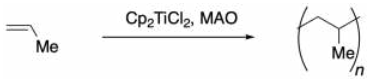
a. $ZrCl_4$
b. EtLi
c. $Mg(OEt)_2$
d. Al_2O_3
e. $AlMe_3$
f. $CrCl_6$
g. VCl_5
h. MgO

As indicated previously, once an alkene binds at the transition metal, an initial alkyl that was previously transfered from the aluminum is able to participate in a 1,2-insertion reaction. As a result, the alkene is incorporated into the alkyl chain. Subsequent alkene association and 1,2-insertion steps serve to extend the chain, eventually into oligomers and then polymers.

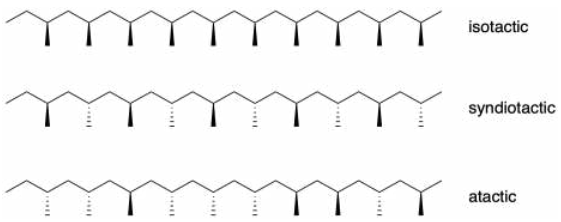


Homogeneous catalysts have also been used commercially for these polymerizations. These systems have been developed more recently by Walter Kaminsky at University of Hamburg, Germany and Hans-Herbert Brintzinger at University of Konstanz,

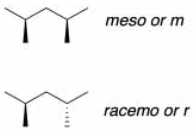
Germany. These soluble catalysts have expanded the scope of stereochemical control over the polymerization of propene and other terminal alkenes or 1-olefins.



When propene is enchained into a polymer, a new chiral center is formed at every position where a methyl group branches from the backbone. Rather than trying to assign each of these chiral centers with stereochemical configurations (*R*) or (*S*), we instead describe the relative stereochemical relationships along the backbone. The term used to describe these relationships is "tacticity". If there is no apparent relationship between the projection of the methyl groups along the backbone, the polymer is termed "atactic". If the methyl groups alternate, pointing first one direction, then the other, all the way along the chain, then the polymer is termed "syndiotactic". If the methyl groups all project the same direction, the polymer is described as "isotactic".



Tacticity in polymers is frequently determined by NMR spectroscopy. Because diastereomers have different physical properties, they display slightly different shifts in the ^{1}H or ^{13}C NMR spectrum. In a polymer chain, we think about chiral centers in pairs, which we call "diads", because every pair of chiral centers has two possible diastereochemical relationships and therefore two possible chemical shifts. If the methyl groups are on the same side, the chiral centers have a "meso" relationship, whereas if they are on opposite sides, they have a "racemo" relationship.



In principle, these are two different stereochemical relationships that could give rise to two different NMR signals. If the polymer is truly isotactic, we might only see the signal that comes from the meso diad, because all of the stereocenters would have that same relationship along the chain. If the polymer is truly syndiotactic, we might see only the signal from the racemo diad, at a slightly different chemcial shift as the meso. On the other hand, we might see two signals, and the relative integration of the two signals might indicate that the polymer is mostly syndiotactic, mostly isotactic, or completely atactic.

Exercise 2.1.2

Label the following diads.

a) 

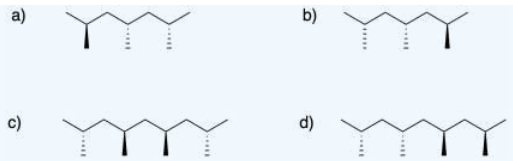
b) 

We can expand from there to think about triads, a sequence of three chiral centers, considering the relationship between the first pair of chiral centers in the triad and then the next pair. We would then describe these relationships as mm, for two meso relationships in a row; rr, for two racemic relationships in a row; or mr, for a meso and a racemo relationship. We might be able to detect different signals for all of these relationships.

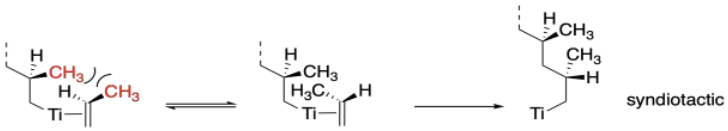
Given a big enough magnetic field strength an an NMR spectrometer, we may even be able to detect the difference between diads and tetrads, allowing us to see more detail along different segments of the polymer backbone.

Exercise 2.1.1

Label the following triads and tetrads.

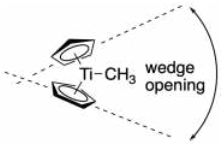


Control over polymer stereochemistry typically occurs in one of two ways. The first way is called chain end control. Given an existing stereocenter at the end of the chain, the approach of the next monomer will be influenced by how that existing chiral center projects in space. As a result, the last chiral center influences how the next one is formed. Conceptually, this idea is the same as saying that in a simple organic reaction, an existing chiral center may force an incoming group to one face of a molecule rather than another, leading to preferential formation of a particular stereochemistry where the new bond is made. In the case of polymers, it means the very first insertion reaction, when the first chiral center forms, determines all of the subsequent stereochemistries along the chain. Of course, there isn't a simple way to predict what that stereochemistry will be: syndiotactic or isotactic. However, the drawing below shows how such an interaction could lead to a syndiotactic polymer.

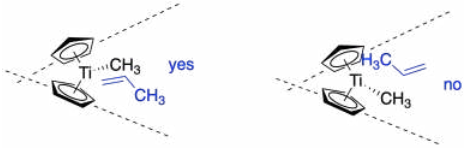


The second mechanism is called site control. In site control, the specific shape of the reagent or catalyst that facilitates the reaction also determines the stereochemictry. This idea is also seen in organic reactions. Chiral reagents or catalysts, whether for hydrogenations, hydroborations, or other reactions, will fit with the substrate in one way more easily than another, leading to preferential formation of one stereochemistry and not the other.

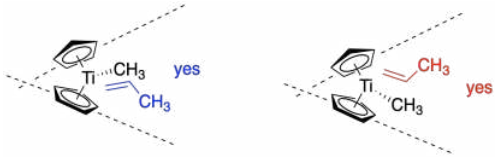
Site control is a topic of interest in homegeneous catalysis, so let's look at how it would work in a titanocene. The first basic lesson in titanocene chemistry is that the two cyclopentadienyls form an angle with each other, so that the molecule takes on a little bit of a wedge shape. One end of the titanocenes are closed together more, and the other end is more open. It's kind of like a clam shell.



If another molecule, such as a propene, approaches to bind to the titanium, it will have to negotiate the wedge shape to minimize steric interactions. For example, keeping the methyl group away from the titanium, toward the opening on the wedge, would cause less crowding than if the methyl spun around to project deeper inside the wedge.



When discussing the formation of a new chiral center, the key idea is whether a new group will bind to one face of a molecule or the other face. We are going to show one face of the propene in blue and the other in red to emphasize this difference. So far, the methyl of the propene will remain further away from the titanium, but there is nothing to prevent the propene from flipping over; the methyl group could be either up or down in the picture.



Much of the focus in these homogeneous catalysts has been on developing some kind of asymmetry in the catalyst. The catalyst shown below has C_s symmetry. The top is now different from the bottom. Specifically, the bottom is much more crowed, so that it

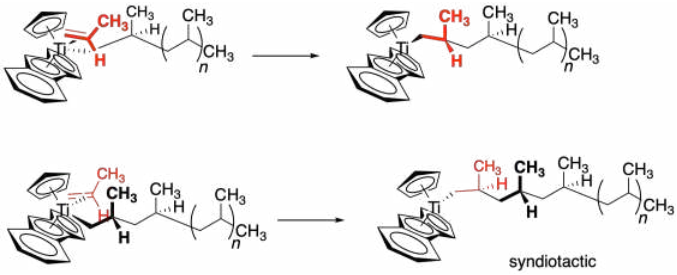
is no longer very likely that the propene would approach with its methyl group down. It would be much easier to come in with its methyl group pointed up in this picture.



To add one more wrinkle, the propene isn't going to bind in the middle of the wedge, but will be off to one side or the other. That's because there should already be an alkyl group on the metal, which we have shown in this case as a simple methyl group. The propene could approach from the near side, in front of the methyl (shown on the left), or from the far side, behind the methyl (shown on the right).

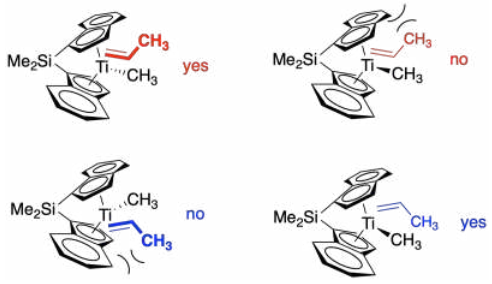


If the propene is on the near side from our perspective, it is actually presenting its blue face to the alkyl chain. When the 1,2-insertion occurs, the alkyl will bond to the blue face, pushing the methyl and hydrogen of the propene towards us (seen in the top picture). However, if the propene is on the far side from our perspective, it really is presenting its red face to the alkyl chain. When the 1,2-insertion occurs, the alkyl will bond to the red face, pushing the methyl and hydrogen of the propene away from us.

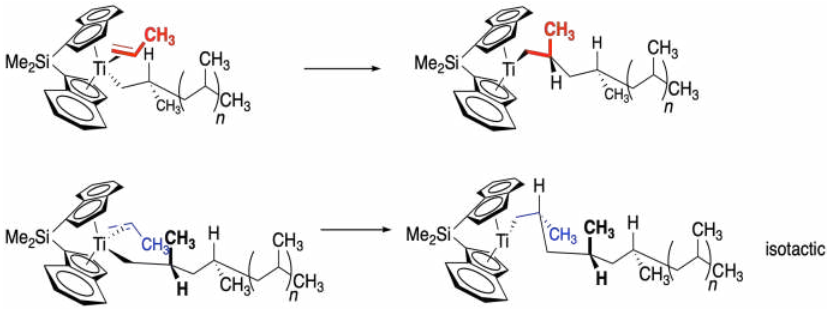


Which one really happens? Both. During the insertion, the alkyl chain shifts over to the coordinated olefin, opening up a coordination site. Notice in the top picture above, the propene is on a wedge and the alkyl is on a dash. After the insertion, the alkyl chain is on a wedge and a new coordination site opens up behind it. A new propene moves into that site. As a result, the new propene approaches first from one side, then the other, alternative every time. This windshield washer mechanism results in a syndiotactive stereochemistry.

What is we change the shape of the catalyst? In the picture below, we have a catalyst with C_2 symmetry. With this symmetry, the propene can approach with its methyl up only if it comes from the front. With its methyl down, it can only approach from the rear.



If you think about it, that means the propene is always presenting the same face to the metal. It only binds to the titanium through the blue face. That means the alkyl chain always binds to the blue face. If the alkyl always binds to the same face, it is always forming a new chiral center with the same configuration. It's making an isotactic polymer.



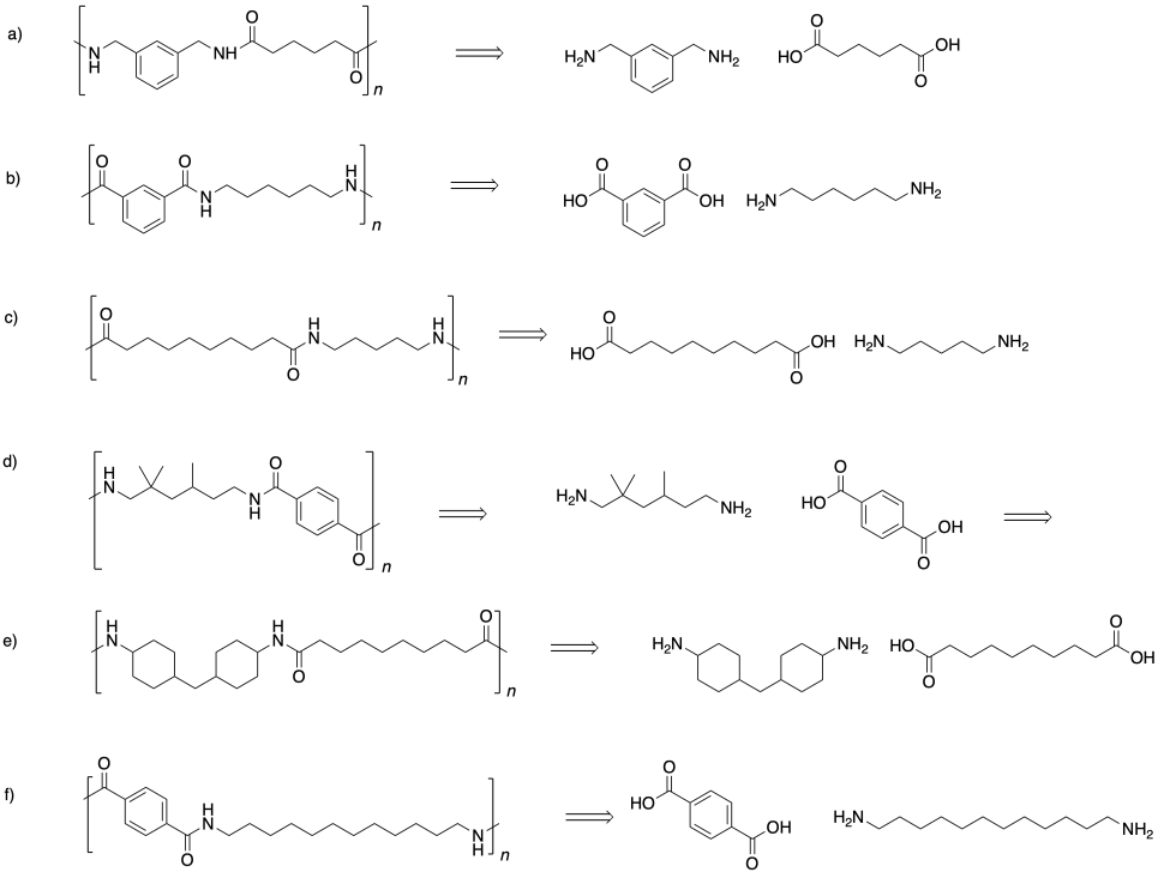
This page titled 11.5.2.1: Ziegler-Natta Polymerization is shared under a CC BY-NC 3.0 license and was authored, remixed, and/or curated by Chris Schaller via source content that was edited to the style and standards of the LibreTexts platform.

- **2.1: Ziegler-Natta Polymerization** by Chris Schaller is licensed CC BY-NC 3.0. Original source: https://employees.csbsju.edu/cschaller/Advanced/Polymers/Polycontents.htm.

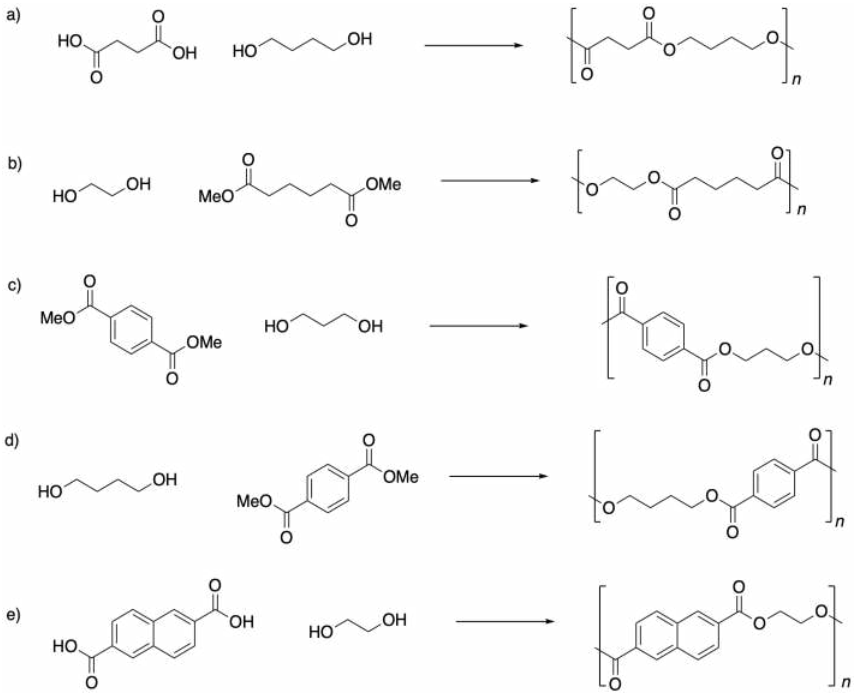
11.5.2.2: Solutions to Selected Problems

SM11. Solutions to Selected Problems

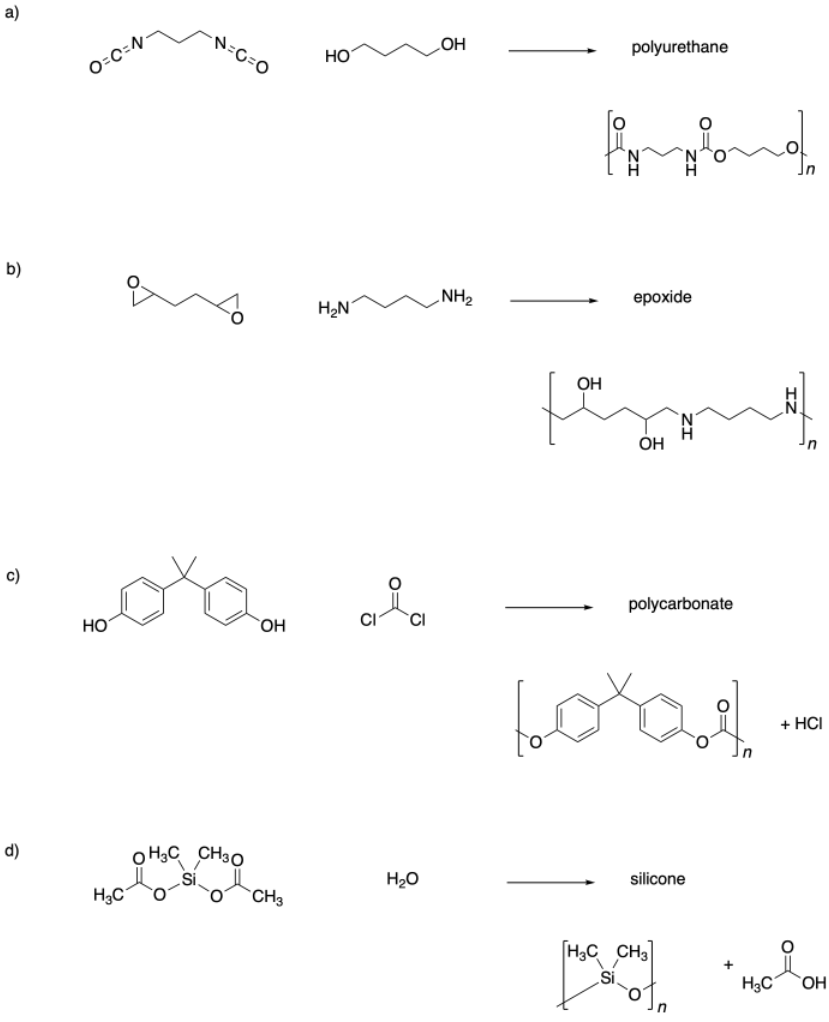
Problem SM1.1.



Problem SM1.2.

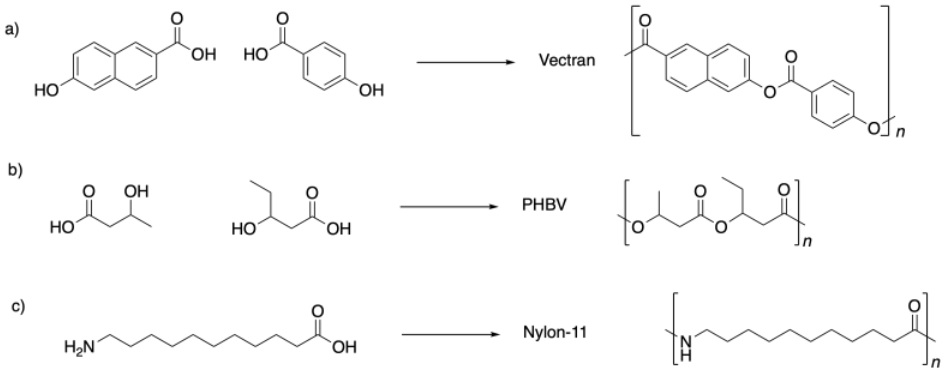


Problem SM1.3.



https://chem.libretexts.org/@go/page/438137

Problem SM1.4.



Problem SM1.5.

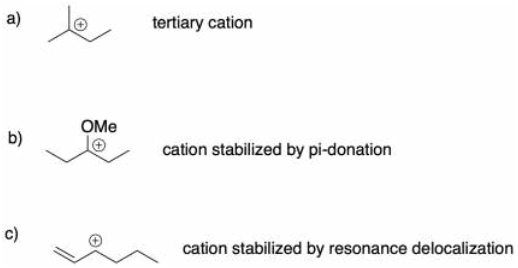
a) After seven steps, the polymer will be 2^7 = 128 units long; MW = 128 x 150 g/mol = 19,200 g/mol.

b) After sixteen steps, the polymer will be 2^{16} = 65,536 units long; MW = [(120 + 130)/2] x 65,360 g/mol = 8,192,000 g/mol.

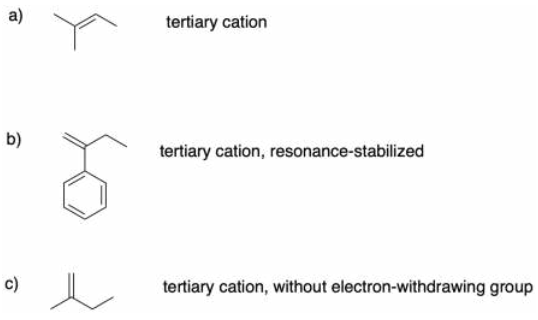
c) After ten steps, the polymer will be 2^{10} = 1,024 units long; MW = [(100 + 105)/2] x 1,024 g/mol = 104,960 g/mol. One condensation will occur at the two ends of each monomer, except for the ones on the ends, but that's a loss of approximately 1,023 x 15 = 15,345 g/mol. The net molecular weight is 104,960 - 15,345 g/mol = 89,615 g/mol.

d) Chain growth occurs linearly, so the molecular weight is 30 x 105 g/mol + 65 g/mol (end group) = 3,215 g/mol.

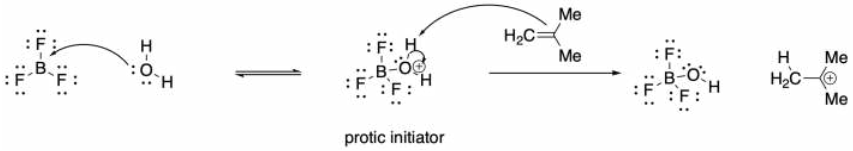
Problem SM2.1.



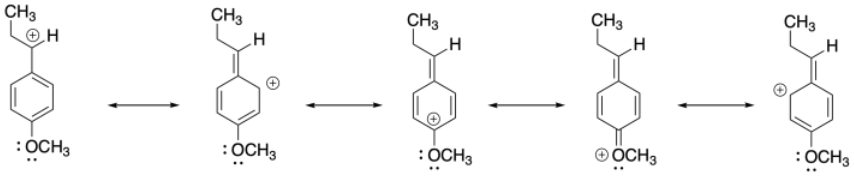
Problem SM2.2.



Problem SM2.3.



Problem SM2.4.



Problem SM2.5.

These large, highly charged anions are not very soluble, limiting their interaction with the growing polymer chains.

Problem SM3.1.

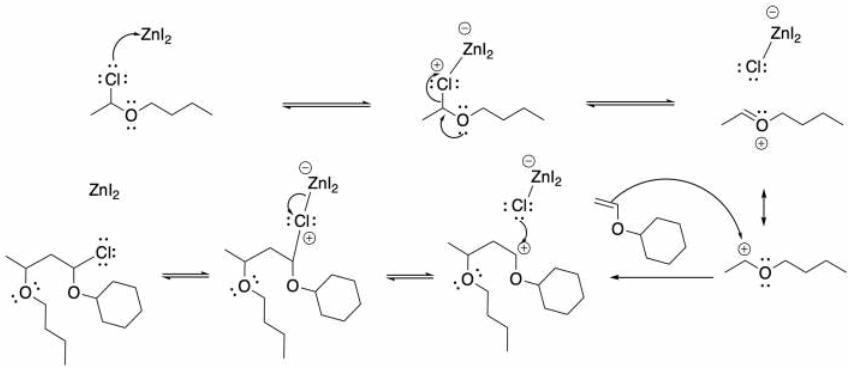
a) $GaCl_3$

b) $SnCl_4$

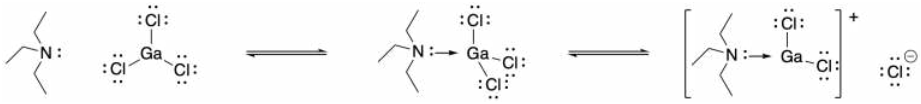
c) $ZnCl_2$

d) $FeCl_3$

Problem SM3.2.

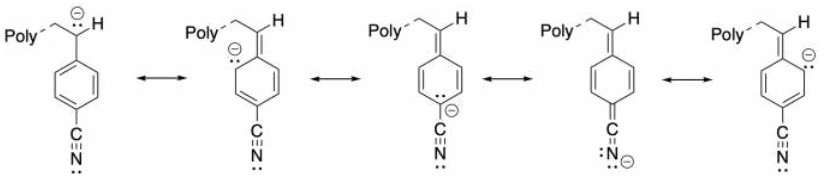


Problem SM3.3.



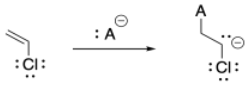
Problem SM4.1.

The additional resonance stabilization of the anion by the nitrile group makes anionic polymerization proceed smoothly.

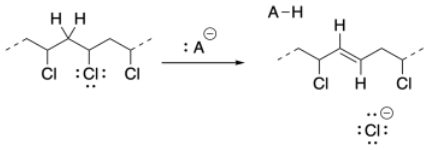


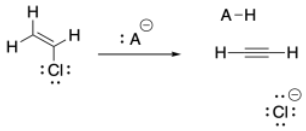
Problem SM4.2.

a) Vinyl chloride's electronegative chlorine might stabilize an anion on the adjacent carbon. However, that inductive effect may be offset by lone pair repulsion between carbon and chlorine.



b) Under these strongly basic conditions, 1,2-elimination may result from the growing polymer chain. Very basic conditions may even result in 1,2-elimination from viyl chloride to give acetylene (ethyne).





Problem SM5.1.

a) Li^+, Na^+, K^+

b) Be^{2+}, Mg^{2+}, Ca^{2+}

Problem SM5.2.

a) K^+, Na^+, Li^+

b) Ca^{2+}, Mg^{2+}, Be^{2+}

Problem SM5.3.

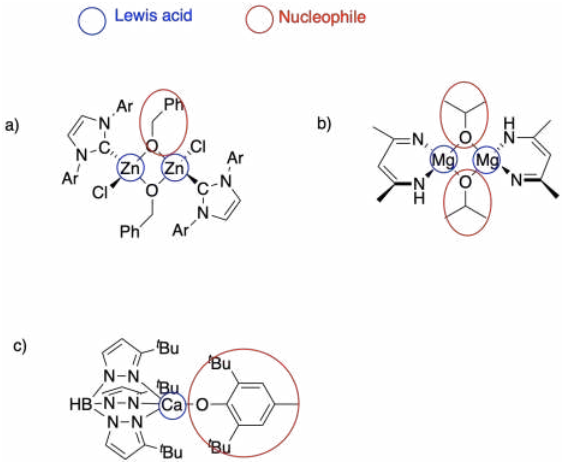
a) Et_3Al

b) Et_2Zn

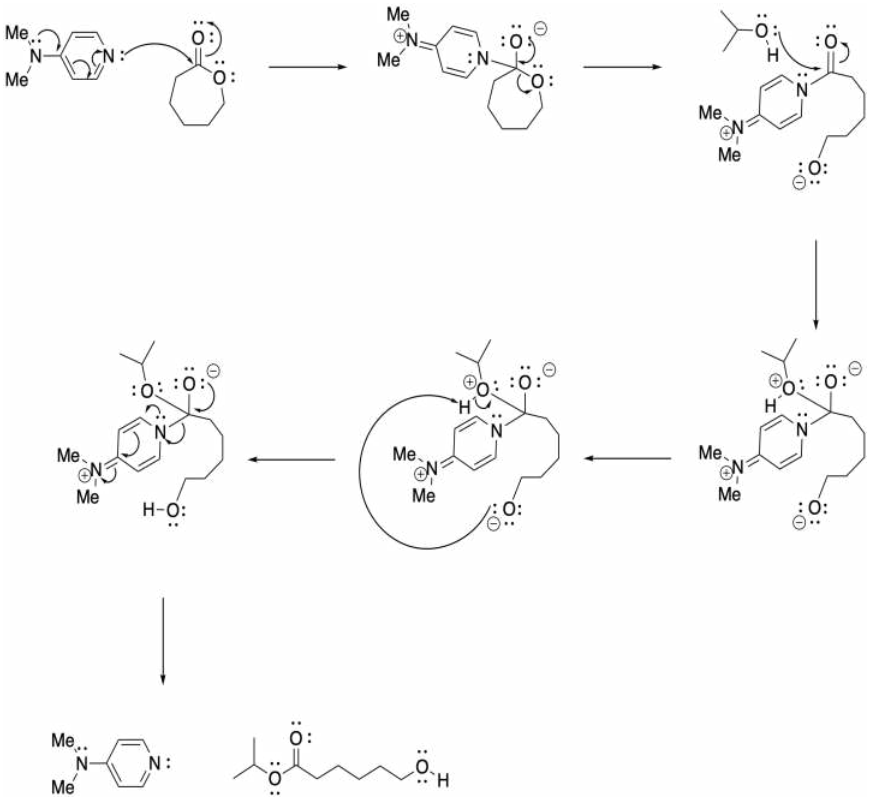
c) Ph_3B

d) $(CH_3O)_2AlCH_3$

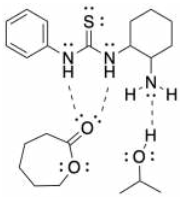
Problem SM6.1.



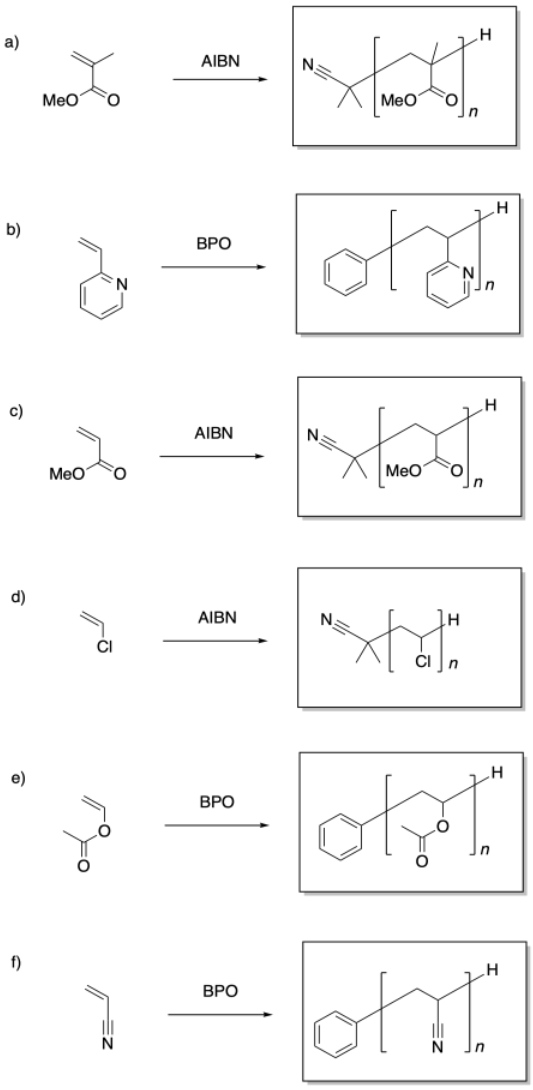
Problem SM6.2.



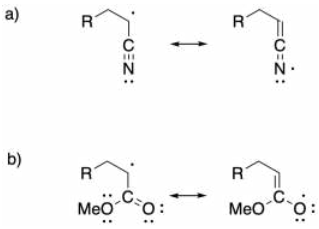
Problem SM6.3.



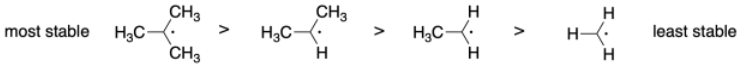
Problem SM7.1.



Problem SM7.2.

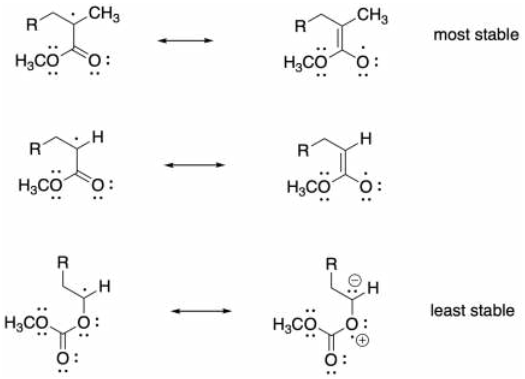


Problem SM7.3.



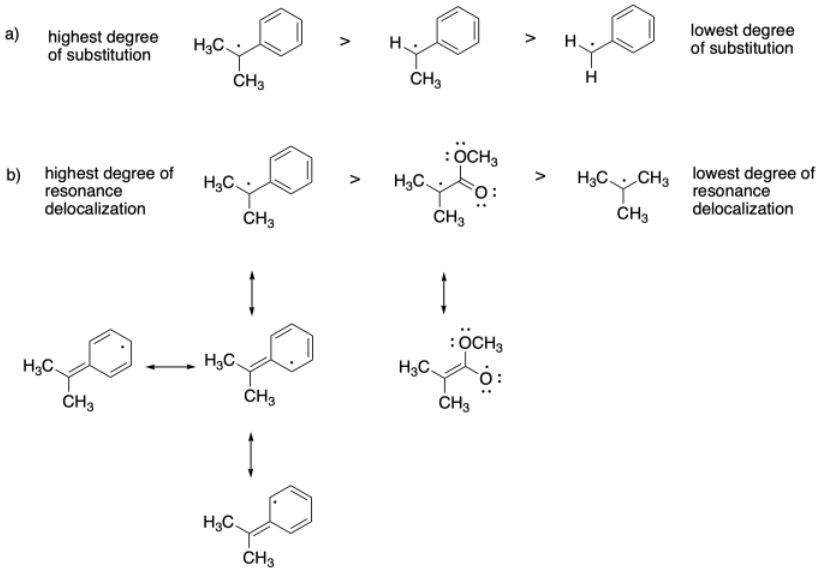
Problem SM8.1.

The more stable the radical, the more rapidly it will form from the monomer, leading to faster polymerization.



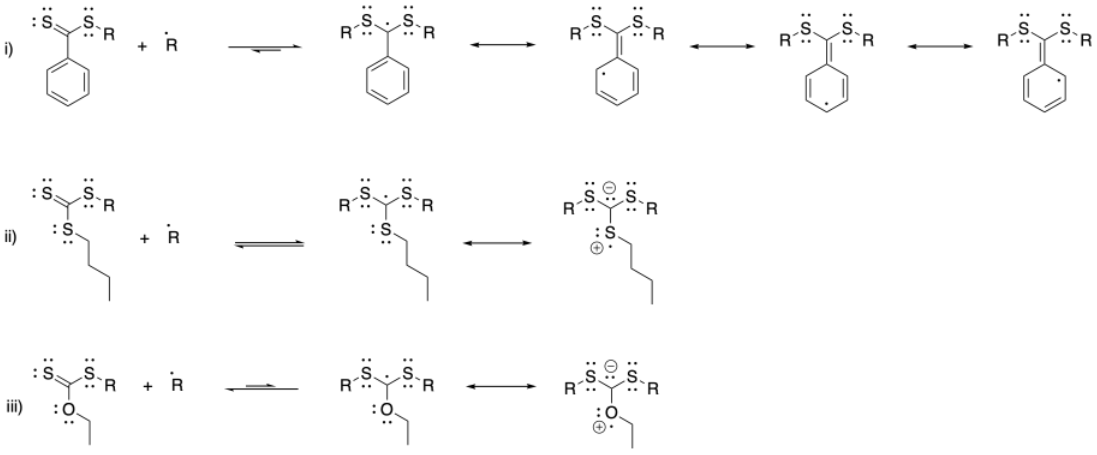
Problem SM8.2.

The more stable the radical generated upon fragmentation of R, the more the equilibrium will shift toward growing phase.



Problem SM8.3.

The more stable the radical formed, the more the equilibrium will shift toward the dormant phase.



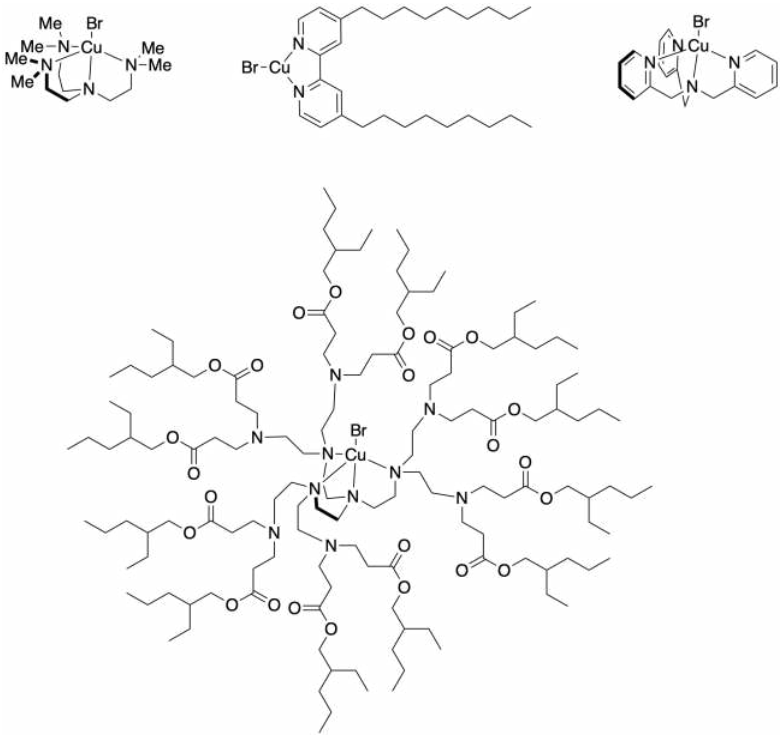
Problem SM8.4.

a) With a fast-polymerizing monomer like this one, we need a chain control agent that will provide a similarly stable radical, so that there is an appreciable equilibrium allowing chains to move into the dormant phase; hence the phenyl substituent. However, to get

into a new growing phase, we need an R group that fragments very easily, such as this disubstituted benzyl.

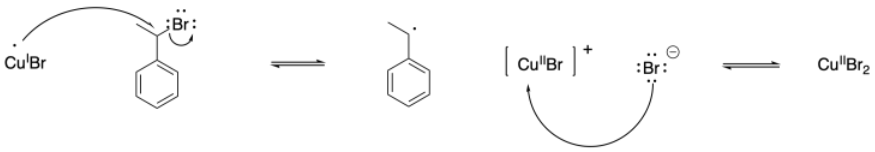
b) With a monomer on the lower end of radical stability, we need a chain transfer agent that isn't terribly stable as a radical, or else the chains will shift completely into the dormant phase. We also need an R group that will fragment at a rate comparable to the original radical chain, so we have one that will form a modestly stable radical.

Problem SM9.1.

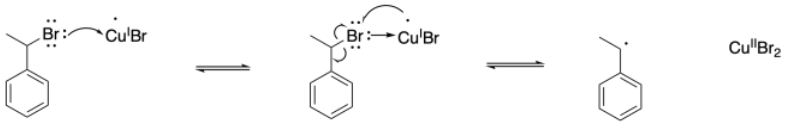


Problem SM9.2.

a)



b)

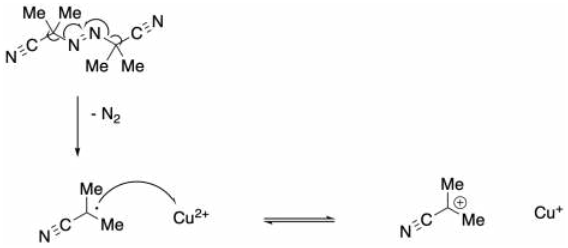


Problem SM9.3.



Problem SM9.4.

a)



b) The radical generated in the first step may initiate new polymer chains instead.

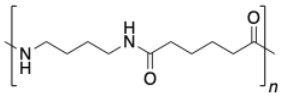
This page titled 11.5.2.2: Solutions to Selected Problems is shared under a CC BY-NC 3.0 license and was authored, remixed, and/or curated by Chris Schaller via source content that was edited to the style and standards of the LibreTexts platform.

- **2.2: Solutions to Selected Problems** by Chris Schaller is licensed CC BY-NC 3.0. Original source: https://employees.csbsju.edu/cschaller/Advanced/Polymers/Polycontents.htm.

11.5.2.3: Step Growth and Chain Growth

Step growth and chain growth are two broad classes of polymerization methods. They use monomers with distinct characteristics and display some different growth patterns.

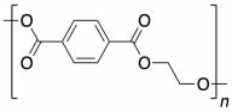
Condensation polymerizations take place via a step-growth process. In a classis condensation reaction, a carboxylic acid reacts with a neutral nucleophile, such as an alcohol or an amine. Substitution leads to formation of either an ester (from an alcohol nucleophile) ar an amide (from an amine nucleophile), with water as a side-product. For example, nylon-6,6 is a condensation polymer.



Nylon-6,6 is produced via a condensation reaction between 1,6-hexanedioic acid (or adipic acid) and 1,6-hexanediamine (or hexamethylenediamine). The amine end group of the nucleophile loses a proton and the carboxylic acid loses an OH group, for the formal loss of one water molecule each time an amide bond forms.

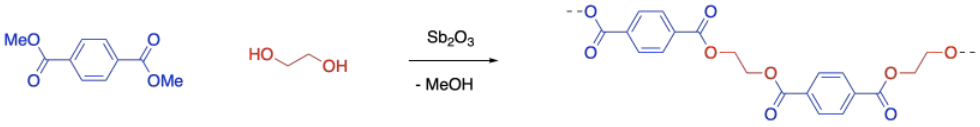


Poly(ethyleneterephthalate) or PETE is a very common example of a polyester.



poly(ethyleneterephthalate)

PETE is formed from the reaction of dimethyl terephthalate with 1,2-ethanediol (or ethylene glycol). Once again, a condensation reaction takes place, with a small molecule formed as a side product. An OMe group is displaced fron the carboxyl electrophile and a proton is lost from the nucleophilic alcohol group, adding up to the formal loss of methanol.



It's worth talking about the conditions used for these reactions. On paper, we might think about using more reactive monomers, such as acyl halide electrophiles, in order to have much faster reactions. However, these reactions are either exothermic in the case of the polyamide or thermoneutral in the case of the polyester, which is formed through a trans-esterification. Both reactions occur in equilibrium. Although they may be relatively slow, they should still get to product eventually, especially if the equilibrium can be shifted to the right. In both of these cases, that shift can be acheived through removal of the water or methanol side-products, which are relatively volatile compared to the other reactants.

Note also that the neutral nucleophile and the relatively poor leaving groups in these cases suggest the reaction will be pretty slow. To speed things up, a Lewis acid may be added (such as the antimony oxide, Sb_2O_3, employed in the second example).

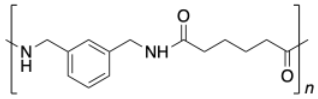
The monomers used in step-growth polymerization usually have a couple of characteristics that we can see in these examples. Most often, there are two different monomers. Neither monomer would undergo polymerization on its own, but the two monomers are complementary to each other, so that each provides the other with an appropriate reactive partner.

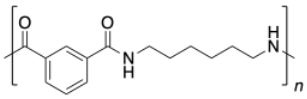
More importantly, each of the monomers we have seen here is mutlifunctional. In this context, functionality describes the number of reactive functional groups. Each of the monomers we have seen so far contains two functional groups; they each have a functionality of two, or they are each difunctional. Once a functional group has reacted on a difunctional monomer, it still has another one that can react. Every monomer can therefore make bonds with two others, allowing for chain formation.

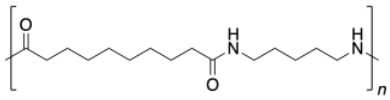
This higher functionality is essential for step-growth polymerization. It isn't limited to difunctional monomers. Monomers could be trifunctional, tetrafunctional, and so on, leading to more highly branched or chemically crosslinked polymers, rather than simple chains.

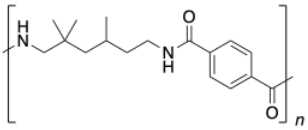
Problem SM1.1.

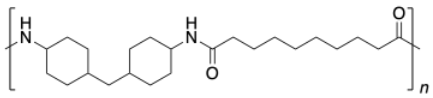
Identify the monomers that would be used to produce these polymers.

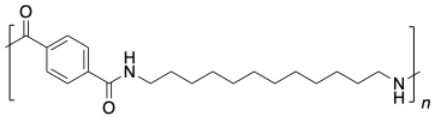
a)  MXDX

b)  Nylon-6I

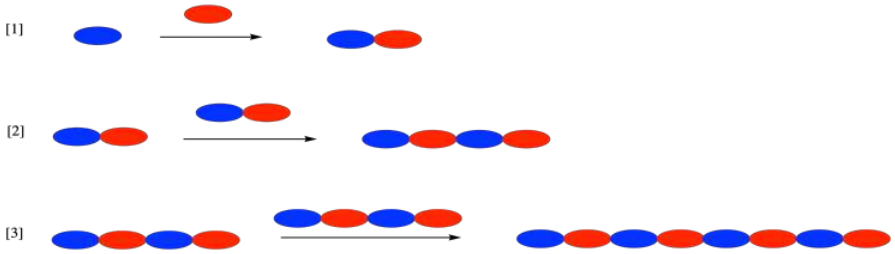
c)  Nylon-510

d)  TMDT

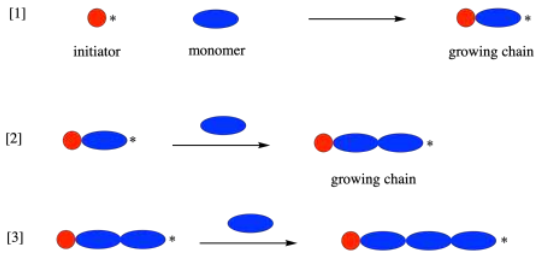
e)  PACM12

f)  Nylon-12T

Because of difunctionality in the monomers, condensation polymers can grow in two directions at once. Two complementary monomers connect with each other to form a dimer. Now, suppose all the monomers are reacting at roughly similar rates (not quite true if you know about polymer molecular weight distribution, but close enough). When one end of the dimer goes to react again, chances are it will find another dimer, because most of the monomers have already reacted. That reaction will form a tetramer. The typical tetramer reacting another time will find another tetramer, forming an octamer, and so on.

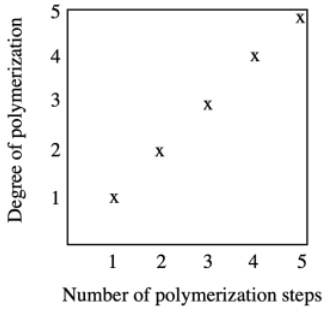


Most of the subsequent chapters in this text deal with a variety of ways of carrying out chain polymerizations. In chain polymerization, we usually start with just one kind of monomer, which is again unreactive by itself. This time, instead of adding a complementary monomer, we add an initiator. The initiator converts one monomer molecule into a reactive intermediate, capable of reacting with another monomer to form a new reactive intermediate, and so on. This is a chain reaction.

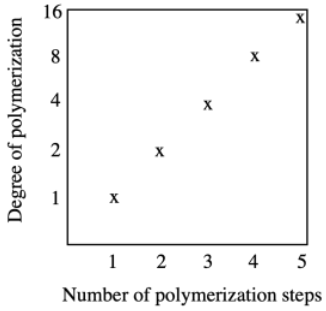


Notice the difference from step growth. In chain growth, the polymer chain always grows one monomer at a time. In step growth, the polymer chain doubles with each step. As a result, the rate of growth of the polymer chain is very different in these two cases.

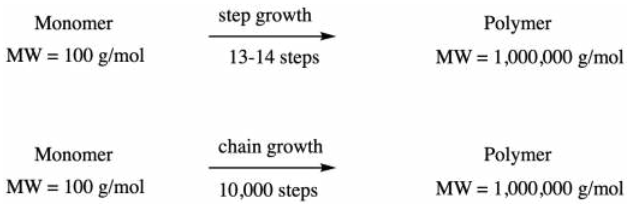
Chain growth results in a steady increase in chain length with every coupling step. Growth is linear.



Chain growth is exponential, with chain length doubling at every coupling step. Notice that the y axis on this graph is logarithmic rather than linear.



What are the consequences of these two growth patterns? Let's take a look at how many steps it would take to form a high molecular weight polymer, maybe with a molecular weight of one million g/mol (sometimes expressed as one million Da in polymer chemistry; Da stands for Dalton). Starting with a monomer of molecular weight 100 g/mol and using step growth, in which chain length doubles every time a reaction takes place, it will take only thirteen or fourteen steps to reach a molecular weight of a million Da, because 2^{13} = 8,192 repeat units. Using chain growth, it would take ten thousand steps to reach the same molecular weight, assuming a monomer of similar size.

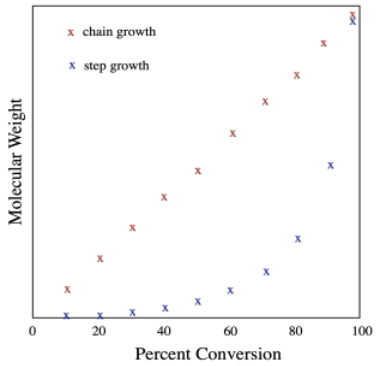


That's a very approximate calculation, and it neglects the weight of side products during condensation polymerization, but we are looking at differences that are orders of magnitude apart.

Why is this difference significant? For one thing, it doesn't matter that much if a condensation reaction is slow. If it only takes twenty (or even thirty) steps to reach a molecular weight of a million (not unheard of in a commercial polymer, but still pretty

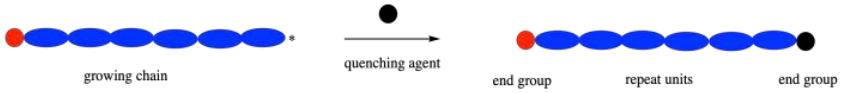
high), then there's no hurry. In chain polymerization, there is a much higher premium on speed. We need very fast reactions or sometimes very fast catalysts that can turn around and enchain monomer after monomer reliably.

If we take these two broad methods and look at them in a different way, we get new information. If, instead of thinking about the number of bonding events or reaction steps, we focus on the percent conversion, we get a graph that looks like this.

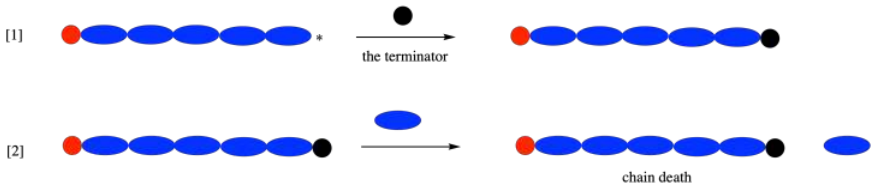


Looked at in this way, we see the linear nature of chain growth. Every time a new monomer is added, the polymer chain grows by the same amount (the weight or length of one new repeat unit, depending on whether we are thiniing in terms of molecular weight or chain length). Step growth works exponentially: doubling, quadrupling, and so on. Both modes of polymerization proceed, ideally, until all of the monomer has completely reacted; in other words, to 100% conversion. But what happens if growth is suddenly arrested because of some unwanted side reaction? In step growth, such an event happening even in the very late stages of polymerization might result in a chain length that is only half what we had expected. Such disastrous results in chain growth would result only if growth stopped after only consuming half the monomer. Arresting chain growth at 80 or 90% conversion still results in pretty long polymer chains, even if they aren't the expected length. Because of this feature, step growth polymerization requires very reliable chemistry. Otherwise, step growth would always result in relatively short chains.

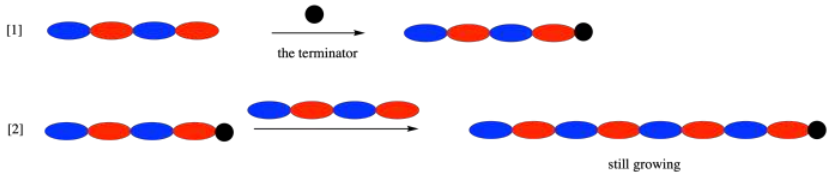
In either case, it's useful to know that polymerization is often followed by a quenching reaction to arrest the process once the polymer has reached the desired chain length. Usually that results in a polymer with two different groups at the end of the chain. The choice of those groups can occasionally be useful in modifying the properties of the polymer.



Imagine a case, however, in which this termination happens accidentally. In a chain growth, the polymer has a reactive intermediate at one end only. If something caps that end of the polymer chain, it stops growing altogether. Unexpected terminations can be a significant problems in chain growth.



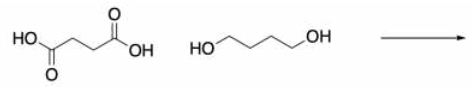
Of course, they are also a problem in step growth, but remember that in step growth the polymer is growing from two ends. If one end gets capped, the other end can keep growing. The polymer will grow more slowly, but it won't stop altogether.

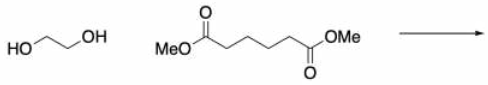


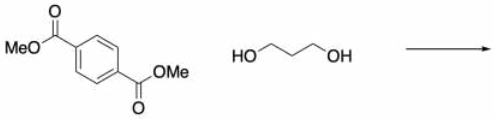
As a result, there is a great deal of interest in developing more reliable ways of carrying out chain growth. That's especially important because one wrong step and chain growth stops altogether. Chain growth is, in fact, a crucial way of making polymers, despite what may seem like some limitations here. A key reason is that step growth is mostly limited to condensation polymerization of carboxyloid compounds such as polyamides and polyesters, as well as a few related materials such as polyurethanes. Chain growth is used to polmerize a wide array of compounds that contain carbob-carbon double bonds (alkenes or olefins) as well as a variety of cyclic monomers. Both approaches are needed to make a range of useful materials.

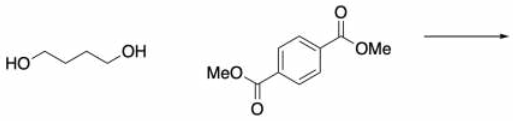
Problem SM1.2.

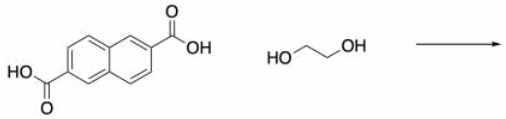
Provide structures of the polyesters made from the monomers as indicated.

a) 

b) 

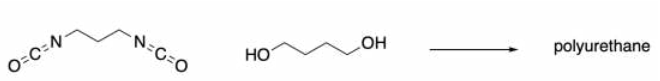
c) 

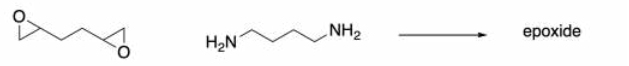
d) 

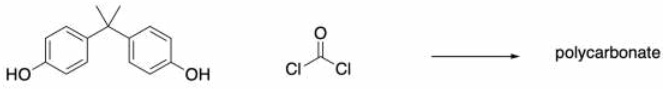
e) 

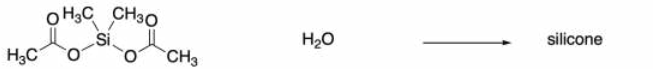
Problem SM1.3.

The following difunctional monomers would undergo polymerization together; in some cases the reaction happens without condensation of a side product. Show the product structures that result.

a) 

b) 

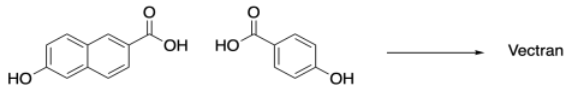
c) 

d) 

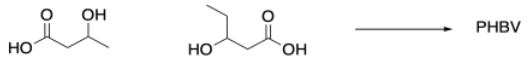
Problem SM1.4.

A few polymers are obtained from difunctional monomers that contain both nucleophilic and electrophilic sides. Show the polymers that result in these cases.

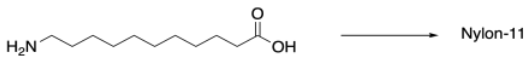
a)



b)



c)



Problem SM1.5.

Calculate the molecular weight of the polymer in each of the following cases.

a) Step polymerization involving monomers of molecular weight 150 g/mol, allowed to undergo seven polymerization steps.

b) Step polymerization involving monomers of 120 and 130 g/mol, allowed to undergo sixteen polymerization steps.

c) Step polymerization involving monomers of 100 and 105 g/mol, allowed to undergo ten polymerization steps, producing a condensation product with molecular weight 15 g/mol.

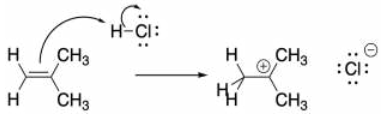
d) Chain polymerization of a monomer with molecular weight 105 g/mol, allowed to undergo thirty polymerization steps, using an initiator with molecular weight 65.

This page titled 11.5.2.3: Step Growth and Chain Growth is shared under a CC BY-NC 3.0 license and was authored, remixed, and/or curated by Chris Schaller via source content that was edited to the style and standards of the LibreTexts platform.

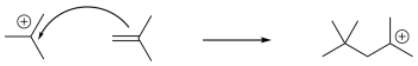
- **2.3: Step Growth and Chain Growth** by Chris Schaller is licensed CC BY-NC 3.0. Original source: https://employees.csbsju.edu/cschaller/Advanced/Polymers/Polycontents.htm.

11.5.2.4: Cationic Polymerization

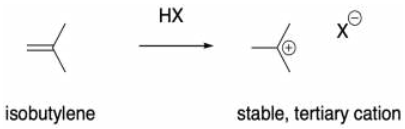
Alkenes, or olefins, are probably the most common polymer feedstock. The pi bonds of alkenes are inherently nucleophilic. The addition of an electrophile to an alkene results in cleavage of the pi bond, with the electrons drawn to the electrophile, and consequently a cation can be left on one end of the former double bond.



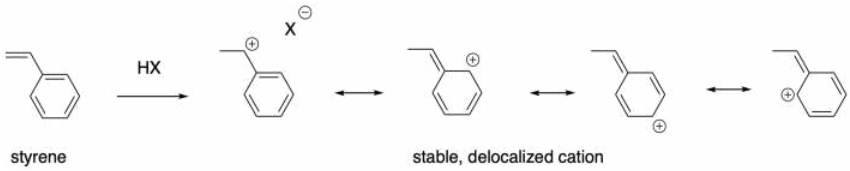
If the resulting cation interacts with another alkene, another electrophilic reaction occurs, and so on, leading to polymerization. Because of the presence of a key cationic intermediate along the reaction pathway, this method of polymerization is termed **cationic polymerization**. It is an example of a chain reaction that is initiated by a cationic species.



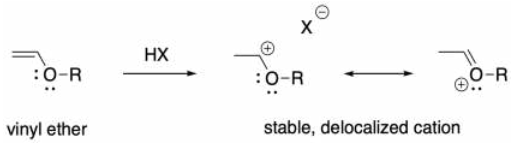
It stands to reason that alkenes that form stable cations would be particularly susceptible to polymerization via cationic methods. Cations are high-energy intermediates, so if a cation is relatively easy to form then the barrier for the process is lowered considerably. Isobutylene, $(CH_3)_2C=CH_2$, is a good example of an alkene that would form a stable cation upon protonation. The relative stability of more-substituted cations dictates that the positive charge is found at a tertiary position.



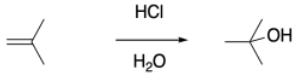
Degree of substitution is just one way that carbocations can be stabilized. Conjugation is also a major factor in cation stability. Alkenes that give rise to delocalized cations are also good candidates for cationic polymerizaton. Styrene, $PhCH=CH_2$, as well as butadiene, $CH_2=CHCH=CH_2$, and the related natural product isoprene, $CH_2=C(CH_3)CH=CH_2$, can all be polymerized using cationic methods.



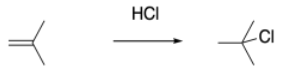
These examples are stabilized by allylic delocalization: the cation is part of a system that contains a $C=C-C^+$ feature, which is delocalized as $^+C-C=C$. Cations can also be stabilized via pi-donation. Oxygen and nitrogen are particularly good pi-donors towards carbocations, so oxygen and nitrogen substituents on alkenes render these compounds susceptible to cationic polymerization. Vinyl ethers, for example, can be polymerized this way.



The obvious way to initiate these polymerizations is through addition of a strong acid. Protonation of the alkene should certainly result in formation of a carbocation. However, most common strong acids are mineral acids, typically found in aqueous media. The presence of nucleophilic water would quickly cap the carbocation before polymerization could take place.

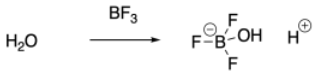


Of course, hydrogen chloride does not require water as a solvent. The addition of dry HCl gas to the olefin of interest should result in cation formation without subsequent hydration. Unfortunately, just the presence of the chloride ion, which can also act as a nucleophile, dooms polymerization to an early death.

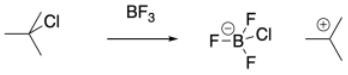


There are other, less nucleophilic acids that are not as strongly prone to classical addition across an alkene compared to the extent that we associate with HCl. Sulfuric acid and various sulfonic acids come to mind. Even in these cases, however, polymerization is limited by eventual collapse of the nucleophile with the cationic chain end.

Instead of using strong Brønsted acids to inititate polymerization, it is actually very common to use Lewis acids. Lewis acids cannot initiate cationic polymerization directly, but they can co-initiate the reaction in the presence of a water impurity, for example. The Lewis acid activates the water towards release of a proton. The proton then initiates the reaction. Traces of HCl can also act as the initiator when a Lewis acid co-initiator is employed, because the Lewis acid ties up the chloride ion so that it cannot connect with the growing cationic chain end.



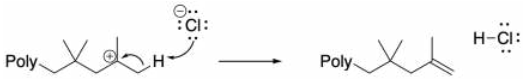
Protic initiators are not strictly required for cationic polymerization. Strong Lewis acids are also capable of activating alkyl halides. The carbocation that results can then initiate the polymerization chain reaction.



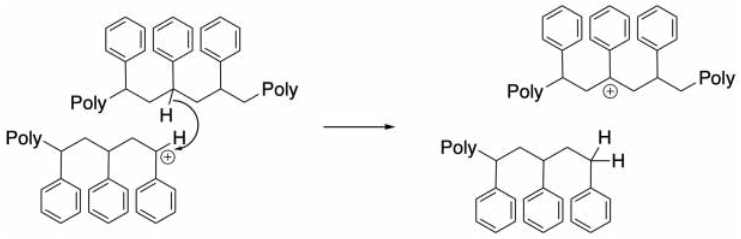
Even in these systems, there are chain-termination events that destroy the reactive intermediate and stop polymerization. As indicated previously, combination of a nucleophilic anion with the cationic chain end is a common fate of growing polymers. Halide ions, released in equilibrium from the Lewis acid-base complex, are still a possible problem, even though this event is much less likely in the presence of Lewis acidic co-initiators. Other, similar anions, such as hydroxide anions in water-initiated polymerizations, can play a similar role.



Anionic species can also carry out beta-eliminations on cationic chain ends. Beta-elimination results in the loss of the cationic intermediate, replacing it with a cain-end elkene. That event results in the production of a new initiator, and although it could be argued that the initiator might just re-initiate the same polymer chain, given relative concentrations it is much more likely that the initiator transfers the proton to a new monomer. In that case, a new growing chain starts from scratch and begins to accumulate monomers.



Surprisingly, chain-transfer events are another common mode of termination. In these cases, a hydride must be transferred from one chain to another, or from one position along the backbone to the growing chain end. This unusual hydride transfer is probably facilitated by very close contact distance between two chains, or between two segments of one chain, in a concentrated polymerization milieu. As a result, one chain end stops growing, and the chain begins growing from a new position along its backbone. This event results in chain branching, changing the morphology and properties of the polymer.



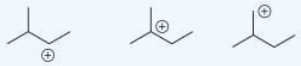
Normally, assuming a relatively rapid initiation step (formation of a cation from the first monomer), growth of tandem polymer chains will proceed at roughly the same rate, so that all of the chains reach similar lengths by the time all monomers have been consumed. What happens if some of those chains die prematurely? Other chains continue to grow to longer lengths. As a result, there is a wider distribution of chain lengths, or molecular weights, than there would be otherwise. A wider molecular weight distribution means that physical properties of the material may be less reproducible.

In a typical polymerization process, the reaction is followed by quenching, in which some agent is added that will stop further polymerization. In cationic polymerizations, quenching might be accomplished through addition of aqueous acid, because either the water or the conjugate of the acid will destroy the cation. The material is usually precipitated in a solvent that can dissolve any remaining monomer, but not polymer. Because some chains may have died very early, they might also remain in solution, leaving only larger chains in the precipitate.

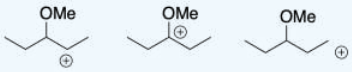
Exercise 2.4.1

Choose the most stable cation from each of the following groups. Provide a reason for the stability of that cation.

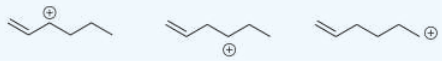
a)



b)



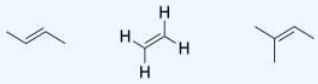
c)



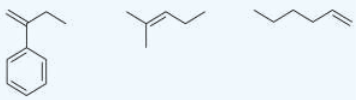
Exercise 2.4.2

In each group, select the alkene most suitable for cationic polymerization.

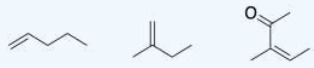
a)



b)



c)

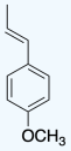


Exercise 2.4.3

Provide a mechanism for the formation of a protic initiator from the interaction of boron trifluoride with water.

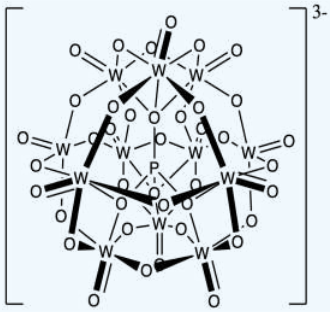
Exercise 2.4.4

Anethole in a naturally-occuring compound that has been used in cationic polymerizations. Show why anethole should be a good monomer for this method.



Exercise 2.4.5

Phosphotungstates such as $H_3PW_{12}O_{40}$ have been used as cationic initiators and do not show much termination by the counterion, below. Propose a reason for the low nucleophilicity of this counterion for the growing cationic chain.

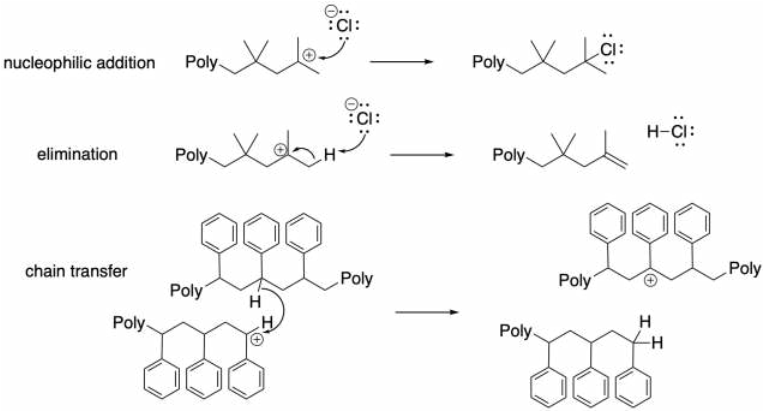


This page titled 11.5.2.4: Cationic Polymerization is shared under a CC BY-NC 3.0 license and was authored, remixed, and/or curated by Chris Schaller via source content that was edited to the style and standards of the LibreTexts platform.

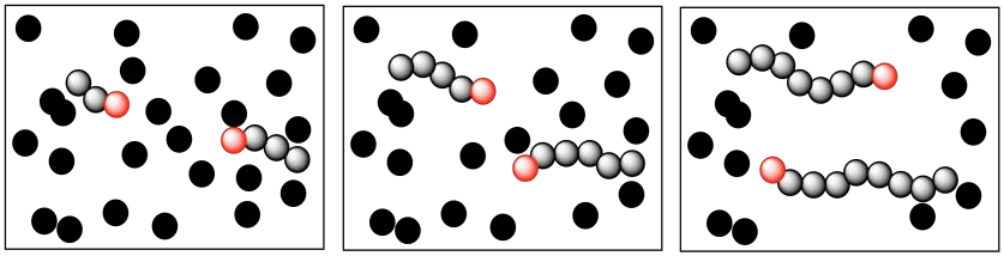
- **2.4: Cationic Polymerization** by Chris Schaller is licensed CC BY-NC 3.0. Original source: https://employees.csbsju.edu/cschaller/Advanced/Polymers/Polycontents.htm.

11.5.2.5: Living Cationic Polymerization

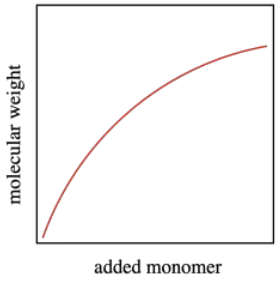
Alkenes are a common polymer feedstock, used to make a range of very familiar plastics in everyday use. Because their properties depend strongly on their molecular weights and molecular weight distributions, it is very important to be able to control the growth of these long-chain polymers from their alkene monomers. Termination events, such as combination of the cation with a nucleophile, elimination, or chain transfer, all contribute to a widening disperity between chains that have undergone these events and those that continue to grow.



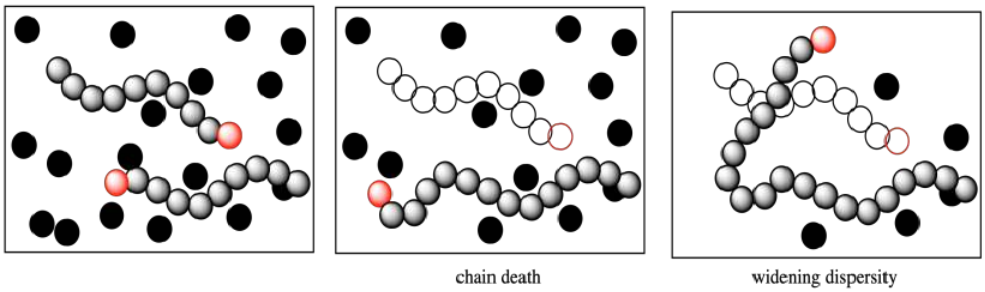
In any polymerization, as in any other reaction, we are dealing with thousands of reactions involving thousands of different molecules all happening at the same time. Several reactive chains growing in tandem would be expected to grow at similar rates, and ultimately they would reach similar degrees of polymerization. That means they would all have the same number of monomers incorporated into the final polymer chain and so they would all have similar molecular weight.



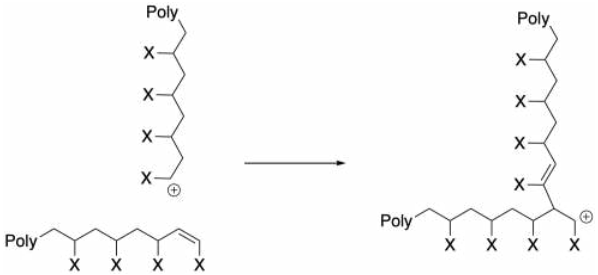
What happens when one of these growing chains undergoes some kind of termination event? Chain death, as this problem is commonly called, has a couple of direct consequences. Obviously, the chain that stopped growing does not keep up with the others, so its molecular weight is lower than the rest. That fact alone might lead us to believe the average molecular weight would be lower than we had expected in this polymerization. If we added more and more polymer to the polymerization over time, we wouldn't expect the molecular weight to keep increasing, because the reactive sites keep getting quenched.



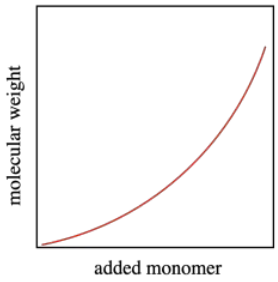
More subtly, that growing chain had been slated to enchain a certain number of monomers, some of which are still left in the system when it dies. What happens to them? Of course, the other growing chains will each get some extra monomers. That means the dispersity problem gets even worse; one chain stops growing and is shorter than anticipated, but others gobble up the extra monomers and become longer than anticipated. Dispersity, the distribution of molecular weights, gets wider.



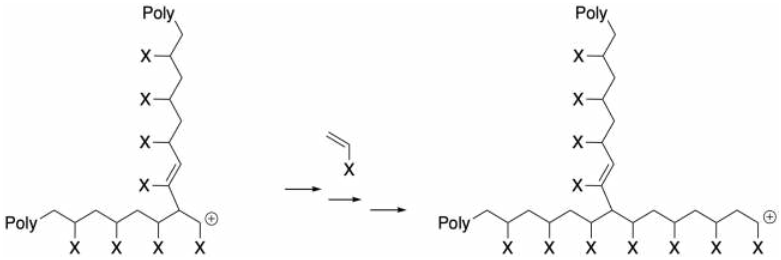
The problem can be even worse when a termination occurs through elimination, resulting in the formation of a new alkene. Because that new alkene is already found at the end of a polymer chain, when it combines with a cationic chain end the polymer molecular weight effectively doubles.



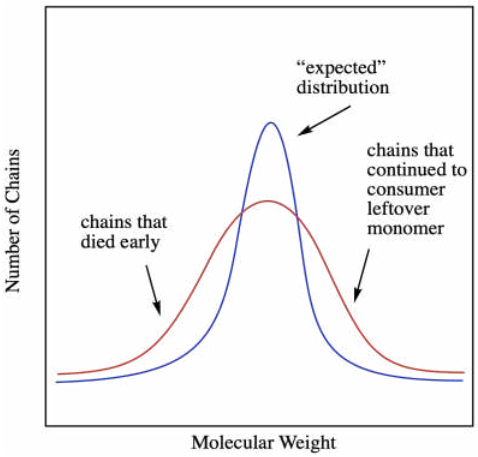
In other words, although we would reasonably expect molecular weight to stop increasing as chains die, resulting in lower molecular weight than expected, the opposite can also happen. We can observe an increase in molecular weight, because the chains that are left are consuming all of the monomer, becoming much bigger, and occasionally two chains are combining to dramatically increase molecular weight. Molecular weight increase is proceeding in an uncontrolled and somewhat unpredictable way.



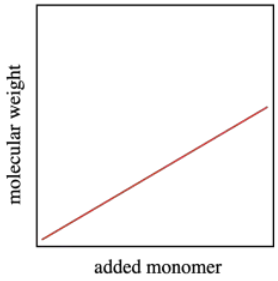
Furthermore, the reaction of a cationic growing chain with a macroalkene results in a sudden shift in polymer morphology. Instead of a straight chain, we now have a dramatically branched polymer. That change in morphology has a severe impact of polymer properties.



All of these factors mean that the distribution of molecular weights gets broader when chain reactions undergo unexpected termination. The term for the width of molecular weight distribution is dispersity (D), sometimes called polydispersity index (PDI). In the graph below, the red line describes a sample from a polymerization that was not as well controlled as the one described by the blue line. There are a lot more polymer chains that are both longer and shorter than the average.



In an ideal polymerization, growing chains wouldn't die unexpectedly. They would continue to grow, and we could easily predict how long each chain would become based on how much monomer and initiator we added. Each initiator molecule would start one growing chain, and each growing chain would enchain its portion of the monomers. The molecular weight would be predicted easily because the polymer chains would grow linearly with added monomer. A polymerization in which there is a linear relationship between added monomer and molecular weight, even as the molecular weight becomes very high, is called a "living polymerization".



A second feature of living polymerization is that dispersity (or PDI) stays relatively constant throughout the course of a reaction. Because there are no chain terminations, the reactive chains all continue to grow at the same pace, and the polymers that result are of uniform molecular weight.

In order to achieve a living cationic polymerization, we would have to prevent unwanted terminations steps. There are a variety of systems that accomplish this goal, but they share some common features. Essentially, these methods intentionally allow a nucleophile to combine with the cationic chain end, but use a Lewis acid to reactivate the resulting compound and regenerate the growing chain end.

Like other cationic polymerizations, these processes could be initiated by addition of a protic acid to an alkene to generate a cation. That initial cation would then begin reacting with the nucleophilic alkenes around it, generating subsequent cations that sustain a chain reaction. In practice, it's instead very common to add an ionizable compound, such as a tertiary alkyl halide, along with a Lewis acid co-initiator. The Lewis acid promotes ionization of the initiator, forming a cation.

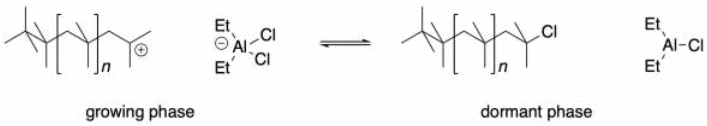


Once that cation has formed, regardless of how it got there, it can begin to react with the monomers around it. The chain reaction will continue, consuming more and more monomers, resulting in a longer growing chain with higher molecular weight.



Lewis acid-base adducts always form reversibly, however. At some point, the adduct can give back to the cationic chain end the same anionic group that it once extracted from the initiator. The chain stops growing, because it no longer contains a reactive site.

However, just as the Lewis acid once extracted an anionic group from the initiator, it can extract it from this polymer chain. When it does, the cationic chain end will start reacting with more monomers, and the chain will grow again.



Living cationic polymerization depends on an equilibrium between a reactive, growing phase and an unreactive, dormant phase. There is an inherent trade-off here. The concentration of reactive cationic chain ends is lowered because a large fraction of the chains are always dormant. That low concentration of cations means there is less opportunity for chain termination events; that's helpful in keeping dispersity low. On the other hand, that low concentration of cations also means the polymer grows much more slowly than it would otherwise.

This trade-off works to our advantage because of kinetic conditions that hold true throughout most of the duration of the polymerization. Termination steps depend on the collision between two species that are both held at relatively low concentration, whether it is a cationic chain end and an anionic base or two different growing chains. Propagation depends on the concentration of reactive chain ends and the concentration of monomer. Although one of those concentrations is very low, the other one is very high all the way up until nearly the end of the polymerization. That means propagation remains fast relative to termination.

For example, if your target is a polymer of molecular weight 100,000 Da and the monomers have molecular weight of 100 Da, then you would conduct the polymerization with one initiator for every thousand monomers. Each time a monomer was consumed, the relative monomer concentration would change very, very little, and it would remain high enough to keep the polymerization reaction moving forward at a reasonable pace. Only near the end of the polymerization would the monomer concentration drop significantly enough to slow the reaction down drastically.

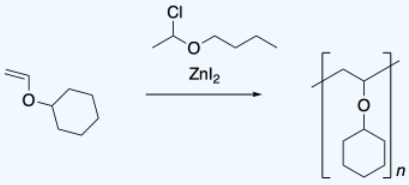
Exercise 2.5.1

Choose the best Lewis acid from each of the following pairs.

a. NCl_3 $GaCl_3$
b. $SnCl_4$ Cl_2
c. CCl_4 $ZnCl_2$
d. $FeCl_3$ $XeCl_2$

Exercise 2.5.2

Provide a mechanism for this polymerization. Show chain control using equilibriu between a growing phase and a dormant phase.



Exercise 2.5.3

Living cationic polymerizations are sometimes promoted when a weakly basic molecule is added to the reaction mixture. Although different reasons have been proposed for the role of the Lewis base, it is well-established that adding a neutral Lewis base to a Lewis acid can result in a more active, cationic Lewis acid. Show how this stronger Lewis acid forms using triethylamine and gallium chloride.

This page titled 11.5.2.5: Living Cationic Polymerization is shared under a CC BY-NC 3.0 license and was authored, remixed, and/or curated by Chris Schaller via source content that was edited to the style and standards of the LibreTexts platform.

- **2.5: Living Cationic Polymerization** by Chris Schaller is licensed CC BY-NC 3.0. Original source: https://employees.csbsju.edu/cschaller/Advanced/Polymers/Polycontents.htm.

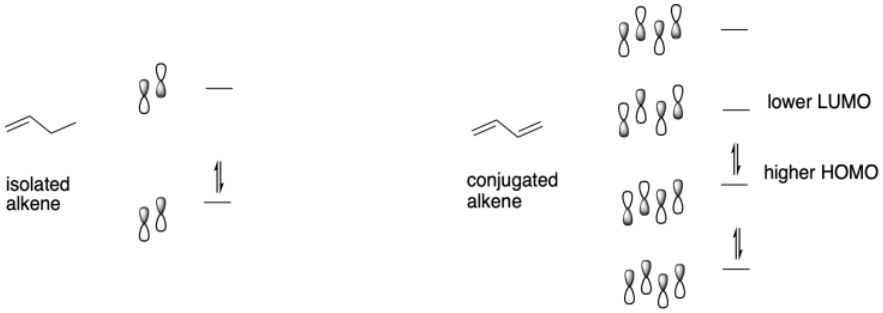
11.5.2.6: Anionic Polymerization

If you have studied some organic chemistry, then it seems obvious that cationic methods would be employed for the polymerisation of alkenes. After all, alkenes are nucleophilic, and so they should react readily with cationic initiators. It might be surprising that there are a number of alkene polymerisations that work very well using anionic initiators.

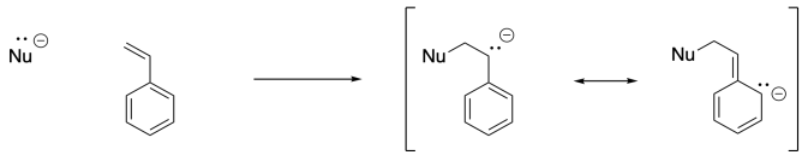
One of the most common scenarios for this approach is in the polymerisation of conjugated hydrocarbons, such as styrene. From the point of view of Lewis structures, this seems like a funny combination. There is no obvious electrophile in an alkene; not even in a conjugated one. Why would it interact with an anionic initiator?



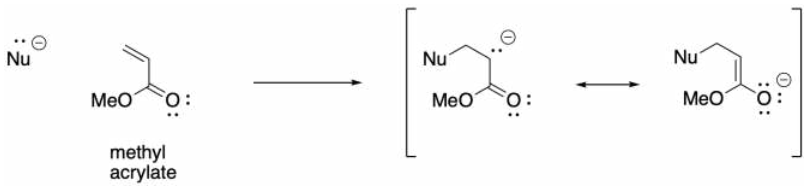
A molecular orbital treatment of conjugated systems provides an answer. When alkenes are conjugated, several things happen. There is at least one extended π-bonding orbital that moves to lower energy because of conjugation, and we think of that factor to explain the relative stability of conjugated alkenes toward electrophiles, compared to the reactivity of isolated alkenes. At the same time, there are also π-bonding orbitals that are raised a little in energy as well as corresponding π*- or π-antibonding orbitals that are lowered in energy by conjugation. This feature explains the well-known shift in optical absorption of conjugated alkenes toward the visible region of the spectrum; we see that in brightly coloured compounds such as carotene and xanthophylls in autumn leaves. It is partly that lowering of the Lowest Unnocupied Molecular Orbital (LUMO) that leads to the increased electophilicity of conjugated alkenes compared to regular alkenes.



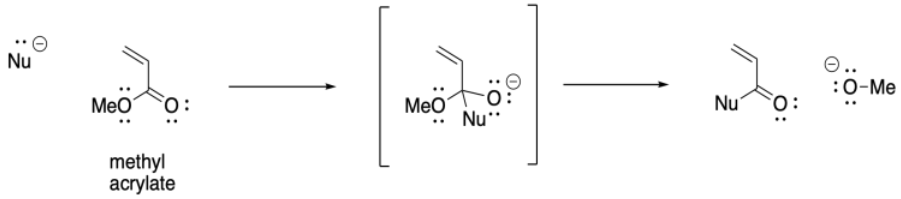
Once an anionic initiator has added to a conjugated alkene, the conjugated alkene itself becomes an anion. That leads to the second part of the explanation. If you look at the anion that results, you will find resonance stabilisation. That delocalisation is always a powerful factor that allows ions to form more easily. In fact, we can easily choose an anionic initiator that is more reactive than that delocalised one, so that there is a driving force toward polymer initiation. Alkyllithiums, such as butyllithium, are good candidates.



There may be other alkenes that come to mind as being potentially suitable for anionic polymerisation. Again, if you have studied organic chemistry, you might thing of 1,4-addition of nucleophiles to conjugated enones. Anionnic initiation of these kinds of monomers is also possible. Acrylate polymerisation, involving monomers that contain a C=C-CO_2 unit, is commercially very important.



The 1,4-addition of anionic initiators does not proceed as smoothly as we might expect, however. This approach is prone to a number of side reactions. For example, Claisen condensations result in the loss of an alkoxide leaving group and chain death.



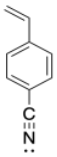
On the other hand, the presence of α-hydrogens along the polymer can lead to a different problem, with equilibrium proton transfer resulting from "back-biting". This phenomenon leads to uncontrolled branching of the polymer chain.



The potential for side reactions means that anionic polymerisations are prone to poor molecular weight control. Chains that die early will have lower molecular weight than those that continue to grow, leading to broad molecular weight distributions. Like cationic polymerisations, anionic polymerisations can be greatly enhanced through the use of living methods.

Problem SM4.1.

Anionic polymerization of *p*-substituted styrene proceeds very well when the substituent is an electron-withdrawing group such as nitrile. Explain the reason for the success of this approach.



Problem SM4.2.

Vinyl chloride (CH2=CHCl) might be expected to be a good candidate for anionic polymerization, but side reactions make it unsuitable.

a) Explain why the resulting anion might be expected to show some stability.

b) Show the side reaction that would result under anionic polymerization conditions.

This page titled 11.5.2.6: Anionic Polymerization is shared under a CC BY-NC 3.0 license and was authored, remixed, and/or curated by Chris Schaller via source content that was edited to the style and standards of the LibreTexts platform.

- **2.6: Anionic Polymerization** by Chris Schaller is licensed CC BY-NC 3.0. Original source: https://employees.csbsju.edu/cschaller/Advanced/Polymers/Polycontents.htm.

11.5.2.7: Living Anionic Polymerization

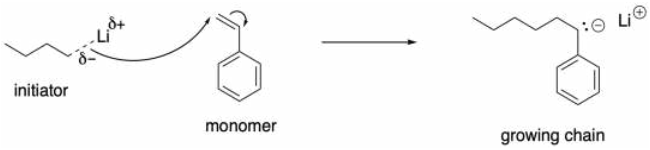
Unwanted side reactions in anionic polymerization, such as back-biting or Claisen reactions with acrylate chains, lead to early chain death and a broadening of the molecular weight distribution. This problem is intrinsic to polymer growth. Because reactive chain ends are needed to enchain additional monomers, there is always the potential that these relatively high-energy species will go off track and lead to different products.

Living polymerization describes any system in which early chain death is limited, so that polymer chains can continue to grow uniformly. In these systems, the molecular weight increases linearly with the percent conversion of monomer to polymer. In addition, dispersity remains low even at high percent conversion.

The reactive chain ends in anionic polymerizations are nucleophilic carbon anions. If you have studied these kinds of compounds before, the idea of covalency might come to mind. Carbon anions are easier to work with if they are not really anions, but instead share their electrons with their counterions to some degree. So, for example, we might choose to employ lithium counterions with these anionic chain ends, rather than sodium or potassium. The smaller, more electronegative lithium (at least compared to sodium or potassium) can form a polar covalent bond with carbon, stabilizing the nucleophile.



Of course, even an alkyllithium is a strong enough nucleophile to initiate anionic polymerization, provided the resulting anion is more stable than the initial one. In general, it can initiate the formation of growing chains if the resulting anion is delocalized.



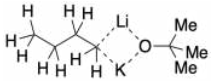
We can think of the growing chains as being in equilibrium between having covalent lithium-carbon bonds and forming ion pairs. The ion pair would be more ready to react with the next monomer. That equilibrium could form a basis for a dormant state and a growing state. Just as in living cationic polymerization, the growing state is necessary for polymer chain growth but is susceptible to unwanted side reactions. The dormant state protects the growing chain by limiting the growing chain concentration, consequently limiting the degree of side reactions.



So, just using a lithium counterion, for instance, might be expected to promote living polymerization, keeping dispersity low. For that reason, it may be surprising that one of the strategies used for chain control in anionic polymerizations is to add potassium alkoxides along with the alkyllithium initiator. If lithium bases have greater covalency and offer greater control, why would you add potassium bases?

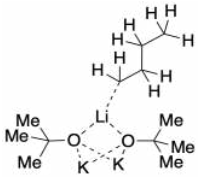
That question has even more merit if you explore the history of mixed-metal bases. Schlosser's base is a well-precedented example. Typically, it's a mixture of butylllithium and potassium tert-butoxide. Developed by Manfred Schlosser at EPF (ETH) Lausanne in Switzerland, mixtures of alkylithiums and potassium alkoxides form powerful bases capable of deprotonating hydrocarbons such as toluene. The mechanism of achieving such high base strength is believed to involve transfer of an alkyl anion from lithium to potassium. From the point of view of making growing chains more covalent, providing a dormant state, this doesn't seem like a good idea. Nevertheless, it works. How?

One of the other features of these mixtures (Schlosser called them LiCKOR bases, noting the mix of lithium and potassium components) is a high level of aggregation. Aggregates are clusters of molecules that stick together. For Schlosser's base, the simplext aggregate would be one alkylithium molecule bound to one potassium tert-butoxide molecule.



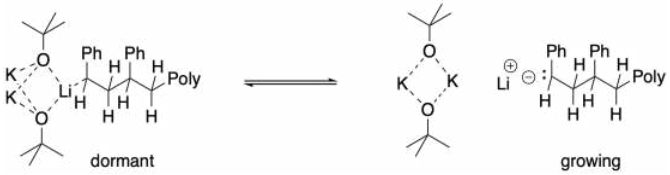
What holds aggregates like this together? The anions can bridge between alkali metals. With the alkoxide ion, that's easy to imagine: the oxygen atom has more than one lone pair, so it can donate one to lithium and one to potassium. It's a little harder to see how the alkyl anion, with only one lone pair, could do that. However, that sort of interaction in which one lone pair is shared between two or more lithium ions, although rare, is pretty well-documented in some alkyllithiums. It's like the alkyl anion has been caught midway between two lithiums, transferring from one to another.

Bigger aggregates could form if additional molecules stuck together. We can easily picture this happening if one alkyllithium combined with two potassium alkoxides.

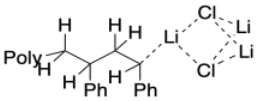


You can probably imagine even larger aggregates. Maybe two alkoxides come together with one alkyllithium, held together by bridging oxygens. In fact, these structures seem to be very dynamic. They can come apart in solution, and they can come together to make even bigger structures. In reality, a number of different aggregation states will exist in equilibrium with each other, and some might contain eight or twelve alkali cations together with their accompanying anions.

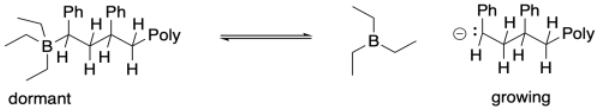
So, what is the role of aggregation in producing a dormant state? It may cap the end of the growing chain temporarily, so that the anionic chain end is less likely to interact with monomers. Reaction would occur only when the aggregate broke up, freeing an anionic chain end.



Aggregate formation can also be promoted by other anions, including simple halides such as chloride and fluoride. As a result, the addition of simple lithium salts can be effectine in promoting living anionic polymerization. The alkoxide base needn't play a role.



An alternative strategy for living anionic polymerization involves the addition of Lewis acidic compounds as chain control agents. In these cases, the equilibrium between dormant and growing chains would involve coordination of the anionic chain end to the Lewis acidic atom. Because Lewis acid-base complexes occur in equilibrium, some fraction of the polymers would always exist in the growing phase, but a greater fraction would always be found in the dormant phase.



Exercise 2.7.1

Rank the following ions in terms of covalency with oxygen (most covalent to least covalent).

a. Na^+, Li^+, K^+
b. Mg^{2+}, Ca^{2+}, Be^{2+}

Exercise 2.7.2

Coordination number can vary with the size of a cation. Rank the following ions from largest to smallest.

a. Na^+, Li^+, K^+
b. Mg^{2+}, Ca^{2+}, Be^{2+}

Exercise 2.7.3

Which compounds would be expected to stabilize growing anionic chains?

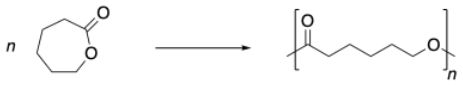
a. Et_3N or Et_3Al
b. Et_2Zn or Et_2O
c. Ph_3B or Ph_3N
d. $(CH_3O)_2AlCH_3$ or $(CH_3O)_2CHCH_3$

This page titled 11.5.2.7: Living Anionic Polymerization is shared under a CC BY-NC 3.0 license and was authored, remixed, and/or curated by Chris Schaller via source content that was edited to the style and standards of the LibreTexts platform.

- **2.7: Living Anionic Polymerization** by Chris Schaller is licensed CC BY-NC 3.0. Original source: https://employees.csbsju.edu/cschaller/Advanced/Polymers/Polycontents.htm.

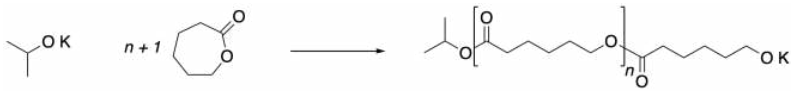
11.5.2.8: Ring-Opening Polymerization

On an earlier page, we saw that polyesters and polyamides are typically obtained via condensation polymerization. Ring-opening polymerization (ROP) offers a second approach to these kinds of materials. Using this method, cyclic esters (lactones) or amides (lactams) are opened up to make extended chain structures. The reaction is typically driven by the release of ring strain. For example, caprolactone is ring-opened to produce polycaprolactone.



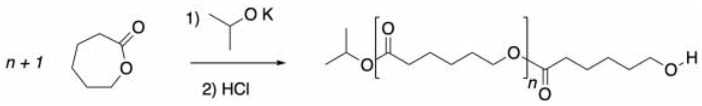
Caprolactone and other ROP monomers are different from the monomers used in condensation polymerization in a couple of ways. First of all, ROP monomers contain only one functional group, not two. Furthermore, they don't need a complementary monomer. These monomers just react with each other. Also, when they react, they don't form a new functional group, as was sometimes the case in condensation reactions. The monomers were esters and the products are esters, too. This swapping of esters leads to the more specific term "ring-opening trans-esterification polymerization" (ROTEP) when lactone monomers are used.

Let's take a look at how these monomers can be enchained together without the need for complementary monomers. The transformation is instead carried out using a chain reaction. An initiator is needed. In this case, an alkoxide nucleophile can be added to open the first monomer, but when that happens, the substitution reaction at the carboxyloid carbon displaces an alkoxide leaving group. The new alkoxide can then add to the next monomer, propagating the chain reaction.

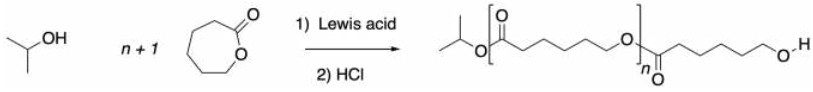


In this drawing, you can explicitly see the new ester linkage formed between two monomers, replacing the ester linkage in the monomer.

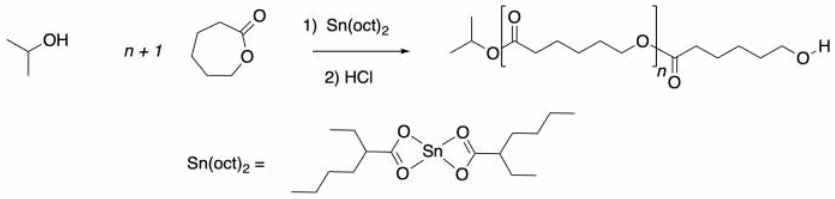
Ring-opening polymerizations like this one are typically quenched with acid to convert the alkoxide nucleophile into a less reactive alcohol, arresting polymerization.



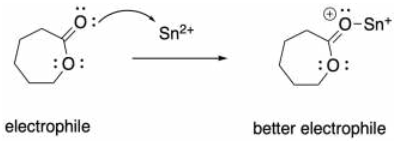
Caprolactone and other cyclic esters can be polymerized via anionic methods, but that isn't the only way. It's very common for these polymerizations to be performed via Lewis acid catalysis instead.



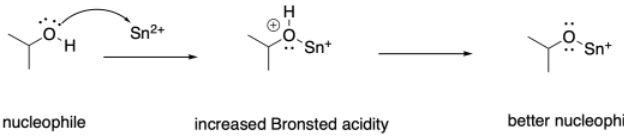
A range of Lewis acids can be used for this purpose, and common examples include iron, zinc, tin and aluminum compounds. This example uses the commercially available tin octoate as a catalyst.



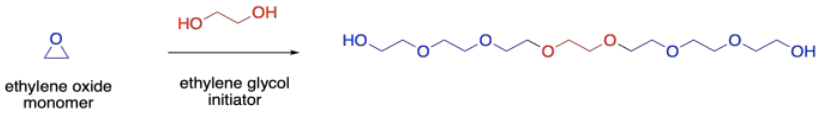
The role of the Lews acid can be twofold. It can accelerate the reaction via electrophilic activation, in which it binds the carbonyl oxygen of the ester, making it more electrophilic.



In addition, when neutral alcohols bind to Lewis acids such as tin octoate, they are more easily deprotonated, becoming better nucleophiles. Both of these effects probably add up to very rapid ring-opening polymerization under these conditions.



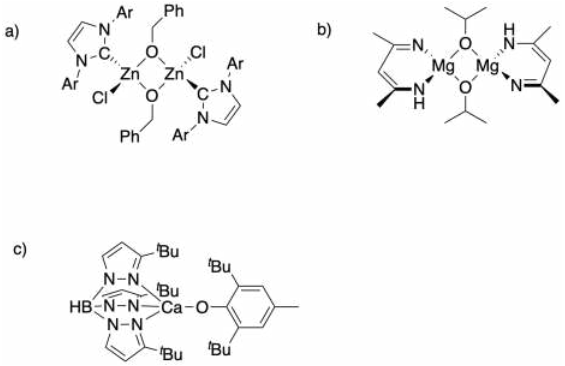
Usually, ring-opened polymers grown either through anionic or Lewis acid conditions have a single growing end, but that doesn't have to be the case. If a difunctional initiator is used instead of a simple alcohol, two monomers would be initiated, allowing growth in two different directions. For example, ring-opening polymerization of ethylene oxide is often accomplished with ethylene glycol as an initiator. The ethylene glycol unit becomes enchained in the middle of the polymer chain, rather than at the end.



This type of structure, with two growing ends, is sometimes called a "telechelic" polymer. It can be very useful in the synthesis of triblock copolymers, because a different kind of monomer can be added to both ends of an existing polymer, leading to an ABA structure.

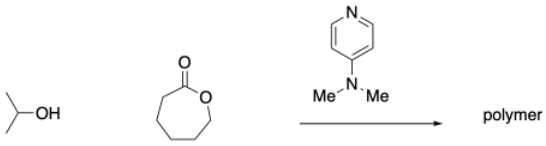
Problem SM6.1.

Some catalysts for ring-opening polymerization contain both a Lewis acid and a nucleophile for initiation of chain growth. Identify these two components in the following catalysts.



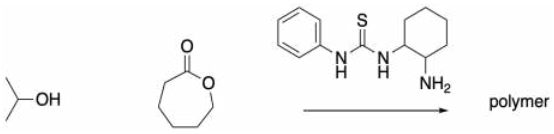
Problem SM6.2.

Some organocatalysts promote ring-opening polymerization of cyclic esters through nucleophilic catalysis, acting as an initial nucleophile. Show the mechanism for the following reaction.



Problem SM6.3.

Some organocatalysts can activate both the nucleophile and the electrophile, and also use a catalytic approximation strategy. Provide a structure that illustrates these features in the following system.

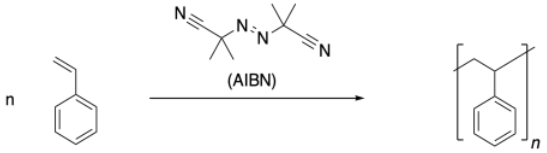


This page titled 11.5.2.8: Ring-Opening Polymerization is shared under a CC BY-NC 3.0 license and was authored, remixed, and/or curated by Chris Schaller via source content that was edited to the style and standards of the LibreTexts platform.

- **2.8: Ring-Opening Polymerization** by Chris Schaller is licensed CC BY-NC 3.0. Original source: https://employees.csbsju.edu/cschaller/Advanced/Polymers/Polycontents.htm.

11.5.2.9: Radical Polymerization

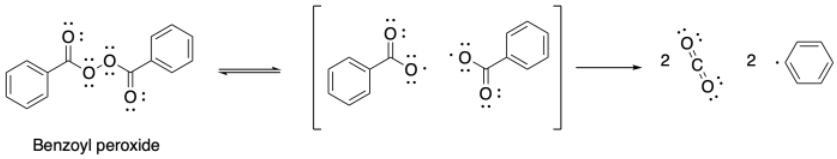
Radical polymerization is a very common approach to making polymers. There are a number of very reliable methods of carrying out radical polymerization, leading to high molecular weight materials. A typical example is the formation of polystyrene under the influence of the radical initiator, azoisobutyronitrile (AIBN).



Radical reactions start with an initiation reaction, in which radicals first come into being. When AIBN is used as an initiator, the compound decomposes partly because of the strong N-N triple bond that is formed, and partly because of the relatively stable radical that results. This radical is both tertiary and delocalized.



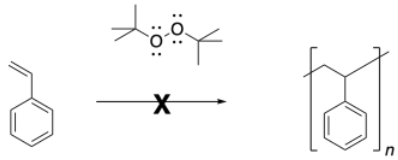
Other initiators can also be used in radical polymerizations. Benzoyl peroxide (BPO) is one common example. In this case, the initiation reaction is sparked by the weak O-O single bond. The benzoate radical that forms from that homolysis further decomposes via decarboxylation, rapidly giving rise to a phenyl radical.



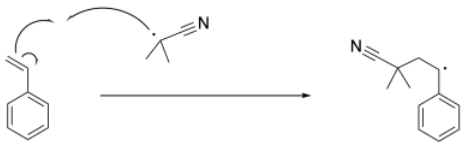
Phenyl radicals and isobutyronitrile radicals are both able to initiate the polymerization of styrene. Not just any radical will peform that task. Simple peroxides are not very good at initiating radical polymerization, despite the fact that they also contain O-O bonds that are readily cleaved.



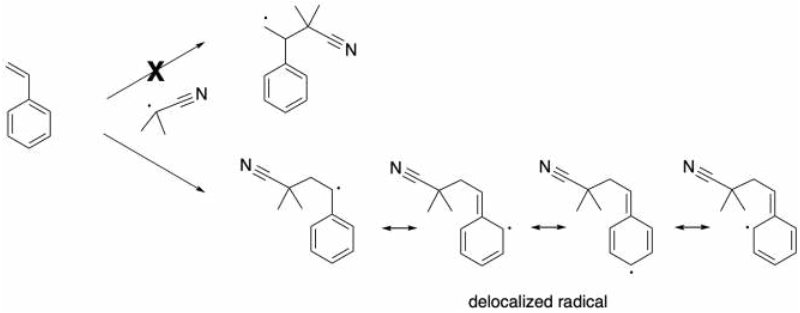
Oxygen-centered radicals do not typically add to double bonds. It's much more common to see them abstract hydrogen atoms. Accordingly, tert-butyl peroxides and other such peroxides would not be used to initiate the polymerization of styrene.



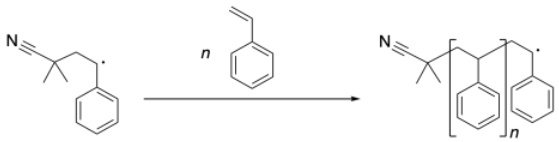
The radical formed via initiation induces cleavage of the pi bond in styrene, resulting in a benzylic radical. This is an example of a propagation step, because old radicals have disappeared and new radicals have appeared.



Note that this step takes place with regioselectivity. There are two possible radicals that could result, but only one actually forms. That's the more stable one. It is stabilized by delocalization because of the benzene ring.

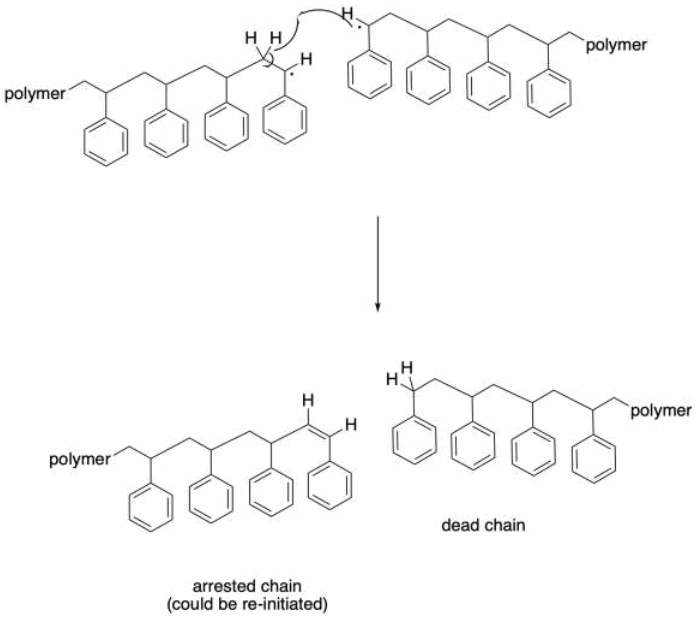


Once that benzylic radical forms, it can continue to propagate, enchaining more styrene molecules. Each time a new styrene molecule is enchained, it forms a new benzylic radical.

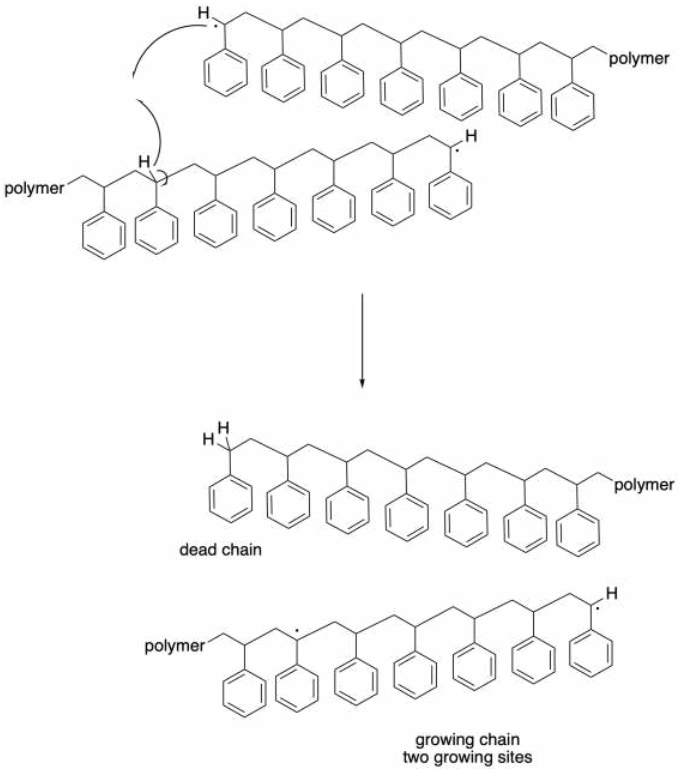


Eventually, radical reactions undergo termination, in which two radicals combine in some way so that neither one is a radical anymore. The most obvious way for that to happen is if two growing chains meet head-to-head, with two benzylic radicals connecting to make a bond.

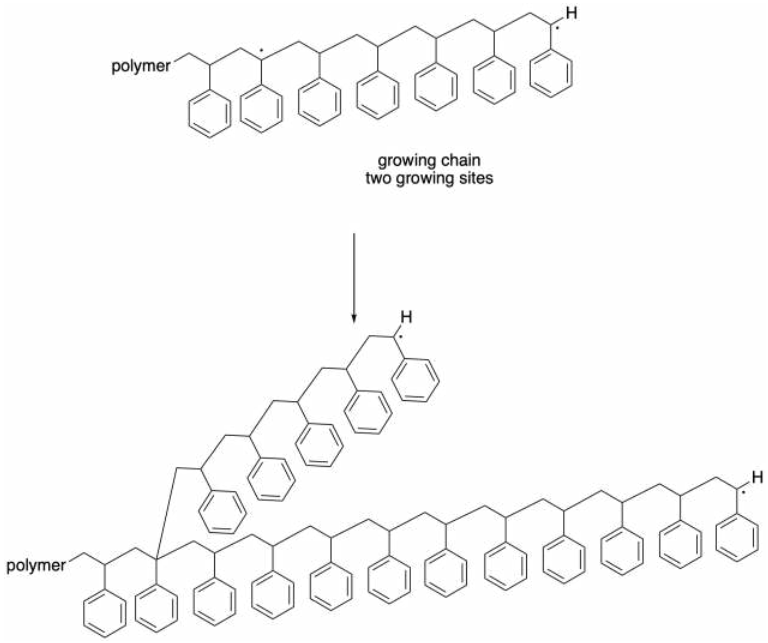
Other termination events are also prevalent in radical polymerizations. Hydrogen atom abstraction is pretty common, with one growing radical stealing a hydrogen atom alpha to the radilca at the head of another chain. The reason that may happen is that it results in the formation of two new bonds: a C-H bond and a C-C pi bond. In that case, both chains stop growing. The one that contains the new pi bond could eventually be re-initiated, of course, but in the meantime it will lag behind most of the other chains that will continue to grow without it. That lag will lead to a broadening molecular weight disctribution.



Partly because of the immense size of the molecules involved, hydrogen atom abstraction need to necessarily take place alpha to another radical. One growing chain may pass another in such a way that its benzylic radical grazes a hydrogen atom along the backbone of another. Hydrogen atom abstraction may occur more randomly in this case, although it may still result in a new benzylic radical.



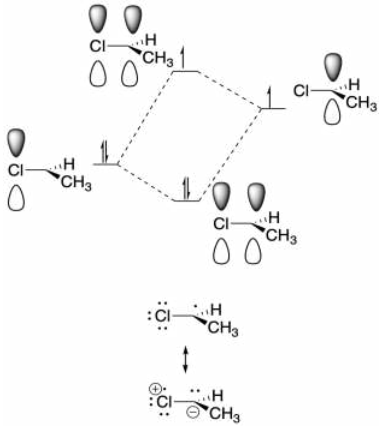
In this case, one chain becomes dead; it stops growing altogether, just like one of the chains in the previous case. However, the other chain continues to grow. In fact, with two radical sites, it will begin to grow twice as quickly as the rest of thegrowing chains. Once again, this development leads to a dramatic broadening of the molecular weight distribution. What's more, this "back-biting" event leads to a change in morphology of the growing chain. Because it is now growing from two different sites, this chain becomes branched, unlike all of the other chains that are growing in a linear fashion. Not only do we now have chains of vastly different lengths, but we also have chains of vastly different shapes, and their properties are becoming less well-defined.



These termination steps are important because they result in the death of growing chains and therefore have an impact on the polymers that result. In later sections, we will see some strategies that limit these termination steps, leading to more uniform molecular weight distribution and more reliable polymer properties.

So far, we have focused on polystyrene as an example of radical polymerization, because of the obvious stability of the benzylic radical. Other monomers can also be polymerized under similar conditions. Like styrene, they may give rise to resonance-delocalized radicals. In other cases, the radical stability may be less obvious, such as in the case of vinyl chloride. Vinyl chloride (CH_2=CHCl) is a pretty candidate for radical polymerization because radicals are stabilized by adjacent halogen atoms.

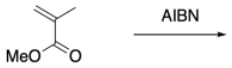
That may come as a surprise. This stability results from a hyperconjugation effect, in which overlap between the radical electron and a nonbonding pair on the halogen results in a net stabilization. This idea is similar to the one behind the stability of highly substituted radicals, such as radicals on tertiary carbons.



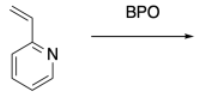
Problem SM7.1.

Show the polymers that would result from radical polymerization of the following monomers.

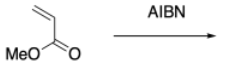
a)



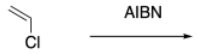
b)



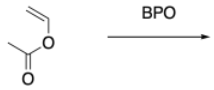
c)



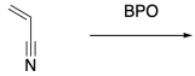
d)



e)



f)



Problem SM7.2.

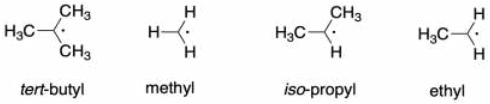
Show why radicals formed from the following monomers are relatively stable:

a) acrylonitrile, CH_2=CHCN

b) methyl acrylate, CH_2=$CHCO_2Me$

Problem SM7.3.

Apart from resonance delocalization, degree of substitution is also a modest stabilizing factor for radicals. Indicate the order of stability of the following radicals:



This page titled 11.5.2.9: Radical Polymerization is shared under a CC BY-NC 3.0 license and was authored, remixed, and/or curated by Chris Schaller via source content that was edited to the style and standards of the LibreTexts platform.

- **2.9: Radical Polymerization** by Chris Schaller is licensed CC BY-NC 3.0. Original source: https://employees.csbsju.edu/cschaller/Advanced/Polymers/Polycontents.htm.

11.5.2.10: Living Radical Polymerization- RAFT

The termination of radical polymerizations can lead to broadening molecular weight distributions and divergent morphology, with branched structures eventually adding in to the mixture of linear chains that were already growing. There are several methods commonly used to prevent these random terminations. All of them work by keeping the concentration of growing chains low. That strategy limits the chance that radical chain ends encounter other chains and undergo termination reactions.

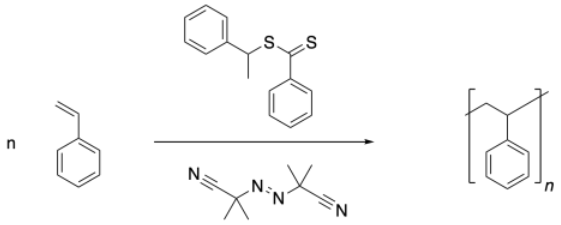
The underlying argument for this strategy is that the kinetics of chain growth and chain termination steps depend differently on the concentration of growing chains. A propagation step requires only one growing chain to encounter a highly abundant monomer molecule. A termination typically requires two growing chains to encounter each other. Consequently,

Rate propagation = k [polymer$^{\cdot}$][monomer]

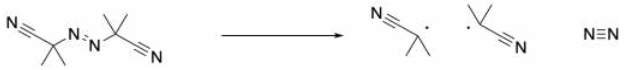
Rate termination = k [polymer$^{\cdot}$][polymer$^{\cdot}$] = [polymer$^{\cdot}$]^2

There is a trade-off. Limiting the concentration of growing chains results in slower polymer growth. At the same time, it results in dramatically slower rates of chain termination.

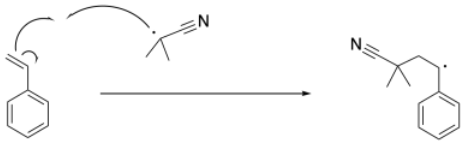
Reversible addition-fragmentation chain transfer (RAFT) polymerization is a common strategy used to limit the concentration of polymer chains at any given time, while ensuring a steady supply of these growing chains in the long run. The strategy has been described as putting growing chains in suspended animation, waking them up periodically to continue polymerization. The key component of this strategy is the chain transfer agent, sometimes called a chain control agent. Usually, these chain transfer agents are thiocarbonylthio compounds like the one shown below.



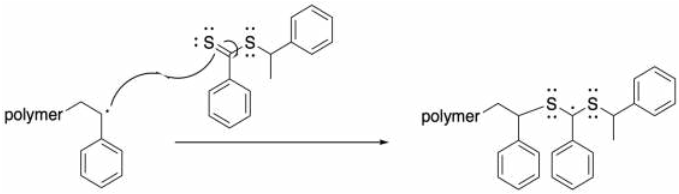
Note that the conditions are otherwise very similar to a regular radical polymerization. The process starts with initiation of radicals, in this case through decomposition of the AIBN.



The isobutyronitrile radical then propagates the radical to the first styrene molecule. So far, nothing different has happened compared to a regular radical polymerization. The resulting benzylic radical propagates with additional styrene monomers, one at a time, enchaining them into the polymer.



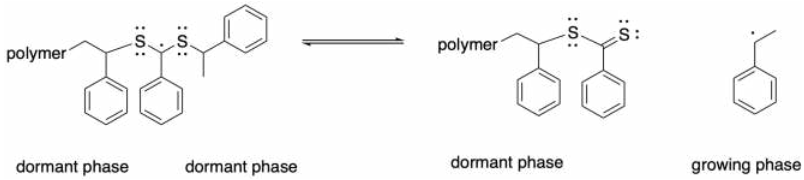
After a few of those propagation events, the growing chain encounters a molecule of the chain transfer agent. Insetad of adding to the pi bond of the styrene, the radical adds to the pi bond of the thiocarbonyl. The new radical is centered on the carbon between the sulfur atoms. If you have encountered sulfur and phosphorus chemistry before, you will know that these large main group atoms have a knack for stabilizing species next to them that would otherwise be very reactive. That's true with radicals, too. The result is that the radical has found a stable resting state. While it sits there, no polymerization can occur, but no terminations will happen, either.



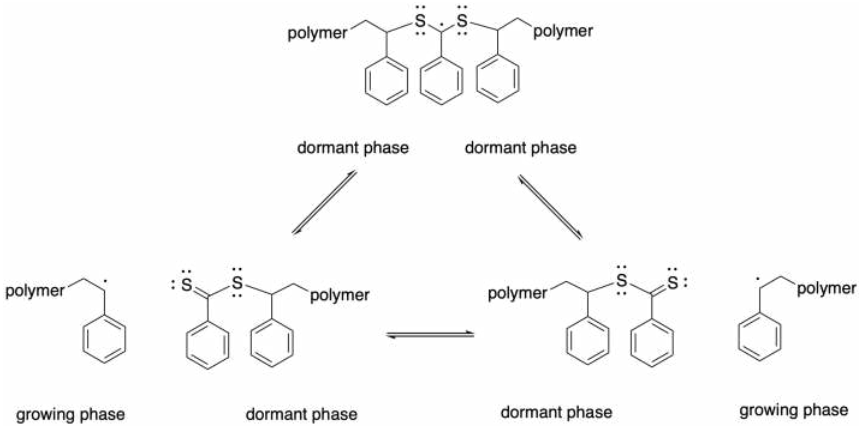
This step happens reversibly, so the growing chain can be released again. It is useful to think of this equilibrium as partitioning the polymers between a growing phase, in which chains can grow but they may also die, and a dormant phase, in which chains are safely sleeping but will not grow.



The structure of these particular chain transfer agents leads to a second possible equilibrium. Rather than releasing the original growing chain from the dormant phase, a radical could be released by cleaving the other sulfur-carbon bond, forming a new thiocarbonyl. The radical that is released is then free to propagate, forming a new polymer chain.



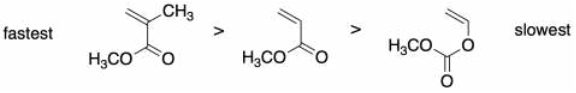
As a result, we can think of this chain control agent as participating in multiple equilibria, with two chains that can each be either dormant or growing. The quilibrium constants are typically chosen so that the chains spend more of their time in a dromant state, but at any given time one of them may be released and start growing again.



As a result, the rate of termination is cut down drastically. Molecular weight distribution (or dispersity) is much narrower and consequently the polymer has much more well-defined properties. Furthermore, the low chance of termination means that the polymer chain can continue to grow until it reaches very high molecular weight.

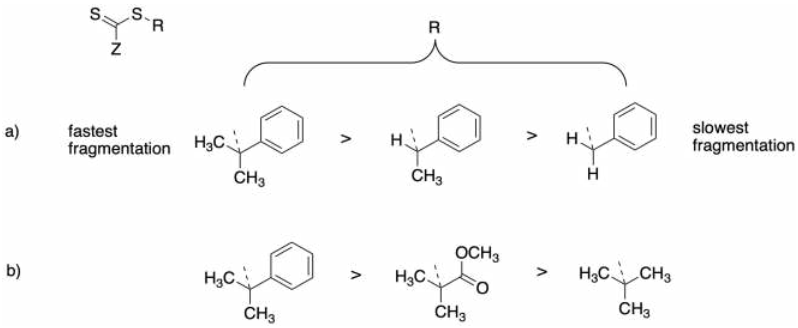
Problem SM8.1.

Relative rates are very important in controlling polymerization via RAFT. Rationalize the relative radical polymerization rates for the monomers below.



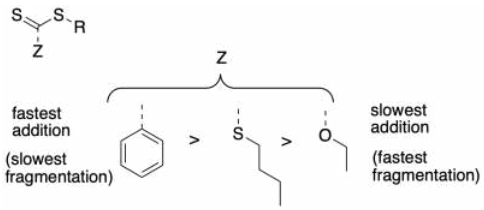
Problem SM8.2.

Relative rates of fragmentation of the chain control agent are important in releasing the growing phase during polymerization. Rationalize the relative fragmentation rates for the chain control agents below.



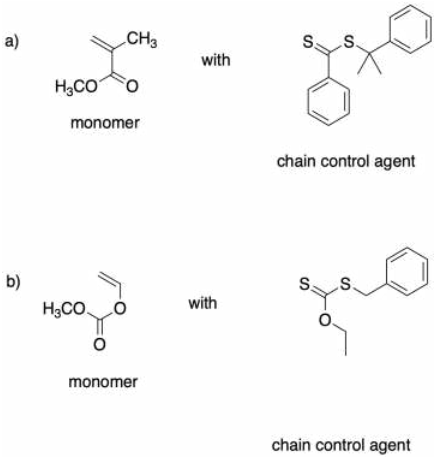
Problem SM8.3.

Relative rates of addition of radical to the chain control agent are important in controlling the concentration of the growing phase during polymerization. Rationalize the relative addition rates for the chain control agents below.



Problem SM8.4.

Effective chain control by RAFT requires selective matching between monomer and chain control agent so that there is an appreciable equilibrium between growing phase and dormant phase. Explain the choice of reagents here.



This page titled 11.5.2.10: Living Radical Polymerization- RAFT is shared under a CC BY-NC 3.0 license and was authored, remixed, and/or curated by Chris Schaller via source content that was edited to the style and standards of the LibreTexts platform.

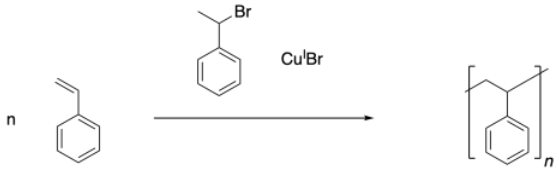
- **2.10: Living Radical Polymerization- RAFT** by Chris Schaller is licensed CC BY-NC 3.0. Original source: https://employees.csbsju.edu/cschaller/Advanced/Polymers/Polycontents.htm.

11.5.2.11: Living Radical Polymerization- ATRP

SM9. Living Radical Polymerization: ATRP

Atom transfer radical polymerization (ATRP) is another common method of carrying out living polymerization. This method, like RAFT and other methods, sets up an equilibrium between a dormant phase of polymer chains and a growing phase. In the dormant phase, radicals have been trapped and are protected from termination, but are also unable to participate in polymerization. In the growing phase, radical chains have been released and can continue to grow by adding monomers in a radical mechanism. The idea is to release just a few radical chains at a time, recapturing them before they have a chance to undergo chain termination events.

ATRP is initiated in a very different way from other radical polymerizations. It does not depend on a typical initiator such as AIBN or benzoyl peroxide. Instead, the initiator is an alkyl halide. On its own, the alkyl halide seems more suited for polar reactions such as nucleophilic substitutions than radical reactions. The second component of the chain control agent, usually a copper(I) halide, is required in order to activate the initiator, turning it into a radical. Polymerization ensues.

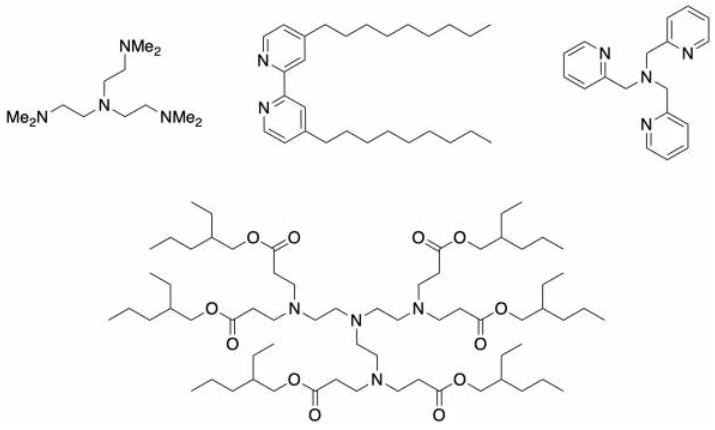


In the initiation step, a halogen atom is transferred from the alkyl halide to the copper(I) ion, leaving behind a radical. In formal terms, the copper has become copper(II), so mechanistically this step appears to involve an electron transfer.



Because the halogen atom on the alkyl halide has lone pairs, it is likely that the electron transfer takes place via an inner-sphere mechanism after the alkyl halide has coordinated to the copper. However, if something prevents the alkyl halide from coordinating to the copper, an outer-sphere electron transfer would still be possible.

There is always an additional component to the chain control system. The copper salts themselves are pretty insoluble. A chelating ligand is added to bind the copper ion and help get it into solution, where it can much more readily participate in the polymerization reaction. A few examples of these ligands are shown below.



Problem SM9.1.

Show CuBr binding with each of the ligands shown above.

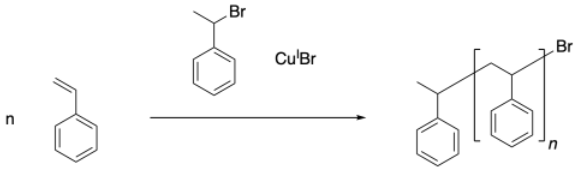
Problem SM9.2.

Show a mechanism of initiator activation via

a) outer-sphere electron transfer

b) inner-sphere electron transfer

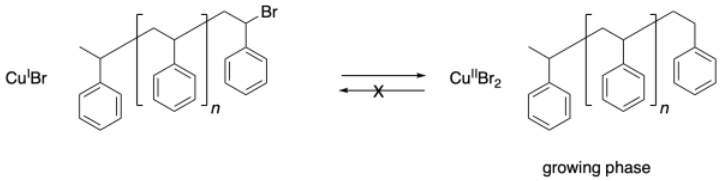
Once the initiator has been activated, it can add to the first styrene molecule. The radical continues to propagate, building up a long polymer chain. In the final polymer, both end groups come from the initiator.



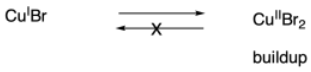
Chain control once again relies on an equilibrium between a dormant phase and a growing phase. In the dormant phase, the radical chain end has been capped with a bromine atom. In the growing phase, the radical chain end is free and able to add to additional monomers.



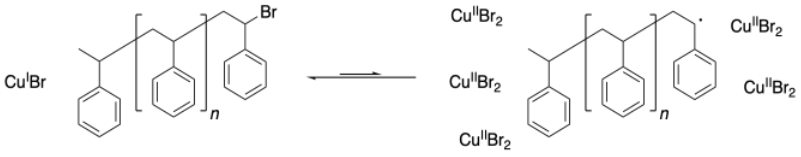
One problem that can arise in living polymerizations is that at some point a termination may still occur. Of course, that results in a dead chain that will no longer grow. An additional consequence is that the chain can no longer go back into the dormant phase, and if the chain cannot go back, then neither can the copper(II).



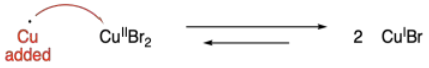
Thus there is a buildup of copper(II) in the system.



What happens when there is a buildup of copper(II)? The job of copper(II) is to deactivate the radical, sending it back into the dormant phase. If copper(II) starts building up, the equilibrium shifts, driving all of the polymer chains into the dormant phase. Polymerization grinds to a stop.



There are a couple of clever solutions to this problem. Perhaps the simplest method uses copper metal to reduce the copper(II) to copper(I). This method has been coined "supplemental activation reducing agent" or SARA.



Problem SM9.3.

In addition to SARA, there are other methods of converting deactivated copper back into its active form in order to shift chains back into the growing phase. Initiators for continuous activator regeneration (ICAR) uses organic reducing agents to convert Cu^{II} back into Cu^{I}. Provide a mechanism for this reaction using phenylhydrazine ($PhNHNH_2$) as the reducing agent.

Problem SM9.4.

Activators regenerated by electron transfer (ARGET) is a similar method to SARA and ICAR, but relies on the addition of the thermal initiator, AIBN, to the polymerization.

a) Provide a mechanism for how AIBN regenerates Cu^{I} ion.

b) Explain the disadvantageous side reaction that can result under these conditions.

This page titled 11.5.2.11: Living Radical Polymerization- ATRP is shared under a CC BY-NC 3.0 license and was authored, remixed, and/or curated by Chris Schaller via source content that was edited to the style and standards of the LibreTexts platform.

- **2.11: Living Radical Polymerization- ATRP** by Chris Schaller is licensed CC BY-NC 3.0. Original source: https://employees.csbsju.edu/cschaller/Advanced/Polymers/Polycontents.htm.

SECTION OVERVIEW

11.5.3: Kinetics and Thermodynamics of Polymerization

11.5.3.1: Thermodynamics of Polymerization

11.5.3.2: Kinetics of Step-Growth Polymerization

11.5.3.3: Kinetics of Chain Polymerization

11.5.3.4: Kinetics of Catalytic Polymerization

11.5.3.5: Solutions to Selected Problems

This page titled 11.5.3: Kinetics and Thermodynamics of Polymerization is shared under a CC BY-NC 3.0 license and was authored, remixed, and/or curated by Chris Schaller via source content that was edited to the style and standards of the LibreTexts platform.

11.5.3.1: Thermodynamics of Polymerization

Polymerization is the process of taking individual monomers and enchaining them into a macromolecule. Thermodynamically, there are always two factors to consider in a reaction: enthalpic contributions and entropic contributions.

$$\Delta G = \Delta H - T\Delta S$$

Entropic changes in chain polymerizations tend to be qualitatively similar in different cases. Because a large number of monomers are being enchained together in a macromolecule, the number of degrees of freedom is always decreasing, regardless of the specific polymerization process under consideration. Consequently, the entropy change associated with polymerization is always negative.

$$\Delta S = k_B \ln\left(\frac{W_f}{W_i}\right)$$

in which k_B is Boltzmann's constant and W is the number of microstates available in the final or initial state. If $W_f < W_i$, then $\Delta S < 0$ because the natural log of a fraction is a negative number.

Free energy correlates positively with enthalpy and negatively with entropy. That means that a negative entropy change translates into a positive, and unfavorable, free energy change. Polymerization is always entropically disfavored, regardless of the circumstances. However, because entropy changes are generally rather small compared to enthalpy changes, polymerization proceeds despite this handicap. The entropy factor begins to dominate the equation only at higher temperatures, because the entropy contribution scales with temperature (in Kelvin) in the expression for free energy.

As a result, thermodynamically, chain polymerizations should be run under cooler conditions in order to maximize the degree of polymerization. Nevertheless, there are certain polymerizations (such as ring-opening polymerization of cyclic esters) that are frequently run at elevated temperatures because of a significant barrier to the reaction. Of course, in these cases there tends to be a maximum extent of polymerization before the process bottoms out in an equilibrium between polymer and monomer.

In general, this entropic problem in entropy gives rise to the term "**ceiling temperature**", which is the temperature above which polymerization of a particular monomer will not occur.

In condensation polymerizations, the entropy of reaction is more subtle. The formation of condensation side products, such as water or methanol, means that there are not overall changes in the number of molecules before and after polymerization. For example, *n* co-monomers are converted into 1 polymer chain and *n*-1 water molecules. There may still be entropy changes in the reaction, but the sign of the entropy change is not as easy to predict compared to chain polymerization.

Since the entropy for chain polymerizations is always positive, then all chain polymerizations must be exothermic, because otherwise they would never proceed. The reasons for these enthalpically-favored reactions varies from one case to another.

In olefin polymerization (alkene polymerization), the enthalpy of reaction has been measured in a wide range of cases; it is usually around -20 kcal/mol. This negative ΔH value can be partly attributed to the exchange of one C=C π bond for one C-C σ bond for every alkene monomer enchained. The strength of an average C=C double bond is approximately 147 kcal/mol, whereas the strength of an average C-C bond is about 83 kcal/mol. By difference, the strength of a C=C π bond is about 64 kcal/mol. Thus, it costs 64 kcal/mol to break the π bond but we drop 83 kcal/mol for each σ bond made, for a net decrease of around 20 kcal/mol.

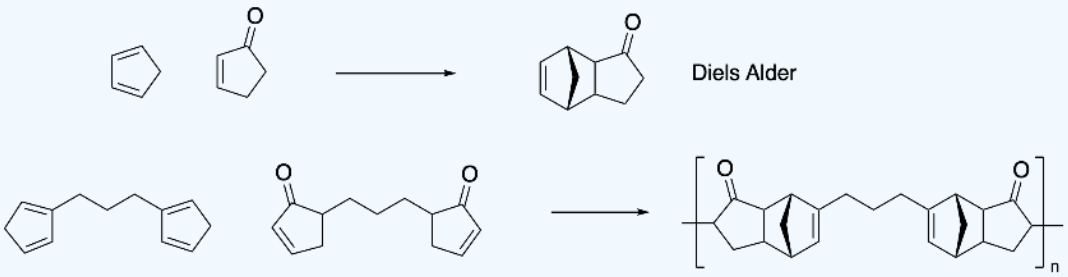
Bond	Bond Energy (kcal/mol)	Bond	Bond Energy (kcal/mol)	Bond	Bond Energy (kcal/mol)
C-C	83	C-N	73	C=C	147
C-O	86	C-Cl	81	C=O	178
N-H	93	Cl-H	102	O-H	111

To be sure, there are other factors that contribute to the enthalpy change. C-H bond strengths change significantly with hybridization changes. Intramolecular steric interactions are drastically different in standard monomers compared to polymers. In alkene polymerization in particular, phase changes between gas phase or liquid phase starting material and solid product is

appreciable, although still small compared to the bond strength issues. Nevertheless, at first glance we would expect a moderately exothermic reaction, and that's what has been measured experimentally.

? Exercise 11.5.3.1.1

Diels Alder polymerization depends on a [4+2] cycloaddition. Thermodynamic studies on the parent reaction indicate ΔH = -40 kcal/mol. Explain this observation in terms of bond strengths.



Taking a second example, the ring-opening polymerization of cyclic esters is considered to be exothermic because of ring strain. Values of ΔH are strongly dependent upon ring size, which is intimately connected with ring strain. For γ-butyrolactone, a five-membered ring containing a carbonyl, ΔH = -1 kcal/mol; that's not enough to compensate for a negative entropy of reaction, so that this monomer can only be polymerized at low temperatures. On the other hand, for δ-valerolactone, ΔH = -3 kcal/mol, whereas for ε-caprolactone, ΔH = -7 kcal/mol. These six- and seven-membered lactones are much more readily polymerized because of increasing ring strain.

? Exercise 11.5.3.1.2

The Ceiling temperature can be calculated from an assumption that $\Delta G = 0$, at which point polymerization is readily reversible. A kinetic approach to equilibrium gives the relation:

$$T_c = \frac{\Delta H}{\Delta S + R \log[M]}$$

in which R is the ideal gas constant, 1.98 cal K^{-1} mol^{-1} (or 8.314 J K^{-1} mol^{-1})

Calculate the ceiling temperature for caprolactone polymerization if ΔH = -7 kcal mol^{-1} and ΔS = -8.6 cal K^{-1} mol^{-1}. The concentration of neat caprolactone is 8.7 M. (Data from: Olsen, P.; Odelius, K.; Albertsson, A.-C. *Biomacromolecules* **2016**, *17*, 699-719.)

Given a less pronounced entropic bias against condensation polymerization, endothermicity becomes less crucial. Indeed, some condensation polymerizations are effected through simple trans-esterifications, which ought to be close to thermoneutral. As pointed out in the condensation section, these reactions are frequently driven to completion by removal of the condensation side product, small molecules such as methanol or water.

? Exercise 11.5.3.1.2

Some polyamides are made industrially from the corresponding difunctional amines and acid chlorides, releasing HCl. Calculate the enthalpy change for this reaction

This page titled 11.5.3.1: Thermodynamics of Polymerization is shared under a CC BY-NC 3.0 license and was authored, remixed, and/or curated by Chris Schaller via source content that was edited to the style and standards of the LibreTexts platform.

- **3.1: Thermodynamics of Polymerization** by Chris Schaller is licensed CC BY-NC 3.0. Original source: https://employees.csbsju.edu/cschaller/Advanced/Polymers/Polycontents.htm.

11.5.3.2: Kinetics of Step-Growth Polymerization

KP2. Kinetics of Step-Growth Polymerization

It is important to understand how reactions proceed over time. This information can tell us how long it will take for a polymer to reach an optimum length. It can also provide insight into how the polymerization occurs, just as kinetics can provide insight into other reaction mechanisms.

Condensation polymers grow through a a step-growth process. The reaction generally involves substitution at a carboxyloid. For example, polyester formation often involves the substitution of an alcohol functional group at a carboxylic acid, making an ester. The drawing below illustrates that action using ethylene glycol and oxalic acid, to use common names prevalent in industry. Oxalic acid is not typically used in making polyesters, but it is drawn here as a very simple example structure.



M1 M2 P

If you know some basic kinetics, you know that we can express the rate of a reaction as the rate of change of product concentration per change in time. In this case, the product is the polymer, abbreviated P. Alternatively, we could express the rate of the reaction as the rate of change of monomer concentration per change in time. Just by looking at the equation of reaction, we expect that every time a polymer molecule is made, a monomer molecule is used up. In this case, we have a co-polymer, made of two different monomers, so that's why we could express the reaction rate as the rate of change of either monomer concentration. The negative sign in the rate suggests we are looking at the rate of disappearance of monomer; as polymer appears, monomer disappears.

$$\text{Rate} = \frac{d[P]}{dt}$$

$$= -\frac{d[M1]}{dt}$$

$$= -\frac{d[M2]}{dt}$$

If you know something about organic reaction mechanisms, you may know that the very first step in an esterification is the donation of a lone pair from an alcohol oxygen on the diol to a carbonyl carbon on the dicarboxylic acid. (It could actually be the second step, but we'll get to that later.) That first step in the mechanism is an elementary reaction. All of the other steps you would draw in a mechanism are also elementary reactions. The nice thing about elementary reactions is that we always know the rate law of each one: it's a rate constant times the concentrations of all of the species leading into that step. In this case, this first step is also the rate-determining step, so the entire reaction is governed by the rate law of that first step. It requires both monomers, so we get a simple rate law.

$$\text{Rate} = k\,[M1]\,[M2]$$

$$\text{but if } [M1] = [M2] = [M]$$

$$\text{then Rate} = k\,[M]^2$$

Note that, based on the stoichiometry (the ratio of monomers in the equation of reaction), we would probably run this polymerization with equal amounts of diol and dicarboxylic acid. Instead of worrying about M1 and M2 separately, we can call them both [M].

So, what we have here is a simple second-order rate law. This form of the rate law is called the differential rate law, because it is expressed in terms of the rate of change of one thing with the rate of change of the other. If that isn't exactly what you are interested in, and you just want to see what happens to concentrations over time, you may want to integrate this expression to obtain the integrated from of the rate law.

$$\text{Rate} = -\frac{d[M]}{dt} = k[M]^2$$

$$-\frac{d[M]}{[M]^2} = k\,dt$$

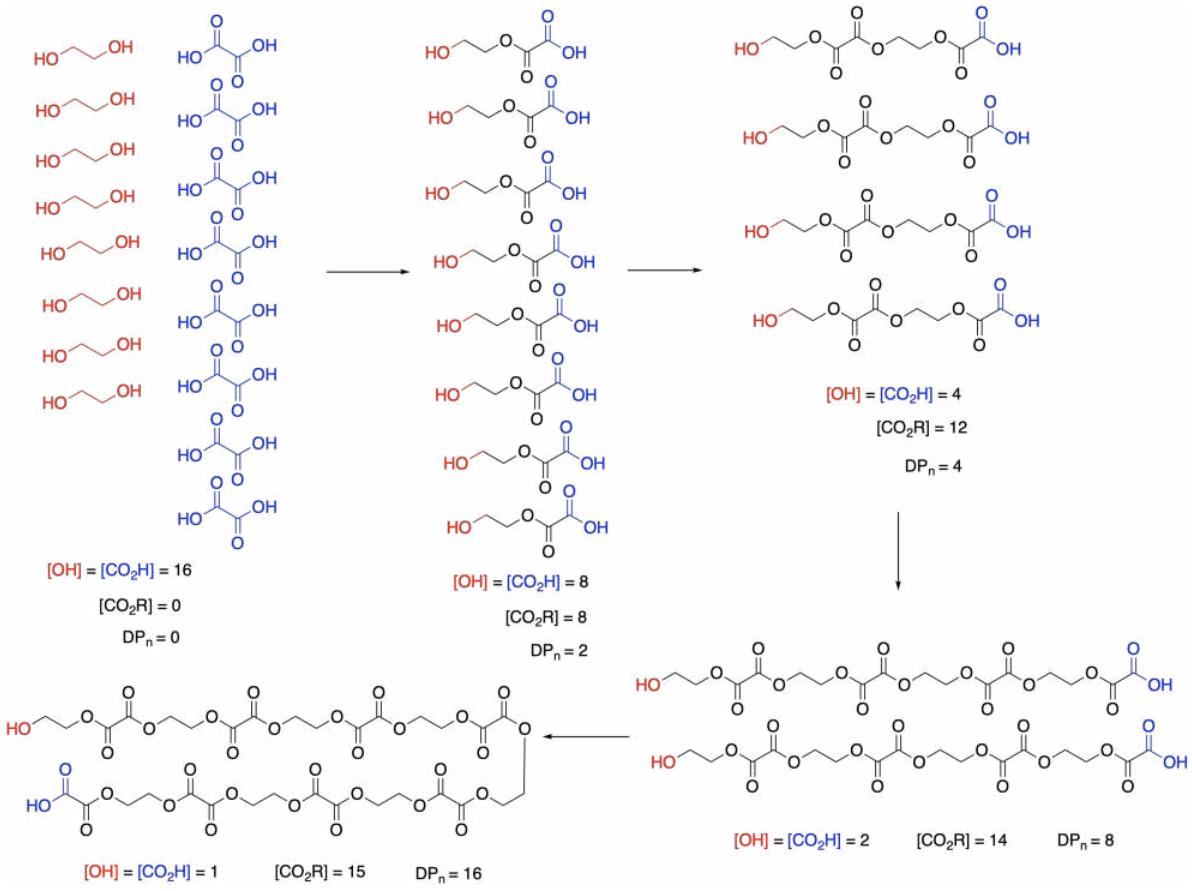
Integrating:

$$\int_{c_0}^{c_t} -\frac{d[M]}{[M]^2} = \int_{t=0}^{t} k\,dt$$

$$\frac{1}{[M]} - \frac{1}{[M]_0} = k\,t$$

If we were to measure monomer concentration periodically during the polymerization and plot its inverse over time, we would obtain a straight line. The slope of the line would be the rate constant, and the intercept would reflect the inverse of the monomer concentration with which we had started the reaction.

At this point, we need to pause and talk about what we actually mean by monomer concentration. Because of a very specific feature of condensation polymerizations, it isn't really the concentration of ethylene glycol or oxalic acid. Take a look at this drawing of this step-growth process and we will talk about why that is.



Remember that, in step-growth polymerization, the majority of molecules are probably reacting at roughly similar rates. Two monomers link together to form dimers, two dimers form tetramers, two tetramers form octamers, and so on. It won't go as perfectly as we see in this picture; there will inevitably be some stragglers that throw the averages off. But notice what this means: the monomers disappear right away. Nobody is really interested in how quickly the monomers turn into dimers. They want to know how the gowth of the polymer chain is progressing.

So, in the above expression, [M] doesn't refer to the concentrations of those two monomers at all. It refers to the concentration of the reactive functional groups in those monomers. After all, once the monomers are gone, the same esterification reaction keeps happening, and it's really the concentration of alcohol and carboxylic acid groups that matters, whether they are found on monomers, dimers, tertramers, or whatever. In these rate expressions, sometimes people will explicitly use [OH] and [CO_2H] in the rate expression, underscoring that they are really following the disappearance of those functional groups.

And notice what's happening to those functional groups. Their concentration is smoothly dropping over time. Furthermore, ester concentration, representing the new functional group in the polymer, is growing in at the same rate. [OH] and [CO_2H] drop by 8 (or in half) in the first step; [CO_2R] increases by 8, and so on. SO the rate of consumption of reactant functional groups equals the rate of appearance of product functional groups.

The other thing we are interested in here is the degree of polymerization: the number of monomers incorporated into the chain. The polymer is growing at a certain rate, but how long is it getting? Just looking at the simple scheme of polymer growth above, we see the average degree of polymerization increasing (written as *DP* or sometimes as X_n; a bar over the symbol signals that we are looking at an average). If you look carefully, you will see that the degree of polymerization is always the original monomer concentration divided by the remaining monomer concentration. That turns out to be a very important relationship.

$$\text{degree of polymerization } DP_n = \bar{X}_n = \frac{[M]_0}{[M]}$$

Note that this relationship is just the inverse of the fraction of monomer remaining (or, really, the fraction of those monomer functional groups left over).

$$\text{fraction monomer remaining} = \frac{[M]}{[M]_0}$$

The opposite quantity is the fraction of monomer converted. That describes the functional groups already converted into esters. Because we are dealing with fractions, the fraction converted is just one minus the fraction remaining. If we do a little algebra, we get a variation on that piece of information.

$$\text{fraction monomer converted } p = 1 - \frac{[M]}{[M]_0}$$

$$\text{or } 1 - p = \frac{[M]}{[M]_0}$$

$$\text{or } \frac{1}{1 - p} = \frac{[M]_0}{[M]}$$

Why did we do that last part? Because now we have arrived back at the expression for degree of polymerization. So, now we have an equivalent way of expressing degree of polymerization in terms of the fraction converted. This relationship is called the Carothers equation, in honor of Wallace Carothers, the DuPont chemist who invented nylon.

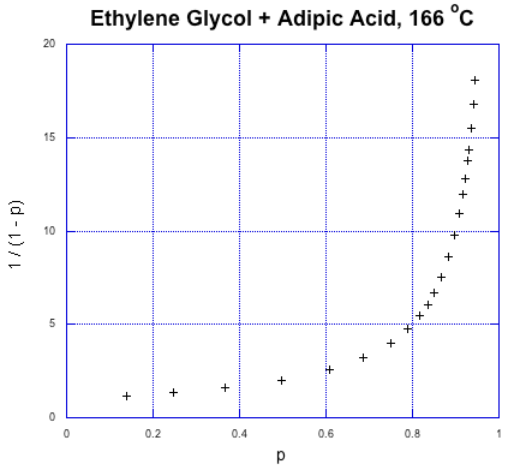
$$\text{but } \bar{X}_n = \frac{[M]_0}{[M]}$$

$$\bar{X}_n = \frac{1}{1 - p} \quad \text{(Carothers Equation)}$$

Problem KP2.1.

Predict the degree of polymerization if 75% of monomer end groups have been converted to polymer.

So, what does that relationship look like? Here's some data from Paul Flory, another DuPont chemist and Nobel laureate, obtained during the period between the World Wars when this kind of chemistry was just getting started (Flory, P. J. *J. Am. Chem. Soc.* **1937**, *59*, 466-470).



That's fraction converted on the x axis and the expression for degree of polymerization on the y axis. This is exponential growth. The degree of polymerization is starting to shoot upward dramatically. We already knew that from our introduction to step growth, but what stands out from the data is how a higher degree of polymerization, and high molecular weight, doesn't really occur until very late in the reaction. If we need high molecular weight condensation polymers, the chemistry better be pretty reliable; otherwise, if things go wrong, we'll be left with some short-chain goo instead of long-chain materials.

Now let's take these new relationships and look at them in the context of our second-order kinetics. We're starting with that same integrated rate law, but we have mulitplied everything on both sides of the equation by the starting monomer concentration. That's fair game in algebra, remember. The reason for doing that is to get a term that resembles our relationships that describe degree of polymerization.

$$\frac{[M]_0}{[M]} - \frac{[M]_0}{[M]_0} = [M]_0 k t$$

$$\frac{[M]_0}{[M]} - 1 = [M]_0 k t$$

$$\text{but} \quad p = 1 - \frac{[M]}{[M]_0}$$

$$\text{or} \quad 1 - p = \frac{[M]}{[M]_0}$$

$$\text{or} \quad \frac{1}{1 - p} = \frac{[M]_0}{[M]}$$

$$\text{so} \quad \frac{1}{1 - p} - 1 = [M]_0 k t$$

So far, we have taken the ratio we obtained in the first line and worked out its relationship to fraction converted, which we substituted in the last line. Now we bring in the Carothers equation to recall that this is really telling us how degree of polymerization changes over time. This relationship indicates the degree of polymerization should increase linearly over time.

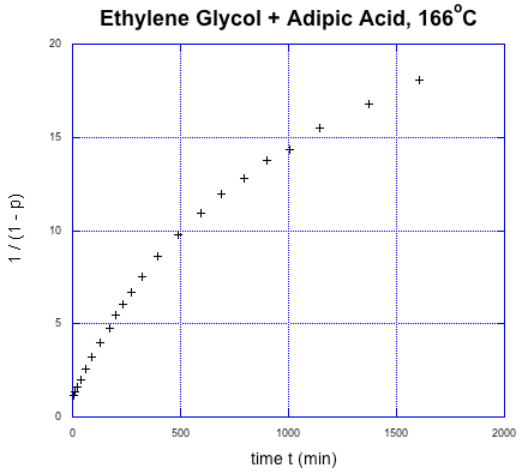
$$DP_n = X_n = \frac{[M]_0}{[M]}$$

$$\text{and} \quad \frac{[M]_0}{[M]} - 1 = [M]_0 k t$$

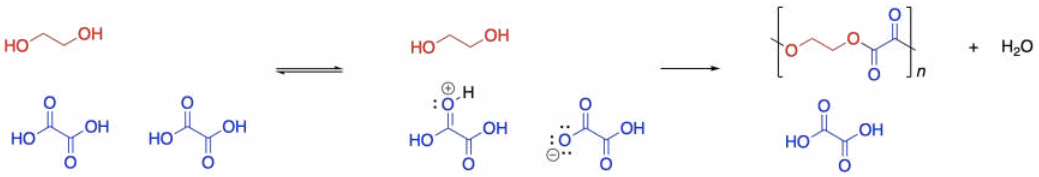
$$\text{so} \quad X_n - 1 = [M]_0 k t$$

This relationship indicates the degree of polymerization should increase linearly over time. Once again, we're going to use Flory's data to illustrate the relationship, using the fraction conversion data. He could measure that data easily, and knew how it was related

to degree of polymerization.



It was supposed to be linear. But don't worry; Flory knew what went wrong. You might know, too, if you remember a few things about substitution at carboxloids. The trouble is, we are dealing with a neutral nucleophile and a fairly unreactive electrophile. That reaction should be really slow. It isn't that slow, thoough, because it is self-catalyzed. One carboxylic acid monomer can activate another, making it a better electrophile.



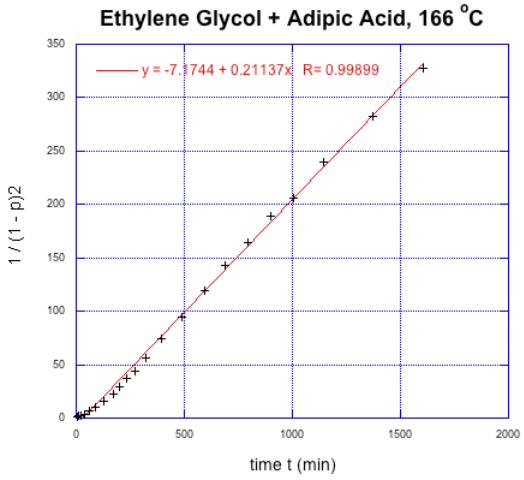
That means the coupling of the alcohol with the carboxylic acid isn't the first elementary step of the reaction, but the second. Before the alcohol and carboxylic acid can come together, two carboxylic acids need to have collided already. That means we have a third order reaction. As it happens, the integrated form of a third order rate law isn't all that much more complicated, and we can do some similar algebra with it to see how the degree of polymerization would vary with time given this new information.

$$\frac{1}{[M]^2} - \frac{1}{[M]_0^2} = 2kt$$

$$\frac{[M]_0^2}{[M]^2} - \frac{[M]_0^2}{[M]_0^2} = 2[M]_0^2 kt$$

$$\frac{1}{(1-p)^2} - 1 = 2[M]_0^2 kt$$

We can take Flory's data again and give it this new treatment.



This time, we get a linear relationship. That correction illustrates one of the fundamental uses of kinetics, which is a tool that lets us probe how reactions happen. In this very specific case, kinetics showed that there was an extra (pre-rate determining) step in the reaction. In addition, we found that it is the square of the degree of polymerization that is increasing linearly with time.

Problem KP2.2.

Given an initial alcohol group concentration [M]0 = 17 M, determine the rate constant from Flory's data in $L^2mol^{-2}s^{-1}$.

Flory also established a statistical basis for predicting molecular weights and molecular weight distributions in polymers. For example, once we have the degree of polymerization, it is a simple step to calculate the approximate molecular weight. That's just the degree of polymerization times the molecular weight of the monomer; in other words, the number of monomers in the chain times the weight of each one. (This approach neglects any small molecules such as water that are lost during the condensation reaction.)

$M_n = DP \times M_0$

$M_n = M_0 / (1 - p)$

This is called the number average molecular weight. It's based on taking one average value for the chain length and converting that into the chain molecular weight. Of course, some chains may be much shorter (Flory actually shows, based on probability, that there will be a number of monomers left over) and as such they contribute less to the overall sample.

A second way to approach the average chain molecular weight is to assess the fraction of the total weight contributed by each chain length. The average chain molecular weight would then be given by:

$M_w = \Sigma\, \pi_x x M_0$

in which π_x is the fraction of chains of length x.

What is the fraction of chains of length x? The approach starts with considering the probability that a chain will be *x* units long. As noted above, a chain x units long has x-1 ester linkages and 2 unreacted chain ends. We know the probability of a chain end being converted to a polymer linkage is p, and in a chain x units long that will have to happen x-1 times, for a probability p^{x-1}. We also know that the probability of a functional group being left unreacted is 1-p, and that has to happen twice here, for a probability $(1-p)^2$. The probability of having a chain of length x is:

$\pi_x = x\, p^{x-1}(1-p)^2$

That means:

$M_w = \Sigma\, x\, p^{x-1}(1-p)^2\, xM_0$

$M_w = (1-p)^2 M_0\, \Sigma\, x^2\, p^{x-1}$

The series on the right is reducible to:

$\Sigma\ x^2\ p^{x-1} = (1 + p) / (1 - p)^3$

So that:

$M_w = (1\text{-}p)^2 M_0 (1 + p) / (1 - p)^3$

$M_w = M_0 (1 + p) / (1 - p)$

That provides a straightforward prediction of the weight-average molecular weight based on the fraction converted in condensation polymerization. Although M_n and M_w presented here are essentially theoretical predictions of molecular weight, these quantities can also be measured experimentally using different methods.

The ratio between these two quantities has always been used as an expression of the breadth of the molecular weight distribution, called the polydispersity index or simply the dispersity:

$D = M_w/M_n$

In the case of condensation polymerization,

$D = [M_0 (1 + p) / (1 - p)]/[M_0 / (1 - p)]$

$D = 1 + p$

Because p is always a fraction, the result is that the dispersity of a condensation polymerization is statistically expected to be less than 2.0.

Problem KP2.3.

Given 99% conversion of monomers with average molecular weight 120 g/mol, calculate M_w, M_n and D.

This page titled 11.5.3.2: Kinetics of Step-Growth Polymerization is shared under a CC BY-NC 3.0 license and was authored, remixed, and/or curated by Chris Schaller via source content that was edited to the style and standards of the LibreTexts platform.

- **3.2: Kinetics of Step-Growth Polymerization** by Chris Schaller is licensed CC BY-NC 3.0. Original source: https://employees.csbsju.edu/cschaller/Advanced/Polymers/Polycontents.htm.

11.5.3.3: Kinetics of Chain Polymerization

The polymerization of alkenes occurs in a very different way than monomers that undergo condensation reactions. Whether it occurs through an anionic, cationic, or radical mechanism, polymerization of alkenes involves a chain reaction. Chain reactions are classically illustrated by radical chemistry, so we will look at a treatment of radical chain polymerization to see some of the factors that influence polymerization rates.

A typical radical polymerization starts with the thermal decomposition of a radical initiator to provide two radicals. The rate of decomposition depends only on the decomposition rate constant and the concentration of the initiator.

$$\mathrm{I} \xrightarrow{k_d} 2\,\mathrm{R}^{\cdot}$$

$$\frac{-\,d[\mathrm{I}]}{dt} = \frac{1}{2}\frac{d[\mathrm{R}^{\cdot}]}{dt} = k_d[\mathrm{I}]$$

Once the radicals have been generated, they are able to undergo radical addition to a monomer double bond. Of course, radical addition to a double bond results in a new radical where the double bond used to be. Although this is formally a radical propagation step, in polymer chemistry it is termed the initiation step, because it is the first time a monomer has undergone radical addition. This step consumes the first monomer and produces a new radical species which will become the growing radical chain. It requires a collision between the radical and a monomer, so the rate of initiation depends on those two concentrations and the chain initiation rate constant, k_i.

$$\mathrm{R}^{\cdot} + \mathrm{M} \xrightarrow{k_i} \mathrm{M}^{\cdot}$$

$$\frac{-\,d[\mathrm{M}]}{dt} = \frac{d[\mathrm{M}^{\cdot}]}{dt} = k_i[\mathrm{R}^{\cdot}][\mathrm{M}]$$

That rate law depends on a reactive intermediate. It's not a very helpful rate law, because the reactive intermediate isn't something that we have directly measured out and added to the reaction, and it might not even occur at high enough levels that we can measure its concentration as the reaction progresses. We usually look for ways to express the rate law in ways that do not include reactive intermediates. In this particular situation, the way of getting around this situation is to assume that the decomposition of the initiator is the rate determining step. Making the radicals in the first place is probably the slow part because it is heavily dependent on bond breaking, which is energy intensive. Once we have radical, it probably undergoes addition to a monomer fairly quickly, initiating chain growth. If that's true, we can assume that the chain initiation step proceeds very quickly afterward, so that the rate really depends only on the rate of the decomposition step.

$$k_i >> k_d$$

$$\frac{d[\mathrm{M}^{\cdot}]}{dt} = \frac{d[\mathrm{R}^{\cdot}]}{dt} = 2\,k_d[\mathrm{I}]$$

In practice, polymer chemists add another factor to the rate law. This factor, f, takes into account the fact that only some of the radicals from the initiator actually react with monomers to initiate growing chains. The rest decay through some other side reactions. Usually, f is assumed to be around 0.5.

$$\frac{d[\mathrm{M}^{\cdot}]}{dt} = 2\,f\,k_d[\mathrm{I}]$$

$$f = 0.3 \text{ to } 0.8$$

Once the first monomer has been initiated into a radical, it can react with another monomer to enchain it and make a new radical. This is the principal propagation step of the chain reaction. That step will keep repeating, adding more monomers into the chain. The rate constant for this step, k_{prop} or k_p, is identical no matter how many monomers have been enchained, but is distinct from k_i because of the different nature of the radical intermediates in the two different steps. For example, the radical obtained from addition to styrene looks pretty similar whether it is the first in the chain or the tenth. Each time, the rate of consumption of monomer depends on the propagation rate constant, the concentration of the monomer, and the concentration of the propagating radical. Notice that in the rate law we just write that propagating radical the same way (M dot) no matter how long the chain grows.

$$\mathrm{M^{\cdot} + M \xrightarrow{k_p} M\text{-}M^{\cdot}}$$

$$-\frac{d[M]}{dt} = k_p\,[M][M^{\cdot}]$$

There is one last process, or group of processes, to complete the chain reaction cycle. In termination, two radicals combine in some way to form closed-shell products. There are a variety of ways that can happen in a radical polymerization. The simplest event conceptually is coupling, in which two radical chains come together and form a bond. That idea is shown below.

$$\mathrm{M^{\cdot} + M^{\cdot} \xrightarrow{k_t} M\text{-}M}$$

$$-\frac{d[M^{\cdot}]}{dt} = 2\,\frac{d[M\text{-}M]}{dt} = 2\,k_t\,[M^{\cdot}]^2$$

Of course, that rate depends on the termination rate constant and the concentrations of both growing chains. The same would be true if the reaction terminated by conproportionation, in which one radical abstracted an alpha hydrogen from the other, forming one saturated and one unsaturated product.

Once again, these last two rates -- of propagation and of termination -- depend on concentrations of reactive intermediates, which we do not typically know. This time we will use a very standard assumption, which is that the concentration of this reactive species remains constant, being consumed as soon as it is generated. The usual way that we apply the steady state approximation is to assume zero change in concentration of the reactive intermediate. That means that the sum of all the rates for processes generating the intermediate equal the sum of all the rates consuming the intermediate. In polymer chemistry, we take a slight shortcut, and just assume that the rate of appearance of the radical in the first place equals its rate of disappearance. We already have expressions for both of those rates.

$$\mathrm{Rate_{term} = Rate_{init}}$$

$$2\,k_t\,[M^{\cdot}]^2 = 2\,f\,k_d\,[I]$$

$$[M^{\cdot}] = \left(\frac{f\,k_d\,[I]}{k_t}\right)^{1/2}$$

By rearranging, we can get an expression for the reactive chain end concentration. Then we can just substitute the result into our expression for propagation rate:

$$-\frac{d[M]}{dt} = k_p\,[M][M^{\cdot}]$$

$$= k_p[M]\left(\frac{f\,k_d\,[I]}{k_t}\right)^{1/2}$$

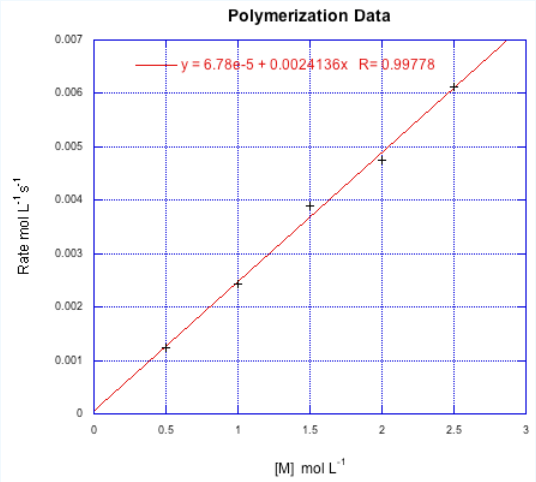
The result sums up the factors that control the growth rate for the polymer. The growth rate increases linearly with the concentration of monomer, and as the square root of the initiator concentration. The rest of the factors are just constants, so we can think of the rate law as one combined constant and those two concentration dependences. Sometimes an aggregate constant of this type is just designated k'.

Note that the propagation rate varies linearly with the concentration of growing chains, but that the termination rate varies with square of the concentration of growing chains. That difference is significant, and it underlies the strategy of living polymerization, which is to keep the concentration of growing chains low. Doing so has the adverse affect of slowing the rate of propagation, but the effect on the termination rate is much greater, making this trade-off worth it to achieve enhanced molecular weight control.

Example 11.5.3.3.1

Suppose the following data were obtained for a radical polymerization conducted at various starting concentrations of monomer. If all of the data were conducted at an initiator concentration of 0.25 mmol L^{-1}, calculate k'.

Solution



Kinetics can also be used to establish a theoretical polymer chain length. This quantity is called kinetic chain length, represented by "vee bar". In principle, it's just the ratio of the chain propagation rate to the chain initiation rate. That should tell us the number of monomers per each chain initiated. Because of our earlier assumption about the initiation rate equaling the termination rate, we can substitute the terms for those two rates and simplify the result.

$$\bar{\nu} = \frac{\text{Rate}_{\text{prop}}}{\text{Rate}_{\text{init}}}$$

but at steady state $\text{Rate}_{\text{init}} = \text{Rate}_{\text{term}}$

$$\bar{\nu} = \frac{\text{Rate}_{\text{prop}}}{\text{Rate}_{\text{term}}}$$

$$\bar{\nu} = \frac{k_p[\text{M}][\text{M}^{\cdot}]}{2k_t[\text{M}^{\cdot}]^2} = \frac{k_p[\text{M}]}{2k_t[\text{M}^{\cdot}]}$$

Substituting our earlier expression for the concentration of the growing radical chain ends gives a new expression.

$$\bar{\nu} = \frac{k_p[\text{M}]}{2(fk_tk_d[\text{I}])^{1/2}}$$

That means that we can theoretically control the length of polymer chains, because the average length should vary linearly with the concentration of monomer and inversely with the square root of initiator concentration.

As chain reactions, cationic and anionic polymerizations have some characteristics in common with radical polymerizations. One key difference is that the initiator does not fragment into two pieces, each capable of initiating a chain; instead, one added initiator starts polymerization of one chain, without the prior decompositions step seen in radical reactions. Also, termination steps in radical reactions are dominated by radical recombinations (as well as other variations), but in anionic and cationic terminations it is more likely that the growing chain encounters an impurity and reacts with that.

Example 11.5.3.3.2

Given that for a cationic polymerization:

$$\text{Rate}_{\text{init}} = k_i\,[\text{M}][\text{I}] \text{ and } \text{Rate}_{\text{term}} = k_t[\text{M}^+]$$

Provide a steady state expression for the concentration of growing cationic chain.

Example 11.5.3.3.3

If the propagation step in a cationic polymerization is written as follows:

$M^+ + M \rightarrow M\text{-}M^+$

Provide the rate expression for cationic polymerization.

Example 11.5.3.3.4

By analogy to radical polymerization, the kinetic chain length in cationic polymerization can be expressed as the ratio of propagation rate to initiation rate. Provide an expression in terms of constants and known concentrations.

Example 11.5.3.3.5

In a living polymerization, chain length simplifies to $[M]_0/[I]_0$ because all initiation leads to polymerization and there are no terminations steps. Given a radical polymerization with $[M]_0$ = 4.5 M and $[I]_0$ = 1.25 mM, compare chain length in the following situations:

a. a living polymerization
b. a non-living polymerization with f = 0.5; $k_p = k_t$ = 0.003 $M^{-1}s^{-1}$; k_d = 0.0001 s^{-1}.
c. a non-living polymerization with f = 0.5; k_p = 0.003 $M^{-1}s^{-1}$; k_t = 0.3 $M^{-1}s^{-1}$; k_d = 0.0001 s^{-1}.
d. a non-living polymerization with f = 0.5; k_p = 0.003 $M^{-1}s^{-1}$; k_t = 0.003 $M^{-1}s^{-1}$; k_d = 0.1 s^{-1}.

This page titled 11.5.3.3: Kinetics of Chain Polymerization is shared under a CC BY-NC 3.0 license and was authored, remixed, and/or curated by Chris Schaller via source content that was edited to the style and standards of the LibreTexts platform.

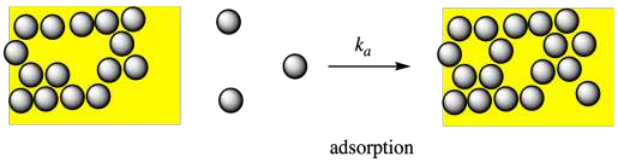
- **3.3: Kinetics of Chain Polymerization** by Chris Schaller is licensed CC BY-NC 3.0. Original source: https://employees.csbsju.edu/cschaller/Advanced/Polymers/Polycontents.htm.

11.5.3.4: Kinetics of Catalytic Polymerization

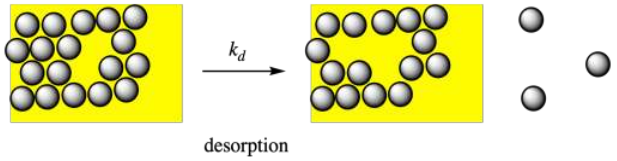
KP4. Kinetics of Catalytic Polymerization

The Ziegler-Natta polymerization of alkenes is conducted under catalytic conditions. In most cases, the process involves heterogeneous catalysis, in which the reaction takes place on the surface of a solid. The kinetics of catalyzed reactions have some features that are different from other reactions and that are worth exploring.

The fact that the reaction is taking place on the surface of a solid is a key feature that must be stressed in the kinetics of heterogeneous catalysis. The treatment of rates therefore uses an approach developed by Irving Langmuir, a long-time scientist at General Electric who was awarded the Nobel Prize for the study of surfaces. One of the things that makes metal catalysts so useful is their ability to adsorb molecules on their surfaces (think of the precious metals used in catalytic hydrogenation, adsorbing alkenes and hydrogen; or the iron in the Haber-Bosch synthesis of ammonia, adsorbing dinitrogen and hydrogen, to cite two important examples). "Adsorption" refers to the adhesion of molecules to a surface. Langmuir thought of this adsorption process as a dynamic one, with molecules landing on and sticking to open spots on a surface even as other molecules lifted off to create vacancies.



Desorption, on the other hand, refers to the process of molecules leaving the surface.



In terms of kinetics, the rate of desorption of a molecule would depend on some rate constant, k_d, and the fraction of the surface covered by these molecules, θ (that's the Greek letter, theta). The greater the surface fraction covered by molecules, the greater the chance that you will encounter one desorbing.

$\text{Rate}_d = k_d\,\theta$

On the other hand, the rate os adsorption of a molecule onto a surface will depend on some rate constant k_a, the concentration of the molecule to be adsorbed, and the fraction of the surface still available. That last part is 1 - θ, because the fraction covered plus the fraction uncovered would equal the whole. Note that Langmuir was interested in gas phase molecules adsorbing onto a surface, and so he expressed things in terms of pressure rather than concentration.

$\text{Rate}_a = k_a\,(1 - \theta)\,[M]$

At equilibrium, these two rates will equal each other:

$k_d\,\theta = k_a\,[M] - k_a\,\theta\,[M]$

$\theta\,(k_d + k_a\,[M]) = k_a\,[M]$

$\theta = k_a\,[M] / (k_d + k_a\,[M])$

Now we have an expression for the fraction of the surface covered by the substrate. This term is called the "Langmuir isotherm" and it shows up in various surface and catalytic phenomena. It is usually expressed slightly differently, in terms of an equilibrium constant for adsorption:

$$\theta = \frac{K_{eq}[M]}{1 + K_{eq}[M]} \qquad K_{eq} = \frac{k_a}{k_d}$$

The rate of a reaction catalyzed on that surface will depend on the catalyst concentration as well as a rate constant for enchainment, k_{prop} or simply k_p, and the amount of surface covered by monomer (unbound monomer will not undergo propagation). An additional factor, x*, takes into account the fact that only a fraction of the catalyst is active.

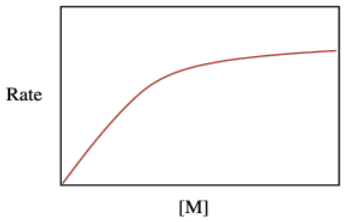
$$\text{Rate}_p = k_p[\text{Cat}]x^*\theta \qquad \begin{matrix}[\text{Cat}] = \text{catalyst concentration} \\ x^* = \text{fraction of catalyst that is active}\end{matrix}$$

$$\text{Rate}_p = \frac{k_p K_{eq}[\text{M}][\text{Cat}]x^*}{1 + K_{eq}[\text{M}]}$$

Superficially, the form of the rate law has something in common with the Michaelis-Menten equation, with which you may already be familiar. The Michaelis-Menten equation relates the rate of an enzyme-catalyzed reaction to enzyme concentration, the rate constant for the catalytic reaction, and rate constants for reversible substrate binding with the enzyme.

$$\text{Rate} = \frac{k_{cat}[\text{E}]_0[\text{S}]}{1 + K_m[\text{S}]} \qquad K_\text{m} = \frac{k_r + k_{cat}}{k_f}$$

Maybe that resemblance shouldn't be too surprising. After all, both equations describe catalytic processes, in which either the surface or the binding site must accomodate the substrate so as to carry out a subsequent series of reactions. Both equations take the form of a saturation curve, indicating that the rate of reaction will level out if the surface or binding site becomes fully occupied.



Problem KP4.1.

One way to evaluate multi-term relationships is to consider what happens under different conditions. What happens to the rate law for catalytic polymerization if monomer concentration is very low, so that $1 >> K_{eq}[\text{M}]$?

Problem KP4.2.

What happens to the rate law for catalytic polymerization if monomer concentration is very high, so that $K_{eq}[\text{M}] >> 1$?

This page titled 11.5.3.4: Kinetics of Catalytic Polymerization is shared under a CC BY-NC 3.0 license and was authored, remixed, and/or curated by Chris Schaller via source content that was edited to the style and standards of the LibreTexts platform.

- **3.4: Kinetics of Catalytic Polymerization** by Chris Schaller is licensed CC BY-NC 3.0. Original source: https://employees.csbsju.edu/cschaller/Advanced/Polymers/Polycontents.htm.

11.5.3.5: Solutions to Selected Problems

KP5. Solutions to Selected Problems

Problem KP1.1.

Two C-C σ bonds and one new π bond are made. Three old π bonds are lost.

ΔH = bonds broken - bonds made

ΔH = (3 x 64) - ((2 x 83) + 64) kcal/mol

ΔH = -38 kcal/mol

Problem KP1.2.

$T_c = \Delta H / (\Delta S + R\log[M])$

T_c = - 7,000 cal mol^{-1} (-8.6 cal K^{-1} mol^{-1} + 1.98 cal K^{-1} mol^{-1} log(8.7))

T_c = - 7,000 (-8.6 + 1.98 (0.939)) K

T_c = - 7,000 (-6.74) K

T_c = 1038 K = 765 °C

Problem KP1.3.

For each amide bond, a C-N bond and a H-Cl bond are made. A C-Cl and a N-H bond are lost.

ΔH = bonds broken - bonds made

= (C-Cl + N-H) - (C-N + H-Cl)

ΔH = (81 + 93) - (73 + 102) kcal/mol

ΔH = -1 kcal/mol

Problem KP2.1.

75% conversion means 0.75 in terms of fractions.

DP = 1 / (1 - p)

DP = 1 / (1 - 0.75)

DP = 1 / 0.25

DP = 4

Problem KP2.2.

slope = 2 $[M]_0$ k = 0.717 s^{-1}

k = 0.717 s^{-1} / (2 x 17 mol L^{-1})

k = 0.021 L $mol^{-1}s^{-1}$

Problem KP2.3.

$M_n = M_0 / (1 - p)$

= 120 g/mol / (1 - 0.99)

= 120 g/mol / 0.01

= 12,000 g/mol

$M_w = M_0(1 + p) / (1 - p)$

= 120 g/mol (1 + 0.99) / (1 - 0.99)

= 120 g/mol (1.99) / 0.01

= 23,800 g/mol

D = 1 + p

= 1 + 0.99

= 1.99

Problem KP3.1.

Rate = k' [M][I]$^{1/2}$

slope = k' [I]$^{1/2}$

0.0024136 s = k' (0.00025)$^{1/2}$

k' = 0.015 s^{-1}

Problem KP3.2.

At steady state:

Rate$_{init}$ = Rate$_{term}$

k_i [M][I] = k_t[M$^+$]

Rearranging:

[M$^+$] = (k_i/k_t) [M][I]

Problem KP3.3.

Rate$_{prop}$ = k_p [M$^+$][M]

Substituting the steady state expression for [M$^+$]:

Rate = ($k_i k_p/k_t$) [M]^2[I]

Problem KP3.4.

$\bar{v}$ = Rate$_{prop}$/Rate$_{init}$

$\bar{v}$ = k_p [M$^+$][M] / k_i [M][I] = (k_p / k_i)[M$^+$] / [I]

but [M$^+$] is not a known quantity. Alternatively, at steady state, Rate$_{init}$ = Rate$_{term}$

$\bar{v}$ = Rate$_{prop}$/Rate$_{term}$

$\bar{v}$ = k_p [M$^+$][M] / k_t [M$^+$] = (k_p / k_t)[M]

Problem KP3.5.

a) $\bar{v}$ = [M]$_0$/[I]$_0$ = 4.5 / 1.25 x 10^{-3} = 3,400

b) $\bar{v}$ = (k_p/2f k_t k_d)([M]/[I]$^{1/2}$)

$\bar{v}$ = (0.003 / 2(0.5)(0.003)(0.0001))(4.5/(1.25 x 10^{-3})$^{1/2}$) = (1/0.0001)(4.5/0.035) = 128/0.0001 = 1,280,000

c) $\bar{v}$ = (k_p/2f k_t k_d)([M]/[I]$^{1/2}$)

$\bar{v}$ = (0.003 / 2(0.5)(0.03)(0.0001))(4.5/(1.25 x 10^{-3})$^{1/2}$) = (0.01/0.0001)(4.5/0.035) = 128/0.01 = 12,800

d) $\bar{v}$ = (k_p/2f k_t k_d)([M]/[I]$^{1/2}$)

$\bar{v}$ = (0.003 / 2(0.5)(0.003)(0.1))(4.5/(1.25 x 10^{-3})$^{1/2}$) = (1/0.1)(4.5/0.035) = 128/0.1 = 1,280

Problem KP4.1.

The key point is that, when two terms are added together and one is much larger than the other, the sum is approximately the same as the larger of the two terms. You can ignore the smaller one.

$$\text{Rate}_p = \frac{k_p K_{eq}[M][Cat]x^*}{1 + \cancel{K_{eq}[M]}} \quad \sim 0$$

$$\text{Rate}_p = \frac{k_p K_{eq}[M][Cat]x^*}{1}$$

$$\text{Rate}_p = k_p K_{eq}[M][Cat]x^*$$

Problem KP4.2.

$$\text{Rate}_p = \frac{k_p K_{eq}[M][Cat]x^*}{\cancel{1} + K_{eq}[M]} \quad \sim 0$$

$$\text{Rate}_p = \frac{k_p K_{eq}[M][Cat]x^*}{K_{eq}[M]}$$

$$\text{Rate}_p = k_p[Cat]x^*$$

This page titled 11.5.3.5: Solutions to Selected Problems is shared under a CC BY-NC 3.0 license and was authored, remixed, and/or curated by Chris Schaller via source content that was edited to the style and standards of the LibreTexts platform.

- **3.5: Solutions to Selected Problems** by Chris Schaller is licensed CC BY-NC 3.0. Original source: https://employees.csbsju.edu/cschaller/Advanced/Polymers/Polycontents.htm.

SECTION OVERVIEW

11.5.4: Polymer Properties

11.5.4.1: Molecular Weight of Polymers

11.5.4.2: Viscosity of Polymers

11.5.4.3: Rheology

11.5.4.4: Glass Transition

11.5.4.5: Crystallinity in Polymers

11.5.4.6: Microphase Separation

11.5.4.7: Stress-Strain Relationships

11.5.4.8: Storage and Loss Modulus

11.5.4.9: Modulus, Temperature, Time

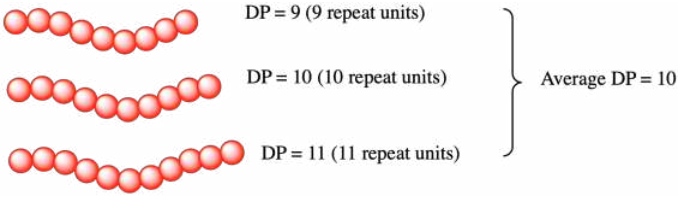
11.5.4.10: Chapter Solutions

This page titled 11.5.4: Polymer Properties is shared under a CC BY-NC 3.0 license and was authored, remixed, and/or curated by Chris Schaller via source content that was edited to the style and standards of the LibreTexts platform.

11.5.4.1: Molecular Weight of Polymers

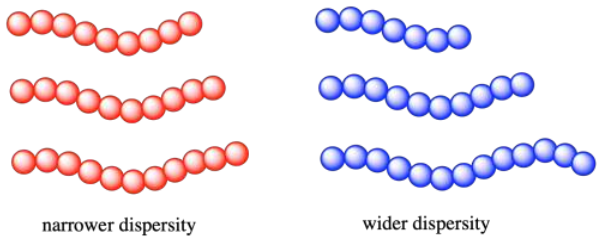
Molecular weight is one of the most central aspects of polymer properties. Of course, all molecules have molecular weights of their own. It might seem obvious that molecular weight is an essential property of any molecular compound. In polymers, molecular weight takes on added significance. That's because a polymer is a large molecule made up of repeating units, but how many repeating units? Thirty? A thousand? A million? Any of those possibilities might still be considered a representative of the same material, but their molecular weights would be very different, and so would their properties.

That variation introduces some unique aspects of polymer molecular weight. Because polymers are assembled from smaller molecules, the length (and consequently the molecular weight) of a polymer chain depends on the number of monomers that have been enchained into the polymer. The number of enchained monomers in an average polymer chain in a material is called the *degree of polymerization* (DP).



Notice that key point: it is just an average. In any given material, there will be some chains that have added more monomers and some chains that have added fewer. Why the difference? First of all, polymer growth is a dynamic process. It requires monomers to come together and react. What if one monomer starts reacting, forming a growing chain, before any of the others get started? With its head start, this chain will become longer than the rest. What if something goes wrong with one of the growing chains, and it can no longer add new monomers? That chain experienced an early death, and it will never grow as long as the others.

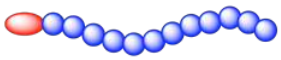
As a result, when we are speaking about the molecular weight of a polymer, we are always talking about an average value. Some chains in the material will be longer (and heavier) and some chains in the material will be shorter (and lighter). As with any group of measurements, it's helpful to know how widely distributed the individual values really are. In polymer chemistry, the width of the distribution of molecular weights is described by the *dispersity* (Đ, also called, in older texts, the polydispersity or the polydispersity index, PDI). The dispersity of a polymer sample if often between 1 and 2 (although it can be even higher than 2). The closer it is to 1, the narrower the distribution. That is, a dispersity of 1.0 would mean that all of the chains in a sample are exactly the same length, with the same molecular weight.



The original idea of dispersity was based on alternative methods of measuring the molecular weight (or the chain length) of a polymer sample. One set of methods gave something called the *number average molecular weight* (symbol M_n). These methods essentially took the weight of a sample, counted the molecules in a sample, and therefore found the average weight of each molecule in that sample. A classic example of this approach is a colligative properties experiment, such as a freezing point depression. You know that impurities in a liquid tend to disrupt intermolecular interactions and lower the freezing point of the liquid. You may also know that the amount by which the freezing gets lowered depends on the number of molecules or ions that get dissolved. Hence, if you weigh a sample of polymer, dissolve it in a solvent, and measure the freezing point, you could figure out the number of molecules dissolved and consequently arrive at M_n.

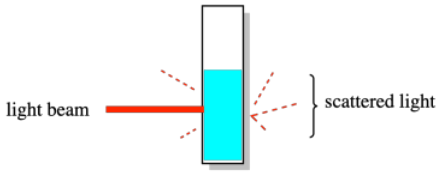
That's not so easy in practice; freezing point depressions are very small. They're not used very often anymore. A very common example of the kind of measurement widely used to determine M_n today is end group analysis. In end group analysis, we use ^{1}H NMR measurements to determine the ratio of a specific proton in the repeat units to a specific proton in the end group. Remember,

the end group might be something like the initiator, which only added onto the first monomer to get the polymerization going. By the end of the polymerization, it is still found at the end of the polymer chain, so it is an end group. There is only one of them per chain, whereas there are lots of monomers enchained in the polymer, so the ratio of those enchained monomers to the end group tells us how long the chain is.



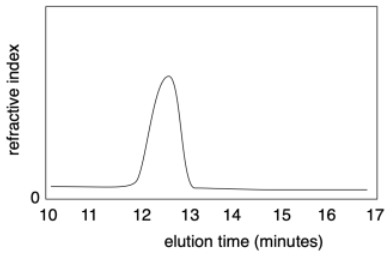
DP = ratio of repeat units to end group

The other set of methods upon which dispersity was based gave something called the *weight average molecular weight* (symbol M_w). The classic example was a light-scattering experiment. In this experiment, a solution of polymer was exposed to a beam of light and the resulting scattered light -- coming from the sample in different directions -- was analyzed to determine the size of the polymer chains in the solution. The results were more heavily influenced by the larger molecules in solution. As a result, this measurement of molecular weight was always higher than measurements based on counting every single molecule.

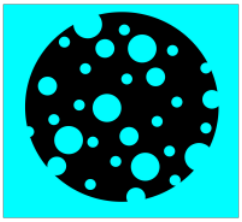


The resulting ratio, Đ = M_w / M_n, became known as the polydispersity index or, more recently, the dispersity. Because M_w was always more strongly influenced by longer chains, it was a little bigger than M_n and therefore the dispersity was always bigger than 1.0.

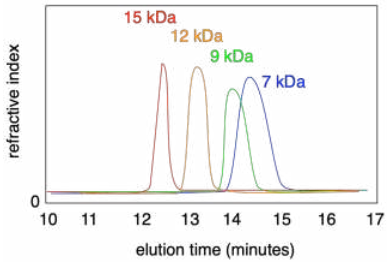
Nowadays, both molecular weight and dispersity are most commonly measured using gel permeation chromatography (GPC), synonymous with size-exclusion chromatography (SEC). This method is a high-performance liquid chromatography (HPLC) technique. Solvent containing a sample of polymer is pumped through a specialized chromatography column capable of separating molecules based on their size differences. As sample emerges from the column, it is detected and recorded. Most commonly, the presence of sample in the solvent emerging from the column causes a slight change in the refractive index. A graph of refractive index versus time presents a record of the amount of sample emerging from the column at a given time. Because the column separated molecules based on size, the time axis corresponds indirectly with chain length of molecular weight.



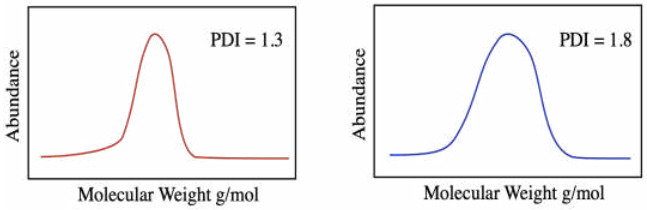
How can the column separate molecules based on size? The column is packed with a porous material, usually insoluble polymer beads. The pore sizes vary. These pores a crucial to separation because molecules flowing through the column may tarry in the pores. Smaller molecules could become delayed in any of the pores in the material, whereas larger molecules will only be delayed in the very largest pores. Consequently, a longer elution time corresponds to a lower molecular weight.



If you injected a series of different polymers into a GPC, each having a different molecular weight distribution, you would observe each one eluting at a different time. What's more, each peak may be broader or narrower, depending on the dispersity of that particular sample.



The wider the peak in GPC, the broader the distribution of molecular weights; the narrower the peaks, the more uniform are the chains. Normally a software package analyzes the curve to determine the dispersity.



Note that the x axis on a GPC trace is most commonly labeled as "elution time" and it normally runs left to right. However, often the x axis is labeled "molecular wright" because that is really the quantity we are interested in. In fact, sometimes the axis is reversed, so that peaks with higher molecular weights appear to the right, because it can feel more natural to look at it that way. You need to look carefully at the data to see how it is displayed.

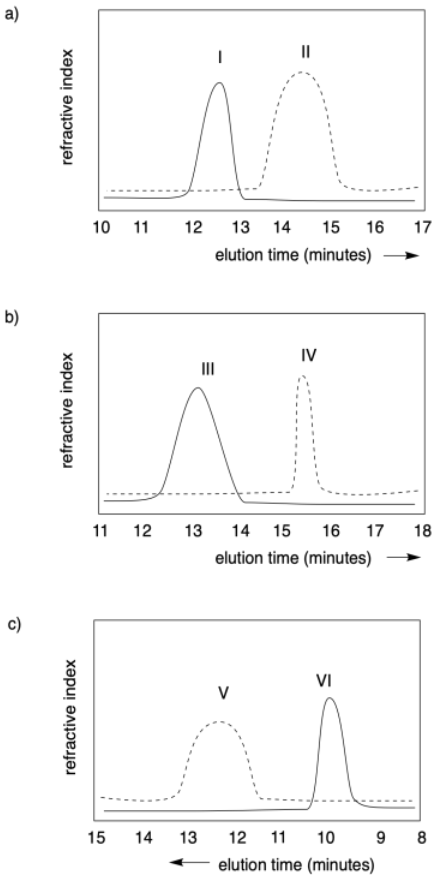
There are some problems with relying on GPC for molecular weight measurements. The main difficulty is that polymers in solution tend to coil into balls, and those coils will contain greater or lesser amounts of solvent, depending on how strongly the polymer and solvent interact with each other. If it interacts more strongly with the solvent, it will pull lots more solvent molecules inside its coils. The coil has to get bigger to make room for those internal solvent molecules. If it doesn't interact strongly with the solvent, it will mostly just stick to itself, blocking the solvent molecules out. There is a broad range of behaviors in between.



As a result, different polymers may swell to different extents in different solvents. That matters because GPC is really using size of the polymer coil as an index of its molecular weight, so comparing GPC traces of two different kinds of polymers has to be done with caution.

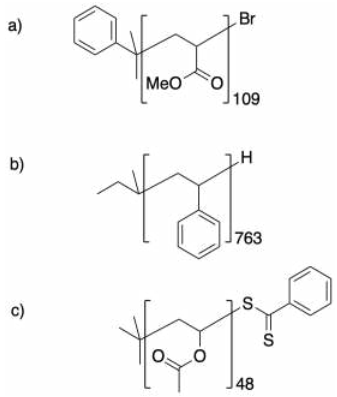
Problem CP1.1.

In each of the following cases, state which polymer has the higher molecular weight, and which one has a narrower dispersity



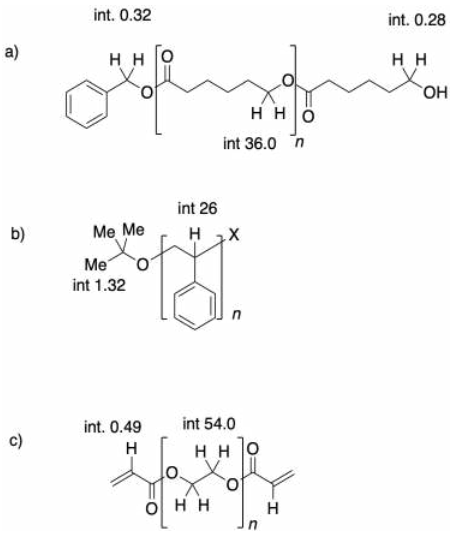
Problem CP1.2.

Calculate the molecular weight of the following samples.



Problem CP1.3.

Use NMR end group analysis to determine the degrees of polymerization in the following samples.



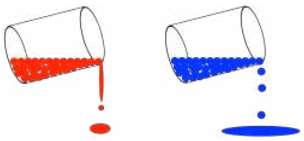
This page titled 11.5.4.1: Molecular Weight of Polymers is shared under a CC BY-NC 3.0 license and was authored, remixed, and/or curated by Chris Schaller via source content that was edited to the style and standards of the LibreTexts platform.

- **4.1: Molecular Weight of Polymers** by Chris Schaller is licensed CC BY-NC 3.0. Original source: https://employees.csbsju.edu/cschaller/Advanced/Polymers/Polycontents.htm.

11.5.4.2: Viscosity of Polymers

Polymers have come to occupy a very important niche in the materials we use every day. What makes them unique? Why do they have properties that aren't easily replicated by other materials?

Let's start with a property that you are probably familiar with. *Viscosity* is a term we use to describe the "thickness" of different liquids. For example, we say that honey is more viscous than water. Motor oil is more viscous than gasoline. When we say that, we mean that water is much easier to stir or to pour than honey. The honey moves more slowly. It resists the movement of the spoon when we stir it. Viscosity is often described in very general terms as "resistance to flow". The honey doesn't flow very easily, especially compared to something like water.

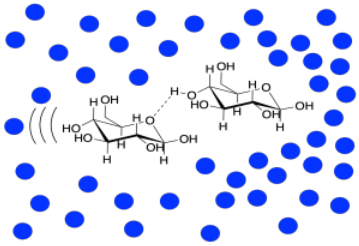


Now, honey isn't a polymer. It's a very concentrated solution. It contains a little bit of water and a whole lot of sugars, plus other small molecules produced by the plants from which the bees gathered the nectar to make the honey. The sugars aren't polymers, either; they are simple monosaccharides such as glucose and fructose. Nevertheless, this high viscosity is something honey has in common with polymer solutions, as well as with some *oligomers*, which are short-chain polymers that can be liquids instead of solids.

Why is honey so viscous? Partly it's just that the sugar molecules in the water are much larger than the water molecules, so they experience a lot more drag as they move through the solution compared to just plain water.



The strong intermolecular attractions between the individual sugar molecules are also a major factor. Sugars are covered in OH or hydroxyl groups that are capable of strong hydrogen bonds. As these molecules move past each other in the very concentrated solution, they cling to each other, slowing down the flow of the liquid.

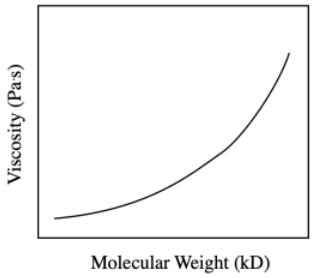


The motor oil example works in a similar way. Motor oil and gasoline are composed of the same class of compounds, hydrocarbons, composed of carbon chains covered in hydrogen atoms. They're very similar to each other. The intermolecular attractions between the molecules are much weaker than those between sugar molecules; they're just London dispersion forces. The major difference between motor oil and gasoline is that the motor oil contains much longer hydrocarbon chains. The molecules are bigger, and so they experience more drag as they move through the liquid. The amount of intermolecular interactions is also crucial in determining how tightly two molecules hold onto each other, and this factor is especially important in very weak London dispersion forces, where a small advantage goes a long way. Those longer hydrocarbon chains in the motor oil cling to each other much more strongly than the shorter ones in the gasoline, so gasoline flows much more easily than motor oil.

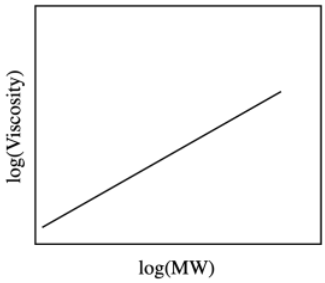
For similar reasons, oligomers and polymers, if they are liquids, also display high viscosity. The extended contact between their long molecular chains leads to enhanced intermolecular attractions that contribute to a resistance to flow. Increased drag is also a

factor; even in solution, these very large molecules encounter more resistance as they move past solvent molecules compared to the resistance smaller molecules would experience.

In fact, viscosity measurements of polymer solutions are another way to determine the size of the polymer -- leading to the chain length and the molecular weight. The larger the polymer, the more drag and also the more intermolecular attraction, and so the higher the viscosity.



So, the viscosity increases with the molecular weight, but not necessarily in a linear way. That can make it more difficult to use a graph like this to predict molecular weight from a viscosity measurement. One common thing to do in this situation is to take the log of the values. That approach will often give a straight line when two things are related.



Often in nature one physical property that depends on another will follow a "power law". That means that one quantity depends on the other raised to some exponent. In this case, the relationship is described by the **Mark-Houwink equation**:

$$[\eta] = KM^{\alpha} \tag{11.5.4.2.1}$$

In this equation, [η] is the intrinsic viscosity; that's the viscosity attributed to the solute, rather than the viscosity of the solvent itself. *M* is the molecular weight. *K* and α are constants for a particular polymer.

If you take the log of both sides of the equation -- that's OK to do mathematically, just like you could multiply both sides of an equation by four or subtract three from both sides and still have an equivalent expression -- you get:

$$\log[\eta] = log(KM^{a}) \tag{11.5.4.2.2}$$

If you take the log of two things multiplied together, it's the same as adding the individual logs of both things.

$$\log[\eta] = \log K + \log(M^{a}) \tag{11.5.4.2.3}$$

And if you take the log of something raised to an exponent, the exponent just comes down to become a coefficient.

$$\log[\eta] = \log K + \alpha \log M \tag{11.5.4.2.4}$$

or

$$\log[\eta] = \alpha \log M + \log K \tag{11.5.4.2.5}$$

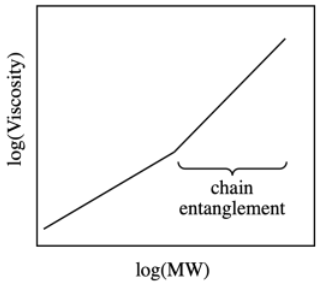
That looks like an equation for a straight line:

$$y = mx + b. \tag{11.5.4.2.6}$$

Here, you plot $\log[\eta]$ on the y axis, $\log M$ on the x axis, and you get a straight line with those constants, α and K, as the slope and y-intercept, respectively.

This approach does not yield an absolute measurement. You couldn't take two completely different polymers, take viscosity measurements, and make conclusions about which one had a higher average molecular weight. However, if you took a series of polymers of the same kind and measured their viscosities in solution, you would be able to deduce which ones were longer and which ones were shorter.

In fact, the dependence of viscosity on the molecular weight of polymers is more complicated than this graph suggests. If you deal with large enough polymers, the graph starts to look like this one:



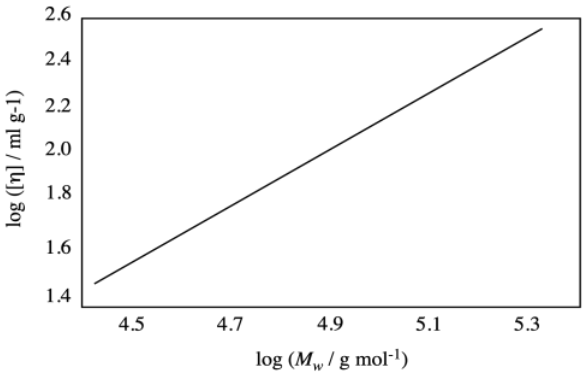
Why does it bend? Remember, polymers in solution are coiled up into balls. A longer chain just corresponds to a bigger coil. At some point, these chains become big enough that they aren't likely to stay coiled independently of each other. They become more and more likely to interact with each other. They become entangled with each other.



There are plenty of other factors you would have to take into account in using viscosity to assess molecular weight. One of them is concentration, for example. The more concentrated a polymer solution, the more large molecules you have exerting drag and interacting with each other. Higher concentration leads to a higher viscosity measurement. Consequently, you would have to make sure you accounted for the polymer concentrations if you used this method.

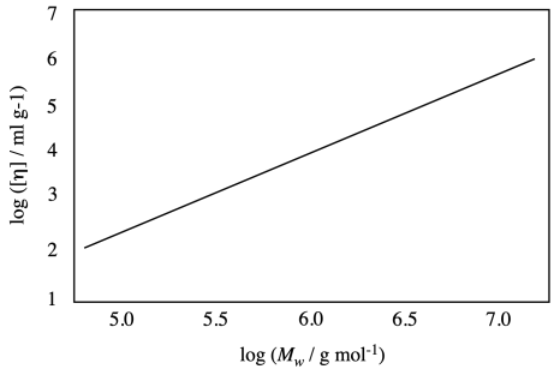
Problem PP2.1.

Estimate the values of α and *K* for the polymer that provided the plot below.



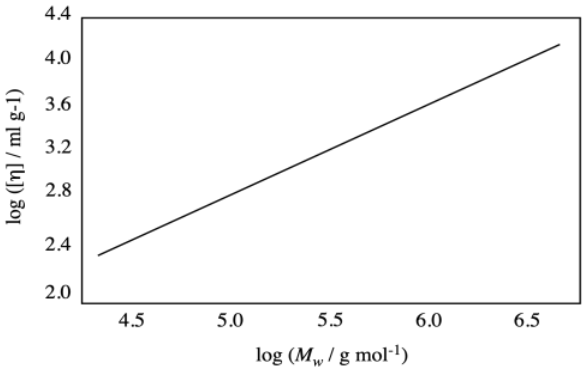
Problem PP2.2.

Suppose you have a polymer described by the plot below. If your sample has a molecular weight of 1 million g/mol, what would you expect for intrinsic viscosity under the conditions of this experiment?



Problem PP2.3.

Suppose you have a calibration plot, below, for a particular polymer. If you measure the intrinsic viscosity of a sample and find that the value is 800 ml / g, what is the molecular weight of the sample?



Problem PP2.4.

Ethanol (CH_3CH_2OH) has an "absolute viscosity" of 1.095 centipoise, whereas ethylene glycol ($HOCH_2CH_2OH$) has an absolute viscosity of 16.2 centipoise. Explain why the two values are so different.

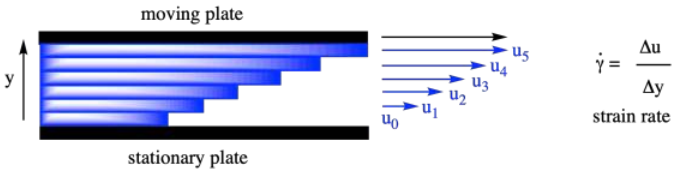
This page titled 11.5.4.2: Viscosity of Polymers is shared under a CC BY-NC 3.0 license and was authored, remixed, and/or curated by Chris Schaller via source content that was edited to the style and standards of the LibreTexts platform.

- **4.2: Viscosity of Polymers** by Chris Schaller is licensed CC BY-NC 3.0. Original source: https://employees.csbsju.edu/cschaller/Advanced/Polymers/Polycontents.htm.

11.5.4.3: Rheology

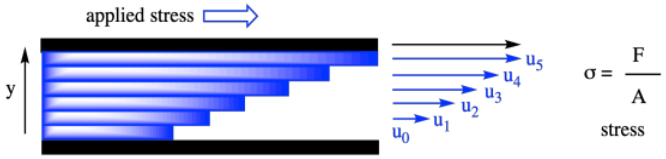
Viscosity measurements are the realm of a field of science called *rheology*. Rheology is, literally, the study of flow. Another very simple definition, attributed to chemical engineer Chris Macosko at University of Minnesota, is the study of "what happens when you squish stuff". There's an element of force or pressure that comes into play here, too.

One of the common ways of assessing properties in rheology is to place a sample between two parallel plates and move one plate with respect to the other. One plate says still and the other one moves. What happens to the liquid between the plates? There ought to be some friction between the stationary plate and the liquid that will keep the liquid still. There also ought to be some friction between the moving plate and the liquid that will make the liquid move along at the same speed as that plate. So at one extreme, the liquid is moving along with the sliding plate and at the other extreme the liquid is perfectly still. If we imagine that the liquid in between these two extremes is divided into very thin layers, then each layer must be moving at a slightly different speed than the next.

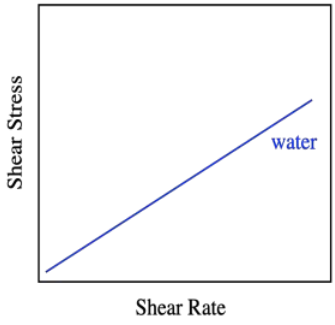


In the diagram, the symbol, *u*, stands for the speed of the layer of liquid. The arrow beside the layer is meant to convey its relative speed: the top layer is moving the fastest, the next layer is a little slower, and so on; the bottom layer isn't moving at all. There is an important quantity, called the strain rate or shear rate (given as a symbol the Greek letter gamma, γ, with a dot on top) that describes how the speed of the liquid moving along the x-axis (left to right) changes, layer by layer, in the y-direction.

What does this picture have to do with viscosity? Well, in order to get that top plate to move, we have to apply some sort of force to it. In rheology the force is given per unit area (like pressure); this force per unit area is described as the stress (given as a symbol the Greek letter sigma, σ).

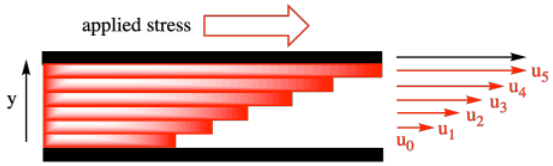


What if we wanted to slide the plate even faster? What would happen to the liquid? Well, the shear rate would go up. The top layer would be moving even faster, and the bottom layer would still be stationary. And what would we have to do to get that faster shear rate? We would have to push the top plate a little harder. The result is a graph that looks like this:

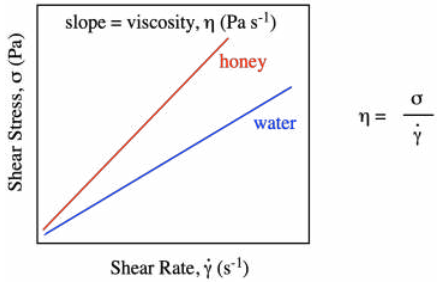


The graph says that shear stress and shear rate are directly related. The stress is called "shear stress" because of the direction of the force parallel to the liquid, causing shear strain. When we increase the shear rate, the shear stress also increases proportionally. So, if we did this experiment using water as the liquid between the plates, we would get a linear relationship between shear stress and shear rate. That's how Sir Isaac Newton described the behavior of liquids, so when we see that linear relationship between stress and strain, we describe the liquid as a *Newtonian liquid*.

What happens if we do the experiment with honey instead of water? What would happen, for example, if we exerted a certain stress to get a certain shear rate with the water, and we wanted to get the same shear rate using honey? Well, the honey is thicker than the water. It's not going to move as easily. We will have to apply a greater stress in order to achieve the same shear rate that we measured with water.

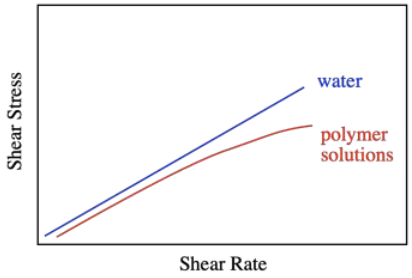


That would be true for every possible shear rate. If we were to graph shear stress vs. shear strain with honey, we would get a linear relationship, just like we did with water, but the value of shear stress would always be higher than for water. The slope of the line for honey would be greater than the slope of the line for water.

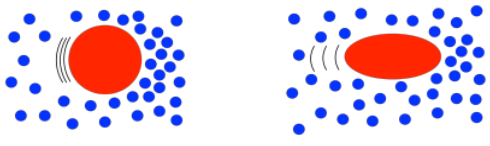


Viscosity is formally defined as the slope of that line. Honey, being thicker than water, requires higher and higher stresses to achieve the same strain rates that you would get using lower stresses with water. In the simple kitchen analog of the experiment, you have to push the spoon harder to stir the honey than you do if you are just stirring water.

Honey and water are Newtonian liquids. The relationship is simple: increase the shear stress and you increase the shear rate. Not all liquids behave that way. Polymer solutions don't, for example. They display a non-linear relationship, in which the shear stresses needed to get higher shear rates are just not as high as you would expect.

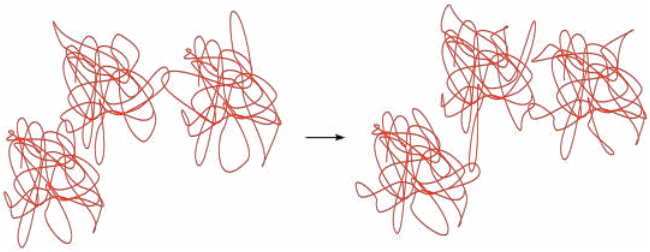


That behavior is described as **shear thinning**. What makes polymer solutions do that? Remember that, in solution, an individual polymer molecule tends to coil up into a ball. Normally, those balls are spherical. At high shear rates, they distort into ellipses. That reduces the amount of drag, making the solution a little less viscous than you would expect. The shear stress still increases with higher shear rates, but not as much as if it were a Newtonian fluid.



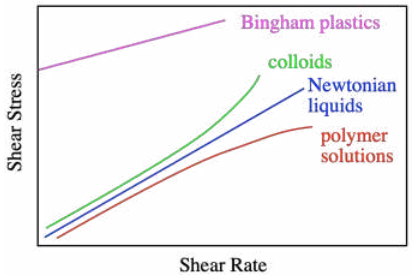
That's not all. Remember, polymers display chain entanglement, especially when they are very large. Chain entanglement increases the viscosity of the solution. These chains are mobile because the polymer is constantly undergoing conformational changes. As the

solution gets sheared, some of the polymer chains may wiggle loose from their neighbors, but random conformational changes will always result in new entanglements right away.



But what happens at a very high rate of shear strain? The polymer chains still become untangled, but they don't have time to form new entanglements, because everything is whizzing by too quickly. Without those entanglements, viscosity doesn't increase as sharply as you would expect.

Some liquids behave just like water, but polymer solutions do not. That's a consequence of the enormously long chain structures of the polymers. It's worth pointing out that there are other things that don't behave in the "normal" way. Colloids often display shear thickening. You can see examples of this in videos of people running across wading pools filled with corn starch and water, a colloidal mixture in which the solid cornstarch particles are just suspended in the water, not dissolved. If you walk across the pool, you sink. If you run, you stay on top. That's shear thickening, and it has to do with how those solid particles move during shearing. When you walk, they just slide past each other, but when you run, they all collide, and come to a stop.



A Bingham plastic, on the other hand, actually appears to be a solid until you give it a good shove; then it flows like a liquid. Peanut butter behaves sort of like that.

Exercise 4.3.1

Honey is a Newtonian fluid, but molasses undergoes shear thinning. What might you deduce about the composition of molasses and honey?

This page titled 11.5.4.3: Rheology is shared under a CC BY-NC 3.0 license and was authored, remixed, and/or curated by Chris Schaller via source content that was edited to the style and standards of the LibreTexts platform.

- **4.3: Rheology** by Chris Schaller is licensed CC BY-NC 3.0. Original source: https://employees.csbsju.edu/cschaller/Advanced/Polymers/Polycontents.htm.

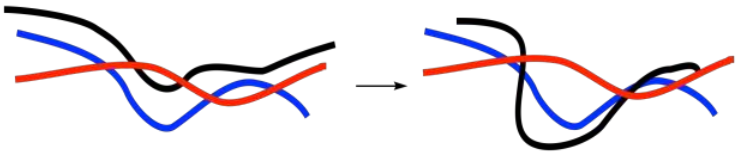
11.5.4.4: Glass Transition

The glass transition is probably the most commonly-cited characteristic of a polymeric material. At the glass transition temperature, the physical nature of the material changes subtly. It goes from being a rubbery, flexible material at higher temperature, above the glass transition, to a glassy, harder material at a lower temperature. The material is still a solid either way, but there is a definite change in how it responds to stimuli.

A material could certainly be useful in either state. We might want a plastic to be more rigid, like a water bottle or a rod for a shower curtain. Alternatively, we might want it to be softer, like a seat cushion. Either way, it might be helpful to know the temperature at which the material will change from one type to the other.

The glass transition is a little like what happens to gummy bears when you put them in ice cream. Straight from the bag, gummy bears are chewy, but they don't feel like they will break your teeth. Put them on ice cream and that changes. They become much harder to chew.

The classic explanation for the glass transition is based on the idea of **chain flow**. Polymers are long-chain molecules and, given a little energy, the chains move around. They wiggle. They undergo bond rotations, switching from one conformation to another. A block of material contains piles of chains, like a nest of snakes. Chain ends and loops squirm past each other continuously.

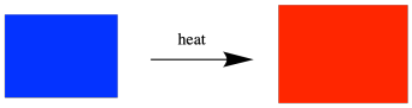


Chain flow allows a material to adapt when forces are exerted on it. We can bend an eraser because the chains in the rubber slide over each other and adopt a new shape. At least, that's what happens at room temperature. It might not work if the eraser were accidentally dropped in some liquid nitrogen, which is very, very cold.

As a block of material cools down, it contracts. The molecules become packed more closely together. At some point, the free volume -- that's the amount of volume in the material that is not actually taken up by the molecules -- becomes too small to allow chains to move past each other. All of those chains need a little room around them if they are going to undergo conformational changes, and conformational changes are how polymer chains move. Without that extra room, the material suddenly becomes less flexible.



If we start in the glassy state and increase the temperature, the volume of the material is expanding, and the free volume is increasing, too. At some point, the free volume becomes great enough that chains can slip past each other. The material becomes more flexible. It becomes rubbery.

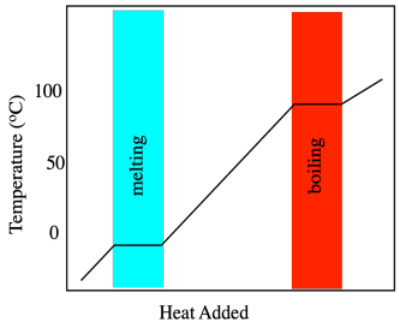


Now, this transition is not the same thing as melting. The chains are not completely overcoming their interactions with each other and gaining freedom of movement in any direction. The chains are still highly entangled. Portions of the chain are sliding past each other but overall things have not changed that drastically. The block of polymer does not turn into a gooey puddle of liquid.

Well, if a material can change from glassy to rubbery at a certain temperature, there will be consequences in how the material behaves. For example, the tires on your car are meant to be rubbery and flexible; that factor helps them grip the road. If the weather gets too cold and your tires become glassy, the tires no longer have the same amount of flexibility, and you don't have as much traction. "All-weather tires" are composed of a rubber that has a very low glass transition temperature, helping to avoid this

problem. ("Snow tires" are a different thing; they have patterns in the treads that help channel away the snow in order to improve traction.) Knowing when this change will occur would be very useful. So, how do we determine the glass transition?

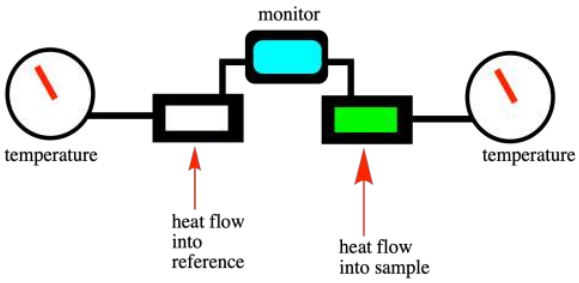
Phase changes, such as melting points, are measured using **calorimetry**, so let's start there. When a solid is heated, its temperature increases. That seems simple enough. Temperature is basically a measure of heat content, so as heat flows in, the measured temperature rises. This simple relationship breaks down at the melting point. At that point, heat flowing into the material is consumed by the breaking of intermolecular forces. Overcoming these attractions costs extra energy. Consequently, there is a point at which the temperature rise in the material stalls out temporarily while it melts.



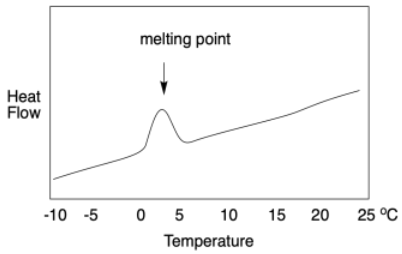
This extra heat needed to melt the material is called the heat of melting or, more commonly, the heat of fusion. Heat of fusion actually refers to the opposite process as the material is cooled and frozen. As heat is carried away from a cooling material, it cools down gradually, but there comes a point at which those strong intermolecular interactions form, giving off some extra heat. The fusion temperature is the same as the melting temperature, and the heat of fusion is the same as the heat of melting, but in one case the heat is added and in another case the heat is given off. In principle, if we just heat something up and look for that stalling point in the temperature, we can find the temperature of the phase transition.

Differential scanning calorimetry

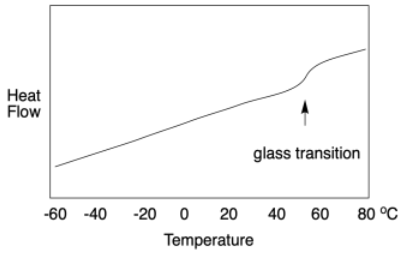
Differential scanning calorimetry (DSC) is a technique that is commonly used to measure phase transitions, including the glass transition temperature. It is based on the same ideas but the experiment is run in a slightly different way. In DSC, we have two tiny sample chambers side by side. One contains the material we are interested in and the other (empty) one is used as a reference. The instrument heats both samples at a constant rate, all the while maintaining both of them at the same temperature. Consequently, it may actually add more heat to one chamber than the other, so that they both reach 30.5 °C at the same time, then 30.6 °C, and so on. Once we reach the melting point of the sample of interest, heat flow into that sample must be increased so that it can keep up with the reference. Past that point, the heat flow drops back to a more normal level.



If we look at a DSC scan, we see a graph of heat flow on the y-axis and temperature on the x-axis. The heat flow usually stays pretty constant as the temperature increases. At the melting point, heat flow increases, but then it drops back down once the melting point has been overcome. It may not drop back to the same level as before, however, because the heat flow that is recorded is related to the heat capacity of the material. The solid and the liquid usually respond differently to heat. In general, because the molecules in a liquid can freely rotate, they have something else to do with added heat. Liquids thus have a slightly higher heat capacity than their corresponding solids.



All of that explanation hopefully prepares us for a DSC study of the glass transition temperature. It works the same way, but only up to a point. If we look at a DSC scan, we still see heat flow on the y-axis and temperature on the x-axis. At the glass transition, heat flow bumps up slightly -- and remains there. It looks very different from a melting point. A DSC scan of a melting point shows a "peak" at the transition temperature. A DSC scan of a glass transition point shows only a little step, like a riverbank

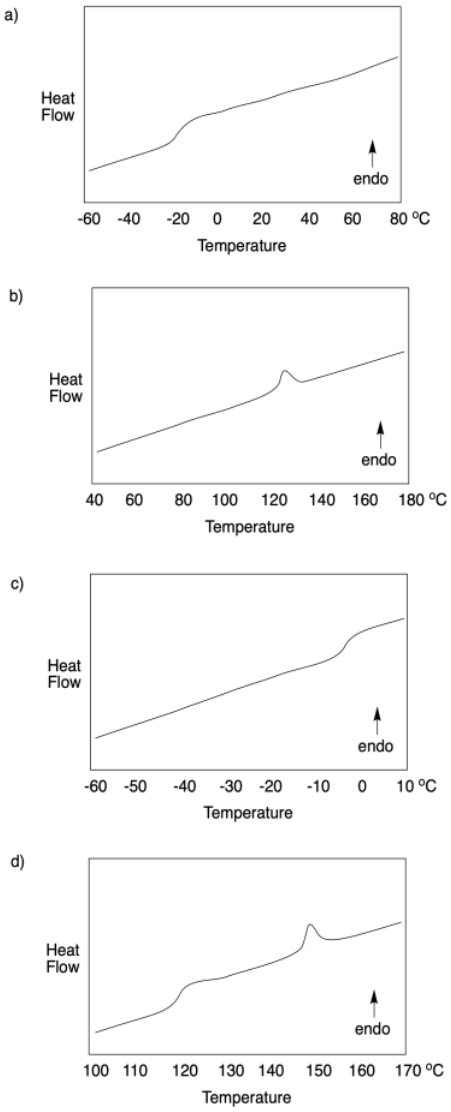


Why is it different? Well, the glass transition is not really a phase change like the melting point or boiling point. It does not involve a physical change of state. It was a solid before and it is a solid afterward. No intermolecular interactions must suddenly be overcome to free the molecules from each other. Instead, it's just a volume change. The free volume became great enough that the chains can slip past each other, but the chains are still clinging together in a solid-state. Now, that additional movement does have consequences. The material becomes more flexible. If heat flows in, there is more freedom of motion into which the heat can be distributed. In other words, there is a slight increase in heat capacity, and that's what we observe in DSC.

> One practical note: DSC scans can actually be displayed in two different ways. The y-axis can either display heat flowing in or heat flowing out. That means melting points can look like peaks or like valleys, depending on how the data is displayed. Often the data are labeled with an arrow that says "endo" to tell you which direction along the y-axis means more heat is flowing in (or possibly "exo", meaning which direction means heat is flowing out). You need to look carefully if things seem backward.

Problem CP4.1.

For each DSC trace, state what sort of transition is occurring at what temperature.



Why does the glass transition temperature vary from one kind of polymer to another? What structural factors influence the glass transition temperature? This structure-property relationship isn't a straightforward one, as there seem to be a number of different variables involved. However, the simplest of these factors is just molecular weight. The higher the molecular weight of a polymer, the higher its glass transition temperature. This relationship is true only up to a certain point, however. The non-linear dependence of the glass transition temperature of molecular weight is described by the **Flory-Fox equation**:

$$T_g = T_{g(\infty)} - \frac{K}{M_n} \tag{11.5.4.4.1}$$

Here, $T_{g(\infty)}$ refers to the glass transition temperature of an infinitely long chain of the polymer. K is a constant for a particular polymer, such as polystyrene or polyethylene.

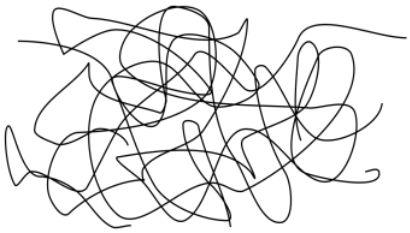
A plot of T_g *vs.* M_n resembles a saturation curve; the line rises sharply, gradually stalling out and continuing parallel to the x-axis. In other words, although this relationship of increasing glass transition temperature with increasing molecular weight holds true at relatively low molecular weights, the glass transition temperature remains constant once a threshold molecular weight has been reached.

This page titled 11.5.4.4: Glass Transition is shared under a CC BY-NC 3.0 license and was authored, remixed, and/or curated by Chris Schaller via source content that was edited to the style and standards of the LibreTexts platform.

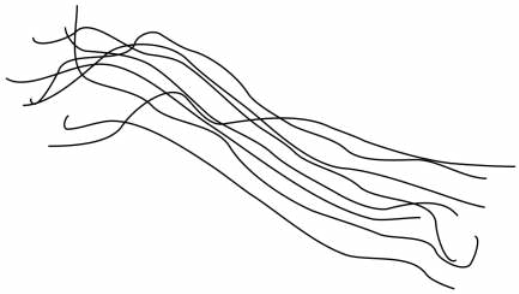
- **4.4: Glass Transition** by Chris Schaller is licensed CC BY-NC 3.0. Original source: https://employees.csbsju.edu/cschaller/Advanced/Polymers/Polycontents.htm.

11.5.4.5: Crystallinity in Polymers

We often think of polymers in the form of plastics: solid materials that serve some structural function, like a water bottle or some Venetian blinds. Polymers are different from many other such solids. Metals, for instance, have crystalline structures, in which atoms form a regularly repeating pattern, row upon row. Polymers, in contrast, are generally somewhat *amorphous*. Think of a strainer filled with cooked spaghetti, the long chains of pasta looping over each other randomly. That's how the molecules of amorphous or "shapeless" polymers tend to distribute themselves.



Polymers are capable of forming more ordered structures. If they aligned instead with their long chains parallel to each other, they would be able to get much closer together, and intermolecular attractions between the chains would be much stronger. The energy of the system would decrease, so this more crystalline structure should be inherently favored.



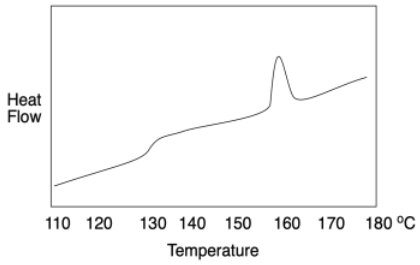
So why doesn't that always happen? Think about a polymer cooling from a completely melted state, in which case the structure is certainly amorphous. As it cools, the material becomes less like a liquid, and then less soft. With small molecules, that transition is relatively abrupt, as the molecules slide into place, guided by their strengthening intermolecular attractions. The molecules just have to rotate a little to face the correct direction, or maybe budge a little to the side. With polymers, the transition is much more gradual, because those great, long chains have to slide over each other and uncoil in order to lie parallel. At some point, there just isn't enough energy for them to keep working their way into the optimal alignment. As a result, many polymers are semi-crystalline, with regions called *lamellae* where portions of chains have aligned parallel to each other, but also with large amorphous areas that are much more randomly oriented.



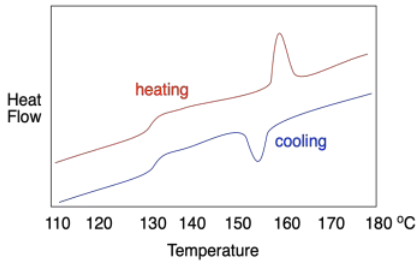
As a result, a polymer sample might be 80% amorphous with only 20% of its chain lengths aligned in crystalline lamellae. Even so, those crystalline domains exert a strong influence on the properties of the polymer. Because of the stronger intermolecular attractions between these closer chains, the chains are much less able to slide past each other. The result is a material that is stronger and more rigid, and that can be very important for reliable structural materials.

How do we know whether a polymer sample contains crystalline domains? We can use differential scanning calorimetry to observe the transition between an ordered crystalline phase and a disordered melt phase with added heat. As we saw when we were looking

at glass transition, a melting point shows up as a peak on a DSC trace. You can look for it at a temperature above T_g, which you will recall looks more like a step in the baseline. Below T_g, the chains are not mobile enough to move out of alignment with each other. In the example below, you can see T_g at about 128 °C as well as a melting point, T_m, when attractions between chains in the lamellae are overcome, at 155-160 °C.



If this were a regular molecular or elemental solid, the melting point would be the same as the fusion point; the material would melt at the same temperature during warming as it froze during cooling. In polymers, it usually doesn't work out that way, and a *hysteresis* is observed. In hysteresis, a sample has changed because of previous events, leading to results that don't seem to be reproducible in the way that we would normally expect. In general, the crystallization temperature, T_c, is lower than the melting temperature, T_m. That's because, as the material melts, the chains move out of alignment with each other and, because of chain entanglement, they are hindered from getting back into alignment with each other again, leading to a delay in crystallization.

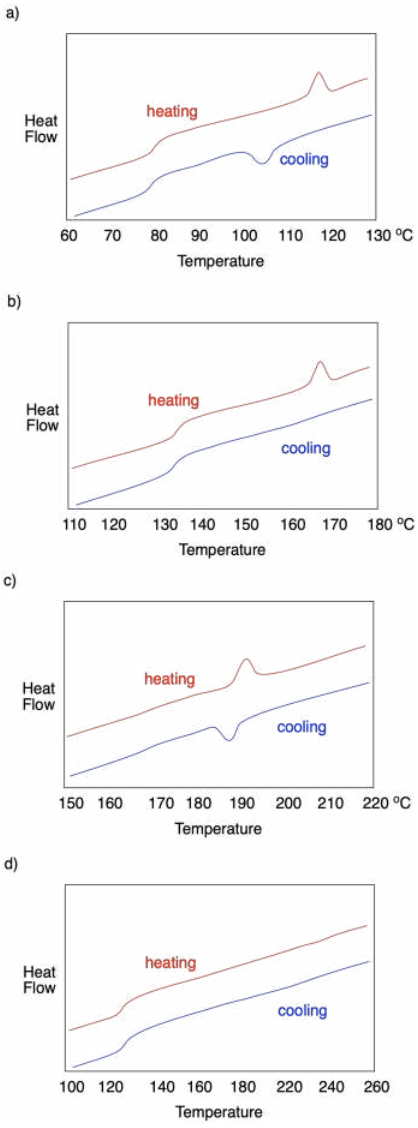


Example 4.5.1

Dec 31, 2019, 7:15 PM

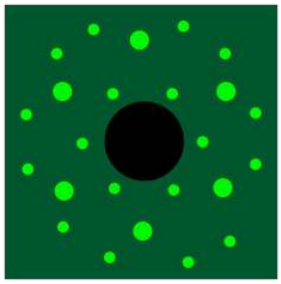
Problem PP5.1.

Describe what is observed in each of the following DSC traces.



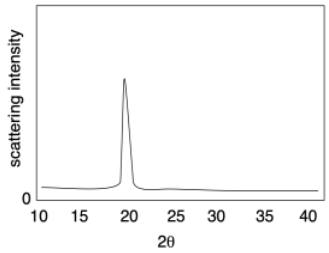
Crystallinity can also be probed in other ways. The classic approach is through X-ray diffraction. When X-rays pass through ordered materials, they give rise to diffraction patterns, bright spots in space where ricocheting X-rays have constructively interfered with each other, shining starkly amid the blackness where the X-rays have undergone destructive interference.

The drawing below is a cartoon of an X-ray diffraction pattern. It might be captured by a digital camera or, in earlier days, a sheet of photographic film. The bright spots result from X-rays scattering out from the middle, where they have encountered the sample. In the middle, the black circle blocks the original X-ray beam, which would otherwise be too bright to allow observation of those spots around it.



The data from an X-ray diffraction experiment is fed into a program that can mathematically deconvolute why the spots showed up where they did. The process has been compared to throwing a stone over your shoulder into a pond, then watching the ripples to decide where the stone must be. With one stone, that should be pretty easy. You would find the stone at the center of a circle of ripples. With two or more stones, interference patterns make the ripples more complex, and so it may take more work to determine where each stone lies in the pond.

The picture below illustrates the results of a relatively simple X-ray diffraction experiment commonly used with crystalline polymer samples. The technique is called wide-angle X-ray scattering, or WAXS. It simply reports the angle at which scattering intensity is observed relative to the initial X-ray beam. That angle corresponds to a distance between atoms in the sample, which in this case usually corresponds to a distance between parallel polymer chains. Sometimes there can be more than one peak, but this example is a simple one to start with.



The relationship between this scattering angle and an interatomic distance is given by Bragg's Law, a fundamental starting point in X-ray crystallography first expressed by Sir William Bragg and his son, Sir Lawrence Bragg. The law states that:

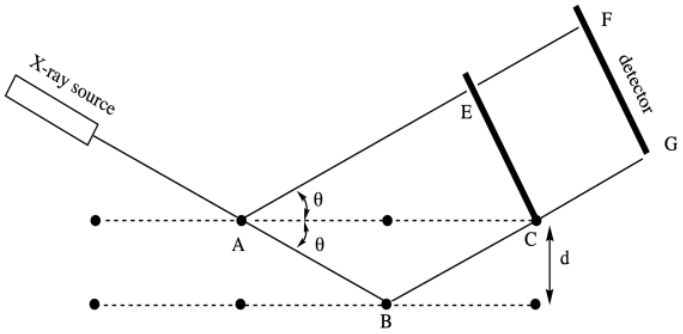
$$n\lambda = 2d\sin\theta \tag{11.5.4.5.1}$$

in which n is an integer (typically assumed to be 1), lambda is the wavelength of the X-ray used (commonly 1.541 Å, although others are possible), d is the distance between regularly repeating atoms and θ is the scattering angle.

Rearranging Equation 11.5.4.5.1, we find:

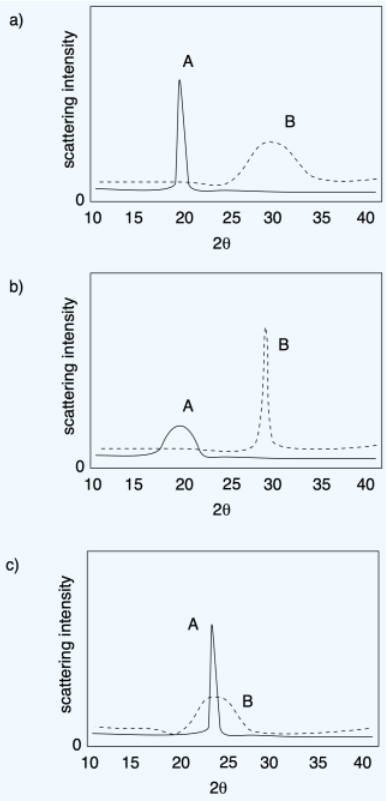
$$d = \frac{1.541}{2\sin\theta} \tag{11.5.4.5.2}$$

In other words, the distance between atoms is inversely proportional to the scattering angle. The greater the angle, the smaller the distance.



Example 4.5.1

In each of the following cases, determine which sample (A or B) has a higher crystalline content.



This page titled 11.5.4.5: Crystallinity in Polymers is shared under a CC BY-NC 3.0 license and was authored, remixed, and/or curated by Chris Schaller via source content that was edited to the style and standards of the LibreTexts platform.

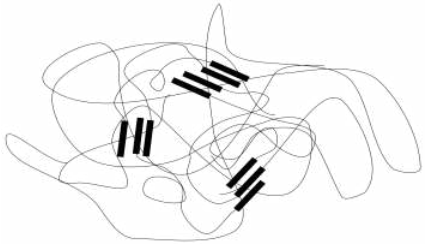
- **4.5: Crystallinity in Polymers** by Chris Schaller is licensed CC BY-NC 3.0. Original source: https://employees.csbsju.edu/cschaller/Advanced/Polymers/Polycontents.htm.

11.5.4.6: Microphase Separation

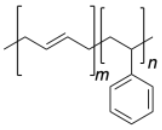
Crystalline domains provide additional strength to polymer materials. The strong attraction possible between closely-aligned chains results in long segments of the polymer being held more firmly in position. Consequently, chain flow is more limited, and the material becomes more rigid.

Sometimes, more rigid segments of a polymer are deliberately built into the structure. For example, in block co-polymers, softer, more flexible blocks are often paired with harder, more rigid blocks. The *soft segments* may have greater conformational flexibility, or weaker intermolecular attractions between themselves, or both. The *hard segments* may be more conformationally rigid or they may have stronger intermolecular attractions, such as strong dipoles or hydrogen bonds.

If the block lengths are the right size, the two segments are able to separate into two phases. As a result of stronger intermolecular attractions, lengths of chains containing hard segments cluster together, pushing out the soft segments that would otherwise get in the way of these intermolecular attractions. This phenomenon is called *microphase separation*. The result is that the material contains islands of strength and rigidity in a matrix of flexible polymer chains. That can be a very useful combination. The flexible chains of the soft segments allow the polymer to be distorted, bent or compressed, but the hard segments put limits on that flexibility, keeping the material firmly together.

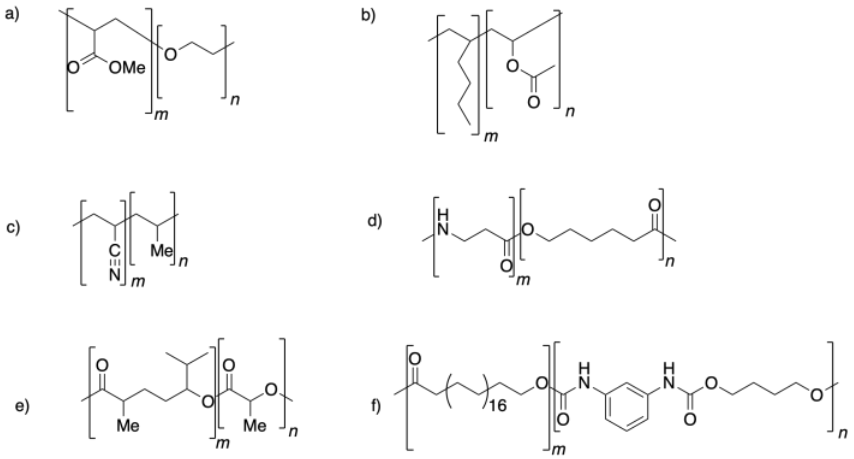


Because we are usually dealing with very large numbers of enchained monomers, the difference between the two kinds of segments need not even be dramatic. A copolymer of butadiene and styrene, both hydrocarbons, can form microphase separated materials. In this case, intermolecular attractions are dominated by weak London dispersion forces, but the aromatic groups of the styrene, with their delocalized pi systems, have London dispersion forces that are slightly stronger. As a result, the polystyrene blocks can cluster together, surrounded by the softer polybutadiene blocks.



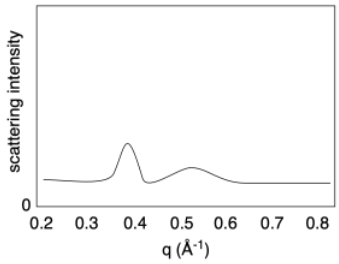
Problem PP6.1.

Identify the hard segment and the soft segment in each of the following block-co-polymers.



Sometimes, the separation between these phases can be directly observed via microscopy. Tunneling electron microscopy (TEM) is a technique that can generate images of a cross-sectional slice of the material. The material is generally stained with a heavy metal, such as osmium, that binds preferentially to one phase or the other. The stained phase shows up darker under TEM than the phase that isn't stained.

X-ray diffraction techniques can often be used to measure distances between hard segments. Small-angle X-ray scattering (SAXS) is very similar to wide-angle X-ray scattering (WAXS). Because of the inverse relationship between scattering angle and distance, SAXS is used to probe regularly repeating structures at greater distances than those seen in WAXS. That makes it possible to see peaks if the hard segments are distributed regularly enough within the soft matrix.



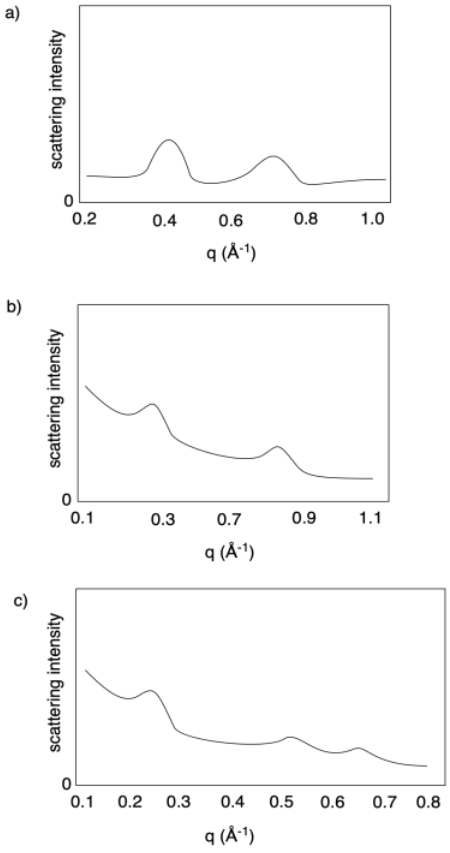
Note that, in SAXS, the x-axis is usually labeled as q, the scattering vector:

$$q = 4\pi\sin\theta / \lambda$$

But since $d = 2\sin\theta/\lambda$ then $q = 2\pi/d$ or $d = 2\pi/q$. That gives us a pretty straightforward way of calculating distances between regularly-spaced hard segments (or any other regularly-spaced objects). Once again, just as in WAXS, there is an inverse relationship between the quantity shown on the x-axis and distances through space.

Problem PP6.2.

Calculate the approximate distances revealed in the following SAXS results.



This page titled 11.5.4.6: Microphase Separation is shared under a CC BY-NC 3.0 license and was authored, remixed, and/or curated by Chris Schaller via source content that was edited to the style and standards of the LibreTexts platform.

- **4.6: Microphase Separation** by Chris Schaller is licensed CC BY-NC 3.0. Original source: https://employees.csbsju.edu/cschaller/Advanced/Polymers/Polycontents.htm.

11.5.4.7: Stress-Strain Relationships

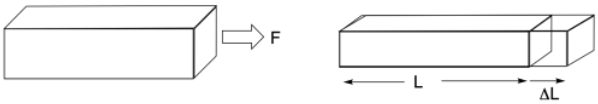
If you think about materials made from polymers, a couple of things might readily come to mind. You might think about the ubiquitous use of plastics in structures around us, such as automobile bumpers. You might think about a rubber band that you use to fasten something more firmly, either at home or in the lab. In either case, the function of the material relies on its response to stimuli. Do we want it to be flexible, to change shape, but then snap back to where it came from? Exactly how much flexibility do we need? Where is the trade-off between flexibility and strength?

These questions are important in polymer chemistry. Consequently, we often need to probe how materials behave under different conditions so that we know how they can be employed most effectively.

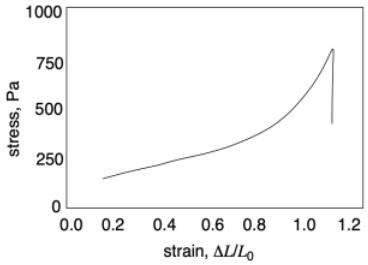
Tensile testing is one of the simplest ways to probe how a material responds to stress. Remember, the stress in this context means the force exerted on the material per unit of cross-sectional area. As such, it has units of pressure, such as Pascals (Pa). To do the experiment, the two ends of a sample are attached to two clamps, one of which is movable. The movable clamp is then pulled so that the sample becomes stretched. The force required to pull the sample is recorded and, given the cross-sectional area of the sample perpendicular to the force, the force is converted into units of strain.



The experiment also measures the distance that the sample is stretched (the strain). That distance is usually expressed as a ratio, comparing the change in length to the original length of the sample. It can be written either as a fraction or as a percent.



In the rough sketch below, we can see what typically happens in such an experiment. The sample stretches (the strain increases), and it gets harder to stretch as seen by the increasing force (and therefore increasing stress) that is needed to keep stretching it. Eventually, the stress plummets, because of the sample breaks.



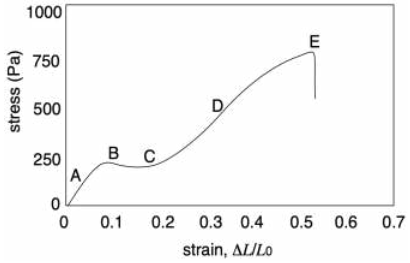
Already in this graph, we can see a couple of important pieces of information we can learn from tensile testing. Number one, how far can we stretch this material before it breaks? That quantity is called "strain at break". In this sample the strain at break looks like about 1.1 or 110%; that means the sample was stretched to twice its original length, and then some. Number two, how much stress can the sample support without breaking? That quantity is called "ultimate tensile strength". In this sample, the ultimate tensile strength is just over 750 Pa.

If we look more closely at the graph from another sample, we will get a third important quantity, and see some additional features. The important quantity can be derived from the first part of the curve (A), in which stress increases linearly with strain. In this linear region, the material is behaving as a "Hookean solid", meaning it obeys Hooke's Law. Hooke's Law says that stress and strain should be directly proportional. In his original words, the extension is proportional to the force:

$F = kx$

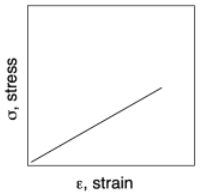
in which F is the force, x is the extension of the solid, and k is the proportionality constant.

Hooke's Law is commonly applied to the behavior of mechanical springs, but it also holds for other solid materials. The slope in the linear region of the graph (A) would equal that proportionality constant, k, because the graph shows the ratio of F/x. In materials science, this slope is more commonly called "Young's modulus". It is a measure of the inherent stiffness of the material.



Young's modulus: $E = \sigma/\varepsilon$

in which σ = stress and ε = extensional strain.



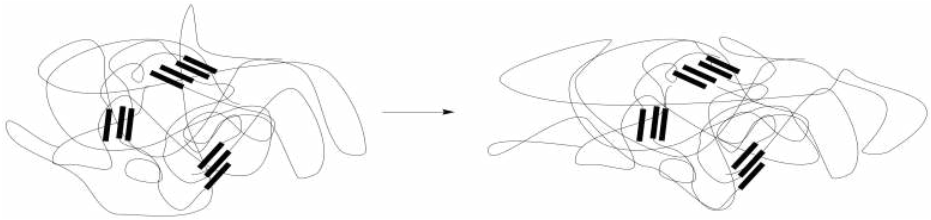
The extensional strain is just the strain observed by stretching the material. In the graph shown above, Young's modulus is around:

250 Pa / 0.1 = 2,500 Pa.

This initial region of the curve, in which Hooke's Law is obeyed, is sometimes called the "linear elastic region". The word "elastic" does have an immediate connotation in everyday English, bringing to mind a rubber band that can be stretched, so we think of the stretching part when we hear the word "elastic". However, the returning motion is an essential feature of elastic behavior. The rubber band always comes back to its original shape. Likewise, within the linear elastic region, any solid material returns to its original shape after it is deformed under stress.

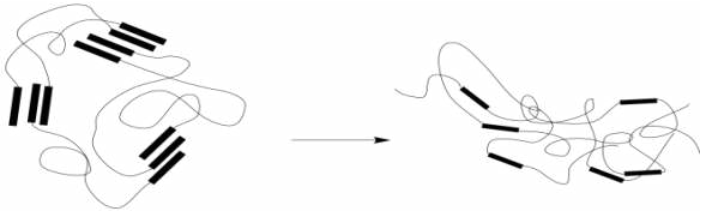
With most solids, such as aluminum or concrete, the linear elastic region spans a very narrow range of strains. Just by looking, we wouldn't notice these materials being deformed. However, this linear stress-strain relationship is typical of solids. In rheology, that behavior is described as elastic. Of course, with many polymers, a sample can be stretched so far that you can see the change with the naked eye, and it still returns to that original shape.

What makes polymers different? The long-chain structure of polymers does make them behave differently from other materials. These chains can undergo conformational change: each bond along the chain can rotate, converting the polymer chain into a slightly different shape. That ability gives a "soft material" a great deal of flexibility. The conformations of chains can adapt to accommodate stress, moving the chains into new shapes that offer lower-energy packing between each other. When the stress is removed, the chains eventually slide back into their original conformations. They return to their equilibrium shapes.



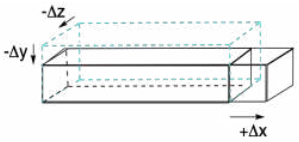
The presence of physical or chemical crosslinks help the material return to its original shape, functioning as anchor points so that the chains don't stray too far. Those interactions might be found in hard-phase interactions in a microphase separated material, as illustrated here, although they could also be found in a homogeneous material.

The linear elastic region isn't all we see in the stress-strain curve above. At point (B), the linear relationship is suddenly lost. The stress might even drop, as seen in this particular case. This feature on the graph is called the "yield point". The stress being experienced by the material, and the resulting strain, has become sufficient to overcome the natural elastic behavior of the solid. As noted previously, physical crosslinks such as hydrogen bonds help to reinforce the elastic behavior of a polymer sample. If, at some point, those interactions are overcome, the chains will start to slide more readily past each other.



As a result, the material loses its elasticity. When the stress is released, the material will still spring back as the chains settle into a new conformational equilibrium. However, that equilibrium will not be the same as the one before. New physical crosslinks will form as groups form intermolecular interactions with the nearest neighbors they encounter. It isn't likely that these will always be the same groups that they were interacting with before. As a result, the material will settle into a slightly different shape. You have probably seen this happen before when a rubber band has been stretched too far, too often, or for too long. Chains have dropped their old interactions and picked up new ones that formed more easily in the extended shape.

At point (C) of the example graph, the slope of the curve starts to increase. The same change in stress results in smaller and smaller changes in strain; the material is getting stiffer. This phenomenon is called "strain hardening". This feature would not always be observed, but if it did happen, what would explain it? In polymers, one explanation may lay in the fact that the volume of the material should remain constant as it is stretched. If the sample is getting longer, that means it is also getting narrower.



As a consequence of that narrowing cross-section, chains become compressed together. At some point, physical crosslinks begin occurring between neighboring chains. These crosslinks don't occur in equilibrium positions, with polymer chains coiled around each other like they were in the original sample. These crosslinks occur when chains are extended, lying parallel to each other, at closer contact distances than normal.



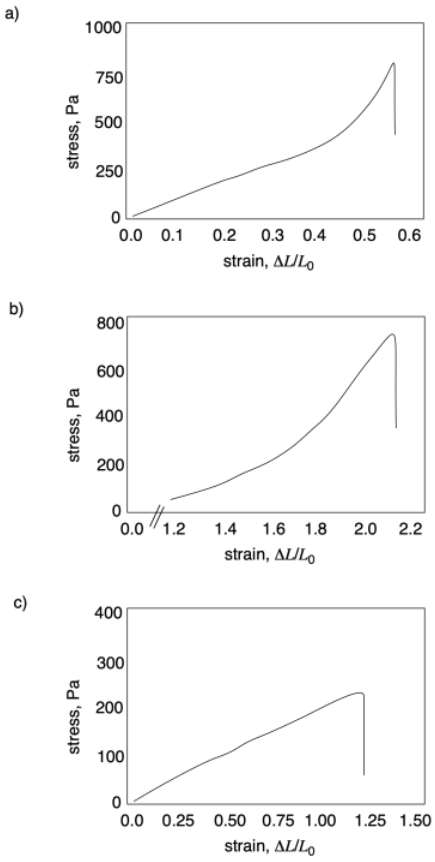
We can see the opposite sort of thing happening at (D), when the slope of the curve is decreasing instead of increasing. This phenomenon is called "strain-softening". Again, it might not be observed in all samples. When it does happen, what causes it? In this case, the answer is simpler. Having overcome the interactions that held the chains together, there is nothing left to resist further deformation. As the chains begin to disentangle from each other, it becomes even easier to pull them apart, facilitating the extension or stretching of the sample.



Eventually, at the breaking point (E), the chains start to lose contact with each other at some location in the sample, resulting in a catastrophic rupture of the sample.

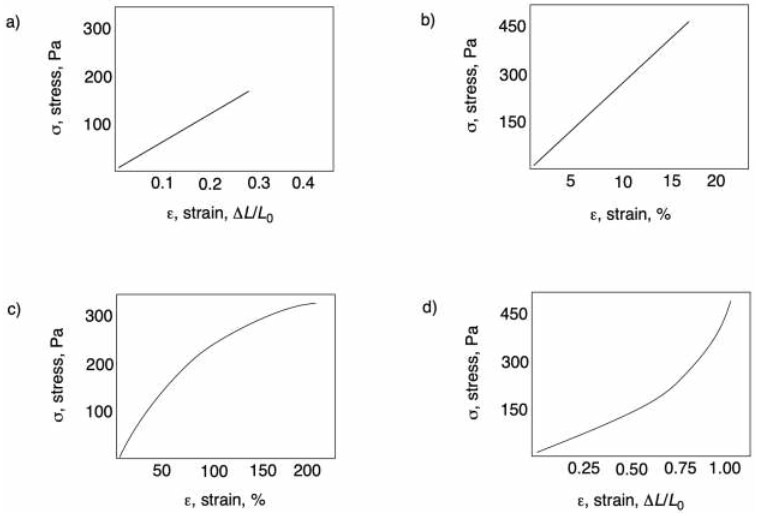
Problem PP7.1.

In each of the following curves, estimate ultimate tensile strength and strain at break.



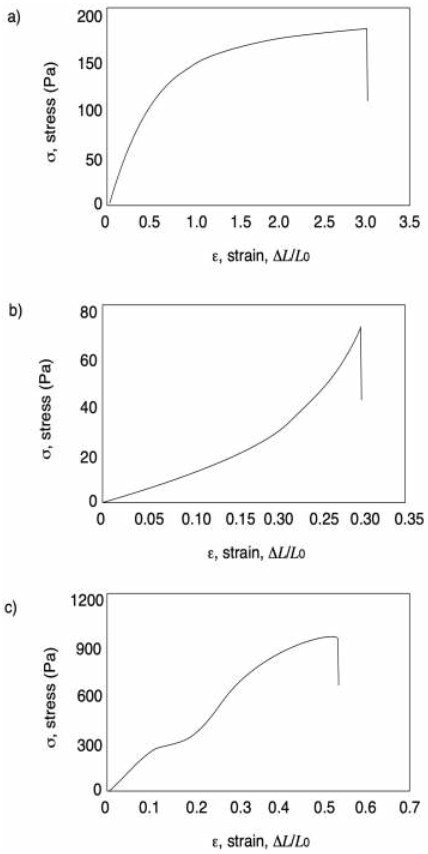
Problem PP7.2.

In each of the following curves, calculate Young's modulus.



Problem PP7.3.

In each of the following curves, identify any diagnostic features.

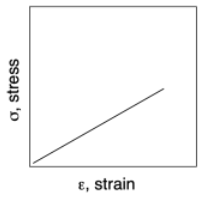


This page titled 11.5.4.7: Stress-Strain Relationships is shared under a CC BY-NC 3.0 license and was authored, remixed, and/or curated by Chris Schaller via source content that was edited to the style and standards of the LibreTexts platform.

- **4.7: Stress-Strain Relationships** by Chris Schaller is licensed CC BY-NC 3.0. Original source: https://employees.csbsju.edu/cschaller/Advanced/Polymers/Polycontents.htm.

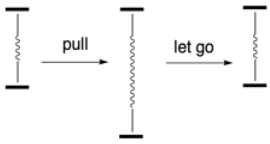
11.5.4.8: Storage and Loss Modulus

We saw earlier that the inherent stiffness of a material can be assessed by its Young's modulus. The Young's modulus is the ratio of the stress-induced in a material under an applied strain. The strain is the amount of deformation in the material, such as the change in length in an extensional experiment, expressed as a fraction of the beginning length. The stress is the force exerted on the sample divided by the cross-sectional area of the sample. If the strain is limited to a very small deformation, then it varies linearly with stress. If we graph the relationship, then the slope of the line gives us Young's modulus, *E*. That's the proportionality constant between stress and strain in Hooke's Law.

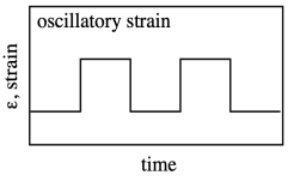


$$E = \sigma / \varepsilon$$

Hooke's Law is sometimes used to describe the behavior of mechanical springs. The modulus can be thought of the resistance to stretching a spring; the more resistance the spring offers, the greater the force needed to stretch it. The same force is what snaps the spring back into place once you let it go.

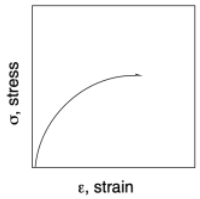


In the experiments we saw earlier, we didn't let go. We continued to stretch the material farther and farther, applying generally increasing stress until the material finally broke. Now we will look at a much more limited approach. Instead of stretching the material as far as we can, we will only stretch it a tiny bit, then release the stress so that it snaps back to its original length. We can then stress it again and release it again. We can keep repeating. Instead of a continuously increasing strain, this sample is subjected to an oscillatory strain, one that repeats in a cycle.

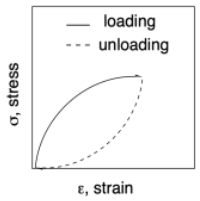


This approach is called dynamic mechanical analysis. We can use dynamic mechanical analysis to measure the modulus of the material. Instead of continuously moving all the way through the linear elastic region, beyond which Hooke's law breaks down, we carefully keep the sample in the Hookean region for the entire experiment. Now, one experiment should be good enough to extract the modulus, but we are letting go and doing it over again. Why?

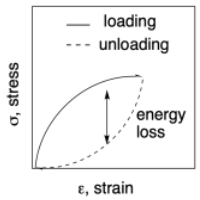
The principle reason for running the experiment this way is to get some additional information. We can get this information because polymers don't quite follow Hooke's Law perfectly. In reality, even within the linear elastic region, the stress-strain curve is not quite linear. In the picture below, the curvature is exaggerated quite a bit, just for illustrative purposes.



Even if the relationship is not quite linear, then as we release the strain, the stress in the material should simply follow the curve back down to zero. It does not. Instead, there is a phenomenon called hysteresis at work. Hysteresis just means that a property of the material depends on how the material came to be in its current situation. In this case, Hooke's Law seems to imply that a specific sample subjected to a specific strain would experience a specific stress (or vice versa). However, it depends whether we are stretching the sample or letting it relax again. As we let the sample relax back to its initial length, the strain is different from what we saw when we were stretching it. Typically, it's lower. Again, we can see this in the curve below, where the curvature has been exaggerated.



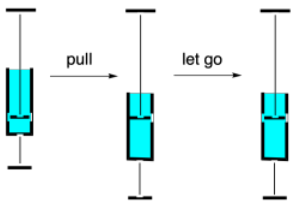
The difference between the loading curve (when the stress was first applied) and the unloading curve (when the stress was removed) represents an energy loss. A force was applied to move a sample or a portion of a sample, some distance. When the sample snapped back the same distance, the force was unequal to the one that was initially applied. Some energy was therefore lost.



The slope of the loading curve, analogous to Young's modulus in a tensile testing experiment, is called the storage modulus, *E*'. The storage modulus is a measure of how much energy must be put into the sample in order to distort it. The difference between the loading and unloading curves is called the loss modulus, *E*''. It measures energy lost during that cycling strain.

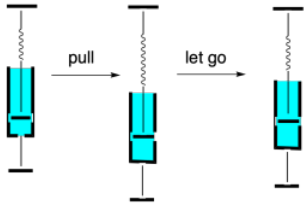
Why would energy be lost in this experiment? In a polymer, it has to do chiefly with chain flow. The resistance to deformation in a polymer comes from entanglement, including both physical crosslinks and more general occlusions as chains encounter each other while undergoing conformational changes to accommodate the new shape of the material. Once the stress is removed, the material springs back to its equilibrium shape, but there is no reason chains would have to follow the exact same conformational pathway to return to their equilibrium conformations. Because they have moved out of their original positions, they are able to follow a lower-energy pathway back to their starting point, a pathway in which there is less resistance between neighboring chains.

For that reason, stretching a polymer is not quite the same as stretching a mechanical spring. A "spring-and-dashpot" analogy is often invoked to describe soft materials. Whereas a spring simply bounces back to its original shape after being pulled, a dashpot does not. If you don't know what a dashpot is, picture the hydraulic arms that support the hatchback on a car when you open it upward. There is some resistance to opening the hatchback because a piston is being pulled through a hydraulic fluid as the arm stretches. When we stop lifting, the arms stay at that length, because the hydraulic fluid also resists the movement of the piston back to its original position. The dashpot has a tendency to stay put rather than spring back.



Polymers display a little of both properties. They have an elastic element, rooted in entanglement, that makes them resist deformation and return to their original shapes. They also have a viscous element, rooted in chain flow. That viscous element means that, when we distort polymeric materials, they might not return to exactly the same form as when they started out. Taken

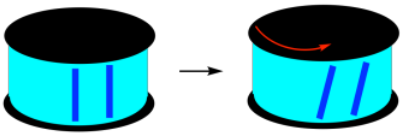
together, these behaviors are described as viscoelastic properties. Many materials have viscoelastic properties, meaning they display some aspects of elastic solids and some aspects of viscous liquids.



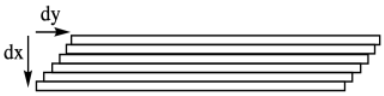
So far, we have concentrated on extensional deformations of materials: we have been looking at what happens when we stretch them. It's worth looking at another type of deformation because it is very commonly used in materials testing. This second approach uses shear instead of an extension to probe how the material will respond. A shear force is applied unevenly to a material so that it tilts or twists rather than stretching.



One of the reasons this approach is used so often is because it is very easy to do. A sample is sandwiched between two plates. The bottom plate is held in place while the top plate is twisted, shearing the material held in between.



If we take a closer look at a layer of the sample, maybe at the surface, along the edge of the sandwich, we can imagine breaking it down into individual layers. Under shear strain, those layers move different amounts. The top layer, right beneath that top plate moves the most. The bottom layer, sitting on the stationary lower plate, doesn't move at all. In between, each layer moves a little further than the one beneath it. This gradation of deformation across the sample is very much like what we saw in the analysis of the viscosity of liquids. The difference is that viscosity looks at the variation of strain with time. Nevertheless, modulus in solids is roughly analogous to viscosity in liquids.



We can use this parallel plate geometry to obtain values for storage modulus and loss modulus, just like we can via an extensional geometry. The values we get are not quite the same. For this reason, modulus obtained from shear experiments is given a different symbol than modulus obtained from extensional experiments. In a shear experiment,

$G = \sigma / \varepsilon$

That means storage modulus is given the symbol G' and loss modulus is given the symbol G''. Apart from providing a little more information about how the experiment was actually conducted, this distinction between shear modulus and extension modulus is important because the resulting values are quite different. In general, the value of the storage modulus obtained from an extensional experiment is about three times larger than the value of storage modulus obtained from a shear experiment.

$E' = 3\ G'$

The reason for the difference is that extension actually involves deformation of the material in three directions. As the material is stretched in one direction (let's say it's the y-direction), in order to preserve the constant volume of the material (there is still the same amount of stuff before and after stretching), the material compresses in both the other two directions (x and z).

Problem PP8.1.

Metric prefixes are frequently encountered when reading about modulus. Rank the following units of stress from smallest to largest, and in each case provide a conversion factor to Pa.

GPa kPa MPa Pa

This page titled 11.5.4.8: Storage and Loss Modulus is shared under a CC BY-NC 3.0 license and was authored, remixed, and/or curated by Chris Schaller via source content that was edited to the style and standards of the LibreTexts platform.

- **4.8: Storage and Loss Modulus** by Chris Schaller is licensed CC BY-NC 3.0. Original source: https://employees.csbsju.edu/cschaller/Advanced/Polymers/Polycontents.htm.

11.5.4.9: Modulus, Temperature, Time

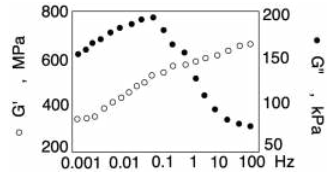
The storage modulus measures the resistance to deformation in an elastic solid. It's related to the proportionality constant between stress and strain in Hooke's Law, which states that extension increases with force. In the dynamic mechanical analysis, we look at the stress (σ), which is the force per cross-sectional unit area, needed to cause an extension in the sample, or the strain (ε).

$$E = \frac{\sigma}{\varepsilon} \tag{11.5.4.9.1}$$

Alternatively, in a shear experiment:

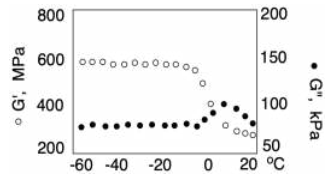
$$G = \frac{\sigma}{\varepsilon} \tag{11.5.4.9.2}$$

The dynamic mechanical analysis differs from simple tensile testing by performing the experiment cyclically. The sample is stretched and released (or sheared and released). It can then be subjected to additional stress and released again. There is an element of time involved here. Specifically, because the experiment is cyclic, it can be carried out at different frequencies. When you do that, and you plot the resulting modulus against frequency, you can get additional information about the sample. The results would typically be presented in a graph like this one:



What the graph tells us is that frequency clearly matters. When the experiment is run at higher frequencies, the storage modulus is higher. The material appears to be stiffer. In contrast, the loss modulus is lower at those high frequencies; the material behaves much less like a viscous liquid. In particular, the sharp drop in loss modulus is related to the relaxation time of the material. In this context, that's the time it takes the chains to flow into new conformations in response to the applied stress. If they don't have time to flow, then that viscous response of the material is lost. The material behaves much more like an elastic solid when subjected to high-frequency cyclic deformation. That's important to know, because a material might be subjected to vibrations or other stimuli during everyday use, and its properties might change accordingly.

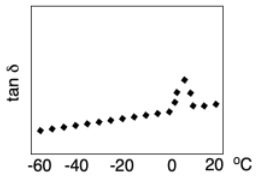
Another variation on this kind of experiment is called dynamic mechanical thermal analysis. Instead of changing the frequency of the stimulus throughout the experiment, the frequency is held constant and the temperature is changed instead. As a result, we can again see how the material responds under different conditions, which might tell us how it will behave in everyday applications. The result of the experiment might be a graph like the one below:



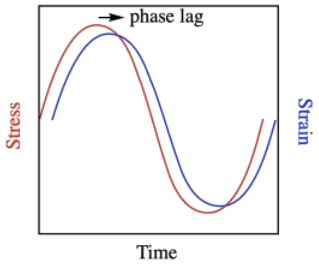
At this point, you are already familiar with the glass transition. It shouldn't be surprising that the properties are dependent on temperature. At the glass transition temperature, the expanding volume of the material with increasing temperature becomes sufficient to allow chain flow. As a result, the material suddenly behaves much more like a viscous liquid. Loss modulus increases. The stiffness of the material drops as the entangled chains not longer resist deformation as strongly. Storage modulus decreases.

The dynamic mechanical thermal analysis thus provides an alternative way to determine the glass transition temperature. Because it is actually measuring a different physical phenomenon than differential scanning calorimetry, the T_g obtained from a DMTA experiment may not agree exactly with one obtained from a DSC experiment. Nevertheless, it is often useful to have different ways of assessing properties.

In order to facilitate the analysis of the T_g in this experiment, a different quantity is usually displayed. Tan delta is just the ratio of the loss modulus to the storage modulus. It peaks at the glass transition temperature.



The term "tan delta" refers to a mathematical treatment of storage modulus; it's what happens in-phase with (or at the same time as) the application of stress, whereas loss modulus happens out-of-phase with the application of stress. Because it would take some time for the chains to move into new confirmation when they are subjected to stress, the strain actually lags behind the stress in these experiments.

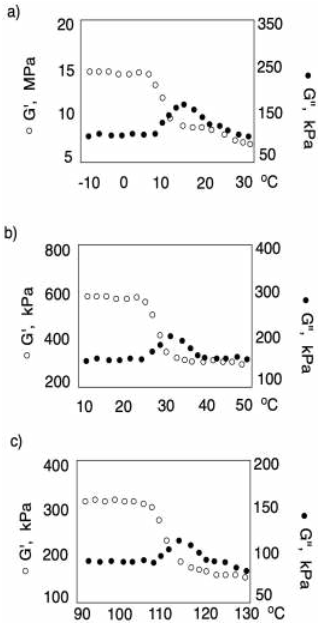


Delta refers to the phase lag, the amount of time between application of stress and the observation of maximum strain. You may remember that a sine curve and cosine curve are out of phase with each other. Storage modulus is described as being proportional to *cosδ* whereas loss modulus is proportional to *sinδ*. The ratio of *cosδ* to *sinδ* is just *tanδ*.

Why does *tanδ* peak at the glass transition temperature? Clearly, as chains begin to move more freely, loss modulus increases. Consequently, the material also becomes less stiff and more rubbery. The storage modulus drops. If tan delta is the ratio of loss modulus to storage modulus, it should increase at that point -- and it does. Why does it drop again? That's because loss modulus refers to an energy loss, but because the material has gotten softer, less stress (and less energy) is put into the sample in the first place, so the energy loss also gets smaller. As a result, tan delta goes up at the glass transition but drops again shortly beyond that point.

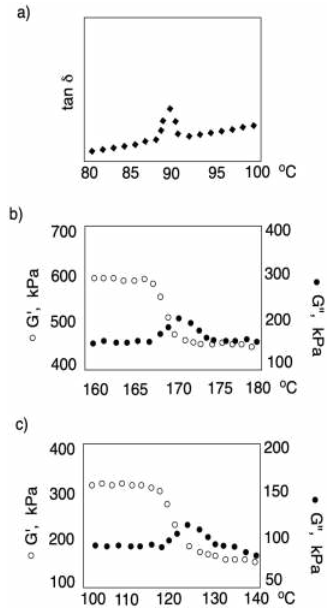
Problem PP9.1.

Estimate the storage and loss, modulus in the glassy phase and rubbery phase in each of the following cases.



Problem PP9.2.

Estimate T_g in each of the following cases.



This page titled 11.5.4.9: Modulus, Temperature, Time is shared under a CC BY-NC 3.0 license and was authored, remixed, and/or curated by Chris Schaller via source content that was edited to the style and standards of the LibreTexts platform.

- **4.9: Modulus, Temperature, Time** by Chris Schaller is licensed CC BY-NC 3.0. Original source: https://employees.csbsju.edu/cschaller/Advanced/Polymers/Polycontents.htm.

11.5.4.10: Chapter Solutions

Problem PP1.1.

a) With a shorter elution time, **I** has a higher molecular weight than **II**. The narrower peak means that **I** has a narrower dispersity than **II**.

b) With a shorter elution time, **III** has a higher molecular weight than **IV**. The wider peak means that **III** has a broader dispersity than **IV**.

c) With a higher elution time, **V** has a lower molecular weight than **VI**. The wider peak means that **V** has a broader dispersity than **VI**.

Problem PP1.2.

a) repeat unit: 109 x ($C_4H_6O_2$) = 109 x 86.09 g/mol = 9,383.81 g/mol

end groups: C_9H_{11} + Br = 119.19 + 79.9 = 199.09 g/mol

total: 9,383.81 + 199.09 = 9,582.90 g/mol

b) repeat unit: 763 x (C_8H_8) = 763 x 104.15 g/mol = 79,466.45 g/mol

end groups: C_4H_9 + H = 57.12 + 1.008 = 58.13 g/mol

total: 79,466.45 + 58.13 = 79,524.58 g/mol

c) repeat unit: 48 x ($C_4H_6O_2$) = 48 x 86.09 g/mol = 4,132.32 g/mol

end groups: C_4H_9 + $C_7H_5S_2$ = 57.12 + 153.26 = 210.38 g/mol

total: 4,132.32 + 210.38 = 4,342.70 g/mol

Problem PP1.3.

The ratio of the repeat unit integral per proton to the end group proton per integral gives the degree of polymerization. We could take the entire integration of the end group and divide it by the entire number of protons in that group, or select one position to represent the end group. Similarly, we can select one position to represent the repeat unit.

a) repeat unit integral per proton = 36.0 / 2H = 18

end group integral per proton = 0.32 / 2H = 0.16

degree of polymerization = 18/0.16 = 112

b) repeat unit integral per proton = 26.0 / 1H = 26

end group integral per proton = 1.32 / 9H = 0.15

degree of polymerization = 26/0.15 = 173

c) repeat unit integral per proton = 54.0 / 4H = 13.5

end group integral per proton = 0.49 / 1H = 0.49

degree of polymerization = 13.5/0.49 = 28

Problem PP2.1.

α is the slope, which is [rise]/[run]. That's approximately [4.0-2.4]/[6.6-4.4] = 1.6/2.2 = 0.73.

K is the y-intercept. The equation for a straight line is y = mx +b; in this case, y = 0.73x + b. If we choose a point on the line, such as (x,y) = (4.9, 2.0), we can substitute those values on for x and y to get b.

So 2.0 = 0.73(4.9) + b, or b = 2.0 - 3.56 = -1.56.

Problem PP2.2.

If the molecular weight is a million g/mol, then log(M_w) = 6. Interpolating, log([η]) = 4, or [η] = 10,000 ml/g.

Problem PP2.3.

If the intrinsic viscosity, [η] = 800 ml/g, then log([η]) = 2.9. Interpolating, log(M_w) = 5.1, or M_w = 126,000 g/mol.

Problem PP2.4.

Ethylene glycol can form hydrogen bonds at either end of the molecule, forming a supramolecular assembly much like a polymer. As a result, it has a much greater drag in solution, higher viscosity.

Problem PP3.1.

Honey is a concentrated solution of simple sugars, which are small molecules. Molasses, although similar to honey in some ways, also contain starches, which are polymers. This polymeric content leads to shear-thinning behavior.

Problem PP4.1.

a) There is a glass transition at around -18°C.

b) There is a melting point at around 125°C.

c) There is a glass transition at around -4°C.

d) There is a glass transition at around 117°C and a melting point at around 146°C.

Problem PP5.1.

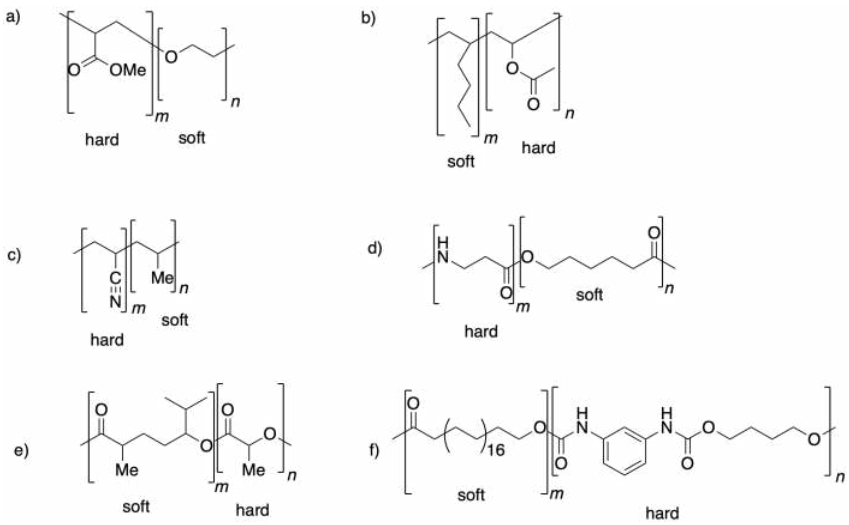
a) T_g is observed at around 78°C, T_m is observed at around 117°C and T_c is observed at around 104°C.

b) T_g is observed at around 134°C and T_m is observed at around 167°C, but T_c is not observed; the sample failed to crystallize, but remained an amorphous solid.

c) T_m is observed at around 194°C and T_c is observed at around 187°C. T_g is not observed, and probably occurs below 150°C

d) T_g is observed at around 123°C, but T_m is not observed. The experiment checked much higher than T_g (over a hundred degrees), so the material may be an amorphous solid.

Problem PP6.1.



Problem PP6.2.

a) d = (2 x 3.14) / 0.40 = 16 Å; d = (2 x 3.14) / 0.70 = 9.0 Å

b) d = (2 x 3.14) / 0.25 = 25 Å; d = (2 x 3.14) / 0.85 = 7.4 Å

c) d = (2 x 3.14) / 0.25 = 25 Å; d = (2 x 3.14) / 0.52 = 12 Å; d = (2 x 3.14) / 0.66 = 10 Å

Problem PP7.1.

a) ultimate tensile strength = 800 Pa; strain at break = 55%

b) ultimate tensile strength = 750 Pa; strain at break = 215%

c) ultimate tensile strength = 220 Pa; strain at break = 120%

Problem PP7.2.

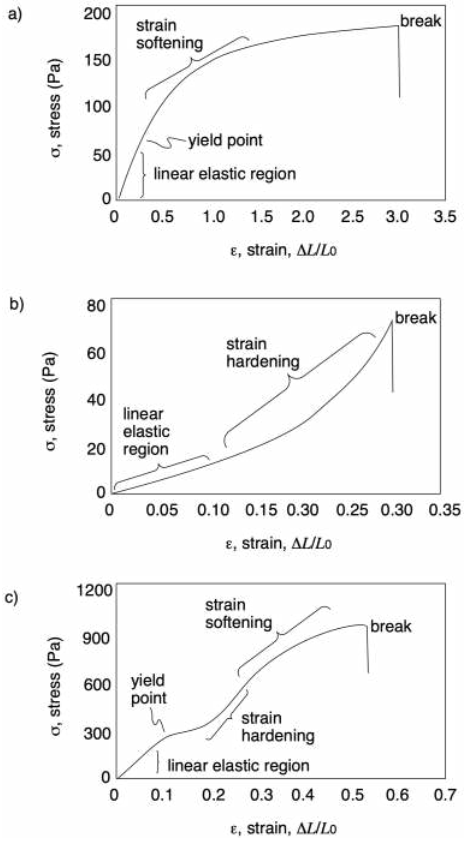
a) E = σ / ε = 180 Pa / 0.30 = 600 Pa

b) E = σ / ε = 450 Pa / 0.15 = 3,000 Pa

c) E = σ / ε = 50 Pa / 0.25 = 200 Pa

d) E = σ / ε = 75 Pa / 0.30 = 250 Pa

Problem PP7.3.



Problem PP8.1.

1 Pa = 1 Pa

1 kPa = 1,000 Pa

1 MPa = 1,000,000 Pa

1GPa = 1,000,000,000 Pa

Problem PP9.1.

a) glassy: storage modulus = 15 MPa; loss modulus = 70 kPa

rubbery: storage modulus = 7 MPa; loss modulus = 80 kPa

b) glassy: storage modulus = 600 kPa; loss modulus = 140 kPa

rubbery: storage modulus = 130 kPa; loss modulus = 150 kPa

c) glassy: storage modulus = 320 kPa; loss modulus = 80 kPa

rubbery: storage modulus = 70 kPa; loss modulus = 70 kPa

Problem PP9.2.

a) 89 °C

b) 170 °C

c) 124 °C

This page titled 11.5.4.10: Chapter Solutions is shared under a CC BY-NC 3.0 license and was authored, remixed, and/or curated by Chris Schaller via source content that was edited to the style and standards of the LibreTexts platform.

- **4.10: Chapter Solutions** by Chris Schaller is licensed CC BY-NC 3.0. Original source: https://employees.csbsju.edu/cschaller/Advanced/Polymers/Polycontents.htm.

CHAPTER OVERVIEW

Back Matter

Detailed Licensing

Detailed Licensing

Overview

Title: 11.5: Polymer Chemistry (Schaller)

Webpages: 44

Applicable Restrictions: Noncommercial

All licenses found:

- CC BY-NC 3.0: 90.9% (40 pages)
- CC BY-NC 4.0: 4.5% (2 pages)
- Undeclared: 4.5% (2 pages)

By Page

- 11.5: Polymer Chemistry (Schaller) - *CC BY-NC 3.0*
  - Front Matter - *CC BY-NC 4.0*
    - Licensing - *Undeclared*
  - 11.5.1: Monomers and Polymers - *CC BY-NC 3.0*
    - 11.5.1.1: Difunctional Carboxyloids - *CC BY-NC 3.0*
    - 11.5.1.2: Cyclic Carboxyloids - *CC BY-NC 3.0*
    - 11.5.1.3: Olefins - *CC BY-NC 3.0*
    - 11.5.1.4: Cyclic Olefins - *CC BY-NC 3.0*
    - 11.5.1.5: Coordination Polymers - *CC BY-NC 3.0*
    - 11.5.1.6: Supramolecular Assemblies - *CC BY-NC 3.0*
    - 11.5.1.7: Other Polymers - *CC BY-NC 3.0*
    - 11.5.1.8: Polymer Topology - *CC BY-NC 3.0*
    - 11.5.1.E: Solutions for Selected Problems - *CC BY-NC 3.0*
  - 11.5.2: Synthetic Methods in Polymer Chemistry - *CC BY-NC 3.0*
    - 11.5.2.1: Ziegler-Natta Polymerization - *CC BY-NC 3.0*
    - 11.5.2.2: Solutions to Selected Problems - *CC BY-NC 3.0*
    - 11.5.2.3: Step Growth and Chain Growth - *CC BY-NC 3.0*
    - 11.5.2.4: Cationic Polymerization - *CC BY-NC 3.0*
    - 11.5.2.5: Living Cationic Polymerization - *CC BY-NC 3.0*
    - 11.5.2.6: Anionic Polymerization - *CC BY-NC 3.0*
    - 11.5.2.7: Living Anionic Polymerization - *CC BY-NC 3.0*
    - 11.5.2.8: Ring-Opening Polymerization - *CC BY-NC 3.0*
    - 11.5.2.9: Radical Polymerization - *CC BY-NC 3.0*
    - 11.5.2.10: Living Radical Polymerization- RAFT - *CC BY-NC 3.0*
    - 11.5.2.11: Living Radical Polymerization- ATRP - *CC BY-NC 3.0*
  - 11.5.3: Kinetics and Thermodynamics of Polymerization - *CC BY-NC 3.0*
    - 11.5.3.1: Thermodynamics of Polymerization - *CC BY-NC 3.0*
    - 11.5.3.2: Kinetics of Step-Growth Polymerization - *CC BY-NC 3.0*
    - 11.5.3.3: Kinetics of Chain Polymerization - *CC BY-NC 3.0*
    - 11.5.3.4: Kinetics of Catalytic Polymerization - *CC BY-NC 3.0*
    - 11.5.3.5: Solutions to Selected Problems - *CC BY-NC 3.0*
  - 11.5.4: Polymer Properties - *CC BY-NC 3.0*
    - 11.5.4.1: Molecular Weight of Polymers - *CC BY-NC 3.0*
    - 11.5.4.2: Viscosity of Polymers - *CC BY-NC 3.0*
    - 11.5.4.3: Rheology - *CC BY-NC 3.0*
    - 11.5.4.4: Glass Transition - *CC BY-NC 3.0*
    - 11.5.4.5: Crystallinity in Polymers - *CC BY-NC 3.0*
    - 11.5.4.6: Microphase Separation - *CC BY-NC 3.0*
    - 11.5.4.7: Stress-Strain Relationships - *CC BY-NC 3.0*
    - 11.5.4.8: Storage and Loss Modulus - *CC BY-NC 3.0*
    - 11.5.4.9: Modulus, Temperature, Time - *CC BY-NC 3.0*
    - 11.5.4.10: Chapter Solutions - *CC BY-NC 3.0*
  - Back Matter - *CC BY-NC 4.0*
    - Detailed Licensing - *Undeclared*

SECTION OVERVIEW

11.6: Synthetic Polymers

11.6.1: Introduction

11.6.2: Chain-Growth Polymers—Addition Polymers

11.6.3: Anionic Polymerization of Epoxides

11.6.4: Ziegler–Natta Catalysts and Polymer Stereochemistry

11.6.5: Natural and Synthetic Rubbers

11.6.6: Step-Growth Polymers—Condensation Polymers

11.6.7: Polymer Structure and Properties

11.6.8: Green Polymer Synthesis

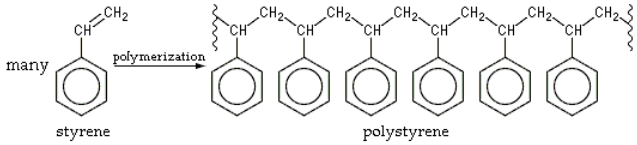
11.6.9: Polymer Recycling and Disposal

11.6: Synthetic Polymers is shared under a CC BY-NC-SA 4.0 license and was authored, remixed, and/or curated by LibreTexts.

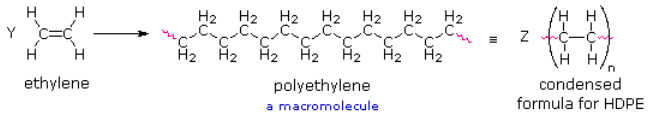
11.6.1: Introduction

Polymers are long chain, giant organic molecules are assembled from many smaller molecules called **monomers**. Polymers consist of many repeating monomer units in long chains, sometimes with *branching* or *cross-linking* between the chains. A polymer is analogous to a necklace made from many small beads (monomers). A chemical reaction forming polymers from monomers is called **polymerization**, of which there are many types. A common name for many synthetic polymer materials is plastic, which comes from the Greek word "plastikos", suitable for molding or shaping.

In the following illustrated example, many monomers called styrene are polymerized into a long chain polymer called polystyrene. The squiggly lines indicate that the polymer molecule extends further at both the left and right ends. In fact, polymer molecules are often hundreds or thousands of monomer units long.



The repeating structural unit of most simple polymers not only reflects the monomer(s) from which the polymers are constructed, but also provides a concise means for drawing structures to represent these macromolecules. For polyethylene, arguably the simplest polymer, this is demonstrated by the following equation. Here ethylene (ethene) is the monomer, and the corresponding linear polymer is called high-density polyethylene (HDPE). HDPE is composed of macromolecules in which n ranges from 10,000 to 100,000 (molecular weight 2×10^5 to 3×10^6).



If Y and Z represent moles of monomer and polymer respectively, Z is approximately 10^{-5} Y. This polymer is called polyethylene rather than polymethylene, $(-CH_2-)_n$, because ethylene is a stable compound (methylene is not), and it also serves as the synthetic precursor of the polymer. The two open bonds remaining at the ends of the long chain of carbons (colored magenta) are normally not specified, because the atoms or groups found there depend on the chemical process used for polymerization. The synthetic methods used to prepare this and other polymers will be described later in this chapter

Introduction

Many objects in daily use from packing, wrapping, and building materials include half of all polymers synthesized. Other uses include textiles, many electronic appliance casings, CD's, automobile parts, and many others are made from polymers. A quarter of the solid waste from homes is plastic materials - some of which may be recycled as shown in the table below.

Some products, such as adhesives, are made to include monomers which can be polymerized by the user in their application.

Polyurethane Foam



Types of Polymers

There are many types of polymers including synthetic and natural polymers.

Natural biopolymers

- Polypeptides in proteins - silk, collagen, keratin.
- Polysaccharides (Carbohydrate chains) - cellulose, starch, glycogen
- Nucleic acids - DNA and RNA

Synthetic polymers

- Plastics
- Elastomers - solids with rubber-like qualities
  - Rubber (carbon backbone often from hydrocarbon monomers)
  - silicones (backbone of alternating silicon and oxygen atoms).
- Fibers
- Solid materials of intermediate characteristics
- Gels or viscous liquids

Classification of Polymers

- Homopolymers: These consist of chains with identical bonding linkages to each monomer unit. This usually implies that the polymer is made from all identical monomer molecules. These may be represented as : -[A-A-A-A-A-A]- Homopolymers are commonly named by placing the prefix poly in front of the constituent monomer name. For example, polystyrene is the name for the polymer made from the monomer styrene (vinylbenzene).
- Copolymers: These consist of chains with two or more linkages usually implying two or more different types of monomer units. These may be represented as : -[A-B-A-B-A-B]-

Polymers classified by mode of polymerization

- Addition Polymers: The monomer molecules bond to each other without the loss of any other atoms. Addition polymers from alkene monomers or substituted alkene monomers are the biggest groups of polymers in this class. Ring opening polymerization can occur without the loss of any small molecules.
- Condensation Polymers: Usually two different monomer combine with the loss of a small molecule, usually water. Most polyesters and polyamides (nylon) are in this class of polymers. Polyurethane Foam in graphic above.

Polymers classified by Physical Response to Heating

Thermoplastics

Plastics that soften when heated and become firm again when cooled. This is the more popular type of plastic because the heating and cooling may be repeated and the thermoplastic may be reformed.

Thermosets

These are plastics that soften when heated and can be molded, but harden permanently. They will decompose when reheated. An example is Bakelite, which is used in toasters, handles for pots and pans, dishes, electrical outlets and billiard balls.

Contributors

- Charles Ophardt, Professor Emeritus, Elmhurst College; Virtual Chembook
- William Reusch, Professor Emeritus (Michigan State U.), Virtual Textbook of Organic Chemistry

11.6.1: Introduction is shared under a CC BY-NC-SA 4.0 license and was authored, remixed, and/or curated by LibreTexts.

11.6.2: Chain-Growth Polymers—Addition Polymers

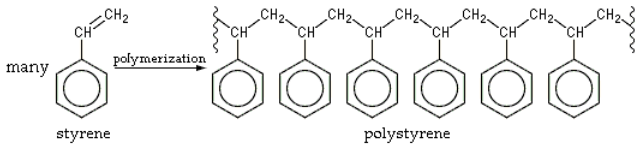
Polymers are long chain giant organic molecules are assembled from many smaller molecules called **monomers**. **Polymers** consist of many repeating monomer units in long chains. A polymer is analogous to a necklace made from many small beads (monomers). Many monomers are alkenes or other molecules with double bonds which react by **addition** to their unsaturated double bonds.

Introduction

The electrons in the double bond are used to bond two monomer molecules together. This is represented by the red arrows moving from one molecule to the space between two molecules where a new bond is to form. The formation of polyethylene from ethylene (ethene) may be illustrated in the graphic on the left as follows. In the complete polymer, all of the double bonds have been turned into single bonds. No atoms have been lost and you can see that the monomers have just been joined in the process of addition. A simple representation is -[A-A-A-A-A]-. Polyethylene is used in plastic bags, bottles, toys, and electrical insulation.

- **LDPE - Low Density Polyethylene:** The first commercial polyethylene process used peroxide catalysts at a temperature of 500 C and 1000 atmospheres of pressure. This yields a transparent polymer with highly branched chains which do not pack together well and is low in density. LDPE makes a flexible plastic. Today most LDPE is used for blow-molding of films for packaging and trash bags and flexible snap-on lids. LDPE is recyclable plastic #4.
- **HDPE - High Density Polyethylene:** An alternate method is to use Ziegler-Natta aluminum titanium catalysts to make HDPE which has very little branching, allows the strands to pack closely, and thus is high density. It is three times stronger than LDPE and more opaque. About 45% of the HDPE is blow molded into milk and disposable consumer bottles. HDPE is also used for crinkly plastic bags to pack groceries at grocery stores. HDPE is recyclable plastic #2.

Other Addition Polymers

- **PVC** (polyvinyl chloride), which is found in plastic wrap, simulated leather, water pipes, and garden hoses, is formed from vinyl chloride (H_2C=CHCl). The reaction is shown in the graphic on the left. Notice how every other carbon must have a chlorine attached.
- **Polypropylene:** The reaction to make polypropylene (H_2C=$CHCH_3$) is illustrated in the middle reaction of the graphic. Notice that the polymer bonds are always through the carbons of the double bond. Carbon #3 already has saturated bonds and cannot participate in any new bonds. A methyl group is on every other carbon.
- **Polystyrene:** The reaction is the same for polystrene where every other carbon has a benzene ring attached. Polystyrene (PS) is recyclable plastic #6. In the following illustrated example, many styrene monomers are polymerized into a long chain polystyrene molecule. The squiggly lines indicate that the polystyrene molecule extends further at both the left and right ends.
- 

- Blowing fine gas bubbles into liquid polystyrene and letting it solidify produces *expanded polystyrene*, called *Styrofoam* by the Dow Chemical Company.
- **Polystyrene with DVB:** Cross-linking between polymer chains can be introduced into polystyrene by copolymerizing with ***p*-divinylbenzene** (**DVB**). DVB has vinyl groups (-CH=CH_2) at each end of its molecule, each of which can be polymerized into a polymer chain like any other vinyl group on a styrene monomer.

Other addition polymers

Table 1: Links to various polymers with Chime molecule - Macrogalleria at U. Southern Mississippi

Monomer	Polymer Name	Trade Name	Uses
$F_2C=CF_2$	polytetrafluoroethylene	Teflon	Non-stick coating for cooking utensils, chemically-resistant specialty plastic parts, Gore-Tex
$H_2C=CCl_2$	polyvinylidene dichloride	Saran	Clinging food wrap
$H_2C=CH(CN)$	polyacrylonitrile	Orlon, Acrilan, Creslan	Fibers for textiles, carpets, upholstery
$H_2C=CH(OCOCH_3)$	polyvinyl acetate		Elmer's glue - Silly Putty Demo
$H_2C=CH(OH)$	polyvinyl alcohol		Ghostbusters Demo
$H_2C=C(CH_3)COOCH_3$	polymethyl methacrylate	Plexiglass, Lucite	Stiff, clear, plastic sheets, blocks, tubing, and other shapes

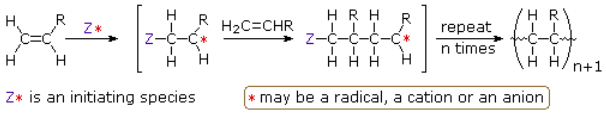
Addition polymers from conjugated dienes

Polymers from conjugated dienes usually give elastomer polymers having rubber-like properties.

Table 2. Addition homopolymers from conjugated dienes

Monomer	Polymer name	Trade name	Uses
$H_2C=CH-C(CH_3)=CH_2$	polyisoprene	natural or some synthetic rubber	applications similar to natural rubber
$H_2C=CH-CH=CH_2$	polybutadiene	polybutadiene synthetic rubber	select synthetic rubber applications
$H_2C=CH-CCl=CH_2$	polychloroprene	Neoprene	chemically-resistant rubber

All the monomers from which addition polymers are made are alkenes or functionally substituted alkenes. The most common and thermodynamically favored chemical transformations of alkenes are addition reactions. Many of these addition reactions are known to proceed in a stepwise fashion by way of reactive intermediates, and this is the mechanism followed by most polymerizations. A general diagram illustrating this assembly of linear macromolecules, which supports the name chain growth polymers, is presented here. Since a pi-bond in the monomer is converted to a sigma-bond in the polymer, the polymerization reaction is usually exothermic by 8 to 20 kcal/mol. Indeed, cases of explosively uncontrolled polymerizations have been reported.



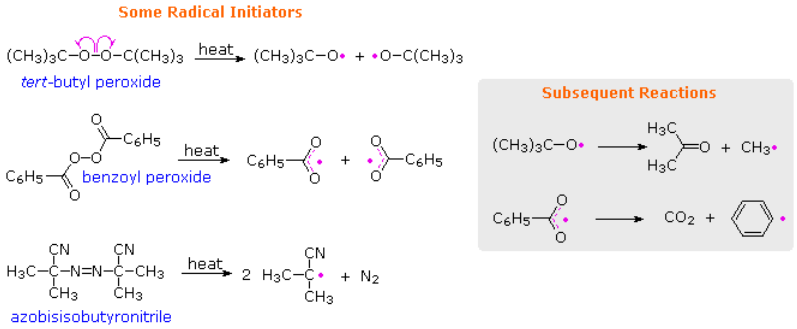
It is useful to distinguish four polymerization procedures fitting this general description.

• Radical Polymerization The initiator is a radical, and the propagating site of reactivity (*) is a carbon radical.
• Cationic Polymerization The initiator is an acid, and the propagating site of reactivity (*) is a carbocation.
• Anionic Polymerization The initiator is a nucleophile, and the propagating site of reactivity (*) is a carbanion.
• Coordination Catalytic Polymerization The initiator is a transition metal complex, and the propagating site of reactivity (*) is a terminal catalytic complex.

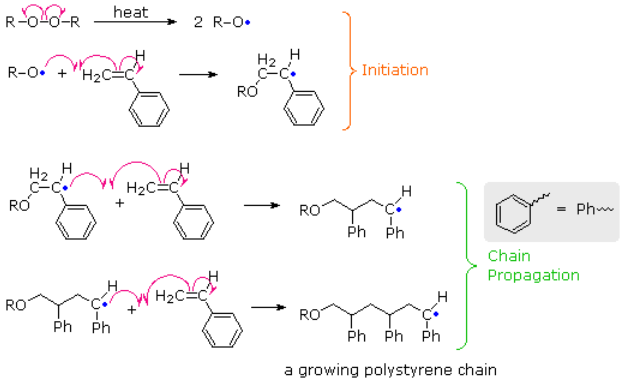
Radical Chain-Growth Polymerization

Virtually all of the monomers described above are subject to radical polymerization. Since this can be initiated by traces of oxygen or other minor impurities, pure samples of these compounds are often "stabilized" by small amounts of radical inhibitors to avoid unwanted reaction. When radical polymerization is desired, it must be started by using a radical initiator, such as a peroxide or

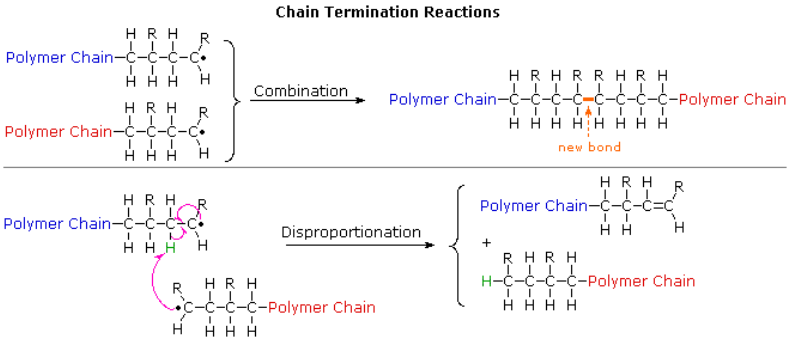
certain azo compounds. The formulas of some common initiators, and equations showing the formation of radical species from these initiators are presented below.



By using small amounts of initiators, a wide variety of monomers can be polymerized. One example of this radical polymerization is the conversion of styrene to polystyrene, shown in the following diagram. The first two equations illustrate the initiation process, and the last two equations are examples of chain propagation. Each monomer unit adds to the growing chain in a manner that generates the most stable radical. Since carbon radicals are stabilized by substituents of many kinds, the preference for head-to-tail regioselectivity in most addition polymerizations is understandable. Because radicals are tolerant of many functional groups and solvents (including water), radical polymerizations are widely used in the chemical industry.



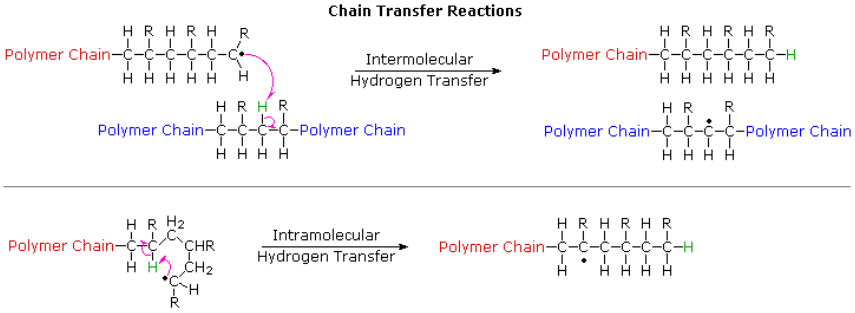
In principle, once started a radical polymerization might be expected to continue unchecked, producing a few extremely long chain polymers. In practice, larger numbers of moderately sized chains are formed, indicating that chain-terminating reactions must be taking place. The most common termination processes are Radical Combination and Disproportionation. These reactions are illustrated by the following equations. The growing polymer chains are colored blue and red, and the hydrogen atom transferred in disproportionation is colored green. Note that in both types of termination two reactive radical sites are removed by simultaneous conversion to stable product(s). Since the concentration of radical species in a polymerization reaction is small relative to other reactants (e.g. monomers, solvents and terminated chains), the rate at which these radical-radical termination reactions occurs is very small, and most growing chains achieve moderate length before termination.



The relative importance of these terminations varies with the nature of the monomer undergoing polymerization. For acrylonitrile and styrene combination is the major process. However, methyl methacrylate and vinyl acetate are terminated chiefly by

disproportionation.

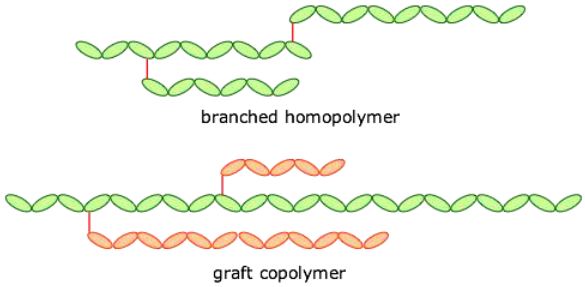
Another reaction that diverts radical chain-growth polymerizations from producing linear macromolecules is called chain transfer. As the name implies, this reaction moves a carbon radical from one location to another by an intermolecular or intramolecular hydrogen atom transfer (colored green). These possibilities are demonstrated by the following equations



Chain transfer reactions are especially prevalent in the high pressure radical polymerization of ethylene, which is the method used to make LDPE (low density polyethylene). The 1º-radical at the end of a growing chain is converted to a more stable 2º-radical by hydrogen atom transfer. Further polymerization at the new radical site generates a side chain radical, and this may in turn lead to creation of other side chains by chain transfer reactions. As a result, the morphology of LDPE is an amorphous network of highly branched macromolecules.

Chain topology

Polymers may also be classified as straight-chained or branched, leading to forms such as these:



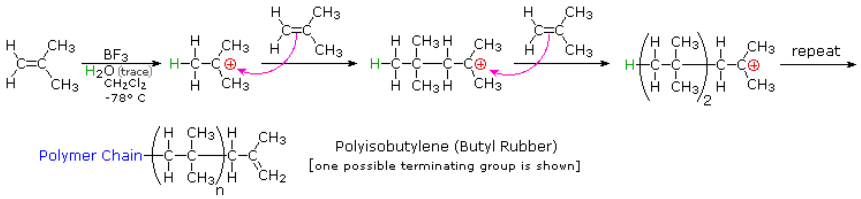
The monomers can be joined end-to-end, and they can also be *cross-linked* to provide a harder material:



If the cross-links are fairly long and flexible, adjacent chains can move with respect to each other, producing an *elastic* polymer or

Cationic Chain-Growth Polymerization

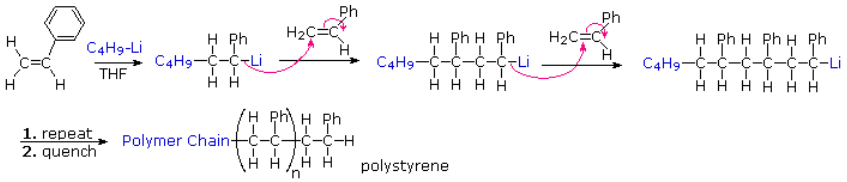
Polymerization of isobutylene (2-methylpropene) by traces of strong acids is an example of cationic polymerization. The polyisobutylene product is a soft rubbery solid, Tg = _70º C, which is used for inner tubes. This process is similar to radical polymerization, as demonstrated by the following equations. Chain growth ceases when the terminal carbocation combines with a nucleophile or loses a proton, giving a terminal alkene (as shown here).



Monomers bearing cation stabilizing groups, such as alkyl, phenyl or vinyl can be polymerized by cationic processes. These are normally initiated at low temperature in methylene chloride solution. Strong acids, such as HClO4 , or Lewis acids containing traces of water (as shown above) serve as initiating reagents. At low temperatures, chain transfer reactions are rare in such polymerizations, so the resulting polymers are cleanly linear (unbranched).

Anionic Chain-Growth Polymerization

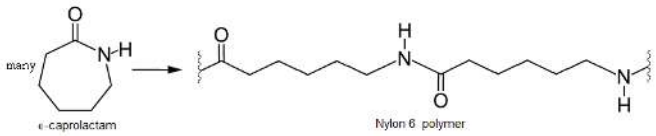
Treatment of a cold THF solution of styrene with 0.001 equivalents of n-butyllithium causes an immediate polymerization. This is an example of anionic polymerization, the course of which is described by the following equations. Chain growth may be terminated by water or carbon dioxide, and chain transfer seldom occurs. Only monomers having anion stabilizing substituents, such as phenyl, cyano or carbonyl are good substrates for this polymerization technique. Many of the resulting polymers are largely isotactic in configuration, and have high degrees of crystallinity.



Species that have been used to initiate anionic polymerization include alkali metals, alkali amides, alkyl lithiums and various electron sources. A practical application of anionic polymerization occurs in the use of superglue. This material is methyl 2-cyanoacrylate, CH2=C(CN)CO2CH3. When exposed to water, amines or other nucleophiles, a rapid polymerization of this monomer takes place.

Ring opening polymerization

In this kind of polymerization, molecular rings are opened in the formation of a polymer. Here epsilon-caprolactam, a 6-carbon cyclic monomer, undergoes ring opening to form a Nylon 6 homopolymer, which is somewhat similar to but not the same as Nylon 6,6 alternating copolymer.



Addition Copolymerization

Most direct copolymerizations of equimolar mixtures of different monomers give statistical copolymers, or if one monomer is much more reactive a nearly homopolymer of that monomer. The copolymerization of styrene with methyl methacrylate, for example, proceeds differently depending on the mechanism. Radical polymerization gives a statistical copolymer. However, the product of cationic polymerization is largely polystyrene, and anionic polymerization favors formation of poly(methyl methacrylate). In cases where the relative reactivities are different, the copolymer composition can sometimes be controlled by continuous introduction of a biased mixture of monomers into the reaction.

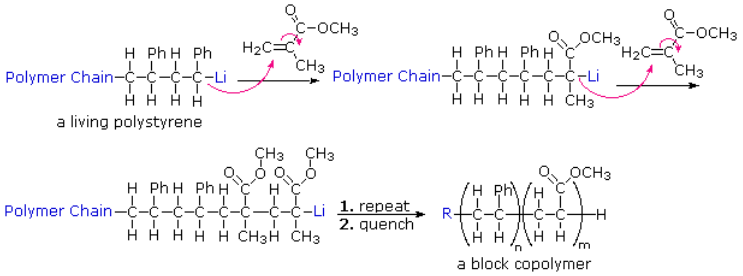
Formation of alternating copolymers is favored when the monomers have different polar substituents (e.g. one electron withdrawing and the other electron donating), and both have similar reactivities toward radicals. For example, styrene and acrylonitrile copolymerize in a largely alternating fashion.

Some Useful Copolymers			
Monomer A	**Monomer B**	**Copolymer**	**Uses**
$H_2C=CHCl$	$H_2C=CCl_2$	Saran	films & fibers
$H_2C=CHC_6H_5$	$H_2C=C-CH=CH_2$	SBR styrene butadiene rubber	tires
$H_2C=CHCN$	$H_2C=C-CH=CH_2$	Nitrile Rubber	adhesives hoses
$H_2C=C(CH_3)_2$	$H_2C=C-CH=CH_2$	Butyl Rubber	inner tubes
$F_2C=CF(CF_3)$	$H_2C=CHF$	Viton	gaskets

A terpolymer of acrylonitrile, butadiene and styrene, called ABS rubber, is used for high-impact containers, pipes and gaskets.

Block Copolymerization

Several different techniques for preparing block copolymers have been developed, many of which use condensation reactions (next section). At this point, our discussion will be limited to an application of anionic polymerization. In the anionic polymerization of styrene described above, a reactive site remains at the end of the chain until it is quenched. The unquenched polymer has been termed a living polymer, and if additional styrene or a different suitable monomer is added a block polymer will form. This is illustrated for methyl methacrylate in the following diagram.



Contributors

Charles Ophardt (Professor Emeritus, Elmhurst College); Virtual Chembook

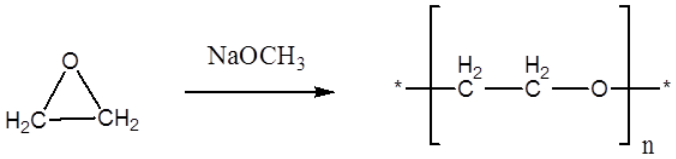
- William Reusch, Professor Emeritus (Michigan State U.), Virtual Textbook of Organic Chemistry

11.6.2: Chain-Growth Polymers—Addition Polymers is shared under a CC BY-NC-SA 4.0 license and was authored, remixed, and/or curated by LibreTexts.

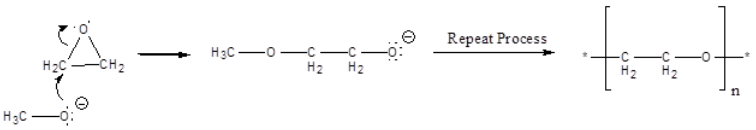
11.6.3: Anionic Polymerization of Epoxides

Another type of anionic polymerization involves an epoxide and forms a polyether. The strained three-memebered epoxide ring is easily opened by nuleophiles, typically a hydroxide or an alkoxy group. Note! This polymerization is different to the other chain-growth polymerizations discussed because the process forms a C-O bond in the polymer chain.

Reaction



Mechanism



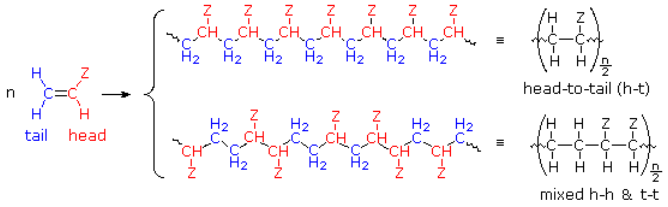
Contributors

- Prof. Steven Farmer (Sonoma State University)

11.6.3: Anionic Polymerization of Epoxides is shared under a CC BY-NC-SA 4.0 license and was authored, remixed, and/or curated by LibreTexts.

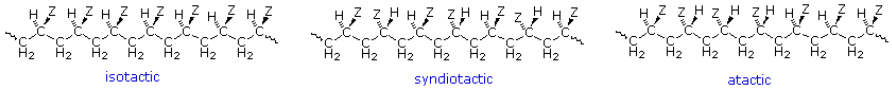
11.6.4: Ziegler–Natta Catalysts and Polymer Stereochemistry

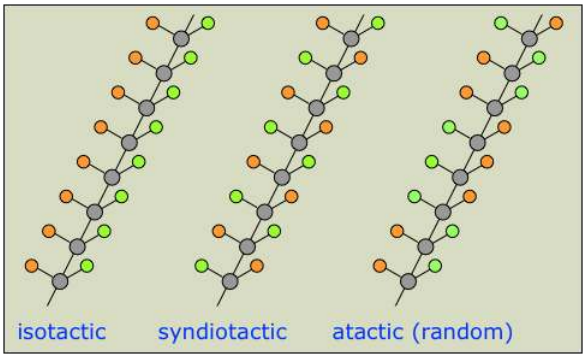
Symmetrical monomers such as ethylene and tetrafluoroethylene can join together in only one way. Monosubstituted monomers, on the other hand, may join together in two organized ways, described in the following diagram, or in a third random manner. Most monomers of this kind, including propylene, vinyl chloride, styrene, acrylonitrile and acrylic esters, prefer to join in a head-to-tail fashion, with some randomness occurring from time to time. The reasons for this regioselectivity will be discussed in the synthetic methods section.



Regioisomeric Polymers from Substituted Monomers

If the polymer chain is drawn in a zig-zag fashion, as shown above, each of the substituent groups (Z) will necessarily be located above or below the plane defined by the carbon chain. Consequently we can identify three configurational isomers of such polymers. If all the substituents lie on one side of the chain the configuration is called isotactic. If the substituents alternate from one side to another in a regular manner the configuration is termed syndiotactic. Finally, a random arrangement of substituent groups is referred to as atactic. Examples of these configurations are shown here.





Many common and useful polymers, such as polystyrene, polyacrylonitrile and poly(vinyl chloride) are atactic as normally prepared. Customized catalysts that effect stereoregular polymerization of polypropylene and some other monomers have been developed, and the improved properties associated with the increased crystallinity of these products has made this an important field of investigation. The following values of Tg have been reported.

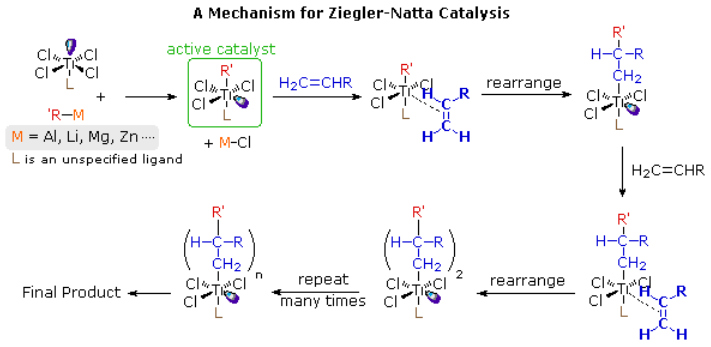
Polymer	T_g atactic	T_g isotactic	T_g syndiotactic
PP	–20 ºC	0 ºC	–8 ºC
PMMA	100 ºC	130 ºC	120 ºC

The properties of a given polymer will vary considerably with its tacticity. Thus, atactic polypropylene is useless as a solid construction material, and is employed mainly as a component of adhesives or as a soft matrix for composite materials. In contrast, isotactic polypropylene is a high-melting solid (ca. 170 ºC) which can be molded or machined into structural components.

Ziegler-Natta Catalytic Polymerization

An efficient and stereospecific catalytic polymerization procedure was developed by Karl Ziegler (Germany) and Giulio Natta (Italy) in the 1950's. Their findings permitted, for the first time, the synthesis of unbranched, high molecular weight polyethylene (HDPE), laboratory synthesis of natural rubber from isoprene, and configurational control of polymers from terminal alkenes like propene (e.g. pure isotactic and syndiotactic polymers). In the case of ethylene, rapid polymerization occurred at atmospheric pressure and moderate to low temperature, giving a stronger (more crystalline) product (HDPE) than that from radical polymerization (LDPE). For this important discovery these chemists received the 1963 Nobel Prize in chemistry.

Ziegler-Natta catalysts are prepared by reacting certain transition metal halides with organometallic reagents such as alkyl aluminum, lithium and zinc reagents. The catalyst formed by reaction of triethylaluminum with titanium tetrachloride has been widely studied, but other metals (e.g. V & Zr) have also proven effective. The following diagram presents one mechanism for this useful reaction. Others have been suggested, with changes to accommodate the heterogeneity or homogeneity of the catalyst. Polymerization of propylene through action of the titanium catalyst gives an isotactic product; whereas, a vanadium based catalyst gives a syndiotactic product.



Contributors

- William Reusch, Professor Emeritus (Michigan State U.), Virtual Textbook of Organic Chemistry

11.6.4: Ziegler–Natta Catalysts and Polymer Stereochemistry is shared under a CC BY-NC-SA 4.0 license and was authored, remixed, and/or curated by LibreTexts.

11.6.5: Natural and Synthetic Rubbers

Rubber is an example of an elastomer type polymer, where the polymer has the ability to return to its original shape after being stretched or deformed. The rubber polymer is coiled when in the resting state. The elastic properties arise from the its ability to stretch the chains apart, but when the tension is released the chains snap back to the original position. The majority of rubber polymer molecules contain at least some units derived from conjugated diene monomers (see Polymerization of Conjugated Dienes). Such conjugated diene monomers have a constructive backbone of at least four carbon atoms with a double-single-double bond reactive core (C=C-C=C). Most if not practically all such dienes undergo 1,4-addition to the polymer chain, where 1 and 4 refer to the 1st and 4th carbons of the backbone unit, which become single-bonded to the rest of the polymer chain. The diene's double bonds turn into single bonds, and the single bond between them turns into a Z or E configured double bond, depending on the polymerization conditions. The unit's backbone thus becomes like this (-C-C=C-C-). Rubber gets its elasticity when the formed double bond gets the Z configuration. For 1,3-butadiene, Z is equivalent to a *cis* and E is equivalent to a *trans* configuration.

Natural Rubber

Natural rubber is an addition polymer that is obtained as a milky white fluid known as latex from a tropical rubber tree. Natural rubber is from the monomer isoprene (2-methyl-1,3-butadiene), which is a conjugated diene hydrocarbon as mentioned above. In natural rubber, most of the double fonds formed in the polymer chain have the Z configuration, resulting in natural rubber's elastomer qualities.

Charles Goodyear accidentally discovered that by mixing sulfur and rubber, the properties of the rubber improved in being tougher, resistant to heat and cold, and increased in elasticity. This process was later called vulcanization after the Roman god of fire. Vulcanization causes shorter chains to cross link through the sulfur to longer chains. The development of vulcanized rubber for automobile tires greatly aided this industry.

Synthetic Rubber

Important conjugated dienes used in synthetic rubbers include isoprene (2-methyl-1,3-butadiene), 1,3-butadiene, and chloroprene (2-chloro-1,3-butadiene). Polymerized 1,3-butadiene is mostly referred to simply as polybutadiene. Polymerized chloroprene was developed by DuPont and given the trade name *Neoprene*.

In a number of cases, monomers which are not dienes are also used for certain types of synthetic rubber, often copolymerized with dienes. Some of the most commercially important addition polymers are the copolymers. These are polymers made by polymerizing a mixture of two or more monomers. An example is *styrene-butadiene rubber* (SBR) - which is a copolymer of 1,3-butadiene and styrene which is mixed in a 3 to 1 ratio, respectively.

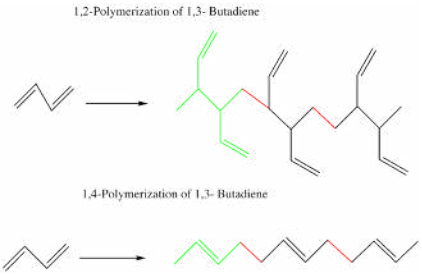
SBR rubber was developed during World War II when important supplies of natural rubber were cut off. SBR is more resistant to abrasion and oxidation than natural rubber and can also be vulcanized. More than 40% of the synthetic rubber production is SBR and is used in tire production. A tiny amount is used for bubble-gum in the unvulcanized form.

Nitrile rubber is copolymerized from butadiene and acrylonitrile (H_2C=CH-CN). *Butyl rubber* is copolymerized from isobutylene [which is methylpropene $H_2C=C(CH_3)_2$] and a small percentage of isoprene. *Silicone rubber* and other compounds, chemically called *polysiloxanes*, are not from conjugated dienes but have repeating units like -O-SiR_2- where R is some organic radical group like methyl. There is a separate page on Silicone Polymers.

Conjugated dienes (alkenes with two double bonds and a single bond in between) can be polymerized to form important compounds like rubber. This takes place, in different forms, both in nature and in the laboratory. Interactions between double bonds on multiple chains leads to cross-linkage which creates elasticity within the compound.

Polymerization of 1,3-Butadiene

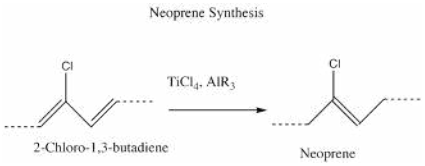
For rubber compounds to be synthesized, 1,3-butadiene must be polymerized. Below is a simple illustration of how this compound is formed into a chain. The 1,4 polymerization is much more useful to polymerization reactions.



Above, the green structures represent the base units of the polymers that are synthesized and the red represents the bonds between these units which form these polymers. Whether the 1,3 product or the 1,4 product is formed depends on whether the reaction is thermally or kinetically controlled.

Synthetic Rubber

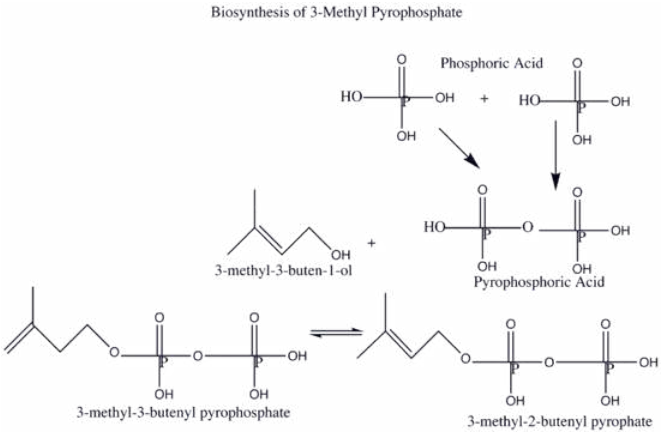
The most important synthetic rubber is Neoprene which is produced by the polymerization of 2-chloro-1,3-butadiene.



In this illustration, the dashed lines represent repetition of the same base units, so both the products and reactants are polymers. The reaction proceeds with a mechanism similar to the Friedel-Crafts mechanism. Cross-linkage between the chlorine atom of one chain and the double bond of another contributes to the overall elasticity of neoprene. This cross-linkage occurs as the chains lie next to each other at random angles, and the attractions between double bonds prevent them from sliding back and forth.

Natural Rubber

The synthesis of rubber in nature in somewhat similar the artificial synthesis of rubber except that it takes place within a plant. Instead of the 2-chloro-1,3-butadiene used in the synthesis of neoprene, natural rubber is synthesized from 2-methyl-1,3-butadiene. As an electrophile, the plant synthesizes the pyrophosphate 3-methyl-3-butenyl pyrophosphate is from phosphoric acid and 3-methyl-3-buten-1-ol. This pyrophosphate then catalyzes the reaction that leads to natural rubber.



The 3-methyl-3-butenyl pyrophosphate (OPP) is then used in the polymerization of natural rubber as it pulls electrons off 2-methyl-1,3-butadiene (see questions section for this process.)

Outside links

- "Dienes," http://en.wikipedia.org/wiki/Diene
- "Rubber," http://en.wikipedia.org/wiki/Rubber
- "Neoprene," http://en.wikipedia.org/wiki/Neoprene

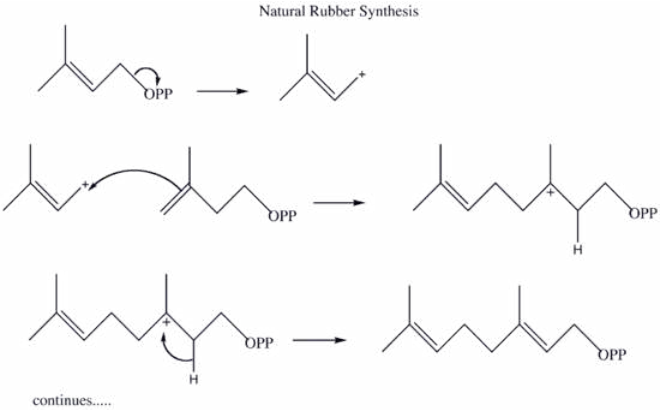
References

1. Vollhardt, Peter, and Neil E. Schore. Organic Chemistry: Structure and Function. New York: W. H. Freeman & Company, 2007.
2. Buehr, Walter. Rubber: Natural and Synthetic. Morrow, 1964.

Problem

Draw out the mechanism for the natural synthesis of rubber from 3-methyl-3-butenyl pyrophosphate and 2-methyl-1,3-butadiene. Show the movement of electrons with arrows.

Answer



Contributors

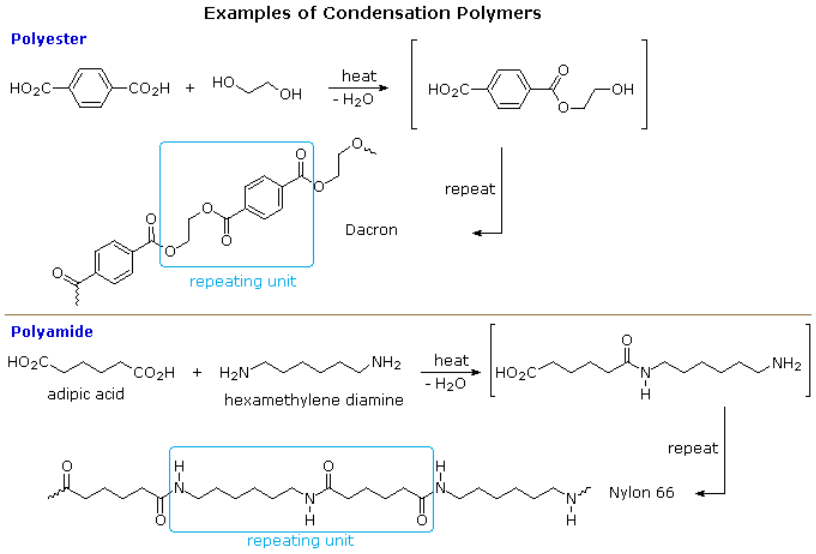
- Charles Ophardt, Professor Emeritus, Elmhurst College; Virtual Chembook
- User:H Padleckas

11.6.5: Natural and Synthetic Rubbers is shared under a CC BY-NC-SA 4.0 license and was authored, remixed, and/or curated by LibreTexts.

11.6.6: Step-Growth Polymers—Condensation Polymers

A large number of important and useful polymeric materials are not formed by chain-growth processes involving reactive species such as radicals, but proceed instead by conventional functional group transformations of polyfunctional reactants. These polymerizations often (but not always) occur with loss of a small byproduct, such as water, and generally (but not always) combine two different components in an alternating structure. The polyester Dacron and the polyamide Nylon 66, shown here, are two examples of synthetic condensation polymers, also known as step-growth polymers. In contrast to chain-growth polymers, most of which grow by carbon-carbon bond formation, step-growth polymers generally grow by carbon-heteroatom bond formation (C-O & C-N in Dacron & Nylon respectively). Although polymers of this kind might be considered to be alternating copolymers, the repeating monomeric unit is usually defined as a combined moiety.

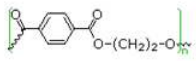
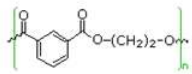
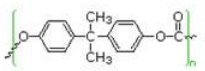
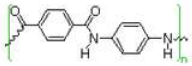
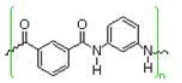
Examples of naturally occurring condensation polymers are cellulose, the polypeptide chains of proteins, and poly(β-hydroxybutyric acid), a polyester synthesized in large quantity by certain soil and water bacteria. Formulas for these will be displayed below by clicking on the diagram.



Characteristics of Condensation Polymers

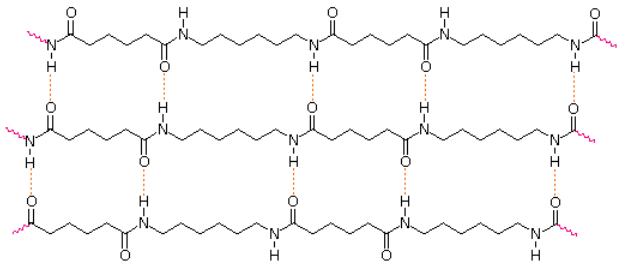
Condensation polymers form more slowly than addition polymers, often requiring heat, and they are generally lower in molecular weight. The terminal functional groups on a chain remain active, so that groups of shorter chains combine into longer chains in the late stages of polymerization. The presence of polar functional groups on the chains often enhances chain-chain attractions, particularly if these involve hydrogen bonding, and thereby crystallinity and tensile strength. The following examples of condensation polymers are illustrative.

Note that for commercial synthesis the carboxylic acid components may actually be employed in the form of derivatives such as simple esters. Also, the polymerization reactions for Nylon 6 and Spandex do not proceed by elimination of water or other small molecules. Nevertheless, the polymer clearly forms by a step-growth process. Some Condensation Polymers

Formula	Type	Components	T_g ºC	T_m ºC
~[CO(CH$_2$)$_4$CO-OCH$_2$CH$_2$O]$_n$~	polyester	HO$_2$C-(CH$_2$)$_4$-CO$_2$H HO-CH$_2$CH$_2$-OH	< 0	50
	polyester Dacron, Mylar	para HO$_2$C-C$_6$H$_4$-CO$_2$H HO-CH$_2$CH$_2$-OH	70	265
	polyester	meta HO$_2$C-C$_6$H$_4$-CO$_2$H HO-CH$_2$CH$_2$-OH	50	240
	polycarbonate Lexan	(HO-C$_6$H$_4$-)$_2$C(CH$_3$)$_2$ (Bisphenol A) X$_2$C=O (X = OCH$_3$ or Cl)	150	267
~[CO(CH$_2$)$_4$CO-NH(CH$_2$)$_6$NH]$_n$~	polyamide Nylon 66	HO$_2$C-(CH$_2$)$_4$-CO$_2$H H$_2$N-(CH$_2$)$_6$-NH$_2$	45	265
~[CO(CH$_2$)$_5$NH]$_n$~	polyamide Nylon 6 Perlon		53	223
	polyamide Kevlar	para HO$_2$C-C$_6$H$_4$-CO$_2$H para H$_2$N-C$_6$H$_4$-NH$_2$	---	500
	polyamide Nomex	meta HO$_2$C-C$_6$H$_4$-CO$_2$H meta H$_2$N-C$_6$H$_4$-NH$_2$	273	390

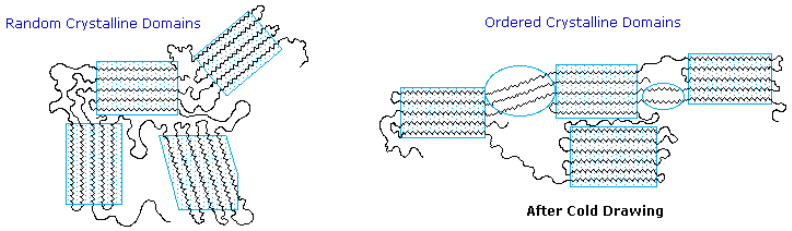
The difference in Tg and Tm between the first polyester (completely aliphatic) and the two nylon polyamides (5th & 6th entries) shows the effect of intra-chain hydrogen bonding on crystallinity. The replacement of flexible alkylidene links with rigid benzene rings also stiffens the polymer chain, leading to increased crystalline character, as demonstrated for polyesters (entries 1, 2 &3) and polyamides (entries 5, 6, 7 & 8). The high Tg and Tm values for the amorphous polymer Lexan are consistent with its brilliant transparency and glass-like rigidity. Kevlar and Nomex are extremely tough and resistant materials, which find use in bullet-proof vests and fire resistant clothing.

Interchain Hydrogen Bonding Enhances Crystallinity

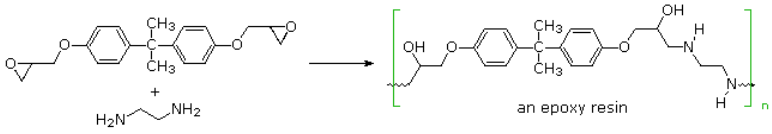


Many polymers, both addition and condensation, are used as fibers The chief methods of spinning synthetic polymers into fibers are from melts or viscous solutions. Polyesters, polyamides and polyolefins are usually spun from melts, provided the Tm is not too high. Polyacrylates suffer thermal degradation and are therefore spun from solution in a volatile solvent. Cold-drawing is an important physical treatment that improves the strength and appearance of these polymer fibers. At temperatures above T_g, a thicker than desired fiber can be forcibly stretched to many times its length; and in so doing the polymer chains become untangled, and tend to align in a parallel fashion. This cold-drawing procedure organizes randomly oriented crystalline domains, and also aligns amorphous domains so they become more crystalline. In these cases, the physically oriented morphology is stabilized and retained in the final product. This contrasts with elastomeric polymers, for which the stretched or aligned morphology is unstable relative to the amorphous random coil morphology.

This cold-drawing treatment may also be used to treat polymer films (e.g. Mylar & Saran) as well as fibers.

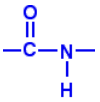


Step-growth polymerization is also used for preparing a class of adhesives and amorphous solids called epoxy resins. Here the covalent bonding occurs by an S_N2 reaction between a nucleophile, usually an amine, and a terminal epoxide. In the following example, the same bisphenol A intermediate used as a monomer for Lexan serves as a difunctional scaffold to which the epoxide rings are attached. Bisphenol A is prepared by the acid-catalyzed condensation of acetone with phenol.



What are polyamides?

Polyamides are polymers where the repeating units are held together by amide links. An amide group has the formula - $CONH_2$. An amide link has this structure:



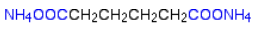
In an amide itself, of course, the bond on the right is attached to a hydrogen atom.

Nylon

In nylon, the repeating units contain chains of carbon atoms. (That is different from Kevlar, where the repeating units contain benzene rings - see below.) There are various different types of nylon depending on the nature of those chains.

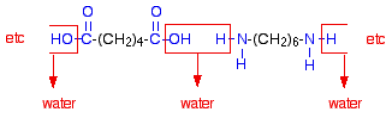
Nylon-6,6

Nylon-6,6 is made from two monomers each of which contain 6 carbon atoms - hence its name. One of the monomers is a 6 carbon acid with a -COOH group at each end - hexanedioic acid. The other monomer is a 6 carbon chain with an amino group, $-NH_2$, at each end. This is 1,6-diaminohexane (also known as hexane-1,6-diamine).

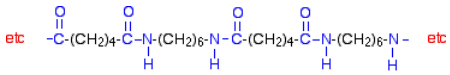


When these two compounds polymerise, the amine and acid groups combine, each time with the loss of a molecule of water. This is known as condensation polymerization. Condensation polymerization is the formation of a polymer involving the loss of a small molecule. In this case, the molecule is water, but in other cases different small molecules might be lost.

The diagram shows the loss of water between two of the monomers:

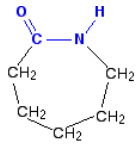


This keeps on happening, and so you get a chain which looks like this:



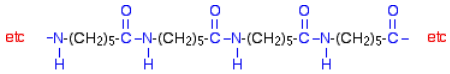
Nylon-6

Iit is possible to get a polyamide from a single monomer. Nylon-6 is made from a monomer called caprolactam.



caprolactam

Notice that this already contains an amide link. When this molecule polymerizes, the ring opens, and the molecules join up in a continuous chain.



Kevlar

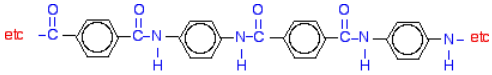
Kevlar is similar in structure to nylon-6,6 except that instead of the amide links joining chains of carbon atoms together, they join benzene rings. The two monomers are benzene-1,4-dicarboxylic acid and 1,4-diaminobenzene.



benzene-1,4-dicarboxylic acid

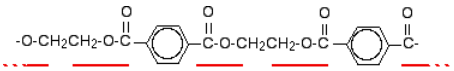
1,4-diaminobenzene

If you line these up and remove water between the -COOH and -NH_2 groups in the same way as we did with nylon-6,6, you get the structure of Kevlar:



What is a polyester?

A polyester is a polymer (a chain of repeating units) where the individual units are held together by ester linkages.



ester linkages

The diagram shows a very small bit of the polymer chain and looks pretty complicated. But it is not very difficult to work out - and that's the best thing to do: work it out, not try to remember it. You will see how to do that in a moment.

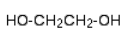
The usual name of this common polyester is poly(ethylene terephthalate). The everyday name depends on whether it is being used as a fibre or as a material for making things like bottles for soft drinks. When it is being used as a fiber to make clothes, it is often just called *polyester*. It may sometimes be known by a brand name like *Terylene*. When it is being used to make bottles, for example, it is usually called *PET*.

Making polyesters as an example of condensation polymerisation

In condensation polymerisation, when the monomers join together a small molecule gets lost. That's different from addition polymerisation which produces polymers like poly(ethene) - in that case, nothing is lost when the monomers join together. A polyester is made by a reaction involving an acid with two -COOH groups, and an alcohol with two -OH groups. In the common polyester drawn below.



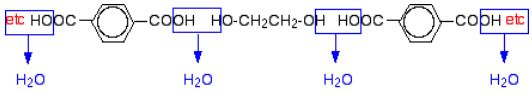
benzene-1,4-dicarboxylic acid



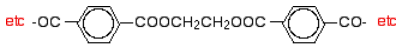
ethane-1,2-diol

Figure: The acid is benzene-1,4-dicarboxylic acid (old name: terephthalic acid) and the alcohol is ethane-1,2-diol (old name: ethylene glycol).

Now imagine lining these up alternately and making esters with each acid group and each alcohol group, losing a molecule of water every time an ester linkage is made.



That would produce the chain shown above (although this time written without separating out the carbon-oxygen double bond - write it whichever way you like).



Contributors

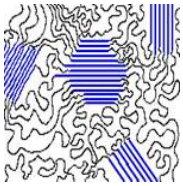
- William Reusch, Professor Emeritus (Michigan State U.), Virtual Textbook of Organic Chemistry
- Jim Clark (Chemguide.co.uk)

11.6.6: Step-Growth Polymers—Condensation Polymers is shared under a CC BY-NC-SA 4.0 license and was authored, remixed, and/or curated by LibreTexts.

11.6.7: Polymer Structure and Properties

A comparison of the properties of polyethylene (both LDPE & HDPE) with the natural polymers rubber and cellulose is instructive. As noted above, synthetic HDPE macromolecules have masses ranging from 105 to 106 amu (LDPE molecules are more than a hundred times smaller). Rubber and cellulose molecules have similar mass ranges, but fewer monomer units because of the monomer's larger size. The physical properties of these three polymeric substances differ from each other, and of course from their monomers.

- HDPE is a rigid translucent solid which softens on heating above 100º C, and can be fashioned into various forms including films. It is not as easily stretched and deformed as is LDPE. HDPE is insoluble in water and most organic solvents, although some swelling may occur on immersion in the latter. HDPE is an excellent electrical insulator.
- LDPE is a soft translucent solid which deforms badly above 75º C. Films made from LDPE stretch easily and are commonly used for wrapping. LDPE is insoluble in water, but softens and swells on exposure to hydrocarbon solvents. Both LDPE and HDPE become brittle at very low temperatures (below -80º C). Ethylene, the common monomer for these polymers, is a low boiling (-104º C) gas.
- Natural (latex) rubber is an opaque, soft, easily deformable solid that becomes sticky when heated (above. 60º C), and brittle when cooled below -50º C. It swells to more than double its size in nonpolar organic solvents like toluene, eventually dissolving, but is impermeable to water. The C5H8 monomer isoprene is a volatile liquid (b.p. 34º C).
- Pure cellulose, in the form of cotton, is a soft flexible fiber, essentially unchanged by variations in temperature ranging from -70 to 80º C. Cotton absorbs water readily, but is unaffected by immersion in toluene or most other organic solvents. Cellulose fibers may be bent and twisted, but do not stretch much before breaking. The monomer of cellulose is the $C_6H_{12}O_6$ aldohexose D-glucose. Glucose is a water soluble solid melting below 150º C.



To account for the differences noted here we need to consider the nature of the aggregate macromolecular structure, or morphology, of each substance. Because polymer molecules are so large, they generally pack together in a non-uniform fashion, with ordered or crystalline-like regions mixed together with disordered or amorphous domains. In some cases the entire solid may be amorphous, composed entirely of coiled and tangled macromolecular chains. Crystallinity occurs when linear polymer chains are structurally oriented in a uniform three-dimensional matrix. In the diagram on the right, crystalline domains are colored blue.
Increased crystallinity is associated with an increase in rigidity, tensile strength and opacity (due to light scattering). Amorphous polymers are usually less rigid, weaker and more easily deformed. They are often transparent.

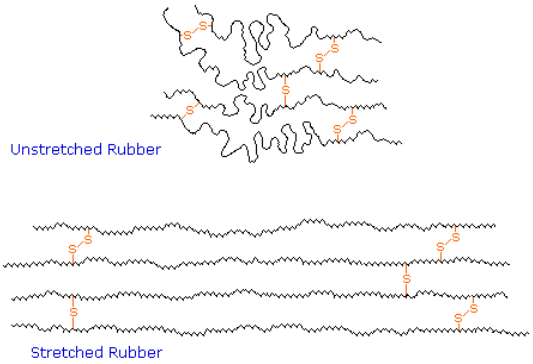
Three factors that influence the degree of crystallinity are:
i) Chain length
ii) Chain branching
iii) Interchain bonding

The importance of the first two factors is nicely illustrated by the differences between LDPE and HDPE. As noted earlier, HDPE is composed of very long unbranched hydrocarbon chains. These pack together easily in crystalline domains that alternate with amorphous segments, and the resulting material, while relatively strong and stiff, retains a degree of flexibility. In contrast, LDPE is composed of smaller and more highly branched chains which do not easily adopt crystalline structures. This material is therefore softer, weaker, less dense and more easily deformed than HDPE. As a rule, mechanical properties such as ductility, tensile strength, and hardness rise and eventually level off with increasing chain length.

The nature of cellulose supports the above analysis and demonstrates the importance of the third factor (iii). To begin with, cellulose chains easily adopt a stable rod-like conformation. These molecules align themselves side by side into fibers that are stabilized by inter-chain hydrogen bonding between the three hydroxyl groups on each monomer unit. Consequently, crystallinity is

high and the cellulose molecules do not move or slip relative to each other. The high concentration of hydroxyl groups also accounts for the facile absorption of water that is characteristic of cotton.

Natural rubber is a completely amorphous polymer. Unfortunately, the potentially useful properties of raw latex rubber are limited by temperature dependence; however, these properties can be modified by chemical change. The cis-double bonds in the hydrocarbon chain provide planar segments that stiffen, but do not straighten the chain. If these rigid segments are completely removed by hydrogenation (H2 & Pt catalyst), the chains lose all constrainment, and the product is a low melting paraffin-like semisolid of little value. If instead, the chains of rubber molecules are slightly cross-linked by sulfur atoms, a process called vulcanization which was discovered by Charles Goodyear in 1839, the desirable elastomeric properties of rubber are substantially improved. At 2 to 3% crosslinking a useful soft rubber, that no longer suffers stickiness and brittleness problems on heating and cooling, is obtained. At 25 to 35% crosslinking a rigid hard rubber product is formed. The following illustration shows a cross-linked section of amorphous rubber. By clicking on the diagram it will change to a display of the corresponding stretched section. The more highly-ordered chains in the stretched conformation are entropically unstable and return to their original coiled state when allowed to relax



Contributors

- William Reusch, Professor Emeritus (Michigan State U.), Virtual Textbook of Organic Chemistry

11.6.7: Polymer Structure and Properties is shared under a CC BY-NC-SA 4.0 license and was authored, remixed, and/or curated by LibreTexts.

11.6.8: Green Polymer Synthesis

11.6.8: Green Polymer Synthesis is shared under a CC BY-NC-SA 4.0 license and was authored, remixed, and/or curated by LibreTexts.

11.6.9: Polymer Recycling and Disposal

Most plastics crumble into ever-tinier fragments as they are exposed to sunlight and the elements. Except for the small amount that's been incinerated–and it's a very small amount–every bit of plastic ever made still exists, unless the material's molecular structure is designed to favor biodegradation. Unfortunately, cleaning up the garbage patch is not a realistic option, and unless we change our disposal and recycling habits, it will undoubtedly get bigger. One sensible solution would require manufacturers to use natural biodegradable packaging materials whenever possible, and consumers to conscientiously dispose of their plastic waste. Thus, instead of consigning all plastic trash to a land fill, some of it may provide energy by direct combustion, and some converted for reuse as a substitute for virgin plastics. The latter is particularly attractive since a majority of plastics are made from petroleum, a diminishing resource with a volatile price.

The energy potential of plastic waste is relatively significant, ranging from 10.2 to 30.7MJ kg Ã , suggesting application as an energy source and temperature stabilizer in municipal incinerators, thermal power plants and cement kilns. The use of plastic waste as a fuel source would be an effective means of reducing landfill requirements while recovering energy. This, however, depends on using appropriate materials. Inadequate control of combustion, especially for plastics containing chlorine, fluorine and bromine, constitutes a risk of emitting toxic pollutants.

Whether used as fuels or a source of recycled plastic, plastic waste must be separated into different categories. To this end, an identification coding system was developed by the Society of the Plastics Industry (SPI) in 1988, and is used internationally. This code, shown on the right, is a set of symbols placed on plastics to identify the polymer type, for the purpose of allowing efficient separation of different polymer types for recycling. The abbreviations of the code are explained in the following table.

PETE	HDPE	V	LDPE
polyethylene terephthalate	high density polyethylene	polyvinyl chloride	low density polyethylene

PP	PS	OTHER
polypropylene	polystyrene	polyesters, acrylics polyamides, teflon etc.



Despite use of the recycling symbol in the coding of plastics, there is consumer confusion about which plastics are readily recyclable. In most communities throughout the United States, PETE and HDPE are the only plastics collected in municipal recycling programs. However, some regions are expanding the range of plastics collected as markets become available. (Los Angeles, for example, recycles all clean plastics numbered 1 through 7) In theory, most plastics are recyclable and some types can be used in combination with others. In many instances, however, there is an incompatibility between different types that necessitates their effective separation. Since the plastics utilized in a given manufacturing sector (e.g. electronics, automotive, etc.) is generally limited to a few types, effective recycling is often best achieved with targeted waste streams.

Recycled Plastics

Recycle Code	Abbreviation and Chemical Name of Plastic	Types of Uses and Examples
1	PET - polyethylene terephthalate	Many types of clear plastic consumer bottles, including clear, 2-liter beverage bottles
2	HDPE - High density polyethylene	Milk jugs, detergent bottles, some water bottles, some grocery plastic bags
3	PVC - Polyvinyl chloride	Plastic drain pipe, shower curtains, some water bottles
4	LDPE - Low density polyethylene	Plastic garbage and other bags, garment bags, snap-on lids such as coffee can lids
5	PP - Polypropylene	Many translucent (or opaque) plastic containers; containers for some products such as yogurt, soft butter, or margarine; aerosol can tops; rigid bottle caps; candy wrappers; bottoms of bottles
6	PS - Polystyrene	Hard clear plastic cups, foam cups, eating utensils, deli food containers, toy model kits, some packing popcorn
7	Other	Polycarbonate is a common type, Biodegradable, Some packing popcorn

11.6.9: Polymer Recycling and Disposal is shared under a CC BY-NC-SA 4.0 license and was authored, remixed, and/or curated by LibreTexts.

12: Reading

12: Reading is shared under a not declared license and was authored, remixed, and/or curated by LibreTexts.

CHAPTER OVERVIEW

Back Matter

Index

Glossary

Detailed Licensing

Index

A

acid–base titrations
8.2.8: pH Calculations for Acid–Base Titrations
addition polymer
1.4.10: Synthetic Macromolecules- Some Applied Organic Chemistry
1.4.11: Addition Polymers
adhesive force
4.2: Properties of Liquids
6.3: Properties of Liquids
alkali metal
1.1.2: Groups of Related Elements
alkaline earth metal
1.1.2: Groups of Related Elements
allotropes
1.4.8: Diamond and Graphite
amorphous polymer
11.5.4.5: Crystallinity in Polymers
amorphous solid
5.3: The Solid State of Matter
angle of rotation
10.5: Optical Isomerism in Metal Complexes
angular
1.3.4: Molecules with Lone Pairs
anion
1.2.2: Ionic Bonding
Anionic Polymerization
11.5.2.6: Anionic Polymerization
atomic number
1.1.9: The Nucleus

B

balancing redox reactions
9.2: Balancing Redox Reactions
barrier to rotation
1.3.7: Orbital Descriptions of Multiple Bonds
bent
1.3.4: Molecules with Lone Pairs
bent bond
1.3.7: Orbital Descriptions of Multiple Bonds
benzene ring
1.3.14: Resonance
binary compound
1.2.9: Binary Ionic Compounds and Their Properties
biogenesis
1.3.9.1: Biology - Polarizability of Biologically Significant Atoms
boiling
6.4: Phase Transitions- Overview
Boiling Point
6.5: Phase Transitions
bond energy
1.2.13: The Covalent Bond
bond length
1.2.19: Atomic Sizes
bond line
1.2.14: Covalent Molecules and the Octet Rule
Bragg equation
5.4: Lattice Structures in Crystalline Solids
11.5.4.5: Crystallinity in Polymers

C

calmodulin
11.2.3.4: Calmodulin
capillary action
4.2: Properties of Liquids
6.3: Properties of Liquids
carbonic anhydrase
11.2.2.14: Steady-State and Equilibrium Kinetics of Carbonic Anhydrase-Catalyzed \(CO_{2}/HCO_{3}^{-}\) Interconversion
catalase
11.2.5.1: Catalase and Peroxidase
cathode
1.1.8: The Electron
cathode ray tube
1.1.8: The Electron
cation
1.2.2: Ionic Bonding
cationic polymerization
11.5.2.4: Cationic Polymerization
chain end control
11.5.2.1: Ziegler-Natta Polymerization
chain flow
11.5.4.4: Glass Transition
chain growth polymerization
11.5.2.3: Step Growth and Chain Growth
chalcogen
1.1.2: Groups of Related Elements
chelate
10.2: Ligands
Chelation
10.7: Chelation
chemcases
11.3: Cisplatin - The Invention of an Anticancer Drug
11.3.1: Cisplatin 1. Study of the Effect of Electric Fields on E. coli
11.3.2: Cisplatin 2. Control Experiments for the Effect of Electric Fields on E. coli
11.3.3: Cisplatin 3. Redox Chemistry
11.3.4: Cisplatin 4. Electrochemistry
11.3.5: Cisplatin 5. The Role of Platinum Electrodes
11.3.7: Cisplatin 7. Bioinorganic Chemistry
11.3.8: Cisplatin 8. Discovery of Cisplatin
11.3.9: Cisplatin 9. The Discovery - One Scientist's Story
11.3.10: Cisplatin 10. Research as a Career
11.3.11: Cisplatin 11. Cisplatin as an Anticancer Drug
11.3.12: Cisplatin 12. Modes of Action of Cisplatin
11.3.13: Cisplatin 13. Further Studies/Recent Developments
11.3.14: Cisplatin 14. DNA
11.3.15: Cisplatin 15. FDA Drug Approval Process
11.3.16: Cisplatin 16. Profits from Cisplatin
11.3.17: Cisplatin 17. Drug Resistance
11.3.18: Cisplatin 18. Toxicity
11.3.19: Cisplatin 19. Cancer
11.3.20: Cisplatin 20. Other Treatments for Cancer
chemical property
1.2.12: Chemical Properties
Chemotherapy
11.1.10: Chemotherapy- Pt anticancer agents
chiral
10.5: Optical Isomerism in Metal Complexes
cis configuration
1.3.7: Orbital Descriptions of Multiple Bonds
cohesive force
4.2: Properties of Liquids
6.3: Properties of Liquids
coinage metal
1.1.2: Groups of Related Elements
condensation
6.5: Phase Transitions
condensation polymer
1.4.10: Synthetic Macromolecules- Some Applied Organic Chemistry
1.4.12: Condensation Polymers
coordination compound
10.1: Werner's Theory of Coordination Compounds
coordination number
5.4: Lattice Structures in Crystalline Solids
Coulomb
1.1.8: The Electron
covalent bond
1.2.1: Prelude to Chemical Bonding
1.2.13: The Covalent Bond
covalent compound
1.4.2: Covalent Compounds and Intermolecular Forces
covalent network solid
5.3: The Solid State of Matter
covalent radius
1.2.19: Atomic Sizes
crystal lattice
1.2.2: Ionic Bonding
crystalline solid
5.3: The Solid State of Matter
cubic closest packing
5.4: Lattice Structures in Crystalline Solids
Cytochrome c
11.1.7: Cytochrome C
cytochrome c oxidase
11.1.8: Cytochrome Oxidase

D

degree of polymerization
11.5.4.1: Molecular Weight of Polymers
deposition
6.5: Phase Transitions
descriptive chemistry
1.1.1: Prelude to Atomic Structure
diamond
1.4.8: Diamond and Graphite
differential scanning calorimetry
11.5.4.4: Glass Transition
diffraction
5.4: Lattice Structures in Crystalline Solids
dipole
1.3.9: Polarizability

dipole force
1.4.3: Dipole Forces
dipole moment
1.3.9: Polarizability
1.3.9.1: Biology - Polarizability of Biologically Significant Atoms
diradical
1.3.2: Exceptions to the Octet Rule
Dispersion
4.1: Intermolecular Forces
6.2: Intermolecular Forces Review
dispersion forces
1.4.4: London Forces
double bond
1.2.15.3: Multiple Bonds
dynamic equilibrium
6.5: Phase Transitions

E
electrode
1.1.8: The Electron
electron
1.1.8: The Electron
2.3: Atomic Structure and Isotopes
electron affinity
1.2.3: Energy and the Formation of Ions
1.2.8: Electron Affinities
electron deficient
1.3.2: Exceptions to the Octet Rule
electronegativity
1.3.11: Electronegativity
electropositive
1.3.11: Electronegativity
enantiomers
10.5: Optical Isomerism in Metal Complexes
Exceptions to the Octet Rule
1.3.2.1: Biology- Biologically Active Exceptions to the Octet Rule
Exemplar
11.3.1: Cisplatin 1. Study of the Effect of Electric Fields on E. coli
11.3.2: Cisplatin 2. Control Experiments for the Effect of Electric Fields on E. coli
11.3.3: Cisplatin 3. Redox Chemistry
11.3.4: Cisplatin 4. Electrochemistry
11.3.5: Cisplatin 5. The Role of Platinum Electrodes
11.3.6: Cisplatin 6. Transition Metal Chemistry
11.3.7: Cisplatin 7. Bioinorganic Chemistry
11.3.8: Cisplatin 8. Discovery of Cisplatin
11.3.9: Cisplatin 9. The Discovery - One Scientist's Story
11.3.10: Cisplatin 10. Research as a Career
11.3.11: Cisplatin 11. Cisplatin as an Anticancer Drug
11.3.12: Cisplatin 12. Modes of Action of Cisplatin
11.3.13: Cisplatin 13. Further Studies/Recent Developments
11.3.14: Cisplatin 14. DNA
11.3.15: Cisplatin 15. FDA Drug Approval Process
11.3.16: Cisplatin 16. Profits from Cisplatin
11.3.17: Cisplatin 17. Drug Resistance
11.3.18: Cisplatin 18. Toxicity
11.3.19: Cisplatin 19. Cancer
11.3.20: Cisplatin 20. Other Treatments for Cancer

F
family
1.1.3: The Periodic Table
formal charge
1.3.13: Formal Charge and Oxidation Numbers
Formation Constants
10.7: Chelation
free radical
1.3.2: Exceptions to the Octet Rule
freezing
6.5: Phase Transitions
freezing point
6.5: Phase Transitions

G
galvanic cell
9.3: Galvanic Cells
glass transition
11.5.4.4: Glass Transition
graphite
1.4.8: Diamond and Graphite
group
1.1.3: The Periodic Table

H
Halogen
1.1.2: Groups of Related Elements
hexagonal closest packing
5.4: Lattice Structures in Crystalline Solids
hole
5.4: Lattice Structures in Crystalline Solids
Human Serum Albumin
11.1.1: A Molecular Depot- Human Serum Albumin Carries Essential Cu and Zn in Serum
hydrated cation
8.1.7: Conjugate Acid-Base Pairs and pH
hydride
1.4.5: Hydrogen Bonding- Water
hydrochloric acid
8.1.4: Introduction to Strong Acids and Bases
hydrogen bond
1.4.5: Hydrogen Bonding- Water
hydrogen bonding
1.4.6: Ice and Water
4.1: Intermolecular Forces
6.2: Intermolecular Forces Review
hydrolysis
8.1.7: Conjugate Acid-Base Pairs and pH
hydroxide
8.1.4: Introduction to Strong Acids and Bases

I
induced dipole
4.1: Intermolecular Forces
6.2: Intermolecular Forces Review
instantaneous dipole
4.1: Intermolecular Forces
6.2: Intermolecular Forces Review
intermolecular force
4.1: Intermolecular Forces
6.2: Intermolecular Forces Review
interstitial sites
5.3: The Solid State of Matter
ion pair
1.2.2: Ionic Bonding
ionic bond
1.2.1: Prelude to Chemical Bonding
ionic compound
1.2.17: Polyatomic Ions
ionic crystal lattice
1.2.4: The Ionic Crystal Lattice
ionic formula
1.2.18: Ionic Compounds Containing Polyatomic Ions
ionic radius
1.2.20: Ionic Sizes
ionic solid
5.3: The Solid State of Matter
ionization energy
1.2.3: Energy and the Formation of Ions
1.2.8: Electron Affinities
ionize
1.2.3: Energy and the Formation of Ions
irreversible oxidation
11.2.4.8: General Aspects of the Chemistry of Iron
isomorphous
5.4: Lattice Structures in Crystalline Solids
isotope
2.4: Isotopes

L
lactam
11.5.1.2: Cyclic Carboxyloids
linear
1.3.3: The Shapes of Molecules
London force
1.4.4: London Forces
lone pair
1.2.14: Covalent Molecules and the Octet Rule

M
macromolecular substance
1.4.7: Macromolecular Substances
Marcus Theory
11.2.6.8: Marcus Theory
mass number
2.3: Atomic Structure and Isotopes
mass spectrometry
2.7: Measurement of Atomic Weights
melting
6.4: Phase Transitions- Overview
6.5: Phase Transitions
Melting Point
6.5: Phase Transitions
metal
1.2.7: Ionization of Transition and Inner Transition Elements
metallic solid
5.3: The Solid State of Matter
metalloid
1.2.7: Ionization of Transition and Inner Transition Elements

microphase separation
11.5.4.6: Microphase Separation
molecular geometry
1.3.3: The Shapes of Molecules
1.3.5: Multiple Bonds and Molecular Shapes
molecular solid
5.3: The Solid State of Matter
Molecular Weights of Polymers
11.5.4.1: Molecular Weight of Polymers
multiple bond
1.2.16: Examples of Lewis Structures
1.3.5: Multiple Bonds and Molecular Shapes

N
neutron
2.3: Atomic Structure and Isotopes
Newtonian liquids
11.5.4.3: Rheology
noble gas
1.1.2: Groups of Related Elements
normal boiling point
6.5: Phase Transitions
nuclear reaction
2.5: Transmutation and Radioactivity
nuclidic mass
2.4: Isotopes
Nylon 6
11.5.1.2: Cyclic Carboxyloids

O
octahedral
1.3.3: The Shapes of Molecules
octahedral hole
5.4: Lattice Structures in Crystalline Solids
octet
1.2.10: The Octet Rule
octet rule
1.2.1: Prelude to Chemical Bonding
1.2.10: The Octet Rule
1.3.2: Exceptions to the Octet Rule
Optical isomerism
10.5: Optical Isomerism in Metal Complexes
oxidation number
1.3.13: Formal Charge and Oxidation Numbers
oxyacid
8.1.4: Introduction to Strong Acids and Bases

P
partial covalent character
1.3.9: Polarizability
period
1.1.3: The Periodic Table
periodic law
1.1.3: The Periodic Table
periodic table
1.1.3: The Periodic Table
Periodic Trend
1.2.6: Ionization Energies
PET scan
2.5: Transmutation and Radioactivity
Peterson
11.3: Cisplatin - The Invention of an Anticancer Drug
11.3.1: Cisplatin 1. Study of the Effect of Electric Fields on E. coli
11.3.2: Cisplatin 2. Control Experiments for the Effect of Electric Fields on E. coli
11.3.3: Cisplatin 3. Redox Chemistry
11.3.4: Cisplatin 4. Electrochemistry
11.3.5: Cisplatin 5. The Role of Platinum Electrodes
11.3.6: Cisplatin 6. Transition Metal Chemistry
11.3.7: Cisplatin 7. Bioinorganic Chemistry
11.3.8: Cisplatin 8. Discovery of Cisplatin
11.3.9: Cisplatin 9. The Discovery - One Scientist's Story
11.3.10: Cisplatin 10. Research as a Career
11.3.11: Cisplatin 11. Cisplatin as an Anticancer Drug
11.3.12: Cisplatin 12. Modes of Action of Cisplatin
11.3.13: Cisplatin 13. Further Studies/Recent Developments
11.3.14: Cisplatin 14. DNA
11.3.15: Cisplatin 15. FDA Drug Approval Process
11.3.16: Cisplatin 16. Profits from Cisplatin
11.3.17: Cisplatin 17. Drug Resistance
11.3.18: Cisplatin 18. Toxicity
11.3.19: Cisplatin 19. Cancer
11.3.20: Cisplatin 20. Other Treatments for Cancer
pH
8.1.7: Conjugate Acid-Base Pairs and pH
phase transition
6.4: Phase Transitions- Overview
phosphotungstates
11.5.2.4: Cationic Polymerization
physical property
1.2.11: Physical Properties
pi bond
1.3.8: Sigma and Pi Bonds
polar covalent bond
1.3.10: Polar Covalent Bonds
1.3.12: Polarity in Polyatomic Molecules
polar covalent bonds
1.3.9.1: Biology - Polarizability of Biologically Significant Atoms
polarimeter
10.5: Optical Isomerism in Metal Complexes
Polarizability
1.3.9: Polarizability
4.1: Intermolecular Forces
6.2: Intermolecular Forces Review
polarization
1.3.9: Polarizability
polyatomic ion
1.2.17: Polyatomic Ions
polyatomic ions
1.5.1: Polyatomic Ions
polyatomic molecule
1.3.12: Polarity in Polyatomic Molecules
polymer
1.4.10: Synthetic Macromolecules- Some Applied Organic Chemistry
Polyurethane
1.4.13: Cross-Linking
potassium channels
11.1.9: Potassium Channels
proton
2.3: Atomic Structure and Isotopes

Q
quartz
1.4.9: Silicon Dioxide

R
racemic mixture
10.5: Optical Isomerism in Metal Complexes
radical polymerization
11.5.2.9: Radical Polymerization
Radioactive
1.1.7: Radiation
radioactivity
1.1.7: Radiation
redox cycling
11.1.6: Keep Cu Safe- Intracellular Copper Chaperones
redox reaction
1.3.13: Formal Charge and Oxidation Numbers
relative atomic mass
2.6: Average Atomic Weights
Reorganization energy
11.2.6.8: Marcus Theory
resonance hybrid
1.3.14: Resonance
rheology
11.5.4.3: Rheology

S
second ionization energy
1.2.5: Ions and Noble-Gas Electron Configurations
semimetal
1.2.7: Ionization of Transition and Inner Transition Elements
shear thickening
11.5.4.3: Rheology
shear thinning
11.5.4.3: Rheology
sigma bond
1.3.8: Sigma and Pi Bonds
simple cubic structure
5.4: Lattice Structures in Crystalline Solids
simple cubic unit cell
5.4: Lattice Structures in Crystalline Solids
site control
11.5.2.1: Ziegler-Natta Polymerization
skeleton structure
1.2.15: Writing Lewis Structures for Molecules
skeleton stucture
1.2.16: Examples of Lewis Structures
sodium hydroxide
8.1.4: Introduction to Strong Acids and Bases
Solids, Liquids, and Gases
6.4: Phase Transitions- Overview
sp hybrid orbital
1.3.6: Hybrid Orbitals
sp2 hybrid orbital
1.3.6: Hybrid Orbitals
sp3 hybrid orbital
1.3.6: Hybrid Orbitals
sp3d hybrid orbital
1.3.6: Hybrid Orbitals

sp3d2 hybrid orbital
1.3.6: Hybrid Orbitals
space lattice
5.4: Lattice Structures in Crystalline Solids
step growth polymerization
11.5.2.3: Step Growth and Chain Growth
strong acid
8.1.4: Introduction to Strong Acids and Bases
strong base
8.1.4: Introduction to Strong Acids and Bases
subatomic particle
2.3: Atomic Structure and Isotopes
sublimation
6.5: Phase Transitions
sulfuric acid
8.1.4: Introduction to Strong Acids and Bases
Superoxide dismutase
11.1.5: Antioxidant- Cu/Zn Superoxide dismutase (SOD1)
surface tension
4.2: Properties of Liquids
6.3: Properties of Liquids

T

tetrahedral
1.3.3: The Shapes of Molecules
tetrahedral hole
5.4: Lattice Structures in Crystalline Solids
thermoplastic polymers
11.5.1.8: Polymer Topology
thermosetting polymers
11.5.1.8: Polymer Topology
trans configuration
1.3.7: Orbital Descriptions of Multiple Bonds
transmutation
1.1.7: Radiation
2.5: Transmutation and Radioactivity
trigonal bipyramidal
1.3.3: The Shapes of Molecules
trigonal planar
1.3.3: The Shapes of Molecules
trigonal pyramidal
1.3.4: Molecules with Lone Pairs
triple bond
1.2.15.3: Multiple Bonds
Troponin C
11.2.3.15: Troponin C

U

unit cell
5.4: Lattice Structures in Crystalline Solids
unshared pair
1.2.14: Covalent Molecules and the Octet Rule

V

vacancy
5.3: The Solid State of Matter
valence
1.1.4: Valence
van der Waals force
1.4.4: London Forces
4.1: Intermolecular Forces
6.2: Intermolecular Forces Review
van der Waals radius
1.2.19: Atomic Sizes
vapor pressure
6.5: Phase Transitions
vaporization
6.5: Phase Transitions
virial theorem
1.2.13: The Covalent Bond
viscosity
4.2: Properties of Liquids
6.3: Properties of Liquids

Z

zinc
11.2.2.13: Selecting Zinc

Glossary

Sample Word 1 | Sample Definition 1

Detailed Licensing

Overview

Title: Textbook- Modern Applications of Chemistry

Webpages: 430

Applicable Restrictions: Noncommercial

All licenses found:

- CC BY-NC-SA 4.0: 61.2% (263 pages)
- Undeclared: 25.3% (109 pages)
- CC BY-NC 3.0: 9.3% (40 pages)
- CC BY 4.0: 2.8% (12 pages)
- CC BY-NC 4.0: 1.2% (5 pages)
- CC BY-NC-SA 3.0: 0.2% (1 page)

By Page

- Textbook- Modern Applications of Chemistry - *Undeclared*
  - Front Matter - *Undeclared*
    - TitlePage - *Undeclared*
    - InfoPage - *Undeclared*
    - Table of Contents - *Undeclared*
    - Licensing - *Undeclared*
  - 1: Primer - *Undeclared*
    - 1.1: The Structure of Atoms - *CC BY-NC-SA 4.0*
      - 1.1.1: Prelude to Atomic Structure - *CC BY-NC-SA 4.0*
      - 1.1.2: Groups of Related Elements - *CC BY-NC-SA 4.0*
      - 1.1.3: The Periodic Table - *CC BY-NC-SA 4.0*
      - 1.1.4: Valence - *CC BY-NC-SA 4.0*
      - 1.1.5: Exceptions to the Periodic Law - *CC BY-NC-SA 4.0*
      - 1.1.6: Implications of Periodicity for Atomic Theory - *CC BY-NC-SA 4.0*
      - 1.1.7: Radiation - *CC BY-NC-SA 4.0*
      - 1.1.8: The Electron - *CC BY-NC-SA 4.0*
      - 1.1.9: The Nucleus - *CC BY-NC-SA 4.0*
    - 1.2: Chemical Bonding - Electron Pairs and Octets - *CC BY-NC-SA 4.0*
      - 1.2.1: Prelude to Chemical Bonding - *CC BY-NC-SA 4.0*
      - 1.2.2: Ionic Bonding - *CC BY-NC-SA 4.0*
      - 1.2.3: Energy and the Formation of Ions - *CC BY-NC-SA 4.0*
      - 1.2.4: The Ionic Crystal Lattice - *CC BY-NC-SA 4.0*
      - 1.2.5: Ions and Noble-Gas Electron Configurations - *CC BY-NC-SA 4.0*
      - 1.2.6: Ionization Energies - *CC BY-NC-SA 4.0*
      - 1.2.7: Ionization of Transition and Inner Transition Elements - *CC BY-NC-SA 4.0*
      - 1.2.8: Electron Affinities - *CC BY-NC-SA 4.0*
      - 1.2.9: Binary Ionic Compounds and Their Properties - *CC BY-NC-SA 4.0*
      - 1.2.10: The Octet Rule - *CC BY-NC-SA 4.0*
      - 1.2.11: Physical Properties - *CC BY-NC-SA 4.0*
        - 1.2.11.1: Lecture Demonstrations - *CC BY-NC-SA 4.0*
      - 1.2.12: Chemical Properties - *CC BY-NC-SA 4.0*
      - 1.2.13: The Covalent Bond - *CC BY-NC-SA 4.0*
      - 1.2.14: Covalent Molecules and the Octet Rule - *CC BY-NC-SA 4.0*
      - 1.2.15: Writing Lewis Structures for Molecules - *CC BY-NC-SA 4.0*
        - 1.2.15.1: An Excess of Bonds - *CC BY-NC-SA 4.0*
        - 1.2.15.2: Deciding on a Skeleton Structure - *CC BY-NC-SA 4.0*
        - 1.2.15.3: Multiple Bonds - *CC BY-NC-SA 4.0*
      - 1.2.16: Examples of Lewis Structures - *CC BY-NC-SA 4.0*
      - 1.2.17: Polyatomic Ions - *CC BY-NC-SA 4.0*
      - 1.2.18: Ionic Compounds Containing Polyatomic Ions - *CC BY-NC-SA 4.0*
      - 1.2.19: Atomic Sizes - *CC BY-NC-SA 4.0*
      - 1.2.20: Ionic Sizes - *CC BY-NC-SA 4.0*

- 1.2.21: Periodic Variation of IE and EA - *CC BY-NC-SA 4.0*
  - 1.2.21.1: Lecture Demonstrations - *CC BY-NC-SA 4.0*
- 1.3: Further Aspects of Covalent Bonding - *CC BY-NC-SA 4.0*
  - 1.3.1: Prelude to Covalent Bonding - *CC BY-NC-SA 4.0*
  - 1.3.2: Exceptions to the Octet Rule - *CC BY-NC-SA 4.0*
    - 1.3.2.1: Biology- Biologically Active Exceptions to the Octet Rule - *CC BY-NC-SA 4.0*
  - 1.3.3: The Shapes of Molecules - *CC BY-NC-SA 4.0*
    - 1.3.3.1: Lecture Demonstrations - *CC BY-NC-SA 4.0*
  - 1.3.4: Molecules with Lone Pairs - *CC BY-NC-SA 4.0*
    - 1.3.4.1: Lecture Demonstrations - *CC BY-NC-SA 4.0*
  - 1.3.5: Multiple Bonds and Molecular Shapes - *CC BY-NC-SA 4.0*
  - 1.3.6: Hybrid Orbitals - *CC BY-NC-SA 4.0*
  - 1.3.7: Orbital Descriptions of Multiple Bonds - *CC BY-NC-SA 4.0*
  - 1.3.8: Sigma and Pi Bonds - *CC BY-NC-SA 4.0*
  - 1.3.9: Polarizability - *CC BY-NC-SA 4.0*
    - 1.3.9.1: Biology - Polarizability of Biologically Significant Atoms - *CC BY-NC-SA 4.0*
  - 1.3.10: Polar Covalent Bonds - *CC BY-NC-SA 4.0*
    - 1.3.10.1: Biology- Nonpolar Iodine and Polar Hydrogen Iodide - *CC BY-NC-SA 4.0*
    - 1.3.10.2: Lecture Demonstrations - *CC BY-NC-SA 4.0*
  - 1.3.11: Electronegativity - *CC BY-NC-SA 4.0*
  - 1.3.12: Polarity in Polyatomic Molecules - *CC BY-NC-SA 4.0*
    - 1.3.12.1: Biology- The Hydrophobic Effect and Properties of Small Polyatomic Molecules - *CC BY-NC-SA 4.0*
    - 1.3.12.2: Lecture Demonstrations - *CC BY-NC-SA 4.0*
  - 1.3.13: Formal Charge and Oxidation Numbers - *CC BY-NC-SA 4.0*
  - 1.3.14: Resonance - *CC BY-NC-SA 4.0*
- 1.4: Properties of Organic Compounds - *CC BY-NC-SA 4.0*
  - 1.4.1: Prelude to Organic Compounds - *CC BY-NC-SA 4.0*
  - 1.4.2: Covalent Compounds and Intermolecular Forces - *CC BY-NC-SA 4.0*
  - 1.4.3: Dipole Forces - *CC BY-NC-SA 4.0*
  - 1.4.4: London Forces - *CC BY-NC-SA 4.0*
    - 1.4.4.1: Chapter 8 page 3.jpg - *CC BY-NC-SA 4.0*
    - 1.4.4.2: Atomic Radii - *CC BY-NC-SA 4.0*
    - 1.4.4.3: Atomic sizes on periodic table.jpg - *CC BY-NC-SA 4.0*
    - 1.4.4.4: Ionization Energies - *CC BY-NC-SA 4.0*
      - 1.4.4.4.1: IonizationEnergyAtomicWeight.PNG - *CC BY-NC-SA 4.0*
    - 1.4.4.5: Ionization Energies and Electron Affinities - *CC BY-NC-SA 4.0*
      - 1.4.4.5.1: Electron Affinities - *CC BY-NC-SA 4.0*
        - 1.4.4.5.1.1: Ionization Energies and Electron Affinities.jpg - *CC BY-NC-SA 4.0*
    - 1.4.4.6: Polarizability on London Forces.jpg - *CC BY-NC-SA 4.0*
  - 1.4.5: Hydrogen Bonding- Water - *CC BY-NC-SA 4.0*
    - 1.4.5.1: Atomic Radii and Ionic Radii - *CC BY-NC-SA 4.0*
    - 1.4.5.2: H-Bonding Between 2 HF Molecules.jpg - *CC BY-NC-SA 4.0*
    - 1.4.5.3: Nonmetal hydride bp.jpg - *CC BY-NC-SA 4.0*
  - 1.4.6: Ice and Water - *CC BY-NC-SA 4.0*
    - 1.4.6.1: Ice; a hexagonal crystal.jpg - *CC BY-NC-SA 4.0*
    - 1.4.6.2: Boiling Points of Hydrides - *CC BY-NC-SA 4.0*
  - 1.4.7: Macromolecular Substances - *CC BY-NC-SA 4.0*
  - 1.4.8: Diamond and Graphite - *CC BY-NC-SA 4.0*
  - 1.4.9: Silicon Dioxide - *CC BY-NC-SA 4.0*
  - 1.4.10: Synthetic Macromolecules- Some Applied Organic Chemistry - *CC BY-NC-SA 4.0*
  - 1.4.11: Addition Polymers - *CC BY-NC-SA 4.0*

- 1.4.12: Condensation Polymers - *CC BY-NC-SA 4.0*
- 1.4.13: Cross-Linking - *CC BY-NC-SA 4.0*
- 1.5: Acid and Base Naming - *Undeclared*
  - 1.5.1: Polyatomic Ions - *CC BY-NC 4.0*
  - 1.5.2: Naming Acids - *CC BY-NC 4.0*
  - 1.5.3: Names and Formulas of Bases - *CC BY-NC 4.0*

2: Nuclear Chemistry - *Undeclared*
- 2.1: Components of the Nucleus - *Undeclared*
- 2.2: The Nuclear Atom - *CC BY-NC-SA 4.0*
- 2.3: Atomic Structure and Isotopes - *CC BY-NC-SA 4.0*
- 2.4: Isotopes - *CC BY-NC-SA 4.0*
- 2.5: Transmutation and Radioactivity - *CC BY-NC-SA 4.0*
- 2.6: Average Atomic Weights - *CC BY-NC-SA 4.0*
- 2.7: Measurement of Atomic Weights - *CC BY-NC-SA 4.0*
- 2.8: Nuclear Reactions - *Undeclared*
- 2.9: Nuclear Radiation - *Undeclared*
- 2.10: Rates of Radioactive Decay - *CC BY-NC-SA 4.0*
- 2.11: Stability of the Atomic Nucleus - *Undeclared*
- 2.12: The Origin of the Elements - *Undeclared*
- 2.13: Transmutation of the Elements - *Undeclared*
- 2.14: Nuclear Fission - *Undeclared*
- 2.15: Nuclear Fusion - *Undeclared*
- 2.16: Nuclear Chemistry (Exercises) - *Undeclared*

3: Physical Properties of Gases - *Undeclared*
- 3.1: Properties of Gases - *Undeclared*
- 3.2: Gas Pressure - *Undeclared*
- 3.3: Relationships among Pressure, Temperature, Volume, and Amount - *Undeclared*
- 3.4: The Ideal Gas Law - *Undeclared*
- 3.5: Gas Volumes and Stoichiometry - *Undeclared*
- 3.6: Kinetic Molecular Theory of Gases - *Undeclared*
- 3.7: Connecting Gas Properties to Kinetic Molecular Theory - *Undeclared*
- 3.8: Chapter Problems - *Undeclared*

4: Intermolecular Forces - *Undeclared*
- 4.1: Intermolecular Forces - *CC BY 4.0*
- 4.2: Properties of Liquids - *CC BY 4.0*
- 4.3: Intermolecular Forces and the Solution Process - *Undeclared*

5: Solids - *CC BY 4.0*
- 5.1: Prelude to Liquids and Solids - *CC BY 4.0*
- 5.2: Carbon and Silicon- Network Atomic Solids - *Undeclared*
- 5.3: The Solid State of Matter - *CC BY 4.0*
- 5.4: Lattice Structures in Crystalline Solids - *CC BY 4.0*
- 5.5: Bonding in Metals and Semiconductors - *Undeclared*
- 5.6: Liquids and Solids (Exercises) - *CC BY 4.0*

6: Phases and Phase Transitions - *Undeclared*
- 6.1: Prelude to Liquids and Solids - *CC BY 4.0*
- 6.2: Intermolecular Forces Review - *CC BY 4.0*
- 6.3: Properties of Liquids - *CC BY 4.0*
- 6.4: Phase Transitions- Overview - *CC BY-NC-SA 4.0*
- 6.5: Phase Transitions - *CC BY 4.0*
- 6.6: Vaporization and Vapor Pressure - *CC BY-NC-SA 4.0*
- 6.7: Sublimation and Fusion - *CC BY 4.0*
- 6.8: Heating Curve for Water - *CC BY-NC-SA 4.0*
- 6.9: Phase Diagrams - *CC BY-NC-SA 4.0*
- 6.10: Water - An Extraordinary Substance - *CC BY-NC-SA 4.0*

7: Solutions and their Physical Properties - *Undeclared*
- 7.1: Types of Solutions- Some Terminology - *Undeclared*
- 7.2: Mixtures of Gases - *Undeclared*
- 7.3: Solution Concentration - *Undeclared*
- 7.4: Intermolecular Forces and the Solution Process - *CC BY-NC-SA 3.0*
- 7.5: Solution Formation and Equilibrium - *CC BY-NC-SA 4.0*
- 7.6: Solubilities of Gases - *Undeclared*
- 7.7: Vapor Pressures of Solutions - *Undeclared*
- 7.8: Osmotic Pressure - *Undeclared*
- 7.9: Freezing-Point Depression and Boiling-Point Elevation of Nonelectrolyte Solutions - *Undeclared*
- 7.10: Solutions of Electrolytes - *Undeclared*
- 7.11: Colloidal Mixtures - *Undeclared*
- 7.12: Solubility and Complex-Ion Equilibria - *Undeclared*
  - 7.12.1: Solubility Product Constant, Ksp - *Undeclared*
  - 7.12.2: Relationship Between Solubility and Ksp - *Undeclared*
  - 7.12.3: Common-Ion Effect in Solubility Equilibria - *Undeclared*
  - 7.12.4: Limitations of the Ksp Concept - *Undeclared*
  - 7.12.5: Criteria for Precipitation and its Completeness - *Undeclared*
  - 7.12.6: Fractional Precipitation - *Undeclared*
  - 7.12.7: Solubility and pH - *Undeclared*

- 7.12.8: Equilibria Involving Complex Ions - *Undeclared*
- 7.12.9: Qualitative Cation Analysis - *Undeclared*

8: Acids and Bases - *Undeclared*

- 8.1: Acids and Bases at Equilibrium - *Undeclared*
  - 8.1.1: Arrhenius Theory- A Brief Review - *Undeclared*
  - 8.1.2: Brønsted-Lowry Theory of Acids and Bases - *Undeclared*
  - 8.1.3: Self-Ionization of Water and the pH Scale - *Undeclared*
  - 8.1.4: Introduction to Strong Acids and Bases - *CC BY-NC-SA 4.0*
  - 8.1.5: Strong Acids and Strong Bases - *Undeclared*
  - 8.1.6: Weak Acids and Weak Bases - *Undeclared*
  - 8.1.7: Conjugate Acid-Base Pairs and pH - *CC BY-NC-SA 4.0*
  - 8.1.8: Polyprotic Acids - *Undeclared*
  - 8.1.9: Ions as Acids and Bases - *Undeclared*
  - 8.1.10: Molecular Structure and Acid-Base Behavior - *Undeclared*
  - 8.1.11: Lewis Acids and Bases - *Undeclared*
  - 8.1.12: Common-Ion Effect in Acid–Base Equilibria - *Undeclared*
- 8.2: Additional Aspects of Acid-Base Equilibria - *CC BY-NC-SA 4.0*
  - 8.2.1: Buffer Solutions - *CC BY-NC-SA 4.0*
  - 8.2.2: Acid–Base Indicators - *CC BY-NC-SA 4.0*
  - 8.2.3: Neutralization Reactions and Titration Curves - *CC BY-NC-SA 4.0*
  - 8.2.4: Solutions of Salts of Polyprotic Acids - *CC BY-NC-SA 4.0*
  - 8.2.5: Acid–Base Equilibrium Calculations- A Summary - *CC BY-NC-SA 4.0*
  - 8.2.6: Exercises on Acids and Bases II - *CC BY-NC-SA 4.0*
  - 8.2.7: E3. Solubility Constants for Compounds at 25°C Data Table - *CC BY-NC-SA 4.0*
  - 8.2.8: pH Calculations for Acid–Base Titrations - *CC BY-NC-SA 4.0*

9: Electrochemistry - *Undeclared*

- 9.1: Oxidation-Reduction Reactions - *Undeclared*
- 9.2: Balancing Redox Reactions - *Undeclared*
- 9.3: Galvanic Cells - *Undeclared*
- 9.4: Standard Electrode Potentials - *CC BY-NC-SA 4.0*
- 9.5: Strengths of Oxidants and Reductants - *Undeclared*
- 9.6: E, ΔG, and K (The Big Triangle of Chemistry) - *Undeclared*
- 9.7: Cell Potential as a Function of Concentrations - *Undeclared*
- 9.8: Batteries- Producing Electricity Through Chemical Reactions - *Undeclared*
- 9.9: Corrosion- Unwanted Voltaic Cells - *Undeclared*
- 9.10: Electrolysis- Causing Nonspontaneous Reactions to Occur - *Undeclared*

10: Coordination Chemistry - *Undeclared*

- 10.1: Werner's Theory of Coordination Compounds - *Undeclared*
- 10.2: Ligands - *Undeclared*
- 10.3: Nomenclature - *Undeclared*
- 10.4: Isomerism - *Undeclared*
- 10.5: Optical Isomerism in Metal Complexes - *Undeclared*
- 10.6: Stability Aspects of Complex-Ion Equilibria - *Undeclared*
- 10.7: Chelation - *Undeclared*
- 10.8: Bonding in Octahedral Complex Ions- Crystal Field Theory - *Undeclared*
- 10.9: Bonding in Non-Octahedral Complex Ions- Crystal Field Theory - *Undeclared*
- 10.10: High Spin and Low Spin Complexes - *CC BY-NC-SA 4.0*
- 10.11: Magnetic Behavior of Atoms, Molecules, and Materials - *Undeclared*
- 10.12: Magnetic Behavior of Complex Ions - *Undeclared*
- 10.13: Optical Properties of Coordination Compounds (Color) - *Undeclared*

11: Applications in Polymer and Biological Chemistry - *Undeclared*

- 11.1: Bioinorganic Chemistry - *Undeclared*
  - 11.1.1: A Molecular Depot- Human Serum Albumin Carries Essential Cu and Zn in Serum - *Undeclared*
  - 11.1.2: Iron acquisition in bacteria- Siderophores - *Undeclared*
  - 11.1.3: Fe Wars- Lactoferrin - *Undeclared*
  - 11.1.4: Iron Storage- Ferritin - *Undeclared*
  - 11.1.5: Antioxidant- Cu/Zn Superoxide dismutase (SOD1) - *Undeclared*
  - 11.1.6: Keep Cu Safe- Intracellular Copper Chaperones - *Undeclared*
  - 11.1.7: Cytochrome C - *Undeclared*
  - 11.1.8: Cytochrome Oxidase - *Undeclared*
  - 11.1.9: Potassium Channels - *Undeclared*

- 11.1.10: Chemotherapy- Pt anticancer agents - *Undeclared*
- 11.2: Bioinorganic Chemistry (Bertini et al.) - *CC BY-NC-SA 4.0*
  - Front Matter - *CC BY-NC-SA 4.0*
    - Licensing - *Undeclared*
    - Preface - *Undeclared*
  - 11.2.1: Transition-Metal Storage, Transport, and Biomineralization - *CC BY-NC-SA 4.0*
    - 11.2.1.1: Biological Significance of Iron, Zinc, Copper, Molybdenum, Cobalt, Chromium, Vanadium, and Nickel - *CC BY-NC-SA 4.0*
    - 11.2.1.2: Biological Systems of Metal Storage - *CC BY-NC-SA 4.0*
    - 11.2.1.3: Chemical Properties Relative to Storage and Transport - *CC BY-NC-SA 4.0*
    - 11.2.1.4: Iron Biomineralization - *CC BY-NC-SA 4.0*
    - 11.2.1.5: Transport of Iron - *CC BY-NC-SA 4.0*
    - 11.2.1.6: Transport of Zinc, Copper, Vanadium, Chromium, Molybdenum, and Cobalt - *CC BY-NC-SA 4.0*
  - 11.2.2: The Reaction Pathways of Zinc Enzymes and Related Biological Catalysts - *CC BY-NC-SA 4.0*
    - 11.2.2.1: About Carbonic Anhydrase - *CC BY-NC-SA 4.0*
    - 11.2.2.2: Acid-base Equilibria - *CC BY-NC-SA 4.0*
    - 11.2.2.3: Catalytic Mechanism - *CC BY-NC-SA 4.0*
    - 11.2.2.4: Coordinated Water and NMR - *CC BY-NC-SA 4.0*
    - 11.2.2.5: Coordination Geometries - *CC BY-NC-SA 4.0*
    - 11.2.2.6: Ester Hydrolysis and Phosphoryl Transfer - *CC BY-NC-SA 4.0*
    - 11.2.2.7: Group Transfer and Vitamin B-12 - *CC BY-NC-SA 4.0*
    - 11.2.2.8: Metal Substitution - *CC BY-NC-SA 4.0*
    - 11.2.2.9: Model Chemistry - *CC BY-NC-SA 4.0*
    - 11.2.2.10: Nucleophilic Addition of \(OH^{-}\) and \(H^{-}\) - *CC BY-NC-SA 4.0*
    - 11.2.2.11: Peptide Hydrolysis - *CC BY-NC-SA 4.0*
    - 11.2.2.12: pH Dependence of Inhibitor Binding - *CC BY-NC-SA 4.0*
    - 11.2.2.13: Selecting Zinc - *CC BY-NC-SA 4.0*
    - 11.2.2.14: Steady-State and Equilibrium Kinetics of Carbonic Anhydrase-Catalyzed \(CO_{2}/HCO_{3}^{-}\) Interconversion - *CC BY-NC-SA 4.0*
    - 11.2.2.15: Strategies for the Investigation of Zinc Enzymes - *CC BY-NC-SA 4.0*
    - 11.2.2.16: The Natural Catalysts - *CC BY-NC-SA 4.0*
    - 11.2.2.17: What Do We Learn? - *CC BY-NC-SA 4.0*
  - 11.2.3: Calcium in Biological Systems - *CC BY-NC-SA 4.0*
    - 11.2.3.1: Ca^{2+}-binding Proteins in Microorganisms- The Search for a Prokaryotic Calmodulin - *CC BY-NC-SA 4.0*
    - 11.2.3.2: Basic Facts About Calcium- Its Compounds and Reactions - *CC BY-NC-SA 4.0*
    - 11.2.3.3: Calcium in Mineralized Tissues - *CC BY-NC-SA 4.0*
    - 11.2.3.4: Calmodulin - *CC BY-NC-SA 4.0*
    - 11.2.3.5: Extracellular Calcium Ion-binding Proteins - *CC BY-NC-SA 4.0*
    - 11.2.3.6: Inositol Trisphosphate and the Calcium Ion Messenger System - *CC BY-NC-SA 4.0*
    - 11.2.3.7: Intracellular Calcium Ion Transport - *CC BY-NC-SA 4.0*
    - 11.2.3.8: Measurements of "Free" Calcium Concentrations - *CC BY-NC-SA 4.0*
    - 11.2.3.9: Measurements of Total Calcium Concentrations - *CC BY-NC-SA 4.0*
    - 11.2.3.10: Mitochondrial Calcium Ion Transport - *CC BY-NC-SA 4.0*
    - 11.2.3.11: Molecular Aspects of Calcium Ion-Regulated Intracellular Processes (Part 1) - *CC BY-NC-SA 4.0*
    - 11.2.3.12: Molecular Aspects of Calcium Ion-regulated Intracellular Processes (Part 2) - *CC BY-NC-SA 4.0*
    - 11.2.3.13: Paravalbumin and Calbindins \(D_{9K}\) and \(D_{28K}\) - *CC BY-NC-SA 4.0*
    - 11.2.3.14: The Transport and Regulation of Ca^{2+} Ions in Higher Organisms - *CC BY-NC-SA 4.0*
    - 11.2.3.15: Troponin C - *CC BY-NC-SA 4.0*
  - 11.2.4: Biological and Synthetic Dioxygen Carriers - *CC BY-NC-SA 4.0*

- 11.2.4.1: Biological Dioxygen Transport Systems - *CC BY-NC-SA 4.0*
- 11.2.4.2: Biological Oxygen Carriers - *CC BY-NC-SA 4.0*
- 11.2.4.3: Detailed Structures of Hemoglobins and Model Systems - *CC BY-NC-SA 4.0*
- 11.2.4.4: Dioxygen Carriers and Bioinorganic Chemistry - *CC BY-NC-SA 4.0*
- 11.2.4.5: General Aspects of the Chemistry of Cobalt - *CC BY-NC-SA 4.0*
- 11.2.4.6: General Aspects of the Chemistry of Copper - *CC BY-NC-SA 4.0*
- 11.2.4.7: General Aspects of the Chemistry of Dioxygen - *CC BY-NC-SA 4.0*
- 11.2.4.8: General Aspects of the Chemistry of Iron - *CC BY-NC-SA 4.0*
- 11.2.4.9: General Structural Features that Modulate Ligand Activity - *CC BY-NC-SA 4.0*
- 11.2.4.10: Hazards of Life with Dioxygen - *CC BY-NC-SA 4.0*
- 11.2.4.11: Nature of the Metal-Dioxygen Linkage in Biological Systems - *CC BY-NC-SA 4.0*
- 11.2.4.12: Other Ligands for Biological Oxygen Carriers - *CC BY-NC-SA 4.0*
- 11.2.4.13: Requirements for a Model System for Hemoglobin - *CC BY-NC-SA 4.0*
- 11.2.4.14: Requirements for Effective Oxygen Carriers - *CC BY-NC-SA 4.0*
- 11.2.4.15: Role of the Protein in Effecting Biological Oxygen Transport - *CC BY-NC-SA 4.0*
- 11.2.4.16: Selected Chemistry of Dioxygen, Iron, Copper, and Cobalt - *CC BY-NC-SA 4.0*
- 11.2.4.17: Stereochemical Changes Upon Ligation - *CC BY-NC-SA 4.0*
- 11.2.4.18: Structural Basis of Ligand Affinities of Oxygen Carriers - *CC BY-NC-SA 4.0*
- 11.2.4.19: Structures Relevant to Liganded Hemoglobins - *CC BY-NC-SA 4.0*
- 11.2.4.20: Thermodynamic Factors - *CC BY-NC-SA 4.0*
- 11.2.4.21: Ch. 4 References and Abbreviations - *CC BY-NC-SA 4.0*

- 11.2.5: Dioxygen Reactions - *CC BY-NC-SA 4.0*
  - 11.2.5.1: Catalase and Peroxidase - *CC BY-NC-SA 4.0*
  - 11.2.5.2: Chemistry of Dioxygen - *CC BY-NC-SA 4.0*
  - 11.2.5.3: Copper-zinc Superoxide Dismutase - *CC BY-NC-SA 4.0*
  - 11.2.5.4: Cytochrome c Oxidase - *CC BY-NC-SA 4.0*
  - 11.2.5.5: Dioxygen Toxicity - *CC BY-NC-SA 4.0*
  - 11.2.5.6: Monooxygenases - *CC BY-NC-SA 4.0*
  - 11.2.5.7: Oxygenases - *CC BY-NC-SA 4.0*
- 11.2.6: Electron Transfer - *CC BY-NC-SA 4.0*
  - 11.2.6.1: Biological Redox Components - *CC BY-NC-SA 4.0*
  - 11.2.6.2: Coupling Electron Transfers and Substrate Activation - *CC BY-NC-SA 4.0*
  - 11.2.6.3: Electron-transfer Rates - *CC BY-NC-SA 4.0*
  - 11.2.6.4: Electron-Transfer Theory - *CC BY-NC-SA 4.0*
  - 11.2.6.5: Energy Storage and Release - *CC BY-NC-SA 4.0*
  - 11.2.6.6: Long-range Electron Transfer in Proteins (Part 1) - *CC BY-NC-SA 4.0*
  - 11.2.6.7: Long-range Electron Transfer in Proteins (Part 2) - *CC BY-NC-SA 4.0*
  - 11.2.6.8: Marcus Theory - *CC BY-NC-SA 4.0*
- 11.2.7: Ferrodoxins, Hydrogenases, and Nitrogenases - Metal-Sulfide Proteins - *CC BY-NC-SA 4.0*
  - 11.2.7.1: Iron-sulfur Proteins and Models - *CC BY-NC-SA 4.0*
  - 11.2.7.2: Iron-sulfur Proteins and Models (Part 2) - *CC BY-NC-SA 4.0*
  - 11.2.7.3: Iron-sulfur Proteins and Models (Part 3) - *CC BY-NC-SA 4.0*
  - 11.2.7.4: Iron-sulfur Proteins and Models (Part 4) - *CC BY-NC-SA 4.0*
  - 11.2.7.5: Multisite Redox Enzymes - *CC BY-NC-SA 4.0*
  - 11.2.7.6: Multisite Redox Enzymes (Part 2) - *CC BY-NC-SA 4.0*
  - 11.2.7.7: Multisite Redox Enzymes (Part 3) - *CC BY-NC-SA 4.0*
  - 11.2.7.8: Multisite Redox Enzymes (Part 4) - *CC BY-NC-SA 4.0*
  - 11.2.7.9: Multisite Redox Enzymes (Part 5) - *CC BY-NC-SA 4.0*
  - 11.2.7.10: Multisite Redox Enzymes (Part 6) - *CC BY-NC-SA 4.0*
  - 11.2.7.11: Report on the Nitrogenase Crystal Structure\(\;^{378-381}\) - *CC BY-NC-SA 4.0*

- 11.2.7.12: Rubredoxin- A Single-Fe Tetrathiolate Protein - *CC BY-NC-SA 4.0*
- 11.2.8: Metal/Nucleic Acid Interactions - *CC BY-NC-SA 4.0*
  - 11.2.8.1: The Basics - *CC BY-NC-SA 4.0*
  - 11.2.8.2: The Basics (Part 2) - *CC BY-NC-SA 4.0*
  - 11.2.8.3: A Case Study- Tris(phenanthroline) Metal Complexes - *CC BY-NC-SA 4.0*
  - 11.2.8.4: Applications of Different Metal Complexes that Bind Nucleic Acids - *CC BY-NC-SA 4.0*
  - 11.2.8.5: Applications of Different Metal Complexes that Bind Nucleic Acids (Part 2) - *CC BY-NC-SA 4.0*
  - 11.2.8.6: Nature's Use of Metal/Nucleic-acid Interactions - *CC BY-NC-SA 4.0*
- 11.2.9: Metals in Medicine - *CC BY-NC-SA 4.0*
  - 11.2.9.1: Metal Deficiency and Disease - *CC BY-NC-SA 4.0*
  - 11.2.9.2: Toxic Effects of Metals - *CC BY-NC-SA 4.0*
  - 11.2.9.3: Aspects of Platinum Binding to DNA - *CC BY-NC-SA 4.0*
  - 11.2.9.4: Survey of Metals Used for Diagnosis and Chemotherapy - *CC BY-NC-SA 4.0*
  - 11.2.9.5: Platinum Anticancer Drugs- A Case Study - *CC BY-NC-SA 4.0*
  - 11.2.9.6: Mapping the Major Adducts of cis- and trans-DDP on DNA; Sequence Specificity - *CC BY-NC-SA 4.0*
  - 11.2.9.7: Structure of Platinum-DNA Complexes - *CC BY-NC-SA 4.0*
  - 11.2.9.8: Site-specifically Platinated DNA \(\;^{154}\) - *CC BY-NC-SA 4.0*
  - 11.2.9.9: Bioinorganic Chemistry of Platinum Anticancer Drugs- How Might They Work? - *CC BY-NC-SA 4.0*
  - 11.2.9.10: Bioinorganic Chemistry of Platinum Anticancer Drugs; How Might They Work? (Part 2) - *CC BY-NC-SA 4.0*
  - 11.2.9.11: Design of New Inorganic Anticancer Drugs - *CC BY-NC-SA 4.0*
- Back Matter - *CC BY-NC-SA 4.0*
  - Detailed Licensing - *Undeclared*
- 11.3: Cisplatin - The Invention of an Anticancer Drug - *CC BY-NC-SA 4.0*
  - 11.3.1: Cisplatin 1. Study of the Effect of Electric Fields on E. coli - *CC BY-NC-SA 4.0*
  - 11.3.2: Cisplatin 2. Control Experiments for the Effect of Electric Fields on E. coli - *CC BY-NC-SA 4.0*
  - 11.3.3: Cisplatin 3. Redox Chemistry - *CC BY-NC-SA 4.0*
  - 11.3.4: Cisplatin 4. Electrochemistry - *CC BY-NC-SA 4.0*
  - 11.3.5: Cisplatin 5. The Role of Platinum Electrodes - *CC BY-NC-SA 4.0*
  - 11.3.6: Cisplatin 6. Transition Metal Chemistry - *CC BY-NC-SA 4.0*
  - 11.3.7: Cisplatin 7. Bioinorganic Chemistry - *CC BY-NC-SA 4.0*
  - 11.3.8: Cisplatin 8. Discovery of Cisplatin - *CC BY-NC-SA 4.0*
  - 11.3.9: Cisplatin 9. The Discovery - One Scientist's Story - *CC BY-NC-SA 4.0*
  - 11.3.10: Cisplatin 10. Research as a Career - *CC BY-NC-SA 4.0*
  - 11.3.11: Cisplatin 11. Cisplatin as an Anticancer Drug - *CC BY-NC-SA 4.0*
  - 11.3.12: Cisplatin 12. Modes of Action of Cisplatin - *CC BY-NC-SA 4.0*
  - 11.3.13: Cisplatin 13. Further Studies/Recent Developments - *CC BY-NC-SA 4.0*
  - 11.3.14: Cisplatin 14. DNA - *CC BY-NC-SA 4.0*
  - 11.3.15: Cisplatin 15. FDA Drug Approval Process - *CC BY-NC-SA 4.0*
  - 11.3.16: Cisplatin 16. Profits from Cisplatin - *CC BY-NC-SA 4.0*
  - 11.3.17: Cisplatin 17. Drug Resistance - *CC BY-NC-SA 4.0*
  - 11.3.18: Cisplatin 18. Toxicity - *CC BY-NC-SA 4.0*
  - 11.3.19: Cisplatin 19. Cancer - *CC BY-NC-SA 4.0*
  - 11.3.20: Cisplatin 20. Other Treatments for Cancer - *CC BY-NC-SA 4.0*
- 11.4: Polymeric Materials and Soft Condensed Matter - *CC BY-NC-SA 4.0*
  - 11.4.1: Polymerization Reactions for Synthetic Polymers - *CC BY-NC-SA 4.0*
  - 11.4.2: Natural Polymers - *CC BY-NC-SA 4.0*
- 11.5: Polymer Chemistry (Schaller) - *CC BY-NC 3.0*
  - Front Matter - *CC BY-NC 4.0*
    - Licensing - *Undeclared*
  - 11.5.1: Monomers and Polymers - *CC BY-NC 3.0*
    - 11.5.1.1: Difunctional Carboxyloids - *CC BY-NC 3.0*
    - 11.5.1.2: Cyclic Carboxyloids - *CC BY-NC 3.0*
    - 11.5.1.3: Olefins - *CC BY-NC 3.0*

- 11.5.1.4: Cyclic Olefins - *CC BY-NC 3.0*
- 11.5.1.5: Coordination Polymers - *CC BY-NC 3.0*
- 11.5.1.6: Supramolecular Assemblies - *CC BY-NC 3.0*
- 11.5.1.7: Other Polymers - *CC BY-NC 3.0*
- 11.5.1.8: Polymer Topology - *CC BY-NC 3.0*
- 11.5.1.E: Solutions for Selected Problems - *CC BY-NC 3.0*

- 11.5.2: Synthetic Methods in Polymer Chemistry - *CC BY-NC 3.0*
  - 11.5.2.1: Ziegler-Natta Polymerization - *CC BY-NC 3.0*
  - 11.5.2.2: Solutions to Selected Problems - *CC BY-NC 3.0*
  - 11.5.2.3: Step Growth and Chain Growth - *CC BY-NC 3.0*
  - 11.5.2.4: Cationic Polymerization - *CC BY-NC 3.0*
  - 11.5.2.5: Living Cationic Polymerization - *CC BY-NC 3.0*
  - 11.5.2.6: Anionic Polymerization - *CC BY-NC 3.0*
  - 11.5.2.7: Living Anionic Polymerization - *CC BY-NC 3.0*
  - 11.5.2.8: Ring-Opening Polymerization - *CC BY-NC 3.0*
  - 11.5.2.9: Radical Polymerization - *CC BY-NC 3.0*
  - 11.5.2.10: Living Radical Polymerization-RAFT - *CC BY-NC 3.0*
  - 11.5.2.11: Living Radical Polymerization-ATRP - *CC BY-NC 3.0*
- 11.5.3: Kinetics and Thermodynamics of Polymerization - *CC BY-NC 3.0*
  - 11.5.3.1: Thermodynamics of Polymerization - *CC BY-NC 3.0*
  - 11.5.3.2: Kinetics of Step-Growth Polymerization - *CC BY-NC 3.0*
  - 11.5.3.3: Kinetics of Chain Polymerization - *CC BY-NC 3.0*
  - 11.5.3.4: Kinetics of Catalytic Polymerization - *CC BY-NC 3.0*
  - 11.5.3.5: Solutions to Selected Problems - *CC BY-NC 3.0*
- 11.5.4: Polymer Properties - *CC BY-NC 3.0*
  - 11.5.4.1: Molecular Weight of Polymers - *CC BY-NC 3.0*
  - 11.5.4.2: Viscosity of Polymers - *CC BY-NC 3.0*
  - 11.5.4.3: Rheology - *CC BY-NC 3.0*
  - 11.5.4.4: Glass Transition - *CC BY-NC 3.0*
  - 11.5.4.5: Crystallinity in Polymers - *CC BY-NC 3.0*
  - 11.5.4.6: Microphase Separation - *CC BY-NC 3.0*
  - 11.5.4.7: Stress-Strain Relationships - *CC BY-NC 3.0*
  - 11.5.4.8: Storage and Loss Modulus - *CC BY-NC 3.0*
  - 11.5.4.9: Modulus, Temperature, Time - *CC BY-NC 3.0*
  - 11.5.4.10: Chapter Solutions - *CC BY-NC 3.0*
- Back Matter - *CC BY-NC 4.0*
  - Detailed Licensing - *Undeclared*

- 11.6: Synthetic Polymers - *CC BY-NC-SA 4.0*
  - 11.6.1: Introduction - *CC BY-NC-SA 4.0*
  - 11.6.2: Chain-Growth Polymers—Addition Polymers - *CC BY-NC-SA 4.0*
  - 11.6.3: Anionic Polymerization of Epoxides - *CC BY-NC-SA 4.0*
  - 11.6.4: Ziegler–Natta Catalysts and Polymer Stereochemistry - *CC BY-NC-SA 4.0*
  - 11.6.5: Natural and Synthetic Rubbers - *CC BY-NC-SA 4.0*
  - 11.6.6: Step-Growth Polymers—Condensation Polymers - *CC BY-NC-SA 4.0*
  - 11.6.7: Polymer Structure and Properties - *CC BY-NC-SA 4.0*
  - 11.6.8: Green Polymer Synthesis - *CC BY-NC-SA 4.0*
  - 11.6.9: Polymer Recycling and Disposal - *CC BY-NC-SA 4.0*

- 12: Reading - *Undeclared*
- Back Matter - *Undeclared*
  - Index - *Undeclared*
  - Glossary - *Undeclared*
  - Detailed Licensing - *Undeclared*

Index

A

acid–base titrations
8.2.8: pH Calculations for Acid–Base Titrations
addition polymer
1.4.10: Synthetic Macromolecules- Some Applied Organic Chemistry
1.4.11: Addition Polymers
adhesive force
4.2: Properties of Liquids
6.3: Properties of Liquids
alkali metal
1.1.2: Groups of Related Elements
alkaline earth metal
1.1.2: Groups of Related Elements
allotropes
1.4.8: Diamond and Graphite
amorphous polymer
11.5.4.5: Crystallinity in Polymers
amorphous solid
5.3: The Solid State of Matter
angle of rotation
10.5: Optical Isomerism in Metal Complexes
angular
1.3.4: Molecules with Lone Pairs
anion
1.2.2: Ionic Bonding
Anionic Polymerization
11.5.2.6: Anionic Polymerization
atomic number
1.1.9: The Nucleus

B

balancing redox reactions
9.2: Balancing Redox Reactions
barrier to rotation
1.3.7: Orbital Descriptions of Multiple Bonds
bent
1.3.4: Molecules with Lone Pairs
bent bond
1.3.7: Orbital Descriptions of Multiple Bonds
benzene ring
1.3.14: Resonance
binary compound
1.2.9: Binary Ionic Compounds and Their Properties
biogenesis
1.3.9.1: Biology - Polarizability of Biologically Significant Atoms
boiling
6.4: Phase Transitions- Overview
Boiling Point
6.5: Phase Transitions
bond energy
1.2.13: The Covalent Bond
bond length
1.2.19: Atomic Sizes
bond line
1.2.14: Covalent Molecules and the Octet Rule
Bragg equation
5.4: Lattice Structures in Crystalline Solids
11.5.4.5: Crystallinity in Polymers

C

calmodulin
11.2.3.4: Calmodulin
capillary action
4.2: Properties of Liquids
6.3: Properties of Liquids
carbonic anhydrase
11.2.2.14: Steady-State and Equilibrium Kinetics of Carbonic Anhydrase-Catalyzed \(CO_{2}/HCO_{3}^{-}\) Interconversion
catalase
11.2.5.1: Catalase and Peroxidase
cathode
1.1.8: The Electron
cathode ray tube
1.1.8: The Electron
cation
1.2.2: Ionic Bonding
cationic polymerization
11.5.2.4: Cationic Polymerization
chain end control
11.5.2.1: Ziegler-Natta Polymerization
chain flow
11.5.4.4: Glass Transition
chain growth polymerization
11.5.2.3: Step Growth and Chain Growth
chalcogen
1.1.2: Groups of Related Elements
chelate
10.2: Ligands
Chelation
10.7: Chelation
chemcases
11.3: Cisplatin - The Invention of an Anticancer Drug
11.3.1: Cisplatin 1. Study of the Effect of Electric Fields on E. coli
11.3.2: Cisplatin 2. Control Experiments for the Effect of Electric Fields on E. coli
11.3.3: Cisplatin 3. Redox Chemistry
11.3.4: Cisplatin 4. Electrochemistry
11.3.5: Cisplatin 5. The Role of Platinum Electrodes
11.3.7: Cisplatin 7. Bioinorganic Chemistry
11.3.8: Cisplatin 8. Discovery of Cisplatin
11.3.9: Cisplatin 9. The Discovery - One Scientist's Story
11.3.10: Cisplatin 10. Research as a Career
11.3.11: Cisplatin 11. Cisplatin as an Anticancer Drug
11.3.12: Cisplatin 12. Modes of Action of Cisplatin
11.3.13: Cisplatin 13. Further Studies/Recent Developments
11.3.14: Cisplatin 14. DNA
11.3.15: Cisplatin 15. FDA Drug Approval Process
11.3.16: Cisplatin 16. Profits from Cisplatin
11.3.17: Cisplatin 17. Drug Resistance
11.3.18: Cisplatin 18. Toxicity
11.3.19: Cisplatin 19. Cancer
11.3.20: Cisplatin 20. Other Treatments for Cancer
chemical property
1.2.12: Chemical Properties
Chemotherapy
11.1.10: Chemotherapy- Pt anticancer agents
chiral
10.5: Optical Isomerism in Metal Complexes
cis configuration
1.3.7: Orbital Descriptions of Multiple Bonds
cohesive force
4.2: Properties of Liquids
6.3: Properties of Liquids
coinage metal
1.1.2: Groups of Related Elements
condensation
6.5: Phase Transitions
condensation polymer
1.4.10: Synthetic Macromolecules- Some Applied Organic Chemistry
1.4.12: Condensation Polymers
coordination compound
10.1: Werner's Theory of Coordination Compounds
coordination number
5.4: Lattice Structures in Crystalline Solids
Coulomb
1.1.8: The Electron
covalent bond
1.2.1: Prelude to Chemical Bonding
1.2.13: The Covalent Bond
covalent compound
1.4.2: Covalent Compounds and Intermolecular Forces
covalent network solid
5.3: The Solid State of Matter
covalent radius
1.2.19: Atomic Sizes
crystal lattice
1.2.2: Ionic Bonding
crystalline solid
5.3: The Solid State of Matter
cubic closest packing
5.4: Lattice Structures in Crystalline Solids
Cytochrome c
11.1.7: Cytochrome C
cytochrome c oxidase
11.1.8: Cytochrome Oxidase

D

degree of polymerization
11.5.4.1: Molecular Weight of Polymers
deposition
6.5: Phase Transitions
descriptive chemistry
1.1.1: Prelude to Atomic Structure
diamond
1.4.8: Diamond and Graphite
differential scanning calorimetry
11.5.4.4: Glass Transition
diffraction
5.4: Lattice Structures in Crystalline Solids
dipole
1.3.9: Polarizability
dipole force
1.4.3: Dipole Forces
dipole moment
1.3.9: Polarizability
1.3.9.1: Biology - Polarizability of Biologically Significant Atoms
diradical
1.3.2: Exceptions to the Octet Rule

Dispersion
4.1: Intermolecular Forces
6.2: Intermolecular Forces Review
dispersion forces
1.4.4: London Forces
double bond
1.2.15.3: Multiple Bonds
dynamic equilibrium
6.5: Phase Transitions

E

electrode
1.1.8: The Electron
electron
1.1.8: The Electron
2.3: Atomic Structure and Isotopes
electron affinity
1.2.3: Energy and the Formation of Ions
1.2.8: Electron Affinities
electron deficient
1.3.2: Exceptions to the Octet Rule
electronegativity
1.3.11: Electronegativity
electropositive
1.3.11: Electronegativity
enantiomers
10.5: Optical Isomerism in Metal Complexes
Exceptions to the Octet Rule
1.3.2.1: Biology- Biologically Active Exceptions to the Octet Rule
Exemplar
11.3.1: Cisplatin 1. Study of the Effect of Electric Fields on E. coli
11.3.2: Cisplatin 2. Control Experiments for the Effect of Electric Fields on E. coli
11.3.3: Cisplatin 3. Redox Chemistry
11.3.4: Cisplatin 4. Electrochemistry
11.3.5: Cisplatin 5. The Role of Platinum Electrodes
11.3.6: Cisplatin 6. Transition Metal Chemistry
11.3.7: Cisplatin 7. Bioinorganic Chemistry
11.3.8: Cisplatin 8. Discovery of Cisplatin
11.3.9: Cisplatin 9. The Discovery - One Scientist's Story
11.3.10: Cisplatin 10. Research as a Career
11.3.11: Cisplatin 11. Cisplatin as an Anticancer Drug
11.3.12: Cisplatin 12. Modes of Action of Cisplatin
11.3.13: Cisplatin 13. Further Studies/Recent Developments
11.3.14: Cisplatin 14. DNA
11.3.15: Cisplatin 15. FDA Drug Approval Process
11.3.16: Cisplatin 16. Profits from Cisplatin
11.3.17: Cisplatin 17. Drug Resistance
11.3.18: Cisplatin 18. Toxicity
11.3.19: Cisplatin 19. Cancer
11.3.20: Cisplatin 20. Other Treatments for Cancer

F

family
1.1.3: The Periodic Table
formal charge
1.3.13: Formal Charge and Oxidation Numbers
Formation Constants
10.7: Chelation
free radical
1.3.2: Exceptions to the Octet Rule
freezing
6.5: Phase Transitions
freezing point
6.5: Phase Transitions

G

galvanic cell
9.3: Galvanic Cells
glass transition
11.5.4.4: Glass Transition
graphite
1.4.8: Diamond and Graphite
group
1.1.3: The Periodic Table

H

Halogen
1.1.2: Groups of Related Elements
hexagonal closest packing
5.4: Lattice Structures in Crystalline Solids
hole
5.4: Lattice Structures in Crystalline Solids
Human Serum Albumin
11.1.1: A Molecular Depot- Human Serum Albumin Carries Essential Cu and Zn in Serum
hydrated cation
8.1.7: Conjugate Acid-Base Pairs and pH
hydride
1.4.5: Hydrogen Bonding- Water
hydrochloric acid
8.1.4: Introduction to Strong Acids and Bases
hydrogen bond
1.4.5: Hydrogen Bonding- Water
hydrogen bonding
1.4.6: Ice and Water
4.1: Intermolecular Forces
6.2: Intermolecular Forces Review
hydrolysis
8.1.7: Conjugate Acid-Base Pairs and pH
hydroxide
8.1.4: Introduction to Strong Acids and Bases

I

induced dipole
4.1: Intermolecular Forces
6.2: Intermolecular Forces Review
instantaneous dipole
4.1: Intermolecular Forces
6.2: Intermolecular Forces Review
intermolecular force
4.1: Intermolecular Forces
6.2: Intermolecular Forces Review
interstitial sites
5.3: The Solid State of Matter
ion pair
1.2.2: Ionic Bonding
ionic bond
1.2.1: Prelude to Chemical Bonding
ionic compound
1.2.17: Polyatomic Ions
ionic crystal lattice
1.2.4: The Ionic Crystal Lattice
ionic formula
1.2.18: Ionic Compounds Containing Polyatomic Ions
ionic radius
1.2.20: Ionic Sizes
ionic solid
5.3: The Solid State of Matter
ionization energy
1.2.3: Energy and the Formation of Ions
1.2.8: Electron Affinities
ionize
1.2.3: Energy and the Formation of Ions
irreversible oxidation
11.2.4.8: General Aspects of the Chemistry of Iron
isomorphous
5.4: Lattice Structures in Crystalline Solids
isotope
2.4: Isotopes

L

lactam
11.5.1.2: Cyclic Carboxyloids
linear
1.3.3: The Shapes of Molecules
London force
1.4.4: London Forces
lone pair
1.2.14: Covalent Molecules and the Octet Rule

M

macromolecular substance
1.4.7: Macromolecular Substances
Marcus Theory
11.2.6.8: Marcus Theory
mass number
2.3: Atomic Structure and Isotopes
mass spectrometry
2.7: Measurement of Atomic Weights
melting
6.4: Phase Transitions- Overview
6.5: Phase Transitions
Melting Point
6.5: Phase Transitions
metal
1.2.7: Ionization of Transition and Inner Transition Elements
metallic solid
5.3: The Solid State of Matter
metalloid
1.2.7: Ionization of Transition and Inner Transition Elements
microphase separation
11.5.4.6: Microphase Separation
molecular geometry
1.3.3: The Shapes of Molecules
1.3.5: Multiple Bonds and Molecular Shapes
molecular solid
5.3: The Solid State of Matter
Molecular Weights of Polymers
11.5.4.1: Molecular Weight of Polymers
multiple bond
1.2.16: Examples of Lewis Structures
1.3.5: Multiple Bonds and Molecular Shapes

N

neutron
2.3: Atomic Structure and Isotopes

Newtonian liquids
11.5.4.3: Rheology
noble gas
1.1.2: Groups of Related Elements
normal boiling point
6.5: Phase Transitions
nuclear reaction
2.5: Transmutation and Radioactivity
nuclidic mass
2.4: Isotopes
Nylon 6
11.5.1.2: Cyclic Carboxyloids

O

octahedral
1.3.3: The Shapes of Molecules
octahedral hole
5.4: Lattice Structures in Crystalline Solids
octet
1.2.10: The Octet Rule
octet rule
1.2.1: Prelude to Chemical Bonding
1.2.10: The Octet Rule
1.3.2: Exceptions to the Octet Rule
Optical isomerism
10.5: Optical Isomerism in Metal Complexes
oxidation number
1.3.13: Formal Charge and Oxidation Numbers
oxyacid
8.1.4: Introduction to Strong Acids and Bases

P

partial covalent character
1.3.9: Polarizability
period
1.1.3: The Periodic Table
periodic law
1.1.3: The Periodic Table
periodic table
1.1.3: The Periodic Table
Periodic Trend
1.2.6: Ionization Energies
PET scan
2.5: Transmutation and Radioactivity
Peterson
11.3: Cisplatin - The Invention of an Anticancer Drug
11.3.1: Cisplatin 1. Study of the Effect of Electric Fields on E. coli
11.3.2: Cisplatin 2. Control Experiments for the Effect of Electric Fields on E. coli
11.3.3: Cisplatin 3. Redox Chemistry
11.3.4: Cisplatin 4. Electrochemistry
11.3.5: Cisplatin 5. The Role of Platinum Electrodes
11.3.6: Cisplatin 6. Transition Metal Chemistry
11.3.7: Cisplatin 7. Bioinorganic Chemistry
11.3.8: Cisplatin 8. Discovery of Cisplatin
11.3.9: Cisplatin 9. The Discovery - One Scientist's Story
11.3.10: Cisplatin 10. Research as a Career
11.3.11: Cisplatin 11. Cisplatin as an Anticancer Drug
11.3.12: Cisplatin 12. Modes of Action of Cisplatin
11.3.13: Cisplatin 13. Further Studies/Recent Developments
11.3.14: Cisplatin 14. DNA
11.3.15: Cisplatin 15. FDA Drug Approval Process
11.3.16: Cisplatin 16. Profits from Cisplatin
11.3.17: Cisplatin 17. Drug Resistance
11.3.18: Cisplatin 18. Toxicity
11.3.19: Cisplatin 19. Cancer
11.3.20: Cisplatin 20. Other Treatments for Cancer
pH
8.1.7: Conjugate Acid-Base Pairs and pH
phase transition
6.4: Phase Transitions- Overview
phosphotungstates
11.5.2.4: Cationic Polymerization
physical property
1.2.11: Physical Properties
pi bond
1.3.8: Sigma and Pi Bonds
polar covalent bond
1.3.10: Polar Covalent Bonds
1.3.12: Polarity in Polyatomic Molecules
polar covalent bonds
1.3.9.1: Biology - Polarizability of Biologically Significant Atoms
polarimeter
10.5: Optical Isomerism in Metal Complexes
Polarizability
1.3.9: Polarizability
4.1: Intermolecular Forces
6.2: Intermolecular Forces Review
polarization
1.3.9: Polarizability
polyatomic ion
1.2.17: Polyatomic Ions
polyatomic ions
1.5.1: Polyatomic Ions
polyatomic molecule
1.3.12: Polarity in Polyatomic Molecules
polymer
1.4.10: Synthetic Macromolecules- Some Applied Organic Chemistry
Polyurethane
1.4.13: Cross-Linking
potassium channels
11.1.9: Potassium Channels
proton
2.3: Atomic Structure and Isotopes

Q

quartz
1.4.9: Silicon Dioxide

R

racemic mixture
10.5: Optical Isomerism in Metal Complexes
radical polymerization
11.5.2.9: Radical Polymerization
Radioactive
1.1.7: Radiation
radioactivity
1.1.7: Radiation
redox cycling
11.1.6: Keep Cu Safe- Intracellular Copper Chaperones
redox reaction
1.3.13: Formal Charge and Oxidation Numbers
relative atomic mass
2.6: Average Atomic Weights
Reorganization energy
11.2.6.8: Marcus Theory
resonance hybrid
1.3.14: Resonance
rheology
11.5.4.3: Rheology

S

second ionization energy
1.2.5: Ions and Noble-Gas Electron Configurations
semimetal
1.2.7: Ionization of Transition and Inner Transition Elements
shear thickening
11.5.4.3: Rheology
shear thinning
11.5.4.3: Rheology
sigma bond
1.3.8: Sigma and Pi Bonds
simple cubic structure
5.4: Lattice Structures in Crystalline Solids
simple cubic unit cell
5.4: Lattice Structures in Crystalline Solids
site control
11.5.2.1: Ziegler-Natta Polymerization
skeleton structure
1.2.15: Writing Lewis Structures for Molecules
skeleton stucture
1.2.16: Examples of Lewis Structures
sodium hydroxide
8.1.4: Introduction to Strong Acids and Bases
Solids, Liquids, and Gases
6.4: Phase Transitions- Overview
sp hybrid orbital
1.3.6: Hybrid Orbitals
sp2 hybrid orbital
1.3.6: Hybrid Orbitals
sp3 hybrid orbital
1.3.6: Hybrid Orbitals
sp3d hybrid orbital
1.3.6: Hybrid Orbitals
sp3d2 hybrid orbital
1.3.6: Hybrid Orbitals

space lattice
5.4: Lattice Structures in Crystalline Solids
step growth polymerization
11.5.2.3: Step Growth and Chain Growth
strong acid
8.1.4: Introduction to Strong Acids and Bases
strong base
8.1.4: Introduction to Strong Acids and Bases
subatomic particle
2.3: Atomic Structure and Isotopes
sublimation
6.5: Phase Transitions
sulfuric acid
8.1.4: Introduction to Strong Acids and Bases
Superoxide dismutase
11.1.5: Antioxidant- Cu/Zn Superoxide dismutase (SOD1)
surface tension
4.2: Properties of Liquids
6.3: Properties of Liquids

T

tetrahedral
1.3.3: The Shapes of Molecules
tetrahedral hole
5.4: Lattice Structures in Crystalline Solids
thermoplastic polymers
11.5.1.8: Polymer Topology
thermosetting polymers
11.5.1.8: Polymer Topology
trans configuration
1.3.7: Orbital Descriptions of Multiple Bonds
transmutation
1.1.7: Radiation
2.5: Transmutation and Radioactivity
trigonal bipyramidal
1.3.3: The Shapes of Molecules
trigonal planar
1.3.3: The Shapes of Molecules
trigonal pyramidal
1.3.4: Molecules with Lone Pairs
triple bond
1.2.15.3: Multiple Bonds
Troponin C
11.2.3.15: Troponin C

U

unit cell
5.4: Lattice Structures in Crystalline Solids
unshared pair
1.2.14: Covalent Molecules and the Octet Rule

V

vacancy
5.3: The Solid State of Matter
valence
1.1.4: Valence
van der Waals force
1.4.4: London Forces
4.1: Intermolecular Forces
6.2: Intermolecular Forces Review
van der Waals radius
1.2.19: Atomic Sizes
vapor pressure
6.5: Phase Transitions
vaporization
6.5: Phase Transitions
virial theorem
1.2.13: The Covalent Bond
viscosity
4.2: Properties of Liquids
6.3: Properties of Liquids

Z

zinc
11.2.2.13: Selecting Zinc

Glossary

Sample Word 1 | Sample Definition 1

Detailed Licensing

Overview

Title: CHEM 210D: Modern Applications of Chemistry

Webpages: 450

Applicable Restrictions: Noncommercial

All licenses found:

- CC BY-NC-SA 4.0: 58.4% (263 pages)
- Undeclared: 28.4% (128 pages)
- CC BY-NC 3.0: 8.9% (40 pages)
- CC BY 4.0: 2.7% (12 pages)
- CC BY-NC 4.0: 1.1% (5 pages)
- CC BY-SA 4.0: 0.2% (1 page)
- CC BY-NC-SA 3.0: 0.2% (1 page)

By Page

- CHEM 210D: Modern Applications of Chemistry - *Undeclared*
  - Front Matter - *Undeclared*
    - TitlePage - *Undeclared*
    - InfoPage - *Undeclared*
    - Table of Contents - *Undeclared*
    - Licensing - *Undeclared*
  - 1: AGENDA - *CC BY-SA 4.0*
  - 2: Core Learning Goals - *Undeclared*
    - 2.1: 1. MAT- States of Matter, Interactions, Bonding, and Energy - *Undeclared*
      - Magic Day of Chemistry - *Undeclared*
    - 2.2: 2. SOL- Solutions - *Undeclared*
    - 2.3: 3. AB1- Equilibrium Acids and Bases - *Undeclared*
    - 2.4: 4. AB2- Quantitative Properties of Acid/Base Systems - *Undeclared*
    - 2.5: 5. ECHEM- Electrochemistry and RedOx Reactions - *Undeclared*
    - 2.6: 6. TMC- Transition Metals and their Complexes - *Undeclared*
    - 2.7: 7. APP- Applications in Modern Chemistry - *Undeclared*
  - Textbook- Modern Applications of Chemistry - *Undeclared*
    - Front Matter - *Undeclared*
      - TitlePage - *Undeclared*
      - InfoPage - *Undeclared*
      - Table of Contents - *Undeclared*
      - Licensing - *Undeclared*
    - 1: Primer - *Undeclared*
      - 1.1: The Structure of Atoms - *CC BY-NC-SA 4.0*
        - 1.1.1: Prelude to Atomic Structure - *CC BY-NC-SA 4.0*
        - 1.1.2: Groups of Related Elements - *CC BY-NC-SA 4.0*
        - 1.1.3: The Periodic Table - *CC BY-NC-SA 4.0*
        - 1.1.4: Valence - *CC BY-NC-SA 4.0*
        - 1.1.5: Exceptions to the Periodic Law - *CC BY-NC-SA 4.0*
        - 1.1.6: Implications of Periodicity for Atomic Theory - *CC BY-NC-SA 4.0*
        - 1.1.7: Radiation - *CC BY-NC-SA 4.0*
        - 1.1.8: The Electron - *CC BY-NC-SA 4.0*
        - 1.1.9: The Nucleus - *CC BY-NC-SA 4.0*
      - 1.2: Chemical Bonding - Electron Pairs and Octets - *CC BY-NC-SA 4.0*
        - 1.2.1: Prelude to Chemical Bonding - *CC BY-NC-SA 4.0*
        - 1.2.2: Ionic Bonding - *CC BY-NC-SA 4.0*
        - 1.2.3: Energy and the Formation of Ions - *CC BY-NC-SA 4.0*
        - 1.2.4: The Ionic Crystal Lattice - *CC BY-NC-SA 4.0*
        - 1.2.5: Ions and Noble-Gas Electron Configurations - *CC BY-NC-SA 4.0*
        - 1.2.6: Ionization Energies - *CC BY-NC-SA 4.0*
        - 1.2.7: Ionization of Transition and Inner Transition Elements - *CC BY-NC-SA 4.0*

- 1.2.8: Electron Affinities - *CC BY-NC-SA 4.0*
- 1.2.9: Binary Ionic Compounds and Their Properties - *CC BY-NC-SA 4.0*
- 1.2.10: The Octet Rule - *CC BY-NC-SA 4.0*
- 1.2.11: Physical Properties - *CC BY-NC-SA 4.0*
  - 1.2.11.1: Lecture Demonstrations - *CC BY-NC-SA 4.0*
- 1.2.12: Chemical Properties - *CC BY-NC-SA 4.0*
- 1.2.13: The Covalent Bond - *CC BY-NC-SA 4.0*
- 1.2.14: Covalent Molecules and the Octet Rule - *CC BY-NC-SA 4.0*
- 1.2.15: Writing Lewis Structures for Molecules - *CC BY-NC-SA 4.0*
  - 1.2.15.1: An Excess of Bonds - *CC BY-NC-SA 4.0*
  - 1.2.15.2: Deciding on a Skeleton Structure - *CC BY-NC-SA 4.0*
  - 1.2.15.3: Multiple Bonds - *CC BY-NC-SA 4.0*
- 1.2.16: Examples of Lewis Structures - *CC BY-NC-SA 4.0*
- 1.2.17: Polyatomic Ions - *CC BY-NC-SA 4.0*
- 1.2.18: Ionic Compounds Containing Polyatomic Ions - *CC BY-NC-SA 4.0*
- 1.2.19: Atomic Sizes - *CC BY-NC-SA 4.0*
- 1.2.20: Ionic Sizes - *CC BY-NC-SA 4.0*
- 1.2.21: Periodic Variation of IE and EA - *CC BY-NC-SA 4.0*
  - 1.2.21.1: Lecture Demonstrations - *CC BY-NC-SA 4.0*

- 1.3: Further Aspects of Covalent Bonding - *CC BY-NC-SA 4.0*
  - 1.3.1: Prelude to Covalent Bonding - *CC BY-NC-SA 4.0*
  - 1.3.2: Exceptions to the Octet Rule - *CC BY-NC-SA 4.0*
    - 1.3.2.1: Biology- Biologically Active Exceptions to the Octet Rule - *CC BY-NC-SA 4.0*
  - 1.3.3: The Shapes of Molecules - *CC BY-NC-SA 4.0*
    - 1.3.3.1: Lecture Demonstrations - *CC BY-NC-SA 4.0*
  - 1.3.4: Molecules with Lone Pairs - *CC BY-NC-SA 4.0*
    - 1.3.4.1: Lecture Demonstrations - *CC BY-NC-SA 4.0*
  - 1.3.5: Multiple Bonds and Molecular Shapes - *CC BY-NC-SA 4.0*
  - 1.3.6: Hybrid Orbitals - *CC BY-NC-SA 4.0*
  - 1.3.7: Orbital Descriptions of Multiple Bonds - *CC BY-NC-SA 4.0*
  - 1.3.8: Sigma and Pi Bonds - *CC BY-NC-SA 4.0*
  - 1.3.9: Polarizability - *CC BY-NC-SA 4.0*
    - 1.3.9.1: Biology - Polarizability of Biologically Significant Atoms - *CC BY-NC-SA 4.0*
  - 1.3.10: Polar Covalent Bonds - *CC BY-NC-SA 4.0*
    - 1.3.10.1: Biology- Nonpolar Iodine and Polar Hydrogen Iodide - *CC BY-NC-SA 4.0*
    - 1.3.10.2: Lecture Demonstrations - *CC BY-NC-SA 4.0*
  - 1.3.11: Electronegativity - *CC BY-NC-SA 4.0*
  - 1.3.12: Polarity in Polyatomic Molecules - *CC BY-NC-SA 4.0*
    - 1.3.12.1: Biology- The Hydrophobic Effect and Properties of Small Polyatomic Molecules - *CC BY-NC-SA 4.0*
    - 1.3.12.2: Lecture Demonstrations - *CC BY-NC-SA 4.0*
  - 1.3.13: Formal Charge and Oxidation Numbers - *CC BY-NC-SA 4.0*
  - 1.3.14: Resonance - *CC BY-NC-SA 4.0*
- 1.4: Properties of Organic Compounds - *CC BY-NC-SA 4.0*
  - 1.4.1: Prelude to Organic Compounds - *CC BY-NC-SA 4.0*
  - 1.4.2: Covalent Compounds and Intermolecular Forces - *CC BY-NC-SA 4.0*
  - 1.4.3: Dipole Forces - *CC BY-NC-SA 4.0*
  - 1.4.4: London Forces - *CC BY-NC-SA 4.0*
    - 1.4.4.1: Chapter 8 page 3.jpg - *CC BY-NC-SA 4.0*
    - 1.4.4.2: Atomic Radii - *CC BY-NC-SA 4.0*
    - 1.4.4.3: Atomic sizes on periodic table.jpg - *CC BY-NC-SA 4.0*
    - 1.4.4.4: Ionization Energies - *CC BY-NC-SA 4.0*
      - 1.4.4.4.1: IonizationEnergyAtomicWeight.PNG - *CC BY-NC-SA 4.0*

- 1.4.4.5: Ionization Energies and Electron Affinities - *CC BY-NC-SA 4.0*
  - 1.4.4.5.1: Electron Affinities - *CC BY-NC-SA 4.0*
    - 1.4.4.5.1.1: Ionization Energies and Electron Affinities.jpg - *CC BY-NC-SA 4.0*
- 1.4.4.6: Polarizability on London Forces.jpg - *CC BY-NC-SA 4.0*
- 1.4.5: Hydrogen Bonding- Water - *CC BY-NC-SA 4.0*
  - 1.4.5.1: Atomic Radii and Ionic Radii - *CC BY-NC-SA 4.0*
  - 1.4.5.2: H-Bonding Between 2 HF Molecules.jpg - *CC BY-NC-SA 4.0*
  - 1.4.5.3: Nonmetal hydride bp.jpg - *CC BY-NC-SA 4.0*
- 1.4.6: Ice and Water - *CC BY-NC-SA 4.0*
  - 1.4.6.1: Ice; a hexagonal crystal.jpg - *CC BY-NC-SA 4.0*
  - 1.4.6.2: Boiling Points of Hydrides - *CC BY-NC-SA 4.0*
- 1.4.7: Macromolecular Substances - *CC BY-NC-SA 4.0*
- 1.4.8: Diamond and Graphite - *CC BY-NC-SA 4.0*
- 1.4.9: Silicon Dioxide - *CC BY-NC-SA 4.0*
- 1.4.10: Synthetic Macromolecules- Some Applied Organic Chemistry - *CC BY-NC-SA 4.0*
- 1.4.11: Addition Polymers - *CC BY-NC-SA 4.0*
- 1.4.12: Condensation Polymers - *CC BY-NC-SA 4.0*
- 1.4.13: Cross-Linking - *CC BY-NC-SA 4.0*
- 1.5: Acid and Base Naming - *Undeclared*
  - 1.5.1: Polyatomic Ions - *CC BY-NC 4.0*
  - 1.5.2: Naming Acids - *CC BY-NC 4.0*
  - 1.5.3: Names and Formulas of Bases - *CC BY-NC 4.0*

- 2: Nuclear Chemistry - *Undeclared*
  - 2.1: Components of the Nucleus - *Undeclared*
  - 2.2: The Nuclear Atom - *CC BY-NC-SA 4.0*
  - 2.3: Atomic Structure and Isotopes - *CC BY-NC-SA 4.0*
  - 2.4: Isotopes - *CC BY-NC-SA 4.0*
  - 2.5: Transmutation and Radioactivity - *CC BY-NC-SA 4.0*
  - 2.6: Average Atomic Weights - *CC BY-NC-SA 4.0*
  - 2.7: Measurement of Atomic Weights - *CC BY-NC-SA 4.0*
  - 2.8: Nuclear Reactions - *Undeclared*
  - 2.9: Nuclear Radiation - *Undeclared*
  - 2.10: Rates of Radioactive Decay - *CC BY-NC-SA 4.0*
  - 2.11: Stability of the Atomic Nucleus - *Undeclared*
  - 2.12: The Origin of the Elements - *Undeclared*
  - 2.13: Transmutation of the Elements - *Undeclared*
  - 2.14: Nuclear Fission - *Undeclared*
  - 2.15: Nuclear Fusion - *Undeclared*
  - 2.16: Nuclear Chemistry (Exercises) - *Undeclared*
- 3: Physical Properties of Gases - *Undeclared*
  - 3.1: Properties of Gases - *Undeclared*
  - 3.2: Gas Pressure - *Undeclared*
  - 3.3: Relationships among Pressure, Temperature, Volume, and Amount - *Undeclared*
  - 3.4: The Ideal Gas Law - *Undeclared*
  - 3.5: Gas Volumes and Stoichiometry - *Undeclared*
  - 3.6: Kinetic Molecular Theory of Gases - *Undeclared*
  - 3.7: Connecting Gas Properties to Kinetic Molecular Theory - *Undeclared*
  - 3.8: Chapter Problems - *Undeclared*
- 4: Intermolecular Forces - *Undeclared*
  - 4.1: Intermolecular Forces - *CC BY 4.0*
  - 4.2: Properties of Liquids - *CC BY 4.0*
  - 4.3: Intermolecular Forces and the Solution Process - *Undeclared*
- 5: Solids - *CC BY 4.0*
  - 5.1: Prelude to Liquids and Solids - *CC BY 4.0*
  - 5.2: Carbon and Silicon- Network Atomic Solids - *Undeclared*
  - 5.3: The Solid State of Matter - *CC BY 4.0*
  - 5.4: Lattice Structures in Crystalline Solids - *CC BY 4.0*
  - 5.5: Bonding in Metals and Semiconductors - *Undeclared*
  - 5.6: Liquids and Solids (Exercises) - *CC BY 4.0*
- 6: Phases and Phase Transitions - *Undeclared*
  - 6.1: Prelude to Liquids and Solids - *CC BY 4.0*
  - 6.2: Intermolecular Forces Review - *CC BY 4.0*
  - 6.3: Properties of Liquids - *CC BY 4.0*
  - 6.4: Phase Transitions- Overview - *CC BY-NC-SA 4.0*
  - 6.5: Phase Transitions - *CC BY 4.0*

- 6.6: Vaporization and Vapor Pressure - *CC BY-NC-SA 4.0*
- 6.7: Sublimation and Fusion - *CC BY 4.0*
- 6.8: Heating Curve for Water - *CC BY-NC-SA 4.0*
- 6.9: Phase Diagrams - *CC BY-NC-SA 4.0*
- 6.10: Water - An Extraordinary Substance - *CC BY-NC-SA 4.0*

- 7: Solutions and their Physical Properties - *Undeclared*
  - 7.1: Types of Solutions- Some Terminology - *Undeclared*
  - 7.2: Mixtures of Gases - *Undeclared*
  - 7.3: Solution Concentration - *Undeclared*
  - 7.4: Intermolecular Forces and the Solution Process - *CC BY-NC-SA 3.0*
  - 7.5: Solution Formation and Equilibrium - *CC BY-NC-SA 4.0*
  - 7.6: Solubilities of Gases - *Undeclared*
  - 7.7: Vapor Pressures of Solutions - *Undeclared*
  - 7.8: Osmotic Pressure - *Undeclared*
  - 7.9: Freezing-Point Depression and Boiling-Point Elevation of Nonelectrolyte Solutions - *Undeclared*
  - 7.10: Solutions of Electrolytes - *Undeclared*
  - 7.11: Colloidal Mixtures - *Undeclared*
  - 7.12: Solubility and Complex-Ion Equilibria - *Undeclared*
    - 7.12.1: Solubility Product Constant, Ksp - *Undeclared*
    - 7.12.2: Relationship Between Solubility and Ksp - *Undeclared*
    - 7.12.3: Common-Ion Effect in Solubility Equilibria - *Undeclared*
    - 7.12.4: Limitations of the Ksp Concept - *Undeclared*
    - 7.12.5: Criteria for Precipitation and its Completeness - *Undeclared*
    - 7.12.6: Fractional Precipitation - *Undeclared*
    - 7.12.7: Solubility and pH - *Undeclared*
    - 7.12.8: Equilibria Involving Complex Ions - *Undeclared*
    - 7.12.9: Qualitative Cation Analysis - *Undeclared*

- 8: Acids and Bases - *Undeclared*
  - 8.1: Acids and Bases at Equilibrium - *Undeclared*
    - 8.1.1: Arrhenius Theory- A Brief Review - *Undeclared*
    - 8.1.2: Brønsted-Lowry Theory of Acids and Bases - *Undeclared*
    - 8.1.3: Self-Ionization of Water and the pH Scale - *Undeclared*
    - 8.1.4: Introduction to Strong Acids and Bases - *CC BY-NC-SA 4.0*
    - 8.1.5: Strong Acids and Strong Bases - *Undeclared*
    - 8.1.6: Weak Acids and Weak Bases - *Undeclared*
    - 8.1.7: Conjugate Acid-Base Pairs and pH - *CC BY-NC-SA 4.0*
    - 8.1.8: Polyprotic Acids - *Undeclared*
    - 8.1.9: Ions as Acids and Bases - *Undeclared*
    - 8.1.10: Molecular Structure and Acid-Base Behavior - *Undeclared*
    - 8.1.11: Lewis Acids and Bases - *Undeclared*
    - 8.1.12: Common-Ion Effect in Acid–Base Equilibria - *Undeclared*
  - 8.2: Additional Aspects of Acid-Base Equilibria - *CC BY-NC-SA 4.0*
    - 8.2.1: Buffer Solutions - *CC BY-NC-SA 4.0*
    - 8.2.2: Acid–Base Indicators - *CC BY-NC-SA 4.0*
    - 8.2.3: Neutralization Reactions and Titration Curves - *CC BY-NC-SA 4.0*
    - 8.2.4: Solutions of Salts of Polyprotic Acids - *CC BY-NC-SA 4.0*
    - 8.2.5: Acid–Base Equilibrium Calculations- A Summary - *CC BY-NC-SA 4.0*
    - 8.2.6: Exercises on Acids and Bases II - *CC BY-NC-SA 4.0*
    - 8.2.7: E3. Solubility Constants for Compounds at 25°C Data Table - *CC BY-NC-SA 4.0*
    - 8.2.8: pH Calculations for Acid–Base Titrations - *CC BY-NC-SA 4.0*

- 9: Electrochemistry - *Undeclared*
  - 9.1: Oxidation-Reduction Reactions - *Undeclared*
  - 9.2: Balancing Redox Reactions - *Undeclared*
  - 9.3: Galvanic Cells - *Undeclared*
  - 9.4: Standard Electrode Potentials - *CC BY-NC-SA 4.0*
  - 9.5: Strengths of Oxidants and Reductants - *Undeclared*
  - 9.6: E, ΔG, and K (The Big Triangle of Chemistry) - *Undeclared*
  - 9.7: Cell Potential as a Function of Concentrations - *Undeclared*
  - 9.8: Batteries- Producing Electricity Through Chemical Reactions - *Undeclared*

- 9.9: Corrosion- Unwanted Voltaic Cells - *Undeclared*
- 9.10: Electrolysis- Causing Nonspontaneous Reactions to Occur - *Undeclared*

- 10: Coordination Chemistry - *Undeclared*
  - 10.1: Werner's Theory of Coordination Compounds - *Undeclared*
  - 10.2: Ligands - *Undeclared*
  - 10.3: Nomenclature - *Undeclared*
  - 10.4: Isomerism - *Undeclared*
  - 10.5: Optical Isomerism in Metal Complexes - *Undeclared*
  - 10.6: Stability Aspects of Complex-Ion Equilibria - *Undeclared*
  - 10.7: Chelation - *Undeclared*
  - 10.8: Bonding in Octahedral Complex Ions- Crystal Field Theory - *Undeclared*
  - 10.9: Bonding in Non-Octahedral Complex Ions- Crystal Field Theory - *Undeclared*
  - 10.10: High Spin and Low Spin Complexes - *CC BY-NC-SA 4.0*
  - 10.11: Magnetic Behavior of Atoms, Molecules, and Materials - *Undeclared*
  - 10.12: Magnetic Behavior of Complex Ions - *Undeclared*
  - 10.13: Optical Properties of Coordination Compounds (Color) - *Undeclared*
- 11: Applications in Polymer and Biological Chemistry - *Undeclared*
  - 11.1: Bioinorganic Chemistry - *Undeclared*
    - 11.1.1: A Molecular Depot- Human Serum Albumin Carries Essential Cu and Zn in Serum - *Undeclared*
    - 11.1.2: Iron acquisition in bacteria- Siderophores - *Undeclared*
    - 11.1.3: Fe Wars- Lactoferrin - *Undeclared*
    - 11.1.4: Iron Storage- Ferritin - *Undeclared*
    - 11.1.5: Antioxidant- Cu/Zn Superoxide dismutase (SOD1) - *Undeclared*
    - 11.1.6: Keep Cu Safe- Intracellular Copper Chaperones - *Undeclared*
    - 11.1.7: Cytochrome C - *Undeclared*
    - 11.1.8: Cytochrome Oxidase - *Undeclared*
    - 11.1.9: Potassium Channels - *Undeclared*
    - 11.1.10: Chemotherapy- Pt anticancer agents - *Undeclared*
  - 11.2: Bioinorganic Chemistry (Bertini et al.) - *CC BY-NC-SA 4.0*
    - Front Matter - *CC BY-NC-SA 4.0*
    - Licensing - *Undeclared*
    - Preface - *Undeclared*
  - 11.2.1: Transition-Metal Storage, Transport, and Biomineralization - *CC BY-NC-SA 4.0*
    - 11.2.1.1: Biological Significance of Iron, Zinc, Copper, Molybdenum, Cobalt, Chromium, Vanadium, and Nickel - *CC BY-NC-SA 4.0*
    - 11.2.1.2: Biological Systems of Metal Storage - *CC BY-NC-SA 4.0*
    - 11.2.1.3: Chemical Properties Relative to Storage and Transport - *CC BY-NC-SA 4.0*
    - 11.2.1.4: Iron Biomineralization - *CC BY-NC-SA 4.0*
    - 11.2.1.5: Transport of Iron - *CC BY-NC-SA 4.0*
    - 11.2.1.6: Transport of Zinc, Copper, Vanadium, Chromium, Molybdenum, and Cobalt - *CC BY-NC-SA 4.0*
  - 11.2.2: The Reaction Pathways of Zinc Enzymes and Related Biological Catalysts - *CC BY-NC-SA 4.0*
    - 11.2.2.1: About Carbonic Anhydrase - *CC BY-NC-SA 4.0*
    - 11.2.2.2: Acid-base Equilibria - *CC BY-NC-SA 4.0*
    - 11.2.2.3: Catalytic Mechanism - *CC BY-NC-SA 4.0*
    - 11.2.2.4: Coordinated Water and NMR - *CC BY-NC-SA 4.0*
    - 11.2.2.5: Coordination Geometries - *CC BY-NC-SA 4.0*
    - 11.2.2.6: Ester Hydrolysis and Phosphoryl Transfer - *CC BY-NC-SA 4.0*
    - 11.2.2.7: Group Transfer and Vitamin B-12 - *CC BY-NC-SA 4.0*
    - 11.2.2.8: Metal Substitution - *CC BY-NC-SA 4.0*
    - 11.2.2.9: Model Chemistry - *CC BY-NC-SA 4.0*
    - 11.2.2.10: Nucleophilic Addition of \(OH^{-}\) and \(H^{-}\) - *CC BY-NC-SA 4.0*
    - 11.2.2.11: Peptide Hydrolysis - *CC BY-NC-SA 4.0*
    - 11.2.2.12: pH Dependence of Inhibitor Binding - *CC BY-NC-SA 4.0*
    - 11.2.2.13: Selecting Zinc - *CC BY-NC-SA 4.0*

- 11.2.2.14: Steady-State and Equilibrium Kinetics of Carbonic Anhydrase-Catalyzed \(CO_{2}/HCO_{3}^{-}\) Interconversion - *CC BY-NC-SA 4.0*
- 11.2.2.15: Strategies for the Investigation of Zinc Enzymes - *CC BY-NC-SA 4.0*
- 11.2.2.16: The Natural Catalysts - *CC BY-NC-SA 4.0*
- 11.2.2.17: What Do We Learn? - *CC BY-NC-SA 4.0*

- 11.2.3: Calcium in Biological Systems - *CC BY-NC-SA 4.0*
  - 11.2.3.1: Ca^{2+}-binding Proteins in Microorganisms- The Search for a Prokaryotic Calmodulin - *CC BY-NC-SA 4.0*
  - 11.2.3.2: Basic Facts About Calcium- Its Compounds and Reactions - *CC BY-NC-SA 4.0*
  - 11.2.3.3: Calcium in Mineralized Tissues - *CC BY-NC-SA 4.0*
  - 11.2.3.4: Calmodulin - *CC BY-NC-SA 4.0*
  - 11.2.3.5: Extracellular Calcium Ion-binding Proteins - *CC BY-NC-SA 4.0*
  - 11.2.3.6: Inositol Trisphosphate and the Calcium Ion Messenger System - *CC BY-NC-SA 4.0*
  - 11.2.3.7: Intracellular Calcium Ion Transport - *CC BY-NC-SA 4.0*
  - 11.2.3.8: Measurements of "Free" Calcium Concentrations - *CC BY-NC-SA 4.0*
  - 11.2.3.9: Measurements of Total Calcium Concentrations - *CC BY-NC-SA 4.0*
  - 11.2.3.10: Mitochondrial Calcium Ion Transport - *CC BY-NC-SA 4.0*
  - 11.2.3.11: Molecular Aspects of Calcium Ion-Regulated Intracellular Processes (Part 1) - *CC BY-NC-SA 4.0*
  - 11.2.3.12: Molecular Aspects of Calcium Ion-regulated Intracellular Processes (Part 2) - *CC BY-NC-SA 4.0*
  - 11.2.3.13: Paravalbumin and Calbindins \(D_{9K}\) and \(D_{28K}\) - *CC BY-NC-SA 4.0*
  - 11.2.3.14: The Transport and Regulation of Ca^{2+} Ions in Higher Organisms - *CC BY-NC-SA 4.0*
  - 11.2.3.15: Troponin C - *CC BY-NC-SA 4.0*

- 11.2.4: Biological and Synthetic Dioxygen Carriers - *CC BY-NC-SA 4.0*
  - 11.2.4.1: Biological Dioxygen Transport Systems - *CC BY-NC-SA 4.0*
  - 11.2.4.2: Biological Oxygen Carriers - *CC BY-NC-SA 4.0*
  - 11.2.4.3: Detailed Structures of Hemoglobins and Model Systems - *CC BY-NC-SA 4.0*
  - 11.2.4.4: Dioxygen Carriers and Bioinorganic Chemistry - *CC BY-NC-SA 4.0*
  - 11.2.4.5: General Aspects of the Chemistry of Cobalt - *CC BY-NC-SA 4.0*
  - 11.2.4.6: General Aspects of the Chemistry of Copper - *CC BY-NC-SA 4.0*
  - 11.2.4.7: General Aspects of the Chemistry of Dioxygen - *CC BY-NC-SA 4.0*
  - 11.2.4.8: General Aspects of the Chemistry of Iron - *CC BY-NC-SA 4.0*
  - 11.2.4.9: General Structural Features that Modulate Ligand Activity - *CC BY-NC-SA 4.0*
  - 11.2.4.10: Hazards of Life with Dioxygen - *CC BY-NC-SA 4.0*
  - 11.2.4.11: Nature of the Metal-Dioxygen Linkage in Biological Systems - *CC BY-NC-SA 4.0*
  - 11.2.4.12: Other Ligands for Biological Oxygen Carriers - *CC BY-NC-SA 4.0*
  - 11.2.4.13: Requirements for a Model System for Hemoglobin - *CC BY-NC-SA 4.0*
  - 11.2.4.14: Requirements for Effective Oxygen Carriers - *CC BY-NC-SA 4.0*
  - 11.2.4.15: Role of the Protein in Effecting Biological Oxygen Transport - *CC BY-NC-SA 4.0*
  - 11.2.4.16: Selected Chemistry of Dioxygen, Iron, Copper, and Cobalt - *CC BY-NC-SA 4.0*
  - 11.2.4.17: Stereochemical Changes Upon Ligation - *CC BY-NC-SA 4.0*
  - 11.2.4.18: Structural Basis of Ligand Affinities of Oxygen Carriers - *CC BY-NC-SA 4.0*
  - 11.2.4.19: Structures Relevant to Liganded Hemoglobins - *CC BY-NC-SA 4.0*

- 11.2.4.20: Thermodynamic Factors - *CC BY-NC-SA 4.0*
- 11.2.4.21: Ch. 4 References and Abbreviations - *CC BY-NC-SA 4.0*

- 11.2.5: Dioxygen Reactions - *CC BY-NC-SA 4.0*
  - 11.2.5.1: Catalase and Peroxidase - *CC BY-NC-SA 4.0*
  - 11.2.5.2: Chemistry of Dioxygen - *CC BY-NC-SA 4.0*
  - 11.2.5.3: Copper-zinc Superoxide Dismutase - *CC BY-NC-SA 4.0*
  - 11.2.5.4: Cytochrome c Oxidase - *CC BY-NC-SA 4.0*
  - 11.2.5.5: Dioxygen Toxicity - *CC BY-NC-SA 4.0*
  - 11.2.5.6: Monooxygenases - *CC BY-NC-SA 4.0*
  - 11.2.5.7: Oxygenases - *CC BY-NC-SA 4.0*
- 11.2.6: Electron Transfer - *CC BY-NC-SA 4.0*
  - 11.2.6.1: Biological Redox Components - *CC BY-NC-SA 4.0*
  - 11.2.6.2: Coupling Electron Transfers and Substrate Activation - *CC BY-NC-SA 4.0*
  - 11.2.6.3: Electron-transfer Rates - *CC BY-NC-SA 4.0*
  - 11.2.6.4: Electron-Transfer Theory - *CC BY-NC-SA 4.0*
  - 11.2.6.5: Energy Storage and Release - *CC BY-NC-SA 4.0*
  - 11.2.6.6: Long-range Electron Transfer in Proteins (Part 1) - *CC BY-NC-SA 4.0*
  - 11.2.6.7: Long-range Electron Transfer in Proteins (Part 2) - *CC BY-NC-SA 4.0*
  - 11.2.6.8: Marcus Theory - *CC BY-NC-SA 4.0*
- 11.2.7: Ferrodoxins, Hydrogenases, and Nitrogenases - Metal-Sulfide Proteins - *CC BY-NC-SA 4.0*
  - 11.2.7.1: Iron-sulfur Proteins and Models - *CC BY-NC-SA 4.0*
  - 11.2.7.2: Iron-sulfur Proteins and Models (Part 2) - *CC BY-NC-SA 4.0*
  - 11.2.7.3: Iron-sulfur Proteins and Models (Part 3) - *CC BY-NC-SA 4.0*
  - 11.2.7.4: Iron-sulfur Proteins and Models (Part 4) - *CC BY-NC-SA 4.0*
  - 11.2.7.5: Multisite Redox Enzymes - *CC BY-NC-SA 4.0*
  - 11.2.7.6: Multisite Redox Enzymes (Part 2) - *CC BY-NC-SA 4.0*
  - 11.2.7.7: Multisite Redox Enzymes (Part 3) - *CC BY-NC-SA 4.0*
  - 11.2.7.8: Multisite Redox Enzymes (Part 4) - *CC BY-NC-SA 4.0*
  - 11.2.7.9: Multisite Redox Enzymes (Part 5) - *CC BY-NC-SA 4.0*
  - 11.2.7.10: Multisite Redox Enzymes (Part 6) - *CC BY-NC-SA 4.0*
  - 11.2.7.11: Report on the Nitrogenase Crystal Structure\(\;^{378-381}\) - *CC BY-NC-SA 4.0*
  - 11.2.7.12: Rubredoxin- A Single-Fe Tetrathiolate Protein - *CC BY-NC-SA 4.0*
- 11.2.8: Metal/Nucleic Acid Interactions - *CC BY-NC-SA 4.0*
  - 11.2.8.1: The Basics - *CC BY-NC-SA 4.0*
  - 11.2.8.2: The Basics (Part 2) - *CC BY-NC-SA 4.0*
  - 11.2.8.3: A Case Study- Tris(phenanthroline) Metal Complexes - *CC BY-NC-SA 4.0*
  - 11.2.8.4: Applications of Different Metal Complexes that Bind Nucleic Acids - *CC BY-NC-SA 4.0*
  - 11.2.8.5: Applications of Different Metal Complexes that Bind Nucleic Acids (Part 2) - *CC BY-NC-SA 4.0*
  - 11.2.8.6: Nature's Use of Metal/Nucleic-acid Interactions - *CC BY-NC-SA 4.0*
- 11.2.9: Metals in Medicine - *CC BY-NC-SA 4.0*
  - 11.2.9.1: Metal Deficiency and Disease - *CC BY-NC-SA 4.0*
  - 11.2.9.2: Toxic Effects of Metals - *CC BY-NC-SA 4.0*
  - 11.2.9.3: Aspects of Platinum Binding to DNA - *CC BY-NC-SA 4.0*
  - 11.2.9.4: Survey of Metals Used for Diagnosis and Chemotherapy - *CC BY-NC-SA 4.0*
  - 11.2.9.5: Platinum Anticancer Drugs- A Case Study - *CC BY-NC-SA 4.0*
  - 11.2.9.6: Mapping the Major Adducts of cis- and trans-DDP on DNA; Sequence Specificity - *CC BY-NC-SA 4.0*
  - 11.2.9.7: Structure of Platinum-DNA Complexes - *CC BY-NC-SA 4.0*

- 11.2.9.8: Site-specifically Platinated DNA \ (\;^{154}\) - *CC BY-NC-SA 4.0*
- 11.2.9.9: Bioinorganic Chemistry of Platinum Anticancer Drugs- How Might They Work? - *CC BY-NC-SA 4.0*
- 11.2.9.10: Bioinorganic Chemistry of Platinum Anticancer Drugs; How Might They Work? (Part 2) - *CC BY-NC-SA 4.0*
- 11.2.9.11: Design of New Inorganic Anticancer Drugs - *CC BY-NC-SA 4.0*

- Back Matter - *CC BY-NC-SA 4.0*
  - Detailed Licensing - *Undeclared*

- 11.3: Cisplatin - The Invention of an Anticancer Drug - *CC BY-NC-SA 4.0*
  - 11.3.1: Cisplatin 1. Study of the Effect of Electric Fields on E. coli - *CC BY-NC-SA 4.0*
  - 11.3.2: Cisplatin 2. Control Experiments for the Effect of Electric Fields on E. coli - *CC BY-NC-SA 4.0*
  - 11.3.3: Cisplatin 3. Redox Chemistry - *CC BY-NC-SA 4.0*
  - 11.3.4: Cisplatin 4. Electrochemistry - *CC BY-NC-SA 4.0*
  - 11.3.5: Cisplatin 5. The Role of Platinum Electrodes - *CC BY-NC-SA 4.0*
  - 11.3.6: Cisplatin 6. Transition Metal Chemistry - *CC BY-NC-SA 4.0*
  - 11.3.7: Cisplatin 7. Bioinorganic Chemistry - *CC BY-NC-SA 4.0*
  - 11.3.8: Cisplatin 8. Discovery of Cisplatin - *CC BY-NC-SA 4.0*
  - 11.3.9: Cisplatin 9. The Discovery - One Scientist's Story - *CC BY-NC-SA 4.0*
  - 11.3.10: Cisplatin 10. Research as a Career - *CC BY-NC-SA 4.0*
  - 11.3.11: Cisplatin 11. Cisplatin as an Anticancer Drug - *CC BY-NC-SA 4.0*
  - 11.3.12: Cisplatin 12. Modes of Action of Cisplatin - *CC BY-NC-SA 4.0*
  - 11.3.13: Cisplatin 13. Further Studies/Recent Developments - *CC BY-NC-SA 4.0*
  - 11.3.14: Cisplatin 14. DNA - *CC BY-NC-SA 4.0*
  - 11.3.15: Cisplatin 15. FDA Drug Approval Process - *CC BY-NC-SA 4.0*
  - 11.3.16: Cisplatin 16. Profits from Cisplatin - *CC BY-NC-SA 4.0*
  - 11.3.17: Cisplatin 17. Drug Resistance - *CC BY-NC-SA 4.0*
  - 11.3.18: Cisplatin 18. Toxicity - *CC BY-NC-SA 4.0*
  - 11.3.19: Cisplatin 19. Cancer - *CC BY-NC-SA 4.0*
  - 11.3.20: Cisplatin 20. Other Treatments for Cancer - *CC BY-NC-SA 4.0*
- 11.4: Polymeric Materials and Soft Condensed Matter - *CC BY-NC-SA 4.0*
  - 11.4.1: Polymerization Reactions for Synthetic Polymers - *CC BY-NC-SA 4.0*
  - 11.4.2: Natural Polymers - *CC BY-NC-SA 4.0*
- 11.5: Polymer Chemistry (Schaller) - *CC BY-NC 3.0*
  - Front Matter - *CC BY-NC 4.0*
    - Licensing - *Undeclared*
  - 11.5.1: Monomers and Polymers - *CC BY-NC 3.0*
    - 11.5.1.1: Difunctional Carboxyloids - *CC BY-NC 3.0*
    - 11.5.1.2: Cyclic Carboxyloids - *CC BY-NC 3.0*
    - 11.5.1.3: Olefins - *CC BY-NC 3.0*
    - 11.5.1.4: Cyclic Olefins - *CC BY-NC 3.0*
    - 11.5.1.5: Coordination Polymers - *CC BY-NC 3.0*
    - 11.5.1.6: Supramolecular Assemblies - *CC BY-NC 3.0*
    - 11.5.1.7: Other Polymers - *CC BY-NC 3.0*
    - 11.5.1.8: Polymer Topology - *CC BY-NC 3.0*
    - 11.5.1.E: Solutions for Selected Problems - *CC BY-NC 3.0*
  - 11.5.2: Synthetic Methods in Polymer Chemistry - *CC BY-NC 3.0*
    - 11.5.2.1: Ziegler-Natta Polymerization - *CC BY-NC 3.0*
    - 11.5.2.2: Solutions to Selected Problems - *CC BY-NC 3.0*
    - 11.5.2.3: Step Growth and Chain Growth - *CC BY-NC 3.0*
    - 11.5.2.4: Cationic Polymerization - *CC BY-NC 3.0*
    - 11.5.2.5: Living Cationic Polymerization - *CC BY-NC 3.0*
    - 11.5.2.6: Anionic Polymerization - *CC BY-NC 3.0*
    - 11.5.2.7: Living Anionic Polymerization - *CC BY-NC 3.0*

- 11.5.2.8: Ring-Opening Polymerization - *CC BY-NC 3.0*
- 11.5.2.9: Radical Polymerization - *CC BY-NC 3.0*
- 11.5.2.10: Living Radical Polymerization-RAFT - *CC BY-NC 3.0*
- 11.5.2.11: Living Radical Polymerization-ATRP - *CC BY-NC 3.0*

- 11.5.3: Kinetics and Thermodynamics of Polymerization - *CC BY-NC 3.0*
  - 11.5.3.1: Thermodynamics of Polymerization - *CC BY-NC 3.0*
  - 11.5.3.2: Kinetics of Step-Growth Polymerization - *CC BY-NC 3.0*
  - 11.5.3.3: Kinetics of Chain Polymerization - *CC BY-NC 3.0*
  - 11.5.3.4: Kinetics of Catalytic Polymerization - *CC BY-NC 3.0*
  - 11.5.3.5: Solutions to Selected Problems - *CC BY-NC 3.0*
- 11.5.4: Polymer Properties - *CC BY-NC 3.0*
  - 11.5.4.1: Molecular Weight of Polymers - *CC BY-NC 3.0*
  - 11.5.4.2: Viscosity of Polymers - *CC BY-NC 3.0*
  - 11.5.4.3: Rheology - *CC BY-NC 3.0*
  - 11.5.4.4: Glass Transition - *CC BY-NC 3.0*
  - 11.5.4.5: Crystallinity in Polymers - *CC BY-NC 3.0*
  - 11.5.4.6: Microphase Separation - *CC BY-NC 3.0*
  - 11.5.4.7: Stress-Strain Relationships - *CC BY-NC 3.0*
  - 11.5.4.8: Storage and Loss Modulus - *CC BY-NC 3.0*
  - 11.5.4.9: Modulus, Temperature, Time - *CC BY-NC 3.0*
  - 11.5.4.10: Chapter Solutions - *CC BY-NC 3.0*
- Back Matter - *CC BY-NC 4.0*
  - Detailed Licensing - *Undeclared*

- 11.6: Synthetic Polymers - *CC BY-NC-SA 4.0*
  - 11.6.1: Introduction - *CC BY-NC-SA 4.0*
  - 11.6.2: Chain-Growth Polymers—Addition Polymers - *CC BY-NC-SA 4.0*
  - 11.6.3: Anionic Polymerization of Epoxides - *CC BY-NC-SA 4.0*
  - 11.6.4: Ziegler–Natta Catalysts and Polymer Stereochemistry - *CC BY-NC-SA 4.0*
  - 11.6.5: Natural and Synthetic Rubbers - *CC BY-NC-SA 4.0*
  - 11.6.6: Step-Growth Polymers—Condensation Polymers - *CC BY-NC-SA 4.0*
  - 11.6.7: Polymer Structure and Properties - *CC BY-NC-SA 4.0*
  - 11.6.8: Green Polymer Synthesis - *CC BY-NC-SA 4.0*
  - 11.6.9: Polymer Recycling and Disposal - *CC BY-NC-SA 4.0*
- 12: Reading - *Undeclared*
- Back Matter - *Undeclared*
  - Index - *Undeclared*
  - Glossary - *Undeclared*
  - Detailed Licensing - *Undeclared*

- Back Matter - *Undeclared*
  - Index - *Undeclared*
  - Glossary - *Undeclared*
  - Detailed Licensing - *Undeclared*